TRIGNOMETRIC HIGHER ORDER SHEAR DEFORMABLE TIMOSHENKO BEAM THEORIES & FORMULATIONS

COMPILED BY

Dr. CHELLAPILLA KAMESWARA RAO

V. Z. Vlasov and N. N. Leont'ev

BEAMS, PLATES AND SHELLS ON ELASTIC FOUNDATIONS

CASE FILE
COPY

TTF 357
(N67-14238)

Translated from Russian

Published for the National Aeronautics and Space Administration, U.S.A.
and the National Science Foundation, Washington, D.C.
by the Israel Program for Scientific Translations

V. Z. VLASOV AND U. N. LEONT'EV

BEAMS, PLATES and SHELLS on ELASTIC FOUNDATIONS

(Balki, plity i obolochki na uprugom osnovanii)

Gosudarstvennoe Izdatel'stvo
Fiziko-Matematicheskoi Literatury
Moskva 1960

Translated from Russian

Israel Program for Scientific Translations
Jerusalem 1966

NASA TT F-357
TT 65-50135 Published Pursuant to an Agreement with
THE NATIONAL AERONAUTICS AND SPACE ADMINISTRATION, U.S.A.
and
THE NATIONAL SCIENCE FOUNDATION, WASHINGTON, D.C.

Copyright © 1966
Israel Program for Scientific Translations Ltd
IPST Cat. No. 1453

Translated by A. Barouch, M.Sc.
Edited by Dip. Ing. T. Pelz, M.Sc.

Printed in Jerusalem by S. Monson
Binding: Wiener Bindery Ltd., Jerusalem

Price: $7.00

Available from the
U.S. DEPARTMENT OF COMMERCE
Clearinghouse for Federal Scientific and Technical Information
Springfield, Va. 22151

IX/18/3

TABLE OF CONTENTS

PREFACE vii

Chapter I. APPLICATION OF THE GENERAL VARIATIONAL METHOD TO THE THEORY OF ELASTIC FOUNDATIONS 1

§ 1. Fundamentals of the variational method used in reducing complex two-dimensional problem in the theory of elasticity to one-dimensional problems 1

§ 2. Two-dimensional deformations of elastic foundations. Calculation models 9

§ 3. Plane model of the elastic foundation with two characteristics 13

§ 4. Single-layer foundation with variable elastic properties 22

§ 5. Double-layer elastic foundation 25

§ 6. Three-dimensional deformations of an elastic foundation 30

§ 7. Three-dimensional model of an elastic foundation with two characteristics 34

§ 8. Thermal stresses in an elastic foundation 40

Chapter II. BENDING OF A BEAM ON AN ELASTIC FOUNDATION 47

§ 1. Differential equation of bending of a beam on an elastic foundation with two characteristics 47

§ 2. Solution of the generalized equation of equilibrium by means of particular integrals 50

§ 3. Solution by the method of initial parameters 53

§ 4. Infinitely long beam 59

§ 5. Rigid beam 65

§ 6. Elastic beam of finite length 75

§ 7. Influence of lateral loading 81

§ 8. Beam on an elastic double-layer foundation 89

Chapter III. BENDING OF A RECTANGULAR PLATE ON AN ELASTIC SINGLE-LAYER FOUNDATION 95

§ 1. Statement of the problem. Differential equations of bending of a plate on a single-layer foundation 95

§ 2. Reducing the problem of the bending of a plate on an elastic foundation to ordinary differential equations 98

§ 3. Generalized internal forces. Boundary conditions at lateral plate edges 107

§ 4. Selecting the function of the lateral distribution of the deflections. Boundary conditions at the longitudinal plate edges 109
§ 5. Selecting the functions of the lateral distribution of the deflections by the statical-equilibrium method 116
§ 6. Plated simply supported at opposite ends 117
§ 7. Solving the differential equation of the bending of a plate by the method of initial parameters 119
§ 8. Determination of initial parameters. Calculation of bending moments end shearing forces 123
§ 9. Cylindrical bending and torsion of a narrow plate. Three-dimensional beam analysis 129
§ 10. Approximate analysis of a plate with free edges in the case of symmetrical loading 138
§ 11. Examples 145
§ 12. General case of loading of a plate having free edges 152
§ 13. General equations for thick plates on elastic single-layer foundations 157

Chapter IV. AXISYMMETRICAL DEFORMATION OF CIRCULAR PLATES ON ELASTIC SINGLE-LAYER FOUNDATIONS 161
§ 1. Statement of the problem. Basic differential relationships 161
§ 2. General integral of the differential equation for a circular plate on a single-layer foundation 163
§ 3. Absolutely rigid plate 169
§ 4. Annular punch 173
§ 5. Infinite plate under the action of a concentrated force 175
§ 6. Elastic plate of finite dimensions 178

Chapter V. AXISYMMETRICAL DEFORMATION OF A SHALLOW SPHERICAL SHELL ON A SINGLE-LAYER ELASTIC FOUNDATION 184
§ 1. Basic differential equations of the theory of shallow spherical shells 184
§ 2. Differential equations of a spherical shell on an elastic single-layer foundation 188
§ 3. General solution for axisymmetrical deformations 189
§ 4. Shallow spherical shell subjected to a uniformly distributed load . . 193
§ 5. Shallow spherical shell subjected to a contour load 198
§ 6. Approximate analysis of a shallow spherical shell on an elastic foundation 201
§ 7. Application of the above method to the analysis of the bottom of cylindrical reservoirs 208

Chapter VI. DYNAMICS AND STABILITY OF BEAMS AND PLATES ON ELASTIC FOUNDATIONS 213
§ 1. Differential equation of the vibrations of a beam on an elastic single-layer foundation 213

§ 2. Free vibrations of a beam 215
§ 3. Action of a momentary impulse 222
§ 4. Forced vibrations of a beam 225
§ 5. Dynamical analysis of beams considered as systems with finite numbers of degrees of freedom 227
§ 6. Differential equation of vibrations of a plate resting on an elastic single-layer foundation 232
§ 7. Approximate analysis of an infinite plate in the case of concentrated impact 234
§ 8. Plate with simple supports along the edges 242
§ 9. Vibrations of a plate with free edges 244
§ 10. Buckling of a rectangular plate resting on an elastic single-layer foundation and compressed in one direction 253
§ 11. Buckling of a narrow plate resting on an elastic single-layer foundation 256
§ 12. Buckling of a prestressed plate resting on an elastic foundation . . . 262

Chapter VII. METHOD OF INITIAL FUNCTIONS. APPLICATION OF THE METHOD TO THE THEORY OF THICK PLATES AND TO THE THEORY OF ELASTIC FOUNDATIONS 265
§ 1. General solution of the three-dimensional problem of the theory of elasticity 265
§ 2. Solving the equations of the theory of elasticity by the method of initial functions 267
§ 3. Basic properties of the linear transformation matrices in the method of initial functions 275
§ 4. General method of reducing the three-dimensional problem of the theory of elasticity to a two-dimensional problem 277
§ 5. Thick plate subjected to a load symmetrical with respect to its middle plane 278
§ 6. Thick plate subjected to a load antisymmetrical with respect to the middle plane 281
§ 7. Deformation of an elastic foundation, due to a load applied to its surface 284
§ 8. Contact between a plate and an elastic foundation 286
§ 9. Theory of plates and shells of variable thickness, subjected to arbitrary surface loads 287
§ 10. General solution of the two-dimensional problem of the theory of elasticity 290
§ 11. Bending of a thick plate in the case of plane strain. Approximate solution 294
§ 12. Use of trigonometric series in the solution of the two-dimensional problem 298
§ 13. Exact solution for a rectangular strip with arbitrary boundary at the longitudinal edges and homogeneous boundary conditions at the lateral edges 306

§ 14. Other homogeneous boundary conditions of the mixed type at the lateral strip edges 310
§ 15. Three- and two-dimensional problems of the theory of thick multilayer plates 313
§ 16. Elastic multilayer foundation 322

APPENDIX 325
BIBLIOGRAPHY 347
INDEX 354

FOREWORD

The theory of beams and plates on elastic foundations occupies a prominent place in contemporary structural mechanics. A very large number of studies have been devoted to this subject, and valuable practical methods for the analysis of beams and plates on elastic foundations have been worked out.

However, the existing calculation methods fall short of perfection, and leave unanswered many problems of practical importance. The large majority of these methods are too cumbrous for practical use; in addition, the assumptions made as regards the strains and stresses in natural soil cannot be fully ccepted. Complex three-dimensional structures on elastic foundations cannot be analyzed by existing methods. The hypothesis of a foundation modulus, by which the elastic foundation is considered as a system of separate unconnected springs, thus simplifying considerably the analysis of structures on elastic foundations, leads frequently to incorrect results.

On the other hand, by means of the hypothesis of an elastic isotropic semi-infinite space, we can describe correctly the physical properties of a natural foundation. This, however, leads to cumbrous calculations; as a result, practical solutions have been obtained only for a very restricted range of problems.

Establishing more accurate foundation models, and developing simplified methods for analyzing complex three-dimensional structures, taking into account the elasticity of the soil, are among the problems which the modern theory of structures on elastic foundations has to solve.

It can be expected that higher accuracy will be obtained by making allowance for the elastic-plastic deformation of the soil.

Approximate methods are obviously best suited for analyzing complex three-dimensional engineering structures on elastic foundations, since they lead to relatively simple expressions.

A new theory for analyzing structures on elastic foundations, based on Vlasov's general variational method, is proposed in the book. This theory is more accurate than the well-known theory of Winkler and Zimmermann, but is simpler than the theory of the elastic semi-infinite space.

This theory considers the elastic foundation (and, in general, the non-homogeneous foundation) as a single- or double-layer model whose properties are described by two or more generalized elastic characteristics. This model was proposed in 1949 by Vlasov in his book "Structural Mechanics of Thin-Walled Three-Dimensional Systems." The theory of the single-layer foundation was further developed by Leont'ev /11, 55/, Ruchkin /68/, Kosab'yan /45/, Cheche /81, 82/, etc.

The basic differential equation describing the state of strain of a loaded single-layer foundation has the same form as the solutions obtained by

Filonenko-Borodich /75, 76/ and Wieghardt. The models of Wieghardt and of Filonenko-Borodich are therefore mathematically equivalent to the single-layer model used here. An elastic-foundation model similar to the single-layer model was also considered by Pasternak /62/.

A merit of the theory proposed here is that the solution of many problems of practical importance is reduced to solving ordinary differential equations whose integrals can be found from tables. The simplicity of the mathematical methods and the clearness of the mathematical model make this theory very adaptable; not only the basic problems of beams and plates on elastic foundation, but also various more complex problems can be solved with its aid. These problems include the analysis of shells, taking into account additional transverse loads and the deformation of the underlying foundation, and problems of the dynamics and stability of structures on elastic foundations. The proposed theory can be applied to the determination of the stresses and strains in single- and multilayer strata of horizontal or inclined excavations.

The authors do not claim to have solved completely all problems of practical interest; nor do they consider that the methods proposed by them are universally applicable. Many problems are examined for the first time in this book, and, as a result, have not been worked out to the stage of formulas and tables for ready use. However, the extensive material, collected so far on the analysis of structures on elastic single-layer foundations, makes publication of such a book necessary. The authors hope that the book will be of use both for engineering practice and for further investigations.

The book consists of seven chapters. The first six chapters are devoted to problems of beams, plates, and spherical shells on elastic foundations, and to the dynamics and stability of such structures. Chapters I to III are mainly based on Leont'ev's thesis /55/; Chapters IV and V make use of the results of Ruchkin's studies /68/, kindly placed by him at the disposal of the authors. The last chapter (Chapter VII) describes a new approach to contact problems, based on the method of initial functions /10, 13, 14/, with whose aid complex three-dimensional problems of the theory of elasticity are reduced to two-dimensional problems; several examples illustrating this method are given. The bibliography indicates the main sources which were used by the authors in writing this book. The list given is, of course, incomplete. More complete bibliographies on the subject of structures on elastic foundations are given in /42, 50, and 64/.

This book is intended not only for research engineers, but also for engineers working in design and planning firms. Tables, dimensionless diagrams, and practical examples have been introduced in order to simplify practical calculations. The basic aim of the book is, however, to make available to the engineer an efficient variational method, with whose aid he himself will be able in each case to select a certain scheme of calculations, establish the corresponding model of the elastic foundation, and solve the problem by relatively simple mathematical means.

Chapters I, II, III, IV, V, and VI of this book were written by N.N. Leont'ev, and Chapter VII by V.Z. Vlasov. The editor was V.Z. Vlasov.

The authors acknowledge the help of V.P. Ruchkin, V.V. Vlasov, E.I. Silkin, A.N. Elpat'evskii, and L.V. Kosab'yan in the work on the manuscript, and of V.V. Petrov and D.N. Sobolev in preparing the manuscript for print.

V.Z. Vlasov, N.N. Leont'ev

Chapter I

APPLICATION OF THE GENERAL VARIATIONAL METHOD TO THE THEORY OF ELASTIC FOUNDATIONS

§ 1. FUNDAMENTALS OF THE VARIATIONAL METHOD USED IN REDUCING COMPLEX TWO-DIMENSIONAL PROBLEMS IN THE THEORY OF ELASTICITY TO ONE-DIMENSIONAL PROBLEMS

1

Consider a thin rectangular plate loaded by forces acting in its plane (Figure 1, a). Assume that the plate is deformed without bending, so that its state of stress is determined by normal stresses σ_x, σ_y and shearing stresses τ_{xy}, τ_{yx} only. The stresses σ_x, σ_y, τ_{xy}, τ_{yx} are independent of the coordinate z, it being assumed that the plate thickness δ is very small. In the theory of elasticity this is called a problem of plane stress.

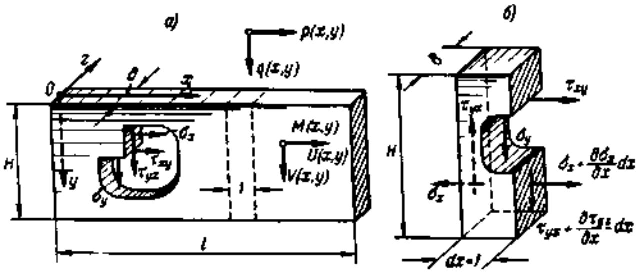

FIGURE 1.

Problems of plane stress are two-dimensional since the displacements, strains, and stresses are functions of the two coordinates x and y only. Two basic methods are available for solving such problems: the method of stresses and the method of displacements. The first method uses as basic unknowns the stresses $\sigma_x(x, y)$, $\sigma_y(x, y)$, $\tau_{xy}(x, y)$, $\tau_{yx}(x, y)$, which are determined from the conditions of continuity of the deformations. This method is similar to the method of forces used widely in the structural mechanics of statically indeterminate strut systems. The second method adopts as basic unknowns the displacements $u(x, y)$, $v(x, y)$, determined from the conditions of equilibrium of the elastic system. This method corresponds to the method of strains in structural mechanics.

We shall use here the method of displacements, adopting as principal unknowns the displacements $u(x, y)$ and $v(x, y)$ of a certain point $M(x, y)$ of the plate. The x-direction will be called longitudinal, and the y-direction, transverse. The displacements $u(x, y)$ and $v(x, y)$ will accordingly be called longitudinal and transverse displacements respectively. These displacements will be considered as positive if they are in the positive direction of the corresponding coordinate axis.

In the two-dimensional case, the stresses and strains are related as follows:

$$\left.\begin{aligned}\sigma_x &= \frac{E}{1-\nu^2}(\varepsilon_{xx} + \nu\varepsilon_{yy}),\\ \sigma_y &= \frac{E}{1-\nu^2}(\varepsilon_{yy} + \nu\varepsilon_{xx}),\\ \tau_{xy} &= \tau_{yx} = \frac{E}{2(1+\nu)}\varepsilon_{xy},\end{aligned}\right\} \qquad (1.1)$$

where E = modulus of elasticity, ν = Poisson's ratio for the material of the plate, $\varepsilon_{xx} = \varepsilon_{xx}(x, y)$ and $\varepsilon_{yy} = \varepsilon_{yy}(x, y)$ = strains in the longitudinal and transverse directions respectively, $\varepsilon_{xy} = \varepsilon_{xy}(x, y)$ = shearing strain.

The strain components ε_{xx}, ε_{yy}, ε_{xy}, are related to the unknown displacements u and v as follows:

$$\varepsilon_{xx} = \frac{\partial u}{\partial x}, \quad \varepsilon_{yy} = \frac{\partial v}{\partial y}, \quad \varepsilon_{xy} = \frac{\partial u}{\partial y} + \frac{\partial v}{\partial x}. \qquad (1.2)$$

The system (1.1) and (1.2) defines the states of stress and strain in the plate; when the displacements u and v are known, the problem can be considered solved.

2

In order to obtain a simple approximate solution, the unknown functions $u(x, y)$ and $v(x, y)$ are expanded in finite series:

$$\left.\begin{aligned}u(x, y) &= \sum_{i=1}^{m} U_i(x)\varphi_i(y) \qquad (i = 1, 2, 3, \ldots, m),\\ v(x, y) &= \sum_{k=1}^{n} V_k(x)\psi_k(y) \qquad (k = 1, 2, 3, \ldots, n).\end{aligned}\right\} \qquad (1.3)$$

The functions $\varphi_i(y)$, $\psi_k(y)$ are assumed to be known, and the functions $U_i(x)$, $V_k(x)$ to be unknown. It is often convenient to introduce dimensionless functions $\varphi_i(y)$, $\psi_k(y)$; the functions $U_i(x)$ and $V_k(x)$ will then have the dimension of length (displacement).

Because of the dimensions and physical meaning of expressions (1.3), the functions $U_i(x)$, $V_k(x)$ can be called generalized displacements. Indeed, each of the m functions $U_i(x)$, calculated for a given section $x = \text{const}$ of the plate, determines in a generalized form the magnitude of the longitudinal displacement $u_i(x, y)$ in this section. Similarly, each of the n functions $V_k(x)$ determines the magnitude of the transverse displacement $v_k(x, y)$ for the entire section $x = \text{const}$. The distributions of the longitudinal and transverse displacements over the sections $x = \text{const}$ are given respectively by the functions $\varphi_i(y)$ and $\psi_k(y)$, which are therefore called functions of the transverse distribution of the displacements.

Provided they are linearly independent and express the physical meaning of the problem, the functions $\varphi_i(y)$ and $\psi_k(y)$ approximating the state of strain in the plate in the transverse direction, can be chosen in different ways. Some examples will make this point clear. Consider the bending of a narrow plate (beam) with free lengthwise ends. Assume that the sections remain plane during bending and that no transverse elongation takes place. The unknown displacements $u(x, y)$ and $v(x, y)$ can be represented in this case in the form:

$$\left.\begin{aligned} u(x, y) &= U_1(x)\varphi_1(y) = U_1(x)\cdot y, \\ v(x, y) &= V_1(x)\psi_1(y) = V_1(x)\cdot 1 \end{aligned}\right\} \tag{1.4}$$

(the coordinate y is measured from the center of the cross section). The functions of the transverse distribution of the displacements are therefore in this case:

$$\varphi_1(y) = y, \quad \psi_1(y) = 1,$$

the remaining functions $\varphi_i(y)$ and $\psi_k(y)$ (i = 2 ... m, k = 2 ... n) are zero.

It follows from (1.4) that the generalized displacement $U_1(x)$ represents the angle of inclination of the section, and the generalized displacement $V_1(x)$, the plate deflection.

A second term can be added to the elementary solution (1.4), known from the theory of the strength of materials, for the bending of a narrow beam acted upon by a load antisymmetrical with respect to the x-axis (Figure 2);

$$\left.\begin{aligned} u(x, y) &= U_1(x)\, y + U_2(x)\sin\frac{2\pi y}{H}, \\ v(x, y) &= V_1(x)\, 1 + V_2(x)\cos\frac{\pi y}{H}. \end{aligned}\right\} \tag{1.5}$$

The following expressions have thus been selected for the functions $\varphi_i(y)$, $\psi_k(y)$:

$$\begin{aligned} \varphi_1(y) &= y, & \varphi_2(y) &= \sin\frac{2\pi y}{H}, \\ \psi_1(y) &= 1, & \psi_2(y) &= \cos\frac{\pi y}{H}. \end{aligned}$$

The first right-hand terms in (1.5) represent the displacements when the sections are assumed to remain plane; the second terms are introduced to correct the inaccuracies due to this assumption and that of zero transverse elongations.

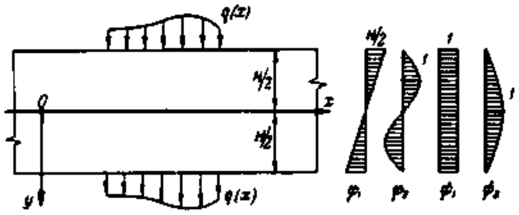

FIGURE 2.

A different procedure can be adopted to find a more accurate solution for a narrow beam. We imagine the beam to be divided into horizontal strips each of which is assumed to remain plane, although this assumption is not valid for the cross section as a whole. As an example, Figure 3 represents a plate with free upper edge and built-in lower edge (immovable both horizontally and vertically). This plate is divided into three parts along its height. It is assumed that the sections of each part remain plane, and that the transverse strains $\varepsilon_y = \frac{\partial v}{\partial y}$ are constant [over each section of the parts]. Equations (1.3) can then be written in the form:

$$\left.\begin{aligned} u(x, y) &= U_1(x)\varphi_1(y) + U_2(x)\varphi_2(y) + U_3(x)\varphi_3(y), \\ v(x, y) &= V_1(x)\psi_1(y) + V_2(x)\psi_2(y) + V_3(x)\psi_3(y). \end{aligned}\right\} \quad (1.6)$$

The functions $\varphi_1(y)$, $\varphi_2(y), \ldots, \psi_2(y)$, $\psi_3(y)$ are represented in Figure 3. It is seen that in the range of variation of y, the functions of the transverse distribution of the displacements satisfy the continuity equations and the geometrical boundary conditions for $y = 0$ and $y = H$. The generalized displacement $U_1(x)$ determines the horizontal displacement on the plate surface, and the generalized displacement $V_1(x)$ equals the deflection of the upper edge of the plate. The remaining generalized displacements determine the displacements of the interior points of the plate along the lines $y = h_1$ and $y = h_2$.

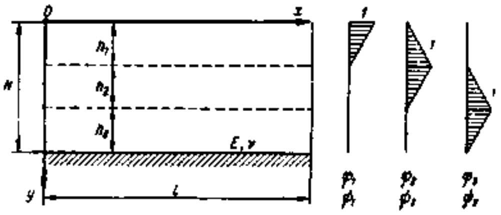

FIGURE 3.

The accuracy of the calculation increases with the number of parts into which the plate is divided (i.e. with the number of terms in (1.3)); the exact solution of the two-dimensional problem is obtained by passing to the limit $n \to \infty$ and $m \to \infty$.

The manner in which, in this example, the functions $\varphi_i(y)$ and $\psi_k(y)$ were chosen for a homogeneous isotropic thin plate may also be applied to a thin plate consisting of several horizontal layers having different elastic coefficients E and ν and thicknesses δ.

Depending on the problem and the accuracy required, the functions $\varphi_i(y)$, and $\psi_k(y)$ can be obtained as linearly independent and continuous functions of the coordinate y by many other methods also.

The representation of the unknown displacements by means of finite series (1.3) is equivalent to reducing the plate to a system having a finite number of degrees of freedom in the transverse direction and an infinite number of degrees of freedom in the longitudinal direction. Such systems can be called discrete-continuous, in contrast to the two-dimensional models of thin plates whose behavior is described by partial differential equations, in which the plates are considered as two-dimensional deformable solids possessing an infinite number of degrees of freedom in both the x- and y-directions.

It also follows from the series expansions (1.3) that the two-dimensional problem of the theory of elasticity has been reduced to a one-dimensional problem, since it suffices to determine m functions $U_i(x)$ and n functions $V_k(x)$ of the same variable in order to obtain the longitudinal and transverse displacements $u(x, y)$ and $v(x, y)$.

3.

The functions $U_i(x)$ and $V_k(x)$ can be obtained from the equilibrium conditions for an elementary strip of length $dx = 1$, delimited by the sections $x = \text{const}$ and $x + dx = \text{const}$ (Figure 1, b). In accordance with Lagrange's principle of virtual displacements, the equilibrium conditions are obtained by equating to zero the total work of all internal and external forces acting on this strip over any virtual displacement.

In accordance with (1.3), the virtual longitudinal displacements of the elementary strip are $\bar{u}_j = \varphi_j(y)$ for $U_j = 1$, where j can have m different values. The virtual transverse displacements of the strip are given in the form $\bar{v}_h = \psi_h(y)$ for $V_h = 1$, the subscript h denoting any of the n virtual displacements. Thus the vertical strip considered possesses $(m + n)$ degrees of freedom in the plane of the plate, m corresponding to longitudinal displacements (parallel to the x-axis), and n to transverse displacements (parallel to the y-axis).

The external forces acting on this strip are caused by the normal stresses σ_x, $\sigma_x + \frac{\partial \sigma_x}{\partial x} dx$, by the shearing stresses τ_{yx}, $\tau_{yx} + \frac{\partial \tau_{yx}}{\partial x} dx$, due to the interaction between the strip and the remainder of the plate, and by the given distributed load whose x and y components [per unit height] are $p(x, y)$ and $q(x, y)$ respectively. The internal forces acting in the strip are caused by the normal stresses σ_y and the shearing stresses τ_{xy}. The work done by all the external and internal forces of the strip over any of the $m + n$ virtual displacements is given by the following expressions:

$$\int \frac{\partial \sigma_x}{\partial x} \varphi_j \, dF - \int \tau_{xy} \varphi_j' \, dF + \int p(x, y) \varphi_j \, dy = 0 \quad (j = 1, 2, 3, \ldots, m), \tag{1.7}$$

$$\int \frac{\partial \tau_{yx}}{\partial x} \psi_h \, dF - \int \sigma_y \psi_h' \, dF + \int q(x, y) \psi_h \, dy = 0 \quad (h = 1, 2, 3, \ldots, n), \tag{1.8}$$

where $dF = \delta dy$ = element of plate cross section, δ = plate thickness.

In each equation (1.7) the total work done by all external and internal forces acting on the elementary strip in the longitudinal direction has been equated to zero. The first term represents the work of the external forces $\frac{\partial \sigma_x}{\partial x} dx dF$. The second term represents the work of the internal shearing forces $\tau_{xy} dF$. By virtue of (1.2) and (1.3), the shearing strains are given by the derivative $\varphi_j'(y)$ when $U_j = 1$. In each equation (1.8) the total work done by all forces acting on the elementary strip in the transverse direction has been equated to zero. As in (1.7), the first term represents the work of the external forces $\frac{\partial \tau_{yx}}{\partial x} dF$; the second term represents the work of the internal normal forces $\sigma_y dF$.

The last terms in equations (1.7) and (1.8) correspond to the virtual work done by the given loads.

The following expressions are obtained by inserting (1.2) and (1.3) into (1.1):

$$\left.\begin{aligned}
\sigma_x &= \frac{E}{1-\nu^2}\Big[\sum_{i=1}^{m} U'_i\varphi_i + \nu\sum_{k=1}^{n} V_k\psi'_k\Big],\\
\sigma_y &= \frac{E}{1-\nu^2}\Big[\sum_{k=1}^{n} V_k\psi'_k + \nu\sum_{i=1}^{m} U'_i\varphi_i\Big],\\
\tau_{xy} = \tau_{yx} &= \frac{E}{2(1+\nu)}\Big[\sum_{i=1}^{m} U_i\varphi'_i + \sum_{k=1}^{n} V'_k\psi_k\Big].
\end{aligned}\right\} \quad (1.9)$$

Substitution of (1.9) in (1.7) and (1.8) leads to a system of ordinary differential equations in $U_i(x)$ and $V_k(x)$; this system consists of m equations corresponding to the m degrees of freedom of the strip in the longitudinal direction, and n equations corresponding to the n degrees of freedom of the strip in the transverse direction. This system can be written down as follows:

$$\left.\begin{aligned}
&\sum_{i=1}^{m} a_{ji}U''_i - \frac{1-\nu}{2}\sum_{i=1}^{m} b_{ji}U_i + \sum_{k=1}^{n}\Big(\nu t_{jk} - \frac{1-\nu}{2}c_{jk}\Big)V'_k + \frac{1-\nu^2}{E}p_j = 0\\
&\qquad\qquad (j = 1, 2, 3, \ldots, m),\\
&-\sum_{i=1}^{m}\Big(\nu t_{hi} - \frac{1-\nu}{2}c_{hi}\Big)U'_i + \frac{1-\nu}{2}\sum_{k=1}^{n} r_{hk}V''_k -\\
&\qquad - \sum_{k=1}^{n} s_{hk}V_k + \frac{1-\nu^2}{E}q_h = 0 \qquad (h = 1, 2, 3, \ldots, n).
\end{aligned}\right\} \quad (1.10)$$

When the functions $\varphi_i(y)$, $\varphi_j(y)$ $(i, j = 1, 2, 3, \ldots, m)$, and $\psi_k(y)$, $\psi_h(y)$, $(k, h = 1, 2, 3, \ldots, n)$ have been chosen, and their derivatives are thus known, the coefficients in (1.10) are obtained from the following equations:

$$\left.\begin{aligned}
a_{ji} = a_{ij} &= \int\varphi_j\varphi_i\,dF, & r_{hk} = r_{kh} &= \int\psi_h\psi_k\,dF,\\
b_{ji} = b_{ij} &= \int\varphi'_j\varphi'_i\,dF, & s_{hk} = s_{kh} &= \int\psi'_h\psi'_k\,dF,\\
c_{jk} &= \int\varphi'_j\psi_k\,dF, & c_{hi} &= \int\psi_h\varphi'_i\,dF,\\
t_{jk} &= \int\varphi_j\psi'_k\,dF, & t_{hk} &= \int\psi'_h\varphi_k\,dF.
\end{aligned}\right\} \quad (1.11)$$

The integrals are taken over the entire width of the strip; in the general case δ can be a function of y.

The expressions (1.11) can be easily obtained from graphs of the functions $\varphi_i(y)$, $\psi_k(y)$, and their first derivatives.

If $p(x, y)$, and $q(x, y)$, are given the free terms $p_j = p_j(x)$ $(j = 1, 2, 3, \ldots, m)$, and $q_h = q_h(x)$ $(h = 1, 2, 3, \ldots, n)$ in (1.10) are obtained from the equations:

$$p_j = \int p(x, y)\varphi_j\,dy, \qquad q_h = \int q(x, y)\psi_h\,dy. \qquad (1.12)$$

The loads $p(x, y)$ and $q(x, y)$ are considered positive when acting in the positive directions of the coordinate axes.

In the general case it is assumed that the loads $p(x, y)$ and $q(x, y)$ are distributed over the plate height as arbitrary functions of y. Expressions (1.12) may also apply to the external load acting at the longitudinal edges of the plate, which in the general case consists of given shearing and normal forces. In accordance with the physical meaning of these expressions (virtual work done by the loads), the concentrated forces must be included. Thus, if shearing and normal forces $p(x, 0)$, $q(x, 0)$ per unit length act at the upper edge of the plate in addition to the loads $p(x, y)$ and $q(x, y)$, we obtain for (1.12):

$$\left.\begin{aligned} p_i &= p(x)\varphi_i(0) + \int p(x, y)\varphi_i(y)\,dy, \\ q_h &= q(x)\psi_h(0) + \int q(x, y)\psi_h(y)\,dy. \end{aligned}\right\} \qquad (1.13)$$

Such integrals, extended both over distributed and concentrated loads, are called Stieltjes integrals.

4

The most efficient modern method of integrating a symmetrical system of ordinary differential equations with constant coefficients is Krylov's method, by which such a system can quickly be reduced to a single equivalent differential equation. In our case, the order of this equation will be $2(m+n)$. Hence, the unknown functions $U_i(x)$, $V_k(x)$ satisfying (1.10) will contain $2(m+n)$ arbitrary integration constants. The number of these constants is equal to the number of independent geometrical conditions to which the end sections $x=0$ and $x=l$ of the plate can be subjected (l = plate length in the longitudinal direction).

The position after deformation of all points of an arbitrary section $x = \text{const}$ is in fact defined by $m+n$ independent magnitudes: m functions $U_i(x)$ determine the positions of these points in the longitudinal direction (displacement from the plane $x = \text{const}$), and n functions $V_k(x)$ determine these positions along the height. Hence, $m+n$ magnitudes can be arbitrarily specified for one end section of the plate. The number of independent conditions for the two end sections $x=0$ and $x=l$ is thus $2(m+n)$, which is equal to the number of arbitrary integration constants. By varying these constants we can obtain a solution for the most varied geometrical boundary conditions in respect to the longitudinal and transverse displacements. Consider a plate with the boundary conditions at $x=0$ and $x=l$ given as stresses or, in the case of a mixed boundary problem, partially as displacements.

When the functions $\varphi_i(y)$ and $\psi_k(y)$ have been selected, the stresses σ_x and τ_{yx} at $x = \text{const}$ can be expressed through $m+n$ independent generalized statical magnitudes. The virtual work done by the normal and shearing forces $\sigma_x dF$ and $\tau_{yx} dF$ over any of the $m+n$ virtual displacements of the points of the section considered is:

$$\left.\begin{aligned} T_j(x) &= \int \sigma_x \varphi_j\,dF \qquad (j = 1, 2, 3, \ldots, m), \\ S_h(x) &= \int \tau_{yx} \psi_h\,dF \qquad (h = 1, 2, 3, \ldots, n), \end{aligned}\right\} \qquad (1.14)$$

where $dF = \delta\,dy$.

The integrals in (1.14) are taken over the entire cross section of the plate. The magnitudes $T_j(x)$ and $S_h(x)$ represent generalized longitudinal and transverse (shearing) forces acting in the section $x = \text{const}$ of the plate. Considering these magnitudes as internal forces, we can express them through the functions $U_i(x)$ and $V_k(x)$. It follows from (1.9), (1.11), and (1.14) that:

$$\left.\begin{aligned} T_j(x) &= E\Big(\sum_{i=1}^{m} a_{ji}U_i' + \nu \sum_{k=1}^{n} t_{jk}V_k\Big) \qquad (i,\ j = 1, 2, 3, \ldots, m),\\ S_h(x) &= G\Big(\sum_{i=1}^{m} c_{hi}U_i + \sum_{k=1}^{n} r_{hk}V_k'\Big) \qquad (h,\ k = 1, 2, 3, \ldots, n). \end{aligned}\right\} \tag{1.15}$$

Using (1.15), it becomes possible to impose $2(m+n)$ generalized boundary conditions expressed as stresses on the plate edges $x = 0$ and $x = l$.

Let a given system of distributed normal force $p^0(x_0, y)$ and distributed shearing forces $q^0(x_0, y)$ act at edge $x = x_0$ (Figure 4).

We imagine an elementary strip dx to be cut from the plate; from the principle of virtual displacements, we obtain the following equilibrium conditions:

$$\left.\begin{aligned} &\int (\sigma_x^0\delta - p^0)\varphi_j\,dy = 0 \qquad (j = 1, 2, 3, \ldots, m),\\ &\int (\tau_{yx}^0\delta - q^0)\psi_h\,dy = 0 \qquad (h = 1, 2, 3, \ldots, n). \end{aligned}\right\} \tag{1.16}$$

Inserting (1.14) into (1.16) yields:

$$S_h^0(x) = \int q^0\psi_h\,dy, \qquad T_j^0(x) = \int p^0\varphi_j\,dy, \tag{1.17}$$

We have thus obtained the relationship between the generalized forces (1.15) and the specified external loads at $x = x_0$.

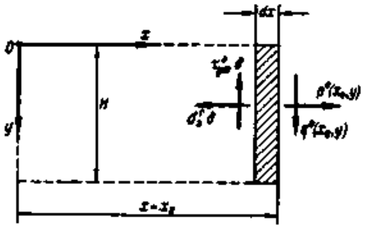

FIGURE 4.

After obtaining the general integral of (1.10), it is possible, with the aid of (1.17) and (1.15), to determine the strains and stresses in the plate for any boundary conditions at $x = 0$ and $x = l$, expressed as stresses, displacements, or both.

§ 2. TWO-DIMENSIONAL DEFORMATIONS OF ELASTIC FOUNDATIONS. CALCULATION MODELS

Consider now the inverse two-dimensional problem. Let the elastic foundation be a compressible layer of thickness H placed on a rigid foundation (Figure 5). The dimensions of this compressible layer in the z-direction are assumed to be large. We also assume that the external load is independent of the z coordinate and acts in planes parallel to the xy plane. The thickness of the elastic foundation, its support conditions, the elastic constants and all the other conditions are constant in the z-direction. In the theory of elasticity this is called plane strain, since the displacements of all points occur in planes perpendicular to the z-axis.

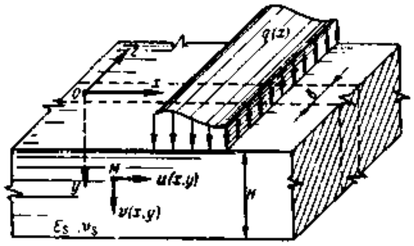

FIGURE 5.

We imagine a narrow plate of thickness δ to be cut from the elastic foundation by two planes parallel to the xy plane (Figure 5). The stresses σ_x, σ_y, τ_{xy}, τ_{yx}, the strain components $\varepsilon_{xx}, \varepsilon_{yy}, \varepsilon_{xy}$, and the displacements u and v of this plate are functions of x and y only, and are, as in plane stress, related by (1.1) and (1.2). In the case of plane strain, the following have to be substituted for E and ν in (1.1):

$$E_0 = \frac{E_S}{1-\nu_S^2}, \quad \nu_0 = \frac{\nu_S}{1-\nu_S}, \tag{2.1}$$

where E_S and ν_S are the modulus of elasticity and Poisson's ratio for the foundation material (soil) respectively.

In order to determine the strains and stresses in the plate by the method of displacements, we express $u(x, y)$ and $v(x, y)$ by expansions (1.3). As in section 1, we obtain the following system of $(m+n)$ ordinary differential equations in $U_i(x)$ and $V_k(x)$ from the conditions of equilibrium of an elementary strip of width $dx = 1$ (Figure 1):

$$\left.\begin{aligned}
&\sum_{i=1}^{m} a_{ji}U_i'' - \frac{1-\nu_0}{2}\sum_{i=1}^{m} b_{ji}U_i + \sum_{k=1}^{n}\left(\nu_0 t_{jk} - \frac{1-\nu_0}{2}c_{jk}\right)V_k' + \\
&\qquad\qquad + \frac{1-\nu_0^2}{E_0}p_j = 0 \qquad (j = 1, 2, 3, \ldots, m), \\
&-\sum_{i=1}^{m}\left(\nu_0 t_{hi} - \frac{1-\nu_0}{2}c_{hi}\right)U_i' + \frac{1-\nu_0}{2}\sum_{k=1}^{n} r_{hk}V_k'' - \sum_{k=1}^{n} s_{hk}V_k + \\
&\qquad\qquad + \frac{1-\nu_0^2}{E_0}q_h = 0 \qquad (h = 1, 2, 3, \ldots, n).
\end{aligned}\right\} \tag{2.2}$$

The system (2.2) differs from (1.10) only by the elastic constants. The coefficients $a_{jl}, b_{jl}, \dots, c_{hl}, t_{hl}$ are again determined from (1.11) and depend only on the functions $\varphi_i(y)$ and $\psi_k(y)$.

As before, the free terms p_i and q_h represent the work done over the displacements $\varphi_i(y)$ and $\psi_h(y)$ respectively, by the given horizontal and vertical distributed loads $p(x, y)$ and $q(x, y)$, and are obtained in the general case from (1.13).

The volume forces distributed over the foundation are usually neglected when the deformation of an elastic foundation is considered; only surface forces (the loads applied to the foundation surface) are taken into consideration. The free terms in (2.2) are in this case:

$$\left.\begin{aligned} p_i &= p(x)\cdot\varphi_i(0), \\ q_h &= q(x)\cdot\psi_h(0), \end{aligned}\right\} \qquad (2.3)$$

where $p(x)$ and $q(x)$ are the shearing and normal surface forces respectively; $\varphi_i(0)$ and $\psi_h(0)$ are the values of the functions $\varphi_i(y)$ and $\psi_h(y)$ at the foundation surface $y = 0$.

After the functions $U_i(x)$ and $V_k(x)$ have been determined from (2.2) and the corresponding boundary conditions, the displacements of the elastic foundation $u(x, y)$ and $v(x, y)$ can be found from (1.3), and the stresses $\sigma_x, \sigma_y, \tau_{xy}$ from (1.9); the elastic constants are given by (2.1).

The system of ordinary differential equations (2.2) thus defines the plane strain of an elastic foundation considered as a linearly deformable medium of finite thickness H. Because of the limited number of terms in expansions (1.3) the solution obtained will be an approximation of the exact solution of the theory of elasticity. At the same time, the system (2.2) can be considered as defining a generalized model of the elastic foundation, based on the general variational method. Different models can be obtained by selecting different expressions for the functions $\varphi_i(y)$ and $\psi_k(y)$. Although only approximations from the point of view of the theory of elasticity, these models are nevertheless sufficiently accurate for practical application. Their accuracy can be increased at will by increasing the number of terms in (1.3).

Increasing the number of terms in (1.3) is, however, undesirable, since an increase in the order of the differential equations (2.2) results. The accuracy of the solution can also be increased by a better selection of the functions $\varphi_i(y)$ and $\psi_k(y)$. Since this selection is based on experimental data or on a more rigorous theoretical analysis, a sufficiently accurate solution can be obtained even with a minimum number of terms in (1.3).

Consider for example an elastic foundation in which the horizontal displacements are either zero or negligible. In this case:

$$\left.\begin{aligned} u(x, y) &= 0, \\ v(x, y) &= \sum_{k=1}^{n} V_k(x)\psi_k(y). \end{aligned}\right\} \qquad (2.4)$$

System (2.2) then becomes:

$$\frac{1-\nu_0}{2}\sum_{k=1}^{n} r_{hk}V_k'' - \sum_{k=1}^{n} s_{hk}V_k + \frac{1-\nu_0^2}{E_0}q_h = 0, \qquad (2.5)$$

where

$$r_{hk} = \int \varphi_h \varphi_k \, dF, \quad s_{hk} = \int \varphi_h' \varphi_k' \, dF.$$

In this model the load may spread due to cohesion: reactions may appear even outside the region of load application. The model described by (2.5) can be represented schematically as a system of elementary elastic columns (springs) mutually interacting as a result of internal friction and adhesion (Figure 6).

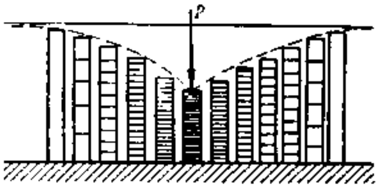

FIGURE 6.

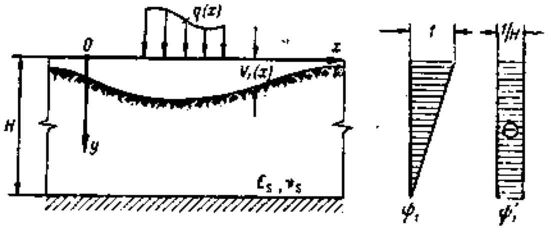

FIGURE 7.

The properties of this model depend on the functions $\varphi_k(y)$ and on the number of terms in (2.4). Since this is a particular case of the generalized model described by (2.2), we can obtain from it even simpler models of the elastic foundation by the introduction of additional hypotheses. Assuming, for example, that the elastic foundation forms a thin compressible layer whose base is fixed, we can write:

$$v(x, y) = V_1(x) \varphi_1(y), \tag{2.6}$$

$$\varphi_1(y) = \frac{H-y}{H}. \tag{2.7}$$

The function $V_1(x)$ thus represents the settling of the foundation surface (Figure 7).

From (2.6) and (2.7) we obtain for (2.5) the single differential equation:

$$\frac{1-\nu_0}{2} r_{11} V_1'' - s_{11} V_1 + \frac{1-\nu_0^2}{E_0} q_1 = 0, \tag{2.8}$$

where

$$\left.\begin{aligned} r_{11} &= \int_0^H \varphi_1^2 dF = \frac{\delta H}{3}, \\ s_{11} &= \int_0^H \varphi_1'^2 dF = \frac{\delta}{H}. \end{aligned}\right\} \tag{2.9}$$

Assuming that the external distributed load $q(x)$ is applied only to the foundation surface, the term q_1 given by (2.3) will be:

$$q_1 = q(x).$$

The model described by (2.8) can be called a model with two characteristics, or simply a single-layer model (/11/).

The stresses in this model are obtained approximately by substituting (2.4), (2.6), and (2.7) in (1.9):

$$\left.\begin{aligned}\sigma_y &= \frac{E_0}{(1-\nu_0^2)} V_1\psi_1' = -\frac{E_0}{(1-\nu_0^2)H} V_1(x),\\ \tau_{yx} = \tau_{xy} &= \frac{E_0}{2(1+\nu_0)} V_1'\psi_1 = \frac{E_0}{2(1+\nu_0)} \frac{H-y}{H} V_1'(x).\end{aligned}\right\} \tag{2.10}$$

The normal stresses σ_y thus remain constant over the height of the foundation, while the shearing stresses τ_{yx} vary linearly.

If the thickness H of the compressible layer is large, the behavior of the elastic foundation will be described only approximately by (2.7) since in this case σ_y cannot be assumed to remain constant over the height. In order to increase the accuracy without increasing the number of terms in (2.6), it is necessary to select for ψ_1 an expression more closely describing the actual decrease of the displacements and stresses with depth. We may, for instance, write (Figure 8)

$$\psi_1 = \frac{\operatorname{sh}\gamma(H-y)}{\operatorname{sh}\gamma H}, \tag{2.11}$$

where γ is a constant determining the rate of decrease of the displacements with depth. In this case the solution is given by (2.8), but the coefficients r_{11} and s_{11} are found from (2.11).

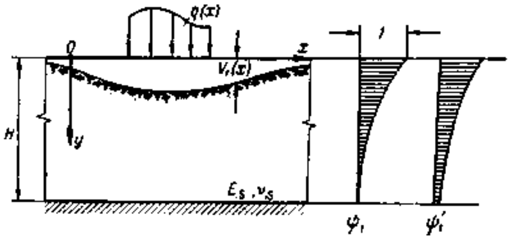

FIGURE 8.

If horizontal displacements in the foundation cannot be neglected, and if the foundation is sufficiently thin and fixed to its base, we can write:

$$u(x, y) = U_1\varphi_1, \quad v(x, y) = V_1\psi_1, \tag{2.12}$$

where

$$\varphi_1 = \frac{H-y}{H}, \quad \psi_1 = \frac{H-y}{H}.$$

System (2.2) then becomes:

$$\left.\begin{aligned}a_{11}U_1' - \frac{1-\nu_0}{2} b_{11}U_1 + \left(\nu_0 t_{11} - \frac{1-\nu_0}{2} c_{11}\right) V_1' + \frac{1-\nu_0^2}{E_0} p_1 = 0,\\ -\left(\nu_0 t_{11} - \frac{1-\nu_0}{2} c_{11}\right) U_1' - \frac{1-\nu_0}{2} r_{11}V_1 - s_{11}V_1 + \frac{1-\nu_0^2}{E_0} q_1 = 0.\end{aligned}\right\} \tag{2.13}$$

The coefficients in (2.13) can be found by inserting (2.12) into (1.11). We can also write:

$$\varphi_1 = \frac{\operatorname{sh}\gamma(H-y)}{\operatorname{sh}\gamma H}, \quad \psi_1 = \frac{\operatorname{sh}\gamma(H-y)}{\operatorname{sh}\gamma H} \tag{2.14}$$

or other suitable expressions.

If the foundation consists of several horizontal layers having different elastic properties, the functions $\varphi_i(y)$, $\psi_k(y)$ can be selected as in section 1 (Figure 3). The modulus of elasticity can then be assumed to vary over the height. This model of the elastic foundation is thus called a multilayer model. A multilayer model can be used for a homogeneous elastic foundation when the thickness H is considerable; the solution obtained is far more accurate than that obtained from the single-layer model described by (2.8) or (2.13).

By selecting the functions $\varphi_i(y)$ and $\psi_k(y)$ differently, we obtain from (2.2) an infinity of different models of the elastic foundation describing with sufficient accuracy the peculiarities of the problem under consideration. Since the selection of the correct model of the elastic foundation is very important in the design of structures resting on such foundations, the advantages of the general variational method are obvious.

Most models obtained by this method are simpler than the model of an elastic semi-infinite plane based on the methods of Zhemochkin and Gorbunov-Posadov. Henceforth only the simplest, i.e., the single-layer model, will be considered. This simple model makes better allowance for the elastic properties of the soil than the well-known model of Winkler and Zimmermann, while permitting the design of beams, plates, and more intricate structures resting on elastic foundations by simple mathematical methods.

§ 3. PLANE MODEL OF THE ELASTIC FOUNDATION WITH TWO CHARACTERISTICS

1. Basic differential relationships

Let the elastic foundation be a compressible layer of thickness H (Figure 9). Assume that the displacements in this layer due to the surface load, are approximately:

$$u(x, y) = 0, \quad v(x, y) = V_1(x)\psi_1(y), \tag{3.1}$$

where $\psi_1(y)$ is a function of y, selected according to the nature of the problem.

According to (1.2) and (3.1) the strain components are as follows:

$$\left.\begin{aligned} \varepsilon_{yy} &= V_1(x)\psi_1'(y), \\ \varepsilon_{xy} &= V_1'(x)\psi_1(y), \\ \varepsilon_{xx} &= 0, \end{aligned}\right\} \tag{3.2}$$

The normal and shearing stresses are obtained from (1.9):

$$\left.\begin{aligned}\sigma_y &= \frac{E_0}{(1-\nu_0^2)} V_1(x)\,\psi_1'(y),\\ \tau_{yx} &= \frac{E_0}{2(1+\nu_0)} V_1'(x)\,\psi_1(y).\end{aligned}\right\} \tag{3.3}$$

The constants E_0 and ν_0 are as follows [cf. (2.1)]:

$$E_0 = \frac{E_s}{1-\nu_s^2}, \quad \nu_0 = \frac{\nu_s}{1-\nu_s}, \tag{3.4}$$

where E_s and ν_s are the modulus of elasticity and Poisson's ratio respectively for the material of the foundation.

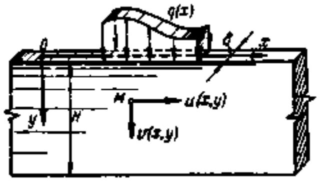

FIGURE 9.

The system (2.2) is in this case reduced to a single equation [cf. (2.8)] containing the only given function of y, $\psi_1(y)$:

$$\frac{1-\nu_0}{2} r_{11} V_1'' - s_{11} V_1 + \frac{1-\nu_0^2}{E_0} q_1 = 0. \tag{3.5}$$

The free term in (3.5) represents the work done by the distributed surface load $q(x)$ and is:

$$q_1(x) = q(x)\,\psi_1(0). \tag{3.6}$$

The coefficients in (3.5) are:

$$\left.\begin{aligned}r_{11} &= \int_0^H \psi_1^2(y)\,dF,\\ s_{11} &= \int_0^H \psi_1'^2(y)\,dF,\end{aligned}\right\} \tag{3.7}$$

where $dF = \delta\,dy$.

After multiplying each term by $\frac{E_0}{1-\nu_0^2}$, (3.5) can be written:

$$2tV_1'' - kV_1 + q_1 = 0, \tag{3.8}$$

where

$$\left.\begin{aligned}k &= \frac{E_0 s_{11}}{1-\nu_0^2}\\ t &= \frac{E_0 r_{11}}{4(1+\nu_0)}.\end{aligned}\right\} \tag{3.9}$$

Differential equation (3.8) relates the vertical displacements of the foundation to the load applied at its surface. It differs from the well-known relationship obtained by assuming a direct proportionality (foundation-modulus hypothesis) by the presence of a term containing the second derivative of the generalized displacement V_1. This term, multiplied by 2t, makes allowance for the shearing stresses in the elastic foundation.

This model of the elastic foundation thus differs basically from the Winkler-Fuss model*. Since allowance is made for the shearing stresses, the load can spread, i.e., displacements occur not only directly beneath the load, but also at other points (Figure 6).

The properties of the elastic foundation satisfying (3.8) are defined by the two integral characteristics (3.9). The characteristic k determines the compressive strain in the elastic foundation; it is thus similar to the foundation modulus. The characteristic t determines the shearing strain in the elastic foundation; it thus defines the load-spreading capacity of the foundation**.

The solution of (3.8) requires the establishment of boundary conditions; these should be given in integral form, either as generalized forces or as generalized displacements.

From (3.1) and (3.3), we obtain:

$$\left.\begin{aligned} T_i &= \int \sigma_x \varphi_i \, dF = 0, \\ S_1 &= \int \tau_{yx} \psi_1 \, dF = \frac{E_0 b}{2(1+\nu_0)} V_1' \int \psi_1^2 \, dy = 2tV_1'. \end{aligned}\right\} \tag{3.10}$$

2. Selecting the function of the transverse distribution of the displacements

The distribution of the displacements and normal stresses over the height H of the elastic foundation, and thus the basic properties of this foundation, are determined by the function $\psi_1(y)$. In the previous section the following function was chosen for a sufficiently thin compressible layer, throughout which the normal stresses σ_y are constant:

$$\psi_1(y) = \frac{H-y}{H}. \tag{3.11}$$

The foundation is assumed to be fixed on its base (Figure 7). The strain in the y direction is constant:

$$\varepsilon_{yy} = -V_1(x)\frac{1}{H};$$

the normal stresses are also constant over the layer height:

$$\sigma_y = -\frac{E_0}{H(1-\nu_0^2)} V_1(x). \tag{3.12}$$

---

* The hypothesis of the foundation modulus, usually called "Winkler hypothesis", was first proposed by the Russian academician Fuss in 1801.

** Pasternak proposed to call the characteristics k and t "the two foundation moduli"; the single-layer model would thus be called "the model with two foundation moduli" /62/. Equation (3.8) is identical with the solution obtained by Filonenko-Borodich for his simplest model of the elastic foundation /76/, and also with Wieghardt's solution.

We then obtain for the coefficients (3.7) [cf. (2.9)]:

$$\left.\begin{aligned} r_{11} &= \int_0^H \varphi_1^2\,dF = \frac{\delta H}{3}, \\ s_{11} &= \int_0^H \varphi_1'^2\,dF = \frac{\delta}{H}, \end{aligned}\right\} \tag{3.13}$$

the constants in (3.9) become:

$$\left.\begin{aligned} k &= \frac{E_0\delta}{H(1-\nu_0^2)}, \\ t &= \frac{E_0\delta H}{12(1+\nu_0)}. \end{aligned}\right\} \tag{3.14}$$

From (3.10) we obtain:

$$S_1 = \frac{E_0\delta H}{6(1+\nu_0)} V_1'(x) = 2tV_1'(x). \tag{3.15}$$

Expressions (3.14) and (3.11) are valid also for elastic foundations of considerable thickness, consisting of several compressible layers having different elastic properties, and in particular for a semi-infinite elastic plane. In this case, H in (3.11) and (3.14) defines the height of an equivalent layer throughout which the normal stresses σ_y are assumed to be constant (Figure 10). This height can be determined by comparing the displacements of the foundation surface, given by (3.8), with the actual displacements.

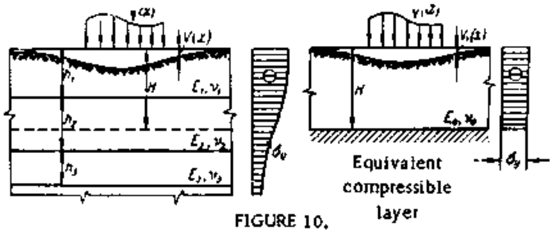

FIGURE 10.

If the concept of equivalent layer is undesirable, we can choose the following expression for $\varphi_1(y)$ when the elastic foundation is deep:

$$\varphi_1(y) = \frac{\operatorname{sh}\gamma(H-y)}{\operatorname{sh}\gamma H}, \tag{3.16}$$

where H is the depth of the subsoil (for a semi-infinite elastic plane $H \to \infty$), and γ is a coefficient depending on the elastic properties of the foundation and determining the rate of decrease of the displacements over the depth of the foundation.

In accordance with (3.16), the normal stresses in the foundation are:

$$\sigma_y = -\frac{E_0\gamma}{(1-\nu_0^2)} V_1(x) \frac{\operatorname{ch}\gamma(H-y)}{\operatorname{sh}\gamma H}. \tag{3.17}$$

and the elastic constants in (3.8) become:

$$k = \frac{E_0\delta}{H(1-\nu_0^2)}\psi_k, \quad t = \frac{E_0\delta H}{12(1+\nu_0)}\psi_t, \tag{3.18}$$

where

$$\left.\begin{aligned} \psi_k &= \frac{\gamma H}{2}\,\frac{\operatorname{sh}\gamma H \operatorname{ch}\gamma H + \gamma H}{\operatorname{sh}^2\gamma H}, \\ \psi_t &= \frac{3}{2}\,\frac{1}{\gamma H}\,\frac{\operatorname{sh}\gamma H \operatorname{ch}\gamma H - \gamma H}{\operatorname{sh}^2\gamma H} \end{aligned}\right\} \tag{3.19}$$

We again obtain:

$$S_1 = \int_0^H \tau_{yx}\psi_1\,dF = 2tV_1''(x), \tag{3.20}$$

where t is given by (3.18).

In this case the normal stresses σ_y are not constant, but vary as the hyperbolic cosine (Figures 8 and 14). The characteristics (3.18) define the elastic properties of the soil more accurately than the characteristics (3.14).

When $H \to \infty$ the characteristics (3.14) tend toward infinitely and zero respectively, while the characteristics (3.18) remain finite. Hence, (3.16) and (3.18) are valid even when the thickness of the elastic layer becomes infinite; expression (3.16) can be used for the approximate calculation of structures on a semi-infinite elastic plane.

Similar results can be obtained when the function $\psi_1(y)$ is an exponential function:

$$\psi_1(y) = e^{-\gamma y}, \tag{3.21}$$

which also adequately describes the decrease of the displacements and stresses over the depth of the elastic foundation.

Depending on the nature of the problem, many analytical expressions in addition to (3.11), (3.16), and (3.21) can be selected, either based on experimental data or on solutions obtained by the methods of the theory of elasticity.

3. Action of a concentrated vertical force.

We shall determine the displacements of an elastic foundation, due to a concentrated force P acting at the origin of coordinates (Figure 11). In this case we obtain from (3.8) the following homogeneous differential equation for the displacements $V_1(x)$:

$$2tV_1'' - k_1V_1 = 0. \tag{3.22}$$

The coefficients are obtained from (3.9) and (3.7).

The general integral of (3.22) is:

$$V_1(x) = C_1e^{-\alpha x} + C_2e^{\alpha x}, \tag{3.23}$$

where

$$\alpha = \sqrt{\frac{k}{2t}}. \tag{3.24}$$

For reasons of symmetry we need consider only the right-hand half of the foundation. One of the integration constants in (3.23) is determined from the condition that the foundation displacement at infinity must be zero:

$$\text{at } x \to \infty \qquad V_1(x) \to 0. \tag{3.25}$$

Hence

$$C_2 = 0.$$

The second integration constant is found from the conditions at $x = 0$.

We can define the generalized shearing force $S_1(x)$ as the work done by all forces acting at the section $x = \text{const}$ over the virtual displacements $\bar{v}_1(x, y) = 1 \cdot \psi_1(y)$ when $V_1(x) = 1$. It has a discontinuity at those sections where concentrated forces act on the elastic-foundation surface (Figure 11).

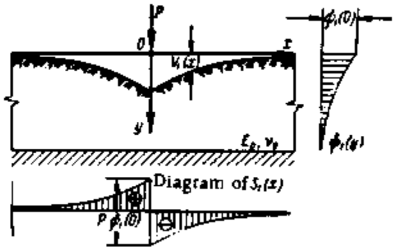

FIGURE 11.

Taking into account the symmetry of the problem we find [from (3.10)] that:

$$\text{at } x = 0 \qquad S_1(0) = -\frac{P}{2}\psi_1(0), \tag{3.26}$$

where $\psi_1(0)$ is the value of $\psi_1(y)$ at the foundation surface.

From (3.10) and (3.26) we obtain:

$$2\alpha t C_1 = \frac{P}{2}\psi_1(0),$$

whence

$$C_1 = \frac{P}{4}\frac{\psi_1(0)}{\alpha t}. \tag{3.27}$$

The displacement of any point of the elastic foundation can now be written:

$$v(x, y) = P\frac{\psi_1(0)}{4\alpha t}e^{-\alpha x}\psi_1(y). \tag{3.28}$$

where

$$\left.\begin{aligned} &\alpha=\sqrt{\frac{k}{2t}}, \quad k=\frac{E_0 s_{11}}{1-\nu_0^2}, \quad t=\frac{E_0 r_{11}}{4(1+\nu_0)},\\ &r_{11}=\delta\int_0^H \varphi_1^2(y)\,dy, \qquad s_{11}=\delta\int_0^H \varphi_1'^2(y)\,dy. \end{aligned}\right\} \tag{3.29}$$

If the linear expression (3.11) is selected for the function of the transverse distribution of the displacements, (3.28) becomes:

$$v(x, y)=\frac{3(1-\nu_0^2)}{\sqrt{6(1-\nu_0)}}\frac{P}{E_0\delta}e^{-\alpha x}\frac{H-y}{H}, \tag{3.30}$$

where

$$\alpha=\sqrt{\frac{k}{2t}}=\frac{1}{H}\frac{\sqrt{6(1-\nu_0)}}{(1-\nu_0)}.$$

As an example, Figure 12 shows the dimensionless displacements $\bar{V}(x)$ of the foundation surface as a function of x/H, obtained from (3.30) for $\nu_0=0$.

The actual displacements of the foundation surface are:

$$V_1(x)=\frac{P}{E_0\delta}\bar{V}(x).$$

It is seen that the displacements decrease rapidly with increasing distance from the point of load application.

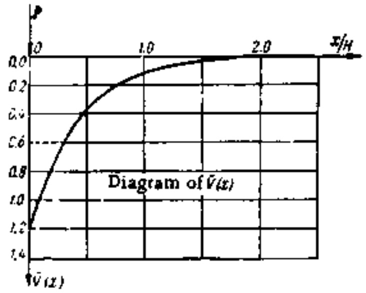

FIGURE 12.

When the function $\varphi_1(y)$ is given by (3.16), expression (3.28) becomes:

$$v(x, y)=\frac{3(1-\nu_0^2)}{\sqrt{6(1-\nu_0)}}\frac{1}{\psi_t\psi_\alpha}\frac{P}{E_0\delta}e^{-\alpha x}\frac{\operatorname{sh}\gamma(H-y)}{\operatorname{sh}\gamma H}, \tag{3.31}$$

where

$$\left.\begin{aligned} &\alpha=\sqrt{\frac{k}{2t}}=\frac{1}{H}\frac{\sqrt{6(1-\nu_0)}}{(1-\nu_0)}\psi_\alpha,\\ &\psi_t=\frac{3}{2}\frac{1}{\gamma H}\frac{\operatorname{sh}\gamma H\operatorname{ch}\gamma H-\gamma H}{\operatorname{sh}^2\gamma H},\\ &\psi_\alpha=\gamma H\sqrt{\frac{1}{3}\frac{\operatorname{sh}\gamma H\operatorname{ch}\gamma H+\gamma H}{\operatorname{sh}\gamma H\operatorname{ch}\gamma H-\gamma H}}. \end{aligned}\right\} \tag{3.32}$$

[cf. (3.18), (3.19)]

We can write (3.31) in the form:

$$v(x, y) = \frac{P}{E_0 \delta} \bar{V}(x) \psi_1(y), \tag{3.33}$$

and plot diagrams of the dimensionless displacement

$$\bar{V}(x) = \frac{3(1-\nu_0^2)}{\sqrt{6(1-\nu_0)}} \frac{1}{\psi_1 \psi_\alpha} e^{-\alpha x} \tag{3.34}$$

for different values of the parameter $\bar{\gamma} = \gamma H$. Such curves are drawn in Figure 13 for $\bar{\gamma} = 1$, $\bar{\gamma} = 2$, $\bar{\gamma} = 1$ (for $\nu_0 = 0$). Figure 14 shows the function $\varphi_1(y)$, plotted for the same values of $\bar{\gamma}$, and also the distribution of the normal stresses σ_y over the foundation height, obtained from (3.17).

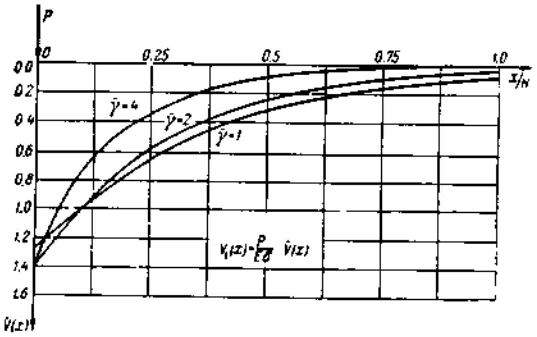

FIGURE 13.

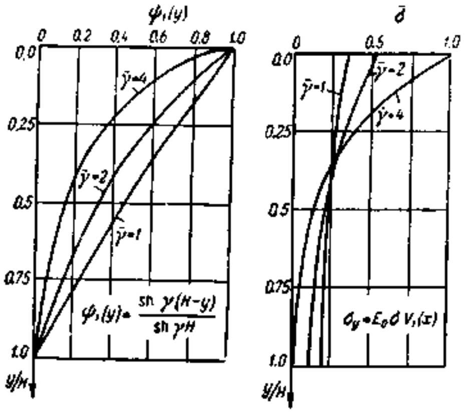

FIGURE 14.

It is seen that an increase in the parameter $\bar{\gamma}$ causes the displacements and normal stresses to decrease more rapidly with increasing depth.

The normal-stress diagrams also show that the proposed model of the elastic foundation is to a certain degree artificial: it gives finite (nonzero) values for the normal stresses at points on the foundation surface which carry no load. This is a result of employing the variational method, which applies the equilibrium conditions in integral form without providing for their fulfilment at every single point of the system.

Since the subject of this book is the analysis of structures on elastic foundations, and not the stresses in the elastic foundation itself, these shortcomings may be ignored.

4. Case of a distributed load

The displacements of an elastic foundation, due to a load $q(x)$ distributed over its surface are best obtained from (3.28), which for $y=0$ determines the displacements of the elastic foundation, due to a concentrated force P. If we put $P=1$, the curve of displacements becomes an influence line and can be used to determine the displacements of any point of the surface at any load.

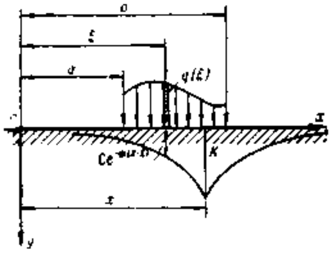

FIGURE 15.

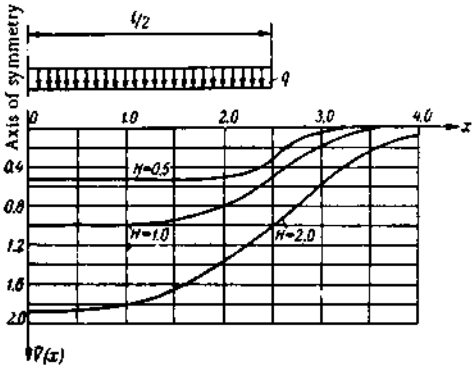

FIGURE 16.

If the applied load $q(\xi)$ is a known function of the distance ξ from the coordinate origin, we obtain for the foundation displacements at point K (Figure 15) [whose coordinates are $(x, 0)$]:
at $a \leqslant x \leqslant b$

$$V_1(x) = C_1\left[\int_a^x q(\xi)\, e^{-\alpha(x-\xi)}\, d\xi + \int_x^b q(\xi)\, e^{\alpha(x-\xi)}\, d\xi\right]; \tag{3.35}$$

at $x > b$

$$V_1(x) = C_1\int_a^b q(\xi)\, e^{-\alpha(x-\xi)}\, d\xi; \tag{3.36}$$

at $x < a$

$$V_1(x) = C_1\int_a^b q(\xi)\, e^{\alpha(x-\xi)}\, d\xi. \tag{3.37}$$

where

$$C_1 = \frac{\psi_1(0)}{4\alpha t}. \qquad (3.38)$$

In the particular case of a uniformly distributed load q, (3.35) becomes: at $a < x < b$

$$V_1(x) = \frac{qC_1}{\alpha}[2 - e^{-\alpha(x-a)} - e^{\alpha(x-b)}]. \qquad (3.39)$$

We assume that the displacement decreases linearly with increasing depth:

$$\psi_1 = \frac{H-y}{H},$$

the constant C_1 is then found from (3.14):

$$C_1 = \frac{3(1+\nu_0)}{\alpha E t H},$$

and (3.39) becomes:

$$V_1(x) = \frac{q}{2k}[2 - e^{-\alpha(x-a)} - e^{\alpha(x-b)}], \qquad (3.40)$$

where

$$k = \frac{Et}{H(1-\nu_0^2)}.$$

Figure 16 shows the dimensionless displacements $\bar{V}(x)$ obtained from (3.40) for several values of H (for $\nu_0 = 0$). The actual displacements are:

$$V_1(x) = \frac{q}{E_0 t}\bar{V}(x).$$

It is seen that with decreasing H the behavior of the foundation approaches that of the Winkler model. With increasing H the displacement curve becomes smoother, and the absolute values of the displacements increase.

§ 4. SINGLE-LAYER FOUNDATION WITH VARIABLE ELASTIC PROPERTIES

1

The determination of the strains and stresses of an elastic foundation subjected to a load becomes considerably more difficult when the elastic properties of the foundation vary.

Consider an elastic foundation whose thickness H varies linearly in the x-direction (Figure 17).

We shall express the displacement of a point $M(x, y)$ of the foundation as before:

$$u(x, y) = 0, \quad v(x, y) = V_1(x)\psi_1(x, y). \qquad (4.1)$$

It will be assumed that the function $\psi_1(x, y)$ varies linearly:

$$\psi_1(x, y) = \frac{H-y}{H}, \tag{4.2}$$

where

$$H = H_0 - \theta_0 x, \tag{4.3}$$

and $\theta_0 = \operatorname{tg} \beta_0$ (Figure 17).

The condition of equilibrium of an elementary strip of width $dx = 1$, cut from the foundation, is derived from (1.7), (1.8), [(1.9)], (4.1), (4.2), and (4.3). We obtain:

$$\frac{1-\nu_0}{6}\delta H(x) V'' - \frac{1-\nu_0}{6}\delta\theta_0 V' - \frac{\delta}{H(x)}\left[1 + \frac{\theta_0^2(1-\nu_0)}{6}\right]V + \frac{1-\nu_0^2}{E_0}q = 0. \tag{4.4}$$

According to (4.1), the generalized shearing force is:

$$S = \int_0^H \tau_{yx}\psi_1 \, dF. \left(V_1(x) = 1\right) \tag{4.5}$$

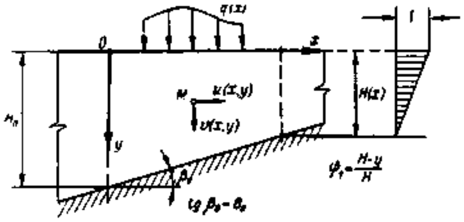

FIGURE 17.

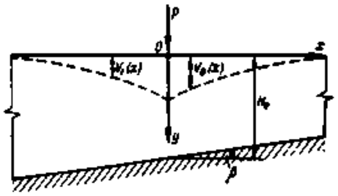

FIGURE 18.

Inserting (4.1) and (4.2) into the last expression of (1.1) yields:

$$\tau_{yx} = \frac{E_0}{2(1+\nu_0)}\frac{\partial v}{\partial x} = \frac{E_0}{2(1+\nu_0)}\left[V_1'\frac{H-y}{H} - \frac{\theta_0 y}{H^2}V_1\right], \tag{4.6}$$

where $H = H_0 - \theta_0 x$.

Substituting (4.6) and (4.2) in (4.5) and integrating, we find:

$$S_1 = \frac{E_0\delta}{12(1+\nu_0)}[2H(x)V_1' - \theta_0 V_1]. \tag{4.7}$$

2

Consider the particular case of a concentrated force P acting on the surface of the elastic foundation at the origin of coordinates (Figure 18). The following homogeneous differential equation is obtained:

$$\frac{1-\nu_0}{6}H(x)V_1'' - \frac{1-\nu_0}{6}\theta_0 V_1' - \frac{1}{H(x)}\left[1 + \frac{\theta_0^2(1-\nu_0)}{6}\right]V_1 = 0. \tag{4.8}$$

This is an Eulerian differential equation and can be written in the following form after cancellation and multiplying each term by $\frac{6H(x)}{1-\nu_0}$:

$$H^2(x)V_1'' + nH(x)V_1' + mV_1 = 0, \tag{4.9}$$

where

$$n = -\theta_0, \; m = -\left(\theta_0^2 + \frac{6}{1-\nu_0}\right).$$

Substituting $V = H^{\lambda}$ in (4.9) we obtain an equation with constant coefficients

$$V_1'' + (n-1)V_1' + mV_1 = 0. \tag{4.10}$$

The roots of the auxiliary equation

$$\lambda^2 + (n-1)\lambda + m = 0$$

are

$$\lambda_{1,2} = -\frac{n-1}{2} \pm \sqrt{\frac{(n-1)^2}{4} - m}. \tag{4.11}$$

Since m must be negative, both roots (4.11) are real:

$$\lambda_1 = -r_1, \quad \lambda_2 = r_2. \tag{4.12}$$

The general integral of (4.8) is:

$$V_1 = C_1(H_0 - \theta_0 x)^{-r_1} + C_2(H_0 - \theta_0 x)^{r_2}. \tag{4.13}$$

Since the displacements of the foundation [at $x = \frac{H_0}{\theta_0}$ and] at infinity are zero, the constant C_2 must be zero for $x < 0$ while the constant C_1 must be zero for $x > 0$. Hence:

$$V_I = C_1(H_0 - \theta_0 x)^{-r_1}, \qquad V_{II} = C_2(H_0 - \theta_0 x)^{r_2}, \tag{4.14}$$

where V_I and V_{II} are the displacements of the surface of the elastic foundation to the left and to the right, respectively, of the point where the force acts (Figure 18).

To determine the constants of integration, we note that:

at $x = 0$

$$V_I = V_{II}, \quad S_I - S_{II} = P, \tag{4.15}$$

where S_I and S_{II} are the generalized shearing forces to the left and right, respectively, of $x = 0$.

Substituting (4.14) in (4.7) yields:

$$S_I = \frac{-E_0\delta(2r_1+1)\theta_0}{12(1+\nu_0)H^{r_1}}C_1, \qquad S_{II} = \frac{E_0\delta(2r_2-1)H^{r_2}\theta_0}{12(1+\nu_0)}C_2. \tag{4.16}$$

By inserting (4.14) and (4.16) into (4.15) we obtain the integration constants:

$$C_1 = -\frac{6(1+\nu_0)H_0^{r_1}}{E_0\delta\theta_0(r_1+r_2)}P, \quad C_2 = -\frac{6(1+\nu_0)H_0^{-r_2}}{E_0\delta\theta_0(r_1+r_2)}P. \tag{4.17}$$

Lastly, by inserting (4.2), (4.14), and (4.17) into (4.1) we find the vertical displacement of any point of the elastic foundation:

at $x < 0$

$$-v(x, y) = \frac{6(1+\nu_0)H_0^{r_1}}{E_0\delta\theta_0(r_1+r_2)} PH^{-r_1}(x)\frac{H(x)-y}{H(x)};$$

at $x > 0$

$$-v(x, y) = \frac{6(1+\nu_0)H_0^{-r_2}}{E_0\delta\theta_0(r_1+r_2)} PH^{r_2}(x)\frac{H(x)-y}{H(x)},$$

where r_1 and r_2 are determined by (4.11).

§ 5. DOUBLE-LAYER ELASTIC FOUNDATION

1

Consider an elastic foundation of thickness $H = h_1 + h_2$, undergoing plane deformations (Figure 19). The two layers have different moduli of elasticity and Poisson ratios.

In accordance with (1.3), the displacements of a point of the elastic foundation are given by the following expressions:

$$\left.\begin{aligned} &u(x, y) = 0,\\ &v(x, y) = V_1(x)\psi_1(y) + V_2(x)\psi_2(y),\end{aligned}\right\} \tag{5.1}$$

where $\psi_1(y)$ and $\psi_2(y)$ are the functions of the transverse distribution of the displacements, and $V_1(x)$, $V_2(x)$ are the generalized vertical displacements.

The functions $\psi_1(y)$, $\psi_2(y)$ are chosen according to the nature of the problem. In particular, expressions (3.11), (3.16), or (3.21) can be used.

If the upper layer is thin and the lower layer thick, we can write (Figure 20):

$$\left.\begin{aligned} &\text{at } 0 \leqslant y \leqslant h_1 \qquad \psi_1 = \frac{h_1 - y}{h_1}, \quad \psi_2 = \frac{y}{h_1};\\ &\text{at } h_1 \leqslant y \leqslant H \qquad \psi_1 = 0, \qquad \psi_2 = \frac{\operatorname{sh}\gamma(H-y)}{\operatorname{sh}\gamma h_2},\end{aligned}\right\} \tag{5.2}$$

where γ is a coefficient determining the rate of decrease of the displacements with depth.

In this case, the generalized displacements $V_1(x)$ and $V_2(x)$ define the vertical displacements respectively of the surface of the elastic foundation and of the boundary between the two layers.

From (2.2), (5.1), and (5.2) we obtain the following two differential equations for the determination of the functions $V_1(x)$ and $V_2(x)$:

$$\left.\begin{aligned} &\frac{1-\nu_1}{2}(r_{11}V_1'' + r_{12}V_2'') - (s_{11}V_1 + s_{12}V_2) + \frac{1-\nu_1^2}{E_1}q = 0,\\ &\frac{E_1}{2(1+\nu_1)}r_{12}V_1'' + \left[\frac{E_1}{2(1+\nu_1)}r_{22} + \frac{E_2}{2(1+\nu_2)}r_{22}'\right]V_2'' - \frac{E_1}{1-\nu_1^2}s_{12}V_1 -\\ &\qquad - \left[\frac{E_1}{1-\nu_1^2}s_{22} + \frac{E_2}{1-\nu_2^2}s_{22}'\right]V_2 = 0,\end{aligned}\right| \tag{5.3}$$

where

$$\left.\begin{aligned} r_{11}&=\int_0^{h_1}\psi_1^2\,dF=\frac{\delta h_1}{3}, & s_{11}&=\int_0^{h_1}\psi_1'^2\,dF=\frac{\delta}{h_1},\\ r_{12}&=\int_0^{h_1}\psi_1\psi_2\,dF=\frac{\delta h_1}{6}, & s_{12}&=\int_0^{h_1}\psi_1'\psi_2'\,dF=-\frac{\delta}{h_1},\\ r_{22}&=\int_0^{h_1}\psi_2^2\,dF=\frac{\delta h_1}{3}, & s_{22}&=\int_0^{h_1}\psi_2'^2\,dF=\frac{\delta}{h_1},\\ r_{22}&=\int_{h_1}^{H}\psi_2^2\,dF=\frac{\delta h_2}{3}\psi_t, & s_{22}'&=\int_{h_1}^{H}\psi_2'^2\,dF=\frac{\delta}{h_2}\psi_k. \end{aligned}\right\} \tag{5.4}$$

The elastic constants E_1. E_2, ν_1 and ν_2, entering in (5.3) define the properties of the elastic foundation in plane strain. For a soil block, these are:

$$\left.\begin{aligned} E_1&=\frac{E_{1.s}}{1-\nu_{1.s}^2}, & \nu_1&=\frac{\nu_{1.s}}{1-\nu_{1.s}},\\ E_2&=\frac{E_{2.s}}{1-\nu_{2.s}^2}, & \nu_2&=\frac{\nu_{2.s}}{1-\nu_{2.s}}, \end{aligned}\right\} \tag{5.5}$$

where $E_{1.s}, E_{2.s}, \nu_{1.s}, \nu_{2.s}$, are the moduli of elasticity and Poisson ratios of the first and second layers respectively.

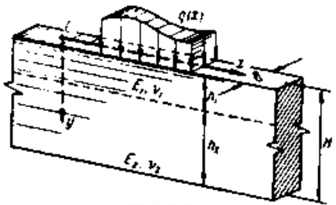

FIGURE 19.

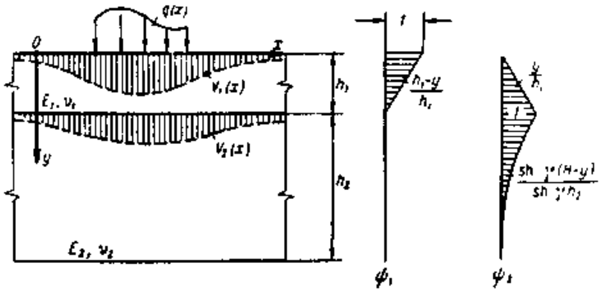

FIGURE 20.

Substituting (5.4) in (5.3), we obtain:

$$\left.\begin{aligned} 2t_1V_1''-k_1V_1+t_1V_2''+k_1V_2+q=0,\\ t_1V_1''+k_1V_1+2(t_1+t_2)V_2''-(k_1+k_2)V_2=0, \end{aligned}\right\} \tag{5.6}$$

where

$$k_1=\frac{E_1\delta}{h_1(1-\nu_1^2)}, \qquad t_1=\frac{E_1h_1\delta}{12(1+\nu_1)}. \tag{5.7}$$

$$k_2=\frac{E_2\delta}{h_2(1-\nu_2^2)}\psi_k, \qquad t_2=\frac{E_2h_2\delta}{12(1+\nu_2)}\psi_t. \tag{5.8}$$

and ψ_k and ψ_t are known from (3.19).

The coefficients k_1 and k_2 determine the compressive strains of the upper and lower layers respectively, while the coefficients t_1 and t_2 define their shearing strains.

In order to solve system (5.6), we introduce a function $F(x)$. The displacements $V_1(x)$ and $V_2(x)$ are then expressed through $F(x)$ and its derivatives in such a way that when these expressions are inserted into the second equation (5.6), the latter becomes an identity. The expressions which satisfy this condition are:

$$\left.\begin{aligned} V_1(x) &= (k_1 + k_2)\,F(x) - 2\,(t_1 + t_2)\,F''(x), \\ V_2(x) &= k_1 F(x) + t_1 F''(x). \end{aligned}\right\} \qquad (5.9)$$

Substituting these expressions in the first equation of (5.6) yields:

$$t_1\,(3t_1 + 4t_2)\,F^{IV} - 2\,(3t_1k_1 + t_1k_2 + t_2k_1)\,F'' + k_1k_2F = q\,(x). \qquad (5.10)$$

Differential equation (5.10) defines the stresses and strains in a double-layer elastic foundation. In order to solve specific problems it is necessary to add to this equation the relevant boundary conditions which are given in a generalized form in this method. We therefore introduce generalized internal forces corresponding to the generalized displacements $V_1(x)$ and $V_2(x)$. Since an elementary transverse strip cut from the foundation possesses two degrees of freedom in its plane, it follows from (1.14) that:

$$\left.\begin{aligned} S_1 &= \int_0^H \tau_{yx}\psi_1\,dF, \\ S_2 &= \int_0^H \tau_{yx}\psi_2\,dF, \end{aligned}\right\} \qquad (5.11)$$

where $dF = \delta\,dy$.

By (5.1) and (5.2) the shearing stresses τ_{yx} are:

at $0 \leqslant y \leqslant h_1$

$$\tau_{yx} = \frac{E_1}{2\,(1 + \nu_1)}\left(V_1'\,\frac{h_1 - y}{h_1} + V_2'\,\frac{y}{h_1}\right);$$

at $h_1 \leqslant y \leqslant H$

$$\tau_{yx} = \frac{E_2}{2\,(1 + \nu_2)}\,V_2'\,\frac{\operatorname{sh}\gamma\,(H - y)}{\operatorname{sh}\gamma h_2}. \qquad (5.12)$$

Substituting (5.12) in (5.11) and integrating over the entire height of the elastic foundation, we obtain:

$$\left.\begin{aligned} S_1 &= t_1\,(2V_1' + V_2'), \\ S_2 &= t_1V_1' + 2\,(t_1 + t_2)\,V_2'. \end{aligned}\right\} \qquad (5.13)$$

Using (5.9), S_1 and S_2 can be expressed through $F(x)$:

$$\left.\begin{aligned} S_1 &= t_1\,[-(3t_1 + 4t_2)\,F''' + (3k_1 + 2k_2)\,F'], \\ S_2 &= (3t_1k_1 + t_1k_2 + 2t_2k_1)\,F'. \end{aligned}\right\} \qquad (5.14)$$

2

The double-layer model can be called a foundation with four elastic characteristics. It permits a higher accuracy than the single-layer model characterized by only two independent parameters k and t (cf. section 3)

Different schemes of the elastic foundation can be obtained according to the selection of the parameters k_1, k_2, t_1, and t_2. Only one such scheme will be considered.

It is seen from (5.7) that when both h_1 and E_1 decrease, t_1 tends toward zero while k_1 remains finite. If we assume that a thin compressible soil layer near the surface of the elastic foundation has a modulus of elasticity considerably smaller than the lower layers, we can write for the first layer

$$t_1 = 0, \quad k_1 = K, \tag{5.15}$$

where K is a coefficient analogous to the foundation modulus and depends on the properties of the elastic foundation near the surface.

The double-layer foundation thus consists of an upper layer subject only to compressive stresses, ($t_1 = 0$), similar in this sense to the Winkler foundation, while the lower layer is subject to both compressive and shearing stresses.

Substituting (5.15) in (5.9), (5.13), and (5.14) yields:

$$V_1 = (K + k_2) F - 2t_2 F'', \qquad V_2 = KF; \tag{5.16}$$

$$S_1 = 0, \qquad S_2 = S = 2t_2 V_2' = 2Kt_2 F'. \tag{5.17}$$

Inserting (5.15) into (5.10) yields:

$$-2t_2 F'' + k_2 F = \frac{q(x)}{K}. \tag{5.18}$$

Unlike (5.10), (5.18) can be applied to a double-layer foundation with upper Winkler layer. The term "double-layer foundation" will henceforth be applied only to this particular case of a double-layer model.

3

Let a concentrated force P act on the elastic foundation at the origin of coordinates (Figure 21). The following homogeneous differential equation is then obtained for the determination of $F(x)$:

$$-2t_2 F'' + k_2 F = 0. \tag{5.19}$$

Equation (5.19) is identical with (3.22). The following solution is obtained by analogy with (3.31):

$$F(x) = \frac{3(1-\nu_2^2)}{\sqrt{6(1-\nu_2)}} \frac{1}{\psi_t \psi_\alpha} \frac{P}{E_2 \delta K} e^{-\alpha_2 x}, \tag{5.20}$$

where

$$\alpha_2 = \sqrt{\frac{k_2}{2t_2}} = \frac{1}{h_2} \frac{\sqrt{6(1-\nu_2)}}{1-\nu_2} \phi_\alpha, \tag{5.21}$$

while ϕ_t and ϕ_α are given by (3.32).

Substitution of (5.20) in the second equation (5.16) yields:

$$V_2 = \frac{3(1-\nu_2^2)}{\sqrt{6(1-\nu_2)}} \frac{1}{\psi_t \psi_\alpha} \frac{P}{E_2 \delta} e^{-\alpha_2 x}. \tag{5.22}$$

which is identical with (3.31). By substituting (5.20) in the first equation (5.16) it is seen that, except at the point where the force acts:

$$V_1 = V_2$$

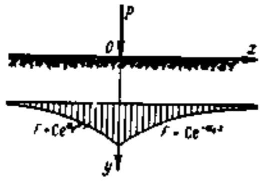

FIGURE 21.

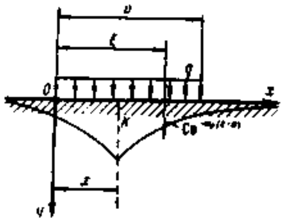

FIGURE 22.

4

When a uniformly distributed load q acts on a double-layer foundation (Figure 22), it is easiest to obtain the solution by using function (5.20), which for $P = 1$ represents an influence line.

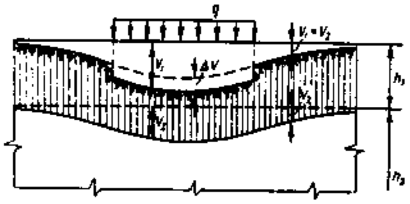

FIGURE 23.

By analogy with (3.36) and (3.40) we find:

at $0 \leqslant x \leqslant b$
$$F = \frac{q}{2Kk_2}\left[2 - e^{-\alpha_0 x} - e^{\alpha_0(x-b)}\right];$$

at $x > b$
$$F = \frac{q}{2Kk_2}\left[e^{-\alpha_0(x-b)} - e^{-\alpha_0 x}\right]. \qquad (5.23)$$

Substituting (5.23) in (5.16) yields:

at $0 \leqslant x \leqslant b$
$$\left.\begin{aligned} V_1 &= \frac{q(K+k_2)}{Kk_2} - \frac{q}{2k_2}\left(e^{-\alpha_0 x} + e^{\alpha_0(x-b)}\right), \\ V_2 &= \frac{q}{k_2} - \frac{q}{2k_2}\left(e^{-\alpha_0 x} + e^{\alpha_0(x-b)}\right); \end{aligned}\right\} \qquad (5.24)$$

at $x > b$
$$V_1 = V_2 = \frac{q}{2k_2}\left(e^{\alpha_0(x-b)} - e^{-\alpha_0 x}\right). \qquad (5.25)$$

It is seen from (5.24) and (5.25) that the surface layer exhibits no strains outside the zone of load application (this corresponds to the postulation of the foundation modulus), since here $V_1 = V_2$. Within the zone of load application, we have:

$$\Delta V = V_1 - V_2 = \frac{q}{K}. \tag{5.26}$$

The function V_2 is everywhere continuous, while V_1 has a discontinuity at the borders of the zone of load application (Figure 23).

§ 6. THREE-DIMENSIONAL DEFORMATIONS OF AN ELASTIC FOUNDATION

Consider now a three-dimensional elastic foundation of thickness H placed above an incompressible layer (Figure 24). Let an external load, whose $x, y\ z$ components are respectively $p(x, y, z)$, $g(x, y, z)$, and $q(x, y, z)$, act on this foundation. As in the two-dimensional problem, we shall use the method of displacements to determine the stresses and strains in the elastic foundation. The unknowns will be the displacements $u(x, y, z)$, $v(x, y, z)$, $w(x, y, z)$ of a point $M(x, y, z)$ of the foundation. The displacements will be considered positive when their directions coincide with the positive directions of the corresponding coordinate axes.

By analogy with the two-dimensional problem, the unknown displacements u, v, w are represented by the following expansions:

$$\left.\begin{aligned} u(x, y, z) &= \sum_{i=1}^{m} u_i(x, y)\varphi_i(z) \qquad (i = 1, 2, 3, \ldots, m),\\ v(x, y, z) &= \sum_{g=1}^{l} v_g(x, y)\chi_g(z) \qquad (g = 1, 2, 3, \ldots, l),\\ w(x, y, z) &= \sum_{k=1}^{n} w_k(x, y)\psi_k(z) \qquad (k = 1, 2, 3, \ldots, n). \end{aligned}\right\} \tag{6.1}$$

The functions $\varphi_i(z)$, $\chi_g(z)$, $\psi_k(z)$ in (6.1) determine the variation with height of the horizontal and vertical displacements. They are assumed to be known dimensionless, linearly independent functions. The functions $u_i(x, y)$, $v_g(x, y)$, $w_k(x, y)$, which have the dimensions of length, are the unknowns. In accordance with their physical meaning, they will be called generalized displacements.

The normal and shearing stresses in the elastic foundation are in the three-dimensional case:

$$\left.\begin{aligned} \sigma_x &= \frac{E_0}{1-\nu_0^2}\left[\frac{\partial u}{\partial x} + \nu_0\left(\frac{\partial v}{\partial y} + \frac{\partial w}{\partial z}\right)\right],\\ \sigma_y &= \frac{E_0}{1-\nu_0^2}\left[\frac{\partial v}{\partial y} + \nu_0\left(\frac{\partial w}{\partial z} + \frac{\partial u}{\partial x}\right)\right],\\ \sigma_z &= \frac{E_0}{1-\nu_0^2}\left[\frac{\partial w}{\partial z} + \nu_0\left(\frac{\partial u}{\partial x} + \frac{\partial v}{\partial y}\right)\right],\\ \tau_{zy} = \tau_{yz} &= \frac{E_0}{2(1+\nu_0)}\left[\frac{\partial w}{\partial y} + \frac{\partial v}{\partial z}\right],\\ \tau_{zx} = \tau_{xz} &= \frac{E_0}{2(1+\nu_0)}\left[\frac{\partial u}{\partial z} + \frac{\partial w}{\partial x}\right],\\ \tau_{xy} = \tau_{yx} &= \frac{E_0}{2(1+\nu_0)}\left[\frac{\partial v}{\partial x} + \frac{\partial u}{\partial y}\right]. \end{aligned}\right\} \tag{6.2}$$

where

$$E_0 = \frac{E_s}{1-\nu_s^2}, \qquad \nu_0 = \frac{\nu_s}{1-\nu_s}, \tag{6.3}$$

E_s and ν_s are respectively modulus of elasticity and Poisson's ratio for the elastic foundation.

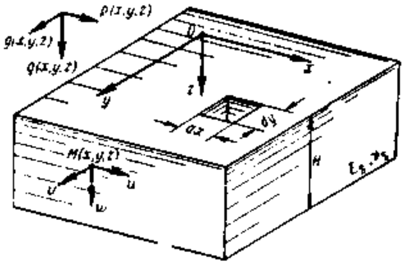

FIGURE 24.

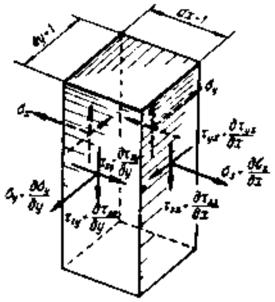

dy=1
dx=1
σ_y
σ_x
$\tau_{yz}+\frac{\partial\tau_{yz}}{\partial x}$
$\sigma_x+\frac{\partial\sigma_x}{\partial x}$
$\sigma_y+\frac{\partial\sigma_y}{\partial y}$
$\tau_{xy}+\frac{\partial\tau_{xy}}{\partial y}$
$\tau_{xz}+\frac{\partial\tau_{xz}}{\partial x}$

FIGURE 25.

Substitution of (6.1) in (6.2) gives the following expressions for the stresses as functions of the generalized displacements:

$$\left.\begin{aligned}
\sigma_x &= \frac{E_0}{1-\nu_0^2}\left[\sum_{i=1}^{m}\frac{\partial u_i}{\partial x}\varphi_i + \nu_0\left(\sum_{g=1}^{l}\frac{\partial v_g}{\partial y}\varkappa_g + \sum_{k=1}^{n} w_k\psi_k'\right)\right],\\
\sigma_y &= \frac{E_0}{1-\nu_0^2}\left[\sum_{g=1}^{l}\frac{\partial v_g}{\partial y}\varkappa_g + \nu_0\left(\sum_{k=1}^{n} w_k\psi_k' + \sum_{i=1}^{m}\frac{\partial u_i}{\partial x}\varphi_i\right)\right],\\
\sigma_z &= \frac{E_0}{1-\nu_0^2}\left[\sum_{k=1}^{n} w_k\psi_k + \nu_0\left(\sum_{i=1}^{m}\frac{\partial u_i}{\partial x}\varphi_i + \sum_{g=1}^{l}\frac{\partial v_g}{\partial y}\varkappa_g\right)\right],
\end{aligned}\right\} \tag{6.4}$$

$$\left.\begin{aligned}
\tau_{zy} = \tau_{yz} &= \frac{E_0}{2(1+\nu_0)}\left[\sum_{k=1}^{n}\frac{\partial w_k}{\partial y}\psi_k + \sum_{g=1}^{l} v_g\varkappa_g'\right],\\
\tau_{zx} = \tau_{xz} &= \frac{E_0}{2(1+\nu_0)}\left[\sum_{i=1}^{m} u_i\varphi_i' + \sum_{k=1}^{n}\frac{\partial w_k}{\partial x}\psi_k\right],\\
\tau_{xy} = \tau_{yx} &= \frac{E_0}{2(1+\nu_0)}\left[\sum_{g=1}^{l}\frac{\partial v_g}{\partial x}\varkappa_g + \sum_{i=1}^{m}\frac{\partial u_i}{\partial y}\varphi_i\right].
\end{aligned}\right\} \tag{6.5}$$

In order to determine the functions $u_i(x, y)$, $v_g(x, y)$, $w_k(x, y)$, we cut from the foundation an elementary column of height H and sides $dx = 1$, $dy = 1$, (Figures 24 and 25). This column possesses $(m+l+n)$ degrees of freedom in the three directions. The generalized equilibrium conditions of the elementary column (considered as virtual displacements) can therefore be written in the form:

$$\left.\begin{aligned}
&\int \frac{\partial \sigma_x}{\partial x}\varphi_j\,dz-\int \tau_{xz}\varphi_j'\,dz+\int \frac{\partial \tau_{xy}}{\partial y}\varphi_j\,dz+\int p\varphi_j\,dz=0\\
&\qquad (j=1,\ 2,\ 3,\ \ldots,\ m),\\
&\int \frac{\partial \sigma_y}{\partial y}\varkappa_f\,dz-\int \tau_{yz}\varkappa_f'\,dz+\int \frac{\partial \tau_{yx}}{\partial x}\varkappa_f\,dz+\int q\varkappa_f\,dz=0\\
&\qquad (f=1,\ 2,\ 3,\ \ldots,\ l),\\
&\int \frac{\partial \tau_{zx}}{\partial x}\psi_h\,dz-\int \sigma_z\psi_h'\,dz+\int \frac{\partial \tau_{zy}}{\partial y}\psi_h\,dz+\int q\psi_h\,dz=0\\
&\qquad (h=1,\ 2,\ 3,\ \ldots,\ n).
\end{aligned}\right\} \tag{6.6}$$

[cf. (1.7), (1.8)]

Each equation (6.6) states that the total work done by all external and internal forces acting on the elementary column over the corresponding virtual displacement equals zero:

$$\bar{u}_j(x,\ y,\ z)=\varphi_j(z),$$
$$\bar{v}_f(x,\ y,\ z)=\varkappa_f(z),$$
$$\bar{w}_h(x,\ y,\ z)=\psi_h(z)$$

for

$$u_j(x,\ y)=1,$$
$$v_f(x,\ y)=1,\quad w_h(x,\ y)=1.$$

The terms behind the minus sign correspond to the work of the internal forces. The other terms represent the work done by the forces external relative to the column.

Substitution of (6.4) and (6.5) in (6.6) yields the following system of partial differential equations for the functions $u_i(x,\ y)$, $v_g(x,\ y)$, $w_k(x,\ y)$:

$$\left.\begin{aligned}
&\sum_{i=1}^{m} a_{ji}\left(\frac{\partial^2 u_i}{\partial x^2}+\frac{1-\nu_0}{2}\frac{\partial^2 u_i}{\partial y^2}\right)-\frac{1-\nu_0}{2}\sum_{i=1}^{m} b_{ji}u_i+\\
&+\frac{1+\nu_0}{2}\sum_{g=1}^{l} t_{jg}\frac{\partial^2 v_g}{\partial x\,\partial y}+\sum_{k=1}^{n}\left(\nu_0 d_{jk}-\frac{1-\nu_0}{2}c_{jk}\right)\frac{\partial w_k}{\partial x}+\frac{1-\nu_0^2}{E_0}p_j=0\\
&\qquad (j=1,\ 2,\ 3,\ \ldots,\ m),\\
&\sum_{g=1}^{l} m_{fg}\left(\frac{\partial^2 v_g}{\partial y^2}+\frac{1-\nu_0}{2}\frac{\partial^2 v_g}{\partial x^2}\right)-\frac{1-\nu_0}{2}\sum_{g=1}^{l} n_{fg}v_g+\\
&+\frac{1+\nu_0}{2}\sum_{i=1}^{m} t_{fi}\frac{\partial^2 u_i}{\partial x\,\partial y}+\sum_{k=1}^{n}\left(\nu_0 l_{fk}-\frac{1-\nu_0}{2}k_{fk}\right)\frac{\partial w_k}{\partial y}+\frac{1-\nu_0^2}{E_0}g_f=0\\
&\qquad (f=1,\ 2,\ 3,\ \ldots,\ l),\\
&-\sum_{i=1}^{m}\left(\nu_0 d_{hi}-\frac{1-\nu_0}{2}c_{hi}\right)\frac{\partial u_i}{\partial x}-\sum_{g=1}^{l}\left(\nu_0 l_{hg}-\frac{1-\nu_0}{2}k_{hg}\right)\frac{\partial v_g}{\partial y}+\\
&\qquad+\frac{1-\nu_0}{2}\sum_{k=1}^{n} r_{hk}\left(\frac{\partial^2 w_k}{\partial x^2}+\frac{\partial^2 w_k}{\partial y^2}\right)-\sum_{k=1}^{n} s_{hk}w_k+\frac{1-\nu_0^2}{E_0}q_h=0\\
&\qquad (h=1,\ 2,\ 3,\ \ldots,\ n).
\end{aligned}\right\} \tag{6.7}$$

The coefficients in (6.7) are:

$$\left.\begin{aligned}
a_{ji} &= a_{ij} = \int \varphi_j\varphi_i\,dz, & m_{fg} &= m_{gf} = \int \varkappa_f\varkappa_g\,dz,\\
b_{ji} &= b_{ij} = \int \varphi_j'\varphi_i'\,dz, & n_{fg} &= n_{gf} = \int \varkappa_f'\varkappa_g'\,dz,\\
c_{jk} &= \int \varphi_j'\psi_k\,dz, & k_{fk} &= \int \varkappa_f'\psi_k\,dz,\\
d_{jk} &= \int \varphi_j\psi_k'\,dz, & l_{fk} &= \int \varkappa_f\psi_k'\,dz,\\
r_{hk} &= \int r_{kh} = \int \psi_h\psi_k\,dz, & c_{hi} &= \int \psi_h\varphi_i'\,dz,\\
s_{hk} &= s_{kh} = \int \psi_h'\psi_k'\,dz, & d_{hi} &= \int \psi_h'\varphi_i\,dz,\\
k_{hg} &= \int \psi_h\varkappa_g'\,dz, & t_{fi} &= \int \varkappa_f\varphi_i\,dz,\\
l_{hg} &= \int \psi_h'\varkappa_g\,dz, & t_{jg} &= \int \varphi\,\varkappa_g\,dz.
\end{aligned}\right\} \qquad (6.8)$$

The definite integrals are taken over the entire height H of the elastic foundation.

The free terms in (6.7) represent the work done by the known external load over the corresponding virtual displacements:

$$\left.\begin{aligned}
p_i &= \int p(x,\ y,\ z)\,\varphi_i(z)\,dz,\\
g_f &= \int g(x,\ y,\ z)\,\varkappa_f(z)\,dz,\\
q_h &= \int q(x,\ y,\ z)\,\psi_h(z)\,dz.
\end{aligned}\right\} \qquad (6.9)$$

When an external load acts on the elastic foundation, the integrals (6.9) are to be considered as Stieltjes integrals (cf. explanations to (1.12), (1.13)). If no body forces act, i.e., if the external load consists only of [distributed] surface forces $p(x, y), g(x, y), q(x, y)$, expressions (6.9) become:

$$\left.\begin{aligned}
p_i &= p(x,\ y)\,\varphi_i(0),\\
g_f &= g(x,\ y)\,\varkappa_f(0),\\
q_h &= q(x,\ y)\,\psi_h(0),
\end{aligned}\right\} \qquad (6.10)$$

Differential equations (6.7) describe completely the states of strain and stress of an elastic foundation having a finite thickness H. The elastic foundation is considered to be an infinitely thick slab secured to its supporting surface and capable of sustaining normal and tangential loads.

The solution (6.7) for a thick isotropic plate is approximate from the viewpoint of the theory of elasticity. Its accuracy increases with the number of terms in (6.1). The differential equations (6.7) define at the same time a generalized three-dimensional model of the elastic foundation, whose properties depend on the number of terms in (6.1) and on the properties of the functions $\varphi_i(z)$, $\varkappa_g(z)$, $\psi_k(z)$. Different schemes, corresponding in varying degrees to the actual foundation, can be obtained by selecting different expressions for the functions φ_i, $\varkappa_g$, ψ_h.

The selection of these functions was discussed in detail in section 2, dealing with the plane strain of an elastic foundation. We repeat that this selection must be specific to the problem considered (e.g., according to an experimental law). In this case even the simplest model described by a minimum number of functions φ_i, $\varkappa_g$, ψ_k will be closer to reality than the model based on the postulation of the foundation modulus.

§ 7. THREE-DIMENSIONAL MODEL OF AN ELASTIC FOUNDATION WITH TWO CHARACTERISTICS

1

Consider an elastic foundation of finite thickness H (Figure 26). Let the horizontal displacements of the foundation vanish everywhere:

$$u(x,\ y,\ z) = 0, \quad v(x,\ y,\ z) = 0, \tag{7.1}$$

and let the vertical displacements be*:

$$w(x,\ y,\ z) = w(x,\ y)\psi(z), \tag{7.2}$$

where $\psi(z)$ is the function of the transverse distribution of the displacements, chosen in accordance with the nature of the problem.

By (7.1) and (7.2), only a single equation of (6.7) remains:

$$\frac{1-\nu_0}{2} r_{11}\nabla^2 w(x,\ y) - s_{11} w(x,\ y) + \frac{1-\nu_0^2}{E_0} q_1 = 0, \tag{7.3}$$

where

$$\nabla^2 w(x,\ y) = \frac{\partial^2 w(x,\ y)}{\partial x^2} + \frac{\partial^2 w(x,\ y)}{\partial y^2}, \tag{7.4}$$

$$r_{11} = \int_0^H \psi^2(z)\,dz, \qquad s_{11} = \int_0^H \psi'^2(z)\,dz. \tag{7.5}$$

The free term in (7.3) represents the work done by the known [external] load $q(x,\ y,\ z)$ over the virtual displacement $\bar{w}(x, y, z) = \psi(z)$ (for $w(x, y) = 1$) and is:

$$q_1 = \int_0^H q(x,\ y,\ z)\psi(z)\,dz. \tag{7.6}$$

If the external load consists only of surface forces $q(x,\ y)$, this becomes:

$$q_1 = q(x,\ y)\psi(0) \tag{7.7}$$

where $\psi(0)$ is the value of $\psi(z)$ at the surface of the elastic foundation.

Equation (7.3) can be rewritten as follows:

$$2t\nabla^2 w(x,\ y) - kw(x,\ y) + q_1 = 0. \tag{7.8}$$

---

* The subscript 1 in $w(x,\ y)$ and $\psi(z)$ will henceforth be omitted.

where

$$k = \frac{E_0 s_{11}}{1 - \nu_0^2}, \qquad t = \frac{E_0 r_{11}}{4(1 + \nu_0)}. \tag{7.9}$$

The coefficient k characterizes the compressive strain in the elastic foundation, and is thus analogous to the foundation modulus. The coefficient t characterizes the shearing strain in the elastic foundation.

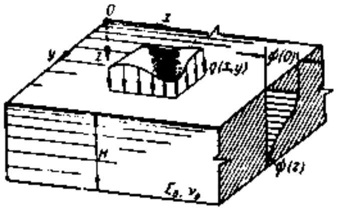

FIGURE 26.

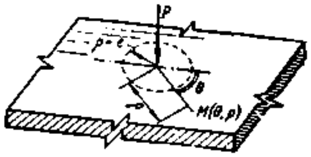

FIGURE 27.

The partial differential equation (7.8) differs from the relationship derived from the postulation of the foundation modulus by the term:

$$2t\nabla^2 w(x, y),$$

which makes allowance for the shearing stresses. In order to determine coefficients (7.9), we must specify $\phi(z)$. Assume that, in accordance with the problem, this function has the form:

$$\phi(z) = \frac{\operatorname{sh} \gamma (H - z)}{\operatorname{sh} \gamma H}, \tag{7.10}$$

where γ is a coefficient determining the variation with depth of the displacements.

Substitution of (7.10) in (7.9) yields [cf. (3.19)]:

$$\left. \begin{aligned} k &= \frac{E_0}{H(1 - \nu_0^2)} \phi_k, \\ t &= \frac{E_0 H}{12(1 + \nu_0)} \phi_t, \end{aligned} \right\} \tag{7.11}$$

where

$$\left. \begin{aligned} \phi_k &= \frac{\gamma H}{2} \left[\frac{\operatorname{sh} \gamma H \operatorname{ch} \gamma H + \gamma H}{\operatorname{sh}^2 \gamma H} \right], \\ \phi_t &= \frac{3}{2} \frac{1}{\gamma H} \left[\frac{\operatorname{sh} \gamma H \operatorname{ch} \gamma H - \gamma H}{\operatorname{sh}^2 \gamma H} \right]. \end{aligned} \right\} \tag{7.12}$$

The elastic constants E_0 and ν_0 are (see (6.3)):

$$E_0 = \frac{E_s}{1 - \nu_s^2}, \qquad \nu_0 = \frac{\nu_s}{1 - \nu_s}. \tag{7.13}$$

We shall now calculate the displacements of an elastic foundation, due to a concentrated force P acting at the origin of the polar system of coordinates (θ, ρ) (Figure 27). [For $P \neq 0$], the following homogeneous differential equation is obtained:

$$\nabla^2 W - \alpha^2 W = 0, \qquad (7.14)$$

where

$$\alpha = \sqrt{\frac{k}{2t}}. \qquad (7.15)$$

Since the load is symmetrical with respect to the coordinate origin, the generalized vertical displacements will be independent of the angle θ. The Laplacian operator is in this case:

$$\nabla^2 W(\rho) = \frac{d^2 W(\rho)}{d\rho^2} + \frac{1}{\rho}\frac{dW(\rho)}{d\rho}. \qquad (7.16)$$

By introducing a new variable

$$\xi = i\alpha\rho \qquad (7.17)$$

we can reduce (7.14) to a Bessel equation of the imaginary argument ξ:

$$\frac{d^2 W}{d\xi^2} + \frac{1}{\xi}\frac{dW}{d\xi} + W = 0. \qquad (7.18)$$

The general solution of (7.18) is*:

$$W = C_1 I_0(\alpha\rho) + C_2 K_0(\alpha\rho), \qquad (7.19)$$

where $I_0(\alpha\rho)$ and $K_0(\alpha\rho)$ are modified zero-order Bessel functions of the first and second kind respectively, while C_1 and C_2 are arbitrary integration constants. Curves of $I_0(\alpha\rho)$ and $K_0(\alpha\rho)$, as functions of the argument $(\alpha\rho)$ are shown in Figure 28. It is seen that the behavior of these functions is similar to that of exponential functions.

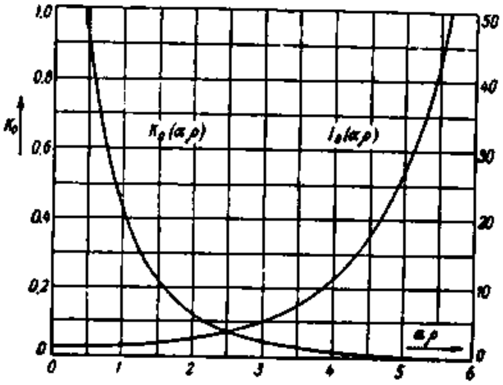

FIGURE 28.

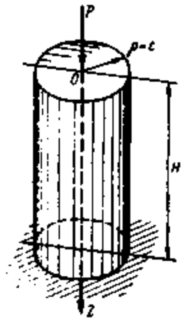

FIGURE 29.

---

* See, e. g., G. N. Watson. Theory of Bessel Functions.—Cambridge. 1923.

Since $I_0(\alpha\rho)$ and $K_0(\alpha\rho)$ are real for all values of ρ, the integration constants C_1 and C_2 will also be real. They can be found by considering the physical aspects of the problem. Since at infinity the displacements of the elastic foundation vanish, we obtain the following boundary condition:

$$\text{at } \rho\to\infty \qquad W\to 0. \tag{7.20}$$

Since I_0 tends to infinity with ρ, it follows from (7.20) that:

$$C_1 = 0. \tag{7.21}$$

To determine C_2 from the equilibrium conditions, we cut an elementary cylinder of radius $\rho=\varepsilon$ ($\varepsilon\to 0$) from the elastic foundation (Figures 27 and 29). The equilibrium conditions for this cylinder can be written in the form:

$$\int_0^{2\pi}\rho\,d\theta\int_0^H \tau_{z\rho}\psi(z)\,dz + P\psi(0) = 0. \tag{7.22}$$

This equation represents the work done by the shearing stresses $\tau_{z\rho}$, distributed over the envelope of the cylinder, and by the external force P over the virtual displacement $\bar{w}(\rho, z)=\phi(z)$ (for $W(\rho)=1$).

By analogy with (6.2), the shearing stresses $\tau_{z\rho}$ are expressed in the cylindrical system of coordinates (z, ρ) as follows:

$$\tau_{z\rho} = \frac{E_0}{2(1+\nu_0)}\frac{dW(\rho)}{d\rho}\phi(z). \tag{7.23}$$

Substitution of (7.23), (7.19), and (7.21) in (7.22) yields:

$$\int_0^{2\pi} 2\alpha t C_2 K_1(\alpha\rho)\rho\,d\theta = P\phi(0), \tag{7.24}$$

where, for $\alpha\rho \leqslant 1$

$$K_1(\alpha\rho)\approx\frac{1}{\alpha\rho},$$

[and t is given by (7.26)].

Integrating (7.24) we obtain for C_2:

$$C_2 = \frac{P\psi(0)}{4\pi t}, \tag{7.25}$$

where

$$t = \frac{E_0 r_{11}}{4(1+\nu_0)}, \quad r_{11} = \int_0^H \phi^2(z)\,dz. \tag{7.26}$$

From (7.19), (7.21), (7.25), and (7.2), we obtain the vertical displacement of any point of the elastic foundation:

$$w(\rho, z) = \frac{P\psi(0)}{4\pi t}K_0(\alpha\rho)\psi(z). \tag{7.27}$$

If, for instance, $\phi(z)$ is given by (7.10), expression (7.27) becomes:

$$w(\rho, z) = \frac{3P(1+\nu_0)}{\pi E_0 H\psi_i}K_0(\alpha\rho)\frac{\operatorname{sh}\gamma(H-z)}{\operatorname{sh}\gamma H}, \tag{7.28}$$

where [cf. (3.32)]

$$\left.\begin{aligned} \alpha &= \sqrt{\frac{k}{2t}} = \frac{1}{H}\cdot\frac{\sqrt{6(1-\nu_0)}}{1-\nu_0}\,\psi_\alpha, \\ \psi_t &= \frac{3}{2}\,\frac{1}{\gamma H}\left[\frac{\operatorname{sh}\gamma H\operatorname{ch}\gamma H-\gamma H}{\operatorname{sh}^2\gamma H}\right], \\ \psi_\alpha &= \gamma H\sqrt{\frac{1}{3}\,\frac{\operatorname{sh}\gamma H\operatorname{ch}\gamma H+\gamma H}{\operatorname{sh}\gamma H\operatorname{ch}\gamma H-\gamma H}}. \end{aligned}\right\} \tag{7.29}$$

If $\psi(z)$ is given by:

$$\psi(z) = e^{-\gamma z} \tag{7.30}$$

we obtain for an elastic semi-infinite space ($H \to \infty$):

$$w(\rho,\ z) = \frac{2P\gamma(1+\nu_0)}{\pi E_0}K_0(\alpha\rho)\,e^{-\gamma z}, \tag{7.31}$$

where

$$\alpha = \sqrt{\frac{k}{2t}} = \gamma\,\frac{\sqrt{2(1-\nu_0)}}{1-\nu_0},$$

and γ is a coefficient of dimension 1/L which determines the variation of the displacements with depth.

As an example, Figure 30 shows displacements of the surface of the elastic foundation in units of $\frac{P}{\pi E_0}$, obtained from (7.31) for $\nu_0 = 0$. The Boussinesq curve corresponding to $\nu_0 = 0$ has also been plotted for comparison. It is seen that the cohesion of the elastic layer decreases with increasing γ, and the properties of the foundation approach those assumed by Winkler. On the other hand, when γ decreases the elastic foundation has a higher load-distributing capacity.

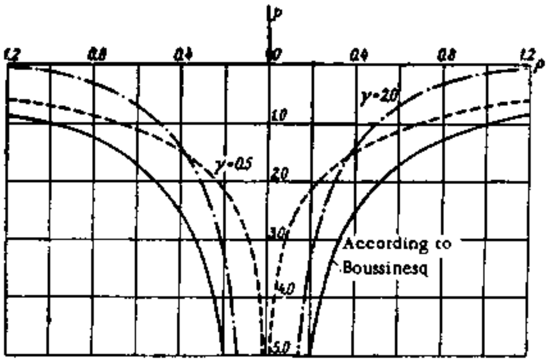

FIGURE 30.

Consider now an elastic foundation acted upon by a load, uniformly distributed within a circle of radius R (Figure 31).

Two regions exist in this case and, by (7.8), two differential equations:

$$\left.\begin{aligned} &\text{at } 0 \leqslant \rho \leqslant R && \frac{d^2W_1}{d\rho^2}+\frac{1}{\rho}\frac{dW_1}{d\rho}-\alpha^2W_1=-\frac{q}{2t}, \\ &\text{at } R \leqslant \rho < \infty && \frac{d^2W_2}{d\rho^2}+\frac{1}{\rho}\frac{dW_1}{d\rho}-\alpha^2W_2=0. \end{aligned}\right\} \qquad (7.32)$$

The solutions of these equations are:

$$\left.\begin{aligned} W_1 &= C_1I_0(\alpha\rho)+C_2K_0(\alpha\rho)+\frac{q}{k}, \\ W_2 &= C_3I_0(\alpha\rho)+C_4K_0(\alpha\rho) \end{aligned}\right\} \qquad (7.33)$$

where k is given by (7.9).

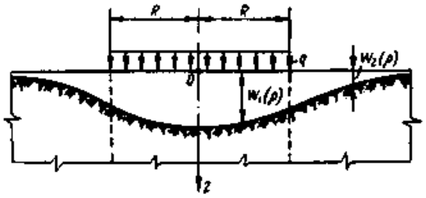

FIGURE 31.

The following boundary conditions are deduced from the nature of the problem for the determination of the integration constants C_1, C_2, C_3, C_4:

$$\left.\begin{aligned} &\text{at } \rho = 0 && \frac{dW_1}{d\rho}=0, \\ &\text{at } \rho \to \infty && W_2=0, \end{aligned}\right\} \qquad (7.34)$$

$$\left.\begin{aligned} &\text{at } \rho = R && W_1=W_2, \\ & && \frac{dW_1}{d\rho}=\frac{dW_2}{d\rho}. \end{aligned}\right\} \qquad (7.35)$$

It follows immediately from (7.34) that:

$$C_2 = C_3 = 0. \qquad (7.36)$$

After substitution of (7.33), we can write (7.35) as follows:

$$\left.\begin{aligned} C_1I_0(\alpha R)-C_4K_0(\alpha R) &= -\frac{q}{k}, \\ C_1I_1(\alpha R)+C_4K_1(\alpha R) &= 0, \end{aligned}\right\} \qquad (7.37)$$

where I_1, K_1 are the first-order modified Bessel functions.

Solving the system (7.37) we obtain for C_1 and C_4:

$$\left.\begin{aligned} C_1 &= -\frac{q}{k}\,\frac{K_1(\alpha R)}{I_0(\alpha R)K_1(\alpha R)+I_1(\alpha R)K_0(\alpha R)}, \\ C_4 &= \frac{q}{k}\,\frac{I_1(\alpha R)}{I_0(\alpha R)K_1(\alpha R)+I_1(\alpha R)K_0(\alpha R)}. \end{aligned}\right\} \qquad (7.38)$$

Finally:

$$\left.\begin{aligned} W_1(\rho) &= C_1 I_0(\alpha\rho) + \frac{q}{k}, \\ W_2(\rho) &= C_4 K_0(\alpha\rho). \end{aligned}\right\} \qquad (7.39)$$

This problem could have been solved by proceeding from (7.27) which, for $z=0$ and $P=1$, defines the influence surface for the displacements. We then obtain for the displacement at $z=0$:

$$W(0) = \frac{q\psi(0)}{4\pi t}\int_0^{2\pi}\int_0^R K_0(\alpha\rho)\,\rho\,d\rho\,d\theta = \frac{q\psi(0)}{k}\left[1-\alpha R K_0(\alpha R)\right]. \qquad (7.40)$$

§ 8. THERMAL STRESSES IN AN ELASTIC FOUNDATION

1

In the design of foundations for heavy structures, it may be necessary to determine the stresses and strains caused by temperature variations. This problem is also encountered in the design of thick slabs and beams on rigid or elastic foundations.

Consider an elastic layer on a rigid foundation (Figure 5), and let this layer be in a state of plane strain as a result of a two-dimensional temperature field. In the general case the temperature is a function of the coordinates x, y and the time t:

$$T = T(x, y, t).$$

The problem will be solved by the variational method. The unknown displacements $u(x, y, t)$, $v(x, y, t)$ are expressed as finite series:

$$\left.\begin{aligned} u(x, y, t) &= \sum_{i=1}^{m} U_i(x, t)\,\varphi_i(y) \qquad (i = 1, 2, 3, \ldots, m), \\ v(x, y, t) &= \sum_{k=1}^{n} V_k(x, t)\,\psi_k(y) \qquad (k = 1, 2, 3, \ldots, n), \end{aligned}\right\} \qquad (8.1)$$

where the functions $U_i(x, t)$, $V_k(x, t)$ are the unknowns, while the functions $\varphi_i(y)$, $\psi_k(y)$ are chosen according to the nature of the problem.

The following system of $m+n$ equations is obtained as before ((1.7) and (1.8)) by considering the generalized equilibrium conditions of an elementary column of height H and measuring $1\times\delta$ in plan, and assuming that no surface or body forces act on the elastic foundation:

$$\left.\begin{aligned} &\int \frac{\partial\sigma_x}{\partial x}\varphi_i\,dF - \int \tau_{xy}\varphi'\,dF = 0 \qquad (j = 1, 2, 3, \ldots, m), \\ &\int \frac{\partial\tau_{yx}}{\partial x}\psi_h\,dF - \int \sigma_y\psi_h'\,dF = 0 \qquad (h = 1, 2, 3, \ldots, n), \end{aligned}\right\} \qquad (8.2)$$

where $dF = \delta\, dy$

The strain components are:

$$\varepsilon_{xx} = \frac{\partial u}{\partial x}, \quad \varepsilon_{yy} = \frac{\partial v}{\partial y}, \quad \varepsilon_{xy} = \frac{\partial u}{\partial y} + \frac{\partial v}{\partial x} ;$$

the stresses σ_x, σ_y, τ_{xy} are, in the case of plane strain caused by temperature variations:

$$\left.\begin{aligned} \sigma_x &= \frac{E_0}{1-\nu_0^2}\left(\frac{\partial u}{\partial x} + \nu_0 \frac{\partial v}{\partial y}\right) - \frac{\alpha E_0 T}{1-\nu_0}, \\ \sigma_y &= \frac{E_0}{1-\nu_0^2}\left(\frac{\partial v}{\partial y} + \nu_0 \frac{\partial u}{\partial x}\right) - \frac{\alpha E_0 T}{1-\nu_0}, \\ \tau_{xy} &= \frac{E_0}{2(1+\nu_0)}\left(\frac{\partial u}{\partial y} + \frac{\partial v}{\partial x}\right), \end{aligned}\right\} \tag{8.3}$$

where α is the coefficient of linear expansion; $T = T(x, y, t)$ is the temperature at point (x, y) and time t; E_0 and ν_0 are elastic constants defined by (2.1).

The following system of $m+n$ ordinary differential equations in the unknowns $U_i(x, t)$, $V_k(x, t)$ is obtained by first inserting (8.1) into (8.3), and then the resulting expressions into (8.2):

$$\left.\begin{aligned} &\sum_{i=1}^{m} a_{ji} U_i'' - \frac{1-\nu_0}{2} \sum_{i=1}^{m} b_{ji} U_i + \sum_{k=1}^{n} \left(\nu_0 t_{jk} - \frac{1-\nu_0}{2} c_{jk}\right) V_k' - \\ &\qquad\qquad - \alpha(1+\nu_0) X_{jT} = 0 \\ &\qquad (j = 1, 2, 3, \ldots, m), \\ &- \sum_{i=1}^{m} \left(\nu_0 t_{hi} - \frac{1-\nu_0}{2} c_{hi}\right) U_i' + \frac{1-\nu_0}{2} \sum_{k=1}^{n} r_{hk} V_k'' - \\ &\qquad\qquad - \sum_{k=1}^{n} s_{hk} V_k + \alpha(1+\nu_0) Y_{hT} = 0 \\ &\qquad (h = 1, 2, 3, \ldots, n). \end{aligned}\right\} \tag{8.4}$$

The coefficients a_{ji}, b_{ji}, …, r_{hk}, s_{hk} in (8.4) are given as before by (1.11) as functions of $\varphi_i(y)$, $\psi_k(y)$. The free terms X_{jT} and Y_{hT} are:

$$X_{jT} = \int \frac{\partial T}{\partial x} \varphi_j dF, \quad Y_{hT} = \int T \psi_h' dF. \tag{8.5}$$

Equations (8.4), together with the corresponding boundary conditions, completely define the temperature equilibrium of a layer of finite thickness H in a state of plane strain. This method can also be applied to the design of elastic foundations and thick plates in a state of three-dimensional stress. The three-dimensional thermo-elastic problem can be reduced to a two-dimensional problem by the method used in section 6 for an elastic foundation subjected to an external load.

2

As an example, consider an elastic layer of finite length in the x direction, which is in a state of plane strain (Figure 32). Let the layer be rigidly connected to its base, so that the displacements $u(x, y)$ and $v(x, y)$ in the plane of contact between layer and base vanish.

Taking only the first three terms in (8.1), we obtain the following approximations:

$$\left.\begin{aligned} u(x,\ y,\ t) &= U_1(x,\ t)\varphi_1(y) + U_2(x, t)\varphi_2(y) + U_3(x, t)\varphi_3(y), \\ v(x,\ y,\ t) &= V_1(x,\ t)\psi_1(y) + V_2(x, t)\psi_2(y) + V_3(x, t)\psi_3(y). \end{aligned}\right\} \tag{8.6}$$

The functions $\varphi_1(y)$, $\varphi_2(y)$, $\varphi_3(y)$, $\psi_1(y)$, $\psi_2(y)$, $\psi_3(y)$ are represented in Figure 33. From (1.11) and Figure 33, we obtain the coefficients in (8.4):

$$\left.\begin{aligned} & a_{11} = r_{11} = \frac{\delta H}{9}, \\ & a_{12} = a_{21} = r_{12} = r_{21} = a_{23} = a_{32} = r_{23} = r_{32} = \frac{\delta H}{18}, \\ & a_{13} = a_{31} = r_{13} = r_{31} = 0, \\ & a_{22} = a_{33} = \frac{2\delta H}{9}, \\ & b_{11} = s_{11} = \frac{3\delta}{H}, \\ & b_{12} = b_{21} = s_{12} = s_{21} = b_{23} = b_{32} = s_{23} = s_{32} = -\frac{3\delta}{H}, \\ & b_{13} = b_{31} = s_{13} = s_{31} = 0, \\ & b_{22} = b_{33} = \frac{6\delta}{H}, \\ & c_{11} = c_{12} = t_{11} = t_{21} = c_{23} = t_{32} = -\frac{\delta}{2}, \\ & c_{13} = t_{13} = c_{22} = t_{22} = c_{31} = t_{31} = c_{33} = t_{33} = 0, \\ & c_{21} = t_{12} = c_{32} = t_{23} = \frac{\delta}{2}. \end{aligned}\right\} \tag{8.7}$$

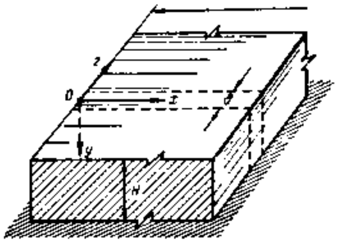

FIGURE 32.

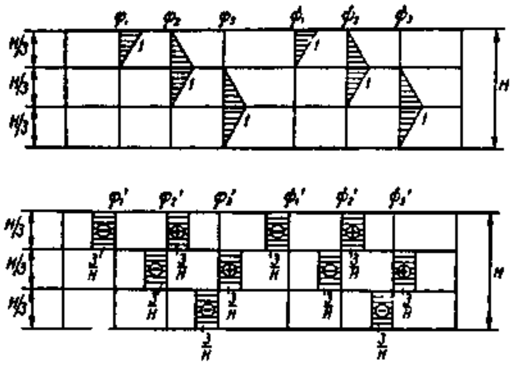

FIGURE 33.

By substituting these values in (8.4), a system of six differential equations in the six unknowns U_1, U_2, U_3, V_1, V_2, V_3 can be represented in the form of Table 1. In this table D and D^2 denote respectively the first and second - order differential operators on the function given at the head of the column. The terms A_1, A_2, A_3, B_1, B_2, B_3, in the last column on the right of Table 1 are:

$$\left.\begin{aligned} A_1 &= \alpha(1+\nu_0)\int \frac{\partial T}{\partial x}\varphi_1\,dy, & B_1 &= -\alpha(1+\nu_0)\int T\psi_1'\,dy, \\ A_2 &= \alpha(1+\nu_0)\int \frac{\partial T}{\partial x}\varphi_2\,dy, & B_2 &= -\alpha(1+\nu_0)\int T\psi_2'\,dy, \\ A_3 &= \alpha(1+\nu_0)\int \frac{\partial T}{\partial x}\varphi_3\,dy, & B_3 &= -\alpha(1+\nu_0)\int T\psi_3'\,dy. \end{aligned}\right\} \tag{8.8}$$

TABLE 1

U_1	U_2	U_3	V_1	V_2	V_3	
$\frac{H}{9}D^2-$ $-\frac{3}{2}\frac{1-\nu_0}{H}$	$\frac{H}{18}D^2+$ $+\frac{3}{2}\frac{1-\nu_0}{H}$	$-$	$\frac{1-3\nu_0}{4}D$	$\frac{1+\nu_0}{4}D$	$-$	A_1
$\frac{H}{18}D^2+$ $+\frac{3}{2}\frac{1-\nu_0}{H}$	$2\Big(\frac{H}{9}D^2-$ $-\frac{3}{2}\frac{1-\nu_0}{H}\Big)$	$\frac{H}{18}D^2+$ $+\frac{3}{2}\frac{1-\nu_0}{H}$	$-\frac{1+\nu_0}{4}D$	$-$	$\frac{1+\nu_0}{4}D$	A_2
$-$	$\frac{H}{18}D^2+$ $+\frac{3}{2}\frac{1-\nu_0}{H}$	$2\Big(\frac{H}{9}D^2-$ $-\frac{3}{2}\frac{1-\nu_0}{H}\Big)$	$-$	$-\frac{1+\nu_0}{4}D$	$-$	A_3
$-\frac{1-3\nu_0}{4}D$	$\frac{1+\nu_0}{4}D$	$-$	$\frac{1-\nu_0}{18}HD^2-\frac{3}{H}$	$\frac{1-\nu_0}{36}HD^2+\frac{3}{H}$	$-$	B_1
$-\frac{1+\nu_0}{4}D$	$-$	$\frac{1+\nu_0}{4}D$	$\frac{1-\nu_0}{36}HD^2+\frac{3}{H}$	$2\left(\frac{1-\nu_0}{18}HD^2-\frac{3}{H}\right)$	$\frac{1-\nu_0}{36}HD^2+\frac{3}{H}$	B_2
$-$	$-\frac{1+\nu_0}{4}D$	$-$	$-$	$\frac{1-\nu_0}{36}HD^2+\frac{3}{H}$	$2\left(\frac{1-\nu_0}{18}HD^2-\frac{3}{H}\right)$	B_3

When the function $T=T(x, y, t)$ is known, the differential equations in Table 1 can be integrated by usual methods. In accordance with the variational method described above, the boundary conditions at $x=0$ and $x=l$ have to be given in generalized form. Thus, in the case of free ends they can be written in the form (cf. (1.14)):

$$\int \sigma_x \varphi_i \, dF = 0, \qquad \int \tau_{xy} \psi_h \, dF = 0. \tag{8.9}$$

When the ends are built-in, and both horizontal and vertical displacements are prevented in sections $x=0$ and $x=l$, the generalized displacements must be zero:

$$U_i = 0, \quad V_k = 0. \tag{8.10}$$

We shall later discuss the case when diaphragms, rigid in their plane and flexible outside their plane, are located at $x=0$ and $x=l$. Such diaphragms prevent only vertical displacements. The stresses σ_x in the end sections then vanish. These boundary conditions are written as follows in a generalized form:

$$\int \sigma_x \varphi_i \, dF = 0, \quad V_k = 0. \tag{8.11}$$

Let the function $T(x, y, t)$ be expressed as a trigonometric series:

$$T(x, y, t) = \sum_{n=1}^{\infty} T_n(y, t) \sin \frac{(2n-1)\pi x}{l}. \tag{8.12}$$

The Fourier coefficients are:

$$T_n(y, t) = \frac{2}{l} \int_0^l T(x, y, t) \sin \frac{(2n-1)\pi x}{l}\, dx. \tag{8.13}$$

It will be assumed that the boundary conditions of the problem are given by (8.11). In this case, the solution of the differential equations in Table 1 can be approximated by trigonometric series. Writing the unknown functions $U_i(x, t)$, $V_k(x, t)$ in the form:

$$\left.\begin{aligned} U_i(x, t) &= \sum_{n=1}^{\infty} U_{in}(t) \cos \frac{(2n-1)\pi x}{l}, \\ V_k(x, t) &= \sum_{n=1}^{\infty} V_{kn}(t) \sin \frac{(2n-1)\pi x}{l}. \end{aligned}\right\} \tag{8.14}$$

it is easily seen that they satisfy (8.11).

Substitution of (8.12) and (8.14) in Table 1 yields a system of algebraic equations for the determination of the coefficients $U_{in}(t)$, $V_{kn}(t)$ in (8.14). Six equations in six unknowns $U_{1n}, U_{2n}, U_{3n}, V_{1n}, V_{2n}, V_{3n}$ correspond to each value of n (Table 2). The free terms in these equations are:

$$\left.\begin{aligned} A_{in} &= (2n-1)\pi(1+\nu_0)\alpha \int_0^H T_n(y, t)\varphi_i\, dy \qquad (i = 1, 2, 3), \\ B_{kn} &= -(1+\nu_0)\alpha l \int_0^H T_n(y, t)\psi_k\, dy \qquad (k = 1, 2, 3). \end{aligned}\right\} \tag{8.15}$$

The solution of this problem has thus been reduced to solving a system of algebraic equations. This must be done in a generalized form, since the free terms A_{in}, B_{kn} are functions of t.

After $U_{1n}(t)$, $U_{2n}(t)$, $U_{3n}(t)$, $V_{1n}(t)$, $V_{2n}(t)$, $V_{3n}(t)$ have been determined, the displacements of the elastic layer can be obtained for any instant from (8.14) and (8.6). The stresses are found from (8.3), after insertion of (8.6) and (8.14). The following expressions are obtained for the normal and shearing stresses of the elastic layer:

$$\begin{aligned} \sigma_x = \frac{E_0}{1-\nu_0^2} \sum_{n=1}^{\infty} \Bigg[&-\frac{(2n-1)\pi}{l} \sum_{i=1}^{3} U_{in}(t)\varphi_i(y) + \\ &+ \nu_0 \sum_{k=1}^{3} V_{kn}(t)\psi_k(y) - \alpha(1+\nu_0) T_n(y, t) \Bigg] \sin \frac{(2n-1)\pi x}{l}, \end{aligned} \tag{8.16}$$

TABLE 2

No.	U_{1n}	U_{2n}	U_{3n}	V_{1n}	V_{2n}	V_{3n}	Free
1	$-\left[\frac{(2n-1)^2\pi^2}{9}\frac{H}{l}+ + \frac{3}{2}(1-\nu_0)\frac{l}{H}\right]$	$-\left[\frac{(2n-1)^2\pi^2}{18}\frac{H}{l}- - \frac{3}{2}(1-\nu_0)\frac{l}{H}\right]$		$\frac{\pi}{4}(2n-1)(1-3\nu_0)$	$\frac{\pi}{4}(2n-1)(1+\nu_0)$	—	A_{1n}
2	$-\left[\frac{(2n-1)^2\pi^2}{18}\frac{H}{l}- - \frac{3}{2}(1-\nu_0)\frac{l}{H}\right]$	$-2\left[\frac{(2n-1)^2\pi^2}{9}\frac{H}{l}+ + \frac{3}{2}(1-\nu_0)\frac{l}{H}\right]$	$-\left[\frac{(2n-1)^2\pi^2}{18}\frac{H}{l}- - \frac{3}{2}(1-\nu_0)\frac{l}{H}\right]$	$-\frac{\pi}{4}(2n-1)(1+\nu_0)$	—	$\frac{\pi}{4}(2n-1)(1+\nu_0)$	A_{2n}
3	—	$-\left[\frac{(2n-1)^2\pi^2}{18}\frac{H}{l}- - \frac{3}{2}(1-\nu_0)\frac{l}{H}\right]$	$-2\left[\frac{(2n-1)^2\pi^2}{9}\frac{H}{l}+ + \frac{3}{2}(1-\nu_0)\frac{l}{H}\right]$	—	$-\frac{\pi}{4}(2n-1)(1+\nu_0)$	—	A_{3n}
4	$\frac{\pi}{4}(2n-1)(1-3\nu_0)$	$-\frac{\pi}{4}(2n-1)(1+\nu_0)$	—	$-\left[\frac{\pi^2(2n-1)^2(1-\nu_0)}{18}\times \times\frac{H}{l}+3\frac{l}{H}\right]$	$-\left[\frac{\pi^2(2n-1)^2(1-\nu_0)}{36}\times \times\frac{H}{l}-3\frac{l}{H}\right]$	—	B_{1n}
5	$\frac{\pi}{4}(2n-1)(1+\nu_0)$	—	$-\frac{\pi}{4}(2n-1)(1+\nu_0)$	$-\left[\frac{\pi^2(2n-1)^2(1-\nu_0)}{36}\times \times\frac{H}{l}-3\frac{l}{H}\right]$	$-2\left[\frac{\pi^2(2n-1)^2(1-\nu_0)}{18}\times \times\frac{H}{l}+3\frac{l}{H}\right]$	$-\left[\frac{\pi^2(2n-1)^2(1-\nu_0)}{36}\times \times\frac{H}{l}-3\frac{l}{H}\right]$	B_{2n}
6	—	$\frac{\pi}{4}(2n-1)(1+\nu_0)$	—	—	$-\left[\frac{\pi^2(2n-1)^2(1-\nu_0)}{36}\times \times\frac{H}{l}-3\frac{l}{H}\right]$	$-2\left[\frac{\pi^2(2n-1)^2(1-\nu_0)}{18}\times \times\frac{H}{l}+3\frac{l}{H}\right]$	B_{3n}

$$\sigma_y = \frac{E_0}{1-\nu_0^2}\sum_{n=1}^{\infty}\left[\sum_{k=1}^{s} V_{kn}(t)\,\psi_k'(y) - \nu_0\frac{(2n-1)\pi}{l}\sum_{i=1}^{s} U_{in}(t)\,\varphi_i(y) - \right.$$

$$\left. - \alpha(1+\nu_0)\,T_n(y,\ t)\right]\sin\frac{(2n-1)\pi x}{l} \qquad (8.16)\ \text{cont'd}$$

$$\tau_{xy} = \frac{E_0}{2(1+\nu_0)}\sum_{n=1}^{\infty}\left[\sum_{i=1}^{s} U_{in}(t)\,\varphi_i'(y) + \right.$$

$$\left. + \frac{(2n-1)\pi}{l}\sum_{k=1}^{s} V_{kn}'(t)\,\psi_k(y)\right]\cos\frac{(2n-1)\pi x}{l} \ .$$

From (8.16), we can determine the stresses in any section of the elastic layer for the duration of temperature variation, provided $T(x,\ y,\ t)$ is known. It is thus possible to find the stresses in a block of concrete caused by the temperature variation during the setting and hardening of the concrete, or by its contraction, if the latter can be analytically expressed.*

---

* See, e.g., Cheche's papers /81, 82/.

Chapter II

BENDING OF A BEAM ON AN ELASTIC FOUNDATION

§ 1. DIFFERENTIAL EQUATION OF BENDING OF A BEAM ON AN ELASTIC FOUNDATION WITH TWO CHARACTERISTICS

Consider a beam lying on the surface of a single-layer elastic foundation. Let an external load $p(x)$ act on the beam (Figure 34). It will be assumed that the sections remain plane during bending, and that friction between the beam and the foundation can be neglected. The differential equation of bending of the beam is then:

$$EJV^{\mathrm{IV}}(x) = p(x) - q(x), \tag{1.1}$$

where $q(x)$ is the reaction of the elastic foundation (= load acting on foundation), and $V(x)$ is the beam deflection [V^{IV} represents $\frac{d^4V}{dx^4}$].

Equation (1.1) contains two unknown functions $V(x)$ and $q(x)$. In order to determine them it is necessary to establish the relationship between the load acting on the foundation and the displacements. This relationship is obtained from the condition that the deflection of the beam is everywhere equal to the vertical displacement of the foundation.

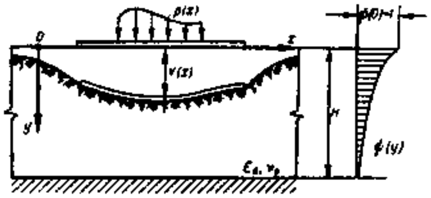

FIGURE 34.

The equation of equilibrium for a single-layer foundation is* [cf. (3.7), (3.8), (3.9) of Chapter I]:

$$-2tV'' + kV = q(x)\psi(0), \tag{1.2}$$

---

* The subscript 1 is henceforth omitted in $V(y)$ and $\psi(y)$.

where

$$\left.\begin{aligned} k &= \frac{E_0\delta}{1-\nu_0^2}\int_0^H \psi'^2(y)\,dy\,, \\ t &= \frac{E_0\delta}{4(1+\nu_0)}\int_0^H \psi^2(y)\,dy. \end{aligned}\right\} \tag{1.3}$$

It is most convenient to select the function $\phi(y)$ in such a way that $\phi(0) = 1$. The generalized displacement $V(x)$ will then represent the displacement of the surface of the elastic foundation, and equation (1.2) becomes:

$$-2tV'' + kV = q(x). \tag{1.4}$$

Since the deflection of the beam equals the vertical displacement of the surface of the elastic foundation, equations (1.1) and (1.4) can be considered together:

$$\left.\begin{aligned} -2tV'' + kV &= q(x), \\ EJV^{IV} &= p(x) - q(x). \end{aligned}\right\} \tag{1.5}$$

Elimination of $q(x)$ from these two equations yields:

$$EJV^{IV} - 2tV'' + kV = p(x). \tag{1.6}$$

This equation differs from the equation, derived by postulating the foundation modulus, by the term containing the second derivative which makes allowance for the influence of shearing stresses in the elastic foundation.

We introduce the dimensionless coordinate $\eta = \frac{x}{L}$, where:

$$L = \sqrt[3]{\frac{2EJ(1-\nu_0^2)}{E_0\delta}}, \tag{1.7}$$

is the "elastic characteristic of the beam."*

Equation (1.6) then becomes:

$$\frac{d^4V}{d\eta^4} - 2r^2\frac{d^2V}{d\eta^2} + s^4V = \frac{pL^4}{EJ}. \tag{1.8}$$

where

$$\left.\begin{aligned} r^2 &= \frac{tL^2}{EJ} = \frac{1}{2}\frac{1-\nu_0}{L}\int_0^H \psi_1^2\,dy\,, \\ s^4 &= \frac{kL^4}{EJ} = 2L\int_0^H \psi_1'^2\,dy\,. \end{aligned}\right\} \tag{1.9}$$

Equation (1.8) represents the generalized equilibrium conditions of the elastic layer together with the beam lying on its surface. Hence, $V(\eta)$ is the generalized vertical displacement.

---

* A similar expression was adopted by Gorbunov-Posadov for analyzing a beam of infinite length /25, 26/.

To the generalized displacement $V(\eta)$ and slope $\varphi(\eta)=\frac{1}{L}V'(\eta)$ (in this case, these magnitudes represent the actual displacement and slope of the beam) there corresponds a generalized shearing force representing the shearing stresses. This force is distinct from the shearing force Q acting on the beam. In accordance with the variational method employed before (cf. second equation (1.14) of Chapter I) (see table on page 82):

$$N(\eta)=-\frac{EJ}{L^3}[V'''(\eta)-2r^2V'(\eta)]. \tag{1.10}$$

This expression must be taken into account for the boundary conditions which, as mentioned in Chapter I, have to be in integral form.

When $V(\eta)$ has been determined, the reactions $q(\eta)$ can be found from (1.4). The bending moments and shearing forces are:

$$M=-EJ\frac{d^2V}{dx^2}=-\frac{EJ}{L^2}\frac{d^2V}{d\eta^2}, \tag{1.11}$$

$$Q=-EJ\frac{d^3V}{dx^3}=-\frac{EJ}{L^3}\frac{d^3V}{d\eta^3}. \tag{1.12}$$

The solution obtained corresponds to the two-dimensional problem of the theory of elasticity. Hence, (1.6) (or (1.8)) is valid both for a beam lying on a vertical foundation of equal width δ (Figure 35), and for strips of width δ cut in the transverse direction from a long plate (Figure 36) lying on an elastic foundation. These two cases correspond respectively to plane stress and plane strain.

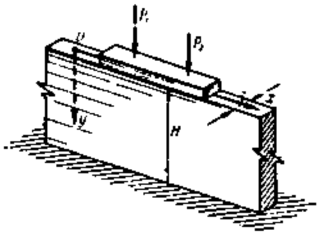

FIGURE 35.

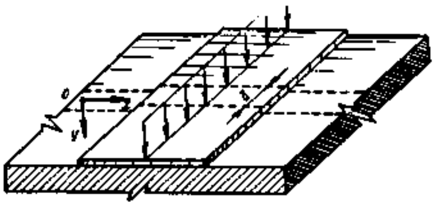

FIGURE 36.

In the case of plane strain, we have:

$$E_0=\frac{E_s}{1-\nu_s^2},\qquad \nu_0=\frac{\nu_s}{1-\nu_s}, \tag{1.13}$$

where E_s, ν_s are respectively the modulus of elasticity and Poisson's ratio for the elastic foundation.

Furthermore, in (1.11) and (1.12), the equivalent moment of inertia J of the strip is:

$$J=\frac{\delta h^3}{12(1-\mu^2)},$$

where μ is Poisson's ratio for the material of the strip.

2. SOLUTION OF THE GENERALIZED EQUATION OF EQUILIBRIUM BY MEANS OF PARTICULAR INTEGRALS

1

To solve (1.8), we must first find the general integral of the corresponding homogeneous equation:

$$\frac{d^4V}{d\eta^4} - 2r^2\frac{d^2V}{d\eta^2} + s^4V = 0. \qquad (2.1)$$

which is:

$$V(\eta) = C_1\Phi_1 + C_2\Phi_2 + C_3\Phi_3 + C_4\Phi_4. \qquad (2.2)$$

where C_1, C_2, C_3, C_4 are integration constants and $\Phi_1, \Phi_2, \Phi_3, \Phi_4$, are roots of the auxiliary equation:

$$k^4 - 2r^2k^2 + s^4 = 0 \ * \qquad (2.3)$$

Since neither s nor r can be negative, the ratio $\frac{s}{r}$ is always positive. The solution of the auxiliary equation is:

1) for $s > r$

$$k = \pm\bar{\alpha} \pm \bar{\beta}i, \qquad (2.4)$$

where $\bar{\alpha}$ and $\bar{\beta}$ are real and positive:

$$\bar{\alpha} = \sqrt{\frac{s^2 + r^2}{2}}, \quad \bar{\beta} = \sqrt{\frac{s^2 - r^2}{2}}; \qquad (2.5)$$

2) for $s = r$

$$\left.\begin{aligned} k_1 &= k_2 = r, \\ k_3 &= k_4 = -r; \end{aligned}\right\} \qquad (2.6)$$

3) for $s < r$

$$\left.\begin{aligned} k_1 &= -k_2 = \lambda_1 = \sqrt{r^2 + \sqrt{r^4 - s^4}}, \\ k_3 &= -k_4 = \lambda_2 = \sqrt{r^2 - \sqrt{r^4 - s^4}}. \end{aligned}\right\} \qquad (2.7)$$

The functions $\Phi_1, \Phi_2, \Phi_3, \Phi_4$, their first three derivatives, and their first integrals denoted by $\Phi_i^{(1)}$ corresponding respectively to (2.5), (2.6), and (2.7), are given in Table 3. The derivatives are expressed linearly through $\Phi_1, \Phi_2, \Phi_3, \Phi_4$.

The first case is the most important for the analysis of beams on single-layer foundations. When $s > r$, the functions in Table 3 differ from those for the bending of a beam on an elastic Winkler foundation by the arguments $\bar{\alpha}$ and $\bar{\beta}$ of the hyperbolic and trigonometric functions. These functions can be characterized by the ratio between the real and imaginary parts of the complex root (2.4):

$$\gamma = \frac{\bar{\beta}}{\bar{\alpha}} = \sqrt{\frac{s^2 - r^2}{s^2 + r^2}}, \qquad (2.8)$$

---

* [k in this equation should not be confused with the characteristic k introduced in (3.9) of Chapter I.]

TABLE 3

Relative magnitude of s and r	Function and its derivatives	Φ_1 (odd)	Φ_2 (even)	Φ_3 (odd)	Φ_4 (even)
$s > r$	Φ	$\operatorname{sh} \bar\alpha\eta \cos \bar\beta\eta$	$\operatorname{ch} \bar\alpha\eta \cos \bar\beta\eta$	$\operatorname{ch} \bar\alpha\eta \sin \bar\beta\eta$	$\operatorname{sh} \bar\alpha\eta \sin \bar\beta\eta$
	Φ'	$\bar\alpha\Phi_2 - \bar\beta\Phi_4$	$\bar\alpha\Phi_1 - \bar\beta\Phi_3$	$\bar\alpha\Phi_4 + \bar\beta\Phi_2$	$\bar\alpha\Phi_3 + \bar\beta\Phi_1$
	Φ''	$(\bar\alpha^2 - \bar\beta^2)\,\Phi_1 - 2\bar\alpha\bar\beta\Phi_3$	$(\bar\alpha^2 - \bar\beta^2)\,\Phi_2 - 2\bar\alpha\bar\beta\Phi_4$	$(\bar\alpha^2 - \bar\beta^2)\,\Phi_3 + 2\bar\alpha\bar\beta\Phi_1$	$(\bar\alpha^2 - \bar\beta^2)\,\Phi_4 + 2\bar\alpha\bar\beta\Phi_2$
	Φ'''	$\bar\alpha\,(\bar\alpha^2 - 3\bar\beta^2)\,\Phi_2 +$ $+ \bar\beta\,(\bar\beta^2 - 3\bar\alpha^2)\,\Phi_4$	$\bar\alpha\,(\bar\alpha^2 - 3\bar\beta^2)\,\Phi_1 +$ $+ \bar\beta\,(\bar\beta^2 - 3\bar\alpha^2)\,\Phi_3$	$\bar\alpha\,(\bar\alpha^2 - 3\bar\beta^2)\,\Phi_4 -$ $- \bar\beta\,(\bar\beta^2 - 3\bar\alpha^2)\,\Phi_2$	$\bar\alpha\,(\bar\alpha^2 - 3\bar\beta^2)\,\Phi_3 -$ $- \bar\beta\,(\bar\beta^2 - 3\bar\alpha^2)\,\Phi_1$
$s = r$	Φ	$\operatorname{sh} r\eta$	$\operatorname{ch} r\eta$	$\eta \operatorname{ch} r\eta$	$\eta \operatorname{sh} r\eta$
	Φ'	$r\Phi_2$	$r\Phi_1$	$\Phi_2 + r\Phi_4$	$\Phi_1 + r\Phi_3$
	Φ''	$r^2\Phi_1$	$r^2\Phi_2$	$2r\Phi_1 + r^2\Phi_3$	$2r\Phi_2 + r^2\Phi_4$
	Φ'''	$r^3\Phi_2$	$r^3\Phi_1$	$3r^2\Phi_2 + r^3\Phi_4$	$3r^2\Phi_1 + r^3\Phi_3$
$s < r$	Φ	$\operatorname{sh} \lambda_1\eta$	$\operatorname{ch} \lambda_1\eta$	$\operatorname{sh} \lambda_2\eta$	$\operatorname{ch} \lambda_2\eta$
	Φ'	$\lambda_1\Phi_2$	$\lambda_1\Phi_1$	$\lambda_2\Phi_4$	$\lambda_2\Phi_3$
	Φ''	$\lambda_1^2\Phi_1$	$\lambda_1^2\Phi_2$	$\lambda_2^2\Phi_3$	$\lambda_2^2\Phi_4$
	Φ'''	$\lambda_1^3\Phi_2$	$\lambda_1^3\Phi_1$	$\lambda_2^3\Phi_4$	$\lambda_2^3\Phi_3$
$s = 0$	Φ	η	1	$\operatorname{sh} r_1\eta$	$\operatorname{ch} r_1\eta$
	Φ'	$\Phi_2 = 1$	0	$r_1\Phi_4$	$r_1\Phi_3$
	Φ''	0	0	$r_1^2\Phi_3$	$r_1^2\Phi_4$
	Φ'''	0	0	$r_1^3\Phi_4$	$r_1^3\Phi_3$
$s > r$	$\Phi^{(1)}$	$\dfrac{\bar\alpha\Phi_2 + \bar\beta\Phi_4}{\bar\alpha^2 + \bar\beta^2}$	$\dfrac{\bar\alpha\Phi_1 + \bar\beta\Phi_3}{\bar\alpha^2 + \bar\beta^2}$	$\dfrac{\bar\alpha\Phi_4 - \bar\beta\Phi_2}{\bar\alpha^2 + \bar\beta^2}$	$\dfrac{\bar\alpha\Phi_3 - \bar\beta\Phi_1}{\bar\alpha^2 + \bar\beta^2}$
$s = r$	$\Phi^{(1)}$	$\dfrac{1}{r}\,\Phi_2$	$\dfrac{1}{r}\,\Phi_1$	$\dfrac{1}{r}\,\Phi_4 - \dfrac{1}{r^2}\,\Phi_2$	$\dfrac{1}{r}\,\Phi_3 - \dfrac{1}{r^2}\,\Phi_1$
$s < r$	$\Phi^{(1)}$	$\dfrac{1}{\lambda_1}\,\Phi_2$	$\dfrac{1}{\lambda_1}\,\Phi_1$	$\dfrac{1}{\lambda_2}\,\Phi_4$	$\dfrac{1}{\lambda_2}\,\Phi_3$
$s = 0$	$\Phi^{(1)}$	$\dfrac{1}{2}\,\Phi_1^2 = \dfrac{\eta^2}{2}$	Φ_1	$\dfrac{1}{r_1}\,\Phi_4$	$\dfrac{1}{r_1}\,\Phi_3$

This ratio varies between 0 and 1. For $\gamma = 0$ the functions Φ ($i = 1 \ldots 4$) degenerate into hyperbolic functions, multiplied by 1 or η. For $\gamma = 1$ they reduce to the functions of the bending of a beam on an elastic Winkler foundation.

The functions Φ_1, Φ_2, Φ_3, Φ_4, are tabulated in the appendix (Tables 1, 2, 3, 4) for values of γ between 0.0 and 1.0. In these tables $z = \bar{\alpha}\eta$.

2

The general solution of the nonhomogeneous equation (1.8) is equal to the sum of the general homogeneous solution (2.2) and of a particular solution V_0:

$$V(\eta) = C_1\Phi_1 + C_2\Phi_2 + C_3\Phi_3 + C_4\Phi_4 + V_0. \qquad (2.9)$$

When the distributed load is either constant or varies according to a linear law $p(\eta) = a + b\eta$, we can write:

$$V_0 = \frac{pL^4}{EJs^4}. \qquad (2.10)$$

Although this method of determining $V(\eta)$ is very simple in principle, it involves cumbersome calculations. Even when the function $p(\eta)$ is defined by a single analytical expression for the entire beam, a system of four algebraic equations has to be solved in order to determine the four integration constants C_1, C_2, C_3, C_4. If the load varies according to different laws in different zones of the beam or includes concentrated forces, the general integral (2.9) will contain different integration constants in each zone, their total number being four times that of the zones. In the relatively simple problems represented in Figure 37, we have to find 12 constants by setting up 12 algebraic equations. Hence, the method described is only practical when the external load is given by a single analytical expression valid for the entire beam.

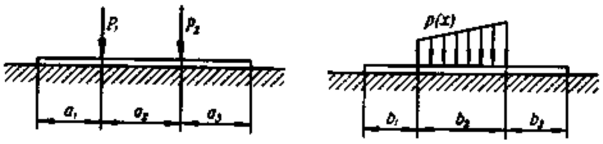

FIGURE 37.

To solve the problem considered in a practical and general manner, we shall apply Puzyrevskii-Krylov's method of the initial parameters (this method was first suggested by Cauchy) in the form proposed by Vlasov. This method requires the determination of only two integration constants irrespective of the load distribution*

---

* The method of initial parameters as applied to the analysis of beams (both ordinary and on elastic Winkler foundations) is explained in /73/ and in /47/.

§ 3. SOLUTION BY THE METHOD OF INITIAL PARAMETERS

1. General integral of the homogeneous equation

It will be assumed that the load consists of concentrated forces and moments. Between their points of application the bending of the beam is determined by the homogeneous equation (2.1) whose general integral (2.2) is written:

$$V = C_1K_1 + C_2K_2 + C_3K_3 + C_4K_4, \tag{3.1}$$

where K_1, K_2, K_3, K_4 are independent linear functions of $\Phi_1, \Phi_2, \Phi_3, \Phi_4$. The system K_1, K_2, K_3, K_4 can accordingly be called the fundamental system.

We choose the fundamental system in such a way that when $\eta = 0$, the generalized geometrical and statical magnitudes V, φ, M, N, expressed through the functions K_1, K_2, K_3, K_4 and their derivatives, form a unit matrix:

i	$V(0) = K_i(0)$	$\varphi(0) = \frac{1}{L} K_i'(0)$	$M(0) = -\frac{EJ}{L^2} K_i''(0)$	$N(0) = -\frac{EJ}{L^3}[K_i'''(0) - 2r^2K_i'(0)]$
1	1	0	0	0
2	0	1	0	0
3	0	0	1	0
4	0	0	0	1

Hence:

$$C_1 = V_0, \quad C_2 = \varphi_0, \quad C_3 = M_0, \quad C_4 = N_0,$$

[the subscript "O" denotes the values for $\eta = 0$].

The functions K_1, K_2, K_3, K_4 thus express the influence of unit initial parameters on the deflection, i.e., they are influence coefficients. Writing:

$$K_1 = K_{VV}, \quad K_2 = K_{V\varphi}, \quad K_3 = K_{VM}, \quad K_4 = K_{VN},$$

we obtain:

$$V(\eta) = V_0K_{VV} + \varphi_0K_{V\varphi} + M_0K_{VM} + N_0K_{VN}. \tag{3.2}$$

Inserting (3.2) into (1.10) and (1.11), the following system is obtained, including (3.2):

$$\left.\begin{aligned} V(\eta) &= V_0K_{VV} + \varphi_0K_{V\varphi} + M_0K_{VM} + N_0K_{VN}, \\ \varphi(\eta) &= V_0K_{\varphi V} + \varphi_0K_{\varphi\varphi} + M_0K_{\varphi M} + N_0K_{\varphi N}, \\ M(\eta) &= V_0K_{MV} + \varphi_0K_{M\varphi} + M_0K_{MM} + N_0K_{MN}, \\ N(\eta) &= V_0K_{NV} + \varphi_0K_{N\varphi} + M_0K_{NM} + N_0K_{NN}. \end{aligned}\right\} \tag{3.3}$$

The 16 influence functions K_{VV}, $K_{V\varphi}, \ldots, K_{NN}$, in (3.3) form a matrix for the direct linear transformation of V_0, φ_0, M_0, N_0 into $V_\eta, \varphi_\eta, M_\eta, N_\eta$. After the initial parameters have been determined, the problem can be considered as solved.

Any section $\eta = t$ in which V_t, φ_t, M_t, N_t are known can be taken as initial section. The values of $V_\eta, \varphi_\eta, M_\eta, N_\eta$ in a section situated at a distance $\eta - t$ from the initial section will be determined by the same influence functions, provided the homogeneous differential equation of bending (2.1) is valid between these two sections:

$$\left.\begin{aligned} V_\eta &= V_t K_{VV} + \varphi_t K_{V\varphi} + M_t K_{VM} + N_t K_{VN}, \\ \varphi_\eta &= V_t K_{\varphi V} + \varphi_t K_{\varphi\varphi} + M_t M_{\varphi M} + N_t K_{\varphi N}, \\ M_\eta &= V_t K_{MV} + \varphi_t K_{M\varphi} + M_t K_{MM} + N_t K_{MN}, \\ N_\eta &= V_t K_{NV} + \varphi_t K_{N\varphi} + M_t K_{NM} + N_t K_{NN}. \end{aligned}\right\} \tag{3.4}$$

The influence functions $K_{VV}, \ldots, K_{NN}$ are here functions of the argument $(\eta - t)$, while $\Phi_1, \ldots, \Phi_4$ become $\Phi_1(\eta - t), \ldots, \Phi_4(\eta - t)$.

A very important property of matrices (3.4) and (3.3) is their symmetrical structure, as a result of which there are only 10 distinct influence functions. The four functions forming the secondary diagonal are not repeated. The remaining 12 functions, arranged symmetrically to this diagonal, are equal by pairs:

$$\left.\begin{aligned} K_{MM} &= K_{\varphi\varphi}, \quad & K_{\varphi N} &= K_{VM}, \quad & K_{MN} &= K_{V\varphi}, \\ K_{NN} &= K_{VV}, \quad & K_{N\varphi} &= K_{MV}, \quad & K_{NM} &= K_{\varphi V}. \end{aligned}\right\} \tag{3.5}$$

This property is derived from the reciprocity theorem of Maxwell and Betti.*

2. Effect of external load. General integral of the nonhomogeneous equation

Consider a beam of length l, acted upon by concentrated forces $P_1, P_2, \ldots, P_n$ (Figure 38) at points whose dimensionless coordinates are respectively $t_1, t_2, \ldots, t_n$.

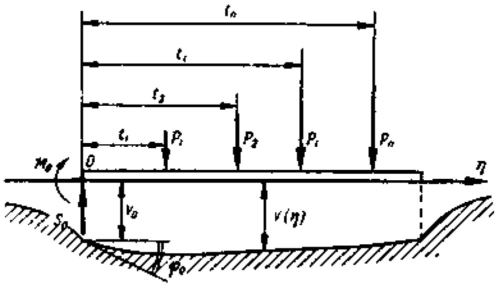

FIGURE 38.

---

* For a detailed discussion of influence functions forming matrices of direct and inverse transformation, cf. V. Z. Vlasov, "Tonkostennye uprugie sterzhni" (Thin-walled Elastic Bars).—Gostekhizdat. 1940. [Translated by IPST, No. 428.], and "Stroitel'naya mekhanika tonkostennykh prostranstvennykh sistem" (Structural Mechanics of Thin-walled Three-dimensional Systems).—Stroiizdat. 1949.

For $0 < \eta < t_1$ the kinematic and statical factors are determined by the initial parameters and influence functions:

$$\left.\begin{aligned}
V(\eta) &= V_0 K_{VV}(\eta) + \varphi_0 K_{V\varphi}(\eta) + M_0 K_{VM}(\eta) + N_0 K_{VN}(\eta),\\
\varphi(\eta) &= V_0 K_{\varphi V}(\eta) + \varphi_0 K_{\varphi\varphi}(\eta) + M_0 K_{\varphi M}(\eta) + N_0 K_{\varphi N}(\eta),\\
M(\eta) &= V_0 K_{MV}(\eta) + \varphi_0 K_{M\varphi}(\eta) + M_0 K_{MM}(\eta) + N_0 K_{MN}(\eta),\\
N(\eta) &= V_0 K_{NV}(\eta) + \varphi_0 K_{N\varphi}(\eta) + M_0 K_{NM}(\eta) + N_0 K_{NN}(\eta).
\end{aligned}\right\} \tag{3.6}$$

These expressions remain valid as long as the homogeneous differential equation (2.1) holds true, i.e., as long as $V(\eta)$, $\varphi(\eta)$, $M(\eta)$, $N(\eta)$ are continuous.

If one of these functions has a discontinuity at $\eta = t_k$, i.e., if a concentrated load acts at this point, the influence of this load must be taken into account for $\eta > t_k$, in accordance with the principle of superposition following from the linearity of (3.6). This influence is equal to the magnitude of the discontinuity multiplied by the corresponding influence function, calculated for the coordinate $(\eta - t_k)$.

Thus, $V(\eta)$, $\varphi(\eta)$, $M(\eta)$ remain continuous at all points where a concentrated force P_1 acts, only $N(\eta)$ increasing by $(-P_1)$. Hence, for $t_1 < \eta < t_2$ (Figure 38):

$$\left.\begin{aligned}
V(\eta) &= V_0 K_{VV}(\eta) + \varphi_0 K_{V\varphi}(\eta) + M_0 K_{VM}(\eta) + N_0 K_{VN}(\eta) -\\
&\qquad - P_1 K_{VN}(\eta - t_1),\\
\varphi(\eta) &= V_0 K_{\varphi V}(\eta) + \varphi_0 K_{\varphi\varphi}(\eta) + M_0 K_{\varphi M}(\eta) + N_0 K_{\varphi N}(\eta) -\\
&\qquad - P_1 K_{\varphi N}(\eta - t_1),\\
M(\eta) &= V_0 K_{MV}(\eta) + \varphi_0 K_{M\varphi}(\eta) + M_0 K_{MM}(\eta) + N_0 K_{MN}(\eta) -\\
&\qquad - P_1 K_{MN}(\eta - t_1),\\
N(\eta) &= V_0 K_{NV}(\eta) + \varphi_0 K_{N\varphi}(\eta) + M_0 K_{NM}(\eta) + N_0 K_{NN}(\eta) -\\
&\qquad - P_1 K_{NN}(\eta - t_1).
\end{aligned}\right\} \tag{3.7}$$

For $t_i < \eta < t_{i+1}$ we have:

$$\left.\begin{aligned}
V(\eta) &= V_0 K_{VV}(\eta) + \varphi_0 K_{V\varphi}(\eta) + M_0 K_{VM}(\eta) + N_0 K_{VN}(\eta) -\\
&\qquad - \sum_{k=1}^{i} P_k K_{VN}(\eta - t_k),\\
\varphi(\eta) &= V_0 K_{\varphi V}(\eta) + \varphi_0 K_{\varphi\varphi}(\eta) + M_0 K_{\varphi M}(\eta) + N_0 K_{\varphi N}(\eta) -\\
&\qquad - \sum_{k=1}^{i} P_k K_{\varphi N}(\eta - t_k),\\
M(\eta) &= V_0 K_{MV}(\eta) + \varphi_0 K_{M\varphi}(\eta) + M_0 K_{MM}(\eta) + N_0 K_{MN}(\eta) -\\
&\qquad - \sum_{k=1}^{i} P_k K_{MN}(\eta - t_k),\\
N(\eta) &= V_0 K_{NV}(\eta) + \varphi_0 K_{N\varphi}(\eta) + M_0 K_{NM}(\eta) + N_0 K_{NN}(\eta) -\\
&\qquad - \sum_{k=1}^{i} P_k K_{NN}(\eta - t_k).
\end{aligned}\right\} \tag{3.8}$$

A distributed load $p(t)$ (Figure 39) can be considered as a system of elementary concentrated forces; we obtain for the loaded part of the beam:

$$\left.\begin{aligned}
V(\eta) &= V_0K_{VV}(\eta) + \varphi_0K_{V\varphi}(\eta) + M_0K_{VM}(\eta) + \\
&\quad + N_0K_{VN}(\eta) - \int_a^\eta p(t)\,K_{VN}(\eta - t)\,dt, \\
\varphi(\eta) &= V_0K_{\varphi V}(\eta) + \varphi_0K_{\varphi\varphi}(\eta) + M_0K_{\varphi M}(\eta) + \\
&\quad + N_0K_{\varphi N}(\eta) - \int_a^\eta p(t)\,K_{\varphi N}(\eta - t)\,dt, \\
M(\eta) &= V_0K_{MV}(\eta) + \varphi_0K_{M\varphi}(\eta) + M_0K_{MM}(\eta) + \\
&\quad + N_0K_{MN}(\eta) - \int_a^\eta p(t)\,K_{MN}(\eta - t)\,dt, \\
N(\eta) &= V_0K_{NV}(\eta) + \varphi_0K_{N\varphi}(\eta) + M_0K_{NM}(\eta) + \\
&\quad + N_0K_{NN}(\eta) - \int_a^\eta p(t)\,K_{NN}(\eta - t)\,dt.
\end{aligned}\right| \qquad (3.9)$$

When distributed and concentrated loads act simultaneously, the integrals in (3.9) are Stieltjes integrals, i.e., the terms under the summation signs in (3.8) have to be added to them.

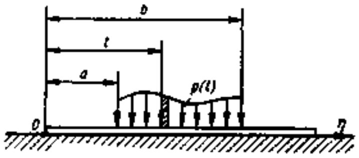

FIGURE 39.

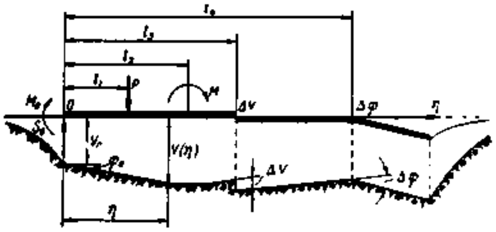

FIGURE 40.

In the most general case of arbitrary external influences, the solution of the nonhomogeneous differential equation (1.8) can be represented in the form:

$$\left.\begin{aligned}
V(\eta) &= V_0K_{VV} + \varphi_0K_{V\varphi} + M_0K_{VM} + N_0K_{VN} - F_V, \\
\varphi(\eta) &= V_0K_{\varphi V} + \varphi_0K_{\varphi\varphi} + M_0K_{\varphi M} + N_0K_{\varphi N} - F_\varphi, \\
M(\eta) &= V_0K_{MV} + \varphi_0K_{M\varphi} + M_0K_{MM} + N_0K_{MN} - F_M, \\
N(\eta) &= V_0K_{NV} + \varphi_0K_{N\varphi} + M_0K_{NM} + N_0K_{NN} - F_N,
\end{aligned}\right| \qquad (3.10)$$

where F_V, F_φ, F_M, F_N are known functions depending on the load and its distribution. These "loads" need not be vertical forces and moments; they may also be breaks and abrupt bends in the beam.

For the case represented in Figure 40, we obtain for F_V and F_M:

$$\left.\begin{array}{l}
\text{at } 0<\eta<t_1 \quad F_V=F_M=0;\\
\text{at } t_1<\eta<t_2 \quad F_V=PK_{VN}(\eta-t_1),\\
\qquad\qquad\qquad\quad F_M=PK_{MN}(\eta-t_1);\\
\text{at } t_2<\eta<t_3 \quad F_V=PK_{VN}(\eta-t_1)-MK_{VM}(\eta-t_2),\\
\qquad\qquad\qquad\quad F_M=PK_{MN}(\eta-t_1)-MK_{MM}(\eta-t_2);\\
\text{at } t_3<\eta<t_4\\
F_V=PK_{VN}(\eta-t_1)-MK_{VM}(\eta-t_2)-\Delta VK_{VV}(\eta-t_3),\\
F_M=PK_{MN}(\eta-t_1)-MK_{MM}(\eta-t_2)-\Delta VK_{MV}(\eta-t_3);\\
\text{at } t_4<\eta\\
F_V=PK_{VN}(\eta-t_1)-MK_{VM}(\eta-t_2)-\Delta VK_{VV}(\eta-t_3)-\\
\qquad\qquad\qquad\qquad\qquad\qquad -\Delta\varphi K_{V\varphi}(\eta-t_4),\\
F_M=PK_{MN}(\eta-t_1)-MK_{MM}(\eta-t_2)-\Delta VK_{MV}(\eta-t_3)-\\
\qquad\qquad\qquad\qquad\qquad\qquad -\Delta\varphi K_{M\varphi}(\eta-t_4).
\end{array}\right| \tag{3.11}$$

The initial parameters V_0, φ_0, M_0, N_0 can be obtained very simply by this method, the initial section of the beam being chosen arbitrarily. Thus, by selecting one of the beam ends as initial section $(\eta=0)$, we automatically determine two of the four parameters. The other two initial parameters can always be found from two equations defining the boundary conditions at the other end of the beam.

Thus, for a simply supported beam, we obtain respectively for $\eta=0$ and $\eta=\frac{l}{L}$:

$$V_0=0, \qquad M_0=0; \tag{3.12}$$

$$V\left(\frac{l}{L}\right)=0, \qquad M\left(\frac{l}{L}\right)=0. \tag{3.13}$$

Substitution of (3.10) and (3.12) in (3.13) yields:

$$V\left(\frac{l}{L}\right)=\varphi_0K_{V\varphi}+N_0K_{VN}-F_V=0,$$

$$M\left(\frac{l}{L}\right)=\varphi_0K_{M\varphi}+N_0K_{MN}-F_M=0,$$

where

$$K_{V\varphi},\ K_{VN},\ K_{M\varphi},\ K_{MN},\ F_V,\ F_M$$

are determined for

$$\eta=\frac{l}{L}(x=l)$$

3. Determination of the influence functions

The functions $K_{VV}, K_{V\varphi}, \ldots, K_{NN}$ in (3.10) were assumed to be known. It will be shown now how these functions are determined for the most important case $s > r$.

We proceed from the homogeneous differential equation (2.1) whose general integral, determining the generalized deflection $V(\eta)$, is

$$V(\eta) = C_1\Phi_1 + C_2\Phi_2 + C_3\Phi_3 + C_4\Phi_4. \tag{3.14}$$

The other kinematic and statical factors are linear functions of the derivatives of $V(\eta)$:

$$\left.\begin{aligned} \varphi(\eta) &= \frac{1}{L}V', \\ M(\eta) &= -\frac{EJ}{L^2}V'', \\ N(\eta) &= -\frac{EJ}{L^3}[V''' - 2r^2V']. \end{aligned}\right\} \tag{3.15}$$

Substitution in (3.15) of (3.14) and the initial conditions (for $\eta = 0$) [cf. Table 3]

$$\begin{gathered} \Phi_2 = 1, \quad \Phi_1 = \Phi_3 = \Phi_4 = 0, \\ V = V_0, \quad \varphi = \varphi_0, \quad M = M_0, \quad N = N_0, \end{gathered}$$

TABLE 4.

Influence functions

	V_0	φ_0	M_0	N_0
V_η	$K_{VV} = \Phi_2 - \frac{r^2}{2\bar\alpha\bar\beta}\Phi_4$	$K_{V\varphi} = \frac{L}{2\bar\alpha\bar\beta}(\bar\beta\Phi_1 + \bar\alpha\Phi_3)$	$K_{VM} = -\frac{L^2}{2\bar\alpha\bar\beta EJ}\Phi_4$	$K_{VN} =$ $= \frac{L^3}{2\bar\alpha\bar\beta s^2 EJ}(\bar\beta\Phi_1 - \bar\alpha\Phi_3)$
φ_η	$K_{\varphi V} = \frac{s^2}{2\bar\alpha\bar\beta L}(\bar\beta\Phi_1 - \bar\alpha\Phi_3)$	$K_{\varphi\varphi} = \Phi_2 + \frac{r^2}{2\bar\alpha\bar\beta}\Phi_4$	$K_{\varphi M} = -\frac{L}{2\bar\alpha\bar\beta EJ}(\bar\alpha\Phi_3 + \bar\beta\Phi_1)$	$K_{\varphi N} = K_{VM}$
M_η	$K_{MV} = \frac{EJ}{2\bar\alpha\bar\beta L^2}s^4\Phi_4$	$K_{M\varphi} = -\frac{EJ}{2\bar\alpha\bar\beta L}[(3\bar\alpha^2 -$ $- \bar\beta^2)\bar\beta\Phi_1 - (\bar\alpha^2 - 3\bar\beta^2)\bar\alpha\Phi_3]$	$K_{MM} = K_{\varphi\varphi}$	$K_{MN} = K_{V\varphi}$
N_η	$K_{NV} = \frac{EJs^2}{2\bar\alpha\bar\beta L^3}[(s^2 -$ $- 2r^2)\bar\beta\Phi_1 - (s^2 - 2r^2)\bar\alpha\Phi_3]$	$K_{N\varphi} = K_{MV}$	$K_{NM} = K_{\varphi V}$	$K_{NN} = K_{VV}$

yields the following expressions for the integration constants C_1, C_2, C_3, C_4:

$$\left.\begin{aligned}
C_1 &= \frac{1}{2\bar{\alpha}\,\bar{\beta}s^2}\left[s^2\bar{\beta}L\varphi_0 + \bar{\beta}\,\frac{L^2}{EJ}\,N_0\right],\\
C_2 &= V_0,\\
C_3 &= \frac{1}{2\bar{\alpha}\,\bar{\beta}s^2}\left[s^2\bar{\alpha}L\varphi_0 - \bar{\alpha}\,\frac{L^2}{EJ}\,N_0\right],\\
C_4 &= -\frac{1}{2\bar{\alpha}\,\bar{\beta}}\left[r^2V_0 + \frac{L^2}{EJ}\,M_0\right].
\end{aligned}\right\} \qquad (3.16)$$

Substituting these values in (3.14) and (3.15), we can express $V(\eta)$, $\varphi(\eta)$, $M(\eta)$, $N(\eta)$ through the initial parameters V_0, φ_0, M_0, N_0 and the influence functions $K_{VV}, K_{V\varphi}, \ldots, K_{NN}$, given in Table 4.

The influence functions for the two other cases:

$$s = r \text{ and } s < r,$$

can be similarly determined.

§ 4. INFINITELY LONG BEAM

1

Consider an infinitely long beam. If a concentrated force P (Figure 41) acts at the origin of coordinates, we obtain the following homogeneous differential equation [for all points except the origin]:

$$\frac{d^4V}{d\eta^4} - 2r^2\frac{d^2V}{d\eta^2} + s^4V = 0. \qquad \text{[cf. (2.1)]} \qquad (4.1)$$

Assuming $s > r$, the general integral of (4.1) has the form

$$V(\eta) = C_1e^{-\bar{\alpha}\eta}\sin\bar{\beta}\eta + C_2e^{-\bar{\alpha}\eta}\cos\bar{\beta}\eta + C_3e^{\bar{\alpha}\eta}\sin\bar{\beta}\eta + C_4e^{\bar{\alpha}\eta}\cos\bar{\beta}\eta, \qquad (4.2)$$

where $\bar{\alpha}$ and $\bar{\beta}$ are given by (2.5).

For reasons of symmetry we consider only that part of the beam for which $x > 0$.

Since for $\eta \to \infty$ $\qquad V \to 0,$

we obtain $\qquad C_3 = C_4 = 0. \qquad (4.3)$

Substitution of (4.3) in (4.2) yields:

$$V(\eta) = C_1F_1 + C_2F_2, \qquad (4.4)$$

where

$$\left.\begin{aligned}
F_1 &= e^{-\bar{\alpha}\eta}\sin\bar{\beta}\eta,\\
F_2 &= e^{-\bar{\alpha}\eta}\cos\bar{\beta}\eta.
\end{aligned}\right\} \qquad (4.5)$$

The integration constants C_1 and C_2 can be determined from the conditions at the origin:

at $\eta = 0$
$$\left.\begin{aligned} \varphi(0) &= \frac{1}{L}\frac{dV}{d\eta} = 0, \\ N(0) &= -\frac{EJ}{L^3}\left[\frac{d^3V}{d\eta^3} - 2r^2\frac{dV}{d\eta}\right] = -\frac{P}{2}, \end{aligned}\right\} \tag{4.6}$$

where $\varphi(0)$ is the slope and $N(0)$ the generalized shearing force for $\eta = 0$.*

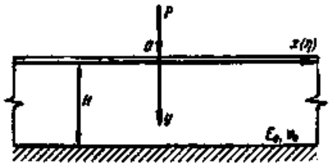

FIGURE 41.

Substitution of (4.4) in (4.6) yields:

$$\left.\begin{aligned} C_1F_1'(0) + C_2F_2'(0) &= 0, \\ C_1F_1'''(0) + C_2F_2'''(0) &= \frac{PL^3}{2EJ}. \end{aligned}\right\} \tag{4.7}$$

By solving (4.7) we obtain the integration constants:

$$\left.\begin{aligned} C_1 &= \frac{PL^3}{2EJ}\,\frac{F_2'(0)}{F_1'''(0)F_2'(0) - F_2'''(0)F_1'(0)}, \\ C_2 &= \frac{-PL^3}{2EJ}\,\frac{F'(0)}{F_1'''(0)F_2'(0) - F_2'''(0)F_1'(0)}, \end{aligned}\right\} \tag{4.8}$$

where $F_1'(0)$, $F_1'''(0)$, $F_2'(0)$, $F_2'''(0)$ are the first and third derivatives of F_1, and F_2 at $\eta = 0$.

By substituting (4.8) in (4.4) and taking (1.7), (1.9), and (2.5) into account we obtain finally:

$$V(\eta) = \frac{P(1-\nu_0^2)}{E_0\delta}\,\frac{1}{2\bar{\alpha}\,\bar{\beta}s^3}\,[\alpha F_1(\eta) + \bar{\beta}F_2(\eta)]. \tag{4.9}$$

Expressions (1.11) and (1.12) for the bending moments and shearing forces respectively then become:

$$M(\eta) = \frac{PL}{4}\left[\frac{F_2(\eta)}{\bar{\alpha}} - \frac{F_1(\eta)}{\bar{\beta}}\right], \tag{4.10}$$

$$Q(\eta) = -\frac{P}{2}\left[F_2(\eta) - \frac{r^2}{2\bar{\alpha}\,\bar{\beta}}F_1(\eta)\right]. \tag{4.11}$$

---

* The following ordinary boundary conditions correspond to the generalized conditions (4.6):

$$\varphi(0) = \frac{1}{L}\,\frac{dV}{d\eta} = 0,$$
$$Q(0) = -\frac{EJ}{L^3}\,\frac{d^3V}{d\eta^3} = -\frac{P}{2}.$$

The reactions of the elastic foundation are, by (1.4),

$$q(\eta)=\frac{P}{4\bar{\alpha}\bar{\beta}L}\left[\bar{\beta}(s^2+2r^2)F_2(\eta)+\bar{\alpha}(s^2-2r^2)F_1(\eta)\right]. \tag{4.12}$$

Expressions (4.9) through (4.12) make possible rapid calculation of the stresses and strains in an infinite beam [on an elastic foundation]. They can be written in the following concise form, similar to that for an [ordinary] infinite beam (cf., for instance, /25/):

$$\left.\begin{aligned} V(\eta)&=\frac{P(1-\nu_0^2)}{E_0 b}\bar{v}(\eta), & M(\eta)&=PL\bar{m}(\eta),\\ Q(\eta)&=-P\bar{Q}(\eta), & q(\eta)&=\frac{P}{L}\bar{q}(\eta),\end{aligned}\right\} \tag{4.13}$$

where

$$\left.\begin{aligned} \bar{v}(\eta)&=\frac{1}{2\bar{\alpha}\bar{\beta}s^2}[\bar{\alpha}F_1(\eta)+\bar{\beta}F_2(\eta)],\\ \bar{m}(\eta)&=\frac{1}{4}\left[\frac{F_2(\eta)}{\bar{\alpha}}-\frac{F_1(\eta)}{\bar{\beta}}\right],\\ \bar{Q}(\eta)&=\frac{1}{2}\left[F_2(\eta)-\frac{r^2}{2\bar{\alpha}\bar{\beta}}F_1(\eta)\right],\\ \bar{q}(\eta)&=\frac{1}{4\bar{\alpha}\bar{\beta}}[\bar{\beta}(s^2+2r^2)F_2(\eta)+\bar{\alpha}(s^2-2r^2)F_1(\eta)].\end{aligned}\right\} \tag{4.14}$$

The following relationships exist between these functions:

$$\left.\begin{aligned} \bar{v}'(\eta)&=-\bar{\varphi}(\eta)^{*}, & \bar{m}'(\eta)&=-\bar{Q}(\eta),\\ \bar{\varphi}'(\eta)&=\bar{m}(\eta), & \bar{Q}'(\eta)&=-\bar{q}(\eta).\end{aligned}\right\} \tag{4.15}$$

2

Expressions (4.9) through (4.12), or (4.13), are quite general. They are valid for any function $\phi(y)$, the accuracy being equal to that with which k, t, s^2, r^2, $\bar{\alpha}$, $\bar{\beta}$ have been determined.

Consider the case for which:

$$\phi(y)=\frac{\operatorname{sh}\gamma\frac{H-y}{L}}{\operatorname{sh}\gamma\frac{H}{L}}, \tag{4.16}$$

where L is defined by (1.7), and γ is a coefficient depending on the properties of the elastic foundation.

---

* $\bar{\varphi}(\eta)=\frac{1}{2\bar{\alpha}\bar{\beta}}F_1(\eta)$ is the dimensionless slope whose dimensional value is: $\varphi(\eta)=-\frac{P(1-\nu_0^2)}{E_0 bL}\bar{\varphi}(\eta)$.

The constants entering in (4.9) through (4.12) are:

$$\left.\begin{aligned} &k=\frac{E_0\delta}{H\left(1-\nu_0^2\right)}\psi_k, \qquad t=\frac{E_0\delta H}{12\left(1+\nu_0\right)}\psi_t,\\ &s^4=2\frac{L}{H}\psi_k, \qquad r^2=2\frac{1-\nu_0}{12}\,\frac{H}{L}\psi_t,\\ &\bar{\alpha}=\sqrt{\frac{s^2+r^2}{2}}, \qquad \bar{\beta}=\sqrt{\frac{s^2-r^2}{2}},\\ &\psi_k=\frac{1}{2}\,\frac{\gamma H}{L}\,\frac{\operatorname{sh}\frac{\gamma H}{L}\operatorname{ch}\frac{\gamma H}{L}+\frac{\gamma H}{L}}{\operatorname{sh}^2\frac{\gamma H}{L}},\\ &\psi_t=\frac{3}{2}\,\frac{L}{\gamma H}\,\frac{\operatorname{sh}\frac{\gamma H}{L}\operatorname{ch}\frac{\gamma H}{L}-\frac{\gamma H}{L}}{\operatorname{sh}^2\frac{\gamma H}{L}}. \end{aligned}\right\} \qquad (4.17)$$

[cf. (2.5) of this chapter and (3.18), (3.19) of Chapter I]

If the elastic foundation is a semi-infinite plane ($H\to\infty$), expressions (4.17) reduce to:

$$\left.\begin{aligned} &k=\frac{E_0\delta}{2\left(1-\nu_0^2\right)}\,\frac{\gamma}{L},\\ &t=\frac{E_0\delta}{8\left(1+\nu_0\right)}\,\frac{L}{\gamma},\\ &s^4=\gamma,\\ &r^2=\frac{1-\nu_0}{4\gamma}. \end{aligned}\right\} \qquad (4.18)$$

Curves of $\bar{v}$, $\bar{m}$, $\bar{Q}$ and $\bar{q}$, calculated from (4.14) and (4.18) for $H\to\infty$, $\nu_0 = 0.3$, and $\gamma = 1.0$, $\gamma = 1.5$, are shown in Figures 42, 43, 44, 45. The abscissae are the dimensionless distances $\eta=\frac{x}{L}$, measured from the origin.

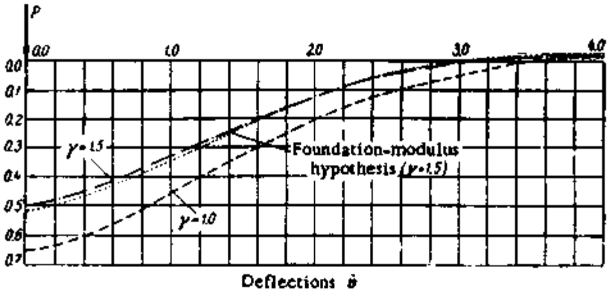

FIGURE 42.

These curves have been plotted only for positive values of η since [obviously] $\bar{v}$, $\bar{m}$, and $\bar{q}$ are even functions of η, only $\bar{Q}$ being an odd function. The dimensional functions V, M, Q and q are obtained from (4.13).

When γ increases, the bending moment at $\eta = 0$ decreases. This is due to the larger reactions near the point of action of the force. In addition, the deflections of the beam are considerably less.

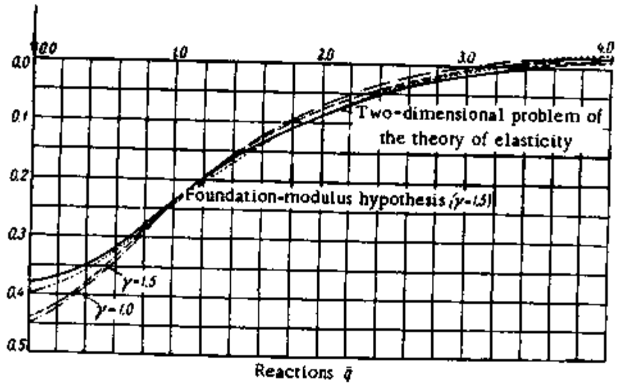

Reactions $\bar{q}$
FIGURE 43.

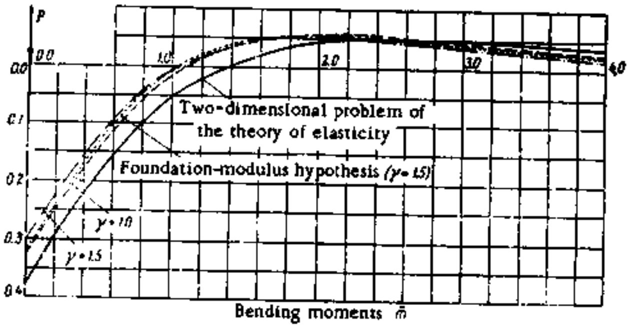

Bending moments $\bar{m}$
FIGURE 44.

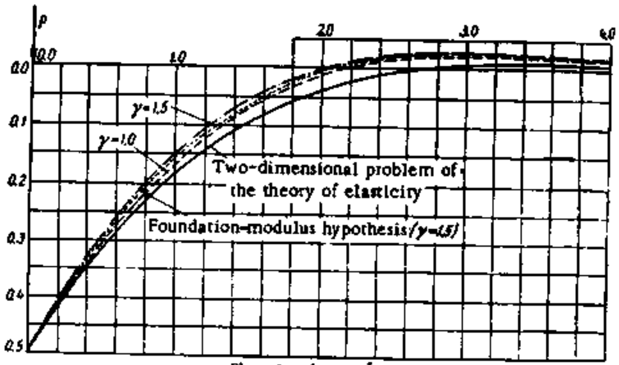

Shearing forces $\bar{\delta}$
FIGURE 45.

Curves obtained by Gersevanov and Macheret (cf. /21, 25/) for an infinite beam on an elastic semi-infinite plane*, and also those obtained by postulating a foundation modulus, have been plotted in Figures 43, 44, and 45 for comparison. The foundation modulus is assumed to be:

$$k = \frac{E_0 b}{2(1-\nu_0^2)} \frac{\gamma}{L} \tag{4.19}$$

where

$$\gamma = 1.5; \qquad \nu_0 = 0.3, \qquad L = \sqrt[3]{\frac{2EJ(1-\nu_0^2)}{bE_0}}.$$

Comparison with the results, obtained when the foundation modulus is postulated, shows (see the curve for $\gamma = 1.5$ in Figure 44) that when allowance is made for shearing stresses in the elastic foundation, the maximum bending moment decreases. The difference is of the order of 4% for the values of γ considered.

When $\phi(y)$ is given by (4.16), the solution presented here gives for $\gamma = 1.0$ and 1.5 lower absolute values of the maximum bending moment than the solution of the two-dimensional problem of the theory of elasticity. The difference is of the order of 15 to 20%, becoming less when γ decreases.

3

Consider an infinite beam on which a positive moment M_0 acts in a clockwise direction (Figure 46).

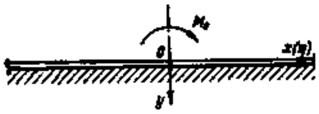

FIGURE 46.

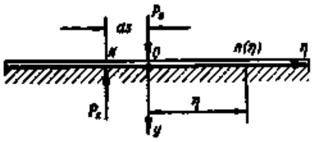

FIGURE 47.

Let two equal and opposite forces P be applied at points O and K situated at a distance ds from each other (Figure 47). We shall determine the deflections of the beam due to this couple. The first equation (4.13) becomes:

$$V_{P_O}(\eta) = \frac{P_O(1-\nu_0^2)}{E_0 b}\,\bar{v}(\eta),$$

$$V_{P_K}(\eta) = -\frac{P_K(1-\nu_0^2)}{E_0 b}\,\bar{v}(\eta + ds).$$

The total deflection of the beam at point $n(\eta)$ is:

$$V(\eta) = V_{P_O} + V_{P_K} = -\frac{P(1-\nu_0^2)}{E_0 b}\,[\bar{v}(\eta + ds) - \bar{v}(\eta)]. \tag{4.20}$$

---

* This was not done in Figure 42, since the vertical displacements cannot be determined in the two-dimensional problem of the theory of elasticity.

Let ds tend to zero and P to infinity so that the product $Pds = M_0$ remains finite and constant. By multiplying and dividing the right side of (4.20) by $ds\,[= L d\eta]$, we obtain in the limit:

$$V(\eta) = -\frac{M_0(1-\nu_0^2)}{E_0\delta L}\bar{v}'(\eta) = \frac{M_0(1-\nu_0^2)}{E_0\delta L}\bar{v}_M(\eta). \tag{4.21}$$

Similarly:

$$\left.\begin{aligned} \varphi(\eta) &= \frac{M_0(1-\nu_0^2)}{E_0\delta L^2}\bar{\varphi}'(\eta) = \frac{M_0(1-\nu_0^2)}{E_0\delta L^2}\bar{\varphi}_M(\eta),\\ M(\eta) &= -M_0\bar{m}'(\eta) = M_0\bar{m}_M(\eta),\\ Q(\eta) &= \frac{M_0}{L}\bar{Q}'(\eta) = -\frac{M}{L}\bar{Q}_M(\eta),\\ q(\eta) &= -\frac{M_0}{L^2}\bar{q}'(\eta) = \frac{M_0}{L^2}\bar{q}_M(\eta). \end{aligned}\right| \tag{4.22}$$

By (4.15):

$$\left.\begin{aligned} \bar{v}_M(\eta) &= \bar{\varphi}(\eta), & \bar{m}_M(\eta) &= \bar{Q}(\eta),\\ \bar{\varphi}_M(\eta) &= \bar{m}(\eta), & \bar{Q}_M(\eta) &= \bar{q}(\eta). \end{aligned}\right\} \tag{4.23}$$

By differentiating the last equation (4.14) we obtain:

$$\bar{q}_M(\eta) = r^2F_2(\eta) + \frac{s^4-2r^4}{4\bar{\alpha}\bar{\beta}}F_1(\eta). \tag{4.24}$$

§ 5. RIGID BEAM

The case of an infinitely rigid beam is very important in the theory of beams of finite length. Analysis of such beams reduces to finding the reactions $q(x)$; the other unknowns can be found by means of the ordinary equations of statics.

It is convenient to resolve the external load into symmetrical and antisymmetrical components and to carry out the calculations separately. The final result is then obtained by superposition.

1. Symmetrical loading

The deflection of a rigid beam under the action of a symmetrical load is constant:

$$V(x) = C_0. \tag{5.1}$$

The vertical displacements of the surface of the elastic foundation are also constant beneath the beam, as follows from (1.4):

$$q(x) = kC_0. \tag{5.2}$$

The reactions of the elastic foundation are thus determined in a manner similar to Winkler's method. The only difference is that in our case $V(x)$ has no discontinuity at the beam ends, as would happen if the foundation modulus were postulated. In other words, the elastic single-layer foundation is strained even beyond the edges of the beam (Figure 48).

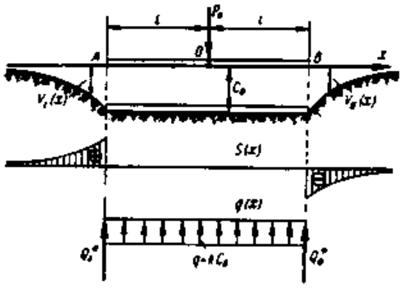

FIGURE 48.

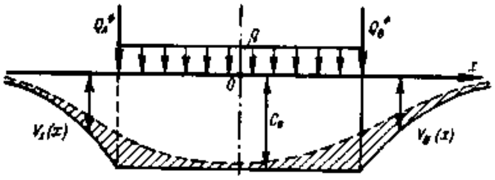

FIGURE 49.

In section 3 of Chapter I we introduced the generalized shearing force:

$$S(x) = \int_0^H \tau_{yx}\psi(y)\,dF = 2tV'(x) \tag{5.3}$$

[cf. (3.10) of Chapter I]

which is discontinuous at points where concentrated forces act at the surface of the elastic foundation.

In accordance with (5.1), S becomes zero beneath the beam. Beyond the edges of the beam, the generalized shearing force is, however, different from zero, so that $S(x)$ has discontinuities at $x=-l$ and $x=l$. Hence, concentrated reactions Q^Φ arise at the beam ends, which are due to stresses in the elastic foundation beyond the beam edges.

The existence of concentrated reactions Q^Φ can be proved also by different reasoning. The assumption that only distributed reactions, given by (5.2), act on the bottom of the rigid beam leads to a contradiction: the vertical displacements of the surface of a single-layer foundation acted upon by a uniformly distributed load are not constant (cf. (3.39) Chapter I). In order that condition (5.1) be satisfied beneath the beam, concentrated forces must act at the beam ends, causing additional displacements of the foundation surface (the hatched part of the displacement diagram in Figure 49).

In the general case the concentrated reactions Q^Φ are equal to the difference between the values of S to the left and to the right of the beam end:

$$\left.\begin{aligned} Q_A^\Phi &= S_0(-l) - S_b(-l), \\ Q_B^\Phi &= S_b(l) - S_0(l), \end{aligned}\right\} \tag{5.4}$$

where S_0 = generalized shearing force acting in the free foundation, S_b = generalized shearing force acting in the foundation beneath the beam.

The sign of Q^Φ is determined in a similar manner as the sign of the reactions $q(x)$, being positive for forces acting upward.

The stresses in the elastic foundation beyond the beam edges are given by:

$$-2tV'' + kV = 0. \tag{5.5}$$

Solving (5.5) for V, we obtain:

$$\left.\begin{aligned} &\text{at } x \leqslant -l \qquad V_{\mathrm{I}} = C_0 e^{\alpha(x+l)}, \\ &\text{at } x \geqslant l \qquad V_{\mathrm{II}} = C_0 e^{-\alpha(x-l)}. \end{aligned}\right\} \tag{5.6}$$

Taking (5.1), (5.6), and (5.3) into account, we obtain from (5.4):

$$Q_A^0 = Q_B^0 = 2\alpha t C_0, \tag{5.7}$$

where

$$\alpha = \sqrt{\frac{k}{2t}}. \tag{5.8}$$

The displacement C_0 is found from the equilibrium condition of the beam by equating the projection of all vertical forces to zero. The forces acting on the beam are the known external load P_0, the uniform reaction q, and the two forces Q_A^0 and Q_B^0; therefore [by (5.2)]

$$C_0 = \frac{P_0}{2(kl + 2\alpha t)}. \tag{5.9}$$

Substitution of (5.9) in (5.2) and (5.7) yields:

$$q = \frac{P_0}{2l}\,\frac{1}{1 + 2\,\frac{\alpha t}{kl}}, \tag{5.10}$$

$$Q_A^0 = Q_B^0 = \frac{P_0}{2}\,\frac{1}{1 + \frac{kl}{2\alpha t}}. \tag{5.11}$$

The constant C_0 could also have been determined from the generalized (variational) equilibrium condition for the entire system (beam and elastic foundation), obtained by equating to zero the total work done by all external and internal forces in the system over the virtual displacement $\bar{v}(x, y) = 1 \cdot \psi(y)$:

$$-\int_{-\infty}^{+\infty}\int_0^H \sigma_y \psi'(y)\, dF\, dx + P_0 \psi(0) = 0, \tag{5.12}$$

where $dF = b\,dy$, and σ_y is the normal stress, given by the first equation (3.3) of Chapter I.

Substituting (3.3) of Chapter I in (5.12), taking into account (1.3), (5.1), (5.6), and noting that $\psi(0) = 1$, we obtain:

$$C_0 k \left[\int_{-\infty}^{-l} e^{\alpha(x+l)}\, dx + \int_{-l}^{+l} dx + \int_l^{\infty} e^{-\alpha(x-l)}\, dx \right] = P_0, \tag{5.12'}$$

or

$$C_0 k\left[2l + \frac{2}{\alpha}\right] = 2C_0[kl + 2\alpha t[= P_0, \qquad (5.12'')$$

from which we again obtain (5.9).

From (5.12') or (5.12") and (5.7) it is seen that each reaction Q^* is equal in magnitude to k times the volume of the displacements in the elastic foundation beyond the corresponding beam end:

$$\left.\begin{aligned} Q_A^* &= k\int_{-\infty}^{-l} C_0 e^{\alpha(x+l)}\,dx = 2\alpha t C_0,\\ Q_B^* &= k\int_{l}^{\infty} C_0 e^{-\alpha(x-l)}\,dx = 2\alpha t C_0. \end{aligned}\right\} \qquad (5.7')$$

A similar result is obtained if the displacements given by (5.1) and (5.6) for $C_0 = 1$ are considered as virtual displacements. Unlike (5.12), the work done by the internal forces is in this case the sum of the work done by the normal stresses σ_y and by the shearing stresses τ_{yx}. The final result will again be given by (5.12").

2. Antisymmetrical loading

The deflection of the beam due to an antisymmetrical load is:

$$V(x) = \theta_0 x, \qquad (5.13)$$

where $\theta_0 = \operatorname{tg}\varphi_0$ = the slope of the beam (Figure 50).

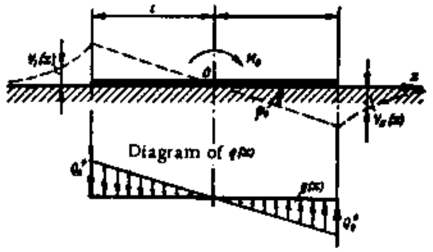

FIGURE 50.

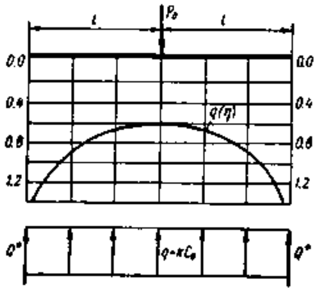

FIGURE 51.

It follows in this case from (1.4) that:

$$q(x) = k\theta_0 x. \qquad (5.14)$$

In order to determine the concentrated reactions Q^*, we calculate the generalized shearing forces $S(x)$.

Proceeding from (5.3), and noting that the displacements of the foundation beyond the beam ends are:

$$\left.\begin{aligned} &\text{at } x \leqslant -l \qquad V_{\rm I} = -\theta_0 l e^{\alpha(x+l)};\\ &\text{at } x \geqslant l \qquad V_{\rm II} = \theta_0 l e^{-\alpha(x-l)}, \end{aligned}\right\} \qquad (5.15)$$

we obtain the following expressions for the generalized shearing force:

$$\left.\begin{aligned} &\text{at } x \leqslant -l && S = -2\alpha t\theta_0 l e^{\alpha(x+l)};\\ &\text{at } -l < x < l && S = 2t\theta_0;\\ &\text{at } x \geqslant l && S = -2\alpha t\theta_0 l e^{-\alpha(x-l)}.\end{aligned}\right\} \tag{5.16}$$

The concentrated reactions at the beam ends can now be determined from (5.4):

$$-Q_A^{\Phi} = Q_B^{\Phi} = 2t(1+\alpha l)\,\theta_0, \tag{5.17}$$

where

$$\alpha = \sqrt{\frac{k}{2t}}.$$

From the equilibrium condition for the beam, obtained by equating to zero the sum of all moments acting on the beam about its center, we find:

$$\theta_0 = \frac{3M_0}{2l\,[kl^3 + 6t(1+\alpha l)]}. \tag{5.18}$$

Substitution of (5.18) in (5.14) and (5.17) leads to the following expressions for the reactions:

$$q = \frac{3M_0}{2l^3\left[1 + 6\frac{t}{l^2k}(1+\alpha l)\right]}\,x, \tag{5.19}$$

$$Q^{\Phi} = \frac{M_0}{2l\left[1 + \frac{kl^3}{6t(1+\alpha l)}\right]}, \tag{5.20}$$

where M_0 is the sum of the external moments about the coordinate origin.

Expressions (5.10), (5.11) (for symmetrical loading), and (5.19), (5.20) (for antisymmetrical loading), give the complete solution for a rigid beam, since the bending moments and shearing forces can be determined by known methods once the reactions have been determined.

3. Calculation examples and analysis of results

The exact solution of the problem of a plane symmetrically loaded punch, obtained by Sadovskii, is:

$$q(\eta) = \frac{P_0}{\pi l\sqrt{1-\eta^2}}, \tag{5.21}$$

where $\eta = \frac{x}{l}$ (Figure 51).

The reactions given by (5.21) are also shown in Figure 51. It can be seen that they increase to infinity toward the punch ends.

The elastic foundation is not considered by us to be a semi-infinite plane but a single-layer model whose properties are determined by two parameters k and t, in which concentrated forces Q^{Φ} correspond to the infinitely large reactions $q(\eta)$ obtained for the exact solution.

The concentrated reactions Q^* are obviously not real forces acting in the elastic foundation at the beam ends. Their appearance is due to the stresses in the elastic foundation beyond the punch ends. They should therefore be considered as fictitious forces by which allowance is made for the influence of the free foundation on the stresses in the punch.

We put:

$$\psi(y)=\frac{\operatorname{sh}\gamma\frac{H-y}{l}}{\operatorname{sh}\frac{\gamma H}{l}}, \tag{5.22}$$

where l is the half-length of the beam, and γ a coefficient characterizing the variation with depth of the vertical displacements in the foundation.

In accordance with (1.3) and (5.22), the elastic parameters of the foundation are:

$$\left.\begin{aligned} k=\frac{E_0 b}{H(1-\nu_0^2)}\phi_k,\qquad t=\frac{E_0 bH}{12(1+\nu_0)}\phi_t,\\ \alpha=\frac{1}{H}\frac{\sqrt{6(1-\nu_0)}}{1-\nu_0}\phi_\alpha, \end{aligned}\right\} \tag{5.23}$$

where

$$\left.\begin{aligned} \phi_k&=\frac{1}{2}\frac{\gamma H}{l}\frac{\operatorname{sh}\frac{\gamma H}{l}\operatorname{ch}\frac{\gamma H}{l}+\frac{\gamma H}{l}}{\operatorname{sh}^2\frac{\gamma H}{l}},\\ \phi_t&=\frac{3}{2}\frac{l}{\gamma H}\frac{\operatorname{sh}\frac{\gamma H}{l}\operatorname{ch}\frac{\gamma H}{l}-\frac{\gamma H}{l}}{\operatorname{sh}^2\frac{\gamma H}{l}},\\ \phi_\alpha&=\frac{\gamma H}{l}\sqrt{\frac{1}{3}\frac{\operatorname{sh}\frac{\gamma H}{l}\operatorname{ch}\frac{\gamma H}{l}+\frac{\gamma H}{l}}{\operatorname{sh}\frac{\gamma H}{l}\operatorname{ch}\frac{\gamma H}{l}-\frac{\gamma H}{l}}}. \end{aligned}\right\} \tag{5.24}$$

[cf. (3.18), (3.19), (3.32) of Chapter I]

Substitution of (5.23) in (5.10), (5.11), (5.19), and (5.20) yields:

for the symmetrical load,

$$\left.\begin{aligned} q&=\frac{P_0}{2l}\frac{1}{1+\frac{\sqrt{2(1-\nu_0)}}{2\gamma}\sqrt{\frac{\operatorname{sh}\frac{\gamma H}{l}\operatorname{ch}\frac{\gamma H}{l}-\frac{\gamma H}{l}}{\operatorname{sh}\frac{\gamma H}{l}\operatorname{ch}\frac{\gamma H}{l}+\frac{\gamma H}{l}}}},\\ Q^*&=\frac{P_0}{2}\frac{1}{1+\frac{2\gamma}{\sqrt{2(1-\nu_0)}}\sqrt{\frac{\operatorname{sh}\frac{\gamma H}{l}\operatorname{ch}\frac{\gamma H}{l}+\frac{\gamma H}{l}}{\operatorname{sh}\frac{\gamma H}{l}\operatorname{ch}\frac{\gamma H}{l}-\frac{\gamma H}{l}}}}; \end{aligned}\right\} \tag{5.25}$$

for the antisymmetrical load,

$$\left.\begin{aligned} q &= \frac{M_0}{l^3}\,\frac{1}{\dfrac{2}{3}+\dfrac{1-\nu_0}{\gamma^2}\,\dfrac{\operatorname{sh}\frac{\gamma H}{l}\operatorname{ch}\frac{\gamma H}{l}-\frac{\gamma H}{l}}{\operatorname{sh}\frac{\gamma H}{l}\operatorname{ch}\frac{\gamma H}{l}+\frac{\gamma H}{l}}+\dfrac{\sqrt{2(1-\nu_0)}}{\gamma}\sqrt{\dfrac{\operatorname{sh}\frac{\gamma H}{l}\operatorname{ch}\frac{\gamma H}{l}-\frac{\gamma H}{l}}{\operatorname{sh}\frac{\gamma H}{l}\operatorname{ch}\frac{\gamma H}{l}+\frac{\gamma H}{l}}}}\,x, \\ Q^{\Phi} &= \frac{M_0}{2l}\,\frac{1+\gamma\dfrac{\sqrt{2(1-\nu_0)}}{1-\nu_0}\sqrt{\dfrac{\operatorname{sh}\frac{\gamma H}{l}\operatorname{ch}\frac{\gamma H}{l}+\frac{\gamma H}{l}}{\operatorname{sh}\frac{\gamma H}{l}\operatorname{ch}\frac{\gamma H}{l}-\frac{\gamma H}{l}}}}{1+\dfrac{2}{3}\,\dfrac{\gamma^2}{1-\nu_0}\,\dfrac{\operatorname{sh}\frac{\gamma H}{l}\operatorname{ch}\frac{\gamma H}{l}+\frac{\gamma H}{l}}{\operatorname{sh}\frac{\gamma H}{l}\operatorname{ch}\frac{\gamma H}{l}-\frac{\gamma H}{l}}+\gamma\dfrac{\sqrt{2(1-\nu_0)}}{1-\nu_0}\sqrt{\dfrac{\operatorname{sh}\frac{\gamma H}{l}\operatorname{ch}\frac{\gamma H}{l}+\frac{\gamma H}{l}}{\operatorname{sh}\frac{\gamma H}{l}\operatorname{ch}\frac{\gamma H}{l}-\frac{\gamma H}{l}}}}\end{aligned}\right\}\qquad(5.26)$$

Consider the case of symmetrical loading, for which curves of the dimensionless magnitudes $\bar{q}$ and $\bar{Q}^{\Phi}$ are given in Figures 52 and 53. for $\nu_0 = 0.3$ and $\gamma = 1.0$; $\gamma = 1.5$; $\gamma = 2.0$. The dimensionless reactions q and Q^{Φ} are obtained from:

$$q = \frac{P_0}{2l}\bar{q}, \quad Q^{\Phi} = \frac{P_0}{2}\bar{Q}^{\Phi}. \qquad (5.27)$$

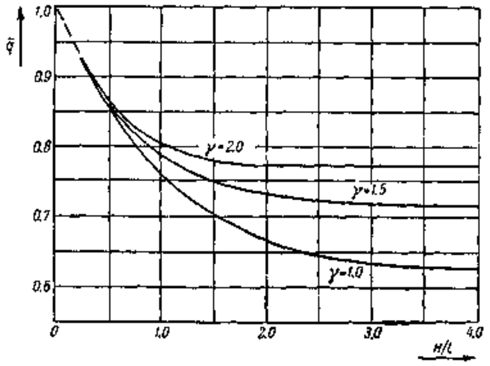

FIGURE 52.

It can be seen that for ratios of $\frac{H}{l}$ above 1.5 to 2.0 the reactions remain constant for the values of γ considered. When $\frac{H}{l}$ exceeds this value, therefore, the elastic foundation behaves like an elastic semi-infinite plane $(H = \infty)$. It can also be seen that when γ increases, the concentrated reactions at the beam ends decrease, the foundation behaving more like Winkler's model.

In order to compare (5.25) with the exact solution given by the theory of elasticity, we determined the bending moment m_0 at the center of the beam, due to the reactions q [(5.10)] and Q^{Φ} [(5.11)] alone:

$$m_0 = \frac{ql^2}{2} + Q^{\Phi}l = \frac{P_0 l}{4}\,\frac{kl + 4\alpha l}{kl + 2\alpha l}. \qquad (5.28)$$

Insertion of (5.23) and (5.24) yields:

$$m_0 = \frac{P_0 l}{2} \frac{3\gamma + \sqrt{6(1-\nu_0)} \sqrt{3 \frac{\operatorname{sh}\bar{\gamma}\operatorname{ch}\bar{\gamma} - \bar{\gamma}}{\operatorname{sh}\bar{\gamma}\operatorname{ch}\bar{\gamma} + \bar{\gamma}}}}{6\gamma + \sqrt{6(1-\nu_0)} \sqrt{3 \frac{\operatorname{sh}\bar{\gamma}\operatorname{ch}\bar{\gamma} - \bar{\gamma}}{\operatorname{sh}\bar{\gamma}\operatorname{ch}\bar{\gamma} + \bar{\gamma}}}}, \tag{5.29}$$

with $\bar{\gamma} = \gamma \frac{H}{l}$.

In the case of an elastic semi-infinite plane $\left(\frac{H}{l} = \infty\right)$, (5.29) reduces to:

$$m_0 = P_0 l \bar{m}_0, \tag{5.30}$$

where

$$\bar{m}_0 = \frac{1}{2} \frac{\gamma + \sqrt{2(1-\nu_0)}}{2\gamma + \sqrt{2(1-\nu_0)}}. \tag{5.31}$$

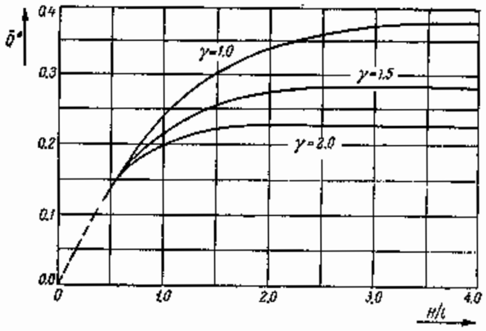

FIGURE 53.

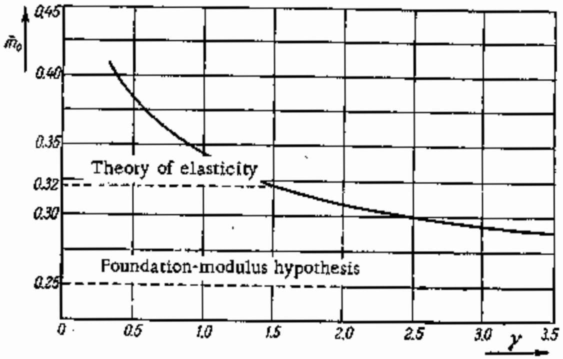

FIGURE 54.

The value of $\bar{m}_0$ given by (5.31) has been plotted in Figure 54 for $\nu_0 = 0.3$ as a function of γ. It is seen that $m_0 = 0.32$ for $\gamma = 1.5$, which is Gorbunov-Posadov's result for a rigid beam /26/. With increasing γ the value of $\bar{m}_0$ approaches 0.25 asymptotically, which is the solution when the foundation modulus is postulated.

The reactions thus obtained for $\gamma = 1.5$ are therefore equal to those obtained in the two-dimensional solution (5.21) for the moments in the center of the beam, due to these reactions. Since, for a rigid beam acted upon by a symmetrical load, q is uniquely determined by P_0 and l, the bending-moment diagram, obtained by the method proposed by us, will be similar to that obtained in the two-dimensional solution given by the theory of elasticity.

As an example, Figures 55 and 56 show curves of M and Q corresponding to the three most important cases of loading of a rigid beam for $\gamma = 1.5$. Comparison with the exact solution* (broken curves and numbers in parentheses) shows that the results differ only near the beam ends.

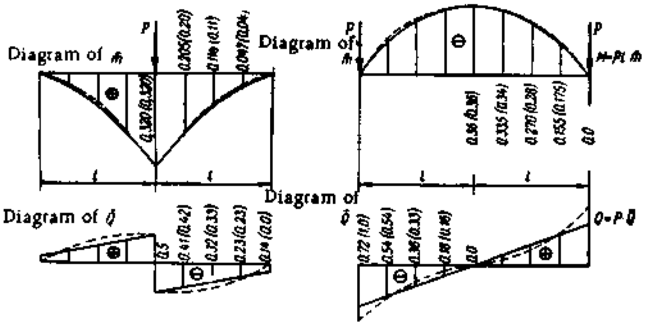

FIGURE 55.

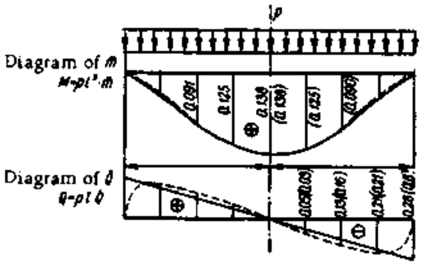

FIGURE 56.

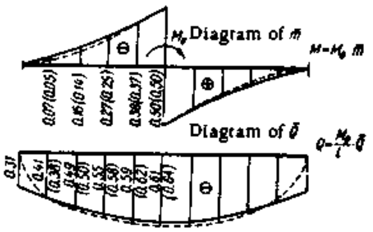

FIGURE 57.

A similar comparison for the case of antisymmetrical loading shows that the results obtained for $\gamma = 1.5$ are very similar (Figure 57).

---

* See Gorbunov-Posadov Raschet konstruktsii na uprugom osnovanii (Analysis of Structures on Elastic Foundations). — Gosstroiizdat, Part 1, Chapter 1, § 6. 1953.

4. Allowance for plastic deformations beneath the beam ends

It was assumed until now that the vertical displacements $V(x)$ of the surface of the elastic foundation are continuous. This necessitated the assumption of concentrated reactions Q^{Φ} beneath the beam ends.

Under actual conditions these intense reactions cause plastic deformations beneath the beam ends, leading to considerable changes in the general stress pattern in beam and foundation. The methods of the theory of elasticity no longer apply to the soil in this case and a special analysis, in which allowance is made for the elastic-plastic deformations of the foundation, becomes necessary.

The approximative method proposed can, however, be applied to this case. Assume that plastic deformations have occurred beneath the ends of a symmetrically loaded beam, as a result of which $V(x)$ has discontinuities at $x = l$ and $x = -l$, equal to:

$$c = (1 - \beta) C_0, \tag{5.32}$$

where β is a coefficient characterizing the settling tendency of the elastic foundation (Figure 58).

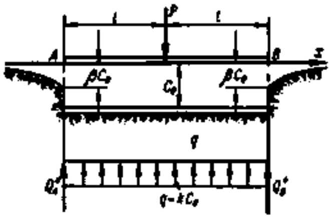

FIGURE 58.

As before, the reactions consist of the uniform reaction q and the fictitious forces Q^{Φ}, where by (5.2)

$$q = kC_0. \tag{5.33}$$

According to (5.3) and (5.4):

$$Q_A^{\Phi} = Q_B^{\Phi} = 2\alpha l \beta C_0 \tag{5.34}$$

From the equilibrium condition of the beam we find:

$$C_0 = \frac{P_0}{2(kl + 2\alpha\beta l)}. \qquad \text{[cf. (5.9)]} \tag{5.35}$$

Substitution of (5.35) in (5.33) and (5.34) yields:

$$\left.\begin{aligned} q &= \frac{P_0}{2l} \frac{1}{1 + 2\frac{\alpha\beta l}{kl}}, \\ Q^{\Phi} &= \frac{P_0}{l} \frac{1}{1 + \frac{kl}{2\alpha\beta l}}. \end{aligned}\right\} \qquad \text{[cf. (5.10), (5.11)]} \tag{5.36}$$

When $\beta = 0$, the elastic foundation is not strained beyond the beam ends; this corresponds to Winkler's model. For $\beta = 1$, (5.35) becomes identical with (5.9).

Similar considerations apply to the case of antisymmetrical loading.

§ 6. ELASTIC BEAM OF FINITE LENGTH

1

The differential equation of the bending of a beam on a single-layer elastic foundation is (cf. (1.8)):

$$\frac{d^4V}{d\eta^4} - 2r^2\frac{d^2V}{d\eta^2} + s^4V = \frac{pL^4}{EJ}. \tag{6.1}$$

Here $\eta = \frac{x}{L}$ and

$$L = \sqrt[3]{\frac{2EJ(1-\nu_0^2)}{E_0 b}}, \tag{6.2}$$

where b = beam width.

The coefficients in (6.1) are [cf. (1.9)]:

$$\left.\begin{aligned} r^2 &= \frac{1}{2}\,\frac{1-\nu_0}{L}\int\limits_0^H \psi_1^2\,dy,\\ s^4 &= 2L\int\limits_0^H \psi_1'^2\,dy. \end{aligned}\right\} \tag{6.3}$$

The general solution of the problem can be presented in the form [cf. (3.10)]:

$$\left.\begin{aligned} V(\eta) &= V_0K_{VV} + \varphi_0K_{V\varphi} + M_0K_{VM} + N_0K_{VN} - F_V,\\ \varphi(\eta) &= V_0K_{\varphi V} + \varphi_0K_{\varphi\varphi} + M_0K_{\varphi M} + N_0K_{\varphi N} - F_\varphi,\\ M(\eta) &= V_0K_{MV} + \varphi_0K_{M\varphi} + M_0K_{MM} + N_0K_{MN} - F_M,\\ N(\eta) &= V_0K_{NV} + \varphi_0K_{N\varphi} + M_0K_{NM} + N_0K_{NN} - F_N, \end{aligned}\right\} \tag{6.4}$$

where $K_{VV}, K_{V\varphi}, \ldots, K_{NM}, K_{NN}$ are the influence functions, given in Table 2; F_V, F_φ, F_M, F_N are functions depending on the external load (cf. e.g., (3.11)).

2.

To determine the initial parameters V_0, φ_0, M_0, N_0, it is necessary to consider the boundary conditions at the beam ends.

If the beam ends are prevented from moving downward, the boundary conditions can be written in the usual way:

a) for simply supported ends:

$$V = 0, \quad M = 0; \tag{6.5'}$$

b) for built-in ends:

$$V = 0, \quad \varphi = 0. \tag{6.5''}$$

If the beam ends are free to move downward, the compatibility conditions for the beam and the elastic foundation must be taken into account when establishing the boundary conditions. The vertical displacements $V(x)$ of the free parts (I) and (II) of the foundation (Figure 59) are determined except for the constants D_1 and D_2 ; the vertical displacements of the foundation beneath the beam are determined except for four constants C_1, C_2, C_3, C_4 (cf. (2.9)). Six independent conditions (three for each end of the beam) have therefore to be established in order to determine these constants.

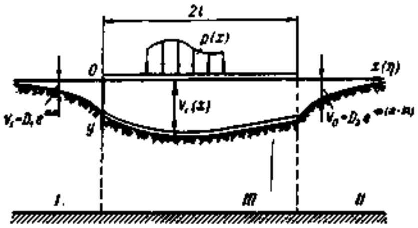

FIGURE 59.

An obvious condition for each end free of load is:

$$M = 0. \tag{6.6'}$$

The two other conditions can be written as follows:

$$\begin{gathered} V_0 = V_b; \\ S = N \text{ at } x = 0 \text{ (or } x = 2l), \end{gathered} \tag{6.6''}$$

where V_0 = vertical displacement of foundation, V_b = vertical displacement of beam, S = generalized shearing force in free parts (I, II) of foundation, and N = generalized shearing force in the foundation beneath beam (part III).

We note that (6.6'') corresponds to the conditions for a rigid beam.

Only simply supported beams will be considered henceforth, since these are of the greatest practical interest while their analysis is the most complicated.

3

By placing the origin of coordinates at the left end of the beam (Figure 59) we find from (6.6) and (5.3):

$$M_0 = 0, \quad N_0 = S(0) = 2\alpha t V_0 \tag{6.7}$$

The system (6.4) now becomes:

$$\left.\begin{aligned}V(\eta)&=(K_{VV}+2\alpha tK_{VN})V_0+K_{V\varphi}\varphi_0-F_V,\\ \varphi(\eta)&=(K_{\varphi V}+2\alpha tK_{\varphi N})V_0+K_{\varphi\varphi}\varphi_0-F_\varphi,\\ M(\eta)&=(K_{MV}+2\alpha tK_{MN})V_0+K_{M\varphi}\varphi_0-F_M,\\ N(\eta)&=(K_{NV}+2\alpha tK_{NN})V_0+K_{N\varphi}\varphi_0-F_N.\end{aligned}\right\}\tag{6.8}$$

The boundary conditions at the otner end of the beam are:

$$M\left(\frac{2l}{L}\right)=0,\quad N\left(\frac{2l}{L}\right)=-2\alpha lV\left(\frac{2l}{L}\right),\tag{6.9}$$

from which the other two initial parameters V_0 and φ_0 are obtained:

$$\left.\begin{aligned}V_0&=\frac{a_1F_M\left(\frac{2l}{L}\right)-a_2\left[F_N\left(\frac{2l}{L}\right)+2\alpha lF_V\left(\frac{2l}{L}\right)\right]}{a_1^2-a_2a_3},\\ \varphi_0&=-\frac{a_3F_M\left(\frac{2l}{L}\right)-a_1\left[F_N\left(\frac{2l}{L}\right)+2\alpha lF_V\left(\frac{2l}{L}\right)\right]}{a_1^2-a_2a_3}.\end{aligned}\right\}\tag{6.10}$$

The coefficients in (6.10) are:

$$\left.\begin{aligned}a_1&=K_{MV}\left(\frac{2l}{L}\right)+2\alpha tK_{MN}\left(\frac{2l}{L}\right),\\ a_2&=K_{M\varphi}\left(\frac{2l}{L}\right),\\ a_3&=K_{NV}\left(\frac{2l}{L}\right)+4\alpha tK_{NN}\left(\frac{2l}{L}\right)+(2\alpha t)^2K_{VN}\left(\frac{2l}{L}\right).\end{aligned}\right\}\tag{6.11}$$

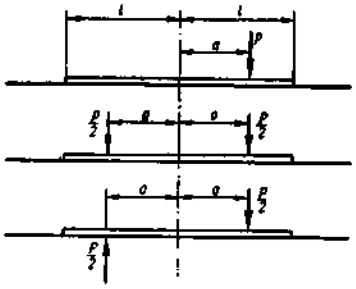

FIGURE 60.

Equations (6.8) and (6.10) represent the required solution when the bending of a beam of finite length, placed on an elastic foundation and acted upon by external loads, is considered.

When the beam is long, the origin of coordinates should be placed at the beam center, and the load should be resolved into symmetrical and antisymmetrical components (Figure 60); this increases the accuracy of the results. The method of solution is similar to that employed above.

In this case the following formulas are obtained:

a) for the symmetrical load:

$$\left.\begin{aligned} V(\eta) &= K_{VV}V_0 + K_{VM}M_0 - F_V, \\ \varphi(\eta) &= K_{\varphi V}V_0 + K_{\varphi M}M_0 - F_\varphi, \\ M(\eta) &= K_{MV}V_0 + K_{MM}M_0 - F_M, \\ N(\eta) &= K_{NV}V_0 + K_{NM}M_0 - F_N, \end{aligned}\right\} \tag{6.12}$$

where

$$V_0 = \frac{b_1 F_M\left(\frac{l}{L}\right) - b_2\left[F_N\left(\frac{l}{L}\right) + 2\alpha l F_V\right]}{b_1 b_4 - b_2 b_3},$$

$$M_0 = -\frac{b_3 F_M\left(\frac{l}{L}\right) - b_4\left[F_N\left(\frac{l}{L}\right) + 2\alpha l F_V\right]}{b_1 b_4 - b_2 b_3};$$

b) for the antisymmetrical load:

$$\left.\begin{aligned} V(\eta) &= K_{V\varphi}\varphi_0 + K_{VN}N_0 - F_V, \\ \varphi(\eta) &= K_{\varphi\varphi}\varphi_0 + K_{\varphi N}N_0 - F_\varphi, \\ M(\eta) &= K_{M\varphi}\varphi_0 + K_{MN}N_0 - F_M, \\ N(\eta) &= K_{N\varphi}\varphi_0 + K_{NN}N_0 - F_N, \end{aligned}\right\} \tag{6.13}$$

where

$$\varphi_0 = \frac{b_1 F_M\left(\frac{l}{L}\right) - b_2\left[F_N\left(\frac{l}{L}\right) + 2\alpha l F_V\left(\frac{l}{L}\right)\right]}{b_1 b_6 - b_2 b_5},$$

$$N_0 = -\frac{b_5 F_M\left(\frac{l}{L}\right) - b_6\left[F_N\left(\frac{l}{L}\right) + 2\alpha l F_V\left(\frac{l}{L}\right)\right]}{b_1 b_6 - b_2 b_5}.$$

The coefficients in (6.12) and (6.13) are:

$$\left.\begin{aligned} b_1 &= K_{NM}\left(\frac{l}{L}\right) + 2\alpha l K_{VM}\left(\frac{l}{L}\right), & b_4 &= K_{MV}\left(\frac{l}{L}\right), \\ b_2 &= K_{MM}\left(\frac{l}{L}\right), & b_5 &= K_{N\varphi}\left(\frac{l}{L}\right) + 2\alpha l K_{V\varphi}\left(\frac{l}{L}\right), \\ b_3 &= K_{NV}\left(\frac{l}{L}\right) + 2\alpha l K_{VV}\left(\frac{l}{L}\right), & b_6 &= K_{M\varphi}\left(\frac{l}{L}\right). \end{aligned}\right\} \tag{6.14}$$

Both (6.12) and (6.13) include only loads acting either to the right or to the left of the origin.

The equilibrium condition of the beam, the contact condition of equal vertical displacements of beam and foundation, and the continuity condition of foundation displacements are all satisfied by (6.8), (6.12), and (6.13). The statical boundary conditions are, however, only approximately satisfied: when the bending moments M vanish, the shearing forces Q at the beam ends differ from zero in the general case. This is explained by the properties of the model adopted for the elastic foundation, which is characterized by two generalized parameters k and t.

4

Analysis of these results shows that the elastic properties of both beam and foundation are characterized by a single magnitude:

$$\lambda = \frac{l}{L}, \tag{6.15}$$

which represents the reduced half-length of the beam.

In the two-dimensional problem of the theory of elasticity (solved, e.g., by the method of Gorbunov-Posadov), a magnitude called the index of beam flexibility is introduced as principal elastic characteristic, being defined as follows:

$$t = \frac{\pi E_0 \delta l^3}{4(1-\nu_0^2)EJ}, \tag{6.16}$$

where l = half-length of beam, δ = width of beam.

By comparing (6.2), (6.15), and (6.16) the following relationship between λ and t is obtained:

$$\lambda = \sqrt[3]{\frac{2t}{\pi}}. \tag{6.17}$$

Several examples will now be discussed in order to show the effect of λ on the results. It will be assumed that the elastic foundation is a semi-infinite plane ($H = \infty$), and that $\phi(y)$ is given by (4.16).

The dimensionless reactions $\bar{q}$ and bending moments $\bar{m}$, calculated by (6.12) for two beams, each loaded at the center by a concentrated force P, are shown in Figures 61 and 62. The elastic characteristics of these beams are respectively: $\lambda = 1.24$ ($t = 3.0$), and $\lambda = 1.64$ ($t = 7.0$). The calculations were performed for $\gamma = 1.0$ and $\gamma = 1.5$, for $\nu_0 = 0$, and $H = \infty$. Curves of $\bar{q}$ and $\bar{m}$, plotted on the basis of Gorbunov-Posadov's data /26/ for t = 3.0 and t = 7.0, have been drawn for comparison in the same figures (full lines). The actual reactions and bending moments are respectively:

$$q = \bar{q}\frac{P}{l}, \quad M = \bar{m}Pl.$$

It is seen that the concentrated reactions Q^{ϕ} at the beam ends vary inversely with λ, as do the bending moments. This variation is more pronounced when the value of λ is less. On the other hand, the more flexible or longer the beam, i.e., the larger the value of γ, the larger are the reactions near the point of application of the load, leading to a reduction in the bending moment at the beam center.

The dimensionless reactions $\bar{q}$ obtained by Gorbunov-Posadov's method are almost equal to those obtained by our method for $\gamma = 1.0$ and $\gamma = 1.5$ along the entire beam, except near its ends. As a result, satisfactory agreement is also observed for the corresponding bending-moment diagrams.

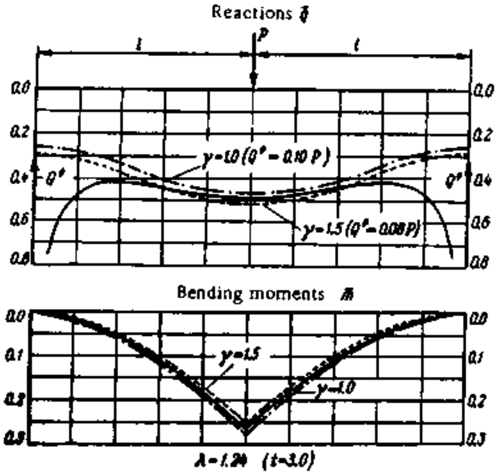

FIGURE 61

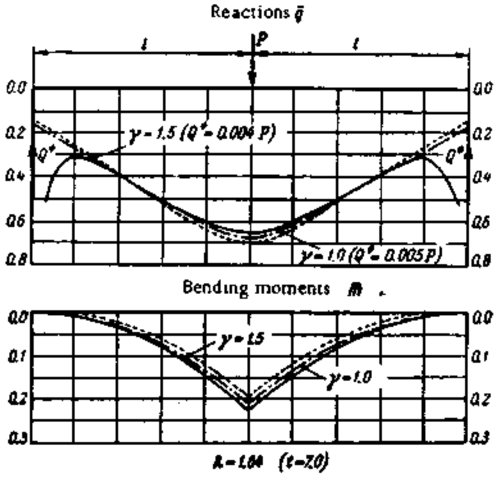

FIGURE 62

For $\gamma = 1.5$, the bending moments for both finite elastic and infinite beams, determined by our method, are slightly less than those obtained when solving the two-dimensional problem of the theory of elasticity.

The dimensionless deflections and bending moments of a rigid beam (broken lines, numbers in parentheses) and of an elastic beam of reduced half-length $\lambda = 0.86$ $(t = 1)$, are shown in Figure 63 for $\gamma = 1.5$, $\nu_0 = 0.3$, $H = \infty$. Comparison of these diagrams shows that (5.23) can be used for beams when $0 < \lambda < 0.86$. Such beams can be considered to be rigid.

A similar comparison, performed in Figure 64 for an elastic beam loaded by a concentrated force, and for an infinite beam, represented by broken lines and numbers in parentheses, shows that the results become practically identical for $\lambda = 1.85$ $(t = 10)$: the difference between the maximum bending moments is only 5%*.

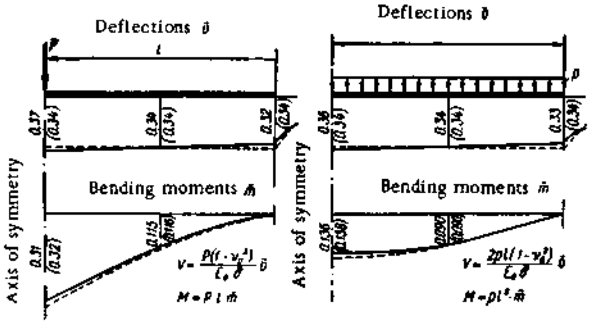

FIGURE 63.

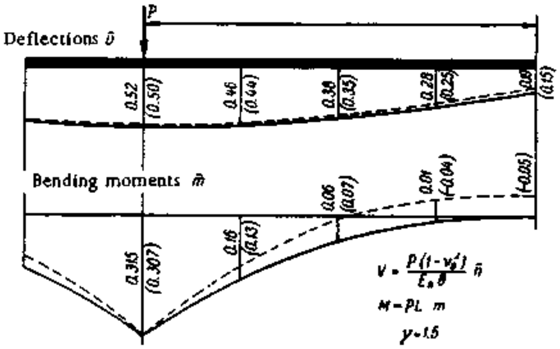

FIGURE 64.

This enables us to establish the values of λ at which transition from the finite-beam model to that of an infinitely long rigid beam occurs.

When a concentrated force acts, these values are as follows:

(λ < 0.86 — rigid beam,
0.86 < λ < 1.85 — finite [elastic] beam,
λ > 1.85 — infinite beam.

The boundaries thus defined are identical with those obtained by the methods of the theory of elasticity, and in particular, by Gorbunov-Posadov's method.

§ 7. INFLUENCE OF LATERAL LOADING

1

The method explained above can be applied to many problems connected with beams on elastic foundations. Such a problem is, e.g., that of a load applied to the elastic foundation beyond the edges of a rigid beam.

---

* The comparison was performed for $\gamma = 1.5$, $H = \infty$, $\nu_0 = 0.3$.

Let a concentrated force G act on the elastic foundation at a distance a from the beam end (Figure 65). The following expressions are obtained for the vertical displacements of the surface of the elastic foundation in sections I, II, III, IV (Figure 65) (see sections 3 of Chapter I and 5 of Chapter II):

$$\left.\begin{aligned} V_I &= D_1 e^{\alpha(x+l)}, \\ V_{II} &= C_0 + \theta_0 x, \\ V_{III} &= D_2 e^{\alpha(l-x)} + D_3 e^{-\alpha(l-x)}, \\ V_{IV} &= D_4 e^{\alpha(l+a-x)}, \end{aligned}\right\} \qquad (7.1)$$

where $\alpha = \sqrt{\frac{k}{2t}}$.

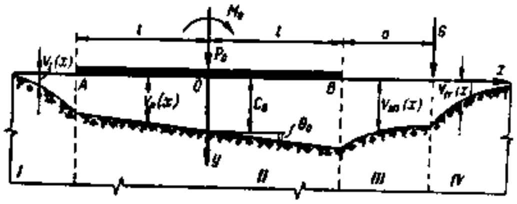

FIGURE 65.

The solution of this problem thus reduces to determining the six constants D_1, D_2, D_3, D_4, C_0 and θ_0.

Since the surface of the elastic foundation is assumed to be continuous, the following four independent conditions are obtained for the boundaries of parts I, II, III, and IV:

$$\left.\begin{aligned} &\text{at } x=-l & V_I &= V_{II}, \\ &\text{at } x=l & V_{II} &= V_{III}, \\ &\text{at } x=l+a & V_{III} &= V_{IV}, \\ & & S_{III}-S_{IV} &= G, \end{aligned}\right\} \qquad (7.2)$$

where S_{III} and S_{IV} are the generalized shearing forces in parts III and IV respectively*.

With the aid of (7.1) and (5.3), conditions (7.2) can be written in the form:

$$\left.\begin{aligned} D_1 &= C_0 - \theta_0 l, \\ D_2 + D_3 &= C_0 + \theta_0 l, \\ D_2 e^{-\alpha a} + D_3 e^{\alpha a} - D_4 &= 0, \\ -D_2 e^{-\alpha a} + D_3 e^{\alpha a} + D_4 &= \frac{G}{2\alpha t}. \end{aligned}\right\} \qquad (7.3)$$

---

[*] The last equation (7.2) states that $S(x)$ has a discontinuity of magnitude G at $x = l + a$. It is again assumed that $\phi(0) = 1$.

Solving (7.3) for D_1, D_2, D_3, D_4 we find:

$$\left.\begin{aligned} D_1 &= C_0 - \theta_0 l, \\ D_2 &= C_0 + \theta_0 l - \frac{G}{4\alpha t e^{\alpha a}}, \\ D_3 &= \frac{G}{4\alpha t e^{\alpha a}}, \\ D_4 &= (C_0 + \theta_0 l)\, e^{-\alpha a} + \frac{G}{4\alpha t} - \frac{G}{4\alpha t e^{2\alpha a}}. \end{aligned}\right\} \qquad (7.4)$$

We determine C_0 and θ_0 from the equilibrium conditions of a beam acted upon by the external load and the reactions $q(x)$ and Q^{Φ} of the elastic foundation.

The distributed reactions $q(x)$ are, in accordance with (1.4) and (7.1):

$$q = k\,(C_0 + \theta_0 x). \qquad (7.5)$$

The concentrated reactions Q^{Φ} are by (5.4):

$$\left.\begin{aligned} Q_A^{\Phi} &= S_I(-l) - S_{II}(-l), \\ Q_B^{\Phi} &= S_{II}(l) - S_{III}(l). \end{aligned}\right\} \qquad (7.6)$$

The generalized shearing forces entering have to be obtained from (5.3) with the aid of (7.1) and (7.4); substitution of the expressions obtained in (7.6) yields:

$$\left.\begin{aligned} Q_A^{\Phi} &= 2t\,[\alpha C_0 - (1 + \alpha l)\,\theta_0], \\ Q_B^{\Phi} &= 2t\,[\alpha C_0 + (1 + \alpha l)\,\theta_0] - \frac{G}{e^{\alpha a}}. \end{aligned}\right\} \qquad (7.7)$$

The equilibrium conditions of the beam, obtained by separately equating to zero the sum of the vertical projections of all forces and the sum of all moments about the beam center, yield:

$$\left.\begin{aligned} C_0 &= \frac{P_{\phi} + \dfrac{G}{e^{\alpha a}}}{2\,(kl + 2\alpha t)}, \\ \theta_0 &= \frac{3\left(M_0 + \dfrac{G}{e^{\alpha a}}\, l\right)}{2l\,[kl^2 + 6t\,(1 + \alpha l)]}. \end{aligned}\right\} \qquad (7.8)$$

Expressions (7.8) differ from (5.9) and (5.18) only by the presence of a term in the numerator containing G, through which allowance is made for the lateral load.

Analysis of (7.7) shows that this lateral load affects the concentrated reactions at the beam ends, thus altering the stress pattern. The influence of the load G decreases rapidly when the distance a is increased. When this load is distributed instead of being concentrated, allowance can be made for it in a similar way.

Consider two elastic beams of length $2l_1$ and $2l_2$ respectively, arranged in line and each acted upon by an external load. The displacements are shown in Figure 66.

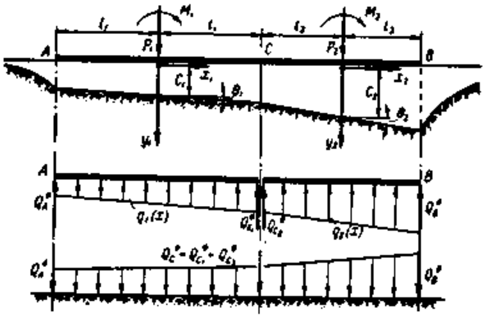

FIGURE 66.

Clockwise rotation will be taken as positive direction for the angles θ_1, θ_2 and external moments M_1 and M_2. For each beam a separate coordinate frame, with origin at the beam center, will be used.

The results of the previous example will be used to determine C_1, θ_1, C_2 and θ_2. The distributed reactions $q_1(x)$ and $q_2(x)$, acting on the first and second beam respectively, are:

$$\left.\begin{aligned} q_1(x) &= (C_1+\theta_1 x)\,k, \\ q_2(x) &= (C_2+\theta_2 x)\,k. \end{aligned}\right\} \qquad (7.9)$$

The concentrated reactions Q_A^{ϕ} and Q_B^{ϕ} are:

$$\left.\begin{aligned} Q_A^{\phi} &= 2l\,[\alpha C_1-(1+\alpha l)\,\theta_1], \\ Q_B^{\phi} &= 2l\,[\alpha C_2+(1+\alpha l)\,\theta_2], \end{aligned}\right\} \qquad (7.10)$$

where $\alpha=\sqrt{\frac{k}{2t}}$.

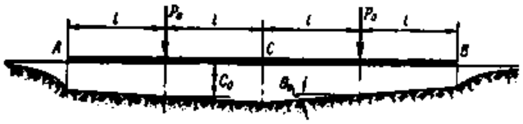

FIGURE 67.

The solution of this problem thus reduces to the determination of the six constants: C_1, θ_1, C_2, θ_2, $Q_{C_1}^{\phi}$ and $Q_{C_2}^{\phi}$. Therefore, a system of six algebraic equations has to be set up, which is represented in Table 5; the symbols used in it are identical with those appearing in Figure 66.

The first four equations in the table define the equilibrium conditions of each beam separately; the last two represent the continuity conditions of the vertical displacements of the foundation at the point where the two beams adjoin:

$$\text{at } x_1 = l_1 \ (x_2 = -l_2): V_1 = V_2, \ S_1 = S_2.$$

The general solution is not given here, since it is much simpler to perform the calculations in each particular case by direct substitution of the numerical values in the equations.

Henceforth, only the case of two beams having equal lengths $2l$ and each acted upon at its center by a load P_0 will be considered (Figure 67).

From Table 5, equations (7.10), and the conditions of symmetry, we obtain:

$$\left.\begin{aligned} C_0 &= \frac{\left(\frac{kl^3}{3t} + \alpha l + 2\right)P_0}{2kl\left(\frac{kl^3}{3t} + \frac{4\alpha l}{3} + 2\frac{\alpha t}{kl} + 2\right)}, \\ \theta_0 &= \frac{\alpha P_0}{2kl\left(\frac{kl^3}{3t} + \frac{4\alpha l}{3} + 2\frac{\alpha t}{kl} + 2\right)}, \\ Q^{\phi}_{C_1} = Q^{\phi}_{C_2} &= \frac{\alpha t P_0}{kl\left(\frac{kl^3}{3t} + \frac{4\alpha l}{3} + 2\frac{\alpha t}{kl} + 2\right)}, \\ Q^{\phi}_{A} = Q^{\phi}_{B} &= \frac{\alpha t\left(\frac{kl^3}{3t} + 1\right)P_0}{kl\left(\frac{kl^3}{3t} + \frac{4\alpha l}{3} + 2\frac{\alpha t}{kl} + 2\right)}. \end{aligned}\right\} \qquad (7.11)$$

TABLE 5.

No.	C_1	C_2	θ_1	θ_2	$Q^{\phi}_{C_1}$	$Q^{\phi}_{C_2}$	Right-hand part
1	$2(kl_1 + \alpha t)$	—	$-2t(1 + \alpha l_1)$	—	1	—	P_1
2	$-2\alpha t l_1$	—	$2l_1\left[(1 + \alpha l_1)t + \frac{kl_1^3}{3}\right]$	—	l_1	—	M_1
3	—	$2(kl_2 + \alpha t)$	—	$2t(1 + \alpha l_2)$	—	1	P_2
4	—	$2\alpha t l_2$	—	$2l_2\left[(1 + \alpha l_2)t + \frac{kl_2^3}{3}\right]$	—	$-l_2$	M_2
5	1	-1	l_1	l_2	—	—	0
6	—	—	$2t$	$-2t$	-1	-1	0

Let $\phi(y)$ be given by (5.22). The characteristics k, t, and α of the elastic foundation are then obtained from (5.23) and (5.24). We further assume that the elastic foundation is a semi-infinite plane ($H \to \infty$); in this case:

$$\left.\begin{aligned} k &= \frac{E_0 b}{t(1-\nu_0^2)}\,\frac{\gamma}{2}, \\ t &= \frac{E_0 b t}{12(1-\nu_0)}\,\frac{3}{2\gamma}, \\ \alpha &= \frac{\gamma}{t}\,\frac{\sqrt{2(1-\nu_0)}}{1-\nu_0}. \end{aligned}\right\} \tag{7.12}$$

Substitution of (7.12) in (7.11) yields:

$$\left.\begin{aligned} C_0 &= \frac{P_0(1-\nu_0^2)}{E_0 b}\times \\ &\times\frac{\gamma^3+\frac{3}{4}\gamma\sqrt{2(1-\nu_0)}+\frac{3}{2}(1-\nu_0)}{\gamma\left[\gamma^3+\gamma\sqrt{2(1-\nu_0)}+\frac{3}{8\gamma}(1-\nu_0)\sqrt{2(1-\nu_0)}+\frac{3}{2}(1-\nu_0)\right]}, \\ \theta_0 &= \frac{P_0(1-\nu_0^2)}{E_0 b t}\times \\ &\times\frac{3\sqrt{2(1-\nu_0)}}{4\left[\gamma^3+\gamma\sqrt{2(1-\nu_0)}+\frac{3}{8\gamma}(1-\nu_0)\sqrt{2(1-\nu_0)}+\frac{3}{2}(1-\nu_0)\right]}, \\ Q^{\phi}_{C_1} &= Q^{\phi}_{C_2} = \\ &= \frac{P_0\,3(1-\nu_0)\sqrt{2(1-\nu_0)}}{16\gamma\left[\gamma^3+\gamma\sqrt{2(1-\nu_0)}+\frac{3}{8\gamma}(1-\nu_0)\sqrt{2(1-\nu_0)}+\frac{3}{2}(1-\nu_0)\right]}, \\ Q^{\phi}_{A} &= Q^{\phi}_{B} = \\ &= \frac{P_0\sqrt{2(1-\nu_0)}\left[\gamma^3+\frac{3}{4}(1-\nu_0)\right]}{4\gamma\left[\gamma^3+\gamma\sqrt{2(1-\nu_0)}+\frac{3}{8\gamma}(1-\nu_0)\sqrt{2(1-\nu_0)}+\frac{3}{2}(1-\nu_0)\right]}, \end{aligned}\right\} \tag{7.13}$$

and

$$q_1(x) = \frac{P_0}{2t}\,\frac{\gamma^3+\frac{3}{4}\gamma\sqrt{2(1-\nu_0)}+\frac{3}{2}(1-\nu_0)+\frac{3}{4}\gamma\sqrt{2(1-\nu_0)}\,\frac{x}{t}}{\gamma^3+\gamma\sqrt{2(1-\nu_0)}+\frac{3}{8\gamma}(1-\nu_0)\sqrt{2(1-\nu_0)}+\frac{3}{2}(1-\nu_0)}. \tag{7.14}$$

The dimensionless bending moments and shearing forces acting on the left beam, obtained from (7.13) and (7.14) for $\gamma = 1.5$, $\nu_0 = 0.3$, and a uniformly distributed load p are shown in Figure 68. The actual bending moments and shearing forces are respectively:

$$M = pt^2\overline{m}, \quad Q = pt\overline{Q}. \tag{7.15}$$

The same figure also shows the results obtained from (5.25) by neglecting the lateral load (broken lines, numbers in parentheses). It is seen that this additional load has a considerable influence, reducing the positive bending moments and the shearing forces.

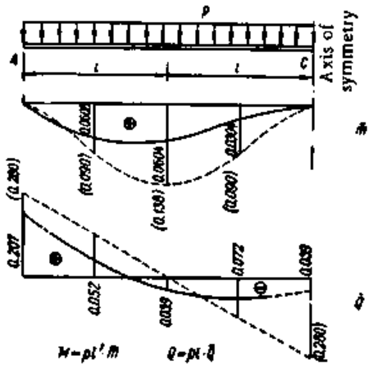

FIGURE 68.

3

The influence of a lateral load can be similarly treated in the case of elastic beams of finite length $2l$. Consider beams having dimensionless lengths $\lambda_1 = \frac{l_1}{L_1}$ and $\lambda_2 = \frac{l_2}{L_2}$, placed in line on an elastic foundation (Figure 69).

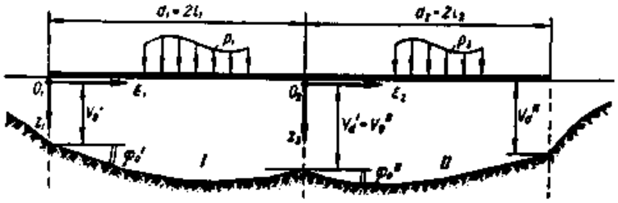

FIGURE 69.

The origin of coordinates for each beam is located at its left end. The boundary conditions are, in accordance with (6.7):

$$\left.\begin{array}{lll}
\text{at } \eta_1 = 0 & \text{a) } M_0^{\mathrm{I}} = 0 \quad \text{b) } N_0^{\mathrm{I}} = 2\alpha t V_0^{\mathrm{I}}; & \\
 & (\eta_2 = 0) & \\
\text{at } \eta_1 = \frac{2l_1}{L_1} & \text{c) } M_d^{\mathrm{I}} = M_0^{\mathrm{II}} = 0; \quad \text{d) } V_d^{\mathrm{I}} = V_0^{\mathrm{II}}; \text{ e) } N_d^{\mathrm{I}} = N_0^{\mathrm{II}}; & \\
\text{at } \eta_2 = \frac{2l_2}{L_2} & \text{f) } M_d^{\mathrm{II}} = 0; \quad \text{g) } N_d^{\mathrm{II}} = +2\alpha t V_d^{\mathrm{II}}, &
\end{array}\right\} \qquad (7.16)$$

where

$$L_1 = \sqrt[3]{\frac{2E_1J_1(1-\nu_0^2)}{E_0\delta}}, \quad L_2 = \sqrt[3]{\frac{2E_2J_2(1-\nu_0^2)}{E_0\delta}}.$$

The superscripts I and II indicate the corresponding beam.

The kinematic and statical magnitudes corresponding to the first beam are then determined except for the two parameters V_0^I and φ_0^I, as are those corresponding to the second beam, except for the three parameters V_0^{II}, φ_0^{II}, N_0^{II}.

Since V_0^{II} and N_0^{II} can be expressed through V_0^I and φ_0^I (cf. (7.16d, e and also, below, (7.17), (7.18)) the problem reduces to determining V_0^I, φ_0^I, φ_0^{II}. A system of three algebraic equations can be obtained from (7.16c, f, g), for the determination of these parameters.

This system is given in Table 6, where the following symbols are used:

$$K_V^{II} = K_{NV}^{II} - 2\alpha t K_{VV}^{II},$$
$$K_N^{II} = K_{NN}^{II} - 2\alpha t K_{VN}^{II},$$
$$K_\varphi^{II} = K_{N\varphi}^{II} - 2\alpha t K_{V\varphi}^{II},$$

TABLE 6

No.	Boundary condition	V_0^I	φ_0^I	φ_0^{II}	Right-hand side
1	$M_{d_1}^I = 0$	$K_{MV}^I(d_1) + 2\alpha t K_{MN}^I(d_1)$	$K_{M\varphi}^I(d_1)$	—	$F_M^I(d_1)$
2	$M_{d_2}^{II} = 0$	$[K_{VV}^I(d_2) + 2\alpha t K_{VM}^I(d_2)] \times$ $\times K_{MV}^{II}(d_2) + [K_{NV}^I(d_2) +$ $+ 2\alpha t K_{NN}^I(d_2)] K_{MN}^{II}(d_2)$	$K_{V\varphi}^I(d_1) K_{MV}^{II}(d_2) +$ $+ K_{N\varphi}^I(d_1) K_{MN}^{II}(d_2)$	$K_{M\varphi}^{II}(d_2)$	$F_V^I(d_1) K_{MV}^{II}(d_2) +$ $+ F_N^I(d_1) K_{MN}^{II}(d_2) +$ $+ F_M^{II}(d_2)$
3	$N_{d_1}^{II} = 2\alpha t V_{d_2}^{II}$	$[K_{VV}^I(d_1) + 2\alpha t K_{VN}^I(d_1)] \times$ $\times K_V^{II}(d_2) + [K_{NV}^I(d_1) +$ $+ 2\alpha t K_{NN}^I(d_1)] K_N^{II}(d_2)$	$K_{V\varphi}^I(d_1) K_V^{II}(d_2) +$ $+ K_{N\varphi}^I(d_1) K_N^{II}(d_2)$	$K_\varphi^{II}(d_2)$	$F_V^I(d_1) K_V^{II}(d_2) +$ $+ F_N^I(d_1) K_N^{II}(d_2) +$ $+ F_N^{II} - 2\alpha t F_V^{II}$

The general solution of this system is [cf. (6.4)]:
for the first beam

$$\left.\begin{aligned}
V^I(\eta) &= (K_{VV}^I + 2\alpha t K_{VN}^I) V_0^I + K_{V\varphi}^I \varphi_0^I - F_V^I,\\
\varphi^I(\eta) &= (K_{\varphi V}^I + 2\alpha t K_{\varphi N}^I) V_0^I + K_{\varphi\varphi}^I \varphi_0^I - F_\varphi^I,\\
M^I(\eta) &= (K_{MV}^I + 2\alpha t K_{MN}^I) V_0^I + K_{M\varphi}^I \varphi_0^I - F_M^I,\\
N^I(\eta) &= (K_{NV}^I + 2\alpha t K_{NN}^I) V_0^I + K_{N\varphi}^I \varphi_0^I - F_N^I;
\end{aligned}\right\} \qquad (7.17)$$

for the second beam

$$\left.\begin{aligned} V^{\text{II}}(\eta) &= K^{\text{II}}_{VV}V^{\text{II}}_0 + K^{\text{II}}_{V\varphi}\varphi^{\text{II}}_0 + K^{\text{II}}_{VN}N^{\text{II}}_0 - F^{\text{II}}_V,\\ \varphi^{\text{II}}(\eta) &= K^{\text{II}}_{\varphi V}V^{\text{II}}_0 + K^{\text{II}}_{\varphi\varphi}\varphi^{\text{II}}_0 + K^{\text{II}}_{\varphi N}N^{\text{II}}_0 - F^{\text{II}}_\varphi,\\ M^{\text{II}}(\eta) &= K^{\text{II}}_{MV}V^{\text{II}}_0 + K^{\text{II}}_{M\varphi}\varphi^{\text{II}}_0 + K^{\text{II}}_{MN}N^{\text{II}}_0 - F^{\text{II}}_M,\\ N^{\text{II}}(\eta) &= K^{\text{II}}_{NV}V^{\text{II}}_0 + K^{\text{II}}_{N\varphi}\varphi^{\text{II}}_0 + K^{\text{II}}_{NN}N^{\text{II}}_0 - F^{\text{II}}. \end{aligned}\right\} \tag{7.18}$$

It can be shown that, as in the case of rigid beams, the lateral load reduces the concentrated reactions at the beam ends, thus considerably altering the stresses in the beam.

§ 8. BEAM ON AN ELASTIC DOUBLE-LAYER FOUNDATION

1

Consider a rigid beam of length $2l$ and width δ lying on a double-layer foundation and carrying an external load (Figure 70). Equations (5.1) and (5.15) of Chapter I are assumed to hold true for the elastic foundation; in other words, we are considering an elastic foundation with upper Winkler layer, whose properties are described by (5.16) and (5.18) of Chapter I.

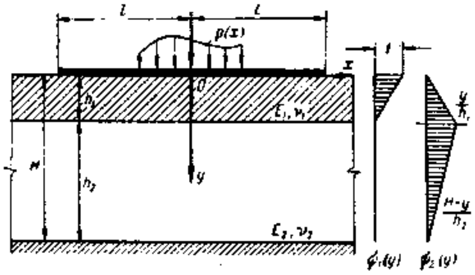

FIGURE 70.

In contrast to (5.2) of Chapter I, $\psi_2(y)$ is assumed to vary linearly over the entire height of the foundation (cf. Figure 70)*. From (5.4) and (5.15) of Chapter I, we obtain:

$$\left.\begin{aligned} k_1 &= K, \quad & k_2 &= \frac{E_2\delta}{h_2(1-\nu_2^2)},\\ t_1 &= 0, \quad & t_2 &= \frac{E_2\delta h_2}{12(1+\nu_2)}. \end{aligned}\right\} \tag{8.1}$$

[cf. (5.7) of Chapter I]

Since the deflections of a rigid beam are equal to zero, the displacement of the surface of the elastic foundation beneath the beam (part III in Figure 71) is:

$$V_1 = C_0 + \theta_0 x. \tag{8.2}$$

---

* This derivation remains valid for any other function $\psi_2(y)$, since the latter determines only the coefficients k_2 and t_2.

where C_0 = vertical displacement of beam center, ϑ_0 = slope of beam.
From the first equation (5.16) of Chapter I and (8.2) we obtain:

$$-2t_2F'' + (K + k_2)F = C_0 + \vartheta_0 x. \qquad (8.3)$$

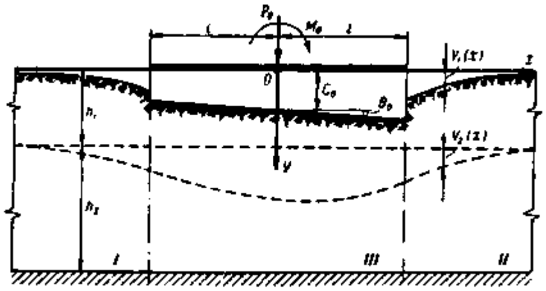

FIGURE 71.

The general integral of this equation is:

$$F(x) = C_1 \operatorname{ch} \beta x + C_2 \operatorname{sh} \beta x + \frac{C_0 + \theta_0 x}{K + k_2}, \qquad (8.4)$$

where

$$\beta = \sqrt{\frac{K + k_2}{2t_2}}. \qquad (8.5)$$

The constants of integration C_1 and C_2 are found from the conditions at the boundaries of the parts shown in Figure 71, which are:

$$\text{at } x = -l \qquad V_2^{I} = V_2^{III}, \quad S_2^{I} = S_2^{III}; \qquad (8.6)$$

$$\text{at } x = l \qquad V_2^{III} = V_2^{II}, \quad S_2^{III} = S_2^{II}, \qquad (8.7)$$

where the superscripts I, II, III indicate the corresponding part of the foundation.

Proceeding from (5.22) of Chapter I, we obtain:

$$\left.\begin{aligned} V_2^{I} &= D_1 e^{\alpha_2(x+l)}, \\ V_2^{II} &= D_2 e^{-\alpha_2(x-l)}, \end{aligned}\right\} \qquad (8.8)$$

where

$$\alpha_2 = \sqrt{\frac{k_2}{2t_2}}.$$

By virtue of (5.17) of Chapter I, we obtain:

$$\left.\begin{aligned} S_2^{I} &= 2\alpha_2 t_2 D_1 e^{\alpha_2(x+l)}, \\ S_2^{II} &= -2\alpha_2 t_2 D_2 e^{-\alpha_2(x-l)}, \\ S_2^{III} &= 2Kt_2(C_1\beta \operatorname{sh} \beta x + C_2\beta \operatorname{ch} \beta x). \end{aligned}\right| \qquad (8.9)$$

Substitution of (8.4), (8.8), and (8.9) in the boundary conditions (8.6), (8.7) yields the following system of four algebraic equations by which the integration constants can be determined:

$$\left.\begin{aligned} &-C_1 \operatorname{ch}\beta l + C_2 \operatorname{sh}\beta l + \frac{1}{K} D_1 = \frac{C_0 - \theta_0 l}{K + k_2}, \\ &-C_1 \operatorname{sh}\beta l + C_2 \operatorname{ch}\beta l - \frac{a_2}{\beta K} D_1 = 0, \\ &-C_1 \operatorname{ch}\beta l - C_2 \operatorname{sh}\beta l + \frac{1}{K} D_2 = \frac{C_0 + \theta_0 l}{K + k_2}, \\ &-C_1 \operatorname{sh}\beta l - C_2 \operatorname{ch}\beta l + \frac{a_1}{\beta K} D_2 = 0, \end{aligned}\right\} \qquad (8.10)$$

By solving (8.10) we obtain C_1, C_2, D_1, and D_2 as functions of C_0 and θ_0. The vertical displacement C_0 of the beam center, and the slope θ_0 are found from the equilibrium conditions of the beam:

$$\sum Y = 0, \quad \sum M = 0.$$

We finally obtain:

$$\left.\begin{aligned} C_1 &= -\frac{1}{lKk_2 \operatorname{ch}\beta l\left[\lambda \frac{\operatorname{th}\beta l}{\beta l} + B_1\right]} \frac{P_0}{2}, \\ C_2 &= -\frac{1}{l^2Kk_2 \operatorname{ch}\beta l\left[\frac{\lambda}{\beta l}\left(1 - \frac{\operatorname{th}\beta l}{\beta l}\right) + \frac{B_2}{3}\right]} \frac{M_0}{2}, \\ D_1 &= \frac{K}{K + k_2} \frac{(C_0 - \theta_0 l)\left[\operatorname{th}^2\beta l + 2\sqrt{1+\lambda}\operatorname{th}\beta l + 1\right] - \frac{C_0 + \theta_0 l}{\operatorname{ch}^2\beta l}}{2B_1B_3}, \\ D_2 &= \frac{K}{K + k_2} \frac{(C_0 + \theta_0 l)\left[\operatorname{th}^2\beta l + 2\sqrt{1+\lambda}\operatorname{th}\beta l + 1\right] - \frac{C_0 - \theta_0 l}{\operatorname{ch}^2\beta l}}{2B_1B_3}, \\ C_0 &= \frac{K + k_2}{lKk_2} \frac{B_1}{\lambda \frac{\operatorname{th}\beta l}{\beta l} + B_1} \frac{P_0}{2}, \\ l\theta_0 &= \frac{K + k_2}{l^2Kk_2} \frac{B_2}{\frac{\lambda}{\beta l}\left(1 - \frac{\operatorname{th}\beta l}{\beta l}\right) + \frac{B_2}{3}} \frac{M_0}{2}, \end{aligned}\right\} \qquad (8.11)$$

where P_0 = sum of vertical loads, M_0 = sum of moments about beam center, considered as positive when acting clockwise, and:

$$\left.\begin{aligned} B_1 &= 1 + \sqrt{1+\lambda}\operatorname{th}\beta l, \\ B_2 &= \sqrt{1+\lambda} + \operatorname{th}\beta l, \\ B_3 &= \frac{\sqrt{1+\lambda}}{1+\lambda}\operatorname{th}\beta l + 1, \\ \lambda &= \frac{K}{k_2}. \end{aligned}\right\} \qquad (8.12)$$

From (8.11), the generalized displacements V_1, V_2, and the function F can be found by (5.16) of Chapter I, and (8.2) and (8.4) of this Chapter.

The reactions of the elastic foundation are obtained from (5.18) of Chapter I[*], which, after substituting in it (8.4), yields:

$$q(x) = K\left[\frac{k_2}{K+k_2}(C_0+\theta_0 x) - K(C_1 \operatorname{ch}\beta x + C_2 \operatorname{sh}\beta x)\right]. \tag{8.13}$$

The solution presented satisfies not only the equilibrium conditions of the beam and the condition of equal vertical displacements of beam and foundation, but also the statical boundary conditions: thus, the bending moments and shearing forces at simply supported beam ends, at which no loads act, are zero. This is due to the fact that the concentrated reactions Q^{Φ} existing in a single-layer foundation are absent in the double-layer model.

2

The case of symmetrical loading of a rigid beam will now be considered in more detail. Putting $M_0 = 0$ in (8.11) we obtain from (8.13):

$$q(x) = \frac{P_0}{2l}\,\frac{1+\sqrt{1+\lambda}\,\operatorname{th}\beta l - \lambda\dfrac{\operatorname{ch}\beta x}{\operatorname{ch}\beta l}}{1+\sqrt{1+\lambda}\,\operatorname{th}\beta l + \lambda\dfrac{\operatorname{th}\beta l}{\beta l}}, \tag{8.14}$$

where

$$\lambda = \frac{K}{k_2}, \quad \beta = \sqrt{\frac{K+k_2}{2t_2}}. \tag{8.15}$$

If $\psi_2(y)$ is linear (cf. Figure 70), the coefficients k_2 and t_2 are given by (8.1), the substitution of which in (8.15) finally yields:

$$q(x) = \frac{P_0}{2l}\,\bar{q}(x), \tag{8.16}$$

where

$$\bar{q}(x) = \frac{1+\sqrt{1+\lambda}\,\operatorname{th}\left(\dfrac{l}{h_2}\sqrt{6\dfrac{1+\lambda}{1-\nu_0}}\right) - \lambda\dfrac{\operatorname{ch}\left(\dfrac{x}{h_2}\sqrt{6\dfrac{1+\lambda}{1-\nu_0}}\right)}{\operatorname{ch}\left(\dfrac{l}{h_2}\sqrt{6\dfrac{1+\lambda}{1-\nu_0}}\right)}}{1+\sqrt{1+\lambda}\,\operatorname{th}\left(\dfrac{l}{h_2}\sqrt{6\dfrac{1+\lambda}{1-\nu_0}}\right) - \lambda\dfrac{\operatorname{th}\left(\dfrac{l}{h_2}\sqrt{6\dfrac{1+\lambda}{1-\nu_0}}\right)}{\dfrac{l}{h_2}\sqrt{6\dfrac{1+\lambda}{1-\nu_0}}}}. \tag{8.17}$$

Curves of the dimensionless function $\bar{q}(x)$ are given in Figure 72 for $\frac{l}{h_2} = 1$, $\nu_0 = 0$, and different values of $\lambda = \frac{K}{k_2}$.

It is seen that in all cases the reactions increase from the center toward the ends of the beam where they remain finite, varying directly with λ; when $\lambda = 0$ ($k_2 = \infty$) the double-layer foundation degenerates into an elastic

---

[*] When $q(x)$ is known, the bending moments and shearing forces of a rigid beam are obtained by the known methods of the strength of materials.

Winkler foundation. On the other hand, when $\lambda \to \infty$, the model becomes similar in its behavior to an elastic semi-infinite plane.

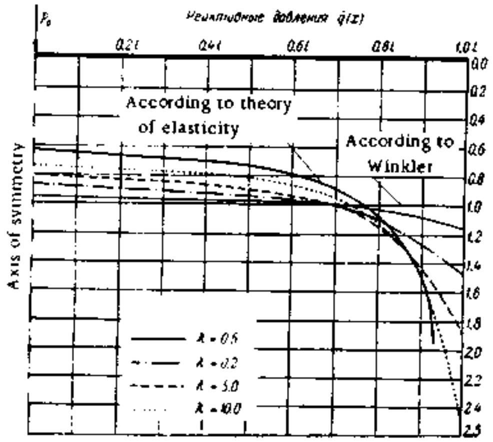

FIGURE 72.

3

When analyzing an elastic beam of finite length, the differential equation of the bending of the beam [cf. (1.1)],

$$EJV_1^{IV} = p - q \tag{8.18}$$

has to be taken into account together with (5.16) and (5.18) of Chapter I, which determine the deformations of the elastic double-layer foundation. Since it is assumed that the beam deflections are equal to the vertical displacements V_1 of the surface of the elastic foundation at the same points, the first equation (5.16) of Chapter I can be inserted into (8.18). From this, and from (5.18) of Chapter I, we then obtain:

$$\left.\begin{aligned} EJ\left[-2t_2F^{VI} + (K + k_2)F^{IV}\right] = p - q, \\ -2Kt_2F'' + Kk_2F = q. \end{aligned}\right\} \tag{8.19}$$

Elimination of $q(x)$ yields:

$$-EJ\frac{2t_2}{K}F^{VI} + EJ\frac{K+k_2}{K}F^{IV} - 2t_2F'' + k_2F = \frac{p(x)}{K}. \tag{8.20}$$

Equation (8.20) is a sixth-order ordinary differential equation with constant coefficients and can easily be integrated. The boundary conditions are given by (8.6) and (8.7). By including the statical conditions $M = 0$ and $Q = 0$, four independent equations can be established for each beam end; this number corresponds to the total number of integration constants*.

---

* The function $F(x)$ is determined for the entire beam length except for six constants which corresponds to the order of (8.20). Beyond the beam ends $F(x)$ is determined except for two constants (cf. (8.8)).

After $F(x)$ has been determined from (8.20) and the corresponding boundary conditions, the beam deflection and the reactions of the elastic foundation can be obtained from (5.16) and (5.18) of Chapter I; the bending moments and shearing forces are given by (1.11) and (1.12) of this chapter.

Chapter III

BENDING OF A RECTANGULAR PLATE ON AN ELASTIC SINGLE-LAYER FOUNDATION

§1. STATEMENT OF THE PROBLEM. DIFFERENTIAL EQUATIONS OF BENDING OF A PLATE ON A SINGLE-LAYER FOUNDATION

Consider a rectangular plate on an elastic foundation whose properties are described by (7.8) of Chapter I (Figure 73). The assumptions usually made in the theory of bending of thin plates will be deemed to apply to this case. Friction and adhesion between the plate and the surface of the elastic foundation will be neglected.

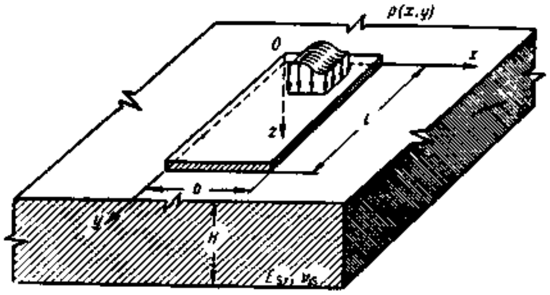

FIGURE 73.

The differential equation of bending of the plate, referred to cartesian coordinates, then becomes:

$$\nabla^2\nabla^2 w(x, y) = \frac{p^*}{D}. \tag{1.1}$$

(∇^2 denotes the Laplace operator) or, in expanded form:

$$\frac{\partial^4 w}{\partial x^4} + 2\frac{\partial^4 w}{\partial x^2\,\partial y^2} + \frac{\partial^4 w}{\partial y^4} = \frac{p^*}{D}, \tag{1.2}$$

where $w = w(x, y)$ = vertical displacements of the plate surface, $p^* = p^*(x, y) =$ distributed load on the plate, $D = \frac{Eh^3}{12(1-\mu^2)}$ = flexural rigidity of the plate.

Although (1.2) is known as the equation of bending of thin plates, it can be applied to the analysis of most rectangular plates. It was shown by academician Galerkin /17/ that (1.2) is valid even when the ratio of the plate thickness to the smallest dimension in plan equals 1:3.

Since the plate lies on an elastic foundation, the distributed load consists of the given surface forces $p^*(x, y)$ and the reactions $q(x, y)$ of the elastic foundation:

$$p^*(x, y) = p(x, y) - q(x, y). \tag{1.3}$$

Since the reactions are unknown functions of the coordinates x, y, our problem consists in determining their distribution as well as the vertical displacements $w(x, y)$ of the plate. In addition, the equilibrium conditions of the plate and the condition of equal vertical displacements of the plate and the elastic-foundation surface have to be fulfilled.

It was established above (cf. (7.8), Chapter I) that the strains of a single-layer foundation under the action of a load distributed over its surface are given by the following differential equation:

$$-2t\nabla^2 w(x, y) + kw(x, y) = q(x, y)\psi(0), \tag{1.4}$$

where

$$\nabla^2 = \frac{\partial^2}{\partial x^2} + \frac{\partial^2}{\partial y^2}$$

is the Laplace operator.

$$k = \frac{E_0}{1-\nu_0^2}\int_0^H \psi'^2\,dz,$$

$$t = \frac{E_0}{4(1+\nu_0)}\int_0^H \psi^2\,dz$$

are the elastic characteristics of the single-layer foundation.

$\psi(z)$ = function of transverse distribution of displacements.

The deflections of the plate and the vertical displacements of the surface of the single-layer foundation are assumed to be equal. In addition, the load $q(x, y)$ acting on the foundation represents the reaction of the foundation on the plate. Hence, (1.2) and (1.4) have to be considered simultaneously.

Assume that $\psi(0) = 1$. Substitution of [(1.3) and] (1.4) in (1.1) yields:

$$\nabla^2\nabla^2 w - 2r^2\nabla^2 w + s^4 w = \frac{p}{D}, \tag{1.5}$$

where r^2 and s^4 are the generalized elastic characteristics of plate and foundation, defined as follows:

$$\left.\begin{aligned} r^2 &= \frac{E_0}{4(1+\nu_0)D}\int_0^H \psi^2(z)\,dz = \frac{t}{D},\\ s^4 &= \frac{E_0}{(1-\nu_0^2)D}\int_0^H \psi'^2(z)\,dz = \frac{k}{D},\end{aligned}\right\} \tag{1.6}$$

Also,

$$E_0 = \frac{E_s}{1-\nu_s^2}, \quad \nu_0 = \frac{\nu_s}{1-\nu_s}, \tag{1.7}$$

where E_s and ν_s are respectively the modulus of elasticity and Poisson's ratio for the material of the foundation (soil).

Differential equation (1.5) differs from that derived from the hypothesis of Winkler and Zimmermann by the additional term containing r^2, which makes allowance for the shearing stresses in the elastic foundation.

After $w(x, y)$ has been determined from (1.5) and the boundary conditions, the reactions $q(x, y)$ can be found from (1.4), the moments and shearing forces being given (Figure 74) by the known formulas of the theory of bending of plates:

$$\left.\begin{aligned} M_x &= -D\left(\frac{\partial^2 w}{\partial x^2} + \mu\frac{\partial^2 w}{\partial y^2}\right), \\ M_y &= -D\left(\frac{\partial^2 w}{\partial y^2} + \mu\frac{\partial^2 w}{\partial x^2}\right), \\ H = H_x &= -H_y = -D(1-\mu)\frac{\partial^2 w}{\partial x\,\partial y}, \\ N_x &= -D\frac{\partial}{\partial x}\left(\frac{\partial^2 w}{\partial x^2} + \frac{\partial^2 w}{\partial y^2}\right), \\ N_y &= -D\frac{\partial}{\partial y}\left(\frac{\partial^2 w}{\partial x^2} + \frac{\partial^2 w}{\partial y^2}\right). \end{aligned}\right| \tag{1.8}$$

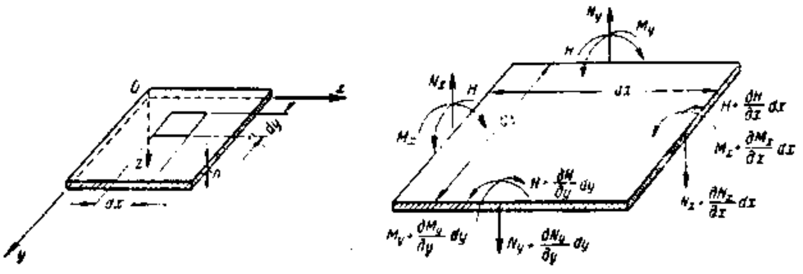
0
x
dy
z
h
dx
y
N_y
M_y
H
N_x
H
dx
$H+\frac{\partial H}{\partial x}dx$
M_x
$M_x+\frac{\partial M_x}{\partial x}dx$
$H+\frac{\partial H}{\partial y}dy$
$N_x+\frac{\partial N_x}{\partial x}dx$
$M_y+\frac{\partial M_y}{\partial y}dy$
$N_y+\frac{\partial N_y}{\partial y}dy$

FIGURE 74.

Following Kirchhoff, the shearing forces N_x, N_y, and the torque H at the plate edges are usually replaced by the reduced shearing forces Q_x and Q_y which, for a rectangular plate, are:

$$\left.\begin{aligned} Q_x &= -D\left[\frac{\partial^3 w}{\partial x^3} + (2-\mu)\frac{\partial^3 w}{\partial x\,\partial y^2}\right], \\ Q_y &= -D\left[\frac{\partial^3 w}{\partial y^3} + (2-\mu)\frac{\partial^3 w}{\partial x^2\,\partial y}\right]. \end{aligned}\right\} \tag{1.9}$$

§ 2. REDUCING THE PROBLEM OF THE BENDING OF A PLATE ON AN ELASTIC FOUNDATION TO ORDINARY DIFFERENTIAL EQUATIONS

1. General considerations

The problem of the bending of a plate on an elastic foundation can only be solved in closed form for a relatively small number of boundary conditions. In most cases the deflections $w(x, y)$ cannot be given as a finite polynomial in x and y.

Approximations, based on series expansions, are therefore mostly used to solve problems concerning the bending of plates. One example is the solution by single or double trigonometric series (the problems of Maurice Lévy and Navier respectively).

Although simple and convenient for practical calculations, this method is only applicable to certain particular boundary conditions. The more general method of reduction to ordinary differential equations will accordingly be used here.

The general variational method of reduction to ordinary differential equations, as applied to the problem of the bending of a rectangular plate, is discussed thoroughly in "Structural Mechanics of Thin-Walled Three-Dimensional Systems", by V. Z. Vlasov. Only the application of this method to the analysis of thin plates on elastic foundations will be dealt with here. No restrictions are imposed on the boundary conditions at the longitudinal and lateral edges of the plate, whose thickness may vary exponentially in one or both directions.

2. Reducing the two-dimensional problem to a one-dimensional problem

We shall consider the x-axis to lie in the lateral, and the y-axis, in the longitudinal direction of the plate (Figure 75).

The unknown deflections of the plate $w(x, y)$ will be represented as a finite series:

$$w(x, y) = \sum_{k=1}^{n} W_k(y)\chi_k(x). \qquad (2.1)$$

in which the dimensionless functions $\chi_k(x)$ determine the lateral distribution of the deflection of the plate, and are assumed to be known. The unknown functions $W_k(y)$, which have the dimension of length, can, in accordance with their physical meaning, be called generalized deflections.

Different expressions may be chosen for the functions $\chi_k(x)$, provided they are linearly independent and satisfy the boundary conditions at the longitudinal edges of the plate. The simplest example of such a system, satisfying the boundary conditions:

$$\chi_k(0) = \chi_k(b) = 0.$$

is a series in $\sin\frac{k\pi x}{b}$, where k is an integer and assumes all values between 1 and n.

The introduction of the finite expansion (2.1) is equivalent to reducing the plate to a system having a finite number of degrees of freedom in the lateral direction and an infinite number of degrees of freedom in the longitudinal direction. It is also equivalent to reducing the two-dimensional problem of the theory of elasticity to a one-dimensional problem, since the deflections $w(x, y)$ are obtained by determining the n functions of the single variable $W_k(y)$.

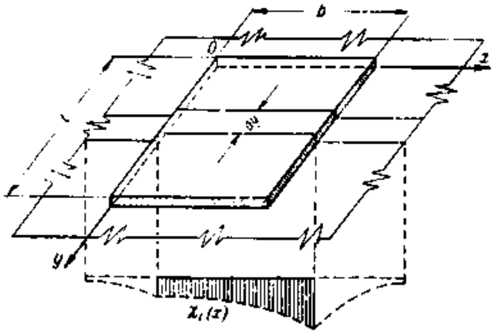

FIGURE 75.

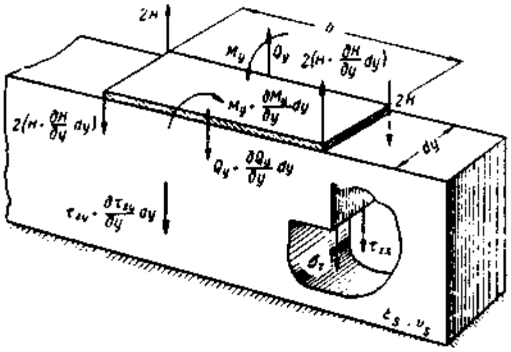
2H
b
M_y
Q_y
$2(H+\frac{\partial H}{\partial y}dy)$
2H
$M_y+\frac{\partial M_y}{\partial y}dy$
$2(H+\frac{\partial H}{\partial y}dy)$
dy
$Q_y+\frac{\partial Q_y}{\partial y}dy$
$\tau_{zy}+\frac{\partial \tau_{zy}}{\partial y}dy$
τ_{zx}
σ_z
E_s, ν_s

FIGURE 76.

To determine the unknown functions $W_k(y)$, we consider the equilibrium of an elementary slab (composed of elements of plate and foundation) bounded by the cross sections $y = \text{const}$ and $y + dy = \text{const}$ (Figures 75 and 76). In accordance with the principle of virtual displacements, the equilibrium conditions will be expressed by equating to zero the total work done by all external and internal forces acting on this slab over any virtual displacement.

Let the i-th virtual displacement of the plate element be a cylindrical bending in the vertical plane. The deflections of the upper surface are determined by one of the functions $\chi_i(x)$, while the corresponding generalized deflection $W_i(y) = 1$. Since all the virtual displacements of the plate are defined by the n linearly independent functions $\chi_i(x)$, $(i = 1 \ldots n)$, n independent conditions of equilibrium can be established, from which the n unknown functions $W_k(y)$ $(k = 1 \ldots n)$ may be determined.

3. Generalized equilibrium conditions of the elementary slab

The elementary slab defined above consists of a compressible layer belonging to the elastic foundation and of an element lying on it (Figure 76).

To establish the generalized conditions of equilibrium, we consider separately the forces acting on the respective elements of the plate and of the elastic foundation.

In addition to the given external load, moments M_y, $M_y + \frac{\partial M_y}{\partial y} dy$, and forces Q_y, $Q_y + \frac{\partial Q_y}{\partial y} dy$, due to the remainder of the plate, act on the sections $y = \text{const}$ and $y + dy = \text{const}$ respectively of the plate element. At the corners, concentrated vertical forces $2H$ and $2\left(H + \frac{\partial H}{\partial y} dy\right)$ act, which, according to Kirchhoff, result from replacing the torques by statically equivalent additional shearing forces.

All these forces, with the positive directions shown in Figure 76, are external forces relative to the plate element. The internal forces are due to the stresses in the longitudinal sections $x = \text{const}$; these stresses can be reduced to bending moments M_x and reduced shearing forces Q_x.

The external forces acting on the element of the elastic foundation are the normal and shearing stresses acting on the vertical edges $y = \text{const}$ and $y + dy = \text{const}$. The internal forces are due to the normal stresses σ_x, σ_z, and the shearing stresses τ_{zx} and τ_{xz}.

In order to establish the generalized equilibrium conditions for the system considered, the work done by each of these forces separately will now be calculated.

The work of the internal forces acting on the plate element is equal to the work done by the bending moments M_x and shearing forces Q_x in the corresponding deformations of the element. On the strength of the assumption usually made in the theory of bending of plates, the work done by the shearing forces Q_x will be equal to zero; the work done by the bending moments is:

$$\int M_x \chi_i'' \, dx. \tag{2.2}$$

where the integral is taken from 0 to b.

The work done by the external forces acting on the plate element consists of:

a) Work done by the given external load

$$G_i = \int p(x, y) \chi_i(x) \, dx, \tag{2.3}$$

where the integral contains not only the distributed load $p(x, y)$, but also the concentrated shearing forces and moments, and is understood as a Stieltjes integral. We can therefore rewrite (2.3) as follows:

$$G_i = \int p(x, y) \chi_i(x) \, dx + \sum p_c(y) \chi_i(c) + \sum m_c(y) \chi_i'(c), \tag{2.4}$$

where $p_c(y)$ and $m_c(y)$ are the concentrated shearing loads and moments respectively, acting along the lines $x = x_c$ which include the reduced shearing forces $Q_x(0)$, $Q_x(b)$ and the bending moments $M_x(0)$, $M_x(b)$.

b) Work done by the reduced shearing forces

$$Q_y \text{ and } Q_y + \frac{\partial Q_y}{\partial y}\,dy:$$

$$\int \frac{\partial Q_y}{\partial y} \chi_i(x)\,dx. \tag{2.5}$$

c) Work done by the concentrated shearing forces

$$2H \text{ and } 2\left(H + \frac{\partial H}{\partial y}\,dy\right)$$

$$-2\left[\frac{\partial H}{\partial y}\chi_i\right]^{*}. \tag{2.6}$$

Henceforth, the brackets with an asterisk will denote the difference between the values of the magnitude inside the brackets at $x = 0$ and $x = b$ respectively.

The work done by the bending moments M_y over the virtual displacements $\chi_i(x)$ ($W_i(y) = 1$) is zero.

In accordance with the assumption made for a single-layer foundation,

$$u(x, y, z) = 0, \quad v(x, y, z) = 0,$$

the work done by the internal and external forces acting on the element of the elastic foundation is represented by the work done by the normal stresses σ_z and the shearing stresses τ_{zx}, τ_{zy} (at y = const), and $\tau_{zy} + \frac{\partial \tau_{zy}}{\partial y}\,dy$ (at $y + dy$ = const) in compressive and shearing deformations respectively. This work will be denoted by $R_i(y)$.

The integral equilibrium condition of the slab element is thus:

$$\int M_x \chi_i''\,dx + \int \frac{\partial Q_y}{\partial y} \chi_i\,dx - 2\left[\frac{\partial H}{\partial y}\chi_i\right]^{*} + R_i + G_i = 0 \tag{2.7}$$

$$(i = 1, 2, 3, \ldots, n).$$

4. Work done by the external and internal forces acting on the elastic foundation

Consider first the most important case of free longitudinal plate edges.

From the condition of continuity of the vertical displacements $w(x, y)$ over the surface of the entire elastic foundation, we obtain for the region beyond the plate edges:

$$w(x, y) = \sum_{k=1}^{n} W_k(y)\,\chi_{0k}(x). \tag{2.8}$$

where $W_k(y)$ are the generalized vertical displacements, and the dimensionless functions $\chi_{0k}(x)$ are:

$$\left.\begin{array}{ll} \text{at } x \leqslant 0 & \chi_{0k} = \chi_k(0)\,e^{ax}, \\ \text{at } x \geqslant b & \chi_{0k} = \chi_k(b)\,e^{-a(x-b)}, \end{array}\right\} \tag{2.9}$$

where $\alpha = \sqrt{\frac{k}{2t}}$, k and t = generalized characteristics of the elastic foundation (cf. (1.4)).

This means that the element cut from the elastic foundation behaves exactly like the plane single-layer model considered earlier: the vertical displacements of the surface vary exponentially. Each virtual displacement

$$w_i(x,\ y) = 1 \cdot \chi_i(x)$$

corresponds to a uniquely defined displacement of the surface of the elastic foundation beyond the plate edges.

The displacements of an elastic single-layer foundation are determined by (7.2) of Chapter I. Therefore, the virtual displacements of the surface of the elastic foundation

$$\bar{w}_i(x,\ y) = 1 \cdot \chi_i(x)$$

correspond to the virtual displacements inside the elastic foundations:

$$w_i(x,\ y,\ z) = 1 \cdot \chi(x)\psi(z). \tag{2.10}$$

The work done by the shearing stresses τ_{zy} and $\tau_{zy} + \frac{\partial \tau_{zy}}{\partial y} dy$, distributed along the edges $y = \text{const}$ and $y + dy = \text{const}$, over the virtual displacements given by (2.10) is:

$$\int\limits_{-\infty}^{+\infty} dx \int\limits_{0}^{H} \frac{\partial \tau_{zy}}{\partial y} \chi_i(x)\psi(z)\, dz. \tag{2.11}$$

The work done by the internal stresses σ_z and τ_{zx} in the deformations corresponding to the virtual displacements (2.10) is respectively:

$$\left.\begin{aligned} &-\int\limits_{-\infty}^{+\infty} dx \int\limits_{0}^{H} \sigma_z \chi_i(x)\psi'(z)\, dz, \\ &-\int\limits_{-\infty}^{+\infty} dx \int\limits_{0}^{H} \tau_{zx} \chi_i'(x)\psi(z)\, dz. \end{aligned}\right\} \tag{2.12}$$

where, in accordance with (6.4), (6.5), (7.1), and (7.2) of Chapter I and (2.1) of this chapter,

$$\left.\begin{aligned} \sigma_z &= \frac{E_0}{1-\nu_0^2}\psi'(z) \sum_{k=1}^{n} W_k(y)\chi_k(x), \\ \tau_{zy} &= \frac{E_0}{2(1+\nu_0)}\psi(z) \sum_{k=1}^{n} W_k'(y)\chi_k(x), \\ \tau_{zx} &= \frac{E_0}{2(1+\nu_0)}\psi(z) \sum_{k=1}^{n} W_k(y)\chi_k'(x). \end{aligned}\right\} \tag{2.13}$$

Only the stresses in the foundation directly below the plate can be calculated by (2.13). In order to determine the normal and shearing stresses beyond the boundaries of the plate, the functions $\chi_k(x)$ and $\chi_k'(x)$ in (2.13) have to be replaced by $\chi_{0k}(x)$ and $\chi_{0k}'(x)$ respectively.

Substitution of (2.13) in (2.11) and (2.12) yields, after integration:

$$\begin{aligned} R_i(y) = \sum_{k=1}^{n} \left\{ 2t \int \chi_k \chi_i \, dx + \frac{t}{\alpha} [[\chi_k \chi_i]] \right\} W_k'' - \\ - \sum_{k=1}^{n} \left\{ k \int \chi_k \chi_i \, dx + 2t \int \chi_k' \chi_i' \, dx + 2\alpha t [[\chi_k \chi_i]] \right\} W_k, \end{aligned} \tag{2.14}$$

where

$$\left. \begin{aligned} k &= \frac{E_0}{1-\nu_0^2} \int_0^H \psi'^2(z) \, dz, \\ t &= \frac{E_0}{4(1+\nu_0)} \int_0^H \psi^2(z) \, dz, \\ \alpha &= \sqrt{\frac{k}{2t}}. \end{aligned} \right\} \tag{2.15}$$

The integrals in (2.14) are taken from 0 to b. The double brackets denote the sum of the values, at $x=0$ and $x=b$, of the magnitude inside the brackets.

When the longitudinal edges of the plate are built-in or simply supported $(\chi_k(0) = \chi_k(b) = 0)$, and the elastic foundation is not strained beyond the plate boundaries, (2.14) reduces to:

$$R_i(y) = \sum_{k=1}^{n} \left\{ 2t \int \chi_k \chi_i \, dx \, W_k'' - \left(k \int \chi_k \chi_i \, dx + 2t \int \chi_k' \chi_i' \, dx \right) W_k \right\}. \tag{2.16}$$

A particular case of (2.14) is obtained when one plate edge is free and the other built-in.

5. Second method for obtaining the generalized equilibrium conditions

We shall show now how the strains of the elastic foundation beneath the plate can be taken into account in a different way.

As before it will be assumed that the deflections of the plate are given by (2.1). The generalized deflections $W_k(y)$ will be determined from the equilibrium conditions for a plate element bounded by the planes $y = \text{const}$, $y + dy = \text{const}$ (Figure 77). It will be assumed that the plate element is acted upon by reactions of the elastic foundation, in addition to the external load and to the forces transmitted from the remainder of the plate.

Let the i-th virtual displacement of the plate element be a cylindrical bending, the deflections of the element being determined by the functions $\chi_i(x)$ $(W_i(y) = 1)$; the generalized equilibrium conditions of the plate element are then, [cf. (2.7)]:

$$\int M_x \chi_i'' \, dx + \int \frac{\partial Q_y}{\partial y} \chi_i \, dx - 2 \left[\frac{\partial H}{\partial y} \chi_i \right]^* + R_i + G_i = 0.$$

where $G_i = G_i(y)$ = work done by external load, and $R_i = R_i(y)$ = work done by reactions of the elastic foundation over the virtual displacements:

$$\bar{w}_i(x, y) = 1 \cdot \chi_i(x).$$

The reactions of the elastic foundation consist, as in the case of a beam in a state of plane strain, of the distributed reactions $q(x, y)$ and the fictitious forces $Q^{\Phi}(y)$* acting at the plate edges (Figure 77).

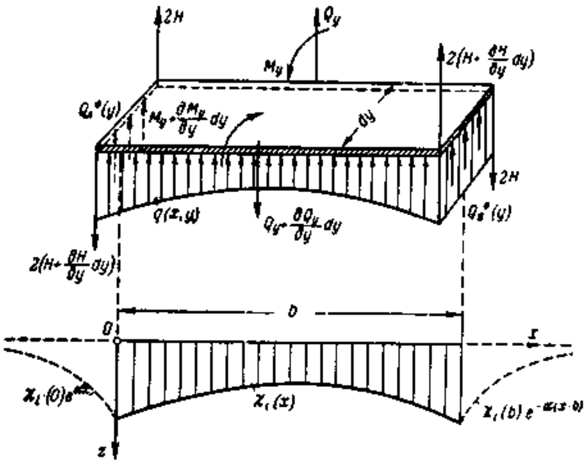
2H
Q_y
M_y
$2(H+\frac{\partial H}{\partial y}dy)$
$Q_0^{\Phi}(y)$
$M_y+\frac{\partial M_y}{\partial y}dy$
dy
2H
$q(x,y)$
$Q_y+\frac{\partial Q_y}{\partial y}dy$
$Q_b^{\Phi}(y)$
$2(H+\frac{\partial H}{\partial y}dy)$
b
0
x
$\chi_i(0)e^{\alpha x}$
$\chi_i(x)$
$\chi_i(b)e^{-\alpha(x-b)}$
z

FIGURE 77.

We obtain from (2.1) and (1.4):

$$q(x, y) = k\sum_{k=1}^{n} W_k\chi_k - 2t\sum_{k=1}^{n} W_k\chi_k'' - 2t\sum_{k=1}^{n} \ddot{W}_k\chi_k. \qquad (2.17)$$

where k and t are given by (2.15).

The work done by the distributed reactions (2.17) over the displacement χ_i is then:

$$\begin{aligned} -\int q(x, y)\chi_i\,dx = 2\sum_{k=1}^{n} t\int \chi_k\chi_i\,dx\,\ddot{W}_k - \\ -\sum_{k=1}^{n}\left(k\int \chi_k\chi_i\,dx + 2t\int \chi_k'\chi_i'\,dx - 2t\,[\chi_k'\chi_i]^*\right)W_k. \end{aligned} \qquad (2.18)$$

By the concentrated forces Q^{Φ} allowance is made for the influence of the free foundation beyond the plate edges. In other words, these forces result from the work done by all the forces acting on the element of the foundation over the virtual displacement χ_{oi} of the foundation beyond the plate edges.

---

* $Q^{\Phi}(y)$ are given as forces per unit length.

We thus obtain:

$$\left.\begin{aligned} Q_A^{\phi} &= -2t \sum_{k=1}^{n} \left\{ W_k \left[\chi_k'(0) - \alpha\chi_k(0)\right] + \frac{1}{2\alpha}\chi_k(0) W_k^{\cdot\cdot} \right\}, \\ Q_B^{\phi} &= 2t \sum_{k=1}^{n} \left\{ W_k \left[\chi_k'(b) + \alpha\chi_k(b)\right] - \frac{1}{2\alpha}\chi_k(b) W_k^{\cdot\cdot} \right\}. \end{aligned}\right| \qquad (2.19)$$

The work done by these reactions over the virtual edge displacements $\chi_i(0)$ and $\chi_i(b)$ respectively is:

$$-\left[Q_A^{\phi}\chi_i(0) + Q_B^{\phi}\chi_i(b)\right] = -\sum_{k=1}^{n} \left\{ \left(2t\left[\chi_k'\chi_i\right]^* + 2\alpha t\left[\left[\chi_k\chi_i\right]\right]\right) W_k - \frac{t}{\alpha}\left[\left[\chi_k\chi_i\right]\right] W_k^{\cdot\cdot} \right\}. \qquad (2.20)$$

Finally adding together (2.18) and (2.20), we obtain:

$$\begin{aligned} R_i(y) = \sum_{k=1}^{n} &\left\{ 2t\int \chi_k\chi_i\,dx + \frac{t}{\alpha}\left[\left[\chi_k\chi_i\right]\right] \right\} W_k^{\cdot\cdot} - \\ &- \left\{ k\int \chi_k\chi_i\,dx + 2t\int \chi_k'\chi_i'\,dx + 2\alpha t\left[\left[\chi_k\chi_i\right]\right] \right\} W_k. \end{aligned} \qquad (2.21)$$

which coincides with (2.14).

6. Solution of the ordinary differential equation

The forces and moments M_x, H, Q_y and their derivatives entering in (2.7) are by (1.8), (1.9), and (2.1):

$$\left.\begin{aligned} M_x &= -D\sum_{k=1}^{n}\left(\mu W_k^{\cdot\cdot}\chi_k + W_k\chi_k''\right), \\ H &= -D\sum_{k=1}^{n}(1-\mu) W_k^{\cdot}\chi_k', \\ \frac{\partial H}{\partial y} &= -D\sum_{k=1}^{n}(1-\mu) W_k^{\cdot\cdot}\chi_k', \\ Q_y &= -D\sum_{k=1}^{n}\left(W_k^{\cdot\cdot\cdot}\chi_k + (2-\mu) W_k^{\cdot}\chi_k''\right), \\ \frac{\partial Q_y}{\partial y} &= -D\sum_{k=1}^{n}\left(W_k^{IV}\chi_k + (2-\mu) W_k^{\cdot\cdot}\chi_k''\right). \end{aligned}\right\} \qquad (2.22)$$

Substitution of (2.22) in (2.7) yields:

$$\begin{aligned} &\sum_{k=1}^{n} W_k^{IV}\int \chi_k\chi_i\,dx + \sum_{k=1}^{n} W_k^{\cdot\cdot}(2-\mu)\int \chi_k''\chi_i\,dx - \\ &\quad - 2\sum_{k=1}^{n} W_k^{\cdot\cdot}(1-\mu)\left[\chi_k'\chi_i\right]^* + \sum_{k=1}^{n} W_k^{\cdot\cdot}\mu\int \chi_k\chi_i''\,dx + \\ &\quad\quad + \sum_{k=1}^{a} W_k\int \chi_k''\chi_i''\,dx - \frac{R_i}{D} - \frac{G_i}{D} = 0. \end{aligned} \qquad (2.23)$$

Integrating by parts:

$$\left.\begin{aligned}\int \chi_k'' \chi_i \, dx &= [\chi_k' \chi_i]^* - \int \chi_k' \chi_i' \, dx, \\ \int \chi_k \chi_i'' \, dx &= [\chi_k \chi_i']^* - \int \chi_k' \chi_i' \, dx,\end{aligned}\right\} \tag{2.24}$$

and inserting (2.21), equation (2.23) becomes:

$$\sum_{k=1}^{n} a_{ik} W_k^{IV} - 2 \sum_{k=1}^{n} (b_{ik} + \rho_{ik}^0) W_k'' + \sum_{k=1}^{n} (c_{ik} + s_{ik}^0) W_k - G_i = 0 \tag{2.25}$$

$$(i = 1, 2, 3, \ldots, n);$$

where

$$\left.\begin{aligned} a_{ik} &= \sum D \int \chi_k \chi_i \, dx, \\ b_{ik} &= \sum D \left\{ \int \chi_k' \chi_i' \, dx - \frac{\mu}{2} [\chi_k \chi_i' + \chi_k' \chi_i]^* \right\}, \\ c_{ik} &= \sum D \int \chi_k' \chi_i' \, dx, \\ \rho_{ik}^0 &= t \int \chi_k \chi_i \, dx + \frac{t}{2\alpha} [[\chi_k \chi_i]], \\ s_{ik}^0 &= k \left\{ \int \chi_k \chi_i \, dx + \frac{2t}{k} \int \chi_k' \chi_i' \, dx + \frac{2\alpha t}{k} [[\chi_k \chi_i]] \right\} \end{aligned}\right\} \tag{2.26}$$

Here $D = \frac{Eh^3}{12(1-\mu^2)}$ = flexural rigidity of plate; μ = Poisson's ratio of plate material; $E_0 = \frac{E_s}{1-\nu_s^2}$, $\nu_0 = \frac{\nu_s}{1-\nu_s}$ = elastic constants of foundation material.

Expressions (2.26) are applicable to a plate whose thickness varies stepwise in the x direction. The integrals are calculated for each part whose flexural rigidity D is uniform; the expression in brackets with asterisk then denotes the difference between the values of $(\chi_k \chi_i' + \chi_k' \chi_i)$ at the ends of each part. The summation is extended over all such parts.

The coefficients in (2.25) evidently depend only on the functions $\chi_k(x)$. These coefficients are symmetrical:

$$a_{ik} = a_{ki}, \quad b_{ik} = b_{ki}, \quad c_{ik} = c_{ki}, \quad \rho_{ik}^0 = \rho_{ki}^0, \quad s_{ik}^0 = s_{ki}^0, \tag{2.27}$$

in accordance with the reciprocity theorem of Maxwell and Betti.

The free term in (2.25) represents the functions $G_i(y)$, obtained from (2.4) as the generalized load per unit length corresponding to the virtual displacements $\chi_i(x)$.

By letting i assume successively different integral values between 1 and n, we obtain a system of n ordinary differential equations with constant coefficients for the determination of the n unknown functions W_k. By virtue of (2.27), this system has a symmetrical structure. All the equations will be of the fourth order in each unknown function.

7. Determining the moments and shearing forces

Solving the system (2.25) for given boundary conditions at $x = 0$ and $x = b$ we obtain all the functions $W_k(y)$; the function $w(x, y)$ can then be determined by (2.1).

We can then rewrite (1.8) and (1.9) as follows:

$$\left.\begin{aligned}
M_x &= -D\sum_{k=1}^{n}(\mu W''_k\chi_k + W_k\chi''_k), && \text{(a)}\\
M_y &= -D\sum_{k=1}^{n}(W''_k\chi_k + \mu W_k\chi''_k), && \text{(b)}\\
H = H_x = -H_y &= -D\sum_{k=1}^{n}(1-\mu)W'_k\chi'_k, && \text{(c)}\\
N_x &= -D\sum_{k=1}^{n}(W''_k\chi'_k + W_k\chi'''_k), && \text{(d)}\\
N_y &= -D\sum_{k=1}^{n}(W'''_k\chi_k + W'_k\chi''_k), && \text{(e)}\\
Q_x &= -D\sum_{k=1}^{n}\{(2-\mu)W''_k\chi'_k + W_k\chi'''_k\}, && \text{(f)}\\
Q_y &= -D\sum_{k=1}^{n}\{W'''_k\chi_k + (2-\mu)W'_k\chi''_k\}. && \text{(g)}
\end{aligned}\right\} \qquad (2.28)$$

§3. GENERALIZED INTERNAL FORCES. BOUNDARY CONDITIONS AT THE LATERAL PLATE EDGES

As already mentioned above, the functions $W_i(y)$ represent the generalized plate deflections corresponding to the virtual displacements $\chi_i(x)$. The derivative of the generalized deflection therefore defines the generalized slope $\varphi_i(y)$. The geometrical magnitudes $W_i(y)$ and $\varphi_i(y)$ correspond to the generalized bending moments $M_i(y)$ and the generalized shearing forces $N_i(y)$, exactly as in the theory of the bending of beams.

The generalized bending moments M_i represent the work done by all the bending moments M_y acting in the section $y = \mathrm{const}$ over the corresponding virtual rotations $\frac{\partial \bar{w}_i}{\partial y} = \varphi_i\chi_i$ $(\varphi_i = 1)$; the generalized shearing forces N_i represent the work done by the shearing forces N_y, the twisting moments H, and the shearing stresses τ_{zy} acting in the section $y = \mathrm{const}$ over the virtual displacements $\bar{w}_i = W_i\chi_i$ $(W_i = 1)$.

The shearing stresses τ_{zy}, acting in the section $y = \mathrm{const}$ of the elastic foundation, are, by virtue of (6.5), (7.2) of Chapter I, and (2.1) of this chapter:

$$\tau_{zy} = \frac{E_0}{2(1+\nu_0)}\frac{\partial w}{\partial y}\psi(z) = \frac{E_0}{2(1+\nu_0)}\psi(z)\sum_{k=1}^{n}W'_k(y)\chi_k(x). \qquad (3.1)$$

The work of these stresses over any virtual displacement of the elastic foundation must be calculated over the entire cross section $y = \mathrm{const}$, i.e., for $-\infty \leqslant x \leqslant +\infty$ and $0 \leqslant z \leqslant H$.

The i-th virtual displacement of an arbitrary point $M(x, y, z)$ of a single-layer foundation is:

$$w_i(x, y, z) = W_i(y)\chi_i(x)\phi(z). \tag{3.2}$$

With $W_i(y) = 1$ the virtual work done by the shearing stresses τ_{zy} is therefore :

$$\iint \tau_{zy}\chi_i(x)\phi(z)\,dx\,dz. \tag{3.3}$$

Substituting (2.9), (2.15) and (3.1) in (3.3), and integrating, we obtain the following expression for the virtual work done by the shearing stresses acting in the section $y = \text{const}$:

$$\sum_{k=1}^{n}\left\{2t\int \chi_k\chi_i\,dx + \frac{t}{a}\,[|\chi_k\chi_i|]\right\}W_k'. \tag{3.4}$$

[The integration limits are in fact: $x = 0$ and $x = b$]

By (2.1), [(2.24)], (2.28 b, c, e,), and (3.4), the generalized moments and shearing forces acting in the section $y = \text{const}$ are:

$$M_i = -\sum_{k=1}^{n}\left\{\left(\sum D\int \chi_k\chi_i\,dx\right)W_k'' - \mu\sum D\left(\int \chi_k'\chi_i'\,dx - |\chi_k'\chi_i|^{*}\right)W_k\right\} \tag{3.5}$$

$$\begin{aligned} N_i = &-\sum_{k=1}^{n}\left(\sum D\int \chi_k\chi_i\,dx\right)W_k''' + \\ &+\sum_{k=1}^{n}\left\{(2-\mu)\sum D\left(\int \chi_k'\chi_i'\,dx - |\chi_k'\chi_i|^{*}\right) + 2t\int \chi_k\chi_i\,dx + \right. \\ &\left. + \frac{t}{a}\left|\left[|\chi_k\chi_i|\right]\right|\right\}W_k' \end{aligned} \tag{3.6}$$

$$(i = 1, 2, \ldots, n),$$

[where the second term on the right includes the virtual work done by the force $\frac{dH}{dx}$].

The boundary conditions for $y = 0$ and $y = b$ can now be expressed in integral form with the aid of (3.5) and (3.6).

Since (2.25) is a system of order $4n$, the functions W_k are determined except for $4n$ constants. It is therefore necessary to add $4n$ boundary conditions to (2.25) in order to obtain a complete solution. It is seen from (2.1), (3.5), and (3.6) that $2n$ boundary conditions can be specified at each edge $y = 0$, $y = l$. If the plate is built-in, the boundary conditions are given as generalized displacements; when the edges are free the boundary conditions are given as generalized forces, and when the edges are simply supported, the boundary conditions are given partly as forces and partly as displacements.

§ 4. SELECTING THE FUNCTION OF THE LATERAL DISTRIBUTION OF THE DEFLECTIONS. BOUNDARY CONDITIONS AT THE LONGITUDINAL PLATE EDGES

The functions $\chi_k(x)$, which determine the lateral distribution of the displacements of the plate, can be selected in different ways provided they satisfy the geometrical boundary conditions at the longitudinal plate edges and are linearly independent. Several methods for selecting the functions χ_k, and the corresponding properties of the matrix of (2.25), will now be considered.

1. Eigenfunctions of the transverse vibrations of a beam

The eigenfunctions of the transverse vibrations of a beam having uniform cross section can be selected as functions $\chi_k(x)$, when the boundary conditions for the beam are similar to those at the longitudinal plate edges.

We begin with a short discussion of the theory of eigenfunctions*. The free vibrations of a single-span massive beam of length b are described by the differential equation:

$$X^{\mathrm{IV}} = \frac{\mu^4}{b^4} X, \tag{4.1}$$

where $X = X(x)$ is the deflection of the beam axis at x, and μ = parameter characterizing frequency of natural vibrations of beam.

The general integral of (4.1) is:

$$X(x) = C_1 \sin\frac{\mu x}{b} + C_2 \cos\frac{\mu x}{b} + C_3 \operatorname{sh}\frac{\mu x}{b} + C_4 \operatorname{ch}\frac{\mu x}{b}. \tag{4.2}$$

The constants C_1, C_2, C_3, C_4 and the parameter μ are determined from the boundary conditions at the beam ends $x = 0$ and $x = b$. The form of the function $X(x)$ depends therefore on these conditions.

Some particular boundary conditions will be considered.

1. Both beam ends simply supported.

In this case the boundary conditions for $X(x)$ are:

$$\begin{aligned} &\text{at } x = 0 \qquad X(0) = X''(0) = 0, \\ &\text{at } x = b \qquad X(b) = X''(b) = 0. \end{aligned} \tag{4.3}$$

Substitution of (4.2) yields:

$$\left.\begin{aligned} C_2 + C_4 &= 0, \\ -C_2 + C_4 &= 0, \\ C_1 \sin\mu + C_2 \cos\mu + C_3 \operatorname{sh}\mu + C_4 \operatorname{ch}\mu &= 0, \\ -C_1 \sin\mu - C_2 \cos\mu + C_3 \operatorname{sh}\mu + C_4 \operatorname{ch}\mu &= 0. \end{aligned}\right\} \tag{4.4}$$

---

* For a more thorough treatment of this problem, see Vlasov, V. Z. "Structural Mechanics of Thin-Walled Three-Dimensional Systems", see also section 2 of Chapter VI.

The first two equations give $C_2 = C_4 = 0$. The remaining two equations then reduce to:

$$\left.\begin{aligned} C_1 \sin\mu + C_3 \operatorname{sh}\mu = 0, \\ -C_1 \sin\mu + C_3 \operatorname{sh}\mu = 0. \end{aligned}\right\} \tag{4.5}$$

Since, for a nontrivial solution, all constants cannot vanish simultaneously, the determinant of (4.5) must be equal to zero. The following transcendental equation is then obtained for μ:

$$\sin\mu = 0,$$

which has an infinite number of real roots $\mu_m (m = 1, 2, 3, \ldots)$ equal to:

$$\pi,\ 2\pi,\ 3\pi,\ \ldots,\ m\pi. \tag{4.6}$$

In accordance with (4.6) we obtain a complete system of eigenfunctions:

$$X_m(x) = \sin\frac{m\pi x}{b} \qquad (m = 1,\ 2,\ 3,\ \ldots),$$

which determine an infinite number of modes of the natural vibrations.

2. Both beam ends built-in. The boundary conditions are in this case:

$$\left.\begin{aligned} &\text{at } x = 0 \qquad X(0) = X'(0) = 0, \\ &\text{at } x = b \qquad X(b) = X'(b) = 0. \end{aligned}\right\} \tag{4.7}$$

Substitution of (4.2) yields, as before, a system of algebraic equations in the integration constants C_1, C_2, C_3, C_4. Equating the determinant of this system to zero, we obtain:

$$\cos\mu \operatorname{ch}\mu = 1,$$

The roots of this equation are:

$$0;\ 4.730;\ 7.853;\ 10.996;\ \ldots;\ \frac{2m+1}{2}\pi. \tag{4.8}$$

The eigenfunctions $X_m(x)$ determined by (4.8) are in this case:

$$X_m(x) = \sin\frac{\mu_m x}{b} - \operatorname{sh}\frac{\mu_m x}{b} - \alpha_m\left(\cos\frac{\mu_m x}{b} - \operatorname{ch}\frac{\mu_m x}{b}\right),$$

where

$$\alpha = \frac{\sin\mu_m - \operatorname{sh}\mu_m}{\cos\mu_m - \operatorname{ch}\mu_m}.$$

No further cases will be discussed. Proceeding from (4.2) and the specified boundary conditions of the problem, the eigenfunctions $X_m(x)$ can be determined for continuous multi-span beams. In each case a system of homogeneous equations will be obtained for the determination of the integration constants. By equating to zero the determinant of this system we obtain a transcendental equation for the parameter μ, whose roots define, together with the boundary conditions, all the eigenfunctions corresponding to the problem considered.

Table 7 contains the eigenfunctions of $\xi\ \frac{x}{b}$ for the six basic cases of boundary conditions of a single-span beam, together with the corresponding transcendental equations and some of their roots.

TABLE 7

	Beam supports	Boundary conditions		Eigen-function $X(\xi)$	Coefficient α	Transcendental equation	Roots of transcendental equation				
		at $x=0$	at $x=l$				μ_1	μ_2	μ_3	μ_4	general formula for μ_n $(n>4)$
1	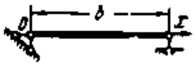	$X=0$ $X''=0$	$X=0$ $X''=0$	$\sin\mu\xi$	—	$\sin\mu=0$	$\pi=$ $=3.1416$	2π	3π	4π	$n\pi$
2	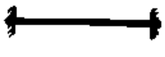	$X=0$ $X'=0$	$X=0$ $X'=0$	$\sin\mu\xi-$ $-\operatorname{sh}\mu\xi-$ $-\alpha(\cos\mu\xi-$ $-\operatorname{ch}\mu\xi)$	$\frac{\sin\mu-\operatorname{sh}\mu}{\cos\mu-\operatorname{ch}\mu}$	$\cos\mu\operatorname{ch}\mu=$ $=1$	4.7300	7.8532	10.9956	14.1372	$\frac{2n+1}{2}\pi$
3	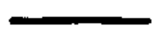	$X''=0$ $X'''=0$	$X''=0$ $X'''=0$	$\sin\mu\xi+$ $+\operatorname{sh}\mu\xi-$ $-\alpha(\cos\mu\xi+$ $+\operatorname{ch}\mu\xi)$	$\frac{\sin\mu-\operatorname{sh}\mu}{\cos\mu-\operatorname{ch}\mu}$	$\cos\mu\operatorname{ch}\mu=$ $=1$	4.7300	7.8532	10.9956	14.1372	$\frac{2n+1}{2}\pi$
4	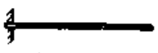	$X=0$ $X'=0$	$X''=0$ $X'''=0$	$\sin\mu\xi-$ $-\operatorname{sh}\mu\xi-$ $-\alpha(\cos\mu\xi-$ $-\operatorname{ch}\mu\xi)$	$\frac{\sin\mu+\operatorname{sh}\mu}{\cos\mu+\operatorname{ch}\mu}$	$\cos\mu\operatorname{ch}\mu=$ $=-1$	1.8751	4.6941	7.8548	10.9955	$\frac{2n-1}{2}\pi$
5	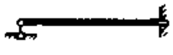	$X=0$ $X''=0$	$X=0$ $X'=0$	$\sin\mu\xi-$ $-\alpha\operatorname{sh}\mu\xi$	$\frac{\sin\mu}{\operatorname{sh}\mu}$	$\operatorname{tg}\mu=$ $=\operatorname{th}\mu$	3.9266	7.0685	10.2102	13.3520	$\frac{4n+1}{4}\pi$
6	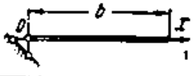	$X=0$ $X''=0$	$X''=0$ $X'''=0$	$\sin\mu\xi+$ $+\alpha\operatorname{sh}\mu\xi$	$\frac{\sin\mu}{\operatorname{sh}\mu}$	$\operatorname{tg}\mu=$ $=\operatorname{th}\mu$	3.9266	7.0685	10.2102	13.3520	$\frac{4n+1}{4}\pi$

In order to simplify the use of the eigenfunctions, values of $X_m(x)$ and of their first three derivatives, multiplied by constant factors:

$$\frac{b}{\mu_m}X_m'(b),\ \frac{b^2}{\mu_m^2}X_m''(x),\ \frac{b^3}{\mu_m^3}X_m'''(x),$$

are given in Tables 5 to 10 of the appendix for nine intermediate sections and the two end sections $x=0$ and $x=b$ of the beam.

The eigenfunctions determined in this way possess some properties which have very important practical applications. Firstly, they are orthogonal over the entire length of the beam:

$$\int_0^b X_m(x)\,X_n(x)\,dx=0. \qquad (m\neq n)$$

The second derivatives of the eigenfunctions are also orthogonal:

$$\int_0^b X''_m(x)\,X''_n(x)\,dx = 0. \qquad (m \neq n)$$

It then follows from (4.1) that all even derivatives of these functions are orthogonal.

The corresponding integrals for $m=n$ are different from zero and independent of the boundary conditions at $x=0$; they can be expressed through the function and its derivatives at $x=b$ only:

$$\int_0^b X_m^2(x)\,dx = \frac{b}{4}\left[X_m^2 - 2X'_m X'''_m + (X''_m)^2\right]_{x=b}.$$

Returning to the problem of a plate on an elastic foundation, we take as eigenfunctions $\chi_k(x)$ the functions of the lateral distribution of the deflections $X_k(x)$.

The solution of (2.25) is simplified when $\chi_k = X_k$. Thus, for the symmetrical problem (cases 1, 2, and 3 in Table 7), the system (2.25) can be divided into two independent sub-systems, each containing only even or only odd terms of (2.1). The system (2.25) cannot be divided when schemes 4, 5, or 6 in Table 7 apply.

Furthermore, by virtue of the orthogonality of the eigenfunctions and their second derivatives, the coefficients a_{ik} and c_{ik} vanish for $i \neq k$.

2. Trigonometric functions

The problem considered is solved most easily when the longitudinal plate edges are simply supported (case 1 in Table 7). In this case the eigenfunctions degenerate into the trigonometric functions $\sin\frac{k\pi x}{b}$, all derivatives of which are orthogonal. Hence, since $\chi_k = \sin\frac{k\pi x}{b} = 0$ at $x=0$ and $x=b$, all coefficients (2.26) vanish for $i \neq k$. System (2.25) then reduces to separate independent equations of the fourth order in $W_k(y)$.

Trigonometric functions may also be used when the longitudinal plate edges are free, or when one edge is simply supported while the other is free (cases 3 and 6 in Table 7). The elastic line can in this case be approximated by a series consisting of the first (linear) terms of the eigenfunctions and of the trigonometric functions $\sin\frac{k\pi x}{b}$.

The function $w(x, y)$ for a plate with free ends (case 3) is then:
for symmetrical loading

$$w(x, y) = W_0(y)\,1 + W_1(y)\sin\frac{\pi x}{b} + W_3(y)\sin\frac{3\pi x}{b} + \ldots; \qquad (4.9)$$

for antisymmetrical loading

$$w(x, y) = W_0(y)\left(1 - \frac{2x}{b}\right) + W_2(y)\sin\frac{2\pi x}{b} + W_4(y)\sin\frac{4\pi x}{b} + \ldots \qquad (4.10)$$

For a plate simply supported at one of its edges (case 6) we obtain:

$$w(x,\ y) = W_0(y)\frac{x}{b} + W_1(y)\sin\frac{\pi x}{b} + W_2(y)\sin\frac{2\pi x}{b} + \ldots \tag{4.11}$$

When the functions $\chi_k(x)$ are defined by (4.9) or (4.10), and $D = \mathrm{const}$ system (2.25) can be represented in the form of Tables 8 and 9 for symmetrical and antisymmetrical loading respectively.

TABLE 8

Matrix of ordinary differential equations for symmetrical loading

$$w_{xy} = W_0 \cdot 1 + \sum_{k=1}^{n} W_k \sin\frac{k\pi x}{b} \quad \text{при } k = 1,\ 3,\ 5,\ \ldots,\ n$$

i	W_0	W_1	W_3	…	W_n	Free term	Displacement
0	$a_{00}D^4 - 2\rho^0_{00}D^2 + s^0_{00}$	$a_{01}D^4 - 2(b_{01} + \rho^0_{01})D^2 + s^0_{01}$	$a_{03}D^4 - 2(b_{03} + \rho^0_{03})D^2 + s^0_{03}$	…	$a_{0n}D^4 - 2(b_{0n} + \rho^0_{0n})D^2 + s^0_{0n}$	G_0	$\chi_0 = 1$ 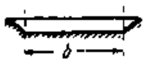
1	•	$a_{11}D^4 - 2(b_{11} + \rho^0_{11})D^2 + (s^0_{11} + c_{11})$	0	…	0	G_1	$\chi_1 = \sin\frac{\pi x}{b}$ 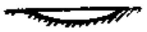
3	•	0	$a_{33}D^4 - 2(b_{33} + \rho^0_{33})D^2 + (s^0_{33} + c_{33})$	…	0	G_3	$\chi_3 = \sin\frac{3\pi x}{b}$ 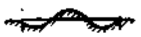
…	…	…	…	…	…	…	…
n	•	0	0	…	$a_{nn}D^4 - 2(b_{nn} + \rho^0_{nn})D^2 + (s^0_{nn} + c_{nn})$	G_n	$\chi_n = \sin\frac{n\pi x}{b}$

The only nonzero terms in these matrices are those of the principal diagonal, the first row, and the first column.

The symbols D^4 and D^2 in these tables denote respectively the fourth and second derivative of the function indicated at the head of the column. The coefficients:

$$a_{00},\ \rho^0_{00},\ s^0_{00},\ a_{01},\ \ldots,\ c_{nn},\ s^0_{nn}$$

are obtained from (2.26), by substituting in them the expressions:
for a symmetrical load,

$$\chi_0 = 1,\ \chi_n = \sin\frac{n\pi x}{b} \qquad (\text{at } n = 1,\ 3,\ 5,\ 7,\ \ldots);$$

for an antisymmetrical load,

$$\chi_0 = 1 - \frac{2x}{b},\ \chi_m = \sin\frac{m\pi x}{b} \qquad (\text{at } m = 2,\ 4,\ 6,\ \ldots).$$

The free terms in the last column but one of each table represent the work done by the external load over the corresponding displacement $W_i\chi_i$ when $W_i = 1$.

These examples show that in order to obtain a complete solution it is necessary to solve an infinite number of ordinary differential equations.

TABLE 9

Matrix of ordinary differential equations for antisymmetrical loading

$$w(x, y) = W_0\left(1-\frac{2x}{b}\right)+\sum_{k=2}^{m} W_k \sin\frac{k\pi x}{b} \quad \text{при } k = 2, 4, 6, \ldots, m$$

i	W_0	W_2	W_4	…	W_m	Free term	Displacements
0	$a_{00}D^4-2(b_{00}+\rho^0_{00})D^2+s_{00}$	$a_{02}D^4-2(b_{02}+\rho^0_{02})D^2+s^0_{02}$	$a_{04}D^4-2(b_{04}+\rho^0_{04})D^2+s^0_{04}$	…	$a_{0m}D^4-2(b_{0m}+\rho^0_{0m})D^2+s^0_{0m}$	G_0	$\chi_0 = 1-\frac{2x}{b}$ 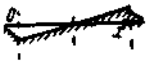
2	•	$a_{22}D^4-2(b_{22}+\rho^0_{22})D^2+(c_{22}+s^0_{22})$	0	…	0	G_2	$\chi_2 = \sin\frac{2\pi x}{b}$ 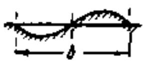
4	•	•	$a_{44}D^4-2(b_{44}+\rho^0_{44})D^2+(c_{44}+s^0_{44})$	…	0	G_4	$\chi_4 = \sin\frac{4\pi x}{b}$ 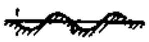
…	…	…	…	…	…	…	…
	•	•	•	…	$a_{mm}D^4-2(b_{mm}+\rho_{mm})D^2+(c_{mm}+s_{mm})$	G_n	$\chi_m = \sin\frac{m\pi x}{b}$ при $m = 2, 4, 6$.

Since, however, the series representing trigonometric functions or eigenfunctions converge rapidly, it suffices in practice to take a small number of terms in (2.1). Thus, if the load distribution is nearly uniform in the x-direction, two or three terms in (4.9) and (4.10) are sufficient in order to obtain satisfactory accuracy. This is also true for the other methods of plate support.

When only a limited number of terms are taken in (2.1), the bending moments M_x and shearing forces N_x and Q_x can be determined directly from the equilibrium conditions instead of from (2.28).

3. Fulfilling the statical [equilibrium] conditions at the longitudinal edges

As already stated, the functions $\chi_k(x)$ are selected in order to satisfy the geometrical boundary conditions at the longitudinal plate edges. The fulfilment of the statical [equilibrium] conditions depends on the type of the boundary conditions and the form of the functions $\chi_k(x)$, and is, as a rule, only approximate; this does not, however, introduce large errors in the calculations.

The statical [equilibrium] conditions at $x=0$ and $x=b$ are particular cases of the conditions of equilibrium which, generally speaking, must be fulfilled at all points. On the other hand, the equilibrium conditions were included only in an integral form when establishing (2.25). In this solution, as usual for variational methods, the average deviation from the exact solution and from the strict fulfillment of the equilibrium conditions is small; at certain points, however, and particularly at the boundaries $x=0$, $x=b$; the equilibrium conditions may not be satisfied.

The following examples will make this point clear.

a) In the case of free plate end $x=0$, functions $X_k(x)$, can be selected as eigenfunctions which satisfy the following boundary conditions:

at $x=0$ $$X''(0)=X'''=0,\ X(0)\neq 0,\ X'(0)\neq 0.$$

The following expressions are then obtained from (2.28a) and (2.28f):

$$\left.\begin{aligned} M_x(0) &= -D\sum_{k=1}^{n}\mu W_k''\chi_k,\\ Q_x(0) &= -D\sum_{k=1}^{n}(2-\mu)W_k''\chi_k'. \end{aligned}\right\} \qquad (4.12)$$

These equations are identical with the statical boundary conditions only for certain values of M_x and Q_x; in particular, they are not identical with the homogeneous boundary conditions:

$$M_x(0)=0,\ Q_x(0)=0 \qquad (4.13)$$

Hence, the statical boundary conditions at the free ends are only approximately satisfied in the general case, the accuracy depending on the number of terms taken in the series expansions.

b) When the plate is supported on hinges at $x=0$, the eigenfunctions must satisfy the condition:

$$\chi(0)=0,\ \chi''(0)=0.$$

It then follows from (2.28a) that:

$$M_x(0)=0. \qquad (4.14)$$

The homogeneous boundary condition (4.14) is thus identically satisfied in this case. If an external moment is applied at $x=0$, the resulting non-homogeneous boundary condition will not be satisfied, irrespective of the number of terms taken in the expansion. This contradiction is, however, purely formal, since in a section an infinitesimal distance from the boundary section we shall obtain a value for M_x which is very close to the actual value by taking a sufficient number of terms in the series expansion.

It will be shown in section 5 how the statical [boundary] conditions at the longitudinal edges can be approximated with a minimum number of terms, by means of a different selection or an extension of the system of functions $\chi_k(x)$.

§ 5. SELECTING THE FUNCTIONS OF THE LATERAL DISTRIBUTION OF THE DEFLECTIONS BY THE STATICAL-EQUILIBRIUM METHOD

Eigenfunctions or trigonometric functions are not the only possible choice for the functions $\chi_k(x)$. They can also be obtained by means of the statical-equilibrium method.

We consider the plate element of width dy as an ordinary beam, its elastic line being determined by the boundary conditions. Different elastic lines can be obtained by varying the point of application of a concentrated force acting on this beam; these lines, which are third-order curves, are then taken as functions $\chi_k(x)$ (Figure 78).

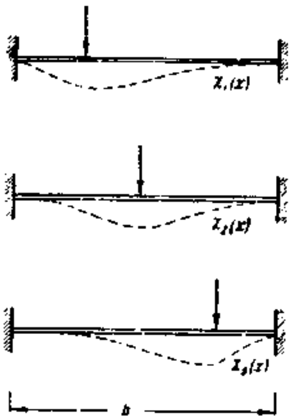

FIGURE 78.

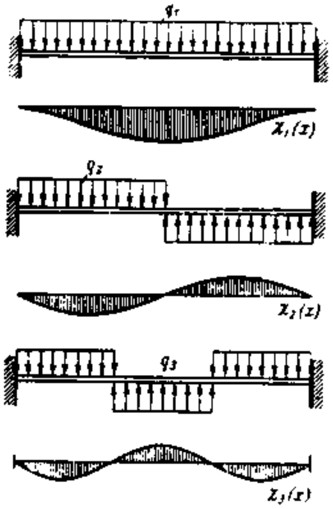

FIGURE 79.

In the same way we can apply a distributed load to the beam. By assuming different laws of variation with x of this load, we can obtain different forms of the functions χ_k from the differential equation:

$$\chi_k^{IV} = \frac{p}{EJ}$$

and the boundary conditions. A certain function χ_k will correspond to each type of loading. With a uniformly distributed load, of differing intensity in different parts of the beam (positive or negative) (Figure 79), the deflections χ_k of each part are represented by fourth-order parabolas when the rigidity EJ of each part is uniform. Since the functions $\chi_k(x)$ and their derivatives may be expressed differently in different parts of the beam, we shall consider the integrals on the right sides of (2.26) as the sum of the integrals taken over all these parts.

This method is more general than the method of eigenfunctions. This follows from the following property of the eigenfunctions:

$$\chi^{IV}(x) = k\chi(x).$$

In the particular case when the load varies like the ordinates of the elastic line, the eigenfunctions themselves will represent the elastic line.

Further, when a shearing force $Q(x)$ acts at the free end $x=0$, or when a moment M_x is applied at a free or hinged end, the elastic lines of the beam, due to a force $Q_x(0)=1$ and moment $M_x(0)=1$ respectively, can be included in functions $\chi_k(x)$. A better approximation to the exact solution at, and near, the free end $x=0$ is thus obtained than by taking a finite number of terms in the expansions of the eigenfunctions.

This method is also simpler than the method of eigenfunctions, used when analyzing complex structures, such as continuous plates and plates of variable thickness whose rigidities vary exponentially in the x direction.

An elementary strip of width dy of such a structure can, depending on the cross section of this structure, be considered either as a stepped or as a continuous beam. By applying an external load to such a beam, we obtain the functions $\chi_k(x)$ by the known methods of the theory of structures.

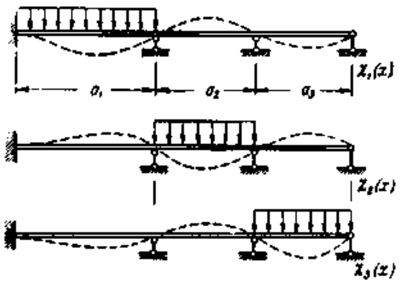

FIGURE 80.

Different functions $\chi_k(x)$, approximating the deflections $w(x)$ for $y=\text{const}$, are obtained by varying the external load. Figure 80 shows the functions $\chi_k(x)$ obtained as deflections of a continuous beam under the action of three types of loads, approximating the deflections of a continuous plate built-in along the edge $x=0$ and having rigid supports parallel to the y axis at $x=a_1$, $x=a_1+a_2$, and $x=a_1+a_2+a_3$.

§ 6. PLATE SIMPLY SUPPORTED AT OPPOSITE ENDS

1

Consider a rectangular plate on an elastic foundation, simply supported along the longitudinal edges (Figure 81).

The functions of the lateral distribution of the deflections are assumed to be:

$$\chi_n(x)=\sin\frac{n\pi x}{b}. \qquad (6.1)$$

Because of the orthogonality of these functions and their derivatives, we find that all coefficients (2.26) having different subscripts vanish, while those with equal subscripts become:

$$\left.\begin{aligned} a_{nn} = D\frac{b}{2}, \qquad b_{nn} = D\frac{n^2\pi^2}{2b}, \qquad c_{nn} = D\frac{n^4\pi^4}{2b^3}, \\ \rho^0_{nn} = t\frac{b}{2}, \qquad s^0_{nn} = k\frac{b}{2}\left[1 + \frac{2t}{k}\frac{n^2\pi^2}{b^2}\right] \end{aligned}\right\} \tag{6.2}$$

System (2.25) thus reduces to n independent equations:

$$a_{nn}W_n^{IV} - 2(b_{nn} + \rho^0_{nn})W_n'' + (c_{nn} + s^0_{nn})W_n = G_r, \tag{6.3}$$

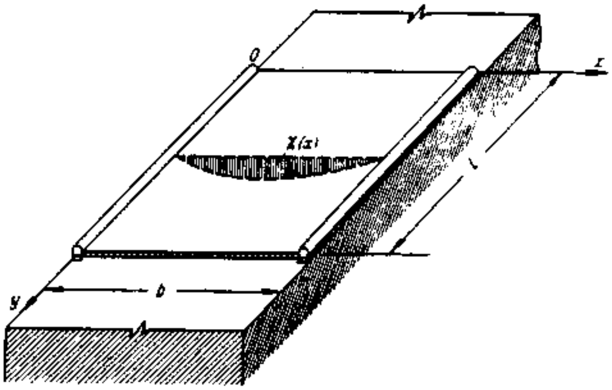

FIGURE 81.

The subscript n will henceforth be omitted. It should be kept in mind that the coefficients (6.2) and the function W correspond to a certain value of n in (2.1).

2

It is convenient to write (6.3) in dimensionless coordinates. Introducing a new variable $\eta = \frac{y}{l}$ and noting that:

$$\frac{dW}{dy} = \frac{1}{l}\frac{dW}{d\eta}, \qquad \frac{d^2W}{dy^2} = \frac{1}{l^2}\frac{d^2W}{d\eta^2} \text{ etc.}$$

we can rewrite (6.3) in the form:

$$W^{IV} - 2r^2W'' + s^4W = \frac{l^4}{a}G. \tag{6.4}$$

where

$$\left.\begin{aligned} r^2 = \frac{b + \rho^0}{a}l^2, \\ s^4 = \frac{c + s^0}{a}l^4. \end{aligned}\right\} \tag{6.5}$$

Substitution of (6.2) in (6.5) yields:

$$\left.\begin{aligned} r^2 &= n^2\pi^2\frac{l^2}{b^2} + \frac{1}{2\alpha^2L^2}\left(\frac{l}{L}\right)^2, \\ s^4 &= n^4\pi^4\frac{l^4}{b^4} + \left[1 - \frac{n^2\pi^2}{\alpha^2b^2}\right]\left(\frac{l}{L}\right)^4, \end{aligned}\right\} \tag{6.6}$$

where

$$L = \sqrt[4]{\frac{D}{k}}$$

l = plate length, b = plate width:

$$\alpha = \sqrt{\frac{k}{2t}}.$$

Introducting the notations,

$$r_1^2 = n^2\pi^2\frac{l^2}{b^2}, \quad r_0^2 = \frac{l^2}{2\alpha^2L^4}, \tag{6.7}$$

we obtain:

$$r^2 = r_1^2 + r_0^2,$$

It is seen that (6.4) has the same form as the differential equation of the bending of a beam (1.8) of Chapter II, differing only in the values of the constants r^2 and s^4. It follows that methods similar to those used for two-dimensional analysis of beams can be applied to this problem (cf. sections 2, 3, 6, of Chapter II).

§ 7. SOLVING THE DIFFERENTIAL EQUATION OF THE BENDING OF A PLATE BY THE METHOD OF INITIAL PARAMETERS

When an arbitrary external load is applied to the plate, equation (6.4) is most simply solved by the method of initial parameters.

The general solution is then:

$$\left.\begin{aligned} W(\eta) &= K_{WW}W_0 + K_{W\varphi}\varphi_0 + K_{WM}M_0 + K_{WN}N_0 - F_W, \\ \varphi(\eta) &= K_{\varphi W}W_0 + K_{\varphi\varphi}\varphi_0 + K_{\varphi M}M_0 + K_{\varphi N}N_0 - F_\varphi, \\ M(\eta) &= K_{MW}W_0 + K_{M\varphi}\varphi_0 + K_{MM}M_0 + K_{MN}N_0 - F_M, \\ N(\eta) &= K_{NW}W_0 + K_{N\varphi}\varphi_0 + K_{NM}M_0 + K_{NN}N_0 - F_N, \end{aligned}\right\} \tag{7.1}$$

where K_{WW}, $K_{W\varphi}, \ldots, K_{NN}$ = influence functions; W_0, φ_0, M_0, N_0 = generalized deflection, generalized slope, generalized bending moment, generalized shearing force respectively (at $y = 0$); $F_W, \ldots, F_N$ = load functions.

In order to determine the influence functions in (7.1) we have to find the solution of the homogeneous equation corresponding to (6.4), which is:

$$W(\eta) = C_1\Phi_1 + C_2\Phi_2 + C_3\Phi_3 + C_4\Phi_4, \tag{7.2}$$

where $C_1, C_2, \ldots, C_4$ = integration constants; $\Phi_1, \ldots, \Phi_4$ = functions depending on the roots of the auxiliary equation, i.e., on the coefficients r^2 and s^4.

The case:

$$s > r.$$

is that most frequently met.

The functions $\Phi_1, \ldots, \Phi_4$ are in this case (cf. Table 3, p. 51):

$$\left.\begin{aligned} \Phi_1 &= \operatorname{sh}\bar{\alpha}\eta\cos\bar{\beta}\eta, & \Phi_2 &= \operatorname{ch}\bar{\alpha}\eta\cos\bar{\beta}\eta, \\ \Phi_3 &= \operatorname{ch}\bar{\alpha}\eta\sin\bar{\beta}\eta, & \Phi_4 &= \operatorname{sh}\bar{\alpha}\eta\sin\bar{\beta}\eta, \end{aligned}\right\} \tag{7.3}$$

$$\bar{\alpha} = \sqrt{\frac{s^2 + r^2}{2}}, \quad \beta = \sqrt{\frac{s^2 - r^2}{2}}. \tag{7.3'}$$

Since W is a function of the dimensionless coordinate $\eta = \frac{y}{l}$, the generalized slope φ is:

$$\varphi = \frac{dW}{dy} = \frac{1}{l} W'. \tag{7.4}$$

We then obtain from (3.5), (3.6), and (6.1) the generalized bending moment M and the generalized shearing force N:

$$\left.\begin{aligned} M &= -\frac{a}{l^2}\left(W'' - \mu\frac{bl^2}{a}W\right), \\ N &= -\frac{a}{l^3}\left\{W''' - \left[(2-\mu)\frac{bl^2}{a} + \frac{2\rho^0 l^2}{a}\right]W'\right\}, \end{aligned}\right\} \tag{7.5}$$

where μ = Poisson's ratio for material of plate; a, b, and ρ^0 are given by (6.2).

Substituting (6.2) and (6.7) in (7.5), we obtain:

$$\left.\begin{aligned} M &= -\frac{a}{l^2}(W'' - \mu r_1^2 W), \\ N &= -\frac{a}{l^3}\{W''' - [(2-\mu)r_1^2 + 2r_0^2]W'\}. \end{aligned}\right\} \tag{7.6}$$

We then obtain from (7.2), (7.3), (7.4), and (7.6):

$$\left.\begin{aligned} W &= C_1\Phi_1 + C_2\Phi_2 + C_3\Phi_3 + C_4\Phi_4, \\ l\varphi &= C_1(\bar{\alpha}\Phi_2 - \bar{\beta}\Phi_4) + C_2(\bar{\alpha}\Phi_1 - \bar{\beta}\Phi_3) + C_3(\bar{\alpha}\Phi_4 + \bar{\beta}\Phi_2) + \\ &\qquad + C_4(\alpha\Phi_3 + \bar{\beta}\Phi_1) \\ \frac{l^2}{a}M &= -C_1\{[(1-\mu)r_1^2 + r_0^2]\Phi_1 - 2\bar{\alpha}\bar{\beta}\Phi_3\} - C_2\{[(1-\mu)r_1^2 + \\ &\quad + r_0^2]\Phi_2 - 2\bar{\alpha}\bar{\beta}\Phi_4\} - C_3\{[(1-\mu)r_1^2 + r_0^2]\Phi_3 + \\ &\quad + 2\bar{\alpha}\bar{\beta}\Phi_1\} - C_4\{[(1-\mu)r_1^2 + r_0^2]\Phi_4 + 2\bar{\alpha}\bar{\beta}\Phi_2\} \\ \frac{l^3}{a}N &= C_1\{\bar{\alpha}[s^2 - \mu r_1^2]\Phi_2 + \bar{\beta}[s^2 + \mu r_1^2]\Phi_4\} + \\ &+ C_2\{\bar{\alpha}[s^2 - \mu r_1^2]\Phi_1 + \bar{\beta}[s^2 + \mu r_1^2]\Phi_3\} - C_3\{\bar{\beta}[s^2 + \mu r_1^2]\Phi_2 - \\ &- \bar{\alpha}[s^2 - \mu r_1^2]\Phi_4\} - C_4\{\bar{\beta}[s^2 + \mu r_1^2]\Phi_1 - \bar{\alpha}[s^2 - \mu r_1^2]\Phi_3\}. \end{aligned}\right\} \tag{7.7}$$

For $\eta = 0$ these expressions become:

$$\left.\begin{aligned} W_0 &= C_2, \\ l\varphi_0 &= \alpha C_1 + \bar{\beta} C_3, \\ \frac{l^2}{a} M_0 &= -C_2[(1-\mu) r_1^2 + r_0^2] - 2\alpha\beta C_4, \\ \frac{l^3}{a} N_0 &= C_1\bar{\alpha}[s^2 - \mu r_1^2] - C_3\bar{\beta}[s^2 + \mu r_1^2]. \end{aligned}\right\} \tag{7.8}$$

Solving (7.8) for C_1, C_2, C_3, C_4 yields:

$$\left.\begin{aligned} C_1 &= \frac{1}{2\bar{\alpha}\bar{\beta}s^2}\left[(s^2 + \mu r_1^2)\bar{\beta} l\varphi_0 + \bar{\beta}\,\frac{l^3}{a} N_0\right], \\ C_2 &= W_0, \\ C_3 &= \frac{1}{2\bar{\alpha}\bar{\beta}s^2}\left[(s^2 - \mu r_1^2)\bar{\alpha} l\varphi_0 - \bar{\alpha}\,\frac{l^3}{a} N_0\right], \\ C_4 &= -\frac{1}{2\bar{\alpha}\bar{\beta}}\left\{[(1-\mu) r_1^2 + r_0^2] W_0 + \frac{l^2}{a} M_0\right\}. \end{aligned}\right\} \tag{7.9}$$

where $\bar{\alpha}$ and $\bar{\beta}$ are given by (7.3'), and s, r_1, and r_0 by (6.6) and (6.7).

TABLE 10.

	W_0	φ_0	M_0	N_n
W_η	$K_{WW} = \frac{1}{2\bar{\alpha}\bar{\beta}}\{2\bar{\alpha}\bar{\beta}\Phi_2 - [(1-\mu) r_1^2 + r_0^2]\Phi_4\}$	$K_{W\varphi} = \frac{l}{2\bar{\alpha}\bar{\beta}s^2}[(s^2 + \mu r_1^2)\bar{\beta}\Phi_1 + (s^2 - \mu r_1^2)\bar{\alpha}\Phi_3]$	$K_{WM} = -\frac{l^2}{2a\bar{\alpha}\bar{\beta}}\Phi_4$	$K_{WN} = \frac{l^3}{2a\bar{\alpha}\bar{\beta}s^2} \times (\bar{\beta}\Phi_1 - \bar{\alpha}\Phi_3)$
φ_η	$K_{\varphi W} = \frac{1}{2l\bar{\alpha}\bar{\beta}}[(s^2 + \mu r_1^2)\bar{\beta}\Phi_1 - (s^2 - \mu r_1^2)\bar{\alpha}\Phi_3]$	$K_{\varphi\varphi} = \frac{1}{2\bar{\alpha}\bar{\beta}}\{2\bar{\alpha}\bar{\beta}\Phi_2 + [(1-\mu) r_1^2 + r_0^2]\Phi_4\}$	$K_{\varphi M} = -\frac{l}{2a\bar{\alpha}\bar{\beta}} \times (\bar{\alpha}\Phi_3 + \bar{\beta}\Phi)$	$K_{\varphi N} = K_{WM}$
M_η	$K_{MW} = \frac{a}{2l^2\bar{\alpha}\bar{\beta}}\{s^4 - \mu r_1^2[(2-\mu) r_1^2 + 2r_0^2]\}\Phi_4$	$K_{M\varphi} = -\frac{a}{2\bar{\alpha}\bar{\beta}s^2 l}\{\bar{\beta}[(s^2 + \mu r_1^2) \times [(1+\mu) r_1^2 + r_0^2] + (s^2 - \mu r_1^2)[s^2 + r^2]]\Phi_1 + \alpha\{(s^2 - \mu r_1^2)[(1-\mu) r_1^2 + r_0^2] - (s^2 + \mu r_1^2)[s^2 - r^2]\}\Phi_3\}$	$K_{MM} = K_{\varphi\varphi}$	$K_{MN} = K_{W\varphi}$
N_η	$K_{NW} = \frac{a}{2\bar{\alpha}\bar{\beta}l^3}\{\bar{\beta}[(s^2 + r^2)(s^2 - \mu r_1^2) + [(1-\mu) r_1^2 + r_0^2](s^2 + \mu r_1^2)]\Phi_1 + \bar{\alpha}[(s^2 - r^2)(s^2 + \mu r_1^2) - [(1-\mu) r_1^2 + r_0^2](s^2 - \mu r_1^2)]\Phi_3\}$	$K_{N\varphi} = K_{MW}$	$K_{NM} = K_{\varphi W}$	$K_{NN} = K_{WW}$

By substituting (7.9) in (7.7) the solution of the homogeneous equation corresponding to (6.4) can be expressed through the initial parameters and influence functions (the functions $F_W, \ldots, F_N$ do not appear in the expressions obtained). The influence functions are given in Table 10.

In order to take into account the external load, represented by the right-side of (6.4), we subtract from the expressions (7.7) terms corresponding to the functions $F_W, \ldots, F_N$, which depend on the applied load and its distribution over the plate. This dependence was discussed in section 3 of Chapter II. One example of the application of this method will be given here.

Let a load as shown in Figure 82 act on the plate. It is seen that in part $0 < \eta < t_1$ the homogeneous differential equation is applicable so that all unknowns are determined by the initial parameters

$$\left.\begin{aligned} W(\eta) &= K_{WW}(\eta)\,W_0 + K_{W\varphi}(\eta)\,\varphi_0 + K_{WM}(\eta)\,M_0 + K_{WN}(\eta)\,N_0,\\ \varphi(\eta) &= K_{\varphi W}(\eta)\,W_0 + K_{\varphi\varphi}(\eta)\,\varphi_0 + K_{\varphi M}(\eta)\,M_0 + K_{\varphi N}(\eta)\,N_0,\\ M(\eta) &= K_{MW}(\eta)\,W_0 + K_{M\varphi}(\eta)\,\varphi_0 + K_{MM}(\eta)\,M_0 + K_{MN}(\eta)\,N_0,\\ N(\eta) &= K_{NM}(\eta)\,W_0 + K_{N\varphi}(\eta)\,\varphi_0 + K_{NM}(\eta)\,M_0 + K_{NN}(\eta)\,N_0. \end{aligned}\right\} \tag{7.10}$$

For $t_1 < \eta < t_2$ the following expressions have to be subtracted from the respective equations (7.10):

$$\left.\begin{aligned} F_W &= G_1 K_{WN}(\eta - t_1), \qquad & F_M &= G_1 K_{MN}(\eta - t_1),\\ F_\varphi &= G_1 K_{\varphi N}(\eta - t_1), \qquad & F_N &= G_1 K_{NN}(\eta - t_1); \end{aligned}\right\} \tag{7.11}$$

where

$$G_1 = \sum P_c \chi(c) = P_1 \chi(c_1) + P_2 \chi(c_2),$$

and $\chi(c)$ = value of $X(x)$ at the point of application of the concentrated force.

For $t_2 < \eta < t_3$ the load functions are:

$$\left.\begin{aligned} F_W &= G_1 K_{WN}(\eta - t_1) + G_3 K_{WN}(\eta - t_2),\\ F_\varphi &= G_1 K_{\varphi N}(\eta - t_1) + G_3 K_{\varphi N}(\eta - t_2),\\ F_M &= G_1 K_{MN}(\eta - t_1) + G_3 K_{MN}(\eta - t_2),\\ F_N &= G_1 K_{NN}(\eta - t_1) + G_3 K_{NN}(\eta - t_2), \end{aligned}\right\} \tag{7.12}$$

where

$$G_3 = P_3 \chi(c_3).$$

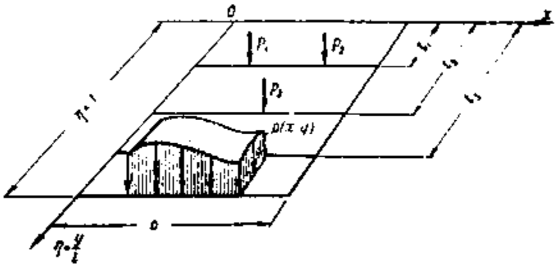

FIGURE 82.

For $t_3 < \eta < 1$ the load functions are:

$$\left.\begin{aligned}
F_W &= G_1K_{WN}(\eta - t_1) + G_3K_{WN}(\eta - t_2) + \\
&\qquad + \int_0^\eta G_4(t)\,K_{WN}(\eta - t)\,dt, \\
F_\varphi &= G_1K_{\varphi N}(\eta - t_1) + G_3K_{\varphi N}(\eta - t_2) + \\
&\qquad + \int_0^\eta G_4(t)\,K_{\varphi N}(\eta - t)\,dt, \\
F_M &= G_1K_{MN}(\eta - t_1) + G_3K_{MN}(\eta - t_2) + \\
&\qquad + \int_0^\eta G_4(t)\,K_{MN}(\eta - t)\,dt, \\
F_N &= G_1K_{NN}(\eta - t_1) + G_3K_{NN}(\eta - t_2) + \\
&\qquad + \int_0^\eta G_4(t)\,K_{NN}(\eta - t)\,dt,
\end{aligned}\right\} \qquad (7.13)$$

where

$$G_4 = \int_0^b p(x, \eta)\,\chi(x)\,dx.$$

§8. DETERMINATION OF INITIAL PARAMETERS. CALCULATION OF BENDING MOMENTS AND SHEARING FORCES

Since the origin can be in any plate cross section, two of the four initial parameters W_0, φ_0, M_0, N_0 in (7.1) are usually determined directly from the boundary conditions (cf. sections 3, 6 of Chapter II). The two other parameters are determined, irrespective of the applied external load, by solving simultaneously two equations written for a different cross section ($\eta = \text{const}$) of the plate. This will be illustrated by several examples.

Simply supported lateral plate edges

The load applied along the η axis will be divided into symmetrical and antisymmetrical components. The origin of coordinates lies in the center section of the plate (Figure 83).

The boundary conditions for symmetrical loading (Figure 83, a), are:

$$\eta = \frac{y}{l} = 0 \qquad\qquad \varphi_0 = 0, \quad N_0 = 0, \qquad (8.1)$$

the general solution then becomes:

$$\left.\begin{aligned}
W(\eta) &= W_0K_{WW}(\eta) + M_0K_{WM}(\eta) - F_W(\eta), \\
\varphi(\eta) &= W_0K_{\varphi W}(\eta) + M_0K_{\varphi M}(\eta) - F_\varphi(\eta), \\
M(\eta) &= W_0K_{MW}(\eta) + M_0K_{MM}(\eta) - F_M(\eta), \\
N(\eta) &= W_0K_{NW}(\eta) + M_0K_{NM}(\eta) - F_N(\eta).
\end{aligned}\right\} \qquad (8.2)$$

where the functions $F_{W,\eta} \dots F_N$ correspond to the load on only one half of the plate ($\eta > 0$). The parameters W_0 and M_0 are determined from the boundary conditions at the lateral edge:

$$\text{at} \quad \eta = \frac{1}{2}\left(\eta = -\frac{1}{2}\right): \; W = 0, \; M = 0. \tag{8.3}$$

Substitution of (8.3) in (8.2) yields:

$$\left.\begin{aligned} W\left(\tfrac{1}{2}\right) &= W_0 K_{WW}\left(\tfrac{1}{2}\right) + M_0 K_{WM}\left(\tfrac{1}{2}\right) - F_W\left(\tfrac{1}{2}\right) = 0, \\ M\left(\tfrac{1}{2}\right) &= W_0 K_{MW}\left(\tfrac{1}{2}\right) + M_0 K_{MM}\left(\tfrac{1}{2}\right) - F_M\left(\tfrac{1}{2}\right) = 0. \end{aligned}\right\} \tag{8.4}$$

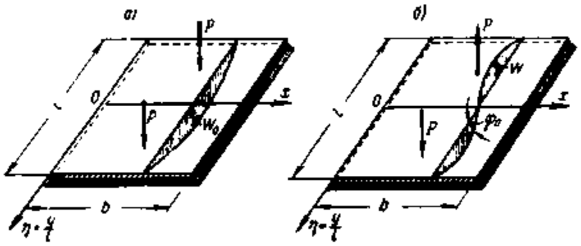

FIGURE 83.

The solution of system (8.4) is:

$$\left.\begin{aligned} W_0 &= \frac{F_W\left(\frac{1}{2}\right) K_{MM}\left(\frac{1}{2}\right) - F_M\left(\frac{1}{2}\right) K_{WM}\left(\frac{1}{2}\right)}{K_{WW}\left(\frac{1}{2}\right) K_{MM}\left(\frac{1}{2}\right) - K_{WM}\left(\frac{1}{2}\right) K_{MW}\left(\frac{1}{2}\right)}, \\ M_0 &= \frac{F_M\left(\frac{1}{2}\right) K_{WW}\left(\frac{1}{2}\right) - F_W\left(\frac{1}{2}\right) K_{MW}\left(\frac{1}{2}\right)}{K_{WW}\left(\frac{1}{2}\right) K_{MM}\left(\frac{1}{2}\right) - K_{WM}\left(\frac{1}{2}\right) K_{MW}\left(\frac{1}{2}\right)}, \end{aligned}\right\} \tag{8.5}$$

For antisymmetrical loading (Figure 83, b), the boundary conditions at $\eta = 0$ are:

$$\text{at} \quad \eta = \frac{y}{l} = 0 \; : \; W_0 = 0, \quad M_0 = 0. \tag{8.6}$$

The general solution for this case is:

$$\left.\begin{aligned} W(\eta) &= \varphi_0 K_{W\varphi}(\eta) + N_0 K_{WN}(\eta) - F_W(\eta), \\ \varphi(\eta) &= \varphi_0 K_{\varphi\varphi}(\eta) + N_0 K_{\varphi N}(\eta) - F_\varphi(\eta), \\ M(\eta) &= \varphi_0 K_{M\varphi}(\eta) + N_0 K_{MN}(\eta) - F_M(\eta), \\ N(\eta) &= \varphi_0 K_{N\varphi}(\eta) + N_0 K_{NN}(\eta) - F_N(\eta), \end{aligned}\right\} \tag{8.7}$$

where the functions $F_W(\eta), \dots, F_N(\eta)$ again correspond to the load on only one half of the plate.

The boundary conditions (8.3) yield:

$$\left.\begin{aligned} W\left(\tfrac{1}{2}\right) &= \varphi_0 K_{W\varphi}\left(\tfrac{1}{2}\right) + N_0 K_{WN}\left(\tfrac{1}{2}\right) - F_W\left(\tfrac{1}{2}\right) = 0, \\ M\left(\tfrac{1}{2}\right) &= \varphi_0 K_{M\varphi}\left(\tfrac{1}{2}\right) + N_0 K_{MN}\left(\tfrac{1}{2}\right) - F_M\left(\tfrac{1}{2}\right) = 0, \end{aligned}\right\} \qquad (8.8)$$

whence

$$\left.\begin{aligned} \varphi_0 &= \frac{F_W\left(\frac{1}{2}\right)K_{MN}\left(\frac{1}{2}\right) - F_M\left(\frac{1}{2}\right)K_{WN}\left(\frac{1}{2}\right)}{K_{W\varphi}\left(\frac{1}{2}\right)K_{MN}\left(\frac{1}{2}\right) - K_{WN}\left(\frac{1}{2}\right)K_{M\varphi}\left(\frac{1}{2}\right)}, \\ N_0 &= \frac{F_M\left(\frac{1}{2}\right)K_{W\varphi}\left(\frac{1}{2}\right) - F_W\left(\frac{1}{2}\right)K_{M\varphi}\left(\frac{1}{2}\right)}{K_{W\varphi}\left(\frac{1}{2}\right)K_{MN}\left(\frac{1}{2}\right) - K_{WN}\left(\frac{1}{2}\right)K_{M\varphi}\left(\frac{1}{2}\right)}. \end{aligned}\right\} \qquad (8.9)$$

Built-in lateral plate edges

In this case (Figure 84), the boundary conditions at $\eta = 0$ for symmetrical and antisymmetrical loading are given by (8.1) and (8.6) respectively. The solution of the problem is given by (8.2) for symmetrical and (8.7) for antisymmetrical loading.

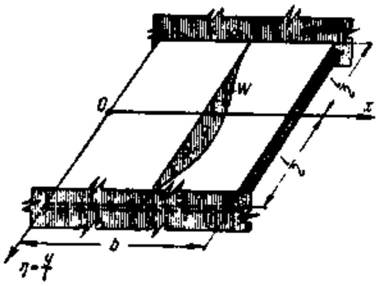

FIGURE 84.

The boundary conditions at the built-in lateral plate edges are:

$$\eta = \frac{1}{2}\ \left(\eta = -\frac{1}{2}\right) \qquad W = 0, \quad \varphi = 0. \qquad (8.10)$$

The initial parameters are determined from (8.10) and (8.2) or (8.7): for symmetrical loading:

$$\left.\begin{aligned} W_0 &= \frac{F_W K_{\varphi M} - F_\varphi K_{WM}}{K_{WW}K_{\varphi M} - K_{WM}K_{\varphi W}}, \\ M_0 &= \frac{F_\varphi K_{WW} - F_W K_{\varphi W}}{K_{WW}K_{\varphi M} - K_{WM}K_{\varphi W}}; \end{aligned}\right\} \qquad (8.11)$$

for antisymmetrical loading

$$\left.\begin{aligned}\varphi_0 &= \frac{F_W K_{\varphi N} - F_\varphi K_{WN}}{K_{W\varphi} K_{\varphi N} - K_{WN} K_{\varphi\varphi}},\\ N_0 &= \frac{F_\varphi K_{W\varphi} - F_W K_{\varphi\varphi}}{K_{W\varphi} K_{\varphi N} - K_{WN} K_{\varphi\varphi}},\end{aligned}\right\} \tag{8.12}$$

where

$$K_{\varphi M},\ K_{WM},\ \ldots,\ K_{\varphi\varphi},\ K_{\varphi N},\ F_W,\ F_\varphi$$

are the values of the corresponding functions at $\eta = \frac{1}{2}$.

Free lateral plate edges

The boundary conditions at the free plate edges are (Figure 85):

$$\left.\begin{aligned}W\left(\tfrac{1}{2}\right) &= W_f,\\ N\left(\tfrac{1}{2}\right) &= S_f,\\ M\left(\tfrac{1}{2}\right) &= 0.\end{aligned}\right\} \tag{8.13}$$

where W_f = vertical displacement of foundation at $\eta = \frac{y}{l} = \frac{1}{2}$, S_f = generalized shearing force exerted by foundation in this section.

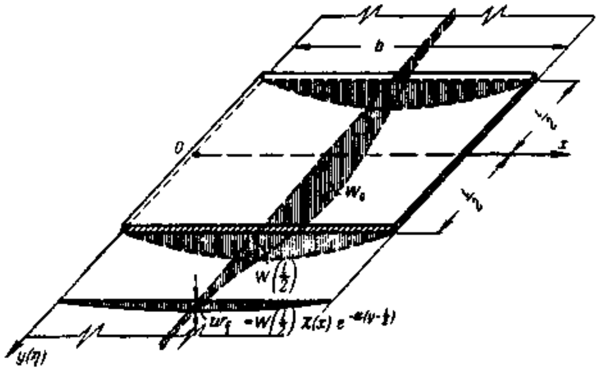

b
0
x
$l/2$
$l/2$
W_0
$W\left(\frac{1}{2}\right)$
$W_f = W\left(\frac{1}{2}\right) X(x)\, e^{-\alpha(y-\frac{1}{2})}$
$y(\eta)$

FIGURE 85.

The first condition (8.13) is purely geometrical and expresses the equality of the vertical depressions of plate and foundation surface. The second and third conditions are statical equilibrium conditions, similar to the corresponding conditions for the free end of a beam of finite length on an elastic single-layer foundation (cf. section 6 of Chapter II).

The vertical displacements of the free foundation surface ($|\eta| > \frac{1}{2}$) can be approximated by an exponential function (Figure 85):

$$w_{\mathrm{f}} = W_{\mathrm{f}}(y)\chi(x) = W_{\mathrm{f}}\left(\frac{l}{2}\right)\chi(x)\, e^{-\alpha\left(y-\frac{l}{2}\right)}, \tag{8.14}$$

where $\alpha = \sqrt{\frac{k}{2t}}$, and $\chi(x)$ is given by (6.1). The first boundary condition (8.13) is then satisfied by (8.14).

The generalized shearing force S_{f} in the free foundation, determined by the work done by the shearing stresses τ_{zy} over the corresponding virtual displacements, is given by (3.4). Since in this case $\chi(x)$ differs from zero only when $0 < x < b$, (3.4) reduces to:

$$S_{\mathrm{f}} = 2t \sum_{k=1}^{n} W'_{\mathrm{f}} \int_0^b \chi_k \chi_i \, dx. \tag{8.15}$$

Substituting (6.1) in (8.15) and taking (8.14) into account, we obtain for $y > \frac{l}{2}$

$$S_{\mathrm{f}} = -\alpha t b W_{\mathrm{f}}\left(\frac{l}{2}\right) e^{-\alpha\left(y-\frac{l}{2}\right)}. \tag{8.16}$$

The values of this expression at $y = \frac{l}{2}$ $\left(\eta = \frac{1}{2}\right)$ is:

$$S_{\mathrm{f}} = -\alpha t b W_{\mathrm{f}}\left(\frac{1}{2}\right).$$

Since

$$W\left(\frac{1}{2}\right) = W_{\mathrm{f}}\left(\frac{1}{2}\right),$$

we can write (8.13) as follows:

$$\left.\begin{aligned} N\left(\frac{1}{2}\right) &= -\alpha t b W\left(\frac{1}{2}\right), \\ M\left(\frac{1}{2}\right) &= 0. \end{aligned}\right\} \tag{8.17}$$

For symmetrical loading, the general solution is as before (cf. (8.2)):

$$\left.\begin{aligned} W(\eta) &= W_0 K_{WW}(\eta) + M_0 K_{WM}(\eta) - F_W(\eta), \\ \varphi(\eta) &= W_0 K_{\varphi W}(\eta) + M_0 K_{\varphi M}(\eta) - F_{\varphi}(\eta), \\ M(\eta) &= W_0 K_{MW}(\eta) + M_0 K_{MM}(\eta) - F_M(\eta), \\ N(\eta) &= W_0 K_{NW}(\eta) + M_0 K_{NM}(\eta) - F_N(\eta). \end{aligned}\right| \tag{8.18}$$

Substitution of (8.17) in (8.18) yields:

$$\left.\begin{aligned} W_0 &= \frac{(K_{NM} + \alpha t b K_{WM}) F_M - K_{MM}(F_N + \alpha t b F_W)}{K_{MW}(K_{NM} + \alpha t b K_{WM}) - K_{MM}(K_{NW} + \alpha t b K_{WW})}, \\ M_0 &= \frac{K_{MW}(F_N + \alpha t b F_W) - (K_{NW} + \alpha t b K_{WW}) F_M}{K_{MW}(K_{NM} + \alpha t b K_{WM}) - K_{MM}(K_{NW} + \alpha t b K_{WW})}. \end{aligned}\right| \tag{8.19}$$

For antisymmetrical loading we obtain:

$$\left.\begin{aligned} W(\eta) &= \varphi_0 K_{W\varphi}(\eta) + N_0 K_{WN}(\eta) - F_W(\eta), \\ \varphi(\eta) &= \varphi_0 K_{\varphi\varphi}(\eta) + N_0 K_{\varphi N}(\eta) - F_\varphi(\eta), \\ M(\eta) &= \varphi_0 K_{M\varphi}(\eta) + N_0 K_{MN}(\eta) - F_M(\eta), \\ N(\eta) &= \varphi_0 K_{N\varphi}(\eta) + N_0 K_{NN}(\eta) - F_N(\eta). \end{aligned}\right\} \tag{8.20}$$

Substitution of (8.17) in (8.20) yields:

$$\left.\begin{aligned} \varphi_0 &= \frac{(K_{NN} + \alpha t b K_{WN}) F_M - K_{MN}(F_N + \alpha t b F_W)}{K_{M\varphi}(K_{NN} + \alpha t b K_{WN}) - K_{MN}(K_{N\varphi} + \alpha t b K_{W\varphi})}, \\ N_0 &= \frac{K_{M\varphi}(F_N + \alpha t b F_W) - (K_{N\varphi} + \alpha t b K_{W\varphi}) F_M}{K_{M\varphi}(K_{NN} + \alpha t b K_{WN}) - K_{MN}(K_{N\varphi} + \alpha t b K_{W\varphi})}. \end{aligned}\right\} \tag{8.21}$$

The values of $K_{NN}(\eta)$. , $K_{W\varphi}(\eta)$ $F_W,(\eta)$ $F_N(\eta)$ in (8.19) and (8.21) are taken for $\eta = \frac{1}{2}$ $\left(y = \frac{l}{2}\right)$. As before:

$$\alpha = \sqrt{\frac{k}{2t}}, \quad k = \frac{E_0}{(1-\nu_0^2)} \int_0^H \psi'^2 \, dz, \quad t = \frac{F_0}{4(1+\nu_0)} \int_0^H \psi^2 \, dz, \tag{8.22}$$

where

$$E_0 = \frac{E_s}{1-\nu_s^2}, \quad \nu_0 = \frac{\nu_s}{1-\nu_s}.$$

Different boundary conditions at the lateral edges

If the boundary conditions at the two lateral edges differ, the x axis is placed along one of these edges (Figure 86). The initial parameters can then be determined in exactly the same way as for a symmetrical plate. From (8.17), we obtain for the free edge $\eta = 0$:

$$M_0 = 0, \quad N_0 = \alpha t b W_0. \tag{8.23}$$

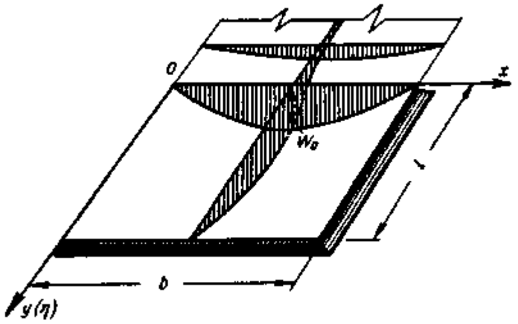

FIGURE 86.

The general solution is then:

$$\left.\begin{aligned} W(\eta) &= (K_{WW} + \alpha tbK_{WN})\,W_0 + K_{W\varphi}\varphi_0 - F_W, \\ \varphi(\eta) &= (K_{\varphi W} + \alpha tbK_{\varphi N})\,W_0 + K_{\varphi\varphi}\varphi_0 - F_\varphi, \\ M(\eta) &= (K_{MW} + \alpha tbK_{MN})\,W_0 + K_{M\varphi}\varphi_0 - F_M, \\ N(\eta) &= (K_{NM} + \alpha tbK_{NN})\,W_0 + K_{N\varphi}\varphi_0 - F_N. \end{aligned}\right\} \qquad (8.24)$$

The values of W_0 and φ_0 can now be determined from the boundary conditions at $\eta = 1$ $(y = l)$. Thus, if this end is simply supported the boundary conditions become:

$$\text{at } \eta = 1: \qquad W = 0, \quad M = 0. \qquad (8.25)$$

From (8.24) and (8.25) we then obtain:

$$\left.\begin{aligned} W_0 &= \frac{K_{M\varphi}F_W - K_{W\varphi}F_M}{K_{M\varphi}(K_{WW} + \alpha tbK_{WN}) - K_{W\varphi}(K_{MW} + \alpha tbK_{MN})}, \\ \varphi_0 &= \frac{(K_{WW} + \alpha tbK_{WN})\,F_M - (K_{MW} + \alpha tbK_{MN})\,F_W}{K_{M\varphi}(K_{WW} + \alpha tbK_{WN}) - K_{M\varphi}(K_{MW} + \alpha tbK_{MN})}, \end{aligned}\right\} \qquad (8.26)$$

where the functions $K_{M\varphi}, K_{W\varphi}, \ldots, F_W, F_M$ are taken at $\eta = 1$ $(y = l)$. In this case the functions F_W, F_M correspond to the load on the entire plate $(0 \leqslant \eta \leqslant 1)$.

Calculating the bending moments and shearing forces

When the generalized plate deflection $W(\eta)$ has been determined, the bending moments and shearing forces can be found from (2.28). Noting that $W(\eta)$ is a function of $\eta = \frac{y}{l}$, and taking (6.1) into account, we obtain for each term of (2.1):

$$\left.\begin{aligned} M_x &= -D\left[\frac{\mu}{l^2}\,W''(\eta) - \left(\frac{n\pi}{b}\right)^2 W(\eta)\right]\sin\frac{n\pi x}{b}, \\ M_y &= -D\left[\frac{1}{l^2}\,W''(\eta) - \mu\left(\frac{n\pi}{b}\right)^2 W(\eta)\right]\sin\frac{n\pi x}{b}, \\ H = H_x &= -H_y = -D\,\frac{1-\mu}{l}\,\frac{n\pi}{b}\,W'(\eta)\cos\frac{n\pi x}{b}, \\ N_x &= -D\left[\frac{1}{l^2}\,\frac{n\pi}{b}\,W''(\eta) - \left(\frac{n\pi}{b}\right)^3 W(\eta)\right]\cos\frac{n\pi x}{b}, \\ N_y &= -D\left[\frac{1}{l^3}\,W'''(\eta) - \frac{1}{l}\left(\frac{n\pi}{b}\right)^2 W'(\eta)\right]\sin\frac{n\pi x}{b}. \end{aligned}\right\} \qquad (8.27)$$

§ 9. CYLINDRICAL BENDING AND TORSION OF A NARROW PLATE. THREE-DIMENSIONAL BEAM ANALYSIS

1

Consider a narrow rectangular plate loaded symmetrically with respect to the y axis (Figure 87).

If we assume that the cross section of this plate (which in the general case is of varying thickness) is not deformed, only the translational displacement

$$\chi_0 = 1. \tag{9.1}$$

remains from all the possible displacements χ_i of an elementary strip of width $dy = 1$. The coefficients (2.26) entering in (2.25) then become:

$$\left.\begin{aligned} a_{00} &= \sum D_m b_m, & b_{00} &= c_{00} = 0, \\ r_{00}^0 &= t\left(b + \frac{1}{\alpha}\right), & s_{00}^0 &= kb + 4\alpha t, \end{aligned}\right\} \tag{9.2}$$

where

$$D_m = \frac{Eh_m^3}{12(1-\mu^2)}$$

is the flexural rigidity of the plate for a part of length b_m of the cross section (Figure 88).

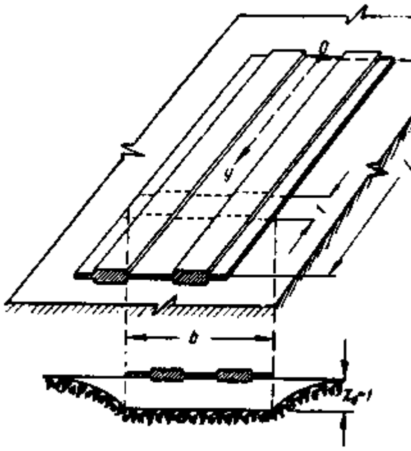

FIGURE 87.

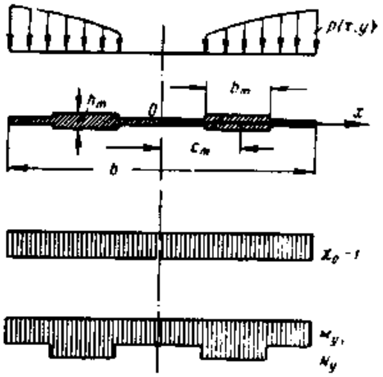

FIGURE 88.

Since

$$D_m b_m = \frac{EJ_m}{1-\mu^2},$$

we obtain

$$a_{00} = \frac{E}{1-\mu^2} \sum J_m = \frac{EJ}{1-\mu^2}, \tag{9.3}$$

where J is the total moment of inertia of the cross section relative to the x axis.

Substituting (9.2) and (9.3) in (2.25), we obtain:

$$\begin{aligned} &W^{IV} - 2r^2W'' + s^4W = \\ &= \frac{Q(1-\mu^2)l}{EJ}, \end{aligned} \tag{9.4}$$

where

$$\left.\begin{aligned} r^2 &= \frac{1-\mu^2}{EJ}\, t\left(b+\frac{1}{\alpha}\right), \\ s^4 &= \frac{1-\mu^2}{EJ}\,(kb+4\alpha t). \end{aligned}\right\} \tag{9.5}$$

In this case, the value of G is that of the actual load, as can be seen from (2.4) and (9.1).

The differential equation (9.4) of the cylindrical bending of a plate has the same form as the equation of the bending of a beam in the two-dimensional problem ((1.8) of Chapter II); it differs from it in that Poisson's ratio μ enters in (9.4). The values of the coefficients s^4 and r^2 are also different. Through the terms

$$\frac{1-\mu^2}{EJ}4\alpha t,\ \frac{1-\mu^2}{EJ}\frac{t}{\alpha}$$

entering in these coefficients, allowance is made for the fictitious reactions Q^{Φ} distributed over the longitudinal plate edges, i.e., for the three-dimensional state of stress in the elastic foundation.

We then obtain from (3.5) and (3.6):

$$\left.\begin{aligned} M &= -\frac{EJ}{1-\mu^2}W'', \\ N &= -\frac{EJ}{1-\mu^2}W''' + 2tb\left(1+\frac{1}{\alpha b}\right)W'. \end{aligned}\right\} \tag{9.6}$$

We can now integrate (9.4) by the methods of sections 2 and 3 of Chapter II. When the generalized deflection of the plate has been determined, the actual bending moments M_y and shearing forces N_y are obtained from (2.28 b, e), which in this case reduce to:

$$M_y = -DW'', \quad N_y = -DW'''. \tag{9.7}$$

It is seen from (9.7) that the bending moments M_y and shearing forces N_y in each cross section are proportional to the flexural rigidities D_m (Figure 89).

2

Consider now the same plate acted upon by an antisymmetrical load (Figure 89). Putting

$$\chi_1 = x, \quad \chi'(x) = 1, \tag{9.8}$$

where $\chi_1(x)$ has the dimension of length, the generalized deflection becomes:

$$W(y) = \frac{w(x,y)}{x}$$

which is a dimensionless magnitude, being the angle of twist of the plate:

$$\theta = \theta(y).$$

By (2.4) and (9.8), the generalized load is:

$$G = \int p(x, y)\, x\, dx + \sum p_c x_c = m(y) \tag{9.9}$$

and represents the twisting moment $m(y)$.

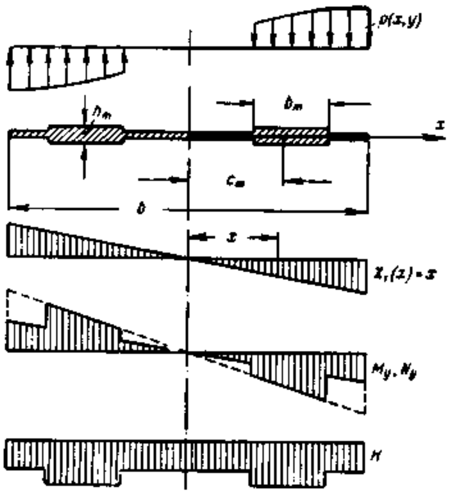

FIGURE 89.

The coefficients of (2.25) are again obtained from (2.26):

$$\left.\begin{aligned}
a_{11} &= \sum D_m \int x^2\, dx = \frac{EJ}{1-\mu^2}\rho^2,\\
b_{11} &= (1-\mu)\sum D_m b_m = \frac{EJ}{1+\mu},\\
c_{11} &= 0,\\
\rho_{11}^0 &= \frac{tb^3}{12}\left(1 + \frac{3}{\alpha b}\right),\\
s_{11}^0 &= \frac{kb^3}{12}\left(1 + \frac{12}{\alpha^2 b^2} + \frac{6}{\alpha b}\right),
\end{aligned}\right\} \tag{9.10}$$

where

$$\alpha = \sqrt{\frac{k}{2t}},$$

k and t = constants characterizing the compressive and shearing strains respectively of the elastic foundation, J = total moment of inertia of plate cross section relative to x axis; ρ = radius of inertia of rigidity diagram (Figure 89):

$$\rho^2 = \frac{1}{12}\,\frac{\Sigma D_m b_m (12c_m^2 + b_m^2)}{\Sigma D_m b_m} \tag{9.11}$$

[where c_m is the distance between the origin and the centroid of that part of the cross section whose rigidity is D_m].

For a plate of uniform thickness:

$$\rho^2 = \frac{b^2}{12}.$$

Equation (2.25) then becomes:

$$a_{11}\theta^{IV} - 2(b_{11} + \rho_{11}^0)\theta'' + s_{11}^0\theta - m = 0. \tag{9.12}$$

The generalized bending moment M and shearing force N are, by (3.5) and (3.6):

$$M = -\frac{EJ}{1-\mu^2}\rho^2\theta'', \tag{9.13}$$

$$N = -\frac{EJ}{1-\mu^2}\rho^2\theta''' + \frac{tb^3}{6}\left[1 + \frac{3}{ab}\right]\theta'. \tag{9.14}$$

where ρ^2 is defined by (9.11).

The actual bending moments M_y, torques H, and shearing forces N_y are by (2.28):

$$\left.\begin{aligned} M_y &= -Dx\theta'', \\ H &= -D(1-\mu)\theta', \\ N_y &= -Dx\theta'''. \end{aligned}\right\} \tag{9.15}$$

The distribution of M_y and N_y over the cross section $y = \text{const}$ is thus similar to that of $\chi_1 = x$ multiplied by the flexural rigidity D; while the twisting moments are directly proportional to the flexural rigidities D (Figure 89).

Together with (9.13) and (9.14), (9.12) determines the deformation of the plate, characterized by the presence of bending moments M_y in addition to the twisting moments H.

The generalized moment (9.13) represents in this case a bimoment, i.e., a system of normal stresses acting in the section $y = \text{const}$, statically equivalent to a zero force. The generalized shearing force determines the total twisting moment acting in the section $y = \text{const}$, due both to the shearing forces N_y and to the reactions of the elastic foundation; these are respectively given by the first and the second term of the right side of (9.14).

3

We can apply (9.4) to the three-dimensional problem of the bending of a beam by putting $\mu = 0$, and considering EJ as the rigidity of the beam. The free term G then represents the load per unit length.

Exactly as in the two-dimensional problem (cf. Chapter II), the beams can be classified as long, short, or rigid, depending on their rigidity.

Long beams acted upon by concentrated forces and moments can be analyzed by the method developed in section 4 of Chapter II. In the three-dimensional problems the generalized shearing force N entering in the boundary conditions is determined by the second equation (9.6), while r^4 and s^4 are given by (9.5).

Short beams acted upon by aribrary external loads are most simply analyzed by the method of initial parameters (section 3 of Chapter II, and section 7 of this chapter). When solving (9.4), the influence functions must be obtained from (9.5) and (9.6). The initial parameters are determined from the boundary conditions, given in generalized form, which, for free beam ends, correspond to (8.13).

In the case of rigid beams we can proceed directly from the equilibrium conditions of a beam acted upon by the known external load and by the reactions of the elastic foundation (cf. section 5 of Chapter II). Thus, for a symmetrical load, we obtain:

$$W(y) = C_0. \tag{9.16}$$

The reactions of the elastic foundation consist of the reactions q distributed over the surface supporting the beam, the reactions Q_l^{*} distributed along the longitudinal edges and the concentrated reactions T^{*} applied at the beam ends (Figure 90). The concentrated reaction T^{*} are introduced in order to make allowance for the effect of the deformation of the elastic foundation beyond the beam ends ($y < 0$, $y > l$) on the stresses in the beam.

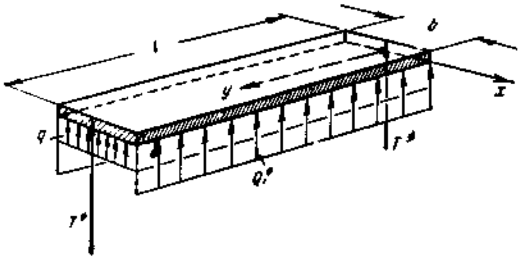

FIGURE 90.

From (2.17), (2.19), (9.1), and (9.16), we obtain:

$$q = kC_0, \quad Q_l^{*} = 2\alpha t C_0. \tag{9.17}$$

The concentrated reactions T^{*} are obtained by assuming that for $y < 0$ and $y > l$, the vertical displacements of the surface of the elastic foundation decrease exponentially. Thus, for $y < 0$ we have (Figure 91):

$$\left.\begin{array}{l}
\text{at } x \leqslant -\frac{b}{2} \\
\qquad w(x, y) = C_0 e^{\alpha\left(x+\frac{b}{2}\right)} e^{\alpha y}, \\
\text{at } -\frac{b}{2} \leqslant x \leqslant \frac{b}{2} \\
\qquad w(x, y) = C_0 e^{\alpha y}, \\
\text{at } x \geqslant \frac{b}{2} \\
\qquad w(x, y) = C_0 e^{-\alpha\left(x-\frac{b}{2}\right)} e^{\alpha y}.
\end{array}\right\} \tag{9.18}$$

We assume that the work done by the reactions T^{Φ} over the displacement $\overline{C}_0 = 1$ is equal to the work done by all the internal forces in the elastic foundation in the region $y < 0$ over the virtual displacements (9.18) when $C_0 = 1$. We thus define the fictitious force T^{Φ} as the virtual work done by the normal and shearing stresses $\sigma_z, \tau_{zx}, \tau_{zy}$ in the elastic foundation in the region $y < 0$. We then obtain:

$$T^{\Phi} = C_0(2\alpha tb + 3t). \qquad (9.19)$$

Strictly speaking, the concentrated reactions T^{Φ} consist of the reactions Q_x^{Φ} distributed over the lateral edges of the beam and the concentrated reactions R^{Φ} at the corners (cf. section 10). However, since the beam is by definition rigid in the lateral direction, we can introduce the resultant concentrated force T^{Φ}.

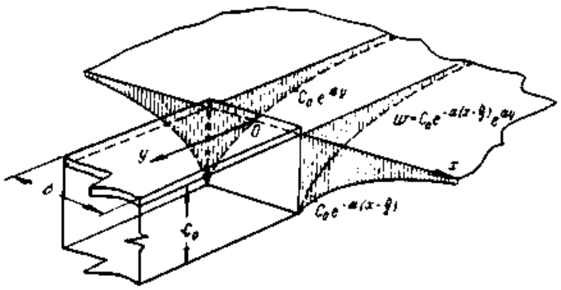

FIGURE 91.

The equilibrium condition of the beam is obtained by equating to zero the vertical projection of all forces acting on the beam. Taking (9.17) and (9.19) into account, we obtain:

$$[kbl + 4\alpha tl + 4\alpha tb + 6t]\,C_0 = P_0,$$

whence

$$C_0 = \frac{P_0}{[kbl + 4\alpha t(l+b) + 6t]}, \qquad (9.20)$$

where P_0 = resultant vertical load acting on beam; l = beam length; b = beam width.

When C_0 has been obtained, the reactions of the foundation are found from (9.17) and (9.19); the bending moments and shearing forces are then determined by the known methods of the strength of materials.

The analysis of a rigid beam acted upon by an antisymmetrical load is performed similarly. If the origin of coordinates is placed at the beam center, the vertical displacements are:

$$W(y) = \theta_0 y,$$

where θ_0 is the slope of the beam, whose value can be determined by equating to zero the sum of all moments about the origin, acting on the beam:

$$\sum M_0 = 0$$

(cf. section 5 of Chapter II).

4

Consider a symmetrically loaded rigid beam. Assume that:

$$\phi(z) = \frac{\operatorname{sh} \gamma \frac{H-z}{b}}{\operatorname{sh} \gamma \frac{H}{b}}. \tag{9.21}$$

Substitution of (9.20) in (9.17) and (9.19) yields:

$$\left.\begin{aligned}
q &= \frac{P_0}{lb}\,\frac{1}{\left[1+\frac{2}{\alpha b}\left(1+\frac{b}{l}\right)+\frac{3}{\alpha^2 lb}\right]},\\
Q_l^{\phi} &= \frac{P_0}{b}\,\frac{1}{\alpha l\left[1+\frac{2}{\alpha b}\left(1+\frac{b}{l}\right)+\frac{3}{\alpha^2 lb}\right]},\\
T^{\phi} &= P_0\,\frac{\left[1+\frac{3}{2\alpha b}\right]}{\alpha l\left[1+\frac{2}{\alpha b}\left(1+\frac{b}{l}\right)+\frac{3}{\alpha^2 lb}\right]}.
\end{aligned}\right\} \tag{9.22}$$

When $\phi(z)$ is given by (9.21), the coefficient $\alpha = \sqrt{\frac{k}{2t}}$ entering in (9.22) (cf. (5.23), (5.24) of Chapter II) becomes:

$$\alpha = \frac{\gamma}{b}\sqrt{\frac{2}{1-\nu_0}}\sqrt{\frac{\operatorname{sh}\frac{\gamma H}{b}\cdot\operatorname{ch}\frac{\gamma H}{b}+\frac{\gamma H}{b}}{\operatorname{sh}\frac{\gamma H}{b}\cdot\operatorname{ch}\frac{\gamma H}{b}-\frac{\gamma H}{b}}}. \tag{9.23}$$

If the single-layer foundation is an elastic semi-infinite space $\left(\frac{H}{b}\to\infty\right)$, we obtain:

$$\left.\begin{aligned}
q &= \frac{P_0}{lb}\,\frac{1}{\left[1+\frac{2}{\gamma}\sqrt{\frac{1-\nu_0}{2}}\left(1+\frac{b}{l}\right)+\frac{3}{2\gamma^3}\,\frac{b}{l}\;1-\nu_0)\right]},\\
Q_l^{\phi} &= \frac{P_0}{b}\,\frac{1}{\gamma\frac{l}{b}\sqrt{\frac{2}{1-\nu_0}}\left[1+\frac{2}{\gamma}\sqrt{\frac{1-\nu_0}{2}}\left(1+\frac{b}{l}\right)+\frac{3}{2\gamma^2}\,\frac{b}{l}\,(1-\nu_0)\right]},\\
T^{\phi} &= P_0\,\frac{1+\frac{3}{2\gamma}\sqrt{\frac{1-\nu_0}{2}}}{\gamma\frac{l}{b}\sqrt{\frac{2}{1-\nu_0}}\left[1+\frac{2}{\gamma}\sqrt{\frac{1-\nu_0}{2}}\left(1+\frac{b}{l}\right)+\frac{3}{2\gamma^3}\,\frac{b}{l}\,(1-\nu_0)\right]}.
\end{aligned}\right\} \tag{9.24}$$

Figures 92 and 93 show the dimensionless bending moments $\overline{M}$ for two cases of loading, obtained from (9.24) for $\gamma = 1.5$; $\nu_0 = 0.3$; $\frac{l}{b} = 5$, and $\frac{l}{b} = 10$. Results obtained by Gorbunov-Posadov for the two- and three-dimensional rigid-beam problem ($\frac{l}{b} = 10$), are also given:

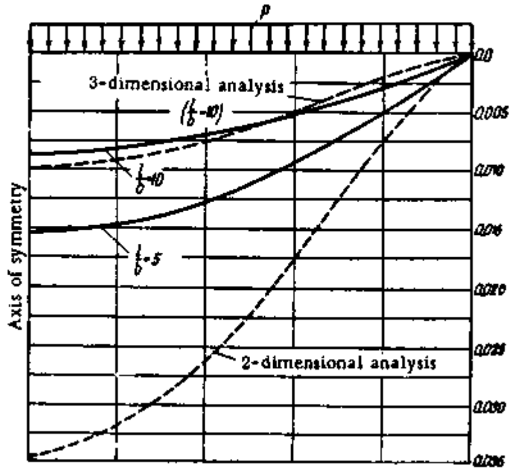

FIGURE 92.

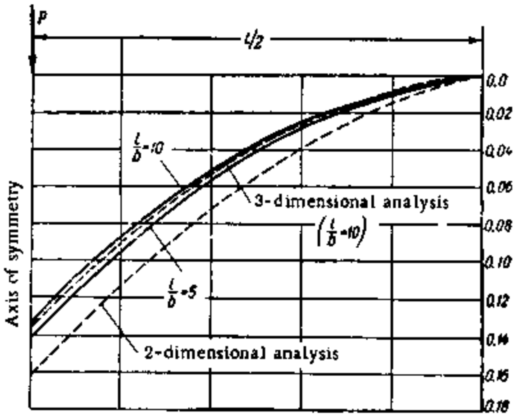

FIGURE 93.

The actual bending moments are:

$$M = \overline{M}pl^2,$$

for a uniformly distributed load, and

$$M = \overline{M}Pl.$$

for a concentrated load.

It is seen that the respective curves obtained by the two- and the three-dimensional analysis differ considerably: the maximum moment obtained by the two-dimensional analysis (for $\frac{l}{b} = 10$ and a uniformly distributed load) is almost 3.5 times the maximum moment obtained by the three-dimensional analysis.

It is also seen that the bending moments vary inversely with $\frac{l}{b}$: the wider the beam, the smaller the difference between the results obtained by two- and three-dimensional analysis.

A comparison of the results obtained by the method proposed and by Gorbunov-Posadov (for $\frac{l}{b} = 10$) shows that the difference between the maximum bending moments is relatively small (about 15% for a uniformly distributed load, and about 1.5% for a concentrated load).

§ 10. APPROXIMATE ANALYSIS OF A PLATE WITH FREE EDGES IN THE CASE OF SYMMETRICAL LOADING

1

Let a symmetrical load $p(x, y)$ be applied to a rectangular plate with free edges on a single-layer elastic foundation (Figure 94). The origin of coordinates is at the center of the plate. The differential equation of the bending of a plate on a single-layer elastic foundation is:

$$D\nabla^2\nabla^2 w - 2t\nabla^2 w + kw = p(x, y), \quad \text{[cf. (1.5)]} \qquad (10.1)$$

where $w(x, y)$ is the unknown deflection function of the plate, and

$$k = \frac{E_0}{(1-\nu_0^2)}\int_0^H \psi'^2\,dz, \quad t = \frac{E_0}{4(1+\nu_0)}\int_0^H \psi^2\,dz \quad \text{[cf. (1.6)]}. \qquad (10.2)$$

If $p(x, y)$ is distributed nearly uniformly over the plate a simple approximate solution can be obtained by writing:

$$w(x\ y) = C_0 + C_1\cos\frac{\pi x}{2b} + C_2\cos\frac{\pi y}{2l} + C_3\cos\frac{\pi x}{2b}\cos\frac{\pi y}{2l}, \qquad (10.3)$$

where C_0, C_1, C_2, C_3 are constants having the dimension of length.

The first term in (10.3) determines the translational displacement of the entire plate, the second and third terms represent the cylindrical bending of the plate in the x and y directions respectively, while the fourth term defines the three-dimensional bending.

The coefficients C_i in (10.3) are determined by Bubnov and Galerkin's variational method based on the equilibrium conditions, i.e., equating the total work done by all external and internal forces acting on the plate over each virtual displacement to zero:

$$\left.\begin{aligned} &\bar{w}_0 = 1, && \bar{w}_2 = \cos\frac{\pi y}{2l}, \\ &\bar{w}_1 = \cos\frac{\pi x}{2b}, && \bar{w}_3 = \cos\frac{\pi x}{2b}\cos\frac{\pi y}{2l}. \end{aligned}\right\} \qquad (10.4)$$

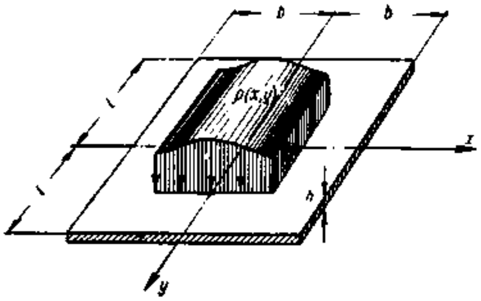

FIGURE 94.

2. Determining the reactions of the elastic foundation

An analysis of (10.1) shows that the first term depends on the internal forces in the plate, while the other terms depend on the reactions of the elastic foundation, distributed over the surface supporting the plate and caused by the compressive and shearing strains in the elastic foundation.

In addition to these forces and to the distributed load $p(x, y)$, reactions Q^{*}, distributed along its edges act on the plate. These reactions are introduced to make allowance for the three-dimensional deformation of the elastic foundation beyond the plate edges. In the case of rectangular or polygon-shaped plates, concentrated reactions R^{*} arise at the plate corners (Figure 95). In order to determine the reactions Q^{*} and R^{*} we shall assume that the vertical displacements w_{f} of the elastic-foundation surface beyond the plate edges obey the following law (Figure 96)*:

in the positive direction of the x axis

$$w_{\mathrm{f}}(x, y) = w_l(y)\, e^{-\alpha(x-b)} \tag{10.5}$$

in the positive direction of the x axis

$$w_{\mathrm{f}}(x, y) = w_b(x)\, e^{-\alpha(y-l)}, \tag{10.6}$$

where $\alpha = \sqrt{\frac{k}{2t}}$, $w_l(y)$ and $w_b(x)$ are respectively the vertical displacements of the longitudinal and lateral plate edges. The following law is also assumed for the vertical displacements of the foundation in the region $x > b$, $y > l$:

$$w_{\mathrm{f}}(x, y) = w_c\, e^{-\alpha(x-b)}\, e^{-\alpha(y-l)}, \tag{10.7}$$

where w_c is the vertical displacement of the plate corner.

It was shown in section 2 of this chapter that if the distribution of the vertical displacements of the foundation beyond the plate edges is given by (10.5), the fictitious reactions $Q_l^{\dagger}$ at the longitudinal plate edges will be given by (2.19), which can be written in the form:

$$Q_l^{\dagger} = 2t\left[\alpha w_l + \left(\frac{\partial w}{\partial x}\right)_l - \frac{1}{2\alpha}\left(\frac{\partial^2 w}{\partial y^2}\right)_l\right], \tag{10.8}$$

---

[*] These expressions are only approximate, since in the three-dimensional problem the vertical displacements of the foundation beyond the plate edges obey a more complex law (see for instance section 7 of Chapter I).

where the derivatives of $w(x, y)$ are taken at $x = \pm b$.

The fictitous reactions Q_b^* distributed over the lateral plate edges are obtained similarly. Defining these reactions as the work done by all forces in a strip of unit width, cut from the elastic foundation, over the virtual displacement of the elastic foundation beyond the plate edges, we obtain:

$$Q_b^* = 2l\left[\alpha w_b + \left(\frac{\partial w}{\partial y}\right)_b - \frac{1}{2\alpha}\left(\frac{\partial^2 w}{\partial x^2}\right)_b\right], \tag{10.9}$$

where the derivatives of $w(x, y)$ are taken at $y = \pm l$.

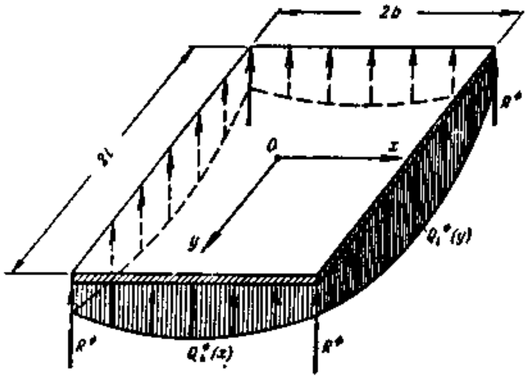

FIGURE 95.

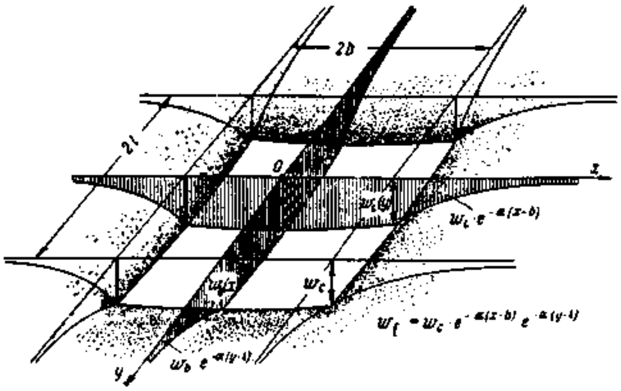

FIGURE 96.

The concentrated fictitious reactions R^* are determined by the vertical displacements of the elastic foundation beyond the plate edges in the regions:

$(x \leqslant -b,\ y \leqslant -b),\ (x \leqslant -b,\ y \geqslant l),\ (x \geqslant b,\ y \leqslant -l),\ (x \geqslant b,\ y \geqslant l).$

These reactions are defined as the work done by all the internal forces in the elastic foundation in the corresponding regions:

$$R^{\Phi} = \frac{3}{2} t w_c, \qquad (10.10)$$

where t is given by (2.15) and w_c is the vertical displacement of the corresponding plate corner.

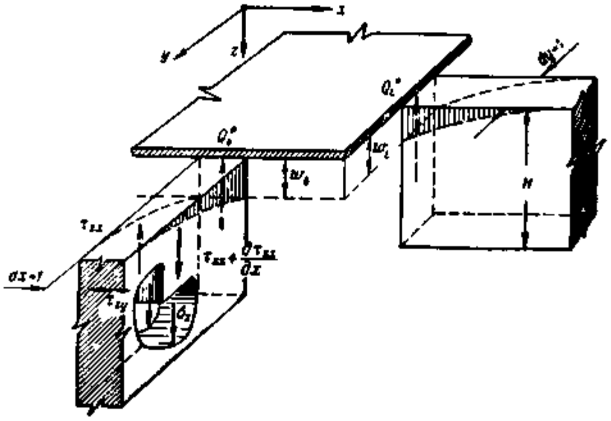

FIGURE 97.

Indeed, for $x \geqslant b$,[$y \geqslant t$], the vertical displacements $w_f(x, y)$ of the surface of the elastic foundation are given by (10.7). The virtual displacements of the elastic foundation are therefore:

$$\bar{w}(x, y, z) = \bar{w}_f(x, y)\psi(z) = 1 \cdot e^{-\alpha(x-b)} e^{-\alpha(y-t)} \psi(z). \text{ [when } w_c = 1 \text{]} \qquad (10.11)$$

The internal forces in the elastic foundation are the stresses $\sigma_z, \tau_{zx}, \tau_{zy}$:

$$\left.\begin{aligned} \sigma_z &= \frac{E_0}{1-\nu_0^2}\psi'(z)\, w_f(x, y), \\ \tau_{zy} &= \frac{E_0}{2(1+\nu_0)}\psi(z)\frac{\partial w_f(x, y)}{\partial y}, \\ \tau_{zx} &= \frac{E_0}{2(1+\nu_0)}\psi(z)\frac{\partial w_f(x, y)}{\partial x}. \end{aligned}\right\} \qquad \text{[cf. (2.13)]} \qquad (10.12)$$

The work done by these stresses over the virtual displacements (10.11) for $x \geqslant b$, $y \geqslant t$ is:

$$R^{\Phi} = \int_b^{\infty}\int_t^{\infty}\int_0^{H}\left(\sigma_z \bar{w}_f \psi' + \tau_{zx}\frac{\partial \bar{w}_f}{\partial x}\psi + \tau_{zy}\frac{\partial \bar{w}_f}{\partial y}\psi\right)dx\,dy\,dz, \text{ [cf. (2.11), (2.12)]} \qquad (10.13)$$

where

$$\bar{w}_f(x, y) = e^{-\alpha(x-b)} e^{-\alpha(y-t)}.$$

Substituting (10.12) in (10.13) and integrating we obtain (10.10).

The reactions R^{φ} given by (10.10) are relatively small and their influence on the strains of the plate is insignificant. Furthermore, plastic deformation occurs in practice near the plate corners. The reactions R^{φ} can therefore be neglected.

3. Variational equilibrium conditions

The following four algebraic equations in the four integration constants appearing in (10.3) are obtained by forming the expressions for the work done by all external and internal forces in the plate over the virtual displacements (10.4):

$$\left.\begin{aligned}
&\iint [kw - p]\,dx\,dy + 2\int Q_b^{\varphi}\,dx + 2\int Q_l^{\varphi}\,dy + 4R^{\varphi} = 0,\\
&\iint\left[D\frac{\partial^4 w}{\partial x^4} - 2t\frac{\partial^2 w}{\partial x^2} + kw - p\right]\cos\frac{\pi x}{2b}\,dx\,dy +\\
&\qquad\qquad + 2\int Q_b\cos\frac{\pi x}{2b}\,dx = 0,\\
&\iint\left[D\frac{\partial^4 w}{\partial y^4} - 2t\frac{\partial^2 w}{\partial y^2} + kw - p\right]\cos\frac{\pi y}{2l}\,dx\,dy +\\
&\qquad\qquad + 2\int Q_l\cos\frac{\pi y}{2l}\,dy = 0,\\
&\iint\left[D\left(\frac{\partial^4 w}{\partial x^4} + 2\frac{\partial^4 w}{\partial x^2\partial y^2} + \frac{\partial^4 w}{\partial y^4}\right) - 2t\left(\frac{\partial^2 w}{\partial x^2} - \frac{\partial^2 w}{\partial y^2}\right) +\right.\\
&\qquad\qquad \left. + kw - p\right]\cos\frac{\pi x}{2b}\cos\frac{\pi y}{2l}\,dx\,dy = 0,
\end{aligned}\right\}\qquad (10.14)$$

where w is given by (10.3); $p = p(x, y)$ is the known external load and Q_l^{φ}, Q_b^{φ}, R^{φ} are given by (10.8), (10.9), and (10.10) respectively. The integrals in (10.14) are definite and have the following limits: $-b \leqslant x \leqslant b$, $-l \leqslant y \leqslant l$. When concentrated external loads are present, these integrals are to be understood as Stieltjes integrals.

The first equation (10.14) defines the work done by all forces external with respect to the plate over the vertical displacement $\bar{w}_0 = 1$. In the term containing k allowance is made for the compressive strains in the elastic foundation.

The second equation (10.14) defines the work done by all forces during the cylindrical bending of the plate in the z plane. By the terms containing D and t allowance is made for the work done by the bending moments M_x, and by the shearing strains in the elastic foundation respectively.

Similarly, the third equation defines the work done by all forces during cylindrical bending of the plate in the yz plane. In this equation, the term containing D corresponds to the work done by the bending moments M_y.

The last equation (10.14) corresponds to three-dimensional bending of the plate, similar to the bending of a plate simply supported along the edges. In this case, the work done by the internal forces consists of the work done by the bending moments M_x and M_y, and the twisting moments H.

Substitution of (10.3), (10.8), (10.9), and (10.10) in (10.14) yields the system of four algebraic equations (10.15) from which the coefficients

C_0, C_1, C_2, C_3 can be obtained:

TABLE 11

C_0	C_1	C_2	C_3	Free term	Virtual displacements
k_{00}	k_{10}	k_{20}	k_{30}	G_0	$\overline{w}_0$ 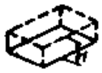
•	n_{11}	n_{21}	n_{31}	G_1	$\overline{w}_1$ 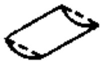
•	•	n_{22}	n_{32}	G_2	$\overline{w}_2$ 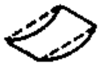
•	•	•	n_{33}	G_3	$\overline{w}_3$ 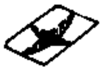

(10.15)

Here

$$\left.\begin{aligned} k_{00} &= 4\left[lbk + 2\alpha t\,(l + b) + \frac{3}{2}\,t\right],\\ k_{10} &= \frac{8}{\pi}\,[lbk + 2\alpha tb],\\ k_{20} &= \frac{8}{\pi}\,[lbk + 2\alpha tl],\\ k_{30} &= \frac{16}{\pi^2}\,lbk; \end{aligned}\right\} \tag{10.16}$$

$$\left.\begin{aligned} n_{11} &= 2\left[lbk + \frac{\pi^2}{2}\,\frac{l}{b}\,t + \frac{\pi^4}{16}\,\frac{l}{b^3}\,D + 2\alpha tb + \frac{\pi^2}{4}\,\frac{t}{\alpha b}\right],\\ n_{21} &= \frac{16}{\pi^2}\,lbk,\\ n_{31} &= \frac{4}{\pi}\left[lbk + \frac{\pi^2}{2}\,\frac{l}{b}\,t + \frac{\pi^4}{16}\,\frac{l}{b^3}\,D\right],\\ n_{22} &= 2\left[lbk + \frac{\pi^2}{2}\,\frac{b}{l}\,t + \frac{\pi^4}{16}\,\frac{b}{l^3}\,D + 2\alpha tl + \frac{\pi^2}{4}\,\frac{t}{\alpha l}\right],\\ n_{32} &= \frac{4}{\pi}\left[lbk + \frac{\pi^2}{2}\,\frac{b}{l}\,t + \frac{\pi^4}{16}\,\frac{b}{l^3}\,D\right],\\ n_{33} &= lbk + \frac{\pi^2}{2}\left(\frac{l}{b} + \frac{b}{l}\right)t + \frac{\pi^4}{16}\,D\left(\frac{l}{b^3} + \frac{2}{lb} + \frac{b}{l^3}\right), \end{aligned}\right\} \tag{10.17}$$

and

$$D = \frac{Eh^3}{12\,(1 - \mu^2)}$$

is the flexural rigidity of the plate, while k and t are given by (10.2).

It is seen that the coefficients (10.16) determine the work done by the reactions of the elastic foundation, while the coefficients (10.17) determine the work done by the reactions and the internal forces in the plate. These coefficients are symmetrical:

$$\left.\begin{array}{lll} k_{10} = k_{01}, & k_{20} = k_{02}, & k_{30} = k_{03}, \\ n_{12} = n_{21}, & n_{13} = n_{31}, & n_{23} = n_{32}, \end{array}\right\} \qquad (10.18)$$

in accordance with Maxwell and Betti's reciprocity theorem.

The matrix of (10.15) is symmetrical by virtue of (10.18), which considerably simplifies the determination of the unknown constants when more than four terms are taken in (10.3).

The free terms on the right sides of (10.15) (Table 11) represent the work done by the known external load over the corresponding displacements (10.4), and are obtained in the form:

$$G_i = \iint p(x,\ y)\, \bar{w}_i\, dx\, dy. \qquad (10.19)$$

4.

System (10.15) could have been obtained without introducing the fictitious reactions Q_l^ϕ, Q_b^ϕ, R^ϕ, had we followed the procedure in section 2 in deriving the generalized equilibrium conditions of an elementary strip of width dy, in which we considered the work done by all internal forces, including those acting in the elastic foundation beyond the plate edges. The final result would have been the same, since the fictitious forces Q_l^ϕ, Q_b^ϕ, R^ϕ were defined as the work done by all the internal forces acting in the elastic foundation beyond the plate edges, and were only introduced to simplify the expressions.

5

After the constants C_0, C_1, C_2, C_3 have been determined from (10.15), the plate deflections can be obtained from (10.3), the bending moments and shearing forces being given by (1.8). Substitution of (10.3) in (1.8) yields:

$$\left.\begin{array}{l} M_x = D\frac{\pi^2}{4b^2}\left[\mu\frac{b^2}{l^2}C_2\cos\frac{\pi y}{2l} + C_1\cos\frac{\pi x}{2b} + \right. \\ \qquad \left. + \left(1+\mu\frac{b^2}{l^2}\right)C_3\cos\frac{\pi x}{2b}\cos\frac{\pi y}{2l}\right], \\ M_y = D\frac{\pi^2}{4b^2}\left[\frac{b^2}{l^2}C_2\cos\frac{\pi y}{2l} + \mu C_1\cos\frac{\pi x}{2b} + \right. \\ \qquad \left. + \left(\frac{b^2}{l^2}+\mu\right)C_3\cos\frac{\pi x}{2b}\cos\frac{\pi y}{2l}\right]. \end{array}\right\} \qquad (10.20)$$

From (10.15) we obtain as particular cases approximate solutions for a plate simply supported along its entire contour, or only along either its lateral or its longitudinal edges. In this case we have to substitute $C_0 = C_1 = C_2 = 0$, $C_0 = C_1 = 0$, or $C_0 = C_2 = 0$ respectively in (10.3).

If a higher accuracy is desired, or if the external load has a pronounced nonuniform distribution, a larger number of terms must be taken in (10.3) (cf. section 12). We must then set up a system of algebraic equations similar to (10.15), each equation of which defines the work done by all external and internal forces acting on the plate over the corresponding displacements.

§ 11. EXAMPLES

1

Consider a rectangular plate, for which we assume that:

$$\psi(z)=\frac{\operatorname{sh}\gamma\frac{H-z}{b}}{\operatorname{sh}\frac{\gamma H}{b}} \tag{11.1}$$

where γ = coefficient depending on elastic properties of foundation; b = plate half-width.

The generalized characteristics of the elastic foundation are in this case: [cf. (5.23) and (5.24) of Chapter II]

$$\left.\begin{aligned}
k&=\frac{E_0\gamma}{2b(1-\nu_0^2)}\cdot\frac{\operatorname{sh}\frac{\gamma H}{b}\operatorname{ch}\frac{\gamma H}{b}+\frac{\gamma H}{b}}{\operatorname{sh}^2\frac{\gamma H}{b}},\\
t&=\frac{E_0 b}{8\gamma(1+\nu_0)}\cdot\frac{\operatorname{sh}\frac{\gamma H}{b}\operatorname{ch}\frac{\gamma H}{b}-\frac{\gamma H}{b}}{\operatorname{sh}^2\frac{\gamma H}{b}},\\
\alpha&=\frac{\gamma}{b}\sqrt{\frac{2}{1-\nu_0}\,\frac{\operatorname{sh}\frac{\gamma H}{b}\operatorname{ch}\frac{\gamma H}{b}+\frac{\gamma H}{b}}{\operatorname{sh}\frac{\gamma H}{b}\operatorname{ch}\frac{\gamma H}{b}-\frac{\gamma H}{b}}}.
\end{aligned}\right\} \tag{11.2}$$

where

$$\left.\begin{aligned}
E_0&=\frac{E_s}{1-\nu_s^2},\\
\nu_0&=\frac{\nu_s}{1-\nu_s}
\end{aligned}\right\} \tag{11.3}$$

(E_s and ν_s are, as before, the modulus of elasticity and Poisson's ratio for the elastic foundation respectively).

Substituting (11.2) in (10.16) and (10.17), and multiplying (10.15) by $\frac{1-\nu_0^2}{E_0 b}$, we obtain:

$$\left.\begin{aligned}
k_{00} &= 4\left[\frac{\gamma}{2}\,\frac{l}{b}\,m_k + \frac{1}{4}\left(1+\frac{l}{b}\right)\sqrt{6(1-\nu_0)}\,m_t m_\alpha + \right.\\
&\qquad\qquad\left. + \frac{3}{16}\,\frac{1-\nu_0}{\gamma}\,m_t\right],\\
k_{10} &= \frac{8}{\pi}\left[\frac{\gamma}{2}\,\frac{l}{b}\,m_k + \frac{1}{4}\sqrt{6(1-\nu_0)}\,m_t m_\alpha\right],\\
k_{20} &= \frac{8}{\pi}\left[\frac{\gamma}{2}\,\frac{l}{b}\,m_k + \frac{1}{4}\,\frac{l}{b}\sqrt{6(1-\nu_0)}\,m_t m_\alpha\right],\\
k_{30} &= \frac{16}{\pi^2}\,\frac{\gamma}{2}\,\frac{l}{b}\,m_k;
\end{aligned}\right\}\qquad(11.4)$$

$$\left.\begin{aligned}
n_{11} &= 2\left[\frac{\gamma}{2}\,\frac{l}{b}\,m_k + \frac{\pi^2}{16}\,\frac{1-\nu_0}{\gamma}\,\frac{l}{b}\,m_t + \frac{\pi^4}{16r}\left(\frac{l}{b}\right)^2 + \right.\\
&\qquad\left. + \frac{1}{4}\sqrt{6(1-\nu_0)}\,m_t m_\alpha + \frac{\pi^2}{32}\,\frac{(1-\nu_0)^2}{\gamma^2\sqrt{6(1-\nu_0)}}\,\frac{m_t}{m_\alpha}\right],\\
n_{21} &= \frac{16}{\pi^2}\,\frac{\gamma}{2}\,\frac{l}{b}\,m_k,\\
n_{31} &= \frac{4}{\pi}\left[\frac{\gamma}{2}\,\frac{l}{b}\,m_k + \frac{\pi^2}{16}\,\frac{1-\nu_0}{\gamma}\,\frac{l}{b}\,m_t + \frac{\pi^4}{16r}\left(\frac{l}{b}\right)^2\right],\\
n_{22} &= 2\left[\frac{\gamma}{2}\,\frac{l}{b}\,m_k + \frac{\pi^2}{16}\,\frac{1-\nu_0}{\gamma}\,\frac{b}{l}\,m_t + \frac{\pi^4}{16r}\,\frac{b}{l} + \right.\\
&\qquad\left. + \frac{1}{4}\sqrt{6(1-\nu_0)}\,\frac{l}{b}\,m_t m_\alpha + \frac{\pi^2}{32}\,\frac{(1-\nu_0)^2}{\gamma^2\sqrt{6(1-\nu_0)}}\,\frac{m_t}{m_\alpha}\,\frac{b}{l}\right],\\
n_{32} &= \frac{4}{\pi}\left[\frac{\gamma}{2}\,\frac{l}{b}\,m_k + \frac{\pi^2}{16}\,\frac{1-\nu_0}{\gamma}\,\frac{b}{l}\,m_t + \frac{\pi^4}{16r}\,\frac{b}{l}\right],\\
n_{33} &= \left[\frac{\gamma}{2}\,\frac{l}{b}\,m_k + \frac{\pi^2}{16}\,\frac{1-\nu_0}{\gamma}\left(1+\frac{l^2}{b^2}\right)\frac{b}{l} + \frac{\pi^4}{16r}\left(1+\frac{l^2}{b^2}\right)^2\frac{b}{l}\right],
\end{aligned}\right\}\qquad(11.5)$$

where

$$\left.\begin{aligned}
m_k &= \frac{\operatorname{sh}\frac{\gamma H}{b}\operatorname{ch}\frac{\gamma H}{b} + \frac{\gamma H}{b}}{\operatorname{sh}^2\frac{\gamma H}{b}},\\
m_t &= \frac{\operatorname{sh}\frac{\gamma H}{b}\operatorname{ch}\frac{\gamma H}{b} - \frac{\gamma H}{b}}{\operatorname{sh}^2\frac{\gamma H}{b}},\\
m_\alpha &= \sqrt{\frac{1}{3}\,\frac{\operatorname{sh}\frac{\gamma H}{b}\operatorname{ch}\frac{\gamma H}{b} + \frac{\gamma H}{b}}{\operatorname{sh}\frac{\gamma H}{b}\operatorname{ch}\frac{\gamma H}{b} - \frac{\gamma H}{b}}}.
\end{aligned}\right\}\qquad(11.6)$$

and

$$r = \frac{\pi E_0 l^3 b}{D(1-\nu_0^2)}\qquad(11.7)$$

is the "flexibility index" of the plate.*

---

* A similar value for r is used by Gorbunov-Posadov /25, 26/.

The free terms in (10.15) are by (10.19):

$$\left.\begin{aligned}
G_1 &= \frac{1-\nu_0^2}{E_0 b}\iint p(x,\ y)\,dx\,dy,\\
G_2 &= \frac{1-\nu_0^2}{E_0 b}\iint p(x,\ y)\ \cos\frac{\pi x}{2b}\,dx\,dy,\\
G_3 &= \frac{1-\nu_0^2}{E_0 b}\iint p(x,y)\ \cos\frac{\pi y}{2l}\,dx\,dy,\\
G_4 &= \frac{1-\nu_0^2}{E_0 b}\iint p(x,\ y)\cos\frac{\pi x}{2b}\cos\frac{\pi y}{2l}\,dx\,dy.
\end{aligned}\right\} \tag{11.8}$$

2. Approximative analysis for a uniformly distributed load

Consider a rectangular plate acted upon by a uniformly distributed load of intensity p (Figure 98). We assume that:

$$l = 2b, \qquad \gamma = 1.5, \qquad r = 1.0, \qquad \nu_0 = 0.4. \tag{11.9}$$

and that the plate lies on an elastic foundation of infinite thickness, $H = \infty$.

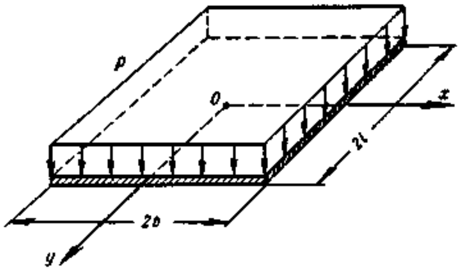

FIGURE 98.

Substitution of (11.9) in (11.4) and (11.5) yields:

$$\left.\begin{aligned}
&k_{00} = 9.58, &&n_{11} = 310.4, &&n_{22} = 23.50,\\
&k_{10} = 4.51, &&n_{21} = 2.44, &&n_{32} = 14.22,\\
&k_{20} = 5.23, &&n_{31} = 197.8; &&n_{33} = 241.1.\\
&k_{30} = 2.44;
\end{aligned}\right\} \tag{11.10}$$

The load terms (11.8) become for $p = \text{const}$:

$$\left.\begin{aligned}
G_0 &= 4\,\frac{1-\nu_0^2}{E_0}pl,\\
G_1 &= \frac{8}{\pi}\,\frac{1-\nu_0^2}{E_0}pl,\\
G_2 &= \frac{8}{\pi}\,\frac{1-\nu_0^2}{E_0}pl,\\
G_3 &= \frac{16}{\pi^2}\,\frac{1-\nu_0^2}{E_0}pl.
\end{aligned}\right\} \tag{11.11}$$

The following formulas are obtained for C_0, C_1, C_2, C_3 by substituting (11.10) and (11.11) in (10.15) and solving:

$$\left.\begin{aligned} C_0 &= 408\cdot 10^{-3}\,\frac{1-\nu_0^2}{E_0}\,pl, \\ C_1 &= 2{,}37\cdot 10^{-3}\,\frac{1-\nu_0^2}{E_0}\,pl, \\ C_2 &= 17{,}4\cdot 10^{-3}\,\frac{1-\nu_0^2}{E_0}\,pl, \\ C_3 &= 0{,}4\cdot 10^{-3}\,\frac{1-\nu_0^2}{E_0}\,pl. \end{aligned}\right\} \tag{11.12}$$

Hence,

$$w(x, y) = \left[408 + 2{,}37\cos\frac{\pi x}{2b} + 17{,}4\cos\frac{\pi y}{2l} - 0{,}4\cos\frac{\pi x}{2l}\cos\frac{\pi y}{2l}\right]\frac{pl\,(1-\nu_0^2)}{E_0}\cdot 10^{-3}. \tag{11.13}$$

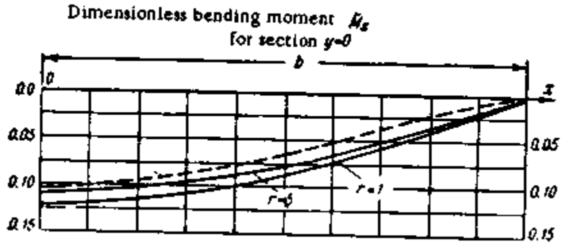

FIGURE 99.

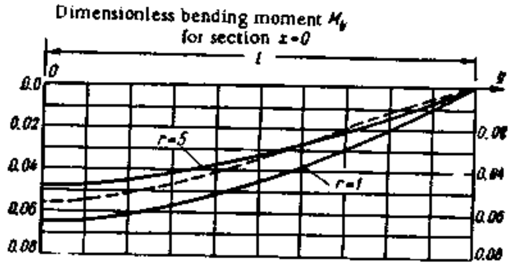

FIGURE 100.

Figures 99 and 100 show the dimensionless bending moments $\overline{M}_x$ and $\overline{M}_y$, at $y=0$ and $x=0$ respectively, determined from (10.20) and (11.12) for $\mu=0$. The actual bending moments are:

$$M_x = \overline{M}_x pb^2, \quad M_y = \overline{M}_y pl^2.$$

Bending moments, obtained for $r=5$ by this method, as well as by Gorbunov-Posadov's method for a rigid plate (broken line) are also shown.*

---

* See Gorbunov-Posadov, M.I. Raschet konstruktsii na uprugom osnovanii (Analyzing Structures on Elastic Foundations), p. 457. 1953.

In view of the approximative character of our method, and taking into account that according to Gorbunov-Posadov, plates are rigid when

$$r < \frac{8}{\sqrt{\frac{l}{b}}},$$

the agreement between the results obtained by the two methods can be considered as satisfactory.

3. Approximative analysis of the foundation slab of a spillway dam

Figure 101 shows a section of a spillway dam of light-weight design. The foundation of this section is a rectangular concrete slab of constant rigidity having piers at its lateral edges. One of the most critical stages is the period when the slab and piers have already been erected, but the spillway sections are not yet in place. This case will now be considered.

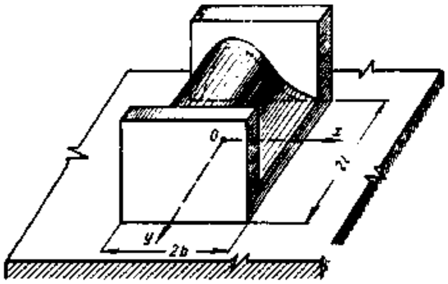

FIGURE 101.

Since the rigidity of the piers in their planes is very large, the lateral plate edges can be considered as unbendable. The joint between the slab and the piers can be considered as a hinged support. Applying (10.3) to the slab deflections, we must put $C_1 = 0$. We then obtain Table 12 from (10.15).

TABLE 12

C_0	C_2	C_3	Free term	Virtual displacements
k_{00}	k_{02}	k_{03}	G_0	$\bar{w}_0$ 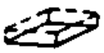
•	n_{22}	n_{23}	G_2	$\bar{w}_2$ 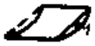
•	•	n_{33}	G_3	$\bar{w}_3$ 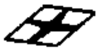

The coefficients in Table 12 are given, as before, by (11.4), (11.5). Assuming that a load p is uniformly distributed over the entire slab and a load g is uniformly distributed along the lateral edges (Figure 102), we obtain:

$$\left.\begin{aligned} G_0 &= 4(pl+g)\frac{1-\nu_0^2}{E_0}, \\ G_2 &= \frac{8}{\pi}pl\frac{1-\nu_0^2}{E_0}, \\ G_3 &= \frac{16}{\pi^2}pl\frac{1-\nu_0^2}{E_0}. \end{aligned}\right\} \tag{11.14}$$

After the constants C_0, C_2, C_3 have been determined from the equations in Table 12, we obtain for the slab deflections:

$$w(x,\ y) = C_0 + C_2\cos\frac{\pi y}{2l} + C_3\cos\frac{\pi x}{2b}\cos\frac{\pi y}{2l}; \tag{11.15}$$

The bending moments are therefore by (10.20):

$$\left.\begin{aligned} M_x &= D\frac{\pi^2}{4b^2}\left[\mu\frac{b^2}{l^2}C_2\cos\frac{\pi y}{2l} + \left(1+\mu\frac{b^2}{l^2}\right)C_3\cos\frac{\pi x}{2b}\cos\frac{\pi y}{2l}\right], \\ M_y &= D\frac{\pi^2}{4b^2}\left[\frac{b^2}{l^2}C_2\cos\frac{\pi y}{2l} + \left(\frac{b^2}{l^2}+\mu\right)C_3\cos\frac{\pi x}{2b}\cos\frac{\pi y}{2l}\right]. \end{aligned}\right\} \tag{11.16}$$

4. Taking into account additional loads transmitted by the adjacent sections

Consider now the case when a system of slabs, loaded symmetrically and arranged in a row, lies on a soil foundation. We thus consider not a separate section, but the dam as a whole (Figure 103, a). If the base of each section is an absolutely rigid plate, no shearing forces will act in the elastic foundation at the boundaries between the different sections. The concentrated reactions Q_b^0 at the lateral plate edges will therefore vanish, as can be seen from (10.9).

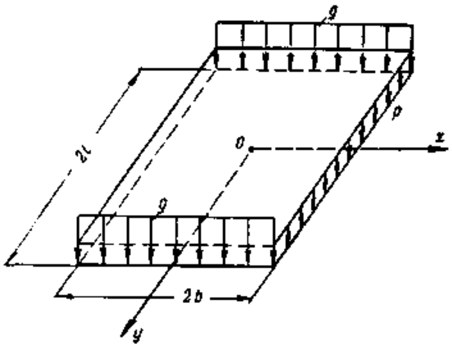

FIGURE 102.

If each plate lying on the elastic foundation has a finite but sufficiently large rigidity, the shearing forces acting in the elastic foundation at the boundaries of the different sections will be small, so that the concentrated reactions Q_b^Φ may be neglected. In this case we shall be able to disregard the influence exerted by the adjacent sections, and analyze such plates according to the scheme in Figure 103, b.

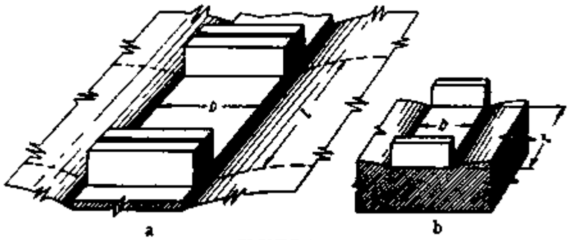

FIGURE 103.

By expressing the deflection of each plate in the form (10.3), we obtain, as before, the system of algebraic equations (10.15) (Table 11). Since, however, Q_b^Φ and R^Φ are zero, the coefficients of this system are:

$$\left.\begin{aligned}
k_{00} &= 4\left[\frac{\gamma}{2}\frac{l}{b}m_k + \frac{1}{4}\frac{l}{b}\sqrt{6(1-\nu_0)}m_t m_a\right],\\
k_{10} &= \frac{8}{\pi}\left[\frac{\gamma}{2}\frac{l}{b}m_k\right],\\
k_{20} &= \frac{8}{\pi}\left[\frac{\gamma}{2}\frac{l}{b}m_k + \frac{1}{4}\frac{l}{b}\sqrt{6(1-\nu_0)}m_t m_a\right],\\
k_{30} &= \frac{16}{\pi^2}\frac{\gamma}{2}\frac{l}{b}m_k;
\end{aligned}\right\} \qquad (11.17)$$

$$\left.\begin{aligned}
n_{11} &= 2\left[\frac{\gamma}{2}\frac{l}{b}m_k + \frac{\pi^2}{16}\frac{1-\nu_0}{\gamma}\frac{l}{b}m_t + \frac{\pi^6}{16r}\left(\frac{l}{b}\right)^3\right],\\
n_{21} &= \frac{16}{\pi^2}\frac{\gamma}{2}\frac{l}{b}m_k,\\
n_{31} &= \frac{4}{\pi}\left[\frac{\gamma}{2}\frac{l}{b}m_k + \frac{\pi^2}{16}\frac{1-\nu_0}{\gamma}\frac{l}{b}m_t + \frac{\pi^6}{16r}\left(\frac{l}{b}\right)^3\right],\\
n_{22} &= 2\left[\frac{\gamma}{2}\frac{l}{b}m_k + \frac{\pi^2}{16}\frac{1-\nu_0}{\gamma}\frac{b}{l}m_t + \frac{\pi^6}{16r}\frac{b}{l} + \right.\\
&\left.\quad + \frac{1}{4}\sqrt{6(1-\nu_0)}\frac{l}{b}m_t m_a + \frac{\pi^2}{32}\frac{1-\nu_0^2}{\gamma^2\sqrt{6(1-\nu_0)}}\frac{m_t}{m_a}\frac{b}{l}\right],\\
n_{32} &= \frac{4}{\pi}\left[\frac{\gamma}{2}\frac{l}{b}m_k + \frac{\pi^2}{16}\frac{1-\nu_0}{\gamma}\frac{b}{l}m_t + \frac{\pi^6}{16r}\frac{b}{l}\right],\\
n_{33} &= \left[\frac{\gamma}{2}\frac{l}{b}m_k + \frac{\pi^2}{16}\frac{1-\nu_0}{\gamma}m_t\left(1+\frac{l^2}{b^2}\right)\frac{b}{l} + \right.\\
&\left.\qquad + \frac{\pi^6}{16r}\left(1+\frac{l^2}{b^2}\right)\frac{b}{l}\right],
\end{aligned}\right\} \qquad (11.18)$$

where m_k, m_t, m_a and r are given by (11.6) and (11.7).

The free terms are, as before:

$$G_i = \frac{1-\nu_0^2}{E_0 b}\iint p(x, y)\,\bar{w}_i\,dx\,dy. \qquad (11.19)$$

If we assume that the lateral plate edges do not bend, due to the presence of perfectly rigid piers, the deflections will be given by (11.15). The constants C_0, C_1, C_2 are determined, as before, by the system of algebraic equations in Table 12, the coefficients being given by (11.17) and (11.18).

By making allowance for the additional loads transmitted from the adjacent sections, marked reduction of the positive, and an increase in the negative, bending moments M_y may result, the general deformation pattern changing considerably.

§ 12. GENERAL CASE OF LOADING OF A PLATE HAVING FREE EDGES

1. Method of solution

Consider the general case of loading of a rectangular plate lying freely on an elastic foundation. Let the external load consist of concentrated vertical forces P and of forces $p(x, y)$ distributed over the plate.

To solve this problem we have to find the deflections $w(x, y)$ from (10.1) for given boundary conditions. When the plate edges are neither built-in nor loaded, the statical boundary conditions are [by (1.8) and (1.9)]:

$$\text{at } x = \pm\frac{b}{2} \qquad \left.\begin{aligned} M_x &= -D\left(\frac{\partial^2 w}{\partial x^2} + \mu\frac{\partial^2 w}{\partial y^2}\right) = 0, \\ Q_x &= -D\left[\frac{\partial^3 w}{\partial x^3} + (2-\mu)\frac{\partial^3 w}{\partial x\,\partial y^2}\right] = Q_l^{\phi}, \end{aligned}\right\} \tag{12.1}$$

$$\text{at } y = \pm\frac{l}{2} \qquad \left.\begin{aligned} M_y &= -D\left(\frac{\partial^2 w}{\partial y^2} + \mu\frac{\partial^2 w}{\partial x^2}\right) = 0, \\ Q_y &= -D\left[\frac{\partial^3 w}{\partial y^3} + (2-\mu)\frac{\partial^3 w}{\partial x^2\,\partial y}\right] = Q_b^{\phi}, \end{aligned}\right\} \tag{12.2}$$

where Q_l^{ϕ}, Q_b^{ϕ}, determining the strain of the elastic foundation beyond the plate edges, are given by (10.8) and (10.9) respectively.

The problem will be solved by Bubnov and Galerkin's variational method, in which the deflection function $w(x, y)$ is represented as a series each term of which satisfies the boundary conditions:

$$w(x, y) = \sum_{1}^{m}\sum_{1}^{n} C_{mn}\varphi_{mn}(x, y), \tag{12.3}$$

where $\varphi_{mn}(x, y)$ are known functions, and C_{mn} are constants which have to be determined.

The functions φ_{mn} can be selected arbitrarily, provided they are linearly independent and satisfy the geometrical boundary conditions of the problem. Rigorous fulfilment of the statical boundary conditions is not required, since, when setting up the Lagrange equations, the equilibrium conditions are approximately satisfied at all points of the plate.

We represent the functions φ_{mn} as trigonometric functions, together with linear terms defining the translational displacements of the entire plate. We thus satisfy the geometrical boundary conditions, since at the plate edges $w \neq 0$, $\frac{\partial w}{\partial n} \neq 0$, and also, for $\mu = 0$, the first of each statical condition (12.1) and (12.2). The remaining statical conditions are fulfilled only approximately.

Proceeding from Lagrange's principle of virtual displacements, we can establish a system of algebraic equations for determining the constant coefficients C_{mn} in (12.3); in each equation the work done by all external and internal forces acting on the plate over the virtual displacement φ_{ik} is equated to zero:

$$\sum_{1}^{m}\sum_{1}^{n} C_{mn}\Big\{\iint [D\nabla^2\nabla^2\varphi_{mn} - 2t\nabla^2\varphi_{mn} + k\varphi_{mn} - p]\,\varphi_{ik}\,dx\,dy + \\ + \oint [Q_{mn}(s) + Q^{\Phi}(s)]\,\varphi_{ik}(s)\,ds\Big\} = 0 \qquad (12.4)$$

$$(i = 1,\ 2,\ 3, \ldots,\ m; \qquad k = 1,\ 2,\ 3, \ldots,\ n),$$

where $\varphi_{mn}(s)$, $\varphi_{ik}(s)$ are the values of the corresponding functions at the contour.

The double integral in (12.4) defines the work done by the internal forces acting in the plate (bending and twisting moments), the work done by the shearing and compressive stresses in the elastic foundation beneath the plate, and the work done by the external load. The contour integral defines the work done by the shearing forces acting on the plate edges over their virtual displacements. The first term represents the work done by Kirchhoff's reduced shearing forces (cf. (1.9)), which appear at the plate edges because the static-equilibrium conditions (12.1), (12.2) are only approximately satisfied. The second term represents the work done by the reactions (10.8), (10.9), acting at the plate edges and determining the deformation of the elastic foundation beyond them.

As already stated, the concentrated reactions R^{Φ} acting at the plate corners (given by (10.10)) can in practice be neglected, so that the work done by them is not taken into account in (12.4).

The integrals in (12.4) are taken over the entire area and the entire contour of the plate respectively. In the presence of concentrated external loads, these integrals are to be understood as Stieltjes integrals. Thus, for a finite number of concentrated forces, the integrals should be replaced by the sums of the products of each force by the function φ_{ik} at its point of action.

We can rewrite (12.4) in canonical form:

$$\left.\begin{array}{l}
\delta_{00,00}C_{00} + \delta_{00,10}C_{10} + \ldots + \delta_{00,mn}C_{mn} = \Delta_{00},\\
\delta_{10,00}C_{00} + \delta_{10,10}C_{10} + \ldots + \delta_{10,mn}C_{mn} = \Delta_{10},\\
\cdot\ \cdot\ \cdot\ \cdot\ \cdot\ \cdot\ \cdot\ \cdot\ \cdot\ \cdot\ \cdot\ \cdot\ \cdot\ \cdot\ \cdot\ \cdot\ \cdot\ \cdot\\
\delta_{ik,00}C_{00} + \delta_{ik,10}C_{10} + \ldots + \delta_{ik,mn}C_{mn} = \Delta_{ik},\\
\cdot\ \cdot\ \cdot\ \cdot\ \cdot\ \cdot\ \cdot\ \cdot\ \cdot\ \cdot\ \cdot\ \cdot\ \cdot\ \cdot\ \cdot\ \cdot\ \cdot\ \cdot\\
\delta_{mn,00}C_{00} + \delta_{mn,10}C_{10} + \ldots + \delta_{mn,mn}C_{mn} = \Delta_{mn}.
\end{array}\right\} \qquad (12.5)$$

where

$$\delta_{ik,mn} = \iint [D\nabla^2\nabla^2\varphi_{mn} - 2t\nabla^2\varphi_{mn} + k\varphi_{mn}]\,\varphi_{ik}\,dx\,dy + \\ + \oint [Q_{mn}(s) + Q^{\Phi}(s)]\,\varphi_{ik}(s)\,ds. \tag{12.6}$$

These coefficients are symmetrical ($\delta_{ik,mn} = \delta_{mn,ik}$) by virtue of Maxwell and Betti's reciprocity theorem; the matrix of (12.5) is therefore symmetrical.

The free terms in (12.5) are:

$$\Delta_{ik} = \iint p(x,\ y)\,\varphi_{ik}\,dx\,dy \tag{12.7}$$

and represent the work done by the external load over each virtual displacement.

In the solution of practical problems it is convenient to resolve the external load into four symmetrical and antisymmetrical components. For example, Figure 104 represents the resolution of a concentrated force applied at $x = a$, $y = c$.

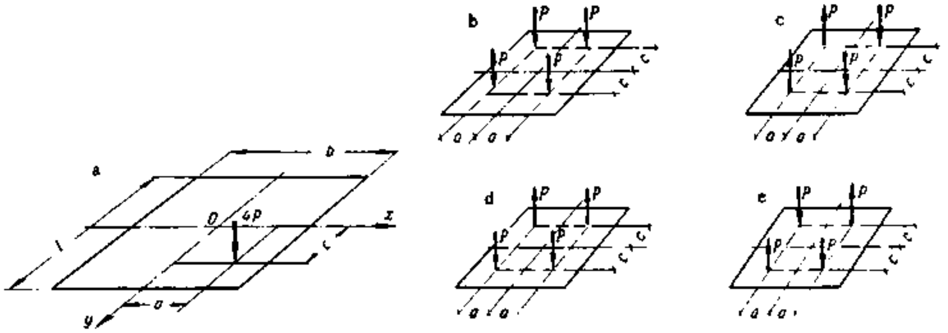

FIGURE 104.

The calculations are considerably reduced when each load component is analyzed separately.

2. Symmetrical load

When the load is symmetrical with respect to both axes (Figure 104, b), (12.3) becomes:

$$w(x,\ y) = C_{00} + \sum_{1}^{m} C_{m0}\cos\frac{m\pi x}{b} + \sum_{1}^{n} C_{0n}\cos\frac{n\pi y}{l} + \sum_{1}^{m}\sum_{1}^{n} C_{mn}\cos\frac{m\pi x}{b}\cos\frac{n\pi y}{l} \tag{12.8}$$

$$(m, n = 1, 3, 5, 7, \ldots, (2k-1)).$$

By forming the expressions for the work done by all forces acting on the plate over each virtual displacement, we obtain the coefficients (12.6). When these are inserted into (12.5), we can solve this system for the unknown constants C_{00}, C_{m0}, C_{0n}, C_{mn}.

Table 13 presents the matrix of the algebraic equations when nine terms ($m = 3$, $n = 3$) are taken in (12.8), corresponding to nine possible displacements of the plate: translational displacement of the entire plate, four displacements characterizing cylindrical bending in the xz and yz planes respectively, and four displacements similar to the deflection of a plate simply supported along the contour.

It can be seen that the matrix is symmetrical about the principal diagonal. It is therefore necessary to obtain 29 dimensionless coefficients.

The magnitudes α, β, k, t and D entering in these coefficients are determined by the formulas:

$$\left.\begin{aligned} &\alpha = \sqrt{\frac{k}{2t}},\ \beta = \frac{b}{l}, \\ &k = \frac{E_0}{1-\nu_0^2}\int_0^H \psi'^2\,dz, \\ &t = \frac{E_0}{4(1+\nu_0)}\int_0^H \psi^2\,dz, \\ &D = \frac{Eh^3}{12(1-\mu^2)}. \end{aligned}\right| \qquad (12.9)$$

Here l and b = length and width of plate respectively; D = flexural rigidity of plate; k and t = generalized characteristics of elastic foundation; $\psi = \psi(z)$ = function describing the distribution of displacements over the depth of the elastic foundation;

and

$$E_0 = \frac{E_s}{1-\nu_s^2}, \qquad \nu_0 = \frac{\nu_s}{1-\nu_s}. \qquad (12.10)$$

The free terms are:

$$A_{ik} = \frac{1}{klb}\iint p(x,\ y)\,\varphi_{ik}\,dx\,dy. \qquad (12.11)$$

When concentrated loads are present, the integrals in (12.11) are to be understood as Stieltjes integrals.

3. Load symmetrical with respect to one, and antisymmetrical with respect to the other axis

If the external load is symmetrical with respect to the x axis and antisymmetrical with respect to the y axis (Figure 104, c), we can write:

$$\begin{aligned} w(x,\ y) = C_{00}\frac{2x}{b} + \sum_2^m C_{m0}\sin\frac{m\pi x}{b} + \frac{2x}{b}\sum_1^n C_{0n}\cos\frac{n\pi y}{l} + \\ + \sum_2^m\sum_1^n C_{mn}\sin\frac{m\pi x}{b}\cos\frac{n\pi y}{l} \end{aligned} \qquad (12.12)$$

$$(m = 2,\ 4,\ 6,\ \ldots;\qquad n = 1,\ 3,\ 5,\ \ldots).$$

The first term defines the rotation of the entire plate about the y axis. The single series defines the cylindrical bending in the xz plane, and the deformation of the longitudinal plate edges respectively. The double series defines the displacements corresponding to a plate, simply supported along its contour. Inserting (12.12) into (12.6) all the coefficients of the solving system (12.5) can be found. Exactly as for symmetrical loading, we restrict ourselves to nine terms in (12.12) $(m=2; 4; n=1; 3)$. The system of nine algebraic equations thus obtained is presented in Table 14. The free terms in these equations represent the work done by the known external load over the corresponding virtual displacements and are obtained from (12.11). The magnitudes α, β, k and D are given by (12.9).

In the similar case of a load, symmetrical with respect to the y axis and antisymmetrical with respect to the x axis (Figure 104, d), we can write:

$$w(x, y) = C_{00}\frac{2y}{l} + \frac{2y}{l}\sum_{1}^{m} C_{m0}\cos\frac{m\pi x}{b} + \\ + \sum_{2}^{n} C_{0n}\sin\frac{n\pi y}{l} + \sum_{1}^{m}\sum_{2}^{n} C_{mn}\cos\frac{m\pi x}{b}\sin\frac{n\pi y}{l} \qquad (12.13)$$

$$(m = 1, 3, 5, \ldots; \quad n = 2, 4, 6, \ldots).$$

The matrix of the algebraic equations for this case $(m=1; 3; n=2; 4)$ is represented in Table 15.

4. Antisymmetrical load

When the load is antisymmetrical with respect to both axes (Figure 104,e), we can write:

$$w(x, y) = C_{00}\frac{4xy}{lb} + \frac{2y}{l}\sum_{2}^{m} C_{m0}\sin\frac{m\pi x}{b} + \\ \frac{2x}{b}\sum_{2}^{n} C_{0n}\sin\frac{n\pi y}{l} + \sum_{2}^{m}\sum_{2}^{n} C_{mn}\sin\frac{m\pi x}{b}\sin\frac{n\pi y}{l} \qquad (12.14)$$

$$(m, n = 2, 4, 6, 8, \ldots).$$

The first term defines the deformation of the entire plate, in which the edges remain straight. The single series defines the deformations of the plate edges. The double series defines the displacements corresponding to a plate, simply supported along its contour.

The coefficients in (12.5) are again obtained from (12.6), the free terms being given by (12.7). The matrix obtained when only the first nine terms are taken in (12.14) is given in Table 16. The elastic characteristics are determined, as before, by (12.9), and the free terms by (12.11). Tables 13 through 16 permit approximate analysis of a rectangular plate acted upon by an arbitrary external load.

It can be seen that in the general case we have to solve four system of algebraic equations, each containing nine unknowns and having the same structure as the system of canonical equations of the theory of frames. The Gauss method is recommended for this.

After the deflections of the plate have been determined from (12.8), (12.12), (12.13), and (12.14), the bending moments and shearing forces are determined from (1.8) and (1.9). The accuracy of the solution obtained depends on the type of loading and on the number of terms taken in (12.8), (12.12), (12.13), and (12.14). Since trigonometric series converge rapidly in the case of nearly uniformly distributed loads, only nine terms were taken in each series. This approximation is thus satisfactory in practice if the external load is distributed over part of the plate. When greater accuracy is required, the obtained solutions can be extended on the basis of (12.5) and (12.6). If, on the other hand, a lesser accuracy is sufficient, a smaller number of terms can be taken as, for example, in (10.3).

The functions φ_{mn} can also be expressed in different ways, provided the boundary conditions of the problem are satisfied. For example, a high accuracy can be obtained with a small number of terms in (12.3), when the functions φ_{mn} are formed by means of the eigenfunctions of the transverse vibrations of a beam (Table 7) p. 111. Various polynomials may also be chosen as functions φ_{mn} *.

13. GENERAL EQUATIONS FOR THICK PLATES ON ELASTIC SINGLE-LAYER FOUNDATIONS

Consider the three-dimensional deformation of a thick plate on a single-layer foundation (Figure 105).

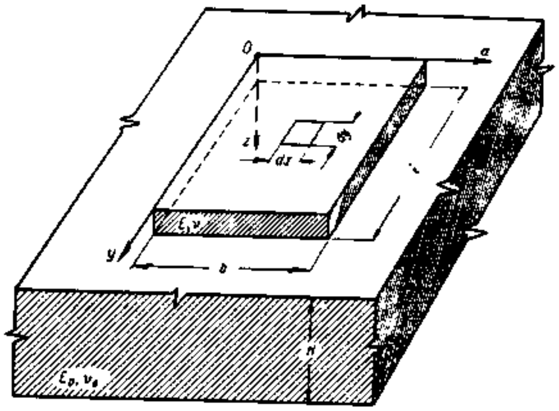

FIGURE 105.

In accordance with the general variational method, the unknown displacements of plate and foundation are assumed to be:

$$\left.\begin{aligned} u(x, y, z) &= u_1(x, y)\varphi_1(z), \\ v(x, y, z) &= v_1(x, y)\varphi_1(z), \\ w(x, y, z) &= w_1(x, y)\phi_1(z) + w_2(x, y)\phi_2(z), \end{aligned}\right\} \qquad (13.1)$$

---

* Some problems of the analysis of rectangular plates on elastic foundations are discussed by Kosab'yan in /46/.

where

$$u_1(x,\ y),\ v_1(x,\ y),\ w_1(x,\ y),\ w_2(x,\ y)$$

are unknown functions of x and y,
and

$$\left.\begin{array}{ll}\text{at } z<h & \begin{array}{l}\varphi_1(z)=\dfrac{h-2z}{2},\\ \psi_1(z)=\dfrac{h-z}{h}, \quad \psi_2(z)=1;\end{array}\\ \\ \text{at } z>h & \begin{array}{l}\varphi_1(z)=0,\\ \psi_1(z)=0, \quad \psi_2(z)=\dfrac{H+h-z}{H}\end{array}\end{array}\right\} \qquad (13.2)$$

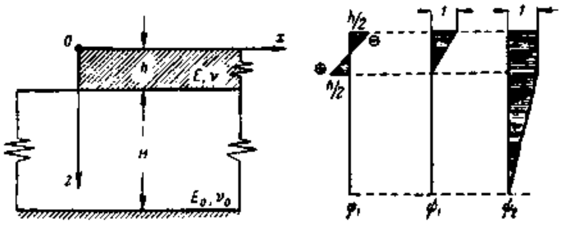

FIGURE 106.

It is seen from (13.2) that $\varphi_1(z)$ and $\psi_1(z)$ define the deformation of a plate on an absolutely rigid foundation. It is assumed that the surface of the foundation is perfectly smooth: no friction or adhesion exists between the plate and the foundation. In contrast to thin plates, vertical compression is taken into account by introducing the function $\psi_1(z)$.

The function $\psi_2(z)$ permits us to make allowance for the elasticity of the foundation: it defines the latter as a single-layer model subjected to both normal stresses σ_z (characteristic of the Winkler foundation) and shearing stresses τ_{zx}, τ_{zy}. For $z>h$, the function $\psi_2(z)$ may be defined in any other way such as a decreasing exponential function or a hyperbolic-sine function (see (11.1)).

The solution given is approximate from the viewpoint of the rigorous mathematical theory of elasticity. The system considered has a finite number of degrees of freedom in the z direction; the horizontal displacements of the elastic foundation are neglected. The solution is, nevertheless, considerably more accurate than that obtained by analyzing a plate on an elastic Winkler foundation, both as regards the strains in the plate itself, as well as those in the elastic foundation.

To determine the unknown functions $u_1(x,y)$, $v_1(x,y)$, $w_1(x,\ y)$, $w_2(x,\ y)$, consider the generalized equilibrium conditions of an elementary column cut from the plate and the elastic foundation (Figure 105). The equilibrium conditions are obtained by equating to zero the work done by all external and internal forces acting on this column over each virtual displacement:

$$\left.\begin{array}{ll}\bar{u}_1(x,\ y,\ z)=\varphi_1(z), & \bar{v}_1(x,\ y,\ z)=\varphi_1(z),\\ \bar{w}_1(x,\ y,\ z)=\psi_1(z), & \bar{w}_2(x,\ y,\ z)=\psi_2(z)\\ \text{for} & \\ \quad u_1(x,\ y)=1, & v_1(x,\ y)=1,\\ \quad w_1(x\ y)=1, & w_2(x,\ y)=1,\end{array}\right\} \qquad (13.3)$$

In the general case these equilibrium conditions can be expressed in the form of (6.6) of Chapter I. Substituting (13.1) and (13.3), we obtain:

for $dx = dy = 1$

$$\left.\begin{aligned}
&\int \frac{\partial \sigma_x}{\partial x}\varphi_1\,dz - \int \tau_{xz}\varphi_1'\,dz + \int \frac{\partial \tau_{xy}}{\partial y}\varphi_1\,dz + \int p\varphi_1\,dz = 0,\\
&\int \frac{\partial \sigma_y}{\partial y}\varphi_1\,dz - \int \tau_{yz}\varphi_1'\,dz + \int \frac{\partial \tau_{yx}}{\partial x}\varphi_1\,dz + \int g\varphi_1\,dz = 0,\\
&\int \frac{\partial \tau_{zx}}{\partial x}\varphi_1\,dz - \int \sigma_z\psi_1'\,dz + \int \frac{\partial \tau_{zy}}{\partial y}\psi_1\,dz + \int q\psi_1\,dz = 0,\\
&\int \frac{\partial \tau_{zx}}{\partial x}\psi_2\,dz - \int \sigma_z\psi_2'\,dz + \int \frac{\partial \tau_{zy}}{\partial y}\psi_2\,dz + \int q\psi_2\,dz = 0.
\end{aligned}\right| \qquad (13.4)$$

The integrals in equations (13.4) are taken over the entire height of the elementary column: $0 \leqslant z \leqslant h + H$. The stresses $\sigma_x, \sigma_y, \sigma_z, \tau_{xz}, \tau_{yz}, \tau_{xy}$ are determined by substituting (13.1) in (6.2) of Chapter I, and assuming that the elementary column consists of two layers, whose elastic characteristics are E and ν for $z < h$, and E_0 and ν_0 for $z > h$.

We assume that no body forces act on plate and elastic foundation, and that a vertical surface load $q(x, y)$ is applied to the plate. In this case the load terms in (13.4) are:

$$\left.\begin{aligned}
&\int p\varphi_1\,dz = 0, && \int g\varphi_1\,dz = 0,\\
&\int q\psi_1\,dz = q\psi_1(0) = q, && \int q\psi_2\,dz = q\psi_2(0) = q.
\end{aligned}\right\} \qquad (13.5)$$

Substituting (6.2) of Chapter I in (13.4) and taking (13.5) into account, we obtain:

$$\left.\begin{aligned}
&a_{11}\frac{\partial^2 u_1}{\partial x^2} + a_{11}\frac{1-\nu}{2}\frac{\partial^2 u_1}{\partial y^2} - b_{11}\frac{1-\nu}{2}u_1 + a_{11}\frac{1+\nu}{2}\frac{\partial^2 v_1}{dx\,\partial y} -\\
&\qquad - c_{11}\frac{1-\nu}{2}\frac{\partial w_1}{\partial x} - c_{12}\frac{1-\nu}{2}\frac{\partial w_2}{\partial x} = 0,\\
&a_{11}\frac{1+\nu}{2}\frac{\partial^2 u_1}{\partial x\,\partial y} + a_{11}\frac{1-\nu}{2}\frac{\partial^2 v_1}{\partial x^2} + a_{11}\frac{\partial^2 v_1}{\partial y^2} - b_{11}\frac{1-\nu}{2}v_1 -\\
&\qquad - c_{11}\frac{1-\nu}{2}\frac{\partial w_1}{\partial y} - c_{12}\frac{1-\nu}{2}\frac{\partial w_2}{\partial y} = 0,\\
&\left(\frac{1-\nu}{2}c_{11} - \nu d_{11}\right)\frac{\partial u_1}{\partial x} + \left(\frac{1-\nu}{2}c_{11} - \nu d_{11}\right)\frac{\partial v_1}{\partial x} +\\
&\qquad + \frac{1-\nu}{2}r_{11}\frac{\partial^2 w_1}{\partial x^2} + \frac{1-\nu}{2}r_{11}\frac{\partial^2 w_1}{\partial y^2} - s_{11}w_1 +\\
&\qquad + \frac{1-\nu}{2}r_{12}\frac{\partial^2 w_2}{\partial x^2} + \frac{1-\nu}{2}r_{12}\frac{\partial^2 w_2}{\partial y^2} - s_{12}w_2 + \frac{1-\nu^2}{E}q = 0,\\
&\left[\frac{E}{2(1+\nu)}c_{12} - \frac{E}{1-\nu^2}d_{12}\right]\frac{\partial u_1}{\partial x} + \left[\frac{E}{2(1+\nu)}c_{12} - \frac{E}{1-\nu^2}d_{12}\right]\frac{\partial v_1}{\partial x} +\\
&\qquad + \frac{E}{2(1+\nu)}r_{12}\frac{\partial^2 w_1}{dx^2} + \frac{E}{2(1+\nu)}r_{12}\frac{\partial^2 w_1}{\partial y^2} -\\
&\qquad - \frac{E}{1-\nu^2}s_{12}w_1 + \left[\frac{E}{2(1+\nu)}r_{22} + \frac{E_0}{2(1+\nu_0)}r_{22}^0\right]\frac{\partial^2 w_2}{\partial x^2} +\\
&+ \left[\frac{E}{2(1+\nu)}r_{22} + \frac{E_0}{2(1+\nu_0)}r_{22}^0\right]\frac{\partial^2 w_2}{\partial y^2} - \frac{E_0}{1-\nu_0^2}s_{22}^0 w_2 + q = 0,
\end{aligned}\right| \qquad (13.6)$$

where

$$u_1 = u_1(x,\ y),\quad v_1 = v_1(x,\ y),\quad w_1 = w_1(x,\ y),\quad w_2 = w_2(x,\ y);$$

$E,\ \nu,\ E_0,\ \nu_0$ = modulus of elasticity and Poisson's ratio for the plate and the elastic foundation, respectively; $q = q(x,\ y)$ = vertical load acting on the plate.

From (13.2), we obtain for the coefficients in (13.6):

$$\left.\begin{aligned}
a_{11} &= \int \varphi_1^2\,dz = \frac{h^3}{12}, & s_{11} &= \int (\psi_1')^2\,dz = \frac{1}{h},\\
b_{11} &= \int (\varphi_1')^2\,dz = h, & s_{12} &= \int \psi_1'\psi_2'\,dz = 0\\
c_{11} &= \int \varphi_1\psi_1\,dz = -\frac{h}{2}, & s_{22}^0 &= \int (\psi_2')^2\,dz = \frac{1}{H},\\
& & r_{11} &= \int \psi_1^2\,dz = \frac{h}{3},\\
c_{12} &= \int \varphi_1'\psi_2\,dz = -h, & r_{12} &= \int \psi_1\psi_2\,dz = \frac{h}{2},\\
d_{11} &= \int \varphi_1\psi_1'\,dz = 0, & r_{22} &= \int_0^h \psi_2^2\,dz = h,\\
d_{12} &= \int \varphi_1\psi_2'\,dz = 0, & r_{22}^0 &= \int_h^{h+H} \psi_2^2\,dz = \frac{H}{3}.
\end{aligned}\right|\qquad (13.7)$$

Substitution of (13.7) in (13.6) yields the system of differential equations given in Table 17 where the symbols $D_x,\ D_y,\ D_x^2,\ D_y^2$ represent differential operators and indicate that the function written at the top of the column is to be differentiated once or twice by x or y respectively.

This system of four differential equations in the four unknown functions $u_1,\ v_1,\ w_1, w_2$, describes the problem of the bending of a thick plate on an elastic foundation completely. When these functions have been determined, the displacements and stresses in the plate and the elastic foundation can be obtained from (13.1) of this chapter and (6.2) of Chapter I respectively.

TABLE 17

No	u_1	v_1	w_1	w_2	Load term
1	$D_x^2 + \frac{1-\nu}{2} D_y^2 - \frac{6(1-\nu)}{h^2}$	$\frac{1+\nu}{2} D_{xy}^2$	$\frac{3(1-\nu)}{h^2} D_x$	$\frac{6(1-\nu)}{h^2} D_x$	0
2	$\frac{1+\nu}{2} D_{xy}^2$	$\frac{1-\nu}{2} D_x^2 + D_y^2 - \frac{6(1-\nu)}{h^2}$	$\frac{3(1-\nu)}{h^2} D_y$	$\frac{6(1-\nu)}{h^2} D_y$	0
3	$-\frac{1}{2} D_x$	$-\frac{1}{2} D_y$	$\frac{1}{3} D_x^2 + \frac{1}{3} D_y^2 - \frac{2}{(1-\nu) h^2}$	$\frac{1}{2}(D_x^2 + D_y^2)$	$-\frac{2(1+\nu)}{Eh} q$
4	$-D_x$	$-D_y$	$\frac{1}{2}(D_x^2 + D_y^2)$	$\left(1 + \frac{1}{2}\frac{E_0}{E}\frac{1+\nu}{1+\nu_0}\frac{H}{h}\right) D_x^2 + \left(1 + \frac{1}{2}\frac{E_0}{E}\frac{1+\nu}{1+\nu_0}\frac{H}{h}\right) D_y^2 - 2\frac{E_0}{E}\frac{1+\nu}{1+\nu_0}\frac{1}{Hh}$	$-\frac{2(1+\nu)}{Eh} q$

Chapter IV

AXISYMMETRICAL DEFORMATION OF CIRCULAR PLATES ON ELASTIC SINGLE-LAYER FOUNDATIONS

§ 1. STATEMENT OF THE PROBLEM. BASIC DIFFERENTIAL RELATIONSHIPS

1

Consider a circular plate of uniform thickness h resting on an elastic foundation possessing two characteristics (Figure 107). Let the external load be applied symmetrically relative to the plate center, so that the plate is subjected to an axisymmetrical deformation. Polar coordinates (θ, ρ) will be used, the origin of coordinates being placed at the plate center, and the distance from the center to a given point denoted by ρ. The differential equation of bending of a plate resting on an elastic single-layer foundation (cf. (1.5) of Chapter III) is in polar coordinates:

$$\nabla_\rho^2 \nabla_\rho^2 W - 2r^2 \nabla_\rho^2 W + s^4 W = \frac{p}{D}, \tag{1.1}$$

where

$$\left.\begin{aligned} r^2 &= \frac{E_0}{4(1+\nu_0) D} \int_0^H \psi^2(z)\, dz, \\ s^4 &= \frac{E_0}{(1-\nu_0^2) D} \int_0^H \psi'^2(z)\, dz, \end{aligned}\right\} \tag{1.2}$$

and $D = \frac{Eh^3}{12(1-\mu^2)}$ = flexural rigidity of plate.

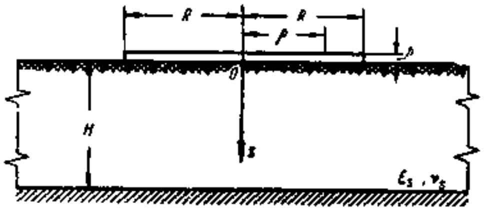

FIGURE 107.

By virtue of the axial symmetry, the plate deflections $W = W(\rho)$ are independent of the polar angle θ, and the Laplacian of W becomes:

$$\nabla_\rho^2 W = \frac{dW^2(\rho)}{d\rho^2} + \frac{1}{\rho}\frac{dW(\rho)}{d\rho}. \tag{1.3}$$

The problem stated is thus completely described by (1.1) and the corresponding boundary conditions. Equation (1.1) differs from the equation of bending of a circular plate on an elastic Winkler foundation by the term:

$$-2r^2\nabla_\rho^2 W$$

through which allowance is made for the work done by the shearing stresses acting in the single-layer foundation.

2

In the case of axisymmetrical bending, radial bending moments M_ρ and shearing forces Q_ρ appear in the cylindrical plate sections $\rho = \text{const}$ (Figure 108). In the radial sections $\theta = \text{const}$ only bending moments M_θ act. The radial and peripheral moments and shearing forces are:

$$\left.\begin{aligned} M_\rho &= -D\left(\frac{d^2W}{d\rho^2} + \frac{\mu}{\rho}\frac{dW}{d\rho}\right) = -D\left[\nabla_\rho^2 W - \frac{1-\mu}{\rho}\frac{dW}{d\rho}\right],\\ M_\theta &= -D\left(\mu\frac{d^2W}{d\rho^2} + \frac{1}{\rho}\frac{dW}{d\rho}\right) = -D\left[\mu\nabla_\rho^2 W + \frac{1-\mu}{\rho}\frac{dW}{d\rho}\right],\\ Q_\rho &= -D\frac{d}{d\rho}\left(\frac{d^2W}{d\rho^2} + \frac{1}{\rho}\frac{dW}{d\rho}\right) = -D\frac{d}{d\rho}\nabla_\rho^2 W. \end{aligned}\right\} \tag{1.4}$$

Shearing forces Q_ρ acting on areas having positive outer normals are considered as positive if their direction coincides with the positive direction of the z axis. Bending moments M_ρ and M_θ causing tension in the lower part of the plate are considered as positive.

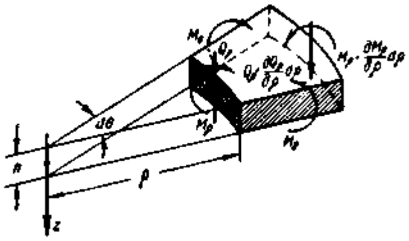
M_θ
Q_ρ
$Q_\rho + \frac{\partial Q_\rho}{\partial\rho}d\rho$
$M_\rho + \frac{\partial M_\rho}{\partial\rho}d\rho$
$d\theta$
M_ρ
M_θ
h
ρ
z

FIGURE 108.

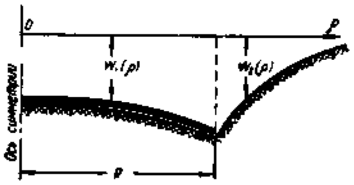

FIGURE 109.

3

We now introduce the generalized shearing force (per unit length) which for $\rho \leqslant R$ defines the shearing stresses in the plate and elastic foundation, acting in the cylindrical sections $\rho = \text{const}$, (cf. (1.10) of Chapter II):

$$N_\rho = -D\left(\frac{d}{d\rho}\nabla_\rho^2 W - 2r^2\frac{dW}{d\rho}\right). \tag{1.5}$$

where

$$r^2 = \frac{t}{D} = \frac{E_0}{4(1+\nu_0)D}\int_0^H \psi^2(z)\,dz.$$

The sign of the forces N_ρ is determined as for the forces Q_ρ.

The generalized shearing force acting in the foundation beyond the plate edge ($\rho \geqslant R$) will be denoted by S_ρ in order to distinguish it from N_ρ. Its value is by (1.5) (cf. (3.10) of Chapter I):

$$S_\rho = 2t\frac{dW}{d\rho}. \qquad (1.6)$$

Consider thus a plate with a free edge on which no forces act (Figure 109). The boundary conditions for $\rho = R$ are:

$$M_\rho(R) = 0, \quad W_1(R) = W_2(R), \quad N_\rho(R) = S_\rho(R), \qquad (1.7)$$

where W_1 and W_2 are the vertical displacements of plate and surface of elastic foundation for $\rho \leqslant R$ and $\rho > R$ respectively.

The last two conditions (1.7) describe the continuity of the deformed surface of the elastic foundation; through them allowance is made for strains of the elastic foundation beyond the plate edge.

Substitution of (1.5) and (1.6) in the last condition (1.7) yields:

$$-D\frac{d}{d\rho}\nabla_\rho^2 W_1 + 2t\frac{dW_1}{d\rho} = 2t\frac{dW_2}{d\rho}.$$

In virtue of (1.4), this boundary condition can be written:

$$Q_\rho(R) = -D\frac{d}{d\rho}\nabla_\rho^2 W_1 = 2t\left(\frac{dW_2}{d\rho} - \frac{dW_1}{d\rho}\right). \qquad (1.8)$$

A fictitious contour force $Q^\Phi = Q_\rho(R)$ thus appears at a free plate edge on which no forces act, due to the coherence of the single-layer foundation and to its capacity for taking up shearing stresses.

We can rewrite (1.8) in the following form*:

$$Q^\Phi = S_{\rho_2} - S_{\rho_1}, \qquad (1.9)$$

where S_{ρ_1} and S_{ρ_2} are the generalized shearing forces in the elastic foundation, obtained for sections $\rho \quad R-\varepsilon$ and $\rho = R+\varepsilon$) respectively, when $\varepsilon \to 0$.

§2. GENERAL INTEGRAL OF THE DIFFERENTIAL EQUATION FOR A CIRCULAR PLATE ON A SINGLE-LAYER FOUNDATION

1

We replace ρ by the dimensionless coordinate $\xi = \frac{\rho}{L_0}$, where:

$$L_0 = \sqrt[4]{\frac{D}{k}}. \qquad (2.1)$$

---

* The fictitious forces Q^Φ were similarly defined in the analysis of beams (see section 5, Chapter II).

and $k = \frac{E_0}{1-\nu_0^2}\int\limits_0^H \psi'^2(z)\,dz$ defines the compressive strain of the soil, D = = flexural rigidity of plate.

We can now write (1.1) in the form:

$$\nabla_\xi^2\nabla_\xi^2 W - 2r_0^2\nabla_\xi^2 W + W = \frac{pL_0^4}{D}, \tag{2.2}$$

where

$$r_0^2 = \frac{tL_0^2}{D} = \frac{E_0 L_0}{4(1+\nu_0)D}\int\limits_0^H \psi^2(z)\,dz, \tag{2.3}$$

and

$$\nabla_\xi^2 = \frac{d^2}{d\xi^2} + \frac{1}{\xi}\frac{d}{d\xi}. \tag{2.4}$$

2

When no surface load acts, (2.2) reduces to the homogeneous equation:

$$\nabla_\xi^2\nabla_\xi^2 W - 2r_0^2\nabla_\xi^2 W + W = 0. \tag{2.5}$$

This can be reduced to an equivalent system of two second-order differential equations. Let $W = W(\xi)$ be a particular solution of (2.5) satisfying at the same time the differential equation

$$\nabla_\xi^2 W + \lambda W = 0, \tag{2.6}$$

where λ is a constant to be determined.

It follows from (2.6) that

$$\left.\begin{aligned} \nabla_\xi^2 W &= -\lambda W, \\ \nabla_\xi^2\nabla_\xi^2 W &= \lambda^2 W. \end{aligned}\right\} \tag{2.7}$$

Substitution of these expressions in (2.5) yields the following equation for λ:

$$\lambda^2 + 2r_0^2\lambda + 1 = 0. \tag{2.8}$$

Its roots are

$$\left.\begin{aligned} \lambda_1 &= -r_0^2 + \sqrt{(r_0^2)^2 - 1}, \\ \lambda_2 &= -r_0^2 - \sqrt{(r_0^2)^2 - 1}. \end{aligned}\right\} \tag{2.9}$$

For actual soils

$$0 \leqslant r_0^2 < 1. \tag{2.10}$$

The case $r_0^2 = 0$ is limiting; it characterizes the absence of shearing forces in the elastic foundation $(t = 0)$.

The roots of (2.8) are therefore conjugate complex numbers:

$$\left.\begin{aligned}\lambda_1 &= a = -a_1 + b_1 i,\\ \lambda_2 &= \bar{a} = -a_1 - b_1 i,\end{aligned}\right\} \tag{2.11}$$

where

$$a_1 = r_0^2, \quad b_1 = \sqrt{1 - (r_0^2)^2}.$$

The complex numbers (2.11) may have the following values (Figure 110):

$$\left.\begin{aligned}\pi > \arg a \geqslant \frac{\pi}{2},\\ -\pi < \arg \bar{a} \leqslant -\frac{\pi}{2}\end{aligned}\right\} \tag{2.12}$$

In accordance with Viéte's theorem, their modulus is equal to the free term in (2.8), i.e., to unity:

$$|a| = 1 \quad |\bar{a}| = 1. \tag{2.13}$$

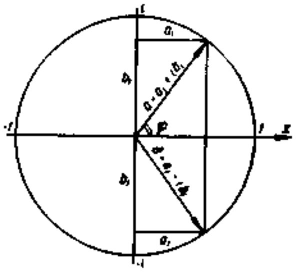

FIGURE 110.

Proceeding from (2.6), we find that the following two independent second-order differential equations correspond to the conjugate complex roots (2.11):

$$\left.\begin{aligned}\frac{d^2W_1}{d\xi^2} + \frac{1}{\xi}\frac{dW_1}{d\xi} + aW_1 = 0,\\ \frac{d^2W_2}{d\xi^2} + \frac{1}{\xi}\frac{dW_2}{d\xi} + \bar{a}W_2 = 0.\end{aligned}\right\} \tag{2.14}$$

3

The general integral of (2.2) can now be written in the form:

$$W = W_1 + W_2 + W_p, \tag{2.15}$$

where W_1 and W_2 satisfy the first and the second equations (2.14) respectively and W_p is a particular integral of the nonhomogeneous equation (2.2).

By introducing the new variables:

$$u = \sqrt{a}\,\xi, \quad v = \sqrt{\bar{a}}\,\xi, \tag{2.16}$$

we can transform (2.14) into zero-order Bessel equations:

$$\left.\begin{aligned} \frac{d^2W_1}{du^2} + \frac{1}{u}\frac{dW_1}{du} + W_1 = 0, \\ \frac{d^2W_2}{dv^2} + \frac{1}{v}\frac{dW_2}{dv} + W_2 = 0. \end{aligned}\right\} \tag{2.17}$$

The solution of (2.17) can be represented in the following form* :

$$\left.\begin{aligned} W_1(\xi) = B_1J_0(\sqrt{a}\,\xi) + B_2H_0^{(1)}(\sqrt{a}\,\xi), \\ W_2(\xi) = B_3J_0(\sqrt{\bar{a}}\,\xi) + B_4H_0^{(2)}(\sqrt{\bar{a}}\,\xi), \end{aligned}\right\} \tag{2.18}$$

where

$$J_0(\sqrt{a}\,\xi) \text{ and } J_0(\sqrt{\bar{a}}\,\xi)$$

are zero-order Bessel functions of the first kind in $\sqrt{a}\,\xi$ and $\sqrt{\bar{a}}\,\xi$; and:

$$H_0^{(1)}(\sqrt{a}\,\xi) \text{ and } H_0^{(2)}(\sqrt{\bar{a}}\,\xi)$$

are zero-order Hankel functions of the first and second kind respectively, also in $\sqrt{a}\,\xi$ and $\sqrt{\bar{a}}\,\xi$.

Using (2.18), we can write (2.15) in the following final form:

$$\begin{aligned} W = B_1J_0(\sqrt{a}\,\xi) + B_2H_0^{(1)}(\sqrt{a}\,\xi) + \\ + B_3J_0(\sqrt{\bar{a}}\,\xi) + B_4H_0^{(2)}(\sqrt{\bar{a}}\,\xi) + W_p. \end{aligned} \tag{2.19}$$

For the solution of practical problems it is convenient to write:

$$\left.\begin{aligned} \sqrt{a} = e^{i\varphi} = \cos\varphi + i\sin\varphi, \\ \sqrt{\bar{a}} = e^{-i\varphi} = \cos\varphi - i\sin\varphi, \end{aligned}\right\} \tag{2.20}$$

where

$$\varphi = \frac{1}{2}\arg a$$

and the modulus of the complex numbers $\sqrt{a}$ and $\sqrt{\bar{a}}$ is equal to unity in accordance with (2.13).

It can be seen from (2.12) and (2.20) that the functions:

$$J_0(\sqrt{a}\,\xi), \quad H_0^{(1)}(\sqrt{a}\,\xi), \quad J_0(\sqrt{\bar{a}}\,\xi), \quad H_0^{2}(\sqrt{\bar{a}}\,\xi)$$

are determined in the regions:

$$\frac{\pi}{2} > \varphi \geqslant \frac{\pi}{4}, \quad -\frac{\pi}{2} < \varphi \leqslant -\frac{\pi}{4}. \tag{2.21}$$

In the particular case $t = 0$, $(r_0^x = 0)$, these functions are determined along a line forming an angle $\varphi = \frac{\pi}{4}$ with the axis of real magnitudes.

---

* For a thorough treatment of the theory of Bessel functions, see /4/.

4

Since the functions

$$J_0(\sqrt{a}\xi),\ H_0^{(1)}(\sqrt{a}\xi),\ J_0(\sqrt{\bar{a}}\xi),\ H_0^{(2)}(\sqrt{\bar{a}}\xi)$$

are complex while the plate-deflection function W must be real, the constants C_1, C_2, C_3, C_4 must be complex. In order to express the solution through real functions, we write (2.19) in a different form:

$$W = C_1u_0(\xi) + C_2v_0(\xi) + C_3f_0(\xi) + C_4g_0(\xi) + W_p, \tag{2.22}$$

where, as before, W_p is a particular integral of the nonhomogeneous equation (2.2), and

$$\left.\begin{aligned}
u_0(\xi) &= \operatorname{Re} J_0(\sqrt{a}\xi) = \frac{J_0(\sqrt{a}\xi) + J_0(\sqrt{\bar{a}}\xi)}{2},\\
v_0(\xi) &= \operatorname{Im} J_0(\sqrt{a}\xi) = \frac{J_0(\sqrt{a}\xi) - J_0(\sqrt{\bar{a}}\xi)}{2i},\\
f_0(\xi) &= \operatorname{Re} H_0^{(1)}(\sqrt{a}\xi) = \frac{H_0^{(1)}(\sqrt{a}\xi) + H_0^{(2)}(\sqrt{\bar{a}}\xi)}{2},\\
g_0(\xi) &= \operatorname{Im} H_0^{(2)}(\sqrt{\bar{a}}\xi) = \frac{H_0^{(1)}(\sqrt{a}\xi) - H_0^{(2)}(\sqrt{\bar{a}}\xi}{2i}.
\end{aligned}\right\} \tag{2.23}$$

It is seen from (2.23) that $u_0(\xi)$ and $f_0(\xi)$ represent the real, $v_0(\xi)$ and $g_0(\xi)$, the imaginary parts of the zero-order Bessel and Hankel functions. Since these functions are real, the constants C_1, C_2, C_3, C_4 will also be real. The behavior of functions $u_0(\xi)$ and $v_0(\xi)$ resembles that of the functions $e^{\xi}\cos\xi$, $e^{\xi}\sin\xi$ appearing in the theory of beams on elastic Winkler foundations: they remain finite when $\xi\to 0$, and tend to infinity when $\xi\to\infty$.

At $\xi\to 0$, the function $f_0(\xi)$ has a singularity of the type $\xi^2\ln\xi$; the function $g_0(\xi)$ becomes infinite when $\xi\to 0$. Both functions tend to zero when $\xi\to\infty$, resembling the functions $e^{-\xi}\cos\xi$, $e^{-\xi}\sin\xi$.

5

The following expressions are obtained for the slopes, bending moments, and shearing forces in the plate by substituting (2.22) into (1.4) and using the known rules of differentiation of cylindrical functions:

$$\left.\begin{aligned}
\frac{dW}{d\rho} &= -\frac{1}{L_0}\left[C_1\theta_1(\xi) + C_2\theta_2(\xi) + C_3\theta_3(\xi) + C_4\theta_4(\xi) - \frac{dW_p}{d\xi}\right],\\
M_\rho &= \frac{D}{L_0^2}\Big\{C_1[M_1(\xi) - (1-\mu)\overline{M}_1(\xi)] + C_2[M_2(\xi) -\\
&\quad - (1-\mu)\overline{M}_2(\xi)] + C_3[M_3(\xi) - (1-\mu)\overline{M}_3(\xi)] +\\
&\quad + C_4[M_4(\xi) - (1-\mu)\overline{M}_4(\xi)] - \left[\nabla_\xi^2 - \frac{1-\mu}{\xi}\frac{d}{d\xi}\right]W_p\Big\},\\
M_\theta &= \frac{D}{L_0^2}\Big\{C_1[\mu M_1(\xi) + (1-\mu)\overline{M}_1(\xi)] + C_2[\mu M_2(\xi) +\\
&\quad + (1-\mu)\overline{M}_2(\xi)] + C_3[\mu M_3(\xi) + (1-\mu)\overline{M}_3(\xi)] +\\
&\quad + C_4[\mu M_4(\xi) + (1-\mu)\overline{M}_4(\xi)] - \left[\mu\nabla_\xi^2 + \frac{1-\mu}{\xi}\frac{d}{d\xi}\right]W_p\Big\},\\
Q_\rho &= -\frac{D}{L_0^3}\left[C_1Q_1(\xi) + C_2Q_2(\xi) + C_3Q_3(\xi) + C_4Q_4(\xi) + \frac{d}{d\xi}\nabla_\xi^2 W_p\right].
\end{aligned}\right\} \tag{2.24}$$

where

$$\left.\begin{aligned}\theta_1(\xi) &= u_1(\xi)\cos\varphi - v_1(\xi)\sin\varphi,\\ \theta_2(\xi) &= u_1(\xi)\sin\varphi + v_1(\xi)\cos\varphi,\\ \theta_3(\xi) &= f_1(\xi)\cos\varphi - g_1(\xi)\sin\varphi,\\ \theta_4(\xi) &= f_1(\xi)\sin\varphi + g_1(\xi)\cos\varphi;\end{aligned}\right\} \qquad (2.25)$$

$$\left.\begin{aligned}M_1(\xi) &= u_0(\xi)\cos 2\varphi - v_0(\xi)\sin 2\varphi,\\ M_2(\xi) &= u_0(\xi)\sin 2\varphi + v_0(\xi)\cos 2\varphi,\\ M_3(\xi) &= f_0(\xi)\cos 2\varphi - g_0(\xi)\sin 2\varphi,\\ M_4(\xi) &= f_0(\xi)\sin 2\varphi + g_0(\xi)\cos 2\varphi;\end{aligned}\right\} \qquad (2.26)$$

$$\left.\begin{aligned}\bar{M}_1(\xi) &= \frac{1}{\xi}\,[u_1(\xi)\cos\varphi - v_1(\xi)\sin\varphi],\\ \bar{M}_2(\xi) &= \frac{1}{\xi}\,[u_1(\xi)\sin\varphi + v_1(\xi)\cos\varphi],\\ \bar{M}_3(\xi) &= \frac{1}{\xi}\,[f_1(\xi)\cos\varphi - g_1(\xi)\sin\varphi],\\ \bar{M}_4(\xi) &= \frac{1}{\xi}\,[f_1(\xi)\sin\varphi + g_1(\xi)\cos\varphi];\end{aligned}\right\} \qquad (2.27)$$

$$\left.\begin{aligned}Q_1(\xi) &= u_1(\xi)\cos 3\varphi - v_1(\xi)\sin 3\varphi,\\ Q_2(\xi) &= u_1(\xi)\sin 3\varphi + v_1(\xi)\cos 3\varphi,\\ Q_3(\xi) &= f_1(\xi)\cos 3\varphi - g_1(\xi)\sin 3\varphi,\\ Q_4(\xi) &= f_1(\xi)\sin 3\varphi + g_1(\xi)\cos 3\varphi,\end{aligned}\right\} \qquad (2.28)$$

and

$$\varphi = \frac{1}{2}\arg a; \qquad (2.29)$$

the complex number a is given by (2.11).

The functions $u_1(\xi)$, $v_1(\xi)$, and $f_1(\xi)$, $g_1(\xi)$ represent the real and the imaginary parts of the first-order Bessel and Hankel functions respectively, and are determined from the functions

$$J_1(\sqrt{a}\xi),\ J_1(\sqrt{\bar{a}}\xi),\ H_1^{(1)}(\sqrt{a}\xi),\ H_1^{(2)}(\sqrt{\bar{a}}\xi)$$

in a manner similar to (2.23).

6

Expressions (2.22) and (2.24) are the general solution to the problem of the axisymmetrical deformation of a circular plate on a single-layer foundation. The integration constants C_1, C_2, C_3, C_4 must be determined from the boundary conditions. Establishing the latter presents no difficulty in the usual cases of plate support (simple support or built-in edge). Thus, for a simple support along the edge,

$$\left.\begin{aligned}W = \left(\frac{R}{L_0}\right) &= 0,\\ M_\rho\left(\frac{R}{L_0}\right) &= 0;\end{aligned}\right\} \qquad (2.30)$$

for a built-in edge

$$\left.\begin{aligned} W = \left(\frac{R}{L_0}\right) &= 0, \\ \left(\frac{dW}{d\rho}\right)_{\text{при}\ \xi=\frac{R}{L_0}} &= 0. \end{aligned}\right\} \quad (2.31)$$

If the plate is freely supported on the elastic foundation, the coherence of the soil and the possibility of strains appearing in it beyond the region of load application necessitate a consideration of an infinite region lying beyond the plate edge. As was shown in section 1 of this chapter, this is expressed through a fictitious shearing force Q^* acting along the plate edge, which has to be taken into account in the boundary conditions.

§ 3. ABSOLUTELY RIGID PLATE

Consider a circular plate under the action of an axisymmetrical load whose resultant is P_0. Let the plate be so rigid that its deformations can be neglected: it can then be considered as a circular punch whose displacement is $W_1 = C_0$ (Figure 111).

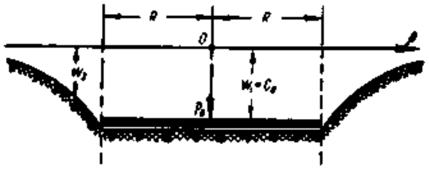

FIGURE 111.

The states of strain and stress of the elastic foundation beyond the plate edges ($R \leqslant \rho < \infty$) are determined in the general case by (7.8) of Chapter I. When no surface loads act within the region considered, this equation reduces to the homogeneous equation:

$$\frac{d^2W_2}{d\rho^2} + \frac{1}{\rho}\frac{dW_2}{d\rho} - \alpha^2 W_2 = 0, \quad (3.1)$$

where $\alpha = \sqrt{\frac{k}{2t}}$, and $W_2 = W_2(\rho)$ is a function characterizing the vertical displacements of the foundation beyond the plate edges.

The solution of (3.1) (cf. section 7 of Chapter I) is:

$$W_2 = C_1 I_0(\alpha\rho) + C_2 K_0(\alpha\rho). \quad (3.2)$$

The problem is thus reduced to determining the integration constants C_1 and C_2, as well as the vertical displacement of the plate C_0, from the boundary and equilibrium conditions of the plate.

Since the deformed surface of the elastic foundation is assumed to be continuous, while the vertical displacements of the foundation are equal to zero at infinity, the boundary conditions are:

$$\left.\begin{aligned} &\text{at } \rho = R: && W_2 = C_0; \\ &\text{at } \rho \to \infty: && W_2 \to 0. \end{aligned}\right\} \tag{3.3}$$

Taking into account the behavior of the function $I_0(\alpha\rho)$ at infinity, the second condition yields:

$$C_1 = 0. \tag{3.4}$$

The first condition gives then:

$$C_2 = \frac{C_0}{K_0(\alpha R)}. \tag{3.5}$$

To determine C_0, the equilibrium condition of the system (plate +elastic foundation) will now be formulated by equating to zero the total work done by all external and internal forces acting on the system over the virtual displacement:

$$\bar{w}(\rho, z) = 1 \cdot \psi(z),$$

We obtain:

$$\begin{aligned} -\left[\int_0^H \int_0^{2\pi} \int_0^P \sigma_{z_1} \psi'(z)\, \rho\, d\rho\, d\theta\, dz + \int_0^H \int_0^{2\pi} \int_R^\infty \sigma_{z_2} \psi'(z)\, \rho\, d\rho\, d\theta\, dz\right] + \\ + P_0 \psi(0) = 0, \end{aligned} \tag{3.6}$$

where σ_{z_1} and σ_{z_2} are the normal stresses appearing in the elastic foundation beneath the plate and beyond its edges respectively. According to (6.4) of Chapter I, these stresses are:

$$\left.\begin{aligned} \sigma_{z_1} &= \frac{E_0}{1 - \nu_0^2} C_0 \psi'(z), \\ \sigma_{z_2} &= \frac{E_0}{1 - \nu_0^2} W_2(\rho) \psi'(z). \end{aligned}\right\} \tag{3.7}$$

Substitution of these expressions in (3.6) yields, after integrating between the limits shown:

$$kC_0\left[\pi R^2 + 2\pi R^2 \frac{K_1(\alpha R)}{\alpha R K_0(\alpha R)}\right] = P_0,$$

or finally:

$$C_0 = \frac{P_0}{\pi R^2 k \left[1 + 2\frac{K_1(\alpha R)}{\alpha R K_0(\alpha R)}\right]}, \tag{3.8}$$

where, as before:

$$k = \frac{E_0}{1 - \nu_0^2} \int_0^H \psi'^2\, dz. \tag{3.9}$$

The reactions of the elastic foundation can be obtained from (7.8) of Chapter I by putting $W_1 = C_0$:

$$q = kC_0 = \frac{P_0}{\pi R^2\left[1 + 2\frac{K_1(\alpha R)}{\alpha R K_0(\alpha R)}\right]}. \qquad (3.10)$$

In addition to the distributed reactions (3.10), fictitious reactions Q^{Φ}, whose dimensions are kg/cm or t/m, act along the contour of the circular plate (Figure 112). These are due to the strains of the elastic foundation beyond the plate edges and correspond to the infinitely large pressures beneath the edges of the circular punch, found by the exact methods of the theory of elasticity.

The fictitious reactions Q^{Φ} can be determined from (1.8), putting $W_1 = C_0$:

$$Q^{\Phi} = 2t\left(\frac{dW_2}{d\rho}\right)_{\rho=R}. \qquad (3.11)$$

Substitution of (3.2), (3.4), (3.5), and (3.8) leads to the following final expression for Q^{Φ}:

$$Q^{\Phi} = \frac{P_0}{\pi R\left[1 + 2\frac{K_1(\alpha R)}{\alpha R K_0(\alpha R)}\right]}\,\frac{K_1(\alpha R)}{\alpha R K_0(\alpha R)}. \qquad (3.12)$$

The reactions of the elastic foundation, obtained from (3.10) and (3.12), satisfy the static-equilibrium condition of the plate $\sum Z = 0$. It is easily seen that:

$$\pi R^2 q + 2\pi R Q^{\Phi} = P_0. \qquad (3.13)$$

This solution is true for any function $\psi(z)$, with the same accuracy as that with which:

$$\alpha = \sqrt{\frac{k}{2t}} \qquad (3.14)$$

has been obtained. In many practical problems it is convenient to select $\psi(z)$ in the linear form (2.7) of Chapter I, or in the form:

$$\psi(z) = \frac{\operatorname{sh}\frac{\gamma(H-z)}{R}}{\operatorname{sh}\frac{\gamma H}{R}}, \qquad (3.15)$$

where H = thickness of compressible soil layer, R = plate radius, and γ = dimensionless coefficient depending on the elastic properties of the foundation. When $\psi(z)$ is given by (3.15), the integral characteristics of the elastic foundation are [cf. (7.11) of Chapter I]:

$$\left.\begin{aligned} k &= \frac{E_0}{(1-\nu_0^2)H}\psi_k, \\ t &= \frac{E_0 H}{12(1+\nu_0)}\psi_t, \\ \alpha &= \frac{1}{H}\sqrt{\frac{6}{1-\nu_0}}\psi_\alpha, \end{aligned}\right\} \qquad (3.16)$$

where [cf. Chapter I, (7.12)]:

$$\left.\begin{aligned}
\psi_k &= \frac{1}{2}\frac{\gamma H}{R}\left[\frac{\operatorname{sh}\frac{\gamma H}{R}\operatorname{ch}\frac{\gamma H}{R}+\frac{\gamma H}{R}}{\operatorname{sh}^2\frac{\gamma H}{R}}\right],\\
\psi_l &= \frac{3}{2}\frac{R}{\gamma H}\left[\frac{\operatorname{sh}\frac{\gamma H}{R}\operatorname{ch}\frac{\gamma H}{R}-\frac{\gamma H}{R}}{\operatorname{sh}^2\frac{\gamma H}{R}}\right],\\
\varphi_a &= \frac{\gamma H}{R}\sqrt{\frac{1}{3}\,\frac{\operatorname{sh}\frac{\gamma H}{R}\operatorname{ch}\frac{\gamma H}{R}+\frac{\gamma H}{R}}{\operatorname{sh}\frac{\gamma H}{R}\operatorname{ch}\frac{\gamma H}{R}-\frac{\gamma H}{R}}}.
\end{aligned}\right\} \qquad (3.17)$$

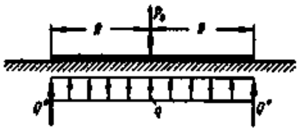

FIGURE 112.

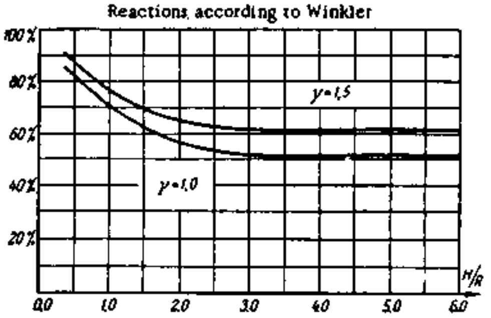

FIGURE 113.

Curves of q as a function of the reduced thickness $\frac{H}{R}$ are easily plotted, using (3.10), (3.16), and (3.17), as in Figure 113 for $\nu_0 = 0.4$ and $\gamma = 1.0$, $\gamma = 1.5$. In this diagram the ordinate defines the ratio (in %) between q and the corresponding values of the reactive pressure as given by Winkler. It is seen that for a single-layer foundation acting like the base of a press, q is less than the value according to Winkler. This is due to the fictitious forces Q^* acting along the contour, which characterize the state of strain of the single-layer foundation beyond the plate edges; they are equivalent to the infinite stresses obtained in the exact solution of the theory of elasticity:

These curves also show that q becomes practically constant for $\frac{H}{R} > 2.5$, so that, for $\frac{H}{R} > 2.5$, the foundation can be considered as a semi-infinite elastic space ($H = \infty$). For $\frac{H}{R} < 1.0$, on the other hand, the single-layer foundation approximates Winkler's model in its behavior, the distributed reactions q increase while the concentrated reactions Q^* decrease.

After the reactions of the elastic foundation have been found, the bending moments and shearing forces acting on the rigid plate can be determined by the ordinary methods applied to symmetrically loaded circular plates. In this case the external load consists of the given actual load and the reactions of the elastic foundation.

The following expressions are thus obtained for the radial bending moments at the plate center, induced by the distributed reactions q and the concentrated reaction Q^{Φ}:

$$M_q(0) = qR^2\overline{M}_q(0), \quad M_Q(0) = PR\overline{M}_Q(0), \tag{3.18}$$

where, using the same notations as in (3.10) and (3.12):

$$\left.\begin{aligned} \overline{M}_q(0) &= \frac{(3+\mu)\dfrac{K_1(\alpha R)}{\alpha RK_0(\alpha R)}}{8\left[1+2\dfrac{K_1(\alpha R)}{\alpha RK_0(\alpha R)}\right]}, \\ \overline{M}_Q(0) &= -\frac{3+\mu}{8\left[1+2\dfrac{K_1(\alpha R)}{\alpha RK_0(\alpha R)}\right]} \end{aligned}\right| \tag{3.19}$$

Curves of $\overline{M}_q(0)$ and $\overline{M}_Q(0)$ as functions of $\frac{H}{R}$, obtained from these formulas, have been plotted in Figure 114 for the function $\phi(z)$ given by (3.15). The elastic characteristics of the foundation are defined by (3.16) and (3.17). The following numerical values were used: $\nu_0 = 0.4$, $\mu = 1/4$, $\gamma = 1.0$ and $\gamma = 1.5$.

It is seen that the radial bending moments at the plate center increase with the depth of the elastic layer, tending toward a finite value; for $\gamma = 1.5$ and $\frac{H}{R} > 2.0$ the solution presented is practically identical with the solution given by the theory of the semi-infinite elastic space; for $\gamma = 1.0$ the difference is about 20 to 25%.

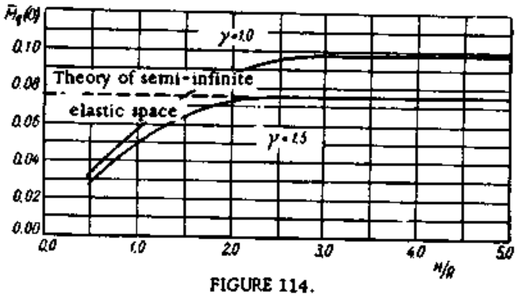

FIGURE 114.

§ 4. ANNULAR PUNCH

Consider an annular punch subjected to an axisymmetrical load P, distributed along the circumference of the circle $\rho = R$ (Figure 115), whose resultant is:

$$P_0 = 2\pi RP.$$

The inner and outer radii of the annulus will be denoted by R_1 and R_2 respectively. The following notations will be used for the vertical displacements of the elastic-foundation surface: $W_1(\rho)$ = vertical displacement inside annulus, $W_2 = C_0$ = vertical displacement beneath annulus, $W_3(\rho)$ = vertical displacement outside annulus.

The homogeneous differential equation (3.2) holds true for $0 \leqslant \rho \leqslant R_1$ and $R_2 \leqslant \rho < \infty$; the vertical displacements in these regions are thus:

$$\left.\begin{aligned} W_1(\rho) &= C_1 I_0(\alpha\rho) + C_2 K_0(\alpha\rho), \\ W_3(\rho) &= C_3 I_0(\alpha\rho) + C_4 K_0(\alpha\rho). \end{aligned}\right\} \tag{4.1}$$

The boundary conditions are:

$$\left.\begin{aligned} &\text{at } \rho = 0: && \frac{dW_1}{d\rho} = 0; \\ &\text{at } \rho = R_1: && W_1 = C_0; \\ &\text{at } \rho = R_2: && W_3 = C_0; \\ &\text{at } \rho \to \infty: && W_3 = 0. \end{aligned}\right\} \tag{4.2}$$

The constants C_1, C_2, C_3, C_4 are, by (4.1) and (4.2):

$$\left.\begin{aligned} &C_1 = \frac{C_0}{I_0(\alpha R_1)}, \quad C_4 = \frac{C_0}{K_0(\alpha R_2)}, \\ &C_2 = C_3 = 0. \end{aligned}\right\} \tag{4.3}$$

The vertical displacements of the surface of the elastic foundation are, therefore:

$$\left.\begin{aligned} W_1(\rho) &= \frac{C_0}{I_0(\alpha R_1)} I_0(\alpha\rho), \\ W_2(\rho) &= C_0, \\ W_3(\rho) &= \frac{C_0}{K_0(\alpha R_2)} K_0(\alpha\rho). \end{aligned}\right\} \tag{4.4}$$

We determine C_0 by the equilibrium conditions of the system considered, applying Lagrange's principle of virtual displacements. We obtain by analogy with (3.6):

$$\begin{gathered} -\left[\int\limits_0^H \int\limits_0^{2\pi} \int\limits_0^{R_1} \sigma_{z_1} \psi'(z)\, \rho\, d\rho\, d\theta\, dz + \int\limits_0^H \int\limits_0^{2\pi} \int\limits_{R_1}^{R_2} \sigma_{z_2} \psi'(z)\, \rho\, d\rho\, d\theta\, dz + \right. \\ \left. + \int\limits_0^H \int\limits_0^{2\pi} \int\limits_{R_2}^{\infty} \sigma_{z_3} \psi'(z)\, \rho\, d\rho\, d\theta\, dz \right] + P_0 \psi_1(0) = 0. \end{gathered} \tag{4.5}$$

The expression in brackets appears with the minus sign since it represents the work done by the internal forces.

Substituting the values of the normal stresses, given by expressions similar to (3.7), and integrating, we obtain:

$$C_0 = \frac{P_0}{k\left[\pi(R_2^2 - R_1^2) + 2\pi R_1^2 \frac{I_1(\alpha R_1)}{I_0(\alpha R_1)\, \alpha R_1} + 2\pi R_2^2 \frac{K_1(\alpha R_2)}{K_0(\alpha R_2)\, \alpha R_2}\right]}. \tag{4.6}$$

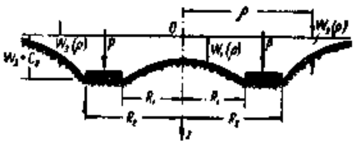

FIGURE 115.

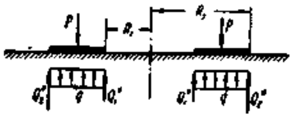

FIGURE 116.

Using (4.4) and (4.6), the reactions of the elastic foundation are, by (7.8) of Chapter I and (1.9) of this chapter:

$$q = \frac{P_0}{\pi (R_2^2 - R_1^2)\left[1 + 2\left(\frac{R_1^2}{R_2^2 - R_1^2}\frac{I_1(\alpha R_1)}{\alpha R_1 I_0(\alpha R_1)} + \frac{R_2^2}{R_2^2 - R_1^2}\frac{K_1(\alpha R_2)}{\alpha R_2 K_0(\alpha R_2)}\right)\right]},$$

$$Q_1^{\phi} = \frac{P_0 R_1 \frac{I_1(\alpha R_1)}{\alpha R_1 I_0(\alpha R_1)}}{\pi (R_2^2 - R_1^2)\left[1 + 2\left(\frac{R_1^2}{R_2^2 - R_1^2}\frac{I_1(\alpha R_1)}{\alpha R_1 I_0(\alpha R_1)} + \frac{R_2^2}{R_2^2 - R_1^2}\frac{K_1(\alpha R_2)}{\alpha R_2 K_0(\alpha R_2)}\right)\right]},$$

$$Q_2^{\phi} = \frac{P_0 R_2 \frac{K_1(\alpha R_2)}{\alpha R_2 K_0(\alpha R_2)}}{\pi (R_2^2 - R_1^2)\left[1 + 2\left(\frac{R_1^2}{R_2^2 - R_1^2}\frac{I_1(\alpha R_1)}{\alpha R_1 I_0(\alpha R_1)} + \frac{R_2^2}{R_2^2 - R_1^2}\frac{K_1(\alpha R_2)}{\alpha R_2 K_0(\alpha R_2)}\right)\right]}.$$

Here, Q_1^{ϕ} and Q_2^{ϕ} are fictitious forces acting along the inner and outer punch contours respectively (Figure 116).

5. INFINITE PLATE UNDER THE ACTION OF A CONCENTRATED FORCE

Consider an infinite plate loaded by a concentrated force P (Figure 117). The origin of coordinates is located at the point of application of the force. The problem is then one of axisymmetrical loading, and can be described by the homogeneous differential equation:

$$D\nabla_\rho^2\nabla_\rho^2 W - 2t\nabla_\rho^2 W + kW = 0. \qquad (5.1)$$

As was shown in section 2, the solution of (5.1) can be represented in the form:

$$W = C_1 u_0(\xi) + C_2 v_0(\xi) + C_3 f_0(\xi) + C_4 g_0(\xi), \text{ [cf. (2.22)]} \qquad (5.2)$$

where

$$\xi = \frac{\rho}{L_0}, \text{ and } L_0 = \sqrt[4]{\frac{D}{k}}.$$

The solution thus reduces to determining the integration constants C_1, C_2, C_3, C_4.

All forces and displacements must tend to zero when $\xi \to \infty$. Since the functions $u_0(\xi)$ and $v_0(\xi)$ tend to infinity when $\xi \to \infty$, then

$$C_1 = C_2 = 0. \tag{5.3}$$

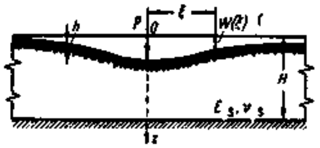

FIGURE 117.

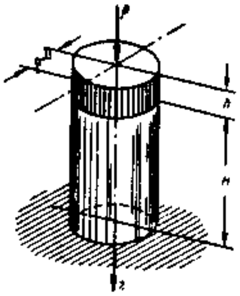

FIGURE 118.

The plate deflection must remain finite at the origin ($\xi = 0$). Since the function $f_0(\xi)$ remains finite when $\xi \to 0$, while $g_0(\xi)$ tends to infinity, the coefficient of $g_0(\xi)$ must be zero: $C_4 = 0$.

It therefore follows that:

$$W = C_3 f_0(\xi). \tag{5.4}$$

To determine the constant C_3, consider the equilibrium condition of an infinitesimal cylinder ($\rho \to 0$) cut out of the plate and the elastic foundation at the origin of coordinates (Figure 118). Applying the variational principle, we obtain:

$$\int_0^{2\pi} N_\rho \rho \, d\theta + P = 0, \tag{5.5}$$

where N_ρ = generalized shearing force, given by (1.5).

The generalized equilibrium condition (5.5) could also have been written in the form:

$$\int_0^{2\pi} Q_\rho \rho d\theta + P = 0, \tag{5.6}$$

since, for reasons of symmetry, we have:

at $\rho = 0$ $$\frac{dW}{d\rho} = 0. \tag{5.7}$$

The last equation (2.24) yields for the shearing force:

$$Q_\rho = -\frac{D}{L_0^3} C_3 Q_3(\xi). \tag{5.8}$$

Substituting (5.8) in (5.6) and integrating, we obtain:

$$C_3 = \frac{PL_0^2}{4D \sin 2\varphi}. \tag{5.9}$$

From (5.4) and (2.24), we finally obtain the displacements, moments, and forces for an infinite plate:

$$\left.\begin{aligned}
W &= \frac{PL_0^2}{4D\sin 2\varphi} f_0(\xi),\\
\frac{dW}{d\rho} &= -\frac{PL_0}{4D\sin 2\varphi}\theta_3(\xi),\\
M_\rho &= \frac{P}{4\sin 2\varphi}[M_3(\xi)-(1-\mu)\overline{M}_3(\xi)],\\
M_\theta &= \frac{P}{4\sin 2\varphi}[\mu M_3(\xi)+(1-\mu)\overline{M}_3(\xi)],\\
Q_\rho &= -\frac{P}{4L_0\sin 2\varphi}Q_3(\xi),
\end{aligned}\right\}\tag{5.10}$$

The functions θ_3, M_3, $\overline{M}_3$, Q_3 are given by (2.25) through (2.28), or, in expanded form, by the following series:

$$\left.\begin{aligned}
\theta_3(\xi) &= \left(1-\frac{2\varphi}{\pi}\right)\sum_{m=0}^{\infty}\frac{(-1)^m}{m!\,(m+1)!}\left(\frac{\xi}{2}\right)^{2m+1}\cos 2(m+1)\varphi -\\
&\quad -\frac{2}{\pi}\left(\ln\frac{\xi}{2}+c\right)\sum_{m=0}^{\infty}\frac{(-1)^m}{m!\,(m+1)!}\left(\frac{\xi}{2}\right)^{2m+1}\sin 2(m+1)\varphi +\\
&\quad +\frac{\xi}{2\pi}\sin 2\varphi+\frac{1}{\pi}\sum_{m=1}^{\infty}\frac{(-1)^m}{m!\,(m+1)!}\times\\
&\quad \times\left(\frac{\xi}{2}\right)^{2m+1}\sin 2(m+1)\varphi\left(1+\frac{1}{2}+\ldots+\frac{1}{m}\right),\\
M_3(\xi) &= \left(1-\frac{2\varphi}{\pi}\right)\sum_{m=0}^{\infty}\frac{(-1)^m}{(m!)^2}\left(\frac{\xi}{2}\right)^{2m}\sin 2(m+1)\varphi -\\
&\quad -\frac{2}{\pi}\left(\ln\frac{\xi}{2}+c\right)\sum_{m=0}^{\infty}\frac{(-1)^m}{(m!)^2}\left(\frac{\xi}{2}\right)^{2m}\sin 2(m+1)\varphi -\\
&\quad -\frac{2}{\pi}\sum_{m=1}^{\infty}\frac{(-1)^m}{(m!)^2}\left(\frac{\xi}{2}\right)^{2m}\sin 2(m+1)\varphi\left(1+\frac{1}{2}+\right.\\
&\quad \left.+\frac{1}{3}+\ldots+\frac{1}{m}\right),\\
\overline{M}_3(\xi) &= \left(1-\frac{2\varphi}{\pi}\right)\sum_{m=0}^{\infty}\frac{(-1)^m}{m!\,(m+1)!}\left(\frac{\xi}{2}\right)^{2m}\cos 2(m+1)\varphi -\\
&\quad -\frac{2}{\pi}\left(\ln\frac{\xi}{2}+c\right)\sum_{m=0}^{\infty}\frac{(-1)^m}{m!\,(m+1)!}\left(\frac{\xi}{2}\right)^{2m}\sin 2(m+1)\varphi +\\
&\quad +\frac{\sin 2\varphi}{\pi}+\frac{1}{\pi}\sum_{m=1}^{\infty}\frac{(-1)^m}{m!\,(m+1)!}\times\\
&\quad \times\left(\frac{\xi}{2}\right)^{2m}\sin 2(m+1)\varphi\left(1+\frac{1}{2}+\ldots+\frac{1}{m}\right),\\
Q_3(\xi) &= \left(1-\frac{2\varphi}{\pi}\right)\sum_{m=0}^{\infty}\frac{(-1)^m}{(m!)^2}\left(\frac{\xi}{2}\right)^{2m+1}\cos 2(m+2)\varphi -\\
&\quad -\frac{2}{\pi}\left(\ln\frac{\xi}{2}+c\right)\sum_{m=0}^{\infty}\frac{(-1)^m}{m!\,(m+1)!}\left(\frac{\xi}{2}\right)^{2m+1}\sin 2(m+2)\varphi -\\
&\quad -\frac{2}{\pi\xi}\sin 2\varphi-\frac{\xi}{2\pi}\sin 4\varphi+\frac{1}{\pi}\sum_{m=1}^{\infty}\frac{(-1)^m}{m!\,(m+1)!}\times\\
&\quad \times\left(\frac{\xi}{2}\right)^{2m+1}\sin 2(m+2)\varphi\left(1+\frac{1}{2}+\ldots+\frac{1}{m}\right).
\end{aligned}\right\}\tag{5.11}$$

Taking a finite number of terms in (5.11), it is possible to determine, with sufficient accuracy, the displacements, moments, and forces in the most highly loaded sections (for $\rho \to 0$).

At $\varphi = 45°$, i.e., if no shearing forces act in the elastic foundation, the solution obtained coincides with Hertz's solution for an infinite plate on an elastic Winkler foundation.

§ 6. ELASTIC PLATE OF FINITE DIMENSIONS

The general solution for a circular plate on an elastic foundation was given in section 2 of this chapter. We shall now give some examples which clarify the general theory.

For practical calculations, tables of Bessel functions of the first kind, of a complex argument, and tables of the functions:

$$\theta_1(\xi),\ \theta_2(\xi),\ M_1(\xi),\ M_2(\xi),\ \overline{M}_1(\xi),\ \overline{M}_2(\xi),$$

which define the states of strain and stress of the plate, are given in Table 12 of the appendix. The tables have been compiled for $45° \leqslant \varphi \leqslant 65°$, and give the various functions for:

$$\xi = \frac{\rho}{L_0} = 0;\ 0{,}05;\ 0{,}10;\ 0{,}15;\ \ldots;\ 1{,}0.$$

When the dimensions and physical properties of the plates are such that the argument ξ of the corresponding functions is not contained in the tables, reference has to be made to /4/ and /86/. After the Bessel functions have been determined, the functions:

$$\theta_1(\xi),\ \theta_2(\xi),\ \ldots,\ \overline{M}_2(\xi),$$

are obtained from (2.25) through (2.28).

In addition, series defining all the required magnitudes are given in the examples below in order to permit calculations for:

$$\xi_R = \frac{R}{L_0} > 1{,}0$$

without having recourse to tables.

1. Circular plate under the action of a uniformly distributed load.

Consider a circular plate of radius R, subjected to a uniformly distributed load p, lying on an elastic single-layer foundation (Figure 119).

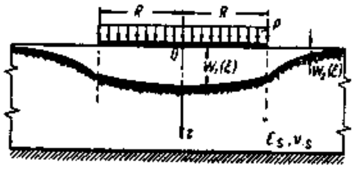

FIGURE 119.

The differential equation of bending is:

$$\nabla_\xi^2\nabla_\xi^2 W_1 - 2r_0^2\nabla_\xi^2 W_1 + W_1 = \frac{pL_0^4}{D}, \tag{6.1}$$

where $\xi = \frac{\rho}{L_0}$, and

$$r_0^2 = \frac{tL_0^2}{D}, \quad L_0 = \sqrt[4]{\frac{D}{k}}. \tag{6.2}$$

The following homogeneous differential equation holds true beyond the plate edges:

$$\nabla_\xi^2 W_2 - \alpha_0^2 W_2 = 0, \tag{6.3}$$

where

$$\alpha_0^2 = \alpha^2 L_0^2 = \frac{kL_0^2}{2t} \tag{6.4}$$

and

$$\nabla_\xi^2 = \frac{d^2}{d\xi^2} + \frac{1}{\xi}\frac{d}{d\xi}. \tag{6.5}$$

The general solution of (6.1) and (6.3) is:

$$W_1 = C_1 u_0(\xi) + C_2 v_0(\xi) + C_3 f_0(\xi) + C_4 g_0(\xi) + \frac{p}{k}, \tag{6.6}$$

$$W_2 = C_5 I_0(\alpha_0\xi) + C_6 K_0(\alpha_0\xi), \tag{6.7}$$

where $\frac{p}{k}$ = particular integral of the nonhomogeneous differential equation (6.1); $I_0(\alpha_0\xi)$, $K_0(\alpha_0\xi)$ = modified zero-order Bessel functions of the first and second kind, of the argument $\alpha_0\xi$; $C_1, \ldots, C_6$ = integration constants.

To determine these six integration constants, the following six independent boundary conditions are used:

at $\rho = 0 \quad (\xi = 0)$:

$$\frac{dW_1}{d\rho} = 0, \quad \int_0^{2\pi} Q_\rho \rho \, d\theta = 0; \tag{6.8}$$

at $\rho = R \quad \left(\xi = \frac{R}{L_0}\right)$:

$$\left.\begin{aligned} &M_\rho = 0,\\ &Q_\rho = 2t\left(\frac{dW_2}{d\rho} - \frac{dW_1}{d\rho}\right), \quad W_1(R) = W_2(R); \end{aligned}\right\} \tag{6.9}$$

at $\rho \to \infty \quad (\xi \to \infty)$:

$$W_2(\rho) = 0. \tag{6.10}$$

Conditions (6.8) state that the slope and the shearing force vanish at the plate center; condition (6.10), states that the vertical displacements of the elastic foundation vanish at infinity. Expressions (6.9) are the boundary conditions at the free plate edge $\rho = R$; the second condition (6.9) accounts for the effect of the free foundation beyond the plate edges on the stresses in the plate (cf. (1.8)).

Recalling the considerations which led to (3.4), (5.4), [and (5.9)], we obtain:

$$C_3 = C_4 = C_5 = 0, \tag{6.11}$$

The plate deflections W_1 and the vertical displacements W_2 of the free foundation surface are then:

$$W_1 = C_1 u_0(\xi) + C_2 v_0(\xi) + \frac{p}{k}. \tag{6.12}$$

$$W_2 = C_6 K_0(\alpha_0 \xi). \tag{6.13}$$

From the third condition (6.9) we obtain:

$$C_6 = \frac{C_1 u_0(\xi_R) + C_2 v_0(\xi_R) + \frac{p}{k}}{K_0(\alpha_0 \xi_R)}, \tag{6.14}$$

where $\xi_R = \frac{R}{L_0}$.

The remaining two constants C_1 and C_2 can be determined from the first two conditions (6.9), rewritten with the aid of (1.4) in the following form:

$$\left.\begin{aligned} \nabla_\xi^2 W_1 - \frac{1-\mu}{\xi}\frac{dW_1}{d\xi} &= 0, \\ \frac{d}{d\xi}\nabla_\xi^2 W_1 &= -\frac{2tL_0^2}{D}\left[\frac{dW_2}{d\xi} - \frac{dW_1}{d\xi}\right]. \end{aligned}\right\} \tag{6.15}$$

Substituting (6.12) and (6.13) in (6.15) and using the rules of differentiation of cylindrical functions, we obtain:

$$\left.\begin{aligned} m_1 C_1 + m_2 C_2 &= 0, \\ n_1 C_1 + n_2 C_2 &= G_p, \end{aligned}\right\} \tag{6.16}$$

where:

$$\left.\begin{aligned} m_1 &= M_1(\xi_R) - (1-\mu)\overline{M}_1(\xi_R), \\ m_2 &= M_2(\xi_R) - (1-\mu)\overline{M}_2(\xi_R), \\ n_1 &= Q_1(\xi_R) + \frac{\theta_1(\xi_R)}{\alpha_0^2} - u_0(\xi_R)\frac{K_1(\alpha_0\xi_R)}{\alpha_0 K_0(\alpha_0\xi_R)}, \\ n_2 &= Q_2(\xi_R) + \frac{\theta_2(\xi_R)}{\alpha_0^2} - v_0(\xi_R)\frac{K_1(\alpha_0\xi_R)}{\alpha_0 K_0(\alpha\xi_R)}, \\ G_p &= \frac{p}{k}\frac{K_1(\alpha_0\xi_R)}{\alpha_0 K_0(\alpha_0\ _R)}. \end{aligned}\right\} \tag{6.17}$$

The solution of system (6.16) is:

$$\left.\begin{aligned} C_1 &= -\frac{G_p m_2}{m_1 n_2 - m_2 n_1}, \\ C_2 &= \frac{G_p m_1}{m_1 n_2 - m_2 n_1}. \end{aligned}\right\} \tag{6.18}$$

The displacements, moments, and forces in the circular plate are then:

$$\left.\begin{aligned}
W_1 &= C_1 u_0(\xi) + C_2 v_0(\xi) + \frac{p}{R},\\
\frac{dW_1}{d\rho} &= -\frac{1}{L_0}[C_1\theta_1(\xi) + C_2\theta_2(\xi)],\\
M_\rho &= \frac{D}{L_0^2}[C_1 L_1(\xi) + C_2 L_2(\xi)],\\
M_\theta &= \frac{D}{L_0^2}[C_1 \overline{L}_1(\xi) + C_2 \overline{L}_2(\xi)],\\
Q_\rho &= -\frac{D}{L_0^3}[C_1 Q_1(\xi) + C_2 Q_2(\xi)].
\end{aligned}\right\} \tag{6.19}$$

where

$$\left.\begin{aligned}
u_0(\xi) &= \sum_{m=0}^{\infty} \frac{(-1)^m}{(m!)^2}\left(\frac{\xi}{2}\right)^{2m} \cos 2m\varphi,\\
v_0(\xi) &= \sum_{m=0}^{\infty} \frac{(-1)^m}{(m!)^2}\left(\frac{\xi}{2}\right)^{2m} \sin 2m\varphi,\\
\theta_1(\xi) &= \sum_{m=0}^{\infty} \frac{(-1)^m}{(m!)(m+1)!}\left(\frac{\xi}{2}\right)^{2m+1} \cos 2(m+1)\varphi,\\
\theta_2(\xi) &= \sum_{m=0}^{\infty} \frac{(-1)^m}{m!(m+1)!}\left(\frac{\xi}{2}\right)^{2m+1} \sin 2(m+1)\varphi,\\
M_1(\xi) &= \sum_{m=0}^{\infty} \frac{(-1)_m}{(m!)^2}\left(\frac{\xi}{2}\right)^{2m} \cos 2(m+1)\varphi,\\
M_2(\xi) &= \sum_{m=0}^{\infty} \frac{(-1)^m}{(m!)^2}\left(\frac{\xi}{2}\right)^{2m} \sin 2(m+1)\varphi,\\
\overline{M}_1(\xi) &= \frac{1}{2}\sum_{m=0}^{\infty} \frac{(-1)^m}{m!(m+1)!}\left(\frac{\xi}{2}\right)^{2m} \cos 2(m+1)\varphi,\\
\overline{M}_2(\xi) &= \frac{1}{2}\sum_{m=0}^{\infty} \frac{(-1)^m}{m!(m+1)!}\left(\frac{\xi}{2}\right)^{2m} \sin 2(m+1)\varphi,\\
Q_1(\xi) &= \sum_{m=0}^{\infty} \frac{(-1)^m}{m!(m+1)!}\left(\frac{\xi}{2}\right)^{2m+1} \cos 2(m+2)\varphi,\\
Q_2(\xi) &= \sum_{m=0}^{\infty} \frac{(-1)^m}{m!(m+1)!}\left(\frac{\xi}{2}\right)^{2m+1} \sin 2(m+2)\varphi,\\
L_1(\xi) &= M_1(\xi) - (1-\mu)\overline{M}_1(\xi),\\
L_2(\xi) &= M_2(\xi) - (1-\mu)\overline{M}_2(\xi),\\
\overline{L}_1(\xi) &= \mu M_1(\xi) + (1-\mu)\overline{M}_1(\xi),\\
\overline{L}_2(\xi) &= \mu M_2(\xi) + (1-\mu)\overline{M}_2(\xi).
\end{aligned}\right\} \tag{6.20}$$

2. Circular plate under the action of a uniformly distributed edge load

If a circular plate is subjected to the action of an edge load P_4(Figure 120), expression (6.1) reduces to a homogeneous differential equation. The general solution of the problem considered is therefore:

$$\left.\begin{aligned}
W_1 &= C_1 u_0(\xi) + C_2 v_0(\xi) + C_3 f_0(\xi) + C_4 g_0(\xi),\\
W_2 &= C_5 I_0(\alpha_0\xi) + C_6 K_0(\alpha_0\xi).
\end{aligned}\right\} \tag{6.21}$$

The boundary conditions are given, as in the first example, by (6.8) through (6.10), only the second condition (6.9) being replaced by:

$$\rho = R \qquad Q_\rho = 2t\left(\frac{dW_2}{d\rho} - \frac{dW_1}{d\rho}\right) + P_k. \tag{6.22}$$

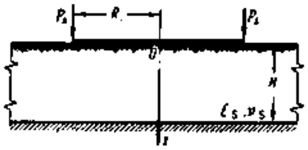

FIGURE 120.

By analogy with (6.11) and (6.14), we obtain:

$$C_3 = C_4 = C_5 = 0, \qquad C_6 = \frac{C_1 u_0(\xi_R) + C_2 v_0(\xi_R)}{K_0(\alpha_0 \xi_R)}. \tag{6.23}$$

The plate deflections W_1 and the vertical displacements W_2 of the free foundation surface ($\rho > R$) are then:

$$W_1 = C_1 u_0(\xi) + C_2 v_0(\xi), \qquad W_2 = C_6 K_0(\alpha_0 \xi). \tag{6.24}$$

From (6.22) and the first condition (6.9), we obtain:

$$\left.\begin{aligned} \nabla_\xi^2 W_1 - \frac{1-\mu}{\xi}\frac{dW_1}{d\xi} &= 0, \\ \frac{d}{d\xi}\nabla_\xi^2 W_1 + \frac{2tL_0^2}{D}\left(\frac{dW_2}{d\xi} - \frac{dW_1}{d\xi}\right) + \frac{P_k L_0^3}{D} &= 0. \end{aligned}\right\} \tag{6.25}$$

Substitution of (6.24) in (6.25) leads to a system of two algebraic equations in the constants C_1 and C_2:

$$m_1 C_1 + m_2 C_2 = 0, \qquad n_1 C_1 + n_2 C_2 = G_{P_k}, \tag{6.26}$$

where m_1, m_2, n_1, n_2 are determined from (6.17), while

$$G_{P_k} = -\frac{P_k L_0^3}{D}. \tag{6.27}$$

The integration constants C_1 and C_2 are thus again given by (6.18), with G_p replaced by G_{P_k}. The plate deflections are determined from the first equation (6.24), while the slopes, bending moments, and shearing forces are given by (6.19).

3. Circular plate under the action of moments distributed along the edge

Consider the plate shown in Figure 121. It can be seen that all the results obtained before also apply in this case. In fact, the general solution for $0 \leqslant \xi \leqslant \xi_R$ and $\xi_R \leqslant \xi < \infty$ can be written in the form (6.21), whence, as above:

$$\left.\begin{aligned} &C_3 = C_4 = C_5 = 0, \\ &C_6 = \frac{C_1 u_0(\xi_R) + C_2 v_0(\xi_R)}{K_0(\alpha_0 \xi_R)}. \end{aligned}\right\} \tag{6.28}$$

The integrations constants C_1 and C_2 are determined from the boundary conditions:

$$\rho = R \ (\xi = \xi_R) \quad M = M_k, \quad Q = 2t\left(\frac{dW_2}{d\rho} - \frac{dW_1}{d\rho}\right). \tag{6.29}$$

From (1.4) and (6.21), taking (6.28) into account, we obtain:

$$m_1 C_1 + m_2 C_2 = G_M, \quad n_1 C_1 + n_2 C_2 = 0. \tag{6.30}$$

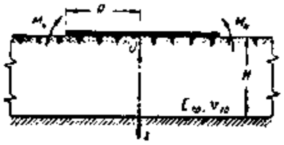

Рис. 121.

The coefficients in (6.3) are obtained, as before, from (6.17), while:

$$G_M = -\frac{M_k L_0^2}{D}. \tag{6.31}$$

Thus, the constants C_1 and C_2 are:

$$C_1 = \frac{m_2 G_M}{m_1 n_2 - n_1 m_2}, \quad C_2 = -\frac{n_1 G_M}{m_1 n_2 - n_1 m_2}. \tag{6.32}$$

Chapter V

AXISYMMETRICAL DEFORMATION OF A SHALLOW SPHERICAL SHELL ON A SINGLE-LAYER ELASTIC FOUNDATION

§ 1. BASIC DIFFERENTIAL EQUATIONS OF THE THEORY OF SHALLOW SPHERICAL SHELLS

1

A shallow shell is a thin-walled three-dimensional structure whose height is small in comparison with its dimensions in plan. A shell is called shallow if the ratio of its height to its smallest dimension in plan l_{min} is less than $^1/_5$.

Since for $\frac{f}{l_{min}} < \frac{1}{5}$ the shell curvatures are very small, we can apply Euclidian plane geometry to the middle surface of a shallow shell. This assumption is equivalent to replacing the first fundamental form [also known as ground form] of the shallow-shell surface by the corresponding fundamental form for a plane. This also means that the Gauss curvature:

$$K = k_1 k_2 = \frac{1}{R_1 R_2},$$

is very small for shallow shells and can be approximated to zero.

An additional assumption, made when considering the general equations of equilibrium of a shallow shell, is that only the principal moment terms, which do not contain as factors surface curvatures and curvature derivatives, need be taken into account. All other moment terms are neglected as being very small and having an insignificant effect on the internal forces and bending moments of the shell*.

2

Consider a shallow shell having the form of a spherical surface of radius R (Figure 122). Let ρ and θ be the polar coordinates measured in the plane of the shell base. It will be assumed that the projection of the shell apex on this plane coincides with the origin of the ρ, θ coordinate system. On the strength of the geometrical hypotheses underlying the general theory of shallow shells, all points of the middle surface of the shell will be defined by the coordinates ρ and θ.

---

* The general theory of shallow shells was first expounded by V. Z. Vlasov. For a detailed treatment of this theory, see /8/.

Let the shell considered be subjected only to the action of a normal load Z, positive when directed along the outer normal (Figure 122). In this case all statical and geometrical equations characterizing the states of stress and strain of the shallow spherical shell can be reduced to the following system of two differential equations:

$$\left.\begin{aligned} &\frac{R}{Eh}\nabla^2\nabla^2\Phi - \nabla^2 w = 0,\\ &\frac{1}{R}\nabla^2\Phi + D\nabla^2\nabla^2 w - Z = 0,\end{aligned}\right\} \qquad (1.1)$$

where $w = w(\rho, \theta)$ = radial displacement of shell (positive if directed along the outer normal), and $\Phi = \Phi(\rho, \theta)$ = stress function determining membrane forces acting in shell:

$$\left.\begin{aligned} N_\rho &= \frac{1}{\rho}\frac{\partial\Phi}{\partial\rho} + \frac{1}{\rho^2}\frac{\partial^2\Phi}{\partial\theta^2},\\ N_\theta &= \frac{\partial^2\Phi}{\partial\rho^2},\\ S &= -\frac{1}{\rho}\frac{\partial^2\Phi}{\partial\rho\,\partial\theta} + \frac{1}{\rho^2}\frac{\partial\Phi}{\partial\theta}.\end{aligned}\right\} \qquad (1.2)$$

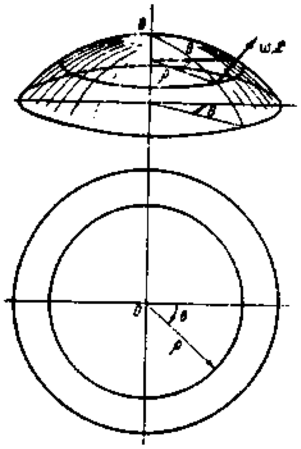

FIGURE 122.

The symbol ∇^2 in (1.1) denotes the second-order differential operator:

$$\nabla^2 = \frac{1}{\rho}\left[\frac{\partial}{\partial\rho}\left(\rho\frac{\partial}{\partial\rho}\right) + \frac{1}{\rho}\frac{\partial^2}{\partial\theta^2}\right]. \qquad (1.3)$$

The magnitudes h and D represent the shell thickness and its flexural rigidity respectively:

$$D = \frac{Eh}{12(1-\mu^2)}. \qquad (1.4)$$

The first equation (1.1) has a geometrical meaning: it expresses the condition of continuity of the deformations; the second equation has a statical meaning: it characterizes the equilibrium condition of the shell in the radial direction.

We introduce the scalar function $F=F(\rho,\theta)$, which satisfies the following relationships:

$$\left.\begin{aligned} w &= \nabla^2\nabla^2 F, \\ \Phi &= \frac{Eh}{R}\nabla^2 F, \end{aligned}\right\} \tag{1.5}$$

The first equation (1.1) is then satisfied identically. Substituting (1.5) in the second equation (1.1) yields:

$$D\nabla^2\nabla^2\nabla^2\nabla^2 F + \frac{Eh}{R^2}\nabla^2\nabla^2 F - Z = 0, \tag{1.6}$$

or

$$D\nabla^2\nabla^2 w + \frac{Eh}{R^2}w - Z = 0. \tag{1.7}$$

The radial displacements w of a spherical shell are thus determined by a fourth-order differential equation having the same form as the equation of bending of a plate on an elastic Winkler foundation whose foundation modulus is

$$k = \frac{Eh}{R^2}.$$

Hence, with respect to the strains due to the deflections w, complete analogy exists between a shallow spherical shell and a circular plate on an elastic foundation, suitably supported along the edge. Exactly as in the case of bending of a circular plate, the additional curvatures $\varkappa_\rho, \varkappa_\theta$ and the twist τ are:

$$\left.\begin{aligned} \varkappa_\rho &= \frac{\partial^2 w}{\partial\rho^2}, \\ \varkappa_\theta &= \frac{1}{\rho^2}\frac{\partial^2 w}{\partial\theta^2} + \frac{1}{\rho}\frac{\partial w}{\partial\rho}, \\ \tau &= \frac{1}{\rho}\frac{\partial^2 w}{\partial\rho\,\partial\theta} - \frac{1}{\rho^2}\frac{\partial w}{\partial\theta}. \end{aligned}\right| \tag{1.8}$$

3

The internal forces and moments acting in sections $\rho = \text{const}$, $\theta = \text{const}$, of a shallow spherical shell can be divided into two groups: the normal (membrane) forces N_ρ, N_θ, S, corresponding to deformation without bending, and the bending moments M_ρ, M_θ, torques H, and shearing forces Q_ρ, Q_θ due to bending. The positive directions of these forces and moments for surfaces with positive outer normals are shown in Figure 123.

As already mentioned, the first group of forces is determined by the stress function $\Phi = \Phi(\rho,\theta)$ with the aid of (1.2). The second group is determined by the displacement function $w=w(\rho,\theta)$. By virtue of the analogy noted above, these forces and moments are calculated in the same way as in the case of bending of a circular plate:

$$\left.\begin{aligned} M_\rho &= -D(\varkappa_\rho + \mu\varkappa_\theta), \\ M_\theta &= -D(\varkappa_\theta + \mu\varkappa_\rho), \\ H &= D(1-\mu)\tau, \end{aligned}\right\} \tag{1.9}$$

$$\left.\begin{aligned} Q_\rho &= -D\frac{\partial}{\partial\rho}\nabla^2 w, \\ Q_\theta &= -D\frac{1}{\rho}\frac{\partial}{\partial\theta}\nabla^2 w, \end{aligned}\right\} \tag{1.10}$$

where $\varkappa_\rho, \varkappa_\theta, \tau$ are defined by (1.8), and ∇^2 by (1.3).

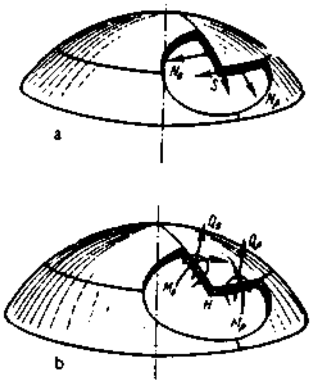

FIGURE 123.

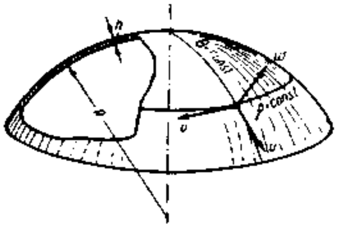

FIGURE 124.

We determine the tangential displacements $u(\rho, \theta)$ and $v(\rho, \theta)$ in the directions of the tangents to the curves $\rho = \text{const}$, $\theta = \text{const}$ respectively (Figure 124), from the relationships between the membrane forces N_ρ, N_θ, S and the strains:

$$N_\rho = \frac{Eh}{(1-\mu^2)}(\varepsilon_\rho + \mu\varepsilon_\theta), \quad N_\theta = \frac{Eh}{(1-\mu^2)}(\varepsilon\ + \mu\varepsilon_\rho), \quad S = \frac{Eh}{2(1+\mu)}\omega, \tag{1.11}$$

where $\varepsilon_\rho, \varepsilon_\theta, \omega$ are the tensile (compressive) and shearing strain respectively, determined by the displacements u, v, and w as follows:

$$\left.\begin{aligned} \varepsilon_\rho &= \frac{\partial u}{\partial\rho} + \frac{w}{R}, \\ \varepsilon_\theta &= \frac{1}{\rho}\frac{\partial v}{\partial\theta} + \frac{u}{\rho} + \frac{w}{R}, \\ \omega &= \frac{1}{\rho}\frac{\partial u}{\partial\theta} + \frac{\partial v}{\partial\rho} - \frac{v}{R}. \end{aligned}\right\} \tag{1.12}$$

When the stress function Φ and the displacement function w have been determined from (1.1), and then $\varepsilon_\rho, \varepsilon_\theta$, and w from (1.2) and (1.11), u and v can be found from (1.12).

§ 2. DIFFERENTIAL EQUATIONS OF A SPHERICAL SHELL ON AN ELASTIC SINGLE-LAYER FOUNDATION

Let a shallow spherical shell lie on an elastic foundation whose properties are described by the differential equation:

$$2t\nabla^2 w - kw + q = 0, \tag{2.1}$$

where ∇^2 is defined by (1.3), k and t are the generalized characteristics of the elastic foundation, and q is the load per unit area, acting on the foundation.

Since the radial displacements w of the shell and of the elastic foundation are equal along the entire area of contact (Figure 125), (1.7) and (2.1) can be considered simultaneously:

$$D\nabla^2\nabla^2 w + \frac{Eh}{R^2} w - Z = 0, \quad 2t\nabla^2 w - kw + q = 0. \tag{2.2}$$

The external load on the shell consists of the known forces p and the foundation reactions q [all referred to unit area]:

$$Z = p - q; \tag{2.3}$$

eliminating q from (2.2), we obtain:

$$D\nabla^2\nabla^2 w - 2t\nabla^2 w + \left(k + \frac{Eh}{R^2}\right) w = p. \tag{2.4}$$

This equation has the same form as the equation of bending of a thin plate on a single-layer foundation (cf. for instance (1.1) of Chapter IV), differing from it only in the coefficient of w. This coefficient is larger by Eh/R^2 than the corresponding coefficient in (1.1) of Chapter IV.

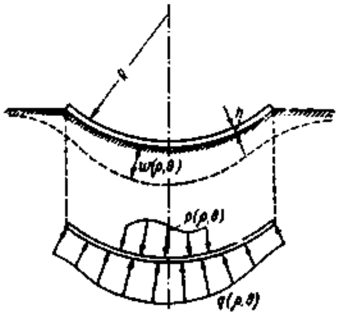

FIGURE 125.

The problem of bending of a spherical shell on a single-layer elastic foundation is thus similar to the corresponding problem of a circular plate, discussed in Chapter IV.

To determine the stresses and displacements when the membrane problem is considered (in which bending stresses are neglected), we use the first equation (1.1):

$$\frac{R}{Eh}\nabla^2\nabla^2\Phi = \nabla^2 w. \tag{2.5}$$

This is a nonhomogeneous biharmonic equation, the function w being assumed known (it can be determined from (2.4)). Having determined the function Φ from (2.5) and the corresponding boundary conditions, the normal forces, moments, strains, and displacements of the spherical shell can be found from (1.2), (1.11), (1.12).

If the problem is axisymmetrical, all derivatives with respect to θ vanish in the equations determining the states of stress and strain of the shell. The Laplacian then reduces to:

$$\nabla^2 = \frac{d^2}{d\rho^2} + \frac{1}{\rho}\frac{d}{d\rho}, \tag{2.6}$$

while (1.9) and (1.10) become (taking (1.8) into account):

$$\left.\begin{aligned} M_\rho &= -D\left[\nabla^2 W - \frac{(1-\mu)}{\rho}\frac{dW}{d\rho}\right], \\ M_\theta &= -D\left[\mu\nabla^2 W + \frac{(1-\mu)}{\rho}\frac{dW}{d\rho}\right], \\ Q_\rho &= -D\frac{d}{d\rho}\nabla^2 W, \\ Q_\theta &= H = 0. \end{aligned}\right\} \tag{2.7}$$

Equation (1.2) and (1.12) respectively take the form:

$$N_\rho = \frac{1}{\rho}\frac{d\Phi}{d\rho}, \qquad N_\theta = \frac{d^2\Phi}{d\rho^2}, \qquad S = 0; \tag{2.8}$$

$$\varepsilon_\rho = \frac{du}{d\rho} + \frac{W}{R}, \qquad \varepsilon_\theta = \frac{u}{\rho} + \frac{W}{R} \qquad \omega = 0, \tag{2.9}$$

where $W = W(\rho)$, $\Phi = \Phi(\rho)$, depend on ρ only.

§ 3. GENERAL SOLUTION FOR AXISYMMETRICAL DEFORMATIONS

1. Bending of shells

Exactly as in bending of a plate, we replace ρ by the dimensionless coordinate $\xi = \frac{\rho}{L_0}$, where

$$L_0 = \sqrt[4]{\frac{DR^2}{Eh + kR^2}} \tag{3.1}$$

Equation (2.4) then becomes:

$$\nabla_\xi^2\nabla_\xi^2 W - 2r^2\nabla_\xi^2 W + W = \frac{pL_0^4}{D}, \tag{3.2}$$

where

$$r^2 = \frac{tL_0^2}{D}, \tag{3.3}$$

and

$$\nabla_\xi^2 = \frac{d^2}{d\xi^2} + \frac{1}{\xi}\frac{d}{d\xi} \qquad (3.4)$$

By analogy with the integral of (2.2) of Chapter IV, the general integral of (3.2) can be presented in the form:

$$W = C_1 u_0(\xi) + C_2 v_0(\xi) + C_3 f_0(\xi) + C_4 g_0(\xi) + W_p, \qquad (3.5)$$

where

$$u_0(\xi),\ v_0(\xi),\ f_0(\xi),\ g_0(\xi)$$

are respectively the real and imaginary parts of the zero-order Bessel and Hankel functions, and W_p is a particular integral of (3.2). On the basis of the general solution of (3.2), all statical and kinematic magnitudes referring to the state of bending stress of the shell are determined from (2.24) of Chapter IV, with L_0 defined by (3.1).

2. Deformation without bending of shells

We determine the stress function $\Phi = \Phi(\rho)$ with the aid of (2.5). Replacing the variable ρ by the dimensionless coordinate $\xi = \rho / L_0$, where L_0 is defined by (3.1), (2.5) becomes:

$$\nabla_\xi^2 \nabla_\xi^2 \Phi = \frac{EhL_0^2}{R} \nabla_\xi^2 W. \qquad (3.6)$$

The function $W = W(\xi)$ is defined by (3.5), and the Laplacian by (3.4).

The general solution of (3.6) is then:

$$\Phi = \frac{EhL_0^2}{R}(\Phi_0 + \Phi_W), \qquad (3.7)$$

where $\Phi_0 = \Phi_0(\xi)$ is the general solution of the homogeneous biharmonic equation corresponding to (3.6) and $\Phi_W = \Phi_W(\xi)$ is a particular integral of the nonhomogeneous equation:

$$\nabla_\xi^2 \nabla_\xi^2 \Phi_W = \nabla_\xi^2 W. \qquad (3.8)$$

The solution of the homogeneous biharmonic equation is for the axi-symmetrical case is:

$$\Phi_0 = C_5 + C_6 \xi^2 + C_7 \xi^2 \ln \xi + C_8 \ln \xi, \qquad (3.9)$$

where C_5, C_6, C_7, C_8 are constants.

The particular integral of the nonhomogeneous biharmonic equation (3.8) is:

$$\Phi_W = -[C_1 \varphi_1(\xi) + C_2 \varphi_2(\xi) + C_3 \varphi_3(\xi) + C_4 \varphi_4(\xi)] + \Phi_p, \qquad (3.10)$$

where Φ_p is a particular integral corresponding to the particular integral W_p of (3.5) and:

$$\left.\begin{aligned}\varphi_1(\xi) &= u_0(\xi)\cos 2\varphi + v_0(\xi)\sin 2\varphi,\\ \varphi_2(\xi) &= -u_0(\xi)\sin 2\varphi + v_0(\xi)\cos 2\varphi,\\ \varphi_3(\xi) &= f_0(\xi)\cos 2\varphi + g_0(\xi)\sin 2\varphi,\\ \varphi_4(\xi) &= -f_0(\xi)\sin 2\varphi + g_0(\xi)\cos 2\varphi.\end{aligned}\right\} \qquad (3.11)$$

Here as before:

$$\varphi = \arg(\sqrt{a}) = \frac{1}{2}\arg a,$$

where a is a complex number defined by (2.11) of Chapter IV in accordance with expressions (3.3) and (3.1) of this chapter.

It is easily seen by direct substitution that (3.10) does in fact satisfy the nonhomogeneous equation (3.8).

In accordance with (3.9) and (3.10), the general integral of (3.6) is therefore:

$$\begin{aligned}\Phi = \frac{EhL_0^2}{R}[&-C_1\varphi_1(\xi) - C_2\varphi_2(\xi) - C_3\varphi_3(\xi) - C_4\varphi_4(\xi) +\\ &+ C_5 + C_6\xi^2 + C_7\xi^2\ln\xi + C_8\ln\xi + \Phi_p].\end{aligned} \qquad (3.12)$$

Substituting this in (2.8) yields the following expressions for the normal forces:

$$\begin{aligned}N_\rho = \frac{Eh}{R}\Big[&C_1n_1(\xi) + C_2n_2(\xi) + C_3n_3(\xi) + C_4n_4(\xi) +\\ &+ 2C_6 + C_7(1 + 2\ln\xi) + C_8\frac{1}{\xi^2} + \frac{1}{\xi}\frac{d\Phi_p}{d\xi}\Big],\end{aligned} \qquad (3.13)$$

$$\begin{aligned}N_\theta = \frac{Eh}{R}\Big\{&C_1[u_0(\xi) - n_1(\xi)] + C_2[v_0(\xi) - n_2(\xi)] +\\ &+ C_3[f_0(\xi) - n_3(\xi)] + C_4[g_0(\xi) - n_4(\xi)] + 2C_6 +\\ &+ C_7(3 + 2\ln\xi) - C_8\frac{1}{\xi^2} + \frac{d^2\Phi_p}{d\xi^2}\Big\},\end{aligned} \qquad (3.14)$$

where

$$\left.\begin{aligned}n_1(\xi) &= \frac{1}{\xi}[u_1(\xi)\cos\varphi + v_1(\xi)\sin\varphi],\\ n_2(\xi) &= \frac{1}{\xi}[-u_1(\xi)\sin\varphi + v_1(\xi)\cos\varphi],\\ n_3(\xi) &= \frac{1}{\xi}[f_1(\xi)\cos\varphi + g_1(\xi)\sin\varphi],\\ n_4(\xi) &= \frac{1}{\xi}[-f_1(\xi)\sin\varphi + g_1(\xi)\cos\varphi],\end{aligned}\right\} \qquad (3.15)$$

and u_1, v_1, f_1, g_1 are respectively the real and imaginary parts of the first-order Bessel and Hankel functions.

To obtain the deformations of the shell, we rewrite (2.9) in dimensionless coordinates:

$$\left.\begin{aligned}\varepsilon_\rho &= \frac{1}{L_0}\frac{du}{d\xi} + \frac{W}{R},\\ \varepsilon_\theta &= \frac{1}{L_0}\frac{u}{\xi} + \frac{W}{R}.\end{aligned}\right\} \qquad (3.16)$$

From these expressions and from (1.11) we obtain:

$$N_\rho + N_\theta = \frac{Eh}{1-\mu}(\varepsilon_\rho + \varepsilon_\theta) = \frac{Eh}{1-\mu}\left[\frac{1}{L_0}\left(\frac{du}{d\xi} + \frac{u}{\xi}\right) + \frac{2W}{R}\right]. \tag{3.17}$$

On the other hand, (2.8), written in dimensionless coordinates, and (3.7) lead to:

$$N_\rho + N_\theta = \frac{1}{L_0^2}\nabla_\xi^2\Phi = \frac{Eh}{R}\nabla_\xi^2(\Phi_0 + \Phi_W). \tag{3.18}$$

Since, by (3.8):

$$\nabla_\xi^2\Phi_W = W, \tag{3.19}$$

we can rewrite (3.18) in the form:

$$N_\rho + N_\theta = \frac{Eh}{R}(\nabla_\xi^2\Phi_0 + W). \tag{3.20}$$

Equating the right sides of (3.17) and (3.20) yields:

$$\frac{Eh}{R}[\nabla_\xi^2\Phi_0 + W] = \frac{Eh}{1-\mu}\left[\frac{1}{L_0}\left(\frac{du}{d\xi} + \frac{u}{\xi}\right) + \frac{2W}{R}\right], \tag{3.21}$$

or

$$\frac{du}{d\xi} + \frac{u}{\xi} = \frac{L_0}{R}[(1-\mu)\nabla_\xi^2\Phi_0 - (1+\mu)W]. \tag{3.22}$$

This equation establishes the relationship between the unknown tangential displacement u and the known functions Φ_0 and W. Substitution of (3.9) and (3.5) in (3.22) yields finally:

$$\begin{aligned}\frac{du}{d\xi} + \frac{u}{\xi} = \frac{L_0}{R}\{(1-\mu)[4C_6 + 4C_7(\ln\xi + 1)] - \\ - (1+\mu)[C_1u_0(\xi) + C_2v_0(\xi) + C_3f_0(\xi) + C_4g_0(\xi) + W_p]\}.\end{aligned} \tag{3.23}$$

The general solution of (3.23) is:

$$\begin{aligned}u = \frac{L_0}{R}\Big\{-(1+\mu)\Big[C_1\chi_1(\xi) + C_2\chi_2(\xi) + C_3\chi_3(\xi) + C_4\chi_4(\xi) + \\ + A_1\frac{1}{\xi}\Big] + (1-\mu)[2C_6\xi + C_7(2\xi\ln\xi + \xi)] + u_p\Big\},\end{aligned} \tag{3.24}$$

where

$$A_1\frac{L_0(1+\mu)}{R}\frac{1}{\xi}$$

is the integral of the homogeneous equation corresponding to (3.23), determined up to the constant factor $\frac{L_0(1+\mu)}{R}$; u_p is a particular integral corresponding to the function W_p; and:

$$\left.\begin{aligned}\chi_1(\xi) &= u_1(\xi)\cos\varphi + v_1(\xi)\sin\varphi, \\ \chi_2(\xi) &= -u_1(\xi)\sin\varphi + v_1(\xi)\cos\varphi, \\ \chi_3(\xi) &= f_1(\xi)\cos\varphi + g_1(\xi)\sin\varphi, \\ \chi_4(\xi) &= -f_1(\xi)\sin\varphi + g_1(\xi)\cos\varphi.\end{aligned}\right| \tag{3.25}$$

Due to the summation of (3.13) and (3.14), the constant C_8 no longer appears in (3.23). On the other hand, a new constant A_1 appears in (3.24) It is seen that these two constants are identical by substituting the solution:

$$u_0 = -\frac{L_0(1+\mu)}{R} A_1 \frac{1}{\xi} \tag{3.26}$$

into the following equation, obtained from (1.11) and (3.16):

$$N_\rho = \frac{Eh}{1-\mu^2}\left[\frac{1}{L_0}\left(\frac{du}{d\xi} + \mu\frac{u}{\xi}\right) + (1+\mu)\frac{W}{R}\right]. \tag{3.27}$$

The first term of this equation, which only depends on u_0, then becomes:

$$N_\rho^0 = \frac{Eh}{R} A_1 \frac{1}{\xi^2}. \tag{3.28}$$

Comparing this with [the coefficient of $\frac{1}{\xi^2}$] in (3.13) we find that:

$$A_1 = C_8.$$

The analysis of a shallow spherical shell thus reduces to determining eight integration constants whose number corresponds to the order of the initial system of differential equations (1.1). The first four (C_1, C_2, C_3, C_4) determine the bending of the shell, while the last four (C_5, C_6, C_7, C_8) determine its deformation without bending.

The constant C_5 does not influence the states of stress and strain of the shell, and it can therefore be disregarded. The logarithmic terms in (3.13), (3.14), (3.24), must also vanish, since the logarithm is multivalued for doubly-connected regions which the shell may form, and does not therefore fulfill the requirement of uniqueness. Hence, the constant C_7 must be zero.

There remain thus six unknown constants. To determine them, three boundary conditions are required for each edge of the shell. Of each group of three, two will determine the bending deformation, and one the deformation without bending.

The boundary conditions corresponding to the bending deformation can be given in displacements W, W' (geometrical conditions), in forces and moments M_ρ, Q_ρ (statical conditions), or partly in forces and partly in displacements (mixed conditions).

The boundary conditions corresponding to the deformation without bending are determined either from the tangential displacements u or the value of the normal forces N_ρ.

§ 4. SHALLOW SPHERICAL SHELL SUBJECTED TO A UNIFORMLY DISTRIBUTED LOAD

1

Consider a shallow spherical shell on an elastic foundation, subjected to a uniformly distributed load p (Figure 126). Let the shell edges be free, so that the elastic foundation can be deformed beyond the limits of the structure. In accordance with (3.5), the normal displacements of the shell are:

$$W_1 = C_1 u_0(\xi) + C_2 v_0(\xi) + C_3 f_0(\xi) + C_4 g_0(\xi) + W_p, \qquad (4.1)$$

where

$$W_p = \frac{pR^2}{Eh + kR^2}$$

is a particular integral of (3.2).

The following differential equation holds true for the region beyond the limits of the structure: [cf. (6.3) of Chapter IV]

$$\nabla_\xi^2 W_2 - \alpha_0^2 W_2 = 0, \qquad (4.2)$$

The general integral of this equation can be represented in the form:

$$W_2 = B_1 I_0(\alpha_0\xi) + B_2 K_0(\alpha_0\xi), \qquad (4.3)$$

where

$$\alpha_0^2 = \alpha^2 L_0^2 = \frac{kL_0^2}{2t}, \quad L_0 = \sqrt[4]{\frac{DR^2}{Eh + kR^2}}. \qquad (4.4)$$

Here, B_1, and B_2 are integration constants, while $I_0(\alpha_0\xi)$ and $K_0(\alpha_0\xi)$ are modified zero-order Bessel and Hankel functions of the argument $\alpha_0\xi$.

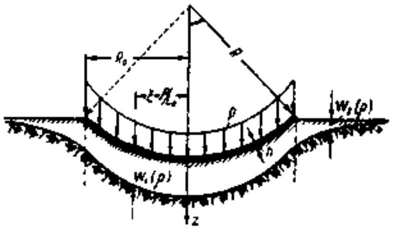

FIGURE 126.

The solution contains therefore six integration constants which are determined from the following boundary conditions (cf. the case of a circular plate, (6.8) through (6.10) of Chapter IV):

$$\left.\begin{array}{lll}
\text{at } \rho=0 \ (\xi=0): & \text{a) } \dfrac{dW_1}{d\rho} = 0, \ \text{b) } \displaystyle\int_0 Q_\rho \rho \, d\theta = 0; & \\
\text{at } \rho = R_0 \ \left(\xi = \dfrac{R_0}{L_0}\right): & \text{c) } M_\rho = 0, \Big| \ \text{d) } Q_\rho = 2t\left(\dfrac{dW_2}{d\rho} - \dfrac{dW_1}{d\rho}\right)\cos\varphi, & \\
 & \text{e) } W_1(R_0) = W_2(R_0); & \\
\text{at } \rho\to\infty \ (\xi\to\infty): & \text{f) } W_2(\rho) = 0. &
\end{array}\right\} \qquad (4.5)$$

The fourth boundary condition of (4.5) differs from the corresponding condition in (6.9) of Chapter IV by the coefficient $\cos\beta$, where β is half the central angle subtended by the shell. The reason for this is that the fictitious shearing force acting on the shell is equal to the projection of the fictitious shearing force acting on a circular plate, onto the normal to the middle surface of the shell at the edge.

Conditions a), b), and f) yield:

$$C_3 = C_4 = B_1 = 0, \tag{4.6}$$

so that the normal displacements of the shell are:

$$W_1 = C_1 u_0(\xi) + C_2 v_0(\xi) + \frac{pR^2}{Eh + kR^2}. \tag{4.7}$$

Condition e) yields:

$$B_2 = \frac{C_1 u_0(\xi_R) + C_2 v_0(\xi_R) + \dfrac{pR^2}{Eh + kR^2}}{K_0(\alpha_0 \xi_R)}, \tag{4.8}$$

where

$$\xi_R = \frac{R_0}{L_0}.$$

Substitution of expressions (2.7) for M_ρ and Q_ρ in conditions c) and d) yields:

$$\text{at} \quad \rho = R_0 \quad \left(\xi = \frac{R_0}{L_0}\right): \qquad \left.\begin{aligned} -\frac{D}{L_0^2}\left[\nabla_\xi^2 W_1 - \frac{1-\mu}{\xi}\frac{dW_1}{d\xi}\right] &= 0, \\ \frac{d}{d\xi}\nabla_\xi^2 W_1 + \frac{2tL_0^2}{D}\left[\frac{dW_2}{d\xi} - \frac{dW_1}{d\xi}\right]\cos\beta &= 0. \end{aligned}\right\} \tag{4.9}$$

Substitution of (4.3), (4.6), (4.7), and (4.8) leads to the following two simultaneous equations in C_1 and C_2:

$$a_1 C_1 + a_2 C_2 = 0, \quad b_1 C_1 + b_2 C_2 = G_p, \tag{4.10}$$

where

$$\left.\begin{aligned} a_1 &= M_1(\xi_R) - (1-\mu)\overline{M}_1(\xi_R), \\ a_2 &= M_2(\xi_R) - (1-\mu)\overline{M}_2(\xi_R), \\ b_1 &= \left\{Q_1(\xi_R) + \frac{2tL_0^2}{D}\left[\theta_1(\xi_R)\cos\beta - u_0(\xi_R)\frac{K_1(\alpha_0\xi_R)\,\alpha_0\cos\beta}{K_0(\alpha_0\xi_R)}\right]\right\}, \\ b_2 &= \left\{Q_2(\xi_R) + \frac{2tL_0^2}{D}\left[\theta_2(\xi_R)\cos\beta - v_0(\xi_R)\frac{K_1(\alpha_0\xi_R)\,\alpha_0\cos\beta}{K_0(\alpha_0\xi_R)}\right]\right\}, \end{aligned}\right\} \tag{4.11}$$

$$G_p = \frac{pR^2}{Eh + kR^2}\,\frac{K_1(\alpha_0\xi_R)}{K_0(\alpha_0\xi_R)}. \tag{4.12}$$

The functions:

$$M_1, \quad M_2, \quad \overline{M}_1, \quad \overline{M}_2, \quad Q_1, \quad Q_2, \quad \theta_1, \quad \theta_2$$

appearing in (4.11) are given by (2.25) through (2.28) or series (6.20) of Chapter IV (see also (6.16) and (6.17) of Chapter IV.)

The solution of (4.10) is;

$$C_1 = -\frac{G_\rho a_2}{a_1 b_2 - a_2 b_1}, \quad C_2 = \frac{G_\rho a_1}{a_1 b_2 - a_2 b_1}. \tag{4.13}$$

The slopes, moments, and shearing forces of the shell are then by (4.7) [cf. (6.19) of Chapter IV]:

$$\left.\begin{aligned} W_1' &= -\frac{1}{L_0}[C_1\theta_1(\xi) + C_2\theta_2(\xi)],\\ M_\rho &= \frac{D}{L_0^2}[C_1 L_1(\xi) + C_2 L_2(\xi)],\\ M_\theta &= \frac{D}{L_0^2}[C_1\overline{L}_1(\xi) + C_2\overline{L}_2(\xi)],\\ Q_\rho &= -\frac{D}{L_0^3}[C_1 Q_1(\xi) + C_2 Q_2(\xi)]. \end{aligned}\right\} \tag{4.14}$$

2

Consider the state of plane stress of the shallow shell. By virtue of (4.7), the stress function Φ defined by (3.12) takes the form:

$$\begin{aligned} \Phi = \frac{EhL_0^2}{R}\Big[&-C_1\varphi_1(\xi) - C_2\varphi_2(\xi) + C_5 + C_6\xi^2 +\\ &+ C_7\xi^2\ln\xi + C_8\ln\xi + \frac{pR^2}{Eh+kR^2}\frac{\xi^2}{4}\Big]. \end{aligned} \tag{4.15}$$

The functions $\varphi_1(\xi), \varphi_2(\xi)$ are given here by (3.11) or by the corresponding series:

$$\left.\begin{aligned} \varphi_1(\xi) &= \sum_{m=0}^{\infty}\frac{(-1)^m}{(m!)^2}\left(\frac{\xi}{2}\right)^{2m}\cos 2(m-1)\varphi,\\ \varphi_2(\xi) &= \sum_{m=0}^{\infty}\frac{(-1)^m}{(m!)^2}\left(\frac{\xi}{2}\right)^{2m}\sin 2(m-1)\varphi. \end{aligned}\right\} \tag{4.16}$$

As already stated, the constants C_5 and C_7 in (4.15) vanish; we thus obtain:

$$\Phi = \frac{EhL_0^2}{R}\left[-C_1\varphi_1(\xi) - C_2\varphi_2(\xi) + C_6\xi^2 + C_8\ln\xi + \frac{pR^2}{Eh+kR^2}\frac{\xi^2}{4}\right]. \tag{4.17}$$

From (3.13) and (3.14) follows:

$$N_\rho = \frac{Eh}{R}\left[C_1 n_1(\xi) + C_2 n_2(\xi) + 2C_6 + C_8\frac{1}{\xi^2} + \frac{1}{2}\frac{pR^2}{Eh+kR^2}\right], \tag{4.13}$$

$$N_\theta = \frac{Eh}{R}\left\{C_1[u_0(\xi) - n_1(\xi)] + C_2[v_0(\xi) - n_2(\xi)] + 2C_6 - C_8\frac{1}{\xi^2} + \frac{1}{2}\frac{pR^2}{Eh+kR^2}\right\}, \tag{4.19}$$

where $n_1(\xi)$, and $n_2(\xi)$ are defined by (3.15), or by the corresponding series:

$$\left.\begin{aligned} n_1(\xi) &= \frac{1}{2}\sum_{m=0}^{\infty}\frac{(-1)^m}{m!\,(m+1)!}\left(\frac{\xi}{2}\right)^{2m}\cos 2m\varphi, \\ n_2(\xi) &= \frac{1}{2}\sum_{m=0}^{\infty}\frac{(-1)^m}{m!\,(m+1)!}\left(\frac{\xi}{2}\right)^{2m}\sin 2m\varphi. \end{aligned}\right\} \tag{4.20}$$

Hence, (3.24) becomes:

$$u = \frac{L_0}{R}\Big\{-(1+\mu)\Big[C_1\chi_1(\xi) + C_2\chi_2(\xi) + C_5\frac{1}{\xi} + \\ + \frac{1}{2}\frac{pR^2}{Eh + kR^2}\xi\Big] + 2C_6(1-\mu)\xi\Big\}, \tag{4.21}$$

where $\chi_1(\xi)$, $\chi_2(\xi)$ are defined by (3.25), or by the series:

$$\left.\begin{aligned} \chi_1(\xi) &= \sum_{m=0}^{\infty}\frac{(-1)^m}{m!\,(m+1)!}\left(\frac{\xi}{2}\right)^{2m+1}\cos 2m\varphi, \\ \chi_2(\xi) &= \sum_{m=0}^{\infty}\frac{(-1)^m}{m!\,(m+1)!}\left(\frac{\xi}{2}\right)^{2m+1}\sin 2m\varphi. \end{aligned}\right\} \tag{4.22}$$

The constants C_1 and C_2 in (4.17), (4.18), (4.19), and (4.21) are obtained from (4.14), while the constants C_5 and C_6 have to be determined from the boundary conditions for the tangential strains, which are:

$$\begin{aligned} &\text{at } \rho=0 \quad (\xi=0): && u = 0; \\ &\text{at } \rho = R_0 \quad \left(\xi = \frac{R_0}{L_0}\right): && N_\rho = -Q^\Phi \sin\beta = -\frac{2l}{L_0}[W_2' - W_1']\sin\beta. \end{aligned} \tag{4.23}$$

The first condition states that the tangential displacements vanish at the shell apex; this is a consequence of the axial symmetry. By the second condition allowance is made for the existence along the shell contour of fictitious forces:

$$N^\Phi = -Q^\Phi \sin\beta, \tag{4.24}$$

equal in magnitude to the projection of the fictitious shearing forces acting on a circular plate, onto the tangent to the middle surface of the shell at the contour. The minus sign results from the convention according to which a negative value of N^Φ corresponds to a positive shearing force at the contour.

The first condition (4.23) yields:

$$C_5 = 0. \tag{4.25}$$

The second condition yields:

$$C_6 = \frac{1}{2}\left[\frac{RN^\Phi}{Eh} - C_1 n_1(\xi_R) - C_2 n_2(\xi_R) - \frac{1}{2}\frac{pR^2}{Eh + kR^2}\right]. \tag{4.26}$$

where

$$N^{\Phi} = -\frac{2t}{L_0}\sin\beta \times$$

$$\times\left[C_1\theta_1(\xi_R) + C_2\theta_2(\xi_R) - \frac{C_1u_0(\xi_R) + C_2v_0(\xi_R) + \frac{pR^2}{Eh + kR^2}}{K_0(\alpha_0\xi_R)}\alpha_0K_1(\alpha_0\xi_R)\right]. \qquad (4.27)$$

§ 5. SHALLOW SPHERICAL SHELL SUBJECTED TO A CONTOUR LOAD

1

Let a shell on an elastic foundation be subjected to a vertical contour load P_k [per unit length] (Figure 127).

The differential equation (3.2), is homogeneous in this case; its solution is:

$$W_1 = C_1u_0(\xi) + C_2v_0(\xi) + C_3f_0(\xi) + C_4g_0(\xi). \qquad (5.1)$$

For the region beyond the limits of the shell ($R_0 \leqslant \rho \leqslant \infty$) we have:

$$W_2 = B_1I_0(\alpha_0\xi) + B_2K_0(\alpha_0\xi). \qquad (5.2)$$

The constants in (5.1) and (5.2) are determined from the boundary conditions which can be formulated as in (4.5) with the exception of condition d), which is replaced by the following, having the same physical meaning:

at $\rho = R_0 \quad \left(\xi = \frac{R_0}{L_0}\right) \qquad Q_\rho = \left[2t\left(\frac{dW_2}{d\rho} - \frac{dW_1}{d\rho}\right) + P_k\right]\cos\beta, \qquad (5.3)$

where P_k is the vertical load per unit length of the contour.

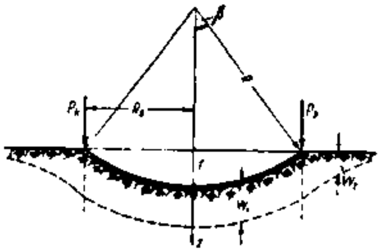

FIGURE 127.

Conditions a, b, e, and f of (4.5) yield:

$$\left.\begin{aligned} &C_3 = C_4 = B_1 = 0,\\ &B_2 = \frac{C_1u_0(\xi_R) + C_2v_0(\xi_R)}{K_0(\alpha_0\xi_R)}.\end{aligned}\right\} \qquad (5.4)$$

Using (4.9), (5.1), (5.2), and (5.4), the following two simultaneous equations in C_1 and C_2 are obtained from conditions c) and d):

$$\left.\begin{aligned} a_1C_1 + a_2C_2 &= 0, \\ b_1C_1 + b_2C_2 &= G_P. \end{aligned}\right\} \tag{5.5}$$

Their solution is:

$$C_1 = -\frac{G_P a_2}{a_1b_2 - a_2b_1}, \quad C_2 = \frac{G_P a_1}{a_1b_2 - a_2b_1}, \tag{5.6}$$

where $a_1, a_2, b_1\ b_2$ are defined by (4.11), while:

$$G_P = -\frac{P_k L_0^3}{D}\cos\beta. \tag{5.7}$$

The normal displacements are thus:

$$W_1 = C_1u_0\ (\xi) + C_2v_0(\xi). \tag{5.8}$$

The slopes moments, and shearing forces are given by (4.14), the constants C_1 and C_2 being obtained from (5.6).

The normal forces are in the case considered [cf. (3.13) and (3.14)]:

$$\left.\begin{aligned} N_\rho &= \frac{Eh}{R}\left[C_1n_1(\xi) + C_2n_2(\xi) + 2C_6 + C_5\frac{1}{\xi^2}\right], \\ N_\theta &= \frac{Eh}{R}\left\{C_1[u_0(\xi) - n_1(\xi)] + C_2[v_0(\xi) - n_2(\xi)] + 2C_6 - C_5\frac{1}{\xi^2}\right\}, \end{aligned}\right\} \tag{5.9}$$

the tangential displacements being [cf. (3.24)]:

$$u = \frac{L_0}{R}\left\{-(1+\mu)\left[C_1\chi_1(\xi) + C_2\chi_2(\xi) + C_5\frac{1}{\xi}\right] + 2C_6(1-\mu)\xi\right\}. \tag{5.10}$$

The boundary conditions are:

$$u(0) = 0, \quad N_\rho(R_0) = N^\Phi - P_k\sin\beta, \tag{5.11}$$

where N^Φ is the fictitious normal contour force given by (4.24). In the case considered [(cf. 4.27)]:

$$N^\Phi = -\frac{2t}{L_0}\left\{C_1\theta_1(\xi_R) + C_2\theta_2(\xi_R) - \frac{C_1u_0(\xi_R) + C_2v_0(\xi_R)}{K_0(a_0\xi_R)}a_0K_1(a_0\xi_R)\right]\sin\beta. \tag{5.12}$$

The first and second boundary conditions (5.11) yield respectively:

$$C_5 = 0. \tag{5.13}$$

$$C_6 = \frac{1}{2}\left[\frac{(N^\Phi - P_k\ \sin\beta)R}{Eh} - C_1n_1(\xi_R) - C_2n_2(\xi_R)\right]. \tag{5.14}$$

2

If a horizontal load N_k is applied to [unit length of] the shell contour (Figure 128), the problem is solved in exactly the same way, the only difference being in the boundary condition (5.3), which become:

$$Q_\rho(R_0) = 2f\left(\frac{dW_2}{d\rho} - \frac{dW_1}{d\rho}\right)\cos\beta - N_k\sin\beta. \qquad (5.15)$$

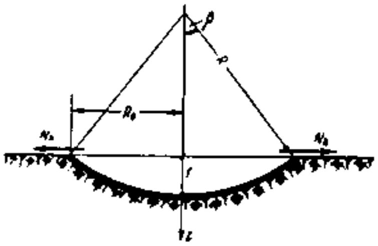

FIGURE 128.

The integration constants C_1 and C_2 are again determined by (5.6), the load term G_P being now:

$$G_N = \frac{N_k L_0^3}{D}\sin\beta. \qquad (5.16)$$

The forces are obtained from (5.9) and the displacements from (5.10). The corresponding boundary conditions are:

$$u(0) = 0, \quad N_\rho(R_0) = N^\Phi - N_k\cos\beta, \qquad (5.17)$$

which yield the following values for the integration constants C_5 and C_6:

$$\left.\begin{aligned} &C_5 = 0,\\ &C_6 = \frac{1}{2}\left[\frac{(N^\Phi - N_k\cos\beta)\,R}{Eh} - C_1 n_1(\xi_R) - C_2 n_2(\xi_R)\right]. \end{aligned}\right\} \qquad (5.18)$$

Here N^Φ is the fictitious contour force, determined by (5.12).

3

Let the shell be subjected to moments M_k applied to [unit length of] its contour (Figure 129).

It is easily seen that the solution can in this case also be presented in the form of (5.1) and (5.2). The boundary conditions are given by (4.5), with the exception of condition c) which is to be replaced by:

$$M_\rho(R_0) = M_k. \qquad (5.19)$$

We obtain:

$$\left.\begin{aligned} &C_3 = C_4 = B_1 = 0, \\ &B_2 = \frac{C_1 u_0(\xi_R) + C_2 v_0(\xi_R)}{K_0(a_0 \xi_R)}. \end{aligned}\right\} \tag{5.20}$$

The following two simultaneous equations are obtained in C_1 and C_2:

$$\left.\begin{aligned} &a_1 C_1 + a_2 C_2 = G_M, \\ &b_1 C_1 + b_2 C_2 = 0, \end{aligned}\right\} \tag{5.21}$$

The magnitudes a_1, a_2, b_1, and b_2 are defined by (4.11), while:

$$G_M = \frac{M_k L_0^2}{D}. \tag{5.22}$$

The solution of (5.21) is:

$$C_1 = \frac{G_M b_2}{a_1 b_2 - a_2 b_1}, \quad C_2 = -\frac{G_M b_1}{a_1 b_2 - a_2 b_1}. \tag{5.23}$$

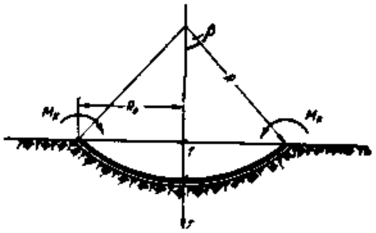

FIGURE 129.

The forces and displacements are in this case again given by (5.9) and (5.10), with $C_5 = 0$ and:

$$C_6 = \frac{1}{2}\left[\frac{RN^{\Phi}}{Eh} - C_1 n_1(\xi_R) - C_2 n_2(\xi_R)\right]. \tag{5.24}$$

§ 6. APPROXIMATIVE ANALYSIS OF A SHALLOW SPHERICAL SHELL ON AN ELASTIC FOUNDATION

1

Taking into account its small deformability in relation to that of the elastic foundation, we shall consider the shallow shell as a rigid punch.

The reactions of the elastic foundation are then determined by (3.10) and (3.12) of Chapter IV, valid for a circular punch of radius R_0 (Figure 130, a):

$$q = \frac{P_0}{\pi R_0^2 \left[1 + 2\frac{K_1(\alpha R_0)}{K_0(\alpha R_0)\,\alpha R_0}\right]}, \tag{6.1}$$

$$Q^{\Phi} = \frac{P_0}{\pi R_0 \left[1 + 2\frac{K_1(\alpha R_0)}{K_0(\alpha R_0)\,\alpha R_0}\right]} \frac{K_1(\alpha R_0)}{K_0(\alpha R_0)\,\alpha R_0}, \tag{6.2}$$

where P_0 is the resultant of the given vertical load.

The analysis of a shell on an elastic foundation thus reduces to determining the strains and stresses in the shell subjected to a given external load and to the reactions q and Q^{Φ} of the elastic foundation, all these forces being in equilibrium. For a uniformly distributed external load p, the system is shown in Figure 130, b, where:

$$p^* = p - q, \tag{6.3}$$

and

$$Q^{\Phi} = \frac{\pi R_0^2 p^*}{2\pi R_0} = \frac{p^* R_0}{2}. \tag{6.4}$$

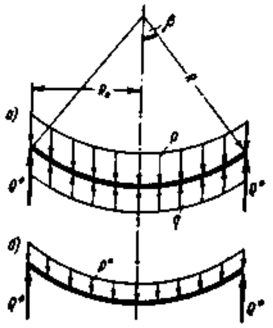

FIGURE 130.

2

It was shown in section 1 that the problem of a shallow spherical shell subjected to a vertical distributed load p^* reduces to integrating the two differential equations [cf. (1.1), (1.7)]:

$$\left.\begin{aligned} D\nabla^2\nabla^2 W + \frac{Eh}{R^2} W - p^* = 0,\\ \frac{R}{Eh}\nabla^2\nabla^2\Phi - \nabla^2 W = 0,\end{aligned}\right\} \tag{6.5}$$

the first of which yields the displacement function W, and the second the stress function Φ.

We introduce the dimensionless coordinates:

$$\xi = \frac{\rho}{L_0},$$

where

$$L_0 = \sqrt[4]{\frac{DR^2}{Eh}}, \tag{6.6}$$

We can then rewrite (6.5) as follows:

$$\nabla_\xi^2 \nabla_\xi^2 W + W = \frac{p^* L_0^4}{D}, \tag{6.7}$$

$$\nabla_\xi^2 \nabla_\xi^2 \Phi = \frac{EhL_0^2}{R} \nabla_\xi^2 W, \tag{6.8}$$

where

$$\nabla_\xi^2 = \frac{d^2}{d\xi^2} + \frac{1}{\xi}\frac{d}{d\xi}. \tag{6.9}$$

3

The homogeneous equation obtained from (6.7) for $p^* = 0$ can be reduced to an equivalent system of two second-order equations:

$$\left.\begin{aligned} \frac{d^2W}{d\xi^2} + \frac{1}{\xi}\frac{dW}{d\xi} + iW = 0, \\ \frac{d^2W}{d\xi^2} + \frac{1}{\xi}\frac{dW}{d\xi} - iW = 0. \end{aligned}\right\} \tag{6.10}$$

The general integral of this system is:

$$W = A_1 J_0(\xi\sqrt{i}) + A_2 J_0(\xi\sqrt{-i}) + A_3 H_0^{(1)}(\xi\sqrt{i}) + A_4 H_0^{(2)}(\xi\sqrt{-i}), \tag{6.11}$$

where $J_0(\xi\sqrt{i})$ and $J_0(\xi\sqrt{-i})$ are zero-order Bessel functions of the first kind, of the arguments $(\xi\sqrt{i})$ and $(\xi\sqrt{-i})$; $H_0^{(1)}(\xi\sqrt{i})$ and $H_0^{(2)}(\xi\sqrt{-i})$ are respectively zero-order Hankel functions of the first and second kind, of the same arguments.

The only difference between (6.11) and (2.19) of Chapter IV is in the arguments of the functions considered. Integral (6.11) is a particular case of the more general solution (2.19) of Chapter IV, since the straight lines along which the Bessel and Hankel functions in (6.11) are determined make angles of 45° with the real axis in the complex plane:

$$\left.\begin{aligned} \varphi = \arg\sqrt{i} = 45^\circ, \\ \varphi = \arg\sqrt{-i} = -45^\circ. \end{aligned}\right\} \tag{6.12}$$

It is convenient to express (6.11) through real functions:

$$W = C_1 u_0(\xi) + C_2 v_0(\xi) + C_3 f_0(\xi) + C_4 g_0(\xi), \tag{6.13}$$

where

$$\left.\begin{aligned} u_0(\xi) &= \operatorname{Re} J_0(\sqrt{i}\,\xi), & f_0(\xi) &= \operatorname{Re} H_0^{(1)}(\sqrt{i}\,\xi),\\ v_0(\xi) &= \operatorname{Im} J_0(\sqrt{i}\,\xi), & g_0(\xi) &= \operatorname{Im} H_0^{(2)}(\sqrt{-i}\,\xi). \end{aligned}\right\} \tag{6.14}$$[*]

The following relationships are obtained from (2.20) of Chapter IV and (6.12) of this chapter :

$$\nabla^2 u_0 = v_0, \quad \nabla^2 v_0 = -u_0, \quad \nabla^2 f_0 = g_0, \quad \nabla^2 g_0 = -f_0. \tag{6.15}$$

The general integral of the nonhomogeneous equation (6.7) is then:

$$W = C_1 u_0(\xi) + C_2 v_0(\xi) + C_3 f_0(\xi) + C_4 g_0(\xi) + W_p, \tag{6.16}$$

where W_p is a particular integral of (6.7).

For instance, if $p^* = \text{const}$ we can put:

$$W_p = \frac{p^* R^2}{Eh} \tag{6.17}$$

From the boundary conditions a) and b) of (4.5) we obtain:

$$C_3 = C_4 = 0. \tag{6.18}$$

Substitution of (6.17) and (6.18) in (6.16) yields:

$$W = C_1 u_0(\xi) + C_2 v_0(\xi) + \frac{p^* R^2}{Eh}. \tag{6.19}$$

We then obtain for $p^* = \text{const}$ from (2.7), using (6.15) and (6.19):

$$\left.\begin{aligned} \frac{dW}{d\rho} &= \frac{1}{L_0}[C_1 u_0'(\xi) + C_2 v_0'(\xi)],\\ M_\rho &= -\frac{D}{L_0^2}\left\{C_1\left[v_0(\xi) - (1-\mu)\frac{u_0'(\xi)}{\xi}\right] + \right.\\ &\qquad \left. + C_2\left[-u_0(\xi) - (1-\mu)\frac{v_0'(\xi)}{\xi}\right]\right\},\\ M_\theta &= -\frac{D}{L_0^2}\left\{C_1\left[\mu v_0(\xi) + (1-\mu)\frac{u_0'(\xi)}{\xi}\right] + \right.\\ &\qquad \left. + C_2\left[-\mu u_0(\xi) + (1-\mu)\frac{v_0(\xi)}{\xi}\right]\right\},\\ Q_\rho &= -\frac{D}{L_0^3}[C_1 v_0'(\xi) - C_2 u_0'(\xi)]. \end{aligned}\right\} \tag{6.20}$$

---

[*] These functions are known as Thomson functions. They, and their derivatives, are tabulated in the appendix (Table 11).

These expressions could also have been obtained from (4.14) by substituting in them (2.25) through (2.28) of Chapter IV, taking into account (6.12).

Equations (4.17), (4.18), (4.19), (4.21) are again valid. Taking into account (4.25), they become in the case considered:

$$\Phi = \frac{EhL_0^2}{p}\left[-C_1 v_0(\xi) + C_2 u_0(\xi) + C_4\xi^2 + \frac{\rho^* R^2}{Eh}\frac{\xi^4}{4}\right], \qquad (6.21)$$

$$N_{\varphi} = \frac{Eh}{R}\left[-C_1\frac{v_0'(\xi)}{\xi} + C_2\frac{u_0'(\xi)}{\xi} + 2C_4 + \frac{1}{2}\frac{\rho^* R^2}{Eh}\right], \qquad (6.22')$$

$$N_{\theta} = \frac{Eh}{R}\left\{C_1\left[u_0(\xi) + \frac{v_0'(\xi)}{\xi}\right] + C_2\left[v_0(\xi) - \frac{u_0'(\xi)}{\xi}\right] + 2C_4 + \frac{1}{2}\frac{\rho^* R^2}{Eh}\right\}, \qquad (6.22'')$$

$$u = \frac{L_0}{R}\left\{-(1+\mu)\left[-C_1 v_0'(\xi) + C_2 u_0'(\xi)\right] + \right.$$
$$\left. + 2C_4(1-\mu)\xi - \frac{(1+\mu)}{2}\frac{\rho^* R^2}{Eh}\xi\right\}. \qquad (6.23)$$

These expressions contain three integration constants which are determined from the boundary conditions at the shell contour.

5

Consider as numerical example the shallow spherical shell shown in Figure 131.

Let the geometrical and physical characteristics of the shell and the elastic foundation be as follows*:

$$\left.\begin{aligned} R &= 13.5 \text{ m},\\ h &= 0.46 \text{ m},\\ R_0 &= 5.1 \text{ m},\\ E_{0s} &= 4\cdot 10^3 \text{ cm/m}^2,\\ \nu_s &= 0.4,\\ H/R_0 &= 1.0,\\ f &= 1.0 \text{ m},\\ E &= 2\cdot 10^6 \text{ cm/m}^2,\\ \mu &= 0.167,\\ \gamma &= 1.55,\\ P &= 1.0 \text{ cm/m},\\ D &= 16.2\cdot 10^4 \text{ cm/m}. \end{aligned}\right\} \qquad (6.24)$$

We then obtain from (3.16) and (3.17) of Chapter IV:

$$\left.\begin{aligned} &k = 1.6\cdot 10^3 \text{ m/m}^3 \quad 2t = 1.85\cdot 10^3 \text{ m/m},\\ &\alpha = 0.93 \text{ 1/m}, \quad \alpha R_0 = 4.72. \end{aligned}\right\} \qquad (6.25)$$

By (6.1) and (6.2), the reactions of the elastic foundation are:

$$q = 0.269 \text{ m/m}^2 \qquad Q^0 = 0.315 \text{ m/m}, \qquad (6.26)$$

---

* It is assumed that the function $\psi(z)$ determining the vertical distribution of the displacements in the elastic foundation is given by (3.15) of Chapter IV.

Their substitution in (6.3) yields:

$$p^* = -0.269 \text{ m/m}^2. \tag{6.27}$$

Insertion of the values (6.24) into (6.6) gives:

$$L_0 = 1.34 \text{ m}, \quad \xi_R = \frac{R_0}{L_0} = 3{,}8. \tag{6.28}$$

The functions entering in (6.19) through (6.23) are for $\xi_R = 3.8$:

$$\left.\begin{aligned} u_0 &= -1.967, & u_0' &= -2.822, \\ v_0 &= -2.345, & v_0' &= 0.0526 \\ \frac{u_0'}{\xi_R} &= -0.742, & \frac{v_0'}{\xi_R} &= 0.138. \end{aligned}\right\} \tag{6.29}$$

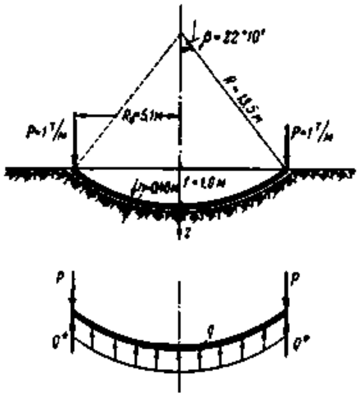

FIGURE 131.

The boundary conditions are in the case considered:

at $\rho = R_0\left(\xi_R = \frac{R_0}{L_0}\right)$:

$$\begin{aligned} M_\rho &= 0, \\ Q_\rho &= (P - Q^\Phi)\cos\beta, \\ N_\rho &= -(P - Q^\Phi)\sin\beta, \end{aligned} \tag{6.30}$$

or [by (6.20) and (6.22')):

$$\left.\begin{aligned} & C_1\left[v_0(\xi_R) - (1-\mu)\frac{u_0'(\xi_R)}{\xi_R}\right] + \\ & \qquad + C_2\left[-u_0(\xi_R) - (1-\mu)\frac{v_0'(\xi_R)}{\xi_R}\right] = 0, \\ & C_1 v_0'(\xi_R) - C_2 u_0'(\xi_R) = -\frac{L_0^2 (P - Q^\Phi)\cos\beta}{D}, \\ & -C_1\frac{v_0'(\xi_R)}{\xi_R} + C_2\frac{u_0'(\xi_R)}{\xi_R} + 2C_4 + \frac{1}{2}\frac{p^* R^2}{Eh} = \\ & \qquad = -\frac{R(P - Q^\Phi)}{Eh}\sin\beta. \end{aligned}\right\} \tag{6.31}$$

Substitution of (6.26), (6.28), (6.29) in (6.31) yields finally:

$$C_1 = -3.68\cdot 10^{-6}\ \mathrm{m},\ C_3 = -3.26\cdot 10^{-6}\ \mathrm{m},\ C_4 = -0.948\cdot 10^{-6}\,\mathrm{m}, \qquad (6.32)$$

The moments M_ρ and M_θ, and the forces N_ρ and N_θ, obtained from (6.20) and (6.22) for the numerical values (6.32), have been plotted in Figures 132 through 135.

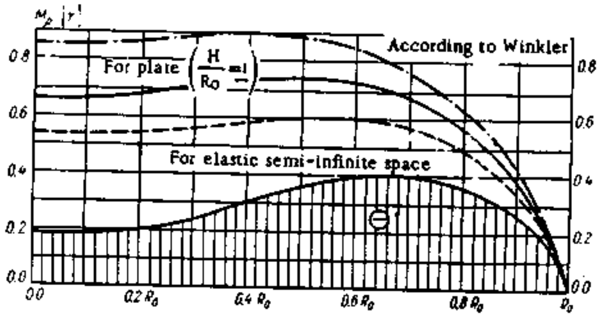

FIGURE 132.

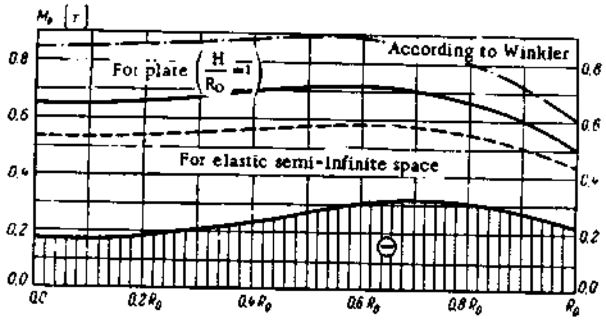

FIGURE 133.

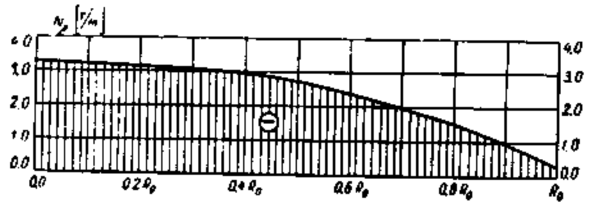

FIGURE 134.

Figures 132 and 133 also show values of the moments M_ρ and M_θ, calculated for a circular plate of radius $R = R_0$, with the same values of the characteristics of the elastic foundation and of the structure. The calculations were performed by three different methods: the method employed in Chapter IV (for $H/R_0 = 1$, $\gamma = 1.55$), the method of the elastic semi-infinite space /26/, and by Winkler's method, the foundation modulus being :

$$k = 1.6\cdot 10^3\ \mathrm{m/m^3}.$$

Comparison of these curves shows that the bending moments M_ρ, and M_θ acting on a shallow spherical shell are considerably smaller than those acting on a circular plate.

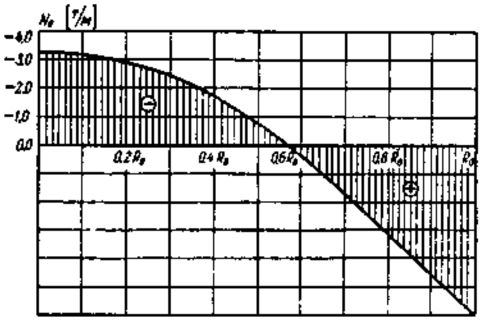

FIGURE 135.

§ 7. APPLICATION OF THE ABOVE METHOD TO THE ANALYSIS OF THE BOTTOMS OF CYLINDRICAL RESERVOIRS

The preceding sections dealt with some problems concerning a shallow spherical shell on an elastic foundation. It was assumed that the shell edges are free and that the shell is acted upon either by a uniformly distributed or by a contour load (Figures 126 through 129).

We shall now consider the case when the spherical shell forms the bottom of a cylindrical reservoir on an elastic foundation (Figure 136).

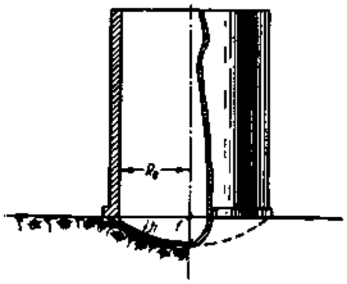

FIGURE 136.

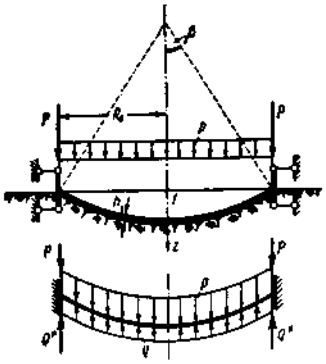

FIGURE 137.

The bottom is usually secured to the cylinder by a supporting ring and can be assumed in a first approximation to be a spherical shell built-in along its contour. In other words, we consider the system shown schematically in Figure 137, disregarding the remainder of the structure. In this figure, the contour forces P represent the load transmitted to the shell by the reservoir walls, while the uniformly distributed load p represents the pressure of the liquid in the reservoir. The reactions q and Q^{ϕ} of the elastic foundation are obtained from (6.1) and (6.2), assuming that in relation to the elastic foundation the shell can be considered as a rigid punch.

As before, the stresses and strains of the shell are determined by (6.19) through (6.23). These contain the three integration constants C_1, C_2, and C_4, which can be determined from the following boundary conditions:

$$\text{at } \rho = R_0 \left(\xi = \frac{R_0}{L_0}\right) \qquad W = 0, \quad W' = 0, \quad u = 0. \tag{7.1}$$

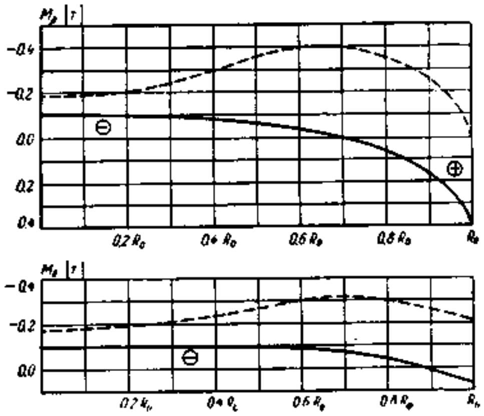

FIGURE 138.

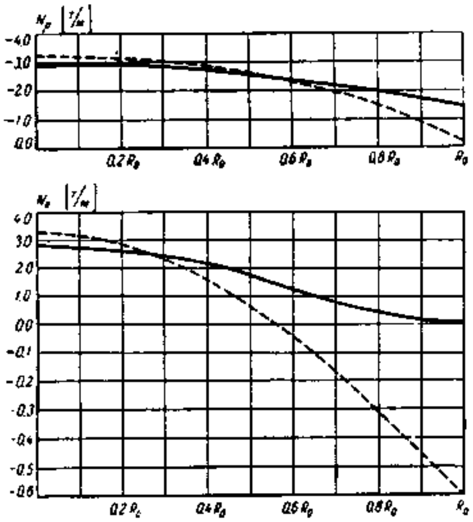

FIGURE 139.

These conditions yield:

$$\left.\begin{aligned} &C_1u_0(\xi_R)+C_2v_0(\xi_R)=-\frac{p^*R^2}{Eh},\\ &C_1u_0'(\xi_R)+C_2v_0'(\xi_R)=0,\\ &-(1+\mu)[-C_1v_0'(\xi_R)+C_2u_0'(\xi_R)]+2C_4(1-\mu)\xi_R-\\ &\qquad-\frac{(1+\mu)}{2}\frac{p^*R^2}{Eh}\xi_R=0, \end{aligned}\right\}\qquad(7.2)$$

where $p^*=p-q$.

The solution of these equations is:

$$\left.\begin{aligned} &C_1=-\frac{v_0'(\xi_R)}{[u_0(\xi_R)v_0'(\xi_R)-u_0'(\xi_R)v_0(\xi_R)]}\frac{p^*R^2}{Eh},\\ &C_2=\frac{u_0'(\xi_R)}{[u_0(\xi_R)v_0'(\xi_R)-u_0'(\xi_R)v_0(\xi_R)]}\frac{p^*R^2}{Eh},\\ &C_4=\frac{(1+\mu)}{4(1-\mu)}\left\{\frac{2[u_0'^2(\xi_R)+v_0'^2(\xi_R)]}{\xi_R[u_0(\xi_R)v_0'(\xi_R)-u_0'(\xi_R)v_0(\xi_R)]}+1\right\}\frac{p^*R^2}{Eh}. \end{aligned}\right\}\qquad(7.3)$$

The bending moments $\dot{M}_\rho$ and M_φ, and the forces N_ρ and N_φ, calculated by means of (7.3), (6.20), and (6.22) for a reservoir bottom subjected only to a contour load P, have been plotted in Figures 138 and 139. The values of the elastic constants of the soil and the structure are given by (6.24). The results obtained for a shell with free edges have been plotted in broken line in the same figures.

It is seen that reinforcing the shell along its contour by a rigid ring preventing radial displacement and rotation, reduces to a certain degree the values of M_ρ, M_φ, and N_ρ, while the tension N_φ at the shell contour becomes considerably less. This is very important when a shell forms the bottom of a reservoir.

2

If the supporting ring prevents only radial displacement, the shell can be analyzed according to the scheme shown in Figure 140.

The boundary conditions are in this case:

$$\text{at}\ \rho=R_0\quad\left(\xi=\frac{R_0}{L_0}\right)\ :\qquad W=0,\quad M_\rho=0,\quad u=0.\qquad(7.4)$$

or

$$\left.\begin{aligned} &C_1u_0(\xi_R)+C_2v_0(\xi_R)=-\frac{p^*R^2}{Eh},\\ &C_1\left[v_0(\xi_R)-(1-\mu)\frac{u_0'(\xi_R)}{\xi_R}\right]+\\ &\qquad+C_2\left[-u_0(\xi_R)-(1-\mu)\frac{v_0'(\xi_R)}{\xi_R}\right]=0,\\ &-(1+\mu)[-C_1v_0'(\xi_R)+C_2u_0'(\xi_R)]+\\ &\qquad+2C_4(1-\mu)\xi_R-\frac{(1+\mu)}{2}\frac{p^*R^2}{Eh}\xi_R=0. \end{aligned}\right\}\qquad(7.5)$$

The integration constants are thus:

$$\left.\begin{aligned}
C_1 &= \frac{K_1}{[u_0(\xi_R)K_1+v_0(\xi_R)K_2]}\frac{p^*R^2}{Eh},\\
C_2 &= \frac{K_2}{[u_0(\xi_R)K_1+v_0(\xi_R)K_2]}\frac{p^*R^2}{Eh},\\
C_4 &= \frac{(1+\mu)}{4(1-\mu)}\left[\frac{-v_0'(\xi_R)K_1-u_0'(\xi_R)K_2}{\xi_R[u_0(\xi_R)K_1+v_0(\xi_R)K_2]}+1\right]\frac{p^*R^2}{Eh},
\end{aligned}\right\} \quad (7.6)$$

where

$$K_1 = u_0(\xi_R)+(1-\mu)\frac{v_0'(\xi_R)}{\xi_R},$$

$$K_2 = v_0(\xi_R)+(1-\mu)\frac{u_0'(\xi_R)}{\xi_R}.$$

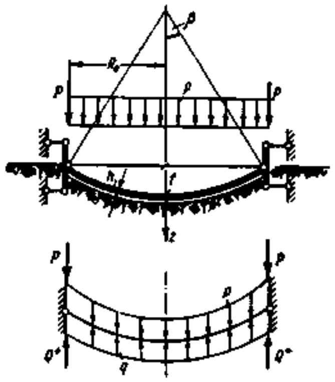

FIGURE 140.

3.

To obtain a more accurate solution it is necessary to make allowance for the effect of the cylindrical reservoir walls on the strains of the bottom. This can be done by the methods used to analyze statically indeterminate systems, i.e., the method of forces or the method of displacements (strains).

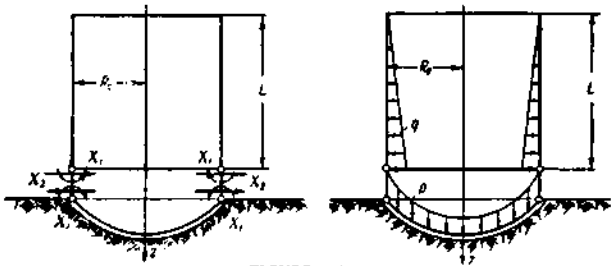

FIGURE 141.

In the first method, a cut is made in the zone where the bottom joins the cylindrical reservoir wall, and the constraints there are replaced by unknown forces [and moments] (Figure 141). In accordance with the convention adopted for the signs, the canonical equations expressing the continuity of the deformations are:

$$\left.\begin{aligned}(\Delta^{c}_{11}+\Delta^{b}_{11})\,X_1+(\Delta^{c}_{12}-\Delta^{b}_{12})\,X_2-\Delta^{c}_{1q}+\Delta^{b}_{1p}-\Delta^{b}_{1P}=0,\\(\Delta^{c}_{21}+\Delta^{b}_{21})\,X_1+(\Delta^{c}_{22}+\Delta^{b}_{22})\,X_2-\Delta^{c}_{2q}+\Delta^{b}_{2p}+\Delta^{b}_{2P}=0.\end{aligned}\right\}\qquad(7.7)$$

The first equation states that there is no relative rotation at the cut; the second states that there is no relative displacement in the direction of X_2.

The coefficients and load terms in (7.7) are given in absolute values. The first subscript indicates the place and direction of the displacement. the second subscript, its cause. The superscript "c" refers to the cylindrical reservoir wall, the superscript "b" to the bottom.

The load terms:

$$\Delta^{c}_{1q},\ \Delta^{c}_{2q},\ \Delta^{b}_{1p},\ \Delta^{b}_{2p}$$

define the absolute values of the displacements due to the external loads q and p, while the load terms Δ^{b}_{1P}, Δ^{b}_{2P} correspond to the displacements due to the contour load P transmitted by the reservoir wall to the bottom.

All coefficients and load terms with superscript "b" can be obtained from (6.19), (6.20), and (6.23).

To obtain the coefficients with superscript "c", it is necessary to consider the axisymmetrical deformation of a cylindrical shell subjected both to an external radial load q and to contour forces X_2 and moments X_1. This problem reduces to solving a fourth-order differential equation identical in form with the differential equation of the bending of a beam on an elastic Winkler foundation.

This problem is discussed in detail in many books* so that the coefficients with superscript "c" can be found without difficulty.

The same procedure is adopted when the reservoir bottom is a circular plate instead of a spherical shell. The coefficients with superscript "b" are in this case obtained from the formulas of sections 3 and 6 of Chapter IV.

---

* See for instance /8/.

Chapter VI

DYNAMICS AND STABILITY OF BEAMS AND PLATES ON ELASTIC FOUNDATIONS

§ 1. DIFFERENTIAL EQUATION OF THE VIBRATIONS OF A BEAM ON AN ELASTIC SINGLE-LAYER FOUNDATION

Consider a beam of width b on an elastic foundation, subjected to an external load $p(x, t)$ varying with time (Figure 142). This is the case of dynamic loading, where the inertia forces acting in the deformed system become significant.

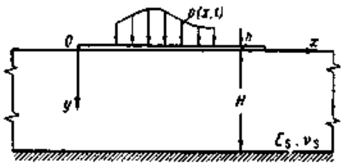

FIGURE 142.

The differential equation of motion of the beam is:

$$EJV^{IV}(x, t) = p(x, t) - m_1 \frac{\partial^2 V(x, t)}{\partial t^2} - q(x, t), \qquad (1.1)$$

where EJ = rigidity of beam, $J = \frac{bh^3}{12(1-\mu^2)}$,

m_1 = mass of beam per unit length,

$q(x, t)$ = distributed reaction of foundation, due to elasticity and inertia of soil.

To determine the reactions $q(x, t)$, we cut out an elementary column from the elastic foundation (cf. sections 2 and 3 of Chapter I), and consider the equilibrium conditions of this column, applying Lagrange's principle of virtual displacements. Assuming that no horizontal displacements occur in the single-layer foundation and that the vertical displacements are described by the function $\psi(y)$, the virtual work done by all external and internal forces acting on this column becomes:

$$\frac{E_0 b}{2(1+\nu_0)} V'' \int_0^H \psi^2(y)\, dy - \frac{E_0 b}{1-\nu_0^2} V \int_0^H \psi'^2(y) dy - \overline{m}_0 b \int_0^H \psi^2(y)\, dy \frac{\partial^2 V}{\partial t^2} + q(x, t) = 0, \qquad (1.2)$$

where $q(x,t)$ = load per unit length, applied to surface of elastic foundation (foundation reaction); $\overline{m}_0 = \frac{\gamma_0}{g}$ = mass per unit volume of foundation (γ_0 = specific weight of soil, g = gravitational acceleration); also,

$$E_0 = \frac{E_s}{1-\nu_s^2}, \quad \nu_0 = \frac{\nu_s}{1-\nu_s}, \tag{1.3}$$

where E_s and ν_s = modulus of elasticity and Poisson's ratio of elastic foundation respectively.

We introduce the symbols:

$$\left.\begin{aligned} k &= \frac{E_0\delta}{1-\nu_0^2}\int_0^H \psi'^2(y)\,dy, \\ t &= \frac{E_0\delta}{4(1+\nu_0)}\int_0^H \psi^2(y)\,dy, \\ m_0 &= \overline{m}\delta\int_0^H \psi^2(y)\,dy, \end{aligned}\right\} \tag{1.4}$$

Equation (1.2) then becomes:

$$2tV'' - kV - m_0\frac{\partial^2 V}{\partial t^2} + q(x,t) = 0. \tag{1.5}$$

This is the differential equation of the vibrations of a single-layer foundation under the action of a load $q(x,t)$. Eliminating $q(x,t)$ between (1.1) and (1.5), we obtain:

$$V^{\mathrm{IV}} - 2r^2V'' + s^4V + m^*\frac{\partial^2 V}{\partial t^2} = \frac{p(x,t)}{EJ}, \tag{1.6}$$

where

$$\left.\begin{aligned} s^4 &= \frac{k}{EJ} = \frac{E_0\delta}{EJ(1-\nu_0^2)}\int_0^H \psi'^2(y)\,dy, \\ r^2 &= \frac{t}{EJ} = \frac{E_0\delta}{4EJ(1+\nu_0)}\int_0^H \psi^2(y)\,dy, \\ m^* &= \frac{m_1+m_0}{EJ} = \left(\frac{\gamma\delta}{g}h + \frac{\gamma_0\delta}{g}\int_0^H \psi^2(y)\,dy\right)\frac{1}{EJ} \end{aligned}\right\} \tag{1.7}$$

(γ and γ_0 = specific weights of materials of beam and elastic foundation respectively).

The partial differential equation (1.6) thus shows that not only the beam, but also the elastic foundation vibrates.

§ 2. FREE VIBRATIONS OF A BEAM

1

When $p(x,t) = 0$, (1.6) reduces to:

$$V^{IV} - 2r^2 V'' + s^4 V = -m^* \frac{\partial^2 V}{dt^2}. \tag{2.1}$$

This equation describes the free vibrations of the beam when it is disturbed from its state of equilibrium and then left to itself.

We assume a solution in the form of a product of two functions, one of which depends only on x, the other only on t:

$$V = X(x)\,T(t). \tag{2.2}$$

Substitution of (2.2) in (2.1) yields:

$$\frac{X^{IV} - 2r^2 X'' + s^4 X}{X} = -\frac{m^* T''}{T}. \tag{2.3}$$

Since its left-hand side is a function of x only, and its right-hand side of t only, (2.3) will hold in the general case only if each side is equal to the same constant. Denoting this constant by $m^*\omega^2$, we obtain:

$$T'' + \omega^2 T = 0, \tag{2.4}$$

$$X^{IV} - 2r^2 X'' + (s^4 - m^*\omega^2)\,X = 0. \tag{2.5}$$

The solution of (2.1) thus reduces to integrating two ordinary differential equations.

Equation (2.4) has the same form as the equation of free vibrations of a system with one degree of freedom: it describes a simple harmonic motion with frequency ω. The solution of this equation is:

$$T = A \sin \omega t + B \cos \omega t, \tag{2.6}$$

where A and B = constants determined from initial conditions.

The mode of the free vibrations of the beam is determined by (2.5), which can also be written thus:

$$X^{IV} - 2r^2 X'' - (\lambda^4 - r^4)\,X = 0, \tag{2.7}$$

where

$$\lambda^4 = r^4 - s^4 + m^*\omega^2. \tag{2.8}$$

The general integral of (2.7) is:

$$X(x) = C_1 \operatorname{sh} \alpha x + C_2 \operatorname{ch} \alpha x + C_3 \sin \beta x + C_4 \cos \beta x,$$

where $C_1, \ldots, C_4$ are constants, and:

$$\alpha^2 = \lambda^2 + r^2, \quad \beta^2 = \lambda^2 - r^2. \tag{2.9}$$

Since ω is still unknown, the parameter λ^2, on which α and β depend, will also be unknown.

The general solution of (2.7) contains therefore the five unknowns C_1, C_2, C_3, C_4, and λ, which can be determined from the statical, kinematic, or mixed-type boundary conditions at the beam ends. Only two conditions can be formulated for each end. When no external forces act, the boundary conditions are homogeneous, containing only the values of the function $X(x)$ or of its derivatives at $x=0$ and $x=l$.

By expanding the boundary conditions at the beam ends $x=0$ and $x=l$ with the aid of the formulas:

$$\left.\begin{aligned} X(x) &= C_1 \operatorname{sh} \alpha x + C_2 \operatorname{ch} \alpha x + C_3 \sin \beta x + C_4 \cos \beta x, \\ X'(x) &= C_1 \alpha \operatorname{ch} \alpha x + C_2 \alpha \operatorname{sh} \alpha x + C_3 \beta \cos \beta x - C_4 \beta \sin \beta x, \\ X''(x) &= C_1 \alpha^2 \operatorname{sh} \alpha x + C_2 \alpha^2 \operatorname{ch} \alpha x - C_3 \beta^2 \sin \beta x - C_4 \beta^2 \cos \beta x, \\ X'''(x) &= C_1 \alpha^3 \operatorname{ch} \alpha x + C_2 \alpha^3 \operatorname{sh} \alpha x - C_3 \beta^3 \cos \beta x + C_4 \beta^3 \sin \beta x, \end{aligned}\right\} \tag{2.10}$$

we obtain, putting $x=0$ and $x=l$, a system of four linear equations in the four integration constants $C_1, \ldots, C_4$. Since the boundary conditions are homogeneous, the four equations formed will also be homogeneous. In the general case we obtain:

$$\left.\begin{aligned} a_{11}(\lambda) C_1 + a_{12}(\lambda) C_2 + a_{13}(\lambda) C_3 + a_{14}(\lambda) C_4 &= 0, \\ a_{21}(\lambda) C_1 + a_{22}(\lambda) C_2 + a_{23}(\lambda) C_3 + a_{24}(\lambda) C_4 &= 0, \\ a_{31}(\lambda) C_1 + a_{32}(\lambda) C_2 + a_{33}(\lambda) C_3 + a_{34}(\lambda) C_4 &= 0, \\ a_{41}(\lambda) C_1 + a_{42}(\lambda) C_2 + a_{43}(\lambda) C_3 + a_{44}(\lambda) C_4 &= 0, \end{aligned}\right\} \tag{2.11}$$

where the coefficients $a_{ik}(\lambda)$ $(i, k = 1, 2, 3, 4)$ are functions of λ. By equating to zero the determinant of system (2.11), we obtain an equation in λ:

$$\Delta(\lambda) = \begin{vmatrix} a_{11}(\lambda) & a_{12}(\lambda) & a_{13}(\lambda) & a_{14}(\lambda) \\ a_{21}(\lambda) & a_{22}(\lambda) & a_{23}(\lambda) & a_{24}(\lambda) \\ a_{31}(\lambda) & a_{32}(\lambda) & a_{33}(\lambda) & a_{34}(\lambda) \\ a_{41}(\lambda) & a_{42}(\lambda) & a_{43}(\lambda) & a_{44}(\lambda). \end{vmatrix} = 0. \tag{2.12}$$

This equation is called characteristic equation of the homogeneous boundary-value problem, i.e., the problem described by the homogeneous differential equation (2.7) and the homogeneous boundary conditions (2.11). Since λ depends on the vibration frequency ω, equation (2.12) will also be the equation of the natural frequencies of the system.

Since by virtue of (2.9) and (2.10) the parameter λ^2 appears in the arguments of the hyperbolic and trigonometric functions, the characteristic equation (2.12) will be transcendental, yielding an infinite set of values for λ_n^2. It is easily seen that all these values are real, irrespective of the type of boundary-value problem to which the equation corresponds.

The parameters λ_n^2 $(n = 1, 2, 3, \ldots)$ determined by (2.12) are called eigenvalues of the homogeneous boundary-value problem.

Applying the method described here to determine λ^2 thus yields an infinite set of real eigenvalues $\lambda_1^2, \lambda_2^2, \lambda_3^2, \ldots$ To each eigenvalue λ_n^2 there corresponds, in accordance with (2.8), a certain vibration frequency; hence, an infinite set of natural frequencies will correspond to the infinite set of eigenvalues λ_n^4 $(n=1,2,3,\ldots)$.

From (2.8) we obtain:

$$\omega_n^2 = \frac{\lambda^4 + s^4 - r^4}{m^4}. \tag{2.13}$$

Similarly, in accordance with (2.9), a pair of numbers α_n and β_n, which determine the function $X_n(x)$, will correspond to each eigenvalue λ_n^4. We thus obtain an infinite set of functions $X_n(x)$ $(n=1,2,3,\ldots)$ which satisfy all the conditions of the given homogeneous boundary-value problem. These functions are called eigenfunctions (cf. section 4 of Chapter III).

Since the constants $C_1,\ldots,C_4$ are determined by (2.11) up to one common constant factor, each eigenfunction $X_n(x)$ will also be determined up to one constant factor.

2

The eigenfunctions possess the property of orthogonality:

$$\int_0^l X_i X_k \, dx = 0. \quad [i \neq k] \tag{2.14}$$

This can be proved as follows:

Since X_i and X_k are solutions of (2.7), we have:

$$\left.\begin{aligned} (\lambda_i^4 - r^4) X_i &= X_i^{IV} - 2r^2 X_i'', \\ (\lambda_k^4 - r^4) X_k &= X_k^{IV} - 2r^2 X_k'', \end{aligned}\right\} \tag{2.15}$$

where λ_i^4 and λ_k^4 = eigenvalues corresponding to eigenfunctions X_i and X_k

We multiply the first equation (2.15) by X_k, the second by X_i, subtract one from the other, and integrate the resulting equation between $x=0$ and $x=l$. This yields:

$$(\lambda_i^4 - \lambda_k^4) \int_0^l X_i X_k \, dx = \int_0^l X_i^{IV} X_k \, dx - \int_0^l X_k^{IV} X_i \, dx - 2r^2 \left(\int_0^l X_i'' X_k \, dx - \int_0^l X_k'' X_i \, dx \right). \tag{2.16}$$

Integrating the right-hand side by parts, we obtain:

$$(\lambda_i^4 - \lambda_k^4) \int_0^l X_i X_k \, dx = [X_i''' X_k - X_k''' X_i - X_i'' X_k' + X_k'' X_i' - 2r^2 (X_i' X_k - X_k' X_i)]_0^l, \tag{2.17}$$

where the symbol $[\;]_0^l$ denotes the difference between the values for $x=l$ and for $x=0$ of the expression in brackets.

The right-hand side of (2.17) is proportional to the work done in state "i" by the generalized boundary moments and forces M and Q over the boundary displacements corresponding to another state k, and is zero in the case of homogeneous boundary conditions, irrespective of the type of support. Hence:

$$(\lambda_i^4 - \lambda_k^4) \int_0^l X_i X_k \, dx = 0.$$

Since the eigenvalues λ_i^2 and λ_k^2 are distinct when $i \neq k$, it follows that:

$$\lambda_i^4 - \lambda_k^4 \neq 0$$

and therefore:

$$\int_0^l X_i X_k \, dx = 0,$$

which proves the orthogonality of the eigenfunctions.

Exactly as in the case of vibrations of a simple beam (cf. section 4 of Chapter III) all even derivatives of the functions X_i and X_k also possess the property of orthogonality:

$$\int_0^l X_i^{(2m)} X_k^{(2m)} \, dx = 0. \tag{2.18}$$

Here, $X^{(2m)}$ denotes the derivative of order $2m \, (m = 1, 2, 3, \ldots)$. This can be proved for any value of m in the same way as the orthogonality of the eigenfunctions themselves was demonstrated.

3

Some examples of the determination of the eigenfunctions and the natural frequencies of a beam on an elastic single-layer foundation will now be given.

a) Let the beam ends have simple supports. The boundary conditions are then:

at $X' = 0$ and $X = l$ $$X = X'' = 0. \tag{2.19}$$

The following system of equations in $C_1, \ldots, C_4$ are obtained from these boundary conditions and from (2.10):

$$\begin{aligned} C_2 + C_4 &= 0, \\ \alpha^2 C_2 - \beta^2 C_4 &= 0, \\ C_1 \operatorname{sh} \alpha l + C_2 \operatorname{ch} \alpha l + C_3 \sin \beta l + C_4 \cos \beta l &= 0, \\ C_1 \alpha^2 \operatorname{sh} \alpha l + C_2 \alpha^2 \operatorname{ch} \alpha l - C_3 \beta^2 \sin \beta l - C_4 \beta^2 \cos \beta l &= 0. \end{aligned}$$

The first two equations yield:

$$C_2 = C_4 = 0.$$

The remaining two equations then reduce to:

$$\left.\begin{aligned} \operatorname{sh}\alpha l C_1 + \sin\beta l C_3 = 0, \\ \alpha^2 \operatorname{sh}\alpha l C_1 - \beta^2 \sin\beta l C_3 = 0. \end{aligned}\right\} \qquad (2.20)$$

Equating to zero the determinant of this system, we obtain:

$$(\alpha^2 + \beta^2)\operatorname{sh}\alpha l \sin\beta l = 0$$

or

$$\sin\beta l = 0, \qquad (2.21)$$

whose roots are:

$$\beta_n = \frac{n\pi}{l}. \ \text{[where } n \text{ is an integer]} \qquad (2.22)$$

Substitution of (2.22) in the second equation (2.9) yields all the eigenvalues of the given problem:

$$\lambda_n^2 = \frac{n^2\pi^2}{l^2} + r^2. \qquad (2.23)$$

Substituting (2.23) in (2.13), we obtain finally:

$$\omega_n = \sqrt{\frac{1}{m^*}\left[s^4 + 2r^2\left(\frac{n\pi}{l}\right)^2 + \left(\frac{n\pi}{l}\right)^4\right]}. \qquad (2.24)$$

This is a general formula for the natural frequencies of the system. For instance, putting $s = r = 0$, we obtain as a particular case the natural frequency of a simple single-span beam. Putting only $r = 0$, we obtain the frequencies of a beam on a Winkler foundation of modulus k.

Having determined the eigenvalues λ_n^2 and frequencies ω_n, we can find the eigenfunctions X_n. According to (2.21):

$$\sin\beta l = 0.$$

Substitution of this in (2.20) yields:

$$C_1 = 0.$$

Hence, in the case considered three constants vanish:

$$C_1 = C_2 = C_4 = 0. \qquad (2.25)$$

The constant C_3 remains indeterminate.

Substitution of (2.25) in the first equation (2.10) yields the eigenfunctions $X_n(x)$, determined up to a constant factor. Taking this factor as unity, we obtain:

$$X_1 = \sin\frac{\pi x}{l}, \quad X_2 = \sin\frac{2\pi x}{l}, \quad X_3 = \sin\frac{3\pi x}{l}, \ldots \qquad (2.26)$$

b) If the beam end $x = 0$ is simply supported while the end $x = l$ is built in, the boundary conditions will be:

$$\left.\begin{array}{ll} \text{at } x = 0 \qquad & X = X'' = 0, \\ \text{at } x = l \qquad & X = X' = 0, \end{array}\right\} \tag{2.27}$$

whence:

$$\left.\begin{aligned} C_2 + C_4 &= 0, \\ \alpha^2 C_2 - \beta^2 C_4 &= 0, \\ \operatorname{sh}\alpha l C_1 + \operatorname{ch}\alpha l C_2 + \sin\beta l C_3 + \cos\beta l C_4 &= 0, \\ \alpha \operatorname{ch}\alpha l C_1 + \alpha \operatorname{sh}\alpha l C_2 + \beta\cos\beta l C_3 - \beta\sin\beta l C_4 &= 0. \end{aligned}\right\} \tag{2.28}$$

Thus:

$$\left.\begin{aligned} C_2 = C_4 &= 0, \\ \operatorname{sh}\alpha l C_1 + \sin\beta l C_3 &= 0, \\ \alpha\operatorname{ch}\alpha l C_1 + \beta\cos\beta l C_3 &= 0. \end{aligned}\right\} \tag{2.29}$$

The corresponding characteristic equation is:

$$\beta \operatorname{sh}\alpha l \cos\beta l - \alpha \operatorname{ch}\alpha l \sin\beta l = 0. \tag{2.30}$$

Substitution of:

$$\alpha = \sqrt{\lambda^2 + r^2}, \quad \beta = \sqrt{\lambda^2 - r^2},$$

yields:

$$\sqrt{\lambda^2 - r^2}\operatorname{th}\sqrt{\lambda^2 + r^2}\, l = \sqrt{\lambda^2 + r^2}\operatorname{tg}\sqrt{\lambda^2 - r^2}\, l. \tag{2.31}$$

If r^2 is given, the transcendental equation (2.31) determines all the eigenvalues $\lambda_1^2, \lambda_2^2, \lambda_3^2, \ldots$ of the boundary-value problem considered, whence all the natural frequencies $\omega_1, \omega_2, \omega_3, \ldots$ of the beam are determined by (2.13).

The eigenfunctions $X_n(x)$ corresponding to the eigenvalues λ_n^2 and boundary conditions (2.27) are:

$$\begin{gathered} X_n(x) = \sin\sqrt{\lambda_n^2 - r^2}\, l \operatorname{sh}\sqrt{\lambda_n^2 + r^2}\, x - \operatorname{sh}\sqrt{\lambda_n^2 + r^2}\, l \sin\sqrt{\lambda_n^2 - r^2}\, x \\ (n = 1, 2, 3, \ldots). \end{gathered} \tag{2.32}$$

It is easily seen that these functions satisfy the boundary conditions (2.27).

The functions $X_n(x)$ obtained depend also on the elastic characteristic r. By successively assigning different values to this parameter we obtain different families of eigenfunctions with corresponding eigenvalues, determined for a given r^2 by (2.23); all the functions corresponding to this value of r^2 will be orthogonal. The family of functions obtained for $r^2 = 0$ corresponds to the vibrations of a simple beam with one end simply supported and the other built-in (cf. section 4 of Chapter III).

c) When both beam ends are built in, the boundary conditions are:

$$\begin{array}{ll} \text{at } x=0 & \left.\begin{array}{ll} X=0, & X'=0; \\ X=0, & X'=0. \end{array}\right\} \\ \text{at } x=l & \end{array} \tag{2.33}$$

The characteristic equation, obtained in the same way as in the preceding examples, is:

$$\cos\sqrt{\lambda^2-r^2}\,l\,\operatorname{ch}\sqrt{\lambda^2+r^2}\,l-\frac{r^2}{\sqrt{\lambda^4-r^4}}\sin\sqrt{\lambda^2-r^2}\,l\,\operatorname{sh}\sqrt{\lambda^2+r^2}\,l=1. \tag{2.34}$$

The eigenfunctions are:

$$\begin{aligned} X_n(x) = (\operatorname{ch}\alpha_n l-\cos\beta_n l)(\beta_n\operatorname{sh}\alpha_n x-\alpha_n\sin\beta_n x)- \\ -(\beta_n\operatorname{sh}\alpha_n l-\alpha_n\sin\beta_n l)(\operatorname{ch}\alpha_n x-\cos\beta_n x), \end{aligned} \tag{2.35}$$

where

$$\alpha_n=\sqrt{\lambda_n^2+r^2},\quad \beta_n=\sqrt{\lambda_n^2-r^2}.$$

Putting $r=0$, we obtain the eigenfunctions and eigenvalues of a simple built-in beam.

The above method can also be applied to other boundary conditions.

4

Proceeding from the properties of the general integral of a homogeneous linear differential equation, the following general expression is obtained for the free vibrations of a beam on an elastic single-layer foundation:

$$V(x,t)=\sum_{n=1}^{\infty}X_nT_n=\sum_{n=1}^{\infty}X_n(A_n\sin\omega_n t+B_n\cos\omega_n t), \tag{2.36}$$

where A_n and B_n = integration constants.

This expression can also be written in the following form:

$$V(x,t)=\sum_{n=1}^{\infty}C_nX_n\sin\omega_n(t-\phi_n), \tag{2.37}$$

where the integration constants are now C_n and ϕ_n, the latter characterizing the phase shift.

It follows from (2.36) that the elastic line of a freely vibrating beam represents the geometrical sum of an infinite set of curves of the form:

$$X_n(A_n\sin\omega_n t+B_n\cos\omega_n t),$$

which are called principal modes of the transverse vibrations of a beam. Each curve is described by the corresponding function X_n and oscillates at the frequency ω_n. The beam axis therefore changes its shape continuously.

After the beam deflections have been determined in form (2.36), the velocity at each point is obtained from:

$$\frac{\partial V}{\partial t}=\sum_{n=1}^{\infty}X_n\omega_n(A_n\cos\omega_n t-B_n\sin\omega_n t). \tag{2.38}$$

The bending moments and shearing forces are:

$$M(x, t) = -EJ\sum_{n=1}^{\infty} X''_n\,(A_n \sin \omega_n t + B_n \cos \omega_n t). \tag{2.39}$$

$$Q(x, t) = -EJ\sum_{n=1}^{\infty} X'''_n\,(A_n \sin \omega_n t + B_n \cos \omega_n t). \tag{2.40}$$

The diagrams of these magnitudes also change their shape continuously. The maximum bending moments and shearing forces are obtained at different beam sections and times.

§ 3. ACTION OF A MOMENTARY IMPULSE

Let an impulse of intensity $p(x)$ per unit length act for an infinitely short time on an elastic beam of length l resting on a single-layer foundation. At the instant at which the load disappears the displacements are still infinitesimal, but the velocities are already finite.

After the load has been removed, the beam will vibrate freely, its deflections being:

$$V(x, t) = \sum_{n=1}^{\infty} X_n\,(A_n \sin \omega_n t + B_n \cos \omega_n t). \tag{3.1}$$

Assume that the eigenfunctions X_n of the bar and the corresponding frequencies ω_n have already been determined from the boundary conditions. We obtain the coefficients A_n and B_n from the initial conditions, which, according to our assumptions, are:

$$\left.\begin{aligned} V(x, 0) &= 0, \\ \frac{\partial V(x, 0)}{\partial t} &= v_0, \end{aligned}\right\} \tag{3.2}$$

where v_0 = initial velocity at section x.

The first condition (3.2) yields $B_n = 0$. To make use of the second condition, we express the initial velocity of a beam element of length dx in the form:

$$v_0 = \frac{p(x)}{m}, \tag{3.3}$$

where m = reduced mass per unit length of system, which, by the last expression (1.7), is:

$$m = m_1 + m_0 = \frac{\gamma\delta}{g} + \frac{\gamma_0\delta}{g}\int_0^R \phi^2(y)\,dy.$$

Since for $B_n = 0$:

$$\frac{\partial V}{\partial t} = \sum_{n=1}^{\infty} X_n A_n \omega_n \cos \omega_n t,$$

the second condition (3.2) becomes:

$$\frac{p(x)}{m}=\sum_{n=1}^{\infty} A_n \omega_n X_n. \tag{3.4}$$

The determination of the coefficients A_n thus reduces to expanding the function $\frac{p(x)}{m}$ in a series of the eigenfunctions X_n.

We multiply both sides of (3.4) by one of the eigenfunctions and integrate the resulting expression over the entire beam length:

$$\frac{1}{m}\int_0^l p(x)\, X_k\, dx=\sum_{n=1}^{\infty} \omega_n A_n \int_0^l X_n X_k\, dx. \tag{3.5}$$

Because of the orthogonality of the eigenfunctions, all integrals on the right-hand side vanish for $n \neq k$. The only nonzero integral is:

$$\omega_k A_k \int_0^l X_k^2\, dx. \tag{3.6}$$

Equation (3.5) thus reduces to:

$$\frac{1}{m}\int_0^l p(x)\, X_k\, dx=\omega_k A_k \int_0^l X_k^2\, dx,$$

whence:

$$A_k=\frac{\int_0^l p(x)\, X_k\, dx}{m\omega_k \int_0^l X_k^2\, dx}. \tag{3.7}$$

The solution finally obtained is thus:

$$V(x, t)=\frac{1}{m}\sum_{n=1}^{\infty} \frac{\int_0^l p(x)\, X_n\, dx}{\omega_n \int_0^l X_n^2\, dx} X_n \sin \omega_n t. \tag{3.8}$$

The bending moments and shearing forces are:

$$\left.\begin{aligned} M(x,t) &= -\frac{EJ}{m}\sum_{n=1}^{\infty}\frac{\int\limits_0^l p(x)\,X_n\,dx}{\omega_n\int\limits_0^l X_n^2\,dx}\,X_n''\sin\omega_n t,\\ Q(x,t) &= -\frac{EJ}{m}\sum_{n=1}^{\infty}\frac{\int\limits_0^l p(x)\,X_n\,dx}{\omega_n\int\limits_0^l X_n^2\,dx}\,X_n'''\sin\omega_n t. \end{aligned}\right\} \tag{3.9}$$

We thus see that each component of the impulse

$$p_n(x) = mA_n\omega_n X_n$$

causes a simple harmonic motion of mode X_n, frequency ω_n, and amplitude A_nX_n.

Series (3.8) for the deflections converges relatively slowly; series (3.9) for the bending moments and shearing forces converge even more slowly. This may cause considerable difficulties in practice. However, in these expressions no allowance has been made for the damping of the vibrations, which is considerably more rapid for the high-frequency vibrations than for the low-frequency vibrations; most high-frequency vibrations are already completely damped at the instant when the deflection corresponding to the fundamental mode attains its maximum.

As a result, it is sufficient to take the first terms of (3.8) and (3.9) in order to obtain a satisfactory approximation.

Consider, for example, a single-span beam with simple supports resting on an elastic foundation (Figure 143). Let a momentary impulse p, uniformly distributed over the span, be applied to the beam. The eigenfunctions are in this case given by (2.26), and the natural frequencies by (2.24). To determine the coefficients A_n, we substitute (2.26) in (3.7) and obtain:

$$A_n = \frac{p\int\limits_0^l \sin\frac{n\pi}{l}x\,dx}{m\omega_n\int\limits_0^l \sin^2\frac{n\pi}{l}x\,dx} = \frac{4p}{n\pi m\omega_n}. \tag{3.10}$$

Substituting these expressions in (3.8) yields:

$$\begin{aligned} V(x,t) &= \frac{4p}{\pi m}\sum_{n=1}^{\infty}\frac{1}{n\omega_n}\sin\frac{n\pi}{l}x\sin\omega_n t =\\ &= \frac{4p}{\pi m}\left[\frac{1}{\omega_1}\sin\frac{\pi x}{l}\sin\omega_1 t + \frac{1}{3\omega_3}\sin\frac{3\pi x}{l}\sin\omega_3 t + \dots\right]. \end{aligned} \tag{3.11}$$

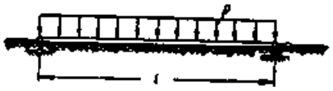

FIGURE 143.

Only odd values of n appear in (3.11), since a uniform impulse will cause the beam to vibrate symmetrically with respect to its center section.

§ 4. FORCED VIBRATIONS OF A BEAM

Consider an external load acting on a beam resting on an elastic foundation:

$$p(x, t) = p(x) f(t). \tag{4.1}$$

Assume that the variation of p is not accompanied by any noticeable variation of the mass of the system, i.e., m remains constant during the motion.

This problem reduces to integrating the nonhomogeneous differential equation (1.6). Its solution is the sum of the general solution of the corresponding homogeneous equation and of a particular solution of the nonhomogeneous equation. The general solution of the homogeneous equation is:

$$V(x, t) = \sum_{n=1}^{\infty} X_n (A_n \sin \omega_n t + B_n \cos \omega_n t), \tag{4.2}$$

where A_n and B_n are found by expanding the given initial values of V and $\frac{\partial V}{\partial t}$ in series of the eigenfunctions X_n, as shown in the preceding section for the case of a momentary impulse.

To determine a particular solution of (1.6), we expand $p(x)$ in a series of the eigenfunctions X_n:

$$p(x) = \sum_{n=1}^{\infty} C_n X_n. \tag{4.3}$$

The coefficients C_n can be determined by multiplying both sides of (4.3) by X_k and integrating over the entire beam length. Because of the orthogonality of the eigenfunctions, we obtain:

$$C_k = \frac{\int\limits_0^l p(x) X_k \, dx}{\int\limits_0^l X_k^2 \, dx}. \tag{4.4}$$

If the external load also includes concentrated forces P, the integral in the numerator of (4.4) is to be understood as a Stieltjes integral. We can therefore rewrite (4.4) as follows:

$$C_k = \frac{\int\limits_0^l p(x)\, X_k\, dx + \sum P\overline{X}_k}{\int\limits_0^l X_k^2\, dx}, \tag{4.5}$$

where $\overline{X}_k$ = values of functions X_k at points of application of forces P.

Each function X_n can be considered as an elastic line induced by a distributed static load of intensity $\omega_n^2 m X_n$. The static load $C_n X_n$ will obviously induce an elastic line whose ordinates are $\frac{C_n}{\omega_n^2 m} X_n$. A dynamic load causes at time t the displacements[*]

$$V(x, t) = \omega \int\limits_0^t V_{st}(u) \sin \omega (t - u)\, du, \tag{4.6}$$

In the case considered the static load is $C_n X_n f(t)$. Hence:

$$V_n(x, t) = \frac{C_n}{m\omega_n} X_n \int\limits_0^t f(u) \sin \omega_n (t - u)\, du. \tag{4.7}$$

Hence by (4.3):

$$V(x, t) = \sum_{n=1}^{\infty} \frac{C_n}{m\omega_n} X_n \int\limits_0^t f(u) \sin \omega_n (t - u)\, du. \tag{4.8}$$

The general solution of (1.6) is the sum of (4.2) and (4.8):

$$V(x, t) = \sum_{n=1}^{\infty} X_n \left[A_n \sin \omega_n t + B_n \cos \omega_n t + \frac{C_n}{m\omega_n} \int\limits_0^t f(u) \sin \omega_n (t - u)\, du \right]. \tag{4.9}$$

The bending moments and shearing forces are calculated by the known formulas of strength of materials:

$$M = -EJ \frac{\partial^2 V}{\partial x^2}, \quad Q = -EJ \frac{\partial^3 V}{\partial x^3}; \tag{4.10}$$

the velocity is found by differentiating (4.9) with respect to t:

$$v = \frac{\partial V}{\partial t} = \sum_{n=1}^{\infty} X_n \left[A_n \omega_n \cos \omega_n t - B_n \omega_n \sin \omega_n t \;\; \frac{C_n}{m} \int\limits_0^t f(u) \cos \omega_n (t - u)\, du \right]. \tag{4.11}$$

---

[*] See for instance, Rabinovich, I. M., Kurs stroitel'noi mekhaniki (A Course in Structural Mechanics), part II. 1954.

§ 5. DYNAMICAL ANALYSIS OF BEAMS CONSIDERED AS SYSTEMS WITH FINITE NUMBERS OF DEGREES OF FREEDOM

From the viewpoint of structural dynamics, the beams considered by us represent systems with infinitely large numbers of degrees of freedom. The deformed axis of such a system can acquire an infinitely large number of different shapes under the action of the various static and dynamic loads. The exact dynamical analysis of elastic beams, which takes into account the entire frequency spectrum, thus leads in general to an infinite series of the eigenfunctions of the given boundary-value problem.

However, it can frequently be assumed that the beam considered has a finite number of degrees of freedom. If a beam resting on an elastic foundation is so rigid that it does not become bent, it can be considered as a system with two degrees of freedom. Elastic beams can also be considered as systems with finite numbers of degrees of freedom. In this case some basic forms are selected from the infinitely large number of forms which the elastic line of the beam may assume, and only these forms are considered in the calculations. Any function approximating the elastic line of the beam and satisfying the geometrical boundary conditions can be taken as vibrational mode. This considerably simplifies the solution of the dynamical problem while being satisfactory for practical needs.

1

We consider first the vibrations of a rigid beam on an elastic single-layer foundation (Figure 144). Let the deflections of the beam be:

$$V = CT(t). \tag{5.1}$$

The equilibrium conditions of the beam are obtained by equating to zero the work done by all the forces acting on the beam over the virtual displacement $\overline{V} = 1$. The inertia forces per unit beam length are:

$$m_1 = \frac{\partial^2 V}{\partial t^2} = m_1 C T''. \tag{5.2}$$

In addition to these forces, there act on the beam also the reactions q and Q^* of the elastic foundation.

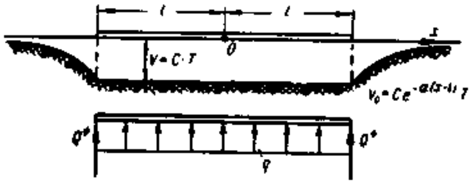

FIGURE 144.

In the general case, when allowance is made for the inertia of the foundation, the distributed reactions q are by (1.5):

$$q = -2t\frac{\partial^2 V}{\partial x^2} + kV + m_0\frac{\partial^2 V}{\partial t^2}. \qquad (5.3)$$

Substitution of (5.1) yields:

$$q = kCT + m_0CT''. \qquad (5.4)$$

To determine the fictitious reactions Q^Φ, it is necessary to calculate the work done by the normal and shearing stresses, and also by the inertia forces in the elastic foundation beyond the beam ends. The virtual displacements to the right of the beam are:

$$\bar{V}_0 = e^{-\alpha(x-l)}.$$

We then obtain:

$$Q^\Phi = \left(2\alpha tT + m_0\frac{\alpha t}{k}T''\right)C = \left(2\alpha tT + \frac{m_0}{2\alpha}T''\right)C, \qquad (5.5)$$

where:

$$\left.\begin{aligned} k &= \frac{E_0\delta}{1-\nu_0^2}\int_0^H \psi'^2(y)\,dy, \\ t &= \frac{E_0\delta}{4(1+\nu_0)}\int_0^H \psi^2(y)\,dy, \\ \alpha &= \sqrt{\frac{k}{2t}}. \end{aligned}\right\} \qquad (5.6)$$

Equation (5.5) for the concentrated reactions, valid for the dynamical problem, differs from (5.7) of Chapter II by the presence of a second term representing the inertia forces in the elastic foundation.

Equating to zero the work done by all the forces acting on the beam, we obtain:

$$(2lk + 4\alpha t)T + \left(2lm_0 + 2lm_1 + 2m_0\frac{\alpha t}{k}\right)T'' = 0, \qquad (5.7)$$

or

$$T'' + \frac{k\left(1 + \frac{1}{\alpha l}\right)}{m_1\left(1 + \frac{m_0}{m_1} + \frac{m_0}{m_1}\frac{1}{2\alpha l}\right)}T = 0. \qquad (5.8)$$

Thus, a rigid beam on an elastic foundation performs a simple harmonic motion at a frequency of

$$\omega = \sqrt{\frac{k}{m_1}\,\frac{1 + \frac{1}{\alpha l}}{1 + \frac{m_0}{m_1} + \frac{m_0}{m_1}\frac{1}{2\alpha l}}}. \qquad (5.9)$$

The vertical displacement of the beam at any instant is

$$V = C_1 \sin \omega t + C_2 \cos \omega t, \tag{5.10}$$

where C_1 and C_2 = constants determined from initial conditions.

2

We consider as a second example the free vibrations of an elastic beam of length $2l$ resting on a single-layer foundation (Figure 145). Let the motion be symmetrical with respect to the section $x = 0$. The elastic line of the beam is then approximately defined as follows:

$$X(x) = \sum_{i=0}^{n} A_i \cos \frac{i\pi x}{2l} \qquad (i = 0,\ 1,\ 3,\ 5, \ldots, n). \tag{5.11}$$

The first term of this series ($i = 0$) corresponds to the displacements of a rigid beam; the other terms correspond to a symmetrical bending. It can be seen that the function $X(x)$ satisfies the geometrical conditions of the problem and one of the statical boundary conditions ($M = 0$ at $x = \pm l$). The second boundary conditions ($Q = 0$ at $x = \pm l$) is not satisfied.

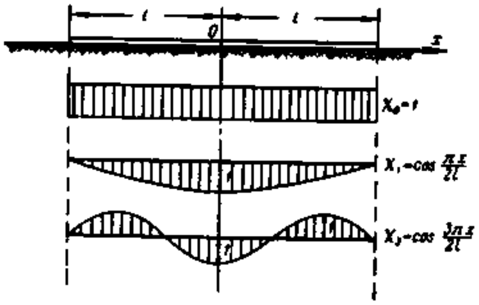

FIGURE 145.

To find the natural frequencies ω_i of the beam, corresponding to modes (5.11), we obtain the equilibrium conditions for the beam by means of the principle of virtual displacements. Taking (1.7) into account, (2.5) can be written as follows:

$$EJX^{IV} - 2tX'' + (k - m\omega^2)X = 0. \tag{5.12}$$

Substitution of (5.11) yields:

$$\sum_{i=0}^{n} A_i \left[EJ \left(\frac{i\pi}{2l}\right)^4 + 2t \left(\frac{i\pi}{2l}\right)^2 + (k - m\omega^2) \right] \cos \frac{i\pi x}{2l} = 0. \tag{5.13}$$

For each value of i, the first term corresponds to bending of the beam; the second and third terms containing the coefficients k and t depend on the reactions of the elastic foundation, distributed over the bottom of the beam; the last term depends on the inertia forces.

In addition to these loads, concentrated reactions Q^{Φ} will also act on the ends of the beam when the latter is forced into the soil like a rigid body. These reactions are determined from (5.5)*:

$$Q^{\Phi} = \left(2\alpha t - \frac{m_0}{2\alpha}\omega^2\right) A_0. \tag{5.14}$$

The following system of algebraic equations is obtained by calculating the work done by all these forces over each virtual displacement of the beam:

$$\left.\begin{aligned}
&\int_{-l}^{l}\sum_{i=0}^{n}(k - m\omega^2) A_i \cos\frac{i\pi x}{2l}\,dx + 2Q^{\Phi} = 0,\\
&\int_{-l}^{l}\sum_{i=0}^{n}\left[EJ\left(\frac{i\pi}{2l}\right)^4 + 2t\left(\frac{i\pi}{2l}\right)^2 + k - m\omega^2\right]\times\\
&\qquad\qquad\times A_i\cos\frac{i\pi x}{2l}\cos\frac{\pi x}{2l}\,dx = 0,\\
&\cdots\cdots\cdots\cdots\cdots\cdots\cdots\cdots\\
&\int_{-l}^{l}\sum_{i=0}^{n}\left[EJ\left(\frac{i\pi}{2l}\right)^4 + 2t\left(\frac{i\pi}{2l}\right)^2 + k - m\omega^2\right]\times\\
&\qquad\qquad\times A_i\cos\frac{i\pi x}{2l}\cos\frac{n\pi x}{2l}\,dx = 0\\
&\qquad(i = 0, 1, 3, 5, 7, \ldots, n),
\end{aligned}\right| \tag{5.15}$$

or, after the corresponding integrations are performed:

$$\left.\begin{aligned}
&\left[k\left(1 + \frac{1}{\alpha l}\right) - \left(m_1 + m_0 + m_0\frac{1}{2\alpha l}\right)\omega^2\right]A_0 +\\
&\qquad\qquad + \sum_{i=1}^{n} A_i\frac{2}{i\pi}(k - m\omega^2)(-1)^{\frac{i-1}{2}} = 0,\\
&\frac{2}{\pi}(k - m\omega^2)A_0 + \frac{1}{2}\left(EJ\frac{\pi^4}{16l^4} +\right.\\
&\qquad\qquad \left.+ 2t\frac{\pi^2}{4l^2} + k - m\omega^2\right)A_1 = 0,\\
&\cdots\cdots\cdots\cdots\cdots\cdots\cdots\cdots\\
&\frac{2}{n\pi}(k - m\omega^2)(-1)^{\frac{n-1}{2}}A_0 +\\
&\qquad + \frac{1}{2}\left(EJ\frac{n^4\pi^4}{16l^4} + 2t\frac{n^2\pi^2}{4l^2} + k - m\omega^2\right)A_n = 0\\
&\qquad(i = 1, 3, 5, 7, \ldots, n).
\end{aligned}\right| \tag{5.16}$$

The $\frac{n+3}{2}$ homogeneous algebraic equations (5.16) become identitites for $A_0 = A_1 = A_3 = \ldots = A_n = 0$. This trivial solution corresponds to the case when the beam does not vibrate. A nontrivial solution is obtained by equating to zero the determinant of the coefficients of the constants A_i. This yields an equation of order $\frac{n+3}{2}$ in the unknown ω^2, whose solution gives all the natural frequencies ω_i corresponding to the vibrational modes (5.11).

---

* It is assumed that the elastic foundation beyond the beam ends performs harmonic motion of frequency ω.

The vibration frequency ω_0 of a rigid beam, given by (5.9), is a particular case. This solution is also applicable to the natural vibrations of a beam on simple supports. In this case, the first term $(i=0)$ in (5.11) and the corresponding terms in (5.16) are discarded. Since in practice only the lowest frequencies are of interest, it is sufficient in the general case of a beam lying freely on the foundation to take only the first two or three terms in (5.11). The low frequencies are therefore obtained from a quadratic or cubic equation.

It was assumed in the above examples that the beam vibrates symmetrically with respect to the section $x=0$. In the general case, due to the orthogonality of the symmetrical and antisymmetrical modes of vibration, the problem can be divided into two independent parts corresponding respectively to the symmetrical and to the antisymmetrical modes. The frequencies corresponding to the antisymmetrical modes can be determined by the same method as described above.

3

Let a beam with free ends be subjected to the action of a momentary impulse of intensity $p(x)$ per unit length.

The initial conditions are:

$$\left.\begin{aligned} &V(x,\ 0)=0,\\ &\frac{\partial V(x,\ 0)}{\partial t}=\frac{p(x)}{m}. \end{aligned}\right\} \tag{5.17}$$

From (5.11) and the first condition (5.17), the beam deflections are approximately given by:

$$V(x,\ t)=\sum_{i=0}^{n} A_i \cos\frac{i\pi x}{2l}\sin\omega_i t, \tag{5.18}$$

where the vibration frequency ω_i is determined from (5.16).

The second condition (5.17) yields:

$$\frac{p(x)}{m}=\sum_{i=0}^{n} A_i\omega_i\cos\frac{i\pi x}{2l}. \tag{5.19}$$

The coefficients A_i are determined by expanding the function $\frac{p(x)}{m}$ in a series of $\cos\frac{i\pi x}{2l}\ (i=0,\ 1,\ 3,\ 5,\ldots)$. Multiplying in turn both sides of (5.19) by $\cos\frac{i\pi x}{2l}\ (i=0,\ 1,\ 3,\ 5,\ldots)$ and integrating the resulting expressions from $x=0$

to = , we obtain:

$$\left.\begin{aligned}
&A_0\omega_0 + \sum_{i=1}^{n} A_i\omega_i \frac{2}{i\pi}(-1)^{\frac{i-1}{2}} = \frac{1}{ml}\int_0^l p(x)\,dx,\\
&\frac{4}{\pi}A_0\omega_0 + A_1\omega_1 = \frac{2}{ml}\int_0^l p(x)\cos\frac{\pi x}{2l}\,dx,\\
&\dots\dots\dots\dots\dots\dots\dots\dots\dots\\
&\frac{4}{n\pi}A_0\omega_0(-1)^{\frac{n-1}{2}} + A_n\omega_n = \frac{2}{ml}\int_0^l p(x)\cos\frac{n\pi x}{2l}\,dx\\
&\qquad (i = 1,\ 3,\ 5,\ 7,\dots,n),
\end{aligned}\right\} \tag{5.20}$$

from which all coefficients A_i in (5.18) can be found.

After the beam deflections have been determined in the form (5.18), the bending moments and shearing forces corresponding to $i \geqslant 1$ can be calculated by means of (4.10). The forces and moments corresponding to rigid-body motion of the beam (the first term in (5.18)) are determined by the reactions of the elastic foundation which can be found from (5.4) and (5.5) when A_0 is known. The bending moments and shearing forces of the beam can then be calculated by the usual methods.

§ 6. DIFFERENTIAL EQUATION OF VIBRATIONS OF A PLATE RESTING ON AN ELASTIC SINGLE-LAYER FOUNDATION

During bending vibrations, a plate resting on an elastic foundation can be considered as being in static equilibrium, the plate elements being acted upon by inertia forces $\left(-m_1\frac{\partial^2 w}{\partial t^2}\right)$ in addition to a distributed load $p^*(x, y, t)$. The differential equation of plate vibrations can thus be obtained from (1.1) of Chapter III in the form:

$$D\nabla^2\nabla^2 w(x, y, t) = p^*(x, y, t) - m_1\frac{\partial^2 w(x, y, t)}{\partial t^2}, \tag{6.1}$$

where m_1 = mass per unit plate area; $p^*(x, y, t)$ = distributed load, consisting of given forces $p(x, y, t)$ per unit area and of reactions $q(x, y, t)$ of elastic foundation:

$$p^*(x, y, t) = p(x, y, t) - q(x, y, t). \tag{6.2}$$

The inertia of the elastic foundation must be taken into account when calculating the reactions $q(x, y, t)$.

To determine the latter, we cut out from the elastic foundation an elementary column of cross section $dx = 1$, $dy = 1$ and consider its equilibrium conditions, applying Lagrange's principle of virtual displacements (cf. section 6 of Chapter I).

Assume that no horizontal displacements occur in the elastic foundation, and that the z-distribution of the vertical displacements is given by a single function $\psi(z)$ *:

$$\left.\begin{aligned} u(x, y, z, t) &= 0, \\ v(x, y, z, t) &= 0, \\ w(x, y, z, t) &= w(x, y, t)\,\psi(z). \end{aligned}\right\} \qquad (6.3)$$

Taking into account the inertia of the elastic foundation, the generalized equilibrium conditions of the elementary column are:

$$\int_0^H \frac{\partial\tau_{zx}}{\partial x}\psi\,dz - \int_0^H \sigma_z\psi'\,dz + \int_0^H \frac{\partial\tau_{zy}}{\partial y}\psi\,dz - \int_0^H \bar{m}_0 \frac{\partial^2 w(x, y, t)}{\partial t^2}\psi^2 dz + q(x, y, t) = 0, \qquad (6.4)$$

where $q(x, y, t)$ = load applied to unit area of elastic-foundation surface, $\bar{m}_0 = \frac{\gamma_0}{g}$ = mass per unit volume of elastic foundation, γ_0 = specific weight of soil, g = gravitational acceleration, and H = thickness of compressible layer.

By substituting in (6.4) the values of the normal and shearing stresses of the elastic foundation $\sigma_z, \tau_{zx}, \tau_{zy}$ (determined from (6.2) of Chapter I), we obtain after some transformations:

$$-2t\nabla^2 w(x, y, t) + kw(x, y, t) + m_0 \frac{\partial^2 w(x, y, t)}{\partial t^2} = q(x, y, t), \qquad (6.5)$$

where

$$\left.\begin{aligned} k &= \frac{E_0}{1-\nu_0^2}\int_0^H \psi'^2(z)\,dz, \\ t &= \frac{E_0}{4(1+\nu_0)}\int_0^H \psi^2(z)\,dz, \\ m_0 &= \bar{m}_0\int_0^H \psi^2(z)\,dz. \end{aligned}\right| \qquad (6.6)$$

The partial differential equation (6.5) describes the vibrations of the elastic foundation, due to a load $q(x, y, t)$. This equation can be considered together with (6.1), since the plate deflections are equal to the vertical displacements of the surface of the elastic foundation beneath the plate, and since the load $q(x, y, t)$ on the foundation equals the reactions of the elastic foundation on the plate.

Eliminating $q(x, y, t)$ between (6.1) and (6.5), we obtain:

$$\nabla^2\nabla^2 w - 2r^2\nabla^2 w + s^4 w + m^4 \frac{\partial^2 w}{\partial t^2} = \frac{p}{D}, \qquad (6.7)$$

---

* The function $\psi(z)$ is selected in such a way that $\psi(0) = 1$.

where:

$$\left.\begin{aligned} s^4 &= \frac{k}{D} = \frac{E_0}{(1-\nu_0^2)D}\int_0^H \psi'^2(z)\,dz, \\ r^2 &= \frac{t}{D} = \frac{E_0}{4(1+\nu_0)D}\int_0^H \psi^2(z)\,dz, \\ m^* &= \frac{m_1+m_0}{D} = \left(\frac{\gamma h}{g} + \frac{\gamma_0}{g}\int_0^H \psi^2(z)\,dz\right)\frac{1}{D} \end{aligned}\right\} \tag{6.8}$$

Here, D = flexural rigidity of plate, γ and γ_0 = specific weights of plate material and of soil respectively, h = plate thickness, g = gravitational acceleration, and:

$$E_0 = \frac{E_s}{1-\nu_s^2}, \qquad \nu_0 = \frac{\nu_s}{1-\nu_s}. \tag{6.9}$$

In the case of free vibrations, when no external load $p(x, y, t)$ acts, (6.7) reduces to:

$$\nabla^2\nabla^2 w - 2r^2\nabla^2 w + s^4 w = -m^*\frac{\partial^2 w}{\partial t^2}. \tag{6.10}$$

§ 7. APPROXIMATIVE ANALYSIS OF AN INFINITE PLATE IN THE CASE OF CONCENTRATED IMPACT*

Consider an infinite plate resting on an elastic single-layer foundation (Figure 146). Let the concentrated force $P(t)$, shown in Figure 147 as a function of t, be applied suddenly at some point of the plate, inducing a vibrational motion of the plate. The problem is to determine the stresses and strains of the plate during impact $(0 \leqslant t \leqslant \tau)$ and during the ensuing free vibrations of the plate $(\tau \leqslant t < \infty)$.

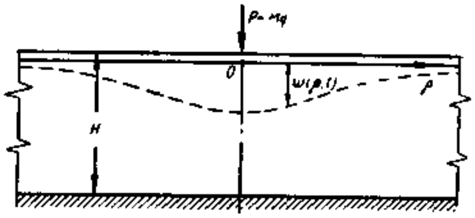

FIGURE 146.

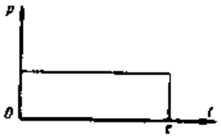

FIGURE 147.

We introduce a system of polar coordinates. Let the origin be at the point of application of the force. Obviously, the plate deflections will depend

---

[*] The calculation given in this section was performed by E. I. Silkin at the Institute of Mechanics of the USSR Academy of Sciences.

only on the space coordinate ρ and on the time t, i.e.:

$$w = w(\rho, t).$$

The fundamental equation describing the free vibrations of the plate is:

$$\nabla_\rho^2 \nabla_\rho^2 w - 2r^2 \nabla_\rho^2 w + s^4 w = -m^* \frac{\partial^2 w}{\partial t^2}, \tag{7.1}$$

where

$$\left.\begin{aligned} \nabla_\rho^2 &= \frac{\partial^2}{\partial\rho^2} + \frac{1}{\rho}\frac{\partial}{\partial\rho}, \\ \nabla_\rho^2 \nabla_\rho^2 &= \frac{\partial^4}{\partial\rho^4} + \frac{2}{\rho}\frac{\partial^3}{\partial\rho^3} - \frac{1}{\rho^2}\frac{\partial^2}{\partial\rho^2} + \frac{1}{\rho^3}\frac{\partial}{\partial\rho}. \end{aligned}\right\} \tag{7.2}$$

1. Solution of the fundamental differential equation

We present the solution of the homogeneous equation corresponding to (7.1) in the form:

$$w(\rho, t) = W(\rho)\, T(t), \tag{7.3}$$

where $W(\rho)$ = function of ρ only, and $T(t)$ = function of t only.
Substitution of (7.3) in (7.1) yields:

$$\frac{\nabla^2\nabla^2 W - 2r^2\nabla^2 W}{W} = -\frac{m^* T'' + s^4 T}{T}. \tag{7.4}$$

Since the two sides of (7.4) are functions of different variables, each of them must be equal to the same constant in order that the equation be satisfied in the general case:

$$\frac{\nabla^2\nabla^2 W - 2r^2\nabla^2 W}{W} = -\frac{m^* T'' + s^4 T}{T} = \lambda^4, \tag{7.5}$$

where λ^4 = parameter to be determined.
It follows from (7.5) that:

$$m^* T'' + (s^4 + \lambda^4)\, T = 0, \tag{7.6}$$

$$\nabla^2\nabla^2 W - 2r^2\nabla^2 W - \lambda^4 W = 0. \tag{7.7}$$

Putting

$$\frac{s^4 + \lambda^4}{m^*} = \omega^2, \tag{7.8}$$

(7.6) then becomes:

$$T'' + \omega^2 T = 0, \tag{7.9}$$

whose solution is:

$$T = D_1 \sin \omega t + D_2 \cos \omega t, \tag{7.10}$$

where D_1 and D_2 = integration constants.

Equation (7.7) determines the mode of the free vibrations of the plate. We assume a solution of the form:

$$\nabla^2 W = nW. \tag{7.11}$$

Substitution of (7.11) in (7.7) yields:

$$n^2 - 2r^2 n - \lambda^4 = 0,$$

whence:

$$n = r^2 \pm \sqrt{r^4 + \lambda^4}. \tag{7.12}$$

It is seen from (7.11) and (7.12) that the fourth-order differential equation (7.7) is equivalent to the two second-order differential equations:

$$\left.\begin{aligned} \nabla^2 W + \left(\sqrt{r^4 + \lambda^4} - r^2\right) W = 0, \\ \nabla^2 W - \left(\sqrt{r^4 + \lambda^4} + r^2\right) W = 0. \end{aligned}\right\} \tag{7.13}$$

These two equations can be reduced to the same form:

$$\frac{d^2 W}{dx^2} + \frac{1}{x}\frac{dW}{dx} + W = 0. \tag{7.14}$$

by putting in the first

$$x = \rho \sqrt{\sqrt{r^4 + \lambda^4} - r^2}$$

and in the second

$$x = i\rho \sqrt{\sqrt{r^4 + \lambda^4} + r^2},$$

Equations (7.13) are thus reduced to two zero-order Bessel equations of a real and an imaginary argument respectively.

Considering again the variable ρ, the solution of (7.7) can be represented as Bessel functions of the first and second kinds of a real and an imaginery arguments*:

$$\begin{aligned} W(\rho) = A_1 J_0\left(\rho \sqrt{\sqrt{r^4 + \lambda^4} - r^2}\right) + A_2 Y_0\left(\rho \sqrt{\sqrt{r^4 + \lambda^4} - r^2}\right) + \\ + A_3 I_0\left(\rho \sqrt{\sqrt{r^4 + \lambda^4} + r^2}\right) + A_4 K_0\left(\rho \sqrt{\sqrt{r^4 + \lambda^4} + r^2}\right), \end{aligned} \tag{7.15}$$

where J_0 and Y_0 = Bessel functions of a real argument, of the first and second kind respectively; I_0 and K_0 = Bessel functions, of an imaginary argument, of the first and second kind respectively (modified Bessel functions); A_1, A_2, A_3, A_4 = integration constants.

By (7.3), (7.10), and (7.15), the general solution of (7.1) is:

$$w(\rho, t) = [D_1 \sin \omega t + D_2 \cos \omega t][A_1 J_0 + A_2 Y_0 + A_3 I_0 + A_4 K_0]. \tag{7.16}$$

---

* In section 2 of Chapter IV the solution of a similar equation was presented in a different form. See also section 7 of Chapter I and section 6 of Chapter V.

2. Determining the integration constants from the initial and boundary conditions

To determine the six integration constants in (7.16) it is necessary to consider the initial and boundary conditions for the plate. Physical considerations impose the following boundary conditions on the function $w(\rho,\ t)$:

$$\left.\begin{aligned}&\text{at }\ \rho\to 0: && w\neq\infty;\\ &\text{at }\ \rho\to\infty: && w\to 0.\end{aligned}\right\}\tag{7.17}$$

Since for $\rho=0$ the functions Y_0 and K_0 tend to infinity, while for $\rho\to\infty$ the function I_0 tends to infinity (Figures 28, 148, and 149), we must have:

$$A_2=A_3=A_4=0,\tag{7.18}$$

Let no deflections occur before impact:

$$\text{at } t=0: \qquad w=0.\tag{7.19}$$

Hence, $D_2=0$, and (7.16) reduces to:

$$w(\rho,\ t)=C\sin\omega t\cdot J_0\left(\rho\sqrt{\sqrt{r^4+\lambda^4}-r^2}\right),\tag{7.20}$$

where C is a constant. To determine its value, let the striking body of mass M have a velocity V_0 at the instant of impact ($t=0$) If the rigidity of the plate is small, we can write:

$$\text{at } t=0 \text{ and } \rho=0: \qquad \frac{\partial w}{\partial t}=V_0.\tag{7.21}$$

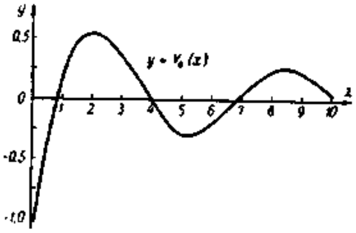

FIGURE 148.

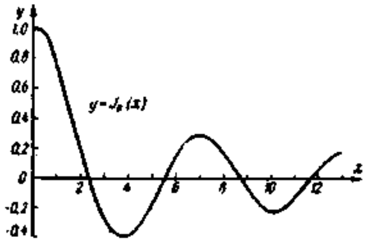

FIGURE 149.

This equation states that the velocities of the striking body and the plate are equal at the point and time of impact.

Since

$$\frac{\partial w}{\partial t}=C\omega\cos\omega t\cdot J_0\left(\rho\sqrt{\sqrt{r^4+\lambda^4}-r^2}\right)$$

and

$$J_0(0)=1,$$

we can rewrite (7.21) as follows:

$$C\omega = V_0,$$

whence:

$$C = \frac{V_0}{\omega}. \tag{7.22}$$

Substitution of (7.22) in (7.20) yields:

$$w(\rho,\ t) = \frac{V_0}{\omega}\sin\omega t\cdot J_0\left(\rho\sqrt{\sqrt{r^4+\lambda^4}-r^2}\right). \tag{7.23}$$

In the case of a massive plate, the coefficient C can be found by equating the momentums of the striking body and the plate at the time of impact:

$$\begin{aligned}\frac{PV_0}{g} = \frac{P}{g}C\omega\cos\omega t\cdot J_0(0)\Big|_{t=0} + \\ +\int_0^{\mu_1} 2\pi m C\omega\cos\omega t\cdot J_0\left(\rho\sqrt{\sqrt{r^4+\lambda^4}-r^2}\right)\rho\,d\rho\Big|_{t=0} + \\ +\sum_{n=1}\int_{\mu_n}^{\mu_{n+1}} 2\pi m C\omega\cos\omega t\cdot J_0\left(\rho\sqrt{\sqrt{r^4+\lambda^4}-r^2}\right)\rho\,d\rho\Big|_{t=0},\end{aligned} \tag{7.24}$$

where m = mass per unit area of plate and elastic foundation, determined from the last expression (6.8):

$$m = m^*D = \frac{\gamma h}{g} + \frac{\gamma_0}{g}\int_0^H \psi^2(z)\,dz; \tag{7.25}$$

and $\mu_1, \mu_2, \ldots, \mu_n$ = roots of the function:

$$J_0\left(\rho\sqrt{\sqrt{r^4-\lambda^4}-r^2}\right),$$

plotted in Figure 149.

The absolute value of the integrals has to be taken in (7.24). The summation in the last term is extended over all half-waves of the function:

$$J_0\left(\rho\sqrt{\sqrt{r^4+\lambda^4}-r^2}\right),$$

which lie inside the zone of motion of the plate, i.e., that part of the plate which acquires a velocity at the time of impact. The boundaries of this zone can be determined experimentally. Assume as a first approximation that the influence of the impact extends only over a distance corresponding to the first half-wave of J_0. We then obtain for $t = 0$:

$$\frac{PV_0}{g} = \frac{P}{g}C\omega + 2\pi C\omega m\int_0^{\mu_1}\rho J_0\left(\rho\sqrt{\sqrt{r^4+\lambda^4}-r^2}\right)d\rho. \tag{7.26}$$

The integral is equal to:

$$\int_0^{\mu_1}\rho J_0\left(\rho\sqrt{\sqrt{r^4+\lambda^4}-r^2}\right)d\rho = \frac{1}{\left(\sqrt{r^4+\lambda^4}-r^2\right)}\int_0^{\mu_1} xJ_0(x)\,dx = \frac{xJ_1(x)}{\left(\sqrt{r^4+\lambda^4}-r^2\right)}\Bigg|_0^{\mu_1}$$

or, since the first root of $J_0(x)$ is $\mu_1 = 2.4048$ and $J_1(\mu_1) = 0.5191$,

$$\int_0^{\mu_1} \rho J_0\left(\rho\sqrt{\sqrt{r^4+\lambda^4}-r^2}\right)d\rho = \frac{1,250}{\sqrt{r^4+\lambda^4}-r^2}.$$

Substituting this value in (7.26), we obtain:

$$C = \frac{PV_0(\sqrt{r^4+\lambda^4}-r^2)}{\omega\left[P(\sqrt{r^4+\lambda^4}-r^2)+2,5\pi mg\right]}. \tag{7.27}$$

Substitution of (7.27) in (7.20) then yields:

$$w(\rho,\ t) = \frac{PV_0(\sqrt{r^4+\lambda^4}-r^2)}{\omega\left[P(\sqrt{r^4+\lambda^4}-r^2)+2,5\pi mg\right]}\sin\omega t\cdot J_0\left(\rho\sqrt{\sqrt{r^4+\lambda^4}-r^2}\right). \tag{7.28}$$

3. Obtaining the parameter λ determining the vibration frequency ω of the plate

The parameter λ appearing in (7.23) and (7.28) is related to the vibration frequency ω of the plate by (7.8), and is determined by considering the equilibrium condition of a cylindrical element cut out of the plate near the point of impact (Figure 150).

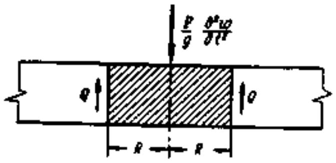

FIGURE 150.

Neglecting the foundation reactions and inertia, the equilibrium condition of this element is approximately given by:

$$2\pi RQ = \frac{P}{g}\frac{\partial^2 w}{\partial t^2}, \tag{7.29}$$

where R = radius of cut-out element and Q = shearing force acting along its edge:

$$Q = -D\frac{\partial}{\partial\rho}\left(\frac{\partial^2 w}{\partial\rho^2}+\frac{1}{\rho}\frac{\partial w}{\partial\rho}\right). \tag{7.30}$$

Introducing the coordinate R, defined by:

$$R = \rho\sqrt{\sqrt{r^4+\lambda^4}-r^2}. \tag{7.31}$$

we can rewrite (7.30) as follows:

$$Q = -D\left(\sqrt{r^4+\lambda^4} - r^2\right)^{3/2}\left(\frac{\partial^3 w}{\partial R^3} - \frac{1}{R^2}\frac{\partial w}{\partial R} + \frac{1}{R}\frac{\partial^2 w}{\partial R^2}\right). \tag{7.32}$$

Substitution of (7.20) yields:

$$Q = -D\left(\sqrt{r^4+\lambda^4} - r^2\right)^{3/2} C\sin\omega t\left[J_0'''(R) - \frac{1}{R^2}J_0'(R) + \frac{1}{R}J_0''(R)\right]. \tag{7.33}$$

Since:

$$J_0' = -J_1,\ J_0'' = \frac{J_1}{R} - J_0,\quad J_0''' = \frac{RJ_0 - J_1}{R^2} - \frac{J_1}{R^2} + J_1,$$

(7.33) can be rewritten as follows:

$$Q = -D\left(\sqrt{r^4+\lambda^4} - r^2\right)^{3/2} C\sin\omega t\cdot J_1(R). \tag{7.34}$$

The function $J_1(R)$ has been plotted in Figure 151. It is seen that (7.34) is not valid at $\rho = 0$. We therefore exclude the zone inside the radius $R = 1.8$ from our consideration. [For $R = 1.8$], we then obtain:

$$Q = -0.582\,D\left(\sqrt{r^4+\lambda^4} - r^2\right)^{3/2} C\sin\omega t. \tag{7.35}$$

Substituting (7.35) and (7.20) in (7.29), and taking (7.8) and (6.8) into account, we obtain:

$$\left(\sqrt{r^4+\lambda^4} - r^2\right)^{3/2} = \frac{\dfrac{P\left(s^4+\lambda^4\right)}{H}}{19.4\left[\gamma h + \gamma_0\int\limits_0 \psi^2(z)\,dz\right]}. \tag{7.36}$$

After λ^4 has been determined from (7.36), the frequency of the plate vibrations during the impact can be calculated by (7.8).

4. Free plate vibrations

At the instant at which the impact ends ($t = \tau$) the plate has already acquired finite displacements and velocities, and it continues thereafter to vibrate freely. The displacement and velocity at the beginning of the free vibrations are, by (7.20):

$$\left.\begin{aligned} w &= C\sin\omega\tau J_0,\\ \frac{\partial w}{\partial t} &= C\omega\cos\omega\tau\cdot J_0. \end{aligned}\right\} \tag{7.37}$$

Taking into account the boundary conditions at the origin of coordinates and at infinity, the solution of (7.1) is:

$$\begin{aligned} w(\rho, t) &= \left[D_1\sin\omega^*(t-\tau) + D_2\cos\omega^*(t-\tau)\right]A_1 J_0^* = \\ &= \left[C_1\sin\omega^*(t-\tau) + C_2\cos\omega^*(t-\tau)\right]J_0^* \end{aligned} \tag{7.38}$$

where ω^* is the frequency of the free vibrations, and λ^* determines the argument of the function J_0^*. The constants C_1 and C_2 are found from the initial conditions. Putting $t=\tau$ in (7.38), we obtain:

$$\left.\begin{aligned} w &= C_2 J_0^*, \\ \frac{\partial w}{\partial t} &= \omega^* C_1 J_0^*. \end{aligned}\right\} \qquad (7.39)$$

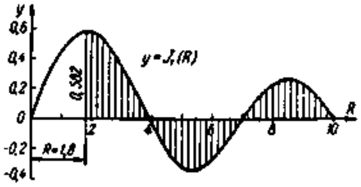

FIGURE 151.

Solving (7.37) and (7.39) for C_1 and C_2 yields:

$$\left.\begin{aligned} C_1 &= C\frac{\omega}{\omega^*}\cos\omega\tau\frac{J}{J_0^*}, \\ C_2 &= C\sin\omega\tau\frac{J_0}{J_0^*}, \end{aligned}\right\} \qquad (7.40)$$

where C is given by (7.22) in the case of a flexible plate, and by (7.27) in the case of a massive plate.

Substitution of (7.40) in (7.38) yields:

$$w(\rho, t) = \left[\frac{\omega}{\omega^*}\cos\omega\tau\sin\omega^*(t-\tau) + \sin\omega\tau\cos\omega^*(t-\tau)\right] CJ_0. \qquad (7.41)$$

We obtain the parameter ω^* from (7.1), assuming its solution to be of the form:

$$\nabla^2 w = \alpha w, \qquad (7.42)$$

where α has to be determined.

Substitution of (7.42) in (7.1) yields:

$$\alpha^2 w - 2r^2\alpha w + s^4 w = -m^*\frac{\partial^2 w}{\partial t^2}. \qquad (7.43)$$

Inserting into this (7.41), we obtain:

$$\alpha^2 - 2r^2\alpha + s^4 = m^*\omega^{*2}, \qquad (7.44)$$

where ω^* is to be considered as a function of α, whose extremum is given by:

$$\frac{d\omega^*}{d\alpha} = 0, \qquad (7.45)$$

or

$$\frac{d\omega^*}{d\alpha} = \frac{\alpha - r^2}{m^* \sqrt{\frac{\alpha^2 - 2r^2\alpha + s^4}{m^*}}} = 0.$$

This condition is fulfilled for:

$$\alpha = r^2.$$

Substitution of this value of α in (7.44) yields:

$$\omega^* = \sqrt{\frac{s^4 - r^4}{m^*}}, \tag{7.46}$$

where, as before:

$$m^* = \frac{m_1 + m_0}{D} = \left[\frac{\gamma h}{g} + \frac{\gamma_0}{g}\int_0^H \psi^2(z)\,dz\right]\frac{1}{D}.$$

§ 8. PLATE WITH SIMPLE SUPPORTS ALONG THE EDGES

2

Let the deflections of a freely vibrating plate with simple supports, resting on an elastic foundation (Figure 152) be given by:

$$w(x, y, t) = w(x, y)\,T(t). \tag{8.1}$$

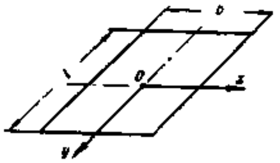

FIGURE 152.

The differential equation describing the shape of the deformed plate surface is, as before:

$$\nabla^2\nabla^2 w - 2r^2\nabla^2 w + (s^4 - m^*\omega^2)\,w = 0, \tag{8.2}$$

whose solution can be represented as follows:

$$w(x, y) = \sum_{i=1}^{\infty}\sum_{n=1}^{\infty} A_{in}\cos\frac{i\pi x}{b}\cos\frac{n\pi y}{l}. \tag{8.3}$$

Each term of this series satisfies the boundary conditions at the plate edges [when i and n are odd]:

at $x = \pm\frac{b}{2}$: $\quad w = 0, \quad \frac{\partial^2 w}{\partial x^2} = 0;$

at $y = \pm\frac{l}{2}$: $\quad w = 0, \quad \frac{\partial^2 w}{\partial y^2} = 0.$

We determine the natural frequencies ω by substituting (8.3) in (8.2), multiplying the result by $\cos\frac{j\pi x}{b}\cos\frac{h\pi x}{l}$ (j and h are arbitrary integers), and integrating over the plate surface:

$$\int_{-\frac{b}{2}}^{\frac{b}{2}}\int_{-\frac{l}{2}}^{\frac{l}{2}}\sum_{i=1}^{\infty}\sum_{n=1}^{\infty} A_{in}\left[\left(\frac{i^2\pi^2}{b^2}+\frac{n^2\pi^2}{l^2}\right)^2+2r^2\left(\frac{i^2\pi^2}{b^2}+\frac{n^2\pi^2}{l^2}\right)+s^4-m^*\omega^2\right]\times \\ \times\cos\frac{i\pi x}{b}\cos\frac{n\pi y}{l}\cos\frac{j\pi x}{b}\cos\frac{h\pi y}{l}\,dx\,dy=0. \tag{8.4}$$

Equation (8.4) defines the work done by all generalized forces acting on plate and elastic foundation over the virtual displacements of the plate. Because of the orthogonality of the trigonometric functions, all integrals for which $i \neq j$ and $n \neq h$ are equal to zero, and (8.4) reduces to:

$$A_{in}\iint\left[\left(\frac{i^2\pi^2}{b^2}+\frac{n^2\pi^2}{l^2}\right)^2+2r^2\left(\frac{i^2\pi^2}{b^2}+\frac{n^2\pi^2}{l^2}\right)+s^4-m^*\omega^2\right]\times \\ \times\cos^2\frac{i\pi x}{b}\cos^2\frac{n\pi y}{l}\,dx\,dy=0. \tag{8.5}$$

In order that the solution be nontrivial, we must have:

$$\left(\frac{i^2\pi^2}{b^2}+\frac{n^2\pi^2}{l^2}\right)^2+2r^2\left(\frac{i^2\pi^2}{b^2}+\frac{n^2\pi^2}{l^2}\right)+s^4-m^*\omega^2=0,$$

whence:

$$\omega_{in}=\sqrt{\frac{1}{m^*}\left[\left(\frac{i^2\pi^2}{b^2}+\frac{n^2\pi^2}{l^2}\right)^2+2r^2\left(\frac{i^2\pi^2}{b^2}+\frac{n^2\pi^2}{l^2}\right)+s^4\right]}. \tag{8.6}$$

The entire frequency spectrum is obtained by assigning in turn different integral values to i and n. The principal vibration modes corresponding to these frequencies are:

$$w_{in}=A_{in}\cos\frac{i\pi x}{b}\cos\frac{n\pi y}{l}. \tag{8.7}$$

2

The coefficients A_{in} are determined from the initial conditions of the problem. Let a momentary impulse of intensity $p(x, y)$ per unit area act on the plate. Since there are no displacements at $t = 0$, the deflection function can be written:

$$w(x, y, t)=\sum_{i=1}^{\infty} \sum_{n=1}^{\infty} A_{in} \cos \frac{i\pi x}{b} \cos \frac{n\pi y}{l} \sin \omega_{in} t, \tag{8.8}$$

whence:

$$\frac{\partial w}{\partial t}=\sum_{i=1}^{\infty} \sum_{n=1}^{\infty} A_{in} \omega_{in} \cos \frac{i\pi x}{b} \cos \frac{n\pi y}{l} \cos \omega_{in} t. \tag{8.9}$$

The initial velocity at $t=0$ is:

$$\left(\frac{\partial w}{\partial t}\right)_{t=0}=\sum_{i=1}^{\infty} \sum^{\infty} A_{in} \omega_{in} \cos \frac{i\pi x}{b} \cos \frac{n\pi y}{l}=\frac{p(x, y)}{m}. \tag{8.10}$$

We multiply (8.10) by $\cos \frac{j\pi x}{b} \cos \frac{h\pi y}{l}$ and integrate the result over the plate surface. Because of the orthogonality of the trigonometric functions this yields:

$$A_{in} \omega_{in} \int_{-b/2}^{b/2} \int_{-l/2}^{l/2} \cos^2 \frac{i\pi x}{b} \cos^2 \frac{n\pi y}{l} \, dx \, dy=\frac{1}{m} \int_{-b/2}^{b/2} \int_{-l/2}^{l/2} p(x, y) \cos \frac{i\pi x}{b} \cos \frac{n\pi y}{l} \, dx \, dy,$$

whence:

$$A_{in}=\frac{4 \int_{-b/2}^{b/2} \int_{-l/2}^{l/2} p(x, y) \cos \frac{i\pi x}{b} \cos \frac{n\pi y}{l} \, dx \, dy}{m \; \omega_{in} \, lb} \tag{8.11}$$

Thus, finally:

$$w(x, y, t)=\frac{4}{m \, lb} \sum_{i=1}^{\infty} \sum_{n=1}^{\infty} \frac{\int_{-b/2}^{b/2} \int_{-l/2}^{l/2} p(x, y) \cos \frac{i\pi x}{b} \cos \frac{n\pi y}{l} \, dx \, dy}{\omega_{in}} \times \cos \frac{i\pi x}{b} \cos \frac{n\pi y}{l} \sin \omega_{in} t. \tag{8.12}$$

Substituting (8.12) in (1.8) of Chapter III, we obtain the values of the bending moments and shearing forces appearing in the plate due to the momentary impulse $p(x, y)$.

§ 9. VIBRATIONS OF A PLATE WITH FREE EDGES

1

The natural frequencies of a plate resting freely on an elastic foundation

(Figure 153) are determined by separating the variables in (6.10):

$$T'' + \omega^2 T = 0, \tag{9.1}$$

$$D\nabla^2\nabla^2 w - 2t\nabla^2 w + (k - m\omega^2)\, w = 0. \tag{9.2}$$

The shape of the deformed surface of the plate can be represented in the following form:

$$w(x, y) = \sum_1^m \sum_1^n C_{mn}\, \varphi_{mn}(x, y), \tag{9.3}$$

where $\varphi_{mn}(x, y)$ = linearly independent functions, selected in advance according to the geometrical boundary conditions, and C_{mn} = constant coefficients. For the functions φ_{mn} we shall choose trigonometric functions together with linear terms corresponding to rigid-body displacements of the plate:

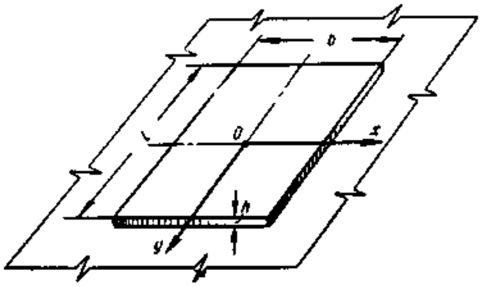

FIGURE 153.

The frequencies corresponding to the vibrational modes (9.3) are determined from the equilibrium conditions, applying Lagrange's principle of virtual displacements. For this we calculate the work done by all external and internal forces acting on the plate over any virtual displacement, in the same way as in section 12 of Chapter III. Substitution of (9.3) in (9.2) then yields the following system of algebraic equations:

$$\begin{gathered}\sum_1^m \sum_1^n C_{mn} \Big\{ \iint [D\nabla^2\nabla^2 \varphi_{mn} - 2t\nabla^2\varphi_{mn} + (k - m\omega^2)\, \varphi_{mn}]\, \varphi_{ik}\, dx\, dy + \\ + \oint [Q_{mn}(s) + Q\Phi(s)]\, \varphi_{ik}\, ds \Big\} = 0 \\ (i = 1, 2, 3, \ldots, m; \qquad k = 1, 2, 3, \ldots, n),\end{gathered} \tag{9.4}$$

The terms under the double integral sign in (9.4) represent the work done by the internal forces acting in the plate, the reactions of the elastic foundation, and the inertia forces arising in the plate and the elastic foundation. The contour integral represents the work done by the shearing forces acting on the plate edges. The first term determines the work done by Kirchhoff's reduced additional shearing forces (cf. (1.9) of Chapter III), which appear at the plate edges as a result of the approximate fulfilment of the static-equilibrium conditions by the functions $\varphi(x, y)$. The second term represents the work done by the reactions, distributed over the plate edges, determined by the deformations of the elastic foundation beyond the plate edges. Using (10.8) and (10.9) of Chapter III, and taking into account the work done by the inertia forces acting on the elastic foundation beyond the plate edges (cf. for instance (5.5) and (5.14)), we obtain:

$$\left.\begin{aligned} Q_l{}^{\Phi} &= 2t\left[\left(\alpha - m_0\frac{\omega^2}{4\alpha t}\right)w_l + \left(\frac{\partial w}{\partial x}\right)_l - \frac{1}{2\alpha}\left(\frac{\partial^2 w}{\partial y^2}\right)_l\right], \\ Q_b{}^{\Phi} &= 2t\left[\left(\alpha - m_0\frac{\omega^2}{4\alpha t}\right)w_b + \left(\frac{\partial w}{\partial y}\right)_b - \frac{1}{2\alpha}\left(\frac{\partial^2 w}{\partial x^2}\right)_b\right], \end{aligned}\right\} \tag{9.5}$$

where the subscripts l and b correspond to the longitudinal $(x = \pm b)$ and lateral $(y = \pm l)$ edges respectively.

Equations (9.4) holds true even when the postulation of a foundation modulus is acceptable; in this case the terms containing Q^{Φ} and t should be discarded, the characteristic k being taken as foundation modulus.

Equations (9.4) can be represented in the following form:

$$\left.\begin{aligned} \delta_{00,\,00}C_{00} + \delta_{00,\,10}C_{10} + \ldots + \delta_{00,\,mn}C_{mn} &= 0, \\ \delta_{10,\,00}C_{00} + \delta_{10,\,10}C_{10} + \ldots + \delta_{10,\,mn}C_{mn} &= 0. \\ \ldots\ldots\ldots\ldots\ldots\ldots\ldots\ldots\ldots & \\ \delta_{ik,\,00}C_{00} + \delta_{ik,\,10}C_{10} + \ldots + \delta_{ik,\,mn}C_{mn} &= 0, \\ \ldots\ldots\ldots\ldots\ldots\ldots\ldots\ldots\ldots & \\ \delta_{mn,\,00}C_{00} + \delta_{mn,\,10}C_{10} + \ldots + \delta_{mn,\,mn}C_{mn} &= 0, \end{aligned}\right\} \tag{9.6}$$

where:

$$\begin{aligned} \delta_{ik,\,mn} = \iint [D\nabla^2\nabla^2\varphi_{mn} - 2t\nabla^2\varphi_{mn} + (k - m\omega^2)\varphi_{mn}]\varphi_{ik}\,dx\,dy + \\ + \oint [Q_{mn}(s) + Q^{\Phi}(s)]\varphi_{ik}(s)\,ds. \end{aligned} \tag{9.7}$$

Integration in (9.7) is extended over the entire surface and the entire contour of the plate respectively. These integrals represent the virtual work done by the forces corresponding to one state of the system over the displacements corresponding to another state. Hence, by the reciprocity theorem:

$$(\delta_{ik,\,mn} = \delta_{mn,\,ik})$$

and the matrix of (9.6) will be symmetrical.

System (9.6) will have a nontrivial solution if its determinant vanishes:

$$\begin{vmatrix} \delta_{00,\,00} & \delta_{00,\,10} & \ldots & \delta_{00,\,mn} \\ \delta_{10,\,00} & \delta_{10,\,10} & \ldots & \delta_{10,\,mn} \\ \ldots & \ldots & \ldots & \ldots \\ \delta_{mn,\,00} & \delta_{mn,\,10} & \ldots & \delta_{mn,\,mn} \end{vmatrix} = 0. \tag{9.8}$$

Expansion of (9.8) leads to an equation of $(m+n)$-th degree in ω^2, whose solution will give all the $m+n$ frequencies corresponding to the vibrational modes (9.3). The natural vibrations of the plate are thus:

$$w(x, y, t) = \sum_1^m \sum_1^n C_{mn} \varphi_{mn}(x, y) \sin \omega_{mn}(t - \phi_{mn}), \tag{9.9}$$

where ϕ_{mn} = constant determining the phase shift.

If the shape of the deformed surface of the plate is described by trigonometric functions, their orthogonality enables the general problem of the motion of a plate on an elastic foundation to be divided into four independent problems corresponding to the symmetrical and antisymmetrical vibrations relative to the x and y axes respectively. Each of these problems will now be treated separately.

2

In the case of symmetrical vibrations, (9.3) becomes:

$$\begin{gathered} w(x, y) = C_{00} + \sum_1^m C_{m0} \cos\frac{m\pi x}{b} + \sum_1^n C_{0n} \cos\frac{n\pi y}{l} + \\ + \sum_1^m \sum_1^n C_{mn} \cos\frac{m\pi x}{b} \cos\frac{n\pi y}{l} \\ (m\ \ n = 1, 3, 5, \ldots, (2k-1)). \end{gathered} \tag{9.10}$$

This means that:

$$\left.\begin{aligned} &\varphi_{00} = 1, \quad \varphi_{m0} = \cos\frac{m\pi x}{b}, \\ &\varphi_{0n} = \cos\frac{n\pi y}{l}, \quad \varphi_{mn} = \cos\frac{m\pi x}{b}\cos\frac{n\pi y}{l}, \end{aligned}\right\} \tag{9.11}$$

where m and n = odd integers.

Substitution of (9.11) in (9.7) yields all the coefficients in (9.6). For example, when four terms $(m = 1,\ n = 1)$, corresponding to the four possible modes of plate vibration shown, are taken in (9.10), the matrix of the algebraic equations is given in Table 18. This matrix is symmetrical. It is formed by calculating 10 dimensionless coefficients, using the following symbols:

$$\left.\begin{aligned} &\alpha = \sqrt{\frac{k}{2t}}, \qquad \beta = \frac{b}{l}, \\ &D = \frac{Eh^3}{12(1-\mu^2)}, \\ &k = \frac{E_0}{1-\nu_0^2} \int_0^H \psi'^2(z)\, dz, \\ &t = \frac{E_0}{4(1+\nu_0)} \int_0^H \psi^2(z)\, dz, \\ &m_0 = \bar{m}_0 \int_0^H \psi^2(z)\, dz, \end{aligned}\right\} \tag{9.12}$$

Here l and b = length and width of the plate respectively, D = flexural rigidity of plate, m_0 = reduced mass of elastic foundation, k and t = generalized characteristics of elastic foundation, $\phi = \phi(t)$ = function representing distribution of displacements over thickness of elastic foundation.

By equating to zero the determinant of this matrix we obtain an algebraic equation of the fourth degree in ω^2, from which the natural frequencies of the plate, corresponding to the four assumed modes, can be obtained.

If the plate is considered to be perfectly rigid, all terms except the first in (9.10) vanish. From Table 18, we obtain for this case:

$$l + \frac{2}{\alpha b}(l + \beta) - \frac{m_0}{k}\left(l + \frac{m_1}{m_0} + \frac{1+\beta}{\alpha b}\right)\omega^2 = 0$$

or

$$\omega_{00} = \sqrt{\frac{k}{m_0} \frac{1 + \frac{2}{\alpha b}(l + \beta)}{1 + \frac{m_1}{m_0} + \frac{1+\beta}{\alpha b}}}. \tag{9.13}$$

3

In the case of antisymmetrical vibrations, (9.3) becomes:

a) for vibrations symmetrical with respect to the x axis and antisymmetrical with respect to the y axis:

$$w(x, y) = C_{00}\frac{2x}{b} + \sum_{2}^{m} C_{m0} \sin\frac{m\pi x}{b} + \frac{2x}{b}\sum_{1}^{n} C_{0n} \cos\frac{n\pi y}{l} + \\ + \sum_{2}^{m}\sum_{1}^{n} C_{mn} \sin\frac{m\pi x}{b}\cos\frac{n\pi y}{l} \tag{9.14}$$
$$(m = 2, 4, 6, \ldots; n = 1, 3, 5, \ldots);$$

b) for vibrations symmetrical with respect to the y axis and antisymmetrical with respect to the x axis:

$$w(x, y) = C_{00}\frac{2y}{l} + \frac{2y}{l}\sum_{1}^{m} C_{m0} \cos\frac{m\pi x}{b} + \sum_{2}^{n} C_{0n} \sin\frac{n\pi y}{l} + \\ + \sum_{1}^{m}\sum_{2}^{n} C_{mn} \cos\frac{m\pi x}{b}\sin\frac{n\pi y}{l} \tag{9.15}$$
$$(m = 1, 3, 5, \ldots; n = 2, 4, 6, \ldots);$$

c) for vibrations antisymmetrical with respect to both axes:

$$w(x, y) = C_{00}\frac{4xy}{lb} + \frac{2y}{l}\sum_{2}^{m} C_{m0} \sin\frac{m\pi x}{b} + \\ + \frac{2x}{b}\sum_{2}^{n} C_{0n} \sin\frac{n\pi y}{l} + \sum_{2}^{m}\sum_{2}^{n} C_{mn} \sin\frac{m\pi x}{b}\sin\frac{n\pi y}{l} \tag{9.16}$$
$$(n, m = 2, 4, 6, 8, \ldots).$$

TABLE 18

	C_{00}	C_{10}	C_{01}	C_{11}	Virtual displacements
0—0	$1+\frac{2}{\alpha b}(1+\beta)-$ $-\frac{m_0}{k}\left(1+\frac{m_1}{m_0}+\frac{1+\beta}{\alpha\beta}\right)\omega^2$	$\frac{2}{\pi}\Big[1+\frac{2}{\alpha b}\beta-$ $-\frac{m_0}{k}\left(1+\frac{m_1}{m_0}+\frac{\beta}{\alpha b}\right)\omega^2\Big]$	$\frac{2}{\pi}\Big[1+\frac{2}{\alpha b}-\frac{m_0}{k}\times$ $\times\left(1+\frac{m_1}{m_0}+\frac{1}{\alpha b}\right)\omega^2\Big]$	$\frac{4}{\pi^2}\left(1-\frac{m_1+m_0}{k}\omega^2\right)$	$\bar{w}_{00}=1$ 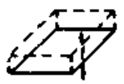
1—0	•	$\frac{1}{2}\Big[\frac{\pi^4 D}{kb^4}+\frac{\pi^2}{\alpha^2 b^2}+1+\frac{2}{\alpha b}\beta+$ $+\frac{\pi^2}{\alpha^2 b^2}\beta-\frac{m_0}{k}\left(1+\frac{m_1}{m_0}+\frac{\beta}{\alpha\beta}\right)\omega^2\Big]$	$\frac{4}{\pi^2}\left(1-\frac{m_1+m_0}{k}\omega^2\right)$	$\frac{1}{\pi}\Big[\frac{\pi^4 D}{kb^4}+\frac{\pi^2}{\alpha^2 b^2}+1-$ $-\frac{m_1+m_0}{k}\omega^2\Big]$	$\bar{w}_{10}=\cos\frac{\pi x}{b}$ 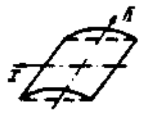
0—1	•	•	$\frac{1}{2}\Big[\frac{\pi^4 D}{kb^4}\beta^4+\frac{\pi^2}{\alpha^2 b^2}\beta^2+$ $+1+\frac{2}{\alpha b}+\frac{\pi^2}{\alpha^2 b^2}\beta^2-$ $-\frac{m_0}{k}\left(1+\frac{m_1}{m_0}+\frac{1}{\alpha b}\right)\omega^2\Big]$	$\frac{1}{\pi}\Big[\frac{\pi^4 D}{kb^4}\beta^4+\frac{\pi^2}{\alpha^2 b^2}\beta^2+$ $+1-\frac{m_1+m_0}{k}\omega^2\Big]$	$\bar{w}_{01}=\cos\frac{\pi y}{l}$ 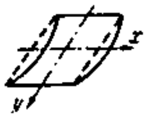
1—1	•	•	•	$\frac{1}{4}\Big[(1+\beta^2)^2\frac{\pi^4 D}{kb^4}+$ $+(1+\beta^2)\frac{\pi^2}{\alpha^2 b^2}+1-$ $-\frac{m_1+m_0}{k}\omega^2\Big]$	$\bar{w}_{11}=\cos\frac{\pi x}{b}\cos\frac{\pi y}{l}$ 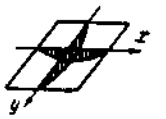

TABLE 19

	C_{00}	C_{20}	C_{01}	C_{21}	Virtual displacements
0—0	$\frac{1}{3}\left[1+\frac{6}{\alpha b}\left(1+\frac{\beta}{3}\right)+\frac{12}{\alpha^2 b^2}-\right.$ $\left.-\frac{m_0}{k}\left(1+\frac{m_1}{m_0}+\frac{3+\beta}{\alpha b}\right)\omega^2\right]$	$\frac{1}{\pi}\left[1+\frac{2}{\alpha b}\beta-\right.$ $\left.-\frac{m_0}{k}\left(1+\frac{m_1}{m_0}+\frac{\beta}{\alpha b}\right)\omega^2\right]$	$\frac{2}{3\pi}\left[1+\frac{6}{\alpha b}+\frac{12}{\alpha^2 b^2}-\right.$ $\left.-\frac{m_0}{k}\left(1+\frac{m_1}{m_0}+\frac{3}{\alpha b}\right)\omega^2\right]$	$\frac{2}{\pi^2}\left(1-\frac{m_1+m_0}{k}\omega^2\right)$	$\overline{w}_{00}=\frac{2x}{b}$ 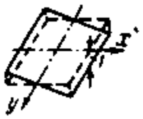
2—0	•	$\frac{1}{2}\left[16\frac{\pi^4 D}{kb^4}+4\frac{\pi^2}{\alpha^2 b^2}+1+\frac{2}{\alpha b}\beta+\right.$ $\left.+4\frac{\pi^2}{\alpha^2 b^2}\beta-\frac{m_0}{k}\left(1+\frac{m_1}{m_0}+\frac{\beta}{\alpha b}\right)\omega^2\right]$	$\frac{2}{\pi^2}\left(1-\frac{m_1+m_0}{k}\omega^2\right)$	$\frac{1}{\pi}\left[16\frac{\pi^4 D}{kb^4}+4\frac{\pi^2}{\alpha^2 b^2}+1-\right.$ $\left.-\frac{m_1+m_0}{k}\omega^2\right]$	$\overline{w}_{20}=\sin\frac{2\pi x}{b}$ 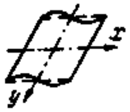
0—1	•	•	$\frac{1}{6}\left[\frac{\pi^4 D}{kb^4}\beta^4+\frac{\pi^2}{\alpha^2 b^2}\beta^2+1+\right.$ $+12(2-\mu)\frac{\pi^2 D}{kb^4}\beta^2+$ $+\frac{6}{\alpha b}+\frac{12}{\alpha^2 b^2}+$ $+3\frac{\pi^2}{\alpha^2 b^2}\beta^2-\frac{m_0}{k}\times$ $\left.\times\left(1+\frac{m_1}{m_0}+\frac{3}{\alpha b}\right)\omega^2\right]$	$\frac{1}{2\pi}\left[\frac{\pi^4 D}{kb^4}\beta^4+\frac{\pi^2}{\alpha^2 b^2}\beta^2+\right.$ $\left.+1-\frac{m_1+m_0}{k}\omega^2\right]$	$\overline{w}_{01}=\frac{2x}{b}\cos\frac{\pi y}{l}$ 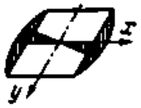
2—1	•	•	•	$\frac{1}{4}\left[(4+\beta^2)^2\frac{\pi^4 D}{kb}+\right.$ $+(4+\beta^2)\frac{\pi^2}{\alpha^2 b^2}+1-$ $\left.-\frac{m_1+m_0}{k}\omega^2\right]$	$\overline{w}_{21}=\sin\frac{2\pi x}{b}\cos\frac{\pi y}{l}$ 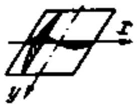

TABLE 20

	C_{00}	C_{10}	C_{02}	C_{12}	Virtual displacements
0—0	$\frac{1}{3}\left[1+\frac{6}{\alpha b}\left(\beta+\frac{1}{3}\right)+\frac{12}{\alpha^2 b^2}\beta^2-\frac{m_0}{k}\left(1+\frac{m_1}{m_0}+\frac{3\beta+1}{\alpha b}\right)\omega^2\right]$	$\frac{2}{3\pi}\left[1+\frac{6}{\alpha b}\beta+\frac{12}{\alpha^2\beta^2}\beta^2-\frac{m_0}{k}\left(1+\frac{m_1}{m_0}+\frac{3\beta}{\alpha b}\right)\omega^2\right]$	$\frac{1}{\pi}\left[1+\frac{2}{\alpha b}-\frac{m_0}{k}\times\left(1+\frac{m_1}{m_0}+\frac{1}{\alpha b}\right)\omega^2\right]$	$\frac{2}{\pi^2}\left(1-\frac{m_1+m_0}{k}\omega^2\right)$	$\bar{w}_{00}=\frac{2y}{l}$ 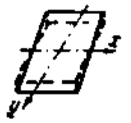
1—0	•	$\frac{1}{6}\left[\frac{\pi^4 D}{kb^4}+\frac{\pi^2}{\alpha^2 b^2}+1+12(2-\nu)\frac{\pi^2 D}{kb^4}\beta^2+\frac{6}{\alpha b}\beta+\frac{12}{\alpha^2 b^2}\beta^2+3\frac{\pi^2}{\alpha^2 b^2}\beta-\frac{m_0}{k}\left(1+\frac{m_1}{m_0}+\frac{3\beta}{\alpha b}\right)\omega^2\right]$	$\frac{2}{\pi^2}\left(1-\frac{m_1+m_0}{k}\omega^2\right)$	$\frac{1}{2\pi}\left[\frac{\pi^4 D}{kb^4}+\frac{\pi^2}{\alpha^2 b^2}+1-\frac{m_1+m_0}{k}\omega^2\right]$	$\bar{w}_{10}=\frac{2y}{l}\cos\frac{\pi x}{b}$ 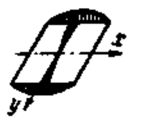
0—2	•	•	$\frac{1}{2}\left[16\frac{\pi^4 D}{kb^4}\beta^4+4\frac{\pi^2}{\alpha^2 b^2}\beta^2+1+\frac{2}{\alpha b}+4\frac{\pi^2}{\alpha^2 b^2}\beta^2-\frac{m_0}{k}\left(1+\frac{m_1}{m_0}+\frac{1}{\alpha b}\right)\omega^2\right]$	$\frac{1}{\pi}\left[16\frac{\pi^4 D}{kb^4}\beta^4+4\frac{\pi^2}{\alpha^2 b^2}\beta^2+1-\frac{m_1+m_0}{k}\omega^2\right]$	$\bar{w}_{02}=\sin\frac{2\pi y}{l}$ 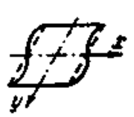
1—2	•	•	•	$\frac{1}{4}\left[(1+4\beta^2)^2\frac{\pi^4 D}{kb^4}+(1+4\beta^2)\frac{\pi^2}{\alpha^2 b^2}+1-\frac{m_1+m_0}{k}\omega^2\right]$	$\bar{w}_{12}=\cos\frac{\pi x}{b}\sin\frac{2\pi y}{l}$ 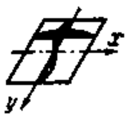

TABLE 21

	C_{00}	C_{20}	C_{02}	C_{22}	Virtual displacements
0—0	$\frac{1}{9}\Big[288(1-\mu)\frac{D}{kb^4}\beta^2+1+ + \frac{6}{\alpha\beta}(1+\beta)+\frac{12}{\alpha^2b^2}(1+\beta^2)- -\frac{m_0}{k}\Big(1+\frac{m_1}{m_0}+\frac{3(1+\beta)}{\alpha b}\Big)\omega^2\Big]$	$\frac{1}{3\pi}\Big[1+\frac{6}{\alpha b}\beta+\frac{12}{\alpha^2b^2}\beta^2- -\frac{m_0}{k}\Big(1+\frac{m_1}{m_0}+\frac{3\beta}{\alpha\beta}\Big)\omega^2\Big]$	$\frac{1}{3\pi}\Big[1+\frac{6}{\alpha b}+\frac{12}{\alpha^2b^2}- -\frac{m_0}{k}\Big(1+\frac{m_1}{m_0}+\frac{3}{\alpha b}\Big)\omega^2\Big]$	$\frac{1}{\pi^2}\Big(1-\frac{m_1+m_0}{k}\omega^2\Big)$	$\bar{w}_{00}=\frac{4xy}{lb}$ 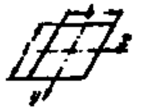
2—0	•	$\frac{1}{6}\Big[16\frac{\pi^4D}{kb^4}+4\frac{\pi^2}{\alpha^2b^2}+1+ +48(2-\mu)\frac{\pi^2D}{kb^4}\beta^2+\frac{6}{\alpha b}\beta+ +\frac{12}{\alpha^2b^2}\beta^2+12\frac{\pi^2}{\alpha^2b^2}\beta- -\frac{m_0}{k}\Big(1+\frac{m_1}{m_0}+\frac{3\beta}{\alpha b}\Big)\omega^2\Big]$	$\frac{1}{\pi^2}\Big(1-\frac{m_1+m_0}{k}\omega^2\Big)$	$\frac{1}{2\pi}\Big(16\frac{\pi^4D}{kb^4}+4\frac{\pi^2}{\alpha^2b^2}+ +1-\frac{m_1+m_0}{k}\omega^2\Big)$	$\bar{w}_{20}=\frac{2y}{l}\sin\frac{2\pi x}{b}$
0—2	•	•	$\frac{1}{6}\Big[16\frac{\pi^4D}{kb^4}\beta^4+4\frac{\pi^2}{\alpha^2b^2}\beta^2+ +1+48(2-\mu)\times \times\frac{\pi^2D}{kb^4}\beta^2+\frac{6}{\alpha b}+ +\frac{12}{\alpha^2b^2}+12\frac{\pi^2}{\alpha^2b^2}\beta^2- -\frac{m_0}{k}\Big(1+\frac{m_1}{m_0}+\frac{3}{\alpha b}\Big)\omega^2\Big]$	$\frac{1}{2\pi}\Big(16\frac{\pi^4D}{kb^4}\beta^4+4\frac{\pi^2}{\alpha^2b^2}+ +1-\frac{m_1+m_0}{k}\omega^2\Big)$	$\bar{w}_{02}=\frac{2x}{b}\sin\frac{2\pi y}{l}$
2—2	•	•		$\frac{1}{4}\Big[16(1+\beta^2)^2\frac{\pi^4D}{kb^4}+ +4(1+\beta^2)\frac{\pi^2}{\alpha^2b^2}+1- -\frac{m_1+m_0}{k}\omega^2\Big]$	$\bar{w}_{22}=\sin\frac{2\pi x}{b}\sin\frac{2\pi y}{l}$

The coefficients in (9.6) are again obtained from (9.7).

Considering only the first four terms in (9.14), (9.15), and (9.16), we can represent (9.6) for the cases a, b, and c, by the matrices given in Tables 19, 20, and 21 respectively, where α, β, k, D, and m_0, are given, as before, by (9.12). Equating to zero the determinants of these matrices, we obtain equations of the fourth degree in ω^2 which yield four natural frequencies for each case considered.

Taking only the first (linear) terms in (9.14) and (9.15), we find from Tables 19 and 20 the frequencies of a rigid plate:

in the case of vibrations antisymmetrical with respect to the y axis

$$\omega_{00} = \sqrt{\frac{k}{m_0}\frac{1+\frac{6}{\alpha b}\left(1+\frac{\beta}{3}\right)+\frac{12}{\alpha^2 b^2}}{1+\frac{m_1}{m_0}+\frac{3+\beta}{\alpha b}}}; \tag{9.17}$$

in the case of vibrations antisymmetrical with respect to the x axis

$$\omega_{ee} = \sqrt{\frac{k}{m_0}\frac{1+\frac{6}{\alpha b}\left(\frac{1}{3}+\beta\right)+\frac{12}{\alpha^2 b^2}\beta^2}{1+\frac{m_1}{m_0}+\frac{1+3\beta}{\alpha b}}}. \tag{9.18}$$

The first approximation in the case of vibrations antisymmetrical with respect to both axes (Table 21) is:

$$\omega_{ee} = \sqrt{\frac{k}{m_0}\frac{288\,(1-\mu)\frac{D}{kb^4}\beta^2+1+\frac{6}{\alpha b}(1+\beta)+\frac{12}{\alpha^2 b^2}\,(1+\beta^2)}{1+\frac{m_1}{m_0}+\frac{3+3\beta}{\alpha b}}} \tag{9.19}$$

§ 10. BUCKLING OF A RECTANGULAR PLATE RESTING ON AN ELASTIC SINGLE-LAYER FOUNDATION AND COMPRESSED IN ONE DIRECTION

Consider a rectangular plate resting on an elastic single-layer foundation and loaded by axial compressive forces $N(x)$ per unit width (Figure 154).

The differential equation of the deflections of this plate is:

$$D\nabla^2\nabla^2 w - 2t\nabla^2 w + kw = -N(x)\frac{\partial^2 w}{\partial y^2}, \tag{10.1}$$

where D = flexural rigidity of the plate, and k and t = generalized characteristics of the elastic foundation. The compressive forces are considered positive in (10.1).

We represent the plate deflections by the finite series

$$w(x, y) = \sum_{k=1}^{n} W_k(y)\,\chi_k(x) \tag{10.2}$$

and assume as before (cf. section 2 of Chapter III) that the functions $\chi_k(x)$ are known; the functions $W_k(y)$ are considered as unknowns. We can then write (10.1) as follows: [cf. (2.25) of Chapter III]:

$$\sum_{k=1}^{n} a_{ik} W_k^{\mathrm{IV}} - \sum_{k=1}^{n} [2(b_{ik} + \rho_{ik}^0) - N_{ik}] W_k'' + \sum_{k=1}^{n} (c_{ik} + s_{ik}^0) W_k = 0 \qquad (10.3)$$

$$(i = 1, 2, 3, \ldots, n).$$

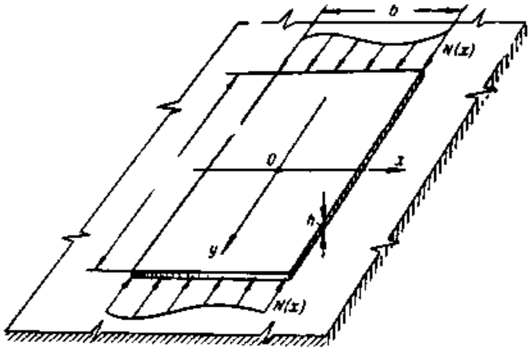

FIGURE 154.

The coefficients a_{ik}, b_{ik}, c_{ik}, ρ_{ik}^0, s_{ik}^0 in (10.3) depend on the selected system of functions $\chi_k(x)$ and on the values of the elastic constants of plate and foundation: [cf. (2.26) of Chapter III]:

$$\left.\begin{aligned} a_{ik} &= \Sigma D \int \chi_k \chi_i \, dx, \\ b_{ik} &= \Sigma D \left\{ \int \chi_k' \chi_i' \, dx - \frac{\mu}{2} [\chi_k \chi_i' + \chi_k' \chi_i]^* \right\}, \\ c_{ik} &= \Sigma D \int \chi_k'' \chi_i'' \, dx, \\ \rho_{ik}^0 &= t \int \chi_k \chi_i \, dx + \frac{t}{2a} [[\chi_k \chi_i]], \\ s_{ik}^0 &= k \left\{ \int \chi_k \chi_i \, dx + \frac{2t}{k} \int \chi_k' \chi_i' dx + \frac{2at}{k} [[\chi_k \chi_i]] \right\} \end{aligned}\right\} \qquad (10.4)$$

The magnitudes N_{ik}, which depend on the compressive load $N(x)$, are:

$$N_{ik} = \int N(x) \chi_i \chi_k \, dx. \qquad (10.5)$$

If the external load is uniformly distributed, i.e., if $N(x) = \mathrm{const}$, equation (10.3) can be written in the form:

$$\sum_{k=1}^{n} a_{ik} W_k^{\mathrm{IV}} - \sum_{k=1}^{n} \left[2(b_{ik} + \rho_{ik}^0) - \frac{P}{bD} a_{ik} \right] W_k'' + \sum_{k=1}^{n} (c_{ik} + s_{ik}^0) W_k = 0, \qquad (10.6)$$

where P = total compressive load and b = plate width.

By assigning to i successively all values from 1 to n we obtain from (10.6) or (10.3) a complete system of ordinary homogeneous differential equations in the unknown functions $W_k(y)\ (k = 1, 2, \ldots, n)$. With the functions $\chi_k(x)\ (k = 1, 2, \ldots, n)$ known, these equations can be solved up to a parameter P (N in the general case), representing the unknown critical force. By adding to (10.6) the homogeneous boundary conditions at $y = \pm b/_2$ for the functions $W_k(y)$, we obtain, from the conditions of the existence of nontrivial solutions, an infinite set of values for P. Since the system (10.6) has a symmetrical structure, the eigenvalues will always be real in the homogeneous boundary-value problem considered.

The best way to solve ordinary differential equations with constant coefficients is Krylov's method, which was developed for the case of small vibrations of systems with many degrees of freedom.

If $l \gg b$, the solution of (10.6) can be represented in the form:

$$W_k(y) = C_k \sin\frac{\pi y}{\lambda} \quad (k = 1, 2, 3, \ldots, n), \tag{10.7}$$

where the C_k = constants, and λ = length of the sine half-wave corresponding to buckling in the y direction.

Substituting (10.7) in (10.6) and equating to zero the determinant of the equations obtained (the C_k being considered as unknowns), we obtain a characteristic equation of order n in P, whose roots will be real. Since two unknowns, the force P and the half-wave length λ, are interrelated by the characteristic equation for finite values of n, these unknowns have to be found from condition:

$$\frac{dP}{d\lambda} = 0.$$

In practice it is sufficient to take only the first terms of (10.3). Buckling in the direction of the plate width is in this case characterized by the function $\chi(x)$, and the differential equation becomes:

$$AW^{\text{IV}} + (N_{11} - 2B)\, W'' + CW = 0, \tag{10.8}$$

where $W = W(y)$ = unknown generalized deflection; and:

$$\left.\begin{aligned}
A &= D\int \chi^2\, dx,\\
B &= D\left\{\int \chi'^2\, dx - \mu\,[\chi\chi']^*\right\} + t\int \chi^2\, dt + \frac{t}{2a}[[\chi^2]],\\
C &= D\int \chi''^2\, dx + k\left\{\int \chi^2\, dx + \frac{2t}{k}\int \chi'^2\, dx + \frac{2\alpha t}{k}[[\chi^2]]\right\},\\
N_{11} &= \int N(x)\,\chi^2\, dx.
\end{aligned}\right\} \tag{10.9}$$

For $(l \ll b)$ we can represent the solution of (10.8) in the form (10.7). We obtain:

$$A\left(\frac{\pi}{\lambda}\right)^4 - (N_{11} - 2B)\left(\frac{\pi}{\lambda}\right)^2 + C = 0. \tag{10.10}$$

It can be seen from (10.10) that the generalized compressive force N_{11} is a function of λ. To determine the minimum (critical) value of n_{11}, we differentiate (10.10) with respect to λ and equate the result to zero. We obtain:

$$\lambda = \pi \sqrt[4]{\frac{A}{C}}. \tag{10.11}$$

The critical value of N_{11} is then:

$$N_{11} = 2(B + \sqrt{AC}). \tag{10.12}$$

If $N(x) = \text{const}$, we can rewrite (10.12) as follows:

$$P = \frac{2Db}{A}(B + \sqrt{AC}), \tag{10.13}$$

where P = total compressive load.

Introducing the generalized geometrical characteristics:

$$r^2 = \frac{Bl^2}{A}, \quad s^4 = \frac{Cl^4}{A}, \tag{10.14}$$

we can represent (10.11) and (10.13) in the following form:

$$\lambda = \frac{\pi}{s} l, \qquad P = \frac{EF}{6(1-\mu^2)} \frac{h^2}{l^2} (r^2 + s^2), \tag{10.15}$$

where F = area of plate cross section, h = plate thickness, and l = plate length. If the plate length l is of the order of the width b, but less than the wave length λ obtained from (10.11), then l has to be taken as wave length, and the critical compressive force is then determined from (10.10). If $\frac{l}{n} > \lambda > \frac{l}{n+1}$, we put $\lambda = \frac{l}{n}$ and $\frac{l}{n+1}$ in (10.10); the lower value obtained for N_{11} is the critical one.

§ 11. BUCKLING OF A NARROW PLATE RESTING ON AN ELASTIC SINGLE-LAYER FOUNDATION

Equations (10.3) are easiest to solve when the plate cross section can be considered as undeformable. This assumption is justified for sufficiently long plates with free edges (Figure 154), or with one edge simply supported (Figure 156), and also in many other cases when an elementary transverse strip of width dy, cut out from the plate, can be deformed (Figure 155). In this case we choose as functions $\chi_k(x)$ the displacements of the strip considered as a combination of rigid links.

We shall now consider some examples.

1. Rectangular plate simply supported along a longitudinal edge

Consider a rectangular plate of uniform thickness h, loaded by a centrally applied compressive force $P = Nb$ (Figure 156). Rigid-body rotation of the plate about the supported edge is taken as the virtual displacement depending on the x coordinate:

$$\chi = x.$$

This problem is described by (10.8), where

$$\left.\begin{aligned} A &= D\frac{b^3}{3},\\ B &= Db(1-\mu) + \frac{tb^3}{3}\left(1 + \frac{3}{2ab}\right),\\ C &= \frac{kb^3}{3}\left[1 + \frac{3}{ab}\left(1 + \frac{1}{ab}\right)\right],\\ N_{11} &= \frac{Pb^2}{3},\end{aligned}\right\} \qquad (11.1)$$

so that (10.8) becomes:

$$W^{\mathrm{IV}} + \left[\frac{P}{Db} - \frac{6}{b^2}(1-\mu) - \frac{2t}{D}\left(1 + \frac{3}{ab}\right)\right]W'' + \frac{k}{D}\left[1 + \frac{3}{ab}\left(1 + \frac{1}{ab}\right)\right]W = 0. \qquad (11.2)$$

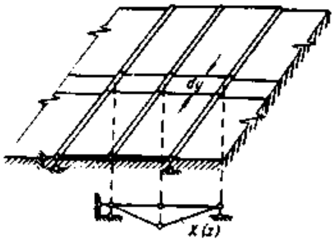

FIGURE 155.

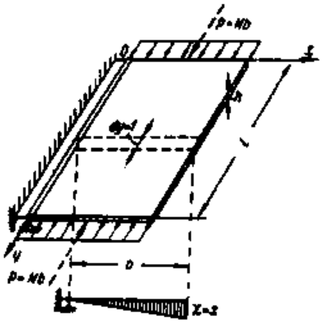

FIGURE 156.

Let the lateral plate edges $y = 0$ and $y = l$ be simply supported. The solution of (11.1) can then be represented in the form:

$$W = C\sin\frac{\pi y}{l}. \qquad (11.3)$$

Plates having undeformable cross sections can only buckle in the form of one half-wave, so that λ in (10.7) is always equal to the plate length l.

Substituting (11.3) in (11.2) and dividing by $C\sin\frac{\pi y}{l}$, which is different from zero, we obtain:

$$\frac{\pi^4}{l^4} - \left[\frac{P}{Db} - \frac{6}{b^2}(1-\mu) - \frac{2t}{D}\left(1 + \frac{3}{ab}\right)\right]\frac{\pi^2}{l^2} + \frac{k}{D}\left[1 + \frac{3}{ab}\left(1 + \frac{1}{ab}\right)\right] = 0,$$

whence:

$$P_{\mathrm{cr}} = \frac{\pi^2 EJ}{l^2(1-\mu^2)} + \frac{6EJ}{b^2(1+\mu)} + 2tb\left(1 + \frac{3}{ab}\right) + \frac{kl^2b}{\pi^2}\left[1 + \frac{3}{ab}\left(1 + \frac{1}{ab}\right)\right]. \qquad (11.4)$$

where $J = \frac{bh^3}{12}$ = moment of inertia of the plate cross section.

For $\mu = 0$, the first term of (11.4) is identical with the expression for the critical Euler load. The second term is due to the increase in the critical force, caused by the fastening of the longitudinal edge of the plate. The last terms of (11.4) takes into account the supporting effect of the elastic foundation.

If the plate lies on a foundation for which a foundation modulus can be postulated, the terms containing t and α in (11.4) (determined by the shearing strains of the elastic foundation) should be discarded. We then obtain:

$$P_{cr} = \frac{\pi^2 EJ}{l^2(1-\mu)} + \frac{6EJ}{b^2(1+\mu)} + \frac{kbl^2}{\pi^2}, \tag{11.5}$$

where k = foundation modulus.

2. Rectangular plate with free longitudinal edges

Consider a rectangular plate loaded by axial forces whose transverse distribution is linear (Figure 157). These forces can be reduced to a centrally applied compressive force P (considered positive) and a bending moment M acting in the plane of the plate. We assumed that the plate consists of longitudinal strips of different thickness and that in the general case it has no longitudinal axis of symmetry.

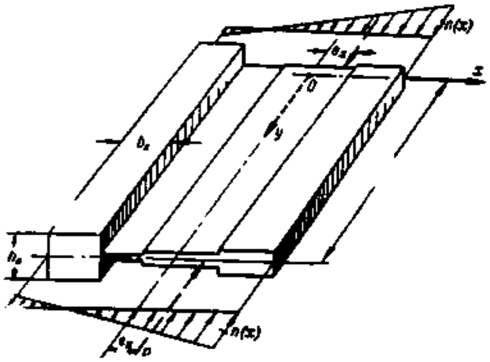

FIGURE 157.

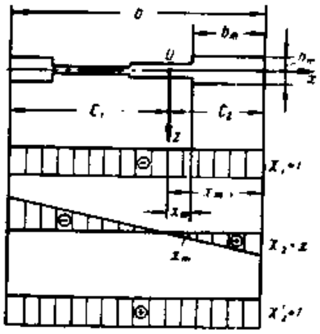

FIGURE 158.

The virtual displacements of a transverse strip, cut out from the plate, are taken as the translatory displacement $\chi_1 = 1$ and the rotation $\gamma_2 = x$ about an axis passing through the centroid of the plate cross section (Figure 158).

The plate deflections are then:

$$w(x, y) = W_1\chi_1 + W_2\chi_2 = W_1 + W_2 x, \tag{11.6}$$

where W_1 and W_2 = generalized deflections. The functions W_1, which has the dimension of length, corresponds to the cylindrical bending of the plate in the longitudinal direction; the dimensionless function W_2 defines the angle of rotation about the axis through the centroid of the cross section. It is thus assumed that both flexural and torsional buckling of the plate is possible.

In the case considered (10.3) takes the form:

$$\left.\begin{aligned}&a_{11}W_1^{IV}+a_{12}W_2^{IV}+[N_{11}-2(b_{11}+\rho_{11}^0)]W_1''+[N_{12}-\\&\quad-2(b_{12}+\rho_{12}^0)]W_2''+(c_{11}+s_{11}^0)W_1+(c_{12}+s_{12}^0)W_2=0,\\&a_{21}W_1^{IV}+a_{22}W_2^{IV}+[N_{21}-2(b_{21}+\rho_{21}^0)]W_1''+[N_{22}-\\&\quad-2(b_{22}+\rho_{22}^0)]W_2''+(c_{21}+s_{21}^0)W_1+(c_{22}+s_{22}^0)W_2=0,\end{aligned}\right\}\tag{11.7}$$

where by (10.4),

$$\left.\begin{aligned}&a_{11}=\sum D_m b_m,\qquad a_{12}=\sum D_m\frac{x_{m+1}^2-x_m^2}{2},\\&a_{22}=\sum D_m\frac{1}{3}(x_{m+1}-x_m)(x_m^2+x_{m+1}x_m+x_{m+1}^2),\\&b_{11}=b_{12}=0,\qquad b_{22}=\sum D_m b_m,\\&c_{11}=c_{12}=c_{21}=0,\\&\rho_{11}^0=tb\left(1+\frac{1}{ab}\right),\qquad \rho_{12}^0=\frac{t}{2}(c_2^2-c_1^2)\left(1+\frac{1}{ab}\right),\\&\rho_{22}^0=tb\left[\frac{1}{3}(c_1^2+c_2^2-c_1c_2)+\frac{1}{2ab}(c_1^2+c_2^2)\right],\\&s_{11}^0=kb\left(1+\frac{2}{ab}\right),\qquad s_{12}^0=\frac{k}{2}(c_2^2-c_1^2)\left(1+\frac{2}{ab}\right),\\&s_{22}^0=kb\left[\frac{1}{3}(c_1^2+c_2^2-c_1c_2)+\frac{1}{ab}(c_1^2+c_2^2)+\frac{1}{a^2}\right].\end{aligned}\right\}\tag{11.8}$$

The summation in these expressions is extended over all the longitudinal strips.

Here $D=\frac{Eh^3}{12(1-\mu^2)}$ = flexural rigidity; b = overall width of the plate; k and t = compression and shear characteristics of elastic foundation respectively.

According to (10.5) we have:

$$\left.\begin{aligned}N_{11}&=\int N(x)\chi_1^2\,dx,\\N_{12}&=\int N(x)\chi_1\chi_2\,dx,\\N_{22}&=\int N(x)\chi_2^2\,dx.\end{aligned}\right\}\tag{11.9}$$

We can write:

$$N(x)=n(x)h,\tag{11.10}$$

where the normal stresses $N(x)$ are given by:

$$n(x)=\frac{P}{F}+\frac{M}{J_y}x.\tag{11.11}$$

Here F = the area, and $J_2 = \int x^2 dF$, the moment of inertia of the plate cross section; $M = Pe_x$, where e_x = eccentricity of applied force P.

Substituting (11.10) and (11.11) in (11.9), with $\chi_1 = 1$ and $\chi_2 = x$, we obtain:

$$\left.\begin{aligned} N_{11} &= \int nh\,dx = P, \\ N_{12} &= \int nxh\,dx = M, \\ N_{22} &= \int nx^2h\,dx = \frac{PJ_2}{F} + \frac{MJ_3}{J_2}, \end{aligned}\right\} \qquad (11.12)$$

where

$$J_3 = \int x^3 dF, \quad dF = h\,dx. \qquad (11.13)$$

Substitution of (11.8) and (11.12) in (11.7) yields finally:

$$\left.\begin{aligned} a_{11}W_1^{IV} + (P - 2\rho_{11}^0)W_1'' + s_{11}^0 W_1 + a_{12}W_2^{IV} + (M - 2\rho_{12}^0)W_2'' + \\ + s_{12}^0 W_2 = 0, \\ a_{21}W_1^{IV} + (M - 2\rho_{21}^0)W_1'' + s_{21}^0 W_1 + a_{22}W_2^{IV} + \\ + \left[\frac{PJ_2}{F} + \frac{MJ_3}{J_2} - 2(b_{22} + \rho_{22}^0)\right]W_2'' + s_{22}^0 W_2 = 0. \end{aligned}\right\} \qquad (11.14)$$

Several examples will be given to illustrate the procedure adopted.

3. Rectangular plate of uniform section

If a rectangular plate of uniform thickness h has free longitudinal edges and is loaded by a centrally applied compressive force P (Figure 159), (11.8) and (11.12) reduce to:

$$\left.\begin{aligned} & a_{11} = Db = \frac{EJ}{1-\mu^2}, \quad a_{12} = b_{11} = b_{12} = c_{11} = c_{12} = c_{22} = 0, \\ & a_{22} = D\frac{b^3}{12} = \frac{EJb^2}{12(1-\mu^2)}, \quad b_{22} = Db = \frac{EJ}{1-\mu^2}, \\ & \rho_{11}^0 = tb\left(1 + \frac{1}{\alpha b}\right), \quad \rho_{12}^0 = s_{12}^0 = 0, \quad \rho_{22}^0 = \frac{tb^3}{12}\left(1 + \frac{3}{\alpha b}\right), \\ & s_{11}^0 = kb\left(1 + \frac{2}{\alpha b}\right), \quad s_{22}^0 = \frac{kb^3}{12}\left(1 + \frac{6}{\alpha b} + \frac{12}{\alpha^2 b^2}\right), \\ & N_{11} = P, \quad N_{12} = 0, \quad N_{22} = \frac{PJ_2}{F} = \frac{Pb^2}{12}. \end{aligned}\right\} \qquad (11.15)$$

System (11.14) can in this case be separated into two independent equations:

$$a_{11}W_1^{IV} + (P - 2\rho_{11}^0)W_1'' + s_{11}^0 W_1 = 0, \qquad (11.16)$$

corresponding to flexural buckling,

and

$$a_{22}W_2^{IV} + \left[P\frac{b^2}{12} - 2(b_{22} + \rho_{22}^0)\right]W_2'' + s_{22}^0 W_2 = 0, \qquad (11.17)$$

corresponding to torsional buckling.

Let the lateral plate edges be simply supported.

Substituting
$$W_1 = C_1 \sin\frac{\pi x}{l}, \quad W_2 = C_2 \sin\frac{\pi x}{l} \tag{11.18}$$

in (11.16) and (11.17), we obtain the following expressions for the critical forces:

$$P_1 = \frac{EJ\pi^2}{l^2(1-\mu^2)} + 2tb\left(1+\frac{1}{ab}\right) + k\frac{bl^2}{\pi^2}\left(1+\frac{2}{ab}\right), \tag{11.19}$$

$$P_2 = \frac{EJ\pi^2}{l^2(1-\mu^2)} + \frac{24EJ}{b^2(1-\mu^2)} + 2tb\left(1+\frac{3}{ab}\right) + k\frac{bl^2}{\pi^2}\left(1+\frac{6}{ab}+\frac{12}{a^2b^2}\right). \tag{11.20}$$

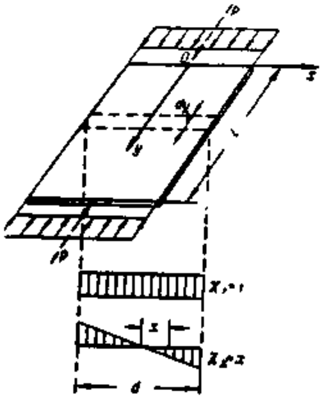

FIGURE 159.

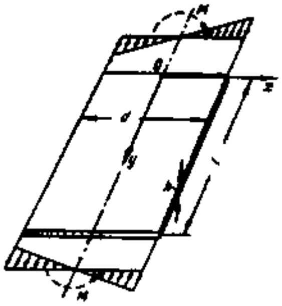

FIGURE 160.

It can be seen that in the case considered, the smaller critical force is given by (11.19), which corresponds to flexural buckling; in other words, torsional buckling is impossible in the symmetrical case. Let a moment M act on the same plate (Figure 160). The coefficients will have the values given by (11.15), except for N_{ik}. Here:

$$N_{11} = 0, \; N_{12} = M, \; N_{22} = M\frac{J_3}{J_2}. \tag{11.21}$$

For a symmetrical plate:

$$J_3 = \int x^3 \, dF = 0$$

so that $N_{22} = 0$. Hence, the system of equations (11.14) reduces to:

$$\left.\begin{aligned} a_{11}W_1^{\mathrm{IV}} - 2\rho_{11}^0 W_1' + s_{11}^0 W_1 + MW_2' = 0, \\ MW_1' + a_{22}W_2^{\mathrm{IV}} - 2(b_{22}+\rho_{22}^0)W_2' + s_{22}^0 W_2 = 0. \end{aligned}\right\} \tag{11.22}$$

When the lateral edges are simply supported, the solution of (11.22) can again be presented in the form (11.18).

Substitution of (11.18) in (11.22) yields the following expression for the critical moment:

$$M = \sqrt{\left(a_{11} + 2\rho_{11}^{0}\frac{l^2}{\pi^2} + s_{11}^{0}\frac{l^4}{\pi^4}\right)\left[a_{22} + 2\left(b_{22} + \rho_{22}^{0}\right)\frac{l^2}{\pi^2} + s_{22}^{0}\frac{l^4}{\pi^4}\right]}. \qquad (11.23)$$

In this case, mixed flexural-torsional buckling takes places.

§ 12. BUCKLING OF A PRESTRESSED PLATE RESTING ON AN ELASTIC FOUNDATION

1

Consider a prestressed rectangular plate, compressed by a reinforcement rod lying in the longitudinal section $x = e_x$ (Figure 161). The rod is extended by a force $R = n_1 \Delta F$, where ΔF = cross-sectional area of bar.

The normal-stress diagram for the plate cross section $y = \text{const}$ is shown in Figure 161. With the exception of the vicinity of the rod, the normal-stress distribution is given by:

$$n_1 = \frac{R}{F} + \frac{Re_x}{J}x, \qquad (12.1)$$

where R = tensile force acting on the reinforcement rod.

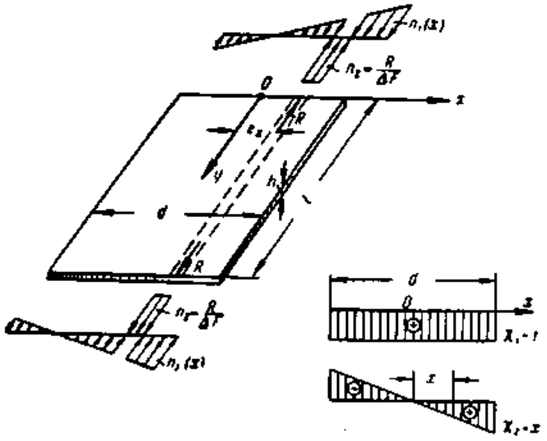

FIGURE 161.

The state of stress thus corresponds to a balanced (in static equilibrium) system of forces, i.e.:

$$\int_0^d n(x)\,dF = P = 0, \quad \int_0^d n(x)\,x\,dF = M = 0. \qquad (12.2)$$

If we assume that the plate cross section is not deformed, the solution will be given as before by (11.14). Those coefficients which do not depend on the compressive load are for a plate of uniform thickness determined by (11.15).

The coefficients which depend on the external load are obtained from (11.9), where the integrals are to be understood as Stieltjes integrals. The integration yields:

$$\left.\begin{aligned} N_{11} &= \int n(x)\,dF = \int n_1\,dF - n_2\,\Delta F = 0, \\ N_{12} &= \int n(x)\,x\,dF = \int n_1 x\,dF - n_2\,\Delta F e_x = 0, \\ N_{22} &= \int n(x)\,x^2\,dF = \frac{RJ_2}{F} + \frac{Re_x J_3}{J_2} - Re_x^2, \end{aligned}\right\} \qquad (12.3)$$

where

$$J_2 = \int x^2\,dF, \quad J_3 = \int x^3\,dF, \quad dF = h\,dx.$$

Substitution of (11.15) and (12.3) in (11.7) yields:

$$\left.\begin{aligned} a_{11}W_1^{IV} - 2\rho_{11}^0 W_1'' + s_{11}^0 W_1 &= 0, \\ a_{22}W_2^{IV} + [N_{22} - 2(b_{22} + \rho_{22}^0)]\,W_2'' + s_{22}^0 W_2 &= 0, \end{aligned}\right\} \qquad (12.4)$$

where for a plate of uniform thickness:

$$N_{22} = R\left(\frac{b^2}{12} - e_x^2\right). \qquad (12.5)$$

The first equation (12.4) is independent of the load and therefore:

$$W_1 = 0.$$

Buckling of the plate is thus determined by the second equation (12.4), in which W_2 appears. Since the generalized displacement W_2 represents a rotation, torsional buckling will take place. It follows that no flexural buckling occurs in a prestressed plate.

Assuming that the lateral edges of the plate are simply supported, the solution of the second equation (12.4) has the form:

$$W_2 = C\sin\frac{\pi x}{l}. \qquad (12.6)$$

Substitution of (12.6) in the second equation (12.4) gives the following value for the critical force:

$$R_{\text{cr}} = \frac{1}{\frac{b^2}{12} - e_x^2}\left[a_{22}\frac{\pi^2}{l^2} + 2(b_{22} + \rho_{22}^0) + s_{22}^0\frac{l^2}{\pi^2}\right]. \qquad (12.7)$$

where a_{22}, b_{22}, ρ_{22}^0, s_{22}^0 are given by (11.15).

2

Consider a prestressed plate of uniform thickness, subjected to a compressive load applied at an eccentricity e_p (Figure 162).

The differential equations of buckling in this general case, which is a combination of the two previous ones, are:

$$\left.\begin{aligned} &a_{11}W_1^{\mathrm{IV}} + (P - 2\rho_{11}^0)\,W_1'' + s_{11}^0 W_1 + Pe_p W_2'' = 0,\\ &Pe_p W_1'' + a_{22}W_2^{\mathrm{IV}} + \left[(P+R)\frac{b^2}{12} - Re_x^2 - 2\,(b_{22} + \rho_{22}^0)\right]W_2'' +\\ &\qquad\qquad + s_{22}^0 W_2 = 0. \end{aligned}\right\} \qquad (12.8)$$

In the particular case when the external load is applied centrally ($e_p = 0$), the system of equations (12.8) can be separated into two independent equations, corresponding to flexural and to torsional buckling respectively.

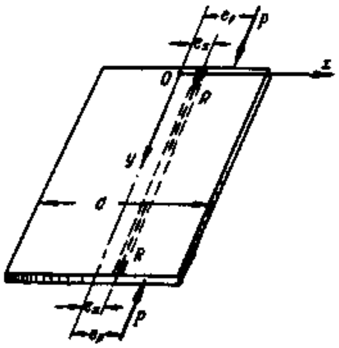

FIGURE 162.

3

In all the above examples it was assumed that the plate is simply supported at the lateral edges $y = 0$ and $y = l$. With other methods of support (built-in edges, free edges, etc.), the critical force is determined from the general integral of the corresponding homogeneous differential equation satisfying the boundary conditions. This yields a system of homogeneous algebraic equations in the integration constants, since the boundary conditions are also homogeneous in buckling problems. Equating to zero the determinant of this system (considering only the nontrivial solution) we obtain a transcendental equation in the parameter characterizing the compressive load. This equation has an infinite number of roots, the smallest of which determines the critical value of the compressive forces.

Chapter VII

METHOD OF INITIAL FUNCTIONS. APPLICATION OF THE METHOD TO THE THEORY OF THICK PLATES AND TO THE THEORY OF ELASTIC FOUNDATIONS

§ 1. GENERAL SOLUTION OF THE THREE-DIMENSIONAL PROBLEM OF THE THEORY OF ELASTICITY

1

The general problem of the equilibrium of a solid isotropic elastic body undergoing small deformations is described in cartesian coordinates by the differential equations:

$$\left.\begin{aligned} &\frac{\partial\sigma_x}{\partial x}+\frac{\partial\tau_{xy}}{\partial y}+\frac{\partial\tau_{xz}}{\partial z}+a=0,\\ &\frac{\partial\sigma_y}{\partial y}+\frac{\partial\tau_{yz}}{\partial z}+\frac{\partial\tau_{yx}}{\partial x}+b=0,\\ &\frac{\partial\sigma_z}{\partial z}+\frac{\partial\tau_{zx}}{\partial x}+\frac{\partial\tau_{zy}}{\partial y}+c=0,\end{aligned}\right\} \tag{1.1}$$

$$\left.\begin{aligned} \sigma_x&=\frac{2G}{1-2\nu}\left[(1-\nu)\frac{\partial u}{\partial x}+\nu\left(\frac{\partial v}{\partial y}+\frac{\partial w}{\partial z}\right)\right],\\ \sigma_y&=\frac{2G}{1-2\nu}\left[(1-\nu)\frac{\partial v}{\partial y}+\nu\left(\frac{\partial w}{\partial z}+\frac{\partial u}{\partial x}\right)\right],\\ \sigma_z&=\frac{2G}{1-2\nu}\left[(1-\nu)\frac{\partial w}{\partial z}+\nu\left(\frac{\partial u}{\partial x}+\frac{\partial v}{\partial y}\right)\right],\\ \tau_{xy}&=\tau_{yx}=G\left(\frac{\partial u}{\partial y}+\frac{\partial v}{\partial x}\right),\\ \tau_{yz}&=\tau_{zy}=G\left(\frac{\partial v}{\partial z}+\frac{\partial w}{\partial y}\right),\\ \tau_{zx}&=\tau_{xz}=G\left(\frac{\partial w}{\partial x}+\frac{\partial u}{\partial z}\right),\end{aligned}\right\} \tag{1.2}$$

where $\sigma_x, \sigma_y, \ldots, \tau_{yz}, \tau_{zx}$ = components of the stress tensor; u, v, w = components of displacement vector of point considered; a, b, c = components of vector of the body force per unit volume at this point; $G=\frac{E}{2(1+\nu)}$ = modulus of elasticity in shear; ν = Poisson's ratio*.

---

* Equations (1.2) were already given in section 6 of Chapter I. The magnitudes introduced there were different, being the elastic constants E_0 and ν_0 of a three-dimensional body (the elastic foundation), defined by (6.3) of Chapter I.

As already mentioned earlier, two methods of solving the general problem are used in the theory of elasticity, namely the method of displacements and the method of stresses. The first method, in which the basic functions are the displacements $u = u(x, y, z)$, $v = v(x, y, z)$, $w = w(x, y, z)$, was used in the preceding chapters when considering the strains in the elastic foundation in the two-dimensional and three-dimensional cases. In the second method the basic functions are the stresses $\sigma_x = \sigma_x(x, y, z), \ldots, \tau_{xz} = \tau_{xz}(x, y, z)$.

In addition, it is also possible to apply a mixed method, as will be done by us in the solution of the general three-dimensional problem of the theory of elasticity.

Let the basic unknown functions be the displacements $u = u(x, y, z)$, $v = v(x, y, z)$, $w = w(x, y, z)$ and the stresses $\tau_{xz}, \tau_{yz}, \sigma_z$. The components u, v, w of the displacement vector will be considered positive if they coincide with the positive directions of the coordinate axes x, y, z.

Similarly, the components $\tau_{xz}, \tau_{yz}, \sigma_z$ of the stress vector acting on an elementary surface, whose outer normal is directed along the z axis, will be considered positive if they coincide with the positive directions of the x, y, z axes respectively. To simplify the notation, the displacements u, v, w will be replaced henceforth by the magnitudes:

$$U = Gu, \quad V = Gv, \quad W = Gw, \tag{1.3}$$

also called displacements.

The unknown stresses will be denoted:

$$\tau_{xz} = X, \quad \tau_{yz} = Y, \quad \sigma_z = Z. \tag{1.4}$$

Eliminating between (1.1) and (1.2) the stresses $\sigma_x, \sigma_y, \tau_{xy} = \tau_{yx}$ we obtain the system of six fundamental equations of the mixed method. Substituting (1.3) and (1.4), these equations can be presented in the form:

$$\left.\begin{aligned}
\frac{\partial U}{\partial z} &= -\frac{\partial W}{\partial x} + X,\\
\frac{\partial V}{\partial z} &= -\frac{\partial W}{\partial y} + Y,\\
\frac{\partial W}{\partial z} &= -\frac{\nu}{1-\nu}\left(\frac{\partial U}{\partial x} + \frac{\partial V}{\partial y}\right) + \frac{1-2\nu}{2(1-\nu)}Z,\\
\frac{\partial Z}{\partial z} &= -\frac{\partial X}{\partial x} - \frac{\partial Y}{\partial y} - c,\\
\frac{\partial Y}{\partial z} &= -\frac{1+\nu}{1-\nu}\frac{\partial^2 U}{\partial x\,\partial y} - \left(\frac{\partial^2 V}{\partial x^2} + \frac{2}{1-\nu}\frac{\partial^2 V}{\partial y^2}\right) - \frac{\nu}{1-\nu}\frac{\partial Z}{\partial y} - b,\\
\frac{\partial X}{\partial z} &= -\frac{1+\nu}{1-\nu}\frac{\partial^2 V}{\partial x\,\partial y} - \left(\frac{\partial^2 U}{\partial y^2} + \frac{2}{1-\nu}\frac{\partial^2 U}{\partial x^2}\right) - \frac{\nu}{1-\nu}\frac{\partial Z}{\partial x} - a.
\end{aligned}\right| \tag{1.5}$$

The remaining stresses are:

$$\left.\begin{aligned}
\sigma_x &= \frac{2}{1-2\nu}\left[(1-\nu)\frac{\partial U}{\partial x} + \nu\left(\frac{\partial V}{\partial y} + \frac{\partial W}{\partial z}\right)\right],\\
\sigma_y &= \frac{2}{1-2\nu}\left[(1-\nu)\frac{\partial V}{\partial y} + \nu\left(\frac{\partial W}{\partial z} + \frac{\partial U}{\partial x}\right)\right],\\
\tau_{xy} &= \tau_{yx} = \frac{\partial U}{\partial y} + \frac{\partial V}{\partial x}.
\end{aligned}\right| \tag{1.6}$$

From (1.5) and the boundary conditions, the six unknown geometrical and statical magnitudes characterizing the states of strain and stress can be obtained.

3

The mixed method of representing the general equations of equilibrium of an isotropic elastic body can also be applied to dynamical problems of the theory of elasticity. The unknown functions U, V, W, X, Y, Z depend in this case on the variables x, y, z, t; in (1.5), the expressions for the inertia forces

$$-\frac{m}{G}\frac{\partial^2 U}{\partial t^2}, \quad -\frac{m}{G}\frac{\partial^2 V}{\partial t^2}, \quad -\frac{m}{G}\frac{\partial^2 W}{\partial t^2}, \tag{1.7}$$

have to be added.

§ 2. SOLVING THE EQUATIONS OF THE THEORY OF ELASTICITY BY THE METHOD OF INITIAL FUNCTIONS

1

Consider two planes in the body: the plane $z=0$ and a plane $z=\text{const}$, parallel to it. The part of the body included between these planes represents a layer of thickness $z=\text{const}$. When z is fixed the unknowns in (1.5) depend only on x and y. Thus, the magnitudes U, V, W, X, Y, Z determine the displacement and stress vectors at any point (x, y) of the fixed plane $z=\text{const}$. The magnitudes $U_0, V_0, W_0, X_0, Y_0, Z_0$ corresponding to $z=0$, will henceforth be called geometrical and statical initial functions.

The positive directions of displacements and stresses for points of the lower plane $z=\text{const}$ and of the upper plane $z=0$ are shown in Figure 163 (the z axis is directed downward).

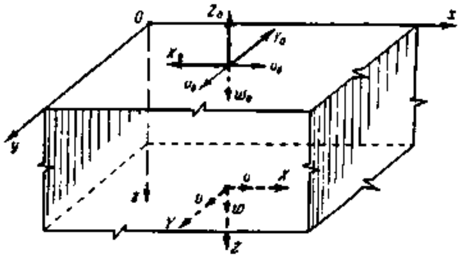

FIGURE 163.

For any plane $z=\text{const}$, the vector components are positive if they act along the positive directions of the coordinate axes. The same rule is also applied to the components U_0, V_0, W_0. The components X_0, Y_0, Z_0 are positive when their directions are opposed to those of the positive coordinates axes.

We assume a general solution of (1.5) in the form of Maclaurin series in z:

$$\left.\begin{aligned}
U &= U_0 + z\left(\frac{\partial U}{\partial z}\right)_0 + \frac{z^2}{2!}\left(\frac{\partial^2 U}{\partial z^2}\right)_0 + \dots \\
V &= V_0 + z\left(\frac{\partial V}{\partial z}\right)_0 + \frac{z^2}{2!}\left(\frac{\partial^2 V}{\partial z^2}\right)_0 + \dots \\
&\dots\dots\dots\dots\dots\dots\dots\dots \\
Z &= Z_0 + z\left(\frac{\partial Z}{\partial z}\right)_0 + \frac{z^2}{2!}\left(\frac{\partial^2 Z}{\partial z^2}\right)_0 + \dots
\end{aligned}\right| \qquad (2.1)$$

The following symbols will be used for the partial derivatives of any function $F = F(x, y, z)$:

$$\left.\begin{array}{lll}
\dfrac{\partial F}{\partial x} = \alpha F, & \dfrac{\partial F}{\partial y} = \beta F, & \dfrac{\partial F}{\partial z} = rF; \\
\dfrac{\partial^2 F}{\partial x^2} = \alpha^2 F, & \dfrac{\partial^2 F}{\partial y^2} = \beta^2 F, & \dfrac{\partial^2 F}{\partial z^2} = r^2 F; \\
\dots\dots\dots & \dots\dots\dots & \dots\dots\dots \\
\dfrac{\partial^n F}{\partial x^n} = \alpha^n F, & \dfrac{\partial^n F}{\partial y^n} = \beta^n F, & \dfrac{\partial^n F}{\partial z^n} = r^n F;
\end{array}\right| \qquad (2.2)$$

in general:

$$\frac{\partial^{k+l+m} F}{\partial x^k \partial y^l \partial z^m} = \alpha^k \beta^l r^m F.$$

These symbols are those used in the so-called symbolic method, which makes possible the application of the methods of linear algebra to differentiation and transformation of equations.

We can then rewrite (1.5) as follows:

$$\left.\begin{aligned}
rU &= -\alpha W + X, \\
rV &= -\beta W + Y, \\
rW &= -\frac{\nu}{1-\nu}(\alpha U + \beta V) + \frac{1-2\nu}{2(1-\nu)} Z, \\
rZ &= -\alpha X - \beta Y - c, \\
rY &= -\frac{1+\nu}{1-\nu}\alpha\beta U - \left(\alpha^2 V + \frac{2}{1-\nu}\beta^2 V\right) - \frac{\nu}{1-\nu}\beta Z - b, \\
rX &= -\frac{1+\nu}{1-\nu}\alpha\beta V - \left(\beta^2 U + \frac{2}{1-\nu}\alpha^2 U\right) - \frac{\nu}{1-\nu}\alpha Z - a.
\end{aligned}\right| \qquad (2.3)$$

The body forces a, b, c will henceforth be assumed to vanish.

Multiplying (2.3) by r, and eliminating the terms containing $rU, rV, \dots, rX$, we obtain the second derivatives with respect to z of the unknown functions:

$$\left.\begin{aligned}
r^2 U &= -\left(\frac{2-\nu}{1-\nu}\alpha^2 + \beta^2\right) U - \frac{1}{1-\nu}\alpha\beta V - \frac{1}{2(1-\nu)}\alpha Z, \\
r^2 V &= -\frac{1}{1-\nu}\alpha\beta U - \left(\frac{2-\nu}{1-\nu}\beta^2 + \alpha^2\right) V - \frac{1}{2(1-\nu)}\beta Z, \\
r^2 W &= \frac{\nu}{1-\nu}(\alpha^2 + \beta^2) W - \frac{1}{2(1-\nu)}\alpha X - \frac{1}{2(1-\nu)}\beta Y,
\end{aligned}\right| \qquad (2.4)$$

$$\left.\begin{aligned}
r^2Z &= \frac{2}{1-\nu}(\alpha^2+\beta^2)\alpha U+\frac{2}{1-\nu}(\alpha^2+\beta^2)\beta V+\frac{\nu}{1-\nu}(\alpha^2+\beta^2)Z,\\
r^2Y &= \frac{2}{1-\nu}(\alpha^2+\beta^2)\beta W-\frac{1}{1-\nu}\alpha\beta X-\left(\frac{2-\nu}{1-\nu}\beta^2+\alpha^2\right)Y,\\
r^2X &= \frac{2}{1-\nu}(\alpha^2+\beta^2)\alpha W-\left(\frac{2-\nu}{1-\nu}\alpha^2+\beta^2\right)X-\frac{1}{1-\nu}\alpha\beta Y.
\end{aligned}\right\} \qquad (2.4)$$

The third derivatives with respect to z are obtained by multiplying (2.4) by r and eliminating the terms containing $rU, rV, \ldots, rX$ with the aid of (2.3). Higher derivatives are obtained in the same way.

3

Equations (2.3) and (2.4) are true for any values of the independent variables x, y, z. Putting $z=0$, we obtain the partial derivatives in the right-hand sides of (2.1). Grouping together the differential operations performed on the same functions ($U_0, V_0, \ldots, X_0$) we obtain the unknown functions $U, V, \ldots, X$, expressed through the initial functions $U_0, V_0, \ldots, X_0$ and their partial derivatives.

These formulas can be written in the form

$$\left.\begin{aligned}
U &= L_{UU}U_0+L_{UV}V_0+\ldots+L_{UX}X_0,\\
V &= L_{VU}U_0+L_{VV}V_0+\ldots+L_{VX}X_0,\\
&\cdots\cdots\cdots\cdots\cdots\cdots\\
X &= L_{XU}U_0+L_{XV}V_0+\ldots+L_{XX}X_0,
\end{aligned}\right\} \qquad (2.5)$$

where $L_{UU}, L_{UV}, \ldots, L_{XX}$ = linear differential operators with respect to the initial functions $U_0(x,y), V_0(x,y), \ldots, X_0(x,y)$, depending on z and containing partial derivatives with respect to x and y for $z=0$. These operators can be represented as follows:

$$\left.\begin{aligned}
L_{UU} = L_{XX} &= 1-\frac{z^2(2-\nu)}{2(1-\nu)}\alpha^2-\frac{z^2}{2}\beta^2+\frac{z^4(3-\nu)}{24(1-\nu)}\gamma^2\alpha^2+\\
&\quad+\frac{z^4}{24}\gamma^2\beta^2-\frac{z^6(4-\nu)}{720(1-\nu)}\gamma^4\alpha^2-\frac{z^6}{720}\gamma^4\beta^2+\ldots\\
L_{UV} = L_{YX} &= -\frac{z^2}{2(1-\nu)}\alpha\beta+\frac{z^4}{12(1-\nu)}\gamma^2\alpha\beta-\\
&\quad-\frac{z^6}{240(1-\nu)}\gamma^4\alpha\beta+\ldots\\
L_{UW} = L_{ZX} &= -\alpha z+\frac{z^3(2-\nu)}{6(1-\nu)}\gamma^2\alpha-\frac{z^5(3-\nu)}{120(1-\nu)}\gamma^4\alpha+\\
&\quad+\frac{z^7(4-\nu)}{5040(1-\nu)}\gamma^6\alpha+\ldots\\
L_{UZ} = L_{WX} &= -\frac{z^2}{4(1-\nu)}\alpha+\frac{z^4}{24(1-\nu)}\gamma^2\alpha-\\
&\quad-\frac{z^6}{480(1-\nu)}\gamma^4\alpha+\frac{z^8}{20\,160(1-\nu)}\gamma^6\alpha+\ldots\\
L_{UY} = L_{VX} &= -\frac{z^3}{12(1-\nu)}\alpha\beta-\frac{z^5}{120(1-\nu)}\gamma^2\alpha\beta-\\
&\quad-\frac{z^7}{3360(1-\nu)}\gamma^4\alpha\beta+\ldots
\end{aligned}\right\} \qquad (2.6)$$

$$
\left.\begin{aligned}
L_{UX} &= z - \frac{z^3(3-2\nu)}{12(1-\nu)}\alpha^2 - \frac{z^3}{6}\beta^2 + \frac{z^5(2-\nu)}{120(1-\nu)}\gamma^2\alpha^2 + \\
&\quad + \frac{z^5}{120}\gamma^2\beta^2 - \frac{z^7(5-2\nu)}{10\,080(1-\nu)}\gamma^4\alpha^2 - \frac{z^7}{5040}\gamma^4\beta^2 + \dots \\
L_{VU} = L_{XY} &= -\frac{z^2}{2(1-\nu)}\alpha\beta + \frac{z^4}{12(1-\nu)}\gamma^2\alpha\beta - \\
&\quad - \frac{z^6}{240(1-\nu)}\gamma^4\alpha\beta + \dots \\
L_{VV} = L_{YY} &= 1 - \frac{z^2(2-\nu)}{2(1-\nu)}\beta^2 - \frac{z^2}{2}\alpha^2 + \frac{z^4(3-\nu)}{24(1-\nu)}\gamma^2\beta^2 + \\
&\quad + \frac{z^4}{24}\gamma^2\alpha^2 - \frac{z^6(4-\nu)}{720(1-\nu)}\gamma^4\beta^2 - \frac{z^6}{720}\gamma^4\alpha^2 + \dots \\
L_{VW} = L_{ZY} &= -{}'z\beta + \frac{z^3(2-\nu)}{6(1-\nu)}\gamma^2\beta - \frac{z^5(3-\nu)}{120(1-\nu)}\gamma^4\beta + \\
&\quad + \frac{z^7(4-\nu)}{5040(1-\nu)}\gamma^6\beta - \dots \\
L_{VZ} = L_{WY} &= -\frac{z^2}{4(1-\nu)}\beta + \frac{z^4}{24(1-\nu)}\gamma^2\beta - \\
&\quad - \frac{z^6}{480(1-\nu)}\gamma^4\beta + \frac{z^8}{20\,160(1-\nu)}\gamma^6\beta - \dots \\
L_{VY} &= z - \frac{z^3(3-2\nu)}{12(1-\nu)}\beta^2 - \frac{z^3}{6}\alpha^2 + \frac{z^5(2-\nu)}{120(1-\nu)}\gamma^2\beta^2 + \\
&\quad + \frac{z^5}{120}\gamma^2\alpha^2 - \frac{z^7(5-2\nu)}{10\,080(1-\nu)} - \frac{z^7}{5040}\gamma^4\alpha^2 + \dots \\
L_{WU} = L_{XZ} &= -\frac{z\nu}{1-\nu}\alpha + \frac{z^3(1+\nu)}{6(1-\nu)}\gamma^2\alpha - \frac{z^5(2+\nu)}{120(1-\nu)}\gamma^4\alpha + \\
&\quad + \frac{z^7(3+\nu)}{5040(1-\nu)}\gamma^6\alpha - \dots \\
L_{WV} = L_{YZ} &= -\frac{z\nu}{1-\nu}\beta + \frac{z^3(1+\nu)}{6(1-\nu)}\gamma^2\beta - \\
&\quad - \frac{z^5(2+\nu)}{120(1-\nu)}\gamma^4\beta + \frac{z^7(3+\nu)}{5040(1-\nu)}\gamma^6\beta - \dots \\
L_{WW} = L_{ZZ} &= 1 + \frac{z^2\nu}{2(1-\nu)}\gamma^2 - \frac{z^4(1+\nu)}{24(1-\nu)}\gamma^4 + \\
&\quad + \frac{z^6(2+\nu)}{720(1-\nu)}\gamma^6 - \dots \\
L_{WZ} &= \frac{z(1-2\nu)}{2(1-\nu)} + \frac{z^3\nu}{6(1-\nu)}\gamma^2 - \frac{z^5(1+2\nu)}{240(1-\nu)}\gamma^4 - \\
&\quad - \frac{z^7(1+\nu)}{5040(1-\nu)}\gamma^6 - \dots \\
L_{ZU} = L_{XW} &= \frac{z^2}{1-\nu}\gamma^2\alpha - \frac{z^4}{6(1-\nu)}\gamma^4\alpha + \frac{z^6}{120(1-\nu)}\gamma^6\alpha - \dots \\
L_{ZV} = L_{YW} &= \frac{z^2}{1-\nu}\gamma^2\beta - \frac{z^4}{6(1-\nu)}\gamma^4\beta + \frac{z^6}{120(1-\nu)}\gamma^6\beta - \dots \\
L_{ZW} &= -\frac{z^3}{3(1-\nu)}\gamma^4 + \frac{z^5}{30(1-\nu)}\gamma^6 - \frac{z^7}{840(1-\nu)}\gamma^8 + \dots \\
L_{YU} = L_{XV} &= -\frac{z(1+\nu)}{1-\nu}\alpha\beta + \frac{z^3(3+\nu)}{6(1-\nu)}\gamma^2\alpha\beta - \\
&\quad - \frac{z^5(5+\nu)}{120(1-\nu)}\gamma^4\alpha\beta + \frac{z^7(7+\nu)}{5040(1-\nu)}\gamma^6\alpha\beta - \dots \\
L_{YV} &= -\frac{2z}{1-\nu}\beta^2 - z\alpha^2 + \frac{2z^3}{3(1-\nu)}\gamma^2\beta^2 + \frac{z^3}{6}\gamma^2\alpha^2 - \\
&\quad - \frac{z^5}{20(1-\nu)}\gamma^4\beta^2 - \frac{z^5}{120}\gamma^4\alpha^2 + \frac{z^7}{630(1-\nu)}\gamma^6\beta^2 + \frac{z^7}{5040}\gamma^6\alpha^2 - \dots \\
L_{XU} &= -\frac{2z}{1-\nu}\alpha^2 - z\beta^2 + \frac{2z^3}{3(1-\nu)}\gamma^2\alpha^2 + \frac{z^3}{6}\gamma^2\beta^2 - \\
&\quad - \frac{z^5}{20(1-\nu)}\gamma^4\alpha^2 - \frac{z^5}{120}\gamma^4\beta^2 + \frac{z^7}{630(1-\nu)}\gamma^6\alpha^2 + \frac{z^7}{5040}\gamma^6\beta^2 - \dots
\end{aligned}\right\} \qquad (2.6)
$$

The symbols $\gamma^2, \gamma^4, \ldots, \gamma^{2n}$ denote two-dimensional harmonic, biharmonic, and n-harmonic differential operators in the x, y plane.

These operators are related to the single-term operators:

$$\alpha^2 = \frac{\partial^2}{\partial x^2}, \quad \beta^2 = \frac{\partial^2}{\partial y^2}$$

as follows:

$$\gamma^2 = \alpha^2 + \beta^2, \quad \gamma^4 = (\alpha^2 + \beta^2)^2, \ldots, \gamma^{2n} = (\alpha^2 + \beta^2)^n.$$

4

Considering the differential operators

$$\alpha, \alpha^2, \beta, \beta^2, \alpha\beta, \gamma^2, \gamma^4, \ldots, \gamma^{2n}$$

in the right-hand sides of (2.6) as algebraic magnitudes, i.e. performing on them the operations of addition, subtraction, multiplication, and division, we can represent the operators $L_{UU}, L_{UV}, L_{UW}, \ldots, L_{XY}, L_{XX}$ in (2.5) in closed form as trigonometric functions of the argument $\gamma z = z\sqrt{\frac{\partial^2}{\partial x^2} + \frac{\partial^2}{\partial y^2}}$.

Using the series developments of the trigonometric functions:

$$\sin\varphi = \varphi - \frac{\varphi^3}{3!} + \frac{\varphi^5}{5!} - \ldots, \quad \cos\varphi = 1 - \frac{\varphi^2}{2!} + \frac{\varphi^4}{4!} - \ldots$$

$$\frac{1}{2}(\sin\varphi - \varphi\cos\varphi) = \frac{\varphi^3}{3!} - \frac{2\varphi^5}{5!} - \frac{3\varphi^7}{7!} - \ldots,$$

$$\frac{1}{2}(\sin\varphi + \varphi\cos\varphi) = \varphi - \frac{2\varphi^3}{3!} + \frac{3\varphi^5}{5!} - \ldots,$$

$$\frac{1}{2}(\varphi\sin\varphi + 2\cos\varphi) = 1 - \frac{\varphi^4}{4!} + \frac{2\varphi^6}{6!} - \frac{3\varphi^8}{8!} + \ldots,$$

$$\frac{1}{2}(3\sin\varphi - \varphi\cos\varphi) = \varphi - \frac{\varphi^5}{5!} + \frac{2\varphi^7}{7!} - \frac{3\varphi^9}{9!} + \ldots$$

where we write $\varphi = \gamma z$, we can represent the series (2.6) in the form:

$$\left.\begin{aligned}
L_{XX} &= L_{UU} = \cos\gamma z - \frac{1}{2(1-\nu)}\frac{\alpha^2 z}{\gamma}\sin\gamma z,\\
L_{VX} &= L_{UV} = -\frac{1}{2(1-\nu)}\frac{\alpha\beta z}{\gamma}\sin\gamma z,\\
L_{ZX} &= L_{UW} = -\frac{1}{2(1-\nu)}\frac{\alpha}{\gamma}[(1-2\nu)\sin\gamma z + \gamma z\cos\gamma z],\\
L_{WX} &= L_{UZ} = -\frac{1}{4(1-\nu)}\frac{\alpha z}{\gamma}\sin\gamma z,\\
L_{VX} &= L_{UY} = -\frac{1}{4(1-\nu)}\frac{\alpha\beta}{\gamma^3}(\sin\gamma z - \gamma z\cos\gamma z),\\
L_{UX} &= \frac{1}{\gamma}\sin\gamma z - \frac{1}{4(1-\nu)}\frac{\alpha^2}{\gamma^3}(\sin\gamma z - \gamma z\cos\gamma z),\\
L_{XY} &= L_{VU} = -\frac{1}{2(1-\nu)}\frac{\alpha\beta z}{\gamma}\sin\gamma z,\\
L_{YY} &= L_{VV} = \cos\gamma z - \frac{1}{2(1-\nu)}\frac{\beta^2 z}{\gamma}\sin\gamma z,\\
L_{ZY} &= L_{\ W} = -\frac{1}{2(1-\nu)}\frac{\beta}{\gamma}[(1-2\nu)\sin\gamma z + \gamma z\cos\gamma z],
\end{aligned}\right| \qquad (2.7)$$

$$\left.\begin{aligned}
L_{WY} &= L_{VZ} = -\frac{1}{4(1-\nu)}\frac{\beta z}{\gamma}\sin\gamma z,\\
L_{XZ} &= L_{WU} = \frac{1}{2(1-\nu)}\frac{\alpha}{\gamma}\left[(1-2\nu)\sin\gamma z-\gamma z\cos\gamma z\right],\\
L_{YZ} &= L_{WV} = \frac{1}{2(1-\nu)}\frac{\beta}{\gamma}\left[(1-2\nu)\sin\gamma z-\gamma z\cos\gamma z\right],\\
L_{ZZ} &= L_{WW} = -\frac{1}{1-\nu}\gamma(\sin\gamma z-\gamma z\cos\gamma z),\\
L_{WZ} &= \frac{1}{4(1-\nu)}\frac{1}{\gamma}\left[(3-4\nu)\sin\gamma z-\gamma z\cos\gamma z\right],\\
L_{XW} &= L_{ZU} = \frac{1}{1-\nu}\alpha\gamma z\sin\gamma z,\\
L_{YW} &= L_{ZV} = \frac{1}{1-\nu}\beta\gamma z\sin\gamma z,\\
L_{ZW} &= -\frac{1}{1-\nu}\gamma(\sin\gamma z-\gamma z\cos\gamma z),\\
L_{XV} &= L_{YU} = -\frac{1}{1-\nu}\frac{\alpha\beta}{\gamma}(\nu\sin\gamma z+\gamma z\cos\gamma z),\\
L_{YV} &= -\frac{\alpha^2}{\gamma}\sin\gamma z-\frac{1}{1-\nu}\frac{\beta^2}{\gamma}(\sin\gamma z+\gamma z\cos\gamma z),\\
L_{XU} &= -\frac{\beta^2}{\gamma}\sin\gamma z-\frac{1}{1-\nu}\frac{\alpha^2}{\gamma}(\sin\gamma z+\gamma z\cos\gamma z).
\end{aligned}\right\}\qquad(2.7)$$

We have thus two forms of representing the differential operators $L_{UU}, L_{UV}, \ldots, L_{XX}$: a purely differential form given by the infinite series (2.6), and an integral-differential form, given by the transcendental equations (2.7), which contain operators of the form:

$$\gamma=(\alpha^2+\beta^2)^{1/2}=\left(\frac{\partial^2}{\partial x^2}+\frac{\partial^2}{\partial y^2}\right)^{1/2}\qquad\frac{1}{\gamma}=(\alpha^2+\beta^2)^{-1/2},$$
$$\frac{1}{\gamma^3}=(\alpha^2+\beta^2)^{-3/2},$$

where, as before:

$$\alpha^2+\beta^2=\frac{\partial^2}{\partial x^2}+\frac{\partial^2}{\partial y^2}.$$

5

Using (2.5) and (2.6) to express $U(x,y,z)$, $V(x,y,z),\ldots,X(x,y,z)$ through $U_0(x,y), V_0(x,y),\ldots,X_0(x,y)$ and their partial derivatives, as well as through z, we obtain by means of (1.6) the remaining stresses σ_x, σ_y, and $\tau_{xy}=\tau_{yx}$, acting on surfaces parallel to the z axis:

$$\left.\begin{aligned}
\sigma_x &= A_UU_0+A_VV_0+\ldots+A_XX_0,\\
\sigma_y &= B_UU_0+B_VV_0+\ldots+B_XX_0,\\
\tau_{xy}=\tau_{yx} &= C_UU_0+C_VV_0+\ldots+C_XX_0,
\end{aligned}\right\}\qquad(2.8)$$

where

$$\left.\begin{aligned}
A_U &= \frac{2}{1-\nu}\alpha - \frac{z^2}{1-\nu}(2\alpha^2+\beta^2)\alpha + \frac{z^4}{12(1-\nu)}(3\alpha^2+\beta^2)\gamma^2\alpha - \\
&\qquad - \frac{z^6}{360(1-\nu)}(4\alpha^2+\beta^2)\gamma^4\alpha + \ldots, \\
A_V &= \frac{2\nu}{1-\nu}\beta - \frac{z^2}{1-\nu}[(1+\nu)\alpha^2+\nu\beta^2]\beta + \frac{z^4}{12(1-\nu)} \times \\
&\times [(2+\nu)\alpha^2+\nu\beta^2]\gamma^2\beta - \frac{z^6}{360(1-\nu)}[(3+\nu)\alpha^2+\nu\beta^2]\gamma^4\beta + \ldots, \\
A_W &= -\frac{2z}{1-\nu}(\alpha^2+\nu\beta^2) + \frac{z^3}{3(1-\nu)}(2\alpha^2+\nu\beta^2)\gamma^2 - \\
&- \frac{z^5}{60(1-\nu)}(3\alpha^2+\nu\beta^2)\gamma^4 + \frac{z^7}{2520(1-\nu)}(4\alpha^2+\nu\beta^2)\gamma^6 - \ldots, \\
A_Z &= \frac{\nu}{1-\nu} - \frac{z^2}{2(1-\nu)}[(1+\nu)\alpha^2+\nu\beta^2] + \frac{z^4}{24(1-\nu)} \times \\
&\times [(2+\nu)\alpha^2+\nu\beta^2]\gamma^2 - \frac{z^6}{720(1-\nu)}[(3+\nu)\alpha^2+\nu\beta^2]\gamma^4 + \ldots, \\
A_Y &= \frac{z\nu}{1-\nu}\beta - \frac{z^3}{6(1-\nu)}[(1+\nu)\alpha^2+\nu\beta^2]\beta + \frac{z^5}{120(1-\nu)} \times \\
&\times [(2+\nu)\alpha^2+\nu\beta^2]\gamma^2\beta - \frac{z^7}{5040(1-\nu)}[(3+\nu)\alpha^2+\nu\beta^2]\gamma^4\beta + \ldots, \\
A_X &= \frac{z(2-\nu)}{1-\nu}\alpha - \frac{z^3}{6(1-\nu)}[(3-\nu)\alpha^2+(2-\nu)\beta^2]\alpha + \\
&\qquad + \frac{z^5}{120(1-\nu)}[(4-\nu)\alpha^2+(2-\nu)\beta^2]\gamma^2\alpha - \\
&\qquad - \frac{z^7}{5040(1-\nu)}[(5-\nu)\alpha^2+(2-\nu)\beta^2]\gamma^4\alpha - \ldots, \\
B_U &= \frac{2\nu}{1-\nu}\alpha - \frac{z^2}{1-\nu}[\nu\alpha^2+(1+\nu)\beta^2]\alpha + \frac{z^4}{12(1-\nu)} \times \\
&\times [\nu\alpha^2+(2+\nu)\beta^2]\gamma^2\alpha - \frac{z^6}{360(1-\nu)}[\nu\alpha^2+(3+\nu)\beta^2]\gamma^4\alpha + \ldots, \\
B_V &= \frac{2}{1-\nu}\beta - \frac{z^2}{1-\nu}(\alpha^2+2\beta^2)\beta + \frac{z^4}{12(1-\nu)}(\alpha^2+3\beta^2)\gamma^2\beta - \\
&\qquad - \frac{z^6}{360(1-\nu)}(\alpha^2+4\beta^2)\gamma^4\beta + \ldots, \\
B_W &= -\frac{2z}{1-\nu}(\nu\alpha^2+\beta^2) + \frac{z^3}{3(1-\nu)}(\nu\alpha^2+2\beta^2)\gamma^2 - \\
&- \frac{z^5}{60(1-\nu)}(\nu\alpha^2+3\beta^2)\gamma^2 + \frac{z^7}{2520(1-\nu)}(\nu\alpha^2+4\beta^2)\gamma^6 - \ldots, \\
B_Z &= \frac{\nu}{1-\nu} - \frac{z^2}{2(1-\nu)} - \frac{z^2}{2(1-\nu)}[\nu\alpha^2+(1+\nu)\beta^2] + \\
&\qquad + \frac{z^4}{24(1-\nu)}[\nu\alpha^2+(2+\nu)\beta^2]\gamma^2 - \frac{z^6}{720(1-\nu)} \times \\
&\qquad \times [\nu\alpha^2+(3+\nu)\beta^2]\gamma^4 + \ldots, \\
B_Y &= \frac{z(2-\nu)}{1-\nu}\beta - \frac{z^3}{6(1-\nu)}[(2-\nu)\alpha^2+(3-\nu)\beta^2]\beta + \\
&\qquad + \frac{z^5}{120(1-\nu)}[(2-\nu)\alpha^2+(4-\nu)\beta^2]\gamma^2\beta - \\
&\qquad - \frac{z^7}{5040(1-\nu)}[(2-\nu)\alpha^2+(5-\nu)\beta^2]\gamma^4\beta + \ldots, \\
B_X &= \frac{z\nu}{1-\nu}\alpha - \frac{z^3}{6(1-\nu)}[\nu\alpha^2+(1+\nu)\beta^2]\alpha + \frac{z^5}{120(1-\nu)} \times \\
&\times [\nu\alpha^2+(2+\nu)\beta^2]\gamma^2\alpha - \frac{z^7}{5040(1-\nu)}[\nu\alpha^2+(3+\nu)\beta^2]\gamma^4\alpha + \ldots, \\
C_U &= \beta - \frac{z^2}{2}\left(\frac{3-\nu}{1-\nu}\alpha^2+\beta^2\right)\beta + \frac{z^4}{24}\left(\frac{5-\nu}{1-\nu}\alpha^2+\beta^2\right)\gamma^2\beta - \\
&\qquad - \frac{z^6}{720}\left(\frac{7-\nu}{1-\nu}\alpha^2+\beta^2\right)\gamma^4\beta + \ldots,
\end{aligned}\right\} \qquad (2.9)$$

$$
\left.\begin{aligned}
C_V &= \alpha - \frac{z^2}{2}\left(\alpha^2 + \frac{3-\nu}{1-\nu}\beta^2\right)\alpha + \frac{z^4}{24}\left(\alpha^2 + \frac{5-\nu}{1-\nu}\beta^2\right)\gamma^2\alpha - \\
&\qquad - \frac{z^6}{720}\left(\alpha^2 + \frac{7-\nu}{1-\nu}\beta^2\right)\gamma^4\alpha + \ldots, \\
C_W &= -2z\alpha\beta + \frac{z^3(1-\nu)}{3(1-\nu)}\gamma^2\alpha\beta - \frac{z^5(3-\nu)}{60(1-\nu)}\gamma^4\alpha\beta + \\
&\qquad + \frac{z^7(4-\nu)}{2520(1-\nu)}\gamma^6\alpha\beta - \ldots, \\
C_Z &= -\frac{z^2}{2(1-\nu)}\alpha\beta + \frac{z^4}{12(1-\nu)}\gamma^2\alpha\beta - \frac{z^6}{240(1-\nu)}\gamma^4\alpha\beta + \ldots, \\
C_Y &= z\alpha - \frac{z^3}{6}\left(\alpha^2 + \frac{2-\nu}{1-\nu}\beta^2\right)\alpha + \frac{z^5}{120}\left(\alpha^2 + \frac{3-\nu}{1-\nu}\beta^2\right)\gamma^2\alpha - \\
&\qquad - \frac{z^7}{5040}\left(\alpha^2 + \frac{4-\nu}{1-\nu}\beta^2\right)\gamma^4\alpha + \ldots, \\
C_X &= z\beta - \frac{z^3}{6}\left(\frac{2-\nu}{1-\nu}\alpha^2 + \beta^2\right)\beta + \frac{z^5}{120}\left(\frac{3-\nu}{1-\nu}\alpha^2 + \beta^2\right)\gamma^2\beta - \\
&\qquad - \frac{z^7}{5040}\left(\frac{4-\nu}{1-\nu}\alpha^2 + \beta^2\right)\gamma^4\beta + \ldots
\end{aligned}\right| \tag{2.9}
$$

Using (2.7) we can represent these operators in the following closed form:

$$
\left.\begin{aligned}
A_U &= \frac{2}{1-\nu}\alpha\cos\gamma z - \frac{z\alpha^3}{\gamma(1-\nu)}\sin\gamma z, \\
A_W &= -\frac{(\alpha^2 + 2\nu\beta^2)}{(1-\nu)\gamma}\sin\gamma z - \frac{z\alpha^2}{1-\nu}\cos\gamma z, \\
A_V &= \frac{2\nu}{1-\nu}\beta\cos\gamma z - \frac{z\alpha^2\beta}{\gamma(1-\nu)}\sin\gamma z, \\
A_Z &= \frac{\nu}{1-\nu}\cos\gamma z - \frac{z}{2(1-\nu)\gamma}\alpha^2\sin\gamma z, \\
A_Y &= \frac{\beta}{\gamma(1-\nu)}\left(\nu - \frac{\alpha^2}{2\gamma^2}\right)\sin\gamma z + \frac{z\alpha^2\beta}{2(1-\nu)\gamma^2}\cos\gamma z, \\
A_X &= \frac{z\alpha^3}{2(1-\nu)\gamma^2}\cos\gamma z + \frac{\alpha}{(1-\nu)\gamma}\left[(2-\nu) - \frac{\alpha^2}{2\gamma^2}\right]\sin\gamma z, \\
B_U &= \frac{2\nu}{1-\nu}\alpha\cos\gamma z - \frac{z\alpha\beta^2}{(1-\nu)\gamma}\sin\gamma z, \\
B_W &= -\frac{2\nu\alpha^2 + \beta^2}{(1-\nu)\gamma}\sin\gamma z - \frac{z\beta^2}{1-\nu}\cos\gamma z, \\
B_V &= \frac{2\beta}{1-\nu}\cos\gamma z - \frac{z\beta^3}{\gamma(1-\nu)}\sin\gamma z, \\
B_Z &= \frac{\nu}{1-\nu}\cos\gamma z - \frac{z}{2(1-\nu)\gamma}\beta^2\sin\gamma z, \\
B_Y &= \frac{\beta}{\gamma(1-\nu)}\left[(2-\nu) - \frac{\beta^2}{2\gamma^2}\right]\sin\gamma z + \frac{z\beta^3}{2(1-\nu)\gamma^2}\cos\gamma z, \\
B_X &= \frac{\alpha}{\gamma(1-\nu)}\left(\nu - \frac{\beta^2}{2\gamma^2}\right)\sin\gamma z + \frac{z\alpha\beta^2}{3(1-\nu)\gamma^2}\cos\gamma z, \\
C_U &= \beta\cos\gamma z - \frac{z\alpha^2\beta}{(1-\nu)\gamma}\sin\gamma z, \\
C_W &= -\frac{\alpha\beta}{(1-\nu)\gamma}[(1-2\nu)\sin\gamma z + \gamma z\cos\gamma z], \\
C_V &= \alpha\cos\gamma z - \frac{z\alpha\beta^2}{(1-\nu)\gamma}\sin\gamma z, \\
C_Y &= \frac{\alpha}{\gamma}\sin\gamma z - \frac{1}{2(1-\nu)}\frac{\alpha\beta^2}{\gamma^2}(\sin\gamma z - \gamma z\cos\gamma z), \\
C_Z &= -\frac{\alpha\beta z}{2(1-\nu)\gamma}\sin\gamma z \\
C_X &= \frac{\beta}{\gamma}\sin\gamma z - \frac{\alpha^2\beta}{3(1-\nu)\gamma^2}(\sin\gamma z - \gamma z\cos\gamma z).
\end{aligned}\right| \tag{2.10}
$$

These expressions could also have been obtained directly from (1.5), (2.5), and (2.7).

§ 3. BASIC PROPERTIES OF THE LINEAR TRANSFORMATION MATRICES IN THE METHOD OF INITIAL FUNCTIONS

1

Equations (2.5) represent a general solution of the three-dimensional problem of the theory of elasticity. When the operators $L_{UU}, L_{UV}, \ldots, L_{XX}$ are defined either by the infinite series (2.6) or by the transcendental equations (2.7), we obtain a one-to-one correspondence between the six initial functions $U_0(x, y), V_0(x, y), \ldots, X_0(x, y)$, corresponding to points of the plane $z=0$, and the six unknown functions $U(x, y), V(x, y), \ldots, X(x, y)$ corresponding to points of any fixed plane $z = \text{const}$.

Equations (2.5) thus represent the general law of transformation of the initial into the unknown functions. An identical transformation corresponds to a unit matrix whose principal diagonal consists of unit elements, all other elements being zero. This property follows also from (2.7).

TABLE 22

	U	V	W	Z	Y	X
U	L_{UU}	L_{UV}	L_{UW}	L_{UZ}	L_{UY}	L_{UX}
V	L_{VU}	L_{VV}	L_{VW}	L_{VZ}	L_{VY}	L_{VX}
W	L_{WU}	L_{WV}	L_{WW}	L_{WZ}	L_{WY}	L_{WX}
Z	L_{ZU}	L_{ZV}	L_{ZW}	L_{ZZ}	L_{ZY}	L_{ZX}
Y	L_{YU}	L_{YV}	L_{YW}	L_{YZ}	L_{YY}	L_{YX}
X	L_{XU}	L_{XV}	L_{XW}	L_{XZ}	L_{XY}	L_{XX}
σ_x	A_U	A_V	A_W	A_Z	A_Y	A_X
σ_y	B_U	B_V	B_W	B_Z	B_Y	B_X
$\tau_{xy} = \tau_{yx}$	C_U	C_V	C_W	C_Z	C_Y	C_X

The transformation of the initial into the unknown functions is called direct transformation. The set of 36 operators $L_{UU}, L_{UV}, \ldots, L_{XX}$ forms the matrix of this direct linear transformation, given in Tables 22 and 23. If $U, V, \ldots, X$ are considered as given and $U_0, V_0, \ldots, X_0$ as unknown in (2.5), we obtain the inverse transformation. In this case the problem reduces to integrating a system of six compatible partial differential equations of an infinitely high order in the limit.

This seemingly complex problem is solved very simply by taking into consideration the physical meaning of the method of initial functions. Taking any plane $z = \text{const}$ as initial, the functions $U, V, \ldots, X$ as given (transformable), and the functions $U_0, V_0, \ldots, X_0$ as unknown (transformed), we assign a negative value to the coordinate z in (2.5). Taking into account that the operators $L_{UU}, L_{UV}, \ldots, L_{XX}$ are even functions of z and thus retain their sign, while the remaining operators $L_{UW}, L_{UY}, \ldots, L_{XY}$, are odd functions of z and change sign, we obtain:

$$\left.\begin{aligned}
U_0 &= L_{UU}U + L_{UV}V - L_{UW}W + L_{UZ}Z - L_{UY}Y - L_{UX}X,\\
V_0 &= L_{VU}U + L_{VV}V - L_{VW}W + L_{VZ}Z - L_{VY}Y - L_{VX}X,\\
W_0 &= -L_{WU}U - L_{WV}V + L_{WW}W - L_{WZ}Z + L_{WY}Y + L_{WX}X,\\
Z_0 &= L_{ZU}U + L_{ZV}V - L_{ZW}W + L_{ZZ}Z - L_{ZY}Y - L_{ZX}X,\\
Y_0 &= -L_{YU}U - L_{YV}V + L_{YW}W - L_{YZ}Z + L_{YY}Y + L_{YX}X,\\
X_0 &= -L_{XU}U - L_{XV}V + L_{XW} - L_{XZ}Z - L_{XY}Y + L_{XX}X.
\end{aligned}\right\} \quad (3.1)$$

2

Substitution in (2.5) of the functions $U_0, V_0, \ldots, X_0$ defined by (3.1), transforms the former into identities. It follows that transformations (2.5) and (3.1) are orthogonal. This property, observed in problems concerning thin-walled bars and shells, and known from Krylov's method of initial parameters in the analysis of beams on elastic foundations, is expressed mathematically as follows: the sum of the products of the corresponding elements in a line of the direct transformation (2.5) and in a column of the inverse transformation (3.1) equals unity, provided line and column have the same ordinal number.

The determinant formed by the operators in transformations (2.5) or (3.1) is equal to unity. This property, just as the property of orthogonality of transformations (2.5) and (3.1), is strictly fulfilled in the limit, when the operators $L_{UU}, L_{UV}, \ldots, L_{XX}$ are defined by (2.7).

TABLE 23

	U	V	W	Z	Y	X
U	$\cos\gamma z - \frac{1}{2(1-\nu)} \times \frac{\alpha^2 z}{\gamma}\sin\gamma z$	$-\frac{1}{2(1-\nu)} \times \frac{\alpha\beta z}{\gamma}\sin\gamma z$	$-\frac{\alpha}{2(1-\nu)\gamma} \times [(1-2\nu) \times \sin\gamma z + \gamma z\cos\gamma z]$	$-\frac{\alpha z}{4(1-\nu)\gamma} \times \sin\gamma z$	$-\frac{\alpha\beta}{4(1-\nu)\gamma^3} \times (\sin\gamma z - \gamma z\cos\gamma z)$	$\frac{1}{\gamma}\sin\gamma z - \frac{1}{4(1-\nu)}\frac{\alpha^2}{\gamma^3} \times (\sin\gamma z - \gamma z\cos\gamma z)$
V	$-\frac{\alpha\beta z}{2(1-\nu)\gamma}\sin\gamma z$	$\cos\gamma z - \frac{\beta^2 z}{2(1-\nu)\gamma} \times \sin\gamma z$	$-\frac{\beta}{2(1-\nu)\gamma} \times [(1-2\nu) \times \sin\gamma z + \gamma z\cos\gamma z]$	$-\frac{\beta z}{4(1-\nu)\gamma} \times \sin\gamma z$	$\frac{1}{\gamma}\sin\gamma z - \frac{1}{4(1-\nu)} \times \frac{\beta^2}{\gamma^3}(\sin\gamma z - \gamma z\cos\gamma z)$	
W	$\frac{1}{2(1-\nu)}\frac{\alpha}{\gamma} \times [(1-2\nu)\sin\gamma z - \gamma z\cos\gamma z]$	$\frac{1}{2(1-\nu)}\frac{\beta}{\gamma} \times [(1-2\nu) \times \sin\gamma z - \gamma z\cos\gamma z]$	$\frac{1}{2(1-\nu)}[\gamma z\sin\gamma z - 2(1-\nu)\cos\gamma z]$	$\frac{1}{4(1-\nu)\gamma} \times [(3-4\nu)\sin\gamma z - \gamma z\cos\gamma z]$		
Z	$\frac{\alpha\gamma z}{1-\nu}\sin\gamma z$	$\frac{\beta\gamma z}{1-\nu}\sin\gamma z$	$\frac{\gamma}{1-\nu} \times (\gamma z\cos\gamma z - \sin\gamma z)$			
Y	$-\frac{\alpha\beta}{(1-\nu)\gamma} \times (\nu\sin\gamma z + \gamma z\cos\gamma z)$	$-\frac{\alpha^2}{\gamma}\sin\gamma z - \frac{\beta^2}{(1-\nu)\gamma} \times (\sin\gamma z + \gamma z\cos\gamma z)$				
X	$-\frac{\beta^2}{\gamma}\sin\gamma z - \frac{\alpha^2}{(1-\nu)\gamma} \times (\sin\gamma z + \gamma z\cos\gamma z)$					

In addition to the properties listed, the operators in transformation (2.5) obey the following law:

$$L_{VU} = L_{XY}, \quad L_{UV} = L_{YX}, \text{etc.} \tag{3.2}$$

Hence, the matrices (2.5) and (3.1) are symmetrical with respect to the secondary diagonal.

The equality of the operators L_{VU} and L_{UV}, and of the operators L_{XY} and L_{YX} symmetrical to them, is due to the isotropy of the elastic body with respect to the z axis. Thus:

$$\left.\begin{aligned} &L_{YU} = L_{XV},\ L_{ZU} = L_{XW},\ L_{WU} = L_{XZ},\ L_{VU} = L_{XY},\\ &L_{UU} = L_{XX},\ L_{UV} = L_{YX},\ L_{UW} = L_{ZX},\ L_{UZ} = L_{WX},\ L_{UY} = L_{VX}.\end{aligned}\right\} \tag{3.3}$$

§ 4. GENERAL METHOD OF REDUCING THE THREE-DIMENSIONAL PROBLEM OF THE THEORY OF ELASTICITY TO A TWO-DIMENSIONAL PROBLEM

The six initial two-dimensional functions $U_0(x, y)$, $V_0(x, y), \ldots, X_0(x, y)$ are obtained by integrating (1.5) by the method of expanding the unknown functions in powers of z. The initial functions are determined by the boundary conditions for $z = 0$ and $z = h = \text{const}$ or, in the general case, for $z = h(x, y)$. These functions are determined at each of these planes. The boundary conditions may be purely statical, purely geometrical, or mixed.

In the case of statical boundary conditions, three components of the stress vector are given at the boundary surface. The unknown functions are in this case the components $U_0(x, y)$, $V_0(x, y)$, $W_0(x, y)$ of the displacement vector of the plane $z = 0$. A system of three differential equations for these functions is obtained from the statical boundary conditions at $z = h(x, y)$.

In the case of purely geometrical conditions, the displacement components are given, the stress components $X_0(x, y)$, $Y_0(x, y)$, $Z_0(x, y)$ being unknown. A system of three linear differential equations for these three unknown functions is obtained from the geometrical boundary conditions at $z = h(x, y)$.

In the mixed problem, the boundary conditions at $z = 0$ are given partly in displacements and partly in stresses. Three conditions altogether are given for each point of the plane $z = 0$. Three differential equations for the remaining three unknown functions are obtained from the three conditions at $z = h(x, y)$.

Expanding, according to the general method of initial functions, the boundary conditions for $z = 0$ and $z = h(x, y)$, we can always reduce the three-dimensional problem of the theory of elasticity to a two-dimensional problem described by a system of three linear differential equations in three unknown initial functions of x and y *.

These equations will have variable coefficients in the case of an elastic layer of variable thickness $h = h(x, y)$. If the thickness is constant, the coefficients will also be constant.

The order of the differential equations depends on the number of terms retained in (2.6).

---

* A similar method, though formulated differently, was proposed by A.N. Lur'e /56/.

The boundary conditions for $z=0$ and $z=h(x, y)$ are satisfied exactly during the reduction of the three-dimensional to a two-dimensional problem. The boundary conditions at the lateral cylindrical surface are satisfied when integrating the differential equations of the two-dimensional problem. These conditions are satisfied up to the terms of (2.6) which have been discarded.

If in (2.6) we use only terms linear in z for the displacements, up to z^2 for the shearing stresses X and Y, and the first terms in z^3 for the normal stress Z, we obtain a solution which satisfies the boundary conditions on the lateral surface only in Saint-Venant's sense.

We arrive in this case at the general moment theory of thick plates, independent of Kirchhoff and Love's hypothesis. If terms of higher order are retained in (2.6), a more accurate theory of thick plates is obtained. In this case there appears on the lateral surface, in addition to the axial forces and moments considered in problems of plane stress and bending of a plate, also an equilibrium system of stresses, which can be reduced to generalized forces of the same nature as bimoments.

It is thus possible to develop by the method of initial functions a general bimoment theory of thick plates and shells, independent of Kirchoff and Love's hypothesis, by means of which the boundary-value problem can be solved with the required accuracy.

§ 5. THICK PLATE SUBJECTED TO A LOAD SYMMETRICAL WITH RESPECT TO ITS MIDDLE PLANE

1

Let a plate of uniform thickness $2h$ be subjected to surface loads (normal and shearing forces in the general case) acting at the planes $z=\pm h$, symmetrically with respect to the middle plane of the plate (Figure 164).

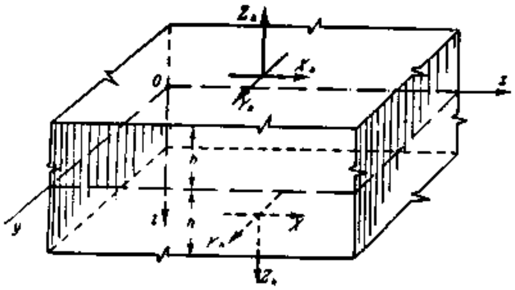

FIGURE 164.

We use the middle plane of the plate as reference plane. The z axis is directed downward, the x axis to the right, and the y axis in such way that the coordinate system xyz is right-handed. Due to symmetry, there will be no vertical displacements and shearing stresses in the middle plane of the plate; the three functions W_0, X_0, Y_0 will therefore vanish. The unknown functions will be the horizontal displacements $U_0(x, y)$ and $V_0(x, y)$, and the normal stress $Z_0(x, y)$.

Inserting $W_0 = X_0 = Y_0 = 0$ into (2.5) yields:

$$\left.\begin{aligned} U &= L_{UU} U_0 + L_{UV} V_0 + L_{UZ} Z_0, \\ V &= L_{VU} U_0 + L_{VV} V_0 + L_{VZ} Z_0, \\ W &= L_{WU} U_0 + L_{WV} V_0 + L_{WZ} Z_0, \\ Z &= L_{ZU} U_0 + L_{ZV} V_0 + L_{ZZ} Z_0, \\ Y &= L_{YU} U_0 + L_{YV} V_0 + L_{YZ} Z_0, \\ X &= L_{XU} U_0 + L_{XV} V_0 + L_{XZ} Z_0. \end{aligned}\right\} \tag{5.1}$$

The unknown functions $U_0(x, y)$, $V_0(x, y)$, $Z_0(x, y)$ are found by solving the system of three differential equations, obtained from (5.1) by equating the stress components X, Y, Z for $z = h$ to the given functions $Z_h(x, y)$, $Y_h(x, y)$, $X_h(x, y)$:

$$\left.\begin{aligned} L_{ZU}(h) U_0 + L_{ZV}(h) V_0 + L_{ZZ}(h) Z_0 &= Z_h, \\ L_{YU}(h) U_0 + L_{YV}(h) V_0 + L_{YZ}(h) Z_0 &= Y_h, \\ L_{XU}(h) U_0 + L_{XV}(h) V_0 + L_{XZ}(h) Z_0 &= X_h, \end{aligned}\right\} \tag{5.2}$$

where $L_{ZU}(h)$, $L_{ZV}(h), \ldots, L_{XZ}(h)$ = differential operators determined from (2.6) for $z = h$. When X_h, Y_h, Z_h are known, (5.2) forms a system of compatible partial differential equations in x and y.

2

The equilibrium of a plate subjected only to a normal load $Z_h(x, y)$, symmetrical with respect to the middle plane, will now be considered in more detail. The last two equations (5.2) are in this case homogeneous ($X_h = Y_h = 0$) and will be satisfied if we introduce the function $F = F(x, y)$ satisfying the equations:

$$\left.\begin{aligned} U_0 &= (L_{XV} L_{YZ} - L_{YV} L_{XZ})_h F, \\ V_0 &= -(L_{XU} L_{YZ} - L_{YU} L_{XZ})_h F, \\ Z_0 &= (L_{XU} L_{YV} - L_{YU} L_{XV})_h F, \end{aligned}\right\} \tag{5.3}$$

where the differential operators in parentheses are formed by the rules of symbolic differentiation for $z = h$. Substituting (5.3) in the first equation (5.2) we obtain:

$$\begin{aligned} [L_{ZU}(L_{XV} L_{YZ} - L_{YV} L_{XZ}) - L_{ZV}(L_{XU} L_{YZ} - L_{YU} L_{XZ}) + \\ + L_{ZZ}(L_{XU} L_{YV} - L_{YU} L_{XV})]_h F = Z_h, \end{aligned} \tag{5.4}$$

where the differential operator in brackets is determined approximately by (2.6) and exactly by (2.7), when $z = h$ is substituted.

The order of this equation depends on the number of terms taken in (2.6), which in turn depends on the relative thickness of the plate and the required accuracy of the solution. If for a plate of medium thickness only the first terms are taken in (2.6), we obtain the approximate theory of the equilibrium of a symmetrically loaded plate.

To obtain the exact theory, the exact values of the differential operators determined from (2.7) for $z = h$ should be substituted in (5.4). In this case, we obtain for F a transcendental equation in which the arguments of the trigonometric functions contain partial derivatives of F with respect to x and y. This equation can be written in the form:

$$\frac{\gamma^2}{1-\nu}\sin\gamma h\,[\sin\gamma h\cos\gamma h+\gamma h]\,F = Z_h. \tag{5.5}$$

Furthermore:

$$\left.\begin{aligned}
U_0 &= \frac{\alpha\sin\gamma h}{2(1-\nu)}[(1-2\nu)\sin\gamma h-\gamma h\cos\gamma h]\,F,\\
V_0 &= \frac{\beta\sin\gamma h}{2(1-\nu)}[(1-2\nu)\sin\gamma h-\gamma h\cos\gamma h]\,F,\\
Z_0 &= \frac{\gamma^2\sin\gamma h}{1-\nu}(\sin\gamma h+\gamma h\cos\gamma h)\,F.
\end{aligned}\right\} \tag{5.6}$$

The order of (5.5) can be reduced by writing:

$$\Phi = \frac{\gamma\sin\gamma h}{1-\nu}F. \tag{5.7}$$

Equations (5.5) and (5.6) then become:

$$\gamma\left[\gamma h+\frac{\sin 2\gamma h}{2}\right]\Phi = Z_h, \tag{5.8}$$

$$\left.\begin{aligned}
U_0 &= \frac{\alpha}{2}\left[(1-2\nu)\frac{\sin\gamma h}{\gamma}-h\cos\gamma h\right]\Phi,\\
V_0 &= \frac{\beta}{2}\left[(1-2\nu)\frac{\sin\gamma h}{\gamma}-h\cos\gamma h\right]\Phi,\\
Z_0 &= \gamma\,[\sin\gamma h+\gamma h\cos\gamma h]\,\Phi.
\end{aligned}\right\} \tag{5.9}$$

If the trigonometric functions in (5.8) and (5.9) are expanded in powers of their argument, the transcendental equation (5.8) becomes an ordinary differential equation. Writing again $\gamma^2 = \alpha^2+\beta^2 = \nabla^2$, we obtain:

$$\left[2h\nabla^2-\frac{2}{3}h^3\nabla^2\nabla^2+\frac{2}{15}h^5\nabla^2\nabla^2\nabla^2-\ldots\right]\Phi = Z_h. \tag{5.10}$$

Expressions (5.9) can then be written as follows:

$$\left.\begin{aligned}
U_0 &= \alpha h\left[-\nu+\frac{1+\nu}{6}h^2\nabla^2-\frac{2+\nu}{120}h^4\nabla^2\nabla^2+\ldots\right]\Phi,\\
V_0 &= \beta h\left[-\nu+\frac{1+\nu}{6}h^2\nabla^2-\frac{2+\nu}{120}h^4\nabla^2\nabla^2+\ldots\right]\Phi,\\
Z_0 &= h\;\left[2-\frac{2}{3}h^2\nabla^2+\frac{1}{20}h^4\nabla^2\nabla^2-\ldots\right]\nabla^2\Phi.
\end{aligned}\right\} \tag{5.11}$$

Equations (5.8) or (5.10) describe exactly the states of strain and stress of a symmetrically loaded thick plate. After the function Φ has been determined from these equations and the boundary conditions on the lateral surface of the plate, the initial functions U_0, V_0, Z_0 can be obtained from (5.11), while the displacements U, V, W and the stresses Z, Y, X are found from (5.1). The remaining stresses σ_x, σ_y, τ_{xy} are then determined from (2.8).

An approximate solution is obtained by taking a finite number of terms in (5.10) and (5.11) or, which is the same, in (2.6). Thus, retaining only the first two terms in (5.10), we obtain:

$$\nabla^2\nabla^2\Phi - \frac{3}{h^2}\nabla^2\Phi = -\frac{3}{2h^3}Z_h. \tag{5.12}$$

The unknown initial functions are in this case:

$$U_0 = -\nu h\frac{\partial\Phi}{\partial x}, \quad V_0 = -\nu h\frac{\partial\Phi}{\partial y}, \quad Z_0 = 2h\nabla^2\Phi. \tag{5.13}$$

If the load acting on the plate is axisymmetrical, an ordinary differential equation in polar coordinates is obtained in both the exact and the approximate solution.

§ 6. THICK PLATE SUBJECTED TO A LOAD ANTISYMMETRICAL WITH RESPECT TO THE MIDDLE PLANE

1

If a plate of thickness $2h$ is subjected to a load consisting of normal and shearing stresses (Figure 165), applied antisymmetrically with respect to the middle plane $z=0$ at the boundary planes $z=\pm h$, the horizontal displacements and the normal stress at the middle plane will be equal to zero. Taking $z=0$ as reference plane, and putting in (2.5) $U_0=V_0=Z_0=0$, we obtain:

$$\left.\begin{aligned} U&=L_{UW}W_0+L_{UY}Y_0+L_{UX}X_0, & Z&=L_{ZW}W_0+L_{ZY}Y_0+L_{ZX}X_0,\\ V&=L_{VW}W_0+L_{VY}Y_0+L_{VX}X_0, & Y&=L_{YW}W_0+L_{YY}Y_0+L_{YX}X_0,\\ W&=L_{WW}W_0+L_{WY}Y_0+L_{WX}X_0, & X&=L_{XW}W_0+L_{XY}Y_0+L_{XX}X_0. \end{aligned}\right\} \tag{6.1}$$

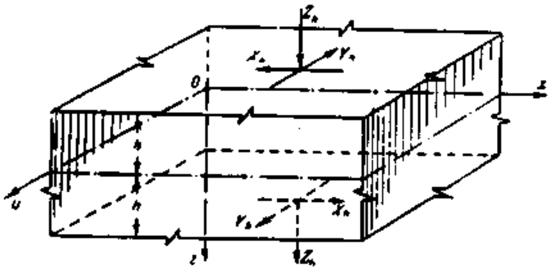

FIGURE 165.

The unknown initial functions are in this case the displacement $W_0 = W_0(x, y)$ and the stresses $X_0 = X_0(x, y)$ and $Y_0 = Y_0(x, y)$.

The following system of three differential equations is obtained for these three unknown functions from the statical boundary conditions:

$$\left.\begin{aligned} L_{XW} W_0 + L_{XX} X_0 + L_{XY} Y_0 &= X_h, \\ L_{YW} W_0 + L_{YX} X_0 + L_{YY} Y_0 &= Y_h, \\ L_{ZW} W_0 + L_{ZX} X_0 + L_{ZY} Y_0 &= Z_h, \end{aligned}\right\} \qquad (6.2)$$

where $z = h$ has to be substituted in the operators $L_{XW}, L_{XX}, \ldots, L_{ZY}$.

If only a vertical load $Z_h = Z_h(x, y)$ acts on the plate, the first two equations (6.2) will be homogeneous. These equations can be satisfied by introducing a function $F = F(x, y)$ which satisfies the equations:

$$\left.\begin{aligned} W_0 &= (L_{XX} L_{YY} - L_{YX} L_{XY})_h F, \\ X_0 &= -(L_{XW} L_{YY} - L_{YW} L_{XY})_h F, \\ Y_0 &= (L_{XW} L_{YX} - L_{YW} L_{XX})_h F, \end{aligned}\right\} \qquad (6.3)$$

(The subscript h indicates that the differential operators in parentheses are determined for $z = h$).

Substitution of (6.3) in the third equation (6.2) yields:

$$\begin{aligned} [L_{ZW}(L_{XX} L_{YY} - L_{YX} L_{XY}) - L_{ZX}(L_{XW} L_{YY} - L_{YW} L_{XY}) + \\ + L_{ZY}(L_{XW} L_{YX} - L_{YW} L_{XW})]_h F = Z_h. \end{aligned} \qquad (6.4)$$

2

The order of (6.3) and (6.4) depends on the required degree of accuracy.

Expanding the differential operators in (6.3) according to (2.6) and substituting $z = h$ yields:

$$\left.\begin{aligned} W_0 &= \left[1 - \frac{h^2(2-\nu)}{2(1-\nu)} \nabla^2 + \frac{h^4(3-\nu)}{24(1-\nu)} \nabla^2\nabla^2 - \ldots\right] F, \\ X_0 &= \left[-\frac{h^2}{1-\nu} \nabla^2 + \frac{h^4}{6(1-\nu)} \nabla^2\nabla^2 - \ldots\right] \alpha F, \\ Y_0 &= \left[-\frac{h^2}{1-\nu} \nabla^2 + \frac{h^4}{6(1-\nu)} \nabla^2\nabla^2 - \ldots\right] \beta F, \end{aligned}\right\} \qquad (6.5)$$

where, in accordance with the symbolic notation used:

$$\nabla^2 = \frac{\partial^2}{\partial x^2} + \frac{\partial^2}{\partial y^2}, \quad \alpha F = \frac{\partial F}{\partial x}, \quad \beta F = \frac{\partial F}{\partial y}. \qquad (6.6)$$

The following differential equation is obtained for the function F:

$$\begin{aligned} \left[\frac{2h^3}{3(1-\nu)} - \frac{2h^5}{15(1-\nu)} \nabla^2 + \frac{4h^7}{315(1-\nu)} \nabla^2\nabla^2 - \right. \\ \left. - \frac{2h^9}{2835(1-\nu)} \nabla^2\nabla^2\nabla^2 + \ldots\right] \nabla^2\nabla^2 F = Z_h. \end{aligned} \qquad (6.7)$$

The fundamental equation of the problem considered is (6.7), which determines the function $F = F(x, y)$. The order of this equation depends on the required degree of accuracy.

To obtain an approximate solution, we retain only the first terms in (6.5) and (6.7), obtaining:

$$\left.\begin{aligned} W_0 = F, \quad X_0 = -\frac{h^2}{1-\nu}\nabla^2\frac{\partial F}{\partial x}, \qquad Y_0 = -\frac{h^2}{1-\nu}\nabla^2\frac{\partial F}{\partial y},\\ \nabla^2\nabla^2 F = \frac{3(1-\nu)}{2h^3}Z_h. \end{aligned}\right\} \tag{6.8}$$

Writing, in accordance with (1.3):

$$W_0 = \frac{E}{2(1+\nu)}w,$$

where $w = w(x, y)$ = actual vertical displacement of the points of the middle plane, and eliminating $F(x, y)$ from (6.8), we obtain:

$$\left.\begin{aligned} X_0 = -\frac{Eh^2}{2(1-\nu^2)}\nabla^2\frac{\partial w}{\partial x}, \quad Y_0 = -\frac{Eh^2}{2(1-\nu^2)}\nabla^2\frac{\partial w}{\partial y},\\ \nabla^2\nabla^2 w = \frac{3(1-\nu^2)}{Eh^3}Z_h. \end{aligned}\right\} \tag{6.9}$$

Equations (6.9) and (6.8) correspond to the moment theory of the bending of plates which is a particular case of the general bimoment theory which is independent of Kirchhoff and Love's hypothesis. The moment theory holds true for sufficiently thin plates and distributed antisymmetrical loads. If the thickness of the plate is not small in relation to its other dimensions, and if the plate is subjected to local (concentrated) loads, the more general bimoment theory corresponding to (6.7) has to be applied. When the plate is of medium thickness, the first two or three terms (depending on the problem and the required accuracy) in (6.7) will be sufficient. The fundamental function $F = F(x, y)$ is invariant with respect to coordinate transmations.

The exact transcendental form of (6.4) and (6.7) is:

$$\frac{\gamma}{1-\nu}[\gamma h - \sin\gamma h\cos\gamma h]F = Z_h. \tag{6.10}$$

while (6.5) takes the form:

$$\left.\begin{aligned} W_0 = \left[\cos\gamma h - \frac{\gamma h}{2(1-\nu)}\sin\gamma h\right]F,\\ Y_0 = -\frac{\beta\gamma h}{1-\nu}\sin\gamma hF, \quad X_0 = -\frac{\alpha\gamma h}{1-\nu}\sin\gamma hF. \end{aligned}\right\} \tag{6.11}$$

§ 7. DEFORMATION OF AN ELASTIC FOUNDATION, DUE TO A LOAD APPLIED TO ITS SURFACE

1

Consider an elastic layer of finite thickness H, lying on an incompressible base and subjected to normal and shearing surface forces Z_H, X_H, Y_H (Figure 166). It will be assumed that at the plane of contact of this layer with the subsoil, the shearing stresses X and Y, and the vertical displacements W vanish. This means that the elastic layer can slide freely along the contact surface, as shown schematically in Figure 166.

Taking the plane of contact as reference plane, we again obtain expressions (5.1) for the displacements and stresses of the elastic layer. The problem considered is thus identical with the problem of a thick plate subjected to a symmetrical load.

In the general case, when surface forces Z_H, X_H, Y_H are present, the system of differential equations determining the solution is written in form (5.2). In the absence of shearing loads ($X_H = Y_H = 0$), we obtain again:

$$\begin{aligned}[L_{ZU}(L_{XV}L_{YZ} - L_{YV}L_{XZ}) - L_{ZV}(L_{XU}L_{YZ} - L_{YU}L_{XZ}) +& \\ + L_{ZZ}(L_{XU}L_{YV} - L_{YU}L_{XV})]_H F = -Z_H&\end{aligned} \tag{7.1}$$

or

$$\left[2H\nabla^2 - \frac{2}{3}H^3\nabla^2\nabla^2 + \frac{2}{15}H^5\nabla^2\nabla^2\nabla^2 - \ldots\right]\Phi = -Z_H. \tag{7.2}$$

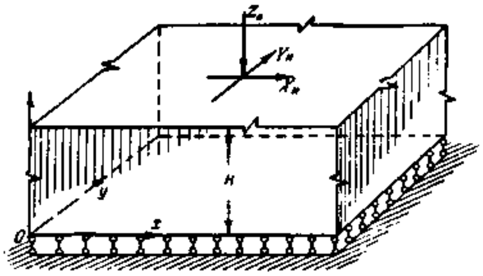

FIGURE 166.

Retaining only the first terms in (7.2), we obtain the differential equation of the approximate theory of an elastic foundation of finite thickness H:

$$\nabla^2\nabla^2\Phi - \frac{3}{H^2}\nabla^2\Phi + \frac{3}{2H^3}Z_H = 0, \quad \nabla^2 = \frac{\partial^2}{\partial x^2} + \frac{\partial^2}{\partial y^2}. \tag{7.3}$$

The foundation model described by (7.3) corresponds in its behavior better to the elastic layer than the single-layer model considered before, since both vertical and horizontal displacements are taken into account.

Let the elastic layer, subjected to surface loads Z_H, X_H, Y_H, be fixed rigidly along the reference plane $z = 0$ (Figure 167). In this case, the three initial functions U_0, V_0, W_0 will be equal to zero. The unknown functions will be the normal and shearing stresses Z_0, Y_0, X_0.

We obtain from (2.5):

$$\left.\begin{aligned} U &= L_{UZ} Z_0 + L_{UY} Y_0 + L_{UX} X_0, \\ V &= L_{VZ} Z_0 + L_{VY} Y_0 + L_{VX} X_0, \\ W &= L_{WZ} Z_0 + L_{WY} Y_0 + L_{WX} X_0, \\ Z &= L_{ZZ} Z_0 + L_{ZY} Y_0 + L_{ZX} X_0, \\ Y &= L_{YZ} Z_0 + L_{YY} Y_0 + L_{YX} X_0, \\ X &= L_{XZ} Z_0 + L_{XY} Y_0 + L_{XX} X_0 \end{aligned}\right\} \qquad (7.4)$$

The functions $Z_0(x, y)$, $Y_0(x, y)$, $X_0(x, y)$ are determined from the boundary conditions at $z = h$:

$$\left.\begin{aligned} L_{ZZ}(H) Z_0 + L_{ZY}(H) Y_0 + L_{ZX}(H) X_0 &= -Z_H, \\ L_{YZ}(H) Z_0 + L_{YY}(H) Y_0 + L_{YX}(H) X_0 &= Y_H, \\ L_{XZ}(H) Z_0 + L_{XY}(H) Y_0 + L_{XX}(H) X_0 &= X_H. \end{aligned}\right\} \qquad (7.5)$$

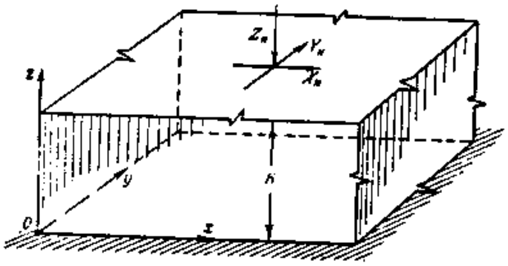

FIGURE 167.

This system of three partial differential equations in x and y represents the solving system of the problem considered.

In the particular case when only normal surface forces Z_H act on the elastic layer ($X_H = Y_H = 0$), we introduce the function $F = F(x, y)$ satisfying the equations:

$$\left.\begin{aligned} Z_0 &= (L_{XY} L_{YX} - L_{YY} L_{XX})_H F, \\ Y_0 &= -(L_{XZ} L_{YX} - L_{YZ} L_{XX})_H F, \\ X_0 &= (L_{XZ} L_{YY} - L_{YZ} L_{XY})_H F. \end{aligned}\right\} \qquad (7.6)$$

Substitution of (7.6) in (7.5) transforms the last two equations (7.5) into identities, and the first one into:

$$\begin{aligned} [L_{ZZ}(L_{XY} L_{YX} - L_{YY} L_{XX}) - L_{ZY}(L_{XZ} L_{YX} - L_{YZ} L_{XX}) + \\ + L_{ZX}(L_{XZ} L_{YY} - L_{YZ} L_{XY})]_H F = -Z_H. \end{aligned} \qquad (7.7)$$

This equation describes the states of stress and strain of a foundation rigidly fixed along the plane $z=0$. The order of this equation depends on the number of terms taken in (2.6). Substitution in (7.7) of the exact values of the differential operators, given by formulas (2.7) for $z=H$, yields:

$$\left[\frac{H^2}{4(1-\nu)^2}\gamma^2-\cos^2\gamma H-\frac{(1-2\nu)^2}{4(1-\nu)^2}\sin^2\gamma H\right]F=-Z_H. \tag{7.8}$$

while (7.6) becomes:

$$\left.\begin{aligned}Z_0&=\cos\gamma H\left[\frac{H\gamma}{2(1-\nu)}\sin\gamma H-\cos\gamma H\right]F,\\ Y_0&=\frac{\beta\cos\gamma H}{2\gamma(1-\nu)}[\gamma H\cos\gamma H-(1-2\nu)\sin\gamma H]F,\\ X_0&=\frac{\alpha\cos\gamma H}{2\gamma(1-\nu)}[(1-2\nu)\sin\gamma H-\gamma H\cos\gamma H]F.\end{aligned}\right\} \tag{7.9}$$

§ 8. CONTACT BETWEEN A PLATE AND AN ELASTIC FOUNDATION

Consider a plate subjected to a distributed load $p(x, y)$ and resting on an elastic foundation representing a compressible layer of finite thickness H (Figure 168).

The plane along which the elastic foundation rests on the underlying subsoil is taken as reference plane. We assume that the displacements at $z=0$ vanish: $U_0=V_0=W_0=0$. The states of stress and strain of the elastic foundation are then given by (7.4).

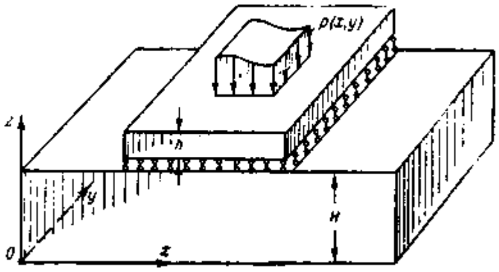

FIGURE 168.

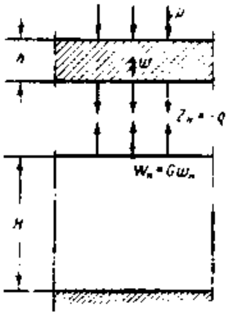

FIGURE 169.

The functions Z_0, Y_0, X_0 are determined from the boundary conditions at $z=H$. Assuming that there is no friction or adhesion between plate and elastic foundation, we obtain:

$$X_H=Y_H=0. \tag{8.1}$$

The differential equation of bending of the plate on the elastic foundation is:

$$D\nabla^2\nabla^2w(x, y)=p(x, y)-q(x, y). \tag{8.2}$$

where $p(x, y)$ = given distributed load, $q(x, y)$ = reactions of elastic foundation.

According to our assumptions, the plate deflections $w(x, y)$ equal the vertical displacements of the elastic-foundation surface $w_H(x, y)=\frac{1}{G}W_H(x, y)$. It follows that $W_H = Gw$ (the positive directions of the deflections and displacements are shown in Figure 169). Furthermore, the reactions $q(x, y)$ represent a surface load $Z_H(x, y)$ with respect to the elastic foundation. In accordance with the convention adopted for the signs, the normal stresses at the surface of the elastic foundation are:

$$Z_H(x, y) = -\frac{D}{G}\nabla^2\nabla^2 W_H(x, y) - p(x, y). \tag{8.3}$$

Substitution of (7.4) in (8.1) and (8.3) yields:

$$\left.\begin{aligned}
&L_{ZZ}(H)Z_0 + L_{ZY}(H)Y_0 + L_{ZX}(H)X_0 =\\
&\qquad = -\frac{D}{G}\nabla^2\nabla^2\left[L_{WZ}(H)Z_0 + L_{WY}(H)Y_0 + L_{WX}(H)X_0\right] - p,\\
&L_{YZ}(H)Z_0 + L_{YY}(H)Y_0 + L_{YX}(H)X_0 = 0,\\
&L_{XZ}(H)Z_0 + L_{XY}(H)Y_0 + L_{XX}(H)X_0 = 0,
\end{aligned}\right\} \tag{8.4}$$

or

$$\left.\begin{aligned}
&\left[L_{ZZ}(H) + \frac{D}{G}\gamma^4 L_{WZ}(H)\right]Z_0 + \left[L_{ZY}(H) + \frac{D}{G}\gamma^4 L_{WY}(H)\right]Y_0 +\\
&\qquad + \left[L_{ZX}(H) + \frac{D}{G}\gamma^4 L_{WX}(H)\right]X_0 = -p,\\
&L_{YZ}(H)Z_0 + L_{YY}(H)Y_0 + L_{YX}(H)X_0 = 0,\\
&L_{XZ}(H)Z_0 + L_{XY}(H)Y_0 + L_{XX}(H)X_0 = 0.
\end{aligned}\right\} \tag{8.5}$$

The differential operators $L_{ZZ}(H)$, $L_{WZ}(H)$, ..., $L_{XX}(H)$ are defined by (2.6) or (2.7) for $z = H$.

Introducing the function $F(x, y)$ satisfying (7.6), system (8.5) is reduced to the single equation:

$$\begin{aligned}
&\Big[\left(L_{ZZ} + \frac{D}{G}\gamma^4 L_{WZ}\right)(L_{XY}L_{YX} - L_{YY}L_{XX}) -\\
&\qquad - \left(L_{ZY} + \frac{D}{G}\gamma^4 L_{WY}\right)(L_{XZ}L_{YX} - L_{YZ}L_{XX}) +\\
&\qquad + \left(L_{ZX} + \frac{D}{G}\gamma^4 L_{WX}\right)(L_{XZ}L_{YY} - L_{YZ}L_{XY})\Big]_H F = -p.
\end{aligned} \tag{8.6}$$

This is the exact equation of bending of a plate resting on an elastic foundation considered as an isotropic layer of finite thickness H. Approximate solutions are obtained by taking a finite number of terms in (2.6), the order of (8.6) depending on this number, i.e., on the accuracy required of the solution.

§ 9. THEORY OF PLATES AND SHELLS OF VARIABLE THICKNESS, SUBJECTED TO ARBITRARY SURFACE LOADS

Consider the general equilibrium problem of a plate of variable thickness $h = h(x, y)$. This problem has considerable practical importance in the design of shallow shell-type roofings of variable thickness, having plane upper surfaces (Figure 170).

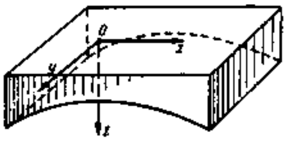

FIGURE 170.

Choosing such a surface as reference plane ($z=0$) and considering the surface load acting on it to be given, we obtain the stress components X_0, Y_0, Z_0 in (2.5) as known functions of x and y. The unknown initial functions in this region are the three displacements

$$U_0 = U_0(x,\ y),\quad V_0 = V_0(x,\ y),\quad W_0 = W(x,\ y).$$

Hence, the displacements

$$U = U(x,\ y,\ z),\quad V = V(x,\ y,\ z),\quad W = W(x,\ y,\ z)$$

and the stresses

$$X = X(x,\ y,\ z),\quad Y = Y(x,\ y,\ z),\quad Z = Z(x,\ y,\ z),$$
$$\sigma_x = \sigma_x(x,\ y,\ z),\quad \sigma_y = \sigma_y(x,\ y,\ z),\quad \tau_{xy} = \tau_{xy}(x,\ y,\ z)$$

at any point x, y, z are determined except for the three unknown initial functions $U_0(x,\ y)$, $V_0(x,\ y)$, $W_0(x,\ y)$. Substituting $z = h(x,\ y)$ in the general solution, we obtain the three components of the displacement vector and the six different components of the stress tensor for the points of the surface $h = h(x,\ y)$ forming the lower surface of the plate or shell. At $z = h(x,\ y)$, the stresses X, Y, Z, (σ_x, σ_y, τ_{xy}) must be in equilibrium with the given surface load applied to the lower surface $h = h(x,\ y)$.

Denoting by X_ν, Y_ν, Z_ν the components of this given surface load in the fixed cartesian reference frame x, y, z, the equilibrium conditions of an elementary tetrahedron, whose inclined surface forms part of the boundary surface $h = h(x,\ y)$, can be represented in the following form:

$$X_\nu = \sigma_x \cos(\nu,\ x) + \tau_{xy}\cos(\nu,\ y) + X\cos(\nu,\ z)\qquad (x,\ y,\ z), \tag{9.1}$$

where

$$\left.\begin{aligned}\cos(\nu,\ x) &= \frac{\partial h}{\partial x}\,\frac{1}{\sqrt{\left(\frac{\partial h}{\partial x}\right)^2+\left(\frac{\partial h}{\partial y}\right)^2+1}},\\ \cos(\nu,\ y) &= \frac{\partial h}{\partial y}\,\frac{1}{\sqrt{\left(\frac{\partial h}{\partial x}\right)^2+\left(\frac{\partial h}{\partial y}\right)^2+1}},\\ \cos(\nu,\ z) &= -\frac{1}{\sqrt{\left(\frac{\partial h}{\partial x}\right)^2+\left(\frac{\partial h}{\partial y}\right)^2+1}}.\end{aligned}\right\} \tag{9.2}$$

= cosines of angles between outer normal to element of surface $h = h(xy)$, and coordinate axes x, y, z respectively.

For $h = h(x, y)$ the statical boundary conditions are given by (9.1), which after insertion of (9.2) become:

$$\left.\begin{aligned}
X_\nu &= \frac{1}{\sqrt{\left(\frac{\partial h}{\partial x}\right)^2 + \left(\frac{\partial h}{\partial y}\right)^2 + 1}}\left(\sigma_x \frac{\partial h}{\partial x} + \tau_{xy}\frac{\partial h}{\partial y} - X\right),\\
Y_\nu &= \frac{1}{\sqrt{\left(\frac{\partial h}{\partial x}\right)^2 + \left(\frac{\partial h}{\partial y}\right)^2 + 1}}\left(\tau_{yx} \frac{\partial h}{\partial x} + \sigma_y\frac{\partial h}{\partial y} - Y\right),\\
Z_\nu &= \frac{1}{\sqrt{\left(\frac{\partial h}{\partial x}\right)^2 + \left(\frac{\partial h}{\partial y}\right)^2 + 1}}\left(\tau_{zx} \frac{\partial h}{\partial x} + \tau_{zy}\frac{\partial h}{\partial y} - Z\right).
\end{aligned}\right\} \tag{9.3}$$

When the initial functions X_0, Y_0, Z_0 are known we obtain, by substituting in (9.3) the stress values given by (2.5) and (2.8), a system of three linear partial differential equations with variable coefficients, for the unknown functions $U_0(x, y), V_0(x, y), W_0(x, y)$. The order of these equations depends on the number of terms retained in (2.6).

We shall consider in detail the moment theory of plates and shells of variable thickness $h = h(x, y)$, assuming that the displacement W is constant over the shell thickness (i.e., does not depend on z), and that the displacements U and V vary linearly. Furthermore, the law of variation of the shearing stresses X and Y is given by a parabola of the second degree in Z, and of the normal stress Z, by a cubic parabola [the stresses σ_x, σ_y, and τ_{xy} vary linearly]. The following approximations then obtained from (2.5) and (2.8):

$$\left.\begin{aligned}
U &= U_0 - z\frac{\partial W_0}{\partial x} + zY_0,\; V = V_0 - z\frac{\partial W_0}{\partial y} + zY_0,\; W = W_0,\\
X &= -z\left(\frac{2}{1-\nu}\frac{\partial^2 U_0}{\partial x^2} + \frac{\partial^2 U_0}{\partial y^2}\right) - \frac{1+\nu}{1-\nu}z\frac{\partial^2 V_0}{\partial x\,\partial y} -\\
&\quad - \frac{2-\nu}{2(1-\nu)}z^2\frac{\partial^2 X_0}{\partial x^2} - \frac{z^2}{2}\frac{\partial^2 X_0}{\partial y^2} - \frac{1}{2(1-\nu)}z^2\frac{\partial^2 Y_0}{\partial x\,\partial y} +\\
&\quad + \frac{1}{1-\nu}z^2\nabla^2\frac{\partial W_0}{\partial x} + X_0 - \frac{\nu}{1-\nu}z\frac{\partial Z_0}{\partial x},\\
Y &= -\frac{1+\nu}{1-\nu}z\frac{\partial^2 U_0}{\partial x\,\partial y} - z\left(\frac{2}{1-\nu}\frac{\partial^2 V_0}{\partial y^2} + \frac{\partial^2 V_0}{\partial x^2}\right) -\\
&\quad - \frac{2-\nu}{2(1-\nu)}z^2\frac{\partial^2 Y_0}{\partial y^2} - \frac{z^2}{2}\frac{\partial^2 Y_0}{\partial x^2} - \frac{1}{2(1-\nu)}z^2\frac{\partial^2 X_0}{\partial x\,\partial y} +\\
&\quad + \frac{1}{1-\nu}z^2\nabla^2\frac{\partial W_0}{\partial y} + Y_0 - \frac{\nu}{1-\nu}z\frac{\partial Z_0}{\partial y},\\
Z &= \frac{1}{1-\nu}z^2\nabla^2\left(\frac{\partial U_0}{\partial x} + \frac{\partial V_0}{\partial y}\right) - \frac{1}{3(1-\nu)}z^3\nabla^2\nabla^2 W_0 -\\
&\quad - z\left(\frac{\partial X_0}{\partial x} + \frac{\partial Y_0}{\partial y}\right) + Z_0 + \frac{z^2\nu}{2(1-\nu)}\nabla^2 Z_0 +\\
&\quad + \frac{2-\nu}{6(1-\nu)}z^3\nabla^2\left(\frac{\partial X_0}{\partial x} + \frac{\partial Y_0}{\partial y}\right),\\
\sigma_x &= \frac{2}{1-\nu}\left(\frac{\partial U_0}{\partial x} + \nu\frac{\partial V_0}{\partial y}\right) - \frac{2}{1-\nu}z\left(\frac{\partial^2 W_0}{\partial x^2} + \nu\frac{\partial^2 W_0}{\partial y^2}\right) +\\
&\quad + \frac{2-\nu}{1-\nu}z\frac{\partial X_0}{\partial x} + \frac{\nu}{1-\nu}z\frac{\partial Y_0}{\partial y} + \frac{\nu}{1-\nu}Z_0,\\
\sigma_y &= \frac{2}{1-\nu}\left(\nu\frac{\partial U_0}{\partial x} + \frac{\partial V_0}{\partial y}\right) - \frac{2}{1-\nu}z\left(\nu\frac{\partial^2 W_0}{\partial x^2} + \frac{\partial^2 W_0}{\partial y^2}\right) +\\
&\quad + \frac{\nu}{1-\nu}z\frac{\partial X_0}{\partial x} + \frac{2-\nu}{1-\nu}z\frac{\partial Y_0}{\partial y} + \frac{\nu}{1-\nu}Z_0,\\
\tau_{xy} &= \frac{\partial U_0}{\partial y} + \frac{\partial V_0}{\partial x} - 2z\frac{\partial^2 W_0}{\partial x\,\partial y} + z\left(\frac{\partial X_0}{\partial y} + \frac{\partial Y_0}{\partial x}\right).
\end{aligned}\right\} \tag{9.4}$$

It is easily seen that the stresses given by (9.4) satisfy (1.1). Substitution of these values in (9.3) yields a system of differential equations for determining the unknown functions $U_0(x, y)$, $V_0(x, y)$, $W_0(x, y)$.

Equations (9.3) and (9.4) describe the general moment theory of a plate or shell of variable thickness $h = h(x, y)$. This theory, based on more general assumptions than Kirchhoff and Love's hypothesis that linear elements remain normal to the middle surface, makes it possible to determine the stresses and strains of a plate or shell for an arbitrary law of variation of its thickness, i.e., for any shape of the lower surface $h = h(x, y)$ of the shell. Equations (9.3) must be supplemented by the corresponding boundary conditions, given for the unknown functions U_0, V_0, W_0 in accordance with the model adopted.

The exact solution of this boundary-value problem for plates of variable thickness $h = h(x, y)$ is very difficult and can hardly be carried out by the methods available at present. Bubnov and Galerkin's variational method is the best existing method for the approximate integration of equations with variable coefficients.

§ 10. GENERAL SOLUTION OF THE TWO-DIMENSIONAL PROBLEM OF THE THEORY OF ELASTICITY

It was shown above that the solution by the method of initial functions of the general three-dimensional problem of the theory of elasticity reduces to determining the six initial functions U_0, V_0, W_0, X_0, Y_0, Z_0. Since the two-dimensional problem is a particular case of the general three-dimensional problem, four initial functions will be sufficient to determine the states of stress and strain of the body, these being the displacements $u_0(x)$, $v_0(x)$ and the stresses $\tau^0_{xy}(x)$, $\sigma^0_y(x)$ at $y = 0$ (Figure 171). This can be proved by taking the displacements $u(x, y)$, $v(x, y)$ and the stresses $\tau_{xy}(x, y)$, $\sigma_y(x, y)$ as unknowns, and representing them as infinite series in powers of y.

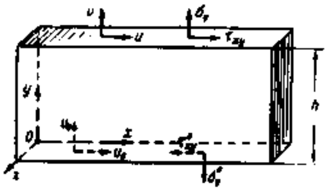

FIGURE 171.

In the two-dimensional case the equilibrium equations (1.1) of an elastic isotropic body become, when no volume forces act:

$$\frac{\partial \sigma_x}{\partial x} + \frac{\partial \tau_{xy}}{\partial y} = 0, \qquad \frac{\partial \sigma_y}{\partial y} + \frac{\partial \tau_{yx}}{\partial x} = 0. \tag{10.1}$$

The relationships between stresses and displacements for the case of plane strain are:

$$\left.\begin{aligned}\sigma_x &= \frac{2G}{1-2\nu}\left[(1-\nu)\frac{\partial u}{\partial x}+\nu\frac{\partial v}{\partial y}\right],\\ \sigma_y &= \frac{2G}{1-2\nu}\left[(1-\nu)\frac{\partial v}{\partial y}+\nu\frac{\partial u}{\partial x}\right],\\ \tau_{xy} = \tau_{yx} &= G\left(\frac{\partial u}{\partial y}+\frac{\partial v}{\partial x}\right),\end{aligned}\right\} \qquad (10.2)$$

where

$$G = \frac{E}{2(1+\nu)}.$$

Introducing the symbols:

$$\left.\begin{aligned} U &= Gu, & V &= Gv,\\ X &= \tau_{xy}, & Y &= \sigma_y,\\ \frac{\partial}{\partial x} &= \alpha, & \frac{\partial}{\partial y} &= \beta,\end{aligned}\right\} \qquad (10.3)$$

we can rewrite (10.1) and (10.2) in the form:

$$\left.\begin{aligned}\beta U &= -\alpha V + X,\\ \beta V &= -\frac{\nu}{1-\nu}\alpha U + \frac{1-2\nu}{2(1-\nu)}Y,\\ \beta Y &= -\alpha X,\\ \beta X &= -\frac{2}{1-\nu}\alpha^2 U - \frac{\nu}{1-\nu}\alpha V,\end{aligned}\right\} \qquad (10.4)$$

whence

$$\sigma_x = \frac{2}{1-2\nu}\left[(1-\nu)\alpha U + \nu\beta V\right]. \qquad (10.5)$$

Expanding, as in (2.1), the unknown magnitudes in Maclaurin series of powers of Y, we obtain the following solution of system (10.4):

$$\left.\begin{aligned} U &= L_{UU}U_0 + L_{UV}V_0 + L_{UY}Y_0 + L_{UX}X_0,\\ V &= L_{VU}U_0 + L_{VV}V_0 + L_{VY}Y_0 + L_{VX}X_0,\\ Y &= L_{YU}U_0 + L_{YV}V_0 + L_{YY}Y_0 + L_{YX}X_0,\\ X &= L_{XU}U_0 + L_{XV}V_0 + L_{XY}Y_0 + L_{XX}X_0,\end{aligned}\right\} \qquad (10.6)$$

where L_{UU}, L_{UV}, ..., L_{XY}, L_{XX} are, as before, the linear differential operators on the initial functions $U_0(x)$, $V_0(x)$, $Y_0(x)$, $X_0(x)$; these operators, which are functions of y and contain derivatives with respect to x, can be represented either by infinite series (Table 24) or in transcendental form (Table 25). The bottom lines of Tables 24 and 25 give the operators obtained from (10.5) entering in the expression for σ_x:

$$\sigma_x = A_U U_0 + A_V V_0 + A_Y Y_0 + A_X X_0. \qquad (10.7)$$

TABLE 24

	U_0	V_0	Y_0	X_0
U	$L_{UU} = 1 - \frac{y^2(2-\nu)}{2(1-\nu)}\alpha^2 + \frac{y^4(3-\nu)}{24(1-\nu)}\alpha^4 - \frac{y^6(4-\nu)}{720(1-\nu)}\alpha^6 + \ldots$	$L_{UV} = -y\alpha + \frac{y^3(2-\nu)}{6(1-\nu)}\alpha^3 - \frac{y^5(3-\nu)}{120(1-\nu)}\alpha^5 + \frac{y^7(4-\nu)}{5040(1-\nu)}\alpha^7 - \ldots$	$L_{UY} = -\frac{y^2}{4(1-\nu)}\alpha + \frac{y^4}{24(1-\nu)}\alpha^3 - \frac{y^6}{480(1-\nu)}\alpha^5 + \frac{y^8}{20160(1-\nu)}\alpha^7 - \ldots$	$L_{UX} = y - \frac{y^3(3-2\nu)}{12(1-\nu)}\alpha^2 + \frac{y^5(2-\nu)}{120(1-\nu)}\alpha^4 - \frac{y^7(5-2\nu)}{10080(1-\nu)}\alpha^6 + \ldots$
V	$L_{VU} = -\frac{y\nu}{1-\nu}\alpha + \frac{y^3(1+\nu)}{6(1-\nu)}\alpha^3 - \frac{y^5(2+\nu)}{120(1-\nu)}\alpha^5 + \frac{y^7(3+\nu)}{5040(1-\nu)}\alpha^7 - \ldots$	$L_{VV} = 1 + \frac{y^2\nu}{2(1-\nu)}\alpha^2 - \frac{y^4(1+\nu)}{24(1-\nu)}\alpha^4 + \frac{y^6(2+\nu)}{720(1-\nu)}\alpha^6 - \ldots$	$L_{VY} = \frac{y(1-2\nu)}{2(1-\nu)} + \frac{y^3\nu}{6(1-\nu)}\alpha^2 - \frac{y^5(1+2\nu)}{240(1-\nu)}\alpha^4 + \frac{y^7(1+\nu)}{5040(1-\nu)}\alpha^6 - \ldots$	$L_{VX} = L_{UY}$
Y	$L_{YU} = \frac{y^2}{1-\nu}\alpha^2 - \frac{y^4}{6(1-\nu)}\alpha^4 + \frac{y^6}{120(1-\nu)}\alpha^6 - \ldots$	$L_{YV} = -\frac{y^3}{3(1-\nu)}\alpha^3 + \frac{y^5}{30(1-\nu)}\alpha^5 - \frac{y^7}{840(1-\nu)}\alpha^7 + \ldots$	$L_{YY} = L_{VV}$	$L_{YX} = L_{UV}$
X	$L_{XU} = -\frac{2y}{1-\nu}\alpha^2 + \frac{2y^3}{3(1-\nu)}\alpha^4 - \frac{y^5}{20(1-\nu)}\alpha^6 + \frac{y^7}{630(1-\nu)}\alpha^8 - \ldots$	$L_{XV} = L_{YU}$	$L_{XY} = L_{VU}$	$L_{XX} = L_{UU}$
σ_x	$A_U = \frac{2}{1-\nu}\alpha - \frac{2y^2}{1-\nu}\alpha^3 + \frac{y^4}{4(1-\nu)}\alpha^5 - \frac{y^6}{90(1-\nu)}\alpha^7 + \ldots$	$A_V = -\frac{2y}{1-\nu}\alpha^2 + \frac{2y^3}{3(1-\nu)}\alpha^4 - \frac{y^5}{20(1-\nu)}\alpha^6 + \frac{y^7}{630(1-\nu)}\alpha^8 - \ldots$	$A_Y = \frac{\nu}{1-\nu} - \frac{y^2(1+\nu)}{2(1-\nu)}\alpha^2 + \frac{y^4(2+\nu)}{24(1-\nu)}\alpha^4 - \frac{y^6(3+\nu)}{720(1-\nu)}\alpha^6 + \ldots$	$A_X = \frac{y(2-\nu)}{1-\nu}\alpha - \frac{y^3(3-\nu)}{6(1-\nu)}\alpha^3 + \frac{y^5(4-\nu)}{120(1-\nu)}\alpha^5 - \frac{y^7(5-\nu)}{5040(1-\nu)}\alpha^7 + \ldots$

TABLE 25

	U_0	V_0	Y_0	X_0
U	$L_{UU} = \cos\alpha y - \frac{\alpha y}{2(1-\nu)}\sin\alpha y$	$L_{UV} = -\frac{1-2\nu}{2(1-\nu)}\sin\alpha y - \frac{\alpha y}{2(1-\nu)}\cos\alpha y$	$L_{UY} = -\frac{y}{4(1-\nu)}\sin\alpha y$	$L_{UX} = \frac{1}{\alpha}\sin\alpha y - \frac{1}{4(1-\nu)}\frac{1}{\alpha}\times$ $\times(\sin\alpha y - \alpha y\cos\alpha y)$
V	$L_{VU} = \frac{1-2\nu}{2(1-\nu)}\sin\alpha y - \frac{\alpha y}{2(1-\nu)}\cos\alpha y$	$L_{VV} = \frac{\alpha y}{2(1-\nu)}\times$ $\times\sin\alpha y + \cos\alpha y$	$L_{VY} = \frac{3-4\nu}{4(1-\nu)\alpha}\sin\alpha y - \frac{y}{4(1-\nu)}\cos\alpha y$	$L_{VX} = L_{UY}$
Y	$L_{YU} = \frac{\alpha^2 y}{1-\nu}\sin\alpha y$	$L_{YV} = -\frac{\alpha}{1-\nu}\times$ $\times(\sin\alpha y - \alpha y\cos\alpha y)$	$L_{YY} = L_{VV}$	$L_{YX} = L_{UV}$
X	$L_{XU} = -\frac{\alpha}{1-\nu}\times$ $\times(\sin\alpha y + \alpha y\cos\alpha y)$	$L_{XV} = L_{YU}$	$L_{XY} = L_{VU}$	$L_{XX} = L_{UU}$
σ_x	$A_U = \frac{2\alpha}{1-\nu}\cos\alpha y - \frac{y\alpha^2}{1-\nu}\sin\alpha y$	$A_V = -\frac{\alpha}{1-\nu}\times$ $\times(\sin\alpha y + y\alpha\cos\alpha y)$	$A_Y = \frac{\nu}{1-\nu}\cos\alpha y - \frac{y\alpha}{2(1-\nu)}\sin\alpha y$	$A_X = \frac{y\alpha}{2(1-\nu)}\cos\alpha y + \frac{3-2\nu}{2(1-\nu)}\sin\alpha y$

Equations (10.2) through (10.5) and Tables 24, 25 correspond to the case of plane strain. The corresponding expressions for plane stress are obtained from them by replacing the modulus of elasticity E and Poisson's ratio ν by $\frac{E(1+2\nu)}{(1+\nu)^2}$, and $\frac{\nu}{1+\nu}$, respectively. Performing this substitution in Table 25 yields the matrix of linear transformation of the functions $U_0(x)$ $V_0(x)$, $Y_0(x)$, $X_0(x)$ into the functions $U(x, y)$, $V(x, y)$, $Y(x, y)$, $X(x, y)$ for the case of plane stress, given in Table 26.

Equations (10.6) represent the law of transformation of the initial into the unknown functions and give the general solution of the two-dimensional problem of the theory of elasticity. These equations are symmetrical with respect to the secondary diagonal:

$$L_{UY} = L_{VX},\ L_{UV} = L_{YX},\ L_{VV} = L_{YY},\ L_{UU} = L_{XX},$$
$$L_{VU} = L_{XY},\ L_{YU} = L_{XV}.$$

The initial functions U_0, V_0, Y_0, X_0, which in (10.6) constitute four arbitrary functions obtained by integrating (10.4), are determined by the boundary conditions at $y = 0$ and $y = h = \text{const}$. Two functions can be prescribed for every plane $y = \text{const}$.

Since two initial functions are always known from the beginning, the solution of the two-dimensional problem reduces to the determination of two initial functions from the boundary conditions for $y = h$. These boundary conditions yield a system of two ordinary differential equations, which, in the general case, are of infinitely high order. When the problem is solved by approximation, the order of these equations depends on the number of terms retained in Table 24.

TABLE 26

	U_0	V_0	Y_0	X_0
U	$L_{UU}=\cos \alpha y-\frac{1+\nu}{2}\alpha y \sin \alpha y$	$L_{UV}=-\frac{1}{2}[(1-\nu)\sin \alpha y+(1+\nu)\alpha y \cos \alpha y]$	$L_{UY}=-\frac{1+\nu}{4}y \sin \alpha y$	$L_{UX}=\frac{3-\nu}{4\alpha}\sin \alpha y+\frac{1+\nu}{4}y \cos \alpha y$
V	$L_{VU}=\frac{1}{2}[(1-\nu)\sin \alpha y-(1+\nu)\alpha y \cos \alpha y]$	$L_{VV}=\frac{1+\nu}{2}\alpha y \sin \alpha y+\cos \alpha y$	$L_{VY}=L_{UX}$	$L_{VX}=L_{UY}$
Y	$L_{YU}=(1+\nu)\alpha^2 y \sin \alpha y$	$L_{YV}=(1+\nu)\alpha \times (\alpha y \cos \alpha y-\sin \alpha y)$	$L_{YY}=L_{VV}$	$L_{YX}=L_{UV}$
X	$L_{XU}=-(1+\nu)\alpha \times (\sin \alpha y+\alpha y \cos \alpha y)$	$L_{XV}=L_{YU}$	$L_{XY}=L_{VU}$	$L_{XX}=L_{UU}$
σ_x	$A_U=(1+\nu)\alpha \times (2\cos \alpha y-\alpha y \sin \alpha y)$	$A_V=-(1+\nu)\alpha \times (\sin \alpha y+\alpha y \cos \alpha y)$	$A_Y=\nu \cos \alpha y-\frac{1+\nu}{2}\alpha y \sin \alpha y$	$A_X=\frac{1}{2}[(1+\nu)\alpha y \cos \alpha y+(3+\nu)\sin \alpha y]$

§ 11. BENDING OF A THICK PLATE IN THE CASE OF PLANE STRAIN. APPROXIMATE SOLUTION

Consider the bending of a thick plate in the case of plane strain (Figure 172). Let the external load consist only of normal forces $p(x)$ disposed antisymmetrically with respect to the middle surface $y=0$.

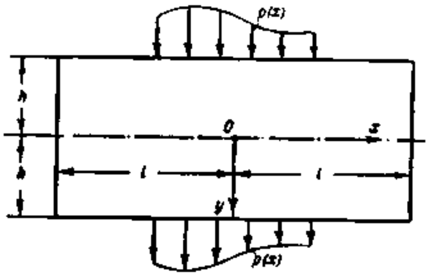

FIGURE 172.

Taking $y = 0$ as reference plane, we obtain:

$$U_0 = Y_0 = 0, \tag{11.1}$$

so that (10.6) reduces to:

$$\left.\begin{aligned} U &= L_{UV}V_0 + L_{UX}X_0, \\ V &= L_{VV}V_0 + L_{VX}X_0, \\ Y &= L_{YV}V_0 + L_{YX}X_0, \\ X &= L_{XV}V_0 + L_{XX}X_0. \end{aligned}\right\} \tag{11.2}$$

From the boundary conditions for $y = h$, namely: $Y_h = p(x)$, $X_h = 0$, we obtain:

$$\left.\begin{aligned} L_{YV}(h)V_0 + L_{YX}(h)X_0 &= p, \\ L_{XV}(h)V_0 + L_{XX}(h)X_0 &= 0. \end{aligned}\right\} \tag{11.3}$$

We introduce the function F satisfying the equation:

$$L_{XX}(h)F = V_0, \qquad L_{XV}(h)F = -X_0 \tag{11.4}$$

Substitution of these expressions transforms the second equation (11.3) into an identity, while the first becomes:

$$(L_{YV}L_{XX} - L_{YX}L_{XV})_h F = p. \tag{11.5}$$

The solution is obtained by rewriting (11.5) either as ordinary differential equation, in which case the operators are given in Table 24, or as transcendental equation, Table 25 being used instead. The second method is more convenient, since transition from the transcendental integral-differential to the ordinary form is easy.

Substitution in (11.5) of the value given in Table 25 yields:

$$\frac{\alpha}{1-\nu}[\alpha h - \sin\alpha h \cos\alpha h]F = p, \tag{11.6}$$

while (11.4) becomes:

$$\left.\begin{aligned} V_0 &= \left[\cos\alpha h - \frac{1}{2(1-\nu)}\alpha h \sin\alpha h\right]F, \\ X_0 &= -\frac{1}{1-\nu}\alpha^2 h \sin\alpha h \cdot F. \end{aligned}\right\} \tag{11.7}$$

Expanding the trigonometric functions in (11.6) and (11.7) in power series, we obtain:

$$\frac{2h^3}{3(1-\nu)}\alpha^4\left[1 - \frac{h^2}{5}\alpha^2 + \frac{2h^4}{105}\alpha^4 - \frac{h^6}{945}\alpha^6 + \ldots\right]F = p \tag{11.8}$$

$$\left.\begin{aligned} V_0 &= \left[1 - \frac{2-\nu}{2(1-\nu)}h^2\alpha^2 + \frac{3-\nu}{24(1-\nu)}h^4\alpha^4 - \frac{4-\nu}{720(1-\nu)}h^6\alpha^6 + \ldots\right]F, \\ X_0 &= -\frac{h^2}{1-\nu}\alpha^3\left[1 - \frac{h^2}{6}\alpha^2 + \frac{h^4}{120}\alpha^4 - \frac{h^6}{5040}\alpha^6 + \ldots\right]F. \end{aligned}\right\} \tag{11.9}$$

Equation (11.6) or (11.8) represents the exact solution of the problem considered. To obtain approximate solutions, we retain in (11.8) only a finite number of terms. Thus, if only the first term is used, (11.8) and (11.9) reduce to:

$$\frac{2h^3}{3(1-\nu)}F^{\mathrm{IV}}=p, \tag{11.10}$$

$$\left.\begin{aligned} V_0 &= F, \\ X_0 &= -\frac{h^2}{1-\nu}F'''. \end{aligned}\right\} \tag{11.11}$$

Thus, in a first approximation, F equals V_0, i.e., the vertical displacements of the middle surface of the plate, while (11.10) becomes the ordinary equation of the bending of a beam in the case of plane strain. The first approximation thus yields the elementary solution corresponding to the hypothesis of plane sections. The matrix of the initial functions or, which is the same, of (11.2), is in this case given by Table 27.

TABLE 27

	V_0	X_0
U	$-y\alpha$	—
V	1	—
Y	$-\frac{y^3}{3(1-\nu)}\alpha^4$	$-y\alpha$
X	$\frac{y^2}{1-\nu}\alpha^3$	1
σ_x	$-\frac{2y}{1-\nu}\alpha^2$	—

It is seen that the horizontal displacements vary linearly with y; the vertical displacements are constant; the laws of variation of the normal stresses $\sigma_y = Y$ and the shearing stresses $\tau_{xy} = X$, are respectively parabolas of the third and second degree.

Substitution of (11.11) in Table 27 yields:

$$\left.\begin{aligned} &U = -yV_0', \qquad V = V_0, \\ &(1-\nu)Y = \frac{y}{3}(3h^2-y^2)V_0^{\mathrm{IV}}, \\ &(1-\nu)X = (y^2-h^2)V_0''' \\ &(1-\nu)\sigma_x = -2yV_0'. \end{aligned}\right\} \tag{11.12}$$

The function V_0 is determined from (11.10) and the boundary conditions at the plate edges $x = \pm l$. Two conditions can be formulated at each edge, in agreement with (11.12) and (11.10). For a free edge, not under load, this solution makes it possible to eliminate the stresses only in the sense of Saint-Venant, i.e., by equating to zero the moment and the shearing force $(V_0'' = 0,\ V_0''' = 0)$.

In a second approximation we obtain from (11.8) and (11.9):

$$F^{\mathrm{VI}} - \frac{5}{h^2} F^{\mathrm{IV}} = -\frac{15}{2h^2} p (1 - \nu), \tag{11.13}$$

$$\left.\begin{aligned} V_0 &= F - \frac{2-\nu}{2(1-\nu)} h^2 F'', \\ X_0 &= -\frac{1}{1-\nu} h^2 F''' + \frac{1}{6(1-\nu)} h^4 F^{\mathrm{V}}. \end{aligned}\right\} \tag{11.14}$$

We assume that the vertical displacements are constant:

$$V = V_0. \tag{11.15}$$

Substituting (11.14) and (11.1) in Table 24, and retaining (in accordance with the order of (11.13)) in the expression obtained for U, the terms containing F' and F'', in the expression for Y, the terms containing F^{IV} and F^{VI}, in the expression for X, the terms containing F''' and F^{V}, and in the expression for σ_x, the terms containing F'' and F^{IV}, we can represent the unknown displacements and stresses of the plate in the form:

$$\left.\begin{aligned} U &= -yF' + \frac{2-\nu}{6(1-\nu)} y \left[y^2 - \frac{3\nu}{2-\nu} h^2 \right] F''', \\ (1-\nu) Y &= \frac{y}{3} (3h^2 - y^2) F^{\mathrm{IV}} - \frac{y}{30} (5h^4 - y^4) F^{\mathrm{VI}}, \\ (1-\nu) X &= (y^2 - h^2) F''' - \frac{y^4 - h^4}{6} F^{\mathrm{V}}, \\ (1-\nu) \sigma_x &= -2y F'' + \frac{2}{3} y^3 F^{\mathrm{IV}}. \end{aligned}\right\} \tag{11.16}$$

The first terms in (11.16) are identical with (11.12). The additional terms take into account the deviation from the hypothesis of plane sections.

The general integral of (11.13) is:

$$F = C_1 + C_2 x + C_3 x^2 + C_4 x^3 + C_5 \operatorname{sh} \frac{\sqrt{5}}{h} x + C_6 \operatorname{ch} \frac{\sqrt{5}}{h} x + G, \tag{11.17}$$

where G = particular integral of (11.13), depending on external load, and $C_1, \ldots, C_6$ = constants.

To determine the six integration constants we require three boundary conditions at each lateral edge of the plate. For built-in edges $(V = 0,\ U = 0)$, we obtain from (11.14), (11.15), and (11.16):

$$\left.\begin{aligned} &F - \frac{2-\nu}{2(1-\nu)} h^2 F'' = 0, \\ &F' = 0, \qquad F'' = 0. \end{aligned}\right\} \tag{11.18}$$

If a membrane, rigid in its plane but flexible in bending, is placed at the edge ($V=0$, $\sigma_x=0$), the boundary conditions will be:

$$F=0, \quad F''=0, \quad F^{IV}=0. \tag{11.19}$$

Finally, for a free edge not under load ($\sigma_x=0$, $\tau_{xy}=0$), the boundary conditions will be:

$$\left.\begin{aligned} F''=0, \quad F^{IV}=0, \\ \int_0^h \left[(y^2-h^2)F''' - \frac{y^4-h^4}{6}F^V\right]dy=0. \end{aligned}\right\} \tag{11.20}$$

The plate can therefore be analyzed in a second approximation for any boundary conditions at the lateral edges $x=\pm l$. After determining the integration constants from these conditions, and then the function F from (11.17), we can find the displacements and stresses in the plate from (11.16). This procedure is applicable to thick plates, for which the deviation from the hypothesis of plane sections is considerable. If in (11.16) Poisson's ratio ν is replaced by $\frac{\nu}{1+\nu}$, we obtain the equation of bending of a high beam (beam-wall) for the case of plane stress.

Higher-order approximations for greater accuracy can be obtained by increasing the number of terms retained in the expansions. This, however, increases the order of the differential equations and makes their solution more laborious. The second approximation is quite satisfactory in practice.

In this section we have considered only the bending of a thick plate for arbitrary boundary conditions at its lateral edges $x=\pm l$, showing how this problem can be solved by approximations. The same procedure is possible in many other problems of plane stress or strain involving massive structures (see sections 5, 6, 7, and 8). In all these cases the fundamental solution is obtained from the boundary conditions at the longitudinal edges of the plate; an approximate solution is then obtained by retaining a number of terms depending on the accuracy required.

§ 12. USE OF TRIGONOMETRIC SERIES IN THE SOLUTION OF THE TWO-DIMENSIONAL PROBLEM*

1

We shall now consider problems of the theory of rectangular plates whose boundary conditions can be expressed with the aid of trigonometric series. Let the plate edges $x=0$ and $x=l$ (Figure 173) be rigidly connected to thin membranes perfectly rigid with respect to displacements in their plane, but freely displaceable out of their plane. These boundary conditions are formulated as follows:

---

* This and the following sections are based in part on V.V. Vlasov's Candidate's Thesis, Metod nachal'nykh funktsii v ploskoi zadache teorii uprugosti (The Method of Initial Functions in the Two-dimensional Problem of the Theory of Elasticity), 1958, and on his papers /13, 14/.

at $x = 0$ and $x = l$: $\quad V = Y = \sigma_x = 0.$ (12.1)

It follows from (12.1) and (10.1), (10.2) that

$$\left.\begin{aligned} U(x, y) &= \sum_{n=1}^{\infty} f_{1n}(y)\cos\alpha_n x, \quad & Y(x, y) &= \sum_{n=1}^{\infty} f_{3n}(y)\sin\alpha_n x, \\ V(x, y) &= \sum_{n=1}^{\infty} f_{2n}(y)\sin\alpha_n x, \quad & X(x, y) &= \sum_{n=1}^{\infty} f_{4n}(y)\cos\alpha_n x, \\ \sigma_x(x, y) &= \sum_{n=1}^{\infty} f_{5n}(y)\sin\alpha_n x, \end{aligned}\right\} \qquad (12.2)$$

where $\alpha_n = \frac{n\pi}{l}$, l = plate length in x direction.

Equations (12.2) represent Filon's solution. If, on the other hand, U and X are expressed by sine series, and V, Y, and σ_x by cosine series, we obtain Ribière's solution satisfying the boundary conditions:

at $x = 0$ and $x = l$: $\quad U = X = 0.$ (12.3)

We shall use (12.2), assuming all the initial functions U_0, V_0, X_0, and Y_0 to be known for $y = 0$, being represented by trigonometric series with constant coefficients:

$$\left.\begin{aligned} U_0 &= \sum_{n=1}^{\infty} u_n \cos\alpha_n x, \quad & Y_0 &= \sum_{n=1}^{\infty} y_n \sin\alpha_n x, \\ V_0 &= \sum_{n=1}^{\infty} v_n \sin\alpha_n x, \quad & X_0 &= \sum_{n=1}^{\infty} x_n \cos\alpha_n x. \end{aligned}\right\} \qquad (12.4)$$

The states of stress and strain of the plate can be expressed through the initial functions which satisfy (12.1), by substituting (12.4) in the general integrals of displacements and stresses, written in the form of Table 25. For example, the first term in the expression for U becomes:

$$\left(\cos\alpha_n y - \frac{1}{2(1-\nu)}\alpha_n y \sin\alpha_n y\right) U_0(x) =$$
$$= \sum_{n=1}^{\infty} u_n \sum_{m=0}^{\infty}\left[\frac{(\alpha_n y)^{2m}}{(2m)!} + \frac{1}{2(1-\nu)}\frac{(\alpha_n y)^{2m+2}}{(2m+1)!}\right]\cos\alpha_n x =$$
$$= \sum_{n=1}^{\infty} u_n\left(\operatorname{ch}\alpha_n y + \frac{1}{2(1-\nu)}\alpha_n y \operatorname{sh}\alpha_n y\right)\cos\alpha_n x.$$

The same procedure is applied to the other terms in Table 25. We obtain:

$$\left.\begin{aligned}
U &= \frac{1}{1-\nu}\sum_{n=1}^{\infty}\Big\{u_n\Big[(1-\nu)\operatorname{ch}\alpha_n y+\frac{1}{2}\alpha_n y\operatorname{sh}\alpha_n y\Big]-\\
&\quad-\frac{v_n}{2}[(1-2\nu)\operatorname{sh}\alpha_n y+\alpha_n y\operatorname{ch}\alpha_n y]-\frac{1}{4}y_n y\operatorname{sh}\alpha_n y+\\
&\quad+\frac{x_n}{4}\Big[\frac{3-4\nu}{\alpha_n}\operatorname{sh}\alpha_n y+y\operatorname{ch}\alpha_n y\Big]\Big\}\cos\alpha_n x.\\
V &= \frac{1}{1-\nu}\sum_{n=1}^{\infty}\Big\{\frac{u_n}{2}[\alpha_n y\operatorname{ch}\alpha_n y-(1-2\nu)\operatorname{sh}\alpha_n y]+\\
&\quad+v_n\Big[(1-\nu)\operatorname{ch}\alpha_n y-\frac{1}{2}\alpha_n y\operatorname{sh}\alpha_n y\Big]+\frac{y_n}{4}\Big[\frac{3-4\nu}{\alpha_n}\operatorname{sh}\alpha_n y-\\
&\quad-y\operatorname{ch}\alpha_n y\Big]+\frac{1}{4}x_n y\operatorname{sh}\alpha_n y\Big\}\sin\alpha_n x,\\
Y &= \frac{1}{1-\nu}\sum_{n=1}^{\infty}\Big\{u_n\alpha_n^2 y\operatorname{sh}\alpha_n y+v_n\alpha_n(\operatorname{sh}\alpha_n y-\alpha_n y\operatorname{ch}\alpha_n y)+\\
&\quad+y_n\Big[(1-\nu)\operatorname{ch}\alpha_n y-\frac{1}{2}\alpha_n y\operatorname{sh}\alpha_n y\Big]+\frac{x_n}{2}\Big[(1-2\nu)\operatorname{sh}\alpha_n y+\\
&\quad+\alpha_n y\operatorname{ch}\alpha_n y\Big]\Big\}\sin\alpha_n x,\\
X &= \frac{1}{1-\nu}\sum_{n=1}^{\infty}\Big\{u_n\alpha_n(\operatorname{sh}\alpha_n y+\alpha_n y\operatorname{ch}\alpha_n y)-v_n\alpha_n^2 y\operatorname{sh}\alpha_n y\\
&\quad+\frac{y_n}{2}[(1-2\nu)\operatorname{sh}\alpha_n y-\alpha_n y\operatorname{ch}\alpha_n y]+\\
&\quad+x_n\Big[(1-\nu)\operatorname{ch}\alpha_n y+\frac{1}{2}\alpha_n y\operatorname{sh}\alpha_n y\Big]\Big\}\cos\alpha_n x,\\
\sigma_x &= \frac{1}{1-\nu}\sum_{n=1}^{\infty}\Big\{-u_n\alpha_n(2\operatorname{ch}\alpha_n y+\alpha_n y\operatorname{sh}\alpha_n y)+\\
&\quad+v_n\alpha_n(\operatorname{sh}\alpha_n y+\alpha_n y\operatorname{ch}\alpha_n y)+y_n\Big(\nu\operatorname{ch}\alpha_n y+\\
&\quad+\frac{1}{2}\alpha_n y\operatorname{sh}\alpha_n y\Big)-\frac{x_n}{2}[(3-2\nu)\operatorname{sh}\alpha_n y+\alpha_n y\operatorname{ch}\alpha_n y]\Big\}\sin\alpha_n x.
\end{aligned}\right\}\tag{12.5}$$

These general expressions are valid for any boundary conditions at the longitudinal plate edges $y = 0$ and $y = h$.

Replacing Poisson's ratio ν by $\frac{\nu}{1+\nu}$, we obtain the general solution for plane stress under boundary conditions (12.1).

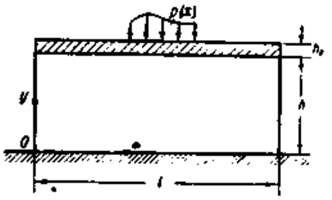

FIGURE 173.

Similar expressions can be obtained when the boundary conditions are given by (12.3).

Several examples will now be considered:

2

Let a plane punch be pressed into a rectangular plate (Figure 173) at the boundary plane $y=h$. It will be assumed that the normal plate displacements under the punch are known functions of x, being zero at the other boundary plane of the plate ($y=0$), and that the shearing stresses X vanish at $y=0$ and $y=h$. Hence, by (12.2):

at $y=h$:
$$V(x)=\sum_{n=1}^{\infty}\delta_n\sin\alpha_n x.$$

The following boundary conditions are therefore obtained:

$$\left.\begin{aligned}
&\text{at } y=0 \qquad && V_0=X_0=0;\\
&\text{at } y=h \qquad && V=\sum_{n=1}^{\infty}\delta_n\sin\alpha_n x, \quad X=0.
\end{aligned}\right\}\qquad(12.6)$$

The initial functions U_0 and Y_0 are determined from the boundary conditions at $y=h$. Putting in (12.5) $v_n=x_n=0$ in accordance with (12.6), and substituting the expressions for V and X at $y=h$ in these boundary conditions, we obtain for each term of the series the following two equations with two unknowns u_n and y_n:

$$\begin{aligned}
&2\left[\beta_n\operatorname{ch}\beta_n-(1-2\nu)\operatorname{sh}\beta_n\right]u_n+h\left(\frac{3-4\nu}{\beta_n}\operatorname{sh}\beta_n-\operatorname{ch}\beta_n\right)y_n=\\
&\qquad\qquad=4(1-\nu)\delta_n,\\
&2\beta_n(\operatorname{sh}\beta_n+\beta_n\operatorname{ch}\beta_n)u_n+h\left[(1-2\nu)\operatorname{sh}\beta_n-\beta_n\operatorname{ch}\beta_n\right]y_n=0,
\end{aligned}$$

where $\beta_n=\frac{n\pi h}{l}$.

After the unknowns u_n, y_n have been determined from these equations, we can rewrite (12.5) as follows:

$$\left.\begin{aligned}
U&=-\sum_{n=1}^{\infty}\frac{\delta_n\cos\beta_n\xi}{2\Delta_n}\left\{\left[(1-2\nu)\operatorname{sh}\beta_n-\beta_n\operatorname{ch}\beta_n\right]\operatorname{ch}\beta_n\eta+\beta_n\operatorname{sh}\beta_n(\eta\operatorname{sh}\beta_n\eta)\right\},\\
V&=\sum_{n=1}^{\infty}\frac{\delta_n\sin\beta_n\xi}{2\Delta_n}\left\{\left[2(1-\nu)\operatorname{sh}\beta_n+\beta_n\operatorname{ch}\beta_n\right]\operatorname{sh}\beta_n\eta-\beta_n\operatorname{sh}\beta_n(\eta\operatorname{ch}\beta_n\eta)\right\},\\
Y&=\sum_{n=1}^{\infty}\frac{\delta_n\beta_n\sin\beta_n\xi}{h\Delta_n}\left\{(\operatorname{sh}\beta_n+\beta_n\operatorname{ch}\beta_n)\operatorname{ch}\beta_n\eta-\beta_n\operatorname{sh}\beta_n\times(\eta\operatorname{sh}\beta_n\eta)\right\},\\
X&=\sum_{n=1}^{\infty}\frac{\delta_n\beta_n^2\cos\beta_n\xi}{h\Delta_n}\left\{\operatorname{ch}\beta_n\operatorname{sh}\beta_n\eta-\operatorname{sh}\beta_n(\eta\operatorname{sh}\beta_n\eta)\right\},\\
\sigma_x&=\sum_{n=1}^{\infty}\frac{\delta_n\beta_n\sin\beta_n\xi}{h\Delta_n}\left\{(\operatorname{sh}\beta_n-\beta_n\operatorname{ch}\beta_n)\operatorname{ch}\beta_n\eta+\beta_n\operatorname{sh}\beta_n(\eta\operatorname{sh}\beta_n\eta)\right\},
\end{aligned}\right\}\qquad(12.7)$$

where $\eta = \frac{y}{h}$, $\xi = \frac{x}{h}$ = dimensionless coordinates, and $\Delta_n = (1-\nu)\,\mathrm{sh}^2\beta_n$.

The magnitude $(1-\nu)$, which depends on Poisson's ratio, enters in the expressions for the stresses Y, X, σ_x only as a factor which can be written before the summation sign. If we assume that at $y=0$ and $y=h$ the displacements U and not the stresses X vanish, more complex expressions will be obtained for the stresses and displacements, and Poisson's ratio will not appear before the summation sign. In the case of boundary conditions of the mixed type (12.6) we thus obtain a peculiar generalization of M. Lévy's theorem for rectangular plates.

3

Consider as second example a double-layer plate subjected to a vertical load

$$p = \sum_{n=1}^{\infty} p_n \sin \alpha_n x.$$

We denote the elastic characteristics and thicknesses of the upper and lower layers by G_1, ν_1, h_1 and G, ν, h respectively. The directions of the coordinate axes are shown in Figure 173. It will be assumed that the upper layer behaves like a thin plate. The following boundary conditions will be assumed for the lower layer:

$$\left.\begin{aligned} &\text{at } y=0: && V_0 = X_0 = 0; \\ &\text{at } y=h: && X=0, \quad \frac{D}{G}\frac{d^4\Psi}{dx^4} + Y = -p, \end{aligned}\right\} \qquad (12.8)$$

where D = flexural rigidity of plate.

The last condition (12.8) expresses the fact that since the upper layer behaves like a thin plate, the load transmitted to the lower layer is determined from the equations of cylindrical bending of a plate. The coefficients u_n and y_n in (12.4) are found from (12.8).

We then obtain:

$$\left.\begin{aligned} U &= -\sum_{n=1}^{\infty} \frac{hp_n \cos\beta_n\xi}{2\beta_n\Delta_n}\Big\{[\beta_n\,\mathrm{ch}\,\beta_n - (1-2\nu)\,\mathrm{sh}\,\beta_n]\,\mathrm{ch}\,\beta_n\eta - \\ &\qquad - \beta_n\,\mathrm{sh}\,\beta_n\,(\eta\,\mathrm{sh}\,\beta_n\eta)\Big\}, \\ V &= -\sum_{n=1}^{\infty} \frac{hp_n \sin\beta_n\xi}{2\beta_n\Delta_n}\Big\{[2(1-\nu)\,\mathrm{sh}\,\beta_n + \beta\ \mathrm{ch}\,\beta_n]\,\mathrm{sh}\,\beta_n\eta - \\ &\qquad - \beta_n\,\mathrm{sh}\,\beta_n\,(\eta\,\mathrm{ch}\,\beta_n\eta)\Big\}, \\ Y &= -\sum_{n=1}^{\infty} \frac{p_n \sin\beta_n\xi}{\Delta_n}\Big\{(\mathrm{sh}\,\beta_n + \beta_n\,\mathrm{ch}\,\beta_n)\,\mathrm{ch}\,\beta_n\eta - \\ &\qquad - \beta_n\,\mathrm{sh}\,\beta_n\,(\eta\,\mathrm{sh}\,\beta_n\eta)\Big\}, \\ X &= \sum_{n=1}^{\infty} \frac{p_n\beta_n \cos\beta_n\xi}{\Delta_n}\Big\{\mathrm{ch}\,\beta_n\,\mathrm{sh}\,\beta_n\eta - \mathrm{sh}\,\beta_n\,(\eta\,\mathrm{ch}\,\beta_n\eta)\Big\}, \\ \sigma_x &= -\sum_{n=1}^{\infty} \frac{p_n \sin\beta_n\xi}{\Delta_n}\Big\{(\mathrm{sh}\,\beta_n - \beta_n\,\mathrm{ch}\,\beta_n)\,\mathrm{ch}\,\beta_n\eta + \\ &\qquad + \beta_n\,\mathrm{sh}\,\beta_n\,(\eta\,\mathrm{sh}\,\beta_n\eta)\Big\}, \end{aligned}\right\} \qquad (12.9)$$

where

$$\Delta_n = \beta_n + \frac{1}{2}\operatorname{sh} 2\beta_n + \frac{(1-\nu)D}{Gh^3}\beta_n^3 \operatorname{sh}^2 \beta_n. \qquad (12.10)$$

4

A solution in trigonometric series can also be obtained by proceeding from the fundamental differential equation of the problem instead of from (12.2) and (12.4). This will be illustrated by the above example of the bending of a thick plate.

The fundamental equation for F is in this case [cf. (11.6)]:

$$\frac{\alpha}{1-\nu}[\alpha h - \sin\alpha h\cos\alpha h] F = p(x). \qquad (12.11)$$

For simplicity, only the case of a load symmetrical with respect to the y axis will be considered.

The origin of coordinates is placed at the center of the plate. We assume a solution of (12.11) for the boundary conditions (12.1) in the form:

$$F = \sum_{1}^{\infty} A_n \cos\frac{n\pi x}{2l} \qquad (n = 1, 3, 5, \ldots, (2m-1)). \qquad (12.12)$$

We expand $p(x)$ in a cosine series:

$$p(x) = \sum_{n=1}^{\infty} p_n \cos\frac{n\pi x}{2l} \qquad (n = 1, 3, 5, \ldots, (2m-1)), \qquad (12.13)$$

where:

$$p_n = \frac{4}{l}\int_0^{l/2} p(x)\cos\frac{n\pi x}{2l}\,dx.$$

Substitution of (12.12) and (12.13) in (12.11) yields:

$$A_n = -\frac{4(1-\nu)\int_0^{l/2} p(x)\cos\lambda_n x\,dx}{\frac{\pi\pi}{2}\left[\lambda_n h - \frac{1}{2}\sin 2\lambda_n h\right]}, \qquad (12.14)$$

where

$$\lambda_n = \frac{n\pi}{2l} \qquad (n = 1, 3, 5, \ldots, (2m-1)).$$

From (11.7) and (12.12) we now obtain:

$$\left.\begin{aligned} V_0 &= \sum_{n=1}^{\infty} A_n\left[\operatorname{ch}\lambda_n h + \frac{\lambda_n h}{2(1-\nu)}\operatorname{sh}\lambda_n h\right]\cos\lambda_n x, \\ X_0 &= -\sum_{n=1}^{\infty}\frac{A_n}{1-\nu}\lambda_n^2 h\operatorname{sh}\lambda_n h\sin\lambda_n x. \end{aligned}\right\} \qquad (12.15)$$

Substitution of (12.5) in Table 25 yields:

$$\left.\begin{aligned}
U &= \frac{1}{2(1-\nu)}\sum_{n=1}^{\infty} A_n[(1-2\nu)\operatorname{ch}\lambda_n h\operatorname{sh}\lambda_n y -\\
&\qquad -\lambda_n h\operatorname{sh}\lambda_n h\operatorname{sh}\lambda_n y+\lambda_n y\operatorname{ch}\lambda_n h\operatorname{ch}\lambda_n y]\sin\lambda_n x,\\
V &= \frac{1}{2(1-\nu)}\sum_{n=1}^{\infty} A_n[2(1-\nu)\operatorname{ch}\lambda_n h\operatorname{ch}\lambda_n y-\lambda_n y\operatorname{ch}\lambda_n h\operatorname{sh}\lambda_n y+\\
&\qquad +\lambda_n h\operatorname{sh}\lambda_n h\operatorname{ch}\lambda_n y]\cos\lambda_n x,\\
Y &= \sum_{n=1}^{\infty}\frac{A_n\lambda_n}{1-\nu}[\lambda_n h\operatorname{sh}\lambda_n y\operatorname{sh}\lambda_n h+\operatorname{ch}\lambda_n h\operatorname{sh}\lambda_n y-\\
&\qquad -\lambda_n y\operatorname{ch}\lambda_n h\operatorname{ch}\lambda_n y]\cos\lambda_n x,\\
X &= \sum_{n=1}^{\infty}\frac{A_n\lambda_n^2}{1-\nu}[y\operatorname{sh}\lambda_n y\operatorname{ch}\lambda_n h-h\operatorname{ch}\lambda_n y\operatorname{sh}\lambda_n h]\sin\lambda_n x,\\
\sigma_x &= \sum_{n=1}^{\infty}\frac{A_n\lambda_n}{1-\nu}[\operatorname{sh}\lambda_n y\operatorname{ch}\lambda_n h+\lambda_n y\operatorname{ch}\lambda_n y\operatorname{ch}\lambda_n h-\\
&\qquad -\lambda_n h\operatorname{sh}\lambda_n y\operatorname{sh}\lambda_n h]\cos\lambda_n x.
\end{aligned}\right\}\qquad (12.16)^*$$

5

We shall now give the exact solution in trigonometric series for a plate subjected to a load symmetrical with respect to both x and y axes (Figure 174).

The solving equation is in this case:

$$\frac{\alpha}{1-\nu}\left[\alpha h+\frac{\sin 2\alpha h}{2}\right]F=-p(x), \qquad (12.17)$$

where

$$\alpha=\frac{\partial}{\partial x}.$$

We assume a solution in the form:

$$F=\sum_{n=1}^{\infty}A_n\cos\frac{n\pi x}{2l}\qquad (n=1,3,5,\ldots,(2m-1)). \qquad (12.18)$$

Expanding $p(x)$ in a series of $\cos\frac{n\pi x}{2l}$, we obtain:

$$A_n=\frac{4(1-\nu)\int\limits_0^{l/n}p(x)\cos\lambda_n x\,dx}{\frac{n\pi}{2}\left[\lambda_n h+\frac{\sin 2\lambda_n h}{2}\right]}, \qquad (12.19)$$

where

$$\lambda_n=\frac{n\pi}{2l}\qquad (n=1,3,5,\ldots,(2m-1)).$$

---

* [The hyperbolic functions used in this section should apparently be trigonometric functions.]

Furthermore:

$$\left.\begin{aligned} U_0 &= -\frac{1}{2(1-\nu)}\sum_{n=1}^{\infty} B_n \sin\lambda_n x, \\ Y_0 &= -\frac{1}{1-\nu}\sum_{n=1}^{\infty} C_n \cos\lambda_n x, \end{aligned}\right\} \tag{12.20}$$

where

$$\left.\begin{aligned} B_n &= A_n[(1-2\nu)\,\mathrm{sh}\,\lambda_n h - \lambda_n h\,\mathrm{ch}\,\lambda_n h], \\ C_n &= A_n\lambda_n[\mathrm{sh}\,\lambda_n h + \lambda_n h\,\mathrm{ch}\,\lambda_n h]. \end{aligned}\right\} \tag{12.21}$$

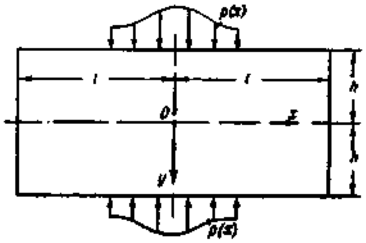

FIGURE 174.

The stresses and displacements of the plate are:

$$\left.\begin{aligned} U &= -\frac{1}{2(1-\nu)}\sum_{n=1}^{\infty}(B_n\,\mathrm{ch}\,\lambda_n y + \\ &\qquad + A_n\lambda_n y\,\mathrm{sh}\,\lambda_n h\,\mathrm{sh}\,\lambda_n y)\sin\lambda_n x, \\ V &= \sum_{n=1}^{\infty} A_n\Big[-\mathrm{sh}\,\lambda_n h\,\mathrm{sh}\,\lambda_n y - \frac{\lambda_n y}{2(1-\nu)}\,\mathrm{ch}\,\lambda_n h\,\mathrm{sh}\,\lambda_n y + \\ &\qquad + \frac{\lambda_n y}{2(1-\nu)}\,\mathrm{sh}\,\lambda_n h\,\mathrm{ch}\,\lambda_n y\Big]\cos\lambda_n x, \\ (1-\nu)Y &= \sum_{n=1}^{\infty}\{A_n\lambda_n^2 y\,\mathrm{sh}\,\lambda_n h\,\mathrm{sh}\,\lambda_n y - C_n\,\mathrm{ch}\,\lambda_n y\}\cos\lambda_n x, \\ (1-\nu)X &= \sum_{n=1}^{\infty} A_n\lambda_n^2(h\,\mathrm{ch}\,\lambda_n h\,\mathrm{sh}\,\lambda_n y - y\,\mathrm{sh}\,\lambda_n h\,\mathrm{ch}\,\lambda_n y)\sin\lambda_n x, \\ (1-\nu)\,\sigma_x &= \sum_{n=1}^{\infty} A_n\lambda_n(-\mathrm{sh}\,\lambda_n h\,\mathrm{ch}\,\lambda_n y + \lambda_n h\,\mathrm{ch}\,\lambda_n h\,\mathrm{ch}\,\lambda_n y - \\ &\qquad - \lambda_n y\,\mathrm{sh}\,\lambda_n h\,\mathrm{sh}\,\lambda_n y)\cos\lambda_n x. \end{aligned}\right| \tag{12.22}$$

§ 13. EXACT SOLUTION FOR A RECTANGULAR STRIP WITH ARBITRARY BOUNDARY CONDITIONS AT THE LONGITUDINAL EDGES AND HOMOGENEOUS BOUNDARY CONDITIONS AT THE LATERAL EDGES

In the preceding section, exact solutions for rectangular plates undergoing plane strain were given for the case where the boundary conditions at the lateral edges can be expressed with the aid of trigonometric series. This section will deal with the problem of finding exact solutions for a rectangular strip with arbitrary boundary conditions at $x=0$ and $x=l$ (Figure 175), and homogeneous boundary conditions at $y=0$ and $y=h$.

We first assume homogeneous boundary conditions of the mixed type, i.e., for $y=0$ and $y=h$:

$$u=\sigma_y=0. \tag{13.1}$$

This means that at the lateral edges $y=0$ and $y=h$ the strip is held by membranes rigid in their plane and flexible out of it. The initial functions U_0 and Y_0 vanish in this case.

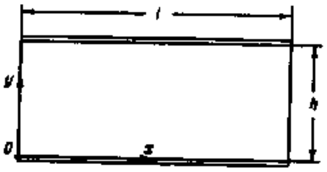

FIGURE 175.

Inserting into (13.1) the values of the operators given in Table 26, we obtain a system of two differential equations of infinitely high order in the two unknown initial functions V_0 and X_0:

$$\left.\begin{aligned}&-[(1-\nu)\sin\alpha h+(1+\nu)\alpha h\cos\alpha h]\,V_0+\\&\qquad+\frac{1}{2}\left[\frac{3-\nu}{\alpha}\sin\alpha h+(1+\nu)h\cos\alpha h\right]X_0=0,\\&2(1+\nu)\alpha(\alpha h\cos\alpha h-\sin\alpha h)\,V_0-\\&\qquad-[(1-\nu)\sin\alpha h+(1+\nu)\alpha h\cos\alpha h]\,X_0=0.\end{aligned}\right\} \tag{13.2}$$

We introduce a function $F(x)$ satisfying the equations:

$$\left.\begin{aligned}V_0&=-\left(\frac{1-\nu}{1+\nu}\sin\alpha h+\alpha h\cos\alpha h\right)F,\\X_0&=-2\alpha(\alpha h\cos\alpha h-\sin\alpha h)\,F.\end{aligned}\right\} \tag{13.3}$$

The second equation (13.2) is then transformed into an identity, while the first becomes:

$$(\sin^2\alpha h)\,F=0. \tag{13.4}$$

We assume a solution in the form:

$$F = Ce^{kx}. \tag{13.5}$$

Substitution of (13.5) in (13.4) leads to a transcendental equation in k:

$$\sin^2 kh = 0, \tag{13.6}$$

whose roots are:

$$k_n = \frac{n\pi}{h},$$

where n = positive integer.

The general solution of (13.4) is thus:

$$F = \sum_{n=0}^{\infty} A_n \operatorname{ch} k_n x + B_n \operatorname{sh} k_n x + C_n x \operatorname{ch} k_n x + D_n x \operatorname{sh} k_n x, \tag{13.7}$$

where A_n, B_n, C_n, D_n = arbitrary constants.

Substituting (13.7) in (13.3), we find the initial functions V_0 and X_0. Introducing these values into Table 26, we obtain the stresses and displacements of the plate when the boundary conditions are given by (13.1). For practical calculations it is more convenient to substitute first (13.3) in Table 26, simplify the results, and then use (13.7). We obtain:

$$\left.\begin{aligned}
U = {} & \sum_{n=1}^{\infty} (-1)^n h \Big\{ k_n A_n \operatorname{ch} k_n x + k_n B_n \operatorname{sh} k_n x + \\
& + \left[-\frac{1-\nu}{1+\nu} \operatorname{sh} k_n x + k_n x \operatorname{ch} k_n x \right] C_n + \\
& + \left[-\frac{1-\nu}{1+\nu} \operatorname{ch} k_n x + k_n x \operatorname{sh} k_n x \right] D_n \Big\} \sin k_n y, \\
V = {} & \sum_{n=1}^{\infty} (-1)^n h \Big\{ k_n A_n \operatorname{sh} k_n x + k_n B_n \operatorname{ch} k_n x + \\
& + \left(\frac{2}{1+\nu} \operatorname{ch} k_n x + k_n x \operatorname{sh} k_n x \right) C_n + \\
& + \left(\frac{2}{1+\nu} \operatorname{sh} k_n x + k_n x \operatorname{ch} k_n x \right) D_n \Big\} \cos k_n y, \\
Y = {} & -2 \sum_{n=1}^{\infty} (-1)^n k_n h\, k_n A_n \{ \operatorname{sh} k_n x + k_n B_n \operatorname{ch} k_n x + \\
& + (2 \operatorname{ch} k_n x + k_n x \operatorname{sh} k_n x) C_n + \\
& + (2 \operatorname{sh} k_n x + k_n x \operatorname{ch} k_n x) D_n \} \sin k_n y, \\
X = {} & 2 \sum_{n=1}^{\infty} (-1)^n k_n h \{ k_n A_n \operatorname{ch} k_n x + k_n B_n \operatorname{sh} k_n x + \\
& + (\operatorname{sh} k_n x + k_n x \operatorname{ch} x_n k) C_n + \\
& + (\operatorname{ch} k_n x + k_n x \operatorname{sh} k_n x) D_n \} \cos k_n y, \\
\sigma_x = {} & 2 \sum_{n=1}^{\infty} (-1)^n k_n h \{ k_n A_n \operatorname{sh} k_n x + k_n B_n \operatorname{ch} k_n x + \\
& + k_n x C_n \operatorname{sh} k_n x + k_n x D_n \operatorname{ch} k_n x \} \sin k_n y.
\end{aligned}\right| \tag{13.8}$$

The elementary solution in polynomials, corresponding to the zero roots of (13.6), no longer appears in the general solution (13.8) which thus represents incomplete expressions for the displacements and stresses. This elementary solution cannot be obtained in a general form by introducing the function F, since V_0 and X_0 are expressed through F by differentiations in which part of the solution in polynomials drops out.

In order to find the elementary solution, we replace the trigonometric functions in (13.2) by their expansions in infinite series. Taking only the first terms, we obtain a system of two first-order differential equations in the unknown functions V_0 and X_0:

$$-\alpha V_0 + X_0 = 0, \quad \alpha X_0 = 0. \tag{13.9}$$

It follows from (13.9) that:

$$X_0 = A_0, \quad V_0 = A_0 x + B_0. \tag{13.10}$$

Substitution of (13.10) in (10.6) [using Table 26 and taking account of (13.1)], yields:

$$U = Y = \sigma_x = 0, \quad V = A_0 x + B_0, \quad X = A_0. \tag{13.11}$$

This result corresponds to pure shear of the plate. The constant B_0 determines the rigid-body displacement of the plate in the y direction.

Adding together (13.8) and (13.11), we obtain a general solution for the displacements and stresses of the strip. To each value of n there correspond distinct states of stress and strain. The infinite set of these states forms the exact solution of the problem for boundary conditions (13.1). All individual solutions are orthogonal.

The solution obtained contains $4n + 2$ constants which have to be determined from the boundary conditions at $x = 0$ and $x = l$. Two boundary conditions can be formulated for each edge. Expanding the statical or geometrical magnitudes given at these edges into Fourier sine or cosine series in the interval $(0, h)$ in accordance with (13.8) and (13.11), and equating the resulting expressions to the known corresponding displacements and stresses at $x = 0$ and $x = l$, we obtain for any $n \neq 0$ a system of four algebraic equations in the unknown constants A_n, B_n, C_n and D_n. When these constants are determined the problem is completely solved.

It is often advisable to introduce other constants having a clearer physical meaning. Taking $x = 0$ as base plane of the strip, and assuming as before that boundary conditions (13.1) are fulfilled at $y = 0$ and $y = h$, we obtain as initial functions:

$$U^* = U(0, y), \quad V^* = V(0, y), \quad X^* = X(0, y), \quad \sigma_x^* = \sigma_x(0, y),$$

which, as follows from (13.8) and (13.11), must satisfy the following relationships:

$$\left.\begin{aligned} U^* &= \sum_{n=1}^{\infty} u_n^* \sin k_n y, & V^* &= \sum_{n=0}^{\infty} v_n^* \cos k_n y, \\ X^* &= \sum_{n=0}^{\infty} x_n^* \cos k_n y, & \sigma_x^* &= \sum_{n=1}^{\infty} \sigma_n^* \sin k_n y \end{aligned}\right\} \tag{13.2}$$

Here u_n^*, v_n^*, x_n^*, σ_n^* are the Fourier coefficients of the trigonometric series for the initial functions. In order to express A_n B_n, C_n and D_n throught them we set $x=0$ in (13.8) and (13.11), and equate the results obtained to the corresponding expressions (13.12). We obtain:

$$\left.\begin{aligned}
&u_n^* = (-1)^n h\left(k_n A_n - \frac{1-\nu}{1+\nu} D_n\right),\\
&v_n^* = (-1)^n h\left(k_n B_n + \frac{2}{1+\nu} C_n\right),\\
&x_n^* = (-1)^n 2k_n h\,(k_n A_n + D_n),\\
&\sigma_n^* = (-1)^n 2k_n^2 h B_n,
\end{aligned}\right\} \qquad (13.13)$$

$$B_0 = v_0^* \quad A_0 = x_0^*. \qquad (13.14)$$

It follows from (13.13) that:

$$\left.\begin{aligned}
&A_n = (-1)^n \frac{1+\nu}{4hk_n}\left(2u_n^* + \frac{1-\nu}{1+\nu}\frac{x_n^*}{k_n}\right),\\
&B_n = (-1)^n \frac{\sigma_n^*}{2k_n^2 h},\\
&C_n = (-1)^n \frac{1+\nu}{2h}\left(v_n^* - \frac{\sigma_n^*}{2k_n}\right)\\
&D_n = (-1)^n \frac{1+\nu}{4h}\left(\frac{x_n^*}{k_n} - 2u_n^*\right)
\end{aligned}\right\} \qquad (13.15)$$

Substitution of (13.14) and (13.15) in (13.8) and (13.11) yields the following general expressions for the stresses and displacements:

$$\left.\begin{aligned}
U = {}& \sum_{n=1}^{\infty}\left\{\frac{v_n^*}{2}[(1+\nu)k_n x\,\mathrm{ch}\,k_n x - (1-\nu)\,\mathrm{sh}\,k_n x] + u_n^*\left(\mathrm{ch}\,k_n x - \frac{1+\nu}{2}k_n x\,\mathrm{sh}\,k_n x\right) + \right.\\
&\left. + \frac{1+\nu}{4}x_n^* x\,\mathrm{sh}\,k_n x + \frac{\sigma_n^*}{4}\left[\frac{3-\nu}{k_n}\,\mathrm{sh}\,k_n x - (1+\nu)\,x\,\mathrm{ch}\,k_n x\right]\right\}\sin k_n y,\\
V = {}& v_0^* + x_0^* x + \sum_{n=1}^{\infty}\left\{v_n^*\left(\mathrm{ch}\,k_n x + \frac{1+\nu}{2}k_n x\,\mathrm{sh}\,k_n x\right) - \right.\\
&- \frac{u_n^*}{2}[(1-\nu)\,\mathrm{sh}\,k_n x + (1+\nu)k_n x\,\mathrm{ch}\,k_n x] - \frac{x_n^*}{4}\left[\frac{3-\nu}{k_n}\times\right.\\
&\left.\left.\times\,\mathrm{sh}\,k_n x + (1+\nu)\,x\,\mathrm{ch}\,k_n x\right] - \frac{1+\nu}{4}\sigma_n^* x\,\mathrm{sh}\,k_n x\right\}\cos k_n y,\\
Y = {}& \sum_{n=1}^{\infty}\left\{-(1+\nu)v_n^* k_n(2\,\mathrm{ch}\,k_n x + k_n x\,\mathrm{sh}\,k_n x) + (1+\nu)u_n^* k_n(\mathrm{sh}\,k_n x + k_n x\,\mathrm{ch}\,k_n x) - \right.\\
&\left. - \frac{x_n^*}{2}[(3+\nu)\,\mathrm{sh}\,k_n x + (1+\nu)k_n x\,\mathrm{ch}\,k_n x] + \sigma_n^*\left(\nu\,\mathrm{ch}\,k_n x + \frac{1+\nu}{2}k_n x\,\mathrm{ch}\,k_n x\right)\right\}\sin k_n y,\\
X = {}& x_0^* + \sum_{n=1}^{\infty}\left\{(1+\nu)v_n^* k_n(\mathrm{sh}\,k_n x + k_n x\,\mathrm{ch}\,k_n x) - (1+\nu)u_n^* k_n^2 x\,\mathrm{sh}\,k_n x + \right.\\
&\left. + x_n^*\left(\mathrm{ch}\,k_n x + \frac{1+\nu}{2}k_n x\,\mathrm{sh}\,k_n x\right) + \frac{\sigma_n^*}{2}[(1-\nu)\,\mathrm{sh}\,k_n x - (1+\nu)k_n x\,\mathrm{ch}\,k_n x]\right\}\cos k_n y,\\
\sigma_x = {}& \sum_{n=1}^{\infty}\left\{(1+\nu)v_n^* k_n^2 x\,\mathrm{sh}\,k_n x + (1+\nu)u_n^* k_n(\mathrm{sh}\,k_n x - k_n x\,\mathrm{ch}\,k_n x) + \right.\\
&\left. \frac{x_n^*}{2}[(1-\nu)\,\mathrm{sh}\,k_n x + (1+\nu)k_n x\,\mathrm{ch}\,k_n x] + \sigma_n^*\left(-\frac{1+\nu}{2}k_n x\,\mathrm{sh}\,k_n x + \mathrm{ch}\,k_n x\right)\right\}\sin k_n y.
\end{aligned}\right\} \qquad (13.16)$$

We can thus determine the stresses and strains of a strip in the case of plane stress with arbitrary statical, geometrical, or mixed boundary conditions at $x=0$ and $x=l$. The solution by trigonometric series (13.16) is a generalization of Filon's solution.

We could also have obtained (13.16) in a simpler way by direct substitution of (13.12) in Table 26, rewritten in terms of the variable x.

The method used to obtain (13.16) from (13.8) is a generalization of Cauchy and Krylov's method of initial parameters.

§ 14. OTHER HOMOGENEOUS BOUNDARY CONDITIONS OF THE MIXED TYPE AT THE LATERAL STRIP EDGES

Consider now a different kind of homogeneous boundary conditions of the mixed type (Figure 176). It will be assumed that at $y=0$ and $y=h$;

$$V = \tau_{xy} = 0. \tag{14.1}$$

We obtain in this case:

$$V_0 = X_0 = 0.$$

By satisfying the boundary conditions at $y=h$ we obtain, [using Table 26], a system of two differential equations of infinitely high order in the unknown initial functions U_0 and Y_0:

$$\left.\begin{aligned} &[(1-\nu)\sin\alpha h-(1+\nu)\alpha h\cos\alpha h]\,U_0+\\ &\qquad+\frac{1}{2}\left[(3-\nu)\frac{\sin\alpha h}{\alpha}-(1+\nu)\,h\cos\alpha h\right]Y_0=0,\\ &-2(1+\nu)\,\alpha\,(\sin\alpha h+\alpha h\cos\alpha h)\,U_0+\\ &\qquad+[(1-\nu)\sin\alpha h-(1+\nu)\,\alpha h\cos\alpha h]\,Y_0=0. \end{aligned}\right\} \tag{14.2}$$

We introduce a function $F(x)$ satisfying the equations:

$$\left.\begin{aligned} U_0&=\left(\frac{1-\nu}{1+\nu}\sin\alpha h-\alpha h\cos\alpha h\right)F,\\ Y_0&=2\alpha\,(\sin\alpha h+\alpha h\cos\alpha h)\,F, \end{aligned}\right\} \tag{14.3}$$

This transforms the second equation (14.2) into an identity. The first equation is again reduced to (13.4).

Since (13.1) and (14.1) have the same solving equations, the considerations of the preceding section apply also to this problem. As a result, we again obtain (13.7) for the solving function F.

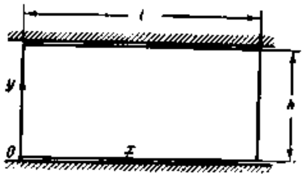

FIGURE 176

To determine the general integrals for the displacements and stresses, we have, as before, to find an elementary solution in polynomials, proceeding from the system:

$$\left.\begin{aligned} -2\nu\alpha U_0 + (1-\nu)Y_0 &= 0, \\ 2(1+\nu)\alpha^2 U_0 + \nu\alpha Y_0 &= 0, \end{aligned}\right\} \qquad (14.4)$$

obtained from (14.2) by retaining only the first terms.

We obtain from (14.4):

$$U_0 = \frac{1-\nu}{2} B_0 x + A_0, \quad Y_0 = \nu B_0. \qquad (14.5)$$

Substitution of this in (10.6) [using Table 26, and taking account of (14.1)] yields:

$$U = \frac{1-\nu}{2} B_0 x + A_0, \quad Y = \nu B_0, \quad \sigma_x = B_0. \qquad (14.6)$$

Expressions (14.6) represent an elementary solution corresponding to a uniformly distributed load $\sigma_x = B_0$. The constant A_0 does not affect the states of stress and strain of the plate but determines rigid-body displacement of the strip in the x direction.

Expressions (14.5), (14.3), (13.7), and (10.6) yield:

$$\left.\begin{aligned}
U = {} & A_0 + \frac{1-\nu}{2} B_0 x - \sum_{n=1}^{\infty} (-1)^n h \Big[k_n \operatorname{sh} k_n x A_n + \\
& + k_n \operatorname{ch} k_n x B_n + \left(\frac{2\nu}{1+\nu} \operatorname{ch} k_n x + k_n x \operatorname{sh} k_n x\right) C_n + \\
& + \left(\frac{2\nu}{1+\nu} \operatorname{sh} k_n x + k_n x \operatorname{ch} k_n x\right) D_n\Big] \cos k_n y, \\
V = {} & \sum_{n=1}^{\infty} (-1)^n h \Big\{k_n \operatorname{ch} k_n x A_n + k_n \operatorname{sh} k_n x B_n + \\
& + \left[\frac{3+\nu}{1+\nu} \operatorname{sh} k_n x + k_n x \operatorname{ch} k_n x\right] C_n + \\
& + \left[\frac{3+\nu}{1+\nu} \operatorname{ch} k_n x + k_n x \operatorname{sh} k_n x\right] D_n\Big\} \sin k_n y, \\
Y = {} & \nu B_0 + 2\sum_{n=1}^{\infty} (-1)^n k_n h [k_n \operatorname{ch} k_n x A_n + k_n \operatorname{sh} k_n x B_n + \\
& + (3 \operatorname{sh} k_n x + k_n x \operatorname{ch} k_n x) C_n + \\
& + (3 \operatorname{ch} k_n x + k_n x \operatorname{sh} k_n x) D_n] \cos k_n y, \\
X = {} & 2\sum_{n=1}^{\infty} (-1)^n k_n h [k_n \operatorname{sh} k_n x A_n + k_n \operatorname{ch} k_n x B_n + \\
& + (2 \operatorname{ch} k_n x + k_n x \operatorname{sh} k_n x) C_n + \\
& + (2 \operatorname{sh} k_n x + k_n x \operatorname{ch} k_n x) D_n] \sin k_n y, \\
\sigma_x = {} & B_0 - 2\sum_{n=1}^{\infty} (-1)^n k_n h [k_n \operatorname{ch} k_n x A_n + k_n \operatorname{sh} k_n x B_n + \\
& + (\operatorname{sh} k_n x + k_n x \operatorname{ch} k_n x) C_n + \\
& + (\operatorname{ch} k_n x + k_n x \operatorname{sh} k_n x) D_n] \cos k_n y.
\end{aligned}\right| \qquad (14.7)$$

As in the preceding section, the general solution (14.7) represents an infinite set of distinct orthogonal states. Any boundary conditions for $x=0$ and $x=l$ can be satisfied by a suitable choice of the constants A_0, B_0, A_n, B_n, C_n, D_n $(n=1,\ 2,\dots,\infty)$. We can also in this case introduce constants having a clearer physical meaning by taking $x=0$ as base plane, and the magnitudes $U(0,y)=U^*$, $V(0,y)=V^*$, $X(0,y)=X^*$, $\sigma_x(0,y)=\sigma_x^*$ as initial functions.

It follows from (14.7) that when the boundary conditions are given by (14.1), we can write:

$$\left.\begin{aligned} U^*=\sum_{n=0}^{\infty}u_n^*\cos k_ny, \quad X^*=\sum_{n=1}^{\infty}x_n^*\sin k_ny,\\ V^*=\sum_{n=1}^{\infty}v_n^*\sin k_ny, \quad \sigma_x^*=\sum_{n=0}^{\infty}\sigma_n^*\cos k_ny.\end{aligned}\right\} \tag{14.8}$$

Inserting $x=0$ into (14.7) and equating the results to the corresponding equations (14.8), we obtain:

$$\left.\begin{aligned} &A_n=-(-1)^n\frac{1+\nu}{2k_nh}\left[v_n^*+\frac{3+\nu}{2(1+\nu)}\frac{\sigma_n^*}{k_n}\right],\\ &B_n=-(-1)^n\frac{1+\nu}{k_nh}\left[u_n^*+\frac{\nu}{2(1+\nu)\,k_n}x_n^*\right],\\ &C_n=(-1)^n\frac{1+\nu}{2h}\left(\frac{x_n^*}{2k_n}+u_n^*\right),\\ &D_n=(-1)^n\frac{1+\nu}{2h}\left(v_n^*+\frac{1}{2}\frac{\sigma_n^*}{k_n}\right),\\ &A_0=u_0^*,\quad B_0=\sigma_0^*.\end{aligned}\right\} \tag{14.9}$$

Substitution of (14.9) in (14.7) then yields expressions similar to (13.16) for the displacements and stresses expressed through the initial functions (14.8):

$$\left.\begin{aligned} U=u_0^*+\frac{1-\nu}{2}\sigma_0^*x+\sum_{n=1}^{\infty}\Big\{u_n^*\left(\operatorname{ch}k_nx-\frac{1+\nu}{2}k\ x\operatorname{sh}k_nx\right)+\\ +\frac{v_n^*}{2}[(1-\nu)\operatorname{sh}k_nx-(1+\nu)k_nx\operatorname{ch}k_nx]-\\ -\frac{1+\nu}{4}x_n^*x\operatorname{sh}k_nx+\\ +\frac{\sigma_n^*}{4}\left[(3-\nu)\frac{\operatorname{sh}k_nx}{k_n}-(1+\nu)x\operatorname{ch}k_nx\right]\Big\}\cos k_ny,\\ V=\sum_{n=1}^{\infty}\Big\{\frac{u_n^*}{2}[(1-\nu)\operatorname{sh}k_nx+(1+\nu)k_nx\operatorname{ch}k_nx]+\\ +v_n^*\left(\operatorname{ch}k_nx+\frac{1+\nu}{2}k\ x\operatorname{sh}k_nx\right)+\\ +\frac{x_n^*}{4}\left[\frac{3-\nu}{k_n}\operatorname{sh}k_nx+(1+\nu)x\operatorname{ch}k_nx\right]+\\ +\frac{1+\nu}{4}\sigma_n^*x\operatorname{sh}k_nx\Big\}\sin k_ny,\end{aligned}\right| \tag{14.10}$$

$$\left.\begin{aligned}
Y = {} & \nu\sigma_0^* + \sum_{n=1}^{\infty} \Big\{(1+\nu) u_n^* k_n (\operatorname{sh} k_n x + k_n x \operatorname{ch} k_n x) + \\
& + (1+\nu) v_n^* k_n (2 \operatorname{ch} k_n x + k_n x \operatorname{sh} k_n x) + \\
& + \frac{\lambda_n^*}{2} [(3+\nu) \operatorname{sh} k_n x + (1+\nu) k_n x \operatorname{ch} k_n x] + \\
& + \sigma_n^* \left(\nu \operatorname{ch} k_n x + \frac{1+\nu}{2} k_n x \operatorname{sh} k_n x\right)\Big\} \cos k_n y, \\
\lambda = {} & \sum_{n=1}^{\infty} \Big\{(1+\nu) u_n^* k_n^2 x \operatorname{sh} k_n x + (1+\nu) v_n^* k_n (\operatorname{sh} k_n x + \\
& + k_n x \operatorname{ch} k_n x) + x_n^* \left(\operatorname{ch} k_n x + \frac{1+\nu}{2} k_n x \operatorname{sh} k_n x\right) - \\
& - \frac{\sigma_n^*}{2} [(1-\nu) \operatorname{sh} k_n x - (1+\nu) k_n x \operatorname{ch} k_n x]\Big\} \sin k_n y, \\
\sigma_x = {} & \sigma_0^* + \sum_{n=1}^{\infty} \Big\{(1+\nu) u_n^* k_n (\operatorname{sh} k_n x - k_n x \operatorname{ch} k_n x) - \\
& - (1+\nu) v_n^* k_n^2 x \operatorname{sh} k_n x - \frac{x_n^*}{2} [(1-\nu) \operatorname{sh} k_n x + \\
& + (1+\nu) k_n x \operatorname{ch} k_n x] + \\
& + \sigma_n^* \left(\operatorname{ch} k_n x - \frac{1+\nu}{2} k_n \operatorname{sh} k_n x\right)\Big\} \cos k_n y.
\end{aligned}\right\} \qquad (14.10)$$

Equations (13.16) and (14.10) represent general solutions in trigonometric series of the two-dimensional problem of the theory of elasticity. They are generalizations of Filon's and Ribière's solutions, since the latter do not actually contain general integrals for the displacements, while (13.16) and (14.10) determine both the states of stress and strain in the strip. It is thus possible to obtain a solution for problems (13.1) and (14.1) not only when the boundary conditions for $x = 0$ and $x = l$ are statical, but also if they are geometrical or of the mixed type.

These examples do not exhaust the problems of the theory of rectangular thin plates which can be solved by the exact methods of mathematical analysis. Similar exact solutions can be obtained for homogeneous statical boundary conditions at the longitudinal edges of the strip (see /15/) or other types of boundary conditions. From these homogeneous solutions it is easy to obtain relatively simple approximations for rectangular thin plates undergoing plane strain, with arbitrary boundary conditions on all four sides of the plate. The same procedure can be applied in the presence of body forces and temperature stresses.

§ 15. THREE- AND TWO-DIMENSIONAL PROBLEMS OF THE THEORY OF THICK MULTILAYER PLATES

1

Consider a thick plate consisting of several horizontal layers having different elastic characteristics (Figure 177). Let h be the total thickness of the plate, and h_m, ν_m, G_m, be respectively the thickness and elastic constants of the m-th layer. The coordinate axes are directed as shown in Figure 177. It will be assumed that the displacement and stress vectors vary continuously at the contact plane of two layers.

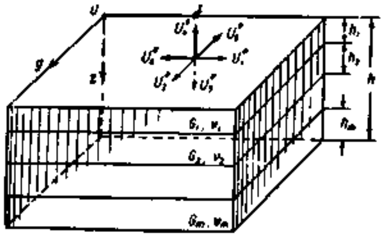

FIGURE 177.

The unknown magnitudes:

$$u, \quad v, \quad w, \quad \sigma_z, \quad \tau_{xz}, \quad \tau_{yz}$$

will be denoted as follows:

$$\left.\begin{array}{lll} u(x, y, z) = U_1, & v(x, y, z) = U_2, & w(x, y, z) = U_3, \\ \sigma_z(x, y, z) = U_4, & \tau_{xz}(x, y, z) = U_5, & \tau_{yz}(x, y, z) = U_6. \end{array}\right\} \qquad (15.1)$$

The initial functions $u_0, v_0, w_0, Z_0, X_0, Y_0$ then become:

$$\left.\begin{array}{lll} u_0(x, y) = U_1^0, & v_0(x, y) = U_2^0 & w_0(x, y) = U_3^0, \\ Z_0(x, y) = U_4^0, & X_0(x, y) = U_5^0 & Y_0(x, y) = U_6^0. \end{array}\right\} \qquad (15.2)$$

When no body forces are present, we can rewrite (2.5) as follows:

$$U_i = \sum_{k=1}^{6} L_{ik}(z) U_k^0 \qquad (i = 1, 2, \ldots, 6). \qquad (15.3)$$

Substituting $\nu = \nu_1$, $G = G_1$, $z \leqslant h_1$ we determine the displacements and stresses in the first layer. These expressions contain only three of the six initial functions (15.2), since three of the latter are already known from the boundary conditions at $z = 0$. To determine the unknown magnitudes of the second layer we first obtain the displacements and stresses at the contact plane of the first and second layers at $z = h_1$, which form the initial functions for the second layer. Then, substituting in (15.3) $\nu = \nu_2$, $G = G_2$, and the expressions for the initial functions of the second layer, we determine the displacements and stresses in the second layer:

$$U_1 = \sum_{k=1}^{6} L_{ik}^{*}(z) U_k^{*} \qquad (i = 1, 2, \ldots, 6), \qquad (15.4)$$

where:

$$L^{*}_{ik}(z)=\sum_{j=1}^{6} L^{(2)}_{ij}(z)\,L^{(1)}_{jk}(h_1) \qquad (h_1\leqslant z\leqslant h_2). \tag{15.5}$$

We denote by $L^{(1)}_{jk}(h_1)$ and $L^{(2)}_{ij}(z)$ respectively, the operators L_{ik} in (15.3) corresponding to the first layer at $z=h_1$ and to the second layer at any arbitrary value of z:

$$\left.\begin{aligned} L^{(1)}_{jk}(h_1) &= L_{jk}(\nu_1, G_1, h_1),\\ L^{(2)}_{ij}(z) &= L_{ij}(\nu_2, G_2, z) \qquad (h_1\leqslant z\leqslant h_2). \end{aligned}\right\} \tag{15.6}$$

The matrix $\|L_{ik}(z)\|$ is thus the product of the matrix $\|L^{(2)}_{ij}(z)\|$ and the matrix $\|L^{(1)}_{jk}(h_1)\|$, and is therefore a function of the three initial functions corresponding to $z=0$. Similarly, the matrix $\|L_{ik}(z)\|$ for the displacements and stresses in the m-th layer of the plate is the product of the matrices:

$$\|L^{(j)}_{ik}(h_j)\| \ (j=1, 2, \ldots, m-1) \text{ and } \|L^{(m)}_{ik}(z)\| (h_{m-1}\leqslant z\leqslant h_m).$$

Determining in this way the displacements and stresses at the bottom $z=h$ of the plate, and inserting the boundary conditions for this plane, we obtain the system of differential equations of the three-dimensional problem considered, from which the three unknown initial functions can be obtained, and thus the states of strain and stress of the multilayer plate determined.

2

Consider the case of plane strain of a multilayer plate (Figure 178). We introduce the following symbols:

$$\left.\begin{aligned} &u(x, y)=U_1, \quad v(x, y)=U_2,\\ &\sigma_y(x, y)=U_3, \quad \tau_{xy}(x, y)=U_4, \quad \sigma_x(x, y)=U_6. \end{aligned}\right\} \tag{15.7}$$

$$\left.\begin{aligned} &u_0(x)=U^0_1, \quad v_0(x)=U^0_2,\\ &Y_0(x)=U^0_3, \quad X_0(x)=U^0_4. \end{aligned}\right\} \tag{15.8}$$

We can then rewrite (10.6) as follows:

$$U_i=\sum_{k=1}^{4} L_{ik}(y)\,U^0_k \qquad (i=1, 2, 3, 4). \tag{15.9}$$

The displacements and stresses in the m-th layer of the plate are:

$$U_i=\sum_{k=1}^{4} L^{*}_{ik}(y)\,U^0_k \qquad (i=1, 2, 3, 4), \tag{15.10}$$

where the matrix $\| L_{ik}^{*}(y) \|$ is the product of the matrices:

$$\| L_{ik}^{(j)}(h_j) \| \qquad (j = 1, 2, \ldots, m-1) \text{ and } \| L_{ik}^{(m)}(y) \| \qquad (h_{m-1} \leqslant y \leqslant h_m).$$

and contains only two of the four initial functions. The other two initial functions are determined directly from the boundary conditions at $y = 0$.

Inserting (15.9) into the boundary conditions at $y = h$ yields a system of two ordinary differential equations of infinitely high order with constant coefficients whose solution determines the two remaining initial functions.

We shall consider now in more detail problems with boundary conditions for the longitudinal plate edges $x = 0$ and $x = l$. Let the initial functions be represented by the following series with constant coefficients:

$$\left.\begin{aligned} U_1^0 &= \sum_{n=1}^{\infty} u_{1n}^0 \sin \alpha_n x, & U_3^0 &= \sum_{n=0}^{\infty} u_{3n}^0 \cos \alpha_n x, \\ U_2^0 &= \sum_{n=0}^{\infty} u_{2n}^0 \cos \alpha_n x, & U_4^0 &= \sum_{n=1}^{\infty} u_{4n}^0 \sin \alpha_n x, \end{aligned}\right| \tag{15.11}$$

where

$$\alpha_n = \frac{n\pi}{l}.$$

The boundary conditions at the plate edges $x = 0$ and $x = l$ are:

$$U_1 = U_4 = 0 \quad (u = \tau_{xy} = 0). \tag{15.12}$$

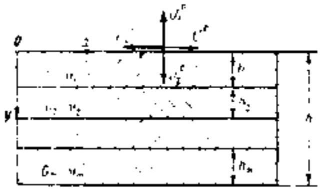

FIGURE 178

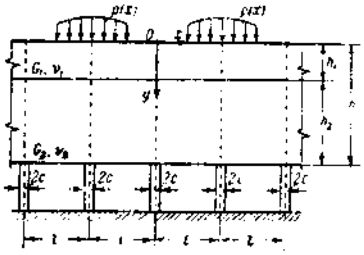

FIGURE 179.

These conditions are satisfied for each span of a multispan plate resting on an infinite number of identical and equidistant supports and subjected to a load symmetrical with respect to the ends of each span (Figure 179).

As already mentioned (see section 12), the representation of the initial functions in the form (15.11) corresponds to Ribière's solution. Interchanging the sines and cosines yields Filon's solution which corresponds to the following boundary conditions:

$$U_2 = U_4 = 0. \tag{15.13}$$

Substituting (15.11) in (15.9) and inserting the values of the operators L_{ik} given in Table 25, we obtain:

$$\begin{aligned}
U_1 = \sum_{n=1}^{\infty} \Big\{ & u_{1n}^0 \Big[\operatorname{ch} \alpha_n y + \frac{1}{2(1-\nu)} \alpha_n y \operatorname{sh} \alpha_n y\Big] + \frac{u_{2n}^0}{2(1-\nu)} \times \\
& \times [(1-2\nu) \operatorname{sh} \alpha_n y + \alpha_n y \operatorname{ch} \alpha_n y] + \frac{u_{3n}^0}{4G(1-\nu)} y \operatorname{sh} \alpha_n y + \\
& + \frac{u_{4n}^0}{4G(1-\nu)} \Big[\frac{3-4\nu}{\alpha_n} \operatorname{sh} \alpha_n y + y \operatorname{ch} \alpha_n y\Big]\Big\} \sin \alpha_n x, \\
U_2 = u_{20}^0 = {} & \frac{u_{30}^0 (1-2\nu)}{2(1-\nu)} y + \\
& + \sum_{n=1}^{\infty} \Big\{\frac{u_{1n}^0}{2(1-\nu)} [(1-2\nu) \operatorname{sh} \alpha_n y - \alpha_n y \operatorname{ch} \alpha_n y] + \\
& + u_{2n}^0 \Big[\operatorname{ch} \alpha_n y - \frac{1}{2(1-\nu)} \alpha_n y \operatorname{sh} \alpha_n y\Big] + \frac{u_{3n}^0}{4G(1-\nu)} \times \\
& \times \Big(\frac{3-4\nu}{\alpha_n} \operatorname{sh} \alpha_n y - y \operatorname{ch} \alpha_n y\Big) - \frac{u_{4n}^0}{4G(1-\nu)} y \operatorname{sh} \alpha_n y\Big\} \cos \alpha_n x, \\
U_3 = u_{30}^0 + \sum_{n=1}^{\infty} \Big\{ & -\frac{u_{1n}^0 G}{1-\nu} \alpha_n^2 y \operatorname{sh} \alpha_n y + \\
& + \frac{u_{2n}^0 G}{1-\nu} \alpha_n (\operatorname{sh} \alpha_n y - \alpha_n y \operatorname{ch} \alpha_n y) + \\
& + u_{3n}^0 \Big(\operatorname{ch} \alpha_n y - \frac{1}{2(1-\nu)} \alpha_n y \operatorname{sh} \alpha_n y\Big) - \\
& - \frac{u_{4n}^0}{2(1-\nu)} \Big[(1-2\nu) \operatorname{sh} \alpha_n y + \alpha_n y \operatorname{ch} \alpha_n y\Big]\Big\} \cos \alpha_n x, \\
U_4 = \sum_{n=1}^{\infty} \Big\{ & \frac{u_{1n}^0 G}{1-\nu} \alpha_n (\operatorname{sh} \alpha_n y + \alpha_n y \operatorname{ch} \alpha_n y) + \frac{u_{2n}^0 G}{1-\nu} \alpha_n^2 y \operatorname{sh} \alpha_n y - \\
& - \frac{u_{3n}^0}{2(1-\nu)} [(1-2\nu) \operatorname{sh} \alpha_n y - \alpha_n y \operatorname{ch} \alpha_n y] + \\
& + u_{4n}^0 \Big[\operatorname{ch} \alpha_n y + \frac{1}{2(1-\nu)} \alpha_n y \operatorname{sh} \alpha_n y\Big]\Big\} \sin \alpha_n x, \\
U_5 = \frac{u_{30}^0 \nu}{1-\nu} + \sum_{n=1}^{\infty} \Big\{ & \frac{u_{1n}^0 G}{1-\nu} \alpha_n (2 \operatorname{ch} \alpha_n y + \alpha_n y \operatorname{sh} \alpha_n y) + \\
& + \frac{u_{2n}^0 G}{1-\nu} \alpha_n (\operatorname{sh} \alpha_n y + \alpha_n y \operatorname{ch} \alpha_n y) + \\
& + \frac{u_{3n}^0}{1-\nu} \Big(\nu \operatorname{ch} \alpha_n y + \frac{1}{2} \alpha_n y \operatorname{sh} \alpha_n y\Big) + \\
& + \frac{u_{4n}^0}{2(1-\nu)} [(3-2\nu) \operatorname{sh} \alpha_n y + \alpha_n y \operatorname{ch} \alpha_n y]\Big\} \cos \alpha_n x.
\end{aligned} \tag{15.14}$$

Putting $\nu = \nu_1$, $G = G_1$, we obtain from these expressions the stresses and strains in the first layer of the plate. The coefficients u_{in}^0 ($i = 1, 2, 3, 4$) represent unknown magnitudes determined from the boundary conditions at $y = 0$ and $y = h$.

Substituting (15.11) in (15.10), we obtain the displacements and stresses in the m-th layer. These can also be determined by a different and simpler procedure. Each term of any series (15.11) is orthogonal in the interval $(0, l)$ to all other terms of the same series. Expressions (15.14) can therefore be considered as an infinite set of independent and orthogonal states of stress and strain. The displacements and stresses in the m-th layer are therefore, in accordance with (15.14):

$$u_{in} = \sum_{k=1}^{4} a_{ik}^{(n)*}(y)\, u_{kn}^{0} \qquad (i = 1, 2, \ldots, 5), \tag{15.15}$$

where the matrix $\| a_{ik}^{(n)*}(y) \|$ is the product of the matrices:

$$\| a_{ik}^{(n)}(\nu_j, G_j, h_j) \| \quad (j = 1, 2, \ldots, m-1) \text{ and } \| a_{ik}^{(n)}(\nu_m, G_m, y) \|.$$

Consider as example the equilibrium of a double-layer plate subjected to a vertical uniformly distributed load p, acting on the upper surface of the plate (Figure 179). We denote by $2c$ the width of the plate supports, and by l the distance between the support centers; the coordinates are directed as shown.

It will be assumed that due to the external load only normal stresses U_3, distributed uniformly over the plate width, arise in the supports. Thus, for $y = h$, the stresses U_3 are constant $= \left(-\frac{1}{2}\frac{pl}{c}\right)$ at the supports and zero between them.

The boundary conditions at the upper plane $y=0$ are:

$$U_3^0 = u_{30}^0 = -p, \quad U_4^0 = 0.$$

The normal load acting on the lower plane of the plate can be represented as a Fourier series in the interval $(0, l)$:

$$U_3(x, h) = -p\left(1 + \sum_{n=2,4,6}^{\infty} \frac{2}{c\alpha_n} \sin \alpha_n c \cos \alpha_n x\right). \tag{15.16}$$

The first term of this series corresponds to the load $U_{30}(h) = -p$. The combined action of this load and the load $U_{30}^0 = -p$ causes a uniform compression of the plate. The loads represented by the remaining terms of the series are statically equivalent to zero in the interval $(0, l)$.

Substituting (15.15) and (15.16) in the boundary conditions for $y = h$, we obtain:

$$\left.\begin{aligned} &a_{31}^{(n)*} u_{1n}^{0} + a_{33}^{(n)*} u_{3n}^{0} = -\frac{2p}{c\alpha_n} \sin \alpha_n c, \\ &a_{41}^{(n)*} u_{1n}^{0} + a_{43}^{(n)*} u_{3n}^{0} = 0, \end{aligned}\right\} \tag{15.17}$$

where:

$$a_{ik}^{(n)*} = \sum_{j=1}^{4} a_{ij}^{(n)}(\nu_2, G_2, h_2)\, a_{jk}^{(n)}(\nu_1, G_1, h_1). \tag{15.18}$$

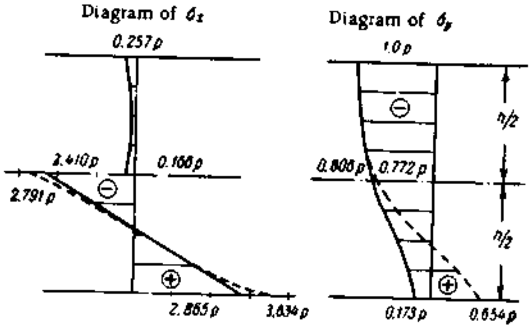

FIGURE 180.

All the unknown coefficients u_{1n}^0 and u_{2n}^0 $(n = 2, 4, 6, \ldots)$ can be obtained from (15.17). It is then possible to determine the stresses and strains in the plate.

The normal stresses $U_2 = \sigma_y$ and $U_6 = \sigma_x$ in the middle section $x = \frac{1}{2}l$ of the span are given in Figure 180. The plate considered has the following dimensions and elastic characteristics:

$$h_1 = h_2 = \frac{3}{2}l, \quad G_2 = 10G_1, \quad \nu_1 = \nu_2 = 0.3.$$

Two curves have been plotted in each graph; the full line represents the sum of three terms of series (15.16), while the broken line represents two terms of the series. It is seen from the diagrams that the normal stress σ_x has a discontinuity at the contact plane of the layers.

It was assumed that there are no relative displacements between the points of the lower and the upper layer at the contact plane. We shall now assume that the contact plane is perfectly smooth, so that the shearing stresses $U_4 = \tau_{xy}$ vanish there. The displacements $U_1 = u$ are discontinuous, while the displacements $U_3 = v$ and normal stresses $U_2 = \sigma_y$ are continuous across this plane.

Representing the initial function of the lower layer by the series:

$$U_1^{0'}(x) = \sum_{n=2,4,6}^{\infty} u_{1n}^{0'} \sin \alpha_n x, \tag{15.19}$$

we obtain from the boundary conditions:

$$\left.\begin{aligned} &a_{41}^{(n)}(\nu_1, G_1, h_1)\,u_{1n}^0 + a_{42}^{(n)}(\nu_1, G_1, h_1)\,u_{2n}^0 = 0, \\ &a_{31}^{(n)*}u_{1n}^0 + a_{32}^{(n)*}u_{2n}^0 + a_{31}^{(n)}(\nu_2, G_2, h_2)\,u_{1n}^{0'} = -\frac{2p}{c\alpha_n}\sin \alpha_n c, \\ &a_{41}^{(n)*}u_{1n}^0 + a_{42}^{(n)*}u_{2n}^0 + a_{41}^{(n)}(\nu_2, G_2, h_2)\,u_{1n}^0 = 0, \end{aligned}\right\} \tag{15.20}$$

where the coefficients $a_{ik}^{(n)*}$ are determined by (15.18).

The first and third equations (15.20) state that U_4 vanishes at the contact plane of the layers and at the bottom of the plate. The second equation expresses the equilibrium condition with respect to U_2 at the plate bottom. These equations are sufficient for determining the stresses and strains in the plate.

The stresses $U_3 = \sigma_y$ and $U_6 = \sigma_x$ in the middle section of the plate have been plotted in Figure 181. The dimensions and elastic characteristics are the same as in the preceding example. The diagrams represent the sums of two terms of (15.16). The distributions of the normal stresses over the middle section are practically linear. The stresses σ_x have a discontinuity at the contact plane of the layers.

3.

A solution by trigonometric series is also possible in the three-dimensional problem, provided one of the following conditions is fulfilled at the longitudinal edges of the plate: 1) the shearing stresses in, and the displacements normal to, the boundary plane vanish or, 2) the normal stresses in, and the tangential displacements of, the boundary plane vanish in the two-dimensional problem. The boundary conditions of the first kind correspond to (15.12), and those of the second kind, to (15.13).

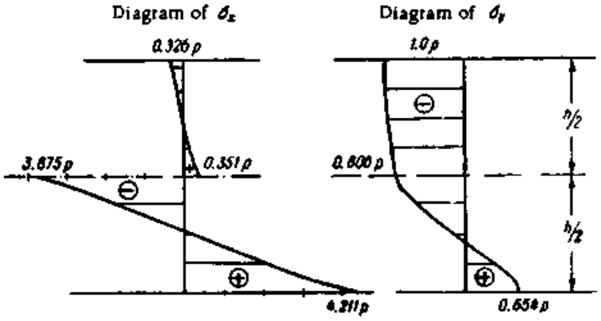

FIGURE 181.

When boundary conditions of the first type obtain on all sides of the plate $(x=0,\ x=a,\ y=0,\ y=b)$, the initial functions can be represented in the form:

$$\left.\begin{aligned}
U_1^0 &= \sum_{n=1}^{\infty}\sum_{m=0}^{\infty} u_{1nm}^0 \sin\alpha_n x \cos\beta_m y, & U_4^0 &= \sum_{n=0}^{\infty}\sum_{m=0}^{\infty} u_{4nm}^0 \cos\alpha_n x \cos\beta_m y,\\
U_2^0 &= \sum_{n=0}^{\infty}\sum_{m=1}^{\infty} u_{2nm}^0 \cos\alpha_n x \sin\beta_m y, & U_5^0 &= \sum_{n=0}^{\infty}\sum_{m=1}^{\infty} u_{5nm}^0 \cos\alpha_n x \sin\beta_m y,\\
U_3^0 &= \sum_{n=0}^{\infty}\sum_{m=0}^{\infty} u_{3nm}^0 \cos\alpha_n x \cos\beta_m y, & U_6^0 &= \sum_{n=1}^{\infty}\sum_{m=0}^{\infty} u_{6nm}^0 \sin\alpha_n x \cos\beta_m y,
\end{aligned}\right\} \tag{15.21}$$

where

$$\alpha_n = \frac{n\pi}{a}, \quad \beta_m = \frac{m\pi}{b}.$$

If boundary conditions of the second type are fulfilled on all sides, it is necessary to interchange sines and cosines in (15.21). If conditions of the first type are fulfilled on two opposite sides, and conditions of the second type on the remaining sides, the trigonometric functions of one argument are unchanged, while in those of the other sines and cosines have to be interchanged.

In the three-dimensional case, the stresses and strains in a multilayer plate are determined in the same way as in the two-dimensional case. The unknown coefficients in (15.21) are found from the boundary conditions at $z=0$ and $z=h$.

The stresses and strains in a plate, corresponding to (15.21) can be represented as follows. Consider an [infinite] multilayer plate supported by a large number of rows of columns (Figure 182) arranged in two orthogonal directions. The distances between the centers of adjacent columns are uniform, being a in one direction and b in the other.

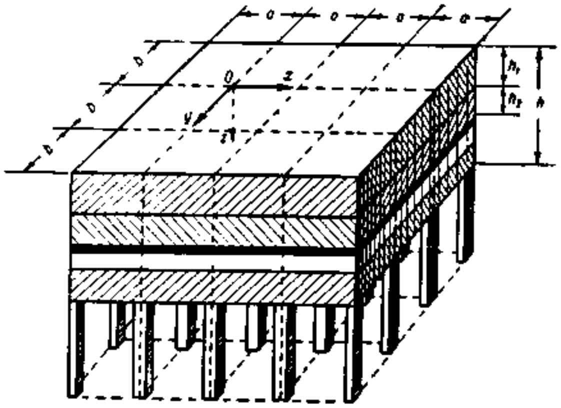

FIGURE 182.

The planes passing through the centers of the columns in the direction of the rows form two families of orthogonal planes of symmetry. If an external load, symmetrical with respect to all these planes, acts on the plate, all plate elements which form rectangular plates supported on four adjacent columns, will be under the same conditions. Boundary conditions of the first type will be fulfilled on all sides of each plate; the initial functions determining the stresses and strains in the plate are then given by (15.21). If the load acting on the plate is antisymmetrical with respect to all planes of both families, boundary conditions of the second type will be fulfilled on all sides of each plate element; the initial functions are then obtained from (15.21) by interchanging the sines and cosines. If, finally, the load acting on the plate is symmetrical with respect to all planes of one family and antisymmetrical with respect to the other, the problem will be of the mixed type: the functions of one argument in (15.21) remain unchanged while sines and cosines are interchanged in the functions of the other argument. The general case of a continuous plate subjected to an arbitrary external load can be considered as a combination of the above-mentioned symmetrical and antisymmetrical loads.

§ 16. ELASTIC MULTILAYER FOUNDATION

The above theory of thick multilayer plates can also be applied to determine the stresses and strains appearing in an elastic multilayer foundation when an external load is applied to its surface (Figure 183).

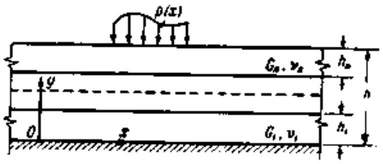

FIGURE 183.

The displacements and stresses in the first layer, which is in a state of plane strain, can be represented in the form:

$$U_i = \sum_{k=1}^{4} \int_{-\infty}^{\infty} [A_{ik}(y, \alpha) f_i(x, \alpha) u_k^0(\alpha) + B_{ik}(y, \alpha) g_i(x, \alpha) u_k^{0*}(\alpha)]\, d\alpha \qquad (16.1)$$

$$(i = 1, 2, \ldots, 5),$$

where $f_i(x, \alpha) = \sin \alpha x$ for $i = 1, 4$; $f_i(x, \alpha) = \cos \alpha x$, for $i = 2, 3, 5$; $g_i(x, \alpha) = \cos \alpha x$ for $i = 1, 4$; $g_i(x, \alpha) = \sin \alpha x$ for $i = 2, 3, 5$; the functions A_{ik} are those entering in (15.14):

$$A_{11} = \operatorname{ch} \alpha y + \frac{\alpha y \operatorname{sh} \alpha y}{2(1 - \nu_1)}, \qquad A_{23} = \frac{1}{4G(1 - \nu_1)} \left(\frac{3 - 4\nu_1}{\alpha} \operatorname{sh} \alpha y - y \operatorname{ch} \alpha y \right)$$

etc.; the functions B_{ik} are determined from expressions similar to (15.14) but corresponding to a different representation of the initial functions (Filon's form).

When the displacements and stresses across the contact planes of the layers are continuous, the stresses and displacements in the m-th layer of an infinite plate are:

$$U_i = \sum_{k=1}^{4} \int_{-\infty}^{\infty} [A_{ik}^* f_i u_k^0 + B_{ik}^* g_i u_k^{0*}]\, d\alpha, \qquad (16.2)$$

where the matrices $\| A_{ik}^* \|$ and $\| B_{ik}^* \|$ are the products of the matrices:

$$\| A_{ik}^{(j)}(\alpha, h_j, \nu_j, G_j) \| \text{ and } \| A_{ik}^{(m)}(\alpha, y, \nu_m, G_m) \|,$$

$$\| B_{ik}^{(j)}(\alpha, h_j, \nu_j, G_j) \| \text{and} \| B_{ik}^{(m)}(\alpha, y, \nu_m, G_m) \|$$

$$(j = 1, 2, \ldots, m - 1), \qquad (h_{m-1} \leqslant y \leqslant h_m).$$

respectively.

The unknown functions u_k^0 and u_k^{0*} have to be found from the boundary conditions at $y=0$ and $y=h$.

Consider as example an infinite elastic foundation, on a bounded region of which acts an external load (Figure 183). It will be assumed that this foundation lies on a rigid subsoil, and that there is no friction between the foundation and the subsoil. In this case the vertical displacements U_2 and the shearing stresses U_4 vanish for $y=0$, so that in (16.2) we must put: $u_2^0=u_2^{0*}=u_4^0=u_4^{0*}=0$. To determine the unknown functions $u_1^0,\ u_1^{0*},\ u_3^0,\ u_3^{0*}$, we shall use the statical boundary conditions for $y=h$. Let only a normal distributed load $p(x)$, differing from zero in the interval $a_1\leqslant x\leqslant a_2$, act at $y=h$ (Figure 183). We represent $p(x)$ as a Fourier integral:

$$p(x)=\frac{1}{2\pi}\int_{-\infty}^{\infty}d\alpha\int_{a_1}^{a_2}p(\lambda)\cos\alpha(\lambda-x)\,d\lambda. \tag{16.3}$$

Equating the expressions for the stresses U_3 and U_4, obtained from (16.2) for $y=h$, to the boundary value (16.3) and to zero respectively, we obtain:

$$\left.\begin{aligned}&\sum_{i=1,3}A_{3i}^{*}(\alpha h)\,u_i^0=-\frac{1}{2\pi}\int_{a_1}^{a_2}p(\lambda)\cos\alpha\lambda\,d\lambda; &&\sum_{i=1,3}A_{4i}^{*}(\alpha h)\,u_i^0=0;\\&\sum_{i=1,3}B_{3i}^{*}(\alpha h)\,u_i^{0*}=-\frac{1}{2\pi}\int_{a_1}^{a_2}p(\lambda)\sin\alpha\lambda\,d\lambda; &&\sum_{i=1,3}B_{4i}^{*}(\alpha h)\,u_i^{0*}=0.\end{aligned}\right\} \tag{16.4}$$

Having found u_i^0 and u_i^{0*} $(i=1,3)$, from (16.4) we determine the stresses and strains in the plate from (16.2). The expressions for the displacements and stresses cannot be obtained in finite form, since the integrals (16.2) cannot be expressed in elementary functions and must be evaluated numerically.

The three-dimensional equilibrium problem of a multilayer foundation extending to infinity in two directions can be similarly treated. We proceed in this case from the sum of the four different representations of the initial functions. One representation is (15.21), while the others are obtained from (15.21) by suitably interchanging sines and cosines. In order to satisfy the boundary conditions for $z=h$ it is necessary to use a double Fourier integral.

TABLE 1

Function $\Phi_{1}(z)=\operatorname{sh} z\cos\gamma z$, where $z=\bar{\alpha}\eta$

z \ γ	0.1	0.2	0.3	0.4	0.5	0.6	0.7	0.8	0.9
0	0	0	0	0	0	0	0	0	0
0.05	0.05000	0.05000	0.04999	0.04999	0.04998	0.04998	0.04997	0.04996	0.04995
0.10	0.10019	0.10018	0.10015	0.10012	0.10007	0.10002	0.09995	0.09988	0.09979
0.15	0.15058	0.15053	0.15045	0.15033	0.15017	0.14999	0.14977	0.14952	0.14923
0.20	0.20130	0.20118	0.20098	0.20070	0.20033	0.19989	0.19937	0.19877	0.19809
0.25	0.25253	0.25229	0.25190	0.25135	0.25063	0.24977	0.24875	0.24757	0.24624
0.30	0.30438	0.30397	0.30329	0.30233	0.30110	0.29960	0.29783	0.29579	0.29349
0.35	0.35697	0.35631	0.35522	0.35370	0.35173	0.34934	0.34652	0.34328	0.33961
0.40	0.41042	0.40943	0.40780	0.40550	0.40256	0.39898	0.39475	0.38990	0.38443
0.45	0.46486	0.46345	0.46110	0.45782	0.45360	0.44848	0.44243	0.43551	0.45096
0.50	0.52045	0.51849	0.51525	0.51071	0.50490	0.49782	0.48950	0.47996	0.46922
0.55	0.57727	0.57466	0.57029	0.56422	0.55642	0.54695	0.53582	0.52308	0.50875
0.60	0.63550	0.63207	0.62636	0.61840	0.60822	0.59584	0.58132	0.56470	0.54606
0.65	0.69527	0.69087	0.68354	0.67333	0.66027	0.64443	0.62586	0.60465	0.58088
0.70	0.75672	0.75116	0.74191	0.72904	0.71259	0.69265	0.66932	0.64271	0.61295
0.75	0.82000	0.81308	0.80158	0.78559	0.76517	0.74046	0.71157	0.67869	0.64198
0.80	0.88527	0.87677	0.87154	0.84333	0.81800	0.78774	0.75246	0.71235	0.66769
0.85	0.95266	0.94233	0.92519	0.89182	0.87105	0.83444	0.79180	0.74345	0.68972
0.90	1.02236	1.00993	0.98933	0.96072	0.92433	0.88046	0.82946	0.77175	0.70778
0.95	1.09451	1.07969	1.05512	1.02104	0.97774	0.92565	0.86518	0.79695	0.72149
1.00	1.16933	1.16353	1.12271	1.08243	1.03133	0.96994	0.89884	0.81877	0.73052
1.05	1.24694	1.22631	1.19214	1.14489	1.08812	1.01190	0.93014	0.83690	0.73445
1.10	1.32758	1.30346	1.26358	1.20843	1.13867	1.05515	0.95888	0.85101	0.73326
1.15	1.41139	1.38337	1.33704	1.27309	1.19229	1.09578	0.98474	0.86074	0.72534
1.20	1.49861	1.46620	1.41270	1.33887	1.24582	1.13483	1.00750	0.86570	0.71145
1.25	1.58941	1.55212	1.49059	1.40581	1.29909	1.17211	1.02601	0.86552	0.69070
1.30	1.68404	1.64131	1.57065	1.47389	1.35205	1.20739	1.04238	0.85975	0.66262
1.35	1.78270	1.73391	1.65538	1.54310	1.40455	1.24047	1.05380	0.84796	0.62669
1.40	1.88568	1.83015	1.73880	1.61344	1.45648	1.27104	1.06073	0.82966	0.58237
1.45	1.99310	1.93015	1.82666	1.68486	1.50766	1.29886	1.06277	0.80438	0.52911
1.50	2.10537	2.03419	1.91731	1.75738	1.55795	1.32858	1.05947	0.77157	0.46633
1.55	2.22261	2.09738	2.01072	1.83091	1.60714	1.34488	1.05036	0.73067	0.39343
1.60	2.34721	2.25688	2.10888	1.90705	1.65648	1.36358	1.03586	0.68170	0.31008
1.65	2.47338	2.37216	2.20646	1.98087	1.70144	1.37582	1.01281	0.62230	0.21486
1.70	2.60748	2.49417	2.30895	2.05716	1.74606	1.38464	0.98327	0.55357	0.10791
1.75	2.74774	2.62123	2.40064	2.13422	1.78862	1.38834	0.94578	0.47429	−0.01172
1.80	2.89286	2.75358	2.52353	2.21195	1.82888	1.38673	0.89977	0.38372	−0.14470
1.85	3.04832	2.89142	2.63575	2.29021	1.86642	1.37902	0.84451	0.28119	−0.29171
1.90	3.20933	3.03501	2.75146	2.35889	1.90102	1.36475	0.77939	0.16592	−0.45346
1.95	3.37793	3.18466	2.87060	2.44781	1.93219	1.34337	0.70358	0.03719	−0.63066
2.00	3.55458	3.34055	2.99339	2.52687	1.95959	1.31423	0.61646	−0.10590	−0.82402
2.05	3.73956	3.50301	3.10058	2.60579	1.98274	1.27666	0.51709	−0.26412	−1.03427
2.10	3.93350	3.67232	3.24978	2.68443	2.00116	1.22996	0.40472	−0.43834	−1.26210
2.15	4.13668	3.84875	3.38350	2.76255	2.01429	1.17338	0.27840	−0.62941	−1.50822
2.20	4.34969	4.03257	3.52107	2.83985	2.02174	1.10616	0.13723	−0.83829	−1.77339
2.25	4.57290	4.22416	3.66240	2.91607	2.02269	1.02741	−0.01970	−1.06583	−2.05820
2.30	4.80697	4.42376	3.80763	2.99091	2.01670	0.93624	−0.19348	−1.31303	−2.36347
2.35	5.05016	4.63179	3.95659	3.06402	2.00292	0.83173	−0.38516	−1.58087	−2.68966
2.40	5.30957	4.84849	4.10957	3.13499	1.98074	0.71290	−0.59576	−1.87027	−3.03758
2.45	5.57919	5.07431	4.26623	3.20344	1.94925	0.57873	−0.82642	−2.18223	−3.40766
2.50	5.86210	5.30953	4.42687	3.26892	1.90775	0.42799	−1.07845	−2.51779	−3.80055
2.55	6.15862	5.55456	4.59123	3.33099	1.85525	0.25961	−1.35284	−2.87790	−4.21674
2.60	6.46972	5.80982	4.75935	3.38901	1.79084	0.07230	−1.65112	−3.26355	−4.65659
2.65	6.79584	6.07564	4.93115	3.44247	1.71345	−0.13520	−1.97442	−3.67583	−5.12050
2.70	7.13793	6.35242	5.10662	3.49079	1.62204	−0.36424	−2.32416	−4.11566	−5.60891
2.75	7.49655	6.64058	5.28546	3.53325	1.51534	−0.61629	−2.70189	−4.58403	−6.12180
2.80	7.87293	6.94069	5.46778	3.56906	1.39238	−0.81002	−3.10842	−5.08194	−6.65962
2.85	8.26730	7.25289	5.65319	3.59750	1.25157	−1.19532	−3.54581	−5.61029	−7.22196

γ z	0.1	0.2	0.3	0.4	0.5	0.6	0.7	0.8	0.9
2.90	8.68123	7.57796	5.84188	3.61784	1.09168	−1.52563	−4.01547	−6.17010	−7.80934
2.95	9.11516	7.91621	6.03314	3.62895	0.91124	−1.88526	−4.51876	−6.76203	−8.42094
3.00	9.57047	8.26815	6.22721	3.63007	0.70866	−2.27606	−5.05752	−7.38707	−9.05686
3.05	10.04774	8.63418	6.42342	3.62000	0.48225	−2 69997	−5.63294	−8.04607	−9.71624
3.10	10.54843	9.01490	6.62183	3.59763	0.23028	−3 15889	−6.24701	−8.73943	−10.39890
3.15	11.07336	9.41081	6.81606	3.56177	−0.04892	−3.65482	−6.90096	−9.46811	−11.10341
3.20	11.62428	9.82242	7.02326	3.51114	−0.35758	−4.18993	−7.59685	−10.23253	−11.82927
3.25	12.20160	10.25015	7.22537	3.44427	−0.69761	−4.76636	−8.33604	−11.03313	−12.57552
3.30	12.80738	10.69479	7.42810	3.35983	−1.07112	−5.36645	−9.12047	−11.87028	−13.33901
3.35	13.44242	11.15675	7.36047	3.25599	−1.48060	−6.05250	−9.95143	−12.74411	−14.11966
3.40	14.10859	11.63681	7.83242	3.13135	−1.92814	−6.76704	−10.83103	−13.65499	−14.91552
3.45	14.80615	12.13509	8.03268	2.98386	−2.41663	−7.53249	−11.76030	−14.60255	−15.72362
3.50	15.53965	12.65246	8.23112	2.81175	−2.94872	−8.35155	−12.74163	−15.58680	−16.54197
3.55	16.30772	13.18962	8.42657	2.61284	−3.52681	−9.22679	−13.77574	−16.60721	−17.36725
3.60	17.11336	13.74719	8.61848	2.38479	−4.15446	−10.16123	−14.86516	−17.66339	−18.19696
3.65	17.95784	14.32540	8.80552	2.12563	−4.83434	−11.15761	−16.01041	−18.75430	−19.02671
3.70	18.84359	14.92543	8.98715	1.83256	−5.57003	−12.21873	−17.21375	−19.87902	−19.85355
3.75	19.77199	15.54752	9.16184	1.50314	−6.36465	−13.34785	−18.47581	−21.03608	−20.67251
3.80	20.74572	16.19250	9.32871	1.13417	−7.22211	−14.54809	−19.79852	−22.22414	−21.47912
3.85	21.76625	16.86075	9.48736	0.72313	−8.14585	−15.82244	−21.18216	−23.41778	−22.26815
3.90	22.83704	17.55315	9.63323	0.26665	−9.14015	−17.17414	−22.62890	−24.68542	−23.03433
3.95	23.95877	18.27058	9.76778	−0.23881	−10.20878	−18.60674	−24.13866	−25.95365	−23.77083
4.00	25.13565	19.01316	9.88877	−0.79686	−11.35670	−20.12331	−25.71311	−27.24325	−24.47251
4.05	26.38305	19.78177	9.98392	−1.41098	−12.58750	−21.72760	−27.35201	−28.55126	−25.13082
4.10	27.66204	20.57702	10.08130	−2.08569	−13.90873	−23.42279	−29.05613	−29.87351	−25.73892
4.15	29.01701	21.39985	10.14882	−2.82496	−15.31867	−25.21255	−30.82539	−31.20590	−26.12927
4.20	30.43847	22.25023	10.19471	−3.63325	−16.82951	−27.10023	−32.66062	−32.54361	−26.77021
4.25	31.92756	23.12937	10.21578	−4.51527	−18.44307	−29.08957	−34.55984	−33.88206	−27.17503
4.30	33.48928	24.03792	10.20996	−5.47673	−20.16644	−31.18438	−36.52442	−35.21501	−27.49380
4.35	35.12521	24.97606	10.17433	−6.52260	−22.00409	−33.38766	−38.55151	−36.53586	−27.71408
4.40	36.84079	25.94430	10.10571	−7.65848	−23.96331	−35.70350	−40.64193	−37.83841	−27.82675
4.45	38.63817	26.94355	10.00072	−8.89029	−26.04930	−38.13518	−42.79222	−39.11504	−27.81611
4.50	40.52296	27.97432	9.85611	−10.22408	−28.26954	−40.68587	−45.00121	−40.35690	−27.67685
4.55	42.49703	29.03708	9.66751	−11.66829	−30.63003	−43.35051	−47.26550	−41.55555	−27.38829
4.60	44.56695	30.13175	9.43215	−13.22809	−33.13885	−46.15954	−49.58444	−42.70082	−26.93962
4.65	46.73528	31.25916	9.14460	−14.91193	−35.80139	−49.08927	−51.95098	−43.78207	−26.31484
4.70	49.00875	32.42019	8.80054	−16.72708	−38.62729	−52.15078	−54.46493	−44.78877	−25.50014
4.75	51.38955	33.61402	8.39541	−18.68222	−41.62283	−55.34880	−56.81814	−45.70843	−24.47719
4.80	53.88572	34.84139	7.92303	−20.78564	−44.79654	−58.68340	−59.30666	−46.52672	−23.23084
4.85	56.49994	36.10361	7.37911	−23.04742	−48.15772	−62.16105	−61.82639	−47.23167	−21.74264
4.90	59.24067	37.39897	6.75641	−25.47672	−51.71414	−65.78156	−64.36824	−47.80653	−19.99464
4.95	62.11104	38.72870	6.04834	−28.08394	−55.47333	−69.54706	−66.92416	−48.23565	−17.96785
5.00	65.11925	40.09199	5.24913	−30.87966	−59.44716	−73.46043	−69.48834	−48.50219	−15.64204
5.05	68.26951	41.48935	4.34973	−33.87499	−63.64207	−77.52282	−72.04822	−48.58808	−12.99892
5.10	71.57158	42.92048	3.34510	−37.08234	−68.07066	−81.73482	−74.59685	−48.47241	−10.01152
5.15	75.02932	44.38410	2.22343	−40.51314	−72.13951	−86.09819	−77.11912	−48.13608	−6.66598
5.20	78.65344	45.88042	0.97884	−44.18195	−77.66282	−90.61251	−79.60781	−47.55714	−2.93471
5.25	82.44813	47.40872	−0.40018	−48.10236	−82.84640	−95.27670	−82.04319	−46.71222	1.20149
5.30	86.42415	48.96811	−1.92318	−52.28761	−88.30426	−100.09179	−84.41582	−45.57649	5.76755
5.35	90.58638	50.55720	−3.60130	−56.75312	−94.04447	−105.05476	−86.70498	−44.12540	10.78600
5.40	94.94931	52.17668	−5.44427	−61.51652	−100.08141	−110.16516	−88.89840	−42.33204	16.28189
5.45	99.51624	53.82317	−7.46674	−66.59204	−106.42205	−115.41915	−90.96486	−40.16633	22.27687
5.50	104.30064	55.49520	−9.67985	−71.99940	−113.08248	−120.82217	−92.90797	−37.59996	28.79731
5.55	109.31016	57.19076	−12.74078	−77.75530	−120.06896	−126.34031	−94 68256	−34.60179	35.86609
5.60	114.55917	58.90888	−14.73790	−83.67971	−127.33884	−131.99873	−96.27454	−31.13917	43.50831
5.65	120.05195	60.36286	−17.60880	−90.39219	−135.07799	−137.35514	−97.66570	−27.17793	52.45681
5.70	125.80683	62.40132	−20.73369	−97.31462	−143.12450	−143.67740	−98.80147	−22.68378	60.60664
5.75	131.82992	64.17122	−24.12803	−104.66842	−151.54265	−149.68205	−99.67912	−17.61806	70.10779
5.80	138.13992	65.95031	−27.81097	−112.47588	−160.35236	−155.78106	−100.25986	−11.94517	80.27692
5.85	144.74345	67.73618	−31.79946	−120.76017	−169.55661	−161.96613	−100.50616	−5.62168	92.02674
5.90	151.66098	69.52451	−36.11836	−129.54900	−179.17729	−168.22260	−100.38820	−1.38896	102.69704
5.95	158.91886	71.31240	−40.78503	−138.86788	−189.21598	−174.53559	−99.86154	9.13135	114.98707
6.00	166.48194	73.09278	−45.82923	−148.74127	−199.69451	−180.88829	−98.89189	17.64990	128.02532
6.05	174.41552	74.85978	−51.27074	−159.20055	−210.61336	−187.26183	−97.43095	26.98616	142.88289
6.10	182.72274	76.60912	−57.13861	−170.27668	−221.99369	−193.63728	−95.43537	37.71910	156.40166
6.15	191.41393	78.33169	−63.45936	−181.99510	−233.83501	−199.99143	−92.85484	48.30579	171.65394
6.20	200.51847	80.02212	−70.26326	−191.39116	−246.15161	−206.29593	−89.64054	60.38368	187.93125
6.25	210.04306	81.66900	−77.57990	−207.49963	−258.96660	−212.63320	−85.73602	73.46949	204.89921
6.30	220.01447	83.27021	−85.44577	−221.35412	−272.27414	−218.65849	−81.08648	87.61488	222.68014
6.35	230.73290	84.91484	−94.01163	−236.28727	−286.45433	−224.92918	−75.72347	103.00238	241.56937
6.40	241.36929	86.28027	−102.96036	−251.44715	−300.40710	−230.46689	−69.30226	119.29138	260.66739
6.45	253.10847	87.77662	−112.82488	−268.09688	−315.64004	−236.36844	−62.11387	137.09078	281.21333
6.50	264.75237	88.96249	−123.11078	−284.97506	−330.61787	−241.42258	−53.76993	155.81572	301.85056
6.55	277.61038	90.26258	−134.44346	−303.51120	−346.94296	−246.78423	−44.47143	176.24394	324.00713
6.60	290.35838	91.21779	−146.23956	−322.27248	−362.94522	−251.17421	−33.90988	197.60057	346.11525

TABLE 2

Function $\Phi_3(z) = \operatorname{ch} z \cos\gamma z$, where $z = \frac{\lambda}{a}\eta$

γ / z	0.1	0.2	0.3	0.4	0.5	0.6	0.7	0.8	0.9
0	1	1	1	1	1	1	1	1	1
0.05	1.00119	1.00115	1.00109	1.00100	1.00088	1.00075	1.00058	1.00040	1.00017
0.10	1.00495	1.00480	1.00460	1.00419	1.00381	1.00320	1.00253	1.00179	1.00092
0.15	1.01119	1.01084	1.01027	1.00948	1.00844	1.00720	1.00571	1.00402	1.00209
0.20	1.01987	1.01925	1.01823	1.01681	1.01500	1.01273	1.01010	1.00704	1.00359
0.25	1.03108	1.03012	1.02850	1.02625	1.02334	1.01982	1.01564	1.01085	1.00540
0.30	1.04487	1.04346	1.04111	1.03782	1.03360	1.02845	1.02237	1.01538	1.00747
0.35	1.06122	1.05928	1.05503	1.05050	1.04566	1.03857	1.02918	1.02053	1.00966
0.40	1.08020	1.07761	1.07330	1.06726	1.05952	1.05009	1.03897	1.02619	1.01177
0.45	1.10184	1.09850	1.09292	1.08515	1.07515	1.06301	1.04868	1.03227	1.01373
0.50	1.12622	1.12199	1.11497	1.10516	1.09257	1.07727	1.05926	1.03861	1.01537
0.55	1.15334	1.14812	1.14770	1.12726	1.11169	1.09277	1.07052	1.04508	1.01644
0.60	1.18334	1.16509	1.16631	1.15149	1.13253	1.10948	1.08244	1.05150	1.01679
0.65	1.21620	1.20850	1.19568	1.17782	1.15497	1.12727	1.09478	1.05769	1.01610
0.70	1.25209	1.24289	1.22759	1.20629	1.17907	1.1460[illegible]	1.10747	1.06345	1.01421
0.75	1.29103	1.28014	1.26203	1.23686	1.20470	1.16580	1.12031	1.06855	1.01076
0.80	1.33315	1.32035	1.31247	1.26954	1.23185	1.18629	1.13315	1.07275	1.00550
0.85	1.37852	1.36358	1.33877	1.29049	1.26043	1.20746	1.14576	1.07579	0.99805
0.90	1.42730	1.40993	1.38117	1.34123	1.29043	1.22918	1.15798	1.07741	0.98811
0.95	1.47951	1.45948	1.42627	1.38020	1.32167	1.25126	1.16951	1.07728	0.97528
1.00	1.53536	1.51233	1.47417	1.42127	1.35418	1.27356	1.18021	1.07508	0.95919
1.05	1.59494	1.56855	1.52485	1.46440	1.39180	1.29428	1.18972	1.07046	0.93940
1.10	1.65844	1.62831	1.57849	1.50959	1.42245	1.31811	1.19785	1.06310	0.91600
1.15	1.72593	1.69166	1.63501	1.55681	1.45800	1.33998	1.20420	1.05256	0.88698
1.20	1.79764	1.75876	1.69460	1.60692	1.49441	1.36127	1.20854	1.03844	0.85342
1.25	1.87367	1.82971	1.75717	1.65724	1.53143	1.38174	1.20951	1.02031	0.81423
1.30	1.95427	1.90467	1.82291	1.71039	1.56900	1.40114	1.20965	0.99771	0.76895
1.35	2.03958	1.98376	1.89185	1.76545	1.60694	1.41922	1.20564	0.97015	0.71760
1.40	2.12986	2.06714	1.96396	1.82237	1.64509	1.43564	1.19809	0.93710	0.65779
1.45	2.22520	2.15493	2.03938	1.88106	1.68323	1.45012	1.18653	0.89805	0.59072
1.50	2.32599	2.24735	2.11823	1.94154	1.72109	1.46228	1.17049	0.85242	0.51520
1.55	2.43232	2.34450	2.20043	2.00266	1.75278	1.47177	1.14947	0.79961	0.43050
1.60	2.54455	2.44663	2.28618	2.06738	1.79574	1.47822	1.12295	0.73901	0.33615
1.65	2.66282	2.55384	2.37546	2.13259	1.83175	1.48119	1.09039	0.66996	0.23132
1.70	2.78754	2.66640	2.46339	2.19922	1.86663	1.48026	1.05117	0.59180	0.11537
1.75	2.91887	2.78447	2.55015	2.26707	1.90002	1.47480	1.00468	0.50353	−0.01245
1.80	3.05725	2.90628	2.66531	2.33592	1.93163	1.46464	0.95033	0.40528	−0.15283
1.85	3.20288	3.03803	2.76939	2.40633	1.96105	1.44894	0.88733	0.29545	−0.30650
1.90	3.35621	3.17391	2.87739	2.47731	1.98802	1.42721	0.81506	0.17352	−0.47421
1.95	3.51750	3.31625	2.91750	2.54892	2.01203	1.39887	0.73266	0.02872	−0.65672
2.00	3.68722	3.46521	3.10509	2.62116	2.03272	1.36327	0.63946	−0.10986	−0.85477
2.05	3.86738	3.62108	3.20509	2.69362	2.04957	1.31969	0.53452	−0.27303	−1.06913
2.10	4.05326	3.78413	3.34873	2.76616	2.06208	1.26741	0.41704	−0.45169	−1.30053
2.15	4.25047	3.95463	3.47658	2.83855	2.06970	1.20566	0.28606	−0.64673	−1.54971
2.20	4.45782	4.13282	3.60860	2.91044	2.07200	1.13366	0.14065	−0.85913	−1.81748
2.25	4.67565	4.31907	3.74468	2.98160	2.06814	1.05050	−0.04029	−1.08978	−2.10445
2.30	4.90460	4.51360	3.88496	3.05165	2.05765	0.95526	−0.19741	−1.33970	−2.41147
2.35	5.14503	4.71682	4.02922	3.12027	2.03969	0.84700	−0.39224	−1.60989	−2.73904
2.40	5.39769	4.92896	4.17777	3.18702	2.01362	0.72474	−0.60565	−1.90131	−3.08800
2.45	5.66290	5.15044	4.33024	3.25150	1.97850	0.58741	−0.83882	−2.21497	−3.45879
2.50	5.94163	5.38157	4.48693	3.31327	1.93363	0.43380	−1.09308	−2.55195	−3.85212
2.55	6.23417	5.62271	4.64756	3.37186	1.87801	0.26279	−1.36944	−2.91321	−4.26847
2.60	6.54150	5.87428	4.81216	3.42661	1.81071	0.07311	−1.66944	−3.29976	−4.70825
2.65	6.86398	6.13660	4.98063	3.47701	1.73065	−0.13656	−1.99423	−3.71271	−5.17188
2.70	7.20271	6.41007	5.15296	3.52247	1.63676	−0.36755	−2.34525	−4.15301	−5.65980
2.75	7.55808	6.69508	5.32884	3.56225	1.52778	−0.62135	−2.72383	−4.62166	−6.17205
2.80	7.93137	6.99221	5.50837	3.59555	1.32019	−0.89947	−3.13150	−5.11966	−6.70006
2.85	8.32286	7.30164	5.69118	3.62168	1.25998	−1.20335	−3.56964	−5.64790	−7.27050

x \ τ	0.1	0.2	0.3	0.4	0.5	0.6	0.7	0.8	0.9
2.90	8.73395	7.62392	5.87735	3.63982	1.09831	−1.53490	−4.03986	−6.20758	−7.85677
2.95	9.16523	7.95970	6.06628	3.64889	0.91626	−1.89562	−4.54358	−6.79918	−8.46720
3.00	9.61804	8.30924	6.25816	3.64812	0.71219	−2.28737	−5.08266	−7.42379	−9.10187
3.05	10.09286	8.67300	6.45230	3.63628	0.48441	−2.71210	−5.65827	−8.08225	−9.75992
3.10	10.59134	9.05157	6.64877	3.61226	0.23122	−3.17174	−6.27241	−8.77497	−10.44120
3.15	11.11410	9.44543	6.84114	3.54787	−0.04910	−3.66827	−6.92636	−9.50295	−11.14426
3.20	11.66298	9.85512	7.04664	3.52283	−0.35877	−4.20388	−7.62215	−10.26660	−11.86866
3.25	12.23835	10.28102	7.24713	3.45464	−0.69971	−4.78071	−8.36114	−11.06636	−12.61339
3.30	12.84227	10.72392	7.44833	3.36898	−1.07390	−5.40113	−9.14532	−11.90262	−13.37535
3.35	13.47556	11.18426	7.64928	3.26401	−1.48425	−6.06743	−9.97597	−12.77553	−14.15447
3.40	14.14006	11.66257	7.84989	3.01361	−1.93244	−6.78213	−10.85519	−13.68545	−14.94879
3.45	14.83603	12.15958	8.04889	2.98988	−2.42151	−7.54769	−11.78403	−14.63202	−15.75535
3.50	15.56801	12.67558	8.24614	2.65115	−2.95411	−8.36662	−12.76488	−15.61524	−16.57216
3.55	16.33465	13.21140	8.44048	2.61716	−3.53283	−9.24202	−13.97270	−16.63464	−17.39593
3.60	17.13893	13.76773	8.63136	2.38835	−4.16066	−10.17641	−14.88737	−17.68978	−18.22415
3.65	17.98212	14.34477	8.81742	2.12851	−4.84088	−11.17270	−16.03206	−18.77986	−19.05244
3.70	18.86664	14.94367	8.99814	1.83480	−5.57684	−12.23368	−17.23481	−19.90333	−19.87783
3.75	19.79175	15.56473	9.17198	1.50480	−6.37169	−13.36262	−18.49626	−20.84664	−20.69539
3.80	20.76649	16.20671	9.33806	1.13531	−7.22934	−14.56286	−19.81351	−22.24639	−21.50063
3.85	21.78597	16.87603	9.49596	0.72379	−8.15323	−15.83878	−21.20135	−23.46251	−22.28832
3.90	22.85577	17.56755	9.64113	0.26688	−9.14765	−17.18823	−22.64746	−24.70567	−23.05322
3.95	23.97654	18.28412	9.77500	−0.23899	−10.21636	−18.62054	−24.15656	−25.97289	−23.78846
4.00	25.15252	19.02592	9.89541	−0.79740	−11.36432	−20.13682	−25.73036	−27.26153	−24.48893
4.05	26.39907	19.79378	9.99995	−1.41183	−12.59510	−21.74072	−27.36852	−28.56850	−25.14599
4.10	27.67724	20.58833	10.08684	−2.08684	−13.91437	−23.43566	−29.07209	−29.83992	−25.75306
4.15	29.03144	21.41049	10.15386	−2.82637	−15.32629	−25.22509	−30.84071	−31.22141	−26.14225
4.20	30.45215	22.26023	10.19930	−3.63489	−16.83708	−27.11242	−32.67531	−32.55825	−26.78225
4.25	31.94968	23.14539	10.22286	−4.51840	−18.45585	−29.10972	−34.58377	−34.25622	−27.19385
4.30	33.50162	24.04677	10.21372	−5.47874	−20.17287	−31.19586	−36.53787	−35.22798	−27.50393
4.35	35.13691	24.98438	10.17771	−6.52477	−22.01142	−33.39873	−38.56435	−36.54802	−27.72331
4.40	36.85189	25.95212	10.10876	−7.66079	−23.97053	−35.71425	−40.65418	−37.84981	−27.83514
4.45	38.64871	26.95090	10.00345	−8.89271	−26.05641	−38.14558	−42.80389	−39.12572	−27.82570
4.50	40.53298	27.98123	9.85854	−10.22721	−28.27652	−40.69591	−45.01232	−40.36686	−27.68368
4.55	42.50653	29.04356	9.66967	−11.67090	−30.63688	−43.36920	−47.27606	−41.56483	−27.39441
4.60	44.07849	30.13784	9.43405	−13.23078	−33.14555	−46.16886	−49.59446	−42.70945	−26.94506
4.65	46.74282	31.31717	9.14627	−14.91466	−35.80794	−49.09825	−51.96047	−43.79007	−26.31965
4.70	49.01685	32.42555	8.80110	−16.72984	−38.63368	−52.15940	−54.37392	−44.79618	−25.50435
4.75	51.39724	33.67685	8.39667	−18.68502	−41.62849	−55.35688	−56.82665	−45.71527	−24.48085
4.80	53.89291	34.84668	7.92423	−20.78880	−44.80331	−58.69229	−59.31568	−46.53374	−23.23436
4.85	56.50687	36.10803	7.38001	−23.01831	−48.16363	−62.16867	−61.83397	−47.23746	−21.74530
4.90	59.24635	37.40256	6.75706	−25.47916	−51.71910	−65.78787	−64.37441	−47.81111	−19.99656
4.95	62.11727	38.73259	6.04894	−28.08676	−55.47889	−69.55404	−66.93088	−48.31108	−17.96965
5.00	65.12517	40.09564	5.24962	−30.88247	−59.45236	−73.42258	−69.49465	−48.50659	−15.64346
5.05	68.27512	41.49276	4.35008	−33.87777	−63.64730	−77.52139	−72.05414	−48.59207	−12.99799
5.10	71.57690	42.92367	3.34535	−37.08509	−68.07572	−81.74089	−74.60239	−48.47601	−10.01227
5.15	75.03436	44.38708	2.22358	−40.51586	−72.74439	−86.10097	−77.12430	−48.13932	−6.66642
5.20	78.65823	45.88321	0.97890	−44.09400	−77.66750	−90.61803	−79.61266	−47.56003	−2.93489
5.25	82.45267	47.41136	0.40020	−48.10501	−82.85097	−95.28105	−82.04771	−46.71480	1.20155
5.30	86.48845	48.97055	1.92328	−52.29021	−88.30866	−100.09677	−84.42003	−45.57876	5.76784
5.35	90.59099	51.61283	−3.60148	−56.75600	−94.04925	−105.06010	−86.70939	−44.12764	10.78655
5.40	94.95310	52.17881	−5.44449	−61.51903	−100.08549	−110.16965	−88.90203	−42.33377	16.28256
5.45	99.51992	53.82515	−7.46702	−66.59450	−106.42598	−115.42341	−90.96822	−40.16782	22.27769
5.50	104.30412	55.49706	−9.68017	−72.00180	−113.08626	−120.81621	−92.91108	−37.60121	27.57979
5.55	109.29647	57.18560	−12.73919	−77.75556	−120.05392	−126.32449	−94.67071	−34.59745	35.86160
5.60	114.56230	58.91049	−14.73709	−83.88201	−127.40232	−132.00234	−96.27717	−31.14003	43.50350
5.65	120.05493	60.36435	−17.60923	−90.39443	−135.08134	−137.35854	−97.65817	−27.17860	52.45811
5.70	125.80964	62.40272	−20.73416	−97.31680	−143.12770	−143.68061	−98.80368	−22.68429	60.60800
5.75	131.83250	64.17252	−24.12851	−104.67054	−151.54511	−149.68508	−99.68114	−17.61842	70.10921
5.80	138.14248	65.95152	−27.81148	−112.47794	−160.35530	−155.78391	−100.26170	−11.94539	80.27839
5.85	144.74585	67.73731	−31.79999	−120.76217	−169.55943	−161.96882	−100.50782	−5.62177	91.13242
5.90	151.66325	69.52556	−36.11890	−129.55094	−179.17998	−168.22513	−100.38970	1.38898	102.69858
5.95	158.92101	71.31337	−40.78558	−139.82915	−189.21854	−174.54715	−99.86289	9.13147	115.98864
6.00	166.48399	73.09368	−45.82979	−148.74309	−199.69647	−180.89052	−98.89312	17.65012	128.02690
6.05	174.41745	74.86061	−51.27131	−159.20231	−210.61570	−187.26390	−97.43203	26.98646	142.88448
6.10	182.72458	76.60990	−57.13919	−170.27840	−221.99593	−193.63923	−95.43634	37.19141	156.40324
6.15	191.41568	78.33241	−63.45994	−181.99676	−233.83714	−199.99324	−92.85568	48.32967	171.76695
6.20	200.52012	80.92277	−70.26384	−194.39276	−246.16366	−206.29763	−89.64128	60.38418	187.93280
6.25	210.04462	81.67021	−77.58048	−207.50117	−258.96859	−212.53110	−85.73662	73.47003	204.90074
6.30	220.01596	83.27077	−85.44634	−221.35561	−272.27598	−218.65997	−81.08703	87.61647	222.68165
6.35	230.74236	84.92843	−94.01549	−236.29696	−286.45174	−224.93840	−75.72658	103.00660	241.57928
6.40	241 38666	86.28648	−102.96777	−251.46525	−300.42874	−230.48348	−69.30725	119.29996	260.68616
6.45	253.11772	87.77983	− 112.82901	−268.10668	−315.65198	−236.37709	−62.11614	137.09580	281.22361
6.50	264.75357	88.96289	−123.11134	−284.97725	−330.61937	−241.42368	−53.77017	155.81643	301.85193
6.55	277.61152	90.26295	−134.44401	−303.51245	−346.94439	−246.78524	−44.47161	176.24467	324.00846
6.60	290.35946	91.18137	−146.24010	−322.27367	−362 94656	−251.17514	−33.91000	197 60130	346.11653

TABLE 3

Function $\Phi_9(z) = \mathrm{ch}\, z \sin \gamma z$, where $z = \bar{\alpha}\eta$

z \ γ	0.1	0.2	0.3	0.4	0.5	0.6	0.7	0.8	0.9
0	0	0	0	0	0	0	0	0	0
0.05	0.00501	0.01000	0.01502	0.02002	0.02503	0.03004	0.03504	0.04004	0.04503
0.10	0.01001	0.02002	0.03004	0.04003	0.05004	0.06003	0.07002	0.08000	0.09000
0.15	0.01517	0.03034	0.04549	0.06064	0.07577	0.09090	0.10600	0.12106	0.13610
0.20	0.02040	0.04080	0.06116	0.08151	0.10183	0.12211	0.14234	0.16252	0.18290
0.25	0.02578	0.05155	0.07727	0.10139	0.12859	0.15413	0.17958	0.20491	0.22942
0.30	0.03136	0.06268	0.09395	0.12514	0.15621	0.18715	0.21791	0.24848	0.27883
0.35	0.03713	0.07421	0.11118	0.14805	0.18471	0.22116	0.25732	0.29319	0.32869
0.40	0.04323	0.08639	0.12941	0.17224	0.21478	0.25697	0.29876	0.34007	0.38083
0.45	0.04962	0.09913	0.14844	0.19746	0.24607	0.29419	0.34172	0.38854	0.43459
0.50	0.05636	0.11257	0.16851	0.22403	0.27897	0.33323	0.38666	0.43912	0.49048
0.55	0.06350	0.12680	0.18972	0.25208	0.31423	0.37430	0.43381	0.49200	0.54870
0.60	0.07108	0.14191	0.21223	0.28179	0.35033	0.41760	0.48339	0.54695	0.60950
0.65	0.07916	0.15799	0.23615	0.31333	0.38916	0.46337	0.53561	0.60559	0.67300
0.70	0.08779	0.17515	0.26165	0.34688	0.43040	0.51181	0.59072	0.66673	0.73947
0.75	0.09701	0.19348	0.28884	0.38260	0.48067	0.56315	0.64915	0.73103	0.80901
0.80	0.10687	0.21308	0.31791	0.42071	0.52082	0.61760	0.71043	0.79871	0.88187
0.85	0.11744	0.23406	0.34899	0.46139	0.57046	0.67541	0.77547	0.86995	0.95814
0.90	0.12881	0.25657	0.38225	0.50483	0.62335	0.73681	0.83570	0.94495	1.03797
0.95	0.14098	0.28069	0.41787	0.55127	0.67971	0.80201	0.91709	1.02389	1.12145
1.00	0.15405	0.30656	0.45602	0.60091	0.73980	0.87128	0.99408	1.10694	1.20874
1.05	0.16808	0.33433	0.49689	0.65396	0.80382	0.94485	1.07546	1.19424	1.29985
1.10	0.18317	0.36412	0.54067	0.71069	0.87212	1.02300	1.16152	1.28600	1.39493
1.15	0.19938	0.39557	0.58759	0.77132	0.94484	1.10593	1.25236	1.38228	1.49391
1.20	0.21675	0.43039	0.63784	0.83659	1.02237	1.19931	1.34829	1.48327	1.59693
1.25	0.23543	0.46719	0.69167	0.90536	1.10489	1.28722	1.44944	1.58905	1.70384
1.30	0.25549	0.50668	0.74932	0.97930	1.19277	1.38610	1.55603	1.69971	1.81472
1.35	0.27703	0.54902	0.81102	1.05827	1.28623	1.49083	1.66825	1.81536	1.92940
1.40	0.30014	0.59442	0.87075	1.14254	1.38565	1.60165	1.78632	1.93602	2.04785
1.45	0.32496	0.64306	0.94766	1.23241	1.49125	1.71886	1.91032	2.06173	2.16984
1.50	0.35194	0.69518	1.02323	1.32826	1.60350	1.84271	2.04053	2.19254	2.29536
1.55	0.38006	0.75101	1.10335	1.43044	1.72259	1.97348	2.17702	2.32838	2.42390
1.60	0.41064	0.81079	1.19022	1.53926	1.84897	2.11143	2.31998	2.46926	2.55545
1.65	0.44339	0.87475	1.28235	1.65512	1.98290	2.25687	2.46946	2.61507	2.68909
1.70	0.47849	0.94322	1.38073	1.87852	2.12486	2.41004	2.62573	2.76570	2.82597
1.75	0.51609	1.01642	1.48565	1.90959	2.27513	2.57120	2.78871	2.92116	2.96413
1.80	0.55633	1.00467	1.59767	2.04900	2.43417	2.74066	2.95859	3.08093	3.10371
1.85	0.59941	1.17805	1.71705	2.19719	2.60229	2.91866	3.13536	3.24510	3.24403
1.90	0.64547	1.26770	1.84431	2.35454	2.78005	3.10545	3.31913	3.41332	3.38468
1.95	0.69476	1.36316	1.97987	2.52160	2.96770	3.30133	3.50975	3.58526	3.52478
2.00	0.74744	1.46508	2.12420	2.69885	3.16578	3.50652	3.70746	3.76058	3.66382
2.05	0.80376	1.57384	2.27802	2.88681	3.37463	3.72125	3.91192	3.93888	3.80057
2.10	0.86392	1.68988	2.44158	3.08602	3.59486	3.94576	4.12326	4.11961	3.93498
2.15	0.92822	1.81368	2.61562	3.29711	3.82676	4.18030	4.34118	4.30233	4.06527
2.20	0.99685	1.94566	2.80068	3.52067	4.07133	4.25502	4.56576	4.48637	4.18941
2.25	1.07016	2.08636	2.99733	3.75730	4.32771	4.68011	4.79647	4.67114	4.31020
2.30	1.14838	2.23627	3.20639	4.00761	4.50777	4.94579	5.03384	4.85578	4.42248
2.35	1.23183	2.39600	3.42833	4.27237	4.88141	5.22222	5.27587	5.03960	4.52616
2.40	1.32089	2.56609	3.66414	4.55220	5.17930	5.50949	5.52383	5.22139	4.61994
2.45	1.41584	2.74722	3.91439	4.84789	5.49175	5.80767	5.77667	5.38499	4.70219
2.50	1.51713	2.94000	4.18001	5.16013	5.81941	6.11689	6.03410	5.57608	4.77235
2.55	1.62508	3.14514	4.46109	5.48980	6.16272	6.43724	6.29731	5.74634	4.82563
2.60	1.74018	3.36339	4.76051	5.83759	6.52235	6.76860	6.55992	5.91023	4.86326
2.65	1.86272	3.59550	5.07722	6.20452	6.89854	7.11106	6.82699	6.06640	4.88219
2.70	1.99340	3.84241	5.41296	6.59130	7.29201	7.46443	7.09596	6.21329	4.88047
2.75	2.13248	4.10483	5.76855	6.99892	7.70313	7.82870	7.36575	6.34938	4.85568
2.80	2.28072	4.38377	6.14531	7.42828	8.13265	8.20354	7.63550	6.42419	4.80581
2.85	2.43845	4.68011	6.54416	7.88038	8.58070	8.58894	7.90405	6.58162	4.72807

γ s	0.1	0.2	0.3	0.4	0.5	0.6	0.7	0.8	0.9
2.90	2.60631	4.09497	7.01212	8.35625	9.04813	8.98442	8.17040	6.67944	4.62027
2.95	2.78504	5.32946	7.41330	8.85698	9.53509	9.38967	8.43291	6.74765	4.47931
3.00	2.97519	5.68460	7.88630	9.38348	10.04239	9.80439	8.69050	6.80030	4.30279
3.05	3.17747	6.06174	8.40741	9.93695	10.57013	10.22730	8.94124	6.82963	4.08726
3.10	3.39272	6.46204	8.91522	10.51849	11.11905	10.65962	9.18402	6.83272	3.83013
3.15	3.62280	6.88673	9.47419	11.12942	11.68923	11.09903	9.41633	6.80712	3.52800
3.20	3.86501	7.33759	10.06510	11.77086	12.28137	11.54515	9.63667	6.74979	3.17757
3.25	4.12362	7.81576	10.68938	12.44395	12.89545	11.99711	9.84244	6.65746	2.76630
3.30	4.39876	8.32296	11.34891	13.15014	13.53227	12.45403	10.03188	6.52702	2.31789
3.35	4.69105	8.86085	12.04510	13.89050	14.19129	12.91464	10.20170	6.35494	1.80145
3.40	5.01693	9.43106	12.78058	14.66066	14.87365	13.37783	10.35018	6.13763	1.22240
3.45	5.33208	10.03573	13.55646	15.47992	15.57878	13.84198	10.47372	5.87128	0.57672
3.50	5.68282	10.67654	14.37580	16.33169	16.30749	14.30582	10.58948	5.55173	0.13938
3.55	6.05520	11.35654	15.23956	17.22329	17.05884	14.76745	10.63396	5.17474	—0.92993
3.60	6.45104	12.07506	16.14931	18.15639	17.83390	15.22488	10.66408	4.73605	—1.79923
3.65	6.87121	12.83747	17.11200	19.13232	18.63143	15.67631	10.65544	4.23084	—2.75126
3.70	7.31775	13.64494	18.12539	20.15263	19.45247	16.11940	10.60448	3.65462	—3.79000
3.75	7.79141	14.52132	19.19315	21.21891	20.29548	16.55134	10.50681	3.00195	—4.92028
3.80	8.29413	15.40548	20.31858	22.33293	21.15715	16.96991	10.35775	2.26793	—6.14546
3.85	8.82835	16.36428	21.50589	23.40209	22.04784	17.37203	10.15251	1.44687	—7.47058
3.90	9.39500	17.37900	22.75298	24.70987	22.95586	17.75412	9.88827	0.53352	—8.89930
3.95	9.99607	18.45298	24.06772	25.97627	23.88354	18.11346	9.55316	—0.47824	—10.43586
4.00	10.62437	19.58983	25.45236	27.29649	24.83137	18.44562	9.14798	—1.59398	—12.08444
4.05	11.31131	20.79251	26.90921	28.67270	25.79851	18.74711	8.66419	—2.82051	—13.84876
4.10	12.02942	22.06496	28.44287	30.10630	26.77913	19.01332	8.09597	—4.16372	—15.73292
4.15	12.79100	23.41074	30.05552	31.59861	27.77640	19.23955	7.43599	—5.62999	—17.73992
4.20	13.59906	24.83423	31.75283	33.15189	28.78862	19.42109	6.67780	—7.22642	—19.87432
4.25	14.45965	26.34727	33.54641	34.77736	29.82023	19.55775	5.81528	—8.96175	—22.14415
4.30	15.36444	27.93141	35.41337	36.44720	30.84535	19.62729	4.83596	—10.83586	—24.53475
4.35	16.32743	29.61448	37.38454	38.19239	31.88537	19.64163	3.73663	—12.86318	—27.06657
4.40	17.34920	31.39345	39.45749	40.00451	32.93147	19.58455	2.50703	—15.04787	—29.73649
4.45	18.43200	33.27360	41.63407	41.88585	33.97798	19.45324	1.13856	—17.39791	—32.54482
4.50	19.57979	35.26091	43.92118	43.83700	35.02414	19.23813	—0.37857	—19.91965	—35.49498
4.55	20.79590	37.36032	46.32206	45.85973	36.06161	18.93191	—2.05375	—22.62109	—38.58500
4.60	22.08526	39.57886	48.84427	47.95529	37.09697	18.52565	—3.89670	—25.50886	—41.81798
4.65	23.45114	41.92254	51.49085	50.12536	38.11425	18.10657	—5.91796	—28.59039	—45.19112
4.70	24.89904	44.39814	54.26891	52.37107	39.11529	17.37749	—8.12907	—31.87302	—48.70458
4.75	26.43264	47.01280	57.18267	54.69280	40.09226	16.61533	—10.54092	—35.36335	—52.35493
4.80	28.05744	49.77343	60.24044	57.09250	41.04049	15.71358	—13.16533	—39.06824	—56.14161
4.85	29.77811	52.68911	63.44551	59.56963	41.95315	14.66102	—16.01324	—42.99430	—60.05827
4.90	31.60168	55.76609	66.80650	62.12564	42.82406	13.41497	—19.10081	—47.14769	—64.06083
4.95	33.53285	59.01621	70.33054	64.76305	43.64643	12.05342	—22.43383	—51.53568	—68.26434
5.00	35.57848	62.44545	74.02368	67.47911	44.41243	10.47251	—26.03137	—56.16209	—72.54245
5.05	37.74339	66.06497	77.89192	70.27463	45.11185	8.68769	—29.90528	—61.03382	—76.92302
5.10	40.03759	69.88495	81.94593	73.15075	45.73757	6.68414	—34.07026	—66.15413	—81.40054
5.15	42.46527	73.91524	85.18846	76.10606	46.27788	4.44630	—38.53973	—71.52785	—85.95998
5.20	45.03665	78.16697	90.63344	79.13952	46.72434	1.95689	—43.32810	—77.15816	—90.59175
5.25	47.75722	82.65277	95.28385	82.25162	47.06354	—0.60135	—48.40664	—83.04916	—95.27623
5.30	50.63939	87.38509	100.15287	85.43977	47.28367	—3.84656	—53.92099	—89.20018	—100.00462
5.35	53.68948	92.37488	105.24334	88.70284	47.37108	—7.19770	—59.75513	—95.61516	—104.75155
5.40	56.91811	97.63780	110.57152	92.03831	47.31330	—10.87681	—65.97160	—102.29185	—109.50210
5.45	60.33435	103.18709	116.14032	95.44425	47.09250	—14.90262	—72.57999	—109.22960	—114.22818
5.50	63.95008	109.03777	121.96506	98.91837	46.69534	—19.30040	—79.60328	—116.42637	—118.91003
5.55	67.76486	115.18706	128.02845	102.43947	46.09436	—24.21423	—87.03568	—123.85921	—123.49784
5.60	71.82488	161.70706	134.40917	106.05187	45.29569	—29.29840	—94.94125	—131.58047	—128.02296
5.65	76.10719	128.55961	141.05011	109.70232	44.53431	—34.94838	—103.28721	—139.52487	—132.39191
5.70	80.63961	135.78146	147.99033	113.40351	42.95968	—41.06783	—112.11090	—147.70341	—136.59289
5.75	85.43245	143.39178	155.23061	117.14874	41.38561	—47.68520	—121.42021	—156.10564	—140.66144
5.80	90.50621	151.41070	162.79293	120.92873	39.51245	—54.82858	—131.20694	—164.65584	—144.32736
5.85	95.87047	159.85935	170.67927	124.73804	37.31084	—62.52528	—141.56516	—173.52835	—147.77376
5.90	101.54686	168.75991	178.90985	128.56898	34.75548	—70.80867	—152.43166	—182.51462	—150.88572
5.95	107.54760	178.13375	187.49164	132.40923	31.81720	—79.70995	—163.84076	—191.66148	—153.60215
6.00	113.86041	188.00704	196.44078	136.25065	28.48611	—89.26320	—175.81132	—200.94105	—155.87778
6.05	120.60993	198.40542	205.76382	140.08107	24.66655	—99.50171	—188.34540	—210.33368	—157.64792
6.10	127.70991	209.35357	215.70485	143.88794	20.38918	—110.46182	—201.46854	—219.80676	—158.85069
6.15	135.09903	220.88173	225.60174	147.65368	15.59430	—122.17877	—215.17741	—229.32805	—159.43494
6.20	143.15404	233.01706	236.14356	151.36574	10.24429	—134.69104	—229.48896	—238.86109	—159.31874
6.25	151.54263	245.79282	247.11376	155.00815	4.29693	—148.03825	—244.40454	—248.36736	—158.42968
6.30	160.41509	259.24161	258.53386	158.56081	—2.28983	—162.26119	—259.93321	—257.80393	—156.69565
6.35	170.01148	273.74609	270.75383	162.21269	—9.57294	—177.61825	—276.42594	—264.60020	—154.22759
6.40	179.72337	288.30975	282.78142	165.32624	—17.56806	—193.50657	—292.85399	—276.28706	—150.36333
6.45	190.43458	304.35324	296.07320	168.68285	—26.38906	—210.85911	—310.60286	—285.55051	—145.75911
6.50	201.26899	320.45286	308.94568	171.44064	—35.98424	—228.73275	—328.19493	—292.81035	—139.60024
6.55	213.24250	333.22089	323.20682	174.42065	—46.58147	—248.27300	—347.21743	—302.45527	—132.49976
6.60	225.35119	356.05136	337.20348	176.72456	—57.98074	—268.33229	—365.98986	—309.91302	—123.67632

TABLE 4

Function $\Phi_4(z) = \operatorname{sh} z \, \sin \gamma z$, where $z = \bar{\alpha}\eta$

z \ γ	0.1	0.2	0.3	0.4	0.5	0.6	0.7	0.8	0.9
0	0	0	0	0	0	0	0	0	0
0.05	0.00025	0.00050	0.00075	0.00100	0.00125	0.00150	0.00175	0.00200	0.00225
0.10	0.00100	0.00200	0.00301	0.00401	0.00501	0.00601	0.00701	0.00801	0.00901
0.15	0.00226	0.00452	0.00677	0.00903	0.01128	0.01354	0.01578	0.01808	0.02027
0.20	0.00403	0.00805	0.01207	0.01609	0.02010	0.02410	0.02809	0.03208	0.03601
0.25	0.00631	0.01262	0.01892	0.02522	0.03149	0.03775	0.04398	0.05019	0.05636
0.30	0.00913	0.01826	0.02737	0.03645	0.04551	0.05452	0.06348	0.07238	0.08122
0.35	0.01250	0.02498	0.03743	0.04984	0.06219	0.07446	0.08664	0.09871	0.11066
0.40	0.01643	0.03282	0.04917	0.06544	0.08160	0.09763	0.11351	0.12921	0.14469
0.45	0.02093	0.04182	0.06262	0.08331	0.10382	0.12412	0.14417	0.16392	0.18335
0.50	0.02604	0.05202	0.07787	0.10353	0.12892	0.15399	0.17868	0.20293	0.22666
0.55	0.03178	0.06347	0.09496	0.12617	0.15728	0.18734	0.21713	0.24626	0.27464
0.60	0.03817	0.07621	0.11398	0.15133	0.18814	0.22427	0.25960	0.29399	0.32733
0.65	0.04525	0.09032	0.13500	0.17912	0.22247	0.26559	0.30619	0.34620	0.38474
0.70	0.05305	0.10586	0.15813	0.20964	0.26012	0.30932	0.35701	0.40295	0.44691
0.75	0.06162	0.12289	0.18346	0.24301	0.30530	0.35768	0.41231	0.46431	0.51384
0.80	0.07097	0.14149	0.21110	0.27937	0.34585	0.41011	0.47175	0.53038	0.58560
0.85	0.08116	0.16176	0.24117	0.31886	0.39423	0.46676	0.53590	0.60120	0.66214
0.90	0.09226	0.18378	0.27380	0.36161	0.44650	0.52777	0.60476	0.67687	0.74350
0.95	0.10430	0.20765	0.30913	0.40782	0.50284	0.59331	0.67844	0.75745	0.82962
1.00	0.11732	0.23348	0.34729	0.45765	0.56343	0.66356	0.75709	0.84304	0.92057
1.05	0.13140	0.26138	0.38847	0.51127	0.62843	0.73870	0.84081	0.93367	1.01624
1.10	0.14663	0.29148	0.43280	0.56891	0.69813	0.81891	0.92980	1.02944	1.11664
1.15	0.16305	0.32401	0.48051	0.63075	0.77265	0.90433	1.02413	1.13037	1.25307
1.20	0.18070	0.35880	0.53174	0.69704	0.85230	0.99531	1.12400	1.23653	1.33128
1.25	0.19971	0.39631	0.58673	0.76801	0.93727	1.09193	1.22954	1.34797	1.44553
1.30	0.22016	0.43662	0.64571	0.84389	1.02784	1.19444	1.34087	1.46468	1.56378
1.35	0.24214	0.47987	0.70888	0.92498	1.12423	1.30306	1.45814	1.58672	1.68639
1.40	0.26573	0.52627	0.77650	1.01154	1.22679	1.41802	1.58152	1.71406	1.81306
1.45	0.29106	0.57598	0.84881	1.10386	1.33570	1.53957	1.71106	1.84668	1.94351
1.50	0.31820	0.62904	0.92617	1.20228	1.45140	1.66793	1.84698	1.98457	2.07764
1.55	0.34729	0.68627	1.00677	1.30711	1.57407	1.80333	1.98933	2.12764	2.23753
1.60	0.37879	0.74791	1.09791	1.41988	1.70557	1.94768	2.14005	2.27776	2.35726
1.65	0.41185	0.81252	1.19112	1.53737	1.84183	2.09631	2.29377	2.42903	2.49778
1.70	0.44759	0.88229	1.29154	1.66355	1.98761	2.25437	2.45612	2.58706	2.64343
1.75	0.48584	0.95683	1.39855	1.79764	2.14175	2.42046	2.62522	2.74981	2.79035
1.80	0.52674	1.03635	1.51269	1.94001	2.30469	2.59488	2.80121	2.91704	2.93861
1.85	0.57048	1.12149	1.63419	2.09117	2.47672	2.77782	2.98406	3.08851	3.08749
1.90	0.61722	1.21222	1.76360	2.25150	2.65839	2.96955	3.17387	3.26394	3.23656
1.95	0.66719	1.30907	1.90131	2.42154	2.84994	3.17033	3.37049	3.44300	3.38492
2.00	0.72055	1.41237	2.04787	2.60176	3.05189	3.38038	3.57409	3.62530	3.53202
2.05	0.77755	1.52252	2.20374	2.79268	3.26459	3.59992	3.78436	3.81045	3.67665
2.10	0.83840	1.63995	2.36944	2.99484	3.48864	3.82917	4.00143	3.99789	3.81872
2.15	0.90336	1.76511	2.54559	3.20884	3.72431	4.06838	4.22496	4.18715	3.95643
2.20	0.97267	1.89846	2.73274	3.43527	3.97258	4.31769	4.45501	4.37755	4.08779
2.25	1.04665	2.04052	2.93146	3.67473	4.23261	4.57727	4.69106	4.56849	4.21548
2.30	1.12552	2.19176	3.14257	3.92784	4.50626	4.84735	4.93316	4.75913	4.33445
2.35	1.20963	2.35281	3.36653	4.19535	4.79341	5.12806	5.18076	4.94875	4.44456
2.40	1.29982	2.46953	3.60432	4.47788	5.09474	5.41955	5.43365	5.13634	4.54451
2.45	1.39491	2.70661	3.85652	4.77623	5.41057	5.72181	5.69128	5.30538	4.63268
2.50	1.49683	2.90065	4.12406	5.09106	5.74152	6.03501	5.95334	5.50145	4.70748
2.55	1.60538	3.10703	4.40761	5.42326	6.08603	6.35923	6.22099	5.67670	4.76714
2.60	1.72106	3.32648	4.70627	5.77353	6.45077	6.69433	6.48793	5.84537	4.80989
2.65	1.84422	3.55978	5.02878	6.14289	6.83001	7.04041	6.75917	6.00613	4.88389
2.70	1.97547	3.80785	5.36428	6.53202	7.22644	7.39730	7.03217	6.15742	4.83850
2.75	2.11512	4.07141	5.72159	6.94195	7.64042	7.76497	7.30579	6.29769	4.81615
2.80	2.26392	4.35147	6.10003	7.37355	8.07273	8.14310	7.57925	6.42509	4.77040
2.85	2.42217	4.64886	6.50047	7.82777	8.52342	8.53160	7.85128	6.53768	4.69650

z \ γ	0.1	0.2	0.3	0.4	0.5	0.6	0.7	0.8	0.9
2.90	2.59058	4.96482	6.92449	8.30580	8.99352	8.93019	8.13014	6.63368	4.59238
2.95	2.76982	5.30034	7.37280	8.80858	9.48297	9.33837	8.38683	6.71078	4.45483
3.00	2.96048	5.65649	7.84730	9.33705	9.99272	9.75590	8.64752	6.76666	4.28144
3.05	3.16325	6.03461	8.36978	9.89247	10.52282	10.18152	8.90122	6.79906	4.06896
3.10	3.37898	6.43586	8.87910	10.47588	11.07401	10.61644	9.14682	6.80504	3.81462
3.15	3.60835	6.86148	9.43946	11.08862	11.64638	11.05834	9.38181	6.78217	3.51506
3.20	3.85219	7.31324	10.03170	11.73180	12.24061	11.50684	9.60469	6.72740	3.16703
3.25	4.11124	7.79229	10.65728	12.40659	12.85672	11.96108	9.81289	6.63746	2.76700
3.30	4.38681	8.30034	11.31807	13.11441	13.49551	12.42019	10.00463	6.50928	2.31159
3.35	4.67951	8.83906	12.01548	13.85634	14.15639	12.88289	10.17661	6.33932	1.79702
3.40	5.00576	9.41007	12.75213	14.63403	14.84065	13.34805	10.32715	6.12397	1.21968
3.45	5.32135	10.01552	13.52915	15.44874	15.54740	13.81410	10.45262	5.85948	0.57556
3.50	5.67247	10.65709	14.34941	16.30193	16.27778	14.27976	10.55023	5.54161	−0.13912
3.55	6.04522	11.33682	15.21444	17.19490	17.03071	14.74310	10.61643	5.16621	−0.92840
3.60	6.44142	12.05707	16.12704	18.12930	17.80729	15.20216	10.64817	4.72899	−1.79655
3.65	6.86193	12.82013	17.08890	19.10649	18.60628	15.65515	10.64106	4.22512	−2.74754
3.70	7.30881	13.62827	18.10325	20.12802	19.42871	16.09971	10.59152	3.65016	−3.78537
3.75	7.78279	14.48402	19.17192	21.19544	20.27304	16.53304	10.49520	2.99863	−4.91484
3.80	8.28613	15.39007	20.29826	22.31059	21.13596	16.95293	10.34739	2.26566	−6.13962
3.85	8.82036	16.34947	21.48442	23.47485	22.02788	17.35631	10.14332	1.44556	−7.46382
3.90	9.38731	17.36476	22.73933	24.68969	22.93704	17.73957	9.87817	0.53308	−8.89201
3.95	9.98866	18.43931	24.04988	25.95702	23.86584	18.10004	9.54602	−0.47789	−10.42813
4.00	10.62724	19.57670	25.43530	27.27818	24.81472	18.43325	9.14185	−1.59291	−12.07633
4.05	11.30444	20.77989	26.89297	28.65540	25.78094	18.73579	8.65896	−2.81880	−13.84040
4.10	12.02282	22.05284	28.42725	30.06977	26.76443	19.00288	8.09152	−4.16143	−15.72428
4.15	12.78480	23.39911	30.04059	31.68292	27.76260	19.22999	7.43230	−5.62710	−17.73110
4.20	13.59295	24.82307	31.73856	33.13699	28.77568	19.41236	6.67480	−7.22317	−19.86539
4.25	14.44964	26.32903	33.52319	34.75329	29.79960	19.54421	5.81126	−8.95554	−22.12882
4.30	15.35879	27.92118	35.40033	36.43378	30.83400	19.62006	4.83418	−10.83187	−24.52572
4.35	16.32199	29.60462	37.37210	38.17967	31.87475	19.63404	3.73539	−12.85889	−27.05756
4.40	17.34398	31.38399	39.44560	39.99246	32.92155	19.57865	2.50627	−15.04334	−29.72753
4.45	18.42697	33.26452	41.62271	41.87442	33.96871	19.44793	1.13825	−17.39317	−32.53594
4.50	19.57496	35.25221	43.91034	43.82618	35.01549	19.23339	−0.37847	−19.91473	−35.48622
4.55	20.79078	37.35197	46.31171	45.84948	36.05376	18.92768	−2.05329	−22.61694	−38.57638
4.60	22.08080	39.57086	48.83440	47.94560	37.06947	18.52211	−3.89591	−25.50371	−41.80953
4.65	23.44685	41.91487	51.48143	50.11620	38.10728	18.00736	−5.91688	−28.58517	−45.18286
4.70	24.89493	44.39080	54.25994	52.36241	39.10882	17.37461	−8.12772	−31.86775	−48.69652
4.75	26.42868	47.00577	57.17411	54.68461	40.08625	16.61284	−10.53934	−35.35806	−52.34710
4.80	28.05318	49.76587	60.23129	57.08332	41.03426	15.71119	−13.16333	−39.06232	−56.13309
4.85	29.77446	52.68266	63.43774	59.56233	41.94801	14.65923	−16.01128	−42.98903	−60.05091
4.90	31.59865	55.76074	66.80009	62.11968	42.81995	13.44368	−19.09696	−47.14317	−64.09497
4.95	33.53372	59.01029	70.32348	64.75653	43.64205	12.05221	−22.43158	−51.53051	−68.25749
5.00	35.57524	62.43977	74.01696	67.47298	44.40839	10.47156	−26.02900	−56.15699	−72.61007
5.05	37.74028	66.05954	77.88556	70.26885	45.10814	8.68697	−29.90282	−61.02880	−76.91670
5.10	40.03462	69.87976	81.93984	73.14581	45.73417	6.68364	−34.06773	−66.14922	−81.39449
5.15	42.46241	73.91028	86.18268	76.10094	46.27475	4.44600	−38.53714	−71.52304	−85.95421
5.20	45.03390	78.16221	90.62792	79.13470	46.72150	1.95677	−43.32546	−77.15346	−90.58623
5.25	47.75459	82.64822	95.27860	82.24709	47.06095	−0.80131	−48.49397	−83.04459	−95.27098
5.30	50.63087	87.38073	100.14788	85.43551	47.28131	−3.84637	−53.91831	−89.19574	−99.99963
5.35	53.68875	92.37019	105.23799	88.69833	47.36868	−7.19733	−59.75210	−95.61030	−104.74623
5.40	56.91579	97.63381	110.59670	92.03456	47.31137	−10.87637	−65.96891	−102.28768	−109.49763
5.45	60.33213	103.18328	116.13603	95.44072	47.09076	−14.90206	−72.57731	−109.22556	−114.22396
5.50	63.94794	109.03412	121.96098	98.91506	46.69378	−19.29975	−80.82406	−116.42247	−118.90605
5.55	67.51612	115.20209	128.04446	102.45231	46.10013	−24.08865	−87.04658	−123.87473	−123.51331
5.60	71.82292	121.70374	134.40549	106.04897	45.29445	−29.29760	−94.93865	−131.57687	−128.01946
5.65	76.10530	128.55643	141.04662	109.69961	44.33370	−34.94752	−103.28465	−139.52141	−132.38863
5.70	80.63800	135.77843	147.98702	113.40098	42.93872	−41.06691	−112.10839	−147.70011	−136.60478
5.75	85.27362	143.38889	155.22747	117.14637	41.38177	−47.68423	−121.41775	−156.10248	−140.65859
5.80	90.50455	151.40793	162.78995	120.92652	39.51172	−54.82757	−131.19874	−164.71558	−144.32472
5.85	95.86888	159.85670	170.67644	124.73597	37.31002	−62.52424	−141.56281	−173.52547	−147.77131
5.90	101.54536	168.75738	178.90717	128.56705	34.75496	−70.82586	−152.42937	−182.51188	−150.88345
5.95	107.54614	178.13134	187.48910	132.40744	31.81677	−79.70877	−163.83854	−191.65855	−153.60007
6.00	113.85901	188.00473	196.43836	136.24917	28.46576	−89.20211	−175.80916	−200.93858	−155.87586
6.05	120.60860	198.40322	205.76154	140.07952	24.60628	−99.50061	−188.34331	−210.33133	−157.64618
6.10	127.70862	209.35145	215.47974	143.88649	20.38897	−110.46070	−201.46650	−219.80454	−158.85600
6.15	135.09780	220.87972	225.59969	147.65234	15.59415	−122.17766	−215.17546	−229.32597	−159.43350
6.20	143.15286	233.01514	236.14162	151.36449	10.24421	−134.68993	−229.48707	−238.85912	−159.34743
6.25	151.54150	245.79099	247.11192	155.00699	4.27100	−148.03721	−244.40282	−248.36551	−158.42845
6.30	160.41400	259.23985	258.53191	158.55974	−7.73562	−162.26010	−258.84232	−257.80219	−156.69459
6.35	170.00452	273.73487	270.74273	162.20604	−9.57255	−177.61097	−276.41461	−267.45539	−154.22127
6.40	179.71043	288.28900	282.76107	165.31433	−17.56480	−193.49264	−292.83290	−276.26717	−150.35251
6.45	190.42762	304.34211	296.06237	168.67668	−26.38810	−210.85140	−310.59151	−285.54008	−145.75378
6.50	201.26807	320.45121	308.94428	171.43987	−35.98408	−228.73171	−328.19344	−293.80902	−139.59961
6.55	213.24162	338.21950	323.20549	174.42014	−46.58128	−248.27198	−347.21600	−302.45053	−132.49713
6.60	225.35036	356.05004	337.20224	176.72390	−57.98052	−268.33130	−365.98851	−309.91188	−123.67586

TABLE 5 $X(\xi) = \sin \mu\xi$. Both beam ends simply supported (case 1)

$\mu_1 = 3.1416$ First term of expansion			$\mu_2 = 6.2832$ Second term of expansion		
$\xi = \frac{x}{b}$	$X = -\left(\frac{b}{\mu_1}\right)^2 X''$	$\frac{b}{\mu_1}X' = -\left(\frac{b}{\mu_1}\right)^3 X'''$	$\xi = \frac{x}{b}$	$X = -\left(\frac{b}{\mu_2}\right)^2 X''$	$\frac{b}{\mu_2}X' = -\left(\frac{b}{\mu_2}\right)^3 X'''$
0.0	0.0000	1.0000	0.0	0.0000	1.0000
0.1	0.3090	0.9511	0.1	0.5878	0.8090
0.2	0.5878	0.8090	0.2	0.9511	0.3090
0.3	0.8090	0.5878	0.3	0.9511	−0.3090
0.4	0.9511	0.3090	0.4	0.5878	−0.8090
0.5	1.0000	0.0000	0.5	0.0000	−1.0000
0.6	0.9511	−0.3090	0.6	−0.5878	−0.8090
0.7	0.8090	−0.5878	0.7	−0.9511	−0.3090
0.8	0.5878	−0.8090	0.8	−0.9511	0.3090
0.9	0.3090	−0.9511	0.9	−0.5878	0.8090
1.0	0.0000	−1.0000	1.0	0.0000	1.0000

$\mu_3 = 9.4248$ Third term of expansion			$\mu_4 = 12.5664$ Fourth term of expansion		
$\xi = \frac{x}{b}$	$X = -\left(\frac{b}{\mu_3}\right)^2 X''$	$\frac{b}{\mu_3}X' = -\left(\frac{b}{\mu_3}\right)^3 X'''$	$\xi = \frac{x}{b}$	$X = -\left(\frac{b}{\mu_4}\right)^2 X''$	$\frac{b}{\mu_4}X' = -\left(\frac{b}{\mu_4}\right)^3 X'''$
0.0	0.0000	1.0000	0.0	0.0000	1.0000
0.1	0.8090	0.5878	0.1	0.9511	0.3090
0.2	0.9511	−0.3090	0.2	0.5878	−0.8090
0.3	0.3090	−0.9511	0.3	−0.5878	−0.8090
0.4	−0.5878	−0.8090	0.4	−0.9511	0.3090
0.5	−1.0000	0.0000	0.5	0.0000	1.0000
0.6	−0.5878	0.8090	0.6	0.9511	0.3090
0.7	0.3090	0.9511	0.7	0.5878	−0.8090
0.8	0.9511	0.3090	0.8	−0.5878	−0.8090
0.9	0.8090	−0.5878	0.9	−0.9511	0.3090
1.0	0.0000	−1.0000	1.0	0.0000	1.0000

TABLE 6

$X(\xi) = \sin\mu\xi - \text{ch}\,\mu\xi - \alpha(\cos\mu\xi - \text{ch}\,\mu\xi)$. Both beam ends built in (case 2)

$\mu_1 = 4.7300$ First term of expansion ($\alpha_1 = 1.01781$)					$\mu_2 = 7.8532$ Second term of expansion ($\alpha_2 = 0.999223$)				
$\xi = \frac{x}{b}$	X	$\frac{b}{\mu_1}X'$	$\left(\frac{b}{\mu_1}\right)^2 X''$	$\left(\frac{b}{\mu_1}\right)^3 X'''$	$\xi = \frac{x}{b}$	X	$\frac{b}{\mu_2}X'$	$\left(\frac{b}{\mu_2}\right)^2 X''$	$\left(\frac{b}{\mu_2}\right)^3 X'''$
0.0	0.0000	0.0000	2.0356	−2.0000	0.0	0.0000	0.0000	1.9984	−2.0000
0.1	0.1925	0.7395	1.0934	−1.9682	0.1	0.4551	0.9569	0.4551	−1.8705
0.2	0.6304	1.0416	0.1989	−1.7792	0.2	1.2053	0.7902	−0.7931	−1.2099
0.3	1.1155	0.9494	−0.5536	−1.3636	0.3	1.5044	−0.0978	−1.3229	−0.1001
0.4	1.4814	0.5570	−1.0591	−0.7431	0.4	1.0351	−1.0506	−0.9665	0.9462
0.5	1.6164	0.0000	−1.2372	0.0000	0.5	0.0000	−1.4530	0.0000	1.3742
0.6	1.4814	−0.5570	−1.0591	0.7431	0.6	−1.0351	−1.0506	0.9665	0.9462
0.7	1.1155	−0.9494	−0.5536	1.3636	0.7	−1.5044	−0.0978	1.3229	−0.1001
0.8	0.6304	−1.0416	0.1989	1.7792	0.8	−1.2053	0.7902	0.7931	−1.2099
0.9	0.1925	−0.7395	1.0934	1.9682	0.9	−0.4551	0.9569	−0.4551	−1.8705
1.0	0.0000	0.0000	2.0356	2.0000	1.0	0.0000	0.0000	−1.9984	−2.0000

$\mu_3 = 10.9960$ Third term of expansion ($\alpha_3 = 1.000034$)					$\mu_4 = 14.1370$ Fourth term of expansion ($\alpha_4 = 0.99900$)				
$\xi = \frac{x}{b}$	X	$\frac{b}{\mu_3}X'$	$\left(\frac{b}{\mu_3}\right)^2 X''$	$\left(\frac{b}{\mu_3}\right)^3 X'''$	$\xi = \frac{x}{b}$	X	$\frac{b}{\mu_4}X'$	$\left(\frac{b}{\mu_4}\right)^2 X''$	$\left(\frac{b}{\mu_4}\right)^3 X'''$
0.0	0.0000	0.0000	2.0000	−2.0000	0.0	0.0000	0.0000	2.0000	−2.0000
0.1	0.7705	1.0120	−0.1047	−1.6777	0.1	1.0711	0.9031	−0.5829	−1.3913
0.2	1.5080	0.1094	−1.2861	−1.3307	0.2	1.3244	−0.6923	−1.2052	0.5730
0.3	0.8671	−1.1817	−0.7924	1.1088	0.3	−0.4075	−1.3644	0.4365	1.3352
0.4	−0.6306	−1.2699	−0.6579	1.2481	0.4	−1.3966	0.1967	1.4033	−0.2042
0.5	−1.4060	0.0000	1.4224	0.0000	0.5	0.0000	1.4123	0.0000	−1.4156
0.6	−0.6306	1.2699	0.6579	−1.2481	0.6	1.3966	0.1967	−1.4033	−0.2042
0.7	0.8671	1.1817	−0.7924	−1.1088	0.7	0.4075	−1.3644	−0.4365	1.3352
0.8	1.5080	−0.1094	−1.2861	1.3307	0.8	−1.3244	−0.6923	1.2052	0.5730
0.9	0.7705	−1.0120	−0.1047	1.5777	0.9	−1.0711	0.9031	0.5829	−1.3913
1.0	0.0000	0.0000	2.0000	2.0000	1.0	0.0000	0.0000	−2.0000	−2.0000

TABLE 7

$X(\xi) = \sin \mu\xi + \operatorname{ch} \mu\xi - \alpha (\cos \mu\xi + \operatorname{ch} \mu\xi)$. Both beam ends free (case 3)

$\mu_1 = 4.7300$ First term of expansion ($\alpha_1 = 1.01781$)					$\mu_2 = 7.8532$ Second term of expansion ($\alpha_2 = 0.999223$)				
$\xi = \frac{x}{b}$	X	$\frac{b}{\mu_1} X'$	$\left(\frac{b}{\mu_1}\right)^2 X''$	$\left(\frac{b}{\mu_1}\right)^3 X'''$	$\xi = \frac{x}{b}$	X	$\frac{b}{\mu_2} X'$	$\left(\frac{b}{\mu_2}\right)^2 X''$	$\left(\frac{b}{\mu_2}\right)^3 X'''$
0.0	−2.0356	2.0000	0.0000	0.0000	0.0	−1.9984	2.0000	0.0000	0.0000
0.1	−1.0934	1.9682	−0.1925	−0.7395	0.1	−0.4551	1.8705	−0.4551	−0.9569
0.2	−0.1989	1.7792	−0.6304	−1.0416	0.2	0.7931	1.2099	−1.2053	−0.7902
0.3	0.5536	1.3636	−1.1155	−0.9494	0.3	1.3229	0.1001	−1.5044	0.0978
0.4	1.0591	0.7431	−1.4814	−0.5570	0.4	0.9665	−0.9462	−1.0351	1.0506
0.5	1.2372	0.0000	−1.6164	0.0000	0.5	0.0000	−1.3742	0.0000	1.4530
0.6	1.0591	−0.7431	−1.4814	0.5570	0.6	−0.9665	−0.9462	1.0351	1.0506
0.7	0.5536	−1.3636	−1.1155	0.9494	0.7	−1.3229	0.1001	1.5044	0.0978
0.8	−0.1989	−1.7792	−0.6304	1.0416	0.8	−0.7931	1.2009	1.2053	−0.7902
0.9	−1.0934	−1.9682	−0.1925	0.7395	0.9	0.4551	1.8705	0.4551	−0.9569
1.0	−2.0356	−2.0000	0.0000	0.0000	1.0	1.9984	2.0000	0.0000	0.0000

$\mu_3 = 10.996$ Third term of expansion ($\alpha_3 = 1.000034$)					$\mu_4 = 14.137$ Fourth term of expansion ($\alpha_4 = 0.999999$)				
$\xi = \frac{x}{b}$	X	$\frac{b}{\mu_3} X'$	$\left(\frac{b}{\mu_3}\right)^2 X''$	$\left(\frac{b}{\mu_3}\right)^3 X'''$	$\xi = \frac{x}{b}$	X	$\frac{b}{\mu_4} X'$	$\left(\frac{b}{\mu_4}\right)^2 X''$	$\left(\frac{b}{\mu_4}\right)^3 X'''$
0.0	−2.0000	2.0000	0.0000	0.0000	0.0	−2.0000	2.0000	0.0000	0.0000
0.1	0.1047	1.6777	−0.7705	−1.0120	0.1	0.5829	1.3913	−1.0711	−0.9031
0.2	1.2861	0.3307	−1.5080	−0.1094	0.2	1.2052	−0.5730	−1.3244	0.6923
0.3	0.7924	−1.1088	−0.8671	1.1817	0.3	−0.4365	−1.3352	0.4075	1.3644
0.4	−0.6579	−1.2481	0.6306	1.2699	0.4	−1.4033	0.2042	1.3966	−0.1967
0.5	−1.4224	0.0000	1.4060	0.0000	0.5	0.0000	1.4156	0.0000	−1.4123
0.6	−0.6579	1.2481	0.6306	−1.2699	0.6	1.4033	0.2042	−1.3966	−0.1967
0.7	0.7924	1.1088	−0.8671	−1.1817	0.7	0.4365	−1.3352	−0.4075	1.3644
0.8	1.2861	−0.3307	−1.5080	0.1094	0.8	−1.2052	−0.5730	1.3244	0.6923
0.9	0.1047	−1.6777	−0.7705	1.0120	0.9	−0.5829	1.3913	1.0711	−0.9031
1.0	−2.0000	−2.0000	0.0000	0.0000	1.0	2.0000	2.0000	0.0000	0.0000

TABLE 8

$X(\xi) = \sin\,\mu\xi - \mathrm{ch}\,\mu\xi - \alpha\,(\cos\mu\xi - \mathrm{ch}\,\mu\xi)$. One beam end built in, the other free (case 4)

$\mu_1 = 1.8751$
First term of expansion ($\alpha_1 = 1.362223$)

$\xi = \frac{x}{b}$	X	$\frac{b}{\mu_1} X'$	$\left(\frac{b}{\mu_1}\right)^2 X''$	$\left(\frac{b}{\mu_1}\right)^3 X'''$
0.0	0.0000	0.0000	2.7244	−2.0000
0.1	0.4560	0.4747	2.3504	−1.9971
0.2	0.1740	0.8813	1.9764	−1.9777
0.3	0.3712	1.2665	1.6107	−1.9276
0.4	0.6262	1.4857	1.2563	−1.8347
0.5	0.9250	1.6898	0.9250	−1.6898
0.6	1.2563	1.8347	0.6262	−1.4857
0.7	1.6107	1.9276	0.3712	−1.2665
0.8	1.9764	1.9777	0.1740	−0.8813
0.9	2.3504	1.9971	0.0456	−0.4747
1.0	2.7244	2.0000	0.0000	0.0000

$\mu_2 = 4.6941$
Second term of expansion ($\alpha_2 = 0.981868$)

$\xi = \frac{x}{b}$	X	$\frac{b}{\mu_2} X'$	$\left(\frac{b}{\mu_2}\right)^2 X''$	$\left(\frac{b}{\mu_2}\right)^3 X'''$
0.0	0.0000	0.0000	1.9637	−2.0000
0.1	0.1816	0.7014	1.0293	−1.9703
0.2	0.5914	0.9728	0.1372	−1.7936
0.3	1.0330	0.8515	−0.6223	−1.4104
0.4	1.3423	0.4227	−1.1579	−0.8443
0.5	1.4014	−0.1895	−1.4014	−0.1895
0.6	1.1579	−0.8443	−1.3423	0.4227
0.7	0.6223	−1.4104	−1.0330	0.3515
0.8	−0.1372	−1.7936	−0.5914	0.9723
0.9	−1.0293	−1.9703	−0.1816	0.7014
1.0	−1.9637	−2.0000	0.0000	0.0000

$\mu_3 = 7.8548$
Third term of expansion ($\alpha_3 = 1.00078$)

$\xi = \frac{x}{b}$	X	$\frac{b}{\mu_3} X'$	$\left(\frac{b}{\mu_3}\right)^2 X''$	$\left(\frac{b}{\mu_3}\right)^3 X'''$
0.0	0.0000	0.0000	2.0016	−2.0000
0.1	0.4560	0.9593	0.4583	−1.8702
0.2	1.2100	0.7945	−0.7904	−1.2066
0.3	1.5137	−0.0699	−1.3158	−0.0916
0.4	1.0547	−1.0327	−0.9501	0.9541
0.5	0.0395	−1.4147	0.0395	1.4147
0.6	−0.9501	−0.9641	1.0547	1.0327
0.7	−1.3158	0.0916	1.5137	0.0699
0.8	−0.7904	1.2066	1.2100	−0.7945
0.9	0.4583	1.8702	0.4560	−0.9593
1.0	2.0016	2.0000	0.0000	0.0000

$\mu_4 = 10.9956$
Fourth term of expansion ($\alpha_4 = 0.999967$)

$\xi = \frac{x}{b}$	X	$\frac{b}{\mu_4} X'$	$\left(\frac{b}{\mu_4}\right)^2 X''$	$\left(\frac{b}{\mu_4}\right)^3 X'''$
0.0	0.0000	0.0000	1.9999	−2.0000
0.1	0.7704	1.0119	−0.1048	−1.6777
0.2	1.5076	0.1090	−1.2863	−0.3309
0.3	0.8661	−1.1826	−0.7933	1.1079
0.4	−0.6334	−1.2725	0.6552	1.2453
0.5	−1.4141	−0.0081	1.4141	−0.0081
0.6	−0.6552	1.2453	0.6334	−1.2725
0.7	0.7933	1.1079	−0.8661	−1.1826
0.8	1.2863	−0.3309	−1.5076	0.1090
0.9	0.1048	−1.6777	−0.7704	1.0119
1.0	−1.9999	−2.0000	0.0000	0.0000

TABLE 9

$X(\xi) = \sin \mu\xi - \alpha \operatorname{ch} \mu\xi$. One beam end built in, the other simply supported (case 5)

$\mu_1 = 3.9266$ First term of expansion ($\alpha_1 = -0.0278749$)					$\mu_2 = 7.0685$ Second term of expansion ($\alpha_2 = 0.00122285$)				
$\xi = \frac{x}{b}$	X	$\frac{b}{\mu_1} X'$	$\left(\frac{b}{\mu_1}\right)^2 X''$	$\left(\frac{b}{\mu_1}\right)^3 X'''$	$\xi = \frac{x}{b}$	X	$\frac{b}{\mu_2} X'$	$\left(\frac{b}{\mu_2}\right)^2 X''$	$\left(\frac{b}{\mu_2}\right)^3 X'''$
0.0	0.0000	1.0279	0.0000	−0.9721	0.0	0.0000	0.9988	0.0000	−1.0012
0.1	0.3939	0.9539	−0.3714	−0.8938	0.1	0.6496	0.7588	−0.6505	−0.7618
0.2	0.7310	0.7443	−0.6826	−0.6705	0.2	0.9854	0.1535	−0.9901	−0.1588
0.3	0.9648	0.4323	−0.8829	−0.3332	0.3	0.8475	−0.5279	−0.8574	0.5178
0.4	1.0642	0.0698	−0.9358	−0.0702	0.4	0.2991	−0.9613	−0.3197	0.9406
0.5	1.0214	−0.2810	−0.8268	0.4834	0.5	−0.3996	−0.9464	0.3579	0.9046
0.6	0.8529	−0.5586	−0.5615	0.8553	0.6	−0.9323	−0.4968	0.8487	0.4132
0.7	0.5995	−0.7052	−0.1657	1.1426	0.7	−1.0569	0.1504	0.8869	−0.3204
0.8	0.3230	−0.6774	0.3198	1.3226	0.8	−0.7555	0.6323	0.4179	−0.9800
0.9	0.0965	−0.4495	0.8539	1.4015	0.9	−0.2714	0.6489	−0.4249	−1.3452
1.0	0.0000	0.0000	1.4136	1.4147	1.0	0.0000	0.0000	−1.4141	−1.4143

$\mu_3 = 10.2102$ Third term of expansion ($\alpha_3 = 0.0000528346$)					$\mu_4 = 13.3520$ Fourth term of expansion ($\alpha_4 = 0.00000224861$)				
$\xi = \frac{x}{b}$	X	$\frac{b}{\mu_3} X'$	$\left(\frac{b}{\mu_3}\right)^2 X''$	$\left(\frac{b}{\mu_3}\right)^3 X'''$	$\xi = \frac{x}{b}$	X	$\frac{b}{\mu_4} X'$	$\left(\frac{b}{\mu_4}\right)^2 X''$	$\left(\frac{b}{\mu_4}\right)^3 X'''$
0.0	0.0000	1.0000	0.0000	−1.0000	0.0	0.0000	1.0000	0.0000	−1.0000
0.1	0.8527	0.5226	−0.8525	−0.5224	0.1	0.9723	0.2336	−0.9723	−0.2336
0.2	0.8912	−0.4537	−0.8908	0.4542	0.2	0.4543	−0.8908	−0.4543	0.8908
0.3	0.0821	−0.9961	−0.0809	0.9972	0.3	−0.7634	−0.6461	0.7632	0.6459
0.4	−0.8051	−0.5895	0.8062	0.5926	0.4	−0.8096	0.5870	0.8092	−0.5874
0.5	−0.9193	0.3869	0.9279	−0.3783	0.5	0.3856	0.9214	−0.3874	−0.9232
0.6	−0.1406	1.0002	0.1645	−0.9763	0.6	0.9845	−0.1588	−0.9912	0.1520
0.7	0.7954	0.0804	−0.7291	−0.6141	0.7	0.0618	−1.0101	−0.0876	0.9843
0.8	1.0424	−0.2188	−0.8586	0.4027	0.8	−1.0004	−0.3601	0.9009	0.2606
0.9	0.4876	−0.7176	0.0223	1.2275	0.0	−0.7064	0.6676	0.3328	−1.0412
1.0	0.0000	0.0000	1.4142	1.4142	1.0	0.0000	0.0000	−1.4145	−1.4139

TABLE 10

$X(\xi) = \sin \mu\xi + \alpha \operatorname{sh} \mu\xi$. One beam end simply supported, the other free (case 6)

$\mu_1 = 3.9266$ First term of expansion ($\alpha_1 = 0.0278749$)					$\mu_2 = 7.0685$ Second term of expansion ($\alpha_2 = 0.00122295$)				
$\xi = \frac{x}{b}$	X	$\frac{b}{\mu_1} X'$	$\left(\frac{b}{\mu_1}\right)^2 X''$	$\left(\frac{b}{\mu_1}\right)^3 X'''$	$\xi = \frac{x}{b}$	X	$\frac{b}{\mu_2} X'$	$\left(\frac{b}{\mu_2}\right)^2 X''$	$\left(\frac{b}{\mu_2}\right)^3 X'''$
0.0	0.0000	0.9721	0.0000	−1.0279	0.0	0.0000	1.0012	0.0000	−0.9988
0.1	0.3714	0.8938	−0.3939	−0.9539	0.1	0.6505	0.7618	−0.6486	−0.7588
0.2	0.6826	0.6705	−0.7310	−0.7443	0.2	0.9901	0.1588	−0.9854	−0.1535
0.3	0.8829	0.3332	−0.9648	−0.4323	0.3	0.8574	−0.5178	−0.8475	0.5279
0.4	0.9358	−0.0702	−1.0642	−0.0698	0.4	0.3197	−0.9406	−0.2991	0.9613
0.5	0.8288	−0.4834	−1.0214	0.2810	0.5	−0.3579	−0.9046	0.3996	0.9484
0.6	0.5615	−0.8553	−0.8529	0.5586	0.6	−0.8487	−0.4132	0.9323	0.4968
0.7	0.1657	−1.1426	−0.5995	0.7052	0.7	−0.8869	0.3204	1.0569	−0.1504
0.8	−0.3198	−1.3226	−0.3230	0.6774	0.8	−0.4179	0.9800	0.7555	−0.6323
0.9	−0.8539	−1.4015	−0.0965	0.4495	0.9	0.4249	1.3452	0.2714	−0.6489
1.0	−1.4136	−1.4147	0.0000	0.0000	1.0	1.4141	1.4143	0.0000	0.0000

$\mu_3 = 10.2102$ Third term of expansion ($\alpha_3 = -0.0000520346$)					$\mu_4 = 13.3520$ Fourth term of expansion ($\alpha_4 = 0.0000022486$)				
$\xi = \frac{x}{b}$	X	$\frac{b}{\mu_3} X'$	$\left(\frac{b}{\mu_3}\right)^2 X''$	$\left(\frac{b}{\mu_3}\right)^3 X'''$	$\xi = \frac{x}{b}$	X	$\frac{b}{\mu_4} X'$	$\left(\frac{b}{\mu_4}\right)^2 X''$	$\left(\frac{b}{\mu_4}\right)^3 X'''$
0.0	0.0000	1.0000	0.0000	−1.0000	0.0	0.0000	1.0000	0.0000	−1.0000
0.1	0.8525	−0.5224	−0.8527	−0.5226	0.1	0.9723	0.2336	−0.9723	−0.2336
0.2	0.8908	−0.4542	−0.8912	0.4537	0.2	0.4543	−0.8908	−0.4543	0.8908
0.3	0.0809	−0.9272	−0.0821	0.9961	0.3	−0.7632	−0.6459	0.7634	0.6461
0.4	−0.8082	−0.5926	0.8051	0.5895	0.4	−0.8092	0.5874	0.8096	−0.5870
0.5	−0.9279	0.3783	0.9193	−0.3869	0.5	0.3874	0.9232	−0.3856	−0.9214
0.6	−0.1645	0.9763	0.1406	−1.0002	0.6	0.9912	−0.1520	−0.9845	0.1588
0.7	0.7291	0.6141	−0.7954	−0.6804	0.7	0.0876	−0.9843	−0.0618	1.0101
0.8	0.8586	−0.4027	−1.0424	0.2188	0.8	−0.9009	−0.2606	1.0004	0.3601
0.9	−0.0223	−1.2275	−0.4876	0.7176	0.9	−0.3328	1.0412	0.7064	−0.6676
1.0	−1.4142	−1.4142	0.0000	0.0000	1.0	1.4145	1.4139	0.0000	0.0000

TABLE 11
Thomson functions

ξ	$u_0(\xi)$	$v_0(\xi)$	$f_0(\xi)$	$g_0(\xi)$	ξ	$u_0(\xi)$	$v_0(\xi)$	$f_0(\xi)$	$g_0(\xi)$
0.00	1.0000	−0.0000	0.5000	− ∞	0.82	0.9929	−0.1680	0.3560	−0.2760
0.02	1.0000	−0.0001	0.4997	−2.5643	0.84	0.9922	−0.1762	0.3514	−0.2641
0.04	1.0000	−0.0004	0.4989	−2.1232	0.86	0.9915	−0.1847	0.3469	−0.2526
0.06	1.0000	−0.0009	0.4978	−1.8653	0.88	0.9906	−0.1934	0.3423	−0.2415
0.08	1.0000	−0.0016	0.4963	−1.6825	0.90	0.9898	−0.2023	0.3377	−0.2308
0.10	1.0000	−0.0025	0.4946	−1.5409	0.92	0.9888	−0.2113	0.3332	−0.2205
0.12	1.0000	−0.0036	0.4926	−1.4254	0.94	0.9878	−0.2206	0.3286	−0.2105
0.14	1.0000	−0.0049	0.4904	−1.3279	0.96	0.9867	−0.2301	0.3241	−0.2008
0.16	1.0000	−0.0064	0.4880	−1.2436	0.98	0.9856	−0.2397	0.3196	−0.1915
0.18	1.0000	−0.0081	0.4854	−1.1695	1.00	0.9844	−0.2496	0.3151	−0.1825
0.20	1.0000	−0.0100	0.4826	−1.1033	1.10	0.9771	−0.3017	0.2929	−0.1419
0.22	1.0000	−0.0121	0.4797	−1.0437	1.20	0.9676	−0.3587	0.2713	−0.1076
0.24	0.9999	−0.0144	0.4767	−0.9894	1.30	0.9554	−0.4204	0.2504	−0.0786
0.26	0.9999	−0.0169	0.4735	−0.9397	1.40	0.9401	−0.4867	0.2302	−0.0542
0.28	0.9999	−0.0196	0.4701	−0.8938	1.50	0.9211	−0.5576	0.2110	−0.0337
0.30	0.9999	−0.0225	0.4667	−0.8513	1.60	0.8979	−0.6327	0.1926	−0.0166
0.32	0.9998	−0.0256	0.4632	−0.8117	1.70	0.8700	−0.7120	0.1752	−0.0023
0.34	0.9998	−0.0289	0.4595	−0.7747	1.80	0.8367	−0.7953	0.1588	0.0094
0.36	0.9997	−0.0324	0.4558	−0.7400	1.90	0.7975	−0.8821	0.1433	0.0189
0.38	0.9997	−0.0361	0.4520	−0.7073	2.00	0.7517	−0.9723	0.1289	0.0265
0.40	0.9996	−0.0400	0.4480	−0.6765	2.20	0.6377	−1.1610	0.1026	0.0371
0.42	0.9995	−0.0441	0.4441	−0.6473	2.4	0.4890	−1.3575	0.0804	0.0429
0.44	0.9994	−0.0484	0.4400	−0.6198	2.6	0.3001	−1.5569	0.0614	0.0446
0.46	0.9993	−0.0529	0.4359	−0.5935	2.8	0.0651	−1.7529	0.0455	0.0447
0.48	0.9992	−0.0576	0.4318	−0.5686	3.0	−0.2214	−1.9376	0.0326	0.0427
0.50	0.9990	−0.0625	0.4275	−0.5449	3.2	−0.5644	−2.1016	0.0220	0.0394
0.52	0.9989	−0.0676	0.4233	−0.5223	3.4	−0.9680	−2.2334	0.0137	0.0356
0.54	0.9987	−0.0729	0.4190	−0.5006	3.6	−1.4353	−2.3199	0.0072	0.0314
0.56	0.9985	−0.0784	0.4146	−0.4800	3.8	−1.9674	−2.3454	0.0022	0.0260
0.58	0.9982	−0.0841	0.4102	−0.4602	4.0	−2.5634	−2.2927	−0.0014	0.0230
0.60	0.9980	−0.0900	0.4058	−0.4413	4.2	−3.2195	−2.1472	−0.0039	0.0192
0.62	0.9977	−0.0961	0.4014	−0.4231	4.4	−3.9283	−1.8726	−0.0056	0.0156
0.64	0.9974	−0.1024	0.3969	−0.4057	4.6	−4.6784	−1.4610	−0.0066	0.0125
0.66	0.9070	−0.1089	0.3924	−0.3889	4.8	−5.4531	−0.8837	−0.0071	0.0097
0.68	0.9967	−0.1156	0.3879	−0.3729	5.0	−6.2301	−0.1160	−0.0071	0.0073
0.70	0.9962	−0.1224	0.3834	−0.3574	5.2	−6.9803	0.8658	−0.0069	0.0053
0.72	0.9958	−0.1295	0.3788	−0.3425	5.4	−7.6674	2.0845	−0.0065	0.0037
0.74	0.9953	−0.1368	0.3743	−0.3282	5.6	−8.2466	3.5597	−0.0059	0.0023
0.76	0.9948	−0.1443	0.3697	−0.3144	5.8	−8.6644	5.3068	−0.0053	0.0012
0.78	0.9942	−0.1520	0.3651	−0.3011	6.0	−8.8583	7.3347	−0.0046	0.0004
0.80	0.9936	−0.1599	0.3606	−0.2883					

TABLE 12

Kinematic and force factors for a circular plate

ξ	$u_0(\xi)$	$v_0(\xi)$	$\theta_1(\xi)$	$\theta_2(\xi)$	$M_1(\xi)$	$M_2(\xi)$	$\overline{M}_1(\xi)$	$\overline{M}_2(\xi)$	$Q_1(\xi)$	$Q_2(\xi)$
$\varphi = 46°$										
0.00	1.0000	0.0000	0.0000	0.0000	−0.0349	0.9994	−0.0174	0.4947	0.0000	0.0000
0.05	1.0000	−0.0006	−0.0009	0.0250	−0.0343	0.9995	−0.0172	0.4997	−0.0249	−0.0017
0.10	1.0000	−0.0024	−0.0016	0.0500	−0.0324	0.9996	−0.0168	0.4997	−0.0499	−0.0034
0.15	1.0002	−0.0056	−0.0024	0.0749	−0.0293	0.9998	−0.0160	0.4998	−0.0748	−0.0050
0.20	1.0003	−0.0100	−0.0030	0.0999	−0.0249	1.0001	−0.0149	0.4999	−0.0998	−0.0065
0.25	1.0005	−0.0156	−0.0034	0.1249	−0.0193	1.0004	−0.0155	0.5000	−0.1248	−0.0077
0.30	1.0007	−0.0225	−0.0035	0.1500	−0.0125	1.0009	−0.0118	0.5001	−0.1498	−0.0088
0.35	1.0009	−0.0306	−0.0034	0.1751	−0.0044	1.0013	−0.0098	0.5002	−0.1748	−0.0095
0.40	1.0010	−0.0400	−0.0030	0.2002	0.0050	1.0018	−0.0074	0.5003	−0.1999	−0.0100
0.45	1.0012	−0.0506	−0.0021	0.2253	0.0157	1.0023	−0.0018	0.5005	−0.2250	−0.0100
0.50	1.0012	−0.0626	−0.0009	0.2504	0.0275	1.0029	−0.0018	0.5006	−0.2501	−0.0097
0.55	1.0012	−0.0770	0.0008	0.2754	0.0406	1.0033	0.0015	0.5008	−0.2753	−0.0069
0.60	1.0011	−0.0900	0.0030	0.3005	0.0551	1.0037	0.0050	0.5009	−0.3004	−0.0065
0.65	1.0011	−0.1058	0.0058	0.3257	0.0708	1.0040	0.0089	0.5010	−0.3257	−0.0056
0.70	1.0006	−0.1227	0.0092	0.3509	0.0877	1.0042	0.0133	0.5012	−0.3510	−0.0030
0.75	1.0000	−0.1404	0.0132	0.3760	0.1058	1.0043	0.0178	0.5013	−0.3762	0.0001
0.80	0.9992	−0.1602	0.0180	0.4012	0.1253	1.0044	0.0227	0.5014	−0.4015	0.0040
0.85	0.9982	−0.1810	0.0236	0.4263	0.1459	1.0039	0.0277	0.5015	−0.4269	0.0089
0.90	0.9969	−0.2029	0.0300	0.4514	0.1680	1.0033	0.0333	0.5015	−0.4522	0.0141
0.95	0.9951	−0.2261	0.0371	0.4764	0.1912	1.0025	0.0391	0.5015	−0.4778	0.0204
1.00	0.9932	−0.2504	0.0453	0.5015	0.2151	1.0012	0.0452	0.5015	−0.4923	0.0276
$\varphi = 47°$										
0.00	1.0000	0.0000	0.0000	0.0000	−0.0698	0.9976	−0.0349	0.4988	0.0000	0.0000
0.05	1.0000	0.0006	−0.0017	0.0249	−0.0692	0.9977	−0.0347	0.4988	−0.0247	−0.0035
0.10	1.0001	0.0024	−0.0034	0.0499	−0.0673	0.9979	−0.0343	0.4989	−0.0495	−0.0069
0.15	1.0004	0.0056	−0.0050	0.0748	−0.0642	0.9984	−0.0335	0.4990	−0.0743	−0.0102
0.20	1.0007	0.0100	−0.0065	0.0999	−0.0599	0.9990	−0.0324	0.4991	−0.0991	−0.0134
0.25	1.0011	0.0156	−0.0077	0.1248	−0.0543	0.9997	−0.0310	0.4993	−0.1240	−0.0165
0.30	1.0016	0.0224	−0.0088	0.1498	−0.0475	1.0006	−0.0293	0.4996	−0.1488	−0.0193
0.35	1.0021	0.0305	−0.0096	0.1750	−0.0395	1.0017	−0.0273	0.4999	−0.1738	−0.0218
0.40	1.0026	0.0399	−0.0100	0.2000	−0.0301	1.0028	−0.0250	0.5001	−0.1989	−0.0239
0.45	1.0029	0.0506	−0.0101	0.2253	−0.0196	1.0040	−0.0224	0.5005	−0.2239	−0.0257
0.50	1.0034	0.0624	−0.0096	0.2504	−0.0077	1.0053	−0.0194	0.5008	−0.2490	−0.0272
0.55	1.0039	0.0756	−0.0089	0.2756	0.0054	1.0067	−0.0162	0.5012	−0.2744	−0.0281
0.60	1.0043	0.0901	−0.0075	0.3010	0.0197	1.0081	−0.0127	0.5016	−0.2997	−0.0286
0.65	1.0048	0.1058	−0.0056	0.3263	0.0354	1.0095	−0.0087	0.5020	−0.3251	−0.0283
0.70	1.0048	0.1227	−0.0031	0.3518	0.0523	1.0109	−0.0045	0.5025	−0.3506	−0.0276
0.75	1.0049	0.1409	0.0000	0.3772	0.0703	1.0124	0.0001	0.5029	−0.3763	−0.0262
0.80	1.0049	0.1604	0.0040	0.4027	0.0898	1.0136	0.0049	0.5034	−0.4019	−0.0242
0.85	1.0045	0.1811	0.0087	0.4283	0.1107	1.0147	0.0101	0.5038	−0.4276	−0.0213
0.90	1.0040	0.2032	0.0140	0.4538	0.1326	1.0157	0.0156	0.5041	−0.4537	−0.0156
0.95	1.0030	0.2265	0.0203	0.4796	0.1559	1.0165	0.0214	0.5045	−0.4796	−0.0131
1.00	1.0018	0.2511	0.0275	0.5052	0.1810	1.0170	0.0265	0.5050	−0.5056	−0.0078
$\varphi = 48°$										
0.00	1.0000	0.0000	0.0000	0.0000	−0.1045	0.9945	−0.0522	0.4977	0.0000	0.0000
0.05	1.0000	0.0006	−0.0026	0.0249	−0.1039	0.9946	−0.0520	0.4977	−0.0244	−0.0052
0.10	1.0002	0.0024	−0.0051	0.0497	−0.1021	0.9950	−0.0516	0.4978	−0.0488	−0.0103
0.15	1.0006	0.0506	−0.0076	0.0746	−0.0990	0.9957	−0.0508	0.4980	−0.0734	−0.0154
0.20	1.0010	0.0099	−0.0100	0.0996	−0.0947	0.9966	−0.0498	0.4982	−0.0979	−0.0203
0.25	1.0016	0.0155	−0.0122	0.1245	−0.0892	0.9977	−0.0484	0.4985	−0.1225	−0.0251
0.30	1.0022	0.0224	−0.0139	0.1495	−0.0825	0.9991	−0.0467	0.4989	−0.1472	−0.0296
0.35	1.0030	0.0304	−0.0157	0.1746	−0.0745	1.0007	−0.0447	0.4993	−0.1720	−0.0339
0.40	1.0038	0.0399	−0.0170	0.1997	−0.0653	1.0024	−0.0424	0.4997	−0.1968	−0.0378
0.45	1.0047	0.0504	−0.0179	0.2250	−0.0548	1.0044	−0.0398	0.5001	−0.2218	−0.0414

ξ	$u_0(\xi)$	$v_0(\xi)$	$\theta_1(\xi)$	$\theta_2(\xi)$	$M_1(\xi)$	$M_2(\xi)$	$\overline{M}_1(\xi)$	$\overline{M}_2(\xi)$	$Q_1(\xi)$	$Q_2(\xi)$
0.50	1.0056	0.0623	−0.0185	0.2501	−0.0431	1.0066	−0.0369	0.5007	−0.2468	−0.0446
0.55	1.0065	0.0755	−0.0185	0.2756	−0.0301	1.0089	−0.0336	0.5014	−0.2721	−0.0473
0.60	1.0074	0.0899	−0.0182	0.3009	−0.0159	1.0113	−0.0301	0.5021	−0.2975	−0.0495
0.65	1.0083	0.1056	−0.0171	0.3265	−0.0003	1.0148	−0.0263	0.5028	−0.3229	−0.0512
0.70	1.0091	0.1226	−0.0155	0.3522	0.0164	1.0164	−0.0220	0.5035	−0.3485	−0.0522
0.75	1.0099	0.1407	−0.0132	0.3778	0.0344	1.0190	−0.0176	0.5042	−0.3743	−0.0527
0.80	1.0105	0.1603	−0.0102	0.4036	0.0539	1.0217	−0.0128	0.5050	−0.4003	−0.0524
0.85	1.0109	0.1812	−0.0064	0.4229	0.0746	1.0242	−0.0076	0.5058	−0.4265	−0.0514
0.90	1.0111	0.2033	0.0001	0.4555	0.0966	1.0268	−0.0022	0.5065	−0.4528	−0.0496
0.95	1.0111	0.2267	0.0035	0.4876	0.1198	1.0293	0.0006	0.5074	−0.4793	−0.0470
1.00	1.0107	0.2514	0.0097	0.5077	0.1444	1.0314	0.0097	0.5082	−0.5059	−0.0435
$\varphi = 49°$										
0.00	1.0000	0.0000	0.0000	0.0000	−0.1392	0.9903	−0.0696	0.4951	0.0000	0.0000
0.05	1.0000	−0.0006	−0.0035	0.0248	−0.1386	0.9905	−0.0695	0.4051	−0.0240	−0.0068
0.10	1.0003	−0.0024	−0.0069	0.0495	−0.1368	0.9910	−0.0690	0.4953	−0.0480	−0.0128
0.15	1.0007	−0.0056	−0.0102	0.0743	−0.1338	0.9918	−0.0682	0.4955	−0.0722	−0.0205
0.20	1.0013	−0.0099	−0.0134	0.0991	−0.1296	0.9930	−0.0672	0.4958	−0.0963	−0.0272
0.25	1.0021	−0.0155	−0.0165	0.1241	−0.1242	0.9946	−0.0658	0.4962	−0.1206	−0.0337
0.30	1.0028	−0.0223	−0.0198	0.1491	−0.1176	0.9964	−0.0642	0.4966	−0.1449	−0.0338
0.35	1.0038	−0.0304	−0.0218	0.1740	−0.1079	0.9985	−0.0622	0.4972	−0.1693	−0.0468
0.40	1.0049	−0.0397	−0.0240	0.1992	−0.1006	1.0009	−0.0600	0.4977	−0.1935	−0.0515
0.45	1.0061	−0.0503	−0.0258	0.2245	−0.0902	1.0036	−0.0574	0.4985	−0.2186	−0.0568
0.50	1.0073	−0.0622	−0.0273	0.2496	−0.0787	1.0066	−0.0545	0.4993	−0.2434	−0.0618
0.55	1.0087	−0.0753	−0.0283	0.2752	−0.0656	1.0098	−0.0513	0.5001	−0.2684	−0.0662
0.60	1.0100	−0.0896	−0.0287	0.3006	−0.0519	1.0133	−0.0479	0.5010	−0.2937	−0.0703
0.65	1.0112	−0.1054	−0.0286	0.3263	−0.0366	1.0169	−0.0440	0.5020	−0.3192	−0.0737
0.70	1.0125	−0.1213	−0.0279	0.3552	−0.0200	1.0207	−0.0400	0.5029	−0.3447	−0.0767
0.75	1.0138	−0.1406	−0.0267	0.3781	−0.0020	1.0245	−0.0355	0.5040	−0.3707	−0.0790
0.80	1.0149	−0.1602	−0.0246	0.4042	0.0171	1.0285	−0.0308	0.5051	−0.3968	−0.0805
0.85	1.0160	−0.1810	−0.0219	0.4306	0.0376	1.0326	−0.0257	0.5063	−0.4231	−0.0814
0.90	1.0168	−0.2032	−0.0182	0.4568	0.0594	1.0367	−0.0202	0.5074	−0.4498	−0.0815
0.95	1.0174	−0.2266	−0.0140	0.4835	0.0826	1.0407	−0.0145	0.5087	−0.4757	−0.0809
1.00	1.0178	−0.2515	−0.0085	0.5100	0.1070	1.0447	−0.0084	0.5099	−0.5038	−0.0795
$\varphi = 50°$										
0.00	1.0000	0.0000	0.0000	0.0000	−0.1736	0.9848	−0.0868	0.4924	0.0000	0.0000
0.05	1.0001	−0.0006	−0.0043	0.0245	−0.1730	0.9850	−0.0867	0.4924	−0.0233	−0.0085
0.10	1.0004	−0.0024	−0.0087	0.0491	−0.1713	0.9856	−0.0862	0.4926	−0.0469	−0.0170
0.15	1.0010	−0.0055	−0.0129	0.0738	−0.1683	0.9866	−0.0855	0.4929	−0.0705	−0.0255
0.20	1.0017	−0.0098	−0.0168	0.0986	−0.1643	0.9881	−0.0845	0.4932	−0.0941	−0.0338
0.25	1.0026	−0.0154	−0.0208	0.1233	−0.1588	0.9829	−0.0831	0.4937	−0.1178	−0.0418
0.30	1.0038	−0.0222	−0.0248	0.1485	−0.1524	0.9922	−0.0815	0.4943	−0.1419	−0.0502
0.35	1.0051	−0.0302	−0.0278	0.1731	−0.1448	0.9994	−0.0796	0.4950	−0.1658	−0.0575
0.40	1.0066	−0.0395	−0.0309	0.1939	−0.1358	0.9980	−0.0774	0.4957	−0.1899	−0.0648
0.45	1.0082	−0.0501	−0.0336	0.2241	−0.1258	1.0014	−0.0749	0.4966	−0.2141	−0.0719
0.50	1.0099	−0.0619	−0.0360	0.2494	−0.1144	1.0052	−0.0721	0.4976	−0.2386	−0.0783
0.55	1.0118	−0.0749	−0.0379	0.2748	−0.1019	1.0093	−0.0690	0.4987	−0.2633	−0.0849
0.60	1.0137	−0.0893	−0.0392	0.3004	−0.0881	1.0138	−0.0655	0.4999	−0.2883	−0.0907
0.65	1.0157	−0.1049	−0.0399	0.3262	−0.0730	1.0184	−0.0618	0.5010	−0.3135	−0.0960
0.70	1.0177	−0.1218	−0.0404	0.3521	−0.0567	1.0228	−0.0577	0.5024	−0.3390	−0.1008
0.75	1.0197	−0.1401	−0.0402	0.3784	−0.0391	1.0285	−0.0534	0.5037	−0.3645	−0.1050
0.80	1.0217	−0.1596	−0.0389	0.4047	−0.0203	1.0338	−0.0487	0.5052	−0.39 1	−0.1071
0.85	1.0236	−0.1805	−0.0371	0.4306		1.0393	−0.0437	0.5066	−0.4176	−0.1113
0.90	1.0254	−0.2027	−0.0345	0.4572		1.0450	−0.0385	0.5082	−0.4443	−0.1135
0.95	1.0271	−0.2263	−0.0311	0.4843		1.0507	−0.0328	0.5099	−0.4714	−0.1147
1.00	1.0285	−0.2511	−0.0267	0.5114		1.0565	−0.0268	0.5116	−0.4990	−0.1153
$\varphi = 51°$										
0.00	1.0000	0.0000	0.0000	0.0000	−0.2079	0.9781	−0.1039	0.4890	−0.0000	0.0000
0.05	1.0001	0.0006	−0.0052	0.0244	−0.2073	0.9783	−0.1038	0.4891	−0.0228	−0.0102
0.10	1.0005	0.0024	−0.0104	0.0489	−0.2056	0.9791	−0.1033	0.4892	−0.0457	−0.0203
0.15	1.0012	0.0055	−0.0154	0.0733	−0.2028	0.9804	−0.1026	0.4896	−0.0686	−0.0303
0.20	1.0021	0.0098	−0.0204	0.0980	−0.1988	0.9832	−0.1016	0.4900	−0.0916	−0.0405
0.25	1.0032	0.0153	−0.0259	0.1227	−0.1936	0.9844	−0.1003	0.4906	−0.1147	−0.0500
0.30	1.0046	0.0220	−0.0297	0.1474	−0.1873	0.9871	−0.0987	0.4913	−0.1380	−0.0596

ξ	$u_0(\xi)$	$v_0(\xi)$	$\theta_1(\xi)$	$\theta_2(\xi)$	$M_1(\xi)$	$M_2(\xi)$	$\overline{M}_1(\xi)$	$\overline{M}_2(\xi)$	$Q_1(\xi)$	$Q_2(\xi)$
0.35	1.0062	0.0300	—0.0340	0.1723	—0.1798	0.9913	—0.0969	0.4921	—0.1614	—0.0690
0.40	1.0080	0.0393	—0.0380	0.1972	—0.1712	0.9947	—0.0948	0.4931	—0.1850	—0.0776
0.45	1.0100	0.0498	—0.0416	0.2224	—0.1613	0.9992	—0.0922	0.4940	—0.2088	—0.0869
0.50	1.0121	0.0615	—0.0449	0.2476	—0.1502	1.0027	—0.0895	0.4952	—0.2330	—0.1008
0.55	1.0144	0.0745	—0.0476	0.2731	—0.1380	1.0087	—0.0865	0.4965	—0.2572	—0.1033
0.60	1.0169	0.0888	—0.0500	0.2987	—0.1245	1.0141	—0.0832	0.4978	—0.2818	—0.1109
0.65	1.0194	0.1044	—0.0517	0.3247	—0.1098	1.0188	—0.0795	0.4993	—0.3069	—0.1181
0.70	1.0221	0.1213	—0.0529	0.3507	—0.0938	1.0259	—0.0755	0.5009	—0.3320	—0.1247
0.75	1.0247	0.1394	—0.0535	0.3770	—0.0766	1.0322	—0.0713	0.5026	—0.3577	—0.1308
0.80	1.0274	0.1590	—0.0534	0.4035	—0.0581	1.0383	—0.0668	0.5044	—0.3836	—0.1362
0.85	1.0300	0.1799	—0.0526	0.4304	—0.0382	1.0448	—0.0619	0.5063	—0.4100	—0.1410
0.90	1.0326	0.2021	—0.0509	0.4509	—0.0170	1.0519	—0.0567	0.5082	—0.4369	—0.1451
0.95	1.0351	0.2256	—0.0486	0.4848	—0.0055	1.0593	—0.0536	0.5102	—0.4641	—0.1484
1.00	1.0433	0.2505	—0.0454	0.5123	—0.0004	1.0668	—0.0453	0.5123	—0.4917	—0.1509
$\varphi = 52^\circ$										
0.00	1.0000	0.0000	0.0000	0.0000	—0.2419	0.9703	—0.1209	0.4851	0.0000	0.0000
0.05	1.0001	0.0006	—0.0060	0.0242	—0.2414	0.9705	—0.1208	0.4852	—0.0200	—0.0117
0.10	1.0006	0.0024	—0.0120	0.0485	—0.2398	0.9714	—0.1204	0.4854	—0.0441	—0.0235
0.15	1.0013	0.0054	—0.0179	0.0729	—0.2369	0.9729	—0.1197	0.4858	—0.0601	—0.0350
0.20	1.0024	0.0153	—0.0238	0.0972	—0.2331	0.9753	—0.1187	0.4863	—0.0886	—0.0466
0.25	1.0038	0.0207	—0.0293	0.1218	—0.2281	0.9775	—0.1175	0.4869	—0.1106	—0.0580
0.30	1.0053	0.0218	—0.0348	0.1463	—0.2219	0.9808	—0.1159	0.4877	—0.1335	—0.0692
0.35	1.0072	0.0298	—0.0399	0.1713	—0.2148	0.9845	—0.1142	0.4887	—0.1518	—0.0802
0.40	1.0093	0.0400	—0.0449	0.1960	—0.2063	0.9888	—0.1121	0.4898	—0.1793	—0.0909
0.45	1.0117	0.0494	—0.0494	0.2210	—0.1968	0.9936	—0.1096	0.4909	—0.2000	—0.1014
0.50	1.0142	0.0610	—0.0536	0.2463	—0.1861	0.9989	—0.1070	0.4923	—0.2259	—0.1115
0.55	1.0169	0.0742	—0.0572	0.2716	—0.1742	1.0051	—0.1040	0.4938	—0.2468	—0.1213
0.60	1.0199	0.0892	—0.0606	0.2973	—0.1612	1.0110	—0.1008	0.4955	—0.2728	—0.1307
0.65	1.0229	0.1038	—0.0633	0.3231	—0.1468	1.0178	—0.0973	0.4972	—0.3013	—0.1369
0.70	1.0262	0.1206	—0.0654	0.3494	—0.1313	1.0250	—0.0935	0.4990	—0.3231	—0.1480
0.75	1.0294	0.1387	—0.0670	0.3758	—0.1145	1.0325	—0.0894	0.5010	—0.3473	—0.1560
0.80	1.0328	0.1582	—0.0680	0.4025	—0.0964	1.0406	—0.0849	0.5031	—0.3741	—0.1633
0.85	1.0362	0.1790	—0.0671	0.4295	—0.0771	1.0489	—0.0801	0.5053	—0.3951	—0.1699
0.90	1.0395	0.2011	—0.0677	0.4569	—0.0464	1.0576	—0.0751	0.5076	—0.4270	—0.1761
0.95	1.0429	0.2247	—0.0663	0.4845	—0.0344	1.0663	—0.0697	0.5100	—0.4547	—0.1814
1.00	1.0477	0.2496	—0.0640	0.5125	—0.0110	1.0756	—0.0640	0.5125	—0.4818	—0.1861
$\varphi = 53^\circ$										
0.00	1.0000	0.0000	0.0000	0.0000	—0.2756	0.9613	—0.1378	0.4806	0.0000	0.0000
0.05	1.0002	0.0006	—0.0069	0.0240	—0.2751	0.9616	—0.1377	0.4807	—0.0200	—0.0132
0.10	1.0007	0.0024	—0.0138	0.0481	—0.2735	0.9626	—0.1373	0.4809	—0.0424	—0.0265
0.15	1.0015	0.0054	—0.0205	0.0722	—0.2708	0.9643	—0.1366	0.4813	—0.0602	—0.0396
0.20	1.0027	0.0096	—0.0272	0.0964	—0.2671	0.9666	—0.1357	0.4819	—0.0852	—0.0527
0.25	1.0043	0.0150	—0.0336	0.1207	—0.2623	0.9696	—0.1345	0.4827	—0.1107	—0.0656
0.30	1.0061	0.0216	—0.0399	0.1451	—0.2564	0.9731	—0.1330	0.4836	—0.1284	—0.0784
0.35	1.0082	0.0295	—0.0459	0.1696	—0.2496	0.9774	—0.1313	0.4846	—0.1520	—0.0909
0.40	1.0107	0.0386	—0.0517	0.1944	—0.2414	0.9822	—0.1293	0.4859	—0.1726	—0.1033
0.45	1.0134	0.0490	—0.0572	0.2193	—0.2322	0.9877	—0.1270	0.4872	—0.1942	—0.1154
0.50	1.0164	0.0606	—0.0622	0.2444	—0.2219	0.9938	—0.1245	0.4888	—0.2178	—0.1272
0.55	1.0196	0.0735	—0.0669	0.2697	—0.2142	1.0005	—0.1216	0.4904	—0.2377	—0.1387
0.60	1.0213	0.0876	—0.0712	0.2954	—0.1978	1.0077	—0.1185	0.4923	—0.2643	—0.1498
0.65	1.0267	0.1030	—0.0749	0.3213	—0.1830	1.0153	—0.1151	0.4943	—0.2826	—0.1604
0.70	1.0305	0.1197	—0.0790	0.3475	—0.1689	1.0237	—0.1113	0.4965	—0.3124	—0.1708
0.75	1.0344	0.1378	—0.0804	0.3741	—0.1527	1.0324	—0.1074	0.4987	—0.3393	—0.1805
0.80	1.0385	0.1571	—0.0824	0.4008	—0.1352	1.0417	—0.1031	0.5011	—0.3626	—0.1898
0.85	1.0427	0.1778	—0.0837	0.4100	—0.1164	1.0515	—0.0986	0.5036	—0.3881	—0.1985
0.90	1.0468	0.1998	—0.0843	0.4557	—0.0964	1.0616	—0.0936	0.5063	—0.4148	—0.2066
0.95	1.0511	0.2234	—0.0840	0.4857	—0.0748	1.0720	—0.0884	0.5091	—0.4390	—0.2141
1.00	1.0553	0.2482	—0.0829	0.5120	—0.0522	1.0829	—0.0829	0.5120	—0.4693	—0.2208
$\varphi = 54^\circ$										
0.00	1.0000	0.0000	0.0000	0.0000	—0.3090	0.9511	—0.1545	0.4755	0.0000	0.0000
0.05	1.0002	0.0006	—0.0077	0.0238	—0.3085	0.9515	—0.1544	0.4756	—0.0202	—0.0149
0.10	1.0008	0.0023	—0.0154	0.0475	—0.3070	0.9525	—0.1540	0.4759	—0.0404	—0.0299
0.15	1.0017	0.0053	—0.0230	0.0714	—0.3045	0.9544	—0.1534	0.4763	—0.0609	—0.0447
0.20	1.0031	0.0095	—0.0305	0.0954	—0.3009	0.9570	—0.1525	0.4770	—0.0813	—0.0595
0.25	1.0048	0.0148	—0.0378	0.1195	—0.2964	0.9603	—0.1513	0.4778	—0.1019	—0.0741
0.30	1.0068	0.0215	—0.0449	0.1437	—0.2907	0.9642	—0.1500	0.4788	—0.1227	—0.0887
0.35	1.0093	0.0292	—0.0519	0.1680	—0.2840	0.9690	—0.1483	0.4800	—0.1438	—0.1030

ξ	$u_0(\xi)$	$v_0(\xi)$	$\theta_1(\xi)$	$\theta_2(\xi)$	$M_1(\xi)$	$M_2(\xi)$	$\overline{M}_1(\xi)$	$\overline{M}_2(\xi)$	$Q_1(\xi)$	$Q_2(\xi)$
0.40	1.0121	0.0382	−0.0581	0.1925	−0.2763	0.9744	−0.1464	0.4814	−0.1655	−0.1173
0.45	1.0151	0.0485	−0.0649	0.2173	−0.2678	0.9804	−0.1442	0.4828	−0.1866	−0.1312
0.50	1.0185	0.0600	−0.0703	0.2424	−0.2578	0.9872	−0.1418	0.4846	−0.2090	−0.1448
0.55	1.0223	0.0727	−0.0765	0.2675	−0.2467	0.9947	−0.1388	0.4865	−0.2309	−0.1584
0.60	1.0262	0.0868	−0.0816	0.2931	−0.2346	1.0028	−0.1362	0.4885	−0.2536	−0.1712
0.65	1.0304	0.1021	−0.0863	0.3191	−0.2214	1.0116	−0.1327	0.4907	−0.2767	−0.1838
0.70	1.0348	0.1187	−0.0905	0.3452	−0.2069	1.0208	−0.1292	0.4931	−0.3003	−0.1962
0.75	1.0393	0.1367	−0.0941	0.3718	−0.1912	1.0307	−0.1254	0.4957	−0.3245	−0.2081
0.80	1.0441	0.1559	−0.0970	0.3987	−0.1744	1.0412	−0.1213	0.4084	−0.3492	−0.2195
0.85	1.0491	0.1765	−0.0994	0.4261	−0.1563	1.0521	−0.1169	0.5012	−0.3745	−0.2304
0.90	1.0541	0.1985	−0.1010	0.4539	−0.1370	1.0639	−0.1123	0.5042	−0.4003	−0.2407
0.95	1.0591	0.2219	−0.1019	0.4821	−0.1163	1.0759	−0.1072	0.5074	−0.4270	−0.2506
1.00	1.0643	0.2466	−0.1019	0.5108	−0.0943	1.0884	−0.1018	0.5107	−0.4542	−0.2597
$\varphi = 55°$										
0.00	1.0000	0.0000	0.0000	0.0000	−0.3420	0.9397	−0.1710	0.4698	0.0000	0.0000
0.05	1.0002	−0.0006	−0.0085	0.0234	−0.3415	0.9401	−0.1709	0.4699	−0.0191	−0.0160
0.10	1.0008	−0.0023	−0.0170	0.0470	−0.3401	0.9412	−0.1705	0.4702	−0.0383	−0.0321
0.15	1.0019	−0.0053	−0.0255	0.0706	−0.3376	0.9433	−0.1699	0.4707	−0.0586	−0.0481
0.20	1.0034	−0.0094	−0.0339	0.0942	−0.3344	0.9461	−0.1691	0.4714	−0.0770	−0.0641
0.25	1.0053	−0.0147	−0.0420	0.1181	−0.3300	0.9496	−0.1680	0.4723	−0.0965	−0.0798
0.30	1.0076	−0.0212	−0.0500	0.1420	−0.3247	0.9539	−0.1667	0.4732	−0.1164	−0.0955
0.35	1.0103	−0.0289	−0.0577	0.1662	−0.3183	0.9592	−0.1652	0.4747	−0.1304	−0.1111
0.40	1.0134	−0.0378	−0.0654	0.1905	−0.3110	0.9651	−0.1634	0.4762	−0.1566	−0.1265
0.45	1.0168	−0.0480	−0.0725	0.2151	−0.3026	0.9719	−0.1613	0.4779	−0.1773	−0.1418
0.50	1.0206	−0.0593	−0.0795	0.2407	−0.2933	0.9794	−0.1590	0.4797	−0.1981	−0.1578
0.55	1.0247	−0.0720	−0.0860	0.2651	−0.2827	0.9875	−0.1563	0.4818	−0.2197	−0.1714
0.60	1.0292	−0.0859	−0.0920	0.2904	−0.2713	0.9965	−0.1535	0.4841	−0.2414	−0.1858
0.65	1.0340	−0.1010	−0.0977	0.3162	−0.2597	1.0061	−0.1504	0.4866	−0.2637	−0.2000
0.70	1.0390	−0.1175	−0.1029	0.3424	−0.2449	1.0165	−0.1471	0.4892	−0.2865	−0.2138
0.75	1.0442	−0.1353	−0.1075	0.3690	−0.2300	1.0275	−0.1434	0.4990	−0.3100	−0.2268
0.80	1.0497	−0.1544	−0.1115	0.3960	−0.2139	1.0392	−0.1395	0.4950	−0.3339	−0.2402
0.85	1.0554	−0.1749	−0.1150	0.4234	−0.1965	1.0516	−0.1353	0.4981	−0.3585	−0.2528
0.90	1.0612	−0.1967	−0.1171	0.4513	−0.1781	1.0645	−0.1308	0.5015	−0.3838	−0.2649
0.95	1.0671	−0.2200	−0.1232	0.4826	−0.1582	1.0780	−0.1261	0.5050	−0.4110	−0.2814
1.00	1.0732	−0.2447	−0.1203	0.5087	−0.1380	1.0922	−0.1210	0.5087	−0.4366	−0.2876
$\varphi = 56°$										
0.00	1.0000	0.0000	0.0000	0.0000	−0.3764	0.9272	−0.1873	0.4636	0.0000	0.0000
0.05	1.0002	−0.0006	−0.0094	0.0232	−0.3760	0.9276	−0.1872	0.4636	−0.0180	−0.0174
0.10	1.0009	−0.0023	−0.0188	0.0464	−0.3746	0.9289	−0.1869	0.4640	−0.0359	−0.0347
0.15	1.0021	−0.0052	−0.0281	0.0698	−0.3724	0.9311	−0.1863	0.4646	−0.0541	−0.0520
0.20	1.0037	−0.0093	−0.0373	0.0930	−0.3692	0.9341	−0.1855	0.4653	−0.0723	−0.0693
0.25	1.0058	−0.0145	−0.0463	0.1162	−0.3652	0.9380	−0.1845	0.4663	−0.0907	−0.0864
0.30	1.0083	−0.0210	−0.0553	0.1403	−0.3601	0.9428	−0.1833	0.4675	−0.1094	−0.1035
0.35	1.0113	−0.0285	−0.0640	0.1642	−0.3542	0.9484	−0.1818	0.4689	−0.1282	−0.1205
0.40	1.0147	−0.0374	−0.0724	0.1882	−0.3472	0.9548	−0.1800	0.4705	−0.1475	−0.1376
0.45	1.0185	−0.0473	−0.0806	0.2125	−0.3394	0.9721	−0.1781	0.4726	−0.1670	−0.1540
0.50	1.0227	−0.0587	−0.0884	0.2372	−0.3306	0.9702	−0.1760	0.4743	−0.1859	−0.1704
0.55	1.0273	−0.0711	−0.0959	0.2622	−0.3207	0.9791	−0.1735	0.4766	−0.2073	−0.1867
0.60	1.0323	−0.0848	−0.1030	0.2875	−0.3099	0.9889	−0.1709	0.4791	−0.2280	−0.2027
0.65	1.0376	−0.0998	−0.1097	0.3131	−0.2979	1.0095	−0.1680	0.4818	−0.2494	−0.2185
0.70	1.0428	−0.1162	−0.1159	0.3392	−0.2849	1.0108	−0.1647	0.4847	−0.2713	−0.2340
0.75	1.0491	−0.1338	−0.1215	0.3658	−0.2708	1.0328	−0.1613	0.4877	−0.2938	−0.2492
0.80	1.0552	−0.1527	−0.1268	0.3928	−0.2555	1.0356	−0.1576	0.4910	−0.3170	−0.2640
0.85	1.0617	−0.1732	−0.1314	0.4204	−0.2391	1.0592	−0.1537	0.4945	−0.3408	−0.2784
0.90	1.0682	−0.1947	−0.1352	0.4482	−0.2215	1.0635	−0.1494	0.4981	−0.3653	−0.2926
0.95	1.0751	−0.2179	−0.1385	0.4768	−0.2025	1.0884	−0.1449	0.5019	−0.3906	−0.3062
1.00	1.0820	−0.2424	−0.1409	0.5060	−0.1823	1.0942	−0.1400	0.5059	−0.4155	−0.3199
$\varphi = 57°$										
0.00	1.0000	0.0000	0.0000	0.0000	−0.4067	0.9135	−0.2033	0.4567	0.0000	0.0000
0.05	1.0002	−0.0006	−0.0102	0.0228	−0.4063	0.9140	−0.2032	0.4568	−0.0167	−0.0186
0.10	1.0010	−0.0022	−0.0203	0.0457	−0.4050	0.9154	−0.2029	0.4572	−0.0335	−0.0373
0.15	1.0023	−0.0051	−0.0304	0.0686	−0.4030	0.9177	−0.2024	0.4577	−0.0503	−0.0558
0.20	1.0041	−0.0091	−0.0404	0.0917	−0.4000	0.9209	−0.2016	0.4585	−0.0674	−0.0743
0.25	1.0063	−0.0143	−0.0502	0.1189	−0.3963	0.9251	−0.2007	0.4596	−0.0845	−0.0928

ξ	$u_0(\xi)$	$v_0(\xi)$	$\theta_1(\xi)$	$\theta_2(\xi)$	$M_1(\xi)$	$M_2(\xi)$	$\overline{M}_1(\xi)$	$\overline{M}_2(\xi)$	$Q_1(\xi)$	$Q_2(\xi)$
0.30	1.0090	−0.0206	−0.0599	0.1382	−0.3916	0.9302	−0.1996	0.4609	−0.1019	−0.1113
0.35	1.0122	−0.0282	−0.0694	0.1619	−0.3860	0.9362	−0.1982	0.4624	−0.1195	−0.1296
0.40	1.0161	−0.0368	−0.0786	0.1857	−0.3795	0.9431	−0.1965	0.4641	−0.1376	−0.1478
0.45	1.0202	−0.0467	−0.0877	0.2097	−0.3722	0.9509	−0.1948	0.4661	−0.1559	−0.1659
0.50	1.0247	−0.0578	−0.0964	0.2342	−0.3640	0.9596	−0.1927	0.4683	−0.1746	−0.1838
0.55	1.0297	−0.0702	−0.1048	0.2589	−0.3548	0.9693	−0.1905	0.4706	−0.1939	−0.2016
0.60	1.0352	−0.0837	−0.1126	0.2840	−0.3446	0.9798	−0.1880	0.4733	−0.2135	−0.2191
0.65	1.0410	−0.0986	−0.1204	0.3095	−0.3334	0.9911	−0.1853	0.4762	−0.2337	−0.2365
0.70	1.0473	−0.1147	−0.1276	0.3355	−0.3211	1.0034	−0.1823	0.4792	−0.2546	−0.2538
0.75	1.0538	−0.1322	−0.1343	0.3620	−0.3079	1.0164	−0.1790	0.4826	−0.2761	−0.2707
0.80	1.0607	−0.1509	−0.1405	0.3889	−0.2936	1.0303	−0.1756	0.4863	−0.2982	−0.2873
0.85	1.0677	−0.1711	−0.1460	0.4164	−0.2782	1.0450	−0.1719	0.4898	−0.3210	−0.3037
0.90	1.0757	−0.1926	−0.1510	0.4444	−0.2615	1.0606	−0.1679	0.4938	−0.3447	−0.3197
0.95	1.0829	−0.2154	−0.1555	0.4731	−0.2436	1.0770	−0.1637	0.4980	−0.3690	−0.3353
1.00	1.0908	−0.2399	−0.1590	0.5023	−0.2245	1.0941	−0.1591	0.5023	−0.3942	−0.3506
$\varphi = 58°$										
0.00	1.0000	0.0000	0.0000	0.0000	−0.4384	0.8988	−0.2192	0.4494	0.0000	0.0000
0.05	1.0003	−0.0006	−0.0110	0.0225	−0.4380	0.8993	−0.2191	0.4495	−0.0153	−0.0197
0.10	1.0010	−0.0022	−0.0219	0.0449	−0.4369	0.9007	−0.2188	0.4499	−0.0309	−0.0395
0.15	1.0025	−0.0050	−0.0328	0.0676	−0.4349	0.9032	−0.2183	0.4505	−0.0463	−0.0592
0.20	1.0044	−0.0090	−0.0435	0.0903	−0.4323	0.9067	−0.2177	0.4514	−0.0621	−0.0789
0.25	1.0068	−0.0140	−0.0542	0.1131	−0.4287	0.9111	−0.2168	0.4545	−0.0778	−0.0986
0.30	1.0098	−0.0203	−0.0648	0.1361	−0.4245	0.9165	−0.2158	0.4538	−0.0939	−0.1180
0.35	1.0133	−0.0277	−0.0751	0.1594	−0.4194	0.9229	−0.2145	0.4554	−0.1103	−0.1375
0.40	1.0173	−0.0362	−0.0852	0.1829	−0.4134	0.9302	−0.2130	0.4573	−0.1270	−0.1570
0.45	1.0218	−0.0400	−0.0951	0.2067	−0.4066	0.9386	−0.2113	0.4594	−0.1441	−0.1763
0.50	1.0268	−0.0570	−0.1047	0.2308	−0.3989	0.9478	−0.2094	0.4617	−0.1615	−0.1955
0.55	1.0322	−0.0691	−0.1141	0.2554	−0.3904	0.9581	−0.2074	0.4643	−0.1795	−0.2147
0.60	1.0382	−0.0825	−0.1265	0.2802	−0.3810	0.9693	−0.2051	0.4670	−0.1979	−0.2337
0.65	1.0446	−0.0971	−0.1316	0.3055	−0.3706	0.9814	−0.2025	0.4701	−0.2170	−0.2525
0.70	1.0514	−0.1130	−0.1398	0.3314	−0.3593	0.9945	−0.1998	0.4734	−0.2355	−0.2712
0.75	1.0585	−0.1303	−0.1476	0.3577	−0.3470	1.0085	−0.1968	0.4769	−0.2568	−0.2898
0.80	1.0661	−0.1488	−0.1549	0.3620	−0.3336	1.0235	−0.1936	0.4807	−0.2778	−0.3082
0.85	1.0741	−0.1687	−0.1617	0.4120	−0.3192	1.0392	−0.1902	0.4847	−0.2996	−0.3762
0.90	1.0823	−0.1901	−0.1679	0.4400	−0.3037	1.0561	−0.1864	0.4889	−0.3221	−0.3440
0.95	1.0908	−0.2127	−0.1734	0.4687	−0.2870	1.0737	−0.1825	0.4934	−0.3455	−0.3617
1.00	1.0996	−0.2369	−0.1784	0.4986	−0.2691	1.0922	−0.1783	0.4081	−0.3695	−0.3790
$\varphi = 59°$										
0.00	1.0000	0.0000	0.0000	0.0000	−0.4695	0.8829	−0.2347	0.4414	0.0000	0.0000
0.05	1.0003	−0.0005	−0.0117	0.0221	−0.4692	0.8834	−0.2346	0.4415	−0.0140	−0.0207
0.10	1.0011	−0.0022	−0.0235	0.0441	−0.4681	0.8850	−0.2344	0.4419	−0.0280	−0.0414
0.15	1.0026	−0.0050	−0.0351	0.0664	−0.4664	0.8874	−0.2339	0.4426	−0.0421	−0.0622
0.20	1.0050	−0.0088	−0.0466	0.0887	−0.4639	0.8912	−0.2333	0.4435	−0.0564	−0.0829
0.25	1.0073	−0.0140	−0.0582	0.1112	−0.4607	0.8958	−0.2325	0.4446	−0.0709	−0.1035
0.30	1.0107	−0.0200	−0.0695	0.1338	−0.4568	0.9015	−0.2316	0.4461	−0.0856	−0.1241
0.35	1.0143	−0.0272	−0.0807	0.1567	−0.4522	0.9083	−0.2304	0.4477	−0.1006	−0.1448
0.40	1.0186	−0.0356	−0.0917	0.1799	−0.4467	0.9161	−0.2290	0.4497	−0.1158	−0.1654
0.45	1.0234	−0.0452	−0.1024	0.2034	−0.4406	0.9248	−0.2276	0.4519	−0.1315	−0.1859
0.50	1.0288	−0.0560	−0.1129	0.2272	−0.4336	0.9346	−0.2258	0.4543	−0.1476	−0.2063
0.55	1.0355	−0.0680	−0.1232	0.2514	−0.4258	0.9455	−0.2240	0.4571	−0.1641	−0.2268
0.60	1.0411	−0.0811	−0.1331	0.2761	−0.4172	0.9573	−0.2219	0.4600	−0.1813	−0.2471
0.65	1.0481	−0.0955	−0.1427	0.3011	−0.4076	0.9702	−0.2195	0.4633	−0.1989	−0.2673
0.70	1.0554	−0.1112	−0.1519	0.3268	−0.3973	0.9840	−0.2170	0.4667	−0.2172	−0.2875
0.75	1.0632	−0.1282	−0.1608	0.3528	−0.3860	0.9989	−0.2143	0.4704	−0.2361	−0.3075
0.80	1.0715	−0.1466	−0.1691	0.3796	−0.3738	1.0147	−0.2113	0.4744	−0.2558	−0.3275
0.85	1.0801	−0.1662	−0.1769	0.4069	−0.3603	1.0317	−0.2082	0.4787	−0.2763	−0.3472
0.90	1.0893	−0.1873	−0.1843	0.4349	−0.3460	1.0495	−0.2048	0.4832	−0.2975	−0.3668
0.95	1.0986	−0.2097	−0.1910	0.4636	−0.3306	1.0683	−0.2012	0.4879	−0.3197	−0.3863
1.00	1.1083	−0.2336	−0.1972	0.4929	−0.3140	1.0881	−0.1973	0.4929	−0.3427	−0.4056
$\varphi = 60°$										
0.00	1.0000	0.0000	0.0000	0.0000	−0.5000	0.8660	−0.2500	0.4330	0.0000	0.0000
0.05	1.0003	−0.0005	−0.0125	0.0216	−0.4957	0.8664	−0.2499	0.4331	−0.0125	−0.0108
0.10	1.0012	−0.0022	−0.0250	0.0432	−0.4988	0.8680	−0.2497	0.4335	−0.0250	−0.0216
0.15	1.0028	−0.0049	−0.0374	0.0650	−0.4973	0.8708	−0.2493	0.4342	−0.0377	−0.0324
0.20	1.0050	−0.0087	−0.0498	0.0870	−0.4950	0.8745	−0.2488	0.4352	−0.0505	−0.0433

ξ	$u_0(\xi)$	$v_0(\xi)$	$\theta_1(\xi)$	$\theta_2(\xi)$	$M_1(\xi)$	$M_2(\xi)$	$\overline{M}_1(\xi)$	$\overline{M}_2(\xi)$	$Q_1(\xi)$	$Q_2(\xi)$
0.25	1.0078	-0.0136	-0.0620	0.1090	-0.4921	0.8793	-0.2481	0.4364	-0.0634	-0.0541
0.30	1.0112	-0.0196	-0.0741	0.1312	-0.4886	0.8853	-0.2472	0.4379	-0.0766	-0.0649
0.35	1.0152	-0.0267	-0.0862	0.1537	-0.4839	0.8924	-0.2462	0.4396	-0.0901	-0.0757
0.40	1.0198	-0.0350	-0.0979	0.1765	-0.4796	0.9005	-0.2449	0.4416	-0.1040	-0.0865
0.45	1.0250	-0.0444	-0.1096	0.1996	-0.4740	0.9097	-0.2436	0.4439	-0.1182	-0.0974
0.50	1.0307	-0.0550	-0.1210	0.2232	-0.4678	0.9200	-0.2420	0.4465	-0.1328	-0.1082
0.55	1.0371	-0.0667	-0.1322	0.2471	-0.4607	0.9314	-0.2404	0.4494	-0.1479	-0.1190
0.60	1.0440	-0.0797	-0.1430	0.2768	-0.4530	0.9438	-0.2385	0.4525	-0.1636	-0.1298
0.65	1.0514	-0.0939	-0.1535	0.2962	-0.4444	0.9573	-0.2365	0.4558	-0.1798	-0.1405
0.70	1.0593	-0.1093	-0.1633	0.3215	-0.4350	0.9719	-0.2341	0.4595	-0.1966	-0.1513
0.75	1.0678	-0.1261	-0.1736	0.3476	-0.4237	0.9876	-0.2317	0.4634	-0.2142	-0.1621
0.80	1.0767	-0.1441	-0.1832	0.3741	-0.4135	1.0043	-0.2289	0.4676	-0.2324	-0.1728
0.85	1.0861	-0.1635	-0.1921	0.4012	-0.4015	1.0222	-0.2261	0.4721	-0.2514	-0.1835
0.90	1.0959	-0.1842	-0.2000	0.4290	-0.3884	1.0410	-0.2230	0.4768	-0.2713	-0.1941
0.95	1.1061	-0.2064	-0.2086	0.4576	-0.3743	1.0611	-0.2198	0.4816	-0.2920	-0.2047
1.00	1.1167	-0.2300	-0.2161	0.4870	-0.3591	1.0821	-0.2162	0.4871	-0.3138	-0.2153
$\varphi = 61°$										
0.00	1.0000	0.0000	0.0000	0.0000	-0.5299	0.8480	-0.2649	0.4240	0.0000	0.0000
0.05	1.0003	-0.0005	-0.0132	0.0218	-0.5296	0.8486	-0.2648	0.4241	-0.0109	-0.0225
0.10	1.0013	-0.0021	-0.0265	0.0425	-0.5288	0.8502	-0.2646	0.4246	-0.0220	-0.0449
0.15	1.0030	-0.0048	-0.0396	0.0638	-0.5274	0.8531	-0.2643	0.4253	-0.0331	-0.0674
0.20	1.0053	-0.0085	-0.0528	0.0852	-0.5255	0.8570	-0.2638	0.4262	-0.0443	-0.0899
0.25	1.0083	-0.0132	-0.0658	0.1069	-0.5230	0.8620	-0.2632	0.4275	-0.0558	-0.1124
0.30	1.0119	-0.0192	-0.0788	0.1287	-0.5199	0.8682	-0.2625	0.4290	-0.0675	-0.1350
0.35	1.0161	-0.0262	-0.0915	0.1508	-0.5163	0.8755	-0.2616	0.4309	-0.0794	-0.1576
0.40	1.0210	-0.0343	-0.1042	0.1732	-0.5120	0.8840	-0.2604	0.4330	-0.0917	-0.1802
0.45	1.0265	-0.0435	-0.1167	0.1959	-0.5071	0.8936	-0.2593	0.4354	-0.1043	-0.2028
0.50	1.0327	-0.0539	-0.1290	0.2170	-0.5015	0.9043	-0.2579	0.4380	-0.1174	-0.2254
0.55	1.0395	-0.0654	-0.1410	0.2425	-0.4954	0.9161	-0.2565	0.4410	-0.1309	-0.2482
0.60	1.0468	-0.0781	-0.1529	0.2665	-0.4885	0.9292	-0.2548	0.4442	-0.1450	-0.2708
0.65	1.0547	-0.0921	-0.1644	0.2910	-0.4808	0.9433	-0.2529	0.4477	-0.1597	-0.2937
0.70	1.0633	-0.1073	-0.1757	0.3161	-0.4725	0.9586	-0.2509	0.4516	-0.1750	-0.3165
0.75	1.0722	-0.1236	-0.1865	0.3418	-0.4634	0.9749	-0.2488	0.4557	-0.1930	-0.3393
0.80	1.0819	-0.1414	-0.1972	0.3681	-0.4535	0.9926	-0.2463	0.4600	-0.2077	-0.3621
0.85	1.0919	-0.1605	-0.2073	0.3950	-0.4425	1.0112	-0.2439	0.4647	-0.2262	-0.3851
0.90	1.1026	-0.1809	-0.2170	0.4227	-0.4308	1.0311	-0.2411	0.4697	-0.2435	-0.4081
0.95	1.1136	-0.2027	-0.2260	0.4511	-0.4182	1.0521	-0.2382	0.4749	-0.2617	-0.4309
1.00	1.1252	-0.2260	-0.2349	0.4805	-0.4045	1.0742	-0.2350	0.4805	-0.2829	-0.4539
$\varphi = 62°$										
0.00	1.0000	0.0000	0.0000	0.0000	-0.5592	0.8290	-0.2796	0.4145	0.0000	0.0000
0.05	1.0003	-0.0005	-0.0132	0.0207	-0.5590	0.8296	-0.2795	0.4146	-0.0094	-0.0232
0.10	1.0013	-0.0020	-0.0265	0.0415	-0.5583	0.8313	-0.2794	0.4151	-0.0188	-0.0464
0.15	1.0030	-0.0046	-0.0396	0.0624	-0.5571	0.8342	-0.2791	0.4158	-0.0283	-0.0695
0.20	1.0053	-0.0083	-0.0527	0.0834	-0.5555	0.8383	-0.2787	0.4168	-0.0380	-0.0928
0.25	1.0083	-0.0129	-0.0658	0.1045	-0.5533	0.8435	-0.2782	0.4181	-0.0477	-0.1161
0.30	1.0119	-0.0187	-0.0788	0.1259	-0.5507	0.8499	-0.2775	0.4197	-0.0578	-0.1394
0.35	1.0161	-0.0256	-0.0916	0.1476	-0.5475	0.8574	-0.2768	0.4216	-0.0682	-0.1629
0.40	1.0211	-0.0338	-0.1043	0.1695	-0.5438	0.8662	-0.2758	0.4238	-0.0788	-0.1862
0.45	1.0266	-0.0426	-0.1160	0.1918	-0.5396	0.8760	-0.2748	0.4262	-0.0899	-0.2098
0.50	1.0327	-0.0527	-0.1363	0.2144	-0.5348	0.8871	-0.2736	0.4290	-0.1013	-0.2334
0.55	1.0395	-0.0640	-0.1415	0.2376	-0.5295	0.8994	-0.2724	0.4320	-0.1133	-0.2571
0.60	1.0468	-0.0765	-0.1535	0.2612	-0.5235	0.9125	-0.2709	0.4355	-0.1257	-0.2809
0.65	1.0549	-0.0902	-0.1653	0.2864	-0.5169	0.9275	-0.2693	0.4391	-0.1387	-0.3047
0.70	1.0634	-0.1050	-0.1768	0.3103	-0.5096	0.9434	-0.2676	0.4430	-0.1524	-0.3287
0.75	1.0725	-0.1212	-0.1881	0.3354	-0.5017	0.9604	-0.2657	0.4473	-0.1667	-0.3528
0.80	1.0822	-0.1385	-0.1989	0.3615	-0.4931	0.9785	-0.2637	0.4518	-0.1817	-0.3770
0.85	1.0924	-0.1572	-0.2094	0.3881	-0.4835	0.9981	-0.2615	0.4567	-0.1976	-0.4013
0.90	1.1031	-0.1774	-0.2195	0.4155	-0.4732	1.0186	-0.2590	0.4618	-0.2163	-0.4256
0.95	1.1143	-0.1987	-0.2293	0.4439	-0.4621	1.0406	-0.2565	0.4672	-0.2318	-0.4501
1.00	1.1261	-0.2216	-0.2387	0.4729	-0.4500	1.0037	-0.2538	0.4729	-0.2503	-0.4748
$\varphi = 63°$										
0.00	1.0000	0.0000	0.0000	0.0000	-0.5878	0.8090	-0.2939	0.4045	0.0000	0.0000
0.05	1.0004	-0.0005	-0.0147	0.0202	-0.5876	0.8096	-0.2939	0.4046	-0.0077	-0.0238
0.10	1.0014	-0.0020	-0.0294	0.0405	-0.5870	0.8114	-0.2937	0.4051	-0.0156	-0.0475
0.15	1.0033	-0.0045	-0.0440	0.0609	-0.5861	0.8143	-0.2935	0.4058	-0.0234	-0.0714
0.20	1.0059	-0.0081	-0.0586	0.0814	-0.5847	0.8185	-0.2931	0.4069	-0.0315	-0.0953
0.25	1.0092	-0.0126	-0.0732	0.1020	-0.5830	0.8238	-0.2927	0.4082	-0.0396	-0.1192

ξ	$u_0(\xi)$	$v_0(\xi)$	$\theta_1(\xi)$	$\theta_2(\xi)$	$M_1(\xi)$	$M_2(\xi)$	$\overline{M}_1(\xi)$	$\overline{M}_2(\xi)$	$Q_1(\xi)$	$Q_2(\xi)$
0.30	1.0132	−0.0183	−0.0877	0.1229	−0.5808	0.8304	−0.2922	0.4098	−0.0480	−0.1432
0.35	1.0179	−0.0250	−0.1021	0.1441	−0.5783	0.8392	−0.2910	0.4118	−0.0567	−0.1672
0.40	1.0234	−0.0328	−0.1162	0.1656	−0.5754	0.8471	−0.2907	0.4140	−0.0657	−0.1924
0.45	1.0295	−0.0415	−0.1305	0.1874	−0.5720	0.8573	−0.2899	0.4165	−0.0751	−0.2158
0.50	1.0364	−0.0515	−0.1414	0.2096	−0.5684	0.8687	−0.2889	0.4194	−0.0849	−0.2402
0.55	1.0440	−0.0625	−0.1583	0.2324	−0.5643	0.8813	−0.2879	0.4226	−0.0951	−0.2646
0.60	1.0523	−0.0747	−0.1719	0.2555	−0.5597	0.8952	−0.2867	0.4260	−0.1059	−0.2894
0.65	1.0612	−0.0880	−0.1853	0.2793	−0.5548	0.9103	−0.2854	0.4297	−0.1171	−0.3143
0.70	1.0709	−0.1072	−0.1987	0.3036	−0.5495	0.9266	−0.2839	0.4338	−0.1291	−0.3392
0.75	1.0810	−0.1185	−0.2117	0.3287	−0.5437	0.9442	−0.2823	0.4381	−0.1417	−0.3644
0.80	1.0919	−0.1355	−0.2244	0.3543	−0.5376	0.9681	−0.2806	0.4428	−0.1550	−0.3898
0.85	1.1035	−0.1538	−0.2368	0.3807	−0.5310	0.9862	−0.2787	0.4478	−0.1691	−0.4154
0.90	1.1156	−0.1735	−0.2489	0.4078	−0.5239	1.0047	−0.2767	0.4531	−0.1839	−0.4412
0.95	1.1284	−0.1945	−0.2607	0.4359	−0.5165	1.0273	−0.2746	0.4587	−0.1997	−0.4672
1.00	1.1417	−0.2169	−0.2721	0.4647	−0.5085	1.0513	−0.2722	0.4647	−0.2163	−0.4933
					$\varphi = 64°$					
0.00	1.0000	−0.0000	−0.0000	0.0000	−0.6157	0.7880	−0.3078	0.3940	0.0000	0.0000
0.05	1.0004	−0.0005	−0.0154	0.0197	−0.6156	0.7886	−0.3078	0.3941	−0.0060	−0.0242
0.10	1.0015	−0.0019	−0.0308	0.0395	−0.6145	0.7904	−0.3077	0.3946	−0.0121	−0.0485
0.15	1.0035	−0.0044	−0.0461	0.0593	−0.6143	0.7934	−0.3075	0.3954	−0.0183	−0.0729
0.20	1.0061	−0.0079	−0.0615	0.0793	−0.6133	0.7977	−0.3072	0.3964	−0.0246	−0.0972
0.25	1.0096	−0.0123	−0.0768	0.0994	−0.6119	0.8032	−0.3069	0.3978	−0.0310	−0.1217
0.30	1.0136	−0.0178	−0.0919	0.1198	−0.6103	0.8098	−0.3065	0.3994	−0.0378	−0.1462
0.35	1.0186	−0.0243	−0.1071	0.1405	−0.6083	0.8178	−0.3060	0.4014	−0.0447	−0.1709
0.40	1.0245	−0.0319	−0.1221	0.1615	−0.6060	0.8270	−0.3054	0.4037	−0.0520	−0.1957
0.45	1.0310	−0.0405	−0.1371	0.1828	−0.6034	0.8374	−0.3047	0.4063	−0.0596	−0.2206
0.50	1.0383	−0.0501	−0.1519	0.2046	−0.6006	0.8490	−0.3040	0.4093	−0.0677	−0.2458
0.55	1.0463	−0.0610	−0.1667	0.2268	−0.5974	0.8620	−0.3031	0.4124	−0.0761	−0.2709
0.60	1.0549	−0.0729	−0.1812	0.2496	−0.5937	0.8761	−0.3021	0.4159	−0.0851	−0.2965
0.65	1.0643	−0.0859	−0.1958	0.2728	−0.5899	0.8916	−0.3011	0.4198	−0.0946	−0.3222
0.70	1.0745	−0.1001	−0.2099	0.2968	−0.5858	0.9083	−0.2999	0.4239	−0.1047	−0.3481
0.75	1.0853	−0.1158	−0.2239	0.3213	−0.5811	0.9254	−0.2986	0.4284	−0.1153	−0.3743
0.80	1.0969	−0.1323	−0.2379	0.3465	−0.5763	0.9458	−0.2972	0.4332	−0.1248	−0.4007
0.85	1.1091	−0.1502	−0.2513	0.3725	−0.5712	0.9664	−0.2958	0.4383	−0.1389	−0.4275
0.90	1.1220	−0.1692	−0.2647	0.3994	−0.5656	0.9886	−0.2940	0.4438	−0.1519	−0.4544
0.95	1.1355	−0.1900	−0.2776	0.4271	−0.5596	1.0120	−0.2926	0.4496	−0.1657	−0.4818
1.00	1.1498	−0.2119	−0.2903	0.4556	−0.5533	1.0367	−0.2906	0.4557	−0.1802	−0.5093
					$\varphi = 65°$					
0.00	1.0000	0.0000	0.0000	0.0000	−0.2588	0.7680	−0.3214	0.3830	0.0000	0.0000
0.05	1.0004	−0.0005	−0.0161	−0.0190	−0.2586	0.7685	−0.3214	0.3831	−0.0043	−0.0245
0.10	1.0016	−0.0019	−0.0322	−0.0382	−0.2578	0.7694	−0.3213	0.3836	−0.0087	−0.0493
0.15	1.0036	−0.0043	−0.0481	−0.0576	−0.2565	0.7715	−0.3212	0.3844	−0.0132	−0.0749
0.20	1.0064	−0.0077	−0.0659	−0.0770	−0.2546	0.7758	−0.3210	0.3855	−0.0177	−0.0998
0.25	1.0100	−0.0120	−0.0818	−0.0974	−0.2523	0.7814	−0.3207	0.3868	−0.0221	−0.1262
0.30	1.0144	−0.0174	−0.0961	−0.1165	−0.2493	0.7881	−0.3204	0.3885	−0.0257	−0.1495
0.35	1.0196	−0.0237	−0.1121	−0.1366	−0.2458	0.7962	−0.3201	0.3905	−0.0327	−0.1736
0.40	1.0256	−0.0310	−0.1279	−0.1571	−0.2417	0.8055	−0.3196	0.3928	−0.0356	−0.1990
0.45	1.0324	−0.0394	−0.1436	−0.1780	−0.2371	0.8161	−0.3191	0.3955	−0.0415	−0.2244
0.50	1.0400	−0.0488	−0.1593	−0.2022	−0.2317	0.8280	−0.3186	0.3985	−0.0476	−0.2500
0.55	1.0483	−0.0593	−0.1748	−0.2209	−0.2259	0.8411	−0.3179	0.4017	−0.0544	−0.2759
0.60	1.0575	−0.0709	−0.1903	−0.2433	−0.2193	0.8556	−0.3172	0.4054	−0.0614	−0.3021
0.65	1.0674	−0.0837	−0.2056	−0.2660	−0.2122	0.8712	−0.3164	0.4092	−0.0690	−0.3285
0.70	1.0780	−0.0976	−0.2209	−0.2895	−0.2043	0.8884	−0.3156	0.4135	−0.0772	−0.3552
0.75	1.0895	−0.1126	−0.2359	−0.3134	−0.1958	0.9068	−0.3146	0.4180	−0.0859	−0.3822
0.80	1.1016	−0.1289	−0.2508	−0.3383	−0.1865	0.9266	−0.3136	0.4229	−0.0954	−0.4096
0.85	1.1145	−0.1465	−0.2655	−0.3639	−0.1764	0.9478	−0.3124	0.4282	−0.1056	−0.4372
0.90	1.1282	−0.1653	−0.2800	−0.3895	−0.1654	0.9703	−0.3111	0.4337	−0.1165	−0.4653
0.95	1.1425	−0.1855	−0.2943	−0.4176	−0.1537	0.9943	−0.3098	0.4395	−0.1281	−0.4939
1.00	1.1576	−0.2071	−0.3083	−0.4458	−0.1410	1.0198	−0.3084	0.4455	−0.1434	−0.5228

BIBLIOGRAPHY

1. Antonevich, P.G. K raschetu balok i plit, opirayushchikhsya na uprugoe osnovanie (Analysis of Beams and Plates on Elastic Foundations). —Izvestiya Tomskogo Politekhnicheskogo Instituta, No. 76. 1954.
2. Akhsharumov, R.T. Ob odnom metode rascheta pryamougol'nykh plastin na uprugom osnovanii (A Method of Analyzing Rectangular Plates on Elastic Foundations). — Sbornik trudov Erevanskogo politekhnicheskogo instituta, No. 4. 1950.
3. Bezukhov, N.I. Teoriya uprugosti i plastichnosti (Theory of Elasticity and Plasticity). — Moskva, Gostekhizdat. 1953.
4. Watson, G.N. Theory of Bessel Functions. — Cambridge. 1948.
5. Viksne, V.P. O kolebaniyakh balok lezhashchikh na uprugo-massivnom osnovanii (Vibration of Beams on Massive Elastic Foundations). — In: Sbornik "Voprosy dinamiki i dinamicheskoi prochnosti", No. 2. Izd. AN LatvSSR, Riga. 1953.
6. Vinokurov, L.P. Opredelenie otporov uprugogo poluprostranstva pod nagruzhennym fundamentom pri uchete sovmestnoi raboty neskol' kikh fundamentov i obrazovaniya uchastkov plasticheskikh otporov (Determining the Reactions of an Elastic Semi-infinite Space Under a Loaded Foundation, Taking account of the Joint Deformation of Several Foundations and the Formation of Zones of Plastic Reactions). — Trudy Khar'kovskogo Inzhenerno-stroitel'nogo Instituta, No. 5. 1957.
7. Vlasov, V.Z. Nekotorye novye zadachi po teorii tonkostennykh konstruktsii (Some New Problems of the Theory of Thin-walled Structures). Collection of papers (edited by V.V. Burgman), No. 1. Moskva. 1948.
8. Vlasov, V.Z. Obshchaya teoriya obolochek i ee prilozhenie v tekhnike (General Theory of Shells and Its Application in Engineering). — Moskva-Leningrad, Gostekhizdat. 1949.
9. Vlasov, V.Z. Prostranstvennye konstruktivnye oblegchennye formy gidrotekhnicheskikh sooruzhenii i metody ikh rascheta (Three-dimensional Light-Weight Shapes of Hydrotechnical Structures, and Methods for Their Analysis). —Izvestiya AN SSSR, OTN, No. 10. 1951.
10. Vlasov, V.Z. Metod nachal'nykh funktsii v zadachakh teorii uprugosti (Method of Initial Functions in Problems of the Theory of Elasticity). — Izvestiya AN SSSR, OTN, No. 7. 1955.

11. Vlasov, V.Z. and N.N. Leont'ev. Tekhnicheskaya teoriya rascheta fundamentov na uprugom osnovanii (Technical Theory of the Analysis of Structures on Elastic Foundations). — Trudy Moskovskogo Inzheneznostroitel'nogo Instituta, Collection, No. 14. 1956.

12. Vlasov, V.Z. Tonkostennye prostranstvennye sistemy (Thin-walled Three-dimensional Systems). — Moskva, Gosstroiizdat. 1958.

13. Vlasov, V.V. Metod nachal'nykh funktsii v ploskoi zadache teorii uprugosti (Method of Initial Functions in the Two-dimensional Problem of the Theory of Elasticity). — Izvestiya MVO SSSR, No. 2. 1958.

14. Vlasov, V.V. Metod nachal'nykh funktsii v zadachakh ravnovesiya tolstykh mnogosloinykh plit (Method of Initial Functions in Problems of Equilibrium of Thick Multilayer Plates). —Izvestiya AN SSSR, OTN, No. 7. 1958.

15. Vlasov, V.V. Metod nachal'nykh funktsii v ploskoi zadache teorii uprugosti (Method of Initial Functions in the Two-dimensional Problem of the Theory of Elasticity). — Thesis, Moskva. 1958.

16. Galerkin, B.G. Uprugie pryamougol'nye i treugol'nye svobodno opertye tolstye plity, podverzhennye izgibu (Elastic Rectangular and Triangular Freely Supported Thick Plates Subjected to Bending). —Doklady AN SSSR, No. 10. 1931.

17. Galerkin, B.G. Napryazhennoe sostoyanie pri izgibe pryamougol'noi plity po teorii tolstykh plit i teorii plit tonkikh (State of Stress in the Bending of a Rectangular Plate, According to the Theory of Thick Plates and the Theory of Thin Plates). — Trudy Lenigradskogo Instituta Sooruzhenii, No. 2. 1935.

18. Galin, L.A. O gipoteze Tzimmermana-Vinklera dlya balok (On the Zimmermann-Winkler Hypothesis for Beams). — Prikladnaga Matematika i Mekhanika, Vol. 7, No. 4. 1943.

19. Galin, L.A. Kontaktnye zadachi teorii uprugosti (Contact Problems of the Theory of Elasticity). — Moskva, Gostekhizdat. 1953.

20. Gastev, V.A. Raschet tonkikh plastinok na uprugom osnovanii, nagruzhennykh po pryamougol'nym ploshchadkam (Analyzing Thin Plates Loaded on Rectangular Elementary Areas and Resting on Elastic Foundations). — Trudy Leningradskogo Instituta Inzhenerov Promyshlennogo Stroitel'stva, No. 1. 1934.

21. Gersevanov, N.M. and Ya. A. Macheret. K vorposu o beskonechno dlinnoi balke na uprugoi pochve, nagruzhennoi siloi (On the Problem of an Infinitely Long Beam on an Elastic Soil, Loaded by a Force). — Gidrotekhnicheskoe Stroitel'stvo, No. 10. 1953.

22. Gil'man, L.S. K voprosu ob opredelenii napryazhenii na poverkhnosti uprugoi sredy (Determining the Stresses at the Surface of an Elastic Medium). —Trudy Leningradskogo Instituta Inzhenerov Promyshlennogo Stroitel'stva, No. 1. 1934.

23. Gorbunov-Posadov, M.I. Plity na uprugom osnovanii (Plates on Elastic Foundations). — Moskva, Stroiizdat. 1941.

24. Gorbunov-Posadov, M.I. Osadki fundamentov na sloe grunta, podstilaemom skal'nykh osnovaniem (Settling of Structures on Soil Layers Resting on Rock Foundations). — Moskva, Stroiizdat. 1946.

25. Gorbunov-Posadov, M.I. Balki i plity na uprugom osnovanii (Beams and Plates on Elastic Foundations). — Moskova, Stroiizdat. 1949.
26. Gorbunov-Posadov, M.I. Raschet konstruktsii na uprugom osnovanii (Analyzing Structures on Elastic Foundations). — Moskva, Gosudarstvennoe izdatel'stvo literatury po stroitel'stvu i arkhitekture. 1953.
27. Didov, B.V. Razrabotka metoda rascheta plity na uprugom osnovanii po Tsimmermanu (Developing Zimmermann's Method for Analyzing Plates on Elastic Foundations). — Sbornik trudov laboratorii osnovanii i fundamentov VODGEO, No. 9. 1938.
28. Dinnik, A.N. Kruglaya plastinka na uprugom osnovanii (Circular Plate on an Elastic Foundation). — Izvestiya Kievskogo politekhnicheskogo instituta. 1910.
29. Dinnik, A.N. Prilozhenie funktsii Besselya k zadacham teorii uprugosti (Use of Bessel Functions in Problems of the Theory of Elasticity). — Part I. Kiev. 1913.
30. Egorov, K.E. Raspredelenie napryazhenii i peremeshchenii v dvykhsloinom osnovanii lentochnogo fundamenta (Distribution of Stresses and Displacements in a Double-layer Strip-type Foundation). — Sbornik trudov nauchno-issledovatel'skogo sektora tresta glubinnykh rabot, No. 10. 1939.
31. Zhemochkin, B.N. 1. Ploskaya zadacha rascheta beskonechno dlinnoi balki na uprugom osnovanii; 2. Raschet balok na uprugom poluprostranstve i poluploskosti (1. Two-dimensional Problem of Analyzing an Infinitely Long Beam on an Elastic Foundation; 2. Analyzing Beams on an Elastic Semi-infinite Space or Plane). — Moskva, Izd. VIA. 1937
32. Zhemochkin, B.N. and A.P. Sinitsyn. Prakticheskie metody rascheta fundamentnykh balok i plit na uprugom osnovanii (bez gipotezy Vinklera) (Practical Methods for Analyzing Beams and Plates on Elastic Foundations (without using Winkler's Hypothesis)). — Moskva, Stroiizdat. 1947.
33. Zavriev, K.S. Svobodnye kolebaniya balok na uprugom osnovanii (Free Vibrations of Beams on Elastic Foundations). — Soobshcheniya AN GruzSSR, 1945.
34. Ishkova, A.G. Tochnoe reshenie zadachi ob izgibe krugloi plastinki, lezhashchei na uprugom poluprostranstve, pod deistviem simmetrichnoi ravnomerno raspredelennoi nagruzki (Exact Solution of the Problem of the Bending of a Circular Plate Resting on an Elastic Semi-infinite Space, Under the Action of a Uniformly Distributed Symmetrical Load). — Doklady AN SSSR, Vol. 4, No. 2. 1947.
35. Kantorovich, L.V. and V.I. Krylov. Priblizhennye metody vysshego analiza (Approximative Methods of Higher Analysis). — Moskva-Leningrad, Gostekhizdat. 1950.
36. Kiselev, V.A. Razvitie metoda deformatsii na ramy na sploshnom uprugom osnovanii (Developing the Method of Deformations on a Frame on a Continuous Plastic Foundation). — Proekt i Standart, No. 10. 1933.
37. Kiselev, V.A. Balki i ramy na uprugom osnovanii (Beams and Frames on Elastic Foundations). — Moskva-Leningrad, ONTI. 1936.

38. Klein, G.K. Uchet neodnorodnosti, razryvnosti deformatsii i drugikh mekhanicheskikh svoistv grunta pri raschete sooruzhenii na sploshnom osnovanii (Taking into Account the Nonhomogeneity, the Discontinuity of the Deformations, and other Mechanical Properties of the Soil when Analyzing Structures on a Continuous Foundation). — Trudy Moskovskogo Inzhenerno-stroitel'nogo Instituta, Sbornik, No. 14. 1956.

39. Klishevich, G.V. Raschet balok na uprugom osnovanii i primenenie ego k raschetam gidrotekhnicheskikh sooruzhenii (Analyzing Beams on Elastic Foundations and Applications in the Design of Hydrotechnical Structures). — Moskva-Leningrad, Gosenergoizdat. 1932.

40. Klubin, P.I. O raschete dnishch shlyuzov i dokov (Analysis of Floors, Locks, and Docks). — Izvestiya AN SSSR, OTN, No. 3. 1953.

41. Korenev, B.G. Ob izgibe neogranichennoi plity, lezhashchei na uprugom osnovanii (Bending of an Infinite Plate Lying on an Elastic Foundation). — Doklady AN SSSR, Vol. 79, No. 3. 1951.

42. Korenev, B.G. Voprosy rascheta balok i plit na uprugom osnovanii (Problems of the Analysis of Beams and Plates on Elastic Foundations). — Moskva Gosstroiizdat. 1954.

43. Korenev, B.G. Konstruktsii, lezhashchie na uprugom osnovanii (Structures on Elastic Foundations). —Stroitel'naya mekhanika v SSSR 1917-1957. Moskva. 1957.

44. Kornevits, E.F. and G.V. Ender. Raschet sploshnykh dnishch sukhikh dokov (Analyzing Continuous Floors of Dry Docks). — Moskva, Gosstroiizdat. 1940.

45. Kosab'yan, L.V. Raschet pryamougol'nykh plit na uprugom odnosloinom osnovanii (Analyzing Rectangular Plates on Elastic Single-Layer Foundations). Thesis. 1956.

46. Krechmer, V.B. Raschety i proektirovanie ploskikh zhelezobetonnykh fundamentov (Analysis and Design of Plane Reinforced-Concrete Foundations) Part I. —ONTI, Moskva-Leningrad. 1936.

47. Krylov, A.N. O raschete balok, lezhashchykh na uprugom osnovanii (Analyzing Beams on Elastic Foundations). — Izd. AN SSSR, Moskva. 1930.

48. Krylov, A.N. Vibratsiya sudov (Vibrations of Ships). — Izd. AN SSSR, Moskva-Leningrad. 1936.

49. Kuznetsov, V.I. Uprugoe osnovanie (Elastic Foundations). — Gosudarstvenuse izdatel'stvo literatury po stroitel'stvu i arkhitekture, Moskva. 1952.

50. Kuznetsov, V.I. Raboty sovetskikh uchenykh v oblasti teorii rascheta konstruktsii na uprugom osnovanii (Soviet Studies in the Field of the Analysis of Structures on Elastic Foundations). — Trudy Instituta Istorii Tekhniki AN SSSR, No. 8. 1954.

51. Kuz'min, R.O. Besselevy funktsii (Bessel Functions). — Moskva-Leningrad, ONTI. 1935.

52. Leonov, M.Ya. K teorii rascheta uprugikh osnovanii (Contribution to the Theory of Elastic Foundations). —Prikladnaya Matematika i Mekhanika, Vol. 3, No. 2. 1939.

53. Leonov, M.Ya. K raschetu fundamentnykh plit (Analyzing Base Plates) — Prikladnaya Matematika i mekhanika, Vol. 4, No. 3. 1940.

54. Leont'ev, N.N. Prakticheskii metod rascheta tonkostennoi tsilindricheskoi truby na uprugom osnovanii (Practical Method of Analyzing a Thin-Walled Cylindrical Pipe on an Elastic Foundation). — Trudy Moskovskogo Inzhenerno-stroitel'nogo Instituta, Sbornik, No. 27. 1957.

55. Leont'ev, N.N. Prilozhenie variatsionnogo metoda V.Z. Vlasova k raschetu fundamentov gidrotekhnicheskikh sooruzhenii (Application of Vlasov's Variational Method to the Analysis of the Foundations of Hydrotechnical Structures). — Thesis. 1952.

56. Lur'e, A.I. Prostranstvennye zadachi teorii uprugosti (Three-dimensional Problems of the Theory of Elasticity). — Moskva, Gostekhizdat. 1955.

57. Love, A.E.H. Mathematical Theory of Elasticity — Cambridge, 1927 [Russian Translation, Moskva-Leningrad, ONTI. 1935].

58. Maliev, L.S. Balki na uprugom osnovanii s peremennym po ikh dline koeffitsientom posteli (Beams on Elastic Foundations whose Foundation Moduli vary along their Length). — Trudy Leningradskogo Instituta Inzhenerov Promyshlennogo Stroitel'stva, No. 6, Leningrad, GONTI. 1938.

59. Muskhelishvili, A.I. Nekotorye osnovnye zadachi matematicheskoi teorii uprugosti (Some Basic Problems of the Mathematical Theory of Elasticity), Third edition. — Moskva, Izd. AN SSSR. 1949.

60. Nikol'skii, A.I. Universal'nyi metod rascheta sooruzhenii na szhimaemykh gruntakh (Universal Method of Analyzing Structures on Compressible Soils). — In: Sbornik Svir'stroya, XIII-XIV. 1937.

61. Pasternak, P.L. Staticheskaya teoriya gibkikh balok i plit na uprugom osnovanii (Statistical Theory of Flexible Beams and Plates on Elastic Foundations). — Beton und Stahl, Nos. 9-10, Berlin. 1926.

62. Pasternak, P.L. Osnovy novogo metoda rascheta fundamentov na uprugom osnovanii pri pomoshchi dvukh koeffitsientov posteli (Fundamentals of a New Method of Analyzing Structures on an Elastic Foundation by Means of Two Foundation Moduli). — Moskva-Leningrad, Gosudarstvennoe izdatel'stvo literatury po stroitel'stvu i arkhitekture. 1954.

63. Puzyrevskii, N.P. Fundamenty (Foundations). — Moskva, Gosstroiizdat. 1944.

64. Rabinovich, I.M. Dostizheniya stroitel'noi mekhaniki sterzhnevykh sistem v SSSR (Achievements of Structural Mechanics of Bar (Lattice) Systems in the USSR). — Moskva, Izd. Akademi arkhitektury SSSR. 1949.

65. Rabinovich, I.M. Kurs stroitel'noi mekhaniki (A Course in Structural Mechanics). Part II. — Moskva, Gosudarstvennoe izdatel'stvo literatury po stroitel'stvu i arkhitekture. 1954.

66. Rudnev, V.I. Noveishie metody rascheta balok na sploshnom uprugom osnovanii (Recent Methods of Analyzing Beams on Continuous Elastic Foundations). — Trudy VIOS, Osnovaniya i Fundamenty, Collection, No. 2. Stroiizdat. 1934.

67. Rudnev, V.I. Priblizhennyi metod rascheta balki na sploshnom uprugom osnovanii bez gipotezy Vinklera (Approximative Method of Analyzing Beams on Continuous Elastic Foundations without Using Winkler's Hypothesis). — Sbornik NIS Fundamentstroya, No. 8. 1937.

68. Ruchkin, V.P. Raschet dnishch rezervuarov na sploshnom uprugom osnovanii (Analyzing the Floors of Reservoirs on Continuous Elastic Foundations). — Thesis. 1956.

69. Simvulidi, I.A. Raschet balok, lezhashchikh na sploshnom uprugom osnovanii, bez gipotezy Vinklera (Analyzing Beams on Continuous Elastic Foundations, without Using Winkler's Hypothesis). — Metrostroi, No. 5. 1936.

70. Snitko, N.K. Raschet balok na uprugom osnovanii peremennogo secheniya (Analyzing Beams on Variable-Section Elastic Foundations). — Vestnik Inzhenerov i Tekhnikov, No. 8. 1935.

71. Timoshenko, S. Theory of Elasticity. — [Translated into Russian. 1937.]

72. Umanskii, A.A. O raschete balok na uprugom osnovanii (Analyzing Beams on Elastic Foundations). — Moskva, Stroiizdat. 1933.

73. Umanskii, A.A. Spetsial'nyi kurs stroitel'noi mekhaniki (A Special Course in Structural Mechanics). Part I. — Moskva-Leningrad, Gosstroiizdat. 1935.

74. Urban, I.V. Temperaturnye napryazheniya v balke, lezhashchei na sploshnom uprugom osnovanii (Temperature Stresses in a Beam Lying on a Continuous Elastic Foundation). — Trudy Moskovskogo Instituta Inzhenerov Transporta, No. 54. Transzheldorizdat. 1937.

75. Filonenko-Borodich, M.M. Nekotorye priblizhennye teorii uprugogo osnovaniya (Some Approximative Theories of Elastic Foundations). — Uchenye Zapiski MGU, No. 46. 1940.

76. Filonenko-Borodich, M.M. Prosteishaya model' uprugogo osnovaniya, sposobnaya raspredelyat' nagruzku (A Very Simple Model of an Elastic Foundation Capable of Spreading the Load). — Sbornik trudov Moskovskogo elektromekhnidieskogo instituta inzhenerov transporta, No. 53. Transzheldorizdat. 1945.

77. Filonenko-Borodich, M.M. Teoriya uprugosti (Theory of Elasticity), 4th edition, Moskva, Fizmatgiz, 1959. [Translated into English. Peace Edition.]

78. Florin, V.A. Opredelenie reaktsii poluploskosti posredstvom primeneniya stroki Maklorena (Determining the Reactions of a Semi-Infinite Plane by Means of Maclaurin Series). — Sbornik Gidroenergoproekta, No. 2. 1937.

79. Florin, V.A. Raschety osnovanii gidrotekhnicheskikh sooruzhenii (Analyzing the Foundations of Hydrotechnical Structures). — Moskva, Stroiizdat. 1948.

80. Tsytovich, N.A. Mekhanika gruntov (Soil Mechanics), 3rd edition. — Moskva, Stroiizdat. 1951.

81. Cheche, A.A. Primenenie variatsionnogo metoda V.Z. Vlasova k resheniyu nekotorykh prakticheskikh zadach termouprugosti (Application of Vlasov's Variational Method to the Solution of Some Practical Problems in Thermoelasticity). Thesis. 1952.

82. Cheche, A.A. Raschet betonnykh blokov i massivnykh plit na zhestkom i uprugom osnovaniiakh ot temperaturnykh vozdeistvii s primeneniem metoda prof V. Z. Vlasova (Analysis of Temperature Stresses in Concrete Blocks and Massive Plates on Rigid and Elastic Foundations by Means of Vlasov's Method).— Sbornik nauchnykh rabot Belorusskogo politekhnicheskogo instituta No. 54, Minsk. 1956.

83. Shapiro, G.S. Izgib polubeskonechnoi plity, lezhashchei na uprugom osnovanii (Bending of Semi-infinite Plate on an Elastic Foundation).— Prikladanaya Matematika i Mekhanika, Vol. 7, No. 4. 1943.

84. Shekhter, O.Ya. O vliyanii moshchnosti sloya na raspredelenie napryazhenii v fundamentnoi balke (Influence of the Soil Thickness on the Stress Distribution in a Foundation Beam).— Sbornik trudov NIS tresta glubinnykh rabot, No. 10. 1939.

85. Shekhter, O.Ya. Raschet beskonechnoi plity, lezhashchei na uprugom osnovanii konechnoi i beskonechnoi moshchnosti i nagruzhennoi sosredotochennoi siloi (Analyzing an Infinite Plate Resting on an Elastic Foundation of Finite or Infinite Thickness and Loaded by a Concentrated Force).— Sbornik trudov NIS fundamentstroya, No. 10. 1939.

86. Shpil'rein, Ya.N. Tablitsy spetsial'nykh funktsii (Tables of Special Functions). 1933.

87. Shtaerman, I.Ya. Kontaktnye zadachi teorii uprugosti (Contact Problems of the Theory of Elasticity).— Moskva-Leningrad, Gostekhizdat. 1949.

88. Shtaerman, I.Ya. Raspredelenie davleniya pod fundamentom pri nalichii plasticheskoi zony (Pressure Distribution under a Foundation in the Presence of a Plastic Zone).— Trudy Moskovskogo Inzhenerno-stroitel'nogo Instituta, Collection, No. 14. 1956.

89. Jahnke, E. and F. Emde. Tablitsy funktsii s formulami i krivymi (Tables of Functions with Formulas and Graphs). 1953. [Translated from German].

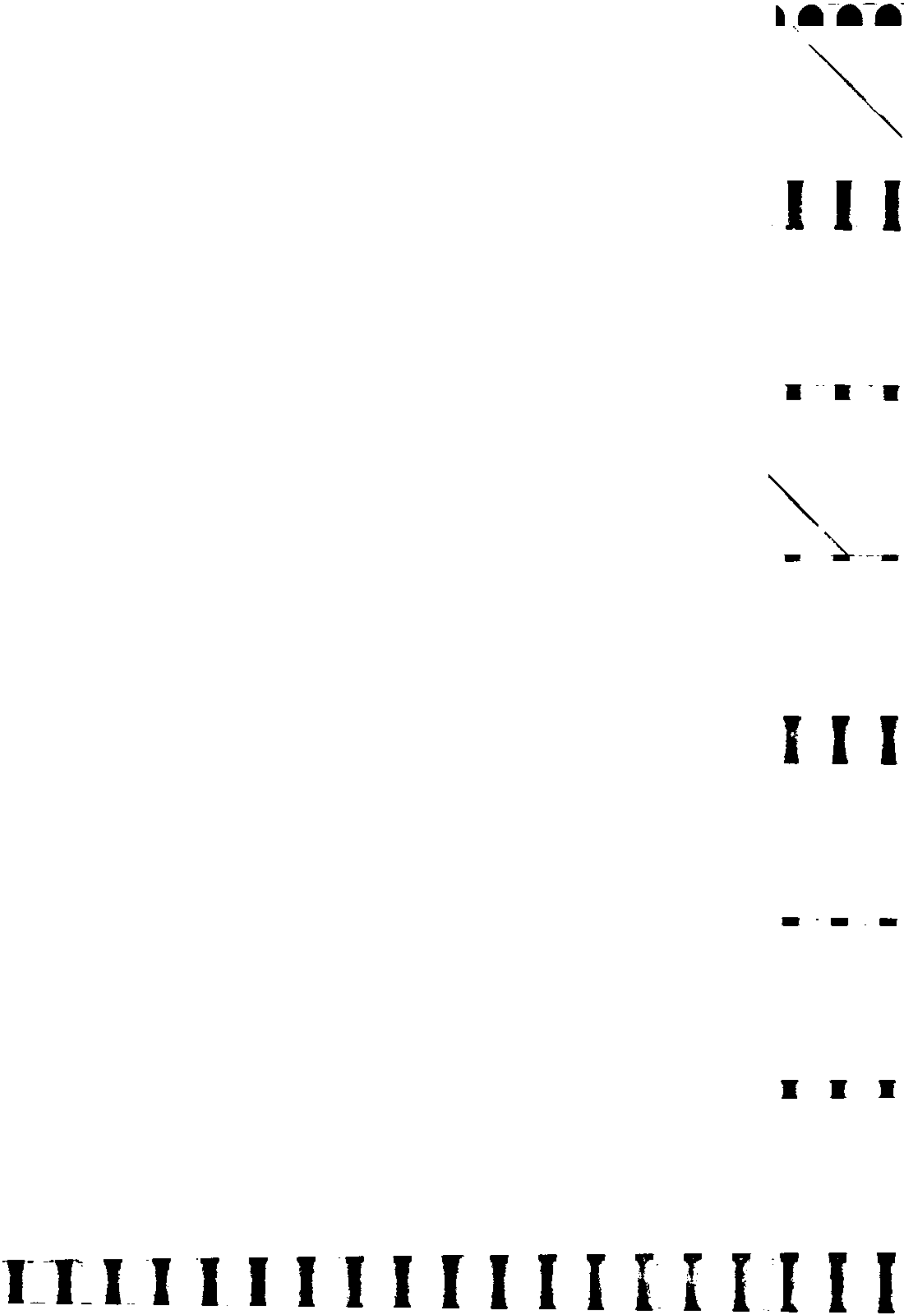

SUBJECT INDEX

Assumption of equality to zero of transverse elongations, 3
Beam, infinite, 59, 81
—, finite, 81, 92
—, long, 133
—, rigid, 65, 81, 89, 133, 228
—, short, 133
Bending, axisymmetrical, 162
—, cylindrical, 129
—, of a beam, 3
—, of a thick plate, 294, 303
—, of a narrow plate, 3
Bessel functions, 166
Betti theorem, 106
Bimoment, 278
Bottom of a cylindrical reservoir, 208
Boundary condition, geometrical, 277
——, kinematic, 216
——, mixed, 216, 277
Bubnov-galerkin method, 138, 152, 290
Buckling, flexural, 260
—, torsional, 260
Characteristic numbers, 217
—of elastic, 9, 26, 49, 50
—of a beam, elastic, 49, 75
—of a foundation, generalized, 96
-of a plate, generalized, 96
—of a single-layer foundation, 96
Components of displacement vector, 265
—of intensity vector, 265
—of stress tensor, 265
Concentrated reactions, 71, 74
Contact plane, 284, 319
Deflection, generalized, 48, 98, 107
—of a beam, 64
Deformation of a shell, 186, 189, 190
——with bending, 187, 190
Differential operators, biharmonic, 271
——, harmonic, 271
——, polyharmonic, 271
Discrete-continuous system, 15
Displacement, 2, 30, 265
—, dynamic, 226
—, generalized, 2, 3, 30, 48
—, longitudinal, 2
— of a shell, 187
——, normal, 185
Elastic foundation, double-layer, 27
—layer of finite thickness, 284
——of uniform thickness, 277
——of variable thickness, 277
—line, 226
Equation, biharmonic, 190
—, characteristic, of a homogeneous boundary value problem, 216
—, geometrical, of a shell, 186
—of a spherical shell, 188
—of a beam bending, 47
—of bending of a circular plate, 161
——of thin plates, 95, 97,
Equilibrium conditions, 5, 31, 138
——, generalized, 48, 99, 103
——, variational, 142
Factors, kinematic, 55, 58
Factors, static, 55, 58
Fictitious reactions, 140, 144
Flexibility index of beam, 79,
——of plate, 146
Force, critical, 255, 256, 258, 261
—, —, Euler, 258
—, external, 5
—, fictitious, 104, 199
—, generalized, 8, 27
—, —, compressive, 256
—, —, internal, 107
—, —, shearing, 8, 23, 49, 60, 66, 97, 107
—, inertia, 228, 232, 267
—, internal, 5
—, surface, 10
Forces and moments, annular (peripheral), 162
——, generalized, 53
——in a shell, 186
—, internal normal, 5

—, —shearing, 5
Foundation, elastic double-layer, 25, 89
—, — multilayer, 322
—, —single-layer, 95
—, —three-dimensional, 30
—modulus, 15, 64
—with two characteristics, 34
Fourier coefficients, 309
Frequency of free vibrations of a plate, 241, 244
—of natural vibrations of a beam, 109
—of vibrations, 216, 220, 231
Function, hyperbolic-trigonometric, 172
—of bending of a beam on an elastic foundation, 50
Functions, eigen, 217, 220
—, initial, 290
—of beam bending, 52
——vibrations, 109
—of natural vibrations, 216
—of transverse distribution of the displacements, 2, 4, 15
—, trigonometric, 112
Fundamental system of functions, 110
Gauss curvature, 184
Gorbunov-Posadov method, 73, 81
Hankel functions, 166
——, modified, 194
Hypothesis, foundation modulus, 15
Hypothesis, Kirchoff-Love, 283
Influence coefficient, 53
—functions, 54, 58
Initial parameters, 53, 55, 57, 75, 123
Integral-differential form of operators, 272, 295
Laplace operator, 95
Laplacian, 36, 162
Length, characteristic, 75
Levy problem, 98
Load, 56
—, antisymmetrical, 3, 68, 113, 123, 155
Loading, antisymmetrical, 68
—, symmetrical, 65
Maclaurin series, 268
Matrix of direct transformation, 54, 275
—, transformation, 54
—, unitary, 53
Method, mixed, 266
—of Cauchy-Krylor, 310
—of displacements, 2, 211, 265
—of forces, 212
—of foundation modulus, 64, 207
—of fundamental functions, 116
—of initial functions, 267
——parameters, 52, 75, 119
—of krylov, 7, 255
—of strains, 211
—of stresses, 266
—of trigonometric series, 320
—, symbolic, 268
Model of elastic foundation, multilayer, 13
———, plane, generalized, 10, 13
———with two characteristics, 13, 34
————foundation moduli, 15
—of Winkler-Fuchs, 15
Modulus of elasticity, 2
Moment, bending, 60, 97, 137
—, generalized, 187
—of inertia, 258, 260
—, torsional (torque), 97
Momentary impulse, 222, 224, 231
Navier theorem, 98
Number of degrees of freedom, 5, 31
Orthogonality of eigenfunctions, 217
Plate, circular, 161, 163, 168, 181, 182
—, finite, 178
—, infinite, 175
—, multilayer, 313, 321
—, multispan, 316
—, rectangular, 117, 256, 260, 298, 301
—, rigid, 169
—, thick, 157
—undergoing plane stress, 301
Poisson ratio, 2
Problem, axisymmetrical, 175
—, temperature, 40
—, three-dimensional, 265
—, two-dimensional, 1, 290
—, Vlasov, 98
Principle of virtual displacements, 8

Properties of a foundation, 15, 34
Punch, annular, 173
—, circular, 169
—, symmetrical, 69
Reaction, uniform, 67, 74
Rectangular strip, 306
Reduced half-length of beam, 80
Reduction of three-dimensional to two-dimensional problem, 277
— of two-dimensional to one-dimensional problem, 98, 99
Rigidity of a cylindrical plate, 138
Shell, cylindrical, 212, 212
—, spherical shallow, 184
Slope, 199
Solution, Filon, 310, 313, 316
—, Filonenko-Borodich, 15
—, Ribiere, 299, 313, 316
—, Sadovskii, 69
—, Wieghardt, 15
State of plane stress of a shell, 196
— of strain, 5, 9
— of stress, 9
— —, plane, 49, 293
Stieljes integral, 7, 33
Strain, bending, 186
—, compression, 187
—, plane, 9
—, temperature, 40
—, transverse, 5
—, shearing, 1, 186
Stresses, 31
—, normal, 1, 5, 30
—, shearing, 5, 30, 107
Stresses, thermal (temperature), 41
Theory of plates, approximate, 280
— —, bimoment, 278, 283
— —, exact, 280
— —, moment, 283
Thomas function, 204
Torsion of a narrow plate, 129
Transformation, direct, 275
—, inverse, 275
Two-dimensional problem of the theory of elasticity, 5
Vibration, simple harmonic, 215
Vibrations, antisymmetrical, 248, 253
—, free, 240
—, of a beam, 213, 215, 229
—, —, forced, 225
—, of an elastic beam, 229
—, of a foundation, 213
—, of a plate, 232
—, of a rigid beam, 227
—, symmetrical, 247
Vertical displacements of the foundation surface, 74
Vietes theorem, 165
Wieghardt solution, 15
Winkler hypothesis, 15
Winkler-Zimmerman hypothesis, 97
— - — model, 13
Work forces, 5, 32
— of internal forces, 100, 142
— done by external load, 100, 142
— — stresses, 37, 102, 141
—, virtual, 5, 7, 107

AIAA 82-4118

Toward a New Engineering Theory of Bending: Fundamentals

Lawrence W. Rehfield* and Pappu L. N. Murthy†
Georgia Institute of Technology, Atlanta, Ga.

The classical engineering theory of bending due to Bernoulli and Euler serves as a cornerstone for structural analysis and design. Limitations of this theory, however, become apparent in flexural wave propagation studies; it predicts infinite phase velocity as the wavelength becomes shorter. This theoretical deficiency is corrected by Timoshenko theory which accounts for transverse shear deformation. A thorough study of exact elasticity solutions reveals that there are two additional effects that are the same order as transverse shear in bending behavior. A new theory accounting for them is presented, along with several applications. The new equations are no more complicated than those of Timoshenko-type theory, yet they yield solutions which are exact or indistinguishable from exact in the examples studied.

Downloaded by UNIVERSITY OF MIAMI on December 31, 2014 | http://arc.aiaa.org | DOI: 10.2514/3.7938

Introduction

THE classical engineering theory of bending due to Bernoulli and Euler dates back to 1705 and precedes the theory of elasticity by over 100 years.[1] It has long been recognized as a convenient approximation for slender beams and serves as a cornerstone for structural analysis and design. Extensions due to Kirchhoff and Love expand the scope of this first approximation theory to plates and shells.

Limitations of Bernoulli-Euler theory become apparent in studying the propagation of elastic flexural waves of short wavelength. It predicts infinite phase velocity for harmonic waves as the wavelength becomes shorter. This result is, of course, physically absurd. This theoretical deficiency is corrected by the theory proposed by Timoshenko.[2] In Timoshenko theory, the influence of transverse shear deformations are accounted for, which results in a finite limit for phase velocity.

There have been a number of attempts to improve upon Timoshenko theory. Most of them are founded on the original Timoshenko assumptions,[2] which are that cross sections remain plane after bending and that shear of cross sections relative to one another is permitted to occur. The differences in various proposed equations are due primarily to the selection of the transverse shear contribution to the response according to different ad hoc criteria. An historical sketch of the development of engineering bending theory and a discussion of attempts at refinement appear in Ref. 3. The emergence of laminated, fiber reinforced advanced composite materials for structural applications and their unusual properties provides the motivation for the present work.

Use of fiber reinforced resin matrix composite materials in aerospace vehicles is increasing. This is primarily due to their superior mechanical properties and the ease with which they can be tailored to a specific application. The directional nature of their properties, however, poses unique challenges for the analyst. Consider, for example, a single layer or lamina made of a composite material. The extensional modulus along the direction of fibers is usually very large relative to the extensional moduli in the lateral directions and the shear moduli. This is a marked departure from conventional isotropic materials. Consequently, the relative importance of physical effects is influenced by the directional nature of properties and their relative magnitude. Transverse shear deformations, for example, are much more pronounced for composite structures.

This work has two primary objectives. The first is to delineate some features of bending behavior in a way which is new and informative. An analysis of bending behavior is described which utilizes an exact solution from the theory of elasticity for isotropic materials. A unique feature is the use of tracer constants in order to track the contributions due to various physical effects throughout the course of the analysis. With the aid of insight from this analysis, the second objective, the basis of a new engineering theory, is achieved. The new theory is applied to elementary static applications for beam-type structures which illustrate its use and permit comparisons with exact solutions to establish its validity.

The scope of this work is restricted to static, planar bending situations. In its present form, the theory applies to beams with thin rectangular cross sections which respond to planar bending in plane stress or to infinitely wide plates which respond in plane strain (cylindrical bending). All equations will be written for plane stress and treated as exact, although plane stress is an approximate state that is valid for thin cross sections.[4] The planar bending restriction is not intrinsic to the subjects being considered. This context is simply a basic step to take prior to confronting the additional complexities of fully three-dimensional behavior. Both isotropic and orthotropic materials are considered. Beams of orthotropic material are the simplest type of structures where composite material behavior can be studied.

Preliminary Analysis

Introductory Remarks

As a first, important step in an analysis of bending behavior, a plane stress elasticity solution for a simply supported beam under uniformly distributed loading is studied. It is possible to identify the individual contributions due to various factors affecting beam response. An assessment of their relative importance, therefore, can be made.

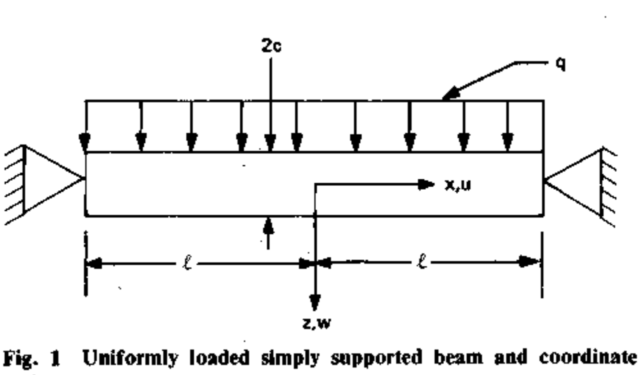

Fig. 1 **Uniformly loaded simply supported beam and coordinate system.**

Received Feb. 9, 1981; revision received Sept. 24, 1981. Copyright © 1982 by L. W. Rehfield and P. L. N. Murthy. Published by the American Institute of Aeronautics and Astronautics, with permission.

*Professor, School of Aerospace Engineering. Associate Fellow AIAA.

†Graduate Research Assistant, School of Aerospace Engineering.

Downloaded by UNIVERSITY OF MIAMI on December 31, 2014 | http://arc.aiaa.org | DOI: 10.2514/3.7938

Problem Definition and Solution

The two-dimensional elasticity solution for a simply supported beam under uniformly distributed loading is given in the text by Timoshenko and Goodier.[4] It is valid for very thin rectangular beams in the plane stress form. For infinitely wide plates, the same solution remains valid if a transformation of elastic constants for plane strain is employed.

The beam and coordinate system are shown in Fig. 1. The length of the beam is 2ℓ and the depth is $2c$. The width of the beam is taken as unity for convenience. The beam is bent by a uniformly distributed load of intensity q applied to its upper surface. The midspan of the beam centroidal axis is chosen as the origin for the coordinate axes x and z. $z=+c$ and $z=-c$ correspond to the bottom and top surfaces of the beam. The notation and convention are shown.

For the stresses, the usual convention and notation are followed: σ_{xx} is the axial stress, σ_{zz} the transverse normal stress, and σ_{xz} the transverse shear stress. They are given by the following expressions.

$$\sigma_{xx}=\frac{q}{2I}(\ell^2-x^2)z+\underline{\frac{q}{2I}\left(\frac{2z^3}{3}-\frac{2c^2z}{5}\right)} \tag{1}$$

$$\sigma_{zz}=-\frac{q}{2I}\left(\frac{z^3}{3}-c^2z+\frac{2c^3}{3}\right) \tag{2}$$

$$\sigma_{xz}=-\frac{q}{2I}(c^2-z^2)x \tag{3}$$

These stresses satisfy all the governing differential equations and the stress boundary conditions on the upper and lower surfaces. On the ends $x=\pm\ell$, the stress boundary conditions are satisfied in an overall Saint Venant sense. I is the second moment of the cross-sectional area and is $2c^3/3$ for the rectangular section under consideration.

As an aid in this analysis, three tracer constants, α_a, α_n, and α_s, are introduced. They are defined and used so as to facilitate keeping track of three distinct contributions to the response. The first term of Eq. (1) corresponds to the bending stress given by classical Bernoulli-Euler theory. The underlined term is a stress contribution which will be called the "nonclassical axial stress." It produces no resultant force or moment and is, therefore, a self-equilibrating stress. α_a is the tracer constant associated with this contribution. If $\alpha_a=1$, this contribution is fully accounted for. If $\alpha_a=0$ in the following, however, it is ignored and the Bernoulli-Euler axial stress distribution is recovered. For example, the axial stress is written using this convention in the form

$$\sigma_{xx}=\frac{q}{2I}(\ell^2-x^2)z+\alpha_a\frac{q}{2I}\left(\frac{2}{3}z^3-\frac{2}{5}c^2z\right) \tag{1a}$$

α_n and α_s are defined analogously and are associated with contributions due to σ_{zz} and σ_{xz}, respectively.

The displacement components u and w are shown in Fig. 1. Expressions for them can be obtained by using Hooke's law and the strain displacement relations. The following boundary conditions at the ends $x=+\ell$ and $x=-\ell$ are imposed:

$$w(\ell,0)=w(-\ell,0)=0 \tag{4}$$

They represent support conditions applied at the beam axis. Also, from the symmetry requirement

$$u(0,0)=0 \tag{5}$$

These conditions are sufficient to prevent rigid body motion.

The expressions for u and w are

$$u(x,z)=\frac{q}{2EI}\left[\left(\ell^2x-\frac{x^3}{3}\right)z+\alpha_a\left(\frac{2}{3}z^3-\frac{2c^2z}{5}\right)x\right.$$
$$\left.+\alpha_n\nu\left(\frac{z^3}{3}-c^2z+\frac{2c^3}{3}\right)x\right] \tag{6}$$

$$w(x,z)=w(x,0)-\frac{q}{2EI}\left[\left(\frac{z^4}{12}-\frac{c^2z^2}{2}+\frac{2c^3z}{3}\right)\alpha_n\right.$$
$$\left.+\nu(\ell^2-x^2)\frac{z^2}{2}+\nu\alpha_a\left(\frac{z^4}{6}-\frac{c^2z^2}{5}\right)\right] \tag{7}$$

In Eq. (7), $w(x,0)$ is the vertical deflection of the beam centroidal axis due to bending. It is given by the equation

$$w(x,0)=\delta-\frac{q}{2EI}\left[\frac{\ell^2x^2}{2}-\frac{x^4}{12}+\left[(1+\nu)\alpha_s\right.\right.$$
$$\left.\left.-\left(\frac{\alpha_a}{5}+\frac{\alpha_n\nu}{2}\right)\right]c^2x^2\right] \tag{8}$$

where

$$\delta=\frac{5q\ell^4}{24EI}\left[1+\frac{12c^2}{5\ell^2}\left[(1+\nu)\alpha_s-\frac{\alpha_a}{5}-\frac{\alpha_n\nu}{2}\right]\right] \tag{9}$$

δ is the deflection at the midspan of the beam.

Analysis of Beam Response

The major differences between the classical Bernoulli-Euler theory and the elasticity solution can be clearly identified in Eq. (9). The bracketed term represents the correction to the former due to the presence of contributions identified by the tracer constants α_s, α_a, and α_n. Note that the contributions due to all three effects—transverse shear, nonclassical axial stress, and transverse normal strain—are of the same order of magnitude. A static version of Timoshenko's theory[2] includes only the terms associated with α_s.

The corrections shown in Eq. (9) were known to earlier authors.[5,6] However, they did not differentiate among the various contributions. This differentiation provides the key ingredient for the establishment of a rational engineering theory. Goodier[7] suspected that the other influences beside transverse shear were important, but offered no means of estimating them quantitatively and no concrete examples of their contribution to beam response. The approach adopted here makes the matter transparent and settles the issue for this example.

Conclusions

On the basis of the foregoing analysis, the following conclusions are reached.

1) A Timoshenko-type transverse shear theory does not contain the necessary physical ingredients to treat problems with distributed loadings.

2) Transverse shear, nonclassical axial stress, and transverse normal strain make contributions to the response that are of the same order of magnitude. A theory that is purported to be more accurate or complete than classical theory must, therefore, correctly account for all of these influences.

Foundations of a New Theory

Objectives

An engineering theory is one in which assumptions or approximations are introduced in order to simplify the governing equations or facilitate their solution. Hopefully,

Downloaded by UNIVERSITY OF MIAMI on December 31, 2014 | http://arc.aiaa.org | DOI: 10.2514/3.7938

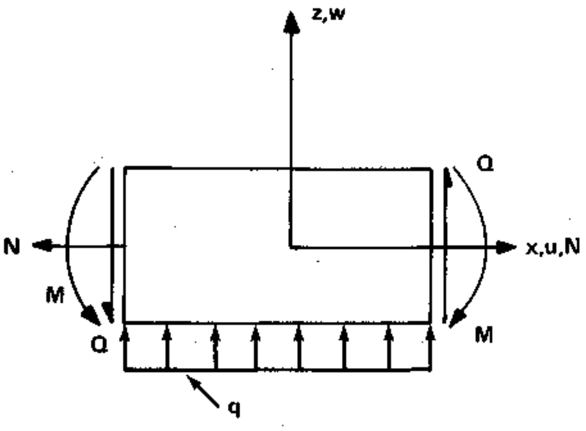

Fig. 2 Sign convention.

only a little accuracy is sacrificed for a considerable reduction in computational labor. The intent is to encompass the heart of the problem under consideration. The primary objective of this work is the development of a foundation for such a theory for bending that is consistent, reliable, and simple to use. Furthermore, it must account for the three effects that were clearly identified previously: transverse shear strain, nonclassical axial stress, and transverse normal strain.

The standard of comparison for results that is used herein is the plane stress solution to the equations of elasticity theory for the problem in question.

A second objective is to obtain stress estimates that are improvements over those provided by classical bending theory. This must be accomplished if the influence of nonclassical axial stress is to be properly accounted for.

Statically Equivalent Stresses

Equilibrium of a beam element is governed by overall equations containing resultant axial force, shear force, and bending moment. The sign convention and notation for these appear in Fig. 2. The equilibrium equations are

$$N_{,x}=0 \tag{10}$$

$$Q_{,x}+q=0 \tag{11}$$

$$M_{,x}-Q=0 \tag{12}$$

The force and moment resultants are defined in terms of stresses as

$$N=\int_{-c}^{c}\sigma_{xx}\mathrm{d}z \tag{13}$$

$$Q=\int_{-c}^{c}\sigma_{xz}\mathrm{d}z \tag{14}$$

$$M=\int_{-c}^{c}\sigma_{xx}z\mathrm{d}z \tag{15}$$

In the preceding, a rectangular cross section of unit width is assumed as before.

According to classical theory, the stresses are

$$\sigma_{xx}=(N/A)+(Mz/I) \tag{16}$$

$$\sigma_{xz}=(Q/2I)(c^2-z^2) \tag{17}$$

$$\sigma_{zz}=\frac{Q_{,x}}{2I}\left(\frac{z^3}{3}-c^2z+\frac{2}{3}c^3\right) \tag{18}$$

A is the cross-sectional area, which is $2c$ for the rectangular cross section under consideration. These stresses are statically equivalent to the applied loads and satisfy the stress equations of equilibrium. In addition, Eqs. (13-15) are satisfied, as are appropriate stress conditions at $z=c$ and $z=-c$.

The stresses, just given, although not exact, serve as a first approximation. They will be used subsequently to develop approximations for the displacement components.

Kinematics

Classical Bernoulli-Euler theory is based upon a kinematic assumption that is equivalent to ignoring, and hence setting to zero, transverse normal strain and transverse shear strain. Timoshenko-type shear deformation theories account for transverse shear strain but still do not permit transverse normal strain. On the basis of the previous analysis of the simply supported beam example, it appears necessary to completely abandon the Bernoulli-Euler kinematic assumption. In order to obtain some simplification from the complete elasticity equations, however, an assumption that facilitates the analysis is required.

The central assumption that replaces the Bernoulli-Euler hypothesis in the present development is that the statically equivalent stresses in Eqs. (16-18) can be used to estimate the transverse normal strain and transverse shear strain. Note that this is an assumption regarding stresses. It is not a kinematic assumption. This is in sharp contrast to classical and Timoshenko-type shear deformation theories.

The development will be carried out for orthotropic materials with principle material directions corresponding to axes of the beam. The appropriate form of Hooke's law for plane stress (beams of thin rectangular cross section) is

$$\epsilon_{xx}=(1/E_{11})(\sigma_{xx}-\nu_{13}\sigma_{zz}) \tag{19}$$

$$\epsilon_{zz}=\frac{\sigma_{zz}}{E_{33}}-\frac{\nu_{13}}{E_{11}}\sigma_{xx} \tag{20}$$

$$\gamma_{xz}=\sigma_{xz}/G_{13} \tag{21}$$

ϵ_{xx}, ϵ_{zz}, γ_{xz} are the axial strain, transverse normal strain, and transverse shear strain, respectively. E_{11} and E_{33} are elastic moduli associated with the x and z directions. ν_{13} is Poisson's ratio and G_{13} the transverse shear modulus. In addition, the strain components are related to the displacement components by the following strain displacement relations.

$$u_{,x}=\epsilon_{xx};\qquad w_{,z}=\epsilon_{zz};\qquad u_{,z}+w_{,x}=\gamma_{xz} \tag{22}$$

Equations (16), (18), (20), and (22) permit the transverse normal strain to be approximated as

$$w_{,z}\cong-\frac{\nu_{13}}{E_{11}}\left(\frac{N}{A}+\frac{Mz}{I}\right)+\underline{\frac{Q_{,x}}{2E_{33}I}\left(\frac{z^3}{3}-c^2z+\frac{2}{3}c^3\right)} \tag{23}$$

Integration of this equation results in the following expression for the lateral displacement component w:

$$w=W(x)-\frac{\nu_{13}}{E_{11}}\left(\frac{Nz}{A}+\frac{Mz^2}{2I}\right)+\underline{\frac{Q_{,x}}{2E_{33}I}\left(\frac{z^4}{12}-\frac{c^2z^2}{2}+\frac{2}{3}c^3z\right)} \tag{24}$$

$W(x)$ is the lateral deflection of the beam axis ($z=0$), which is an unknown function to be determined.

The axial component of displacement u can be estimated as follows. Equations (17), (21), and (22) permit $u_{,z}$ to be ex-

Downloaded by UNIVERSITY OF MIAMI on December 31, 2014 | http://arc.aiaa.org | DOI: 10.2514/3.7938

pressed as

$$u_{,z}=\sigma_{xz}/G_{13}-w_{,x}=\frac{Q}{2G_{13}I}(c^2-z^2)-W_{,x}+\frac{\nu_{13}}{2E_{11}I}Qz^2$$
$$-\frac{Q_{,xx}}{2E_{33}I}\left(\frac{z^4}{12}-\frac{c^2z^2}{2}+\frac{2}{3}c^3z\right) \tag{25}$$

This expression is integrated to yield

$$u=U(x)-zW_{,x}+\frac{\nu_{13}}{E_{11}I}Q\frac{z^3}{6}+\frac{Q}{2G_{13}I}\left(c^2z-\frac{z^3}{3}\right)$$
$$\underline{-\frac{Q_{,xx}}{2E_{33}I}\left(\frac{z^5}{60}-\frac{c^2z^3}{6}+\frac{1}{3}c^3z^2\right)} \tag{26}$$

$U(x)$ is the axial deflection of the beam axis, which is an unknown function to be determined.

The static displacement field is completely described by Eqs. (24) and (26). This approximate displacement field was determined by estimating precisely the strains that are ignored in classical theory. U and W, the axis displacement components, emerge as natural kinematic variables. If $\nu_{13}\to 0$ and $E_{33}\to\infty$ in Eqs. (24) and (26), a transverse shear theory is obtained that includes the effects of cross section warping. If, in addition, $G_{13}\to\infty$, then the classical Bernoulli-Euler kinematic assumption is recovered.

Considerable simplification is achieved if the underlined terms in Eqs. (24) and (26) are neglected. These terms are associated with higher derivatives of the shear force Q than the remaining terms. This simplification is adopted here. Its full implication will be discussed in a future paper. The accuracy of this approximation is related to how rapidly the applied load q varies with x.

Refined Axial Stress Distribution

The axial stress σ_{xx} is the largest and most important stress component. An accurate knowledge of it is often all that is needed in a practical application. A refined estimate that improves Eq. (16) is central, therefore, to the improvements that are sought.

Equations (18), (19), and (26) can be utilized to produce a refined axial stress expression.

$$\sigma_{xx}=E_{11}u_{,x}+\nu_{13}\sigma_{zz}=E_{11}\left[U_{,x}-zW_{,xx}+\frac{\nu_{13}}{E_{11}I}Q_{,x}\frac{z^3}{6}\right.$$
$$\left.+\frac{Q_{,x}}{2G_{13}I}\left(c^2z-\frac{z^3}{3}\right)\right]+\nu_{13}\frac{Q_{,x}}{2I}\left(\frac{z^3}{3}-c^2z+\frac{2}{3}c^3\right) \tag{27}$$

In the preceding, contributions due to the underlined terms in Eq. (26) are not included. Notice that the stress distribution throughout the thickness is not linear as in the classical approximation Eq. (16).

Relationships for the axial force and bending moment are obtained by using Eqs. (13), (15), and (27). The results are

$$N=\left(E_{11}U_{,x}+\frac{\nu_{13}c^3}{3I}Q_{,x}\right)A \tag{28}$$

$$M=-E_{11}IW_{,xx}+\left(\frac{4}{5}k_x+\frac{\nu_{13}}{2}\right)c^2Q_{,x} \tag{29}$$

The parameter k_x is $(E_{11}/2G_{13}-\nu_{13})$; it is unity for an isotropic material. Equations (28) and (29) permit Eq. (27) to be rewritten as

$$\sigma_{xx}=\frac{N}{A}+\frac{Mz}{I}+\underline{\frac{Q_{,x}}{3I}k_x\left(\frac{3}{5}c^2z-z^3\right)} \tag{27a}$$

The underlined term is the nonclassical axial stress contribution, which is the desired refinement.

Summary

The governing equations for the new theory can be summarized now. They encompass four categories. Overall beam-type equations consist of the equilibrium Eqs. (10-12) and the constitutive Eqs. (28) and (29). In addition, two sets of equations provide the distributions of stresses and displacements throughout the structure. The first set for stresses consists of Eqs. (27a), (17), and (18). The second for displacements is composed of Eqs. (24) and (26) with the underlined terms omitted.

The preceding collection of equations requires the specification of boundary conditions. A virtual work development based upon U and W as displacements to be varied yields the classical boundary conditions as options. Thus, N or U, Q or W, and M or $W_{,x}$ must be specified at the ends of the beam.

It is often convenient to introduce an intermediate kinematic variable that is related to rotation of the beam cross section. Three commonly used variables are considered next. The first is the rotation of the cross section at the beam axis ϕ_1.

$$\phi_1=u_{,z}(x,0)=\frac{Qc^2}{2G_{13}I}-W_{,x} \tag{30}$$

Another is the rotation-related variable ϕ_2, which is defined by the following equation:

$$\phi_2=\frac{1}{I}\int_{-c}^{c}uz\,\mathrm{d}z=-W_{,x}+\frac{3}{10A}\left(\frac{\nu_{13}}{E_{11}}+\frac{4}{G_{13}}\right)Q \tag{31}$$

This variable naturally arises in Reissner's development of plate bending theory[8] based upon the complementary energy principle.

The third is the mean rotation of the cross section ϕ_3.

$$\phi_3=\frac{1}{2c}\int_{-c}^{c}u_{,z}\mathrm{d}z=\frac{1}{2c}[u(x,c)-u(x,-c)]$$
$$=\frac{Qc^2}{3I}\left(\frac{1}{G_{13}}+\frac{\nu_{13}}{2E_{11}}\right)-W_{,x} \tag{32}$$

In a Timoshenko-type theory, since u is linear in z, all of the preceding definitions are equivalent. Equation (30) is the actual definition used in the original paper.[2] These variables permit different models for simulating clamped end conditions to be defined.

Discussion

The development of the equations requires no ad hoc kinematic assumptions or use of a variational principle. The central assumption is that the transverse normal and shear strain components can be estimated from classical stresses. The equations have the following properties:

1) Stress and displacement distributions throughout the structure are found in terms of the response variables associated with the axis.

Downloaded by UNIVERSITY OF MIAMI on December 31, 2014 | http://arc.aiaa.org | DOI: 10.2514/3.7938

2) Nonclassical axial stress and cross section warping effects, transverse shear strain and transverse normal strain are all accounted for in a rational manner.

3) The equations can be shown to yield exact results for the case of uniformly distributed lateral loading.

4) For nonuniform loading, some of the equations are approximate: the stresses are not exactly in equilibrium and the stresses and displacements are not exactly compatible.

5) The equations are as simple to apply as static Timoshenko-type shear deformation theories.

Items 1-3 and 5 are strong points in favor of the new equations. Item 4 imposes some limitations on the validity of the theory, which will be thoroughly discussed in a future paper, but it is responsible for the simplicity that is achieved. The level of stress approximation which results is analogous to that suggested by Seewald[6] for isotropic materials.

In the process of solving a particular bending problem, the only apparent difference from application of a static Timoshenko-type shear deformation theory is the value for the coefficient of the $Q_{,x}$ term in Eq. (29). As the applications will demonstrate, this seemingly minor difference, together with the use of Eqs. (24), (26), and (27a), produces substantially improved results.

Applications

Introductory Remarks

In order to illustrate the theory, three elementary applications for uniform beams subjected to uniformly distributed loading applied to the upper surface, analogous to the situation shown in Fig. 1, will be presented. One special case of a linearly varying load is studied to illustrate a particular point. Comparisons are made with the exact solution, classical Bernoulli-Euler theory and the original static Timoshenko theory[2] in each case.

Solutions are derived for orthotropic beams, and corresponding results for isotropic beams are obtained by specialization. Poisson's ratio is taken to be 0.3 throughout. For orthotropic beams, E_{11}/G_{13} is taken to be 30; this is a typical value for a modern graphite/epoxy composite material.

In presenting results, appropriate response variables are nondimensionalized with respect to the corresponding values obtained from Bernoulli-Euler theory. This practice permits easy recognition of departures from classical theory predictions.

Response can be separated into bending and stretching. Stretching is governed by Eqs. (10) and (28), bending by Eqs. (11), (12), and (29). The bending problem involving *M, Q,* and *W* must be solved first. *N* and *U*, stretching variables, are determined secondarily. For the present purposes, only the bending portion of the response is discussed.

Simply Supported Beam

The exact solution for a simply supported (SS) isotropic beam was presented earlier. The precise boundary conditions that have been imposed at the ends are

$$\text{SS:}\quad M=0,\quad W=0 \tag{33}$$

Such a beam is shown in Fig. 1. It is a statically determinate structure, so the moment and shear distributions are known.

The response of the beam is defined if the axis lateral deflection $W(x)$ is found. For this type of end restraint, W can be expressed as

$$W=\delta-\frac{q}{4E_{11}I}\left[\left(\ell^2x^2-\frac{x^4}{6}\right)+\frac{K}{2}H^2x^2\right] \tag{34}$$

In Eq. (34) the constant K is

$$K=\tfrac{1}{2}\left(\alpha_s\frac{E_{11}}{G_{13}}-\alpha_n\nu_{13}\right)-\alpha_a\frac{k_x}{5} \tag{35}$$

The tracer constants introduced earlier are utilized to identify the origin of the various contributions to K. δ is the maximum or midspan deflection, which is

$$\delta=\frac{5q\ell^4}{24E_{11}I}\left[1+\frac{12}{5}K\left(\frac{H}{L}\right)^2\right] \tag{36}$$

$L=2\ell$ is the total length of the beam and $H=2c$ the depth of the cross section.

The solution by the present theory corresponds to $\alpha_a=\alpha_n=\alpha_s=1$ in Eq. (35); it is exact for this problem. If K is set to zero in Eqs. (34) and (36), then the Bernoulli-Euler result is obtained. If $\alpha_a=\alpha_n=0$ and $\alpha_s=1$ in Eq. (35), the static Timoshenko theory prediction is recovered. Timoshenko theory overestimates the deflection (underestimates stiffness) for this case.

Cantilever Beam

For a cantilever beam, it is convenient to take the origin of coordinates, $x=0$, at the free end. $x=L$ corresponds to the clamped end. Unlike the more elementary theories, the present theory does not suggest a unique, simple model for a clamped or fixed end. Three rotation variables were introduced earlier in Eqs. (30-32). Three clamping models, based upon these variables, will be discussed.

All results can be cast in a common format. The three clamping models are denoted C1, C2, and C3. They correspond to the following conditions:

$$\text{C1:}\quad W=0,\qquad \phi_1=0 \tag{37}$$

$$\text{C2:}\quad W=0,\qquad \phi_2=0 \tag{38}$$

$$\text{C3:}\quad W=0,\qquad \phi_3=0 \tag{39}$$

These models do not eliminate cross section warping, but they permit solutions by elementary means. The cantilever beam is statically determinate with M and Q vanishing at the free end. At the fixed end, one of the definitions of clamping just given must be imposed. The rotation variables can be expressed in the common form

$$\phi_i=K_i\frac{Qc^2}{E_{11}I}-W_{,x};\qquad i=1,2,3 \tag{40}$$

The constants K_1-K_3 are

$$K_1=\frac{\alpha_s}{2}\frac{E_{11}}{G_{13}} \tag{41}$$

$$K_2=\frac{1}{2}\left[\alpha_s\frac{E_{11}}{G_{13}}-\frac{\alpha_a}{5}\left(\frac{E_{11}}{G_{13}}-\nu_{13}\right)\right] \tag{42}$$

$$K_3=\frac{1}{2}\left[\alpha_s\frac{E_{11}}{G_{13}}-\frac{\alpha_a}{3}\left(\frac{E_{11}}{G_{13}}-\nu_{13}\right)\right] \tag{43}$$

The lateral deflection can be conveniently expressed as follows:

$$W=\delta_i-\frac{q}{E_{11}I}\left[\left(\frac{L^3}{6}+(K_i-K)c^2L\right)x+\frac{KH^2}{8}x^2-\frac{x^4}{24}\right];\qquad i=1,2,3 \tag{44}$$

Downloaded by UNIVERSITY OF MIAMI on December 31, 2014 | http://arc.aiaa.org | DOI: 10.2514/3.7938

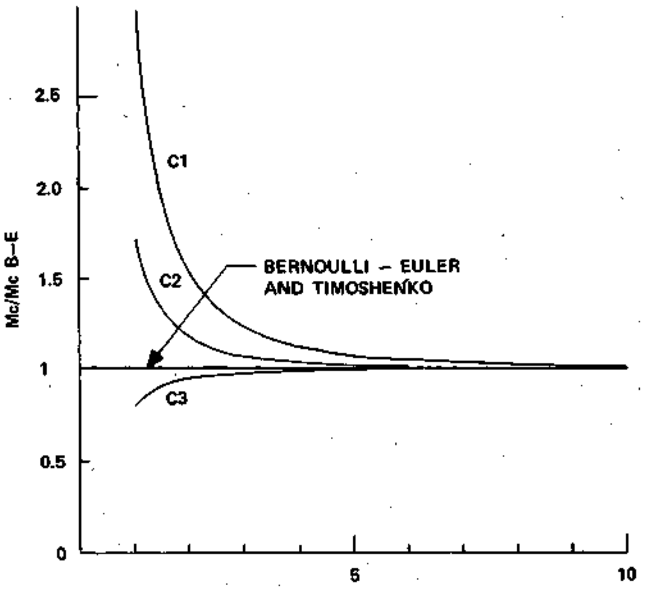

Fig. 3 Central moment ratio for a clamped isotropic beam.

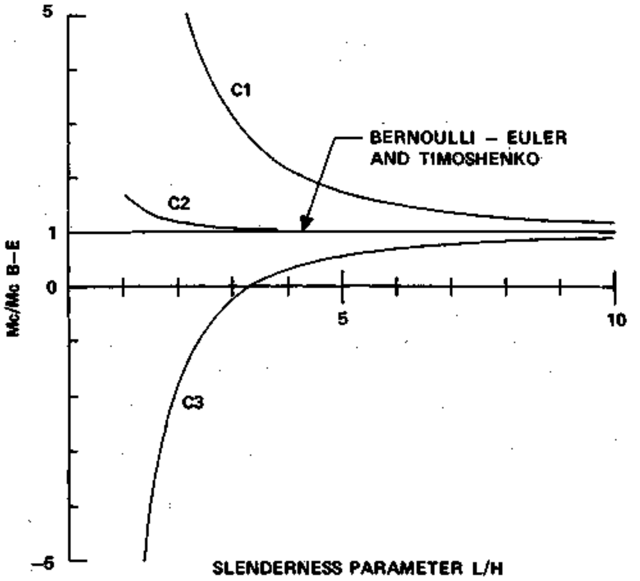

Fig. 4 Central moment ratio for a clamped orthotropic beam.

The constants δ_i $(i=1,2,3)$ are the beam tip deflections; they are found from

$$\delta_i = \frac{qL^4}{8E_{11}I}\left[1+(2K_i-K)\left(\frac{H}{L}\right)^2\right]; \qquad i=1,2,3 \tag{45}$$

The constant K is defined in Eq. (35).

The present theory solutions correspond to setting all the tracer constants to unity; they are exact for the end conditions imposed. The designation C1, C2, and C3 has been chosen to correspond to the order of increasing stiffness of the end restraint. Differences in response due to the definition of clamping imposed are minor in this case.

If K_i and K are set to zero in the preceding equations, the Bernoulli-Euler results are obtained. This approximation overestimates stiffness. The Timoshenko theory results ($\alpha_s=1$ and $\alpha_a=\alpha_n=0$), interestingly enough, overestimate stiffness in this case.

Bernoulli-Euler theory tends to always overestimate stiffness. Timoshenko theory, however, in light of the results presented here, may either provide an overestimate or underestimate of stiffness, depending upon the problem under consideration.

A related problem is a cantilever beam subjected to a linearly varying distributed load that varies from zero at the free end to q at the fixed end. The exact solution is given in Ref. 4. For an isotropic beam with C1 restraint at the fixed end, the tip deflection is

$$\delta = \frac{qL^4}{30EI}\left\{1+\frac{H^2}{4L^2}\left[2\alpha_a+5\alpha_n+5\alpha_s(1+\nu)\right] \underline{-\frac{\alpha_s}{4}(1+\nu)\left(\frac{H}{L}\right)^4}\right\} \tag{46}$$

If the present theory is used, the underlined term is not obtained. For $L/H>2$, this term is negligible. For practical purposes, therefore, the present theory results are indistinguishable from the exact ones.

Clamped Beam

Unlike the previous examples, the clamped beam is statically indeterminate. Three solutions corresponding to the three clamping models have been determined. They may be expressed in a common form. It is convenient to place the origin of coordinates at midspan and use the semilength ℓ. The bending moment distribution is

$$M=(q/2)(\ell^2-x^2)-M_0 \tag{47}$$

M_0 is the end fixing moment, which is positive if it tends to reduce the end rotation due to the uniform load.

The expression for the lateral axis deflection is

$$W=\frac{1}{E_{11}I}\left[\frac{q}{4}\left(\frac{5}{6}\ell^4-\ell^2x^2+\frac{x^4}{6}\right)+\left(\frac{KH^2q}{8}-\frac{M_0}{2}\right)(\ell^2-x^2)\right] \tag{48}$$

The redundant end fixing moment is different for each clamping model. It can be written in the common form

$$M_0=\frac{qL^2}{12}\left[1+3\left(\frac{H}{L}\right)^2(K-K_i)\right]; \qquad i=1,2,3 \tag{49}$$

The occurrence of different end moment values is due to the statically indeterminate nature of the structure. The present theory yields the exact solutions to this problem for each form of clamping.

A central moment ratio as a function of beam slenderness is plotted in Figs. 3 and 4 for isotropic and orthotropic materials, respectively. The notation B-E refers to the value from Bernoulli-Euler theory. Bernoulli-Euler and Timoshenko theories give identical predictions. The present theory, however, which agrees with the exact solutions, predicts behavior that differs for each clamping model. Departures from classical theory are much greater for beams made of the typical orthotropic material. This is because the transverse shear stiffness to extensional stiffness ratio is low for this material, which accentuates the nonclassical effects.

It is apparent that predictions for shorter beams, the class of structures for which improved predictions are the most needed, are sensitive to the precise conditions used to model restraint. Consequently, care must be devoted to matching mathematical descriptions of boundary restraint with practical end restraint achieved in tests or structural assemblies. The clamped end condition is an extreme example as cross section warping cannot be fully eliminated by elementary means.

Downloaded by UNIVERSITY OF MIAMI on December 31, 2014 | http://arc.aiaa.org | DOI: 10.2514/3.7938

Concluding Remarks

A systematic analysis employing tracer constants has been presented which adds quantitative proof to the earlier statements of Goodier. There are two additional effects, transverse normal strain and nonclassical axial stress, in addition to transverse shear strain, which must be included in a refined bending theory. New equations for planar bending are developed which 1) include all the essential physical effects, 2) provide predictions which are exact or indistinguishable from exact solutions for a variety of examples, 3) provide information which is not discernible by other engineering theories, and 4) are as simple to apply as static Timoshenko-type theory.

Further consideration must be given to the modeling of boundary conditions which restrain local cross section warping. This will be the subject of a forthcoming paper.

Acknowledgments

This work was sponsored by AFOSR under Contract F49620-78-C-0085. The authors acknowledge the enormous debt due to their predecessors. Discussions with Mr. R. R. Valisetty have been extremely helpful. Professor C. Virgil Smith suggested the boundary condition C3.

References

[1] Love, A. E. H., *A Treatise on the Mathematical Theory of Elasticity*, 4th ed., Cambridge University Press, Cambridge, England, 1952.

[2] Timoshenko, S. P., "On the Correction for Shear of the Differential Equation for Transverse Vibrations of Prismatic Bars," *Philosophical Magazine*, Ser. 6, Vol. 41, 1921, pp. 744-746.

[3] Rehfield, L. W. and Murthy, P. L. N., "Toward A New Engineering Theory of Bending," AFOSR Tech. Rept., number to be assigned, Jan. 1981.

[4] Timoshenko, S. P. and Goodier, J. N., *Theory of Elasticity*, 3rd ed., McGraw Hill Book Co., New York, 1970, pp. 274-277.

[5] Von Kármán, Th., "Über die Grundlagen der Balkentheorie," *Abhandlungen aus dem Aerodynamischen Institut an der Technischen Hochschule Aachen*, Vol. 7, 1927, pp. 3-10.

[6] Seewald, Von F., "Die Spannungen and Formänderungen von Balken mit rechteckigem Querschnitt," *Abhandlungen aus dem Aerodynamischen Institut an der Technischen Hochschule Aachen*, Vol. 7, 1927, pp. 11-33.

[7] Goodier, J. N., "On the Problems of the Beam and Plate in the Theory of Elasticity," *Transactions of the Royal Society of Canada, Third Series*, Vol. 32, Sec. 3, 1938, pp. 65-68.

[8] Reissner, E., "On Bending of Elastic Plates," *Quarterly of Applied Mathematics*, Vol. 5, 1947, pp. 55-68.

From the AIAA Progress in Astronautics and Aeronautics Series . . .

AEROTHERMODYNAMICS AND PLANETARY ENTRY—v. 77

HEAT TRANSFER AND THERMAL CONTROL—v. 78

Edited by A. L. Crosbie, University of Missouri-Rolla

The success of a flight into space rests on the success of the vehicle designer in maintaining a proper degree of thermal balance within the vehicle or thermal protection of the outer structure of the vehicle, as it encounters various remote and hostile environments. This thermal requirement applies to Earth-satellites, planetary spacecraft, entry vehicles, rocket nose cones, and in a very spectacular way, to the U.S. Space Shuttle, with its thermal protection system of tens of thousands of tiles fastened to its vulnerable external surfaces. Although the relevant technology might simply be called heat-transfer engineering, the advanced (and still advancing) character of the problems that have to be solved and the consequent need to resort to basic physics and basic fluid mechanics have prompted the practitioners of the field to call it thermophysics. It is the expectation of the editors and the authors of these volumes that the various sections therefore will be of interest to physicists, materials specialists, fluid dynamicists, and spacecraft engineers, as well as to heat-transfer engineers. Volume 77 is devoted to three main topics, Aerothermodynamics, Thermal Protection, and Planetary Entry. Volume 78 is devoted to Radiation Heat Transfer, Conduction Heat Transfer, Heat Pipes, and Thermal Control. In a broad sense, the former volume deals with the external situation between the spacecraft and its environment, whereas the latter volume deals mainly with the thermal processes occurring within the spacecraft that affect its temperature distribution. Both volumes bring forth new information and new theoretical treatments not previously published in book or journal literature.

Volume 77—444 pp., 6×9, illus., $30.00 Mem., $45.00 List
Volume 78—538 pp., 6×9, illus., $30.00 Mem., $45.00 List

TO ORDER WRITE: Publications Dept., AIAA, 1290 Avenue of the Americas, New York, N.Y. 10104

Downloaded from ascelibrary.org by New York University on 05/18/15. Copyright ASCE. For personal use only; all rights reserved.

TECHNICAL THEORY OF BEAMS WITH NORMAL STRAIN

By Mohammed H. Baluch,[1] Abul K. Azad,[2] M. ASCE,
and Mohamed A. Khidir[3]

INTRODUCTION

A theory which takes into account the influence of transverse normal strain on the bending of isotropic and nonisotropic plates was formulated recently and applied to plates in cylindrical bending (1) in addition to studying the classical wave propagation problem in such plates (5).

The work presented in this paper includes an extension and application of the refined theory to isotropic beams. The features of this work include: (1) Establishment of the fact that the refined theory, when applied to beams, is of fourth order in bending and second order in a plane problem, yielding a combined sixth order problem; and (2) the nature of the boundary conditions. The boundary conditions are specified in the exact sense and in the average sense, both in terms of stress resultants and displacement resultants.

GOVERNING EQUATIONS

The equations may be deduced from the plate equations as given in Ref. 5 by initially assuming a parabolic variation for the shear stress τ_{xz} and then using equilibrium to obtain a cubic variation for the transverse normal stress σ_z subject to the boundary conditions $\sigma_z(x, +h/2) = 0$; $\sigma_z(x, -h/2) = -p$. Consequently, an expression for the transverse normal strain ϵ_z is obtained by using Hooke's constitutive equation, together with a linear approximation for the normal stress $\sigma_x (= 12\ M_x z/h^3)$. Integrating the expression for ϵ_z for transverse displacement

$$w(x,z) = -\frac{p}{4E}\left[2z - \frac{3z^2}{h} + \frac{2z^4}{h^3}\right] - \frac{6\nu M_x}{Eh^3} z^2 + w_o(x) \quad \ldots\ldots\ldots\ldots\ldots\ldots (1)$$

is obtained; in which w_o is the transverse displacement of the surface $z = 0$; M_x = moment per unit width; E = modulus of elasticity; ν = Poisson's ratio; and h = beam depth. Further, using strain-displacement relation for γ_{xz}, the displacement along the beam axis becomes

---

[1] Assoc. Prof., Dept. of Civil Engrg., Univ. of Petroleum & Minerals, UPM Box 57, Dhahran Airport Box 144, Dhahran, Saudi Arabia.

[2] Assoc. Prof., Dept. of Civil Engrg., Univ. of Petroleum & Minerals, Dhahran, Saudi Arabia.

[3] Grad. Research Asst., Dept. of Civil Engrg., Univ. of Petroleum & Minerals, Dhahran, Saudi Arabia.

Note.—Discussion open until January 1, 1985. To extend the closing date one month, a written request must be filed with the ASCE Manager of Technical and Professional Publications. The manuscript for this paper was submitted for review and possible publication on October 28, 1983. This paper is part of the *Journal of Engineering Mechanics*, Vol. 110, No. 8, August, 1984. ©ASCE, ISSN 0733-9399/84/0008-1233/$01.00. Paper No. 19033.

$$u(x,z) = -z\frac{dw_o}{dx} + \frac{Q_x}{2G}\frac{z}{h}\left[3 - \left(\frac{2z}{h}\right)^2\right] + \frac{1}{4E}\frac{dp}{dx}\left[z^2 - \frac{z^3}{h} + \frac{2z^5}{5h^3}\right]$$

$$+ \frac{2\nu}{Eh^3}\frac{dM_x}{dx}z^3 + u_o(x) \tag{2}$$

in which u_0 is the u displacement of the surface $z = 0$; Q_x = shear per unit width; G = shear modulus. Using the cubic variation for σ_z and Eq. 2 for displacement u in the stress-strain relation describing ϵ_x, an expression for σ_x is obtained as

$$\sigma_x = E\left\{-z\frac{d^2w_o}{dx^2} + \frac{1}{2G}\frac{dQ_x}{dx}\frac{z}{h}\left[3 - \left(\frac{2z}{h}\right)^2\right] + \frac{1}{4E}\frac{d^2p}{dx^2}\left[z^2 - \frac{z^3}{h} + \frac{2z^5}{5h^3}\right]\right.$$

$$\left. + \frac{2\nu}{Eh^3}\frac{d^2M_x}{dx^2}z^3\right\} + \frac{Edu_o}{dx} - \frac{\nu p}{4}\left[2 - 3\left(\frac{2z}{h}\right) + \left(\frac{2z}{h}\right)^3\right] \tag{3}$$

Using Eq. 3 in the definitions for the stress resultants $M_x = \int_{-h/2}^{+h/2}\sigma_x z\,dz$; $N_x = \int_{-h/2}^{+h/2}\sigma_x\,dz$ yields

$$M_x = EI\left[\frac{d\phi_x}{dx} + \frac{6\nu}{5Eh}p\right] \tag{4}$$

$$N_x = Eh\frac{du_o}{dx} - \frac{\nu ph}{2} + \frac{h^3}{48}\frac{d^2p}{dx^2} \tag{5}$$

in which $$\phi_x = -\frac{dw_o}{dx} + \frac{Q_x}{S} - \frac{1}{N}\frac{dp}{dx} + \frac{1}{R}\frac{dM_x}{dx} \tag{6}$$

and $S = 5Eh/[12(1+\nu)]$; $N = 1{,}120E/39h$; $R = 10Eh/3\nu$; $I = h^3/12$. Also required are the equilibrium equations $dQ_x/dx + p = 0$; $dM_x/dx = Q_x$; and $dN_x/dx = 0$.

BOUNDARY CONDITIONS

An interpretation for the term ϕ_x is first given. The line of reasoning used is basically that originally given by Green (3) for a Reissner plate model. Defining the average rotation of a section x = constant by ψ_x, one equates the work of the resultant couple displacing through the average rotation to the work of the corresponding stress σ_x due to displacement u, i.e.

$$\int_{-h/2}^{+h/2}\sigma_x u\,dz = M_x\psi_x \tag{7}$$

The stress expression to be used for σ_x in Eq. 7 is the linear expression used as input stress in the iteration that yields displacement u as given by Eq. 2. On substitution of appropriate expressions into Eq. 7, with subsequent integration, yields for ψ_x the same expression as that given for ϕ_x in Eq. 6. Thus, ϕ_x is the rotation of any vertical element of the beam.

Consequently, if a beam has a fixed support at $x = L$, the boundary

Downloaded from ascelibrary.org by New York University on 05/18/15. Copyright ASCE. For personal use only; all rights reserved.

Downloaded from ascelibrary.org by New York University on 05/18/15. Copyright ASCE. For personal use only; all rights reserved.

conditions would be $w_o(L) = 0$; $\phi_x(L) = 0$. If the beam is simply supported at $x = L$, the boundary conditions would be $w_o(L) = 0$; $M_x(L) = 0$. Also, the stretch effect has increased the order of the system by two, as indicated by substitution of Eq. 5 into the equilibrium equation $dN_x/dx = 0$. The boundary conditions on u_o are $u_o(L) = 0$ if the edge $x = L$ is fixed and $N_x(L) = 0$ if the edge $x = L$ is free.

An alternative boundary condition may be derived in terms of a displacement resultant function. Introducing an average transverse displacement $\bar{w}$ and equating work

$$\int_{-h/2}^{+h/2} \tau_{xz} w dz = Q_x \bar{w} \qquad (8)$$

yields for $\bar{w}$ the expression

$$\bar{w} = w_o + \frac{p}{N} - \frac{M_x}{R} \qquad (9)$$

It is noted that while the transverse shear modifies the rotation of the bending theory from $-dw_o/dx$ to $-dw_o/dx + Q_x/S$, the transverse normal strain modifies the displacement from w_o to $w_o + p/N - M_x/R$ [yielding a rotation $-d/dx\,(w_o + p/N - M_x/R) + Q_x/S$ as given by Eq. 6].

APPLICATION

Substituting the known beam moment function (Fig. 1) into Eq. 4 and integrating yields

$$\phi_x = \frac{1}{EI} p \frac{Lx^2}{4} - p \frac{x^3}{6} - \frac{6\nu}{5Eh} px + C_1 \qquad (10)$$

Substituting Eq. 10 into Eq. 6 and integrating with respect to x, together with the boundary conditions $w_o(0) = 0$ and $w_o(L) = 0$, yields

$$w_o = p\frac{x}{2}(L - x)\bar{R} + p\frac{x}{24EI}(x^3 - 2Lx^2 + L^3) + \frac{3\nu p x}{5Eh}(x - L) \qquad (11)$$

in which $\bar{R} = R + S/SR$. For the stretch of the middle surface, on successive integration of the second order equation on u_o, together with boundary conditions of free stretch at the two ends and $u_o(L/2) = 0$, one obtains, $u(x, o) = u_o = \nu p/2E(x - L/2)$, which is identical to the exact solution as given in Eq. 4.

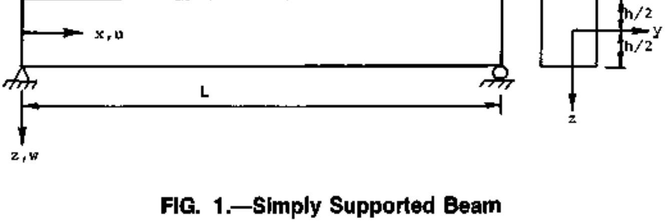

FIG. 1.—Simply Supported Beam

J. Eng. Mech. 1984.110:1233-1237.

Downloaded from ascelibrary.org by New York University on 05/18/15. Copyright ASCE. For personal use only; all rights reserved.

TABLE 1.—Values of $w_o EI/pL^4$ (ν = 0.3)

h/L (1)	Exact solution (2)	Present theory Eq. 11 (3)	Present theory Eq. 12 (4)	Shear deformation theory (5)
0.025	0.0130393	0.0130393	0.0130394	0.0130411
0.100	0.0133176	0.0133176	0.0133174	0.0133458
0.200	0.0142083	0.0142083	0.0142037	0.0143208
0.300	0.0156926	0.0156926	0.0156692	0.0159458
0.400	0.0177708	0.0177708	0.0176965	0.0182208
0.500	0.0204426	0.0204426	0.0202613	0.0211458

In the shear deformation theory, u_o is identically zero at all points of the beam.

The substitution of various functions and their derivatives in Eq. 3 yields for the flexural stress at $x = L/2$; $\sigma_x = p\, z/h\, [3/2(L/h)^2 - 3/5] + 4p(z/h)^3$ which is identical to the exact expression given in Eq. 4.

The alternate formulation for the case studied is made in terms of the boundary condition on the displacement resultant $\bar{w}$. The boundary conditions to be satisfied in this case are $\bar{w}(o) = \bar{w}(L) = 0$ and lead to

$$w_o\left(x=\frac{L}{2}\right)=\frac{pL^4}{EI}\left[\frac{5}{384}+\left(\frac{24+15\nu}{960}\right)\left(\frac{h}{L}\right)^2-\frac{39}{13{,}440}\left(\frac{h}{L}\right)^4\right] \quad \ldots\ldots\ldots\ldots (12)$$

Table 1 shows a comparison of w_o at midspan as given by Eqs. 11 and 12, the exact theory and the shear deformation theory (2). The table indicates that the point boundary condition (Eq. 11) yields results identical to the exact solution, inasmuch as the elasticity boundary condition on w is in a point sense. However, results from Eq. 12, although a correction over the shear deformation theory, are not identical to the exact solution inasmuch as an average (but consistent) displacement boundary condition has been used rather than the displacement of a specific point.

CONCLUSIONS

The results for the case presented indicate a verification of the refined theory developed and interpreted in this work. Differences due to use of point boundary conditions as compared to resultant boundary conditions have also been addressed.

ACKNOWLEDGMENT

The support of the University of Petroleum and Minerals, Dhahran, Saudi Arabia, in the pursuit of this work is acknowledged.

APPENDIX.—REFERENCES

1. Baluch, M. H., and Voyiadjis, G. Z., "A Refined Theory for the Bending of Plates," 15th International Congress of Theoretical and Applied Mechanics, Aug., 1980, Toronto, Canada.
2. Reismann, H., and Pawlik, P. S., *Elasticity, Theory and Applications,* John Wiley & Sons, Inc., New York, N.Y., 1980, pp. 226–229.

3. Timoshenko, S. P., and Woinowsky-Krieger, S., *Theory of Plates and Shells*, McGraw-Hill, Tokyo, Japan, 1959, p. 168.
4. Venkatraman, B., and Patel, S. A., *Structural Mechanics with Introduction to Elasticity and Plasticity*, McGraw-Hill Book Co., New York, N.Y., 1970.
5. Voyiadjis, G. Z., and Baluch, M. H., "Refined Theory for Flexural Motions of Isotropic Elastic Plates," *Journal of Sound and Vibration*, Vol. 76, No. 1, 1981, pp. 57–64.

Downloaded from ascelibrary.org by New York University on 05/18/15. Copyright ASCE. For personal use only; all rights reserved.

NONLINEAR ANALYSIS OF LOOSELY CLAMPED PLATES

By Robert Schmidt,[1] M. ASCE

INTRODUCTION

One of the few analytical methods available for the analysis of flexure of plates with moderately large deflections is the so-called perturbation method (1,3,5–11,13), the main feature of which is the representation of a dependent variable as a power series in a constant (perturbation) parameter. In the geometrically nonlinear theory of plates, the central deflection (3,5–7,10,13), edge rotation (9), load (11), and $(1 - \nu)$, where ν is Poisson's ratio, (8) have been used in the role of the perturbation parameter. The asymptotic solutions in (6,7,10,13) have indicated that $(1 - \nu^2)$ is a suitable parameter for loosely clamped circular plates with finite axisymmetric deflections. Herein, in order to demonstrate the utility of this new parameter, an analysis of a uniformly loaded circular plate with movable clamped edge is carried out. Furthermore, deviating from the usual practice of obtaining the necessary linearized equations from the nonlinear differential equations, the derivations make use of the energy integrals.

EQUATIONS

With the dimensionless independent variable $s = r/a$, the potential energy integral V can be written as (12)

$$V = \pi \int_0^1 \left\{ D \left[s(\beta')^2 + \frac{\beta^2}{s} + 2\nu\beta\beta' \right] + K[a^2 s e^2 - (1 - \nu)(2uu' + au\beta^2)] \right.$$

---

[1] Prof., Dept. of Mech. Engrg., Univ. of Detroit, Detroit, Mich. 48221.

Note.—Discussion open until January 1, 1985. To extend the closing date one month, a written request must be filed with the ASCE Manager of Technical and Professional Publications. The manuscript for this paper was submitted for review and possible publication on December 6, 1983. This paper is part of the *Journal of Engineering Mechanics*, Vol. 110, No. 8, August, 1984. ©ASCE, ISSN 0733-9399/84/0008-1237/$01.00. Paper No. 19033.

J. Eng. Mech. 1984.110:1233-1237.

MECHANICS RESEARCH COMMUNICATIONS Vol.12(1), 1-9, 1985. Printed in the USA.
0093-6413/85 $3.00 + .00 Copyright (c) 1985 Pergamon Press Ltd.

ON BICKFORD'S CONSISTENT HIGHER ORDER BEAM THEORY

Mark Levinson
Department of Mechanical Engineering, University of Maine at Orono
Orono, Maine, U.S.A.

(Received 2 July 1984; accepted for print 25 January 1985)

Introduction

Recently Bickford [1] used Hamilton's principle to derive a consistent, higher order theory of the elastodynamics of beams based upon the kinematic and stress assumptions previously used by Levinson [2] for beams of rectangular cross section. In [2] the usual beam equations of motion [3] were used to obtain a higher order beam theory. This latter theory provided a fourth order system of differential equations not too unlike the equations of Timoshenko beam theory with the difference being that in the new theory the shear stress boundary conditions on the lateral surfaces of the beam were satisfied. Bickford's consistent theory is a sixth order system of differential equations requiring the specification, provided by the variational formulation, of three boundary conditions at each end of the beam. A vectorial formulation of Bickford's theory is achieved in [1] by defining *a posteriori*, a "... higher order moment resultant" but, as Bickford himself notes, "It remains to be seen whether or not there can be developed a rational method for constructing the vectorial equations without knowing, *a priori*, the variational equations." This latter point is of no consequence since the validity of the variational equations is unquestioned.

It would seem that Bickford's work has relegated the earlier work of the present writer to the status of an intellectual artifact in the history of applied mechanics whose importance is limited to providing the motivation for the work of Bickford; from a certain theoretical point of view this is clearly so. What is vexatious, however, is that Bickford's theory, in the two elastostatic and one elastodynamic problems which he considers, provides inferior results in two cases and essentially the same results in the remaining case when compared to the results given by the present writer's theory, exact elasticity solutions being available for purposes of comparison in all three of the examples considered. Bickford [2] makes comparisons only with Timoshenko beam theory and the theory of elasticity and one of the latter comparisons is erroneous.

It is the purpose of this paper, therefore, to bring to the attention of the applied mechanics community the observation that a theoretically superior beam theory does not, in three often used comparison examples, always provide better or even equally good, results when compared with a supposedly inferior theory. This question is considered in the discussion at the end of this paper.

The Various Theories

Bickford's (variationally) consistent beam theory is based upon the kinematic assumptions, previously used in [2], that

$$u(x,z,t) = z\left(1 - \frac{4}{3}\frac{z^2}{h^2}\right)\psi - \frac{4}{3}\frac{z}{h}\frac{\partial w}{\partial x}$$

and (1)

$$w(x,z,t) = w(x,t)$$

where u and w are displacement components in the x and z directions respectively. $\psi(x,t)$ represents the rotation, at the neutral surface, of a cross-section of the beam; the comparable quantity in Timoshenko beam theory is an averaged rotation of the cross-section [4]. u and w as given lead, upon use of the strain-displacement relations and Hooke's law, to the vanishing of the shear stress at $z = \pm\frac{h}{2}$ where h is the depth of the beam of narrow, rectangular cross-section whose width conveniently may be taken as unity. Furthermore, Bickford assumed the beam to be in a one-dimensional state of stress as was also done in [2].

By making use of the above assumptions and Hamilton's Principle, Bickford obtained the following consistent boundary value problem for the linear elastodynamics of a beam of rectangular cross-section. The equations of motion are

$$\alpha(\psi + w') + \frac{\partial}{\partial x}\left[\beta(16\,w'' - 68\psi')\right] = \frac{\partial}{\partial t}\left[\gamma(16\,\dot{w}' - 68\dot{\psi})\right]$$

and (2)

$$\frac{\partial}{\partial x}\left[\alpha(\psi + w')\right] - \frac{\partial^2}{\partial x^2}\left[\beta(5w'' - 16\;')\right] = \rho A\ddot{w} - \frac{\partial^2}{\partial t\,\partial x}\left[\gamma(5\dot{w}' - 16\dot{\psi})\right] - p(x,t)$$

and the boundary conditions given by Bickford are

$$\alpha(w' + \psi) - \frac{\partial}{\partial x}\left[\beta(5w'' - 16\psi')\right] - \frac{\partial}{\partial t}\left[\gamma(5w'' - 16\dot{\psi})\right]\quad \delta w\Big|_0^{\ell} = 0\ ,$$

$$\beta(16\psi' - 5w'')\delta w'\Big|_0^{\ell} = 0\ , \qquad (3)$$

and

$$\beta(16w'' - 68\psi')\delta\psi\Big|_0^{\ell} = 0$$

where ρ is the density of the beam and p(x,t) is the transverse loading acting on the beam of length ℓ. Furthermore,

$$(\ \ )' \equiv \frac{\partial(\ )}{\partial x}\ ,\ (\dot{\ }) \equiv \frac{\partial(\ )}{\partial t}\ ,\ \alpha = \frac{8AG}{15}\ ,$$

(4)

$$\beta = \frac{EI}{105}\ ,\ \gamma = \frac{\rho I}{105}\ ,\ A = h,\ \text{and}\ I = \frac{h^3}{12}$$

with E and G being the elastic and shear modulii of the beam's material respectively.

The above theory, of sixth order in x, is the one provided by the calculus of variations which is consistent with the kinematic assumptions (1).

The work of Levinson [2] done earlier, was based upon the kinematic assumptions (1) and the usual notions of transverse shear force Q and bending moment M. These are related by the beam equations of motion [3]

$$\begin{gathered} Q' = \rho A\ddot{w} - p \\ \text{and} \\ M' - Q = \int_A \rho\ddot{u}z\,dA. \end{gathered} \tag{5}$$

The analysis [2] led to the following boundary value problem for the linear elastodynamics of a beam of narrow rectangular cross-section.

$$\begin{gathered} \frac{2}{3}AG(\psi + w') + \frac{1}{5}\frac{\partial}{\partial x}\left[EI(w'' - 4\psi')\right] = \frac{1}{5}\rho I(\ddot{w}' - 4\ddot{\psi}) \\ \text{and} \\ \frac{2}{3}\frac{\partial}{\partial x}\left[AG(\psi + w')\right] = \rho A\ddot{w} - p(x,t) \end{gathered} \tag{6}$$

are the governing differential equations while the boundary conditions to be satisfied at each end of the beam are

$$\begin{gathered} Q = \frac{2}{3}AG(\psi + w') \text{ or } w \text{ specified} \\ \text{and} \\ M = \frac{1}{5}EI(4\psi' - w'') \text{ or } \psi \text{ specified.} \end{gathered} \tag{7}$$

The approximate theory represented by equations (6) and (7), which is of the fourth order in x, clearly is different from Bickford's approximate theory given in equations (2) and (3). Furthermore, the former theory cannot be obtained from Bickford's theory by an approximation procedure of any sort. Note, however, that the former theory, equations (6) and (7), is mathematically well-posed. From an energy viewpoint, *i.e.* being consistent with Hamilton's principle, Bickford's theory is to be preferred. We note that Bickford was able, *a posteriori*, to provide a vectorial, *i.e.* dynamic equilibrium, derivation by introducing a "...higher order moment resultant"

$$M = -\int_A z^3\sigma_{xx}\,dA = \frac{EIh^2}{10}(5w'' - 16\psi') \tag{8}$$

and manipulating the stress equations of motion of the plane mechanics of a continuous media in less than obvious ways. In fact, Bickford himself noted that "It remains to be seen whether or not there can be developed a rational method for constructing the vactorial equations without knowing, *a priori*, the variational equations."

Since some comparisons with the results of the now classical Timoshenko beam theory will be made later in this paper, it is appropriate to give the equations of that theory here for reference purposes. They are, in the notation used in this paper,

$$\kappa^2 AG(\psi + w') - \frac{\partial}{\partial x}(EI\psi') = -\rho I\ddot{\psi}$$

and (9)

$$\kappa^2 \frac{\partial}{\partial x}[AG(\psi + w')] = \rho A\ddot{w} - p(x,t)$$

while the appropriate boundary conditions are

$$Q = \kappa^2 AG(\psi + w') \text{ or } w \text{ specified}$$

and (10)

$$M = EI\psi' \text{ or } \psi \text{ specified}$$

at each end of the beam. κ^2 is the so-called Timoshenko shear coefficient and ψ here represents an averaged rotation of a beam cross-section; this latter matter is discussed in some detail in [4].(1) Note that the mathematical structure of the boundary value problem given by equations (9) and (10) is the same as that of the one given by equations (6) and (7).

We now proceed to compare the predictions of the various approximate theories with those of the linear theory of elasticity for several particular problems. These comparisons will lead to an unexpected conundrum which will be examined in later discussion.

Some Examples and Comparisons

We now give some results for three standard problems, all used for illustrative purposes by Bickford, as given by (a) Bickford's theory, (b) the theory given in [2], and (c) Timoshenko beam theory. These results are then compared with those provided by the classical, linear theory of elasticity; Bickford did not provide all of these comparisons. The problems considered are the elastostatic ones for the end loaded cantilever and the uniformly loaded, simply supported beam while the third one is the elastodynamic problem for the first family of flexural frequencies of simply supported beams (or its travelling wave equivalent).

---

(1) The theory given in [2] primarily was devised so as to have a beam theory which included shear deflection and rotatory inertia effects but did not require, as does Timoshenko beam theory, an adscitious shear coefficient.

1. The End Loaded Cantilever

For our purposes it is sufficient to give the expressions for $w(x)$ provided by the various beam theories as well as $w(x,0)$ from the theory of elasticity. The loaded end of the beam is taken to be at $x = 0$ and the beam is fixed at $x = \ell$ while $-h/2 \leq z \leq h/2$. w_b, w_ℓ, w_t, w_e, and $\overline{w}$ are the deflections given by Bickford's theory, Levinson's theory, Timoshenko's theory, linear elasticity for the case of plane stress, and Bernoulli-Euler (or technical) beam theory, respectively.

$$w_b = \overline{w} + \frac{1}{5}\frac{P\ell^3}{EI}(1+\nu)\left(\frac{h}{\ell}\right)^2\left(1 - \frac{x}{\ell} - \frac{\sinh\lambda\ell - \sinh\lambda x}{\lambda\ell\cosh\lambda\ell}\right) \tag{11}$$

where

$$\lambda = \frac{420}{(1+\nu)h} \qquad (12)^{(2)}$$

and

$$\overline{w} = \frac{P\ell^3}{6EI}\left(\frac{x^3}{\ell^3} - 3\frac{x}{\ell} + 2\right). \tag{13}$$

$$w_\ell = \overline{w} + \frac{1}{4}\frac{P\ell^3}{EI}(1+\nu)\left(\frac{h}{\ell}\right)^2\left(1 - \frac{x}{\ell}\right), \tag{14}$$

$$w_t = \overline{w} + \frac{1}{5}\frac{P\ell^3}{EI}(1+\nu)\left(\frac{h}{\ell}\right)^2\left(1 - \frac{x}{\ell}\right), \tag{15}$$

and

$$w_e(x,0) = \overline{w} + \frac{1}{4}\frac{P\ell^3}{EI}(1+\nu)\left(\frac{h}{\ell}\right)^2\left(1 - \frac{x}{\ell}\right) \text{ from [5].} \tag{16}$$

It already is apparent from this problem that Bickford's (variationally) consistent beam theory [1] provides a result for the beam deflection which is inferior, when compared to the one given by the linear theory of elasticity, to the prediction of the theory given in [2]. In fact, for this example the latter theory gives the exact deflection curve for the neutral surface. Indeed, for the deflection of the loaded end, Bickford provides an approximation which is very slightly inferior to the one given by Timoshenko beam theory [3](3) due to the hyperbolic term which at $x = 0$ becomes

$$\frac{(1+\nu)}{420}\left(\frac{h}{\ell}\right)\tanh\left[\frac{420}{(1+\nu)}\left(\frac{\ell}{h}\right)\right] \approx \frac{(1+\nu)}{420}\left(\frac{h}{\ell}\right) << 1 \tag{17}$$

for realistic values of h/ℓ.

---

(2) Unfortunately [1] has a number of typographical errors so that as given there is not quite right.

(3) We use $\kappa^2 = 5/6$ throughout this paper although, for the rectangular beam, work of Cowper [4] suggests that $\kappa^2 = 10(1+\nu)/(12+11\nu)$; for $\nu = 0.3$ this provides $\kappa^2 = 0.850$.

2. The Uniformly Loaded, Simply Supported Beam

In this case we only present the various predictions for the central deflection of the beam which occupies the interval $0 \leq x \leq \ell$

$$w_b(\frac{\ell}{2}) = \bar{w} + \frac{5}{24}\,\frac{p_0\ell^4}{EI}\,[\frac{3}{25}(1+\nu)(\frac{h}{\ell})^2 - \frac{2}{875}(1+\nu)^2(\frac{h}{\ell})^4] \tag{18}$$

where now

$$\bar{w} = \frac{5}{384}\,\frac{p_0\ell^4}{EI}\ , \tag{19}$$

$$w_\ell(\frac{\ell}{2}) = \bar{w} + \frac{1}{40}\,\frac{p_0\ell^4}{EI}\,(1+\nu)(\frac{h}{\ell})^2\ , \tag{20}$$

$$w_t(x) \equiv w_\ell(x)\ , \tag{21}$$

and

$$w_e(\frac{\ell}{2},0) \approx \bar{w} + \frac{1}{32}\,\frac{p_0\ell^4}{EI}\,(\frac{4}{5} + \frac{\nu}{2})(\frac{h}{\ell})^2 \quad \text{from [5].} \tag{22}$$

For this problem all of the beam theories *overestimate* the "shear correction" term. For $\nu = 0.3$ the order $(h/\ell)^2$ term is about 9.5% too large and the (h/ℓ) term of Bickford's theory will decrease this overestimate by $\frac{(1+\nu)^2}{2100}\,(\frac{h}{\ell})^2$ which is negligibly small for meaningful values of h/ℓ , *i.e.* much less than 1% of the "shear correction" term.

We note that Bickford erroneously claims that the order $(h/\ell)^2$ term in his result is the same as the corresponding term in the elasticity solution [5] whereas, in fact, it is exactly the same as the *approximate* order $(h/\ell)^2$ term provided by the beam theories of Timoshenko and the present writer. Consequently, all of the beam theories incorporating the deflection due to shear (and rotatory inertia in the dynamic case) provide virtually identical results.

Finally, we come to the third example.

3. The Natural Frequencies of Simply Supported Beams

This example may be viewed either in terms of standing flexural waves (natural frequencies) of a beam of length ℓ or of travelling flexural waves (phase velocities). We confine our discussion of this problem to the lower branch of the flexural frequency curve since all of the beam theories provide comparable, and not especially good, approximations to the known elasticity results for the upper branch of the frequency curve; this has been noted by Bickford.

Since, as observed in [2], the equations for flexural waves in beams are identical for Timoshenko beam theory and the present writer's theory provided that $\kappa^2 = 5/6$ we only need comment on the results given in [1] and by Cowper in [6] for Bickford's and Timoshenko's beam theories respectively. In both of those papers it is noted that Timoshenko beam theory (and, consequently, the theory of the present writer) provides an excellent approximation to the results of the linear theory of elasticity for the lower branch of the flexural frequency curve. Bickford notes, however, that while his beam theory provides a comparable approximation for low frequencies it provides a decidedly inferior approximation for high frequencies. In fact, Bickford's theory provides a lower branch of the frequency curve which is asymptotically incorrect for high frequencies whereas Timoshenko beam theory (and, therefore, the theory of the present writer) is asymptotically correct.

We have, then, another example for which Bickford's (variationally) consistent higher order beam theory provides results inferior to those given by the lower order, but consistent, theory of Timoshenko and the (variationally) inconsistent higher order theory of the present writer.

Discussion

In this paper we have reviewed the beam theories of Bickford [1] and the present writer [2] as well as the now classical Timoshenko beam theory and have noted that in the fundamental sense of (variational) consistency Bickford's theory is the superior one of the more recent theories mentioned. However, in the three examples of (1) the end loaded cantilever, (2) the uniformly loaded, simply supported beam, and (3) the natural frequencies of a simply supported beam, common test cases for all of which plane stress linear elasticity solutions exist, unexpected results were encountered.

In the first example the (variationally) inconsistent theory given in [2] provided the exact deflection curve of the neutral axis given by the linear theory of elasticity and, in fact, the exact stress field. On the other hand, the theory of Bickford predicted an approximate centerline deflection which is very slightly inferior to the one given by Timoshenko beam theory, that theory giving a "shear correction" term which is 20% too small. For the second example all three beam theories being compared provided essentially the same, good approximation to the elasticity result. In this case Bickford's theory provided a result for the "shear correction" term which was a fraction of a percent better than the result given by the other two theories due to an additional term having no counterpart in the elasticity solution.

Finally, in the third example, one of elastodynamics, Timoshenko beam theory and the theory of the present writer provided the same excellent approximation to the elasticity predictions for the lower branch of the frequency curve for a simply supported beam while Bickford's theory provided a good approximation only at low frequencies and that theory even was asymptotically incorrect at high frequencies.

We are left, then, with the vexatious situation that Bickford's (variationally) consistent beam theory is, for certain common examples, inferior to or, at best, equivalent to both the (variationally) inconsistent theory of the present writer [2] and to Timoshenko beam theory. This goes against our intuitive belief that (variationally) consistent approximate theories are best. The explanation would seem to be that whereas (variationally) consistent approximate theories provide the best approximations to the functionals (energies) of a problem they may not provide the best approximations to quantities of more direct interest such as deflections, frequencies, etc. It then may become necessary to evaluate the worth of an approximate theory by its performance over a spectrum of criteria rather than the single criterion of (variational) consistency. Perhaps it is too early yet to relegate the theory of the present writer [2] to the status of an artifact in the history of applied mechanics. This view would be consistent with the views expressed in recent work of Irritier [8] and Bert [9] concerning the plate theory extension [10,11,12] of the beam theory given in [2].

Recently, Reddy [13] was motivated by that plate theory [10] to derive a (variationally) consistent plate theory analogous to Bickford's beam theory. It will be of interest to compare the actual performance, in particular cases, of Reddy's plate theory and the one given in [10].

References

1. W.B. Bickford, A Consistent Higher Order Beam Theory, Developments in Theoretical and Applied Mechanics, 11, 137 (1982).
2. M. Levinson, A New Rectangular Beam Theory, J. Sound Vib., 74, 81 (1981).
3. H. Reismann and P.S. Pawlik, Elastokinetics, West Publishing Co., St. Paul, (1974).
4. G.R. Cowper, The Shear Coefficient in Timoshenko's Beam Theory, J. Appl. Mechs., 33, 335 (1966).

5. S.P. Timoshenko and J.N. Goodier, Theory of Elasticity, 3rd ed., McGraw-Hill Book Co. (1970).

6. G.R. Cowper, On the Accuracy of Timoshenko's Beam Theory, ASCE J. Eng. Mechs., 94, 1447 (1968).

7. M. Levinson, Further Results of a New Beam Theory, J. Sound Vib., 77, 440 (1981).

8. H. Irretier, The Influence of Mid-Plane Normal Stress and Cross Section Deformation in Free Vibrating Plates, Mechs. Res. Comm., 10, 53 (1983).

9. C.W. Bert, Comparison of New Plate Theories Applied to Laminated Composites, Mechanics of Composite Materials, ASME Winter Annual Meeting, Boston, (1983).

10. M. Levinson, An Accurate, Simple Theory of the Statics and Dynamics of Elastic Plates, Mechs. Res. Comm., 7, 343 (1980).

11. M. Levinson and D.W. Cooke, Thick Rectangular Plates - I. The Generalized Navier Solution, Int. J. Mech. Sci., 25, 199 (1983).

12. D.W. Cooke and M. Levinson, Thick Rectangular Plates - II. The Generalized Lévy Solution, Int. J. Mech. Sci., 25, 207 (1983).

13. J.N. Reddy, A Simple Higher-Order Theory for Laminated Composite Plates, J. Appl. Mechs., to appear.

ResearchGate

See discussions, stats, and author profiles for this publication at: https://www.researchgate.net/publication/248122582

Toward a Consistent Design of Structural Concrete

Article *in* Pci Journal · May 1987

DOI: 10.15554/pcij.05011987.74.150

CITATIONS
767

READS
11,105

4 authors, including:

Michael D. Kotsovos
National Technical University of Athens

161 PUBLICATIONS **4,003** CITATIONS

SEE PROFILE

Some of the authors of this publication are also working on these related projects:

structural assessment of existing bridges and buildings View project

All content following this page was uploaded by Michael D. Kotsovos on 28 September 2017.

The user has requested enhancement of the downloaded file.

READER COMMENTS

Toward a Consistent Design of Structural Concrete*

by Jörg Schlaich, Kurt Shäfer and Mattias Jennewein

Comments by Michael D. Kotsovos and Authors

MICHAEL D. KOTSOVOS†

I would like to congratulate the authors for an interesting and comprehensive design proposal. In general terms, I share their view with regard to the significant contribution that the use of strut-and-tie models may have towards the development of a unified design concept for structural concrete. However, I believe that *only* models which provide a realistic description of structural behavior may lead to efficient design procedures.

The authors, on the other hand, appear to hold the view that it is sufficient for design purposes to use the theory of elasticity (adapted, if necessary, to conform with practical considerations) as a guide for developing strut-and-tie models which will provide an internal structural system sutiable for modeling any type of concrete structure. They consider that a structure under increasing load will adapt itself to the assumed internal structural system and that such a system can easily lead to an understanding of structural behavior.

The basis of their argument appears to lie on the widely accepted view that the truss analogy provides a rational tool for the design of reinforced concrete beams in flexure, shear and torsion. Their paper, therefore, describes an attempt to generalize the truss analogy in order to apply it in the form of strut-and-tie models to other structural members.

However, the truss analogy does not appear to provide, in general, a realistic description of the causes of the observed behavior of structural concrete. There has been recent published experimental evidence which indicates that a reinforced concrete beam subjected to combined flexure and shear does not have to behave as a truss in order to attain its flexural capacity.[28] This is clearly indicated in Figs. A and B which show that, in contrast with predictions based on the truss analogy, the unconventionally reinforced concrete beams D, in Fig. C, and C and D, in Fig. D, exhibit strength and deformational characteristics similar to those of Beams B (also shown in Figs. C and D) which are reinforced in compliance with the truss model.

---

* PCI JOURNAL, V. 32, No. 3, May-June 1987, pp. 74-150.

† Department of Civil Engineering, Imperial College of Science and Technology, London, England.

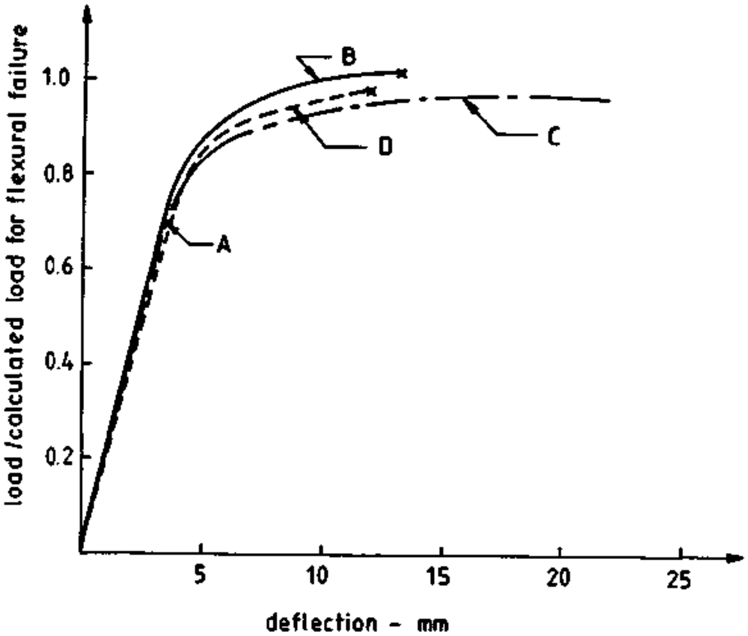

Fig. A. Load deflection curves of beams with $a/d = 1.5$.

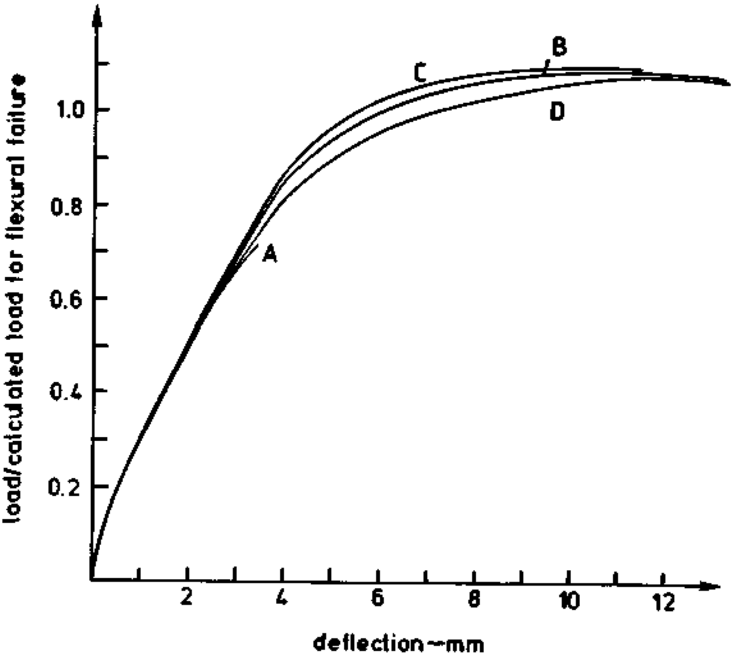

Fig. B. Load deflection curves of beams with $a/d = 3.3$.

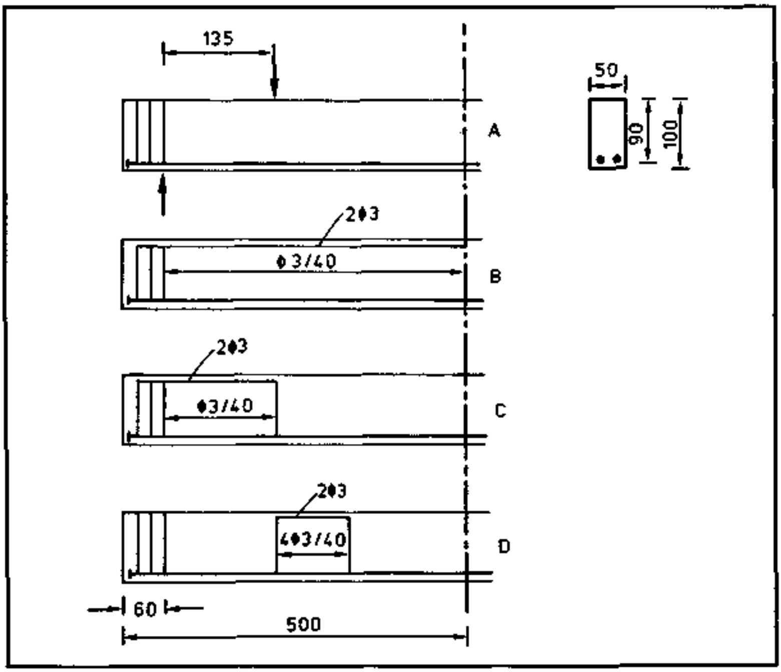

Fig. C. Design details of beams with a/d = 1.5.

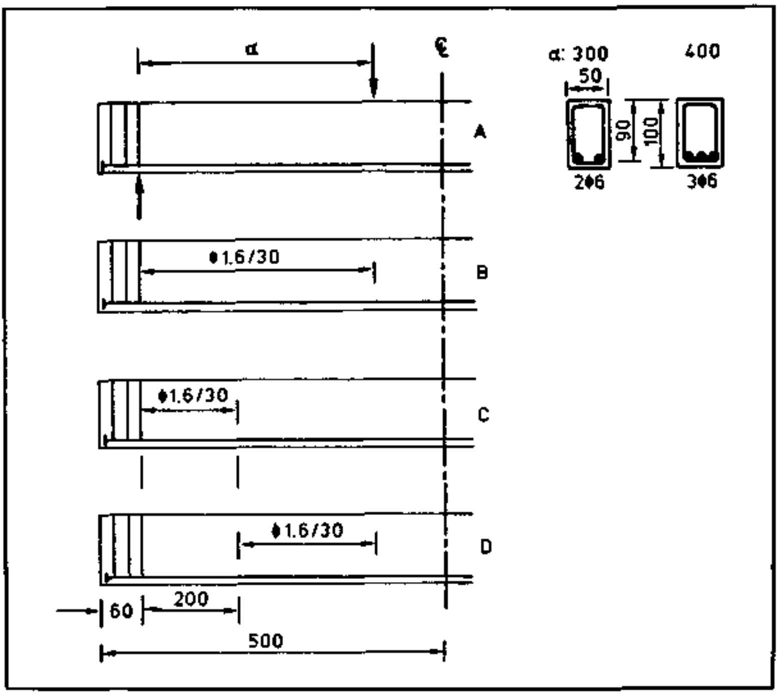

Fig. D. Design details of beams with a/d = 3.3.

It could be argued, however, that although the unconventionally reinforced concrete beams could not have behaved as trusses, the above results cannot disprove the view that Beams B (which were designed in compliance with the truss analogy) behaved as such. The truss analogy forms the basis of current code provisions for shear design and it is generally expected that compliance with these provisions always leads to safe design solutions. And yet, there is published ex-

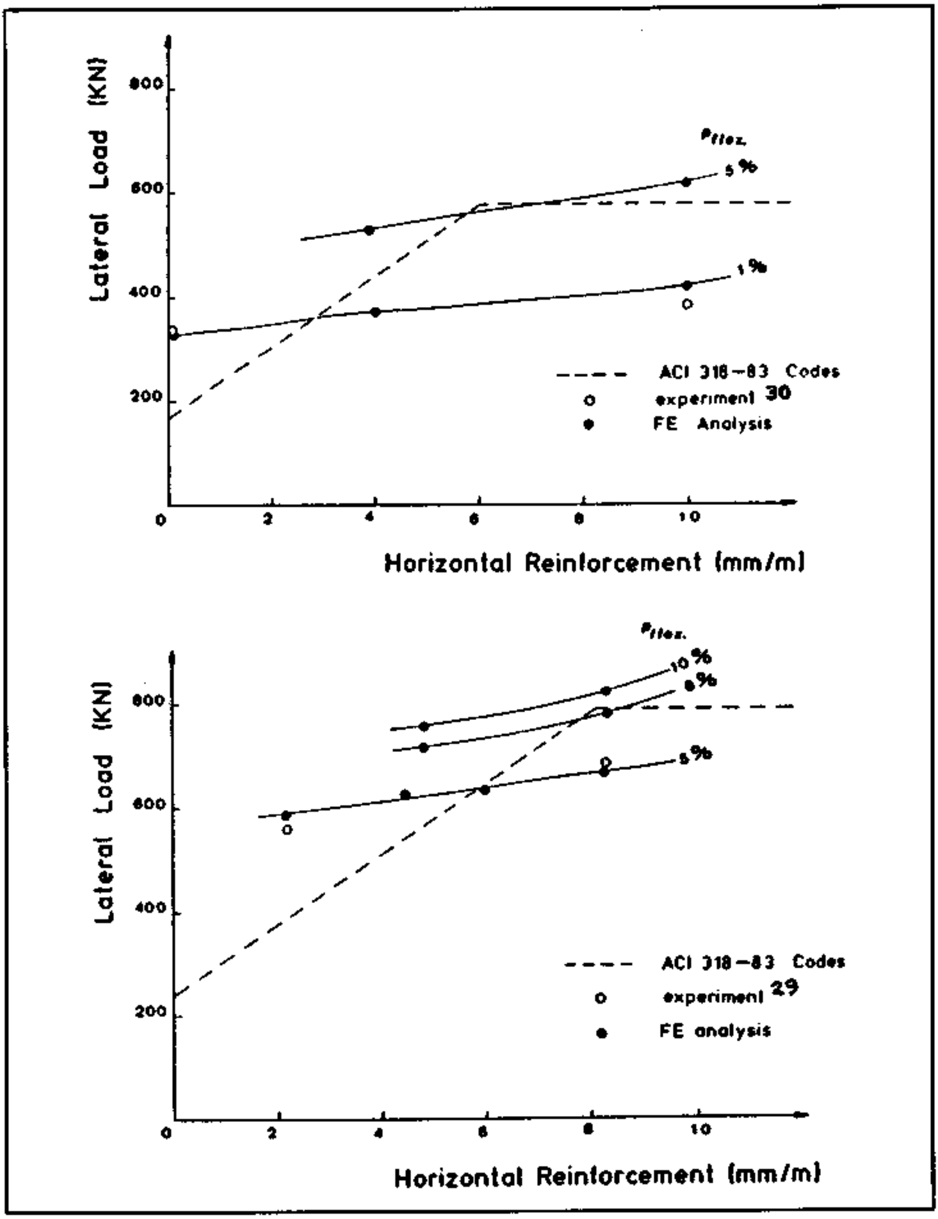

Fig. E. Relation between shear capacity and amount of transverse reinforcement.

perimental evidence which indicates that this is not always the case.[29,30]

Fig. E indicates that code provisions for earthquake resistant design[31] predict a linear increase in shear capacity with increasing percentage of transverse reinforcement, from a lower level representing the contribution of concrete to shear resistance, to a "plateau" corresponding to "crushing" of the concrete struts of the truss model. The figure also includes experimental values obtained from tests on structural walls[29,30] and clearly indicates that, for certain percentages of tensile reinforcement, the code provisions overestimate considerably the wall capacity for the upper range of values of the percentage of transverse reinforcement. It may also be interesting to note in the figure that the experimental results correlate very closely with results obtained by finite element analysis.[32]

The above results shed doubt on the validity of current concepts with regard to not only the ability of the truss analogy to realistically represent structural behavior, but also the view that a structure under increasing load will respond in the way prescribed by the physical model used to design it. Designing in compliance with the truss analogy appears to lead to overreinforced (in the transverse direction) structural members in which the presence of excess steel is likely to give rise to high secondary stresses within concrete for compatibility of deformation purposes. The development of such stresses in critical regions may be the cause of "prema-

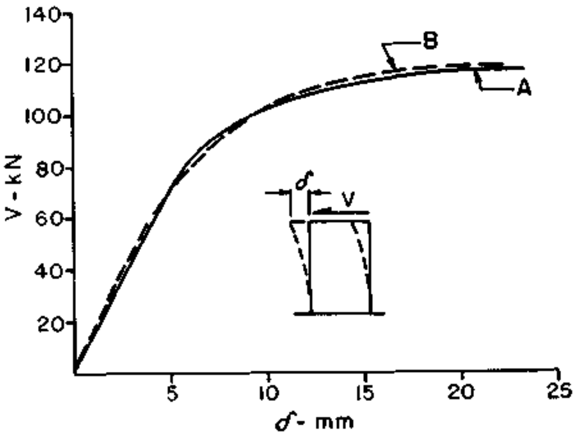

Specimen	Flange	Web	
	ρ_{fl}	ρ_v	ρ_h
A	0.033	0.011	0.007
B	0.033	0.011	0.0025

Fig. F. Effect of web reinforcement on the strength and deformational characteristics of structural walls. Note that ρ_{fl}, ρ_v, and ρ_h denote percentages of vertical flange, and vertical and horizontal web reinforcement, respectively.

ture" failure similar to that exhibited by the walls with a high percentage of transverse reinforcement discussed above.

The amount of transverse reinforcement, assessed on the basis of current code provisions, appears to be excessive even for the case where the use of the truss analogy yields safe design solutions. This is clearly indicated in Fig. F which shows that a reduction of the amount of web reinforcement by more than 60 percent has virtually no effect on the deformational and strength characteristics of the structural wall with geometry and tension reinforcement as indicated also in Fig. F.[33] Similar results have also been obtained from tests on both reinforced and prestressed concrete beams subjected to combined flexure and shear during an ongoing research program concerned with the development of design methods.[34]

It may be concluded from the above that structural concrete should not be expected, in general, to behave in the way it is modeled to behave. It would appear that the main reason for this lies in the fact that modeling is usually based on concepts which do not give full consideration to important aspects of concrete behavior. For example, the theory of elasticity, proposed by the authors as a basis for the development of strut-and-tie models, cannot provide any detailed information with regard to the strength and deformation characteristics of concrete at the material level. Despite the vast amount of such information produced to date, only recently attempts have started to use it in design.[34-37]

I believe, therefore, that design methods have reached the stage where no improvement is any more possible without attempting to implement in design information on the properties of concrete as a material. Such an attempt has already begun and led to the introduction of concepts which appear to provide a realistic description of the causes of the observed behavior of structural concrete.[33-37] These concepts are currently discussed in CEB Task Group 24 and research work[34] is in progress which explores possibilities of using them as a basis for the development of physical models which may be employed in design in a way similar to that stipulated by the authors.

REFERENCES

28. Kotsovos, M. D., "Shear Failure of RC Beams: A Reappraisal of Current Concepts," Contributions to a Joint Meeting on Fundamental Developments in Design Models, Organized by CEB Commissions II and IV, Karlsruhe, November 1986; CEB Bulletin d'Information No. 178/179, March 1987, pp. 103-111.
29. Cardenas, A. E.; Russell, H. G.; and Corley, W. G.; "Strength of Low Rise Structural Walls," Reinforced Concrete Subjected to Wind and Earthquake Forces, ACI SP-63, American Concrete Institute, Detroit, Michigan, 1980, pp. 221-241.
30. Maier, J., and Thürliman, B., "Bruchversuche an Stahlbetonscheiben," Institut für Baustatic und Konstruction, Eifgenossishe Technische Hochschule Zurich, January 1985, 130 pp.
31. ACI Committee 318, "Building Code Requirements for Reinforced Concrete (ACI 318-83)," American Concrete Institute, Detroit, Michigan, 1983, 111 pp.
32. Lefas, I. D., and Kotsovos, M. D., "Behaviour of RC Structural Walls — A New Interpretation," Colloquium on Computational Mechanics of Reinforced Concrete, Delft, August 1987.
33. Lefas, I. D., "Behaviour of Reinforced Concrete Structural Walls," PhD Thesis, University of London (in preparation).
34. Kotsovos, M. D., "The Use of Fundamental Properties of Concrete for the Design of Prestressed Concrete Beams," SERC Research Grant, GR/E/07333, Civil Engineering Department, Imperial College, London.
35. Kotsovos, M. D., "Consideration of Triaxial Stress Conditions in Design: A Necessity," *ACI Structural Journal,* V. 84, No. 3, May-June 1987, pp. 266-273.

36. Kotsovos, M. D. "Compressive Force Path Concept: Basis for Reinforced Concrete Ultimate Limit State Design," *ACI Structural Journal*, V. 85, No. 1, January-February 1988, pp. 68-75.

37. Kotsovos, M. D.; Bobrowski, J.; and Eibl, J.; "Behaviour of Reinforced Concrete T-Beams in Shear," *The Structural Engineer*, V. 65B, No. 1, March, 1987, pp. 1-10.

AUTHORS' CLOSURE by JÖRG SCHLAICH, KURT SCHÄFER and MATTIAS JENNEWEIN*

We wish to express our appreciation to Professor Kotsovos for preparing his comments and also we wish to thank the numerous other colleagues who have verbally commented on our paper. We, therefore, take it as an indication of consent that there were no further written discussions.

Unfortunately, Professor Kotsovos' contribution does not really discuss the method given in our paper. He presents some interesting test results and compares them with a code. From his comparison, he directly concludes that certain code rules are not adequate and safe. Inadvertently, this conclusion is transferred to the method presented in the paper instead of comparing results derived by the method with the tests. But the assumption that codes for beams and in particular those for shear walls are in agreement with the method is not true.

Furthermore, in defense of the codes it must also be stated that no test results we know of, including those cited in the discussion, have disproved a code, which is based on the truss model when applied to a B-region (with linear strain distribution). But applying regular truss models and corresponding code rules to D-regions (with nonlinear strain distribution) conflicts with one of the basic principles of the method (see Section 2 of our paper). In D-regions individual modeling is required. Inadequate applications of the truss model were in fact the starting point for expanding it to a more general method.

Some comments on individual paragraphs of the discussion may support what is said above:

Beams D in Figs. C and D are not conventionally reinforced with stirrups in the shear span and therefore the regular truss model or corresponding code rules do not apply. A code which gives safe results for given requirements such as distributed stirrup reinforcement should not be blamed for showing wrong results if these requirements are not fulfilled.

The more flexible strut-and-tie method, as contrasted with the rigid truss model, is capable of dealing with such irregularities as well. If the truss model is adjusted to the chosen reinforcement, the tested beams' capacity can be explained. A model shows — in contrast to a thoughtless application of a code formula — that shear forces can, for example, be transferred by an inclined strut over a considerable length of a beam without any stirrups.

Furthermore, a second load path with concrete ties contributes to the shear capacity as shown for B-regions in Fig. 30 of our paper. However, the load bearing capacity depends also on the nodes joining the struts and the chords: compatibility stresses may cause a shear crack to penetrate into a node and separate there the chords from the web (see Fig. 34). The importance of a minimum stirrup reinforcement to prevent such separation is outlined on page 115 of the paper. The stirrups in the node region explain the difference between failure loads of Beams A and D.

---

*Institute of Reinforced Concrete, University of Stuttgart, Stuttgart, FRG.

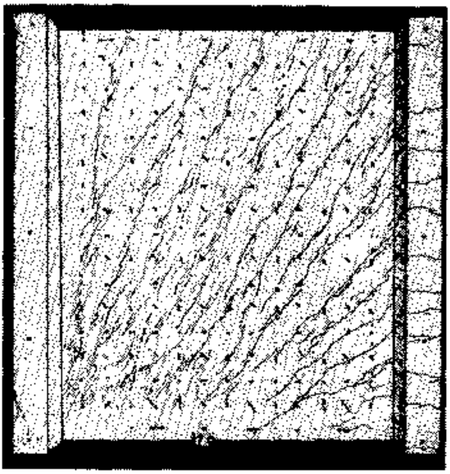

Fig. G. Crack pattern of Specimen S2.

Professor Kotsovos derives from comparison of test results and code provisions that the truss analogy gives unsafe results. First of all it must be stated, that the test panels[29,30,33] mentioned in the discussion are D-regions for which the standard truss model normally does not apply. So it is wrong to argue on this basis. We investigated the three square panels[30] using the method described in our paper. The predicted failure loads are not beyond 84 percent of the measured ultimate load for Panel S1 and 90 percent for Panels S2 and S3. Hence, all predictions according to the strut-and-tie method are safe, contrary to Professor Kotsovos' implication. A numerical analysis for Panel S2 will be given here as an example.

Fig. G shows the crack pattern of the test specimen and Fig. H gives an optimized, yet simple strut-and-tie-model. (Other models, especially the standard truss model, give more conservative predictions.) The nodes are not critical (smeared nodes in the panel). From the geometry of the model and the capacity of the ties T_{1u} and T_{2u}, the ultimate load F_h and all the strut and tie forces can be analyzed consecutively from simple

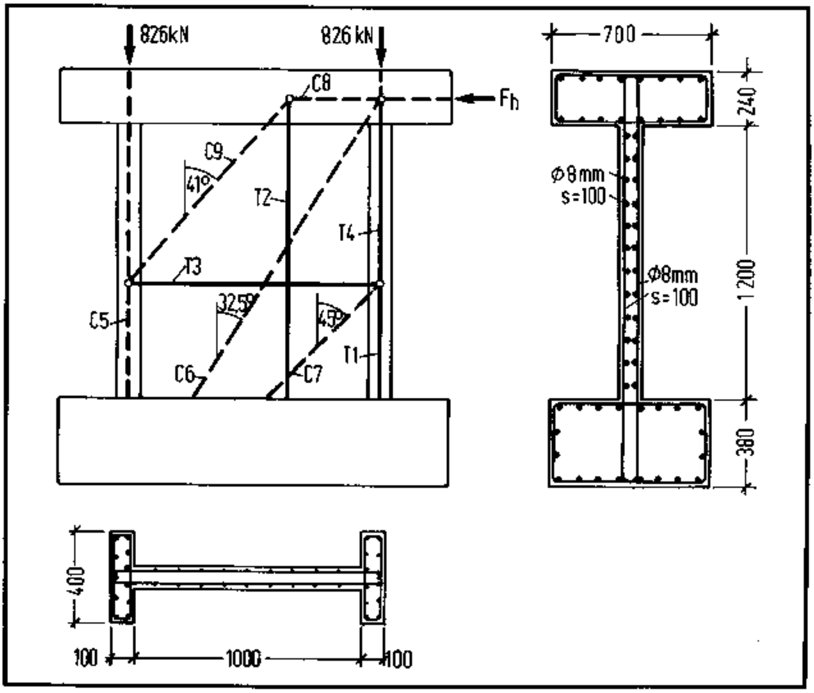

Fig. H. Strut-and-tie model and dimensions of Specimen S2.

equilibrium conditions, followed by a check of their capacity:

$$T_1 = T_{1u} = f_{sy} \cdot A_{s1} = 57{,}4 \text{ kN/cm}^2 \cdot 5{,}5 \text{ cm}^2 = 316 \text{ kN}$$
$$T_2 = T_{2u} = 57{,}4 \cdot 6{,}0 = 344 \text{ kN}$$
$$C_8 = T_{2u} \tan 41^\circ = 299 \text{ kN}$$
$$T_3 = C_8 = 299 \text{ kN} < T_{3u}$$
$$T_{3u} = 57{,}4 \cdot 6{,}0 = 344 \text{ kN}$$
$$T_4 = T_1 - T_3 \cos 45^\circ = 17 \text{ kN} < T_{4u}$$
$$F_h = C_8 + (T_4 + 826 \text{ kN}) \tan 32{,}5^\circ = \underline{836 \text{ kN}}$$
$$C_5 = T_2 + 826 \text{ kN} = 1170 \text{ kN} \approx C_{5u}$$
$$C_{5u} = 0{,}8 f_c' A_{c5} = 0{,}8 \cdot 36400 \cdot 0{,}1 \cdot 0{,}4 = 1165 \text{ kN}$$
$$C_6 = 1000 \text{ kN} \approx C_{6u} = 0{,}8 \cdot 36400 \cdot 0{,}1 \cdot 0{,}35 = 1027 \text{ kN}$$
$$C_7 = 424 \text{ kN} < C_{7u} = 0{,}8 \cdot 36400 \cdot 0{,}1 \cdot 0{,}2 = 582 \text{ kN}$$

The predicted load $F_h = 836$ kN corresponds to 90 percent of the measured ultimate load $F_u = 928$ kN. The two structures compared in Fig. F of the discussion carry the shear force by two load paths similar to those drawn in Fig. H: A direct strut C_6 and the strut-tie combination C_9, T_3, C_7. No horizontal reinforcement beyond the minimum reinforcement is necessary for the direct strut. If the struts are strong enough, the behavior of the beam is controlled by the chord reinforcement and vertical reinforcement and not much difference can be expected in their behavior if these reinforcements are the same as given in Fig. F.

The authors believe that this discussion supports their view that strut-and-tie models (correctly applied) provide a rational and practical tool for the design of reinforced and prestressed concrete beams and that experimental evidence supports their view. It also shows that code rules may be misinterpreted if their basis is not clearly defined.

* * *

DISCUSSION NOTE

The Editors welcome discussion of papers published in the PCI JOURNAL. The comments must be confined to the scope of the article being discussed. Please note that discussion of papers appearing in this issue must be received at PCI Headquarters by August 1, 1989.

Journal of Sound and Vibration (1988) **126**(2), 309-326

A HIGHER ORDER BEAM FINITE ELEMENT FOR BENDING AND VIBRATION PROBLEMS†

P. R. Heyliger

Fracture and Deformation Division, National Bureau of Standards, Boulder, Colorado 80303, *U.S.A.*

AND

J. N. Reddy

Department of Engineering Science and Mechanics, Virginia Polytechnic Institute and State University, Blacksburg, Virginia 24061, *U.S.A.*

(*Received* 11 *November* 1987, *and in revised form* 18 *April* 1988)

The finite element equations for a variationally consistent higher order beam theory are presented for the static and dynamic behavior of rectangular beams. The higher order theory correctly accounts for the stress-free conditions on the upper and lower surfaces of the beam while retaining the parabolic shear strain distribution. The need for a shear correction coefficient is therefore eliminated. Full integration of the shear stiffness terms is shown to result in the recovery of the Kirchhoff constraint for thin beams without introducing spurious locking constraints. The accuracy of this formulation is demonstrated by using several numerical examples for the cases of small and large displacements. For a hinged-hinged beam, the linear thickness-shear mode frequency can be matched with the Timoshenko frequency to yield a shear coefficient of 0·824. Matching the bending frequencies between the two theories indicates a shear coefficient for the Timoshenko theory that changes with mode number and slenderness ratio. The influence of in-plane inertia and slenderness ratio on the non-linear frequency is examined for beams with a number of different support conditions.

1. INTRODUCTION

Historically, investigations of problems in beam bending have been limited to the elementary Bernoulli-Euler theory and the shear deformation theory of Timoshenko [1, 2]. The primary deficiency of Timoshenko's theory is the presence of the shear correction coefficient k, which is introduced to correct the contradictory shear stress distribution over the cross-section of the beam. Recently, Levinson [3] and Bickford [4] considered a shear deformation theory for rectangular beams that correctly accounts for the stress-free boundary conditions on the upper and lower surfaces of the beam while retaining the parabolic distribution of the transverse shear strain. This was accomplished by expanding the axial displacement of a point on the beam cross-section as a cubic function of the beam thickness co-ordinate. Expansion of the displacement components in terms of the thickness co-ordinate had been proposed for shells by Basset [5], Hildebrand, Reissner and Thomas [6] and Hencky [7]. Although a cubic displacement field was used to derive strains, Levinson employed the equations of equilibrium of the first-order shear deformation theory. The cubic displacement field of Levinson was used by Reddy to develop a variationally consistent higher order plate theory [8, 9].

---

† Contribution of NBS not subject to copyright.

0022-460X/88/200309+18 $03.00/0

© 1988 Academic Press Limited

Complicated problems in beam bending are frequently solved by using approximate numerical techniques such as the finite element method. The element equations for the Bernoulli-Euler and Timoshenko theories are well established [10-12]. The objectives of this paper are to present a higher order beam finite element for the static and dynamic behavior of rectangular beams obtained by using the variationally consistent higher order theory of Reddy [8, 9, 13], and to determine the numerical accuracy of this formulation. The effect of the order of integration for this element is briefly discussed, and several numerical examples are presented.

2. GOVERNING EQUATIONS

The displacement field for the higher order theory can be written for a beam of height h as (see the papers by Levinson [3] and Reddy [8])

$$u_1 = u(x,t) + z[\psi(x,t) - \tfrac{4}{3}(z/h)^2(\psi + \partial w/\partial x)], \qquad u_2 = 0, \quad u_3 = w(x,t), \tag{1}$$

where x and z are the axial and thickness co-ordinates of the beam, u and w are the axial and transverse displacements of the beam centerline, and ψ represents the rotation of a normal to the axis of the beam.

The von Kármán strains are included in the subsequent derivation to account for the possibility of moderately large deflections and rotations. The non-zero strain components are given by (see references [9, 13])

$$\begin{gathered}\varepsilon_1 = \varepsilon_{11} = \frac{\partial u}{\partial x} + z\left[\frac{\partial \psi}{\partial x} - \frac{4}{3}\left(\frac{z}{h}\right)^2\left(\frac{\partial \psi}{\partial x} + \frac{\partial^2 w}{\partial x^2}\right)\right] + \frac{1}{2}\left(\frac{\partial w}{\partial x}\right)^2, \\ \varepsilon_4 = 2\varepsilon_{13} = \left(\psi + \frac{\partial w}{\partial x}\right)\left(1 - 4\frac{z^2}{h^2}\right).\end{gathered} \tag{2}$$

Hamilton's principle (see reference [13]) is used to obtain the equations of motion for the displacement field given by equation (1). This can be expressed as

$$\begin{aligned}0 = &-\int_0^t \left[\int_{-h/2}^{h/2}\int_0^b\int_0^L (\sigma_1 \delta\varepsilon_1 + \sigma_4 \delta\varepsilon_4)\,\mathrm{d}x\,\mathrm{d}y\,\mathrm{d}z\right]\mathrm{d}t + \int_0^t\int_0^L q\,\delta w\,\mathrm{d}x\,\mathrm{d}t \\ &+ \int_0^t\int_0^L f\,\delta u\,\mathrm{d}x\,\mathrm{d}t + \tfrac{1}{2}\delta\int_0^t\int_{-h/2}^{h/2}\int_0^b\int_0^L \rho[\dot u_1^2 + \dot u_3^2]\,\mathrm{d}x\,\mathrm{d}y\,\mathrm{d}z\,\mathrm{d}t,\end{aligned} \tag{3}$$

where b and L are the width and length of the beam, q and f are the distributed transverse and axial loads acting on the beam, and $\dot u_1 = \partial u_1/\partial t$. The one-dimensional stress-strain relations are

$$\sigma_1 = E\varepsilon_1, \qquad \sigma_4 = G\varepsilon_4, \tag{4}$$

where E is the Young's modulus and G is the shear modulus of the beam material. Performing the integration over the area of cross-section of the beam, and letting $I = bh^3/12$ and $A = bh$ gives the variational form of the equations of motion as

$$\begin{aligned}0 = -\int_0^t\int_0^L \Bigg\{ &AE\left[\frac{\partial u}{\partial x} + \frac{1}{2}\left(\frac{\partial w}{\partial x}\right)^2\right]\frac{\partial \delta u}{\partial x} + AE\left[\frac{\partial u}{\partial x} + \frac{1}{2}\left(\frac{\partial w}{\partial x}\right)^2\right]\frac{\partial w}{\partial x}\frac{\partial \delta w}{\partial x} \\ &+ EI\frac{\partial \psi}{\partial x}\frac{\partial \delta\psi}{\partial x} - \frac{16}{105}EI\left[\left(\frac{\partial \psi}{\partial x} + \frac{\partial^2 w}{\partial x^2}\right)\frac{\partial \delta\psi}{\partial x} + \left(\frac{\partial \delta\psi}{\partial x} + \frac{\partial^2 \delta w}{\partial x^2}\right)\frac{\partial \psi}{\partial x}\right] \\ &+ \frac{EI}{21}\left(\frac{\partial \psi}{\partial x} + \frac{\partial^2 w}{\partial x^2}\right)\left(\frac{\partial \delta\psi}{\partial x} + \frac{\partial^2 \delta w}{\partial x^2}\right) + \tfrac{8}{15}GA\left(\psi + \frac{\partial w}{\partial x}\right)\left(\delta\psi + \frac{\partial \delta w}{\partial x}\right)\end{aligned}$$

$$
\left. - q\,\delta w - f\,\delta u \right\} \mathrm{d}x\,\mathrm{d}t
$$

$$
+ \int_0^t \int_0^L \left\{ \rho A\,\ddot{u}\,\delta u + \rho \left[\frac{68}{105} I\ddot{\psi} - \frac{16}{105} I \frac{\partial \ddot{w}}{\partial x} \right] \delta\psi \right.
$$

$$
\left. + \rho \left[\frac{I}{21} \frac{\partial \ddot{w}}{\partial x} - \frac{16}{105} I\ddot{\psi} \right] \frac{\partial \delta w}{\partial x} + \rho A\,\ddot{w}\,\delta w \right\} \mathrm{d}x\,\mathrm{d}t. \tag{5}
$$

Integrating the appropriate terms in equation (5) by parts and collecting the coefficients of δu, δw and $\delta\psi$ gives the equations of motion:

$$
\frac{\partial}{\partial x} \left\{ AE \left[\frac{\partial u}{\partial x} + \frac{1}{2} \left(\frac{\partial w}{\partial x} \right)^2 \right] \right\} + f = A\rho \frac{\partial^2 u}{\partial t^2}, \tag{6a}
$$

$$
\frac{\partial}{\partial x} \left\{ AE \frac{\partial w}{\partial x} \left[\frac{\partial u}{\partial x} + \frac{1}{2} \left(\frac{\partial w}{\partial x} \right)^2 \right] + \tfrac{8}{15} GA \left(\psi + \frac{\partial w}{\partial x} \right) \right\} - \frac{\partial^2}{\partial x^2} \left[\tfrac{1}{21} EI \frac{\partial^2 w}{\partial x^2} - \tfrac{16}{105} EI \frac{\partial \psi}{\partial x} \right] + q
$$

$$
= \rho A \frac{\partial^2 w}{\partial t^2} - \frac{\partial}{\partial x} \left[\tfrac{1}{21} \rho I \frac{\partial^3 w}{\partial t^2 \partial x} - \tfrac{16}{105} \rho I \frac{\partial^2 \psi}{\partial t^2} \right], \tag{6b}
$$

$$
- \frac{\partial}{\partial x} \left[\tfrac{68}{105} EI \frac{\partial \psi}{\partial x} - \tfrac{16}{105} EI \frac{\partial^2 w}{\partial x^2} \right] + \tfrac{8}{15} GA \left(\psi + \frac{\partial w}{\partial x} \right) = - \tfrac{68}{105} EI \frac{\partial^2 \psi}{\partial t^2} + \tfrac{16}{105} \rho I \frac{\partial^3 w}{\partial x \partial t^2}. \tag{6c}
$$

The appropriate boundary conditions are as follows:

natural boundary conditions:	essential boundary conditions:
$AE[\partial u/\partial x + \frac{1}{2}(\partial w/\partial x)^2]$	u
$AE \frac{\partial w}{\partial x} \left[\frac{\partial u}{\partial x} + \frac{1}{2} \left(\frac{\partial w}{\partial x} \right)^2 \right] + \tfrac{8}{15} GA \left(\psi + \frac{\partial w}{\partial x} \right)$ $- \tfrac{1}{21} EI \frac{\partial^2 w}{\partial x^2} + \tfrac{16}{105} EI \frac{\partial \psi}{\partial x} - \rho I \left[\frac{1}{21} \frac{\partial^3 w}{\partial t^2 \partial x} - \frac{16}{105} \frac{\partial^2 \psi}{\partial t^2} \right]$	w
$\tfrac{1}{21} EI \frac{\partial^2 w}{\partial x^2} - \tfrac{16}{105} EI \frac{\partial \psi}{\partial x}$	$\frac{\partial w}{\partial x}$
$\tfrac{68}{105} EI \frac{\partial \psi}{\partial x} - \tfrac{16}{105} EI \frac{\partial^2 w}{\partial x^2}$	ψ. (7)

The displacement field given in equations (2) correctly accounts for the parabolic distribution of the transverse shear strain and the stress free conditions on the upper and lower surfaces of the beam. Therefore, there is no need for the shear correction coefficient in the present theory. One disadvantage of using the higher order displacement field when compared to the Timoshenko theory is the presence of the higher order derivative of the transverse deflection, which requires the development of a C^1-element (see reference [10]).

3. FINITE ELEMENT MODEL

The variational statement in equation (5) requires that the transverse displacement w be twice differentiable and C^1-continuous, whereas the axial displacement u and rotation ψ must be only once differentiable and C^0-continuous. The generalized displacements u, w and ψ are approximated by using the following interpolation (see reference [10]):

$$
u(x, t) = \sum_{j=1}^{n} u_j(t) N_j(x), \qquad \psi(x, t) = \sum_{j=1}^{n} \psi_j(t) N_j(x), \qquad w(x, t) = \sum_{j=1}^{m} \Delta_j(t) \phi_j(x). \tag{8}
$$

Here N_j are the Lagrange interpolation functions and ϕ_j are the Hermite interpolation functions. In the present discussion, linear interpolation functions are used for u and $\psi (n=2)$ and the Hermite cubic interpolation functions are used for $w (m=4)$. This implies that (see reference [10])

$$\Delta_1 = w_1, \qquad \Delta_3 = \theta_1 = -(\mathrm{d}w/\mathrm{d}x)|_{x=x_e}, \qquad \Delta_2 = w_2, \qquad \Delta_4 = -(\mathrm{d}w/\mathrm{d}x)|_{x=x_{e+1}}, \quad (9)$$

where (x_e, x_{e+1}) are the global nodal co-ordinates of the eth element. Substitution of equation (8) into equation (5) yields the element equation

$$[K]\{\bar{\Delta}\}+[M]\ddot{\bar{\Delta}}\}=\{F\}, \quad (10)$$

where $[K]$ is the element stiffness matrix, $[M]$ is the element mass matrix, $\{F\}$ is the total force vector and $\{\bar{\Delta}\}$ is the vector of nodal values, $\{\Delta\}=\{u_1 \ \Delta_1 \ \Delta_2 \ \psi_1 \ u_2 \ \Delta_3 \ \Delta_4 \ \psi_2\}$. The explicit entries of these matrices are given in the Appendix.

4. CONSISTENCY OF THE THEORY

The performance of the Timoshenko beam element is improved if the stiffness terms due to shear are evaluated by using reduced integration. This helps to prevent the locking that occurs when the beam is thin [11, 12]. In this section, the effects of integration are examined for the higher order element. For the static, linear (small displacement) case, the axial displacements are uncoupled from the transverse displacement and rotation components. The strain energy expression can be written for the static case as

$$U=\int_0^L \int_A \left\{ \tfrac{1}{2} G\left(1-4\frac{z^2}{h^2}\right)\left(\psi+\frac{\mathrm{d}w}{\mathrm{d}x}\right)^2 + \tfrac{1}{2} Ez\left[\frac{\mathrm{d}\psi}{\mathrm{d}x}-\frac{4}{3}\left(\frac{z}{h}\right)^2\left(\frac{\mathrm{d}\psi}{\mathrm{d}x}+\frac{\mathrm{d}^2 w}{\mathrm{d}x^2}\right)\right]^2\right\} \mathrm{d}A\, \mathrm{d}x. \quad (11)$$

When using the interpolations specified above, the exactly integrated element matrices are given by (see the Appendix)

$$\begin{bmatrix} [K^{22}][K^{23}] \\ [K^{32}][K^{33}] \end{bmatrix} = [K_1]+[K_2] = \frac{2EI}{105L^3}\begin{bmatrix} 30 & -30 & -15L & -15L & 0 & 0 \\ -30 & 30 & 15L & 15L & 0 & 0 \\ -15L & 15L & 10L^2 & 5L^2 & 8L^2 & -8L^2 \\ -15L & 15L & 5L^2 & 10L^2 & -8L^2 & 8L^2 \\ 0 & 0 & 8L^2 & -8L^2 & 34L^2 & -34L^2 \\ 0 & 0 & -8L^2 & 8L^2 & -34L^2 & 34L^2 \end{bmatrix}$$

$$+\frac{8GA}{15}\begin{bmatrix} 1{\cdot}2/L & -1{\cdot}2/L & -0{\cdot}1 & -0{\cdot}1 & -0{\cdot}5 & -0{\cdot}5 \\ -1{\cdot}2/L & 1{\cdot}2/L & 0{\cdot}1 & 0{\cdot}1 & 0{\cdot}5 & 0{\cdot}5 \\ -0{\cdot}1 & 0{\cdot}1 & 2L/15 & -L/30 & -L/12 & -L/12 \\ -0{\cdot}1 & 0{\cdot}1 & -L/30 & 2L/30 & L/12 & -L/12 \\ -0{\cdot}5 & 0{\cdot}5 & -L/12 & L/12 & L/3 & L/6 \\ -0{\cdot}5 & 0{\cdot}5 & -L/12 & -L/12 & L/6 & L/3 \end{bmatrix}, \quad (12)$$

where $[K_1]$ represents the bending stiffness matrix and $[K_2]$ represents the shear stiffness matrix. Here L denotes the element length. As the beam becomes thin, the elementary bending theory should be recovered from the higher order theory by enforcing the

Kirchhoff constraint For the Timoshenko element, reduced integration is required to recover the Kirchhoff constraint while eliminating the spurious constraints that arise if full integration is used [12].

For the higher order beam element, full integration should be used in evaluating the stiffness terms due to shear. This may be verified by noting that as the coefficient GAL^2/EI becomes large, the shear related terms corresponding to the matrix $[K_2]$ act as constraints [12]. For the matrix $[K_2]$ given in equation (12), there are three constraints corresponding to $[K_2]$ being of rank three. Enforcing these constraints is equivalent to letting the strain energy due to shear, U_G, approach zero as the beam becomes thin. Hence, in the limit,

$$U_G=\int_0^L\int_A\left[\tfrac{1}{2}G\left(1-4\frac{z^2}{h^2}\right)\left(\psi+\frac{\mathrm{d}w}{\mathrm{d}x}\right)^2\right]\mathrm{d}A\,\mathrm{d}x=0. \tag{13}$$

This implies that

$$(\psi+\partial w/\partial x)=0 \qquad \text{for all } x \text{ in } [0, L). \tag{14}$$

This can be written for a given element as

$$\psi_1N_1+\psi_2N_2+w_1\frac{\mathrm{d}\phi_1}{\mathrm{d}x}+\theta_1\frac{\mathrm{d}\phi_3}{\mathrm{d}x}+w_2\frac{\mathrm{d}\phi_2}{\mathrm{d}x}+\theta_2\frac{\mathrm{d}\phi_4}{\partial x}=0, \tag{15}$$

or

$$\psi_1\left(1-\frac{x}{L}\right)+\psi_2\left(\frac{x}{L}\right)+w_1\left(\frac{-6x}{L^2}+\frac{6x^2}{L^3}\right)+\theta_1\left(-1+\frac{4x}{L}-\frac{3x^2}{L^2}\right)+w_2\left(\frac{6x}{L^2}-\frac{6x^2}{L^3}\right)$$
$$+\theta_2\left(\frac{-3x^2}{L^2}+\frac{2x}{L}\right)=0. \tag{16}$$

Since this is true for any x, equation (16) implies that

$$\theta_1=\psi_1, \qquad \theta_2=\psi_2, \qquad (w_1-w_2)/L=(\theta_1+\theta_2)/2. \tag{17}$$

These equations represent the Kirchhoff constraints and correspond to the three constraints of the matrix $[K_2]$. This demonstrates that, in contrast to the Timoshenko element, so spurious constraints arise from the fully integrated shear stiffness matrix. The element equations given in equation (12) should therefore yield accurate numerical values for thin and thick beams. In a similar vein, Phan and Reddy [14] reported that the order of integration had little effect on the numerical results for a plate element of this type.

5. DISCUSSION OF NUMERICAL RESULTS

5.1. STATIC ANALYSIS

Several example problems are considered to demonstrate the accuracy of the finite element model based on the higher order theory. The linear cases of a cantilevered beam under an end load p and a simply supported beam under a uniform load q are considered first. The exact solutions [4] for the maximum displacements for these two cases, when using the higher order theory, are given by

$$w_E^c=\frac{1}{3}\frac{pL^3}{EI}+\frac{1}{5}\frac{pL^3}{EI}(1+\nu)\left(\frac{h}{L}\right)^2\left(1-\frac{1}{\lambda L}\tanh\lambda L\right), \qquad \lambda=\frac{420}{(1+\nu)h}, \tag{18}$$

and

$$w_E^{ss}=\frac{5}{384}\frac{qL^4}{EI}+\frac{5}{24}\frac{qL^4}{EI}\left[\tfrac{3}{25}(1+\nu)\left(\frac{h}{L}\right)^2-\tfrac{2}{875}(1+\nu)^2\left(\frac{h}{L}\right)^4\right], \tag{19}$$

where the subscript E denotes an exact solution and the superscripts c and ss represent the cantilevered and simply supported beam solutions, respectively. These problems have been solved for several values of h and L, with $b = 1$, $E = 29\,000$, $\nu = 0{\cdot}3$, $p = 100{\cdot}0$ and $q = 10{\cdot}0$. The results are given in Table 1 for a varying number, N, of uniform elements. The finite element results are in excellent agreement with the exact solutions for both cases.

Although the results obtained by using the higher order beam element given in Table 1 represent both thick and thin beam geometries, a direct comparison with the C^0-continuous Timoshenko beam element is useful to show the effects of integration order as discussed earlier. A tip-loaded ($p = 1{\cdot}0$) cantilevered beam with the properties $b = 1{\cdot}0$, $E = 2{\cdot}6$, $\nu = 0{\cdot}3$, $L = 4$, and $h = 0{\cdot}554256$ is considered as an example. The shear correction coefficient was taken as 0·85 for the Timoshenko element. The tip deflections for the Timoshenko element are shown in Table 2 as obtained by using exact (w_{TE}) and reduced (w_{TR}) integration, along with results from the exactly integrated higher order beam element (w_{HOE}). The values for the Timoshenko element are taken from the paper by Prathap and Bhashyam [12]. Also shown in Table 2 are the exact solutions for the two theories, which are given by

$$w_T = (pL^3/3EI)(1 + 3EI/KGAL^2) \tag{20}$$

for the Timoshenko theory and by equation (18) for the higher order theory. The higher order beam element gives excellent results when full integration is used. The Timoshenko element requires reduced integration in order to obtain acceptable results.

TABLE 1

Linear solution for cantilevered and simply supported beams; maximum displacements for (a) cantilevered and (b) simply supported beams

(a)

Length (L)	Height (h)	Maximum displacement (eq. (18))	Finite element solution $N = 2$	$N = 4$	$N = 8$	$N = 16$
160	12	32·838	30·838	32·368	32·742	32·823
80		4·1585	3·9234	4·1105	4·1506	4·1567
40		0·54668	0·52266	0·54249	0·54540	0·54588
12		0·024518	0·023551	0·023741	0·023874	0·023931
160	1	56 498·0	52 968·0	55616·0	56 278·0	56 444·0
80		7062·9	6621·8	6952·9	7035·6	7056·3
40		883·19	828·15	869·53	879·87	882·44
12		23·964	22·513	23·627	23·897	23·953

(b)

Length (L)	Height (h)	Maximum displacement (eq. (19))	Finite element solution $N = 2$	$N = 4$	$N = 8$	$N = 16$
160	12	20·721	19·779	20·529	20·691	20·717
80		1·3488	1·3011	1·3415	1·3478	1·3486
40		0·097712	0·096033	0·097481	0·097670	0·097703
12		0·0022204	0·0022234	0·0022206	0·0022204	0·0022204
160	1	35 314·0	33 549·0	34 873·0	35 205·0	35 287·0
80		2207·8	2097·7	2180·4	2201·1	2206·3
40		138·15	131·31	136·49	137·77	138·08
12		1·1366	1·0860	1·1267	1·1351	1·1364

TABLE 2

Comparison of displacements calcuated by using Timoshenko and higher order beam elements

N	$w_{TE}(FEM)$	$w_{TR}(FEM)$	$w_{HOE}(FEM)$
2	111·6	550·6	553·3
3	202·9	570·7	573·1
4	284·2	577·7	579·9
5	349·0	581·0	582·9
6	398·4	582·8	584·4
7	435·6	584·2	585·3
8	463·5	584·6	585·8
9	485·0	585·2	586·1
Exact	586·8		586·9

As a final example for the static case, we consider the moderately large deflection of a cantilevered beam ($L = 10$, $h = b = 1$, $E = 12\,000$, $\nu = 0{\cdot}3$) under a uniformly distributed load Q. The full equations must now be solved iteratively to account for the non-linear ($\mathrm{d}w/\mathrm{d}x$) terms in the stiffness matrix. Direct iteration was used in the present case. The loading was applied in 16 equal increments with an error tolerance of 0·001 being used. The non-dimensionalized tip displacement W/D is plotted against the non-dimensionalized load parameter $K = QD^3/EI$ in Figure 1, where D represents the deformed length of the beam. The results are compared with two solutions obtained by using a displacement and mixed updated Lagrangian formulation of the plane elasticity equations [15]. The agreement among the formulations is very good.

5.2. LINEAR VIBRATIONS

Of the numerous authors who have studied the linear and non-linear vibrations of beams [16–42], nearly all have used the Euler–Bernoulli or Timoshenko theories. Several

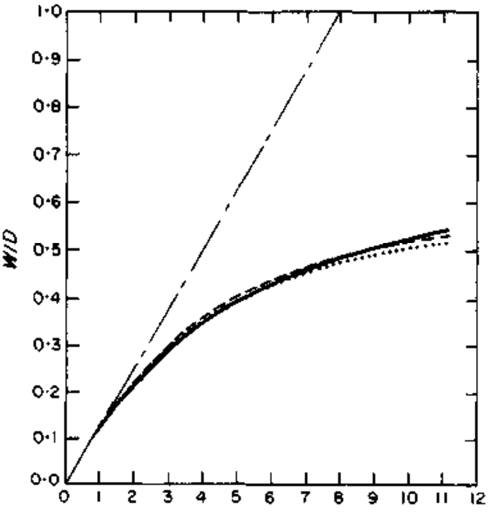

Figure 1. Non-dimensionalized tip displacement for uniformly loaded cantilever beam. ——, Beam theory; · · · · ·, elasticity solution; - - -, mixed elasticity solution; — - —, linear solution.

exceptions exist, including the works of Krishna Murty [26, 27] and Levinson [3], who presented results for the linear vibrations of rectangular beams using higher order theories similar to but substantially different from the theory considered in this paper. Most of the finite element models developed for Timoshenko beams possess a two node-two degree of freedom structure based on the requirements of the variational principle for the Timoshenko displacement field [23-25]. A Timoshenko element with a higher-order approximation was developed by Thomas and Abbas [24], but the C^1-continuity implied by this element was not required from variational considerations. An advantage of the higher order theory is the appearance of the primary variables u, w, $\mathrm{d}w/\mathrm{d}x$ and ψ as a natural consequence of the variational principle used to obtain the governing equations.

Estimates for the shear correction used in Timoshenko's theory range from 0·822 to 0·870 for beams with rectangular cross-section [43-47]. These are based upon both static and dynamic considerations. Most recent investigations of Timoshenko beam vibrations have used either $k = 5/6$ (see reverences [39, 49]) or $k = 0{\cdot}85$ (see references [42, 48, 50]). Without exception, the shear coefficient in these works is assumed to be constant. Several authors have commented that the shear coefficient should change with mode number [44, 45] because of the change in the shear stress distribution at higher frequencies [51]. Although a second advantage of the higher order theory is the accurate modeling of the parabolic shear stress distribution, this assumption is valid only for static problems and dynamic problems with long wavelength - low frequency deformation fields. At higher frequencies, this is a very poor approximation and the resulting frequencies computed by the higher order theory reflect this deficiency [4]. These considerations should not apply to the discussion of non-linear vibrations, where the fundamental mode shape is the quantity of interest.

The next two sections contain several numerican examples of rectangular beam vibration results obtained by using the higher order shear deformation theory. The Poisson ratio is taken to be 0·3 in all examples. Exact (linear) frequencies have been computed for a hinged-hinged beam. The structure of the resulting eigenvalue problem is identical to that obtained when using the Timoshenko theory, thus providing opportunities for a number of worthwhile comparisons. The finite element model of the equations of motion for the higher order theory has been used to compute the linear and non-linear frequencies for beams with a variety of support conditions. The effects of in-plane inertia and slenderness ratio of non-linear frequency are examined. Results are compared with existing solutions whenever possible.

Natural vibrations of a hinged-hinged beam can be obtained by beginning with the following representation of the displacement field:

$$w = A_w \sin(n\pi x/L) \sin \omega t, \qquad \psi = A_\psi \cos(n\pi x/L) \sin \omega t. \tag{21}$$

Here L and ω are the length and natural frequency of the beam, respectively. Substitution of equations (21) into equations (6b, c) and neglecting the non-linear terms leads to

$$[K]\{A\} - \omega^2[M]\{A\} = \{0\}, \tag{22}$$

where

$$\begin{gathered} K_{11} = \tfrac{8}{15}GA(n\pi/L)^2 + \tfrac{1}{21}EI(n\pi/L)^4, \qquad K_{22} = \tfrac{8}{15}GA + \tfrac{68}{105}EI(n\pi/L)^2, \\ K_{12} = K_{21} = \tfrac{8}{15}GA(n\pi/L) - \tfrac{16}{105}EI(n\pi/L)^3, \\ M_{11} = \rho A + \tfrac{1}{21}\rho I(n\pi/L)^2, \qquad M_{12} = M_{21} = \tfrac{16}{105}\rho I(n\pi/L), \qquad M_{22} = \tfrac{68}{21}\rho I. \end{gathered} \tag{23}$$

The corresponding entries for the Timoshenko theory are given by

$$\begin{gathered} K_{11} = KGA(n\pi/L)^2, \qquad K_{22} = KGA + EI(n\pi/L)^2, \qquad K_{12} = K_{21} = KGA(n\pi/L) \\ M_{11} = \rho A, \qquad M_{12} = M_{21} = 0, \qquad M_{22} = \rho I. \end{gathered} \tag{24}$$

The exact solution for the circular frequency of the thickness-shear mode ($n=0$) for thin rectangular bars can be written as [52]

$$\omega=\sqrt{(\pi^2/12)(G/\rho r)}=\sqrt{0{\cdot}8225(G/\rho r)}, \tag{25}$$

where r is the radius of gyration.

The corresponding value given by the higher order theory is

$$\omega=\tfrac{105}{68}\,\tfrac{8}{15}\,(G/\rho r)=\sqrt{0{\cdot}8235(G/\rho r)}. \tag{26}$$

The higher order theory gives the thickness-shear mode frequency to within 0·07 percent, an accuracy not achieved by the Timoshenko theory unless k is specified to be near 0·8225. In fact, this strategy was used by Mindlin and Deresiewicz [45] and Goodman and Sutherland [44] to obtain the value of k of 0·822 for rectangular cross-sections. Using this value in a comparison of Timoshenko and higher order beams with $b=h=\rho=E=1{\cdot}0$, $\nu=0{\cdot}3$ and $L=4{\cdot}0$ yields excellent agreement (within 0·06 percent) between the two theories for the thickness-shear mode and the remaining second spectrum frequencies. However, this value does not consistently yield the best results for either vibration or static bending problems, as indicated from the differing values of k obtained for these cases by earlier workers [43–47].

A plane stress elasticity solution for the fundamental frequency of a hinged-hinged beam was given by Cowper [47] as the lowest root of the equation

$$2(1-\nu)\alpha\beta\tan h(\alpha)=[(\pi h/2L)^2+\alpha^2][(2\beta L/\pi h)^2-\nu]\tan h(\beta) \tag{27}$$

where

$$\alpha^2=(\pi h/2L)^2-(1+\nu)\rho\omega^2h^2/2E, \qquad \beta^2=(\pi h/2L)^2-(1-\nu^2)\rho\omega^2h^2/4E. \tag{28}$$

For the hinged-hinged beam considered, the non-dimensional frequency given by equation (27) is 9·0143, compared to the Euler-Bernoulli value of 9·8696. The higher order theory gives a value of 8·9922, with the Timoshenko theory yielding values of 8·9832 ($k=0{\cdot}822$), 8·9912 ($k=5/6$) and 9·0136 ($k=0{\cdot}867$). For this mode, the assumed value of k clearly makes little difference in the results for the bending frequency. However, as indicated by equation (26), the error in the thickness-shear mode frequency is proportional to $\sqrt{k}$. The higher order theory yields acceptable results for both frequency spectra without having to use a shear coefficient based on the relative importance of the flexural and thickness-shear motions.

The Timoshenko and higher order theories give comparable bending frequencies for a variety of slenderness ratios when k is taken at 5/6. If these frequencies are to be matched more closely, however, there is a small but noticeable increase in the value of k. This behavior is shown in Figure 2 for three different slenderness ratios. The bending frequencies from the two theories have been matched to four significant figures. As the beam becomes thick, the value of k used in the Timoshenko theory increases with mode number. Regardless of slenderness ratio, the best value of k used to match the fundamental frequency is near 5/6. Although the change in k is significant, the changes in frequency induced by maintaining a constant shear correction coefficient for the higher modes in Figure 2 are minimal. For example, the difference in frequency for mode 5 of $L/\rho=13{\cdot}856$ is only 1·23 percent if k is kept constant at 5/6. If k is taken as 0·863 as shown in Figure 2, the difference is within 0·02 percent. Again, we note that the parabolic shear distribution is only valid for lower frequencies. The work of Prescott indicates that the parabolic shear stress distribution for a beam of rectangular cross-section does not begin to change until the wavelength is approximately equal to the depth of the beam [51]. The modes represented in this figure fall within these limits.

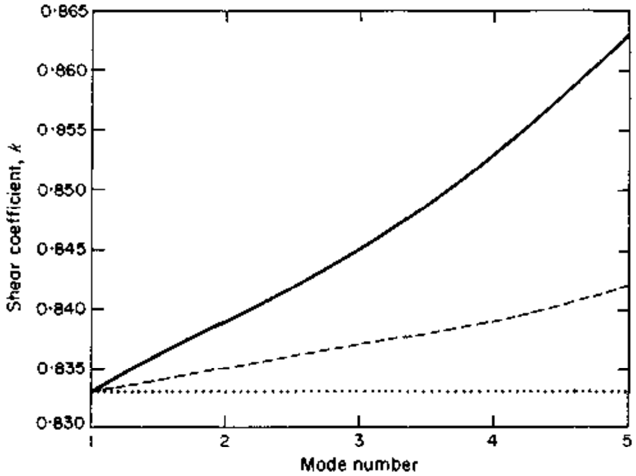

Figure 2. Variation of shear coefficient with mode number for hinged-hinged beam. ——, $L/\rho = 13{\cdot}856$; - - -, $L/\rho = 27{\cdot}713$; · · · · ·, $L/\rho = 110{\cdot}85$.

It is informative to consider the solution of the equations of Levinson's theory [3] for the hinged-hinged beam. The equations of motion are (being the same as those of the Reissner-Mindlin theory, except that the resultants are computed by using the displacement in equation (1))

$$\frac{2}{3}\frac{\partial}{\partial x}\left[AG\left(\psi+\frac{\partial w}{\partial x}\right)\right]=\rho A\frac{\partial^2 w}{\partial t^2}$$

$$\tfrac{2}{3}AG\left(\psi+\frac{\partial w}{\partial x}\right)+\frac{1}{5}\frac{\partial}{\partial x}\left[EI\frac{\partial^2 w}{\partial x^2}-4EI\frac{\partial \psi}{\partial x}\right]=\tfrac{1}{5}\rho I\frac{\partial^2}{\partial t^2}\left(\frac{\partial w}{\partial x}-4\psi\right) \qquad (29)$$

Substitution of equations (21) into equations (29) yields

$$\begin{bmatrix} \tfrac{2}{3}AG\left(\frac{n\pi}{L}\right)^2 & \tfrac{2}{3}AG\left(\frac{n\pi}{L}\right) \\ \tfrac{2}{3}AG\left(\frac{n\pi}{L}\right)-\tfrac{1}{5}EI\left(\frac{n\pi}{L}\right)^3 & \tfrac{2}{3}AG+\tfrac{4}{5}EI\left(\frac{n\pi}{L}\right)^2 \end{bmatrix}\begin{Bmatrix} A_w \\ A_\psi \end{Bmatrix}=\omega^2\begin{bmatrix} \rho A & 0 \\ -\tfrac{1}{5}\rho I\left(\frac{n\pi}{L}\right) & \tfrac{4}{5}\rho I \end{bmatrix}\begin{Bmatrix} A_w \\ A_\psi \end{Bmatrix}. \qquad (30)$$

Note that the coefficient matrices in Levinson's theory are unsymmetric because the equations of motion are not derived by using the virtual work statements (see references [8, 9]). The shear correction coefficient for $n=0$ is $k=5/6=0{\cdot}8333$ as opposed to 0·8225 (exact) and 0·8235 (present higher order theory). In any case, the frequencies obtained by equation (30) are not nearly as good as those obtained in the present theory.

5.3. NON-LINEAR VIBRATIONS

The problems considered in this section are assumed to be governed by the assumptions of moderately large bending theory, in which the axial force generated by the stretching of the neutral axis is accounted for by including the non-linear (von Kármán) strain components in the expression for the strain energy. A number of authors have provided solutions for this class of problem using continuum [32–36] and finite element approaches [20, 21, 28–31, 37–42]. Several of these investigations have included the effects of shear deformation according to the Timoshenko theory [20, 21, 39, 42]. This section contains results from the solution of equation (5) for the non-linear frequencies obtained by using the finite element model described by equation (10). The effects of shear deformation and rotary inertia are accounted for and no simplifications are made regarding the behavior of the non-linear stretching force. Results of numerical examples are presented to demonstrate the effects of longitudinal inertia and slenderness ratio for beams with different support conditions.

We first consider several linear vibration examples to assess the accuracy of the finite element model given by equation (10). For thin beams, the Euler–Bernoulli behavior should be recovered from the higher-order theory yielding the corresponding thin beam frequencies [53]. Table 3 shows the convergence of the higher order element for a very thin beam with a variety of support conditions. Also shown are the values obtained for Euler–Bernoulli beam elements. The results for the higher order beam converge to the exact thin beam solutions, although not as rapidly as do the results for the Euler–Bernoulli beam elements. The frequencies are within 2 and 0·5 percent for the 8 and 16 element idealizations, respectively.

TABLE 3

Convergence of higher order beam elements for thin beam frequencies

Number of elements:	4		8		16		ω_{Exact}
Support conditions:	ω_{HOT}	ω_{EB}	ω_{HOT}	ω_{EB}	ω_{HOT}	ω_{EB}	[53]
Hinged–hinged	9·9356	9·8698	9·8822	9·8696	9·8768	9·8696	9·8696
Clamped–clamped	23·128	22·375	22·556	22·373	22·419	22·373	22·373
Clamped–hinged	16·613	15·428	15·697	15·419	15·486	15·418	15·418
Clamped–free	3·5601	3·5161	3·5266	3·5161	3·5197	3·5160	3·5160

The non-linear algebraic equations given in equation (10) evaluated at the point of reversal of motion have been solved by using the direct iteration technique used in reference [38]. Following Woinowsky-Krieger [32], the frequency of vibration for the in-plane displacement u will be twice that of the transverse displacement frequency ω. Hence the relation $\ddot{u} = -2\omega^2 u$ is introduced into the appropriate mass matrix entries when the in-plane inertia is to be taken into account. If the in-plane inertia is neglected, the terms in the mass matrix correspond to the case in which u displacmeents are set equal to zero.

The non-linear frequencies have been computed for a number of values of (a/ρ) for hinged–hinged, clamped–clamped and hinged–hinged beams, where a is the amplitude and ρ is the radius of gyration. The amplitude a is measured at mid-span for these beams. The converged frequencies are expressed as the ratio $(\omega_{NL}/\omega_L)^2$, where ω_L is the linear frequency obtained at the first iteration. Convergence is assumed to be met when the non-linear frequency and normalized eigenvector have satisfied the following convergence norms [41, 54]:

$$\|\varepsilon\|_\infty = \mathrm{Max}_i \left|\frac{\Delta r_i(j)}{r_i}\right|, \qquad \|\varepsilon\|_1 = \frac{1}{N}\sum_{i=1}^{N}\left|\frac{\Delta r_i(j)}{r_i}\right|,$$

$$\|\varepsilon\|_2 = \left\{\frac{1}{N}\sum_{i=1}^{N}\left|\frac{\Delta r_i(j)}{r_i}\right|^2\right\}^{1/2}, \qquad \|\varepsilon\|_f = \left|\frac{\Delta\lambda_n}{\lambda_n}\right|.$$

Here $\|\varepsilon\|_\infty$ is the maximum norm, $\|\varepsilon\|_1$ is the modified absolute norm, $\|\varepsilon\|_2$ is the modified Euclidean norm, $\|\varepsilon\|_f$ is the frequency norm, $\Delta r_i(j)$ is the change in the ith eigenvector

TABLE 4

Convergence of $(\omega_{NL}/\omega_L)^2$ for a thin hinged-hinged beam

	Number of elements			Exact
(a/ρ)	4	8	16	[32]
0·4	1·0399	1·0399	1·0396	1·0400
1·0	1·2489	1·2465	1·2465	1·2500
1·5	1·5596	1·5553	1·5537	1·5625
2·0	1·9938	1·9867	1·9841	2·0000
2·5	2·5507	2·5414	2·5385	2·5625

TABLE 5

Non-linear frequencies of a hinged-hinged beam

	$L/\rho = 13·856$				$L/\rho = 27·713$			
	$\ddot{u} = 0$		$\ddot{u} = -2\omega^2 u_0$		$\ddot{u} = 0$		$\ddot{u} = -2\omega^2 u$	
(a/ρ)	Present	[42]	Present	[42]	Present	[42]	Present	[42]
0·1	1·00287	1·00278	1·00281	1·00277	1·00257	1·00250	1·00256	1·00249
0·2	1·01148	1·01117	1·01124	1·01105	1·01029	1·01000	1·01023	1·00998
0·4	1·04593	1·04469	1·04494	1·04412	1·04115	1·04003	1·04091	1·03991
0·6	1·10330	1·10589	1·10097	1·09942	1·09262	1·09009	1·09205	1·08980
0·8	1·18362	1·17887	1·17923	1·17666	1·16461	1·16019	1·16353	1·15964
1·0	1·28686	1·27955	1·27948	1·27586	1·25723	1·25003	1·25542	1·24940
1·5	1·64478	1·62854	1·62473	1·61839	1·57835	1·56269	1·57362	1·56043
2·0	2·14550	2·11719	2·10026	2·09478	2·02769	2·00027	2·01710	1·99549
2·5	2·78825	2·74542	2·69961	2·70223	2·60493	2·56303	2·58427	2·55219
3·0	3·57361	3·50999	3·41251	3·43368	3·31011	3·25088	3·27355	3·23187
3·5	4·50072	4·43412	4·22079	4·27866	4·14347	4·06309	4·08435	4·03499
4·0	5·57054	—	5·10121	—	5·10388	5·00470	5·01183	4·95729
Linear	$\omega_{\text{Exact}} = 8·9922$		$\omega_{FEM} = 8·9946$		$\omega_{\text{Exact}} = 9·6206$		$\omega_{FEM} = 9·6251$	

	$L/\rho = 55·426$				$L/\rho = 110·85$				
	$\ddot{u} = 0$		$\ddot{u} = -2\omega^2 u$		$\ddot{u} = 0$		$\ddot{u} = -2\omega^2 u$		Exact
(a/ρ)	Present	[42]	Present	[42]	Present	[42]	Present	[42]	[32]
0·1	1·00250	1·00243	1·00249	1·00243	1·00248	1·00241	1·00247	1·00241	1·0025
0·2	1·00998	1·00972	1·00997	1·00971	1·00990	1·00964	1·00990	1·00964	1·0100
0·4	1·03994	1·03887	1·03987	1·03884	1·03961	1·03858	1·03959	1·03857	1·0400
0·6	1·08988	1·08747	1·08973	1·08739	1·08914	1·08681	1·08911	1·08679	1·0900
0·8	1·15975	1·15552	1·15948	1·15517	1·15844	1·15435	1·15837	1·15431	1·1600
1·0	1·24953	1·24302	1·24908	1·24278	1·24749	1·24119	1·24738	1·24113	1·2500
1·5	1·56143	1·54642	1·56019	1·54578	1·55685	1·54235	1·55655	1·54219	1·5625
2·0	1·99737	1·97183	1·99507	1·97042	1·98931	1·96452	1·98863	1·96417	2·0000
2·5	2·55783	2·51880	2·55255	2·51616	2·54530	2·50739	2·54398	2·50671	2·5625
3·0	3·24249	3·18524	3·23324	3·18045	3·22450	3·16909	3·22219	3·16789	3·2500
3·5	4·05149	3·97465	4·03642	3·96684	4·02583	3·95464	4·02207	3·95269	4·0625
4·0	4·98362	4·88489	4·96050	4·87288	4·95159	4·85904	4·94583	4·85603	5·0000
Linear	$\omega_{\text{Exact}} = 9·8051$		$\omega_{FEM} = 9·8137$		$\omega_{\text{Exact}} = 9·8533$		$\omega_{FEM} = 9·8662$		

TABLE 6

Non-linear frequencies of a clamped-clamped beam

	$L/\rho = 13{\cdot}856$		$L/\rho = 27{\cdot}713$		$L/\rho = 110{\cdot}85$		Continuum solutions	
(a/ρ)	$\ddot{u} = 0$	$\ddot{u} = -2\omega^2 u$	$\ddot{u} = 0$	$\ddot{u} = -2\omega^2 u$	$\ddot{u} = 0$	$\ddot{u} = -2\omega^2 u$	[32]	[34]
0·1	1·00093	1·00091	1·00067	1·00067	1·00060	1·00060	1·0006	1·0006
0·2	1·00373	1·00364	1·00268	1·00266	1·00241	1·00241	1·0024	1·0024
0·4	1·01491	1·01457	1·01072	1·01065	1·00964	1·00964	1·0096	1·0096
0·6	1·03355	1·03276	1·02411	1·02396	1·02170	1·02169	1·0216	1·0216
0·8	1·05963	1·05818	1·04282	1·04280	1·03856	1·03854	1·0383	1·0384
1·0	1·09312	1·09105	1·06698	1·06679	1·06023	1·06020	1·0598	1·0599
1·5	1·20917	1·20388	1·15067	1·14956	1·13525	1·13518	1·1343	1·1349
2·0	1·37215	1·35941	1·26643	1·26428	1·23987	1·23974	1·2382	1·2398
2·5	1·57985	1·55573	1·41379	1·41003	1·37349	1·37326	1·3708	1·3750
3·0	1·83305	1·78986	1·59208	1·58596	1·53588	1·53551	1·5320	1·5396
3·5	2·13107	2·05671	1·80081	1·79129	1·72816	1·72759	1·7211	1·7350
4·0	2·47420	2·34674	2·03936	2·02538	1·94646	1·94563	1·9377	1·9592
Linear	$\omega_{HOT} = 16{\cdot}716$	$\omega_T = 17{\cdot}024$	$\omega_{HOT} = 20{\cdot}390$	$\omega_T = 21{\cdot}194$	$\omega_{HOT} = 22{\cdot}368$	$\omega_T = 23{\cdot}337$		

TABLE 7

Non-linear frequencies of a clamped-hinged beam

	$L/\rho = 13{\cdot}856$		$L/\rho = 27{\cdot}713$		$L/\rho = 110{\cdot}85$		Continuum solutions	
(a/ρ)	$\ddot{u} = 0$	$\ddot{u} = 2\omega^2 u$	$\ddot{u} = 0$	$\ddot{u} = -2\omega^2 u$	$\ddot{u} = 0$	$\ddot{u} = -2\omega^2 u$	[32]	[34]
0·1	1·00175	1·00162	1·00144	1·00141	1·00137	1·00137	1·0013	1·0013
0·2	1·00698	1·00647	1·00578	1·00565	1·00548	1·00547	1·0053	1·0053
0·4	1·02789	1·02583	1·02310	1·02256	1·02190	1·02187	1·0213	1·0214
0·6	1·06264	1·05790	1·05185	1·05062	1·04919	1·04911	1·0479	1·0481
0·8	1·11121	1·10241	1·09187	1·08967	1·08718	1·08704	1·0850	1·0854
1·0	1·17373	1·15897	1·14291	1·13954	1·13576	1·13553	1·1323	1·1335
1·5	1·38336	1·34923	1·31771	1·30980	1·30206	1·30155	1·2947	1·3004
2·0	1·67298	1·59357	1·55719	1·54234	1·53019	1·52925	1·5175	1·5340
2·5	2·03974	—	1·85983	1·83384	1·81785	1·81635	1·7978	1·8344
3·0	2·48337	—	2·22378	2·18223	2·16354	2·16092	2·1331	2·2015
3·5	3·00356	—	2·62890	2·58536	2·56799	2·56324	2·5217	2·6354
Linear	$\omega_{HOT} = 12{\cdot}751$	$\omega_T = 12{\cdot}974$	$\omega_{HOT} = 14{\cdot}674$	$\omega_T = 14{\cdot}999$	$\omega_{HOT} = 15{\cdot}619$	$\omega_T = 15{\cdot}873$		

component for iteration j, N is the total number of degrees of freedom, and $\Delta\lambda_n$ is the change in the eigenvalue λ_n calculated during iteration j. In all examples, eight uniform elements were used with a tolerance limit of 0·001 for each of the convergence norms.

A convergence study was performed for the non-linear vibration of a hinged–hinged beam as described by using higher order elements for several (a/ρ) ratios. Table 4 shows the ratios $(\omega_{NL}/\omega_L)^2$ computed by the finite element discretizations of 4, 8 and 16 uniform elements. These are compared with the exact solutions given by Woinowsky-Krieger [32]. The converged values are slightly below the exact values, with the difference increasing as (a/ρ) increases. However, most values are well within 1 percent for the 8 and 16 element models.

The computed values of $(\omega_{NL}/\omega_L)^2$ for the hinged–hinged beam are shown in Table 5. The results are compared with those given by Sarma and Varadan [42], who used linear Timoshenko elements with a shear coefficient of 0·85 and the same direct iteration technique used in this study. There is good agreement between the results of these two theories with the higher order theory giving, in general, slightly larger values than those given by the Timoshenko model. The influence of in-plane inertia is also slightly larger for the higher order model. For most cases this softening effect is fairly small but it does increase with amplitude. As the slenderness ratio (L/ρ) is increased, the beams should behave according to the E(uler)Bernoulli theory. The corresponding values of $(\omega_{NL}/\omega_L)^2$ for $\ddot{u}=0$ may be compared accordingly with the continuum solution [32] which is shown in the table. Also shown are the exact and computed linear frequencies expressed in non-dimensional form.

Results for the clamped–clamped and clamped–hinged beams are given in Tables 6 and 7. The continuum solutions for the Euler–Bernoulli beam are included in the tables [32, 34, 42] as are the linear higher order and Timoshenko frequencies [42]. The general trends for these beams are the same as for the hinged–hinged beam in that the effect of in-plane inertia is small for most cases but becomes larger as the slenderness ratio decreases and the amplitude increases. The convergence criteria were not met for higher amplitudes of the clamped–hinged beam when in-plane inertia was accounted for. The thin beam results for $L/\rho = 110{\cdot}85$ are in good agreement with the continuum solutions.

6. SUMMARY

A finite element model for the static and dynamic response of rectangular beams using a higher order shear deformation theory has been presented. The theory correctly accounts for the parabolic shear distribution across the beam cross-section and satisfies the stress free conditions on the upper and lower surfaces of the beam. The theory therefore needs no shear correction coefficient. Geometric non-linearity is accounted for using the von Kármán strain components. Unlike the minimum ordered Timoshenko beam element, the shear stiffness terms of the minimum order higher order element does not require reduced integration to obtain acceptable results. The exact integration of these terms results in the recovery of the Kirchhoff constraint in the case of thin beams without introducing spurious locking constraints.

Examples have been presented for static and dynamic cases. Comparisons have been made with results from elasticity solutions and the Timoshenko beam theory. In general, the agreement is good. Results for the linear vibration of a simply supported beam indicate that the shear correction coefficient used in the Timoshenko theory must increase with mode number if the bending frequencies are to be matched with those from the higher order theory. However, a constant value for k of $\pi^2/12$ yields excellent agreement between the second spectra frequencies. For higher modes, the higher order theory provides a poor approximation to the true shear stress distribution which changes from parabolic to a distribution with maxima near the upper and lower surfaces and a minimum at the neutral axis. For static and low frequency deformation fields, the higher order theory may yield more accurate and more consistent results than the Timoshenko theory because it does not require a shear coefficient that is frequently problem dependent.

ACKNOWLEDGMENTS

Portions of this research were performed by the first author under a postdoctoral research program at the National Bureau of Standards, Boulder, Colorado. The first author gratefully acknowledges this support and the continued encouragement of Dr R. D. Kriz. The helpful comments of Dr R. Sweet are appreciated. The second author gratefully acknowledges the support of this research by the Alexander von Humboldt Research Foundation.

REFERENCES

1. S. P. TIMOSHENKO 1921 *Philosophical Magazine* **41**, 744–746. On the correction for shear of the differential equation for transverse vibrations of prismatic bars.
2. S. P. TIMOSHENKO 1922 *Philosophical Magazine* **43**, 125–131. On the transverse vibration of bars of uniform cross-section.
3. M. LEVINSON 1981 *Journal of Sound and Vibration* **74**, 81–87. A new rectangular beam theory.
4. W. B. BICKFORD 1982 *Developments in Theoretical and Applied Mechanics* **11**, 137–150. A consistent higher order beam theory.
5. A. B. BASSET 1890 *Philosophical Transactions of the Royal Society (London), Series A*, **181**(6) 433–480. On the extension and flexure of cylindrical and spherical thin elastic shells.
6. F. B. HILDEBRAND, E. REISSNER and G. B. THOMAS 1947 *NACA Technical Note* 1033. Notes on the foundations of the theory of small displacements of orthotropic shells.
7. H. HENCKY 1947 *Ingenier-Archiv* **16**, 72–76. Über die berucksichtitung der schubverzerrungen in ebenen platten.
8. J. N. REDDY 1984 *American Society of Mechanical Engineers, Journal of Applied Mechanics* **54**, 745–752. A simple higher-order theory for laminated composite plates.
9. J. N. REDDY 1984 *International Journal of Solids and Structures* **20**, 881–896. A refined nonlinear theory of plates with transverse shear deformation.
10. J. N. REDDY 1984 *An Introduction to the Finite Element Method*. New York: McGraw-Hill.
11. T. J. R. HUGHES, R. L. TAYLOR and W. KANOKNUKULCHAI 1977 *International Journal of Numerical Methods in Engineering* **11**, 1529–1543. A simple and efficient finite element for plate bending.
12. G. PRATHAP and G. R. BHASHYAM 1982 *International Journal of Numerical Methods in Engineering* **18**, 195–210. Reduced integration and the shear-flexible beam element.
13. J. N. REDDY 1984 *Energy and Variational Methods in Applied Mechanics*. New York: John Wiley.
14. N. D. PHAN and J. N. REDDY 1985 *International Journal of Numerical Methods in Engineering* **12**, 2201–2219, Analysis of laminated composite plates using a higher-order shear deformation theory.
15. P. R. HEYLIGER and J. N. REDDY (1988) *International Journal of Nonlinear Mechanics* **23**, 131–145. On a mixed finite element model for large deformation analysis of elastic solids.
16. R. A. ANDERSON 1953 *American Society of Mechanical Engineers, Journal of Applied Mechanics* **20**, 504–510. Flexural vibrations in uniform beams according to the Timoshenko theory.
17. R. W. TRAILL-NASH and A. R. COLLAR 1953 *Quarterly Journal of Mechanics and Applied Mathematics* **6**, 186–222. The effect of shear flexibility and rotary inertia on the bending vibration of beams.
18. C. L. DOLPH 1954 *Quarterly Journal of Applied Mathematics* **12**, 175–187. On the Timoshenko theory of transverse beam vibrations.
19. T. C. HUANG 1961 *American Society of Mechanical Engineers, Journal of Applied Mechanics* **28**, 579–584. The effect of rotatory inertia and of shear deformation on the frequency and normal mode equations of uniform beams with simple end conditions.

20. K. KAPUR 1966 *Journal of the Acoustic Society of America* **40**, 1058–1063. Vibrations of a Timoshenko beam using a finite element approach.
21. S. B. DONG and J. A. WOLF, JR 1973 *Journal of the Acoustical Society of America* **53**, 120–127. Effect of transverse shear deformation on vibrations of planar structure composed of beam type elements.
22. B. DOWNS 1976 *Journal of Applied Mechanics* **43**, 671–674. Vibration of a uniform, simply supported Timoshenko beam without transverse deflection.
23. D. L. THOMAS, J. M. WILSON and R. R. WILSON 1973 *Journal of Sound and Vibration* **31**, 315–330. Timoshenko beam finite elements.
24. J. THOMAS and B. A. H. ABBAS 1975 *Journal of Sound and Vibration* **41**, 291–299. Finite element model for the dynamic analysis of Timonshenko beams.
25. D. J. DAWE 1978 *Journal of Sound and Vibration* **60**, 11–20. A finite element for vibration analysis of Timoshenko beams.
26. A. V. KRISHNA MURTY 1970 *American Institute of Aeronautics and Astronautics Journal* **8**, 34–38. Vibrations of short beams.
27. A. V. KRISHNA MURTY 1985 *Journal of Sound and Vibration* **101**, 1–12. On the shear deformation theory for dynamic analysis of beams.
28. C. MEI 1972 *American Institute of Aeronautics and Astronautics Journal* **10**, 355–357. Nonlinear vibrations of beams by matrix displacement method.
29. C. MEI 1973 *Journal of Computers and Structures* **3**, 163–174. Finite element displacement method for large amplitude free flexural vibrations of beams and plates.
30. G. V. RAO, I. S. RAJU and K. K. RAJU 1976 *American Institute of Aeronautics and Astronautics Journal* **14**, 685–687. Nonlinear vibrations of beams considering shear deformation and rotary inertia.
31. G. V. RAO, K. K. RAJU and I. S. RAJU 1976 *Journal of Computers and Structures* **6**, 169–172. Finite element formulation for the large amplitude free vibrations of beams and orthotropic circular plates.
32. S. WOINOWSKY-KRIEGER 1950 *Journal of Applied Mechanics* **17**, 35–36. The effect of an axial force on the vibration of hinged bars.
33. D. BURGREEN 1951 *Journal of Applied Mechanics* **18**, 135–139. Free vibrations of a pin-ended column with constant distance between pin ends.
34. D. A. EVENSON 1968 *American Institute of Aeronautics and Astronautics Journal* **6**, 370–372. Nonlinear vibrations of beams with various boundary conditions.
35. A. V. SRINIVASAN 1965 *American Institute of Aeronautics and Astronautics Journal* **3**, 1951–1953. Large amplitude free oscillations of beams and plates.
36. J. D. RAY and C. W. BERT 1961 *Journal of Engineering and Industry* **91**, 977–1004, Nonlinear vibrations of a beam with pinned ends.
37. G. PRATHAP and T. K. VARADAN 1978 *Journal of Computers and Structures* **9**, 219–222. The large amplitude vibration of hinged beams.
38. G. R. BHASHYAM and G. PRATHAP 1980 *Journal of Sound and Vibration* **72**, 191–203. Galerkin finite element method for nonlinear beam vibrations.
39. J. N. REDDY and I. R. SINGH 1981 *International Journal of Numerical Methods in Engineering* **17**, 829–852. Large deflections and large-amplitude free vibrations of straight and curved beams.
40. B. S. SARMA and T. K. VARADAN 1983 *Journal of Sound and Vibration* **86**, 61–70. Lagrange-type formulation for finite element analysis for nonlinear beam vibrations.
41. B. S. SARMA and T. K. VARADAN 1984 *International Journal of Numerical Methods in Engineering* **20**, 353–387. Ritz finite element approach to nonlinear vibrations of beams.
42. B. S. SARMA and T. K. VARADAN 1985 *Communications on Applied Numerical Methods* **1**, 23–32. Ritz finite element approach to nonlinear vibration of a Timoshenko beam.
43. R. D. MINDLIN 1951 *Journal of Applied Mechanics* **18**, 31–38. Influence of rotatory inertia and shear on flexural vibrations of isotropic, elastic plates.
44. L. E. GOODMAN and J. G. SUTHERLAND 1951 *Journal of Applied Mechanics* **18**, 217–218. Discussion of "Natural frequencies of continuous beams of uniform span length," by R. S. Ayre and L. S. Jacobson.
45. R. D. MINDLIN and H. DERESIEWICZ 1954 *Proceedings of the Second U. S. National Congress of Applied Mechanics*, 175–178. Timoshenko's shear coefficient for flexural vibrations of beams.
46. G. R. COWPER 1966 *Journal of Applied Mechanics* **33**, 335–340. The shear coefficient in Timoshenko's beam theory.
47. G. R. COWPER 1968 *Journal of the Engineering Mechanics Division* **94**, 1447–1453. On the accuracy of Timoshenko's beam theory.

48. G. R. BHASHYAM and G. PRATHAP 1981 *Journal of Sound and Vibration* **76**, 407–420. The second frequency spectrum of Timoshenko beams.
49. M. LEVINSON and D. W. COOKE 1982 *Journal of Sound and Vibration* **84**, 319–326. On the two frequency spectra of Timoshenko beams.
50. N. G. STEPHEN 1982 *Journal of Sound and Vibration* **80**, 578–582. The second frequency spectrum of Timoshenko beams.
51. J. PRESCOTT 1942 *Philosophical Magazine* **33**, 703–754. Elastic waves and vibrations of thin rods.
52. H. LAMB 1945 *Hydrodynamics* (second edition) New York: Dover Publications.
53. D. YOUNG and R. P. FELGAR, JR 1949 *University of Texas Publication No.* 4913. Tables of characteristic functions representing the normal modes of vibration of a beam.
54. R. H. MALLET and P. V. MARCAL 1968 *American Society of Civil Engineers, Journal of the Structural Division* **94**, 2081–2109. Finite element analysis of nonlinear structures.

APPENDIX

The finite element equations (10) may be written as

$$\begin{bmatrix} [K^{11}] & [K^{12}] & [0] \\ [K^{21}] & [K^{22}] & [K^{23}] \\ [0] & [K^{32}] & [K^{33}] \end{bmatrix} \begin{Bmatrix} \{u\} \\ \{\Delta\} \\ \{\psi\} \end{Bmatrix} + \begin{bmatrix} [M^{11}] & [0] & [0] \\ [0] & [M^{22}] & [M^{23}] \\ [0] & [M^{32}] & [M^{33}] \end{bmatrix} \begin{Bmatrix} \{\ddot{u}\} \\ \{\ddot{\Delta}\} \\ \{\ddot{\psi}\} \end{Bmatrix} = \begin{Bmatrix} \{F^1\} \\ \{F^2\} \\ \{F^3\} \end{Bmatrix},$$

where

$$K_{ij}^{11} = \int_L AE \frac{\mathrm{d}N_i}{\mathrm{d}x}\frac{\mathrm{d}N_j}{\mathrm{d}x}\,\mathrm{d}x, \qquad K_{ij}^{12} = \int_L \frac{AE}{2}\left(\frac{\mathrm{d}w}{\mathrm{d}x}\right)\frac{\mathrm{d}N_i}{\mathrm{d}x}\frac{\mathrm{d}\phi_j}{\mathrm{d}x}\,\mathrm{d}x,$$

$$K_{ij}^{21} = \int_L AE\left(\frac{\mathrm{d}w}{\mathrm{d}x}\right)\frac{\mathrm{d}\phi_i}{\mathrm{d}x}\frac{\mathrm{d}N_j}{\mathrm{d}x}\,\mathrm{d}x,$$

$$K_{ij}^{22} = \int_L \left[\tfrac{1}{2}AE\left(\frac{\mathrm{d}w}{\mathrm{d}x}\right)^2\frac{\mathrm{d}\phi_i}{\mathrm{d}x}\frac{\mathrm{d}\phi_j}{\mathrm{d}x} + \tfrac{8}{15}GA\frac{\mathrm{d}\phi_i}{\mathrm{d}x}\frac{\mathrm{d}\phi_j}{\mathrm{d}x} + \tfrac{1}{21}EI\frac{\mathrm{d}^2\phi_i}{\mathrm{d}x^2}\frac{\mathrm{d}^2\phi_j}{\mathrm{d}x^2}\right]\mathrm{d}x,$$

$$K_{ij}^{23} = \int_L \left[\tfrac{8}{15}GA\frac{\mathrm{d}\phi_i}{\mathrm{d}x}N_j - \tfrac{16}{105}EI\frac{\mathrm{d}^2\phi_i}{\mathrm{d}x^2}\frac{\mathrm{d}N_j}{\mathrm{d}x}\right]\mathrm{d}x = K_{ji}^{32},$$

$$K_{ij}^{33} = \int_L \left[\tfrac{68}{105}EI\frac{\mathrm{d}N_i}{\mathrm{d}x}\frac{\mathrm{d}N_j}{\mathrm{d}x} + \tfrac{8}{15}GAN_iN_j\right]\mathrm{d}x,$$

$$M_{ij}^{11} = \int_L \rho AN_iN_j\,\mathrm{d}x, \qquad M_{ij}^{22} = \int_L \left[\tfrac{1}{2}\rho I\frac{\mathrm{d}\phi_i}{\mathrm{d}x}\frac{\mathrm{d}\phi_j}{\mathrm{d}x} + \rho_A\phi_i\phi_j\right]\mathrm{d}x,$$

$$M_{ij}^{23} = \int_L -\tfrac{16}{105}\rho I\frac{\mathrm{d}\phi_i}{\mathrm{d}x}N_j\,\mathrm{d}x = M_{ji}^{32},$$

$$M_{ij}^{33} = \int_L \tfrac{68}{105}\rho IN_iN_j\,\mathrm{d}x, \qquad F_i^1 = \int_L fN_i\,\mathrm{d}x, \qquad F_i^2 = \int_L q\phi_i\,\mathrm{d}x, \qquad F_i^3 = 0.$$

INTERNATIONAL JOURNAL FOR NUMERICAL METHODS IN ENGINEERING, VOL. 33, 1553–1572 (1992)

AN ASSESSMENT OF FOUR-NODED PLATE FINITE ELEMENTS BASED ON A GENERALIZED THIRD-ORDER THEORY

R. C. AVERILL* AND J. N. REDDY†

Department of Engineering Science and Mechanics, Virginia Polytechnic Institute and State University, Blacksburg, Virginia 24061, U.S.A.

SUMMARY

Plate finite elements based on the generalized third-order theory of Reddy and the first-order shear deformation theory are analysed and compared on the basis of thick and thin plate modelling behaviour, distortion sensitivity, overall accuracy, reliability and efficiency. In particular, several four-noded Reddy-type elements and the nine-noded Lagrangian and heterosis (Mindlin-type) plate elements are analysed to assess their behaviour in bending, vibration and stability of isotropic and laminated composite plates. A four-noded Reddy-type element is identified which is free of all spurious stiffness and zero energy modes, computationally efficient, and suitable for use in any general-purpose finite element program.

1. INTRODUCTION

A great deal of effort has been spent on developing accurate and efficient plate finite elements based on the first-order shear deformation theory, often known as the Mindlin plate theory,[1] with only limited success. It is universally agreed that isoparametric, displacement-based plate finite elements of the first-order shear deformation plate theory are among the simplest available in terms of formulation, implementation and application to various plate structures. Unfortunately, the accuracy of the low-order elements of this type (i.e. those with nine or fewer nodes) is less than satisfactory when the span-to-thickness ratio of the elements is large. Under such circumstances, the shearing strains are required to vanish, and the plate elements based on the first-order theory become excessively stiff, yielding displacements that are too small compared to the true solution. This type of behaviour, known as shear locking, has plagued shear deformable elements since their inception (see Zienkiewicz *et al.*[2] and Pawsey and Clough[3]).

It should be emphasized, though, that even relatively thick elements may be required to model a state of zero (or very small) transverse shearing strain. While cases of pure bending are seldom encountered in real structures, there certainly may be regions within a structure where the values of the transverse shearing strains (or other strain components) change from positive to negative, or vice versa, requiring that the strain components be very small. In order for an element to be reliable for all applications, it must be able to accommodate these vanishing strain components while maintaining an accurate representation of the non-vanishing components. In fact, shear locking is due to the inability of shear deformable elements to accurately model the curvatures

---

*NASA Graduate Student Researcher

†Clifton C. Garvin Professor

0029–5981/92/111553–20$10.00
© 1992 by John Wiley & Sons, Ltd.

Received September 1990
Revised March 1991

within an element under a state of zero transverse shearing strain. This argument may be modified and extended to account for membrane locking in curved elements, as well as the poor behaviour of all elements which contain multi-strain fields (e.g. plane stress and plane strain elements).

The various means employed to alleviate shear locking in plate elements include reduced integration, mixed formulations, hybrid formulations, assumed strain techniques and discrete Kirchhoff methods, to name only a few. Of the large number of new displacement-based elements in the literature, only a few have been reasonably successful,[4–6] and there is still much room for improvement in terms of accuracy, ease of implementation and computational efficiency.

After many unsuccessful attempts to develop a general plate element, it became clear to many researchers that a better understanding of locking phenomena and the effects of reduced integration was necessary in order to give guidelines for the development of new elements and to allow a more complete analysis of existing elements. To demonstrate why shear deformable plate elements become overly stiff, early investigators presented a penalty formulation of the equations of plate bending.[7] As will be shown in the next section, as the span-to-thickness ratio of a plate tends towards infinity (or a large number), a constraint condition is imposed which requires the product of the shear stiffness matrix and the displacement vector to be zero. Therefore, in order to obtain a non-trivial solution, it was concluded that the shear stiffness matrix must be singular. These observations led to explanations of locking behaviour based upon measures of singularity of the shear stiffness matrix,[8] the number of independent shear constraints imposed on an element in the thin plate limit[9, 10] and other criteria. However, the exact cause of the poor behaviour of shear deformable elements in thin plate or beam applications was identified by Prathap and Bhashyam,[11] who demonstrated that locking is a function of the type of constraints that arise when an element is very thin. These investigators developed a method of identifying the actual constraints that arise under full or reduced integration, and, by deriving the constraints in terms of the nodal degrees of freedom, were able to classify them as being either proper Kirchhoff constraints that enforce a condition of zero transverse shearing strain or spurious constraints that cause locking. Prathap and his co-workers have also contributed significantly to the understanding of locking, field-consistency and stress oscillations in finite element models of beams, plates and shells.[6, 12, 13]

Recently, the present authors presented a new analytical technique for identifying the exact form of the shear constraints that are imposed on an element when its side-to-thickness ratio is very large.[14] The technique yields results that are equivalent to those obtained by Prathap and Bhashyam[11] for Timoshenko beam elements, but the new method is much simpler both in concept and in application to two-dimensional elements, especially when high orders of interpolation and/or Gaussian quadrature are employed. By applying the technique to several popular Mindlin plate elements, it was shown that, if the form of the shear constraints in an element is known, the performance of that element when used to model thin structures can be determined *a priori*. Furthermore, by studying the form of the constraints, a more complete understanding of the locking behaviour of plate elements was gained, resulting in new insights and definitive conclusions regarding the origin of locking phenomena and the effects of reduced integration.[14]

In the present study, the improved technique for identifying shear constraints has been applied to plate elements based on a generalized form of the third-order theory of plate bending presented by Reddy.[15] Third-order shear deformation plate theories and their associated plate finite elements have been much maligned in the past owing to the misconception that their formulation and implementation are overly complicated and that their use is unjustifiably expensive. In order to clear up this misconception, it is demonstrated through numerous numerical examples that selected elements based upon third-order plate theories not only are comparable, and in some cases superior, to the best Mindlin-type elements in terms of accuracy, but also are extremely efficient in terms of computational cost.

2. A GENERALIZED THIRD-ORDER THEORY OF PLATE BENDING

The analysis of plate structures entails two important aspects: the selection of an appropriate plate theory, and the implementation of a suitable numerical model to solve the governing differential equations of the theory. It is well known by now that the classical theory of thin plates introduced by Kirchhoff[16] is inadequate for modelling laminated composite plates, even if the plate is fairly thin. The Kirchhoff assumptions amount to treating plates as being infinitely rigid in the transverse direction, with all of the transverse normal and shearing effects being neglected. As a result, this theory underestimates deflections and overestimates natural frequencies and buckling loads. Since laminated composite materials are often very flexible in transverse shear, the transverse shearing strains and stresses must be taken into account if an accurate representation of the behaviour of the plate is to be achieved.

Numerous plate theories which include transverse shear deformations are presented in the literature, but the one most commonly used is the first-order shear deformation theory.[1] In this theory, the in-plane displacements are expanded up to the first term in the thickness co-ordinate, and the rotations of normals to the mid-surface are assumed to be independent of the transverse deflection. This theory yields a constant value of transverse shearing strain through the thickness of the plate, and thus requires shear correction factors in order to ensure the proper amount of transverse shear energy (i.e. equivalent to a parabolic distribution of shearing strain through the thickness).

Reddy's third-order plate theory[15,17] allows for a quadratic distribution of transverse shearing strain through the thickness of the plate by assuming a cubic expansion of the in-plane displacements in the thickness co-ordinate. The form of the assumed displacement functions is simplified by enforcing traction-free boundary conditions at the top and bottom surfaces of the plate. No shear correction factors are needed, because a correct representation of the transverse shearing strain is given. The first- and third-order plate theories contain the same number of dependent variables, but the variationally consistent form of Reddy's theory involves additional high-order stress resultants and material stiffness coefficients compared to the first-order theory.

Various other theories which utilize assumed displacement fields either the same or similar to that in Reddy's theory[15] have been presented in the literature. While several authors have claimed that these theories are in some way new, Reddy[15] has demonstrated that all third-order displacement expansions which satisfy traction-free boundary conditions on the top and bottom surfaces of the plate are in fact the same. The displacement field for these theories can be written in a general form as (from Reddy[15]):

$$\begin{aligned} u &= u^0 - z\frac{\partial w^0}{\partial x} + z\left[1 - \frac{4}{3}\left(\frac{z}{h}\right)^2\right]\hat{\phi}_x \\ v &= v^0 - z\frac{\partial w^0}{\partial y} + z\left[1 - \frac{4}{3}\left(\frac{z}{h}\right)^2\right]\hat{\phi}_y \qquad (1) \\ w &= w^0 \end{aligned}$$

where u^0, v^0 and w^0 are the displacements of the mid-surface of the plate in the x, y and z directions, respectively. The different forms of the displacement field are obtained by making the appropriate change of variables for the generalized rotations $\hat{\phi}_x$ and $\hat{\phi}_y$. For example, the rotation functions (ψ_x, ψ_y) used by Reddy in his first paper[17] can be obtained from the relations

$$\psi_x = \hat{\phi}_x - \frac{\partial w^0}{\partial x}, \quad \psi_y = \hat{\phi}_y - \frac{\partial w^0}{\partial y} \tag{2}$$

Even though the displacement expansions of all the theories are equivalent, two different forms of the governing equations have been presented: those that utilize the equilibrium equations of the first-order theory and those derived using a variational principle such as the principle of total potential energy. Further discussion and the appropriate substitutions for other theories are given by Reddy.[15]

While the equivalence of the various plate theories is an important theoretical consideration, from a practical point of view it is important to identify which form of the theory yields the optimal finite element model.

In order to facilitate the model formulation and to ensure symmetry of the stiffness matrix, we will consider only the energy-consistent form of the general theory. It is easy to show that forms of the theory that utilize the equilibrium equations of the first-order theory give rise to an unsymmetric stiffness matrix. Ultimately, considerations of consistent strain interpolation will dictate the final form of the model, so that excess stiffness or shear locking will be eliminated. The linear strains for the general theory are:

$$\begin{aligned}
\varepsilon_x &= \varepsilon_x^0 + z\kappa_x^0 + z^3\kappa_x^2 \\
\varepsilon_y &= \varepsilon_y^0 + z\kappa_y^0 + z^3\kappa_y^2 \\
\varepsilon_z &= 0 \\
\gamma_{yz} &= \gamma_{yz}^0 + z^2\kappa_{yz}^2 \\
\gamma_{xz} &= \gamma_{xz}^0 + z^2\kappa_{xz}^2 \\
\gamma_{xy} &= \gamma_{xy}^0 + z\kappa_{xy}^0 + z^3\kappa_{xy}^2
\end{aligned} \tag{3a}$$

where

$$\begin{aligned}
&\varepsilon_x^0 = \frac{\partial u^0}{\partial x}, \quad \kappa_x^0 = \frac{\partial \hat{\phi}_x}{\partial x} - \frac{\partial^2 w^0}{\partial x^2}, \quad \kappa_x^2 = -\frac{4}{3h^2}\frac{\partial \hat{\phi}_x}{\partial x} \\
&\varepsilon_y^0 = \frac{\partial v^0}{\partial x}, \quad \kappa_y^0 = \frac{\partial \hat{\phi}_y}{\partial y} - \frac{\partial^2 w^0}{\partial y^2}, \quad \kappa_y^2 = -\frac{4}{3h^2}\frac{\partial \hat{\phi}_y}{\partial y} \\
&\gamma_{yz}^0 = \hat{\phi}_y, \quad \kappa_{yz}^2 = -\frac{4}{h^2}\hat{\phi}_y \\
&\gamma_{xz}^0 = \hat{\phi}_x, \quad \kappa_{xz}^2 = -\frac{4}{h^2}\hat{\phi}_x \\
&\gamma_{xy}^0 = \frac{\partial u^0}{\partial y} + \frac{\partial v^0}{\partial x}, \quad \kappa_{xy}^0 = \frac{\partial \hat{\phi}_x}{\partial y} + \frac{\partial \hat{\phi}_y}{\partial x} - 2\frac{\partial^2 w^0}{\partial x \partial y} \\
&\kappa_{xy}^2 = -\frac{4}{3h^2}\left(\frac{\partial \hat{\phi}_x}{\partial y} + \frac{\partial \hat{\phi}_y}{\partial x}\right)
\end{aligned} \tag{3b}$$

The total potential energy of the plate may now be written as

$$\Pi = U_{\mathrm{m}} + U_{\mathrm{b}} + U_{\mathrm{s}} - V \tag{4a}$$

where

$$U_{\mathrm{m}} = \frac{1}{2}\int_{\Omega} \{N_x \varepsilon_x^0 + N_y \varepsilon_y^0 + N_{xy}\gamma_{xy}^0\}\,\mathrm{d}x\,\mathrm{d}y \tag{4b}$$

$$U_{\mathrm{b}} = \frac{1}{2}\int_{\Omega} \{M_x \kappa_x^0 + M_y \kappa_y^0 + M_{xy}\kappa_{xy}^0 + P_x \kappa_x^2 + P_y \kappa_y^2 + P_{xy}\kappa_{xy}^2\}\,\mathrm{d}x \tag{4c}$$

$$U_{\mathrm{s}} = \frac{1}{2}\int_{\Omega} \{Q_y \gamma_{yz}^0 + Q_x \gamma_{xz}^0 + R_y \kappa_{yz}^2 + R_x \kappa_{xz}^2\}\,\mathrm{d}x\,\mathrm{d}y \tag{4d}$$

are the internal strain energies of the plate due to stretching, bending and shearing, respectively, and

$$V = \int_{\Omega} p(x, y) w^0\,\mathrm{d}x\,\mathrm{d}y \tag{4e}$$

is the potential energy of the distributed transverse load p. Minimization of (4) with respect to u^0, v^0, w^0, $\hat{\phi}_x$ and $\hat{\phi}_y$ and subsequent integration by parts yields the variationally consistent equilibrium equations and corresponding boundary conditions. The equilibrium equations of the generalized theory are

$$\begin{aligned} N_{x,x} + N_{xy,y} &= 0 \\ N_{xy,x} + N_{y,y} &= 0 \end{aligned} \tag{5}$$

$$\begin{aligned} M_{x,xx} + M_{y,yy} + 2M_{xy,xy} + p &= 0 \\ M_{x,x} + M_{xy,y} - Q_x + \frac{4}{h^2}R_x - \frac{4}{3h^2}(P_{x,x} + P_{xy,y}) &= 0 \\ M_{xy,x} + M_{y,y} - Q_y + \frac{4}{h^2}R_y - \frac{4}{3h^2}(P_{xy,x} + P_{y,y}) &= 0 \end{aligned} \tag{6}$$

and the displacement and force boundary conditions are given by:

Displacements	Forces
u^0	$N_x \hat{n}_x + N_{xy}\hat{n}_y$
v^0	$N_{xy}\hat{n}_x + N_y \hat{n}_y$
w^0	$\bar{Q}_x \hat{n}_x + \bar{Q}_y \hat{n}_y$
$\dfrac{\partial w^0}{\partial x}$	$M_x \hat{n}_x + M_{xy}\hat{n}_y$
$\dfrac{\partial w^0}{\partial y}$	$M_{xy}\hat{n}_x + M_y \hat{n}_y$
$\hat{\phi}_x$	$\bar{M}_x \hat{n}_x + \bar{M}_{xy}\hat{n}_y$
$\hat{\phi}_y$	$\bar{M}_{xy}\hat{n}_x + \bar{M}_y \hat{n}_y$

(7)

where

$$\bar{Q}_x = Q_x - \frac{4}{h^2}R_x + \frac{4}{3h^2}(P_{x,x} + P_{xy,y})$$

$$\bar{Q}_y = Q_y - \frac{4}{h^2}R_y + \frac{4}{3h^2}(P_{xy,x} + P_{y,y})$$

$$\bar{M}_x = M_x - \frac{4}{3h^2}P_x$$

$$\bar{M}_y = M_y - \frac{4}{3h^2}P_y$$

$$\bar{M}_{xy} = M_{xy} - \frac{4}{3h^2}P_{xy}$$

As discussed in References 8 and 14, it is illuminating to rewrite the potential energy (4) for the special case of uniform, isotropic plates in terms of new, non-dimensional variables. The non-dimensionalized potential energy, neglecting membrane effects, takes the form[8, 14]

$$\Pi = Eh^3\{\bar{U}_b + \lambda\bar{U}_s\} \tag{8a}$$

where

$$\lambda = \frac{G}{E}\left(\frac{a}{h}\right)^2 \tag{8b}$$

E is Young's modulus, G is the shearing modulus, a is the length along a side of the plate and h is the thickness of the plate. The bending energy, a function of the curvature strains in (3b), is a rather long expression, and will not be presented explicitly here. The energy related to shear is given by[18]

$$\bar{U}_s = \frac{1}{2}\int_\Omega \frac{8}{15}[\hat{\phi}_x^2 + \hat{\phi}_y^2]\,\mathrm{d}\bar{x}\,\mathrm{d}\bar{y} \tag{9}$$

where $\bar{x}$ and $\bar{y}$ are the non-dimensional mid-plane co-ordinates. As can be seen in (8), the shearing energy is prefixed by a term, λ, which behaves as a penalty parameter. This term tends towards infinity as the plate thickness is decreased, and, in the thin plate limit (i.e. as $a/h \to \infty$), the penalty parameter enforces the Kirchhoff constraints

$$\hat{\phi}_x = 0 \qquad \hat{\phi}_y = 0 \tag{10}$$

When these constraints are enforced, it can be shown that the potential energy given by (4) or (8) reduces to that of the classical plate theory, which neglects the transverse shearing strains.

The finite element model obtained by minimizing the potential energy in (8) can be written as

$$([\bar{K}_b] + \lambda[\bar{K}_s])\{\bar{u}\} = \{\bar{F}\} \tag{11}$$

where $[\bar{K}_b]$ is the bending stiffness matrix, $[\bar{K}_s]$ is the shearing stiffness matrix, $\{\bar{u}\}$ is the displacement vector and $\{\bar{F}\}$ is the load vector. In the thin plate limit (i.e. when λ tends towards infinity), $[\bar{K}_s]\{\bar{u}\}$ must vanish identically in order for the potential energy to remain bounded. This is equivalent to satisfying the Kirchhoff constraints in (10), which imply that the shearing strain in each element should vanish as its thickness is decreased. Furthermore, each element must be able to model a state of zero transverse shearing strain without adversely modifying the form of the bending energy. The inability of an element to fulfill this requirement leads to the behaviour known as locking. Fortunately, it is now possible to predict *a priori* whether or not an element will lock in thin plate applications, so that reliable elements may be identified.

3. SHEARING CONSTRAINTS IN THIN ELEMENTS

The technique presented by Averill and Reddy[14] for determining the exact form of the shearing constraints in thin shear deformable elements will now be employed to predict the behaviour of elements based upon the generalized form of Reddy's third-order plate theory. In the finite element model, the Kirchhoff constraints in (10) are approximated within each element according to the assumed form of the displacement field and the interpolation functions used to approximate each variable. For example, the constraints imposed on a thin element which utilizes the same displacement field as Reddy[17] (see equations (2)) are

$$\begin{aligned} \sum_{i=1}^{m} \psi_{xi} M_i(x, y) + \sum_{i=1}^{n} w_i \frac{\partial N_i(x, y)}{\partial x} &= 0 \\ \sum_{i=1}^{m} \psi_{yi} M_i(x, y) + \sum_{i=1}^{n} w_i \frac{\partial N_i(x, y)}{\partial y} &= 0 \end{aligned} \tag{12}$$

where ψ_{xi}, ψ_{yi} and w_i are the rotations and the transverse deflection at the ith nodal point, and M_i and N_i are the interpolation functions for the rotations and transverse deflection, respectively. The conditions in (12) must be satisfied exactly at the Gaussian integration points that are used to integrate the shearing stiffness matrix. Thus, we have

$$\begin{aligned} \sum_{i=1}^{m} \psi_{xi} M_i(x_k, y_k) + \sum_{i=1}^{n} w_i \frac{\partial N_i(x_k, y_k)}{\partial x} &= 0 \\ \sum_{i=1}^{m} \psi_{yi} M_i(x_k, y_k) + \sum_{i=1}^{n} w_i \frac{\partial N_i(x_k, y_k)}{\partial y} &= 0 \end{aligned} \tag{13}$$

for $k = 1, 2, \ldots, \mathrm{NGP}$, where NGP is the number of Gauss points and (x_k, y_k) are the coordinates of the kth Gauss point. By expanding (13) and performing the necessary algebraic simplifications, the shearing constraints can be interpreted as discretized equivalents of either the true Kirchhoff constraints or some other condition that will cause locking.

To demonstrate more fully, we will consider the element described above based on the displacement field used by Reddy and in which w^0 is approximated by the non-conforming cubic interpolation functions of Melosh,[19] while the variation of ψ_x and ψ_y is governed by the Lagrangian bilinear interpolation functions. When the stiffness coefficients are integrated exactly (i.e. using a 4×4 mesh of integration points), the following shear constraints arise:

$$\psi_{x1} + \theta_{x1} = 0 \qquad \psi_{y1} + \theta_{y1} = 0 \tag{14a}$$

$$\psi_{x2} + \theta_{x2} = 0 \qquad \psi_{y2} + \theta_{y2} = 0 \tag{14b}$$

$$\psi_{x3} + \theta_{x3} = 0 \qquad \psi_{y3} + \theta_{y3} = 0 \tag{14c}$$

$$\psi_{x4} + \theta_{x4} = 0 \qquad \psi_{y4} + \theta_{y4} = 0 \tag{14d}$$

$$\frac{w_2 - w_1}{a} = \frac{\theta_{x1} + \theta_{x2}}{2} \qquad \frac{w_3 - w_1}{b} = \frac{\theta_{y1} + \theta_{y3}}{2} \tag{14e}$$

$$\frac{w_4 - w_3}{a} = \frac{\theta_{x3} + \theta_{x4}}{2} \qquad \frac{w_4 - w_2}{b} = \frac{\theta_{y2} + \theta_{y4}}{2} \tag{14f}$$

$$\frac{\theta_{x3} - \theta_{x1}}{b} = \frac{\theta_{x4} - \theta_{x2}}{b} \qquad \frac{\theta_{y2} - \theta_{y1}}{a} = \frac{\theta_{y4} - \theta_{y3}}{a} \tag{14g}$$

where

$$\theta_{xi} = \left.\frac{\partial w^0}{\partial x}\right|_{(x_i, y_i)}, \quad \theta_{yi} = \left.\frac{\partial w^0}{\partial y}\right|_{(x_i, y_i)} \tag{15}$$

and (x_i, y_i) are the co-ordinates of the ith node. The four sets of expressions (14a)–(14d) are true Kirchhoff constraints which relate the rotations ψ_x and ψ_y to the slopes $\partial w^0/\partial x$ and $\partial w^0/\partial y$, respectively. However, the remaining constraints (14e)–(14g) contain only terms which appear in the approximation of w^0. The effect of these constraints is to restrict the originally cubic variation of the transverse deflection to a quadratic one. At the element level, this implies that the curvature strains are constant, as is the case for four-noded Mindlin-type elements. At the global level, however, the slopes are required to be continuous at the nodes and tangential to (but not normal to) the inter-element boundaries, which imposes additional constraints on the approximation of the deflection. While it is possible for the slopes to be continuous when the deflection varies quadratically, the resulting solution will not likely resemble the true solution, so that the results obtained in practice will always be too stiff. It should be noted, however, that the locking constraints (14g) and two of the four constraints (14e), (14f) are satisfied exactly for the case of cylindrical bending, so that the element may be expected to give better results for this type of deformation than for deformations which involve curvature about two axes.

The use of a 2 × 2 integration rule to evaluate the stiffness coefficients yields only limited improvement in the thin plate modelling capabilities and a 3 × 3 rule gives no improvement at all. The shear constraints that are present in this case are given in Reference 18, where it is shown that the locking constraints are less severe than in the exactly integrated element, but still cause the element to be too stiff when used to model thin structures. The shear constraints for a conforming element are also given in Reference 18. These constraints, while slightly different in form, lead to the same conclusions regarding locking behaviour in thin plate applications. Numerical examples will be presented in the next section to verify these predictions of element behaviour based on the form of the shear constraints.

It has been shown by many researchers that the shearing strains must be interpolated consistently in order to eliminate all spurious stiffness effects (see References 11, 12 and 18). For the element just discussed, a consistent interpolation scheme would be one in which the rotations ψ_x and ψ_y vary according to the derivatives of the deflection field $\partial w^0/\partial x$ and $\partial w^0/\partial y$, respectively. While such an interpolation scheme is possible, it would be inconvenient to implement and would lead to a computationally inefficient element. Therefore, a new approach should be sought.

A more desirable consistent finite element approximation of the shearing strains is easily identified by examining the generalized form of the shearing strains in (3b). The consistency criteria may be satisfied identically by letting the generalized rotations $\hat{\phi}_x$ and $\hat{\phi}_y$ each be equal to a single variable, say ϕ_x and ϕ_y. If these rotational degrees of freedom are then approximated by the bilinear Lagrangian interpolation functions, the shear constraints which arise in thin elements are:

$$\phi_{xi} = 0 \qquad \phi_{yi} = 0 \qquad \text{for } i = 1, 2, 3, 4 \tag{16}$$

When these constraints are enforced, the shearing energy will vanish, and the bending energy will reduce precisely to that of the classical plate theory. This form of the third-order theory was first used by Bhimaraddi and Stevens,[20] and a finite element based upon this form was developed by Ren and Hinton.[21] The latter investigators demonstrated that their plate element does not lock at all in thin plate applications, and yields accurate results for both thick and thin rectangular plate structures. The behaviour of many shear deformable elements was analysed by Asdal and Kosmatka,[22] where it was found that the element of Ren and Hinton shows the best overall behaviour for rectangular plates. This element employs the non-conforming cubic interpolation functions of Melosh[19] for approximating the transverse deflection and the bilinear Lagrange interpolation functions for the rotational degrees of freedom. A 4 × 4 Gaussian integration rule is required to integrate the stiffness coefficients exactly. While the element has been shown to behave well in thick and thin geometries, its sensitivity to distortion and its computational efficiency have yet to be investigated. Perhaps this is why the element has not received widespread acclaim.

In the next section, this and new elements based on the third-order plate theory will be examined thoroughly and compared to the most popular Mindlin-type elements.

4. NUMERICAL EVALUATION OF THE ELEMENTS

4.1. Preliminary comments

In this section, the overall behaviour of several shear deformable plate elements will be evaluated. The criteria to be tested are: accuracy, distortion sensitivity, efficiency and rank sufficiency. Each of the elements to be tested allows for a linear distribution of the strain components within the element.

Of the Reddy-type elements to be evaluated, four are based on the original theory of Reddy,[17] and four are based on the modified form of the theory[15] in which $\hat{\phi}_x = \phi_x$ and $\hat{\phi}_y = \phi_y$. The notation used to designate these elements is as follows. The number preceding the name specifies the number of nodes in the element (always four in this study). The following three or four letters describe the theory upon which the element is based (RED for Reddy's theory and MRED for the modified form of the theory in which $\hat{\phi}_x = \phi_x$ and $\hat{\phi}_y = \phi_y$). The final one or two letters before the hyphen denote whether the element is conforming (C) or non-conforming (NC). Lastly, the letter after the hyphen describes the type of integration used to evaluate the stiffness coefficients (F for a uniform 4 × 4 mesh of full integration points and R for a uniformly reduced 2 × 2 mesh). For example, 4MREDC-F and 4MREDNC-R are the conforming and non-conforming elements based on the modified form of Reddy's theory which employ uniform full (4 × 4) and reduced (2 × 2) integrations, respectively.

Many elements based on the first-order plate theory have been developed and tested, but none surpass the overall accuracy and economy of the Lagrangian nine-noded element with selectively-reduced integration[8] (hereafter called the 9MIN-S element). This element contains one zero energy mode, which precludes its use in general-purpose finite element codes, but it is well suited for benchmark testing. For this reason, the 9MIN-S element has been chosen by the authors as the standard element against which the merits (i.e. accuracy and efficiency) of other elements should be measured. The other Mindlin-type element to be tested is the heterosis element with selectively-reduced integration,[23] and denoted by 9HET-S. The reasons for the excellent behaviour of these two elements has been explained in detail[14] based upon the form of the shear constraints that arise in thin element situations.

A numerical procedure that can be used to immediately screen out many elements (and to discover new ones, as will be seen) is the elemental stiffness rank test. An eigenvalue analysis of the stiffness matrix of each element is performed in order to determine the number of zero energy modes which are present under various numerical integration rules. The results are presented in

Table I. Eigenvalue analysis of the Reddy-type elements

Element	Numerical integration grid			Number of zero eigenvalues	
D.O.F. per node	Name of integration rule	Bending terms	Transverse shearing terms	K_s	$K_b + K_s$
4REDC	full	4×4	4×4	6	3
w $w_{,x}$ $w_{,y}$ $w_{,xy}$	selective	4×4	2×2	16	3
ψ_x ψ_y	reduced	2×2	2×2	16	3
4REDNC	full	4×4	4×4	6	3
w $w_{,x}$ $w_{,y}$	selective	4×4	2×2	12	3
ψ_x ψ_y	reduced	2×2	2×2	12	3
4MREDC	full	4×4	4×4	16	3
w $w_{,x}$ $w_{,y}$ $w_{,xy}$	selective	4×4	2×2	16	3
φ_x φ_y	reduced	2×2	2×2	16	4
4MREDNC	full	4×4	4×4	12	3
w $w_{,x}$ $w_{,y}$	selective	4×4	2×2	12	3
φ_x φ_y	reduced	2×2	2×2	12	3

Table I. The elemental stiffness matrix $K = K_b + K_s$ should contain three zero eigenvalues, which correspond to the rigid body modes. Any additional zero eigenvalues are due to zero energy modes or mechanisms. It is often stated that certain zero energy modes are eliminated in the assembled stiffness matrix by the application of appropriate boundary conditions. However, experience has shown that, in plates with unconstrained interior boundaries such as holes and in many linear buckling problems (see Section 4.4), zero energy modes may contaminate the solution despite sufficiently constrained exterior boundaries. Thus, elements which possess a rank deficient stiffness matrix should be avoided altogether in general-purpose finite element programs unless care has been taken to suppress all possible mechanisms. As seen in Table I, a fortuitous property exists in all but one of the Reddy-type elements. That is, the entire stiffness matrix may be integrated by a uniform 2×2 integration rule without the introduction of zero energy modes. This property is easily explained by noting that nearly all of the terms in the stiffness matrix are integrated exactly by the 2×2 rule. Only a few of the terms in the bending stiffness matrix and in the mass and stability matrices will be approximated by performing the integrations in this way. Furthermore, the 2×2 integration points correspond to the optimum strain sampling points for the C^1-cubic interpolation functions (see page 282 of Reference 24). It will be demonstrated below that the elements which utilize 4×4 and 2×2 integration rules yield nearly identical results. Thus, the application of reduced integration to these elements should not be looked upon as a trick, but simply as a mild approximation which reduces the stiffness computation time by as much as 75 per cent. These elements will be evaluated and discussed further in the sequel.

To assess the behaviour of the elements in a variety of applications, problems of plate bending, vibration and buckling will be analysed for assorted boundary conditions and material properties. The three types of materials to be used are:

Material 1: $E = 10{\cdot}0\times10^6, \quad \nu = 0{\cdot}3, \quad \rho = 1$

Material 2: $$E_1 = 25{\cdot}0\times10^6,\quad E_2 = 1{\cdot}0\times10^6$$
$$G_{12} = G_{13} = 0{\cdot}5\times10^6,\quad G_{23} = 0{\cdot}2\times10^6$$
$$\nu_{12} = \nu_{13} = 0{\cdot}25,\quad \rho = 1$$

Material 3: $$E_1 = 40{\cdot}0\times10^6,\quad E_2 = 1{\cdot}0\times10^6,\quad G_{12} = G_{13} = 0{\cdot}6\times10^6$$
$$G_{23} = 0{\cdot}5\times10^6,\quad \nu_{12} = \nu_{13} = 0{\cdot}25,\quad \rho = 1$$

Computations were carried out in double precision on an IBM 3090 computer. All results are normalized by the exact solution of the problem discussed.

4.2. Bending analysis

The first two numerical examples are designed to assess the ability of the elements to model thin plate structures and thus to verify the role that shear constraints play in determining the behaviour of thin shear deformable elements. The deflections of a cantilever isotropic beam under a tip load and a clamped isotropic plate under a uniform load are investigated for a wide range of plate span-to-thickness ratios. For the cantilever beam, a 5×1 mesh of elements is used, and a 4×4 mesh is employed for a quarter model of the clamped plate. All results are normalized by the exact solutions for thin plates.[16] These standard test cases demonstrate the behaviour of thin plate elements in deformations with single and double curvature, respectively. It can be seen in Tables II and III that all of the elements considered yield excellent results except for those based on the original form of Reddy's theory, which does not employ consistent interpolation of the shearing strains. When used to model the cantilever beam, these elements exhibit a small amount of excess stiffness due to the spurious constraints. However, the elements lock completely when modelling the clamped plate. These results are in complete agreement with the predictions made in Section 3 based on the form of the shearing constraints. Because the elements based on the original form of the theory behave poorly when applied to thin structures, they will not be considered further.

Next, the accuracy of the remaining elements in modelling the bending of simply-supported laminated plates will be investigated. Table IV shows the results of a square (0/90/90/0) laminate subjected to a sinusoidal load for two values of the plate span-to-thickness ratio. For a co-ordinate system with its origin at a corner of the plate, the following normalized deflection and stresses are given:

$$\begin{gathered}\bar{w}\left(\frac{a}{2},\frac{a}{2},0\right),\quad \bar{\sigma}_x\left(\frac{a}{2},\frac{a}{2},\frac{h}{2}\right),\quad \bar{\sigma}_y\left(\frac{a}{2},\frac{a}{2},\frac{h}{4}\right)\\ \bar{\sigma}_{xy}\left(0,0,\frac{h}{2}\right),\quad \bar{\sigma}_{yz}\left(\frac{a}{2},0,0\right),\quad \bar{\sigma}_{xz}\left(0,\frac{a}{2},0\right)\end{gathered}\tag{17}$$

where the results are normalized by the exact solution of Phan and Reddy.[25] The stresses are computed in each element at the reduced integration point nearest the desired location in the plate. For $a/h = 100$, the Mindlin-type elements yield the most accurate deflections, while the most accurate in-plane stresses are given by the Reddy-type elements, especially 4MREDNC-F and 4MREDNC-R, which give nearly identical results. For the thicker plate, $a/h = 10$, the solution given by the Mindlin-type elements seems to converge to about 7–10 per cent below the closed form solution. The Reddy-type elements, on the other hand, yield excellent results for nearly all stresses and displacements, converging rapidly from above in each case. The prediction

Table II. Normalized tip deflection of an isotropic, cantilever beam with an end load

a/h	9MIN-S	9HET-S	4REDC-F	4REDC-R	4REDNC-F	4REDNC-R	4MREDC-F	4MREDNC-F	4MREDNC-R
5	1·024	1·023	1·010	1·014	1·009	1·013	1·012	1·012	1·012
10	1·000	0·999	0·984	0·990	0·984	0·989	0·989	0·990	0·990
50	0·993	0·986	0·971	0·975	0·972	0·976	0·981	0·982	0·982
100	0·993	0·985	0·965	0·969	0·966	0·975	0·981	0·982	0·982
500	0·993	0·984	0·929	0·941	0·932	0·974	0·981	0·982	0·982
1000	0·993	0·984	0·915	0·936	0·917	0·974	0·981	0·982	0·982

Table III. Normalized centre deflection of an isotropic, clamped plate subjected to a uniform load

a/h	9MIN-S	9HET-S	4REDC-F	4REDC-R	4REDNC-F	4REDNC-R	4MREDC-F	4MREDNC-F	4MREDNC-R
5	1·725	1·724	1·662	1·682	1·666	1·686	1·600	1·635	1·635
10	1·195	1·194	1·159	1·186	1·163	1·190	1·167	1·191	1·191
50	1·013	1·011	0·922	0·946	0·926	0·946	1·022	1·041	1·041
100	1·007	1·003	0·818	0·879	0·818	0·872	1·017	1·036	1·036
500	1·005	0·998	0·199	0·373	0·190	0·318	1·016	1·035	1·035
1000	1·005	0·998	0·060	0·140	0·056	0·110	1·015	1·035	1·035

Table IV. Maximum deflection and stresses in a simply-supported (0/90/90/0) laminate subjected to a sinusoidal load (Material 2)

a/h	Element	Mesh	$\bar{W}$	$\bar{\sigma}_x$	$\bar{\sigma}_y$	$\bar{\sigma}_{xy}$	$\bar{\sigma}_{yz}$	$\bar{\sigma}_{xz}$
	9MIN-S	2 × 2	0·928	0·888	0·903	0·869	0·878	0·613
		4 × 4	0·927	0·908	0·923	0·894	0·897	0·627
	9HET-S	2 × 2	0·926	0·888	0·903	0·869	0·878	0·613
		4 × 4	0·927	0·908	0·923	0·894	0·897	0·627
10	4MREDC-F	2 × 2	1·033	1·046	1·001	0·817	1·049	0·926
		4 × 4	1·004	1·019	1·001	0·768	1·082	0·989
	4MREDNC-F	2 × 2	1·094	1·007	1·005	1·080	1·099	1·016
		4 × 4	1·024	1·002	1·003	1·021	1·076	1·004
	4MREDNC-R	2 × 2	1·094	1·008	1·007	1·080	1·098	1·016
		4 × 4	1·024	1·002	1·003	1·021	1·076	1·004
	9MIN-S	2 × 2	0·999	0·970	0·969	0·971	0·873	0·593
		4 × 4	0·999	0·992	0·992	0·993	0·896	0·609
	9HET-S	2 × 2	0·995	0·968	0·968	0·969	0·898	0·598
		4 × 4	0·998	0·992	0·992	0·993	0·896	0·610
100	4MREDC-F	2 × 2	1·089	1·055	1·056	0·912	1·096	0·953
		4 × 4	1·013	1·023	1·010	0·895	1·021	0·990
	4MREDNC-F	2 × 2	1·097	1·014	1·006	1·060	1·034	1·018
		4 × 4	1·024	1·004	1·004	1·018	1·007	1·005
	4MREDNC-R	2 × 2	1·097	1·014	1·008	1·060	1·032	1·018
		4 × 4	1·024	1·004	1·004	1·018	1·006	1·005

of $\bar{\sigma}_{xy}$ given by MREDC-F is less than satisfactory, but no explanation for this single anomalous result can be provided. Because the Mindlin theory accounts for only a constant value of transverse shearing strain through the thickness of the plate, it is not capable of predicting accurate values of the transverse shearing stresses via the constitutive equations. However, Reddy's theory, and the associated finite elements, predict very accurately the transverse shearing stresses due to the parabolic variation of transverse shearing strains through the thickness. The 4MREDNC-F and 4MREDNC-R elements give extremely accurate results for all of the stress values, even for a coarse 2 × 2 mesh. It should be emphasized that, for a value of span-to-thickness ratio that is usually associated with thin plate behaviour, $a/h = 10$, the Mindlin-type elements are still not capable of capturing the appropriate in-plane deformations (and hence stresses) for this laminate.

Having demonstrated the accuracy of the elements for the single case of a laminated plate, we will turn our attention to two element properties that have as yet been untested—distortion sensitivity and computational efficiency. Because this is the first attempt in the literature to use the Reddy-type elements in a non-rectangular geometry, a few comments concerning the construction of the element stiffness matrices may be in order. A subparametric formulation is employed, where the bilinear interpolation functions are used for the co-ordinate transformation and for the approximation of the generalized rotations ϕ_x and ϕ_y. The transverse deflection is approximated by either bicubic conforming or cubic non-conforming functions. In all cases, the interpolation functions are given in the local (or natural) co-ordinates.

In order to determine how accurate the elements are in non-rectangular configurations, the distorted meshes in Figure 1 will be used to analyse a clamped, isotropic plate with a concentrated load at the centre of the plate. Again, results are normalized by the exact solution for thin plates.[16] Figure 2 shows that the 9MIN-S element is virtually oblivious to the mesh distortions. The

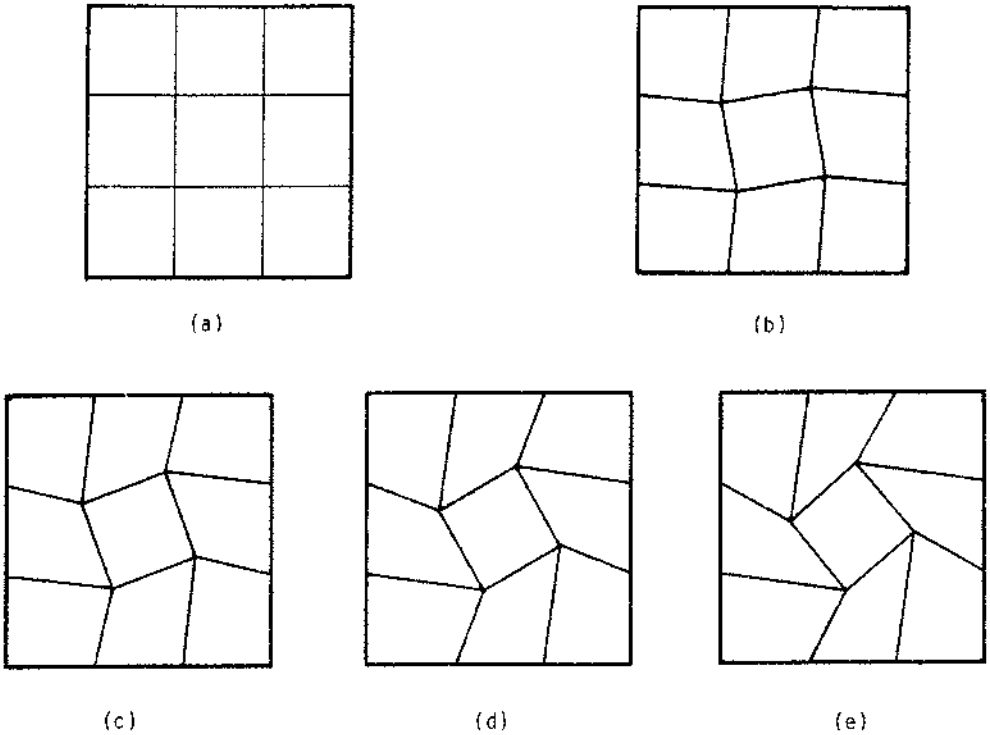

Figure 1. The 3 × 3 meshes used to investigate the distortion sensitivity: (a) undistorted; (b) $\theta = 10$; (c) $\theta = 20$; (d) $\theta = 30$; and (e) $\theta = 40$

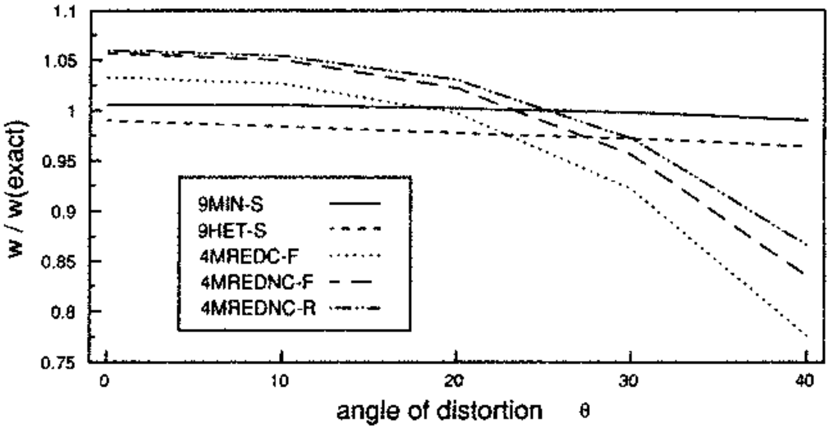

Figure 2. Effect of mesh distortion on the modelling of a clamped isotropic plate with concentrated load at the centre

excellent results for this isoparametric element cast doubts on the true effect of the assumed natural co-ordinate strain formulations,[26] which claim to yield superior results for distorted meshes. The behaviour of 9HET-S is more than satisfactory, but not as good as 9MIN-S. The 4MREDNC-R element yields very good results for an angle of distortion up to 30 degrees, with the other Reddy-type elements giving slightly inferior results. The behaviour of these elements when $\theta = 40$ is a little less than satisfactory, but this is indeed an extreme case which would not (or should not) be encountered in most analyses. The superior behaviour of the Mindlin-type elements over the Reddy-type elements in this example may be attributed to the poor geometric modelling of the Hermite interpolation functions used in the Reddy-type elements.

In order to assess the efficiency of each element, the problem of the simply-supported (0/90/90/0) laminate under a sinusoidal load is revisited, with the VS FORTRAN Version II Interactive Debugger (IAD)[27] being employed to determine the execution time of each subroutine in the finite element programs. IAD samples the program every 10 msec during execution to record the statement being executed. Because a sample interval of 10 msec is not small enough to measure precise execution times, the results of this test should not be interpreted as being exact. However, the amount of error is not enough to skew the outcome even slightly, making this test a good measure of the relative efficiency of the elements. The two programs written for the Mindlin- and Reddy-type finite element models are essentially identical, except for the computation of the stiffness matrices and some parts of the pre- and post-processing. The solution is obtained using a banded equation solving routine. Results are presented in Table V for two sizes of the mesh. Because the Reddy-type elements all have only four nodes, the bandwidth and the total number of equations are less in these elements than in the nine-noded Mindlin-type elements. Thus, the CPU time required to solve the assembled set of equations is approximately four to eight times less for the same size meshes of elements based on the third-order theory than the meshes of the Mindlin-type elements. As far as computation of the elemental stiffness matrices and assembly of the global system of equations is concerned, the Mindlin-type elements are substantially more efficient than the exactly integrated Reddy-type elements. However, it is seen that a nearly 75 per cent savings in assembly time can be obtained by using reduced integration to evaluate the elemental stiffness

Table V. CPU time (sec) required to evaluate the structure in Table III

Mesh		9MIN-S	9HET-S	4MREDC-F	4MREDNC-F	4MREDNC-R
	total nodes	81	81	25	25	25
	total equations	243	227	150	125	125
	half bandwidth	63	59	42	35	35
4 × 4	$\bar{w}$	0·999	0·998	1·013	1·024	1·024
	time to assemble (sec)	0·54	0·46	1·50	1·07	0·29
	time to solve (sec)	0·76	0·62	0·27	0·16	0·16
	total cpu time (sec)	1·36	1·15	1·79	1·26	0·47
	total nodes	169	169	49	49	49
	total equations	507	471	294	245	245
	half bandwidth	87	81	54	45	45
6 × 6	$\bar{w}$	0·999	0·999	1·003	1·011	1·011
	time to assemble (sec)	1·24	1·20	3·36	2·41	0·64
	time to solve (sec)	3·26	2·60	0·74	0·42	0·42
	total cpu time (sec)	4·61	3·93	4·16	2·87	1·11

coefficients instead of an exact integration rule, making assembly of the 4MREDNC-R element much less than that of either 9MIN-S or 9HET-S. Thus, for the 4 × 4 mesh, the 4MREDNC-R element requires less than half the total CPU time of its nearest competitor, 9HET-S, and this ratio decreases to just above one-fourth for the 6 × 6 mesh. For the larger mesh, the 4MREDNC-F element is also cheaper than either of the Mindlin-type elements, but still 2·5 times more expensive than its reduced-integrated counterpart. It is interesting to note that the 4 × 4 mesh of 9MIN-S elements and the 6 × 6 mesh of 4MREDNC-R elements have approximately the same number of total equations, and the model with 4MREDNC-R elements is still the least expensive of the two. Therefore, the prevailing conclusion that elements based on the third-order theory (and requiring C^1-continuity) are unduly expensive is proven to be incorrect.

4.3. Free vibration analysis

The ability of the elements to predict the lowest natural frequency of thick and thin simply-supported (0/90/90/0) laminates (Material 3) is now evaluated. The results are presented in Table VI for various meshes and span-to-thickness ratios. All of the elements give solutions that converge rapidly to the closed form solution,[28] except for 4MREDC-F, which appears to diverge with mesh refinement for $a/h = 5$. The Mindlin-type elements converge most rapidly, but the non-conforming Reddy-type elements also yield excellent results.

4.4. Buckling analysis

In order to examine the ability of the elements to model linear stability (buckling) problems, a (0/90/0) laminate consisting of layers of Material 3 will be examined for a variety of boundary conditions. Two opposite sides of the plate are simply-supported, and the remaining two sides are either simply-supported (S), clamped (C) or free (F). Because the principal buckling modes in square, orthotropic laminates are not necessarily symmetric, a full plate finite element model is employed. It was found that the models using the 9MIN-S element were contaminated by spurious mechanisms for most of the boundary conditions considered, so these results are not given. Table VII shows the results for biaxial in-plane loading ($\bar{N} = \bar{N}_x = \bar{N}_y$), which are normalized by the closed form solutions obtained by Khdeir.[29] In addition, the CPU times required to obtain the solutions for the plate which is simply-supported on all four sides are presented. The 9HET-S element converges very rapidly towards the analytical solution for the

Table VI. Normalized natural frequency of a simply-supported (0/90/90/0) laminate (Material 3)

a/h	Mesh	9MIN-S	9HET-S	4MREDC-F	4MREDNC-F	4MREDNC-R
5	2 × 2	0·988	0·988	0·997	0·939	0·939
	4 × 4	0·988	0·988	0·985	0·970	0·970
	6 × 6	0·988	0·988	0·983	0·977	0·977
10	2 × 2	0·992	0·992	0·978	0·946	0·946
	4 × 4	0·992	0·992	0·988	0·978	0·978
	6 × 6	0·992	0·992	0·989	0·984	0·984
100	2 × 2	1·005	1·006	0·970	0·960	0·960
	4 × 4	1·004	1·004	1·000	0·992	0·992
	6 × 6	1·004	1·004	1·003	0·999	0·999

lowest buckling load, while the 4MREDNC-F and 4MREDNC-R elements require a slightly more refined mesh to yield satisfactory results. Despite requiring more elements than the heterosis element, the efficiency of the Reddy-type elements is duly noted in the final column of results.

5. IMPLEMENTATION AND USE OF REFINED PLATE ELEMENTS

The overall accuracy and efficiency of the 4MREDNC-F and 4MREDNC-R plate elements have been firmly established, but questions remain about the convenience of using these elements in general-purpose programs. One of the main obstacles is the fact that these elements have five bending degrees of freedom per node, instead of the usual three engineering degrees freedom—one deflection and two rotations. Because the refined elements require C^1-continuity of the transverse deflection, there are two additional rotational degrees of freedom corresponding to the derivatives of the deflection. In this section, it will be shown how this problem can be overcome and be viewed as an advantage instead of a hindrance.

It is common for the user of a commercial finite element code to be unaware of all the details involved in the computation and assembly of a finite element stiffness matrix. Likewise, the user need not worry about every step taken during the pre-processing portion of the program. Therefore, it is proposed that two of the four rotational degrees of freedom may be 'invisible' to the user. This causes no problem with the application of boundary conditions, because there are no conceivable cases where one member of the two sets of rotations ($\partial w^0/\partial x$, ϕ_x) and ($\partial w^0/\partial y$, ϕ_y) will be constrained without the status of the other also being implied. This is clear from the form of the boundary conditions given in (7), where it is seen that if M_x is unknown, both ϕ_x and $\partial w^0/\partial x$ must be specified, and likewise for the respective y-components. Therefore, either both members of a set of rotations must be specified as boundary conditions, or neither member can be specified (when the applied moment is known). In most problems, both members of a set of rotations will be constrained to zero because of conditions at the boundary of a structure. In this case, when the one 'visible' member of the set of rotations is constrained to zero, a simple pre-processing step can add this boundary condition to the other member. In the case where the slope, $\partial w/\partial n$, of a boundary must be specified as some non-zero quantity, the additional rotation, ϕ_n,

Table VII. Normalized buckling loads and CPU times for a square (0/90/0) laminate (Material 3)

Element	Full plate mesh	SS	SC	CC	FF	SS CPU time (sec)
9HET-S	4 × 4	1·027	1·008	0·986	0·954	5·12
	6 × 6	1·027	1·006	0·986	0·953	59·84
	8 × 8	1·023	1·006	0·986	0·953	326·15
4MREDNC-F	4 × 4	0·847	0·842	0·852	0·968	1·80
	6 × 6	0·921	0·921	0·927	0·963	9·96
	8 × 8	0·953	0·954	0·958	0·959	48·84
	10 × 10	0·969	0·970	0·973	0·957	180·25
4MREDNC-R	4 × 4	0·850	0·844	0·855	0·968	0·96
	6 × 6	0·921	0·921	0·927	0·963	7·97
	8 × 8	0·953	0·954	0·958	0·959	44·93
	10 × 10	0·969	0·970	0·973	0·957	177·88

must be specified as zero at that point. Therefore, it is suggested that the 'visible' rotations be the familiar slopes of the deflection, and the 'invisible' rotations, which can be specified during pre-processing based on the other boundary conditions, be the ϕ_x and ϕ_y degrees of freedom. The same technique can be employed when a force boundary condition, a moment in this case, is applied. According to the variationally consistent form of the boundary conditions in (7), the value of the moment should be added to the force vector in the equations corresponding to both members of the set of rotations that are in the same direction as the moment. Again, this modification can be made to the boundary condition data during pre-processing.

It should be noted that ϕ_x and ϕ_y are not true rotations, but are actually measures of the transverse shearing strain. Therefore, when ϕ_x and ϕ_y are specified to be zero, as at clamped boundaries, the shearing strain is automatically zero at these points. This is an unfortunate property of the plate theory, but it clearly has no deleterious effects on the numerical results, as seen herein.

The existence of the slope degrees of freedom in the refined plate elements is actually advantageous in terms of applying physically consistent boundary conditions. To explain this further, consider the definitions of the infinitesimal rotations of a point in an elastic continuum

$$\omega_{yz} = \frac{1}{2}\left(\frac{\partial v}{\partial z} - \frac{\partial w}{\partial y}\right) \qquad \omega_{xz} = \frac{1}{2}\left(\frac{\partial u}{\partial z} - \frac{\partial w}{\partial x}\right) \tag{18}$$

In the first-order theory, these rotations are given by

$$\omega_{yz} = \frac{1}{2}\left(\psi_y - \frac{\partial w^0}{\partial y}\right) \qquad \omega_{xz} = \frac{1}{2}\left(\psi_x - \frac{\partial w^0}{\partial x}\right) \tag{19}$$

while in the generalized third-order theory, they are

$$\begin{aligned} \omega_{yz} &= \frac{1}{2}\left[\hat{\phi}_y - 2\frac{\partial w^0}{\partial y} - 4\left(\frac{z}{h}\right)^2 \hat{\phi}_y\right] \\ \omega_{xz} &= \frac{1}{2}\left[\hat{\phi}_x - 2\frac{\partial w^0}{\partial x} - 4\left(\frac{z}{h}\right)^2 \hat{\phi}_x\right] \end{aligned} \tag{20}$$

In the displacement finite element model of the first-order theory, no boundary condition can be imposed on $\partial w^0/\partial x$ or $\partial w^0/\partial y$. Therefore, the rotation of a point in the plate can never be specified to be identically zero, as is required at some clamped boundaries. The zero rotation condition is satisfied only for very thin structures, where the Kirchhoff constraints impose the conditions

$$\psi_x = -\frac{\partial w^0}{\partial x} \qquad \psi_y = -\frac{\partial w^0}{\partial y} \tag{21}$$

on the finite element degrees of freedom. However, in the displacement finite element models based on the third-order theory, the rotation of a point in the plate can be specified to be exactly zero, as is physically appropriate. While the specification of the derivatives of w^0 may be unnecessary for the majority of structures (those which are thin), the inability to adequately restrain the rotations of a Mindlin-type plate places restrictions on the thick plate modelling capability of the theory (note the differences in deflection given by the finite element models of the two theories in Tables II and III for $a/h = 5$).

When using refined plate theories or their associated finite element models, questions often emerge about the meaning of the higher-order stress resultants such as P_x, P_y, P_{xy}, R_x and R_y in

(6). These terms arise naturally in the variational formulation of the theory and must be included, but their physical meaning and significance are difficult to interpret. The one thing that is understood is that these types of loads are not applied externally to engineering structures. Therefore, it is customary to simply assume that they are either zero or unknown (when the corresponding displacement is specified). In this way, the question of their physical meaning need not be addressed directly, with the understanding that they are a necessary component of the mathematical formulation of the problem.

As a final note, the 4MREDNC-R element appears to be ideally suited to be used as a flat, four-noded shell element for applications in which the membrane and bending coupling are not significant. The entire elemental stiffness matrix (membrane, bending and shearing portions) may be integrated using a uniform 2×2 rule, yielding a very efficient and accurate element.

6. CONCLUSIONS

The misunderstanding surrounding plate finite elements based on the third-order plate theories has been addressed, with the intent of demonstrating the accuracy and efficiency of these elements. Some of the advantages of these elements over the most commonly used finite elements based on the first-order shear deformation theory have been shown. These include: parabolic distribution of the shearing strains and quadratic variation of transverse shearing stresses through the thickness so that no shear correction factors are needed, improved modelling of in-plane deformations for thick and laminated plates, and better modelling of physically appropriate boundary conditions. Properties of the third-order theory elements that were previously not widely known have been illuminated: comparable, and often superior, accuracy and efficiency compared to the best known quadratic Mindlin-type elements (especially the element herein called MREDNC-R), and suitability for general use in a commercial finite element program.

ACKNOWLEDGEMENT

The support of this research by NASA (Headquarters) through Grant NGT–50404 is gratefully acknowledged.

REFERENCES

1. R. D. Mindlin, 'Influence of rotatory inertia and shear on flexural motions of isotropic, elastic plates', *J. Appl. Mech. ASME*, **18**, 31–38 (1951).
2. O. C. Zienkiewicz, R. L. Taylor and J. M. Too, 'Reduced integration technique in general analysis of plates and shells', *Int. j. numer. methods eng.*, **3**, 275–290 (1971).
3. S. F. Pawsey and R. W. Clough, 'Improved numerical integration of thick shell finite elements', *Int. j. numer. methods eng.*, **3**, 575–586 (1971).
4. K. J. Bathe and E. N. Dvorkin, 'A four-node plate bending element based on Mindlin/Reissner plate theory and a mixed interpolation', *Int. j. numer. methods eng.*, **21**, 367–383 (1985).
5. J. Donea and L. G. Lamain, 'A modified representation of transverse shear in C^0 quadrilateral plate elements', *Comp. Methods Appl. Mech. Eng.*, **63**, 183–207 (1987).
6. G. Prathap and B. R. Somashekar, 'Field- and edge-consistency synthesis of a 4-noded quadrilateral plate bending element', *Int. j. numer. methods eng.*, **26**, 1693–1708 (1988).
7. O. C. Zienkiewicz and E. Hinton, 'Reduced integration, function smoothing and non-conformity in finite element analysis (with special reference to thick plates)', *J. Franklin Inst.*, **32**, 443–461 (1976).
8. E. D. L. Pugh, E. Hinton and O. C. Zienkiewicz, 'A study of quadrilateral plate bending elements with "reduced" integration', *Int. j. numer. methods eng.*, **12**, 1059–1079 (1978).
9. T. J. R. Hughes, M. Cohen and M. Haroun, 'Reduced and selective integration techniques in the finite element analysis of plates', *Nucl. Eng. Des.*, **46**, 203–222 (1978).
10. D. S. Malkus and T. J. R. Hughes, 'Mixed finite element methods—reduced and selective integration techniques: a unification of concepts', *Comp. Methods Appl. Mech. Eng.*, **15**, 63–81 (1978).

11. G. Prathap and G. R. Bhashyam, 'Reduced integration and the shear-flexible beam element', *Int. j. numer. methods eng.*, **18**, 195–210 (1982).
12. G. Prathap and C. R. Babu, 'Field-consistency and violent stress oscillations in the finite element method', *Int. j. numer. methods eng.*, **24**, 2017–2033 (1987).
13. G. Prathap and B. P. Naganarayana, 'Analysis of locking and stress oscillations in a general curved beam element', *Int. j. numer. methods eng.*, **30**, 177–200 (1990).
14. R. C. Averill and J. N. Reddy, 'Behavior of plate elements based on the first-order shear deformation theory', *Eng. Comput.*, **7**, 57–74 (1990).
15. J. N. Reddy, 'A general nonlinear third-order theory of plates with moderate thickness', *Int. J. Non-Linear Mech.*, **25**, 677–686 (1990).
16. S. Timoshenko and S. Woinowsky-Krieger, *Theory of Plates and Shells*, McGraw-Hill, New York, 1959.
17. J. N. Reddy, 'A simple higher-order theory for laminated composite plates', *J. Appl. Mech. ASME*, **51**, 745–752 (1984).
18. R. C. Averill, 'On the behavior of shear deformable plate elements', *M.S. Thesis*, Virginia Polytechnic Institute and State University, Blacksburg, VA, 1989.
19. R. J. Melosh, 'Basis for derivation of matrices for the direct stiffness method', *AIAA J.*, **1**, 1631–1637 (1963).
20. A. Bhimaraddi and L. K. Stevens, 'A higher order theory for free vibration of orthotropic, homogeneous, and laminated rectangular plates', *J. Appl. Mech. ASME*, **51**, 195–198 (1984).
21. J. G. Ren and E. Hinton, 'The finite element analysis of homogeneous and laminated composite plates using a simple higher order theory', *Commun. appl. numer. methods*, **2**, 217–228 (1986).
22. B. Asdal and J. B. Kosmatka, 'Static and free vibration analysis of advanced composites using shear-deformable rectangular plate finite elements', *CCMS-88-06*, *VPI-E-88-11*, Virginia Polytechnic Institute and State University, Blacksburg, VA, May, 1988.
23. T. J. R. Hughes and M. Cohen, 'The "heterosis" finite element for plate bending', *Comp. Struct.*, **9**, 445–450 (1978).
24. O. C. Zienkiewicz, *The Finite Element Method*, McGraw-Hill, London, 1977.
25. N. D. Phan and J. N. Reddy, 'Analysis of laminated composite plates using a higher-order shear deformation theory', *Int. j. numer. methods eng.*, **21**, 2201–2219 (1985).
26. K. C. Park and G. M. Stanley, 'A curved C^0 shell element based on assumed natural-coordinate strains', *J. Appl. Mech. ASME*, **53**, 278–290 (1986).
27. *IBM FORTRAN Version 2 Interactive Debug Guide and Reference, Document No. SC26-4223-2*, Release 3, 1988.
28. J. N. Reddy and N. D. Phan, 'Stability and vibration of isotropic, orthotropic and laminated plates according to a higher-order shear deformation theory', *J. Sound Vib.*, **98**, 157–170 (1985).
29. A. A. Khdeir, 'Free vibration and buckling of symmetric cross-ply laminated plates by an exact method', *J. Sound Vib.*, **126**, 447–461 (1988).

OBSERVATIONS ON HIGHER-ORDER BEAM THEORY

By A. Bhimaraddi[1] and K. Chandrashekhara[2]

ABSTRACT: A parabolic shear-deformation beam theory assuming a higher-order variation for axial displacement has been recently presented. In this theory, the axial displacement variation can be selected so that it results in a suitable admissible transverse shear-strain variation across the depth of the beam. This paper examines several transverse shear-strain variations that can go with the aforementioned higher-order theory. Apart from the usual simple parabolic variation, six other shear-strain variations are considered: the sinusoidal variation, cubic, quartic, quintic, and sixth-order polynomials. All these variations for transverse shear-strain satisfy the requirement that the shear strain be zero at the extreme fibers ($z = \pm h/2$) and nonzero elsewhere along the depth of the beam. Comparison of the results from this paper with results from others show that the simple parabolic distribution for transverse shear strain gives most accurate results. Also, Timoshenko's theory (with a shear factor of five-sixths) and the current formulation which uses the parabolic shear-strain distribution, give identical values for deflections.

INTRODUCTION

Timoshenko (1921) was the first to recognize the importance of including shear deformation effects in the dynamic response calculations of elastic beams. In his formulation, Timoshenko retained all of the assumptions of classical Euler-Bernoulli beam theory except he does not assume that cross sections remained normal to the deformed neutral surface. Thus, Timoshenko's theory assumes that cross sections remain plane, but no longer remain normal to the deformed neutral surface. This assumption led to the prediction of constant shear strain across the cross section and is in contradiction to that predicted by the theory of elasticity, which predicts a parabolic variation with zero values at the extreme fibers. To correct this inherent deficiency, Timoshenko introduced the shear correction factor (or the Timoshenko shear coefficient). It is well known that the value of this factor varies from problem to problem; see Mindlin and Deresiewicz (1954) and Cowper (1966) for more details. A large amount of literature available on the calculation of this factor indicates its importance and its influence on the results of the Timoshenko beam theory. Some discussion of the available literature on shear-factor computation may be found in Bhimaraddi (1985). Therefore, it must be understood here that the accuracy and reliability of the results from the Timoshenko beam theory depend to a very large extent on a proper selection of the shear coefficient.

In a pursuit to advance a shear deformation beam theory that accounted for a parabolic shear-strain variation across the cross section with zero values at the extreme fibers (and therefore obviated the use of shear correction factor), Levinson (1981a, b) proposed a new beam theory. Levinson (1981a,

---

[1] Prin. Res. Engr., Diversified Computer Engrg. and Develop., 11 W. 14 Mile Road, Suite 205, Clawson, MI 48107.

[2] Assoc. Prof., Dept. of Mech. and Aerosp. Engrg. and Engrg. Mech., Univ. of Missouri, Rolla, MO 65401-0249.

Note. Discussion open until March 1, 1994. To extend the closing date one month, a written request must be filed with the ASCE Manager of Journals. The manuscript for this technical note was submitted for review and possible publication on December 6, 1991. This technical note is part of the ***Journal of Aerospace Engineering***, Vol. 6, No. 4, October, 1993. ©ASCE, ISSN 0893-1321/93/0004-0408/$1.00 + $.15 per page. Technical note No. 2363.

J. Aerosp. Eng. 1993.6:408-413.

Downloaded from ascelibrary.org by Northeastern Univ Library on 10/10/14. Copyright ASCE. For personal use only; all rights reserved.

b) showed that his theory predicts better results when compared with elasticity solutions than Timoshenko's theory. However, due to the type of formulation followed (vectorial approach) by Levinson (1981b), his theory is variationally inconsistent (see Bickford 1982). Bickford (1982) reformulated Levinson's theory using a variational principle and also showed how one could obtain the correct and variationally consistent equations using the vectorial approach. Thus, the resulting differential equation for consistent beam theory is of the sixth order, whereas that for the inconsistent beam theory is of the fourth order.

Bhimaraddi (1985, 1988) has presented a beam theory that is very similar in all respects to that of Bickford (1982) but uses a slightly different set of ad hoc displacement forms. There are, however, two main differences in the formulations of Bhimaraddi and Bickford: (1) The classical Euler-Bernoulli beam theory comes out readily as a special case in Bhimaraddi's formulation, whereas this is not so in Bickford's formulation; and (2) any suitable distribution to shear strains can be used (see the ξ function later) in Bhimaraddi's formulation with no additional alterations being required in the subsequent derivations that follow once the ad hoc displacements are written. In Bhimaraddi (1985, 1988) the shear-strain distribution has been assumed to be a symmetric parabola with zero values at the extreme fibers. It is the purpose of this paper to examine how the other shear-strain distributions affect the response of beams. In what follows we briefly describe the current formulation.

BASIC EQUATIONS

We consider a rectangular cross-section beam of unit width with depth h and length L. Displacements at any point, following Bhimaraddi (1985), are written as

$$u(x, z) = \xi(z)\phi(x) - z\frac{\partial w}{\partial x} \quad \text{(1a)}$$

$$w(x, z) = w(x) \quad \text{(1b)}$$

where u and w = the displacements along the axial (x) and lateral (z) direction, respectively; ϕ = the shear rotation in addition to the flexural rotation ($\partial w/\partial x$); and ξ is a function of the z-coordinate. ϕ and w are functions of x only. In Bhimaraddi (1985, 1988), a parabolic variation ($d\xi/dz = 1 - 4z^2/h^2$) for shear strain was used, and it was only suggested that almost any function (ξ) whose first derivative vanishes at $z = \pm h/2$ and is nonzero elsewhere can be used. Using the preceding displacement field given by (1a) and (1b), the normal and shear strains can be written as

$$\varepsilon = \xi\phi' - zw'' \quad \text{(2a)}$$

$$\gamma = \xi^*\phi \quad \text{(2b)}$$

where $\xi^* = d\xi/dz$; and various forms for the ξ functions and their first derivatives are listed in Table 1. A detailed discussion on the selection of the displacement fields for the more general problem of a curved beam may be found in Bhimaraddi (1988). Stresses are related to strains as

$$\sigma = E\varepsilon \quad \text{(3a)}$$

$$\tau = \gamma G \quad \text{(3b)}$$

Downloaded from ascelibrary.org by Northeastern Univ Library on 10/10/14. Copyright ASCE. For personal use only; all rights reserved.

Downloaded from ascelibrary.org by Northeastern Univ Library on 10/10/14. Copyright ASCE. For personal use only; all rights reserved.

TABLE 1. Various ξ Functions and Their First Derivatives

S1 number (1)	ξ function (2)	$d\xi/dz = \xi^*$ function (3)
Theory 1	$z - (4z^3/3h^2)$	$1 - (4z^2/h^2)$
Theory 2	$z - (16z^5/5h^4)$	$1 - (16z^4/h^4)$
Theory 3	$z + (z^2/2h) - (4z^3/3h^2) - (z^4/h^3)$	$1 + (z/h) - (4z^2/h^2) - (4z^3/h^3)$
Theory 4	$z - (z^2/2h) - (4z^3/3h^2) + (z^4/h^3)$	$1 - (z/h) - (4z^2/h^2) + (4z^3/h^3)$
Theory 5	$z - (8z^3/3h^2) + (16z^5/5h^4)$	$1 - (8z^2/h^2) + (16z^4/h^4)$
Theory 6	$z - (4z^3/h^2) + (48z^5/5h^4) - (64z^7/7h^6)$	$1 - (12z^2/h^2) + 48(z^4/h^4) - 64(z^6/h^6)$
Theory 7	$(h/\pi)\cos\{(\pi/2)[1 - (2z/h)]\}$	$\sin\{(\pi/2)[1 - (2z/h)]\}$

$$G = \frac{E}{2(1 + \mu)} \quad \text{(3c)}$$

where E, G, and μ = the Young's modulus, shear modulus, and the Poisson's ratio of an isotropic material, respectively.

Using the principle of the stationary total potential energy, one obtains the following differential equations governing the static response of the beam

$$\alpha\phi'' - \beta w''' - \frac{6\delta}{h^2(1 - \mu)}\phi = 0 \quad \text{(4a)}$$

$$w^{iv} - \beta\phi''' = -\frac{q}{EI} \quad \text{(4b)}$$

where q = the applied lateral load on the beam; $I = h^3/12$; and α, β, and δ and the stress resultants are defined as

$$\int_{-h/2}^{h/2} (\xi^2, z\xi, \xi^{*2})\, dz = (I\alpha, I\beta, h\delta) \quad \text{(5a)}$$

$$\int_{-h/2}^{h/2} (z, \xi)\sigma\, dz = (M, \bar{M}); \quad Q = M' \quad \text{(5b)}$$

Substituting stress-strain relations [(3a)–(3c)] and strain-displacement relations [(2a) and (2b)] in stress-resultant definitions [(5a) and (5b)] and integrating, one obtains the following.

$$M = EI(w'' - \beta\phi') \quad \text{(6a)}$$

$$\bar{M} = EI(\alpha\phi' - \beta w'') \quad \text{(6b)}$$

$$Q = EI(w''' - \beta\phi'') \quad \text{(6c)}$$

Eliminating ϕ from (4a) and (4b), we obtain a single governing equation in terms of w as

$$w^{vi} - \lambda^2 w^{iv} = -\lambda^2 \frac{q}{EI} + \left(\frac{\alpha}{\alpha - \beta^2}\right)\frac{q''}{EI} \quad \text{(7a)}$$

where

$$\lambda^2 = \frac{6\delta}{(\alpha - \beta^2)(1 + \mu)h^2} \quad \text{.......................................} \quad (7b)$$

All other quantities can also be expressed in terms of w as

$$\lambda^2\beta(\alpha - \beta^2)\phi = \alpha w^{v} - \beta^2 w''' - \frac{\alpha^2}{\lambda^2(\alpha - \beta^2)EI} q' \quad \text{...............} \quad (8a)$$

$$M = \frac{EI}{\lambda^2}\left(\lambda^2 w'' - w^{iv} + \frac{\alpha}{\alpha - \beta^2}\frac{q}{EI}\right) \quad \text{.........................} \quad (8b)$$

$$\bar{M} = \frac{\alpha EI}{\beta\lambda^2}\left(w^{iv} - \frac{\beta^2\lambda^2}{\alpha} w'' - \frac{\alpha}{\alpha - \beta^2}\frac{q}{EI}\right) \quad \text{.....................} \quad (8c)$$

$$Q = \frac{EI}{\lambda^2}\left(\lambda^2 w''' - w^{v} + \frac{\alpha}{\alpha - \beta^2}\frac{q'}{EI}\right) \quad \text{.........................} \quad (8d)$$

The following boundary conditions are to be used for different types of supports:

- Simply supported end:

  $$w = M = \bar{M} = 0 \quad \text{....................................} \quad (9a)$$

- Free end

  $$M = Q = \bar{M} = 0 \quad \text{....................................} \quad (9b)$$

- Fixed end:

  $$w = w' = \phi = 0 \quad \text{....................................} \quad (9c)$$

Thus, we have reduced the problem of calculating the static response of a beam to the problem of finding the solution of a sixth-order differential equation [(7*a*)] with appropriate boundary conditions [(9*a*)–(9*c*)].

RESULTS

One can obtain the tip deflection of a cantilever and the central deflection (at $x = 0$) of simply supported and clamped beams as

$$w_{tip} = \frac{PL^3}{3EI}\left[1 + \frac{1}{2}\frac{\beta^2}{\delta}(1 + \mu)\frac{h^2}{L^2}\right] \qquad \text{(cantilever with tip load } P\text{)}$$

$$\text{...} \quad (10a)$$

$$w_{tip} = \frac{q_0 L^4}{8EI}\left[1 + \frac{2}{3}\frac{\beta^2}{\delta}(1 + \mu)\frac{h^2}{L^2}\right] \qquad \text{(cantilever with uniform load } q_0\text{)}$$

$$\text{...} \quad (10b)$$

Downloaded from ascelibrary.org by Northeastern Univ Library on 10/10/14. Copyright ASCE. For personal use only; all rights reserved.

Downloaded from ascelibrary.org by Northeastern Univ Library on 10/10/14. Copyright ASCE. For personal use only; all rights reserved.

$$w_{\text{center}} = \frac{5q_0L^4}{384EI}\left[1 + \frac{8}{5}\frac{\beta^2}{\delta}(1 + \mu)\frac{h^2}{L^2}\right]$$

(simply supported beam with uniform load q_0) . . . . (10*c*)

$$w_{\text{center}} = \frac{q_0L^4}{384EI}\left[1 + \frac{8\beta^2}{\delta}(1 + \mu)\frac{h^2}{L^2}\right]$$

(clamped beam with uniform load q_0) . . . . (10*d*)

While arriving at these expressions, we have observed that λL is too large (and therefore $\tanh \lambda L \simeq 1$, $1/\lambda L \simeq 0$, and $\sinh \lambda L \simeq \cosh \lambda L$). This is a very good approximation for most problems of practical interest. In (10*a*)–(10*d*), the second term in the bracketed quantity represents the effects of shear deformation, while the first term is the solution to the Euler-Bernoulli theory. Furthermore, in (10*a*)–(10*d*), the shear deformation effects are proportional to β^2/δ. In a more general fashion, one can write (10*a*)–(10*d*) as

$$w = w_c\left[1 + (1 + \mu)\frac{h^2}{L^2}\cdot w_s\right] \qquad (11)$$

where w_c = the deflection corresponding to the Euler-Bernoulli beam theory; and w_s = the proportionality constant due to shear deformation effects.

Table 2 shows w_s values for different beam problems, along with various theories considered. One may observe from this table that, for various ξ functions considered, a symmetric parabolic distribution for shear strain (theory 1) gives the greatest value for w_s followed by the sinusoidal distribution (theory 7). Thus, it is interesting to note that a simple parabolic distribution is a good enough approximation. Comparing with the other theories, Table 2 shows that the current parabolic distribution (theory 1) and Timoshenko's (1921) theory (with shear coefficient, $\kappa^2 = 5/6$) give identical results for all the problems considered. In general, Levinson's (1981a, b) inconsistent beam theory gives higher w_s values than the present formulation and Timoshenko's theory.

TABLE 2. Values of w_s for Various Theories Considered

Theory (1)	Cantilever (top load) (2)	Cantilever (uniform load) (3)	Simple support (4)	Clamped (5)
Theory 1	0.6	0.8	1.92	9.6
Theory 2	0.58776	0.78367	1.88082	9.40408
Theory 3	0.57931	0.77241	1.85379	9.26897
Theory 4	0.57931	0.77241	1.85379	9.26897
Theory 5	0.57857	0.77143	1.85143	9.25714
Theory 6	0.54476	0.72635	1.74324	8.71619
Theory 7	0.59913	0.79885	1.91723	9.58613
Timoshenko (1921)	0.6	0.8	1.92	9.6
Levinson (1981a, b; 1988)	0.75	1.2	1.92	12.0
Elasticity (Timoshenko and Goodier 1970)	0.75	—	1.93846[a]	—

[a] $w_s = (48/25)[1 + (25/24)\mu]/(1 + \mu)$ and $\mu = 0.3$.

Downloaded from ascelibrary.org by Northeastern Univ Library on 10/10/14. Copyright ASCE. For personal use only; all rights reserved.

CONCLUSIONS

In this paper the effect of shear deformation on the static response of beams of rectangular cross section has been considered using various distribution functions for shear strain. Numerical results indicate that the simple parabolic distribution gives the best results. The deflection values obtained using the parabolic shear-strain distribution are identical to those of Timoshenko's (1921) theory with shear factor equal to five-sixths. The major disadvantage of Timoshenko's theory lies in the use of the proper value for the shear factor and the theories which do not use shear factor should be considered, even if they are more complicated than Timoshenko's theory.

APPENDIX. REFERENCES

Bickford, W. B. (1982). "A consistent higher order beam theory." *Devel. in Theoretical and Appl. Mech.*, SECTAM, 11, 137–150.

Bhimaraddi, A. (1985). "Static and dynamic response of plates and shells," PhD thesis, University of Melbourne, Melbourne, Australia.

Bhimaraddi, A. (1988). "Generalized analysis of shear deformable rings and curved beams." *Int. J. Solids and Struct.*, 24(4), 363–373.

Cowper, G. R. (1966). "The shear coefficient in Timoshenko's beam theory." *J. Appl. Mech.*, 33(2), 335–340.

Levinson, M. (1981a). "Further results of a new beam theory." *J. Sound and Vib.*, 77(3), 440–444.

Levinson, M. (1981b). "A new rectangular beam theory." *J. Sound and Vib.*, 74(1), 81–87.

Levinson, M. (1985). "On Bickford's consistent higher order beam theory." *Mech. Res. Commun.*, 12(1), 1–9.

Mindlin, R. D., and Deresiewicz, H. (1984). "Timoshenko's shear coefficient for flexural vibrations of beams." *Proc. 2nd U.S. Nat. Congress of Appl. Mech.*, American Society of Mechanical Engineers, 175–178.

Timoshenko, S. P. (1921). "On the correction for shear of the differential equation for transverse vibrations of prismatic bars." *Philosophical Magazine*, 41, 744–746.

Timoshenko, S. P., and Goodier, J. N. (1970). *Theory of elasticity*. 3rd Ed., McGraw-Hill Book Co., New York, N.Y.

AN INTRODUCTION TO THE FINITE ELEMENT METHOD

McGraw-Hill Series in Mechanical Engineering

Consulting Editors
Jack P. Holman, *Southern Methodist University*
John R. Lloyd, *Michigan State University*

Anderson: *Modern Compressible Flow: With Historical Perspective*
Arora: *Introduction to Optimum Design*
Bray and Stanley: *Nondestructive Evaluation: A Tool for Design, Manufacturing, and Service*
Culp: *Principles of Energy Conversion*
Dally: *Packaging of Electronic Systems: A Mechanical Engineering Approach*
Dieter: *Engineering Design: A Materials and Processing Approach*
Eckert and Drake: *Analysis of Heat and Mass Transfer*
Edwards and McKee: *Fundamentals of Mechanical Component Design*
Gebhart: *Heat Conduction and Mass Transfer*
Heywood: *Internal Combustion Engine Fundamentals*
Hinze: *Turbulence*
Howell and Buckius: *Fundamentals of Engineering Thermodynamics*
Hutton: *Applied Mechanical Vibrations*
Juvinall: *Engineering Considerations of Stress, Strain, and Strength*
Kane and Levinson: *Dynamics: Theory and Applications*
Kays and Crawford: *Convective Heat and Mass Transfer*
Kimbrell: *Kinematics Analysis and Synthesis*
Martin: *Kinematics and Dynamics of Machines*
Modest: *Radiative Heat Transfer*
Norton: *Design of Machinery*
Phelan: *Fundamentals of Mechanical Design*
Raven: *Automatic Control Engineering*
Reddy: *An Introduction to the Finite Element Method*
Rosenberg and Karnopp: *Introduction to Physics*
Schlichting: *Boundary-Layer Theory*
Shames: *Mechanics of Fluids*
Sherman: *Viscous Flow*
Shigley: *Kinematic Analysis of Mechanisms*
Shigley and Mischke: *Mechanical Engineering Design*
Shigley and Uicker: *Theory of Machines and Mechanisms*
Stiffler: *Design with Microprocessors for Mechanical Engineers*
Stoecker and Jones: *Refrigeration and Air Conditioning*
Ullman: *The Mechanical Design Process*
Vanderplaats: *Numerical Optimization: Techniques for Engineering Design, with Applications*
White: *Viscous Fluid Flow*
Zeid: *CAD/CAM Theory and Practice*

Also Available from McGraw-Hill

Schaum's Outline Series in Mechanical Engineering

Most outlines include basic theory, definitions, and hundreds of solved problems and supplementary problems with answers.

Titles on the Current List Include:

Acoustics
Basic Equations of Engineering
Continuum Mechanics
Engineering Economics
Engineering Mechanics, 4th edition
Fluid Dynamics, 2d edition
Fluid Mechanics & Hydraulics, 2d edition
Heat Transfer
Introduction to Engineering Calculations
Lagrangian Dynamics
Machine Design
Mathematical Handbook of Formulas & Tables
Mechanical Vibrations
Operations Research
Statistics & Mechanics of Materials
Strength of Materials, 2d edition
Theoretical Mechanics
Thermodynamics, 2d edition

Schaum's Solved Problems Books

Each title in this series is a complete and expert source of solved problems containing thousands of problems with worked out solutions.

Related Titles on the Current List Include:

3000 Solved Problems in Calculus
2500 Solved Problems in Differential Equations
2500 Solved Problems in Fluid Mechanics and Hydraulics
1000 Solved Problems in Heat Transfer
3000 Solved Problems in Linear Algebra
2000 Solved Problems in Mechanical Engineering Thermodynamics
2000 Solved Problems in Numerical Analysis
700 Solved Problems in Vector Mechanics for Engineers: Dynamics
800 Solved Problems in Vector Mechanics for Engineers: Statistics

Available at your College Bookstore. A complete list of Schaum titles may be obtained by writing to:
Schaum Division
McGraw-Hill, Inc.
Princeton Road, S-1
Hightstown, NJ 08520

AN INTRODUCTION TO THE FINITE ELEMENT METHOD

Second Edition

J. N. Reddy
Oscar S. Wyatt Chair in Mechanical Engineering
Texas A&M University
College Station, Texas 77843

O.D.T.Ü. KÜTÜPHANESİ
M.E.T.U. LIBRARY

McGraw-Hill, Inc.
New York St. Louis San Francisco Auckland Bogotá
Caracas Lisbon London Madrid Mexico Milan Montreal
New Delhi Paris San Juan Singapore Sydney Tokyo Toronto

This book was set in Times Roman.
The editors were John J. Corrigan and John M. Morriss;
the production supervisor was Louise Karam.
The cover was designed by Joseph Gillians.
Project supervision was done by The Universities Press.
R. R. Donnelley & Sons Company was printer and binder.

TA 347.F5
R4
1993

TA347.F5 R4 1993 METU LIBRARY
An introduction to the finite element metho
0020046676

269154

AN INTRODUCTION TO THE FINITE ELEMENT METHOD

Copyright © 1993, 1984 by McGraw-Hill, Inc. All rights reserved. Printed in the United States of America. Except as permitted under the United States Copyright Act of 1976, no part of this publication may be reproduced or distributed in any form or by any means, or stored in a data base or retrieval system, without the prior written permission of the publisher.

2 3 4 5 6 7 8 9 0 DOC/DOC 9 9 8 7 6 5 4 3

ISBN 0-07-051355-4

Library of Congress Cataloging-in-Publication Data

Reddy, J. N. (John N.)
An introduction to the finite element method/J. N. Reddy.—2nd ed.
p. cm.—(McGraw-Hill series in mechanical engineering)
Includes bibliographical references and index.
ISBN 0-07-051355-4
1. Finite element method. I. Series.
TA347.F5R4 1993
620'.001'51535—dc20 92-29532

ABOUT THE AUTHOR

J. N. Reddy is the inaugural holder of the *Oscar S. Wyatt, Jr, Endowed Chair* in Mechanical Engineering at Texas A&M University. Prior to the current appointment, he was the *Clifton C. Garvin Chaired Professor* of Engineering Science and Mechanics at Virginia Polytechnic Institute and State University. After receiving his Ph.D. in Applied Mechanics in 1974, he joined Lockheed Missiles and Space Company in Huntsville, Alabama, as a research scientist. In 1975, he joined the School of Aerospace, Mechanical and Nuclear Engineering at the University of Oklahoma. In 1980, he was appointed as a professor of Engineering Science and Mechanics at Virginia Polytechnic Institute and State University.

Dr. Reddy has authored and coauthored over 150 journal papers and seven books on the theory and applications of the finite element method in solid and structural mechanics, fluid mechanics and heat transfer, and on the development of refined theories and finite element models of laminated composite plates and shells.

Dr. Reddy has taught many short courses on the finite element method to industry and government, and has received Certificates of Teaching Excellence from Virginia Polytechnic Institute and State University.

Dr. Reddy serves on the editorial boards of a dozen journals, including *Journal of Applied Mechanics, Meccanica, International Journal for Numerical Methods in Engineering, International Journal of Numerical Methods in Fluids, Journal of Non-Linear Mechanics,* and *Journal of Composites Technology and Research.* He has received the College of Engineering Research Award from the University of Oklahoma and the Alumni Research Award from the Virginia Polytechnic Institute and State University. Dr. Reddy was awarded the *1983 Walter L. Huber Research Prize* of the American Society of Civil Engineers and *1992 Worcester Reed Warner Medal* of the American Society of Mechanical Engineers. He is a Fellow of the American Academy of Mechanics, the American Society of Mechanical Engineers, the American Society of Civil Engineers, and the Aeronautical Society of India.

TO MY FAMILY
Aruna, Anita, and Anil

CONTENTS

Preface to the Second Edition xvii
Preface to the First Edition xix

Part 1 Preliminaries

1 Introduction 3
1.1 General Comments 3
1.2 Historical Background 5
1.3 The Basic Concept of the Finite Element Method 5
1.3.1 General Comments 5
1.3.2 Approximation of the Circumference of a Circle 6
1.3.3 Approximate Determination of the Center of Mass 8
1.3.4 Solution of Differential Equation 10
1.3.5 Some Remarks 13
1.4 The Present Study 15
1.5 Summary 15
References for Additional Reading 16

2 Integral Formulations and Variational Methods 18
2.1 Need for Weighted-Integral Forms 18
2.2 Some Mathematical Concepts and Formulae 20
2.2.1 Boundary, Initial, and Eigenvalue Problems 20
2.2.2 Integral Relations 22
2.2.3 Functionals 26
2.2.4 The Variational Symbol 27
2.3 Weak Formulation of Boundary Value Problems 28
2.3.1 Introduction 28
2.3.2 Weighted-Integral and Weak Formulations 28
2.3.3 Linear and Bilinear Forms and Quadratic Functionals 33
2.3.4 Examples 35

2.4 Variational Methods of Approximation 40
2.4.1 Introduction 40
2.4.2 The Rayleigh–Ritz Method 40
2.4.3 The Method of Weighted Residuals 51
2.5 Summary 57
Problems 59
References for Additional Reading 63

Part 2 Finite Element Analysis of One-Dimensional Problems

3 Second-Order Boundary Value Problems 67
3.1 Introduction 67
3.2 Basic Steps of Finite Element Analysis 70
3.2.1 Model Boundary Value Problem 70
3.2.2 Discretization of the Domain 72
3.2.3 Derivation of Element Equations 72
3.2.4 Connectivity of Elements 89
3.2.5 Imposition of Boundary Conditions 95
3.2.6 Solution of Equations 95
3.2.7 Postprocessing of the Solution 96
3.2.8 Radially Symmetric Problems 103
3.3 Applications 105
3.3.1 Heat Transfer 105
3.3.2 Fluid Mechanics 117
3.3.3 Solid Mechanics 123
3.4 Summary 127
Problems 128
References for Additional Reading 141

4 Bending of Beams 143
4.1 Introduction 143
4.2 The Euler–Bernoulli Beam Element 143
4.2.1 Governing Equation 143
4.2.2 Discretization of the Domain 144
4.2.3 Derivation of Element Equations 144
4.2.4 Assembly of Element Equations 151
4.2.5 Imposition of Boundary Conditions 154
4.2.6 Solution 156
4.2.7 Postprocessing of the Solution 158
4.2.8 Examples 160
4.3 Plane Truss and Euler–Bernoulli Frame Elements 167
4.4 The Timoshenko Beam and Frame Elements 177
4.4.1 Governing Equations 177
4.4.2 Weak Form 177
4.4.3 Finite Element Model 178
4.5 Inclusion of Constraint Equations 187
4.6 Summary 191

Problems 192
References for Additional Reading 198

5 Finite Element Error Analysis 199

5.1 Approximation Errors 199
5.2 Various Measures of Errors 200
5.3 Convergence of Solution 201
5.4 Accuracy of the Solution 202
5.5 Summary 207
Problems 207
References for Additional Reading 208

6 Eigenvalue and Time-Dependent Problems 209

6.1 Eigenvalue Problems 209
6.1.1 Introduction 209
6.1.2 Formulation of Eigenvalue Problems 210
6.1.3 Finite Element Models 213
6.1.4 Applications 216
6.2 Time-Dependent Problems 224
6.2.1 Introduction 224
6.2.2 Semidiscrete Finite Element Models 225
6.2.3 Time Approximations 227
6.2.4 Mass Lumping 232
6.2.5 Applications 233
6.3 Summary 241
Problems 241
References for Additional Reading 245

7 Numerical Integration and Computer Implementation 246

7.1 Isoparametric Formulations and Numerical Integration 246
7.1.1 Background 246
7.1.2 Natural Coordinates 248
7.1.3 Approximation of Geometry 249
7.1.4 Isoparametric Formulations 251
7.1.5 Numerical Integration 251
7.2 Computer Implementation 258
7.2.1 Introductory Comments 258
7.2.2 General Outline 259
7.2.3 Preprocessor 260
7.2.4 Calculation of Element Matrices (Processor) 262
7.2.5 Assembly of Element Equations (Processor) 265
7.2.6 Imposition of Boundary Conditions (Processor) 267
7.2.7 Solution of Equations and Postprocessing 269
7.3 Applications of the Computer Program FEM1DV2 270
7.3.1 General Comments 270
7.3.2 Illustrative Examples 271
7.4 Summary 286
Problems 287
References for Additional Reading 291

Part 3 Finite Element Analysis of Two-Dimensional Problems

8 Single-Variable Problems

8 Single-Variable Problems 295
8.1 Introduction 295
8.2 Boundary Value Problems 297
8.2.1 The Model Equation 297
8.2.2 Finite Element Discretization 298
8.2.3 Weak Form 299
8.2.4 Finite Element Model 301
8.2.5 Interpolation Functions 303
8.2.6 Evaluation of Element Matrices and Vectors 311
8.2.7 Assembly of Element Equations 318
8.2.8 Postprocessing 322
8.2.9 Axisymmetric Problems 323
8.2.10 An Example 324
8.3 Some Comments on Mesh Generation and Imposition of Boundary Conditions 334
8.3.1 Discretization of a Domain 334
8.3.2 Generation of Finite Element Data 336
8.3.3 Imposition of Boundary Conditions 339
8.4 Applications 340
8.4.1 Heat Transfer 340
8.4.2 Fluid Mechanics 353
8.4.3 Solid Mechanics 365
8.5 Eigenvalue and Time-Dependent Problems 370
8.5.1 Introduction 370
8.5.2 Parabolic Equations 372
8.5.3 Hyperbolic Equations 379
8.6 Summary 384
Problems 386
References for Additional Reading 402
9 Interpolation Functions, Numerical Integration, and Modeling Considerations 404
9.1 Library of Elements and Interpolation Functions 404
9.1.1 Introduction 404
9.1.2 Triangular Elements 405
9.1.3 Rectangular Elements 411
9.1.4 The Serendipity Elements 417
9.2 Numerical Integration 421
9.2.1 Preliminary Comments 421
9.2.2 Coordinate Transformations 423
9.2.3 Integration over a Master Rectangular Element 429
9.2.4 Integration over a Master Triangular Element 433
9.3 Modeling Considerations 439
9.3.1 Preliminary Comments 439
9.3.2 Element Geometries 439
9.3.3 Mesh Generation 441
9.3.4 Load Representation 446
9.4 Summary 448

Problems 448
References for Additional Reading 453

10 Plane Elasticity 455

10.1 Introduction 455
10.2 Governing Equations 456
  10.2.1 Assumptions of Plane Elasticity 456
  10.2.2 Basic Equations 457
10.3 Weak Formulations 459
  10.3.1 Preliminary Comments 459
  10.3.2 Principle of Virtual Displacements in Matrix Form 459
  10.3.3 Weak Form of the Governing Differential Equations 461
10.4 Finite Element Model 461
  10.4.1 Matrix Form of the Model 461
  10.4.2 Weak Form Model 464
  10.4.3 Eigenvalue and Transient Problems 465
10.5 Evaluation of Integrals 465
10.6 Assembly and Boundary and Initial Conditions 468
10.7 Examples 469
10.8 Summary 476
Problems 476
References for Additional Reading 480

11 Flows of Viscous Incompressible Fluids 482

11.1 Preliminary Comments 482
11.2 Governing Equations 483
11.3 Velocity–Pressure Finite Element Model 484
11.4 Penalty–Finite Element Model 488
  11.4.1 Penalty Function Method 488
  11.4.2 Formulation of the Flow Problem as a Constrained Problem 489
  11.4.3 Lagrange Multiplier Formulation 491
  11.4.4 Penalty Function Formulation 491
  11.4.5 Computational Aspects 492
11.5 Examples 494
11.6 Summary 502
Problems 503
References for Additional Reading 506

12 Bending of Elastic Plates 508

12.1 Introduction 508
12.2 Classical Plate Model 510
  12.2.1 Displacement Field 510
  12.2.2 Virtual Work Statement 510
  12.2.3 Finite Element Model 514
12.3 Shear Deformable Plate Model 516
  12.3.1 Displacement Field 516
  12.3.2 Virtual Work Statement 517
  12.3.3 Finite Element Model 518
  12.3.4 Shear Locking and Reduced Integration 519
12.4 Eigenvalue and Time-Dependent Problems 520

12.5 Examples 522
12.6 Summary 529
Problems 529
References for Additional Reading 531

13 Computer Implementation 533
13.1 Introduction 533
13.2 Preprocessor 534
13.3 Element Computations: Processor 535
13.4 Applications of the Computer Program FEM2DV2 540
13.4.1 Introduction 540
13.4.2 Description of Mesh Genrators 548
13.4.3 Applications (Illustrative Examples) 551
13.5 Summary 563
Problems 570
References for Additional Reading 575

Part 4 Advanced Topics

14 Weighted-Residual Finite Element Models, and Finite Element Models of Nonlinear and Three-Dimensional Problems 579
14.1 Introduction 579
14.2 Alternative Formulations 580
14.2.1 Introductory Comments 580
14.2.2 Weighted-Residual Finite Element Models 580
14.2.3 Mixed Formulations 590
14.3 Nonlinear Problems 594
14.3.1 General Comments 594
14.3.2 Large-Deflection Bending of (Euler–Bernoulli) Beams 595
14.3.3 Solution Methods for Nonlinear Algebraic Equations 597
14.3.4 The 2-D Navier–Stokes Equations 598
14.4 Three-Dimensional Problems 599
14.5 Summary 601
Problems 602
References for Additional Reading 606

Appendixes

1 Fortran Listing of FEM1DV2 609

2 Fortran Listing of FEM2DV2 640

Index 679

PREFACE TO THE SECOND EDITION

This second edition has the same objectives as the first, namely, an introduction to the finite element method as applied to linear, one- and two-dimensional problems of engineering and applied sciences. The revisions are mainly in the form of additional details, expansion of the topics discussed, and the addition of a few topics to make the coverage more complete.

The major organizational change from the first edition is the division of its five chapters into fourteen chapters here. These chapters are grouped into four parts. This reorganization should aid instructors in selecting suitable material for courses. Other organizational changes include putting problem sets at the ends of the chapters, providing a chapter summary for each, and reviewing pertinent equations and text in each chapter instead of referring to several chapters back. In addition, example problems in Chapters 3 and 8 are presented in separate sections on heat transfer, fluid flow, and solid mechanics.

Additional details are provided on the construction of the weak forms, time approximations (e.g., accuracy and stability of schemes, and mass lumping), alternative finite element formulations, and nonlinear finite element models. The new topics include sections on trusses and frames, the Timoshenko beam element, eigenvalue problems, and classical plate bending elements. All these changes are also reflected in the revised computer programs FEM1DV2 and FEM2DV2 (revised versions of the FEM1D, FEM2D and PLATE programs in the first edition). Therefore the sections on computer implementation and applications of FEM1DV2 and FEM2DV2 have also been modified extensively. These changes are accompanied by the addition of several figures, tables, and examples.

These extensive changes have resulted in a second edition that is 60% larger. In the interest of keeping the cost of the book within reasonable limits while retaining the basic approach and technical details, certain portions of the original manuscript have been omitted. More specifically, answers to selective problems have been included at the end of the problem statements themselves, rather than in a separate section. Interested readers and instructors can obtain a copy of the excutable programs on a diskette from the author. Fortran source programs can also be purchased from the author.

There is no doubt that this edition is more complete and thorough than the first. It can be used as a textbook for an introductory and/or intermediate level course on the finite element method at senior undergraduate as well as graduate levels. Students of engineering and applied sciences should feel comfortable with the coverage in the book.

The author gratefully acknowledges help in reading the manuscript and suggestions for constructive changes from several colleagues. These include: Hasan Akay, Purdue University at Indianapolis, Norman Knight, Jr, Clemson University; J. K. Lee, Ohio State University; William Rule, University of Alabama; Martin Sadd, University of Rhode Island; John Whitcomb, Texas A&M University, and the author's research students: Ronald Averill, Filis Kokkinos, Y. S. N. Reddy, and Donald Robbins. It is a great pleasure to acknowledge typing of the manuscript by Mrs Vanessa McCoy, without whose patience and cooperation this work would not have been completed.

J. N. Reddy

PREFACE TO THE FIRST EDITION

The motivation which led to the writing of the present book has come from my many years of teaching finite-element courses to students from various fields of engineering, meteorology, geology and geophysics, physics, and mathematics. The experience gained as a supervisor and consultant to students and colleagues in universities and industry, who have asked for explanations of the various mathematical concepts related to the finite-element method, helped me introduce the method as a variationally based technique of solving differential equations that arise in various fields of science and engineering. The many discussions I have had with students who had no background in solids and structural mechanics gave rise to my writing a book that should fill the rather unfortunate gap in the literature.

The book is designed for senior undergraduate and first-year graduate students who have had a course in linear algebra as well as in differential equations. However, additional courses (or exposure to the topics covered) in mechanics of materials, fluid flow, and heat transfer should make the student feel more comfortable with the physical examples discussed in the book.

In the present book, the finite-element method is introduced as a variationally based technique of solving differential equations. A continuous problem described by a differential equation is put into an equivalent variational form, and the approximate solution is assumed to be a linear combination, $\sum c_j\phi_j$, of approximation functions ϕ_j. The parameters c_j are determined using the associated variational form. The finite-element method provides a systematic technique for deriving the approximation functions for simple subregions by which a geometrically complex region can be represented. In the finite-element method, the approximation functions are piecewise polynomials (i.e., polynomials that are defined only on a subregion, called an element).

The approach taken in the present book falls somewhere in the middle of the approaches taken in books that are completely mathematical and those approaches that are more structural-mechanics-oriented. From my own experience as an engineer and self-taught applied mathematician, I know how unfortunate outcomes may be arrived at if one follows a "formula" without deeper insight into the problem and its approximation. Even the best theories lead ultimately to some sort of guidelines (e.g., which variational formulation is suitable, what kind of element is desirable, what is the quality of the approximation, etc.). However, without a certain theoretical knowledge of variational methods one cannot fully understand various formulations, finite-element models, and their limitations.

In the present study of variational and finite-element methods, advanced mathematics are intentionally avoided in the interest of simplicity. However, a minimum of mathematical machinery that seemed necessary is included in Chapters 1 and 2. In Chapter 2, considerable attention is devoted to the construction of variational forms since this exercise is repeatedly encountered in the finite-element formulation of differential equations. The chapter is concerned with two aspects: first, the selection of the approximation functions that meet the specified boundary condtions; second, the technique of obtaining algebraic equations in terms of the undetermined parameters. Thus, Chapter 2 not only equips readers with certain concepts and tools that are needed in Chapters 3 and 4, but it also motivates them to consider systematic methods of constructing the approximation functions, which is the main feature of the finite-element method.

In introducing the finite element method in Chapters 3 and 4, the traditional solid mechanics approach is avoided in favor of the "differential equation" approach, which has broader interpretations than a single special case. However, when specific examples are considered, the physical background of the problem is stated. Since a large number of physical problems are described by second- and fourth-order ordinary differential equations (Chapter 3), and by the Laplace operator in two dimensions (Chapter 4), considerable attention is devoted to the finite-element formulation, the derivation of the interpolation functions, and the solution of problems described by these equations. Representative examples are drawn from various fields of engineering, especially from heat transfer, fluid mechanics, and solid mechanics. Since this book is intended to serve as a textbook for a first course on the finite-element method, advanced topics such as nonlinear problems, shells, and three-dimensional analyses are omitted.

Since the practice of the finite-element method ultimately depends on one's ability to implement the technique on a digital computer, examples and exercises are designed to let the reader actually compute the solutions of various problems using computers. Ample discussion of the computer implementation of the finite-element method is given in Chapters 3 and 4. Three model programs (FEM1D, FEM2D, and PLATE) are described, and their application is illustrated via several examples. The computer programs are very easy to understand because they are designed along the same lines as the theory presented in the book. The programs are available for mainframe and IBM PC compatibles from the author for a small charge.

Numerous examples, most of which are applications of the concepts to specific problems in various fields of engineering and applied science, are provided throughout the book. The conclusion of the examples are indicated by the symbol ■. At approprate intervals in the book an extensive number of exercise problems is included to test and extend the understanding of the concepts discussed. For those who wish to gain additional knowledge of the topics covered in the book, many reference books and research papers are listed at the end of each chapter.

There are several sections that can be skipped in a first reading of the book (such sections are marked with an asterisk); these can be filled in wherever needed later. The material is intended for a quarter or a semester course, although it is better suited for a semester course.

The following schedule of topics is suggested for a first course using the present textbook:

Undergraduate		Graduate	
Chapter 1	Self-study	Chapter 1	Self-study
Chapter 2	Section 2.1 (self) Section 2.2 Sections 2.3.1–2.3.3	Chapter 2	Section 2.1 (self) Section 2.2 Section 2.3
Chapter 3	Sections 3.1–3.4 Sections 3.6–3.7	Chapter 3	Sections 3.1–3.7
Chapter 4	Sections 4.1–4.4 Section 4.7 Sections 4.8.1–4.8.4	Chapter 4	Sections 4.1–4.8
		Chapter 5	Term Paper

Due to the intimate relationship between Sections 3.5 and 4.6, 3.6 and 4.7, and 3.7 and 4.8, they can be covered simultaneously. Also, it is suggested that Sections 3.6 and 3.7 (hence, 4.7 and 4.8) be covered after Section 3.2.

The author wishes to thank all those students and colleagues who have contributed by their advice and criticism to the improvement of this work. The author is also thankful to Vanessa McCoy for skillful typing of the manuscript, to Mr. N. S. Putcha and Mr. K. Chandrashekhara for proofreading the pages, and to the editors Michael Slaughter and Susan Hazlett for their help and cooperation in publishing the mauscript.

J. N. Reddy

Tejashwina vadheetamasthu
(May what we study be well studied)

PART
1
PRELIMINARIES

CHAPTER
1

INTRODUCTION

1.1 GENERAL COMMENTS

Virtually every phenomenon in nature, whether biological, geological, or mechanical, can be described with the aid of the laws of physics, in terms of algebraic, differential, or integral equations relating various quantities of interest. Determining the stress distribution in a pressure vessel with oddly shaped holes and numerous stiffeners and subjected to mechanical, thermal, and/or aerodynamic loads, finding the concentration of pollutants in seawater or in the atmosphere, and simulating weather in an attempt to understand and predict the mechanics of formation of tornadoes and thunderstorms are a few examples of many important practical problems.

Most engineers and scientists studying physical phenomena are involved with two major tasks:

1. Mathematical formulation of the physical process
2. Numerical analysis of the mathematical model

The mathematical formulation of a physical process requires background in related subjects (e.g., laws of physics) and, most often, certain mathematical tools. The formulation results in mathematical statements, often differential equations, relating quantities of interest in the understanding and/or design of the physical process. Development of the mathematical model of a process is achieved through assumptions concerning how the process works. In a numerical simulation, we use a numerical method and a computer to evaluate the mathematical model and estimate the characteristics of the process.

While the derivation of the governing equations for most problems is not unduly difficult, their solution by exact methods of analysis is a formidable task. In such cases, approximate methods of analysis provide alternative means of finding solutions. Among these, the finite difference method and the variational methods such as the Rayleigh–Ritz and Galerkin methods are most frequently used in the literature.

In the finite difference approximation of a differential equation, the derivatives in the latter are replaced by difference quotients (or the function is expanded in a Taylor series) that involve the values of the solution at discrete mesh points of the domain. The resulting algebraic equations are solved, after imposing the boundary conditions, for the values of the solution at the mesh points.

In the solution of a differential equation by a variational method, the equation is put into an equivalent weighted-integral form and then the approximate solution over the domain is assumed to be a linear combination ($\sum_j c_j\phi_j$) of appropriately chosen approximation functions ϕ_j and undetermined coefficients, c_j. The coefficients c_j are determined such that the integral statement equivalent to the original differential equation is satisfied. Various variational methods, e.g., the Rayleigh–Ritz, Galerkin, and least-squares methods, differ from each other in the choice of the integral form, weight functions, and/or approximation functions. A more complete discussion of variational methods will be given in Chapter 2. They suffer from the disadvantage that the approximation functions for problems with arbitrary domains are difficult to construct.

The finite element method overcomes the disadvantage of the traditional variational methods by providing a systematic procedure for the derivation of the approximation functions over subregions of the domain. The method is endowed with three basic features that account for its superiority over other competing methods. First, a geometrically complex domain of the problem is represented as a collection of geometrically simple subdomains, called *finite elements*. Second, over each finite element, the approximation functions are derived using the basic idea that any continuous function can be represented by a linear combination of algebraic polynomials. Third, algebraic relations among the undetermined coefficients (i.e., nodal values) are obtained by satisfying the governing equations, often in a weighted-integral sense, over each element. Thus, the finite element method can be viewed, in particular, as an element-wise application of the Rayleigh–Ritz or weighted-residual methods. In it, the approximation functions are often taken to be algebraic polynomials, and the undetermined parameters represent the values of the solution at a finite number of preselected points, called *nodes*, on the boundary and in the interior of the element. The approximation functions are derived using concepts from interpolation theory, and are therefore called *interpolation functions*. One finds that the degree of the interpolation functions depends on the number of nodes in the element and the order of the differential equation being solved.

1.2 HISTORICAL BACKGROUND

The idea of representing a given domain as a collection of discrete parts is not unique to the finite element method. It was recorded that ancient mathematicians estimated the value of π by noting that the perimeter of a polygon inscribed in a circle approximates the circumference of the latter. They predicted the value of π to accuracies of almost 40 significant digits by representing the circle as a polygon of a finitely large number of sides. In modern times, the idea found a home in aircraft structural analysis, where, for example, wings and fuselages are treated as assemblages of stringers, skins, and shear panels. In 1941, Hrenikoff introduced the so-called framework method, in which a plane elastic medium was represented as a collection of bars and beams. The use of piecewise-continuous functions defined over a subdomain to approximate an unknown function can be found in the work of Courant (1943), who used an assemblage of triangular elements and the principle of minimum total potential energy to study the St Venant torsion problem. Although certain key features of the finite element method can be found in the works of Hrenikoff (1941) and Courant (1943), its formal presentation is attributed to Argyris and Kelsey (1960) and Turner, Clough, Martin, and Topp (1956). The term "finite element" was first used by Clough in 1960. Since its inception, the literature on finite element applications has grown exponentially, and today there are numerous journals that are primarily devoted to the theory and application of the method. A review of the historical developments and the basic theory of the finite element method can be found in more than three dozen textbooks that are exclusively devoted to its introduction and application. The selective finite element books listed in References for Additional Reading at the end of this chapter are only for additional information on certain topics (e.g., three-dimensional problems, shells, structural dynamics, plasticity, and mathematics of finite elements). For the beginner, it is not necessary to consult these; the present book provides complete details of the method as applied to linear field problems, with examples from fluid mechanics, heat transfer, and solid mechanics.

1.3 THE BASIC CONCEPT OF THE FINITE ELEMENT METHOD

1.3.1 General Comments

The most distinctive feature of the finite element method that separates it from others is the division of a given domain into a set of simple subdomains, called *finite elements*. Any geometric shape that allows computation of the solution or its approximation, or provides necessary relations among the values of the solution at selected points, called *nodes,* of the subdomain, qualifies as a finite element. Other features of the method include seeking continuous, often polynomial, approximations of the solution over each element in terms of nodal values, and assembly of element equations by imposing the interelement continuity of the solution and balance of interelement forces. Here the basic ideas underlying the finite element method are introduced via two simple examples:

1. Determination of the circumference of a circle using a finite number of line segments
2. Determination of the center of mass (or gravity) of an irregular body

The first example is an expansion of an article written by the author in 1978 for a student magazine at the University of Oklahoma. Ideas expressed in the second can be found in books on statics of rigid bodies.

1.3.2 Approximation of the Circumference of a Circle

Consider the problem of determining the perimeter of a circle of radius R (see Fig. 1.1*a*). Ancient mathematicians estimated the value of the circumference

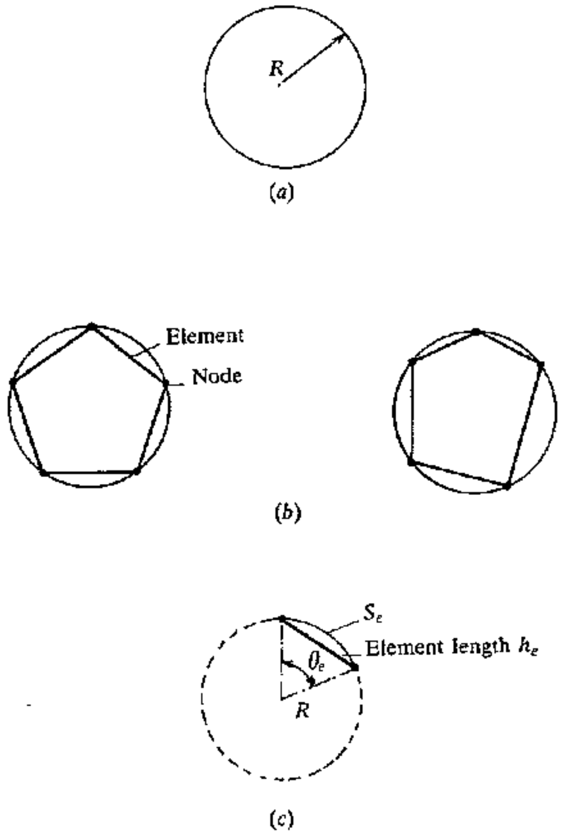

FIGURE 1.1
Approximation of the circumference of a circle by line elements: (*a*) Circle of radius R; (*b*) uniform and nonuniform meshes used to represent the circumference of the circle; (*c*) a typical element.

by approximating it by line segments, whose lengths they were able to measure. The approximate value of the circumference is obtained by summing the lengths of the line segments used to represent it. Although this is a trivial example, it illustrates several (but not all) ideas and steps involved in the finite element analysis of a problem. We outline the steps involved in computing an approximate value of the circumference of the circle. In doing so, we introduce certain terms that are used in the finite element analysis of any problem.

1. *Finite element discretization.* First, the domain (i.e., the circumference of the circle) is represented as a collection of a finite number n of subdomains, namely, line segments. This is called *discretization of the domain.* Each subdomain (i.e., line segment) is called an *element.* The collection of elements is called the *finite element mesh.* The elements are connected to each other at points called *nodes.* In the present case, we discretize the circumference into a mesh of five ($n = 5$) line segments. The line segments can be of different lengths. When all elements (i.e., line segments) are of the same length, the mesh is said to be *uniform*; otherwise, it is called a *nonuniform* mesh (see Fig. 1.1*b*).
2. *Element equations.* A typical element (i.e., line segment, Ω^e) is isolated and its required properties, i.e., length, are computed by some appropriate means. Let h_e be the length of element Ω^e in the mesh. For a typical element Ω^e, h_e is given by (see Fig. 1.1*c*)
$$h_e = 2R \sin \tfrac{1}{2}\theta_e \tag{1.1}$$
where R is the radius of the circle and $\theta_e < \pi$ is the angle subtended by the line segment. The above equations are called *element equations.* Ancient mathematicians most likely made measurements, rather than using (1.1), to find h_e.
3. *Assembly of element equations and solution.* The approximate value of the circumference (or perimeter) of the circle is obtained by putting together the element properties in a meaningful way; this process is called the *assembly* of the element equations. It is based, in the present case, on the simple idea that the total perimeter of the polygon (assembled elements) is equal to the sum of the lengths of individual elements:
$$P_n = \sum_{e=1}^{n} h_e \tag{1.2}$$
Then P_n represents an approximation to the actual perimeter, p. If the mesh is uniform, or h_e is the same for each of the elements in the mesh, then $\theta_e = 2\pi/n$, and we have
$$P_n = n\left(2R \sin \frac{\pi}{n}\right) \tag{1.3}$$
4. *Convergence and error estimate.* For this simple problem, we know the exact solution: $p = 2\pi R$. We can estimate the error in the approximation and show that the approximate solution P_n converges to the exact p in the

limit as $n \to \infty$. Consider the typical element Ω^e. The error in the approximation is equal to the difference between the length of the sector and that of the line segment (see Fig. 1.1c):

$$E_e = |S_e - h_e| \tag{1.4}$$

where $S_e = R\theta_e$ is the length of the sector. Thus, the error estimate for an element in the mesh is given by

$$E_e = R\left(\frac{2\pi}{n} - 2\sin\frac{\pi}{n}\right) \tag{1.5}$$

The total error (called *global* error) is given by multiplying E_e by n:

$$E = 2R\left(\pi - n\sin\frac{\pi}{n}\right) = 2\pi R - P_n \tag{1.6}$$

We now show that E goes to zero as $n \to \infty$. Letting $x = 1/n$, we have

$$P_n = 2Rn\sin\frac{\pi}{n} = 2R\frac{\sin \pi x}{x}$$

and

$$\lim_{n\to\infty} P_n = \lim_{x\to 0}\left(2R\frac{\sin \pi x}{x}\right) = \lim_{x\to 0}\left(2\pi R\frac{\cos \pi x}{1}\right) = 2\pi R \tag{1.7}$$

Hence, E_n goes to zero as $n \to \infty$. This completes the proof of convergence.

In summary, it is shown that the circumference of a circle can be approximated as closely as we wish by a finite number of piecewise-linear functions. As the number of elements is increased, the approximation improves, i.e., the error in the approximation decreases.

1.3.3 Approximate Determination of the Center of Mass

Another elementary example to illustrate the finite element concept is provided by the calculation of the center of mass of a continuous body. It should be recalled, from a first course on statics of rigid bodies, that the calculation of the center of an irregular mass or the centroid of an irregular volume makes use of the so-called method of composite bodies, in which a body is conveniently divided (mesh discretization) into several parts (elements) of simple shape for which the mass and the center of mass (element properties) can be computed readily. The center of mass of the whole body is then obtained using the moment *principle of Varignon* (a basis for the assembly of element properties):

$$(m_1 + m_2 + \ldots + m_n)\bar{X} = m_1\bar{x}_1 + m_2\bar{x}_2 + \ldots + m_n\bar{x}_n \tag{1.8}$$

where $\bar{X}$ is the x coordinate of the center of mass of the whole body, m_e is the mass of the eth part, and $\bar{x}_e$ is the x coordinate of the center of mass of the eth part. Similar expressions hold for the y and z coordinates of the center of mass of the whole body. Analogous relations hold for composite lines, areas, and volumes, wherein the masses are replaced by lengths, areas, and volumes, respectively.

When a given body is not expressible in terms of simple geometric shapes (elements) for which the mass and the center of mass can be represented mathematically, it is necessary to use a method of approximation to represent the properties of an element. As an example, consider the problem of finding the centroid $(\bar{X}, \bar{Y})$ of the irregular area (region) shown in Fig. 1.2. The region can be divided into a finite number of rectangular strips (elements), a typical element having width h_e and height b_e. The area of the eth strip is given by $A_e = h_e b_e$. The area A_e is an approximation of the true area of the element because b_e is an estimated average height of the element. The coordinates of the centroid of the region are obtained by applying the moment principle:

$$\bar{X} = \frac{\sum_e A_e \bar{x}_e}{\sum_e A_e}, \qquad \bar{Y} = \frac{\sum_e A_e \bar{y}_e}{\sum_e A_e}$$

where $\bar{x}_e$ and $\bar{y}_e$ are the coordinates of the centroid of the eth element with respect to the coordinate system used for the whole body. When the center of mass is required, A_e in the above equations is replaced by the mass $m_e = \rho_e A_e$, ρ_e being the mass density of the eth element; for a homogeneous body, ρ_e is the same for all elements.

It should be noted that the accuracy of the approximation will be improved by increasing the number of strips (decreasing their width) used. Rectangular elements are used in the present discussion for the sake of simplicity only; one may choose to use elements of any size and shape that approximate the given area to a satisfactory accuracy. For example, a trapezoidal element will require two heights to compute the area:

$$A_e = \tfrac{1}{2} h_e (b_e + b_{e+1})$$

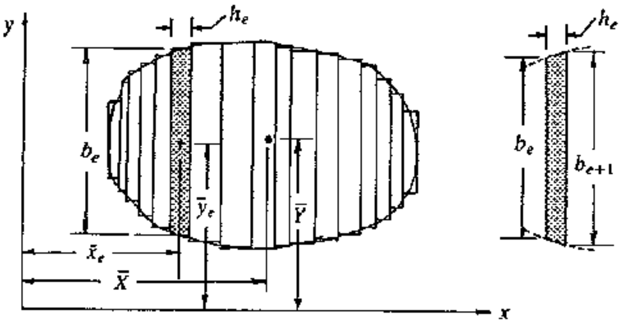

FIGURE 1.2
Approximate determination of the mass or geometric centroid of an irregular region by dividing it into a set of rectangular or trapezoidal subregions.

where b_e and b_{e+1} are the left and right heights, respectively, of the eth element.

The two examples considered above illustrate how the idea of piecewise approximation is used to approximate irregular geometries and calculate required quantities. In the first example, the circumference of a circle is approximated by a collection of line segments, whose measure is available. In the second, the geometric centroid or mass centroid of an irregular domain is located by approximating its geometry as a collection of strips that allow computation of their areas. Rectangles and trapezoids provide examples of the element geometries. Thus, subdividing a geometrically complex domain into parts that allow the evaluation of desired quantities is a very natural and practical approach. The idea can be extended to approximate functions representing physical quantities. For example, the temperature variation in a two-dimensional domain can be viewed as a curved surface, and it can be approximated over any part of the domain, i.e., over a subdomain or element, by a function of desired degree. Figure 1.3 shows a curved surface over a triangular subregion approximated by a planar surface, i.e., a linear polynomial. Such ideas form the basis of finite element approximations. The next example illustrates this idea for a one-dimensional continuous system.

1.3.4 Solution of Differential Equation

Consider the temperature variation in a composite cylinder consisting of two coaxial layers in perfect thermal contact (see Fig. 1.4). Heat dissipation from a wire (with two insulations) carrying an electric current and heat flow across a thick-walled composite circular cylindrical tube are typical examples. The temperature T is a function of the radial coordinate r. The variation of T with r is, in general, nonuniform. We wish to determine an approximation $T_e(r)$ to $T(r)$ over the thicknesses of the cylinder. The exact solution is determined by solving the differential equation

$$-\frac{1}{r}\frac{d}{dr}\left(rk\frac{dT}{dr}\right)=q(r) \tag{1.9a}$$

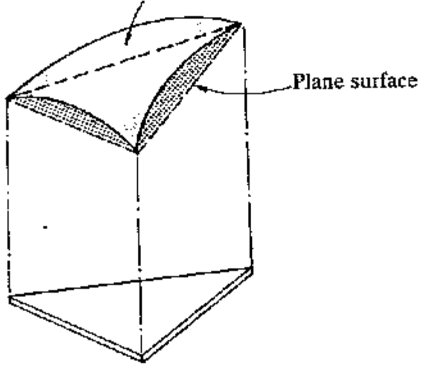

FIGURE 1.3
Approximation of curved surface (or a nonuniform function) over a triangular region by a planar surface.

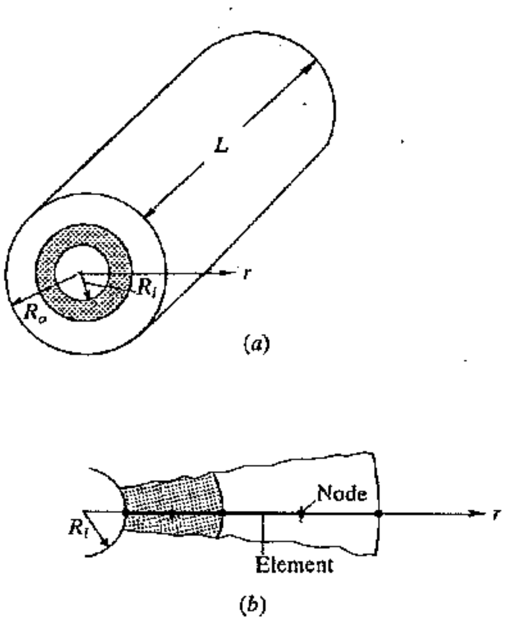

FIGURE 1.4
(*a*) Coaxial (composite) cylinder made of two different materials. (*b*) Finite element representation of a radial line of the cylinder.

subject to appropriate boundary conditions, for example, insulated at $r = R_i$ and subjected to a temperature T_o at $r = R_o$:

$$kr\frac{dT}{dr} = 0 \quad \text{at } r = R_i; \qquad T(r) = T_o \quad \text{at } r = R_o \tag{1.9b}$$

where k is the thermal conductivity, which varies from layer to layer, R_i and R_o are the inner and outer radii of the cylinder, and q is the rate of energy generation in the medium. Note that the temperature is independent of the circumferential coordinate (because of the axisymmetric geometry, boundary conditions, and loading), and it has the same variation along any radial line. When it is difficult to obtain an exact solution of the problem (1.9), either because of complex geometry and material properties or because $q(r)$ is a complicated function that does not allow exact evaluation of its integral, we seek an approximate one. In the finite element method, the domain (R_i, R_o) is divided into N subintervals, and the approximate solution is sought in the form

$$\begin{aligned}
T_1(r) &= \sum_{j=1}^{n} T_j^1 \psi_j^1(r) \quad (R_i \leq r \leq R_i + h_1;\ \text{first interval}) \\
T_2(r) &= \sum_{j=1}^{n} T_j^2 \psi_j^2(r) \quad (R_i + h_1 \leq r \leq R_i + h_1 + h_2;\ \text{second interval}) \qquad (1.10) \\
&\vdots \\
T_N(r) &= \sum_{j=1}^{n} T_j^N \psi_j^N(r) \quad (R_i + h_1 + \cdots + h_{N-1} \leq r \leq R_o;\ N\text{th interval})
\end{aligned}$$

where h_e denotes the length of the eth interval, T_j^e is the value of the temperature $T_e(r)$ at the jth geometric point of the eth interval, and ψ_j^e are polynomials on the eth interval. The continuous function $T(r)$ is approximated in each interval by a desired degree of polynomial, and the polynomial is expressed in terms of the values of the function at a selected number of points in the interval. The number of points is equal to the number of parameters in the polynomial. For example, a linear polynomial approximation of the temperature over the interval requires two values, and hence two points are identified in the interval. The endpoints of the interval are selected for this purpose because the two points also define the length of the interval (see Fig. 1.5*a*). For higher-order polynomial approximation, additional points are identified interior to the interval (see Fig. 1.5*b*). The intervals are called *finite elements*, the points used to express the polynomial approximation of the function are called *nodes*, T_j^e are called *nodal values*, and ψ_j^e are called *finite element approximation functions*. The nodal values T_j^e are determined such that $T_e(r)$ satisfies the differential equation (1.9*a*) and boundary conditions (1.9*b*) in some sense. Usually, the differential equation is satisfied in a weighted-integral sense, and boundary conditions on the function itself are satisfied exactly.

The piecewise (i.e., element-wise) approximation of the solution allows us to include any discontinuous data, such as the material properties, and to use meshes of many lower-order elements or a mesh of few higher-order elements to represent large gradients of the solution. Polynomial approximations of the form (1.10) can be derived systematically for any assumed degree of variation.

The satisfaction of the differential equation in a weighted-integral sense leads, for steady-state problems, to algebraic relations among nodal temperatures T_j^e and heats Q_j^e of the element. The algebraic equations of all elements are assembled (i.e., related to each other) such that the temperature is continuous and the heats are balanced at nodes common to elements. The

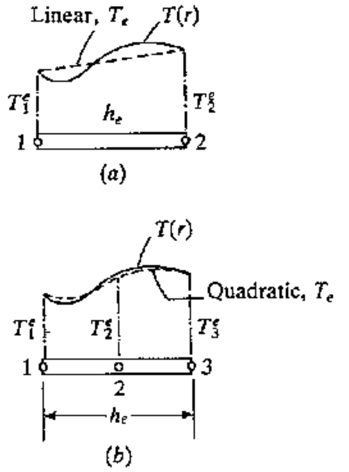

FIGURE 1.5
(*a*) Linear approximation of a function $T(r)$. (*b*) Quadratic approximation of a function $T(r)$.

assembled equations are solved for the nodal values after imposing the boundary conditions of the problem.

1.3.5 Some Remarks

In summary, in the finite element method, a given domain is divided into subdomains, called finite elements, and an approximate solution to the problem is developed over each of these. The subdivision of a whole into parts has two advantages:

1. It allows accurate representation of complex geometries and inclusion of dissimilar materials.
2. It enables accurate representation of the solution within each element, to bring out local effects (e.g., large gradients of the solution).

The three fundamental steps of the finite element method that are illustrated via the examples are:

1. Divide the whole into parts (both to represent the geometry and solution of the problem).
2. Over each part, seek an approximation to the solution as a linear combination of nodal values and approximation functions.
3. Derive the algebraic relations among the nodal values of the solution over each part, and assemble the parts to obtain the solution to the whole.

Although the above examples illustrate the basic idea of the finite element method, there are several other features that are either not present or not apparent from the discussion of the examples.
Some remarks are in order.

1. One can discretize a domain, depending on its shape, into a mesh of more than one type of element. For example, in the approximation of an irregular domain, one can use a combination of rectangles and triangles.
2. If more than one type of element is used in the representation of the domain, one of each kind should be isolated and its equations developed.
3. The governing equations are generally more complex than those considered in the first two examples. They are usually differential equations. In most cases, the equations cannot be solved over an element for two reasons. First, they do not permit the exact solution. It is here that the variational methods come into play. Second, the discrete equations obtained in the variational methods cannot be solved independent of the remaining elements, because the assemblage of the elements is subjected to certain continuity, boundary, and/or initial conditions.
4. There are two main differences in the form of the approximate solution used in the finite element method and that used in the classical variational

methods (i.e., variational methods applied to the whole domain). First, instead of representing the solution u as a linear combination ($u = \sum_j c_j\phi_j$) in terms of arbitrary parameters c_j as in the variational methods, in the finite element method the solution is often represented as a linear combination ($u = \sum_j u_j\psi_j$) in terms of the values u_j of u (and possibly its derivatives as well) at the nodal points. Second, the approximate functions in the finite element method are often polynomials that are derived using interpolation theory. However, the finite element method is *not* restricted to the use of approximations that are linear combinations of nodal values u_j and interpolation functions ψ_j that are algebraic polynomials. One can use, in addition to nodal values, nodeless variables (as in the Rayleigh–Ritz method) to represent the approximation of a function.

5. The number and the location of the nodes in an element depend on (*a*) the geometry of the element, (*b*) the degree of the polynomial approximation, and (*c*) the integral form of the equations. By representing the required solution in terms of its values at the nodes, one obtains directly the approximate solution at the nodes.
6. The assembly of elements, in a general case, is based on the idea that the solution (and possibly its derivatives for higher-order equations) is continuous at the interelement boundaries.
7. In general, the assemblage of finite elements is subjected to boundary and/or initial conditions. The discrete equations associated with the finite element mesh are solved only after the boundary and/or initial conditions have been imposed.
8. There are three sources of error in a finite element solution: (*a*) those due to the approximation of the domain (this was the only error present in the first two examples); (*b*) those due to the approximation of the solution; and (*c*) those due to numerical computation (e.g., numerical integration and round-off errors in a computer). The estimation of these errors, in general, is not a simple matter. However, under certain conditions, they can be estimated for a given element and problem (see Chapter 5).
9. The accuracy and convergence of the finite element solution depends on the differential equation, its integral form, and the element used. "Accuracy" refers to the difference between the exact solution and the finite element solution, while "convergence" refers to the accuracy as the number of elements in the mesh is increased.
10. For time-dependent problems, a two-stage formulation is usually followed. In the first stage, the differential equations are approximated by the finite element method to obtain a set of ordinary differential equations in time. In the second, the differential equations in time are solved exactly or further approximated by either variational methods or finite difference methods to obtain algebraic equations, which are then solved for the nodal values (see Chapter 6).
11. When the continuity conditions of assembly are replaced by contact conditions, the method is known as the *discrete element method* (DEM). In

the discrete element method, individual elements can have finite motions (e.g., displacements and rotations). Such methods have applications in rock mechanics (mining and tunneling), ice mechanics, and other fields where a continuum is disintegrated during deformation or the original medium is a collection of individual particles (e.g., granular media and molecular biology).

1.4 THE PRESENT STUDY

This is a book on the finite element method and its applications to linear problems in engineering and applied sciences. Most introductory finite element textbooks written for use in engineering schools are intended for students of solid and structural mechanics, and these introduce the method as an offspring of matrix methods of structural analysis. A few texts that treat the method as a variationally based technique leave the variational formulations and the associated methods of approximation either to an appendix or to self-study by the student. This book is written to introduce the finite element method as a numerical technique that employs the philosophy of constructing piecewise approximations of solutions to problems described by differential equations. This viewpoint makes the student aware of the generality of the finite element concept, irrespective of the student's background. It also enables the student to see the mathematical structure common to various physical theories, and thereby to gain additional insight into various engineering problems.

1.5 SUMMARY

In a numerical simulation of a physical process, we employ a numerical method and computer to evaluate a mathematical model of the process. The finite element method is a powerful numerical technique devised to evaluate complex physical processes. The method is characterized by three features:

1. The domain of the problem is represented by a collection of simple subdomains, called finite elements. The collection of finite elements is called the finite element mesh.
2. Over each finite element, the physical process is approximated by functions of desired type (polynomials or otherwise), and algebraic equations relating physical quantities at selective points, called nodes, of the element are developed.
3. The element equations are assembled using continuity and/or "balance" of physical quantities.

In the finite element method, in general, we seek an approximate solution u to a differential equation in the form

$$u \approx \sum_{j=1}^{n} u_j \psi_j + \sum_{j=1}^{m} c_j \phi_j$$

where u_j are the values of u at the element nodes, ψ_j are the interpolation functions, c_j are the nodeless coefficients, and ϕ_j are the associated approximation functions. Direct substitution of such approximations into the governing differential equations does not always result, for an arbitrary choice of the data of the problem, in a necessary and sufficient number of equations for the undetermined coefficients u_j and c_j. Therefore, a procedure whereby a necessary and sufficient number of equations can be obtained is needed. One such procedure is provided by a weighted-integral form of the governing differential equation. Chapter 2 is devoted to the study of weighted-integral formulations of differential equations and their solution by variational methods of approximation.

There is only one *method of finite elements*, and it is characterized by the three features stated above. Of course, there can be more than one *finite element model* of the same problem. The type of model depends on the differential equations and methods used to derive the algebraic equations (i.e., the weighted-integral form used) for the undetermined coefficients over an element. Although the Rayleigh–Ritz method and polynomial approximations are used frequently to generate the finite element equations, any appropriate method or combination of methods, can be used, in principle, to generate the algebraic equations. In this spirit, the collocation method, subdomain method, boundary integral methods, and so on can be used to generate the algebraic equations among discrete values of the primary and secondary variables.

REFERENCES FOR ADDITIONAL READING

Papers

Argyris, J. H., and S. Kelsey: *Energy Theorems and Structural Analysis*, Butterworth Scientific Publications, London, 1960.

Clough, R. W.: "The Finite Element Method in Plane Stress Analysis," *Journal of Structures Division, ASCE, Proceedings of 2d Conference on Electronic Computation*, pp. 345–378, 1960.

Courant, R.: "Variational Methods for the Solution of Problems of Equilibrium and Vibration," *Bulletin of the American Mathematical Society*, vol. 49, pp. 1–43, 1943.

Hrenikoff, A.: "Solution of Problems in Elasticity by the Framework Method," *Transactions of the ASME, Journal of Applied Mechanics*, vol. 8, pp. 169–175, 1941.

Reddy, J. N.: "The Finite Element Method: A Child of the Computer Age," *Sooner Shamrock* (Engineering Student Magazine at the University of Oklahoma), pp. 23–26, Fall 1978.

Turner, M., R. W. Clough, H. H. Martin, and L. Topp: "Stiffness and Deflection Analysis of Complex Structures," *Journal of Aeronautical Science*, vol. 23, pp. 805–823, 1956.

Books

Bathe, K. J.: *Finite Element Procedures in Engineering Analysis*, Prentice-Hall, Englewood Cliffs, NJ, 1982.

Becker, E. B., G. F. Carey, and J. T. Oden: *Finite Elements, An Introduction*, vol. I, Prentice-Hall, Englewood Cliffs, NJ, 1976.

Cook, R. D., D. S. Malkus, and M. E. Plesha: *Concepts and Applications of Finite Element Analysis*, 3d ed., John Wiley, New York, 1989.

Desai, C. S., and J. F. Abel: *Introduction to the Finite Element Method*, Van Nostrand Reinhold, New York, 1972.

Gallagher, R. H.: *Finite Element Analysis Fundamentals,* Prentice-Hall, Englewood Cliffs, NJ, 1975.

Hughes, T. J. T.: *The Finite Element Method,* Prentice-Hall, Englewood Cliffs, NJ, 1987.

Irons, B. M., and S. Ahmad: *Techniques of Finite Elements,* Ellis Horwood, Chichester, U.K., 1979.

Owen, D. R. J., and E. Hinton: *Finite Elements in Plasticity: Theory and Practice,* Pineridge Press, Swansea, U.K., 1980.

Rao, S. S.: *The Finite Element Method in Engineering,* Pergamon Press, Oxford, 1982.

Reddy, J. N.: *Applied Functional Analysis and Variational Methods in Engineering,* McGraw-Hill, New York, 1986; Krieger, Melbourne, FL, 1991.

Strang, G., and G. Fix: *An Analysis of the Finite Element Method,* Prentice-Hall, Englewood Cliffs, NJ, 1973.

Zienkiewicz, O. C., and R. L. Taylor: *The Finite Element Method,* vol. 1, *Basic Formulation and Linear Problems,* McGraw-Hill, London, 1989.

—— and ——: *The Finite Element Method,* vol. 2, *Solid and Fluid Mechanics, Dynamics and Non-Linearity,* McGraw-Hill, London, 1991.

CHAPTER 2

INTEGRAL FORMULATIONS AND VARIATIONAL METHODS

2.1 NEED FOR WEIGHTED-INTEGRAL FORMS

In the finite element method, we use an integral statement to develop algebraic relations among the coefficients u_j of the approximation

$$u \approx \sum_{j=1}^{n} u_j \psi_j \tag{2.1}$$

where u represents the solution of a particular differential equation. The use of an integral statement equivalent to the governing differential equation is necessitated by the fact that substitution of (2.1) into the governing differential equation does not always result in the required number of linearly independent algebraic equations for the unknown coefficients u_j. One way to insure that there are exactly the same number n of equations as there are unknowns is to require *weighted integrals* of the error in the equation to be zero. A more detailed discussion of this idea is given in the next few paragraphs.

Suppose that we wish to determine an approximate solution of the equation

$$-\frac{d}{dx}\left(x\frac{du}{dx}\right)+u=0 \quad \text{for } 0<x<1 \tag{2.2a}$$

$$u(0)=1, \qquad \left.\left(x\frac{du}{dx}\right)\right|_{x=1}=0 \tag{2.2b}$$

We seek an approximate solution, over the entire domain $\Omega=(0,1)$, in the form

$$u\approx U_N\equiv\sum_{j=1}^{N}c_j\phi_j(x)+\phi_0(x) \tag{2.3}$$

where the c_j are coefficients to be determined, and $\phi_j(x)$ and $\phi_0(x)$ are functions preselected such that the specified boundary conditions of the problem are satisfied by the N-parameter approximate solution U_N. For example, we could take $N=2$ and write the approximate solution of (2.2) in the form ($\phi_1=x^2-2x$, $\phi_2=x^3-3x$, $\phi_0=1$)

$$u\approx U_N=c_1(x^2-2x)+c_2(x^3-3x)+1$$

which satisfies the boundary conditions (2.2*b*) of the problem for any values of c_1 and c_2. The constants c_1 and c_2 are to be determined such that the approximate solution U_N in (2.3) satisfies (2.2*a*) in some sense. If we require U_N to satisfy (2.2*a*) in the exact sense, we obtain

$$-\frac{dU_N}{dx}-x\frac{d^2U_N}{dx^2}+U_N=-2c_1(x-1)-3c_2(x^2-1)-2c_1x-6c_2x^2$$
$$+c_1(x^2-2x)+c_2(x^3-3x)+1=0$$

Since this expression must be zero for any value of x, the coefficients of the various powers of x must be zero:

$$\begin{aligned}1+2c_1+3c_2&=0\\-(6c_1+3c_2)&=0\\c_1-9c_2&=0\\c_2&=0\end{aligned}$$

The above relations are inconsistent; hence, there is *no solution* to the equations. On the other hand, we can require the approximate solution U to satisfy the differential equation (2.2*a*) in the weighted-integral sense,

$$\int_0^1 wR\,dx=0 \tag{2.4a}$$

where R is called the *residual*,

$$R\equiv-\frac{dU_N}{dx}-x\frac{d^2U_N}{dx^2}+U_N$$

and w is called a *weight function*. From (2.4a), we obtain as many linearly independent equations as there are independent functions for w. For example, if we take $w = 1$ and $w = x$, we obtain

$$0 = \int_0^1 1R\,dx = (1 + 2c_1 + 3c_2) + \tfrac{1}{2}(-6c_1 - 3c_2) + \tfrac{1}{3}(c_1 - 9c_2) + \tfrac{1}{4}c_2$$

$$0 = \int_0^1 xR\,dx = \tfrac{1}{2}(1 + 2c_1 + 3c_2) + \tfrac{1}{3}(-6c_1 - 3c_2) + \tfrac{1}{4}(c_1 - 9c_2) + \tfrac{1}{5}c_2$$

or

$$\begin{aligned} \tfrac{2}{3}c_1 + \tfrac{5}{4}c_2 &= 1 \\ \tfrac{3}{4}c_1 + \tfrac{31}{20}c_2 &= \tfrac{1}{2} \end{aligned} \tag{2.4b}$$

which provide two linearly independent equations for c_1 and c_2 (giving $c_1 = \frac{222}{23}$ and $c_2 = -\frac{100}{23}$).

Thus, integral statements of the type in (2.4a) provide means for obtaining as many algebraic equations as there are unknown coefficients in the approximation. This chapter deals with the construction of different types of integral statements used in different variational methods. A variational method is one in which approximate solutions of the type $u \approx \sum_j c_j\phi_j + \phi_0$ are sought, and the coefficients c_j are determined, as shown above, using an integral statement. The variational methods differ from each other in the choice of the weight function w and the integral statement used, which in turn dictates the choice of the approximation functions ϕ_j. In the finite element method, a given domain is viewed as an assemblage of subdomains (i.e., elements), and an approximate solution is sought over each subdomain in the same way as in variational methods. Therefore, it is informative to study variational methods before we study the finite element method.

Our goal in this chapter is to illustrate the basic steps in the integral formulations and the associated approximations of various boundary problems. Toward this goal, we first introduce necessary terminology and notation.

2.2 SOME MATHEMATICAL CONCEPTS AND FORMULAE

2.2.1 Boundary, Initial, and Eigenvalue Problems

DOMAIN AND BOUNDARY. The objective of most analyses is to determine unknown functions, called *dependent variables*, that satisfy a given set of differential equations in a given domain or region and some boundary conditions on the boundary of the domain. A domain is a collection of points in space with the property that if P is a point in the domain then all points sufficiently close to P belong to the domain. This definition implies that a domain consists only of internal points. If any two points of the domain can be joined by a line lying entirely within it then the domain is said to be *convex* and *simply connected*. The boundary of a domain is the set of points such that, in any neighborhood of each of these points, there are points that belong to the domain as well as points that do not. Note from the definition that the points on the boundary do not belong to the domain. We shall use the symbol Ω to denote an arbitrary domain and Γ to denote its boundary.

A function of several variables is said to be of class $C^m(\Omega)$ in a domain Ω if all its partial derivatives up to and including the mth order exist and are *continuous* in Ω. Thus, if f is of class C^0 in two dimensions then f is continuous (i.e., $\partial f/\partial x$ and $\partial f/\partial y$ exist but may not be continuous). The letters x and y will always be used for rectangular coordinates of a point in two dimensions.

When the dependent variables are functions of one independent variable (say, x), the domain is a line segment (i.e., one-dimensional) and the endpoints of the domain are called boundary points. When the dependent variables are functions of two independent variables (say, x and y), the (two-dimensional) domain is a surface (most often a plane) and the boundary is the closed curve enclosing it. It is not uncommon to find problems in which the dependent variable and possibly its derivatives are specified at points interior to the domain (e.g., bending of continuous beams).

A differential equation is said to describe a *boundary value problem* if the dependent variable and possibly its derivatives are required to take specified values on the boundary. An *initial value problem* is one in which the dependent variable and possibly its derivatives are specified initially (i.e., at time $t=0$). Initial value problems are generally time-dependent problems. Examples of boundary and initial value problems are given below.

BOUNDARY VALUE PROBLEM

$$-\frac{d}{dx}\left(a\frac{du}{dx}\right)=f \quad \text{for } 0<x<1 \tag{2.5}$$

$$u(0)=d_0, \qquad \left(a\frac{du}{dx}\right)\bigg|_{x=1}=g_0 \tag{2.6}$$

INITIAL VALUE PROBLEM

$$\rho\frac{d^2u}{dt^2}+au=f \quad \text{for } 0<t\leqslant t_0 \tag{2.7}$$

$$u(0)=u_0, \qquad \left(\frac{du}{dt}\right)\bigg|_{t=0}=v_0 \tag{2.8}$$

BOUNDARY AND INITIAL VALUE PROBLEM

$$-\frac{\partial}{\partial x}\left(a\frac{\partial u}{\partial x}\right)+\rho\frac{\partial u}{\partial t}=f(x,t) \quad \text{for } \begin{cases}0<x<1\\ 0<t\leqslant t_0\end{cases} \tag{2.9}$$

$$u(0,t)=d_0(t), \qquad \left(a\frac{\partial u}{\partial x}\right)\bigg|_{x=1}=g_0(t), \qquad u(x,0)=u_0(x) \tag{2.10}$$

The conditions in (2.6) are called *boundary conditions,* while those in (2.8) are called *initial conditions.* When any of the specified values (i.e., d_0, g_0, u_0, and v_0) are nonzero, the conditions are said to be *nonhomogeneous*; otherwise, they are said to be *homogeneous.* For example, $u(0) = d_0$ is a nonhomogenous boundary condition, and the associated homogeneous boundary condition is $u(0) = 0$. The set of specified quantities (e.g., a, g_0, d_0, ρ, u_0, and v_0) is called the *data* of the problem. Differential equations in which the right-hand side f is zero are called *homogeneous differential equations.*

EIGENVALUE PROBLEM. The problem of determining the values of the constant λ such that

$$\begin{aligned} -\frac{d}{dx}\left(a\frac{du}{dx}\right) &= \lambda u \quad \text{for } 0<x<1 \\ u(0)=0, \quad \left(a\frac{du}{dx}\right)\bigg|_{x=1} &= 0 \end{aligned} \tag{2.11}$$

is called the *eigenvalue problem* associated with the differential equation (2.5). The values of λ for which (2.11) can be satisfied are called *eigenvalues,* and the associated functions u are called *eigenfunctions.*

The *classical* (or exact) *solution* of a differential equation is the function that identically satisfies the differential equation and the specified boundary and/or initial conditions.

2.2.2 Integral Relations

Integration by parts is frequently used in the integral formulation of differential equations. In two-dimensional cases, integration by parts is better known as the gradient and divergence theorems. In this section, we derive some useful identities for future use.

INTEGRATION-BY-PARTS FORMULAE. Let u, v, and w be sufficiently differentiable functions of the coordinate x. Then the following integration-by-parts formula holds:

$$\begin{aligned} \int_a^b w\frac{dv}{dx}\,dx &= \int_a^b w\,dv = -\int_a^b v\,dw + [wv]_a^b \\ &= -\int_a^b v\frac{dw}{dx}\,dx + w(b)v(b) - w(a)v(a) \end{aligned} \tag{2.12}$$

This identity can easily be established. First, note the following identity from the product rule of differentiation:

$$\frac{d}{dx}(wv) = \frac{dw}{dx}v + w\frac{dv}{dx}$$

Therefore

$$w\frac{dv}{dx}=\frac{d}{dx}(wv)-\frac{dw}{dx}v$$

Integrating both sides over the interval (a, b), we obtain

$$\begin{aligned}\int_a^b w\frac{dv}{dx}\,dx &= \int_a^b \left[\frac{d}{dx}(wv)-\frac{dw}{dx}v\right]dx\\ &= \int_a^b \frac{d}{dx}(wv)\,dx - \int_a^b \frac{dw}{dx}v\,dx\\ &= [wv]_a^b - \int_a^b \frac{dw}{dx}v\,dx\end{aligned}$$

which is the same as (2.12).

Next, consider the expression

$$\begin{aligned}\int_a^b w\frac{d^2u}{dx^2}\,dx &= \int_a^b w\frac{d}{dx}\left(\frac{du}{dx}\right)dx\\ &= \int_a^b w\frac{dv}{dx}\,dx, \qquad v\equiv\frac{du}{dx}\end{aligned}$$

Using (2.12), we obtain

$$\begin{aligned}\int_a^b w\frac{d^2u}{dx^2}\,dx &= -\int_a^b v\frac{dw}{dx}\,dx + w(b)v(b) - w(a)v(a)\\ &= -\int_a^b \frac{du}{dx}\frac{dw}{dx}\,dx + w(b)\frac{du}{dx}(b) - w(a)\frac{du}{dx}(a) \qquad (2.13a)\end{aligned}$$

or

$$-\int_a^b \frac{du}{dx}\frac{dw}{dx}\,dx = \int_a^b w\frac{d^2u}{dx^2}\,dx + w(a)\frac{du}{dx}(a) - w(b)\frac{du}{dx}(b) \qquad (2.13b)$$

Similarly,

$$\begin{aligned}\int_a^b v\frac{d^4w}{dx^4}\,dx &= \int_a^b v\frac{d^2}{dx^2}\left(\frac{d^2w}{dx^2}\right)dx\\ &= \int_a^b v\frac{d^2u}{dx^2}\,dx, \qquad \text{where } u\equiv\frac{d^2w}{dx^2}\end{aligned}$$

Using (2.13a) with $w=v$, we can write the right-hand side as

$$-\int_a^b \frac{du}{dx}\frac{dv}{dx}\,dx + v(b)\frac{du}{dx}(b) - v(a)\frac{du}{dx}(a) \qquad (2.14a)$$

We use (2.13b) with $w=u$ and $u=v$ to write (2.14a) as

$$\int_a^b u\frac{d^2v}{dx^2}\,dx + u(a)\frac{dv}{dx}(a) - u(b)\frac{dv}{dx}(b) + v(b)\frac{du}{dx}(b) - v(a)\frac{du}{dx}(a) \qquad (2.14b)$$

and, finally, replacing u by its actual value $u = d^2w/dx^2$, we arrive at

$$\int_a^b v\frac{d^4w}{dx^4}\,dx = \int_a^b \frac{d^2w}{dx^2}\frac{d^2v}{dx^2}\,dx + \frac{d^2w}{dx^2}(a)\frac{dv}{dx}(a) - \frac{d^2w}{dx^2}(b)\frac{dv}{dx}(b) + v(b)\frac{d^3w}{dx^3}(b) - v(a)\frac{d^3w}{dx^3}(a) \tag{2.15}$$

Equations (2.13*a*) and (2.15) are useful in the weak formulation (see Section 2.3) of second- and fourth-order differential equations, respectively.

Let ∇ and ∇^2 denote, respectively, the gradient operator and the Laplacian operator in the two-dimensional cartesian rectangular coordinate system (x, y):

$$\nabla = \hat{\mathbf{i}}\frac{\partial}{\partial x} + \hat{\mathbf{j}}\frac{\partial}{\partial y}, \qquad \nabla^2 = \nabla\cdot\nabla = \frac{\partial^2}{\partial x^2} + \frac{\partial^2}{\partial y^2} \tag{2.16}$$

where $\hat{\mathbf{i}}$ and $\hat{\mathbf{j}}$ denote the unit basis vectors along the x and y coordinates, respectively. The caret "$\hat{\ }$" over the vectors indicates that they are of unit length. If $F(x, y)$ and $G(x, y)$ are scalar functions of class $C^0(\Omega)$ in the two-dimensional domain Ω, the following gradient and divergence theorems hold.

GRADIENT THEOREM

$$\int_\Omega \operatorname{grad} F\,dx\,dy \equiv \int_\Omega \nabla F\,dx\,dy = \oint_\Gamma \hat{\mathbf{n}}F\,ds$$

or $\qquad$ (2.17*a*)

$$\int_\Omega \left(\hat{\mathbf{i}}\frac{\partial F}{\partial x} + \hat{\mathbf{j}}\frac{\partial F}{\partial y}\right)dx\,dy = \oint_\Gamma (n_x\hat{\mathbf{i}} + n_y\hat{\mathbf{j}})F\,ds$$

The second equation implies (because two vectors are equal if and only if their components are equal) that the following relations hold:

$$\int_\Omega \frac{\partial F}{\partial x}\,dx\,dy = \oint_\Gamma n_xF\,ds, \qquad \int_\Omega \frac{\partial F}{\partial y}\,dx\,dy = \oint_\Gamma n_yF\,ds \tag{2.17b}$$

DIVERGENCE THEOREM

$$\int_\Omega \operatorname{div}\mathbf{G}\,dx\,dy \equiv \int_\Omega \nabla\cdot\mathbf{G}\,dx\,dy = \oint_\Gamma \hat{\mathbf{n}}\cdot\mathbf{G}\,ds$$

or $\qquad$ (2.18)

$$\int_\Omega \left(\frac{\partial G_x}{\partial x} + \frac{\partial G_y}{\partial y}\right)dx\,dy = \oint_\Gamma (n_xG_x + n_yG_y)\,ds$$

Here the dot denotes the scalar product of vectors, $\hat{\mathbf{n}}$ denotes the unit vector normal to the surface Γ of the domain Ω, n_x and n_y (G_x and G_y) are the rectangular components of $\hat{\mathbf{n}}$ ($\mathbf{G}$), and the circle on the boundary integral

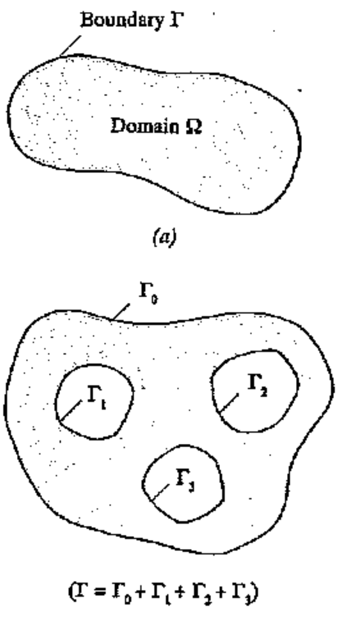

(b) FIGURE 2.1

indicates that the integration is taken over the entire boundary (see Fig. 2.1). The direction cosines n_x and n_y of the unit vector $\hat{\mathbf{n}}$ can be written as

$$n_x = \cos(x, \hat{\mathbf{n}}), \qquad n_y = \cos(y, \hat{\mathbf{n}}) \tag{2.19}$$

where $\cos(x, \hat{\mathbf{n}})$ is the cosine of the angle between the positive x direction and the unit vector $\hat{\mathbf{n}}$.

The following identities, which can be derived using the gradient and divergence theorems, will be useful in the sequel. Let w and G be scalar functions defined in a two-dimensional domain Ω. Then

$$\int_\Omega (\nabla G) w \, dx \, dy = -\int_\Omega (\nabla w) G \, dx \, dy + \int_\Gamma \hat{\mathbf{n}} w G \, ds \tag{2.20a}$$

and

$$\boxed{-\int_\Omega (\nabla^2 G) w \, dx \, dy = \int_\Omega \nabla w \cdot \nabla G \, dx \, dy - \oint_\Gamma \frac{\partial G}{\partial n} w \, ds} \tag{2.20b}$$

where $\partial/\partial n$ denotes the normal derivative operator,

$$\frac{\partial}{\partial n} = \hat{\mathbf{n}} \cdot \nabla = n_x \frac{\partial}{\partial x} + n_y \frac{\partial}{\partial y} \tag{2.21}$$

The following component form of (2.20*a*), with an appropriate change of variables, is useful in the sequel:

$$\boxed{\begin{aligned}\int_\Omega w\frac{\partial G}{\partial x}\,dx\,dy &= -\int_\Omega \frac{\partial w}{\partial x}G\,dx\,dy + \oint_\Gamma n_x wG\,ds \\ \int_\Omega w\frac{\partial G}{\partial y}\,dx\,dy &= -\int_\Omega \frac{\partial w}{\partial y}G\,dx\,dy + \oint_\Gamma n_y wG\,ds\end{aligned}} \qquad \begin{aligned}(2.22a)\\(2.22b)\end{aligned}$$

Equations (2.22*a*, *b*) can easily be established by means of (2.17*b*).

2.2.3 Functionals

An integral expression of the form

$$I(u) = \int_a^b F(x, u, u')\,dx, \qquad u = u(x), \qquad u' = \frac{du}{dx}$$

where the integrand $F(x, u, u')$ is a given function of the arguments x, u, and du/dx, is called a *functional*. The value $I(u)$ of the integral depends on u; hence the notation $I(u)$ is appropriate. However, for a given u, $I(u)$ represents a scalar value. We shall use the term *functional* to describe functions defined by integrals whose arguments themselves are functions. Loosely speaking, a functional is a "function of functions." Mathematically, a functional is an operator I mapping u into a scalar $I(u)$.

A functional $l(u)$ is said to be *linear* in u if and only if it satisfies the relation

$$l(\alpha u + \beta v) = \alpha l(u) + \beta l(v) \tag{2.23}$$

for any scalars α and β and dependent variables u and v. A functional $B(u, v)$ is said to be *bilinear* if it is linear in each of its arguments u and v:

$$\begin{aligned}&B(\alpha u_1 + \beta u_2, v) = \alpha B(u_1, v) + \beta B(u_2, v)\\ &\qquad\qquad\text{(linearity in the first argument)}\\ &B(u, \alpha v_1 + \beta v_2) = \alpha B(u, v_1) + \beta B(u, v_2)\\ &\qquad\qquad\text{(linearity in the second argument)}\end{aligned} \tag{2.24}$$

where u, u_1, u_2, v, v_1, and v_2 are dependent variables. A bilinear form $B(u, v)$ is said to be *symmetric* in its arguments u and v if

$$B(u, v) = B(v, u) \tag{2.25}$$

for all u and v.

An example of a linear functional is

$$l(v) = \int_0^L vf\,dx + \frac{dv}{dx}(L)M_0$$

where $f = f(x)$ and M_0 are known quantities. An example of a bilinear functional is

$$B(v, w) = \int_0^L a \frac{dv}{dx}\frac{dw}{dx}\, dx$$

where $a = a(x)$ is a known function.

2.2.4 The Variational Symbol

Consider the function $F = F(x, u, u')$. For an arbitrary fixed value of the independent variable x, F depends on u and u'. The change αv in u, where α is a constant and v is a function, is called the *variation* of u and is denoted by δu:

$$\delta u = \alpha v \tag{2.26}$$

The operator δ is called the *variational symbol*. The variation δu of a function u represents an admissible change in the function $u(x)$ at a *fixed* value of the independent variable x. If u is specified at a point (usually on the boundary), the variation of u is zero there because the specified value cannot be varied. thus the variation of a function u should satisfy the homogeneous form of the boundary conditions for u. The variation δu in u is a *virtual* change. Associated with this change in u (i.e., u going to $u + \alpha v$), there is a change in F. In analogy with the total differential of a function of two variables, the *first variation* of F at u is defined by

$$\delta F = \frac{\partial F}{\partial u}\delta u + \frac{\partial F}{\partial u'}\delta u' \tag{2.27}$$

Note the analogy between the first variation, (2.27), and the total differential of F,

$$dF = \frac{\partial F}{\partial x}dx + \frac{\partial F}{\partial u}du + \frac{\partial F}{\partial u'}du' \tag{2.28}$$

Since x is not varied during the variation of u to $u + \delta u$, $dx = 0$ and the analogy between ∂F and dF becomes apparent. That is, δ *acts as a differential operator with respect to dependent variables.* It can easily be verified that the laws of variation of sums, products, ratios, powers, and so forth are completely analogous to the corresponding laws of differentiation. For example, if $F_1 = F_1(u)$ and $F_2 = F_2(u)$ then

$$\begin{aligned}
&1.\ \delta(F_1 \pm F_2) = \delta F_1 \pm \delta F_2\\
&2.\ \delta(F_1F_2) = F_2\,\delta F_1 + F_1\,\delta F_2\\
&3.\ \delta\left(\frac{F_1}{F_2}\right) = \frac{F_2\,\delta F_1 - F_1\,\delta F_2}{F_2^2}\\
&4.\ \delta[(F_1)^n] = n(F_1)^{n-1}\,\delta F_1
\end{aligned} \tag{2.29}$$

Furthermore, the variational operator can commute with differential and integral operators (as long as the coordinates x and y are the fixed, Lagrangian coordinates):

$$\frac{d}{dx}(\delta u) = \frac{d}{dx}(\alpha v) = \alpha \frac{dv}{dx} = \alpha v' = \delta u' = \delta\left(\frac{du}{dx}\right) \tag{2.30a}$$

$$\delta \int_a^b u(x)\,dx = \int_a^b \delta u(x)\,dx \tag{2.30b}$$

2.3 WEAK FORMULATION OF BOUNDARY VALUE PROBLEMS

2.3.1 Introduction

Recall from Section 2.1 that the motivation for integral formulations of boundary value problems comes from the fact that variational methods of approximation, e.g., the Ritz, Galerkin, least-squares, collocation, or, in general, weighted-residual methods, are based on weighted-integral statements of the governing equations. Since the finite element method is a technique for constructing approximation functions required in an element-wise application of any variational method, it is necessary to study the weighted-integral formulation and the weak formulation of differential equations. In addition to the above reason, weak formulations also facilitate, in a natural way, the classification of boundary conditions into *natural* and *essential* boundary conditions, which play a crucial role in the derivation of the approximation functions and the selection of the nodal degrees of freedom of the finite element model.

In this section, our primary objectives will be to construct the weak form of a given differential equation and to classify the boundary conditions associated with the equation. A *weak form* is a weighted-integral statement of a differential equation in which the differentiation is distributed among the dependent variable and the weight function and includes the natural boundary conditions of the problem.

2.3.2 Weighted-Integral and Weak Formulations

Consider the problem of solving the differential equation

$$-\frac{d}{dx}\left[a(x)\frac{du}{dx}\right] = q(x) \quad \text{for } 0 < x < L \tag{2.31a}$$

for the solution $u(x)$, subject to the boundary conditions

$$u(0) = u_0, \qquad \left(a\frac{du}{dx}\right)\bigg|_{x=L} = Q_0 \tag{2.31b}$$

Here a and q are known functions of the coordinate x, u_0 and Q_0 are known values, and L is the length of the one-dimensional domain. The functions a and q, and constants u_0 and Q_0, along with the length L of the domain, are the data of the problem. The solution u is the *dependent variable* of the problem. When the specified values are nonzero ($u_0 \neq 0$ or $Q_0 \neq 0$), the boundary conditions are said to be nonhomogeneous; when the specified values are zero the boundary conditions are said to be homogeneous. The homogeneous form of the boundary condition $u(0) = u_0$ is $u(0) = 0$, and the homogeneous form of the boundary condition $(a\,du/dx)|_{x=L} = Q_0$ is $(a\,du/dx)|_{x=L} = 0$.

Equations of the type (2.31*a*) arise, for example, in the study of heat conduction in a heat exchanger fin or a long axisymmetric cylinder. Other examples are included in Table 3.2. In the former case, $a = kA$, with k being the thermal conductivity and A the cross-sectional area, and L being the length of the fin. For the axisymmetric case, $a = 2\pi Lkx$, x being the radial coordinate r and L the length of the cylinder (see Fig. 1.4). In both cases, q denotes the heat generation term, u_0 is the specified temperature, and Q_0 is the specified heat. Other physical problems are also described by the same equation, but with different meanings for the variables (see Table 3.2).

It should be recalled that the sole purpose of developing a weighted-integral statement of a differential equation is to have the means to obtain N linearly independent algebraic relations among the coefficients c_j of the approximation

$$u \approx U_N = \sum_{j=1}^{N} c_j \phi_j(x) + \phi_0(x) \tag{2.32}$$

This is accomplished by choosing N linearly independent weight functions in the integral statement, as will be seen shortly.

There are three steps in the development of the weak form, if it exists, of any differential equation. These steps are illustrated by means of the model differential equation and boundary conditions in (2.31).

Step 1. Move all expressions of the differential equation to one side, multiply the entire equation with a function w, called the *weight function,* and integrate over the domain $\Omega = (0, L)$ of the problem:

$$0 = \int_0^L w\left[-\frac{d}{dx}\left(a\frac{du}{dx}\right) - q\right] dx \tag{2.33}$$

We shall call the statement in (2.33) the *weighted-integral* or *weighted-residual* statement equivalent to the original equation (2.31a). The expression in the square brackets is not identically zero when u is replaced by its approximation. Mathematically, (2.33) is a statement that the error in the differential equation (due to the approximation of the solution) is zero in the weighted-integral sense. When u is the exact solution, (2.33) is trivial. The integral statement (2.33) allows us to choose N linearly independent functions for w and obtain N equations for $c_1, c_2, \ldots, c_N$ of (2.32).

Note that the weighted-integral statement of any differential equation can be developed. The weight function w in (2.33) can be any nonzero, integrable function. In general, the weight function w in the integral statement is subject to less stringent continuity requirements than the dependent variable u. The weighted-integral statement is equivalent only to the differential equation, and it does not include any boundary conditions.

Step 2. While the weighted-integral statement (2.33) allows us to obtain the necessary number N of algebraic relations among c_j for N different choices of the weight function w, it requires that the approximation functions ϕ_j be such that U_N [see (2.32)] is differentiable as many times as called for in the original differential equation and satisfies the specified boundary conditions. If this is not a concern, one can proceed with the integral statement (2.33) and obtain the necessary algebraic equations for c_j. Approximate methods based on weighted-integral statements of the form (2.33) are known as *weighted-residual* methods (see Section 2.4.3). If the differentiation is distributed between the approximate solution U_N and the weight function w, the resulting integral form will require weaker continuity conditions on ϕ_j, and hence the weighted-integral statement is called the *weak form*. As will be seen shortly, the weak formulation has two desirable characteristics. First, it requires weaker (i.e., less) continuity of the dependent variable, and often it results in a symmetric set of algebraic equations in the coefficients. Second, the *natural* boundary conditions of the problem are included in the weak form, and therefore the approximate solution U_N is required to satisfy only the *essential* boundary conditions of the problem. These two features of a weak form play an important role in the development of finite element models of a problem.

The equal distribution of differentiation among the weight function and the dependent variable is possible only if the derivatives appearing in the differential equation are of even order, as is the case with most problems studied in this book. The trading of differentiability from the dependent variable to the weight function is dictated by the need to include physically meaningful boundary terms into the weak form, regardless of the effect on the continuity requirements. On the other hand, trading of differentiation from the dependent variable to the weight function should not be performed if it leads to boundary terms that are not physically meaningful.

Returning to the integral statement (2.33), we integrate the first term of the expression by parts to obtain

$$\begin{aligned} 0 &= \int_0^L \left\{ w\left[-\frac{d}{dx}\left(a\frac{du}{dx}\right)\right] - wq \right\} dx \\ &= \int_0^L \left(\frac{dw}{dx}a\frac{du}{dx} - wq\right) dx - \left[wa\frac{du}{dx}\right]_0^L \end{aligned} \tag{2.34}$$

where the integration-by-parts formula [see (2.12) or (2.13a)]

$$\int_0^L w\,dv = -\int_0^L v\,dw + [wv]_0^L \tag{2.35}$$

with $v = -a\,du/dx$ is used on the first term to arrive at the second line of (2.34). The reader is asked to verify (2.34) either directly or by the use of (2.35). Note that now the weight function w is required to be differentiable at least once.

An important part of Step 2 is to identify the two types of boundary conditions associated with *any* differential equation: *natural* and *essential*. The classification is important for both the variational methods of approximation considered in this chapter and the finite element formulations presented in Chapters 3–5. The following rule is used to identify the natural boundary conditions and their form. After trading differentiation between the weight function and the variable, i.e., after completing Step 2, examine all boundary terms of the integral statement. The boundary terms will involve both the weight function and the dependent variable. Coefficients of the weight function and its derivatives in the boundary expressions are termed the *secondary variables* (SV). Specification of secondary variables on the boundary constitutes the *natural boundary conditions* (NBC). For the case at hand, the boundary term is $w(a\,du/dx)$. The coefficient of the weight function is $a\,du/dx$. Hence the secondary variable is of the form [see (2.34)] $a\,du/dx$.

The secondary variables always have physical meaning, and are often quantities of interest. In the case of heat transfer problems, the secondary variable represents heat, Q. We shall denote the secondary variable by

$$Q \equiv \left(a\frac{du}{dx}\right)n_x \tag{2.36}$$

where n_x denotes the direction cosine,

n_x = cosine of the angle between the x axis and the normal to the boundary

For one-dimensional problems, the normal at the boundary points is always along the length of the domain. Thus, $n_x = -1$ at the left end and $n_x = 1$ at the right end of the domain: $n_x(0) = -1$ and $n_x(L) = 1$.

The dependent variable of the problem, expressed in the same form as the weight function appearing in the boundary term, is called the *primary variable* (PV), and its specification on the boundary constitutes the *essential boundary condition* (EBC). For the case under consideration, the weight function appears in the boundary expression [see (2.34)] as w. Therefore, the dependent variable u is the primary variable, and the essential boundary condition involves specifying u at the boundary points.

It should be noted that the number and form of the primary and secondary variables depend on the order of the differential equation. The number of primary and secondary variables is always the same, and with each primary variable there is an associated secondary variable (e.g., displacement and force, temperature and heat, and so on). Only one of the pair, either the primary or the secondary variable, may be specified at a point of the boundary. Thus, a given problem can have its specified boundary conditions in one of three categories: (i) all specified boundary conditions are EBC; (ii) some of the specified boundary conditions are EBC and the remaining are NBC; or (iii) all specified boundary conditions are NBC. For a single second-order equation, as in the present case, there is one primary variable u and one secondary variable Q. At a boundary point, only one of the pair (u, Q) can be specified. For a fourth-order equation, such as that for the classical (i.e., Euler–Bernoulli) theory of beams, there are two of each kind (i.e., two PVs and two SVs), as will be illustrated later (see Example 2.2). In general, a $2m$th-order differential equation has m PVs and m SVs, i.e., m pairs of primary and secondary variables.

In the notation of (2.36), (2.34) takes the form

$$\begin{aligned}0 &= \int_0^L \left(a\frac{dw}{dx}\frac{du}{dx} - wq\right) dx - \left[wa\frac{du}{dx}\right]_0^L\\ &= \int_0^L \left(a\frac{dw}{dx}\frac{du}{dx} - wq\right) dx - \left(wa\frac{du}{dx}n_x\right)\bigg|_{x=0} - \left(wa\frac{du}{dx}n_x\right)\bigg|_{x=L}\\ &= \int_0^L \left(a\frac{dw}{dx}\frac{du}{dx} - wq\right) dx - (wQ)_0 - (wQ)_L \qquad (2.37)\end{aligned}$$

Equation (2.37) is called the *weak form* of the differential equation (2.31). "Weak" refers to the reduced (i.e., weakened) continuity of u, which is required to be twice-differentiable in the weighted-integral form (2.33) but only once-differentiable in (2.37).

Step 3. The third and last step of the weak formulation is to impose the actual boundary conditions of the problem under consideration. It is here that we require the weight function w to vanish at boundary points where the essential boundary conditions are specified; i.e., w is required to satisfy the *homogeneous form* of the specified essential boundary conditions of the problem. This requirement on w might seem arbitrary for a reader not familiar with variational calculus. In weak formulations, the weight function has the meaning of a *virtual* change (or variation) of the primary variable. If a primary variable is specified at a point, the virtual change there must be zero. For more detailed discussions of this, the reader may consult books on variational methods [see Reddy (1986)]. For the problem at hand, the boundary conditions are given in (2.31*b*). By the rules of classification of the boundary conditions, $u = u_0$ is the essential boundary condition and $(a\, du/dx)|_{x=L} = Q_0$ is the natural boundary condition. Thus, the weight function w is required to satisfy

$$w(0) = 0, \quad \text{because } u(0) = u_0$$

Since $w(0) = 0$ and

$$Q(L) = \left(a\frac{du}{dx}n_x\right)\bigg|_{x=L} = \left(a\frac{du}{dx}\right)\bigg|_{x=L} = Q_0$$

(2.37) reduces to the expression

$$0=\int_0^L \left(a\frac{dw}{dx}\frac{du}{dx}-wq\right)dx-w(L)Q_0 \tag{2.38}$$

which is the weak form equivalent to the original differentiatl equation (2.31*a*) and the natural boundary condition (2.31*b*). This completes the steps involved in the development of the weak or *variational form* of a differential equation.

The terms "variational form" and "weak form" will be used interchangeably. The weak form of a differential equation is a weighted-integral statement equivalent to the differential equation *and* the specified natural boundary conditions of the problem. Note that the weak form exists for all problems—linear or nonlinear—that are described by second- and higher-order differential equations. When the differential equation is linear and of even order, the resulting weak form will have a *symmetric* bilinear form in the dependent variable u and weight function w.

In summary, there are three steps in the development of a weak form. In the first, we put all expressions of the differential equation on one side (so that the other side is equal to zero), then multiply the entire equation by a weight function and integrate over the domain of the problem. The resulting expression is called the *weighted-integral form* of the equation. In the second step, we use integration by parts to distribute differentiation evenly between the dependent variable and the weight function, and use the boundary terms to identify the form of the primary and secondary variables. In the third step, we modify the boundary terms by restricting the weight function to satisfy the homogeneous form of the specified essential boundary conditions and replacing the secondary variables by their specified values.

It should be recalled that a weighted-integral statement or the weak form of a differential equation is needed to obtain as many algebraic equations as there are unknown coefficients in the approximation of the dependent variables of the equation. For different choices of the weight function, different algebraic equations can be obtained. Because of the restrictions placed on the weight function in Step 3 of the variational formulation, it must belong to the same space of functions as the approximation functions (i.e., $w \sim \phi_i$).

2.3.3 Linear and Bilinear Forms and Quadratic Functionals

It is informative, although not necessary for the use of variational methods or the finite element method, to see the relation between the weak form and the minimum of a quadratic functional associated with the differential equation. The weak form (2.38) contains two types of expressions: those involving both the dependent variable u and the weight function w, and those involving only the latter. We shall denote these two types of expressions by $B(w, u)$ and $l(w)$, respectively:

$$B(w, u) = \int_0^L a \frac{dw}{dx}\frac{du}{dx}\,dx, \qquad l(w) = \int_0^L wq\,dx + w(L)Q_0 \tag{2.39}$$

Hence, the weak statement (2.38) can be expressed in the form

$$0 = B(w, u) - l(w) \tag{2.40}$$

which is termed the *variational* (or weak) *problem* associated with the equations (2.31). Using the definitions of linear and bilinear forms from Section 2.2.3, it can be verified that $B(w, u)$ is bilinear and symmetric in w and u and that $l(w)$ is linear [see (2.23) and (2.24)]. The *variational problem* associated with (2.31*a*, *b*) can be stated as one of finding the solution u such that

$$B(w, u) = l(w) \tag{2.41}$$

holds for any w that satisfies the homogeneous form of the specified essential boundary conditions and continuity conditions implied by the weak form. The function w can be viewed as a variation (or increment) of the actual solution u^*,

$$u = u^* + w \tag{2.42}$$

and u is the variational solution, i.e., the solution of (2.41). Since both u and u^* must satisfy any specified essential boundary condition (in addition, u^* also satisfies any specified natural boundary condition), it follows that w must satisfy the homogeneous form of the specified essential boundary condition. Thus, in the notation of (2.26), w is the variation (see Section 2.2.4) of the solution:

$$w = \delta u$$

Then (2.40) can be written as

$$0 = B(\delta u, u) - l(\delta u)$$

If $B(\cdot\,,\ \cdot)$ is symmetric, we can write

$$\begin{aligned} &= \delta[\tfrac{1}{2}B(u, u)] - \delta[l(u)] \\ &= \delta I(u) \end{aligned} \tag{2.43a}$$

where

$$\boxed{I(u) = \tfrac{1}{2}B(u, u) - l(u)} \tag{2.43b}$$

In arriving at the second line of (2.43*a*), the following identities are used:

$$\begin{aligned} B(\delta u, u) &= \int_0^L a \frac{d\delta u}{dx}\frac{du}{dx}\,dx = \delta \int_0^L \frac{a}{2}\left[\left(\frac{du}{dx}\right)^2\right] dx \\ &= \tfrac{1}{2}\delta \int_0^L a \frac{du}{dx}\frac{du}{dx}\,dx = \tfrac{1}{2}\,\delta[B(u, u)] \end{aligned} \tag{2.44a}$$

$$
\begin{aligned}
l(\delta u) &= \int_0^L \delta u\, q\, dx + \delta u(L)\, Q_0 \\
&= \delta\left[\int_0^L uq\, dx + u(L)Q_0\right] = \delta[l(u)] \qquad (2.44b)
\end{aligned}
$$

Note that the key step in the derivation of the functional $I(u)$ from the weak form is the linearity and symmetry of the bilinear form $B(w, u)$. The relation $B(\delta u, u) = \frac{1}{2}\,\delta B(u, u)$ holds only if $B(w, u)$ is bilinear and symmetric in w and u. Thus, whenever $B(w, u)$ is bilinear and symmetric, and $l(w)$ is linear, the associated quadratic functional is given by (2.43*b*). When $B(w, u)$ is not linear in w and u, but is symmetric, the functional $I(u)$ can be derived, but not from (2.43*b*). The interested reader can consult the books by Oden and Reddy (1976) and Reddy (1986).

Equation (2.43*a*) represents the necessary condition for the functional $I(u)$ to have an extremum value. For solid mechanics problems, $I(u)$ represents the total potential energy functional, and (2.43*a*) is the statement of the *total potential energy principle*:

> Of all admissible functions u, that which makes the total potential energy $I(u)$ a minimum also satisfies the differential equation and natural boundary condition in (2.31).

In other words, the weak form of a differential equation is the same as the statement of the total potential energy principle. For problems outside solid mechanics, the functional $I(u)$ may not have the meaning of energy, but it is still useful for mathematical analysis (e.g., in considering the existence and uniqueness of solutions).

As noted earlier, every differential equation admits a weighted-integral statement, and a weak form exists provided the equation is of order two or higher. However, not all equations admit the functional formulation. In order for the functional to exist, the associated bilinear form should be symmetric in its arguments. On the other hand, variational methods and the finite element method do not require a functional; an integral statement or a weak form of the equation to be solved is sufficient. If one has a functional at hand, the weak form is obtained by taking its first variation.

2.3.4 Examples

Now we consider some representative examples of differential equations in one and two dimensions, and formulate their variational equations. These examples are of primary interest in the study of the finite element method.

Example 2.1. Consider the differential equation

$$
-\frac{d}{dx}\left(a\frac{du}{dx}\right) - cu + x^2 = 0 \quad \text{for } 0 < x < 1 \qquad (2.45a)
$$

subject to the boundary conditions

$$u(0)=0, \qquad \left(a\frac{du}{dx}\right)\bigg|_{x=1}=1 \tag{2.45b}$$

The data are [cf. (2.31)] $q=-x^2$, $Q_0=1$, and $u_0=0$.

Following the three steps outlined above for the construction of variational statements, we obtain

$$\begin{aligned}
&(1)\quad 0=\int_0^1 w\left[-\frac{d}{dx}\left(a\frac{du}{dx}\right)-cu+x^2\right]dx \\
&(2)\quad 0=\int_0^1\left(a\frac{dw}{dx}\frac{du}{dx}-cwu+wx^2\right)dx-\left(wa\frac{du}{dx}\right)\bigg|_0^1
\end{aligned} \tag{2.46}$$

From the boundary term, it is clear that the specification of u is an essential boundary condition, and the specification of $a\,du/dx$ is a natural boundary condition. Since $a\,du/dx=1$ at $x=1$ and $w=0$ at $x=0$ (because u is specified there), we obtain the weak form

$$(3)\quad 0=\int_0^1\left(a\frac{dw}{dx}\frac{dv}{dx}-cwu\right)dx+\int_0^1 wx^2\,dx-w(1) \tag{2.47a}$$

$$0=B(w,u)-l(w) \tag{2.47b}$$

where

$$\begin{aligned}
B(w,u)&=\int_0^1\left(a\frac{dw}{dx}\frac{du}{dx}-cwu\right)dx \\
l(w)&=-\int_0^1 wx^2\,dx+w(1)
\end{aligned} \tag{2.47c}$$

Since $B(\cdot,\cdot)$ is bilinear and symmetric, and $l(\cdot)$ is linear, we can compute the quadratic functional from (2.43):

$$I(u)=\frac{1}{2}\int_0^1\left[a\left(\frac{du}{dx}\right)^2-cu^2+2ux^2\right]dx-u(1) \tag{2.48}$$

Equations of the type of (2.45) arise in the study of the deflection of a cable or of heat transfer in a fin ($c=0$). In the former case, u denotes the transverse deflection and a the tension in the cable. The first two terms in the quadratic functional represent the elastic strain energy, while the last term represents the work done by the distributed force in moving through the displacement u.

The next example illustrates the variational formulation of a fourth-order differential equation in one dimension.

Example 2.2. Consider the problem of finding the solution w to the differential equation

$$\frac{d^2}{dx^2}\left[b(x)\frac{d^2w}{dx^2}\right]-f(x)=0 \quad \text{for } 0<x<L \tag{2.49}$$

subject to the boundary conditions

$$w(0)=\left(\frac{dw}{dx}\right)\bigg|_{x=0}=0, \qquad \left(b\frac{d^2w}{dx^2}\right)\bigg|_{x=L}=M_0, \qquad \left[\frac{d}{dx}\left(b\frac{d^2w}{dx^2}\right)\right]\bigg|_{x=L}=0 \tag{2.50}$$

This equation arises, for example, in the study of the elastic bending of beams (under the Euler–Bernoulli hypothesis). In this case, w denotes the transverse deflection of the beam, L is the total length of the beam, $b(x) \geqslant 0$ is the flexural rigidity of the beam (i.e., the product of modulus of elasticity E and moment of inertia I: $b = EI$), $f(x)$ is the transverse distributed load, and M_0 is the bending moment. The solution w is the *dependent variable* of the problem, and all other quantities (L, b, f, M_0) that are known in advance are the *data* of the problem.

Since the equation contains a fourth-order derivative, we should integrate it twice by parts to distribute the derivatives equally between the dependent varaible w and the weight function v. In this case, v must be twice differentiable and satisfy the homogeneous form of EBC. Multiplying (2.49) by v, and integrating the first term by parts twice with respect to x, we obtain [see (2.15)]

$$0=\int_0^L v\left[\frac{d^2}{dx^2}\left(b\frac{d^2w}{dx^2}\right)-f\right]dx \tag{2.51}$$

$$\begin{aligned}0&=\int_0^L\left[\left(-\frac{dv}{dx}\right)\frac{d}{dx}\left(b\frac{d^2w}{dx^2}\right)-vf\right]dx+\left[v\frac{d}{dx}\left(b\frac{d^2w}{dx^2}\right)\right]\Bigg|_0^L\\&=\int_0^L\left(b\frac{d^2v}{dx^2}\frac{d^2w}{dx^2}-vf\right)dx+\left[v\frac{d}{dx}\left(b\frac{d^2w}{dx^2}\right)-\frac{dv}{dx}b\frac{d^2w}{dx^2}\right]\Bigg|_0^L\end{aligned} \tag{2.52}$$

From the last line, it follows that the specification of w and dw/dx constitutes the essential (geometric or static) boundary conditions, and the specification of

$$\frac{d}{dx}\left(b\frac{d^2w}{dx^2}\right)\equiv V \text{ (shear force)} \tag{2.53a}$$

and

$$b\left(\frac{d^2w}{dx^2}\right)\equiv M \text{ (bending moment)} \tag{2.53b}$$

constitutes the natural boundary conditions. In the present case, the specified essential boundary conditions are (because of the clamped condition)

$$w(0)=\left(\frac{dw}{dx}\right)\bigg|_{x=0}=0$$

Hence, the weight function v is required to satisfy the conditions

$$v(0)=\left(\frac{dv}{dx}\right)\bigg|_{x=0}=0 \tag{2.54}$$

The natural boundary conditions are

$$\left[\frac{d}{dx}\left(b\frac{d^2w}{dx^2}\right)\right]_{x=L}=0, \quad \left(b\frac{d^2w}{dx^2}\right)\bigg|_{x=L}=M_0 \tag{2.55}$$

Using (2.54) and (2.55) in (2.52), we obtain

$$0=\int_0^L\left(b\frac{d^2v}{dx^2}\frac{d^2w}{dx^2}-vf\right)dx-\left(\frac{dv}{dx}\right)\bigg|_{x=L}M_0 \tag{2.56a}$$

or

$$B(v,w)=l(v) \tag{2.56b}$$

where

$$B(v, w) = \int_0^L b \frac{d^2 v}{dx^2} \frac{d^2 w}{dx^2}\, dx$$

$$l(v) = \int_0^L vf\, dx + \left(\frac{dv}{dx}\right)\bigg|_{x=L} M_0 \tag{2.56c}$$

The quadratic form, commonly known as the *total potential energy* of the beam, is obtained using (2.56*c*) and (2.43*b*):

$$I(w) = \int_0^L \left[\frac{b}{2}\left(\frac{d^2 w}{dx^2}\right)^2 - wf\right] dx - \left(\frac{dw}{dx}\right)\bigg|_{x=L} M_0 \tag{2.57}$$

Note that for the fourth-order equation, the essential boundary conditions involve not only the dependent variable but also its first derivative. As pointed out earlier, at any boundary point, only one of the two boundary conditions (essential or natural) can be specified. For example, if the transverse deflection is specified at a boundary point then one cannot specify the shear force V at the same point, and vice versa. Similar comments apply to the slope dw/dx and the bending moment M. Note that in the present case, w and dw/dx are the primary variables, and V and M are the secondary variables.

The next example is concerned with a second-order differential equation governing conductive and convective heat transfer in two dimensions. It should be noted that the boundary condition for a convective boundary contains both primary and secondary variables.

Example 2.3. Consider steady heat conduction in a two-dimensional domain Ω, enclosed by lines AB, BC, CD, DE, EF, FG, GH, and HA (see Fig. 2.2). The governing equation is

$$-k\left(\frac{\partial^2 T}{\partial x^2} + \frac{\partial^2 T}{\partial y^2}\right) = q_0 \quad \text{in } \Omega \tag{2.58}$$

where q_0 is the uniform heat generation, k is the conductivity of the isotropic material of the domain, and T is the temperature. We wish to construct the weak form of the

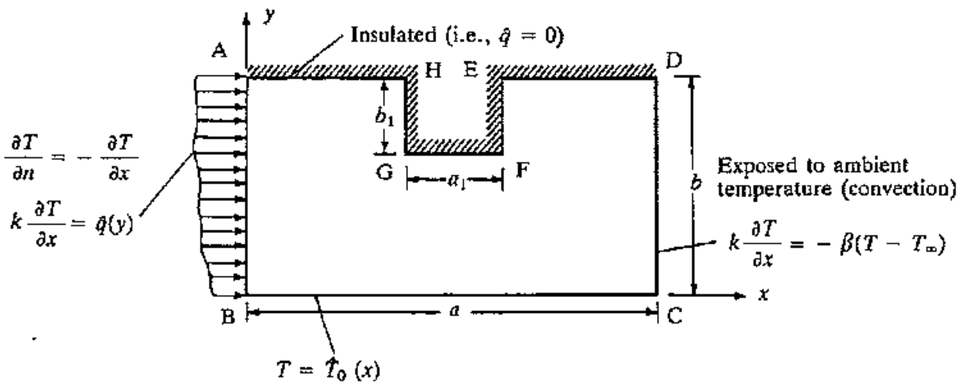

y
Insulated (i.e., $\hat{q} = 0$)
A
H
E
D
b_1
G
a_1
F
$\frac{\partial T}{\partial n} = -\frac{\partial T}{\partial x}$
$k\frac{\partial T}{\partial x} = \hat{q}(y)$
b
Exposed to ambient temperature (convection)
$k\frac{\partial T}{\partial x} = -\beta(T - T_\infty)$
x
B
a
C
$T = \hat{T}_0(x)$

FIGURE 2.2
Conduction and convection heat transfer in two-dimensional domains.

equation. Equation (2.58), known as the Poisson equation, arises in many fields of engineering (see Table 8.1).

Proceeding as described earlier, we have

$$0=\int_\Omega w\left[-k\left(\frac{\partial^2 T}{\partial x^2}+\frac{\partial^2 T}{\partial y^2}\right)-q_0\right]dx\,dy$$

where w denotes the weight function. Using (2.22) [with $G=\partial T/\partial x$ in (2.22a) and $G=\partial T/\partial y$ in (2.22b)], we obtain

$$0=\int_\Omega\left[k\left(\frac{\partial w}{\partial x}\frac{\partial T}{\partial x}+\frac{\partial w}{\partial y}\frac{\partial T}{\partial y}\right)-wq_0\right]dx\,dy-\oint_\Gamma wk\left(\frac{\partial T}{\partial x}n_x+\frac{\partial T}{\partial y}n_y\right)ds \tag{2.59}$$

The reader should verify the last step [i.e. the application of (2.22)]. From the boundary expression, it follows that the secondary variable of the problem is of the form

$$k\left(\frac{\partial T}{\partial x}n_x+\frac{\partial T}{\partial y}n_y\right)=k\frac{\partial T}{\partial n}\equiv q_n$$

and the primary variable is T. The secondary variable q_n denotes the total flux across (i.e., along the normal to) the boundary. In general, q_n is composed of fluxes due to conduction, convection, and radiation.

The boundary Γ of the domain consists of several line segments, and they are subject to different types of boundary conditions (see Fig. 2.2):

on $\Gamma_1=\text{AB}$ $(n_x=-1,\ n_y=0)$: specified heat flux, $\hat{q}(y)$
on $\Gamma_2=\text{BC}$ $(n_x=0,\ n_y=-1)$: specified temperature, $\hat{T}_0(x)$
on $\Gamma_3=\text{CD}$ $(n_x=1,\ n_y=0)$: convective boundary with ambient temperature T_∞ and film coefficient β; $k\,\partial T/\partial n+\beta(T-T_\infty)=0$ (2.60)
on $\Gamma_4=\text{DEFGHA}$: insulated boundary, $\partial T/\partial n=0$

Using the boundary information, the boundary integral in (2.59) can be simplified as follows (note that $w=0$ on Γ_2):

$$\begin{aligned}\oint_\Gamma w\left(k\frac{\partial T}{\partial n}\right)ds&=\int_{\Gamma_1} wq_n\,ds+\int_{\Gamma_2}0\left(k\frac{\partial T}{\partial n}\right)ds\\&\quad-\int_{\Gamma_3} w[\beta(T-T_\infty)]\,ds+\int_{\Gamma_4} w0\,ds\\&=-\int_0^b w(0,y)\hat{q}(y)\,dy-\beta\int_0^b w(a,y)[T(a,y)-T_\infty]\,dy\end{aligned} \tag{2.61}$$

Substituting (2.61) into (2.59), we obtain the weak form

$$\begin{aligned}0=&\int_\Omega\left[k\left(\frac{\partial w}{\partial x}\frac{\partial T}{\partial x}+\frac{\partial w}{\partial y}\frac{\partial T}{\partial y}\right)-wq_0\right]dx\,dy+\int_0^b w(0,y)\hat{q}(y)\,dy\\&+\beta\int_0^b w(a,y)[T(a,y)-T_\infty]\,dy\end{aligned} \tag{2.62}$$

Collecting terms involving both w and T into $B(\cdot,\cdot)$, and those involving only w into $l(\cdot)$, we can write (2.62) in the form

$$B(w,T)=l(w) \tag{2.63a}$$

where

$$\begin{aligned} B(w, T) &= \int_\Omega k\left(\frac{\partial w}{\partial x}\frac{\partial T}{\partial x} + \frac{\partial w}{\partial y}\frac{\partial T}{\partial y}\right) dx\, dy + \beta \int_0^b w(a, y)T(a, y)\, dy \\ l(w) &= \int_\Omega w q_0\, dx\, dy - \int_0^b w(0, y)\hat{q}(y)\, dy + \beta \int_0^b w(a, y)T_\infty\, dy \end{aligned} \tag{2.63b}$$

The quadratic functional is given by

$$\begin{aligned} I(T) = \frac{k}{2}\int_\Omega \left[\left(\frac{\partial T}{\partial x}\right)^2 + \left(\frac{\partial T}{\partial y}\right)^2\right] dx\, dy - \int_\Omega T q_0\, dx\, dy \\ + \int_0^b T(0, y)\hat{q}(y)\, dy + \beta \int_0^b \tfrac{1}{2}[T^2(a, y) - 2T(a, y)T_\infty]\, dy \end{aligned} \tag{2.63c}$$

Note that the boundary integrals in this example are defined along the y and x axes, respectively. This is because the boundaries are parallel to either the x or the y axis.

2.4 VARIATIONAL METHODS OF APPROXIMATION

2.4.1 Introduction

Our objective in this section is to study the variational methods of approximation. These include the Rayleigh–Ritz, Galerkin, Petrov–Galerkin, least-squares, and collocation methods. In all these, we seek an approximate solution in the form of a linear combination of suitable approximation functions ϕ_j and undetermined parameters c_j: $\Sigma_j c_j \phi_j$. The parameters c_j are determined such that the approximate solution satisfies the weighted-integral form or weak form of the governing equation or minimizes the quadratic functional associated with the equation studied. Various methods differ from each other in the choice of weight function w and approximation functions ϕ_j.

The primary objective of this section is to present a number of classical variational methods. The finite element method makes use of variational methods to formulate the discrete equations over an element. As we shall see in Chapters 3–14, the choice of the approximation functions in the finite element methods is different from that in the classical variational methods.

2.4.2 The Rayleigh–Ritz Method

In the Rayleigh–Ritz method, the coefficients c_j of the approximation are determined using the weak form of the problem, and the choice of weight functions is restricted to the approximation functions, $w = \phi_i$. Recall that the weak form contains both the governing differential equation and the natural boundary conditions of the problem, and it places less stringent continuity requirements on the approximate solution than the original differential equation or its weighted-integral form. The method is described below for a linear variational problem.

Consider the variational problem of finding the solution u such that

$$B(w, u) = l(w) \tag{2.64}$$

for all sufficiently differentiable functions w that satisfy the homogeneous form of any specified essential boundary conditions on u. When the functional B is bilinear and symmetric and l is linear, the problem in (2.64) is equivalent to minimization of the quadratic functional

$$I(u) = \tfrac{1}{2}B(u, u) - l(u) \tag{2.65}$$

In the Rayleigh–Ritz method, we seek an approximate solution to (2.64) in the form of a finite series

$$\boxed{u_N = \sum_{j=1}^{N} c_j\phi_j + \phi_0} \tag{2.66}$$

where the constants c_j, called the *Ritz coefficients*, are chosen such that (2.64) holds for $w = \phi_i$ $(i = 1, 2, \ldots, N)$; i.e., (2.64) holds for N different choices of w, so that N independent algebraic equations in c_j are obtained. The requirements on ϕ_j and ϕ_0 will be discussed shortly. The ith algebraic equation is obtained by substituting ϕ_i for w:

$$B\left(\phi_i, \sum_{j=1}^{N} c_j\phi_j + \phi_0\right) = l(\phi_i) \quad (i = 1, 2, \ldots, N)$$

If B is bilinear, the summation and constants c_j can be taken outside the operator. We have

$$\sum_{j=1}^{N} B(\phi_i, \phi_j)c_j = l(\phi_i) - B(\phi_i, \phi_0) \tag{2.67a}$$

or

$$\sum_{j=1}^{N} B_{ij}c_j = F_i, \qquad B_{ij} = B(\phi_i, \phi_j), \qquad F_i = l(\phi_i) - B(\phi_i, \phi_0) \tag{2.67b}$$

which represents the ith algebraic equation in a system of N linear algebraic equations in N constants c_j. The columns (and rows) of the matrix coefficients $B_{ij} = B(\phi_i, \phi_j)$ must be linearly independent in order that the coefficient matrix in (2.67) can be inverted.

For symmetric bilinear forms, the Rayleigh–Ritz method can also be viewed as one that seeks a solution of the form in (2.66) in which the parameters are determined by minimizing the quadratic functional corresponding to the symmetric bilinear form, that is, the functional $I(u)$ in (2.65). After substituting u_N from (2.66) for u into (2.65) and integrating, the functional $I(u)$ becomes an ordinary (quadratic) function of the parameters $c_1, c_2, \ldots$. Then the necessary condition for the minimization of $I(c_1, c_2, \ldots, c_N)$ is that its partial derivatives with respect to each of the parameters be zero:

$$\frac{\partial I}{\partial c_1}=0, \quad \frac{\partial I}{\partial c_2}=0, \quad \ldots, \quad \frac{\partial I}{\partial c_N}=0 \tag{2.68}$$

Thus there are N linear algebraic equations in N unknowns, c_j ($j=1,2,\ldots,N$). These equations are exactly the same as those in (2.67) for all problems for which the variational problem (2.64) is equivalent to $\delta I=0$. Of course, when $B(\cdot,\cdot)$ is not symmetric, we do not have a quadratic functional. In other words, (2.67) is more general than (2.68), and they are the same when $B(\cdot,\cdot)$ is bilinear and symmetric. In most problems of interest in the present study, we shall have a symmetric bilinear form.

Returning to the Rayleigh–Ritz approximation u_N in (2.66), we note that u_N must satisfy the specified essential boundary conditions of the problem; any specified natural boundary conditions are already included in the variational problem (2.64). The particular form of u_N in (2.66) facilitates satisfaction of specified boundary conditions. If we were to use the form

$$u_N=\sum_{j=1}^{N} c_j\phi_j(x)$$

then it would not be easy to satisfy nonhomogeneous boundary conditions. For example, suppose that u_N is required to satisfy the condition $u_N(x_0)=u_0$ at a boundary point $x=x_0$:

$$\sum_{j=1}^{N} c_j\phi_j(x_0)=u_0$$

Since c_j are unknown parameters to be determined, it is not easy to choose $\phi_j(x)$ such that this relation holds. If $u_0=0$ then any ϕ_j such that $\phi_j(x_0)=0$ would meet the requirement. By writing the approximate solution u_N in the form (2.66), a sum of homogeneous and nonhomogeneous parts, the nonhomogeneous essential boundary conditions can be satisfied by ϕ_0, $\phi_0(x_0)=u_0$, and ϕ_j are required to satisfy the homogeneous form of the same boundary condition, $\phi_j(x_0)=0$. In this way, u_N satisfies the specified boundary conditions:

$$\begin{aligned} u_N(x_0)&=\sum_{j=1}^{N} c_j\phi_j(x_0)+\phi_0(x_0)\\ &=0+u_0 \end{aligned}$$

If all specified essential boundary conditions are homogeneous (i.e., the specified value u_0 is zero) then ϕ_0 is taken to be zero and ϕ_j must still satisfy the same conditions, $\phi_j(x_0)=0$. Since ϕ_i satisfy the homogeneous essential boundary conditions, the choice $w=\phi_i$ is consistent with the requirements of a weight function. The approximation functions ϕ_i satisfy the following conditions:

1. (*a*) ϕ_i should be such that $B(\phi_i, \phi_j)$ is well defined and nonzero [i.e., sufficiently differentiable as required by the bilinear form $B(\cdot, \cdot)$].
   (*b*) ϕ_i must satisfy at least the homogeneous form of the essential boundary conditions of the problem. (2.69)
2. For any N, the set $\{\phi_i\}_{i=1}^N$ along with the columns (and rows) of $B(\phi_i, \phi_j)$ must be linearly independent.
3. $\{\phi_i\}$ must be complete. For example, when ϕ_i are algebraic polynomials, completeness requires that the set $\{\phi_i\}$ should contain all terms of the lowest order admissible, and up to the highest order desired.

The only role that ϕ_0 plays is to satisfy the specified nonhomogeneous essential boundary conditions of the problem. Any low-order function that satisfies the specified essential boundary conditions should be used. If all specified essential boundary conditions are homogeneous then $\phi_0 = 0$ and

$$F_i = l(\phi_i) - B(\phi_i, \phi_0) = l(\phi_i) \tag{2.70}$$

Next, we consider a few examples of the application of the Rayleigh–Ritz method.

Example 2.4. Consider the differential equation [cf. Example 2.1, with $a = c = 1$]

$$-\frac{d^2u}{dx^2} - u + x^2 = 0 \quad \text{for } 0 < x < 1 \tag{2.71}$$

We consider two sets of boundary conditions:

$$\textbf{set 1:} \quad u(0) = 0, \quad u(1) = 0 \tag{2.72a}$$

$$\textbf{set 2:} \quad u(0) = 0, \quad \left(\frac{du}{dx}\right)\bigg|_{x=1} = 1 \tag{2.72b}$$

Set 1. The bilinear functional and the linear functional are [see (2.47*c*)]

$$B(w, u) = \int_0^1 \left(\frac{dw}{dx}\frac{du}{dx} - wu\right) dx, \qquad l(w) = -\int_0^1 wx^2\, dx \tag{2.73}$$

Since both boundary conditions $[u(0) = u(1) = 0]$ are of the essential type, we must select ϕ_i in the N-parameter Ritz approximation to satisfy the conditions $\phi_i(0) = \phi_i(1) = 0$. We choose the following functions: $\phi_0 = 0$ and

$$\phi_1 = x(1-x), \quad \phi_2 = x^2(1-x), \quad \ldots, \quad \phi_N = x^N(1-x) \tag{2.74}$$

It should be pointed out that if one selects, for example, the functions $\phi_1 = x^2(1-x)$, $\phi_2 = x^3(1-x)$, etc. [not including $x(1-x)$], requirement 3 in the conditions (2.69) is violated, because the set cannot be used to generate the linear term x if the exact solution contains it. As a rule, one must start with the lowest-order admissible function and include all admissible, higher-order functions up to the desired degree.

The N-parameter Rayleigh–Ritz solution for the problem is of the form

$$u_N = c_1\phi_1 + c_2\phi_2 + \ldots + c_N\phi_N = \sum_{j=1}^{N} c_j\phi_j \tag{2.75}$$

Substituting this into the variational problem $B(w, u) = l(w)$, we obtain

$$\int_0^1 \left[\frac{d\phi_i}{dx}\left(\sum_{j=1}^{N} c_j \frac{d\phi_j}{dx}\right) - \phi_i\left(\sum_{j=1}^{N} c_j\phi_j\right)\right] dx = -\int_0^1 \phi_i x^2\, dx$$

$$\sum_{j=1}^{N} c_j \int_0^1 \left(\frac{d\phi_i}{dx}\frac{d\phi_j}{dx} - \phi_i\phi_j\right) dx = -\int_0^1 \phi_i x^2\, dx$$

or

$$\sum_{j=1}^{N} c_j B(\phi_i, \phi_j) = l(\phi_i) \tag{2.76a}$$

where the coefficients $B(\phi_i, \phi_j)$ and $l(\phi_i)$ are defined by

$$B(\phi_i, \phi_j) = \int_0^1 \left(\frac{d\phi_i}{dx}\frac{d\phi_j}{dx} - \phi_i\phi_j\right) dx, \qquad l(\phi_i) = -\int_0^1 x^2\phi_i\, dx \tag{2.76b}$$

The same result can be obtained using (2.65) [instead of (2.64)]. We have

$$I(u) = \frac{1}{2}\int_0^1 \left[\left(\frac{du}{dx}\right)^2 - u^2 + 2x^2u\right] dx$$

Substituting for $u \approx u_N$ from (2.75) into the above functional, we obtain

$$I(c_j) = \frac{1}{2}\int_0^1 \left[\left(\sum_{j=1}^{N} c_j\frac{d\phi_j}{dx}\right)^2 - \left(\sum_{j=1}^{N} c_j\phi_j\right)^2 + 2x^2\left(\sum_{j=1}^{N} c_j\phi_j\right)\right] dx \tag{2.77}$$

The necessary conditions for the minimization of I, which is a quadratic function of the variables $c_1, c_2, \ldots, c_N$, are

$$\frac{\partial I}{\partial c_i} = 0 = \int_0^1 \left[\frac{d\phi_i}{dx}\left(\sum_{j=1}^{N} c_j\frac{d\phi_j}{dx}\right) - \phi_i\left(\sum_{j=1}^{N} c_j\phi_j\right) + \phi_i x^2\right] dx$$

$$= \sum_{j=1}^{N} B_{ij}c_j - F_i$$

where

$$B_{ij} = \int_0^1 \left(\frac{d\phi_i}{dx}\frac{d\phi_j}{dx} - \phi_i\phi_j\right) dx, \qquad F_i = -\int_0^1 x^2\phi_i\, dx$$

which are the same as those in (2.76). Equations (2.76a, b) hold for any choice of admissible approximation functions ϕ_i.

For the choice of approximation functions in (2.74), the matrix coefficients $B_{ij} = B(\phi_i, \phi_j)$ and vector coefficients $F_i = l(\phi_i) - B(\phi_i, \phi_0) = l(\phi_i)$ can be computed using

$$\phi_i = x^i(1 - x) = x^i - x^{i+1}$$

$$\frac{d\phi_i}{dx} = ix^{i-1} - (i + 1)x^i$$

We have

$$B_{ij} = \int_0^1 \{[ix^{i-1} - (i+1)x^i][jx^{j-1} - (j+1)x^j] - (x^i - x^{i+1})(x^j - x^{j+1})\}\, dx$$

$$= \frac{2ij}{(i+j)[(i+j)^2 - 1]} - \frac{2}{(i+j+1)(i+j+2)(i+j+3)} \tag{2.78a}$$

$$F_i = -\int_0^1 x^2(x^i - x^{i+1})\, dx = -\frac{1}{(3+i)(4+i)} \tag{2.78b}$$

Equation (2.76) can be written in matrix form as

$$[B]\{c\} = \{F\} \tag{2.79}$$

For example, when $N = 2$, (2.79) becomes

$$\frac{1}{420}\begin{bmatrix} 126 & 63 \\ 63 & 52 \end{bmatrix}\begin{Bmatrix} c_1 \\ c_2 \end{Bmatrix} = -\frac{1}{60}\begin{Bmatrix} 3 \\ 2 \end{Bmatrix}$$

and the use of Cramer's rule to solve the equations gives

$$c_1 = -\tfrac{10}{123} = -0.0813, \qquad c_2 = -\tfrac{21}{123} = -0.1707.$$

The two-parameter Rayleigh–Ritz solution is given by

$$u_2 = c_1\phi_1 + c_2\phi_2 = (-\tfrac{10}{123})(x - x^2) + (-\tfrac{21}{123})(x^2 - x^3)$$
$$= -\tfrac{1}{123}(10x + 11x^2 - 21x^3)$$

The exact solution of (2.71) and (2.72*a*) is given by

$$u(x) = \frac{\sin x + 2\sin(1-x)}{\sin 1} + x^2 - 2 \tag{2.80}$$

The values of the Ritz coefficients for various values of N can be obtained by solving (2.79). A comparison of the Rayleigh–Ritz solution (2.75) with the exact solution (2.80) is presented in Table 2.1 and Fig. 2.3.

Set 2. For the second set of boundary conditions (2.72*b*), the bilinear form is the same as that given in (2.73) and (2.76*b*). The linear form is given by ($\phi_0 = 0$)

$$l(w) = -\int_0^1 wx^2\, dx + w(1) \tag{2.81a}$$

and we therefore have

$$F_i = -\int_0^1 x^2\phi_i\, dx + \phi_i(1) \tag{2.81b}$$

In this case, the ϕ_i should be selected to satisfy the condition $\phi_i(0) = 0$, because the only EBC is at $x = 0$. The following choice of ϕ_i meets the requirements:

$$\phi_i = x^i \tag{2.82}$$

The coefficients B_{ij} and F_i can be computed using (2.82) in (2.76*b*) and (2.81*b*) respectively:

$$\begin{aligned} B_{ij} &= \int_0^1 (ijx^{i+j-2} - x^{i+j})\, dx = \frac{ij}{1+j-1} - \frac{1}{i+j+1} \\ F_i &= -\int_0^1 x^{i+2}\, dx + 1 = -\frac{1}{i+3} + 1 \end{aligned} \tag{2.83}$$

TABLE 2.1
Comparison of the Rayleigh–Ritz and exact solutions of the equation

$$-\frac{d^2u}{dx^2}-u+x^2=0 \quad \text{for } 0<x<1; \qquad u(0)=u(1)=0$$

Ritz coefficients†	x	Rayleigh–Ritz solution, $-10u$			Exact solution
		$N=1$	$N=2$	$N=3$	
$N=1$:	0.0	0.0	0.0	0.0	0.0
$c_1=-0.1667$	0.1	0.1500	0.0885	0.0954	0.0955
$N=2$:	0.2	0.2667	0.1847	0.1890	0.1890
$c_1=-0.0813$	0.3	0.3500	0.2783	0.2766	0.2764
$c_2=-0.1707$	0.4	0.4000	0.3590	0.3520	0.3518
$N=3$:	0.5	0.4167	0.4167	0.4076	0.4076
$c_1=-0.0952$	0.6	0.4000	0.4410	0.4340	0.4342
$c_2=-0.1005$	0.7	0.3500	0.4217	0.4200	0.4203
$c_3=-0.0702$	0.8	0.2667	0.3486	0.3529	0.3530
	0.9	0.1500	0.2115	0.2183	0.2182
	1.0	0.0	0.0	0.0	0.0

†The four-parameter Rayleigh–Ritz solution coincides with the exact solution up to four decimal places.

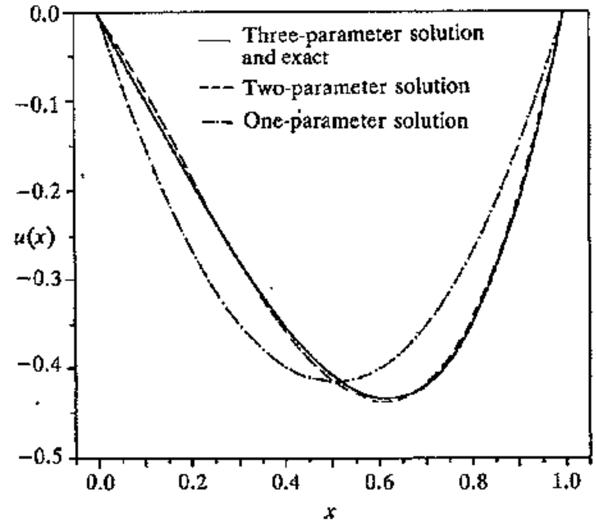

FIGURE 2.3
Comparison of the Rayleigh–Ritz solution with the exact solution of (2.71) and (2.72a). The three-parameter solution and the exact solution do not differ on the scale of the plot.

TABLE 2.2
Comparison of the Rayleigh–Ritz and exact solutions of the equation

$$-\frac{d^2u}{dx^2} - u + x^2 = 0 \quad \text{for } 0 < x < 1; \qquad u(0) = 0, \qquad \left(\frac{du}{dx}\right)\bigg|_{x=1} = 1$$

Ritz coefficients†	x	Rayleigh–Ritz solution, u			Exact solution
		$N=1$	$N=2$	$N=3$	
$N=1$:	0.0	0.0	0.0	0.0	0.0
$c_1 = 1.1250$	0.1	0.1125	0.1280	0.1271	0.1262
$N=2$:	0.2	0.2250	0.2530	0.2519	0.2513
$c_1 = 1.2950$	0.3	0.3375	0.3749	0.3740	0.3742
$c_2 = -0.15108$	0.4	0.4500	0.4938	0.4934	0.4944
$N=3$:	0.5	0.5625	0.6097	0.6099	0.6112
$c_1 = 1.2831$	0.6	0.6750	0.7226	0.7234	0.7244
$c_2 = -0.11424$	0.7	0.7875	0.8325	0.8337	0.8340
$c_3 = -0.02462$	0.8	0.9000	0.9393	0.9407	0.9402
	0.9	1.0125	1.0431	1.0443	1.0433
	1.0	1.1250	1.1439	1.1442	1.1442

† The four-parameter Rayleigh–Ritz solution coincides with the exact solution up to four decimal places.

The exact solution in the present case is given by

$$u(x) = \frac{2\cos(1-x) - \sin x}{\cos 1} + x^2 - 2 \tag{2.84}$$

A comparison of the Rayleigh–Ritz solution with the exact solution is presented in Table 2.2.

Example 2.5. Consider the problem of finding the transverse deflection of a cantilever beam under a uniform transverse load of intensity f_0 per unit length and end moment M_0 using Euler–Bernoulli beam theory (see Example 2.2). The governing equations of this theory are

$$\frac{d^2}{dx^2}\left(EI\frac{d^2w}{dx^2}\right) - f_0 = 0 \quad \text{for } \begin{cases} 0 < x < L \\ EI > 0 \end{cases} \tag{2.85}$$

$$w(0) = \left(\frac{dw}{dx}\right)\bigg|_{x=0} = 0, \qquad \left(EI\frac{d^2w}{dx^2}\right)\bigg|_{x=L} = M_0, \qquad \left[\frac{d}{dx}\left(EI\frac{d^2w}{dx^2}\right)\right]\bigg|_{x=L} = 0 \tag{2.86}$$

The variational form of (2.85) (which includes the specified NBC) was derived in Example 2.2, and is given by (2.56).

We now construct an N-parameter Ritz solution using the variational form, (2.56), $B(v, w) = l(v)$, where

$$B(v, w) = \int_0^L EI\frac{d^2v}{dx^2}\frac{d^2w}{dx^2}\,dx, \qquad l(v) = \int_0^L f_0 v\,dx + \left(M_0\frac{dv}{dx}\right)\bigg|_{x=L} \tag{2.87}$$

Note that the specified EBC, $w(0)=0$ and $(dw/dx)|_{x=0}$ are homogeneous. Therefore, $\phi_0=0$. We select algebraic approximation functions ϕ_i that satisfy the continuity conditions and boundary conditions $\phi_i(0)=\phi_i'(0)=0$. The lowest-order algebraic function that meets these conditions is $\phi_1=x^2$. The next function in the sequence is $\phi_2=x^3$. Thus we have

$$\phi_1=x^2, \quad \phi_2=x^3, \quad \ldots, \quad \phi_N=x^{N+1}$$

The N-parameter Rayleigh–Ritz approximation is

$$w_N(x)=\sum_{j=1}^{N} c_j\phi_j, \qquad \phi_j=x^{j+1} \tag{2.88}$$

Substituting (2.88) for w and $v=\phi_i$ into (2.87), we obtain

$$\begin{aligned} B_{ij}&=\int_0^L EI(i+1)ix^{i-1}(j+1)jx^{j-1}\,dx=\frac{EIij(i+1)(j+1)L^{i+j-1}}{i+j-1} \\ F_i&=\frac{f_0(L)^{i+2}}{i+2}+M_0(i+1)L^i \end{aligned} \tag{2.89}$$

For $N=2$ (i.e., the two-parameter solution), we have

$$\begin{aligned} EI(4Lc_1+6L^2c_2)&=\tfrac{1}{3}f_0L^3+2M_0L \\ EI(6L^2c_1+12L^3c_2)&=\tfrac{1}{4}f_0L^4+3M_0L^2 \end{aligned} \tag{2.90a}$$

or, in matrix form,

$$EI\begin{bmatrix} 4L & 6L^2 \\ 6L^2 & 12L^3 \end{bmatrix}\begin{Bmatrix} c_1 \\ c_2 \end{Bmatrix}=\frac{f_0L^3}{12}\begin{Bmatrix} 4 \\ 3L \end{Bmatrix}+M_0L\begin{Bmatrix} 2 \\ 3L \end{Bmatrix} \tag{2.90b}$$

Solving for c_1 and c_2, we obtain

$$c_1=\frac{5f_0L^2+12M_0}{24EI}, \qquad c_2=\frac{-f_0L}{12EI}$$

and the solution (2.88) becomes

$$w_2(x)=\frac{5f_0L^2+12M_0}{24EI}x^2-\frac{f_0L}{12EI}x^3 \tag{2.91}$$

For the three-parameter approximation ($N=3$), we obtain the matrix equation

$$EI\begin{bmatrix} 4 & 6L & 8L^2 \\ 6L & 12L^2 & 18L^3 \\ 8L^2 & 18L^2 & \frac{144}{5}L^4 \end{bmatrix}\begin{Bmatrix} c_1 \\ c_2 \\ c_3 \end{Bmatrix}=\begin{Bmatrix} \frac{1}{3}f_0L^2+2M_0 \\ \frac{1}{4}f_0L^3+3M_0L \\ \frac{1}{5}f_0L^4+4M_0L^2 \end{Bmatrix} \tag{2.92}$$

The solution of this when substituted into (2.88) for $N=3$, gives

$$w_3(x)=\frac{f_0x^2}{24EI}(6L^2-4Lx+x^2)+\frac{M_0x^2}{2EI} \tag{2.93}$$

which coincides with the exact solution of (2.85) and (2.86). If we try to compute the four-parameter solution without knowing that the three-parameter solution is exact, the parameters c_j ($j>3$) will be zero. Figure 2.4 shows a comparison of the Rayleigh–Ritz solution with the exact solution.

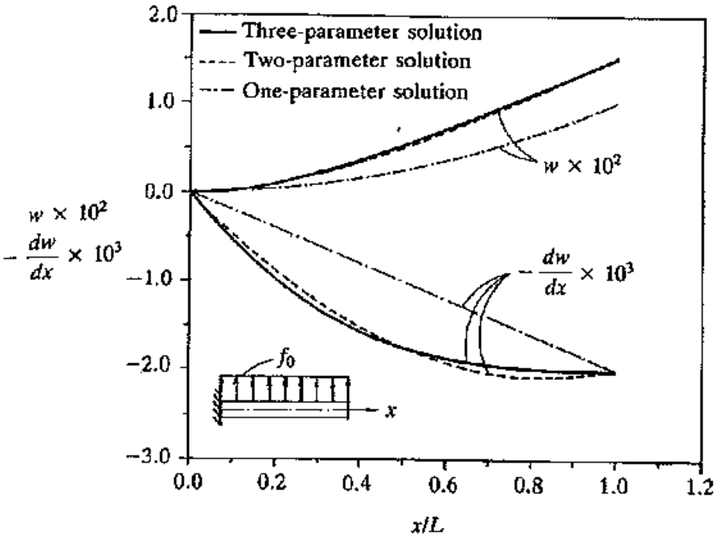

FIGURE 2.4
Comparison of the Rayleigh–Ritz solution with the exact solution of a cantilever beam under a uniform transverse load (Euler–Bernoulli beam theory).

The next example deals with two-dimensional heat conduction in a square region. Note that the dependent variable, namely the temperature, is denoted by T, consistent with the standard notation used in heat transfer books.

Example 2.6. Consider the Poisson equation in a unit square region:

$$-k\nabla^2 T = q_0 \quad \text{in } \Omega = \{(x, y): 0 < (x, y) < 1\} \tag{2.94a}$$

$$\begin{aligned} T &= 0 \quad \text{on sides } x = 1 \text{ and } y = 1 \\ \frac{\partial T}{\partial n} &= 0 \quad \text{on sides } x = 0 \text{ and } y = 0 \end{aligned} \tag{2.94b}$$

where q_0 is the rate of uniform heat generation in the region. The variational problem is of the form (see Example 2.3)

$$B(w, T) = l(w) \tag{2.95a}$$

where the bilinear and linear functionals are

$$\begin{aligned} B(w, T) &= \int_0^1 \int_0^1 k\left(\frac{\partial w}{\partial x}\frac{\partial T}{\partial x} + \frac{\partial w}{\partial y}\frac{\partial T}{\partial y}\right) dx\, dy \\ l(\overset{w}{v}) &= \int_0^1 \int_0^1 w q_0\, dx\, dy \end{aligned} \tag{2.95b}$$

We consider an N-parameter approximation of the form

$$T_N = \sum_{i,j=1}^{N} c_{ij} \cos \alpha_i x \cos \alpha_j y, \qquad \alpha_i = \tfrac{1}{2}(2i - 1)\pi \tag{2.96}$$

Note that (2.96) involves a double summation. Since the boundary conditions are homogeneous, we have $\phi_0 = 0$. Incidentally, ϕ_i also satisfies the natural boundary conditions of the problem. While the choice $\hat{\phi}_i = \sin i\pi x \sin i\pi y$ meets the essential boundary conditions, it is not complete, because it cannot be used to generate the solution that *does not* vanish on the sides $x = 0$ and $y = 0$. Hence, $\hat{\phi}_i$ are not admissible.

The coefficients B_{ij} and F_i can be computed by substituting (2.96) into (2.95*b*). Since the double Fourier series has two summations [see (2.96)], we introduce the notation

$$\begin{aligned} B_{(ij)(kl)} &= k \int_0^1 \int_0^1 [(\alpha_i \sin \alpha_i x \cos \alpha_j y)(\alpha_k \sin \alpha_k x \cos \alpha_l y) \\ &\quad + (\alpha_j \cos \alpha_i x \sin \alpha_j y)(\alpha_l \cos \alpha_k x \sin \alpha_l y)]\, dx\, dy \\ &= \begin{cases} 0 & \text{if } i \neq k \text{ or } j \neq l \\ \frac{1}{4}k(\alpha_i^2 + \alpha_j^2) & \text{if } i = k \text{ and } j = l \end{cases} \end{aligned} \tag{2.97a}$$

$$F_{ij} = q_0 \int_0^1 \int_0^1 \cos \alpha_i x \cos \alpha_j y\, dx\, dy = \frac{q_0}{\alpha_i \alpha_j} \sin \alpha_i \sin \alpha_j \tag{2.97b}$$

In evaluating the integrals, the following orthogonality conditions were used

$$\int_0^1 \sin \alpha_i x \sin \alpha_j x\, dx = \begin{cases} 0 & \text{if } i \neq j \\ \frac{1}{2} & \text{if } i = j \end{cases}$$

$$\int_0^1 \cos \alpha_i x \cos \alpha_j x\, dx = \begin{cases} 0 & \text{if } i \neq j \\ \frac{1}{2} & \text{if } i = j \end{cases}$$

Owing to the diagonal form of the coefficient matrix (2.97*a*), we can readily solve for the coefficients c_{ij}:

$$c_{ij} = \frac{F_{ij}}{B_{(ij)(ij)}} = \frac{4q_0}{k} \frac{\sin \alpha_i \sin \alpha_j}{(\alpha_i^2 + \alpha_j^2)\alpha_i \alpha_j} \tag{2.98}$$

The one- and two-parameter Rayleigh–Ritz solutions are

$$T_1 = \frac{32 q_0}{k\pi^4} \cos \tfrac{1}{2}\pi x \cos \tfrac{1}{2}\pi y \tag{2.99}$$

$$\begin{aligned} T_2 = \frac{q_0}{k} [0.3285 \cos \tfrac{1}{2}\pi x \cos \tfrac{1}{2}\pi y - 0.0219(\cos \tfrac{1}{2}\pi x \cos \tfrac{3}{2}\pi y \\ + \cos \tfrac{3}{2}\pi x \cos \tfrac{1}{2}\pi y) + 0.0041 \cos \tfrac{3}{2}\pi x \cos \tfrac{3}{2}\pi y] \end{aligned} \tag{2.100}$$

If algebraic polynomials are to be used in the approximation of T, one can choose $\phi_1 = (1 - x)(1 - y)$ or $\phi_1 = (1 - x^2)(1 - y^2)$, both of which satisfy the (homogeneous) essential boundary conditions. However, the choice $\phi_1 = (1 - x^2)(1 - y^2)$ also meets the natural boundary conditions of the problem. The one-parameter Ritz solution for the choice $\phi_1 = (1 - x^2)(1 - y^2)$ is

$$T_1(x, y) = \frac{5q_0}{16k}(1 - x^2)(1 - y^2) \tag{2.101}$$

The exact solution of (2.94*a*, *b*) is

$$T(x, y) = \frac{q_0}{2k}\left[(1 - y^2) + 4 \sum_{n=1}^{\infty} \frac{(-1)^n \cos \alpha_n y \cosh \alpha_n x}{\alpha_n^3 \cosh \alpha_n}\right] \tag{2.102}$$

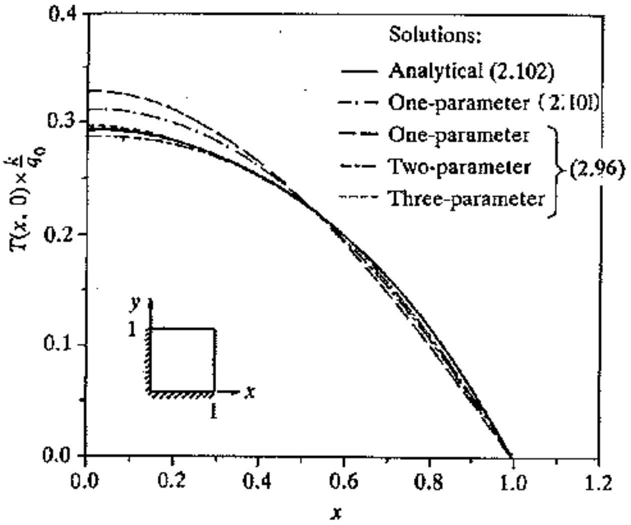

FIGURE 2.5
Comparison of the Rayleigh–Ritz solutions with the analytical solution of the Poisson equation (2.94) in two dimensions.

where $\alpha_n = \frac{1}{2}(2n-1)\pi$. The Rayleigh–Ritz solutions (2.99), (2.100), and (2.101) are compared with the exact solution (2.102) in Fig. 2.5. The analytical solution is evaluated using 20 terms of the series (2.102).

2.4.3 The Method of Weighted Residuals

As noted in Section 2.3.2, one can always write the weighted-integral form of a differential equation, whether the equation is linear or nonlinear (in the dependent variables). The weak form can be developed if the equations are second-order or higher, even if they are nonlinear. However, it is not always possible to construct a functional whose first variation is equal to the variational form. The Rayleigh–Ritz method can also be applied to all problems, including nonlinear problems, that have weak forms. In this method, the weight functions are necessarily equated to those used in the approximation. The weighted-residual method is a generalization of the Rayleigh–Ritz method in that the weight functions can be chosen from an independent set of functions, and it requires only the weighted-integral form to determine the parameters. The method of weighted residuals can be used to approximate the weighted-integral form of any equation. Since the latter form does not include any of the specified boundary conditions of the problem, the approximation functions should be selected such that the approximate solution satisfies both the natural and essential boundary conditions. In addition, the weight functions can be selected independently of the approximation functions, but are required to be linearly independent (so that the resulting algebraic equations are linearly independent). This flexibility is advantageous in certain nonlinear problems.

In this section, we discuss the general method of weighted residuals first, and then consider certain special cases that are known by specific names (e.g., the Galerkin and least-squares methods). Although a limited use of the weighted-residual method is made in this book (see Chapter 14), it is informative to have a knowledge of this method for use in the formulation of certain nonlinear problems readers might encounter in their work.

The method of weighted residuals can be described in its generality by considering the operator equation

$$A(u)=f \quad \text{in } \Omega, \tag{2.103}$$

where A is an operator (linear or nonlinear), often a differential operator, acting on the dependent variable u, and f is a known function of the independent variables. Some examples of such operators are provided by

$$\begin{aligned}
&1.\ A(u)=-\frac{d}{dx}\left(a\frac{du}{dx}\right)+cu\\
&2.\ A(u)=\frac{d^2}{dx^2}\left(b\frac{d^2u}{dx^2}\right)\\
&3.\ A(u)=-\left[\frac{\partial}{\partial x}\left(k_x\frac{\partial u}{\partial x}\right)+\frac{\partial}{\partial y}\left(k_y\frac{\partial u}{\partial y}\right)\right]\\
&4.\ A(u)=-\frac{d}{dx}\left(u\frac{du}{dx}\right)\\
&5.\ A(u,v)=u\frac{\partial u}{\partial x}+v\frac{\partial u}{\partial y}+\frac{\partial^2 u}{\partial x^2}+\frac{\partial}{\partial y}\left(\frac{\partial u}{\partial y}+\frac{\partial v}{\partial x}\right)
\end{aligned} \tag{2.104}$$

For an operator A to be *linear* in its arguments, it must satisfy the relation

$$A(\alpha u+\beta v)=\alpha A(u)+\beta A(v) \tag{2.105}$$

for any scalars α and β and dependent variables u and v. It can be easily verified that all operators in (2.104), except for 4 and 5, are linear. When an operator does not satisfy the condition (2.105), it is said to be *nonlinear.*

The function u is not only required to satisfy the operator equation (2.103), it is also required to satisfy the boundary conditions associated with the operator equation. From the examples considered so far, the boundary conditions associated with the operators defined in 1, 2, and 3 of (2.104) are obvious [see Examples 2.1–2.3].

In the weighted-residual method, the solution u is approximated, in much the same way as in the Rayleigh–Ritz method, by the expression

$$u_N=\sum_{j=1}^{N}c_j\phi_j+\phi_0 \tag{2.106}$$

except that the requirements on ϕ_0 and ϕ_j for the weighted-residual method are more stringent than those for the Rayleigh–Ritz method. Substitution of the approximate solution u_N into the left-hand side of (2.103) gives a function $f_N \equiv A(u_N)$ that, in general, is not equal to the specified function f. The difference $A(u_N) - f$, called the *residual* of the approximation, is nonzero:

$$R \equiv A(u_N) - f = A\left(\sum_{j=1}^{N} c_j\phi_j + \phi_0\right) - f \neq 0 \qquad (2.107)$$

Note that the residual R is a function of position as well as of the parameters c_j. In the weighted-residual method, as the name suggests, the parameters c_j are determined by requiring the residual R to vanish in the weighted-integral sense:

$$\boxed{\int_\Omega \psi_i(x, y)R(x, y, c_j)\,dx\,dy = 0 \quad (i = 1, 2, \ldots, N)} \qquad (2.108)$$

where Ω is a two-dimensional domain and ψ_i are *weight functions*, which, in general, are not the same as the approximation functions ϕ_i. The set $\{\psi_i\}$ must be a linearly independent set; otherwise, the equations provided by (2.108) will not be linearly independent and hence will not be solvable.

The requirements on ϕ_0 and ϕ_j for the weighted-residual method are different from those for the Rayleigh–Ritz method, which is based on the weak (integral) form of the differential equation. The differentiability requirement on ϕ_j in the weighted-residual method is dictated by the integral statement (2.108), as opposed to the weak form in the Rayleigh–Ritz method. Thus, ϕ_j must have nonzero derivatives up to the order appearing in the operator equation (2.103). Since the weighted-integral form (2.108) does not include any of the specified (either essential or natural) boundary conditions, we must also require u_N in (2.106) to satisfy all specified boundary conditions of the problem. Consequently, ϕ_0 is required to satisfy all specified boundary conditions, and ϕ_j are required to satisfy the homogeneous form of all specified boundary conditions of the problem. These requirements on ϕ_0 and ϕ_j will increase the order of the polynomial expressions used for the weighted-residual method. In general, the ϕ_j used in this method are higher-order functions than those used in the Rayleigh–Ritz method, and the functions used in the latter may not satisfy the continuity (i.e. differentiability) requirements of the weighted-residual method. Various special cases of the weighted-residual method are discussed in the following paragraphs.

THE PETROV–GALERKIN METHOD. The weighted-residual method is referred to as the *Petrov–Galerkin method* when $\psi_i \neq \phi_i$. When the operator A is linear, (2.108) can be simplified to the form

$$\sum_{j=1}^{N}\left[\int_\Omega \psi_i A(\phi_j)\,dx\,dy\right]c_j = \int_\Omega \psi_i[f - A(\phi_0)]\,dx\,dy$$

or

$$\sum_{j=1}^{N} A_{ij}c_j = F_i \tag{2.109}$$

Note that the coefficient matrix $[A]$ is not symmetric:

$$A_{ij} = \int_{\Omega} \psi_i A(\phi_j)\,dx\,dy \neq A_{ji} \tag{2.110}$$

THE GALERKIN METHOD. For the choice of weight function ψ_i equal to the approximation function ϕ_i, the weighted-residual method is better known as the Galerkin method. The algebraic equations of the Galerkin approximation are

$$\sum_{j=1}^{N} A_{ij}c_j = F_i \tag{2.111a}$$

where

$$A_{ij} = \int_{\Omega} \phi_i A(\phi_j)\,dx\,dy, \qquad F_i = \int_{\Omega} \phi_i[f - A(\phi_0)]\,dx\,dy \tag{2.111b}$$

Once again, we note that A_{ij} is not symmetric.

In general, the Galerkin method is *not* the same as the Rayleigh–Ritz method. This should be clear from the fact that the former uses the weighted-integral form whereas the latter uses the weak (or variational) form to determine the coefficients c_j. Consequently, the approximation functions used in the Galerkin method are required to be of higher order than those in the Rayleigh–Ritz method.

If the equation permits, and one wishes, the differentiation can be transferred from the solution u to the weight function $w = \phi_i$; and one thereby obtains the weak form to relax the continuity requirements on the approximation functions and include the specified natural boundary conditions of the problem.

The Rayleigh–Ritz and Galerkin methods yield the same solutions in two cases: (i) when the specified boundary conditions of the problem are all of the essential type, and therefore the requirements on ϕ_i in the two methods become the same and the weighted-integral form reduces to the weak form; and (ii) when the approximation functions of the Galerkin method are used in the Rayleigh–Ritz method. The reader is urged to keep the distinction between the Rayleigh–Ritz and Galerkin methods in mind.

THE LEAST-SQUARES METHOD. In this method, we determine the parameters c_j by minimizing the integral of the square of the residual (2.107):

$$\frac{\partial}{\partial c_i}\int_{\Omega} R^2(x, y, c_j)\,dx\,dy = 0$$

or

$$\int_\Omega \frac{\partial R}{\partial c_i} R\,dx\,dy = 0 \tag{2.112a}$$

Comparison of (2.112*a*) with (2.108) shows that $\psi_i = \partial R/\partial c_i$. If A is a linear operator, $\psi_i = A(\phi_i)$, and (2.112*a*) becomes

$$\sum_{j=1}^{N} \left[\int_\Omega A(\phi_i)A(\phi_j)\,dx\,dy\right]c_j = \int_\Omega A(\phi_i)[f - A(\phi_0)]\,dx\,dy$$

or

$$\sum_{j=1}^{N} A_{ij}c_j = F_i \tag{2.112b}$$

where

$$A_{ij} = \int_\Omega A(\phi_i)A(\phi_j)\,dx,\,dy \quad F_i = \int_\Omega A(\phi_i)[f - A(\phi_0)]\,dx\,dy \tag{2.112c}$$

Note that the coefficient matrix A_{ij} is symmetric, but it involves the same order of differentiation as in the governing differential equation.

THE COLLOCATION METHOD. In the collocation method, we seek an approximate solution u_N to (2.103) in the form of (2.106) by requiring the residual in the equation to be identically zero at N selected points $\mathbf{x}^i = (x^i, y^i)$ $(i = 1, 2, \ldots, N)$ in the domain Ω:

$$R(x^i, y^i, c_j) = 0 \quad (i = 1, 2, \ldots, N) \tag{2.113}$$

The selection of the points $\mathbf{x}^i$ is crucial in obtaining a well-conditioned system of equations and ultimately in obtaining an accurate solution. The collocation method can be shown to be a special case of (2.108) with $\psi_i = \delta(\mathbf{x} - \mathbf{x}^i)$, where $\delta(\mathbf{x})$ is the *Dirac delta function,* which is defined by

$$\int_\Omega f(\mathbf{x})\delta(\mathbf{x} - \boldsymbol{\xi})\,dx\,dy = f(\boldsymbol{\xi}) \tag{2.114}$$

With this choice of weight functions, the weighted-residual statement becomes

$$\int_\Omega \delta(\mathbf{x} - \mathbf{x}^i)R(\mathbf{x}, c_j)\,dx\,dy = 0$$

or

$$R(\mathbf{x}^i, c_j) = 0 \tag{2.115}$$

We consider an example to illustrate the use of various cases of the weighted-residual method.

Example 2.7. Consider the differential equation [see Example 2.4 with Set 2 boundary conditions]:

$$-\frac{d^2u}{dx^2} - u + x^2 = 0, \qquad u(0) = 0, \qquad u'(1) = 1 \tag{2.116}$$

For a weighted-residual method, ϕ_0 and ϕ_i should satisfy the following conditions:

$\phi_0(0) = 0, \quad \phi_0'(1) = 1$ (satisfy actual boundary conditions)

$\phi_i(0) = 0, \quad \phi_i'(1) = 0$ (satisfy homogeneous form of the specified boundary conditions)

For a choice of algebraic polynomials, we assume $\phi_0(x) = a + bx$ and use the two conditions on ϕ_0 to determine the constants a and b. We obtain

$$\phi_0(x) = x$$

Since there are two homogeneous conditions, we must assume at least a three-parameter polynomial to obtain a nonzero function, $\phi_1 = a + bx + cx^2$. Using the conditions on ϕ_i, we obtain

$$\phi_1 = -cx(2 - x)$$

The constant c can be set equal to unity because it will be absorbed into the parameter c_1. For ϕ_2, we can assume one of the forms

$$\phi_2 = a + bx + dx^3 \quad \text{or} \quad \phi_2 = a + cx^2 + dx^3$$

with $d \neq 0$; ϕ_2 does not contain all-order terms in either case, but the approximate solution is complete because $\{\phi_1, \phi_2\}$ contains all terms up to degree three. For the first choice of ϕ_2, we obtain

Second

$$\phi_2 = x^2(1 - \tfrac{2}{3}x)$$

The residual in the approximation of the equation is

$$\begin{aligned} R &= -\left(0 + \sum_{i=1}^{N} c_i \frac{d^2\phi_i}{dx^2}\right) - \left(\phi_0 + \sum_{i=1}^{N} c_i\phi_i\right) + x^2 \\ &= c_1(2 - 2x + x^2) + c_2(-2 + 4x - x^2 + \tfrac{2}{3}x^3) - x + x^2 \end{aligned} \tag{2.117}$$

We next consider various methods.

The Petrov–Galerkin method. Let the weight functions be

$$\psi_1 = x, \qquad \psi_2 = x^2 \tag{2.118}$$

Then

$$\int_0^1 xR\,dx = 0, \qquad \int_0^1 x^2R\,dx = 0$$

or

$$\tfrac{7}{12}c_1 + \tfrac{13}{60}c_2 - \tfrac{1}{12} = 0, \qquad \tfrac{11}{30}c_1 + \tfrac{11}{45}c_2 - \tfrac{1}{20} = 0 \tag{2.119}$$

Solving for c_i, we obtain $c_1 = \frac{103}{682}$ and $c_2 = -\frac{15}{682}$; the solution becomes

$$u_{PG} = 1.302053x - 0.173021x^2 - 0.014663x^3 \tag{2.120}$$

The Galerkin method. Taking $\psi_i = \phi_i$, we have

$$\int_0^1 x(2-x)R\,dx = 0, \qquad \int_0^1 x^2(1-\tfrac{2}{3}x)R\,dx = 0$$

or

$$\tfrac{4}{5}c_1 + \tfrac{28}{45}c_2 - \tfrac{7}{60} = 0, \qquad \tfrac{17}{90}c_1 + \tfrac{29}{315}c_2 - \tfrac{1}{36} = 0 \tag{2.121}$$

Hence, the solution becomes (with $c_1 = \frac{623}{4306}$, $c_2 = \frac{21}{4306}$),

$$u_G = 1.2894x - 0.1398x^2 - 0.00325x^3 \tag{2.122}$$

The least-squares method. Taking $\psi_i = \partial R/\partial c_i$, we have

$$\int_0^1 (2-2x+x^2)R\,dx = 0, \qquad -\int_0^1 (2-4x+x^2-\tfrac{2}{3}x^3)R\,dx = 0$$

or

$$\tfrac{28}{15}c_1 - \tfrac{47}{90}c_2 - \tfrac{13}{60} = 0, \qquad -\tfrac{47}{90}c_1 + \tfrac{253}{315}c_2 + \tfrac{1}{36} = 0 \tag{2.123}$$

The least-squares approximation of (2.116) is given by (with $c_1 = \frac{1292}{9935}$ and $c_2 = \frac{991}{19870}$)

$$u_{LS} = 1.2601x - 0.08017x^2 - 0.03325x^3 \tag{2.124}$$

The collocation method. Choosing the points $x = \frac{1}{3}$ and $x = \frac{2}{3}$ as the collocation points, we evaluate the residuals at these points and set them equal to zero:

$$\begin{aligned} R(\tfrac{1}{3}) = 0: &\quad 117c_1 - 61c_2 = 18 \\ R(\tfrac{2}{3}) = 0: &\quad 90c_1 + 34c_2 = 18 \end{aligned} \tag{2.125}$$

The solution is given by ($c_1 = \frac{1710}{9468}$ and $c_2 = \frac{486}{9468}$)

$$u_C = 1.3612x - 0.12927x^2 - 0.03422x^3 \tag{2.126}$$

The four approximate solutions are compared in Table 2.3 with the exact solution (2.84). For this problem, the Petrov–Galerkin method gives the most accurate solution.

2.5 SUMMARY

In this chapter, we have studied two major topics that are of immediate interest in the study of the finite element method in the forthcoming chapters:

1. Weighted-integral and weak formulations of differential equations
2. Solution of boundary value problems by the Rayleigh–Ritz and weighted-residual (e.g., the Galerkin, least-squares, and collocation) methods

The weighted-integral statements are required in order to generate the necessary and sufficient number of algebraic equations to solve for the parameters c_i in the approximate solution. Thus the algebraic equations are equivalent to minimizing the error introduced in the approximation of the differential equation in a weighted-integral sense.

In studying the two topics, a three-step procedure for developing the weak form of a differential equation is presented, and procedures for obtaining

TABLE 2.3
Comparison of the Rayleigh–Ritz, weighted-residual, and exact solutions of the boundary value problem in (2.116)

	Solution, $u(x)$†					
x	u_{exact}	u_{RR}	u_{PG}	u_G	u_{LS}	u_C
0.0	0.0000	0.0000	0.0000	0.0000	0.0000	0.0000
0.1	0.1262	0.1280	0.1285	0.1275	0.1252	0.1348
0.2	0.2513	0.2529	0.2536	0.2523	0.2485	0.2668
0.3	0.3742	0.3749	0.3754	0.3741	0.3699	0.3958
0.4	0.4943	0.4938	0.4941	0.4932	0.4891	0.5216
0.5	0.6112	0.6097	0.6096	0.6093	0.6058	0.6440
0.6	0.7244	0.7226	0.7221	0.7226	0.7200	0.7628
0.7	0.8340	0.8324	0.8317	0.8329	0.8314	0.8778
0.8	0.9402	0.9393	0.9384	0.9404	0.9397	0.9887
0.9	1.0433	1.0431	1.0424	1.0448	1.0449	1.0954
1.0	1.1442	1.1439	1.1437	1.1463	1.1467	1.1977

† Subscripts are as follows: *RR*, Rayleigh–Ritz; *PG*, Petrov–Galerkin; *G*, Galerkin; *LS*, least-squares; *C*, collocation.

algebraic equations in terms of the unknown parameters of the approximate solution are developed. These topics are immediately applicable in the finite element method, which is a piecewise (or element-wise) application of a variational method. Thus, the material covered in this chapter constitutes the heart of the finite element method. A few remarks are in order on the variational methods of approximation studied here.

The traditional variational methods (e.g., the Rayleigh–Ritz, Galerkin, and least-squares) presented in Section 2.4 provide a simple means of finding spatially continuous approximate solutions to physical problems. The approximate solutions obtained via these methods are continuous functions of position in the domain.

The main disadvantage, from the practical point of view, of variational methods that prevents them from being competitive with traditional finite difference methods is the difficulty encountered in selecting the approximation functions. Apart from the properties the functions are required to satisfy, there exists no unique procedure for constructing them. The selection process becomes more difficult or even impossible when the domain is geometrically complex and/or the boundary conditions are complicated.

From the preceding discussion, it is apparent that the variational methods can provide a powerful means of finding approximate solutions—provided one can find a way to systematically construct approximation functions, for almost any geometry, that depend only on the differential equation being solved and not on the boundary conditions of the problem. This property enables one to develop a computer program for a particular class of problem (each problem in the class differs from the others only in the data), that is, a *general-purpose* computer program. Since the functions must be constructed for a geometrically complex domain, it seems that (recall the discussion of the method of composites for the determination of the center of mass of an irregular shape from Chapter 1) the region must be represented (or approximated if required) as an assemblage of simple geometric shapes for which the construction of approximation functions becomes simpler. The finite element method to be discussed in the forthcoming chapters is based on these ideas.

In this method, a given domain is represented (discretized) by a collection of geometrically simple shapes (elements), and on each element of the collection, the governing equation is *formulated* using any one of the variational methods. The approximation functions are systematically generated for each (typical) element using the essential boundary conditions. The elements are *connected* together by imposing the continuity of the dependent variables across the interelement boundaries. The remaining chapters of this book are devoted to the introduction of the finite element method and its use in the analysis of several model differential equations representing mathematical models for many physical processes.

PROBLEMS

Sections 2.1–2.3

In Problems 2.1–2.9, construct the weak forms and, whenever possible, quadratic functionals.

2.1. *One-dimensional heat conduction/convection:*

$$-\frac{d}{dx}\left(a\frac{du}{dx}\right)+cu=q \quad \text{for } 0<x<1$$

$$u(0)=u_0, \quad \left[a\frac{du}{dx}+\beta(u-u_\infty)\right]\bigg|_{x=1}=Q_0 \quad \text{at } x=1$$

where a and q are functions of x, and β, c, u_∞, and Q_0 are constants.

2.2. *Beam on elastic foundation:*

$$\frac{d^2}{dx^2}\left(b\frac{d^2w}{dx^2}\right)+kw=f \quad \text{for } 0<x<L$$

$$w=b\frac{d^2w}{dx^2}=0 \quad \text{at } x=0,\ L$$

where $b=EI$ and f are functions of x, and k is a constant (foundation modulus).

2.3. *Longitudinal deformation of a bar with an end spring:*

$$-\frac{d}{dx}\left(a\frac{du}{dx}\right)=q \quad \text{for } 0<x<L$$

$$u(0)=0, \quad \left(a\frac{du}{dx}+ku\right)\bigg|_{x=L}=P$$

where a and q are functions of x, and k and P are constants.

2.4. *The Timoshenko (shear-deformable) beam theory:*

$$\left.\begin{aligned} &-\frac{d}{dx}\left[GKA\left(\frac{dw}{dx}+\Psi\right)\right]=f \\ &-\frac{d}{dx}\left(EI\frac{d\Psi}{dx}\right)+GKA\left(\frac{dw}{dx}+\Psi\right)=0 \end{aligned}\right\} \quad \text{for } 0<x<L$$

$$w(0)=w(L)=0, \qquad \left(EI\frac{d\Psi}{dx}\right)\bigg|_{x=0}=\left(EI\frac{d\Psi}{dx}\right)\bigg|_{x=L}=0$$

where G, K, A, E, I, and f are functions of x.

2.5. *A nonlinear equation:*

$$-\frac{d}{dx}\left(u\frac{du}{dx}\right)+f=0 \quad \text{for } 0<x<1$$

$$\left(\frac{du}{dx}\right)\bigg|_{x=0}=0, \qquad u(1)=\sqrt{2}$$

2.6. *The Euler–Bernoulli–von Kármán nonlinear theory of beams:*

$$-\frac{d}{dx}\left\{a\left[\frac{du}{dx}+\frac{1}{2}\left(\frac{dw}{dx}\right)^2\right]\right\}=q \quad \text{for } 0<x<L$$

$$\frac{d^2}{dx^2}\left(b\frac{d^2w}{dx^2}\right)-\frac{d}{dx}\left\{a\frac{dw}{dx}\left[\frac{du}{dx}+\frac{1}{2}\left(\frac{dw}{dx}\right)^2\right]\right\}=f$$

$$u=w=0 \quad \text{at } x=0, L; \qquad \left(\frac{dw}{dx}\right)\bigg|_{x=0}=0; \qquad \left(b\frac{d^2w}{dx^2}\right)\bigg|_{x=L}=M_0$$

where a, b, q, and f are functions of x, and M_0 is a constant. Here u denotes the axial displacement and w the transverse deflection of the beam.

2.7. *A second-order equation:*

$$-\frac{\partial}{\partial x}\left(a_{11}\frac{\partial u}{\partial x}+a_{12}\frac{\partial u}{\partial y}\right)-\frac{\partial}{\partial y}\left(a_{21}\frac{\partial u}{\partial x}+a_{22}\frac{\partial u}{\partial y}\right)+f=0 \quad \text{in } \Omega$$

$$u=u_0 \quad \text{on } \Gamma_1$$

$$\left(a_{11}\frac{\partial u}{\partial x}+a_{12}\frac{\partial u}{\partial y}\right)n_x+\left(a_{21}\frac{\partial u}{\partial x}+a_{22}\frac{\partial u}{\partial y}\right)n_y=t_0 \quad \text{on } \Gamma_2$$

where $a_{ij}=a_{ji}$ $(i,j=1,2)$ and f are given functions of position (x,y) in a two-dimensional domain Ω, and u_0 and t_0 are known functions on portions Γ_1 and Γ_2 of the boundary Γ: $\Gamma_1+\Gamma_2=\Gamma$.

2.8. *Navier–Stokes equations for two-dimensional flow of viscous, incompressible fluids* (primitive variables):

$$\left.\begin{aligned} &u\frac{\partial u}{\partial x}+v\frac{\partial u}{\partial y}=-\frac{1}{\rho}\frac{\partial P}{\partial x}+\nu\left(\frac{\partial^2 u}{\partial x^2}+\frac{\partial^2 u}{\partial y^2}\right) \\ &u\frac{\partial v}{\partial x}+v\frac{\partial v}{\partial y}=-\frac{1}{\rho}\frac{\partial P}{\partial y}+\nu\left(\frac{\partial^2 v}{\partial x^2}+\frac{\partial^2 v}{\partial y^2}\right) \\ &\frac{\partial u}{\partial x}+\frac{\partial v}{\partial y}=0 \end{aligned}\right\} \quad \text{in } \Omega \qquad \text{(i)}$$

$$u = u_0, \qquad v = v_0 \quad \text{on } \Gamma_1 \tag{ii}$$

$$\left.\begin{aligned} \nu\left(\frac{\partial u}{\partial x} n_x + \frac{\partial u}{\partial y} n_y\right) - \frac{1}{\rho} P n_x = \hat{t}_x \\ \nu\left(\frac{\partial v}{\partial x} n_x + \frac{\partial v}{\partial y} n_y\right) - \frac{1}{\rho} P n_y = \hat{t}_y \end{aligned}\right\} \quad \text{on } \Gamma_2 \tag{iii}$$

2.9. *Two-dimensional flow of viscous, incompressible fluids* (stream function–vorticity formulation):

$$\left.\begin{aligned} -\nabla^2 \psi - \zeta = 0 \\ -\nabla^2 \zeta + \frac{\partial \psi}{\partial x}\frac{\partial \zeta}{\partial y} - \frac{\partial \psi}{\partial y}\frac{\partial \zeta}{\partial x} = 0 \end{aligned}\right\} \quad \text{in } \Omega$$

Assume that all essential boundary conditions are specified to be zero.

Section 2.4

2.10. Compute the coefficient matrix and the right-hand side of the N-parameter Rayleigh–Ritz approximation of the equation

$$-\frac{d}{dx}\left[(1+x)\frac{du}{dx}\right] = 0 \quad \text{for } 0 < x < 1$$

$$u(0) = 0, \qquad u(1) = 1$$

Use algebraic polynomials for the approximation functions. Specialize your result for $N = 2$ and compute the Ritz coefficients.

Answer: $c_1 = \frac{55}{131}$ and $c_2 = -\frac{20}{131}$.

2.11. Use trigonometric functions for the two-parameter approximation of the equation in Problem 2.10, and obtain the Ritz coefficients.

2.12. A steel rod of diameter $D = 2$ cm, length $L = 25$ cm, and thermal conductivity $k = 50\ \text{W m}^{-1}\ {}^\circ\text{C}^{-1}$ is exposed to ambient air at $T_\infty = 20^\circ\text{C}$ with a heat-transfer coefficient $\beta = 64\ \text{W m}^{-2}\ {}^\circ\text{C}^{-1}$. Given that the left end of the rod is maintained at a temperature of $T_0 = 120^\circ\text{C}$ and the other end is exposed to the ambient temperature, determine the temperature distribution in the rod using a two-parameter Rayleigh–Ritz approximation with polynomial approximation functions. The equation governing the problem is given by (see Problem 2.1)

$$-\frac{d^2\theta}{dx^2} + c\theta = 0 \quad \text{for } 0 < x < 25 \text{ cm}$$

where $\theta = T - T_\infty$, T is the temperature, and c is given by

$$c = \frac{\beta P}{Ak} = \frac{\beta \pi D}{\frac{1}{4}\pi D^2 k} = \frac{4\beta}{kD} = 256\ \text{m}^{-2}$$

P being the perimeter and A the cross-sectional area of the rod. The boundary conditions are

$$\theta(0) = T(0) - T_\beta = 100^\circ\text{C}, \qquad \left.\left(k\frac{d\theta}{dx} + \beta\theta\right)\right|_{x=L} = 0$$

Answer: For $L = 0.25$ m, $\phi_0 = 100$, $\phi_i = x^i$, the Ritz coefficients are $c_1 = -1019.469$, $c_2 = 2508.217$.

2.13. Set up the equations for the N-parameter Rayleigh–Ritz approximation of the following equations associated with a simply supported beam and subjected to a uniform transverse load $f = f_0$:

$$\frac{d^2}{dx^2}\left(EI\frac{d^2w}{dx^2}\right) = f_0 \quad \text{for } 0 < x < L$$

$$w = EI\frac{d^2w}{dx^2} = 0 \quad \text{at } x = 0, L$$

(a) Use algebraic polynomials.
(b) Use trigonometric functions.

Compare the two-parameter Rayleigh–Ritz solutions with the exact solution.

Answer: (a) $c_1 = -7\alpha L$, $c_2 = -2\alpha$ $(\alpha = \frac{1}{180} f_0 L)$.

2.14. Repeat Problem 2.13 for $f = f_0 \sin(\pi x/L)$.

2.15. Repeat Problem 2.13 for $f = F_0\delta(x - \frac{1}{2}L)$, where $\delta(x)$ is the Dirac delta function (i.e., a point load F_0 is applied at the center of the beam).

2.16. Develop the N-parameter Rayleigh–Ritz solution for a simply supported beam under uniform transverse load using Timoshenko beam theory. The governing equations are given in Problem 2.4. Use trigonometric functions to approximate w and Ψ.

2.17. Solve the Poisson equation governing heat conduction in a square region (see Example 2.6):

$$-k\nabla^2 T = q_0$$

$$T = 0 \quad \text{on sides } x = 1 \text{ and } y = 1$$

$$\frac{\partial T}{\partial n} = 0 \text{ (insulated)} \quad \text{on sides } x = 0 \text{ and } y = 0$$

using a one-parameter Rayleigh–Ritz approximation of the form

$$T_1(x, y) = c_1(1 - x^2)(1 - y^2)$$

Answer: $c_1 = \dfrac{5q_0}{16k}$.

2.18. Solve Problem 2.12 using a two-parameter Galerkin approximation with algebraic approximation functions.

2.19. Consider the (Neumann) boundary value problem

$$-\frac{d^2u}{dx^2} = f \quad \text{for } 0 < x < L$$

$$\left(\frac{du}{dx}\right)\bigg|_{x=0} = \left(\frac{du}{dx}\right)\bigg|_{x=L} = 0$$

Find a two-parameter Galerkin approximation of the problem using trigonometric approximation functions, when (a) $f = f_0 \cos(\pi x/L)$ and (b) $f = f_0$.

Answer: (a) $\phi_i = \cos(i\pi x/L)$, $c_1 = f_0L^2/\pi^2$, $c_i = 0$ for $i \neq 1$.

2.20. Find a one-parameter approximate solution of the nonlinear equation

$$-2u\frac{d^2u}{dx^2} + \left(\frac{du}{dx}\right)^2 = 4 \quad \text{for } 0 < x < 1$$

subject to the boundary conditions $u(0) = 1$ and $u(1) = 0$, and compare it with the exact solution $u_0 = 1 - x^2$. Use (*a*) the Galerkin method, (*b*) the least-squares method, and (*c*) the Petrov–Galerkin method with weight function $w = 1$.

Answer: (*a*) $(c_1)_1 = 1$, $(c_1)_2 = -2$.

2.21. Give a one-parameter Galerkin solution of the equation

$$-\nabla^2 u = 1 \quad \text{in } \Omega \ (= \text{unit square})$$

$$u = 0 \quad \text{on } \Gamma$$

Use (*a*) algebraic and (*b*) trigonometric approximation functions. What would be the one-parameter Rayleigh–Ritz solution of this problem?

Answer: (*b*) $c_{ij} = \dfrac{16}{\pi^4}\dfrac{1}{ij(i^2+j^2)} \quad (i, j \text{ odd})$

$$\phi_{ij} = \sin i\pi x \sin j\pi y$$

2.22. Repeat Problem 2.21 for an equilateral triangular domain.

Hint: Use the product of equations of the lines representing the sides of the triangle for the approximation function.

Answer: $c_1 = -\frac{1}{2}$.

2.23. Consider the differential equation

$$-\frac{d^2u}{dx^2} = \cos \pi x \quad \text{for } 0 < x < 1$$

subject to the following three sets of boundary conditions:

(1) $u(0) = 0, \quad u(1) = 0$

(2) $u(0) = 0, \quad \left(\dfrac{du}{dx}\right)\Big|_{x=1} = 0$

(3) $\left(\dfrac{du}{dx}\right)\Big|_{x=0} = 0, \quad \left(\dfrac{du}{dx}\right)\Big|_{x=1} = 0$

Determine a three-parameter solution, with trigonometric functions, using (*a*) the Rayleigh–Ritz method, (*b*) the least-squares method, and (*c*) collocation at $x = \frac{1}{4}$, $\frac{1}{2}$, and $\frac{3}{4}$, and compare with the exact solutions:

(1) $u_0 = \pi^{-2}(\cos \pi x + 2x - 1)$

(2) $u_0 = \pi^{-2}(\cos \pi x - 1)$

(3) $u_0 = \pi^{-2} \cos \pi x$

Answer: (1) $c_i = \dfrac{4}{\pi^3 i(i^2 - 1)}$.

REFERENCES FOR ADDITIONAL READING

Variational formulations and methods

Becker, M.: *The Principles and Applications of Variational Methods*, MIT Press, Cambridge, MA 1964.

Biot, M. A.: *Variational Principles in Heat Transfer*, Clarendon, London, 1972.

Finlayson, B. A.: *The Method of Weighted Residuals and Variational Principles*, Academic Press, New York, 1972.

Forray, M. J.: *Variational Calculus in Science and Engineering*, McGraw-Hill, New York, 1968.

Hildebrand, F. B.: *Methods of Applied Mathematics*, 2d ed., Prentice-Hall, New York, 1965.

Lanczos, C.: *The Variational Principles of Mechanics,* The University of Toronto Press, Toronto, 1964.

Langhaar, H. L.: *Energy Methods in Applied Mechanics,* John Wiley, New York, 1962.

Leipholz, H.: *Direct Variational Methods and Eigenvalue Problems in Engineering,* Noordhoff, Leyden, 1977.

Lippmann, H.: *Extremum and Variational Principles in Mechanics,* Springer-Verlag, New York, 1972.

Mikhlin, S. G.: *Variational Methods in Mathematical Physics,* Pergamon Press, New York, 1964.

———: *The Numerical Performance of Variational Methods,* Wolters-Noordhoff, Groningen, 1971.

Oden, J. T., and J. N. Reddy: *Variational Methods in Theoretical Mechanics,* Springer-Verlag, New York, 1976; 2d ed., 1983.

Reddy, J. N.: *Energy and Variational Methods in Applied Mechanics,* John Wiley, New York, 1984.

———: *Applied Functional Analysis and Variational Methods in Engineering,* McGraw-Hill, New York, 1986; Krieger, Melbourne, FL, 1991.

——— and M. L. Rasmussen: *Advanced Engineering Analysis,* John Wiley, New York, 1982; Krieger, Melbourne, FL, 1990.

Rektorys, K.: *Variational Metnods in Mathematics, Science and Engineering,* Reidel, Boston, 1977.

Schechter, R. S.: *The Variational Methods in Engineering,* McGraw-Hill, New York, 1967.

Washizu, K.: *Variational Methods in Elasticity and Plasticity,* 2d ed., Pergamon Press, New York, 1975; 3d ed., 1982.

Weinstock, R.: *Calculus of Variations with Applications to Physics and Engineering,* McGraw-Hill, New York, 1952.

PART
2

FINITE ELEMENT ANALYSIS OF ONE-DIMENSIONAL PROBLEMS

CHAPTER 3

SECOND-ORDER BOUNDARY VALUE PROBLEMS

3.1 INTRODUCTION

The traditional variational methods (e.g., the Rayleigh–Ritz, Galerkin, and least-squares) described in Chapter 2 cease to be effective because of a serious shortcoming, namely, the difficulty in constructing the approximation functions. The approximation functions, apart from satisfying continuity, linear independence, completeness, and essential boundary conditions, are arbitrary; the selection becomes even more difficult when the given domain is geometrically complex. Since the quality of the approximation is directly affected by the choice of the approximation functions, it is discomforting to know that there exists no systematic procedure to construct them. Because of this shortcoming, despite the simplicity in obtaining approximate solutions, the traditional variational methods of approximation were never regarded as competitive computationally when compared with traditional finite difference schemes.

Ideally speaking, an effective computational method should have the following features:

1. It should have a sound mathematical as well as physical basis (i.e., yield convergent solutions and be applicable to practical problems).
2. It should not have limitations with regard to the geometry, the physical composition of the domain, or the nature of the "loading."

3. The formulative procedure should be independent of the shape of the domain and the specific form of the boundary conditions.
4. The method should be flexible enough to allow different degrees of approximation without reformulating the entire problem.
5. It should involve a systematic procedure that can be automated for use on digital computers.

The finite element method is a technique in which a given domain is represented as a collection of simple domains, called *finite elements,* so that it is possible to systematically construct the approximation functions needed in a variational or weighted-residual approximation of the solution of a problem over each element. Thus, the finite element method differs from the traditional Rayleigh–Ritz, Galerkin, least-squares, collocation, and other weighted-residual methods in the manner in which the approximation functions are constructed. But this difference is responsible for the following three basic features of the finite element method:

1. *Division of whole into parts,* which allows representation of geometrically complex domains as collections of geometrically simple domains that enable a systematic derivation of the approximation functions.
2. *Derivation of approximation functions* over each element; the approximation functions are often algebraic polynomials that are derived using interpolation theory.
3. *Assembly of elements,* which is based on continuity of the solution and balance of internal fluxes; the assemblage of elements represents a discrete analog of the original domain, and the associated system of algebraic equations represents a numerical analog of the mathematical model of the problem being analyzed.

These three features, which constitute three major steps of the finite element formulation, are closely related. The geometry of the elements used to represent the domain of a problem should be such that the approximation functions can be uniquely derived. The approximation functions depend not only on the geometry but also on the number and location of points, called *nodes,* in the element and the quantities to be interpolated (e.g., solution, or solution and its derivatives). Once the approximation functions have been derived, the procedure to obtain algebraic relations among the unknown coefficients (which give the values of the solution at the nodes of the finite elements) is exactly the same as that used in the Rayleigh–Ritz and weighted-residual methods. Hence, a careful reading of Chapter 2 makes the present reading easier.

The finite element method not only overcomes the shortcomings of the traditional variational methods, but it is also endowed with the features of an

TABLE 3.1
Steps involved in the finite element analysis of a typical problem

1. Discretization (or representation) of the given domain into a collection of preselected finite elements. (This step can be postponed until after the finite element formulation of the equation is completed.)
    - *a.* Construct the finite element mesh of preselected elements.
    - *b.* Number the nodes and elements.
    - *c.* Generate the geometric properties (e.g., coordinates and cross-sectional areas) needed for the problem.
2. Derivation of element equations for all typical elements in the mesh.
    - *a.* Construct the variational formulation of the given differential equation over the typical element.
    - *b.* Assume that a typical dependent variable u is of the form

      $$u = \sum_{i=1}^{n} u_i \psi_i$$

      and substitute it into Step 2*a* to obtain element equations in the form

      $$[K^e]\{u^e\} = \{F^e\}$$

    - *c.* Derive or select, if already available in the literature, element interpolation functions ψ_i and compute the element matrices.
3. Assembly of element equations to obtain the equations of the whole problem.
    - *a.* Identify the interelement continuity conditions among the primary variables (relationship between the local degrees of freedom and the global degrees of freedom—connectivity of elements) by relating element nodes to global nodes.
    - *b.* Identify the "equilibrium" conditions among the secondary variables (relationship between the local source or force components and the globally specified source components).
    - *c.* Assemble element equations using Steps 3*a* and 3*b*.
4. Imposition of the boundary conditions of the problem.
    - *a.* Identify the specified global primary degrees of freedom.
    - *b.* Identify the specified global secondary degrees of freedom (if not already done in Step 3*b*).
5. Solution of the assembled equations.
6. Postprocessing of the results.
    - *a.* Compute the gradient of the solution or other desired quantities from the primary degrees of freedom computed in Step 5.
    - *b.* Represent the results in tabular and/or graphical form.

effective computational technique. The basic steps involved in the finite element analysis of a problem are given in Table 3.1.

In the sections that follow, our objective will be to introduce many fundamental ideas that form the basis of the finite element method. In doing so, we postpone some issues of practical and theoretical complexity to later sections of this chapter and to Chapters 4–14. The basic steps of a finite element analysis are introduced via a model second-order differential equation, which is representative of many one-dimensional systems.

3.2 BASIC STEPS OF THE FINITE ELEMENT ANALYSIS

3.2.1 Model Boundary Value Problem

Consider the problem of finding the function $u(x)$ that satisfies the differential equation

$$\boxed{-\frac{d}{dx}\left(a\frac{du}{dx}\right)+cu-q=0 \quad \text{for } 0<x<L} \tag{3.1}$$

and the boundary conditions

$$\boxed{u(0)=u_0, \qquad \left(a\frac{du}{dx}\right)\bigg|_{x=L}=Q_0} \tag{3.2}$$

where $a=a(x)$, $c=c(x)$, $q=q(x)$, u_0, and Q_0 are the data (i.e., known quantities) of the problem. Equation (3.1) arises in connection with the analytical description of many physical processes. For example, conduction and convection heat transfer in a plane wall or fin (1-D heat transfer), flow through channels and pipes, transverse deflection of cables, axial deformation of bars (see Fig. 3.1*a*), and many other physical processes are described by (3.1). Table 3.2 contains a list of several field problems described by (3.1)

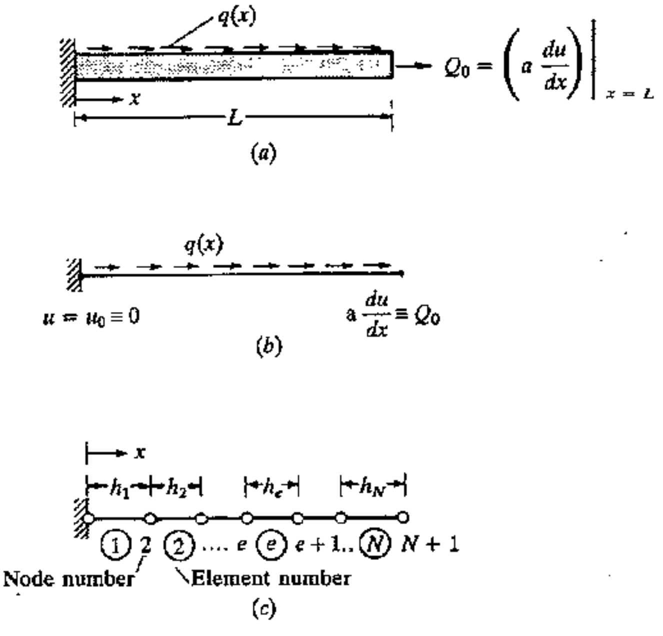
$q(x)$
$Q_0 = \left(a\frac{du}{dx}\right)\Big|_{x=L}$
x
L
(a)
$q(x)$
$u = u_0 \equiv 0$
$a\frac{du}{dx} \equiv Q_0$
(b)
x
h_1
h_2
h_e
h_N
① 2 ② .... e ⓔ e + 1.. Ⓝ N + 1
Node number
Element number
(c)

FIGURE 3.1
Finite element discretization of a one-dimensional domain: (*a*) physical problem; (*b*) mathematical idealization; (*c*) finite element discretization.

TABLE 3.2
Some examples of the second-order equations in one dimension

$$-\frac{d}{dx}\left(a\frac{du}{dx}\right)=q \quad \text{for } 0<x<L$$

Essential boundary condition: $u|_{x=0}=u_0$. **Natural boundary condition:** $(a\,du/dx)|_{x=L}=Q_0$

Field	**Primary variable** u	a	**Source term** q	**Secondary variable** Q_0
1. Transverse deflection of a cable	Transverse deflection	Tension in cable	Distributed transverse load	Axial force
2. Axial deformation of a bar	Longitudinal displacement	EA (E = modulus, A = cross-sectional area)	Friction or contact force on surface of bar	Axial force
3. Heat transfer	Temperature	Thermal conductivity	Heat generation	Heat
4. Flow through pipes	Hydrostatic pressure	$\pi D^4/128\mu$ (D = diameter, μ = viscosity)	Flow source (generally zero)	Flow rate
5. Laminar incompressible flow through a channel under constant pressure gradient	Velocity	Viscosity	Pressure gradient	Axial stress
6. Flow through porous media	Fluid head	Coefficient of permeability	Fluid flux	Flow (seepage)
7. Electrostatics	Electrostatic potential	Dielectric constant	Charge density	Electric flux

when $c(x)=0$. The mathematical structure common to apparently different fields is brought out in this table. Thus, if we can develop a numerical procedure by which (3.1) can be solved for all possible boundary conditions, the procedure can be used to solve all field problems listed in Table 3.2, as well as many others. This fact provides us with the motivation to use (3.1) as the model second-order equation in one dimension. A step-by-step procedure (see Table 3.1) for the formulation and solution of (3.1) by the finite element method is presented next.

3.2.2 Discretization of the Domain

The domain of the problem in the present case consists of all points between $x=0$ and $x=L$: $\Omega=(0, L)$; see Fig. 3.1(b). The domain Ω is divided into a set of line elements, a typical element being of length h_e and located between points A and B. The collection of such elements is called the *finite element mesh* of the domain (see Fig. 3.1c). The reason for dividing the domain into finite elements is twofold: first, to represent the geometry of the domain; and, second, to approximate the solution over each element of the mesh in order to better represent the solution over the entire domain. Approximation of the domain in the present case is not a concern, since it is a straight line. If the domain is a curve then approximation by a set of straight or curved line elements is necessary to represent it. Approximation of the solution over each element of the mesh is simpler than its approximation over the entire domain. Recall that in the traditional variational methods, the solution is required to satisfy the boundary conditions of the problem. This places severe restrictions on the choice of approximation functions, especially when discontinuities exist in the geometry, material properties, and/or loading of the problem (see Chapter 2 for details).

To connect the elements and impose continuity of the solution at nodes common to elements, we identify the endpoints of each line element as the *element nodes*. Depending on the degree of polynomial approximation used to represent the solution, additional nodes may be identified inside the element. The nodes play the role of interpolation points, as will be seen shortly, in constructing the approximation functions over an element.

The number of elements used in a problem depends mainly on the element type and accuracy desired. Whenever a problem is solved by the finite element method for the first time, one is required to investigate the convergence characteristics of the finite element approximation by gradually *refining the mesh* (i.e., increasing the number of elements) and comparing the solution with those obtained by *higher-order* elements. The *order* of an element refers to the degree of polynomial used to represent the solution over the element.

3.2.3 Derivation of Element Equations

The derivation of finite element equations, i.e., algebraic equations that relate the primary variables to the secondary variables at the nodes of the elements, involves three steps:

1. Construct the weighted-residual or weak form of the differential equation.
2. Assume the form of the approximate solution over a typical finite element.
3. Derive the finite element equations by substituting the approximate solution into the weighted-residual or weak form.

A typical element $\Omega^e = (x_A, x_B)$, whose endpoints have the coordinates $x = x_A$ and $x = x_B$, is isolated from the mesh (see Fig. 3.2*a*). We seek an approximate solution to the governing differential equation over the element, using the Rayleigh–Ritz method discussed in Chapter 2. In principle, any method that allows the derivation of necessary algebraic relations among the nodal values of the dependent variable can be used. In this book we develop the algebraic equations using the Rayleigh–Ritz method, which is based on the weak form of the differential equation. The equations resulting from the application of a variational method are relations between the *primary* variables (i.e., those involved in the specification of the essential boundary conditions) and the *secondary* variables (i.e., those involved in the specification of the natural boundary conditions). The three steps in the derivation of finite element equations of a *typical element* of the mesh are discussed next.

STEP 1: WEAK FORM. In the finite element method, we seek an approximate solution to (3.1) over each finite element. The polynomial approximation of

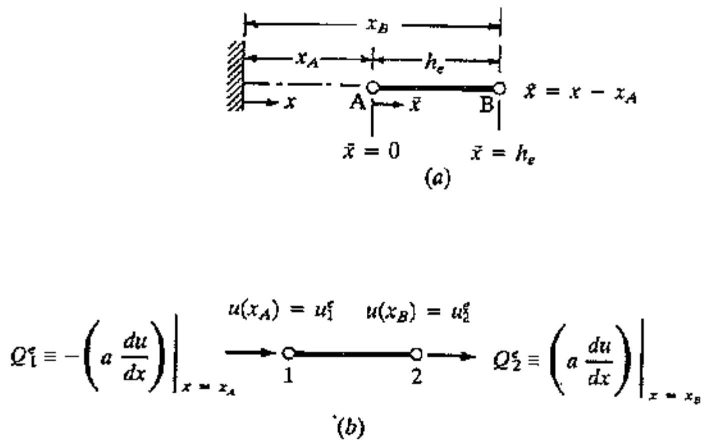

FIGURE 3.2.
Finite element discretization of a one-dimensional domain for the model problem in (3.1). (*a*) A typical finite element from the finite element mesh in Fig. 3.1(*c*); x = global coordinate, $\bar{x}$-local coordinate. (*b*) A typical element, with the definition of the primary (u) and secondary (Q) variables at the element nodes.

the solution within a typical finite element Ω^e is of the form

$$\boxed{U^e = \sum_{j=1}^{n} u_j^e \psi_j^e(x)} \tag{3.3}$$

where u_j^e are the values of the solution at the nodes of the finite element and ψ_j^e are the approximation functions over the element. The coefficients u_j^e are determined such that (3.1) is satisfied in a weighted-integral sense. As discussed in Chapter 2 (which should be consulted for additional details), the necessary and sufficient number of algebraic relations among the u_j^e can be obtained by recasting the differential equation (3.1) in a weighted-integral form:

$$0 = \int_{x_A}^{x_B} w\left[-\frac{d}{dx}\left(a\frac{du}{dx}\right) + cu - q\right] dx \tag{3.4}$$

where $w(x)$ denotes the weight function and $\Omega^e = (x_A, x_B)$ is the domain of a typical element (see Fig. 3.2*a*). For $u \approx U^e$ and each independent choice of w, we obtain an independent algebraic equation relating all u_j^e of the element. A total of n independent equations are required to solve for n values u_j^e. When w is selected to be ψ_i^e and (3.4) is used to obtain the ith equation of the required n equations, the resulting finite element model (i.e., system of algebraic equations among the nodal values) is termed the *Galerkin finite element model*. Since (3.4) contains the second derivative of U^e, the approximation functions ψ_j^e must be twice differentiable. In addition, if the secondary variables are to be included in the model, ψ_j^e must be at least cubic. Similar arguments apply for cases of the weighted-residual methods discussed in Chapter 2. For additional details of the weighted residual finite element models, see Reddy (1986) and Chapter 14.

To weaken the continuity required of the functions $\psi_j^e(x)$, we trade the differentiation in (3.4) from u to w such that both u and w are differentiated equally, once each in the present case. The resulting integral form is termed the *weak form* of (3.1). This form is not only equivalent to (3.1) but it also contains the natural boundary conditions of the problem. The three-step procedure of constructing the weak form of (3.1) was presented in Chapter 2, and is revisited in the next few paragraphs.

The first step is to multiply the governing differential equation with a weight function w and integrate over a *typical element*. The second step is to trade differentiation from u to w, using integration by parts. This is achieved as follows. Consider the identity

$$-w\left[\frac{d}{dx}\left(a\frac{du}{dx}\right)\right] = -\frac{d}{dx}\left(wa\frac{du}{dx}\right) + a\frac{dw}{dx}\frac{du}{dx} \tag{3.5a}$$

which is simply the product rule of differentiation applied to the product of two functions, $a\,du/dx$ and w. Integrating this identity over the element domain,

we obtain

$$-\int_{x_A}^{x_B} w\left[\frac{d}{dx}\left(a\frac{du}{dx}\right)\right]dx = -\int_{x_A}^{x_B} \frac{d}{dx}\left(wa\frac{du}{dx}\right)dx + \int_{x_A}^{x_B} a\frac{dw}{dx}\frac{du}{dx}\,dx$$

$$= -\left[wa\frac{du}{dx}\right]_{x_A}^{x_B} + \int_{x_A}^{x_B} a\frac{dw}{dx}\frac{du}{dx}\,dx \qquad (3.5b)$$

Substituting (3.5*b*) into (3.4), we arrive at the result [cf. (2.34)]

$$0 = \int_{x_A}^{x_B}\left(a\frac{dw}{dx}\frac{du}{dx} + cwu - wq\right)dx - \left[wa\frac{du}{dx}\right]_{x_A}^{x_B} \qquad (3.6)$$

The third and last step is to identify the primary and secondary variables of the variational (or weak) form. This requires us to classify the boundary conditions of each differential equation into *essential* (or geometric) and *natural* (or force) boundary conditions. The classification is made uniquely by examining the boundary term appearing in the weak form (3.6),

$$\left[wa\frac{du}{dx}\right]_{x_A}^{x_B}$$

As a rule, the coefficient of the weight function in the boundary expression is called the *secondary variable,* and its specification constitutes the *natural boundary condition.* The dependent unknown *in the same form as the weight function* in the boundary expression is termed the *primary variable,* and its specification constitutes the *essential boundary condition.* For the model equation at hand, the primary and secondary variables are

$$u \quad \text{and} \quad a\frac{du}{dx} \equiv Q$$

In writing the final form of the variational (or weak) statement, we assume that all boundary conditions at the element level are of the natural type, so that they can be included in the variational statement:

$$\boxed{-Q_A = \left(a\frac{du}{dx}\right)\bigg|_{x_A}, \qquad Q_B = \left(a\frac{du}{dx}\right)\bigg|_{x_B}.} \qquad (3.7)$$

The primary and secondary variables at the nodes are shown on the typical element in Fig. 3.2(*b*). Students of engineering recognize that this figure is the *free-body diagram* of the typical element, with its internal forces (i.e., reactions) Q_1^e and Q_2^e. The quantities $Q_1^e \equiv Q_A$ and $Q_2^e \equiv Q_B$ have the meaning of forces in the axial deformation of bars; Q_1^e is a compressive force while Q_2^e is a tensile force (algebraically, both are positive, as shown in Fig. 3.2*b*). For heat conduction problems Q_1^e and Q_2^e denote the heats conducting *into* the body. The arrow on the second node should be reversed for heat transfer problems, because the Fourier heat conduction law relating the gradient of temperature to the heat flux contains a negative sign (implying heat flows from hot to cold). For additional details on heat transfer, see Section 3.3.1. With the notation in (3.7), the variational form becomes

$$\boxed{0=\int_{x_A}^{x_B}\left(a\frac{dw}{dx}\frac{du}{dx}+cwu-wq\right)dx-w(x_A)Q_A-w(x_B)Q_B} \tag{3.8}$$

This completes the three-step procedure of constructing the weak form. The weak form in (3.8) contains two types of expressions: those containing both w and u; and those containing only w. We group the former type into a single expression, called the *bilinear form*:

$$B(w,u)\equiv\int_{x_A}^{x_B}\left(a\frac{dw}{dx}\frac{du}{dx}+cwu\right)dx \tag{3.9a}$$

We denote all terms containing only w (but not u) by $l(w)$, called the *linear form*:

$$l(w)=\int_{x_A}^{x_B} wq\,dx+w(x_A)Q_A+w(x_B)Q_B \tag{3.9b}$$

The variational statement (3.8) can now be expressed as

$$B(w,u)=l(w) \tag{3.10}$$

which is called the *variational problem* associated with (3.1). As will be seen later, the bilinear form results directly in the element coefficient matrix, and the linear form leads to the right-hand-side column vector of the finite element equations.

Those who have a background in applied mathematics or solid and structural mechanics will appreciate the fact that the variational problem (3.10) is nothing but the statement of the minimization of a quadratic functional or of total potential energy $I(u)$:

$$\delta I=0$$

where δ is the variational symbol (see Section 2.3.3) and I is the quadratic functional defined by [see (2.43*b*)]

$$I(u)=\tfrac{1}{2}B(u,u)-l(u) \tag{3.11}$$

Equation (3.11) holds only when $l(u)$ is linear in u, and $B(w,u)$ is bilinear and symmetric in u and w,

$$B(w,u)=B(u,w)$$

When (3.1) describes the axial deformation of a bar, $\frac{1}{2}B(u,u)$ represents the elastic strain energy stored in the bar, $l(u)$ represents the work done by applied forces, and $I(u)$ represents the total potential energy of the bar element. It is important to note that finite element formulations do not require the existence of the functional $I(u)$. What is needed is a way to obtain exactly n algebraic equations among the u_j^e of (3.3) such that the governing differential equation is satisfied over the element in some meaningful way. In the present study, we use the weak form of the differential equation, i.e., (3.8) or (3.10), and the Rayleigh–Ritz method to obtain the n algebraic equations among the nodal variables u_i^e and Q_i^e.

STEP 2: APPROXIMATION OF THE SOLUTION. Recall that the weak form over an element is equivalent to the differential equation and the natural boundary conditions of the element. The essential boundary conditions of the element, say $u(x_A) = u_A$ and $u(x_B) = u_B$, are not included in the weak form. Hence, they must be included in the approximation of $u(x)$. Thus, the approximation of $u(x)$ must be an interpolant, i.e., must be equal to u_A at x_A and u_B at x_B. Since the weak form contains the first-order derivatives of u, any continuous function would be a candidate for the finite element solution. Let us denote the finite element solution over element $\Omega^e = (x_A, x_B)$ by U^e. Then we seek the approximate solution U^e in the form of algebraic polynomials. The reason for this choice is twofold: first, the interpolation theory of numerical analysis can be used to develop the approximation functions systematically over an element; second, numerical evaluation of integrals of algebraic polynomials is easy.

As in variational methods, the approximation solution U^e must fulfill certain requirements in order that it be convergent to the actual solution u as the number of elements is increased. These are:

1. The approximate solution should be continuous over the element, and differentiable, as required by the weak form.
2. It should be a *complete* polynomial, i.e., include all lower-order terms up to the highest order used.
3. It should be an interpolant of the primary variables at the nodes of the finite element.

(3.12)

The reason for the first requirement is obvious; it ensures a nonzero coefficient matrix. The second requirement is necessary in order to capture all possible states, i.e., constant, linear and so on, of the actual solution. For example, if a linear polynomial without the constant term is used to represent the temperature distribution in a one-dimensional system, the approximate solution can never be able to represent a uniform state of temperature in the element. The third requirement is necessary in order to satisfy the essential boundary conditions of the element and to enforce continuity of the primary variables at points common to several elements.

For the variational statement at hand, the minimum polynomial order is linear. A *complete* linear polynomial is of the form

$$U^e = a + bx \tag{3.13}$$

where a and b are constants. This expression meets the first two requirements in (3.12). To satisfy the third

$$U^e(x_A) = u_1^e, \qquad U^e(x_B) = u_2^e \tag{3.14}$$

we express the constants a and b in (3.13) in terms of u_1^e and u_2^e. Equations (3.14) provide two relations between (a, b) and (u_1^e, u_2^e):

$$\begin{aligned} u_1^e &= a + bx_A \\ u_2^e &= a + bx_B \end{aligned} \tag{3.15a}$$

or, in matrix form,

$$\begin{Bmatrix} u_1^e \\ u_2^e \end{Bmatrix} = \begin{bmatrix} 1 & x_A \\ 1 & x_B \end{bmatrix} \begin{Bmatrix} a \\ b \end{Bmatrix} \tag{3.15b}$$

Inverting (3.15*b*) by Cramer's rule, we obtain

$$\begin{aligned} a &= \begin{vmatrix} u_1^e & x_A \\ u_2^e & x_B \end{vmatrix} \bigg/ \begin{vmatrix} 1 & x_A \\ 1 & x_B \end{vmatrix} = \frac{1}{h_e}(u_1^e x_B - u_2^e x_A) \equiv \frac{1}{h_e}(\alpha_1^e u_1^e + \alpha_2^e u_2^e) \\ b &= \begin{vmatrix} 1 & u_1^e \\ 1 & u_2^e \end{vmatrix} \bigg/ \begin{vmatrix} 1 & x_A \\ 1 & x_B \end{vmatrix} = \frac{1}{h_e}(u_2^e - u_1^e) \equiv \frac{1}{h_e}(\beta_1^e u_1^e + \beta_2^e u_2^e) \end{aligned} \tag{3.15c}$$

where $h_e = x_B - x_A$ and

$$\alpha_i^e = (-1)^j x_j^e, \quad \beta_i^e = (-1)^i; \quad x_1^e = x_A, \quad x_2^e = x_B \tag{3.15d}$$

In (3.15*d*), i and j permute in a natural order:

$$\text{if} \quad i = 1 \quad \text{then} \quad j = 2; \quad \text{if} \quad i = 2 \quad \text{then} \quad j = 1$$

The α_i^e and β_i^e are introduced to show the typical form of the interpolation functions. Substitution of (3.15*c*) into (3.13) yields

$$\begin{aligned} U^e(x) &= \frac{1}{h_e}[(\alpha_1^e u_1^e + \alpha_2^e u_2^e) + (\beta_1^e u_1^e + \beta_2^e u_2^e)x] \\ &= \frac{1}{h_e}(\alpha_1^e + \beta_1^e x)u_1^e + \frac{1}{h_e}(\alpha_2^e + \beta_2^e x)u_2^e \end{aligned}$$

That is,

$$\boxed{U^e(x) = \psi_1^e(x)u_1^e + \psi_2^e(x)u_2^e = \sum_{j=1}^{2} \psi_j^e(x)u_j^e} \tag{3.16a}$$

where

$$\boxed{\psi_1^e(x) = \frac{1}{h_e}(\alpha_1^e + \beta_1^e x) = \frac{x_B - x}{x_B - x_A}, \qquad \psi_2^e(x) = \frac{1}{h_e}(\alpha_2^e + \beta_2^e x) = \frac{x - x_A}{x_B - x_A}} \tag{3.16b}$$

which are called the linear *finite element approximation functions*.

For the linear interpolation (3.16), we label the endpoints as nodes 1 and 2, and rename the secondary variables as

$$Q_A = Q_1^e, \quad Q_B = Q_2^e \tag{3.17}$$

The global node numbers for elements connected in series can be related to the element node numbers. For linear elements, the global node numbers of element Ω^e are e and $e+1$, and the global coordinates of the element nodes are x_e and x_{e+1} (i.e., $x_A = x_e$ and $x_B = x_{e+1}$).

Note that the element interpolation functions ψ_i^e in (3.16*b*) are expressed in terms of the *global coordinate* x (i.e., the coordinate of the problem), but they are defined only on the element domain $\Omega^e = (x_A, x_B) = (x_e, x_{e+1})$. If we choose to express them in terms of a coordinate $\bar{x}$ with origin fixed at node 1 of the element, ψ_i^e of (3.16*b*) take the forms

$$\boxed{\psi_1^e(\bar{x}) = 1 - \frac{\bar{x}}{h_e}, \qquad \psi_2^e(\bar{x}) = \frac{\bar{x}}{h_e}} \tag{3.18}$$

The coordinate $\bar{x}$ is termed the *local* or *element coordinate*. The functions ψ_i^e are shown in Fig. 3.3(*a*). Note that ψ_1^e is equal to 1 at node 1 and zero at node 2, and ψ_2^e is equal to 1 at node 2 and zero at node 1. These properties of ψ_i^e are known as the interpolation properties.

The global interpolation functions Φ_I can be defined in terms of the element interpolation functions corresponding to the global node I (see Fig.

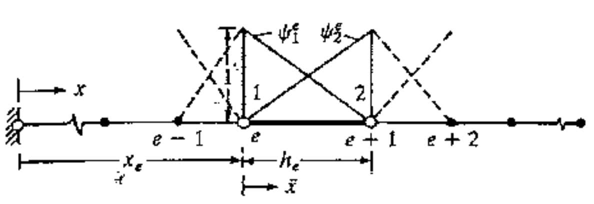

$$\psi_1^e = 1 - \bar{x}/h_e$$
$$\psi_2^e = \bar{x}/h_e$$

(*a*)

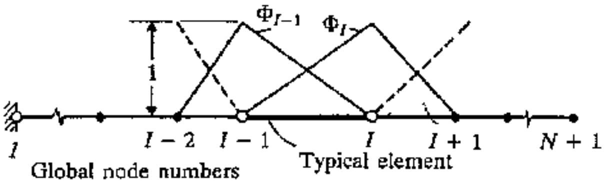

$$\Phi_I = \begin{cases} \psi_2^{I-1} & \text{for } x_{I-1} \le x \le x_I \\ \psi_1^I & \text{for } x_I \le x \le x_{I+1} \end{cases}$$

(*b*)

FIGURE 3.3
(*a*) Local and (*b*) global interpolation functions for the two-node (linear) element ($x_A = x_e$, $x_B = x_{e+1}$).

3.3*b*). Since $U^e(x)$ of (3.16*a*) is an interpolant of $u(x)$ over the element Ω^e, ψ_i^e are also called *interpolation functions*. Interpolation functions derived using the dependent unknown—not its derivatives—at the nodes (i.e., interpolation functions with C^0 continuity) are called the *Lagrange family of interpolation functions*. When the dependent unknown and its derivatives at the nodes are used to derive the interpolation functions, the resulting interpolation functions are known as the *Hermite family of interpolation functions* (see the classical beam element in Chapter 4).

Note that ψ_i^e are derived systematically; starting with an assumed degree of algebraic polynomial for the dependent unknown and determining the coefficients of the polynomial in terms of the primary degrees of freedom, we expressed the dependent variable as a linear combination of approximation functions and the primary nodal variables. The key in the procedure is to select the number and the location of nodes in the element so that the geometry of the latter is uniquely defined. The number of nodes must be sufficient to allow the assumed degree of interpolation of the solution in terms of the primary variables. For a linear polynomial approximation, two nodes with one primary unknown per node are sufficient to define the geometry of the element, provided the two nodes are the endpoints of the element. Since a quadratic polynomial is uniquely defined by three parameters, a total of three nodal points must be identified in the element. To define the geometry of the element, two of the nodes must be the endpoints of the element. The third can be identified inside the element.

Returning to the linear approximation (3.13), which is recast as (3.16*a*), we note that the true solution is approximated over each element by a linear polynomial $U^e(x)$ (see Fig. 3.4*a*). The error in the approximation, $E = u(x) - U^e(x)$, can be reduced by either decreasing the element size h_e or increasing the degree of the approximation (see Fig. 3.4*b*).

A quadratic approximation is of the form

$$U^e(x) = a + bx + cx^2 \tag{3.19}$$

which requires three nodes in order to rewrite U^e in terms of the values of $u(x)$ at the nodes. Two of the nodes are identified as the endpoints of the element to define the geometry, and the third node is taken interior to the element. In theory, the third node can be placed at any interior point. However, the midpoint of the element, being equidistant from the end nodes, is the best choice. Other choices (e.g., quarter-point) are dictated by special considerations (e.g., to have a certain degree of singularity in the derivative of the solution). Thus, we identify three nodes in the element of length h_e (see Fig. 3.5*a*) and rewrite $U^e(x)$ in terms of the three nodal values, (u_1^e, u_2^e, u_3^e). We have

$$\begin{aligned} u_1^e &= U^e(x_1^e) = a + bx_1^e + c(x_1^e)^2 \\ u_2^e &= U^e(x_2^e) = a + bx_2^e + c(x_2^e)^2 \\ u_3^e &= U^e(x_3^e) = a + bx_3^e + c(x_3^e)^2 \end{aligned} \tag{3.20a}$$

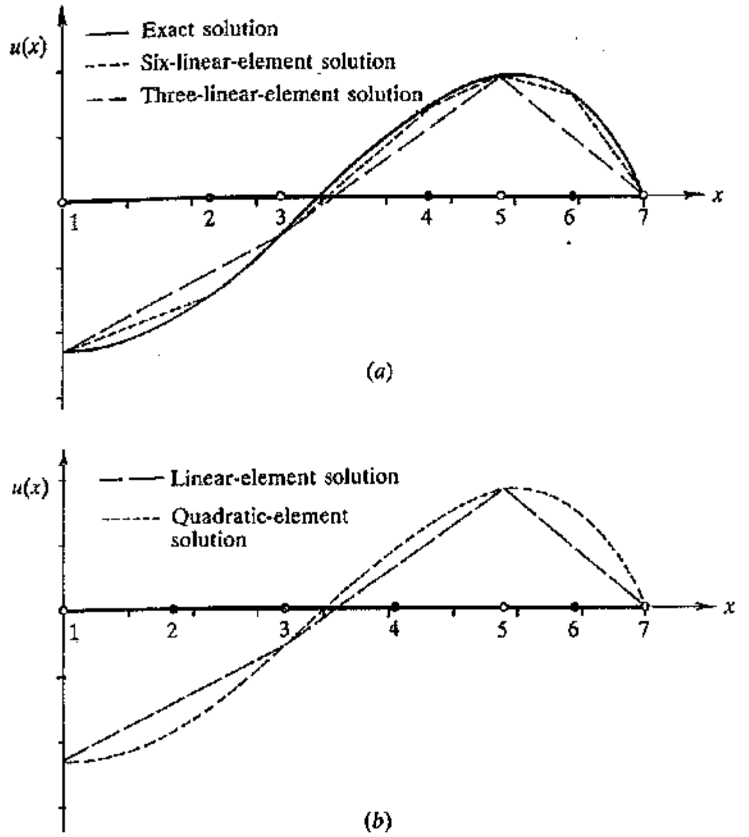

FIGURE 3.4
Refinements of finite element solutions; (*a*) mesh refinement using linear elements; (*b*) quadratic element solution using three elements.

or, in matrix form,

$$\begin{Bmatrix} u_1^e \\ u_2^e \\ u_3^e \end{Bmatrix} = \begin{bmatrix} 1 & x_1^e & (x_1^e)^2 \\ 1 & x_2^e & (x_2^e)^2 \\ 1 & x_3^e & (x_3^e)^2 \end{bmatrix} \begin{Bmatrix} a \\ b \\ c \end{Bmatrix} \tag{3.20b}$$

where x_i^e is the global coordinate of the ith node of the element Ω^e. Inverting the above relations, we obtain

$$\begin{aligned} a &= \frac{1}{D^e}\sum_{i=1}^{3} \alpha_i^e u_i^e, \qquad \alpha_i^e = x_j^e (x_k^e)^2 - x_k^e (x_j^e)^2 \\ b &= \frac{1}{D^e}\sum_{i=1}^{3} \beta_i^e u_i^e, \qquad \beta_i^e = (x_j^e)^2 - (x_k^e)^2 \\ c &= \frac{1}{D^e}\sum_{i=1}^{3} \gamma_i^e u_i^e, \qquad \gamma_i^e = -(x_j^e - x_k^e), \qquad D^e = \sum_{i=1}^{3} \alpha_i^e \end{aligned} \tag{3.21}$$

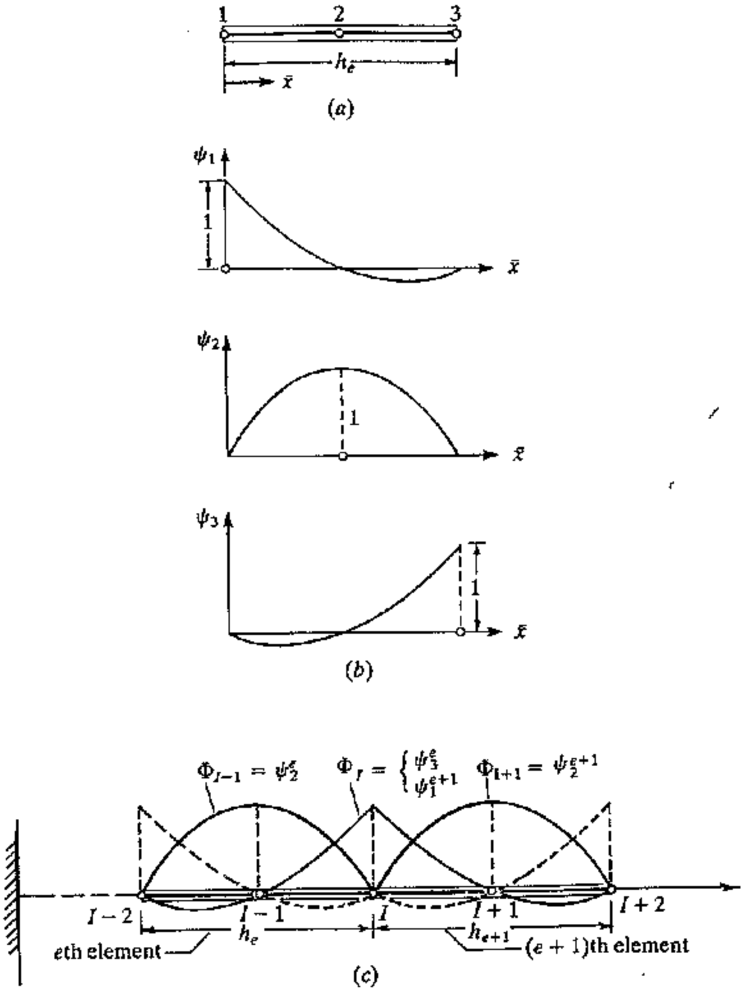

FIGURE 3.5
One-dimensional Lagrange quadratic element and its interpolation functions: (*a*) geometry of the element; (*b*) interpolation functions; (*c*) global interpolation functions corresponding to the quadratic interpolation functions. Here I denotes the global node number, e the element number, and i the element node number.

and (3.19) takes the form

$$U^e(x) = \psi_1^e(x)u_1^e + \psi_2^e(x)u_2^e + \psi_3^e(x)u_3^e = \sum_{j=1}^{3} \psi_j^e(x)u_j^e \qquad (3.22)$$

where ψ_j^e are the *quadratic Lagrange interpolation functions*,

$$\psi_i^e(x) = \frac{1}{D^e}(\alpha_i^e + \beta_i^e x + \gamma_i^e x^2) \quad (i = 1, 2, 3) \qquad (3.23)$$

Here D^e denotes the determinant of the matrix in (3.20b), and α_i^e, β_i^e, and γ_i^e are defined by (3.21). The subscripts used in (3.21) permute in a natural order:

$$\begin{aligned} &\text{if} \quad i=1 \quad \text{then} \quad j=2 \text{ and } k=3 \\ &\text{if} \quad i=2 \quad \text{then} \quad j=3 \text{ and } k=1 \\ &\text{if} \quad i=3 \quad \text{then} \quad j=1 \text{ and } k=2 \end{aligned} \tag{3.24}$$

For example, α_2^e, β_3^e, and γ_1^e are given by

$$\alpha_2^e = x_3^e(x_1^e)^2 - x_1^e(x_3^e)^2, \qquad \beta_3^e = (x_1^e)^2 - (x_2^e)^2, \qquad \gamma_1^e = x_3^e - x_2^e$$

The quadratic interpolation functions can be expressed in terms of a *local coordinate* $\bar{x}$, with origin fixed at node 1, the left end of the element. The global coordinate x is related to the local coordinate $\bar{x}$ by the relation

$$x = x_1^e + \bar{x} \tag{3.25}$$

where $x_1^e = x_A$ is the global coordinate of the first node of the element Ω^e. For a quadratic element with the interior node, node 2, located at $\bar{x} = \alpha h_e$, we have

$$\begin{aligned} \psi_1^e(\bar{x}) &= \left(1 - \frac{\bar{x}}{h}\right)\left(1 - \frac{1}{\alpha}\frac{\bar{x}}{h}\right) \\ \psi_2^e(\bar{x}) &= \frac{1}{\alpha(1-\alpha)}\frac{\bar{x}}{h}\left(1 - \frac{\bar{x}}{h}\right) \\ \psi_3^e(\bar{x}) &= -\frac{\alpha}{(1-\alpha)}\frac{\bar{x}}{h}\left(1 - \frac{1}{\alpha}\frac{\bar{x}}{h}\right) \end{aligned} \tag{3.26}$$

where $0 < \alpha < 1$ and $x_2^e = x_1^e + \alpha h_e$. For $\alpha = \frac{1}{2}$, i.e., when node 2 is placed at the midpoint of the element, (3.26) becomes

$$\boxed{\begin{aligned} \psi_1^e(\bar{x}) &= \left(1 - \frac{\bar{x}}{h}\right)\left(1 - \frac{2\bar{x}}{h}\right) \\ \psi_2^e(\bar{x}) &= 4\frac{\bar{x}}{h}\left(1 - \frac{\bar{x}}{h}\right) \\ \psi_3^e(\bar{x}) &= -\frac{\bar{x}}{h}\left(1 - \frac{2\bar{x}}{h}\right) \end{aligned}} \tag{3.27}$$

Plots of the quadratic interpolation functions are given in Fig. 3.5(*b*). The function ψ_i^e is equal to 1 at node i and zero at the other two nodes, but varies quadratically between the nodes.

All Lagrange family of interpolation functions satisfy the following properties, known as the *interpolation properties*:

$$\boxed{\begin{array}{ll}(1) & \psi_i^e(x_j^e)=\delta_{ij}\equiv\begin{cases}0 & \text{if } i\neq j\\ 1 & \text{if } i=j\end{cases}\\[2ex] (2) & \displaystyle\sum_{j=1}^{n}\psi_j^e(x)=1, \quad \text{hence} \quad \sum_{j=1}^{n}\frac{d\psi_j^e}{dx}=0\end{array}} \tag{3.28}$$

where $n-1$ is the degree of interpolation polynomials and x_j^e is the global coordinate of node j in the element Ω^e. It can be verified that the linear interpolation functions in (3.16) and quadratic interpolation functions in (3.26) and (3.27) satisfy the two properties in (3.28). The first is a direct result of the requirement $U^e(x_j^e)=u_j^e$, and the second comes from the inclusion of a constant term in the polynomial. For example, if the approximation U^e is to represent a uniform state of solution, $U^e=U_0^e=$ constant, then all $u_i^e=U_0^e$, and we have

$$U_0^e=\sum_{j=1}^{n}U_0^e\psi_j^e(x)$$

or

$$1=\sum_{j=1}^{n}\psi_j^e(x)$$

The interpolation properties (3.28) can be used to construct the Lagrange interpolation functions of any degree. For example, the quadratic interpolation functions (3.27) can be derived using property (1) of (3.28). Since $\psi_1^e(\bar{x})$ must vanish at nodes 2 and 3, i.e., at $\bar{x}=\frac{1}{2}h_e$ and $x=h_e$, it is of the form

$$\psi_1^e(\bar{x})=C(\bar{x}-\tfrac{1}{2}h_e)(\bar{x}-h_e)$$

The constant C is to be determined such that ψ_1^e is equal to 1 at $\bar{x}=0$:

$$1=C(0-\tfrac{1}{2}h_e)(0-h_e) \quad \text{or} \quad C=2/h_e^2$$

This gives

$$\psi_1^e(\bar{x})=\frac{2}{h_e^2}(\bar{x}-\tfrac{1}{2}h_e)(\bar{x}-h_e)=\left(1-\frac{\bar{x}}{h_e}\right)\left(1-\frac{2\bar{x}}{h_e}\right)$$

which is the same as in (3.27). The other two interpolation functions can be derived in a similar manner.

Although a detailed discussion is presented here on how to construct the Lagrange interpolation functions for one-dimensional elements, they are readily available in books on numerical analysis, and their derivation is independent of the physics of the problem to be solved. Their derivation depends only on the geometry of the element and the number and location of the nodes. The number of nodes must be equal to the number of terms in the polynomial. Thus, the interpolation functions derived above are useful not only in the finite element approximation of the problem at hand, but also in all problems that admit Lagrange interpolation of the variables, i.e., all problems for which the primary variables are the dependent unknowns of the governing equations.

STEP 3: FINITE ELEMENT MODEL. The weak form (3.8) or (3.10) is equivalent to the differential equation (3.1) over the element Ω^e and also contains the natural boundary conditions (3.7). Further, the finite element approximations (3.16*a*) or (3.22) satisfy the essential boundary conditions (3.14) of the element. The substitution of (3.16*a*) or (3.22) into (3.8) will give the necessary algebraic equations among the nodal values u_i^e and Q_i^e of the element Ω^e. In order to formulate the finite element model based on the weak form (3.8), it is *not* necessary to decide *a priori* the degree of approximation of U^e. The model can be developed for an arbitrary degree of interpolation:

$$\boxed{u \approx U^e = \sum_{j=1}^{n} u_j^e \psi_j^e(x)} \tag{3.29}$$

where ψ_j^e are the Lagrange interpolation functions of degree $n-1$. When $n > 2$, the weak form in (3.8) must be modified to include nonzero secondary variables, if any, at interior nodes:

$$\boxed{0 = \int_{x_A}^{x_B} \left(a \frac{dw}{dx}\frac{du}{dx} + cwu \right) dx - \int_{x_A}^{x_B} wq \, dx - \sum_{i=1}^{n} w(x_i^e) Q_i^e} \tag{3.30}$$

where x_i^e is the global coordinate of the ith node of element Ω^e. If nodes 1 and n denote the endpoints of the element then Q_1^e and Q_n^e represent the unknown point sources, and all other Q_i^e are always known (i.e., applied point sources).

Following the Rayleigh–Ritz procedure developed in Section 2.4.2, we substitute (3.29) for u and $\psi_1^e, \psi_2^e, \ldots, \psi_n^e$ for w into the weak form (3.30) to obtain n algebraic equations:

$$\begin{aligned}
0 &= \int_{x_A}^{x_B} \left[a \frac{d\psi_1^e}{dx} \left(\sum_{j=1}^{n} u_j^e \frac{d\psi_j^e}{dx} \right) + c\psi_1^e \left(\sum_{j=1}^{n} u_j^e \psi_j^e(x) \right) - \psi_1^e q \right] dx - \sum_{j=1}^{n} \psi_1^e(x_j^e) Q_j^e \\
0 &= \int_{x_A}^{x_B} \left[a \frac{d\psi_2^e}{dx} \left(\sum_{j=1}^{n} u_j^e \frac{d\psi_j^e}{dx} \right) + c\psi_2^e \left(\sum_{j=1}^{n} u_j^e \psi_j^e(x) \right) - \psi_2^e q \right] dx - \sum_{j=1}^{n} \psi_2^e(x_j^e) Q_j^e \\
&\vdots \\
0 &= \int_{x_A}^{x_B} \left[a \frac{d\psi_i^e}{dx} \left(\sum_{j=1}^{n} u_j^e \frac{d\psi_j^e}{dx} \right) + c\psi_i^e \left(\sum_{j=1}^{n} u_j^e \psi_j^e(x) \right) - \psi_i^e q \right] dx - \sum_{j=1}^{n} \psi_i^e(x_j^e) Q_j^e \\
&\qquad\qquad\qquad\qquad (i\text{th equation}) \\
&\vdots \\
0 &= \int_{x_A}^{x_B} \left[a \frac{d\psi_n^e}{dx} \left(\sum_{j=1}^{n} u_j^e \frac{d\psi_j^e}{dx} \right) + c\psi_n^e \left(\sum_{j=1}^{n} u_j^e \psi_j^e(x) \right) - \psi_n^e q \right] dx - \sum_{j=1}^{n} \psi_n^e(x_j^e) Q_j^e
\end{aligned} \tag{3.31a}$$

Note that the numbering of the algebraic equations follows that of the primary variables in the element. The ith algebraic equation can be written as

$$\boxed{0=\sum_{j=1}^{n} K_{ij}^e u_j^e - f_i^e - Q_i^e \quad (i=1,2,\ldots,n).} \tag{3.31b}$$

where

$$\boxed{K_{ij}^e=\int_{x_A}^{x_B}\left(a\frac{d\psi_i^e}{dx}\frac{d\psi_j^e}{dx}+c\psi_i^e\psi_j^e\right)dx=B(\psi_i^e,\psi_j^e), \qquad f_i^e=\int_{x_A}^{x_B} q\psi_i^e\,dx=l(\psi_i^e)} \tag{3.31c}$$

Note that the interpolation property (1) of (3.28) is used to write

$$\sum_{j=1}^{n}\psi_j^e(x_i^e)Q_j^e=Q_i^e \tag{3.32}$$

Equations (3.31a) can be expressed in terms of the coefficients K_{ij}^e, f_i^e, and Q_i^e as

$$\begin{aligned}
K_{11}^e u_1^e + K_{12}^e u_2^e + \ldots + K_{1n}^e u_n^e &= f_1^e + Q_1^e\\
K_{21}^e u_1^e + K_{22}^e u_2^e + \ldots + K_{2n}^e u_n^e &= f_2^e + Q_2^e\\
&\vdots\\
K_{n1}^e u_1^e + K_{n2}^e u_2^e + \ldots + K_{nn}^e u_n^e &= f_n^e + Q_n^e
\end{aligned} \tag{3.33a}$$

In matrix notation, the linear algebraic equations (3.33a) can be written as

$$\boxed{[K^e]\{u^e\}=\{f^e\}+\{Q^e\}} \tag{3.33b}$$

The matrix $[K^e]$ is called the *coefficient matrix*, or *stiffness matrix* in structural mechanics applications. The column vector $\{f^e\}$ is the *source vector*, or *force vector* in structural mechanics problems. Note that (3.33) contains $2n$ unknowns: $(u_1^e, u_2^e, \ldots, u_n^e)$ and $(Q_1^e, Q_2^e, \ldots, Q_n^e)$, called primary and secondary element *nodal degrees of freedom*; hence, it cannot be solved without having an additional n conditions. Some of these are provided by the boundary conditions and the remainder by balance of the secondary variables Q_i^e at nodes common to several elements. This balance can be implemented by putting the elements together (i.e., assembling the element equations). Upon assembly and imposition of boundary conditions, we shall obtain exactly the same number of algebraic equations as the number of unknown primary and secondary degrees of freedom. The ideas underlying the assembly procedure are discussed in the next section.

The coefficient matrix $[K^e]$, which is symmetric, and source vector $\{f^e\}$ can be evaluated for a given element and data (a, c, and q). For element-wise-constant values of a, c, and q (say, a_e, c_e, and q_e) the coefficients K_{ij}^e and f_i^e can easily be evaluated for a typical element.

Linear element. For a mesh of linear elements, the element Ω^e is located between the global nodes $x_A = x_e$ and $x_B = x_{e+1}$ (see Fig. 3.2). Hence,

$$K_{ij}^e = \int_{x_e}^{x_{e+1}} \left(a_e \frac{d\psi_i^e}{dx} \frac{d\psi_j^e}{dx} + c_e \psi_i^e \psi_j^e \right) dx, \qquad f_i^e = \int_{x_e}^{x_{e+1}} q_e \psi_i^e \, dx$$

or, in the local coordinate system $\bar{x}$,

$$K_{ij}^e = \int_0^{h_e} \left(a_e \frac{d\psi_i^e}{d\bar{x}} \frac{d\psi_j^e}{d\bar{x}} + c_e \psi_i^e \psi_j^e \right) d\bar{x}, \qquad f_i^e = \int_0^{h_e} q_e \psi_i^e \, d\bar{x}$$

where $x = x_e + \bar{x}$ and

$$dx = d\bar{x}, \qquad \frac{d\psi_i^e}{dx} = \frac{d\psi_i^e}{d\bar{x}}$$

The ψ_i^e can be expressed in terms of $\bar{x}$ as [see (3.18)]

$$\psi_1^e(\bar{x}) = 1 - \bar{x}/h_e, \qquad \psi_2^e(\bar{x}) = \bar{x}/h_e$$

We can compute K_{ij}^e and f_i^e by evaluating the integrals. We have

$$\begin{aligned}
K_{11}^e &= \int_0^{h_e} \left[a_e \left(-\frac{1}{h_e}\right)\left(-\frac{1}{h_e}\right) + c_e \left(1 - \frac{\bar{x}}{h_e}\right)\left(1 - \frac{\bar{x}}{h_e}\right) \right] d\bar{x} \\
&= \frac{a_e}{h_e} + \tfrac{1}{3} c_e h_e \\
K_{12}^e &= \int_0^{h_e} \left[a_e \left(-\frac{1}{h_e}\right)\frac{1}{h_e} + c_e \left(1 - \frac{\bar{x}}{h_e}\right)\frac{\bar{x}}{h_e} \right] d\bar{x} \\
&= -\frac{a_e}{h_e} + \tfrac{1}{6} c_e h_e = K_{21}^e \quad \text{(by symmetry)} \\
K_{22}^e &= \int_0^{h_e} \left(a_e \frac{1}{h_e}\frac{1}{h_e} + c_e \frac{\bar{x}}{h_e}\frac{\bar{x}}{h_e} \right) d\bar{x} = \frac{a_e}{h_e} + \tfrac{1}{3} c_e h_e
\end{aligned}$$

Similarly,

$$f_1^e = \int_0^{h_e} q_e \left(1 - \frac{\bar{x}}{h_e}\right) d\bar{x} = \tfrac{1}{2} q_e h_e, \qquad f_2^e = \int_0^{h_e} q_e \frac{\bar{x}}{h_e} \, d\bar{x} = \tfrac{1}{2} q_e h_e$$

Thus, for constant q_e, the total source $q_e h_e$ is equally distributed to the two nodes. The coefficient matrix and column vector are

$$\boxed{\begin{aligned} [K^e] &= \frac{a_e}{h_e} \begin{bmatrix} 1 & -1 \\ -1 & 1 \end{bmatrix} + \frac{c_e h_e}{6} \begin{bmatrix} 2 & 1 \\ 1 & 2 \end{bmatrix} \qquad (3.34a) \\ \{f^e\} &= \frac{q_e h_e}{2} \begin{Bmatrix} 1 \\ 1 \end{Bmatrix} \qquad (3.34b) \end{aligned}}$$

If $a = a_e x$ and $c = c_e$, the coefficient matrix $[K^e]$ can be evaluated as

$$[K^e] = \frac{a_e}{h_e} \left(\frac{x_e + x_{e+1}}{2} \right) \begin{bmatrix} 1 & -1 \\ -1 & 1 \end{bmatrix} + \frac{c_e h_e}{6} \begin{bmatrix} 2 & 1 \\ 1 & 2 \end{bmatrix} \qquad (3.35)$$

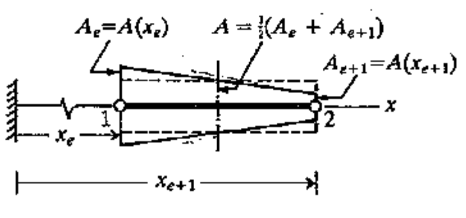

FIGURE 3.6
Approximation of an element with linearly varying cross-section by an equivalent element, with constant cross-section.

The reader should verify this. Note that when a is a linear function of x, this is equivalent to replacing a in the coefficient matrix with its average value [compare (3.34a) with (3.35)]:

$$a_{\text{avg}} = \tfrac{1}{2}(x_e + x_{e+1})a_e \tag{3.36}$$

For example, in the study of bars with linearly varying cross-section

$$a = EA(x) = E\left(A_e + \frac{A_{e+1} - A_e}{h_e}\bar{x}\right),$$

this amounts to replacing the varying cross-section with a constant cross-section within each element, the cross-sectional area of the constant section being the average area of cross section of the linearly varying element (see Fig. 3.6). Here A_e denotes the cross-sectional area at x_e and A_{e+1} is that at $x = x_{e+1}$.

When a, c, and q are algebraic polynomials in x, the evaluation of K_{ij}^e and f_j^e is straightforward. When they are complicated functions of x, numerical evaluation of the integrals in $[K^e]$ and $\{f^e\}$ will be sought. A complete discussion of the numerical evaluation of integrals is presented in Chapter 7.

When a and q are element-wise-constant and $c = 0$, the finite element equations corresponding to the linear element are

$$\frac{a_e}{h_e}\begin{bmatrix} 1 & -1 \\ -1 & 1 \end{bmatrix}\begin{Bmatrix} u_1^e \\ u_2^e \end{Bmatrix} = \frac{q_e h_e}{2}\begin{Bmatrix} 1 \\ 1 \end{Bmatrix} + \begin{Bmatrix} Q_1^e \\ Q_2^e \end{Bmatrix} \tag{3.37a}$$

$$\begin{aligned} \frac{a_e}{h_e}u_1^e - \frac{a_e}{h_e}u_2^e &= \tfrac{1}{2}q_e h_e + Q_1^e \\ -\frac{a_e}{h_e}u_1^e + \frac{a_e}{h_e}u_2^e &= \tfrac{1}{2}q_e h_e + Q_2^e \end{aligned} \tag{3.37b}$$

Quadratic element. For a quadratic-element mesh, the element Ω^e is located between global nodes $x_A = x_{2e-1}$ and $x_B = x_{2e+1}$. Hence,

$$\begin{aligned} K_{ij}^e &= \int_{x_{2e-1}}^{x_{2e+1}} \left(a_e \frac{d\psi_i^e}{dx}\frac{d\psi_j^e}{dx} + c_e\psi_i^e\psi_j^e\right) dx = \int_0^{h_e} \left(a_e \frac{d\psi_i^e}{d\bar{x}}\frac{d\psi_j^e}{d\bar{x}} + c_e\psi_i^e\psi_j^e\right) d\bar{x} \\ f_i^e &= \int_{x_{2e-1}}^{x_{2e+1}} \psi_i^e q_e \, dx = \int_0^{h_e} \psi_i^e q_e \, d\bar{x} \end{aligned} \tag{3.38}$$

where the Lagrange quadratic interpolation functions $\psi_i^e(\bar{x})$ $(i = 1, 2, 3)$ are given in (3.27). Evaluating the integrals in (3.38), we obtain

$$
\begin{aligned}
K_{11}^e &= \int_0^{h_e} \left\{ a_e\left(-\frac{3}{h_e}+\frac{4\bar{x}}{h_e^2}\right)\left(-\frac{3}{h_e}+\frac{4\bar{x}}{h_e^2}\right) \right. \\
&\quad \left. + c_e\left[1-\frac{3\bar{x}}{h_e}+2\left(\frac{\bar{x}}{h_e}\right)^2\right]\left[1-\frac{3\bar{x}}{h_e}+2\left(\frac{\bar{x}}{h_e}\right)^2\right]\right\} d\bar{x} \\
&= \frac{7}{3}\frac{a_e}{h_e}+\frac{2}{15}c_e h_e \\
K_{12}^e = K_{21}^e &= \int_0^{h_e} \left\{ a_e\left(-\frac{3}{h_e}+\frac{4\bar{x}}{h_e^2}\right)\left(\frac{4}{h_e}-\frac{8\bar{x}}{h_e^2}\right) \right. \\
&\quad \left. + c_e\left[1-\frac{3\bar{x}}{h_e}+2\left(\frac{\bar{x}}{h_e}\right)^2\right]\left[4\frac{\bar{x}}{h_e}\left(1-\frac{\bar{x}}{h_e}\right)\right]\right\} d\bar{x} \\
&= -\frac{8}{3}\frac{a_e}{h_e}+\frac{2}{30}c_e h_e
\end{aligned}
$$

and so on. Similarly,

$$
f_1^e = \int_0^{h_e} q_e\left[1-\frac{3\bar{x}}{h_e}+2\left(\frac{\bar{x}}{h_e}\right)^2\right] d\bar{x} = \tfrac{1}{6}q_e h_e = f_3^e \quad \text{(by symmetry)}
$$

$$
f_2^e = \int_0^{h_e} q_e\left[4\frac{\bar{x}}{h_e}\left(1-\frac{\bar{x}}{h_e}\right)\right] d\bar{x} = \tfrac{4}{6}q_e h_e
$$

Note that, for quadratic elements, the total source $q_e h_e$ is not distributed equally between the nodes. The distribution is *not* equivalent to that of two linear elements of lengths $\frac{1}{2}h_e$. Therefore, the computation of f_i^e should be based on the interpolation functions of that element. The sum of f_i^e for *any element* should always be equal to the integral of $q(x)$ over the element:

$$
\sum_{i=1}^{n} f_i^e = \int_{x_A}^{x_B} q(x)\,dx \tag{3.39}
$$

In summary, for element-wise-constant values of a, c, and q, the element matrices of a quadratic element are

$$
[K^e] = \frac{a_e}{3h_e}\begin{bmatrix} 7 & -8 & 1 \\ -8 & 16 & -8 \\ 1 & -8 & 7 \end{bmatrix} + \frac{c_e h_e}{30}\begin{bmatrix} 4 & 2 & -1 \\ 2 & 16 & 2 \\ -1 & 2 & 4 \end{bmatrix} \tag{3.40a}
$$

$$
\{f^e\} = \frac{q_e h_e}{6}\begin{Bmatrix} 1 \\ 4 \\ 1 \end{Bmatrix} \tag{3.40b}
$$

3.2.4 Connectivity of Elements

In deriving the element equations, we isolated a typical element (the *e*th) from the mesh and formulated the variational problem (or weak form) and developed its finite element model. To solve the total problem, we must put the elements back into their original positions. In doing this before discretization, we impose the continuity of the primary variables and balance of the secondary variables at the connecting nodes between elements. Continuity of the primary variables refers here to the single-valued nature of the solution; balance of secondary variables refers to the equilibrium of point sources at the junction of several elements. Thus, the assembly of elements is carried out by imposing the following two conditions:

1. Continuity of primary variables at connecting nodes:

$$u_n^e = u_1^{e+1} \tag{3.41a}$$

i.e., the last nodal value of the element Ω^e is the same as the first nodal value of the adjacent element Ω^{e+1}.

2. Balance of secondary variables at connecting nodes:

$$Q_n^e + Q_1^{e+1} = \begin{cases} 0 & \text{if no external point source is applied} \\ Q_0 & \text{if an external point source of magnitude } Q_0 \text{ is applied} \end{cases} \tag{3.41b}$$

In writing (3.41), it is assumed that elements are connected in a sequence. The continuity of primary variables $u_2^e = u_1^{e+1}$ and balance of secondary variables $Q_2^e + Q_1^{e+1}$ for a mesh of linear elements is illustrated in Fig. 3.7. The balance of secondary variables can be interpreted as the continuity of $a\,du/dx$ (*not* $a\,dU^e/dx$) at the point common to elements Ω^e and Ω^{e+1} (when no change in

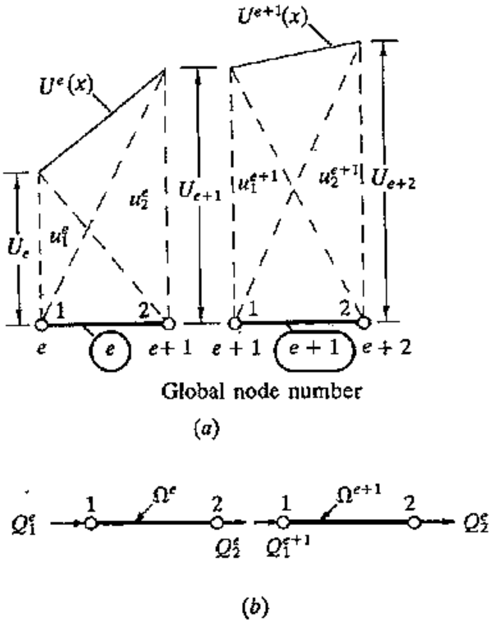

FIGURE 3.7
Assembly of two linear Lagrange elements: (*a*) continuity of the primary variable; (*b*) balance of the secondary variables.

$a\,du/dx$ is imposed externally):

$$\left(a\frac{du}{dx}\right)^{e}=\left(a\frac{du}{dx}\right)^{e+1}$$

or

$$\begin{aligned}\left(a\frac{du}{dx}\right)^{e}+\left(-a\frac{du}{dx}\right)^{e+1}&=0\\ Q_2^e+Q_1^{e+1}&=0\end{aligned}\tag{3.42}$$

The interelement continuity of the primary variables is imposed by renaming the two variables u_n^e and u_1^{e+1} at $x=x_N$ as one and the same, namely the value of u at the global node N:

$$u_n^e=u_1^{e+1}\equiv U_N \tag{3.43}$$

where $N=(n-1)e+1$ is the global node number corresponding to node n of the element Ω^e and node 1 of the element Ω^{e+1}. For example, for a mesh of E linear finite elements ($n=2$), we have

$$\begin{aligned}u_1^1&=U_1\\ u_2^1=u_1^2&=U_2\\ u_2^2=u_1^3&=U_3\\ &\vdots\\ u_2^{E-1}=u_1^E&=U_E\\ u_2^E&=U_{E+1}\end{aligned}\tag{3.44}$$

To enforce balance of the secondary variables Q_i^e, (3.41b), it is clear that we can set $Q_n^e+Q_1^{e+1}$ equal to zero or a specified value only if we have such expressions in our equations. To obtain such expressions, we must add the nth equation of the element Ω^e to the first equation of the element Ω^{e+1}; that is, we add

$$\sum_{j=1}^{n}K_{nj}^e u_j^e=f_n^e+Q_n^e$$

and

$$\sum_{j=1}^{n}K_{1j}^{e+1}u_j^{e+1}=f_1^{e+1}+Q_1^{e+1}$$

to give

$$\begin{aligned}\sum_{j=1}^{n}\left(K_{nj}^e u_j^e+K_{1j}^{e+1}u_j^{e+1}\right)&=f_n^e+f_1^{e+1}+\left(Q_n^e+Q_1^{e+1}\right)\\ &=f_n^e+f_1^{e+1}+Q_0\end{aligned}\tag{3.45}$$

This process reduces the number of equations from $2E$ to $E+1$. The first equation of the first element and the last equation of the last element will remain unchanged, except for renaming of the primary variables. The left-hand side of (3.45) can be written in terms of the global nodal values as

$$
\begin{aligned}
&(K^e_{n1}u^e_1 + K^e_{n2}u^e_2 + \ldots + K^e_{nn}u^e_n) + (K^{e+1}_{11}u^{e+1}_1 + K^{e+1}_{12}u^{e+1}_2 + \ldots + K^{e+1}_{1n}u^{e+1}_n)\\
&\quad = (K^e_{n1}U_N + K^e_{n2}U_{N+1} + \ldots + K^e_{nn}U_{N+n-1})\\
&\qquad + (K^{e+1}_{11}U_{N+n-1} + K^{e+1}_{12}U_{N+n} + \ldots + K^{e+1}_{1n}U_{N+2n-2})\\
&\quad = K^e_{n1}U_N + K^e_{n2}U_{N+1} + \ldots + K^e_{n(n-1)}U_{N+n-2}\\
&\qquad + (K^e_{nn} + K^{e+1}_{11})U_{N+n-1} + K^{e+1}_{12}U_{N+n} + \ldots + K^{e+1}_{1n}U_{N+2n-2}
\end{aligned}
\tag{3.46}
$$

where $N = (n-1)e + 1$.

For a mesh of E linear elements ($n = 2$), we have

$$
\begin{gathered}
K^1_{11}U_1 + K^1_{12}U_2 = f^1_1 + Q^1_1 \quad \text{(unchanged)}\\
K^1_{21}U_1 + (K^1_{22} + K^2_{11})U_2 + K^2_{12}U_3 = f^1_2 + f^2_1 + Q^1_2 + Q^2_1\\
K^2_{21}U_2 + (K^2_{22} + K^3_{11})U_3 + K^3_{12}U_4 = f^2_2 + f^3_1 + Q^2_2 + Q^3_1\\
\vdots\\
K^{E-1}_{21}U_{E-1} + (K^{E-1}_{22} + K^E_{11})U_E + K^E_{12}U_{E+1} = f^{E-1}_2 + f^E_1 + Q^{E-1}_2 + Q^E_1\\
K^E_{21}U_E + K^E_{22}U_{E+1} = f^E_2 + Q^E_2 \quad \text{(unchanged)}
\end{gathered}
\tag{3.47a}
$$

These are called the *assembled equations*. They contain the sum of coefficients and source terms at nodes common to two elements. Note that the numbering of the global equations corresponds to the numbering of the global primary degrees of freedom, U_I. This correspondence carries the symmetry of element matrices to the global matrix. Equations (3.47a) can be expressed in matrix form as

$$
\begin{bmatrix}
K^1_{11} & K^1_{12} & & & & \\
K^1_{21} & K^1_{22} + K^2_{11} & K^2_{12} & & 0 & \\
 & K^2_{21} & K^2_{22} + K^3_{11} & & & \\
\cdots & \cdots & \cdots & \cdots & \cdots & \cdots \\
 & 0 & & & K^{E-1}_{22} + K^E_{11} & K^E_{12}\\
 & & & & K^E_{21} & K^E_{22}
\end{bmatrix}
\begin{Bmatrix} U_1\\ U_2\\ U_3\\ \vdots\\ U_E\\ U_{E+1} \end{Bmatrix}
=
\begin{Bmatrix} f^1_1\\ f^1_2 + f^2_1\\ f^2_2 + f^3_1\\ \vdots\\ f^{E-1}_2 + f^E_1\\ f^E_2 \end{Bmatrix}
+
\begin{Bmatrix} Q^1_1\\ Q^1_2 + Q^2_1\\ Q^2_2 + Q^3_1\\ \vdots\\ Q^{E-1}_2 + Q^E_1\\ Q^E_2 \end{Bmatrix}
\tag{3.47b}
$$

Recall that all the above discussion of assembly is based on the assumption that elements are connected in series. In general, several elements can be connected at a node, and the elements do not have to be consecutively numbered. In that case, the above idea still holds, with the change that coefficients coming from all elements connected at one node will add up. For

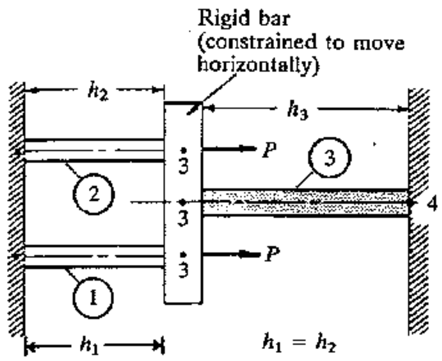

FIGURE 3.8
The geometry and finite element mesh of a bar structure.

example, consider the structure consisting of three bar elements shown in Fig. 3.8. Suppose that the connecting bar is rigid (i.e., not deformable) and is constrained to remain horizontal at all times. Then the continuity and force balance conditions for the structure are

$$u_2^1 = u_1^3 = u_2^2 = U_3, \qquad Q_2^1 + Q_1^3 + Q_2^2 = 2P \tag{3.48}$$

To enforce these conditions, we must add the second equation of element 1, the first equation of element 3, and the second equation of element 2:

$$(K_{21}^1 u_1^1 + K_{22}^1 u_2^1) + (K_{11}^3 u_1^3 + K_{12}^3 u_2^3) + (K_{21}^2 u_1^2 + K_{22}^2 u_2^2)$$
$$= f_2^1 + f_1^3 + f_2^2 + Q_2^1 + Q_1^3 + Q_2^2 \tag{3.49}$$

We note the following correspondence of local and global nodal values (see Fig. 3.8):

$$u_1^1 = U_1, \qquad u_1^2 = U_2, \qquad u_2^1 = u_1^3 = u_2^2 = U_3, \qquad u_2^3 = U_4$$

Hence, (3.49) becomes

$$K_{21}^1 U_1 + K_{21}^2 U_2 + (K_{22}^1 + K_{11}^3 + K_{22}^2) U_3 + K_{12}^3 U_4 = f_2^1 + f_1^3 + f_2^2 + Q_2^1 + Q_1^3 + Q_2^2$$
$$= f_2^1 + f_1^3 + f_2^2 + 2P$$

The other equations remain unchanged, except for renaming of the primary variables. The assembled equations are

$$\begin{bmatrix} K_{11}^1 & 0 & K_{12}^1 & 0 \\ 0 & K_{11}^2 & K_{12}^2 & 0 \\ K_{21}^1 & K_{21}^2 & \hat{K} & K_{12}^3 \\ 0 & 0 & K_{21}^3 & K_{22}^3 \end{bmatrix} \begin{Bmatrix} U_1 \\ U_2 \\ U_3 \\ U_4 \end{Bmatrix} = \begin{Bmatrix} f_1^1 \\ f_1^2 \\ f_2^1 + f_1^3 + f_2^2 \\ f_2^3 \end{Bmatrix} + \begin{Bmatrix} Q_1^1 \\ Q_1^2 \\ Q_2^1 + Q_1^3 + Q_2^2 \\ Q_2^3 \end{Bmatrix} \tag{3.50}$$

where $\hat{K} = K_{22}^1 + K_{11}^3 + K_{22}^2$.

The coefficients of the assembled matrix can be obtained directly. We note that the global coefficient K_{IJ} is a physical property of the system, relating global node I to global node J. For axial deformation of bars, K_{IJ} denotes the force required at node I to induce a unit displacement at node J, while the displacements at all other nodes are zero. Therefore, K_{IJ} is equal to the sum of all K_{ij}^e for which i corresponds to I and j corresponds to J, and i and j are the local nodes of the element Ω^e. Thus, if we have a correspondence between element node numbers and global node numbers then the assembled global coefficients can readily be written in terms of the element coefficients. The correspondence can be expressed through a matrix $[B]$, called the *connectivity matrix*, whose coefficient b_{ij} has the following meaning:

b_{ij} is the global node number corresponding to the jth node of element i

For example, for the structure shown in Fig. 3.8, the matrix $[B]$ is of order 3×2 (3 elements and 2 nodes per element):

$$[B] = \begin{bmatrix} 1 & 3 \\ 2 & 3 \\ 3 & 4 \end{bmatrix}$$

This array can be used in a variety of ways—not only for assembly, but also in the computer implementation of finite element computations. The matrix $[B]$ is used to assemble coefficient matrices as follow:

$K_{11}^1 = K_{11}$, because local node 1 of element 1 corresponds to global node 1

$K_{12}^1 = K_{13}$, because local nodes 1 and 2 of element 1 correspond to global nodes 1 and 3, respectively

and so on. When more than one element is connected at a global node, the element coefficients are to be added. For example, global node 3 appears in all three rows (i.e., elements) of the matrix $[B]$, implying that all three elements are connected at global node 3. More specifically, it indicates that node 2 of element 1, node 2 of element 2, and node 1 of element 3 are the same as global node 3. Hence

$$K_{22}^1 + K_{22}^2 + K_{11}^3 = K_{33}$$

Assembly on paper can be carried out by examining the finite element mesh of the problem. For the mesh shown in Fig. 3.8, we have

$K_{23} = K_{12}^2$, because global node 2 is the same as node 1 and global node 3 is the same as node 2 of element 2

$K_{24} = 0$, because global nodes 2 and 4 do not belong to the same element

$K_{33} = K_{22}^1 + K_{22}^2 + K_{11}^3$

and so on.

In summary, assembly of finite elements is carried out by imposing interelement continuity of primary variables and balance of secondary variables [see (3.41)]. Renaming the elemental primary variables in terms of the global primary variables and using the correspondence between the local and global nodes allows the assembly. When certain primary nodal values are not required to be continuous (by the variational formulation) across elements, such variables may be *condensed* out at the element level before assembling elements.

3.2.5 Imposition of Boundary Conditions

Up to this point, the specific nature of the problem has not been used in the development of the finite element model or in the assembly of finite elements. In other words, the discussion in Sections 3.2.1–3.2.4 is valid for any differential equation that is a special case of the model equation (3.1). One particular problem differs from others in the specification of the data and boundary conditions. Here we discuss how to impose the boundary conditions of a problem on the assembled set of algebraic equations. To this end, we use the problem in Fig. 3.8. Its boundary conditions are evident from the structure. The known primary degrees of freedom (i.e., displacements) are

$$u_1^1 = U_1 = 0, \qquad u_1^2 = U_2 = 0, \qquad u_2^3 = U_4 = 0 \tag{3.51a}$$

The known secondary degrees of freedom (i.e., forces) are

$$Q_2^1 + Q_2^2 + Q_1^3 = 2P \tag{3.51b}$$

The forces Q_1^1, Q_1^2, and Q_2^3 are unknown (reaction forces), and they can be determined in the post-computation, i.e., after the primary degrees of freedom are determined.

Imposing the boundary conditions (3.51) on the assembled system of equations (3.50) and for f_i^e, we obtain

$$\begin{bmatrix} K_{11}^1 & 0 & K_{12}^1 & 0 \\ 0 & K_{11}^2 & K_{12}^2 & 0 \\ K_{21}^1 & K_{21}^2 & K_{22}^1 + K_{22}^2 + K_{11}^3 & K_{12}^3 \\ 0 & 0 & K_{21}^3 & K_{22}^3 \end{bmatrix} \begin{Bmatrix} U_1 = 0 \\ U_2 = 0 \\ U_3 \\ U_4 = 0 \end{Bmatrix} = \begin{Bmatrix} Q_1^1 \\ Q_1^2 \\ 2P \\ Q_2^3 \end{Bmatrix} \tag{3.52}$$

This contains four equations in four unknowns: U_3, Q_1^1, Q_1^2, and Q_2^3.

3.2.6 Solution of Equations

As a standard procedure in finite element analysis, the unknown primary degrees of freedom are determined first by *considering the algebraic equations corresponding to the unknown primary variables.* Thus, in the present case, we consider the third equation in (3.52) to solve for U_3:

$$K_{21}^1 U_1 + K_{21}^2 U_2 + (K_{22}^1 + K_{22}^2 + K_{11}^3) U_3 + K_{12}^3 U_4 = 2P$$

or

$$(K_{22}^1 + K_{22}^2 + K_{11}^3) U_3 = 2P - (K_{21}^1 U_1 + K_{21}^2 U_2 + K_{12}^3 U_4) \tag{3.53}$$

Equation (3.53) is called the *condensed equation* for the unknown U_3. The term in parentheses on the right-hand side is zero because all specified displacements are zero in the present problem. Hence, the solution is given by

$$U_3 = 2P/(K_{22}^1 + K_{22}^2 + K_{11}^3) \tag{3.54a}$$

The unknown secondary variables are determined by considering the remaining equations of (3.52), i.e., those that contain the unknown secondary variables:

$$\begin{Bmatrix} Q_1^1 \\ Q_1^2 \\ Q_2^3 \end{Bmatrix} = \begin{bmatrix} K_{11}^1 & 0 & K_{12}^1 & 0 \\ 0 & K_{11}^2 & K_{12}^2 & 0 \\ 0 & 0 & K_{21}^3 & K_{22}^3 \end{bmatrix} \begin{Bmatrix} U_1 \\ U_2 \\ U_3 \\ U_4 \end{Bmatrix}$$

$$= \begin{Bmatrix} K_{12}^1 U_3 \\ K_{12}^2 U_3 \\ K_{21}^3 U_3 \end{Bmatrix}, \quad \text{because } U_1,\ U_2 \text{ and } U_4 \text{ are zero} \tag{3.54b}$$

It is possible, although not common with computer programs, to move all the unknowns to the left-hand side in (3.52) and solve for them all at once. But this process requires more computational time in practical problems.

In general, the assembled finite element equations can be partitioned conveniently into the following form:

$$\begin{bmatrix} [K^{11}] & [K^{12}] \\ [K^{21}] & [K^{22}] \end{bmatrix} \begin{Bmatrix} \{U^1\} \\ \{U^2\} \end{Bmatrix} = \begin{Bmatrix} \{F^1\} \\ \{F^2\} \end{Bmatrix} \tag{3.55}$$

where $\{U^1\}$ is the column of known primary variables, $\{U^2\}$ is the column of unknown primary variables, $\{F^1\}$ is the column of unknown secondary variables, and $\{F^2\}$ is the column of known secondary variables. Writing (3.55) as two matrix equations, we obtain

$$[K^{11}]\{U^1\} + [K^{12}]\{U^2\} = \{F^1\} \tag{3.56a}$$

$$[K^{21}]\{U^1\} + [K^{22}]\{U^2\} = \{F^2\} \tag{3.56b}$$

From (3.56*b*), we have

$$\boxed{\{U^2\} = [K^{22}]^{-1}(\{F^2\} - [K^{21}]\{U^1\})} \tag{3.56c}$$

Once $\{U^2\}$ is known, $\{F^1\}$ can be computed from (3.56*a*).

3.2.7 Postprocessing of the Solution

The solution of the finite element equations gives the nodal values of the primary unknown (e.g., displacement, velocity, or temperature). Postprocessing of the results includes one or more of the following:

1. Computation of any secondary variables (e.g., the gradient of the solution).
2. Interpretation of the results to check whether the solution makes sense (an understanding of the physical process and experience are the guides when other solutions are not available for comparison).
3. Tabular and/or graphical presentation of the results.

To determine the solution u as a continuous function of position x, we return to the approximation (3.29) over each element:

$$\boxed{u(x) \approx \begin{cases} U^1(x) = \sum_{j=1}^{n} u_j^1 \psi_j^1(x) \\ U^2(x) \approx \sum_{j=1}^{n} u_j^2 \psi_j^2(x) \\ \vdots \\ U^N(x) = \sum_{j=1}^{n} u_j^N \psi_j^N(x) \end{cases}} \tag{3.57}$$

where N is the number of elements in the mesh. Depending on the value of x, the corresponding element equation from (3.57) is used. The derivative of the solution is obtained by differentiating (3.57):

$$\frac{du}{dx} \approx \begin{cases} \sum_{j=1}^{n} u_j^1 \frac{d\psi_j^1}{dx} \\ \sum_{j=1}^{n} u_j^2 \frac{d\psi_j^2}{dx} \\ \vdots \\ \sum_{j=1}^{n} u_j^N \frac{d\psi_j^N}{dx} \end{cases} \tag{3.58}$$

Note that the derivative dU^e/dx of the linear finite element solution U^e is constant within each element, and it is discontinuous at the nodes because the continuity of the derivative of the finite element solution at the connecting nodes is not imposed:

$$\frac{dU^e}{dx} \neq \frac{dU^{e+1}}{dx}$$

The derivative calculated from different elements meeting at a node is always discontinuous in all C^0 approximations (i.e., approximations in which only the function values are interpolated), unless the approximate solution coincides with the actual solution.

The secondary variables Q_i^e can be computed in two different ways. In (3.54b), we determined the unknown secondary variables Q_1^1, Q_1^2, and Q_2^3 from the assembled equations of the problem in Fig. 3.8. Since the assembled equations often represent the equilibrium relations of a system, the Q_i^e computed from them will be denoted by $(Q_i^e)_{\text{equil}}$. The Q_i^e can also be determined using the definitions in (3.7), replacing u with U. We shall denote Q_i^e computed in this way by $(Q_i^e)_{\text{def}}$. Since $(Q_i^e)_{\text{def}}$ are calculated using the approximate U^e, they are not as accurate as $(Q_i^e)_{\text{equil}}$. However, in finite element computer codes, $(Q_i^e)_{\text{def}}$ are calculated instead of $(Q_i^e)_{\text{equil}}$. This is primarily because of computational aspects. Recall that, in arriving at the result (3.54*b*), we used part of the assembled coefficient matrix. In the numerical solution of simultaneous algebraic equations in a computer, the original assembled coefficient matrix is often modified, and therefore the coefficients needed for the determination of the secondary variables are not available, unless they are saved in an additional array. For the problem in Fig. 3.8, we have

$$
\begin{aligned}
(Q_1^1)_{\text{def}} &= -\left(EA\frac{dU}{dx}\right)\bigg|_{x=0} = -EA\frac{U_3-U_1}{h_1} = -\frac{EA}{h_1}U_3 = K_{12}^1U_3 \\
(Q_1^2)_{\text{def}} &= -\left(EA\frac{dU}{dx}\right)\bigg|_{x=0} = K_{12}^2U_3 \\
(Q_2^3)_{\text{def}} &= \left(EA\frac{dU}{dx}\right)\bigg|_{x=h_1+h_3} = EA\frac{U_4-U_3}{h_3} \\
&= -\frac{EAU_3}{h_3} = K_{21}^3U_3
\end{aligned}
\tag{3.59}
$$

where h_1 and h_3 are the lengths of elements 1 and 3, respectively.

The Qs computed using the definitions (3.7) are the same as those derived from the assembled equations for the problem in Fig. 3.8. This equality is *not to be expected in general*. In fact, when the source vector q is not zero, the secondary variables computed from the definitions (3.7) will be in error compared with those computed from the assembled equations. The error decreases as the number of elements or the degree of interpolation is increased.

This completes the basic steps involved in the finite element analysis of the model equation (3.1). A few remarks are in order on the steps described above for the model equation.

Remark 1. Although the Rayleigh–Ritz method was used to set up the element equations, any other method, such as a weighted-residual (e.g., the least-squares or Galerkin) method, could be used.

Remark 2. Steps 1–6 (see Table 3.1) are common for any problem. The derivation of interpolation functions depends only on the element geometry, and on the number and position of nodes in the element. The number of nodes in the element and the degree of approximation used are related.

Remark 3. The finite element equations (3.31) are derived for the linear operator equation

$$A(u) = q, \quad \text{where} \quad A = -\frac{d}{dx}\left(a\frac{d}{dx}\right) + c$$

Hence, they are valid for any physical problem that is described by the operator equation $A(u) = q$ or its special cases. One need only interpret the quantities appropriately. Examples of problems described by this operator are listed in Table 3.2. Thus, a computer program written for the finite element analysis of (3.1) can be used to analyze any of the problems in this table. Also, note that the data $a = a(x)$, $c = c(x)$, and $q = q(x)$ can be different in each of the elements.

Remark 4. Integration of the element matrices in (3.31*c*) can be implemented on a computer using numerical integration (see Chapter 7). When these integrals are algebraically complicated, one has no other choice but numerical integration.

Remark 5. As noted in (3.48) and (3.51*b*), the point sources at the nodes are included in the finite element model via the balance of sources at the nodes. Thus, in constructing finite element meshes, one should include nodes at the locations of point sources. If a point source does not occur at a node, it is possible to "distribute" it to the element nodes. Let Q_0 denote a point source at point x_0, $x_A \leqslant x_0 \leqslant x_B$. The point source Q_0 can be represented as a "function" by

$$q(x) = Q_0\delta(x - x_0)$$

where the Dirac delta function $\delta(\cdot)$ is defined by

$$\int_{-\infty}^{\infty} F(x)\delta(x - x_0)\,dx = F(x_0)$$

The contribution of the function $q(x)$ to the nodes of the element $\Omega^e = (x_A, x_B)$ is computed from [see (3.31*c*)]

$$f_i^e = \int_{x_A}^{x_B} q(x)\psi_i^e(x)\,dx = \int_{x_A}^{x_B} Q_0\delta(x - x_0)\psi_i^e(x)\,dx = Q_0\psi_i^e(x_0) \qquad (3.60)$$

where ψ_i^e are the interpolation functions of the element Ω^e. Thus, the point source Q_0 is distributed to the element node i by the value $Q_0\psi_i^e(x_0)$. Equation (3.60) holds for any element, irrespective of the degree of the interpolation, the nature of the interpolation (i.e., Lagrange or Hermite polynomials), or the dimension (i.e., 1-*D*, 2-*D*, or 3-*D*) of the element. For linear Lagrange interpolation functions in 1-*D*, (3.60) yields

$$f_1^e = Q_0\frac{x_B - x_0}{h_e} = \alpha Q_0, \qquad f_2^e = Q_0\frac{x_0 - x_A}{h_e} = (1 - \alpha)Q_0$$

where $\alpha = (x_B - x_0)/h_e$ is the ratio of the distance between node 2 and the source to the length of the element.

Remark 6. There are three sources of error that may contribute to the inaccuracy of the finite element solution of a problem:

1. *Domain approximation error,* which is due to the approximation of the domain.

2. *Computational errors,* which are due to inexact evaluation of the coefficients K_{ij}^e and f_i^e, or are introduced owing to the finite arithmetic in a computer.
3. *Approximation error,* which is due to approximation of the solution by piecewise polynomials.

Since the geometry of the problem is exactly represented, and the linear approximation is able to represent the exact solution at the nodes (for $a = EA = \text{constant}$, $c = 0$, and $f = 0$), the first and third type of errors are zero in the problem of Fig. 3.8. The only error that can be introduced into the final numerical results is possibly due to the computer evaluation of the coefficients K_{ij}^e and f_i^e and the solution of algebraic equations. Additional discussion of the errors in the finite element approximation is presented in Chapter 5.

Remark 7. The approach used in matrix methods of structural analysis to solve the problem in Fig. 3.8 is not much different than that presented here. The difference lies only in the derivation of the element equations (3.37a). In matrix methods of structural analysis, the element equations are obtained directly from the definitions of stress and strain and their relationship. For example, consider the free-body diagram of a bar element (see Fig. 3.2*b*). From a course on deformable bodies, we have

$$\text{force} = \text{stress} \times \text{area of cross section}$$
$$\text{stress} = \text{Young's modulus} \times \text{strain}$$
$$\text{strain} = \text{elongation/original length}$$

The strain defined above is the average (or engineering) strain. Mathematically, strain is defined as $\varepsilon = du/dx$, u being the displacement, which includes rigid body motion as well as elongation of the bar. Hence, the force at the left end of the bar element is

$$P_1^e = A^e\sigma_1^e = A^eE^e\varepsilon_1^e = A^eE^e\frac{u_1^e - u_2^e}{h_e} = \frac{a_e}{h_e}(u_1^e - u_2^e)$$

where σ is the stress and E is Young's modulus. Similarly, the force at the right end is

$$P_2^e = \frac{a_e}{h_e}(u_2^e - u_1^e)$$

In matrix form, these relations can be expressed as

$$\frac{a_e}{h_e}\begin{bmatrix} 1 & -1 \\ -1 & 1 \end{bmatrix}\begin{Bmatrix} u_1^e \\ u_2^e \end{Bmatrix} = \begin{Bmatrix} P_1^e \\ P_2^e \end{Bmatrix} \tag{3.61}$$

which is the same as (3.37*a*) with $P_i^e = Q_i^e + f_i^e$. Note that in deriving the element equations, we have used knowledge of the mechanics of materials and the assumption that the strain is constant (or the displacement is linear) over the length of the element. Equations of the type (3.61) can also be derived for a spring element, a pipe-flow element, an electrical resistor element, and so on (see the problems at the end of this chapter). If a higher-order representation of the strain (or displacement) is required, we cannot write the force–displacement relations (3.61) directly. We must use the principle of virtual displacements, which is equivalent to the weak form of the governing equation. For more details, see Reddy (1984).

Remark 8. Another interpretation of (3.37) can be given in terms of the finite difference approximation. The axial force at any point x is given by $P(x) = EA\, du/dx$. Using the forward difference approximation, we approximate the derivative du/dx and write

$$-P_1^e \equiv P(x)|_{x_e} = E^eA^e[u(x_{e+1}) - u(x_e)]/h_e \tag{3.62a}$$

$$P_2^e \equiv P(x)|_{x_{e+1}} = E^eA^e[u(x_{e+1}) - u(x_e)]/h_e \tag{3.62b}$$

which are the same as (3.61), with $u_1^e = u(x_e)$ and $u_2^e = u(x_{e+1})$. Note that no approximation of $u(x)$ itself is assumed in writing (3.62). To obtain the value of u at a point other than the nodes (or mesh points), linear interpolation is often used.

Remark 9. For the model problem considered, the element matrices $[K^e]$ in (3.31b) are symmetric: $K_{ij}^e = K_{ji}^e$. This enables one to compute K_{ij}^e ($i = 1, 2, \ldots, n$) for $j \leq i$ only. In other words, one need compute only the diagonal terms and the upper or lower diagonal terms. Because of the symmetry of the element matrices, the assembled global matrix will also be symmetric. Thus, one need store only the upper triangle, including the diagonal, of the assembled matrix in a finite element program. Another property characteristic of the finite element method is the *sparseness* of the assembled matrix. Since $K_{IJ} = 0$ if global nodes I and J do not belong to the same element, the global coefficient matrix is *banded*, i.e., all coefficients beyond a certain distance from the diagonal are zero. The maximum of the distances between the diagonal element, including the latter, of a row and the last nonzero coefficient in that row is called the *half-bandwidth*, and can be computed from the equation

$$\text{half-bandwidth} = \max_{1 \leq i \leq E} (|b_{i1} - b_{in}| + 1) \times \text{NDF}$$

where E is the number of elements in the mesh, NDF is the number of degrees of freedom per node, n is the number of nodes per element, and b_{ij} are the coefficients of the connectivity matrix. When a matrix is banded and symmetric, one need store only the entries in the upper or lower band of the matrix. Equation solvers written for the solution of banded symmetric equations are available for use in such cases. The symmetry of the coefficient matrix depends on the type of the differential equation, its variational form, and the numbering of the finite element equations. The sparseness of the matrix is a result of the finite element interpolation functions, which have nonzero values only over an element of the domain.

Remark 10. The balance (or "equilibrium") of the secondary variables (or "forces") Q_i^e at the interelement boundaries is expressed by (3.41*b*). This amounts to imposing the condition that the secondary variable $a\,du/dx$ at the node, where u is the actual solution, be continuous. However, this does not imply continuity of $a\,dU^e/dx$, where U^e is the finite element solution. Thus, in general, we have

$$Q_2^e + Q_1^{e+1} = 0 \text{ or } Q_0 \tag{3.63a}$$

but

$$\left(a\frac{dU^e}{dx}\right)\bigg|_{x_e} + \left(-a\frac{dU^{e+1}}{dx}\right)\bigg|_{x_e} \neq 0 \text{ or } Q_0 \tag{3.63b}$$

Note. In most books on the finite element method, this point is not made clear to the reader. These books consider the quadratic form (3.11) of the total problem and omit the sum of the interelement contributions (for linear elements),

$$\sum_{e=1}^{N}\left(\sum_{i=1}^{2} Q_i^e u_i^e\right) \tag{i}$$

in the quadratic form of the problem. However, this amounts to imposing equilibrium conditions of the form (3.63*a*). When the secondary variable is specified to be nonzero (say, Q_0) at an interelement boundary (say, at global node 2), we have

$$Q_2^1 + Q_1^2 = Q_0 \tag{ii}$$

In other books, Q_0 is included in the functional as Q_0U_2, where U_2 is the value of u at global node 2.

To fix ideas, consider (3.1). The variational form of this equation over the entire domain is given by (when $c = 0$)

$$0 = \int_0^L \left(a\frac{dv}{dx}\frac{du}{dx} - vq\right)dx - v(x_2)Q_0 \tag{iii}$$

When u is approximated by functions that are defined only on a local interval (which is the case in the finite element method), use of the above variational form implies the omission of the sum of the interelement contributions of (i).

Since ψ_i^e ($e = 1, 2, 3$) is zero in any element Ω^f for $e \neq f$ (see Fig. 3.3*b*), the (global) finite element solution for the entire domain is given by

$$U_e(x) = \sum_{e=1}^{3}\left(\sum_{i=1}^{2} u_i^e\psi_i^e\right) = \sum_{J=1}^{4} U_J\Phi_J(x) \tag{iv}$$

where $\Phi_I(x)$ ($I = 1, 2, 3, 4$) are the piecewise-continuous *global interpolation functions*,

$$\Phi_I(x) = \begin{cases} \psi_2^{(I-1)}(x) & \text{for } x_{I-1} \leq x \leq x_I \\ \psi_1^{(I)}(x) & \text{for } x_I \leq x \leq x_{I+1} \end{cases} \tag{v}$$

Substituting (iv) for u and $v = \Phi_I$ into (iii), we obtain

$$0 = \int_0^L \left[a\frac{d\Phi_I}{dx}\left(\sum_{J=1}^{4} U_J\frac{d\Phi_J}{dx}\right) - \Phi_I q\right]dx - \Phi_I(x_2)Q_0 \tag{vi}$$

Since Φ_I is nonzero only between x_{I-1} and x_{I+1}, the integral becomes

$$0=\int_{x_{I-1}}^{x_{I+1}}\left[a\frac{d\Phi_I}{dx}\left(U_{I-1}\frac{d\Phi_{I-1}}{dx}+U_I\frac{d\Phi_I}{dx}+U_{I+1}\frac{d\Phi_{I+1}}{dx}\right)-\Phi_I q\right]dx-\Phi_I(x_2)Q_0 \quad \text{(vii)}$$

and we have (for a three-element mesh)

$$\begin{aligned}
I=1:&\quad 0=\int_{x_1=0}^{x_2}\left[a\frac{d\Phi_1}{dx}\left(U_1\frac{d\Phi_1}{dx}+U_2\frac{d\Phi_2}{dx}\right)-\Phi_1 q\right]dx-\Phi_1(x_2)Q_0\\
I=2:&\quad 0=\int_{x_1=0}^{x_3}\left[a\frac{d\Phi_2}{dx}\left(U_1\frac{d\Phi_1}{dx}+U_2\frac{d\Phi_2}{dx}+U_3\frac{d\Phi_3}{dx}\right)-\Phi_2 q\right]dx-\Phi_2(x_2)Q_0\\
I=3:&\quad 0=\int_{x_2}^{x_4=L}\left[a\frac{d\Phi_3}{dx}\left(U_2\frac{d\Phi_2}{dx}+U_3\frac{d\Phi_3}{dx}+U_4\frac{d\Phi_4}{dx}\right)-\Phi_3 q\right]dx-\Phi_{\underset{3}{2}}(x_2)Q_0\\
I=4:&\quad 0=\int_{x_3}^{x_4=L}\left[a\frac{d\Phi_4}{dx}\left(U_3\frac{d\Phi_3}{dx}+U_4\frac{d\Phi_4}{dx}\right)-\Phi_4 q\right]dx-\Phi_4(x_2)Q_0
\end{aligned} \quad \text{(viii)}$$

These equations, upon performing the integrations, yield (3.47), with the last column (containing Qs) in the latter replaced by

$$\begin{Bmatrix} 0 \\ Q_0 \\ 0 \\ 0 \end{Bmatrix} \quad \text{(ix)}$$

Although this procedure gives the assembled equations directly, it is algebraically complicated (especially for two-dimensional problems) and not amenable to simple computer implementation.

3.2.8 Radially Symmetric Problems

The equations governing physical processes in cylindrical or spherical geometries are described analytically in terms of cylindrical or spherical coordinates. When the geometry, loading, and boundary conditions are dependent only on the radial direction and independent of the other two coordinates, the governing equations are one-dimensional. The equations governing radially symmetric problems in cylindrical geometries are of the form [an analogue of (3.1)]

$$-\frac{1}{r}\frac{d}{dr}\left[a(r)\frac{du}{dr}\right]=q(r) \quad \text{for } R_i<r<R_o \tag{3.64}$$

where r is the radial coordinate, a and q are known functions of r, and u is the dependent variable. Such equations arise, for example, in connection with radial heat flow in a long circular cylinder of inner radius R_i and outer radius R_o. The radially symmetric conditions require that both a and q be functions only of r. Since the cylinder is long, the temperature distribution at any section along its length (except perhaps at the ends) is the same, and it is sufficient to consider any cross-section away from the ends, i.e., the problem is reduced from a 3-D problem to a 2-D one. Since a and q are independent of the circumferential direction θ, the temperature distribution along any radial line is the same, reducing the 2-D problem to a 1-D one, as described by (3.64).

In developing the weak form of (3.64), we multiply (3.64) with a weight function $w(r)$ and integrate over the volume of the cylinder of unit length.

$$\text{(1)}\quad 0 = \int_V w\left[-\frac{1}{r}\frac{d}{dr}\left(a\frac{du}{dr}\right) - q\right] r\,dr\,d\theta\,dz$$

$$= \int_0^1\int_0^{2\pi}\int_{r_A}^{r_B} w\left[-\frac{1}{r}\frac{d}{dr}\left(a\frac{du}{dr}\right) - q\right] r\,dr\,d\theta\,dz$$

$$= 2\pi\int_{r_A}^{r_B} w\left[-\frac{1}{r}\frac{d}{dr}\left(a\frac{du}{dr}\right) - q\right] r\,dr$$

where (r_A, r_B) is the domain of the element along the radial direction. Next, we carry out the remaining two steps of the variational formulation:

$$\text{(2)}\quad 0 = 2\pi\int_{r_A}^{r_B}\left(a\frac{dw}{dr}\frac{du}{dr} - rwq\right)dr - \left[w2\pi a\frac{du}{dr}\right]_{r_A}^{r_B}$$

$$\text{(3)}\quad 0 = 2\pi\int_{r_A}^{r_B}\left(a\frac{dw}{dr}\frac{du}{dr} - rwq\right)dr - w(r_A)Q_1^e - w(r_B)Q_2^e \tag{3.65a}$$

where

$$Q_1^e \equiv -2\pi\left(a\frac{du}{dr}\right)\bigg|_{r_A}, \qquad Q_2^e \equiv 2\pi\left(a\frac{du}{dr}\right)\bigg|_{r_B} \tag{3.65b}$$

The finite element model is obtained by substituting the approximation

$$u(r) \approx \sum_{j=1}^{n} u_j\psi_j^e(r)$$

into (3.65a):

$$[K^e]\{u^e\} = \{f^e\} + \{Q^e\} \tag{3.66a}$$

where

$$K_{ij}^e = 2\pi\int_{r_A}^{r_B} a\frac{d\psi_i^e}{dr}\frac{d\psi_j^e}{dr}\,dr, \qquad f_i^e = 2\pi\int_{r_A}^{r_B}\psi_i^e q r\,dr \tag{3.66b}$$

and ψ_i^e are the interpolation functions expressed in terms of the radial coordinate r. For example, the linear interpolation functions are of the forms

$$\psi_1^e(r) = (r_B - r)/h_e, \qquad \psi_2^e(r) = (r - r_A)/h_e \tag{3.66c}$$

The explicit forms of the coefficients K_{ij}^e and f_i^e for $a = a_e r$ and $q = q_e$ are given below.

Linear element

$$[K^e] = \frac{2\pi a_e}{h_e}\left(r_A + \tfrac{1}{2}h_e\right)\begin{bmatrix} 1 & -1 \\ -1 & 1 \end{bmatrix}, \qquad \{f^e\} = \frac{2\pi q_e h_e}{6}\begin{Bmatrix} 3r_e + h_e \\ 3r_e + 2h_e \end{Bmatrix}$$

Quadratic element

$$[K^e] = \frac{2\pi a_e}{6h_e}\begin{bmatrix} 3h_e + 14r_A & -(4h_e + 16r_A) & h_e + 2r_A \\ -(4h_e + 16r_A) & 16h_e + 32r_A & -(12h_e + 16r_A) \\ h_e + 2r_A & -(12h_e + 16r_A) & 11h_e + 14r_A \end{bmatrix}$$

$$\{f^e\} = \frac{2\pi q_e h_e}{6}\begin{Bmatrix} r_A \\ 4r_A + 2h_e \\ r_A + h_e \end{Bmatrix}$$

In the next section, we consider several examples to illustrate the steps involved in the finite element analysis of one-dimensional second-order equations arising in heat transfer, fluid mechanics, and solid mechanics. While the notation used for the dependent variables, independent coordinates, and data of problems from various fields is different, the reader should keep the common mathematical structure in mind and not get confused with the change of notation from field to field or problem to problem.

3.3 APPLICATIONS

3.3.1 Heat Transfer

Heat flows from high-temperature regions to low-temperature regions. This transfer of heat within the medium is called *conduction heat transfer*. The Fourier heat conduction law for one-dimensional systems states that the heat flow Q is related to the temperature gradient $\partial T/\partial x$ by the relation (with heat flow in the positive direction of x),

$$Q = -kA\frac{\partial T}{\partial x} \tag{3.67}$$

where k is the thermal conductivity of the material, A the cross-sectional area, and T the temperature. The negative sign in (3.67) indicates that heat flows downhill on the temperature scale. The balance of energy in an element of length dx requires that

energy into the element + energy generated within the element

= change in internal energy + energy out of the element

$$-kA\frac{\partial T}{\partial x} + qA\,dx = \rho cA\frac{\partial T}{\partial t}dx - \left[kA\frac{\partial T}{\partial x} + \frac{\partial}{\partial x}\left(kA\frac{\partial T}{\partial x}\right)dx\right]$$

or

$$\frac{\partial}{\partial x}\left(kA\frac{\partial T}{\partial x}\right) + Aq = \rho cA\frac{\partial T}{\partial t} \tag{3.68}$$

where q is the heat energy generated per unit volume, ρ is the density, c is the specific heat of the material, and t is time. Equation (3.68) governs the transient heat conduction in a slab or fin (i.e., a one-dimensional system) when the heat flow in the normal direction is zero. The following metric units will be used:

T	°C (celsius)
k	$\mathrm{W\,m^{-1}\,{}^\circ C^{-1}}$ (watts per meter per degree Celsius)
q	$\mathrm{W\,m^{-3}}$
ρ	$\mathrm{kg\,m^{-3}}$
c	$\mathrm{J\,kg^{-1}\,{}^\circ C^{-1}}$ (joules per kilogram per degree Celsius or $\mathrm{m^2\,s^{-2}\,{}^\circ C^{-1}}$)

(3.69)

In the case of radially symmetric problems with cylindrical geometries, (3.68) takes a different form (see Section 3.2.8). Consider a long cylinder of inner radius R_i, outer radius R_o, and length L. When L is very large compared with the diameter, it is assumed that heat flows in the radial direction r. Thus, the surface area for heat flow in the cylindrical system is (see Fig. 3.9)

$$A = 2\pi r L \tag{3.70}$$

Hence, the transient radially symmetric heat flow in the cylinder is governed by

$$\frac{\partial}{\partial r}\left(kA\frac{\partial T}{\partial r}\right) + Aq = \rho c A\frac{\partial T}{\partial t} \tag{3.71a}$$

or

$$\boxed{\frac{1}{r}\frac{\partial}{\partial r}\left(kr\frac{\partial T}{\partial r}\right) + q = \rho c\frac{\partial T}{\partial t}} \tag{3.71b}$$

A cylindrical fuel element of a nuclear reactor, a current-carrying electrical wire, and a thick-walled circular tube provide examples of one-dimensional radial systems.

For the radial flow in a sphere, the cross-sectional area is

$$A = 4\pi^2 r^2$$

and the governing equation takes the form

$$\frac{1}{r^2}\frac{\partial}{\partial r}\left(kr^2\frac{\partial T}{\partial r}\right) + q = \rho c\frac{\partial T}{\partial t} \tag{3.72}$$

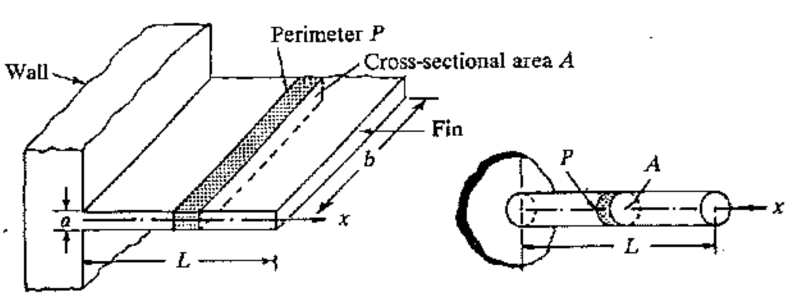

FIGURE 3.9
Convective heat transfer in a fin.

The boundary conditions for heat conduction involve specifying either temperature T or the heat flow Q at a point:

$$T = T_0 \quad \text{or} \quad Q = -kA\frac{\partial T}{\partial x} = Q_0 \tag{3.73}$$

We know that when a heated surface is exposed to a cooling medium, such as air or liquid, the surface will cool faster. We say that the heat is convected away. The *convection heat transfer* between the surface and the medium in contact is given by *Newton's law of cooling*:

$$Q = \beta A(T_s - T_\infty) \tag{3.74}$$

where T_s is the surface temperature, T_∞ is the temperature of the surrounding medium (the *ambient temperature*), A is the surface area, and β is the *convection heat transfer coefficient* or *film conductance* (or film coefficient). The units of β are $\mathrm{W\,m^{-2}\,{}^\circ C^{-1}}$. The heat flow due to conduction and convection at a boundary point must be in balance with the applied flow Q_0:

$$\boxed{\pm kA\frac{\partial T}{\partial x} + \beta A(T - T_\infty) + Q_0 = 0} \tag{3.75}$$

The sign of the first term in (3.75) is negative when the heat flow is from the fluid at T_∞ to the surface at the left end of the element, and it is positive when the heat flow is from the fluid at T_∞ to the surface at the right end.

Convection of heat from a surface to the surrounding fluid can be increased by attaching thin strips of conducting metal to the surface. The metal strips are called *fins*. For a fin with heat flow along its axis, heat can convect across the lateral surface of the fin unless it is insulated (see Fig. 3.9). To account for the convection of heat through the surface, we must add the rate of heat loss by convection to the right-hand side of (3.68):

$$\frac{\partial}{\partial x}\left(Ak\frac{\partial T}{\partial x}\right) + Aq = \rho cA\frac{\partial T}{\partial t} + P\beta(T - T_\infty) \tag{3.76a}$$

where P is the perimeter and β is the film coefficient. Equation (3.76*a*) can be expressed in the alternative form

$$\rho cA\frac{\partial T}{\partial t} - \frac{\partial}{\partial x}\left(kA\frac{\partial T}{\partial x}\right) + P\beta T = Aq + P\beta T_\infty \tag{3.76b}$$

For a steady state, we set the time derivatives in (3.68), (3.71), (3.72), and (3.76) equal to zero. The steady-state equations for various one-dimensional systems are summarized below:

Plane wall and fin

$$-\frac{d}{dx}\left(kA\frac{dT}{dx}\right) + \hat{c}T = Aq + \hat{c}T_\infty, \qquad \hat{c} = P\beta \tag{3.77}$$

Cylindrical system

$$-\frac{1}{r}\frac{d}{dr}\left(2\pi kr\frac{dT}{dr}\right) = 2\pi q \tag{3.78}$$

Spherical system

$$-\frac{1}{r^2}\frac{d}{dr}\left(4\pi^2 kr^2\frac{dT}{dr}\right) = 4\pi^2 q \tag{3.79}$$

For a plane wall and insulated lateral surfaces of a bar, we set $\hat{c} = 0$ in (3.77). The essential and natural boundary conditions associated with these equations are

$$T = T_0, \qquad Q + \beta A(T - T_\infty) + Q_0 = 0 \tag{3.80}$$

The weak form and finite element model of (3.77) can be developed using the ideas presented in Section 3.2.3. Since (3.77) is a special case of the model boundary value problem with $a = kA$, $c = P\beta$, and $q \rightarrow Aq + P\beta T_\infty$, we can immediately write the finite element model of (3.77) from (3.31):

$$[K^e]\{T^e\} = \{f^e\} + \{Q^e\} \tag{3.81a}$$

where

$$K_{ij}^e = \int_{x_A}^{x_B}\left(kA\frac{d\psi_i^e}{dx}\frac{d\psi_j^e}{dx} + P\beta\psi_i^e\psi_j^e\right)dx, \qquad f_i^e = \int_{x_A}^{x_B}\psi_i^e(Aq + P\beta T_\infty)\,dx$$
$$Q_1^e = \left(-kA\frac{dT}{dx}\right)\bigg|_{x_A}, \qquad Q_2^e = \left(kA\frac{dT}{dx}\right)\bigg|_{x_B} \tag{3.81b}$$

where Q_1^e and Q_2^e denote heat flow *into* the element at the nodes.

Equations (3.78) and (3.79) are also special cases of the model boundary value problem. However, in developing the weak forms of (3.78) and (3.79), the integration must be carried over a typical volume element of each system, as illustrated in Section 3.2.8 for a radially symmetric cylindrical problem. The weak form of (3.78) is given in (3.65), and the finite element model is given by (3.66), with $\{u^e\} = \{T^e\}$. Similarly, the weak form of (3.79) can be developed using a volume element of a sphere:

$$dV = r^2\,dr\,d\theta\,d\phi \quad \text{for } 0 \leqslant \theta < 2\pi,\ 0 \leqslant \phi < 2\pi$$

The weak form of (3.79) is

$$0 = (2\pi)^2\int_{r_A}^{r_B}\left(k\frac{dw}{dr}\frac{dT}{dr} - qw\right)r^2\,dr - Q_1^e w(r_A) - Q_2^e w(r_B) \tag{3.82}$$

and the finite element model of (3.79) is

$$[K^e]\{T^e\} = \{f^e\} + \{Q^e\} \tag{3.83a}$$

where

$$K^e_{ij} = (2\pi)^2 \int_{r_A}^{r_B} k \frac{d\psi^e_i}{dr}\frac{d\psi^e_j}{dr} r^2\,dr, \qquad f^e_i = (2\pi)^2 \int_{r_A}^{r_B} q\psi^e_i r^2\,dr$$
$$Q^e_1 = -(2\pi)^2\left(r^2 k \frac{dT}{dr}\right)\Bigg|_{r_A}, \qquad Q^e_2 = (2\pi)^2\left(r^2 k \frac{dT}{dr}\right)\Bigg|_{r_B} \tag{3.83b}$$

In the following examples, we consider some typical applications of the finite element models (3.81) and (3.66).

Example 3.1. Consider a slab of thickness L and constant thermal conductivity k ($\mathrm{W\,m^{-1}\,{}^\circ C^{-1}}$). Suppose that energy at a uniform rate of q_0 ($\mathrm{W\,m^{-3}}$) is generated in the wall. We wish to determine the temperature distribution in the wall when the boundary surfaces of the wall are subject to the following three different sets of boundary conditions:

Set 1 $\quad T(0) = T_1, \quad T(L) = T_2 \qquad (3.84a)$

Set 2 $\quad \left(-k\frac{dT}{dx}\right)\Big|_{x=0} = g_0\ (\mathrm{W\,m^{-2}}), \quad \left[k\frac{dT}{dx} + \beta(T - T_\infty)\right]\Big|_{x=L} = 0 \qquad (3.84b)$

Set 3 $\quad T(0) = T_1, \quad \left(k\frac{dT}{dx}\right)\Big|_{x=L} = g_0\ (\mathrm{W\,m^{-2}}) \qquad (3.84c)$

The governing differential equation for this problem is given by (3.77) with $\hat{c} = 0$. Hence, the finite element model in (3.81) is applicable here. We must select the order of approximation (or type of element) to evaluate the coefficients K^e_{ij} and f^e_i in (3.81b). For the choice of linear elements and the data $a = kA = \text{constant}$ and $q = Aq_0 = \text{constant}$, (3.81$a$) takes the form [see (3.37a)]

$$\frac{kA}{h_e}\begin{bmatrix} 1 & -1 \\ -1 & 1 \end{bmatrix}\begin{Bmatrix} T^e_1 \\ T^e_2 \end{Bmatrix} = \frac{Aq_0h_e}{2}\begin{Bmatrix} 1 \\ 1 \end{Bmatrix} + \begin{Bmatrix} Q^e_1 \\ Q^e_2 \end{Bmatrix}$$

For a uniform mesh of N elements, i.e., a mesh of same-size elements, $h_1 = h_2 = \cdots = L/N = h$, the assembled equations are

$$\frac{kA}{h}\begin{bmatrix} 1 & -1 & & & & \\ -1 & 1+1 & -1 & & 0 & \\ & -1 & 1+1 & & & \\ \cdots & \cdots & \cdots & \cdots & \cdots & \cdots \\ & 0 & & & 1+1 & -1 \\ & & & & -1 & 1 \end{bmatrix}\begin{Bmatrix} U_1 \\ U_2 \\ U_3 \\ \vdots \\ U_N \\ U_{N+1} \end{Bmatrix}$$
$$= \frac{Aq_0h}{2}\begin{Bmatrix} 1 \\ 1+1 \\ 1+1 \\ \vdots \\ 1+1 \\ 1 \end{Bmatrix} + \begin{Bmatrix} Q^1_1 \\ Q^1_2 + Q^2_1 \\ Q^2_2 + Q^3_1 \\ \vdots \\ Q^{N-1}_2 + Q^N_1 \\ Q^N_2 \end{Bmatrix} \tag{3.85}$$

where U_I $(I = 1, 2, \ldots, N+1)$ denotes the temperature at global node I. The assembled equations (3.85) are valid for all three sets of boundary conditions in (3.84). We now specialize the finite element equations (3.85) for each set of boundary conditions.

Set 1. The boundary conditions (3.84*a*) imply that

$$U_1 = T_1, \qquad U_{N+1} = T_2 \tag{3.86a}$$

and the balance of the heats at global nodes 2, 3, . . . , N requires

$$Q_2^{e-1} + Q_1^e = 0 \quad \text{for } e = 2, 3, \ldots, N \tag{3.86b}$$

The condensed equations for the unknown primary variables $U_2, U_3, \ldots, U_N$ are obtained by considering the 2nd, 3rd, . . . , Nth equations of (3.85) (and omitting those corresponding to the known temperatures):

$$\frac{kA}{h}\begin{bmatrix} 2 & -1 & & 0 & \\ -1 & 2 & & & \\ \cdots & \cdots & \cdots & \cdots & \cdots \\ & 0 & & 2 & -1 \\ & & & -1 & 2 \end{bmatrix}\begin{Bmatrix} U_2 \\ U_3 \\ \vdots \\ U_{N-1} \\ U_N \end{Bmatrix} = \frac{Aq_0h}{2}\begin{Bmatrix} 2 \\ 2 \\ \vdots \\ 2 \\ 2 \end{Bmatrix} - \frac{kA}{h}\begin{Bmatrix} -T_1 \\ 0 \\ \vdots \\ 0 \\ -T_2 \end{Bmatrix} \tag{3.87}$$

The unknown secondary variables Q_1^1 and Q_2^N are computed from the first and last of the assembled equations (3.85):

$$(Q_1^1)_{\text{equil}} = -\tfrac{1}{2}Aq_0h + \frac{kA}{h}(U_1 - U_2), \qquad (Q_2^N)_{\text{equil}} = -\tfrac{1}{2}Aq_0h + \frac{kA}{h}(U_{N+1} - U_N) \tag{3.88a}$$

They can also be computed from the definition (3.81*b*):

$$\begin{aligned} (Q_1^1)_{\text{def}} &\equiv -\left(kA\frac{dT}{dx}\right)\bigg|_{x=0} = kA\sum_{j=1}^{2} T_j^1\left(\frac{d\psi_j^1}{dx}\right)\bigg|_{x=0} = -\frac{kA}{h}(U_2 - U_1) \\ (Q_2^N)_{\text{def}} &\equiv +\left(kA\frac{dT}{dx}\right)\bigg|_{x=L} = kA\sum_{j=1}^{2} T_j^N\left(\frac{d\psi_j^N}{dx}\right)\bigg|_{x=L} = \frac{kA}{h}(U_{N+1} - U_N) \end{aligned} \tag{3.88b}$$

The values computed in (3.88*b*) are in error compared with those in (3.88*a*) by the nodal sources, $\tfrac{1}{2}q_0hA$, for $h = L/N$.

For any number of elements, the solution can be computed from (3.87). For this set of boundary conditions and a linear-element mesh, the minimum number of elements is 2.

For $N = 2$ $(h = \tfrac{1}{2}L)$,

$$\frac{kA}{h}\begin{bmatrix} 1 & -1 & 0 \\ -1 & 2 & -1 \\ 0 & -1 & 1 \end{bmatrix}\begin{Bmatrix} T_1 \\ U_2 \\ T_2 \end{Bmatrix} = \frac{Aq_0h}{2}\begin{Bmatrix} 1 \\ 2 \\ 1 \end{Bmatrix} + \begin{Bmatrix} Q_1^1 \\ 0 \\ Q_2^2 \end{Bmatrix}$$

and the solution is

$$U_2 = \frac{q_0h^2}{2k} + \tfrac{1}{2}(T_1 + T_2)$$

$$(Q_1^1)_{\text{equil}} = -q_0hA + \frac{kA}{2h}(T_1 - T_2), \qquad (Q_2^2)_{\text{equil}} = -q_0hA + \frac{kA}{2h}(T_2 - T_1)$$

For $N = 3$ $(h = \frac{1}{3}L)$,

$$\frac{kA}{h}\begin{bmatrix} 1 & -1 & 0 & 0 \\ -1 & 2 & -1 & 0 \\ 0 & -1 & 2 & -1 \\ 0 & 0 & -1 & 1 \end{bmatrix}\begin{Bmatrix} T_1 \\ U_2 \\ U_3 \\ T_2 \end{Bmatrix} = \frac{Aq_0h}{2}\begin{Bmatrix} 1 \\ 2 \\ 2 \\ 1 \end{Bmatrix} + \begin{Bmatrix} Q_1^1 \\ 0 \\ 0 \\ Q_2^3 \end{Bmatrix}$$

or

$$\frac{kA}{h}\begin{bmatrix} 2 & -1 \\ -1 & 2 \end{bmatrix}\begin{Bmatrix} U_2 \\ U_3 \end{Bmatrix} = Aq_0h\begin{Bmatrix} 1 \\ 1 \end{Bmatrix} + \frac{kA}{h}\begin{Bmatrix} T_1 \\ T_2 \end{Bmatrix}$$

$$\begin{Bmatrix} Q_1^1 \\ Q_2^3 \end{Bmatrix}_{\text{equil}} = \frac{kA}{h}\begin{bmatrix} 1 & -1 & 0 & 0 \\ 0 & 0 & -1 & 1 \end{bmatrix}\begin{Bmatrix} T_1 \\ U_2 \\ U_3 \\ T_2 \end{Bmatrix} - \frac{Aq_0h}{2}\begin{Bmatrix} 1 \\ 1 \end{Bmatrix}$$

The solution is given by

$$U_2 = \frac{q_0h^2}{k} + \tfrac{1}{3}(2T_1 + T_2), \qquad U_3 = \frac{q_0h^2}{k} + \tfrac{1}{3}(T_1 + 2T_2)$$

$$(Q_1^1)_{\text{equil}} = -\tfrac{3}{2}q_0hA + \frac{kA}{3h}(T_1 - T_2), \qquad (Q_2^3)_{\text{equil}} = -\tfrac{3}{2}q_0hA + \frac{kA}{3h}(T_2 - T_1)$$

The exact solution of (3.77) (with $\hat{c} = 0$), subject to the boundary conditions (3.84*a*), is

$$T(x) = \frac{q_0L^2}{2k}\left[\frac{x}{L} - \left(\frac{x}{L}\right)^2\right] + (T_2 - T_1)\frac{x}{L} + T_1$$

$$Q(x) = -kA\frac{dT}{dx} = -\frac{q_0LA}{2}\left(1 - 2\frac{x}{L}\right) - \frac{kA}{L}(T_2 - T_1)$$

Note that the finite element solution at the nodes coincides with the exact solution for *any* number of elements. In fact, for constant $a = kA$, it can be shown that the finite element solution at the nodes is exact [see Reddy (1986), pp. 403, 404]; the only error would be that due to the round-off error introduced in electronic computations. The finite element solution, being linear, will not be exact at points other than the nodes.

If we use quadratic elements, we can improve the solution at points between the nodes. Let us consider a mesh of one quadratic element. The element coefficient matrix and source vector are given in (3.40). We have $(c_e = 0)$

$$\frac{kA}{3h}\begin{bmatrix} 7 & -8 & 1 \\ -8 & 16 & -8 \\ 1 & -8 & 7 \end{bmatrix}\begin{Bmatrix} U_1 \\ U_2 \\ U_3 \end{Bmatrix} = \frac{Aq_0h}{6}\begin{Bmatrix} 1 \\ 4 \\ 1 \end{Bmatrix} + \begin{Bmatrix} Q_1^1 \\ 0 \\ Q_3^1 \end{Bmatrix}$$

where $h = L$. The solution is

$$U_2 = \tfrac{4}{16}\frac{Aq_0h}{6}\frac{3h}{Ak} + \tfrac{8}{16}(T_1 + T_2) = \tfrac{1}{8}\frac{q_0h^2}{k} + \tfrac{1}{2}(T_1 + T_2)$$

$$(Q_1^1)_{\text{equil}} = -\tfrac{1}{2}Aq_0h + \frac{kA}{h}(T_1 - T_2), \qquad (Q_3^1)_{\text{equil}} = -\tfrac{1}{2}Aq_0h + \frac{kA}{h}(T_2 - T_1)$$

If we compute the Q_1^1 using the definition (3.81*b*), we obtain

$$
\begin{aligned}
(Q_1^1)_{\text{def}} &\equiv -\left(kA\frac{dT_e}{dx}\right)\bigg|_{x=0} = -kA\sum_{j=1}^{3} T_j^1\left(\frac{d\psi_j^1}{dx}\right)\bigg|_{x=0}\\
&= -kA\left[U_1\left(-\frac{3}{h}+\frac{4x}{h^2}\right)+U_2\left(\frac{4}{h}-\frac{8x}{h^2}\right)+U_3\left(-\frac{1}{h}+\frac{4x}{h^2}\right)\right]_{x=0}\\
&= -\tfrac{1}{2}Aq_0h+\frac{kA}{h}(T_1-T_2)
\end{aligned}
$$

which coincides with the exact value. Recall that $(Q_1^1)_{\text{def}}$ for a linear-element mesh does not coincide with the exact value. Also, the values of $T(x)$ at $x=\frac{1}{4}L$, for example, from the two linear- and one quadratic-element meshes can be computed using the interpolations

$$T(\tfrac{1}{4}L)=\tfrac{1}{16}\frac{q_0L^2}{k}+\tfrac{1}{4}(3T_1+T_2)\qquad\text{(linear element)}$$

$$T(\tfrac{1}{4}L)=\tfrac{3}{32}\frac{qL^2}{k}+\tfrac{1}{4}(3T_1+T_2)\qquad\text{(quadratic element)}$$

The quadratic interpolation gives the exact value. Thus, the finite element solution given by the quadratic element is exact at all points, because the exact solution varies quadratically.

Set 2. In this case, the surface at $x=0$ is subjected to a uniform heat flux g_0 ($\mathrm{W\,m^{-2}}$) (if it is insulated, $g_0=0$), and heat is dissipated by convection into a fluid of temperature T_∞ at the boundary surface at $x=L$. These boundary conditions imply that

$$Q_1^1\equiv\left(-kA\frac{dT}{dx}\right)\bigg|_{x=0}=Ag_0$$

$$Q_2^N\equiv\left(kA\frac{dT}{dx}\right)\bigg|_{x=L}=-A\beta(T-T_\infty)|_{x=L}=-A\beta(U_{N+1}-T_\infty)$$

where A is the cross-sectional area normal to heat flow and β is the heat transfer coefficient. Equations (3.86*b*) are also valid for the present case. For a one-element mesh ($N=1$, $h=L$), the finite element equations are

$$\frac{kA}{h}\begin{bmatrix}1&-1\\-1&1\end{bmatrix}\begin{Bmatrix}U_1\\U_2\end{Bmatrix}=\frac{Aq_0h}{2}\begin{Bmatrix}1\\1\end{Bmatrix}+\begin{Bmatrix}Ag_0\\-A\beta U_2+A\beta T_\infty\end{Bmatrix}$$

or

$$\frac{kA}{h}\begin{bmatrix}1&-1\\-1&1+\beta h/k\end{bmatrix}\begin{Bmatrix}U_1\\U_2\end{Bmatrix}=\begin{Bmatrix}\tfrac{1}{2}Aq_0h+Ag_0\\\tfrac{1}{2}Aq_0h+A\beta T_\infty\end{Bmatrix}$$

Their solution is

$$U_1=-\left(\frac{1+\alpha}{1-\alpha}\right)\frac{q_0h^2}{2k}-\left(\frac{\alpha}{1-\alpha}\right)\frac{g_0h}{k}+T_\infty$$

$$U_2=-\left(\frac{1}{1-\alpha}\right)\frac{q_0h^2}{k}-\left(\frac{1}{1-\alpha}\right)\frac{g_0h}{k}+T_\infty$$

where $\alpha = 1 + \beta h/k$. The exact solution is

$$T(x) = \frac{q_0L^2}{2k}\left(1 + \frac{2k}{\beta L} - \frac{x^2}{L^2}\right) + \frac{g_0L}{k}\left(1 + \frac{k}{\beta L} - \frac{x}{L}\right) + T_\infty$$

The finite element solution agrees with this at the nodes.

Set 3. In this case, the boundary surface at $x = 0$ is maintained at a temperature T_1, while at the other boundary surface, $x = L$, a heat flux at the rate of g_0 is removed. These boundary conditions can be expressed in terms of the primary and secondary variables as

$$U_1 = T_1, \qquad Q_2^N = Ag_0$$

and (3.86*b*) are still valid. For a two-element mesh with $h_1 = h_2 = \frac{1}{2}L = h$, we have

$$\frac{kA}{h}\begin{bmatrix} 1 & -1 & 0 \\ -1 & 2 & -1 \\ 0 & -1 & 1 \end{bmatrix}\begin{Bmatrix} U_1 \\ U_2 \\ U_3 \end{Bmatrix} = \frac{Aq_0h}{2}\begin{Bmatrix} 1 \\ 2 \\ 1 \end{Bmatrix} + \begin{Bmatrix} Q_1^1 \\ 0 \\ Ag_0 \end{Bmatrix}$$

or

$$\frac{kA}{h}\begin{bmatrix} 2 & -1 \\ -1 & 1 \end{bmatrix}\begin{Bmatrix} U_2 \\ U_3 \end{Bmatrix} = \frac{Aq_0h}{2}\begin{Bmatrix} 2 \\ 1 \end{Bmatrix} + \begin{Bmatrix} \dfrac{kA}{h}T_1 \\ Ag_0 \end{Bmatrix}$$

$$(Q_1^1)_{\text{equil}} = -\tfrac{1}{2}Aq_0h + \frac{kA}{h}(U_1 - U_2)$$

We have

$$U_2 = \frac{3}{2}\frac{q_0h^2}{k} + \frac{g_0h}{k} + T_1, \qquad U_3 = 2\frac{q_0h^2}{k} + \frac{2g_0h}{\cancel{K}k} + T_1$$

$$(Q_1^1)_{\text{equil}} = -(2A\overset{q_0}{Q_0}h + Ag_0) \quad [= Q(0)]$$

For a three-element mesh ($h = \frac{1}{3}L$), we have

$$\frac{kA}{h}\begin{bmatrix} 2 & -1 & 0 \\ -1 & 2 & -1 \\ 0 & -1 & 1 \end{bmatrix}\begin{Bmatrix} U_2 \\ U_3 \\ U_4 \end{Bmatrix} = \frac{Aq_0h}{2}\begin{Bmatrix} 2 \\ 2 \\ 1 \end{Bmatrix} + \begin{Bmatrix} 0 \\ 0 \\ Ag_0 \end{Bmatrix} + \frac{kA}{h}\begin{Bmatrix} T_1 \\ 0 \\ 0 \end{Bmatrix}$$

Using *Cramer's rule*, we can solve for U_2, U_3, and U_4:

$$U_2 = \frac{h}{kAD}\begin{vmatrix} F_1 & -1 & 0 \\ F_2 & 2 & -1 \\ F_3 & -1 & 1 \end{vmatrix}, \qquad U_3 = \frac{h}{kAD}\begin{vmatrix} 2 & F_1 & 0 \\ -1 & F_2 & -1 \\ 0 & F_3 & 1 \end{vmatrix}, \qquad U_4 = \frac{h}{kAD}\begin{vmatrix} 2 & -1 & F_1 \\ -1 & 2 & F_2 \\ 0 & -1 & F_3 \end{vmatrix}$$

where

$$D = \begin{vmatrix} 2 & -1 & 0 \\ -1 & 2 & -1 \\ 0 & -1 & 1 \end{vmatrix} = 2 + (-1) = 1$$

and $\{F\} = \{F_1 \quad F_2 \quad F_3\}^T$ is the right-hand-side vector:

$$\{F\} = \begin{Bmatrix} Aq_0h + \dfrac{kAT_1}{h} \\ Aq_0h \\ \frac{1}{2}Aq_0h + Ag_0 \end{Bmatrix}$$

Evaluating the determinants, we obtain

$$U_2 = \frac{h}{kA}(F_1 + F_2 + F_3) = \frac{h}{k}(\tfrac{5}{2}q_0h + g_0) + T_1$$

$$U_3 = \frac{h}{kA}(F_1 + 2F_2 + 2F_3) = \frac{h}{k}(4q_0h + 2g_0) + T_1$$

$$U_4 = \frac{h}{kA}(F_1 + 2F_2 + 3F_3) = \frac{h}{k}(\tfrac{9}{2}q_0h + 3g_0) + T_1$$

$$(Q_1^1)_{\text{equil}} = -\tfrac{1}{2}Aq_0h + \frac{kA}{h}(U_1 - U_2) = -A(g_0 + 3q_0h)$$

$$(Q_1^1)_{\text{def}} = -A(g_0 + \tfrac{5}{2}q_0h)$$

The exact solution of (3.77) with $\hat{c} = 0$ and subject to the boundary conditions (3.84*c*) is given by

$$\begin{aligned} T(x) &= \frac{L^2}{k}\left[\frac{q_0}{2}\left(2\frac{x}{L} - \frac{x^2}{L^2}\right) + \frac{g_0x}{L^2}\right] + T_1 \\ Q(x) &= -kA\frac{dT}{dx} = -A\left[q_0L\left(1 - \frac{x}{L}\right) + g_0\right] \end{aligned} \tag{3.89}$$

Note that the finite element solution at the nodes, for any number of elements, coincides with the exact solution. The exact value of Q_1^1 is

$$(Q_1^1)_{\text{exact}} = -\left(kA\frac{du}{dx}\right)\bigg|_{x=0} = Q(0) = -A(q_0L + g_0)$$

The value of Q_1^1 computed from the assembled equations is the same as the exact one; however, when computed using the definition $Q_1^1 = -kA(dU_e/dx)|_{x=0}$, it is in error by an amount $f_1^1 = \frac{1}{2}Aq_0h$. As the number of elements is increased, the value of $(Q_1^1)_{\text{def}}$ approaches the exact value. Of course, when quadratic elements are used, we shall obtain a more accurate (or even exact) value of $(Q_1^1)_{\text{def}}$.

The next example deals with radially symmetric heat transfer in a cylinder.

Example 3.2. Consider a long solid cylinder of radius R_o in which energy is generated at a constant rate q_0 (W m^{-3}). The boundary surface at $r = R_0$ is maintained at a constant temperature T_0. We wish to calculate the temperature distribution $T(r)$ and heat flux $q(r) = -k\,dT/dr$ (or heat $Q = -Ak\,dT/dr$).

The governing equation for this problem is given by (3.78) with $q = q_0$. The boundary conditions are

$$T(R_0) = T_0, \qquad \left(2\pi kr\frac{dT}{dr}\right)\bigg|_{r=0} = 0 \tag{3.90}$$

The zero-flux boundary condition at $r = 0$ is a result of the radial symmetry at $r = 0$. If the cylinder is hollow with inner radius R_i then the boundary condition at $r = R_i$ can be specified temperature, specified heat flux, or convection boundary condition, depending on the situation.

The finite element model of the governing equation is given in (3.66) (for unit height of the cylinder and $a = kr$):

$$[K^e]\{T^e\} = \{f^e\} + \{Q^e\} \tag{3.91a}$$

where

$$\begin{aligned} K_{ij}^e &= 2\pi\int_{r_A}^{r_B} kr\frac{d\psi_i^e}{dr}\frac{d\psi_j^e}{dr}\,dr, \qquad f_i^e = 2\pi\int_{r_A}^{r_B} \psi_i^e q_0 r\,dr \\ Q_1^e &= -2\pi k\left(r\frac{dT}{dr}\right)\bigg|_{r_A}, \qquad Q_2^e = 2\pi k\left(r\frac{dT}{dr}\right)\bigg|_{r_B} \end{aligned} \tag{3.91b}$$

and (r_A, r_B) are the coordinates of the element $\Omega^e = (r_A, r_B)$.

For the choice of linear interpolation functions ψ_i^e as [see (3.16b) and (3.66c)]

$$\psi_1^e = (r_B - r)/h_e, \qquad \psi_2^e = (r - r_A)/h_e$$

the element equations for a typical linear element are

$$\frac{2\pi k}{h_e}\frac{r_{e+1} + r_e}{2}\begin{bmatrix} 1 & -1 \\ -1 & 1 \end{bmatrix}\begin{Bmatrix} T_1^e \\ T_2^e \end{Bmatrix} = 2\pi q_0\frac{h_e}{6}\begin{Bmatrix} 2r_e + r_{e+1} \\ r_e + 2r_{e+1} \end{Bmatrix} + \begin{Bmatrix} Q_1^e \\ Q_2^e \end{Bmatrix} \tag{3.92}$$

The element equations for individual elements are obtained from these by giving the element length h_e and the global coordinates of the element nodes, $r_e = r_A$ and $r_{e+1} = r_B$.

For the mesh of one linear element, we have $r_1 = 0$, $r_2 = h_e = R_o$, and

$$\pi k\begin{bmatrix} 1 & -1 \\ -1 & 1 \end{bmatrix}\begin{Bmatrix} U_1 \\ U_2 \end{Bmatrix} = \frac{\pi q_0 R_0}{3}\begin{Bmatrix} R_0 \\ 2R_0 \end{Bmatrix} + \begin{Bmatrix} Q_1^1 \\ Q_2^1 \end{Bmatrix}$$

The boundary conditions in (3.90) imply $U_2 = T_0$ and $Q_1^1 = 0$. Hence the temperature at (global) node 1 is

$$U_1 = q_0 R_0^2/3k + T_0$$

and the heat at $r = R_0$ is

$$Q_2^1 = \pi k(U_2 - U_1) - \tfrac{2}{3}\pi q_0 R_0^2 = -\pi q_0 R_0^2$$

The negative sign indicates that heat is removed from the body (because $dT/dr < 0$). The one-element solution as a function of the radial coordinate r is

$$T^1(r) = U_1\psi_1^1(r) + U_2\psi_2^1(r) = \frac{q_0 R_0^2}{3k}\left(1 - \frac{r}{R_0}\right) + T_0 \tag{3.93}$$

and the heat flux is

$$q(r) \equiv -k\frac{dT^1}{dr} = \tfrac{1}{3}q_0 R_0 \tag{3.94}$$

The exact solution of the problem can be obtained by integrating (3.78) and evaluating the constants of integration with the help of the boundary conditions in (3.90):

$$\begin{gathered} T(r)=\frac{q_0R_0^2}{4k}\left[1-\left(\frac{r}{R_0}\right)^2\right]+T_0 \\ q(r)=\tfrac{1}{2}q_0r\ \ (\text{in W m}^{-2}),\qquad Q(R_0)=-\left(2\pi kr\frac{dT}{dr}\right)\bigg|_{R_0}=\pi q_0R_0^2 \end{gathered} \tag{3.95}$$

For a mesh of two linear elements, we take $h_1=h_2=\frac{1}{2}R_0$, $r_1=0$, $r_2=h_1=\frac{1}{2}R_0$, and $r_3=h_1+h_2=R_0$. The two-element assembly gives

$$\pi k\begin{bmatrix} 1 & -1 & 0 \\ -1 & 1+3 & -3 \\ 0 & -3 & 3 \end{bmatrix}\begin{Bmatrix} U_1 \\ U_2 \\ U_3 \end{Bmatrix}=\frac{\pi q_0R_0}{6}\begin{Bmatrix} \frac{1}{2}R_0 \\ R_0+2R_0 \\ \frac{1}{2}R_0+2R_0 \end{Bmatrix}+\begin{Bmatrix} Q_1^1 \\ Q_2^1+Q_1^2 \\ Q_2^2 \end{Bmatrix} \tag{3.96}$$

Imposing the boundary conditions $U_3=T_o$ and $Q_1^1=0$, the condensed equations are

$$\pi k\begin{bmatrix} 1 & -1 \\ -1 & 4 \end{bmatrix}\begin{Bmatrix} U_1 \\ U_2 \end{Bmatrix}=\frac{\pi q_0R_0^2}{12}\begin{Bmatrix} 1 \\ 6 \end{Bmatrix}+\pi k\begin{Bmatrix} 0 \\ 3T_0 \end{Bmatrix} \tag{3.97}$$

Their solution is

$$U_1=\tfrac{5}{18}\frac{q_0R_0^2}{k}+T_0,\qquad U_2=\tfrac{7}{36}\frac{q_0R_0^2}{k}+T_0 \tag{3.98a}$$

From equilibrium, Q_2^2 is computed as

$$Q_2^2=-\tfrac{5}{12}\pi q_0R_0^2+3\pi k(U_3-U_2)=-\pi q_0R_0^2 \tag{3.98b}$$

The finite element solution becomes

$$\begin{aligned} T_{\text{fem}}(r)&=\begin{cases} U_1\psi_1^1+U_2\psi_2^1=\left(\frac{5}{18}\frac{q_0R_0^2}{k}+T_0\right)\frac{R_0-2r}{R_0}+\left(\frac{7}{36}\frac{q_0R_0^2}{k}+T_0\right)\frac{2r}{R_0} \\ U_2\psi_1^2+U_3\psi_2^2=\left(\frac{7}{36}\frac{q_0R_0^2}{k}+T_0\right)\frac{2(R_0-r)}{R_0}+T_0\frac{2r-R_0}{R_0} \end{cases} \\ &=\begin{cases} \frac{q_0R_0^2}{18k}\left(r-\frac{3r}{R_0}\right)+T_0 & \text{for } 0\leqslant r\leqslant\frac{1}{2}R_0 \\ \frac{7}{18}\frac{q_0R_0^2}{k}\left(1-\frac{r}{R_0}\right)+T_0 & \text{for } \frac{1}{2}R_0\leqslant r\leqslant R_0 \end{cases} \end{aligned} \tag{3.99}$$

Note that the heat flow at $r=R_0$ is predicted accurately by both one- and two-element models. The temperature at the center of the cylinder according to the exact solution is $T(0)=q_0R_0^2/4k+T_0$, whereas it is $q_0R_0^2/3k+T_0$ and $q_0R_0^2/18k+T_0$ according to the one- and two-element models, respectively.

The finite element solutions obtained using one-, two-, four-, and eight-element meshes of linear elements are compared with the exact solution in Table 3.3. Convergence of the finite element solutions to the exact solution with an increasing number of elements is clear (see Fig. 3.10). Figure 3.11 shows plots of $q(r)=-dT/dr$, as computed by the finite element interpolation and the exact formula. The figure also shows the plot of the exact $Q=-2\pi kr\,dT/dr$ versus r.

TABLE 3.3
Comparison of the finite element and exact solutions for heat transfer in a radially symmetric cylinder (Example 3.2) ($R_0 = 0.01$ m, $q_0 = 2 \times 10^8$ W m^{-3}, $k = 20$ W m^{-1} °C^{-1}, $T_0 = 100$ °C)

	Temperature $u(r)$†				
r/R_0	One element‡	Two elements	Four elements	Eight elements	Exact
0.00	$\underline{433.33}$	$\underline{377.78}$	$\underline{358.73}$	$\underline{352.63}$	350.00
0.125	391.67	356.24	348.31	$\underline{347.42}$	346.09
0.250	350.00	335.11	$\underline{337.90}$	$\underline{335.27}$	334.38
0.375	308.33	315.28	313.59	$\underline{315.48}$	314.84
0.500	266.67	$\underline{294.44}$	$\underline{289.29}$	$\underline{287.95}$	287.50
0.625	225.00	245.83	249.70	$\underline{252.65}$	252.34
0.750	183.33	197.22	$\underline{210.12}$	$\underline{209.56}$	209.38
0.875	141.67	148.61	155.06	$\underline{158.68}$	158.59
1.000	$\underline{100.00}$	$\underline{100.00}$	$\underline{100.00}$	$\underline{100.00}$	100.00

† The underlined terms are nodal values and others are interpolated values.
‡ Uniform meshes (i.e., equal-length elements) of linear elements.

3.3.2 Fluid Mechanics

All bulk matter in nature exists in one of two forms: solid or fluid. A solid body is characterized by relative immobility of its molecules, whereas a fluid state is characterized by their relative mobility. Fluids can exist either as gases or liquids. The field of fluid mechanics is concerned with the motion of fluids

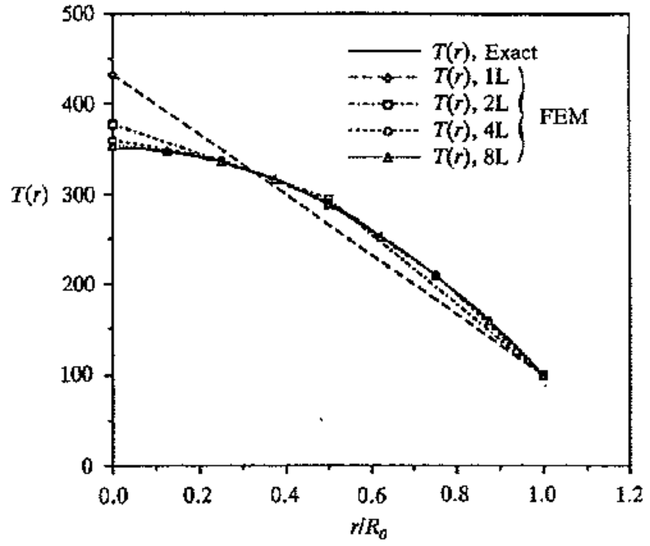

FIGURE 3.10
Comparison of the finite element solutions with the exact solution for heat transfer in a radially symmetric problem with cylindrical geometry (Example 3.2).

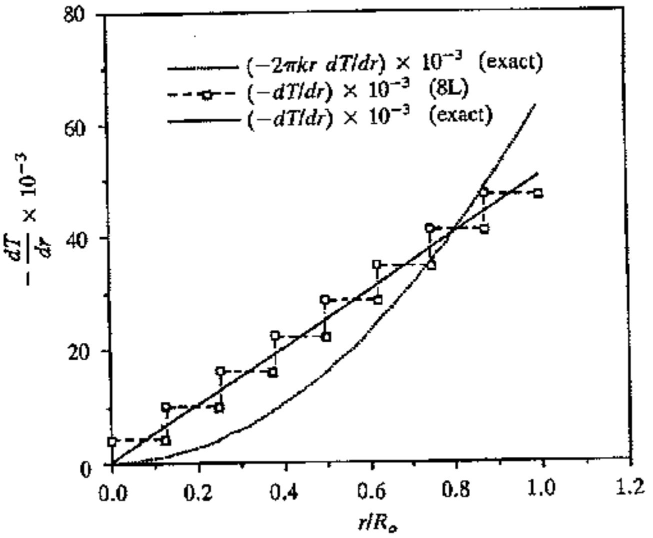

FIGURE 3.11
Comparison of the finite element solution with the exact solution for the temperature gradient in a radially symmetric problem with cylindrical geometry (Example 3.2).

and the conditions affecting the motion. In this section, we review the basic equations of fluid mechanics and develop finite element models of certain one-dimensional fluid systems. Several numerical examples will be discussed.

The basic equations of fluid mechanics are derived from the global laws of conservation of mass, momentum, and energy. Conservation of mass gives the continuity equation, while the conservation of momentum results in the equations of motion. The conservation of energy, considered in the last section, is the first law of thermodynamics and results in (3.68), and (3.77)–(3.79) for various one-dimensional systems when thermal–fluid coupling is omitted. Before we review the basic equations of fluid mechanics, it is informative to consider various types of fluids.

An *ideal* (or *perfect*) *fluid* is one that has zero viscosity and is incompressible. A *real fluid* or *viscous fluid* is one with finite viscosity, and may or may not be incompressible. *Nonviscous fluids* are those with zero viscosity, and again may or may not be incompressible. A viscous fluid is said to be a *Newtonian fluid* if its viscosity coefficient is independent of the velocity gradient (i.e., the viscosity is constant). *Non-Newtonian* fluids are those for which the viscosity is a function of the velocity gradient.

Two different viewpoints are used in the analytical description of the equations of a continuous medium. In the first, one considers the motion of all matter passing through a *fixed spatial location*. Here one is concerned with changes (e.g., in velocity field, pressure, and density) that are taking place in the matter that happens to occupy the fixed spatial location. This viewpoint, known as the *Eulerian description*, is the one that is most commonly used in fluid mechanics. In the study of the motion of fluids, one is interested in the flow characteristics of fluids occuping a fixed region rather than a fixed set of fluid particles. In the other viewpoint, one considers the motion of a *fixed set of material particles* (i.e., fixed matter), irrespective of its spatial location. This viewpoint is known as the *Lagrangian description,* and it is used in the study of the motion of solid bodies.

The conservation of mass in the Eulerian description is expressed as

$$\frac{\partial \rho}{\partial t} + \nabla \cdot (\rho \mathbf{u}) = 0 \tag{3.100a}$$

or, for two-dimensional flow,

$$\frac{\partial \rho}{\partial t} + \frac{\partial}{\partial x}(\rho u) + \frac{\partial}{\partial y}(\rho v) = 0 \tag{3.100b}$$

where ρ is the density (in $\mathrm{kg\,m^{-3}}$) and (u, v) are the velocity components (in $\mathrm{m\,s^{-1}}$) in the x and y directions. All problems of fluid mechanics require that the continuity equation (3.100) be satisfied (because of the Eulerian description). In the steady-state case, we have $\partial/\partial t = 0$, and (3.100*a*,*b*) become

$$\nabla \cdot (\rho \mathbf{u}) = 0, \qquad \frac{\partial}{\partial x}(\rho u) + \frac{\partial}{\partial y}(\rho v) = 0 \tag{3.101a,b}$$

If a fluid is incompressible, the density is constant, and the continuity equations (3.101*a*,*b*) take the forms

$$\boxed{\nabla \cdot \mathbf{u} = 0, \qquad \frac{\partial u}{\partial x} + \frac{\partial v}{\partial y} = 0} \tag{3.102a,b}$$

For flows of incompressible fluids, the conservation of linear momentum results in the following equations of motion:

$$\nabla \cdot \boldsymbol{\sigma} + \mathbf{f} = \rho\left(\frac{\partial \mathbf{u}}{\partial t} + \mathbf{u} \cdot \nabla \mathbf{u}\right) \tag{3.103a}$$

or, for two-dimensional systems,

$$\boxed{\begin{aligned} \frac{\partial \sigma_x}{\partial x} + \frac{\partial \sigma_{xy}}{\partial y} + f_x &= \rho\left(\frac{\partial u}{\partial t} + u\frac{\partial u}{\partial x} + v\frac{\partial u}{\partial y}\right) \\ \frac{\partial \sigma_{xy}}{\partial x} + \frac{\partial \sigma_y}{\partial y} + f_y &= \rho\left(\frac{\partial v}{\partial t} + u\frac{\partial v}{\partial x} + v\frac{\partial v}{\partial y}\right) \end{aligned}} \tag{3.103b}$$

where $(\sigma_x, \sigma_y, \sigma_{xy})$ are the total stress components (in $\mathrm{N\,m^{-2}}$) and (f_x, f_y) are the x and y components of the body force vector (measured per unit volume). The total stress components can be expressed in terms of the viscous stress components $(\tau_x, \tau_y, \tau_{xy})$ and the hydrostatic pressure P (in $\mathrm{N\,m^{-2}}$):

$$\sigma_x = \tau_x - P, \qquad \sigma_y = \tau_y - P, \qquad \sigma_{xy} = \tau_{xy} \tag{3.104}$$

The viscous components of stress are related to the velocity gradients by Newton's law of viscosity. For isotropic, Newtonian fluids, these are

$$\tau_x = 2\mu \frac{\partial u}{\partial x}, \qquad \tau_y = 2\mu \frac{\partial v}{\partial y}, \qquad \tau_{xy} = \mu\left(\frac{\partial u}{\partial y} + \frac{\partial v}{\partial x}\right) \tag{3.105}$$

where μ is the viscosity (in kg m^{-1} s^{-1}) of the fluid. Combining (3.103)–(3.105), we obtain

$$\begin{aligned}
\frac{\partial}{\partial x}\left(2\mu\frac{\partial u}{\partial x} - P\right) + \frac{\partial}{\partial y}\left[\mu\left(\frac{\partial u}{\partial y} + \frac{\partial v}{\partial x}\right)\right] + f_x &= \rho\left(\frac{\partial u}{\partial t} + u\frac{\partial u}{\partial x} + v\frac{\partial u}{\partial y}\right)\\
\frac{\partial}{\partial x}\left[\mu\left(\frac{\partial u}{\partial y} + \frac{\partial v}{\partial x}\right)\right] + \frac{\partial}{\partial y}\left(2\mu\frac{\partial v}{\partial y} - P\right) + f_y &= \rho\left(\frac{\partial v}{\partial t} + u\frac{\partial v}{\partial x} + v\frac{\partial v}{\partial y}\right)
\end{aligned} \tag{3.106}$$

These are known as the *Navier–Stokes equations*. When the viscosity is zero, we have

$$\begin{aligned}
-\frac{\partial P}{\partial x} + f_x &= \rho\left(\frac{\partial u}{\partial t} + u\frac{\partial u}{\partial x} + v\frac{\partial u}{\partial y}\right)\\
-\frac{\partial P}{\partial y} + f_y &= \rho\left(\frac{\partial v}{\partial t} + u\frac{\partial v}{\partial x} + v\frac{\partial v}{\partial y}\right)
\end{aligned} \tag{3.107}$$

which are known as the *Euler equations*.

Conservation of energy for incompressible fluids is expressed by

$$\boxed{\rho c\left(\frac{\partial T}{\partial t} + u\frac{\partial T}{\partial x} + v\frac{\partial T}{\partial y}\right) = k\left(\frac{\partial^2 T}{\partial x^2} + \frac{\partial^2 T}{\partial y^2}\right) + q + \Phi} \tag{3.108}$$

where c is the mean heat capacity at constant volume, q is the internal heat generation, k is the thermal conductivity of the (isotropic) fluid, and Φ is the viscous dissipation,

$$\Phi = \mu\left[\left(\frac{\partial u}{\partial x}\right)^2 + \left(\frac{\partial v}{\partial y}\right)^2\right] + \mu\left(\frac{\partial u}{\partial y} + \frac{\partial v}{\partial x}\right)^2 \tag{3.109}$$

which is zero for nonviscous fluids. For fluids of low viscosity and for velocities less than the sonic velocity, Φ has a magnitude that is small compared with the other terms in the equation.

In summary, the two-dimensional flows of viscous incompressible fluids are governed by (3.102), (3.106), and (3.108). There are four unknowns (u, v, P, T) and four equations. The two-dimensional flows of nonviscous fluids are governed by (3.100), (3.107), and (3.108) (with $\Phi = 0$). There are five unknowns (u, v, T, P, ρ) in four equations. The fifth equation is provided by the equation of state, $F(\rho, T, P) = 0$, which relates the density ρ, temperature T, and pressure P.

For certain flows, the equations can be further simplified to 1-D equations. These are discussed below.

Consider the flow of a viscous, incompressible fluid between two stationary parallel flat walls separated by a distance $2L$. We assume that there are no body forces. The velocity of the fluid at the wall is zero, because of adhesion, and reaches a maximum at the center of the channel. The velocity is constant on a plane parallel to the center plane, with its magnitude being proportional to the distance from the latter; the individual planes slide over each other, the velocity field being purely axial everywhere. Such fluid flows are called *laminar*. At a sufficiently large distance from the entrance, where the velocity is uniform, the velocity distribution becomes independent of the coordinate along the flow direction. The portion of the flow region beyond this distance is called the *hydrodynamically developed* or *fully developed* region, and the flow is called *fully developed flow*. For this case, the governing field equations (3.102), (3.106), and (3.108) can be simplified because of the specific nature of the velocity field:

$$u = u(x, y), \qquad v = 0$$

where the x and y coordinates are chosen along and normal to the flow direction, respectively. The continuity equation (3.012) reduces to

$$\frac{\partial u}{\partial x} = 0, \quad \text{which implies that} \quad u = u(y)$$

The y momentum equation in (3.106), for $f_y = 0$, simplifies to

$$\frac{\partial P}{\partial y} = 0, \quad \text{which implies that} \quad P = P(x)$$

The x momentum equation in (3.106), subject to the requirements $v = 0$, $u = u(y)$, $P = P(x)$, and $f_x = 0$, simplifies to

$$\boxed{\mu \frac{d^2u}{dy^2} = \frac{dP}{dx}} \tag{3.110}$$

The energy equation (3.108) for this problem reduces to

$$\boxed{\rho c u \frac{\partial T}{\partial x} = k\left(\frac{\partial^2 T}{\partial x^2} + \frac{\partial^2 T}{\partial y^2}\right) + \mu\left(\frac{du}{dy}\right)^2} \tag{3.111}$$

In the case of the steady flow of an incompressible, Newtonian fluid inside a circular tube of radius r, (3.110) and (3.111) take the forms

$$\boxed{\begin{aligned} \frac{\mu}{r}\frac{d}{dr}\left(r\frac{du}{dr}\right) &= \frac{dP}{dz} && (3.112) \\ \rho c u \frac{\partial T}{\partial z} &= k\left[\frac{1}{r}\frac{\partial}{\partial r}\left(r\frac{\partial T}{\partial r}\right) + \frac{\partial^2 T}{\partial z^2}\right] + \mu\left(\frac{du}{dr}\right)^2 && (3.113) \end{aligned}}$$

where $u = u(r)$ is the axial velocity, $T = T(r, z)$ is the temperature, $P = P(z)$ is the hydrostatic pressure, and the r and z coordinates are chosen along and normal to the direction of main flow. This flow is also known as *Poiseuille flow*.

This completes the review of the pertinent equations of fluid mechanics that are considered in this chapter. Next, we consider the finite element analysis of one-dimensional problems governed by (3.110)–(3.113).

Example 3.3. Consider parallel flow between two long flat walls separated by a distance $2L$. We wish to determine the velocity distribution $u(y)$ for a given constant pressure gradient dP/dx, using the finite element method. The governing equation (3.110) is a special case of the model equation (3.1) with the following correspondence:

$$q = -\frac{dP}{dx} = \text{constant} \equiv q_0, \qquad a = \mu = \text{constant}, \qquad c = 0, \qquad x = y$$

Hence the finite element model in (3.31) is valid for this problem:

$$[K^e]\{u^e\} = \{f^e\} + \{Q^e\} \tag{3.114a}$$

where

$$K_{ij}^e = \int_{y_A}^{y_B} \mu \frac{d\psi_i^e}{dy}\frac{d\psi_j^e}{dy}\,dy, \qquad f_i^e = \int_{y_A}^{y_B} \left(-\frac{dP}{dx}\right)\psi_i^e\,dy$$
$$Q_1^e = -\left(\mu\frac{du}{dy}\right)\bigg|_A, \qquad Q_2^e = \left(\mu\frac{du}{dy}\right)\bigg|_B \tag{3.114b}$$

For the choice of linear finite elements, (3.114*a*) is the same as (3.37), with $a_e = \mu$ and $q_e = q_0$. For quadratic finite finite elements, $[K^e]$ is given by (3.40*a*) with $c_e = 0$, and $\{f^e\}$ is given by (3.40*b*).

For a two-element mesh of linear elements ($h = L$), we have

$$\frac{\mu}{h}\begin{bmatrix} 1 & -1 & 0 \\ -1 & 2 & -1 \\ 0 & -1 & 1 \end{bmatrix}\begin{Bmatrix} U_1 \\ U_2 \\ U_3 \end{Bmatrix} = \frac{q_0 h}{2}\begin{Bmatrix} 1 \\ 2 \\ 1 \end{Bmatrix} + \begin{Bmatrix} Q_1^1 \\ Q_2^1 + Q_1^2 \\ Q_2^2 \end{Bmatrix}$$

We consider two sets of boundary conditions

$$\begin{aligned} &\textbf{Set 1} \quad u(-L) = u(L) = 0 && \text{or} \quad U_1 = U_3 = 0 \\ &\textbf{Set 2} \quad u(-L) = 0, \quad u(L) = U_0 && \text{or} \quad U_1 = 0, \quad U_3 = U_0 \end{aligned} \tag{3.115}$$

The finite element solutions for these two cases are

$$\begin{aligned} U_2 &= \frac{q_0 L^2}{2\mu} && \text{for Set 1} \\ U_2 &= \frac{q_0 L^2}{2\mu} + \tfrac{1}{2}U_0 && \text{for Set 2} \end{aligned} \tag{3.116}$$

For a one-element mesh of the quadratic element ($h = 2L$), we have

$$\frac{\mu}{6L}\begin{bmatrix} 7 & -8 & 1 \\ -8 & 16 & -8 \\ 1 & -8 & 7 \end{bmatrix}\begin{Bmatrix} U_1 \\ U_2 \\ U_3 \end{Bmatrix} = \frac{q_0 L}{3}\begin{Bmatrix} 1 \\ 4 \\ 1 \end{Bmatrix} + \begin{Bmatrix} Q_1^1 \\ 0 \\ Q_3^1 \end{Bmatrix}$$

and the solution is

$$\begin{aligned} U_2 &= \frac{q_0 L^2}{2\mu} && \text{for Set 1} \\ U_2 &= \frac{q_0 L^2}{2\mu} + \tfrac{1}{2} U_0 && \text{for Set 2} \end{aligned} \tag{3.117}$$

Although the nodal values predicted in the linear- and quadratic-element meshes are the same, they vary linearly and quadratically, respectively, between nodes.

The exact solutions of (3.110) for the two sets of boundary conditions in (3.115) are $(-L \leq y \leq L)$

$$\begin{aligned} u(y) &= \frac{q_0 L^2}{2\mu}\left(1 - \frac{y^2}{L^2}\right) && \text{for Set 1} \\ u(y) &= U_0 \frac{1}{2}\left(1 + \frac{y}{L}\right) + \frac{q_0 L^2}{2\mu}\left(1 - \frac{y^2}{L^2}\right) && \text{for Set 2} \end{aligned} \tag{3.118}$$

Note that the finite element solutions at the nodes are exact, as expected (see the comments made in Example 3.1). The quadratic-element solution agrees with the exact solutions (3.118) for every value of y.

3.3.3 Solid Mechanics

Solid mechanics is that branch of mechanics dealing with the motion and deformation of solid bodies. The Lagrangian description of motion is used to express the global conservation laws. The conservation of mass for solid bodies is trivially satisfied because of the fixed material viewpoint used in the Lagrangian description. The conservation of momentum is nothing but Newton's second law of motion. Under isothermal conditions, the energy equation uncouples from the momentum equations, and we need only consider the equations of motion.

Unlike in fluid mechanics, here the equations governing solid bodies undergoing different forms of deformations are derived directly, without specializing the three-dimensional elasticity equations. Various types of load-carrying members are called by different names, e.g., bars, beams, and plates. A bar is a structural member that is subjected to only axial loads, while a beam is a member that is subjected to bending loads. The equations governing the motion of such structural elements are not obtained directly from (3.103). They are derived either by considering an element of the member with all its proper forces and using Newton's second law, or by using an energy principle. Examples of the governing equations of the bending of beams and bars were discussed in Example 2.2 in Chapter 2. Energy principles provide an alternative to Newton's laws, and they are more suitable for finite element modeling because energy principles are nothing but the weak forms used in the development of the finite element models. Here we illustrate an application of Newton's second law and the energy principle, namely, the *principle of virtual displacements*, to a bar element. Other examples will be presented in connection with the finite element modeling of beams (Chapter 4) and plates (Chapter 12) later in this book.

Consider a material body of length L and cross-sectional area A. Suppose that the material of the body is homogeneous (i.e., material properties are independent of position), the cross-section is either constant or gradually varying in the axial (i.e., lengthwise) direction, and the applied loads are axial and symmetrically positioned with respect to the geometric centroid of the cross-section. Then the axial stress in the member, except near the points of load application, will be uniform. The only nonzero stress component is $\sigma_x = \sigma_x(x, t)$. Such members are called *bars*. For this case, $u = u(x, t)$, $v = 0$, and (3.103) reduce to the single equation (here u denotes the displacement)

$$\frac{\partial \sigma_x}{\partial x} + f_x = \rho \frac{\partial^2 u}{\partial t^2} \tag{3.119}$$

However, the above equation does not include cross-sectional properties of the member, and it is not useful in its present form. The governing equations of bars of axially varying cross-sections can be derived from Newton's second law (e.g., summation of forces along the x direction) applied to an element of the body (see Fig. 3.12); i.e.,

$$\sum F_x = ma$$

giving

$$-\sigma_x A + (\sigma_x + d\sigma_x)(A + dA) + f\,dx = \rho[A + (A + dA)]\frac{dx}{2}\frac{\partial^2 u}{\partial t^2}$$

or

$$\sigma_x\,dA + d\sigma_x\,A + d\sigma_X\,dA + f\,dx = \rho(A + \tfrac{1}{2}\,dA)\,dx\frac{\partial^2 u}{\partial t^2}$$

Dividing throughout by dx and taking the limit $dx \to 0$, we obtain

$$\frac{\partial}{\partial x}(\sigma_x A) + f = \rho A \frac{\partial^2 u}{\partial t^2} \tag{3.120}$$

where f is the body force per unit length.

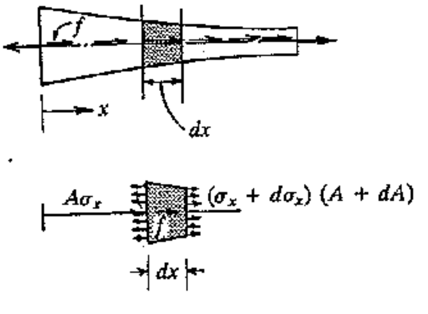

FIGURE 3.12
Axially loaded member and a typical portion of a member of length dx with its axial forces.

From the strain–stress relation $\varepsilon_x = (\sigma_x - \nu\sigma_y)/E$, we have (because $\sigma_y = 0$)

$$\sigma_x = E\varepsilon_x = E\frac{\partial u}{\partial x}$$

Substituting for σ_x from here into (3.120), we obtain

$$\frac{\partial}{\partial x}\left(EA\frac{\partial u}{\partial x}\right) + f = \rho A\frac{\partial^2 u}{\partial t^2}$$

or

$$\boxed{\rho A\frac{\partial^2 u}{\partial t^2} - \frac{\partial}{\partial x}\left(EA\frac{\partial u}{\partial x}\right) = f(x, t)} \tag{3.121}$$

For static problems, this reduces to

$$-\frac{d}{dx}\left(EA\frac{du}{dx}\right) = f(x) \tag{3.122a}$$

Equation (3.122*a*) can be used to determine the displacement $u(x)$ of a material point located at a distance x along the axis of a uniaxially loaded member, called a *bar*. It should be recalled that (3.122*a*) is derived under the assumption that all material points on the line $x = \text{constant}$ move by the same distance $u(x)$ (i.e., the stress at any cross-section is uniform). Equation (3.122*a*) is the same as the model equation (3.1), with $a = EA$ and $q = f(x)$.

The average transverse deflection $u(x)$ of a cable made of elastic material is also governed by an equation of the form (3.122*a*):

$$-\frac{d}{dx}\left(T\frac{du}{dx}\right) = f(x) \tag{3.122b}$$

where T is the uniform tension in the cable and f is the distributed transverse force.

Example 3.4. A bridge is supported by several concrete piers, and the geometry and loads of a typical pier are shown in Fig. 3.13. The load 20 kN m^{-2} represents the weight of the bridge and an assumed distribution of the traffic on the bridge. The concrete weighs approximately 25 kN m^{-3} and its modulus is $E = 28 \times 10^6$ kN m^{-2}. We wish to analyze the pier for displacements and stresses using the finite element method.

The pier is indeed a three-dimensional structure. However, we wish to approximate the deformation and stress fields in the pier as one-dimensional. To this end, we represent the distributed force at the top of the pier as a point force

$$F = (0.5 \times 0.5)20 = 5\ \text{kN}$$

The weight of the concrete is represented as the body force per unit length. The total force at any distance x is equal to the weight of the concrete above that point. The weight at a distance x is equal to the product of the volume of the body above x and the

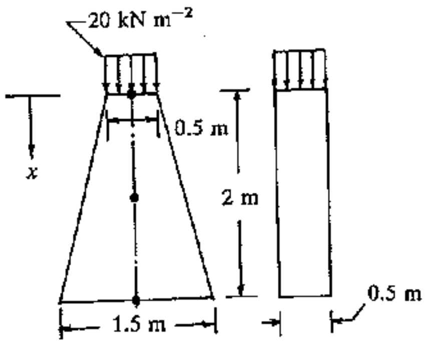

FIGURE 3.13
The geometry and loading in the concrete pier problem of Example 3.4.

specific weight of the concrete:

$$W(x)=0.5\,\frac{0.5+(0.5+0.5x)}{2}\,x\times 25.0=6.25(1+0.5x)x$$

The body force per unit length is computed from

$$f=\frac{dW}{dx}=6.25(1+x)$$

This completes the load representation of the problem.

The governing differential equation for the problem is given by (3.122*a*), with $E=28\times10^6\ \mathrm{kN\,m^{-2}}$ and cross-sectional area $A(x)$:

$$A(x)=(0.5+0.5x)0.5=\tfrac{1}{4}(1+x)$$

Thus

$$-\frac{d}{dx}\left[\tfrac{1}{4}E(1+x)\frac{du}{dx}\right]=6.25(1+x) \tag{3.123a}$$

subject to the boundary conditions

$$\left[\tfrac{1}{4}E(1+x)\frac{du}{dx}\right]\bigg|_{x=0}=-5,\qquad u(2)=0 \tag{3.123b}$$

The finite element model is

$$[K^e]\{u^e\}=\{f^e\}+\{Q^e\} \tag{3.124a}$$

where

$$\begin{gathered}K_{ij}^e=\int_{x_A}^{x_B}EA\frac{d\psi_i^e}{dx}\frac{d\psi_j^e}{dx}\,dx,\qquad f_i^e=\int_{x_A}^{x_B}f(x)\psi_i^e\,dx\\ Q_A^e=\left(-EA\frac{du}{dx}\right)\bigg|_A,\qquad Q_B^e=\left(EA\frac{du}{dx}\right)\bigg|_B\end{gathered} \tag{3.124b}$$

For the choice of linear interpolation functions (3.16*b*), we have

$$K_{11}^e=\int_{x_e}^{x_{e+1}}E\tfrac{1}{4}(1+x)\left(-\frac{1}{h}\right)^2dx=\frac{E}{4h_e}\left[1+\tfrac{1}{2}(x_e+x_{e+1})\right]$$

$$f_1^e=\int_{x_e}^{x_{e+1}}6.25(1+x)\psi_1^e\,dx=6.25h_e\left[\tfrac{1}{2}+\tfrac{1}{6}(x_{e+1}+2x_e)\right]$$

Similarly, other components can be evaluated:

$$\begin{aligned}
[K^e] &= \frac{E}{4h_e}[1+\tfrac{1}{2}(x_e+x_{e+1})]\begin{bmatrix} 1 & -1 \\ -1 & 1 \end{bmatrix} \\
\{f^e\} &= 6.25\frac{h_e}{2}\left(\begin{Bmatrix} 1 \\ 1 \end{Bmatrix} + \frac{1}{3}\begin{Bmatrix} x_{e+1}+2x_e \\ 2x_{e+1}+x_e \end{Bmatrix}\right)
\end{aligned} \tag{3.125}$$

Let us consider a two-element mesh with $h_1 = h_2 = 1\ m$. We have

$$[K^1] = \frac{E}{4}\begin{bmatrix} 1.5 & -1.5 \\ -1.5 & 1.5 \end{bmatrix}, \quad \{f^1\} = \frac{6.25}{6}\begin{Bmatrix} 3+1 \\ 3+2 \end{Bmatrix} = \begin{Bmatrix} 4.167 \\ 5.208 \end{Bmatrix}$$

$$[K^2] = \frac{E}{4}\begin{bmatrix} 2.5 & -2.5 \\ -2.5 & 2.5 \end{bmatrix}, \quad \{f^2\} = \frac{6.25}{6}\begin{Bmatrix} 3+4 \\ 3+5 \end{Bmatrix} = \begin{Bmatrix} 7.292 \\ 8.333 \end{Bmatrix}$$

The assembled equations are

$$E\begin{bmatrix} 0.375 & -0.375 & 0.000 \\ -0.375 & 1.000 & -0.625 \\ 0.000 & -0.625 & 0.625 \end{bmatrix}\begin{Bmatrix} U_1 \\ U_2 \\ U_3 \end{Bmatrix} = \begin{Bmatrix} 4.167 \\ 12.500 \\ 8.333 \end{Bmatrix} + \begin{Bmatrix} Q_1^1 \\ Q_2^1 + Q_1^2 \\ Q_2^2 \end{Bmatrix}$$

The boundary and equilibrium conditions require

$$U_3 = 0, \quad Q_2^1 + Q_1^2 = 0, \quad Q_1^1 = 5\ \text{kN}$$

The condensed equations are

$$E\begin{bmatrix} 0.375 & -0.375 \\ -0.375 & 1.000 \end{bmatrix}\begin{Bmatrix} U_1 \\ U_2 \end{Bmatrix} = \begin{Bmatrix} 9.167 \\ 12.500 \end{Bmatrix}, \quad Q_2^2 = -0.6255U_2 - 8.333$$

and the solution is given by

$$U_1 = 2.111\times10^{-6}\ \text{m}, \quad U_2 = 1.238\times10^{-6}\ \text{m}, \quad Q_2^2 = -30\ \text{kN} \tag{3.126}$$

Hence the stress at the fixed end is given by

$$\sigma_x = Q_2^2/A = -30/0.75 = -40\ \text{kN m}^{-2}$$

The exact solution of (3.123) is

$$u(x) = \frac{1}{E}\left[56.25 - 6.25(1+x)^2 - 7.5\ln\left(\frac{1+x}{3}\right)\right] \tag{3.127}$$

The exact values of u at nodes 1 and 2 are

$$u(0) = 2.08\times10^{-6}\ \text{m}, \quad u(1) = 1.225\times10^{-6}\ \text{m}$$

The four-element model gives 2.008×10^{-6} m and 1.228×10^{-6} m, respectively. The finite element solution at the nodes is not exact because $a = EA$ is not a constant in the problem.

3.4 SUMMARY

In this chapter, the finite element formulation of a second-order differential equation in a single variable has been presented systematically, following a step-by-step procedure. The basic steps of the formulation and analysis of a typical equation are described in Table 3.1. The model equation is representative of the equations arising in various fields of engineering (see Table 3.2). The finite element model is developed following three steps:

1. Weak formulation of the differential equation over an element.
2. Finite element interpolation of the primary variables of the weak fomulation.
3. Finite element formulation over a typical element.

The weak formulation itself involves a three-step procedure, which enables identification of primary variables (i.e., variables that are required to be continuous throughout the domain, including the nodes at which elements are connected). The finite element interpolation functions have been developed here on the basis of continuity, completeness, and linear independence. The finite element model has been developed by substituting appropriate interpolation of the primary variable into the weak form of the differential equation.

Applications of the model to the solution of problems of heat transfer, fluid mechanics, and solid mechanics have been presented. To aid the reader, a brief review of the basic terminology and governing equations of each of the three fields has also been given. The numerical examples should aid the reader in deeper understanding of the steps involved in the finite element analysis of one-dimensional second-order differential equations.

It has been shown that the secondary variables of a problem can be computed using either the global algebraic equations of the finite element mesh (i.e., condensed equations for the secondary variables) or by their original definition through finite element interpolation. The former method gives more accurate results, which will satisfy the equilibrium at interelement nodes, whereas the latter gives less accurate results, which are discontinuous at such nodes. The secondary variables computed using the Lagrange linear elements are element-wise-constant, while they are element-wise-linear for the Lagrange quadratic elements.

PROBLEMS

Many of the following problems are designed for hand calculation while some are intended specifically for computer calculations using the program FEM1DV2. This should give the student deeper understanding of what is involved in the formulation and solution of a problem by the finite element method. The hand calculations can be verified, in most cases, by solving the same problems using FEM1DV2, which is described in Chapter 7.

Section 3.2

3.1. Develop the weak form and the finite element model of the following differential equation over an element:

$$-\frac{d}{dx}\left(a\frac{du}{dx}\right)+\frac{d^2}{dx^2}\left(b\frac{d^2u}{dx^2}\right)+cu=f \quad \text{for } x_A<x<x_B$$

where a, b, c, and f are known functions of position x. Ensure that the element coefficient matrix $[K^e]$ is symmetric. What is the nature of the interpolation functions for the problem?

3.2. Construct the weak form and the finite element model of the differential equation

$$-\frac{d}{dx}\left(a\frac{du}{dx}\right)-b\frac{du}{dx}=f \quad \text{for } 0<x<L$$

over a typical element $\Omega^e=(x_A, x_B)$. Here a, b, and f are known functions of x, and u is the dependent variable. The natural boundary condition should *not* involve the function $b(x)$. What type of interpolation functions can be used for u?

3.3. Construct the weak form and associated finite element model of the equation

$$-\frac{d}{dx}\left(a\frac{du}{dx}\right)+cu=f \quad \text{for } 0<x<L$$

such that the natural boundary condition of the type

$$a\frac{du}{dx}+k(u-u_0)=Q$$

is included in the weak form. Here a, c, and f are known functions of x, while k, u_0, and Q are constants.

3.4. Derive the Lagrange cubic interpolation functions for a four-node (one-dimensional) element (with equally spaced nodes) using the alternative procedure based on interpolation properties (3.28). Use the local coordinate $\bar{x}$ for simplicity.

3.5. Verify (3.34a,b) by actual evaluation of $K_{ij}^e=K_{ji}^e$ and f_i^e.

3.6. Evaluate the following coefficient matrices and source vector using the linear Lagrange interpolation functions:

$$K_{ij}^e=\int_{x_A}^{x_B}(a_0+a_1x)\frac{d\psi_i^e}{dx}\frac{d\psi_j^e}{dx}\,dx$$

$$m_{ij}^e=\int_{x_A}^{x_B}(c_0+c_1x)\psi_i^e\psi_j^e\,dx, \qquad f_i^e=\int_{x_A}^{x_B}(q_0+q_1x)\psi_i^e\,dx$$

where a_0, a_1, c_0, c_1, q_0, and q_1 are constants.

3.7. Verify the coefficients in (3.40a,b) by actual evaluation of $K_{ij}^e=K_{ji}^e$ and f_i^e.

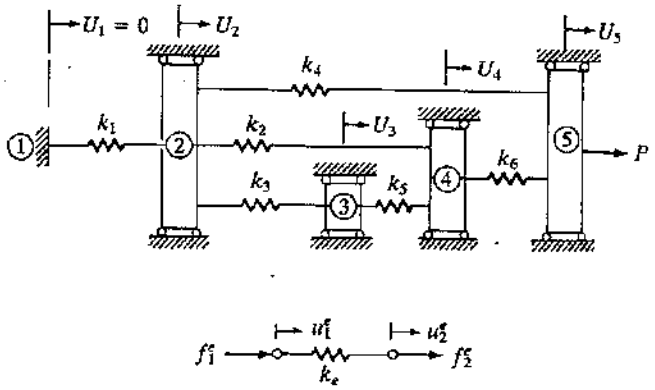

Typical element

FIGURE P3.8

3.8. Consider the system of linear elastic springs shown in Fig. P3.8. Write the force–displacement relationship for a typical (single) spring element, and assemble the element equations to obtain the force–displacement relations for the entire system. Use the boundary conditions to write the condensed equations for the unknown displacements and forces.

3.9. Consider the hydraulic network (the flow is assumed to be laminar) shown in Fig. P3.9. A typical element (which is a circular pipe of constant diameter) with two nodes is also shown in the figure. The unknown primary degree of freedom at each node is the pressure P, and the secondary degree of freedom is the flow (or discharge) Q. The element equations relating the primary variables to the secondary variables are given by

$$\frac{c(d_e)^4}{h_e}\begin{bmatrix} 1 & -1 \\ -1 & 1 \end{bmatrix}\begin{Bmatrix} P_1^e \\ P_2^e \end{Bmatrix}=\begin{Bmatrix} Q_1^e \\ Q_2^e \end{Bmatrix}, \qquad c=\frac{\pi}{128\mu}$$

where d_e is the diameter of the pipe, h_e is its length, and μ is the viscosity of the fluid. Write the condensed equations for the unknown pressures and flows (use the minimum number of elements.)

Answer: $P_1=\frac{39}{14}Qa$, $P_2=\frac{12}{7}Qa$, $P_3=\frac{15}{14}Qa$.

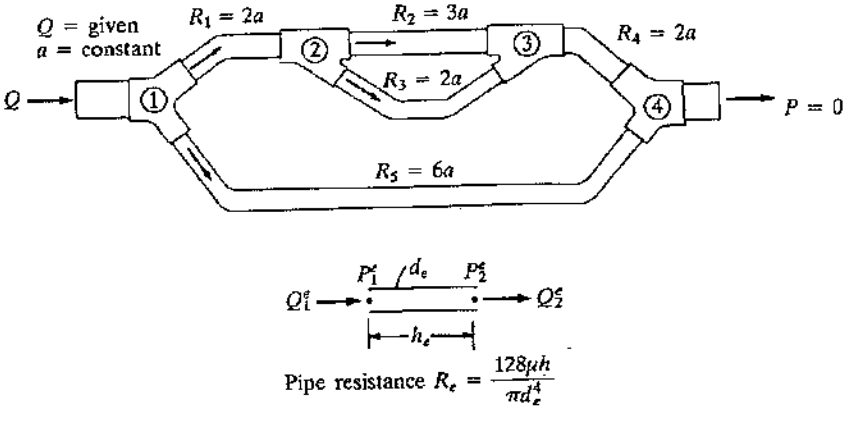

FIGURE P3.9

3.10. Consider the direct current electric network shown in Fig. P3.10. We wish to determine the voltages V and currents I in the network using the finite element method. A typical finite element in this case consists of a resistor R, with the primary degree of freedom being the voltage and the secondary degree of freedom being the current. The element equations are provided by Ohm's law:

$$\frac{1}{R_e}\begin{bmatrix} 1 & -1 \\ -1 & 1 \end{bmatrix}\begin{Bmatrix} V_1^e \\ V_2^e \end{Bmatrix}=\begin{Bmatrix} I_1^e \\ I_2^e \end{Bmatrix}$$

The continuity conditions at the interelement nodes require that the net current flow into any junction (node) always be zero in a closed loop. Set up the algebraic equations (i.e., condensed equations) for the unknown voltages and currents.

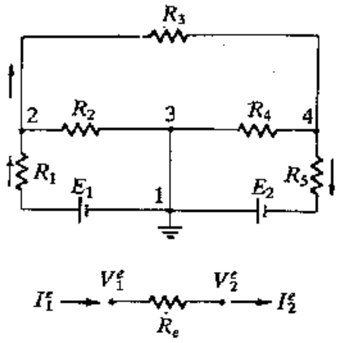

Typical element

FIGURE P3.10

3.11. Consider the composite structure of axially loaded members shown in Fig. P3.11. Write the continuity conditions (i.e., the correspondence of element nodal values to global nodal values) and the equilibrium conditions (i.e., the relationships between Q_i^e at the interelement nodes) for the structure. Derive the assembled coefficient (stiffness) matrix for the structure, and set up the condensed equations for the unknown displacements and forces.

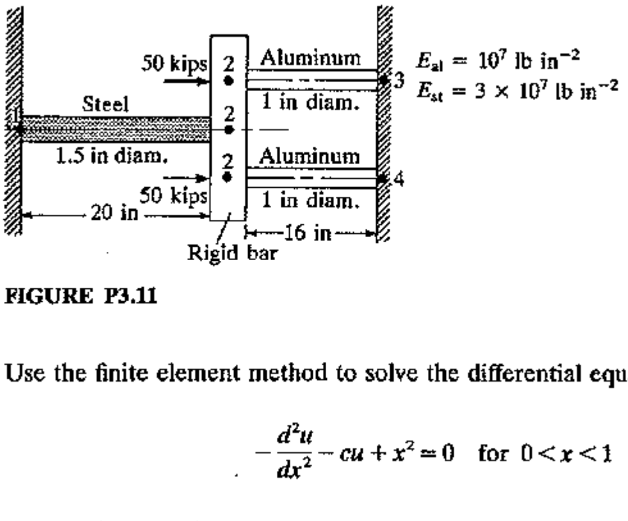

FIGURE P3.11

3.12. Use the finite element method to solve the differential equation

$$-\frac{d^2u}{dx^2} - cu + x^2 = 0 \quad \text{for } 0 < x < 1$$

for the (Dirichlet) boundary conditions $u(0) = 0$ and $u(1) = 0$. Use a uniform mesh of three linear elements, and compare the finite element solution with the exact solution for $c = 1$.

Answer: $U_2 = -0.02999$, $U_3 = -0.04257$, $P_2^3 = 0.12771$.

3.13. Solve the differential equation in Problem 3.12 for the (mixed) boundary conditions

$$u(0) = 0, \qquad \left(\frac{du}{dx}\right)\bigg|_{x=1} = 0$$

Use three linear elements.

Answer: $U_2 = -0.18805$, $U_3 = -0.34144$, $U_4 = -0.40708$, $P_1^1 = 5.6414$.

3.14. Solve the differential equation in Problem 3.12 for the (Neumann) boundary conditions

$$\left(\frac{du}{dx}\right)\bigg|_{x=0} = 1, \quad \left(\frac{du}{dx}\right)\bigg|_{x=1} = \frac{4}{3}$$

Use a uniform mesh of three linear finite elements to solve the problem. Verify your solution with the analytical solution.

Note that for Neumann boundary conditions, none of the primary dependent variables is specified, and therefore the solution can be determined within a constant; the coefficient matrix of the finite element equations for this case remains unaltered. When $c = 0$, the coefficient matrix is singular and cannot be inverted. In such cases, one of the U_i should be set equal to a constant (e.g., zero) to remove the "rigid-body" mode (i.e., to determine the arbitrary constant in the solution).

Answer: $U_1 = -0.56862$, $U_2 = -0.20932$, $U_4 = 0.18696$, $U_5 = 0.61334$.

3.15. The governing equation for an unconfined aquifer with flow in the radial direction is given by the differential equation

$$-\frac{1}{r}\frac{d}{dr}\left(rk\frac{du}{dr}\right) = f$$

where k is the coefficient of permeability, f the recharge, and u the piezometric head. Pumping is considered to be a negative recharge. Consider the following problem. A well penetrates an aquifer and pumping is performed at $r = 0$ at a rate $Q = 150\, m^2 h^{-1}$. The permeability of the aquifer is $k = 25\ \mathrm{m}^3\,\mathrm{h}^{-1}\,\mathrm{m}^{-2}$. A constant head $u_0 = 50$ m exists at a radial distance $L = 200$ m. Determine the piezometric head at radial distances of 0, 10, 20, 40, 80, and 140 m (see Fig. P3.15). You are required to set up the finite element equations for the unknowns using a nonuniform mesh of five linear elements.

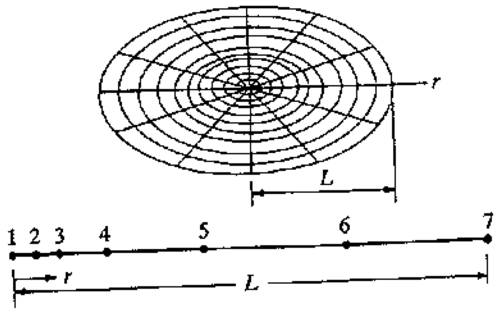

FIGURE P3.15

Section 3.3
Heat transfer

3.16. The following differential equation arises in connection with heat transfer in an insulated rod:

$$-\frac{d}{dx}\left(k\frac{dT}{dx}\right) = q \quad \text{for } 0 < x < L$$

$$T(0) = T_0, \quad \left[k\frac{dT}{dx} + \beta(T - T_\infty) + \hat{q}\right]\bigg|_{x=L} = 0$$

where T is the temperature, k the thermal conductivity, and q the heat generation. Take the following values for the data: $q=0$, $\hat{q}=0$, $L=0.1$ m, $k=0.01$ W m^{-1} °C^{-1}, $\beta = 25$ W m^{-2} °C^{-1}, $T_0 = 50$ °C, and $T_\infty = 5$ °C. Solve the problem using two linear finite elements for temperature values at $x=\frac{1}{2}L$ and L.

Answer: $U_2 = 27.59$ °C, $U_3 = 5.179$ °C, $P_1^1 = 4.482$ W m^{-2} $= -P_2^2$.

3.17. An insulating wall is constructed of three homogeneous layers with conductivities k_1, k_2, and k_3 in intimate contact (see Fig. P3.17). Under steady-state conditions, the temperatures at the boundaries of the layers are characterized by the external surface temperatures T_1 and T_4 and the interface temperatures T_2 and T_3. Formulate the problem to determine the temperatures T_i $(i = 1, \ldots, 4)$ when the ambient temperatures T_0 and T_5 and the (surface) film coefficients β_0 and β_5 are known. Assume that there is no internal heat generation and that the heat flow is one-dimensional $(\partial T/\partial y = 0)$.

Answer: $U_1 = 84.489$ °C, $U_2 = 68.977$ °C, $U_3 = 50.881$ °C, $U_4 = 45.341$ °C, $(P_1^1)_{\text{def}} = 217.16$ W m^{-2}, $(P_2^3)_{\text{def}} = -155.11$ W m^{-2}.

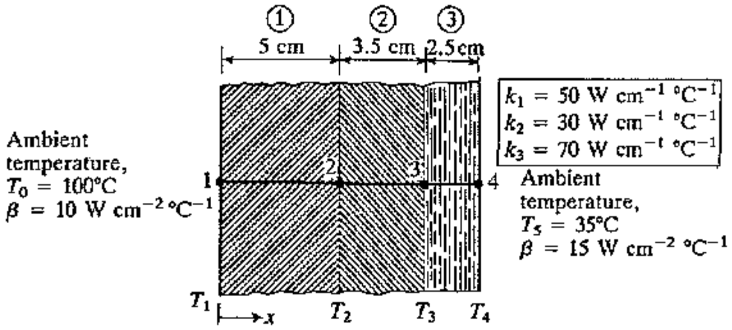
①
②
③
5 cm
3.5 cm
2.5cm
k_1 = 50 W cm^{-1} °C^{-1}
k_2 = 30 W cm^{-1} °C^{-1}
k_3 = 70 W cm^{-1} °C^{-1}
Ambient temperature, T_0 = 100°C
β = 10 W cm^{-2} °C^{-1}
1
2
3
4
Ambient temperature, T_5 = 35°C
β = 15 W cm^{-2} °C^{-1}
T_1
x
T_2
T_3
T_4

FIGURE P3.17

3.18. Consider the rectangular cooling fin shown in Fig. 3.9. The governing equation (i.e., balance of energy) is

$$-\frac{d^2T}{dx^2} + \frac{\beta}{ka}(T - T_\infty) = 0$$

where T is the temperature, k the thermal conductivity, β the film coefficient, a the thickness, and T_∞ the temperature of the surrounding fluid (i.e., ambient temperature). The boundary conditions of the problem are

$$T(0) = T_w \quad \text{(wall temperature)}, \qquad \left(kA\frac{dT}{dx}\right)\Big|_{x=L} = 0$$

The equations can be recast by introducing the following nondimensional quantities:

$$\theta = \frac{T - T_\infty}{T_w - T_\infty}, \qquad \xi = \frac{x}{L}, \qquad N = \left(\frac{\beta L^2}{ka}\right)^{1/2}$$

They then take the forms

$$-\frac{d^2\theta}{d\xi^2} + N^2\theta = 0, \qquad \theta(0) = 1, \qquad \left(\frac{d\theta}{d\xi}\right)\Big|_{\xi=1} = 0$$

Solve the problem using (*a*) two linear elements and (*b*) one quadratic element, and compare the finite solutions at four equal distances with the analytical solution

$$\theta = \cosh N\zeta - (\tanh N) \sinh N\zeta$$

3.19. A steel rod of diameter $D = 2$ cm, length $L = 5$ cm, and thermal conductivity $k = 50\ \mathrm{W\,m^{-1}\,°C^{-1}}$ is exposed to ambient air at $T_\infty = 20\,°\mathrm{C}$ with a heat transfer coefficient $\beta = 100\ \mathrm{W\,m^{-2}\,°C^{-1}}$. If the left end of the rod is maintained at temperature $T_0 = 320\,°\mathrm{C}$ and the other end is insulated (see Fig. P3.19), determine the temperatures at distances 25 mm and 50 mm from the left end, and the heat at the left end. The governing equation of the problem is

$$-\frac{d^2\theta}{dx^2} + N^2\theta = 0 \quad \text{for } 0 < x < L$$

where $\theta = T - T_\infty$, T is the temperature, and N^2 is given by

$$N^2 = \frac{\beta P}{Ak} = \frac{\beta \pi D}{\frac{1}{4}\pi D^2 k} = \frac{4\beta}{kD}$$

The boundary conditions are

$$\theta(0) = T(0) - T_\infty = 300\,°\mathrm{C}, \qquad \left(\frac{d\theta}{dx}\right)\bigg|_{x=L} = 0$$

Use (*a*) two linear elements and (*b*) one quadratic element to solve the problem by the finite element method. The exact solution is

$$\theta(x) = \theta(0)\frac{\cosh N(L - x)}{\cosh NL}$$

Answer: (*a*) $U_1 = 300\,°\mathrm{C}$, $U_2 = 50.272\,°\mathrm{C}$, $U_3 = 15.996\,°\mathrm{C}$, $P_1^1 = 998.9\ \mathrm{W\,m^{-2}}$.
(*b*) $U_2 = 300\,°\mathrm{C}$, $U_2 = 62.658\,°\mathrm{C}$, $U_3 = 34.177\,°\mathrm{C}$, $P_1^1 = 1367\ \mathrm{W\,m^{-2}}$.

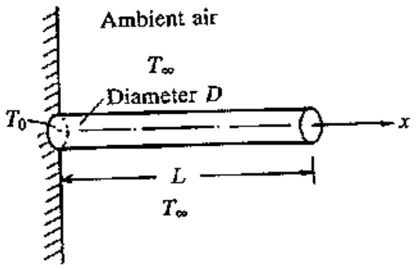

FIGURE P3.19

3.20. Find the temperature distribution in the tapered fin shown in Fig. P3.20. Assume that the temperature at the root of the fin is 250 °F, the conductivity $k = 120\ \mathrm{BTu\,h^{-1}\,ft^{-1}\,°F^{-1}}$, and the film coefficient $\beta = 15\ \mathrm{Btu\,h^{-1}\,ft^{-2}\,°F^{-1}}$, and use three linear elements. The ambient temperature at the top and bottom of the fin is $T_\infty = 75\,°\mathrm{F}$.

Answer: $T_1(\text{tip}) = 166.188\,°\mathrm{F}$, $T_2 = 191.1\,°\mathrm{F}$, $T_3 = 218.87\,°\mathrm{F}$.

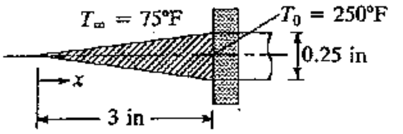

FIGURE P3.20

3.21. Consider steady heat conduction in a wire of circular cross-section with an electrical heat source. Suppose that the radius of the wire is R_0, its electrical conductivity is K_e ($\Omega^{-1}\,\text{cm}^{-1}$), and it is carrying an electric current density of I (A cm^{-2}). During the transmission of an electric current, some of the electrical energy is converted into thermal energy. The rate of heat production per unit volume is given by $q_e = I^2/K_e$. Assume that the temperature rise in the wire is sufficiently small that the dependence of the thermal or electric conductivity on temperature can be neglected. The governing equations of the problem are

$$-\frac{1}{r}\frac{d}{dr}\left(rk\frac{dT}{dr}\right) = q_e \quad \text{for } 0 \leq r \leq R_0, \qquad \left(kr\frac{dT}{dr}\right)\bigg|_{r=0} = 0, \qquad T(R_0) = T_0$$

Determine the distribution of temperature in the wire using (*a*) two linear elements and (*b*) one quadratic element, and compare the finite element solution at eight equal intervals with the exact solution

$$T(r) = T_0 + \frac{q_e R_0^2}{4k}\left[1 - \left(\frac{r}{R_0}\right)^2\right]$$

Also, determine the heat flow $Q = -2\pi R_0 L k (dT/dr)|_{R_0}$ at the surface using (i) the temperature field and (ii) the balance equations.

3.22. Consider a nuclear fuel element of spherical form, consisting of a sphere of "fissionable" material surrounded by a spherical shell of aluminum "cladding" as shown in Fig. P3.22. Nuclear fission is a source of thermal energy, which varies nonuniformly from the center of the sphere to the interface of the fuel element and the cladding. We wish to determine the temperature distribution in the nuclear fuel element and the aluminum cladding.

The governing equations for the two regions are the same, with the exception that there is no heat source term for the aluminum cladding. We have

$$-\frac{1}{r^2}\frac{d}{dr}\left(r^2 k_1 \frac{dT_1}{dr}\right) = q \quad \text{for } 0 \leq r \leq R_F$$

$$-\frac{1}{r^2}\frac{d}{dr}\left(r^2 k_2 \frac{dT_2}{dr}\right) = 0 \quad \text{for } R_F \leq r \leq R_C$$

where subscripts 1 and 2 refer to the nuclear fuel element and cladding, respectively. The heat generation in the nuclear fuel element is assumed to be of the form

$$q_1 = q_0\left[1 + c\left(\frac{r}{R_F}\right)^2\right]$$

where q_0 and c are constants depending on the nuclear material. The boundary conditions are

$$kr^2\frac{dT_1}{dr}=0 \quad \text{at } r=0$$

$$T_1=T_2 \quad \text{at } r=R_F$$

$$T_2=T_0 \quad \text{at } r=R_C$$

Use two linear elements to determine the finite element solution for the temperature distribution, and compare the nodal temperatures with the exact solution

$$T_1-T_0=\frac{q_0R_F^2}{6k_1}\left\{\left[1-\left(\frac{r}{R_F}\right)^2\right]+\tfrac{3}{10}c\left[1-\left(\frac{r}{R_F}\right)^4\right]\right\}+\frac{q_0R_F^2}{3k_2}(1+\tfrac{3}{5}c)\left(1-\frac{R_F}{R_c}\right)$$

$$T_2-T_0=\frac{q_0R_F^2}{3k_2}(1+\tfrac{3}{5}c)\left(\frac{R_F}{r}-\frac{R_F}{R_C}\right)$$

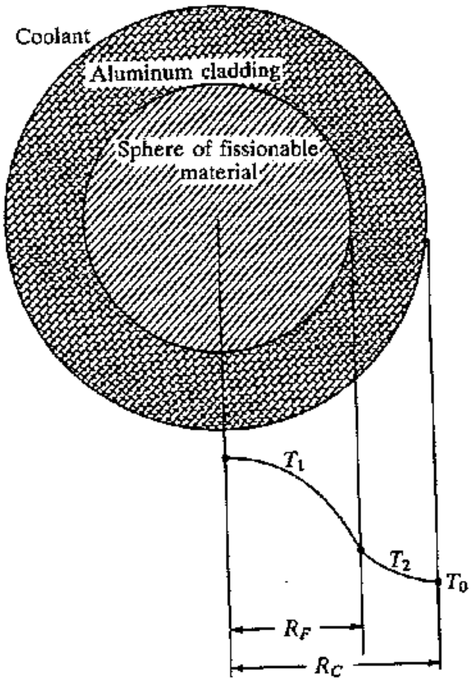

FIGURE P3.22

Fluid mechanics

3.23. Consider the flow of a Newtonian viscous fluid on an inclined flat surface, as shown in Fig. P3.23. Examples of such flow can be found in wetted-wall towers and the application of coatings to wallpaper rolls. The momentum equation, for a fully developed steady laminar flow along the z coordinate, is given by

$$-\mu\frac{d^2w}{dx^2}=\rho g\cos\beta$$

where w is the z component of the velocity, μ is the viscosity of the fluid, ρ is the density, g is the acceleration due to gravity, and β is the angle between the inclined surface and the vertical. The boundary conditions associated with the problem are that the shear stress is zero at $x = 0$ and the velocity is zero at $x = L$:

$$\left(\frac{dw}{dx}\right)\Bigg|_{x=0} = 0, \qquad w(L) = 0$$

Use (*a*) two linear finite elements of equal length and (*b*) one quadratic finite element in the domain $(0, L)$ to solve the problem and compare the two finite element solutions at four points $x = 0, \frac{1}{4}L, \frac{1}{2}L$, and $\frac{3}{4}L$ of the domain with the exact solution

$$w_e = \frac{\rho g L^2 \cos\beta}{2\mu}\left[1 - \left(\frac{x}{L}\right)^2\right]$$

Evaluate the shear stress ($\tau_{xz} = -\mu\, dw/dx$) at the wall using (i) the velocity fields and (ii) the equilibrium equations, and compare with the exact value.

Answer: (*a*) $U_1 = \frac{1}{2}f_0$, $U_2 = \frac{3}{8}f_0$, $f_0 = (\rho g \cos\beta)L^2/\mu$.

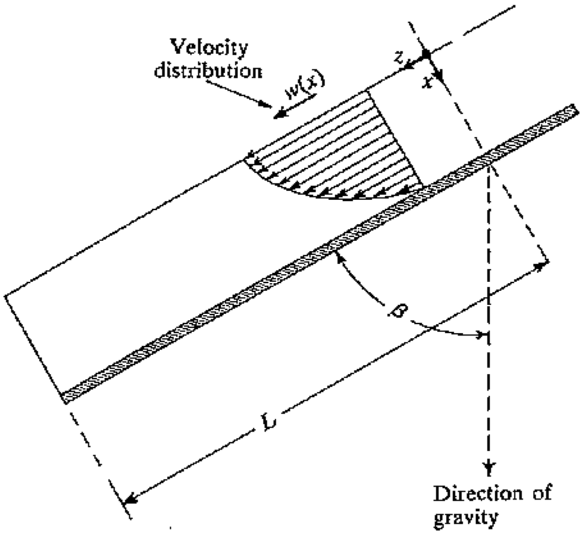

FIGURE P3.23

3.24. Consider the steady laminar flow of a viscous fluid through a long circular cylindrical tube. The governing equation is

$$-\frac{1}{r}\frac{d}{dr}\left(r\mu\frac{dw}{dr}\right) = \frac{P_0 - P_L}{L} \equiv f_0$$

where w is the axial (i.e., z) component of velocity, μ is the viscosity, and f_0 is the gradient of pressure (which includes the combined effect of static pressure and gravitational force). The boundary conditions are

$$\left(r\frac{dw}{dr}\right)\Bigg|_{r=0} = 0, \qquad w(R_0) = 0$$

Using the symmetry and (*a*) two linear elements, (*b*) one quadratic element, determine the velocity field and compare with the exact solution at the nodes:

$$w_e(r)=\frac{f_0R_0^2}{4\mu}\left[1-\left(\frac{r}{R_0}\right)^2\right]$$

3.25. In the problem of the flow of a viscous fluid through a circular cylinder (Problem 3.24), assume that the fluid slips at the cylinder wall; i.e., instead of assuming that $w=0$ at $r=R_0$, use the boundary condition that

$$kw=-\mu\frac{dw}{dr}\quad \text{at } r=R_0$$

in which k is the "coefficient of sliding friction." Solve the problem with two linear elements.

3.26. Consider the steady laminar flow of a Newtonian fluid with constant density in a long annular region between two coaxial cylinders of radii R_i and R_o (see Fig. P3.26). The differential equation for this case is given by

$$-\frac{1}{r}\frac{d}{dr}\left(r\mu\frac{dw}{dr}\right)=\frac{P_1-P_2}{L}\equiv f_0$$

where w is the velocity along the cylinders (i.e. the z component of velocity), μ is the viscosity, L is the length of the region along the cylinders in which the flow is

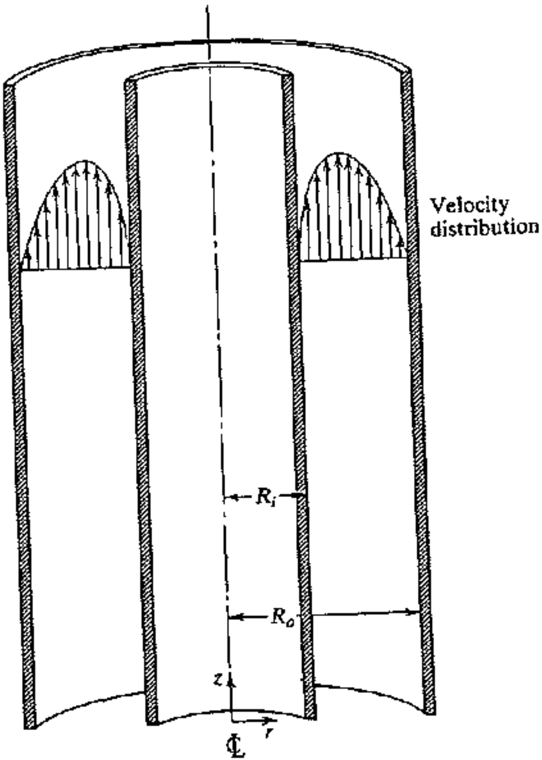

FIGURE P3.26

fully developed, and P_1 and P_2 are the pressures at $z = 0$ and $z = L$, respectively (P_1 and P_2 represent the combined effect of static pressure and gravitational force). The boundary conditions are

$$w = 0 \quad \text{at } r = R_o \text{ and } R_i$$

Solve the problem using (*a*) two linear elements and (*b*) one quadratic element, and compare the finite element solutions with the exact solution at the nodes:

$$w_e(r) = \frac{f_0 R_0^2}{4\mu}\left[1 - \left(\frac{r}{R_o}\right)^2 + \frac{1-k^2}{\ln(1/k)}\ln\left(\frac{r}{R_o}\right)\right]$$

where $k = R_i/R_o$. Determine the shear stress $\tau_{rz} = -\mu\, dw/dr$ at the walls using (i) the velocity field and (ii) the equilibrium equations, and compare with the exact values. (Note that the steady laminar flow of a viscous fluid through a long cylinder or a circular tube can be obtained as a limiting case of $k \rightarrow 0$.)

Answer: $U_2 = 0.40198$, $U_3 = 0.5036$, $U_4 = 0.35811$, $P_1^1 = -1.6079$, $P_2^4 = -2.8705$.

3.27. Consider the steady laminar flow of two immiscible incompressible fluids in a region between two parallel stationary plates under the influence of a pressure gradient. The fluid rates are adjusted such that the lower half of the region is filled with Fluid I (the denser and more viscous fluid) and the upper half is filled with Fluid II (the less dense and less viscous fluid), as shown in Fig. P3.27. We wish to determine the velocity distributions in each region using the finite element method.

The governing equations for each fluid are

$$-\mu_1 \frac{d^2 u_1}{dx^2} = f_0, \qquad -\mu_2 \frac{d^2 u_2}{dx^2} = f_0$$

where $f_0 = (P_0 - P_L)/L$ is the pressure gradient. The boundary conditions are

$$u_1(-b) = 0, \qquad u_2(b) = 0, \qquad u_1(0) = u_2(0)$$

Solve the problem using (*a*) four linear elements and (*b*) two quadratic elements, and compare the finite element solutions with the exact solution at the nodes

$$u_i = \frac{f_0 b^2}{2\mu_i}\left[\frac{2\mu_i}{\mu_1 + \mu_2} + \frac{\mu_1 - \mu_2}{\mu_1 + \mu_2}\frac{y}{b} - \left(\frac{y}{b}\right)^2\right] \quad (i = 1, 2)$$

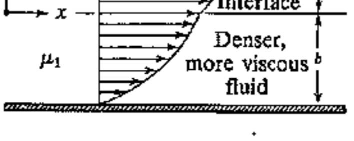

FIGURE P3.27

Solid mechanics

3.28. Find the three-element finite element solution to the stepped-bar problem (axial deformation of a bar). See Fig. P3.28 for the geometry and data.

Answer: $U_2 = 6P/\pi E_a$, $U_3 = 5P/\pi E_a$, $U_4 = \frac{16}{3} P\pi E_a$.

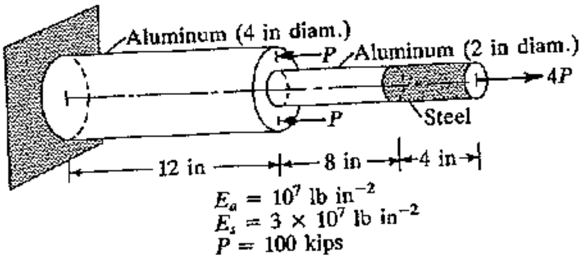

FIGURE P3.28

3.29. The equation governing the axial deformation of an elastic bar in the presence of applied mechanical loads f and P and a temperature change T is

$$-\frac{d}{dx}\left[EA\left(\frac{du}{dx}-\alpha T\right)\right]=f \quad \text{for } 0<x<L$$

where α is the thermal expansion coefficient, E the modulus of elasticity, and A the cross-sectional area. Using three linear finite elements, determine the axial displacements in a nonuniform rod of length 30 in, fixed at the left end and subjected to an axial force $P = 400$ lb and a temperature change of 60 °F. Take $A(x) = 6 - \frac{1}{10}x$ in^2, $E = 30 \times 10^6$ lb in^{-2}, and $\alpha = 12 \times 10^{-6}$ in in^{-1} °F^{-1}.

3.30. Analyze the stepped bar with its right end supported by a linear axial spring (see Fig. P3.30). The boundary condition at $x = 24$ in is

$$EA\frac{du}{dx} + ku = 0$$

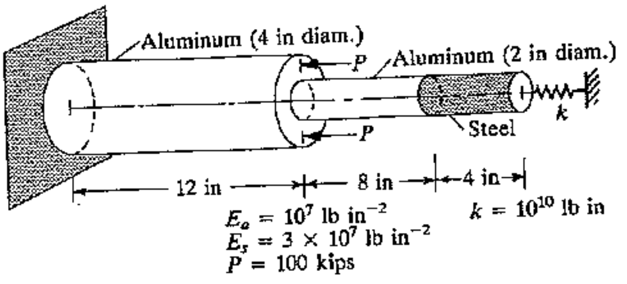

FIGURE P3.30

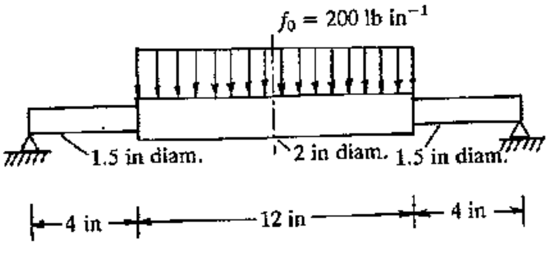

FIGURE P3.31

3.31. Consider the steel ($E = 30 \times 10^6$ psi) beam shown in Fig. P3.31. Determine the transverse deflection using two linear elements. Exploit the symmetry of the beam.

3.32. Determine the axial deformation of a nonuniform bar, $A = A_0 + A_1 x$, under its own weight (f_0 per unit length). Use two linear elements. The bar is fixed at $x = 0$.

3.33. Turbine disks are often thick near their hub and taper down to a smaller thickness at the periphery. The equation governing a variable-thickness $t = t(r)$ disk is

$$\frac{d}{dr}(tr\sigma_r) - t\sigma_\theta + t\rho\omega^2 r^2 = 0$$

where ω^2 is the angular speed of the disk and

$$\sigma_r = c\left(\frac{du}{dr} + \nu\frac{u}{r}\right), \quad \sigma_\theta = c\left(\frac{u}{r} + \nu\frac{du}{dr}\right), \quad c = \frac{E}{1-\nu^2}$$

(*a*) Construct the weak integral form of the governing equation such that the bilinear form is symmetric and the natural boundary condition involves specifying the quantity $tr\sigma_r$.

(*b*) Develop the finite element model associated with the weak form derived in part (*a*).

3.34. Determine the axial deformation of a varying cross-section member (see Fig. P3.34) under its own weight. Use one quadratic element.

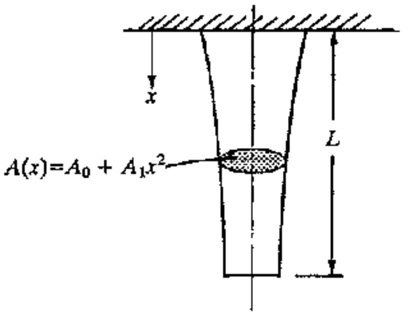

FIGURE P3.34

REFERENCES FOR ADDITIONAL READING

Fluid mechanics

Bird, R. B., W. E. Stewart, and E. N. Lightfoot: *Transport Phenomena*, John Wiley, New York, 1960.

Duncan, W. J., A. S. Thom, and A. D. Young: *Mechanics of Fluids*, 2d ed., Elsevier, New York, 1970.

Harr, M. E.: *Ground Water and Seepage*, McGraw-Hill, New York, 1962.

Shames, I. H.: *Mechanics of Fluids*, McGraw-Hill, New York, 1962.

Vallentine, H. R.: *Applied Hydrodynamics*, Butterworths, London 1959.

Heat transfer

Kreith, F.: *Principles of Heat Transfer*, 3d ed., Harper & Row, New York, 1973.

Myers, G. E.: *Analytical Methods in Conduction Heat Transfer*, McGraw-Hill, New York, 1972.

Nagotov, E. P.: *Applications of Numerical Methods to Heat Transfer*, McGraw-Hill, New York, 1978.

Solid mechanics

Boresi, A. P., and P. P. Lynn: *Elasticity in Engineering Mechanics*, Prentice-Hall, Englewood Cliffs, NJ, 1974.

Dym, C. L., and I. H. Shames: *Solid Mechanics: A Variational Approach*, McGraw-Hill, New York, 1973.

Reddy, J. N.: *Energy and Variational Methods in Applied Mechanics*, John Wiley, New York, 1984.

Timenshenko, S. P., and J. N. Goodier: *Theory of Elasticity*, McGraw-Hill, New York, 1970.

Variational methods

(See also References for Additional Reading in Chapter 2)

Crandall, S. H.: *Engineering Analysis*, McGraw-Hill, New York, 1956.

Mikhlin, S. G.: *Variational Methods in Mathematical Physics*, Pergamon Press, New York, 1964.

———: *The Numerical Performance of Variational Methods*, Wolters-Noordhoff, Groningen, 1971.

Oden, J. T., and J. N. Reddy: *Variational Methods in Theoretical Mechanics*, Springer-Verlag, New York, 1976; 2d ed., 1983.

Reddy, J. N.: *Energy and Variational Methods in Applied Mechanics*, John Wiley, New York, 1984.

———: *Applied Functional Analysis and Variational Methods in Engineering*, McGraw-Hill, New York, 1986; Krieger, Melbourne, FL, 1991.

——— and M. L. Rasmussen: *Advanced Engineering Analysis*, John Wiley, New York, 1982; Krieger, Melbourne, FL, 1990.

Rektorys, K.: *Variational Methods in Mathematics, Science and Engineering*, Reidel, Boston, 1977.

Schechter, R. S.: *The Variational Methods in Engineering*, McGraw-Hill, New York, 1967.

Washizu, K.: *Variational Methods in Elasticity and Plasticity*, 2d ed., Pergamon Press, New York, 1975; 3d ed., 1982.

CHAPTER 4

BENDING OF BEAMS

4.1 INTRODUCTION

Here we consider the finite element formulation of the one-dimensional fourth-order differential equation that arises in the Euler–Bernoulli beam theory and the pair of one-dimensional second-order equations associated with Timoshenko beam theory. The formulations of a fourth-order equation and two coupled second-order equations involve the same steps as described in Section 3.2 for a second-order equation, but the mathematical details are somewhat different, especially in the finite element formulation of the equations.

4.2 THE EULER–BERNOULLI BEAM ELEMENT

4.2.1 Governing Equation

In the Euler–Bernoulli beam theory, it is assumed that plane cross-sections perpendicular to the axis of the beam remain plane and perpendicular to the axis after deformation. In this theory, the transverse deflection w of the beam

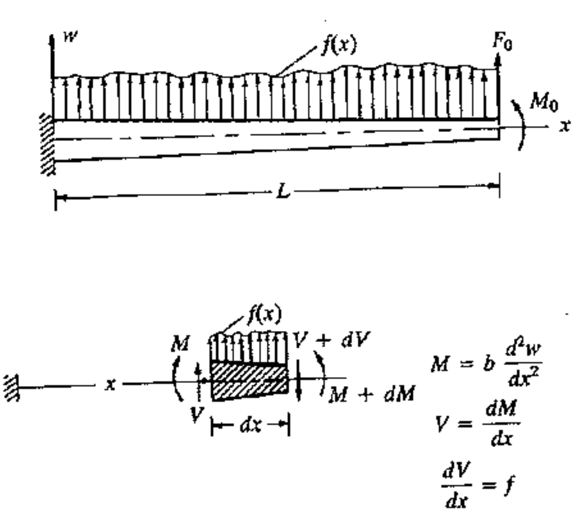

FIGURE 4.1
Bending of beams. The shear force–bending moment–deflection relations and the sign convention.

is governed by the fourth-order differential equation

$$\boxed{\frac{d^2}{dx^2}\left(b\frac{d^2w}{dx^2}\right)=f(x) \quad \text{for } 0<x<L} \tag{4.1}$$

where $b = b(x)$ and $f = f(x)$ are given functions of x (i.e., data), and w is the dependent variable. The sign convention used in the derivation of (4.1) is shown in Fig. 4.1. The function $b = EI$ is the product of the modulus of elasticity E and the moment of inertia I of the beam, f is the transversely distributed load, and w is the transverse deflection of the beam. In addition to satisfying the differential equation (4.1), w must also satisfy appropriate boundary conditions; since the equation is of fourth order, four boundary conditions are needed to solve it. The weak formulation of the equation will provide the form of these four boundary conditions. A step-by-step procedure for the finite-element analysis of (4.1) is presented next.

4.2.2 Discretization of the Domain

The domain of the structure (i.e., length of the beam) is divided into a set (say, N) of line elements, each element having at least the two end nodes (see Fig. 4.2a). Although the element is geometrically the same as that used for bars, the number and form of the primary and secondary unknowns at each node are dictated by the variational formulation of the differential equation (4.1). In most practical problems, the discretization of a given structure into a minimum number of elements is often dictated by the geometry, loading, and material properties.

4.2.3 Derivation of Element Equations

In this step we isolate a typical element $\Omega^e = (x_e, x_{e+1})$ (see Fig. 4.2b) and construct the weak form of (4.1) over the element. The variational formulation

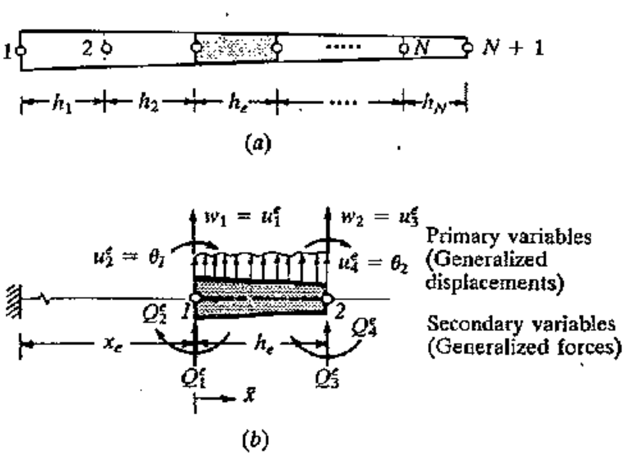

FIGURE 4.2
Discretization of a beam using Euler–Bernoulli beam elements. The generalized displacements and generalized forces are shown on a typical beam element.

provides the primary and secondary variables of the problem. Then suitable approximations for the primary variables are selected, interpolation functions are developed, and the element equations are derived.

WEAK FORM. The weak forms of problems in solid mechanics can be developed either from the principle of virtual work (i.e., the principle of virtual displacements or virtual forces) or from the governing differential equations. Here we start with a given differential equation and using the three-step procedure to obtain the weak form. Following the three-step procedure developed in Chapter 2 and revisited in Section 3.2.3, we write

$$\begin{aligned}0 &= \int_{x_e}^{x_{e+1}} v\left[\frac{d^2}{dx^2}\left(b\frac{d^2w}{dx^2}\right) - f\right] dx\\&= \int_{x_e}^{x_{e+1}} \left[-\frac{dv}{dx}\frac{d}{dx}\left(b\frac{d^2w}{dx^2}\right) - vf\right] dx + \left[v\frac{d}{dx}\left(b\frac{d^2w}{dx^2}\right)\right]_{x_e}^{x_{e+1}}\\&= \int_{x_e}^{x_{e+1}} \left(b\frac{d^2v}{dx^2}\frac{d^2w}{dx^2} - vf\right) dx + \left[v\frac{d}{dx}\left(b\frac{d^2w}{dx^2}\right) - \frac{dv}{dx}b\frac{d^2w}{dx^2}\right]_{x_e}^{x_{e+1}}\end{aligned} \tag{4.2}$$

where $v(x)$ is a weight function that is twice differentiable with respect to x. Note that, in the present case, the first term of the equation is integrated twice by parts to trade two differentiations to the weight function v, while retaining two derivatives of the dependent variable w; i.e., the differentiation is distributed equally between the weight function v and the dependent variable w. Because of the two integrations by parts, there appear two boundary expressions (see Example 2.2), which are to be evaluated at the two boundary points $x = x_e$ and $x = x_{e+1}$. Examination of the boundary terms indicates that the essential boundary conditions involve the specification of the deflection w and slope dw/dx, and the natural boundary conditions involve the specification of the bending moment $b\,d^2w/dx^2$ and shear force $(d/dx)(b\,d^2w/dx^2)$ at the endpoints of the element. Thus, there are two essential boundary conditions and two natural boundary conditions; therefore, we must identify w and dw/dx as the primary varaibles at each node (so that the essential boundary conditions are included in the interpolation). The natural boundary conditions always remain in the weak form and end up on the right-hand side (i.e., the source vector) of the matrix equation. For the sake of mathematical convenience, we introduce the following notation: $\theta = -dw/dx$ and

$$\boxed{\begin{aligned} Q_1^e &\equiv \left[\frac{d}{dx}\left(b\frac{d^2w}{dx^2}\right)\right]\bigg|_{x_e}, & Q_2^e &\equiv \left(b\frac{d^2w}{dx^2}\right)\bigg|_{x_e} \\ Q_3^e &\equiv -\left[\frac{d}{dx}\left(b\frac{d^2w}{dx^2}\right)\right]\bigg|_{x_{e+1}}, & Q_4^e &\equiv -\left(b\frac{d^2w}{dx^2}\right)\bigg|_{x_{e+1}} \end{aligned}} \tag{4.3}$$

where Q_1^e and Q_3^e denote the shear forces, and Q_2^e and Q_4^e denote the bending moments (see Fig. 4.2b). Since the quantities Q_i^e contain bending moments, which can also be viewed as "bending forces," the set $\{Q_1^e, Q_2^e, Q_3^e, Q_4^e\}$ is often referred to as the *generalized forces.* The corresponding displacements and rotations are called the *generalized displacements.*

With the notation in (4.3), the weak form (4.2) can be expressed as

$$\begin{aligned} 0 &= \int_{x_e}^{x_{e+1}} \left(b\frac{d^2v}{dx^2}\frac{d^2w}{dx^2} - vf\right)dx - v(x_e)Q_1^e - \left(-\frac{dv}{dx}\right)\bigg|_{x_e} Q_2^e \\ &\quad - v(x_{e+1})Q_3^e - \left(-\frac{dv}{dx}\right)\bigg|_{x_{e+1}} Q_4^e \\ &\equiv B(v, w) - l(v) \end{aligned} \tag{4.4a}$$

We can identify the bilinear and linear forms of the problem as

$$\begin{aligned} B(v, w) &= \int_{x_e}^{x_{e+1}} b\frac{d^2v}{dx^2}\frac{d^2w}{dx^2}\,dx \\ l(v) &= \int_{x_e}^{x_{e+1}} vf\,dx + v(x_e)Q_1^e + \left(-\frac{dv}{dx}\right)\bigg|_{x_e} Q_2^e \\ &\quad + v(x_{e+1})Q_3^e + \left(-\frac{dv}{dx}\right)\bigg|_{x_{e+1}} Q_4^e \end{aligned} \tag{4.4b}$$

Equation (4.4a) is a statement of the principle of virtual displacements for the Euler–Bernoulli beam theory. The quadratic functional, known as the *total potential energy* of the beam element, is given by [from (2.43b)]

$$\begin{aligned} I_e(w) &= \int_{x_e}^{x_{e+1}} \left[\frac{b}{2}\left(\frac{d^2w}{dx^2}\right)^2 - wf\right]dx - w(x_e)Q_1^e - \left(-\frac{dw}{dx}\right)\bigg|_{x_e} Q_2^e \\ &\quad - w(x_{e+1})Q_3^e - \left(-\frac{dw}{dx}\right)\bigg|_{x_{e+1}} Q_4^e \end{aligned} \tag{4.5}$$

The first term in the square brackets represents the elastic strain energy due to bending, while the second is the work done by the distributed load; the remaining terms account for the work done by the generalized forces Q_i^e in moving through the generalized displacements of the element.

INTERPOLATION FUNCTIONS. The variational form (4.4*a*) requires that the interpolation functions of an element be continuous with nonzero derivatives up to order two. The approximation of the primary variables over a finite element should be such that it satisfies the interpolation properties (i.e., that it satisfies the essential boundary conditions of the element):

$$w(x_e)=w_1, \qquad w(x_{e+1})=w_2; \qquad \theta(x_e)=\theta_1, \qquad \theta(x_{e+1})=\theta_2 \tag{4.6}$$

In satisfying the essential boundary conditions (4.6), the approximation automatically satisfies the continuity conditions. Hence, we pay attention to the satisfaction of (4.6), which form the basis for the interpolation procedure.

Since there is a total of four conditions in an element (two per node), a four-parameter polynomial must be selected for w:

$$w(x)=c_1+c_2x+c_3x^2+c_4x^3 \tag{4.7}$$

Note that the continuity conditions (i.e., the existence of a nonzero second derivative of w in the element) are automatically met. The next step involves expressing c_i in terms of the primary nodal variables (i.e., generalized displacements)

$$u_1^e\equiv w(x_e), \qquad u_2^e\equiv\left(-\frac{dw}{dx}\right)\bigg|_{x=x_e}, \qquad u_3^e\equiv w(x_{e+1}), \qquad u_4^e\equiv\left(-\frac{dw}{dx}\right)\bigg|_{x=x_{e+1}}$$

such that the conditions (4.6) are satisfied:

$$\begin{aligned}
u_1^e&=w(x_e)=c_1+c_2x_e+c_3x_e^2+c_4x_e^3\\
u_2^e&=\left(-\frac{dw}{dx}\right)\bigg|_{x=x_e}=-c_2-2c_3x_e-3c_4x_e^2\\
u_3^e&=w(x_{e+1})=c_1+c_2x_{e+1}+c_3x_{e+1}^2+c_4x_{e+1}^3\\
u_4^e&=\left(-\frac{dw}{dx}\right)\bigg|_{x_{e+1}}=-c_2-2c_3x_{e+1}-3c_4x_{e+1}^2
\end{aligned} \tag{4.8a}$$

or

$$\begin{Bmatrix}u_1^e\\u_2^e\\u_3^e\\u_4^e\end{Bmatrix}=\begin{bmatrix}1 & x_e & x_e^2 & x_e^3\\ 0 & -1 & -2x_e & -3x_e^2\\ 1 & x_{e+1} & x_{e+1}^2 & x_{e+1}^3\\ 0 & -1 & -2x_{e+1} & -3x_{e+1}^2\end{bmatrix}\begin{Bmatrix}c_1\\c_2\\c_3\\c_4\end{Bmatrix} \tag{4.8b}$$

Inverting this matrix equation to express c_i in terms of u_1^e, u_2^e, u_3^e, and u_4^e, and substituting the result into (4.7), we obtain

$$\boxed{w^e(x) = u_1^e\phi_1^e + u_2^e\phi_2^e + u_3^e\phi_3^e + u_4^e\phi_4^e = \sum_{j=1}^{4} u_j^e\phi_j^e} \tag{4.9a}$$

where (with $x_{e+1} = x_e + h_e$)

$$\boxed{\begin{aligned} \phi_1^e &= 1 - 3\left(\frac{x - x_e}{h_e}\right)^2 + 2\left(\frac{x - x_e}{h_e}\right)^3, & \phi_2^e &= -(x - x_e)\left(1 - \frac{x - x_e}{h_e}\right)^2 \\ \phi_3^e &= 3\left(\frac{x - x_e}{h_e}\right)^2 - 2\left(\frac{x - x_e}{h_e}\right)^3, & \phi_4^e &= -(x - x_e)\left[\left(\frac{x - x_e}{h_e}\right)^2 - \frac{x - x_e}{h_e}\right] \end{aligned}} \tag{4.9b}$$

Note that the cubic interpolation functions in (4.9) are derived by interpolating w *and* its derivative at the nodes. Such polynomials are known as the *Hermite family of interpolation functions*, and ϕ_i^e in (4.9b) are called the *Hermite cubic interpolation* (or *cubic spline*) *functions*. Recall that the Lagrange cubic interpolation functions are derived to interpolate a function, but not its derivatives, at the nodes. Hence, a Lagrange cubic element will have four nodes, with the dependent variable, not its derivative, as the nodal degree of freedom. Since the slope (or derivative) of the dependent variable is also required by the weak form to be continuous at the nodes for Euler–Bernoulli beam theory, the Lagrange cubic interpolation of w, although it meets the continuity requirement for w, is *not admissible* in the finite element approximation of Euler–Bernoulli beam theory.

The interpolation functions ϕ_i^e can be expressed in terms of the local coordinate $\bar{x}$:

$$\boxed{\begin{aligned} \phi_1^e &= 1 - 3\left(\frac{\bar{x}}{h_e}\right)^2 + 2\left(\frac{\bar{x}}{h_e}\right)^3, & \phi_2^e &= -\bar{x}\left(1 - \frac{\bar{x}}{h_e}\right)^2 \\ \phi_3^e &= 3\left(\frac{\bar{x}}{h_e}\right)^2 - 2\left(\frac{\bar{x}}{h_e}\right)^3, & \phi_4^e &= -\bar{x}\left[\left(\frac{\bar{x}}{h_e}\right)^2 - \frac{\bar{x}}{h_e}\right] \end{aligned}} \tag{4.10a}$$

The first, second, and third derivatives of ϕ_i^e with respect to $\bar{x}$ are

$$\begin{gathered} \frac{d\phi_1^e}{d\bar{x}} = -\frac{6}{h_e}\frac{\bar{x}}{h_e}\left(1 - \frac{\bar{x}}{h_e}\right), \quad \frac{d\phi_2^e}{d\bar{x}} = -\left[1 + 3\left(\frac{\bar{x}}{h_e}\right)^2 - 4\frac{\bar{x}}{h_e}\right] \\ \frac{d\phi_3^e}{d\bar{x}} = -\frac{d\phi_1^e}{d\bar{x}}, \quad \frac{d\phi_4^e}{d\bar{x}} = -\frac{\bar{x}}{h_e}\left(3\frac{\bar{x}}{h_e} - 2\right) \\ \frac{d^2\phi_1^e}{d\bar{x}^2} = -\frac{6}{h_e^2}\left(1 - 2\frac{\bar{x}}{h_e}\right), \quad \frac{d^2\phi_2^e}{d\bar{x}^2} = -\frac{2}{h_e}\left(3\frac{\bar{x}}{h_e} - 2\right) \\ \frac{d^2\phi_3^e}{d\bar{x}^2} = -\frac{d^2\phi_1^e}{d\bar{x}^2}, \quad \frac{d^2\phi_4^e}{d\bar{x}^2} = -\frac{2}{h_e}\left(3\frac{\bar{x}}{h_e} - 1\right) \\ \frac{d^3\phi_1^e}{d\bar{x}^3} = \frac{12}{h_e^3}, \quad \frac{d^3\phi_2^e}{d\bar{x}^3} = -\frac{6}{h_e^2}, \quad \frac{d^3\phi_3^e}{d\bar{x}^3} = -\frac{12}{h_e^3}, \quad \frac{d^3\phi_4^e}{d\bar{x}^3} = -\frac{6}{h_e^2} \end{gathered} \tag{4.10b}$$

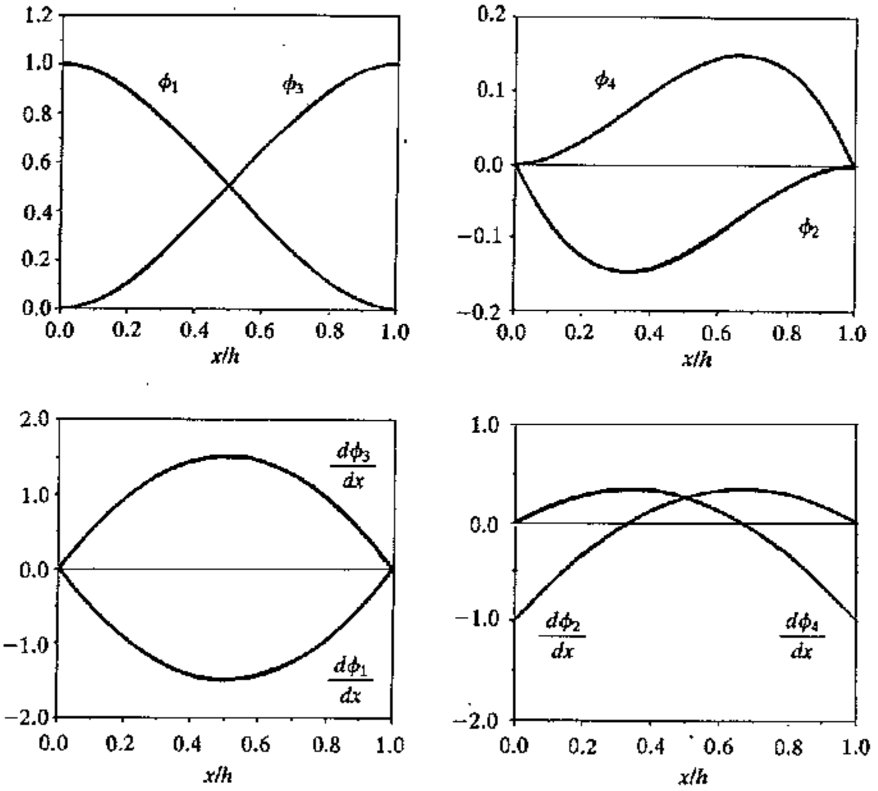

FIGURE 4.3
Hermite cubic interpolation functions and their first derivatives used in the finite element model of Euler–Bernoulli beam theory.

The Hermite cubic interpolation functions (4.9) satisfy the following interpolation properties (see Fig. 4.3):

$$
\begin{aligned}
\phi_1^e(x_e) &= 1, & \phi_i^e(x_e) &= 0 \quad (i \neq 1)\\
\phi_3^e(x_{e+1}) &= 1, & \phi_i^e(x_{e+1}) &= 0 \quad (i \neq 3)\\
\left(-\frac{d\phi_2^e}{dx}\right)\bigg|_{x_e} &= 1, & \left(\frac{d\phi_i^e}{dx}\right)\bigg|_{x_e} &= 0 \quad (i \neq 2)\\
\left(-\frac{d\phi_4^e}{dx}\right)\bigg|_{x_{e+1}} &= 1, & \left(\frac{d\phi_i^e}{dx}\right)\bigg|_{x_{e+1}} &= 0 \quad (i \neq 4)
\end{aligned}
\tag{4.11a}
$$

These can be stated in compact form as $(i, j = 1, 2)$

$$
\boxed{
\begin{gathered}
\phi_{2i-1}^e(\bar{x}_j) = \delta_{ij}, \quad \phi_{2i}^e(\bar{x}_j) = 0, \quad \sum_{i=1}^{2} \phi_{2i-1}^e = 1\\
\left(\frac{d\phi_{2i-1}^e}{dx}\right)\bigg|_{\bar{x}_j} = 0, \quad \left(-\frac{d\phi_{2i}^e}{dx}\right)\bigg|_{\bar{x}_j} = \delta_{ij}
\end{gathered}
}
\tag{4.11b}
$$

where $\bar{x}_1 = 0$ and $\bar{x}_2 = h_e$ are the local coordinates of nodes 1 and 2 of the element $\Omega^e = (x_e, x_{e+1})$.

It should be noted that the order of the interpolation functions derived above is the minimum required for the variational formulation (4.4). If a higher-order (i.e., higher than cubic) approximation of w is desired, one must either identify additional primary unknowns at each of the two nodes or add additional nodes with the two degrees of freedom $(w, -dw/dx)$. For example, if we add d^2w/dx^2 as the primary unknown at each of the two nodes, or add a third node, there will be a total of six conditions, and a fifth-order polynomial is required to interpolate the end conditions (see Problems 4.27 and 4.28). However, continuity of dw^2/dx^2 is not required, in general, and such elements should be used only in problems where d^2w/dx^2 is continuous everywhere.

FINITE ELEMENT MODEL. The finite element model of the Euler–Bernoulli beam is obtained by substituting the finite element interpolation (4.9a) for w and the ϕ_j for the weight function v into the weak form (4.4d). Since there are four nodal variables u_i^e, four different choices are used for v, $v=\phi_1^e$, $v=\phi_2^e$, $v=\phi_3^e$, and $v=\phi_4^e$, to obtain a set of four algebraic equations. The ith algebraic equation of the finite element model is (for $v=\phi_i^e$)

$$0=\sum_{j=1}^{4}\left(\int_{x_e}^{x_{e+1}} b\frac{d^2\phi_i^e}{dx^2}\frac{d^2\phi_j^e}{dx^2}\,dx\right)u_j^e-\int_{x_e}^{x_{e+1}}\phi_i^e f\,dx-Q_i^e \tag{4.12a}$$

or

$$\boxed{\sum_{j=1}^{4}K_{ij}^e u_j^e-F_i^e=0} \tag{4.12b}$$

where

$$\boxed{K_{ij}^e=\int_{x_e}^{x_{e+1}} b\frac{d^2\phi_i^e}{dx^2}\frac{d^2\phi_j^e}{dx^2}\,dx,\qquad F_i^e=\int_{x_e}^{x_{e+1}}\phi_i^e f\,dx+Q_i^e} \tag{4.12c}$$

Note that the coefficients K_{ij}^e are symmetric: $K_{ij}^e=K_{ji}^e$. In matrix notation, (4.12b) can be written as

$$\begin{bmatrix} K_{11}^e & K_{12}^e & K_{13}^e & K_{14}^e \\ K_{21}^e & K_{22}^e & K_{23}^e & K_{24}^e \\ K_{31}^e & K_{32}^e & K_{33}^e & K_{34}^e \\ K_{41}^e & K_{42}^e & K_{43}^e & K_{44}^e \end{bmatrix}\begin{Bmatrix} u_1^e \\ u_2^e \\ u_3^e \\ u_4^e \end{Bmatrix}=\begin{Bmatrix} f_1^e \\ f_2^e \\ f_3^e \\ f_4^e \end{Bmatrix}+\begin{Bmatrix} Q_1^e \\ Q_2^e \\ Q_3^e \\ Q_4^e \end{Bmatrix} \tag{4.13}$$

This represents the finite element model of (4.1). Here $[K^e]$ is the *stiffness matrix* and $\{F^e\}$ is the *force vector* of a beam element. When a transverse point force F_0^e is applied at a point x_0 inside the element, it is distributed to the element nodes by the relation [see Remark 5 in Chapter 3: (3.60)]:

$$F_i^e=F_0^e\phi_i^e(x_0) \tag{4.14}$$

which contains both transverse forces (F_1^e and F_3^e) and bending moments (F_2^e and F_4^e).

For the case in which b $(=EI)$ and f are constant over an element, the element stiffness matrix $[K^e]$ and force vector $\{F^e\}$ have the specific forms (see Fig. 4.2 for the element displacement and force degrees of freedom)

$$\boxed{\begin{aligned}
[K^e] &= \frac{2b}{h^3}\begin{bmatrix} 6 & -3h & -6 & -3h \\ -3h & 2h^2 & 3h & h^2 \\ -6 & 3h & 6 & 3h \\ -3h & h^2 & 3h & 2h^2 \end{bmatrix} \qquad (b = EI = \text{constant}) \\
\{F^e\} &= \frac{fh}{12}\begin{Bmatrix} 6 \\ -h \\ 6 \\ h \end{Bmatrix} + \begin{Bmatrix} Q_1 \\ Q_2 \\ Q_3 \\ Q_4 \end{Bmatrix} \qquad (f = \text{constant})
\end{aligned}} \tag{4.15}$$

It can be verified that the generalized force vector in (4.15) represents the "statically equivalent" forces and moments at nodes 1 and 2 due to the uniformly distributed load over the element. For any given function f, (4.12c) provides a straightforward way of computing the components of the generalized force vector $\{f^e\}$.

4.2.4 Assembly of Element Equations

The assembly procedure for beam elements is the same as that used for bar elements, except that we must take into account the two degrees of freedom at each node. Recall that the assembly of elements is based on: (a) interelement continuity of the primary variables (deflection and slope) and (b) interelement equilibrium of the secondary variables (shear force and bending moment) at the nodes common to elements. To demonstrate the assembly procedure, we select a two-element model (see Fig. 4.4). There are three global nodes and a total of six global generalized displacements and six generalized forces in the problem. The continuity of the primary variables implies the following relation between the element degrees of freedom u_i^e and the global degrees of freedom U_i (see Fig. 4.4):

$$\begin{aligned} &u_1^1 = U_1, \quad u_2^1 = U_2, \quad u_3^1 = u_1^2 = U_3 \\ &u_4^1 = u_2^2 = U_4, \quad u_3^2 = U_5, \quad u_4^2 = U_6 \end{aligned} \tag{4.16}$$

In general, the equilibrium of the generalized forces at a node between two connecting elements Ω^e and Ω^f requires that

$$\begin{aligned} Q_3^e + Q_1^f &= \text{applied external point force} \\ Q_4^e + Q_2^f &= \text{applied external bending moment} \end{aligned} \tag{4.17}$$

If no external applied forces are given, the sum should be equated to zero. In equating the sums to the applied generalized forces (i.e., force or moment), the sign convention for the element force degrees of freedom (see Fig. 4.2)

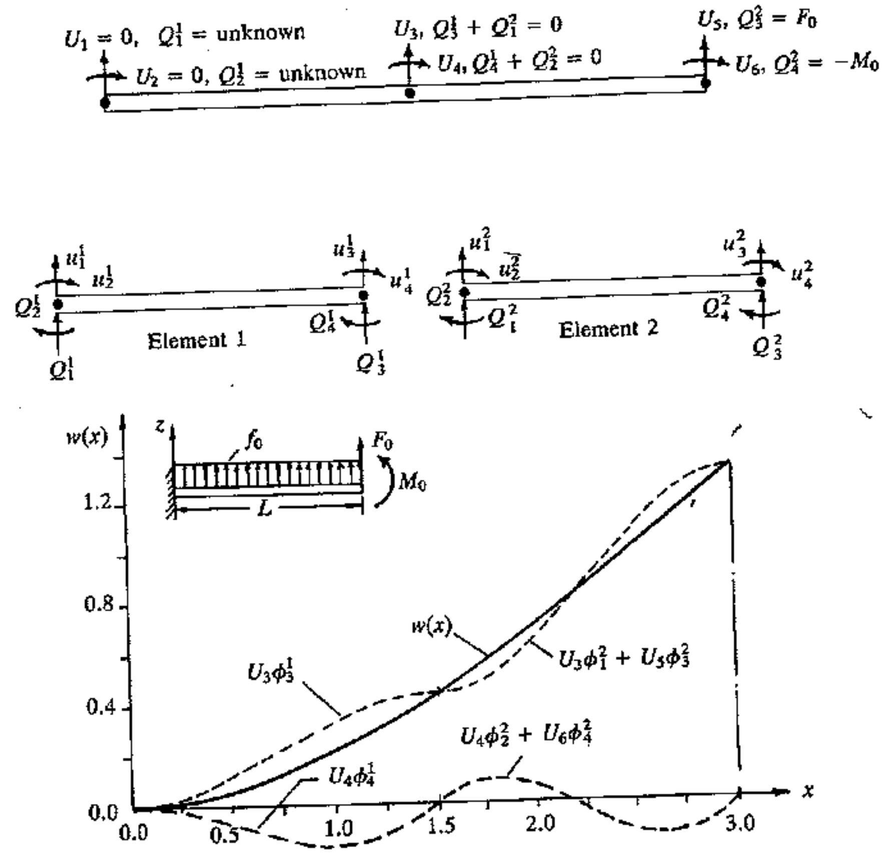
$U_1 = 0,\ Q_1^1 = \text{unknown}$
$U_2 = 0,\ Q_2^1 = \text{unknown}$
$U_3,\ Q_3^1 + Q_1^2 = 0$
$U_4,\ Q_4^1 + Q_2^2 = 0$
$U_5,\ Q_3^2 = F_0$
$U_6,\ Q_4^2 = -M_0$
u_1^1 u_2^1 Q_2^1 Q_1^1
Element 1
u_3^1 u_4^1 Q_4^1 Q_3^1
u_1^2 u_2^2 Q_2^2 Q_1^2
Element 2
u_3^2 u_4^2 Q_4^2 Q_3^2
$w(x)$
z
f_0
F_0
M_0
L
1.2
0.8
0.4
0.0
0.0
0.5
1.0
1.5
2.0
3.0
x
$w(x)$
$U_3\phi_3^1$
$U_3\phi_1^2 + U_5\phi_3^2$
$U_4\phi_2^2 + U_6\phi_4^2$
$U_4\phi_4^1$

FIGURE 4.4
Assembly of two Euler–Bernoulli (or classical) beam finite elements, and the finite element solution as a linear combination of the nodal values and interpolation functions.

should be followed. Forces are taken positive acting upward and moments are taken positive acting clockwise.

To impose the equilibrium of forces in (4.17), it is necessary to add the third and fourth equations (corresponding to the second node) of Ω^e to the first and second equations (corresponding to the first node) of Ω^f. Consequently, the global stiffnesses K_{33}, K_{34}, K_{43}, and K_{44} associated with global node 2 are the superpositions of the element stiffnesses:

$$K_{33} = K_{33}^1 + K_{11}^2, \quad K_{34} = K_{34}^1 + K_{12}^2, \quad K_{43} = K_{43}^1 + K_{21}^2, \quad K_{44} = K_{44}^1 + K_{22}^2 \tag{4.18}$$

In general, the assembled stiffness matrix and force vector for beam elements connected in series have the following forms:

$$
[K]=\left[\begin{array}{cc:cc:cc}
\multicolumn{2}{c}{\overbrace{\hspace{4em}}^{\substack{\text{Global}\\ \text{nodes}\\ 1}}} & \multicolumn{2}{c}{\overbrace{\hspace{10em}}^{2}} & \multicolumn{2}{c}{\overbrace{\hspace{4em}}^{3}} \\
K^1_{11} & K^1_{12} & K^1_{13} & K^1_{14} & & \\
K^1_{21} & K^1_{22} & K^1_{23} & K^1_{24} & & \\ \hdashline
K^1_{31} & K^1_{32} & K^1_{33}+K^2_{11} & K^1_{34}+K^2_{12} & K^2_{13} & K^2_{14} \\
K^1_{41} & K^1_{42} & K^1_{43}+K^2_{21} & K^1_{44}+K^2_{22} & K^2_{23} & K^2_{24} \\ \hdashline
 & & K^2_{31} & K^2_{32} & K^2_{33} & K^2_{34} \\
 & & K^2_{41} & K^2_{42} & K^2_{43} & K^2_{44}
\end{array}\right]
\begin{array}{l}
\\[2em]
\left.\begin{matrix}\\ \\ \end{matrix}\right\} 1 \\
\left.\begin{matrix}\\ \\ \end{matrix}\right\} 2 \\
\left.\begin{matrix}\\ \\ \end{matrix}\right\} 3
\end{array}
\tag{4.19a}
$$

$$
\{F\}=\begin{Bmatrix} F^1_1 \\ F^1_2 \\ F^1_3+F^2_1 \\ F^1_4+F^2_2 \\ F^2_3 \\ F^2_4 \end{Bmatrix}
\tag{4.19b}
$$

The connectivity matrix $[B]$ (which will be used in computer implementation) for the two-element mesh is

$$
[B]=\begin{bmatrix} 1 & 2 \\ 2 & 3 \end{bmatrix}
$$

Since there are two primary degrees of freedom per node, repetition of a number in $[B]$ indicates that the coefficients associated with both degrees of freedom will add up. For example, the repetition of the global node number 2 (which corresponds to global degrees of freedom 3 and 4) in rows 1 and 2 indicates that the global K_{33}, K_{34}, K_{43}, and K_{44} have contributions from both elements 1 and 2.

The assembled system of equations for a mesh of two elements with $h_1=h_2=\frac{1}{2}L=h$, and constant EI and f [hence, $[K^e]$ and $\{f^e\}$ are given by

(4.15)] is

$$\frac{2EI}{h^3}\begin{bmatrix} 6 & -3h & -6 & -3h & 0 & 0 \\ -3h & 2h^2 & 3h & h^2 & 0 & 0 \\ -6 & 3h & 6+6 & 3h-3h & -6 & -3h \\ -3h & h^2 & 3h-3h & 2h^2+2h^2 & 3h & h^2 \\ 0 & 0 & -6 & 3h & 6 & 3h \\ 0 & 0 & -3h & h^2 & 3h & 2h^2 \end{bmatrix}\begin{Bmatrix} U_1 \\ U_2 \\ U_3 \\ U_4 \\ U_5 \\ U_6 \end{Bmatrix}$$

$$=\frac{fh}{12}\begin{Bmatrix} 6 \\ -h \\ 6+6 \\ h-h \\ 6 \\ h \end{Bmatrix}+\begin{Bmatrix} Q_1^1 \\ Q_2^1 \\ Q_3^1+Q_1^2 \\ Q_4^1+Q_2^2 \\ Q_3^2 \\ Q_4^2 \end{Bmatrix} \tag{4.20}$$

The reader is cautioned that (4.20) does not represent the assembled equations of any two beam elements; it is based on the assumption that $h_1 = h_2$, $(EI)_1 = (EI)_2$, and $(f)_1 = (f)_2$. Equations (4.19) are more general.

4.2.5 Imposition of Boundary Conditions

At this step of the analysis, we must specify the particular boundary conditions, i.e., geometric constraints and forces applied, of the particular problem to be analyzed. The type of essential (also known as *geometric*) boundary conditions for a specific beam problem depend on the nature of the geometric support. Table 4.1 contains a list of commonly used geometric supports for beams. For the sake of completeness, the boundary conditions on the axial displacement u are also included. The natural (also called *force*) boundary conditions involve the specification of generalized forces when the corresponding primary variables are not constrained. Here we consider a cantilever beam (i.e., a beam fixed at one end and free at the other) of length L, flexural rigidity EI (= constant), and subjected to a uniformly distributed force f_0, end force F_0, and end moment M_0 (see Fig. 4.4).

First, we write the equilibrium conditions for the generalized forces. At global node 1, Q_1^1 and Q_2^1 (the shear force and the bending moment, respectively; i.e., the reactions at the fixed end) are not known. At global node 2, there are no externally applied shear forces and bending moment. Hence,

$$Q_3^1 + Q_1^2 = 0, \qquad Q_4^1 + Q_2^2 = 0 \tag{4.21a}$$

At global node 3, the shear force is given as F_0, and the bending moment as M_0 (note the sign convention for F_0 and M_0 from Fig. 4.2):

$$Q_3^2 \equiv -\left[\frac{d}{dx}\left(EI\frac{d^2w}{dx^2}\right)\right]\bigg|_{x=L} = F_0, \qquad Q_4^2 \equiv -\left(b\frac{d^2w}{dx^2}\right)\bigg|_{x=L} = -M_0 \tag{4.21b}$$

TABLE 4.1
Types of commonly used support conditions for beams and frames

Type of support	**Displacement boundary conditions**	**Force boundary conditions**
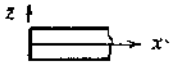 FREE	None	All, as specified
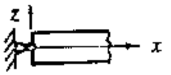 PINNED	$u=0$ $w=0$	Moment is specified
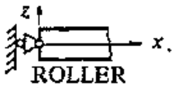 ROLLER (vertical)	$u=0$	Transverse force and moment are specified
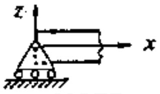 ROLLER (horizontal)	$w=0$	Horizontal force and bending moment are specified
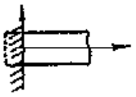 FIXED or CLAMPED	$u=0$ $w=0$ $dw/dx=0$	None specified

Next, we identify and impose the specified generalized displacements. Since the beam is clamped at global node 1, it follows that the deflection w and the slope dw/dx are zero there:

$$u_1^1 \equiv w_1^1 = U_1 = 0, \qquad u_2^1 \equiv \theta_1^1 = U_2 = 0 \tag{4.22}$$

Using (4.21) and (4.22) in (4.20), we obtain

$$\frac{2EI}{h^3}\left[\begin{array}{cc|cccc} 6 & -3h & -6 & -3h & 0 & 0 \\ -3h & 2h^2 & 3h & h^2 & 0 & 0 \\ \hline -6 & 3h & 12 & 0 & -6 & -3h \\ -3h & h^2 & 0 & 4h^2 & 3h & h^2 \\ 0 & 0 & -6 & 3h & 6 & 3h \\ 0 & 0 & -3h & h^2 & 3h & 2h^2 \end{array}\right]\left\{\begin{array}{c} U_1=0 \\ U_2=0 \\ \hline U_3 \\ U_4 \\ U_5 \\ U_6 \end{array}\right\} = \frac{f_0 h}{12}\left\{\begin{array}{c} 6 \\ -h \\ \hline 12 \\ 0 \\ 6 \\ h \end{array}\right\} + \left\{\begin{array}{c} Q_1^1 \\ Q_2^1 \\ \hline 0 \\ 0 \\ F_0 \\ -M_0 \end{array}\right\} \tag{4.23}$$

4.2.6 Solution

Equation (4.23) contains six algebraic equations in six unknowns: $(Q_1^1, Q_2^1, U_3, U_4, U_5, U_6)$. Because the algebraic equations for the unknown generalized displacements (U_3, U_4, U_5, U_6) do not contain the unknown generalized forces (Q_1^1, Q_2^1), equations 3, 4, 5, and 6 of the system (4.23) can be solved independently; the known values of the displacements U_1 and U_2 are used in equations 3 and 4. This provides us with the motivation to partition (shown by dashed lines) the matrix equation (4.23), which can be recast in the form

$$\begin{bmatrix} [K^{11}] & [K^{12}] \\ [K^{21}] & [K^{22}] \end{bmatrix} \begin{Bmatrix} \{U^1\} \\ \{U^2\} \end{Bmatrix} = \begin{Bmatrix} \{F^1\} \\ \{F^2\} \end{Bmatrix} \tag{4.24}$$

where $\{U^1\}$ denotes the column of known generalized displacements, $\{U^2\}$ the column of unknown generalized displacements, $\{F^1\}$ the column of unknown forces, and $\{F^2\}$ the column of known forces. Equation (4.24) can be written, after carrying out the matrix multiplication, in the form [cf. (3.56)]

$$[K^{11}]\{U^1\} + [K^{12}]\{U^2\} = \{F^1\}$$

$$[K^{21}]\{U^1\} + [K^{22}]\{U^2\} = \{F^2\}$$

or

$$[K^{22}]\{U^2\} = \{F^2\} - [K^{21}]\{U^1\} \tag{4.25a}$$

$$\{F^1\} = [K^{11}]\{U^1\} + [K^{12}]\{U^2\} \tag{4.25b}$$

These are the condensed equations for the generalized displacements and forces, respectively. Since $\{U^1\}$ and $\{F^2\}$ are known $(\{U^1\} = \{0\})$, we can use (4.25a) to solve for $\{U^2\}$, and then use (4.25b) to compute the unknown reactions $\{F^1\}$:

$$\{U^2\} = \begin{Bmatrix} U_3 \\ U_4 \\ U_5 \\ U_6 \end{Bmatrix} = \frac{h^3}{2EI} \begin{bmatrix} 12 & 0 & -6 & -3h \\ 0 & 4h^2 & 3h & h^2 \\ -6 & 3h & 6 & 3h \\ -3h & h^2 & 3h & 2h^2 \end{bmatrix}^{-1} \begin{Bmatrix} f_0 h \\ 0 \\ F_0 + \frac{1}{2} f_0 h \\ -M_0 + \frac{1}{12} f_0 h^2 \end{Bmatrix} \tag{4.26}$$

Inverting the matrix (say, by Gaussian elimination) and performing the matrix multiplication (i.e., solving the equations), we obtain

$$\{U^2\} = \frac{h}{6EI}\begin{bmatrix} 2h^2 & -3h & 5h^2 & -3h \\ -3h & 6 & -9h & 6 \\ 5h^2 & -9h & 16h^2 & -12h \\ -3h & 6 & -12h & 12 \end{bmatrix}\begin{Bmatrix} f_0 h \\ 0 \\ F_0 + \frac{1}{2}f_0 h \\ -M_0 + \frac{1}{12}f_0 h^2 \end{Bmatrix}$$

$$= \frac{h}{6EI}\begin{Bmatrix} 5h^2F_0 + 3hM_0 + \frac{17}{4}f_0h^3 \\ -9hF_0 - 6M_0 - 7f_0h^2 \\ 16h^2F_0 + 12hM_0 + 12f_0h^3 \\ -12hF_0 - 12M_0 - 8f_0h^2 \end{Bmatrix} \tag{4.27}$$

The reactions Q_1^1 and Q_2^1 can be obtained by substituting (4.27) into (4.25*b*). The Q_i^e obtained from the element (equilibrium) equations are more accurate than those obtained from the definitions (4.3), wherein the derivatives of w are obtained by differentiation of its finite element interpolation. The reactions from equilibrium $(Q_i^e)_{\text{equil}}$ are

$$\{F^1\} = \begin{Bmatrix} Q_1^1 \\ Q_2^1 \end{Bmatrix} = \frac{2EI}{h^3}\begin{bmatrix} -6 & -3h & 0 & 0 \\ 3h & h^2 & 0 & 0 \end{bmatrix}\begin{Bmatrix} U_3 \\ U_4 \\ U_5 \\ U_6 \end{Bmatrix} - \frac{f_0 h}{12}\begin{Bmatrix} 6 \\ -h \end{Bmatrix}$$

$$= \begin{Bmatrix} -(F_0 + 2f_0h) \\ 2h(F_0 + f_0h) + M_0 \end{Bmatrix} \tag{4.28}$$

It can be verified that the reactions Q_1^1 and Q_2^1 in (4.28) satisfy the static equilibrium equations of the beam:

$$Q_1^1 + (F_0 + 2f_0h) = 0, \qquad Q_2^1 - (2F_0h + 2f_0h^2 + M_0) = 0$$

The reactions Q_1^1 and Q_2^1 can also be computed using the definitions (4.3):

$$Q_1^1 = \frac{d}{dx}\left(EI\frac{d^2w}{dx^2}\right)\bigg|_{x=0}, \qquad Q_2^1 = \left(EI\frac{d^2w}{dx^2}\right)\bigg|_{x=0} \tag{4.29a}$$

From (4.10*b*), we note that the second derivative of the Hermite cubic interpolation functions is linear over the element and the third derivative is constant over the element. Therefore, the reactions, i.e., bending moment and shear force, computed using the definition (4.3) are element-wise linear and constant, respectively. Further, at nodes connecting two elements, they yield discontinuous values because the second and third derivatives of w are not made continuous across the interelement nodes. Substituting (4.10*b*) into (4.29*a*), we obtain the values

$$Q_1^1 = EI\left(U_3\frac{d^3\phi_3^1}{dx^3} + U_4\frac{d^3\phi_4^1}{dx^3}\right)\bigg|_{x=0} = EI\left[U_3\left(-\frac{12}{h_e^3}\right) + U_4\left(-\frac{6}{h_e^2}\right)\right] = -(F_0 + \tfrac{3}{2}f_0h) \tag{4.29b}$$

$$Q_2^1 = EI\left(U_3\frac{6}{h_e^2} + U_4\frac{2}{h_e}\right) = (M_0 + 2F_0h + \tfrac{23}{12}f_0h^2)$$

which are in error by $f_1^e = \frac{1}{2}f_0h$ and $f_2^e = \frac{1}{12}f_0h^2$ compared with those in (4.28).

4.2.7 Postprocessing of the Solution

The finite element solution as a function of position x is given by

$$w^e(x) = \begin{cases} U_3\phi_3^1 + U_4\phi_4^1 & \text{for } 0 \leqslant x \leqslant h \\ U_3\phi_1^2 + U_4\phi_2^2 + U_5\phi_3^2 + U_6\phi_4^2 & \text{for } h \leqslant x \leqslant 2h \end{cases} \tag{4.30a}$$

where [see (4.10*a*)]

$$\begin{aligned} &\phi_3^1 = 3\left(\frac{x}{h}\right)^2 - 2\left(\frac{x}{h}\right)^3, \quad \phi_4^1 = h\left[\left(\frac{x}{h}\right)^2 - \left(\frac{x}{h}\right)^3\right] \\ &\phi_1^2 = 1 - 3\left(1-\frac{x}{h}\right)^2 - 2\left(1-\frac{x}{h}\right)^3, \quad \phi_2^2 = h\left(1-\frac{x}{h}\right)\left(2-\frac{x}{h}\right)^2 \\ &\phi_3^2 = 3\left(1-\frac{x}{h}\right)^2 + 2\left(1-\frac{x}{h}\right)^3, \quad \phi_4^2 = h\left[\left(1-\frac{x}{h}\right)^3 + \left(1-\frac{x}{h}\right)^2\right] \end{aligned} \tag{4.30b}$$

The exact solution of (4.1) subject to the boundary condition (4.21) can be obtained by direct integration, and is given by

$$\left.\begin{aligned} EIw(x) &= \tfrac{1}{24}f_0x^4 - \tfrac{1}{6}(F_0 + f_0L)x^3 + \tfrac{1}{2}(M_0 + F_0L + \tfrac{1}{2}f_0L^2)x^2 \\ EI\theta(x) &= -\tfrac{1}{6}f_0x^3 + \tfrac{1}{2}(F_0 + f_0L)x^2 - (M_0 + F_0L + \tfrac{1}{2}f_0L^2) \\ M(x) &= \tfrac{1}{2}f_0x^2 - (F_0 + f_0L)x + M_0 + F_0L + \tfrac{1}{2}f_0L^2 \end{aligned}\right\} \text{ for } 0 \leqslant x \leqslant L \tag{4.31}$$

The finite element solution (4.30) and the exact solution (4.31) are compared in Table 4.2 for the data

$$f_0 = 24\,\text{kN m}^{-1}, \quad F_0 = 60\,\text{kN}, \quad L = 3\,\text{m}, \quad M_0 = 0\,\text{kN m}$$
$$E = 200 \times 10^6\,\text{kN m}^{-2}, \quad I = 29 \times 10^6\,\text{mm}^4 \quad (EI = 5800\,\text{kN m}^2)$$

As expected, the finite element solution for w and θ coincides with the exact solution at the nodes. At other points, the difference between the finite element and exact solutions is less than 2%.

This completes the finite element formulation and analysis of the fourth-order differential equation (4.1) governing the Euler–Bernoulli beam theory. Whenever the flexural rigidity $b \equiv EI$ is a constant in each element, the

TABLE 4.2
Comparison of the finite element solution with the exact solution of the cantilever beam of Fig. 4.4 (2 elements; $L = 3$ m, $EI = 5800$ kN m^2, $f_0 = 24$ kN m^{-1}, $F_0 = 60$ kN, $M_0 = 0$ kN m)

	w (m)		$-\theta = dw/dx$		M/EI (kN m)	
x (m)	**FEM**	**Exact**	**FEM**	**Exact**	**FEM**	**Exact**
0.00	0.0000†	0.0000	0.0000†	0.0000	0.0489†	0.0497
0.1875	0.0008	0.0008	0.0088	0.0089	0.0452	0.0455
0.3750	0.0033	0.0033	0.0169	0.0171	0.0415	0.0414
0.5625	0.0071	0.0072	0.0244	0.0245	0.0378	0.0375
0.7500	0.0124	0.0124	0.0311	0.0311	0.0341	0.0338
0.9375	0.0188	0.0188	0.0372	0.0371	0.0305	0.0301
1.1250	0.0263	0.0263	0.0426	0.0425	0.0268	0.0266
1.3125	0.0347	0.0347	0.0472	0.0471	0.0231	0.0234
1.5000	0.0439†	0.0439	0.0512†	0.0512	0.0194†	0.0202
1.6875	0.0539	0.0539	0.0546	0.0547	0.0169	0.0171
1.8750	0.0644	0.0644	0.0575	0.0576	0.0144	0.0143
2.0625	0.0754	0.0755	0.0600	0.0600	0.0118	0.0115
2.2500	0.0868	0.0869	0.0620	0.0620	0.0093	0.0089
2.4375	0.0986	0.0987	0.0635	0.0634	0.0068	0.0065
2.6250	0.1106	0.1107	0.0645	0.0644	0.0043	0.0042
2.8025	0.1228	0.1228	0.0651	0.0650	0.0017	0.0020
3.0000	0.1350†	0.1350	0.0652†	0.0652	−0.0008†	0.0000

† Nodal values; all others are computed by interpolation.

element stiffness matrix (4.15) can be used directly. The finite element solution for the generalized displacements at the nodes is exact for all problems for which EI is constant and the applied transverse load f is a polynomial expression. Further, the solution is exact at all points if the distributed load is such that the exact solution is a cubic.

The bending moment at any point in the element Ω^e of the beam can be computed from the formula

$$\boxed{M = EI\frac{d^2w}{dx^2} = EI\sum_{j=1}^{4} u_j^e \frac{d^2\phi_j^e}{dx^2}} \tag{4.32a}$$

For beams of rectangular cross-section with height H (and width B) the maximum bending stress is

$$\boxed{\sigma_x = \mp\frac{MH}{2I} = \mp\frac{EH}{2}\frac{d^2w}{dx^2} = \mp\frac{EH}{2}\sum_{j=1}^{4} u_j^e \frac{d^2\phi_j^e}{dx^2}} \tag{4.32b}$$

The minus sign is for the top and the plus sign for the bottom of the beam.

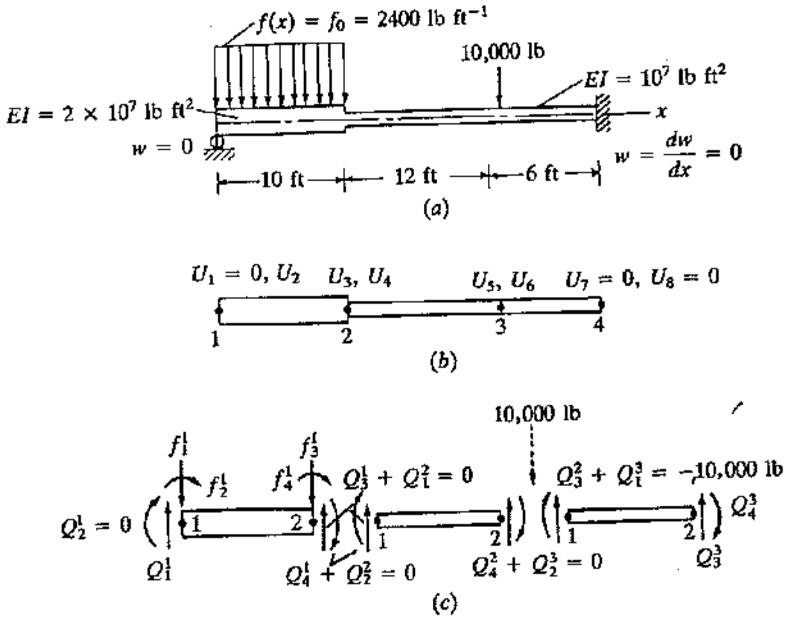

FIGURE 4.5
Finite element mesh and equilibrium conditions for the beam bending problem considered in Example 4.2: (*a*) physical problem; (*b*) finite element mesh of three elements; (*c*) equilibrium conditions among the generalized forces (i.e., secondary variables).

4.2.8 Examples

Example 4.1. Consider the beam shown in Fig. 4.5(*a*). The differential equation (4.1) is valid with the following discontinuous data:

$$EI = \begin{cases} 2 \times 10^7 \text{ lb ft}^2 & \text{for } 0 \leqslant x \leqslant 10 \text{ ft} \\ 10^7 \text{ lb ft}^2 & \text{for } 10 \text{ ft} \leqslant x \leqslant 28\, ft \end{cases} \tag{4.33a}$$

$$f(x) = \begin{cases} -2400 \text{ lb ft}^{-1} & \text{for } 0 \leqslant x \leqslant 10 \text{ ft} \\ 0 & \text{for } 10 \text{ ft} \leqslant x \leqslant 28 \text{ ft} \end{cases} \tag{4.33b}$$

The geometry and loading in the present case require us to use at least three elements (see Fig. 4.5*b*) to represent the domain $\Omega = (0, L)$, $L = 28$ ft. It is possible to use two elements if we choose to distribute the point load $-10{,}000$ lb by (4.14). We shall use three elements to analyze the problem. There are four nodes and eight global degrees of freedom in the mesh of three beam elements.

Since EI and f are element-wise-constant, the element stiffness matrix and the force vector are given by (4.15), with $f_0 = -2400$ lb ft^{-1} in element 1 and $f = 0$ in elements 2 and 3. The point load will be directly included in the global force vector through equilibrium of forces. The assembled equations are

$$10^7\left[\begin{array}{c|cccccc|cc}
0.024 & -0.12 & -0.024 & -0.12 & & & & & \\
\hline
 & 0.80 & 0.12 & 0.40 & & & & & \\
 & & 0.0309 & 0.0783 & -0.00694 & -0.04167 & & & \\
 & & & 1.133 & 0.0417 & 0.167 & & & \\
 & & & & 0.0625 & -0.125 & & -0.0556 & -0.167 \\
 & & & & & 1.0 & & 0.1667 & 0.333 \\
\hline
\text{symmetric} & & & & & & & 0.0556 & 0.1667 \\
 & & & & & & & & 0.6667
\end{array}\right]$$

$$\times\left\{\begin{array}{c} U_1 \\ \hline U_2 \\ U_3 \\ U_4 \\ U_5 \\ U_6 \\ \hline U_7 \\ U_8 \end{array}\right\} = \left\{\begin{array}{c} -12{,}000 \\ \hline 20{,}000 \\ -12{,}000 \\ -20{,}000 \\ 0 \\ 0 \\ \hline 0 \\ 0 \end{array}\right\} + \left\{\begin{array}{c} Q_1^1 \\ \hline Q_2^1 \\ Q_3^1 + Q_1^2 \\ Q_4^1 + Q_2^2 \\ Q_3^2 + Q_1^3 \\ Q_4^2 + Q_2^3 \\ \hline Q_3^3 \\ Q_4^3 \end{array}\right\} \tag{4.34}$$

where the interelement continuity conditions on the primary variables (i.e., displacements and rotations) have already been used. The equilibrium of the secondary variables (i.e., internal forces and moments) is given by

$$Q_2^1 = 0, \quad Q_3^1 + Q_1^2 = 0, \quad Q_4^1 + Q_2^2 = 0, \quad Q_3^2 + Q_1^3 = -10{,}000, \quad Q_4^2 + Q_2^3 = 0 \tag{4.35a}$$

Note that the forces Q_1^1 and Q_3^3 and the moment Q_4^3 (the reactions at the supports) are not known. The boundary conditions on the primary degrees of freedom are

$$w(0) = 0 \Rightarrow U_1 = 0; \quad w(28) = 0 \Rightarrow U_7 = 0; \quad \left(\frac{dw}{dx}\right)\bigg|_{x=28} = 0 \Rightarrow U_8 = 0 \tag{4.35b}$$

Using the known forces and displacements in (4.35), we can partition the global system of equations to obtain the condensed equations for the unknown generalized displacements and forces. Since the specified generalized displacements are all zero, the condensed stiffness matrix associated with the unknown generalized displacements can be obtained by deleting the columns and rows corresponding to the known U_i [see the submatrix enclosed by the dashed lines in (4.34)]:

$$10^6\begin{bmatrix} 8.000 & 1.200 & 4.000 & 0.000 & 0.000 \\ & 0.309 & 0.783 & -0.069 & -0.417 \\ & & 11.333 & 0.417 & 1.667 \\ & \text{symmetric} & & 0.625 & -1.250 \\ & & & & 10.000 \end{bmatrix} \begin{Bmatrix} U_2 \\ U_3 \\ U_4 \\ U_5 \\ U_6 \end{Bmatrix} = \begin{Bmatrix} 20{,}000 \\ -12{,}000 \\ -20{,}000 \\ -10{,}000 \\ 0 \end{Bmatrix} \tag{4.36}$$

The unknown reactions can be computed from the remaining equations, i.e., equations 1, 7, and 8 of (4.34):

$$\begin{Bmatrix} Q_1^1 \\ Q_3^3 \\ Q_4^3 \end{Bmatrix} = \begin{Bmatrix} 12{,}000 \\ 0 \\ 0 \end{Bmatrix} + 10^7 \begin{bmatrix} -0.12 & -0.024 & -0.12 & 0.0 & 0.0 \\ 0.0 & 0.0 & 0.0 & -0.0556 & 0.1667 \\ 0.0 & 0.0 & 0.0 & -0.1667 & 0.3333 \end{bmatrix} \begin{Bmatrix} U_2 \\ U_3 \\ U_4 \\ U_5 \\ U_6 \end{Bmatrix} \tag{4.37}$$

The algebraic equations (4.36) are solved first for the generalized displacements, and then (4.37) are used to obtain the unknown generalized forces of the problem.

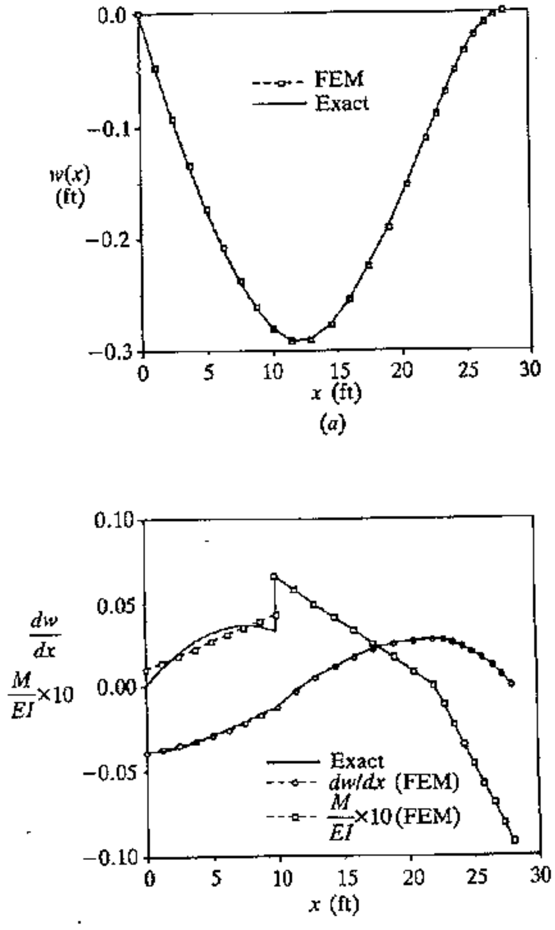

(*a*)

(*b*)

FIGURE 4.6
Comparison of the finite element solutions for deflection, slope, and bending moment of a cantilever beam with the exact solutions (Example 4.2).

Equations (4.36) are solved with the help of a computer; the solution is

$$U_2 = 0.03856, \qquad U_3 = -0.2808\,\text{ft}, \qquad U_4 = 0.01214$$
$$U_5 = -0.1103\,\text{ft}, \qquad U_6 = -0.02752 \tag{4.38a}$$

The reaction forces, from the element equilibrium equations, are

$$Q_1^1 = 18{,}565.54\,\text{lb}, \qquad Q_3^3 = 15{,}434.46\,\text{lb}, \qquad Q_4^3 = 92{,}165\,\text{ft lb} \tag{4.38b}$$

Plots of the finite element solution for the transverse deflection w, rotation $\theta = -dw/dx$, and bending moment $M = EI\,d^2w/dx^2$ are shown in Fig. 4.6. Because of the discontinuity in the loading and the flexural rigidity, the exact solution $w(x)$ is also defined by three separate expressions for the three regions:

$$w(x) = \begin{cases} \frac{1}{12}R_1x^2 - \frac{1}{48}A_0x^4 - A_1x & \text{for } 0 \leqslant x \leqslant 10\,\text{ft} \\ \frac{1}{6}R_1x^3 - \frac{1}{6}A_0h_1(x - \frac{1}{2}h_1)^3 - A_2x + A_3 & \text{for } 10\,\text{ft} \leqslant x \leqslant 22\,\text{ft} \\ \frac{1}{6}R_1x^3 - \frac{1}{6}A_0h_1(x - \frac{1}{2}h_1)^3 - \frac{1}{6}F_0(x - h_1 - h_2)^3 - A_2x + A_3 & \text{for } 22\,\text{ft} \leqslant x \leqslant 28\,\text{ft} \end{cases} \tag{4.39a}$$

where

$$R_1 = 0.001856, \qquad A_0 = 2400 \times 10^{-7}$$
$$A_1 = 0.03856, \qquad A_2 = 0.07497, \qquad A_3 = 0.20943 \tag{4.39b}$$
$$h_1 = 10\,\text{ft}, \qquad h_2 = 12\,\text{ft}$$

In the next example we consider a beam with linearly varying distributed transverse load and with clamped and spring-supported ends. This requires us to evaluate the integral for f_i^e [see (4.12c)], since it is not available when $f(x)$ is a linear function of x.

Example 4.2. Consider a beam that has a clamped support at one end and is spring-supported at the other (see Fig. 4.7). A linearly varying transverse load is applied in the span, 4 ft $\leqslant x \leqslant$ 10 ft. We must use at least two elements, as dictated by the loading. A one-element model could be used when the load is distributed as discussed in Remark 5 in Section 3.2.7. The force vector $\{f^2\}$ due to the distributed load on element 2 can be computed according to (4.12c):

$$f_i^2 = \int_0^6 f(\bar{x})\phi_i^2(\bar{x})\,d\bar{x}, \qquad f(\bar{x}) = -\frac{100}{6}\bar{x} \tag{4.40}$$

and ϕ_i^2 are the Hermite interpolation functions given in (4.10a). Carrying out the integration, we obtain

$$\{f^2\} = \begin{Bmatrix} -90\,\text{lb} \\ 120\,\text{lb ft} \\ -210\,\text{lb} \\ -180\,\text{lb ft} \end{Bmatrix} \tag{4.41}$$

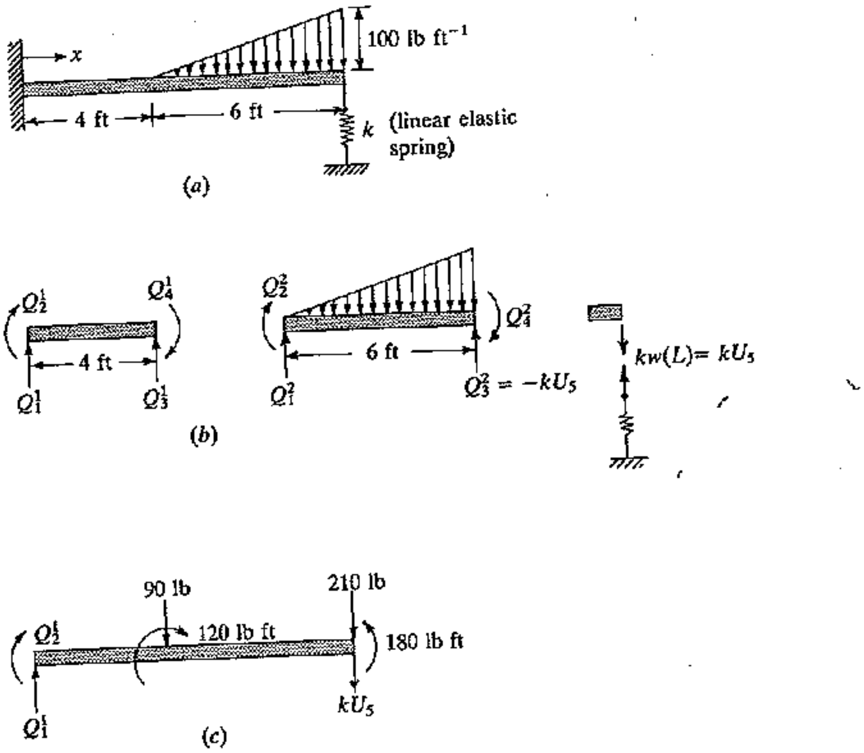

FIGURE 4.7
Finite element analysis of a cantilevered beam with discontinuous loading: (*a*) physical problem; (*b*) finite element discretization and generalized element forces; (*c*) assembly of finite element and generalized global forces (Example 4.3).

The assembled equations are

$$\frac{EI}{144}\begin{bmatrix} 27 & -54 & -27 & -54 & 0 & 0 \\ -54 & 144 & 54 & 72 & 0 & 0 \\ -27 & 54 & 27+8 & 54-24 & -8 & -24 \\ -54 & 72 & 54-24 & 144+96 & 24 & 48 \\ 0 & 0 & -8 & 24 & 8 & 24 \\ 0 & 0 & -24 & 48 & 24 & 96 \end{bmatrix}\begin{Bmatrix} U_1 \\ U_2 \\ U_3 \\ U_4 \\ U_5 \\ U_6 \end{Bmatrix} = \begin{Bmatrix} 0 \\ 0 \\ -90 \\ 120 \\ -210 \\ -180 \end{Bmatrix} + \begin{Bmatrix} Q_1^1 \\ Q_2^1 \\ Q_3^1 + Q_1^2 \\ Q_4^1 + Q_2^2 \\ Q_3^2 \\ Q_4^2 \end{Bmatrix} \tag{4.42}$$

The displacement boundary conditions at $x = 0$ and force boundary conditions at $x = L$ are

$$w(0) = 0, \qquad \left(\frac{dw}{dx}\right)\Big|_{x=0} = 0 \tag{4.43a}$$

$$\left[-\frac{d}{dx}\left(EI\frac{d^2w}{dx^2}\right)\right]\Big|_{x=L} = -kw(L), \qquad \left(EI\frac{d^2w}{dx^2}\right)\Big|_{\substack{x=0\\ L}} = 0$$

which can be expressed in terms of the nodal degrees of freedom as

$$U_1 = 0, \quad U_2 = 0, \quad Q_3^2 = -kU_5, \quad Q_4^2 = 0 \tag{4.43b}$$

The condensed equations for the generalized displacements U_3, U_4, U_5, and U_6 are given by the last four equations of (4.42):

$$\frac{EI}{144}\begin{bmatrix} 35 & 30 & -8 & -24 \\ 30 & 240 & 24 & 48 \\ -8 & 24 & 8+c & 24 \\ -24 & 48 & 24 & 96 \end{bmatrix}\begin{Bmatrix} U_3 \\ U_4 \\ U_5 \\ U_6 \end{Bmatrix} = \begin{Bmatrix} -90 \\ 120 \\ -210 \\ -180 \end{Bmatrix} \tag{4.44}$$

where $c = 144k/EI$. The solution of these equations for different values of k/EI can be computed as follows:

For $k/EI = 0$ (no spring),

$$\begin{aligned} U_3 &= \frac{-0.16\times 10^5}{EI}\ \text{(ft)}, \quad U_4 = \frac{0.72\times 10^4}{EI}\ \text{(rad)} \\ U_5 &= \frac{-0.7108\times 10^5}{EI}\ \text{(ft)}, \quad U_6 = \frac{0.99\times 10^4}{EI}\ \text{(rad)} \end{aligned} \tag{4.45}$$

for $k/EI = 10^{-2}$ (a soft spring),

$$\begin{aligned} U_3 &= \frac{-0.4627\times 10^4}{EI}\ \text{(ft)}, \quad U_4 = \frac{0.1951\times 10^4}{EI}\ \text{(rad)} \\ U_5 &= \frac{-0.164\times 10^5}{EI}\ \text{(ft)}, \quad U_6 = \frac{0.1699\times 10^4}{EI}\ \text{(rad)} \end{aligned} \tag{4.46}$$

for $k/EI = 10^2$ (a hard spring),

$$\begin{aligned} U_3 &= \frac{-0.1216\times 10^4}{EI}\ \text{(ft)}, \quad U_4 = \frac{0.3765\times 10^3}{EI}\ \text{(rad)} \\ U_5 &= \frac{-2.132}{EI}\ \text{(ft)}, \quad U_6 = \frac{-0.7617\times 10^3}{EI}\ \text{(rad)} \end{aligned} \tag{4.47}$$

The solutions coincide with the exact solution at the nodes:

$$w(x) = \begin{cases} \dfrac{1}{EI}\left(\tfrac{1}{6}R_1x^3 + \tfrac{1}{2}M_1x^2\right) & \text{for } 0 \leqslant x \leqslant a \\ \dfrac{1}{EI}\left[\tfrac{1}{6}R_1x^3 + \tfrac{1}{2}M_1x^2 - \dfrac{f_0}{120b}(x-a)^5\right] & \text{for } a \leqslant x \leqslant L \end{cases} \tag{4.48a}$$

where

$$\begin{gathered} R_1 = \left(\frac{f_0 b}{40}\right)\frac{60EI + 10kL^2b - kb^3}{2EI + kL^3}, \quad M_1 = \tfrac{1}{6}f_0b^2 - R_1L \\ f_0 = 100\ \text{lb ft}^{-1}, \quad a = 4\ \text{ft}, \quad b = 6\ \text{ft}, \quad L = 10\ \text{ft} \end{gathered} \tag{4.48b}$$

Figure 4.8 shows plots of the transverse deflection, slope, and bending moment for the case $k/EI = 100$. The finite element solution obtained using two elements is in good agreement with the exact solution. Improvement can be expected if the region $4\ \text{ft} \leqslant x \leqslant 10\ \text{ft}$ is subdivided into two or more elements (note that the particular scale

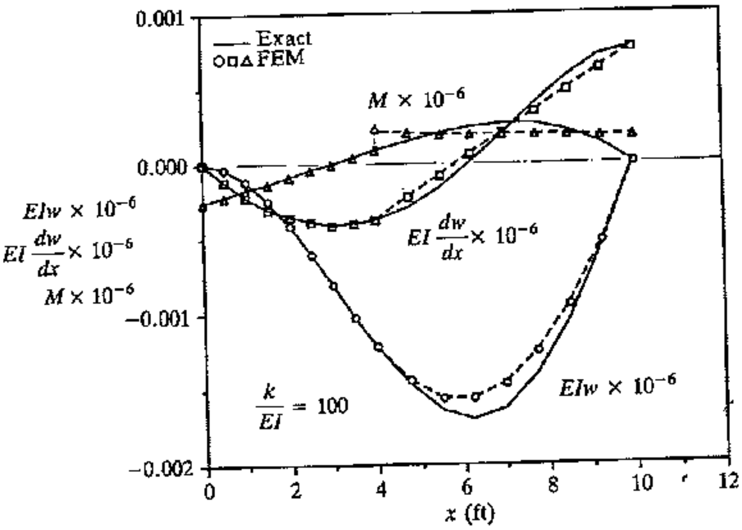

FIGURE 4.8
Comparison of the finite element solutions with the exact solutions for a clamped spring-supported beam (see Fig. 4.7 for the geometry and loading).

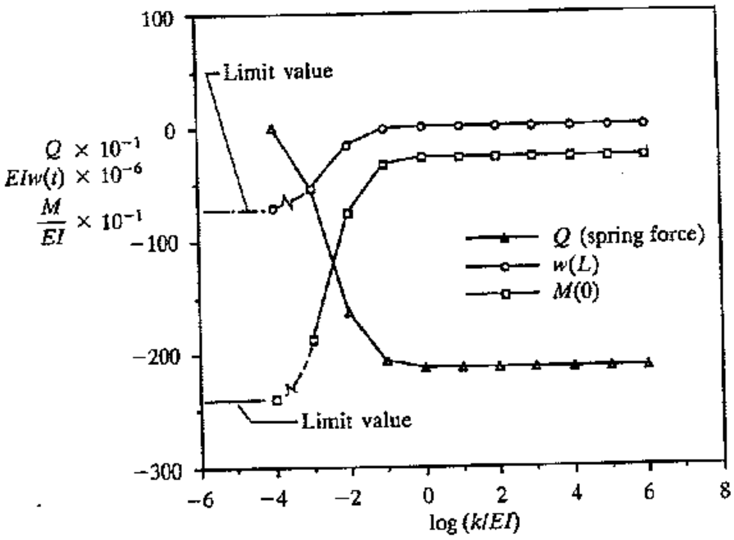

FIGURE 4.9
The effect of spring stiffness on the deflection, bending moment, and spring force for the problem in Example 4.3.

used in Fig. 4.8 brings out the difference between the finite element and exact solutions). The effect of the spring on the end deflection $w(L)$, the bending moment $M(0)$ at the fixed end, and the spring force $Q \equiv Q_3^2 = -kw(L)$ can be seen from the results presented in Fig. 4.9. For $k/EI > 1$, the spring acts essentially like a rigid support.

This completes the development and applications of the Euler–Bernoulli beam element.

4.3 PLANE TRUSS AND EULER-BERNOULLI FRAME ELEMENTS

Structures composed of bar elements and beam elements are classified as truss and frame structures, respectively. By definition, bars can only carry axial loads and deform axially, whereas beams can take transverse loads and bending moments about an axis perpendicular to the plane of the member. All members of a truss are subjected to only axial loads, and no transverse shearing forces and bending moments are experienced by any member. All members are connected to each other through pins that allow free rotation about the pin axis. On the other hand, members of a frame are connected by a rigid connection (e.g., welded or rivetted), so that axial and transverse forces and bending moments can be developed in the members. A truss can be looked upon as a special case of a frame structure. Thus, a typical truss member can be modeled using the bar finite element developed in Section 3.3.3. A member of a frame structure can be modeled by a superposition of the bar element with the beam element of Section 4.2.

The objective of this section is to formulate, with the help of the information from Sections 3.3.3 and 4.2, the truss finite element and frame finite element. The formulation will be based on matrix notation. Since a truss finite element is a special case of the frame element, the derivation is presented for the frame element only.

In many truss and frame structures, the bar and beam structural elements are found in many different orientations (see Fig. 4.10). Analysis of such structures for displacements and stresses requires the setting up of a global coordinate system and referencing of all quantities (i.e. displacements, forces, and stiffnesses) of individual elements to the common (global) coordinate system in order to assemble the elements and impose boundary conditions on the whole structure. When a truss element is oriented at an angle from the global axis, its axial displacements at the nodes have components along the global axes. Thus, every node of a truss will have two displacements in the global coordinates: one along the global x axis and another transverse to the x axis. Therefore, the element will have two degrees of freedom per node in the global coordinate system. In order to facilitate the transformation from element equations to global equations, we append the element equations for the axial displacements to those associated with the transverse displacements. Since there are no stiffnesses associated with the transverse displacements

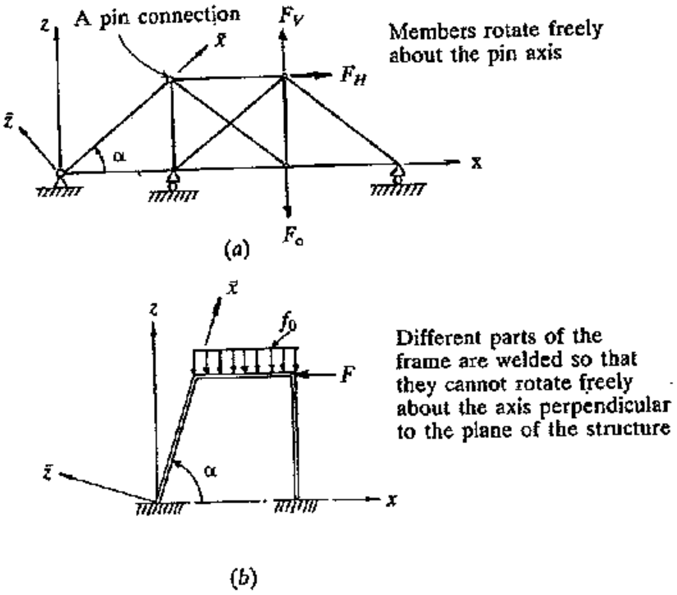
z
A pin connection
$\bar{x}$
F_V
F_H
Members rotate freely about the pin axis
$\bar{z}$
α
x
F_0
(a)
$\bar{x}$
z
f_0
F
Different parts of the frame are welded so that they cannot rotate freely about the axis perpendicular to the plane of the structure
$\bar{z}$
α
x
(b)

FIGURE 4.10
Typical examples of the plane truss and plane frame: (*a*) a plane truss structure (all elements carry only axial loads); (*b*) a typical plane frame structure (all members may carry axial and transverse loads and bending moments).

(because the element experiences axial deformation only), the entries in the stiffness matrix corresponding to the transverse displacements are set equal to zero. For example, when the linear Lagrange interpolation is used for the axial displacement, the element stiffness matrix in the element coordinates for a truss element with two displacements (axial and transverse) per node can be written as

$$[K^e] = \frac{A_e E_e}{h_e}\begin{bmatrix} 1 & 0 & -1 & 0 \\ 0 & 0 & 0 & 0 \\ -1 & 0 & 1 & 0 \\ 0 & 0 & 0 & 0 \end{bmatrix} \tag{4.49}$$

Similarly, a superposition of the bar element of Section 3.3.3 with the beam element of Section 4.2 gives three primary degrees of freedom per node (see Fig. 4.11*a*) of the frame element: $(u, w, -dw/dx)$. When the axial stiffness AE, bending stiffness EI, and axial distributed force q and transverse distributed force f are element-wise-constant, the superposition of the linear bar element with the Hermite cubic Euler–Bernoulli beam element gives the following element equations:

$$[K^e]\{u^e\} = \{F^e\} \tag{4.50a}$$

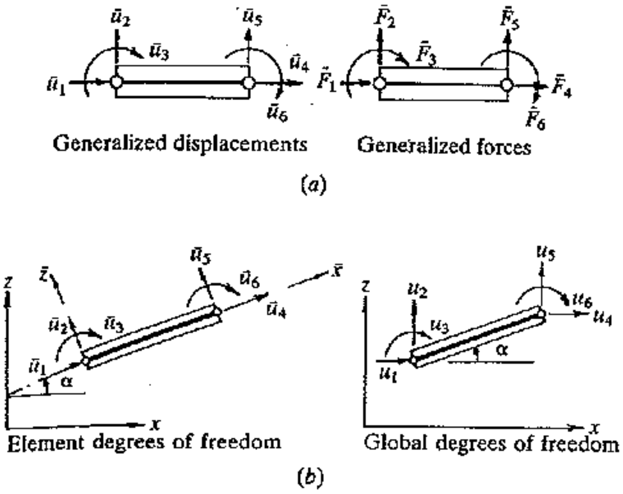

Generalized displacements Generalized forces

(a)

Element degrees of freedom Global degrees of freedom

(b)

FIGURE 4.11
The frame element with primary and secondary variables (or degree of freedom) in the local and global coordinate systems. (a) The generalized displacements and forces in the element coordinate system ($\bar{x}, \bar{y}, \bar{z}$). (b) The generalized displacements in the element coordinate system and global coordinate system (x, y, z); the y axis is into the plane of the paper. The angle of orientation is measured counter-clockwise from the global x axis to the element $\bar{x}$ axis. The truss element is obtained from the frame element by omitting the rotation and moment degrees of freedom at the nodes (also, $\bar{u}_2 = \underset{5}{\bar{u}_{\cancel{4}}} = 0$ for the truss element).

where

$$\{u^e\} = \begin{Bmatrix} u_1 \\ w_1 \\ \theta_1 \\ u_2 \\ w_2 \\ \theta_2 \end{Bmatrix}^e, \qquad \{F^e\} = \begin{Bmatrix} \frac{1}{2}qh \\ \frac{1}{2}fh \\ -\frac{1}{12}fh^2 \\ \frac{1}{2}qh \\ +\frac{1}{2}fh \\ \frac{1}{12}fh^2 \end{Bmatrix} + \begin{Bmatrix} Q_1^e \\ Q_2^e \\ Q_3^e \\ Q_4^e \\ Q_5^e \\ Q_6^e \end{Bmatrix} \tag{4.50b}$$

and $q = q_0$ and $f = f_0$ are constants over an element.

The element stiffness matrix $[K^e]$ is of order 6×6:

$$\boxed{[K] = \frac{2EI}{h^3}\begin{bmatrix} \mu & 0 & 0 & -\mu & 0 & 0 \\ 0 & 6 & -3h & 0 & -6 & -3h \\ 0 & -3h & 2h^2 & 0 & 3h & h^2 \\ -\mu & 0 & 0 & \mu & 0 & 0 \\ 0 & -6 & 3h & 0 & 6 & 3h \\ 0 & -3h & h^2 & 0 & 3h & 2h^2 \end{bmatrix}, \qquad \mu = \frac{Ah^2}{2I}} \tag{4.50c}$$

In the following paragraphs, we develop transformation relations to express the element equations (4.50*c*)—valid in the element coordinate system—to the global coordinate system.

Let $\bar{u}$ and $\bar{w}$ denote the axial and transverse displacements referred to the local coordinate system $(\bar{x}, \bar{z})$. The local coordinates $(\bar{x}, \bar{y}, \bar{z})$ are related to the global coordinates (x, y, z) by (see Fig. 4.11*b*)

$$\begin{Bmatrix} \bar{x} \\ \bar{y} \\ \bar{z} \end{Bmatrix} = \begin{bmatrix} \cos\alpha & 0 & \sin\alpha \\ 0 & 1 & 0 \\ -\sin\alpha & 0 & \cos\alpha \end{bmatrix} \begin{Bmatrix} x \\ y \\ z \end{Bmatrix} \tag{4.51}$$

where the angle α is measured counter-clockwise from x axis to $\bar{x}$ axis. Note that the y and $\bar{y}$ coordinates are parallel to each other, and they are *into* the plane of the paper. The same transformation relations hold for displacements (u, v, w) along the global coordinates (x, y, z) and displacements $(\bar{u}, \bar{v}, \bar{w})$ in the local coordinates $(\bar{x}, \bar{y}, \bar{z})$. Since we are considering 2-D structures, we have $v = \bar{v} = 0$. The rotation $\theta \equiv -dw/dx$ about the y axis remains unchanged: $\theta = \bar{\theta}$. Hence, the relationship between (u, w, θ) and $(\bar{u}, \bar{w}, \bar{\theta})$ can be written as

$$\begin{Bmatrix} \bar{u} \\ \bar{w} \\ \bar{\theta} \end{Bmatrix} = \begin{bmatrix} \cos\alpha & \sin\alpha & 0 \\ -\sin\alpha & \cos\alpha & 0 \\ 0 & 0 & 1 \end{bmatrix} \begin{Bmatrix} u \\ w \\ \theta \end{Bmatrix} \tag{4.52}$$

Therefore, the six element nodal degrees of freedom $\bar{u}_i^e$ in the $(\bar{x}, \bar{y}, \bar{z})$ system are related to the six degrees of freedom u_i^e in the (x, y, z) system by $(\alpha = \alpha^e)$

$$\begin{Bmatrix} \bar{u}_1 \\ \bar{u}_2 \\ \bar{u}_3 \\ \hline \bar{u}_4 \\ \bar{u}_5 \\ \bar{u}_6 \end{Bmatrix}^e = \left[\begin{array}{ccc|ccc} \cos\alpha & \sin\alpha & 0 & & & \\ -\sin\alpha & \cos\alpha & 0 & & 0 & \\ 0 & 0 & 1 & & & \\ \hline & & & \cos\alpha & \sin\alpha & 0 \\ & 0 & & -\sin\alpha & \cos\alpha & 0 \\ & & & 0 & 0 & 1 \end{array}\right] \begin{Bmatrix} u_1 \\ u_2 \\ u_3 \\ \hline u_4 \\ u_5 \\ u_6 \end{Bmatrix}^e \tag{4.53a}$$

or

$$\{\bar{u}^e\} = [T^e]\{u^e\} \tag{4.53b}$$

The inverse of (4.53) is

$$\{u^e\} = [T^e]^{-1}\{\bar{u}^e\} \equiv [R^e]\{\bar{u}^e\}$$

and it can be shown that

$$[R^e] = [T^e]^T \tag{4.54}$$

i.e., the inverse of $[T^e]$ is equal to its transpose.

Analogously to (4.53b), the element force vectors in the local and global coordinate systems are related according to

$$\{\bar{F}^e\} = [T^e]\{F^e\} \tag{4.55}$$

To obtain expressions for the element stiffness matrix and the force vector referred to the global coordinates in terms of the element stiffness matrix and force vector in the local coordinates, we use (4.53)–(4.55) in the element equations

$$[\bar{K}^e]\{\bar{u}^e\} = \{\bar{F}^e\} \tag{4.56}$$

Substituting the transformation equations into (4.56), we obtain

$$[\bar{K}^e][T^e]\{u^e\} = [T^e]\{F^e\}$$

Premultiplying both sides with $[T^e]^{-1} \equiv [T^e]^T$, we obtain

$$[T^e]^T[\bar{K}^e][T^e]\{u^e\} = \{F^e\} \tag{4.57}$$

which gives

$$\boxed{[K^e] = [T^e]^T[\bar{K}^e][T^e], \qquad \{F^e\} = [T^e]^T\{\bar{F}^e\}} \tag{4.58a, b}$$

Thus, if we know the element matrices $[\bar{K}^e]$ and $\{\bar{F}^e\}$ of an element Ω^e in the local coordinate system $(\bar{x}, \bar{y}, \bar{z})$ then the element matrices of the element in the global coordinate system, which is obtained by rotating the element coordinate system through an angle α in the counter-clockwise direction about the y axis, are given by (4.58). Note that the angle α is measured in the counter-clockwise direction from the positive global x axis.

Inserting the element stiffness from (4.50c) for $[\bar{K}^e]$ into (4.58a) and carrying out the indicated matrix multiplications, we arrive at the element stiffness matrix $[K^e]$ referred to the global coordinates:

$$[K^e] = \frac{2EI}{h^3}$$
$$\times \begin{bmatrix} \mu\cos^2\alpha + 6\sin^2\alpha & & & & & \\ (\mu-6)\cos\alpha\sin\alpha & \mu\sin^2\alpha + 6\cos^2\alpha & & \text{symmetric} & & \\ 3h\sin\alpha & -3h\cos\alpha & 2h^2 & & & \\ -(\mu\cos^2\alpha + 6\sin^2\alpha) & -(\mu-6)\sin\alpha\cos\alpha & -3h\sin\alpha & \mu\cos^2\alpha + 6\sin^2\alpha & & \\ -(\mu-6)\cos\alpha\sin\alpha & -(\mu\sin^2\alpha + 6\cos^2\alpha) & 3h\cos\alpha & (\mu-6)\cos\alpha\sin\alpha & \mu\sin^2\alpha + 6\cos^2\alpha & \\ 3h\sin\alpha & -3h\cos\alpha & h^2 & -3h\sin\alpha & 3h\cos\alpha & 2h^2 \end{bmatrix} \tag{4.59a}$$

where

$$\mu = Ah^2/2I \tag{4.59b}$$

Equation (4.58*b*), after multiplication, yields

$$\begin{Bmatrix} F_1 \\ F_2 \\ F_3 \\ F_4 \\ F_5 \\ F_6 \end{Bmatrix}^e = \begin{Bmatrix} \bar{F}_1 \cos\alpha - \bar{F}_2 \sin\alpha \\ \bar{F}_1 \sin\alpha + \bar{F}_2 \cos\alpha \\ \bar{F}_3 \\ \bar{F}_4 \cos\alpha - \bar{F}_5 \sin\alpha \\ \bar{F}_4 \sin\alpha + \bar{F}_5 \cos\alpha \\ \bar{F}_6 \end{Bmatrix}^e \tag{4.60}$$

which is the element force vector referred to the global coordinates.

We next consider an example each of a truss and frame structure.

Example 4.3. Consider the three-member truss shown in Fig. 4.12(*a*). All members of the truss have identical cross-sectional area A and modulus E. The hinged supports at points 1, 2, and 3 allow free rotation of the members about the y axis (taken as positive into the plane of the paper). We wish to determine the horizontal and vertical displacements at the joint 3 and the forces in each member of the structure.

Since all joints are hinged, and the applied forces are acting at the nodes, the members are subjected to only axial forces. Hence, the structure is a truss. We use three finite elements to model the structure. Any further subdivision of the members

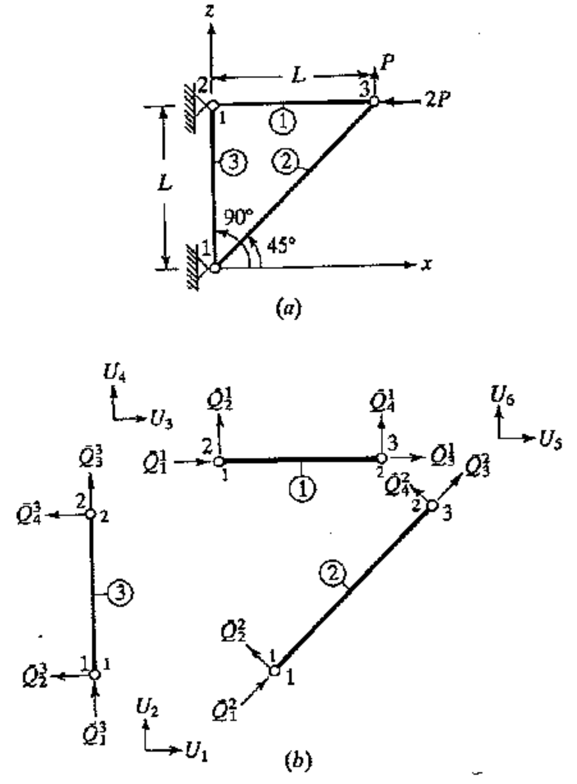

FIGURE 4.12
Geometry and finite element discretization of a plane truss: (*a*) geometry and loading; (*b*) element numbers, global node numbers of element nodes, and element nodal forces in the element coordinates.

does not add to the accuracy, because for all truss problems the finite element solutions are exact. This is a consequence of the fact that all truss members with constant cross-section are governed by the homogeneous differential equation

$$EA\frac{d^2u}{dx^2}=0 \tag{4.61}$$

whose solution is of the form $u(x)=c_1x+c_2$. Thus, linear interpolation of the displacements should give the exact result.

The global node numbers and element numbers are shown in Fig. 4.12(*b*). There are two degrees of freedom, horizontal and vertical displacements, at each node of the element. The element stiffness matrix in the local coordinate system is

$$[\bar{K}^e]=\frac{A_eE_e}{h_e}\begin{bmatrix} 1 & 0 & -1 & 0 \\ 0 & 0 & 0 & 0 \\ -1 & 0 & 1 & 0 \\ 0 & 0 & 0 & 0 \end{bmatrix} \tag{4.62}$$

The (transformed) stiffness matrix of the element Ω_e in the global coordinate system is given by

$$[K^e]=\frac{EA}{h_e}\left[\begin{array}{cc:cc} \cos^2\alpha & \cos\alpha\sin\alpha & -\cos^2\alpha & -\cos\alpha\sin\alpha \\ \cos\alpha\sin\alpha & \sin^2\alpha & -\cos\alpha\sin\alpha & -\sin^2\alpha \\ \hdashline -\cos^2\alpha & -\cos\alpha\sin\alpha & \cos^2\alpha & \cos\alpha\sin\alpha \\ -\cos^2\alpha\sin\alpha & -\sin^2\alpha & \cos\alpha\sin\alpha & \sin^2\alpha \end{array}\right] \tag{4.63}$$

which is obtained from (4.59) by deleting the rows and columns corresponding to the bending degrees of freedom and setting all bending stiffnesses to zero. The element stiffness matrix is 4 × 4 in the global coordinate system because of the horizontal and vertical displacement degrees of freedom at each node. The element data for the problem are as follows.

Element number	Global nodes of the element	Geometric properties	Material property	Orientation
1	2 3	$A, h_1=L$	E	$\alpha=0°$
2	1 3	$A, h_2=\sqrt{2}L$	E	$\alpha=45°$
3	1 2	$A, h_2=L$	E	$\alpha=90°$

The assembled stiffness and force coefficients are given by

$$[K]=\left[\begin{array}{cccccc} 1 & 2 & 3 & 4 & 5 & 6 \\ K_{11}^2+K_{11}^3 & K_{12}^2+K_{12}^3 & K_{13}^3 & K_{14}^3 & K_{13}^2 & K_{14}^2 \\ & K_{22}^2+K_{22}^3 & K_{23}^3 & K_{24}^3 & K_{23}^2 & K_{24}^2 \\ & & K_{33}^3+K_{11}^1 & K_{34}^3+K_{12}^1 & K_{13}^1 & K_{14}^1 \\ & & & K_{44}^3+K_{22}^1 & K_{23}^1 & K_{24}^1 \\ & \text{symmetric} & & & K_{33}^2+K_{33}^1 & K_{34}^2+K_{34}^1 \\ & & & & & K_{44}^2+K_{44}^1 \end{array}\right]\begin{array}{c} \\ 1 \\ 2 \\ 3 \\ 4 \\ 5 \\ 6 \end{array} \tag{4.64}$$

The force vector can be written directly by including the known applied forces:

$$\{F\} = \left\{\begin{array}{l} Q_1^3 + Q_1^2 \\ Q_2^3 + Q_2^2 \\ Q_3^3 + Q_1^1 \\ Q_4^3 + Q_2^1 \\ \cancel{Q_3^1 + Q_3^2} \\ \cancel{Q_4^1 + Q_4^2} \end{array}\right\} \begin{array}{l} \\ \\ \\ \\ \rightarrow -2P \\ \rightarrow P \end{array} \tag{4.65}$$

Substituting the element data into (4.63) and the result into the assembled equations, we obtain

$$[K] = \frac{EA}{L}\begin{bmatrix} 0.3536 & 0.3536 & 0.0 & 0.0 & -0.3536 & -0.3536 \\ & 1.3536 & 0.0 & -1.0 & -0.3536 & -0.3536 \\ & & 1.0 & 0.0 & -1.0 & 0.0 \\ & & & 1.0 & 0.0 & 0.0 \\ & \text{symmetric} & & & 1.3536 & 0.3536 \\ & & & & & 0.3536 \end{bmatrix}$$

The specified displacement degrees of freedom are

$$U_1 = U_2 = U_3 = U_4 = 0 \tag{4.66}$$

The first two correspond to the horizontal and vertical displacements at node 1, and the last two to the horizontal and vertical displacements at node 2. The condensed equations for the unknown displacements and forces are

$$\frac{EA}{L}\begin{bmatrix} 1.3536 & 0.3536 \\ 0.3536 & 0.3536 \end{bmatrix}\begin{Bmatrix} U_5 \\ U_6 \end{Bmatrix} = \begin{Bmatrix} -2P \\ P \end{Bmatrix} \tag{4.67}$$

$$\begin{Bmatrix} Q_1^3 + Q_1^2 \\ Q_2^3 + Q_2^2 \\ Q_3^3 + Q_1^1 \\ Q_4^3 + Q_2^1 \end{Bmatrix} = \frac{EA}{L}\begin{bmatrix} -0.3536 & -0.3536 \\ -0.3536 & -0.3536 \\ -1.0 & 0.0 \\ 0.0 & 0.0 \end{bmatrix}\begin{Bmatrix} U_5 \\ U_6 \end{Bmatrix} \tag{4.68}$$

where, for example, $Q_1^2 + Q_1^3$ is the horizontal force and $Q_2^2 + Q_2^3$ the vertical force at node 1. Solving (4.67) and computing the reaction forces (4.68), we obtain

$$U_5 = -\frac{3PL}{EA}, \qquad U_6 = (3 + 2\sqrt{2})\frac{PL}{EA} = 5.828\frac{PL}{EA} \tag{4.69}$$
$$F_1 \equiv Q_1^2 + Q_1^3 = -P, \qquad F_2 = -P, \qquad F_3 = 3P, \qquad F_4 = 0.0$$

The stress in each element can be computed from the relation

$$\sigma^e = \frac{\bar{Q}_3^e}{A_e}$$

where $\bar{Q}_3^e$ is the axial force at node 2 of the element Ω^e. Note that, for a truss element with constant cross-section, the following relations hold:

$$\bar{Q}_2^e = 0, \qquad \bar{Q}_4^e = 0, \qquad \bar{Q}_1^e = -\bar{Q}_3^e$$

The $\bar{Q}_3^e$ can be determined from the element equilibrium equations

$$\begin{Bmatrix} \bar{Q}_1^e \\ \bar{Q}_2^e \\ \bar{Q}_3^e \\ \bar{Q}_4^e \end{Bmatrix} = \frac{E_e A_e}{h_e} \begin{bmatrix} 1 & 0 & -1 & 0 \\ 0 & 0 & 0 & 0 \\ -1 & 0 & 1 & 0 \\ 0 & 0 & 0 & 0 \end{bmatrix} \begin{Bmatrix} \bar{u}_1^e \\ \bar{u}_2^e \\ \bar{u}_3^e \\ \bar{u}_4^e \end{Bmatrix} \tag{4.70}$$

Hence,

$$\sigma^e = \frac{E_e}{h_e}(\bar{u}_3^e - \bar{u}_1^e), \qquad \bar{u}_1^e = 0$$

From the global displacements U_5 and U_6, we have

$$\bar{u}_3^1 = -\frac{3PL}{AE}, \qquad \bar{u}_3^2 = U_5 \cos\alpha + U_6 \sin\alpha = 2\frac{PL}{AE}, \qquad \bar{u}_3^3 = 0 \tag{4.71}$$

Therefore, we have

$$\sigma^1 = -\frac{3P}{A}, \qquad \sigma^2 = \sqrt{2}\frac{P}{A}, \qquad \sigma^3 = 0 \tag{4.72}$$

The next example deals with a frame structure. It also illustrates how to incorporate a point load between nodes.

Example 4.4. The frame structure shown in Fig. 4.13 is to be analyzed for displacements and forces. Both members of the structure are made of the same material (E) and have the same geometric properties (A, I). The element stiffness matrices and force vectors in the global coordinate system (x, y, z) can be computed from (4.59) and (4.60). The geometric and material properties of each element are as follows.

Element 1

$$\begin{gathered} L = 144\text{ in}, \quad A = 10\text{ in}^2, \quad I = 10\text{ in}^4, \quad \cos\alpha = 0.0, \quad \sin\alpha = 1.0 \\ E = 10^6\text{ psi}, \quad f_1 = \tfrac{1}{72}P\text{ lb in}^{-1} \end{gathered} \tag{4.73}$$

Element 2

$$\begin{gathered} L = 180\text{ in}, \quad A = 10\text{ in}^2, \quad I = 10\text{ in}^2, \quad \cos\alpha = 0.8, \quad \sin\alpha = 0.6 \\ E = 10^6\text{ psi}, \quad f_2 = 0 \end{gathered} \tag{4.74}$$

The load $F_0 = 4P$ at the center of the element is distributed to the nodes according to (4.14).

The assembled stiffness matrix and force vectors are obtained by superposing the last three rows and columns of element 1 on the first three rows and columns of element 2; i.e., the 3 × 3 submatrix associated with rows and columns 4, 5, and 6 of element 1, and the 3 × 3 submatrix associated with rows and columns 1, 2, and 3 of element 2 overlap in the global stiffness matrix.

The known geometric boundary conditions are

$$U_1 = 0, \quad U_2 = 0, \quad U_3 = 0, \quad U_7 = 0, \quad U_8 = 0, \quad U_9 = 0 \tag{4.75a}$$

The force boundary conditions are

$$Q_4^1 + Q_1^2 = 0, \quad Q_5^1 + Q_2^2 = -2P, \quad Q_6^1 + Q_3^2 = 0 \tag{4.75b}$$

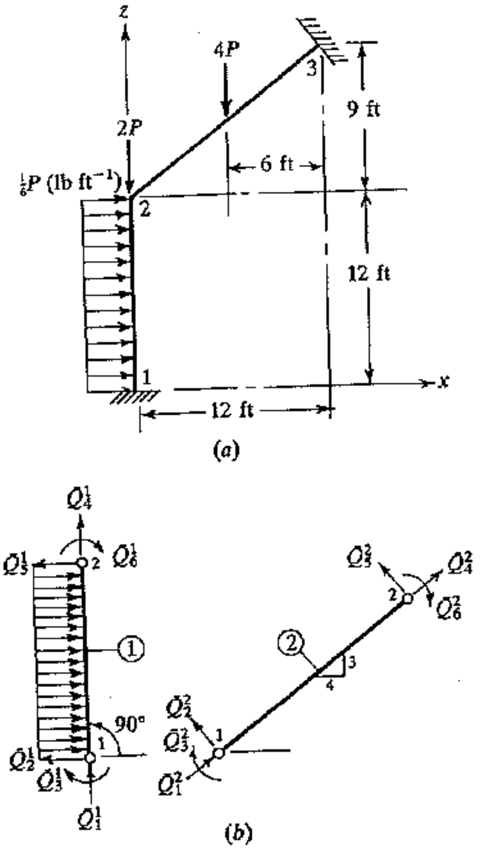

FIGURE 4.13
Geometry, loading and finite element discretization of a plane frame structure: (*a*) geometry and loading; (*b*) finite element discretization, element numbers, and element forces in the element coordinates.

Since all specified values of the known boundary conditions on the primary variables are zero, the condensed equations for the unknown global displacement degrees of freedom are

$$10^5\begin{bmatrix} 0.3560 & 0.2666 & -0.0178 \\ 0.2666 & 0.8846 & -0.0148 \\ -0.0178 & -0.0148 & 5.0000 \end{bmatrix}\begin{Bmatrix} U_4 \\ U_5 \\ U_6 \end{Bmatrix} = \begin{Bmatrix} 1 \\ -4 \\ 48 \end{Bmatrix}P \tag{4.76}$$

whose solution is

$$U_4 = 0.839 \times 10^{-4}P \text{ (in)}, \quad U_5 = -0.681 \times 10^{-4}P \text{ (in)}, \quad U_6 = 0.961 \times 10^{-4}P \text{ (rad)}. \tag{4.77}$$

The reactions and forces in each member in the global coordinates can be computed from the element equations

$$\{Q^e\} = [K^e]\{u^e\} - \{f^e\} \tag{4.78a}$$

The forces $\{Q^e\}$ can be transformed to those in the element coordinate system by means of (4.55):

$$\{\bar{Q}^e\} = [T^e]\{Q^e\} \tag{4.78b}$$

We obtain

$$\{\bar{Q}^1\} = \begin{Bmatrix} 4.731 \\ 0.725 \\ -10.900 \\ -4.731 \\ 1.275 \\ 50.450 \end{Bmatrix} P, \quad \{\bar{Q}^2\} = \begin{Bmatrix} 1.458 \\ -0.180 \\ 21.550 \\ -1.458 \\ 0.180 \\ 10.870 \end{Bmatrix} P \tag{4.79}$$

4.4 THE TIMOSHENKO BEAM AND FRAME ELEMENTS

4.4.1 Governing Equations

Recall that the Euler–Bernoulli beam theory is based on the assumption that plane cross-sections remain plane *and perpendicular* to the longitudinal axis after bending. This assumption implies that all transverse shear strains are zero. When the normality assumption is not used, i.e., plane sections remain plane but not necessarily normal to the longitudinal axis after deformation, the transverse shear strain ϵ_{xz} is not zero. Therefore, the rotation of a transverse normal plane about the y axis is not equal to $-dw/dx$. Beam theory based on these relaxed assumptions is called a *shear deformation beam theory,* most commonly known as the *Timoshenko beam theory*. We denote the rotation about the y axis by an independent function $\Psi(x)$. The governing equilibrium equations of the Timoshenko beam theory are

$$\boxed{\begin{aligned} &\frac{d}{dx}\left[GAK_s\left(\Psi + \frac{dw}{dx}\right)\right] + f = 0 \\ &\frac{d}{dx}\left(EI\frac{d\Psi}{dx}\right) - GAK_s\left(\Psi + \frac{dw}{dx}\right) = 0 \end{aligned}} \qquad \begin{aligned} &(4.80a) \\ &(4.80b) \end{aligned}$$

where G is the shear modulus and K_s is the *shear correction coefficient,* which is introduced to account for the difference in the constant state of shear stress in this theory and the parabolic variation of the actual (i.e., as predicted by equilibrium equations) shear stress through the thickness. When the second equation is substituted into the first for $GAK_s(\Psi + dw/dx)$, and Ψ is replaced with $-dw/dx$, we obtain governing equation (4.1) of the Euler–Bernoulli beam theory.

4.4.2 Weak Form

The weak form of (4.80) over an element $\Omega^e = (x_A, x_B)$ is developed using the usual procedure, now applied to each equation. We multiply (4.80a) wtih a weight function $-w_1$ and (4.80b) with a weight function $-w_2$, and integrate over the element length:

$$0=\int_{x_A}^{x_B} -w_1\left\{\frac{d}{dx}\left[GAK_s\left(\Psi+\frac{dw}{dx}\right)\right]+f\right\}dx$$

$$0=\int_{x_A}^{x_B} -w_2\left[\frac{d}{dx}\left(EI\frac{d\Psi}{dx}\right)-GAK_s\left(\Psi+\frac{dw}{dx}\right)\right]dx$$

Integrating the first term of each integral once by parts, we obtain

$$0=\int_{x_A}^{x_B}\left[\frac{dw_1}{dx}GAK_s\left(\Psi+\frac{dw}{dx}\right)-w_1f\right]dx-\left[w_1GAK_s\left(\Psi+\frac{dw}{dx}\right)\right]_{x_A}^{x_B} \tag{4.81a}$$

$$0=\int_{x_A}^{x_B}\left[\frac{dw_2}{dx}EI\frac{d\Psi}{dx}+w_2GAK_s\left(\Psi+\frac{dw}{dx}\right)\right]dx-\left[w_2EI\frac{d\Psi}{dx}\right]_{x_A}^{x_B} \tag{4.81b}$$

The coefficients of the weight functions w_1 and w_2 in the boundary integrals are

$$GAK_s\left(\Psi+\frac{dw}{dx}\right)\equiv V \quad\text{and}\quad EI\frac{d\Psi}{dx}\equiv M \tag{4.82}$$

where V is the shear force and M is the bending moment; these coefficients constitute the secondary variables of the weak form. The weight functions w_1 and w_2 must have the physical interpretations that give w_1V and w_2M units of work. Clearly, w_1 must be equivalent to (the variation of) the transverse deflection w, and w_2 must be equivalent to (the variation of) the rotation function Ψ:

$$w_1\sim w,\qquad w_2\sim\Psi$$

Hence, the primary variables of the formulation are w and Ψ. Denoting the shear forces and bending moments at the endpoints of the element by the expressions

$$\boxed{\begin{aligned}Q_1^e&\equiv-\left[GAK_s\left(\Psi+\frac{dw}{dx}\right)\right]\Big|_{x_A}, & Q_2^e&\equiv-\left(EI\frac{d\Psi}{dx}\right)\Big|_{x_A}\\ Q_3^e&\equiv\left[GAK_s\left(\Psi+\frac{dw}{dx}\right)\right]\Big|_{x_B}, & Q_4^e&\equiv\left(EI\frac{d\Psi}{dx}\right)\Big|_{x_B}\end{aligned}} \tag{4.83}$$

the weak statements in (4.81) can be written in the final form

$$\boxed{\begin{aligned}0&=\int_{x_A}^{x_B}\left[GAK_s\frac{dw_1}{dx}\left(\Psi+\frac{dw}{dx}\right)-w_1f\right]dx-w_1(x_A)Q_1^e-w_1(x_B)Q_3^e\\ 0&=\int_{x_A}^{x_B}\left[EI\frac{dw_2}{dx}\frac{d\Psi}{dx}+GAK_sw_2\left(\Psi+\frac{dw}{dx}\right)\right]dx-w_2(x_A)Q_2^e-w_2(x_B)Q_4^e\end{aligned}} \tag{4.84}$$

4.4.3 Finite Element Model

A close examination of the terms in (4.84) shows that both w and Ψ are differentiated only once with respect to x. Since the primary variables are the dependent unknowns themselves (and do not include their derivatives), the Lagrange interpolation of w and Ψ is appropriate here. The minimum admissible degree of interpolation is linear, so that $dw/dx \neq 0$ and $d\Psi/dx \neq 0$. The variables w and Ψ do not have the same physical units; they can be interpolated, in general, with different degrees of interpolation.

Let us consider Lagrange interpolation of w and Ψ in the form

$$\boxed{w = \sum_{j=1}^{m} w_j \psi_j^{(1)}, \qquad \Psi = \sum_{j=1}^{n} s_j \psi_j^{(2)}} \tag{4.85}$$

where $\psi_j^{(1)}$ and $\psi_j^{(2)}$ are the Lagrange interpolation functions of degree $m-1$ and $n-1$, respectively. In general, m and n are independent of each other, although $m = n$ is most common. However, when $m = n = 2$ (i.e., linear interpolation is used), the derivative of w is

$$\left(\frac{dw}{dx}\right)^e = \frac{w_2^e - w_1^e}{h_e}$$

which is element-wise-constant. The rotation function Ψ, being linear, is not consistent with that predicted by $w(x)$. For thin beams, the transverse shear deformation is negligible, and we have $\Psi = -dw/dx$, which requires

$$s_1^e \frac{x_B - x}{h_e} + s_2^e \frac{x - x_A}{h_e} = -\frac{w_2^e - w_1^e}{h_e} \tag{4.86a}$$

or, equivalently (by equating like coefficients on both sides),

$$s_1^e x_B - s_2^e x_A = -(w_2^e - w_1^e), \qquad s_2^e - s_1^e = 0 \tag{4.86b}$$

which in turn requires

$$s_1^e = s_2^e = -\frac{w_2^e - w_1^e}{h_e} \tag{4.87}$$

This implies that $\Psi(x)$ is a constant:

$$\Psi(x) = s_1^e \frac{x_B - x}{h_e} + s_2^e \frac{x - x_A}{h_e} = s_1^e \ (= s_2^e) \tag{4.88}$$

However, a constant state of $\Psi(x)$ is not admissible, because the bending energy of the element,

$$\int_{x_A}^{x_B} \frac{EI}{2} \left(\frac{d\Psi}{dx}\right)^2 dx \tag{4.89a}$$

would be zero. This numerical problem is known as *shear locking*.

To circumvent this, two alternative procedures have been developed in the literature:

1. Use a *consistent interpolation* for w and Ψ such that dw/dx and Ψ are polynomials of the same order (i.e., $m = n + 1$).

2. Use equal interpolation (i.e. $m = n$) for w and Ψ, but evaluate the bending energy with actual interpolation of Ψ and the shear energy

$$\int_{x_A}^{x_B} \frac{GAK_s}{2}\left(\frac{dw}{dx} + \Psi\right)^2 dx \tag{4.89b}$$

with a polynomial that is one order lower.

The latter can be achieved computationally without using different interpolations of Ψ in (4.89*a*, *b*). In the numerical evaluation of the integral (4.89*b*), we use a quadrature rule (see Section 7.1 for details) that is necessary to calculate the integral

$$\int_{x_A}^{x_B} GAK_s\left(\frac{dw}{dx}\right)^2 dx \tag{4.89c}$$

exactly. For example, when the linear interpolation of w and Ψ is used, we use a one-point quadrature rule to evaluate (4.89*b*) because a one-point quadrature would give the exact value of the integral (4.89*c*) when GA = constant. A two-point quadrature is needed to evaluate the integral in (4.89*b*) exactly. The use of *reduced integration*, i.e., one-point quadrature on the integral (4.89*b*), would result in the linear term in the approximation of Ψ not contributing to the shear energy. For illustrative purposes, we take a detailed look at the expression

$$\frac{GAK_s}{2}\int_{x_A}^{x_B}\left(\frac{dw}{dx} + \Psi\right)^2 dx = \frac{GAK_s}{2}\left[\left(\frac{dw}{dx} + \Psi\right)^2\Big|_{x=x_A+h_e/2}\right]h_e$$

where $x = x_A + \frac{1}{2}h_e$ is the midpoint of the element and h_e is its length. Substituting (4.85) into this expression (with $m = n = 2$), we have

$$\frac{GAK_s h_e}{2}\left(\frac{w_2^e - w_1^e}{h_e} + s_1^e\frac{x_B - x}{h_e} + s_2^e\frac{x - x_A}{h_e}\right)^2\Bigg|_{x=x_A+h_e/2} = \frac{GAK_s h_e}{2}\left(\frac{w_2^e - w_1^e}{h_e} + \frac{s_1^e + s_2^e}{2}\right)^2 \tag{4.90}$$

which is a weaker requirement than (4.87), i.e., if (4.87) holds then (4.90) also holds, but (4.90) does not imply (4.87). We note that (4.87) must hold only for problems for which the transverse shear energy (4.89) is negligible.

In summary, we use either consistent interpolation ($m = n + 1$) or equal interpolation with reduced integration in the evaluation of the transverse shear stiffness coefficients in the Timoshenko beam element. We consider both forms of elements here.

Substitution of (4.85) for w and Ψ, and $w_1 = \psi_i^{(1)}$ and $w_2 = \psi_i^{(2)}$ into the weak forms (4.84), we obtain the finite element equations:

$$\boxed{\begin{aligned} 0 &= \sum_{j=1}^{m} K_{ij}^{11}w_j + \sum_{j=1}^{n} K_{ij}^{12}s_j - F_i^1 \quad (i = 1, 2, \ldots, m)\\ 0 &= \sum_{j=1}^{m} K_{ij}^{21}w_j + \sum_{j=1}^{n} K_{ij}^{22}s_j - F_i^2 \quad (i = 1, 2, \ldots, n)\end{aligned}} \tag{4.91a}$$

where

$$\boxed{\begin{aligned} K_{ij}^{11} &= \int_{x_A}^{x_B} GAK_s \frac{d\psi_i^{(1)}}{dx}\frac{d\psi_j^{(1)}}{dx}\,dx \\ K_{ij}^{12} &= \int_{x_A}^{x_B} GAK_s \frac{d\psi_i^{(1)}}{dx}\psi_j^{(2)}\,dx = K_{ji}^{21} \\ K_{ij}^{22} &= \int_{x_A}^{x_B} \left(EI\frac{d\psi_i^{(2)}}{dx}\frac{d\psi_j^{(2)}}{dx} + GAK_s\psi_i^{(2)}\psi_j^{(2)}\right) dx \\ F_i^1 &= \int_{x_A}^{x_B} f\psi_i^{(1)}\,dx + Q_{2i-1}, \qquad F_i^2 = Q_{2i} \end{aligned}} \tag{4.91b}$$

Equations (4.91*a*) can be written in matrix form as

$$\begin{bmatrix} [K^{11}] & [K^{12}] \\ [K^{21}] & [K^{22}] \end{bmatrix} \begin{Bmatrix} \{w\} \\ \{s\} \end{Bmatrix} = \begin{Bmatrix} \{F^1\} \\ \{F^2\} \end{Bmatrix} \tag{4.92}$$

A CONSISTENT INTERPOLATION ELEMENT (CIE). To illustrate the use of consistent interpolation, we select $\psi_i^{(1)}$ to be Lagrange quadratic polynomials and $\psi_i^{(2)}$ Lagrange linear polynomials. For this choice of interpolation, $[K^{11}]$ is 3×3, $[K^{12}]$ is 3×2, and $[K^{22}]$ is 2×2. The explicit forms of the matrices, when EI and GAK_s are constant, are

$$\begin{aligned} [K^{11}] &= \frac{GAK_s}{3h_e}\begin{bmatrix} 7 & -8 & 1 \\ -8 & 16 & -8 \\ 1 & -8 & 7 \end{bmatrix}, \quad [K^{12}] = \frac{GAK_s}{6}\begin{bmatrix} -5 & -1 \\ 4 & -4 \\ 1 & 5 \end{bmatrix} \\ [K^{22}] &= \frac{EI}{h_e}\begin{bmatrix} 1 & -1 \\ -1 & 1 \end{bmatrix} + \frac{GAK_s h_e}{6}\begin{bmatrix} 2 & 1 \\ 1 & 2 \end{bmatrix} \end{aligned} \tag{4.93}$$

The element equations become

$$GAK_s\begin{bmatrix} \frac{7}{3h} & -\frac{8}{3h} & \frac{1}{3h} & -\frac{5}{6} & -\frac{1}{6} \\ -\frac{8}{3h} & \frac{16}{3h} & -\frac{8}{3h} & \frac{4}{6} & -\frac{4}{6} \\ \frac{1}{3h} & -\frac{8}{3h} & \frac{7}{3h} & \frac{1}{6} & \frac{5}{6} \\ -\frac{5}{6} & \frac{4}{6} & \frac{1}{6} & \frac{\alpha}{h}+\frac{h}{3} & -\frac{\alpha}{h}+\frac{h}{6} \\ -\frac{1}{6} & -\frac{4}{6} & \frac{5}{6} & -\frac{\alpha}{h}+\frac{h}{6} & \frac{\alpha}{h}+\frac{h}{3} \end{bmatrix} \begin{Bmatrix} w_1 \\ w_3 \\ w_2 \\ s_1 \\ s_2 \end{Bmatrix}^e = \begin{Bmatrix} f_1 \\ f_3 \\ f_2 \\ 0 \\ 0 \end{Bmatrix}^e + \begin{Bmatrix} Q_1 \\ \hat{Q} \\ Q_3 \\ Q_2 \\ Q_4 \end{Bmatrix}^e \tag{4.94}$$

where $\alpha = EI/GAK_s$, $\hat{Q}$ is any specified transverse force at node 3, and

Q_1, Q_3) are shear forces and (Q_2, Q_4) bending moments at the end nodes 1 and 2 of the element.

Note that node 3, which is the middle node of the element, is not connected to other elements, and the only degree of freedom there is the transverse deflection. Thus, there are different number of degrees of freedom at different nodes of the element, and this therefore complicates the assembly of elements and its implementation on a computer. Hence, we eliminate the node 3 dependence in the system of element equations by condensing out w_3. We obtain

$$\boxed{\begin{aligned}&\begin{bmatrix} \frac{GAK_s}{h} & -\frac{GAK_s}{h} & -\frac{1}{2}GAK_s & -\frac{1}{2}GAK_s \\ -\frac{GAK_s}{h} & \frac{GAK_s}{h} & \frac{1}{2}GAK_s & \frac{1}{2}GAK_s \\ -\frac{1}{2}GAK_s & \frac{1}{2}GAK_s & \frac{1}{4}GAK_sh+\frac{EI}{h} & \frac{1}{4}GAK_sh-\frac{EI}{h} \\ -\frac{1}{2}GAK_s & \frac{1}{2}GAK_s & \frac{1}{4}GAK_sh-\frac{EI}{h} & \frac{1}{4}GAK_sh+\frac{EI}{h} \end{bmatrix} \begin{Bmatrix} w_1 \\ w_2 \\ s_1 \\ s_2 \end{Bmatrix}^e \\ &\qquad = \begin{Bmatrix} f_1+\frac{1}{2}\hat{f}_3 \\ f_2+\frac{1}{2}\hat{f}_3 \\ -\frac{1}{8}\hat{f}_3h \\ \frac{1}{8}\hat{f}_3h \end{Bmatrix}^e + \begin{Bmatrix} Q_1 \\ Q_3 \\ Q_2 \\ Q_4 \end{Bmatrix}^e\end{aligned}} \tag{4.95}$$

where $\hat{f}_3 = f_3 + \hat{Q}$. This is obtained by solving the second equation of (4.94) for w_3 and substituting for w_3 in the first four equations of (4.94). The forces f_i are obtained using

$$f_i^e = \int_{x_A}^{x_B} f(x)\psi_i^e\,dx, \qquad \psi_i^e = [\psi_i^{(1)}]^e = \text{quadratic interpolation functions} \tag{4.96}$$

The element equations (4.95) can be assembled in the same manner as the classical beam equations, with two degrees of freedom (w, s) per node. However, it should be noted that w is interpolated with quadratic polynomials.

For constant $f = f_0$, the specified load vector in (4.95) takes the form [because $f_1^e = \frac{1}{6}f_0h$, $f_2^e = \frac{1}{6}f_0h$, $f_3^e = \frac{4}{6}f_0h$, $\hat{Q}_0 = 0$; see (3.40b)]

$$\{f^e\} = \begin{Bmatrix} \frac{1}{2}f_0h \\ \frac{1}{2}f_0h \\ -\frac{1}{12}f_0h^2 \\ \frac{1}{12}f_0h^2 \end{Bmatrix} \tag{4.97}$$

which is precisely the same as that obtained in the classical beam element [see (4.15)].

AN EQUAL INTERPOLATION, REDUCED INTEGRATION ELEMENT (RIE). When equal interpolation is used ($m = n$), all submatrices in (4.92) are of the same order: $n \times n$. The element coefficient matrices K_{ij}^{11} and K_{ij}^{12} are evaluated exactly, as is the first part of K_{ij}^{22}. The second part of K_{ij}^{22} is to be evaluated using reduced integration. For the choice of linear interpolation functions, and for constant values of GAK_s and EI, the matrices have the following explicit values:

$$\begin{aligned} [K^{11}] &= \frac{GAK_s}{h_e}\begin{bmatrix} 1 & -1 \\ -1 & 1 \end{bmatrix}, \qquad [K^{12}] = \frac{GAK_s}{2}\begin{bmatrix} -1 & -1 \\ 1 & 1 \end{bmatrix} \\ [K^{22}] &= \frac{EI}{h_e}\begin{bmatrix} 1 & -1 \\ -1 & 1 \end{bmatrix} + \frac{GAK_s h_e}{4}\begin{bmatrix} 1 & 1 \\ 1 & 1 \end{bmatrix} \end{aligned} \tag{4.98}$$

where one-point integration is used to evaluate the second part of $[K^{22}]$. Note that $[K^{11}]$, $[K^{12}]$, and the first part of $[K^{22}]$ are also evaluated exactly with one-point quadrature when EI and GAK_s are constant. Hence the uniform one-point integration for $[K^{\alpha\beta}]$ satisfies all requirements.

The element equations are

$$\begin{bmatrix} \dfrac{GAK_s}{h} & -\frac{1}{2}GAK_s & -\dfrac{GAK_s}{h} & -\frac{1}{2}GAK_s \\ -\frac{1}{2}GAK_s & \frac{1}{4}GAK_s h + \dfrac{EI}{h} & \frac{1}{2}GAK_s & \frac{1}{4}GAK_s h - \dfrac{EI}{h} \\ -\dfrac{GAK_s}{h} & \frac{1}{2}GAK_s & \dfrac{GAK_s}{h} & \frac{1}{2}GAK_s \\ -\frac{1}{2}GAK_s & \frac{1}{4}GAK_s h - \dfrac{EI}{h} & \frac{1}{2}GAK_s & \frac{1}{4}GAK_s h + \dfrac{EI}{h} \end{bmatrix} \begin{Bmatrix} w_1 \\ s^1 \\ w_2 \\ s_2 \end{Bmatrix}^e = \begin{Bmatrix} f_1 \\ 0 \\ f_2 \\ 0 \end{Bmatrix}^e + \begin{Bmatrix} Q_1 \\ Q_2 \\ Q_3 \\ Q_4 \end{Bmatrix}^e \tag{4.99}$$

It is interesting to note that the element stiffness matrix in (4.99) is the same as that in (4.95) obtained from the consistent interpolation with quadratic approximation of w and linear approximation of Ψ, except that the nodal variables are listed in a different order. The only difference is the load representation. In the consistent interpolation, the load vector is equivalent to that of the Euler–Bernoulli beam theory, whereas, in the equal interpolation with reduced integration element, the load vector does not contain any moment components due to the distributed load.

The quadratic interpolation of both w and Ψ with full integration of the element coefficient matrices also suffers slightly from the shear-locking phenomenon. A uniform two-point quadrature rule has the desired effect on $[K^{11}]$, $[K^{12}]$, and $[K^{22}]$; i.e., $[K^{11}]$, $[K^{12}]$, and the first term of $[K^{22}]$ will be evaluated exactly and the second term of $[K^{22}]$ approximately. As the degree of approximation and/or the number of elements in the mesh is increased, the shear locking will disappear and reduced integration is not necessary.

Example 4.5. Here we reconsider the indeterminate beam problem of Example 4.2 (see Fig. 4.7), and analyze it with the reduced integration element (RIE) and consistent interpolation element (CIE). Unlike the Euler–Bernoulli beam element, the Timoshenko beam element does not yield exact values at the nodes, even when EI and GAK_s are constant. This is because of the coupled nature of the equations relating w and Ψ.

The beam is modeled using two ($h_1 = 4$, $h_2 = 6$) and four ($h_1 = 2$, $h_2 = 2$, $h_3 = 3$, $h_4 = 3$) linear elements with reduced integration. The element equations for a typical element are the same as those in (4.99), where f_i^e for the elements with distributed force are given by

$$f_i^e = \int_{x_e-4}^{x_{e+1}-4} [-\tfrac{100}{6}\bar{x}\psi_i^e(\bar{x})]\,d\bar{x} \quad \text{for } x_e \geq 4 \tag{4.100}$$

where $\bar{x}$ is a coordinate such that $x = \bar{x} + 4$. We obtain

$$\{f^2\} = -\frac{h_2 f_0}{6}\begin{Bmatrix}1\\2\end{Bmatrix}$$

for the two-element case and

$$\{f^3\} = -\frac{h_3 f_0}{12}\begin{Bmatrix}1\\2\end{Bmatrix}, \qquad \{f^4\} = -\frac{h_3 f_0}{12}\begin{Bmatrix}1\\2\end{Bmatrix} - \frac{h_4 f_0}{4}\begin{Bmatrix}1\\1\end{Bmatrix}$$

for the four-element case ($h_3 = h_4$).

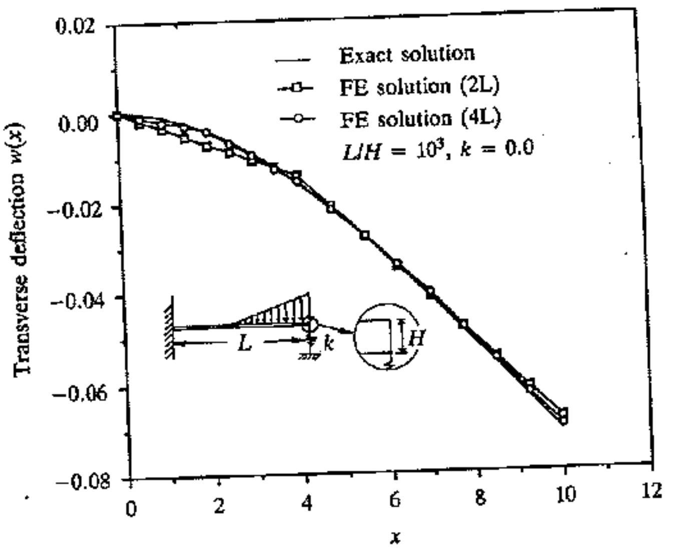

FIGURE 4.14
Comparison of the transverse deflection obtained using Timoshenko beam elements with the exact deflection of a cantilever beam (see Fig. 4.7).

Figure 4.14 shows plots of transverse deflection versus x for the case with $k=0$ (i.e., a centilever beam), beam length-to-height ratio $L/H=10^3$, and $EI=10^6\,\text{ft}^2\,\text{lb}$. The ratio L/H is a measure of the thinness of the beam. When it is large (i.e., for very thin beams), the transverse shear deformation is negligible and the Euler–Bernoulli and Timoshenko beam theories give the same results. For small values of L/H, say 10 (i.e., $GAK_s = 4\times10^6$ lb), Timoshenko beam theory predicts larger deflections, and for the problem at hand the difference is not noticeable enough to be seen if the deflections from both theories were included in Fig. 4.14. The finite element solutions shown in the figure are obtained with the reduced integration elements.

Figure 4.15 contains results of a convergence study, which includes two and four linear and quadratic element meshes for the case of $k/EI=1.0$ and $L/H=10$. The reduced integration elements are used. The scale used for plotting the deflections is such that the difference between the finite element solutions and the exact solution can be seen clearly. The mesh of four quadratic elements gives the converged solution. To show the effect of the transverse shear deformation, the exact solution for the thin beam ($L/H=10^3$) is also shown in Fig. 4.15. It is clear from the results that the convergence is rapid and the quadratic elements yield faster convergence.

The accuracy of the reduced integration element (RIE) relative to the full integration element (FIE) and the consistent interpolation element (CIE) can be seen from the results shown in Fig. 4.16 (for $L/H=10$ and $k/EI=1$). Clearly, the CIE element gives more accurate results, followed by the reduced integration element. Recall that the stiffness matrices of the two elements are identical, the only difference being in their force vectors [see (4.95) and (4.99)]. Of course, in the CIE element, the transverse deflection is interpolated using quadratic functions. The plots shown in Fig. 4.17 indicate that the reduced integration is necessry even for quadratic elements, although they are not as sensitive to locking.

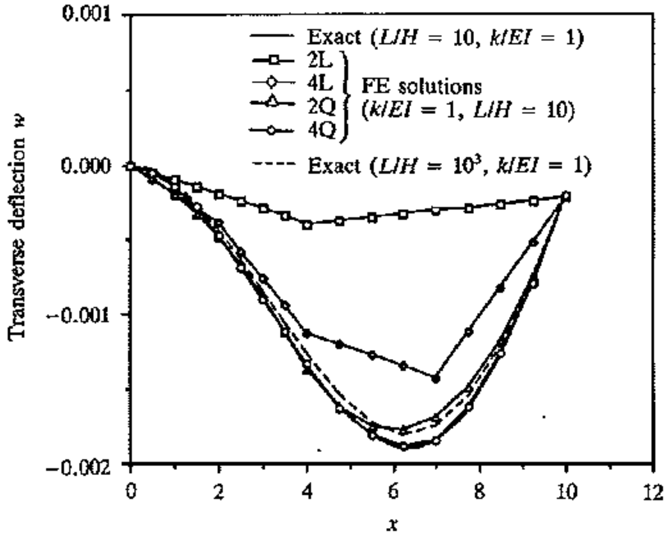

FIGURE 4.15

Convergence of the finite element solution to the exact solution of the beam in Fig. 4.7 ($k/EI=1$); the Timoshenko beam element is used.

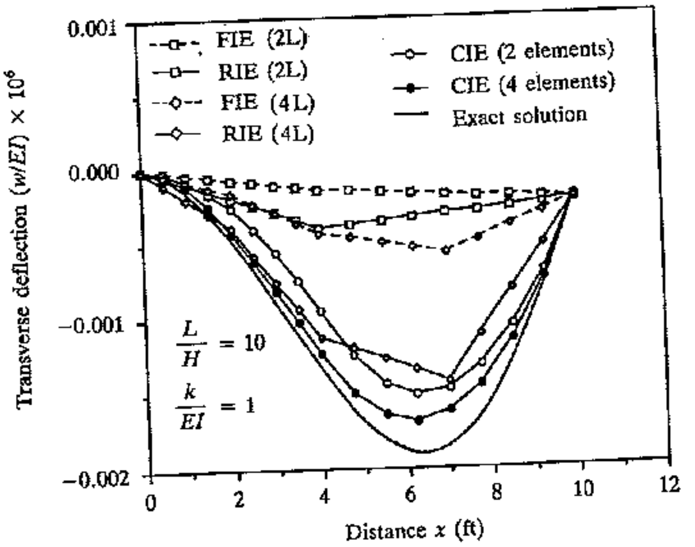

FIGURE 4.16
Comparison of the transverse deflection $w(x)$ obtained with reduced integration elements (RIE), full integration elements (FIE), and consistent interpolation elements (CIE) with the exact solution: 2L, two linear elements; 4L, four linear elements.

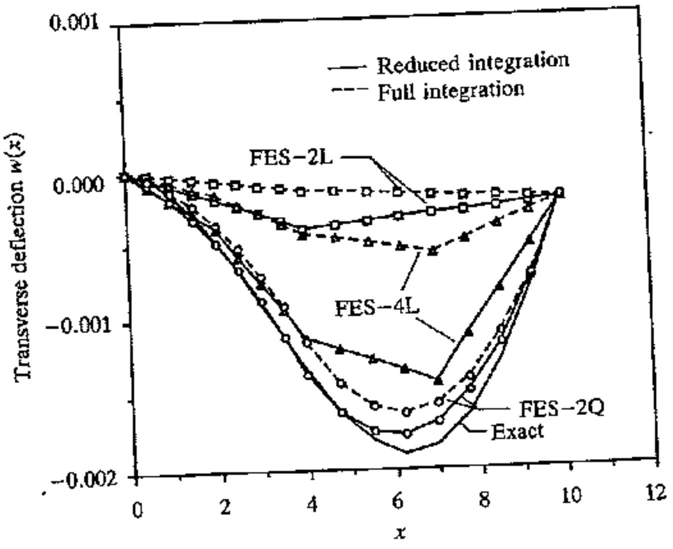

FIGURE 4.17
The effect of full and reduced integration on the accuracy of the finite element solution (FES) obtained using the Timoshenko beam element.

The following general observations can be made about various finite element models based on the Timoshenko beam theory:

1. The reduced integration element (RIE) exhibits less locking compared with the full integration element (FIE).
2. As the number of elements in the mesh is increased or the degree of approximation is increased (i.e., higher-order elements are used), the finite element solutions obtained by both RIE and FIE elements improve; i.e., the effect of locking is reduced with mesh refinements and higher-order elements.
3. The consistent interpolation element (i.e., quadratic approximation of w and linear approximation of Ψ) with full integration yields a more accurate solution than that predicted by the RIE element. This is due to a better representation of the distributed load.
4. The element with quadratic approximation of both w and Ψ and reduced integration of the coefficients yields more accurate results than the consistent interpolation element with quadratic approximation of w and linear approximation of Ψ and with full integration of the coefficients.

The frame element based on shear deformation beam theory can be obtained by superposing the bar and beam stiffnesses.

4.5 INCLUSION OF CONSTRAINT EQUATIONS

When the support plane of a roller support is at an angle to the global coordinate system (see Fig. 4.18), the boundary conditions on the displacements and forces at the roller are

$$u_n^e = 0, \qquad Q_t^e = Q_0 \tag{4.101}$$

where u_n^e is the normal component of the displacement, Q_t^e is the tangential component of the force at node 1 of the element Ω^e, and Q_0 is any specified tangential force. These conditons must be expressed in terms of the global

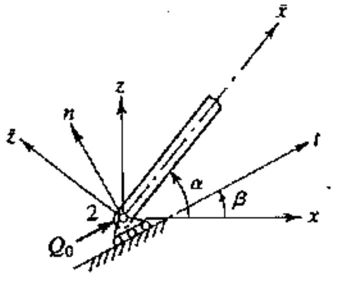

$$u_t = u\cos\beta + w\sin\beta$$
$$u_n = w\cos\beta - u\sin\beta$$

FIGURE 4.18
Transformation of specified boundary conditions from a local coordinate system to the global coordinate system.

components of displacements and forces by means of the transformation (4.53) and (4.55):

$$u_n^e = -u_1^e \sin\beta + u_2^e \cos\beta = 0 \tag{4.102a}$$

$$Q_t^e = Q_1^e \cos\beta + Q_2^e \sin\beta = Q_0 \tag{4.102b}$$

where (u_1^e, u_2^e) and (Q_1^e, Q_2^e) are the x and z components of the displacements and forces at the support.

Equations (4.102) can be incorporated into the global system of equations as follows. Consider the assembled system of equations,

$$\begin{aligned}
K_{11}U_1 + K_{12}U_2 + \cdots + K_{1n}U_n &= F_1 \\
K_{21}U_1 + K_{22}U_2 + \cdots + K_{2n}U_n &= F_2 \\
&\vdots \\
K_{n1}U_1 + K_{n2}U_2 + \cdots + K_{nn}U_n &= F_n
\end{aligned} \tag{4.103}$$

where U_i are the global generalized displacement degrees of freedom and F_i are the sums of the applied (f_i^e) and internal (Q_i^e) generalized force degrees of freedom. Suppose that the roller support is at the first node of the element Ω^e, and that the corresponding displacement degrees of freedom are U_I, U_J, and U_K. The forces Q_1^e, Q_2^e, and Q_3^e corresponding to these displacements end up in the forces F_I, F_J, and F_K, respectively. Hence, to include the force boundary condition of (4.102b), we must add $\cos\beta$ times the Ith global equation to $\sin\beta$ times the Jth equation:

$$(\cos\beta)(K_{I1}U_1 + K_{I2}U_2 + \ldots + K_{II}U_I + K_{IJ}U_J + \ldots + K_{IN}U_N) = (\cos\beta)F_I$$

$$(\sin\beta)(K_{J1}U_1 + K_{J2}U_2 + \ldots + K_{JI}U_I + K_{JJ}U_J + \ldots + K_{JN}U_N) = (\sin\beta)F_J$$

and obtain

$$\begin{aligned}
(K_{I1}\cos\beta + K_{J1}\sin\beta)U_1 + \ldots &+ (K_{IN}\cos\beta + K_{JN}\sin\beta)U_N \\
&= (F_I \cos\beta + F_J \sin\beta) \\
&= (f_1^e \cos\beta + f_2^e \sin\beta) + (Q_1^e \cos\beta + Q_2^e \sin\beta) \\
&= (f_1^e \cos\beta + f_2^e \sin\beta) + Q_0
\end{aligned} \tag{4.104}$$

We replace the Jth equation with this and replace the Ith equation with (4.102a):

$$(\sin\beta)U_I + (-\cos\beta)U_J = 0 \tag{4.105}$$

These modifications of the global set of algebraic equations violate the symmetry of the resulting global stiffness matrix.

To retain the symmetry of the global stiffness matrix, an alternative method of incorporating the conditions (4.102) is presented here. Equations (4.102a) or (4.105) can be viewed as the constraint equations among the global displacements, which have a companion relation among the associated forces, i.e., (4.102b). In the following paragraphs, we present a general procedure by which constraint equations of the type

$$\begin{Bmatrix} \{U^1\} \\ \{U^2\} \end{Bmatrix} = [A]\{U^1\} \tag{4.106a}$$

among the primary variables

$$\{U\} = \begin{Bmatrix} \{U^1\} \\ \{U^2\} \end{Bmatrix} \tag{4.106b}$$

can be implemented in the assembled system of equations (4.103). In (4.106), $\{U^1\}$ denotes the $n \times 1$ vector of generalized nodal displacements that are selected as the independent nodal variables, and $\{U^2\}$ denotes the $m \times 1$ vector of generalized nodal displacements that are selected as the dependent nodal variables. The matrix operator $[A]$ is of order $(n+m) \times n$.

For example, consider a frame problem with N nodes and a total of $3N$ $(= m + n)$ degrees of freedom in the problem. If one of the supports is a roller support, there will be one constraint equation of the type (4.102*a*). If the global node number corresponding to the roller is I then $p = 3(I - 1) + 1$ is the first degree of freedom at the support. Hence, the constraint condition (4.102*a*) can be expressed in terms of the generalized global displacement degrees of freedom U_p and U_{p+1} as

$$-U_p \sin\beta + U_{p+1} \cos\beta = 0 \tag{4.107}$$

Suppose that U_p is selected as the independent variable and U_{p+1} as the dependent variable. Then the number of independent variables is $n = 3N + 2$, and there is only one dependent variable (i.e., $m = 1$). For this case, the constraint (4.106*a*) has the form

$$\begin{Bmatrix} U_1 \\ U_2 \\ \vdots \\ U_p \\ U_{p+2} \\ \vdots \\ U_{m+n} \\ U_{p+1} \end{Bmatrix} = \begin{bmatrix} 1 & 0 & \dots & 0 & 0 & 0 & \dots & 0 \\ 0 & 1 & \dots & 0 & 0 & 0 & \dots & 0 \\ \vdots & \vdots & & \vdots & \vdots & \vdots & & \vdots \\ 0 & 0 & \dots & 0 & 1 & 0 & \dots & 0 \\ 0 & 0 & \dots & & & \ddots & & 0 \\ \vdots & \vdots & & & & & \ddots & \vdots \\ 0 & 0 & \dots & 0 & \underset{p\text{th column}}{\tan\beta} & 0 & \dots & 0 \end{bmatrix} \begin{Bmatrix} U_1 \\ U_2 \\ \vdots \\ U_p \\ U_{p+2} \\ \vdots \\ U_{m+n} \end{Bmatrix} \tag{4.108}$$

Equation (4.106*a*) represents a transformation similar to (4.55*a*), between two sets of global generalized nodal displacements, with $[A]$ being the transformation matrix. Therefore, the discussion presented in the paragraph following (4.58) can be used to transform the equations in $m + n$ variables to those in only n variables.

Consider the assembled equations

$$[K]\{U\} = \{F\} \tag{4.109}$$

which can be rearranged as

$$[\bar{K}]\left\{\begin{matrix}\{U^1\}\\ \{U^2\}\end{matrix}\right\} = \{\bar{F}\} \tag{4.110}$$

where $\{U^1\}$ and $\{U^2\}$ denote the vectors defined in (4.106*a*). Using the transformation (4.106*a*), we obtain

$$[\bar{K}][A]\{U^1\} = \{\bar{F}\} \tag{4.111}$$

To obtain a symmetric coefficient matrix, we premultiply both sides with $[A]^T$, and arrive at

$$[A]^T[\bar{K}][A]\{U^1\} = [A]^T\{\bar{F}\}$$

or

$$[\hat{K}]\{U^1\} = \{\hat{F}\} \tag{4.112a}$$

where

$$[\hat{K}] = [A]^T[\bar{K}][A], \qquad \{\hat{F}\} = [A]^T\{\bar{F}\} \tag{4.112b}$$

Equations (4.112) are now ready for the implementation of boundary conditions and solution.

As an example, consider the frame element in Fig. 4.18. We have one constraint equation,

$$U_5 = U_4 \tan\beta$$

The transformation equation (4.108) has the form

$$\left\{\begin{array}{c} U_1\\ U_2\\ U_3\\ U_4\\ U_6\\ \hdashline U_5 \end{array}\right\} = \left[\begin{array}{ccccc} 1 & 0 & 0 & 0 & 0\\ 0 & 1 & 0 & 0 & 0\\ 0 & 0 & 1 & 0 & 0\\ 0 & 0 & 0 & 1 & 0\\ 0 & 0 & 0 & 0 & 1\\ \hdashline 0 & 0 & 0 & \tan\beta & 0 \end{array}\right] \left\{\begin{array}{c} U_1\\ U_2\\ U_3\\ U_4\\ U_6 \end{array}\right\}$$

and the stiffness matrix $[\bar{K}]$ is the same as $[K]$, with the fifth and sixth rows and columns interchanged:

$$[\bar{K}] = \begin{bmatrix} K_{11}\cdots K_{14} & K_{16} & K_{15}\\ \vdots \qquad \vdots & \vdots & \vdots\\ K_{41}\cdots K_{44} & K_{46} & K_{45}\\ K_{61}\cdots K_{64} & K_{66} & K_{65}\\ K_{51}\cdots K_{54} & K_{56} & K_{55} \end{bmatrix}$$

The transformed stiffness matrix and force vector are, from (4.112b), of order 5×5 and 5×1, respectively. The elements of $[\hat{K}]$ and $\{\hat{F}\}$ are given by

$$\hat{K}_{ij}=\bar{K}_{ij} \quad (i,j=1,2,3,5)$$

$$\left.\begin{aligned}\hat{K}_{4i}&=\bar{K}_{4i}+\bar{K}_{6i}\tan\beta\\ \hat{K}_{i4}&=\bar{K}_{i4}+\bar{K}_{i6}\tan\beta\end{aligned}\right\}\quad (i=1,2,\ldots,5;\, i\neq 4)$$

$$\hat{K}_{44}=\bar{K}_{44}+(\bar{K}_{46}+\bar{K}_{64})\tan\beta+\bar{K}_{66}\tan^2\beta$$

$$\hat{F}_i=\bar{F}_i \quad (i=1,2,3,5), \qquad \hat{F}_4=\bar{F}_4+\bar{F}_6\tan\beta$$

During the imposition of the boundary conditions of the problem, the force $\hat{F}_4$ will be replaced by Q_0.

4.6 SUMMARY

In this chapter, finite element models of the classical (i.e., Euler–Bernoulli) and Timoshenko beam theories have been developed. The classical beam theory is governed by a fourth-order differential equation, and therefore results in a weak form whose primary variables contain the transverse deflection and its first derivative. Therefore, Hermite interpolation of the transverse deflection is required in order to impose the continuity of the deflection and its derivative at the nodes between elements. In the case of the Timoshenko beam theory, there are two second-order equations governing the transverse deflection and the rotation. The weak forms of the equations require Lagrange interpolation of the transverse deflection and rotation. Since the rotation function is like the (negative of the) derivative of the transverse deflection, the degree of the interpolation used for the rotation should be one less than that used for the transverse deflection. Such selective interpolation of the variables is called *consistent interpolation*. When the same interpolation functions are used to approximate the transverse deflection and the rotation, the resulting stiffness matrix is often too stiff—especially when the number of elements used is small—to yield good solutions. This is due to the inconsistency of interpolation of the variables, and the phenomenon is known as *shear locking*. It is overcome by the use of reduced integration to evaluate the stiffness coefficients associated with transverse shear strains. Both reduced integration elements (RIE) and consistent interpolation elements (CIE) have been developed here. It has been shown that consistent interpolation with linear approximation of the rotation and quadratic interpolation of the transverse deflection yields the same stiffness matrix as that obtained with a reduced integration element with linear approximation of the rotation as well as the deflection. However, the load vector of the consistent interpolation element, for a uniformly distributed transverse load, is equal to that of the Hermite cubic element of the classical beam theory.

The plane truss element and frame elements of the classical and Timoshenko beam theories have also been discussed. A plane truss element is a bar element that carries only axial loads and is oriented, in general, at an angle from the horizontal axis (the global x axis is taken to be horizontal). The bar element is first modified by adding columns and rows of zeros corresponding to the transverse displacements, so that it has two degrees of freedom (axial and transverse displacements) per node. The arbitrary plane truss element is then obtained by transforming the stiffness matrix and force vector from element coordinates to global coordinates, which are taken to be horizontal and vertical. Thus, a plane truss element has two degrees of freedom (horizontal and vertical displacements) per node, and carries only axial loads. The frame element is a superposition of the beam and bar elements, and has three degrees of freedom (axial displacement, transverse deflection, and rotation about an axis perpendicular to the plane of axial and transverse coordinates). The general plane frame element is oriented at an angle from the horizontal position, and its equations are obtained by transforming the equations of the frame element in local coordinates.

Finally, a procedure for including constraint conditions among the displacements and/or forces has been presented.

PROBLEMS

4.1–4.16. For the beam problems shown in Figs. P4.1–P4.16, use the Euler–Bernoulli beam element, and give:

(*a*) the assembled stiffness matrix and force vector;
(*b*) the specified global displacements and forces, and the equilibrium conditions;
(*c*) the condensed matrix equations for the primary unknowns (i.e., generalized displacements) and the secondary unknowns (i.e., generalized forces) separately.

Solve for the unknown displacements if there are less than four unknown displacements (use Cramer's rule), and evaluate the bending moment $M^c = EI\, d^2w/dx^2$ at point C using the finite element interpolation of w (when the condensed equations are not solved, express M^c in terms of the nodal values of

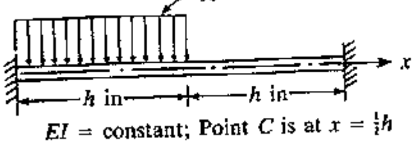

EI = constant; Point C is at $x = \frac{1}{2}h$

FIGURE P4.1

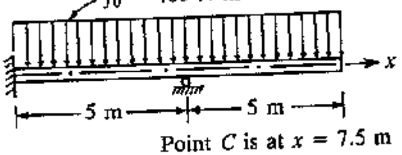

Point C is at $x = 7.5$ m

$E = 200$ GPa, $G = 79$ GPa, $A = 2.86 \times 10^{-3}$ m^2, $I = 20 \times 10^{-6}$ m^4

FIGURE P4.2

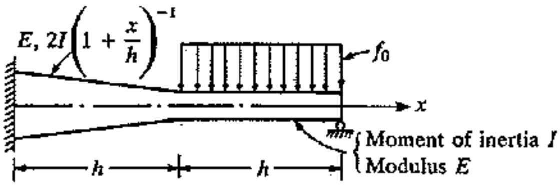

FIGURE P4.3

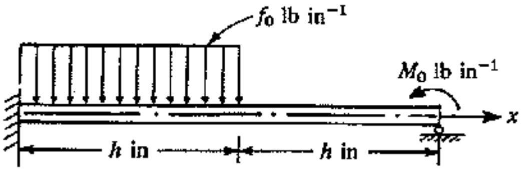

Point C is at $x = \frac{1}{2}h$; EI = constant (lb in^{-2})

FIGURE P4.4

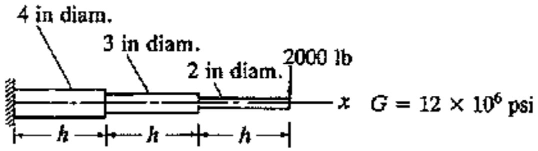

$h = 20$ in $E = 30 \times 10^6$ lb in^{-2}

$A = \pi d^2$; Point C is at $x = \frac{1}{2}h$; $I = \frac{1}{64}\pi d^4$

FIGURE P4.5

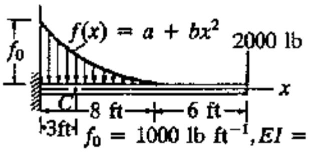

$f_0 = 1000$ lb ft^{-1}, EI = constant

FIGURE P4.6

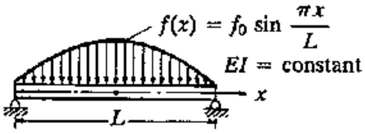

Point C is at $x = \frac{1}{2}L$

FIGURE P4.7

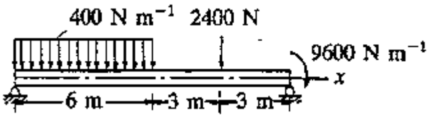

$EI = 20.7 \times 10^7$ N m^2

Point C is at $x = 3$ m

FIGURE P4.8

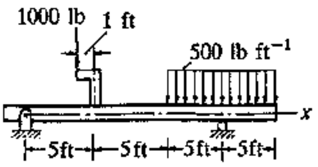

EI = constant

Point C is at x = 2.5 ft

FIGURE P4.9

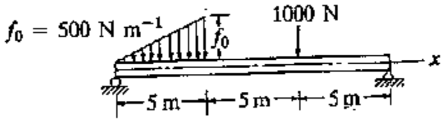

EI = constant

Point C is at $x = 7.5$ m

FIGURE P4.10

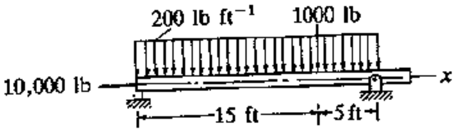

EI = constant

Point C is at $x = 7.5$ ft

FIGURE P4.11

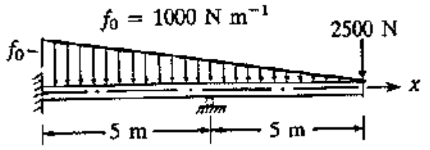

$EI = 2 \times 10^6$ N m^2; Point C is at $x = 7.5$ m

FIGURE P4.12

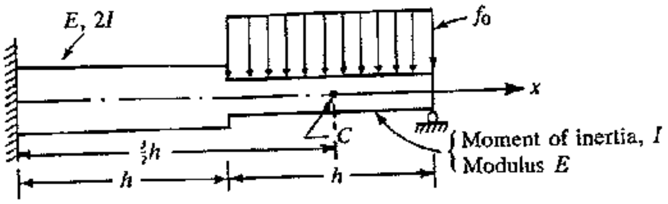

FIGURE P4.13

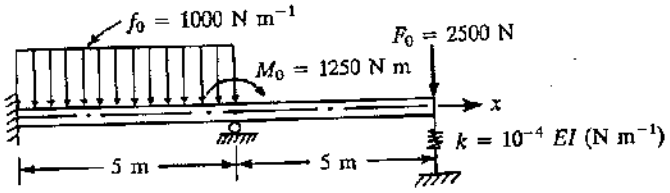

$EI = 2 \times 10^6$ N m^2; Point C is at $x = 7.5$ m

FIGURE P4.14

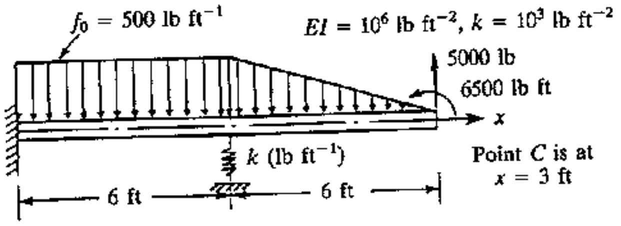

FIGURE P4.15

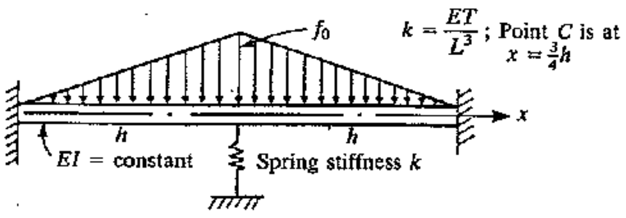

FIGURE P4.16

the appropriate element). Use the minimum number of elements required in each problem.

Answer: (Problem 4.1) $U_3 = f_0h^4/48EI$, $U_4 = -(f_0h^3/96EI)$.

4.17–4.21. Repeat Problems 4.1–4.5 using the Timoshenko beam element (with reduced integration). Use a value of $\frac{5}{6}$ for the shear correction factor. Note that accurate results can be obtained only with a sufficiently large number of elements, when compared with the Euler–Bernoulli element.

4.22. Consider a simply supported beam on an elastic foundation (with foundation modulus k) and subjected to uniform transverse loading. Determine the transverse displacement at midspan using one Euler–Bernoulli beam element.

4.23. Consider the axisymmetric bending of a linear elastic circular plate of constant thickness. The governing differential equation according to the thin plate assumption is (see Section 7.3 for additional details)

$$\frac{1}{r}\frac{d^2}{dr^2}\left(rD_{11}\frac{d^2w}{dr^2} + D_{12}\frac{dw}{dr}\right) - \frac{1}{r}\frac{d}{dr}\left(D_{12}\frac{d^2w}{dr^2} + \frac{D_{22}}{r}\frac{dw}{dr}\right) = f$$

where D_{11}, D_{12}, and D_{22} are the plate material stiffnesses (constant), w is the transverse deflection, and r is the radial coordinate. Develop

(*a*) the weak form of the equation over a typical element $\Omega^e = (r_A, r_B)$; the quantities in parentheses should not be integrated by parts;

(*b*) the finite element model of the equation in the form

$$[K^e]\{u^e\} = \{f^e\} + \{Q^e\}$$

Make sure that $[K^e]$ is symmetric (i.e., the bilinear form in (*a*) should be symmetric). Comment on the interpolation functions that are admissible for the element.

4.24. The differential equations governing axisymmetric bending of circular plates according to thick plate theory are

$$-\frac{1}{r}\frac{d}{dr}\left[rA_{55}\left(\Psi + \frac{dw}{dr}\right)\right] = f$$

$$-\frac{1}{r}\frac{d}{dr}\left[r\left(D_{11}\frac{d\Psi}{dr} + \frac{D_{12}}{r}\Psi\right)\right] + \frac{1}{r}\left(D_{12}\frac{\partial\Psi}{\partial r} + \frac{D_{22}}{r}\Psi\right) + A_{55}\left(\Psi + \frac{dw}{dr}\right) = 0$$

where A_{55}, D_{11}, D_{12}, and D_{22} are plate material stiffnesses, Ψ is the rotation function, w is the transverse deflection, and f is the transverse load. Develop

(*a*) the weak form of the equations over an element;

(*b*) the finite element model of the equations.

4.25. Solve the problem of a thin (radius-to-thickness ratio $r_0/t = 100$) clamped isotropic ($\nu = 0.3$) circular plate with uniformly distributed load using the element developed in Problem 4.23. Exploit symmetry, and use two thin plate (Euler–Bernoulli) elements in the computational domain.

4.26. Solve the circular plate problem of Problem 4.25 using a two-element mesh of Timoshenko elements (use $k = \frac{5}{6}$).

4.27. Consider the fourth-order equation (4.1) and its weak form (4.4). Suppose that a two-node element is employed, with *three* primary variables at each node: (w, θ, κ), where $\theta = dw/dx$ and $\kappa = d^2w/dx^2$. Show that the associated interpolation (Hermite) functions are given by

$$\phi_1 = \frac{2h^5 - 20x^3h^2 + 30x^4h - 12x^5}{2h^5}, \qquad \phi_2 = \frac{2h^5x - 12x^3h^3 + 16x^4h^2 - 6x^5h}{2h^5}$$

$$\phi_3 = \frac{x^2h^5 - 3x^3h^4 + 3x^4h^3 - x^5h^2}{2h^5}, \qquad \phi_4 = \frac{-20x^3h^2 + 30x^4h - 12x^5}{2h^5}$$

$$\phi_5 = \frac{8x^3h^3 - 14x^4h^2 + 6x^5h}{2h^5}, \qquad \phi_6 = \frac{x^3h^4 - 2x^4h^3 + x^5h^2}{2h^5}$$

where x is the element coordinate with the origin at node 1. Also compute the element stiffness matrix and force vector.

4.28. Consider the weak form (4.4*a*) of the Euler–Bernoulli beam element. Use a three-node element with *two* degrees of freedom (w, θ), where $\theta = -dw/dx$. Derive the Hermite interpolation functions for the element. Compute the element stiffness matrix and force vector.

4.29–4.36. For the truss and frame problems shown in Figs. P4.29–P4.36, give (*a*) the transformed element matrices; (*b*) the assembled element matrices; (*c*) the condensed matrix equations for the unknown generalized displacements and forces.

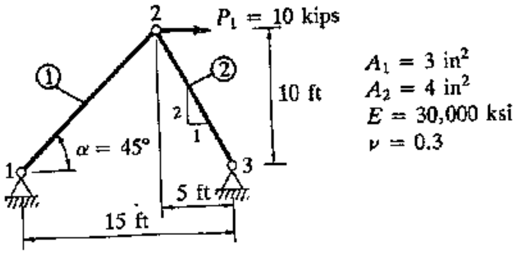

FIGURE P4.29

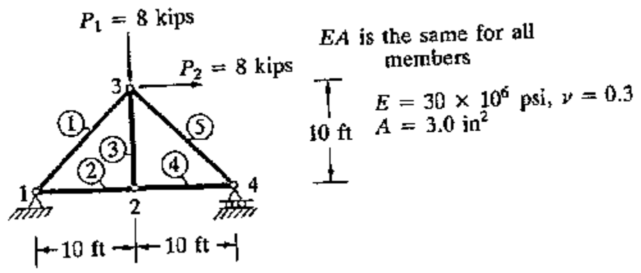

FIGURE P4.30

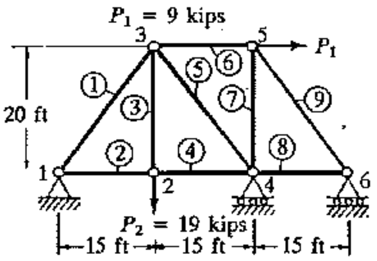

$E = 30 \times 10^6$ psi, $\nu = 0.3$
$A_1 = A_5 = A_9 = 5\ \text{in}^2$
$A_2 = A_4 = A_6 = A_8 = 6\ \text{in}^2$
$A_3 = A_7 = 2\ \text{in}^2$

FIGURE P4.31

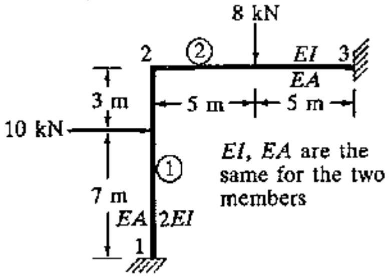

$\nu = 3.0$
$E = 200$ GPa
$A = 10^3\ \text{mm}^2$
$I = 10^3\ \text{mm}^4$

FIGURE P4.32

$\nu = 0.3$
$E = 30 \times 10^6$ psi
$A = 10\ \text{in}^2$
$I = 10\ \text{in}^4$

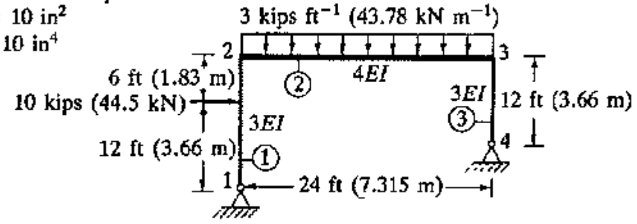

EA is the same for all members

FIGURE P4.33

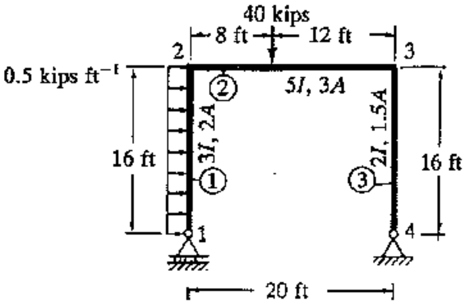

$\nu = 0.3$
$E = 3 \times 10^6$ psi
$I = 100\ \text{in}^4$
$A = 100\ \text{in}^2$

FIGURE P4.34

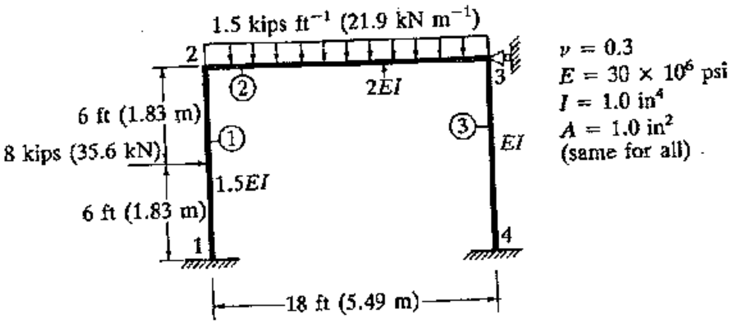

FIGURE P4.35

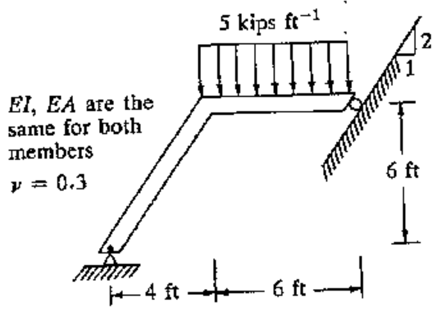

FIGURE P4.36

Answer: (Problem 4.29) $U_3 = 0.022973$ in, $U_4 = -0.002169$ in, $P_1^1 = -9428$ lb, $P_1^2 = 7454$ lb.

REFERENCES FOR ADDITIONAL READING

Budynas, R. G.: *Advanced Strength and Applied Stress Analysis*, McGraw-Hill, New York, 1977.

Dym, C. L., and I. H. Shames: *Solid Mechanics: A Variational Approach*, McGraw-Hill, New York, 1973.

Reddy, J. N.: *Energy and Variational Methods in Applied Mechanics*, John Wiley, New York, 1984.

Timoshenko, S. P., and J. N. Goodier: *Theory of Elasticity*, McGraw-Hill, New York, 1970.

Ugural, A. C., and S. K. Fenster: *Advanced Strength and Applied Elasticity*, Elsevier, New York, 1975.

Volterra, E., and J. H. Gaines: *Advanced Strength of Materials*, Prentice-Hall, Englewood Cliffs, NJ, 1971.

Wang, Chu-Kia, and C. G. Salmon: *Introductory Structural Analysis*, Prentice-Hall, Englewood Cliffs, NJ, 1984.

Willems, N., and W. M. Lucas, Jr.: *Structural Analysis for Engineers*, McGraw-Hill, New York, 1978.

CHAPTER 5

FINITE ELEMENT ERROR ANALYSIS

5.1 APPROXIMATION ERRORS

The errors introduced into the finite element solution of a given differential equation can be attributed to three basic sources:

1. *Domain approximation error,* which is due to the approximation of the domain.
2. *Quadrature and finite arithmetic errors,* which are due to the numerical evaluation of integrals and the numerical computation on a computer.
3. *Approximation error,* which is due to the approximation of the solution (see (iv) in the Note to Remark 10 in Section 3.2.7):

$$u \approx u_h = \sum_{I=1}^{N} U_I \Phi_I \tag{5.1}$$

   where U_I denotes the value of u at global node I, and Φ_I denotes the global interpolation function associated with global node I (see Fig. 3.3*b*).

In the one-dimensional problems discussed thus far, the domains considered have been straight lines. Therefore, no approximation of the domain has been necessary. In two-dimensional problems involving nonrectangular domains (as will be seen in Chapter 8), domain (or boundary) approximation errors are introduced into the finite element solutions. In general, these can be interpreted as errors in the specification of the data of the problem because we are now solving the given differential equation on a modified domain. As we refine the mesh, the domain is more accurately represented, and, therefore, the boundary approximation errors are expected to approach zero.

When finite element computations are performed on a computer, round-off errors in the computation of numbers and errors due to the numerical evaluation of integrals are introduced into the solution. In most linear problems with a reasonably small number of total degrees of freedom in the system, these errors are expected to be small (or zero when only a certain decimal point accuracy is desired).

The error introduced into the finite element solution U^e because of the approximation of the dependent variable u in an element Ω^e is inherent to any problem

$$u \approx u_h = \sum_{e=1}^{N} \sum_{i=1}^{n} u_i^e \psi_i^e = \sum_{I=1}^{M} U_I \Phi_I \tag{5.2}$$

where u_h is the finite element solution over the domain ($u_h = U^e$ in Ω^e), N is the number of elements in the mesh, M is the total number of global nodes, and n is the number of nodes in an element. We wish to know how the error $E = u - u_h$, measured in a meaningful way, behaves as the number of elements in the mesh is increased. It can be shown that the approximation error is zero for the single second-order and fourth-order equations with element-wise-constant coefficients [see (5.30)–(5.35)].

5.2 VARIOUS MEASURES OF ERRORS

There are several ways in which one can measure the "difference" (or distance) between any two functions u and u_h. The *pointwise error* is the difference of u and u_h at each point of the domain. One can also define the difference of u and u_h to be the maximum of all absolute values of the differences of u and u_h in the domain $\Omega = (a, b)$:

$$\|u - u_h\|_\infty = \max_{a \leq x \leq b} |u(x) - u_h(x)| \tag{5.3}$$

This measure of difference is called the *supmetric*. Note that the supmetric is a real number, whereas the pointwise error is a function and does not qualify as a distance or *norm* in a strict mathematical sense. The norm of a function is a non-negative real number.

More generally used measures (or norms) of the difference of two functions are the *energy norm* and the L_2 *norm* (pronounced "L-two norm"). For any square-integrable functions u and u_h defined on the domain $\Omega =$

(a, b), the two norms are defined by

$$\boxed{\begin{aligned} &\text{energy norm} \quad \|u-u_h\|_m = \left(\int_a^b \sum_{i=0}^{m} \left|\frac{d^i u}{dx^i} - \frac{d^i u_h}{dx^i}\right|^2 dx\right)^{1/2} && (5.4) \\ &L_2 \text{ norm} \quad \|u-u_h\|_0 = \left(\int_a^b |u-u_h|^2\, dx\right)^{1/2} && (5.5) \end{aligned}}$$

where $2m$ is the order of the differential equation being solved. The term "energy norm" is used to indicate that this norm contains the same-order derivatives as the quadratic functional (which, for most solid mechanics problems, denotes the energy) associated with the equation. Various measures of the distance between two functions are illustrated in Fig. 5.1. These definitions can easily be modified for two-dimensional domains.

5.3 CONVERGENCE OF SOLUTION

The finite element solution u_h in (5.1) is said to *converge in the energy norm* to the true solution u if

$$\boxed{\|u-u_h\|_m \leq ch^p \quad \text{for } p>0} \qquad (5.6)$$

where c is a constant independent of u and u_h, and h is the characteristic length of an element. The constant p is called the *rate of convergence*. Note that the convergence depends on h as well as on p; p depends on the order of the derivative of u in the weak form and the degree of the polynomials used to approximate u [see (5.15) below]. Therefore, the error in the approximation can be reduced either by reducing the size of the elements or increasing the degree of approximation. Convergence of the finite element solutions with mesh refinements (i.e., more of the same kind of elements are used) is termed *h-convergence*. Convergence with increasing degree of polynomials is called *p-convergence*.

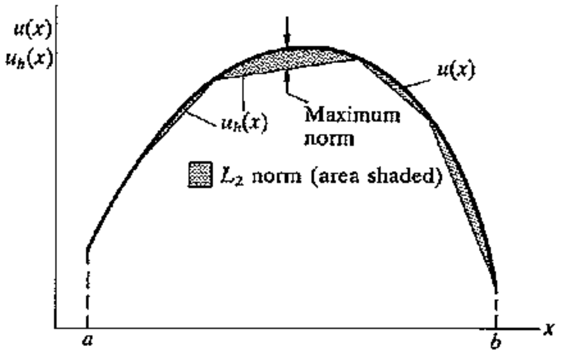

FIGURE 5.1
Different measures of error $E = u - u_h$ between the exact solution u and the finite element solution u_h. The maximum norm and the L_2 norm are illustrated.

5.4 ACCURACY OF THE SOLUTION

Returning to the question of estimating the approximation error, we consider a $2m$th-order differential equation in one dimension ($m = 1$, second-order equations; $m = 2$, fourth-order equations):

$$\sum_{i=1}^{m} (-1)^i \frac{d^i}{dx^i}\left(a_i \frac{d^i u}{dx^i}\right) = f \quad \text{for } 0 < x < L \tag{5.7}$$

where the coefficients $a_1(x)$ and $a_2(x)$ are assumed to be positive. Suppose that the essential boundary conditions of the problem are

$$u(0) = u(L) = 0 \quad (m = 1, 2) \tag{5.8}$$

$$\left(\frac{du}{dx}\right)\bigg|_{x=0} = \left(\frac{du}{dx}\right)\bigg|_{x=L} = 0 \quad (m = 2) \tag{5.9}$$

The variational formulation of (5.7) and (5.9) is given by

$$0 = \int_0^L \left(\sum_{i=1}^{m} a_i \frac{d^i v}{dx^i}\frac{d^i u}{dx^i} - vf\right) dx \tag{5.10}$$

The quadratic functional corresponding to the variational form is

$$I(u) = \int_0^L \frac{1}{2}\left[\sum_{i=1}^{m} a_i \left(\frac{d^i u}{dx^i}\right)^2\right] dx - \int_0^L uf\, dx \tag{5.11}$$

Now consider a finite element discretization of the domain by N elements of equal length h. If u_h denotes the finite element solution in (5.1), we have, from (5.11),

$$I(u_h) = \int_0^L \frac{1}{2}\left[\sum_{i=1}^{m} a_i \left(\frac{d^i u_h}{dx^i}\right)^2\right] dx - \int_0^L u_h f\, dx \tag{5.12}$$

In the following paragraphs, we show that the energy I associated with the finite element solution approaches the true energy from above, and we then give an error estimate. We confine our discussion, for the sake of simplicity, to the second-order equation ($m = 1$).

From (5.11) and (5.12), and

$$f = -\frac{d}{dx}\left(a_1 \frac{du}{dx}\right)$$

we have

$$\begin{aligned} I(u_h) - I(u) &= \int_0^L \frac{1}{2}\left[a_1\left(\frac{du_h}{dx}\right)^2 - a_1\left(\frac{du}{dx}\right)^2 + 2f(u - u_h)\right] dx \\ &= \int_0^L \left[\frac{a_1}{2}\left(\frac{du_h}{dx}\right)^2 - \frac{a_1}{2}\left(\frac{du}{dx}\right)^2 - \frac{d}{dx}\left(a_1 \frac{du}{dx}\right)(u - u_h)\right] dx \end{aligned}$$

$$
\begin{aligned}
&= \int_0^L \left\{ \frac{a_1}{2}\left[\left(\frac{du_h}{dx}\right)^2 - \left(\frac{du}{dx}\right)^2\right] + a_1\frac{du}{dx}\frac{d}{dx}(u-u_h)\right\} dx \\
&= \int_0^L \frac{a_1}{2}\left[\left(\frac{du_h}{dx}\right)^2 + \left(\frac{du}{dx}\right)^2 - 2\frac{du}{dx}\frac{du_h}{dx}\right] dx \\
&= \int_0^L \frac{a_1}{2}\left(\frac{du_h}{dx} - \frac{du}{dx}\right)^2 dx \geq 0
\end{aligned}
\tag{5.13}
$$

Thus,

$$\boxed{I(u_h) \geq I(u)} \tag{5.14}$$

The equality holds only for $u = u_h$. Equation (5.14) implies that the convergence of the energy of the finite element solution to the true energy is from above. Since the relation in (5.14) holds for any u_h, the inequality also indicates that the true solution u minimizes the energy. A similar relation can be established for the fourth-order equation ($m = 2$).

Now suppose that the finite element interpolation functions Φ_I ($I = 1, 2, \ldots, M$) are complete polynomials of degree k. Then the error in the energy norm can be shown to satisfy the inequality [see Reddy (1986, 1991), p. 401]

$$\boxed{\|e\|_m = \|u - u_h\|_m \leq ch^p, \qquad p = k + 1 - m > 0} \tag{5.15}$$

where c is a constant. This estimate implies that the error goes to zero as the pth power of h as h is decreased (or the number of elements is increased). In other words, the logarithm of the error in the energy norm versus the logarithm of h is a straight line whose slope is $k + 1 - m$. The greater the degree of the interpolation functions, the more rapid the rate of convergence. Note also that the error in the energy goes to zero at the rate of $k + 1 - m$; the error in the L_2 norm will decrease even more rapidly, namely, at the rate of $k + 1$, i.e., derivatives converge more slowly than the solution itself.

Error estimates of the type in (5.15) are very useful because they give an idea of the accuracy of the approximate solution, whether or not we know the true solution. While the estimate gives an idea of how rapidly the finite element solution converges to the true solution, it does not tell us when to stop refining the mesh. This decision rests with the analysts, because only they know what a reasonable tolerance is for the problems they are solving.

As an example of estimating the error in the approximation, i.e. (5.15), consider the linear (two-node) element for a second-order equation ($m = 1$). We have for an element

$$u_h = u_1(1 - s) + u_2 s \tag{5.16}$$

where $s = \bar{x}/h$ and $\bar{x}$ is the local coordinate. Since u_2 can be viewed as a function of u_1 via (5.16), one can expand u_2 in a Taylor series around node 1 to obtain

$$u_2 = u_1 + u_1' + \tfrac{1}{2}u_1'' + \ldots \tag{5.17}$$

where $u' \equiv du/ds$. Substituting this into (5.16), we obtain

$$u_h = u_1 + u_1' s + \tfrac{1}{2} u_1'' s + \dots \tag{5.18}$$

Expanding the true solution in a Taylor series about node 1, we obtain

$$u = u_1 + u_1' s + \tfrac{1}{2} u_1'' s^2 + \dots \tag{5.19}$$

Therefore, we have, from (5.18) and (5.19),

$$|u_h - u| \leq \frac{1}{2}(s - s^2) \max_{0 \leq s \leq 1} \left|\frac{d^2u}{ds^2}\right| = \frac{1}{2}(s - s^2) h^2 \max_{0 \leq \bar{x} \leq h} \left|\frac{d^2u}{d\bar{x}^2}\right| \tag{5.20}$$

$$\left|\frac{d}{d\bar{x}}(u_h - u)\right| \leq \frac{1}{2} h \max_{0 \leq \bar{x} \leq h} \left|\frac{d^2u}{d\bar{x}^2}\right| \tag{5.21}$$

These lead to

$$\|u - u_h\|_0 \leq c_1 h^2, \qquad \|u - u_h\|_1 \leq c_2 h \tag{5.22}$$

where the constants c_1 and c_2 depend only on the length L of the domain.

The reader may carry a similar error analysis for the fourth-order equation.

Example 5.1. Here we consider a computational example to verify the error estimates in (5.22). Consider the differential equation

$$-\frac{d^2u}{dx^2} = 2 \quad \text{for } 0 < x < 1 \tag{5.23}$$

with

$$u(0) = u(1) = 0$$

The exact solution is

$$u(x) = x(1 - x) \tag{5.24}$$

while the finite element solutions are, for $N = 2$,

$$u_h = \begin{cases} h^2(x/h) & \text{for } 0 \leq x \leq h \\ h^2(2 - x/h) & \text{for } h \leq x \leq 2h \end{cases}$$

for $N = 3$,

$$u_h = \begin{cases} 2h^2(x/h) & \text{for } 0 \leq x \leq h \\ 2h^2(2 - x/h) + 2h^2(x/h - 1) & \text{for } h \leq x \leq 2h \\ 2h^2(3 - x/h) & \text{for } 2h \leq x \leq 3h \end{cases} \tag{5.25}$$

and, for $N = 4$,

$$u_h = \begin{cases} 3h^2(x/h) & \text{for } 0 \leq x \leq h \\ 3h^2(2 - x/h) + 4h^2(x/h - 1) & \text{for } h \leq x \leq 2h \\ 4h^2(3 - x/h) + 3h^2(x/h - 2) & \text{for } 2h \leq x \leq 3h \\ 3h^2(4 - x/h) & \text{for } 3h \leq x \leq 4h \end{cases}$$

TABLE 5.1
The L_2 error and error in the energy norm of the solution to (5.23) (Example 5.1)

h	$\log_{10} h$	$\|e\|_0$	$\log_{10}\|e\|_0$	$\|e\|_1$	$\log_{10}\|e\|_1$
$\frac{1}{2}$	−0.301	0.04564	−1.341	0.2887	−0.5396
$\frac{1}{3}$	−0.477	0.02028	−1.693	0.1925	−0.7157
$\frac{1}{4}$	−0.601	0.01141	−1.943	0.1443	−0.8406

For the two-element case ($h = 0.5$), the errors are given by

$$\begin{aligned} \|u-u_h\|_0^2 &= \int_0^h (x-x^2-hx)^2\,dx + \int_h^{2h} (x-x^2-2h^2+xh)^2\,dx \\ &= 0.002083 \\ \left\|\frac{du}{dx}-\frac{du_h}{dx}\right\|_0^2 &= \int_0^h (1-2x-h)^2\,dx + \int_h^{2h} (1-2x+h)^2\,dx \\ &= 0.08333 \end{aligned} \tag{5.26}$$

Similar calculations can be performed for $N=3$ and $N=4$. Table 5.1 gives the errors for $N=2$, 3, and 4.

Plots of $\log\|e\|_0$ and $\log\|e\|_1$ versus $\log h$ show that (see Fig. 5.2)

$$\log\|e\|_0 = 2\log h + \log c_1, \qquad \log\|e\|_1 = \log h + \log c_2 \tag{5.27}$$

In other words, the rate of convergence of the finite element solution is 2 in the L_2 norm and 1 in the energy norm, verifying the estimates in (5.22).

Much of the discussion presented in this section can be carried over to curved elements and two-dimensional elements. When the former, i.e.,

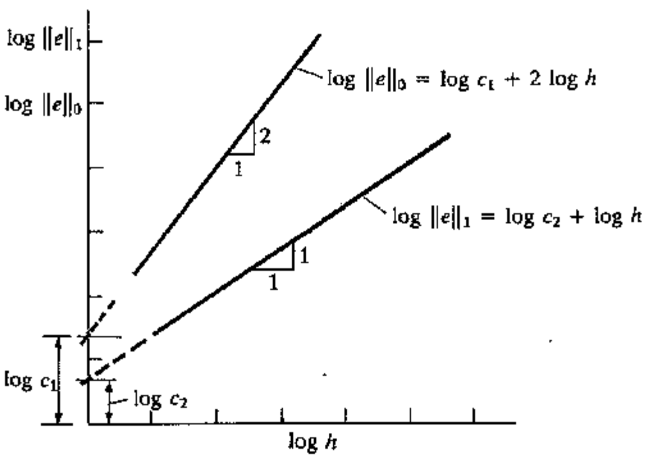

FIGURE 5.2
Plots of the L_2 and energy norms of errors versus the mesh size. The log–log plots give the rates of convergence in the respective norms. The rates of convergence are given by the slopes of the lines (the plots shown are for linear elements).

elements with nonstraight sides, are involved, the error estimate also depends on the Jacobian of the transformation. Because of the introductory nature of the present study, these topics are not discussed here. Interested readers can consult Cairlet (1978), Wait and Mitchell (1985), Oden and Reddy (1982), Strang and Fix (1973), and Reddy (1986, 1991).

As noted earlier, in the case of both second- and fourth-order equations in a single unknown and with constant coefficients, the error between the exact solution and the finite element solution at the nodes is zero. This is not accidental. We can prove that when the coefficients a and b are constant, the finite element solutions of the equations

$$-\frac{d}{dx}\left(a\frac{du}{dx}\right)=f(x) \tag{5.28}$$

$$\frac{d^2}{dx^2}\left(b\frac{d^2u}{dx^2}\right)=f(x) \tag{5.29}$$

coincide with the exact solutions at the nodes. The proof is presented below for the second-order equation.

Consider the equation

$$-a\frac{d^2u}{dx^2}=f \quad \text{for } 0<x<L \tag{5.30}$$

with

$$u(0)=0, \qquad u(L)=0 \tag{5.31}$$

The global finite element solution is given by ($U_1=U_N=0$)

$$u_h=\sum_{I=2}^{N-1} U_I\Phi_I \tag{5.32}$$

where Φ_I are the linear global interpolation functions shown in Fig. 3.3(b). From the definition of the variational problem, we have

$$\int_0^L\left(\frac{d\Phi_I}{dx}\frac{du_h}{dx}-\Phi_I\hat{f}\right)dx=0 \quad \text{for each } I=2,\ldots,N-1 \tag{5.33}$$

where $\hat{f}=f/a$. The exact solution also satisfies this equation. Hence, by subtracting the finite element equation (5.33) from the exact solution, we obtain

$$\int_0^L\left(\frac{du}{dx}-\frac{du_h}{dx}\right)\frac{d\Phi_I}{dx}\,dx=0 \quad (I=2,\ldots,N-1)$$

Since we have $\Phi_I=0$ for $x\geqslant(I+1)h$ and $x\leqslant(I-1)h$, and $d\Phi_I/dx=1/h$ for $(I-1)h\leqslant x\leqslant Ih$ and $d\Phi_I/dx=-1/h$ for $Ih\leqslant x\leqslant(I+1)h$, it follows that

$$\int_{(I-1)h}^{Ih}\left(\frac{du}{dx}-\frac{du_h}{dx}\right)\frac{1}{h}\,dx+\int_{Ih}^{(I+1)h}\left(\frac{du}{dx}-\frac{du_h}{dx}\right)\left(-\frac{1}{h}\right)dx=0 \tag{5.34}$$

for $I = 2, 3, \ldots, N-1$. Denoting $\epsilon(x) = u(x) - u_h(x)$, we have

$$\frac{1}{h}(\epsilon_I - \epsilon_{I-1}) + \left(-\frac{1}{h}\right)(\epsilon_{I+1} - \epsilon_I) = 0$$

or

$$\frac{1}{h}(-\epsilon_{I-1} + 2\epsilon_I - \epsilon_{I+1}) = 0 \quad (I = 2, 3, \ldots, N-1) \tag{5.35}$$

where $\epsilon_I = \epsilon(Ih)$ (i.e., the value of ϵ at $x = Ih$). Since $\epsilon_0 = \epsilon_N = 0$ (because both u and u_h satisfy the essential boundary conditions), it follows from the above homogeneous equations that the solution is trivial: $\epsilon_1 = \epsilon_2 = \ldots = \epsilon_{N-1} = 0$. This implies that the finite element solution coincides with the exact solution at the nodes.

5.5 SUMMARY

Various types of errors in the finite element approximation of differential equations have been discussed and different measures of the error (or difference between two functions) have been defined. Error estimates for the second-order differential equations have been presented. It has been shown that the finite element solutions of differential equations with constant coefficients are exact at the nodes. The proof has been presented for a single second-order differential equation. This result does not hold for coupled second-order differential equations with constant coefficients.

PROBLEMS

5.1. Show that the error estimate for the fourth-order equation (4.1) is given by

$$\|w - w_h\|_2 \leq ch^2$$

where c is a constant, w_h is the finite element solution obtained by using the Hermite cubic interpolation, and w is the exact solution of the problem.

5.2. Consider a Lagrange quadratic element extending between $x = -h$ and $x = h$ and having the three nodes at $x = -h$, $x = \alpha h$, and $x = h$. The transformation between x and a normalized coordinate ξ is given by

$$x = h[\xi + \alpha(1 - \xi^2)]$$

If the dependent variable u is interpolated by a quadratic polynomial in ξ, show that the error $\epsilon = u - u_h$ is given by

$$\|\epsilon\|_1 \leq \frac{c\alpha}{1 - 2\alpha} h$$

Hint: First show that

$$|u - u_h| \leq c \max_{-1 \leq \xi \leq 1} \left|\frac{d^3u}{d\xi^3}\right|$$

and then

$$\frac{d^3u}{d\xi^3} = -6h^2\alpha(1 - 2\alpha\xi)\frac{d^2u}{dx^2} + h^3(1 - 2\alpha\xi)^3\frac{d^3u}{dx^3}, \qquad \frac{d}{dx} = \frac{1}{h(1 - 2\alpha\xi)}\frac{d}{d\xi}$$

5.3. The *error* in the finite element approximation is often measured in terms of the *energy* associated with the problem under consideration. For the second-order problem considered in (3.1), the energy of the problem is given by the functional

$$I = \sum_{e=1}^{N} I_e(u_e) \tag{i}$$

where N is the total number of elements in the finite element mesh and I_e is the functional given in (3.11). The error in the solution is defined to be the difference between the true or exact solution u_0 and the finite element solution u_h, and the error in the energy is defined by

$$E = u_0 - u_h, \qquad \|E\|_1 = \sum_{e=1}^{N} I_e(E) \tag{ii, iii}$$

If the finite element approximation u_h is an interpolant of the true solution u_0, determine the error in the solution and the energy of (3.1) when (*a*) u_h is a linear interpolant and (*b*) u_h is a quadratic interpolant.

Hint: Use pertinent references at the end of the chapter to determine the interpolation error in terms of the mesh parameter (spacing) h, and use the result (iii) to determine the error in the energy in the form

$$\|E_1\| = c_0 h^p$$

where c_0 and p are constants; p determines the rate of convergence ($p > 0$) or divergence ($p < 0$).

REFERENCES FOR ADDITIONAL READING

Ciarlet, P. G.: *The Finite Element Method for Elliptic Problems,* North-Holland, Amsterdam, 1978.

Davies, A. L.: *The Finite Element Method, A First Approach,* Clarendon Press, Oxford, 1980.

Oden, J. T., and J. N. Reddy: *An Introduction to the Mathematical Theory of Finite Elements,* Wiley-Interscience, New York, 1982.

Reddy, J. N.: *Applied Functional Analysis and Variational Methods in Engineering,* McGraw-Hill, New York, 1986; Krieger, Melbourne, FL, 1991.

Rektorys, K.: *Variational Methods in Mathematics, Science and Engineering,* Reidel, Boston, 1977.

Strang, G., and G. J. Fix: *An Analysis of the Finite Element Method,* Prentice-Hall, Englewood Cliffs, NJ, 1973.

Wait, R., and A. R. Mitchell: *Finite Element Analysis and Applications,* John Wiley, New York, 1985.

CHAPTER 6

EIGENVALUE AND TIME-DEPENDENT PROBLEMS

6.1 EIGENVALUE PROBLEMS

6.1.1 Introduction

Determination of the values of the parameter λ such that the equation

$$A(u) = \lambda B(u) \tag{6.1}$$

where A and B denote linear differential operators, has nontrivial solutions u is called an *eigenvalue problem*. The values of λ are called *eigenvalues* and the associated functions u are called *eigenfunctions*. For example, the equation

$$-\frac{d^2u}{dx^2} = \lambda u, \quad \text{with } A = \frac{d^2}{dx^2}, \quad B = 1$$

which arises in connection with the axial oscillations of a bar or the transverse oscillations of a cable, constitutes an eigenvalue problem. Here λ denotes the square of the frequency of vibration ω.

In general, the determination of the eigenvalues is of engineering as well as mathematical importance. In structural problems, the eigenvalues denote either natural frequencies or buckling loads. In fluid mechanics and heat transfer, eigenvalue problems arise in connection with the determination of the homogeneous parts of the solution. In these cases, eigenvalues often denote amplitudes of the Fourier components making up the solution. Eigenvalues are also useful in determining the stability characteristics of temporal schemes, as discussed in Section 6.2.

In this section, we develop finite element models of eigenvalue problems. In view of the close similarity between the equations of eigenvalue and boundary value problems, the steps involved in the construction of their finite element models are entirely analogous. Differential eigenvalue problems are reduced to algebraic eigenvalue problems by means of the finite element approximation. The methods of solution of algebraic eigenvalue problems are then used to solve for the eigenvalues and eigenvectors.

6.1.2 Formulation of Eigenvalue Problems

Consider the parabolic partial differential equation

$$\rho c A \frac{\partial u}{\partial t} - \frac{\partial}{\partial x}\left(kA \frac{\partial u}{\partial x}\right) = q(x, t) \tag{6.2}$$

which governs transient heat transfer in one-dimensional systems (e.g., a plane wall). Here u denotes the temperature, k the thermal conductivity, ρ the density, A the cross-sectional area, c the specific heat, and q the heat generation per unit length. The homogeneous solution (i.e., the solution when $q = 0$) of (6.2) is often sought in the form of a product of a function of x and a function of t (i.e., through the *separation of variables* technique):

$$u(x, t) = S(x)T(t) \tag{6.3}$$

Substitution of this assumed form of solution into the homogeneous form of (6.2) gives

$$\rho c A S \frac{dT}{dt} - \frac{d}{dx}\left(kA \frac{dS}{dx}\right)T = 0$$

Separating the variables (assuming that $\rho c A$ and kA are functions of x only),

$$\frac{1}{T}\frac{dT}{dt} = \frac{1}{\rho c A}\frac{1}{S}\frac{d}{dx}\left(kA \frac{dS}{dx}\right) \tag{6.4}$$

Note that the left-hand side of this equation is a function of t only while the right-hand side is a function of x only. For two functions of two independent variables to always be equal, both must be equal to the same constant, say $-\lambda$:

$$\frac{1}{T}\frac{dT}{dt} = \frac{1}{\rho c A}\frac{1}{S}\frac{d}{dx}\left(kA \frac{dS}{dx}\right) = -\lambda \tag{6.5a}$$

or

$$\frac{dT}{dt} = -\lambda T, \qquad -\frac{d}{dx}\left(kA \frac{dS}{dx}\right) - \lambda \rho c A S = 0 \tag{6.5b}$$

The negative sign in the constant λ is based on the physical requirement that the solution $S(x)$ be harmonic in x while $T(t)$ must decay exponentially with increasing t. The solution of the first equation is $T = T_0 e^{-\lambda t}$. When k, A, ρ, and c are constants, the solution of the second equation is

$$S(x) = B_1 \sin \sqrt{\bar{\lambda}}x + B_2 \cos \sqrt{\bar{\lambda}}x, \qquad \bar{\lambda} = \frac{\rho c}{k}\lambda$$

The constants λ, T_0, B_1, and B_2 are determined with the help of initial and boundary conditions.

In view of the above discussion, the solution of (6.2) is of the form

$$u(x, t) = U(x)e^{-\lambda t} \tag{6.6}$$

This form is consistent with the solutions we derived above, with $U(x) \equiv S(x)T_0$. Substituting (6.6) into the homogeneous form of (6.2), we obtain

$$-\frac{d}{dx}\left(kA\frac{dU}{dx}\right)e^{-\lambda t} - \lambda\rho c A\, U(x)e^{-\lambda t} = 0$$

or

$$\boxed{-\frac{d}{dx}\left(kA\frac{dU}{dx}\right) - \lambda\rho c A\, U = 0} \tag{6.7}$$

We wish to determine λ and nonzero $U(x)$ such that (6.7) holds and the boundary conditions of the problem are met. Equation (6.7) describes an eigenvalue problem, λ being the eigenvalue and $U(x)$ the eigenfunction.

The axial motion of a bar can be described by the hyperbolic equation

$$\rho A\frac{\partial^2 u}{\partial t^2} - \frac{\partial}{\partial x}\left(EA\frac{\partial u}{\partial x}\right) = q(x, t) \tag{6.8}$$

Here u denotes the axial displacement, E the modulus of elasticity, A the cross-sectional area, ρ the density, and q the axial force per unit length.

The natural axial oscillations of the bar are periodic, and they can be determined by assuming a solution of the form

$$u(x, t) = U(x)e^{-i\omega t}, \quad \text{with } i = \sqrt{-1} \tag{6.9}$$

where ω denotes the frequency of natural axial motion (or vibration), and $U(x)$ denotes the configuration of the bar, called the *mode shape*, during the vibration. For each value of ω, there is an associated mode shape. Substitution of (6.9) into the homogeneous form of (6.8) gives

$$\left[-\rho A\omega^2 U - \frac{d}{dx}\left(EA\frac{dU}{dx}\right)\right]e^{-i\omega t} = 0$$

or

$$\boxed{-\frac{d}{dx}\left(EA\frac{dU}{dx}\right)-\lambda\rho AU=0} \tag{6.10}$$

where $\lambda=\omega^2$. Equation (6.10) is an eigenvalue problem, which involves determining the square of natural frequencies λ and mode shapes U. This equation also arises in the solution of (6.8) by means of separation of variables, as discussed in connection with the parabolic equation. Note that (6.7) and (6.10) are of the same form. Only the coefficients are different.

Equations similar to (6.10) can be derived for the transverse vibrations of a beam using the Euler–Bernoulli or the Timoshenko beam theories. For the Euler–Bernoulli beam theory, we assume

$$w(x,t)=W(x)e^{-i\omega t}$$

where ω is the frequency of natural transverse motion and $W(x)$ is the mode shape of the transverse motion. Substitution of this form into the equation of motion of the Euler–Bernoulli beam theory

$$\rho A\frac{\partial^2 w}{\partial t^2}+\frac{\partial^2}{\partial x^2}\left(EI\frac{\partial^2 w}{\partial x^2}\right)=0 \tag{6.11}$$

gives

$$\boxed{\frac{d^2}{dx^2}\left(EI\frac{d^2W}{dx^2}\right)-\lambda\rho AW=0} \tag{6.12}$$

where $\lambda=\omega^2$. For the Timoshenko beam theory, we assume

$$w(x,t)=W(x)e^{-i\omega t},\qquad \Psi(x,t)=S(x)e^{-i\omega t}$$

and substitute into the equations of motion of the theory

$$\begin{aligned}\rho A\frac{\partial^2 w}{\partial t^2}-\frac{\partial}{\partial x}\left[GAK\left(\frac{\partial w}{\partial x}+\Psi\right)\right]&=0\\ \rho I\frac{\partial^2\Psi}{\partial t^2}-\frac{\partial}{\partial x}\left(EI\frac{\partial\Psi}{\partial x}\right)+GAK\left(\frac{\partial w}{\partial x}+\Psi\right)&=0\end{aligned} \tag{6.13}$$

to obtain the eigenvalue problem

$$\boxed{\begin{aligned}-\frac{d}{dx}\left[GAK\left(\frac{dW}{dx}+S\right)\right]-\lambda\rho AW&=0\\ -\frac{d}{dx}\left(EI\frac{dS}{dx}\right)+GAK\left(\frac{dW}{dx}+S\right)-\lambda\rho IS&=0\end{aligned}} \tag{6.14}$$

The study of buckling of beam-columns also leads to an eigenvalue problem. For example, the equation governing the equilibrium of a beam subjected to an axial force P, according to the Euler–Bernoulli beam theory, is

$$\boxed{\frac{d^2}{dx^2}\left(EI\frac{d^2w}{dx^2}\right)+P\frac{d^2w}{dx^2}=0} \tag{6.15}$$

which is an eigenvalue equation with $\lambda = P$ as the eigenvalue, which represents the buckling load. Often one is interested only in the smallest value of λ, called the *critical buckling load.* For the Timoshenko beam theory, the buckling equations are

$$\boxed{\begin{aligned}&-\frac{d}{dx}\left[GAK\left(\frac{dw}{dx}+\Psi\right)\right]+P\frac{d^2w}{dx^2}=0\\&-\frac{d}{dx}\left(EI\frac{d\Psi}{dx}\right)+GAK\left(\frac{dw}{dx}+\Psi\right)=0\end{aligned}} \tag{6.16}$$

This completes the formulation of eigenvalue problems associated with the model problems studied in this book. In the next section, we develop the finite element models of (6.7), (6.10), (6.12), and (6.14)–(6.16).

6.1.3 Finite Element Models

An examination of the eigenvalue equations derived in the previous section shows that they are a special case of the equations studied in Chapters 3 and 4. For example, consider

$$-\frac{d}{dx}\left(a\frac{du}{dx}\right)=f \tag{6.17}$$

The eigenvalue equation associated with this is

$$-\frac{d}{dx}\left(a\frac{dU}{dx}\right)=\lambda c_0 U \tag{6.18}$$

where a and c_0 are quantities that depend on the physical problem: for heat transfer,

$$a = kA, \qquad c_0 = \rho c A$$

where c is the specific heat, while, for a bar,

$$a = EA, \qquad c_0 = \rho A$$

Similarly, the eigenvalue equations associated with the transverse vibrations and buckling of beams are special cases of their static counterparts. Therefore, the finite element models of the eigenvalue equations can readily be developed. It is important to note that the spatial derivative operators of the static (i.e., non-time-dependent) and eigenvalue equations are the same. The difference between (6.17) and (6.18) is that, in place of the source term f, we have $\lambda c_0 U$ in the eigenvalue equations. This difference is responsible for another coefficient matrix, in addition to the usual coefficient matrix $[K^e]$, in the eigenvalue problems. The derivation of the finite element models of eigenvalue equations is presented next.

Over a typical element Ω^e, we seek a finite element approximation of u in the form

$$U=\sum_{j=1}^{n} u_j^e \psi_j^e(x) \tag{6.19}$$

The weak form of (6.18) is

$$0=\int_{x_A}^{x_B}\left(\frac{dw}{dx}a\frac{dU}{dx}-\lambda c_0 wU\right)dx-Q_1 w(x_A)-Q_n w(x_B) \tag{6.20a}$$

where w is the weight function, and Q_1 and Q_n are the usual secondary variables ($Q_i^e=0,\ i\neq 1, n$)

$$Q_1=-\left(a\frac{dU}{dx}\right)\bigg|_{x_A},\qquad Q_n=\left(a\frac{dU}{dx}\right)\bigg|_{x_B} \tag{6.20b}$$

Substitution of the finite element approximation into the weak form gives the finite element model of the eigenvalue equation (6.18):

$$[K^e]\{u^e\}-\lambda[M^e]\{u^e\}=\{Q^e\} \tag{6.21a}$$

where

$$K_{ij}^e=\int_{x_A}^{x_B} a\frac{d\psi_i^e}{dx}\frac{d\psi_j^e}{dx}\,dx,\qquad M_{ij}^e=\int_{x_A}^{x_B} c_0\psi_i^e\psi_j^e\,dx \tag{6.21b}$$

Equation (6.21a) represents the finite element model of the eigenvalue equations (6.18) and (6.10).

The finite element model of (6.12) is

$$[K^e]\{u^e\}-\lambda[M^e]\{u^e\}=\{Q^e\} \tag{6.22a}$$

where $\{u^e\}$ and $\{Q^e\}$ are the columns of nodal generalized displacement and force degrees of freedom of the Euler–Bernoulli beam element:

$$\{u^e\}=\begin{Bmatrix} W_1^e \\ \left(-\dfrac{dW}{dx}\right)_1^e \\ W_2^e \\ \left(-\dfrac{dW}{dx}\right)_2^e \end{Bmatrix};\qquad \{Q^e\}=\begin{Bmatrix} \left[\dfrac{d}{dx}\left(EI\dfrac{d^2W}{dx^2}\right)\right]_1 \\ \left(EI\dfrac{d^2W}{dx^2}\right)_1 \\ \left[-\dfrac{d}{dx}\left(EI\dfrac{d^2W}{dx^2}\right)\right]_2 \\ \left(-EI\dfrac{d^2W}{dx^2}\right)_2 \end{Bmatrix} \tag{6.22b}$$

where the subscripts 1 and 2 refer to element nodes 1 and 2 (at $x=x_A$ and $x=x_B$). The matrices $[K^e]$ and $[M^e]$, known as the *stiffness* and *mass matrices*, are defined by

$$K_{ij}^e=\int_{x_A}^{x_B} EI\frac{d^2\phi_i^e}{dx^2}\frac{d^2\phi_j^e}{dx^2}\,dx, \qquad M_{ij}^e=\int_{x_A}^{x_B}\rho A\phi_i^e\phi_j^e\,dx \tag{6.22c}$$

where ϕ_i^e are the Hermite cubic interpolation functions (see Chapter 4 for details).

The finite element model of (6.14), with equal interpolation of w and S, is

$$\begin{bmatrix}[K^{11}] & [K^{12}]\\ [K^{12}]^T & [K^{22}]\end{bmatrix}\begin{Bmatrix}\{w^e\}\\ \{S^e\}\end{Bmatrix}-\lambda\begin{bmatrix}[M^{11}] & [0]\\ [0] & [M^{22}]\end{bmatrix}\begin{Bmatrix}\{w^e\}\\ \{S^e\}\end{Bmatrix}=\begin{Bmatrix}\{V^e\}\\ \{M^e\}\end{Bmatrix} \tag{6.23a}$$

where

$$K_{ij}^{11}=\int_{x_A}^{x_B} GAK\frac{d\psi_i^e}{dx}\frac{d\psi_j^e}{dx}\,dx, \qquad K_{ij}^{12}=\int_{x_A}^{x_B} GAK\frac{d\psi_i^e}{dx}\psi_j^e\,dx$$

$$K_{ij}^{22}=\int_{x_A}^{x_B}\left(GAK\,\psi_i^e\psi_j^e+EI\frac{d\psi_i^e}{dx}\frac{d\psi_j^e}{dx}\right)dx$$

$$M_{ij}^{11}=\int_{x_A}^{x_B}\rho A\psi_i^e\psi_j^e\,dx, \qquad M_{ij}^{22}=\int_{x_A}^{x_B}\rho I\psi_i^e\psi_j^e\,dx \tag{6.23b}$$

$$V_1^e=\left[-GAK\left(\frac{dW}{dx}+S\right)\right]_1, \qquad V_2^e=\left[GAK\left(\frac{dW}{dx}+S\right)\right]_2$$

$$M_1^e=\left(-EI\frac{dS}{dx}\right)_1, \qquad M_2^e=\left(EI\frac{dS}{dx}\right)_2$$

Note, that for sufficiently large ratios of length L to height H of the beam, the Timoshenko beam element gives the results of the Euler–Bernoulli beam element. For example, for $L/H \geqslant 100$, the effect of shear deformation is negligible, and both elements give approximately the same solution.

The finite element models of (6.15) and (6.16) are the same as those in (6.22*a*) and (6.23*a*), respectively, with $\lambda = P$, and $[M^e]$ and $[M^{11}]$ (and $[M^{22}]=[0]$) replaced by $[G^e]$ and $[G^{11}]$, respectively, where

$$G_{ij}^e=\int_{x_A}^{x_B}\frac{d\phi_i^e}{dx}\frac{d\phi_j^e}{dx}\,dx, \qquad G_{ij}^{11}=\int_{x_A}^{x_B}\frac{d\psi_i^e}{dx}\frac{d\psi_j^e}{dx}\,dx \tag{6.24}$$

The coefficient matrix $[G^e]$ is known as the *stability matrix.*

The numerical form of the stiffness matrices $[K^e]$ were given in the previous sections [see, e.g., (3.34*a*), (3.40*a*), (4.15), and (4.98)]. Expressions for the mass matrices M_{ij}^e and stability matrices G_{ij}^e for the Lagrange elements are also available from the previous derivations [see, e.g., (3.34*a*) and (3.35)]. The mass and stability matrices for the Hermite cubic interpolation,

$$M_{ij}^e=\int_{x_A}^{x_B} c_e\phi_i^e\phi_j^e\,dx, \qquad G_{ij}^e=\int_{x_A}^{x_B} a_e\frac{d\phi_i^e}{dx}\frac{d\phi_j^e}{dx}\,dx \tag{6.25}$$

can be evaluated numerically for element-wise-constant values of c_e and a_e:

$$[M^e] = \frac{ch}{420}\begin{bmatrix} 156 & -22h & 54 & 13h \\ -22h & 4h^2 & -13h & -3h^2 \\ 54 & -13h & 156 & 22h \\ 13h & -3h^2 & 22h & 4h^2 \end{bmatrix} \tag{6.26a}$$

$$[G^e] = \frac{a}{30h}\begin{bmatrix} 36 & -3h & -36 & -3h \\ -3h & 4h^2 & 3h & -h^2 \\ -36 & 3h & 36 & 3h \\ -3h & -h^2 & 3h & 4h^2 \end{bmatrix} \tag{6.26b}$$

The assembly procedure and imposition of boundary conditions in the eigenvalue analysis remains the same as for static problems. The boundary conditions are necessarily homogeneous.

The standard error estimates for the fundamental eigenvalues and eigenfunctions of the problems discussed here are [see Strang and Fix (1973)]

$$\boxed{\begin{gathered} \lambda^{(0)} \leqslant \lambda^h \leqslant \lambda^{(0)} + ch^{2(k+1-m)}[\lambda^{(0)}]^{(k+1)/m} \\ \|\mathbf{u}^0 - \mathbf{u}^h\|_m \leqslant ch^{k+1-m}[\lambda^{(0)}]^{(k+1)/2m} \end{gathered}} \tag{6.27}$$

where $(\lambda^{(0)}, \mathbf{u}^0)$ is the exact solution, $(\lambda^h, \mathbf{u}^h)$ is the finite element solution, m is the order of derivatives appearing in the weak form, k is the degree of polynomials used in $\mathbf{u}^h$, and h is the characteristic length of the element (see Chapter 5 for the notation and definitions of errors).

6.1.4 Applications

Here we consider a couple of examples of eigenvalue problems to illustrate the concepts described in the previous section. We consider one example of a heat-transfer-type problem and one of free vibration of beams.

Example 6.1. Consider a plane wall, initially at a uniform temperature T_0, which has both surfaces suddenly exposed to a fluid at temperature T_∞. The governing differential equation

$$\frac{\partial^2 T}{\partial x^2} = \frac{1}{\alpha}\frac{\partial T}{\partial t}, \qquad \alpha = \frac{k}{\rho c_p} \tag{6.28}$$

and the initial condition is

$$T(x, 0) = T_0$$

where α is the diffusion coefficient, k the thermal conductivity, ρ the density, and c_p the specific heat at constant pressure. Equation (6.28) is also known as the *diffusion equation*.

We consider two sets of boundary conditions.

Set 1. If the heat transfer coefficient at the surfaces of the wall is assumed to be infinite, the boundary conditions can be expressed as

$$T(0,t)=T_\infty, \qquad T(L,t)=T_\infty \quad \text{for } t>0 \tag{6.29a}$$

Set 2. If we assume that the wall at $x=L$ is subjected to ambient temperature, we have

$$T(0,t)=T_\infty, \qquad \left[kA\frac{\partial T}{\partial x}+\beta A(T-T_\infty)\right]\bigg|_{x=L}=0 \tag{6.29b}$$

Equation (6.28) can be normalized while making the boundary conditions homogeneous. Let

$$\bar{x}=\frac{x}{L}, \qquad \bar{t}=\frac{\alpha t}{L^2}, \qquad u=\frac{T-T_\infty}{T_0-T_\infty}$$

The differential equation (6.28), boundary conditions (6.29), and the initial condition become

$$-\frac{\partial^2 u}{\partial x^2}+\frac{\partial u}{\partial t}=0 \tag{6.30a}$$

$$u(0,t)=0, \qquad u(1,t)=0, \qquad u(x,0)=1 \tag{6.30b}$$

$$u(0,t)=0, \qquad \left(\frac{du}{dx}+Hu\right)\bigg|_{x=1}=0, \qquad H=\frac{\beta L}{k} \tag{6.30c}$$

where the bars over x and t are omitted in the interest of brevity.

Solution of (6.30a,b) by separation of variables leads to solution of the eigenvalue problem

$$-\frac{d^2U}{dx^2}-\lambda U=0, \qquad U(0)=0, \qquad U(1)=0 \tag{6.31}$$

The finite element model of this equation is given by (6.21), with $a=1$ and $c_0=1$. For the choice of linear and quadratic interpolation functions, the element equations (6.21a) become [see (3.34) and (3.40)]

$$\left(\frac{1}{h_e}\begin{bmatrix}1 & -1\\ -1 & 1\end{bmatrix}-\frac{\lambda h_e}{6}\begin{bmatrix}2 & 1\\ 1 & 2\end{bmatrix}\right)\begin{Bmatrix}u_1^e\\ u_2^e\end{Bmatrix}=\begin{Bmatrix}Q_1^e\\ Q_2^e\end{Bmatrix} \quad \text{(linear element)}$$

$$\left(\frac{1}{3h_e}\begin{bmatrix}7 & -8 & 1\\ -8 & 16 & -8\\ 1 & -8 & 7\end{bmatrix}-\lambda\frac{h_e}{30}\begin{bmatrix}4 & 2 & -1\\ 2 & 16 & 2\\ -1 & 2 & 4\end{bmatrix}\right)\begin{Bmatrix}u_1^e\\ u_2^e\\ u_3^e\end{Bmatrix}=\begin{Bmatrix}Q_1^e\\ 0\\ Q_3^e\end{Bmatrix} \quad \text{(quadratic element)}$$

For a mesh of two linear elements (the minimum needed), with $h_1=h_2=0.5$, the assembled equations are

$$\left(2\begin{bmatrix}1 & -1 & 0\\ -1 & 2 & -1\\ 0 & -1 & 1\end{bmatrix}-\lambda\frac{1}{12}\begin{bmatrix}2 & 1 & 0\\ 1 & 4 & 1\\ 0 & 1 & 2\end{bmatrix}\right)\begin{Bmatrix}U_1\\ U_2\\ U_3\end{Bmatrix}=\begin{Bmatrix}Q_1^1\\ 0\\ Q_2^2\end{Bmatrix}$$

The Set 1 boundary conditions $U(0)=0$ and $U(1)=0$ require $U_1=U_3=0$. Hence, the eigenvalue problem reduces to the single equation

$$(4-\tfrac{4}{12}\lambda)U_2=0, \qquad \text{or} \quad \lambda_1=12.0, \qquad U_2\neq 0$$

For a mesh of one quadratic element, we have ($h = 1.0$)

$$\tfrac{16}{3} - \tfrac{1}{30}\lambda 16 = 0, \qquad \text{or} \qquad \lambda_1 = 10.0$$

The corresponding eigenfunction amplitude is $U_2 = 1.0$ (or any nonzero constant), so that the eigenfunctions are as follows: for linear elements ($h = 0.5$),

$$U(x) = \begin{cases} U_2\psi_2^1 = \dfrac{x}{h} & \text{for } 0 \le x \le 0.5 \\[2ex] U_2\psi_1^2 = \dfrac{1-x}{h} & \text{for } 0.5 \le x \le 1.0 \end{cases}$$

while, for a quadratic element ($h = 1.0$),

$$U(x) = U_2\psi_2^1 = 4\frac{x}{h}\left(1 - \frac{x}{h}\right) \quad \text{for } 0 \le x \le 1.0$$

The exact eigenvalues are $\lambda_n = (n\pi)^2$ and $\lambda_1 = \pi^2 = 9.8696$. The exact eigenfunctions for Set 1 boundary conditions are $U_n(x) = \sin n\pi x$ and $U_1 = \sin \pi x$.

The eigenvalues and eigenfunctions can be used to construct the solution of the transient problem. For example, the solution of (6.28) with Set 1 boundary conditions is

$$u(x, t) = \sum_{n=1}^{\infty} T_n U_n(x) e^{-\lambda_n t} = \sum_{n=1}^{\infty} T_n \sin n\pi x \, e^{-(n\pi)^2 t}$$

where T_n are constants to be determined using the initial condition of the problem. The finite element solution of the same problem, when one quadratic element is used, is given by

$$u_h(x, t) = 4x(1-x)e^{-10t}T_0$$

For a mesh of two linear elements, the Set 2 boundary conditions translate into $U_1 = 0$ and $Q_2^2 + U_3 = 0$. The condensed equations are

$$\left(2\begin{bmatrix} 2 & -1 \\ -1 & 1 \end{bmatrix} - \frac{\lambda}{12}\begin{bmatrix} 4 & 1 \\ 1 & 2 \end{bmatrix}\right)\begin{Bmatrix} U_2 \\ U_3 \end{Bmatrix} = \begin{Bmatrix} 0 \\ -U_3 \end{Bmatrix}$$

or

$$\left(\begin{bmatrix} 4 & -2 \\ -2 & 3 \end{bmatrix} - \frac{\lambda}{12}\begin{bmatrix} 4 & 1 \\ 1 & 2 \end{bmatrix}\right)\begin{Bmatrix} U_2 \\ U_3 \end{Bmatrix} = \begin{Bmatrix} 0 \\ 0 \end{Bmatrix}$$

The characteristic polynomial of the above eigenvalue problem is obtained by setting the determinant of the coefficient matrix equal to zero:

$$\begin{vmatrix} 4 - 4\bar{\lambda} & -(2+\bar{\lambda}) \\ -(2+\bar{\lambda}) & 3 - 2\bar{\lambda} \end{vmatrix} = 0, \qquad \bar{\lambda} = \tfrac{1}{12}\lambda$$

or

$$7\bar{\lambda}^2 - 24\bar{\lambda} + 8 = 0$$

The roots of this equation are

$$\bar{\lambda}_{1,2} = \frac{12 \pm \sqrt{88}}{7} \qquad (\bar{\lambda}_1 = 0.374167,\ \bar{\lambda}_2 = 3.0544)$$

and the eigenvalues are ($\lambda = 12\bar{\lambda}$)

$$\lambda_1 = 4.4900, \qquad \lambda_2 = 36.6529$$

The eigenvectors are computed from the equations

$$\begin{bmatrix} 4-\frac{4}{12}\lambda_l & -(2+\frac{1}{12}\lambda_l) \\ -(2+\frac{1}{12}\lambda_l) & 3-\frac{2}{12}\lambda_l \end{bmatrix} \begin{Bmatrix} U_2 \\ U_3 \end{Bmatrix}^{(l)} = \begin{Bmatrix} 0 \\ 0 \end{Bmatrix}$$

For example, for $\lambda_1 = 4.4900$, we have

$$2.5033U_2^{(1)} - 2.3742U_3^{(1)} = 0$$

or

$$\{U^{(1)}\} = (1.000, 1.0544) = (0.6881, 0.7256) \ \text{(normalized)}$$

Hence, the eigenfunction corresponding to $\lambda_1 = 4.4900$ ($h = 0.5$) is

$$U^{(1)}(x) = \begin{cases} 0.6881x/h & \text{for } 0 \leqslant x \leqslant 0.5 \\ 0.6881(1-x)/h + 0.7256(2x-1)/2h & \text{for } 0.5 \leqslant x \leqslant 1.0 \end{cases}$$

The exact eigenfunctions for Set 2 boundary conditions are

$$U_n(x) = \sin \sqrt{\lambda_n} x$$

and the eigenvalues λ_n are computed from the equation

$$1 + \sqrt{\lambda_n} \cot \sqrt{\lambda_n} = 0$$

Table 6.1 gives a comparison of the eigenvalues obtained using meshes of linear and quadratic elements with the exact values. Note that the number of eigenvalues we can obtain is equal to the number of unknown nodal values. As the mesh is refined, not only do we increase the number of eigenvalues but we also improve the accuracy of the preceding eigenvalues. Note also that the convergence of the numerical eigenvalues to

TABLE 6.1

Eigenvalues of the heat conduction equation (6.28) for two sets of boundary conditions

Set 1: $U(0) = 0, \quad U(1) = 0$

Set 2 (in parentheses): $U(0) = 0, \quad (dU/dx + U)\big|_{x=1} = 0$

Mesh	λ_1	λ_2	λ_3	λ_4	λ_5	λ_6	λ_7
2L	12.0000 (4.4900)	(36.6529)					
4L	10.3866 (4.2054)	48.0000 (27.3318)	126.756 (85.7864)	(177.604)			
8L	9.9971 (4.1380)	41.5466 (24.9088)	99.4855 (69.1036)	192.000 (143.530)	328.291 (257.580)	507.025 (417.701)	686.512 (607.022)
1Q	10.000 (4.1545)	(38.5121)					
2Q	9.9439 (4.1196)	40.000 (24.8995)	128.723 (81.4446)	(207.653)			
4Q	9.8747 (4.1161)	39.7754 (24.2039)	91.7847 (64.7705)	160.000 (129.261)	308.253 (240.539)	514.891 (405.253)	794.794 (658.137)
Exact	9.8696 (4.1159)	39.4784 (24.1393)	88.8264 (63.6591)	157.9137 (122.889)	246.740 (201.851)	355.306 (300.550)	483.611 (418.987)

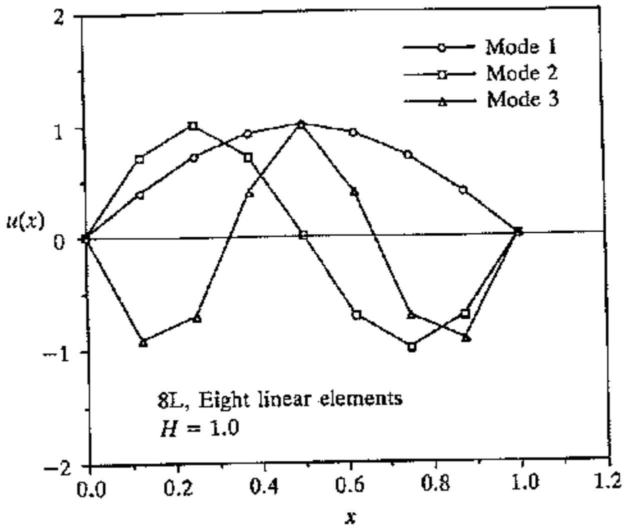

FIGURE 6.1
The first three mode shapes (or eigenvectors) as predicted by the mesh of eight linear elements for the heat transfer problem in Example 6.1, Set 1 boundary conditions.

the exact ones is from the above, i.e., the finite element solution provides an upper bound to the exact eigenvalues. For structural systems, this can be interpreted as follows. According to the principle of total minimum potential energy, any approximate displacement field would overestimate the total potential energy of the system. This is equivalent to approximating the stiffness of the system with a larger value than the actual one. A stiffer system will have larger eigenvalues (or frequencies). The first three mode shapes of the system are shown in Figs. 6.1 and 6.2.

We close this example by noting that the eigenvalue equation (6.31) can also be interpreted as that arising in connection with the axial vibrations of a constant cross-section member. In that case, U denotes the axial displacement and $\lambda = \omega^2\rho/E$, ω being the frequency of vibration. The boundary conditions in (6.30c) can be interpreted as the left end of the bar being fixed and the right end being connected to a linear

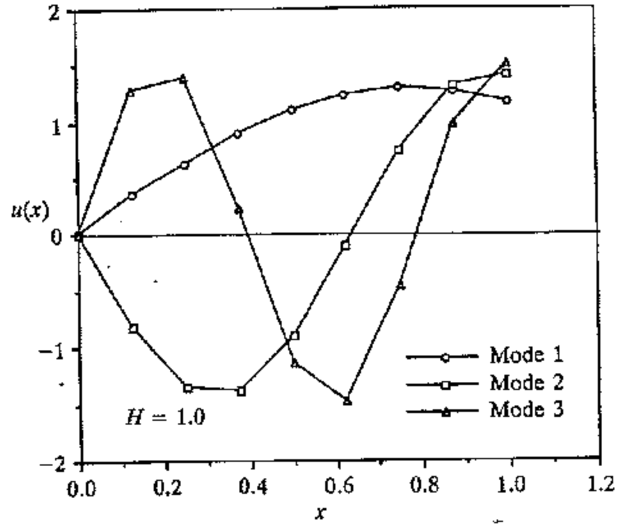

FIGURE 6.2
The first three mode shapes as predicted by a mesh of eight linear elements for the heat transfer problem with convection ($H = 1.0$). See Example 6.1, Set 2 boundary conditions.

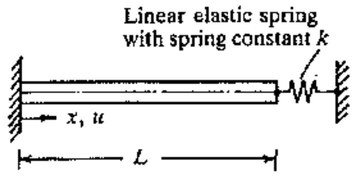

FIGURE 6.3
An elastic bar with an end spring. The axial vibrations in this case can be shown to be governed by the same eigenvalue problem as that used for the heat transfer problem with convective boundary condition at $x = L$ (Set 2 boundary conditions in Example 6.1).

elastic spring (see Fig. 6.3). The constant H is equal to k/EA, k being the spring constant. Thus, the results presented in Table 6.1 can be interpreted as the square of the natural frequencies of a uniform bar (multiplied by ρ/E).

In the next example we study transverse vibrations of cantilever beams using the Timoshenko beam theory. The effect of shear deformation is brought out by considering two different ratios of length to height of the beam. In problems with more than one independent variable and certain coarse meshes, the computed eigenvalues are not always the lowest eigenvalues of the problem. This is due to the restrictions placed by the particular mesh on the mode shapes it can model.

Example 6.2. Consider a uniform beam of rectangular cross-section, length L, width B, and height H. The beam is fixed at one end, say at $x = 0$, and free at the other, $x = L$. We assume that Poisson's ratio is $\nu = 0.25$. We wish to determine the first four natural frequencies associated with the transverse deflection w.

The finite element model of the Timoshenko beam theory is given by (6.23a). The number of eigenvalues we wish to determine dictates the minimum number of elements to be used. If we use one linear element, we shall have four degrees of freedom, with two degrees of freedom at the fixed end being specified as zeros. Thus, we can only obtain two eigenvalues. If two linear elements are used, there are six degrees of freedom, with two of them known to be zero, and we can obtain four eigenvalues. However, the four computed eigenvalues may not be the lowest four. Indeed, a mesh of two linear elements can only represent the first two mode shapes of the cantilever beam (see Fig. 6.4). In order to represent the first four mode shapes, we must use at least four linear elements.

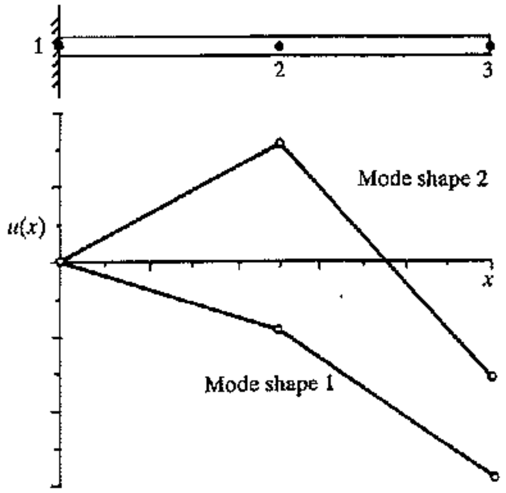

FIGURE 6.4
Two possible nonzero mode shapes that can be represented by a mesh of two linear (Lagrange) elements.

Because of the algebraic complexity of the element matrices for meshes of 4, 8, and 16 linear elements and 2, 4, and 8 quadratic elements that are used to study the convergence characteristics of the eigenvalues of the beam, the element matrices and assembled equations are not presented here. For all meshes used, the boundary conditions at the fixed end require $w(0) = 0$ and $\Psi(0) = 0$, or

$$U_1 = 0, \qquad U_2 = 0$$

The frequencies obtained by solving the resulting eigenvalue problems are shown in Table 6.2 for two different values of the length-to-height ratio L/H. The value $L/H = 100$ makes the effect of shear deformation negligible and yields essentially the Euler–Bernoulli beam theory results. Since the frequencies are normalized, $\bar{\omega} = \omega L^2(\rho A/EI)^{1/2}$, it is necessary only to select the values of ν and L/H. For computational purposes, we take $\nu = 0.25$, $\rho I = 1.0$, $EI = 1.0$, and $L = 1.0$, and compute

$$GAK = \frac{E}{2(1+\nu)} BH \frac{5}{6} = \frac{4EI}{H^2}, \qquad \rho A = \frac{12\rho I}{H^2}$$

where B and H are the width and height, respectively, of the beam. Thus for $L/H = 100$ (or $H = 10^{-2}$), we take $GAK = 4 \times 10^4$ and $\rho A = 12 \times 10^4$, and, for $L/H = 10$, we have $GAK = 4 \times 10^2$ and $\rho A = 12 \times 10^2$.

We note from Table 6.2 that the finite element results converge with h-refinement (i.e., when more of the same kind of elements are used) and also with p-refinement (i.e., when higher-order elements are used). The p-refinement shows more rapid convergence of the fundamental (i.e., first) frequency (see Fig. 6.5). The rates of convergence are consistent with the error estimates in (6.27). The mesh refinements with either more or higher-order elements refine the higher frequencies more than the fundamental frequency (see Table 6.2). Note also that the effect of shear deformation is to reduce the natural frequencies. This is because of the increased flexibility in the Timoshenko beam theory compared with the Euler–Bernoulli beam theory. The first four mode shapes of the cantilever beam, as obtained using the 16-element mesh of linear elements, are shown in Fig. 6.6.

TABLE 6.2
Natural frequencies of a cantilever beam according to the Timoshenko and Euler–Bernoulli beam theories [$\bar{\omega} = \omega L^2(\rho A/EI)^{1/2}$]

	$L/H = 100$				$L/H = 10$			
Mesh	$\bar{\omega}_1$	$\bar{\omega}_2$	$\bar{\omega}_3$	$\bar{\omega}_4$	$\bar{\omega}_1$	$\bar{\omega}_2$	$\bar{\omega}_3$	$\bar{\omega}_4$
4L	3.5406	25.6726	98.3953	417.1330	3.5137	24.1345	80.2244	189.9288
8L	3.5223	22.8851	68.8937	151.8431	3.4956	21.7004	60.6297	119.2798
16L	3.5174	22.2350	63.3413	127.5434	3.4908	21.1257	56.4714	104.6799
2Q	3.5214	23.3226	78.3115	328.3250	3.4947	22.0762	67.0884	181.0682
4Q	3.5161	22.1054	63.3271	133.9828	3.4895	21.0103	56.4572	108.6060
8Q	3.5158	22.0280	61.7325	121.4458	3.4892	20.4421	55.2405	100.7496
Exact TBT†	3.5158	22.0226	61.6179	120.6152	3.4892	20.9374	55.1530	100.2116
Exact EBT†	3.5158	22.0315	61.6774	120.8300	3.5092	21.7425	59.8013	114.2898
Exact EBT‡	3.5160	22.0345	61.6972	120.9019	3.5160	22.0345	61.6972	120.9019

† TBT, Timoshenko beam theory; EBT, Euler–Bernoulli beam theory (with rotary inertia).

‡ Rotory inertia neglected; the results are independent of the ratio L/H.

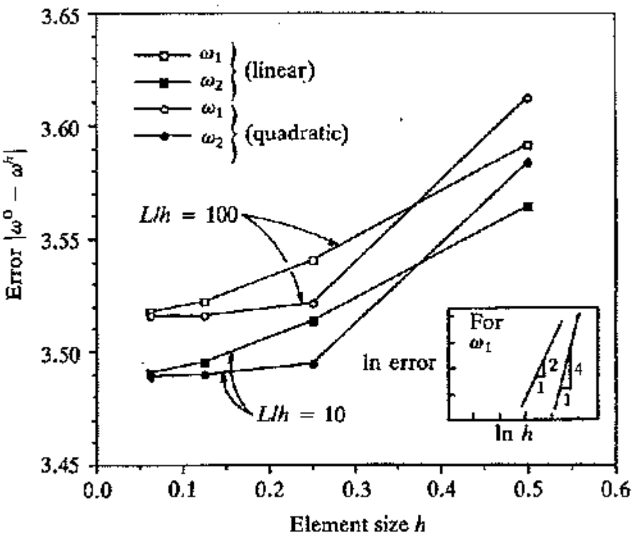

FIGURE 6.5
Plots of error in the frequencies computed using linear and quadratic finite elements (for length-to-height ratios $L/H = 10$ and 100).

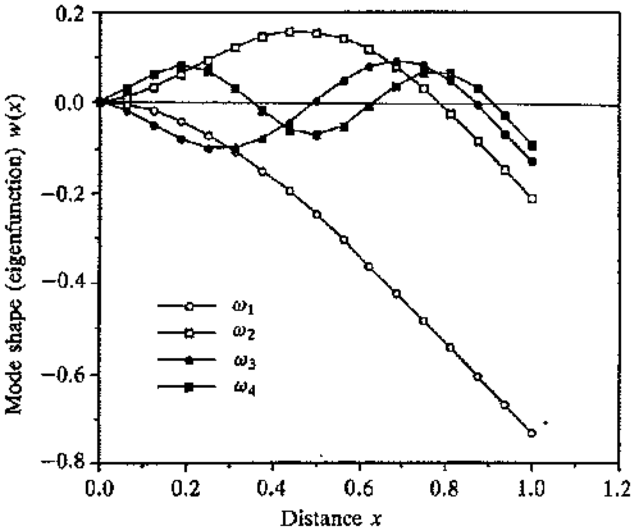

FIGURE 6.6
First four natural mode shapes of a cantilever beam, as predicted using a 16-element mesh of linear Timoshenko beam elements ($L/H = 10$).

6.2 TIME-DEPENDENT PROBLEMS

6.2.1 Introduction

In this section, we develop the finite element models of one-dimensional time-dependent problems and describe time approximation schemes to convert ordinary differential equations in time to algebraic equations. We consider finite element models of the time-dependent version of the differential equations studied in Chapters 3 and 4. These include the second-order (in space) parabolic (i.e., first time derivative) and hyperbolic (i.e., second time derivative) equations and fourth-order hyperbolic equations arising in connection with the bending of beams. Recall that second-order parabolic equations arise in heat transfer and fluid mechanics (see Sections 3.3.1 and 3.3.2), while second- and fourth-order hyperbolic equations arise in solid mechanics problems.

The finite element formulation of time-dependent problems involves two steps:

1. *Spatial approximation*, where the solution u of the equation under consideration is approximated by expressions of the form

$$\boxed{u(x,t) \approx U^e(x,t) = \sum_{j=1}^{n} u_j^e(t)\psi_j^e(x)} \tag{6.32}$$

   and the spatial finite element model of the equation is developed using the procedures of static or steady-state problems, while carrying all time-dependent terms in the formulation. This step results in a set of ordinary differential equations (i.e., a semidiscrete system of equations) in time for the nodal variables $u_j^e(t)$ of the element. Equation (6.32) represents the spatial approximation of u for any time t. When the solution is separable into functions of time only and space only, $u(x,t) = T(t)X(x)$, the approximation (6.32) is clearly justified. Even when the solution is not separable, (6.32) can represent a good approximation of the actual solution, provided a sufficiently small time step is used.
2. *Temporal approximation*, where the system of ordinary differential equations are further approximated in time, often using finite difference formulae for the time derivatives. This step allows conversion of the system of ordinary differential equations into a set of algebraic equations among u_j^e at time $t_{s+1} = (s+1)\,\Delta t$, where Δt is the time increment and s is an integer.

All time approximation schemes seek to find u_j at time t_{s+1} using the known values of u_j from previous times:

$$\text{compute} \quad \{u\}_{s+1} \quad \text{using} \quad \{u\}_s,\ \{u\}_{s-1},\ \ldots$$

Thus, at the end of the two-stage approximation, one has a continuous spatial solution at discrete intervals of time:

$$U^e(x, t_s) = \sum_{j=1}^{n} u_j^e(t_s)\psi_j^e(x) \quad (s = 0, 1, \dots)$$

Here we study the details of these two steps by considering a model differential equation that contains both second- and fourth-order spatial derivatives and first- and second-order time derivatives:

$$\boxed{-\frac{\partial}{\partial x}\left(a\frac{\partial u}{\partial x}\right) + \frac{\partial^2}{\partial x^2}\left(b\frac{\partial^2 u}{\partial x^2}\right) + c_0 u + c_1\frac{\partial u}{\partial t} + c_2\frac{\partial^2 u}{\partial t^2} = f(x, t)} \tag{6.33a}$$

subject to appropriate boundary and initial conditions. The boundary conditions are of the form

$$\begin{gathered}\text{specify} \quad u(x, t) \quad \text{or} \quad -a\frac{\partial u}{\partial x}(x, t) + \frac{\partial}{\partial x}\left(b\frac{\partial^2 u}{\partial x^2}\right) \\ \text{and} \\ \text{specify} \quad \frac{\partial u}{\partial x}(x, t) \quad \text{or} \quad b\frac{\partial^2 u}{\partial x^2}\end{gathered} \tag{6.33b}$$

at $x = 0$, L, and the initial conditions involve specify

$$c_2 u(x, 0) \quad \text{and} \quad c_2\dot{u}(x, 0) + c_1 u(x, 0) \tag{6.33c}$$

where $\dot{u} \equiv \partial u/\partial t$. Equation (6.33*a*) contains, as special cases, time-dependent second- and fourth-order equations. Second-order equations arise, for example, in determining the transverse motion of a cable ($a = T$; $b = 0$, $c_1 = \rho$, $c_2 = 0$, $c_0 = 0$), the longitudinal motion of a rod ($a = EA$, $b = 0$, $c_1 = 0$ if damping is not considered, $c_2 = \rho A$, $c_0 = 0$), and the temperature transients in a fin ($a = kA$, $b = 0$, $c_1 = \rho A$, $c_2 = 0$). A fourth-order equation arises in determining the transverse motion of a beam ($a = 0$, $b = EI$, $c_0 = k$, $c_1 = 0$, $c_2 = \rho A$).

6.2.2 Semidiscrete Finite Element Models

The semidiscrete formulation involves approximation of the spatial variation of the dependent variable, which follows essentially the same steps as described in Section 3.2. The first step involves the construction of the weak form of the equation over a typical element.

Following the three-step procedure of constructing the weak form of a differential equation, we can develop the weak form of (6.33*a*) over an element. Integration by parts is used on the first term once and on the second term twice to distribute the spatial derivatives equally between the weight function w and the dependent variable u:

$$
\begin{aligned}
0 &= \int_{x_A}^{x_B} w\left[-\frac{\partial}{\partial x}\left(a\frac{\partial u}{\partial x}\right)+\frac{\partial^2}{\partial x^2}\left(b\frac{\partial^2 u}{\partial x^2}\right)+c_0 u + c_1\frac{\partial u}{\partial t}+c_2\frac{\partial^2 u}{\partial t^2}-f\right]dx \\
&= \int_{x_A}^{x_B}\left[\frac{\partial w}{\partial x}a\frac{\partial u}{\partial x}+\frac{\partial^2 w}{\partial x^2}b\frac{\partial^2 u}{\partial x^2}+c_0 wu + c_1 w\frac{\partial u}{\partial t}+c_2 w\frac{\partial^2 u}{\partial t^2}-wf\right]dx \\
&\quad+\left[w\left[\left(-a\frac{\partial u}{\partial x}\right)+\frac{\partial}{\partial x}\left(b\frac{\partial^2 u}{\partial x^2}\right)\right]+\frac{\partial w}{\partial x}\left(-b\frac{\partial^2 u}{\partial x^2}\right)\right]_{x_A}^{x_B} \\
&= \int_{x_A}^{x_B}\left(a\frac{\partial w}{\partial x}\frac{\partial u}{\partial x}+b\frac{\partial^2 w}{\partial x^2}\frac{\partial^2 u}{\partial x^2}+c_0 wu + c_1 w\frac{\partial u}{\partial t}+c_2 w\frac{\partial^2 u}{\partial t^2}-wf\right)dx \\
&\quad-\hat{Q}_1 w(x_A)-\hat{Q}_3 w(x_B)-\hat{Q}_2\left(-\frac{\partial w}{\partial x}\right)\Big|_{x_A}-\hat{Q}_4\left(-\frac{\partial w}{\partial x}\right)\Big|_{x_B} \qquad (6.34a)
\end{aligned}
$$

where

$$
\hat{Q}_1=\left[-a\frac{\partial u}{\partial x}+\frac{\partial}{\partial x}\left(b\frac{\partial^2 u}{\partial x^2}\right)\right]\Big|_{x_A}, \qquad \hat{Q}_2=\left(b\frac{\partial^2 u}{\partial x^2}\right)\Big|_{x_A}
$$

$$
\hat{Q}_3=-\left[-a\frac{\partial u}{\partial x}+\frac{\partial}{\partial x}\left(b\frac{\partial^2 u}{\partial x^2}\right)\right]\Big|_{x_B}, \qquad \hat{Q}_4=-\left(b\frac{\partial^2 u}{\partial x^2}\right)\Big|_{x_B} \qquad (6.34b)
$$

Next, we assume that u is interpolated by an expression of the form (6.32). Equation (6.32) implies that, at any arbitrarily fixed time $t>0$, the function u can be approximated by a linear combination of the ψ_j^e, with $u_j^e(t)$ being the value of u at time t at the jth node of the element Ω^e. In other words, the time and spatial variations of u are separable. This assumption is not valid, in general, because it may not be possible to write the solution $u(x, t)$ as the product of a function of time only and a function of space only. However, with sufficiently small time steps, it is possible to obtain accurate solutions to even those problems for which the solution is not separable in time and space. The finite element solution that we obtain at the end of the analysis is continuous in space but not in time. We only obtain the finite element solution in the form

$$
u(x, t_s)=\sum_{j=1}^{n} u_j^e(t_s)\psi_j^e(x)=\sum_{j=1}^{n}(u_j^s)^e\psi_j^e(x) \quad (s=1, 2, \ldots) \qquad (6.35)
$$

where $(u_j^s)^e$ is the value of $u(x, t)$ at time $t=t_s$ and node j of the element Ω^e.

Substituting $w = \psi_i(x)$ and (6.32) into (6.34a), we obtain

$$
\begin{aligned}
0 = \int_{x_A}^{x_B} \Bigg[& a\frac{d\psi_i}{dx}\left(\sum_{j=1}^{n}\frac{d\psi_j}{dx}\right)u_j + b\frac{d^2\psi_i}{dx^2}\left(\sum_{j=1}^{n} u_j\frac{d^2\psi_j}{dx^2}\right) \\
& + c_0\psi_i\left(\sum_{j=1}^{n} u_j\psi_j\right) + c_1\psi_i\left(\sum_{j=1}^{n}\frac{du_j}{dt}\psi_j\right) + c_2\psi_i\left(\sum_{j=1}^{n}\frac{d^2u_j}{dt^2}\psi_j\right) - \psi_i f\Bigg]\,dx \\
& - \hat{Q}_1\psi_i(x_A) - \hat{Q}_3\psi_i(x_B) - \hat{Q}_2\left(-\frac{d\psi_i}{dx}\right)\Bigg|_{x_A} - \hat{Q}_4\left(-\frac{d\psi_i}{dx}\right)\Bigg|_{x_B} \\
= \sum_{j=1}^{n} & \left[(K_{ij}^1 + K_{ij}^2 + M_{ij}^0)u_j + M_{ij}^1\frac{du_j}{dt} + M_{ij}^2\frac{d^2u_j}{dt^2}\right] - F_i
\end{aligned}
\tag{6.36}
$$

In matrix form, we have

$$
[K]\{u\} + [M^1]\{\dot{u}\} + [M^2]\{\ddot{u}\} = \{F\} \tag{6.37a}
$$

where

$$
[K] = [K^1] + [K^2] + [M^0] \tag{6.37b}
$$

$$
\begin{aligned}
M_{ij}^0 &= \int_{x_A}^{x_B} c_0\psi_i\psi_j\,dx \\
M_{ij}^1 &= \int_{x_A}^{x_B} c_1\psi_i\psi_j\,dx, \qquad M_{ij}^2 = \int_{x_A}^{x_B} c_2\psi_i\psi_j\,dx \\
K_{ij}^1 &= \int_{x_A}^{x_B} a\frac{d\psi_i}{dx}\frac{d\psi_j}{dx}\,dx, \qquad K_{ij}^2 = \int_{x_A}^{x_B} b\frac{d^2\psi_i}{dx^2}\frac{d^2\psi_j}{dx^2}\,dx \\
F_i &= \int_{x_A}^{x_B} \psi_i f\,dx + \hat{Q}_i
\end{aligned}
\tag{6.37c}
$$

This completes the semidiscrete finite element formulation of (6.33) over an element.

6.2.3 Time Approximations

As special cases, (6.37a) contains the parabolic equation (set $[M^2] = [0]$) and the hyperbolic equation (set $[M^1] = [0]$). The time approximation of (6.37a) for these two cases will be considered separately: in Case 1, $c_2 = 0$; in Case 2, $c_1 = 0$.

CASE 1: PARABOLIC EQUATIONS. Consider the parabolic equation [set $[M^2]$ equal to zero in (6.37a)]

$$
[M^1]\{\dot{u}\} + [K]\{u\} = \{F\} \tag{6.38a}
$$

subject to the initial condition

$$
\{u\}_0 = \{u_0\} \tag{6.38b}
$$

where $\{u\}_0$ denotes the value of the enclosed quantity u at time $t = 0$, whereas $\{u_0\}$ denotes the column of values u_{j0}.

The most commonly used method for solving (6.38*a*) is the *α family of approximation*, in which a weighted average of the time derivative of a dependent variable is approximated at two consecutive time steps by linear interpolation of the values of the variable at the two steps:

$$(1-\alpha)\{\dot{u}\}_s + \alpha\{\dot{u}\}_{s+1} = \frac{\{u\}_{s+1} - \{u\}_s}{\Delta t_{s+1}} \quad \text{for } 0 \leqslant \alpha \leqslant 1 \tag{6.39a}$$

where $\{\ \}_s$ refers to the value of the enclosed quantity at time $t = t_s = \sum_{i=1}^{s} \Delta t_i$, and $\Delta t_s = t_s - t_{s-1}$ is the sth time step. If the time interval $[0, T_0]$ is divided into equal time steps then $t_s = s\,\Delta t$. Equation (6.39*a*) can be interpreted as

$$\boxed{\begin{aligned} \{u\}_{s+1} &= \{u\}_s + \Delta t\{\dot{u}\}_{s+\alpha} \\ \{\dot{u}\}_{s+\alpha} &= (1-\alpha)\{\dot{u}\}_s + \alpha\{\dot{u}\}_{s+1} \quad \text{for } 0 \leqslant \alpha \leqslant 1 \end{aligned}} \tag{6.39b}$$

For different values of α, we obtain the following well-known numerical integration schemes:

$$\boxed{\alpha = \begin{cases} 0, & \text{the forward difference (or Euler) scheme (conditionally} \\ & \text{stable); order of accuracy} = O(\Delta t) \\ \frac{1}{2}, & \text{the Crank–Nicolson scheme (stable); } O((\Delta t)^2) \\ \frac{2}{3}, & \text{the Galerkin method (stable); } O((\Delta t)^2) \\ 1, & \text{the backward difference scheme (stable); } O(\Delta t) \end{cases}} \tag{6.40}$$

Equation (6.39*a*) can be used to reduce the ordinary differential equations (6.38*a*) to algebraic equations among the u_j at time t_{s+1}. Since (6.38*a*) is valid for any $t > 0$, it is valid for $t = t_s$ and $t = t_{s+1}$ ($[M^1] = [M]$):

$$[M]\{\dot{u}\}_s + [K]_s\{u\}_s = \{F\}_s \tag{6.41a}$$

$$[M]\{\dot{u}\}_{s+1} + [K]_{s+1}\{u\}_{s+1} = \{F\}_{s+1} \tag{6.41b}$$

where it is assumed that the mass matrix is independent of time. After multiplying (6.39*a*) throughout by Δt_{s+1}, we premultiply both sides of the equation with $[M]$ and obtain

$$\Delta t_{s+1}\,\alpha[M]\{\dot{u}\}_{s+1} + \Delta t_{s+1}(1-\alpha)[M]\{\dot{u}\}_s = [M](\{u\}_{s+1} - \{u\}_s)$$

Substituting for $[M]\{\dot{u}\}_{s+1}$ and $[M]\{\dot{u}\}_s$ from (6.41*a*) and (6.41*b*), respectively, in the above equation, we obtain

$$\begin{aligned} \Delta t_{s+1}\,\alpha(\{F\}_{s+1} - [K]_{s+1}\{u\}_{s+1}) + \Delta t_{s+1}(1-\alpha)(\{F\}_s - [K]_s\{u\}_s) \\ = [M](\{u\}_{s+1} - \{u\}_s) \end{aligned}$$

Rearranging the terms into known and unknown ones, we obtain

$$\boxed{[\hat{K}]_{s+1}\{u\}_{s+1} = [\bar{K}]_s\{u\}_s + \{\hat{F}\}_{s,s+1}} \tag{6.42a}$$

where

$$\boxed{\begin{gathered} [\hat{K}]_{s+1} = [M^1] + a_1[K]_{s+1}, \qquad [\bar{K}]_s = [M^1] - a_2[K]_s \\ \{\hat{F}\}_{s,s+1} = \Delta t_{s+1}\left[\alpha\{F\}_{s+1} + (1-\alpha)\{F\}_s\right] \\ a_1 = \alpha\,\Delta t_{s+1}, \qquad a_2 = (1-\alpha)\,\Delta t_{s+1} \end{gathered}} \tag{6.42b}$$

Note that, in deriving (6.42), it has been assumed that $[M^1]$ is independent of time and that the time step is nonuniform.

Equations (6.42) are valid for a typical element. The assembly, imposition of boundary conditions, and solution of the assembled equations are the same as described before for static (or steady-state) problems. Calculation of $[\hat{K}]$ and $\{\hat{F}\}$ at time $t = 0$ requires knowledge of the initial conditions $\{u\}_0$ and the time variation of $\{F\}$. Note that, for $\alpha = 0$ (the forward difference scheme), we obtain $[\hat{K}] = [M^1]$. When the mass matrix $[M^1]$ is diagonal, (6.42a) become *explicit*, and one can solve for $\{u\}_{s+1}$ directly without inverting $[\hat{K}]$. The mass matrix obtained according to the weak form, called the *consistent mass matrix*, is not diagonal. There are several ways to diagonalize mass matrices; these will be described in Section 6.2.4.

Stability and accuracy. Since (6.39a) represents an approximation, which is used to derive (6.42a), error is introduced into the solution $\{u\}_{s+1}$ at each time step. In addition to the truncation error introduced in approximating the derivative, round-off errors can be introduced because of the finite arithmetic used in our computations. Since the solution at time t_{s+1} depends on the solution at time t_s, the error can grow with time. If it grows unboundedly with time, the solution scheme is said to be *unstable*. If it is bounded (i.e., it increases for one time step and decreases for another time step, but never exceeds a certain finite value), the solution scheme is said to be *stable*. The numerical scheme (6.42) is said to be *consistent* with the continuous problem (6.38) if the round-off and truncation errors go to zero as $\Delta t \to 0$. *Accuracy* of a numerical scheme is a measure of the closeness between the approximate solution and the exact solution, whereas *stability* of a solution is a measure of the boundedness of the approximate solution with time. As one might expect, the size of the time step can influence both accuracy and stability. When we construct an approximate solution, we like it to converge to the true solution when the number of elements or the degree of approximation is increased and the time step Δt is decreased. A time approximation scheme is said to be *convergent* if, for fixed t_s and Δt, the numerical value $\{u\}_s$ converges to its true value $\{u(t_s)\}$ as $\Delta t \to 0$. Accuracy is measured in terms of the rate at which the approximate solution converges. If a numerical scheme is stable and consistent, it is also convergent [see Isaacson and Keller (1966)].

A numerical scheme is said to be *conditionally stable* if it is stable only when certain restrictions on the time step are satisfied. For all numerical schemes in which $\alpha < \frac{1}{2}$, the α family of approximations is stable only if the time step satisfies the following (stability) condition:

$$\boxed{\Delta t < \Delta t_{cr} \equiv \frac{2}{(1-2\alpha)\lambda}} \tag{6.43}$$

where λ is the largest eigenvalue of the finite element equations (6.38). Note that the same mesh as that used for the transient analysis must be used to calculate the eigenvalues.

When $\alpha = 0$, the numerical scheme is called an *explicit* scheme. The name comes from the fact that when the mass matrix $[M]$ is diagonal, (6.42) can be solved without inverting $[\hat{K}]$ (because $[\hat{K}] = [M]$ is diagonal). When $\alpha \neq 0$ the scheme is said to be *implicit*, indicating that $[\hat{K}]$ has to be inverted (whether or not $[M]$ is diagonal). Such a classicfication of time integration schemes seems to have originated with finite difference methods. When these methods are used for spatial discretization, the mass matrix $[M]$ ends up as a diagonal matrix. However, in the finite element method, irrespective of the time integration scheme used, the consistent mass matrix $[M]$ is not diagonal and hence it is necessary to invert $[\hat{K}]$. When the consistent mass matrix is replaced by an equivalent diagonal mass matrix (see Section 6.2.4), an explicit scheme results in an explicit set of algebraic equations that can be solved without inverting the coefficient matrix $[\hat{K}]$.

CASE 2: HYPERBOLIC EQUATIONS. For this case $c_1 = 0$ (i.e., $[M^1] = [0]$), and (6.37*a*) takes the form

$$[M^2]\{\ddot{u}\} + [K]\{u\} = \{F\} \tag{6.44}$$

The hyperbolic nature is dictated by $c_2 \neq 0$, not by $c_1 = 0$; in fact, in structural systems, both c_1 and c_2 can be nonzero. For example, consider the case where $[M^1]$ is the damping matrix in a structural system; see Problem 6.24.

There are several numerical integration methods available to integrate second-order (i.e., hyperbolic) equations. Among these, the Newmark family of time integration schemes is widely used in structural dynamics. Other methods, such as the Wilson method and the Houbolt method, can be used to develop the algebraic equations from the second-order differential equations (6.44).

In the Newmark method, the function and its first time derivative are approximated according to

$$\boxed{\begin{aligned}\{u\}_{s+1} &= \{u\}_s + \Delta t\,\{\dot{u}\}_s + \tfrac{1}{2}(\Delta t)^2\{\ddot{u}\}_{s+\gamma}\\ \{\dot{u}\}_{s+1} &= \{\dot{u}\}_s + \{\ddot{u}\}_{s+\alpha}\,\Delta t\end{aligned}} \tag{6.45a}$$

where

$$\boxed{\{\ddot{u}\}_{s+\theta} = (1-\theta)\{\ddot{u}\}_s + \theta\{\ddot{u}\}_{s+1}} \tag{6.45b}$$

and α and γ $(=2\beta)$ are parameters that determine the stability and accuracy of the scheme. The following schemes are special cases of (6.45*a*,*b*):

$$\boxed{\begin{array}{lll} \alpha = \frac{1}{2}, & \gamma = 2\beta = \frac{1}{2}, & \text{the constant-average acceleration method (stable)} \\ \alpha = \frac{1}{2}, & \gamma = 2\beta = \frac{1}{3}, & \text{the linear acceleration method (conditionally stable)} \\ \alpha = \frac{1}{2}, & \gamma = 2\beta = 0, & \text{the central difference method (conditionally stable)} \\ \alpha = \frac{3}{2}, & \gamma = 2\beta = \frac{8}{5}, & \text{the Galerkin method (stable)} \\ \alpha = \frac{3}{2}, & \gamma = 2\beta = 2, & \text{the backward difference method (stable)} \end{array}} \tag{6.45c}$$

For all schemes in which $\gamma < \alpha$ and $\alpha \geqslant \frac{1}{2}$, the stability requirement is

$$\boxed{\Delta t \leqslant \Delta t_{cr} = [\tfrac{1}{2}\omega_{\max}^2(\alpha - \gamma)]^{-1/2}} \tag{6.46}$$

where $\omega_{\max}$ is the maximum natural frequency of the system (6.44).

The use of (6.45) in (6.44) gives the following system of algebraic equations:

$$\boxed{[\hat{K}]_{s+1}\{u\}_{s+1} = \{\hat{F}\}_{s,s+1}} \tag{6.47a}$$

where

$$\boxed{\begin{gathered} [\hat{K}]_{s+1} = [K]_{s+1} + a_3[M]_{s+1} \\ \{\hat{F}\}_{s,s+1} = \{F\}_{s+1} + [M]_{s+1}(a_3\{u\}_s + a_4\{\dot{u}\}_s + a_5\{\ddot{u}\}_s) \\ a_3 = \frac{2}{\gamma(\Delta t)^2}, \quad a_4 = \frac{2}{\gamma\,\Delta t}, \quad a_5 = \frac{1}{\gamma} - 1 \end{gathered}} \tag{6.47b}$$

Again, (6.47) are valid over a typical element.

Note that the calculation of $[\hat{K}]$ and $\{\hat{F}\}$ requires knowledge of the initial conditions $\{u\}_0$, $\{\dot{u}\}_0$, and $\{\ddot{u}\}_0$. In practice, one does not know $\{\ddot{u}\}_0$. As an approximation, it can be calculated from (6.44) (we often assume that the applied force is zero at $t = 0$):

$$\{\ddot{u}\}_0 = [M^2]^{-1}(\{F\}_0 - [K]\{u\}_0) \tag{6.48}$$

At the end of each time step, the new velocity vector $\{\dot{u}\}_{s+1}$ and acceleration vector $\{\ddot{u}\}_{s+1}$ are computed using the equations

$$\boxed{\begin{gathered} \{\ddot{u}\}_{s+1} = a_3(\{u\}_{s+1} - \{u\}_s) - a_4\{\dot{u}\}_s - a_5\{\ddot{u}\}_s \\ \{\dot{u}\}_{s+1} = \{\dot{u}\}_s + a_2\{\ddot{u}\}_s + a_1\{\ddot{u}\}_{s+1} \\ a_1 = \alpha\,\Delta t, \qquad a_2 = (1 - \alpha)\,\Delta t \end{gathered}} \tag{6.49}$$

The remaining procedure stays the same as in static (i.e., non-time-dependent) problems.

6.2.4 Mass Lumping

Recall from the time approximation of parabolic equations that use of the forward difference scheme (i.e., $\alpha = 0$) results in the following time marching scheme [see (6.42)]:

$$[M^e]\{u\}_{s+1} = ([M^e] - \Delta t\,[K^e])\{u\}_s + \Delta t\,\{F^e\}_s \tag{6.50}$$

The mass matrix $[M^e]$ derived from the weighted-integral formulation of the governing equation is called the *consistent mass matrix*, and it is symmetric, positive-definite, and nondiagonal. Solution of the global equations associated with (6.50) requires inversion of the assembled mass matrix. If the mass matrix is diagonal then the assembled equations can be solved explicitly,

$$(U_I)_{s+1} = M_{II}^{-1}\left[M_{II}(U_I)_s - \Delta t \sum_{J=1}^{N} K_{IJ}(U_J)_s + \Delta t\,(F_I)_s\right] \tag{6.51}$$

thus saving computational time. The explicit nature of (6.51) motivated analysts to find rational ways of diagonalizing the mass matrix.

There are several ways of constructing diagonal mass matrices [see Hughes (1987)]. Diagonal mass matrices are known as *lumped mass matrices*. The error estimates in (6.27) are generally not valid for lumped mass matrices. The *row-sum* and *proportional lumping* techniques are discussed here.

ROW-SUM LUMPING. The sum of the elements of each row of the consistent mass matrix is used as the diagonal element:

$$\boxed{M_{ii}^e = \sum_{j=1}^{n} \int_{x_A}^{x_B} \rho \psi_i^e \psi_j^e \, dx = \int_{x_A}^{x_B} \rho \psi_i^e \, dx} \tag{6.52}$$

where the property $\sum_{j=1}^{n} \psi_j^e = 1$ of the interpolation functions is used. When ρ is constant, (6.52) gives

$$[M^e]_L = \frac{\rho h_e}{2}\begin{bmatrix} 1 & 0 \\ 0 & 1 \end{bmatrix} \quad \text{for the Lagrange linear element}$$

$$[M^e]_L = \frac{\rho h_e}{6}\begin{bmatrix} 1 & 0 & 0 \\ 0 & 4 & 0 \\ 0 & 0 & 1 \end{bmatrix} \quad \text{for the Lagrange quadratic element} \tag{6.53a}$$

Compare these lumped mass matrices with the consistent mass matrices

$$[M^e]_C = \frac{\rho h_e}{6}\begin{bmatrix} 2 & 1 \\ 1 & 2 \end{bmatrix} \quad \text{for the Lagrange linear element}$$

$$[M^e]_C = \frac{\rho h_e}{30}\begin{bmatrix} 4 & 2 & -1 \\ 2 & 16 & 2 \\ -1 & 2 & 4 \end{bmatrix} \quad \text{for the Lagrange quadratic element} \tag{6.53b}$$

Here subscripts L and C refer to lumped and consistent mass matrices, respectively.

PROPORTIONAL LUMPING. Here the diagonal elements of the lumped mass matrix are computed to be proportional to the diagonal elements of the consistent mass matrix while conserving the total mass of the element:

$$\boxed{M^e_{ii} = \alpha \int_{x_A}^{x_B} \rho \psi^e_i \psi^e_i \, dx, \qquad \alpha = \left(\int_{x_A}^{x_B} \rho \, dx\right) \Big/ \left(\sum_{i=1}^{n} \int_{x_A}^{x_B} \rho \psi^e_i \psi^e_i \, dx\right)} \tag{6.54}$$

For constant ρ, the proportional lumping gives the same lumped mass matrices as those obtained in the row-sum technique for the Lagrange linear and quadratic elements.

The use of a lumped mass matrix in transient analyses can save computational time in two ways. First, for forward difference schemes, lumped mass matrices result in explicit algebraic equations, not requiring matrix inversions. Second, the critical time step required for conditionally stable schemes is larger, and hence less computational time is required when lumped mass matrices are used. To see this, consider the stability criterion in (6.46) for the case $\alpha = \frac{1}{2}$, $\beta = 0$. For a one linear element model of a uniform bar of stiffness EA and mass ρA, fixed at the left end, the eigenvalue problem with a consistent mass matrix is

$$\left(\frac{EA}{h}\begin{bmatrix} 1 & -1 \\ -1 & 1 \end{bmatrix} - \omega^2 \frac{\rho A h}{6}\begin{bmatrix} 2 & 1 \\ 1 & 2 \end{bmatrix}\right)\begin{Bmatrix} U_1 \\ U_2 \end{Bmatrix} = \begin{Bmatrix} Q^1_1 \\ Q^1_2 \end{Bmatrix}$$

Since $U_1 = 0$ and $Q^1_2 = 0$, we have

$$\omega^2 = \frac{EA}{h} \Big/ \frac{\rho A h}{3} = \frac{3E}{\rho h^2}$$

Substituting this into the critical time step relation (6.46), we have,

$$(\Delta t_{\text{cr}})_C = 2/\omega_{\max} = h(4\rho/3E)^{1/2}$$

If we use the lumped matrix, ω is given by

$$\omega = (2E/\rho)^{1/2}/h$$

and the critical time step is

$$\boxed{(\Delta t_{\text{cr}})_L = h(2\rho/E)^{1/2} > (\Delta t_{\text{cr}})_C} \tag{6.55}$$

6.2.5 Applications

Here we consider two examples of applications of finite element models of one-dimensional problems. Problems are taken from heat transfer and solid mechanics. Other field problems can be related to heat-transfer-type problems.

Example 6.3. Consider the transient heat conduction problem with equation

$$\frac{\partial u}{\partial t} - \frac{\partial^2 u}{\partial x^2} = 0 \quad \text{for } 0 < x < 1 \tag{6.56a}$$

boundary conditions

$$u(0, t) = 0, \quad \frac{\partial u}{\partial t}(1, t) = 0 \tag{6.56b}$$

and initial condition

$$u(x, 0) = 1.0 \tag{6.56c}$$

The problem at hand is a special case of (6.33*a*) with $a = 1$, $b = 0$, $c_0 = 0$, $c_1 = 1$, $c_2 = 0$, and $f = 0$. The finite element model of (6.56*a*) is given by (6.38*a*):

$$[M^e]\{\dot{u}\} + [K^e]\{u\} = \{Q^e\} \tag{6.57a}$$

where

$$M_{ij}^e = \int_{x_A}^{x_B} \psi_i^e \psi_j^e \, dx, \quad K_{ij}^e = \int_{x_A}^{x_B} \frac{d\psi_i^e}{dx}\frac{d\psi_j^e}{dx}\, dx \tag{6.57b}$$

For the choice of linear interpolation functions, (6.57*a*) becomes

$$\frac{h}{6}\begin{bmatrix} 2 & 1 \\ 1 & 2 \end{bmatrix}\begin{Bmatrix} \dot{u}_1 \\ \dot{u}_2 \end{Bmatrix} + \frac{1}{h}\begin{bmatrix} 1 & -1 \\ -1 & 1 \end{bmatrix}\begin{Bmatrix} u_1 \\ u_2 \end{Bmatrix} = \begin{Bmatrix} Q_1 \\ Q_2 \end{Bmatrix} \tag{6.57c}$$

where h is the length of the element. Use of the α-family of approximation (6.39) results in the equation [see (6.42)]

$$\begin{aligned}([M^e] + \Delta t\, \alpha[K^e])\{u^e\}_{s+1} = {} & ([M^e] - \Delta t\,(1-\alpha)[K^e])\{u^e\}_s \\ & + \Delta t(\alpha\{Q^e\}_{s+1} + (1-\alpha)\{Q^e\}_s)\end{aligned} \tag{6.58a}$$

where Δt is the time step.

For a one-element model, we have

$$\begin{aligned}&\begin{bmatrix} \frac{1}{3}h + \alpha\dfrac{\Delta t}{h} & \frac{1}{6}h - \alpha\dfrac{\Delta t}{h} \\ \frac{1}{6}h - \alpha\dfrac{\Delta t}{h} & \frac{1}{3}h + \alpha\dfrac{\Delta t}{h} \end{bmatrix}\begin{Bmatrix} U_1 \\ U_2 \end{Bmatrix}_{s+1} \\ &\quad = \begin{bmatrix} \frac{1}{3}h - (1-\alpha)\dfrac{\Delta t}{h} & \frac{1}{6}h + (1-\alpha)\dfrac{\Delta t}{h} \\ \frac{1}{6}h + (1-\alpha)\dfrac{\Delta t}{h} & \frac{1}{3}h - (1-\alpha)\dfrac{\Delta t}{h} \end{bmatrix}\begin{Bmatrix} U_1 \\ U_2 \end{Bmatrix}_s + \Delta t \begin{Bmatrix} \bar{Q}_1 \\ \bar{Q}_2 \end{Bmatrix}\end{aligned} \tag{6.58b}$$

where $\bar{Q}_i = \alpha(Q_i^1)_{s+1} + (1-\alpha)(Q_i^1)_s$. The boundary conditions of the problem require

$$(U_1)_s = 0, \quad (Q_2^1)_s = 0 \quad \text{for all } s > 0 \text{ (i.e., } t > 0)$$

while the initial condition requires

$$(U_1)_0 = 1, \quad (U_2)_0 = 1 \quad \text{for } t = 0$$

Since the initial condition should be consistent with the boundary conditions, we take $(U_1)_0 = 0.0$. Using the boundary conditions, we can write for the one-element model ($h = 1.0$)

$$\left(\tfrac{1}{3}h + \alpha\frac{\Delta t}{h}\right)(U_2)_{s+1} = \left[\tfrac{1}{3}h - (1-\alpha)\frac{\Delta t}{h}\right](U_2)_s \tag{6.59}$$

which can be solved repeatedly for U_2 at different times, $s = 0, 1, \ldots$.

Repeated use of (6.59) can cause the temporal approximation error to grow with time, depending on the value of α. As noted earlier, the forward difference scheme ($\alpha = 0$) is a conditionally stable scheme. The critical time step is given by

$$\Delta t_{cr} = 2/\lambda_{max}$$

where λ_{max} is the maximum eigenvalue associated with (6.57c):

$$-\lambda[M]\{U\} + [K]\{U\} = \{0\}$$

For the model at hand, this reduces to

$$-\tfrac{1}{3}\lambda h U_2 + h^{-1}U_2 = 0, \quad \text{or} \quad \lambda = 3/h^2 = 3$$

Hence $\Delta t_{cr} = 0.6667$. Thus, in order for the forward difference solution of (6.59) to be stable, the time step should be smaller than $\Delta t_{cr} = 0.6667$; otherwise, the solution will be unstable, as shown in Fig. 6.7.

For unconditionally stable schemes ($\alpha \geq \frac{1}{2}$), there is no restriction on the time step. However, to obtain a sufficiently accurate solution, the time step must be taken as a fraction of Δt_{cr}. Of course, the accuracy of the solution also depends on the mesh size h. As this is decreased (i.e., the number of elements is increased), Δt_{cr} decreases.

Figure 6.8 shows plots of $u(1, t)$ versus time for $\alpha = 0.5$ and $\Delta t = 0.05$. Solutions predicted by meshes of one and two linear elements and the mesh of one quadratic element are compared with the exact solution. The convergence of the solution with increasing number of elements is clear. The finite element solutions obtained with different methods, time steps, and meshes are compared with the exact solution in Table 6.3.

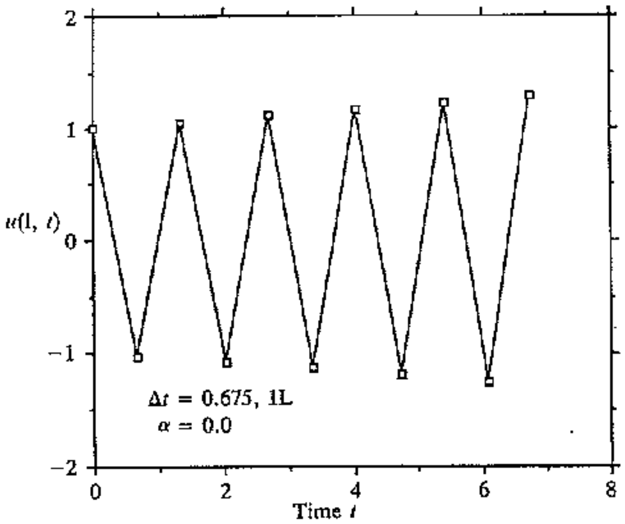

FIGURE 6.7
Transient solution of a parabolic equation according to the forward difference scheme ($\Delta t = 0.675$, one linear element). The solution is unstable because the time step is larger than the critical time step.

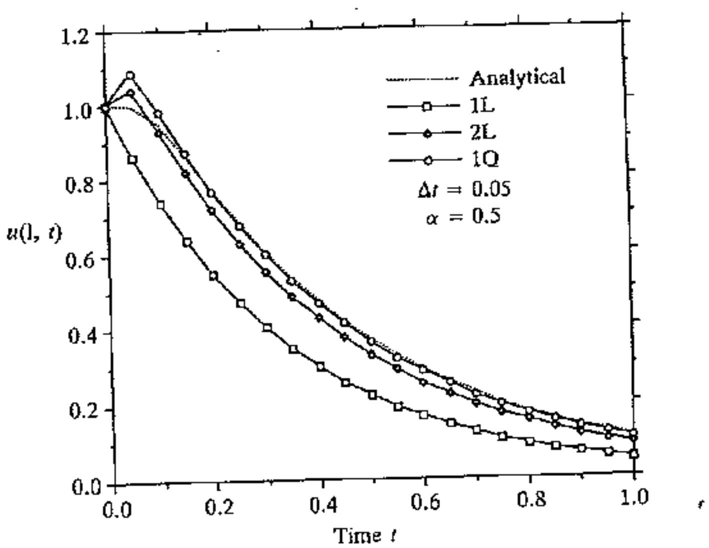

FIGURE 6.8
Transient solution of a parabolic equation according to linear and quadratic finite elements.

TABLE 6.3
A comparison of the finite element solutions obtained using various time approximation schemes and meshes with the analytical solution of a parabolic equation arising in conductive heat transfer

Time t	1L		Linear elements ($\alpha = 0.5$)				Quadratic elements ($\alpha = 0.5$, $t = 0.05$)			Exact solution
	$\alpha = 0$	$\alpha = 1$	1L	2L	4L	8L	1Q	2Q	4Q	
0.00	1.0000	1.0000	1.0000	1.0000	1.0000	1.0000	1.0000	1.0000	1.0000	1.0000
0.05	0.8500	0.8696	0.8605	1.0359	0.9951	0.9933	1.0870	0.9942	0.9928	0.9969
0.10	0.7225	0.7561	0.7404	0.9279	0.9588	0.9554	0.9819	0.9550	0.9549	0.9493
0.15	0.6141	0.6575	0.6371	0.8169	0.8639	0.8707	0.8693	0.8831	0.8725	0.8642
0.20	0.5220	0.5718	0.5482	0.7176	0.7557	0.7694	0.7679	0.7633	0.7731	0.7723
0.25	0.4437	0.4972	0.4717	0.6300	0.6759	0.6824	0.6780	0.6933	0.6855	0.6854
0.30	0.3771	0.4323	0.4059	0.5533	0.5906	0.6037	0.5987	0.6006	0.6070	0.6068
0.35	0.3206	0.3759	0.3492	0.4858	0.5250	0.5325	0.5286	0.5394	0.5358	0.5367
0.40	0.2725	0.3269	0.3005	0.4266	0.4608	0.4713	0.4668	0.4710	0.4741	0.4745
0.45	0.2316	0.2843	0.2586	0.3746	0.4083	0.4158	0.4121	0.4201	0.4188	0.4194
0.50	0.1969	0.2472	0.2225	0.3289	0.3592	0.3676	0.3639	0.3687	0.3701	0.3708
0.55	0.1673	0.2149	0.1914	0.2888	0.3176	0.3247	0.3213	0.3275	0.3273	0.3277
0.60	0.1422	0.1869	0.1647	0.2536	0.2798	0.2868	0.2837	0.2883	0.2890	0.2897
0.65	0.1209	0.1625	0.1418	0.2227	0.2472	0.2535	0.2505	0.2556	0.2556	0.2561
0.70	0.1028	0.1413	0.1220	0.1955	0.2180	0.2238	0.2212	0.2253	0.2258	0.2264
0.75	0.0874	0.1229	0.1050	0.1717	0.1924	0.1979	0.1953	0.1995	0.1996	0.2001
0.80	0.0743	0.1069	0.0903	0.1508	0.1697	0.1747	0.1725	0.1761	0.1764	0.1769
0.85	0.0631	0.0929	0.0777	0.1324	0.1498	0.1544	0.1523	0.1557	0.1559	0.1563
0.90	0.0536	0.0808	0.0669	0.1162	0.1322	0.1363	0.1345	0.1375	0.1378	0.1382
0.95	0.0456	0.0703	0.0575	0.1020	0.1166	0.1205	0.1187	0.1216	0.1218	0.1222
1.00	0.0388	0.0611	0.0495	0.0896	0.1029	0.1065	0.1048	0.1074	0.1076	0.1080

The next example concerns a hyperbolic equation.

Example 6.4. Consider the transverse motion of a beam clamped at both ends, according to the Euler–Bernoulli beam theory,

$$\frac{\partial^2 w}{\partial t^2}+\frac{\partial^4 w}{\partial x^4}=0 \quad \text{for } 0<x<1 \tag{6.60a}$$

$$w(0,t)=0, \quad \frac{\partial w}{\partial x}(0,t)=0, \quad w(1,t)=0, \quad \frac{\partial w}{\partial x}(1,t)=0 \tag{6.60b}$$

$$w(x,0)=\sin \pi x-\pi x(1-x), \quad \frac{\partial w}{\partial t}(x,0)=0 \tag{6.60c}$$

Note that the initial deflection of the beam is consistent with the boundary conditions. The initial slope is given by

$$\frac{\partial w}{\partial x}(x,0)=\pi \cos \pi x-\pi(1-2x) \tag{6.60d}$$

Because of symmetry about $x=0.5$, we consider only half of the beam for finite element modeling. In this case, the boundary condition at $x=0.5$ is $(\partial w/\partial x)(0.5,t)=0$. For a one-element model with the Euler–Bernoulli beam element, we have

$$\frac{h}{420}\begin{bmatrix} 156 & -22h & 54 & 13h \\ -22h & 4h^2 & -13h & -3h^2 \\ 54 & -13h & 156 & 22h \\ 13h & -3h^2 & 22h & 4h^2 \end{bmatrix}\begin{Bmatrix} \ddot{u}_1 \\ \ddot{u}_2 \\ \ddot{u}_3 \\ \ddot{u}_4 \end{Bmatrix} + \frac{2}{h^3}\begin{bmatrix} 6 & -3h & -6 & -3h \\ -3h & 2h^2 & 3h & h^2 \\ -6 & 3h & 6 & 3h \\ -3h & h^2 & 3h & 2h^2 \end{bmatrix}\begin{Bmatrix} u_1 \\ u_2 \\ u_3 \\ u_4 \end{Bmatrix}=\begin{Bmatrix} Q_1 \\ Q_2 \\ Q_3 \\ Q_4 \end{Bmatrix}$$

The boundary conditions for the one-element model translate into

$$U_1=0, \quad U_2=0, \quad U_4=0, \quad Q_3=0 \quad \text{for all } t>0$$

while the initial conditions

$$\left.\begin{matrix} U_1=0, & U_2=0, & U_3=0.2146, & U_4=0 \\ \dot{U}_1=0, & \dot{U}_2=0, & \dot{U}_3=0, & \dot{U}_4=0 \end{matrix}\right\} \quad \text{for } t=0$$

The time marching scheme (6.47a) for this case takes the form

$$(K_{33}+a_3M_{33})(U_3)_{s+1}=(\hat{F}_3)_{s,s+1}\equiv M_{33}(a_3U_3+a_4\dot{U}_3+a_5\ddot{U}_3)_s$$

where a_3, a_4, and a_5 are defined in (6.47b). The second derivative $\ddot{U}_3$ for time $t=0$ (i.e., when $s=0$) is computed from the equation of motion:

$$(\ddot{U}_3)_0=-\frac{K_{33}(U_3)_0}{M_{33}}=-\left(\frac{12}{h^3}\times 0.2146\right)\frac{420}{156h}=-110.932$$

The stability criterion (6.46) requires, for $\gamma<\frac{1}{2}$, that the time step Δt be less than Δt_{cr}. For the present model, $\omega_{\max}$ is computed from the eigenvalue problem

$$(K_{33}-\omega^2M_{33})U_3=0 \quad \text{or} \quad \omega^2=M_{33}/K_{33}=516.923$$

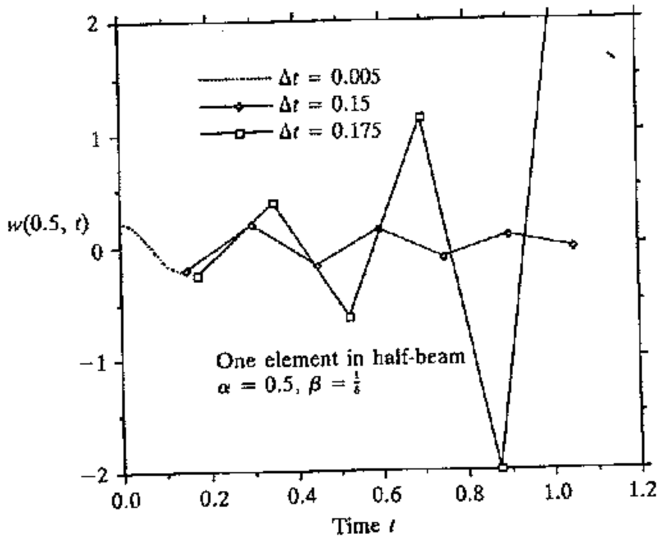

FIGURE 6.9
Transient response of a beam clamped at both ends, according to the linear acceleration method ($\alpha = 0.5$ and $\beta = \frac{1}{6}$). The critical time step for the method using one element is 0.1524. The remainder of the $\Delta t = 0.005$ plot is not shown.

Hence, the critical time step for $\alpha = 0.5$ and $\gamma = \frac{1}{3}$ (i.e., the linear acceleration scheme) is

$$\Delta t_{cr} = \sqrt{12}/\omega_{\max} = 0.15236$$

Although there is no restriction on time integration schemes with $\alpha = 0.5$ and $\gamma > 0.5$, the critical time step provides an estimate of the time step to be used.

Figure 6.9 shows plots of $w(0.5, t)$ versus time for the scheme $\alpha = 0.5$, $\gamma = \frac{1}{3}$. Three different time steps, $\Delta t = 0.175$, 0.150, and 0.005, are used to illustrate the accuracy. For $\Delta t = 0.175 > \Delta t_{cr}$, the solution is unstable, whereas for $\Delta t = 0.15 < \Delta t_{cr}$, it is stable but inaccurate. The period of the solution is given by

$$T = 2\pi/\omega = 0.27635$$

For a time step $\Delta t = 0.005$, the solution is predicted very accurately.

For two- and four-element meshes, the critical steps are computed by computing the maximum eigenvalues of the corresponding discrete systems. The critical time steps for the two meshes are

$$(\Delta t_{cr})_2 = 0.00897, \quad (\Delta t_{cr})_4 = 0.00135$$

where the subscripts refer to the number of elements in the mesh. Figure 6.10 shows a comparison of the transverse deflections obtained with the two Euler–Bernoulli elements ($\Delta t = 0.005$) and the Galerkin method (see Chapter 2) for a complete period (0, 0.28).

The problem can also be analyzed using the Timoshenko beam element, which requires us to select the coefficients GAK, EI, ρA, and ρI consistent with those in the differential equation (6.11). Comparing (6.60a) with (6.11), we have $EI = 1.0$ and

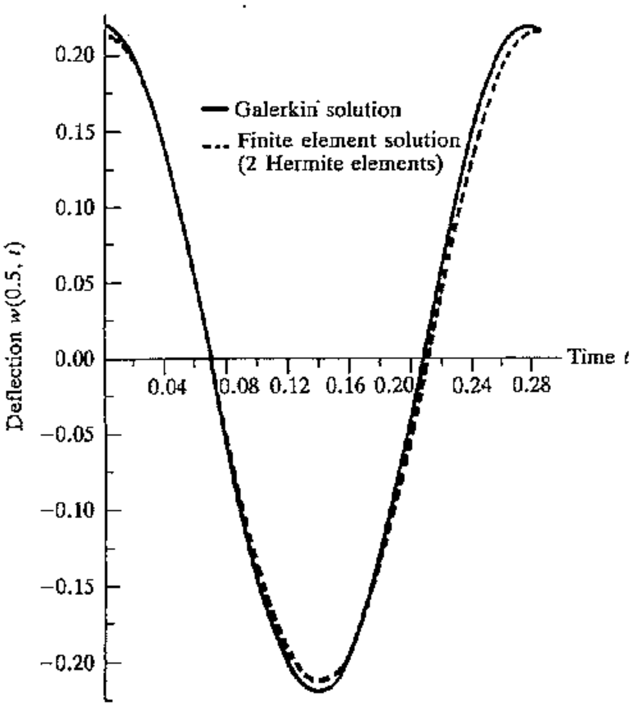

FIGURE 6.10
Transient response of a beam clamped at both ends and subjected to an initial transverse deflection ($\Delta t = 0.005$, $\alpha = 0.5$, and $\beta = 0.25$).

$\rho A = 1.0$. Therefore, GAK can be computed as

$$GAK = \frac{E}{2(1+\nu)} BHK = \frac{EI}{2(1+\nu)} \frac{12}{H^2} \frac{5}{6} = \frac{4}{H^2} EI \tag{6.61}$$

where B is the width and H the height of the beam, and $I = \frac{1}{12}BH^3$, $\nu = 0.25$, and $K = \frac{5}{6}$ are used in arriving at the last expression. Similarly,

$$\rho I = \rho \tfrac{1}{12} BH^3 = \tfrac{1}{12} \rho A H^2 \tag{6.62}$$

For $L/H = 100$ (since $L = 1.0$, $H = 0.01$), the shear deformation effect is small; while for $L/H = 10$ (or $H = 0.1$), it is significant enough to warrant its inclusion in the analysis.

Table 6.4 gives values of $w(0.5, t)$ as obtained using the Euler–Bernoulli and Timoshenko elements for various numbers of elements. The time step is taken to be $\Delta t = 0.005$, which is larger than that required for stability of the four-element mesh of the Euler–Bernoulli beam element when $\gamma = \frac{1}{2}$. Figure 6.11 shows plots of $w(0.5, t)$ obtained with two quadratic Timoshenko elements for $L/H = 100$ and 10. The Timoshenko elements have better stability characteristics (i.e., larger Δt_{cr}) than the Euler–Bernoulli beam element for small ratios L/H. This is because, as L/H is decreased, the $\omega_{\max}$ predicted by the Timoshenko beam theory is smaller than that predicted by the Euler–Bernoulli beam theory. The critical time steps for the mesh of

TABLE 6.4
Effect of mesh and shear deformation on the transient response of a beam clamped at both ends ($\Delta t = 0.005$)

Time	Euler–Bernoulli beam element						Timoshenko element (2Q)		Galerkin in space and exact in time
	$\alpha = 0.25$, $\beta = 1.6$			$\alpha = 0.5$, $\beta = 0.25$			$\alpha = 0.5$, $\beta = 0.25$		
t	1	2	4†	1	2	4	$L/H = 100$	$L/H = 10$	
0.00	0.2146	0.2146	0.2146	0.2146	0.2146	0.2146	0.2146	0.2146	0.2146
0.01	0.2091	0.2098	0.2098	0.2091	0.2098	0.2098	0.2100	0.2116	0.2157
0.02	0.1928	0.1951	0.1950	0.1928	0.1951	0.1951	0.1953	0.1951	0.1988
0.03	0.1666	0.1696	0.1681	0.1667	0.1696	0.1698	0.1695	0.1690	0.1716
0.04	0.1319	0.1346	0.1181	0.1320	0.1348	0.1350	0.1342	0.1427	0.1356
0.05	0.0904	0.0930	−0.0795	0.0905	0.0931	0.0935	0.0929	0.1067	0.0925
0.06	0.0442	0.0481	−1.7165	−0.0443	0.0482	0.0483	0.0484	0.0657	0.0447
0.07	−0.0043	0.0014	−17.877	−0.0041	0.0014	0.0018	0.0016	0.0234	−0.0055
0.08	−0.0525	−0.0462	−179.92	−0.0523	−0.0459	−0.0455	−0.0469	−0.0267	−0.0553
0.09	−0.0980	−0.0926	−1796.9	−0.0978	−0.0923	−0.0916	−0.0937	−0.0706	−0.1023
0.10	−0.1385	−0.1345	·	−0.1383	−0.1342	−0.1336	−0.1349	−0.1100	−0.1441
0.11	−0.1719	−0.1685	·	−0.1717	−0.1685	−0.1682	−0.1680	−0.1461	−0.1783
0.12	−0.1964	−0.1933	·	−0.1963	−0.1933	−0.1932	−0.1931	−0.1717	−0.2034
0.13	−0.2108	−0.2088	·	−0.2108	−0.2088	−0.2087	−0.2100	−0.1969	−0.2179
0.14	−0.2144	−0.2153	·	−0.2144	−0.2150	−0.2148	−0.2169	−0.2110	−0.2211
0.15	−0.2070	−0.2113	Diverged	−0.2071	−0.2112	−0.2111	−0.2117	−0.2146	−0.2129

† $\Delta t_{cr} = 0.00135$

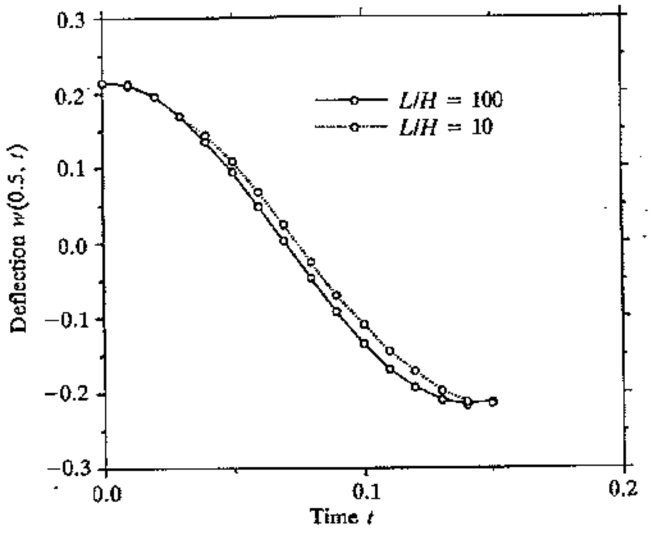

FIGURE 6.11
Transient response of a beam clamped at both ends, according to the Timoshenko beam theory ($\Delta t = 0.005$, two quadratic elements are used, $\alpha = 0.5$, and $\beta = 0.25$).

two quadratic elements are

$$(\Delta t_{cr})_{100} = 0.00665, \quad (\Delta t_{cr})_{10} = 0.00644$$

where the subscripts refer to the ratio L/H. This completes the example.

6.3 SUMMARY

In this chapter eigenvalue problems and their formulation for one-dimensional second- and fourth-order equations (beams) have been discussed, finite element models of the equations have been developed, and applications to heat transfer and the natural vibration of beams have been presented. Except for the solution procedure, the finite element formulation of eigenvalue problems is entirely analogous to boundary value problems.

Finite element models of time-dependent problems described by parabolic and hyperbolic equations have also been presented. A two-step procedure to derive finite element models from differential equations has been described. In the first step, we seek spatial approximations of the dependent variables of the problem as linear combinations of nodal values that are functions of time and interpolation functions that are functions of space. This procedure is entirely analogous to the finite element formulation presented for boundary value problems in Chapters 3 and 4. The end result of this step is a set of ordinary differential equations (in time) among the nodal values. In the second step, the ordinary differential equations are further approximated to replace the time derivatives with the values of the functions at different times.

PROBLEMS

Section 6.1

6.1. Determine the first two longitudinal frequencies of a rod (E, A, L) fixed at one end and spring-supported at the other:

$$-EA\frac{\partial^2 u}{\partial x^2} + \rho A\frac{\partial^2 u}{\partial t^2} = 0 \quad \text{for } 0 < x < L$$

$$u(0) = 0, \quad \left(EA\frac{du}{dx} + ku\right)\Big|_{x=L} = 0$$

Use (*a*) two linear finite elements and (*b*) one quadratic element.

Answer: (a) The characteristic equation is $7\lambda^2 - (10+4c)\lambda + (1+2c) = 0$, $c = kh/EA$, $\lambda = (\rho h^2/6E)\omega^2$.

6.2. Determine the smallest natural frequency of a beam with clamped ends, and of constant cross-sectional area A, moment of inertia I, and length L. Use the symmetry and two Euler–Bernoulli beam elements in the half-beam.

6.3. Re-solve the above problem with two linear Timoshenko beam elements in the half-beam.

6.4. Consider a beam (A, I, E, L) with its left end clamped and its right end supported by an elastic spring. Determine the fundamental natural frequency using (*a*) one Euler–Bernoulli beam and (*b*) one Timoshenko beam element.

6.5. Determine the critical buckling load of a cantilever beam (A, I, L, E) using (a) one Euler–Bernoulli beam element and (b) one Timoshenko beam element.

6.6. Determine the fundamental natural frequency of the truss shown in Fig. P4.24.

6.7. Determine the fundamental natural frequency of the frame shown in Fig. P4.27.

6.8. Determine the first two longitudinal natural frequencies of a rod (A, E, L, m), fixed at one end and with an attached mass m_2 at the other. Use two linear elements.

Hint: Note that the boundary conditions for the problem are $u(0)=0$ and $(EA\,\partial u/\partial x + m_2\,\partial^2 u/\partial t^2)|_{x=L}=0$.

6.9. The equation governing the torsional vibration of a circular rod is

$$-GJ\frac{\partial^2 \phi}{\partial x^2}+mJ\frac{\partial^2 \phi}{\partial t^2}=0$$

where ϕ is the angular displacement, J the moment of inertia, G the shear modulus, and m the density. Determine the fundamental torsional frequency of a rod with disk (J_1) attached at each end. Use the symmetry and (a) two linear elements, (b) one quadratic element.

6.10. The equations governing the motion of a beam according to the Timoshenko beam theory can be written as

$$a^2\frac{\partial^4 w}{\partial x^4}+\frac{\partial^2 w}{\partial t^2}-b^2\left(1+\frac{E}{kG}\right)\frac{\partial^4 w}{\partial x^2\,\partial t^2}+b^2\frac{m}{kG}\frac{\partial^4 w}{\partial t^4}=0$$

where $a^2=EI/mA$ and $b^2=I/A$. Assuming that $b^2m/kG \ll 1$ (i.e., neglecting the last term in the governing equation), formulate the eigenvalue problem for the determination of natural frequencies, and develop the finite element model of the eigenvalue problem.

6.11. Use the finite element model of Problem 6.10 to determine the fundamental frequency of a simply supported beam.

6.12. Find the critical buckling load P_{cr} by determining the eigenvalues of the equation

$$EI\frac{d^4 w}{dx^4}+P_{cr}\frac{d^2 w}{dx^2}=0 \quad \text{for } 0<x<L$$

$$w(0)=w(L)=0, \qquad \left(EI\frac{d^2 w}{dx^2}\right)\bigg|_{x=0}=\left(EI\frac{d^2 w}{dx^2}\right)\bigg|_{x=L}=0$$

Use one Euler–Bernoulli element in the half-beam.

Answer: $P_{cr}=9.9439EI/L^2$.

Section 6.2

6.13. Consider the partial differential equation arising in connection with unsteady heat transfer in an insulated rod:

$$\frac{\partial u}{\partial t}-\frac{\partial}{\partial x}\left(a\frac{\partial u}{\partial x}\right)=f \quad \text{for } 0<x<L$$

$$u(0)=u_0, \qquad \left[a\frac{\partial u}{\partial x}+\beta(u-u_\infty)+\hat{q}\right]\bigg|_{x=L}=0$$

Following the procedure outlined in Section 6.2, derive the semidiscrete variational form, the semidiscrete finite element model, and the fully discretized finite element equations for a typical element.

6.14. Using a two-element (linear) model and the semidiscrete finite element equations derived in Problem 6.13, determine the nodal temperatures as functions of time for the case in which $a = 1$, $f = 0$, $u_0 = 1$, and $\hat{q} = 0$. Use the Laplace transform technique [see Reddy (1986)] to solve the ordinary differential equations in time.

6.15. Consider a uniform bar of cross-sectional area A, modulus of elasticity E, mass density m, and length L. The axial displacement under the action of time-dependent axial forces is governed by the wave equation

$$\frac{\partial^2 u}{\partial t^2} = a^2 \frac{\partial^2 u}{\partial x^2}, \qquad a = \left(\frac{E}{m}\right)^{1/2}$$

Determine the transient response [i.e., find $u(x, t)$] of the bar when the end $x = 0$ is fixed and the end $x = L$ is subjected to a force P_0. Assume zero initial conditions. Use one linear element to approximate the spatial variation of the solution, and solve the resulting ordinary differential equation in time exactly to obtain

$$u_2(x, t) = \frac{P_0 L}{AE}\frac{x}{L}(1 - \cos \alpha t), \qquad \alpha = \sqrt{3}\frac{a}{L}$$

6.16. Re-solve Problem 6.15 with a mesh of two linear elements. Use the Laplace transform method to solve the two ordinary differential equations in time.

6.17. Solve Problem 6.15 when the right end is subjected to an axial force F_0 and supported by an axial spring of stiffness k.
Answer:

$$u_2(t) = c(1 - \cos \beta t), \qquad c = \frac{3F_0}{mAL\beta^2}, \qquad \beta = \sqrt{3}\frac{a}{L}\left(1 + \frac{kL}{EA}\right)^{1/2}$$

6.18. A bar of length L moving with velocity v_0 strikes a spring of stiffness k. Determine the motion $u(x, t)$ from the instant the end $x = 0$ strikes the spring. Use one linear element.

6.19. A uniform rod of length L and mass m is fixed at $x = 0$ and loaded with a mass M at $x = L$. Determine the motion $u(x, t)$ of the system when the mass M is subjected to a force P_0. Use one linear element.
Answer:

$$u_2(t) = c(1 - \cos \lambda t), \qquad c = \frac{P_0 L}{AE}, \qquad \lambda = \sqrt{3}\frac{a}{L}\left(\frac{3M}{AL} + m\right)^{-1}$$

6.20. The flow of liquid in a pipe, subjected to a surge-of-pressure wave (i.e., a water hammer), experiences a surge pressure p, which is governed by the equation

$$\frac{\partial^2 p}{\partial t^2} - c^2 \frac{\partial^2 p}{\partial x^2} = 0, \qquad c^2 = \frac{1}{m}\left(\frac{1}{k} + \frac{D}{bE}\right)^{-1}$$

where m is the mass density and K the bulk modulus of the fluid, D is the diameter and b the thickness of the pipe, and E is the modulus of elasticity of the pipe material. Determine the pressure $p(x, t)$ using one linear finite element, for the following boundary and initial conditions:

$$p(0, t) = p_0, \qquad p(L, t) = 0, \qquad p(x, 0) = p_0$$

6.21. Consider the problem of determining the temperature distribution of a solid cylinder, initially at a uniform temperature T_0 and cooled in a medium of zero temperature (i.e., $T_\infty = 0$). The governing equation of the problem is

$$\rho c \frac{\partial T}{\partial t} - \frac{1}{r}\frac{\partial}{\partial r}\left(rk\frac{\partial T}{\partial r}\right) = 0$$

The boundary conditions are

$$\frac{\partial T}{\partial r}(0, t) = 0, \qquad \left(rk\frac{\partial T}{\partial r} + \beta T\right)\Big|_{r=R} = 0$$

The initial condition is $T(r, t) = T_0$. Determine the temperature distribution $T(r, t)$ using one linear element. Take $R = 2.5$ cm, $T_0 = 130$ °C, $k = 215\ \mathrm{W\,m^{-1}\,°C^{-1}}$, $\beta = 525\ \mathrm{W\,m^{-2}\,°C^{-1}}$, $\rho = 2700\ \mathrm{kg\,m^{-2}}$, and $c = 0.9\ \mathrm{kJ\,kg^{-1}\,°C^{-1}}$. What is the heat loss at the surface?

6.22. Determine the nondimensional temperature $\theta(r, t)$ in the region bounded by two long cylindrical surfaces of radii R_1 and R_2. The dimensionless heat conduction equation is

$$-\frac{1}{r}\frac{\partial}{\partial r}\left(r\frac{\partial \theta}{\partial r}\right) + \frac{\partial \theta}{\partial t} = 0$$

with boundary and initial conditions

$$\frac{\partial \theta}{\partial r}(R_1, t) = 0, \qquad \theta(R_2, t) = 1, \qquad \theta(r, 0) = 0$$

6.23. Show that (6.44) and (6.45) can be expressed in the alternative form [see (6.47)]

$$[H]\{\ddot{u}\}_{s+1} = \{F\}_{s+1} - [K]\{b\}_s$$

where

$$[H] = \beta(\Delta t)^2[K] + [M], \qquad \{b\} = \{u\}_s + \Delta t\,\{\dot{u}\}_s + (\tfrac{1}{2} - \beta)(\Delta t)^2\{\ddot{u}\}_s$$

6.24. Using the Newmark integration scheme (6.45), express the equation

$$[M]\{\ddot{u}\} + [C]\{\dot{u}\} + [K]\{u\} = \{F\}$$

in the form

$$[\hat{K}]\{u\}_{s+1} = \{\hat{F}\}_{s+1}$$

where

$$[\hat{K}] = [K] + a_0[M] + a_5[C]$$

$$\{\hat{F}\}_{s+1} = \{F\}_{s+1} + [M](a_0\{u\}_s + a_1\{\dot{u}\}_s + a_2\{\ddot{u}\}_s) + [C](a_5\{u\}_s + a_6\{\dot{u}\}_s + a_7\{\ddot{u}\}_s)$$

$$a_5 = \frac{\alpha}{\beta\,\Delta t}, \qquad a_6 = \frac{\alpha}{\beta} - 1, \qquad a_7 = \frac{\Delta t}{2}\left(\frac{\alpha}{\beta} - 2\right)$$

6.25. A uniform cantilever beam of length L, moment of inertia I, modulus of elasticity E, and mass m begins to vibrate with initial displacement

$$w(x, 0) = w_0 x^2/L^2$$

and zero initial velocity. Find its displacement at the free end at any subsequent time. Use one Euler–Bernoulli beam element to determine the solution. Solve the resulting differential equations in time using the Laplace transform method.

6.26. Re-solve Problem 6.25 using one Timoshenko element.

6.27. Use the Newmark integration scheme to reduce the ordinary differential equations of time in Problem 6.10 to algebraic equations.

REFERENCES FOR ADDITIONAL READING

Bathe, K.J.: *Finite Element Procedures in Engineering Analysis,* Prentice-Hall, Englewood Cliffs, NJ, 1982.

—— and E. L. Wilson: "Stability and Accuracy Analysis of Direct Integration Methods," *International Journal of Earthquake Engineering and Structural Dynamics,* vol. 1, pp. 283–291, 1973.

Belytschko, T.: "An Overview of Semidiscretization and Time Integration Procedures," in *Computational Methods for Transient Analysis,* eds. T. Belytschko and T. J. R. Hughes, pp. 1–65, North-Holland, Amsterdam, 1983.

Goudreau, G. L., and R. L. Taylor: "Evaluation of Numerical Integration Methods in Elastodynamics," *Journal of Computer Methods in Applied Mechanics and Engineering,* vol. 2, No. 1, pp. 69–97, 1973.

Hilber, H. M.: "Analysis and Design of Numerical Integration Methods in Structural Dynamics," EERC Report no. 77–29, Earthquake Engineering Research Center, University of California, Berkeley, California, November 1976.

Houbolt, J. C.: "A Recurrence Matrix Solution for the Dynamic Response of Elastic Aircraft," *Journal of Aeronautical Science,* vol. 17, pp. 540–550, 1950.

Hughes, T. J. R.: "Analysis of Transient Algorithms with Particular Reference to Stability Behavior," in *Computational Methods for Transient Analysis,* eds. T. Belytschko and T. J. R. Hughes, pp. 67–155, North-Holland, Amsterdam, 1983.

———: *The Finite Element Method,* Prentice-Hall, Englewood Cliffs, NJ, 1987.

——— and W. K. Liu: "Implicit–Explicit Finite Elements in Transient Analysis: Stability Theory," *Journal of Applied Mechanics,* vol. 45, pp. 371–374, 1978.

——— and W. K. Liu: "Implicit–Explicit Finite Elements in Transient Analysis: Implementation and Numerical Examples," *Journal of Applied Mechanics,* vol. 45, pp. 375–378, 1978.

———, Pister, K. S., and Taylor, R. L.: "Implicit–Explicit Finite Elements in Nonlinear Transient Analysis," *Computer Methods in Applied Mechanics and Engineering,* vol. 17/18, pp. 159–182, 1979.

Isaacson, E., and H. B. Keller: *Analysis of Numerical Methods,* John Wiley, New York, 1966.

Krieg, R. D., "Unconditional Stability in Numerical Time Integration Methods," *Transactions of the ASME, Journal of Applied Mechanics,* vol. 40, pp. 417–421, June 1973.

Lanczos, C.: *Applied Analysis,* Prentice-Hall, Englewood Cliffs, NJ, 1956.

Newmark, N. M.: "A Method of Computation for Structural Dynamics," *Journal of Engineering Mechanics Division, ASCE,* vol. 85, pp. 67–94, 1959.

Nickell, R. E.: "On the Stability of Approximation Operators in Problems of Structural Dynamics," *International Journal of Solids and Structures,* vol. 7, pp. 301–319, 1971.

———: "Direct Integration in Structural Dynamics," *Journal of Engineering Mechanics Division, ASCE,* vol. 99, pp. 303–317, 1973.

———: "Nonlinear Dynamics by Mode Superposition," *Journal of Computer Methods in Applied Mechanics and Engineering,* vol. 7, pp. 107–129, 1976.

Park, K. C.: "An Improved Stiffly Stable Method for Direct Integration of Nonlinear Structural Dynamics Equations," *Journal of Applied Mechanics,* vol. 42, pp. 464–470, 1975.

Wilson, E. L., I. Farhoomand, and K. J. Bathe: "Nonlinear Dynamic Analysis of Complex Structures," *International Journal of Earthquake Engineering and Structural Dynamics,* vol. 1, pp. 241–252, 1973.

CHAPTER
7

NUMERICAL INTEGRATION AND COMPUTER IMPLEMENTATION

7.1 ISOPARAMETRIC FORMULATIONS AND NUMERICAL INTEGRATION

7.1.1 Background

Exact evaluation of the integrals appearing in element coefficient matrices and source vectors is not always possible because of the algebraic complexity of the coefficients a, b, and c in differential equations. In such cases, it is natural to seek numerical evaluation of these integral expressions. Numerical evaluation of the coefficient matrices is also useful in problems with constraints, where reduced integration techniques are used (see, e.g., the reduced integration element of the Timoshenko beam theory, Section 4.4).

Numerical evaluation of integrals, called *numerical integration* or *numerical quadrature*, involves approximation of the integrand by a polynomial of sufficient degree, because the integral of a polynomial can be evaluated exactly. For example, consider the integral,

$$\mathscr{I} = \int_{x_A}^{x_B} F(x)\,dx \tag{7.1}$$

We approximate the function $F(x)$ by a polynomial:

$$F(x) \approx \sum_{I=1}^{N} F_I \psi_I(x) \tag{7.2}$$

where F_I denotes the value of $F(x)$ at the Ith point of the interval $[x_A, x_B]$ and $\psi_I(x)$ are polynomials of degree $N-1$. The representation can be viewed as the finite element interpolation of $F(x)$, where F_I is the value of the function at the Ith node. The interpolation can be of the Lagrange type or the Hermite type.

Substitution of (7.2) into (7.1) and evaluation of the integral gives an approximate value of $\mathcal{I}$. For example, suppose that we choose linear interpolation of $F(x)$. Then $N=2$, $\psi_1 = (x_B - x)/h$, $\psi_2 = (x - x_A)/h$, and

$$\mathcal{I} = \tfrac{1}{2}h(F_1 + F_2), \qquad F_1 = F(x_A), \qquad F_2 = F(x_B) \tag{7.3}$$

Thus, the value of the integral is given by the area of a trapezoid used to approximate the area under the function $F(x)$ (see Fig. 7.1). Equation (7.3) is known as the *trapezoidal rule* of numerical integration. If we use the Lagrange quadratic interpolation of $F(x)$, we obtain

$$\begin{aligned} \mathcal{I} &= \tfrac{1}{6}h(F_1 + 4F_2 + F_3), \qquad F_1 = F(x_A), \\ F_2 &= F(x_A + \tfrac{1}{2}h), \qquad F_3 = F(x_B) \end{aligned} \tag{7.4}$$

which is known as *Simpson's one-third rule*.

Equations (7.3) and (7.4) represent the form of numerical quadrature formulae. In general, a quadrature formula has the form

$$\mathcal{I} = \int_{x_A}^{x_B} F(x)\,dx \approx \sum_{I=1}^{I} F(x_I) W_I \tag{7.5}$$

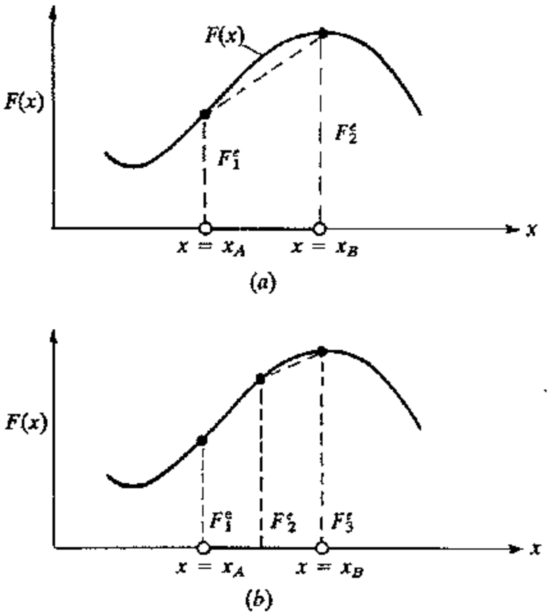

FIGURE 7.1
Approximate evaluation of an integral using the trapezoidal rule: (*a*) Two-point formula; (*b*) three-point formula.

where x_I are called the *quadrature points* and W_I are the *quadrature weights.* These formulae require functional evaluations, multiplications, and additions to obtain the numerical value of the integral. They yield exact values of the integral whenever $F(x)$ is a polynomial of order $r - 1$.

In this section, we describe several numerical integration techniques and formulations in which the geometry as well as the dependent variables are approximated using different degrees of polynomials. We begin with the discussion of a local coordinate system.

7.1.2 Natural Coordinates

Of all the quadrature formulae, as will be discussed in the subsequent sections, the Gauss–Legendre one is the most commonly used. The details of the method itself will be discussed shortly. The formula requires the integral to be cast as one to be evaluated over the interval $[-1, 1]$. This requires the transformation of the problem coordinate x to a local coordinate ξ such that (see Fig. 7.2):

$$\text{when} \quad x = x_A, \quad \xi = -1; \qquad \text{when} \quad x = x_B, \quad \xi = 1$$

The transformation between x and ξ can be represented by the linear "stretch" transformation

$$x = a + b\xi$$

where a and b are constants to be determined such that the above conditions hold:

$$x_A = a + b(-1), \qquad x_B = a + b(1)$$

Solving for a and b, we obtain

$$b = \tfrac{1}{2}(x_B - x_A) = \tfrac{1}{2}h_e, \qquad a = \tfrac{1}{2}(x_B + x_A) = x_A + \tfrac{1}{2}h_e$$

Hence the transformation takes the form

$$x = x_A + \tfrac{1}{2}h_e(1 + \xi) \tag{7.6}$$

where x_A denotes the global coordinate of the left end node of the element Ω^e and h_e is the element length (see Fig. 7.2). The local coordinate ξ is called the *normal coordinate* or *natural coordinate,* and its values always lie between -1 and 1, with its origin at the center of the element.

The local coordinate ξ is useful in two ways: (i) it is convenient in constructing the interpolation functions; (ii) it is required in numerical integration using Gauss–Legendre quadrature.

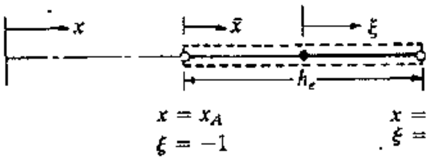

FIGURE 7.2
Global coordinate x, local coordinate $\bar{x}$, and normalized local coordinate ξ.

The derivation of the Lagrange family of interpolation functions in terms of the natural coordinate ξ is made easy by the property 1 in (3.28) of the interpolation functions:

$$\psi_i(\xi_j) = \begin{cases} 1 & \text{if } i = j \\ 0 & \text{if } i \neq j \end{cases} \tag{7.7}$$

where ξ_j is the ξ coordinate of the jth node in the element. For an element with n nodes, ψ_i $(i = 1, 2, \ldots, n)$ are functions of degree $n - 1$. To construct ψ_i satisfying (7.7), we proceed as follows. For each ψ_i, we form the product of $n - 1$ linear functions $\xi - \xi_j$ $(j = 1, 2, \ldots, i-1, i+1, \ldots, n, j \neq i)$:

$$\psi_i = c_i(\xi - \xi_1)(\xi - \xi_2) \cdots (\xi - \xi_{i-1})(\xi - \xi_{i+1}) \cdots (\xi - \xi_n)$$

Note that ψ_i is zero at all nodes except the ith. Next we determine the constant c_i such that $\psi_i = 1$ at $\xi = \xi_i$:

$$c_i = [(\xi_i - \xi_1)(\xi_i - \xi_2) \cdots (\xi_i - \xi_{i-1})(\xi_i - \xi_{i+1}) \cdots (\xi_i - \xi_n)]^{-1}$$

Thus, the interpolation function associated with node i is

$$\psi_i(\xi) = \frac{(\xi - \xi_1)(\xi - \xi_2) \cdots (\xi - \xi_{i-1})(\xi - \xi_{i+1}) \cdots (\xi - \xi_n)}{(\xi_i - \xi_1)(\xi_i - \xi_2) \cdots (\xi_i - \xi_{i-1})(\xi_i - \xi_{i+1}) \cdots (\xi_i - \xi_n)} \tag{7.8}$$

Interpolation functions that satisfy (7.7) are said to belong to the *Lagrange family of interpolation functions*, and the associated finite elements belong to the *Lagrange family of finite elements*. The interpolation functions ψ_i in (3.16*b*) and (3.18) provide an example of the Lagrange interpolation functions ($n = 2$). Figure 7.3 shows the linear, quadratic, and cubic Lagrange interpolation functions expressed in terms of the natural coordinate (for equally spaced nodes).

7.1.3 Approximation of Geometry

Recall from (3.31*c*) and (4.12*c*) that the element matrices involve the derivatives of the interpolation functions with respect to the global coordinate

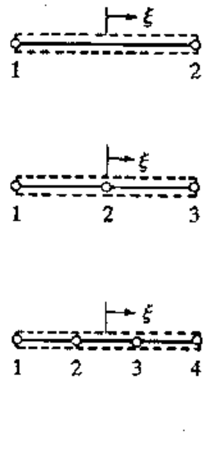

$$\psi_1 = \tfrac{1}{2}(1 - \xi)$$
$$\psi_2 = \tfrac{1}{2}(1 + \xi)$$

$$\psi_1 = -\tfrac{1}{2}\xi(1 - \xi)$$
$$\psi_2 = (1 + \xi)(1 - \xi)$$
$$\psi_3 = \tfrac{1}{2}\xi(1 + \xi)$$

$$\psi_1 = -\tfrac{9}{16}(1 - \xi)(\tfrac{1}{3} + \xi)(\tfrac{1}{3} - \xi)$$
$$\psi_2 = \tfrac{27}{16}(1 + \xi)(1 - \xi)(\tfrac{1}{3} - \xi)$$
$$\psi_3 = \tfrac{27}{16}(1 + \xi)(1 - \xi)(\tfrac{1}{3} + \xi)$$
$$\psi_4 = -\tfrac{9}{16}(\tfrac{1}{3} + \xi)(\tfrac{1}{3} - \xi)(1 + \xi)$$

FIGURE 7.3
Lagrange family of 1-D interpolation functions in terms of the normalized coordinate.

x. A transformation of the form

$$x = f(\xi) \tag{7.9}$$

is required in order to rewrite the integrals in terms of ξ $(-1 \leq \xi \leq 1)$. The function f is assumed to be a one-to-one transformation. An example of $f(\xi)$ is provided by (7.6):

$$f(\xi) = x_A + \tfrac{1}{2}h_e(1 + \xi),$$

In this case, $f(\xi)$ is a linear function of ξ. Hence, a straight line is transformed into a straight line. When f is a nonlinear function, a straight line is mapped into a curve of the same degree as the transformation.

It is natural to think of approximating the geometry in the same way as we approximated a dependent variable. In other words, the transformation $x = f(\xi)$ can be written as

$$x = \sum_{i=1}^{m} x_i^e \hat{\psi}_i^e(\xi) \tag{7.10}$$

where x_i^e is the global coordinate of the ith node of the element Ω^e and $\hat{\psi}_i^e$ are the Lagrange interpolation functions of degree $m-1$. Equation (7.10) represents the shape (or geometry) of an element, and the $\hat{\psi}_i^e$ are therefore called *shape functions*. Equation (7.10) maps a geometric shape from ξ space into x space, i.e., for any given ξ, (7.10) gives the corresponding x. When the element is a straight line, (7.10) is exactly the same as (7.6).

The transformation (7.10) is useful in evaluating integrals by the Gauss quadrature. It should be noted that the transformation is not used to change the actual geometry of the element; the transformation is used to write integral expressions involving x in terms of expressions involving ξ:

$$\int_{x_A}^{x_B} F(x)\, dx = \int_{-1}^{1} \hat{F}(\xi)\, d\xi \tag{7.11}$$

so that the Gauss quadrature can be used to evaluate the integral over $[-1, 1]$.

The differential element dx in the global coordinate system x is related to the differential element $d\xi$ in the natural coordinate system ξ by

$$dx = \frac{dx}{d\xi} d\xi = \mathcal{J}_e\, d\xi$$

where $\mathcal{J}_e$ is called the *Jacobian* of the transformation. We have

$$\mathcal{J}_e = \frac{dx}{d\xi} = \frac{d}{d\xi}\left(\sum_{i=1}^{m} x_i^e \hat{\psi}_i^e\right) = \sum_{i=1}^{m} x_i^e \frac{d\hat{\psi}_i^e}{d\xi} \tag{7.12}$$

For a linear transformation, i.e., when $\hat{\psi}_i^e$ are the linear Lagrange interpolation functions $(m = 2)$, we have

$$\begin{gathered} \hat{\psi}_1 = \tfrac{1}{2}(1 - \xi), \quad \hat{\psi}_2 = \tfrac{1}{2}(1 + \xi) \\ \mathcal{J}_e = x_1^e(-\tfrac{1}{2}) + x_2^e(\tfrac{1}{2}) = \tfrac{1}{2}(x_2^e - x_1^e) = \tfrac{1}{2}h_e \end{gathered} \tag{7.13}$$

It can be shown that $\mathcal{J}_e = \frac{1}{2}h_e$ whenever the element is a straight line, irrespective of the degree of interpolation used in the transformation (7.10).

7.1.4 Isoparametric Formulations

Recall that a dependent variable u is approximated in the element Ω^e by expressions of the form

$$u(x) = \sum_{j=1}^{n} u_j^e \psi_j^e(x) \tag{7.14}$$

In general, the degree of approximation used to describe the coordinate transformation (7.10) is not equal to the degree of approximation (7.14) used to represent a dependent variable, i.e., $\hat{\psi}_i^e \neq \psi_i^e$. In other words, two independent elements can be used in the finite element analysis: one for the approximation of the geometry x and the other for the interpolation of the dependent variable u. Depending on the relationship between the degree of approximation used for the coordinate transformation and that used for the dependent variable, the finite element formulations are classified into three categories:

1. Subparametric formulations: $m < n$
2. Isoparametric formulations: $m = n$ (7.15)
3. Superparametric formulations: $m > n$

In subparametric formulations, the geometry is represented by lower-order elements than those used to approximate the dependent variables. An example of this category is provided by the Euler–Bernoulli beam element, where the Hermite cubic element is used to approximate the transverse deflection, while the geometry is approximated, when straight beams are analyzed, with linear interpolation functions. In isoparametric formulations (the most common in practice), the same element is used to approximate the geometry as well as the dependent unknowns: $\psi_i(x) = \hat{\psi}_i(\xi)$. In the superparametric formulations, the geometry is represented with higher-order elements than those used to approximate the dependent variables. This formulation is seldom used in practice.

7.1.5 Numerical Integration

The evaluation of integrals of the form

$$\int_a^b F(x)\,dx \tag{7.16}$$

by exact means is either difficult or impossible owing to the complicated form of the integrand F. Numerical integration is also required when the integrand is to be evaluated inexactly (as in the Timoshenko beam element) and when the integrand depends on a quantity that is known only at discrete points (e.g., in nonlinear problems).

The basic idea behind all numerical integration techniques is to find a function $P(x)$ that is both a suitable approximation of $F(x)$ and simple to integrate. The interpolating polynomials of degree n, denoted by P_n, which interpolate the integrand at $n+1$ points of the interval $[a, b]$, often produce a suitable approximation and possess the desired property of simple integrability. An illustration of the approximation of the function $F(x)$ by the polynomial $P_4(x)$ that exactly matches the function $F(x)$ at the indicated base points is given in Fig. 7.4(a). The exact value of (7.16) is given by the area under the solid curve, while the approximate value

$$\int_a^b P_4(x)\,dx$$

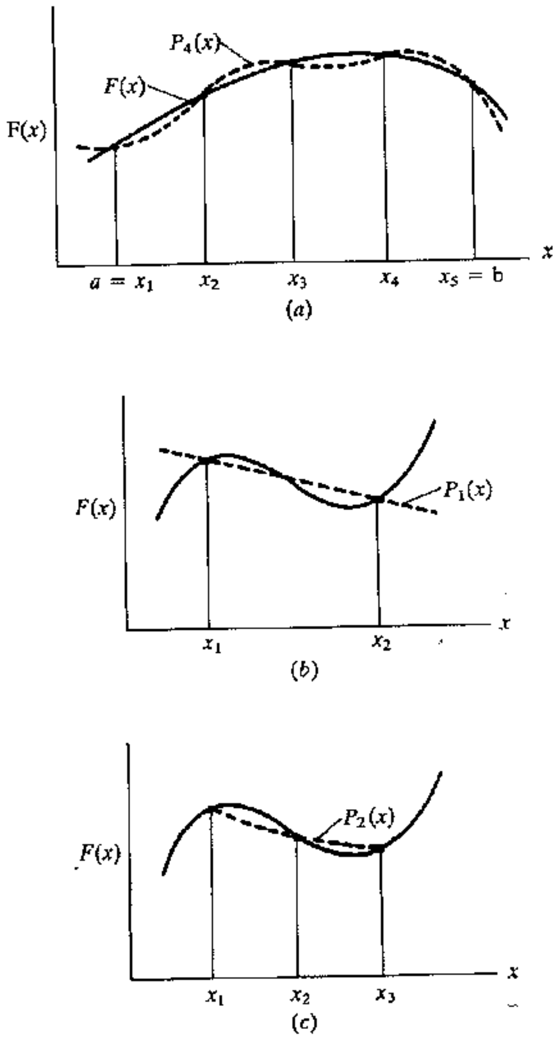

FIGURE 7.4
Numerical integration by the Newton–Cotes quadrature: (a) approximation of a function by $P_4(x)$; (b) the trapezoidal rule; (c) Simpson's rule.

is given by the area under the dashed curve. It should be noted that the difference (i.e., the error in the approximation) $E = F(x) - P_4(x)$ is not always of the same sign, and therefore the overall integration error may be small (because positive errors in one part cancel negative errors in other parts), even when P_4 is not a good approximation of F.

The commonly used integration methods can be classified into two basic groups:

1. The Newton–Cotes formulae that employ values of the function at equally spaced *base points*.
2. The Gauss quadrature formula that employs unequally spaced base points.

These are described here.

THE NEWTON–COTES QUADRATURE. For r equally spaced base points, the Newton–Cotes integration formula is given by

$$\boxed{\int_a^b F(x)\,dx = (b-a)\sum_{I=1}^{r} F(x_I)w_I} \tag{7.17}$$

where w_I are the weighting coefficients and x_I are the base points, which are equally spaced. For $r = 1$, (7.17) gives the rectangle formula. For $r = 2$, it gives the familiar *trapezoidal rule*, in which the required area under the solid curve in Fig. 7.4(b) is approximated by the area under the dotted straight line [i.e., $F(x)$ is approximated by $P_1(x)$]:

$$\int_{a=x_1}^{b=x_2} F(x)\,dx = \tfrac{1}{2}h[F(x_1) + F(x_2)], \qquad E = O(h^3) \tag{7.18}$$

where E denotes the error in the approximation and h is the spacing between two base points. The notation $O(h)$, read as "order of h", is used to indicate the order of the error in terms of the spacing h. For $r = 3$, (7.17) gives the familiar *Simpson's one-third rule* (see Fig. 7.4c):

$$\int_{a=x_1}^{b=x_3} F(x)\,dx = \tfrac{1}{3}h[F(x_1) + 4F(x_2) + F(x_3)], \qquad E = O(h^5) \tag{7.19}$$

The weighting coefficients for $r = 1, 2, \ldots, 7$ are given in Table 7.1. Note that $\sum_{I=1}^{r} w_I = 1$. The base point location for $r = 1$ is $x_1 = a + \frac{1}{2}(b-a) = \frac{1}{2}(a+b)$. For $r > 1$, the base point locations are

$$a_1 = a, \qquad a_2 = a + \Delta x, \quad \ldots, \quad a_r = a + (r-1)\,\Delta x = b$$

where $\Delta x = (b-a)/(r-1)$.

A comment is in order on the use of the Newton–Cotes integration formula (7.17). For even r (i.e., when there is an even number of intervals or an odd number of base points), the formula is exact when $F(x)$ is a polynomial of degree $r+1$ or less; for odd r, the formula is exact for a polynomial of degree r or less. Conversely, a p^{th}-order polynomial is integrated exactly by choosing $r = p + 1$ base points.

TABLE 7.1
Weighting coefficients for the Newton–Cotes formula (7.17)

r	w_1	w_2	w_3	w_4	w_5	w_6	w_7
1	1						
2	$\frac{1}{2}$	$\frac{1}{2}$					
3	$\frac{1}{6}$	$\frac{4}{6}$	$\frac{1}{6}$				
4	$\frac{1}{8}$	$\frac{3}{8}$	$\frac{3}{8}$	$\frac{1}{8}$			
5	$\frac{7}{90}$	$\frac{32}{90}$	$\frac{12}{90}$	$\frac{32}{90}$	$\frac{7}{90}$		
6	$\frac{19}{288}$	$\frac{75}{288}$	$\frac{50}{288}$	$\frac{50}{288}$	$\frac{75}{288}$	$\frac{19}{288}$	
7	$\frac{41}{840}$	$\frac{216}{840}$	$\frac{27}{840}$	$\frac{272}{840}$	$\frac{27}{840}$	$\frac{216}{840}$	$\frac{41}{840}$

THE GAUSS-LEGENDRE QUADRATURE. In the Newton–Cotes quadrature, the base point locations have been specified. If the x_I are not specified then there will be $2r+2$ undetermined parameters, the weights w_I and base points x_I, which define a polynomial of degree $2r+1$. The Gauss–Legendre quadrature is based on this idea. The base points x_I and the weights w_I are chosen so that the sum of the $r+1$ appropriately weighted values of the function yields the integral exactly when $F(x)$ is a polynomial of degree $2r+1$ or less. The Gauss–Legendre quadrature formula is given by (see Fig. 7.5)

$$\boxed{\int_a^b F(x)\,dx = \int_{-1}^{1} \hat{F}(\xi)\,d\xi \approx \sum_{I=1}^{r} \hat{F}(\xi_I)w_I} \tag{7.20}$$

where w_I are the weight factors, ξ_I are the base points [roots of the Legendre

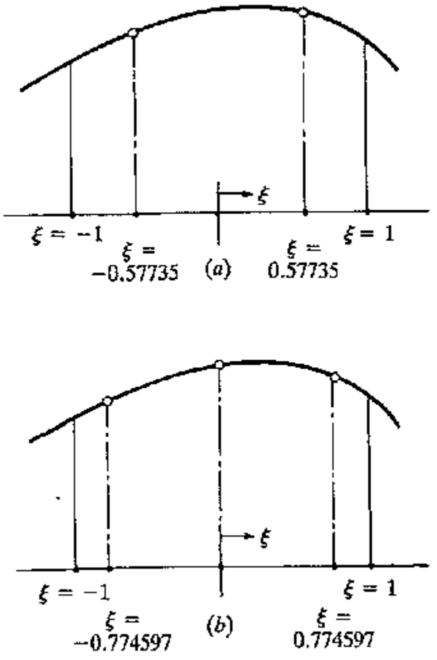

FIGURE 7.5
The two-point (a) and three-point (b) Gauss–Legendre quadratures.

TABLE 7.2
Weights and Gauss points for the Gauss–Legendre quadrature

$$\int_{-1}^{1} F(\xi)\,d\xi = \sum_{i=1}^{r} F(\xi_i)w_i$$

Points ξ_i	r	Weights w_i
0.0000000000	One-point formula	2.0000000000
±0.5773502692	Two-point formula	1.0000000000
0.0000000000	Three-point formula	0.8888888889
±0.7745966692		0.5555555555
±0.3399810435	Four-point formula	0.6521451548
±0.8611363116		0.3478548451
0.0000000000	Five-point formula	0.5688888889
±0.5384693101		0.4786286705
±0.9061798459		0.2369268850
±0.2386191861	Six-point formula	0.4679139346
±0.6612093865		0.3607615730
±0.9324695142		0.1713244924

polynomial $P_{r+1}(\xi)$], and $\hat{F}$ is the transformed integrand

$$\hat{F}(\xi) = F(x(\xi))\mathscr{J}(\xi) \tag{7.21}$$

The weight factors and Gauss points for the Gauss–Legendre quadrature (7.20) are given, for $r = 1, \ldots, 6$, in Table 7.2.

The Gauss–Legendre quadrature is more frequently used than the Newton–Cotes quadrature because it requires fewer base points (hence a saving in computation) to achieve the same accuracy. The error in the approximation is zero if the $(2r+2)$th derivative of the integrand vanishes. In other words, a polynomial of degree p is integrated exactly by employing $r = \frac{1}{2}(p+1)$ Gauss points. When $p+1$ is odd, one should pick the nearest larger integer:

$$r = [\tfrac{1}{2}(p+1)] \tag{7.22}$$

In finite element formulations, we encounter integrals whose integrands F are functions of x, $\psi_i(x)$ and derivatives of $\psi_i(x)$ with respect to x. For the Gauss–Legendre quadrature, we must transform $F(x)\,dx$ to $\hat{F}(\xi)\,d\xi$ to use (7.20). For example, consider the integral

$$K_{ij}^e = \int_{x_A}^{x_B} a(x)\frac{d\psi_i^e}{dx}\frac{d\psi_j^e}{dx}\,dx \tag{7.23}$$

Using the chain rule of differentiation, we have

$$\frac{d\psi_i^e(x)}{dx} = \frac{d\psi_i^e(\xi)}{d\xi}\frac{d\xi}{dx} = \mathscr{J}^{-1}\frac{d\psi_i^e(\xi)}{d\xi} \tag{7.24}$$

Therefore, the integral can be written, with the help of (7.10), as

$$K_{ij}^e = \int_{-1}^{1} a(x(\xi))\,\frac{1}{\mathcal{J}}\frac{d\psi_i^e}{d\xi}\,\frac{1}{\mathcal{J}}\frac{d\psi_j^e}{d\xi}\,\mathcal{J}\,d\xi \tag{7.25}$$

$$\approx \sum_{I=1}^{r} \hat{F}_{ij}^e(\xi_I)\,w_I \tag{7.26}$$

where

$$\hat{F}_{ij}^e = a\,\frac{1}{\mathcal{J}}\frac{d\psi_i^e}{d\xi}\frac{d\psi_j^e}{d\xi}, \qquad \mathcal{J} = \sum_{i=1}^{m} x_i^e\,\frac{d\hat{\psi}_i^e}{d\xi} \tag{7.27}$$

For the isoparametric formulation, we take $\psi_i^e = \hat{\psi}_i^e$. The transformation from x to ξ is not required for the Newton–Cotes quadrature.

As noted earlier, the Jacobian matrix will be the same $(\mathcal{J}_e = \frac{1}{2}h_e)$ when the element is straight, even if the coordinate transformation is quadratic or cubic. However, when the element is curved, the Jacobian is a function of ξ for transformations other than linear.

It is possible to determine the number of Gauss points required to evaluate the finite element matrices

$$K_{ij}^e = \int_{x_A}^{x_B} \frac{d\psi_i^e}{dx}\frac{d\psi_j^e}{dx}\,dx, \qquad M_{ij}^e = \int_{x_A}^{x_B} \psi_i^e\psi_j^e\,dx, \qquad F_i^e = \int_{x_A}^{x_B} \psi_i^e\,dx \tag{7.28}$$

exactly using linear, quadratic, and cubic interpolation functions. For linear interpolation functions, the integrand of K_{ij}^e is constant, requiring only one-point Gauss quadrature. The integrand of the mass matrix M_{ij}^e is quadratic $(p = 2)$, requiring $[r = \frac{1}{2}(p +)1 = \frac{3}{2}]$ two-point quadrature. The coefficients f_i^e are evaluated exactly by one-point quadrature. Similarly, for quadratic and cubic elements, we can estimate the number of Gauss points needed to evaluate K_{ij}^e, M_{ij}^e, and f_i^e exactly. The results are summarized below. Note that, in estimating the quadrature points, it is assumed that the Jacobian is a constant, which holds true when the element is a straight line.

Element type	Number of Gauss quadrature points needed		
	K_{ij}^e	M_{ij}^e	f_i^e
Linear	1	2	1
Quadratic	2	3	2
Cubic	3	4	3

If the matrices in (7.28) have variable coefficients or the elements are curved [and hence $\mathcal{J}_e = \mathcal{J}_e(\xi)$], the degree of the variation of the integrands changes and the number of Gauss points needed to evaluate the integral exactly changes. If the elements are straight, and the coefficients $a = a(x)$ and $c = c(x)$ together with $f = f(x)$ are no more than linear in x, then the number of Gauss points for evaluating the coefficients

$$K_{ij}^e=\int_{x_A}^{x_B} a\frac{d\psi_i^e}{dx}\frac{d\psi_j^e}{dx}\,dx,\qquad M_{ij}^e=\int_{x_A}^{x_B} c\psi_i^e\psi_j^e\,dx \tag{7.29}$$

remain the same as listed in the above table. However, the evaluation of f_i^e requires one point more than before. Conversely, the two-point quadrature for linear elements, three-point quadrature for quadratic elements, and four-point quadrature for cubic elements would exactly evaluate K_{ij}^e with a quadratic variation of $a(x)$, M_{ij}^e with linear variation of $c(x)$, and f_i^e with quadratic variation of $f(x)$.

The use of Gauss quadrature on (7.28) yields the following values (exact up to the fifth decimal place) when the element is straight and the isoparametric formulation is used:

Quadratic (three-point formula)

$$\begin{aligned}
[K]&=\frac{1}{h_e}\begin{bmatrix} 2.33333 & -2.66667 & 0.33333\\ -2.66667 & 5.33333 & -2.66667\\ 0.33333 & -2.66667 & 2.33333\end{bmatrix}\\
[M]&=\frac{h_e}{10}\begin{bmatrix} 1.33333 & 0.66667 & -0.33333\\ 0.66667 & 5.33333 & 0.66667\\ -0.33333 & 0.66667 & 1.333433\end{bmatrix}\\
\{F\}&=h_e\begin{Bmatrix} 0.166667\\ 0.666667\\ 0.166667\end{Bmatrix}
\end{aligned}\tag{7.30}$$

Cubic (four-point formula)

$$\begin{aligned}
[K]&=\frac{1}{h_e}\begin{bmatrix} 3.700 & -4.725 & 1.350 & -0.325\\ -4.725 & 10.800 & -7.425 & 1.350\\ 1.350 & -7.425 & 10.800 & -4.725\\ -0.325 & 1.350 & -4.725 & 3.700\end{bmatrix}\\
[M]&=\frac{h_e}{10}\begin{bmatrix} 0.761905 & 0.589286 & -0.214286 & 0.113095\\ 0.589286 & 3.857143 & -0.482143 & -0.214286\\ -0.214286 & -0.482143 & 3.857143 & 0.589286\\ 0.113095 & -0.214286 & 0.589286 & 0.761905\end{bmatrix}\\
\{F\}&=h_e\begin{Bmatrix} 0.125\\ 0.375\\ 0.375\\ 0.125\end{Bmatrix}
\end{aligned}\tag{7.31}$$

In Section 7.2, we study the computer implementation of the steps involved in the finite element analysis of one-dimensional problems. As a part of the element calculations there, the computer implementation of the numerical integration ideas presented in this section will be studied. A model finite element program (FEM1DV2) for the solution of one-dimensional problems is also described, and its application is demonstrated via several examples. Appendix 1 contains a source listing of program FEM1DV2.

7.2 COMPUTER IMPLEMENTATION

7.2.1 Introductory Comments

Chapters 3–6 were devoted to the finite element formulations of two *classes* of boundary value, initial value, or eigenvalue problems in one dimension:

1. Second-order differential equations (e.g., heat transfer, fluid mechanics, 1-D elasticity, bars, and the Timoshenko beam theory);
2. Fourth-order differential equations governing the Euler–Bernoulli beam theory.

The frame element, obtained by superposing the bar element and the beam element, was discussed in Chapter 4.

By now, it should be clear to the reader that the steps involved in the finite element analysis of a general class of problems (e.g., single second-order, single fourth-order, and a pair of second-order equations) are systematic and can be implemented on a digital computer. Indeed, the success of the finite element method is largely due to the ease with which the analysis of a class of problems, without regard to a specific problem, can be implemented on a digital computer. For different geometries, boundary and initial conditions, and problem data, a specific problem from the general class can be solved by simply supplying the required input data to the program. For example, if we develop a general computer program to solve equations of the form

$$c_1 \frac{\partial u}{\partial t} + c_2 \frac{\partial^2 u}{\partial t^2} - \frac{\partial}{\partial x}\left(a \frac{\partial u}{\partial x}\right) + \frac{\partial^2}{\partial x^2}\left(b \frac{\partial^2 u}{\partial x^2}\right) + cu = f \tag{7.32}$$

then all physical problems described by (3.1) and (4.1) and their time-dependent versions can be solved for any compatible boundary and initial conditions.

The purpose of this section is to discuss the basic steps involved in the development of a computer program for second- and fourth-order one-dimensional differential equations studied in the preceding chapters. The ideas presented here are used in the development of the model program FEM1DV2 (a revised version of FEM1D from the first edition of this book), and they are meant to be illustrative of the steps used in a typical finite element program development. One can make use of the ideas presented here to develop a program of one's own.

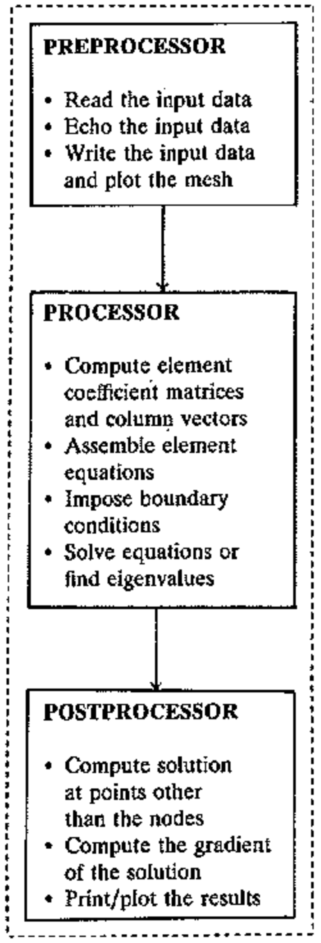
PREPROCESSOR
• Read the input data
• Echo the input data
• Write the input data and plot the mesh
PROCESSOR
• Compute element coefficient matrices and column vectors
• Assemble element equations
• Impose boundary conditions
• Solve equations or find eigenvalues
POSTPROCESSOR
• Compute solution at points other than the nodes
• Compute the gradient of the solution
• Print/plot the results

FIGURE 7.6
The three main functional units of a finite element program.

7.2.2 General Outline

A finite element program consists of three basic parts (see Fig. 7.6):

1. Preprocessor
2. Processor
3. Postprocessor

In the preprocessor part of the program, the input data of the problem are read in and/or generated. This includes the geometry (e.g., length of the domain and boundary conditions), the data of the problem (e.g., coefficients in the differential equation), finite element mesh information (e.g., element type, number of elements, element length, coordinates of the nodes, and connectivity matrix), and indicators for various options (e.g., print, no print, type of field problem analyzed, static analysis, eigenvalue analysis, transient analysis, and degree of interpolation).

In the processor part, all steps in the finite element method, except for postprocessing, discussed in the preceding chapters are performed. These include the following:

1. Generation of the element matrices using numerical integration.
2. Assembly of element equations.
3. Imposition of the boundary conditions.
4. Solution of the algebraic equations for the nodal values of the primary variables.

In the postprocessor part of the program, the solution is computed by interpolation at points other than nodes, secondary variables that are derivable from the solution are computed, and the output data are processed in a desired format for printout and/or plotting.

The preprocessor and postprocessors can be a few Fortran statements to read and print pertinent information, simple subroutines (e.g., subroutines to generate mesh and compute the gradient of the solution), or complex programs linked to other units via disk and tape files. The processor, where typically large amounts of computing time are spent, can consist of several subroutines, each having a special purpose (e.g., a subroutine for the calculation of element matrices, a subroutine for the imposition of boundary conditions, and a subroutine for the solution of the equations). The degree of sophistication and the complexity of a finite element program depend on the general class of problems being programmed, the generality of the data in the equation, and the intended user of the program. It is always desirable to describe, through comment statements, all variables used in the computer program. A flow chart of the computer program FEM1DV2 is presented in Fig. 7.7. In the following sections, a discussion of the basic components of a typical finite element program is presented, and then the basic ideas are illustrated via FORTRAN statements (see Appendix 1).

7.2.3 Preprocessor

The preprocessor unit consists of reading input data and generating finite element mesh, and printing the data and mesh information. The input data to a finite element program consist of element type IELEM (i.e., Lagrange element or Hermite element), number of elements used (NEM), specified boundary conditions on primary and secondary variables (number of boundary conditions, global node number and degree of freedom, and specified values of the degrees of freedom), the global coordinates of nodes X_I, and element properties (e.g., coefficients a_e, b_e, c_e, f_e, etc.). If a uniform mesh is used, the length of the domain should be read in, and global coordinates of the nodes can be generated in the program.

The preprocessor portion that deals with the generation of finite element mesh (when not supplied by the user) can be separated into a subroutine

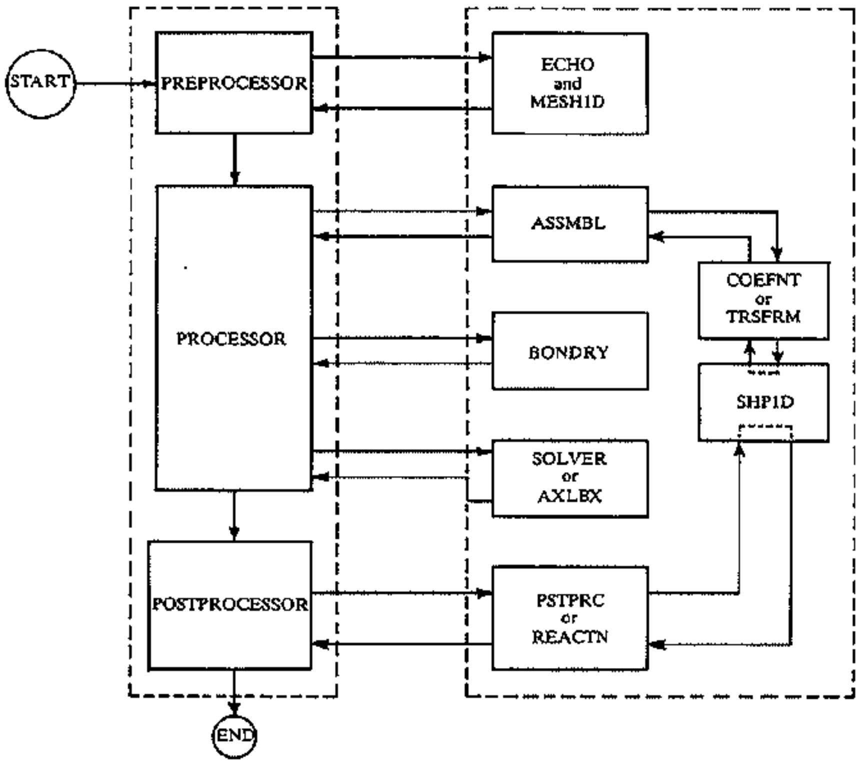

ASSMBL:	Subroutine for the assembly of element equations: upper-banded form for static and transient problems; full matrix form for eigenvalue problems.
AXLBX:	Subroutine for determining eigenvalues and eigenvectors of the equation $[A]\{X\} = L[B]\{X\}$.
BONDRY:	Subroutine for imposing specified boundary conditions of essential type, natural type, and mixed type.
COEFNT:	Subroutine for computing element matrices and vectors for all problems except truss and frame problems.
ECHO:	Subroutine to echo the input file.
MESH1D:	Subroutine to generate the mesh (i.e. global coordinates of the global nodes and the connectivity array).
PSTPRC:	Subroutine to postprocess the solution for all problems, except truss and frame problems.
REACTN:	Subroutine to calculate the reactions for truss and frame problems.
SHP1D:	Subroutine to compute the shape functions and their derivatives.
SOLVER:	Subroutine to solve linear algebraic equations.
TRSFRM:	Subroutine to compute element stiffness matrices and force vectors for truss and frame problems.

FIGURE 7.7
Flow chart of the computer program FEM1DV2 along with the subroutines.

(MESH1D), depending on the convenience and complexity of the program. Mesh generation includes computation of the global coordinates X_I and the connectivity array $[B] = [\text{NOD}]$. Recall that the connectivity matrix describes the relationship between element nodes to global nodes:

NOD(I, J) = global node number corresponding to the Jth node of element I

This array is used in the assembly procedure as well as to transfer information from element to the global system and vice versa. For example, to extract the element nodal coordinates x_i^n of the element Ω^n from the global coordinates X_I, we can use the array NOD:

$$x_i^n = X_I, \qquad I = \text{NOD}(n, i)$$

The arrays {ELX} and {GLX} are used in FEM1DV2 for $\{x_i^n\}$ and $\{X_I\}$, respectively.

7.2.4 Calculation of Element Matrices (Processor)

The most significant part of a processor is where we generate element matrices. The element matrices are computed in various subroutines (COEFNT and TRSFRM), depending on the type of problem being solved. These subroutines typically involve numerical evaluations of the element matrices $[K^e]$ and $[M^e]$ (program variables ELK and ELM) and the element vector $\{f^e\}$ (program variable ELF) for various field problems. The Gauss quadrature described in Section 7.1.5 is used to evaluate element matrices and vectors, and the arrays are assembled as soon as they are computed. Thus, a loop on the number of elements in the mesh (NEM) is used to compute element matrices and assemble them (subroutine ASSMBL). It is here that the connectivity array NOD plays a crucial role. By putting element matrices into global locations one at a time, we avoid the computation of all element matrices at once.

Element matrices for different model equations (MODEL) and type of problem (NTYPE) are generated by assigning values as follows:

1. MODEL = 1, NTYPE = 0: all field problems described by the model equation (3.1), including radially symmetric heat-transfer-type problems.
2. MODEL = 1, NTYPE = 1: radially symmetric elastic disk problems (see Problem 3.33).
3. MODEL = 2, NTYPE = 0 (RIE) or 2 (CIE): the Timoshenko theory of beams.
4. MODEL = 2, NTYPE = 1 (RIE) or 3 (CIE): the Timoshenko theory for bending of circular plates.
5. MODEL = 3, NTYPE = 0: the Euler–Bernoulli theory of beams.
6. MODEL = 3, NTYPE = 1: the Euler–Bernoulli theory for bending of circular plates.

7. MODEL = 4, NTYPE = 0: the two-node truss element.
8. MODEL = 4, NTYPE = 1: the two-node Euler–Bernoulli frame element.
9. MODEL = 4, NTYPE = 2: the two-node, Timoshenko frame element.

The time-dependent option is exercised through variable ITEM:

ITEM = 0	static analysis
ITEM = 1	first-order time derivative (i.e., parabolic) problems
ITEM = 2	second-order time derivative (i.e., hyperbolic) problems

The element matrices are evaluated using the Gauss quadrature, except for MODEL = 4, where the explicit forms of element coefficients are programmed in the interest of computational efficiency.

The element shape functions SF and their derivatives GDSF are evaluated at the Gauss points in subroutine SHP1D. The Gaussian weights and points associated with two-, three-, four-, and five-point integration are stored in arrays GAUSWT and GAUSPT, respectively. The nth column of GAUSWT, for example, contains the weights corresponding to the n-point Gauss quadrature rule:

$$\text{GAUSPT}(i, n) = i\text{th Gauss point corresponding to the } n\text{-point Gauss rule}$$

The variable NGP is used to denote the number of Gauss points, which is selected to achieve good accuracy. As noted earlier, the linear, quadratic, and cubic interpolation functions require two, three, and four quadrature points, respectively, to evaluate the element coefficients exactly. Thus, if IELEM is the element type,

$$\text{IELEM} = \begin{cases} 1 & \text{for linear} \\ 2 & \text{for quadratic} \quad \text{(Lagrange elements)} \\ 3 & \text{for cubic} \end{cases}$$

then NGP = IELEM + 1 would evaluate K_{ij}^e, M_{ij}^e, and f_i^e [see (7.29)] exactly when $c(x)$ is linear, and $a(x)$, $b(x)$, and $f(x)$ are quadratic functions. The Hermite cubic element is identified with IELEM = 0, for which case NGP is taken to be 4.

The coefficients $a(x) = \text{AX}$, $b(x) = \text{BX}$, and $c(x) = \text{CX}$, together with $f(x) = \text{FX}$ in the differential equation (7.32) are assumed to vary with x as follows:

$$\begin{aligned} &\text{AX} = \text{AX0} + \text{AX1} * \text{X} && (a = a_0 + a_1 x) \\ &\text{BX} = \text{BX0} + \text{BX1} * \text{X} && (b = b_0 + b_1 x) \\ &\text{CX} = \text{CX0} + \text{CX1} * \text{X} && (c = c_0 + c_1 x) \\ &\text{FX} = \text{FX0} + \text{FX1} * \text{X} + \text{FX2} * \text{X} * \text{X} && (f = f_0 + f_1 x + f_2 x^2) \end{aligned}$$

For radially symmetric elasticity problems, (AX0, AX1) [or (BX0, BX1) for circular plates] are used to input Young's modulus E and Poisson's ratio ν.

The Gauss quadrature formula (7.20) can be implemented on the computer as follows. Consider K_{ij}^e of the form

$$K_{ij}^e = \int_{x_A}^{x_B} \left[a(x) \frac{d\psi_i^e}{dx}\frac{d\psi_j^e}{dx} + c(x)\psi_i^e\psi_j^e \right] dx \tag{7.33}$$

Let us use the following program variables for the quantities in (7.33):

$$\text{ELK(I, J)} = K_{ij}^e, \quad \text{SF(I)} = \psi_i^e, \quad \text{GDSF(I)} = \frac{d\psi_i^e}{dx}$$

$$\text{AX} = a(x), \quad \text{CX} = c(x), \quad \text{ELX(I)} = x_i^e$$

$$\text{NPE} = n, \quad \text{the number of nodes in the element}$$

After transforming x to ξ,

$$x = \sum_{i=1}^{n} x_i^e \psi_i^e \quad [= -x_A + \tfrac{1}{2}h_e(1+\xi)] \tag{7.34}$$

the coefficients K_{ij}^e in (7.33) take the form [see (7.25)]

$$K_{ij}^e = \int_{-1}^{1} \left[a(\xi) \frac{1}{\mathscr{J}}\frac{d\psi_i^e}{d\xi}\frac{1}{\mathscr{J}}\frac{d\psi_j^e}{d\xi} + c(\xi)\psi_i^e\psi_j^e \right] \mathscr{J}\, d\xi \tag{7.35a}$$

$$= \sum_{I=1}^{\text{NGP}} F_{ij}^e(\xi_I)\mathscr{J}W_I \tag{7.35b}$$

where F_{ij}^e denotes the expression in the square brackets in (7.35a), $\mathscr{J}$ is the Jacobian, and (ξ_I, W_I) are the Gauss points and weights.

Examination of (7.35b) shows that there are three free indices: i, j, and I. We take the Gauss-point loop on I as the outermost one. Inside this loop, we evaluate F_{ij}^e at the Gauss point ξ_I for each i and j, multiply with the Jacobian $\mathscr{J} = \frac{1}{2}h_e$ and the weights W_I, and sum:

$$\text{ELK}(i, j) = \text{ELK}(i, j) + F_{ij}^e(\xi_I)\mathscr{J}W_I \tag{7.36}$$

To accomplish this, we must initialize all arrays that are being evaluated using the Gauss quadrature:

```
   DO 10 J  = 1,NPE
   DO 10 I  = 1,NPE
10 ELK(I,J) = 0.0
```

This initialization is made outside the do-loop on number of Gauss points.

The computation of coefficients F_{ij}^e in (7.35b) requires evaluation of a, c, ψ_i, and $d\psi_i/d\xi$ at the Gauss point ξ_I. Hence, inside the loop on I, we call subroutine SHP1D to evaluate ψ_i, $d\psi_i/dx = (d\psi_i/d\xi)/\mathscr{J}$. We now have all quantities needed to compute K_{ij}^e in (7.35b):

```
      DO 100 NI = 1,NGP
      XI = GAUSPT(NI,NGP)
C
C     Call subroutine SHP1D to evaluate the interpolation functions
C     (SF) and their global derivatives (GDSF) at the Gauss point XI
C
      CALL SHP1D(XI,NPE,SF,GDSF,GJ)
      CONST = GJ*GAUSWT(NI,NGP)
C
      X = 0.0
      DO 20 I=1,NPE
   20 X = X + SF(I)*ELX(I)
C
      AX=AX0 + AX1*X
      CX=CX0 + CX1*X
      DO 30 J = 1,NPE
      ELF(J) = ELF(J) + CONST*SF(J)*FX
      DO 30 I = 1,NPE
   30 ELK(I,J)=ELK(I,J)+CONST*(AX*GDSF(I)*GDSF(J)+CX*SF(I)*SF(J))
```

In the same way, all other coefficients (e.g., M_{ij}^e and f_i^e) can be evaluated. Recall that the element properties (i.e., K_{ij}^e, M_{ij}^e, and f_i^e) are calculated by calling a suitable subroutine (COEFNT or TRSFRM) for the field problem being analyzed within a loop on number of elements. As soon as the element properties are available for a particular element, they are put into their proper locations (i.e., assembled) with the help of array NOD. The assembly is explained in the next section.

7.2.5 Assembly of Element Equations (Processor)

The assembly of element equations should be carried out as soon as they are computed, rather than waiting till element coefficients of all elements are computed. The latter requires storage of the element coefficients of each element. In the former case, we can perform the assembly in the same loop in which a subroutine is called to calculate element matrices.

A feature of the finite element equations that enables us to save storage and computing time is the assembly of element matrices in upper-banded form. When element matrices are symmetric, as is the case in most problems of interest in this book, the resulting global (or assembled) matrix is also symmetric, with many zeros away from the main diagonal. Therefore, it is sufficient to store only the upper *half-band* of the assembled matrix. The half-bandwidth of a matrix is defined as follows. Let N_i be the number of matrix elements between the diagonal element and the last nonzero element in the ith row, after which all elements in that row are zero; the half-bandwidth is the maximum of $(N_i + 1) \times \mathrm{NDF}$, where NDF is the number of degrees of freedom per node:

$$b_i = \max_{1 \leq i \leq n} [(N_i + 1) \times \mathrm{NDF}]$$

where n is the number of rows in the matrix (or equations in the problem). General-purpose equation solvers are available for such banded systems of equations.

The half-bandwidth NHBW of the assembled (i.e., global) finite element matrix can be determined in the finite element program itself. The local nature of the finite element interpolation functions (i.e., ψ_i^e are defined to be nonzero only over the element Ω^e) is responsible for the banded character of the assembled matrix. Recall from earlier discussions that if two global nodes do not belong to the same element then the corresponding entries in the global matrix are zeros:

$$K_{IJ} = 0 \quad \text{if global nodes } I \text{ and } J \text{ do not correspond to local nodes of the same element}$$

This property enables us to determine the half-bandwidth NHBW of the assembled matrix:

$$\text{NHBW} = \max_{\substack{1 \leq N \leq \text{NEM} \\ 1 \leq I,\, J \leq \text{NPE}}} \{\text{abs}\,[\text{NOD}(N, I) - \text{NOD}(N, J)] + 1\} \times \text{NDF} \tag{7.37a}$$

where

$$\begin{aligned} \text{NEM} &= \text{number of elements in the mesh} \\ \text{NPE} &= \text{number of nodes per element} \\ \text{NDF} &= \text{number of degrees of freedom per element} \end{aligned} \tag{7.37b}$$

Clearly, for one-dimensional problems with elements connected in series, the maximum difference between nodes of an element is equal to NPE − 1. Hence,

$$\text{NHBW} = [(\text{NPE} - 1) + 1] \times \text{NDF} = \text{NPE} \times \text{NDF} \tag{7.38}$$

Of course, NHBW is always less than or equal to the total number of primary degrees of freedom, i.e., the number of equations, NEQ, in the finite element mesh of the problem.

The logic for assembling the element matrices K_{ij}^e into the upper-banded form of the global coefficients K_{IJ} is that the assembly can be skipped whenever $J < I$ and $J > \text{NHBW}$. The main diagonal, $I = J$, of the assembled square matrix (i.e., full storage form), becomes the first column of the assembled banded matrix (i.e., banded storage form), as shown in Fig. 7.8. The upper diagonals (parallel to the main diagonal) take the position of respective columns in the banded matrix. Thus, the banded matrix has dimension NEQ × NHBW, where NEQ denotes the total number of equations in the problem.

The element coefficients K_{ij}^n and f_i^n of a typical element Ω^n are to be assembled into the global coefficient matrix $[K]$ and source vector $\{F\}$, respectively. If the ith node of the element is equal to the Ith global node, and the jth node of the element is equal to the Jth global node, we have

$$K_{IJ} = K_{ij}^n, \qquad F_I = F_i^n \quad (\text{for NDF} = 1) \tag{7.39a}$$

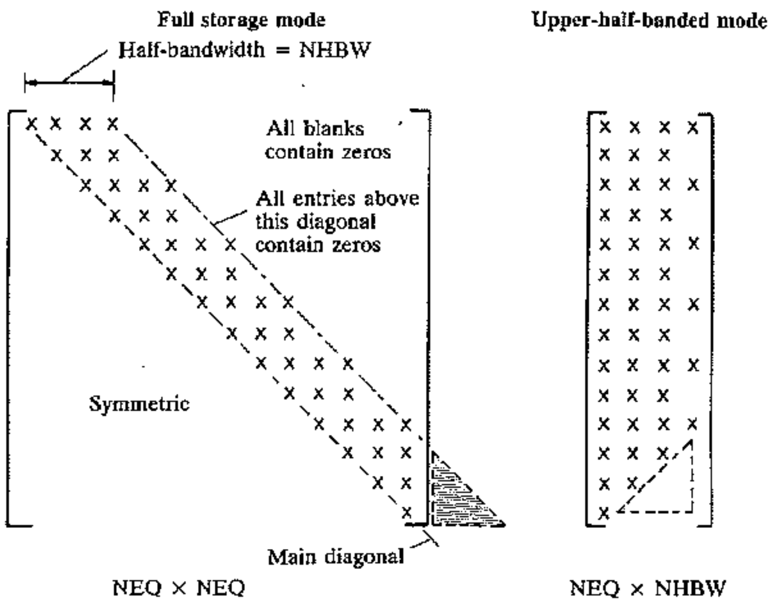

FIGURE 7.8
Finite element coefficient matrix storage in upper-half-banded form.

The values of I and J can be obtained with the help of array NOD:

$$I = \text{NOD}(n, i), \qquad J = \text{NOD}(n, j) \tag{7.39b}$$

Recall that it is possible that the same I and J may correspond to a pair of i and j of some other element Ω^m. In that case, K^m_{ij} will be added to existing coefficients K_{IJ} during the assembly. For NDF > 1, the logic still holds, with the change

$$K_{(\text{NR})(\text{NC})} = K^n_{(i+p-1)(j+q-1)} \quad (p, q = 1, 2, \ldots, \text{NDF}) \tag{7.40a}$$

where

$$\text{NR} = (I-1) \times \text{NDF} + p, \qquad \text{NC} = (J-1) \times \text{NDF} + q \tag{7.40b}$$

and I and J are related to i and j by (7.39*b*). A Fortran listing of the subroutine ASSMBL can be found in FEM1DV2 in Appendix 1.

7.2.6 Imposition of Boundary Conditions (Processor)

Imposition of boundary conditions on the primary and secondary global degrees of freedom can be carried out through a subroutine (BONDRY), which remains unchanged for 2-D or 3-D problems. There are three types of boundary conditions for any problem:

1. Essential boundary conditions, i.e., boundary conditions on primary variables (Dirichlet boundary conditions).

2. Natural boundary conditions, i.e., boundary conditions on secondary variables (Neumann boundary conditions).
3. Mixed boundary conditions (Newton boundary conditions).

The procedure for implementing the boundary conditions on the primary variables involves modifying the assembled coefficient matrix (GLK) and right-hand column vector (GLF) by three operations:

Step 1 moving the known products to the right-hand column of the matrix equation.

Step 2 replacing the columns and rows of GLK corresponding to the known primary variable by zeros, and setting the coefficient on the main diagonal to unity.

Step 3 replacing the corresponding component of the right-hand column by the specified value of the variable.

Consider the following N algebraic equations in full matrix form:

$$\begin{bmatrix} K_{11} & K_{12} & K_{13} & \dots \\ K_{21} & K_{22} & K_{23} & \dots \\ K_{31} & K_{32} & K_{33} & \dots \\ \vdots & \vdots & \vdots & \end{bmatrix} \begin{Bmatrix} U_1 \\ U_2 \\ U_3 \\ \vdots \end{Bmatrix} = \begin{Bmatrix} F_1 \\ F_2 \\ F_3 \\ \vdots \end{Bmatrix}$$

where U_I and F_I are the global primary and secondary degrees of freedom, and K_{IJ} are the assembled coefficients. Suppose that $U_S = \hat{U}_S$ is specified. Recall that when the primary degree of freedom at a node is known, the corresponding secondary degree of freedom is unknown, and vice versa. Set $K_{SS} = 1$ and $F_S = \hat{U}_S$; further, set $K_{SI} = K_{IS} = 0$ for $I = 1, 2, \dots, N$ and $I \neq S$. For $S = 2$, the modified equations are

$$\begin{bmatrix} K_{11} & 0 & K_{13} & K_{14} & \dots & K_{1n} \\ 0 & 1 & 0 & 0 & \dots & 0 \\ K_{31} & 0 & K_{33} & K_{34} & \dots & K_{3n} \\ \vdots & \vdots & \vdots & \vdots & & \vdots \\ K_{n1} & 0 & K_{n3} & K_{n4} & \dots & K_{nn} \end{bmatrix} \begin{Bmatrix} U_1 \\ U_2 \\ U_3 \\ \vdots \\ U_n \end{Bmatrix} = \begin{Bmatrix} \hat{F}_1 \\ \hat{U}_2 \\ \hat{F}_3 \\ \vdots \\ \hat{F}_n \end{Bmatrix}$$

where

$$\hat{F}_i = F_i - K_{i2}\hat{U}_2 \quad (i = 1, 3, 4, 5, \dots, n; i \neq 2)$$

Thus, in general, if $U_S = \hat{U}_S$ is known, we have

$$K_{SS} = 1, \quad F_S = \hat{U}_S; \quad \hat{F}_i = F_i - K_{iS}\hat{U}_S; \quad K_{Si} = K_{iS} = 0$$

where $i = 1, 2, \dots, S - 1, S + 1, \dots, n$ $(i \neq S)$. This procedure is repeated for every specified primary degree of freedom. It enables us to retain the original order of the matrix, and the specified boundary conditions on the primary degrees of freedom are printed as part of the solution. Of course, the logic should be implemented for a banded system of equations.

The specified secondary degrees of freedom (Q_i) are implemented directly by adding their specified values to the computed values. Suppose that the point source corresponding to the Rth secondary degree of freedom is specified to be $\hat{F}_R$. Then

$$F_R = f_R + \hat{F}_R$$

where f_R is the contribution due to the distributed source $f(x)$; f_R is computed as a part of the element computations and assembled.

Mixed-type boundary conditions are of the form

$$a\frac{du}{dx} + k(u - \bar{u}) = 0 \quad (\bar{u} \text{ and } k \text{ are known constants}) \tag{7.41}$$

which contains both the primary variable u and the secondary variable $a\,du/dx$. Thus $a\,du/dx$ at the node P is replaced by $-k_p(u_p - \bar{u}_p)$:

$$Q_p = -k_p(U_p - \bar{U}_p)$$

This amounts to modifying K_{pp} by adding k_p to its existing value,

$$K_{pp} \leftarrow K_{pp} + k_p$$

and adding $k_p\bar{U}_p$ to F_p,

$$F_p \leftarrow F_p + k_p\bar{U}_p$$

All three types of boundary conditions are implemented in subroutine BONDRY for boundary, initial, and eigenvalue problems. The following are used in subroutine BONDRY (see Appendix 1):

NSPV	number of specified primary variables	
NSSV	number of specified secondary variables	
NNBC	number of Newton boundary conditions	
VSPV	column of the specified values $\hat{U}_s$ of primary variables	
VSSV	column of the specified values $\hat{F}_R$ of secondary variables	(7.42)
VNBC	column of the specified values k_p	
UREF	column of the specified values $\bar{U}_p$	
ISPV	array of the global node and degree of freedom at the node that is specified [ISPV(I, 1) = global node of the Ith boundary condition, ISPV(I, 2) = degree of freedom specified at the global node, ISPV(I, 1)]	

Similar definitions are used for ISSV and INBC arrays.

7.2.7 Solution of Equations and Postprocessing

Subroutine SOLVE is used to solve a banded system of equations, and the solution is returned in array GLF. The program performs the Gaussian elimination and back-substitution to compute the solution. For a discussion of the Gaussian elimination used to solve a set of linear algebraic equations, the reader is referred to the book by Carnhan, Luther, and Wilkes (1969). On most computing systems, a variety of equation solvers are available, and one can use any of the programs that suits the needs. See Appendix 1 for a listing of subroutine SOLVER.

Postprocessing involves computation of the solution and its gradient at preselected points of the domain. Subroutine PSTPRC is used to evaluate the solution and its derivatives in any element:

$$u^e(x) = \sum_{j=1}^{n} u_j^e \psi_j^e(x), \qquad \left(\frac{du^e}{dx}\right)\bigg|_x = \sum_{j=1}^{n} u_j^e \left(\frac{d\psi_j^e}{dx}\right)\bigg|_x \tag{7.43a}$$

for the Lagrange elements and

$$w^e(x) = \sum_{j=1}^{n} u_j^e \phi_j^e(x), \qquad \frac{d^m w^e}{dx^m} = \sum_{j=1}^{n} u_j^e \left(\frac{d^m \phi_j^e}{dx^m}\right)\bigg|_x \quad (m = 1, 2, 3) \tag{7.43b}$$

for the Hermite cubic elements. The nodal values u_j^e of the element Ω^e are deduced from the global nodal values U_I as follows:

$$u_j^e = U_I, \qquad I = \text{NOD}(e, j), \qquad \text{when NDF} = 1$$

For NDF > 1, I is given by $I = [\text{NOD}(e, j) - 1] \times \text{NDF}$ and

$$u_{j+p}^e = U_{I+p} \quad (p = 1, 2, \ldots, \text{NDF})$$

The values computed using the derivatives of the solution are often inaccurate because the derivatives of the approximate solution become increasingly inaccurate with increasing order of differentiation. For example, the shear force computed in the Euler–Bernoulli beam theory,

$$V = \frac{d}{dx}\left(b\frac{d^2 w}{dx^2}\right) = \sum_{j=1}^{n} u_j^e \frac{d}{dx}\left(b\frac{d^2\phi_j^e}{dx^2}\right) \tag{7.44}$$

will be in considerable error compared with the true value of V. The accuracy increases, rather slowly, with mesh refinement and higher-order elements. When accurate values of the secondary variables are desired, it is recommended that they be computed from the element equations:

$$Q_i^e = \sum_{j=1}^{n} K_{ij}^e u_j^e - f_i^e \quad (i = 1, 2, \ldots, n) \tag{7.45}$$

However, this requires recomputation or saving of element coefficients K_{ij}^e and f_i^e.

7.3 APPLICATIONS OF THE COMPUTER PROGRAM FEM1DV2

7.3.1 General Comments

The computer program FEM1DV2, which embodies the ideas presented in the previous section, is intended to illustrate the use of the finite element models developed in Chapters 3–6 to a variety of one-dimensional field problems, some of them not discussed in this book. FEM1DV2 is a modified version of

FEM1D from the first edition of this book. It was developed as a learning computational tool for students of the course. In the interest of simplicity and ease of understanding, only the model equations discussed in this book and their immediate extensions are included in the program (see Appendix 1).

Table 7.3 contains a summary of the definitions of coefficients of various model problems and their corresponding program variables. The table can be used as a ready reference to select proper values of AX0, AX1, and so on for different problems.

7.3.2 Illustrative Examples

Here we revisit some of the example problems considered earlier to illustrate the use of FEM1DV2 in their solution. Only certain key observations concerning the input data are made, but complete listings of input files for each problem are given. In the interest of brevity, the output files for most problems are not included. Table 7.4 contains a description of the input variables to program FEM1DV2.

Example 7.1 Steady heat transfer in a fin. The problem is governed by

$$-\frac{d^2\theta}{dx^2}+c\theta=0 \quad \text{for } 0<x<L$$

$$\theta(0)=\theta_0, \quad \left(\frac{d\theta}{dx}\right)\bigg|_{x=L}=0 \qquad \text{(Set 1)}$$

$$\theta(0)=\theta_0, \quad \left(\frac{d\theta}{dx}+\frac{\beta}{k}\theta\right)\bigg|_{x=L}=0 \quad \text{(Set 2)}$$

where θ is the nondimensional temperature, and L, c, θ_0, β, and k are

$$\begin{aligned} &L=0.25\,\text{m}, \quad c=256\,\text{m}^{-2}, \quad \theta_0=100^\circ\text{C}, \\ &\beta=64\,\text{W m}^{-2}\,{}^\circ\text{C}^{-1}, \quad k=50\,\text{W m}^{-1}\,{}^\circ\text{C}^{-1} \end{aligned} \tag{7.46}$$

Thus the problem is governed by the model equation (3.1).

Hence, MODEL = 1, NTYPE = 0, and ITEM = 0 (for a steady-state solution). Since $a=a_0=1.0$ and $c=c_0=P\beta/k=256$ are the same for all elements, we set ICONT = 1, AX0 = 1.0, and CX0 = 256.0. All other coefficients are zero [$b=0$ and f $(=q)=0$] for this problem. For a uniform mesh of four linear elements (NEM = 4, IELEM = 1), the increments DX(I) are [DX(1) is always the coordinate of node 1]:

$$\{\text{DX}\}=\{0.0, 0.0625, 0.0625, 0.0625, 0.0625\}$$

(because $\frac{1}{4}L=0.25/4=0.0625$).

Set 1 boundary conditions are $U_1=0$ and $Q_2^4=0$. Since the natural boundary condition ($Q_2^4=0$) is homogeneous, there is no need to add a zero to the corresponding entry of the source column ($F_5+Q_2^4\rightarrow F_5$). There are no mixed (i.e., convection) boundary conditions. Hence, NSPV = 1, NSSV = 0, and NNBC = 0. The specified boundary condition on the primary variable is at node 1 and degree of freedom 1: ISPV(1, 1) = 1 and ISPV(1, 2) = 1. The specified value is VSPV(1) = 100.0.

TABLE 7.3

Meaning of the program variables AX0, AX1, . . . , for various field problems

Subscripts 0, 1, and 2 on variables denote the constant, linear, and quadratic coefficients of the variables [e.g., f_0, f_1, and f_2 denote the coefficients in $f(x) = f_0 + f_1 x + f_2 x^2$]

Field problem	MODEL	NTYPE	ITEM†	AX0	AX1	BX0	BX1	CX0	CX1	FX0	FX1	FX2	CT0‡	CT1‡
1. Plane wall	1	0	1	k_0	k_1	0.0	0.0	0.0	0.0	f_0	f_1	f_2	ρ_0	ρ_1
2. Heat exchanger fin	1	0	1	$(kA)_0$	$(kA)_1$	0.0	0.0	c_0	c_1	f_0	f_1	f_2	ρ_0	ρ_1
3. Radially symmetric heat transfer	1	0	1	0.0	k_1	0.0	0.0	0.0	0.0	0.0	f_1	f_2	0.0	ρ_1
4. Viscous flow through channels	1	0	1	μ_0	μ_1	0.0	0.0	0.0	0.0	f_0	f_1	f_2	ρ_0	ρ_1
5. Viscous flow through pipes	1	0	1	0.0	μ_1	0.0	0.0	0.0	0.0	0.0	f_1	f_2	0.0	ρ_1
6. Unidirectional seepage	1	0	1	μ_0	μ_1	0.0	0.0	0.0	0.0	f_0	f_1	f_2	ρ_0	ρ_1
7. Radially symmetric seepage (ground water flow)	1	0	1	0.0	μ_1	0.0	0.0	0.0	0.0	0.0	f_1	f_2	0.0	ρ_1
8. Axial deformation of a bar	1	0	2	$(AE)_0$	$(AE)_1$	0.0	0.0	c_0	c_1	f_0	f_1	f_2	$(\rho A)_0$	$(\rho A)_1$
9. Radially symmetric deformation of a disk (plane stress)	1	1	2	E_1	E_2	ν_{12}	H	c_0	c_1	f_0	f_1	f_2	$(\rho A)_0$	$(\rho A)_1$

10. Radially symmetric deformation of a cylinder (plane strain)	1	2	2	E_1	E_2	ν_{12}	H	c_0	c_1	f_0	f_1	f_2	$(\rho A)_0$	$(\rho A)_1$
11. Euler–Bernoulli beam theory	3	0	2	0.0	0.0	$(EI)_0$	$(EI)_1$	c_0	c_1	f_0	f_1	f_2	ρA	ρI
12. Euler–Bernoulli theory for circular plates	3	1	2	E_1	E_2	ν_{12}	H	c_0	c_1	f_0	f_1	f_2	ρA	ρI
13. Timoshenko beam theory (RIE)	2	0	2	$(GAK)_0$	$(GAK)_1$	$(EI)_0$	$(EI)_1$	c_0	c_1	f_0	f_1	f_2	ρA	ρI
14. Timoshenko beam theory (CIE)	2	2	2	$(GAK)_0$	$(GAK)_1$	$(EI)_0$	$(EI)_1$	c_0	c_1	f_0	f_1	f_2	ρA	ρI
15. Timoshenko theory of circular plates (RIE)	2	1	2	E_1	E_2	ν_{12}	H	c_0	c_1	f_0	f_1	G_{13}	ρA	ρI
16. Timoshenko theory of circular plates (CIE)	2	3	2	E_1	E_2	ν_{12}	H	c_0	c_1	f_0	f_1	G_{13}	ρA	ρI
17. Truss	4	0	0	For field problems 17–19, these parameters are not read; instead, $E = \mathrm{SE}$, $A = \mathrm{SA}$, $L = \mathrm{SL}$, and so on are read for each member of the structure: SE = modulus E, SA = cross-sectional area A, SI = moment of inertia I, SL = length L of the member, $CN = \cos\alpha$, SN = $\sin\alpha$, etc. (see Table 7.4)										
18. The Euler–Bernoulli frame element	4	1	0											
19. The Timoshenko frame element	4	2	0											

---

† For time-dependent problems only; when steady-state solutions are required, set ITEM = 0.

‡ For transient analysis only; no transient analysis option is included for truss and frame problems.

TABLE 7.4
Description of the input variables to the program FEM1DV2†

```
 * Data Card 1:

        TITLE - Title of the problem being solved (80 characters)

 * Data Card 2:

        MODEL - Model equation being solved (see below)
        NTYPE - Type of problem solved (see below)

                MODEL=1, NTYPE=0: A problem of MODEL EQUATION 1
                MODEL=1, NTYPE=1: A circular DISK (PLANE STRESS)
                MODEL=1, NTYPE>1: A circular DISK (PLANE STRAIN)
                MODEL=2, NTYPE=0: A Timoshenko BEAM (RIE#) problem
                MODEL=2, NTYPE=1: A Timoshenko PLATE (RIE) problem
                MODEL=2, NTYPE=2: A Timoshenko BEAM (CIE##) problem
                MODEL=2, NTYPE>2: A Timoshenko PLATE (CIE) problem
                MODEL=3, NTYPE=0: A Euler-Bernoulli BEAM problem
                MODEL=3, NTYPE>0: A Euler-Bernoulli Circular plate
                MODEL=4, NTYPE=0: A plane TRUSS problem
                MODEL=4, NTYPE=1: A Euler-Bernoulli FRAME problem
                MODEL=4, NTYPE=2: A Timoshenko (CIE) FRAME problem

                #  - Reduced Integration Element (RIE)
                ## - Consistent Interpolation Element (CIE)

        ITEM  - Indicator for transient analysis:

                ITEM=0, Steady-state solution
                ITEM=1, Transient analysis of PARABOLIC equations
                ITEM=2, Transient analysis of HYPERBOLIC equations
                ITEM=3, Eigenvalue analysis

 * Data Card 3:

        IELEM - Type of finite element:

                IELEM=0, Hermite cubic finite element
                IELEM=1, Linear Lagrange finite element
                IELEM=2, Quadratic Lagrange finite element

        NEM   - Number of elements in the mesh

 * Data Card 4:

        ICONT - Indicator for continuity of data for the problem:

                ICONT=1, Data (AX,BX,CX,FX and mesh) is continuous
                ICONT=0, Data is element dependent

        NPRNT - Indicator for printing of element/global matrices:

                NPRNT=0, Not print element or global matrices
                         but postprocess the solution and print
                NPRNT=1, Print Element 1 coefficient matrices only
                         but postprocess the solution and print
```

---

† SKIP means that you omit the input data. It *does not* mean that you leave a blank. In the "free format" used here, variables of each data card are read from the same line; if the values are not found on the same line, the computer will look for them on the next line(s). Each *data card* should start with a new line. Note that the variable names included in the data sets of Tables 7.5–7.14 are only for the convenience of the reader—they are *not* read by the computer.

TABLE 7.4 (Continued)

NPRNT=2, Print Element 1 and global matrices but
NOT postprocess the solution
NPRNT>2, Not print element or global matrices and
NOT postprocess the solution

SKIP Cards 5 through 15 for TRUSS/FRAME problems (MODEL = 4), and read Cards 5 through 15 only if MODEL.NE.4. SKIP Cards 5 through 9 if data is discontinuous (ICONT = 0)

* Data Card 5:

DX(I) - Array of element lengths. DX(1) denotes the global coordinate of Node 1 of the mesh; DX(I) (I=2,NEM1) denotes the length of the (I-1)st element. Here NEM1=NEM+1, and NEM=number of elements in the mesh.

Cards 6 through 9 define the coefficients in the model equations. All coefficients are expressed in terms of GLOBAL coordinate x. See Table 7.3 for the meaning of the coefficients, especially for deformation of circular plates and Timoshenko elements.

* Data Card 6:

AX0 - Constant term of the coefficient AX
AX1 - Linear term of the coefficient AX

* Data Card 7:

BX0 - Constant term of the coefficient BX
BX1 - Linear term of the coefficient BX

* Data Card 8:

CX0 - Constant term of the coefficient CX
CX1 - Linear term of the coefficient CX

SKIP Card 9 for eigenvalue problems (i.e. ITEM=3)

* Data Card 9:

FX0 - Constant term of the coefficient FX
FX1 - Linear term of the coefficient FX
FX2 - Quadratic term of the coefficient FX

SKIP Cards 10 through 15 if data is continuous (ICONT.NE.0). Cards 10 through 15 are read for each element (i.e., NEM times). All coefficients are expressed in terms of the GLOBAL coord

* Data Card 10:

{GLX} - Global x-coordinates of the FIRST and LAST nodes of the element

* Data Card 11:

{NOD} - Connectivity of the element:
NOD(N,I)=Global node number corresponding to the
I-th node of Element N (I=1,NPE)
NPE denotes the Number of nodes Per Element

* Data Card 12:

{DCAX}- Constant and linear terms of the coefficient AX

* Data Card 13:

{DCBX}- Constant and linear terms of the coefficient BX

TABLE 7.4 (Continued)

```
* Data Card 14:

       {DCCX}- Constant and linear terms of the coefficient CX

* Data Card 15:

       {DCFX}- Constant, linear and quadratic terms of FX

  READ Cards 16 through 21 for TRUSS/FRAME problems (MODEL = 4).
  SKIP Cards 16 through 21 if MODEL.NE.4 ____________________________

* Data Card 16:

       NNM    - Number of nodes in the finite element mesh

  SKIP Cards 17 through 19 for TRUSS problems (NTYPE = 0). Cards
  19 through 19 are read for each element, i.e., NEM times _________

* Data Card 17:

       PR     - Poisson's ratio of the material#
       SE     - Young's modulus of the material
       SL     - Length of the element
       SA     - Cross-ectional area of the element
       SI     - Moment of inertia of the element
       CS     - Cosine of the angle of orientation of the element
       SN     - Sine   of the angle of orientation of the element
                Angle is measured counter-clock-wise from x axis

       # PR is not used for the Euler -Bernoulli element

* Data Card 18:

       HF     - Intensity of the horizontal distributed force
       VF     - Intensity of the transversely distributed force
       PF     - Point load on the element
       XB     - Distance from node 1, along the length of the
                element, to the point of load application, PF
       CNT    - Cosine of the angle of orientation of the load PF
       SNT    - Sine   of the angle of orientation of the load PF
                Angle is measured counter-clock-wise from the
                element x axis
* Data Card 19:

       {NOD} - Connectivity of the element:
               NOD(N,I) = Global node number corresponding to the
                          I-th node of Element N (I=1,NPE)

  READ Cards 20  and 21 only for TRUSS problems (NTYPE = 0). Cards
  20 and 21  are read for each element;i.e. NEM times _______________

* Data Card 20:

       SE     - Young's modulus of the material
       SL     - Length of the element
       SA     - Cross-ectional area of the element
       CS     - Cosine of the angle of orientation of the element
       SN     - Sine   of the angle of orientation of the element
                Angle is measured counter-clock-wise from x axis
       HF     - Intensity of the horizontal distributed force

* Data Card 21:

       {NOD} - Connectivity of the element:
               NOD(N,I) = Global node number corresponding to the
                          Ith node of Element N (I=1,NPE)
```

TABLE 7.4 (Continued)

* Data Card 22:

NSPV - Number of specified PRIMARY degrees of freedom

SKIP Card 23 if no primary variables is specified (NSPV=0). Repeat Card 23 NSPV times

* Data Card 23: (I = 1 to NSPV)

ISPV(I,1) - Node number at which the PV is specified
ISPV(I,2) - Specified local primary DOF at the node
VSPV(I) - Specified value of the primary variable (PV)
(will not read for eigenvalue problems)

SKIP Card 24 for eigenvalue problems (i.e. when ITEM=3)

* Data Card 24:

NSSV - Number of specified (nonzero) SECONDARY variables

SKIP Card 25 if no secondary variable is specified (NSSV=0). Repeat Card 25 NSSV times

* Data Card 25: (I = 1 to NSSV)

ISSV(I,1) - Node number at which the SV is specified
ISSV(I,2) - Specified local secondary DOF at the node
VSSV(I) - Specified value of the secondary variable (PV)

* Data Card 26:

NNBC - Number of the Newton (mixed) boundary conditions

SKIP Card 27 if no mixed boundary condition is specified (NNBC=0). The mixed boundary condition is assumed to be of the form: SV+VNBC *(PV-UREF) = 0. Repeat Card 28 NNBC times

* Data Card 27: (I = 1 to NNBC)

INBC(I,1) - Node number at which the mixed B.C. is specified
INBC(I,2) - Local DOF of the PV and SV at the node
VNBC(I) - Value of the coefficient of the PV in the B.C.
UREF(I) - Reference value of the PV

SKIP Card 28 if ITEM=0 (read only for time-dependent and eigenvalue problems

* Data Card 28:

CT0 - Constant part of CT = CT0 + CT1*X
CT1 - Linear part of CT = CT0 + CT1*X

SKIP remaining cards if steady-state or eigenvalue analysis is to be performed (ITEM=0 or ITEM=3)

* Data Card 29:

DT - Time increment (uniform)
ALFA - Parameter in the time approximation scheme
BETA - Parameter in the time approximation scheme

* Data Card 30:

INCOND- Indicator for initial conditions:
INCOND=0, Homogeneous (zero) initial conditions
INCOND>0, Nonhomogeneous initial conditions
NTIME - Number of time steps for which solution is sought
INTVL - Time step intervals at which solution is to printed

TABLE 7.4 (Continued)

```
    SKIP Cards 31 and 32 if initial conditions are zero (INCOND=0) ___

  * Data Card 31:

          {GU0} - Array of initial values of the primary variables

    SKIP Card 32 for parabolic equations (ITEM=1) __________________

  * Data Card 32:

          {GU1} - Array of initial values of the first time-deriva-
                  tives of the primary variables
```

For Set 2 boundary conditions, we have one essential boundary condition and one mixed boundary condition:

$$U_1 = 0, \qquad Q_2^4 + \frac{\beta}{k}(U_5 - U_\infty) = 0$$

Hence, NSPV = 1, NSSV = 0, and NNBC = 1, and the values in the mixed boundary conditions are input as

$$\text{VNBC}(1) = \beta/k = 1.28, \quad \text{UREF}(1) = U_\infty = 0.0, \quad \text{INBC}(1,1) = 5, \quad \text{INBC}(1,2) = 1.$$

The output file for Set 1 boundary conditions is presented in Table 7.5(*a*). The input files are echoed in the output. The input file for Set 2 boundary conditions is given in Table 7.5(*b*).

Example 7.2 (Example 3.2) Radially symmetric heat transfer in a solid cylinder. The governing equation of the problem is given by [see (3.78)]

$$-\frac{d}{dr}\left(2\pi kr\frac{dT}{dr}\right) = 2\pi q_0 \quad \text{for } 0 < r < R_o \tag{7.47}$$

$$\left(2\pi kr\frac{dT}{dr}\right)\bigg|_{r=0} = 0, \qquad T(R_o) = T_o \tag{7.48}$$

with $k = 20\ \text{W m}^{-1}\ {}^\circ\text{C}^{-1}$, $q_0 = 2\times10^8\ \text{W m}^{-3}$, $T_o = 100^\circ\text{C}$, and $R_o = 0.01$ m (see Table 3.3). We have MODEL = 1, NTYPE = 0, and ITEM = 0 (for a steady-state solution), and the data is continuous (ICONT = 1) in the domain for a mesh of two quadratic elements (IELEM = 2, NEM = 2). The data is

$$a = 2\pi kr \rightarrow a_0 = 0, \quad a_1 = 2\pi k; \quad b = 0 \rightarrow b_0 = 0.0, \quad b_1 = 0.0$$

$$c = 0 \rightarrow c_0 = 0.0, \quad c_1 = 0.0; \quad f = 2\pi q_0 r \rightarrow f_0 = 0.0, \quad f_1 = 2\pi q_0, \quad f_2 = 0.0$$

Thus, we have [for values $k = 20\ \text{W m}^{-1}\ {}^\circ\text{C}^{-1}$, $q_0 = 2\times10^8\ \text{W m}^{-3}$

$$\text{AX0} = 0.0 \quad \text{AX1} = 125.6637, \quad \text{BX0} = 0.0, \quad \text{BX1} = 0.0$$

$$\text{CX0} = 0.0, \quad \text{CX1} = 0.0, \quad \text{FX0} = 0.0, \quad \text{FX1} = 12.5664\text{E}8, \quad \text{FX2} = 0.0$$

The array {DX} and boundary information are given by

$$\{\text{DX}\} = \{0.0, 0.0025, 0.0025, 0.0025, 0.0025\}$$

$$\text{NSPV} = 1, \quad \text{ISPV}(1,1) = 5, \quad \text{ISPV}(1,2) = 1, \quad \text{VSPV}(1) = 100$$

TABLE 7.5
Output from FEM1DV2 for the problem in Example 7.1

(*a*) Set 1 boundary conditions (edited output)

```
    *** ECHO OF THE INPUT DATA STARTS ***

 Example 7.1: Steady heat transfer in a fin (Set 1 boundary conditions)
   1  0  0                                    MODEL, NTYPE, ITEM
   1  4                                       IELEM, NEM
   1  1                                       ICONT, NPRNT
     0.0  0.0625  0.0625  0.0625  0.0625      DX(I)
     1.0  0.0                                 AX0, AX1
     0.0  0.0                                 BX0, BX1
   256.0  0.0                                 CX0, CX1
     0.0  0.0  0.0                            FX0,FX1,FX2
   1                                          NSPV
   1  1  100.0                                ISPV(1,J) {J=1,2}, VSPV(1)
   0                                          NSSV
   0                                          NNBC
    **** ECHO OF THE INPUT DATA ENDS ****
```

```
   ________________________________________________________

   OUTPUT FROM PROGRAM   FEM1DV2  BY  J. N. REDDY
   ________________________________________________________

 Example 7.1: Steady heat transfer in a fin (Set 1 boundary conditions)

   *** ANALYSIS OF MODEL 1, AND TYPE 0 PROBLEM ***

        Element type (0, Hermite,>0, Lagrange)..=   1
        No. of deg. of freedom per node, NDF....=   1
        No. of elements in the mesh, NEM........=   4
        No. of total DOF in the model, NEQ......=   5
        No. of specified primary DOF, NSPV......=   1
        No. of specified secondary DOF, NSSV....=   0
        No. of specified Newton B. C.: NNBC.....=   0

  Boundary information on primary variables:

        1    1    0.10000E+03

  Global coordinates of the nodes, {GLX}:

   0.00000E+00  0.62500E-01  0.12500E+00  0.18750E+00  0.25000E+00

  Coefficients of the differential equation:

        AX0 =  0.1000E+01     AX1 =  0.0000E+00
        BX0 =  0.0000E+00     BX1 =  0.0000E+00
        CX0 =  0.2560E+03     CX1 =  0.0000E+00
        FX0 =  0.0000E+00     FX1 =  0.0000E+00     FX2 =  0.0000E+00

 SOLUTION (values of PVs) at the NODES:

   0.10000E+03  0.35158E+02  0.12504E+02  0.48560E+01  0.30350E+01
```

TABLE 7.5 (Continued)

```
       X          P. Variable  S. Variable

  0.00000E+00  0.10000E+03 -0.10375E+04
  0.78125E-02  0.91895E+02 -0.10375E+04
  0.15625E-01  0.83789E+02 -0.10375E+04
  0.23438E-01  0.75684E+02 -0.10375E+04
  0.31250E-01  0.67579E+02 -0.10375E+04
  0.39063E-01  0.59473E+02 -0.10375E+04
  0.46875E-01  0.51368E+02 -0.10375E+04
  0.54688E-01  0.43263E+02 -0.10375E+04
  0.62500E-01  0.35158E+02 -0.10375E+04
  0.62500E-01  0.35158E+02 -0.36245E+03
  0.70313E-01  0.32326E+02 -0.36245E+03
  0.78125E-01  0.29494E+02 -0.36245E+03
  0.85938E-01  0.26663E+02 -0.36245E+03
  0.93750E-01  0.23831E+02 -0.36245E+03
  0.10156E+00  0.20999E+02 -0.36245E+03
  0.10938E+00  0.18168E+02 -0.36245E+03
  0.11719E+00  0.15336E+02 -0.36245E+03
  0.12500E+00  0.12504E+02 -0.36245E+03
  0.12500E+00  0.12504E+02 -0.12237E+03
  0.13281E+00  0.11548E+02 -0.12237E+03
  0.14063E+00  0.10592E+02 -0.12237E+03
  0.14844E+00  0.96362E+01 -0.12237E+03
  0.15625E+00  0.86801E+01 -0.12237E+03
  0.16406E+00  0.77241E+01 -0.12237E+03
  0.17188E+00  0.67681E+01 -0.12237E+03
  0.17969E+00  0.58120E+01 -0.12237E+03
  0.18750E+00  0.48560E+01 -0.12237E+03
  0.18750E+00  0.48560E+01 -0.29136E+02
  0.19531E+00  0.46284E+01 -0.29136E+02
  0.20313E+00  0.44008E+01 -0.29136E+02
  0.21094E+00  0.41731E+01 -0.29136E+02
  0.21875E+00  0.39455E+01 -0.29136E+02
  0.22656E+00  0.37179E+01 -0.29136E+02
  0.23438E+00  0.34903E+01 -0.29136E+02
  0.24219E+00  0.32626E+01 -0.29136E+02
  0.25000E+00  0.30350E+01 -0.29136E+02
```

(*b*) Set 2 boundary conditions (input data only)

```
Example 7.1: Steady heat transfer in a fin (Set 2 boundary conditions)
  1  0  0                                   MODEL, NTYPE, ITEM
  1  4                                      IELEM, NEM
  1  1                                      ICONT, NPRNT
    0.0  0.0625  0.0625  0.0625  0.0625     DX(I)
    1.0  0.0                                AX0, AX1
    0.0  0.0                                BX0, BX1
  256.0  0.0                                CX0, CX1
    0.0  0.0  0.0                           FX0,FX1,FX2
  1                                         NSPV
  1  1  100.0                               ISPV(1,J), VSPV(1)
  0                                         NSSV
  1                                         NNBC
  5  1  1.28  0.0                           INBC(1,J), VNBC(1), UREF(1)
```

TABLE 7.6
Input file for the problem in Example 7.2

```
Example 7.2: Radially symmetric heat transfer in a solid cylinder
  1  0  0                                       MODEL, NTYPE, ITEM
  2  2                                          IELEM, NEM
  1  1                                          ICONT, NPRNT
    0.0  0.005   0.005                          DX(I)
    0.0  125.6637                               AX0, AX1
    0.0  0.0                                    BX0, BX1
    0.0  0.0                                    CX0, CX1
    0.0  12.56637E8  0.0                        FX0,FX1,FX2
  1                                             NSPV
  5  1  100.0                                   ISPV(1,J), VSPV(1)
  0                                             NSSV
  0                                             NNBC
```

The input file of the problem is presented in Table 7.6 (cf. Table 3.3). Note that the finite element solution obtained with two quadratic elements is more accurate (essentially the same as the exact) than the solution obtained with four linear elements.

The fluid mechanics problem in Example 3.3 is very simple, and the reader should be able to generate the input file very easily to solve it with FEM1DV2.

Example 7.3 Deformation of a rotating disk. For this case, we have MODEL = 1, NTYPE = 1, and ITEM = 0. For a mesh of two quadratic elements (i.e., IEL = 2 and NEM = 2), we use ICONT = 1 and

$$\{DX\} = \{0.0, 0.25R, 0.25R, 0.25R, 0.25R\}$$

where R is the radius of the disk. For a uniform and homogeneous disk of thickness H and made of isotropic material, we take the moduli $E_1 = E_2 = E$. Since we are seeking results in nondimensional form, we take

$$R = 1.0, \quad E = 1.0, \quad \nu = 0.3, \quad H = 1.0$$

Thus, we have

$$\text{AX0}\,(=E_1) = 1.0, \quad \text{AX1}\,(=E_2) = 1.0$$

$$\text{BX0}\,(=\nu_{12}) = 0.3, \quad \text{BX1}\,(=H) = 1.0$$

$$\text{CX0} = 0.0, \quad \text{CX1} = 0.0$$

The body force is $f_r = \rho\omega^2 r = f_0 + f_1 r + f_2 0$. Hence, taking $\rho\omega^2 = 1.0$,

$$\text{FX0} = 0.0, \quad \text{FX1} = 1.0, \quad \text{FX2} = 0.0$$

The boundary conditions are $u(0) = 0$ (by symmetry) and $r\sigma_r = 0$ at $r = R$ (stress-free condition). Since the secondary variable is homogeneous, there is no need to impose it—only the boundary condition on the primary variable is to be imposed. We have

$$\text{NSPV} = 1, \quad \text{NSSV} = 0, \quad \text{NNBC} = 0$$

$$\text{ISPV}(1,1) = 1, \quad \text{ISPV}(1,2) = 1, \quad \text{VSPV}(1) = 0.0$$

The input file for this problem is presented in Table 7.7.

TABLE 7.7
Input file for the problem in Example 7.3

```
Example 7.3: Deformation of a rotating disk
 1  1  0                                        MODEL, NTYPE, ITEM
 2  2                                           IELEM, NEM
 1  1                                           ICONT, NPRNT
   0.0  0.50     0.50                           DX(I)
   1.0  1.0                                     AX0, AX1
   0.3  1.0                                     BX0, BX1
   0.0  0.0                                     CX0, CX1
   0.0  1.0      0.0                            FX0, FX1, FX2
 1                                              NSPV
 1  1   0.0                                     ISPV(1,J), VSPV(1)
 0                                              NSSV
 0                                              NNBC
```

Example 7.4 (Example 4.2) Clamped and spring-supported beam in Fig. 4.7. We solve the problem using the Euler–Bernoulli beam element (MODEL = 3, NTYPE = 0, IELEM = 0) and the Timoshenko beam element (MODEL = 2, NTYPE = 0 or 2, IELEM = 1, 2, or 3).

Since the loading is discontinuous, we set ICONT = 0. A minimum of two elements are required to model the problem (i.e., NEM = 2).

If we take $EI = 1.0\text{E}6$ (i.e., $10^6\ \text{ft}^2\ \text{lb}$) then

$$GAK = \frac{E}{2(1+\nu)} BH \frac{5}{6} = \frac{EI}{1+\nu} \frac{5}{H^2}$$

For $L/H = 10$, we have $H = 1.0$ because $L = 10$ ft. For the choice $\nu = 0.25$, we have

$$GAK = 4EI/H^2 = 4 \times 10^6\ \text{lb}$$

Thus, we use

$$\text{AX0} = 0.0, \quad \text{AX1} = 0.0, \quad \text{BX0}\ (= EI) = 1.0\text{E}6$$
$$\text{BX1} = 0.0, \quad \text{CX0} = 0.0, \quad \text{CX1} = 0.0$$

for the Euler–Bernoulli beam and

$$\text{AX0}\ (= GAK) = 4.0\text{E}6, \quad \text{AX1} = 0.0, \quad \text{BX0}\ (= EI) = 1.0\text{E}6$$
$$\text{BX1} = 0.0, \quad \text{CX0} = 0.0, \quad \text{CX1} = 0.0$$

for the Timoshenko beam.

The distributed transverse load is zero in element 1, and it is

$$f(x) = -\frac{100}{6}(x-4)$$

in element 2. Hence,

$$\text{FX0} = 0.0, \qquad \text{FX1} = 0.0, \qquad \text{FX2} = 0.0 \quad \text{in element 1}$$
$$\text{FX0} = 66.666, \quad \text{FX1} = -16.666, \quad \text{FX2} = 0.0 \quad \text{in element 2}$$

The global coordinates of nodes and the connectivity matrix entries for each element are obvious from the geometry. For the Euler–Bernoulli beam element the number of nodes is always equal to 2 (NPE = 2), whereas for the Timoshenko beam element, the number of nodes depend on the degree of interpolation (or element type) selected: NPE = IELEM + 1.

The boundary conditions for this problem are

$$w(0)=0, \quad \left(\frac{dw}{dx}\right)\bigg|_{x=0}=0, \quad (V+kw)\bigg|_{x=L}=0$$

Therefore, we have (NSSV = 0)

$$\text{NSPV}=2, \quad \text{ISPV}(1,1)=1, \quad \text{ISPV}(1,2)=1, \quad \text{VSPV}(1)=0.0$$
$$\text{ISPV}(2,1)=1, \quad \text{ISPV}(2,2)=2, \quad \text{VSPV}(2)=0.0$$
$$\text{NNBC}=1, \quad \text{INBC}(1,1)=3, \quad \text{INBC}(1,2)=1$$
$$\text{VNBC}(1)\ (=k)=1.0\text{E}6 \quad (\text{for } k/EI=1) \text{ and } 0.0 \ (\text{for } k=0.0)$$
$$\text{UREF}(1)=0.0$$

Tables 7.8 and 7.9 give the input files for the Euler–Bernoulli and Timoshenko elements. Note that the Euler–Bernoulli element is a Hermite cubic element, whereas the Timoshenko element is only a Lagrange linear element.

Example 7.5 (Example 4.4) Analysis of a plane frame. Here we consider the two-member frame structure shown in Fig. 4.13(*a*). We shall analyze it using the Euler–Bernoulli frame element (MODEL = 4, NTYPE = 1) and the Timoshenko frame element (MODEL = 4, NTYPE = 2). The former gives an exact solution for all frame structures with constant cross-section members. The Timoshenko frame element, on the other hand, does not yield accurate results unless several elements per member of the structure are used.

The input files of the problem are presented in Tables 7.10 and 7.11. The eight-element mesh of Timoshenko elements gives results comparable to the two-element mesh with the Euler–Bernoulli frame elements (results are not included here).

The next example deals with the use of FEM1DV2 for time-dependent problems (i.e., ITEM = 1 or 2).

TABLE 7.8
Input file for the problem in Example 7.4

```
Example 7.4: Clamped and spring-supported beam (E-B element; k=1.0E4)
  3  0  0                                  MODEL, NTYPE, ITEM
  0  2                                     IELEM, NEM
  0  1                                     ICONT, NPRNT
    0.0    4.0                             GLX(I)      |
    1       2                              NOD(1,J)    |
    0.0    0.0                             AX0, AX1    |  Data for
    1.0E6  0.0                             BX0, BX1    |  Element 1
    0.0    0.0                             CX0, CX1    |
    0.0    0.0     0.0                     FX0,FX1,FX2 |
    4.0   10.0                             GLX(I)      |
    2       3                              NOD(2,J)    |
    0.0    0.0                             AX0, AX1    |  Data for
    1.0E6  0.0                             BX0, BX1    |  Element 2
    0.0    0.0                             CX0, CX1    |
    66.666667   -16.666667  0.0            FX0,FX1,FX2 |
  2                                        NSPV
  1    1   0.0                             ISPV(1,J), VSPV(1)
  1    2   0.0                             ISPV(2,J), VSPV(2)
  0                                        NSSV
  1                                        NNBC  (with transv. spring)
  3    1   1.0E04   0.0
```

TABLE 7.9
Input file for the problem in Example 7.4

```
Example 7.4:  Clamped and spring-supported beam (TIM element; k=1.0E4)
  2  0  0                                          MODEL, NTYPE, ITEM
  1  2                                             IELEM, NEM
  0  1                                             ICONT, NPRNT
    0.0     4.0                                    GLX(I)        |
    1        2                                     NOD(1,J)      |
    4.0E6  0.0                                     AX0, AX1      |   Data for
    1.0E6  0.0          (L/H = 10)                 BX0, BX1      |   Element 1
    0.0     0.0                                    CX0, CX1      |
    0.0     0.0     0.0                            FX0,FX1,FX2   |
    4.0    10.0                                    GLX(I)        |
    2        3                                     NOD(2,J)      |
    4.0E6  0.0                                     AX0, AX1      |   Data for
    1.0E6  0.0                                     BX0, BX1      |   Element 2
    0.0     0.0                                    CX0, CX1      |
    66.666667   -16.666667  0.0                    FX0,FX1,FX2   |
  2                                                NSPV
  1    1    0.0                                    ISPV(1,J), VSPV(1)
  1    2    0.0                                    ISPV(2,J), VSPV(2)
  0                                                NSSV
  1                                                NNBC  (with tranv. spring)
  3   1     1.0E4   0.0                            INBC(1,J), VNBC(1), UREF(1)
```

Example 7.6 (Example 6.4) Transient heat conduction in a plane wall. Consider the transient heat conduction problem of Example 6.4 [see (6.56)]:

$$\frac{\partial u}{\partial t}-\frac{\partial^2 u}{\partial x^2}=0 \quad \text{for } 0<x<1 \tag{7.49a}$$

$$u(0,t)=0, \qquad \frac{\partial u}{\partial t}(1,t)=0 \qquad \text{(Set 1)} \tag{7.49b}$$

TABLE 7.10
Input file for the problem in Example 7.5

```
Example 7.5:  Analysis of a plane frame  (E-B element)
  4  1  0                                            MODEL, NTYPE, ITEM
  0  2                                               IELEM, NEM
  0  1                                               ICONT, NPRNT
  3                                                  NEM
  0.3   1.0E6  144.0  10.0  10.0  0.0  1.0           PR, SE, SL, SA, SI, CS, SN
  0.0  -0.0138888  0.0  0.0  0.0  0.0                HF, VF, PF, XB, CST, SNT
  1  2                                               NOD(1,J)
  0.3   1.0E6  180.0  10.0  10.0  0.8  0.6
  0.0   0.0     -4.0  90.0   0.6  0.8                Same as above for Element 2
    2     3
    6                                                NSPV
    1     1    0.0             <-----------
    1     2    0.0                         |
    1     3    0.0                         |
    3     1    0.0                         |         ISPV, VSPV
    3     2    0.0                         |
    3     3    0.0             <-----------
    1                                                NSSV
    2     2   -2.0                                   ISSV, VSSV
    0                                                NNBC
```

TABLE 7.11
Input file for the problem in Example 7.5

```
Example 7.5:  Analysis of a plane frame  (TIM element)
  4  2  0                                       MODEL, NTYPE, ITEM
  0  2                                          IELEM, NEM
  0  1                                          ICONT, NPRNT
  3                                             NNM
  0.3   1.0E6  144.0  10.0  10.0  0.0  1.0     PR, SE, SL, SA, SI, CS, SN
  0.0  -0.0138888  0.0  0.0  0.0  0.0           HF, VF, PF, XB, CST, SNT
    1     2                                     NOD(1,J)
  0.3   1.0E6  180.0  10.0  10.0  0.8  0.6
  0.0   0.0     -4.0  90.0  0.6   0.8           Same as above for Element 2
    2     3
    6                                           NSPV
    1     1    0.0              <-----------
    1     2    0.0                          |
    1     3    0.0                          |
    3     1    0.0                          |   ISPV, VSPV
    3     2    0.0                          |
    3     3    0.0              <-----------
    1                                           NSSV
    2     2   -2.0                              ISSV, VSSV
    0                                           NNBC
```

$$u(0, t) = 0, \quad \left(\frac{\partial u}{\partial t} + u\right)\bigg|_{x=1} = 0 \qquad \text{(Set 2)} \tag{7.49c}$$

$$u(x, 0) = 1$$

In Example 6.4, only Set 1 boundary conditions were considered.

We have MODEL = 1, NTYPE = 0, ITEM = 1, ICONT = 1, NSPV = 1, NSSV = 0, and NNBC = 0 for Set 1 and NNBC = 1 for Set 2. The coefficients of the differential equations are ($a = 1.0$, $b = 0.0$, $c = 0.0$, $c_t = 1.0$ and $f = 0$)

$$\begin{aligned} &\text{AX0} = 1.0, \quad \text{AX1} = 0.0, \quad \text{BX0} = 0.0, \quad \text{BX1} = 0.0\\ &\text{CX0} = 0.0, \quad \text{CX1} = 0.0, \quad \text{FX0} = 0.0, \quad \text{FX1} = 0.0\\ &\text{FX2} = 0.0, \quad \text{CT0} = 1.0, \quad \text{CT1} = 0.0 \end{aligned}$$

The boundary and initial conditions (since INCOND = 1) are input as

$$\begin{aligned} &\text{ISPV}(1, 1) = 1, \quad \text{ISPV}(1, 2) = 1, \quad \text{VSPV}(1) = 0.0\\ &\text{GU0(I)} = \{0.0, 1.0, 1.0, \ldots\} \end{aligned}$$

From the discussions of Example 6.4, we use $\Delta t = 0.01$ (DT = 0.01) and print the solution for every time step (i.e., INTVL = 1).

The input file of the problem for Set 1 boundary conditions is presented in Table 7.12.

Example 7.7 (Example 6.2) Natural vibrations of a cantilever beam. For this problem, the boundary conditions are given by

$$w(0) = 0, \quad \left(\frac{dw}{dx}\right)\bigg|_{x=0} = 0 \quad \text{for the Euler–Bernoulli beam theory}$$

$$w(0) = 0, \quad \Psi(0) = 0 \qquad \text{for the Timoshenko beam theory}$$

The input data for all variables is the same as in the static analysis. In addition, we must input c_{t0} and c_{t1}. For the Timoshenko beam theory [see (6.13)], c_{t0} denotes the inertia

TABLE 7.12
Input file for the problem in Example 7.6

```
Example 7.6: Transient heat conduction in a plane wall
  1  0  1                                   MODEL, NTYPE, ITEM
  1  2                                      IELEM, NEM
  1  1                                      ICONT, NPRNT
    0.0   0.5   0.5                         DX(I)
    1.0   0.0                               AX0, AX1
    0.0   0.0                               BX0, BX1
    0.0   0.0                               CX0, CX1
    0.0   0.0   0.0                         FX0,FX1,FX2
    1                                       NSPV
    1  1  0.0                               ISPV(I,J), VSPV(I)
    0                                       NSSV
    0                                       NNBC
    1.0   0.0                               CT0, CT1
    0.05  0.5   0.0                         DT, ALFA, BETA
    1     20    2                           INCOND, NTIME, INTVL
    0.0   1.0   1.0                         GU0(I)
```

ρA, and c_{t1} denotes the rotatory inertia ρI. The eigenvalue solver used in FEM1DV2 requires the matrix $[B]$ in $[A]\{x\} = \lambda[B]\{x\}$ to be positive-definite. Hence, c_{t0} and c_{t1} should be nonzero, otherwise, the mass matrix coefficients associated with Ψ will be zero.

The input files for the natural vibrations of the cantilever beam by the two types of elements are given in Tables 7.13 and 7.14. The reader can investigate the convergence characteristics of the elements in improving the accuracy of the fundamental frequency with the use of FEM1DV2.

7.4 SUMMARY

In this chapter three main items have been discussed: numerical integration of finite element coefficient matrices and vectors, logical units of a typical finite element program and their contents, and applications of the finite element program FEM1DV2. The numerical evaluation of the coefficients is required because of (*a*) variable coefficients of the differential equations modeled and (*b*) special evaluation of the coefficients, as was required for the Timoshenko

TABLE 7.13
Input file for the problem in Example 7.7

```
Example 7.7: Natural vibrations of a cantilever beam (E-B; with RI)
  3  0  3                                     MODEL, NTYPE, ITEM
  0  4                                        IELEM, NEM
  1  1                                        ICONT, NPRNT
    0.0    0.25   0.25   0.25   0.25          DX(I)
    0.0    0.0                                AX0, AX1
    1.0    0.0                                BX0, BX1
    0.0    0.0                                CX0, CX1
    2                                         NSPV
  1  1                                        ISPV(1,J)
  1  2                                        ISPV(2,J)
    0                                         NNBC
    1200.0 1.0                                CT0, CT1  (L/H=10)
```

TABLE 7.14
Input file for the problem in Example 7.7

```
Example 7.7: Natural vibrations of a cantilever beam (TIM element)
  2  0  3                                         MODEL, NTYPE, ITEM
  1  4                                            IELEM, NEM
  1  1                                            ICONT, NPRNT
    0.0    0.25   0.25   0.25   0.25              DX(I)
    4.0E2  0.0                                    AX0, AX1
    1.0    0.0                                    BX0, BX1
    0.0    0.0                                    CX0, CX1
    2                                             NSPV
  1  1                                            ISPV(1,J)
  1  2                                            ISPV(2,J)
    0                                             NNBC
   12.0E2  1.0                                    CT0, CT1  (L/H=10)
```

beam element with equal interpolation. The Newton–Cotes and Gauss–Legendre integration rules have been discussed. The integration rules require the transformation of the integral expressions from the global coordinate system to a local coordinate system. This transformation requires interpolation of the global coordinate x. Depending on the relative degrees of interpolation of the geometry and the dependent variables, the formulations are classified as subparametric, isoparametric, and superparametric.

The three logical units—preprocessor, processor, and postprocessor—have been discussed. The contents of processor, where most finite element calculations are carried out, have been considered in detail. Fortran statements for numerical evaluation of integral expressions, assembly of element coefficients, and imposition of boundry conditions have been discussed.

A description of the finite element computer program FEM1DV2 has been presented, and its application to problems of heat transfer and solid mechanics has been discussed.

PROBLEMS

Section 7.1

In Problems 7.1–7.5, compute the matrix coefficients using (*a*) the Newton–Cotes integration formula and (*b*) the Gauss–Legendre quadrature. Use the appropriate number of integration points, and verify the results with those obtained by the exact integration.

7.1.

$$K_{12}=\int_{x_A}^{x_B}(1+x)\frac{d\psi_1}{dx}\frac{d\psi_2}{dx}\,dx,\qquad G_{12}=\int_{x_A}^{x_B}(1+x)\psi_1\psi_2\,dx$$

where ψ_i are the linear (Lagrange) interpolation functions.

Answer: $K_{12}=-h^{-1}[1+\frac{1}{2}(x_A+x_B)]$, $G_{12}=\frac{1}{6}h(1+x_A+\frac{1}{2}h)$.

7.2. Repeat Problem 7.1 for the quadratic interpolation functions.

7.3.

$$K_{11}=\int_{x_A}^{x_B}\left(\frac{d^2\psi_1}{dx^2}\right)^2 dx, \qquad G_{11}=\int_{x_A}^{x_B}(\psi_1)^2\,dx$$

where ψ_i are the Hermite cubic interpolation functions.

Answer: $r=2$: $K_{11}=12/h^3$ (exact), $G_{11}=0.398148h$.

7.4. Repeat Problem 7.3 for the case in which the interpolation functions are the fifth-order Hermite polynomials of Problem 4.21.

Answer: $K_{11}=\frac{120}{7}h^3$, $G_{11}=\frac{181}{462}h$ (exact for five-point quadrature).

7.5.

$$K_{11}=\int_{x_A}^{x_B}\left(\frac{d\psi_1}{dx}\right)^2 dx$$

where $\psi_1=\sin\left[\frac{1}{4}\pi(\xi+3\xi^2)\right]$. Use three- and five-point Gauss quadrature to compute K_{11}.

Section 7.2

Computer exercises (use FEM1DV2)

7.6. Solve the problem in Example 3.1 (Set 2) using two, four, and six linear elements. Tabulate the results along with the exact solution. Use the following data: $L=0.02$ m, $k=20$ W m^{-1} °C^{-1}, $g_0=10^5$ W m^{-2}, $T_\infty=50$°C, $\beta=500$ W m^{-1} °C^{-1}.

7.7. Solve the problem in Example 3.1 (Set 2) using one, two, and three quadratic elements. Compare the finite element results for the temperature and heat flux with the exact solutions at the nodes.

7.8. Solve the heat transfer problem in Example 3.2 (Set 2), using four linear elements and two quadratic elements, and tabulate them with the exact solution at nodes (see Table 3.3).

7.9. Solve the problem in Example 3.4 using four quadratic elements, and compare the solution with that obtained using eight linear elements and the exact solution.

7.10. Solve the one-dimensional flow problem of Example 3.4 (Set 2), for $dP/dx=-24$, using four linear elements and two quadratic elements. Compare the finite element results with the exact one.

7.11. Solve the Couette flow problem in Example 3.3 using (*a*) four linear elements and (*b*) two quadratic elements. Compare the finite element solution for the temperature with the exact solution.

7.12. Solve the problem of heat flow in a rod (Problem 3.19) using (*a*) four linear elements and (*b*) two quadratic elements, and compare the results with the analytical solution.

7.13. Solve Problem 3.26 using (*a*) four linear elements and (*b*) two quadratic elements, and compare the finite element solution with the exact solution at nodes.

7.14. Solve the problem of axisymmetric deformation of a rotating circular disk using (*a*) four linear elements and (*b*) two quadratic elements (see Example 7.3). Assume that the body force is given by $f=\rho\omega^2 r$.

7.15. Solve Problem 3.28.

7.16. Solve Problem 3.30.

7.17. Solve the problem in Example 3.4 using (*a*) four linear and (*b*) two quadratic elements. Determine the stress at the fixed end.

7.18–7.29. Solve the beam problems 4.1–4.12 using the minimum number of Hermite cubic elements.

7.30. Analyze a clamped circular plate under a uniformly distributed transverse load using the Euler–Bernoulli plate element. Investigate the convergence using two, four, and six elements by comparing with the exact solution

$$w(r) = \frac{q_0 a^4}{64D}\left[1 - \left(\frac{r}{a}\right)^2\right]^2$$

where $D = EH^3/12(1-\nu^2)$, q_0 is the intensity of the distributed load, a is the radius of the plate, H is its thickness, and ν is Poisson's ratio ($\nu = 0.25$).

7.31. Repeat Problem 7.30 with (*a*) two, four, and six linear and (*b*) one, two, and three quadratic Timoshenko plate elements (RIE) for $a/H = 10$ and 100.

7.32. Repeat Problem 7.30 with the Timoshenko plate element (CIE) for $a/H = 10$ and 100.

7.33. Consider an annular plate of outer radius a and and inner radius b, and thickness H. If the plate is simply supported at the outer edge and subjected to a uniformly distributed moment M_0 at the inner edge (see Fig. P7.33), analyze the problem using the Euler–Bernoulli plate element. Investigate the accuracy using two and four elements and comparing with the analytical solution ($\nu = 0.25$)

$$w(r) = \frac{b^2 M_0 (a^2 - r^2)}{2(1+\nu)D(a^2 - b^2)} - \frac{a^2 b^2 M_0}{(1-\nu)D(a^2 - b^2)} \ln\left(\frac{r}{a}\right)$$

See Problem 7.30 for the definition of D.

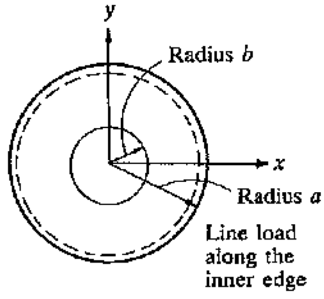

FIGURE P7.33

7.34. Repeat Problem 7.33 with (*a*) two and four linear and (*b*) one and two quadratic Timoshenko (RIE) elements for $a/H = 10$ and 100.

7.35. Consider the simply supported annular plate described in Problem 7.33. Suppose that the inner edge is loaded with a uniformly distributed shearing force Q_0. Use meshes of two and four Euler–Bernoulli plate elements to analyze the problem.

7.36. Analyze Problem 7.35 with (*a*) two and four linear and (*b*) one and two quadratic Timoshenko (RIE) plate elements for $a/H = 10$ and 100.

7.37. Repeat Problem 7.36 with the Timoshenko (CIE) plate element.

7.38. Consider a simply supported circular plate of radius a, loaded at the center with a load P. Analyze the problem with two, four, and six Euler–Bernoulli plate elements and compare with the analytical solution ($\nu = 0.25$)

$$w(r) = \frac{P}{8\pi D}\left[\frac{3+\nu}{2(1+\nu)}(a^2 - r^2) + r^2 \ln\left(\frac{r}{a}\right)\right]$$

Note that $Q_1^1 = P/2\pi$.

7.39. Analyze Problem 7.38 with four and eight linear Timoshenko (RIE) plate elements for $a/H = 10$ and 100.

7.40. Analyze the simply supported annular plate in Problem 7.33 when it is subjected to a uniformly distributed load of intensity q_0. Use the Euler–Bernoulli plate element.

7.41. Analyze the annular plate in Problem 7.40 using two and four Timoshenko (CIE) plate elements.

7.42–7.49. Solve the truss and frame problems in Figs. P4.29–P4.36.

7.50. Consider the axial motion of an elastic bar, governed by the second-order equation

$$EA\frac{\partial^2 u}{\partial x^2} = \rho A\frac{\partial^2 u}{\partial t^2} \quad \text{for } 0 < x < L$$

with the following data: length of bar $L = 500$ mm, cross-sectional area $A = 1\ \text{mm}^2$, modulus of elasticity $E = 20{,}000\ \text{N mm}^{-2}$, density $\rho = 0.008\ \text{N s}^2\ \text{mm}^{-4}$, boundary conditions

$$u(0, t) = 0, \qquad EA\frac{\partial u}{\partial x}(L, t) = 1$$

and zero initial conditions. Using 50 linear elements and $\Delta t = 0.002$ s, determine the axial displacement and plot the displacement as a function of position along the bar for $t = 0.8$ s.

7.51. Consider the following nondimensionalized differential equation governing the plane wall transient [see Myers (1971), p. 101]:

$$-\frac{\partial^2 T}{\partial x^2} + \frac{\partial T}{\partial t} = 0 \quad \text{for } 0 < x < 1$$

with boundary conditions $T(0, t) = 1$ and $T(1, t) = 0$, and initial condition $T(x, 0) = 0$. Solve the problems using (a) four, six, and eight linear elements, and (b) two, three, and four quadratic elements. Compare the finite element solutions with the exact solution.

Note. Program FEM1DV2 cannot be used without modification to solve Problems 7.52–7.54.

7.52. Consider a simply supported beam of length L subjected to a point load

$$P(t) = \begin{cases} P_0 \sin\dfrac{\pi t}{\tau} & \text{for } 0 \leqslant t \leqslant \tau \\ 0 & \text{for } t \geqslant \tau \end{cases}$$

at a distance c from the left end of the beam (assumed to be at rest at $t=0$). The transverse deflection $w(x, t)$ is given by [see Harris and Crede (1961), pp. 8–53]

$$w(x,t)=\begin{cases}\dfrac{2P_0L^3}{\pi^4 EI}\displaystyle\sum_{i=1}^{\infty}\frac{1}{i^4}\sin\frac{i\pi c}{L}\sin\frac{i\pi x}{L}\left[\frac{1}{1-T_i^2/4\tau^2}\left(\sin\frac{\pi t}{\tau}-\frac{T_i}{2\tau}\sin\omega_i t\right)\right] & \text{for } 0\leqslant t\leqslant\tau\\[2ex] \dfrac{2P_0L^3}{\pi^4 EI}\displaystyle\sum_{i=1}^{\infty}\frac{1}{i^4}\sin\frac{i\pi c}{L}\sin\frac{i\pi x}{L}\left[\frac{(T_i/\tau)\cos(\pi\tau/T_i)}{T_i^2/4\tau^2-1}\sin\omega_i(t-\tfrac{1}{2}\tau)\right] & \text{for } t\geqslant\tau\end{cases}$$

where

$$T_i=\frac{2\pi}{\omega_i}=\frac{2L^2}{i^2\pi}\frac{A\rho}{EI}=\frac{T_1}{i^2}$$

Use the data $P_0=1000$ lb, $\tau=20\times10^{-6}$ s, $L=30$ in, $E=30\times10^6$ lb in^{-2}, $\rho=733\times10^{-6}$ lb in^{-3}, $\Delta t=10^{-6}$ s, and assume that the beam is of square cross-section 0.5 in by 0.5 in. Using five Euler–Bernoulli elements in the half-beam, obtain the finite element solution and compare with the series solution at midspan for the case $c=\frac{1}{2}L$.

7.53. Repeat Problem 7.52 for $c=\frac{1}{4}L$ and eight elements in the full span.

7.54. Repeat Problem 7.52 for $P(t)=P_0$ at midspan and eight elements in the full span.

7.55. Consider a cantilevered beam with a point load at the free end. Using the load and data of Problem 7.52, find the finite element solution for the transverse deflection using Euler–Bernoulli beam elements.

7.56. Repeat Problem 7.52 for a clamped beam with the load at the midspan.

7.57–7.61. Solve Problems 7.52–7.56 using Timoshenko beam elements. Use $\nu=0.3$.

REFERENCES FOR ADDITIONAL READING

Fluid mechanics

Bird, R. B., W. E. Stewart, and E. N. Lightfoot: *Transport Phenomena*, John Wiley, New York, 1960.
Duncan, W. J., A. S. Thom, and A. D. Young: *Mechanics of Fluids*, 2d ed., Elsevier, New York, 1970.
Eskinazi, S.: *Principles of Fluid Mechanics*, Allyn and Bacon, Boston, 1962.
Harr, M. E.: *Ground Water and Seepage*, McGraw-Hill, New York, 1962.
Nadai, A.: *Theory of Flow and Fracture of Solids*, vol. II, McGraw-Hill, New York, 1963.
Schlichting, H.: *Boundary-Layer Theory* (translated by J. Kestin), 7th ed., McGraw-Hill, New York, 1979.
Shames, I. H.: *Mechanics of Fluids*, McGraw-Hill, New York, 1962.
Vallentine, H. R.: *Applied Hydrodynamics*, Butterworths, London, 1959.
Verrujit, A.: *Theory of Groundwater Flow*, Gordon and Breach, New York, 1970.

Heat transfer

Carslaw, H. S., and J. C. Jaeger: *Conduction of Heat in Solids*, Clarendon Press, Oxford, 1959.
Holoman, J. P.: *Heat Transfer*, 6th ed., McGraw-Hill, New York, 1986.
Kreith, F.: *Principles of Heat Transfer*, 3rd ed., Harper & Row, New York, 1973.
Myers, G. G.: *Analytical Methods in Conduction Heat Transfer*, McGraw-Hill, New York, 1972.
Özisik, M. N.: *Heat Transfer: A Basic Approach*, McGraw-Hill, New York, 1985.

Plane elasticity

Budynas, R. G.: *Advanced Strength and Applied Stress Analysis,* McGraw-Hill, New York, 1977.

Harris, C. M., and C. E. Crede: *Shock and Vibration Handbook,* vol. 1, McGraw-Hill, New York, 1961.

Ugural, A. C., and S. K. Fenster: *Advanced Strength and Applied Elasticity,* Elsevier, New York, 1975.

Volterra, E., and J. H. Gaines: *Advanced Strength of Materials,* Prentice-Hall, Englewood Cliffs, NJ, 1971.

Time approximations

Bathe, K. J.: *Finite Element Procedures in Engineering Analysis,* Prentice-Hall, Englewood Cliffs, NJ, 1982.

Clough, R. W., and J. Penzien: *Dynamics of Structures,* McGraw-Hill, New York, 1975.

Hughes, T. J. R.: *The Finite Element Method,* Prentice-Hall, Englewood-Cliffs, NJ, 1987.

Numerical integration

Carnahan, B., H. A. Luther, and J. O. Wilker: *Applied Numerical Methods,* John Wiley, New York, 1969.

Loxan, A. N., N. Davids, and A. Levenson: "Table of the Zeros of the Legendre Polynomials of Order 1–16 and the Weight Coefficients for Gauss' Quadrature Formula," *Bulletin of the American Mathematical Society,* vol. 48, pp. 739–743, 1942.

Silvester, P.: "Newton–Cotes Quadrature Formulae for *N*-Dimensional Simplexes," *Proceedings of 2d Canadian Congress of Applied Mechanics, Waterloo, Ontario, 1969.* University of Waterloo, Waterloo, Ontario, 1969.

Stroud, A. H., and D. Secrest: *Gaussian Quadrature Formulas,* Prentice-Hall, Englewood Cliffs, NJ, 1966.

Zienkiewicz, O. C., and R. L. Taylor: *The Finite Element Method,* vols. 1 and 2, McGraw-Hill, 1989 and 1991.

PART 3

FINITE ELEMENT ANALYSIS OF TWO-DIMENSIONAL PROBLEMS

CHAPTER
8

SINGLE-VARIABLE PROBLEMS

8.1 INTRODUCTION

The finite element analysis of two-dimensional problems involves the same basic steps as those described for one-dimensional problems in Chapter 3. The analysis is somewhat complicated by the fact that two-dimensional problems are described by partial differential equations over geometrically complex regions. The boundary Γ of a two-dimensional domain Ω is, in general, a curve. Therefore, the finite elements are simple two-dimensional geometric shapes that can be used to approximate a given two-dimensional domain as well as the solution over it. Thus, in two-dimensional problems, we not only seek an approximate solution to a given problem on a domain but we also approximate the domain by a suitable finite element mesh. Consequently, in the finite element analysis of two-dimensional problems, we shall have approximation errors due to the approximation of the solution as well as discretization errors due to the approximation of the domain. The finite element mesh (discretization) consists of simple two-dimensional elements, such as triangles, rectangles, and/or quadrilaterals, that allow unique derivation of the interpolation functions. The elements are connected to each other at nodal points on the boundaries of the elements. The ability to represent domains with irregular geometries by a collection of finite elements makes the

TABLE 8.1
Some examples of the Poisson equation $-\nabla \cdot (k\nabla u) = f$
Natural boundary condition: $k\,\partial u/\partial n + \beta(u - u_\infty) = q$. Essential boundary condition: $u = \hat{u}$

Field of application	Primary variable u	Material constant k	Source variable f	Secondary variables $q, \frac{\partial u}{\partial x}, \frac{\partial u}{\partial y}$
1. Heat transfer	Temperature T	Conductivity k	Heat source Q	Heat flow q [comes from conduction $k\,\partial T/\partial n$ and convection $h(T - T_\infty)$]
2. Irrotational flow of an ideal fluid	Stream function ψ	Density ρ	Mass production σ (normally zero)	Velocities: $\frac{\partial \psi}{\partial x} = -v,\ \frac{\partial \psi}{\partial y} = u$
	Velocity potential ϕ	Density ρ	Mass production σ (normall zero)	$\frac{\partial \phi}{\partial x} = u,\ \frac{\partial \phi}{\partial y} = v$
3. Groundwater flow	Piezometric head ϕ	Permeability K	Recharge Q (or pumping, $-Q$)	Seepage $q = k\frac{\partial \phi}{\partial n}$ Velocities: $u = -k\frac{\partial \phi}{\partial x},\ v = -k\frac{\partial \phi}{\partial y}$
4. Torsion of members with constant cross-section	Stress function Ψ	$k = 1$	$f = 2$	$G\theta\frac{\partial \Psi}{\partial x} = -\sigma_{yz}$
		G = shear modulus	θ = angle of twist per unit length	$G\theta\frac{\partial \Psi}{\partial y} = \sigma_{xz}$
5. Electrostatics	Scalar potential ϕ	Dielectric constant ε	Charge density ρ	Displacement flux density D_n
6. Magnetostatics	Magnetic potential ϕ	Permeability μ	Charge density ρ	Magnetic flux density B_n
7. Transverse deflection of elastic membranes	Transverse deflection u	Tension T in membrane	Transversely distributed load	Normal force q

method a valuable practical tool for the solution of boundary, initial, and eigenvalue problems arising in various fields of engineering.

The objective of this chapter is to extend the basic steps discussed earlier for one-dimensional problems to two-dimensional boundary value problems involving a single dependent variable. Once again, we describe the basic steps of the finite element analysis with a model second-order partial differential equation, namely the Poisson equation, governing a single variable. This equation arises in a number of fields, including electrostatics, heat transfer, fluid mechanics, and solid mechanics (see Table 8.1).

8.2 BOUNDARY VALUE PROBLEMS

8.2.1 The Model Equation

Consider the problem of finding the solution u of the second-order partial differential equation

$$\boxed{-\frac{\partial}{\partial x}\left(a_{11}\frac{\partial u}{\partial x}+a_{12}\frac{\partial u}{\partial y}\right)-\frac{\partial}{\partial y}\left(a_{21}\frac{\partial u}{\partial x}+a_{22}\frac{\partial u}{\partial y}\right)+a_{00}u-f=0} \tag{8.1}$$

for given data a_{ij} $(i, j = 1, 2)$, a_{00} and f, and specified boundary conditions. The form of the boundary conditions will be apparent from the weak formulation. As a special case, one can obtain the Poisson equation from (8.1) by setting $a_{11} = a_{22} = a$ and $a_{12} = a_{21} = a_{00} = 0$:

$$-\boldsymbol{\nabla}\cdot(a\,\boldsymbol{\nabla}u)=f \quad \text{in } \Omega \tag{8.2}$$

where $\boldsymbol{\nabla}$ is the gradient operator. If $\hat{\mathbf{i}}$ and $\hat{\mathbf{j}}$ denote the unit vectors directed along the x and y axes, respectively, the gradient operator can be expressed as (see Section 2.2.2)

$$\boldsymbol{\nabla}=\hat{\mathbf{i}}\frac{\partial}{\partial x}+\hat{\mathbf{j}}\frac{\partial}{\partial y}$$

and (8.2) in the cartesian coordinate system takes the form

$$-\frac{\partial}{\partial x}\left(a\frac{\partial u}{\partial x}\right)-\frac{\partial}{\partial y}\left(a\frac{\partial u}{\partial y}\right)=f \tag{8.3}$$

In the following, we shall develop the finite element model of (8.1). The major steps are as follows:

1. Discretization of the domain into a set of finite elements.
2. Weak (or weighted-integral) formulation of the governing differential equation.
3. Derivation of finite element interpolation functions.
4. Development of the finite element model using the weak form.
5. Assembly of finite elements to obtain the global system of algebraic equations.

6. Imposition of boundary conditions.
7. Solution of equations.
8. Post-computation of solution and quantities of interest.

Steps 6 and 7 remain unchanged from one-dimensional finite element analysis because at the end of Step 5 we have a set of algebraic equations whose form is independent of the dimension of the domain or nature of the problem. In the following sections, we discuss each step in detail.

8.2.2 Finite Element Discretization

In two dimensions, there is more than one simple geometric shape that can be used as a finite element (see Fig. 8.1). As we shall see shortly, the interpolation functions depend not only on the number of nodes in the element but also on the shape of the element. The shape of the element must be such that its geometry is uniquely defined by a set of points, which serve as the element nodes in the development of the interpolation functions. As will be discussed later in this section, a triangle is the simplest geometric shape, followed by a rectangle.

The representation of a given region by a set of elements (i.e., discretization or *mesh generation*) is an important step in finite element analysis. The choice of element type, number of elements, and density of elements depends on the geometry of the domain, the problem to be analyzed,

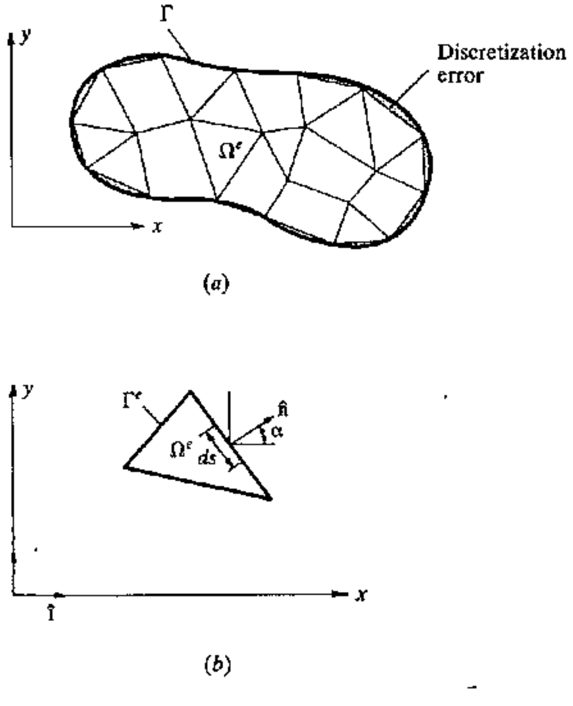

FIGURE 8.1
Finite element discretization of an irregular domain: (*a*) discretization of a domain by triangular and quadrilateral elements; (*b*) a typical triangular element (boundary Γ^e, the unit normal $\hat{n}$ on the boundary of the element).

and the degree of accuracy desired. Of course, there are no specific formulae for obtaining this information. In general, the analyst is guided by his or her technical background, insight into the physics of the problem being modeled (e.g., a qualitative understanding of the solution), and experience with finite element modeling. The general rules of mesh generation for finite element formulations include the following:

1. Select elements that characterize the governing equations of the problem.
2. The number, shape, and type (i.e., linear or quadratic) of elements should be such that the geometry of the domain is represented as accurately as desired.
3. The density of elements should be such that regions of large gradients of the solution are adequately modeled (i.e., more or higher-order elements should be used in regions of large gradients).
4. Mesh refinements should vary gradually from high-density regions to low-density regions. If *transition elements* are used, they should be used away from critical regions (i.e., regions of large gradients). Transition elements are those that connect lower-order elements to higher-order elements (e.g., linear to quadratic).

Additional discussion of finite element meshes and types of elements (linear and higher-order Lagrange elements, transition elements, etc.) will be presented in Chapter 9.

8.2.3 Weak Form

In the development of the weak form, we need only consider an arbitrarily typical element. We assume that Ω^e is such an element, whether triangular or quadrilateral, of the finite element mesh, and we develop the finite element model of (8.1) over Ω^e. Various two-dimensional elements will be discussed in the sequel.

Following the three-step procedure presented in Chapters 2 and 3, we develop the weak form of (8.1) over the typical element Ω^e. The first step is to multiply (8.1) with a weight function w, which is assumed to be once-differentiable with respect to x and y, and then integrate the resulting equation over the element domain Ω^e:

$$0=\int_{\Omega^e} w\left[-\frac{\partial}{\partial x}(F_1)-\frac{\partial}{\partial y}(F_2)+a_{00}u-f\right]dx\,dy \tag{8.4a}$$

where

$$F_1=a_{11}\frac{\partial u}{\partial x}+a_{12}\frac{\partial u}{\partial y},\qquad F_2=a_{21}\frac{\partial u}{\partial x}+a_{22}\frac{\partial u}{\partial y} \tag{8.4b}$$

In the second step, we distribute the differentiation equally between u and w. To achieve this, we integrate the first two terms in (8.4a) by parts. First we note the identities

$$\frac{\partial}{\partial x}(wF_1) = \frac{\partial w}{\partial x}F_1 + w\frac{\partial F_1}{\partial x} \quad \text{or} \quad -w\frac{\partial F_1}{\partial x} = \frac{\partial w}{\partial x}F_1 - \frac{\partial}{\partial x}(wF_1) \tag{8.5a}$$

$$\frac{\partial}{\partial y}(wF_2) = \frac{\partial w}{\partial y}F_2 + w\frac{\partial F_2}{\partial y} \quad \text{or} \quad -w\frac{\partial F_2}{\partial y} = \frac{\partial w}{\partial y}F_2 - \frac{\partial}{\partial y}(wF_2) \tag{8.5b}$$

Next, we recall the component form of the gradient (or divergence) theorem in (2.17b):

$$\boxed{\begin{aligned} \int_{\Omega^e}\frac{\partial}{\partial x}(wF_1)\,dx\,dy &= \oint_{\Gamma^e} wF_1 n_x\,ds \qquad (8.6a)\\ \int_{\Omega^e}\frac{\partial}{\partial y}(wF_2)\,dx\,dy &= \oint_{\Gamma^e} wF_2 n_y\,ds \qquad (8.6b)\end{aligned}}$$

where n_x and n_y are the components (i.e., direction cosines) of the unit normal vector

$$\hat{\mathbf{n}} = n_x\hat{\mathbf{i}} + n_y\hat{\mathbf{j}} = \cos\alpha\hat{\mathbf{i}} + \sin\alpha\hat{\mathbf{j}} \tag{8.7}$$

on the boundary Γ^e, and ds is the arclength of an infinitesimal line element along the boundary (see Fig. 8.1*b*). Using (8.5) and (8.6) in (8.4*a*), we obtain

$$\begin{aligned} 0 = &\int_{\Omega^e}\left[\frac{\partial w}{\partial x}\left(a_{11}\frac{\partial u}{\partial x} + a_{12}\frac{\partial u}{\partial y}\right) + \frac{\partial w}{\partial y}\left(a_{21}\frac{\partial u}{\partial x} + a_{22}\frac{\partial u}{\partial y}\right) + a_{00}wu - wf\right]dx\,dy\\ &- \oint_{\Gamma^e} w\left[n_x\left(a_{11}\frac{\partial u}{\partial x} + a_{12}\frac{\partial u}{\partial y}\right) + n_y\left(a_{21}\frac{\partial u}{\partial x} + a_{22}\frac{\partial u}{\partial y}\right)\right]ds \end{aligned} \tag{8.8}$$

From an inspection of the boundary term in this equation, we note that the specification of u constitutes the essential boundary condition, and hence u is the primary variable. The specification of the coefficient of the weight function in the boundary expression

$$\boxed{q_n \equiv n_x\left(a_{11}\frac{\partial u}{\partial x} + a_{12}\frac{\partial u}{\partial y}\right) + n_y\left(a_{21}\frac{\partial u}{\partial x} + a_{22}\frac{\partial u}{\partial y}\right)} \tag{8.9}$$

constitutes the natural boundary condition; thus, q_n is the secondary variable of the formulation. The function $q_n = q_n(s)$ denotes the projection of the vector $\mathbf{a}_{\chi}\nabla u$ along the unit normal $\hat{\mathbf{n}}$. By definition, q_n is positive outward from the surface as we move counter-clockwise along the boundary Γ^e. The secondary variable q_n is of physical interest in most problems. For example, in the case of heat transfer through an anisotropic medium, a_{ij} are the conductivities of the medium, and q_n is the heat flux normal to the boundary of the element (into the element).

The third and last step of the formulation is to use the definition (8.9) in (8.8) and write the weak form of (8.1) as

$$\boxed{\begin{aligned}0=&\int_{\Omega^e}\left[\frac{\partial w}{\partial x}\left(a_{11}\frac{\partial u}{\partial x}+a_{12}\frac{\partial u}{\partial y}\right)+\frac{\partial w}{\partial y}\left(a_{21}\frac{\partial u}{\partial x}+a_{22}\frac{\partial u}{\partial y}\right)+a_{00}wu-wf\right]dx\,dy\\&-\oint_{\Gamma^e}wq_n\,ds\end{aligned}}\tag{8.10a}$$

or

$$B(w,u)=l(w)\tag{8.10b}$$

where the bilinear form $B(\cdot,\cdot)$ and linear form $l(\cdot)$ are

$$\begin{aligned}B(w,u)&=\int_{\Omega^e}\left[\frac{\partial w}{\partial x}\left(a_{11}\frac{\partial u}{\partial x}+a_{12}\frac{\partial u}{\partial y}\right)+\frac{\partial w}{\partial y}\left(a_{21}\frac{\partial u}{\partial x}+a_{22}\frac{\partial u}{\partial y}\right)+a_{00}wu\right]dx\,dy\\l(w)&=\int_{\Omega^e}wf\,dx\,dy+\oint_{\Gamma^e}wq_n\,ds\end{aligned}\tag{8.10c}$$

The weak form (also called the *variational problem*) in (8.10) forms the basis of the finite element model of (8.1). The quadratic functional associated with the problem can be obtained from (2.43*b*) when $B(\cdot,\cdot)$ is symmetric [see Mikhlin (1964), Reddy and Rasmussen (1982), and Reddy (1986)]:

$$I(u)=\tfrac{1}{2}B(u,u)-l(u)$$

The bilinear form in (8.10*c*) is symmetric when $a_{12}=a_{21}$.

8.2.4 Finite Element Model

The weak form in (8.10) requires that the approximation chosen for u should be at least linear in both x and y so that there are no terms in (8.10) that are identically zero. Since the primary variable is simply the function itself, the Lagrange family of interpolation functions is admissible. Suppose that u is approximated over a typical finite element Ω^e by the expression

$$u(x,y)\approx U^e(x,y)=\sum_{j=1}^{n}u_j^e\psi_j^e(x,y)\tag{8.11}$$

where u_j^e is the value of U^e at the jth node (x_j, y_j) of the element, and ψ_j^e are the Lagrange interpolation functions, with the property

$$\psi_i^e(x_j,y_j)=\delta_{ij}\tag{8.12}$$

The specific form of ψ_i^e will be derived for linear triangular and rectangular elements in Section 8.2.5, and higher-order interpolation functions will be derived in Chapter 9.

Substituting the finite element approximation (8.11) for u into the weak form (8.10), we obtain

$$0=\int_{\Omega^e}\left[\frac{\partial w}{\partial x}\left(a_{11}\sum_{j=1}^{n}u_j\frac{\partial\psi_j}{\partial x}+a_{12}\sum_{j=1}^{n}u_j\frac{\partial\psi_j}{\partial y}\right)\right.$$
$$+\frac{\partial w}{\partial y}\left(a_{21}\sum_{j=1}^{n}u_j\frac{\partial\psi_j}{\partial x}+a_{22}\sum_{j=1}^{n}u_j\frac{\partial\psi_j}{\partial y}\right)$$
$$\left.+a_{00}w\sum_{j=1}^{n}u_j\psi_j-wf\right]dx\,dy-\oint_{\Gamma^e}wq_n\,ds \tag{8.13}$$

This equation must hold for any weight function w. Since we need n independent algebraic equations to solve for the n unknowns $u_1, u_2, \ldots, u_n$, we choose n independent functions for w: $w=\psi_1, \psi_2, \ldots, \psi_n$. This particular choice is a natural one when the weight function is viewed as a virtual variation of the dependent unknown (i.e., $w=\delta u=\sum_{i=1}^{n}\delta u_i\,\psi_i$). For each choice of w, we obtain an algebraic relation among $(u_1, u_2, \ldots, u_n)$. We label the algebraic equation resulting from substitution of ψ_1 for w into (8.13) as the first algebraic equation. The ith algebraic equation is obtained by substituting $w=\psi_i$ into (8.13):

$$0=\sum_{j=1}^{n}\left\{\int_{\Omega^e}\left[\frac{\partial\psi_i}{\partial x}\left(a_{11}\frac{\partial\psi_j}{\partial x}+a_{12}\frac{\partial\psi_j}{\partial y}\right)\right.\right.$$
$$\left.\left.+\frac{\partial\psi_i}{\partial y}\left(a_{21}\frac{\partial\psi_j}{\partial x}+a_{22}\frac{\partial\psi_j}{\partial y}\right)+a_{00}\psi_i\psi_j\right]dx\,dy\right\}u_j$$
$$-\int_{\Omega^e}f\psi_i\,dx\,dy-\oint_{\Gamma^e}\psi_i q_n\,ds\quad(i=1,2,\ldots,n)$$

or

$$\boxed{\sum_{j=1}^{n}K_{ij}^e u_j^e=f_i^e+Q_i^e} \tag{8.14a}$$

where

$$\boxed{\begin{aligned}K_{ij}^e&=\int_{\Omega^e}\left[\frac{\partial\psi_i}{\partial x}\left(a_{11}\frac{\partial\psi_j}{\partial x}+a_{12}\frac{\partial\psi_j}{\partial y}\right)+\frac{\partial\psi_i}{\partial y}\left(a_{21}\frac{\partial\psi_j}{\partial x}+a_{22}\frac{\partial\psi_j}{\partial y}\right)+a_{00}\psi_i\psi_j\right]dx\,dy\\ f_i^e&=\int_{\Omega^e}f\psi_i^e\,dx\,dy,\qquad Q_i^e=\oint_{\Gamma^e}q_n\psi_i^e\,ds\end{aligned}} \tag{8.14b}$$

In matrix notation, (8.14a) takes the form

$$[K^e]\{u^e\}=\{f^e\}+\{Q^e\} \tag{8.14c}$$

Note that $K_{ij}^e=K_{ji}^e$ (i.e., $[K]$ is symmetric) only when $a_{12}=a_{21}$. Equation (8.14c) represents the finite element model of (8.1). This completes the development of the finite element model. Before we discuss assembly of elements, it is informative to consider how the interpolations ψ_i^e are derived for certain basic elements and evaluate the element matrices in (8.14*b*).

8.2.5 Interpolation Functions

The finite element approximation $U^e(x, y)$ of $u(x, y)$ over an element Ω^e must satisfy the following conditions in order for the approximate solution to be convergent to the true one:

1. U^e must be differentiable, as required in the weak form of the problem (i.e., all terms in the weak form are represented as nonzero values).
2. The polynomials used to represent U^e must be complete (i.e., all terms, beginning with a constant term up to the highest order used in the polynomial, should be included in U^e).
3. All terms in the polynomial should be linearly independent.

The number of linearly independent terms in the representation of U^e dictates the shape and number of degrees of freedom of the element. Next, we discuss some of the basic polynomials and associated elements for problems with a single degree of freedom per node.

An examination of the variational form (8.10) and the finite element matrices in (8.14*b*) shows that ψ_i^e should be at least linear functions of x and y. For example, the polynomial

$$U^e(x, y) = c_1 + c_2 x + c_3 y \tag{8.15}$$

contains three linearly independent terms, and it is linear in both x and y. To write the constants c_i $(i = 1, 2, 3)$ in terms of the nodal values of U^e, we must identify three points or nodes in the element Ω^e. These three nodes must also uniquely define the geometry of the element. Obviously, the geometric shape defined by three points in a two-dimensional domain is a triangle. Thus the polynomial (8.15) is associated with a triangular element, and there are three nodes identified, namely, the vertices of the triangle.

On the other hand, the polynomial

$$U^e(x, y) = c_1 + c_2 x + c_3 y + c_4 xy \tag{8.16}$$

contains four linearly independent terms, and is linear in x and y, with a bilinear term in x and y. This polynomial requires an element with four nodes. There are two possible geometric shapes: a triangle with the fourth node at its center (or centroid), or a rectangle with the nodes at the vertices. A triangle with a fourth node at the center does not provide a single-valued variation of u at interelement boundaries, resulting in *incompatible* variations of u there, and is therefore not admissible. The linear rectangular element is a compatible element.

A polynomial with five constants is the incomplete quadratic polynomial

$$U^e(x, y) = c_1 + c_2x + c_3y + c_4xy + c_5(x^2 + y^2) \tag{8.17}$$

which can be used to construct an element with five nodes (e.g., a rectangle with a node at each corner and at its midpoint); however, the element does not give single-valued variation of u. Also, note that the x^2 and y^2 terms cannot be varied independently of each other.

The quadratic polynomial

$$U^e(x, y) = c_1 + c_2x + c_3y + c_4xy + c_5x^2 + c_6y^2 \tag{8.18}$$

with six constants can be used to construct an element with six nodes. For example, a triangle with a node at each vertex and a node at the midpoint of each side is admissible. It is known as the quadratic triangular element. Examples of three-, four-, five-, and six-node elements are shown in Fig. 8.2.

Here we derive the linear interpolation functions for the three-node triangular element and the four-node rectangular element. The procedure used is the same as that for one-dimensional elements. The interpolation functions for linear, quadratic and cubic triangular and rectangular elements can be found in many books, and the present study is intended to illustrate the procedure used to derive the interpolation functions. Additional discussion on the generation of interpolation functions is presented in Chapter 9.

LINEAR TRIANGULAR ELEMENT. Consider the linear approximation (8.15). The set $\{1, x, y\}$ is linearly independent and complete. We must rewrite the approximation (8.15) such that it satisfies the conditions

$$U^e(x_i^e, y_i^e) = u_i^e \quad (i = 1, 2, 3) \tag{8.19}$$

where (x_i^e, y_i^e) $(i = 1, 2, 3)$ are the global coordinates of the three vertices of the triangle Ω^e. In other words, we determine the three constants c_i in (8.15) in

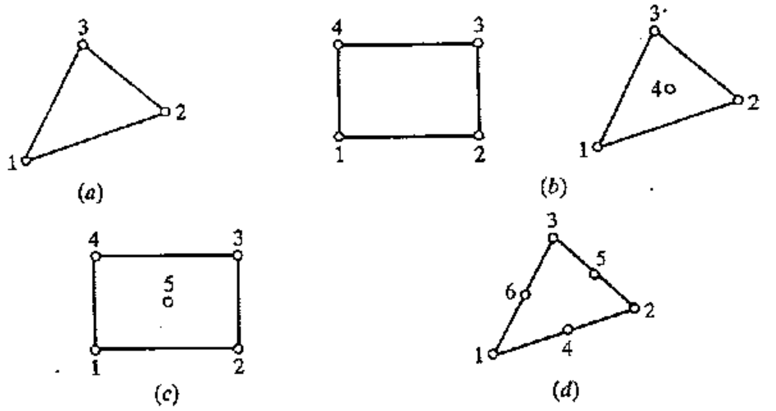

FIGURE 8.2
Finite elements in two dimensions: (a) a three-node element; (b) four-node elements; (c) a five-node element; (d) a six-node element.

terms of u_i^e from (8.19):

$$
\begin{aligned}
u_1 &\equiv u(x_1, y_1) = c_1 + c_2 x_1 + c_3 y_1 \\
u_2 &\equiv u(x_2, y_2) = c_1 + c_2 x_2 + c_3 y_2 \\
u_3 &\equiv u(x_3, y_3) = c_1 + c_2 x_3 + c_3 y_3
\end{aligned} \tag{8.20}
$$

where the element label e on the us, xs, ys, and cs is omitted for simplicity. Throughout the following discussion, this format will be followed. In matrix form, we have

$$
\begin{Bmatrix} u_1 \\ u_2 \\ u_3 \end{Bmatrix} = \begin{bmatrix} 1 & x_1 & y_1 \\ 1 & x_2 & y_2 \\ 1 & x_3 & y_3 \end{bmatrix} \begin{Bmatrix} c_1 \\ c_2 \\ c_3 \end{Bmatrix} \tag{8.21}
$$

Solution of (8.21) for c_i ($i = 1, 2, 3$) requires inversion of the coefficient matrix in (8.21). The inverse does not exist when any two rows or columns of (8.21) are the same. This happens only when all three nodes lie on the same line. Thus, in theory, as long as the three vertices of the triangle are distinct and do not lie on a line, the coefficient matrix is invertible. However, in actual computations, if any two of the three nodes are *very close* relative to the third, or the three nodes are almost on the same line, the coefficient matrix can be *nearly singular* and numerically noninvertible. Hence, one should avoid elements with narrow geometries (see Fig. 8.3) in finite element meshes.

Inverting the coefficient matrix in (8.21), we obtain

$$
[A]^{-1} = \frac{1}{2A_e} \begin{bmatrix} \alpha_1 & \alpha_2 & \alpha_3 \\ \beta_1 & \beta_2 & \beta_3 \\ \gamma_1 & \gamma_2 & \gamma_3 \end{bmatrix}, \quad 2A_e = \alpha_1 + \alpha_2 + \alpha_3 \tag{8.22}
$$

and, solving for c_i in terms of u_i,

$$
\{c\} = [A]^{-1}\{u\},
$$

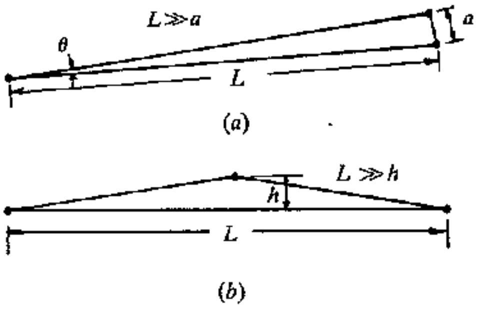

FIGURE 8.3
Triangular geometries that should be avoided in finite element meshes.

we obtain

$$
\begin{aligned}
c_1 &= \frac{1}{2A_e}(\alpha_1 u_1 + \alpha_2 u_2 + \alpha_3 u_3) \\
c_2 &= \frac{1}{2A_e}(\beta_1 u_1 + \beta_2 u_2 + \beta_3 u_3) \qquad (8.23a) \\
c_3 &= \frac{1}{2A_e}(\gamma_1 u_1 + \gamma_2 u_2 + \gamma_3 u_3),
\end{aligned}
$$

where A_e is the area of the triangle (or $2A_e$ is the determinant of $[A]$), and α_i, β_i, and γ_i are the geometric constants

$$
\left.\begin{aligned}
\alpha_i &= x_j y_k - x_k y_j \\
\beta_i &= y_j - y_k \\
\gamma_i &= -(x_j - x_k)
\end{aligned}\right\} \quad (i \neq j \neq k;\ \text{and } i, j \text{ and } k \text{ permute in a natural order}) \qquad (8.23b)
$$

Substituting for c_i from (8.23a) into (8.15), we obtain

$$
\begin{aligned}
U^e(x, y) &= \frac{1}{2A_e}[(\alpha_1 u_1 + \alpha_2 u_2 + \alpha_3 u_3) + (\beta_1 u_1 + \beta_2 u_2 + \beta_3 u_3)x \\
&\quad + (\gamma_1 u_1 + \gamma_2 u_2 + \gamma_3 u_3)y] \\
&= \sum_{i=1}^{3} u_i^e \psi_i^e(x, y) \qquad (8.24)
\end{aligned}
$$

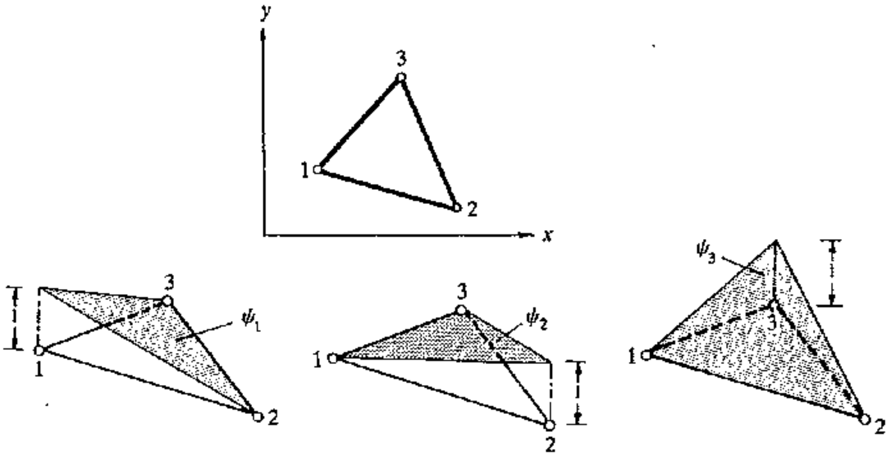

FIGURE 8.4
Linear interpolation functions for the three-node triangular element.

where ψ_i^e are the linear interpolation functions for the triangular element,

$$\boxed{\psi_i^e = \frac{1}{2A_e}(\alpha_i^e + \beta_i^e x + \gamma_i^e y) \quad (i = 1, 2, 3)} \tag{8.25}$$

and α_i, β_i, and γ_i are constants defined in (8.23*b*). The linear interpolation functions ψ_i^e are shown in Fig. 8.4. They have the properties

$$\begin{gathered} \psi_i^e(x_j^e, y_j^e) = \delta_{ij} \quad (i, j = 1, 2, 3) \\ \sum_{i=1}^{3} \psi_i^e = 1, \qquad \sum_{i=1}^{3} \frac{\partial \psi_i^e}{\partial x} = 0, \qquad \sum_{i=1}^{3} \frac{\partial \psi_i^e}{\partial y} = 0 \end{gathered} \tag{8.26}$$

Note that (8.24) determines a plane surface passing through u_1, u_2, and u_3. Hence, use of the linear interpolation functions ψ_i^e of a triangle will result in the approximation of the curved surface $u(x, y)$ by a planar function $U^e = \sum_{i=1}^{3} u_i^e \psi_i^e$ as shown in Fig. 8.5. We consider an example of the computation of ψ_i^e.

Example 8.1. Consider the triangular element shown in Fig. 8.6. Let

$$U(x, y) = c_1 + c_2 x + c_3 y = \{1 \quad x \quad y\} \begin{Bmatrix} c_1 \\ c_2 \\ c_3 \end{Bmatrix}$$

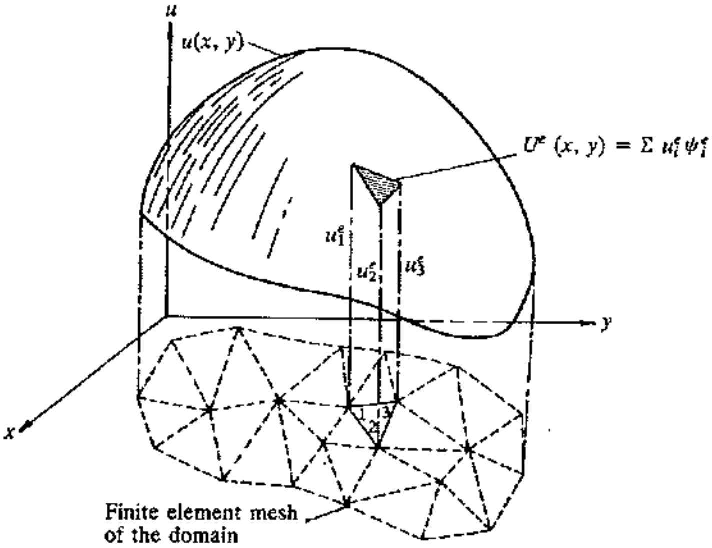
u
u(x, y)
$U^e(x, y) = \Sigma\, u_i^e \psi_i^e$
u_1^e
u_2^e
u_3^e
y
x
1
2
3
Finite element mesh of the domain

FIGURE 8.5
Representation of a continuous function $u(x, y)$ by linear interpolation functions of three-node triangular elements.

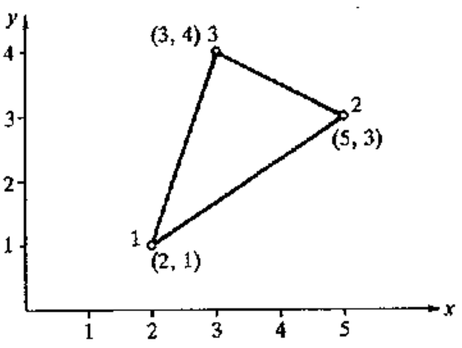

FIGURE 8.6
A triangular element with element nodes and coordinates (for Example 8.1).

Evaluating this polynomial at nodes 1, 2, and 3, we obtain the equations, from (8.21)

$$\begin{Bmatrix} u_1 \\ u_2 \\ u_3 \end{Bmatrix} = \begin{bmatrix} 1 & 2 & 1 \\ 1 & 5 & 3 \\ 1 & 3 & 4 \end{bmatrix} \begin{Bmatrix} c_1 \\ c_2 \\ c_3 \end{Bmatrix}, \qquad \begin{Bmatrix} c_1 \\ c_2 \\ c_3 \end{Bmatrix} = [A]^{-1} \begin{Bmatrix} u_1 \\ u_2 \\ u_3 \end{Bmatrix}$$

where

$$[A]^{-1} = \frac{1}{7} \begin{bmatrix} 11 & -5 & 1 \\ -1 & 3 & -2 \\ -2 & -1 & 3 \end{bmatrix}$$

Substituting into U, we obtain ($[A]^{-1} = [A^*]$)

$$U^e(x, y) = \{1 \quad x \quad y\}[A^*] \begin{Bmatrix} u_1 \\ u_2 \\ u_3 \end{Bmatrix} = \{\psi_1 \quad \psi_2 \quad \psi_3\} \begin{Bmatrix} u_1 \\ u_2 \\ u_3 \end{Bmatrix} = \sum_{i=1}^{3} \psi_i^e u_i^e$$

where

$$\psi_i^e = A_{1i}^* + A_{2i}^* x + A_{3i}^* y$$

and A_{ij}^* are the elements of the inverse matrix $[A]^{-1}$.

Alternatively, from the definitions (8.23*b*), we have

$$\alpha_1 = 5 \times 4 - 3 \times 3 = 11, \quad \alpha_2 = 3 \times 1 - 2 \times 4 = -5, \quad \alpha_3 = 2 \times 3 - 5 \times 1 = 1$$
$$\beta_1 = 3 - 4 = -1, \quad \beta_2 = 4 - 1 = 3, \quad \beta_3 = 1 - 3 = -2$$
$$\gamma_1 = -(5 - 3) = -2, \quad \gamma_2 = -(3 - 2) = -1, \quad \gamma_3 = -(2 - 5) = 3$$
$$2A_e = \alpha_1 + \alpha_2 + \alpha_3 = 7$$

The interpolation functions are

$$\psi_1^e = \tfrac{1}{7}(11 - x - 2y), \qquad \psi_2^e = \tfrac{1}{7}(-5 + 3x - y), \qquad \psi_3^e = \tfrac{1}{7}(1 - 2x + 3y)$$

LINEAR (FOUR-NODE) RECTANGULAR ELEMENT. Here we consider an approximation of the form (8.16) and use a rectangular element with sides a and b (see Fig. 8.7*a*). For the sake of convenience, we choose a local coordinate system $(\bar{x}, \bar{y})$ to derive the interpolation functions. We assume that

$$U(\bar{x}, \bar{y}) = c_1 + c_2\bar{x} + c_3\bar{y} + c_4\bar{x}\bar{y} \tag{8.27}$$

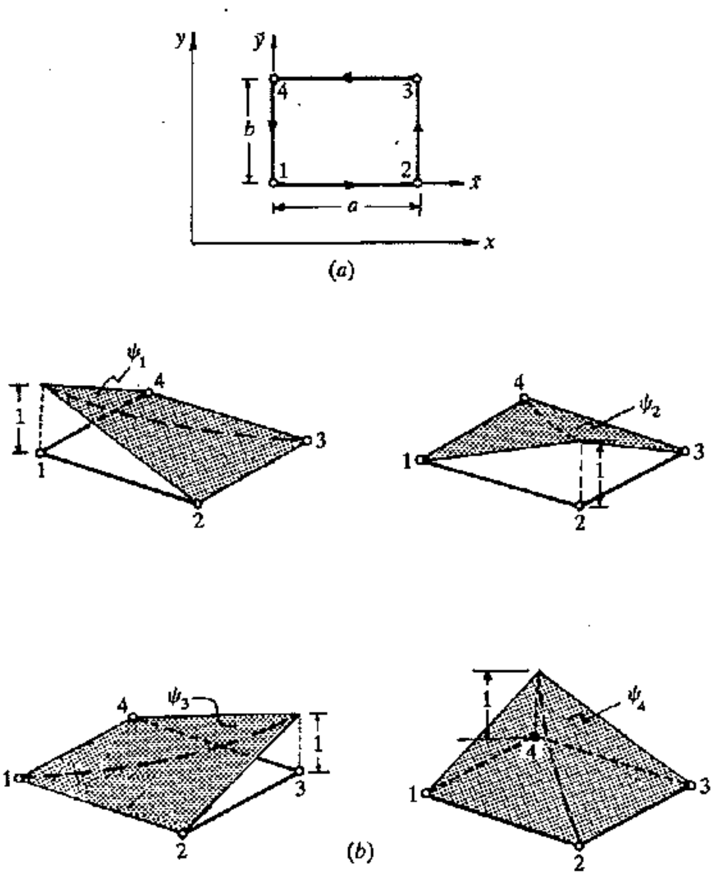

FIGURE 8.7
Linear rectangular element and its interpolation functions: (*a*) geometry of the element; (*b*) interpolation functions.

and require

$$\begin{aligned} u_1 &= U(0, 0) = c_1 \\ u_2 &= U(a, 0) = c_1 + c_2 a \\ u_3 &= U(a, b) = c_1 + c_2 a + c_3 b + c_4 ab \\ u_4 &= U(0, b) = c_1 + c_3 b \end{aligned} \tag{8.28}$$

Solving for c_i $(i = 1, \ldots, 4)$, we obtain

$$\begin{aligned} c_1 &= u_1, \qquad c_2 = \frac{u_2 - u_1}{a} \\ c_3 &= \frac{u_4 - u_1}{b}, \qquad c_4 = \frac{u_3 - u_4 + u_1 - u_2}{ab}, \end{aligned} \tag{8.29}$$

Substituting these into (8.27), we obtain

$$
\begin{aligned}
U(\bar{x},\bar{y}) &= u_1\left(1-\frac{\bar{x}}{a}-\frac{\bar{y}}{b}+\frac{\bar{x}}{a}\frac{\bar{y}}{b}\right)+u_2\left(\frac{\bar{x}}{a}-\frac{\bar{x}}{a}\frac{\bar{y}}{b}\right)+u_3\frac{\bar{x}}{a}\frac{\bar{y}}{b}+u_4\left(\frac{\bar{y}}{b}-\frac{\bar{x}}{a}\frac{\bar{y}}{b}\right)\\
&= u_1\psi_1+u_2\psi_2+u_3\psi_3+u_4\psi_4=\sum_{i=1}^{4}u_i^e\psi_i^e \qquad (8.30)
\end{aligned}
$$

where

$$
\boxed{\begin{aligned}
&\psi_1^e=\left(1-\frac{\bar{x}}{a}\right)\left(1-\frac{\bar{y}}{b}\right), \qquad \psi_2^e=\frac{\bar{x}}{a}\left(1-\frac{\bar{y}}{b}\right)\\
&\psi_3^e=\frac{\bar{x}}{a}\frac{\bar{y}}{b}, \qquad \psi_4^e=\left(1-\frac{\bar{x}}{a}\right)\frac{\bar{y}}{b}
\end{aligned}} \qquad (8.31a)
$$

or, in concise form,

$$
\psi_i^e(\bar{x},\bar{y})=(-1)^{i+1}\left(1-\frac{\bar{x}+\bar{x}_i}{a}\right)\left(1-\frac{\bar{y}+\bar{y}_i}{b}\right) \qquad (8.31b)
$$

where $(\bar{x}_i, \bar{y}_i)$ are the $(\bar{x}, \bar{y})$ coordinates of node i. The interpolation functions are shown in Fig. 8.7(b). We again have

$$
\psi_i^e(\bar{x}_j,\bar{y}_j)=\delta_{ij} \quad (i,j=1,\ldots,4), \qquad \sum_{i=1}^{4}\psi_i^e=1 \qquad (8.32a,b)
$$

where $(\bar{x}_j, \bar{y}_j)$ are the coordinates of node j in the $(\bar{x}, \bar{y})$ system.

Note that the linear interpolation functions for the four-node rectangular element can also be obtained by taking the tensor product of the 1-D linear interpolation functions (3.18) associated with sides 1–2 and 2–3:

$$
\begin{Bmatrix} 1-\dfrac{\bar{x}}{a} \\ \dfrac{\bar{x}}{a} \end{Bmatrix}\begin{Bmatrix} 1-\dfrac{\bar{y}}{b} & \dfrac{\bar{y}}{b} \end{Bmatrix}=\begin{bmatrix} \psi_1 & \psi_4 \\ \psi_2 & \psi_3 \end{bmatrix}. \qquad (8.33)
$$

The procedure given above for the construction of the Lagrange interpolation functions involves the inversion of an $n \times n$ matrix, where n is the number of nodes in the element. When n is large, the inversion becomes very tedious. The alternative procedure discussed in Chapter 3 for one-dimensional elements proves to be algebraically simple. Here we illustrate the alternative procedure for the four-node rectangular element. Equation (8.32a) requires that

$$
\psi_1^e(\bar{x}_i,\bar{y}_i)=0 \quad (i=2,3,4), \qquad \psi_1^e(x_1,y_1)=1
$$

That is, ψ_1^e is identically zero on lines $\bar{x}=a$ and $\bar{y}=b$. Hence, $\psi_1^e(\bar{x},\bar{y})$ must be of the form

$$
\psi_1^e(\bar{x},\bar{y})=c_1(a-\bar{x})(b-\bar{y})
$$

Using the condition $\psi_1^e(x_1, y_1) = \psi_1^e(0, 0) = 1$, we obtain $c_1 = 1/ab$. Hence,

$$\psi_1^e(\bar{x}, \bar{y}) = \frac{1}{ab}(a - \bar{x})(b - \bar{y}) = \left(1 - \frac{\bar{x}}{a}\right)\left(1 - \frac{\bar{y}}{b}\right)$$

Likewise, one can obtain the remaining three interpolation functions.

8.2.6 Evaluation of Element Matrices, and Vectors

The exact evaluation of the element matrices $[K^e]$ and $\{f^e\}$ in (8.14*b*) is, in general, not easy. Therefore, they are evaluated using numerical integration techniques described in Section 7[illegible].5. However, when a_{ij}, a_{00}, and f are element-wise constant, it is possible to evaluate the integrals exactly over the linear triangular and rectangular elements discussed in the previous section. The boundary integral in $\{Q^e\}$ of (8.14*b*) can be evaluated whenever q_n is known. For an interior element (i.e., one that does not have any of its sides on the boundary of the problem), the contribution from the boundary integral cancels with similar contributions from adjoining elements of the mesh (analogous to the Q_i^e in one-dimensional problems). A more detailed discussion is given below.

For the sake of brevity, we rewrite $[K^e]$ in (8.14) as the sum of four basic matrices $[S^{\alpha\beta}]$ $(\alpha, \beta = 0, 1, 2)$:

$$[K^e] = a_{00}[S^{00}] + a_{11}[S^{11}] + a_{12}[S^{12}] + a_{21}[S^{12}]^T + a_{22}[S^{22}] \tag{8.34}$$

where $[\ ]^T$ denotes the transpose of the enclosed matrix, and

$$S_{ij}^{\alpha\beta} = \int_{\Omega^e} \psi_{i,\alpha}\psi_{j,\beta}\, dx\, dy \tag{8.35}$$

with $\psi_{i,\alpha} \equiv \partial\psi_i/\partial x_\alpha$, $x_1 = x$, and $x_2 = y$; $\psi_{i,0} = \psi_i$. All matrices in (8.34) and interpolation functions in (8.35) are understood to be defined over an element; i.e., all expressions and quantities should have the element label *e*, but these are omitted in the interest of brevity. We now proceed to compute the matrices in (8.34) and (8.14*b*) using the linear interpolation functions derived in the previous section.

ELEMENT MATRICES FOR A LINEAR TRIANGULAR ELEMENT. For a triangle, the following exact integral formulae are available for evaluating the integrals. Let

$$I_{mn} \equiv \int_{\Delta} x^m y^n\, dx\, dy \tag{8.36}$$

Then we have (the element label on A is omitted)

$$I_{00} = A \quad \text{(area of the triangle)}$$

$$I_{10} = A\hat{x}, \quad \hat{x} = \tfrac{1}{3}\sum_{i=1}^{3} x_i, \quad I_{01} = A\hat{y}, \quad \hat{y} = \tfrac{1}{3}\sum_{i=1}^{3} y_i$$

$$I_{11} = \frac{A}{12}\left(\sum_{i=1}^{3} x_i y_i + 9\hat{x}\hat{y}\right), \quad I_{20} = \frac{A}{12}\left(\sum_{i=1}^{3} x_i^2 + 9\hat{x}^2\right), \quad I_{02} = \frac{A}{12}\left(\sum_{i=1}^{3} y_i^2 + 9\hat{y}^2\right) \tag{8.37}$$

Using the linear interpolation functions (8.25) in (8.35), and noting that

$$\frac{\partial \psi_i}{\partial x} = \frac{\beta_i}{2A}, \quad \frac{\partial \psi_i}{\partial y} = \frac{\gamma_i}{2A} \tag{8.38}$$

we obtain

$$S_{ij}^{11} = \frac{1}{4A}\beta_i\beta_j, \quad S_{ij}^{12} = \frac{1}{4A}\beta_i\gamma_j, \quad S_{ij}^{22} = \frac{1}{4A}\gamma_i\gamma_j$$

$$S_{ij}^{00} = \frac{1}{4A}\left\{[\alpha_i\alpha_j + (\alpha_i\beta_j + \alpha_j\beta_i)\hat{x} + (\alpha_i\gamma_j + \alpha_j\gamma_i)\hat{y}] + \frac{1}{A}[I_{20}\beta_i\beta_j + I_{11}(\gamma_i\beta_j + \gamma_j\beta_i) + I_{02}\gamma_i\gamma_j]\right\} \tag{8.39}$$

In view of the identity $\alpha_i + \beta_i\hat{x} + \gamma_i\hat{y} = \frac{2}{3}A$ [which follows from (8.23*b*) and (8.37)], for an element-wise-constant value of $f = f_e$, we have

$$f_i^e = \tfrac{1}{2}f_e(\alpha_i + \beta_i\hat{x} + \gamma_i\hat{y}) = \tfrac{1}{3}f_e A_e \tag{8.40}$$

This should be obvious, because for a constant source f_e, the total magnitude of the source on the element is equal to $f_e A_e$, which is distributed equally among the nodes. Once the coordinates of the element nodes are known, one can compute α_i, β_i, and γ_i from (8.23*b*) and substitute into (8.39) to obtain the element matrices, which in turn can be used in (8.34) to obtain the element matrix $[K^e]$. For example, when a_{12}, a_{21}, and a_{00} are zero, and a_{11} and a_{22} are element–wise-constant, we have

$$\boxed{K_{ij}^e = \frac{1}{4A_e}(a_{11}^e\beta_i^e\beta_j^e + a_{22}^e\gamma_i^e\gamma_j^e)} \tag{8.41}$$

ELEMENT MATRICES FOR A LINEAR RECTANGULAR ELEMENT. When a_{ij} $(i, j = 0, 1, 2)$ and f are constants, we can use the interpolation functions of (8.31*a*) expressed in the local coordinates $\bar{x}$ and $\bar{y}$, which are related to the global coordinates by

$$x = \bar{x} + x_1^e, \quad y = \bar{y} + y_1^e, \quad dx = d\bar{x}, \quad dy = d\bar{y} \tag{8.42}$$

where (x_1^e, y_1^e) are the global coordinates of node 1 of the element Ω^e with respect to the global (x, y) coordinate system. For example, we have

$$S_{ij}^{00} = \int_{x_1^e}^{x_1^e+a} \int_{y_1^e}^{y_1^e+b} \psi_i\psi_j\,dx\,dy = \int_0^a \int_0^b \psi_i\psi_j\,d\bar{x}\,d\bar{y}$$

where a and b are the lengths along the $\bar{x}$ and $\bar{y}$ axes of the element. Consider the coefficient

$$\begin{aligned} S_{11}^{00} &= \int_0^a \int_0^b \psi_1\psi_1\,dx\,dy = \int_0^a \int_0^b \left(1-\frac{\bar{x}}{a}\right)\left(1-\frac{\bar{y}}{b}\right)\left(1-\frac{\bar{x}}{a}\right)\left(1-\frac{\bar{y}}{b}\right) d\bar{x}\,d\bar{y} \\ &= \int_0^a \left(1-\frac{\bar{x}}{a}\right)^2 d\bar{x} \int_0^b \left(1-\frac{\bar{y}}{b}\right)^2 d\bar{y} = \frac{a}{3}\frac{b}{3} = \frac{ab}{9} \end{aligned}$$

Similarly, we can evaluate all the matrices $[S^{\alpha\beta}]$ with the aid of the integral identities

$$\begin{gathered} \int_0^a \left(1-\frac{\bar{x}}{a}\right)^2 d\bar{x} = \tfrac{1}{3}a, \qquad \int_0^a \frac{\bar{x}}{a}\left(1-\frac{\bar{x}}{a}\right) d\bar{x} = \tfrac{1}{6}a \\ \int_0^a \left(1-\frac{\bar{x}}{a}\right) d\bar{x} = \tfrac{1}{2}a, \qquad \int_0^a \frac{\bar{x}}{a}\,d\bar{x} = \tfrac{1}{2}a \end{gathered} \tag{8.43}$$

We have

$$\begin{gathered} [S^{11}] = \frac{b}{6a}\begin{bmatrix} 2 & -2 & -1 & 1 \\ -2 & 2 & 1 & -1 \\ -1 & 1 & 2 & -2 \\ 1 & -1 & -2 & 2 \end{bmatrix}, \qquad [S^{12}] = \frac{1}{4}\begin{bmatrix} 1 & 1 & -1 & -1 \\ -1 & -1 & 1 & 1 \\ -1 & -1 & 1 & 1 \\ 1 & 1 & -1 & -1 \end{bmatrix} \\ [S^{22}] = \frac{a}{6b}\begin{bmatrix} 2 & 1 & -1 & -2 \\ 1 & 2 & -2 & -1 \\ -1 & -2 & 2 & 1 \\ -2 & -1 & 1 & 2 \end{bmatrix}, \qquad [S^{00}] = \frac{ab}{36}\begin{bmatrix} 4 & 2 & 1 & 2 \\ 2 & 4 & 2 & 1 \\ 1 & 2 & 4 & 2 \\ 2 & 1 & 2 & 4 \end{bmatrix} \\ \{f\} = \tfrac{1}{4}fab\{1 \quad 1 \quad 1 \quad 1\}^T \end{gathered} \tag{8.44}$$

EVALUATION OF THE BOUNDARY INTEGRALS. Here we consider the evaluation of boundary integrals of the type

$$Q_i^e = \oint_{\Gamma^e} q_n^e \psi_i^e(s)\,ds \tag{8.45}$$

where q_n^e is a known function of the distance s along the boundary Γ^e. It is not necessary to compute such integrals when a portion of Γ^e does not coincide with the boundary Γ of the total domain Ω. On portions of Γ^e that are in the interior of the domain Ω, q_n^e on side (i, j) of the element Ω^e cancels with q_n^f on side (p, q) of the element Ω^f when sides (i, j) of Ω^e and (p, q) of Ω^f are the same (i.e., at the interface of Ω^e and Ω^f). This can be viewed as the equilibrium of the internal "flux" (see Figs. 8.8*b*,*c*). When Γ^e falls on the

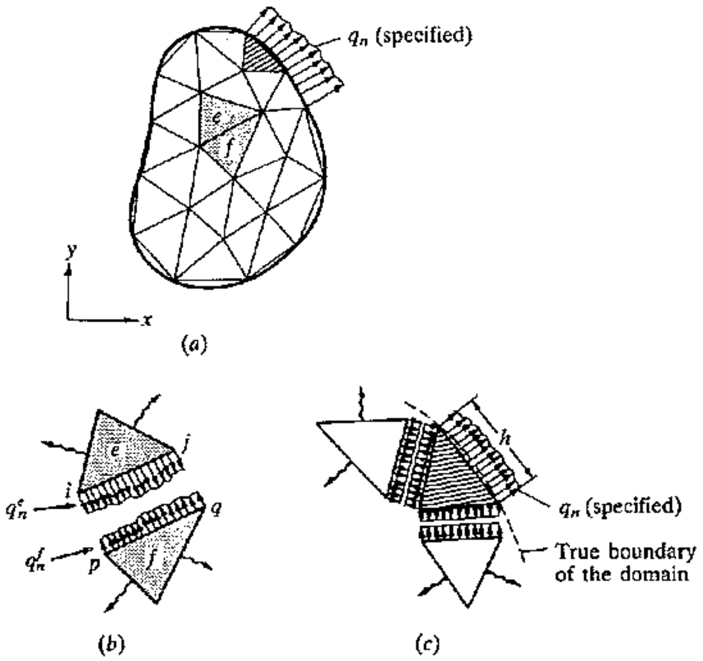

FIGURE 8.8
Computation of boundary forces and equilibrium of secondary variables at interelement boundaries: (*a*) finite element discretization; (*b*) equilibrium of forces at interfaces; (*c*) computation of forces on the true boundary.

boundary of the domain Ω, q_n^e is either known, in general, as a function of s, or is to be determined in the post-computation. In the latter case, the primary variable will be specified on the portion of the boundary where q_n is not specified.

The boundary Γ^e of linear two-dimensional elements is a set of linear one-dimensional elements. Therefore, the evaluation of the boundary integrals in two-dimensional problems amounts to evaluating line integrals. It should not be surprising to the reader that when two-dimensional interpolation functions are evaluated on the boundary, we obtain the corresponding one-dimensional interpolation functions. For example, consider the linear triangular element shown in Fig. 8.9. The linear interpolation functions for this element are given by (8.25). Now let us choose a coordinate system (s, t) with its origin at node 1 and the coordinate s parallel to the side connecting nodes 1 and 2. The two coordinate systems (x, y) and (s, t) are related by

$$x = a_1 + b_1 s + c_1 t$$

$$y = a_2 + b_2 s + c_2 t$$

The constants a_1, b_1, c_1, a_2, b_2, and c_2 can be determined with the following conditions:

$$\begin{aligned} &\text{when } s=0,\ t=0, && x=x_1,\ y=y_1 \\ &\text{when } s=a,\ t=0, && x=x_2,\ y=y_2 \\ &\text{when } s=c,\ t=b, && x=x_3,\ y=y_3 \end{aligned}$$

We obtain

$$\begin{aligned} x(s,t) &= x_1 + (x_2-x_1)\frac{s}{a} + \left[\left(\frac{c}{a}-1\right)x_1 - \frac{c}{a}x_2 + x_3\right]\frac{t}{b} \\ y(s,t) &= y_1 + (y_2-y_1)\frac{s}{a} + \left[\left(\frac{c}{a}-1\right)y_1 - \frac{c}{a}y_2 + y_3\right]\frac{t}{b} \end{aligned} \tag{8.46}$$

These equations allow us to express $\psi_i(x, y)$ as $\psi_i(s, t)$, which can be evaluated on the side connecting nodes 1 and 2 by setting $t = 0$ in $\psi_i(s, t)$:

$$\psi_i(s) \equiv \psi_i(s, 0) = \psi_i(x(s, 0), y(s, 0))$$

$$x(s) = x_1 + (x_2 - x_1)\frac{s}{a}, \qquad y(s) = y_1 + (y_2 - y_1)\frac{s}{a}$$

For instance,

$$\begin{aligned} \psi_1(s) &= \frac{1}{2A}\left\{\alpha_1 + \beta_1\left[\left(1-\frac{s}{a}\right)x_1 + \frac{s}{a}x_2\right] + \gamma_1\left[\left(1-\frac{s}{a}\right)y_1 + \frac{s}{a}y_2\right]\right\} \\ &= \frac{1}{2A}(\alpha_1 + \alpha_2 + \alpha_3)\left(1-\frac{s}{a}\right) = 1 - \frac{s}{a} \end{aligned}$$

where the definitions of α_1, β_1, and γ_1 have been used to rewrite the entire expression. Similarly,

$$\psi_2(s) = \frac{s}{a}, \qquad \psi_3(s) = 0$$

where $a = h_{12}$ is the length of side 1–2. We note that $\psi_1(s)$ and $\psi_2(s)$ are precisely the linear one-dimensional interpolation functions associated with the line element connecting nodes 1 and 2. Similarly, when $\psi_i(x, y)$ are evaluated on side 3–1 of the element, we obtain

$$\psi_1(s) = \frac{s}{h_{13}}, \qquad \psi_2 = 0, \qquad \psi_3(s) = 1 - \frac{s}{h_{13}}$$

where the s coordinate is taken along the side 3–1, with origin at node 3, and h_{13} is the length of side 1–3. Thus evaluation of Q_i^e involves the use of appropriate 1-D interpolation functions and the known variation of q_n on the boundary:

$$\begin{aligned} Q_i^e &= \int_{1-2} \psi_i(s)q_n(s)\,ds + \int_{2-3} \psi_i(s)q_n(s)\,ds + \int_{3-1} \psi_i(s)q_n(s)\,ds \\ &\equiv Q_{i1}^e + Q_{i2}^e + Q_{i3}^e \end{aligned} \tag{8.47}$$

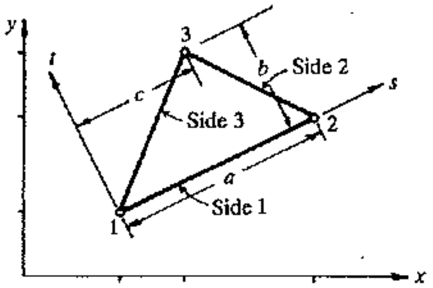

FIGURE 8.9
The linear triangular element in the global (x, y) and local (s, t) coordinate systems.

where $\int_{i-j}$ denotes the integral over the line connecting node i to node j, the s coordinate is taken from node i to node j, with origin at node i, and Q_{iJ}^e is defined as the contribution to Q_i^e from q_n^e on side J (see Fig. 8.9) of the element Ω^e:

$$Q_{iJ}^e = \int_{\text{side } J} \psi_i q_n \, ds \tag{8.48}$$

For example,

$$Q_1^e = \oint_{\Gamma^e} q_n \psi_1(s) \, ds = \int_{1-2} (q_n)_{1-2} \psi_1 \, ds + 0 + \int_{3-1} (q_n)_{3-1} \psi_1 \, ds$$

The contribution from side 2–3 is zero, because ψ_1 is zero on side 2–3 of a triangular element. For a rectangular element, Q_1^e has contributions from sides 1–2 and 4–1, because ψ_1 is zero on sides 2–3 and 3–4.

Example 8.2. Consider the evaluation of the boundary integral Q_i^e in (8.45) for the four cases of $q(s)$ and finite elements shown in Fig. 8.10. For each case, we must use the $q(s)$ and the interpolation functions associated with the type of boundary element (i.e., linear or quadratic).

Case 1. $q(s) = q_0 = \text{constant}$; linear element:

$$Q_i^e = \oint_{\Gamma^e} q_0 \psi_i \, ds = q_0 \int_0^{h_e} \psi_i \, ds + 0 + 0 \quad (i = 1, 2, 3)$$

where

$$\psi_1 = 1 - \frac{s}{h_e}, \qquad \psi_2 = \frac{s}{h_e}, \qquad \psi_3 = 0$$

We have

$$Q_1^e = \tfrac{1}{2} q_0 h_e \; (= Q_{11}^e), \qquad Q_2^e = \tfrac{1}{2} q_0 h_e \; (= Q_{21}^e), \qquad Q_3^e = 0$$

Case 2. $q(s) = q_0 s/h_e$ (linear variation); linear element:

$$Q_i^e = \oint_{\Gamma^e} q_0 \frac{s}{h_e} \psi_i \, ds = \frac{q_0}{h_e} \int_0^{h_e} s \psi_i \, ds \quad (i = 1, 2, 3)$$

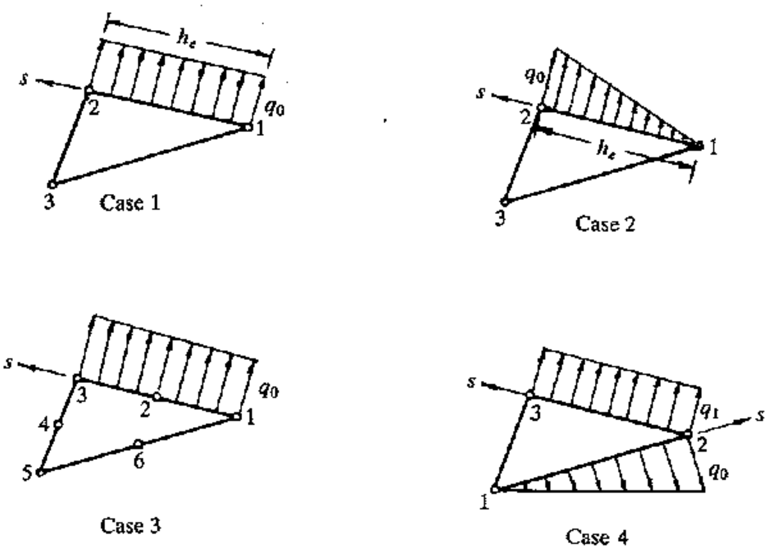

FIGURE 8.10
Evaluation of boundary integrals in the finite element analysis (Example 8.2).

where

$$\psi_1 = 1 - \frac{s}{h_e}, \qquad \psi_2 = \frac{s}{h_e}, \qquad \psi_3 = 0$$

We have

$$Q_1^e = \tfrac{1}{6}q_0 h_e \ (= Q_{11}^e), \qquad Q_2^e = \tfrac{1}{3}q_0 h_e \ (= Q_{21}^e), \qquad Q_3^e = 0$$

Case 3. $q(s) = q_0 =$ constant; quadratic element:

$$Q_i^e = \oint_{\Gamma^e} q_0 \psi_i \, ds \quad (i = 1, 2, \ldots, 6)$$

$$\psi_1 = \left(1 - \frac{s}{h_e}\right)\left(1 - \frac{2s}{h_e}\right), \qquad \psi_2 = \frac{4s}{h_e}\left(1 - \frac{s}{h_e}\right), \qquad \psi_3 = -\frac{s}{h_e}\left(1 - \frac{2s}{h_e}\right)$$

and ψ_4, ψ_5, and ψ_6 are zero on side 1–2–3. We have

$$Q_1^e = \tfrac{1}{6}q_0 h_e \ (= Q_{11}^e), \qquad Q_2^e = \tfrac{4}{6}q_0 h_e \ (= Q_{21}^e), \qquad Q_3^e = \tfrac{1}{6}q_0 h_e \ (= Q_{31}^e)$$

Case 4. $q(s)$ as shown in Fig. 8.10; linear element:

$$Q_i^e = \oint_{\Gamma^e} q(s)\psi_i \, ds = \int_{1-2} q_0 \frac{s}{h_{12}} \psi_i \, ds + \int_{2-3} q_1 \psi_i \, ds + 0$$

$$= Q_{i1}^e + Q_{i2}^e \qquad (Q_{i3}^e = 0)$$

We obtain,

$$Q_1^e = \int_{1-2} q_0 \frac{s}{h_{12}}\left(1 - \frac{s}{h_{12}}\right) ds + 0 + 0 = \tfrac{1}{6} q_0 h_{12} \;\; (= Q_{11}^e)$$

$$\begin{aligned} Q_2^e &= \int_{1-2} q_0 \frac{s}{h_{12}} \frac{s}{h_{12}}\, ds + \int_{2-3} q_1 \left(1 - \frac{s}{h_{23}}\right) ds + 0 \\ &= \tfrac{1}{3} q_0 h_{12} + \tfrac{1}{2} q_1 h_{23} \;\; (= Q_{21}^e + Q_{22}^e) \end{aligned}$$

$$Q_3^e = 0 + \int_{2-3} q_1 \frac{s}{h_{23}}\, ds + 0 = \tfrac{1}{2} q_1 h_{23} \;\; (= Q_{32}^e)$$

8.2.7 Assembly of Element Equations

The assembly of finite element equations is based on the same two principles that were used in one-dimensional problems:

1. Continuity of primary variables
2. "Equilibrium" (or "balance") of secondary variables

We illustrate the procedure by considering a finite element mesh consisting of a triangular element and a quadrilateral element (see Fig. 8.11*a*). Let K_{ij}^1 $(i, j = 1, 2, 3)$ denote the coefficient matrix corresponding to the triangular element, and let K_{ij}^2 $(i, j = 1, \ldots, 4)$ denote the coefficient matrix corresponding to the quadrilateral element. From the finite element mesh shown in Fig. 8.11(*a*), we note the following correspondence (i.e., connectivity relations)

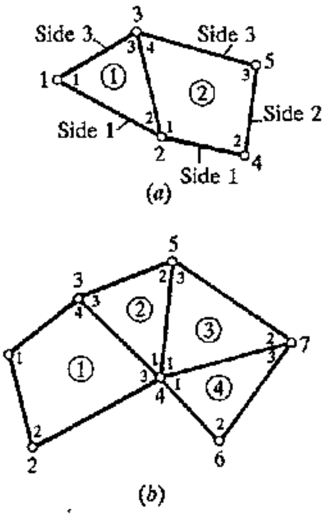

Global →	Local
K_{11}	K_{11}^1
K_{12}	K_{12}^1
K_{22}	$K_{22}^1 + K_{11}^2$
K_{14}	0
K_{15}	0
K_{23}	$K_{23}^1 + K_{14}^2$
K_{14}	K_{13}^1
K_{34}	$K_{43}^1 + K_{31}^2$
K_{17}	0
K_{44}	$K_{33}^1 + K_{11}^2 + K_{11}^3 + K_{11}^4$
K_{45}	$K_{12}^2 + K_{13}^3$
K_{56}	0
K_{47}	$K_{12}^3 + K_{13}^4$

FIGURE 8.11
Assembly of finite element coefficient matrices using the correspondence between global and element nodes (one unknown per node): (*a*) assembly of two elements; (*b*) assembly of several elements.

between the global and element nodes:

$$[B]=\begin{bmatrix}1 & 2 & 3 & \times\\ 2 & 4 & 5 & 3\end{bmatrix} \tag{8.49}$$

where × indicates that there is no entry. The correspondence between the local and global nodal values is (see Fig. 8.11*a*)

$$u_1^1=U_1, \quad u_2^1=u_1^2=U_2, \quad u_3^1=u_4^2=U_3, \quad u_2^2=U_4, \quad u_3^2=U_5 \tag{8.50}$$

which amounts to imposing the continuity of the primary variables at the nodes common to elements 1 and 2.

Note that the continuity of the primary variables at the interelement nodes guarantees the continuity of the primary variable along the entire interelement boundary. For the case in Fig. 8.11(*a*), the requirement

$$u_2^1=u_1^2 \text{ and } u_3^1=u_4^2 \quad \text{guarantees} \quad U^1(s)=U^2(s)$$

on the side connecting global nodes 2 and 3. This can be shown as follows. The solution $U^1(s)$ along the line connecting global nodes 2 and 3 is linear, and is given by

$$U^1(s)=u_2^1\left(1-\frac{s}{h}\right)+u_3^1\frac{s}{h}$$

where s is the local coordinate along side 2–3 with its origin at global node 2 and h is the length of side 2–3 (or side 2). Similarly, the finite element solution along the same line but from element 2 is

$= u_1^2\frac{s}{h} + u_4^2\left(1-\frac{s}{h}\right)$ connectivity is from node 3 to 2 for 2nd element

$$U^2(s)=u_1^2\left(1-\frac{s}{h}\right)+u_4^2\frac{s}{h}$$

Since $u_1^2=u_2^1$ and $u_4^2=u_3^1$, it follows that $U^1(s)=U^2(s)$ for every value of s along the interface of the two elements.

Next we use the balance of secondary variables. At the interface between the two elements, the fluxes from them should be equal in magnitude and opposite in sign. For the two elements in Fig. 8.11(*a*), the interface is along the side connecting global nodes 2 and 3. Hence, the internal flux q_n^1 on side 2–3 of element 1 should balance the flux q_n^2 on side 4–1 of element 2 (recall the sign convention on q_n^e):

$$(q_n^1)_{2-3}=(q_n^2)_{4-1} \quad \text{or} \quad (q_n^1)_{2-3}=(-q_n^2)_{1-4} \tag{8.51}$$

In the finite element method, we impose the above relation in a weighted-integral sense:

$$\int_{h_{23}^1} q_n^1\psi_2^1\,ds=-\int_{h_{14}^2} q_n^2\psi_1^2\,ds, \qquad \int_{h_{23}^1} q_n^1\psi_3^1\,ds=-\int_{h_{14}^2} q_n^2\psi_4^2\,ds \tag{8.52a}$$

where h^e_{pq} denotes the length of the side connecting node p to node q of the element Ω^e. The above equations can be written in the form

$$\int_{h^1_{23}} q^1_n \psi^1_2 \, ds + \int_{h^2_{14}} q^2_n \psi^2_1 \, ds = 0, \qquad \int_{h^1_{23}} q^1_n \psi^1_3 \, ds + \int_{h^2_{14}} q^2_n \psi^2_4 \, ds = 0 \tag{8.52b}$$

or

$$Q^1_{22} + Q^2_{14} = 0, \qquad Q^1_{32} + Q^2_{44} = 0 \tag{8.52c}$$

where Q^e_{iJ} denotes the part of Q^e_i that comes from side J of element e [see (8.48)]:

$$Q^e_{iJ} = \int_{\text{side } J} q^e_n \psi^e_i \, ds$$

The sides of triangular and rectangular elements are numbered as shown in Fig. 8.11. These balance relations must be imposed in assembling the element equations. We note that Q^e_{iJ} is only a portion of Q^e_i [see (8.47)].

The element equations of the two elements are written first. For the model problem at hand, there is only one primary degree of freedom (NDF = 1) per node. For the triangular element, the element equations are of the form

$$\begin{aligned}
K^1_{11}u^1_1 + K^1_{12}u^1_2 + K^1_{13}u^1_3 &= f^1_1 + Q^1_1 \\
K^1_{21}u^1_1 + K^1_{22}u^1_2 + K^1_{23}u^1_3 &= f^1_2 + Q^1_2 \\
K^1_{31}u^1_1 + K^1_{32}u^1_2 + K^1_{33}u^1_3 &= f^1_3 + Q^1_3
\end{aligned} \tag{8.53a}$$

For the rectangular element, the element equations are given by

$$\begin{aligned}
K^2_{11}u^2_1 + K^2_{12}u^2_2 + K^2_{13}u^2_3 + K^2_{14}u^2_4 &= f^2_1 + Q^2_1 \\
K^2_{21}u^2_1 + K^2_{22}u^2_2 + K^2_{23}u^2_3 + K^2_{24}u^2_4 &= f^2_2 + Q^2_2 \\
K^2_{31}u^2_1 + K^2_{32}u^2_2 + K^2_{33}u^2_3 + K^2_{34}u^2_4 &= f^2_3 + Q^2_3 \\
K^2_{41}u^2_1 + K^2_{42}u^2_2 + K^2_{43}u^2_3 + K^2_{44}u^2_4 &= f^2_4 + Q^2_4
\end{aligned} \tag{8.53b}$$

In order to impose the balance of secondary variables in (8.52), we must add the second equation of element 1 to the first equation of element 2, and also add the third equation of element 1 to the fourth equation of element 2:

$$\begin{aligned}
&(K^1_{21}u^1_1 + K^1_{22}u^1_2 + K^1_{23}u^1_3) + (K^2_{11}u^2_1 + K^2_{12}u^2_2 + K^2_{13}u^2_3 + K^2_{14}u^2_4) \\
&\qquad = (f^1_2 + Q^1_2) + (f^2_1 + Q^2_1) \\
&(K^1_{31}u^1_1 + K^1_{32}u^1_2 + K^1_{33}u^1_3) + (K^2_{41}u^2_1 + K^2_{42}u^2_2 + K^2_{43}u^2_3 + K^2_{44}u^2_4) \\
&\qquad = (f^1_3 + Q^1_3) + (f^2_4 + Q^2_4)
\end{aligned}$$

Using the global-variable notation in (8.50), we can rewrite the above equations as follows [this amounts to imposing continuity of the primary variables in (8.50)]:

$$\begin{aligned}
K^1_{21}U_1 + (K^1_{22} + K^2_{11})U_2 + (K^1_{23} + K^2_{14})U_3 + K^2_{12}U_4 + K^2_{13}U_5 &= f^1_2 + f^2_1 + (Q^1_2 + Q^2_1) \\
K^1_{31}U_1 + (K^1_{32} + K^2_{41})U_2 + (K^1_{33} + K^2_{44})U_3 + K^2_{42}U_4 + K^2_{43}U_5 &= f^1_3 + f^2_4 + (Q^1_3 + Q^2_4)
\end{aligned}$$

Now we can impose the conditions in (8.52) by setting appropriate portions of the expressions in parentheses on the right-hand sides of the above equations equal to zero:

$$
\begin{aligned}
Q_2^1 + Q_1^2 &= (Q_{21}^1 + Q_{22}^1 + Q_{23}^1) + (Q_{11}^2 + Q_{12}^2 + Q_{13}^2 + Q_{14}^2) \\
&= Q_{21}^1 + Q_{23}^1 + \underline{(Q_{22}^1 + Q_{14}^2)} + Q_{11}^2 + Q_{12}^2 + Q_{13}^2 \\
Q_3^1 + Q_4^2 &= (Q_{31}^1 + Q_{32}^1 + Q_{33}^1) + (Q_{41}^2 + Q_{42}^2 + Q_{43}^2 + Q_{44}^2) \\
&= Q_{31}^1 + Q_{33}^1 + \underline{(Q_{32}^1 + Q_{44}^2)} + Q_{41}^2 + Q_{42}^2 + Q_{43}^2
\end{aligned}
$$

The underlined terms are zero, by the balance requirement (8.52*c*). The remaining terms of each equation will be either known because q_n is known on the boundary or will remain unknown because the primary variable is specified on the boundary.

In general, when several elements are connected, the assembly of the elements is carried out by putting element coefficients K_{ij}^e, f_i^e, and Q_i^e into proper locations of the global coefficient matrix and right-hand column vectors. This is done by means of the connectivity relations, i.e., the correspondence of the local node number to the global node number. For example, if global node number 3 corresponds to node 3 of element 1 and node 4 of element 2 then we have

$$F_3 = F_3^1 + F_4^2 \equiv f_3^1 + f_4^2 + Q_3^1 + Q_4^2, \qquad K_{33} = K_{33}^1 + K_{44}^2$$

If global node numbers 2 and 3 correspond, respectively, to nodes 2 and 3 of element 1 and nodes 1 and 4 of element 2 then the global coefficients K_{22}, K_{23} and K_{33} are given by

$$K_{22} = K_{22}^1 + K_{11}^2, \qquad K_{23} = K_{23}^1 + K_{14}^2, \qquad K_{33} = K_{33}^1 + K_{44}^2$$

Similarly, the source components of global nodes 2 and 3 are added:

$$F_2 = F_2^1 + F_1^2, \qquad F_3 = F_3^1 + F_4^2$$

For the two-element mesh shown in Fig. 8.11(*a*), the assembled equations are

$$
\begin{bmatrix}
K_{11}^1 & K_{12}^1 & K_{13}^1 & 0 & 0 \\
K_{21}^1 & K_{22}^1 + K_{11}^2 & K_{23}^1 + K_{14}^2 & K_{12}^2 & K_{13}^2 \\
K_{31}^1 & K_{32}^1 + K_{41}^2 & K_{33}^1 + K_{44}^2 & K_{42}^2 & K_{43}^2 \\
0 & K_{21}^2 & K_{24}^2 & K_{22}^2 & K_{23}^2 \\
0 & K_{31}^2 & K_{34}^2 & K_{32}^2 & K_{33}^2
\end{bmatrix}
\begin{Bmatrix} U_1 \\ U_2 \\ U_3 \\ U_4 \\ U_5 \end{Bmatrix}
=
\begin{Bmatrix} F_1^1 \\ F_2^1 + F_1^2 \\ F_3^1 + F_4^2 \\ F_2^2 \\ F_3^2 \end{Bmatrix}
\tag{8.54}
$$

The assembly procedure described above can be used to assemble elements of any shape and type. The procedure can be implemented on a computer, as described for one-dimensional problems, with the help of the array $[B]$ (program variable is NOD). For hand calculations, the procedure described above must be used. For example, consider the finite element mesh shown in Fig. 8.11(*b*). Location (4, 4) of the global coefficient matrix contains $K_{33}^1 + K_{11}^2 + K_{11}^3 + K_{11}^4$. Location 4 in the assembled column vector contains $F_3^1 + F_1^2 + F_1^3 + F_1^4$. Locations (1,5), (1,6), (1,7), (2,5), (2,6), (2,7), (3,6), (3,7), and (5,6) of the global matrix contain zeros because $K_{IJ} = 0$ when global nodes I and J do not correspond to nodes of the same element in the mesh.

This completes the first five steps in the finite element modeling of the model equation (8.1). The next two steps of the analysis, namely, the imposition of boundary conditions and solution of equations, remain the same as for one-dimensional problems. Postprocessing of the solution for two-dimensional problems is discussed next.

8.2.8 Postprocessing

The finite element solution at any point (x, y) in an element Ω^e is given by

$$U^e(x, y) = \sum_{j=1}^{n} u_j^e \psi_j^e(x, y) \tag{8.55}$$

and its derivatives are computed as

$$\frac{\partial U^e}{\partial x} = \sum_{j=1}^{n} u_j^e \frac{\partial \psi_j^e}{\partial x}, \qquad \frac{\partial U^e}{\partial y} = \sum_{j=1}^{n} u_j^e \frac{\partial \psi_j^e}{\partial y} \tag{8.56}$$

Equations (8.55) and (8.56) can be used to compute the solution and its derivatives at any point (x, y) in the element. It is useful to generate, by interpolation from (8.55), information needed to plot contours of U^e and its gradient.

The derivatives of U^e will not be continuous at interelement boundaries, because continuity of the derivatives is not imposed during the assembly procedure. The weak form of the equations suggests that the primary variable is u, which is to be carried as the nodal variable. If additional variables, such as higher-order derivatives of the dependent unknown, are carried as nodal variables in the interest of making them continuous across interelement boundaries, the degree of interpolation (or order of the element) increases. In addition, the continuity of higher-order derivatives that are not identified as the primary variables may violate the physical features of the problem. For example, making $\partial u/\partial x$ continuous will violate the requirement that q_x $(= a_{11}\, \partial u/\partial x)$ be continuous at the interface of two dissimilar materials, because a_{11} is different for the two materials at the interface.

For linear triangular elements, the derivatives are constants within each element:

$$\begin{gathered}\psi_j^e = \frac{1}{2A_e}(\alpha_j + \beta_j x + \gamma_j y) \\ \frac{\partial \psi_j^e}{\partial x} = \frac{1}{2A}\beta_j, \qquad \frac{\partial \psi_j^e}{\partial y} = \frac{1}{2A}\gamma_j \\ \frac{\partial U^e}{\partial x} = \sum_{j=1}^{n} \frac{u_j^e \beta_j}{2A_e}, \qquad \frac{\partial U^e}{\partial y} = \sum_{j=1}^{n} \frac{u_j^e \gamma_j}{2A_e}\end{gathered} \tag{8.57}$$

For linear rectangular elements, $\partial U^e/\partial x$ is linear in $\bar{y}$, and $\partial U^e/\partial y$ is linear in $\bar{x}$ [see (8.31b)]:

$$\begin{aligned} \frac{\partial \psi_j^e}{\partial \bar{x}} &= -\frac{1}{a}\left(1-\frac{\bar{y}+\bar{y}_j}{b}\right), & \frac{\partial \psi_j^e}{\partial \bar{y}} &= -\frac{1}{b}\left(1-\frac{\bar{x}+\bar{x}_j}{a}\right) \\ \frac{\partial U^e}{\partial \bar{x}} &= -\frac{1}{a}\sum_{j=1}^{n} u_j^e\left(1-\frac{\bar{y}+\bar{y}_j}{b}\right), & \frac{\partial U^e}{\partial \bar{y}} &= -\frac{1}{b}\sum_{j=1}^{n} u_j^e\left(1-\frac{\bar{x}+\bar{x}_j}{a}\right) \end{aligned} \tag{8.58}$$

where $\bar{x}$ and $\bar{y}$ are the local coordinates (see Fig. 8.7a). Although $\partial U^e/\partial \bar{x}$ and $\partial U^e/\partial \bar{y}$ are linear functions of y and x, respectively, in each element, they are discontinuous at interelement boundaries. Consequently, quantities computed using derivatives of the finite element solution U^e are discontinuous there. For example, if one computes $q_x^e = a_{11}^e\, \partial U^e/\partial x$ at a node shared by three different elements, three different values of q_x^e are expected. The differences between the three values will diminish as the mesh is refined. Some commercial finite element softwares give a single value of q_x at the node by averaging the values obtained from various elements connected at the node.

8.2.9 Axisymmetric Problems

In studying problems involving cylindrical geometries, it is convenient to use the cylindrical coordinate system (r, θ, z) to formulate the problem. If the geometry, material properties, boundary conditions, and loading (or source) of the problem are independent of the angular coordinate θ, the problem solution will also be independent of θ. Consequently, a three-dimensional problem is reduced to a two-dimensional one in (r, z) coordinates. Here we consider a model axisymmetric problem, develop its weak form, and formulate the finite element model.

MODEL EQUATION. Consider the partial differential equation

$$-\frac{1}{r}\frac{\partial}{\partial r}\left(r\hat{a}_{11}\frac{\partial u}{\partial r}\right) - \frac{\partial}{\partial z}\left(\hat{a}_{22}\frac{\partial u}{\partial z}\right) + \hat{a}_{00}u = \hat{f}(r, z) \tag{8.59}$$

where $\hat{a}_{00}$, $\hat{a}_{11}$, $\hat{a}_{22}$, and $\hat{f}$ are given functions of r and z. This equation arises in the study of heat transfer in cylindrical geometries, as well as in other fields of engineering and applied science. Our objective is to develop the finite element model of the equation based on the weak form of (8.59).

WEAK FORM. Following the three-step procedure, we write the weak form of (8.59):

$$\begin{aligned} &\text{(i)} \quad 0 = \int_{\Omega^e} w\left[-\frac{1}{r}\frac{\partial}{\partial r}\left(r\hat{a}_{11}\frac{\partial u}{\partial r}\right) - \frac{\partial}{\partial z}\left(\hat{a}_{22}\frac{\partial u}{\partial z}\right) + \hat{a}_{00}u - \hat{f}\right] r\,dr\,dz \\ &\text{(ii)} \quad 0 = \int_{\Omega^e} \left(\frac{\partial w}{\partial r} r\hat{a}_{11}\frac{\partial u}{\partial r} + \frac{\partial w}{\partial z} r\hat{a}_{22}\frac{\partial u}{\partial z} + wr\hat{a}_{00}u - wr\hat{f}\right) dr\,dz \\ &\qquad\quad - \oint_{\Gamma^e} w\left(r\hat{a}_{11}\frac{\partial u}{\partial r}n_r + r\hat{a}_{22}\frac{\partial u}{\partial z}n_z\right) ds \\ &\text{(iii)} \quad 0 = \int_{\Omega^e} \left(\hat{a}_{11}\frac{\partial w}{\partial r}\frac{\partial u}{\partial r} + \hat{a}_{22}\frac{\partial w}{\partial z}\frac{\partial u}{\partial z} + \hat{a}_{00}wu - w\hat{f}\right) r\,dr\,dz - \oint_{\Gamma^e} wq_n\,ds \end{aligned} \tag{8.60}$$

where w is the weight function and q_n is the normal flux,

$$q_n = r\left(\hat{a}_{11}\frac{\partial u}{\partial r}n_r + \hat{a}_{22}\frac{\partial u}{\partial z}n_z\right) \tag{8.61}$$

Note that the weak form (8.60) does not differ significantly from that developed for the model equation (8.1) when $a_{12} = a_{21} = 0$. The only difference is the presence of r in the integrand. Consequently, (8.60) can be obtained as a special case of (8.10) for $a_{00} = \hat{a}_{00}x$, $a_{11} = \hat{a}_{11}x$, $a_{22} = \hat{a}_{22}x$, and $f = \hat{f}x$; the coordinates r and z are treated like x and y, respectively.

FINITE ELEMENT MODEL. Let us assume that $u(r, z)$ is approximated by the finite element interpolation U^e over the element Ω^e:

$$u \approx U^e(r, z) = \sum_{j=1}^{n} u_j^e \psi_j^e(r, z) \tag{8.62}$$

The interpolation functions $\psi_j^e(r, z)$ are the same as those developed in (8.25) and (8.31*a*) for linear triangular and rectangular elements, with $x = r$ and $y = z$. Substitution of (8.62) for u and ψ_i^e for w into the weak form gives the ith equation of the finite element model:

$$0 = \sum_{j=1}^{n}\left[\int_{\Omega^e}\left(\hat{a}_{11}\frac{\partial \psi_i^e}{\partial r}\frac{\partial \psi_j^e}{\partial r} + \hat{a}_{22}\frac{\partial \psi_i^e}{\partial z}\frac{\partial \psi_j^e}{\partial z} + \hat{a}_{00}\psi_i^e\psi_j^e\right) r\, dr\, dz\right]u_j^e$$
$$- \int_{\Omega^e} \psi_i^e \hat{f} r\, dr\, dz - \oint_{\Gamma^e} \psi_i^e q_n\, ds \tag{8.63}$$

or

$$0 = \sum_{j=1}^{n} K_{ij}^e u_j^e - f_i^e - Q_i^e \tag{8.64a}$$

where

$$K_{ij}^e = \int_{\Omega^e}\left(\hat{a}_{11}\frac{\partial \psi_i^e}{\partial r}\frac{\partial \psi_j^e}{\partial r} + \hat{a}_{22}\frac{\partial \psi_i^e}{\partial z}\frac{\partial \psi_j^e}{\partial z} + \hat{a}_{00}\psi_i^e\psi_j^e\right) r\, dr\, dz$$
$$f_i^e = \int_{\Omega^e} \psi_i^e \hat{f} r\, dr\, dz, \qquad Q_i^e = \oint_{\Gamma^e} \psi_i^e q_n\, ds \tag{8.64b}$$

Exact evaluation of the integrals in K_{ij}^e and f_i^e for polynomial forms of $\hat{a}_{ij}$ and $\hat{f}$ is possible. However, we evaluate them numerically using the numerical integration methods discussed in Chapter 7 (see Section 7.1.5), and reviewed in Chapter 9. This completes the development of the finite element model of an axisymmetric problem.

8.2.10 An Example

The model equation in (8.1) arises in many fields of engineering and applied sciences, and some examples are given in Table 8.1. The application of the finite element model developed in Sections 8.2.2–8.2.8 to a problem is discussed here. This example will be particularly useful for readers who are interested in the mathematical aspects rather than the physical background of the problem.

Example 8.3. Consider the Poisson equation

$$-\nabla^2 u = f_0 \quad \text{or} \quad -\left(\frac{\partial^2 u}{\partial x^2}+\frac{\partial^2 u}{\partial y^2}\right)=f_0 \quad \text{in } \Omega \tag{8.65}$$

in a square region Ω (see Fig. 8.12*a*). The boundary condition of the problem is

$$u=0 \quad \text{on } \Gamma \tag{8.66}$$

We wish to solve the problem using the finite element method.

A problem possesses symmetry of the solution about a line only when there is symmetry of (*a*) the geometry, (*b*) the material properties, (*c*) the source variation, and

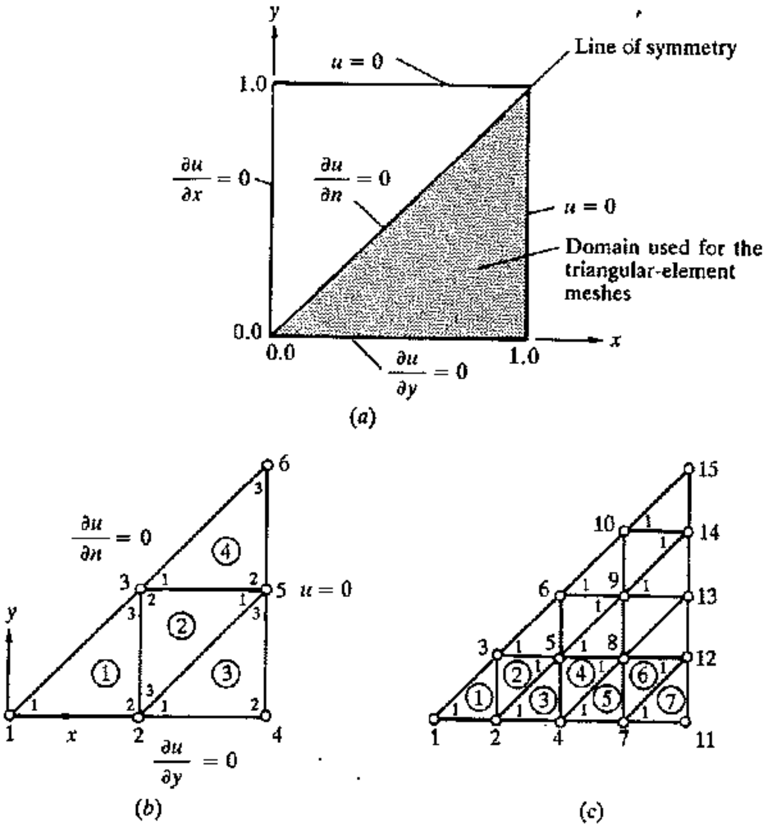

FIGURE 8.12
Finite element analysis of the Poisson equation in a square region: (*a*) geometry and computational domain, and boundary conditions of the problem; (*b*) a coarse finite element mesh of linear triangular elements; (*c*) a refined mesh of linear triangular elements (Example 8.3).

(*d*) the boundary conditions about the line. Whenever a portion of the domain is modeled to exploit symmetries available in the problem, a portion of the boundary of the computational domain is a line of symmetry. On lines of symmetry, the normal derivative of the solution (i.e., the derivative with respect to the coordinate normal to the line of symmetry) is zero:

$$q_n \equiv \frac{\partial u}{\partial n} = \frac{\partial u}{\partial x} n_x + \frac{\partial u}{\partial y} n_y = 0 \tag{8.67}$$

The problem at hand has symmetry about the $x = 0$ and $y = 0$ axes; it is also symmetric about the diagonal line $x = y$ (see Fig. 8.12*a*). We can exploit such symmetries in modeling the problem. Thus, we can use a quadrant for meshes of rectangular elements and an octant for meshes of triangular elements of the domain to analyze the problem. Of course, it is possible to mix triangular and rectangular elements to represent the domain as well as the solution.

Solution by linear triangular elements. Owing to the symmetry along the diagonal $x = y$, we model the triangular domain shown in Fig. 8.12(*a*). As a first choice, we use a uniform mesh of four linear triangular elements to represent the domain (see Fig. 8.12*b*), and then a refined mesh (see Fig. 8.12*c*) to compare the solutions. In the present case, there is no discretization error involved in the problem because the geometry is exactly represented.

Elements 1, 3, and 4 are identical in orientation as well as geometry. Element 2 is geometrically identical with element 1, except that it is oriented differently. If we number the local nodes of element 2 to match those of element 1 then all four elements have the same element matrices, and it is necessary to compute them only for element 1. When the element matrices are calculated on a computer, such considerations are not taken into account. In solving the problem by hand, we use the correspondence between a master element (element 1) and the other elements in the mesh to avoid unnecessary calculations.

We consider element 1 as the typical element, with its local coordinate system $(\bar{x}, \bar{y})$. Suppose that the element dimensions, i.e., length and height, are a and b, respectively. The coordinates of the element nodes are

$$(\bar{x}_1, \bar{y}_1) = (0, 0), \quad (\bar{x}_2, \bar{y}_2) = (a, 0), \quad (\bar{x}_3, \bar{y}_3) = (a, b)$$

Hence, the parameters α_i, β_i, and γ_i are given by

$$\begin{aligned}
&\alpha_1 = \bar{x}_2\bar{y}_3 - \bar{x}_3\bar{y}_2 = ab, \quad \alpha_2 = \bar{x}_3\bar{y}_1 - \bar{x}_1\bar{y}_3 = 0, \quad \alpha_3 = \bar{x}_1\bar{y}_2 - \bar{x}_2\bar{y}_1 = 0\\
&\beta_1 = \bar{y}_2 - \bar{y}_3 = -b, \quad \beta_2 = \bar{y}_3 - \bar{y}_1 = b, \quad \beta_3 = \bar{y}_1 - \bar{y}_2 = 0\\
&\gamma_1 = -(\bar{x}_2 - \bar{x}_3) = 0, \quad \gamma_2 = -(\bar{x}_3 - \bar{x}_1) = -a, \quad \gamma_3 = -(\bar{x}_1 - \bar{x}_2) = a
\end{aligned} \tag{8.68}$$

The element coefficients K_{ij}^e and f_i^e are given by

$$[K^1] = \frac{1}{2ab}\begin{bmatrix} b^2 & -b^2 & 0 \\ -b^2 & a^2 + b^2 & -a^2 \\ 0 & -a^2 & a^2 \end{bmatrix}, \quad \{f^1\} = \frac{f_0 ab}{6}\begin{Bmatrix} 1 \\ 1 \\ 1 \end{Bmatrix} \tag{8.69a}$$

The element matrix in (8.69*a*) is valid for the Laplace operator $-\nabla^2$ on any right-angled triangle with sides a and b in which the right-angle is at node 2, and the diagonal line of the triangle connects node 3 to node 1. Note that the off-diagonal coefficient associated with the nodes on the diagonal line is zero for a right-angled triangle. These observations can be used to write the element matrix associated with the

Laplace operator on *any* right-angled triangle, i.e., for any element-node numbering system. For example, if the right-angled corner is numbered as node 1, and the diagonal-line nodes are numbered as 2 and 3 (following the counter-clockwise numbering scheme), we have (note that a denotes the length of side connecting nodes 1 and 2)

$$[K^e] = \frac{1}{2ab}\begin{bmatrix} a^2+b^2 & -b^2 & -a^2 \\ -b^2 & b^2 & 0 \\ -a^2 & 0 & a^2 \end{bmatrix} \tag{8.69b}$$

For the mesh shown in Fig. 8.12(b), we have

$$[K^1] = [K^2] = [K^3] = [K^4], \qquad \{f^1\} = \{f^2\} = \{f^3\} = \{f^4\}$$

For $a = b$, the coefficient matrix in (8.69a) takes the form

$$[K^e] = \frac{1}{2}\begin{bmatrix} 1 & -1 & 0 \\ -1 & 2 & -1 \\ 0 & -1 & 1 \end{bmatrix} \tag{8.70}$$

The assembled coefficient matrix for the finite element mesh is 6 × 6, because there are six global nodes, with one unknown per node. The assembled matrix can be obtained directly by using the correspondence between the global nodes and the local nodes, expressed through the connectivity matrix

$$[B] = \begin{bmatrix} 1 & 2 & 3 \\ 5 & 3 & 2 \\ 2 & 4 & 5 \\ 3 & 5 & 6 \end{bmatrix} \tag{8.71}$$

The assembled system of equations is

$$\frac{1}{2}\left[\begin{array}{ccc:ccc} 1 & -1 & 0 & 0 & 0 & 0 \\ -1 & 4 & -2 & -1 & 0 & 0 \\ 0 & -2 & 4 & 0 & -2 & 0 \\ \hdashline 0 & -1 & 0 & 2 & -1 & 0 \\ 0 & 0 & -2 & -1 & 4 & -1 \\ 0 & 0 & 0 & 0 & -1 & 1 \end{array}\right]\begin{Bmatrix} U_1 \\ U_2 \\ U_3 \\ U_4 \\ U_5 \\ U_6 \end{Bmatrix} = \frac{f_0}{24}\begin{Bmatrix} 1 \\ 3 \\ 3 \\ 1 \\ 3 \\ 1 \end{Bmatrix} + \left\{\begin{array}{c} Q_1^1 \\ Q_2^1 + Q_3^2 + Q_1^3 \\ Q_3^1 + Q_2^2 + Q_1^4 \\ \hdashline Q_2^3 \\ Q_1^2 + Q_3^3 + Q_2^4 \\ Q_3^4 \end{array}\right\} \tag{8.72}$$

The sums of the secondary variables at global nodes 2, 3, and 5 are

$$\begin{aligned} Q_2^1 + Q_3^2 + Q_1^3 &= \hat{Q}_2 \\ Q_3^1 + Q_2^2 + Q_1^4 &= \hat{Q}_3 \\ Q_1^2 + Q_3^3 + Q_2^4 &= \hat{Q}_5 \end{aligned} \tag{8.73}$$

At nodes 1, 4, and 6, we have $Q_1^1 = \hat{Q}_1$, $Q_2^3 = \hat{Q}_4$, and $Q_3^4 = \hat{Q}_6$.

The specified boundary conditions on the primary degrees of freedom of the problem are

$$U_4 = U_5 = U_6 = 0 \tag{8.74}$$

The specified secondary degrees of freedom are (all due to symmetry)

$$\hat{Q}_1 = 0, \qquad \hat{Q}_2 = 0, \qquad \hat{Q}_3 = 0 \tag{8.75}$$

Since U_4, U_5, and U_6 are known, the secondary variables at these nodes, i.e., $\hat{Q}_4$, $\hat{Q}_5$, and $\hat{Q}_6$, are unknown, and can be obtained in the post-computation.

Since the only unknown primary variables are (U_1, U_2, and U_3), and (U_4, U_5, and U_6) are specified to be zero, the condensed equations for the primary unknowns can be obtained by deleting rows and columns 4, 5, and 6 from the system (8.72). In retrospect, it would have been sufficient to assemble the element coefficients associated with the global nodes 1, 2, and 3, i.e., writing out equations 1, 2 and 3:

$$\begin{bmatrix} K_{11}^1 & K_{12}^1 & K_{13}^1 \\ K_{21}^1 & K_{22}^1+K_{33}^2+K_{11}^3 & K_{23}^1+K_{32}^2 \\ K_{31}^1 & K_{32}^1+K_{23}^2 & K_{33}^1+K_{22}^2+K_{11}^4 \end{bmatrix} \begin{Bmatrix} U_1 \\ U_2 \\ U_3 \end{Bmatrix} = \begin{Bmatrix} f_1^1 \\ f_2^1+f_3^2+f_1^3 \\ f_3^1+f_2^2+f_1^4 \end{Bmatrix} + \begin{Bmatrix} 0 \\ 0 \\ 0 \end{Bmatrix} \tag{8.76}$$

The unknown secondary variables $\hat{Q}_4$, $\hat{Q}_5$, and $\hat{Q}_6$ can be computed either from the equations (i.e., from equilibrium)

$$\begin{Bmatrix} \hat{Q}_4 \\ \hat{Q}_5 \\ \hat{Q}_6 \end{Bmatrix} = -\begin{Bmatrix} f_2^3 \\ f_1^2+f_3^3+f_2^4 \\ f_3^4 \end{Bmatrix} + \begin{bmatrix} 0 & K_{21}^3 & 0 \\ 0 & K_{13}^2+K_{31}^3 & K_{12}^2+K_{21}^4 \\ 0 & 0 & K_{31}^4 \end{bmatrix} \begin{Bmatrix} U_1 \\ U_2 \\ U_3 \end{Bmatrix} \tag{8.77}$$

or from their definitions (8.73) and (8.47). For example, we have,

$$\hat{Q}_4 = Q_2^3 = \int_{1-2} q_n^3 \psi_2^3 \, dx + \int_{2-3} q_n^3 \psi_2^3 \, dy + \int_{3-1} q_n^3 \psi_2^3 \, ds \tag{8.78a}$$

where

$$(q_n^3)_{1-2} = \left(\frac{\partial u}{\partial x} n_x + \frac{\partial u}{\partial y} n_y\right)_{1-2} = 0 \qquad \left(n_x = 0, \quad \frac{\partial u}{\partial y} = 0\right)$$

$$(q_n^3)_{2-3} = \left(\frac{\partial u}{\partial x} n_x + \frac{\partial u}{\partial y} n_y\right)_{2-3} = \frac{\partial u}{\partial x} \qquad (n_x = 1, \ n_y = 0)$$

$$(\psi_2^3)_{2-3} = 1 - \frac{y}{h_{23}}, \qquad (\psi_2^3)_{1-3} = 0$$

Thus,

$$\hat{Q}_4 = Q_{22}^3 = \int_0^{h_{23}} \frac{\partial u}{\partial x}\left(1 - \frac{y}{h_{23}}\right) dy$$

where $\partial u / \partial x$ from the finite element interpolation is

$$\frac{\partial u}{\partial x} = \sum_{j=1}^{3} u_j^3 \frac{\beta_j^3}{2A_3}$$

We obtain ($h_{23} = a$, $\beta_1^3 = -a$, $2A_3 = a^2$, $U_4 = U_5 = 0$)

$$\hat{Q}_4 = \frac{h_{23}}{4A_3} \sum_{j=1}^{3} u_j^3 \beta_j^3 = -0.5 U_2 \tag{8.78b}$$

Using the numerical values of the coefficients K_{ij}^e and f_i^e (with $f_0 = 1$), we write the condensed equations for U_1, U_2, and U_3 as

$$\begin{bmatrix} 0.5 & -0.5 & 0 \\ -0.5 & 2.0 & -1.0 \\ 0 & -1.0 & 2.0 \end{bmatrix} \begin{Bmatrix} U_1 \\ U_2 \\ U_3 \end{Bmatrix} = \frac{1}{24} \begin{Bmatrix} 1 \\ 3 \\ 3 \end{Bmatrix} \tag{8.79}$$

Solving (8.79) for U_i $(i = 1, 2, 3)$, we obtain

$$\begin{Bmatrix} U_1 \\ U_2 \\ U_3 \end{Bmatrix} = \frac{1}{24} \begin{bmatrix} 3 & 1 & 0.5 \\ 1 & 1 & 0.5 \\ 0.5 & 0.5 & 0.75 \end{bmatrix} \begin{Bmatrix} 1 \\ 3 \\ 3 \end{Bmatrix} = \frac{1}{24} \begin{Bmatrix} 7.5 \\ 5.5 \\ 4.25 \end{Bmatrix} = \begin{Bmatrix} 0.31250 \\ 0.22917 \\ 0.17708 \end{Bmatrix} \tag{8.80}$$

and, from (8.77), we have

−0.15625

$$\begin{Bmatrix} Q_{22}^3 \\ Q_{32}^3 + Q_{22}^4 \\ Q_{32}^4 \end{Bmatrix} = -\frac{1}{24} \begin{Bmatrix} 1 \\ 3 \\ 1 \end{Bmatrix} + \begin{bmatrix} 0 & -0.5 & 0 \\ 0 & 0 & -1 \\ 0 & 0 & 0 \end{bmatrix} \begin{Bmatrix} U_1 \\ U_2 \\ U_3 \end{Bmatrix} = \begin{Bmatrix} -0.197917 \\ -0.302083 \\ -0.041667 \end{Bmatrix} \tag{8.81}$$

By interpolation, Q_{22}^3, for example, is equal to $-0.5U_2$, and it differs from Q_{22}^3 computed from equilibrium by the amount f_2^3 $(=\frac{1}{24})$.

Solution by linear rectangular elements. Note that we cannot exploit the symmetry along the diagonal $x = y$ to our advantage when we use a mesh of rectangular elements. Therefore, we use a 2×2 uniform mesh of four linear rectangular elements (see Fig. 8.13) to discretize a quadrant of the domain. Once again, no discretization error is introduced in the present case.

Since all elements in the mesh are identical, we shall compute the element matrices for only one element, say element 1. We have

$$\psi_1 = (1-2\bar{x})(1-2\bar{y}), \qquad \psi_2 = 2\bar{x}(1-2\bar{y}), \qquad \psi_3 = 4\bar{x}\bar{y}, \qquad \psi_4 = (1-2\bar{x})2\bar{y}$$

$$K_{ij}^e = \int_0^{0.5}\int_0^{0.5} \left(\frac{\partial \psi_i}{\partial \bar{x}}\frac{\partial \psi_j}{\partial \bar{x}} + \frac{\partial \psi_i}{\partial \bar{y}}\frac{\partial \psi_j}{\partial \bar{y}} \right) d\bar{x}\, d\bar{y} \tag{8.82}$$

$$f_i^e = \int_0^{0.5}\int_0^{0.5} f_0 \psi_i \, d\bar{x}\, d\bar{y}$$

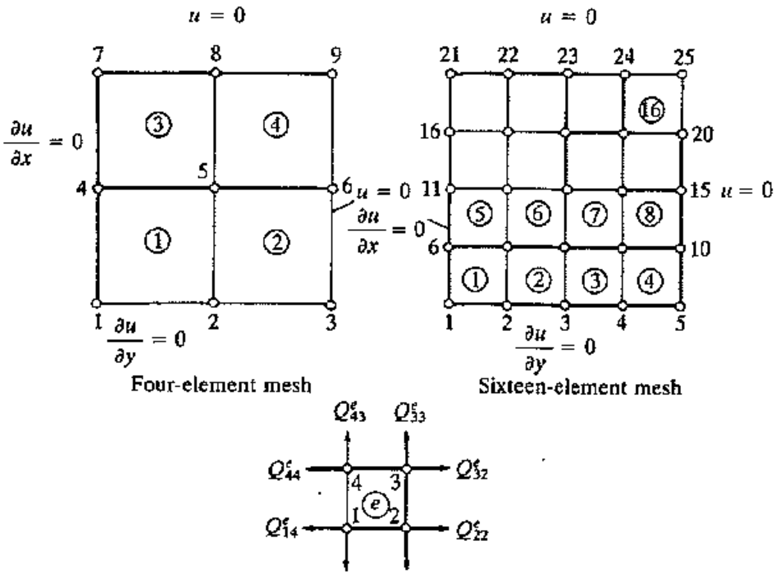

FIGURE 8.13
Finite element discretization of the domain of Example 8.3 by linear rectangular elements.

Evaluating these integrals, we obtain {see (8.44): $[K^e]=[S^{11}]+[S^{22}]$}

$$[K^e]=\frac{1}{6}\begin{bmatrix} 4 & -1 & -2 & -1 \\ -1 & 4 & -1 & -2 \\ -2 & -1 & 4 & -1 \\ -1 & -2 & -1 & 4 \end{bmatrix}, \qquad \{F^e\}=\frac{1}{16}\begin{Bmatrix} 1 \\ 1 \\ 1 \\ 1 \end{Bmatrix}+\begin{Bmatrix} Q_1^e \\ Q_2^e \\ Q_3^e \\ Q_4^e \end{Bmatrix} \tag{8.83a}$$

where

$$\begin{aligned} Q_i^e = &\int_{\bar{x}_1}^{\bar{x}_2} [q_n^{(e)}\psi_i(\bar{x},\bar{y})]_{\bar{y}=0}\,d\bar{x} + \int_{\bar{y}_2}^{\bar{y}_3} [q_n^{(e)}\psi_i(\bar{x},\bar{y})]_{\bar{x}=a}\,d\bar{y} \\ &+ \int_{\bar{x}_3}^{\bar{x}_4} [q_n^{(e)}\psi_i(\bar{x},\bar{y})]_{\bar{y}=b}\,d\bar{x} + \int_{\bar{y}_4}^{\bar{y}_1} [q_n^{(e)}\psi_i(\bar{x},\bar{y})]_{\bar{x}=0}\,d\bar{y} \end{aligned} \tag{8.83b}$$

and $(\bar{x}_i, \bar{y}_i)$ denote the local coordinates of the element nodes (and $a=\bar{x}_2-\bar{x}_1=\bar{x}_3-\bar{x}_4$ and $b=\bar{y}_4-\bar{y}_1=\bar{y}_3-\bar{y}_2$).

The coefficient matrix of the condensed equations for the primary unknowns can be directly assembled. There are four unknowns (at nodes 1, 2, 4, and 5). The condensed equations are

$$\begin{bmatrix} K_{11} & K_{12} & K_{14} & K_{15} \\ K_{21} & K_{22} & K_{24} & K_{25} \\ K_{41} & K_{42} & K_{44} & K_{45} \\ K_{51} & K_{52} & K_{54} & K_{55} \end{bmatrix}\begin{Bmatrix} U_1 \\ U_2 \\ U_4 \\ U_5 \end{Bmatrix}=\begin{Bmatrix} F_1 \\ F_2 \\ F_4 \\ F_5 \end{Bmatrix} \tag{8.84a}$$

where K_{IJ} and F_I are the global coefficients

$$\begin{gathered} K_{11}=K_{11}^1, \quad K_{12}=K_{12}^1, \quad K_{14}=K_{14}^1, \quad K_{15}=K_{13}^1 \\ K_{22}=K_{22}^1+K_{11}^2, \quad K_{24}=K_{24}^1, \quad K_{25}=K_{23}^1+K_{14}^2 \\ K_{44}=K_{44}^1+K_{11}^3, \quad K_{45}=K_{43}^1+K_{12}^3, \quad K_{55}=K_{33}^1+K_{44}^2+K_{11}^4+K_{22}^3 \\ F_1=f_1^1+Q_1^1, \quad F_2=f_2^1+f_1^2+Q_2^1+Q_1^2, \quad F_4=f_4^1+f_1^3+Q_4^1+Q_1^3 \\ F_5=f_3^1+f_4^2+f_1^4+f_2^3+Q_3^1+Q_4^2+Q_1^4+Q_2^3 \end{gathered} \tag{8.84b}$$

The boundary conditions on the secondary variables are

$$Q_1^1=0, \quad Q_2^1+Q_1^2=0, \quad Q_4^1+Q_1^3=0 \tag{8.85a}$$

and the balance of secondary variables at global node 5 requires

$$Q_3^1+Q_4^2+Q_2^3+Q_1^4=0 \tag{8.85b}$$

Thus, we have

$$\frac{1}{6}\begin{bmatrix} 4 & -1 & -1 & -2 \\ -1 & 8 & -2 & -2 \\ -1 & -2 & 8 & -2 \\ -2 & -2 & -2 & 16 \end{bmatrix}\begin{Bmatrix} U_1 \\ U_2 \\ U_4 \\ U_5 \end{Bmatrix}=\frac{1}{16}\begin{Bmatrix} 1 \\ 2 \\ 2 \\ 4 \end{Bmatrix} \tag{8.86}$$

The solution of these equations is

$$U_1=0.31071, \quad U_2=0.24107, \quad U_4=0.24107, \quad U_5=0.19286 \tag{8.87}$$

The secondary variables $\hat{Q}_3$, $\hat{Q}_6$, and $\hat{Q}_9$ at nodes 3, 6, and 9, respectively, can be computed from the equations ($\hat{Q}_3 = Q_2^2$, $\hat{Q}_6 = Q_3^2 + Q_2^4$, $\hat{Q}_9 = Q_3^4$)

$$\begin{Bmatrix} \hat{Q}_3 \\ \hat{Q}_6 \\ \hat{Q}_9 \end{Bmatrix} = -\begin{Bmatrix} f_2^2 \\ f_3^2 + f_2^4 \\ f_3^4 \end{Bmatrix} + \begin{bmatrix} K_{31} & K_{32} & K_{34} & K_{35} \\ K_{61} & K_{62} & K_{64} & K_{65} \\ K_{91} & K_{92} & K_{94} & K_{95} \end{bmatrix} \begin{Bmatrix} U_1 \\ U_2 \\ U_4 \\ U_5 \end{Bmatrix} \tag{8.88a}$$

where

$$\begin{gathered} K_{31} = 0, \quad K_{32} = K_{21}^2, \quad K_{34} = 0, \quad K_{35} = K_{24}^2 \\ K_{61} = 0, \quad K_{62} = K_{31}^2, \quad K_{64} = 0, \quad K_{65} = K_{34}^2 + K_{21}^4 \\ K_{91} = 0, \quad K_{92} = 0, \quad K_{94} = 0, \quad K_{95} = K_{31}^4 \end{gathered} \tag{8.88b}$$

We have

$$\begin{Bmatrix} \hat{Q}_3 \\ \hat{Q}_6 \\ \hat{Q}_9 \end{Bmatrix} = -\frac{1}{16}\begin{Bmatrix} 1 \\ 2 \\ 1 \end{Bmatrix} + \frac{1}{6}\begin{bmatrix} 0 & -1 & 0 & -2 \\ 0 & -2 & 0 & -2 \\ 0 & 0 & 0 & -2 \end{bmatrix} \begin{Bmatrix} U_1 \\ U_2 \\ U_4 \\ U_5 \end{Bmatrix} = -\begin{Bmatrix} 0.16697 \\ 0.26964 \\ 0.12679 \end{Bmatrix} \tag{8.89}$$

The finite element solutions obtained using two different meshes of triangular elements and two different meshes of rectangular elements are compared in Table 8.2 with the 50-term series solution (at $x = 0$ for varying y) in (2.102) (set $k = 1$, $q_0 = f_0 = 1$) and the one-parameter Ritz solution in (2.101); see also Fig. 8.14. The finite element solution obtained using 16 triangular elements (in an octant) is the most accurate one when compared with the series solution. The accuracy of the triangular element mesh is due to the large number of elements it has compared with the number of elements in the rectangular element mesh for the same size of domain.

The solution u and its gradient can be computed at any interior point of the domain. For a point (x, y) in the element Ω^e, we have

$$U(x, y) = \sum_{j=1}^{n} u_j^e \psi_j^e(x, y) \tag{8.90a}$$

$$q_y(x, y) = \frac{\partial U}{\partial y} = \sum_{i=1}^{n} u_i^e \frac{\partial \psi_i^e}{\partial y}, \quad q_x(x, y) = \frac{\partial U}{\partial x} = \sum_{i=1}^{n} u_i^e \frac{\partial \psi_i^e}{\partial x} \tag{8.90b}$$

TABLE 8.2
Comparison of the finite element solutions $u(0, y)$ with the series solution and the Ritz solution of (8.65) (Example 8.3)

	Triangular elements		Rectangular elements			Series
y	4 elements	16 elements	4 elements	16 elements	Ritz (2.101)	solution (2.102)
0.0	0.3125	0.3013	0.3107	0.2984	0.3125	0.2947
0.25	0.2709†	0.2805	0.2759†	0.2824	0.2930	0.2789
0.50	0.2292	0.2292	0.2411	0.2322	0.2344	0.2293
0.75	0.1146†	0.1393	0.1205†	0.1414	0.1367	0.1397
1.0	0.0000	0.0000	0.0000	0.0000	0.0000	0.0000

† Interpolated values.

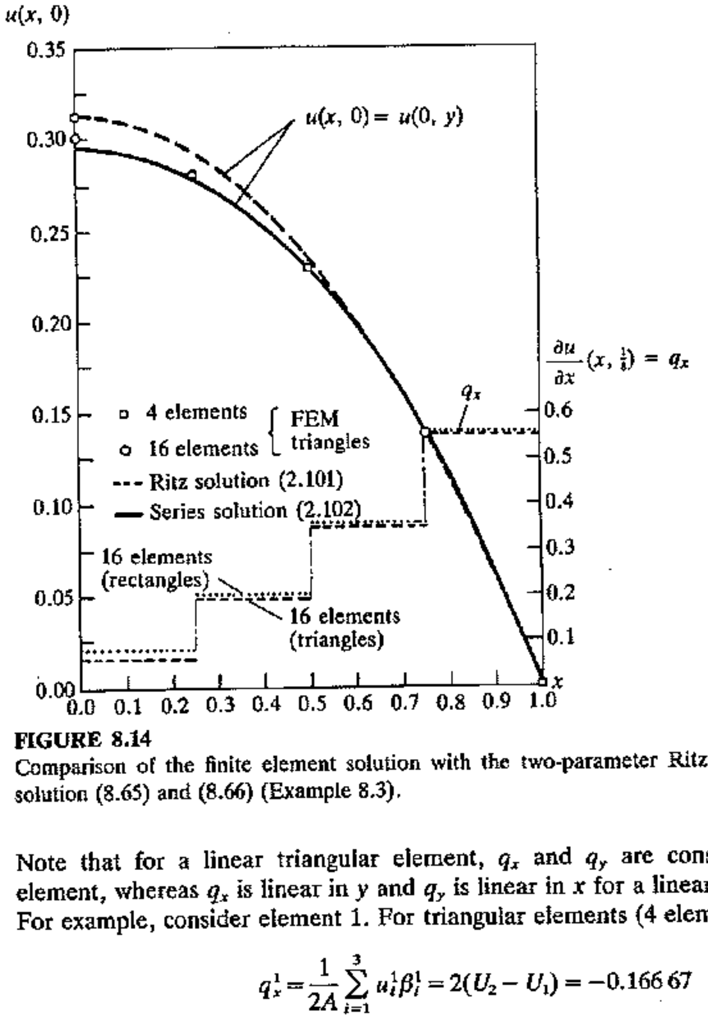

FIGURE 8.14
Comparison of the finite element solution with the two-parameter Ritz solution and the series solution (8.65) and (8.66) (Example 8.3).

Note that for a linear triangular element, q_x and q_y are constants over an entire element, whereas q_x is linear in y and q_y is linear in x for a linear rectangular element. For example, consider element 1. For triangular elements (4 elements),

$$\begin{aligned} q_x^1 &= \frac{1}{2A}\sum_{i=1}^{3} u_i^1 \beta_i^1 = 2(U_2 - U_1) = -0.166\,67 \\ q_y^1 &= \frac{1}{2A}\sum_{i=1}^{3} u_i^1 \gamma_i^1 = 2(U_3 - U_2) = -0.104\,17 \end{aligned} \tag{8.91a}$$

while for rectangular elements (4 elements),

$$\begin{aligned} q_x^1 &= \sum_{i=1}^{4} u_i^1 \frac{\partial \psi_i^1}{\partial x} = -2U_1(1-2y) + 2U_2(1-2y) + 4yU_5 - 4yU_4 \\ q_x^1&(0.25, 0.25) = -0.11785 \\ q_y^1 &= \sum_{i=1}^{4} u_i^1 \frac{\partial \psi_i^1}{\partial y} = -2U_1(1-2x) + 2U_2(1-2x) + 4xU_5 - 4xU_4 \\ q_y^1&(0.25, 0.25) = -0.11785 \end{aligned} \tag{8.91b}$$

Plots of q_x, obtained using the 16-element meshes of linear triangular and rectangular elements, as a function of x (for $y = 0.125$) are also shown in Fig. 8.14.

The computation of *isolines*, i.e., lines of constant u, for linear finite elements is straightforward. Suppose that we wish to find the $u = u_0$ (constant) isoline. On a side of a linear triangle or rectangular element, the solution u varies according to the equation

$$U^e(s) = u_1^e + \frac{u_3^e - u_1^e}{h} s$$

where s is the local coordinate with its origin at node 1 of the side, (u_1^e, u_3^e) are the nodal values (see Fig. 8.15), and h is the length of the side. Then, if $u = u_0$ lies on the line (i.e., $u_1^e < u_0 < u_3^e$ or $u_3^e < u_0 < u_1^e$), the point s_0 at which $U^e(s_0) = u_0$ is given by

$$s_0 = \frac{(u_0 - u_1^e)h}{u_3^e - u_1^e} \tag{8.92}$$

Similar equations apply for other sides of the element. Since the solution varies linearly between any two points of linear elements, the isoline is determined by joining two points on any two sides of the element for which (8.92) gives a positive value (and $s_0 < h$).

For quadratic elements, isolines are determined by finding three points s_i in the element at which $U^e(s_i) = u_0$ $(i = 1, 2, 3)$:

$$\frac{s_0}{h} = \frac{-b \pm (b^2 - 4ac)^{1/2}}{2a} > 0 \tag{8.93a}$$

where

$$c = u_1^e - u_0, \qquad b = -3u_1^e + 4u_2^e - u_3^e, \qquad a = 2(u_1^e - 2u_2^e + u_3^e) \tag{8.93b}$$

Equation (8.93*a*) is to be applied on any three lines in the element until three different values $h > s_0 > 0$ are found.

The computational problem considered here [i.e., (8.65)] has several physical interpretations (see Table 8.1). The problem can be viewed as one of finding the temperature u in a unit square with uniform internal heat generation, where the sides $x = 0$ and $y = 0$ are insulated and the other two sides are at zero temperature (see Section 8.4.1). Another interpretation of the equation is that it defines the torsion of a cylindrical bar of 2 in square cross-section (see Section 8.4.3). In this case, u denotes the stress function Ψ,

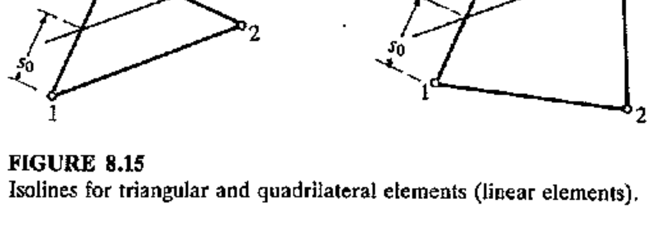

FIGURE 8.15
Isolines for triangular and quadrilateral elements (linear elements).

and the components of the gradient of the solution are the stresses (which are of primary interest):

$$\sigma_{xz} = G\theta \frac{\partial \Psi}{\partial y}, \qquad \sigma_{yz} = -G\theta \frac{\partial \Psi}{\partial x}$$

where G is the shear modulus and θ is the angle of twist per unit length of the bar.

A third interpretation of (8.65) is provided by groundwater (seepage) and potential flow problems. In this case, u is the piezometric head ϕ, stream function ψ or velocity potential ϕ (see Section 8.4.2). The x and y components of the velocity for the groundwater flow are defined as

$$u_1 = -a_{11} \frac{\partial \phi}{\partial x}, \qquad u_2 = -a_{22} \frac{\partial \phi}{\partial y}$$

where a_{11} and a_{22} are the permeabilities of the soil along the x and y directions, respectively.

Examples of each of these field problems will be considered in Section 8.4.

8.3 SOME COMMENTS ON MESH GENERATION AND IMPOSITION OF BOUNDARY CONDITIONS

8.3.1 Discretization of a Domain

The representation of a given domain by a collection of finite elements requires engineering judgement on the part of the finite element practitioner. The number, type (e.g., linear or quadratic), shape (e.g., triangular or rectangular), and density (i.e., mesh refinement) of elements used in a given problem depend on a number of considerations. The first is to discretize the domain as closely as possible with elements that are admissible. As we shall see later, one can use one set of elements for the approximation of a domain and another set for the solution. In discretizing a domain, consideration must be given to an accurate representation of the domain, point sources, distributed sources with discontinuities (i.e., sudden change in the intensity of the source), and material and geometric discontinuities, including a re-entrant corner. The discretization should include, for example, nodes at point sources (so that the point source is accurately lumped at the node), re-entrant corners, and element interfaces where abrupt changes in geometry and material properties occur. A second consideration, which requires some engineering judgement, is to discretize the body or portions of the body into sufficiently small elements so that steep gradients of the solution can be accurately calculated. The engineering judgement should come from both a qualitative understanding of the behavior of the solution and an estimate of the computational costs involved in the mesh refinement (i.e., reducing the size of the elements). For example, consider inviscid flow around a cylinder in a

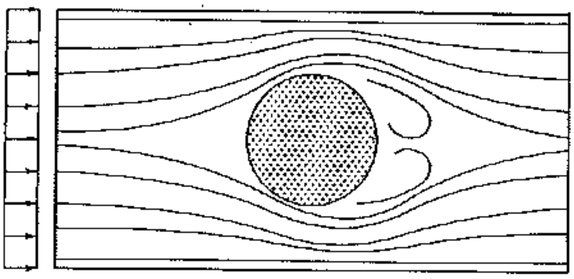

FIGURE 8.16
Flow of an inviscid fluid around a cylinder (streamlines).

channel. The flow entering the channel at the left goes around the cylinder and exits the channel at the right (see Fig. 8.16). Since the section at the cylinder is smaller than the inlet section, it is expected that the flow accelerates in the vicinity of the cylinder. On the other hand, the velocity field far from the cylinder (e.g., at the inlet) is essentially uniform. Such knowledge of the qualitative behavior of the flow allows us to employ a coarse mesh (i.e., elements that are relatively large in size) at sites sufficiently far from the cylinder, and a fine one at closer distances to the cylinder (see Fig. 8.17). Another purpose of using a refined mesh near the cylinder is to accurately represent the curved boundary of the domain there. In general, a refined mesh is required in places where acute changes in geometry, boundary conditions, loading, material properties or solution occur.

A mesh refinement should meet three conditions: (1) all previous meshes should be contained in the refined mesh; (2) every point in the body can be included within an arbitrarily small element at any stage of the mesh refinement; and (3) the same order of approximation for the solution may be retained through all stages of the refinement process. The last requirement eliminates comparison of two different approximations in two different meshes. When a mesh is refined, care should be taken to avoid elements with very large aspect ratios (i.e., the ratio of the smallest to the largest side of the element)

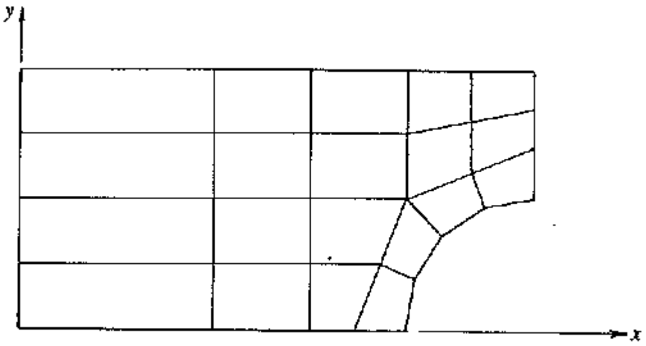

FIGURE 8.17
Finite element mesh considerations for inviscid flow around a cylinder. A typical mesh for a quadrant of the domain.

or small angles. Recall from the element matrices (8.41) and (8.68) that the coefficient matrices depend on the ratios of a to b and b to a. If the value of a/b or b/a is very large, the resulting coefficient matrices are ill-conditioned (i.e., numerically not invertible). Although the safe lower and upper limits on b/a are believed to be 0.1 and 10, respectively, the actual values are much more extreme (say, 1000), and they depend on the nature of the physical phenomenon being modeled. For example, in the inviscid flow problem discussed above, large aspect ratios are allowed at the entrance of the channel.

The words "coarse" and "fine" are relative. In any given problem, one begins with a finite element mesh that is believed to be adequate (based on experience and engineering judgement) to solve the problem at hand. Then, as a second choice, one selects a mesh that consists of a larger number of elements (and includes the first one as a subset) to solve the problem once again. If there is a significant difference between the two solutions, one sees the benefit of mesh refinement, and further refinement may be warranted. If the difference is negligibly small, further refinements are not necessary. Such numerical experiments with mesh refinements are not always feasible in practice, mostly because of the computational costs involved. In cases where computational cost is the prime concern, one must depend on one's judgement concerning what is a reasonably good mesh, which is often dictated by the geometry and qualitative understanding of the variations of the solution and its gradient. Since most practical problems are approximated in their engineering formulations, one should not be overly concerned with the numerical accuracy of the solution. A feel for the relative proportions and directions of various errors introduced into the analysis helps the finite element practitioner to make a decision on when to stop refining a mesh. In summary, scientific (or engineering) knowledge and experience with a given class of problems is an essential part of any approximate analysis.

8.3.2 Generation of Finite Element Data

An important part of finite element modeling is mesh generation, which involves numbering the nodes and elements, and the generation of nodal coordinates and the connectivity matrix. While the task of generating such data is quite simple, the type of the data has an effect on the computational efficiency as well as on accuracy. More specifically, the numbering of the nodes directly affects the bandwidth of the final assembled equations, which in turn increases the storage requirement and computational cost if equation solvers with the Gauss elimination procedure are used. The elements can be numbered arbitrarily, because this has no effect on the half-bandwidth. In a general-purpose program with a preprocessor, options to minimize the bandwidth are included. The saving of computational cost due to a smaller bandwidth in the solution of equations can be substantial, especially in problems where a large number of nodes and degrees of freedom per node are involved. While element numbering does not affect the half-bandwidth, it may affect the computer time required to assemble the global coefficient matrix—usually, a very small percentage of the time required to solve the equations.

The accuracy of the finite element solution can also depend on the choice of the finite element mesh. For instance, if the selected mesh violates the symmetry of the problem, the resulting solution will be less accurate than one obtained using a mesh that agrees with the physical symmetry of the problem. Geometrically, a triangular element has fewer (or no) lines of symmetry compared with a rectangular element, and therefore one should use meshes of triangular elements with care (e.g., one should select a mesh that does not violate the mathematical symmetry present in the problem).

The effect of the finite element meshes shown in Fig. 8.18 on the solution of the Poisson equation in Example 8.3 is investigated. The finite element solutions obtained by the three meshes are compared with the series solution in Table 8.3. Clearly, the solution obtained using mesh 3 is less accurate. This is to be expected, because mesh 3 is symmetric about the diagonal line connecting node 3 to node 7, whereas the mathematical symmetry is about the diagonal line connecting node 1 to node 9 (see Fig. 8.18). Mesh 1 is the most

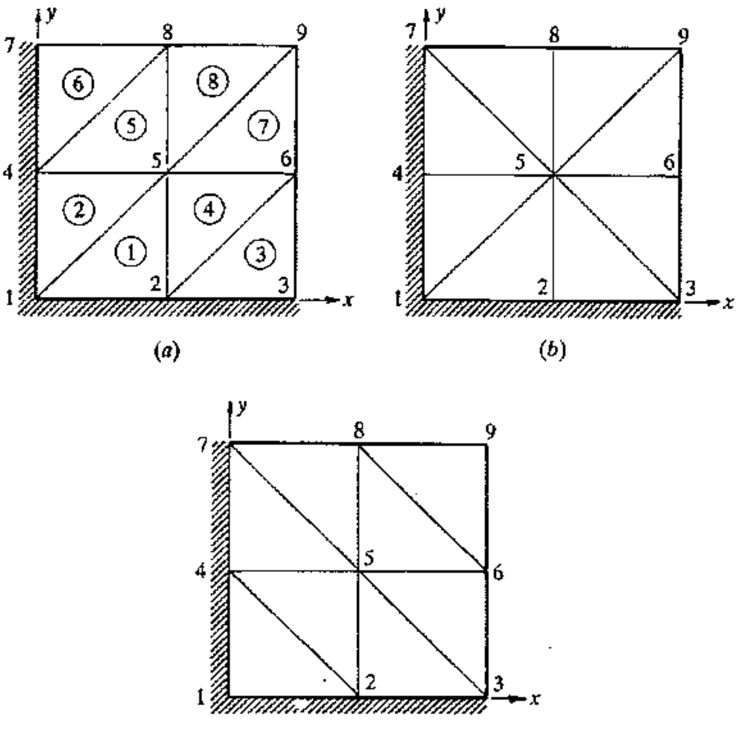

(a)

(b)

(c)

FIGURE 8.18
Various types of triangular-element meshes for the domain of Example 8.3: (a) mesh 1; (b) mesh 2; (c) mesh 3.

TABLE 8.3
Comparison of the finite element solutions obtained using various linear triangular-element meshes† with the series solution of the problem in Example 8.3

Node	Finite element solution			Series solution
	Mesh 1	Mesh 2	Mesh 3	
1	0.31250	0.29167	0.25000	0.29469
2	0.22917	0.20833	0.20833	0.22934
4	0.22917	0.20833	0.20833	0.22934
5	0.17708	0.18750	0.16667	0.18114

† See Fig. 8.18 for the finite element meshes.

desirable of the three, because it does not violate the mathematical symmetry of the problem.

Next, the effect of mesh refinement with rectangular elements is investigated. Four different meshes of rectangular elements are shown in Fig. 8.19. Each mesh contains the previous mesh as a subset. The mesh shown in Fig. 8.19(*c*) is nonuniform; it is obtained by subdividing the first two rows and columns of elements of the mesh shown in Fig. 8.19(*b*). The finite element solutions obtained by these meshes are compared in Table 8.4. The numerical

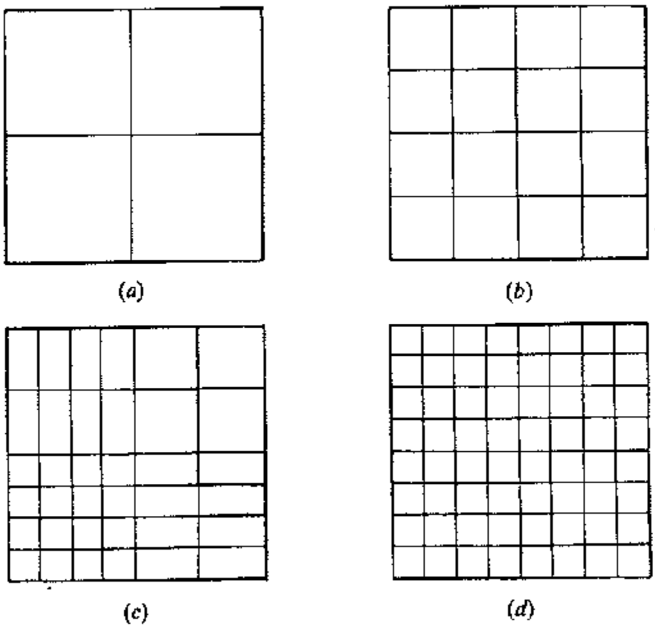

FIGURE 8.19
Mesh refinement; the meshes in (*a*), (*b*), and (*d*) are uniform; the mesh in (*c*) is nonuniform: (*a*) 2 × 2 mesh; (*b*) 4 × 4 mesh; (*c*) 6 × 6 mesh; (*d*) 8 × 8 mesh.

TABLE 8.4
Convergence of the finite element solution (with mesh refinement†) of the problem in Example 8.3

Location		Finite element solution				Series solution
x	y	2×2	4×4	6×6	8×8	
0.0	0.0	0.31071	0.29839	0.29641	0.29560	0.29469
0.125	0.0	—	—	0.29248	0.29167	0.29077
0.250	0.0	—	0.28239	0.28055	0.27975	0.27888
0.375	0.0	—	—	0.26022	0.24943	0.25863
0.50	0.0	0.24107	0.23220	0.23081	0.23005	0.22934
0.625	0.0	—	—	—	0.19067	0.19009
0.750	0.0	—	0.14137	0.14064	0.14014	0.13973
0.875	0.0	—	—	—	0.07709	0.07687
0.125	0.125	—	—	0.28862	0.28781	0.28692
0.250	0.250	—	0.26752	0.26580	0.26498	0.26415
0.375	0.375	—	—	0.22960	0.22873	0.22799
0.50	0.50	0.19286	0.18381	0.18282	0.18179	0.18114
0.625	0.625	—	—	—	0.12813	0.12757
0.750	0.750	—	0.07506	0.07481	0.07332	0.07282
0.875	0.875	—	—	—	0.02561	0.02510

† See Fig. 8.19 for the finite-element meshes.

convergence of the finite element solution of the refined meshes to the series solution is apparent from the results presented.

8.3.3 Imposition of Boundary Conditions

In most problems of interest, one encounters situations where the portion of the boundary on which natural boundary conditions are specified has points in common with the portion of the boundary on which the essential boundary conditions are specified. In other words, at a few nodal points of the mesh, both the primary and secondary degrees of freedom may be specified. Such points are called *singular points*. Obviously, one cannot impose boundary conditions on both the primary and secondary variables at the same point. As a general rule, one should impose the essential boundary condition (i.e., the boundary condition on the primary variables) at the singular points and disregard the natural boundary condition (i.e., the boundary condition on the secondary variables), because the essential boundary conditions are often maintained more strictly than the natural ones. Of course, if the true situation in a problem is that the natural boundary conditions are imposed and the essential boundary conditions are a result of this then consideration must be given to the former.

Another type of singularity that one encounters in the solution of boundary value problems is the specification of two different values of a primary variable at the same boundary point. An example of such a case is provided by the problem in Fig. 8.20, where u is specified to be zero on the

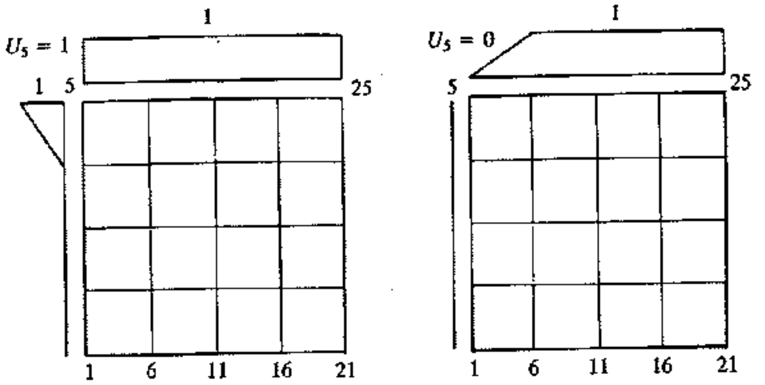

(*a*) 4 × 4 mesh (mesh 1) (*b*)

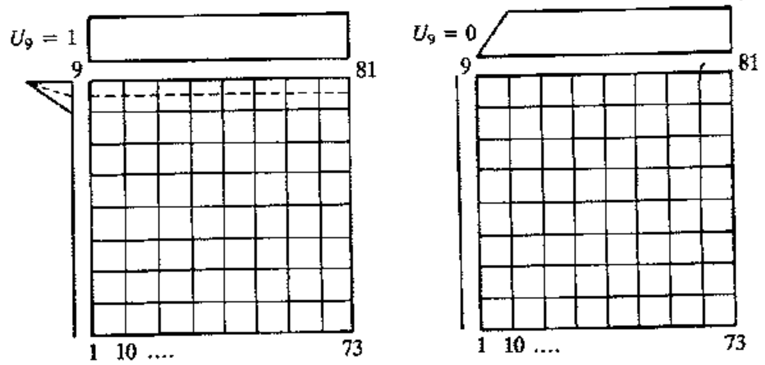

(*c*) 8 × 8 mesh (mesh 2) (*d*)

FIGURE 8.20
Effect of specifying (either of the) two values of a primary variable at a boundary node [node 5 in (*a*) and (*b*) and node 9 in (*c*) and (*d*)].

boundary defined by the line $x = 0$ (for any y), and to be unity on the boundary defined by the line $y = 1$ (for any x). Consequently, at $x = 0$ and $y = 1$, u has two different values. In the finite element analysis, one must make a choice between the two values, or a weighted average of the two values can be used. When a choice is made between two values, often the larger one is imposed. In any case, the true boundary condition is replaced by an approximate condition. The closeness of the approximate boundary condition to the true one depends on the size of the element containing the point (see Fig. 8.20). A mesh refinement in the vicinity of the singular point often yields an acceptable solution.

8.4 APPLICATIONS

8.4.1 Heat Transfer

In Chapter 3, Section 3.3.1, heat transfer (by conduction and convection) in one-dimensional (axial and radially symmetric) systems was considered. Here we consider heat transfer in two-dimensional plane and axisymmetric systems. The derivation of two-dimensional heat transfer equations in plane and axisymmetric geometries follows the same procedure as in one dimension, but considers heat transfer in the two directions. Details of such derivations can be found in textbooks on heat transfer (see the references at the end of the chapter). Here we record the governing equations for various cases, construct their finite element models, and present typical applications.

For heat conduction in plane or axisymmetric geometries, the finite element models developed in Sections 8.2 and 8.3 are immediately applicable with the following interpretation of the variables:

$$\begin{aligned}
u = T &\equiv \text{temperature (in °C)}\\
q_n &\equiv \text{negative of heat flux (in W m}^{-2}\,°\text{C}^{-1})\\
a_{11}, a_{22} &\equiv \text{conductivities (in W m}^{-1}\,°\text{C}^{-1}) \text{ of an orthotropic medium}\\
&\quad\ \text{whose principal material axes coincide with the } (x, y) \text{ axes}\\
f &\equiv \text{internal heat generation (in W m}^{-3}\,°\text{C}^{-1})\\
a_{00} &= 0
\end{aligned} \tag{8.94}$$

For convective heat transfer, i.e., when heat is transferred from one medium to the surrounding medium (often a fluid) by convection, the finite element model developed earlier requires some modification. This is because, in two-dimensional problems, the convective boundary is a curve as opposed to a point in one-dimensional problems. Therefore, the contributions of the convection (or Newton-type) boundary condition to the coefficient matrix and source vector are to be computed by evaluating boundary integrals involving the interpolation functions of elements with convective boundaries. The model to be presented allows the computation of the additional contributions to the coefficient matrix and source vector whenever the element has the convection boundary condition.

PLANE SYSTEMS. The governing equation for steady-state heat transfer in plane systems is a special case of (8.1), and is given by

$$-\frac{\partial}{\partial x}\left(k_x \frac{\partial T}{\partial x}\right) - \frac{\partial}{\partial y}\left(k_y \frac{\partial T}{\partial y}\right) = f(x, y) \tag{8.95}$$

where T is the temperature (in °C), k_x and k_y are the thermal conductivities (in W m^{-1} °C^{-1}) along the x and y directions, respectively, and f is the internal heat generation per unit volume (in W m^{-3}). For a convective boundary, the natural boundary condition is a balance of energy transfer across the boundary due to conduction and/or convection (i.e., Newton's law of cooling):

$$k_x \frac{\partial T}{\partial x} n_x + k_y \frac{\partial T}{\partial y} n_y + \beta(T - T_\infty) = \hat{q}_n \tag{8.96}$$

where β is the convective conductance (or the convective heat transfer coefficient) (in W m^{-2} °C^{-1}), T_∞ is the (ambient) temperature of the surrounding fluid medium, and $\hat{q}_n$ is the specified heat flow. The first two terms account for heat transfer by conduction, the third for heat transfer by convection, while the term on the right-hand side accounts for the specified heat flux, if any. It is the presence of the term $\beta(T - T_\infty)$ that requires some modification of (8.10).

The weak form of (8.95) can be obtained from (8.8). The boundary integral should be modified to account for the convective heat transfer term in (8.96). Instead of replacing the coefficient of w in the boundary integral by q_n, we use (8.96) ($\hat{q}_n$ is replaced by q_n, which is obtained on the element boundary):

$$
\begin{aligned}
0 &= \int_{\Omega^e} \left(k_x \frac{\partial w}{\partial x}\frac{\partial T}{\partial x} + k_y \frac{\partial w}{\partial y}\frac{\partial T}{\partial y} - wf \right) dx\,dy - \oint_{\Gamma^e} w\left(k_x \frac{\partial T}{\partial x} n_x + k_y \frac{\partial T}{\partial y} n_y \right) ds \\
&= \int_{\Omega^e} \left(k_x \frac{\partial w}{\partial x}\frac{\partial T}{\partial x} + k_y \frac{\partial w}{\partial y}\frac{\partial T}{\partial y} - wf \right) dx\,dy - \oint_{\Gamma^e} w[q_n - \beta(T - T_\infty)]\, ds \\
&= B(w, T) - l(w) \qquad (8.97a)
\end{aligned}
$$

where w is the weight function, and $B(\cdot, \cdot)$ and $l(\cdot)$ are the bilinear and linear forms

$$
\begin{aligned}
B(w, T) &= \int_{\Omega^e} \left(k_x \frac{\partial w}{\partial x}\frac{\partial T}{\partial x} + k_y \frac{\partial w}{\partial y}\frac{\partial T}{\partial y} \right) dx\,dy + \oint_{\Gamma^e} \beta w T\, ds \\
l(w) &= \int_{\Omega^e} wf\, dx\,dy + \oint_{\Gamma^e} \beta w T_\infty\, ds + \oint_{\Gamma^e} w q_n\, ds
\end{aligned}
\qquad (8.97b)
$$

The finite element model of (8.58) is obtained by substituting the finite element approximation of the form

$$
T = \sum_{j=1}^{n} T_j^e \psi_j^e(x, y) \qquad (8.98)
$$

for T and ψ_i^e for w into (8.97):

$$
\boxed{\sum_{j=1}^{n} (K_{ij}^e + H_{ij}^e) T_j^e = F_i^e + P_i^e} \qquad (8.99a)
$$

where

$$
\boxed{
\begin{aligned}
K_{ij}^e &= \int_{\Omega^e} \left(k_x \frac{\partial \psi_i}{\partial x}\frac{\partial \psi_j}{\partial x} + k_y \frac{\partial \psi_i}{\partial y}\frac{\partial \psi_j}{\partial y} \right) dx\,dy \\
F_i^e &= \int_{\Omega^e} f\psi_i\, dx\,dy + \oint_{\Gamma^e} q_n^e \psi_i\, ds \equiv f_i^e + Q_i^e \\
H_{ij}^e &= \beta^e \oint_{\Gamma^e} \psi_i \psi_j\, ds, \qquad P_i^e = \beta^e \oint_{\Gamma^e} \psi_i T_\infty\, ds
\end{aligned}
} \qquad (8.99b)
$$

Note that by setting the heat transfer coefficient β equal to zero, we obtain the heat conduction model with no account taken of convection.

The additional coefficients H^e_{ij} and P^e_i due to the convective boundary conditions can be computed by evaluating boundary integrals. These coefficients must be computed only for those elements and boundaries that are subject to the convective boundary condition. The computation of the coefficients for the linear triangular and rectangular elements is presented in the following paragraphs. The coefficients H^e_{ij} and P^e_i for a linear triangular element are defined by

$$\begin{aligned} H^e_{ij} &= \beta^e_{12}\int_0^{h^e_{12}} \psi^e_i\psi^e_j\,ds + \beta^e_{23}\int_0^{h^e_{23}} \psi^e_i\psi^e_j\,ds + \beta^e_{31}\int_0^{h^e_{31}} \psi^e_i\psi^e_j\,ds \\ P^e_i &= \beta^e_{12}T^{12}_\infty\int_0^{h^e_{12}} \psi^e_i\,ds + \beta^e_{23}T^{23}_\infty\int_0^{h^e_{23}} \psi^e_i\,ds + \beta^e_{31}T^{31}_\infty\int_0^{h^e_{31}} \psi^e_i\,ds \end{aligned} \tag{8.100}$$

where β^e_{ij} is the film coefficient (assumed to be constant) for the side connecting nodes i and j of the element Ω^e, T^{ij}_∞ is the ambient temperature on that side, and h^e_{ij} is the length of the side. For a rectangular element, the expressions in (8.100) must be modified to account for four line integrals on four sides of the element.

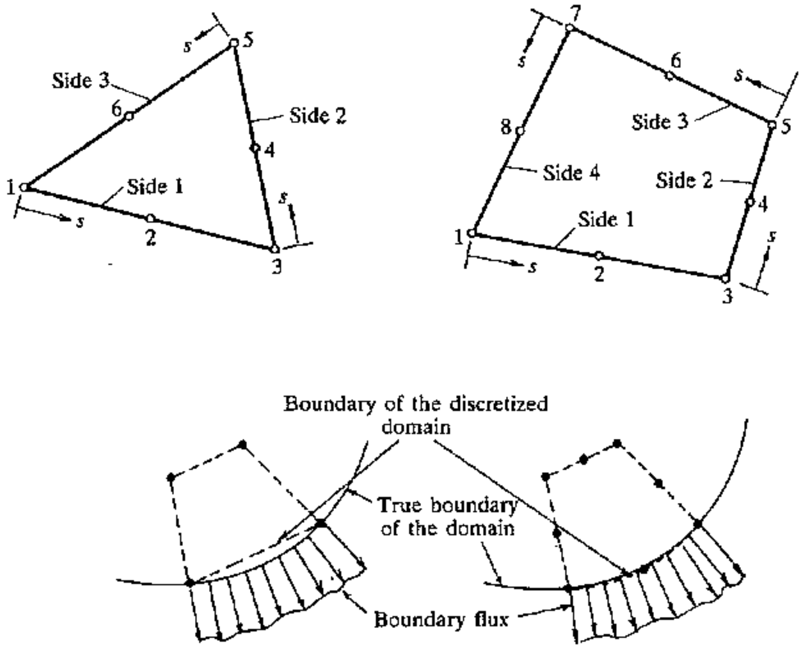

FIGURE 8.21
Triangular and quadrilateral elements, with node numbers and local coordinates for the evaluation of the boundary integrals. Also shown are the boundary approximation and flux representation using linear and quadratic elements.

The boundary integrals are line integrals involving the interpolation functions. The local coordinate s is taken along the side, with its origin at the first node of the side (see Fig. 8.21). As noted earlier, the interpolation functions on any given side are the one-dimensional interpolation functions. Therefore, the evaluation of integrals is made easy. Indeed, the integrals

$$\int_0^{h_{ij}^e} \psi_i^e \psi_j^e \, ds, \qquad \int_0^{h_{ij}^e} \psi_i^e \, ds$$

have been evaluated in Chapter 3 in connection with mass matrix coefficients and source vector coefficients for linear and quadratic elements. We summarize the results here.

For a linear triangular element, the matrices $[H^e]$ and $\{P^e\}$ are given by

$$[H^e] = \frac{\beta_{12}^e h_{12}^e}{6} \begin{bmatrix} 2 & 1 & 0 \\ 1 & 2 & 0 \\ 0 & 0 & 0 \end{bmatrix} + \frac{\beta_{23}^e h_{23}^e}{6} \begin{bmatrix} 0 & 0 & 0 \\ 0 & 2 & 1 \\ 0 & 1 & 2 \end{bmatrix} + \frac{\beta_{31}^e h_{31}^e}{6} \begin{bmatrix} 2 & 0 & 1 \\ 0 & 0 & 0 \\ 1 & 0 & 2 \end{bmatrix} \tag{8.101a}$$

$$\{P^e\} = \frac{\beta_{12}^e T_\infty^{12} h_{12}^e}{2} \begin{Bmatrix} 1 \\ 1 \\ 0 \end{Bmatrix} + \frac{\beta_{23}^e T_\infty^{23} h_{23}^e}{2} \begin{Bmatrix} 0 \\ 1 \\ 1 \end{Bmatrix} + \frac{\beta_{31}^e T_\infty^{31} h_{31}^e}{2} \begin{Bmatrix} 1 \\ 0 \\ 1 \end{Bmatrix} \tag{8.101b}$$

For a quadratic triangular element, we have

$$[H^e] = \frac{\beta_{13}^e h_{13}^e}{30} \begin{bmatrix} 4 & 2 & -1 & 0 & 0 & 0 \\ 2 & 16 & 2 & 0 & 0 & 0 \\ -1 & 2 & 4 & 0 & 0 & 0 \\ 0 & 0 & 0 & 0 & 0 & 0 \\ 0 & 0 & 0 & 0 & 0 & 0 \\ 0 & 0 & 0 & 0 & 0 & 0 \end{bmatrix} + \frac{\beta_{35}^e h_{35}^e}{30} \begin{bmatrix} 0 & 0 & 0 & 0 & 0 & 0 \\ 0 & 0 & 0 & 0 & 0 & 0 \\ 0 & 0 & 4 & 2 & -1 & 0 \\ 0 & 0 & 2 & 16 & 2 & 0 \\ 0 & 0 & -1 & 2 & 4 & 0 \\ 0 & 0 & 0 & 0 & 0 & 0 \end{bmatrix}$$

$$+ \frac{\beta_{51} h_{51}^e}{30} \begin{bmatrix} 4 & 0 & 0 & 0 & -1 & 2 \\ 0 & 0 & 0 & 0 & 0 & 0 \\ 0 & 0 & 0 & 0 & 0 & 0 \\ 0 & 0 & 0 & 0 & 0 & 0 \\ -1 & 0 & 0 & 0 & 4 & 2 \\ 2 & 0 & 0 & 0 & 2 & 16 \end{bmatrix} \tag{8.102a}$$

$$\{P^e\} = \frac{\beta_{13}^e T_\infty^{13} h_{13}^e}{6} \begin{Bmatrix} 1 \\ 4 \\ 1 \\ 0 \\ 0 \\ 0 \end{Bmatrix} + \frac{\beta_{35}^e T_\infty^{35} h_{35}^e}{6} \begin{Bmatrix} 0 \\ 0 \\ 1 \\ 4 \\ 1 \\ 0 \end{Bmatrix} + \frac{\beta_{51}^e T_\infty^{51} h_{51}^e}{6} \begin{Bmatrix} 1 \\ 0 \\ 0 \\ 0 \\ 1 \\ 4 \end{Bmatrix} \tag{8.102b}$$

For a linear rectangular element, the matrix $[H^e]$ is of the form

$$[H^e]=\frac{\beta_{12}^e h_{12}^e}{6}\begin{bmatrix}2&1&0&0\\1&2&0&0\\0&0&0&0\\0&0&0&0\end{bmatrix}+\frac{\beta_{23}^e h_{23}^e}{6}\begin{bmatrix}0&0&0&0\\0&2&1&0\\0&1&2&0\\0&0&0&0\end{bmatrix}$$

$$+\frac{\beta_{34}^e h_{34}^e}{6}\begin{bmatrix}0&0&0&0\\0&0&0&0\\0&0&2&1\\0&0&1&2\end{bmatrix}+\frac{\beta_{41}^e h_{41}^e}{6}\begin{bmatrix}2&0&0&1\\0&0&0&0\\0&0&0&0\\1&0&0&2\end{bmatrix} \tag{8.103a}$$

and $\{P^e\}$ is given by

$$\{P^e\}=\frac{\beta_{12}^e T_\infty^{12} h_{12}^e}{2}\begin{Bmatrix}1\\1\\0\\0\end{Bmatrix}+\frac{\beta_{23}^e T_\infty^{23} h_{23}^e}{2}\begin{Bmatrix}0\\1\\1\\0\end{Bmatrix}+\frac{\beta_{34}^e T_\infty^{34} h_{34}^e}{2}\begin{Bmatrix}0\\0\\1\\1\end{Bmatrix}+\frac{\beta_{41}^e T_\infty^{41} h_{41}^e}{2}\begin{Bmatrix}1\\0\\0\\1\end{Bmatrix} \tag{8.103b}$$

Similar expressions hold for a quadratic rectangular element.

AXISYMMETRIC SYSTEMS. For symmetric heat transfer about the z axis (i.e., independent of the circumferential coordinate), the governing equation is given by

$$-\left[\frac{1}{r}\frac{\partial}{\partial r}\left(rk_r\frac{\partial T}{\partial r}\right)+\frac{\partial}{\partial z}\left(k_z\frac{\partial T}{\partial z}\right)\right]=f(r,z) \tag{8.104}$$

where r is the radial coordinate and z is the axial coordinate. The temperature gradient vector is defined by

$$\mathbf{q}=r\left(k_r\frac{\partial T}{\partial r}\hat{\mathbf{i}}+k_z\frac{\partial T}{\partial z}\hat{\mathbf{j}}\right)$$

and the normal derivative of T (i.e., the negative of the heat flux) across the surface is

$$q_n=r\left(k_r\frac{\partial T}{\partial r}n_r+k_z\frac{\partial T}{\partial z}n_z\right) \tag{8.105}$$

where n_r and n_z are the direction cosines of the unit normal $\hat{\mathbf{n}}$,

$$\hat{\mathbf{n}}=n_r\hat{\mathbf{i}}+n_z\hat{\mathbf{j}}$$

The weak form of (8.104) is given by

$$\begin{aligned}0&=2\pi\int_{\Omega^e}w\left\{-\left[\frac{1}{r}\frac{\partial}{\partial r}\left(k_r r\frac{\partial T}{\partial r}\right)+\frac{\partial}{\partial z}\left(k_z\frac{\partial T}{\partial z}\right)\right]-f\right\}r\,dr\,dz\\&=2\pi\int_{\Omega^e}\left(k_r\frac{\partial w}{\partial r}\frac{\partial T}{\partial r}+k_z\frac{\partial w}{\partial z}\frac{\partial T}{\partial z}-wf\right)r\,dr\,dz-2\pi\oint_{\Gamma^e}wq_n\,ds\end{aligned} \tag{8.106}$$

where the factors of 2π come from the integration with respect to the circumferential coordinate over $(0, 2\pi)$, and q_n is given by (8.105). The convective boundary condition is of the form

$$q_n + r\beta(T - T_\infty) = \hat{q}_n$$

Substituting for $q_n = -r\beta(T - T_\infty) + \hat{q}_n$ in (8.106), we obtain

$$0 = 2\pi \int_{\Omega^e} \left(k_r \frac{\partial w}{\partial r}\frac{\partial T}{\partial r} + k_z \frac{\partial w}{\partial z}\frac{\partial T}{\partial z} - wf \right) r\, dr\, dz - 2\pi \oint_{\Gamma^e} w[-r\beta(T - T_\infty) + \hat{q}_n]\, ds \tag{8.107}$$

The finite element model of this equation is

$$[K^e + H^e]\{T^e\} = \{f^e\} + \{P^e\} + \{Q^e\} \tag{8.108a}$$

where

$$K_{ij}^e = 2\pi \int_{\Omega^e} \left(k_r \frac{\partial \psi_i^e}{\partial r}\frac{\partial \psi_j^e}{\partial r} + k_z \frac{\partial \psi_i^e}{\partial z}\frac{\partial \psi_j^e}{\partial z} \right) r\, dr\, dz$$

$$H_{ij}^e = 2\pi \oint_{\Gamma^e} \beta^e \psi_i^e \psi_j^e r\, ds, \qquad f_i^e = 2\pi \int_{\Omega^e} \psi_i^e f r\, dr\, dz \tag{8.108b}$$

$$Q_i^e = 2\pi \oint_{\Gamma^e} \hat{q}_n \psi_i^e\, ds, \qquad P_i^e = 2\pi \oint_{\Gamma^e} \beta^e T_\infty^e \psi_i^e r\, ds$$

Evaluation of the line integrals in $[H^e]$ and $\{P^e\}$ once again follows along the lines of Example 8.3.

The finite element models in (8.99) and (8.108) are valid for conductive and convective heat transfer boundary conditions. Radiative heat transfer boundary conditions are nonlinear, and therefore are not considered here. For problems with no convective boundary conditions, the convective contributions $[H^e]$ and $\{P^e\}$ to the element coefficients are omitted. Indeed, these contributions have to be included only for those elements whose sides fall on the problem boundary with convective heat transfer specified. For example, if side 2–3 of the element Ω^e is on the boundary with convective boundary conditions then the only contribution to $[H^e]$ and $\{P^e\}$ comes from the second integrals in (8.100).

Next we consider a couple of examples of heat transfer.

Example 8.4. Consider steady-state heat conduction in an isotropic rectangular region of dimensions $3a$ by $2a$ (see Fig. 8.22a). The origin of the x and y coordinates is taken at the lower left corner such that x is parallel to the side $3a$ and y is parallel to the side $2a$. The boundaries $x = 0$ and $y = 0$ are insulated, the boundary $x = 3a$ is maintained at zero temperature, and the boundary $y = 2a$ is maintained at a temperature $T = T_0 \cos(\pi x/6a)$. We wish to determine the temperature distribution using the finite element method in the region and the heat required at the boundary $x = 3a$ to maintain it at zero temperature.

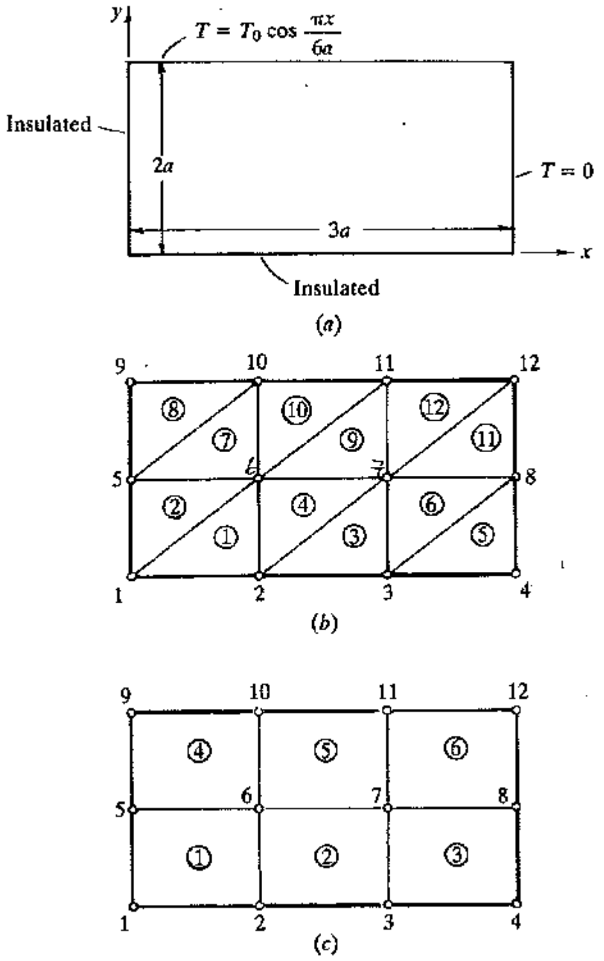

FIGURE 8.22
Finite element analysis of a heat conduction problem over a rectangular domain: (*a*) domain; (*b*) mesh of linear triangular elements; (*c*) mesh of linear rectangular elements.

To analyze the problem, we first note that it is governed by (8.95) with zero internal heat generation, $f = 0$, and no-convection boundary conditions:

$$-k\nabla^2 T = 0 \tag{8.109}$$

Hence, the finite element model of the problem is given by (8.99) with $[H^e]$ and $\{P^e\}$ omitted:

$$[K^e]\{u^e\} = \{Q^e\} \qquad (\{f^e\} = \{0\}) \tag{8.110a}$$

where u_i^e is the temperature at node i of the element Ω^e, and

$$K_{ij}^e = \int_{\Omega^e} k\left(\frac{\partial\psi_i}{\partial x}\frac{\partial\psi_j}{\partial x} + \frac{\partial\psi_i}{\partial y}\frac{\partial\psi_j}{\partial y}\right) dx\,dy, \qquad Q_i^e = \oint_{\Gamma^e} q_n \psi_i\, ds \tag{8.110b}$$

Suppose that we use a 3 × 2 mesh (i.e., 3 subdivisions along the x axis and 2 along the y axis) of linear triangular elements and then a 3 × 2 mesh of linear rectangular elements. Both meshes have the same number of global nodes (12) but differing numbers of elements.

Triangular element mesh (12 elements). The global node numbers, element numbers, and element node numbers used are shown in Fig. 8.22(b). Of course, the global node numbering and element numbering are arbitrary (they do not have to follow any particular pattern), although the global node numbering dictates the size of the half-bandwidth of the assembled equations, which in turn affects the computational time of Gauss elimination methods used in the solution of algebraic equations on a computer. The element node numbering scheme should be that used in the development of element interpolation functions. In the present study, a counter-clockwise numbering system was adopted [see (8.19) and Fig. 8.4]. According to the element node numbering scheme used in Fig. 8.22(a), all elements in the mesh fall into one of two geometric shapes: one with its base at the bottom of the element and another with its base at the top of the element. By renumbering the element nodes, as shown in Fig. 8.12(b), all elements can be made to have a common geometric shape, and thus the element coefficients need to be computed only for a single element. Such considerations are important only when hand calculations are carried out.

For a typical element of the mesh of triangles in Fig. 8.22(b), the element coefficient matrix is [see (8.69a) and (8.70)]

$$[K^e] = \frac{k}{2}\begin{bmatrix} 1 & -1 & 0 \\ -1 & 2 & -1 \\ 0 & -1 & 1 \end{bmatrix}$$

where k is the conductivity of the medium. Note that the element matrix is independent of the size of the element, as long as the latter is a right-angled triangle with base equal to height.

The assembly of the elements (on a computer) follows the logic discussed earlier. The boundary conditions require that

$$\begin{aligned} &U_4 = U_8 = U_{12} = 0, \quad U_9 = T_0, \quad U_{10} = \tfrac{1}{2}\sqrt{3}\,T_0, \quad U_{11} = \tfrac{1}{2}T_0 \\ &F_1 = F_2 = F_3 = F_5 = 0 \quad \text{(zero heat flow due to insulated boundary)} \end{aligned} \tag{8.111}$$

We first write the six finite element equations for the six unknown primary variables. These equations come from nodes 1, 2, 3, 5, 6, and 7:

$$\frac{k}{2}\begin{bmatrix} 2 & -1 & 0 & -1 & 0 & 0 \\ -1 & 4 & -1 & 0 & -2 & 0 \\ 0 & -1 & 4 & 0 & 0 & -2 \\ -1 & 0 & 0 & 4 & -2 & 0 \\ 0 & -2 & 0 & -2 & 8 & -2 \\ 0 & 0 & -2 & 0 & -2 & 8 \end{bmatrix}\begin{Bmatrix} U_1 \\ U_2 \\ U_3 \\ U_5 \\ U_6 \\ U_7 \end{Bmatrix} = \frac{k}{2}\begin{Bmatrix} 0 \\ 0 \\ 0 \\ T_0 \\ \sqrt{3}\,T_0 \\ T_0 \end{Bmatrix} \tag{8.112}$$

The solution of these equations is (in °C)

$$\begin{aligned} &U_1 = 0.6362T_0, \quad U_2 = 0.5510T_0, \quad U_3 = 0.3181T_0 \\ &U_5 = 0.7214T_0, \quad U_6 = 0.6248T_0, \quad U_7 = 0.3607T_0 \end{aligned} \tag{8.113}$$

The exact solution of (8.109) for the boundary conditions shown in Fig. 8.22(a) is

$$T(x, y) = T_0\frac{\cosh(\pi y/6a)\cos(\pi x/6a)}{\cosh\frac{1}{3}\pi} \tag{8.114a}$$

Evaluating the exact solution at the nodes, we have (in °C)

$$\begin{aligned} T_1 &= 0.6249T_0, \quad & T_2 &= 0.5412T_0, \quad & T_3 &= 0.3124T_0 \\ T_5 &= 0.7125T_0, \quad & T_6 &= 0.6171T_0, \quad & T_7 &= 0.3563T_0 \end{aligned} \tag{8.114b}$$

The heat at node 4, for example, can be compared from the fourth finite element equation:

$$\begin{aligned} F_4 = Q_2^5 = K_{41}U_1 + K_{42}U_2 + K_{43}U_3 + K_{44}U_4 + K_{45}U_5 & \\ + K_{46}U_6 + K_{47}U_7 + K_{48}U_8 + \ldots & \end{aligned} \tag{8.115a}$$

Noting that $K_{41} = K_{42} = K_{45} = \ldots = K_{4(12)} = 0$ and $U_4 = U_8 = 0$, we obtain

$$Q_2^5 = -\tfrac{1}{2}k\, U_3 = -0.1591kT_0 \text{ (in W)} \tag{8.115b}$$

Rectangular element mesh (6 elements). For a 3 × 2 mesh of linear rectangular elements (see Fig. 8.22*c*), the element coefficient matrix is given by (8.34) and (8.44) with $a_{00} = 0$, $a_{11} = a_{22} = k$, $a_{12} = 0$, and $a = b = 1$:

$$[K^e] = \frac{k}{6}\begin{bmatrix} 4 & -1 & -2 & -1 \\ -1 & 4 & -1 & -2 \\ -2 & -1 & 4 & -1 \\ -1 & -2 & -1 & 4 \end{bmatrix}, \quad \{f^e\} = \{0\} \tag{8.116}$$

The present mesh of rectangular elements is node-wise-equivalent to the triangular element mesh considered in Fig. 8.22(*b*). Hence the boundary conditions in (8.111) are valid for the present case. The six finite element equations for the unknowns U_1, U_2, U_3, U_5, U_6, and U_7 have the same form as before.

The equations for the unknown temperatures (i.e., the condensed equations for the unknown primary variables) are given by

$$\frac{k}{6}\begin{bmatrix} 4 & -1 & 0 & -1 & -2 & 0 \\ -1 & 8 & -1 & -2 & -2 & -2 \\ 0 & -1 & 8 & 0 & -2 & -2 \\ -1 & -2 & 0 & 8 & -2 & 0 \\ -2 & -2 & -2 & -2 & 16 & -2 \\ 0 & -2 & -2 & 0 & -2 & 16 \end{bmatrix}\begin{Bmatrix} U_1 \\ U_2 \\ U_3 \\ U_5 \\ U_6 \\ U_7 \end{Bmatrix} = \frac{k}{6}\begin{Bmatrix} 0 \\ 0 \\ 0 \\ T_0 + \sqrt{3}\,T_0 \\ 2T_0 + \sqrt{3}\,T_0 + T_0 \\ \sqrt{3}\,T_0 + T_0 \end{Bmatrix} \tag{8.117}$$

Their solution is

$$\begin{aligned} U_1 &= 0.6128T_0, \quad & U_2 &= 0.5307T_0, \quad & U_3 &= 0.3064T_0 \\ U_5 &= 0.7030T_0, \quad & U_6 &= 0.6088T_0, \quad & U_7 &= 0.3515T_0 \end{aligned} \tag{8.118}$$

The value of the heat at node 4 is given by

$$Q_2^3 = K_{43}U_3 + K_{47}U_7 = -\frac{k}{6}U_3 - \frac{2k}{6}U_7 = -0.1682kT_0 \text{ (in W)}$$

We note that the results obtained using the 3 × 2 mesh of rectangular elements is not as accurate as that obtained with 3 × 2 mesh of triangular elements. This is due to the fact that there are only half as many elements in the former case as in the latter.

Table 8.5 gives a comparison of the finite element solutions with the analytical solution (8.114*a*) for two different meshes of linear triangular and rectangular elements, and Fig. 8.23 shows plots of $T(x, 0)$ and $q_x(x, 0)/T_0$, computed using various meshes of

TABLE 8.5
Comparison of the nodal temperatures $T(x, y)/T_0$, obtained using various finite element meshes,† with the analytical solution of (8.109) (Example 8.4)

		Triangles		Rectangles		Analytical solution
x	y	3×2	6×4	3×2	6×4	(8.114a)
0.0	0.0	0.6362	0.6278	0.6128	0.6219	0.6249
0.5	0.0	—	0.6064	—	0.6007	0.6036
1.0	0.0	0.5510	0.5437	0.5307	0.5386	0.5412
1.5	0.0	—	0.4439	—	0.4398	0.4419
2.0	0.0	0.3181	0.3139	0.3064	0.3110	0.3124
2.5	0.0	—	0.1625	—	0.1610	0.1617
0.0	1.0	0.7214	0.7148	0.7030	0.7102	0.7125
0.5	1.0	—	0.6904	—	0.6860	0.6882
1.0	1.0	0.6248	0.6190	0.6088	0.6150	0.6171
1.5	1.0	—	0.5054	—	0.5022	0.5038
2.0	1.0	0.3607	0.3574	0.3515	0.3551	0.3563
2.5	1.0	—	0.1850	—	0.1838	0.1844

† See Fig. 8.22 for the geometry and meshes.

triangular and rectangular elements. Note that Q_i^e are heats (in W) whereas q_x is the flux (in W m^{-1}) in the x direction ($q_x = -k\,\partial T/\partial x$).

Next we consider an example involving convective heat transfer.

Example 8.5. Consider heat transfer in a rectangular region of dimensions a by b, subject to the boundary conditions shown in Fig. 8.24. We wish to write the finite element algebraic equations for the unknown nodal temperatures and heats. For illustrative purposes, a 4 × 2 mesh of rectangular elements is chosen. We assume that the medium is orthotropic, with conductivities k_x and k_y in the x and y directions, respectively. It is assumed that there is no internal heat generation.

The heat transfer in the region is governed by the equation

$$-\frac{\partial}{\partial x}\left(k_x\frac{\partial T}{\partial x}\right)-\frac{\partial}{\partial y}\left(k_y\frac{\partial T}{\partial y}\right)=0$$

The finite element model of the equation is given by

$$[K^e + H^e]\{u^e\} = \{Q^e\} + \{P^e\} \qquad (\{f^e\} = \{0\}) \tag{8.119}$$

where u_i^e denotes the temperature at node i of the element Ω^e.

The element matrices are

$$[K^e]=\frac{k_x r}{6}\begin{bmatrix} 2 & -2 & -1 & 1\\ -2 & 2 & 1 & -1\\ -1 & 1 & 2 & -2\\ 1 & -1 & -2 & 2\end{bmatrix}+\frac{k_y}{6r}\begin{bmatrix} 2 & 1 & -1 & -2\\ 1 & 2 & -2 & -1\\ -1 & -2 & 2 & 1\\ -2 & -1 & 1 & 2\end{bmatrix}$$

$$[H^e]=\frac{\beta_{23}^e h_{23}^e}{6}\begin{bmatrix} 0 & 0 & 0 & 0\\ 0 & 2 & 1 & 0\\ 0 & 1 & 2 & 0\\ 0 & 0 & 0 & 0\end{bmatrix} \qquad (e = 4, 8)$$

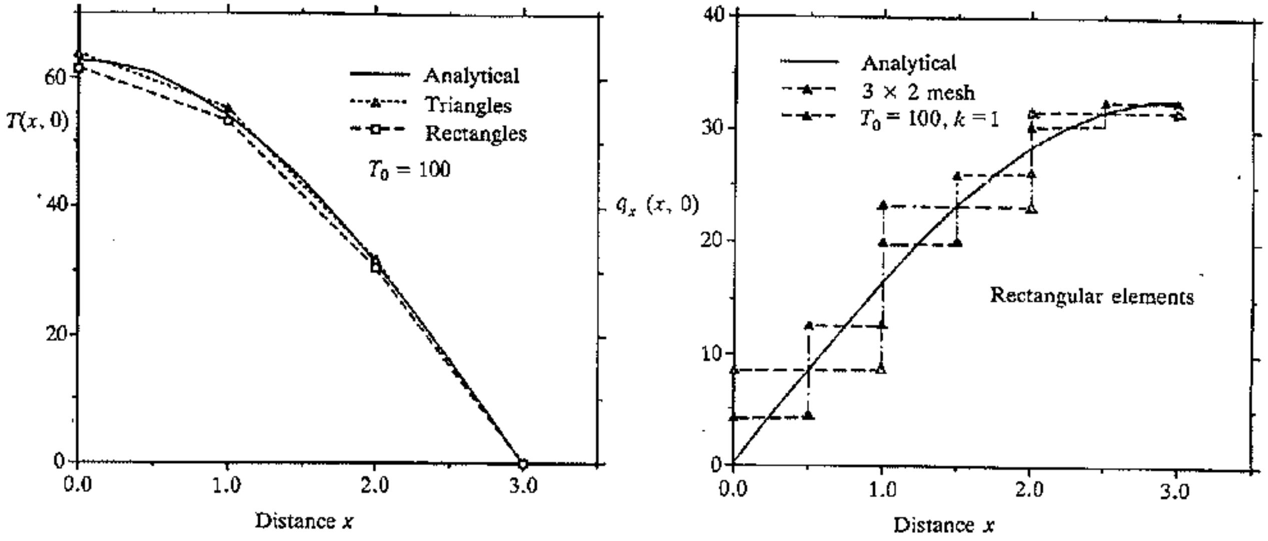

(*a*) (*b*)

FIGURE 8.23
Comparison of the finite element solution with the analytical solution of the heat conduction problem of Example 8.4: (*a*) $T(x, 0)$ versus x; (*b*) $\partial T/\partial x$ versus x.

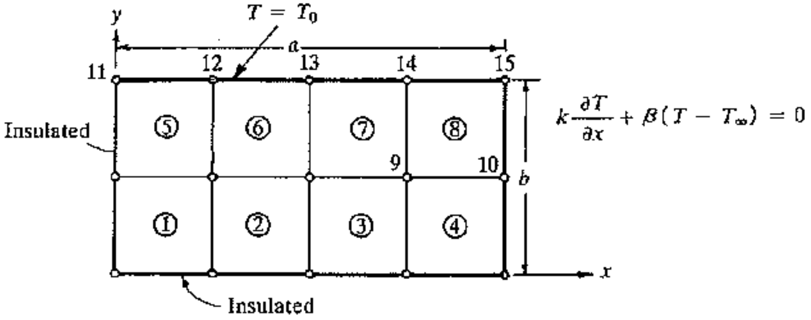

FIGURE 8.24
Domain and boundary conditions for convective heat transfer in a rectangular domain. A mesh of linear rectangular elements is also shown (Example 8.5).

$$\{P^e\} = \frac{\beta^e_{23} T^{23}_\infty h^e_{23}}{2} \begin{Bmatrix} 0 \\ 1 \\ 1 \\ 0 \end{Bmatrix} \quad (e = 4, 8) \tag{8.120}$$

where

$$r = \tfrac{1}{2}b/\tfrac{1}{4}a = 2b/a$$

There are 10 nodal temperatures that are to be determined, and heats at all nodes except nodes 7, 8, 9 and 10 are to be computed. To illustrate the procedure, we write algebraic equations for only representative temperatures and heats.

Node 10 (for temperatures)

$$\begin{aligned} K^4_{31}U_4 + (K^4_{32} + H^4_{32})U_5 + (K^4_{43} + K^8_{21})U_9 \\ + (K^4_{33} + H^4_{33} + K^8_{22} + H^8_{22})U_{10} + K^8_{24}U_{14} + (K^8_{23} + H^8_{23})U_{15} \\ = (Q^4_3 + P^4_3) + (Q^8_2 + P^8_2) = P^4_3 + P^8_2 \quad \text{(known)} \end{aligned}$$

Node 14 (for heat Q_{14})

$$Q_{14} \equiv Q^7_3 + Q^8_4 = K^7_{31}U_8 + (K^7_{32} + K^8_{41})U_9 + K^8_{42}U_{10} + K^7_{34}U_{13} + (K^7_{33} + K^8_{44})U_{14} + K^8_{43}U_{15}$$

From the boundary conditions, we know the temperatures at nodes 11–15 (i.e., $U_{11}, U_{12}, \ldots, U_{15}$ are known). Substituting the values of K^e_{ij}, H^e_{ij}, and P^e_i, we obtain explicit form of the algebraic equations. For example, the algebraic equation corresponding to node 10 is

$$\begin{aligned} -\frac{1}{6}\left(k_x r + \frac{k_y}{r}\right)U_4 + \left[\frac{1}{6}\left(k_x r - \frac{2k_y}{r}\right) + \frac{1}{12}\beta b\right]U_5 + \frac{1}{6}\left[\left(-2k_x r + \frac{k_y}{r}\right) + \left(-2k_x r + \frac{k_y}{r}\right)\right]U_9 \\ + \frac{2}{3}\left[\left(k_x r + \frac{k_y}{r}\right) + \frac{\beta b}{2}\right]U_{10} + \frac{1}{6}\left(-k_x r - \frac{k_y}{r}\right)U_{14} + \frac{1}{6}\left[k_x r - \frac{2k_y}{r} + \frac{1}{2}\beta b\right]U_{15} = \tfrac{1}{2}\beta b T_\infty \end{aligned}$$

8.4.2 Fluid Mechanics

Recall from Section 3.3.2 that there are three basic differential equations of fluid motion. They are as follows [see (3.100), (3.103), and (3.108)]:

Conservation of mass

$$\frac{\partial \rho}{\partial t} + \nabla \cdot \rho(\mathbf{v}) = 0 \tag{8.121}$$

Conservation of linear momentum

$$\rho \frac{D\mathbf{v}}{Dt} = \mathbf{f} - \nabla P + \nabla \cdot \boldsymbol{\tau} \tag{8.122}$$

Conservation of energy

$$\rho \frac{De}{Dt} + P(\nabla \cdot \mathbf{v}) = \nabla \cdot (k\, \nabla T) + \Phi \tag{8.123}$$

Here ρ is the density, $\mathbf{v}$ is the velocity vector, $\mathbf{f}$ is the body force vector, P is the pressure, $\boldsymbol{\tau}$ is the viscous stress tensor, e is the internal energy, k is the thermal conductivity, T is the temperature and Φ is the dissipation,

$$\Phi = \nabla \mathbf{v} : \boldsymbol{\tau}$$

The operator D/Dt denotes the material time derivative,

$$\frac{D}{Dt} = \frac{\partial}{\partial t} + \mathbf{v} \cdot \nabla$$

Equations (8.121)–(8.123) are supplemented with constitutive equations.

A fluid is said to be *incompressible* if the volume change is zero,

$$\nabla \cdot \mathbf{v} = 0 \tag{8.124}$$

and it is termed *inviscid* if the viscosity is zero, $\mu = 0$. A flow with negligible angular velocity is called *irrotational,*

$$\nabla \times \mathbf{v} = 0 \tag{8.125}$$

The irrotational flow of an ideal fluid (i.e., ρ = constant and $\mu = 0$) is called a *potential flow.*

For an ideal fluid ($\boldsymbol{\tau} = \mathbf{0}$), the continuity and momentum equations can be written as

$$\nabla \cdot \mathbf{v} = 0 \tag{8.126a}$$

$$\tfrac{1}{2}\rho \nabla(\mathbf{v} \cdot \mathbf{v}) - \rho[\mathbf{v} \times (\nabla \times \mathbf{v})] = -\nabla \hat{P} \tag{8.126b}$$

where $\nabla \hat{P} = \nabla P - \mathbf{f}$. For irrotational flow, the velocity field $\mathbf{v}$ satisfies (8.125).

For two-dimensional irrotational flows, these equations have the forms

$$\frac{\partial u}{\partial x}+\frac{\partial v}{\partial y}=0 \tag{8.126c}$$

$$\tfrac{1}{2}\rho(u^2+v^2)+\hat{P}=\text{constant} \tag{8.126d}$$

$$\frac{\partial u}{\partial y}-\frac{\partial v}{\partial x}=0 \tag{8.126e}$$

Equations (8.132), (8.133) and (8.126*d*) are used to determine u, v, and $\hat{P}$.

The problem of determining u, v, and $\hat{P}$ is simplified by introducing a function $\psi(x, y)$ such that the continuity equation is identically satisfied:

$$\boxed{u=\frac{\partial \psi}{\partial y}, \qquad v=-\frac{\partial \psi}{\partial x}} \tag{8.127}$$

Then the irrotational flow condition in terms of ψ takes the form

$$\boxed{\frac{\partial^2 \psi}{\partial y^2}+\frac{\partial^2 \psi}{\partial x^2}\equiv\nabla^2\psi=0} \tag{8.128}$$

This equation is used to determine ψ, and then the velocities u and v are determined from (8.127) and $\hat{P}$ from (8.126*d*).

The function ψ has the physical significance that lines of constant ψ are lines across which there is no flow, i.e., they are streamlines of the flow. Hence, $\psi(x, y)$ is called the *stream function*.

In cylindrical coordinates, the continuity equation takes the form

$$\frac{\partial u}{\partial r}+\frac{1}{r}\frac{\partial v}{\partial \theta}=0 \tag{8.129}$$

where u and v are the radial and circumferential velocity components. The stream function $\psi(r, \theta)$ is defined by

$$u=\frac{1}{r}\frac{\partial \psi}{\partial \theta}, \qquad v=-\frac{\partial \psi}{\partial r} \tag{8.130}$$

and (8.128) takes the form

$$\nabla^2\psi\equiv\frac{\partial^2 \psi}{\partial r^2}+\frac{1}{r}\frac{\partial \psi}{\partial r}+\frac{1}{r^2}\frac{\partial^2 \psi}{\partial \theta^2}=0 \tag{8.131}$$

There exists an alternative formulation of the potential flow equations (8.126). We introduce the function $\phi(x, y)$, called the *velocity potential*, such that the condition of irrotational flow is identically satisfied:

$$\boxed{u = -\frac{\partial \phi}{\partial x}, \qquad v = -\frac{\partial \phi}{\partial y}} \tag{8.132}$$

Then the continuity equation (8.126c) in terms of the velocity potential takes the form

$$\boxed{-\nabla^2 \phi = 0} \tag{8.133}$$

Comparing (8.127) with (8.132), we note that

$$-\frac{\partial \phi}{\partial x} = \frac{\partial \psi}{\partial y}, \qquad -\frac{\partial \phi}{\partial y} = -\frac{\partial \psi}{\partial x} \tag{8.134}$$

The velocity potential has the physical significance that lines of constant ϕ are lines along which there is no change in velocity. The equipotential lines and streamlines intersect at right-angles.

Although both ψ and ϕ are governed by the Laplace equation, the boundary conditions on them are different in a flow problem, as should be evident from the definitions (8.127) and (8.132). In this section, we consider applications of the finite element method to potential flows, i.e., the solution of (8.128) and (8.133).

We consider two examples of fluid flow. The first deals with a groundwater flow problem and the second with the flow around a cylindrical body. In discussing these problems, emphasis is placed on certain modeling aspects, data generation, and postprocessing of solutions. Evaluation of element matrices and assembly is amply illustrated in previous examples, and will not be discussed, since it takes substantial space to write the assembled equations even for the crude meshes used in these examples.

Example 8.6 Groundwater flow or seepage. The governing differential equation for a homogeneous aquifer (i.e., one where material properties do not vary with position) of unit depth, with flow in the (x, y) plane, is given by

$$\boxed{-\frac{\partial}{\partial x}\left(a_{11}\frac{\partial \phi}{\partial x}\right) - \frac{\partial}{\partial y}\left(a_{22}\frac{\partial \phi}{\partial y}\right) = f} \tag{8.135}$$

where a_{11} and a_{22} are the coefficients of permeability (in m day^{-1}) along the x and y directions, respectively, ϕ is the piezometric head (in m), measured from a reference level (usually the bottom of the aquifer), and f is the rate of pumping (in m^3 day^{-1} m^{-3}). We know from the previous discussions that the natural and essential boundary conditions associated with (8.135) are

Natural

$$a_{11}\frac{\partial \phi}{\partial x}n_x + a_{22}\frac{\partial \phi}{\partial y}n_y = \phi_n \quad \text{on } \Gamma_1 \tag{8.136a}$$

Essential

$$\phi = \phi_0 \quad \text{on } \Gamma_2 \tag{8.136b}$$

where Γ_1 and Γ_2 are the portions of the boundary Γ of Ω such that $\Gamma_1 + \Gamma_2 = \Gamma$.

Here we consider the following specific problem: find the lines of constant potential ϕ (equipotential lines) in a 3000 m × 1500 m rectangular aquifer Ω (see Fig. 8.25) bounded on the long sides by an impermeable material (i.e., $\partial\phi/\partial n = 0$) and on the short sides by a constant head of 200 m ($\phi_0 = 200$ m). In the way of sources, suppose that a river is passing through the aquifer, infiltrating it at a rate of $0.24\,\text{m}^3\,\text{day}^{-1}\,\text{m}^{-2}$, and that two pumps are located at (1000, 670) and (1900, 900), pumping at rates $Q_1 = 1200\,\text{m}^3\,\text{day}^{-1}\,\text{m}^{-1}$ and $Q_2 = 2400\,\text{m}^3\,\text{day}^{-1}\,\text{m}^{-1}$, respectively. Pumping is considered as a negative point source.

A mesh of 64 triangular elements and 45 nodes is used to model the domain (see Fig. 8.26*a*). The river forms the interelement boundary between elements (33, 35, 37, 39) and (26, 28, 30, 32). In the mesh selected, neither pump is located at a node. This is done intentionally for the purpose of illustrating the calculation of the generalized forces due to a point source within an element. If the pumps are located at a node then the rate of pumping Q_0 is input as the specified secondary variable of the node. When a source (or sink) is located at a point other than a node, we must calculate its contribution to the nodes. Similarly, the source components due to the distributed line source (i.e., the river) should be computed.

First, consider the line source. We can view the river as a line source of constant intensity, $0.24\,\text{m}^3\,\text{day}^{-1}\,\text{m}^{-2}$. Since the length of the river is equally divided by nodes 21–25 (into four parts), we can compute the contribution of the infiltration of the river at each of the nodes 21–25 by evaluating the integrals (see Fig. 8.26*b*):

node 25: $\displaystyle\int_0^h (0.24)\psi_1^1\,ds$

node 24: $\displaystyle\int_0^h (0.24)\psi_2^1\,ds + \int_0^h (0.24)\psi_1^2\,ds$

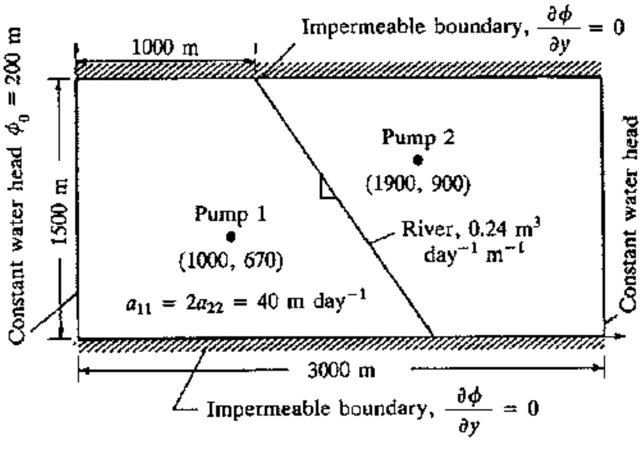
Impermeable boundary, $\dfrac{\partial\phi}{\partial y} = 0$
1000 m
Constant water head $\phi_0 = 200$ m
1500 m
Pump 2
(1900, 900)
Pump 1
(1000, 670)
River, 0.24 m^3 day^{-1} m^{-1}
$a_{11} = 2a_{22} = 40$ m day^{-1}
Constant water head $\phi_0 = 200$ m
3000 m
Impermeable boundary, $\dfrac{\partial\phi}{\partial y} = 0$

FIGURE 8.25
Geometry and boundary conditions for the groundwater flow problem of Example 8.6.

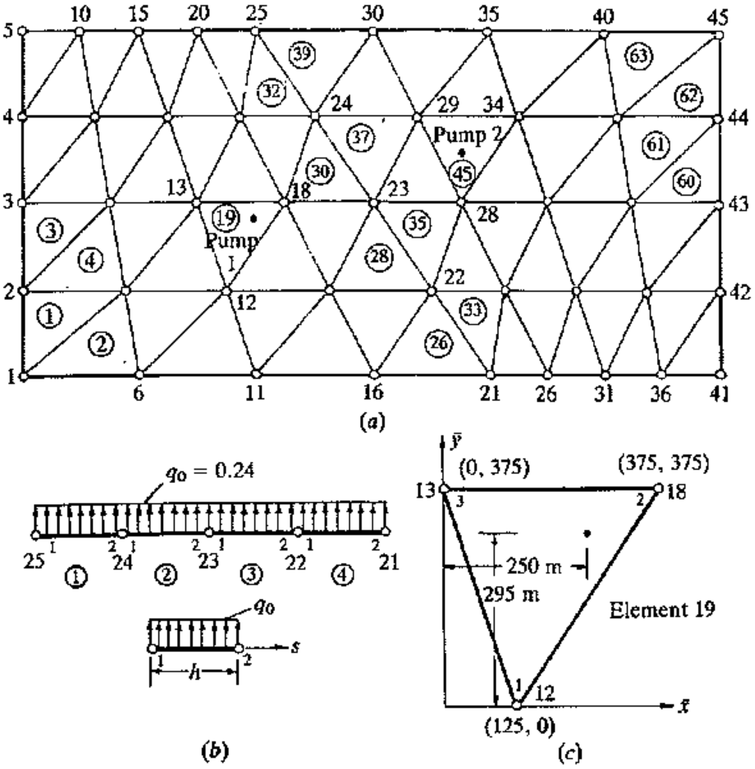

FIGURE 8.26.
Finite element mesh, and computation of force components for the groundwater (seepage) flow: (*a*) finite element mesh of triangular elements (45 nodes and 64 elements); (*b*) computation of global forces due to the infiltration of the river; (*c*) computation of global forces for pump 1, located inside element 19 (Example 8.6).

node 23: $\int_0^h (0.24)\psi_2^2\,ds + \int_0^h (0.24)\psi_1^3\,ds$

node 22: $\int_0^h (0.24)\psi_2^3\,ds + \int_0^h (0.24)\psi_1^4\,ds$

node 21: $\int_0^h (0.24)\psi_2^4\,ds$

For constant intensity q_0 and the linear interpolation functions $\psi_1^e(s) = 1 - s/h$ and $\psi_2^e(s) = s/h$, the contribution of these integrals is well known:

$$\int_0^h q_0\psi_i\,ds = \tfrac{1}{2}q_0h, \qquad h = \tfrac{1}{4}[(1000)^2 + (1500)^2]^{1/2}, \qquad q_0 = 0.24$$

Hence, we have

$$F_{21} = \tfrac{1}{2}q_0h, \qquad F_{22} = F_{23} = F_{24} = q_0h, \qquad F_{25} = \tfrac{1}{2}q_0h.$$

Next, we consider the contribution of the point sources. Since these are located inside an element, we distribute them to the nodes of the element by interpolation (see

Fig. 8.26*c*):

$$\boxed{f_i^e = \int_{\Omega^e} Q_0 \delta(x - x_0, y - y_0)\psi_i^e(x, y)\, dx\, dy = Q_0 \psi_i^e(x_0, y_0)}$$

where the two-dimensional Dirac delta function is defined by

$$\int_{-\infty}^{\infty}\int_{-\infty}^{\infty} F(x, y)\delta(x - x_0, y - y_0)\, dx\, dy = F(x_0, y_0)$$

For example, the source at pump 1 (located at $x_0 = 1000$ m, $y_0 = 670$ m) can be expressed as

$$Q_1(x, y) = -1200\delta(x - 1000, y - 670)$$

The interpolation functions ψ_i^e for element 19 are (in terms of the local coordinates $\bar{x}$ and $\bar{y}$; see Fig. 8.26c)

$$\psi_i(\bar{x}, \bar{y}) = \frac{1}{2A}(\alpha_i + \beta_i \bar{x} + \gamma_i \bar{y})$$

$$A = \tfrac{1}{2}(375)^2, \quad \alpha_1 = (375)^2, \quad \alpha_2 = -375(125), \quad \alpha_3 = 375(125)$$

$$\beta_1 = 0, \quad \beta_2 = 375, \quad \beta_3 = -375, \quad \gamma_1 = -375, \quad \gamma_2 = 125, \quad \gamma_3 = 250$$

We have $\bar{x} = x - 750$ and $\bar{y} = y - 375$, and, therefore,

$$\psi_1(250, 295) = 0.2133, \quad \psi_2 = (250, 295) = 0.5956, \quad \psi_3 = (250, 295) = 0.1911$$

Similar computations can be performed for pump 2.

In summary, the primary variables and nonzero secondary variables are

$$U_1 = U_2 = U_3 = U_4 = U_5 = U_{41} = U_{42} = U_{43} = U_{44} = U_{45} = 200.0$$

$$F_{21} = 54.08, \quad F_{22} = F_{23} = F_{24} = 108.17, \quad F_{25} = 54.08$$

$$F_{12} = -255.6, \quad F_{13} = -229.2, \quad F_{18} = -715.2, \quad F_{28} = -1440.0$$

$$F_{29} = -410.4, \quad F_{34} = -549.6$$

The secondary variables at nodes 6–11, 14–17, 19, 20, 26, 27, 30–33, and 35–40 are zero. This completes the data generation for the problem.

The assembled equations are solved, after imposing the specified boundary conditions, for the values of ϕ at the nodes. The equipotential lines can be determined using (8.92) or a postprocessor. The lines of constant ϕ are shown in Fig. 8.27(*a*) and the velocity vectors in Fig. 8.27(*b*). The greatest drawdown of water occurs at node 28, which has the largest portion of discharge from pump 2.

The solution of the same problem by an alternative mesh that puts pumps 1 and 2 at nodal points is left as an exercise.

Next, we consider an example of irrotational flow of an ideal fluid (i.e., a nonviscous fluid). Examples of physical problems that can be approximated by such flows are provided by flow around bodies such as weirs, airfoils, buildings, and so on, and by flow of water through the earth and dams. The Laplace equations (8.128) and (8.133) governing these flows are special cases of (8.1), and therefore one can use the finite element equations developed earlier to model these problems.

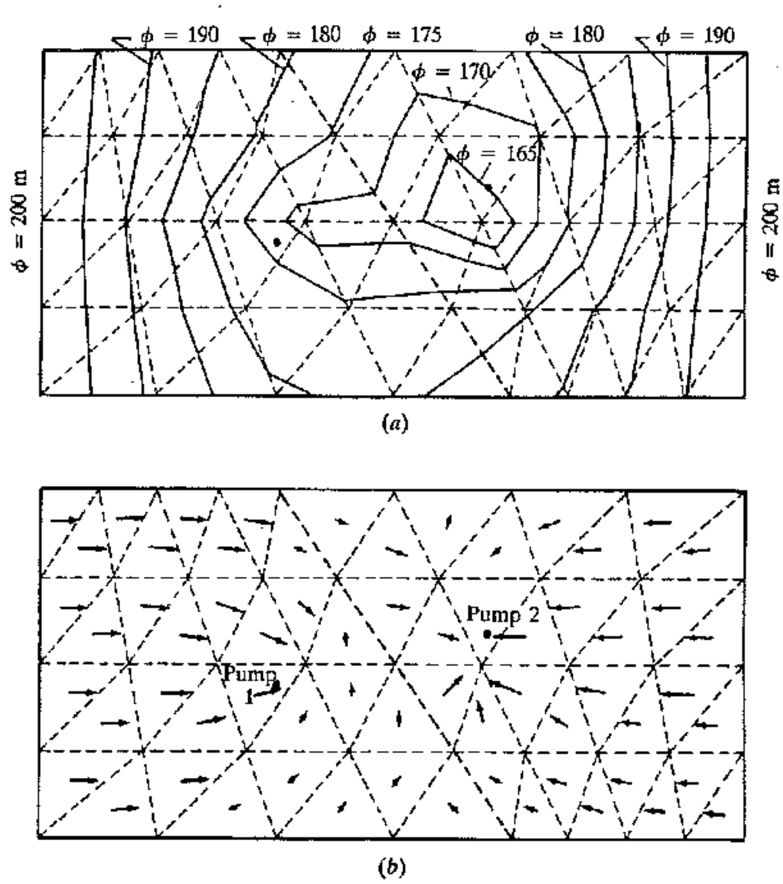

FIGURE 8.27
Plots of constant piezometric head and velocity vector for the groundwater flow: (*a*) lines of constant ϕ; (*b*) plot of velocity vectors (Example 8.6).

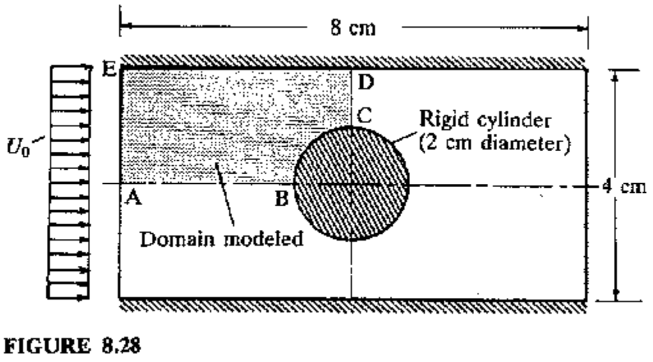

FIGURE 8.28
Domain and boundary conditions for the stream function and velocity potential formulations of irrotational flow about a cylinder (Example 8.7).

Example 8.7 Confined flow around a circular cylinder. The irrotational flow of an ideal fluid about a circular cylinder, placed with its axis perpendicular to the plane of the flow between two *long* horizontal walls (see Fig. 8.28) is to be analyzed using the finite element method. The equation governing the flow is

$$-\nabla^2 u = 0 \quad \text{in } \Omega$$

where u is either (1) the stream function ψ or (2) the velocity potential ϕ. If it is the former, the velocity components $\mathbf{u} = (u_1, u_2)$ of the flow field are given by

$$u_1 = \frac{\partial \psi}{\partial y}, \qquad u_2 = -\frac{\partial \psi}{\partial x}$$

If u is the velocity potential ϕ, the velocity components can be computed from

$$u_1 = -\frac{\partial \phi}{\partial x}, \qquad u_2 = -\frac{\partial \phi}{\partial y}$$

In either case, the velocity field is not affected by a constant term in the solution u. To determine the constant state of the solution, which does not affect the velocity field, we arbitrarily set the functions ψ and ϕ equal to zero (or a constant) on appropriate boundary lines. We analyze the problem using both formulations. For both, symmetry exists about the horizontal and vertical centerlines; therefore, only a quadrant of the flow region is used as the computational domain.

Stream function formulation. The boundary conditions on the stream function ψ can be determined as follows. Streamlines have the property that flow perpendicular to them is zero. Therefore, the fixed walls correspond to streamlines. Note that, for inviscid flows, fluid does not stick to rigid walls. Because of the biaxial symmetry about the horizontal and vertical centerlines, only a quadrant (say, ABCDE in Fig. 8.29) of the domain need to be used in the analysis. The fact that the velocity component perpendicular to the horizontal line of symmetry is zero allows us to use that line as a streamline. Since the velocity field depends on the relative difference of two streamlines, we take the value of the stream function that coincides with the horizontal axis of symmetry (i.e., on ABC) to be zero, and then determine the value of ψ on the upper wall from the condition

$$\frac{\partial \psi}{\partial y} = U_0$$

where U_0 is the inlet horizontal velocity of the field. We determine the value of the stream function on the boundary $x = 0$ by integrating the above equation with respect

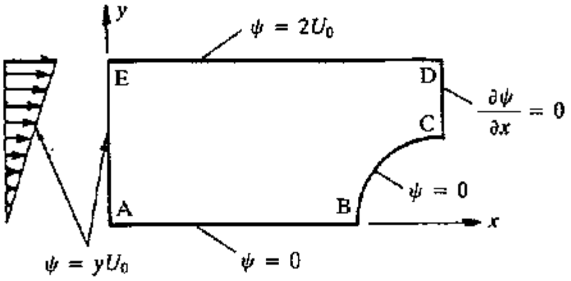

FIGURE 8.29
Computational domain and boundary conditions for the stream function formulation of inviscid flow around a cylinder (see Fig. 8.28).

to y:

$$\int_0^y \frac{d\psi}{dy}\,dy = \int_0^y U_0\,dy + \psi_A = U_0 y + 0 \tag{8.137}$$

because $\psi_A = 0$ from the previous discussion. This gives the boundary condition on AE. Since the line ED is a streamline and its value at the point E is $2U_0$, it follows that $\psi = 2U_0$ on the line ED. Lastly, we assume that the vertical velocity is zero on the line CD (i.e., $U_2 = 0$); hence $\partial\psi/\partial x = 0$ on CD. The boundary conditions are shown on the computational domain in Fig. 8.29.

In selecting a mesh, we should note that the velocity field is uniform (i.e., streamlines are horizontal) at the inlet, and that it has a parabolic profile at the exit (along CD). Therefore, the mesh at the inlet should be uniform, and the mesh close to the cylinder should be relatively more refined to be able to model the curved boundary and capture the rapid change in ψ. Two coarse finite element meshes are used to discuss the boundary conditions, and results for refined meshes will be discussed subsequently. Mesh T1 consists of 32 triangular elements and mesh Q1 consist of 16 quadrilateral elements. Both contain 25 nodes (see Fig. 8.30). The mesh with the solid lines in Fig. 8.30 corresponds to mesh Q1, and that with both the solid and dashed lines corresponds to mesh T1. It should be noted that the discretization error is not zero for this case.

The specified primary degrees of freedom (i.e., nodal values of ψ) for meshes T1 and Q1 are

$$\begin{gathered} U_1 = U_2 = \ldots = U_5 = U_{10} = U_{15} = U_{20} = U_{25} = 0.0 \\ U_6 = 1.0, \qquad U_{11} = U_{16} = U_{21} = 2.0 \end{gathered} \tag{8.138}$$

There are no nonzero specified secondary variables; the secondary variables are specified to be zero at the nodes on the line CD:

$$F_{22} = F_{23} = F_{24} = 0$$

Although the secondary variable is specified to be zero at nodes 21 and 25, where the primary variable is also specified, we choose to impose the boundary conditions on the primary variable instead of the secondary variables.

Table 8.6 gives the values of the stream function and its derivative $\partial\psi/\partial y$ $(= u_1)$ at selected points/elements of the meshes. The finite element program FEM2DV2 (see Chapter 13 for details) is used in the analysis. The stream function values obtained with meshes T1 and Q1 are very close to each other. Recall that the derivative $\partial\psi/\partial y$ is constant in a linear triangular element, whereas it varies linearly with x in a linear

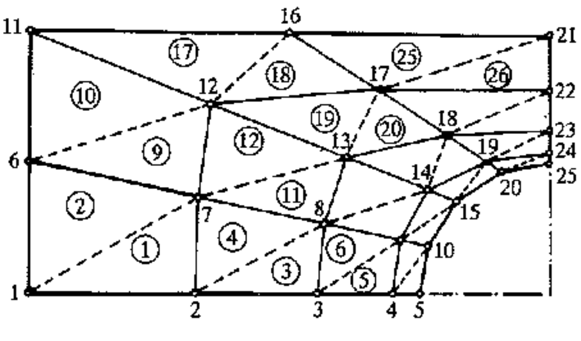

FIGURE 8.30
Meshes T1 and Q1 (remove the dashed lines for the mesh of quadrilaterals) used for inviscid flow around a cylinder.

TABLE 8.6
Finite element results from the stream function formulation of inviscid flow around a cylinder (Example 8.7)

		Stream function		Velocity $u_1 = \partial\psi/\partial y$		Velocity $u_1 = -\partial\phi/\partial x$	
x	y	Mesh T1	Mesh Q1	Mesh T1	Mesh Q1	Mesh T1	Mesh Q1
1.3183	0.7354	0.7092	0.7095	0.9643(1)†	0.9852(1)	0.9922(1)	0.9989(1)
2.2705	0.5444	0.4372	0.4379	0.8032(3)	0.9002(2)	0.9371(3)	0.9408(2)
2.8564	0.4268	0.1667	0.1650	0.3906(5)	0.6432(3)	0.7047(5)	0.7018(3)
1.4112	1.4459	1.4241	1.4270	0.0000(7)	0.2679(4)	0.2999(7)	0.3197(4)
2.4305	1.0457	0.8730	0.8823	0.4469(15)	0.8746(8)	0.6469(15)	0.8364(8)
3.0577	0.7995	0.3357	0.3384	1.636(24)	1.586(12)	1.873(24)	1.453(12)
2.6931	1.5388	1.3758	1.4010	2.544(32)	2.4551(16)	2.163(32)	2.075(16)
3.1937	1.2057	0.7706	0.7980				
3.5018	1.0007	0.2520	0.2658				
4.0000	1.5714	1.2395	1.2065				
4.0000	1.2619	0.6191	0.5796				
4.0000	1.0714	0.1817	0.1588				

† Denotes element number; the derivatives of ψ and ϕ are evaluated at the center of this element.

rectangular element. Therefore, the results for meshes T1 and Q1 will not be the same. The velocities included in Table 8.6 correspond to elements closest to the symmetry line (i.e., the $y = 0$ line) and the surface of the cylinder.

The tangential velocity u_t on the cylinder surface can be computed from the relation

$$u_t(\theta) = u_1 \sin\theta + u_2 \cos\theta = \frac{\partial\psi}{\partial y}\sin\theta - \frac{\partial\psi}{\partial x}\cos\theta \tag{8.139}$$

where θ is the angular distance along the cylinder surface.

Velocity potential formulation. The boundary conditions on the velocity potential ϕ can be derived as follows (see Fig. 8.31). The fact that $u_2 = -\partial\phi/\partial y = 0$ (no penetration) on the upper wall as well as on the horizontal line of symmetry gives the

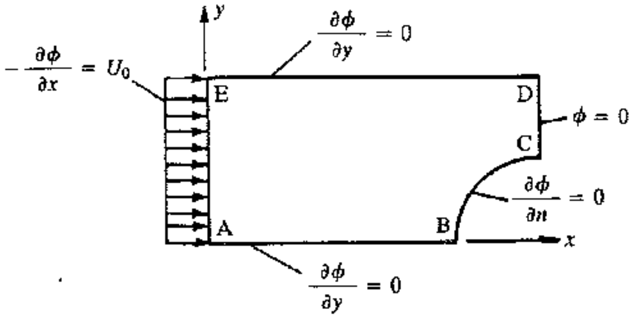
y
$\frac{\partial\phi}{\partial y} = 0$
$-\frac{\partial\phi}{\partial x} = U_0$
E
D
$\phi = 0$
C
$\frac{\partial\phi}{\partial n} = 0$
A
B
x
$\frac{\partial\phi}{\partial y} = 0$

FIGURE 8.31
Computational domain and boundary conditions for the velocity potential formulation of inviscid flow around a cylinder (see Fig. 8.28).

boundary conditions there. Along AE, the velocity $u_1 = -\partial\phi/\partial x$ is specified to be U_0. On the surface of the cylinder, the normal velocity, $u_n = -\partial\phi/\partial n$ is zero. Thus all boundary conditions, so far, are of the flux type. On the boundary CD, we must know either ϕ or $\partial\phi/\partial n = \partial\phi/\partial x$. It is clear that $-\partial\phi/\partial x = u_1$ is not known on CD. Therefore, we assume that ϕ is known, and we set it equal to $\phi_0 =$ constant. The constant ϕ_0 is arbitrary and does not contribute to the velocity field (because $-\partial\phi/\partial x = u_1$ and $-\partial\phi/\partial y = u_2$ are independent of ϕ_0). It should be noted that specification of ϕ at least one point of the mesh is necessary to determine the constant part in the solution for ϕ (i.e., eliminate the rigid body motion). We take $\phi = \phi_0 = 0$ on CD.

The mathematical boundary conditions of the problem must be translated into finite element data. The boundary conditions on the primary variables are from the boundary CD. We have

$$U_{21} = U_{22} = U_{23} = U_{24} = U_{25} = 0.0$$

The only nonzero boundary conditions on the secondary variables come from the boundary AE. There we must evaluate the boundary integral

$$\int_{\Gamma^e} \frac{\partial\phi}{\partial n}\,\psi_i\,ds = U_0 \int_{\mathrm{AE}} \psi_i(y)\,dy$$

We obtain

$$Q_1 = U_0 \int_0^{h_1} \left(1 - \frac{\bar{y}}{h_1}\right) d\bar{y} = \tfrac{1}{2} U_0 h_1 = 0.5 U_0$$

$$Q_2 = U_0 \int_0^{h_1} \frac{\bar{y}}{h}\, d\bar{y} + U_0 \int_0^{h_2} \left(1 - \frac{\bar{y}}{h_2}\right) d\bar{y} = \tfrac{1}{2} U_0 (h_1 + h_2) = U_0$$

$$Q_3 = U_0 \int_0^{h_2} \frac{\bar{y}}{h_2}\, d\bar{y} = \tfrac{1}{2} h_2 U_0 = 0.5 U_0$$

The finite element solutions for $u_1 = -\partial\phi/\partial x$ obtained with meshes T1 and Q1 are listed in Table 8.6. Note that there is a difference between the velocities obtained with the two formulations (for either mesh). This is primarily due to the nature of the boundary value problems in the two formulations. In the stream function formulation, there are more boundary conditions on the primary variable than in the velocity potential formulation.

Contour plots of streamlines, velocity potential, and horizontal velocity $u_1 = \partial\psi/\partial y$ obtained with mesh Q1 (and a plotter routine) are shown in Figs 8.32(*a*–*c*). A plot of the variation of the tangential velocity with the angular distance along the cylinder surface is shown in Fig. 8.33, along with the analytical potential solution

$$u_t = U_0(1 + R^2/r^2)\sin\theta \tag{8.140a}$$

valid on the cylinder surface. The finite element solution of a refined mesh, mesh Q2, is also included in the figure. The angle θ, radial distance r, and tangential velocity u_t can be computed from the relations

$$\theta = \tan^{-1}\left(\frac{y}{4-x}\right), \qquad r = [(4-x)^2 + y^2]^{1/2}, \qquad u_t = u_1 \sin\theta + u_2 \cos\theta \tag{8.140b}$$

The finite element solution is in general agreement with the potential solution of the problem. However, the former is not expected to agree closely, because u_t is evaluated at a radial distance $r > R$, whereas the potential solution is evaluated at $r = R$ only.

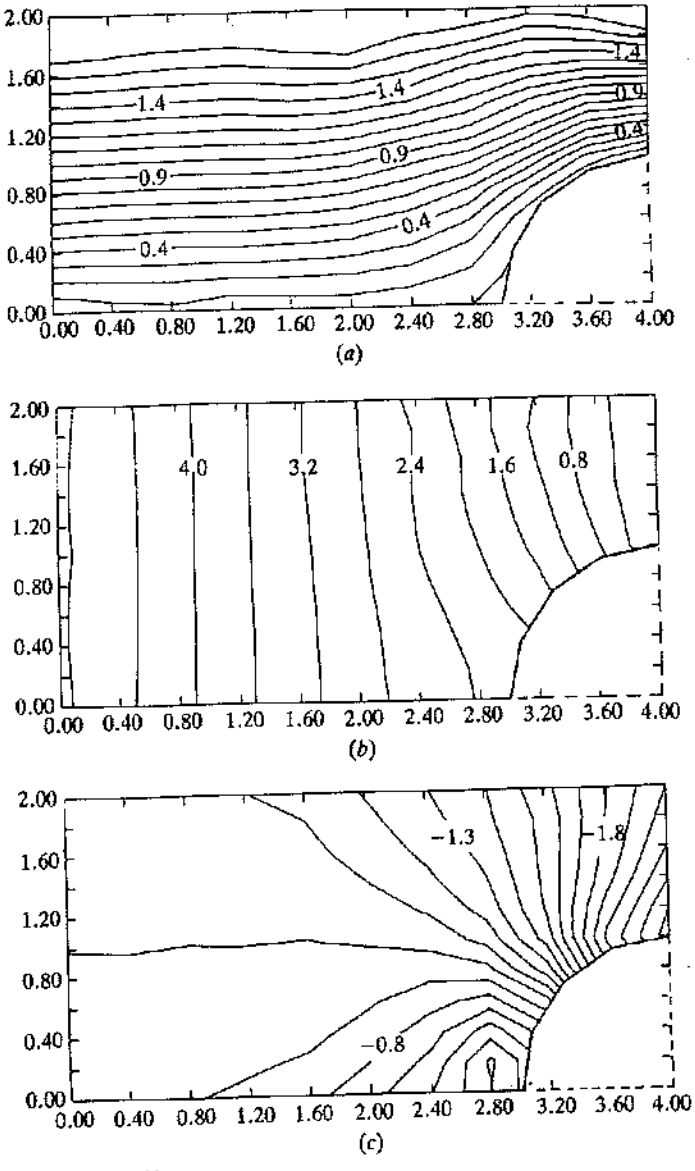

FIGURE 8.32
Contours of (*a*) stream function, (*b*) velocity potential, and (*c*) x component of velocity (with the stream function formulation), as obtained using mesh Q1.

This completes the section on fluid mechanics problems that are cast in terms of a single dependent unknown, such as the stream function or velocity potential. We return to fluid mechanics later in this book to consider two-dimensional flows of viscous incompressible fluids. The governing equations of such problems consist of several dependent variables and as many differential equations (see Chapter 11).

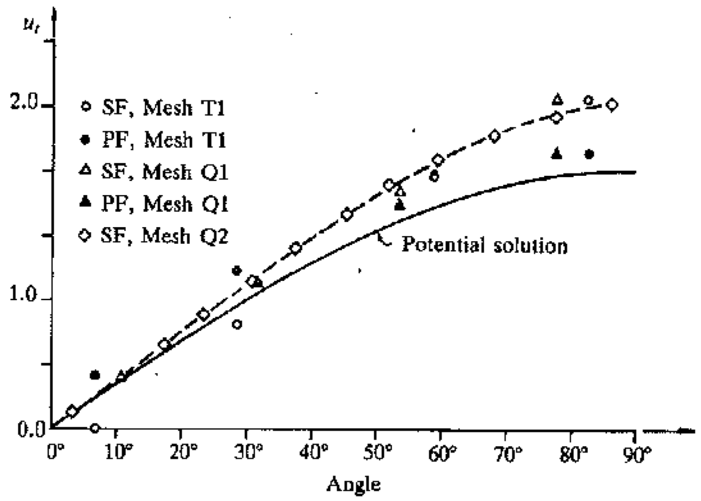

FIGURE 8.33
Variation of the tangential velocity along the cylinder surface: comparison of the finite element results with the potential theory solution (mesh Q2 contains 96 elements and 117 nodes).

8.4.3 Solid Mechanics

In this section, we consider two-dimensional boundary value problems of solid mechanics that are cast in terms of a single dependent unknown. These problems include torsion of cylindrical members and transverse deflection of membranes. The discussion is restricted to small deformations.

TORSION OF CYLINDRICAL BARS. Consider a cylindrical bar (i.e., a long member of uniform cross-section), fixed at one end and twisted by a couple (i.e., a moment or torque) of magnitude M directed along the axis (z) of the bar (see Fig. 8.34*a*). Suppose that the bar is not subjected to any body forces and is free from external forces on the lateral surface. We wish to determine the amount of twist and the associated stress field in the bar. To this end, we first describe the deformation of the bar analytically, and then analyze the equation using the finite element method.

In general, a member of noncircular cross-section subjected to a torsional moment experiences warping at any section. We assume that all cross-sections warp in the same way (which holds true for small twisting moments and deformation). This allows us to take the displacements (u, v, w) along the coordinates (x, y, z) to be of the form (see Fig. 8.34*b*)

$$u = -\theta zy, \qquad v = \theta zx, \qquad w = \theta\phi(x, y) \tag{8.141}$$

where $\phi(x, y)$ is a function to be determined and θ is the angle of twist per unit length of the bar.

The displacement field in (8.141) can be used to compute the strains, and stresses are computed using an assumed constitutive law. The stresses thus

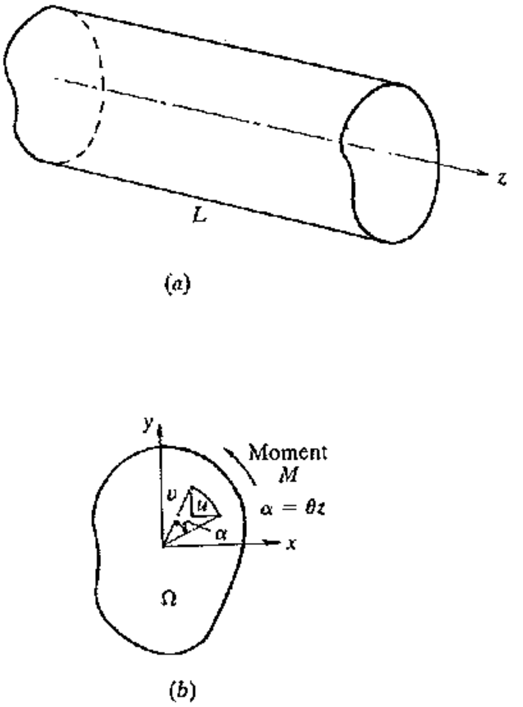

FIGURE 8.34
Torsion of cylindrical members: (*a*) a cylindrical member; (*b*) domain of analysis.

determined must satisfy the three-dimensional equations of stress equilibrium

$$\begin{aligned}
&\frac{\partial \sigma_x}{\partial x}+\frac{\partial \sigma_{xy}}{\partial y}+\frac{\partial \sigma_{xz}}{\partial z}=0\\
&\frac{\partial \sigma_{xy}}{\partial x}+\frac{\partial \sigma_y}{\partial y}+\frac{\partial \sigma_{yz}}{\partial z}=0\\
&\frac{\partial \sigma_{xz}}{\partial x}+\frac{\partial \sigma_{yz}}{\partial y}+\frac{\partial \sigma_z}{\partial z}=0.
\end{aligned} \tag{8.142}$$

and the stress boundary conditions on the lateral surface and at the ends of the cylindrical bar. Calculation of strains and then stresses using the generalized Hooke's law gives the expressions

$$\boxed{\sigma_{xz}=G\theta\left(\frac{\partial \phi}{\partial x}-y\right), \qquad \sigma_{yz}=G\theta\left(\frac{\partial \phi}{\partial y}+x\right)} \tag{8.143}$$

and all other stresses are identically zero. Here G denotes the shear modulus of the material of the bar. Substitution of these stresses into (8.142) gives [the first two equations in (8.142) are identically satisfied, and the third leads to this result]

$$\boxed{\frac{\partial}{\partial x}\left(G\theta\frac{\partial\phi}{\partial x}\right)+\frac{\partial}{\partial y}\left(G\theta\frac{\partial\phi}{\partial y}\right)=0} \tag{8.144}$$

throughout the cross-section Ω of the cylinder. The boundary conditions on the lateral surfaces Γ require that

$$\sigma_{xz}n_x+\sigma_{yz}n_y=0$$

$$\left(\frac{\partial\phi}{\partial x}-y\right)n_x+\left(\frac{\partial\phi}{\partial y}+x\right)n_y=0$$

or

$$\frac{\partial\phi}{\partial n}=yn_x-xn_y \quad \text{on } \Gamma \tag{8.145}$$

Here (n_x, n_y) denote the direction cosines of the unit normal at a point on Γ.

In summary, the torsion of a cylindrical bar is governed by (8.144) and (8.145). The function $\phi(x, y)$ is called the *torsion function* or *warping function.* Since the boundary condition in (8.145) is of the flux type, this function can be determined to within an additive constant. The stresses in (8.143), however, are independent of this constant. The additive constant has the meaning of rigid-body movement of the cylinder as a whole in the z direction. For additional discussion of this topic, the reader is referred to Sokolnikoff (1956).

The Laplace equation (8.144) and the Neumann boundary condition (8.145) governing ϕ are not convenient in the analysis because of the nature and form of the boundary condition, especially for members of irregular cross-section. The theory of analytic functions can be used to rewrite these equations in terms of the function $\Psi(x, y)$, called the *stress function,* which is related to $\phi(x, y)$ by the equations

$$\frac{\partial\Psi}{\partial x}=+\frac{\partial\phi}{\partial x}-x, \qquad \frac{\partial\Psi}{\partial y}=\frac{\partial\phi}{\partial y}-y \tag{8.146}$$

Eliminating ϕ from (8.144) and (8.145) gives, respectively, the results

$$-\left(\frac{\partial^2\Psi}{\partial x^2}+\frac{\partial^2\Psi}{\partial y^2}\right)=2 \tag{8.147}$$

$$\frac{\partial\Psi}{\partial y}n_x-\frac{\partial\Psi}{\partial x}n_y=0 \tag{8.148}$$

The left-hand side of (8.148) denotes the tangential derivative $d\Psi/ds$, and $d\Psi/ds=0$ implies that

$$\Psi=\text{constant} \quad \text{on } \Gamma$$

Since the constant part of Ψ does not contribute to the stress field,

$$\boxed{\sigma_{xz} = G\theta \frac{\partial \Psi}{\partial y}, \qquad \sigma_{yz} = -G\theta \frac{\partial \Psi}{\partial x}} \tag{8.149}$$

we take $\Psi = 0$ on the boundary.

Now the torsion problem can be stated as one of determining the stress function Ψ such that

$$\boxed{\begin{aligned} -\nabla^2 \Psi &= 2 \quad \text{in } \Omega \\ \Psi &= 0 \quad \text{on } \Gamma \end{aligned}} \tag{8.150}$$

Once Ψ has been determined, the stresses can be computed from (8.149) for a given angle of twist per unit length, θ, and shear modulus G.

The finite element model of (8.150) follows immediately from that of (8.1):

$$[K^e]\{u^e\} = \{f^e\} + \{Q^e\} \tag{8.151a}$$

where u_i^e is the value of Ψ at the ith node of Ω^e and

$$\begin{aligned} K_{ij}^e &= \int_{\Omega^e} \left(\frac{\partial \psi_i}{\partial x} \frac{\partial \psi_j}{\partial x} + \frac{\partial \psi_i}{\partial y} \frac{\partial \psi_j}{\partial y} \right) dx\, dy \\ f_i^e &= \int_{\Omega^e} 2\psi_i \, dx\, dy, \qquad Q_i^e = \oint_{\Gamma^e} \frac{\partial \Psi}{\partial n} \psi_i \, ds \end{aligned} \tag{8.151b}$$

Next we consider an example of a torsion problem.

Example 8.8 Torsion of a square cross-section bar. It should be recalled that (8.1) can also be interpreted as the equation associated with the torsion of a square cross-section cylindrical bar of cross-sectional dimensions a by b. Note that the actual problem is antisymmetric as far as the loading and stress distribution are concerned; however, the stress function, being a scalar function governed by the Poisson equation, is symmetric about the x and y axes as well as the diagonal lines. When using rectangular elements, one quadrant of the bar cross-section can be used in the finite element analysis. The biaxial symmetry about the x and y axes requires imposition of the following boundary conditions on Ψ:

$$\frac{\partial \Psi}{\partial x} = 0 \quad \text{on the line } x = 0$$

$$\frac{\partial \Psi}{\partial y} = 0 \quad \text{on the line } y = 0$$

In addition, on the actual boundary we have the boundary condition

$$\Psi = 0 \quad \text{on the lines } x = a,\ y = b$$

The analytical solution of the problem is given by

$$\Psi(x, y) = \tfrac{1}{4}a^2 - x^2 - \frac{8a^2}{\pi^3}\sum_{n=0}^{\infty}\frac{(-1)^n}{(2n+1)^3}\frac{\cosh k_n y \cos k_n x}{\cosh \frac{1}{2}k_n b} \tag{8.152a}$$

$$\sigma_{xz} = -\frac{8aG\theta}{\pi^2}\sum_{n=0}^{\infty}\frac{(-1)^n}{(2n+1)^2}\frac{\sinh k_n y \cos k_n x}{\cosh \frac{1}{2}k_n b} \tag{8.152b}$$

$$\sigma_{yz} = G\theta\left[2x - \frac{8a}{\pi^2}\sum_{n=0}^{\infty}\frac{(-1)^n}{(2n+1)^2}\frac{\cosh k_n y \sin k_n x}{\cosh \frac{1}{2}k_n b}\right] \tag{8.152c}$$

where $k_n = \frac{1}{2}(2n+1)\pi$. The problem is analyzed here for shear stresses σ_{xz} and σ_{yz} [see (8.149)].

Here we investigate the convergence of the finite element solutions using gradually refined meshes of linear and quadratic rectangular elements. The results of this study are summarized in Tables 8.7 and 8.8. The convergence of the finite element solutions for the stress function and stresses to the analytical solutions (8.152) can be seen from these results. The contour lines of the surface $\Psi(x, y) = \text{constant}$, $\sigma_{xz} = \text{constant}$, and $\sigma_{yz} = \text{constant}$ are shown in Fig. 8.35.

TRANSVERSE DEFLECTION OF MEMBRANES. Suppose that a membrane, with fixed edges, occupies a region Ω in the (x, y) plane. Initially, the membrane is stretched so that the tension a in the membrane is uniform and that a is so large that it is not appreciably altered when the membrane is deflected by a distributed normal force $f(x, y)$. The equation governing the transverse deflection u of the membrane is

$$-a\left(\frac{\partial^2 u}{\partial x^2} + \frac{\partial^2 u}{\partial y^2}\right) = f(x, y) \quad \text{in } \Omega \tag{8.153a}$$

TABLE 8.7
Convergence of the finite element solutions for Ψ using linear and quadratic rectangular elements (four-node and nine-node elements) in Example 8.8

		Linear elements			Quadratic elements†		
x	y	2×2	4×4	8×8	1×1	2×2	4×4
0.0000	0.0000	0.15536	0.14920	0.14780	0.14744	0.14730	0.14734
0.0625	0.0000	—	—	0.14583	—	—	0.14538
0.1250	0.0000	—	0.14120	0.13987	—	0.13941	0.13944
0.1875	0.0000	—	—	0.12972	—	—	0.12931
0.2500	0.0000	0.12054	0.11610	0.11502	0.11378	0.11463	0.11467
0.3125	0.0000	—	—	0.09534	—	—	0.09505
0.3750	0.0000	—	0.07069	0.07007	—	0.06983	0.06986
0.4375	0.0000	—	—	0.03854	—	—	0.03844
0.1250	0.2500	—	0.11031	0.10925	—	0.10887	0.10890
0.2500	0.2500	0.09643	0.09191	0.09090	0.09095	0.09056	0.09057
0.3750	0.2500	—	0.05729	0.05660	—	0.05626	0.05636

† The 4 × 4 mesh of nine-node quadratic elements gives a solution that coincides with the analytical solution to five significant decimal places.

TABLE 8.8
Comparison of finite element solutions for the shear stress $\sigma_{yz}(x, y)$ $[= -\sigma_{xz}(y, x)]$, computed using various meshes, with the analytical solution (Example 8.8)

		Mesh			Analytical
x	y	2×2	4×4	8×8	solution
0.03125	↑	—	—	0.0312	0.0312
0.09375		—	—	0.0946	0.0946
0.15625		—	—	0.1612	0.1611
0.21875		—	—	0.2332	0.2331
0.28125	0.03125	—	—	0.3127	0.3124
0.34375		—	—	0.4015	0.4011
0.40625		—	—	0.5013	0.5008
0.46875	↓	—	—	0.6135	0.6128
0.06250	↑	—	0.06175	—	0.0618
0.1875		—	0.1942	—	0.1939
0.3125	0.0625	—	0.3529	—	0.3516
0.4375	↓	—	0.5528	—	0.5504
0.1250	0.1250	0.1179	—	—	0.1193
0.3750	0.1250	0.4339	—	—	0.4272

with

$$u = 0 \quad \text{on } \Gamma \tag{8.153b}$$

Note that this equation and boundary conditions are of the same form as those for the torsion of cylindrical bars [see (8.150)]. The finite element model of the equation is obvious. In view of the close analogy between this problem and the torsion of cylindrical bars, we shall not consider any numerical examples here.

8.5 EIGENVALUE AND TIME-DEPENDENT PROBLEMS

8.5.1 Introduction

This section deals with the finite element analysis of two-dimensional eigenvalue and time-dependent problems involving a single variable. We use the results of Section 6.2 to develop finite element algebraic equations from the semidiscrete finite element models of time-dependent problems. Since the weak form and temporal approximations have already been discussed in detail in Section 6.2, attention is focussed here first on the development of the semidiscrete finite element models and then on the associated eigenvalue and fully discretized models. The examples presented are very simple, because they are designed to illustrate the procedure for eigenvalue and time-dependent problems; solution of two-dimensional problems with complicated geometries requires the use of numerical integration. Chapter 9 is devoted to the discussion of various two-dimensional elements and their interpolation functions and numerical integration methods.

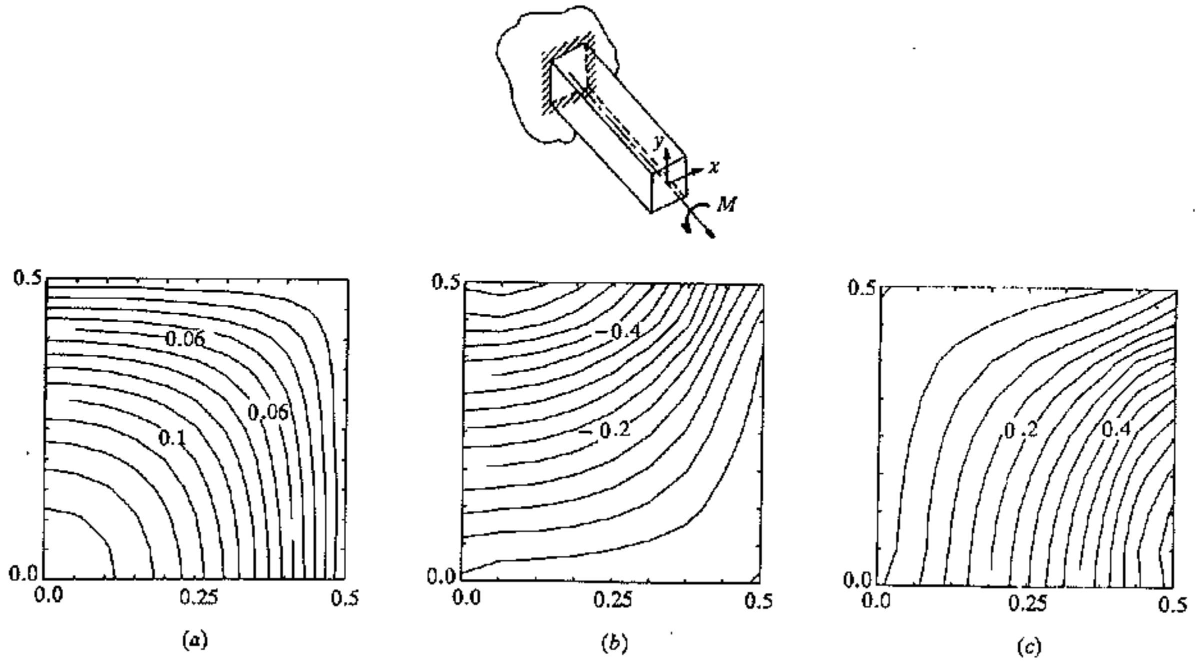

(*a*) (*b*) (*c*)

FIGURE 8.35
Contour plots of the stress function and shear stresses obtained using the 8 × 8 mesh of linear rectangular elements in a quadrant of square cross-section in Example 8.8: (*a*) stress function; (*b*) stress σ_{xz}; (*c*) stress σ_{yz}.

The development of finite element models of eigenvalue and time-dependent problems involves, as described in Section 6.2, two main stages. The first, called *semidiscretization*, is to develop the weak form of the equations over an element and to seek spatial approximations of the dependent variables of the problem. The end result of this step is a set of ordinary differential equations in time among the nodal values of the dependent variables. For transient problems, the second stage consists in time approximation of the ordinary differential equations (i.e., numerical integration of the equations) by finite difference schemes. This step leads to a set of algebraic equations involving the nodal values at time t_{s+1} [$= (s+1)\,\Delta t$, where s is an integer and Δt is the time increment] in terms of known values from the previous time step(s). For eigenvalue problems, the second stage consists in seeking a solution of the form $u_j(t) = U_j e^{-\lambda t}$ for nodal values and determining the eigenvalues λ and eigenfunctions $U_j \psi_j(x, y)$ (no sum on j). The two-stage procedure was clearly illustrated for one-dimensional problems in Sections 6.1 and 6.2. It will be applied here to two-dimensional problems involving a single equation in a single variable. Since the emphasis in this section is on the time approximations, the development of the weak form and spatial finite element model will not be covered explicitly here, and the reader is referred to Sections 8.2 and 8.3 for details.

8.5.2 Parabolic Equations

Consider the partial differential equation governing transient heat transfer and similar problems in a two-dimensional region Ω with total boundary Γ,

$$c\frac{\partial u}{\partial t} - \frac{\partial}{\partial x}\left(a_{11}\frac{\partial u}{\partial x}\right) - \frac{\partial}{\partial y}\left(a_{22}\frac{\partial u}{\partial y}\right) + a_0 u = f(x, y, t) \tag{8.154}$$

with the boundary conditions

$$u = \hat{u} \ \text{ or } \ q_n = \hat{q}_n \quad \text{on } \Gamma \quad (t \geq 0) \tag{8.155a}$$

where

$$q_n = a_{11}\frac{\partial u}{\partial x} n_x + a_{22}\frac{\partial u}{\partial y} n_y \tag{8.155b}$$

The initial conditions (i.e., at $t = 0$) are of the form

$$u(x, y, 0) = u_0(x, y) \quad \text{in } \Omega \tag{8.156}$$

Here t denotes time, and c, a_{11}, a_{22}, a_0, $\hat{u}$, u_0, f, and $\hat{q}_n$ are given functions of position and/or time. Equation (8.154) is a modification of (8.1) in that it contains a time-derivative term, which accounts for time variations of the physical process represented by (8.1).

The weak form of (8.154) and (8.155) over an element Ω^e is obtained by the standard procedure: multiply (8.154) with the weight function $v(x, y)$ and integrate over the element, integrate by parts (spatially) those terms that involve higher-order derivatives using the gradient or divergence theorem, and replace the coefficient of the weight function in the boundary integral with the secondary variable [i.e., use (8.155*b*)]. We obtain

$$0=\int_{\Omega^e}\left[v\left(c\frac{\partial u}{\partial t}+a_0u-f\right)+a_{11}\frac{\partial v}{\partial x}\frac{\partial u}{\partial x}+a_{22}\frac{\partial v}{\partial y}\frac{\partial u}{\partial y}\right]dx\,dy-\oint_{\Gamma^e}q_nv\,ds \tag{8.157}$$

Note that the procedure for obtaining the weak form for time-dependent problems is not very different from that used for steady-state problems in Section 8.2.3. The difference is that all terms of the equations may be functions of time. Also, there is no integration by parts with respect to time, and the weight function v is not a function of time.

The *semidiscrete* finite element model is obtained from (8.157) by substituting a finite element approximation for the dependent variable u. In selecting the approximation for u, once again we assume that the time dependence can be separated from the spatial variation:

$$u(x, y, t)\approx\sum_{j=1}^{n}u_j^e(t)\psi_j^e(x, y) \tag{8.158}$$

where u_j denotes the value of $u(x, y, t)$ at the spatial location (x_j, y_j) at time t. The ith differential equation (in time) of the finite element model is obtained by substituting $v=\psi_i^e(x, y)$ and replacing u by (8.158) in (8.157):

$$0=\sum_{j=1}^{n}\left(M_{ij}^e\frac{du_j^e}{dt}+K_{ij}^eu_j^e\right)-f_i^e-Q_i^e \tag{8.159a}$$

or, in matrix form,

$$[M^e]\{\dot{u}^e\}+[K^e]\{u^e\}=\{f^e\}+\{Q^e\} \tag{8.159b}$$

where a superposed dot on u denotes the time derivative ($\dot{u}=\partial u/\partial t$), and

$$M_{ij}^e=\int_{\Omega^e}c\psi_i\psi_j\,dx\,dy,\qquad K_{ij}^e=\int_{\Omega^e}\left(a_{11}\frac{\partial\psi_i}{\partial x}\frac{\partial\psi_j}{\partial x}+a_{22}\frac{\partial\psi_i}{\partial y}\frac{\partial\psi_j}{\partial y}+a_0\psi_i\psi_j\right)dx\,dy$$
$$f_i^e=\int_{\Omega^e}f(x, y, t)\psi_i\,dx\,dy \tag{8.159c}$$

This completes the semidiscretization step.

EIGENVALUE ANALYSIS. The problem of finding $u_j^e(t)=U_j^e e^{-\lambda t}$ such that (8.159) holds for homogeneous boundary and initial conditions and $f=0$ is called an *eigenvalue problem*. Substituting for $u_j^e(t)$ in (8.159*b*), we obtain

$$\boxed{(-\lambda[M^e]+[K^e])\{u^e\}=\{Q^e\}} \tag{8.160}$$

Upon assembly of the element equations (8.160), the right-hand-side column vector of the condensed equations is zero (because of the homogeneous boundary conditions), giving rise to the global eigenvalue problem

$$([K]-\lambda[M])\{U\}=\{0\} \tag{8.161}$$

The order of the matrix equations is $N \times N$, where N is the number of nodes at which the solution is not known. A nontrivial solution to (8.161) exists only if the determinant of the coefficient matrix is zero:

$$|[K]-\lambda[M]|=0$$

which when expanded, results in an Nth-degree polynomial in λ. The N roots λ_j $(j=1,2,\ldots,N)$ of this polynomial give the first N eigenvalues of the discretized system (the continuous system, in general, has an infinite number of eigenvalues). There exist standard eigenvalue routines for solving (8.161), which give the N eigenvalues and eigenvectors.

TRANSIENT ANALYSIS. Note that the form of (8.159) is the same as the parabolic equation discussed in Section 6.2. The spatial dimension does not appear in (8.159a,b) because it is taken into account in the spatial approximation. Thus, irrespective of the spatial dimension, the finite element model of all problems with a first time derivative is the same. Therefore, the time approximation schemes discussed in Section 6.2.3 for parabolic equations can be readily applied.

Using the α-family of approximation (6.39),

$$\{u\}_{s+1}=\{u\}_s+\Delta t\,[(1-\alpha)\{\dot u\}_s+\alpha\{\dot u\}_{s+1}] \quad (0\leqslant\alpha\leqslant 1) \tag{8.162}$$

we can transform the ordinary differential equations (8.159) into a set of algebraic equations at time t_{s+1}:

$$\boxed{[\hat K]_{s+1}\{u\}_{s+1}=\{\hat F\}_{s,s+1}} \tag{8.163a}$$

where

$$\boxed{\begin{gathered}[\hat K]_{s+1}=[M]+a_1[K]_{s+1}\\ \{\hat F\}=\Delta t\,(\alpha\{F\}_{s+1}+(1-\alpha)\{F\}_s)+([M]-a_2[K]_s)\{u\}_s\\ a_1=\alpha\,\Delta t,\qquad a_2=(1-\alpha)\,\Delta t\end{gathered}} \tag{8.163b}$$

Equation (8.163a), after assembly and imposition of boundary conditions, is solved at each time step for the nodal values u_j at time $t_s=(s+1)\,\Delta t$. At time $t=0$ (i.e., $s=0$), the right-hand side is computed using the initial values $\{u\}_0$; the vector $\{F\}$, which is the sum of the source vector $\{f\}$ and the internal flux vector $\{Q\}$, is always known, for both times t_s and t_{s+1}, at all nodes at which the solution is unknown [because $f(x,t)$ is a *known* function of time, and the sum of Q_j^e at these nodes is zero].

It should be recalled from Section 6.2.3 that, for different values of α, we obtain different well-known approximation schemes, with given order of accuracy:

$$\alpha = \begin{cases} 0, & \text{the forward difference scheme (conditionally stable); } O(\Delta t) \\ \frac{1}{2}, & \text{the Crank–Nicolson scheme (unconditionally stable); } O(\Delta t)^2 \\ \frac{2}{3}, & \text{the Galerkin scheme (unconditionally stable); } O(\Delta t)^2 \\ 1, & \text{the backward difference scheme (unconditionally stable); } O(\Delta t) \end{cases}$$

For the forward difference scheme, the stability requirement is

$$\boxed{\Delta t < \Delta t_{cr} = \frac{2}{(1-2\alpha)\lambda_{\max}}, \qquad \alpha < \tfrac{1}{2}} \tag{8.164}$$

where $\lambda_{\max}$ is the largest eigenvalue of the finite element equations (8.161).

We next consider examples of eigenvalue and time-dependent problems.

Example 8.9 Eigenvalue analysis. Consider the differential equation

$$\frac{\partial u}{\partial t} - \left(\frac{\partial^2 u}{\partial x^2} + \frac{\partial^2 u}{\partial y^2}\right) = f \tag{8.165a}$$

in a square region, subject to the boundary conditions

$$\frac{\partial u}{\partial x}(0, y, t) = 0, \qquad \frac{\partial u}{\partial y}(x, 0, t) = 0, \qquad u(x, 1, t) = 0, \qquad u(1, y, t) = 0 \tag{8.165b}$$

and initial condition

$$u(x, y, 0) = 0 \tag{8.165c}$$

As a first choice, we take a 1 × 1 mesh of triangular (2 elements) and rectangular elements. Alternatively, for the choice of triangles, we can use the diagonal symmetry and model the domain with one triangular element. The triangular element matrices are

$$[K^e] = \frac{1}{2}\begin{bmatrix} 1 & -1 & 0 \\ -1 & 2 & -1 \\ 0 & -1 & 1 \end{bmatrix}, \qquad [M^e] = \frac{1}{24}\begin{bmatrix} 2 & 1 & 1 \\ 1 & 2 & 1 \\ 1 & 1 & 2 \end{bmatrix}$$

The eigenvalue problem becomes

$$\left(-\frac{\lambda}{24}\begin{bmatrix} 2 & 1 & 1 \\ 1 & 2 & 1 \\ 1 & 1 & 2 \end{bmatrix} + \frac{1}{2}\begin{bmatrix} 1 & -1 & 0 \\ -1 & 2 & -1 \\ 0 & -1 & 1 \end{bmatrix}\right)\begin{Bmatrix} U_1 \\ U_2 \\ U_3 \end{Bmatrix} = \begin{Bmatrix} 0 \\ 0 \\ 0 \end{Bmatrix}$$

The boundary conditions require $U_2 = U_3 = 0$. Hence, we have

$$(-\tfrac{1}{12}\lambda + \tfrac{1}{2})U_1 = 0, \qquad \text{or} \quad \lambda = 6$$

The eigenfunction becomes

$$U(x, y) = \psi_1(x, y) = 1 - x$$

which is defined over the octant of the domain. For a quadrant of the domain, by symmetry, it becomes $U(x, y) = (1 - x)(1 - y)$.

For one rectangular element, we have

$$[K^e]=\frac{1}{6}\begin{bmatrix} 4 & -1 & -2 & -1\\ -1 & 4 & -1 & -2\\ -2 & -1 & 4 & -1\\ -1 & -2 & -1 & 4 \end{bmatrix},\qquad [M^e]=\frac{1}{36}\begin{bmatrix} 4 & 2 & 1 & 2\\ 2 & 4 & 2 & 1\\ 1 & 2 & 4 & 2\\ 2 & 1 & 2 & 4 \end{bmatrix}$$

$$\left(-\frac{\lambda}{36}\begin{bmatrix} 4 & 2 & 1 & 2\\ 2 & 4 & 2 & 1\\ 1 & 2 & 4 & 2\\ 2 & 1 & 2 & 4 \end{bmatrix}+\frac{1}{6}\begin{bmatrix} 4 & -1 & -2 & -1\\ -1 & 4 & -1 & -2\\ -2 & -1 & 4 & -1\\ -1 & -2 & -1 & 4 \end{bmatrix}\right)\begin{Bmatrix} U_1\\ U_2\\ U_3\\ U_4 \end{Bmatrix}=\begin{Bmatrix} 0\\ 0\\ 0\\ 0 \end{Bmatrix}$$

Using the boundary conditions $U_2=U_3=U_4=0$, we obtain

$$(-\tfrac{1}{36}\lambda\times 4+\tfrac{4}{6})U_1=0, \qquad \text{or} \quad \lambda=6$$

The eigenfunction over the quadrant of the domain is given by

$$U(x, y)=\psi_1(x, y)=(1-x)(1-y)$$

For this problem, the one-element mesh of triangles in an octant of the domain gives the same solution as the one-element mesh of rectangular elements in a quadrant of the domain.

Table 8.9 gives eigenvalues obtained with various meshes of triangular and rectangular elements, along with the analytical solution of the problem. It is clear that the convergence of the minimum eigenvalue obtained using the finite element method to the analytical value is rapid compared with the convergence of the higher eigenvalues; i.e., the errors in the higher eigenvalues are always larger than that in the minimum eigenvalue. Also, the minimum eigenvalue converges faster with mesh refinements. The mesh used must be such that the required eigenmodes are represented accurately.

Example 8.10. We wish to solve the transient heat conduction equation

$$\frac{\partial T}{\partial t}-\left(\frac{\partial^2 T}{\partial x^2}+\frac{\partial^2 T}{\partial y^2}\right)=1 \tag{8.166a}$$

TABLE 8.9

Comparison of finite element solutions for eigenvalues, obtained using various meshes, with the analytical solution (Example 8.9)

	Triangles				Rectangles				Analytical†
λ	**1×1**	**2×2**	**4×4**	**8×8**	**1×1**	**2×2**	**4×4**	**8×8**	λ_{mn}
$\lambda_1\ (\lambda_{11})$	6.000	5.415	5.068	4.969	6.000	5.193	4.999	4.951	4.935
$\lambda_2\ (\lambda_{13})$	—	32.000	27.250	25.340	—	34.290	27.370	25.330	24.674
$\lambda_3\ (\lambda_{31})$	—	38.200	28.920	25.730	—	34.290	27.370	25.330	24.674
$\lambda_4\ (\lambda_{33})$	—	76.390	58.220	48.080	—	63.380	49.740	45.710	44.413
$\lambda_4\ (\lambda_{15})$	—	—	85.350	69.780	—	—	84.570	69.260	64.152
$\lambda_5\ (\lambda_{51})$	—	—	86.790	69.830	—	—	84.570	69.260	64.152

† The analytical solution is $\lambda_{mn}=\frac{1}{4}\pi^2(m^2+n^2)$ $(m, n=1, 3, 5, \ldots)$.

subject to the boundary conditions, for $t \geq 0$,

$$\begin{aligned} \frac{\partial T}{\partial x}(0, y, t) &= 0, \quad & \frac{\partial T}{\partial y}(x, 0, t) &= 0 \\ T(1, y, t) &= 0, \quad & T(x, 1, t) &= 0 \end{aligned} \tag{8.166b}$$

and the initial condition

$$T(x, y, 0) = 0 \quad \text{for all } (x, y) \text{ in } \Omega \tag{8.166c}$$

We choose a 4×4 mesh of linear triangular elements (see Fig. 8.36) to model the domain, and investigate the stability and accuracy of the Crank–Nicolson method (i.e., $\alpha = 0.5$) and the forward difference scheme ($\alpha = 0.0$) for the temporal approximation. Since the Crank–Nicolson method is unconditionally stable, one can choose any value of Δt. However, for large values of Δt, the solution may not be accurate. The forward difference scheme is conditionally stable; it is stable if $\Delta t < \Delta t_{cr}$, where

$$\Delta t_{cr} = \frac{2}{\lambda_{\max}} = \frac{2}{386.4} = 0.00518$$

where the maximum eigenvalue of (8.166a) for the 4×4 mesh of triangles is 386.4.

The element equations are given by (8.163), with $[M^e]$, $[K^e]$, and $\{f^e\}$ defined by (8.159c), wherein $c = 1$, $a_{11} = 1$, $a_{22} = 1$, $a_0 = 0$, and $f = 1$. The boundary conditions of the problem for the 4×4 mesh are given by

$$U_5 = U_{10} = U_{15} = U_{20} = U_{21} = U_{22} = U_{23} = U_{24} = U_{25} = 0.0$$

Beginning with the initial conditions $U_i = 0$ ($i = 1, 2, \ldots, 25$), we solve the assembled set of equations associated with (8.163).

The forward difference scheme would be unstable for $\Delta t > 0.00518$. To illustrate this point, the equations are solved using $\alpha = 0$, $\Delta t = 0.01$ and $\alpha = 0.5$, $\Delta t = 0.01$. The Crank–Nicolson method gives a stable and accurate solution, while the forward difference scheme yields an unstable solution (i.e., the solution error grows unboundedly with time), as can be seen from Fig. 8.37. For $\Delta t = 0.005$, the forward difference scheme yields a stable solution.

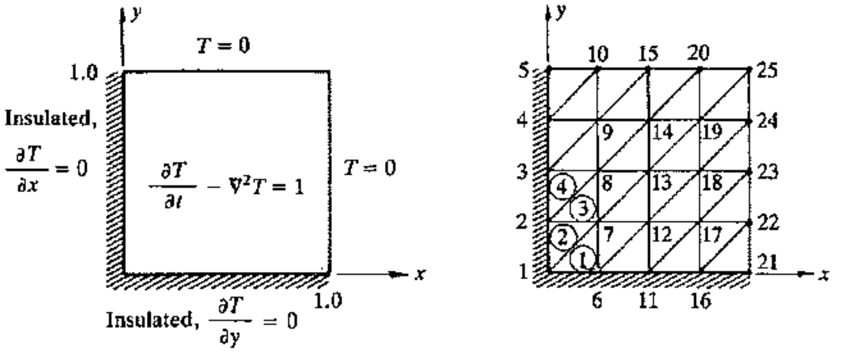

FIGURE 8.36
Domain, boundary conditions, and finite element mesh for the transient heat conduction problem of Example 8.10.

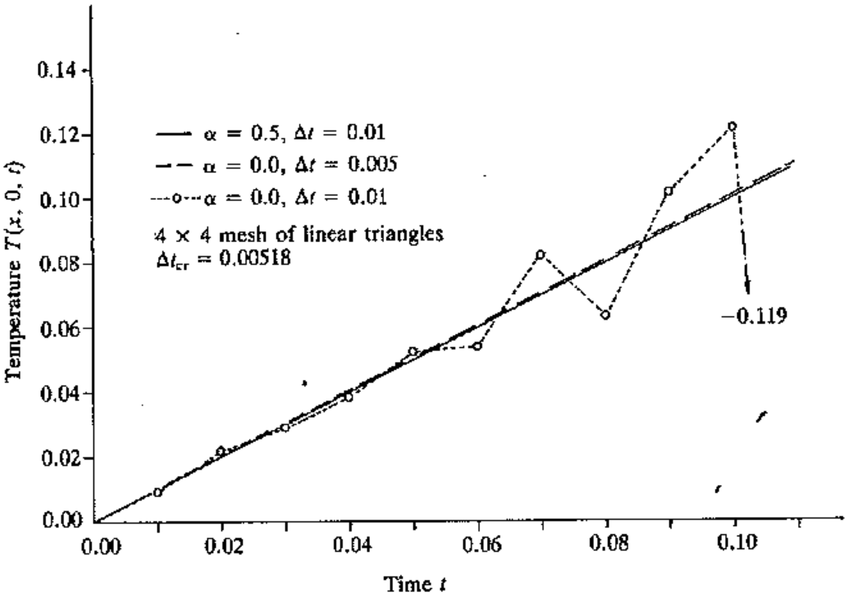

FIGURE 8.37
Stability of the transient solutions of the heat conduction problem in Example 8.10 analyzed using a 4×4 mesh of linear triangular elements and the Crank–Nicolson ($\alpha = 0.5$) and forward difference ($\alpha = 0.0$) time integration schemes.

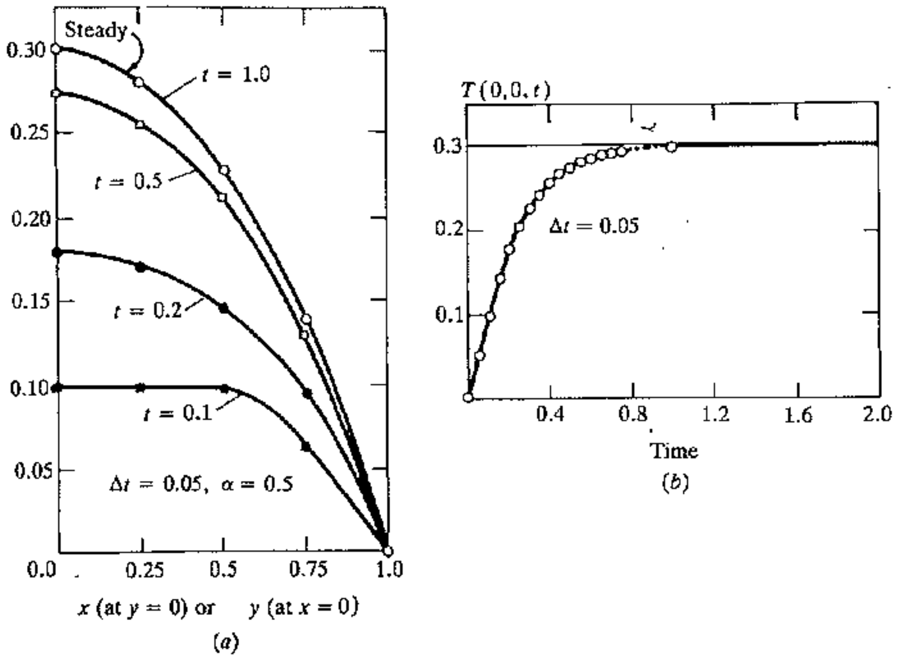

(a)

(b)

FIGURE 8.38
Variation of the temperature as a function of position x and time t for the transient heat conduction problem of Example 8.10.

TABLE 8.10
Comparison of finite difference and finite element solutions with the exact solution of the heat conduction problem in Example 8.10

Node	Exact solution	Finite difference solution	Error	Finite element solution (steady)	Error	Finite element solution (unsteady) at $t = 1.0$
1	0.2947	0.2911	0.0036	0.3013	−0.0066	0.2993
2	0.2789	0.2755	0.0034	0.2805	−0.0016	0.2786
3	0.2293	0.2266	0.0027	0.2292	0.0001	0.2278
4	0.1397	0.1381	0.0016	0.1392	0.0005	0.1385
5	0.0000	0.0000	0.0000	0.0000	0.0000	0.0000
7	0.2642	0.2609	0.0033	0.2645	−0.0003	0.2628
8	0.2178	0.2151	0.0027	0.2172	0.0006	0.2159
9	0.1333	0.1317	0.0016	0.1327	0.0006	0.1320
10	0.0000	0.0000	0.0000	0.0000	0.0000	0.0000
13	0.1811	0.1787	0.0024	0.1801	0.0010	0.1791
14	0.1127	0.1110	0.0017	0.1117	0.0010	0.1111
15	0.0000	0.0000	0.0000	0.0000	0.0000	0.0000
19	0.0728	0.0711	0.0017	0.0715	0.0013	0.0712
20	0.0000	0.0000	0.0000	0.0000	0.0000	0.0000
25	0.0000	0.0000	0.0000	0.0000	0.0000	0.0000

The Crank–Nicolson method gives a stable and accurate solution even for $\Delta t = 0.05$. The temperature $T(x, 0, t)$ is plotted versus x for various values of the time in Fig. 8.38(a). The steady state is reached at time $t = 1.0$. The temperature $T(0, 0, t)$ predicted by the Crank–Nicolson method is plotted versus time in Fig. 8.38(b), which indicates the evolution of the temperature from zero to the steady state. Table 8.10 gives a comparison of the transient solution at $t = 1.0$ with the steady-state finite element, the finite difference, and the analytical solutions. Table 8.11 gives the finite element solutions for temperature predicted by 4 × 4 meshes of triangles and rectangles and various values of Δt and $\alpha = 0.5$.

8.5.3 Hyperbolic Equations

The transverse motion of a membrane, for example, is governed by a partial differential equation of the form

$$c\frac{\partial^2 u}{\partial t^2} - \frac{\partial}{\partial x}\left(a_{11}\frac{\partial u}{\partial x}\right) - \frac{\partial}{\partial y}\left(a_{22}\frac{\partial u}{\partial y}\right) + a_0 u = f(x, y, t) \qquad (8.167a)$$

where $u(x, y, t)$ denotes the transverse deflection, c is the material density of the membrane, a_{11} and a_{22} are the tensions in the x and y directions of the membrane, a_0 is the modulus of the elastic foundation on which the membrane is stretched (often $a_0 = 0$, i.e., there is no foundation), and $f(x, y, t)$ is the transversely distributed force. Equation (8.167a) is known as the *wave equation*, and is classified mathematically as a hyperbolic equation. The function u must be determined such that it satisfies (8.167a) in a region Ω,

TABLE 8.11
Comparison of the transient solutions of (8.166) obtained using a mesh of triangular and rectangular elements ($\alpha = 0.5$) (Example 8.10)

Time	Temperature along the line $y = 0$: $T(x, 0, t) \times 10$				
t	Element†	$x = 0.0$	$x = 0.25$	$x = 0.5$	$x = 0.75$
0.1	T1	0.9758	0.9610	0.9063	0.7104
	R1	0.9684	0.9556	0.8956	0.6887
	T2	0.9928	0.9798	0.9168	0.6415
	R2	0.9841	0.9718	0.9020	0.6323
0.2	T1	1.8003	1.7238	1.4891	0.9321
	R1	1.7723	1.7216	1.4829	0.9367
	T2	1.7979	1.7060	1.4644	0.9462
	R2	1.7681	1.6990	1.4626	0.9469
0.3	T1	2.3130	2.1671	1.7961	1.1466
	R1	2.2747	2.1650	1.8084	1.1499
	T2	2.2829	2.1448	1.7943	1.1249
	R2	2.2479	2.1432	1.8018	1.1319
1.0	T1	2.9960	2.7871	2.2804	1.3843
	R1	2.9648	2.8053	2.3090	1.4059
	T2	2.9925	2.7862	2.2776	1.3849
	R2	2.9621	2.8037	2.3065	1.4053

† T1, triangular element mesh with $\Delta t = 0.1$; T2, triangular element mesh with $\Delta t = 0.05$; R1, rectangular element mesh with $\Delta t = 0.1$; R2, rectangular element mesh with $\Delta t = 0.05$.

together with the following boundary and initial conditions:

$$u = \hat{u} \quad \text{or} \quad q_n = \hat{q}_n \quad \text{on } \Gamma \quad (t \geq 0) \tag{8.167b}$$

$$u(x, y, 0) = u_0(x, y), \qquad \frac{\partial u}{\partial t}(x, y, 0) = v_0(x, y) \tag{8.167c}$$

where $\hat{u}$ and $\hat{q}_n$ are specified boundary values of u and q_n [see (8.155b)], and u_0 and v_0 are specified initial values of u and its time derivative, respectively.

The weak form of (8.167a,b) over a typical element Ω^e is similar to that of (8.154) [see (8.157)], except that here we have the second time derivative of u:

$$0 = \int_{\Omega^e} \left[v\left(c\frac{\partial^2 u}{\partial t^2} + a_0 u - f \right) + a_{11}\frac{\partial v}{\partial x}\frac{\partial u}{\partial x} + a_{22}\frac{\partial v}{\partial y}\frac{\partial u}{\partial y} \right] dx\, dy - \oint_{\Gamma^e} q_n v\, ds \tag{8.168}$$

where $v = v(x, y)$ is the weight function.

The semidiscrete finite element model of (8.167a) is obtained by substituting the finite element approximation (8.158) for u and $v = \psi_i$ into

(8.168):

$$0=\sum_{j=1}^{n}\left(M_{ij}^e\frac{d^2u_j^e}{dt^2}+K_{ij}^e u_j^e\right)-f_i^e-Q_i^e \tag{8.169a}$$

or, in matrix form,

$$[M^e]\{\ddot{u}^e\}+[K^e]\{u^e\}=\{f^e\}+\{Q^e\} \tag{8.169b}$$

The coefficients M_{ij}^e, K_{ij}^e, and f_i^e are the same as those in (8.159*c*).

EIGENVALUE ANALYSIS. The problem of finding $u_j(t)=U_je^{-i\omega t}$ ($i=\sqrt{-1}$) such that (8.169) holds for homogeneous boundary and initial conditions and $f=0$ is called an eigenvalue problem of (8.167). We obtain

$$\boxed{(-\omega^2[M^e]+[K^e])\{u^e\}=\{Q^e\}} \tag{8.170}$$

The eigenvalues ω^2 and eigenfunctions $\sum_{j=1}^{n}U_j\psi_j(x,y)$ are determined from the assembled equations associated with (8.170), after imposing the homogeneous boundary conditions. For a membrane problem, ω denotes the frequency of natural vibration. The number of eigenvalues of the discrete system (8.170) of the problem is equal to the number of unknown nodal values of U in the mesh.

Example 8.11. Consider the free vibrations of a rectangular membrane of homogeneous material, of dimensions a by b (in ft), material density ρ (in slugs ft^{-2}), and fixed on all its edges, i.e., $u=0$ on Γ. Although the problem has symmetry about the horizontal centerline and vertical centerlines of the domain (see Fig. 8.39), use of any symmetry in the finite element analysis will eliminate the unsymmetric modes of vibration of the membrane. For example, if we consider a quadrant of the domain in the finite element analysis, the frequencies ω_{mn} ($m, n \neq 1, 3, 5, \ldots$) and associated eigenfunctions will be missed in the results [i.e., we can only obtain ω_{mn} ($m, n = 1, 3, 5, \ldots$)]. By considering the full domain, the first N frequencies allowed by the mesh can be computed, where N is the number of unknown nodal values in the mesh.

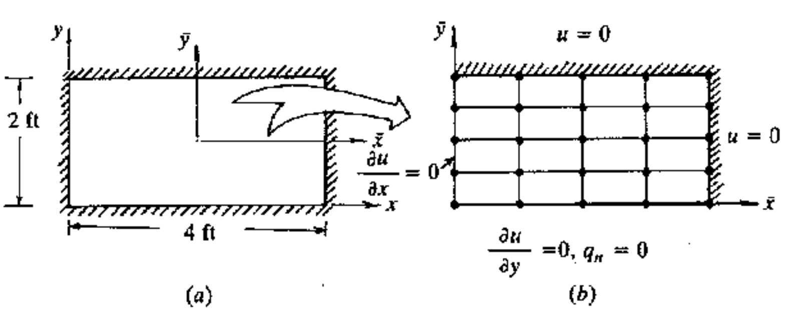
y
$\bar{y}$
2 ft
4 ft
$\bar{x}$
$\frac{\partial u}{\partial x}=0$
x
$\bar{y}$
$u=0$
$u=0$
$\bar{x}$
$\frac{\partial u}{\partial y}=0,\ q_n=0$

(*a*) (*b*)

FIGURE 8.39

Geometry, computational domain, finite element mesh, and boundary conditions for the transient analysis of a rectangular membrane with initial deflection: (*a*) actual geometry; (*b*) computational domain, finite element mesh of rectangular elements, and boundary conditions (4 × 4 mesh of linear elements or 2 × 2 mesh of nine-node quadratic elements).

TABLE 8.12
Comparison of natural frequencies computed using various meshes of linear triangular and rectangular elements with the analytical solution of a rectangular membrane fixed on all its sides ($a_{11} = a_{22} = 12.5$, $\rho = T = 2.5$)

	Triangular (linear)			Rectangular (linear)			
ω_{mn}	2×2	4×4	8×8	2×2	4×4	8×8	Analytical
ω_{11}	5.0000	4.2266	4.0025	4.3303	4.0285	3.9522	3.9270
ω_{21}	—	5.9083	5.2068	—	5.2899	5.0478	4.9673
ω_{31}	—	8.2392	6.8788	—	7.2522	6.6020	6.3321
ω_{12}	—	8.3578	7.5271	—	7.9527	7.4200	7.2410
ω_{22}	—	10.0618	8.4565	—	8.6603	8.0571	7.8540
ω_{41}	—	12.1021	8.8856	—	9.9805	8.5145	7.8540
ω_{32}	—	13.2011	9.9280	—	12.7157	9.1117	8.7810
ω_{51}	—	14.6942	11.1193	—	13.1700	10.5797	9.4574
ω_{42}	—	15.8117	11.4425	—	14.0734	10.7280	9.9346

If only the first eigenvalue ω_{11} is of interest or only symmetric frequencies are required, one can use a quadrant of the domain in the analysis. Indeed the results of Example 8.9 are applicable here, with $\lambda_{mn} = \omega_{mn}^2$. The results presented in Table 8.9 can be interpreted as the squares of the symmetric natural frequencies of a square $a = b = 2$) membrane with $\rho = 1$ and $a_{11} = a_{22} = T = 1$. The exact natural frequencies of a rectangular membrane of dimensions a by b, with tensions $a_{11} = a_{22} = T$ and density ρ are

$$\omega_{mn} = \pi\left(\frac{T}{\rho}\right)^{1/2}\left(\frac{m^2}{a^2} + \frac{n^2}{b^2}\right)^{1/2} \quad (m, n = 1, 2, \ldots)$$

To obtain all frequencies, the full domain must be modeled.

Table 8.12 contains the first nine frequencies of a rectangular membrane of 4 ft by 2 ft, tension $T = 12.5\,\text{lb ft}^{-1}$, and density $\rho = 2.5$ slugs ft^{-2}, computed using various meshes of linear triangular and rectangular elements. The convergence of the finite element results to the analytical solution is clear. The mesh of linear rectangular element yields more accurate results than the mesh of linear triangular elements.

TRANSIENT ANALYSIS. The hyperbolic equation (8.169*b*) can be reduced to a system of algebraic equations by approximating the second time derivative. As discussed in Section 6.2, the Newmark time integration scheme is the most commonly used method, and therefore it is used here. Since the mathematical form of (8.169b) is exactly the same as that in (6.44), the results in (6.47) and (6.49) are immediately applicable to the former. For the sake of convenience, the results are repeated here. The Newmark scheme is

$$\boxed{\begin{aligned} \{u\}_{s+1} &= \{u\}_s + \Delta t\{\dot{u}\}_s + \tfrac{1}{2}(\Delta t)^2\{\ddot{u}\}_{s+\gamma} \\ \{\dot{u}\}_{s+1} &= \{\dot{u}\}_s + \Delta t\{\ddot{u}\}_{s+\alpha} \\ \{\ddot{u}\}_{s+\theta} &= (1-\theta)\{\ddot{u}\}_s + \theta\{\ddot{u}\}_{s+1} \end{aligned}} \qquad (8.171a)$$

where, for example,

$\alpha=\frac{1}{2}$,	$\gamma=\frac{1}{2}$,	the constant-average acceleration method (stable)
$\alpha=\frac{1}{2}$,	$\gamma=\frac{1}{3}$,	the linear acceleration method (conditionally stable)
$\alpha=\frac{1}{2}$,	$\gamma=0$,	the central difference method (conditionally stable)

(8.171*b*)

The stability criterion is

$$\boxed{\Delta t<\Delta t_{\mathrm{cr}}=[\tfrac{1}{2}\omega_{\max}^{2}(\alpha-\gamma)]^{-1/2}, \qquad \alpha\geqslant\tfrac{1}{2}, \qquad \gamma<\alpha} \tag{8.172}$$

where $\omega_{\max}^2$ is the maximum eigenvalue of the corresponding discrete eigenvalue problem (8.170) (i.e., the same mesh and element type used in the transient analysis must be used in the eigenvalue analysis). Note that a more refined mesh will yield a lower maximum eigenvalue and a higher Δt_{cr}.

Time marching scheme

$$[\hat{K}^e]_{s+1}\{u^e\}_{s+1}=\{\hat{F}^e\}_{s,s+1} \tag{8.173a}$$

where (the superscript *e* is omitted for brevity in the following)

$$\boxed{\begin{gathered}[\hat{K}]_{s+1}=[K]_{s+1}+a_3[M]_{s+1}\\ \{\hat{F}\}_{s,s+1}=\{F\}_{s+1}+[M]_{s+1}(a_3\{u\}_s+a_4\{\dot{u}\}_s+a_5\{\ddot{u}\}_s)\\ a_3=\frac{2}{\gamma(\Delta t)^2}, \qquad a_4=\Delta t\, a_3, \qquad a_5=\frac{1}{\gamma}-1\end{gathered}} \tag{8.173b}$$

Once $\{u\}_{s+1}$ has been calculated from (8.173*a*), the velocities and accelerations at time $t_{s+1}=\Delta t\,(s+1)$ are calculated from (6.49):

$$\begin{gathered}\{\ddot{u}\}_{s+1}=a_3(\{u\}_{s+1}-\{u\}_s)-a_4\{\dot{u}\}_s-a_5\{\ddot{u}\}_s\\ \{\dot{u}\}_{s+1}=\{\dot{u}\}_s+a_2\{\ddot{u}\}_s+a_1\{\ddot{u}\}_{s+1}\\ a_1=\alpha\,\Delta t, \qquad a_2=(1-\alpha)\,\Delta t\end{gathered} \tag{8.174}$$

Note that (8.173*a*) is valid for an element. Therefore, the operations indicated in (8.173*b*) are carried out for an element, and $[\hat{K}^e]=\{\hat{F}^e\}$ are assembled as in a static analysis. For the first time step, the initial conditions on u and $\partial u/\partial t$ are used to compute $\{u\}_0$ and $\{\dot{u}\}_0$ for each element of the entire mesh. The acceleration vector $\{\ddot{u}\}_0$ is computed from (8.169*b*) at $t=0$:

$$\{\ddot{u}\}_0=[M]^{-1}(\{F\}_0-[K]\{U\}_0) \tag{8.175}$$

It is often assumed that $\{F\}_0=\{0\}$. If the initial conditions are zero, $\{u\}_0=\{0\}$, and the applied force is assumed to be zero at $t=0$, we then take $\{\ddot{u}\}_0=\{0\}$.

Example 8.12. Consider a homogeneous rectangular membrane of sides $a = 4$ ft and $b = 2$ ft, fixed on all its four edges. Assume that the tension in the membrane is $12.5\ \text{lb ft}^{-1}$ (i.e., $a_{11} = a_{22} = 12.5$) and the density is $\rho = c = 2.5\ \text{slugs ft}^{-2}$. The initial deflection of the membrane is assumed to be

$$u_0(x, y) = 0.1(4x - x^2)(2y - y^2) \tag{8.176}$$

and the initial velocity is $v_0 = 0$. We wish to determine the deflection $u(x, y, t)$ of the membrane as a function of time using the finite element method. The analytical solution of this problem is [see Kreyszig (1988), p. 684],

$$u(x, y, t) = \frac{409.6}{\pi^6} \sum_{m,n=1,3,\ldots} \frac{1}{m^3 n^3} \cos \omega_{mn} t \sin \tfrac{1}{4} m\pi x \sin \tfrac{1}{2} n\pi y \tag{8.177a}$$

$$\omega_{mn} = \tfrac{1}{4}\pi[5(m^2 + 4n^2)]^{1/2} \tag{8.177b}$$

where the origin of the (x, y) coordinate system is located at the lower corner of the domain (see Fig. 8.39*a*).

In the finite element analysis, we can utilize the biaxial symmetry of the problem and model one quadrant of the domain (see Fig. 8.39*b*). We set up a new coordinate system $(\bar{x}, \bar{y})$ for the computational domain. The inital displacement in the new coordinates is given by (8.176), with x and y replaced in terms of $\bar{x}$ and $\bar{y}$:

$$x = \bar{x} + 2, \qquad y = \bar{y} + 1$$

The initial values of $\ddot{u}$ are calculated using (8.175), with $\{F\}_0 = \{0\}$ and $\{u\}_0$ as given in (8.176) by $u_0(x, y)$. At $\bar{x} = 2$ and $\bar{y} = 1$, all nodal values for the function u and its time derivatives are zero.

As for the critical time step, we calculate $\lambda_{\max}$ from the solution of (8.170) using the same mesh as that used for the transient analysis, and then use (8.172) to compute Δt_{cr}. Of course, for $\alpha = \frac{1}{2}$ and $\gamma = \frac{1}{2}$, there is no restriction on the time step for a stable solution. For a 4×4 mesh of linear rectangular elements, $\lambda_{\max} = (14.0734)^2$ (see Table 8.12), and $\Delta t_{cr} = 0.246$ for the linear acceleration scheme ($\alpha = 0.5$, $\gamma = \frac{1}{3}$).

Figure 8.40 shows plots of the center deflection $u(0, 0, t)$ versus time t, and Fig. 8.41 shows the stability of the solutions computed using the constant-average acceleration ($\alpha = 0.5$, $\gamma = 0.5$) and linear acceleration ($\alpha = 0.5$, $\gamma = \frac{1}{3}$) schemes for $\Delta t = 0.25 > \Delta t_{cr}$. Figure 8.40 also shows a comparison of the finite element solutions with the analytical solution (8.177). The finite element solutions are in good agreement with the analytical one.

8.6 SUMMARY

A step-by-step procedure for finite element formulation of second-order differential equations in two dimensions with a single dependent variable has been presented. The Poisson equation in two dimensions has been used to illustrate the steps involved. These include weak formulation of the equation, development of the finite element model, derivation of the interpolation functions for linear triangular and rectangular elements, evaluation of element matrices and vectors, assembly of element equations, solution of equations, and post-computation of the gradient of the solution. A number of illustrative problems of heat transfer (conduction and convection), fluid mechanics and solid mechanics have been discussed. Finally, the eigenvalue and time-

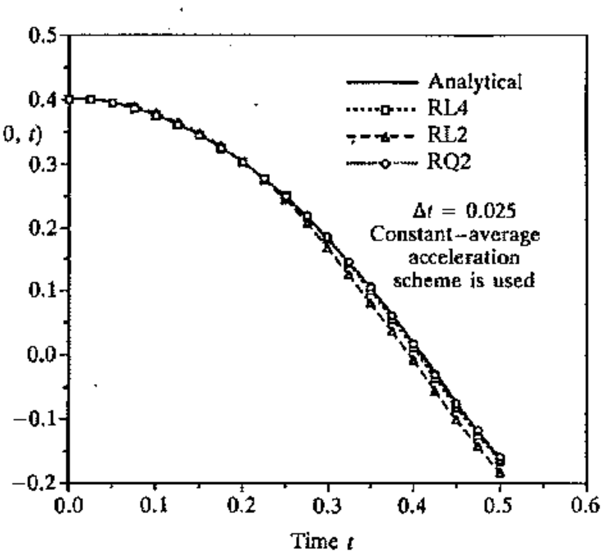

FIGURE 8.40
Comparison of the center deflection obtained using various meshes with the analytical solution of a rectangular membrane with initial deflection: RL4, 4×4 mesh of linear rectangular elements; RL2, 2×2 mesh of linear rectangular elements; RQ2, 2×2 mesh of nine-node quadratic elements.

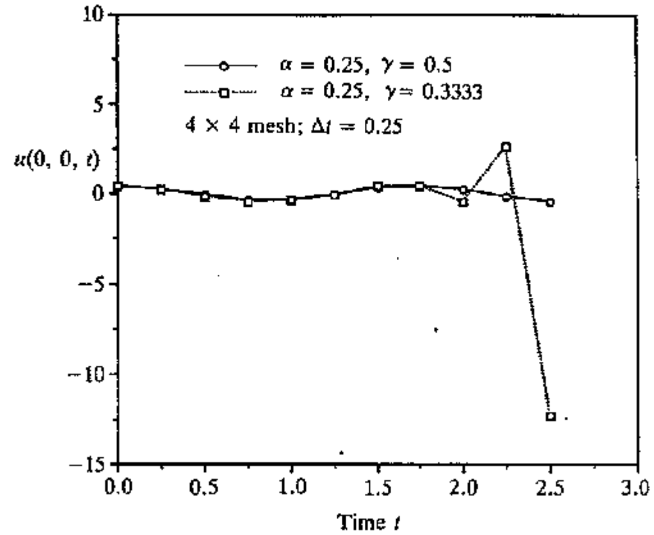

FIGURE 8.41
Stability characteristics of the constant-average acceleration and linear acceleration schemes (a 4×4 mesh of linear rectangular elements is used in a quadrant of the domain).

dependent problems associated with the model equation have also been discussed. This chapter constitutes the heart of the finite element analysis of two-dimensional problems to be discussed in Chapters 10–12.

PROBLEMS

Note that most of the problems given here require hand calculations only. When four or more simultaneous algebraic equations are to be solved, they should be left in matrix form. New problems can be created just by changing data and meshes.

Section 8.2

8.1. The electrostatic potential $\phi(x, y)$ of electrical charges in a region Ω is governed by the Poisson equation

$$-\nabla^2\phi = f(x, y)$$

where f is the distributed electric charge.

(*a*) Develop the finite element model of the equation.

(*b*) Identify the element coefficient matrices for linear triangular and rectangular elements from those available in this book.

(*c*) Write the specified primary and secondary variables at all boundary nodes and their specified values for the problem shown in Fig. P8.1.

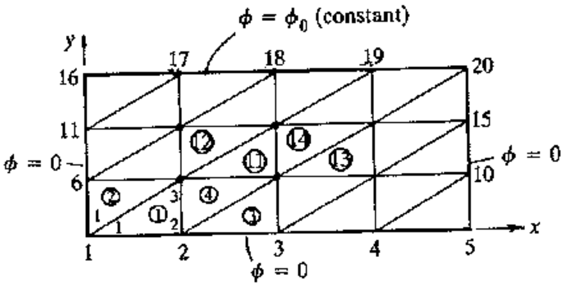

FIGURE P8.1

8.2. Consider the partial differential equation

$$-\nabla^2 u + cu = 0 \quad \text{in } \Omega^e, \qquad \text{with} \quad \frac{\partial u}{\partial n} + ku = 0 \quad \text{on } \Gamma^e$$

Develop the weak form and finite element model of the equation over an element Ω^e.

8.3. Assuming that c and k are constant in Problem 8.2, write the element coefficient matrix and source vector for (*a*) a linear rectangular element and (*b*) a linear triangular element.

8.4. Develop the finite element model of the following differential equation governing an axisymmetric problem,

$$-\frac{1}{r}\left[\frac{\partial}{\partial r}\left(r\frac{\partial u}{\partial r}\right) + \frac{\partial}{\partial z}\left(r\frac{\partial u}{\partial z}\right)\right] = f(r, z)$$

and compute the coefficients K_{ij}^e and f_i^e for a linear triangular element in terms of I_{mn} of (8.36).

8.5. Calculate the linear interpolation functions for the linear triangular and rectangular elements shown in Fig. P8.5.

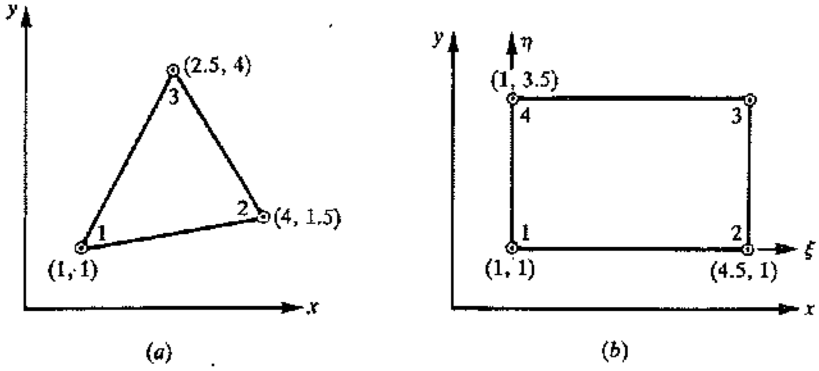

FIGURE P8.5

Answer: $\psi_1 = (12.25 - 2.5x - 1.5y)/8.25$.

8.6. For the linear triangular element shown in Fig. P8.6, show that the element coefficient matrix associated with the Laplace operator $-\nabla^2$,

$$K_{ij}^e = \int_{\Omega^e} \left(\frac{\partial \psi_i^e}{\partial x} \frac{\partial \psi_j^e}{\partial x} + \frac{\partial \psi_i^e}{\partial y} \frac{\partial \psi_j^e}{\partial y} \right) dx\, dy$$

is

$$[K^e] = \frac{1}{2} \begin{bmatrix} \alpha + \beta & -\alpha & -\beta \\ -\alpha & \alpha & 0 \\ -\beta & 0 & \beta \end{bmatrix}, \qquad \alpha = \frac{b}{a}, \qquad \beta = \frac{a}{b}$$

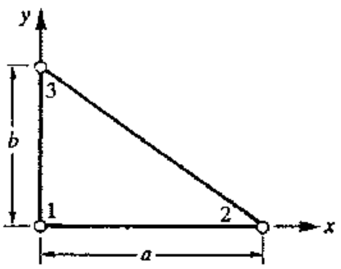

FIGURE P8.6

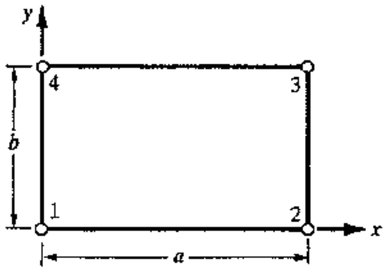

FIGURE P8.7

8.7. For the linear rectangular element shown in Fig. P8.7, show that the element coefficient matrix associated with the Laplace operator is

$$[K^e] = \frac{1}{6} \begin{bmatrix} 2(\alpha+\beta) & -2\alpha+\beta & -(\alpha+\beta) & \alpha-2\beta \\ -2\alpha+\beta & 2(\alpha+\beta) & \alpha-2\beta & -(\alpha+\beta) \\ -(\alpha+\beta) & \alpha-2\beta & 2(\alpha+\beta) & -2\alpha+\beta \\ \alpha-2\beta & -(\alpha+\beta) & -2\alpha+\beta & 2(\alpha+\beta) \end{bmatrix}, \qquad \alpha = \frac{b}{a}, \qquad \beta = \frac{a}{b}$$

8.8. Find the coefficient matrix associated with the Laplace operator when the rectangular element in Fig. P8.7 is divided into two triangles by joining node 1 to node 3.

8.9. The nodal values of an element in the finite element analysis of a field problem $-\nabla^2 u = f_0$ are $U_{10} = 389.79$, $U_{11} = 337.19$, and $U_{12} = 395.08$ (see Fig. P8.9). Find the gradient of the solution in the element. Also determine where the 392 isoline intersects the boundary of the element in Fig. P8.9.

Answer: $\nabla T = 10.76\hat{e}_1 - 105.02\hat{e}_2$.

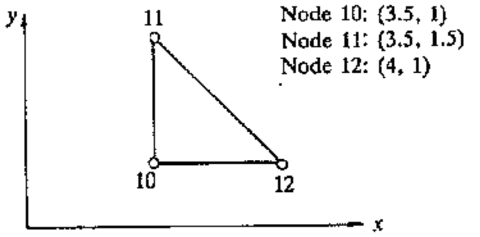

FIGURE P8.9

8.10. If the nodal values of the elements shown in Fig. P8.10 are $u_1 = 0.2645$, $u_2 = 0.2172$, $u_3 = 0.1800$ for the triangular element and $u_1 = 0.2173$, $u_3 = 0.1870$, $u_2 = u_4 = 0.2232$ for the rectangular element, compute u, $\partial u/\partial x$, and $\partial u/\partial y$ at the point $(x, y) = (0.375, 0.375)$.

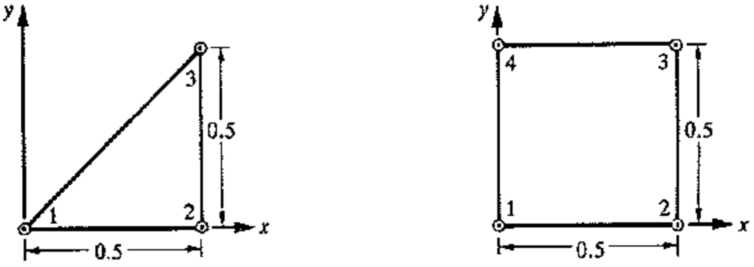

(a)

(b)

FIGURE P8.10

8.11. Compute the element matrices

$$S^{01}_{ij} = \int_0^a \int_0^b \psi_i \frac{d\psi_j}{dx}\,dx\,dy, \qquad S^{02}_{ij} = \int_0^a \int_0^b \psi_i \frac{d\psi_j}{dy}\,dx\,dy$$

where ψ_i are the linear interpolation functions of a rectangular element with sides a and b.

8.12. Give the assembled coefficient matrix for the finite element meshes shown in Fig. P8.12. Assume one degree of freedom per node and let $[K^e]$ denote the element coefficient matrix for the eth element. Your answer should be in terms of element matrices K^e_{ij}.

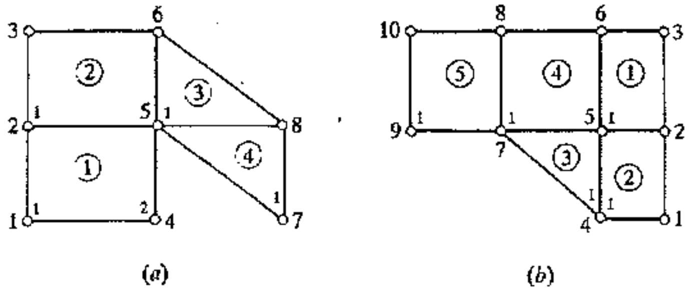

(a) (b)

FIGURE P8.12

8.13. Compute the global source vector corresponding to the nonzero specified boundary flux for the finite element meshes of linear elements shown in Fig. P8.13.

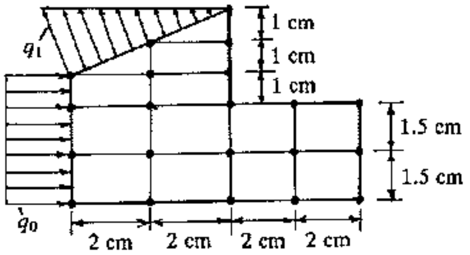

FIGURE P8.13

8.14. Repeat Problem 8.13 for the finite element mesh of quadratic elements shown in Fig. P8.14.

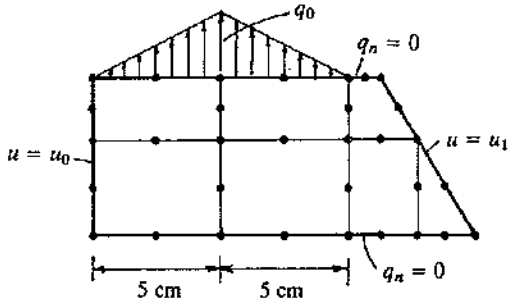

FIGURE P8.14

8.15. A point source of magnitude Q_0 is located at the point $(x, y) = (1.25, 2.5)$ inside the triangular element shown in Fig. P8.5(*a*). Determine the contribution of the point source to the element source vector.

8.16. Repeat Problem 8.15 for the rectangular element in Fig. P8.5(*b*).

8.17. A line source of intensity q_0 is located across the triangular element shown in Fig. 8.17. Compute the element source vector.

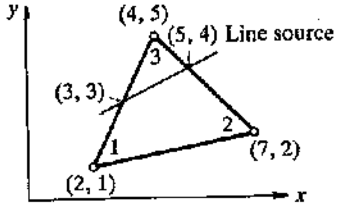

FIGURE P8.17

8.18. Repeat Problem 8.17 when the line source has varying intensity $q(s)=q_0 s/L$, where s is the coordinate along the line source.

8.19. When a_{11} and a_{22} in (8.1) are bilinear functions of the global coordinates x and y, $a_{ij}=a_{ij}^0+a_{ij}^1 x+a_{ij}^2 y$, and $a_{12}=a_{21}=a_{00}=0$, determine the explicit form of the coefficient matrix $[K^e]$ in (8.14b) for the linear triangular element. Express the result in terms of the integrals defined in (8.36).

8.20. Repeat Problem 8.19 for the linear rectangular element with local coordinate system $(\bar{x},\bar{y})$. Use (8.42) and (8.43) to evaluate the integrals. You may also use the coefficient matrices in (8.44).

8.21. Determine the source vector

$$f_i^e=\int_{\Omega^e} f\psi_i\,dx\,dy$$

for linear rectangular elements when f is a function of the form $f=a_0+a_1x+a_2y$, where x and y are the global coordinates.

8.22. Evaluate the coefficient matrix K_{ij}^e and source vector f_i^e in (8.64b) for a linear triangular element when $\hat{a}_{11}$, $\hat{a}_{22}$, and $\hat{f}$ are constant, and $\hat{a}_{00}=0$. Note that the results of Problem 8.19 are useful here.

8.23. Repeat Problem 8.22 for a linear rectangular element.

8.24. For the mesh of linear triangular elements shown in Fig. P8.1, give the condensed set of equations for the unknown nodal values when $f=f_0=$ constant. Use the symmetry of the problem. Write algebraic equations for the secondary variables Q_1^1 and Q_2^1 (from equilibrium).

8.25. Repeat Problem 8.24 with the equivalent mesh of linear rectangular elements.

8.26. Solve the Laplace equation

$$-\left(\frac{\partial^2 u}{\partial x^2}+\frac{\partial^2 u}{\partial y^2}\right)=0 \quad \text{in } \Omega$$

on a rectangle, when $u(0,y)=u(a,y)=u(x,0)=0$ and $u(x,b)=u_0(x)$. Use the symmetry and (a) a mesh of 2×2 triangular elements and (b) a mesh of 2×2 rectangular elements (see Fig. P8.26). Compare the finite element solution with the exact solution

$$u(x,y)=\sum_{n=1}^{\infty} A_n \sin\frac{n\pi x}{a}\sinh\frac{n\pi y}{b}$$

where

$$A_n=\frac{2}{a\sinh(n\pi b/a)}\int_0^a u_0(x)\sin\frac{n\pi x}{a}\,dx$$

Take $a = b = 1$, and $u_0(x) = \sin \pi x$ in the computations. For this case, the exact solution becomes

$$u(x, y) = \frac{\sin \pi x \sinh \pi y}{\sinh \pi}$$

Answer: for a 2×2 mesh of triangles, $U_4 = 0.23025$ and $U_5 = 0.16281$; for a 2×2 mesh of rectangles, $U_4 = 0.15202$ and $U_5 = 0.10750$.

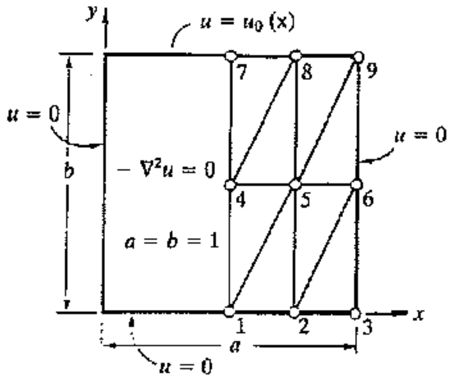

FIGURE P8.26

8.27. Solve Problem 8.26 when $u_0(x) = 1$. The analytical solution is given by

$$u(x, y) = \frac{4}{\pi} \sum_{n=0}^{\infty} \frac{\sin (2n+1)\pi x \sin (2n+1)\pi y}{(2n+1) \sinh (2n+1)\pi}$$

Answer: (*a*) $U_4 = 0.26471$ and $U_5 = 0.20588$.

8.28. Solve Problem 8.26 when $u_0(x) = 4(x - x^2)$.
Answer: $U_4 = 0.23529$ and $U_5 = 0.16912$.

8.29. Solve the Laplace equation for the unit square domain and boundary conditions given in Fig. P8.29. Use one rectangular element.

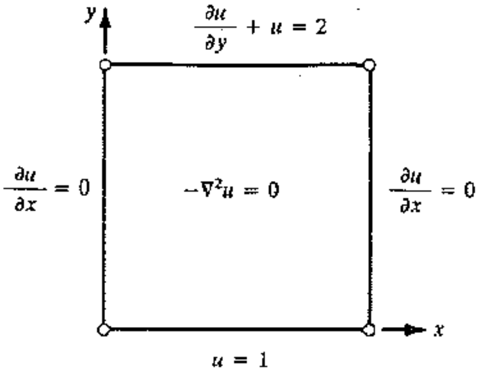

FIGURE P8.29

8.30. Use two triangular elements to solve the problem in Fig. P8.29. Use the mesh obtained by joining points $(1, 0)$ and $(0, 1)$.

8.31. Solve the Poisson equation $-\nabla^2 u = 2$ in the square whose vertices are at $(0, 0)$, $(1, 0)$, $(1, 1)$, and $(0, 1)$. The boundary conditions are $u(0, y) = y^2$, $u(x, 0) = x^2$, $u(1, y) = 1 - y$ and $u(x, 1) = 1 - x$. Use four linear rectangular elements (a 2×2 mesh).

8.32. Solve Problem 8.31 using four triangular elements in the upper half of the triangle because of the symmetry about the $x = y$ lines; join node 2 to 5 in Fig. P8.32.

Answer: $U_3 = 0.5$.

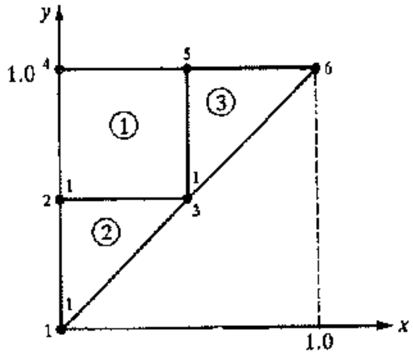

FIGURE P8.32

8.33. Solve Problem 8.31 using the mesh of a rectangle and two triangles, as shown in Fig. P8.32.

Answer: $U_3 = 0.675$.

8.34. Solve the Poisson equation $-\nabla^2 u = 2$ in Ω, with boundary conditions $u = 0$ on Γ_1 and $\partial u/\partial n = 0$ on Γ_2, where Ω is the first quadrant bounded by the parabola $y = 1 - x^2$ and the coordinate axes (see Fig. P8.34), and Γ_1 and Γ_2 are the boundaries shown in Fig. P8.34.

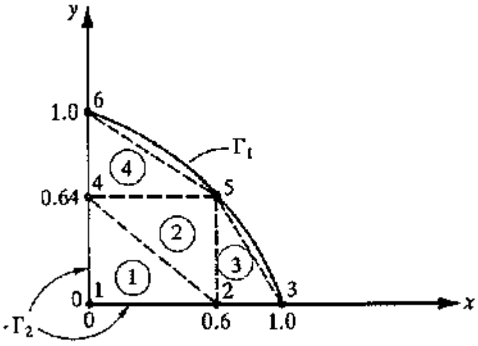

FIGURE P8.34

8.35. Show that a variable approximated by the quadratic interpolation functions of a rectangular element is continuous along interelement boundaries.

8.36. Solve the axisymmetric field problem shown in Fig. P8.36 for the mesh shown there. Note that the problem has symmetry about any line z = constant. Hence, the problem is essentially one-dimensional. Compare the finite element solution with the exact one.

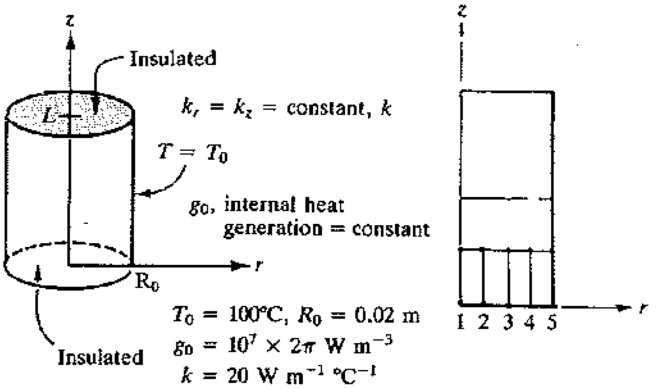
z
Insulated
L
$k_r = k_z$ = constant, k
$T = T_0$
g_0, internal heat generation = constant
r
R_0
T_0 = 100°C, R_0 = 0.02 m
$g_0 = 10^7 \times 2\pi$ W m^{-3}
k = 20 W m^{-1} °C^{-1}
Insulated
z
1 2 3 4 5
r

FIGURE P8.36

8.37. Formulate the axisymmetric field problem shown in Fig. P8.37 for the mesh shown. Compute the secondary variable at $r = \frac{1}{2}R$ using (*a*) equilibrium and (*b*) the definition. Use the element at the left of the node.

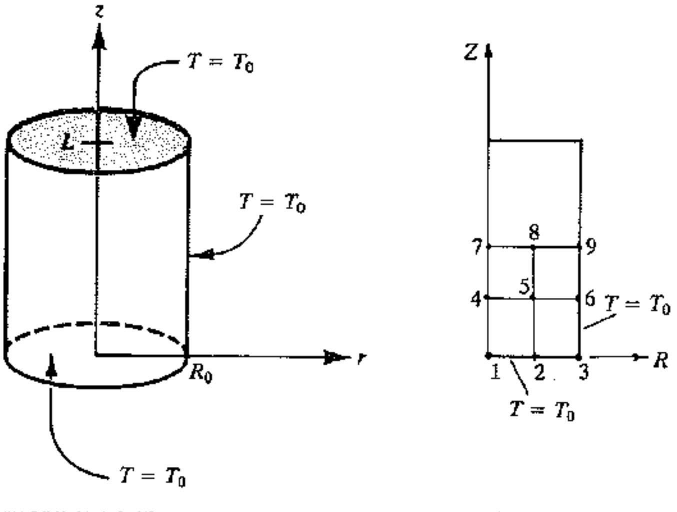

FIGURE P8.37

Section 8.4

8.38. A series of heating cables have been placed in a conducting medium, as shown in Fig. P8.38. The medium has conductivities of $k_x = 10\ \mathrm{W\,cm^{-1}\,°C^{-1}}$ and $k_y =$

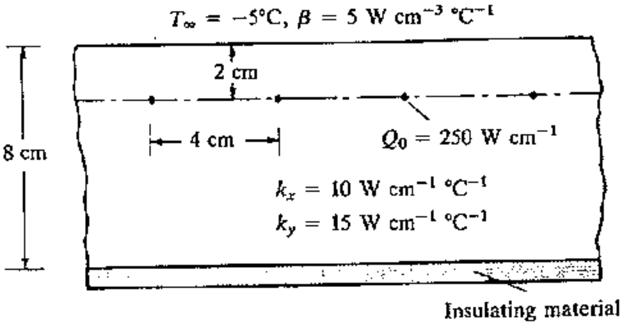
$T_\infty = -5°C$, $\beta = 5$ W cm^{-3} °C^{-1}
2 cm
4 cm
$Q_0 = 250$ W cm^{-1}
8 cm
$k_x = 10$ W cm^{-1} °C^{-1}
$k_y = 15$ W cm^{-1} °C^{-1}
Insulating material

FIGURE P8.38

15 W cm^{-1} °C^{-1}, the upper surface is exposed to a temperature of -5 °C, and the lower surface is bounded by an insulating medium. Assume that each cable is a point source of 250 W cm^{-1}. Take the convection coefficient between the medium and the upper surface to be $\beta = 5$ W cm^{-2} °C^{-1}. Use a 2×8 mesh of linear rectangular (or triangular) elements in the computational domain (use the symmetry available in the problem), and formulate the problem (i.e., give element matrices for a typical element, give boundary conditions on primary and secondary variables, and compute convective boundary contributions).

8.39. Formulate the finite element analysis information to determine the temperature distribution in the molded asbestos insulation shown in Fig. P8.39. Use the symmetry to identify a computational domain and identify the specified boundary conditions at the nodes of the mesh. What is the size of the assembled coefficient matrix?

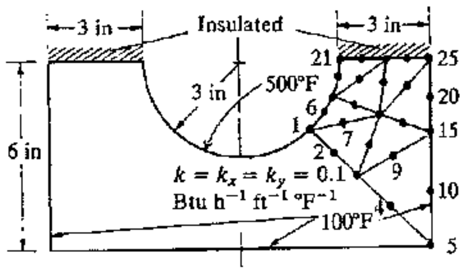

FIGURE P8.39

8.40. Consider steady-state heat conduction in a square region of side $2a$. Assume that the medium has conductivity k (in W m^{-1} °C^{-1}) and uniform heat (energy) generation f_0 (in W m^{-3}). For the boundary conditions and mesh shown in Fig. P8.40, write the finite element algebraic equations for nodes 1, 3, and 7.

8.41. Repeat Problem 8.40 for nodes 4, 5, and 9.

8.42. For the convective heat transfer problem shown in Fig. P8.42, write the four finite element equations for the unknown temperatures. Assume that the thermal conductivity of the material is $k = 5$ W m^{-1} °C^{-1}, the convective heat transfer

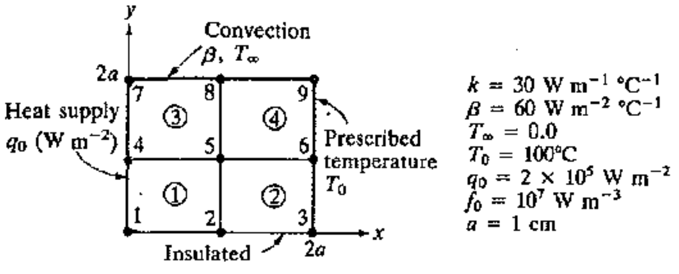

FIGURE P8.40

coefficient on the left surface is $\beta = 30\,\mathrm{W\,m^{-2}\,°C^{-1}}$, and the internal heat generation is zero. Compute the heats at nodes 2, 4, and 9 using (*a*) element equations (i.e., equilibrium) and (*b*) the definition (use the temperature field of elements 1 and 2).

8.43. Write the finite element equations for the unknown temperatures of the problem shown in Fig. P8.43.

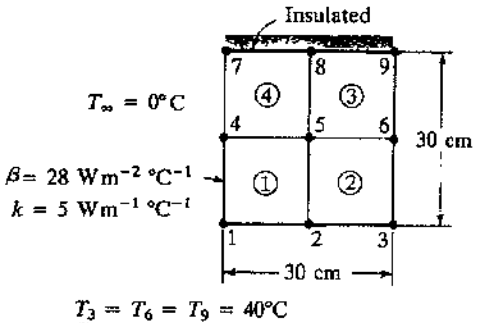

FIGURE P8.42

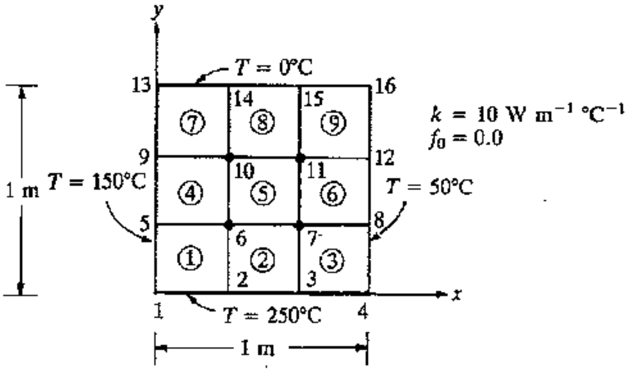

FIGURE P8.43

8.44. Write the finite element equations for the heats at nodes 1 and 13 of Problem 8.43. The answer should be in terms of the nodal temperatures $T_1, T_2, \ldots, T_{16}$.

8.45. Write the finite element equations associated with nodes 13, 16, and 19 for the problem shown in Fig. P8.45.

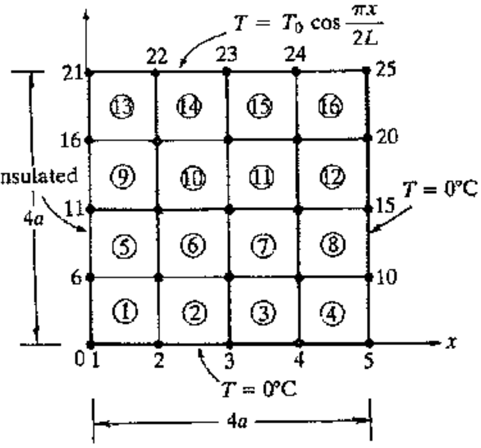

FIGURE P8.45

8.46. The fin shown in Fig. P8.46 has its base maintained at 300°C and is exposed to ambient temperature on its remaining boundary. Write the finite element equations at nodes 7 and 10.

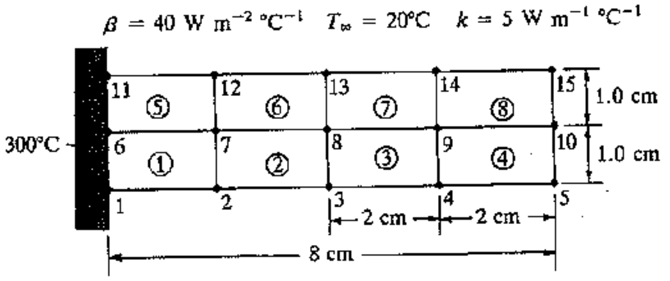

FIGURE P8.46

8.47. Compute the heat loss at nodes 10 and 13 of Problem 8.46.

8.48. Consider the problem of groundwater flow beneath a coffer dam. Formulate it using the velocity potential for finite element analysis. The geometry and boundary conditions are shown in Fig. P8.48.

8.49. Formulate the groundwater flow problem for the domain shown in Fig. P8.49 for finite element analysis. The pump is located at $(826\frac{2}{3}, 400)$.

8.50. Repeat Problem 8.49 for the domain shown in Fig. P8.50.

8.51. Consider steady confined flow through the foundation soil of a dam (see Fig. P8.51). Assuming that the soil is isotropic ($k_x = k_y$), formulate the problem for

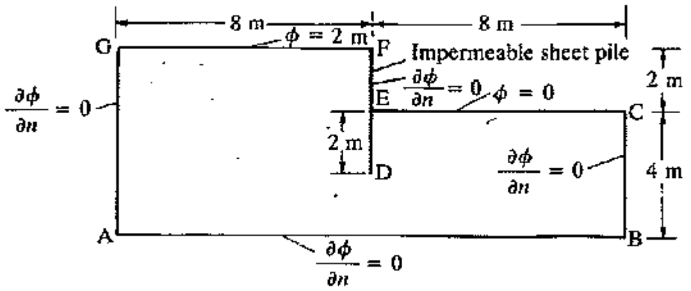
8 m
8 m
$\phi = 2$ m
G
F
Impermeable sheet pile
2 m
$\frac{\partial \phi}{\partial n} = 0$
E
$\frac{\partial \phi}{\partial n} = 0$
$\phi = 0$
C
2 m
D
$\frac{\partial \phi}{\partial n} = 0$
4 m
A
B
$\frac{\partial \phi}{\partial n} = 0$

FIGURE P8.48

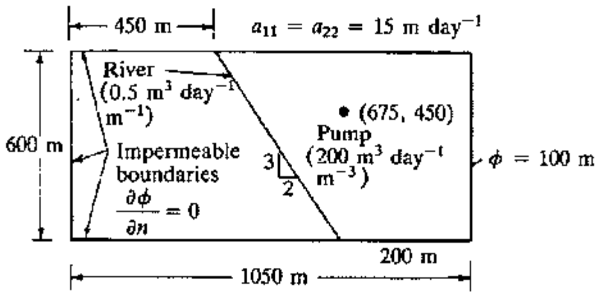
450 m
$a_{11} = a_{22} = 15$ m day^{-1}
River
(0.5 m^3 day^{-1} m^{-1})
600 m
Impermeable boundaries
$\frac{\partial \phi}{\partial n} = 0$
3
2
• (675, 450)
Pump
(200 m^3 day^{-1} m^{-3})
$\phi = 100$ m
200 m
1050 m

FIGURE P8.49

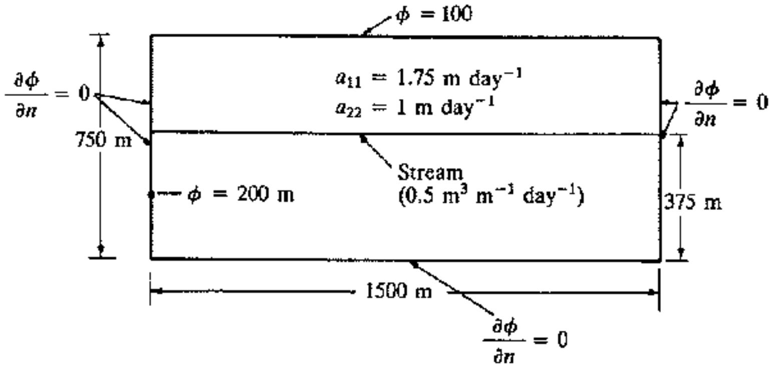
$\phi = 100$
$\frac{\partial \phi}{\partial n} = 0$
$a_{11} = 1.75$ m day^{-1}
$a_{22} = 1$ m day^{-1}
$\frac{\partial \phi}{\partial n} = 0$
750 m
Stream
(0.5 m^3 m^{-1} day^{-1})
$\phi = 200$ m
375 m
1500 m
$\frac{\partial \phi}{\partial n} = 0$

FIGURE P8.50

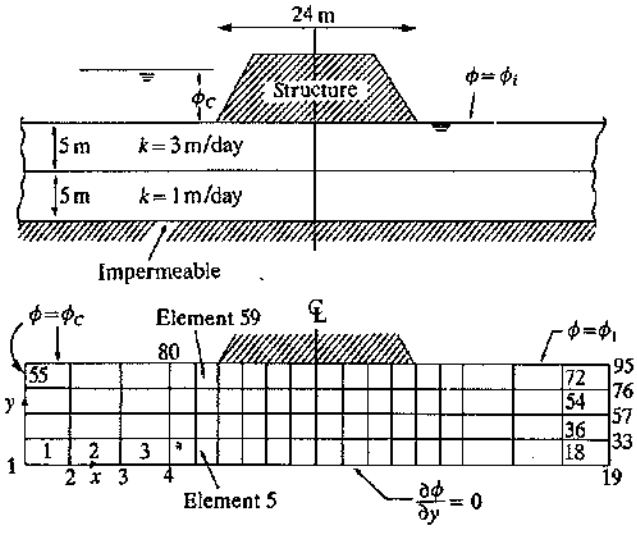

FIGURE P8.51

finite element analysis (identify the specified primary and secondary variables and their contribution to the nodes). In particular, write the finite element equations at nodes 8 and 11. Write the finite element equations for the horizontal velocity component in the fifth and tenth elements.

8.52. Formulate the problem of flow about an elliptical cylinder using (*a*) the stream function and (*b*) the velocity potential. The geometry and boundary conditions are shown in Fig. P8.52.

8.53. Repeat Problem 8.52 for the domain shown in Fig. P8.53.

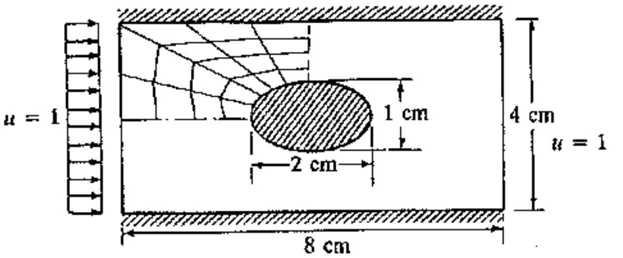

FIGURE P8.52

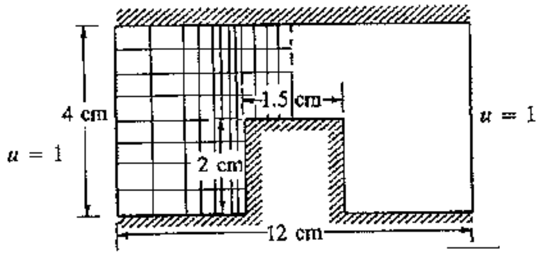

FIGURE P8.53

8.54. The Prandtl theory of torsion of a cylindrical member leads to

$$-\nabla^2 u = 2G\theta \quad \text{in } \Omega; \qquad u = 0 \quad \text{on } \Gamma$$

where Ω is the cross-section of the cylindrical member being twisted, Γ is the boundary of Ω, G is the shear modulus of the material of the member, θ is the angle of twist, and u is the stress function. Solve the equation for the case in which Ω is a circular section (see Fig. P8.54) using the mesh of linear triangular elements. Compare the finite element solution with the exact one (valid for

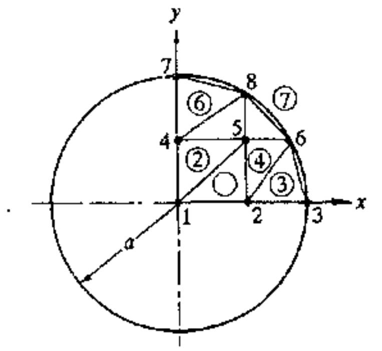

FIGURE P8.54

elliptical sections with axes a and b)

$$u = \frac{G\theta a^2 b^2}{a^2 + b^2}\left(1 - \frac{x^2}{a^2} - \frac{y^2}{b^2}\right)$$

Use $a = 1$, $b = 1$, and $2G\theta = 10$.

8.55. Repeat Problem 8.54 for a member with elliptical section. Use $a = 1$ and $b = 1.5$.

8.56. Repeat Problem 8.54 for the case in which Ω is an equilateral triangle (see Fig. P8.56). The exact solution is

$$u = -G\theta[\tfrac{1}{2}(x^2 + y^2) - \tfrac{1}{2}a(x^3 - 3xy^2) - \tfrac{2}{27}a^2]$$

Take $a = 1$ and $2G\theta = 10$.

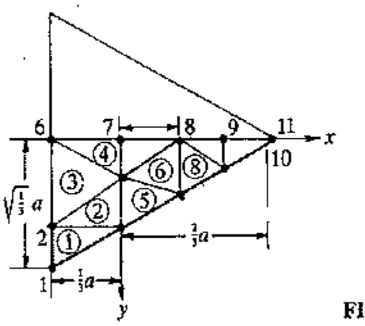

FIGURE P8.56

8.57. Consider the torsion of a hollow member with square cross-section. The stress function Ψ is required to satisfy the Poisson equation (8.150) and the following boundary conditions:

$$\Psi = 0 \quad \text{on the outer boundary}; \qquad \Psi = 2r^2 \quad \text{on the inner boundary}$$

where $r = a/c$ is the ratio of outside to inside dimensions. Formulate the problem for finite element analysis using the mesh shown in Fig. P8.57.

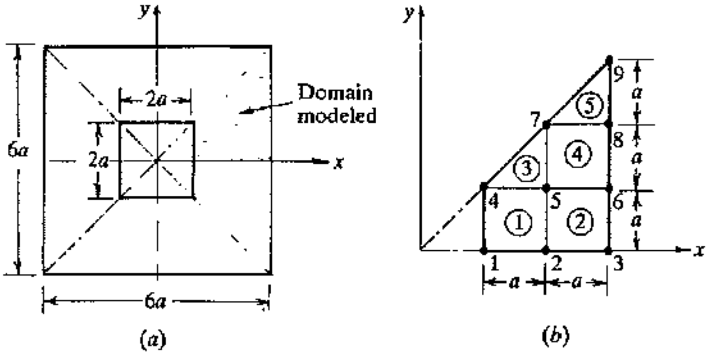

FIGURE P8.57

8.58. Repeat Problem 8.57 with the mesh of linear triangles (join nodes 1 and 5, 2 and 6, and 5 and 8 in Fig. P8.57b).

8.59. The membrane shown in Fig. P8.59 is subjected to a uniformly distributed load of intensity f_0 (in N m^{-2}). Formulate the problem for finite element analysis.

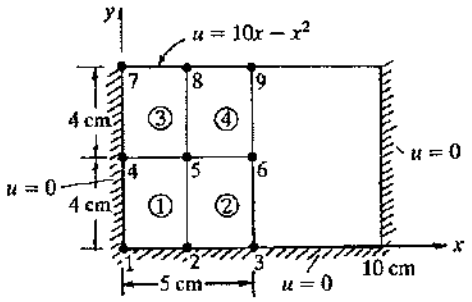

FIGURE P8.59

8.60. Repeat Problem 8.59 for the membrane shown in Fig. P8.60.

Section 8.5

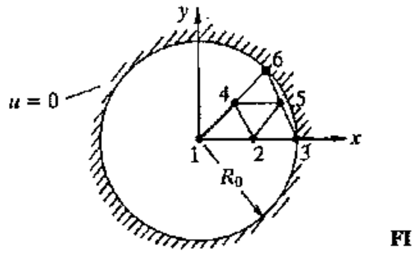

FIGURE P8.60

8.61. Determine the time step for the transient analysis (with $\alpha \leq \frac{1}{2}$) of the problem

$$\frac{\partial u}{\partial t} - \nabla^2 u = 1 \quad \text{in } \Omega; \qquad u = 0 \quad \text{in } \Omega \text{ at } t = 0$$

by determining the minimum eigenvalue of the problem

$$-\nabla^2 u = \lambda u \quad \text{in } \Omega; \; u = 0 \quad \text{on } \Gamma$$

The geometry of the domain and mesh are shown in Fig. P8.26.
Answer: $\lambda = 24$ for a 1×1 mesh.

8.62. Set up the condensed equations for the transient problem in Problem 8.61 for the α family of approximation. Use the finite element mesh shown in Fig. P8.26.

8.63. Set up the condensed equations for the time-dependent analysis of the membrane in Problem 8.60.

8.64. (*Central difference method*) Consider the following matrix differential equation in time:

$$[M]\{\ddot{U}\} + [C]\{\dot{U}\} + [K]\{U\} = \{F\}$$

where the superposed dots indicate differentiation with respect to time. Assume

$$\{\ddot{U}\}_n = \frac{1}{(\Delta t)^2}(\{U\}_{n-1} - 2\{U\}_n + \{U\}_{n+1}), \qquad \{\dot{U}\}_n = \frac{1}{2(\Delta t)}(\{U\}_{n+1} - \{U\}_{n-1})$$

and derive the algebraic equations for the solution of $\{U\}_{n+1}$ in the form

$$[A]\{U\}_{n+1} = \{F\}_n - [B]\{U\}_n - [D]\{U\}_{n-1}$$

Define $[A]$, $[B]$, and $[D]$ in terms of $[M]$, $[C]$, and $[K]$.

8.65. Repeat Problem 8.64 using the Newmark time approximation scheme.

8.66. Consider the first-order differential equation in time

$$a\frac{du}{dt} + bu = f$$

Using linear approximation, $u(t) = u_1\psi_1(t) + u_2\psi_2(t)$, $\psi_1 = 1 - t/\Delta t$, and $\psi_2 = t/\Delta t$, derive the associated algebraic equation and compare it with that obtained using the α family of approximation.

8.67. (*Space–time element*) Consider the differential equation

$$c\frac{\partial u}{\partial t} - \frac{\partial}{\partial x}\left(a\frac{\partial u}{\partial x}\right) = f \quad \text{for } 0 < x < L, \ 0 \leqslant t \leqslant T$$

with

$$u(0, t) = u(L, t) = 0 \quad \text{for } 0 \leqslant t \leqslant T; \qquad u(x, 0) = u_0(x) \quad \text{for } 0 < x < L$$

where $c = c(x)$, $a = a(x)$, $f = f(x, t)$, and u_0 are given functions. Consider the rectangular domain defined by

$$\Omega = \{(x, t): 0 < x < L, \ 0 \leqslant t \leqslant T\}$$

A finite element discretization of Ω by rectangles requires a space–time rectangular element (with y replaced by t). Give a finite element formulation of the equation over a space–time element, and discuss the mathematical and practical limitations of such a formulation. Compute the element matrices for a linear element.

8.68. (*Space-time finite elements*) Consider the time-dependent problem

$$\frac{\partial^2 u}{\partial x^2} = \frac{\partial u}{\partial t} \quad \text{for } 0 < x < 1, \ t > 0$$

$$u(0, t) = 0, \qquad \frac{\partial u}{\partial t}(1, t) = 1, \qquad u(x, 0) = x$$

Use linear rectangular elements in the (x, t) plane to model the problem. Note that the finite element model is given by $[K^e]\{u^e\} = \{Q^e\}$, where

$$K_{ij}^e = \int_0^{\Delta t}\int_{x_A}^{x_B}\left(\frac{\partial \psi_i^e}{\partial x}\frac{\partial \psi_j^e}{\partial x} + \psi_i\frac{\partial \psi_j}{\partial t}\right)dx\,dt$$

$$Q_1^e = \left(-\int_0^{\Delta t}\frac{\partial u}{\partial x}dt\right)\Bigg|_{x=x_A}, \qquad Q_2^e = \left(\int_0^{\Delta t}\frac{\partial u}{\partial x}dt\right)\Bigg|_{x=x_B}$$

8.69. For the heat transfer problem in Problem 8.45, set up the equations (for nodes 13, 16, and 19) for the transient case (see Fig. P8.45).

8.70. The collocation time approximation methods [see Hughes (1987), p. 530] are defined by the following relations:

$$\{\ddot{u}\}_{s+\alpha} = (1-\alpha)\{u\}_s + \alpha\{u\}_{s+1}$$

$$\{\dot{u}\}_{s+\alpha} = \{\dot{u}\}_s + \alpha\,\Delta t\,[(1-\gamma)\{\ddot{u}\}_s + \gamma\{\ddot{u}\}_{s+\alpha}]$$

$$\{u\}_{s+\alpha} = \{u\}_s + \alpha\,\Delta t\,\{\dot{u}\}_s + \tfrac{1}{2}\alpha(\Delta t)^2\,[(1-2\beta)\{\ddot{u}\}_s + 2\beta\{\ddot{u}\}_{s+\alpha}]$$

The collocation scheme contains two of the well-known schemes: $\alpha = 1$ gives the Newmark scheme; $\beta = \frac{1}{6}$, $\gamma = \frac{1}{2}$ gives the Wilson scheme. The collocation scheme is unconditionally stable and second-order-accurate for the following values of the parameters:

$$\alpha \geqslant 1, \qquad \gamma = \tfrac{1}{2}, \qquad \frac{\alpha}{2(1+\alpha)} \geqslant \beta \geqslant \frac{2\alpha^2 - 1}{4(2\alpha^3 - 1)}$$

Formulate the algebraic equations associated with the matrix differential equation

$$[M]\{\ddot{u}\} + [C]\{\dot{u}\} + [K]\{u\} = \{F\}$$

using the collocation scheme.

REFERENCES FOR ADDITIONAL READING

Bird, R. B., W. E. Stewart, and E. N. Lightfoot: *Transport Phenomena*, John Wiley, New York, 1960.

Budynas, R. G.: *Advanced Strength and Applied Stress Analysis*, McGraw-Hill, New York, 1977.

Carslaw, H. S., and J. C. Jaeger: *Conduction of Heat in Solids*, 2d ed., Oxford University Press, Fairlawn, NJ, 1959.

Clough, R. W., and J. Penzien, *Dynamics of Structures*, McGraw-Hill, New York, 1975.

Eskinazi, S.: *Principles of Fluid Mechanics*, Allyn and Bacon, Boston, 1962.

Holman, J. P.: *Heat Transfer*, 6th ed., McGraw-Hill, New York, 1986.

Hughes, J. T. R.: *The Finite Element Method (Linear, Static and Dynamic Finite Element Analysis)*, Prentice-Hall, Englewood Cliffs, NJ, 1987.

Kohler, W., and J. Pittr: "Calculation of Transient Temperature Fields with Finite Elements in Space and Time Dimensions," *International Journal for Numerical Methods in Engineering*, vol. 8, pp. 625–631, 1974.

Kreyszig, E.: *Advanced Engineering Mathematics*, 6th ed., John Wiley, New York, 1988.

Myers, G. E.: *Analytical Methods in Conduction Heat Transfer*, McGraw-Hill, New York, 1971.

Mikhlin, S. G.: *Variational Methods in Mathematical Physics* (translated from the Russian by T. Boddington), Pergamon Press, Oxford, 1964.

———: *The Numerical Performance of Variational Methods* (translated from the Russian by R. S. Anderssen), Wolters–Noordhoff, The Netherlands, 1971.

Oden, J. T., and J. N. Reddy: *Variational Methods in Theoretical Mechanics*, 2d ed., Springer-Verlag, Berlin, 1983.

Özisik, M. N.: *Heat Transfer: A Basic Approach*, McGraw-Hill, New York, 1985.

Reddy, J. N.: *Energy and Variational Methods in Applied Mechanics*, John Wiley, New York, 1984.

———: *Applied Functional Analysis and Variational Methods in Engineering*, McGraw-Hill, New York, 1986; Krieger, Melbourne, FL, 1991.

——— and M. L. Rasmussen: *Advanced Engineering Analysis*, John Wiley, New York, 1982; Krieger, Melbourne, FL, 1990.

Rektorys, K.: *Variational Methods in Mathematics, Science and Engineering*, D. Reidel, Boston, MA, 1980.

———: *The Method of Discretization in Time*, D. Reidel, Boston, MA, 1982.

Schlichting, H.: *Boundary-Layer Theory* (translated by J. Kestin), 7th ed., McGraw-Hill, New York, 1979.

Sobey, R. J.: "Hermitian Space–Time Finite Elements for Estuarine Mass Transport." *International Journal for Numerical Methods in Fluids*, vol. 2, pp. 277–297, 1982.

Sokolnikoff, I. S.: *Mathematical Theory of Elasticity*, McGraw-Hill, New York, 1956.

Timoshenko, S. P., and J. N. Goodier: *Theory of Elasticity*, 3d ed., McGraw-Hill, New York, 1970.

Ugural, A. C., and S. K. Fenster: *Advanced Strength and Applied Elasticity*, Elsevier, New York, 1975.

Volterra, E., and J. H. Gaines: *Advanced Strength of Materials*, Prentice-Hall, Englewood Cliffs, NJ, 1971.

CHAPTER
9

INTERPOLATION FUNCTIONS, NUMERICAL INTEGRATION, AND MODELING CONSIDERATIONS

9.1 LIBRARY OF ELEMENTS AND INTERPOLATION FUNCTIONS

9.1.1 Introduction

In the previous chapter, we studied the finite element analysis of a model second-order equation and its analogues in the fields of heat transfer, fluid mechanics, and solid mechanics. During this study, we developed the interpolation functions for the basic elements, namely, the linear triangular and rectangular elements. These elements, which were developed in connection with the finite element analysis of a second-order partial differential equation in a single variable, are useful in all finite element models that admit Lagrange interpolation of the primary variables of the weak formulation.

The objective of this chapter is to develop a library of two-dimensional triangular and rectangular elements of the Lagrange family, i.e., elements over which only the function—not its derivatives—is interpolated. Once we have elements of different shapes and order at our disposal, we can choose appropriate elements and associated interpolation functions for a given problem. The regularly shaped elements, called *master elements,* for which interpolation functions are developed here, can be used for numerical evaluation of integrals defined on irregular elements. Of course, this requires a transformation of the geometry from the actual element shape to an associated master element. Section 9.2 deals with the transformation and numerical integration. With these preliminary comments, we now proceed to the discussion of interpolation functions for triangular and rectangular master elements.

9.1.2 Triangular Elements

The linear (three-node) triangular element was developed in Section 8.2.5. Higher-order triangular elements (i.e., those with interpolation functions of higher degree) can be systematically developed with the help of the so-called *Pascal's triangle,* which contains the terms of polynomials of various degrees in the two coordinates x and y, as shown in Fig. 9.1. Here x and y denote some local coordinates—they do not, in general, represent the global coordinates of the problem. One can view the position of the terms as the nodes of the triangle, with the constant term and the first and last terms of a given row being the vertices of the triangle. Of course, the shape of the triangle is arbitrary—it is not necessarily an equilateral triangle, as might appear from the position of the terms in Pascal's triangle. For example, a triangular element of order 2 (i.e., one for which the degree of the polynomial is 2) contains six nodes, as can be seen from the top three rows of Pascal's triangle. The position of the six nodes in the triangle is at the three vertices and at the midpoints of the three sides. The polynomial involves six constants, which can be expressed in terms of the nodal values of the variable being interpolated:

$$u = \sum_{i=1}^{6} u_i \psi_i(x, y) \tag{9.1}$$

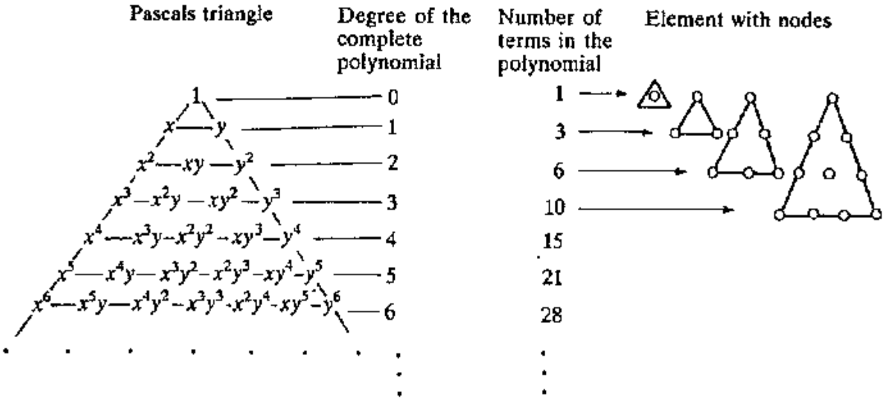

FIGURE 9.1
Pascal's triangle for the generation of the Lagrange family of triangular elements.

where ψ_i are the quadratic interpolation functions obtained following the same procedure as used for the linear element in Section 8.2.5. In general, a pth-order triangular element has n nodes, with

$$n = \tfrac{1}{2}(p+1)(p+2) \tag{9.2}$$

and a complete polynomial of the pth degree is given by

$$u(x, y) = \sum_{i=1}^{n} a_i x^r y^s = \sum_{j=1}^{n} u_j \psi_j, \qquad r + s \leq p \tag{9.3}$$

The location of the entries in Pascal's triangle gives a symmetric location of nodal points in elements that will produce exactly the right number of nodes to define a Lagrange interpolation of any degree. It should be noted that the Lagrange family of triangular elements (of order greater than zero) should be used for second-order problems that require only the dependent variables (not their derivatives) of the problem to be continuous at interelement boundaries. It can easily be seen that the pth-degree polynomial associated with the pth-order Lagrange element, when evaluated on the boundary of the latter, yields a pth-degree polynomial in the boundary coordinate. For example, the quadratic polynomial associated with the quadratic (six-node) triangular element shown in Fig. 9.2 is

$$u^e(x, y) = a_1 + a_2 x + a_3 y + a_4 xy + a_5 x^2 + a_6 y^2 \tag{9.4}$$

The derivatives of u^e are

$$\frac{\partial u^e}{\partial x} = a_2 + a_4 y + 2a_5 x, \qquad \frac{\partial u^e}{\partial y} = a_3 + a_4 x + 2a_6 y \tag{9.5}$$

The element shown in Fig. 9.2(a) is an arbitrary quadratic triangular element. By rotating and translating the (x, y) coordinate system, we obtain the (s, t) coordinate system. Since the transformation from the (x, y) system to the (s, t) system involves only rotation (which is linear) and translation, a kth-degree polynomial in the (x, y) coordinate system is still a kth-degree polynomial in the (s, t) system:

$$u^e(s, t) = \hat{a}_1 + \hat{a}_2 s + \hat{a}_3 t + \hat{a}_4 st + \hat{a}_5 s^2 + \hat{a}_6 t^2 \tag{9.6}$$

where $\hat{a}_i$ $(i = 1, 2, \ldots, 6)$ are constants depending on a_i and the angle of rotation α. Now, by setting $t = 0$, we obtain the restriction of u to side 1–2–3 of the element Ω^e:

$$u^e(s, 0) = \hat{a}_1 + \hat{a}_2 s + \hat{a}_5 s^2 \tag{9.7}$$

which is a quadratic polynomial in s. If a neighboring element Ω^f has its side 5–4–3 in common with side 1–2–3 of the element Ω^e then the function u on side 5–4–3 of the element Ω^f is also a quadratic polynomial:

$$u^f(s, 0) = \hat{b}_1 + \hat{b}_2 s + \hat{b}_5 s^2 \tag{9.8}$$

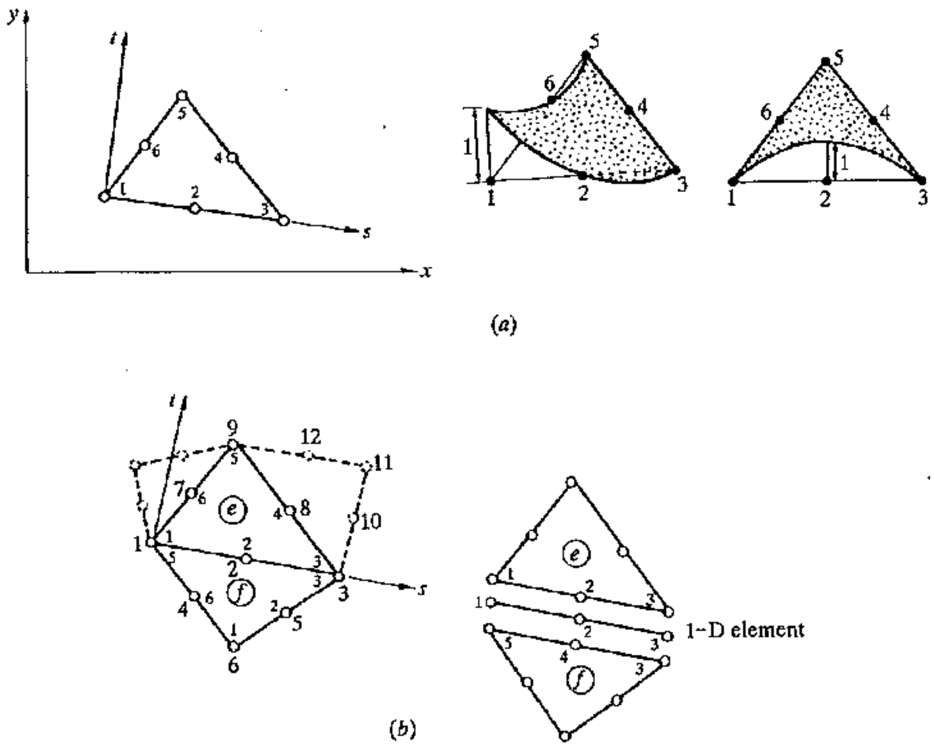

(a)

(b)

FIGURE 9.2
Variation of a function along the interelement boundaries of Lagrange (triangular) elements: (*a*) a typical higher-order element; (*b*) interelement continuity of a quadratic function.

Since the polynomials are uniquely defined by the same nodal values $U_1 = u_1^e = u_5^f$, $U_2 = u_2^e = u_4^f$, and $U_3 = u_3^e = u_3^f$, we have $u^e(s, 0) = u^f(s, 0)$, and hence the function u is uniquely defined on the interelement boundary of the elements Ω^e and Ω^f.

The above ideas can easily be extended to three dimensions, in which case Pascal's triangle takes the form of a Christmas tree and the elements are of a pyramidal shape, called tetrahedral elements. We shall not elaborate on this any further, because the scope of the present study is limited to two-dimensional elements only. An introduction to 3-D elements is presented in Chapter 14.

Recall from (8.19)–(8.25) that the procedure for deriving the interpolation functions involves the inversion of an $n \times n$ matrix, where n is the number of terms in the polynomial used to represent a function. When $n > 3$, this procedure is algebraically very tedious, and therefore one should devise an alternative way of developing the interpolation functions, as was discussed for one-dimensional elements in Chapter 3.

The alternative derivation of the interpolation functions for the higher-order Lagrange family of triangular elements is simplified by use of the *area*

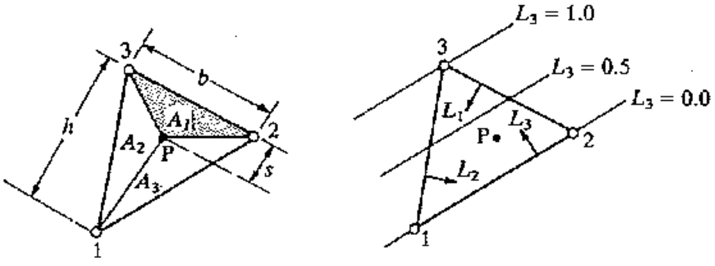

$L_i = \dfrac{A_i}{A}$ ($A = \frac{1}{2}bh$, $A_1 = \frac{1}{2}bs$, $L_1 = A_1/A = s/h$, etc.)

FIGURE 9.3
Definition of the natural coordinates of a triangular element.

coordinates L_i. For triangular elements, it is possible to construct three nondimensionalized coordinates L_i $(i = 1, 2, 3)$, which relate respectively to the sides directly opposite nodes 1, 2, and 3, such that (see Fig. 9.3)

$$\boxed{L_i = \frac{A_i}{A}, \qquad A = \sum_{i=1}^{3} A_i} \tag{9.9}$$

where A_i is the area of the triangle formed by nodes j and k and an arbitrary point P in the element, and A is the total area of the element. For example A_1 is the area of the shaded triangle, which is formed by nodes 2 and 3 and point P. The point P is at a perpendicular distance s from the side connecting nodes 2 and 3. We have $A_1 = \frac{1}{2}bs$ and $A = \frac{1}{2}bh$. Hence,

$$L_1 = A_1/A = s/h$$

Clearly, L_1 is zero on side 2–3 (and hence zero at nodes 2 and 3), and has a value of unity at node 1. Thus, L_1 is the interpolation function associated with node 1. Similarly, L_2 and L_3 are the interpolation functions associated with nodes 2 and 3, respectively. In summary, we have

$$\psi_i = L_i \tag{9.10}$$

for a linear triangular element. We shall use L_i to construct interpolation functions for higher-order triangular elements.

Consider a higher-order element with k nodes (equally spaced) per side (see Fig. 9.4a). Then the total number of nodes in the element is

$$n = \sum_{i=0}^{k-1} (k - i) = k + (k - 1) + \ldots + 1 = \tfrac{1}{2}k(k + 1) \tag{9.11}$$

and the degree of the interpolation functions is $k - 1$. For example, for the quadratic element, we have $k - 1 = 2$ and $n = 6$. Let the corner (i.e., vortex) nodes be denoted by I, J, and K, and let h_I be the perpendicular distance of node I from the side connecting J and K. Then the distance s_p to the pth row

4. L2. L3. L1 [illegible]

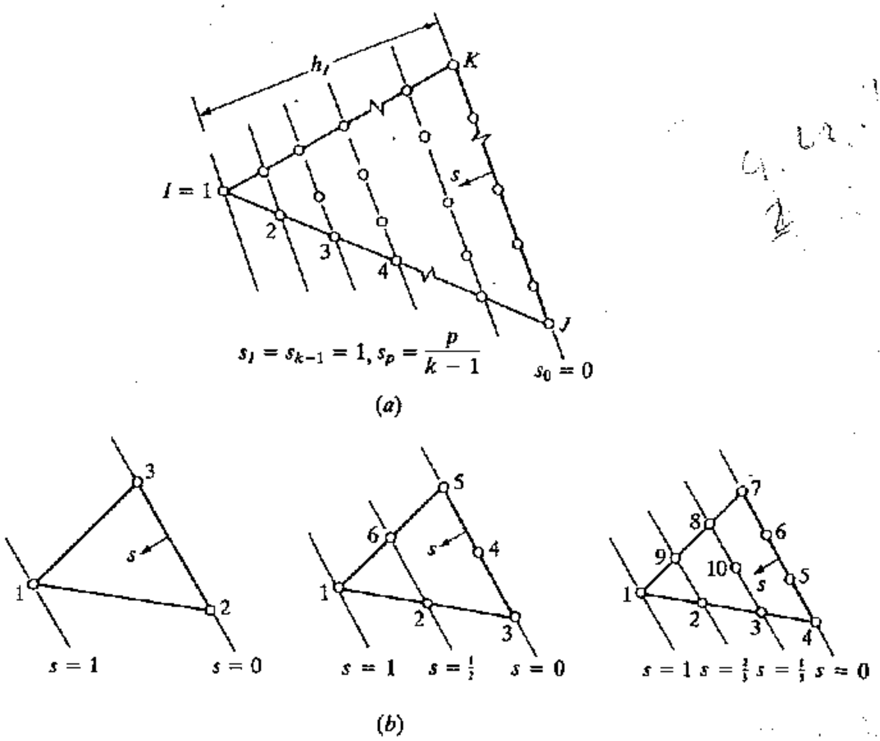

FIGURE 9.4
Construction of the element interpolation functions of the Lagrange triangular elements: (a) an arbitrary $(k-1)$th-order element; (b) linear, quadratic, and cubic elements.

parallel to side J–K (under the assumption that the nodes are equally spaced along the sides and the rows) is given in nondimensional form by

$$s_p = \frac{p}{k-1}, \qquad s_0 = 0, \qquad s_I = s_{k-1} = 1 \tag{9.12}$$

The interpolation function ψ_I should be zero at the nodes on the lines $L_I = 0$, $1/(k-1), \ldots, p/(k-1)$ $(p = 0, 1, \ldots, k-2)$, and ψ_I should be unity at $L_I = S_I$. Thus we have the necessary information for constructing the interpolation function ψ_I:

$$\boxed{\psi_I = \frac{(L_I - s_0)(L_I - s_1)(L_I - s_2) \cdots (L_I - s_{k-2})}{(s_I - s_0)(s_I - s_1)(s_I - s_2) \cdots (s_I - s_{k-2})} = \prod_{p=0}^{k-2} \frac{L_I - s_p}{s_I - s_p}} \tag{9.13}$$

Similar expressions can be derived for nodes located other than at the vertices. In general, ψ_i for node i is given by

$$\psi_i = \prod_{j=1}^{k-1} \frac{f_j}{f_j^i} \tag{9.14}$$

where f_j are functions of L_4, L_2, and L_3, and f_j^i is the value of f_j at node i. The functions f_j are derived from the equations of $k-1$ lines that pass through all the nodes except node i. The procedure is illustrated below via an example.

Example 9.1. First consider the triangular element that has two nodes per side (i.e., $k=2$). This is the linear triangular element with total number of nodes equal to 3 ($n=3$). For node 1 (see Fig. 9.4b), we have $k-2=0$ and

$$s_0=0, \qquad s_1=1, \qquad \psi_1=\frac{L_1-s_0}{s_1-s_0}=L_1 \tag{9.15a}$$

Similarly, for ψ_2 and ψ_3, we obtain

$$\psi_2=L_2, \qquad \psi_3=L_3 \tag{9.15b}$$

Next, consider the triangular element with three nodes per side ($k=3$). The total number of nodes is 6. For node 1, we have

$$\begin{gathered} s_0=0, \quad s_1=\tfrac{1}{2}, \quad s_2=1 \\ \psi_1=\frac{L_1-s_0}{s_2-s_0}\,\frac{L_1-s_1}{s_2-s_1}=L_1(2L_1-1) \end{gathered} \tag{9.16a}$$

The function ψ_2 (see Fig. 9.4b) should vanish at nodes 1, 3, 4, 5, and 6, and should be unity at node 2. Equivalently, ψ_2 should vanish along the lines connecting nodes 1 and 5, and 3 and 5. These two lines are given in terms of L_1, L_2, and L_3 (note that the subscripts on L refer to the nodes in the three-node triangular element) by $L_2=0$ and $L_1=0$. Hence,

$$\psi_2=\frac{L_2-s_0}{s_1-s_0}\,\frac{L_1-s_0}{s_1-s_0}=\frac{L_2-0}{\frac{1}{2}-0}\,\frac{L_1-0}{\frac{1}{2}-0}=4L_1L_2 \tag{9.16b}$$

Similarly,

$$\psi_3=L_2(2L_2-1), \qquad \psi_4=4L_2L_3, \qquad \psi_5=L_3(2L_3-1), \qquad \psi_6=4L_1L_3 \tag{9.16c}$$

As a last example, consider the cubic element (i.e., $k-1=3$). For ψ_1, we note that it must vanish along the lines $L_1=0$, $L_1=\frac{1}{3}$, and $L_1=\frac{2}{3}$. Therefore,

$$\psi_1=\frac{L_1-0}{1-0}\,\frac{L_1-\frac{1}{3}}{1-\frac{1}{3}}\,\frac{L_1-\frac{2}{3}}{1-\frac{2}{3}}=\tfrac{1}{2}L_1(3L_1-1)(3L_1-2)$$

Similarly,

$$\psi_2=\frac{L_2-0}{\frac{1}{3}-0}\,\frac{L_1-0}{\frac{2}{3}-0}\,\frac{L_1-\frac{1}{3}}{\frac{2}{3}-\frac{1}{3}}=\tfrac{9}{2}L_2L_1(3L_1-1)$$

and so on. We have

$$\begin{aligned} \psi_3&=\tfrac{9}{2}L_1L_2(3L_2-1), & \psi_4&=\tfrac{1}{2}L_2(3L_2-1)(3L_2-2) \\ \psi_5&=\tfrac{9}{2}L_2L_3(3L_2-1), & \psi_6&=\tfrac{9}{2}L_2L_3(3L_3-1) \\ \psi_7&=\tfrac{1}{2}L_3(3L_3-1)(3L_3-2), & \psi_8&=\tfrac{9}{2}L_3L_1(3L_3-1) \\ \psi_9&=\tfrac{9}{2}L_1L_3(3L_1-1), & \psi_{10}&=27L_1L_2L_3 \end{aligned} \tag{9.17}$$

In closing this section, it should be pointed out that the area coordinates L_i facilitate not only the construction of the interpolation functions for the higher-order elements but also the integration of functions of L_i over line paths and areas. The following exact integration formulae prove to be useful:

$$\boxed{\begin{aligned} &\int_a^b L_1^m L_2^n \, ds = \frac{m!\,n!}{(m+n+1)!}(b-a) \qquad (9.18a) \\ &\iint_{\text{area}} L_1^m L_2^n L_3^p \, dA = \frac{m!\,n!\,p!}{(m+n+p+2)!} 2A \qquad (9.18b) \end{aligned}}$$

where m, n, and p are arbitrary (positive) integers, A is the area of the domain of integration, and $m!$ denotes the factorial of m. Of course, one should transform the integrals from the x and y coordinates to L_i coordinates using

$$x = \sum_{i=1}^{n} x_i L_i, \qquad y = \sum_{i=1}^{n} y_i L_i \tag{9.19}$$

where (x_i, y_i) are the global coordinates of the ith node of the element.

9.1.3 Rectangular Elements

Analogous to the Lagrange family of triangular elements, the Lagrange family of rectangular elements can be developed from Pascal's triangle in Fig. 9.1 or the rectangular array shown in Fig. 9.5. Since a linear rectangular element has four corners (and hence four nodes), the polynomial should have the first four terms 1, x, y, and xy (which form a parallelogram in Pascal's triangle and a rectangle in the array given in Fig. 9.5). The coordinates (x, y) are usually taken to be the element (i.e., local) coordinates. In general, a pth-order Lagrange rectangular element has n nodes, with

$$n = (p+1)^2 \quad (p = 0, 1, \ldots)$$

and the associated polynomial contains the terms from the pth parallelogram or the pth rectangle in Fig. 9.5. When $p = 0$, it is understood (as in triangular elements) that the node is at the center of the element (i.e., the variable is a constant on the entire element). The Lagrange quadratic rectangular element has nine nodes, and the associated polynomial is given by

$$\begin{aligned} u(x, y) = a_1 + a_2 x + a_3 y + a_4 xy + a_5 x^2 + a_6 y^2 \\ + a_7 x^2 y + a_8 x y^2 + a_9 x^2 y^2 \end{aligned} \tag{9.20a}$$

$$\begin{aligned} \frac{\partial u}{\partial x} &= a_2 + a_4 y + 2a_5 x + 2a_7 xy + a_8 y^2 + 2a_9 x y^2 \\ \frac{\partial u}{\partial y} &= a_3 + a_4 x + 2a_6 y + a_7 x^2 + 2a_8 xy + 2a_9 x^2 y \end{aligned} \tag{9.20b}$$

The polynomial contains the complete polynomial of the second degree plus the third-degree terms x^2y and xy^2 and also an x^2y^2 term. Four of the nine nodes are placed at the four corners, four at the midpoints of the sides, and one at the center of the element. The polynomial is uniquely determined by

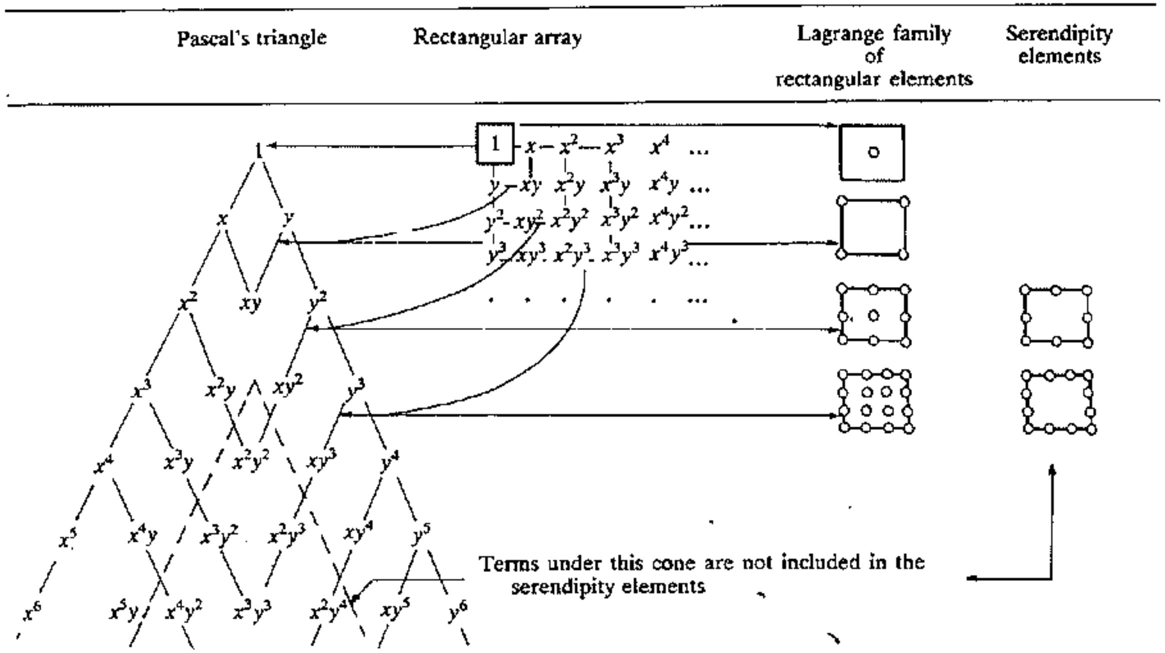
Pascal's triangle
Rectangular array
Lagrange family of rectangular elements
Serendipity elements
1
x y
x^2 xy y^2
x^3 x^2y xy^2 y^3
x^4 x^3y x^2y^2 xy^3 y^4
x^5 x^4y x^3y^2 x^2y^3 xy^4 y^5
x^6 x^5y x^4y^2 x^3y^3 x^2y^4 xy^5 y^6
1 x x^2 x^3 x^4 …
y xy x^2y x^3y x^4y …
y^2 xy^2 x^2y^2 x^3y^2 x^4y^2 …
y^3 xy^3 x^2y^3 x^3y^3 x^4y^3 …
Terms under this cone are not included in the serendipity elements

FIGURE 9.5
Lagrange and serendipity families of rectangular elements.

specifying its values at each of the nine nodes. Moreover, along the sides of the element, the polynomial is quadratic (with three terms—as can be seen by setting $y = 0$), and is determined by its values at the three nodes on that side. If two rectangular elements share a side, and the polynomial is required to have the same values from both elements at the three nodes of the elements, then u is uniquely defined along the entire side (shared by the two elements). Note that the normal derivative of u approximated by the quadratic Lagrange polynomials is quadratic in the tangential direction and linear in the normal direction (i.e., $\partial u/\partial x$ is quadratic in y and linear in x, and $\partial u/\partial y$ is quadratic in x and linear in y). Plots of ψ_1, ψ_2, and ψ_5 (the node numbers correspond to those in Fig. 9.6) of the nine-node rectangular element are shown in Fig. 9.7.

The pth-order Lagrange rectangular element has the pth-degree polynomial

$$\begin{aligned} u(x, y) &= \sum_{i=1}^{n} a_i x^j y^k \quad (j + k \leq p + 1; i, j \leq p) \\ &= \sum_{i=1}^{n} u_i \psi_i \end{aligned} \tag{9.21}$$

and ψ_i are called the pth-order Lagrange interpolation functions.

The Lagrange interpolation functions associated with rectangular elements can be obtained from corresponding one-dimensional Lagrange inter-

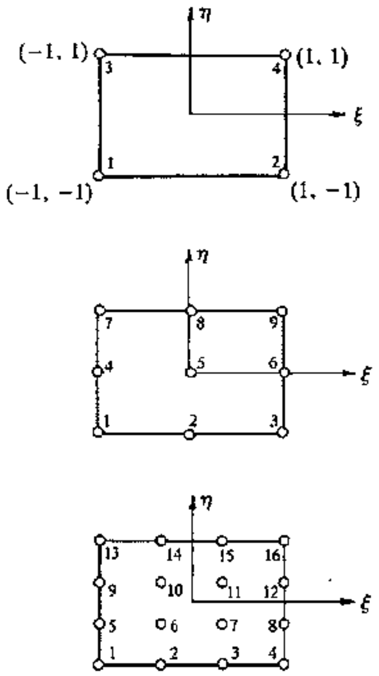

$\psi_1 = \frac{1}{4}(1 - \xi)(1 - \eta)$
$\psi_2 = \frac{1}{4}(1 + \xi)(1 - \eta)$
$\psi_3 = \frac{1}{4}(1 - \xi)(1 + \eta)$
$\psi_4 = \frac{1}{4}(1 + \xi)(1 + \eta)$

$\psi_1 = \frac{1}{4}(\xi^2 - \xi)(\eta^2 - \eta)$, $\psi_2 = \frac{1}{2}(1 - \xi^2)(\eta^2 - \eta)$
$\psi_3 = \frac{1}{4}(\xi^2 + \xi)(\eta^2 - \eta)$, $\psi_4 = \frac{1}{2}(\xi^2 - \xi)(1 - \eta^2)$
$\psi_5 = (1 - \xi^2)(1 - \eta^2)$, $\psi_6 = \frac{1}{2}(\xi^2 + \xi)(1 - \eta^2)$
$\psi_7 = \frac{1}{4}(\xi^2 - \xi)(\eta^2 + \eta)$, $\psi_8 = \frac{1}{2}(1 - \xi^2)(\eta^2 + \eta)$
$\psi_9 = \frac{1}{4}(\xi^2 + \xi)(\eta^2 + \eta)$,

Use (9.25)–(9.27) to develop the interpolation functions.

FIGURE 9.6
Node numbers and interpolation functions for the rectangular elements of the Lagrange family.

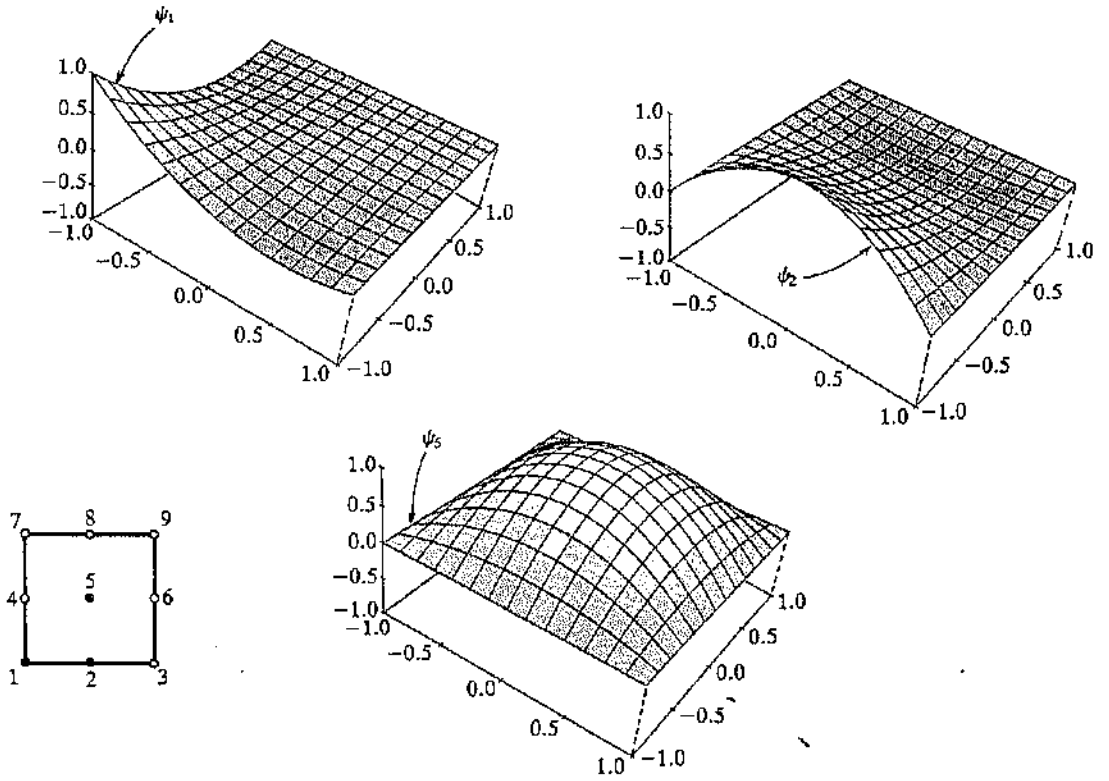

FIGURE 9.7
Geometric variation of the Lagrange interpolation functions at nodes 1, 2, and 5 (see Fig. 9.6) of the nine-node quadratic element.

polation functions by taking the tensor product of the x-direction (one-dimensional) interpolation functions with the y-direction (one-dimensional) interpolation functions. Let the x and y coordinates be taken along element sides, with the origin of the coordinate system at the lower left corner of the rectangle. Then for an element with dimensions a and b along the x and y directions, respectively, the interpolation functions are given as follows:

Linear ($p = 1$)

$$
\begin{aligned}
\begin{bmatrix} \psi_1 & \psi_3 \\ \psi_2 & \psi_4 \end{bmatrix} &= \begin{Bmatrix} 1-\dfrac{x}{a} \\ \dfrac{x}{a} \end{Bmatrix} \left\{ 1-\frac{y}{b} \quad \frac{y}{b} \right\} \\
&= \begin{bmatrix} \left(1-\dfrac{x}{a}\right)\left(1-\dfrac{y}{b}\right) & \left(1-\dfrac{x}{a}\right)\dfrac{y}{b} \\ \dfrac{x}{a}\left(1-\dfrac{y}{b}\right) & \dfrac{x}{a}\dfrac{y}{b} \end{bmatrix}
\end{aligned} \tag{9.22}
$$

Quadratic ($p = 2$)

$$
\begin{aligned}
\begin{bmatrix} \psi_1 & \psi_4 & \psi_7 \\ \psi_2 & \psi_5 & \psi_8 \\ \psi_3 & \psi_6 & \psi_9 \end{bmatrix} &= \begin{Bmatrix} \dfrac{(x-\frac{1}{2}a)(x-a)}{(-\frac{1}{2}a)(-a)} \\ \dfrac{x(x-a)}{\frac{1}{2}a(\frac{1}{2}a-a)} \\ \dfrac{x(x-\frac{1}{2}a)}{a(\frac{1}{2}a)} \end{Bmatrix} \begin{Bmatrix} \dfrac{(y-\frac{1}{2}b)(y-b)}{\frac{1}{2}b^2} \\ \dfrac{y(y-b)}{-\frac{1}{4}b^2} \\ \dfrac{y(y-b/2)}{\frac{1}{2}b^2} \end{Bmatrix}^T \\
&\equiv \{f\}\{g\}^T = \begin{bmatrix} f_1g_1 & f_1g_2 & f_1g_3 \\ f_2g_1 & f_2g_2 & f_2g_3 \\ f_3g_1 & f_3g_2 & f_3g_3 \end{bmatrix}
\end{aligned} \tag{9.23}
$$

where $f_i(x)$ and $g_i(y)$ are the one-dimensional interpolation functions along the x and y directions, respectively. We obtain

$$
\begin{aligned}
&\psi_1 = \left(1-\frac{2x}{a}\right)\left(1-\frac{x}{a}\right)\left(1-\frac{2y}{b}\right)\left(1-\frac{y}{b}\right) \\
&\psi_2 = \frac{4x}{a}\left(1-\frac{x}{a}\right)\left(1-\frac{2y}{b}\right)\left(1-\frac{y}{b}\right), \qquad \psi_3 = \frac{x}{a}\left(\frac{2x}{a}-1\right)\left(1-\frac{2y}{b}\right)\left(1-\frac{y}{b}\right) \\
&\psi_4 = \left(1-\frac{2x}{a}\right)\left(1-\frac{x}{a}\right)\frac{4y}{b}\left(1-\frac{y}{b}\right), \qquad \psi_5 = \frac{4x}{a}\left(1-\frac{x}{a}\right)\frac{4y}{b}\left(1-\frac{y}{b}\right) \\
&\psi_6 = \frac{x}{a}\left(\frac{2x}{a}-1\right)\frac{4y}{b}\left(1-\frac{y}{b}\right), \qquad \psi_7 = \left(1-\frac{2x}{a}\right)\left(1-\frac{x}{a}\right)\frac{y}{b}\left(\frac{2y}{b}-1\right) \\
&\psi_8 = \frac{4x}{a}\left(1-\frac{x}{a}\right)\frac{y}{b}\left(\frac{2y}{b}-1\right), \qquad \psi_9 = \frac{x}{a}\left(\frac{2x}{a}-1\right)\frac{y}{b}\left(\frac{2y}{b}-1\right)
\end{aligned} \tag{9.24}
$$

At *p*th order

$$\begin{bmatrix} \psi_1 & \psi_{p+2} & \cdots & \psi_k \\ \psi_2 & & & \\ \vdots & \ddots & & \vdots \\ \psi_p & & \ddots & \\ \psi_{p+1} & \psi_{2p+2} & \cdots & \psi_n \end{bmatrix} = \begin{Bmatrix} f_1 \\ f_2 \\ \vdots \\ f_{p+1} \end{Bmatrix} \begin{Bmatrix} g_1 \\ g_2 \\ \vdots \\ g_{p+1} \end{Bmatrix}^T \tag{9.25}$$

$$k = (p+1)p + 1, \qquad n = (p+1)^2$$

where $f_i(x)$ and $g_i(y)$ are the pth-order interpolants in x and y, respectively. For example, the polynomial

$$f_i(\xi) = \frac{(\xi - \xi_1)(\xi - \xi_2)\cdots(\xi - \xi_{i-1})(\xi - \xi_{i+1})\cdots(\xi - \xi_{p+1})}{(\xi_i - \xi_1)(\xi_i - \xi_2)\cdots(\xi_i - \xi_{i-1})(\xi_i - \xi_{i+1})\cdots(\xi_i - \xi_{p+1})} \tag{9.26}$$

(where ξ_i is the ξ coordinate of node i) is the pth-degree interpolation polynomial in ξ that vanishes at the points $\xi_1, \xi_2, \ldots, \xi_{i-1}, \xi_{i+1}, \ldots, \xi_{p+1}$. We recall that (x, y) are the element coordinates.

It is convenient (for numerical integration purposes) to express the interpolation functions in (9.25) in terms of the natural coordinates ξ and η:

$$\xi = \frac{2(x - x_1) - a}{a}, \qquad \eta = \frac{2(y - y_1) - b}{b} \tag{9.27}$$

where x_1 and y_1 are the global coordinates of node 1 in the local x and y coordinates. For a coordinate system with origin fixed at node 1 and coordinates parallel to the sides of the element, we have $x_1 = y_1 = 0$. In this case, the quadratic interpolation functions in (9.24) can be written in terms of ξ and η as

$$\begin{aligned} \psi_1 &= \tfrac{1}{4}(1-\xi)(1-\eta)\xi\eta, & \psi_5 &= (1-\xi^2)(1-\eta^2) \\ \psi_2 &= -\tfrac{1}{2}(1-\xi^2)(1-\eta)\eta, & \psi_6 &= \tfrac{1}{2}(1+\xi)(1-\eta^2)\xi \\ \psi_3 &= -\tfrac{1}{4}(1+\xi)(1-\eta)\xi\eta, & \psi_7 &= -\tfrac{1}{4}(1-\xi)(1+\eta)\xi\eta \\ \psi_4 &= -\tfrac{1}{2}(1-\xi)(1-\eta^2)\xi, & \psi_8 &= \tfrac{1}{2}(1-\xi^2)(1+\eta)\eta \\ \psi_9 &= \tfrac{1}{4}(1+\xi)(1+\eta)\xi\eta \end{aligned} \tag{9.28}$$

The reader should be cautioned that the subscripts of ψ_i refer to the node numbering used in Fig. 9.6. For any renumbering of the nodes, the subscripts of the interpolation functions should be changed accordingly.

9.1.4 · The Serendipity Elements

Since the internal nodes of the higher-order elements of the Lagrange family do not contribute to the interelement connectivity, they can be condensed out at the element level so that the size of the element matrices is reduced. The serendipity elements are those rectangular elements that have no interior nodes. In other words, all the node points are on the boundary of the element. The interpolation functions for serendipity elements cannot be obtained using tensor products of one-dimensional interpolation functions. Instead, an alternative procedure that employs the interpolation properties in (8.26) is used. Here we show how to construct the interpolation functions for the eight-node (quadratic) element using the natural coordinates (ξ, η).

The interpolation function for node 1 should be zero at nodes $2, 3, \ldots, 8$, and unity at node 1. Equivalently, ψ_1 should vanish on the sides defined by the equations $1 - \xi = 0$, $1 - \eta = 0$, and $1 + \xi + \eta = 0$ (see Fig. 9.8). Therefore, ψ_1 is of the form

$$\psi_1(\xi, \eta) = c(1 - \xi)(1 - \eta)(1 + \xi + \eta) \tag{9.29a}$$

where c is a constant that should be determined so as to yield $\psi_1(-1, -1) = 1$. We obtain $c = -\frac{1}{4}$, and therefore

$$\psi_1(\xi, \eta) = -\tfrac{1}{4}(1 - \xi)(1 - \eta)(1 + \xi + \eta) \tag{9.29b}$$

Similarly, we obtain

$$\begin{aligned} &\psi_2 = \tfrac{1}{2}(1 - \xi^2)(1 - \eta), && \psi_3 = \tfrac{1}{4}(1 + \xi)(1 - \eta)(-1 + \xi - \eta) \\ &\psi_4 = \tfrac{1}{2}(1 - \xi)(1 - \eta^2), && \psi_5 = \tfrac{1}{2}(1 + \xi)(1 - \eta^2) \\ &\psi_6 = \tfrac{1}{4}(1 - \xi)(1 + \eta)(-1 - \xi + \eta), && \psi_7 = \tfrac{1}{2}(1 - \xi^2)(1 + \eta) \\ &\psi_8 = \tfrac{1}{4}(1 + \xi)(1 + \eta)(-1 + \xi + \eta) && \end{aligned} \tag{9.30}$$

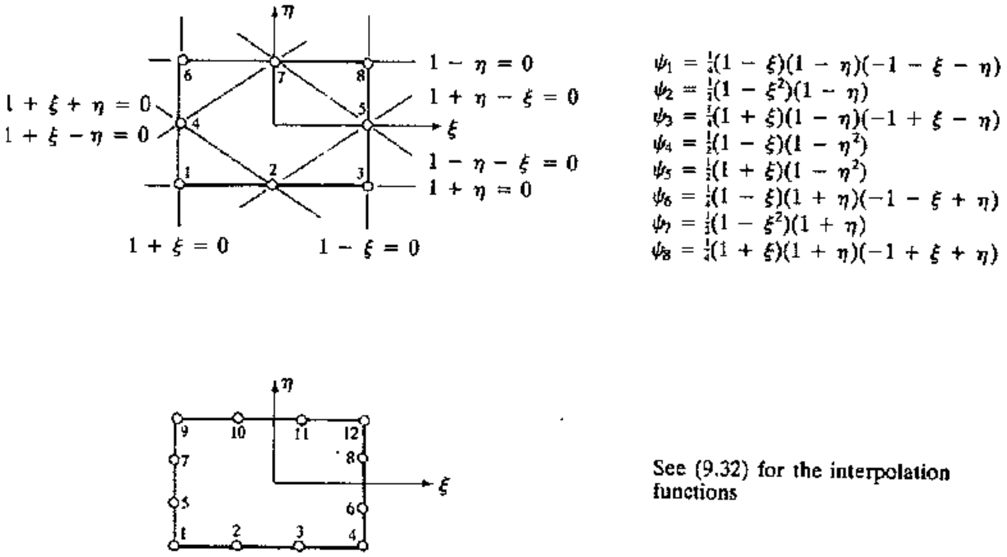

$\psi_1 = \frac{1}{4}(1 - \xi)(1 - \eta)(-1 - \xi - \eta)$
$\psi_2 = \frac{1}{2}(1 - \xi^2)(1 - \eta)$
$\psi_3 = \frac{1}{4}(1 + \xi)(1 - \eta)(-1 + \xi - \eta)$
$\psi_4 = \frac{1}{2}(1 - \xi)(1 - \eta^2)$
$\psi_5 = \frac{1}{2}(1 + \xi)(1 - \eta^2)$
$\psi_6 = \frac{1}{4}(1 - \xi)(1 + \eta)(-1 - \xi + \eta)$
$\psi_7 = \frac{1}{2}(1 - \xi^2)(1 + \eta)$
$\psi_8 = \frac{1}{4}(1 + \xi)(1 + \eta)(-1 + \xi + \eta)$

See (9.32) for the interpolation functions

FIGURE 9.8
Node numbers and interpolation functions for the serendipity family of elements.

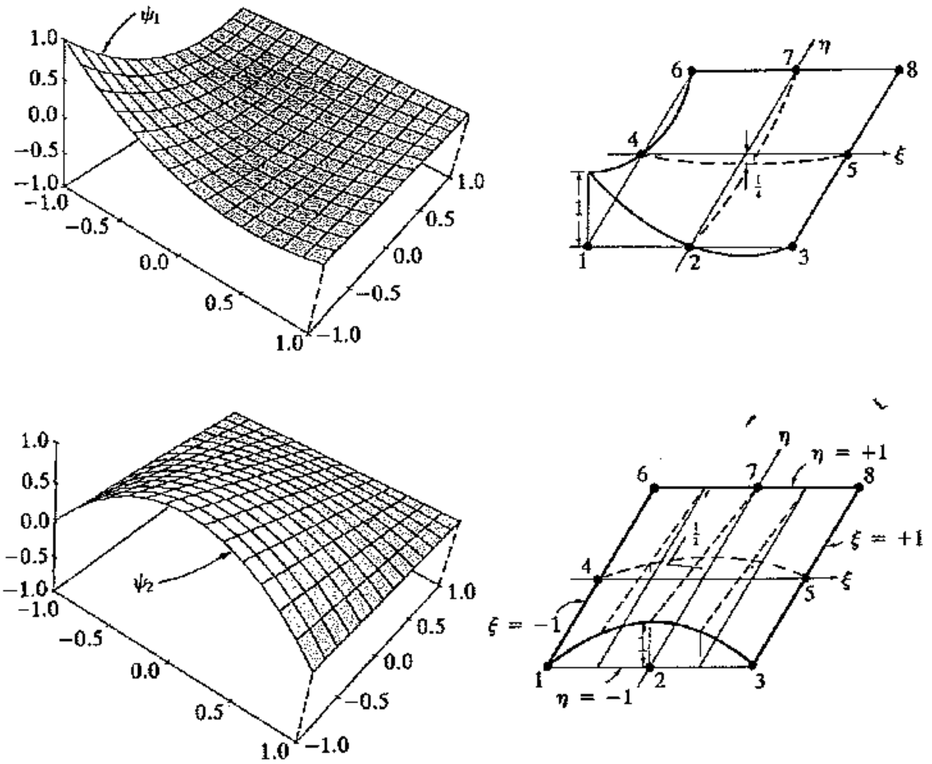

FIGURE 9.9
Geometric variation of the interpolation functions associated with nodes 1 and 2 of the eight-node serendipity element (see Fig. 9.8).

Note that all the ψ_i for the eight-node element have the form

$$\psi_i = c_1 + c_2\xi + c_3\eta + c_4\xi\eta + c_5\xi^2 + c_6\eta^2 + c_7\xi^2\eta + c_8\xi\eta^2 \tag{9.31a}$$

The derivatives of ψ_i with respect to ξ and η are of the form

$$\begin{aligned}\frac{\partial\psi_i}{\partial\xi} &= c_2 + c_4\eta + 2c_5\xi + 2c_7\xi\eta + c_8\eta^2 \\ \frac{\partial\psi_i}{\partial\eta} &= c_3 + c_4\xi + 2c_6\eta + c_7\xi^2 + 2c_8\xi\eta\end{aligned} \tag{9.31b}$$

Plots of ψ_1 and ψ_2 (the node numbers correspond to those in Fig. 9.8) for the eight-node serendipity element are shown in Fig. 9.9. It should be noted that ψ_2 of the nine-node element is zero at the element center, whereas ψ_2 of the eight-node element is nonzero there.

The interpolation functions for the cubic serendipity element, which has 12 nodes, are

$$\begin{aligned}
&\psi_1 = \tfrac{1}{32}(1-\xi)(1-\eta)[-10+9(\xi^2+\eta^2)], \qquad \psi_2 = \tfrac{9}{32}(1-\eta)(1-\xi^2)(1-3\xi)\\
&\psi_3 = \tfrac{9}{32}(1-\eta)(1-\xi^2)(1+3\xi), \qquad \psi_4 = \tfrac{1}{32}(1+\xi)(1-\eta)[-10+9(\xi^2+\eta^2)]\\
&\psi_5 = \tfrac{9}{32}(1-\xi)(1-\eta^2)(1-3\eta), \qquad \psi_6 = \tfrac{9}{32}(1+\xi)(1-\eta^2)(1-3\eta)\\
&\psi_7 = \tfrac{9}{32}(1-\xi)(1-\eta^2)(1+3\eta), \qquad \psi_8 = \tfrac{9}{32}(1+\xi)(1-\eta^2)(1+3\eta)\\
&\psi_9 = \tfrac{1}{32}(1-\xi)(1+\eta)[-10+9(\xi^2+\eta^2)], \qquad \psi_{10} = \tfrac{9}{32}(1+\eta)(1-\xi^2)(1-3\xi)\\
&\psi_{11} = \tfrac{9}{32}(1+\eta)(1-\xi^2)(1+3\xi), \qquad \psi_{12} = \tfrac{1}{32}(1+\xi)(1+\eta)[-10+9(\xi^2+\eta^2)]
\end{aligned} \tag{9.32}$$

The interpolation functions ψ_i for the 12-node element are of the form

$$\psi_i = \text{terms of the form in } (9.31a) + c_9\xi^3 + c_{10}\eta^3 + c_{11}\xi^3\eta + c_{12}\xi\eta^3 \tag{9.33}$$

TABLE 9.1

Interpolation functions for the linear and quadratic Langrange rectangular elements, quadratic serendipity element and Hermite cubic rectangular element†

Element type	Interpolation functions	Remarks
Lagrange elements:		
Linear	$\frac{1}{4}(1+\xi\xi_i)(1+\eta\eta_i)$	Node i ($i = 1, \ldots, 4$)
Quadratic	$\frac{1}{4}\xi\xi_i(1+\xi\xi_i)\eta\eta_i(1+\eta\eta_i)$	Corner node
	$\frac{1}{2}\eta\eta_i(1+\eta\eta_i)(1-\xi^2)$	Side node, $\xi_i = 0$
	$\frac{1}{2}\xi\xi_i(1+\xi\xi_i)(1-\eta^2)$	Side node, $\eta_i = 0$
	$(1-\xi^2)(1-\eta^2)$	Interior node
Seredipity element:		
Quadratic	$\frac{1}{4}(1+\xi\xi_i)(1+\eta\eta_i)(\xi\xi_i+\eta\eta_i-1)$	Corner node
	$\frac{1}{2}(1-\xi^2)(1+\eta\eta_i)$	Side node, $\xi_i = 0$
	$\frac{1}{2}(1+\xi\xi_i)(1-\eta^2)$	Side node, $\eta_i = 0$
Hermite cubic element:		
Interpolation functions for		
variable u	$\frac{1}{16}(\xi+\xi_i)^2(\xi\xi_i-2)(\eta+\eta_i)^2(\eta\eta_i-2)$	For node i ($i = 1, \ldots, 4$)
derivative $\partial u/\partial\xi$	$-\frac{1}{16}\xi_i(\xi+\xi_i)^2(\xi\xi_i-1)(\eta+\eta_i)^2(\eta\eta_i-2)$	
derivative $\partial u/\partial\eta$	$-\frac{1}{16}(\xi+\xi_i)^2(\xi\xi_i-2)\eta_i(\eta+\eta_i)^2(\eta\eta_i-1)$	
derivative $\partial^2 u/\partial\xi\,\partial\eta$	$\frac{1}{16}\xi_i(\xi+\xi_i)^2(\xi\xi_i-1)\eta_i(\eta+\eta_i)^2(\eta\eta_i-1)$	
Interpolation functions for		
variable u	$\frac{1}{2}(\xi_0+1)(\eta_0+1)(2+\xi_0+\eta_0-\xi^2-\eta^2)$	For node i ($i = 1, \ldots, 4$)
derivative $\partial u/\partial\xi$	$\frac{1}{2}\xi_i(\xi_0+1)^2(\xi_0-1)(\eta_0+1)$	
derivative $\partial u/\partial\eta$	$\frac{1}{2}\eta_i(\xi_0+1)(\eta_0+1)^2(\eta_0-1)]$	
	$\xi = (x-x_c)/a, \quad \eta = (y-y_c)/b$ $\xi_0 = \xi\xi_i, \quad \eta_0 = \eta\eta_i$	($2a$ and $2b$ are the sides of the rectangular element)

† See Fig. 9.10 for the coordinate system; (ξ_i, η_i) denote the natural coordinates of the ith node of the element; (x_c, y_c) are the global coordinates of the center of the element.

In the above discussion, we developed only the Lagrange interpolation functions for triangular and rectangular elements. The Hermite family of interpolation functions (which interpolate the function and its derivatives) were not discussed. We recall that such functions are required in the finite element formulation of fourth-order (or higher-order) differential equations (e.g., the Euler–Bernoulli beam theory of Chapter 4 and the classical or Kirchhoff plate theory of Chapter 12). For the sake of completeness, while not presenting the details of the derivation, the Hermite cubic interpolation functions for two rectangular elements are summarized in Table 9.1. The first is based on the interpolation of $(u, \partial u/\partial x, \partial u/\partial y, \partial^2 u/\partial x\, \partial y)$ at each node, and the second is based on the interpolation of $(u, \partial u/\partial x, \partial u/\partial y)$ at each node. The node numbering system in Table 9.1 refers to that used in Fig. 9.10. The notation used in Table 9.1 and Fig. 9.10 is also followed in the computer program FEM2DV2, which will be discussed in Chapter 13.

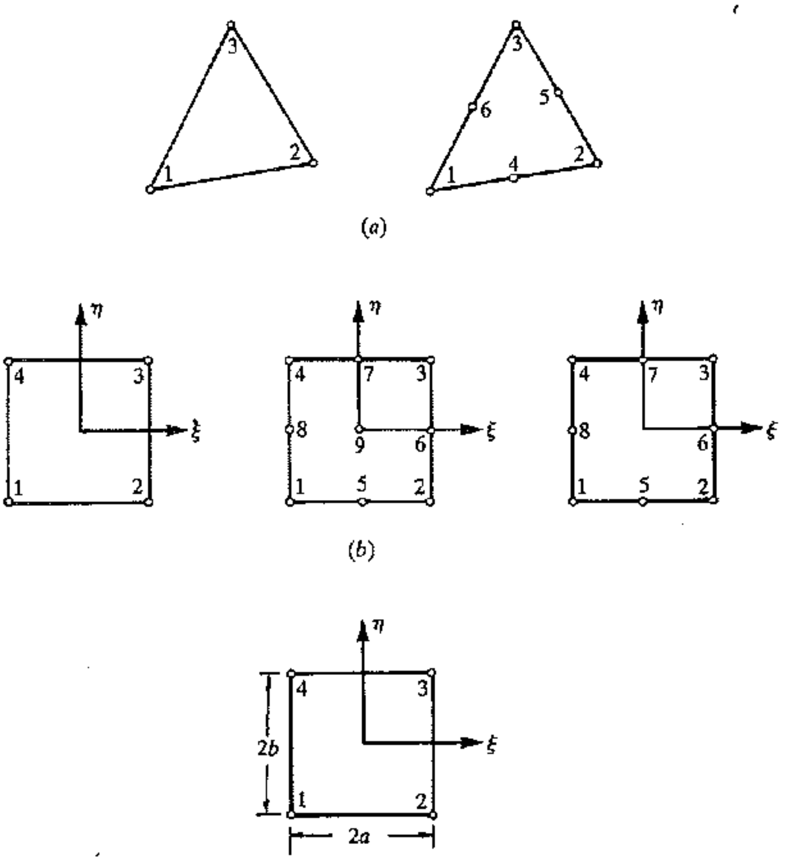

FIGURE 9.10
Triangular and rectangular elements: (*a*) linear and quadratic triangular elements; (*b*) linear and quadratic Lagrange elements; (*c*) Hermite cubic element.

9.2 NUMERICAL INTEGRATION

9.2.1 Preliminary Comments

An accurate representation of domains with curved boundaries can be accomplished by the use of refined meshes and/or curvilinear elements. For example, a nonrectangular region cannot be represented using rectangular elements; however, it can be represented by quadrilateral elements. Since the interpolation functions are easily derivable for a rectangular element, and it is easier to evaluate integrals over rectangular geometries, we transform the finite element integral statements defined over quadrilaterals to a rectangle. The transformation results in complicated expressions in terms of the coordinates used for the rectangular element. Therefore, numerical integration is used to evaluate such expressions. Numerical integration schemes, such as the Gauss–Legendre scheme, require that the integral be evaluated on a specfic domain or with respect to a specific coordinate system. Gauss quadrature, for example, requires that the integral be expressed over a square region $\hat{\Omega}$ of dimension 2 by 2 and that the coordinate system (ξ, η) be such that $-1 \leqslant (\xi, \eta) \leqslant 1$. The transformation of the geometry and the variable coefficients of the differential equation from the problem coordinates (x, y) to the coordinates (ξ, η) results in algebraically complex expressions, and this precludes analytical (i.e., exact) evaluation of the integrals. Thus, the transformation of a given integral expression, defined over the element Ω^e, to one on the domain $\hat{\Omega}$ must be such as to facilitate numerical integration. Each element of the finite element mesh is transformed to $\hat{\Omega}$, only for the purpose of numerically evaluating the integrals. The element $\hat{\Omega}$ is called a *master element*. For example, every quadrilateral element can be transformed to a square element with side 2 that facilitates the use of Gauss–Legendre quadrature to evaluate integrals defined over the quadrilateral element.

The transformation between Ω^e and $\hat{\Omega}$ [or, equivalently, between (x, y) and (ξ, η)] is accomplished by a coordinate transformation of the form

$$\boxed{x = \sum_{j=1}^{m} x_j^e \hat{\psi}_j^e(\xi, \eta), \qquad y = \sum_{j=1}^{m} y_j^e \hat{\psi}_j^e(\xi, \eta)} \tag{9.34}$$

where $\hat{\psi}_j^e$ denote the finite element interpolation functions of the master element $\hat{\Omega}$. Although the Lagrange interpolation of the geometry is implied by (9.34), one can also use Hermite interpolation. Consider, as an example, the master element shown in Fig. 9.11. The coordinates in the master element are chosen to be the natural coordinates (ξ, η) such that $-1 \leqslant (\xi, \eta) \leqslant 1$. This choice is dictated by the limits of integration in the Gauss quadrature rule that is used to evaluate the integrals. For this case, the $\hat{\psi}_j^e$ denote the interpolation functions of the four-node rectangular element shown in Fig. 9.11 (i.e., $m = 4$). The transformation (9.34) maps a point (ξ, η) in the master element $\hat{\Omega}$ onto a point (x, y) in the element Ω^e, and vice versa if the Jacobian of the transformation is positive definite. The transformation maps the line $\xi = 1$ in $\hat{\Omega}$ to the line defined parametrically by $x = x(1, \eta)$ and $y = y(1, \eta)$ in the (x, y)

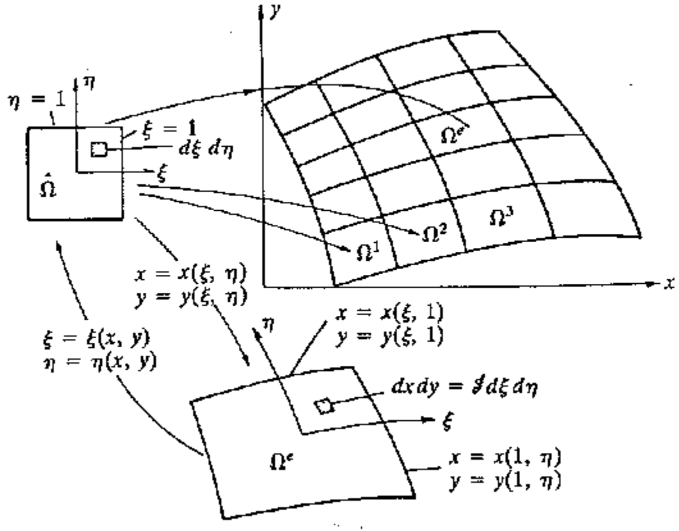

FIGURE 9.11
Generation of a finite element mesh from a master element.

plane. For instance, consider the line $\xi = 1$ in the master element $\hat{\Omega}$. We have

$$\begin{aligned} x(1, \eta) &= \sum_{i=1}^{4} x_i \hat{\psi}_i(1, \eta) = x_1 0 + \tfrac{1}{2}x_2(1-\eta) + \tfrac{1}{2}x_3(1+\eta) + x_4 0 \\ &= \tfrac{1}{2}(x_2 + x_3) + \tfrac{1}{2}(x_3 - x_2)\eta \qquad (9.35) \\ y(1, \eta) &= \sum_{i=1}^{4} y_i \hat{\psi}_i(1, \eta) = \tfrac{1}{2}(y_2 + y_3) + \tfrac{1}{2}(y_3 - y_2)\,\eta \end{aligned}$$

Clearly, x and y are linear functions on η. Therefore, they define a straight line. Similarly, the lines $\xi = -1$ and $\eta = \pm 1$ are mapped into straight lines in the element Ω^e. In other words, the master element $\hat{\Omega}$ is transformed, under the linear transformation, into a quadrilateral element (i.e., a four-sided element whose sides are not parallel) in the (x, y) plane. Conversely, every quadrilateral element of a mesh can be transformed to the same four-noded square (master) element $\hat{\Omega}$ in the (ξ, η) plane (see Fig. 9.6).

In general, the dependent variable(s) of the problem are approximated by expressions of the form

$$u(x, y) = \sum_{j=1}^{n} u_j^e \psi_j^e(x, y) \qquad (9.36)$$

The interpolation functions ψ_j^e used for the approximation of the dependent variable are, in general, different from the $\hat{\psi}_j^e$ used in the approximation of the geometry. Depending on the relative degree of approximations used for the geometry [see (9.34)] and the dependent variable(s) [see (9.36)], the finite element formulations are classified into three categories.

1. *Superparametric* ($m > n$): the approximation used for the geometry is of higher order than that used for the dependent variable.
2. *Isoparametric* ($m = n$): equal degree of approximation is used for both geometry and dependent variables.
3. *Subparametric* ($m < n$): higher-order approximation of the dependent variable is used. (9.37)

For example, in the finite element analysis of the Euler–Bernoulli beams, we used linear Lagrange interpolation of the geometry,

$$x = \sum_{j=1}^{2} x_j \hat{\psi}_j(\xi) = x_A + \tfrac{1}{2}h_e(1+\xi) \tag{9.38}$$

whereas Hermite cubic interpolation was used to approximate the transverse deflection. Such a formulation falls into the subparametric category. Since the axial displacement is approximated by the linear Lagrange interpolation functions, it can be said that the isoparametric formulation is used for the axial displacement. Superparametric formulations are rarely used. Also, the approximation of geometry by the Hermite family of interpolation functions is not common.

9.2.2 Coordinate Transformations

It should be noted that the transformation of a quadrilateral element of a finite element mesh to the master element $\hat{\Omega}$ is solely for the purpose of numerically evaluating the integrals. *No transformation of the physical domain or elements is involved in the finite element analysis.* The resulting algebraic equations of the finite element formulation are always among the nodal values of the physical domain. Different elements of the finite element mesh can be generated from the same master element by assigning the global coordinates of the elements (see Fig. 9.11). Master elements of different order define different transformations and hence different collections of finite element meshes. For example, a cubic-order master rectangular element can be used to generate a mesh of cubic curvilinear quadrilateral elements. Thus, with the help of an appropriate master element, any arbitrary element of a mesh can be generated. However, the transformations of a master element should be such that there are no spurious gaps between elements and no element overlaps. The elements in Figs. 9.6 and 9.8 can be used as master elements.

When a typical element of the finite element mesh is transformed to its master element for the purpose of numerically evaluating integrals, the integrand must also be expressed in terms of the coordinates (ξ, η) of the master element. For example, consider the element coefficients

$$K_{ij}^e = \int_{\Omega^e} \left[a(x,y) \frac{\partial \psi_i^e}{\partial x} \frac{\partial \psi_j^e}{\partial x} + b(x,y) \frac{\partial \psi_i^e}{\partial y} \frac{\partial \psi_j^e}{\partial y} + c(x,y) \psi_i^e \psi_j^e \right] dx\,dy \tag{9.39}$$

The integrand (i.e., the expression in the square brackets under the integral) is a function of the global coordinates x and y. We must rewrite it in terms of ξ and η using the transformation (9.34). Note that the integrand contains not only functions but also derivatives with respect to the global coordinates (x, y). Therefore, we must relate $\partial\psi_i^e/\partial x$ and $\partial\psi_i^e/\partial y$ to $\partial\psi_i^e/\partial\xi$ and $\partial\psi_i^e/\partial\eta$ using the transformation (9.34).

The functions $\psi_i^e(x, y)$ can be expressed in terms of the local coordinates ξ and η by means of (9.34). Hence, by the chain rule of partial differentiation, we have

$$\begin{aligned}\frac{\partial\psi_i^e}{\partial\xi}&=\frac{\partial\psi_i^e}{\partial x}\frac{\partial x}{\partial\xi}+\frac{\partial\psi_i^e}{\partial y}\frac{\partial y}{\partial\xi}\\ \frac{\partial\psi_i^e}{\partial\eta}&=\frac{\partial\psi_i^e}{\partial x}\frac{\partial x}{\partial\eta}+\frac{\partial\psi_i^e}{\partial y}\frac{\partial y}{\partial\eta}\end{aligned}\tag{9.40a}$$

or, in matrix notation,

$$\begin{Bmatrix}\dfrac{\partial\psi_i^e}{\partial\xi}\\ \dfrac{\partial\psi_i^e}{\partial\eta}\end{Bmatrix}=\begin{bmatrix}\dfrac{\partial x}{\partial\xi} & \dfrac{\partial y}{\partial\xi}\\ \dfrac{\partial x}{\partial\eta} & \dfrac{\partial y}{\partial\eta}\end{bmatrix}^e\begin{Bmatrix}\dfrac{\partial\psi_i^e}{\partial x}\\ \dfrac{\partial\psi_i^e}{\partial y}\end{Bmatrix}\tag{9.40b}$$

which gives the relation between the derivatives of ψ_i^e with respect to the global and local coordinates.

The matrix in (9.40*b*) is called the *Jacobian matrix* of the transformation (9.34):

$$[\mathscr{J}]=\begin{bmatrix}\dfrac{\partial x}{\partial\xi} & \dfrac{\partial y}{\partial\xi}\\ \dfrac{\partial x}{\partial\eta} & \dfrac{\partial y}{\partial\eta}\end{bmatrix}^e\tag{9.41}$$

Note from the expression given for K_{ij}^e in (9.39) that we must relate $\partial\psi_i^e/\partial x$ and $\partial\psi_i^e/\partial y$ to $\partial\psi_i^e/\partial\xi$ and $\partial\psi_i^e/\partial\eta$, whereas (9.40) provides the inverse relations. Therefore, (9.40*b*) must be inverted by inverting the Jacobian matrix:

$$\begin{Bmatrix}\dfrac{\partial\psi_i^e}{\partial x}\\ \dfrac{\partial\psi_i^e}{\partial y}\end{Bmatrix}=[\mathscr{J}]^{-1}\begin{Bmatrix}\dfrac{\partial\psi_i^e}{\partial\xi}\\ \dfrac{\partial\psi_i^e}{\partial\eta}\end{Bmatrix}\tag{9.42}$$

This requires that the Jacobian matrix $[\mathscr{J}]$ be nonsingular.

Although it is possible to write the relationship (9.42) directly by means of the chain rule,

$$\begin{aligned}\frac{\partial \psi_i^e}{\partial x}&=\frac{\partial \psi_i^e}{\partial \xi}\frac{\partial \xi}{\partial x}+\frac{\partial \psi_i^e}{\partial \eta}\frac{\partial \eta}{\partial x}\\ \frac{\partial \psi_i^e}{\partial y}&=\frac{\partial \psi_i^e}{\partial \xi}\frac{\partial \xi}{\partial y}+\frac{\partial \psi_i^e}{\partial \eta}\frac{\partial \eta}{\partial y}\end{aligned}\tag{9.43}$$

it is not possible to evaluate $\partial\xi/\partial x$, $\partial\xi/\partial y$, $\partial\eta/\partial x$, and $\partial\eta/\partial y$ directly from the transformation equation (9.34). The transformation equation (9.34) allows direct evaluation of $\partial x/\partial\xi$, $\partial x/\partial\eta$, $\partial y/\partial\xi$ and $\partial y/\partial\eta$, and therefore $[\mathscr{J}]$.

Using the transformation (9.34), we can write

$$\begin{aligned}\frac{\partial x}{\partial \xi}&=\sum_{j=1}^{m} x_j\frac{\partial \hat{\psi}_j^e}{\partial \xi}, & \frac{\partial y}{\partial \xi}&=\sum_{j=1}^{m} y_j\frac{\partial \hat{\psi}_j^e}{\partial \xi}\\ \frac{\partial x}{\partial \eta}&=\sum_{j=1}^{m} x_j\frac{\partial \hat{\psi}_j^e}{\partial \eta}, & \frac{\partial y}{\partial \eta}&=\sum_{j=1}^{m} y_j\frac{\partial \hat{\psi}_j^e}{\partial \eta}\end{aligned}\tag{9.44a}$$

and

$$\begin{aligned}[\mathscr{J}]&=\begin{bmatrix}\dfrac{\partial x}{\partial \xi} & \dfrac{\partial y}{\partial \xi}\\[2mm] \dfrac{\partial x}{\partial \eta} & \dfrac{\partial y}{\partial \eta}\end{bmatrix}=\begin{bmatrix}\sum\limits_{i=1}^{m} x_i\dfrac{\partial \hat{\psi}_i}{\partial \xi} & \sum\limits_{i=1}^{m} y_i\dfrac{\partial \hat{\psi}_i}{\partial \xi}\\ \sum\limits_{i=1}^{m} x_i\dfrac{\partial \hat{\psi}_i}{\partial \eta} & \sum\limits_{i=1}^{m} y_i\dfrac{\partial \hat{\psi}_i}{\partial \eta}\end{bmatrix}\\ &=\begin{bmatrix}\dfrac{\partial \hat{\psi}_1}{\partial \xi} & \dfrac{\partial \hat{\psi}_2}{\partial \xi} & \cdots & \dfrac{\partial \hat{\psi}_m}{\partial \xi}\\[2mm] \dfrac{\partial \hat{\psi}_1}{\partial \eta} & \dfrac{\partial \hat{\psi}_2}{\partial \eta} & \cdots & \dfrac{\partial \hat{\psi}_m}{\partial \eta}\end{bmatrix}\begin{bmatrix}x_1 & y_1\\ x_2 & y_2\\ \vdots & \vdots\\ x_m & y_m\end{bmatrix}\end{aligned}\tag{9.44b}$$

Thus, given the global coordinates (x_j, y_j) of element nodes and the interpolation functions $\hat{\psi}_j^e$ used for geometry, the Jacobian matrix can be evaluated using (9.44*b*). Note that the $\hat{\psi}_j^e$ are different, in general, from the ψ_j^e used in the approximation of the dependent variables.

In order to compute the global derivatives of ψ_i^e (i.e., derivatives of ψ_i^e with respect to x and y) from (9.42), it is necessary to invert the Jacobian matrix. A necessary and sufficient condition for $[\mathscr{J}]^{-1}$ to exist is that the determinant $\mathscr{J}$, called the *Jacobian*, be non-negative at every point (ξ, η) in $\hat{\Omega}$:

$$\mathscr{J}\equiv\det[\mathscr{J}]=\frac{\partial x}{\partial \xi}\frac{\partial y}{\partial \eta}-\frac{\partial x}{\partial \eta}\frac{\partial y}{\partial \xi}>0\tag{9.45}$$

From this it is clear that the functions $\xi=\xi(x, y)$ and $\eta=\eta(x, y)$ must be continuous, differentiable, and invertible. Moreover, the transformation should be algebraically simple so that the Jacobian matrix can be easily evaluated. Transformations of the form (9.34) satisfy these requirements and the requirement that no spurious gaps between elements or overlapping of elements occur. We consider an example to illustrate the invertibility requirements.

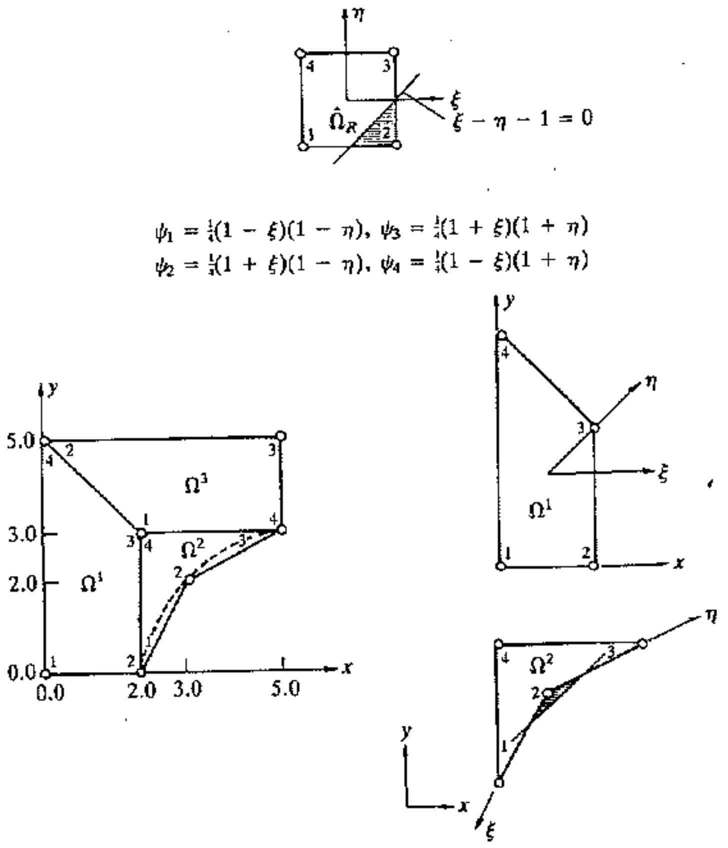

$$\psi_1 = \tfrac{1}{4}(1-\xi)(1-\eta),\quad \psi_3 = \tfrac{1}{4}(1+\xi)(1+\eta)$$
$$\psi_2 = \tfrac{1}{4}(1+\xi)(1-\eta),\quad \psi_4 = \tfrac{1}{4}(1-\xi)(1+\eta)$$

FIGURE 9.12
Examples of transformations of the master rectangular element $\hat{\Omega}_R$.

Example 9.2. Consider the three-element mesh of quadrilaterals shown in Fig. 9.12. The master element is the four-node square. Elements 1 and 2 have counter-clockwise element node numbering consistent with the node numbering in the master element, and element 3 has node numbering opposite to that of the master element. Elements 1 and 3 are *convex* domains in the sense that the line segment connecting any two arbitrary points of a convex domain lies entirely in the element. Clearly, element 2 is not convex, because, for example, the line segment joining nodes 1 and 3 is not entirely inside the element. In the following paragraphs, we investigate the effect of node numbering and element convexity on the transformations from the master element to each of the three elements.

First, we compute the elements of the Jacobian matrix (the interpolation functions are given in Fig. 9.12):

$$\frac{\partial x}{\partial \xi} = \sum_{i=1}^{4} x_i \frac{\partial \hat{\psi}_i}{\partial \xi} = \tfrac{1}{4}[-x_1(1-\eta) + x_2(1-\eta) + x_3(1+\eta) - x_4(1+\eta)]$$
$$\frac{\partial x}{\partial \eta} = \sum_{i=1}^{4} x_i \frac{\partial \hat{\psi}_i}{\partial \eta} = \tfrac{1}{4}[-x_1(1-\xi) - x_2(1+\xi) + x_3(1+\xi) + x_4(1-\xi)] \tag{9.46}$$

$$\frac{\partial y}{\partial \xi}=\sum_{i=1}^{4} y_i\frac{\partial \hat{\psi}_i}{\partial \xi}=\tfrac{1}{4}[-y_1(1-\eta)+y_2(1-\eta)+y_3(1+\eta)-y_4(1+\eta)]$$

$$\frac{\partial y}{\partial \eta}=\sum_{i=1}^{4} y_i\frac{\partial \hat{\psi}_i}{\partial \eta}=\tfrac{1}{4}[-y_1(1-\xi)-y_2(1+\xi)+y_3(1+\xi)+y_4(1-\xi)]$$

Next, we evaluate the Jacobian for each of the elements.

Element 1. We have $x_1=x_4=0$, $x_2=x_3=2$, $y_1=y_2=0$, $y_3=3$, and $y_4=5$. The transformation and Jacobian are given by

$$x=2\hat{\psi}_2+2\hat{\psi}_3=1+\xi,\qquad y=3\hat{\psi}_3+5\hat{\psi}_4=(1+\eta)(2-\tfrac{1}{2}\xi) \tag{9.47a}$$

$$\mathcal{J}=\det[\mathcal{J}]=\begin{vmatrix}1 & -\frac{1}{2}(1+\eta)\\ 0 & 2-\frac{1}{2}\xi\end{vmatrix}=\tfrac{1}{2}(4-\xi)>0 \tag{9.47b}$$

Clearly, the Jacobian is linear in ξ, and, for all values of ξ in $-1\leq\xi\leq 1$, it is positive. Therefore, the transformation (9.47*a*) is invertible.

Element 2. Here we have $x_1=x_4=2$, $x_2=3$, $x_3=5$, $y_1=0$, $y_2=2$, and $y_3=y_4=3$. The transformation and Jacobian are given by

$$x=3+\xi+\tfrac{1}{2}\eta+\tfrac{1}{2}\xi\eta,\qquad y=2+\tfrac{1}{2}\xi+\eta-\tfrac{1}{2}\xi\eta \tag{9.48a}$$

$$\mathcal{J}=\begin{vmatrix}1+\frac{1}{2}\eta & \frac{1}{2}(1-\eta)\\ \frac{1}{2}(1+\xi) & 1-\frac{1}{2}\xi\end{vmatrix}=\tfrac{3}{4}(1+\eta-\xi) \tag{9.48b}$$

The Jacobian is *not* nonzero everywhere in the master element. It is zero along the line $\xi=1+\eta$ shown by the shaded area in the master element in Fig. 9.12. Moreover, this area is mapped into the shaded area outside element 2. Thus, elements with any interior angle greater than π should not be used in any finite element mesh.

Element 3. We have $x_1=2$, $x_2=0$, $x_3=x_4=5$, $y_1=y_4=3$, and $y_2=y_3=5$. The transformation and Jacobian become (note that the nodes are numbered clockwise)

$$x=3-\tfrac{1}{2}\xi+2\eta+\tfrac{1}{2}\xi\eta,\qquad y=4+\xi \tag{9.49a}$$

$$\mathcal{J}=\begin{vmatrix}-\frac{1}{2}(1-\eta) & 1\\ 2+\frac{1}{2}\xi & 0\end{vmatrix}=-(2+\tfrac{1}{2}\xi)<0 \tag{9.49b}$$

The negative Jacobian indicates that a right-hand coordinate system is mapped into a left-hand coordinate system. Such coordinate transformations should be avoided.

The above example illustrates, for the four-node master element, that nonconvex elements are not admissible in finite element meshes. In general, any interior angle θ (see Fig. 9.13) should not be too small or too large, because the Jacobian $\mathcal{J}=(|d\mathbf{r}_1|\,|d\mathbf{r}_2|\sin\theta)/d\xi\,d\eta$ will be very small. Similar restrictions hold for higher-order master elements. Additional restrictions also exist for higher-order elements. For example, for higher-order triangular and rectangular elements, the placing of the side and interior nodes is restricted. For the eight-node rectangular element, it can be shown that the side nodes should be placed at a distance greater than a quarter of the length of the side from either corner node (see Fig. 9.13).

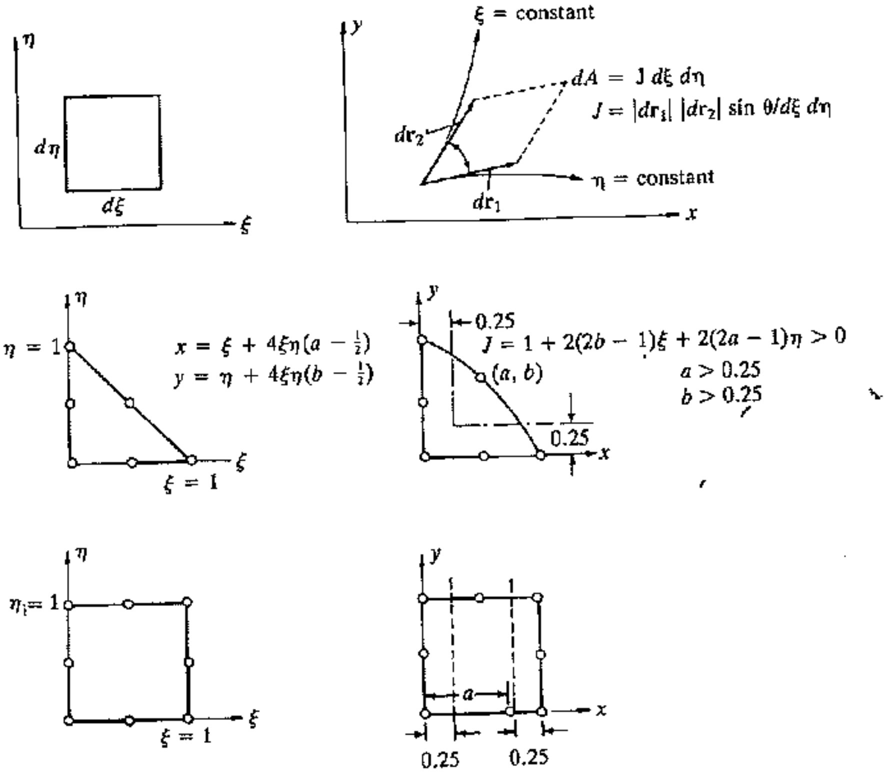

FIGURE 9.13
Some restrictions on element transformations.

Returning to numerical evaluation of integrals, we have, from (9.42),

$$\begin{Bmatrix} \dfrac{\partial \psi_i^e}{\partial x} \\ \dfrac{\partial \psi_i^e}{\partial y} \end{Bmatrix} = [\mathscr{J}]^{-1} \begin{Bmatrix} \dfrac{\partial \psi_i^e}{\partial \xi} \\ \dfrac{\partial \psi_i^e}{\partial \eta} \end{Bmatrix} \equiv [\mathscr{J}^*] \begin{Bmatrix} \dfrac{\partial \psi_i^e}{\partial \xi} \\ \dfrac{\partial \psi_i^e}{\partial \eta} \end{Bmatrix} \tag{9.50}$$

where $\mathscr{J}_{ij}^*$ is the element in position (i, j) of the inverse of the Jacobian matrix,

$$[\mathscr{J}]^{-1} \equiv [\mathscr{J}^*] = \begin{bmatrix} \mathscr{J}_{11}^* & \mathscr{J}_{12}^* \\ \mathscr{J}_{21}^* & \mathscr{J}_{22}^* \end{bmatrix} \tag{9.51}$$

The elemental area $dA = dx\, dy$ in the element Ω^e is transformed to

$$dA \equiv dx\, dy = \mathscr{J}\, d\xi\, d\eta \tag{9.52}$$

in the master element $\hat{\Omega}$.

Equations (9.42), (9.44), (9.51), and (9.52) provide the necessary relations to transform integral expressions on any element Ω^e to an associated master element $\hat{\Omega}$. For instance, consider the integral expression in (9.39) where $a = a(x, y)$, $b = b(x, y)$, and $c = c(x, y)$ are functions of x and y. Suppose that the mesh of finite elements is generated by a master element $\hat{\Omega}$. Under the transformation (9.34), we can write

$$
\begin{aligned}
K_{ij}^e &= \int_{\Omega^e} \left(a \frac{\partial \psi_i}{\partial x}\frac{\partial \psi_j}{\partial x} + b \frac{\partial \psi_i}{\partial y}\frac{\partial \psi_j}{\partial y} + c\psi_i\psi_j \right) dx\, dy \\
&= \int_{\hat{\Omega}} \left[\hat{a} \left(\mathcal{J}_{11}^* \frac{\partial \psi_i}{\partial \xi} + \mathcal{J}_{12}^* \frac{\partial \psi_i}{\partial \eta} \right) \left(\mathcal{J}_{11}^* \frac{\partial \psi_j}{\partial \xi} + \mathcal{J}_{12}^* \frac{\partial \psi_j}{\partial \eta} \right) \right. \\
&\qquad \left. + \hat{b} \left(\mathcal{J}_{21}^* \frac{\partial \psi_i}{\partial \xi} + \mathcal{J}_{22}^* \frac{\partial \psi_i}{\partial \eta} \right) \left(\mathcal{J}_{21}^* \frac{\partial \psi_j}{\partial \xi} + \mathcal{J}_{22}^* \frac{\partial \psi_j}{\partial \eta} \right) + \hat{c}\psi_i\psi_j \right] \mathcal{J}\, d\xi\, d\eta \\
&\equiv \int_{\hat{\Omega}} F(\xi, \eta)\, d\xi\, d\eta
\end{aligned}
\tag{9.53}
$$

where $\mathcal{J}_{ij}^*$ are the elements of the inverse of the Jacobian matrix in (9.51), and $\hat{a} = a(\xi, \eta)$, and so on. Equations (9.42), (9.44), and (9.51)–(9.53) are valid for master elements of both rectangular and triangular geometry. The master triangular and rectangular elements for linear and quadratic triangular and quadrilateral elements are shown in Fig. 9.14.

9.2.3 Integration over a Master Rectangular Element

Quadrature formulae for integrals defined over a rectangular master element $\hat{\Omega}_R$ (such as that shown in Fig. 9.14) can be derived from the one-dimensional quadrature formulae presented in Section 7.1.5. We have

$$
\begin{aligned}
\int_{\hat{\Omega}_R} F(\xi, \eta)\, d\xi\, d\eta &= \int_{-1}^{1} \left[\int_{-1}^{1} F(\xi, \eta)\, d\eta \right] d\xi \approx \int_{-1}^{1} \left[\sum_{J=1}^{N} F(\xi, \eta_J) W_J \right] d\xi \\
&\approx \sum_{I=1}^{M} \sum_{J=1}^{N} F(\xi_I, \eta_J) W_I W_J
\end{aligned}
\tag{9.54}
$$

where M and N denote the number of quadrature points in the ξ and η directions, (ξ_I, η_J) denote the Gauss points, and W_I and W_J denote the corresponding Gauss weights (see Table 7.2). The selection of the number of Gauss points is based on the same formula as that given in Section 7.1.5: a polynomial of degree p is integrated exactly employing $N = \text{int}\,[\frac{1}{2}(p+1)]$; that is, the smallest integer greater than $\frac{1}{2}(p+1)$. In most cases, the interpolation functions are of the same degree in both ξ and η, and therefore one has $M = N$. When the integrand is of different degree in ξ and η, the number of Gauss points is selected on the basis of the largest-degree polynomial. The minimum allowable quadrature rule is one that computes the mass of the element exactly when the density is constant.

Tables 9.2 and 9.3 give information on the selection of the integration order and the location of the Gauss points for linear, quadratic, and cubic elements. The maximum degree of the polynomial refers to the degree of the highest polynomial in ξ or η that is present in the integrands $F(\xi, \eta)$ of the

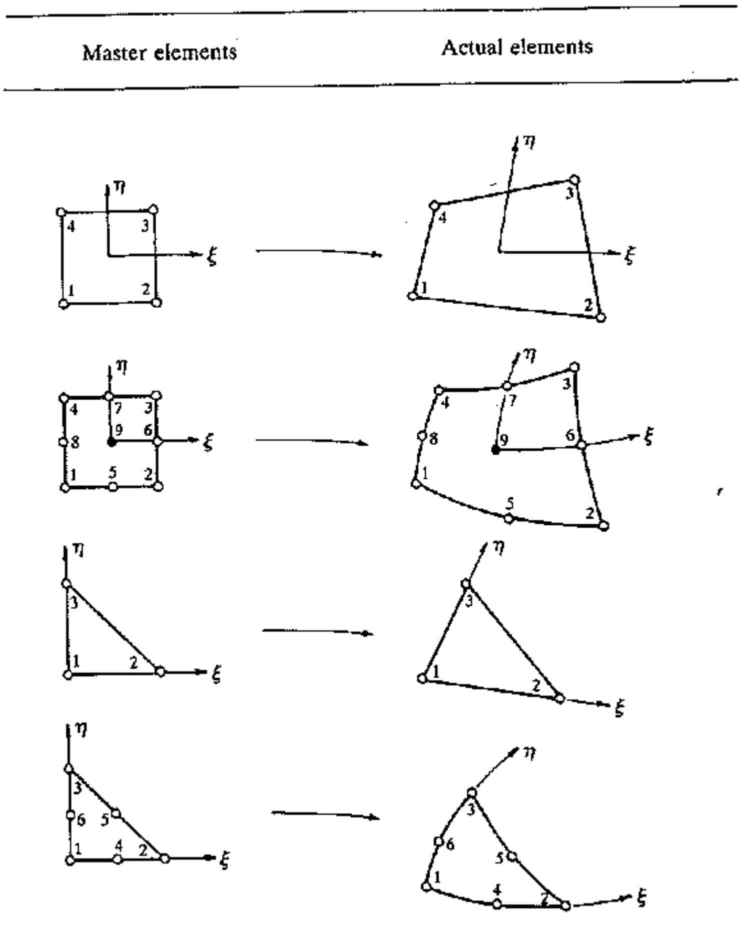

FIGURE 9.14
Linear and quadratic master elements and their transformations.

element matrices of the type in (9.53). Note that the polynomial degree of coefficients as well as $\mathscr{J}_{ij}^*$ and $\mathscr{J}$ should be accounted for in determining the total polynomial degree of the integrand. Of course, the coefficients a, b, and c, and $\mathscr{J}_{ij}^*$ in general, may not be polynomials. In those cases, their functional variations must be approximated by a suitable polynomial (for example, via a binomial series) in order to determine the polynomial degree of the integrand.

The $N \times N$ Gauss point locations are given by the *tensor product* of one-dimensional Gauss points ξ_I:

$$\begin{Bmatrix} \xi_1 \\ \xi_2 \\ \vdots \\ \xi_N \end{Bmatrix} \{\xi_1, \xi_2, \ldots, \xi_N\} \equiv \begin{bmatrix} (\xi_1, \xi_1) & (\xi_1, \xi_2) & \cdots & (\xi_1, \xi_N) \\ (\xi_2, \xi_1) & & \ddots & \vdots \\ \vdots & & & \\ (\xi_N, \xi_1) & & \cdots & (\xi_N, \xi_N) \end{bmatrix} \tag{9.55}$$

The values of ξ_I $(I = 1, 2, \ldots, N)$ are presented in Table 7.2.

TABLE 9.2
Selection of the integration order and location of the Gauss points for linear, quadratic, and cubic quadrilateral elements (nodes not shown)

Element type	Maximum polynomial degree	Order of integration ($r \times r$)	Order of the residual	Location of integration points* in master element
Linear ($r = 2$)	2	2×2	$O(h^4)$	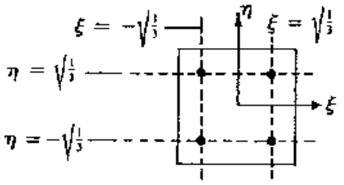 $\xi = -\sqrt{\frac{1}{3}}$ η $\xi = \sqrt{\frac{1}{3}}$ $\eta = \sqrt{\frac{1}{3}}$ ξ $\eta = -\sqrt{\frac{1}{3}}$
Quadratic ($r = 3$)	4	3×3	$O(h^6)$	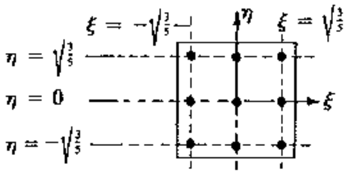 $\xi = -\sqrt{\frac{3}{5}}$ η $\xi = \sqrt{\frac{3}{5}}$ $\eta = \sqrt{\frac{3}{5}}$ $\eta = 0$ ξ $\eta = -\sqrt{\frac{3}{5}}$
Cubic ($r = 4$)	6	4×4	$O(h^8)$	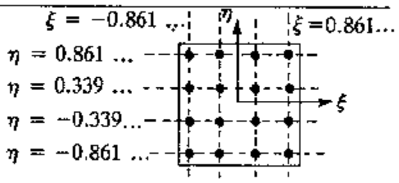 $\xi = -0.861$ ... η $\xi = 0.861$... $\eta = 0.861$ ... $\eta = 0.339$ ... ξ $\eta = -0.339$... $\eta = -0.861$ ...

*See Table 7.2 for the integration points and weights for each coordinate direction.

The following examples illustrate the evaluation of the Jacobian and element matrices on rectangular elements.

Example 9.3. Consider the quadrilateral element Ω^1 shown in Fig. 9.12. We wish to evaluate $\partial\psi_i/\partial x$ and $\partial\psi_i/\partial y$ at $(\xi, \eta) = (0, 0)$ and $(\frac{1}{2}, \frac{1}{2})$ using the isoparametric formulation (i.e., $\hat{\psi}_i = \psi_i$). From (9.44*b*), we have

$$[\mathcal{J}] = \frac{1}{4}\begin{bmatrix} -(1-\eta) & 1-\eta & 1+\eta & -(1+\eta) \\ -(1-\xi) & -(1+\xi) & 1+\xi & 1-\xi \end{bmatrix}\begin{bmatrix} 0.0 & 0.0 \\ 2.0 & 0.0 \\ 2.0 & 3.0 \\ 0.0 & 5.0 \end{bmatrix}$$

$$= \begin{bmatrix} 1 & -\frac{1}{2}(1+\eta) \\ 0 & \frac{1}{2}(4-\xi) \end{bmatrix}$$

The inverse of the Jacobian matrix is given by

$$[\mathcal{J}]^{-1}=\begin{bmatrix} 1 & \dfrac{1+\eta}{4-\xi} \\ 0 & \dfrac{2}{4-\xi} \end{bmatrix}$$

$$\mathcal{J}_{11}^{*}=1, \quad \mathcal{J}_{21}^{*}=0, \quad \mathcal{J}_{12}^{*}=\frac{1+\eta}{4-\xi}, \quad \mathcal{J}_{22}^{*}=\frac{2}{4-\xi}$$

From (9.42), we have

$$\frac{\partial\psi_i}{\partial x}=\frac{\partial\psi_i}{\partial\xi}+\frac{1+\eta}{4-\xi}\frac{\partial\psi_i}{\partial\eta}, \qquad \frac{\partial\psi_i}{\partial y}=\frac{2}{4-\xi}\frac{\partial\psi_i}{\partial\eta}$$

where

$$\psi_i=\tfrac{1}{4}(1+\xi\xi_i)(1+\eta\eta_i), \qquad \frac{\partial\psi_i}{\partial\xi}=\tfrac{1}{4}\xi_i(1+\eta\eta_i), \qquad \frac{\partial\psi_i}{\partial\eta}=\tfrac{1}{4}\eta_i(1+\xi\xi_i) \tag{9.56}$$

(ξ_i, η_i) being the coordinates of the ith node in the master element (see Fig. 9.12):

Node	ξ_i	η_i
1	-1	-1
2	1	-1
3	1	1
4	-1	1

Then we have

$$\frac{\partial\psi_i}{\partial x}=\tfrac{1}{4}\xi_i(1+\eta\eta_i)+\frac{1}{4}\frac{1+\eta}{4-\xi}\eta_i(1+\xi\xi_i)$$

$$\frac{\partial\psi_i}{\partial y}=\frac{1}{4}\frac{2}{4-\xi}\eta_i(1+\xi\xi_i)$$

$(\xi, \eta)\rightarrow$	$(0, 0)$	$(\frac{1}{2}, \frac{1}{2})$
$\dfrac{\partial\psi_i}{\partial x}$	$\frac{1}{4}\xi_i+\frac{1}{16}\eta_i$	$\frac{1}{8}\xi_i(2+\eta_i)+\frac{3}{56}\eta_i(2+\xi_i)$
$\dfrac{\partial\psi_i}{\partial y}$	$\frac{1}{8}\eta_i$	$\frac{1}{14}\eta_i(2+\xi_i)$

Example 9.4. Consider the quadrilateral element in Fig. 9.15. We wish to compute the following element matrices using Gauss quadrature and the isoparametric formulation:

$$\begin{aligned} S_{ij}&=\int_{\Omega}\psi_i\psi_j\,dx\,dy, & S_{ij}^{11}&=\int_{\Omega}\frac{\partial\psi_i}{\partial x}\frac{\partial\psi_j}{\partial x}\,dx\,dy \\ S_{ij}^{22}&=\int_{\Omega}\frac{\partial\psi_i}{\partial y}\frac{\partial\psi_j}{\partial y}\,dx\,dy, & S_{ij}^{12}&=\int_{\Omega}\frac{\partial\psi_i}{\partial x}\frac{\partial\psi_j}{\partial y}\,dx\,dy \end{aligned} \tag{9.57}$$

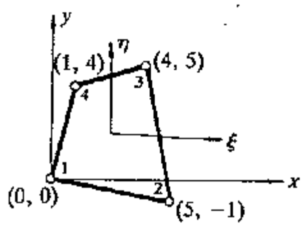

FIGURE 9.15
Geometry of the bilinear element used in Example 9.4

We have

$$[\mathcal{J}]=\frac{1}{4}\begin{bmatrix}8-2\eta & 2\eta\\ -2\xi & 10+2\xi\end{bmatrix}$$

$$\mathcal{J}=(4-\eta)(5+\xi)+\xi\eta=20+4\xi-5\eta$$

$$S_{ij}=\int_{\Omega}\psi_i\psi_j\,dx\,dy=\int_{-1}^{1}\int_{-1}^{1}\psi_i\psi_j\mathcal{J}\,d\xi\,d\eta$$

$$\begin{aligned}S_{ij}^{11}&=\int_{\Omega}\frac{\partial\psi_i}{\partial x}\frac{\partial\psi_j}{\partial x}\,dx\,dy\\ &=\int_{-1}^{1}\int_{-1}^{1}\left(\mathcal{J}_{11}^{*}\frac{\partial\psi_i}{\partial\xi}+\mathcal{J}_{12}^{*}\frac{\partial\psi_i}{\partial\eta}\right)\left(\mathcal{J}_{11}^{*}\frac{\partial\psi_j}{\partial\xi}+\mathcal{J}_{12}^{*}\frac{\partial\psi_j}{\partial\eta}\right)\mathcal{J}\,d\xi\,d\eta\end{aligned} \tag{9.58}$$

and so on, where $\partial\psi_i/\partial\xi$ and $\partial\psi_i/\partial\eta$ are given by (9.56). Note that the integrand of S_{ij} is a polynomial of order $p=3$ in each coordinate. Hence, $N=M=2$ will evaluate S_{ij} exactly. Evaluating the integrals in (9.57) using the 2×2 quadrative rule, we obtain

$$[S^{11}]=\begin{bmatrix}0.40995 & -0.36892 & -0.20479 & 0.16376\\ -0.36892 & 0.34516 & 0.25014 & -0.22639\\ -0.20479 & 0.25014 & 0.43155 & -0.47690\\ 0.16376 & -0.22639 & -0.47690 & 0.53953\end{bmatrix}$$

$$[S^{22}]=\begin{bmatrix}0.26237 & 0.16389 & -0.13107 & -0.29520\\ 0.16389 & 0.22090 & -0.23991 & -0.14489\\ -0.13107 & -0.23991 & 0.27619 & 0.09478\\ -0.29520 & -0.14489 & 0.09478 & 0.34530\end{bmatrix}$$

$$[S^{12}]=\begin{bmatrix}0.24731 & 0.25156 & -0.25297 & -0.24589\\ -0.24844 & -0.25090 & 0.25172 & 0.24762\\ -0.25297 & -0.24828 & 0.24671 & 0.25454\\ 0.25411 & 0.24762 & -0.24546 & -0.25627\end{bmatrix}$$

$$[S]=\begin{bmatrix}2.27780 & 1.25000 & 0.55556 & 1.00000\\ 1.25000 & 2.72220 & 1.22220 & 0.55556\\ 0.55556 & 1.22220 & 2.16670 & 0.97222\\ 1.00000 & 0.55556 & 0.97222 & 1.72222\end{bmatrix}$$

9.2.4 Integration over a Master Triangular Element

In the preceding section, we discussed numerical integration on quadrilateral elements, which can be used to represent very general geometries as well as field variables in a variety of problems. Here we discuss numerical integration on triangular elements. Since quadrilateral elements can be geometrically distorted, it is possible to distort a quadrilateral element to obtain a required triangular element by moving the position of the corner node to one of the neighboring nodes. In actual computation, this is achieved by assigning the same global node number to two corner nodes of the quadrilateral element. Thus, master triangular elements can be obtained in a natural way from associated master rectangular elements. Here we discuss the transformations from an arbitrary triangular element to a master triangular element.

We choose the unit right isosceles triangle (see Fig. 9.16*a*) as the master element. An arbitrary triangular element Ω^e can be generated from the master triangular element $\hat{\Omega}_T$ by a transformation of the form (9.34). The coordinate lines $\xi = 0$ and $\eta = 0$ in $\hat{\Omega}_T$ correspond to the skew curvilinear coordinate lines 1–3 and 1–2 in Ω^e. For the three-node triangular element, the transformation (9.34) is taken to be

$$x = \sum_{i=1}^{3} x_i \hat{\psi}_i(\xi, \eta), \qquad y = \sum_{i=1}^{3} y_i \hat{\psi}_i(\xi, \eta) \tag{9.59}$$

where $\hat{\psi}_i(\xi, \eta)$ are the interpolation functions of the master three-node triangular element (see Fig. 9.16*b*),

$$\hat{\psi}_1 = 1 - \xi - \eta, \qquad \hat{\psi}_2 = \xi, \qquad \hat{\psi}_3 = \eta \tag{9.60}$$

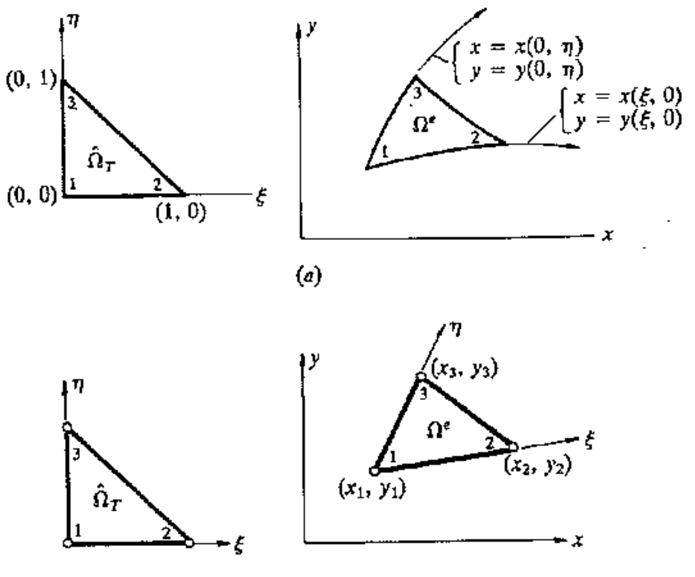

(*a*)

(*b*)

FIGURE 9.16
Triangular master element and its transformations: (*a*) general transformation; (*b*) linear transformation of a master element to a triangular element.

The inverse transformation from the element Ω^e to $\hat{\Omega}_T$ is given by inverting (9.59):

$$\begin{aligned}\xi &= \frac{1}{2A}[(x-x_1)(y_3-y_1)-(y-y_1)(x_3-x_1)]\\ \eta &= \frac{1}{2A}[(x-x_1)(y_1-y_2)+(y-y_1)(x_2-x_1)]\end{aligned} \tag{9.61}$$

where A is the area of Ω^e.

With the help of (9.61), one can show that the interpolation functions in (8.25) are equivalent to the $\hat{\psi}_i$ in (9.60). Moreover, the area coordinates L_i in (9.9) are also equivalent to $\hat{\psi}_i$. The interpolation functions for the linear and higher-order triangular elements can be obtained from the area coordinates, as described in Section 9.1.

The Jacobian matrix for the linear triangular element is

$$[\mathcal{J}] = \begin{bmatrix} x_2-x_1 & y_2-y_1 \\ x_3-x_1 & y_3-y_1 \end{bmatrix} = \begin{bmatrix} \gamma_3 & -\beta_3 \\ -\gamma_2 & \beta_2 \end{bmatrix} \tag{9.62}$$

where β_i and γ_i are the constants defined in (8.23b). The inverse of the Jacobian matrix is given by

$$[\mathcal{J}]^{-1} = \frac{1}{\mathcal{J}}\begin{bmatrix} \beta_2 & \beta_3 \\ \gamma_2 & \gamma_3 \end{bmatrix}, \qquad \mathcal{J} = \beta_2\gamma_3 - \gamma_2\beta_3 = 2A \tag{9.63}$$

The relations (9.42) for the isoparametric formulation with linear triangular elements have the explicit form

$$\begin{aligned}&\frac{\partial\psi_1}{\partial x} = -\frac{\beta_2+\beta_3}{2A} = \frac{\beta_1}{2A}, \qquad \frac{\partial\psi_1}{\partial y} = -\frac{\gamma_2+\gamma_3}{2A} = \frac{\gamma_1}{2A}\\ &\frac{\partial\psi_2}{\partial x} = \frac{\beta_2}{2A}, \quad \frac{\partial\psi_2}{\partial y} = \frac{\gamma_2}{2A}, \quad \frac{\partial\psi_3}{\partial x} = \frac{\beta_3}{2A}, \quad \frac{\partial\psi_3}{\partial y} = \frac{\gamma_3}{2A}\end{aligned} \tag{9.64}$$

In a general case, the derivatives of ψ_i with respect to the global coordinates can be computed from (9.43), which take the form

$$\begin{aligned}\frac{\partial\psi_i}{\partial x} &= \frac{\partial\psi_i}{\partial L_1}\frac{\partial L_1}{\partial x} + \frac{\partial\psi_i}{\partial L_2}\frac{\partial L_2}{\partial x}\\ \frac{\partial\psi_i}{\partial y} &= \frac{\partial\psi_i}{\partial L_1}\frac{\partial L_1}{\partial y} + \frac{\partial\psi_i}{\partial L_2}\frac{\partial L_2}{\partial y}\end{aligned} \tag{9.65a}$$

or

$$\begin{Bmatrix} \dfrac{\partial\psi_i}{\partial x} \\[2mm] \dfrac{\partial\psi_i}{\partial y} \end{Bmatrix} = [\mathcal{J}]^{-1}\begin{Bmatrix} \dfrac{\partial\psi_i}{\partial L_1} \\[2mm] \dfrac{\partial\psi_i}{\partial L_2} \end{Bmatrix}, \qquad [\mathcal{J}] = \begin{bmatrix} \dfrac{\partial x}{\partial L_1} & \dfrac{\partial y}{\partial L_1} \\[2mm] \dfrac{\partial x}{\partial L_2} & \dfrac{\partial y}{\partial L_2} \end{bmatrix} \tag{9.65b}$$

Note that only L_1 and L_2 are treated as linearly independent coordinates, because $L_3 = 1 - L_1 - L_2$.

After transformation, integrals on $\hat{\Omega}_T$ have the form

$$\int_{\hat{\Omega}_T} G(\xi, \eta)\, d\xi\, d\eta = \int_{\hat{\Omega}_T} \hat{G}(L_{\cancel{1}}, L_{\cancel{2}}, L_3)\, dL_{\cancel{1}_3}\, dL_2 \tag{9.66}$$

which can be approximated by the quadrature formula

$$\int_{\hat{\Omega}_T} \hat{G}(L_1, L_2, L_3)\, dL_{\cancel{1}_3}\, dL_2 \approx \frac{1}{2} \sum_{I=1}^{N} W_I \hat{G}(\mathbf{S}_I) \tag{9.67}$$

TABLE 9.3
Quadrature points and weights for triangular elements

Number of integration points	Degree of polynomial and order of the residual	Location of integration points					
		$L_{\cancel{1}3}$	L_2	$L_{\cancel{3}1}$	W	Geometric locations	
1	1 $O(h^2)$	$\frac{1}{3}$	$\frac{1}{3}$	$\frac{1}{3}$	1	a	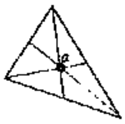
	2	$\frac{1}{2}$	0	$\frac{1}{2}$	$\frac{1}{3}$	a	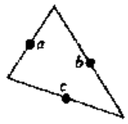
3	$O(h^3)$	$\frac{1}{2}$	$\frac{1}{2}$	0	$\frac{1}{3}$	b	
		0	$\frac{1}{2}$	$\frac{1}{2}$	$\frac{1}{3}$	c	
	3	$\frac{1}{3}$	$\frac{1}{3}$	$\frac{1}{3}$	$-\frac{27}{48}$	a	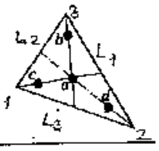
		0.6	0.2	0.2	$\frac{25}{48}$	b	
4	$O(h^4)$	0.2	0.6	0.2	$\frac{25}{48}$	c → d	
		0.2	0.2	0.6	$\frac{25}{48}$	d → c	
		$\frac{1}{3}$	$\frac{1}{3}$	$\frac{1}{3}$	0.225	a	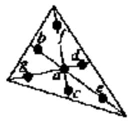
	5	α_1	β_1	β_1		b	
		β_1	α_1	β_1	w_2	c	
7	$O(h^6)$	β_1	β_1	α_1		d	
		α_2	β_2	β_2		e	
		β_2	α_2	β_2	w_3	f	
		β_2	β_2	α_2		g	

$\alpha_1 = 0.797\,426\,985\,353$
$\beta_1 = 0.101\,286\,507\,323$
$W_2 = 0.125\,939\,180\,544$

$\alpha_2 = 0.059\,715\,871\,789$
$\beta_2 = 0.470\,142\,064\,105$
$W_3 = 0.132\,394\,152\,788$

where W_I and $\mathbf{S}_I$ denote the weights and integration points of the quadrature rule. Table 9.3 gives the location of integration points and weights for one-, three-, and four-point quadrature rules over triangular elements. For the evaluation of integrals whose integrands are polynomials of degree higher than five (in any of the area coordinates), the reader should consult books on numerical integration.

Example 9.5. Consider the quadratic triangular element shown in Fig. 9.17. We wish to calculate $\partial\psi_1/\partial x$, $\partial\psi_1/\partial y$, $\partial\psi_4/\partial x$, and $\partial\psi_4/\partial y$ at the point $(x, y) = (2, 4)$ and evaluate the integral of the product $(\partial\psi_1/\partial x)(\partial\psi_4/\partial x)$.

Since the element has straight edges, its geometry is defined by the interpolation functions of the corner nodes (i.e., a subparametric formulation can be used). Note that if the element is curvilinear, we cannot use only three corner nodes to describe the geometry exactly (hence an isoparametric formulation must be used). For the element at hand, we have

$$x = \sum_{i=1}^{3} x_i L_i = 7L_2 + 2L_3 = 2 - 2L_1 + 5L_2$$

$$y = \sum_{i=1}^{3} y_i L_i = 2L_2 + 6L_3 = 6 - 6L_1 - 4L_2 \tag{9.68a}$$

$$[\mathscr{J}] = \begin{bmatrix} -2 & -6 \\ 5 & -4 \end{bmatrix}, \quad [\mathscr{J}]^{-1} = \frac{1}{38}\begin{bmatrix} -4 & 6 \\ -5 & -2 \end{bmatrix}$$

The ψ_i for the quadratic triangular element are given by (9.16), with ψ_2 in (9.16c) being equal to ψ_4 here (compare the node numbering in Figs. 9.17 and 9.4b). The global derivatives of ψ_i are given by (9.65):

$$\begin{Bmatrix} \dfrac{\partial\psi_1}{\partial x} \\ \dfrac{\partial\psi_1}{\partial y} \end{Bmatrix} = \frac{1}{38}\begin{bmatrix} -4 & 6 \\ -5 & -2 \end{bmatrix}\begin{Bmatrix} \dfrac{\partial\psi_1}{\partial L_1} \\ \dfrac{\partial\psi_1}{\partial L_2} \end{Bmatrix} = \begin{Bmatrix} \dfrac{-4(4L_1 - 1)}{38} \\ \dfrac{-5(4L_1 - 1)}{38} \end{Bmatrix} \tag{9.68b}$$

$$\begin{Bmatrix} \dfrac{\partial\psi_4}{\partial x} \\ \dfrac{\partial\psi_4}{\partial y} \end{Bmatrix} = \frac{1}{38}\begin{bmatrix} -4 & 6 \\ -5 & -2 \end{bmatrix}\begin{Bmatrix} \dfrac{\partial\psi_4}{\partial L_1} \\ \dfrac{\partial\psi_4}{\partial L_2} \end{Bmatrix} = \frac{1}{38}\begin{Bmatrix} -16L_2 + 24L_1 \\ -20L_2 - 8L_1 \end{Bmatrix}$$

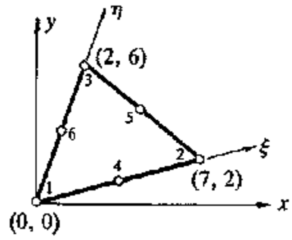

FIGURE 9.17
A quadratic triangular element in the global (x, y) and local coordinate systems (Example 9.5).

where $\psi_1 = L_1(2L_1 - 1)$ and $\psi_4 = 4L_1L_2$ [see (9.16) and Fig. 9.4*b*], so that

$$\frac{\partial\psi_1}{\partial L_1} = 4L_1 - 1, \quad \frac{\partial\psi_1}{\partial L_2} = 0, \quad \frac{\partial\psi_4}{\partial L_1} = 4L_2, \quad \frac{\partial\psi_4}{\partial L_2} = 4L_1$$

For the point (2, 4), the area coordinates L_i can be calculated from (9.68*a*):

$$2 = 7L_2 + 2L_3, \qquad 4 = 2L_2 + 6L_3$$

Once L_2 and L_3 have been computed from the above relations, L_1 is found from the relation $L_1 = 1 - L_2 - L_3$. We obtain

$$L_1 = \tfrac{5}{19}, \qquad L_2 = \tfrac{2}{19}, \qquad L_3 = \tfrac{12}{19}$$

Evaluating $\partial\psi_4/\partial x$ and $\partial\psi_4/\partial y$ at the point (2, 4), we obtain

$$\begin{aligned}
\frac{\partial\psi_1}{\partial x} &= -\frac{2}{19}\left(\frac{20}{19} - 1\right) = -\frac{2}{361}\\
\frac{\partial\psi_1}{\partial y} &= -\frac{5}{38}\left(4 \times \frac{5}{19} - 1\right) = -\frac{5}{722}\\
\frac{\partial\psi_4}{\partial x} &= \frac{-16}{(19)^2} + \frac{60}{(19)^2} = \frac{44}{361}\\
\frac{\partial\psi_4}{\partial y} &= \frac{-20}{(19)^2} + \frac{-20}{(19)^2} = \frac{-40}{361}
\end{aligned} \tag{9.69}$$

The integral of the product $(\partial\psi_1/\partial x)(\partial\psi_4/\partial x)$ over the quadratic element is

$$\int_{\hat{\Omega}_T} \frac{\partial\psi_1}{\partial x}\frac{\partial\psi_4}{\partial x}\,dx\,dy = \frac{-4\mathcal{J}}{361}\int_0^1\int_0^{1-L_2} (4L_1 - 1)(6L_1 - 4L_2)\,dL_1\,dL_2$$

Since the integrand is quadratic in L_1 and bilinear in L_1 and L_2, we use the three-point quadrature (see Table 9.3) to evaluate the integral exactly:

$$\begin{aligned}
&\frac{-4\mathcal{J}}{361}\int_0^1\int_0^{1-L_2} (4L_1 - 1)(6L_1 - 4L_2)\,dL_1\,dL_2\\
&\quad = \frac{1}{2}\frac{(-4)\times 38}{361}\tfrac{1}{3}\left[(\tfrac{4}{2} - 1)(\tfrac{6}{2} - 0) + (\tfrac{4}{2} - 1)(\tfrac{6}{2} - \tfrac{4}{2}) + (0 - 1)(0 - \tfrac{4}{2})\right]\\
&\quad = -\frac{8}{19}
\end{aligned} \tag{9.70}$$

The result can be verified using the exact integration formula in (9.$\overset{18}{81}$):

$$\begin{aligned}
\int_{\hat{\Omega}_T} \frac{\partial\psi_1}{\partial x}\frac{\partial\psi_4}{\partial x}\,dx\,dy &= \frac{4}{361}\left[6 \times \frac{1}{3!} - 4 \times \frac{1}{3!} - 24 \times \frac{2!}{4!} + 16 \times \frac{1}{4!}\right]2A\\
&= -\frac{8}{19}
\end{aligned}$$

The area A of the triangle is equal to 19, and therfore we obtain the same result as above.

9.3 MODELING CONSIDERATIONS

9.3.1 Preliminary Comments

Numerical simulation of a physical process or a system requires (i) a mathematical model that describes the process and (ii) a numerical method to analyze the mathematical model. In the development of a mathematical model, we often make a set of assumptions about the process (e.g., constitutive behavior, loads, and boundary conditions) to derive the mathematical relationships governing the system. The mathematical model is used to gain an understanding of how the corresponding process works. If the relationships are simple, it is possible to obtain *exact* information on quantities of interest. This is known as the *analytical* solution. However, most practical problems are too complicated to allow analytical solutions of the models. Hence, these mathematical models must be studied by numerical methods, such as the finite element method. We use a computer to evaluate a mathematical model *numerically* to *estimate* the quantities that characterize the system.

Finite element analysis is a numerical simulation of a physical process. Therefore, finite element modeling involves assumptions concerning the representation of the system and/or its behavior. Valid assumptions can be made only if one has a qualitative understanding of how the process or system works. A good knowledge of the basic principles governing the process and the finite element theory enable the development of a good numerical model of the actual process.

Here we discuss several aspects of the development of finite element models. Guidelines concerning element geometries, mesh refinements, and load representations are given.

9.3.2 Element Geometries

Recall from Section 9.2 that the numerical evaluation of integrals over actual elements involves a coordinate transformation from the actual element to a master element. The transformation is acceptable if and only if every point in the actual element is mapped uniquely to a point in the master element, and vice versa. Such mappings are termed one-to-one. This requirement can be expressed as [see (9.45)]

$$\mathcal{J}^e \equiv \det[\mathcal{J}^e] > 0 \quad \text{everywhere in the element } \Omega^e \tag{9.71}$$

where $[\mathcal{J}^e]$ is the Jacobian matrix in (9.44*b*). Geometrically, the Jacobian $\mathcal{J}^e$ represents the ratio of an area element in the real element to the corresponding area element in the master element:

$$dA \equiv dx\,dy = \mathcal{J}^e\,d\xi\,d\eta$$

If $\mathcal{J}^e$ is zero then a nonzero area element in the real element is mapped into zero area in the master element, which is unacceptable. Also, if $\mathcal{J}^e < 0$, a right-handed coordinate system is mapped into a left-handed coordinate system.

In general, the Jacobian is a function of ξ and η, implying that the real element is nonuniformly mapped into the master element, i.e., the element is distorted. Excessive distortion of elements is not good, because a nonzero area element can be mapped into a zero or nearly zero area.

To ensure $\mathscr{J}^e > 0$ and keep within the extreme limits of acceptable distortion, certain geometric shapes of elements must be avoided. For example, the interior angle at each vertex of a triangular element should not be equal to either 0° or 180°. Indeed, in practice the angle should reasonably be larger than 0° and less than 180° to avoid numerical ill-conditioning of element matrices. Although the acceptable range depends on the problem, the

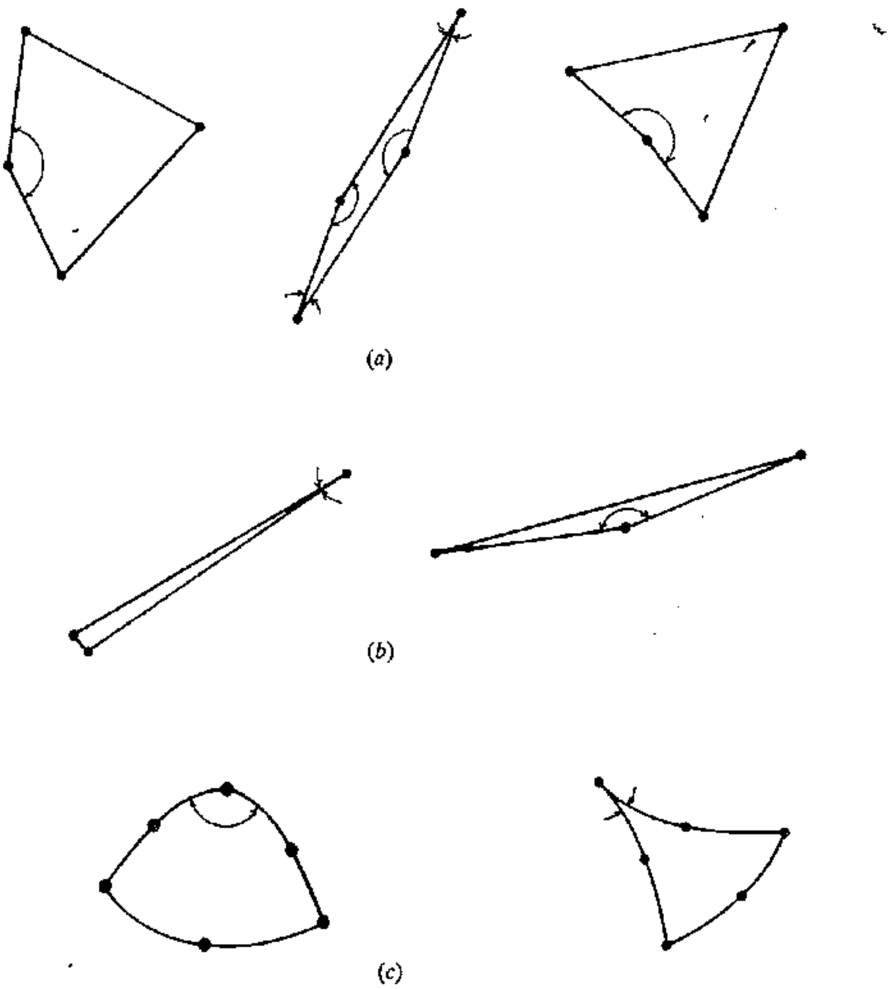

FIGURE 9.18
Finite elements with unacceptable vertex angles: (*a*) linear quadrilateral elements; (*b*) linear triangular elements; (*c*) quadratic quadrilateral and triangular elements. The angles marked are either too small compared with 0° or too large compared with 180°.

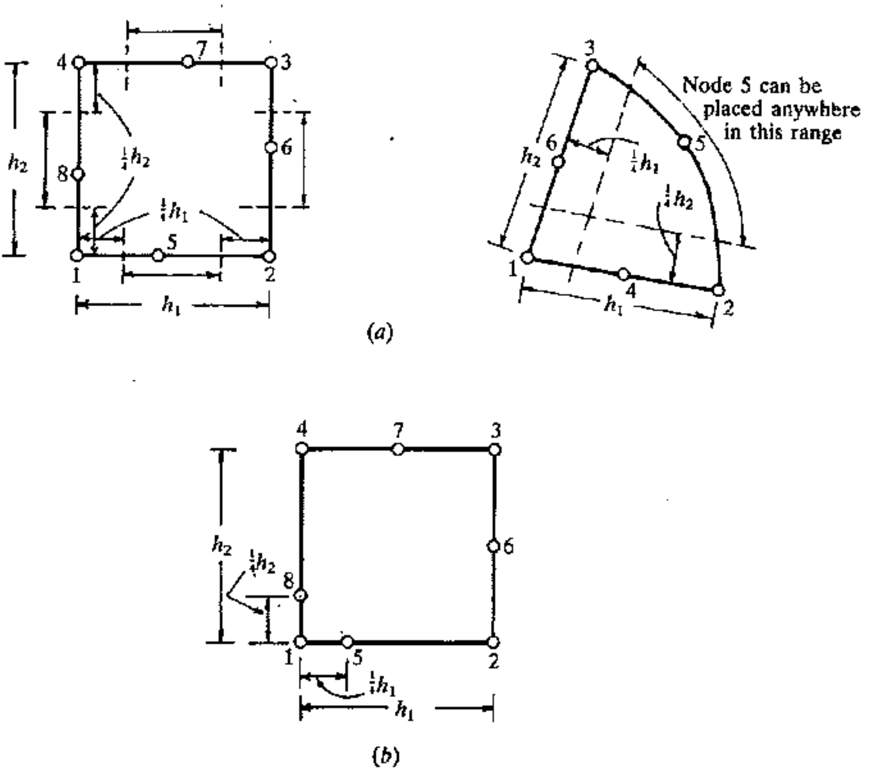

FIGURE 9.19
Range of acceptable locations of the midside nodes for quadratic elements: (*a*) eight-node quadratic element and six-node quadratic triangular element; (*b*) the quarter-point quadrilateral element.

range 15°–165° can be used as a guide. Figure 9.18 shows elements with unacceptable vertex angles for straight- and curved-sided elements.

For higher-order Lagrange elements (also called C^0 elements), the location of the interior nodes contributes to the element distortion, and therefore they are constrained to lie within a certain distance from the vertex nodes. For example, in the case of a quadratic element, the midside node should be at a distance not less than one-quarter of the length of the side from the vertex nodes (see Fig. 9.19). When the midside node is located exactly at a distance of one-quarter of the side length from a vertex, the element exhibits special properties (see Problem 9.20). Such elements, called *quarter-point elements*, are used in fracture mechanics problems to represent an inverse square-root singularity in the gradient of the solution at the nearest vertex node.

(9.21)

9.3.3 Mesh Generation

Generation of a finite element mesh for a given problem should follow the guidelines listed below:

1. The mesh should represent the geometry of the computational domain and load accurately.
2. It should be such that large gradients in the solution are adequately represented.
3. It should not contain elements with unacceptable geometries, especially in regions of large gradients.

Within the above guidelines, the mesh used can be *coarse* (i.e., have few elements) or *refined* (i.e., have many elements), and may consist of one or more orders and types of elements (e.g., linear and quadratic, triangular and quadrilateral). A judicious choice of element order and type could save computational cost while giving accurate results. It should be noted that the choice of elements and mesh is problem-dependent. What works well for one problem may not for another. An analyst with physical insight into the process being simulated can make a better choice of elements and mesh for the problem at hand. One should start with a coarse mesh that meets the three requirements listed above, exploit symmetries available in the problem, and evaluate the results thus obtained in the light of physical understanding and approximate analytical and/or experimental information. These results can be used to guide subsequent mesh refinements and analyses.

Generation of meshes of a single element type is easy because elements of the same degree are compatible with each other (see Fig. 9.20). Mesh refinements involve several options. The mesh can be refined by subdividing existing elements into two or more elements of the same type (see Fig. 9.21*a*). This is called *h-version mesh refinement.* Alternatively, existing elements can be replaced by elements of higher order (see Fig. 9.21*b*). This is called *p-version mesh refinement.* There is also *h, p-version mesh refinement,* in which elements are subdivided into two or more elements in some places and replaced with higher-order elements in other places. Generally, local mesh refinements should be such that elements of very small size are not placed adjacent to those of very large size (see Fig. 9.22).

Combining elements of different *kinds* naturally arises in solid and structural mechanics problems. For example, plate bending elements (2-D) can be connected to a beam element (1-D). If the plate element is based on classical plate theory (see Chapter 12), the beam element should be based on the Euler–Bernoulli beam theory so that they have the same degrees of freedom at the connecting node. When a plane elasticity element (see Chapter 10) is connected to a beam element, which is not compatible with the former in terms of the degrees of freedom at the nodes, one must construct a special element that makes the transition from the 2-D plane elasticity element to the 1-D beam element (see Problem 10.8). Such an element is called a *transition element.*

Combining elements of different order, say a linear to a quadratic element, may be necessary to accomplish local mesh refinements. There are two ways to do this. One way is to use a transition element that has a different number of nodes on different sides (see Fig. 9.23*a*). The other way is to

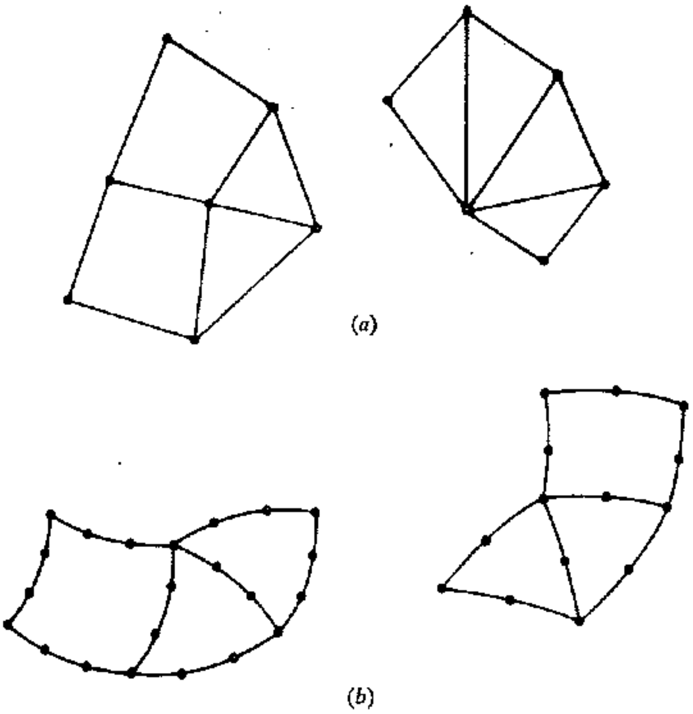

FIGURE 9.20
Connecting elements of the same order. The C^0 elements of the same order ensure the C^0 continuity along the element interfaces: (*a*) linear elements; (*b*) quadratic elements.

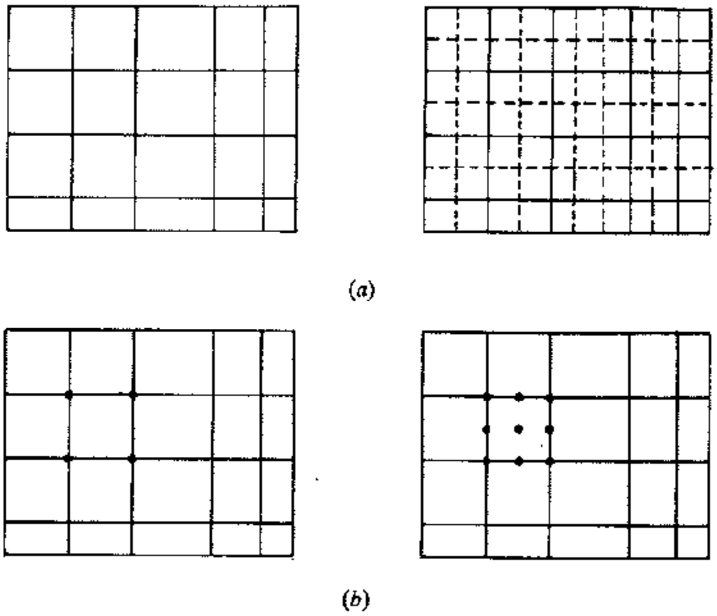

FIGURE 9.21
The h-version (*a*) and p-version (*b*) mesh refinements.

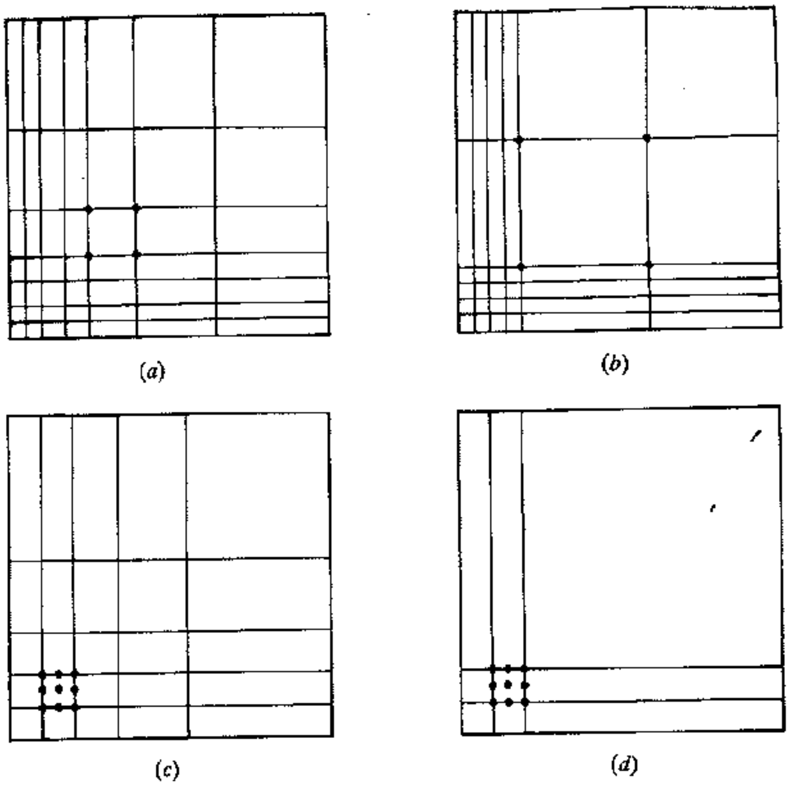

FIGURE 9.22
Finite element mesh refinements. Meshes shown in (*a*) and (*c*) are acceptable, and those shown in (*b*) and (*d*) are unacceptable. The typical element of the mesh is shown in each case.

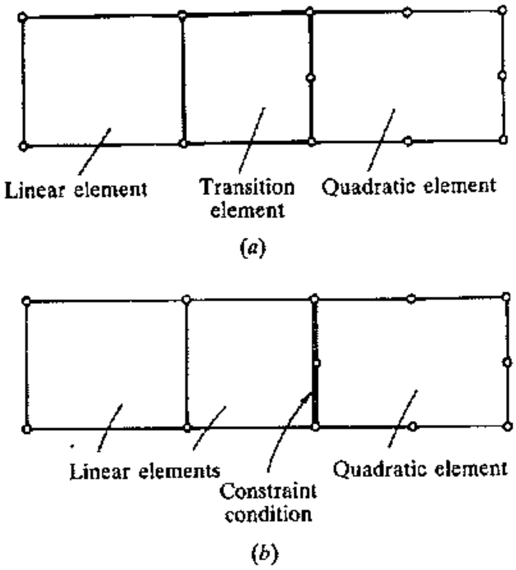

FIGURE 9.23
Combining different order elements: (*a*) use of a transition element that has three sides linear and one side quadratic; (*b*) use of a linear constraint equation to connect a linear side to a quadratic side.

impose a condition that constrains the midside node to have the same value as that experienced at the node by the lower-order element (see Fig. 9.23*b*). However, such combinations do not enforce interelement continuity of the solution. Figure 9.24 shows element connections that do not satisfy C^0 continuity along the connecting sides. Use of transition elements and constraint conditions in local mesh refinements is a common practice. Figure 9.25 shows a few examples of such refinements.

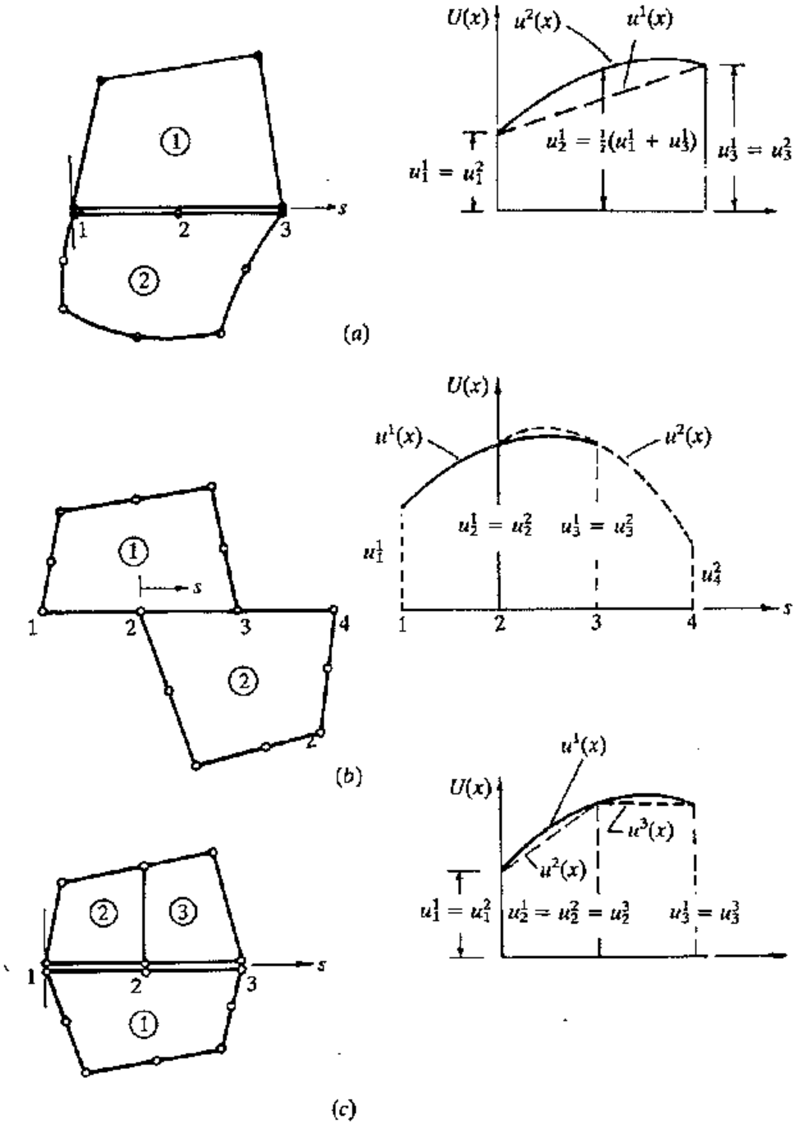

FIGURE 9.24
Various types of incompatible connections of finite elements. In all cases the interelement continuity of the function is violated along the connecting side.

9.3.4 Load Representation

Computation of the nodal contributions of a distributed boundary source was discussed in Chapter 8 [see (8.45)]. The accuracy of the result depends on the element and mesh used to represent the domain. For example, in heat transfer problems, the boundary source is the heat flux across (i.e., normal to) the boundary. Use of linear elements, for example, to represent the boundary will change the actual distribution (see Fig. 9.26). Of course, h-version or p-version mesh refinements will improve the representation of the boundary flux.

Another situation where boundary forces are subject to different approximations is the force due to contact between two bodies. For example, a solid plate in contact with a circular disk generates a reactive force that can be represented either as a point load or a locally distributed force. Representation of the contact force between deformable bodies as a point load is an approximation of the true distribution. A sine distribution might be a more realistic representation of the actual force (see Fig. 9.27).

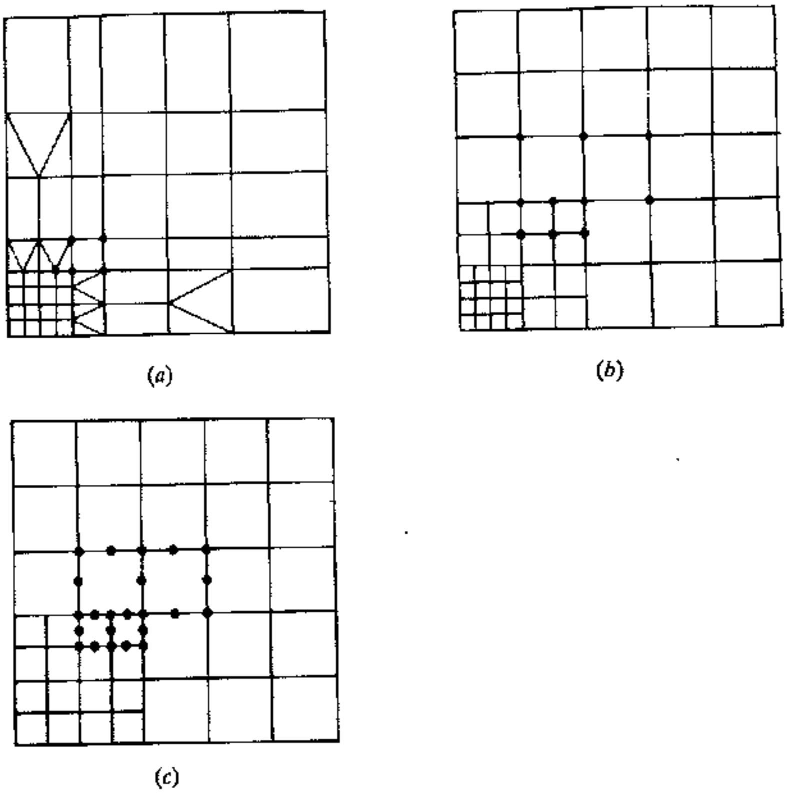
(*a*)

(*b*)

(*c*)

FIGURE 9.25
Some examples of local mesh refinements: (*a*) with compatible (C^0-continuous) elements; (*b*) with transition elements (or constraint conditions are imposed) between linear elements; (*c*) with transition elements between quadratic elements. In (*b*) and (*c*), the transition elements can be between linear and quadratic, and quadratic and cubic elements, respectively.

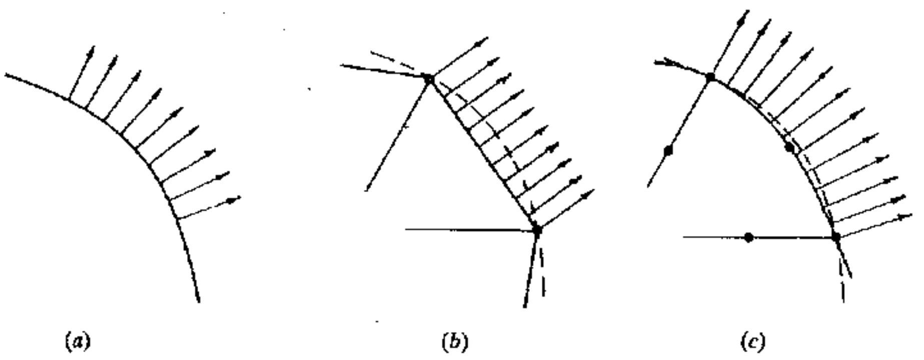

FIGURE 9.26
Approximation of the boundary fluxes in the finite element method: (*a*) actual geometry of the domain and distribution of flux; (*b*) approximation of the domain by linear finite elements and associated representation of the boundary flux; (*c*) approximation of the domain by quadratic finite elements and associated representation of the boundary flux.

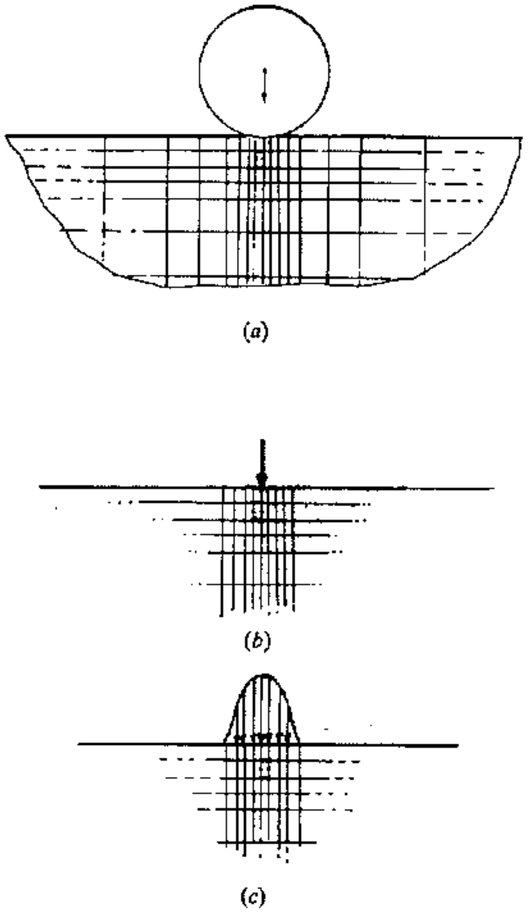

FIGURE 9.27
Representation of contact pressure developed between two bodies: (*a*) geometry of the bodies in contact; (*b*) representation of the contact pressure as a point load; (*c*) representation of the contact pressure as a distributed surface load. In the latter case, often the surface area of the distributed force is unknown.

9.4 SUMMARY

In this chapter three major topics have been discussed: (i) Lagrange interpolation functions for triangular and rectangular elements; (ii) numerical integration to evaluate integral expressions over triangular and rectangular elements; (iii) some modeling guidelines. Interpolation functions for linear, quadratic, and cubic triangular elements have been developed using the area coordinates. Linear, quadratic, and cubic interpolation functions for the Lagrange and serendipity families of rectangular elements have also been developed. A systematic description of the numerical evaluation of integral expressions involving interpolation functions and their derivatives with respect to global coordinates has been presented. This development is suitable for computer implementation, as will be seen in Chapter 13. Modeling is an art that can be improved by experience and understanding of the physical interactions involved in the process. It is necessary to critically evaluate the computed results before using them. The guidelines given are to encourage good modeling practice, and they should be followed to determine the actual "working" model.

PROBLEMS

9.1. Show that the bilinear interpolation functions for the four-node triangular element in Fig. P9.1 are of the form

$$\psi_i = a_i + b_i\xi + c_i\eta + d_i\xi\eta \quad (i = 1, \ldots, 4)$$

where

$$a_1 = 1, \quad a_2 = a_3 = a_4 = 0, \quad -b_1 = b_2 = 1/a, \quad b_3 = b_4 = 0$$

$$c_1 = \frac{6ab - a^2 - 2b^2}{ac(a-2b)}, \quad c_2 = \frac{2b(a+b)}{ac(a-2b)}, \quad c_3 = \frac{a+b}{c(a-2b)}, \quad c_4 = \frac{-9b}{c(a-2b)}$$

$$d_1 = d_2 = d_3 = -\tfrac{1}{3}d_4 = -\frac{3}{c(a-2b)}$$

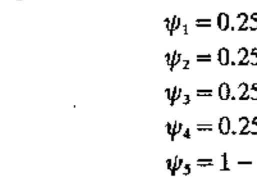

FIGURE P9.1

9.2. Show that the interpolation functions involving the term $\xi^2 + \eta^2$ for the five-node rectangular element shown in Fig. P9.2 are

$$\psi_1 = 0.25(-\xi - \eta + \xi\eta) + 0.125(\xi^2 + \eta^2)$$
$$\psi_2 = 0.25(\xi - \eta - \xi\eta) + 0.125(\xi^2 + \eta^2)$$
$$\psi_3 = 0.25(\xi + \eta + \xi\eta) + 0.125(\xi^2 + \eta^2)$$
$$\psi_4 = 0.25(-\xi + \eta - \xi\eta) + 0.125(\xi^2 + \eta^2)$$
$$\psi_5 = 1 - 0.5(\xi^2 + \eta^2)$$

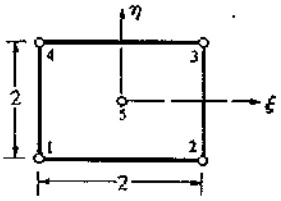

FIGURE P9.2

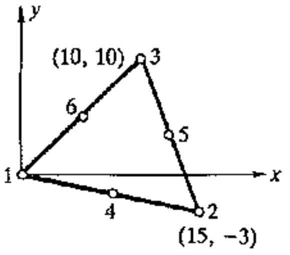

FIGURE P9.3

9.3. Calculate the interpolation functions for the quadratic triangular element shown in Fig. P9.3.

9.4. Determine the interpolation function ψ_{14} for the quartic triangular element shown in Fig. P9.4.

Answer: $32L_1L_2L_3(4L_2 - 1)$.

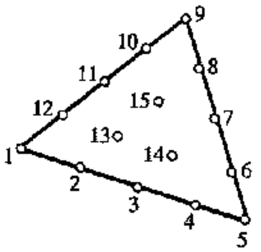

FIGURE P9.4

9.5. Derive the interpolation function of a corner node in a cubic serendipity element.

9.6. Consider the five-node element shown in Fig. P9.6. Using the basic linear and quadratic interpolations along the coordinate directions ξ and η, derive the interpolation functions for the element. Note that the element can be used as a transition element connecting four-node elements to eight- or nine-node elements.

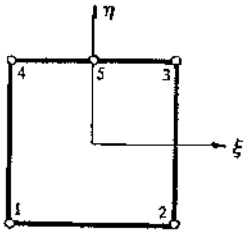

FIGURE P9.6

9.7. (*Nodeless variables*) Consider the four-node rectangular element with interpolation of the form

$$u = \sum_{i=1}^{4} u_i\psi_i + \sum_{i=1}^{4} c_i\phi_i$$

where u_i are the nodal values and c_i are arbitrary constants. Determine the form of ψ_i and ϕ_i for the element.

9.8–9.10. Determine the Jacobian matrix and the transformation equations for the elements shown in Figs. P9.8–P9.10.

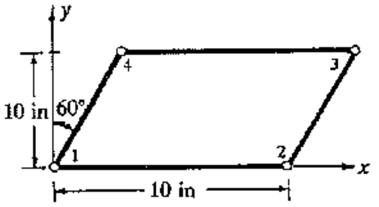

FIGURE P9.8

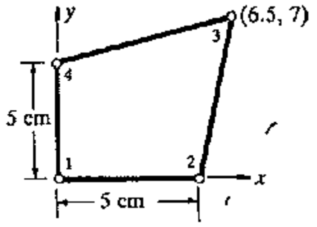

FIGURE P9.9

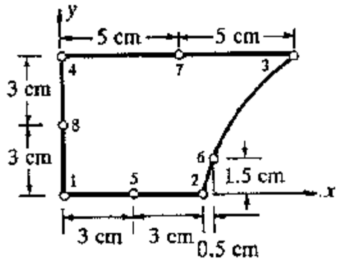

FIGURE P9.10

9.11. Using Gauss quadrature, determine the contribution of a constant distributed source to nodal points of the four-node finite element shown in Fig. P9.9.

Answer: $f_0(7.7083, 8.5417, 9.1667, 8.3333)$.

9.12. Show that the side nodes in the eight-node rectangular element of Fig. 9.13 should be located such that $0.25 < \alpha < 0.75$.

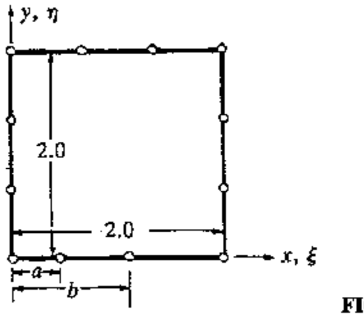

FIGURE P9.13

9.13. For a 12-node serendipity (cubic) element, as illustrated in Fig. P9.13, show that the determinant $\mathcal{J}$ is

$$\mathcal{J} = \tfrac{9}{2}(2 - 10\xi + 9\xi^2)a + \tfrac{9}{2}(-1 + 8\xi - 9\xi^2)b + \tfrac{1}{2}(2 - 18\xi + 27\xi^2)$$

What can you conclude from the requirement $\mathcal{J} > 0$?

9.14. Determine the conditions on the location of node 3 of the quadrilateral element shown in Fig. P9.14. Show that the transformation equations are

$$x = \xi + \xi\eta(a - 2), \qquad y = \eta + \xi\eta(b - 2)$$

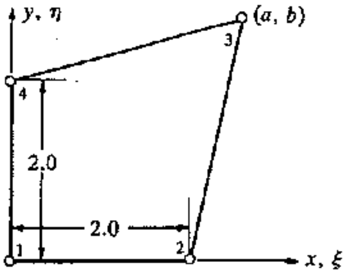

FIGURE P9.14

9.15. Determine the global derivatives of the interpolation functions for node 3 of the element shown in Fig. P9.9.

9.16. Let the transformation between the global coordinates (x, y) and local normalized coordinates (ξ, η) in a Lagrange element Ω^e be

$$x = \sum_{i=1}^{m} x_i \hat{\psi}_i(\xi, \eta), \qquad y = \sum_{i=1}^{m} y_i \hat{\psi}_i(\xi, \eta)$$

where (x_i^e, y_i^e) denote the global coordinates of the element nodes. The differential lengths in the two coordinate systems are related by

$$dx_e = \frac{\partial x_e}{\partial \xi} d\xi + \frac{\partial x_e}{\partial \eta} \partial \eta, \qquad dy_e = \frac{\partial y_e}{\partial \xi} \xi + \frac{\partial y_e}{\partial \eta} d\eta$$

or

$$\begin{Bmatrix} dx_e \\ dy_e \end{Bmatrix} = \begin{bmatrix} \dfrac{\partial x_e}{\partial \xi} & \dfrac{\partial x_e}{\partial \eta} \\ \dfrac{\partial y_e}{\partial \xi} & \dfrac{\partial y_e}{\partial \eta} \end{bmatrix} \begin{Bmatrix} d\xi \\ d\eta \end{Bmatrix} = [\mathcal{T}] \begin{Bmatrix} d\xi \\ d\eta \end{Bmatrix}$$

In the finite element literature the transpose of $[\mathcal{T}]$ is called the Jacobian matrix, $[\mathcal{J}]$. Show that the derivatives of the interpolation function $\psi_i^e(\xi, \eta)$ with respect to the global coordinates (x, y) are related to their derivatives with respect to the local coordinates (ξ, η) by

$$\begin{Bmatrix} \dfrac{\partial \psi_i^e}{\partial x} \\ \dfrac{\partial \psi_i^e}{\partial y} \end{Bmatrix} = [\mathcal{J}]^{-1} \begin{Bmatrix} \dfrac{\partial \psi_i^e}{\partial \xi} \\ \dfrac{\partial \psi_i^e}{\partial \eta} \end{Bmatrix}$$

and

$$\begin{Bmatrix} \dfrac{\partial^2\psi_i^e}{\partial x^2} \\ \dfrac{\partial^2\psi_i^e}{\partial y^2} \\ \dfrac{\partial^2\psi_i^e}{\partial x\,\partial y} \end{Bmatrix} = \begin{bmatrix} \left(\dfrac{\partial x_e}{\partial \xi}\right)^2 & \left(\dfrac{\partial y_e}{\partial \xi}\right)^2 & 2\dfrac{\partial x_e}{\partial \xi}\dfrac{\partial y_e}{\partial \xi} \\ \left(\dfrac{\partial x_e}{\partial \eta}\right)^2 & \left(\dfrac{\partial y_e}{\partial \eta}\right)^2 & 2\dfrac{\partial x_e}{\partial \eta}\dfrac{\partial y_e}{\partial \eta} \\ \dfrac{\partial x_e}{\partial \xi}\dfrac{\partial x_e}{\partial \eta} & \dfrac{\partial y_e}{\partial \xi}\dfrac{\partial y_e}{\partial \eta} & \dfrac{\partial x_e}{\partial \eta}\dfrac{\partial y_e}{\partial \xi} + \dfrac{\partial x_e}{\partial \xi}\dfrac{\partial y_e}{\partial \eta} \end{bmatrix}^{-1}$$

$$\times \left(\begin{Bmatrix} \dfrac{\partial^2\psi_i^e}{\partial \xi^2} \\ \dfrac{\partial^2\psi_i^e}{\partial \eta^2} \\ \dfrac{\partial^2\psi_i^e}{\partial \xi\,\partial \eta} \end{Bmatrix} - \begin{bmatrix} \dfrac{\partial^2 x_e}{\partial \xi^2} & \dfrac{\partial^2 y_e}{\partial \xi^2} \\ \dfrac{\partial^2 x_e}{\partial \eta^2} & \dfrac{\partial^2 y_e}{\partial \eta^2} \\ \dfrac{\partial^2 x_e}{\partial \xi\,\partial \eta} & \dfrac{\partial^2 y_e}{\partial \xi\,\partial \eta} \end{bmatrix} \begin{Bmatrix} \dfrac{\partial \psi_i^e}{\partial x} \\ \dfrac{\partial \psi_i^e}{\partial y} \end{Bmatrix} \right),$$

9.17. (*Continuation of Problem 9.16*) Show that the Jacobian can be computed from the equation

$$[\mathcal{J}] = \begin{bmatrix} \dfrac{\partial \psi_1^e}{\partial \xi} & \dfrac{\partial \psi_2^e}{\partial \xi} & \dots & \dfrac{\partial \psi_n^e}{\partial \xi} \\ \dfrac{\partial \psi_1^e}{\partial \eta} & \dfrac{\partial \psi_2^e}{\partial \eta} & \dots & \dfrac{\partial \psi_n^e}{\partial \eta} \end{bmatrix} \begin{bmatrix} x_1^e & y_1^e \\ x_2^e & y_2^e \\ \vdots & \vdots \\ x_n^e & y_n^e \end{bmatrix}$$

9.18. Consider the quadrilateral element shown in Fig. P9.18. Using the linear interpolation functions of a rectangular element, transform the element to the local coordinate system and sketch the transformed element.

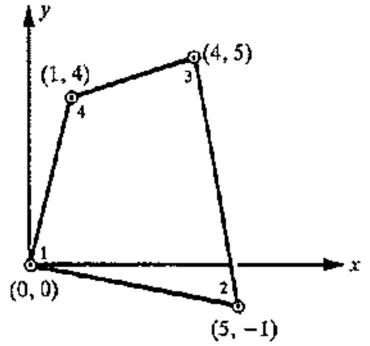

FIGURE P9.18

9.19. For the quadrilateral element Ω^e in Problem 9.18, express the following integral in the local coordinates:

$$K_{ij}^e = \int_{\Omega^e} \left[a\left(\frac{\partial \psi_i^e}{\partial x}\frac{\partial \psi_j^e}{\partial x} + \frac{\partial \psi_i^e}{\partial y}\frac{\partial \psi_j^e}{\partial y} \right) + b\psi_i^e\psi_j^e \right] dx\,dy$$

9.20. Find the Jacobian matrix for the nine-node rectangular element shown in Fig. P9.20. What is the determinant of the Jacobian matrix?

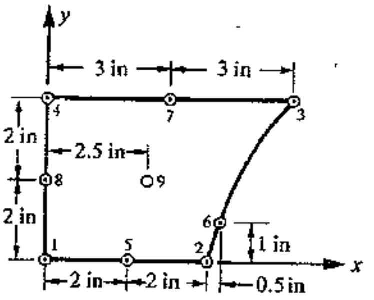

FIGURE P9.20

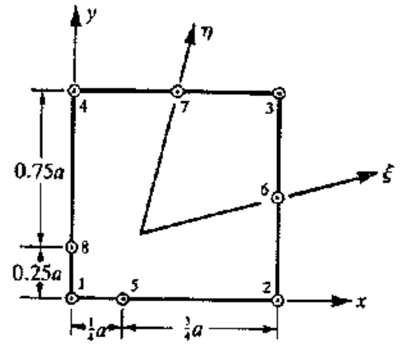

FIGURE P9.21

9.21. For the eight-node element shown in Fig. P9.21, show that the x coordinate along side 1–2 is related to the ξ coordinate by

$$x = -\tfrac{1}{2}\xi(1-\xi)x_1^e + \tfrac{1}{2}\xi(1+\xi)x_2^e + (1-\xi^2)x_5^e$$

and that the relations

$$\xi = 2\left(\frac{x}{a}\right)^{1/2} - 1, \qquad \frac{\partial x}{\partial \xi} = (xa)^{1/2}$$

hold. Also, show that

$$u_e(x,0) = -\left[2\left(\frac{x}{a}\right)^{1/2} - 1\right]\left[1 - \left(\frac{x}{a}\right)^{1/2}\right]u_1^e + \left[-1 + 2\left(\frac{x}{a}\right)^{1/2}\right]\left(\frac{x}{a}\right)^{1/2} u_2^e + 4\left[\left(\frac{x}{a}\right)^{1/2} - \frac{x}{a}\right]u_5^e$$

$$\frac{\partial u_e(x,0)}{\partial x} = \frac{1}{(xa)^{1/2}}\left\{\frac{1}{2}\left[3 - 4\left(\frac{x}{a}\right)^{1/2}\right]u_1^e + \frac{1}{2}\left[-1 + 4\left(\frac{x}{a}\right)^{1/2}\right]u_2^e + 2\left[1 - 2\left(\frac{x}{a}\right)^{1/2}\right]u_5^e\right\}$$

Thus, $\partial u_e/\partial x$ grows at a rate of $(xa)^{-1/2}$ as x approaches zero along side 1–2. In other words, we have a $x^{-1/2}$ singularity at node 1. Such elements are used in fracture mechanics problems.

9.22. Using the tensor product of the one-dimensional Hermite cubic interpolation functions, obtain the Hermite cubic interpolation functions (16 of them) for the four-node rectangular element.

REFERENCES FOR ADDITIONAL READING

Burnett, D. S.: *Finite Element Analysis from Concepts to Applications,* Addison-Wesley, Reading, MA, 1987.

Carnahan, B., H. A. Luther, and J. O. Wilkes: *Applied Numerical Methods,* John Wiley, New York, 1969.

Cowper, G. R.: "Gaussian Quadrature Formulas for Triangles," *International Journal for Numerical Methods in Engineering,* vol. 7, pp. 405–408, 1973.

Fellippa, C. A.: "Refined Finite Element Analysis of Linear and Non-linear Two-Dimensional Structures," Structures Materials Research Report no. 66-22, University of California, Berkeley, October 1966.

Froberg, C. E.: *Introduction to Numerical Analysis,* Addison-Wesley, Reading, MA, 1969.

Hammer, P. C., O. P. Marlowe, and A. H. Stroud: "Numerical Integration over Simplexes and Cones," *Mathematics Tables and Aids to Computation, National Research Council (Washington),* vol. 10, pp. 130–137 , 1956.

Irons, B. M.: "Quadrature Rules for Brick-Based Finite Elements," *International Journal for Numerical Methods in Engineering,* vol. 3, pp. 293–294, 1971.

Loxan, A. N., N. Davids, and A. Levenson: "Table of the Zeros of the Legendre Polynomials of Order 1–16 and the Weight Coefficients for Gauss' Mechanical Quadrature Formula," *Bulletin of the American Mathematical Society,* vol. 48, pp. 739–743, 1942.

Reddy, C. T., and D. J. Shippy: "Alternative Integration Formulae for Triangular Finite Elements," *International Journal for Numerical Methods in Engineering,* vol. 17, pp. 133–139, 1981.

Segerlind, L. J.: *Applied Finite Element Analysis,* John Wiley, New York, 1977.

Silvester, P.: "Newton–Cotes Quadrature Formulae for *N*-Dimensional Simplexes," *Proceedings of 2d Canadian Congress of Applied Mechanics, Waterloo, Ontario, 1969,* University of Waterloo, Waterloo, Ontario, 1969.

Stroud, A. H., and D. Secrest: *Gaussian Quadrature Formulas,* Prentice-Hall, Englewood Cliffs, NJ, 1966.

Zienkiewicz, O. C., and R. L. Taylor: *The Finite Element Method,* vol. 1: *Linear Problems,* McGraw-Hill, New York, 1989.

CHAPTER
10

PLANE ELASTICITY

10.1 INTRODUCTION

In Section 8.4.3, we considered the finite element analysis of second-order problems of solid mechanics that are described by only one dependent unknown. These include the torsion of a cylindrical bar and the deflection of a membrane. The governing equation in each case is the Laplace or Poisson equation for the dependent variable (e.g., stress function or deflection). Here we consider plane elasticity problems described by a pair of *coupled* partial differential equations expressed in terms of two dependent variables representing the two components of the displacement vector. The word "coupled" is used to imply that the same dependent variables appear in more than one equation of the set, and therefore no equation can be solved independent of the other(s) in the set.

The primary objective of this chapter is twofold: first, to describe the weak form and associated finite element model of the plane elasticity equations; and second, to describe how the linear Lagrange elements developed in Section 8.2 can be used in the solution of plane elasticity problems in two dimensions. The treatment of both these subjects proceeds along the same lines as in the one-dimensional problems.

10.2 GOVERNING EQUATIONS

10.2.1 Assumptions of Plane Elasticity

Consider a linear elastic solid Ω of uniform thickness h bounded by two parallel planes (say, by planes $z = -\frac{1}{2}h$ and $z = \frac{1}{2}h$) and any closed boundary Γ. If the thickness h is very large compared with the size of Ω then the problem is considered to be a *plane strain problem,* and if the thickness is small compared with the size of Ω then the problem is considered to be a *plane stress problem.* Both of these problems are simplifications of three-dimensional elasticity problems under the following assumptions on loading: the body forces, if any exist, cannot vary in the thickness direction and cannot have components in the z direction; the applied boundary forces must be uniformly distributed across the thickness (i.e., constant in the z direction); and no loads can be applied on the parallel planes bounding the top and bottom surfaces.

The assumption that the forces are zero on the parallel planes implies that for plane stress problems the stresses in the z direction are negligibly small (see Fig. 10.1):

$$\sigma_{xz} = 0, \qquad \sigma_{yz} = 0, \qquad \sigma_z = 0 \tag{10.1}$$

For plane strain problems, where the body is very thick in the z direction, the assumption is that the strains in the z direction are zero (see Fig. 10.2):

$$\epsilon_{xz} = 0, \qquad \epsilon_{yz} = 0, \qquad \epsilon_z = 0 \tag{10.2}$$

An example illustrating the difference between plane stress and plane strain problems is provided by the bending of a beam of rectangular cross-section. If the beam is narrow then the problem is a plane stress problem, and if it is very wide then the problem is a plane strain problem. The reader should consult the references on advanced strength of materials and elasticity listed at the end of the chapter.

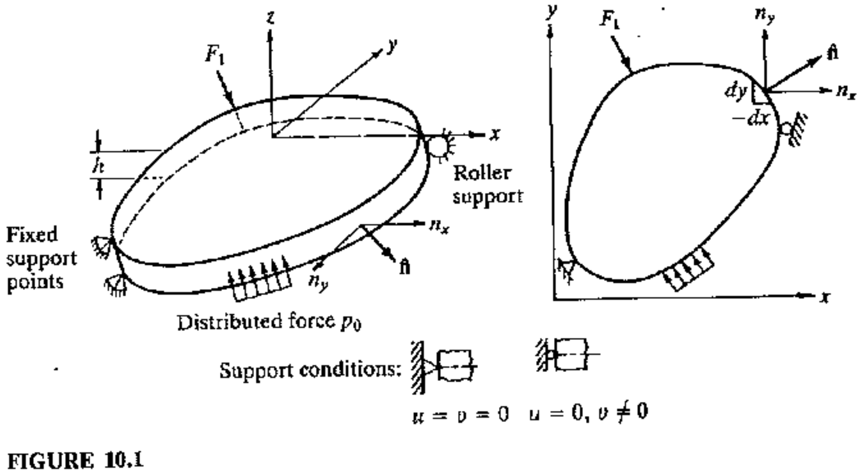

FIGURE 10.1
Plane stress problems in two-dimensional elasticity.

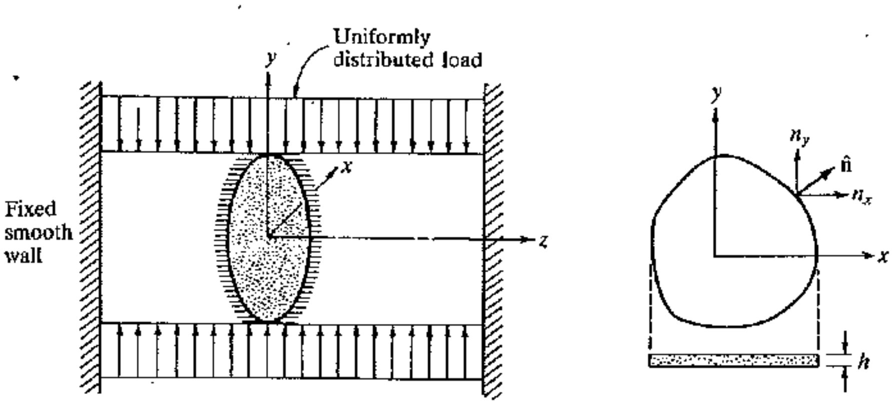

FIGURE 10.2
Plane strain problems in two-dimensional elasticity.

10.2.2 Basic Equations

The governing equations for the two types of plane elasticity problems discussed above are summarized below. The equations of the two classes of problems differ from each other only in the constitutive relations.

EQUATIONS OF MOTION

$$\begin{aligned}\frac{\partial\sigma_x}{\partial x}+\frac{\partial\sigma_{xy}}{\partial y}+f_x&=\rho\frac{\partial^2u}{\partial t^2}\\ \frac{\partial\sigma_{xy}}{\partial x}+\frac{\partial\sigma_y}{\partial y}+f_y&=\rho\frac{\partial^2v}{\partial t^2}\end{aligned}\tag{10.3}$$

where f_x and f_y denote the body forces per unit volume along the x and y directions, respectively, and ρ is the density of the material.

STRAIN-DISPLACEMENT RELATIONS

$$\epsilon_x=\frac{\partial u}{\partial x},\qquad \epsilon_y=\frac{\partial v}{\partial y},\qquad 2\epsilon_{xy}=\frac{\partial u}{\partial y}+\frac{\partial v}{\partial x}\tag{10.4}$$

STRESS-STRAIN (OR CONSTITUTIVE) RELATIONS

$$\begin{Bmatrix}\sigma_x\\ \sigma_y\\ \sigma_{xy}\end{Bmatrix}=\begin{bmatrix}c_{11}&c_{12}&0\\ c_{12}&c_{22}&0\\ 0&0&c_{66}\end{bmatrix}\begin{Bmatrix}\epsilon_x\\ \epsilon_y\\ 2\epsilon_{xy}\end{Bmatrix}\tag{10.5}$$

where c_{ij} ($c_{ji}=c_{ij}$) are the elasticity (material) constants for an orthotropic medium with the material principal directions coinciding with the coordinate axes (x, y, z) used to describe the problem. The c_{ij} can be expressed in terms of the engineering constants (E_1, E_2, ν_{12}, and G_{12}) for an orthotropic material, for plane stress and plane strain given below ($\nu_{12}E_2 = \nu_{21}E_1$):

Plane stress

$$
\begin{aligned}
c_{11} &= \frac{E_1}{1-\nu_{12}\nu_{21}}, \qquad c_{22} = \frac{E_2}{1-\nu_{12}\nu_{21}} \\
c_{12} &= \nu_{21}c_{11} = \nu_{12}c_{22}, \qquad c_{66} = G_{12}
\end{aligned}
\tag{10.6}
$$

Plane strain ($\nu_{23} = \nu_{12}$)

$$
\begin{aligned}
c_{11} &= \frac{E_1(1-\nu_{12})}{1-\nu_{12}-2\nu_{12}\nu_{21}}, \qquad c_{22} = \frac{E_2(1-\nu_{12}\nu_{21})}{(1+\nu_{12})(1-\nu_{12}-2\nu_{12}\nu_{21})} \\
c_{12} &= \frac{\nu_{12}E_2}{1-\nu_{12}-2\nu_{12}\nu_{21}}, \qquad c_{66} = G_{12}
\end{aligned}
\tag{10.7}
$$

For an isotropic material,

$$
E_1 = E_2 = E, \qquad \nu_{12} = \nu_{21} = \nu, \qquad G = \frac{E}{2(1+\nu)}
\tag{10.8}
$$

BOUNDARY CONDITIONS

Natural

$$
\left.
\begin{aligned}
t_x &\equiv \sigma_x n_x + \sigma_{xy} n_y = \hat{t}_x \\
t_y &\equiv \sigma_{xy} n_x + \sigma_y n_y = \hat{t}_y
\end{aligned}
\right\} \quad \text{on } \Gamma_2
\tag{10.9}
$$

Essential

$$
u = \hat{u}, \qquad v = \hat{v} \quad \text{on } \Gamma_1
\tag{10.10}
$$

where (n_x, n_y) are the components (or direction cosines) of the unit normal vector $\hat{\mathbf{n}}$ on the boundary Γ, Γ_1 and Γ_2 are (disjoint) portions of the boundary (Γ_1 and Γ_2 do not overlap except for a small number of discrete points—singular points), $\hat{t}_x$ and $\hat{t}_y$ are specified boundary stresses (or tractions), and $\hat{u}$ and $\hat{v}$ are specified displacements. Only one element of each pair, (u, t_x) and (v, t_y), may be specified at a boundary point.

Equations (10.3) can be expressed in terms of just the displacements u and v by substituting (10.4) into (10.5), and the result into (10.3):

$$
\boxed{
\begin{aligned}
-\frac{\partial}{\partial x}\left(c_{11}\frac{\partial u}{\partial x} + c_{12}\frac{\partial v}{\partial y}\right) - \frac{\partial}{\partial y}\left[c_{66}\left(\frac{\partial u}{\partial y} + \frac{\partial v}{\partial x}\right)\right] &= f_x - \rho\frac{\partial^2 u}{\partial t^2} \\
-\frac{\partial}{\partial x}\left[c_{66}\left(\frac{\partial u}{\partial y} + \frac{\partial v}{\partial x}\right)\right] - \frac{\partial}{\partial y}\left(c_{12}\frac{\partial u}{\partial x} + c_{22}\frac{\partial v}{\partial y}\right) &= f_y - \rho\frac{\partial^2 v}{\partial t^2}
\end{aligned}
}
\tag{10.11}
$$

the boundary stress components (or tractions) can also be expressed in terms of the displacements:

$$
\begin{aligned}
t_x &= \left(c_{11}\frac{\partial u}{\partial x} + c_{12}\frac{\partial v}{\partial y}\right)n_x + c_{66}\left(\frac{\partial u}{\partial y} + \frac{\partial v}{\partial x}\right)n_y \\
t_y &= c_{66}\left(\frac{\partial u}{\partial y} + \frac{\partial v}{\partial x}\right)n_x + \left(c_{12}\frac{\partial u}{\partial x} + c_{22}\frac{\partial v}{\partial y}\right)n_y
\end{aligned}
\tag{10.12}
$$

This completes the review of the governing equations of a plane elastic body undergoing small deformations (i.e., with strains small compared with unity) in the (x, y) plane. The material of the body will be assumed in the present study to be linearly orthotropic.

10.3 WEAK FORMULATIONS

10.3.1 Preliminary Comments

Here we study two different ways of constructing the weak form and associated finite element model of the plane elasticity equations (10.11) and (10.12). The first uses the principle of virtual displacements (or the total potential energy principle), expressed in terms of matrices relating displacements to strains, and strains to stresses. This approach is used in most finite element texts on solid mechanics. The second follows a procedure consistent with the previous sections and employs the weak formulation of (10.11) and (10.12) to construct the finite element model. Of course, both methods give, mathematically, the *same* finite element model, but differ in their algebraic forms.

10.3.2 Principle of Virtual Displacements in Matrix Form

First, we rewrite (10.3)–(10.5) in matrix form:

$$
\begin{bmatrix} \partial/\partial x & 0 & \partial/\partial y \\ \hdashline 0 & \partial/\partial y & \partial/\partial x \end{bmatrix}
\begin{Bmatrix} \sigma_x \\ \sigma_y \\ \sigma_{xy} \end{Bmatrix}
+ \begin{Bmatrix} f_x \\ f_y \end{Bmatrix} = \rho \begin{Bmatrix} \ddot{u} \\ \ddot{v} \end{Bmatrix}
\tag{10.13a}
$$

or

$$
[T^*]\{\sigma\} + \{f\} = \rho\begin{Bmatrix} \ddot{u} \\ \ddot{v} \end{Bmatrix}
\tag{10.13b}
$$

and

$$
\begin{Bmatrix} \epsilon_x \\ \epsilon_y \\ 2\epsilon_{xy} \end{Bmatrix}
= \begin{bmatrix} \partial/\partial x & 0 \\ 0 & \partial/\partial y \\ \partial/\partial y & \partial/\partial x \end{bmatrix}
\begin{Bmatrix} u \\ v \end{Bmatrix}
\tag{10.14a}
$$

or

$$
\{\epsilon\} = [T]\begin{Bmatrix} u \\ v \end{Bmatrix}
\tag{10.14b}
$$

and

$$\{\sigma\} = [C]\{\epsilon\} \tag{10.15}$$

where $[T]$ and $[T^*]$ are matrices of differential operators. Note that $[T]$ is the transpose of $[T^*]$:

$$[T] = [T^*]^T = \begin{bmatrix} \partial/\partial x & 0 \\ 0 & \partial/\partial y \\ \partial/\partial y & \partial/\partial x \end{bmatrix} \tag{10.16}$$

Next, we use the (dynamic version of the) principle of virtual displacements [see Reddy (1984)] applied to a plane elastic body:

$$0 = \int_{V^e} (\sigma_{ij}\,\delta\epsilon_{ij} + \rho\ddot{u}_i\,\delta u_i)\,dV - \oint_{V_e} f_i\,\delta u_i\,dV - \oint_{S^e} \hat{t}_i\,\delta u_i\,ds \tag{10.17}$$

where V^e denotes the volume of element e $[V^e = \Omega^e \times (-\frac{1}{2}h, \frac{1}{2}h)]$, S^e is the boundary of Ω^e, h_e is the thickness of the element, δ denotes the variational operator, σ_{ij} and ϵ_{ij} are the components of stress and strain tensors, respectively, and f_i and $\hat{t}_i$ are the components of the body force and boundary stress vectors, respectively:

$$\sigma_{11} = \sigma_x, \quad \sigma_{12} = \sigma_{xy}, \quad \sigma_{22} = \sigma_y, \quad \text{etc.}$$
$$f_1 = f_x, \quad f_2 = f_y, \quad t_1 = t_x, \quad t_2 = t_y$$

The first term in (10.17) corresponds to the virtual strain energy stored in the body, the second represents the virtual work done by the body forces, and the third represents the virtual work done by the surface tractions. For plane stress problems with thickness h_e, we assume that all quantities are independent of the thickness coordinate z. Hence,

$$\begin{aligned} 0 = h_e \int_{\Omega^e} (\sigma_x\,\delta\epsilon_x + \sigma_y\,\delta\epsilon_y + 2\sigma_{xy}\,\delta\epsilon_{xy} + \rho\ddot{u}\,\delta u + \rho\ddot{v}\,\delta v)\,dx\,dy \\ - h_e \int_{\Omega^e} (f_x\,\delta u + f_y\,\delta v)\,dx\,dy - h_e \oint_{\Gamma^e} (t_x\,\delta u + t_y\,\delta v)\,ds \end{aligned} \tag{10.18}$$

where f_x and f_y are now body forces per unit area, and t_x and t_y are boundary forces per unit length. When the stresses are expressed in terms of strains through (10.5), and strains in terms of displacements by (10.4), (10.18) takes the form of the principle of total minimum potential energy.

Equation (10.18) can be rewritten using the notation introduced in (10.13)–(10.16):

$$\begin{aligned} 0 = h_e \int_{\Omega^e} \left(\begin{Bmatrix} \delta\epsilon_x \\ \delta\epsilon_y \\ 2\,\delta\epsilon_{xy} \end{Bmatrix}^T \begin{Bmatrix} \sigma_x \\ \sigma_y \\ \sigma_{xy} \end{Bmatrix} + \rho \begin{Bmatrix} \delta u \\ \delta v \end{Bmatrix}^T \begin{Bmatrix} \ddot{u} \\ \ddot{v} \end{Bmatrix} \right) dx\,dy \\ - h_e \int_{\Omega^e} \begin{Bmatrix} \delta u \\ \delta v \end{Bmatrix}^T \begin{Bmatrix} f_x \\ f_y \end{Bmatrix} dx\,dy - h_e \oint_{\Gamma^e} \begin{Bmatrix} \delta u \\ \delta v \end{Bmatrix}^T \begin{Bmatrix} t_x \\ t_y \end{Bmatrix} ds \end{aligned} \tag{10.19}$$

10.3.3 Weak Form of the Governing Differential Equations

Here we present an alternative procedure for the weak form of the plane elasticity equations (10.11)–(10.12). The present approach does not assume knowledge of the principles of virtual displacements or the total minimum potential energy (10.17). It is based on the three-step procedure used throughout this book. We begin with the governing differential equations (10.11) of plane elasticity. We use the three-step procedure for each of the two differential equations, multiplying the first equation with a weight function w_1 and integrating by parts to trade the differentiation equally between the weight function and the dependent variables. We have

$$\begin{aligned} 0 = h_e \int_{\Omega^e} \left[\frac{\partial w_1}{\partial x}\left(c_{11}\frac{\partial u}{\partial x} + c_{12}\frac{\partial v}{\partial y}\right) + \frac{\partial w_1}{\partial y} c_{66}\left(\frac{\partial u}{\partial y} + \frac{\partial v}{\partial x}\right) - w_1 f_x + \rho w_1 \ddot{u} \right] dx\, dy \\ - h_e \oint_{\Gamma^e} w_1 \left[\left(c_{11}\frac{\partial u}{\partial x} + c_{12}\frac{\partial v}{\partial y}\right) n_x + c_{66}\left(\frac{\partial u}{\partial y} + \frac{\partial v}{\partial x}\right) n_y \right] ds \qquad (10.20a) \end{aligned}$$

Similarly, for the second equation, we have

$$\begin{aligned} 0 = h_e \int_{\Omega^e} \left[\frac{\partial w_2}{\partial x} c_{66}\left(\frac{\partial u}{\partial y} + \frac{\partial v}{\partial x}\right) + \frac{\partial w_2}{\partial y}\left(c_{12}\frac{\partial u}{\partial x} + c_{22}\frac{\partial v}{\partial y}\right) - w_2 f_y + \rho w_2 \ddot{v} \right] dx\, dy \\ - h_e \oint_{\Gamma^e} w_2 \left[c_{66}\left(\frac{\partial u}{\partial y} + \frac{\partial v}{\partial x}\right) n_x + \left(c_{12}\frac{\partial u}{\partial x} + c_{22}\frac{\partial v}{\partial y}\right) n_y \right] ds \qquad (10.20b) \end{aligned}$$

The last step of the development is to identify the primary and secondary variables of the formulation and rewrite the boundary integrals in terms of the secondary variables. Examination of the boundary integrals in (10.20) reveals that the expressions in the square brackets constitute the secondary variables. By comparing these expressions with those in (10.12), it follows that the boundary forces t_x and t_y are the secondary variables. The weight functions w_1 and w_2 are like the first variations of u and v, respectively. Thus, the final weak form is given by (10.20), with the boundary integrals replaced by

$$h_e \oint_{\Gamma^e} w_1 t_x \, ds, \qquad h_e \oint_{\Gamma^e} w_2 t_y \, ds \qquad (10.21)$$

respectively.

This completes the development of the weak formulation of the plane elasticity equations (10.11) and (10.12). The alternative formulation in (10.20) is exactly the same as that in (10.19); one is in matrix form and the other is in the form of explicit expressions. Therefore, the finite element models developed using the weak forms (10.19) and (10.20) would be the same.

10.4 FINITE ELEMENT MODEL

10.4.1 Matrix Form of the Model

First we develop the finite element model of the plane elasticity equations using the matrix form in (10.19). An examination of the weak form (10.19) or

(10.20) reveals that (i) u and v are the primary variables, which must be carried as the primary nodal degrees of freedom; and (ii) only first derivatives of u and v with respect to x and y appear. Therefore, u and v must be approximated by the Lagrange family of interpolation functions, and at least bilinear (i.e., linear in x and y) interpolation should be used. The simplest elements that satisfy those requirements are the linear triangular and rectangular elements. Although u and v are independent of each other, they are the components of the displacement vector. Therefore, both components should be approximated using the same interpolation.

Let u and v be approximated over Ω^e by the finite element interpolations

$$u \approx \sum_{j=1}^{n} u_j^e \psi_j^e(x, y), \qquad v \approx \sum_{j=1}^{n} v_j^e \psi_j^e(x, y) \tag{10.22}$$

For the moment, we shall not restrict ψ_j^e to any specific element, so that the finite element formulation to be developed is valid for any admissible element. For example, for a linear triangular element ($n = 3$), there are two (u_j^e, v_j^e) degrees of freedom per node and a total of six nodal displacements per element (see Fig. 10.3*a*). For a linear quadrilateral element, there are a total of eight nodal displacements per element (see Fig. 10.3*b*). Since the first derivatives of ψ_i^e for a triangular element are element-wise-constant, all strains $(\epsilon_x, \epsilon_y, \epsilon_{xy})$ computed for the triangular element are element-wise-constant. Therefore, the linear triangular element for plane elasticity is known as the *constant-strain triangular* (*CST*) *element*. For a quadrilateral element, the first derivatives of ψ_i^e are not constant: $\partial\psi_i^e/\partial\xi$ is linear in η and constant in ξ, and $\partial\psi_i^e/\partial\eta$ is linear in ξ and constant in η [see Barlow (1976, 1989)].

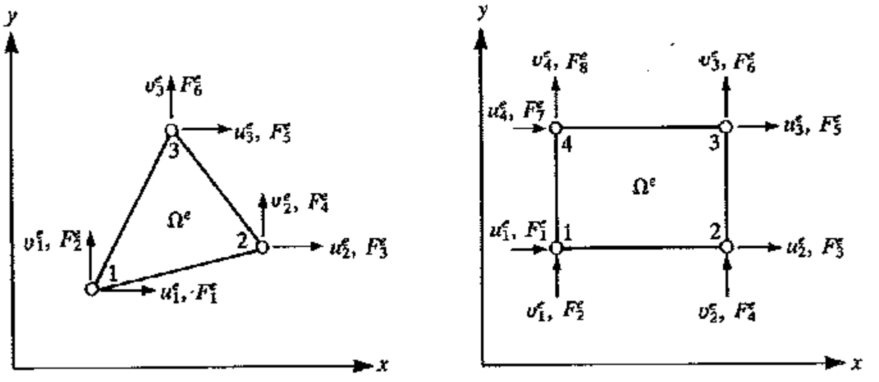

(*a*) (*b*)

FIGURE 10.3
Linear triangular and rectangular elements for plane elasticity problems: (*a*) triangular element; (*b*) rectangular element.

The displacements and strains are (the element label e is omitted in the following)

$$\begin{Bmatrix} u \\ v \end{Bmatrix} = \begin{Bmatrix} \sum_{j=1}^{n} u_j\psi_j \\ \sum_{j=1}^{n} v_j\psi_j \end{Bmatrix} = \begin{bmatrix} \psi_1 & \psi_2 \ldots \psi_n & 0 & 0 \ldots 0 \\ 0 & 0 \ldots 0 & \psi_1 & \psi_2 \ldots \psi_n \end{bmatrix} \begin{Bmatrix} u_1 \\ u_2 \\ \vdots \\ u_n \\ v_1 \\ v_2 \\ \vdots \\ v_n \end{Bmatrix}$$

$$= \begin{bmatrix} \psi_1 & 0 & \psi_2 & 0 \ldots \psi_n & 0 \\ 0 & \psi_1 & 0 & \psi_2 \ldots 0 & \psi_n \end{bmatrix} \begin{Bmatrix} u_1 \\ v_1 \\ u_2 \\ v_2 \\ \vdots \\ u_n \\ v_n \end{Bmatrix} = [\Psi]\{\Delta\} \tag{10.23}$$

$$\begin{Bmatrix} \ddot{u} \\ \ddot{v} \end{Bmatrix} = [\Psi]\{\ddot{\Delta}\} \tag{10.24}$$

and

$$\{\epsilon\} = [B]\{\Delta\}, \qquad \{\sigma\} = [C][B]\{\Delta\} \tag{10.25a}$$

where

$$[B] = [T][\Psi] \tag{10.25b}$$

and $[T]$ is the matrix of differential operators defined in (10.16). We have

$$\begin{Bmatrix} \delta u \\ \delta v \end{Bmatrix} = [\Psi]\{\delta\Delta\}, \qquad \{\delta\epsilon\} = [B]\{\delta\Delta\} \tag{10.26}$$

Substituting these expressions for the displacements and strains into (10.19), we obtain

$$\begin{aligned} 0 &= h_e \int_{\Omega^e} \{\delta\Delta\}^T([B]^T[C][B]\{\Delta\} + \rho[\Psi]^T[\Psi]\{\ddot{\Delta}\})\,dx\,dy \\ &\quad - h_e \int_{\Omega^e} \{\delta\Delta\}^T[\Psi]^T \begin{Bmatrix} f_x \\ f_y \end{Bmatrix} dx\,dy - h_e \oint_{\Gamma^e} \{\delta\Delta\}^T[\Psi]^T \begin{Bmatrix} t_x \\ t_y \end{Bmatrix} ds \\ &= \{\delta\Delta\}^T([K]\{\Delta\} + [M]\{\ddot{\Delta}\} - \{f\} - \{Q\}) \end{aligned} \tag{10.27}$$

Since this equation holds for any *arbitrary* variations $\{\delta\Delta\}$, it follows that the expression in parentheses should be identically zero, giving the result

$$\boxed{[M^e]\{\ddot{\Delta}^e\} + [K^e]\{\Delta^e\} = \{f^e\} + \{Q^e\}} \tag{10.28a}$$

where

$$\boxed{\begin{aligned} &[K^e] = h_e \int_{\Omega^e} [B^e]^T[C^e][B^e]\,dx\,dy, \qquad [M^e] = \rho h_e \int_{\Omega^e} [\Psi^e]^T[\Psi^e]\,dx\,dy \\ &\{f^e\} = h_e \int_{\Omega^e} [\Psi^e]^T \begin{Bmatrix} f_x \\ f_y \end{Bmatrix} dx\,dy, \qquad \{Q^e\} = h_e \oint_{\Gamma^e} [\Psi^e]^T \begin{Bmatrix} t_x \\ t_y \end{Bmatrix} ds \end{aligned}} \tag{10.28b}$$

The element mass matrix $[M^e]$ and stiffness matrix $[K^e]$ are of order $2n \times 2n$ and the element force vector $\{F^e\} = \{f^e\} + \{Q^e\}$ is of order $2n \times 1$.

10.4.2 Weak Form Model

Next we use the weak form (10.20) to construct the finite element model. Substituting (10.22) for u and v, and $w_1 = \psi_i^e$ and $w_2 = \psi_i^e$ [to obtain the ith algebraic equation associated with each of the weak statements in (10.20)], and writing the resulting algebraic equations in matrix form, we obtain

$$\begin{bmatrix} [M] & [0] \\ [0] & [M] \end{bmatrix} \begin{Bmatrix} \{\ddot{u}\} \\ \{\ddot{v}\} \end{Bmatrix} + \begin{bmatrix} [K^{11}] & [K^{12}] \\ [K^{12}]^T & [K^{22}] \end{bmatrix} \begin{Bmatrix} \{u\} \\ \{v\} \end{Bmatrix} = \begin{Bmatrix} \{F^1\} \\ \{F^2\} \end{Bmatrix} \tag{10.29a}$$

where

$$\begin{aligned} M_{ij} &= \int_{\Omega^e} c\psi_i\psi_j\,dx\,dy, \qquad c = \rho h \\ K_{ij}^{11} &= \int_{\Omega^e} h\left(c_{11}\frac{\partial\psi_i}{\partial x}\frac{\partial\psi_j}{\partial x} + c_{66}\frac{\partial\psi_i}{\partial y}\frac{\partial\psi_j}{\partial y}\right) dx\,dy \\ K_{ij}^{12} = K_{ji}^{21} &= \int_{\Omega^e} h\left(c_{12}\frac{\partial\psi_i}{\partial x}\frac{\partial\psi_j}{\partial y} + c_{66}\frac{\partial\psi_i}{\partial y}\frac{\partial\psi_j}{\partial x}\right) dx\,dy \\ K_{ij}^{22} &= \int_{\Omega^e} h\left(c_{66}\frac{\partial\psi_i}{\partial x}\frac{\partial\psi_j}{\partial x} + c_{22}\frac{\partial\psi_i}{\partial y}\frac{\partial\psi_j}{\partial y}\right) dx\,dy \\ F_i^1 &= \int_{\Omega^e} h\psi_i f_x\,dx\,dy + \oint_{\Gamma^e} h\psi_i t_x\,ds, \qquad F_i^2 = \int_{\Omega^e} h\psi_i f_y\,dx\,dy + \oint_{\Gamma^e} h\psi_i t_y\,ds \end{aligned} \tag{10.29b}$$

The coefficient matrix $[K^{12}]$, for example, corresponds to the coefficient of v in the first equation, i.e., the first superscript corresponds to the equation number and the second to the variable number. By expanding (10.28a), one can show that they yield the same equations as (10.29a).

10.4.3 Eigenvalue and Transient Problems

For natural vibration study of plane elastic bodies, (10.28*a*) or (10.29*a*) is reduced to an eigenvalue problem by replacing $\{\Delta\}$ by

$$\{\Delta\} = \{\bar{\Delta}\}e^{-i\omega t} \qquad (i = \sqrt{-1})$$

We obtain [cf. (8.170)]

$$\boxed{(-\omega^2[M^e] + [K^e])\{\bar{\Delta}^e\} = \{Q^e\}} \tag{10.30}$$

For transient analysis, following the discussions of Section 8.5.3, (10.28*a*) or (10.29*a*) can be reduced to a system of algebraic equations by using the Newmark integration scheme (8.171). We have [see Eq. (8.173)]

$$\boxed{[\hat{K}^e]_{s+1}\{\Delta^e\}_{s+1} = \{\hat{F}^e\}_{s,s+1}} \tag{10.31a}$$

where

$$\boxed{\begin{gathered}[\hat{K}^e]_{s+1} = [K^e]_{s+1} + a_3[M^e]_{s+1}\\ \{\hat{F}^e\}_{s,s+1} = \{F^e\}_{s+1} + [M^e]_{s+1}(a_3\{\Delta^e\}_s + a_4\{\dot{\Delta}^e\}_s + a_5\{\ddot{\Delta}^e\}_s)\\ a_3 = \frac{2}{\gamma(\Delta t)^2}, \qquad a_4 = \Delta t\, a_3, \qquad a_5 = \frac{1}{\gamma} - 1\end{gathered}}$$

(10.31*b*)

For additional details, see Sections 6.2.3 and 8.5.3.

10.5 EVALUATION OF INTEGRALS

For the linear triangular (i.e., CST) element, ψ_i^e has the form

$$\psi_i^e = \frac{1}{2A_e}(\alpha_i^e + \beta_i^e x + \gamma_i^e y)$$

where A_e is the area of the triangular element, and $[B^e] = [T][\Psi^e]$ [see (10.23)–(10.25)] is constant. Since $[B^e]$ and $[C^e]$ are independent of x and y, the element stiffness matrix for the CST element is given by

$$[K^e] = h_e A_e [B^e]^T [C^e][B^e] \tag{10.32}$$

For the case in which the body force components f_x and f_y are element-wise-constant (say, equal to f_{x0}^e and f_{y0}^e, respectively), the force vector $\{f^e\}$ has the form

$$\{f^e\} = h_e \int_{\Omega^e} [\Psi^e]^T \begin{Bmatrix} f^e_{x0} \\ f^e_{y0} \end{Bmatrix} dx\,dy = \frac{A_e h_e}{3} \begin{Bmatrix} f^e_{x0} \\ f^e_{y0} \\ f^e_{x0} \\ f^e_{y0} \\ f^e_{x0} \\ f^e_{y0} \end{Bmatrix} \tag{10.33}$$

For a general quadrilateral element, it is not easy to compute the coefficients of the stiffness matrix by exact means. In such cases, we use the numerical integration discussed in Section 9.2. However, for a linear rectangular element of sides a and b, the element coefficient matrices in (8.35) and (8.44) can be used to obtain the stiffness matrix. The load vector for a linear rectangular element is given by

$$\{f^e\}_{8\times 1} = \frac{A_e h_e}{4} \begin{Bmatrix} f^e_{x0} \\ f^e_{y0} \\ f^e_{x0} \\ f^e_{y0} \\ \vdots \end{Bmatrix} \tag{10.34}$$

The vector $\{Q^e\}$ is computed only when the element Ω^e falls on the boundary of the domain on which tractions are specified (i.e., known). Computation of $\{Q^e\}$ involves the evaluation of line integrals (for any type of element), as explained in Section 8.2.6; see also Example 8.2. For plane elasticity problems, the surface tractions t_x and t_y take the place of q_n in single-variable problems [see (8.45)]. Often, in practice, it is convenient to express the surface tractions t_x and t_y in the element coordinates. In that case, $\{Q^e\}$ can be evaluated in the element coordinates and then transformed to the global coordinates for assembly. If $\{\bar{Q}^e\}$ denotes the element traction vector referred to the element coordinates then [see (4.58b)] the corresponding global vector is given by

$$\{Q^e\} = [R^e]^T\{\bar{Q}^e\} \tag{10.35a}$$

where

$$[R^e] = \left[\begin{array}{cc|cc|c} \cos\alpha & \sin\alpha & 0 & 0 & \\ -\sin\alpha & \cos\alpha & 0 & 0 & \\ \hline 0 & 0 & \cos\alpha & \sin\alpha & \\ 0 & 0 & -\sin\alpha & \cos\alpha & \\ \hline & & & & \ddots \end{array}\right]_{2n\times 2n} \tag{10.35b}$$

and α is the angle between the global x axis and t_n.

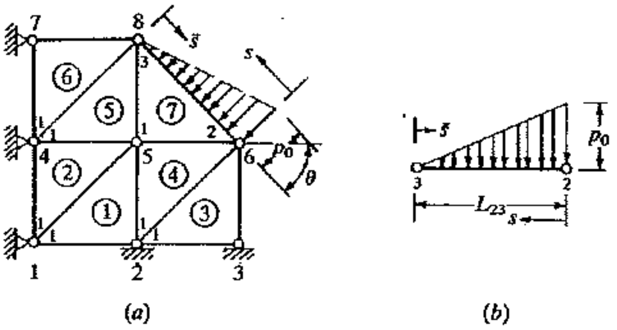

FIGURE 10.4
Computation of boundary force components for plane elasticity problems: (*a*) the constant strain triangle (CST); (*b*) a typical plane elasticity problem; (*c*) computation of the boundary forces.

As a specific example, consider the structure shown in Fig. 10.4(*a*). Side 2–3 of element 7 is subjected to a linearly varying normal force:

$$t_n \neq 0, \qquad t_s = 0$$

where the subscripts n and s refer to normal and tangential directions, respectively. We have for $(e = 7)$

$$\{\bar{Q}^e\} = \oint_{\Gamma^e} [\Psi^e]^T \begin{Bmatrix} t_n \\ t_s \end{Bmatrix} ds = \int_{\Gamma_{12}^e} [\Psi^e]^T \begin{Bmatrix} t_n \\ t_s \end{Bmatrix} ds + \int_{\Gamma_{23}^e} [\Psi^e]^T \begin{Bmatrix} t_n \\ 0 \end{Bmatrix} ds + \int_{\Gamma_{31}^e} [\Psi^e]^T \begin{Bmatrix} t_n \\ t_s \end{Bmatrix} ds \qquad (10.36a)$$

The first and third integrals cannot be evaluated, because we do not know t_n and t_s on these sides of the element. However, by internal stress equilibrium, those portions cancel with like contributions from the neighboring elements (elements 4 and 5) in the assembled force vector of the structure. Thus, we must compute the integral over side 2–3 of the element. We have (for $e = 7$)

$$\{\bar{Q}^e\}_{2\text{-}3} = \int_0^{L_{23}} [\Psi^e]^T \begin{Bmatrix} t_n \\ 0 \end{Bmatrix} ds, \qquad t_n = -p_0\left(1 - \frac{s}{L_{23}}\right) \qquad (10.36b)$$

where the minus sign in front of p_0 is added to account for the direction of the applied traction, which acts toward the body in the present case. The local coordinate system s used in the above expression is chosen along the side connecting node 2 to node 3, with its original at node 2 (see Fig. 10.4*b*). One is not restricted to this choice. If it is considered to be convenient to choose the local coordinate system $\bar{s}$, which is taken along side 3–2, with its origin at node 3 of element 7, we can write

$$\{\bar{Q}^e\}_{2\text{-}3} = \int_0^{L_{23}} [\Psi^e]^T \begin{Bmatrix} t_n \\ 0 \end{Bmatrix} d\bar{s}, \qquad t_n = -\frac{p_0 \bar{s}}{L_{23}} \qquad (10.36c)$$

where $[\Psi^e]$ is now expressed in terms of the local coordinate $\bar{s}$. We have

$$\{\bar{Q}^e\}_{2-3} = \int_0^{L_{23}} \begin{Bmatrix} 0 \\ 0 \\ \psi_2^7 t_n \\ 0 \\ \psi_3^7 t_n \\ 0 \end{Bmatrix} d\bar{s} = -\frac{L_{23} p_0}{6} \begin{Bmatrix} 0 \\ 0 \\ 2 \\ 0 \\ 1 \\ 0 \end{Bmatrix} \tag{10.37a}$$

The global components of this force vector are [set $\alpha = 90° - \theta$ in (10.35*b*)]

$$\{Q^e\}_{2-3} = -\frac{L_{23} p_0}{6} \begin{Bmatrix} 0 \\ 0 \\ 2\sin\theta \\ 2\cos\theta \\ \sin\theta \\ \cos\theta \end{Bmatrix} \tag{10.37b}$$

The same procedure applies to linear quadrilateral elements. In general, the loads due to specified boundary stresses can be computed using an appropriate local coordinate system and one-dimensional interpolation functions. When higher-order elements are involved, the same order one-dimensional interpolation functions must be used.

10.6 ASSEMBLY AND BOUNDARY AND INITIAL CONDITIONS

The assembly procedure for problems with many degrees of freedom is the same as that used when there is a single degree of freedom (see Section 8.2), except that the procedure should be applied to all degrees of freedom at each node. For example, consider the plane elastic structure shown in Fig. 10.4(*a*). There are eight nodes in the mesh; hence, the total size of the assembled stiffness matrix will be 16 × 16, and the force vector will be 16 × 1. The first two rows and columns of the global stiffness matrix correspond to global node 1, which has contributions from node 1 of elements 1 and 2. For instance, we have

$$K_{11} = K_{11}^1 + K_{11}^2, \quad K_{22} = K_{22}^1 + K_{22}^2, \quad K_{12} = K_{12}^1 + K_{12}^2, \quad K_{13} = K_{13}^1,$$
$$K_{33} = K_{33}^1 + K_{11}^3 + K_{11}^4, \quad K_{34} = K_{34}^1 + K_{12}^3 + K_{12}^4, \quad \text{etc.} \tag{10.38}$$

Note that K_{12}, for example, denotes the coupling stiffness coefficient between the first and second global degrees of freedom, both of which are at global node 1. Similar arguments apply for the assembly of the force vector.

With regard to the boundary conditions, the primary degrees of freedom are the displacements and the secondary degrees of freedom are the forces. At any node on the boundary of the domain of a plane elasticity problem, one has the following four distinct possibilities:

Case 1	u and v are specified (and t_x and t_y are unknown)
Case 2	u and t_y are specified (and t_x and v are unknown)
Case 3	t_x and v are specified (and u and t_y are unknown)
Case 4	t_x and t_y are specified (and u and v are unknown)

(10.39)

In general, only one of the quantities of each of the pairs (u, t_x) and (v, t_y) must be specified at a point on the boundary.

For time-dependent problems, the initial displacement and velocity must be specified:

$$\begin{Bmatrix} u \\ v \end{Bmatrix} = \begin{Bmatrix} u_0 \\ v_0 \end{Bmatrix}, \qquad \begin{Bmatrix} \dot{u} \\ \dot{v} \end{Bmatrix} = \begin{Bmatrix} \dot{u}_0 \\ \dot{v}_0 \end{Bmatrix} \tag{10.40}$$

10.7 EXAMPLES

Here we consider a couple of examples of plane elasticity problems to illustrate the load computation and imposition of boundary conditions. The stresses are evaluated at reduced Gauss points of the elements [see Barlow (1976, 1989)]. These examples are actually analyzed using the program FEM2DV2, which is discussed in Chapter 13.

Example 10.1. Consider a thin elastic plate subjected to a uniformly distributed edge load, as shown in Fig. 10.5(*a*). We wish to determine the equilibrium (i.e., static) solution. First we consider a two-element discretization of the plate by triangular elements, and then we perform all the algebra to obtain the nodal displacements.

The assembly of element matrices for elements with two degrees of freedom (DOF) is described in Section 10.6. For the finite element mesh at hand, the correspondence between the global and local nodes and stiffness is as follows:

Nodal correspondence		Stiffness correspondence	
Global (DOF)	Local (DOF)	Global	Local
	1 of element 1 (1, 2)	K_{11}	$K^1_{11}+K^2_{11}$
1 (1, 2)		K_{22}	$K^1_{22}+K^2_{22}$
	1 of element 2 (1, 2)	K_{12}	$K^1_{12}+K^2_{12}$
		K_{33}	K^1_{33}
2 (3, 4)	2 of element 1 (3, 4)	K_{44}	K^1_{44}
		K_{34}	K^1_{34}
	3 of element 1 (5, 6)	K_{55}	$K^1_{55}+K^2_{33}$
3 (5, 6)	2 of element 2 (3, 4)	K_{66}	$K^1_{66}+K^2_{44}$
		K_{56}	$K^1_{56}+K^2_{34}$
		K_{77}	K^2_{55}
4 (7, 8)	3 of element 2 (5, 6)	K_{88}	K^2_{66}
		K_{78}	K^2_{56}

(10.41)

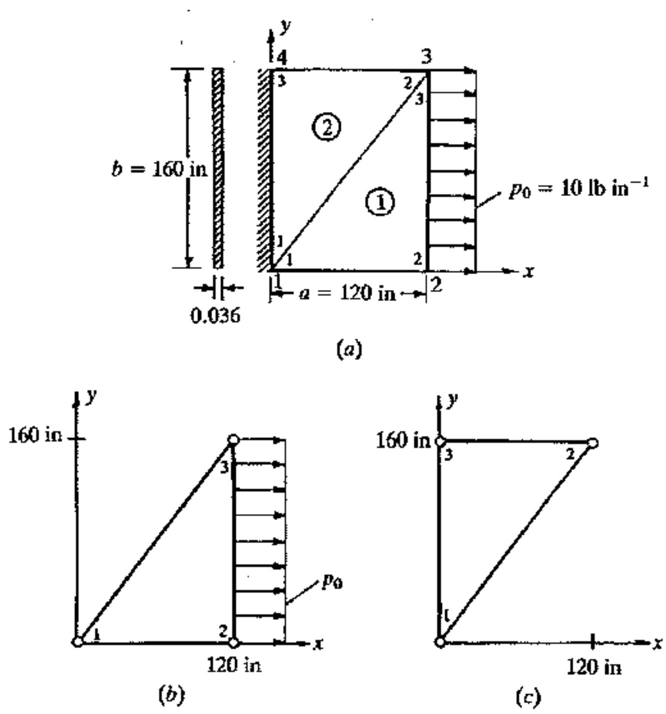

FIGURE 10.5
Geometry and finite element mesh of a plane elasticity problem by the CST elements: (*a*) a plane elasticity problem; (*b*) element 1; (*c*) element 2.

If two global nodes correspond to two (local) nodes of the same element then the corresponding stiffness coefficient is nonzero; otherwise it is zero.

The specified (primary) degrees of freedom are

$$U_1 = V_1 = U_4 = V_4 = 0 \tag{10.42}$$

The known secondary degrees of freedom (forces) are already included in $\{F^1\}$ and $\{F^2\}$. Equilibrium of forces requires that (note that p_0 is the force per unit length)

$$F^1_3 = \tfrac{1}{2}p_0 b, \quad F^1_4 = 0, \quad F^1_5 + F^2_3 = \tfrac{1}{2}p_0 b, \quad F^1_6 + F^2_4 = 0 \tag{10.43}$$

The first two rows and columns and the last two rows and columns of the assembled $[K]$ can be deleted (since the specified boundary conditions are homogeneous) to obtain the condensed form of the matrix equation:

$$\begin{bmatrix} K^1_{33} & K^1_{34} & K^1_{35} & K^1_{36} \\ K^1_{43} & K^1_{44} & K^1_{45} & K^1_{46} \\ K^1_{53} & K^1_{54} & K^1_{55} + K^2_{33} & K^1_{56} + K^2_{34} \\ K^1_{63} & K^1_{64} & K^1_{65} + K^2_{43} & K^1_{66} + K^2_{44} \end{bmatrix} \begin{Bmatrix} U_2 \\ V_2 \\ U_3 \\ V_3 \end{Bmatrix} = \begin{Bmatrix} \frac{1}{2}p_0 b \\ 0 \\ \frac{1}{2}p_0 b \\ 0 \end{Bmatrix} \tag{10.44}$$

or (using $a = 120$ in, $b = 160$ in, $h = 0.036$ in, $\nu = 0.25$, $E = 30 \times 10^6$ lb in^{-2}, and $p_0 =$

10 lb in^{-1})

$$10^4\begin{bmatrix} 93.0 & -36.0 & -16.2 & 14.4 \\ -36.0 & 72.0 & 21.6 & -43.2 \\ -16.2 & 21.6 & 93.0 & 0.0 \\ 14.4 & -43.2 & 0.0 & 72.0 \end{bmatrix}\begin{Bmatrix} U_2 \\ V_2 \\ U_3 \\ V_3 \end{Bmatrix} = \begin{Bmatrix} 800.0 \\ 0.0 \\ 800.0 \\ 0.0 \end{Bmatrix} \tag{10.45}$$

Inverting the matrix, we obtain

$$\begin{Bmatrix} U_2 \\ V_2 \\ U_3 \\ V_3 \end{Bmatrix} = \frac{10^{-6}}{3}\begin{bmatrix} 4.07 & 2.34 & 0.17 & 0.59 \\ 2.34 & 8.65 & -1.6 & 4.72 \\ 0.17 & -1.6 & 3.63 & -0.99 \\ 0.59 & 4.72 & -0.99 & 6.88 \end{bmatrix}\begin{Bmatrix} 800.0 \\ 0.0 \\ 8.00 \\ 0.0 \end{Bmatrix}$$

$$= 10^{-4}\begin{Bmatrix} 11.28 \\ 1.97 \\ 10.10 \\ -1.09 \end{Bmatrix} \text{ in} \tag{10.46}$$

Note that the solution is not symmetric (i.e., $U_2 \neq U_3$, $V_2 \neq -V_3$) about the horizontal centerline. The exact solution should be symmetric about the centerline. This is due to the asymmetry in the finite element discretization.

Table 10.1 gives the finite element solutions (obtained using FEM2DV2) for the displacements at the points (120, 0) and (120, 160) of isotropic and orthotropic plates

TABLE 10.1

Finite element results for a thin plate (plane stress assumption) using various meshes of triangular and rectangular elements and material properties†

Mesh	Material	U_2 ($\times 10^{-4}$)	V_2 ($\times 10^{-4}$)	U_3 ($\times 10^{-4}$)	V_3 ($\times 10^{-4}$)
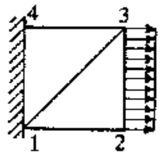	Isotropic: $E = 30 \times 10^6$ lb in^{-2} $\nu = 0.25$ $G = E/2(1+\nu)$	11.291 10.853	1.9637 2.3256	10.113 10.853	−1.08 −2.3256
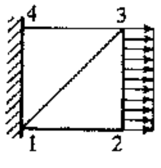	Orthotropic: $E_1 = 31 \times 10^6$ lb in^{-2} $E_2 = 2.7 \times 10^6$ lb in^{-2} $G_{12} = 0.75 \times 10^6$ lb in^{-2} $\nu_{12} = 0.28$	10.767 10.728	1.6662 2.6758	10.650 10.728	−1.579 −2.6758
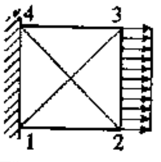	Orthotropic: same as above	10.821 10.778	2.157 2.002	10.821 10.778	−2.157 −2.002

For each mesh, the first row corresponds to triangular elements and the second row to one rectangular element.

TABLE 10.2
Deflections and stresses in an isotropic plate subjected to uniform edge load (Example 10.1)

Mesh		$u(120, 0)$ $(\times 10^{-4})$	$v(120, 0)$ $(\times 10^{-4})$	σ_x	σ_y	σ_{xy}
	1×1	11.291	1.9637	285.9 (80, 53.33)†	14.40 (80, 53.33)	10.80 (80, 53.33)
Triangular	2×2	11.372	2.1745	279.7 (80, 53.33)	69.36 (20, 53.33)	23.20 (40, 26.67)
	4×4	11.284	2.1255	280.0 (80, 53.33)	69.59 (10, 26.67)	35.93 (20, 13.33)
	1×1	10.853	2.3256	277.8 (60, 80)	25.84 (60, 80)	0.0 (60, 80)
Rectangular	2×2	11.078	2.0212	277.8 (30, 40)	37.46 (30, 40)	13.23 (30, 40)
	4×4	11.150	2.0094	280.4 (75, 60)	49.74 (15, 60)	27.73 (15, 20)

† Location of the stress.

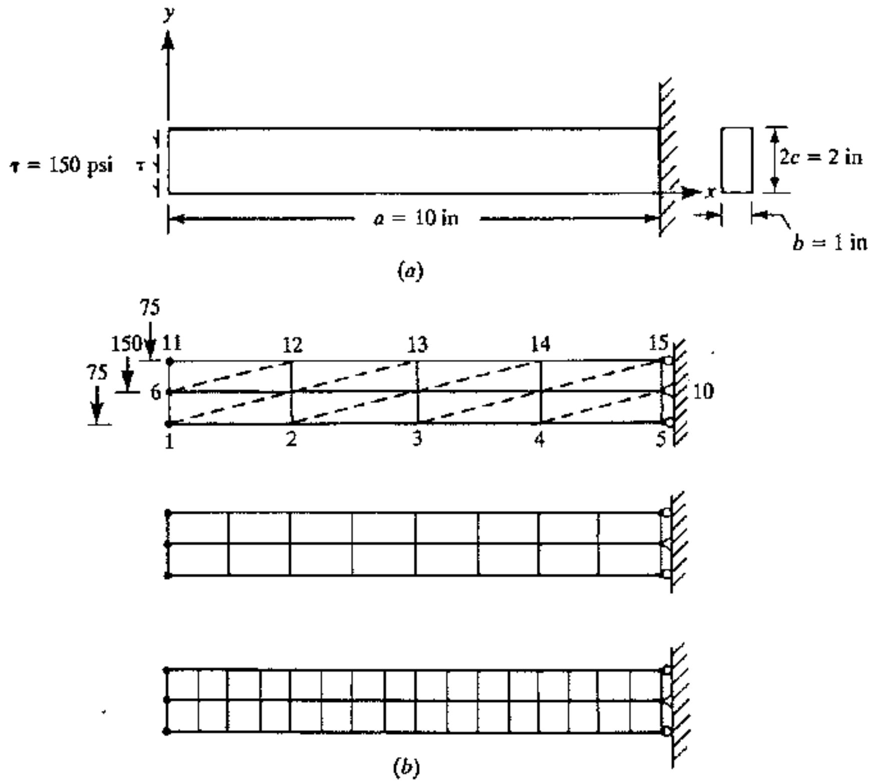

FIGURE 10.6
Finite-element meshes for an end-loaded cantilever beam.

for the meshes shown. Table 10.2 gives the deflections and stresses obtained with refined meshes of triangular and rectangular elements.

Example 10.2. Consider the cantilever beam ($E = 30 \times 10^6$ psi, $\nu = 0.25$, $a = 10$ in, $b = c = 1$ in) shown in Fig. 10.6(*a*). We wish to determine, using the elasticity equations, the maximum deflection and bending stress in the beam when it is subjected to a uniformly distributed shear stress $\tau = 150$ psi. The boundary conditions of the problem are

$$\begin{gathered} u(a, y) = 0, \qquad v(a, c) = 0 \\ t_x = t_y = 0 \quad \text{at } y = 0,\ 2c \text{ for any } x \\ t_x = 0, \qquad t_y = -\tau \quad \text{at } x = 0 \text{ for any } y \\ t_y = 0 \quad \text{at } x = a \text{ and for any } y \neq c \end{gathered} \tag{10.47}$$

We shall solve the problem using the plane stress assumption. The elastic coefficients c_{ij} for the plane stress case are defined (assuming that steel is isotropic) by

$$c_{11} = c_{12} = \frac{E}{1 - \nu^2}, \qquad c_{12} = \frac{E\nu}{1 - \nu^2}, \qquad c_{66} = \frac{E}{2(1 + \nu)}\ (= G) \tag{10.48}$$

Three different finite element meshes, increasingly refined, are shown in Fig. 10.6(*b*). These meshes are those consisting of linear rectangular elements. Equivalent triangular element meshes are obtained by joining node 1 to node 3 of each rectangular element (see the dashed lines). Equivalent meshes of nine-node quadratic Lagrange elements are obtained by considering a 2×2 mesh of linear Lagrange elements as a quadratic element.

For the finite element model, the boundary conditions on the primary and secondary variables, e.g., for the 15-node mesh, are given by

$$\begin{gathered} U_5 = U_{10} = V_{10} = U_{15} = 0.0 \\ F_1^y = -75.0, \qquad F_6^y = -150.0, \qquad F_{11}^y = -75.0 \end{gathered} \tag{10.49}$$

and all other forces are zero on the boundary.

Table 10.3 gives a comparison of the finite element solutions with the elasticity solutions for the tip deflection (i.e., the deflection at the center node of the left end) and bending stress σ_x, obtained using two-dimensional elasticity theory [see Reddy (1984)]. The linear triangular element mesh has the slowest convergence compared with the linear and quadratic rectangular elements.

The final example in this chapter deals with free vibration and transient analysis of a plane elasticity problem. We consider the cantilever beam of Example 10.2.

Example 10.3. Consider the cantilever beam shown in Fig. 10.6*a*. We wish to determine the natural frequencies and transient response using the plane elasticity elements. We use the finite element meshes of linear triangular and rectangular elements shown in Fig. 10.6(*b*) and their nodal equivalent meshes of quadratic elements to analyze the problem. Table 10.4 gives a comparison of the first 10 natural frequencies obtained with various meshes. The convergence of the natural frequencies with mesh refinement is clear.

TABLE 10.3
Comparison of the finite element solution with the elasticity solution for a cantilever beam subjected to a uniform shear load at the free end

	Tip deflection, $-v \times 10^{-2}$			Normal stress σ_x		
Number of nodes	Linear triangles	Linear rectangles	Quadratic rectangles	Linear triangles	Linear rectangles	Quadratic rectangles
15	0.16112	0.31335	0.50310	1209 (15)†	1196 (8.75, 1.5)‡	2196 (8.943, 1.577)
27	0.26623	0.43884	0.51288	2270 (31)	1793 (9.375, 1.5)	2439 (9.471, 1.577)
51	0.316459	0.48779	0.51374	2829 (63)	2056 (9.6875, 1.5)	2526 (9.736, 1.577)
Elasticity§		0.51875 (0.0, 1.0)		2876 (9.583, 1.667)	2180 (9.6875, 1.5)	2528 (9.736, 1.577)

† Element number.
‡ Quadrature points.
§ From Reddy (1984), p. 53: $v(0, 1) = -(PL^3/3EI)[1 + 3(1+\nu)/L^2]$; $\sigma_x = Px(1-y)/I$, $I = \frac{2}{3}$.

For transient analysis with the linear acceleration scheme ($\alpha = 0.5$, $\gamma = \frac{1}{3}$), the time step Δt is given by the inequality

$$\Delta t < \Delta t_{cr} = \left(\frac{12}{\lambda_{\max}}\right)^{1/2} \tag{10.50}$$

For the 4×1 mesh of rectangular elements, for example, we have $\Delta t_{cr} = 1.617 \times 10^{-5}$. Figure 10.7 contains plots of the tip deflection $v(0, 1, t)$ versus time, as predicted using the 4×1 mesh of linear rectangular elements and the following two time integration schemes: (1) $\alpha = \gamma = \frac{1}{2}$ and (2) $\alpha = \frac{1}{2}$, $\gamma = \frac{1}{3}$. The time step used in these computations,

TABLE 10.4
Comparison of first ten frequencies of the cantilever beam of Example 10.3 as computed using various meshes of linear and quadratic triangular and rectangular elements

	Triangular elements				Rectangular elements			
ω	Linear element		Quadratic element		Linear element		Quadratic element	
	4×2	8×2	2×1	4×1	4×2	8×2	2×1	4×1
1	2,019.4	1,583.0	1,186.4	1,156.7	1,465.5	1,242.3	1,169.9	1,151.8
2	9,207.4	8,264.0	7,896.6	6,496.5	8,457.9	6,845.8	7,179.7	6,341.4
3	10,449.6	9,177.7	9,158.2	9,156.0	9,218.4	9,171.7	9,158.2	9,156.0
4	25,339.2	19,540.5	18,369.1	16,219.9	22,334.0	16,887.7	17,890.8	15,572.7
5	29,193.2	27,843.9	27,805.3	27,441.7	29,113.3	27,836.8	27,869.8	27,266.3
6	42,363.4	32,727.8	40,399.2	28,696.9	40,309.7	29,433.6	39,583.7	27,442.2
7	52,937.0	46,840.4	50,469.6	39,762.6	52,991.9	44,231.1	50,964.4	39,302.3
8	67,964.6	48,014.4	66,260.9	45,815.6	66,842.5	47,441.0	67,015.3	45,839.9
9	76,833.2	61,560.4	74,582.1	57,429.5	74,523.3	60,078.3	74,064.6	56,949.9
10	79,443.0	68,257.4	79,241.8	64,867.4	76,515.5	67,813.3	80,029.3	64,636.0

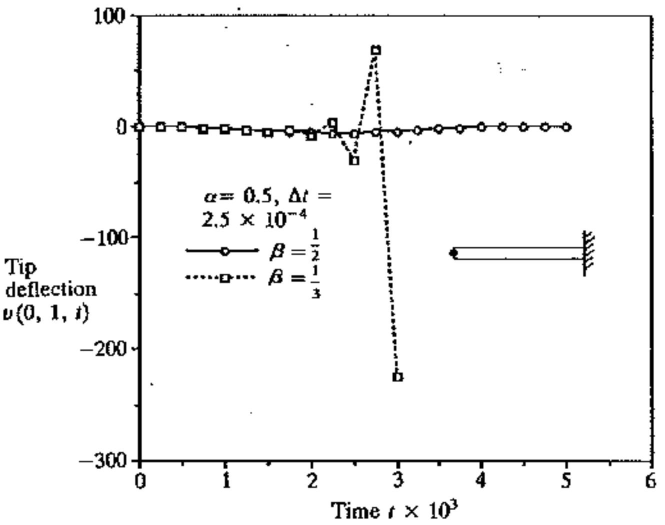

FIGURE 10.7
Stability of the finite element solutions predicted by two different time integration schemes (Example 10.3). The 4×1 mesh of linear rectangular elements is used.

$\Delta t = 2.5 \times 10^{-4} > \Delta t_{cr}$, makes the second scheme yield unstable solutions. It should be noted that if Δt is close to Δt_{cr} but $\Delta t > \Delta t_{cr}$ then the solution predicted by the linear acceleration scheme may be stable for the first several time steps, but it will eventually become unstable. Figures 10.8 and 10.9 show the relative accuracies of solutions predicted by triangular and rectangular elements. It should be noted that the linear triangular element yields a less accurate solution than the linear rectangular element.

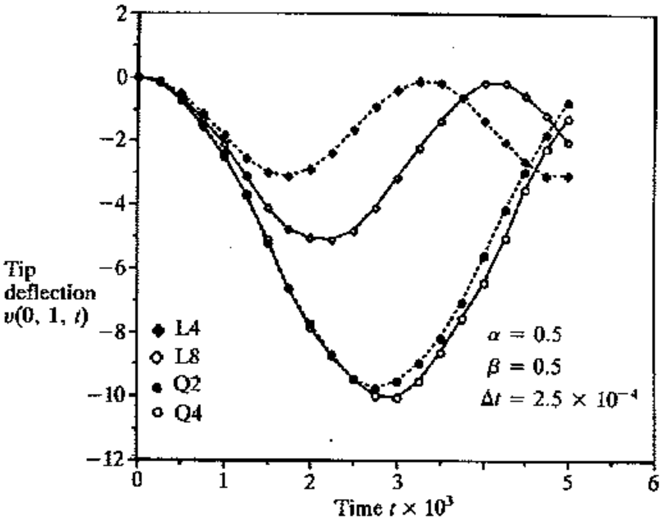

FIGURE 10.8
Tip deflection $v(0, 1, t)$ versus time, as predicted by various meshes of linear (L) and quadratic (Q) triangular elements: L4, 4×2 mesh of linear elements; L8, 8×2 mesh of linear elements; Q2, 2×1 mesh of quadratic elements; Q4, 4×1 mesh of quadratic elements.

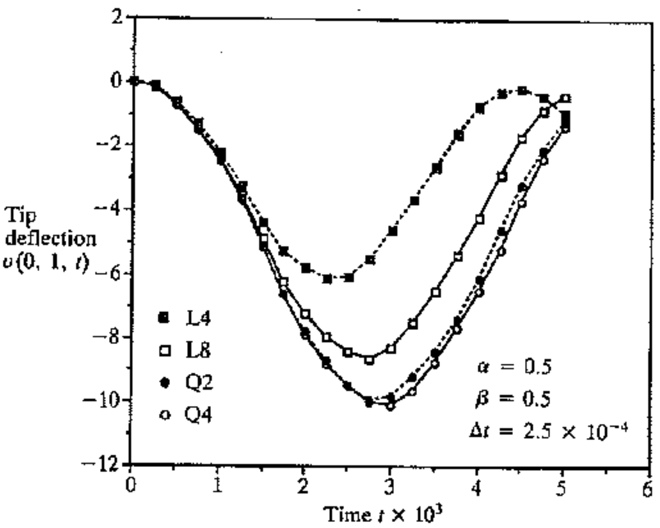

FIGURE 10.9
Tip deflection versus time, as predicted by various meshes of rectangular elements: L4, 4 × 2 mesh of linear elements; L8, 8 × 2 mesh of linear elements; Q2, 2 × 1 mesh of nine-node quadratic elements; Q4, 4 × 1 mesh of nine-node quadratic elements.

10.8 SUMMARY

In this chapter an introduction to the equations of plane elasticity (i.e., two-dimensional problems of elasticity) has been presented, and their finite element models have been formulated. The plane strain and plane stress problems, which differ only in the use of constitutive relations, have been discussed. The governing equations have been expressed in terms of the displacements, and their weak form and finite element model developed in two alternative ways: (i) the matrix formulation, which is standard in most finite element textbooks on solid mechanics; and (ii) the three-step procedure, which is used throughout the book. The eigenvalue and time-dependent problems of plane elasticity have also been discussed. Some numerical examples have been presented to illustrate the evaluation of element stiffness matrices and force vectors.

PROBLEMS

10.1–10.3. Compute the contribution of the surface forces to the global force degrees of freedom in the plane elasticity problems given in Figs. P10.1–P10.3.

10.4–10.6. Give the connectivity matrices and the specified primary degrees of freedom for the plane elasticity problems shown in Figs. P10.1–P10.3. Give only the first three rows of the connectivity matrix.

10.7. Consider a cantilevered beam of length 6 cm, width 2 cm, thickness 1 cm, and material properties $E = 3 \times 10^7$ N cm^{-2} and $\nu = 0.3$, and subjected to a bending moment of 600 N cm at the free end (see Fig. P.10.7). Replace the moment by

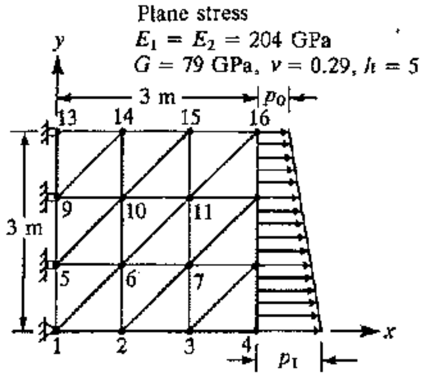

FIGURE P10.1

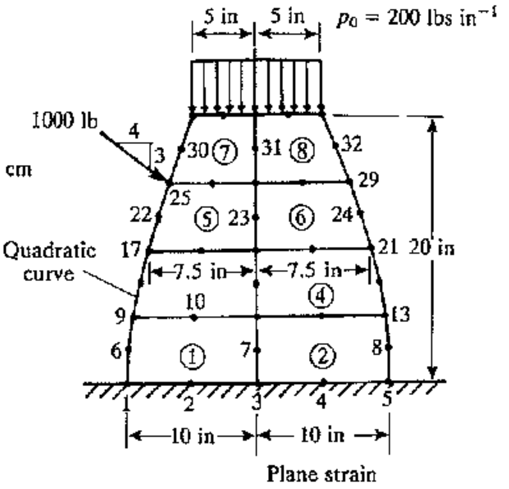

FIGURE P10.2

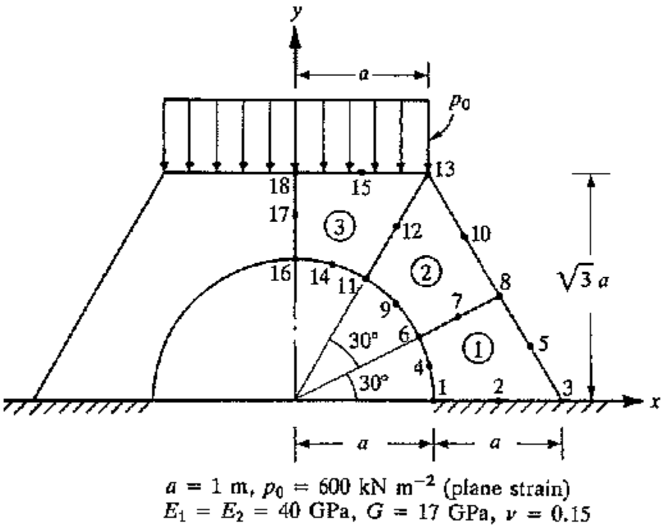
y
a
p_0
13
18
15
17
③
12
10
16
14
11
②
8
$\sqrt{3}\,a$
9
7
30°
6
①
5
4
30°
1
2
3
x
a
a
$a = 1$ m, $p_0 = 600$ kN m^{-2} (plane strain)
$E_1 = E_2 = 40$ GPa, $G = 17$ GPa, $\nu = 0.15$

FIGURE P10.3

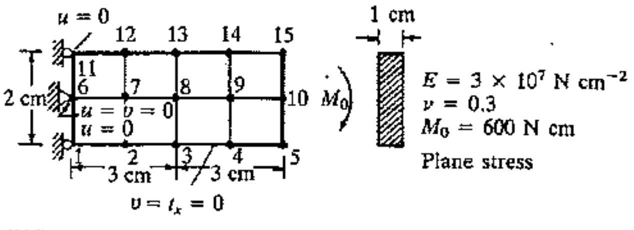

FIGURE P10.7

an equivalent distributed force at $x = 6$ cm, and model the domain by (*a*) a 4×2 mesh of linear rectangular elements and (*b*) quadratic rectangular elements. Identify the specified displacements and global forces.

Answer: $F_5^x = -300$ and $F_{15}^x = 300$.

10.8. Consider the ("transition") element shown in Fig. P10.8. Define the generalized displacement vector of the element by

$$\{u\} = \{u_1, v_1, \theta_1, u_2, v_2, u_3, v_3\}^T$$

and represent the displacement components u and v by

$$u = \psi_1 u_1 + \psi_2 u_2 + \psi_3 u_3 + \tfrac{1}{2} h \eta \psi_1 \theta_1, \qquad v = \psi_1 v_1 + \psi_2 v_2 + \psi_3 v_3$$

where ψ_1 is the interpolation function for the beam, and ψ_2 and ψ_3 are the interpolation functions for nodes 2 and 3:

$$\psi_1 = \tfrac{1}{2}(1 - \xi), \qquad \psi_2 = \tfrac{1}{4}(1 + \xi)(1 - \eta), \qquad \psi_3 = \tfrac{1}{4}(1 + \xi)(1 + \eta)$$

Derive the stiffness matrix for the element.

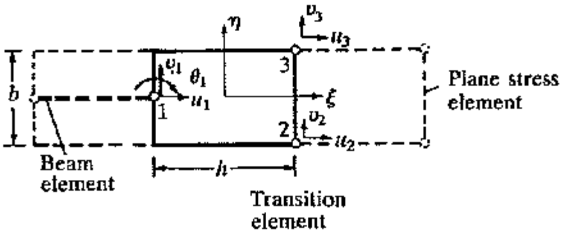

FIGURE P10.8

10.9. Consider the square, isotropic, elastic body of thickness h shown in Fig. P10.9. Suppose that the displacements are approximated by

$$u(x, y) = (1 - x)y u_1 + x(1 - y)u_2, \qquad v(x, y) = 0$$

Assuming that the body is in a state of plane stress, derive the 2×2 stiffness matrix for the unit square:

$$[K]\begin{Bmatrix} u_1 \\ u_2 \end{Bmatrix} = \begin{Bmatrix} F_1 \\ F_2 \end{Bmatrix}$$

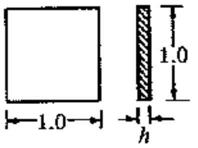

FIGURE P10.9

10.10–10.16. For the plane elasticity problems shown in Figs. P10.10–P10.16, give the boundary degrees of freedom and compute the contribution of the specified forces to the nodes.

Answer: (Problem 10.10) $F_7^y = 200/6$, $F_{11}^y = 800/6$, and $F_{18}^y = F_7^y$.

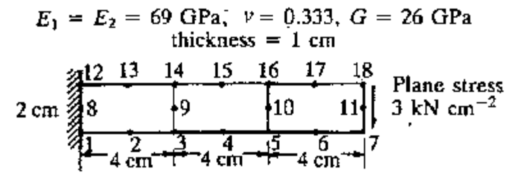

FIGURE P10.10

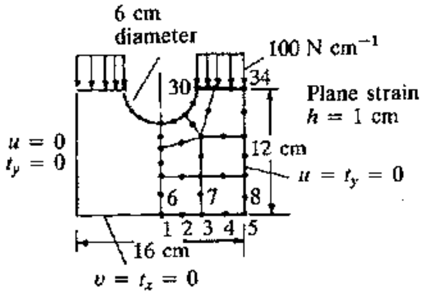

FIGURE P10.11

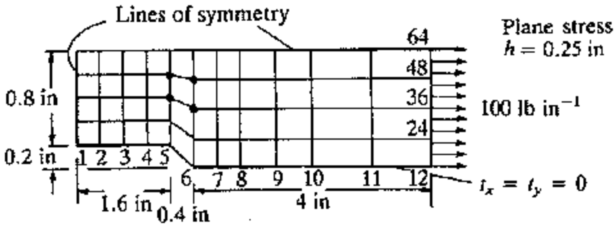

FIGURE P10.12

Fig P10.12

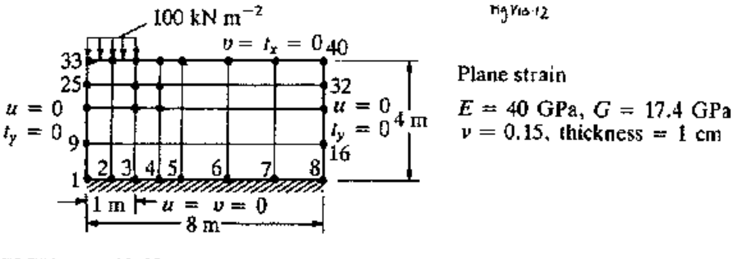

FIGURE P10.13

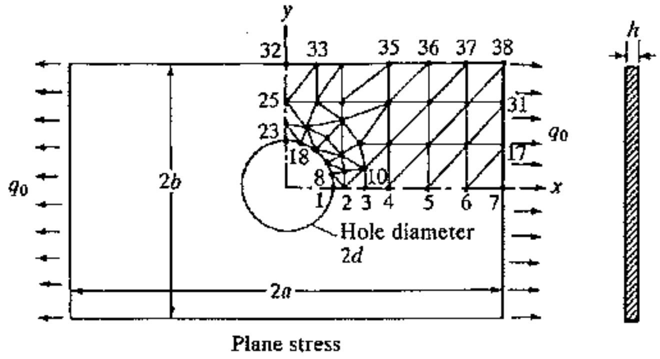

FIGURE P10.14

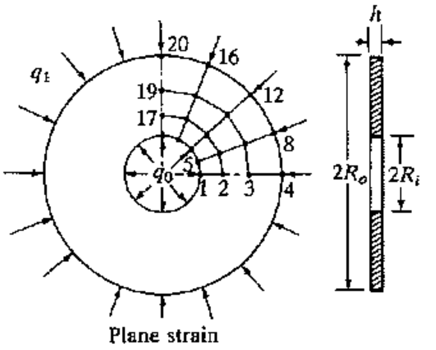

FIGURE P10.15

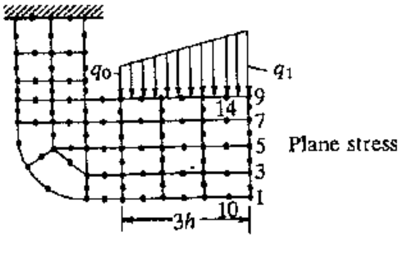

FIGURE P10.16

REFERENCES FOR ADDITIONAL READING

Barlow, J.: "Optimal Stress Locations in Finite Element Models," *International Journal for Numerical Methods in Engineering*, vol. 10, pp. 243–251, 1976.

———: "More on Optimal Stress Points—Reduced Integration, Element Distortions and Error Estimation," *International Journal for Numerical Methods in Engineering*, vol. 28, pp. 1487–1504, 1989.

Budynas, R. G.: *Advanced Strength and Applied Stress Analysis*, McGraw-Hill, New York, 1977.

Dym, C. L., and I. H. Shames: *Solid Mechanics: A Variational Approach*, McGraw-Hill, New York, 1973.

Ugural, A. C., and S. K. Fenster: *Advanced Strength and Applied Elasticity*, Elsevier, New York, 1975.

Volterra, E., and J. H. Gaines: *Advanced Strength of Materials*, Prentice-Hall, Englewood Cliffs, NJ, 1971.

Reddy, J. N.: *Energy and Variational Methods in Applied Mechanics*, John Wiley, New York, 1984.

——— and M. L. Rasmussen: *Advanced Engineering Analysis*, John Wiley, New York, 1982.

Rektorys, K.: *Variational Methods in Mathematics, Science and Engineering*, D. Reidel, Boston, MA, 1980.

———: *The Method of Discretization in Time*, D. Reidel, Boston, MA, 1982.

Timoshenko, S. P., and J. N. Goodier: *Theory of Elasticity*, 3d ed., McGraw-Hill, New York, 1970.

CHAPTER 11

FLOWS OF VISCOUS INCOMPRESSIBLE FLUIDS

11.1 PRELIMINARY COMMENTS

An introduction to fluids and their governing equations was given in Section 3.3.2. The finite element analysis of fluid flow problems that can be described as one-dimensional systems was also discussed there. Two-dimensional flows of inviscid incompressible fluids (i.e., potential flows) were considered in Section 8.4.2. Potential flow problems were cast in terms of either the stream function or the velocity potential, and the governing equation in each case was the Laplace equation (i.e., a second-order partial differential equation in a single variable; see Chapter 8).

In this section, we consider the finite element analysis of two-dimensional flows of viscous incompressible fluids. These problems are governed by a set of coupled partial differential equations in terms of the velocity components and pressure. When the speed of the flow is low, the nonlinear terms due to inertial effects can be neglected. Such a flow is called Stokes flow, and the resulting equations are termed the Stokes equations. Here we describe two different finite element models of Stokes flow. We begin with a review of the pertinent equations governing slow, laminar flows of viscous incompressible fluids (see Section 3.3.2).

11.2 GOVERNING EQUATIONS

Consider the slow flow of a viscous incompressible fluid in a closed domain Ω:

$$\frac{D}{Dt} \equiv \frac{\partial}{\partial t} + \mathbf{v}\cdot\nabla \approx \frac{\partial}{\partial t} \qquad \text{(slow: inertial effects are negligible)}$$

$$\mu \neq 0 \qquad \text{(viscous)}$$

$$\frac{D\rho}{Dt} = 0 \quad (\rho = \text{constant}) \qquad \text{(incompressible)}$$

Suppose that the domain is very long in one direction—say, the z direction. Then, if there is no flow along this direction and the velocity components in the other two directions are independent of z, the flow can be approximated by a two-dimensional model. The governing equations are summarized below [see (3.102)–(3.106)]:

Conservation of linear momentum

$$\boxed{\begin{aligned} &\rho\frac{\partial u}{\partial t} - \frac{\partial}{\partial x}\left(2\mu\frac{\partial u}{\partial x}\right) - \frac{\partial}{\partial y}\left[\mu\left(\frac{\partial u}{\partial y} + \frac{\partial v}{\partial x}\right)\right] + \frac{\partial P}{\partial x} - f_x = 0 \\ &\rho\frac{\partial v}{\partial t} - \frac{\partial}{\partial x}\left[\mu\left(\frac{\partial u}{\partial y} + \frac{\partial v}{\partial x}\right)\right] - \frac{\partial}{\partial y}\left(2\mu\frac{\partial v}{\partial y}\right) + \frac{\partial P}{\partial y} - f_y = 0 \end{aligned}} \tag{11.1}$$

Conservation of mass

$$\boxed{\frac{\partial u}{\partial x} + \frac{\partial v}{\partial y} = 0} \tag{11.2}$$

Here u and v are the velocity components along the x and y directions, respectively, P is the pressure, f_x and f_y are the components of the body force, μ is the viscosity, and ρ is the density of the fluid. The boundary and initial conditions are of the form

$$\left.\begin{aligned} t_x &\equiv 2\mu\frac{\partial u}{\partial x}n_x + \mu\left(\frac{\partial u}{\partial y} + \frac{\partial v}{\partial x}\right)n_y - Pn_x = \hat{t}_x \\ t_y &\equiv \mu\left(\frac{\partial u}{\partial y} + \frac{\partial v}{\partial x}\right)n_x + 2\mu\frac{\partial v}{\partial y}n_y - Pn_y = \hat{t}_y \end{aligned}\right\} \text{ on } \Gamma_1 \tag{11.3a}$$

$$u = \hat{u}, \quad v = \hat{v} \qquad \text{on } \Gamma_2$$

$$u(x, y, 0) = u_0(x, y), \qquad v(x, y, 0) = v_0(x, y) \tag{11.3b}$$

The same four possibilities as given in (10.39) exist for the specification of the boundary conditions in fluid flow problems; i.e. only one element of each of the pairs (u, t_x) and (v, t_y) can be specified at any point on the boundary. The boundary stresses are

$$\boxed{\begin{aligned} t_x &= \left(2\mu\frac{\partial u}{\partial x} - P\right)n_x + \mu\left(\frac{\partial u}{\partial y} + \frac{\partial v}{\partial x}\right)n_y \\ t_y &= \mu\left(\frac{\partial u}{\partial y} + \frac{\partial v}{\partial x}\right)n_x + \left(2\mu\frac{\partial v}{\partial y} - P\right)n_y \end{aligned}} \tag{11.3c}$$

There are three partial differential equations (11.1), (11.2) in three unknowns (u, v and P). It is possible to reduce the number of equations and unknowns by the introduction of the stream function ψ and/or the vorticity ζ:

$$\boxed{\frac{\partial \psi}{\partial x} = -v, \qquad \frac{\partial \psi}{\partial y} = u, \qquad \zeta = \frac{\partial u}{\partial y} - \frac{\partial v}{\partial x} = \nabla^2\psi} \tag{11.4}$$

If both functions are used, the three equations can be reduced to two second-order equations [because the continuity equation (11.2) is identically satisfied by the stream function]. If ζ is not used, the three equations can be reduced to a single fourth-order equation in ψ. Since these alternative formulations are not as physically clear as the original equations (especially for the imposition of boundary conditions), or require higher-order elements (for the fourth-order equation for ψ), we shall confine our attention here to the development of finite element models of (11.1) and (11.2) in terms of the primitive variables (u, v, and P).

In the present study, we shall consider two different finite element models of (11.1) and (11.2). The first is a natural and direct formulation in which the three equations in u, v, P are used in their original form. This formulation is known as the *velocity–pressure formulation.* The other is based on the interpretation that the continuity equation (11.2) is an additional relation among the velocity components (i.e., a constraint on u and v), and this constraint is satisfied in a least-squares (i.e., approximate) sense. This particular method of including the constraint in the formulation is known as the *penalty function method,* and the model is termed as the *penalty finite element model.* It is informative to note that the velocity–pressure formulation is the same as the Lagrange multiplier formulation, wherein the constraint is included by means of the Lagrange multiplier. The Lagrange multiplier turns out to be the negative of the pressure.

11.3 VELOCITY–PRESSURE FINITE ELEMENT MODEL

The weak forms of (11.1) and (11.2) over an element Ω^e can be obtained using the three-step procedure discussed in Chapter 8 and revisited in Chapter 10 for plane elasticity problems. We multiply the three equations in (11.1) and (11.2), with three different weight functions w_1, w_2, and w_3, and integrate over the element:

$$0=\int_{\Omega^e} w_1\left\{\rho\frac{\partial u}{\partial t}-\frac{\partial}{\partial x}\left(2\mu\frac{\partial u}{\partial x}\right)-\frac{\partial}{\partial y}\left[\mu\left(\frac{\partial u}{\partial y}+\frac{\partial v}{\partial x}\right)\right]+\frac{\partial P}{\partial x}-f_x\right\}dx\,dy$$

$$0=\int_{\Omega^e} w_2\left\{\rho\frac{\partial v}{\partial t}-\frac{\partial}{\partial x}\left[\mu\left(\frac{\partial u}{\partial y}+\frac{\partial v}{\partial x}\right)\right]-\frac{\partial}{\partial y}\left(2\mu\frac{\partial v}{\partial y}\right)+\frac{\partial P}{\partial y}-f_y\right\}dx\,dy \qquad (11.5)$$

$$0=\int_{\Omega^e} w_3\left(\frac{\partial u}{\partial x}+\frac{\partial v}{\partial y}\right)dx\,dy$$

where w_1, w_2, and w_3 are the weight functions. The latter can be interpreted physically as follows. Since the first equation is the momentum equation and $f_x\,dx\,dy$ denotes the force, w_1 must be like the x component of velocity (u), so that the product $f_x w_1$ gives the power. Similarly, w_2 must be like the y component of velocity (v). The third equation represents the volume change in an element of dimensions dx and dy. Therefore, w_3 must be like a force that causes the volume change. Volume changes occur under the action of hydrostatic pressure; hence, w_3 is like $-P$:

$$\boxed{w_1 \sim u, \qquad w_2 \sim v, \qquad w_3 \sim -P} \qquad (11.6)$$

This interpretation is useful in developing the finite element model, because w_1, for example, will be replaced by the ith interpolation function used in the approximation of u. Similarly, w_3 will be replaced by the ith interpolation function used in the approximation of P. When different interpolations are used for (u, v) and P, this interpretation becomes necessary.

The second step of the weak formulation for the present case needs some comments. The integration by parts to distribute differentiation equally among the variables (u, v, P) and weight functions (w_1, w_2, w_3) helps relax the continuity requirements on the finite element approximation functions used for u, v, and P. However, in any problem, such trading of differentiability is subject to the restriction that the resulting boundary expressions must be physically meaningful. Otherwise, the secondary variables of the formulation may not be the quantities the physical problem admits as boundary conditions. Examination of the boundary stress components t_x and t_y shows that the pressure term is a part of them [see (11.3c)]. For example, t_x is the x component of the *total* boundary stress, which is the sum of the viscous boundary stress, $2\mu(\partial u/\partial x)n_x + \mu(\partial u/\partial y + \partial v/\partial x)n_y$, and the hydrostatic boundary stress, $-Pn_x$. Therefore, it is necessary that each term, except the body force term, must be integrated by parts in the two momentum equations. By trading the differentiation from P onto w_1 and w_2 in the two momentum equations, we gain both physically meaningful natural boundary conditions and the symmetry of the finite element equations, as we shall see shortly. No integration by parts is used in the continuity equation, because no relaxation of continuity on u and v can be accomplished; further, the resulting boundary conditions are not physically justifiable.

Keeping the above comments in mind, we carry out the remaining two steps of the weak formulation. The result is

$$\begin{aligned}
0 &= \int_{\Omega^e} \left[\rho w_1 \frac{\partial u}{\partial t} + 2\mu \frac{\partial w_1}{\partial x}\frac{\partial u}{\partial x} + \mu \frac{\partial w_1}{\partial y}\left(\frac{\partial u}{\partial y} + \frac{\partial v}{\partial x}\right) \right. \\
&\quad \left. - \frac{\partial w_1}{\partial x} P - w_1 f_x \right] dx\,dy - \oint_{\Gamma^e} w_1 t_x\, ds \\
0 &= \int_{\Omega^e} \left[\rho w_2 \frac{\partial v}{\partial t} + \mu \frac{\partial w_2}{\partial x}\left(\frac{\partial u}{\partial y} + \frac{\partial v}{\partial x}\right) + 2\mu \frac{\partial w_2}{\partial y}\frac{\partial v}{\partial y} \right. \\
&\quad \left. - \frac{\partial w_2}{\partial y} P - w_2 f_y \right] dx\,dy - \oint_{\Gamma^e} w_2 t_y\, ds \\
0 &= -\int_{\Omega^e} w_3 \left(\frac{\partial u}{\partial x} + \frac{\partial v}{\partial y}\right) dx\,dy
\end{aligned} \tag{11.7}$$

Note that there is no boundary integral involving w_3, because no integration by parts is used. This implies that P is *not* a primary variable; it is part of the secondary variables (t_x and t_y). This in turn requires that P not be made continuous across interelement boundaries. If P by itself is not specified in a problem (but t_x and t_y are specified) then P is arbitrarily set equal to a value at some node to determine the constant part of the pressure. Thus, P can be determined only to within an arbitrary constant. The minus sign in the third statement is inserted because $P \sim -w_3$, which makes the resulting finite element model symmetric.

An examination of the weak form reveals that u and v are the primary variables that should be made continuous at interelement boundaries, while P is a nodal variable that is not to be made continuous across the interelement boundaries. Therefore, the Lagrange family of finite elements can be used for (u, v, P). The weak form shows that the minimum continuity requirements on (u, v, P) are

(u, v) linear in x and y

P constant

Thus, there are different continuity requirements on the interpolation of the velocity field and pressure:

$$\boxed{u = \sum_{j=1}^{n} u_j \psi_j^e, \qquad v = \sum_{j=1}^{n} v_j \psi_j^e, \qquad P = \sum_{j=1}^{m} P_j \phi_j^e} \tag{11.8}$$

where ψ_j^e and ϕ_j^e are interpolation functions of different order ($m < n$; $m + 1 = n$). Substituting (11.8) into (11.7), we obtain the finite element model:

$$\begin{bmatrix} [M] & [0] & [0] \\ [0] & [M] & [0] \\ [0] & [0] & [0] \end{bmatrix} \begin{Bmatrix} \{\dot{u}\} \\ \{\dot{v}\} \\ \{\dot{P}\} \end{Bmatrix} + \begin{bmatrix} [K^{11}] & [K^{12}] & [K^{13}] \\ [K^{21}] & [K^{22}] & [K^{23}] \\ [K^{31}] & [K^{32}] & [K^{33}] \end{bmatrix} \begin{Bmatrix} \{u\} \\ \{v\} \\ \{P\} \end{Bmatrix} = \begin{Bmatrix} \{F^1\} \\ \{F^2\} \\ \{0\} \end{Bmatrix} \tag{11.9a}$$

where $(i, j = 1, 2, \ldots, n;\ J = 1, 2, \ldots, m)$

$$M_{ij} = \int_{\Omega^e} \rho \psi_i \psi_j \, dx\, dy$$

$$[K^{11}] = 2\mu[S^{11}] + \mu[S^{22}], \qquad [K^{12}] = \mu[S^{12}]^T, \qquad [K^{21}] = [K^{12}]^T$$

$$[K^{22}] = \mu[S^{11}] + 2\mu[S^{22}], \qquad [K^{33}] = [0] \text{ (zero matrix)}$$

$$S^{11}_{ij} = \int_{\Omega^e} \frac{\partial \psi_i}{\partial x}\frac{\partial \psi_j}{\partial x} dx\, dy, \qquad S^{12}_{ij} = \int_{\Omega^e} \frac{\partial \psi_i}{\partial x}\frac{\partial \psi_j}{\partial y} dx\, dy, \qquad S^{22}_{ij} = \int_{\Omega^e} \frac{\partial \psi_i}{\partial y}\frac{\partial \psi_j}{\partial y} dx\, dy \tag{11.9b}$$

$$F^1_i = \int_{\Omega^e} f_x \psi_i \, dx\, dy + \oint_{\Gamma^e} t_x \psi_i \, ds, \qquad F^2_i = \int_{\Omega^e} f_y \psi_i \, dx\, dy + \oint_{\Gamma^e} t_y \psi_i \, ds$$

$$K^{13}_{iJ} = -\int_{\Omega^e} \frac{\partial \psi_i}{\partial x} \phi_J \, dx\, dy, \qquad K^{23}_{iJ} = -\int_{\Omega^e} \frac{\partial \psi_i}{\partial y} \phi_J \, dx\, dy$$

We note that $[K^{33}] = [0]$, because the continuity equation does not contain P. Therefore, the assembled equations will also have zeros in diagonal elements corresponding to the nodal values of P.

Both triangular and rectangular elements for the velocity–pressure model are shown in Fig. 11.1. Since the pressure does not appear at all nodes and it is not made continuous between elements (i.e., a discontinuous pressure approximation is used), the assembly procedure is applicable to only the velocity degrees of freedom. Thus, a finite element mesh with N global nodes will have a total of $2N + M$ unknowns, where N is the total number of nodes in the mesh and M is the number of pressure degrees of freedom.

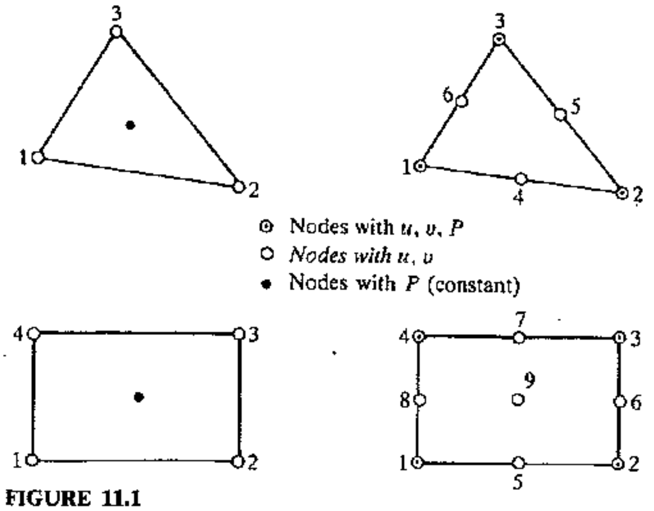

FIGURE 11.1
Linear and quadratic triangular and rectangular finite elements for the pressure–velocity model of incompressible fluid flow.

11.4 PENALTY–FINITE ELEMENT MODEL

11.4.1 Penalty Function Method

The penalty function method, like the Lagrange multiplier method, allows us to reformulate a problem with constraints as one without constraints. The basic idea of the method can be described by considering a constrained algebraic problem:

minimize the function $f(x, y)$ subject to the constraint $G(x, y) = 0$

In the Lagrange multiplier method, the problem is reformulated as one of determining the stationary (or critical) points of the modified function $F_L(x, y)$,

$$F_L(x, y) = f(x, y) + \lambda G(x, y) \tag{11.10}$$

subject to no constraints. Here λ denotes the *Lagrange multiplier*. The solution to the problem is obtained by setting partial derivatives of F_L with respect to x, y, and λ equal to zero:

$$\frac{\partial F_L}{\partial x} = 0, \quad \frac{\partial F_L}{\partial y} = 0, \quad \frac{\partial F_L}{\partial \lambda} = 0 \tag{11.11}$$

which gives three equations in the three unknowns (x, y, λ).

In the penalty function method, the problem is reformulated as one of finding the minimum of the modified function F_P,

$$F_P(x, y) = f(x, y) + \tfrac{1}{2}\gamma[G(x, y)]^2 \tag{11.12}$$

where γ is a preassigned weight parameter, called the *penalty parameter*. The factor $\frac{1}{2}$ in (11.12) is used for convenience: when F_P is differentiated with respect to its arguments, the factor will be cancelled by the power on $G(x, y)$. The solution to the modified problem is given by the following two equations:

$$\frac{\partial F_P}{\partial x} = 0, \quad \frac{\partial F_P}{\partial y} = 0 \tag{11.13a}$$

The solution (x_γ, y_γ) of these will be a function of the penalty parameter γ. The larger the value of γ, the more exactly is the constraint satisfied (in a least-squares sense), and (x_γ, y_γ) approaches the actual solution (x, y) as $\gamma \to \infty$. An approximation to the Lagrange multiplier is computed from the equation (by comparing δF_L with δF_P)

$$\lambda_\gamma = \gamma G(x_\gamma, y_\gamma) \tag{11.13b}$$

We consider a specific example to illustrate the above ideas.

Example 11.1. Minimize the quadratic function

$$f(x, y) = 4x^2 - 3y^2 + 2xy + 6x - 3y + 5 \tag{11.14a}$$

subject to the constraint

$$G(x, y) \equiv 2x + 3y = 0 \tag{11.14b}$$

Geometrically, we see that the inflection point of the surface $f(x, y)$ that is on the line $2x + 3y = 0$ is the solution. We solve the problem using the Lagrange multiplier method and the penalty function method.

Lagrange multiplier method. The modified functional is

$$F_L(x, y) = f(x, y) + \lambda(2x + 3y) \tag{11.15}$$

and we have

$$\begin{aligned}\frac{\partial F_L}{\partial x} &= 8x + 2y + 6 + 2\lambda = 0\\ \frac{\partial F_L}{\partial y} &= -6y + 2x - 3 + 3\lambda = 0\\ \frac{\partial F_L}{\partial \lambda} &= 2x + 3y = 0\end{aligned} \tag{11.16}$$

Solving the three algebraic equations, we obtain

$$x = -3, \qquad y = 2, \qquad \lambda = 7 \tag{11.17}$$

Penalty function method. The modified functional is

$$F_P(x, y) = f(x, y) + \tfrac{1}{2}\gamma(2x + 3y)^2 \tag{11.18}$$

and we have

$$\begin{aligned}\frac{\partial F_P}{\partial x} &= 8x + 2y + 6 + 2\gamma(2x + 3y) = 0\\ \frac{\partial F_P}{\partial y} &= -6y + 2x - 3 + 3\gamma(2x + 3y) = 0\end{aligned} \tag{11.19}$$

The solution of these equations is

$$x_\gamma = \frac{15 - 36\gamma}{-26 + 12\gamma}, \qquad y_\gamma = \frac{18 + 24\gamma}{-26 + 12\gamma} \tag{11.20a}$$

The Lagrange multiplier is given by

$$\lambda_\gamma = \gamma G(x_\gamma, y_\gamma) = \frac{84\gamma}{-26 + 12\gamma} \tag{11.20b}$$

Clearly, in the limit $\gamma \to \infty$, the penalty function solution approaches the exact solution:

$$\lim_{\gamma \to \infty} x_\gamma = -3, \qquad \lim_{\gamma \to \infty} y_\gamma = 2 \qquad \lim_{\gamma \to \infty} \lambda_\gamma = 7$$

An approximate solution (11.20) to the problem can be obtained, to within a desired accuracy, by selecting a finite value of the penalty parameter (see Table 11.1).

11.4.2 Formulation of the Flow Problem as a Constrained Problem

The continuum problem at hand, namely, the flow of a viscous incompressible fluid, can be stated as one of minimizing a functional subjected to a constraint. From the weak form in (11.7), we have the following linear and bilinear forms,

TABLE 11.1
Convergence of the penalty function solution with increasing penalty parameter

γ	x_γ	y_γ	λ_γ	$E_\gamma = 2x_\gamma + 3y_\gamma$
0	−0.5769	−0.6923	0.0000	−3.2308
1	1.5000	−3.0000	−6.0000	−6.0000
10	−3.6702	2.7447	8.9362	0.8936
100	−3.0537	2.0596	7.1550	0.0716
1,000	−3.0053	2.0058	7.0152	0.0068
10,000	−3.0005	2.0006	7.0015	0.0008
∞	−3.0000	2.0000	7.0000	0.0000

for the steady-state case, when the velocity field satisfies the constraint $\partial u/\partial x + \partial v/\partial y = 0$:

$$l(w_1, w_2) = \int_{\Omega^e} (f_x w_1 + f_y w_2)\, dx\, dy + \oint_{\Gamma^e} (t_x w_1 + t_y w_2)\, ds \tag{11.21a}$$

$$B((w_1, w_2), (u, v)) = \mu \int_{\Omega^e} \left[2\left(\frac{\partial w_1}{\partial x}\frac{\partial u}{\partial x} + \frac{\partial w_2}{\partial y}\frac{\partial v}{\partial y} \right) + \left(\frac{\partial w_1}{\partial y} + \frac{\partial w_2}{\partial x} \right)\left(\frac{\partial u}{\partial y} + \frac{\partial v}{\partial x} \right) \right] dx\, dy \tag{11.21b}$$

The pressure term does not appear in the bilinear form, and the third equation in (11.7) is not used, because the continuity equation is identically satisfied by the velocity field (u, v); i.e., (u, v) are subject to the constraint $\partial u/\partial x + \partial v/\partial y = 0$. From the discussion in Chapter 2 [see (2.40)–(2.44)], the quadratic functional is given by

$$\begin{aligned} I((u, v)) &= \tfrac{1}{2}B((u, v), (u, v)) - l((u, v)) \\ &= \mu \int_{\Omega^e} \left[\left(\frac{\partial u}{\partial x}\right)^2 + \left(\frac{\partial v}{\partial y}\right)^2 + \frac{1}{2}\left(\frac{\partial u}{\partial y} + \frac{\partial v}{\partial x}\right)^2 \right] dx\, dy \\ &\quad - \int_{\Omega^e} (f_x u + f_y v)\, dx\, dy - \oint_{\Gamma^e} (t_x u + t_y v)\, ds \end{aligned} \tag{11.22}$$

where the velocity components (u, v) satisfy the continuity equation (11.2).

Now we state that (11.1) and (11.2) governing the steady flow of viscous incompressible fluids are equivalent to minimizing $I(u, v)$ of (11.22) subject to the contsraint

$$G(u, v) \equiv \frac{\partial u}{\partial x} + \frac{\partial v}{\partial y} = 0 \tag{11.23}$$

The constrained problem can be reformulated as an unconstrained problem using the Lagrange multiplier or penalty function methods. These are discussed next.

11.4.3 Lagrange Multiplier Formulation

In the Lagrange multiplier method, the constrained problem is reformulated as one of finding the stationary points of the modified functional

$$I_L(u, v, \lambda) \equiv I(u, v) + \int_{\Omega^e} \lambda G(u, v)\, dx\, dy \tag{11.24}$$

The necessary condition for I_L to have a stationary point is that

$$\begin{gathered} \delta I_L = \delta_u I_L + \delta_v I_L + \delta_\lambda I_L = 0 \\ \text{or} \\ \delta_u I_L = 0, \qquad \delta_v I_L = 0, \qquad \delta_\lambda I_L = 0 \end{gathered} \tag{11.25}$$

where δ_u, δ_v, and δ_λ denote the partial variations (see Section 2.2.4) with respect to u, v, and λ, respectively. The three equations in (11.25) are exactly the same as the weak forms in (11.7), with $\lambda = -P$, $\delta u = w_1$, $\delta v = w_2$, and $\delta\lambda = -w_3$. Therefore, the velocity–pressure finite element model can also be termed the Lagrange multiplier finite element model.

11.4.4 Penalty Function Formulation

In the penalty function method, the constrained problem is reformulated as an unconstrained problem as follows: minimize the modified functional

$$I_P(u, v) \equiv I(u, v) + \tfrac{1}{2}\gamma_e \int_{\Omega^e} [G(u, v)]^2\, dx\, dy \tag{11.26}$$

where the penalty parameter γ_e can be chosen element-wise. The necessary conditions for the minimum of I_P are

$$\delta_u I_P = 0, \qquad \delta_v I_P = 0 \tag{11.27}$$

We have

$$\begin{aligned} \delta_u I_P &= \delta_u I + \gamma_e \int_{\Omega^e} G(u, v)\, \delta_u G(u, v)\, dx\, dy \\ &= \int_{\Omega^e} \left[2\mu \frac{\partial \delta u}{\partial x}\frac{\partial u}{\partial x} + \mu \frac{\partial \delta u}{\partial y}\left(\frac{\partial u}{\partial y} + \frac{\partial v}{\partial x}\right)\right] dx\, dy - \int_{\Omega^e} \delta u\, f_x\, dx\, dy - \oint_{\Gamma^e} \delta u\, t_x\, ds \\ &\quad + \gamma_e \int_{\Omega^e} \frac{\partial \delta u}{\partial x}\left(\frac{\partial u}{\partial x} + \frac{\partial v}{\partial y}\right) dx\, dy = 0 \end{aligned} \tag{11.28a}$$

$$\begin{aligned} \delta_v I_P &= \int_{\Omega^e} \left[2\mu \frac{\partial \delta v}{\partial y}\frac{\partial v}{\partial y} + \mu \frac{\partial \delta v}{\partial x}\left(\frac{\partial u}{\partial y} + \frac{\partial v}{\partial x}\right)\right] dx\, dy - \int_{\Omega^e} \delta v\, f_y\, dx\, dy - \oint_{\Gamma^e} \delta v\, t_y\, ds \\ &\quad + \gamma_e \int_{\Omega^e} \frac{\partial \delta v}{\partial y}\left(\frac{\partial u}{\partial x} + \frac{\partial v}{\partial y}\right) dx\, dy = 0 \end{aligned} \tag{11.28b}$$

These two statements provide the weak forms for the penalty finite element model. We note that the pressure, which is the Lagrange multiplier, does not appear explicitly in the weak form (11.28), although it is a part of the boundary stresses t_x and t_y. The time-derivative terms can be added to (11.28) without affecting the above discussion:

$$\int_{\Omega^e} \rho\, \delta u \frac{\partial u}{\partial t}\, dx\, dy, \qquad \int_{\Omega^e} \rho\, \delta v \frac{\partial v}{\partial t}\, dx\, dy \tag{11.29}$$

The penalty finite element model is obtained from (11.28*a*,*b*) with the inertia terms (11.29) added, by substituting (11.8) for the velocity field, and $\delta u = \psi_i$ and $\delta v = \psi_i$:

$$\begin{bmatrix} [M] & [0] \\ [0] & [M] \end{bmatrix} \begin{Bmatrix} \{\dot{u}\} \\ \{\dot{v}\} \end{Bmatrix} + \begin{bmatrix} [\bar{K}^{11}] & [\bar{K}^{12}] \\ [\bar{K}^{21}] & [\bar{K}^{22}] \end{bmatrix} \begin{Bmatrix} \{u\} \\ \{v\} \end{Bmatrix} = \begin{Bmatrix} \{F^1\} \\ \{F^2\} \end{Bmatrix} \tag{11.30}$$

where F_i^1 and F_i^2 are as defined in (11.9*b*), and

$$\begin{gathered} [\bar{K}^{11}] = [K^{11}] + \gamma[S^{11}], \qquad [\bar{K}^{12}] = [K^{12}] + \gamma[S^{12}], \\ [\bar{K}^{22}] = [K^{22}] + \gamma[S^{22}] \end{gathered} \tag{11.31}$$

The matrices $[K^{\alpha\beta}]$ and $[S^{\alpha\beta}]$ are defined in (11.9*b*).

For the unsteady case, (11.9*a*) or (11.30) are further approximated using a time approximation scheme. First, let us write (11.30) in the concise form

$$[M]\{\dot{\Delta}\} + [K]\{\Delta\} = \{F\} \tag{11.32}$$

where $\{\Delta\}$ denotes the vector of nodal velocities. Using the α family of approximation [see (8.162)–(8.164)], we reduce (11.32) to

$$[\hat{K}]_{s+1}\{\Delta\}_{s+1} = \{\hat{F}\}_{s,s+1} \tag{11.33a}$$

where

$$\begin{gathered} [\hat{K}]_{s+1} = [M] + a_1[K]_{s+1} \\ \{\hat{F}\}_{s+1} = (\alpha\{F\}_{s+1} + (1-\alpha)\{F\}_s)\,\Delta t_{s+1} + ([M] - a_2[K]_s)\{\Delta\}_s \\ a_1 = \alpha\,\Delta t, \qquad a_2 = (1-\alpha)\,\Delta t \end{gathered} \tag{11.33b}$$

The Lagrange multiplier (i.e., the negative of the pressure) for any $t > 0$ is computed from the equation

$$\boxed{\lambda_\gamma = -P_\gamma^e = \gamma G(u_\gamma, v_\gamma) = \gamma\left(\frac{\partial u_\gamma}{\partial x} + \frac{\partial v_\gamma}{\partial y}\right)} \tag{11.34}$$

where (u_γ, v_γ) is the finite element solution of (11.33).

11.4.5 Computational Aspects

Some comments are in order on the numerical evaluation of the integrals and pressure computation in the penalty model. Note that the penalty finite element model for the steady case is of the form

$$(\mu[K^1] + \gamma[K^2])\{\Delta\} = \{F\} \tag{11.35}$$

where $[K^1]$ is the contribution from the viscous terms and $[K^2]$ is from the penalty terms, which come from the incompressibility constraint (11.2). In theory, as we increase the value of γ, the mass conservation constraint is satisfied more exactly. However, in practice, for some large value of γ, the contribution from the viscous terms would be negligibly small compared with the penalty terms in the computer. Thus, in the limit as γ tends to a large number, we have

$$\lim_{\gamma\to\infty}\frac{1}{\gamma}\left((\mu[K^1]+\gamma[K^2])\{\Delta\}-\{F\}\right)=\{0\} \tag{11.36a}$$

or

$$[K^2]\{\Delta\}=\{0\} \quad \text{as } \gamma\to\infty \tag{11.36b}$$

Thus, if $[K^2]$ is a nonsingular (i.e., invertible) matrix, the solution of (11.36*b*) for large γ is trivial: $\{\Delta\}=\{0\}$. While this solution satisfies the continuity equation, it does not satisfy the momentum equations. In this case, the discrete problem (11.35) is said to be overconstrained or "locked." If $[K^2]$ is singular then the sum $\mu[K^1]+\gamma[K^2]$ is nonsingular (because $[K^1]$ is nonsingular), and a nontrivial solution to the problem can be obtained.

The numerical problem described above is eliminated by proper evaluation of the integrals in $[K^1]$ and $[K^2]$. It is found that if the coefficients of $[K^2]$ (i.e., the penalty terms) are evaluated using a numerical integration rule (see Section 9.2) of an order less than that required to integrate them exactly, the finite element equations (11.35) give acceptable solutions for the velocity field. This technique of under-integrating the penalty terms is known in the literature as *reduced integration*.

For a linear rectangular element, for example, the coefficients K^1_{ij} are evaluated using 2×2 Gauss quadrature, and K^2_{ij} are evaluated using 1×1 Gauss quadrature. One-point quadrature yields a singular $[K^2]$. Therefore, (11.36*b*) cannot be inverted, whereas $\mu_e[K^1]+\gamma_e[K^2]$ is nonsingular and can be inverted (after assembly and imposition of boundary conditions) to obtain a good finite element solution of the original problem.

For linear and quadratic triangular elements, it is found that a good solution for the velocity field is obtained without using reduced integration on penalty terms. For example, the four-point integration (i.e., full integration) of $[K^1]$ and $[K^2]$ for the linear triangular element gives exactly the same velocity field as when four-point (2×2) integration is used to evaluate $[K^1]$ and either three- or one-point integration is used for $[K^2]$. Similarly, seven-point integration of $[K^1]$ and $[K^2]$ for the quadratic triangular element gives the same velocity field as that obtained using seven-point integration of $[K^1]$ and three- or four-point integration of $[K^2]$. Since reduced integration saves computational time, it is used to evaluate $[K^2]$ in the present study.

Concerning the post-computation of pressure in the penalty model, in general, the pressure computed from (11.34) at the integration points is not always reliable and accurate. Various techniques have been proposed in the literature to obtain accurate pressure fields. It is found that for both triangular and rectangular elements, the pressure computed at the reduced Gauss

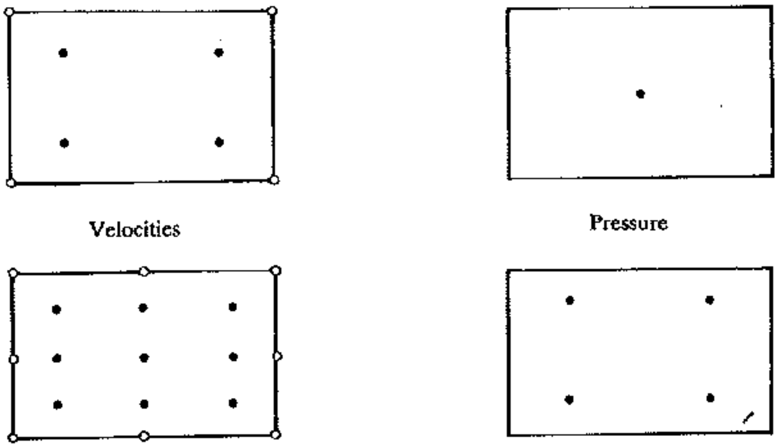

FIGURE 11.2
Finite elements for the approximation of velocities and the post-computation of the pressure (open circles denote nodes and dark circles integration points) in the penalty finite element model. A three-point evaluation of pressure is also suggested when velocities are approximated by quadratic polynomials.

quadrature points (the same integration points that are used to evaluate the penalty terms $[K^2]$) is better than that obtained with full integration points. Thus, pressure should be computed from (11.34) at the Gauss points of the reduced integration. The pressures predicted using the linear elements, especially for coarse meshes, are seldom acceptable. Quadratic elements are known to yield more reliable results. In general, triangular elements do not yield stable solutions for pressures. A mathematical study of the penalty elements (mostly rectangular ones) can be found in the work of Oden (1982).

Figure 11.2 shows linear and quadratic finite elements with integration points for the viscous and penalty terms. Other elements and their convergence and stability characteristics can be found in Oden and Carey (1983). Of these elements, only rectangular ones give stable solutions for pressures; and for uniform meshes and problems with smooth solutions, all elements give good velocity fields. The reader should be cautioned that pressures produced by the penalty elements can be unstable for some problems and coarse meshes, especially when triangular elements are used.

The choice of penalty parameter is largely dictated by the ratio of the magnitude of penalty terms to the viscous terms, the mesh, and the word length in the computer. Generally, a value of $\gamma = 10^4\mu$–$10^{12}\mu$ gives good results. It is found that the pressure is more sensitive to the value of γ than the velocity field, and triangular elements permit a smaller range of γ ($10^4\mu$–$10^8\mu$) than the rectangular elements for good pressures.

11.5 EXAMPLES

Example 11.2. Consider the flow of a viscous incompressible material squeezed between two long parallel plates (see Fig. 11.3*a*). When the length of the plates is very

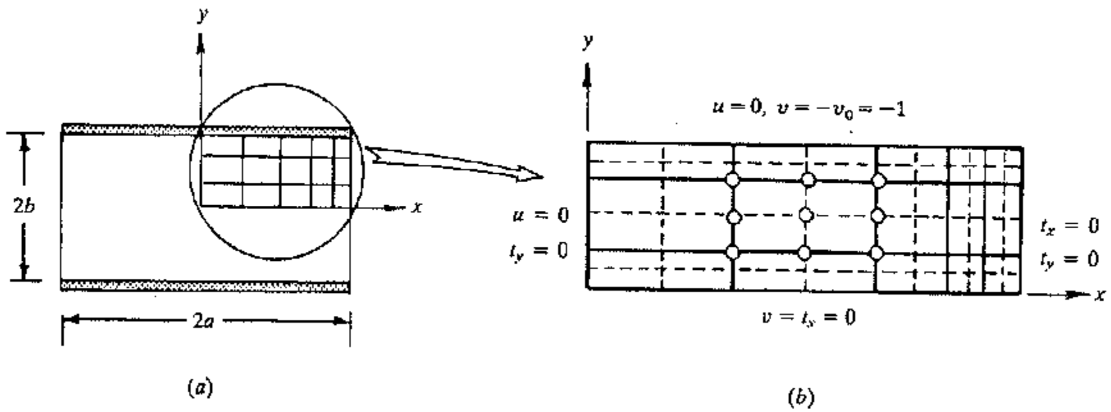

FIGURE 11.3
Boundary conditions and finite element meshes for the problem of an incompressible viscous fluid squeezed between plates: (*a*) geometry of the flow domain; (*b*) finite element mesh of a quadrant.

large compared with both their width and the distance between them, we have a case of plane flow (in the plane formed by the plate width and the distance between them). Assumining that a state of plane flow exists, we determine the velocity and pressure fields. Let V_0 be the velocity with which the two plates are moving toward each other (i.e., squeezing out the fluid), and let $2b$ and $2a$ denote, respectively, the distance between and the width of the plates (see Fig. 11.3a). An approximate analytical solution to this two-dimensional problem is provided by Nadai (1963):

$$
\begin{aligned}
&u=\frac{3V_0x}{2b}\left(1-\frac{y^2}{b^2}\right), \qquad v=-\frac{V_0y}{2b}\left(3-\frac{y^2}{b^2}\right)\\
&P=\frac{P_0}{a^2}(a^2+y^2-x^2), \qquad P_0=\frac{3\mu V_0a^2}{2b^3}\\
&\sigma_x=2\mu\frac{\partial u}{\partial x}-P=\frac{P_0}{a^2}(x^2-3y^2-a^2+2b^2)\\
&\sigma_y=2\mu\frac{\partial v}{\partial y}-P=\frac{P_0}{a^2}(x^2+y^2-a^2-2b^2)\\
&\tau_{xy}=\mu\left(\frac{\partial u}{\partial y}+\frac{\partial v}{\partial x}\right)=\frac{-2P_0xy}{a^2}
\end{aligned}
\tag{11.37}
$$

Owing to the biaxial symmetry of the problem, it suffices to model only a quadrant of the domain. A 5×3 nonuniform mesh of nine-node quadratic elements is used in the velocity–pressure model, and a 10×6 mesh of four-node linear elements and a 5×3 mesh of quadratic elements is used in the penalty model (see Fig. 11.3b). The nonuniform mesh, with smaller elements near the free surface (i.e., at $x=a$), is used to accurately approximate the singularity in the shear stress at the point $(a, b)=(6, 2)$. The mesh used for the penalty model has exactly the same number of nodes as the mesh used for the velocity–pressure model. There are no specified

TABLE 11.2

Comparison of the horizontal velocity $u(x, 0)$ obtained using the penalty model† and the mixed (velocity–pressure) model with the analytical solution

	$\gamma=1.0$		$\gamma=100$		$\gamma=10^8$		Mixed model	Mixed model	
x	4-node	9-node	4-node	9-node	4-node	9-node	8-node	9-node	Analytical solution
1	0.0303	0.0310	0.6563	0.6513	0.7576	0.7505	0.7496	0.7497	0.7500
2	0.0677	0.0691	1.3165	1.3062	1.5135	1.4992	1.5038	1.5031	1.5000
3	0.1213	0.1233	1.9911	1.9769	2.2756	2.2557	2.2563	2.2561	2.2500
4	0.2040	0.2061	2.6960	2.6730	3.0541	3.0238	3.0213	3.0203	3.0000
4.5	0.2611	0.2631	3.0718	3.0463	3.4648	3.4307	3.4331	3.4292	3.3750
5.0	0.3297	0.3310	3.4347	3.3956	3.8517	3.8029	3.8249	3.8165	3.7500
5.25	0.3674	0.3684	3.6120	3.5732	4.0441	3.9944	4.0074	3.9893	3.9375
5.5	0.4060	0.4064	3.7388	3.6874	4.1712	4.1085	4.1450	4.1204	4.1250
5.75	0.4438	0.4443	3.8316	3.7924	4.2654	4.2160	4.2188	4.2058	4.3125
6.0	0.4793	0.4797	3.8362	3.7862	4.2549	4.1937	4.2659	4.2364	4.5000

† The three-point Gauss rule for nonpenalty terms and the two-point Gauss rule for penalty terms are used for quadratic elements.

nonzero secondary variables in the problem. The velocities $u(x, 0)$ obtained using the two models are compared with the analytical solution in Table 11.2. The influence of the penalty parameter on the accuracy of the solution is clear from the results.

Next, a 12×8 mesh of linear elements and a 6×4 mesh of quadratic elements are used to evaluate the relative accuracies of the rectangular and triangular elements. The 12×8 mesh of linear triangular elements with full integration of $[K^1]$ and $[K^2]$ [see (11.35)] and selective integration (i.e., full integration of $[K^1]$ and reduced integration of $[K^2]$) both give the same results for the velocity field. However, in both cases, erroneous results for pressure and stresses are obtained. The 6×4 mesh of quadratic triangular elements with full and selective integrations gives the same velocity fields, while the stresses and pressure are predicted to be the same at the same quadrature points. Both the 12×8 mesh of linear rectangular elements and the 6×4 mesh of nine-node rectangular elements give good results for velocities, pressure, and stresses. Figure 11.4 shows plots of the velocity $u(x, y)$ for $x = 4$ and 6, and Fig. 11.5 shows plots of pressure $P(x, y)$, for $y = \text{constant}$, computed using the quadratic triangular and nine-node rectangular elements. The pressure in the penalty model was computed using (11.34) with the 2×2 Gauss rule for the quadratic rectangular element and the one-point formula for the quadratic triangular element. If the pressure in the penalty model were computed using the full quadrature rule for rectangular elements, we should obtain erroneous values. The linear triangular element with full as well as reduced integrations gives unstable pressures, while the quadratic triangular element with one- or two-point rules yields good results. In general, the same quadrature rule as that used for the evaluation of the penalty terms in the coefficient matrix must be used to evaluate the pressure, and one should avoid using the linear triangular element.

The next example deals with the finite element analysis of a lubrication problem.

Example 11.3 Flow of a viscous lubricant in a slider bearing. The slider (or slipper) bearing consists of a short sliding pad moving at a velocity $u = U_0$ relative to a stationary pad inclined at a small angle with respect to the stationary pad, and the small gap between the two pads is filled with a lubricant (see Fig. 11.6a). Since the ends of the bearing are generally open, the pressure P_0 there is atmospheric. If the upper pad is parallel to the base plate, the pressure everywhere in the gap must be atmospheric

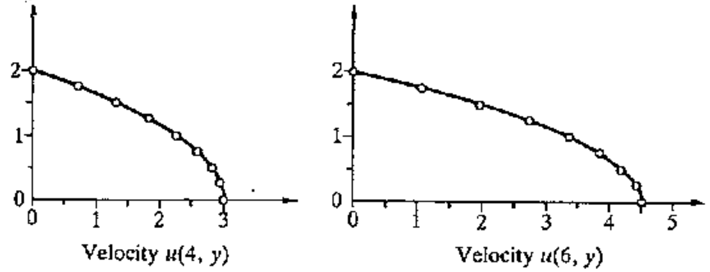

FIGURE 11.4
Horizontal velocity distributions at $x = 3$ and 6 for the problem of a viscous incompressible fluid squeezed between parallel plates (the solid lines represent the analytical solutions and the circles finite element results with all elements for the meshes used).

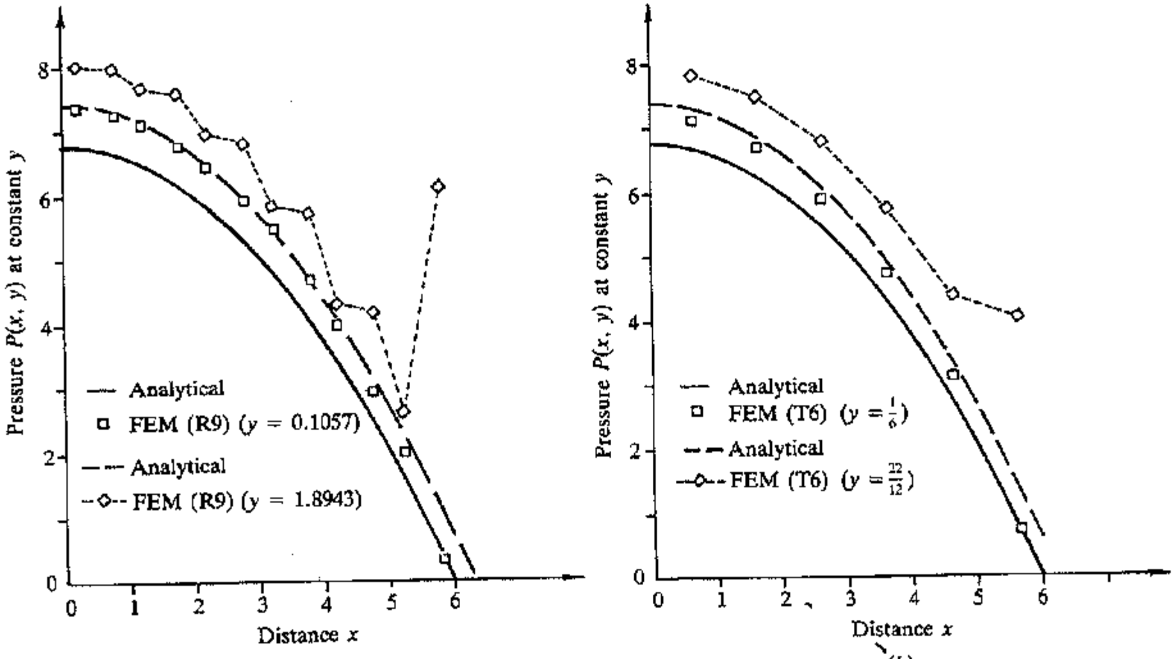

(*a*) (*b*)

FIGURE 11.5
Comparison of the pressure variations computed using the finite element model and Nadai's analytical solution for a viscous fluid squeezed between two parallel plates (Example 11.2).

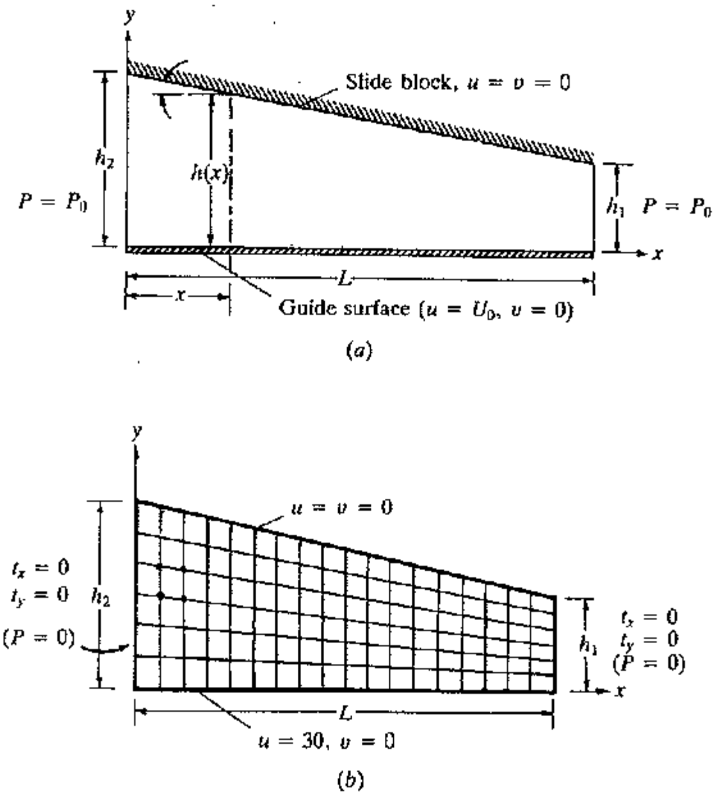

FIGURE 11.6
Finite element analysis of a slider bearing: (*a*) geometry and boundary conditions; (*b*) finite element mesh of linear quadrilateral elements.

(because dP/dx is a constant for flow between parallel plates), and the bearing cannot support any transverse load. If the upper pad is inclined to the base pad, a pressure distribution (in general, a function of x and y) is set up in the gap. For large values of U_0, the pressure generated can be of sufficient magnitude to support heavy loads normal to the base pad.

Analytical solution. Since the width of the gap and the angle of inclination are in general small, it can be assumed with good accuracy that the pressure is not a function of y. Assuming a two-dimensional flow and a small angle of inclination, and neglecting the normal stress gradient (in comparison with the shear stress gradient), the equations governing the motion of the lubricant between the pads can be written as

$$\frac{dP}{dx}=\mu\frac{\partial^2 u}{\partial y^2}, \qquad u=u(x,y), \qquad v=0 \tag{11.38a}$$

with the boundary conditions

$$\begin{aligned} u &= U_0 \quad \text{at } y=0 \\ u &= 0, \quad \text{for } y=h(x) \end{aligned} \tag{11.38b}$$

where

$$h(x) = h_2 + \frac{h_1 - h_2}{L} x \tag{11.38c}$$

The solution (u, P) of (11.38) is

$$u = \left(U_0 - \frac{1}{2\mu} h^2 \frac{dP}{dx} \frac{y}{h}\right)\left(1 - \frac{y}{h}\right), \qquad P = \frac{6\mu U_0 L}{h_2^2 - h_1^2} \frac{(h_2 - h)(h - h_1)}{h^2} \tag{11.39}$$

The shear stress is given by

$$\tau_{xy} = \mu \frac{\partial u}{\partial y} = \frac{dP}{dx}(y - \tfrac{1}{2}h) - \mu \frac{U_0}{h}, \tag{11.40}$$

In our computations, we choose

$$\begin{aligned} h_2 = 2h_1 = 8 \times 10^{-4}\,\text{ft}, &\qquad L = 0.36\,\text{ft}, \\ \mu = 8 \times 10^{-4}\,\text{lbf s ft}^{-2}, &\qquad U_0 = 30\,\text{ft s}^{-1} \end{aligned} \tag{11.41}$$

Finite element solution. It should be pointed out that the assumption concerning the pressure not being a function of y is not necessary in the finite element analysis. First, we use a mesh (mesh 1) of 18×6 linear quadrilateral elements to analyze the problem. The boundary conditions are given in Fig. 11.6(*b*). Figure 11.7 shows plots of the pressure distributions along the length of the bearing for various values of the penalty parameter. The converged pressure is slightly higher than the analytical solution.

To obtain more accurate solutions, a graded mesh (mesh 2) of 128 linear quadrilateral elements (153 nodes) (equivalently, 32 nine-node quadrilateral elements or 64 six-node triangular elements) is used. For this problem, the mesh of quadratic triangular elements gives unstable pressures (see Fig. 11.8), whereas both linear and quadratic elements give excellent results for velocities, pressure, and shear stress.

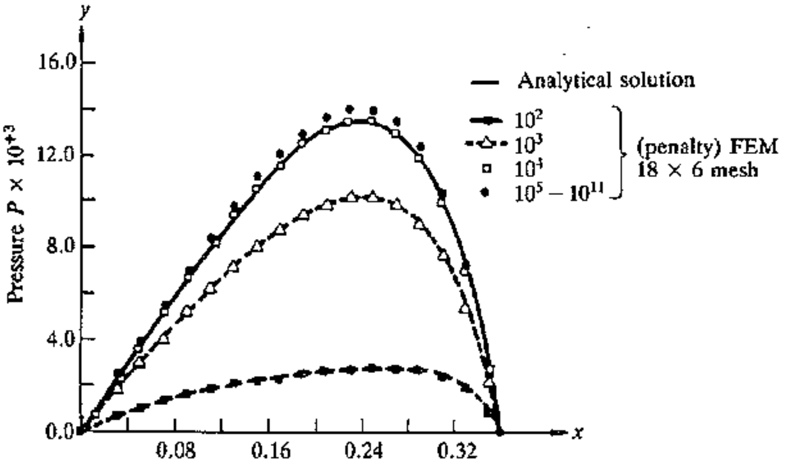

FIGURE 11.7
Influence of the penalty parameter on the variation of the pressure along the length of the slider bearing. A mesh of linear quadrilateral elements is used.

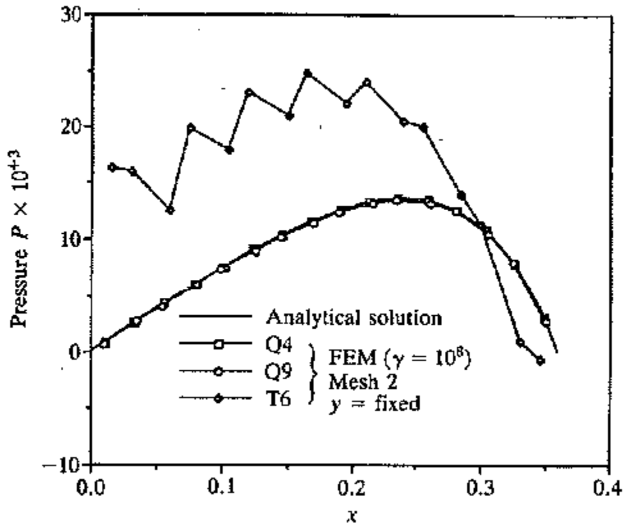

FIGURE 11.8
Variation of pressure $P(x, y_0)$ along the length of the bearing (y_0 is the y coordinate of the first integration point of the first element): Q4, four-node quadrilateral elements; Q9, nine-node quadrilateral elements; T6; six-node triangular element.

Figures 11.9 and 11.10 give a comparison of the finite element solutions (for $\gamma = 10^8$) with the analytical solutions for the horizontal velocity, pressure, and shear stress.

The last example of this section is devoted to the transient analysis of the problem of Example 11.2.

Example 11.4 Time-dependent analysis of fluid squeezed between plates. Consider the unsteady flow of a viscous fluid squeezed between two parallel plates (see Fig.

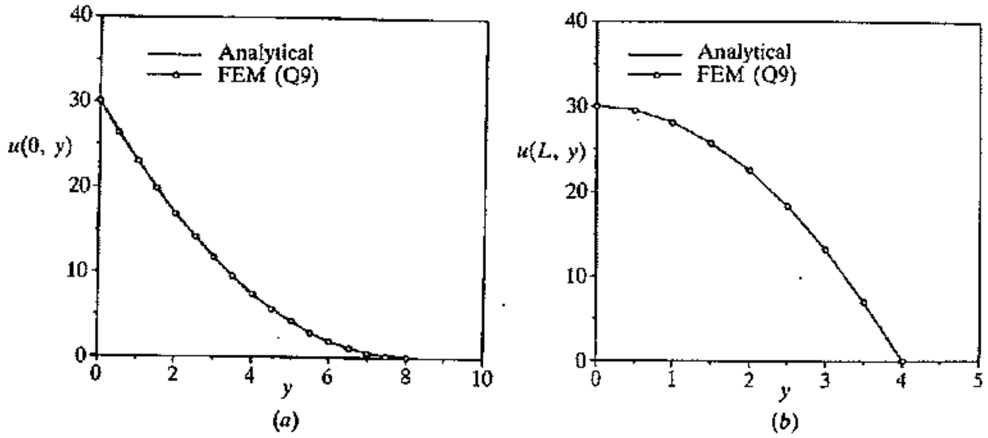

(*a*) (*b*)

FIGURE 11.9
Comparison of the finite element solution $u(x_0, y)$ with the analytical solution of the slider bearing problem in Example 11.3 (the finite element solution is obtained using 32 nine-node rectangular elements).

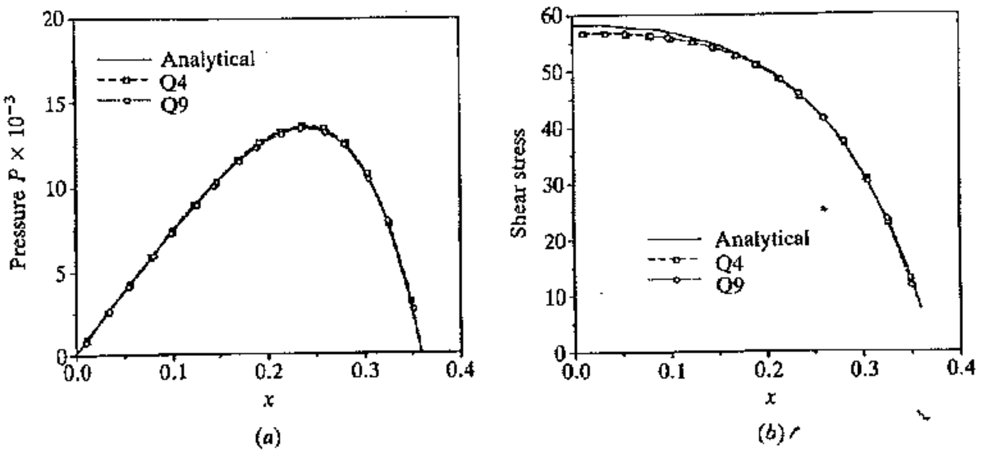

FIGURE 11.10
Comparison of the finite element solutions for pressure and shear stress with the analytical solution of the slider bearing problem of Example 11.3: Q4, four-node quadrilateral element; Q9, nine-node quadrilaterial element. The pressure and shear stress are computed at the Gauss points closest to the bottom wall.

11.3*a*). The flow is induced by the uniform motion of the plates toward each other. The boundary conditions of the model are the same as shown in Fig. 11.3(*b*). The initial boundary conditions are assumed to be zero.

We use the 6×4 mesh of nine-node quadratic elements, employed in Example 11.2, to model the problem. Figure 11.11(*a*) shows plots of the horizontal velocity $u(6, y)$ as a function of y for various times and for two different time steps, and Fig. 11.11(*b*) shows the evolution of the velocity $u(6, 0)$ with time. The transient solution becomes steady around $t = 1.5$ (for a difference of 10^{-3} between the solutions at two consecutive time steps).

11.6 SUMMARY

Finite element models of the equations governing two-dimensional flows of viscous incompressible fluids have been developed. Two different types of finite element models have been presented: (i) the velocity–pressure finite element model, with (u, v, P) as the primary nodal degrees of freedom; and (ii) the penalty finite element model, with (u, v) as the primary nodal degrees of freedom. In the penalty function method, the pressure is calculated from the velocity field in the post-computation. The coefficient matrix in the penalty finite element model is evaluated using mixed integration: full integration for the viscous terms and reduced integration for the penalty terms (i.e., terms associated with the incompressibility or divergence-free condition on the velocity field). Both triangular and rectangular elements have been discussed. In general, triangular elements do not yield accurate pressure fields. The linear and quadratic quadrilateral elements are more reliable for pressure as well as for velocity fields in the penalty finite element model.

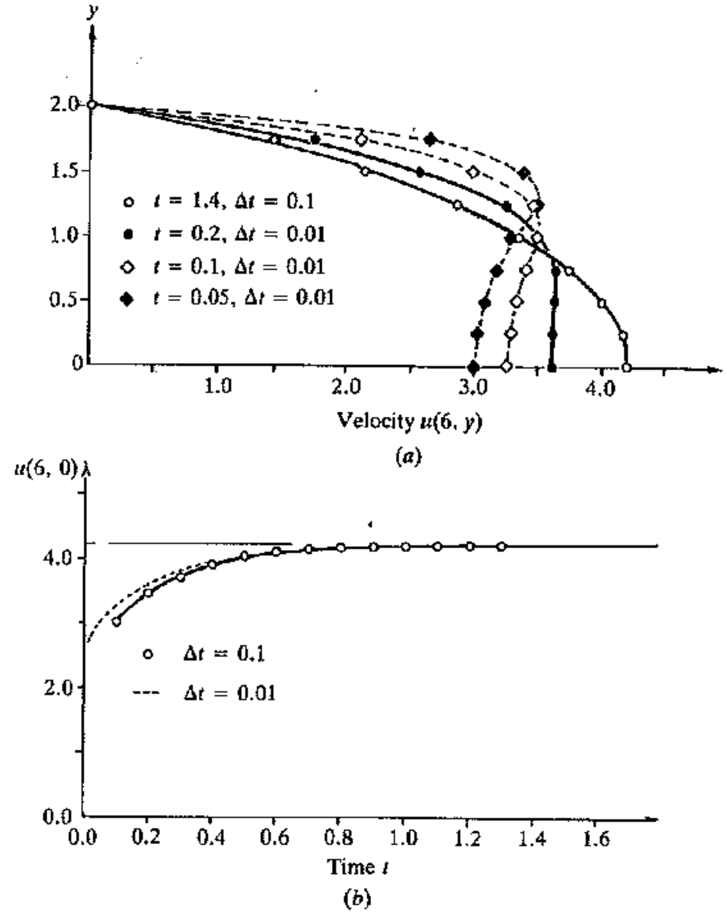

FIGURE 11.11
Transient analysis of a viscous fluid squeezed between parallel plates: (*a*) velocity $u(6, y)$ versus y; (*b*) velocity $u(6, 0)$ versus t.

PROBLEMS

11.1. Consider (11.1) and (11.2) in cylindrical coordinates (r, θ, z). For axisymmetric viscous incompressible flows (i.e., where the flow field is independent of θ), we have

$$\rho \frac{\partial u}{\partial t} = \frac{1}{r}\frac{\partial}{\partial r}(r\sigma_r) - \frac{\sigma_\theta}{r} + \frac{\partial \sigma_{rz}}{\partial z} + f_r \tag{i}$$

$$\rho \frac{\partial w}{\partial t} = \frac{1}{r}\frac{\partial}{\partial r}(r\sigma_{rz}) + \frac{\partial \sigma_{zz}}{\partial z} + f_z \tag{ii}$$

$$\frac{1}{r}\frac{\partial}{\partial r}(ru) + \frac{\partial w}{\partial z} = 0 \tag{iii}$$

where

$$\sigma_r = -P + 2\mu\frac{\partial u}{\partial r}, \quad \sigma_\theta = -P + 2\mu\frac{u}{r}, \quad \sigma_z = -P + 2\mu\frac{\partial w}{\partial z}, \quad \sigma_{rz} = \mu\left(\frac{\partial u}{\partial z} + \frac{\partial w}{\partial r}\right)$$

Develop the semidiscrete finite element model of the equations using the pressure–velocity formulation.

11.2. Develop the semidiscrete finite element model of the equations in Problem 11.1 using the penalty function formulation.

11.3. Write the fully discretized finite element equations of the finite element models in Problems 11.1 and 11.2. Use the α family of approximation.

11.4. The equations governing unsteady slow flow of viscous incompressible fluids in the (x, y) plane can be expressed in terms of the vorticity ζ and stream function ψ:

$$\rho\frac{\partial \zeta}{\partial t} - \mu\nabla^2\zeta = 0, \qquad \zeta - \nabla^2\psi = 0$$

Develop the semidiscrete finite element model of these equations. Discuss the meaning of the secondary variables. Use the α family of approximation to reduce the ordinary differential equations to algebraic equations.

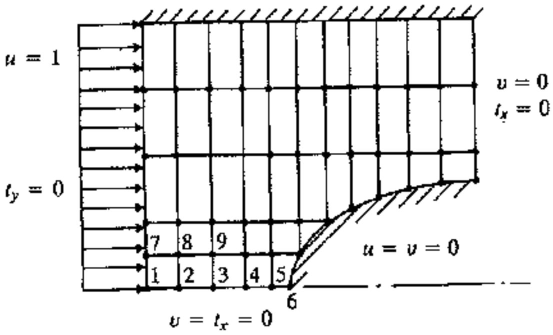

FIGURE P11.5

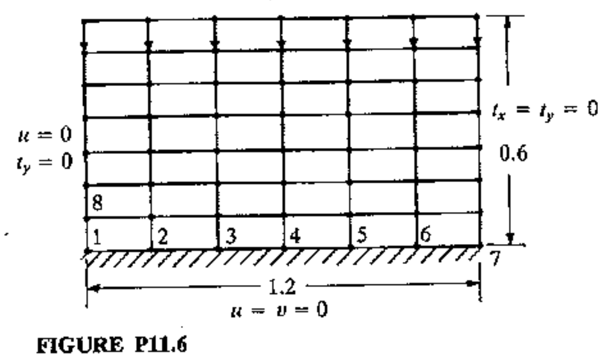

FIGURE P11.6

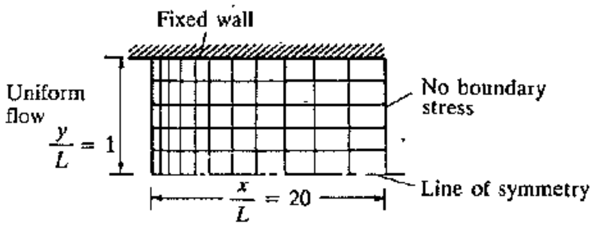

FIGURE P11.7

11.5–11.7. For the viscous flow problems given in Figs. P11.5–P11.7, give the specified primary and secondary degrees of freedom and their values.

11.8. Consider the flow of a viscous incompressible fluid in a square cavity (Fig. P11.8). The flow is induced by the movement of the top wall (or lid) with a constant velocity $u = 1.0$. For a 4×4 mesh of linear elements, identify the primary and secondary degrees of freedom.

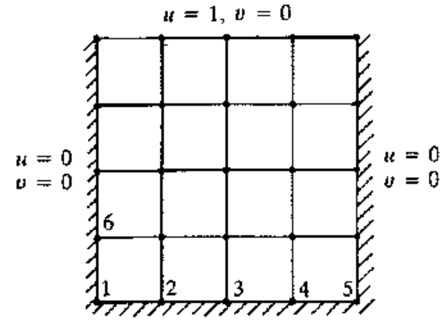

FIGURE P11.8

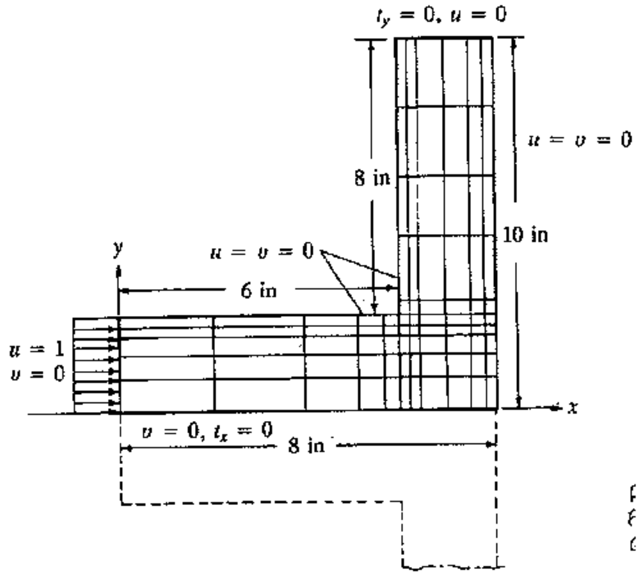

FIGURE P11.9

11.9. Consider the flow of a viscous incompressible fluid in a 90° plane tee. Using the symmetry and the mesh shown in Fig. P11.9, write the specified primary and secondary variables for the computational domain.

11.10. Repeat Problem 11.9 for the geometry shown in Fig. P11.10.

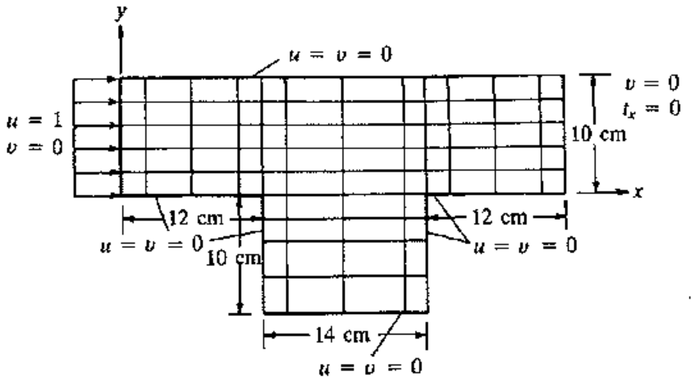

FIGURE P11.10

REFERENCES FOR ADDITIONAL READING

(For references on fluid mechanics, see References for Additional Reading in Chapter 8.)

Babuska, I.: "The Finite Element Method with Lagrange Multipliers," *Numerical Mathematics*, vol. 20, pp. 179–192, 1973*a*.

———: "The Finite Element Method with Penalty," *Mathematics of Computation*, vol. 27, pp. 221–228, 1973*b*.

Bird, R. B., W. E. Stewart, and E. N. Lightfoot: *Transport Phenomena*, John Wiley, New York, 1960.

Ciarlet, P. G.: *The Finite Element Method for Elliptic Problems*, North-Holland, Amsterdam, 1978.

Courant, R.: "Variational Methods for the Solution of Problems of Equilibrium and Vibrations," *Bulletin of the American Mathematical Society*, vol. 49, pp. 1–23, 1943.

Hestenes, M. R.: *Calculus of Variations and Optimal Control*, John Wiley, New York, 1966.

———: *Optimization Theory: The Finite Dimensional Case*, John Wiley, New York, 1975.

Hughes, J. T. R.: *The Finite Element Method (Linear, Static and Dynamic Finite Element Analysis)*, Prentice-Hall, Englewood Cliffs, NJ, 1987).

Ladyzhenskaya, O. A.: *The Mathematical Theory of Viscous Incompressible Flow*, 2d ed. (translated from the Russian by R. A. Silverman), Gordon and Breach, New York, 1969.

Nadai, A.: *Theory of Flow and Fracture of Solids*, vol. II, McGraw-Hill, New York, 1963.

Oden, J. T.: "RIP methods for Stokesian flows," in *Finite Element Method in Flow Problems*, vol. IV, eds. R. H. Gallagher, O. C. Zienkiewicz, J. T. Oden, and D. Norrie, John Wiley, London, 1982.

——— and G. F. Carey: *Finite Elements, Mathematical Aspects*, vol. IV, Prentice-Hall, Englewood Cliffs, NJ, 1983.

Polyak, B. T.: "The Convergence Rate of the Penalty Function Method," *USSR Computational Mathematics and Mathematical Physics*, vol. 11, pp. 1–12, 1971).

Reddy, J. N.: "On the Accuracy and Existence of Solutions to Primitive Variable Models of Viscous Incompressible Fluids, *International Journal of Engineering Science*, vol. 16, pp. 921–929, 1978.

———: "On the Finite Element Method with Penalty for Incompressible Fluid Flow Problems," in *The Mathematics of Finite Elements and Applications* III, ed. J. R. Whiteman, Academic Press, New York, 1979*a*.

———: *Applied Functional Analysis and Variational Methods in Engineering*, McGraw-Hill, New York, 1986; Krieger, Melbourne, FL, 1991.

Schlichting, H.: *Boundary-Layer Theory* (translated by J. Kestin), 7th ed., McGraw-Hill, New York, 1979.

CHAPTER
12

BENDING OF ELASTIC PLATES

12.1 INTRODUCTION

The word "plate" refers to solid bodies that are bounded by two parallel planes whose lateral dimensions are large compared with the separation between them. Geometrically, plates are similar to the plane elastic bodies considered in Chapter 10; however, plates are subjected to transverse loads (i.e., loads perpendicular to the plane of the plate). A plate is a two-dimensional analog of a beam. Therefore, the deformation of a plate can be described by *classical plate theory* or by *first-order shear deformation theory.* Classical plate theory is an extension of the Euler–Bernoulli beam theory to plates, and is known as the *Kirchhoff plate theory.* First-order shear deformation theory is an extension of the Timoshenko beam theory, and is known as the *Hencky–Mindlin plate theory.* A review of these plate theories and other refined theories can be found in Reddy (1984, 1990*a*, *b*).

Classical plate theory is based on the assumptions that a straight line perpendicular to the plane of the plate is (1) inextensible, (2) remains straight, and (3) rotates such that it remains perpendicular to the tangent to the deformed surface (see Fig. 12.1*a*). These assumptions are equivalent to specifying

$$\epsilon_z = 0, \qquad \epsilon_{yz} = 0, \qquad \epsilon_{xz} = 0 \tag{12.1}$$

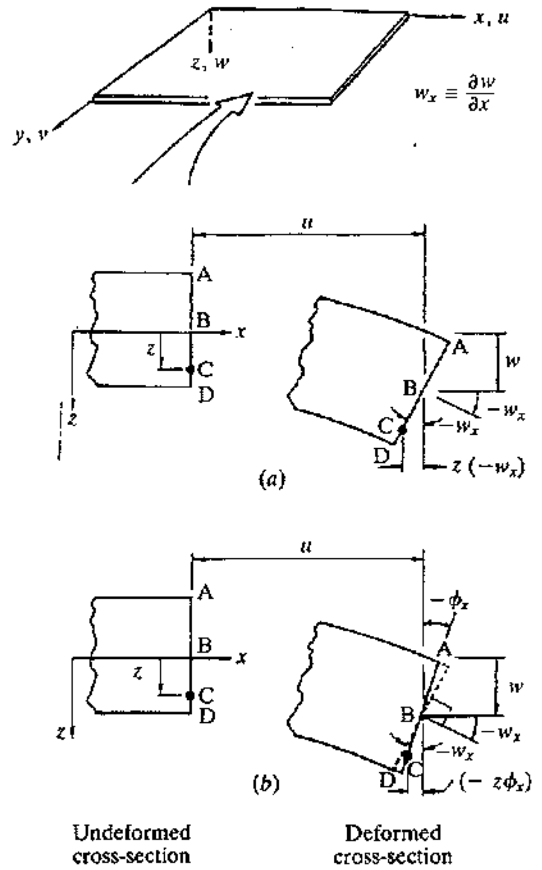

FIGURE 12.1
Geometry of the undeformed and deformed (x, z) plane for (*a*) classical plate theory (CPT) and (*b*) first-order shear deformation plate theory (FSDT).

In the first-order shear deformation theory, the normality condition, assumption (3), is removed (see Fig. 12.1*b*), resulting in a constant state of transverse shear strains through the thickness and zero transverse normal strain:

$$\epsilon_z = 0, \qquad \epsilon_{yz} = \epsilon_{yz}(x, y), \qquad \epsilon_{xz} = \epsilon_{xz}(x, y) \tag{12.2}$$

In this section, we briefly review the governing equations of these two theories and develop their finite element models. Let us consider a plate made up of several finite elements. The volume of a typical element is $V^e = \Omega^e \times (-\frac{1}{2}h_e, \frac{1}{2}h_e)$, where Ω^e denotes the midplane of the element and h_e is its thickness. The boundary of Ω^e is denoted by Γ^e. A plate of nonuniform thickness can be approximated by elements of uniform thickness. We assume that the midplanes of all elements are in the same plane Ω, the midplane of the plate.

12.2 CLASSICAL PLATE MODEL

12.2.1 Displacement Field

The classical theory of plates is based on the displacement field (see Fig. 12.1*a*)

$$\boxed{\begin{aligned}&u_1(x, y, z, t) = u - z\frac{\partial w}{\partial x}, \qquad u_2(x, y, z, t) = v - z\frac{\partial w}{\partial y}\\ &u_3(x, y, z, t) = w(x, y, t)\end{aligned}} \tag{12.3}$$

where (u_1, u_2, u_3) denote the displacements of the point (x, y, z) along the x, y and z directions, and (u, v, w) represent displacements of a point on the midplane $(x, y, 0)$ at time t. The equations of motion of the plate can be derived using the principle of virtual displacements [see Reddy (1984)], which also provides the weak form for the finite element model. For a linear theory based on infinitesimal strains and orthotropic materials, the in-plane displacements (u, v) are uncoupled from the transverse deflection. The in-plane displacements (u, v) are governed by the plane elasticity equations discussed in Chapter 10. Hence, we discuss only the equations governing the (bending) deflection w and the associated finite element model.

The linear strains due to the displacement w in (12.3) are

$$\begin{Bmatrix}\epsilon_x\\ \epsilon_y\\ 2\epsilon_{xy}\end{Bmatrix} = -z\begin{Bmatrix}\dfrac{\partial^2 w}{\partial x^2}\\[2mm] \dfrac{\partial^2 w}{\partial y^2}\\[2mm] 2\dfrac{\partial^2 w}{\partial x\,\partial y}\end{Bmatrix} \tag{12.4}$$

and $\epsilon_{xz} = 0$, $\epsilon_{yz} = 0$, and $\epsilon_z = 0$.

12.2.2 Virtual Work Statement

The principle of virtual displacements for the time-dependent case is

$$\begin{aligned}0 = &\int_{V^e}\left[\rho z^2\left(\frac{\partial \delta w}{\partial x}\frac{\partial^3 w}{\partial x\,\partial t^2} + \frac{\partial \delta w}{\partial y}\frac{\partial^3 w}{\partial y\,\partial t^2}\right) + \rho\,\delta w\frac{\partial^2 w}{\partial t^2}\right.\\ &\left. + \delta\epsilon_x\,\sigma_x + \delta\epsilon_y\,\sigma_y + 2\,\delta\epsilon_{xy}\,\sigma_{xy}\right]dV\\ &- \int_{\Omega^e} f\,\delta w\,dx\,dy - \oint_{\Gamma^e}\left(-M_n\frac{\partial \delta w}{\partial n} + V_n\,\delta w\right)ds\end{aligned} \tag{12.5}$$

Here the first three terms represent the virtual work done by the inertial forces in the three coordinate directions, while the remaining terms in the volume integral represent the virtual strain energy stored in the plate. The last two integrals, one defined on the midplane Ω^e and the other on the boundary Γ^e,

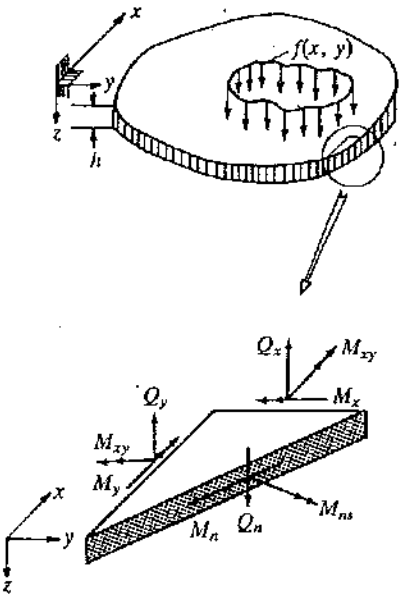

Use the right-hand-rule convention to determine the moment direction (shown with double arrow)

Boundary conditions for plates

Clamped	Simply supported 1	Simply supported 2	Free
$w=0$	$w=0$	$w=0$	$Q_n=0$
$\phi_s=0$	$M_{ns}=0$	$\phi_s=0$	$M_{ns}=0$
$\phi_n=0$	$M_n=0$	$M_n=0$	$M_n=0$

FIGURE 12.2
Geometry, moment, and shear force resultants, and various boundary conditions for a plate element.

denote the virtual work done by the transversely distributed load f and edge loads M_n and V_n (see Fig. 12.2). Since $V^e = \Omega^e \times (-\tfrac{1}{2}h_e, \tfrac{1}{2}h_e)$, and the displacements, strains, and stresses are separable into functions of x and y alone and functions of z,

$$F(x, y, z) = g(x, y)f(z) \tag{12.6a}$$

we can write the volume integral as

$$\int_{V^e} (\cdot)\, dV = \int_{\Omega^e} \int_{-h/2}^{h/2} (\cdot)\, dz\, dx\, dy \tag{12.6b}$$

Substitution of (12.3) and (12.4) for virtual displacements and strains into

(12.5) and integrating with respect to z, we obtain

$$\begin{aligned} 0 = \int_{\Omega^e} \bigg(& \delta w \, I_0 \frac{\partial^2 w}{\partial t^2} + \frac{\partial \delta w}{\partial x} I_2 \frac{\partial^3 w}{\partial x \, \partial t^2} + \frac{\partial \delta w}{\partial y} I_2 \frac{\partial^3 w}{\partial y \, \partial t^2} \\ & - M_x \frac{\partial^2 \delta w}{\partial x^2} - M_y \frac{\partial^2 \delta w}{\partial y^2} - 2M_{xy} \frac{\partial^2 \delta w}{\partial x \, \partial y} - f \, \delta w \bigg) \, dx \, dy \\ & - \oint_{\Gamma^e} \left(-M_n \frac{\partial \delta w}{\partial n} + V_n \, \delta w \right) ds \end{aligned} \tag{12.7}$$

where (M_x, M_y, M_{xy}) are the bending moments (see Fig. 12.2),

$$M_x = \int_{-h/2}^{h/2} \sigma_x z \, dz, \qquad M_y = \int_{-h/2}^{h/2} \sigma_y z \, dz, \qquad M_{xy} = \int_{-h/2}^{h/2} \sigma_{xy} z \, dz \tag{12.8}$$

and I_0 and I_2 are the mass moments of inertia,

$$I_0 = \int_{-h/2}^{h/2} \rho \, dz = \rho h, \qquad I_2 = \int_{-h/2}^{h/2} \rho z^2 \, dz = \tfrac{1}{12} \rho h^3 \tag{12.9}$$

Note that M_n and M_{ns} denote the normal and twisting moments on an edge, and V_n is the shear force. It can be shown that, for a linear orthotropic material, the bending moments are related to the derivatives of the transverse deflection w:

$$\boxed{\begin{aligned} & M_x = -\left(D_{11} \frac{\partial^2 w}{\partial x^2} + D_{12} \frac{\partial^2 w}{\partial y^2} \right), \qquad M_y = -\left(D_{12} \frac{\partial^2 w}{\partial x^2} + D_{22} \frac{\partial^2 w}{\partial y^2} \right) \\ & M_{xy} = -2D_{66} \frac{\partial^2 w}{\partial x \, \partial y} \end{aligned}} \tag{12.10}$$

where D_{ij} are the plate rigidities,

$$\begin{aligned} D_{11} &= \frac{E_1 h^3}{12(1 - \nu_{12}\nu_{21})}, \qquad D_{22} = \frac{E_2 h^3}{12(1 - \nu_{12}\nu_{21})} \\ D_{12} &= \frac{\nu_{12} E_2 h^3}{12(1 - \nu_{12}\nu_{21})}, \qquad D_{66} = \tfrac{1}{12} G_{12} h^3 \end{aligned} \tag{12.11}$$

The boundary forces M_n and V_n can be related to M_x, M_y, and M_{xy} by

$$\begin{aligned} & M_n = M_x n_x^2 + M_y n_y^2 + 2M_{xy} n_x n_y, \qquad V_n = \hat{Q}_n + \frac{\partial M_{ns}}{\partial s} \\ & \hat{Q}_n = Q_x n_x + Q_y n_y + I_2 \left(\frac{\partial^3 w}{\partial x \, \partial t^2} n_x + \frac{\partial^3 w}{\partial y \, \partial t^2} n_y \right) \\ & M_{ns} = (M_y - M_x) n_x n_y + M_{xy} (n_x^2 - n_y^2) \\ & Q_x = \frac{\partial M_x}{\partial x} + \frac{\partial M_{xy}}{\partial y}, \qquad Q_y = \frac{\partial M_{xy}}{\partial x} + \frac{\partial M_y}{\partial y} \end{aligned} \tag{12.12}$$

where (n_x, n_y) are the direction cosines of the unit normal on the boundary Γ^e. Substituting (12.10) into (12.7) yields the weak form of the problem:

$$\begin{aligned}0=\int_{\Omega^e}\bigg[&\delta w\, I_0\frac{\partial^2 w}{\partial t^2}+\frac{\partial \delta w}{\partial x}I_2\frac{\partial^3 w}{\partial x\,\partial t^2}+\frac{\partial \delta w}{\partial y}I_2\frac{\partial^3 w}{\partial y\,\partial t^2}\\&+\left(D_{11}\frac{\partial^2 w}{\partial x^2}+D_{12}\frac{\partial^2 w}{\partial y^2}\right)\frac{\partial^2 \delta w}{\partial x^2}+\left(D_{12}\frac{\partial^2 w}{\partial x^2}+D_{22}\frac{\partial^2 w}{\partial y^2}\right)\frac{\partial^2 \delta w}{\partial y^2}\\&+4D_{66}\frac{\partial^2 w}{\partial x\,\partial y}\frac{\partial^2 \delta w}{\partial x\,\partial y}-\delta w f\bigg]\,dx\,dy\\&-\oint_{\Gamma^e}\left(-M_n\frac{\partial \delta w}{\partial n}+V_n\,\delta w\right)ds\end{aligned}\tag{12.13}$$

It is informative to note that the differential equation governing w is

$$\boxed{\begin{aligned}&\frac{\partial^2}{\partial x^2}\left(D_{11}\frac{\partial^2 w}{\partial x^2}+D_{12}\frac{\partial^2 w}{\partial y^2}\right)+\frac{\partial^2}{\partial y^2}\left(D_{12}\frac{\partial^2 w}{\partial x^2}+D_{22}\frac{\partial^2 w}{\partial y^2}\right)\\&\quad+2\frac{\partial^2}{\partial x\,\partial y}\left(2D_{66}\frac{\partial^2 w}{\partial x\,\partial y}\right)-f+I_0\frac{\partial^2 w}{\partial t^2}-I_2\frac{\partial^2}{\partial t^2}\left(\frac{\partial^2 w}{\partial x^2}+\frac{\partial^2 w}{\partial y^2}\right)=0\end{aligned}}\tag{12.14}$$

Note that the expressions in parentheses in the first three terms are the bending moments $-M_x$, $-M_y$, and $-M_{xy}$, respectively [see (12.10)].

Of course, we can construct the weak form of (12.14) using the three-step procedure. We obtain

$$\begin{aligned}0=\int_{\Omega^e}\bigg[&\frac{\partial^2 v}{\partial x^2}\left(D_{11}\frac{\partial^2 w}{\partial x^2}+D_{12}\frac{\partial^2 w}{\partial y^2}\right)+\frac{\partial^2 v}{\partial y^2}\left(D_{12}\frac{\partial^2 w}{\partial x^2}+D_{22}\frac{\partial^2 w}{\partial y^2}\right)\\&+4D_{66}\frac{\partial^2 v}{\partial x\,\partial y}\frac{\partial^2 w}{\partial x\,\partial y}-vf+I_0 v\frac{\partial^2 w}{\partial t^2}+I_2\left(\frac{\partial v}{\partial x}\frac{\partial^3 w}{\partial x\,\partial t^2}+\frac{\partial v}{\partial y}\frac{\partial^3 w}{\partial y\,\partial t^2}\right)\bigg]\,dx\,dy\\&-\oint_{\Gamma^e}v\left[\left(\frac{\partial M_x}{\partial x}+\frac{\partial M_{xy}}{\partial y}\right)n_x+\left(\frac{\partial M_{xy}}{\partial x}+\frac{\partial M_y}{\partial y}\right)n_y+I_2\left(\frac{\partial^3 w}{\partial x\,\partial t^2}n_x+\frac{\partial^3 w}{\partial y\,\partial t^2}n_y\right)\right]ds\\&+\oint_{\Gamma^e}\left[\frac{\partial v}{\partial x}(M_x n_x+M_{xy}n_y)+\frac{\partial v}{\partial y}(M_{xy}n_x+M_y n_y)\right]ds\end{aligned}\tag{12.15}$$

where v denotes the weight function, which can be interpreted as the first variation, $\delta w = v$. Next, we convert the derivatives with respect to the rectangular coordinates (x, y) to those with respect to the local, normal and tangential, coordinates (n, s). We use the identities

$$\frac{\partial v}{\partial x}=n_x\frac{\partial v}{\partial n}-n_y\frac{\partial v}{\partial s},\qquad \frac{\partial v}{\partial y}=n_x\frac{\partial v}{\partial s}+n_y\frac{\partial v}{\partial n}\tag{12.16}$$

in the boundary integrals of (12.15). The boundary integrals become

$$-\oint_{\Gamma^e} v\hat{Q}_n\, ds + \oint_{\Gamma^e} \left(\frac{\partial v}{\partial n} M_n + \frac{\partial v}{\partial s} M_{ns}\right) ds \tag{12.17}$$

where $\hat{Q}_n$, M_n, and M_{ns} are the quantities defined in (12.12). The second term in the second integral is integrated by parts to yield the final expression

$$-\oint_{\Gamma^e} \left[v\left(\hat{Q}_n + \frac{\partial M_{ns}}{\partial s}\right) - \frac{\partial v}{\partial n} M_n\right] ds \tag{12.18}$$

The expression in parentheses is denoted by V_n, and its specification is known as the *Kirchhoff free-edge condition*. We assumed that $[vM_{ns}]_s = 0$.

12.2.3 Finite Element Model

An examination of the boundary terms in the weak form (12.13) suggests that the essential boundary conditions involve specifying the transverse deflection w and the normal derivative of w, which constitute the primary variables of the problem (cf. the Euler–Bernoulli beam model). Hence, the finite element interpolation of w must be such that w, $\partial w/\partial n$, and $\partial w/\partial s$ are continuous across the interelement boundaries. Note that $\partial/\partial n$ and $\partial/\partial s$ are related to the global derivatives $\partial/\partial x$ and $\partial/\partial y$ by the relations [the inverses of those in (12.16)]

$$\frac{\partial}{\partial n} = n_x \frac{\partial}{\partial x} + n_y \frac{\partial}{\partial y}, \qquad \frac{\partial}{\partial s} = n_x \frac{\partial}{\partial y} - n_y \frac{\partial}{\partial x} \tag{12.19}$$

Thus, the primary variables at the nodes should be [this also follows directly from (12.15)]

$$w, \quad \frac{\partial w}{\partial x}, \quad \frac{\partial w}{\partial y}$$

Finite elements that require continuity of w and its first derivatives are called C^1 elements.

Suppose that w is interpolated by expressions of the form

$$\boxed{w = \sum_{j=1}^{n} \Delta_j \phi_j(x, y)} \tag{12.20}$$

where Δ_j denote the nodal values of w and its derivatives, and $\phi_j(x, y)$ are the Hermite interpolation functions. A rectangular element with four nodes, with $(w, \partial w/\partial x, \partial w/\partial y)$ at each node, requires the 12-term ($n = 12$) polynomial approximation of w to obtain expressions for ϕ_j:

$$\begin{aligned} w &= a_1 + a_2 x + a_3 y + a_4 xy + a_5 x^2 + a_6 y^2 \\ &\quad + a_7 x^2 y + a_8 xy^2 + a_9 x^3 + a_{10} y^3 + a_{11} x^3 y + a_{12} xy^3 \end{aligned} \tag{12.21}$$

The polynomial is *not* a complete fourth-order polynomial; it is a complete third-order polynomial. For a three-node triangular element, the nine-term ($n = 9$) polynomial is selected to obtain ϕ_i:

$$w = a_1 + a_2 x + a_3 y + a_4 xy + a_5 x^2 + a_6 y^2 + a_7(x^2 y + xy^2) + a_8 x^3 + a_9 y^3 \tag{12.22}$$

This is an incomplete third-order polynomial, because x^2y and y^2x do not vary independently.

Some comments are in order on the interelement continuity of w and $\partial w/\partial n$ for the four-node rectangular element ($n = 12$) and three-node triangular element ($n = 9$). First let us consider the rectangular element. We note from (12.21) that w varies as a cubic along any line $x = \text{constant}$ or $y = \text{constant}$. Along a given side, there are two nodes and two values (w and its normal derivative) per node to define the cubic variation uniquely. Hence, w is uniquely defined along the element boundary and is continuous along interelement boundaries. The normal derivative, say, $\partial w/\partial x$ on a line $x = \text{constant}$, also varies as a cubic function of y along the side. Since only two values of $\partial w/\partial x$ are available on the line, the cubic variation cannot be uniquely defined, and the normal slope continuity is not satisfied. In addition, $\partial^2 w/\partial x\,\partial y$ is not single-valued at the corner points of the element. Elements that violate any of the continuity conditions are known as *nonconforming elements*. Thus the four-node rectangular element with w represented by (12.21) is a nonconforming element. We denote it as CPT(N). Despite this deficiency, the element is known to give good results. A similar discussion leads to the conclusion that the three-node triangular element is nonconforming. In addition, the triangular element is found to have convergence problems and singular behavior for certain meshes. The triangular plate bending elements will not be discussed in this study. The four-node element with (w, $\partial w/\partial x$, $\partial w/\partial y$, $\partial^2 w/\partial x\,\partial y$) as nodal degrees of freedom requires a complete quartic polynomial (obtained from the tensor products of the 1-D Hermite cubic polynomials). This element is a conforming element, and it is denoted as CPT(C). The conforming and nonconforming rectangular plate elements are shown in Fig. 12.3(a). The interpolation functions for the two rectangular elements are listed in Table 9.1. For further discussion on various plate bending elements, the reader is referred to Zienkiewicz and Taylor (1991) and references therein.

Substitution of (12.20) for w and $\delta w = \phi_i$ ($i = 1, 2, \ldots, n$) into (12.13) gives the finite element model

$$[M^e]\{\ddot{\Delta}^e\} + [K^e]\{\Delta^e\} = \{f^e\} + \{Q^e\} \tag{12.23a}$$

where

$$\begin{aligned} K_{ij}^e = \int_{\Omega^e} \bigg[& D_{11} \frac{\partial^2 \phi_i}{\partial x^2} \frac{\partial^2 \phi_j}{\partial x^2} + D_{12} \left(\frac{\partial^2 \phi_i}{\partial x^2} \frac{\partial^2 \phi_j}{\partial y^2} + \frac{\partial^2 \phi_i}{\partial y^2} \frac{\partial^2 \phi_j}{\partial x^2} \right) \\ & + D_{22} \frac{\partial^2 \phi_i}{\partial y^2} \frac{\partial^2 \phi_j}{\partial y^2} + 4 D_{66} \frac{\partial^2 \phi_i}{\partial x\,\partial y} \frac{\partial^2 \phi_j}{\partial x\,\partial y} \bigg] \,dx\,dy \end{aligned} \tag{12.23b}$$

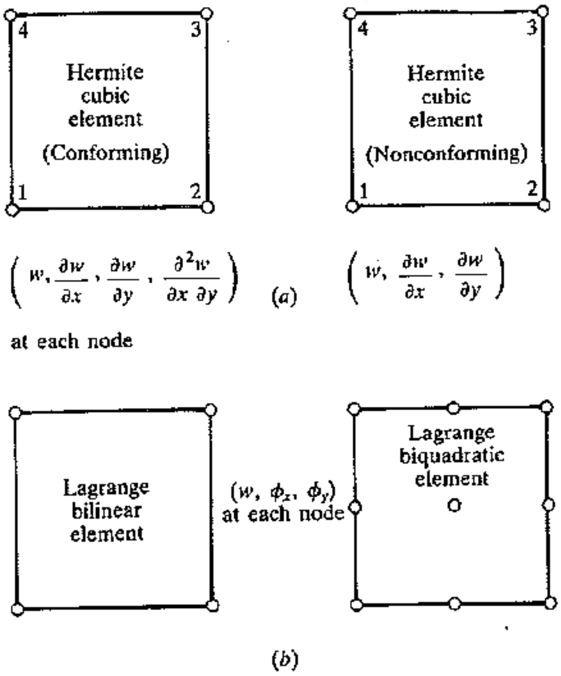
4
3
Hermite cubic element
(Conforming)
1
2
4
3
Hermite cubic element
(Nonconforming)
1
2
$\left(w, \frac{\partial w}{\partial x}, \frac{\partial w}{\partial y}, \frac{\partial^2 w}{\partial x\,\partial y}\right)$
at each node
(a)
$\left(w, \frac{\partial w}{\partial x}, \frac{\partial w}{\partial y}\right)$
Lagrange bilinear element
(w, ϕ_x, ϕ_y)
at each node
Lagrange biquadratic element
(b)

FIGURE 12.3
Finite elements for (*a*) displacement and (*b*) shear deformation models of plates.

$$M^e_{ij} = \int_{\Omega^e}\left[I_0\phi_i\phi_j + I_2\left(\frac{\partial\phi_i}{\partial x}\frac{\partial\phi_j}{\partial x}+\frac{\partial\phi_i}{\partial y}\frac{\partial\phi_j}{\partial y}\right)\right]dx\,dy$$

$$f^e_i = \int_{\Omega^e} f\phi_i\,dx\,dy, \qquad Q^e_i = \oint_{\Gamma^e}\left(-M_n\frac{\partial\phi_i}{\partial n}+V_n\phi_i\right)ds$$

The rotatory inertia, $I_2 = \frac{1}{12}\rho h^3$, where h is the plate thickness, is neglected in most books. This completes the development of the classical plate bending finite element.

12.3 SHEAR DEFORMABLE PLATE MODEL

12.3.1 Displacement Field

Of all the shear deformation plate theories available in the literature [see Reddy (1989, 1990*a*, *b*) for reviews], first-order shear deformation theory (FSDT) is the one most commonly used in the modeling of thick plates. The first-order theory is based on the displacement field (see Fig. 12.1*b*)

$$\boxed{u_1 = u + z\phi_x, \qquad u_2 = v + z\phi_y, \qquad u_3 = w} \tag{12.24}$$

where (u, v, w) are the displacements of a point $(x, y, 0)$, and ϕ_x and ϕ_y are the rotations of the transverse normal about the y and $-x$ axes, respectively. Once again, we develop the equations governing the bending deflections (w, ϕ_x, ϕ_y) only, because the in-plane displacements (u, v) are uncoupled from (w, ϕ_x, ϕ_y).

The bending strains associated with (12.24) are

$$\begin{Bmatrix} \epsilon_x \\ \epsilon_y \\ 2\epsilon_{xy} \\ 2\epsilon_{xz} \\ 2\epsilon_{yz} \end{Bmatrix} = \begin{Bmatrix} z\,\partial\phi_x/\partial x \\ z\,\partial\phi_y/\partial y \\ z(\partial\phi_x/\partial y + \partial\phi_y/\partial x) \\ \phi_x + \partial w/\partial x \\ \phi_y + \partial w/\partial y \end{Bmatrix} \tag{12.25}$$

Note that the transverse shear strains are nonzero and $\epsilon_z = 0$.

12.3.2 Virtual Work Statement

Substituting the displacement field (12.24) and strains (12.25) into the statement of the principle of virtual displacements, we obtain

$$\begin{aligned} 0 = {} & \int_{V^e} \left(\delta\phi_x\, \rho z^2 \frac{\partial^2 \phi_x}{\partial t^2} + \delta\phi_y\, \rho z^2 \frac{\partial^2 \phi_y}{\partial t^2} + \delta w\, \rho \frac{\partial^2 w}{\partial t^2} + \delta\epsilon_x\, \sigma_x + \delta\epsilon_y\, \sigma_y \right. \\ & \left. + 2\,\delta\epsilon_{xy}\, \sigma_{xy} + 2\,\delta\epsilon_{xz}\, \sigma_{xz} + 2\,\delta\epsilon_{yz}\, \sigma_{yz} \right) dV - \int_{\Omega^e} \delta w\, f\, dx\, dy \\ & - \oint_{\Gamma^e} (\delta\phi_n\, M_n + \delta\phi_s\, M_{ns} + \delta w\, Q_n)\, ds \\ = {} & \int_{\Omega^e} \left[I_0\, \delta w \frac{\partial^2 w}{\partial t^2} + I_2 \left(\delta\phi_x \frac{\partial^2 \phi_x}{\partial t^2} + \delta\phi_y \frac{\partial^2 \phi_y}{\partial t^2} \right) + M_x \frac{\partial \delta\phi_x}{\partial x} + M_y \frac{\partial \delta\phi_y}{\partial y} \right. \\ & + M_{xy} \left(\frac{\partial \delta\phi_x}{\partial y} + \frac{\partial \delta\phi_y}{\partial x} \right) + Q_x \left(\delta\phi_x + \frac{\partial \delta w}{\partial x} \right) \\ & \left. + Q_y \left(\delta\phi_y + \frac{\partial \delta w}{\partial y} \right) - \delta w\, f \right] dx\, dy \\ & - \oint_{\Gamma^e} (\delta\phi_n\, M_n + \delta\phi_s\, M_{ns} + \delta w\, Q_n)\, ds \end{aligned} \tag{12.26}$$

where M_n, M_{ns}, and Q_n are defined by (12.12), and

$$\begin{gathered} Q_x = \int_{-h/2}^{h/2} \sigma_{xz}\, dz = A_{55} \left(\phi_x + \frac{\partial w}{\partial x} \right), \qquad Q_y = \int_{-h/2}^{h/2} \sigma_{yz}\, dz = A_{44} \left(\phi_y + \frac{\partial w}{\partial y} \right) \\ M_x = D_{11} \frac{\partial \phi_x}{\partial x} + D_{12} \frac{\partial \phi_y}{\partial y}, \qquad M_y = D_{12} \frac{\partial \phi_x}{\partial x} + D_{22} \frac{\partial \phi_y}{\partial y} \\ M_{xy} = D_{66} \left(\frac{\partial \phi_x}{\partial y} + \frac{\partial \phi_y}{\partial x} \right) \\ Q_n = Q_x n_x + Q_y n_y, \qquad \phi_n = \phi_x n_x + \phi_y n_y, \qquad \phi_s = \phi_y n_x - \phi_x n_y \\ A_{44} = kG_{23} h, \qquad A_{55} = kG_{13} h \end{gathered} \tag{12.27}$$

Here k denotes the shear correction coefficient ($k = \frac{5}{6}$). This coefficient is introduced to account for the discrepancy between the distribution of transverse shear stresses of the first-order theory and the actual distribution (see Section 4.4 on the Timoshenko beam element). Equation (12.26) contains three weak forms for the three displacements (w, ϕ_x, ϕ_y):

$$
\begin{aligned}
0 &= \int_{\Omega^e}\left(I_0\,\delta w\frac{\partial^2 w}{\partial t^2} + Q_x\frac{\partial \delta w}{\partial x} + Q_y\frac{\partial \delta w}{\partial y} - f\,\delta w\right)dx\,dy - \oint_{\Gamma^e}\delta w\,Q_n\,ds\\
0 &= \int_{\Omega^e}\left(I_2\,\delta\phi_x\frac{\partial^2 \phi_x}{\partial t^2} + M_x\frac{\partial \delta\phi_x}{\partial x} + M_{xy}\frac{\partial \delta\phi_x}{\partial y} + Q_x\,\delta\phi_x\right)dx\,dy\\
&\quad - \oint_{\Gamma^e}\delta\phi_x\,(M_n n_x - M_{ns} n_y)\,ds \qquad\qquad (12.28)\\
0 &= \int_{\Omega^e}\left(I_2\,\delta\phi_y\frac{\partial^2 \phi_y}{\partial t^2} + M_{xy}\frac{\partial \delta\phi_y}{\partial x} + M_y\frac{\partial \delta\phi_y}{\partial y} + Q_y\,\delta\phi_y\right)dx\,dy\\
&\quad - \oint_{\Gamma^e}\delta\phi_y\,(M_n n_y + M_{ns} n_x)\,ds
\end{aligned}
$$

The governing differential equations of first-order shear deformation theory are

$$
\boxed{
\begin{aligned}
&\frac{\partial Q_x}{\partial x} + \frac{\partial Q_y}{\partial y} + f = I_0\frac{\partial^2 w}{\partial t^2}\\
&\frac{\partial M_x}{\partial x} + \frac{\partial M_{xy}}{\partial y} - Q_x = I_2\frac{\partial^2 \phi_x}{\partial t^2}\\
&\frac{\partial M_{xy}}{\partial x} + \frac{\partial M_y}{\partial y} - Q_y = I_2\frac{\partial^2 \phi_y}{\partial t^2}
\end{aligned}
}
\qquad (12.29)
$$

where (Q_x, Q_y, M_x, M_{xy}, M_y) are defined in (12.27). The three-step procedure of developing weak forms can be used to develop the weak forms of (12.29), which will be equivalent to those listed in (12.28). To see the equivalence, the following identities must be used:

$$
\begin{aligned}
&M_n n_x - M_{ns} n_y = M_x n_x + M_{xy} n_y \equiv \hat{M}_n\\
&M_n n_y + M_{ns} n_x = M_{xy} n_x + M_y n_y \equiv \hat{M}_{ns} \qquad (12.30)\\
&\phi_x = \phi_n n_x - \phi_s n_y, \qquad \phi_y = \phi_n n_y + \phi_s n_x
\end{aligned}
$$

12.3.3 Finite Element Model

We note from the boundary integrals that the primary variables of the theory are (w, ϕ_x, ϕ_y) and the secondary variables are (Q_n, M_n, M_{ns}) [or a linear combination of Q_x, Q_y, M_x, M_y and M_{xy}; see (12.12)]. Therefore, the Lagrange interpolation of w, ϕ_x and ϕ_y is admissible for the first-order theory.

We assume finite element interpolation of w, ϕ_x, and ϕ_y in the form

$$\boxed{w = \sum_{j=1}^{n} w_j \psi_j^1, \qquad \phi_x = \sum_{j=1}^{m} S_j^x \psi_j^2, \qquad \phi_y = \sum_{j=1}^{m} S_j^y \psi_j^2} \tag{12.31}$$

where ψ_j^1 and ψ_j^2 are interpolation functions used for w and (ϕ_x, ϕ_y), respectively. In general, ψ_j^1 and ψ_j^2 are polynomials of different degree. However, in the present study, we take $\psi_j^1 = \psi_j^2 \equiv \psi_j$. This choice, as discussed for the Timoshenko beam element, requires the use of reduced integration for the evaluation of stiffness coefficients associated with the transverse shear strains. Substituting (12.31) into (12.28), we obtain the finite element model

$$\begin{bmatrix} [M^{11}] & [0] & [0] \\ & [M^{22}] & [0] \\ \text{symmetric} & & [M^{33}] \end{bmatrix} \begin{Bmatrix} \{\ddot{w}\} \\ \{\ddot{S}^x\} \\ \{\ddot{S}^y\} \end{Bmatrix} + \begin{bmatrix} [K^{11}] & [K^{12}] & [K^{13}] \\ & [K^{22}] & [K^{23}] \\ \text{symmetric} & & [K^{33}] \end{bmatrix} \begin{Bmatrix} \{w\} \\ \{S^x\} \\ \{S^y\} \end{Bmatrix} = \begin{Bmatrix} \{F^1\} \\ \{F^2\} \\ \{F^3\} \end{Bmatrix} \tag{12.32a}$$

where

$$\begin{aligned}
&M_{ij}^{11} = I_0 M_{ij}, \qquad M_{ij}^{22} = M_{ij}^{33} = I_2 M_{ij}, \qquad M_{ij} = \int_{\Omega^e} \psi_i \psi_j \, dx\, dy \\
&K_{ij}^{11} = \int_{\Omega^e} \left(A_{55} \frac{\partial \psi_i}{\partial x} \frac{\partial \psi_j}{\partial x} + A_{44} \frac{\partial \psi_i}{\partial y} \frac{\partial \psi_j}{\partial y} \right) dx\, dy \\
&K_{ij}^{12} = \int_{\Omega^e} A_{55} \frac{\partial \psi_i}{\partial x} \psi_j \, dx\, dy, \qquad K_{ij}^{13} = \int_{\Omega^e} A_{44} \frac{\partial \psi_i}{\partial y} \psi_j \, dx\, dy \\
&K_{ij}^{22} = \int_{\Omega^e} \left(D_{11} \frac{\partial \psi_i}{\partial x} \frac{\partial \psi_j}{\partial x} + D_{66} \frac{\partial \psi_i}{\partial y} \frac{\partial \psi_j}{\partial y} + A_{55} \psi_i \psi_j \right) dx\, dy \\
&K_{ij}^{23} = \int_{\Omega^e} \left(D_{12} \frac{\partial \psi_i}{\partial x} \frac{\partial \psi_j}{\partial y} + D_{66} \frac{\partial \psi_i}{\partial y} \frac{\partial \psi_j}{\partial x} \right) dx\, dy \\
&K_{ij}^{33} = \int_{\Omega^e} \left(D_{66} \frac{\partial \psi_i}{\partial x} \frac{\partial \psi_j}{\partial x} + D_{22} \frac{\partial \psi_i}{\partial y} \frac{\partial \psi_j}{\partial y} + A_{44} \psi_i \psi_j \right) dx\, dy \\
&F_i^1 = \int_{\Omega^e} f \psi_i \, dx\, dy + \oint_{\Gamma^e} Q_n \psi_i \, dx, \qquad F_i^2 = \oint_{\Gamma^e} \hat{M}_n \psi_i \, dx, \qquad F_i^3 = \oint_{\Gamma^e} \hat{M}_{ns} \psi_i \, ds
\end{aligned} \tag{12.32b}$$

The element stiffness and mass matrices in (12.32a) are of order $3n \times 3n$, where n is the number of nodes per element. When the four-node rectangular element is used, the element matrices are of order 12×12, while they are 27×27 for the nine-node element (see Fig. 12.3b).

12.3.4 Shear Locking and Reduced Integration

It should be noted that the inclusion of the transverse shear strains (i.e., terms involving A_{44} and A_{55}) in the equations presents computational difficulties when the side-to-thickness ratio of the plate is large (i.e., when the plate becomes thin). For thin plates, the transverse shear strains $2\epsilon_{xz} = \phi_x + \partial w/\partial x$ and $2\epsilon_{yz} = \phi_y + \partial w/\partial y$ are negligible, and consequently the element stiffness matrix becomes stiff and yields erroneous results for the generalized displacements (w_i, S_i^x, S_i^y). This phenomenon is known as *shear locking*, and it can be interpreted as being caused by the inclusion of the following constraints into the variational form [see Reddy (1979, 1980) and Averill and Reddy (1990, 1992)]:

$$\phi_x + \frac{\partial w}{\partial x} = 0, \qquad \phi_y + \frac{\partial w}{\partial y} = 0 \tag{12.33}$$

The energy due to transverse shear strains (i.e., the penalty term) in the total potential energy of the shear deformable plate is given by

$$\frac{1}{2}\int_{\Omega^e}\left[A_{44}\left(\phi_y + \frac{\partial w}{\partial y}\right)^2 + A_{55}\left(\phi_x + \frac{\partial w}{\partial x}\right)^2\right] dx\,dy \tag{12.34}$$

The locking observed in the displacement finite element model of the first-order theory is the result of the fact that the discrete form of (12.33) is not satisfied when the plate is very thin. Of course, when the plate is thick, the relations (12.33) do not have to be satisfied, and the locking does not occur (at least, it is not severe enough to give completely wrong results). However, for thin plates, the constraints (12.33) are valid but not satisfied in the numerical model, and we therefore face the same problem as in the Timoshenko beam model. Therefore, we use the same remedy as before: reduced integration to evaluate stiffness coefficients involving the transverse shear terms. For example, when a four-node rectangular element is used, the one-point Gauss rule should be used to evaluate the shear energy terms (i.e., terms involving A_{44} and A_{55}), while the two-point Gauss rule should be used for all other terms. When an eight- or nine-node rectangular element is used, the two- and three-point Gauss rules should be used to evaluate the shear and bending terms, respectively. For the triangular elements, we use one- and three-point integrations for transverse shear stiffnesses in the linear and quadratic elements, respectively. However, in the present study, we shall not consider triangular plate bending elements.

12.4 EIGENVALUE AND TIME-DEPENDENT PROBLEMS

Equations (12.23*a*) and (12.32*a*) can be reduced to appropriate forms depending on the type of analysis. For static analysis, we set the inertia term $\{\ddot{\Delta}\}$ equal to zero and solve the problem

$$[K]\{\Delta\} = \{F\} \tag{12.35}$$

For natural vibration problems, we replace the inertia term by

$$\{\ddot{\Delta}\} = -\omega^2\{\Delta\} \qquad (\text{or } \{\Delta\} = \{\Delta_0\}e^{-i\omega t})$$

Then (12.23*a*) or (12.32*a*) takes the form of an eigenvalue problem:

$$([K^e] - \omega^2[M^e])\{\Delta_0\} = \{0\} \tag{12.36}$$

For buckling analysis (i.e., to determine the value of the in-plane compressive force at which the plate buckles), we replace the mass matrix in (12.36) with the stability matrix $[G]$, and ω^2 with the buckling load λ. This expression comes from the in-plane force due to the nonlinear inplane strains (underlined):

$$\begin{gathered}\epsilon_x = \underline{\frac{1}{2}\left(\frac{\partial w}{\partial x}\right)^2} - z\frac{\partial^2 w}{\partial x^2}, \qquad \epsilon_y = \underline{\frac{1}{2}\left(\frac{\partial w}{\partial y}\right)^2} - z\frac{\partial^2 w}{\partial y^2}, \\ 2\epsilon_{xy} = \underline{\frac{\partial w}{\partial x}\frac{\partial w}{\partial y}} - 2z\frac{\partial^2 w}{\partial x\,\partial y}\end{gathered} \tag{12.37}$$

For classical plate theory, $[G]$ is given by

$$G_{ij} = \int_{\Omega^e}\left[\bar{N}_x\frac{\partial\phi_i}{\partial x}\frac{\partial\phi_j}{\partial x} + \bar{N}_y\frac{\partial\phi_i}{\partial y}\frac{\partial\phi_j}{\partial y} + \bar{N}_{xy}\left(\frac{\partial\phi_i}{\partial x}\frac{\partial\phi_j}{\partial y} + \frac{\partial\phi_i}{\partial y}\frac{\partial\phi_j}{\partial x}\right)\right]dx\,dy \tag{12.38}$$

where $\bar{N}_x$, $\bar{N}_y$, and $\bar{N}_{xy}$ are the applied in-plane force resultants. The eigenvalue λ represents the ratio of the actual buckling load to the applied in-plane forces:

$$\lambda = N_x/\bar{N}_x = N_y/\bar{N}_y = N_{xy}/\bar{N}_{xy} \tag{12.39}$$

For first-order shear deformation theory, only $[M^{11}]$ in (12.32*a*) is replaced by $[G]$ (with $\phi_i = \psi_i$), and $[M^{22}]$ and $[M^{33}]$ are set equal to zero. Hence, the stability matrix is not positive definite, requiring special eigenvalue solvers for the first-order theory.

To solve a time-dependent problem, one must approximate the time derivatives in (12.23*a*) or (12.32*a*) to obtain algebraic equations relating $\{\Delta\}$ at time $t + \Delta t$ to $\{\Delta\}$ at time t, where Δt is the time step. In the Newmark integration scheme, the vectors $\{\dot{\Delta}\}$ and $\{\ddot{\Delta}\}$ at time $t = (s+1)\,\Delta t$ are approximated by the expressions

$$\begin{aligned}\{\dot{\Delta}\}_{s+1} &= \{\dot{\Delta}\}_s + ((1-\alpha)\{\ddot{\Delta}\}_s + \alpha\{\ddot{\Delta}\}_{s+1})\,\Delta t \\ \{\Delta\}_{s+1} &= \{\Delta\}_s + \{\dot{\Delta}\}_s\,\Delta t + \tfrac{1}{2}((1-\gamma)\{\ddot{\Delta}\}_s + \gamma\{\ddot{\Delta}\}_{s+1})(\Delta t)^2\end{aligned} \tag{12.40}$$

where α and γ are parameters that control the accuracy and stability of the scheme, and the subscript s indicates that the vectors are evaluated at the sth time step (i.e., at time $t = s\,\Delta t$).

Rearranging (12.23*a*) and (12.40), or (12.32*a*) and (12.40), we obtian [see (8.171)–(8.174)]

$$[\hat{K}]_{s+1}\{\Delta\}_{s+1} = \{\hat{F}\}_{s,s+1} \tag{12.41a}$$

where $\{\Delta\}_{s+1}$ denotes the value of $\{\Delta\}$ at time $t = (s+1)\,\Delta t$, s being the time step number, and

$$\begin{aligned}[\hat{K}]_{s+1} &= [K]_{s+1} + a_3[M]_{s+1}\\ \{\hat{F}\}_{s,s+1} &= \{F\}_{s+1} + [M]_{s+1}(a_3\{\Delta\}_s + a_4\{\dot{\Delta}\}_s + a_5\{\ddot{\Delta}\}_s) \qquad (12.41b)\\ a_3 &= \frac{2}{\gamma\,(\Delta t)^2}, \qquad a_4 = a_3\,\Delta t, \qquad a_5 = \frac{1}{\gamma} - 1\end{aligned}$$

Once the solution $\{\Delta\}$ is known at time $t_{s+1} = (s+1)\,\Delta t$, the first and second derivatives of $\{\Delta\}$ (velocity and acceleration) at t_{s+1} can be computed from

$$\begin{aligned}\{\ddot{\Delta}\}_{s+1} &= a_3(\{\Delta\}_{s+1} - \{\Delta\}_s) - a_4\{\dot{\Delta}\}_s - a_5\{\ddot{\Delta}\}_s,\\ \{\dot{\Delta}\}_{s+1} &= \{\dot{\Delta}\}_s + a_2\{\ddot{\Delta}\}_s + a_1\{\ddot{\Delta}\}_{s+1}\end{aligned} \qquad (12.42)$$

where $a_1 = \alpha\,\Delta t$ and $a_2 = (1-\alpha)\,\Delta t$.

12.5 EXAMPLES

Here we consider several numerical examples of plate bending, involving plates with different boundary conditions. Figure 12.2 shows various types of boundary conditions on an edge of a plate element. When the edge is parallel to the x or y axis, the normal and tangential components of a variable become the y and x (or x and y) components, respectively, of the variable. For classical plate theory, ϕ_n and ϕ_s in Fig. 12.2 must be replaced with $-\partial w/\partial n$ and $-\partial w/\partial s$, respectively. In all cases, the stresses are computed at the reduced Gauss points [see Barlow (1976, 1989)].

The first example deals with the effect of reduced integration on the deflections and stresses of a simply supported plate as computed using the shear deformable plate element.

Example 12.1. Consider a simply supported, isotropic, square plate subjected to a uniformly distributed transverse load f_0. We shall solve the problem using the classical and shear deformable plate bending elements. Owing to the biaxial symmetry, we need model only a quadrant of the plate. The essential boundary conditions at simply supported edges ($x = \frac{1}{2}a$ and $y = \frac{1}{2}a$), for the first-order theory, are (see Fig. 12.4)

$$\begin{aligned} w = 0, \quad \phi_y = 0 \quad \text{at } x = \tfrac{1}{2}a\\ w = 0, \quad \phi_x = 0 \quad \text{at } y = \tfrac{1}{2}a\end{aligned} \qquad (12.43)$$

The essential (or geometric) boundary conditions along the symmetry lines ($x = 0$ and $y = 0$) are

$$\phi_x(0, y) = \phi_y(x, 0) = 0 \qquad (12.44)$$

The natural or force boundary conditions, which enter the finite element equations through the forces $\{F^l\}$, are

$$\begin{aligned} Q_n = 0 \quad &\text{along } x = 0 \text{ and } y = 0\\ M_x = 0 \quad &\text{along } y = 0 \text{ and } x = \tfrac{1}{2}a\\ M_y = 0 \quad &\text{along } x = 0 \text{ and } y = \tfrac{1}{2}a\end{aligned} \qquad (12.45)$$

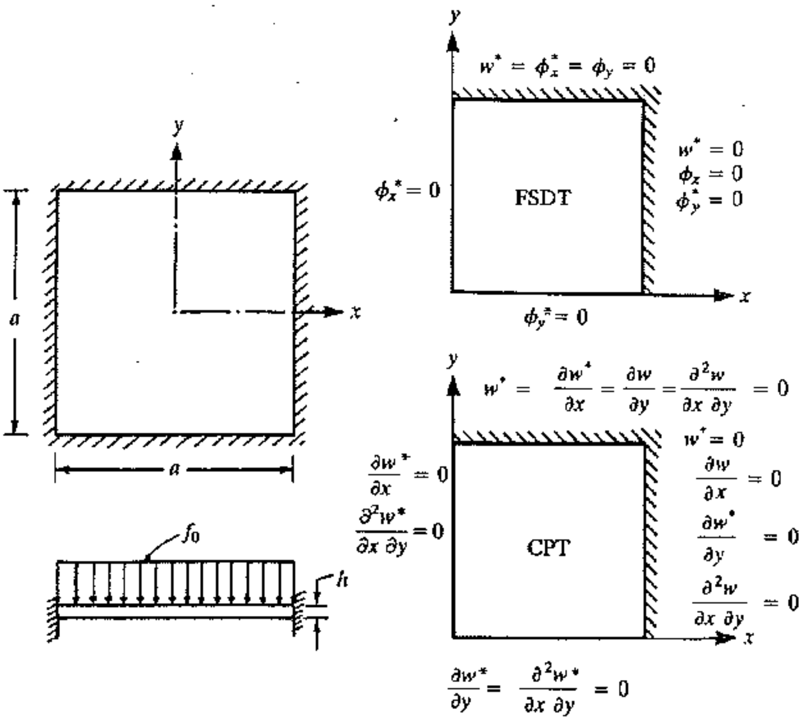
y
x
a
a
f_0
h
y
$w^* = \phi_x^* = \phi_y = 0$
$\phi_x^* = 0$
FSDT
$w^* = 0$
$\phi_x = 0$
$\phi_y^* = 0$
x
$\phi_y^* = 0$
y
$w^* = \frac{\partial w^*}{\partial x} = \frac{\partial w}{\partial y} = \frac{\partial^2 w}{\partial x \partial y} = 0$
$\frac{\partial w^*}{\partial x} = 0$
$\frac{\partial^2 w^*}{\partial x \partial y} = 0$
CPT
$w^* = 0$
$\frac{\partial w}{\partial x} = 0$
$\frac{\partial w^*}{\partial y} = 0$
$\frac{\partial^2 w}{\partial x \partial y} = 0$
x
$\frac{\partial w^*}{\partial y} = \frac{\partial^2 w^*}{\partial x \partial y} = 0$

FIGURE 12.4
Geometry and coordinate system used for a square plate: CPT, classical plate theory; FSDT, first-order shear deformation theory. Boundary conditions for simply supported (quantities with an asterisk only) and clamped edges are shown for both theories. Boundary conditions along the lines of symmetry are also shown.

The essential boundary conditions for a quadrant, when using the classical plate element, are shown in Fig. 12.4.

For a linear (four-node) rectangular element of shear deformation theory, the contribution of a uniformly distributed load f_0 is given by

$$f_i = \int_0^{h_x} \int_0^{h_y} f_0 \psi_i \, dx \, dy = \tfrac{1}{4} h_x h_y f_0 \tag{12.46}$$

where h_x and h_y are the plane-form dimensions of the element. This contribution goes to the first, fourth, seventh, and tenth nodal degrees of freedom of the element (corresponding to w). For classical plate theory, the nodal forces are computed using the definition

$$f_i = \int_{\Omega^e} f_0 \phi_i \, dx \, dy \tag{12.47}$$

Except for the nodal forces given by (12.46) and (12.47), all other specified nodal forces of the problem are zero.

The effect of reduced integration, thickness, and mesh on the center deflection and stress is investigated, and the results are presented in Table 12.1. The nondimen-

TABLE 12.1

The effect of reduced integration, thickness, and mesh refinement on the center deflection and stress† of a simply supported, isotropic ($\nu = 0.25$), square plate under a uniform transverse load f_0 (Example 12.1)

		1×1 linear		2×2 linear		4×4 linear		2×2 quadratic		Exact‡	
a/h	Integration	$\bar{w}$	$\bar{\sigma}_x$	$\bar{w}$	$\bar{\sigma}_x$	$\bar{w}$	$\bar{\sigma}_x$	$\bar{w}$	$\bar{\sigma}_x$	$\bar{w}$	$\bar{\sigma}_x$
10	F	0.964	0.0182	2.474	0.1185	3.883	0.216	4.770	0.2899	4.791	0.2762
	M	3.950	0.0953	4.712	0.2350	4.773	0.2661	4.799	0.2715		
20	F	0.270	0.0053	0.957	0.0476	2.363	0.1375	4.570	0.2683	4.625	0.2762
	M	3.669	0.0954	4.524	0.2350	4.603	0.2660	4.633	0.2715		
40	F	0.0695	0.0014	0.279	0.0140	0.9443	0.0558	4.505	0.2699	4.584	0.2762
	M	3.599	0.0953	4.375	0.2349	4.560	0.2661	4.592	0.2714		
50	F	0.0045	0.0001	0.182	0.0092	0.6515	0.0386	4.496	0.2667	4.579	0.2762
	M	3.590	0.0953	4.472	0.2350	4.555	0.2660	4.587	0.2714		
100	F	0.011	0.0002	0.047	0.0024	0.182	0.0108	4.482	0.2664	4.572	0.2762
	M	3.579	0.0953	4.465	0.235	4.548	0.2661	4.580	0.2715		
CPT(N)		5.643	0.2599	4.857	0.2738	4.643	0.2758	—	—	4.570	0.2762
CPT(C)		4.638	0.2616	4.574	0.2714	4.570	0.2750	—	—	4.570	0.2762

† $\bar{w} = wEh^3 \times 10^2/f_0a^4$, $\bar{\sigma}_x = \sigma_x(A, A, \pm\frac{1}{2}h)h^2/f_0a^2$, $A = \frac{1}{4}a$ (1×1 linear), $\frac{1}{8}a$ (2×2 linear), $\frac{1}{16}a$ (4×4 linear), $0.05283a$ (2×2 quadratic).

‡ From Reddy (1984).

sionalized center displacement and stress are defined as

$$\bar{w} = \frac{w(0, 0)E_2h^3 \times 10^2}{f_0a^4}, \qquad \bar{\sigma}_x = \left(\frac{h}{a}\right)^2 \frac{1}{f_0}\sigma_x(A, A, \pm\tfrac{1}{2}h) \tag{12.48}$$

where A is the Gauss-point location with respect to the (x, y) system located at the center of the plate:

	2×2 Q4	4×4 Q4	2×2 Q9
A	$0.125a$	$0.0625a$	$0.05283a$

where Q4 denotes the four-node rectangular element and Q9 the nine-node rectangular element.

In Table 12.1, F denotes full integration for all terms, and M denotes mixed integration: full integration for bending terms and reduced integration for the shear terms. The following observations can be made from the results of Table 12.1:

1. The nine-node element gives virtually the same results for full (3 × 3 Gauss rule) and mixed (3 × 3 and 2 × 2 Gauss rules) integrations. However, the results obtained using the mixed integration are closest to the exact solution.
2. Full integration gives less accurate results than mixed integration, and the error increases with an increase in side-to-thickness ratio. This implies that mixed integration is essential for thin plates, especially when modeled by lower-order elements.

3. Full integration results in smaller errors for quadratic elements and refined meshes than for linear elements and/or coarse meshes.
4. The conforming plate finite element CPT(C) gives accurate results when compared with the nonconforming plate element CPT(N).

Table 12.2 gives the natural frequencies of the simply supported plate, obtained using various elements and meshes. Note that classical plate theory overpredicts the natural frequencies.

The next example deals with a clamped square plate under a distributed transverse load. The mixed integration rule is used in the evaluation of stiffness coefficients of the FSDT model.

Example 12.2. Consider an isotropic ($\nu = 0.3$) square plate under a uniform load of intensity f_0. We shall consider clamped boundary conditions (see Fig. 12.4). Note that, for the case of the conforming displacement model based on CPT, we must also specify the boundary conditions on the cross-derivative $\partial^2 w/\partial x\,\partial y$. Once again, we exploit the biaxial symmetry and model only a quadrant of the plate.

Table 12.3 gives the center deflection $\bar{w} = w(0,0)D \times 10^2/f_0 a^4$ $[D = Eh^3/12(1-\nu^2)]$ and center normal stress $\bar{\sigma}_x = \sigma_x(A, A) \times 10/f_0$ as obtained using uniform meshes of the two types of elements: CPT(N) and CPT(C). In both models, the point

TABLE 12.2
The first three symmetric vibrational frequencies ($\bar{\omega} \times 10^{-2}$) of an isotropic simply supported square plate obtained using classical and shear deformation theories ($a/h = 10$)

Theory	Mesh	$\bar{\omega}_{11}$	$\bar{\omega}_{13}$	$\bar{\omega}_{33}$
FSDT	1 × 1 Q4	0.0746	—	—
	2 × 2 Q4	0.0608	0.4473	0.4810
	4 × 4 Q4	0.0579	0.2913	0.4654
	1 × 1 Q9	0.0575	0.4030	0.5476
	2 × 2 Q9	0.0570	0.2651	0.4342
	Exact	0.0569	0.2552	0.4217
CPT†	1 × 1 Q4	0.0535 (0.0597)	0.3118 (0.2912)	0.3565 (0.3360)
	2 × 2 Q4	0.0567 (0.0584)	0.2762 (0.4842)	0.4406 (0.4842)
	4 × 4 Q4	0.0579 (0.0584)	0.2792 (0.2821)	0.4665 (0.4900)
	Exact	0.0584	0.2829	0.4943

† Numbers without parentheses are computed using the noncomforming element and those in parentheses are computed using the conforming element $[\bar{\omega} = \omega(\rho/E)^{1/2} a^2/h]$.

TABLE 12.3
Comparison of the center deflection and normal stress of a clamped square plate under a uniformly distributed load as obtained using various finite element meshes (Example 12.2)

Mesh	Displacement model (CPT)	Displacement model (FSDT; $a/h = 10$)	
		Linear	Quadratic
	Center deflection $\bar{w}$		
1×1	0.1943	0.0357	—
2×2	0.1265	0.1459	0.1757
4×4	0.1266	0.1495	0.1586
Exact	0.1266		
	Center stress $\bar{\sigma}_x$		
1×1	2.443	0.000	—
2×2	1.415	1.142	1.321
4×4	1.381	1.333	1.345

$(x, y) = (A, A)$ is defined as follows:

Element type		Location A			
		1×1	$2\times 2\ (1\times 1)$	$4\times 4\ (2\times 2)$	$8\times 8\ (4\times 4)$
CPT model		$0.05635a$	$0.02817a$	$0.01409a$	$0.03125a$
FSDT model	linear	$0.25a$	$0.125a$	$0.0625a$	$0.03125a$
	quadratic	—	$0.1057a$	$0.0528a$	$0.02642a$

The distance is measured from the center of the plate. The numbers in parentheses above denote the mesh of quadratic Q9 (i.e., nine-node) elements. Clearly, both finite element models exhibit good convergence characteristics. The difference between the CPT and FSDT is attributed to the inclusion of transverse shear strains in FSDT.

The next example deals with a simply supported orthotropic plate under a uniformly distributed transverse load.

Example 12.3. Here we consider an orthotropic plate with the following (graphite–epoxy) material properties ($\nu_{21} = \nu_{12}E_2/E_1$):

$$E_1 = 31.8\times 10^6 \text{ psi},\quad E_2 = 1.02\times 10^6 \text{ psi},\quad \nu_{12} = 0.31,\quad G_{12} = G_{23} = G_{13} = 0.96 \text{ psi} \tag{12.49}$$

The nondimensionalized center deflection $\bar{w}$ and normal stress $\bar{\sigma}_x$ obtained using the conforming CPT(C) element and the FSDT element are compared in Table 12.4.

TABLE 12.4
Comparison of the center deflection ($\bar{w} = wH \times 10^3/f_0a^4$) and normal stress ($\bar{\sigma}_x = \sigma_x \times 10\,h^2/f_0a^2$) of a graphite–epoxy, simply supported square plate under a uniform transverse load (Example 12.3)

Mesh	Displacement model (CPT)	Displacement model (FSDT; $a/h = 10$) Linear	Displacement model (FSDT; $a/h = 10$) Quadratic
		Center deflection $\bar{w}$	
2×2	0.9220	1.2545	1.2715
4×4	0.9224	1.2186	1.2147
8×8	0.9224	1.2152	1.2147
Exact†	0.9225	1.215	
		Center stress $\bar{\sigma}_x$	
2×2	7.678	6.277	7.192
4×4	7.616	7.256	7.399
8×8	7.600	7.449	7.478
Exact†	7.595	7.512	

† From Reddy (1984); $H = D_{12} + 2D_{66}$.

The final example deals with the transient response of an isotropic plate subjected to a sudden uniform patch loading.

Example 12.4. Consider an isotropic ($\nu = 0.3$, $\rho = 1.0$), simply supported, rectangular plate ($a/b = \sqrt{2}$, $h/b = 0.2$) under a suddenly applied uniformly distributed load on a square ($c/b = 0.4$) area at the center:

$$a/b = \sqrt{2}, \qquad \Delta t = 0.01$$
$$f = f_0(x, y)H(t), \qquad \text{where } f_0(x, y) = \begin{cases} 1 & \text{for } 0 < x, y \leq 0.2 \\ 0 & \text{for } x, y > 0.2 \end{cases} \tag{12.50}$$

and $H(t)$ is the Heaviside unit step function. The geometry and boundary conditions are shown in Fig. 12.5. A nonuniform mesh of 4×4 nine-node shear deformation elements is used in a quadrant of the plate.

The center deflection and bending moments of the present linear analysis are compared with the analytical thick- and thin-plate solutions of Reismann and Lee (1969) in Fig. 12.6. We note significant difference between the solutions of the two theories. The present finite element solutions for the center deflection and bending moment are in excellent agreement with the thick-plate solution of Reismann and Lee. Since the bending moment in the finite element method is calculated at the Gauss points, it is not expected to match exactly with the analytical solution at the center of the plate.

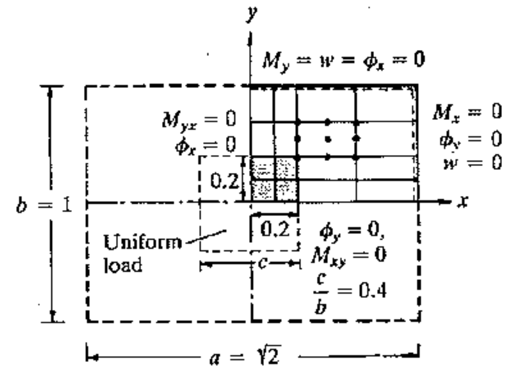

FIGURE 12.5
Domain, boundary conditions, and finite element mesh for the bending of a rectangular plate under a suddenly applied pulse loading at the central square area.

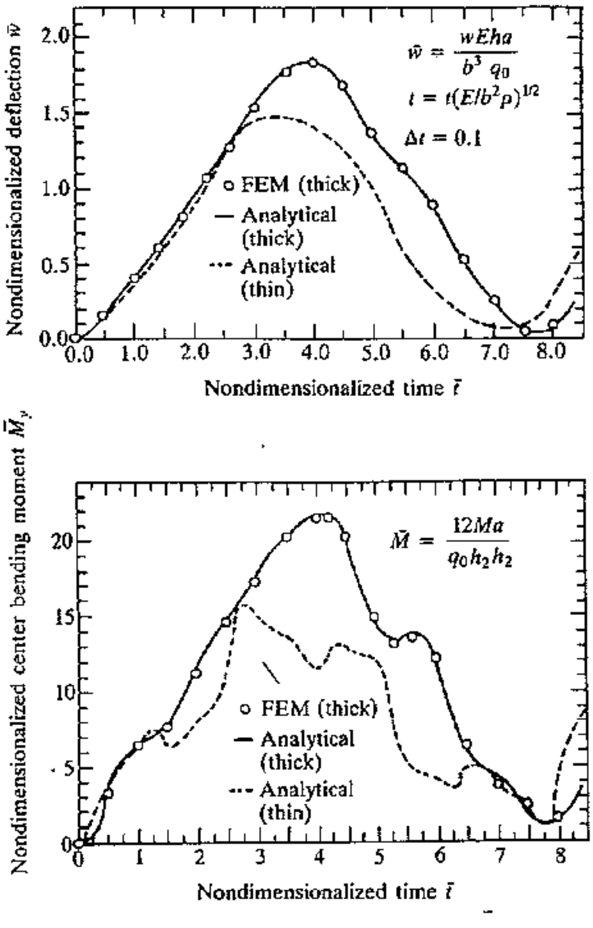

FIGURE 12.6
Comparison of the finite element solution with the analytical solution for a simply supported rectangular isotropic plate under a suddenly applied pulse loading at the central square area.

12.6 SUMMARY

Finite element models of the classical (i.e., Kirchhoff) and first-order shear deformation plate theories have been developed in this chapter. The classical plate theory requires C^1 continuity of the transverse deflection w (i.e., the deflection and its derivatives are continuous between elements), whereas first-order shear deformation theory requires C^0 continuity (i.e., only the variables are continuous between elements) of the generalized displacements (w, ϕ_x, ϕ_y). Triangular and rectangular elements with C^1 continuity have been discussed. Two four-node rectangular elements, one with (w, $\partial w/\partial x$, $\partial w/\partial y$) and another with (w, $\partial w/\partial x$, $\partial w/\partial y$, $\partial^2 w/\partial x\, \partial y$) as degrees of freedom, have been presented. The first does not satisfy continuity of the normal derivative along element sides, and is called a nonconforming element. The second is a conforming element. Linear and quadratic rectangular elements of first-order shear deformation theory have been developed. They require selective evaluation of the stiffness coefficients. The bending stiffness coefficients are evaluated using full integration and the transverse shear stiffness coefficients are evaluated using reduced integration to avoid the shear locking that occurs when these elements are applied to thin plates. Finite element models of vibration, stability, and static and dynamic response have been developed for the two theories.

PROBLEMS

12.1–12.9. For the plate bending problems (CPT and FSDT) given in Figs. P12.1–P12.9, give the specified primary and secondary degrees of freedom and their values for the 4×4 meshes shown. The dashed lines in the figures indicate simply supported boundary conditions: those of types "simply supported 1" and "simply supported 2" (see Fig. 12.2) are indicated by SS-1 and SS-2, respectively. Use E, ν, h, a, and b in formulating the data.

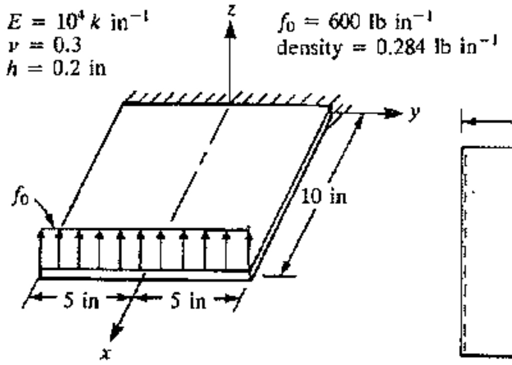

FIGURE P12.1

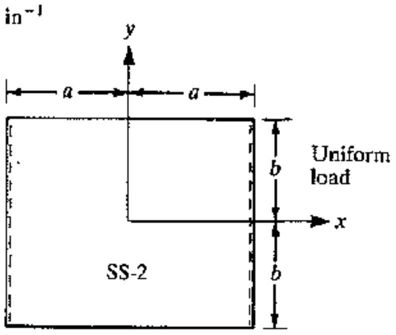

FIGURE P12.2

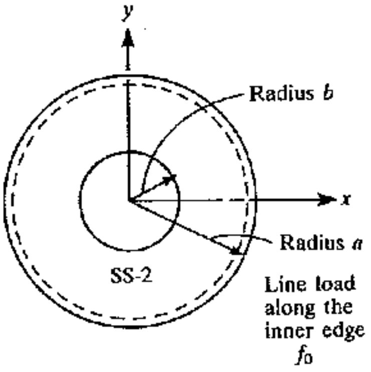

FIGURE P12.3

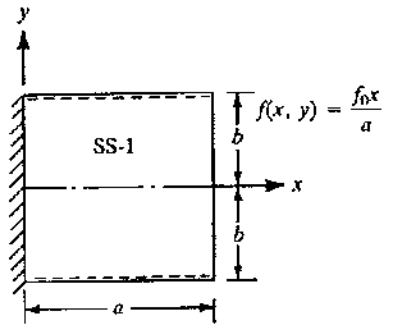

FIGURE P12.4

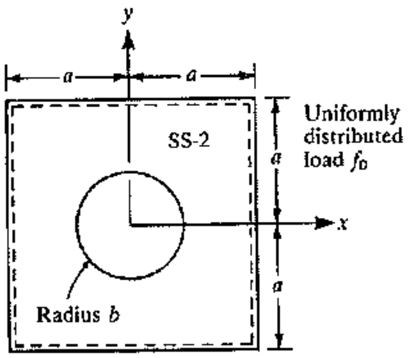

FIGURE P12.5

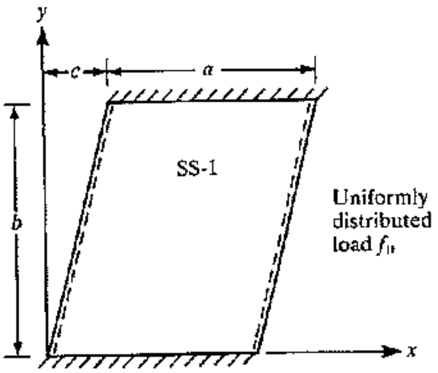

FIGURE P12.6

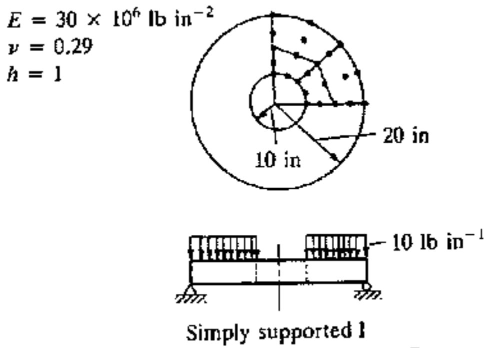

FIGURE P12.7

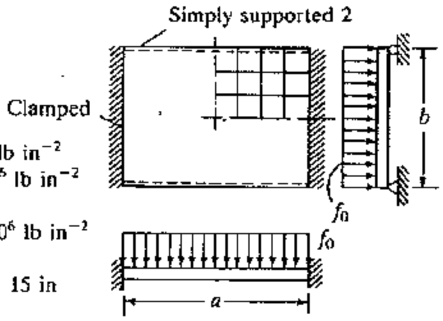

$E_1 = 30 \times 10^6$ lb in^{-2}
$E_2 = 0.75 \times 10^6$ lb in^{-2}
$\nu_{12} = 0.25$
$G_{12} = 0.375 \times 10^6$ lb in^{-2}
$h = 0.1a$
$a = 20$ in, $b = 15$ in

FIGURE P12.8

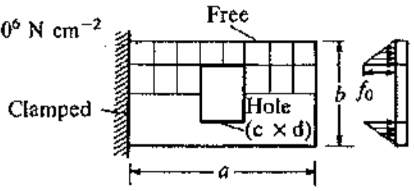

$E = 30 \times 10^6$ N cm^{-2}
$\nu = 0.3$
$h = 1$ cm
$a = 40$ cm
$b = 24$ cm
$c = 10$ cm
$d = 12$ cm

FIGURE P12.9

12.10. Give an algebraic form for the elements of the stiffness matrix (in a local coordinate system) for a thin plane elastic body subjected to both in-plane and transverse loads.

Hint: Combine the element matrices of the plane stress element with the plate bending element—analogous to the construction of a frame element from bar and beam elements.

12.11. Consider an isotropic annular plate ($E = 30 \times 10^6$ lb in^{-2}, $\nu = 0.29$) with the outer edges clamped and subjected to uniform loading (see Fig. P12.7). Formulate the necessary data for the problem.

12.12. Repeat Problem 12.11 for the case in which the plate is subjected to a load varying linearly with radial distance.

REFERENCES FOR ADDITIONAL READING

Averill, R. C., and J. N. Reddy: "On the Behavior of Plate Elements Based on the First-Order Shear Deformation Theory," *Engineering Computations,* vol. 7, pt. 1, pp. 57–74, 1990.

——— and ———: "An Assessment of Four-Noded Plate Finite Elements Based on a Generalized Third-Order Theory," *International Journal for Numerical Methods in Engineering,* vol. 33, pp. 1553–1572, 1992.

Barlow, J.: "Optimal Stress Locations in Finite Element Models," *International Journal for Numerical Methods in Engineering,* vol. 10, pp. 243–251, 1976.

———: "More on Optimal Stress Points—Reduced Integration Element Distortions and Error Estimation," *International Journal for Numerical Methods in Engineering,* vol. 28, pp. 1487–1504, 1989.

Dym, C. L., and I. H. Shames: *Solid Mechanics: A Variational Approach,* McGraw-Hill, New York, 1973.

Goudreau, G. L., and R. L. Taylor: "Evaluation of Numerical Integration Methods in Elastodynamics," *Journal of Computer Methods in Aplied Mechanics and Engineering*, vol. 2, pp. 69–97, 1973.

Hughes, T. J. R., and W. K. Liu: "Implicit–Explicit Finite Elements in Transient Analysis: Stability Theory, and Implementation and Numerical Examples," *Journal of Applied Mechanics*, vol. 45, pp. 371–378, 1978.

Jounson, D. E.: "A Proof of the Stability of the Hubolt Method," *Journal of the American Institute for Aeronautics and Astronautics*, vol. 4, pp. 1450–1451, 1966.

Krieg, R. D.: "Unconditional Stability in Numerical Time Integration Methods," *Journal of Applied Mechanics*, vol. 40, pp. 417–421, 1973.

Lax, P. D., and R. D. Richtmyer: "Survey of the Stability of Finite Difference Equations," *Communications in Pure and Applied Mathematics*, vol. 9, pp. 267–293, 1956.

Leech, J. W.: "Stability of Finite-Difference Equations for the Transient Response of a Flat Plate," *Journal of the American Institute for Aeronautics and Astronautics*, vol. 3, pp. 1172–1173 1965.

Levy, S., and W. D. Kroll: "Errors Introduced by Finite Space and Time Increments in Dynamic Response Computation," *Journal of Research, National Bureau of Standards*, vol. 51, pp. 57–68, 1953.

Nickell, R. E.: "On the Stability of Approximation Operators in Problems of Structural Dynamics," *International Journal for Solids and Structures*, vol. 7, pp. 301–319, 1971.

———: "Direct Integration in Structural Dynamics," *Journal of Engineering Mechanics Division, ASCE*, vol. 99, pp. 303–317, 1973.

Reddy, J. N.: "Simple Finite Elements with Relaxed Continuity for Nonlinear Analysis of Plates," in *Finite Element Methods in Engineering*, eds. A. P. Kabaila and V. A. Pulmano, pp. 265–281, The University of New South Wales, Sydney, 1979.

———: "A Penalty Plate Bending Element for the Analysis of Laminated Anisotropic Composite Plates," *International Journal for Numerical Methods in Engineering*, vol. 15, pp. 1187–1206, 1980.

———: "On the Solutions to Forced Motions of Rectangular Composite Plates," *Journal of Applied Mechanics*, vol. 49, pp. 403–408, 1982.

———: *Energy and Variational Methods in Applied Mechanics*, John Wiley, New York, 1984.

———: "A Review of Refined Theories of Laminated Composite Plates," *Shock and Vibration Digest*, vol. 22, pt. 7, pp. 3–17, 1990*a*.

———: "A General Non-Linear Third-Order Theory of Plates with Moderate Thickness," *Journal of Non-Linear Mechanics*, vol. 25, pp. 677–686, 1990*b*.

Reismann, H., and Y. Lee: "Forced Motions of Rectangular Plates," in *Developments in Theoretical and Applied Mechanics*, vol. 4, ed. D. Frederick, pp. 3–18, Pergamon Press, New York, 1969.

Szilard, R.: *Theory and Analysis of Plates*, Prentice-Hall, Englewood Cliffs, NJ, 1974.

Timoshenko, S., and S. Woinowsky-Krieger: *Theory of Plates and Shells*, 2d ed., McGraw–Hill, New York, 1959.

Tsay, C. S., and J. N. Reddy: "Bending, Stability, and Free Vibration of Thin Orthotropic Plates by Simplified Mixed Finite Elements," *Journal of Sound and Vibration*, vol. 59, pp. 307–311, 1978.

Tsui, T. Y., and P. Tong: "Stability of Transient Solution of Moderately Thick Plate by Finite Difference Method," *Journal of the American Institute for Aeronautics and Astronautics*, vol. 9, pp. 2062–2063, 1971.

Zienkiewicz, O. C., and R. L. Taylor: *The Finite Element Method*, vol. 1: *Linear Problems*, McGraw–Hill, New York, 1989.

——— and ———: *The Finite Element Method*, vol. 2: *Nonlinear Problems*, McGraw–Hill, New York, 1991.

———, ——— and J. M. Too: "Reduced Integration in General Analysis of Plates and Shells," *International Journal for Numerical Methods in Engineering*, vol. 3, pp. 275–290, 1972.

CHAPTER
13

COMPUTER IMPLEMENTATION

13.1 INTRODUCTION

In Chapter 7, we discussed some basic ideas concerning the development of a typical finite element program, and the use of FEM1DV2 in the solution of one-dimensional problems was illustrated via many example problems. Specific details of various logical units of a finite element program for one-dimensional problems were given. Most of the ideas presented there are also valid for two-dimensional problems. The imposition of the boundary conditions and the solution of the equations remain the same as in one-dimensional problems. Here we focus attention on the computer implementation of two-dimensional elements. The use of a model program FEM2DV2 (a revised and combined version of the FEM2D and PLATE programs in the first edition of the book) is discussed. The program FEM2DV2 contains linear and quadratic triangular and rectangular elements, and it can be used for the solution of heat conduction and convection problems, laminar flows of viscous incompressible fluids using the penalty function formulation, plane elasticity problems, and plate bending problems using classical and shear deformation theories. A flow chart of FEM2DV2 is given in Fig. 13.1.

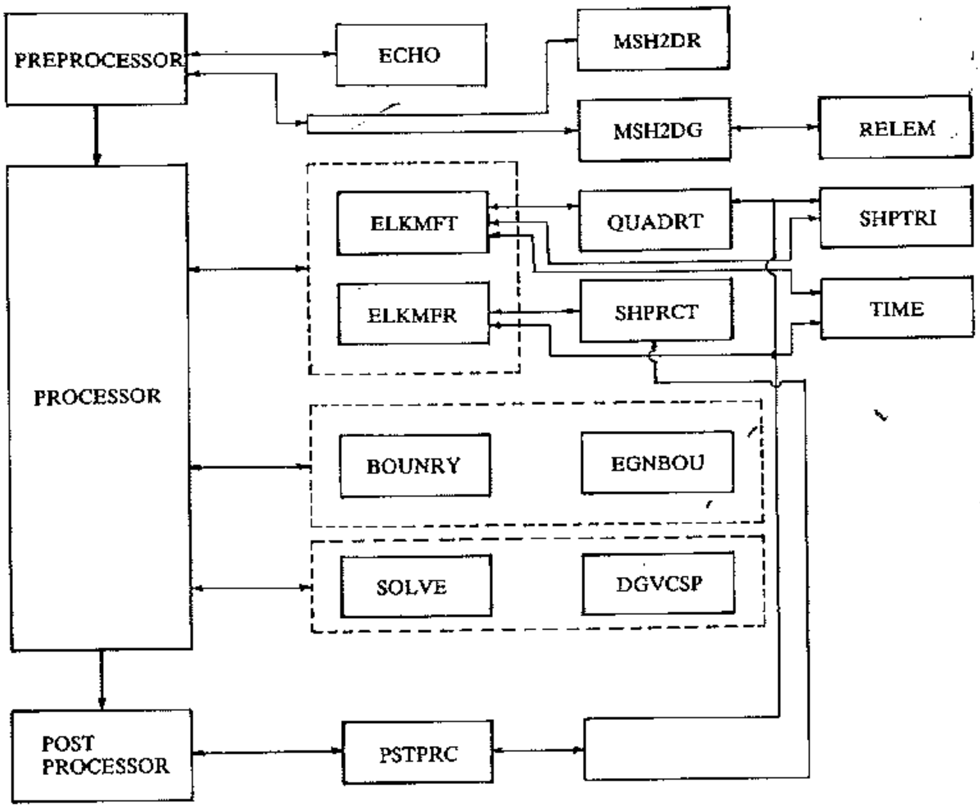

FIGURE 13.1

In two dimensions, the element calculations are more involved than in one dimension, owing to the following considerations:

1. Various geometric shapes of elements.
2. Single as well as multivariable problems.
3. Integrations performed over areas as opposed to along lines (for one-dimensional elements).
4. Mixed-order integrations used in certain formulations (shear-deformable plates and penalty function formulations of viscous incompressible fluids).

13.2 PREPROCESSOR

In the preprocessor unit, the program MSH2DR is used to generate triangular- and rectangular-element meshes of rectangular domains. The subroutine requires minimal input, but is not general enough to generate finite element meshes of arbitrary domains. The subroutine MSH2DG is more general, and can be used to generate meshes for nonrectangular domains. Of course, one

BOUNRY	Subroutine to impose specified boundary conditions on the primary and secondary variables when a steady-state or transient analysis is carried out.
DGVCSP	An IBM system-supplied subroutine to solve an eigenvalue problem of the type $[K]\{U\} = L(M)\{U\}$, where $[K]$ and $[M]$ are positive definite matrices.
ECHO	Subroutine to echo the input data to the program.
EGNBOU	Subroutine to impose specified boundary conditions on the primary variables when an eigenvalue problem is analyzed.
ELKMFR	Subroutine to compute the element $[K]$, $[M]$, and $\{F\}$ matrices and vectors for the rectangular elements.
ELKMFT	Subroutine to compute the element $[K]$, $[M]$, and $\{F\}$ matrices and vectors for the triangular elements.
MSH2DG	Subroutine to generate mesh for general domains.
MSH2DR	Subroutine to generate mesh for rectangular domains only.
PSTPRC	Subroutine to post-complete the solution, gradient of solution, and stresses.
QUADRT	Subroutine to generate the quadrature points and weights for the triangular elements.
RELEM	Subroutine called in MSH2DG to generate element data.
SHPRCT	Subroutine to compute the shape functions for linear and quadratic (eight- and nine-node) rectangular elements.
SHPTRI	Subroutine to compute the shape functions for linear and quadratic triangular elements.
SOLVE	Subroutine to solve a banded, symmetric system of algebraic equations.
TIME	Subroutine to compute the equivalent coefficient matrices and columen vectors for parabolic and hyperbolic equations when time-dependent analysis is carried out.

FIGURE 13.1 (Continued)

can use any other mesh generation program in place of MSH2DR or MSH2DG. The subroutines MSH2DR and MSH2DG generate the connectivity matrix (array NOD) and the global coordinates of the nodes (array GLXY). When the mesh generators cannot be used, the mesh information should be read in.

13.3 ELEMENT COMPUTATIONS: PROCESSOR

Element calculations for linear and quadratic triangular (ELKMFT) and quadrilateral (ELKMFR) elements can be carried out according to the developments presented in Chapters 8 and 9. The principal steps involved are as follows:

1. Development of a subroutine for the evaluation of the interpolation functions and their derivatives with respect to the global coordinates [see (9.42)–(9.45)].

2. Numerical integration of the coefficients of the element matrices using numerical quadrature formulas [see (9.54) and (9.67)].
3. Setting up of the element matrices required for the class of problems being solved (e.g., static, transient, and eigenvalue problems).

The subroutines SHPTRI and SHPRCT (called in a do-loop on the number of quadrature points) contain the expressions of the interpolation functions and their derivatives for various-order triangular (TRI) and rectangular (RCT) elements, respectively. The derivatives of the interpolation functions with respect to global coordinates [(9.42)] are also computed in these subroutines. The Fortran implementation of (9.42)–(9.45) is summarized below.

```
c     ------------------------------------------------------------------
c
c     DEFINITION OF THE VARIABLES
c
c     SF(I)........Interpolation function for node I of the element
c     DSF(J,I).....Derivative of SF(I) with respect to XI if J=1 and
c                  and ETA if J=2
c     GDSF(J,I)....Derivative of SF(I) with respect to  X if J=1 and
c                  and  Y  if J=2
c     ELXY(I,J)....Global coordinates of the element Ith node:
c                  J=1: the x coordinate; J=2: the y coordinate
c     GJ(I,J)......Jacobian matrix
c     GJINV(I,J)...Inverse of the jacobian matrix
c     DET..........Determinant of the Jacobian matrix
c     ------------------------------------------------------------------
c
c     Given the interpolation functions {SF} and their derivatives with
c     respect to the natural coordinates  [DSF], compute  the  Jacobian
c     matrix [GJ] [see Eqn. (9.44b)] and its inverse [GJINV]:
c
      DO 40 I = 1,2
      DO 40 J = 1,2
      GJ(I,J)  = 0.0
      DO 40 K = 1,NPE
   40 GJ(I,J)  = GJ(I,J) + DSF(I,K)*ELXY(K,J)
c
      DET = GJ(1,1)*GJ(2,2)-GJ(1,2)*GJ(2,1)
      GJINV(1,1) = GJ(2,2)/DET
      GJINV(2,2) = GJ(1,1)/DET
      GJINV(1,2) = -GJ(1,2)/DET
      GJINV(2,1) = -GJ(2,1)/DET
c
c     Compute the first derivatives of the interpolation functions with
c     respect to the global coordinates [GDSF] [see Eqn. (9.42)]:
c
          DO 50 I  = 1,2
          DO 50 J  = 1,NPE
          GDSF(I,J) = 0.0
          DO 50 K  = 1, 2
   50     GDSF(I,J) = GDSF(I,J) + GJINV(I,K)*DSF(K,J)
c     ------------------------------------------------------------------
```

The two-dimensional problems of interest to us here require the evaluation of element matrices that involve products of interpolation functions and their derivatives with respect to the global coordinates. Since the integrals are evaluated numerically, the integrands must be evaluated at the quadrature points and summed over the number of integration points. Thus, evaluation of the interpolation functions and their derivatives must be carried out inside the do-loops. To fix ideas, for rectangular elements, we define

SF(I)	interpolation function ψ_I of the Ith node of an element
GDSF(K, I)	global derivative with respect to x_K (i.e., derivative with respect to the global coordinate x_K) of interpolation function ψ_I [GDSF$(K, I) = \partial\psi_I/\partial x_K$, $x_1 = x$, $x_2 = y$]
CONST	product of the Jacobian (i.e., determinant of $[\mathscr{J}]$) with the weights corresponding to the Gauss integration point (ξ_{NI}, η_{NJ}) = DET * GAUSWT(NI, NGP) * GAUSWT(NJ, NGP)

Then $S_{ij}^{00}, S_{ij}^{11}, \ldots$ of (8.35),

$$S_{ij}^{\alpha\beta} = \int_{\Omega^e} \frac{\partial\psi_i}{\partial x_\alpha}\frac{\partial\psi_j}{\partial x_\beta}\,dx\,dy \tag{13.1}$$

are given in Fortran form by

$$\begin{aligned}
&\text{S00(I, J)} = \text{S00(I, J)} + \text{SF(I)} * \text{SF(J)} * \text{CONST}\\
&\text{S11(I, J)} = \text{S11(I, J)} + \text{GDSF(1, I)} * \text{GDSF(1, J)} * \text{CONST}\\
&\text{S12(I, J)} = \text{S12(I, J)} + \text{GDSF(1, I)} * \text{GDSF(2, J)} * \text{CONST}\\
&\text{S22(I, J)} = \text{S22(I, J)} + \text{GDSF(2, I)} * \text{GDSF(2, J)} * \text{CONST}
\end{aligned} \tag{13.2}$$

The summed values of S00(I, J), S11(I, J), ... represent the numerical values of the integral coefficients in (13.1). The Fortran statements listed below summarize the discussion:

```
C     ______________________________________________________________________
C
C     NUMERICAL EVALUATION OF ELEMENT COEFFICIENT MATRICES IN EQ.(13.1)
C        FOR QUADRILATERAL ELEMENTS (WITH ISOPARAMETRIC FORMULATION)
C
C      NPE = Number of nodes per elements
C      IPDF= Number of integration points (i.e., Gauss points)
C     ______________________________________________________________________
C
      DIMENSION  GAUSPT(5,5), GAUSWT(5,5), SF(9), GDSF(2,9), ELXY(9,2),
     1           S00(9,9), S11(9,9), S12(9,9), S21(9,9), S22(9,9)
C
      DATA GAUSPT/5*0.0D0, -0.57735027D0, 0.57735027D0, 3*0.0D0,
     2  -0.77459667D0, 0.0D0, 0.77459667D0, 2*0.0D0, -0.86113631D0,
     3  -0.33998104D0, 0.33998104D0, 0.86113631D0, 0.0D0, -0.90617984D0,
     4  -0.53846931D0, 0.0D0, 0.53846931D0, 0.90617984D0/
C
      DATA GAUSWT/2.0D0, 4*0.0D0, 2*1.0D0, 3*0.0D0, 0.55555555D0,
     2   0.88888888D0, 0.55555555D0, 2*0.0D0, 0.34785485D0,
     3 2*0.65214515D0, 0.34785485D0, 0.0D0, 0.23692688D0,
     4   0.47862867D0, 0.56888888D0, 0.47862867D0, 0.23692688D0/
C
C     Initialize the arrays
C
      DO 120 I = 1,NPE
         DO 120 J = 1,NPE
            S00(I,J)= 0.0
            S11(I,J)= 0.0
```

```
              S12(I,J)= 0.0
              S21(I,J)= 0.0
              S22(I,J)= 0.0
  120 CONTINUE
C
C     DO-loops on numerical (Gauss) integration begin here:______________
C
      DO 200 NI = 1,IPDF
      DO 200 NJ = 1,IPDF
      XI  = GAUSPT(NI,IPDF)
      ETA = GAUSPT(NJ,IPDF)
C
C     SHPRCT (SHaPe functions for ReCTangular elements) is called here
C     to compute {SF} and [GDSF]:
C
      CALL SHPRCT (NPE,XI,ETA,ELXY,DET,SF,GDSF)
      CNST = DET*GAUSWT(NI,IPDF)*GAUSWT(NJ,IPDF)
C
C     Compute Sij(I,J) of Eqn. (13.1):
C
      DO 180 I=1,NPE
         DO 180 J=1,NPE
            S00(I,J) = S00(I,J) + SF(I)*SF(J)*CNST
            S11(I,J) = S11(I,J) + GDSF(1,I)*GDSF(1,J)*CNST
            S12(I,J) = S12(I,J) + GDSF(1,I)*GDSF(2,J)*CNST
            S21(I,J) = S21(I,J) + GDSF(2,I)*GDSF(1,J)*CNST
            S22(I,J) = S22(I,J) + GDSF(2,I)*GDSF(2,J)*CNST
  180    CONTINUE
  200 CONTINUE
C     ____________________________________________________________________
```

To set up the element coefficient matrices of a given problem, we make use of the element matrices defined above. As an example, consider the problem described by (8.1). The element coefficient matrix and the column vectors for the problem are given by (8.14*b*). The element matrix K_{ij} [ELK(I, J)] can be expressed in terms of S_{ij}^{00}, $S_{ij}^{11}, \ldots$ by

$$\begin{aligned}\text{ELK(I, J)} &= \text{A00} * \text{S00(I, J)} + \text{A11} * \text{S11(I, J)} + \text{A12} * \text{S12(I, J)}\\ &\quad + \text{A21} * \text{S12(J, I)} + \text{A22} * \text{S22(I, J)}\end{aligned}$$

where $a_{00} = \text{A00}$, $a_{11} = \text{A11}$, $a_{12} = \text{A12}$, $a_{21} = \text{A21}$, and $a_{22} = \text{A22}$ are the constant coefficients of the differential equation (8.1).

In multivariable problems, the element matrices are themselves defined in terms of submatrices, as was the case for plane elasticity, fluid flow, and plate bending. In such cases, the nodal degrees of freedom should be renumbered to reduce the half-bandwidth of the assembled coefficient matrix. For example, consider the element equations (10.29*a*) associated with plane elasticity problems. The element nodal variables Δ_i are given (say, for a linear rectangular element) by

$$\begin{Bmatrix} \Delta_1 \\ \Delta_2 \\ \Delta_3 \\ \\ \vdots \\ \\ \Delta_8 \end{Bmatrix} = \begin{Bmatrix} u_1 \\ u_2 \\ u_3 \\ u_4 \\ v_1 \\ v_2 \\ v_3 \\ v_4 \end{Bmatrix} \tag{13.3}$$

Thus, at any node, the difference between the label number of the first degree of freedom and that of the second degree of freedom is 4 (in a general case, the difference is n, where n is the number of nodes per element). This difference contributes to an increase in the half-bandwidth of the assembled coefficient matrix. To remedy this situation, we reorder the element nodal degrees of freedom as follows:

$$\begin{Bmatrix} \Delta_1 \\ \Delta_2 \\ \Delta_3 \\ \Delta_4 \\ \vdots \\ \Delta_{2n-1} \\ \Delta_{2n} \end{Bmatrix} = \begin{Bmatrix} u_1 \\ v_1 \\ u_2 \\ v_2 \\ \vdots \\ u_n \\ v_n \end{Bmatrix} \tag{13.4}$$

In reordering the nodal degrees of freedom, we must retain the symmetry, if one is present, of the system of algbebraic equations. This is accomplished by renumbering the equations in the same way as the nodal degrees of freedom. To illustrate how this can be done, we consider a set of four equations in four unknowns:

$$\begin{aligned} S^{11}_{11}u_1 + S^{11}_{12}u_2 + S^{12}_{11}v_1 + S^{12}_{12}v_2 &= F^1_1 \\ S^{11}_{21}u_1 + S^{11}_{22}u_2 + S^{12}_{21}v_1 + S^{12}_{22}v_2 &= F^1_2 \\ S^{21}_{11}u_1 + S^{21}_{12}u_2 + S^{22}_{11}v_1 + S^{22}_{12}v_2 &= F^2_1 \\ S^{21}_{21}u_1 + S^{21}_{22}u_2 + S^{22}_{21}v_1 + S^{22}_{22}v_2 &= F^2_2 \end{aligned} \tag{13.5a}$$

or, in matrix form,

$$\begin{bmatrix} [S^{11}] & [S^{12}] \\ [S^{21}] & [S^{22}] \end{bmatrix} \begin{Bmatrix} \{u\} \\ \{v\} \end{Bmatrix} = \begin{Bmatrix} \{F^1\} \\ \{F^2\} \end{Bmatrix} \tag{13.5b}$$

Now letting

$$\Delta_1 = u_1, \qquad \Delta_2 = v_1, \qquad \Delta_3 = u_2, \qquad \Delta_4 = v_2 \tag{13.6}$$

(i.e., the third nodal variable is renamed as the second, and vice versa) and rearranging (13.5) (i.e., the third equation becomes the second equation, and vice versa), we obtain

$$\begin{aligned} S^{11}_{11}\Delta_1 + S^{12}_{11}\Delta_2 + S^{11}_{12}\Delta_3 + S^{12}_{12}\Delta_4 &= F^1_1 \\ S^{21}_{11}\Delta_1 + S^{22}_{11}\Delta_2 + S^{21}_{12}\Delta_3 + S^{22}_{12}\Delta_4 &= F^2_1 \\ S^{11}_{21}\Delta_1 + S^{12}_{21}\Delta_2 + S^{11}_{22}\Delta_3 + S^{12}_{22}\Delta_4 &= F^1_2 \\ S^{21}_{21}\Delta_1 + S^{22}_{21}\Delta_2 + S^{21}_{22}\Delta_3 + S^{22}_{22}\Delta_4 &= F^2_2 \end{aligned} \tag{13.7a}$$

or, in matrix form,

$$[S]\{\Delta\} = \{F\} \tag{13.7b}$$

where

$$\begin{gathered} S_{ij} = S^{11}_{\alpha\beta}, \qquad S_{i,j+1} = S^{12}_{\alpha\beta}, \qquad S_{i+1,j} = S^{21}_{\alpha\beta}, \qquad S_{i+1,j+1} = S^{22}_{\alpha\beta} \\ F_i = F^1_\alpha, \qquad F_{i+1} = F^2_\alpha \\ i = 2\alpha - 1, \qquad j = 2\beta - 1, \qquad \alpha, \beta = 1, 2 \end{gathered} \tag{13.7c}$$

The above discussion applies to any number of degrees of freedom per node (NDF). Computer implementation of (13.7) is straightforward. An example of this procedure is given by the following Fortran statements, which correspond to (10.29):

```
C     ---------------------------------------------------------------------
C
C        REARRANGING THE ELEMENT EQUATIONS OF MULTIVARIABLE PROBLEMS
C            (Illustrated using the plane elasticity FE model)
C
C        NDF........ = Number of degrees of freedom per node
C        NPE........ = Number of nodes per element
C        CMAT(I,J).. = Matrix of elastic coefficients
C        ELK(I,J)... = Element stiffness matrix coefficients
C
C     ---------------------------------------------------------------------
C
C     Dimension the arrays. For example (NN = NPE*NDF):
C                          ELK(NN,NN),CMAT(3,3)
C
C     Compute the coefficients  ELK11(I,J),  ELK12(I,J),  ELK21(I,J) and
C     ELK22(I,J) of Eqn. (10.29) using  numerical  integration.  We have
C     (the following statements go inside the loops on Gauss quadrature;
C     see the fortran statements for the evaluation of Sij):
C
      DO 140 I=1,NPE
         DO 120 J=1,NPE
            ELK11(I,J) = ELK11(I,J) + CMAT(1,1)*S11 + CMAT(3,3)*S22
            ELK12(I,J) = ELK12(I,J) + CMAT(1,2)*S12 + CMAT(3,3)*S21
            ELK21(I,J) = ELK21(I,J) + CMAT(1,2)*S21 + CMAT(3,3)*S12
            ELK22(I,J) = ELK22(I,J) + CMAT(3,3)*S11 + CMAT(2,2)*S22
  120    CONTINUE
  140 CONTINUE
C
C     We are now ready to rearrange the coefficients
C
      II=1
      DO 180 I=1,NN
         JJ=1
         DO 160 J=1,NN
            ELK(II,JJ)     = ELK11(I,J)
            ELK(II,JJ+1)   = ELK12(I,J)
            ELK(II+1,JJ)   = ELK21(I,J)
            ELK(II+1,JJ+1) = ELK22(I,J)
  160    JJ = NDF*J+1
  180 II = NDF*I+1
C     ---------------------------------------------------------------------
```

13.4 APPLICATIONS OF THE COMPUTER PROGRAM FEM2DV2

13.4.1 Introduction

The computer program FEM2DV2 (see Appendix 2 for the source listing) is developed to solve the following types of problems:

1. Single-variable problems, including convective-type boundary conditions for heat transfer problems,

$$\boxed{c_t\left(\frac{\partial u}{\partial t}+\frac{\partial^2 u}{\partial t^2}\right)-\frac{\partial}{\partial x}\left(a_x\frac{\partial u}{\partial x}\right)-\frac{\partial}{\partial y}\left(a_y\frac{\partial u}{\partial y}\right)+a_0 u=f} \tag{13.8a}$$

   with

$$\begin{gathered} c_t=c_0+c_x x+c_y y, \qquad a_x=a_{10}+a_{1x}x+a_{1y}y,\\ a_y=a_{20}+a_{2x}x+a_{2y}y, \qquad f_0=f_0+f_x x+f_y y\\ a_0=\text{constant}\end{gathered} \tag{13.8b}$$

2. The plane elasticity problems of Chapter 10 [(10.11)]
3. Viscous incompressible fluid flows using the penalty function formulation of Chapter 11 [(11.1) with P replaced by (11.34)]
4. Plate problems using classical and shear deformation theories (only with rectangular elements) of Chapter 12 [(12.29)].

The first category of problems is quite general and includes, as special cases, many other field problems. As a special case, axisymmetric problems can be analyzed. The last three categories are specialized to linear elasticity, linear (i.e., Stokes) viscous incompressible fluid flow, and linear plate bending.

The type of gradient of the solution computed (in subroutine PSTPRC) for single-variable problems differs for different physical problems. For heat transfer problems, we have

$$q_x=-a_x\frac{\partial u}{\partial x}, \qquad q_y=-a_y\frac{\partial u}{\partial y} \tag{13.9}$$

The same definition applies to the velocity potential formulation of inviscid fluid flows (to calculate velocity components). In the stream function formulation, the velocity components (u, v) are defined by

$$u=q_y=a_y\frac{\partial u}{\partial y}, \qquad v=q_x=-a_x\frac{\partial u}{\partial x} \tag{13.10}$$

The (total) stresses for multivariable problems are computed using the constitutive equations, with the strains (or strain rates for fluid flow problems) computed at the reduced Gauss points using the strain–displacement relations. The spatial variation of the derivatives of the solution is dependent on the element type.

For heat transfer problems (i.e., ITYPE = 0), the variable ICONV is used to indicate the presence (ICONV = 1) or absence (ICONV = 0) of convective boundaries. When convective boundaries are involved (i.e., ICONV = 1), the elements whose boundaries coincide with such a boundary will have additional contributions to their coefficient matrices [see (8.99)–(8.103)]. The array IBN is used to store elements that have convective

TABLE 13.1
Description of the input variables to the program FEM2DV2

---

* Data Card 1:

TITLE - Title of the problem being solved (80 characters)

* Data Card 2:

ITYPE - Problem type:
ITYPE = 0, Single variable problems
ITYPE = 1, Viscous incompressible flow problems
ITYPE = 2, Plane elasticity problems
ITYPE = 3, Plate bending problems by the FSDT
ITYPE = 4, Plate bending problems by the CPT(N)
ITYPE = 5, Plate bending problems by the CPT(C)

IGRAD - Indicator for computing the gradient of the solution or stresses in the postprocessor:
IGRAD = 0, No postprocessing is required
IGRAD > 0, Postprocessing is required

When ITYPE=0 and IGRAD=1, the gradient is computed as in Eq. (13.9); for ITYPE=0 and IGRAD > 1, the gradient is computed as in Eq (13.10).

ITEM - Indicator for dynamic analysis:
ITEM = 0, Static analysis is required
ITEM > 0, Either eigenvalue or transient analysis is required:

ITEM = 1, Parabolic equation is analyzed
ITEM = 2, Hyperbolic equation is analyzed

NEIGN - Indicator for eigenvalue analysis:
NEIGN = 0, Static or transient analysis is required
NEIGN > 0, Eigenvalue analysis is required:
NEIGN= 1, Frequency/vibration analysis
NEIGN> 1, Stability analysis of plates

* Data Card 3: SKIP the card if NEIGN = 0

NVALU - Number of eigenvalues to be printed
NVCTR - Indicator for printing eigenvectors:
NVCTR = 0, Do not print eigenvectors
NVCTR ≥ 0, Print eigenvectors

* Data Card 4:

IELTYP - Element type used in the analysis:
IELTYP= 0, Triangular elements
IELTYP> 0, Quadrilateral elements

NPE - Nodes per element:
NPE = 3, Linear triangle (IELTYP=0)
NPE = 4, Linear quadrilateral (IELTYP>0)
NPE = 6, Quadratic triangle (IELTYP=0)
NPE = 8 or 9, Quadratic quadrilateral (IELTYP>0)

TABLE 13.1 (Continued)

MESH - Indicator for mesh generation by the program:
MESH = 0, Mesh is not generated by the program
MESH = 1, Mesh is generated by the program for rectangular domains (by MSH2DR)
MESH > 1, Mesh is generated by the program for general domains (by MSH2DG)

NPRNT - Indicator for printing certain output:
NPRNT = 0, Not print array NOD, element matrices, or global matrices
NPRNT = 1, Print array NOD and Element 1 matrices: [ELK] and {ELF}
NPRNT = 2, Print array NOD and assembled matrices, [GLK] and {GLF}
NPRNT > 2, Combination of NPRNT=1 and NPRNT=2

* Data Card 5: SKIP the card if MESH.EQ.1

NEM - Number of elements in the mesh when the user inputs the mesh or the mesh is generated by MSH2DG

NNM - Number of nodes in the mesh when the user inputs the mesh or the mesh is generated by MSH2DG

* Data Card 6: SKIP the card if MESH.NE.0; otherwise, the card is read in a loop on the number of elements (N=1, NEM)

NOD(N,I)-Connectivity for the N-th element (I=1,NPE)

* Data Card 7: SKIP the card if MESH.NE.0

GLXY(I,J)-Global x and y coordinates of I-th global node in the mesh (J=1, x-coordinate, J=2, y-coordinate)
Loops on I and J are: ((J=1,2), I=1,NNM); the NNM pairs of (x,y)--coordinates are read sequentially

_____ The next FOUR data cards are read in subroutine MSH2DG ______
* * * * * SKIP Cards 8, 9, 10 and 11 unless MESH.GT.1 * * * * *

* Data Card 8:

NRECL - Number of line records to be read in the mesh

* Data Card 9: Read the following variables NRECL times

NOD1 - First global node number of the line segment
NODL - Last global node number of the line segment
NODINC - Node increment on the line
X1 - The global x-coordinate of NOD1
Y1 - The global y-coordinate of NOD1
XL - The global x-coordinate of NODL
YL - The global y-coordinate of NODL
RATIO - The ratio of the first element length to the last element length

* Data Card 10:

NRECEL - Number of rows of elements to be read in the mesh

TABLE 13.1 (Continued)

* Data Card 11: Read the following variables NRECEL times

NEL1 - First element number of the row
NELL - Last element number of the row
IELINC - Increment of element number in the row
NODINC - Increment of global node number in the row
NPE - Number of nodes in each element
NODE(I) - Connectivity array of the first element in the row (I=1,NPE)

* Data Card 12: SKIP the card if MESH.NE.1

NX - Number of elements in the x-direction
NY - Number of elements in the y-direction

* Data Card 13: SKIP the card if MESH.NE.1

X0 - The x-coordinate of global node 1
DX(I) - The x-dimension of the I-th element (I=1,NX)

* Data Card 14: SKIP the card if MESH.NE.1

Y0 - The y-coordinate of global node 1
DY(I) - The y-dimension of the I-th element (I=1,NY)

* Data Card 15:

NSPV - The number of specified primary variables

* Data Card 16: SKIP the card if NSPV.EQ.0

ISPV(I,J)-Node number and LOCAL degree of freedom number of the I-th specified primary variable:
ISPV(I,1)=Node number; ISPV(I,2)=Local DOF number

The loops on I and J are: ((J=1,2),I=1,NSPV)

* Data Card 17: SKIP the card if NSPV.EQ.0 or NEIGN.NE.0

VSPV(I) - Specified value of the I-th primary variable (I=1,NSPV)

* Data Card 18: SKIP the card if NEIGN.NE.0

NSSV - Number of (nonzero) specified secondary variables

* Data Card 19: SKIP the card if NSSV.EQ.0 or NEIGN.NE.0

ISSV(I,J)-Node number and LOCAL degree of freedom number of the I-th specified secondary variable:
ISSV(I,1)=Node number; ISSV(I,2)=Local DOF number

The loops on I and J are: ((J=1,2),I=1,NSSV)

* Data Card 20: SKIP the card if NSSV.EQ.0 or NEIGN.NE.0

VSSV(I) - Specified value of the I-th secondary variable (I=1,NSSV)

TABLE 13.1 (Continued)

```
-------------------------------------------------------------------

Data Cards 21 through 27 are for SINGLE VARIABLE PROBLEMS (ITYPE=0)

* Data Card 21:  SKIP the card if ITYPE.NE.0

        A10   |
        A1X   |  Coefficients of the differential equation
        A1Y   |  a11 = A10 +A1X*X + A1Y*Y

* Data Card 22:  SKIP the card if ITYPE.NE.0

        A20   |
        A2X   |  Coefficients of the differential equation
        A2Y   |  a22 = A20 +A2X*X + A2Y*Y

* Data Card 23:  SKIP the card if ITYPE.NE.0

        A00    -  Coefficient of the differential equation

* Data Card 24:  SKIP the card if ITYPE.NE.0

        ICONV  -  Indicator for convection boundary conditions:
                  ICONV = 0, No convection boundary conditions
                  ICONV > 0, Convection boundary conditions present

* Data Card 25:  SKIP the card if ITYPE.NE.0 or ICONV.EQ.0

        NBE    -  Number elements with convection

* Data Card 26:  SKIP the card if ITYPE.NE.0 or ICONV.EQ.0
                 The following cards are read for each I, I=1,NBE

        IBN(I)  -  I-th element number with convection
        BETA(I) -  Film coefficient for convection on I-th element
        TINF(I) -  Ambient temperature of the I-th element

* Data Card 27:  SKIP the card if ITYPE.NE.0 or ICONV.EQ.0

        INOD(I,J)- Local node numbers of the side with convection
                   (J=1,2; for quadratic elements, give end nodes)
                   Loops on I and J are: ((J=1,2), I=1,NBE)

-------------------------------------------------------------------

_____ Data Card 28 is for VISCOUS FLUID FLOWS (ITYPE = 1) only ____

* Data Card 28:  SKIP the card if ITYPE.NE.1

        AMU    - Viscosity of the fluid
        PENLTY - Value of the penalty parameter

-------------------------------------------------------------------

____ Data Cards 29 & 30 are for PLANE ELASTICITY (ITYPE=2) only ___

* Data Card 29:  SKIP the card if ITYPE.NE.2

        LNSTRS - Flag for PLANE STRESS or PLANE STRAIN problems:
                 LNSTRS=0, Plane strain elastic problems
```

TABLE 13.1 (Continued)

LNSTRS>0, Plane stress elastic problems

* Data Card 30: SKIP the card if ITYPE.NE.2

E1 - Young's moduli along the global x-axis
E2 - Young's moduli along the global y-axis
ANU12 - Poisson's ratio in the xy-plane
G12 - Shear modulus in the xy-plane
THKNS - Thickness of the plane elastic body analyzed

__ Data Card 31 is for PLATE BENDING PROBLEMS (ITYPE=3 to 5) only _

* Data Card 31: SKIP the card unless ITYPE.GE.3

E1 - Young's moduli along the global x-axis
E2 - Young's moduli along the global y-axis
ANU12 - Poisson's ratio in the xy-plane
G12 - Shear modulus in the xy-plane
G13 - Shear modulus in the xz-plane
G23 - Shear modulus in the yz-plane
THKNS - Thickness of the plate analyzed

__________ Remaining data cards are for ALL problem types __________

* Data Card 32: SKIP the card if NEIGN.NE.0

F0
FX
FY
Coefficients to define the source term:
f = F0 + FX*x + FY*y

__________ Cards 33 thru 37 are for DYNAMIC ANALYSIS only __________

* Data Card 33: SKIP the card if ITEM.EQ.0

C0
CX
CY
Coefficients defining the temporal parts of the differential equations:

CT = C0 + CX*x + CY*y, when ITYPE = 0 or 1

CT = (C0 + CX*x + CY*y)*THKNS, when ITYPE = 2

I0 = C0*THKNS
I2 = C0*(THKNS**3)/12
and CX and CY are not used
when ITYPE=3 to 5 and NEIGN.LE.1

C0, CX, and CY denote the buckling parameters when ITYPE.EQ.3 and NEIGN.GT.1

* Data Card 34: SKIP the card if ITEM.EQ.0 or NEIGN.NE.0

NTIME - Number of time steps for the transient solution
NSTP - Time step number at which the source is removed
INTVL - Time step interval at which to print the solution

TABLE 13.1 (Continued)

```
         INTIAL - Indicator for nature of initial conditions:

                  INTIAL=0, Zero initial conditions are used
                  INTIAL>0, Non-zero initial conditions are used

 * Data Card 35:  SKIP the card if ITEM.EQ.0 or NEIGN.NE.0

         DT     - Time step used for the transient solution

         ALFA   - Parameter in the alfa-family of time approximation
                  used for parabolic equations:

                  ALFA=0,   The forward difference scheme (C.S.)@
                  ALFA=0.5, The Crank-Nicolson scheme (stable)
                  ALFA=2/3, The Galerkin scheme (stable)
                  ALFA=1,   The backward difference scheme (stable)

                 @C.S.=Conditionally Stable; For all schemes with
                  ALFA < 0.5, the time step DT is restricted to:
                  DT < 2/[MAXEGN*(1-2*ALFA)], where MAXEGN is the
                  maximum eigenvalue of the discrete problem.

         GAMA   - Parameter in the Newmark time integration scheme
                  used for hyperbolic equations:
                  GAMA=0.5,  Constant-average acceleration (stable)
                  GAMA=1/3,  Linear acceleration scheme (C.S.)@
                  GAMA=0.0,  The central difference scheme (C.S.)

                  ALFA = 0.5 for all schemes; For schemes for which
                  ALFA.LE.0.5 and GAMA < ALFA, DT is restricted to:
                  DT < 2/SQRT{MAXEGN*(ALFA-GAMA)}, MAXEGN being the
                  maximum eigenvalue of the discrete system.

         EPSLN  - A small parameter to check if the solution has
                  reached a steady state

 * Data Card 36:  SKIP the card if ITEM or INTIAL.EQ.0, or NEIGN.NE.0

         GLU(I) - Vector of initial values of the primary variables
                  (I=1,NEQ, NEQ=Number of nodal values in the mesh)

 * Data Card 37:  SKIP if ITEM.LE.1, NEIGN.NE.0, or INTIAL.EQ.0

         GLV(I) - Vector of initial values of the first derivative
                  of the primary variables (velocity)
                  (I=1,NEQ, NEQ=Number of nodal values in the mesh)
```

boundaries, and the array INOD is used to store the pairs of element local nodes (of elements in array IBN) that are on the convective boundary (to specify the side of the element on the convective boundary). If an element has more than one of its sides on the convective boundary, it should be repeated as many times as the number of its sides on the convective boundary.

A complete description of the input variables of the program FEM2DV2 is given in Table 13.1, which contains the values of the key variables for the four classes (ITYPE $= 0, 1, 2, \ldots, 5$) of problems. In the next section, the application of the program FEM2DV2 is illustrated via several examples.

13.4.2 Description of Mesh Generators

In this section, the input data to FEM2DV2 for several example problems is given. The example problems are selected from those discussed in earlier sections of this chapter. A major limitation of the program lies in the mesh generation [i.e., the computation of arrays NOD(I, J) and GLXY(I, J) for arbitrary domains]. For such problems, the user is required to input the mesh information, which can be a tedious job if many elements are used. Of course, the program can be modified to accept any other mesh generation subroutines.

First, let us consider MSH2DR. The program is restricted to rectangular domains with sides parallel to the global x and y axes. The subroutine requires the following input data:

NX	number of elements in the x direction
NY	number of elements in the y direction
(X_0, Y_0)	global coordinates of global node 1, which is located at the lower left corner of the rectangular domain (see Fig. 13.2)
DX(I)	the array of element lengths along the x direction
DY(I)	the array of element lengths along the y direction

The node and element numbering schemes for triangular and rectangular element meshes generated by MSH2DR are shown in Fig. 13.2.

Next, we consider MSH2DG, which is relatively more general than MSH2DR. The program, based on the straight line generation logic used by Akay *et al.* (1987), requires the user to sketch a desired mesh with certain regularity of node and element numbering. It exploits the regularity to generate the mesh. The program MSH2DG requires the following input (except for NEM and NNM, all other variables are read from the subroutine):

NEM	number of total elements in the mesh
NNM	number of total nodes in the mesh
NRECL	number of line-segment records

For each line segment, read the following variables:

NOD1	first node number on the line segment
NODL	last node number on the line segment
NODINC	increment between two consecutive nodes on the line
(X1, Y1)	global coordinates of the first node, NOD1 on the line
(XN, YN)	global coordinates of the last node, NODL on the line
RATIO	ratio of the first element length to the last element length

Similar information on the elements is read:

NRECEL	number of rows of elements

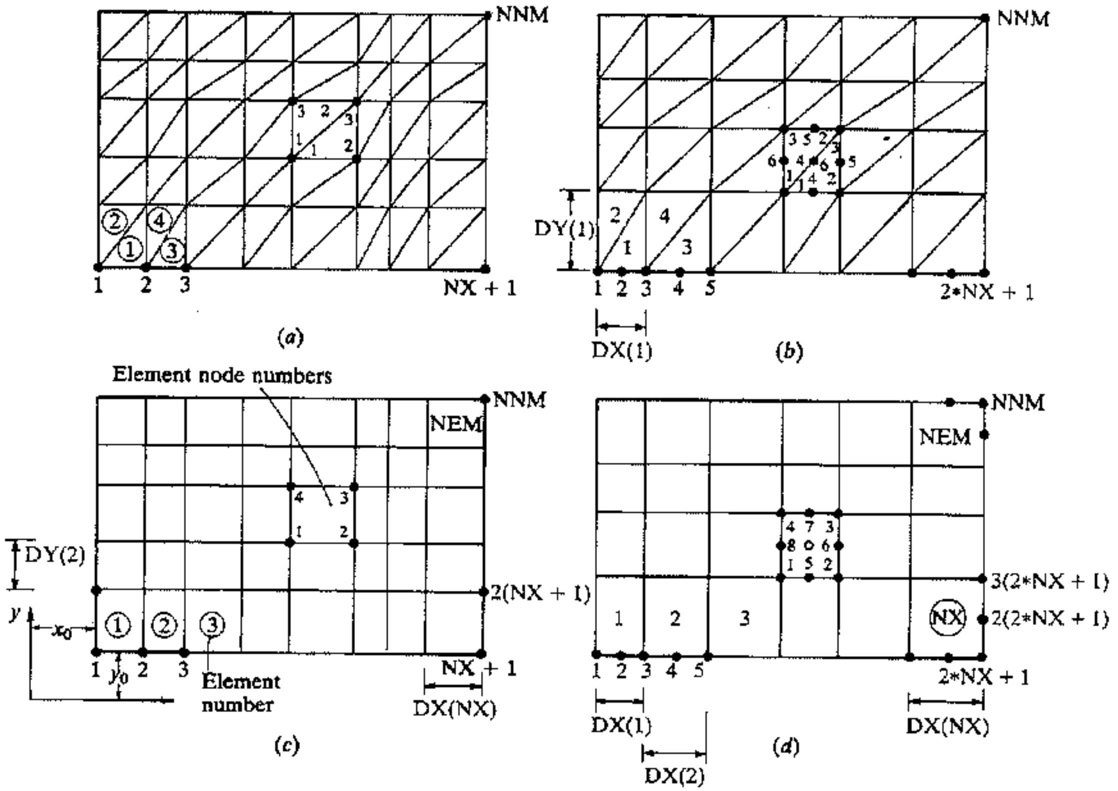

FIGURE 13.2

Global node numbering and element numbering system used in subroutine MSH2DR for the generation of meshes of (*a*) linear triangular elements [NNM = (NX + 1) * (NY + 1)]; (*b*) quadratic triangular elements [NNM = (2 * NX + 1) * (2 * NY + 1)]; (*c*) linear rectangular elements [NNM = (NX + 1) * (NY + 1)]; and (*d*) quadratic rectangular elements. Either the nine- or the eight-node rectangular elements can be used.

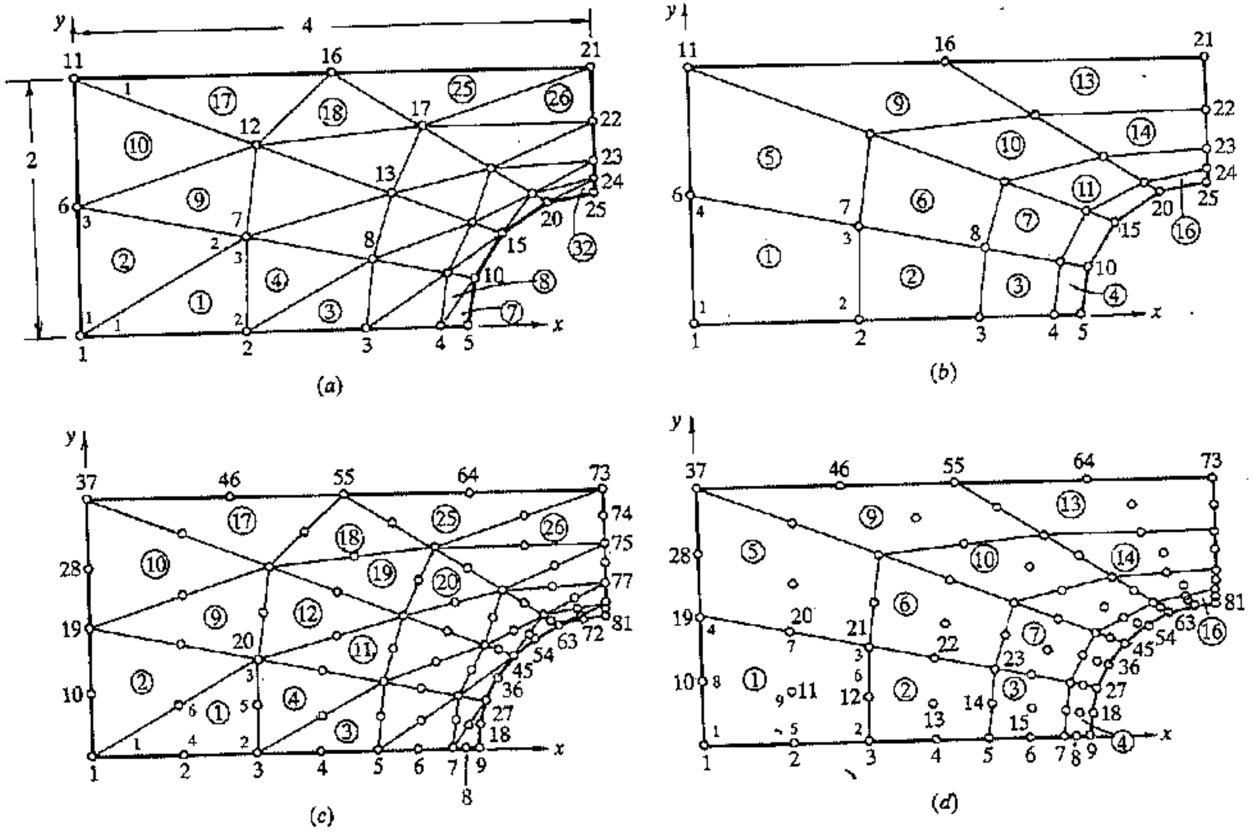

(a) (b) (c) (d)

FIGURE 13.3
Typical examples of mesh generation using subroutine MSH2DG: (*a*) mesh of linear triangular elements; (*b*) mesh of linear quadrilateral elements; (*c*) mesh of quadratic triangles; (*d*) mesh of nine-node quadratic quadrilateral elements (eight-node quadrilaterals can also be generated in the same way). Global node numbers, element numbers, and a typical element node numbering scheme are shown.

For each row of elements, read the following variables:

NEL1	first element number in the row
NELL	last element number in the row
NODINC	increment between respective nodes of consecutive elements in the row
NPE	number of nodes per element
NODE(I)(I = 1, NPE)	nodal connectivity for element NEL1

The type of data being read in MSH2DG should give some indication of the restrictions of the program. The node and element numbering should be regular along the lines and rows being read. Figures 13.3(*a–d*) show typical examples of meshes of linear and quadratic triangular and quadrilateral elements. For each of these meshes, the input data required for MSH2DG is listed in Table 13.2.

13.4.3 Applications (Illustrative Examples)

Example 13.1 Solution of the Poisson equation of Example 8.1. We consider the Poisson equation $-\nabla^2 u = 1$ in a unit square. We represent the domain by linear triangles or rectangles (see Fig. 13.4).

Triangular elements. We use the 2 × 2 mesh shown in Fig. 13.4(*a*). We have

$$\text{ITYPE} = 0, \quad \text{IGRAD} = 1, \quad \text{ITEM} = 0, \quad \text{NEIGN} = 0$$

$$\text{IELTYP} = 0, \quad \text{NPE} = 3, \quad \text{MESH} = 1, \quad \text{NPRNT} = 0$$

Note that we chose to generate the mesh using subroutine MSH2DR. Therefore, we must specify the number of subdivisions and their lengths along each direction:

$$\text{NX} = 2, \quad \text{NY} = 2, \quad \text{X0} = 0.0, \quad \text{Y0} = 0.0$$

$$\text{DX(1)} = 0.5, \quad \text{DX(2)} = 0.5, \quad \text{DY(1)} = 0.5, \quad \text{DY(2)} = 0.5$$

The number of specified primary variables (NSPV), the node numbers and the specified local degree of freedom (ISPV), and their specified values (VSPV) for the problem are

$$\text{NSPV} = 5, \quad \text{ISPV(I, J)} = (3, 1; 6, 1; 7, 1; 8, 1; 9, 1), \quad \text{VSPV(I)} = (0.0, 0.0, 0.0, 0.0, 0.0)$$

There are no specified secondary variables: NSSV = 0.

The coefficients a_x and a_y of the differential equation are unity, $a_0 = 0$, the source term f is unity, and there is no convection:

$$\text{A10} = 1.0, \quad \text{A1X} = 0.0, \quad \text{A1Y} = 0.0, \quad \text{A20} = 1.0, \quad \text{A2X} = 0.0, \quad \text{A2Y} = 0.0$$

$$\text{A00} = 0.0, \quad \text{ICONV} = 0, \quad \text{F0} = 1.0, \quad \text{FX} = 0.0, \quad \text{FY} = 0.0$$

Rectangular elements. For the 2 × 2 (four-element) mesh of rectangular elements (see Fig. 13.4*b*), the data input to the program differs only in the specification of the element type and the number of nodes per element:

$$\text{IELTYP} = 1, \quad \text{NPE} = 4$$

An edited output of the program for the problem is presented in Table 13.3.

TABLE 13.2
The input data to Program FEM2DV2 to generate the finite element meshes shown in Figs. 13.3(*a–d*)

```
(a) Mesh of linear triangles (see Fig.13.3a):
                                                     NEM, NNM
 32  25
                                                     NRECL
  5
  1   5  1  0.0  0.0  3.0      0.0      6.0   |
  6  10  1  0.0  1.0  3.07612  0.38268  6.0   |  NOD1,NODL,NODINC,
 11  15  1  0.0  2.0  3.29289  0.7071   6.0   |  X1,Y1,XL,YL,RATIO
 16  20  1  2.0  2.0  3.61732  0.92388  6.0   |  for each line segment
 21  25  1  4.0  2.0  4.0      1.0      6.0   |
                                                     NRECEL
  8                                           |
  1   7  2  1  3    1  2   7                  |
  2   8  2  1  3    1  7   6                  |  NEL1,NELL,IELINC,NODINC,
  9  15  2  1  3    6  7  12                  |  NPE, NOD(I,J)
 10  16  2  1  3    6 12  11                  |  for each line
 17  23  2  1  3   11 12  16                  |
 18  24  2  1  3   12 17  16                  |
 25  31  2  1  3   16 17  21                  |
 26  32  2  1  3   17 22  21                  |

(b) Mesh of four-node quadrilaterals (see Fig. 13.3b):
                                                     NEM, NNM
 16  25
                                                     NRECL
  5
  1   5  1  0.0  0.0  3.0      0.0      6.0   |
  6  10  1  0.0  1.0  3.07612  0.38268  6.0   |  NOD1,NODL,NODINC,
 11  15  1  0.0  2.0  3.29289  0.7071   6.0   |  X1,Y1,XL,YL,RATIO
 16  20  1  2.0  2.0  3.61732  0.92388  6.0   |  for each line segment
 21  25  1  4.0  2.0  4.0      1.0      6.0   |
                                                     NRECEL
  4                                           |
  1   4  1  1  4    1  2   7   6              |  NEL1,NELL,IELINC,NODINC,
  5   8  1  1  4    6  7  12  11              |  NPE,NOD(I,J)
  9  12  1  1  4   11 12  17  16              |
 13  16  1  1  4   16 17  22  21              |
```

Example 13.2 Heat transfer with convection boundary conditions. Consider a square region of $1\,\text{m} \times 1\,\text{m}$. The left side of the region (i.e., $x = 0$) is maintained at 100°C, while the boundary $y = 1$ m is maintained at 500°C. The boundaries $x = 1$ m and $y = 0$ are exposed to an ambient temperature of 100°C, and the film coefficient $\beta = 10\,\text{W m}^{-2}\,{}^\circ\text{C}^{-1}$. There is no internal heat generation ($f = 0$). The conductivity is taken to be $k_x = k_y = 12.5\,\text{W m}^{-1}\,{}^\circ\text{C}^{-1}$.

The input variables associated with convective boundary conditions are

$$\text{ICONV} = 1, \quad \text{NBE} = 16 \quad \text{(for an } 8 \times 8 \text{ mesh of linear rectangular elements)}$$

$$[\text{IBN(I)}, \text{BETA(I)}, \text{TINF(I)}] = [1, 10.0, 100.0; 2, 10.0, 100.0; \ldots]$$

$$[\text{INOD(I, J)}] = [1, 2; 1, 2; \ldots]$$

$$\text{A10} = 12.5, \quad \text{A1X} = 0.0, \quad \text{A1Y} = 0.0, \quad \text{A20} = 12.5,$$

$$\text{A2X} = 0.0, \quad \text{A2Y} = 0.0, \quad \text{A00} = 0.0$$

Table 13.4 gives the input data for the 8×8 mesh of linear rectangular elements. Figures 13.5 and 13.6 show plots of temperature variations and heat flow

$$q_x = -a_x \frac{\partial T}{\partial x}, \quad q_y = -a_y \frac{\partial T}{\partial y}$$

TABLE 13.2 (Continued)

```
(c) Mesh of quadratic triangles (see Fig. 13.3c):

 32  81                                              NEM, NNM

  9                                                  NRECL
  1   9  1  0.0  0.0  3.0      0.0      6.0  |
 10  18  1  0.0  0.5  3.01921  0.19509  6.0  |
 19  27  1  0.0  1.0  3.07612  0.38268  6.0  |
 28  36  1  0.0  1.5  3.16853  0.55557  6.0  |   NOD1,NODL,NODINC,
 37  45  1  0.0  2.0  3.29289  0.7071   6.0  |   X1,Y1,XL,YL,RATIO
 46  54  1  1.0  2.0  3.44443  0.83147  6.0  |   for each line segment
 55  63  1  2.0  2.0  3.61732  0.92388  6.0  |
 64  72  1  3.0  2.0  3.80491  0.98078  6.0  |
 73  81  1  4.0  2.0  4.0      1.0      6.0  |

  8                                                  NRECEL
  1   7  2  2  6    1  3 21  2 12 11             |
  2   8  2  2  6    1 21 19 11 20 10             |
  9  15  2  2  6   19 21 39 20 30 29             |
 10  16  2  2  6   19 39 37 29 38 28             |   NEL1,NELL,IELINC,NODINC,
 17  23  2  2  6   37 39 55 38 47 46             |   NPE,NOD(I,J)
 18  24  2  2  6   39 57 55 48 56 47             |
 25  31  2  2  6   55 57 73 56 65 64             |
 26  32  2  2  6   57 75 73 66 74 65             |

(d) Mesh of quadratic (nine-node) quadrilaterals (see Fig. 13.3d):

 16  81                                              NEM, NNM

  9                                                  NRECL
  1   9  1  0.0  0.0  3.0      0.0      6.0  |
 10  18  1  0.0  0.5  3.01921  0.19509  6.0  |
 19  27  1  0.0  1.0  3.07612  0.38268  6.0  |
 28  36  1  0.0  1.5  3.16853  0.55557  6.0  |   NOD1,NODL,NODINC,
 37  45  1  0.0  2.0  3.29289  0.7071   6.0  |   X1,Y1,XL,YL,RATIO
 46  54  1  1.0  2.0  3.44443  0.83147  6.0  |   for each line segment
 55  63  1  2.0  2.0  3.61732  0.92388  6.0  |
 64  72  1  3.0  2.0  3.80491  0.98078  6.0  |
 73  81  1  4.0  2.0  4.0      1.0      6.0  |

  4                                                  NRECEL
  1   4  1  2  9    1  3 21 19  2 12 20 10 11
  5   8  1  2  9   19 21 39 37 20 30 38 28 29    NEL1,NELL,IELINC,NODINC,
  9  12  1  2  9   37 39 57 55 38 48 56 46 47    NPE,NOD(I,J)
 13  16  1  2  9   55 57 75 73 56 66 74 64 65
```

along the boundaries. Note that q_x is linear in x and constant in y, and q_y is linear in y and constant in x (for constant a_x and a_y). A nonuniform mesh with smaller elements in the high-gradient region gives more accurate results:

$$\{\mathrm{DY(I)}\} = \{\mathrm{DX(I)}\} = (0.25, 0.125, 0.125, 0.125, 0.125, 0.125, 0.0625, 0.0625)$$

The program can also be used to analyze an axisymmetric problem. For example, consider a finite cylinder of radius $R_0 = 1$ m and length $L = 1$ m. The bottom and top of the cylinder are maintained at $T_0 = 100°C$, while the surface is exposed to an ambient temperature $T_\infty = 100°\mathrm{C}$ ($\beta = 10\,\mathrm{W\,m^{-2}\,°C^{-1}}$). For this case, the governing differential equation is (8.104). The coefficients A10, A1X, A1Y, A20, A2X, A2Y, and A00 are

$$\mathrm{A10} = 0.0, \quad \mathrm{A1X} = 2\pi k_r, \quad \mathrm{A1Y} = 0.0$$

$$\mathrm{A20} = 0.0, \quad \mathrm{A2X} = 2\pi k_z, \quad \mathrm{A2Y} = 0.0$$

$$\mathrm{A00} = 0.0$$

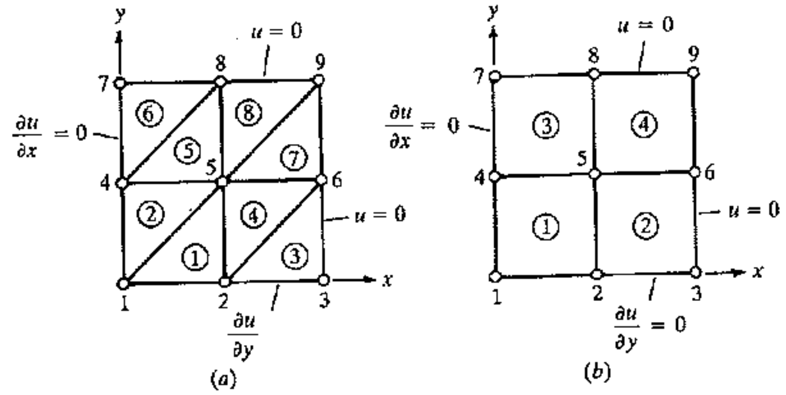

FIGURE 13.4
Finite element meshes of linear triangular and rectangular elements used in Example 13.1: (*a*) 2 × 2 mesh of triangles; (*b*) 2 × 2 mesh of rectangles.

The uniform internal heat generation f_0 (if not zero) is entered as

$$F0 = 0.0, \quad FX = 2\pi f_0, \quad FY = 0.0$$

Example 13.3 Flow about a circular cylinder (Example 8.7). Consider the flow of an inviscid fluid around a cylinder. We shall use the stream function and velocity potential formulations. Since the domain is not rectangular, we should use MSH2DG (i.e., MESH = 2). We consider the mesh of 25 nodes and 32 triangular elements shown in Fig. 13.7(*a*). We have ITYPE = 0 and IGRAD = 1 in the velocity potential formulation, and IGRAD = 2 in the stream function formulation, ITEM = 0, NEIGN = 0 and IELTYP = 0 for triangles, and IELTYP = 1 for quadrilaterals, MESH = 2, NPRNT = 0. The input for MSH2DG is given in Table 13.5 for triangular and quadrilateral elements.

In the stream function formulation, we have NSPV = 13 and NSSV = 0; and in the velocity potential formulation, we have NSPV = 5 and NSSV = 3. The coefficients are

$$A10 = 1.0, \quad A20 = 1.0, \quad A1X = 0.0, \quad A1Y = 0.0, \quad A2X = 0.0, \quad A2Y = 0.0$$
$$A00 = 0.0, \quad F0 = 0.0, \quad FX = 0.0, \quad FY = 0.0$$

The partial input of the problem is given in Table 13.6.

Example 13.4 Eigenvalue and transient analysis (Examples 8.9 and 8.10). We consider the eigenvalue and transient problems discussed in Examples 8.9 and 8.10. The governing differential equation is [see (8.165)]

$$\frac{\partial u}{\partial t} - \left(\frac{\partial^2 u}{\partial x^2} + \frac{\partial^2 u}{\partial y^2}\right) = 1$$

For eigenvalue analysis, we set ITEM = 1 and NEIGN = 1; for the transient analysis, we set ITEM = 1 (parabolic equation) and NEIGN = 0. In addition, we must

TABLE 13.3
Output from FEM2DV2 for the problem in Example 13.1

```
   *** ECHO OF THE INPUT DATA STARTS ***

Example 8.1: Solution of the Poisson equation on a square domain
  0   1   0   0                                       ITYPE,IGRAD,ITEM,NEIGN
  0   3   1   0                                       IELTYP,NPE,MESH,NPRNT

  2   2                                               NX,NY
  0.0  0.5  0.5                                       X0,DX(I)
  0.0  0.5  0.5                                       Y0,DY(I)

  5                                                   NSPV
  3 1     6 1     7 1     8 1     9 1                 ISPV(I,J)
  0.0     0.0     0.0     0.0     0.0                 VSPV(I)

  0                                                   NSSV

  1.0  0.0  0.0                                       A10, A1X, A1Y
  1.0  0.0  0.0                                       A20, A2X, A2Y
  0.0                                                 A00

  0                                                   ICONV

  1.0  0.0  0.0                                       F0,  FX,  FY

   **** ECHO OF THE INPUT DATA ENDS ****

Example 8.1: Solution of the Poisson equation on a square domain
________________________________________________________________________

        OUTPUT  FROM  PROGRAM  *FEM2DV2*   BY  J. N. REDDY
________________________________________________________________________


              ANALYSIS  OF   A  POISSON/LAPLACE  EQUATION

  COEFFICIENTS OF THE DIFFERENTIAL EQUATION:

    Coefficient, A10 .......................=  0.1000E+01
    Coefficient, A1X .......................=  0.0000E+00
    Coefficient, A1Y .......................=  0.0000E+00
    Coefficient, A20 .......................=  0.1000E+01
    Coefficient, A2X .......................=  0.0000E+00
    Coefficient, A2Y .......................=  0.0000E+00
    Coefficient, A00 .......................=  0.0000E+00


  CONTINUOUS SOURCE COEFFICIENTS:

    Coefficient, F0  .......................=  0.1000E+01
    Coefficient, FX  .......................=  0.0000E+00
    Coefficient, FY  .......................=  0.0000E+00


    ******* A STEADY-STATE PROBLEM is analyzed *******
       *** A mesh of   TRIANGLES    is chosen by user ***

    FINITE ELEMENT MESH INFORMATION:

       Element type: 0 = Triangle; >0 = Quad.)..=  0
       Number of nodes per element, NPE ........=  3
       No. of primary deg. of freedom/node, NDF =  1
       Number of elements in the mesh, NEM .....=  8
       Number of nodes in the mesh, NNM ........=  9
       Number of equations to be solved, NEQ ...=  9
       Half bandwidth of the matrix GLK, NHBW ..=  5
```

TABLE 13.3 (Continued)

```
        Mesh subdivisions, NX and NY ...........=   2   2

        No. of specified PRIMARY variables, NSPV =  5

  Node   x-coord.    y-coord.     Speci. primary & secondary variables
                                    (0, unspecified; >0, specified)
                                       Primary DOF  Secondary DOF

    1  0.0000E+00  0.0000E+00              0           0
    2  0.5000E+00  0.0000E+00              0           0
    3  0.1000E+01  0.0000E+00              1           0
    4  0.0000E+00  0.5000E+00              0           0
    5  0.5000E+00  0.5000E+00              0           0
    6  0.1000E+01  0.5000E+00              1           0
    7  0.0000E+00  0.1000E+01              1           0
    8  0.5000E+00  0.1000E+01              1           0
    9  0.1000E+01  0.1000E+01              1           0

  NUMERICAL INTEGRATION DATA:

     Full Integration polynomial degree, IPDF =   3
     Number of full integration points,  NIPF =   4
     Reduced Integration polynomial deg.,IPDR =   1
     No. of reduced integration points, NIPR =    1
     Integ. poly. deg. for stress comp., ISTR =   1
     No. of integ. pts. for stress comp.,NSTR =   1

  S O L U T I O N :

  Node    x-coord.       y-coord.      Primary DOF

    1   0.00000E+00   0.00000E+00   0.31250E+00
    2   0.50000E+00   0.00000E+00   0.22917E+00
    3   0.10000E+01   0.00000E+00   0.00000E+00
    4   0.00000E+00   0.50000E+00   0.22917E+00
    5   0.50000E+00   0.50000E+00   0.17708E+00
    6   0.10000E+01   0.50000E+00   0.00000E+00
    7   0.00000E+00   0.10000E+01   0.00000E+00
    8   0.50000E+00   0.10000E+01   0.00000E+00
    9   0.10000E+01   0.10000E+01   0.00000E+00

 The orientation of  gradient vector is measured from  the positive x-axis

 x-coord.      y-coord.    -a11(du/dx)  -a22(du/dy)   Flux Mgntd  Orientation

0.3333E+00   0.1667E+00   0.1667E+00   0.1042E+00   0.1965E+00      32.01
0.1667E+00   0.3333E+00   0.1042E+00   0.1667E+00   0.1965E+00      57.99
0.8333E+00   0.1667E+00   0.4583E+00   0.0000E+00   0.4583E+00       0.00
0.6667E+00   0.3333E+00   0.3542E+00   0.1042E+00   0.3692E+00      16.39
0.3333E+00   0.6667E+00   0.1042E+00   0.3542E+00   0.3692E+00      73.61
0.1667E+00   0.8333E+00   0.0000E+00   0.4583E+00   0.4583E+00      90.00
0.8333E+00   0.6667E+00   0.3542E+00   0.0000E+00   0.3542E+00       0.00
0.6667E+00   0.8333E+00   0.0000E+00   0.3542E+00   0.3542E+00      90.00
```

TABLE 13.4
Input data for the heat transfer problem in Example 13.2

```
 Example 13.2: Convective heat transfer in a square region
   0   1   0   0                                          ITYPE,IGRAD,ITEM,NEIGN
   1   4   1   0                                          IELTYP,NPE,MESH,NPRNT

   8   8                                                                NX,NY
   0.0  0.125  0.125  0.125  0.125  0.125  0.125  0.125  0.125  X0,DX(I)
   0.0  0.125  0.125  0.125  0.125  0.125  0.125  0.125  0.125  Y0,DY(I)

   17                                                     NSPV
   1 1   10 1   19 1   28 1   37 1   46 1   55 1   64 1    73 1  74 1  75 1
  76 1   77 1   78 1   79 1   80 1   81 1                 ISPV(I,J)
  100.0 100.0 100.0 100.0 100.0 100.0 100.0 100.0  500.0 500.0 500.0
  500.0 500.0 500.0 500.0 500.0 500.0                     VSPV(I)

   0                                                      NSSV

   10.0  0.0  0.0                                         A10, A1X, A1Y
   10.0  0.0  0.0                                         A20, A2X, A2Y
    0.0                                                   A00

   1                                                      ICONV
   16                                                     NBE
   1 10.0 100.0  2 10.0 100.0  3 10.0 100.0  4 10.0 100.0
   5 10.0 100.0  6 10.0 100.0  7 10.0 100.0  8 10.0 100.0
   8 10.0 100.0 16 10.0 100.0 24 10.0 100.0 32 10.0 100.0
  40 10.0 100.0 48 10.0 100.0 54 10.0 100.0 62 10.0 100.0  IBN,BETA,...
   1 2    1 2    1 2    1 2    1 2    1 2    1 2    1 2
   2 3    2 3    2 3    2 3    2 3    2 3    2 3    2 3    INOD(I,J)

   0.0     0.0  0.0                                       F0,  FX,  FY
```

input the following parameters:

$$\text{NTIME} = 20, \quad \text{NSTP} = 21 \ (>\text{NTIME}), \quad \text{INTVL} = 1$$

$$\text{INTIAL} = 0, \quad \text{DT} = 0.05, \quad \text{ALFA} = 0.5, \quad \text{GAMA} = 0.5 \ (\text{not used})$$

$$\text{C0} = 1.0, \quad \text{CX} = 0.0, \quad \text{CY} = 0.0$$

The parameter NSTP allows removal of the source (i.e., f) at a given time step. For example, if NSTP = 5 then, at the fifth time step and at each subsequent time step, f will be set equal to zero.

Table 13.7 gives the input files for the two problems. For a discussion of the results, see Examples 8.9 and 8.10.

The problems in Examples 8.11 and 8.12 can be analyzed using FEM2DV2, with minor changes to the input data in Table 13.7. The data for the hyperbolic problem in Examples 8.11 and 8.12 is given in Table 13.8.

Example 13.5 Deformation of a cantilever plate (Example 10.2). This is a plane elasticity problem, with plane stress assumption (i.e., LNSTRS = 1). Here we consider both triangular and rectangular-element meshes (see Fig. 13.7). MSH2DR can be used to generate the meshes (i.e., MESH = 1). For the 8×2 mesh of linear elements (or the 4×1 mesh of quadratic elements), we have the following input parameters:

$$\text{ITYPE} = 2, \quad \text{IGRAD} = 1 \quad (\text{or} > 0), \quad \text{ITEM} = 0$$

for static analysis and ITEM = 2 for dynamic analysis.

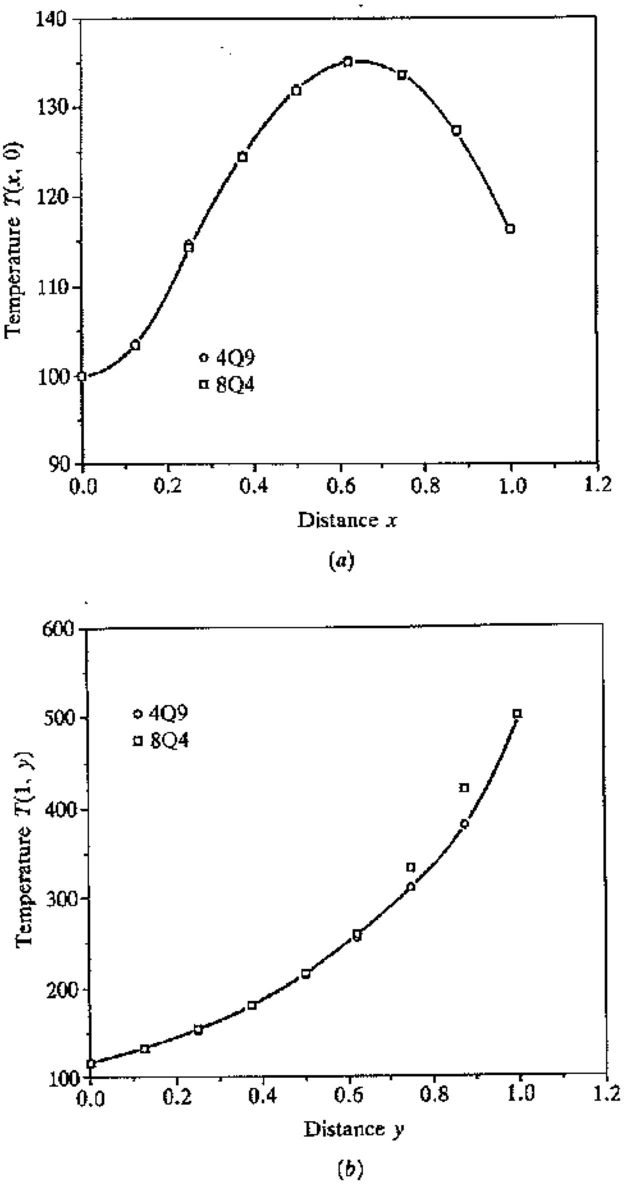

(a)

(b)

FIGURE 13.5
Temperature variations along the boundaries $y = 0$ and $x = 1$ for the convective heat transfer problem of Example 13.2: 4Q9, 4×4 mesh of nine-node quadrilateral elements; 8Q4, 8×8 mesh of four-node quadrilateral elements.

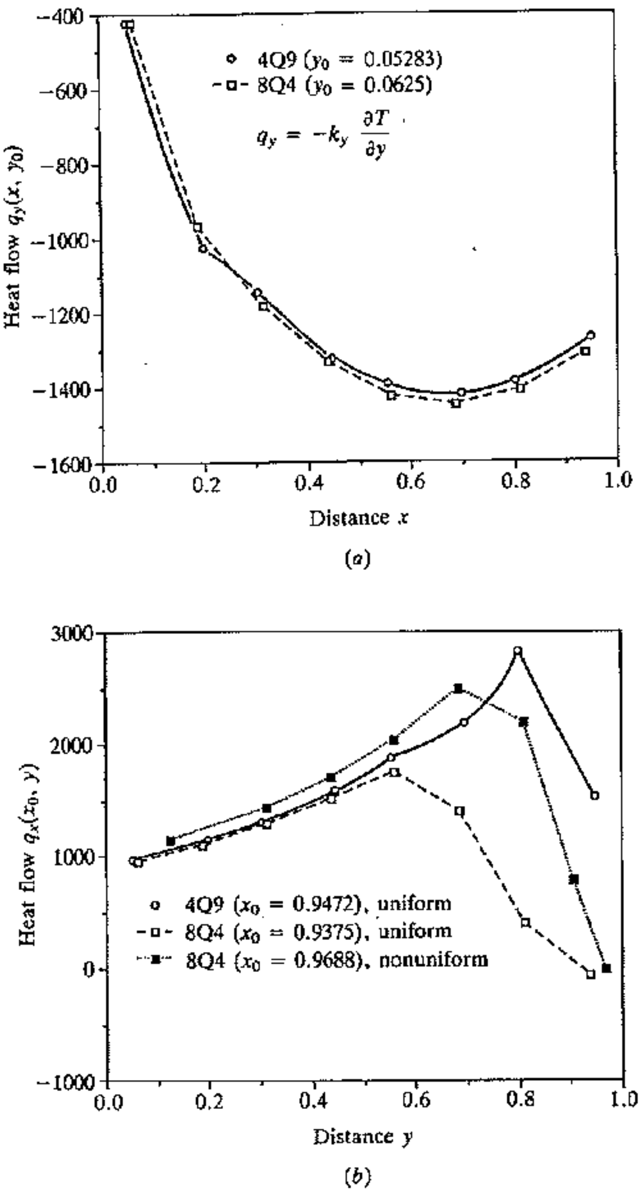

(a)

(b)

FIGURE 13.6
Variations of the heat flow along the horizontal ($x = 0.9472$ and 0.9375) and vertical ($y = 0.05283$ and 0.0625) boundaries (at the Gauss points nearest to the boundaries). See Fig. 13.5 for the explanation of the notation 4Q9 and 8Q4.

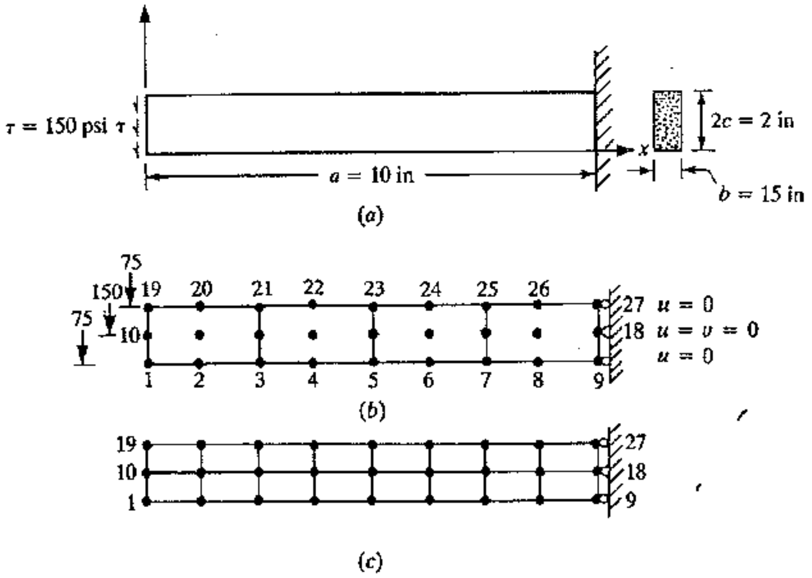

FIGURE 13.7
Bending of a cantilever plate using the elasticity equations: (*a*) geometry and loading; (*b*) mesh of nine-node quadratic elements (4 × 1); (*c*) mesh of linear rectangular elements (8 × 2).

There are four specified primary variables and three nonzero specified forces for the mesh:

$$\text{NSPV} = 4, \quad \text{ISPV(I, J)} = (9, 1; 18, 1; 18, 2; 27, 1)$$

$$\text{VSPV(I)} = (0.0, 0.0, 0.0, 0.0)$$

$$\text{NSSV} = 3, \quad \text{ISSV(I, J)} = (1, 2; 10, 2; 19, 2), \quad \text{VSSV(I)} = (-75.0, -150.0, -75.0)$$

Table 13.9 gives the data sets for natural vibration and transient analysis for the 4 × 1 mesh of nine-node quadratic elements. The data for the static case follows easily from the transient case. The results were discussed in Examples 10.2 and 10.3.

Example 13.6 Viscous fluid squeezed between two parallel plates (Example 11.4). We set up the data for a 12 × 8 uniform mesh of linear rectangular elements and the equivalent 6 × 4 mesh of nine-node elements. Most of the data are exactly the same for both meshes. We have

$$\text{ITYPE} = 1, \quad \text{IGRAD} = 1, \quad \text{ITEM} = 0 \text{ (for static analysis)}$$

$$\text{ITEM} = 1 \text{ (for transient analysis)}, \quad \text{NEIGN} = 0$$

Table 13.10 gives the complete input data for the 6 × 4 mesh of nine-node elements for the transient case.

Example 13.7 Bending of a simply supported isotropic plate under uniform load (Example 12.1). The 4 × 4 mesh of Hermite elements and 2 × 2 mesh of nine-node elements are used to model the square plate. Only rectangular elements are allowed (IELTYP = 1).

Classical plate model (ITYPE = 4 or 5)

$$\text{ITYPE} = 5 \text{ (conforming element)}, \quad \text{IGRAD} = 1$$

TABLE 13.5
Input data required for mesh generation by MSH2DG for the problem of inviscid flow around a circular cylinder

```
(a) Mesh of linear triangles (see Fig.13.3a):

 32  25                                             NEM, NNM

  5                                                 NRECL
  1   5  1  0.0  0.0  3.0      0.0      6.0
  6  10  1  0.0  1.0  3.07612  0.38268  6.0         NOD1,NODL,NODINC,
 11  15  1  0.0  2.0  3.29289  0.7071   6.0         X1,Y1,XL,YL,RATIO
 16  20  1  2.0  2.0  3.61732  0.92388  6.0         for each line segment
 21  25  1  4.0  2.0  4.0      1.0      6.0

  8                                                 NRECEL
  1   7  2  1  3    1  2   7
  2   8  2  1  3    1  7   6
  9  15  2  1  3    6  7  12                        NEL1,NELL,IELINC,NODINC,
 10  16  2  1  3    6 12  11                        NPE, NOD(I,J)
 17  23  2  1  3   11 12  16                        for each line
 18  24  2  1  3   12 17  16
 25  31  2  1  3   16 17  21
 26  32  2  1  3   17 22  21

(b) Mesh of four-node quadrilaterals (see Fig. 13.3b):

 16  25                                             NEM, NNM

  5                                                 NRECL
  1   5  1  0.0  0.0  3.0      0.0      6.0
  6  10  1  0.0  1.0  3.07612  0.38268  6.0         NOD1,NODL,NODINC,
 11  15  1  0.0  2.0  3.29289  0.7071   6.0         X1,Y1,XL,YL,RATIO
 16  20  1  2.0  2.0  3.61732  0.92388  6.0         for each line segment
 21  25  1  4.0  2.0  4.0      1.0      6.0

  4                                                 NRECEL
  1   4  1  1  4    1  2   7   6
  5   8  1  1  4    6  7  12  11                    NEL1,NELL,IELINC,NODINC,
  9  12  1  1  4   11 12  17  16                    NPE,NOD(I,J)
 13  16  1  1  4   16 17  22  21
```

Shear deformation plate model

$$\text{ITYPE} = 3, \qquad \text{IGRAD} = 1$$

The classical plate model has three degrees of freedom per node when the nonconforming element is used (i.e., ITYPE = 4), and four degrees of freedom per node for the conforming element (i.e., ITYPE = 5). This must be taken into consideration in inputting boundary conditions.

Table 13.11 gives the input data for classical and shear deformation plate models. For the nonconforming element, the data is the same as that used for the shear deformation model, except that ITYPE = 4.

For free vibration (NEIGN = 1) and stability analysis (NEIGN = 2), most of the data remain the same. For transient analysis, the time step used for unconditionally stable schemes is arbitrary, but should be small enough to give a complete response curve.

TABLE 13.6
Input data for the problem in Example 13.3 (for triangles)†

```
Example 8.7: Flow around a circular cylinder (Streamfunction)
  0   2   0   0                                      ITYPE,IGRAD,ITEM,NEIGN
  0   3   2   0                                      IELTYP,NPE,MESH,NPRNT
 32  25                                              NEM, NNM

<--------- input data for MSH2DG from Table 13.5 goes here --------->

                                                            NSPV
 13
  1 1    2 1    3 1    4 1    5 1   10 1   15 1   20 1   25 1
  6 1   11 1   16 1   21 1                                  ISPV(I,J)
  0.0    0.0    0.0    0.0    0.0    0.0    0.0    0.0    0.0
  1.0    2.0    2.0    2.0                                  VSPV(I)

  0                                                  NSSV

  1.0  0.0  0.0                                      A10, A1X, A1Y
  1.0  0.0  0.0                                      A20, A2X, A2Y
  0.0                                                A00

  0                                                  ICONV

  0.0  0.0  0.0                                      F0,  FX,  FY
Example 8.7: Flow around a circular cylinder (velocity potential)
  0   1   0   0                                      ITYPE,IGRAD,ITEM,NEIGN
  0   3   2   0                                      IEL, NPE, MESH, NPRNT

 32  25                                              NEM, NNM

<--------- input data for MSH2DG from Table 13.5 goes here --------->

  5                                                  NSPV
 21 1   22 1   23 1   24 1   25 1                    ISPV(I,J)
  0.0    0.0    0.0    0.0    0.0                    VSPV(I)

  3                                                  NSSV
  1 1    6 1   11 1                                  ISSV(I,J)
  0.5    1.0    0.5                                  VSSV(I)

  1.0  0.0  0.0                                      A10, A1X, A1Y
  1.0  0.0  0.0                                      A20, A2X, A2Y
  0.0                                                A00

  0                                                  ICONV

  0.0  0.0  0.0                                      F0,  FX,  FY
```

---

† For the nodal-equivalent mesh of quadrilateral elements, the input data differs only in specifying IELTYP = 1 and NEM = 16, and using the quadrilateral element data for MSH2DG from Table 13.5.

Example 13.8 Dynamic response of a clamped circular plate under suddenly applied uniform transverse loading. Consider a clamped circular plate of radius $R = 100$ in, thickness $h = 20$ in, modulus $E = 100 \text{ lb in}^{-2}$, Poisson ratio $\nu = 0.3$, and density $\rho = 10 \text{ lb s}^2 \text{ in}^{-4}$, subjected to a suddenly applied (i.e., $w = \phi_x = \phi_y = \dot{w} = \dot{\phi}_x = \dot{\phi}_y = 0$ at time $t = 0$) uniform loading of intensity $f_0 = 1 \text{ lb in}^{-2}$. We analyze the problem by modeling one quadrant (using the symmetry) of the plate by five nine-node elements (see Fig. 13.8*a*) and $\Delta t = 2.5$ s. The input data is presented in Table 13.12.

Plots of the center deflection and stress versus time are shown in Fig. 13.8(*b*).

TABLE 13.7
Input data for the eigenvalue and transient analysis of a parabolic equation over a square region ($a = b = 2$)†

```
 Example 8.9: Eigenvalue analysis of a parabolic equation on a square
  0   0   1   1                                     ITYPE,IGRAD,ITEM,NEIGN
 10   0                                             NVALU, NVCTR

  1   4   1   0                                     IELTYP,NPE,MESH,NPRNT

  4   4                                             NX,NY
  0.0  0.25   0.25   0.25   0.25                    X0,DX(I)
  0.0  0.25   0.25   0.25   0.25                    Y0,DY(I)

  9                                                                  NSPV
  5 1  10 1   15 1   20 1   21 1   22 1   23 1   24 1  25 1          ISPV

  1.0   0.0  0.0                                    A10, A1X, A1Y
  1.0   0.0  0.0                                    A20, A2X, A2Y
  0.0                                               A00

  0                                                 ICONV

   1.0  0.0  0.0                                    C0,  CX,  CY
 Example 8.10: Transient analysis of a parabolic equation on a square
  0   0   1   0                                     ITYPE,IGRAD,ITEM,NEIGN
  1   4   1   0                                     IELTYP,NPE,MESH,NPRNT

  4   4                                             NX,NY
  0.0  0.25   0.25   0.25   0.25                    X0,DX(I)
  0.0  0.25   0.25   0.25   0.25                    Y0,DY(I)

  9                                                                  NSPV
  5 1  10 1   15 1   20 1   21 1   22 1   23 1   24 1  25 1          ISPV
  0.0   0.0    0.0    0.0    0.0    0.0    0.0    0.0   0.0          VSPV

  0                                                                  NSSV

  1.0   0.0  0.0                                    A10, A1X, A1Y
  1.0   0.0  0.0                                    A20, A2X, A2Y
  0.0                                               A00

  0                                                 ICONV

   1.0  0.0  0.0                                    F0,  FX,  FY

   1.0  0.0  0.0                                    C0,  CX,  CY

 20    21    1   0                                  NTIME,NSTP,INTVL,INTIAL
 0.05  0.5   0.5  1.0E-3                            DT,ALFA,GAMA,EPSLN
```

---

† Only a quadrant is modeled in the transient as well as the eigenvalue analysis (hence, only symmetric eigenvalues can be obtained).

13.5 SUMMARY

A description of finite element computer program FEM2DV2 and its application to problems discussed in Chapters 8–12 have been presented. The program can be used to analyze two-dimensional field problems and problems of plane elasticity, 2-D flows of viscous incompressible fluids, and plate bending. It allows static, eigenvalue, and time-dependent analyses. Linear and quadratic, and triangular and rectangular elements can be used. The mesh

TABLE 13.8
Input data for the eigenvalue and transient analysis of an hyperbolic equation over a rectangular region ($a = 4$, $b = 2$)†

```
Example 8.11: Natural vibration of a rectangular membrane
                                                        ITYPE,IGRAD,ITEM,NEIGN
  0   0   2   1
  9   0                                                 NVALU, NVCTR
  1   4   1   0                                         IELTYP,NPE,MESH,NPRNT
  4   4                                                 NX,NY
  0.0  1.0    1.0    1.0    1.0                         X0,DX(I)
  0.0  0.5    0.5    0.5    0.5                         Y0,DY(I)
                                                                  NSPV
  16
   1  1   2 1    3 1    4 1    5 1    6 1   10 1   11 1
  15  1  16 1   20 1   21 1   22 1   23 1   24 1   25 1          ISPV
  12.5  0.0  0.0                                        A10, A1X, A1Y
  12.5  0.0  0.0                                        A20, A2X, A2Y
  0.0                                                   A00
  0                                                     ICONV
  2.5  0.0  0.0                                         C0,  CX,  CY

Example 8.12: Transient analysis of an hyperbolic equation (membrane)
                                                        ITYPE,IGRAD,ITEM,NEIGN
  0   0   2   0
  1   4   1   0                                         IELTYP,NPE,MESH,NPRNT
  4   4                                                 NX,NY
  0.0  0.5    0.5    0.5    0.5                         X0,DX(I)
  0.0  0.25   0.25   0.25   0.25                        Y0,DY(I)
                                                                  NSPV
  9
  5 1  10 1   15 1   20 1   21 1   22 1   23 1   24 1  25 1       ISPV
  0.0   0.0    0.0    0.0    0.0    0.0    0.0    0.0   0.0       VSPV
                                                                  NSSV
  0
  12.5  0.0  0.0                                        A10, A1X, A1Y
  12.5  0.0  0.0                                        A20, A2X, A2Y
  0.0                                                   A00
  0                                                     ICONV
  0.0  0.0  0.0                                         F0,  FX,  FY
  2.5  0.0  0.0                                         C0,  CX,  CY
  20    21    1    1                                    NTIME,NSTP,INTVL,INTIAL
  0.025 0.5  0.5  1.0E-3                                DT,ALFA,GAMA,EPSLN
  0.400    0.375    0.300    0.175    0.0
  0.375    0.35156  0.28125  0.16406  0.0
  0.300    0.28125  0.225    0.13125  0.0
  0.175    0.16406  0.13125  0.076563 0.0
  0.0      0.0      0.0      0.0      0.0               Initial cond., GLU(I)
  0.0      0.0      0.0      0.0      0.0
  0.0      0.0      0.0      0.0      0.0
  0.0      0.0      0.0      0.0      0.0
  0.0      0.0      0.0      0.0      0.0
  0.0      0.0      0.0      0.0      0.0               Initial cond., GLV(I)
```

† Only a quadrant is modeled in the transient analysis, and the whole domain is modeled in the eigenvalue analysis.

generators are fairly general for generating finite element meshes for geometrically complex domains. The program FEM2DV2 is a true reflection of the theory presented in Chapters 8–12, and it can be extended to analyze other field problems with appropriate modifications.

TABLE 13.9
Input data for the dynamic analysis of a cantilever beam

```
Example 10.5: Natural vibration of a cantilever beam  by elasticity
  2   0   2   1                                     ITYPE,IGRAD,ITEM,NEIGN
  10  0                                             NVALU,NVCTR
  1   9   1   1                                     IELTYP,NPE,MESH,NPRNT

  4   1                                             NX, NY
  0.0  2.5   2.5   2.5   2.5                        XO, DX(I)
  0.0  2.0                                          YO, DY(I)

  4                                                 NSPV
  9  1  18 1   18 2   27 1                          ISPV

  1                                                 LNSTRS

  30.0E06  30.0E06  0.25  12.0E06  1.0              E1,E2,ANU12,G12,THKNS

  8.8255E-03  0.0   0.0                             CO, CX, CY

Example 10.5: Transient analysis of a cantilever beam by elasticity
  2   1   2   0                                    ITYPE,IGRAD,ITEM,NEIGN
  1   9   1   0                                    IELTYP,NPE,MESH,NPRNT

  4   1                                            NX, NY
  0.0  2.5   2.5   2.5   2.5                       XO,DX(I)
  0.0  2.0                                         YO,DY(I)

  4                                                NSPV
  9  1  18 1   18 2   27 1                         ISPV
  0.0   0.0    0.0    0.0                          VSPV

  3                                                NSSV
  1  2   10  2  19  2                              ISSV
 -75.0  -150.0  -75.0                              VSSV

  1                                                LNSTRS

  30.0E06  30.0E06  0.25  12.0E06  1.0             E1,E2,ANU12,G12,THKNS

   0.0         0.0  0.0                            FO, FX, FY

   8.8255E-03  0.0  0.0                            CO, CX, CY

   20   21   1    0                                NTIME,NSTP,INTVL,INTIAL

  0.25E-03      0.5  0.5  1.0E-3                   DT,ALFA,GAMA,EPSLN
```

TABLE 13.10
Input data for the viscous flow problem in Example 13.6

```
Example 11.5: Transient analysis of fluid squeezed between plates
  1   1   1   0                                 ITYPE,IGRAD,ITEM,NEIGN
  1   9   1   0                                 IEL, NPE, MESH, NPRNT

  6   4                                         NX, NY
  0.0  1.0  1.0  1.0  1.0  1.0  1.0             X0, DX(I)
  0.0  0.5  0.5  0.5  0.5                       Y0, DY(I)

  47                                            NSPV
   1 1   1 2   2  2   3  2   4  2   5  2   6  2  7  2  8  2  9  2
  10 2  11 2  12  2  13  2  14  1  27  1  40  1  53 1  66 1  79 1
  92 1 105 1 105  2 106  1 106  2 107  1 107  2 108 1 108 2 109 1
 109 2 110 1 110  2 111  1 111  2 112  1 112  2 113 1 113 2 114 1
 114 2 115 1 115  2 116  1 116  2 117  1 117  2 ISPV(I,J)

  0.0  0.0   0.0   0.0   0.0   0.0   0.0  0.0  0.0  0.0
  0.0  0.0   0.0   0.0   0.0   0.0   0.0  0.0  0.0  0.0
  0.0  0.0  -1.0   0.0  -1.0   0.0  -1.0  0.0 -1.0  0.0
 -1.0  0.0  -1.0   0.0  -1.0   0.0  -1.0  0.0 -1.0  0.0
 -1.0  0.0  -1.0   0.0  -1.0   0.0  -1.0 VSPV(I)

  0                                             NSSV

  1.0  1.0E8                                    AMU, PENLTY

  0.0  0.0  0.0                                 F0, FX, FY

  1.0  0.0  0.0                                 C0, CX, CY

  20   50   1     0                             NTIME,NSTP,INTVL,INTIAL
  0.1  0.5  0.25  1.0D-3                        DT, ALFA, GAMA, EPSLN
```

TABLE 13.11
Input data for the bending of a simply supported plate

```
Example 12.1: Bending of a simply supported isotropic plate--FSDT
  3   1   0   0                                 ITYPE,IGRAD,ITEM,NEIGN
  1   4   1   0                                 IEL, NPE, MESH, NPRNT

  4   4                                         NX, NY
  0.0  1.25   1.25   1.25   1.25                X0, DX(I)
  0.0  1.25   1.25   1.25   1.25                Y0, DY(I)

  27                                                             NSPV
   1  2   1  3   2  3   3  3   4  3   5  1   5  3   6  2  10 1
  10  3  11  2  15  1  15  3  16  2  20  1  20  3  21  1  21 2
  22  1  22  2  23  1  23  2  24  1  24  2  25  1  25  2  25 3   ISPV

  0.0    0.0    0.0    0.0    0.0    0.0    0.0    0.0    0.0
  0.0    0.0    0.0    0.0    0.0    0.0    0.0    0.0    0.0
  0.0    0.0    0.0    0.0    0.0    0.0    0.0    0.0    0.0   VSPV

  0                                             NSSV

  1.0E7  1.0E7  0.25  0.4E7 0.4E7 0.4E7   1.0   E1, E2, ANU12, G12,...

  1.0   0.0   0.0                               F0, FX, FY
Example 12.1: Bending of a simply supported isotropic plate--CPT(C)
  5   1   0   0                                 ITYPE,IGRAD,ITEM,NEIGN
  1   4   1   0                                 IEL, NPE, MESH, NPRNT

  1   1                                         NX, NY
  0.0  5.0                                      X0, DX(I)
  0.0  5.0                                      Y0, DY(I)

  12                                            NSPV
  1  2   1  3   2  1   2  3   3  1   3  2   4  1   4  2   4  3
  1  4   2  4   3  4                            ISPV(I,J)

  0.0    0.0    0.0    0.0    0.0    0.0    0.0    0.0    0.0
  0.0    0.0    0.0                             VSPV(I)

  0                                             NSSV

  1.0E7  1.0E7  0.25  0.4E7  0.4E7  0.4E7  1.0  E1,E2,ANU12,G12,...

  1.0   0.0   0.0                               F0, FX, FY
```

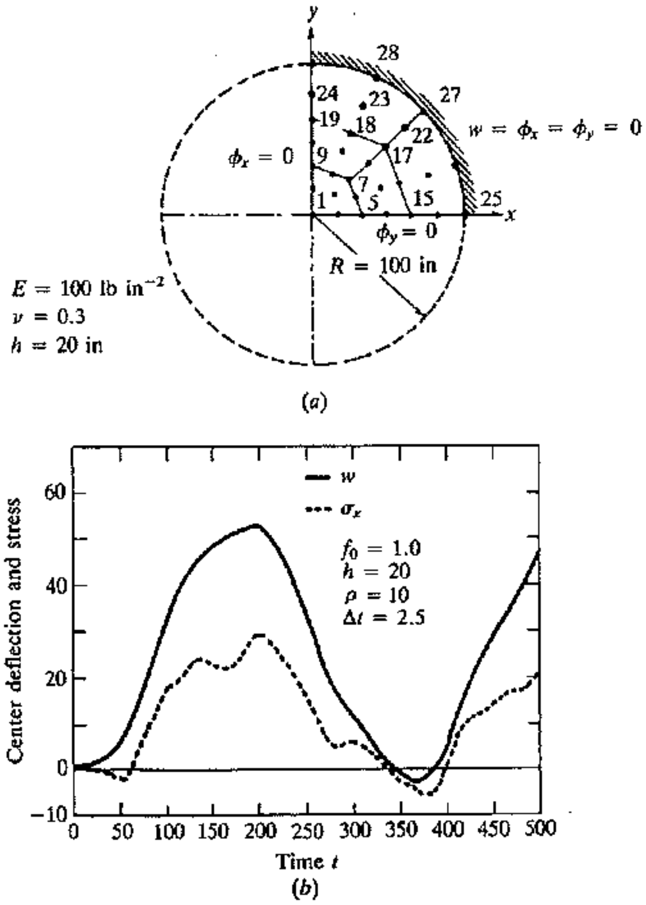

FIGURE 13.8
Clamped circular plate under a suddenly applied uniform load: (*a*) geometry and boundary conditions; (*b*) center deflection and stress versus time.

TABLE 13.12
Input data for the transient analysis of a circular plate

```
Example 13.8: Transient response of a clamped circular plate--FSDT
  3   1   2   0                                         ITYPE,IGRAD,ITEM,NEIGN
  1   9   0   0                                         IEL, NPE, MESH, NPRNT

  5  29                                                 NEM, NNM

  1   5   7   9   2   6   8   4   3                     NOD(1,I), I=1,NPE
  5  15  17   7  10  16  12   6  11                     NOD(2,I), I=1,NPE
  9   7  17  19   8  12  18  14  13                     NOD(3,I), I=1,NPE
 15  25  27  17  20  26  22  16  21                     NOD(4,I), I=1,NPE
 19  17  27  29  18  22  28  24  23                     NOD(5,I), I=1,NPE

 0.0000  0.0000   16.5000 0.0000    11.6673 11.6673
 0.0000  16.5     33.0    0.0       30.488  12.6286
 23.3345 23.3345  12.6286 30.488    0.0     33.0
 49.5    0.0      45.732  18.9428   35.0    35.0
 18.9428 45.732   0.0     49.5      66.0    0.0
 60.976  25.2571  46.669  46.669    25.2571 60.976
 0.0     66.0     83.0    0.0       76.682  31.7627
 58.6898 58.6898  31.7627 76.682    0.0     83.0
 100.0   0.0      92.388  38.2683   70.7107 70.7107
 38.2683 92.388   0.0     100.0                            GLXY(I,J)

  27                                                           NSPV
   1  2   1  3   2  3   4  2   5  3   9  2  10  3  14  2  15 3
  19  2  20  3  24  2  25  1  25  2  25  3  26  1  26  2  26 3
  27  1  27  2  27  3  28  1  28  2  28  3  29  1  29  2  29 3   ISPV

  0.0    0.0    0.0    0.0    0.0    0.0    0.0    0.0    0.0
  0.0    0.0    0.0    0.0    0.0    0.0    0.0    0.0    0.0
  0.0    0.0    0.0    0.0    0.0    0.0    0.0    0.0    0.0    VSPV

  0                                           NSSV

  1.0E2  1.0E2  0.30  0.3845E2  0.3845E2  0.3845E2  20.0  E1,E2,...

  1.0   0.0   0.0                             FO, FX, FY

 10.0   0.0   0.0                             CO, CX, CY

  40    41    10   0                          NTIME,NSTP,INTVL,INTIAL
  2.5   0.5   0.5  1.0E-03                    DT, ALFA, GAMA, EPSLN
```

PROBLEMS

Note that all of the problems must be analyzed using FEM2DV2. The results obtained from the program should be evaluated for their accuracy in the light of analytical solutions for qualitative understanding of the solution of the problem. New problems can be generated from those given here by changing the problem data, mesh, type of element, etc. For time-dependent problems, the time step and number of time steps should be chosen such that the solution pattern is established or a steady state is reached. When specific material properties are not given, use values such that the solution can be interpreted as the nondimensional solution of the problem.

Field problems (Chapter 8)

13.1. Investigate the convergence of the solution to Problem 8.26 using 2 × 2, 4 × 4, and 8 × 8 meshes of linear triangular elements, and compare the results (in graphical or tabular form) with the analytical solution.

13.2. Repeat Problem 13.1 with rectangular elements.

13.3. Repeat Problem 13.1 for the case $u_0 = 1$ (see Problem 8.27 for the analytical solution).

13.4. Repeat Problem 13.3 with rectangular elements.

13.5. Investigate the convergence of the solution to Problem 8.31 using 2 × 2, 4 × 4, and 8 × 8 meshes of linear triangular elements and equivalent meshes of quadratic triangular elements.

13.6. Repeat Problem 13.5 using rectangular elements.

13.7. Analyze the axisymmetric problem in Problem 8.36 using 4 × 1 and 8 × 1 linear rectangular elements, and compare the solution with the exact solution.

13.8. Analyze the axisymmetric problem in Problem 8.37 using 4 × 4 and 8 × 8 meshes of linear rectangular elements.

13.9. Analyze Problem 8.26 for eigenvalues (take $c = 1.0$), using a 2 × 4 uniform mesh of triangular elements. Calculate the critical time step for a parabolic equation.

13.10. Analyze Problem 8.26 using a 2 × 4 mesh of triangles for transient response. Assume zero initial conditions. Use $\alpha = 0.5$ and $\Delta t = 0.01$. Investigate the stability of the solution when $\alpha = 0.0$ and $\Delta t = 0.005$. The number of time steps should be such that the solution reaches its peak value or a steady state.

13.11. Analyze Problem 8.31 for transient response (take $c = 1.0$) using a 4 × 4 mesh of linear rectangular elements and a 2 × 2 mesh of nine-node quadratic rectangular elements. Assume zero initial conditions. Investigate the stability and accuracy of the Crank–Nicolson scheme ($\alpha = 0.5$) and the forward difference scheme ($\alpha = 0$).

13.12. Repeat Problem 13.11 for the axisymmetric problem in Fig. P8.37. Assume zero initial conditions.

Heat transfer (Chapter 8)

13.13. Analyze the heat transfer problem in Problem 8.38 using an 8 × 16 mesh of linear triangular elements and an equivalent mesh of linear rectangular elements.

13.14. Analyze the heat transfer problem in Fig. P8.39.

13.15. Analyze Problem 8.40 for nodal temperatures and heat flow across the boundaries. Use the following data: $k = 30\ \text{W m}^{-1}\,{}^\circ\text{C}^{-1}$, $\beta = 60\ \text{W m}^{-2}\,{}^\circ\text{C}^{-1}$, $T_\infty = 0^\circ\text{C}$, $T_0 = 100^\circ\text{C}$, $q_0 = 200,000\ \text{W m}^{-2}$, $f_0 = 10^7\ \text{W m}^{-3}$, and $a = 1$ cm.

13.16. Repeat Problem 13.15 with an equivalent mesh of triangular elements.

13.17. Analyze Problem 8.46 for nodal temperature and heat flows across the boundary. Take $k = 5\ \text{W m}^{-1}\,{}^\circ\text{C}^{-1}$.

13.18. Repeat Problem 13.17 using equivalent meshes of nine-node rectangular elements.

13.19. Consider heat transfer in a rectangular domain with a central heated circular cylinder (see Fig. P13.19 for the geometry). Analyze the problem using the mesh of linear quadrilateral elements shown in Fig. 13.3(*b*).

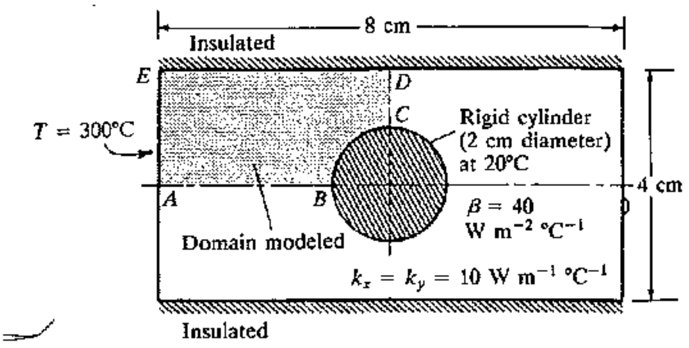

FIGURE P13.19

13.20. Repeat Problem 13.19 with the mesh of quadratic quadrilateral elements shown in Fig. 13.3(*d*).

13.21. Analyze the heat transfer problem in Fig. P8.42 with (*a*) 2×2 and (*b*) 4×4 meshes of linear rectangular elements.

13.22. Repeat Problem 13.21 with triangular elements.

13.23. Analyze the problem in Fig. P8.43 with (a) 3×3, and (b) 6×6 meshes of linear rectangular elements. Take $k = 10\ \text{W m}^{-1}\,{}^\circ\text{C}^{-1}$.

13.24. Repeat Problem 13.23 with linear triangular elements.

13.25. Analyze the heat transfer problem in Fig. P8.45 with a 4×4 mesh of linear rectangular elements and an equivalent mesh of quadratic (nine-node) elements. Take $a = 1$ cm, $T_0 = 100^\circ\text{C}$, and $k = 3\ \text{W m}^{-1}\,{}^\circ\text{C}^{-1}$.

13.26. Determine the transient response of the problem in Fig. P8.43 using a 6×6 mesh of rectangular elements. Use the Crank–Nicolson scheme.

13.27. Analyze the problem in Fig. P8.46 for transient response using (*a*) $\alpha = 0$ and (*b*) $\alpha = 0.5$.

13.28. Analyze the axisymmetric problem in Fig. P8.36 using the Crank–Nicolson method. Use an 8×1 mesh of linear rectangular elements.

Ground water and inviscid flows (Chapter 8)

13.29. Analyze the groundwater flow in Problem 8.50 using a 16×8 mesh of linear rectangular elements, and homogeneous properties $a_{11} = a_{22} = 1\ \text{m day}^{-1}$.

13.30. Repeat Problem 13.29 with a 16 × 18 mesh of linear triangular elements.

13.31. Analyze Problem 8.49 with an 8 × 4 mesh of linear triangular elements.

13.32. Repeat Problem 8.49 with an equivalent mesh of linear quadrilateral elements.

13.33. Repeat Problem 8.49 with an equivalent mesh of quadratic triangular elements.

13.34. Repeat Problem 8.49 with an equivalent mesh of quadratic (nine-node) quadrilateral elements.

13.35. Analyze Problem 8.48 using linear rectangular elements and an equivalent mesh of quadratic rectangular elements. Use an 8 × 6 mesh in the first rectangle and an 8 × 4 mesh in the second. The meshes should be refined in the horizontal direction to have smaller elements around the sheet pile.

13.36. Analyze the flow around cylinder of elliptical cross-section (see Fig. P8.52). Use the symmetry and an appropriate mesh of linear triangular elements. Use the stream function approach.

13.37. Repeat Problem 13.36 using the velocity potential formulation.

13.38. Repeat Problem 13.36 with quadrilateral elements.

13.39. Repeat Problem 13.36 using the velocity potential formulation and quadrilateral elements.

13.40. Analyze the problem in Fig. P8.53 using (*a*) the stream function and (*b*) the velocity potential formulations. Use an 8 × 8 mesh in the first rectangle and a 4 × 4 mesh in the second. Use a nonuniform mesh of linear rectangular elements such that smaller elements are used near the obstruction.

Solid mechanics (Chapter 8)

13.41. Analyze the torsion of a member of circular cross-section (see Fig. P8.54) for the state of shear stress distribution. Investigate the accuracy with mesh refinements (by subdividing the mesh in Fig. P8.54 with horizontal and vertical lines).

13.42. Analyze the torsion problem in Fig. P8.56.

13.43. Analyze the hollow-cross-section torsion problem in Fig. P8.57 using a mesh of (*a*) linear triangular elements in an octant and (*b*) linear rectangular elements in a quadrant. The meshes should be node-wise-equivalent.

13.44. Analyze the rectangular membrane problem in Fig. P8.59 with 4 × 4 and 8 × 8 meshes of linear rectangular elements in the computational domain. Take $a_{11} = a_{22} = 1$.

13.45. Repeat Problem 13.44 with triangular elements.

13.46. Repeat Problem 13.45 with equivalent meshes of quadratic elements.

13.47. Investigate the convergence of the solution of the circular membrane problem in Fig. P8.60 by subdividing each element into three elements. Compare the nodal values of the deflection obtained with the two meshes.

13.48. Determine the eigenvalues of the rectangular membrane in Fig. P8.59 using a 4 × 4 mesh in the half-domain. Use $c = 1.0$.

13.49. Analyze Problem 8.59 (with a 4 × 4 mesh in the half-domain) for transient response. Assume zero initial conditions and (*a*) $\alpha = \frac{1}{2}$, $\gamma = \frac{1}{2}$ and (*b*) $\alpha = \frac{1}{2}$, $\gamma = \frac{1}{3}$. Use $\Delta t \approx \Delta t_{cr}$ and a sufficient number of time steps to plot the results graphically.

13.50. Determine the eigenvalues of the circular membrane problem in Fig. P8.60 with a refined mesh obtained from that shown in the figure by subdividing the elements.

13.51. Determine the transient response of the problem in Fig. P8.60 (see Problem 13.50). Assume zero initial conditions, $c = 1$ and $f_0 = 1$. Use $\alpha = \gamma = 0.5$, $\Delta t = 0.05$, and plot the center deflection versus time t for $t = 0\text{–}2.4$.

Plane elasticity (Chapter 10)

13.52. Analyze the plane elasticity problem in Fig. P10.7 using (*a*) 4×2 and (*b*) 8×4 meshes of linear rectangular elements and equivalent meshes of quadratic (nine-node) elements. Evaluate the results (i.e., displacements and stresses) qualitatively. Use the plane stress assumption.

13.53. Repeat Problem 13.52 using triangular elements.

13.54–13.63. Analyze the plane elasticity problems shown in Figs. P10.1–10.3 and P10.10–P10.16 using suitable meshes of triangular or rectangular elements (the instructor should specify the element type and mesh).

13.64. Analyze the plane elasticity problem in Fig. P10.7 for natural frequencies. Use an 8×4 mesh of linear rectangular elements and an equivalent mesh of quadratic elements. Use a density of 0.0088.

13.65. Repeat Problem 13.64 with triangular elements.

13.66. Analyze Problem 13.64 for its transient response. Use $\alpha = \frac{1}{2}$, $\gamma = \frac{1}{2}$, and $\Delta t = 10^{-5}$. Assume zero initial conditions.

13.67–13.70. Analyze Problems 13.54–13.57 for their transient response. Use $\alpha = \frac{1}{2}$, $\gamma = \frac{1}{2}$, and $\Delta t = \Delta t_{cr}$.

Viscous incompressible fluids (Chapter 11)

13.71. Analyze the viscous flow problem in Problem 11.8 using an 8×8 mesh of linear rectangular elements. Plot the horizontal velocity $u(0.5, y)$ versus y, and the pressure along the top surface of the cavity. Investigate the effect of the penalty parameter on the solution (see Fig. P11.8).

13.72. Repeat Problem 13.71 with nine-node quadratic elements.

13.73. Repeat Problem 13.71 with eight-node quadratic elements.

13.74. Analyze the slider bearing problem of Example 11.4 to investigate the effect of the penalty parameter on the velocity and pressure fields. Use an 8×8 mesh of linear rectangular elements.

13.75. Repeat Problem 13.74 with nine-node quadratic elements.

13.76. Repeat Problem 13.74 with eight-node quadratic elements.

13.77. Analyze the problem of a viscous incompressible fluid being squeezed through a 4:1 contraction, as shown in Fig. P13.77. Take $L_1 = 10$, $L = 6$, $R_1 = 4$, and $R_2 = 1$, and linear quadrilateral elements. The inlet velocity $u(y)$ is the fully developed solution of the flow between parallel plates. Plot the velocity $u(x, y)$ and pressure along the horizontal centerline.

13.78. Analyze the cavity problem in Problem 13.71 for its transient solution. Use $\rho = 1.0$, zero initial conditions, penalty parameter $\gamma = 10^8$, time parameter $\alpha = 0.5$, and a time step of 0.005 to capture the evolution of $u(0.5, y)$ with time.

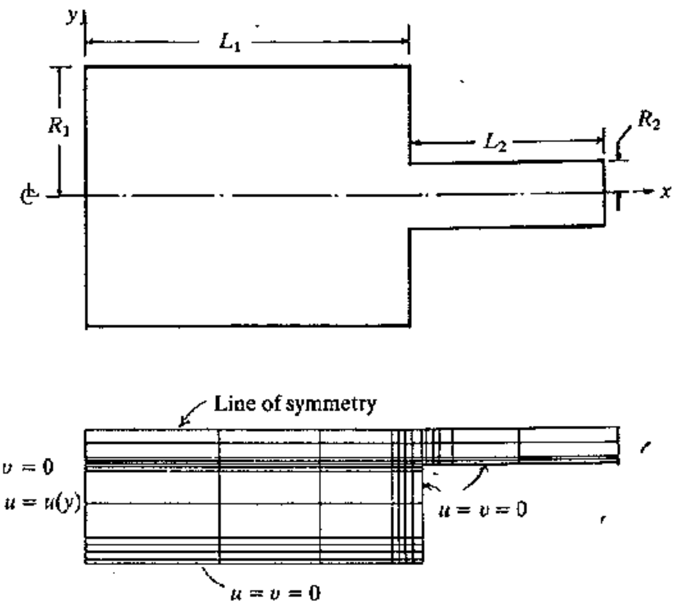

FIGURE P13.77

13.79. Analyze the slider bearing problem of Example 11.4 for its transient solution. Use $\rho = 20$, zero initial conditions, $\gamma = 10^8$, $\alpha = 0.5$, and a time step of 10^{-4}.

Plate bending (Chapter 12)

13.80. Analyze the plate problem in Fig. P12.1 using 2×1, 4×2 and 8×4 meshes of CPT(N) elements in the half-plate, and compare the maximum deflections and stresses.

13.81. Repeat Problem 13.80 with a CPT(C) element.

13.82. Repeat Problem 13.80 with an 8×4 mesh of linear rectangular elements and a 4×2 mesh of nine-node quadratic elements (first-order plate theory).

13.83. Analyze the plate problem in Fig. P12.4 using a 4×4 mesh of CPT(N) elements.

13.84. Repeat Problem 13.83 with CPT(C) elements.

13.85. Repeat Problem 13.83 with a 4×4 mesh of nine-node quadratic elements.

13.86–13.88. Analyze the plate bending problems shown in Figs. P12.7–P12.9 with the CPT(C) elements. Use the mesh shown.

13.89–13.91. Repeat Problems 13.86–13.88 using shear deformation theory. Use linear finite elements.

13.92. Analyze the annular plate in Fig. P12.3 using a four-element mesh (see Fig. P12.7) of CPT(C) elements.

13.93. Repeat Problem 13.92 with four nine-node FSDT elements.

13.94. Analyze the rhombic plate in Fig. P12.6 with a 4×4 mesh of nine-node (FSDT) elements.

13.95. Analyze the plate problem in Fig. P12.1 for its transient response. Use CPT(C) elements and a value of 0.1 for the density.

13.96. Analyze the plate problem in Fig. P12.1 for its transient response using the 4×2 mesh of nine-node quadratic elements (see Problem 13.82) and a value of 0.1 for the density.

13.97. Determine the transient response of the plate in Problem 13.83 with the CPT(C) element.

13.98. Determine the transient response of the plate in Problem 13.83 with the nine-node quadratic element.

13.99. Determine the transient response of the annular plate in Fig. P12.7 using FSDT elements.

REFERENCES FOR ADDITIONAL READING

(See also Chapters 3, 4, 6–12)

Fluid mechanics

Eskinazi, S.: *Principles of Fluid Mechanics,* Allyn and Bacon, Boston 1962.

Bird, R. B., W. E. Stewart, and E. N. Lightfoot: *Transport Phenomena,* John Wiley, New York, 1960.

Duncan, W. J., A. S. Thom, and A. D. Young: *Mechanics of Fluids,* 2d ed., Elsevier, New York, 1970.

Harr, M. E.: *Ground Water and Seepage,* McGraw-Hill, New York, 1962.

Nadai, A.: *Theory of Flow and Fracture of Solids,* vol. II, McGraw-Hill, New York, 1963.

Schlichting, H.: *Boundary-Layer Theory* (translated by J. Kestin), 7th ed., McGraw-Hill, New York, 1979.

Shames, I. H.: *Mechanics of Fluids,* McGraw-Hill, New York, 1962.

Vallentine, H. R.: *Applied Hydrodynamics,* Butterworths, London, 1959.

Verrujit, A.: *Theory of Groundwater Flow,* Gordon and Breach, New York, 1970.

Heat transfer

Carslaw, H. S., and J. C. Jaeger: *Conduction of Heat in Solids,* Clarendon Press, Oxford, 1959.

Holoman, J. P.: *Heat Transfer,* 6th ed., McGraw-Hill, New York, 1986.

Donea, J.: "On the Accuracy of Finite Element Solutions to the Transient Heat-Conduction Equation," *International Journal for Numerical Methods in Engineering,* vol. 8, pp. 103–110, 1974.

Kreith, F.: *Principles of Heat Transfer,* 3d ed., Harper & Row, New York, 1973.

Moore, A. H., B. Kaplan, and D. B. Mitchell: "A Comparison of Crandall and Crank–Nicolson Methods for Solving a Transient Heat Conduction Problem," *International Journal for Numerical Methods in Engineering,* vol. 9, pp. 938–943, 1975.

Myers, G. E.: *Analytical Methods in Conduction Heat Transfer,* McGraw-Hill, New York, 1972.

Özisik, M. N.: *Heat Transfer: A Basic Approach,* McGraw-Hill, New York, 1985.

Wilson, E. L., and R. E. Nickell: "Application of the Finite Element Method to Heat Conduction Analysis," *Journal for Nuclear Engineering and Design,* vol. 4, pp. 276–286, 1966.

Wood, W. L., and R. W. Lewis: "A Comparison of Time Marching Schemes for the Transient Heat Conduction Equation," *International Journal for Numerical Methods in Engineering,* vol. 9, pp. 679–690, 1975.

Plane elasticity

Budynas, R. G.: *Advanced Strength and Applied Stress Analysis,* McGraw-Hill, New York, 1977.

Harris, C. M., and C. E. Crede: *Shock and Vibration Handbook,* vol. 1, McGraw-Hill, New York, 1961.

Ugural, A. C., and S. K. Fenster, *Advanced Strength and Applied Elasticity*, Elsevier, New York, 1975.

Volterra, E., and J. H. Gaines: *Advanced Strength of Materials*, Prentice-Hall, Englewood Cliffs, NJ, 1971.

Plate bending

Dym, C. L., and I. H. Shames: *Solid Mechanics: A Variational Approach*, McGraw-Hill, New York, 1973.

Reddy, J. N.: "A Penalty-Plate Bending Element for the Analysis of Laminated Anisotropic Composite Plates," *International Journal for Numerical Methods in Engineering*, vol. 15, pp. 1187–1206, 1980.

———: "On the Solutions to Forced Motions of Rectangular Composite Plates," *Journal of Applied Mechanics*, vol. 49, pp. 403–408, 1982.

———: *Energy and Variational Methods in Applied Mechanics*, John Wiley, New York, 1984.

Szilard, R.: *Theory and Analysis of Plates*, Prentice-Hall, Englewood Cliffs, NJ, 1974.

Timoshenko, S., and S. Woinowsky-Krieger: *Theory of Plates and Shells*, 2d ed., McGraw-Hill, New York, 1959.

Tsay, C. S., and J. N. Reddy: "Bending, Stability, and Free Vibration of Thin Orthotropic Plates by Simplified Mixed Finite Elements," *Journal of Sound and Vibration*, vol. 59, pp. 307–311, 1978.

Computer Implementation

Akay, H. U., P. G. Willhite, and H. Didandeh: "UCODE2, Version 87.1," Computational Fluid Dynamics Laboratory, Department of Mechanical Engineering, Purdue University at Indianapolis, Indianapolis, 1987.

Bathe, K.-J.: *Finite Element Procedures in Engineering Analysis*, Prentice-Hall, Englewood Cliffs, NJ, 1982.

Burnett, D. S.: *Finite Element Analysis*, Addison-Wesley, Reading, MA, 1987.

Hughes, T. J. R.: *The Finite Element Method*, Prentice-Hall, Englewood Cliffs, NJ, 1987.

Zienkiewicz, O. C., and R. L. Taylor: *The Finite Element Method*, vol. 1, McGraw-Hill, New York, 1989.

PART
4

ADVANCED TOPICS

CHAPTER
14

WEIGHTED-RESIDUAL FINITE ELEMENT MODELS, AND FINITE ELEMENT MODELS OF NONLINEAR AND THREE-DIMENSIONAL PROBLEMS

14.1 INTRODUCTION

The introduction presented in the preceding chapters is sufficient to provide the essential ideas for the development of finite element models and the associated computer programs for most linear boundary and initial value problems, and eigenvalue problems in one and two dimensions. However, there are many additional ideas that deserve some comment. Here we discuss some immediate extensions of the present study to alternative formulations, three-dimensional problems, and nonlinear problems. The discussions are only meant to give some idea of the applicability of the finite element method to these advanced topics, and therefore details are not included here. The topics discussed in this chapter are as follows:

1. Alternative formulations
2. Nonlinear problems
3. Three-dimensional problems

The reader interested in a detailed treatment of any of these topics should consult the books listed in the References at the end of the chapter.

14.2 ALTERNATIVE FORMULATIONS

14.2.1 Introductory Comments

The finite element formulations presented in Chapters 3–12 were based on the weak formulation of the governing differential equations. These models can be termed the *Ritz finite element models* or *weak form finite element models.* In most cases, especially when the governing equations contain derivatives of even order, weak forms can be developed using the three-step procedure. In some cases, the governing equations must be recast in an alternative form that facilitates the use of lower-order interpolations and/or yields better accuracies for the secondary variables, which, as the reader knows, are discontinuous at the interelement boundaries. Here we discuss a couple of such formulations and demonstrate the use of the weighted-residual methods of Section 2.4.3 in the finite element modeling of the equations. More specifically, we shall study the following formulations:

1. Weighted-residual formulations
2. A mixed formulation of the Euler–Bernoulli beam theory

It should be noted that these specific equations have been chosen to illustrate the basic ideas behind the two formulations—the ideas are applicable to other equations, and to two- and three-dimensional problems.

14.2.2 Weighted-Residual Finite Element Models

Here we describe finite element models based on weighted-residual methods. Recall from the preceding chapters that the finite element models presented are based on a weak formulation. In this formulation, integration by parts is used to include the natural boundary conditions in the integral form. Weighted-residual methods are based on a weighted-integral form of a given differential equation. They are the natural and only choice for first-order equations, which do not have a weak formulation. For second- and higher-order equations, we have a choice between the weak formulation and the weighted residual formulation. We begin with the description of weighted-residual finite element models of a first-order equation in one dimension.

1-D FIRST-ORDER EQUATIONS. Consider the first-order equation

$$a\frac{du}{dx}+cu=f \quad \text{for } 0<x<L \tag{14.1}$$

where a, c, and f are given functions of x. An example of a situation in which the above equation arises is given by Newton's law of cooling of a body with temperature u in an environment at temperature u_0:

$$\frac{du}{dt}+k(u-u_0)=0$$

which is the same as (14.1) with $x=t$, $c=k$, $a=1$, and $f=ku_0$.

Since the equation under consideration is of first order, there is no advantage in transferring the derivative to the weight function. Hence, the weighted-integral form to be used here naturally falls under the weighted-residual method. Over an element, we have

$$0 = \int_{x_A}^{x_B} w\left(a\frac{du}{dx} + cu - f\right) dx \tag{14.2}$$

Note that there are no "flux" terms in the equation. When u is approximated by an n-parameter approximation, we need n algebraic equations to solve for the parameters. These n equations are provided by n different (i.e., linearly independent) choices of the weight function w. Different choices of w dictate different methods.

Suppose that u is approximated as

$$u \approx U^e = \sum_{j=1}^{n} u_j^e \psi_j^e(x) \tag{14.3}$$

where u_j^e denote the nodal values of the variable U^e, and $\psi_j^e(x)$ are the interpolation functions. An examination of the weighted-integral statement (14.2) shows that ψ_j should be once-differentiable with respect to x. Hence, the minimum continuity on ψ_j is that they be linear. Consequently, the Lagrange family of interpolation functions are admissible.

The only requirements on the weight function w are (i) that it be integrable in the sense of (14.2), and (ii) that it belong to a linearly independent set $\{w_i\}_{i=1}^{n}$. The ith algebraic equation is obtained by replacing w in (14.2) with w_i. Different choices for the set $\{w_i\}$ have been suggested, and the resulting models bear the names of the original scientists who suggested them. The best-known choices for w_i are

1. The Petrov–Galerkin method: $w_i = \phi_i$ and $\phi_i \neq \psi_i$
2. The Bubnov–Galerkin method: $w_i = \psi_i$
3. The collocation method: $w_i = \delta(x - x_i)$, the Dirac delta function
4. The subdomain method: $w_i = \delta_{ij}$ in the ith subdomain
5. The least-squares method: $w_i = A(\psi_i)$, where A is the operator in the differential equation $Au = f$

(14.4)

The finite element models of (14.1) based on these methods are discussed next.

The Petrov–Galerkin model. Substitute (14.3) for u and $w = \phi_i$ into (14.2) to obtain

$$0 = \sum_{j=1}^{n} K_{ij}u_j - f_i \quad \text{or} \quad [K^e]\{u^e\} = \{f^e\} \tag{14.5a}$$

where

$$K_{ij}^e = \int_{x_A}^{x_B} \left(a\phi_i^e \frac{d\psi_j^e}{dx} + c\phi_i^e\psi_j^e\right) dx, \quad f_i^e = \int_{x_A}^{x_B} \phi_i^e f\, dx \tag{14.5b}$$

The Bubnov–Galerkin model. Here we substitute $w = \psi_i^e$ into (14.2) to obtain the finite element model

$$[K^e]\{u^e\} = \{f^e\} \tag{14.6a}$$

where

$$K_{ij}^e = \int_{x_A}^{x_B} \left(a\psi_i^e \frac{d\psi_j^e}{dx} + c\psi_i^e\psi_j^e \right) dx, \qquad f_i^e = \int_{x_A}^{x_B} f\psi_i^e \, dx \tag{14.6b}$$

Collocation model. In this case, we take $w = \delta(x - x_i)$, the Dirac delta function. The collocation points x_i can be chosen arbitrarily, usually as the quadrature points in $\Omega^e = [x_A, x_B]$. We have

$$K_{ij}^e = a(x_i)\frac{d\psi_j^e}{dx}(x_i) + c(x_i)\psi_j^e(x_i), \qquad f_i^e = f(x_i) \tag{14.7}$$

Subdomain model. In this model, the element domain Ω^e is subdivided further into n subdomains. The weight function for the ith subdomain Ω_i^e is unity over the subdomain and zero outside it:

$$w(x) = \begin{cases} 1 & \text{for } x \in \Omega_i^e \\ 0 & \text{for } x \notin \Omega_i^e \end{cases} \tag{14.8}$$

We obtain

$$K_{ij}^e = \int_{\Omega_i^e} \left(a\frac{d\psi_j^e}{dx} + c\psi_j^e \right) dx, \qquad f_i^e = \int_{\Omega_i^e} f \, dx \tag{14.9}$$

Least-squares model. The weight function in this case is $w \equiv A(\psi_i) = a\,d\psi_i^e/dx + c\psi_i^e$. Consequently, we have

$$K_{ij}^e = \int_{x_A}^{x_B} \left(a\frac{d\psi_i^e}{dx} + c\psi_i^e \right)\left(a\frac{d\psi_j^e}{dx} + c\psi_j^e \right) dx \tag{14.10a}$$

$$f_i^e = \int_{x_A}^{x_B} \left(a\frac{d\psi_i^e}{dx} + c\psi_i^e \right) f \, dx \tag{14.10b}$$

Note that only the least-squares method gives a symmetric coefficient matrix for a single first-order equation. It is possible to obtain a symmetric coefficient matrix in the Galerkin model of a set of first-order equations (see Problem 14.1). Next we consider an example.

Example 14.1. Let us solve (14.1) for the data $a = 1$, $c = 2$, $f = 1$, and $L = 1$, and the boundary condition $u(0) = 1$. We shall use two linear elements in the domain.

For the Bubnov–Galerkin model, we have

$$[K^e] = \frac{1}{2}\begin{bmatrix} -1 & 1 \\ -1 & 1 \end{bmatrix} + \frac{h_e}{3}\begin{bmatrix} 2 & 1 \\ 1 & 2 \end{bmatrix}, \qquad \{f^e\} = \frac{h_e}{2}\begin{Bmatrix} 1 \\ 1 \end{Bmatrix} \tag{14.11}$$

The assembled equations are given by

$$\left(\frac{1}{2}\begin{bmatrix}-1 & 1 & 0\\ -1 & 0 & 1\\ 0 & -1 & 1\end{bmatrix}+\frac{1}{6}\begin{bmatrix}2 & 1 & 0\\ 1 & 4 & 1\\ 0 & 1 & 2\end{bmatrix}\right)\begin{Bmatrix}U_1\\ U_2\\ U_3\end{Bmatrix}=\frac{1}{4}\begin{Bmatrix}1\\ 2\\ 1\end{Bmatrix} \tag{14.12}$$

Using the boundary condition $U_1 = 1$, we obtain from the last two equations

$$\frac{1}{6}\begin{bmatrix}4 & 4\\ -2 & 5\end{bmatrix}\begin{Bmatrix}U_2\\ U_3\end{Bmatrix}=\frac{1}{6}\begin{Bmatrix}5\\ 1.5\end{Bmatrix} \tag{14.13}$$

and their solution is $U_2 = 0.6786$ and $U_3 = 0.5714$. The exact solution is

$$u(x) = u(0)e^{-(c/a)x} + \frac{f}{c}(1 - e^{-(c/a)x}) \tag{14.14}$$

0.6538

The exact values of u at $x = \frac{1}{2}$ and 1 are 0.6389 and 0.5677, respectively.

For the collocation model, we choose $x_1 = \frac{1}{3}h_e$ and $x_2 = \frac{2}{3}h_e$, and obtain

$$[K^e] = \frac{1}{h_e}\begin{bmatrix}-1 & 1\\ -1 & 1\end{bmatrix}+\frac{2}{3}\begin{bmatrix}2 & 1\\ 1 & 2\end{bmatrix}, \qquad \{f^e\} = \begin{Bmatrix}1\\ 1\end{Bmatrix} \tag{14.15}$$

Clearly, the element equations obtained using the collocation points $x_1 = \frac{1}{3}h_e$ and $x_2 = \frac{2}{3}h_e$ are the same as those obtained in the Bubnov–Galerkin method (actually a multiple of $\frac{1}{2}h_e$). Hence, we obtain the same solution as in the Bubnov–Galerkin method.

In the case of the subdomain model, we use $\Omega_1^e = (0, \frac{1}{2}h_e)$ and $\Omega_2^e = (\frac{1}{2}h_e, h_e)$. For this choice, we obtain

$$[K^e] = \frac{1}{2}\begin{bmatrix}-1 & 1\\ -1 & 1\end{bmatrix}+\frac{h_e}{4}\begin{bmatrix}3 & 1\\ 1 & 3\end{bmatrix}, \qquad \underline{\{f^e\} = \frac{3h_e}{8}\begin{Bmatrix}1\\ 1\end{Bmatrix}} \quad ? \tag{14.16}$$

?

The assembled equations become

$$\frac{1}{8}\begin{bmatrix}-1 & 5 & 0\\ -3 & 6 & 5\\ 0 & -3 & 7\end{bmatrix}\begin{Bmatrix}U_1\\ U_2\\ U_3\end{Bmatrix}=\frac{3}{16}\begin{Bmatrix}1\\ 2\\ 1\end{Bmatrix} \tag{14.17}$$

The solution, from the last two equations, is $U_2 = 0.6053$ and $U_3 = 0.4737$.

Last, we consider the least-squares model. We have

$$[K^e] = \frac{1}{h_e}\begin{bmatrix}1 & -1\\ -1 & 1\end{bmatrix}+\frac{4h_e}{6}\begin{bmatrix}2 & 1\\ 1 & 2\end{bmatrix}+\begin{bmatrix}-2 & 0\\ 0 & 2\end{bmatrix} \tag{14.18a}$$

$$\{f^e\} = \begin{Bmatrix}-1\\ 1\end{Bmatrix}+h_e\begin{Bmatrix}1\\ 1\end{Bmatrix} \tag{14.18b}$$

The assembled equations are

$$\frac{1}{3}\begin{bmatrix}-2.5 & -0.5 & 0.0\\ -0.5 & 7.0 & -0.5\\ 0.0 & -0.5 & 9.5\end{bmatrix}\begin{Bmatrix}U_1\\ U_2\\ U_3\end{Bmatrix}=\begin{Bmatrix}-0.5\\ 1.0\\ 1.5\end{Bmatrix} \tag{14.19}$$

TABLE 14.1
Comparison of the numerical solution of (14.1) with the exact solution (Example 14.1)

Nodal values	Bubnov–Galerkin	Collocation	Subdomain	Least-squares	Exact
$u(0.5)$	0.6786	0.6786	0.6053	0.6793	0.6839
$u(1.0)$	0.5714	0.5714	0.4737	0.5094	0.5677

The solution of these equations is

$$U_2 = 0.6793, \qquad U_3 = 0.5094$$

Table 14.1 gives a summary of the solutions obtained using various models.

1-D SECOND-ORDER EQUATIONS. Use of weighted-residual finite element models in the solution of second-order equations is more involved. We describe the finite element models for the model equation

$$-\frac{d}{dx}\left(a\frac{du}{dx}\right) = f \tag{14.20}$$

For the weak formulation of this equation, the approximation functions ψ_i^e must be continuous, as required by the weak form, and they are also required to be the interpolants of u only. The weak form includes the natural boundary conditions associated with the equation, and therefore interpolation of only u (not its derivatives) is required.

In the weighted-residual methods, we use the weighted-integral form of the differential equation without weakening the differentiability on u. Therefore, the continuity conditions on the interpolation functions used in the weighted-residual methods are dictated by the order of the differential equation. For example, the second-order differential equation (14.20) requires the approximation functions to be twice-differentiable with respect to x. In addition, the approximation solution must satisfy the end conditions on the primary and secondary variables (identified with the help of the weak formulation) of the problem. This amounts, for second-order equations, to using approximation functions that make the primary and secondary variables continuous at the nodes connecting two elements (i.e., interelement nodes). For the second-order equation under consideration, the natural boundary condition involves specifying the secondary variable $a\,du/dx$ at the element boundaries. Therefore, the interpolation functions must be selected such that u and $a\,du/dx$ are continuous across an interface between elements. This in turn implies, if a is continuous, that du/dx is continuous throughout the domain $\Omega = (0, L)$. Hence, a C^1 approximation (i.e., Hermite interpolation) of u is required.

Because u and du/dx are required to be continuous across an interface between elements, and a typical element (in one dimension) has two such interfaces, the polynomial approximation of u must involve four parameters, i.e., it must be a cubic polynomial. Thus, the finite element is a line element with two nodes and two degrees of freedom, u and du/dx, at each node. The element is different from the Lagrange cubic element, which has four nodes with one degree of freedom per node. The Lagrange interpolation functions (of any order) do not satisfy the continuity of du/dx across element interfaces, and therefore do not belong to $C^1(0, L)$. The two-node element, with continuous u and du/dx at element interfaces, is the Hermite cubic element developed in Section 4.2 for the Euler–Bernoulli beam element. We have

$$U^e(x) = \sum_{j=1}^{4} u_j^e \psi_j^e(x) \tag{14.21}$$

where u_1^e and u_3^e are the nodal values of U^e, u_2^e and u_4^e are the nodal values of dU^e/dx at the two nodes, and ψ_j^e are the Hermite cubic interpolation functions in (4.10). We consider various weighted-residual finite element models of (14.20).

The weighted-residual form of (14.20) over an element $\Omega^e = (x_A, x_B)$ is

$$0 = \int_{x_A}^{x_B} w\left[-\frac{d}{dx}\left(a\frac{du}{dx}\right) - f\right] dx \tag{14.22}$$

Substituting ϕ_i^e for the weight function w and (14.21) for u, we obtain

$$0 = \sum_{j=1}^{4} K_{ij}^e u_j^e - f_i^e, \quad \text{or} \quad [K^e]\{u^e\} = \{f^e\} \tag{14.23a}$$

where

$$K_{ij}^e = \int_{x_A}^{x_B} \left[-\phi_i^e \frac{d}{dx}\left(a\frac{d\psi_j^e}{dx}\right)\right] dx, \qquad f_i^e = \int_{x_A}^{x_B} \phi_i^e f\, dx \tag{14.23b}$$

Equation (14.23a) is the Petrov–Galerkin model of (14.20) when $\phi_i^e \neq \psi_i^e$.

For different choices of ϕ_i^e in (14.23b), we obtain different finite element models. These are presented below.

The Bubnov–Galerkin model. For $\phi_i^e = \psi_i^e$, (14.23b) becomes

$$K_{ij}^e = \int_{x_A}^{x_B} -\psi_i^e \frac{d}{dx}\left(a\frac{d\psi_j^e}{dx}\right) dx, \qquad f_i^e = \int_{x_A}^{x_B} \psi_i^e f\, dx \tag{14.24}$$

Least-squares model. For $\phi_i^e = A(\psi_i^e) \equiv -(d/dx)(a\, d\psi_i^e/dx)$, we have

$$K_{ij}^e = \int_{x_B}^{x_A} \frac{d}{dx}\left(a\frac{d\psi_i^e}{dx}\right)\frac{d}{dx}\left(a\frac{d\psi_j^e}{dx}\right) dx, \qquad f_i^e = -\int_{x_A}^{x_B} \frac{d}{dx}\left(a\frac{d\psi_i^e}{dx}\right) f\, dx \tag{14.25}$$

Collocation model. For $\phi_i^e = \delta(x - x_i)$, (14.23$b$) takes the form

$$K_{ij}^e = -\left\{\frac{d}{dx}\left[a(x)\frac{d\psi_j^e}{dx}(x)\right]\right\}_{x=x_i}, \qquad f_i^e = f(x_i) \tag{14.26}$$

where x_i are the collocation points.

While the Bubnov–Galerkin and least-squares models have the same form as the Ritz model, i.e., they are defined by integral expressions, the collocation model does not. In the latter, one simply evaluates the coefficient matrices and column vector at the collocation points, instead of evaluating the integral expressions. The number of collocation points should be equal to the number of unknowns, after imposition of the boundary conditions of the problem. For second-order equations, we have two boundary conditions and $2(N+1)$ nodal degrees of freedom for an N-element model. Hence, a total of $2N$ collocation points, two per element, are needed. Also, note that the coefficient matrix in (14.26) is of order 2×4 $(i = 1, 2)$, and there is no overlap of element matrices because there is no summation of equations over the number of elements. However, the continuity conditions on nodal variables are imposed in all other models.

Example 14.2. Consider the boundary value problem

$$-\frac{d}{dx}\left[(1+x)\frac{du}{dx}\right]=0 \quad \text{for } 0<x<1 \tag{14.27a}$$

$$u(0)=0, \qquad \left[(1+x)\frac{du}{dx}\right]\bigg|_{x=1}=1 \tag{14.27b}$$

The exact solution of this problem is

$$u=\ln(1+x) \tag{14.28}$$

We wish to solve the problem using various weighted-residual finite element models.

Consider a two-element discretization of the problem. There are three nodes and six degrees of freedom. The known degrees of freedom for the weighted-residual models are

$$U_1=0, \qquad U_6=0.5 \tag{14.29}$$

whereas, in the four-element Ritz model (i.e., the weak form finite element model) with linear elements, they are

$$U_1=0, \qquad U_5=1.0 \tag{14.30}$$

For the collocation model, the two-point Gauss quadrature points are used as the collocation points. The two- and four-element finite element solutions obtained from three weighted-residual finite element models, all using the Hermite cubics, are compared with the exact solution and the solution of the weak form finite element model in Table 14.2. All models give accurate results.

2-D SECOND-ORDER EQUATIONS. Here we describe the Bubnov–Galerkin, least-squares, and collocation finite element models of a second-order equation in two dimensions. We consider the Poisson equation $(Au=f)$

$$-\frac{\partial}{\partial x}\left(a_{11}\frac{\partial u}{\partial x}\right)-\frac{\partial}{\partial y}\left(a_{22}\frac{\partial u}{\partial y}\right)=f \quad \text{in } \Omega \tag{14.31}$$

TABLE 14.2

Comparison of weighted-residual finite-element solutions† with the exact solution of the problem in (14.27)

x		Exact	Collocation	Bubnov–Galerkin	Least-squares	Ritz
0.00	u	0.00000	0.00000	0.00000	0.00000	0.00000
	u'	1.00000	0.99390 0.99967	0.99604 0.99930	0.99902 0.99993	0.99612 0.99930
0.25	u	0.22314	— 0.22326	— 0.22313	— 0.22315	— 0.22313
	u'	0.80000	— 0.80028	— 0.80004	— 0.79997	— 0.80004
0.50	u	0.40547	0.40487 0.40562	0.40537 0.40546	0.40554 0.40547	0.40538 0.40546
	u'	0.66667	0.66299 0.66646	0.66707 0.66673	0.66645 0.66665	0.66728 0.66674
0.75	u	0.55962	— 0.55975	— 0.55961	— 0.55962	— 0.55961
	u'	0.57143	— 0.57123	— 0.57146	— 0.57142	— 0.57148
1.00	u	0.69315	0.69202 0.69325	0.69309 0.69314	0.69324 0.69315	0.69315 0.69315
	u'	0.50000	0.50000 0.50000	0.50000 0.50000	0.50000 0.50000	0.50102 0.50010

† The first line in each case corresponds to two elements and the second line to four.

In the weighted-residual finite element model, we seek an approximate solution U^e of u in Ω^e in the form

$$U^e = \sum_{j=1}^{16} u_j^e \psi_j^e(x, y) \tag{14.32}$$

where $\psi_j^e(x, y)$ are the conforming Hermite interpolation functions of the four-node rectangular element (see Table 9.1), and u_1^e, u_5^e, u_9^e, and u_{13}^e are the nodal values of U^e at the four nodes of the element, u_2^e, u_6^e, u_{10}^e, and u_{14}^e are the nodal values of $\partial U^e/\partial x$ at the four nodes, and so on. The weighted-residual statement of (14.31) over an element is given by

$$0 = \int_{\Omega^e} w\left[-\frac{\partial}{\partial x}\left(a_{11}\frac{\partial u}{\partial x}\right) - \frac{\partial}{\partial y}\left(a_{22}\frac{\partial u}{\partial y}\right) - f\right] dx\, dy \tag{14.33}$$

Substituting $w = \phi_i^e$ and replacing u by (14.32), we obtain the usual form of the element equations

$$[K^e]\{u^e\} = \{f^e\} \tag{14.34}$$

The specific forms of $[K^e]$ and $\{f^e\}$ are defined below for various models.

The Bubnov–Galerkin model. For $w = \psi_i^e$, the coefficient matrix $[K^e]$ and column vector $\{f^e\}$ are defined by

$$K_{ij}^e = -\int_{\Omega^e} \psi_i^e \left[\frac{\partial}{\partial x}\left(a_{11}\frac{\partial \psi_j^e}{\partial x}\right) + \frac{\partial}{\partial y}\left(a_{22}\frac{\partial \psi_j^e}{\partial y}\right)\right] dx\,dy \tag{14.35a}$$

$$f_i^e = \int_{\Omega^e} \psi_i^e f\,dx\,dy \tag{14.35b}$$

The least-squares model. For $w = A(\psi_i^e)$, where A is the differential operator in (14.31), the coefficients of $[K^e]$ and $\{f^e\}$ are defined by

$$K_{ij}^e = \int_{\Omega^e} \left[\frac{\partial}{\partial x}\left(a_{11}\frac{\partial \psi_i^e}{\partial x}\right) + \frac{\partial}{\partial y}\left(a_{22}\frac{\partial \psi_i^e}{\partial y}\right)\right]\left[\frac{\partial}{\partial x}\left(a_{11}\frac{\partial \psi_j^e}{\partial x}\right) + \frac{\partial}{\partial y}\left(a_{22}\frac{\partial \psi_j^e}{\partial y}\right)\right] dx\,dy \tag{14.36a}$$

$$f_i^e = -\int_{\Omega^e} \left[\frac{\partial}{\partial x}\left(a_{11}\frac{\partial \psi_i^e}{\partial x}\right) + \frac{\partial}{\partial y}\left(a_{22}\frac{\partial \psi_i^e}{\partial y}\right)\right] f\,dx\,dy \tag{14.36b}$$

The collocation model. In this model, we select four collocation points per element and satisfy (14.31) exactly at those four points of each element. For the best results, the Gauss quadrature points are selected. We have

$$K_{ij}^e = \left[-\frac{\partial}{\partial x}\left(a_{11}^e\frac{\partial \psi_j^e}{\partial x}\right) - \frac{\partial}{\partial y}\left(a_{22}^e\frac{\partial \psi_j^e}{\partial y}\right)\right]\Bigg|_{(x,y)=(x_i,y_i)} \tag{14.37a}$$

$$f_i^e = f_e(x_i, y_i) \tag{14.37b}$$

for $i = 1, \ldots, 4$ and $j = 1, 2, \ldots, 16$. Note that the coefficient matrix is rectangular (4×16) and that each coefficient of the global matrix and column vector has a contribution from no more than one element. After imposing the boundary conditions of the problem, the number of linearly independent equations (which is equal to four times the number of elements in the finite element mesh) will be equal to the number of unknown nodal degrees of freedom.

We now consider an application of the weighted-residual models described in (14.35)–(14.37).

Example 14.3. Consider the Dirichlet problem for the Poisson equation [cf. (8.150)]

$$\begin{aligned} -\nabla^2 u &= 2 \quad \text{in } \Omega \\ u &= 0 \quad \text{on } \Gamma \end{aligned} \tag{14.38}$$

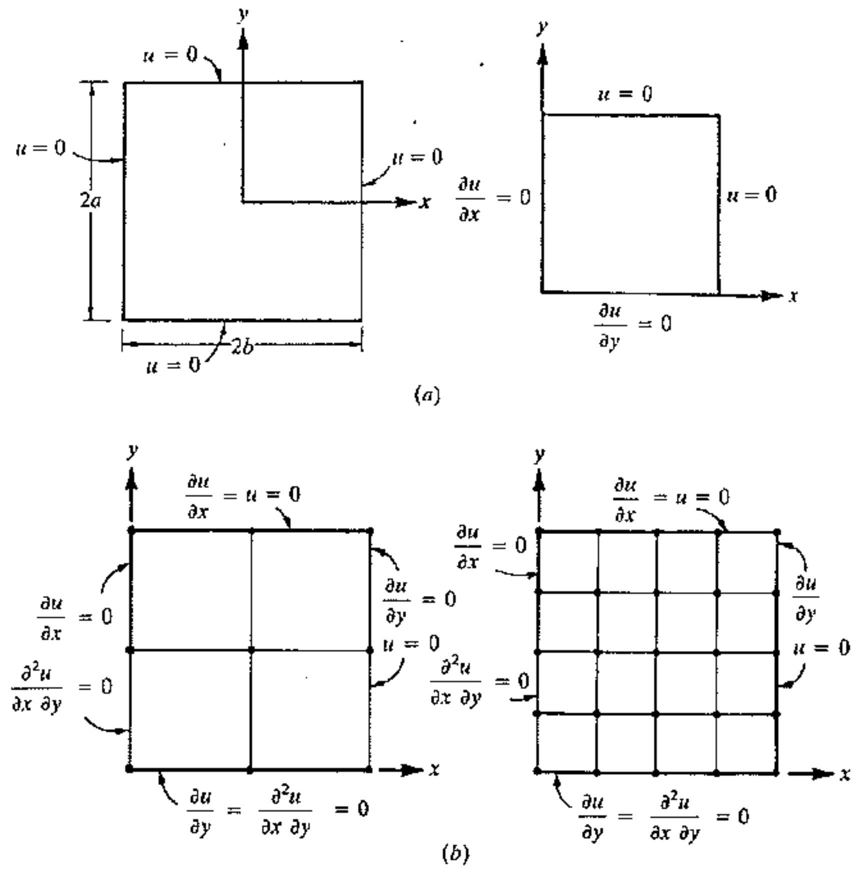
y
u = 0
u = 0
2a
u = 0
x
2b
u = 0
(a)
y
u = 0
$\frac{\partial u}{\partial x} = 0$
u = 0
x
$\frac{\partial u}{\partial y} = 0$
y
$\frac{\partial u}{\partial x} = u = 0$
$\frac{\partial u}{\partial x} = 0$
$\frac{\partial^2 u}{\partial x\, \partial y} = 0$
$\frac{\partial u}{\partial y} = 0$
u = 0
x
$\frac{\partial u}{\partial y} = \frac{\partial^2 u}{\partial x\, \partial y} = 0$
y
$\frac{\partial u}{\partial x} = u = 0$
$\frac{\partial u}{\partial x} = 0$
$\frac{\partial^2 u}{\partial x\, \partial y} = 0$
$\frac{\partial u}{\partial y}$
u = 0
x
$\frac{\partial u}{\partial y} = \frac{\partial^2 u}{\partial x\, \partial y} = 0$
(b)

FIGURE 14.1
(*a*) Domain, boundary conditions, and (*b*) finite element meshes of the problem in Example 14.3.

where Ω is a square region (see Fig. 14.1*a*). The exact solution of this problem is given by (8.152*a*). Exploiting the biaxial symmetry, we model only a quadrant, say the region bounded by the positive axes.

Two different uniform meshes (see Fig. 14.1*b*) of Hermite rectangular elements are used to solve the problem, employing various finite element models. Since the element has u, $\partial u/\partial x$, $\partial u/\partial y$, and $\partial^2 u/\partial x\, \partial y$ as nodal degrees of freedom, we must impose all known boundary values of these quantities (which are not readily known a priori). This can be considered as a drawback of the weighted-residual finite element models (especially, the collocation finite-element model) compared with the Ritz finite element model of a second-order equation, where the only boundary conditions are on u and $\partial u/\partial n$. For the problem at hand, we impose the following boundary conditions: $u = 0$ on the lines $x = 1$ and $y = 1$, $\partial u/\partial x = 0$ on the line $x = 0$, and $\partial u/\partial y = 0$ on the line $y = 0$. The boundary conditions for the weighted residual models are indicated in Fig. 14.1(*b*). For the 2×2 mesh, the number of known boundary conditions is 20, whereas the number of total nodal variables is 36. Thus, for the collocation model, we have 16 unknowns and 16 equations, 4 from each element. Similarly, for the 4×4

mesh, we have 36 boundary conditions among 100 nodal variables, requiring 64 collocation equations, which are provided by the 16 elements.

The finite element solutions obtained from the three finite element models for the two meshes are compared with the exact solution (8.152*a*) in Table 14.3. The collocation finite element solution is relatively more accurate than the other two solutions. The numerical convergence of all three models is apparent from the results.

14.2.3 Mixed Formulations

The equation governing bending of beams according to the Euler–Bernoulli beam theory is

$$\frac{d^2}{dx^2}\left(EI\frac{d^2w}{dx^2}\right) - f = 0 \tag{14.39}$$

TABLE 14.3
Comparison of the various finite element solutions† with the exact solution of the Dirichlet problem for the Poisson equation (14.38) (Example 14.3)

		$u(x, y)$				$\partial u/\partial x$			
x	y	**Exact**	**Bubnov–Galerkin‡**	**Least-squares**	**Col-location**	**Exact**	**Bubnov–Galerkin‡**	**Least-squares**	**Col-location**
0.0	0.0	0.58936	0.58903 0.58935	0.58902 0.58935	0.58932 0.58937	0.00000	0.00000	0.00000	0.00000
0.25	0.0	0.55776	0.55774	0.55774	0.55776	0.25538	0.25568	0.25568	0.25570
0.50	0.0	0.45868	0.45837 0.45866	0.45846 0.45886	0.45862 0.45868	0.54549	0.54436 0.54541	0.54540 0.54543	0.54548 0.54555
0.75	0.0	0.27945	0.27944	0.27945	0.27946	0.90265	0.90176	0.90184	0.90192
1.00	0.00	0.00000	0.00000	0.00000	0.00000	1.33490	1.34628 1.35040	1.34912 1.35064	1.35068 1.35064
0.25	0.25	0.52830	0.52827	0.52827	0.52829	0.23827	0.23680	0.23859	0.23859
0.50	0.25	0.43560	0.43557	0.43558	0.43559	0.51168	0.51162	0.51162	0.51166
0.75	0.25	0.26665	0.26664	0.26665	0.26665	0.85513	0.85416	0.85432	0.85440
1.00	0.25	0.00000	0.00000	0.00000	0.00000	1.28190	1.29712	1.29744	1.29752
0.50	0.50	0.36230	0.36192 0.36226	0.36197 0.36226	0.36225 0.36228	0.40785	0.40744 0.40789	0.40692 0.40783	0.40724 0.40782
0.75	0.50	0.22548	0.22544	0.22545	0.22547	0.70416	0.70317	0.70314	0.70337
1.00	0.50	0.00000	0.00000	0.00000	0.00000	1.1102	1.11576 1.12448	1.1182 1.1252	1.12268 1.12552
0.75	0.75	0.14564	0.14557	0.14557	0.14563	0.42422	0.42355	0.42309	0.42315

† The first line in each case corresponds to the solution obtained using a 2 × 2 mesh and the second to a 4 × 4 mesh.

‡ The Ritz finite-element solution coincides with the Galerkin solution for the same choice of the Hermite interpolation.

The weak form finite element model of this equation requires Hermite cubic interpolation of the transverse deflection w. On the other hand, a weighted-integral finite element model of (14.39) requires the approximation W^e of w to have a nonzero fourth-order derivative, and the element should include w, dw/dx, $EI\,d^2w/dx^2$, and $(d/dx)(EI\,d^2w/dx^2)$ as the nodal degrees of freedom (i.e., seventh-degree Hermite polynomials). To reduce the differentiability requirements on w in the weak form and include the bending moment (or stress) as a nodal degree of freedom, (14.39) can be decomposed into a pair of lower-order equations:

$$\frac{d^2M}{dx^2} - f = 0, \qquad \frac{d^2w}{dx^2} - \frac{M}{b} = 0 \quad (b \neq 0) \tag{14.40}$$

The assumption that the function $b = EI \neq 0$ always holds in practice because neither the modulus of elasticity nor the moment of inertia is zero; in fact, we always have $b > 0$. We can develop either a weak form finite element model or a weighted-integral finite element model of (14.40). Here we discuss the weak form finite element model.

WEAK FORM. The weak form associated with the pair (14.40) over a typical 1-D element (a two-node line element) is given by

$$\begin{aligned} 0 &= \int_{x_A}^{x_B} u\left(\frac{d^2M}{dx^2} - f\right) dx \\ &= -\int_{x_A}^{x_B} \left(\frac{du}{dx}\frac{dM}{dx} + uf\right) dx - u(x_A)\left(\frac{dM}{dx}\right)\bigg|_{x_A} + u(x_B)\left(\frac{dM}{dx}\right)\bigg|_{x_B} \end{aligned} \tag{14.41a}$$

$$\begin{aligned} 0 &= \int_{x_A}^{x_B} v\left(\frac{d^2w}{dx^2} - \frac{M}{b}\right) dx \\ &= -\int_{x_A}^{x_B} \left(\frac{dv}{dx}\frac{dw}{dx} + \frac{vM}{b}\right) dx - v(x_A)\left(\frac{dw}{dx}\right)\bigg|_{x_A} + v(x_B)\left(\frac{dw}{dx}\right)\bigg|_{x_B} \end{aligned} \tag{14.41b}$$

where u and v are the weight functions, which can be viewed as the variations of w and M, respectively ($u \sim \delta w$ and $v \sim \delta M$). The boundary terms in (14.41) indicate that the specifications of w and M constitute the essential boundary conditions, and the specifications of the derivatives dw/dx and dM/dx constitute natural boundary conditions of the problem:

Essential boundary condition

$$\text{specify } w \text{ and } M \text{ (primary variables)} \tag{14.42a}$$

Natural boundary conditions

$$\text{specify } \frac{dw}{dx} \text{ and } \frac{dM}{dx} \text{ (secondary variables)} \tag{14.42b}$$

Note that the natural boundary condition on the bending moment M in the conventional formulation (i.e., the Euler–Bernoulli beam element) becomes

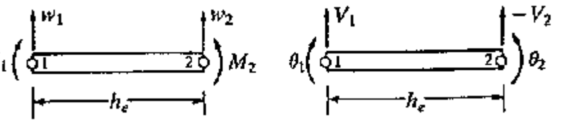

FIGURE 14.2
Generalized displacements and forces for the mixed finite element formulation of the fourth-order equation (14.39) [or the weak form model of (14.40)].

the essential boundary condition in the present formulation. Since both the displacement variable and force variables are used as the nodal degrees of freedom, the finite element model of (14.42) is called a mixed finite element model.

FINITE ELEMENT MODEL. The finite element model of (14.41) is obtained by substituting finite element approximations of the form (see Fig. 14.2 for the nodal variables)

$$w = \sum_{j=1}^{m} w_j \psi_j, \qquad M = \sum_{j=1}^{n} M_j \phi_j \tag{14.43}$$

into the weak forms (14.41). Note that, in general, w and M can be interpolated by different sets of interpolation functions ψ_j and ϕ_j. The finite element equations can be expressed conveniently in the form

$$\begin{bmatrix} [K^{11}] & [K^{12}] \\ [K^{12}]^T & [K^{22}] \end{bmatrix} \begin{Bmatrix} \{w\} \\ \{M\} \end{Bmatrix} = \begin{Bmatrix} \{F^1\} \\ \{F^2\} \end{Bmatrix} \tag{14.44a}$$

where the matrix coefficients $K_{ij}^{\alpha\beta}$ of the matrix $[K^{\alpha\beta}]$ ($\alpha, \beta = 1, 2$) are given by

$$K_{ij}^{11} = 0, \qquad K_{ij}^{12} = \int_{x_A}^{x_B} \frac{d\psi_i}{dx}\frac{d\phi_j}{dx}\,dx = K_{ji}^{21}, \qquad K_{ij}^{22} = \int_{x_A}^{x_B} \frac{1}{b}\,\phi_i\phi_j\,dx$$

$$F_i^1 = \int_{x_A}^{x_B} (-\psi_i f)\,dx - \psi_i(x_A)V_1 - \psi_i(x_B)V_2, \qquad F_i^2 = \phi_i(x_A)\theta_1 + \phi_i(x_B)\theta_2 \tag{14.44b}$$

$$V_1 \equiv \left(\frac{dM}{dx}\right)\bigg|_{x_A}, \qquad V_2 \equiv \left(-\frac{dM}{dx}\right)\bigg|_{x_B}, \qquad \theta_1 \equiv \left(-\frac{dw}{dx}\right)\bigg|_{x_A}, \qquad \theta_2 \equiv \left(\frac{dw}{dx}\right)\bigg|_{x_B}$$

The quantities V_i and θ_i are the secondary variables (shear force and rotation, respectively) associated with w and M at the nodes. It should be pointed out that (14.41) are used in a specific order that gives a symmetric coefficient matrix in (14.44a).

In order to compute the matrix coefficients in (14.44b), we must choose appropriate functions for ψ_i and ϕ_i. For the sake of simplicity, we take $\psi_i = \phi_i$ and ψ_i to be the linear interpolation functions. We obtain ($m = n = 2$), for constant b and f,

$$\begin{aligned} [K^{12}] &= \frac{1}{h_e}\begin{bmatrix} 1 & -1 \\ -1 & 1 \end{bmatrix}, \qquad [K^{22}] = \frac{h_e}{6b_e}\begin{bmatrix} 2 & 1 \\ 1 & 2 \end{bmatrix} \\ \{F^1\} &= \frac{-f_e h_e}{2}\begin{Bmatrix} 1 \\ 1 \end{Bmatrix} - \begin{Bmatrix} V_1 \\ V_2 \end{Bmatrix}, \qquad \{F^2\} = \begin{Bmatrix} \theta_1 \\ \theta_2 \end{Bmatrix} \end{aligned} \tag{14.45}$$

Rearranging the primary variables, the element equations (14.44*a*) can be expressed as

$$\frac{1}{h_e}\begin{bmatrix} 0 & 1 & 0 & -1 \\ 1 & 2\alpha_e & -1 & \alpha_e \\ 0 & -1 & 0 & 1 \\ -1 & \alpha_e & 1 & 2\alpha_e \end{bmatrix}\begin{Bmatrix} w_1 \\ M_1 \\ w_2 \\ M_2 \end{Bmatrix} = -\frac{f_e h_e}{2}\begin{Bmatrix} 1 \\ 0 \\ 1 \\ 0 \end{Bmatrix} + \begin{Bmatrix} -V_1 \\ \theta_1 \\ -V_2 \\ \theta_2 \end{Bmatrix} \tag{14.46}$$

where $\alpha_e = h_e^2/6b_e$.

The usual assembly procedure, which assumes interelement continuity of the primary variables, would result in a continuous bending moment field. This feature is not desirable when the problem involves specified concentrated (i.e., point) moments. Therefore, in general, the moment degrees of freedom should be either eliminated at the element level or not made continuous during the assembly of element equations (14.46). The following example illustrates this point.

Example 14.4. Consider the clamped, simply supported beam shown in Fig. 14.3. We wish to determine its deflection and bending moment using the Euler–Bernoulli beam theory, i.e., (14.40). We take $b = EI =$ constant and $f = 0$. The boundary conditions are

$$w(0) = 0, \qquad \left(EI\frac{d^2w}{dx^2}\right)\Bigg|_{x=h^-}^{x=h^+} = -M_0, \qquad w(2h) = \theta(2h) = 0 \tag{14.47}$$

We wish to analyze the problem using the mixed finite element in (14.44).

For simplicity, we shall use the minimum number of elements that allows us to impose the specified generalized displacements and forces. Thus, we have two elements and three nodes in the mesh. The assembled stiffness matrix is given by

$$\frac{1}{h}\begin{bmatrix} 0 & 1 & 0 & -1 & 0 & 0 \\ 1 & 2\alpha & -1 & \alpha & 0 & 0 \\ 0 & -1 & 0 & 2 & 0 & -1 \\ -1 & \alpha & 2 & 4\alpha & -1 & \alpha \\ 0 & 0 & 0 & -1 & 0 & 1 \\ 0 & 0 & -1 & \alpha & 1 & 2\alpha \end{bmatrix}\begin{Bmatrix} U_1 \\ U_2 \\ U_3 \\ U_4 \\ U_5 \\ U_6 \end{Bmatrix} = \begin{Bmatrix} -V_1^1 \\ \theta_1^1 \\ -V_2^1 - V_1^2 \\ \theta_2^1 + \theta_1^2 \\ -V_2^2 \\ \theta_2^2 \end{Bmatrix} \tag{14.48}$$

The boundary conditions and equilibrium of secondary variables require

$$U_1 = U_2 = U_5 = 0, \qquad -V_2^1 - V_1^2 = 0, \qquad \theta_2^1 + \theta_1^2 = 0, \qquad \theta_2^2 = 0 \tag{14.49}$$

Equations (14.48) become

$$\frac{1}{h}\begin{bmatrix} 0 & 2 & -1 \\ 2 & 4\alpha & \alpha \\ -1 & \alpha & 2\alpha \end{bmatrix}\begin{Bmatrix} U_3 \\ U_4 \\ U_6 \end{Bmatrix} = \begin{Bmatrix} 0 \\ 0 \\ 0 \end{Bmatrix} \tag{14.50}$$

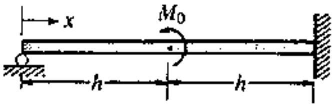

FIGURE 14.3
Clamped, simply supported beam considered in Example 14.4.

If we use the additional boundary condition $U_4 = M_0$, we obtain an inconsistent set of equations. This is the result of the assumption

$$M_2^1 = M_1^2 = U_4 \tag{14.51}$$

used in the assembly. In the present problem, the moment is discontinuous and therefore (14.51) does not hold. The correct condition is

$$M_2^1 - M_1^2 = M_0 \tag{14.52}$$

Suppose that $U_4 = M_1^2 = M_2^1 - M_0$. Then the equations of element 2 become

$$\frac{1}{h}\begin{bmatrix} 0 & 1 & 0 & -1 \\ 1 & 2\alpha & -1 & \alpha \\ 0 & -1 & 0 & 1 \\ -1 & \alpha & 1 & 2\alpha \end{bmatrix} \begin{Bmatrix} w_1^2 \\ M_2^1 - M_0 \\ w_2^2 \\ M_2^2 \end{Bmatrix} = \begin{Bmatrix} -V_1^2 \\ \theta_1^2 \\ -V_2^2 \\ \theta_2^2 \end{Bmatrix} \tag{14.53}$$

The assembled equations for the unknowns, after using the boundary condition (14.52), become

$$\frac{1}{h}\begin{bmatrix} 0 & 2 & -1 \\ 2 & 4\alpha & \alpha \\ -1 & \alpha & 2\alpha \end{bmatrix} \begin{Bmatrix} U_3 \\ M_2^1 \\ U_6 \end{Bmatrix} = \frac{M_0}{h}\begin{Bmatrix} 1 \\ 2\alpha \\ \alpha \end{Bmatrix} \tag{14.54}$$

where the right-hand side comes from the second element when M_1^2 is replaced by $M_1^2 = M_2^1 - M_0$. The solution is

$$U_3 = -\frac{M_0 h^2}{32EI}, \quad M_2^1 = \frac{9M_0}{16}, \quad U_6 = \frac{M_0}{8}, \quad V_1^1 = \frac{9M_0}{16h}, \quad V_2^1 = -\frac{9M_0}{16h} \tag{14.55}$$

Recalling the sign convention for the bending moments in the mixed element (see Fig. 14.2), we note that the solution (14.55) coincides with that given by the conventional model. The reader should verify this statement.

14.3 NONLINEAR PROBLEMS

14.3.1 General Comments

Many engineering problems are described by nonlinear differential equations. Under certain simplifying assumptions, these problems can be described by linear differential equations. For example, the equations governing the large-deflection bending of elastic beams are

$$\boxed{\begin{gathered} -\frac{d}{dx}\left\{EA\left[\frac{du}{dx}+\frac{1}{2}\left(\frac{dw}{dx}\right)^2\right]\right\}-q=0 \\ \frac{d^2}{dx^2}\left(EI\frac{d^2w}{dx^2}\right)-\frac{d}{dx}\left\{EA\frac{dw}{dx}\left[\frac{du}{dx}+\frac{1}{2}\left(\frac{dw}{dx}\right)^2\right]\right\}-f=0 \end{gathered}} \tag{14.56}$$

where u is the longitudinal displacement, w is the transverse deflection, E is the modulus of elasticity, A is the cross-sectional area, q is the axial distributed load, and f is the transverse loading. Under the assumption that the slope

dw/dx is small compared with unity [i.e., $(dw/dx)\,(du/dx)$, $(dw/dx)^2 \approx 0$], (14.56) become uncoupled and reduce to (3.1) and (14.39), respectively. However, when the slope dw/dx is not too small, we must solve the coupled set of nonlinear equations (14.56).

Another example of a nonlinear problem is provided by the equation governing the flow of a viscous incompressible fluid. When the convective effects are larger than the viscous effects, (11.1) should be modified to include the convective terms, that is, the Navier–Stokes equation should be solved:

$$\boxed{\begin{gathered}\rho\left(u\frac{\partial u}{\partial x}+v\frac{\partial u}{\partial y}\right)-\mu\left[2\frac{\partial^2 u}{\partial x^2}+\frac{\partial}{\partial y}\left(\frac{\partial u}{\partial y}+\frac{\partial v}{\partial x}\right)\right]+\frac{\partial P}{\partial x}=f_x\\ \rho\left(u\frac{\partial v}{\partial x}+v\frac{\partial v}{\partial y}\right)-\mu\left[\frac{\partial}{\partial x}\left(\frac{\partial u}{\partial y}+\frac{\partial v}{\partial x}\right)+2\frac{\partial^2 v}{\partial y^2}\right]+\frac{\partial P}{\partial y}=f_y\\ \frac{\partial u}{\partial x}+\frac{\partial v}{\partial y}=0\end{gathered}} \tag{14.57}$$

where ρ is the density of the fluid, and all other symbols have the same meaning as in Chapter 11.

The finite element formulation of nonlinear problems proceeds in much the same way as for linear problems. The main difference lies in the solution of the finite element algebraic equations. Here we describe some details of the formulation, and comment about the solution procedure using equations of large-deflection bending of beams and the Navier–Stokes equations.

14.3.2 Large-Deflection Bending of (Euler–Bernoulli) Beams

Here we use the weak forms of (14.56) to develop the finite element model. These weak forms over an element (x_A, x_B) are

$$0=\int_{x_A}^{x_B}\left\{EA\frac{dv_1}{dx}\left[\frac{du}{dx}+\frac{1}{2}\left(\frac{dw}{dx}\right)^2\right]-v_1 q\right\}dx-Q_1^e v_1(x_A)-Q_4^e v_1(x_B) \tag{14.58a}$$

where v_1 is the weight function ($v_1 \sim \delta u$) and

$$Q_1^e=-\left\{EA\left[\frac{du}{dx}+\frac{1}{2}\left(\frac{dw}{dx}\right)^2\right]\right\}\bigg|_{x_A},\qquad Q_4^e=\left\{EA\left[\frac{du}{dx}+\frac{1}{2}\left(\frac{dw}{dx}\right)^2\right]\right\}\bigg|_{x_B} \tag{14.58b}$$

Similarly,

$$\begin{aligned}0=\int_{x_A}^{x_B}&\left\{EI\frac{d^2v_2}{dx^2}\frac{d^2w}{dx^2}+EA\frac{dv_2}{dx}\frac{dw}{dx}\left[\frac{du}{dx}+\frac{1}{2}\left(\frac{dw}{dx}\right)^2\right]-v_2 f\right\}\\ &-Q_2^e v_2(x_A)-Q_3^e\left(-\frac{dv_2}{dx}\right)\bigg|_{x_A}-Q_5^e v_2(x_B)-Q_6^e\left(-\frac{dv_2}{dx}\right)\bigg|_{x_B}\end{aligned} \tag{14.59a}$$

where v_2 is the weight function ($v_2 \sim \delta w$), and

$$Q_2^e = \left\{ \frac{d}{dx}\left(EI\frac{d^2w}{dx^2}\right) - EA\frac{dw}{dx}\left[\frac{du}{dx} + \frac{1}{2}\left(\frac{dw}{dx}\right)^2\right]\right\}\bigg|_{x_A}, \qquad Q_3^e = \left(EI\frac{d^2w}{dx^2}\right)\bigg|_{x_A}$$

$$Q_5^e = -\left\{ \frac{d}{dx}\left(EI\frac{d^2w}{dx^2}\right) - EA\frac{dw}{dx}\left[\frac{du}{dx} + \frac{1}{2}\left(\frac{dw}{dx}\right)^2\right]\right\}\bigg|_{x_B}, \qquad Q_6^e = -\left(EI\frac{d^2w}{dx}\right)\bigg|_{x_B} \tag{14.59b}$$

The primary variables of the formulation (as in the frame element formulation of the Euler–Bernoulli beam theory) are

$$u, \quad w, \quad -\frac{dw}{dx}$$

From the discussions presented in Chapters 3 and 4, it is clear that we must use a Lagrange interpolation of u and a Hermite interpolation of w:

$$u = \sum_{j=1}^{n} u_j\psi_j(x), \qquad w = \sum_{j=1}^{m} s_j\phi_j(x) \tag{14.60}$$

where ψ_j are the Lagrange interpolation functions of degree $n-1$, and ϕ_j are the Hermite interpolation functions of degree $m-1$. For $n=2$ and $m=4$, the elements used for u and w contain the same number of nodes, which is convenient in the computer implementation of the model (see Fig. 14.4).

Substituting the approximations (14.60) for u and w, and $v_1 = \psi_i^e$ and $v_2 = \phi_i^e$, into (14.58a) and (14.59a), we obtain the finite element model

$$\begin{bmatrix} [K^{11}] & [K^{12}] \\ [K^{21}] & [K^{22}] \end{bmatrix} \begin{Bmatrix} \{u\} \\ \{s\} \end{Bmatrix} = \begin{Bmatrix} \{F^1\} \\ \{F^2\} \end{Bmatrix} \tag{14.61a}$$

where

$$K_{ij}^{11} = \int_{x_A}^{x_B} EA\frac{d\psi_i}{dx}\frac{d\psi_j}{dx}\,dx, \qquad f_i^1 = \int_{x_A}^{x_B} \psi_i q\,dx + Q_{3i-2} \quad (i, j = 1, 2, \ldots, n)$$

$$K_{ij}^{12} = \int_{x_A}^{x_B} \tfrac{1}{2}EA\frac{dw}{dx}\frac{d\psi_i}{dx}\frac{d\phi_j}{dx}\,dx, \qquad K_{ji}^{21} = \int_{x_A}^{x_B} EA\frac{dw}{dx}\frac{d\phi_j}{dx}\frac{d\psi_i}{dx}\,dx$$

$$(i = 1, 2, \ldots, n; j = 1, 2, \ldots, m) \tag{14.61b}$$

$$K_{ij}^{22} = \int_{x_A}^{x_B} EI\frac{d^2\phi_i}{dx^2}\frac{d^2\phi_j}{dx^2}\,dx + \int_{x_A}^{x_B} \tfrac{1}{2}EA\left(\frac{dw}{dx}\right)^2\frac{d\phi_i}{dx}\frac{d\phi_j}{dx}\,dx$$

$$(i, j = 1, 2, \ldots, m)$$

$$F_i^2 = \int_{x_A}^{x_B} \phi_i f\,dx + Q_{i+I}, \quad \begin{cases} I = 1 & \text{if } i = 1 \text{ or } 2 \\ I = 2 & \text{if } i = 3 \text{ or } 4 \end{cases}$$

This completes the finite element model of the nonlinear bending of beams.

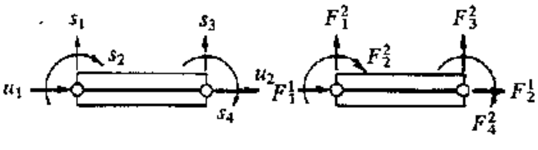

Generalized displacements   Generalized forces

FIGURE 14.4
Nonlinear beam bending element based on linear interpolation of the axial displacement u and Hermite cubic interpolation of the transverse deflection.

14.3.3 Solution Methods for Nonlinear Algebraic Equations

Note that the element stiffness matrix in (14.61*a*) is nonlinear and asymmetric. Therefore, the assembled equations will be nonlinear and asymmetric. The assembled nonlinear equations must be solved, after imposing boundary conditions, using an iterative method, which seeks an approximate solution to the algebraic equations by linearization. The *direct iteration method,* also known as the *Picard method,* is based on the scheme

$$\boxed{[K(\{\Delta\}^r)]\{\Delta\}^{r+1} = \{F\}} \tag{14.62}$$

where $\{\Delta\}^r$ denotes the solution at the rth iteration. Thus, in the direct iteration method, the coefficients K_{ij} (and hence $K_{ij}^{\alpha\beta}$) are evaluated using the solution $\{\Delta\}^r$ from the previous iteration, and the solution at the $(r+1)$th iteration is obtained by solving (14.62):

$$\{\Delta\}^{r+1} = [K(\{\Delta\}^r)]^{-1}\{F\} \tag{14.63}$$

At the beginning of the iteration (i.e., $r=0$), we assume a solution $\{\Delta\}^0$, based on our qualitative understanding of the solution behavior. For example, $\{\Delta\}^0 = \{0\}$ for large-deflection bending would reduce the nonlinear stiffness matrix to a linear one, and (14.63) would yield the linear solution of the problem at the end of the first iteration, $\{\Delta\}^1$. The iteration is continued [i.e., (14.63) is solved in each iteration] until the difference between $\{\Delta\}^r$ and $\{\Delta\}^{r+1}$ reduces to a preselected error tolerance. The *error criterion* is of the form (other criteria can also be used)

$$\boxed{\left(\frac{\sum_{I=1}^{N} |\Delta_I^{r+1} - \Delta_I^r|^2}{\sum_{I=1}^{N} |\Delta_I^{r+1}|^2}\right)^{1/2} < \epsilon \quad (\text{say, } 10^{-3}).} \tag{14.64}$$

where N is the total number of primary unknowns (i.e., generalized displacements) in the finite element mesh.

The other iterative method is the *Newton–Raphson method,* which is based on the Taylor series expansion of the algebraic equations (14.62) about the known solution $\{\Delta\}^r$. To describe the method, we rewrite (14.62) in the form

$$\{R\} \equiv [K]\{\Delta\} - \{F\} = 0 \tag{14.65}$$

where $\{R\}$ denotes the residual. Expanding $\{R\}$ about $\{\Delta\}^r$, we obtain

$$\begin{aligned}\{0\} = \{R\} = \{R\}^r &+ \left(\frac{\partial\{R\}}{\partial\{\Delta\}}\right)^r (\{\Delta\}^{r+1} - \{\Delta\}^r) \\ &+ \frac{1}{2!}\left(\frac{\partial^2\{R\}}{\partial\{\Delta\}^2}\right)^r (\{\Delta\}^{r+1} - \{\Delta\}^r)^2 + \dots\end{aligned} \tag{14.66a}$$

or

$$0 \approx \{R\}^r + [K^T]^r\{\delta\Delta\} + O(\{\delta\Delta\})^2 \tag{14.66b}$$

where $[K^T]$ is the *tangent* (*stiffness*) *matrix*,

$$\boxed{\begin{aligned} &[K^T]^r \equiv \left[\frac{\partial\{R\}}{\partial\{\Delta\}}\right] \quad \text{evaluated at} \quad \{\Delta\} = \{\Delta\}^r \\ &\{\delta\Delta\} = \{\Delta\}^{r+1} - \{\Delta\}^r \quad \text{(incremental solution)} \end{aligned}} \tag{14.66c}$$

For structural problems with variational principles, it can be shown that $[K^T]$ is symmetric even if $[K]$ is not. From (14.66*b*), we have

$$\boxed{\{\delta\Delta\} = -[K^T]^{-1}\{R\}^r = [K^T(\{\Delta\}^r)]^{-1}(\{F\} - [K(\{\Delta\}^r)]\{\Delta\}^r)} \tag{14.67a}$$

and the total solution at the $(r+1)$th iteration is given by

$$\{\Delta\}^{r+1} = \{\Delta\}^r + \{\delta\Delta\} \tag{14.67b}$$

The iteration in (14.66*a*) is continued until the convergence criteria in (14.64) is satisfied or the residual $\{R\}$ [measured in the same way as the solution error in (14.64)] in (14.65) is less than a certain preselected value. For additional details on iterative methods, the References at the end of the chapter.

14.3.4 The 2-D Navier–Stokes Equations

The weak formulation of (14.57) over an element is given by (see Section 11.3 for details)

$$\begin{gathered} \int_{\Omega^e}\left\{w_1\rho\left(u\frac{\partial u}{\partial x} + v\frac{\partial u}{\partial y}\right) + [\cdots]\right\} dx\,dy - \oint_{\Gamma^e} w_1 t_x\,ds = 0 \\ \int_{\Omega^e}\left\{w_2\rho\left(u\frac{\partial v}{\partial x} + v\frac{\partial v}{\partial y}\right) + [\cdots]\right\} dx\,dy - \oint_{\Gamma^e} w_2 t_y\,ds = 0 \\ \int_{\Omega^e} w_3\left(\frac{\partial u}{\partial x} + \frac{\partial v}{\partial y}\right) dx\,dy = 0 \end{gathered} \tag{14.68}$$

where $[\cdots]$ denotes the expressions (omitting the time-derivative terms) in the square brackets of (11.7). The finite element model of these equations is given by

$$\begin{bmatrix} [\bar{K}^{11}] & [K^{12}] & [K^{13}] \\ [K^{12}]^T & [\bar{K}^{22}] & [K^{23}] \\ [K^{13}]^T & [K^{23}]^T & [0] \end{bmatrix} \begin{Bmatrix} \{u\} \\ \{v\} \\ \{P\} \end{Bmatrix} = \begin{Bmatrix} \{F^1\} \\ \{F^2\} \\ \{0\} \end{Bmatrix} \tag{14.69}$$

where $[K^{\alpha\beta}]$ and $\{F^\alpha\}$ $(\alpha, \beta = 1, 2, 3)$ are as defined in (11.9*b*), and

$$\begin{aligned}
\bar{K}_{ij}^{11} &= K_{ij}^{11} + \rho \int_{\Omega^e} \psi_i\left(\bar{u}\frac{\partial \psi_j}{\partial x} + \bar{v}\frac{\partial \psi_j}{\partial y}\right) dx\, dy \\
\bar{K}_{ij}^{22} &= K_{ij}^{22} + \rho \int_{\Omega^e} \psi_i\left(\bar{u}\frac{\partial \psi_i}{\partial x} + \bar{v}\frac{\partial \psi_j}{\partial y}\right) dx\, dy \\
\bar{u} &= \sum_{i=1}^{r} \bar{u}_i\psi_i, \qquad \bar{v} = \sum_{i=1}^{r} \bar{v}_i\psi_i
\end{aligned} \tag{14.70}$$

where $\bar{u}$ and $\bar{v}$ are velocity components that are assumed to be known.

Clearly, the element coefficient matrix, and hence the global coefficient matrix, are unsymmetric, and they depend on the velocity field, which is not known a priori. Therefore, an iterative solution procedure, such as the direct iteration method, is required. At the beginning of the first iteration, the velocity field can be set equal to zero to obtain the linear solution. In the second iteration, the coefficient matrices are evaluated using the velocity field obtained in the first iteration, and the assembled equations are solved again for the nodal velocities. This procedure is repeated until the velocity field obtained at the end of two consecutive iterations differs by a small preassigned number. The convergence criterion can be expressed as

$$\frac{\left[\sum_{i=1}^{N} \left(|U_i^{(r)} - U_i^{(r+1)}|^2 + |V_i^{(r)} - V_i^{(r+1)}|^2\right)\right]^{1/2}}{\left[\sum_{i=1}^{N} \left(|U_i^{(r+1)}|^2 + |V_i^{(r+1)}|^2\right)\right]^{1/2}} \leqslant \epsilon \tag{14.71}$$

where (U_i^r, V_i^r) denote the velocities at node i at the rth iteration. We note that the tangent matrix for the Navier–Stokes equations is not symmetric (because no variational principle exists for this case). The iterative solution methods discussed in Section 14.3.3 are also applicable here.

14.4 THREE-DIMENSIONAL PROBLEMS

Most of the basic ideas covered in Chapters 3 and 8 for one- and two-dimensional problems can be extended to three-dimensional problems. For the sake of completeness, we discuss here the finite element formulation of the Poisson equation in three dimensions, and describe some of the three-dimensional elements.

Consider the Poisson equation

$$-\frac{\partial}{\partial x}\left(k_1\frac{\partial u}{\partial x}\right) - \frac{\partial}{\partial y}\left(k_2\frac{\partial u}{\partial y}\right) - \frac{\partial}{\partial z}\left(k_3\frac{\partial u}{\partial z}\right) = f \quad \text{in } \Omega \tag{14.72a}$$

$$u = \hat{u} \quad \text{on } \Gamma_1, \qquad k_1\frac{\partial u}{\partial x}n_x + k_2\frac{\partial u}{\partial y}n_y + k_3\frac{\partial u}{\partial z}n_z = \hat{q} \quad \text{on } \Gamma_2 \tag{14.72b}$$

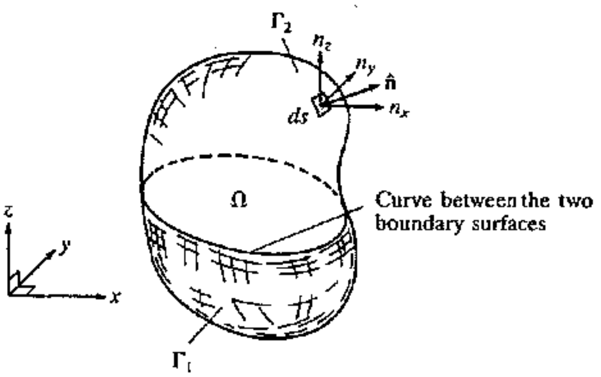

FIGURE 14.5
Three-dimensional domain showing a surface element ds, unit normal and its components $\hat{\mathbf{n}} = (n_x, n_y, n_z)$, and two portions of the boundary Γ.

where $k_i = k_i(x, y, z)$ and $f = f(x, y, z)$ are given functions of position in a three-dimensional domain Ω, and $\hat{u}$ and $\hat{q}$ are specified functions of position on the portions Γ_1 and Γ_2, respectively, of the surface Γ of the domain (see Fig. 14.5). Suppose that the domain Ω is discretized by some three-dimensional elements Ω^e, such as tetrahedral and prism elements (which are the three-dimensional extensions of the triangular and rectangular elements).

The variational formulation of (14.72) over an element Ω^e is given by

$$0 = \int_{\Omega^e} v\left[-\frac{\partial}{\partial x}\left(k_1\frac{\partial u}{\partial x}\right) - \frac{\partial}{\partial y}\left(k_2\frac{\partial u}{\partial y}\right) - \frac{\partial}{\partial z}\left(k_3\frac{\partial u}{\partial z}\right) - f\right] dx\,dy\,dz$$

$$= \int_{\Omega^e}\left[k_1\frac{\partial v}{\partial x}\frac{\partial u}{\partial x} + k_2\frac{\partial v}{\partial y}\frac{\partial u}{\partial y} + k_3\frac{\partial v}{\partial z}\frac{\partial u}{\partial z} - vf\right] dx\,dy\,dz - \oint_{\Gamma^e} vq_n\,ds \qquad (14.73a)$$

where

$$q_n = k_1\frac{\partial u}{\partial x}n_x + k_2\frac{\partial u}{\partial y}n_y + k_3\frac{\partial u}{\partial z}n_z \qquad (14.73b)$$

Clearly, the primary variable is u and the secondary variable is q_n.

Assuming a finite element interpolation of the form

$$u = \sum_{j=1}^{n} u_j\psi_j^e(x, y, z) \qquad (14.74)$$

over the element Ω^e, and substituting $v = \psi_i$ and (14.74) into (14.73a), we obtain

$$\boxed{[K^e]\{u^e\} = \{f^e\} + \{Q^e\}} \tag{14.75a}$$

where

$$\boxed{\begin{gathered} K_{ij}^e = \int_{\Omega^e} \left(k_1 \frac{\partial \psi_i}{\partial x}\frac{\partial \psi_j}{\partial x} + k_2 \frac{\partial \psi_i}{\partial y}\frac{\partial \psi_j}{\partial y} + k_3 \frac{\partial \psi_i}{\partial z}\frac{\partial \psi_j}{\partial z} \right) dx\,dy\,dz \\ f_i^e = \int_{\Omega^e} f\psi_i \,dx\,dy\,dz, \qquad Q_i^e = \oint_{\Gamma^e} q_n \psi_i \,ds \end{gathered}} \tag{14.75b}$$

The interpolation functions ψ_i^e have the same general properties as for two-dimensional elements:

$$\sum_{i=1}^{n} \psi_i^e(x, y, z) = 1, \qquad \psi_i^e(x_j, y_j, z_j) = \delta_{ij} \tag{14.76}$$

The assembly of equations, the imposition of boundary conditions, and the solution of the equations are completely analogous to those described in Chapter 8 for the two-dimensional problems. Next, we comment on the geometry of two linear 3-D elements and the element calculations.

The element matrices in (14.75*b*) require the use of interpolation functions that are at least linear in x, y, and z. Here we consider two linear elements: the tetrahedral element and the prism (or brick) element. These elements are described by approximations of the form

$$\begin{aligned} u(x, y, z) &= a_0 + a_1 x + a_2 y + a_3 z \quad \text{(four-node tetrahedral element)} \\ u(x, y, z) &= a_0 + a_1 x + a_2 y + a_3 z + a_4 yz \\ &\quad + a_5 xz + a_6 xy + a_7 xyz \quad \text{(eight-node prism element)} \end{aligned} \tag{14.77}$$

The interpolation functions can be determined as described in Chapters 8 and 9 for two-dimensional elements.

If the element matrices are to be evaluated numerically, the isoparametric element concept can be used. The geometry of the elements can be described by the transformation equations

$$x = \sum_{i=1}^{n} x_i \hat{\psi}_i(\xi, \eta, \zeta), \qquad y = \sum_{i=1}^{n} y_i \hat{\psi}_i(\xi, \eta, \zeta), \qquad z = \sum_{i=1}^{n} z_i \hat{\psi}_i(\xi, \eta, \zeta) \tag{14.78}$$

Under these transformations, the master tetrahedral and prism elements transform to arbitrary tetrahedral and hexahedral elements, as shown in Fig. 14.6. The definition of the Jacobian matrix and the numerical quadrature rules described in Chapter 9 can easily be extended to the three-dimensional case.

14.5 SUMMARY

Three advanced topics have been discussed briefly in this chapter: (i) weighted-residual and mixed finite element formulations of differential equa-

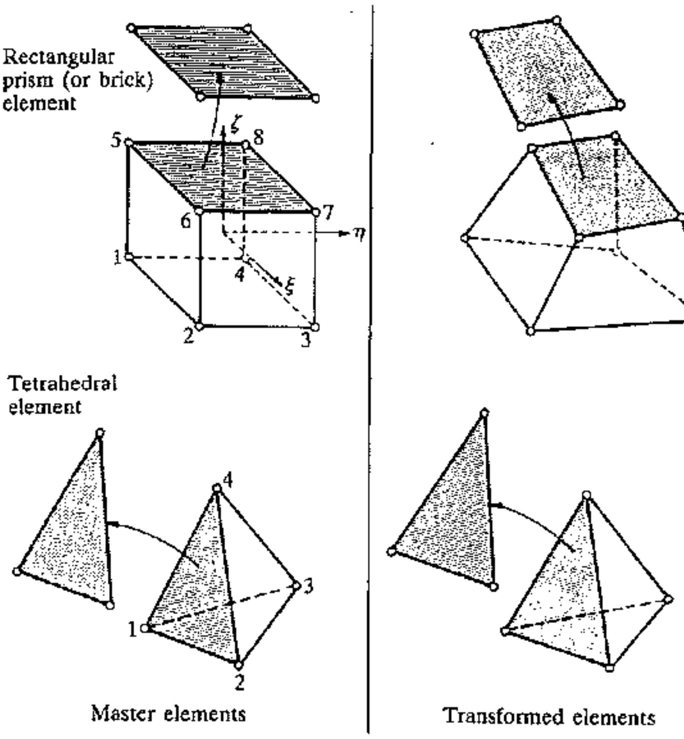

Master elements

Transformed elements

FIGURE 14.6
Linear three-dimensional elements: tetrahedral element and prism element (whose surfaces are two-dimensional triangular and rectangular elements, respectively).

tions; (ii) finite element models of nonlinear equations; and (iii) finite element models of three-dimensional problems. The weighted-residual models discussed include the Petrov–Galerkin model, Bubnov–Galerkin model, collocation model, subdomain model, and least-squares model. First- and second-order differential equations have been considered. Nonlinear finite element models of the Euler–Bernoulli beam theory and the Navier–Stokes equations governing 2-D viscous incompressible flows have been developed. Two iterative schemes, Picard and Newton–Raphson, for solving nonlinear algebraic equations have been discussed. Finally, the finite element formulation of the Poisson equation governing 3-D field problems has been developed. Each of these topics deserves detailed discussion. However, they are not within the scope of the present study. For further study, the reader should consult the books listed in the References.

PROBLEMS

14.1. Consider the second-order equation

$$-\frac{d}{dx}\left(a\frac{du}{dx}\right)=f \qquad \text{(i)}$$

and rewrite it as a pair of first-order equations,

$$-\frac{du}{dx}+\frac{P}{a}=0, \qquad -\frac{dP}{dx}-f=0 \tag{ii}$$

Construct the weighted-residual finite element model of the equations, and specialize it to the Galerkin model. Assume interpolation in the form

$$u=\sum_{j=1}^{m} u_j\psi_j(x), \qquad P=\sum_{j=1}^{n} P_j\phi_j(x) \tag{iii}$$

and use the equations in (ii) in a sequence that yields symmetric element equations:

$$\begin{bmatrix} [K^{11}] & [K^{12}] \\ [K^{12}]^T & [K^{22}] \end{bmatrix} \begin{Bmatrix} \{u\} \\ \{P\} \end{Bmatrix} = \begin{Bmatrix} \{F^1\} \\ \{F^2\} \end{Bmatrix} \tag{iv}$$

The model can also be called a mixed model because (u, P) are of different kinds.

14.2. Evaluate the coefficient matrices $[K^{\alpha\beta}]$ in Problem 14.1 for $a=\text{constant}$ and column vectors $\{F^\alpha\}$ for $f=\text{constant}$. Assume that $\psi_i=\phi_i$ are the linear interpolation functions. Eliminate $\{P\}$ from the two sets of equations (iv) to obtain an equation of the form

$$[K]\{u\}=\{F\}$$

Compare the coefficient matrix $[K]$ and $\{F\}$ with those obtained with the weak form finite element model of (i). What conclusions can you draw?

14.3. Develop the least-squares finite element model of (ii) in Problem 14.1, and compute element coefficient matrices and vectors when $\psi_i=\phi_i$ are the linear interpolation functions.

14.4. Solve the problem in Example 3.1, Set 3 boundary conditions, using two linear elements of the least-squares model developed in Problem 14.3. Compare the results with the exact solution and those of the weak form finite element model.

14.5. For a cantilevered beam of length L and flexural rigidity EI, subjected to a concentrated moment M_0 at $x=\frac{1}{2}L$, obtain the mixed finite element solution and compare it with the exact solution. Do you see any discrepancy in the solutions?

14.6. Consider the pair of equations

$$\nabla u-\mathbf{q}/k=0, \quad \nabla\cdot\mathbf{q}+f=0 \quad \text{in } \Omega$$

where u and $\mathbf{q}$ are the dependent variables, and k and f are given functions of position (x, y) in a two-dimensional domain Ω. Derive the finite element formulation of the equations in the form

$$\begin{bmatrix} [K^{11}] & [K^{12}] & [K^{13}] \\ & [K^{22}] & [K^{23}] \\ \text{symmetric} & & [K^{33}] \end{bmatrix} \begin{Bmatrix} \{u\} \\ \{q^1\} \\ \{q^2\} \end{Bmatrix} = \begin{Bmatrix} \{F^1\} \\ \{F^2\} \\ \{F^3\} \end{Bmatrix}$$

Caution: Do not eliminate the variable u from the given equations.

14.7. Compute the element coefficient matrices $[K^{\alpha\beta}]$ and vectors $\{F^\alpha\}$ of Problem 14.6 using linear triangular elements for all variables. Assume that k is constant.

14.8. Repeat Problem 14.7 with linear rectangular elements.

14.9. Consider the following equations governing a thin, elastic, isotropic plate:

$$-S(M_1-\nu M_2)-\frac{\partial^2 w}{\partial x^2}=0,\qquad -S(M_2-\nu M_1)-\frac{\partial^2 w}{\partial y^2}=0$$

$$\frac{2}{(1+\nu)S}\frac{\partial^4 w}{\partial x^2\,\partial y^2}-\frac{\partial^2 M_1}{\partial x^2}-\frac{\partial^2 M_2}{\partial y^2}-f=0$$

Where M_1 and M_2 are the bending moments, w is the transverse deflection, q is the distributed load, ν is the Poisson ratio, and S is a constant. Give

(*a*) the weak form of the equations, and

(*b*) the finite element model (M_1, M_2, and w are the dependent unknowns) in the form

$$\begin{bmatrix}[K^{11}] & [K^{12}] & [K^{13}]\\ & [K^{22}] & [K^{23}]\\ \text{symmetric} & & [K^{33}]\end{bmatrix}\begin{Bmatrix}\{w\}\\ \{M_1\}\\ \{M_2\}\end{Bmatrix}=\begin{Bmatrix}\{F^1\}\\ \{F^2\}\\ \{F^3\}\end{Bmatrix},$$

14.10. Use the interpolation

$$w=\sum_{j=1}^{4} w_j\psi_j,\qquad M_1=\sum_{j=1}^{2} m_1^j\phi_j^1,\qquad M_2=\sum_{j=1}^{2} m_2^j\phi_j^2$$

with

$$\psi_1=(1-x)(1-y),\qquad \psi_2=x(1-y),\qquad \psi_3=xy,\qquad \psi_4=(1-x)y$$

$$\phi_1^1=1-x,\qquad \phi_2^1=x,\qquad \phi_1^2=1-y,\qquad \phi_2^2=y$$

for a rectangular element with sides a and b to evaluate the matrices $[K^{\alpha\beta}]$ ($\alpha,\beta=1,2,3$) in Problem 14.9.

14.11. Repeat Problem 14.10 for the case in which $\phi_i^1=\phi_i^2=\psi_i$.

14.12. Evaluate the element matrices in (14.61*b*) by assuming that the nonlinear parts in the element coefficients are element-wise-constant.

14.13. Give the finite element formulation of the following nonlinear equation over an element (x_A, x_B):

$$-\frac{d}{dx}\left(u\frac{du}{dx}\right)+1=0\quad\text{for }0<x<1$$

$$\left(\frac{du}{dx}\right)\bigg|_{x=0}=0,\qquad u(1)=\sqrt{2}$$

14.14. Compute the tangent coefficient matrix for the nonlinear problems in Problem 14.13. What restriction(s) should be placed on the initial guess vector?

14.15. Compute the tangent stiffness matrix $[K^T]$ in (14.66*c*) for the Euler–Bernoulli beam element in (14.61*b*).

14.16. Develop the nonlinear finite element model of the Timoshenko beam theory. Equations (14.56) are valid for this case, with the following changes. In place of $(d^2/dx^2)(b\,d^2w/dx^2)$ use $-(d/dx)(b\,d\Psi/dx)+GAk(dw/dx+\Psi)$ and add the following additional equation for w:

$$-\frac{d}{dx}\left[GAk\left(\frac{dw}{dx}+\Psi\right)\right]=f$$

See Section 4.4 for additional details.

14.17. Compute the tangent stiffness matrix for the Timoshenko beam element in Problem 14.16.

14.18. (*Natural convection in flow between heated vertical plates*) Consider the flow of a viscous incompressible fluid in the presence of a temperature gradient between two stationary long vertical plates. Assuming zero pressure gradient between the plates, we can write $u = u(y)$, $v = 0$, $T = T(y)$, and

$$0 = \rho\beta g(T - T_m) + \mu\frac{d^2u}{dy^2}, \qquad 0 = k\frac{d^2T}{dy^2} + \mu\left(\frac{du}{dy}\right)^2$$

where $T_m = \frac{1}{2}(T_0 + T_1)$ is the mean temperature of the two plates, g the gravitational acceleration, ρ the density, β the coefficient of thermal expansion, μ the viscosity, and k the thermal conductivity of the fluid. Give a finite element formulation of the equations and discuss the solution strategy for the computational scheme.

14.19. The equations given in Problem 14.18 are a special case of the more general Navier–Stokes equations (which are nonlinear and coupled) for two-dimensional flow:

(*a*) *Mass continuity*

$$\frac{\partial u}{\partial x} + \frac{\partial v}{\partial y} = 0$$

(*b*) *Conservation of momentum*

$$\rho\left(u\frac{\partial u}{\partial x} + v\frac{\partial u}{\partial y}\right) = -\frac{\partial P}{\partial x} + 2\mu\frac{\partial^2 u}{\partial x^2} + \mu\frac{\partial}{\partial y}\left(\frac{\partial u}{\partial y} + \frac{\partial v}{\partial x}\right) + \rho g\beta(T - T_m)$$

$$\rho\left(u\frac{\partial v}{\partial x} + v\frac{\partial v}{\partial y}\right) = -\frac{\partial P}{\partial y} + \mu\frac{\partial}{\partial x}\left(\frac{\partial u}{\partial y} + \frac{\partial v}{\partial x}\right) + 2\mu\frac{\partial^2 v}{\partial y^2}$$

(*c*) Energy equation

$$\rho c\left(u\frac{\partial T}{\partial x} + v\frac{\partial T}{\partial y}\right) = k\left(\frac{\partial^2 T}{\partial x^2} + \frac{\partial^2 T}{\partial y^2}\right)$$

where c is the specific heat (the x coordinate is taken vertically downward). Construct the finite element model of the equations, and discuss the computational strategy through a flow chart.

14.20. Derive the interpolation functions ψ_1, ψ_5, and ψ_8 for the eight-node prism element using the alternative procedure described in Section 8.2.

14.21. Give the finite element formulation of the heat conduction equation in three dimensions with convective boundary condition. Use a rectangular cartesian system.

14.22. Give the penalty finite element model of the three-dimensional flow equations in cartesian coordinates.

14.23. Repeat Problem 14.21 in cylindrical coordinates.

14.24. Repeat Problem 14.22 in cylindrical coordinates.

14.25. Evaluate the source vector components f_i^e and coefficients K_{ij}^e over a master prism element when f is a constant, f_0, and $k_1 = k_2 = k_3 =$ constant in (14.75*b*).

REFERENCES FOR ADDITIONAL READING

Baker, A. J.: *Finite Element Computational Fluid Mechanics*, McGraw-Hill, New York/Hemisphere, Washington, DC, 1983.

Bathe, K. J.: *Finite Elements in Engineering Analysis*, Prentice-Hall, Englewood Cliffs, NJ, 1982.

Carey, G. F., and J. T. Oden: *Finite Elements: A Second Course*, Prentice-Hall, Englewood Cliffs, NJ, 1983*a*.

——— and ———: *Finite Elements: Computational Aspects*, Prentice-Hall, Englewood Cliffs, NJ, 1983*b*.

Chandrupatla, T. R., and A. D. Belegundu: *Introduction to Finite Elements in Engineering*, Prentice-Hall, Englewood Cliffs, NJ, 1991.

Cook, R. D., S. D. Malkus, and M. E. Plesha: *Concepts and Applications of Finite Analysis*, 3d ed., John Wiley, New York, 1989.

Desai, C. S., and J. F. Abel: *Introduction to the Finite Element Method*, Van Nostrand-Reinhold, New York, 1972.

Gallagher, R. H.: *Finite Element Analysis: Fundamentals*, Prentice-Hall, Englewood Cliffs, NJ, 1975.

Huebner, K. H., and E. A. Thornton: *The Finite Element Method for Engineers*, 2d ed., John Wiley, New York, 1982.

Hughes, T. J. R.: *The Finite Element Method*, Prentice-Hall, Englewood Cliffs, NJ, 1986.

Irons, B., and S. Ahmad: *Techniques of Finite Elements*, Ellis Horwood, Chichester, Sussex/Halsted Press, New York, 1980.

———: "Quadrature Rules for Brick-Based Finite Elements," *International Journal for Numerical Methods in Engineering*, vol. 3, pp. 293–294, 1971.

Oden, J. T.: *Finite Elements of Nonlinear Continua*, McGraw-Hill, New York, 1972.

——— and G. F. Carey: *Finite Elements: Special Problems in Solid Mechanics*, vol. V, Prentice-Hall, Englewood Cliffs, NJ, 1984.

Rao, S. S.: *The Finite Element Method in Engineering*, Pergamon Press, New York, 1982.

Reddy, J. N.: *Energy and Variational Methods in Applied Mechanics*, John Wiley, New York, 1984.

———: *Applied Functional Analysis and Variational Methods in Engineering*, McGraw-Hill, New York, 1986.

Zienkiewicz, O. C., and R. L. Taylor: *The Finite Element Method*, vols. 1 and 2, McGraw-Hill, New York, 1989 and 1991.

APPENDICES

APPENDIX
1

COMPUTER PROGRAM FEM1DV2

```
C       Program Name: FEM1DV2                          Length: 2194 lines F1D00010
C       * * * * * * * * * * * * * * * * * * * * * * * * * * * * * * * * *F1D00020
C       *                    Program  FEM1DV2                            *F1D00030
C       *     (AN IN-CORE FINITE ELEMENT ANALYSIS COMPUTER PROGRAM)      *F1D00040
C       * * * * * * * * * * * * * * * * * * * * * * * * * * * * * * * * *F1D00050
C                                                                         F1D00060
C       |                                                               | F1D00070
C       |  This is a finite element computer program for the analysis   | F1D00080
C       |  of following three model equations and others:               | F1D00090
C       |                                                               | F1D00100
C       |  1. Heat transfer, fluid mechanics, bars, and cables:         | F1D00110
C       |                                                               | F1D00120
C       |           CT.u* + CT.u** - (AX.u')' + CX.u = FX               | F1D00130
C       |                                                               | F1D00140
C       |  2. The Timoshenko beam and circular plate theory:            | F1D00150
C       |                                                               | F1D00160
C       |           CT0.w** - [AX.(w' + s)]' + CX.w = FX                | F1D00170
C       |           CT1.s** - (BX.s')' + AX.(w' + s) = 0                | F1D00180
C       |                                                               | F1D00190
C       |  3. The Euler-Bernoulli beam and circular plate theory:       | F1D00200
C       |                                                               | F1D00210
C       |             CT.w** + (BX.w'')'' + CX.w = FX                   | F1D00220
C       |                                                               | F1D00230
C       | In the above equations  (')  and (*) denote  differentiations | F1D00240
C       | with respect to space x and time t,  and  AX, BX, CX, CT, and | F1D00250
C       | FX are functions of x only:                                   | F1D00260
C       |                                                               | F1D00270
C       |   AX = AX0 + AX1.X,  BX = BX0 + BX1.X,  CX = CX0 + CX1.X      | F1D00280
C       |        CT = CT0 + CT1.X,  FX = FX0 + FX1.X + FX2.X.X          | F1D00290
C       |                                                               | F1D00300
C       |   In addition to the three model equations, other equations   | F1D00310
C       | (for example, disks, trusses, and frames) can be analyzed by  | F1D00320
C       | the program.                                                  | F1D00330
C       |                                                               | F1D00340
```

```
C
C      ______________________________________________________________________
C      .
C      .              KEY VARIABLES USED IN THE PROGRAM
C      .      (see Table 7.4 for a description of other variables)
C      .
C      . NDF....... Number of degrees of freedom per node
C      . NEQ....... Number of equations in the model (before B. C.)
C      . NGP....... Number of Gauss points used in the evaluation of
C      .            the element coeffcients, [ELK], {ELF}, [ELM]
C      . NHBW...... Half bandwidth of global coefficient matrix [GLK]
C      . NN ....... Number of total degrees of freedom in the element
C      . NPE....... Number of nodes per element
C      ______________________________________________________________________
C      .
C      .          DIMENSIONS OF VARIOUS ARRAYS IN THE PROGRAM
C      .
C      . Values of MXELM,MXNOD, etc. in the PARAMETER statement should
C      .         be changed to meet the requirements of problem:
C      .
C      . MXELM..... Maximum number of elements in the mesh:
C      . MXEBC..... Maximum number of speci. primary deg. of freedom
C      . MXMBC..... Maximum number of speci. mixed boundary conditions
C      . MXNBC..... Maximum number of speci. secondary deg. of freedom
C      . MXNEQ..... Maximum number of equations in the FE model
C      . MXNOD..... Maximum number of nodes in the mesh
C      .
C      . NOTE:  The following dimension statement in subroutine JACOBI
C      .        should be modified when MXNEQ is greater than 50:
C      .          DIMENSION  V(50,50),VT(50,50),W(50,50),IH(50)
C      .        The value of MXNEQ should be used in place of '50'
C      ______________________________________________________________________
C      .
C      .               SUBROUTINES USED IN THE PROGRAM
C      .
C      .  ASSMBL, AXLBX, BONDRY COEFNT, ECHO, JACOBI, MESH1D, MTRXML,
C      .    PSTPRC, REACTN, SHP1D, SOLVER, TMSFRC, TMSTRS, TRSFRM
C      ______________________________________________________________________
C
      IMPLICIT REAL*8(A-H,O-Z)
      PARAMETER  (MXELM=20,MXNEQ=50,MXEBC=10,MXNBC=10,MXMBC=10,MXNOD=25)
      DIMENSION  DCAX(MXELM,2),DCBX(MXELM,2),DCCX(MXELM,2),DCFX(MXELM,3)
      DIMENSION  GU0(MXNEQ),GU1(MXNEQ),GU2(MXNEQ),GPU(MXNEQ),DX(MXNOD)
      DIMENSION  IBDY(MXEBC),ISPV(MXEBC,2),ISSV(MXNBC,2),INBC(MXMBC,2)
      DIMENSION  GLM(MXNEQ,MXNEQ),GLF(MXNEQ),GLX(MXNOD),NOD(MXELM,4)
      DIMENSION  CS(MXELM),SN(MXELM),CNT(MXELM),SNT(MXELM),XB(MXELM)
      DIMENSION  EGNVAL(MXNEQ),EGNVEC(MXNEQ,MXNEQ),GLK(MXNEQ,MXNEQ)
      DIMENSION  PR(MXELM),SE(MXELM),SL(MXELM),SA(MXELM),SI(MXELM)
      DIMENSION  HF(MXELM),VF(MXELM),PF(MXELM),F3(MXELM),TITLE(20)
      DIMENSION  UREF(MXMBC),VSPV(MXEBC),VSSV(MXNBC),VNBC(MXMBC)
      COMMON/STF1/ELK(9,9),ELM(9,9),ELF(9),ELX(4),ELU(9),ELV(9),ELA(9)
      COMMON/STF2/A1,A2,A3,A4,A5,AX0,AX1,BX0,BX1,CX0,CX1,CT0,CT1,FX0,
     *             FX1,FX2
      COMMON/IO/IN,IT
C
C               ---------------------------------------------------
C              |                                                   |
C              |        P R E P R O C E S S O R   U N I T          |
C              |                                                   |
C               ---------------------------------------------------
C
      IN=5
      IT=6
      NT=0
      NSSV=0
      JVEC=1
      TIME=0.0D0
      TOLRNS=1.0D-06
      CALL ECHO(IN,IT)
C
      READ(IN,300) TITLE
      READ(IN,*) MODEL,NTYPE,ITEM
      READ(IN,*) IELEM,NEM
      READ(IN,*) ICONT,NPRNT
C
      IF(MODEL.GE.3)THEN
        NPE=2
```

```
         IF(MODEL.EQ.4 .AND. NTYPE.GE.1)THEN                            F1D01100
             NDF=3                                                      F1D01110
         ELSE                                                           F1D01120
             NDF=2                                                      F1D01130
         ENDIF                                                          F1D01140
         IF(MODEL.EQ.4 .AND. NTYPE.EQ.2)THEN                            F1D01150
             IELEM=1                                                    F1D01160
         ELSE                                                           F1D01170
             IELEM=0                                                    F1D01180
         ENDIF                                                          F1D01190
      ELSE                                                              F1D01200
         IF(MODEL.EQ.2)THEN                                             F1D01210
             NDF=2                                                      F1D01220
             IF(NTYPE.GT.1)IELEM=1                                      F1D01230
         ELSE                                                           F1D01240
             NDF=1                                                      F1D01250
         ENDIF                                                          F1D01260
         NPE=IELEM+1                                                    F1D01270
      ENDIF                                                             F1D01280
C                                                                       F1D01290
      NNM = NEM*(NPE-1)+1                                               F1D01300
      NN  = NPE*NDF                                                     F1D01310
      NEM1=NEM + 1                                                      F1D01320
      IF(MODEL.NE.4)THEN                                                F1D01330
C                                                                       F1D01340
C     Data input for BAR-LIKE and BEAM problems (MODEL=1,2, AND 3)      F1D01350
C                                                                       F1D01360
          IF(ICONT.NE.0)THEN                                            F1D01370
              READ(IN,*) (DX(I), I=1,NEM1)                              F1D01380
              CALL MESH1D(NEM,NNM,NPE,NOD,MXELM,MXNOD,DX,GLX)           F1D01390
              READ(IN,*) AX0,AX1                                        F1D01400
              READ(IN,*) BX0,BX1                                        F1D01410
              READ(IN,*) CX0,CX1                                        F1D01420
              IF(ITEM.NE.3)THEN                                         F1D01430
                  READ(IN,*) FX0,FX1,FX2                                F1D01440
              ENDIF                                                     F1D01450
          ELSE                                                          F1D01460
C                                                                       F1D01470
C     Read GLX, NOD, and element-wise continuous coefficients (DC.X)    F1D01480
C                                                                       F1D01490
              DO 10 N=1,NEM                                             F1D01500
              II=(N-1)*(NPE-1)+1                                        F1D01510
              JJ=N*(NPE-1)+1                                            F1D01520
              READ(IN,*) (GLX(K),K=II,JJ)                               F1D01530
              READ(IN,*) (NOD(N,I),I=1,NPE)                             F1D01540
              READ(IN,*) (DCAX(N,I),I=1,2)                              F1D01550
              READ(IN,*) (DCBX(N,I),I=1,2)                              F1D01560
              READ(IN,*) (DCCX(N,I),I=1,2)                              F1D01570
   10         READ(IN,*) (DCFX(N,I),I=1,3)                              F1D01580
          ENDIF                                                         F1D01590
C                                                                       F1D01600
      ELSE                                                              F1D01610
C                                                                       F1D01620
C     Input data for plane TRUSS or FRAME structures (MODEL=4)          F1D01630
C                                                                       F1D01640
          READ(IN,*)NNM                                                 F1D01650
          IF(NTYPE.NE.0)THEN                                            F1D01660
              DO 20 N=1,NEM                                             F1D01670
              READ(IN,*) PR(N),SE(N),SL(N),SA(N),SI(N),CS(N),SN(N)      F1D01680
              READ(IN,*) HF(N),VF(N),PF(N),XB(N),CNT(N),SNT(N)          F1D01690
   20         READ(IN,*) (NOD(N,I),I=1,2)                               F1D01700
          ELSE                                                          F1D01710
              DO 30 N=1,NEM                                             F1D01720
              READ(IN,*) SE(N),SL(N),SA(N),CS(N),SN(N),HF(N)            F1D01730
   30         READ(IN,*) (NOD(N,I),I=1,2)                               F1D01740
          ENDIF                                                         F1D01750
      ENDIF                                                             F1D01760
      NEQ=NNM*NDF                                                       F1D01770
C                                                                       F1D01780
C     Read data on BOUNDARY CONDITIONS of three kinds: Dirichlet (PV)   F1D01790
C               Neumann (SV), and Newton’s (MIXED) types                F1D01800
C                                                                       F1D01810
      READ(IN,*) NSPV                                                   F1D01820
      IF(NSPV.NE.0)THEN                                                 F1D01830
          DO 40 NB=1,NSPV                                               F1D01840
          IF(ITEM.GT.2)THEN                                             F1D01850
              READ(IN,*) (ISPV(NB,J),J=1,2)                             F1D01860
          ELSE                                                          F1D01870
              READ(IN,*) (ISPV(NB,J),J=1,2),VSPV(NB)                    F1D01880
          ENDIF                                                         F1D01890
   40     CONTINUE                                                      F1D01900
      ENDIF                                                             F1D01910
C                                                                       F1D01920
      IF(ITEM.LE.2)THEN                                                 F1D01930
          READ(IN,*) NSSV                                               F1D01940
          IF(NSSV.NE.0)THEN                                             F1D01950
              DO 50 IB=1,NSSV                                           F1D01960
   50         READ(IN,*) (ISSV(IB,J),J=1,2),VSSV(IB)                    F1D01970
          ENDIF                                                         F1D01980
      ENDIF                                                             F1D01990
C                                                                       F1D02000
      READ(IN,*) NNBC                                                   F1D02010
      IF(NNBC.NE.0)THEN                                                 F1D02020
          DO 60 I=1, NNBC                                               F1D02030
   60     READ(IN,*) (INBC(I,J),J=1,2),VNBC(I),UREF(I)                  F1D02040
      ENDIF                                                             F1D02050
C                                                                       F1D02060
      IF(ITEM .NE. 0)THEN                                               F1D02070
C                                                                       F1D02080
C     Input data here for TIME-DEPENDENT problems                       F1D02090
C                                                                       F1D02100
          READ(IN,*) CT0,CT1                                            F1D02110
          IF(ITEM.LE.2)THEN                                             F1D02120
              READ(IN,*) DT,ALFA,GAMA                                   F1D02130
              READ(IN,*) INCOND,NTIME,INTVL                             F1D02140
              A1=ALFA*DT                                                F1D02150
              A2=(1.0-ALFA)*DT                                          F1D02160
              IF(INCOND.NE.0)THEN                                       F1D02170
                  READ(IN,*) (GU0(I),I=1,NEQ)                           F1D02180
              ELSE                                                      F1D02190
                  DO 70 I=1,NEQ                                         F1D02200
   70             GU0(I)=0.0                                            F1D02210
              ENDIF                                                     F1D02220
              IF(ITEM.EQ.2)THEN                                         F1D02230
                  A3=2.0/GAMA/(DT*DT)                                   F1D02240
                  A4=A3*DT                                              F1D02250
                  A5=1.0/GAMA-1.0                                       F1D02260
                  IF(INCOND.NE.0)THEN                                   F1D02270
                      READ(IN,*) (GU1(I),I=1,NEQ)                       F1D02280
                  ELSE                                                  F1D02290
                      DO 80 I=1,NEQ                                     F1D02300
                      GU1(I)=0.0                                        F1D02310
   80                 GU2(I)=0.0                                        F1D02320
                  ENDIF                                                 F1D02330
              ENDIF                                                     F1D02340
          ENDIF                                                         F1D02350
      ENDIF                                                             F1D02360
C                                                                       F1D02370
C     ----------------------------------------------------------------- F1D02380
C      E  N  D     O  F     T  H  E     I  N  P  U  T      D  A  T  A   F1D02390
C     ----------------------------------------------------------------- F1D02400
C     Compute the half BANDWIDTH of the coefficient matrix GLK          F1D02410
C                                                                       F1D02420
      NHBW=0.0                                                          F1D02430
      DO 90 N=1,NEM                                                     F1D02440
      DO 90 I=1,NPE                                                     F1D02450
      DO 90 J=1,NPE                                                     F1D02460
      NW=(IABS(NOD(N,I)-NOD(N,J))+1)*NDF                                F1D02470
   90 IF(NHBW.LT.NW) NHBW=NW                                            F1D02480
C                                                                       F1D02490
C     ----------------------------------------------------------------- F1D02500
C               P  R  I  N  T     T  H  E     I  N  P  U  T     D  A  T  A F1D02510
C     ----------------------------------------------------------------- F1D02520
C                                                                       F1D02530
      WRITE(IT,530)                                                     F1D02540
      WRITE(IT,310)                                                     F1D02550
      WRITE(IT,530)                                                     F1D02560
      WRITE(IT,300) TITLE                                               F1D02570
      WRITE(IT,320) MODEL,NTYPE                                         F1D02580
      WRITE(IT,350) IELEM,NDF,NEM,NEQ,NSPV,NSSV,NNBC                    F1D02590
```

```
C                                                                       F1D02600
      IF(ITEM.NE.0)THEN                                                 F1D02610
          IF(ITEM.LE.2)THEN                                             F1D02620
              WRITE(IT,330)                                             F1D02630
              WRITE(IT,390) CT0,CT1,ALFA,GAMA,DT,NTIME,INTVL            F1D02640
              IF(INCOND.NE.0)THEN                                       F1D02650
                  WRITE(IT,370)                                         F1D02660
                  WRITE(IT,540) (GU0(I),I=1,NEQ)                        F1D02670
                  IF(ITEM.EQ.2)THEN                                     F1D02680
                      WRITE(IT,380)                                     F1D02690
                      WRITE(IT,540) (GU1(I),I=1,NEQ)                    F1D02700
                  ENDIF                                                 F1D02710
              ENDIF                                                     F1D02720
          ELSE                                                          F1D02730
              WRITE(IT,340)                                             F1D02740
              WRITE(IT,400) CT0,CT1                                     F1D02750
          ENDIF                                                         F1D02760
      ENDIF                                                             F1D02770
C                                                                       F1D02780
      IF(NSPV.NE.0)THEN                                                 F1D02790
          WRITE(IT,480)                                                 F1D02800
          DO 100 IB=1,NSPV                                              F1D02810
          IF(ITEM.LE.2)THEN                                             F1D02820
              WRITE(IT,490) (ISPV(IB,J),J=1,2),VSPV(IB)                 F1D02830
          ELSE                                                          F1D02840
              WRITE(IT,490) (ISPV(IB,J),J=1,2)                          F1D02850
          ENDIF                                                         F1D02860
  100     CONTINUE                                                      F1D02870
      ENDIF                                                             F1D02880
C                                                                       F1D02890
      IF(NSSV.NE.0)THEN                                                 F1D02900
          WRITE(IT,500)                                                 F1D02910
          DO 110 IB=1,NSSV                                              F1D02920
  110     WRITE(IT,490) (ISSV(IB,J),J=1,2),VSSV(IB)                     F1D02930
      ENDIF                                                             F1D02940
C                                                                       F1D02950
      IF(NNBC.NE.0)THEN                                                 F1D02960
          WRITE(IT,510)                                                 F1D02970
          DO 120 I=1,NNBC                                               F1D02980
  120     WRITE(IT,490) (INBC(I,J),J=1,2),VNBC(I),UREF(I)               F1D02990
      ENDIF                                                             F1D03000
C                                                                       F1D03010
      IF(MODEL.NE.4)THEN                                                F1D03020
          IF(ICONT.EQ.1)THEN                                            F1D03030
              WRITE(IT,410)                                             F1D03040
              WRITE(IT,540) (GLX(I),I=1,NNM)                            F1D03050
              WRITE(IT,420)                                             F1D03060
              IF(MODEL.NE.3)THEN                                        F1D03070
                  WRITE(IT,440) AX0,AX1,BX0,BX1,CX0,CX1,FX0,FX1,FX2     F1D03080
              ELSE                                                      F1D03090
                  WRITE(IT,445) AX0,AX1,BX0,BX1,CX0,CX1                 F1D03100
              ENDIF                                                     F1D03110
          ELSE                                                          F1D03120
              DO 130 N=1,NEM                                            F1D03130
              II=(N-1)*(NPE-1)+1                                        F1D03140
              JJ=N*(NPE-1)+1                                            F1D03150
              WRITE(IT,430) N,GLX(II),GLX(JJ)                           F1D03160
  130         WRITE(IT,440) (DCAX(N,I),I=1,2),(DCBX(N,I),I=1,2),        F1D03170
     *                      (DCCX(N,I),I=1,2),(DCFX(N,I),I=1,3)         F1D03180
          ENDIF                                                         F1D03190
      ELSE                                                              F1D03200
          DO 140 N=1,NEM                                                F1D03210
          WRITE(IT,460) N                                               F1D03220
          IF(NTYPE.NE.0)THEN                                            F1D03230
              WRITE(IT,450) PR(N),SE(N),SL(N),SA(N),SI(N),CS(N),SN(N),  F1D03240
     *                      HF(N),VF(N),PF(N),XB(N),CNT(N),SNT(N),      F1D03250
     *                      (NOD(N,I),I=1,2)                            F1D03260
          ELSE                                                          F1D03270
              WRITE(IT,470) SE(N),SL(N),SA(N),CS(N),SN(N),HF(N),        F1D03280
     *                      (NOD(N,I),I=1,2)                            F1D03290
          ENDIF                                                         F1D03300
  140     CONTINUE                                                      F1D03310
      ENDIF                                                             F1D03320
C                                                                       F1D03330
```

```
C                                                                       F1D03340
C              P R O C E S S O R   U N I T                              F1D03350
C                                                                       F1D03360
C                                                                       F1D03370
C     TIME MARCHING scheme begins here. For  ITEM=2, initial conditions F1D03380
C     on second derivatives of the solution are computed in the program F1D03390
C                                                                       F1D03400
      IF(ITEM.NE.0)THEN                                                 F1D03410
          IF(ITEM.EQ.1)THEN                                             F1D03420
              NT=NT+1                                                   F1D03430
              TIME=TIME+DT                                              F1D03440
          ENDIF                                                         F1D03450
      ENDIF                                                             F1D03460
C                                                                       F1D03470
      IF(ITEM.GT.2)NHBW=NEQ                                             F1D03480
C                                                                       F1D03490
C     Initialize global matrices and vectors                            F1D03500
C                                                                       F1D03510
  150 DO 160 I=1,NEQ                                                    F1D03520
      GLF(I)=0.0                                                        F1D03530
      DO 160 J=1,NHBW                                                   F1D03540
      IF(ITEM.GT.2)THEN                                                 F1D03550
          GLM(I,J)=0.0                                                  F1D03560
      ENDIF                                                             F1D03570
  160 GLK(I,J)=0.0                                                      F1D03580
C                                                                       F1D03590
C     Do-loop for ELEMENT CALCULATIONS and ASSEMBLY                     F1D03600
C                                                                       F1D03610
      DO 200 NE = 1, NEM                                                F1D03620
      IF(MODEL.NE.4)THEN                                                F1D03630
          IF(ICONT.NE.1) THEN                                           F1D03640
              AX0=DCAX(NE,1)                                            F1D03650
              AX1=DCAX(NE,2)                                            F1D03660
              BX0=DCBX(NE,1)                                            F1D03670
              BX1=DCBX(NE,2)                                            F1D03680
              CX0=DCCX(NE,1)                                            F1D03690
              CX1=DCCX(NE,2)                                            F1D03700
              FX0=DCFX(NE,1)                                            F1D03710
              FX1=DCFX(NE,2)                                            F1D03720
              FX2=DCFX(NE,3)                                            F1D03730
          ENDIF                                                         F1D03740
C                                                                       F1D03750
          L=0                                                           F1D03760
          DO 180 I=1,NPE                                                F1D03770
          NI=NOD(NE,I)                                                  F1D03780
          ELX(I)=GLX(NI)                                                F1D03790
          IF(ITEM.EQ.1 .OR. ITEM.EQ.2)THEN                              F1D03800
              LI=(NI-1)*NDF                                             F1D03810
              DO 170 J=1,NDF                                            F1D03820
              LI=LI+1                                                   F1D03830
              L=L+1                                                     F1D03840
              ELU(L)=GU0(LI)                                            F1D03850
              IF(ITEM.EQ.2 .AND. NT.GT.0)THEN                           F1D03860
                  ELV(L)=GU1(LI)                                        F1D03870
                  ELA(L)=GU2(LI)                                        F1D03880
              ENDIF                                                     F1D03890
  170         CONTINUE                                                  F1D03900
          ENDIF                                                         F1D03910
  180     CONTINUE                                                      F1D03920
C                                                                       F1D03930
          CALL COEFNT(IELEM,ITEM,MODEL,NDF,NPE,TIME,NTYPE,NE,F3,MXELM)  F1D03940
      ELSE                                                              F1D03950
          CALL TRSFRM (MXELM,MXNEQ,NE,NTYPE,PR,SE,SL,SA,SI,CS,SN,       F1D03960
     *                CNT,SNT,HF,VF,PF,XB)                              F1D03970
      ENDIF                                                             F1D03980
C                                                                       F1D03990
      IF(NPRNT .NE.0)THEN                                               F1D04000
          IF(NPRNT .LE.2)THEN                                           F1D04010
              IF(NE.EQ.1 .AND. NT.LE.1)THEN                             F1D04020
                  WRITE(IT,550)                                         F1D04030
                  DO 190 I=1,NN                                         F1D04040
  190             WRITE(IT,540) (ELK(I,J),J=1,NN)                       F1D04050
                  IF(ITEM.GT.2)THEN                                     F1D04060
                      WRITE(IT,360)                                     F1D04070
                      DO 195 I=1,NN                                     F1D04080
  195                 WRITE(IT,540)  (ELM(I,J),J=1,NN)
                  ELSE
                      WRITE(IT,560)
                      WRITE(IT,540)  (ELF(I),I=1,NN)
                  ENDIF
              ENDIF
          ENDIF
      ENDIF
C
C     Assemble element matrices
C
      CALL ASSMBL(NOD,MXELM,MXNEQ,NDF,NPE,NE,ITEM,GLK,GLM,GLF)
C
  200 CONTINUE
      IF(NPRNT.EQ.2)THEN
C
C     Print assembled coefficient matrices if required
C
          WRITE(IT,570)
          DO 210 I=1,NEQ
  210     WRITE(IT,540)  (GLK(I,J),J=1,NHBW)
          IF(ITEM.GT.2)THEN
              WRITE(IT,575)
              DO 215 I=1,NEQ
  215         WRITE(IT,540)  (GLM(I,J),J=1,NHBW)
          ELSE
              WRITE(IT,580)
              WRITE(IT,540)  (GLF(I),I=1,NEQ)
          ENDIF
      ENDIF
C
C     Call subroutine BONDRY to impose essential, natural and Newton's
C     type boundary conditions on the primary and secondary variables.
C
      CALL BONDRY(NEQ,NEQR,NHBW,NSPV,NSSV,NNBC,NDF,DT,ITEM,ALFA,IBDY,
     *            ISPV,ISSV,INBC,UREF,VSPV,VSSV,VNBC,GLK,GLM,GLF,GU0,
     *            MXEBC,MXNBC,MXMBC,MXNEQ)
C
      IF(ITEM.GT.2)THEN
C
C     Call subroutine AXLBX to solve for the eigenvalues and eigenvector
C
          CALL AXLBX(NEQR,GLK,GLM,EGNVAL,EGNVEC,JVEC,NROT,MXNEQ)
C
          WRITE(IT,690) NROT
          DO 230 NVEC=1,NEQR
          FRQNCY=DSQRT(EGNVAL(NVEC))
          WRITE(IT,700)NVEC,EGNVAL(NVEC),FRQNCY
  230     WRITE(IT,540)(EGNVEC(I,NVEC),I=1,NEQR)
          STOP
      ENDIF
C
      IRES = 0
C
C     Call subroutine SOLVER to solve the finite-element equations
C
      CALL SOLVER(MXNEQ,MXNEQ,NEQ,NHBW,GLK,GLF,IRES)
C
      IF(ITEM.EQ.0)THEN
          WRITE(IT,590)
          WRITE(IT,540)  (GLF(NI),NI=1,NEQ)
      ELSE
          IF(NT.EQ.0)THEN
              DO 240 I=1,NEQ
  240         GU2(I)=GLF(I)
              NT=NT+1
              TIME=TIME+DT
              GOTO 150
          ENDIF
C
C     Compute and print current values of GU0, GU1, and GU2
C
          DO 250 I=1,NEQ
          IF(ITEM.EQ.2)THEN
              ACCLRN=A3*(GLF(I)-GU0(I))-A4*GU1(I)-A5*GU2(I)
```

```
             GU1(I)=GU1(I)+A2*GU2(I)+A1*ACCLRN
             GU2(I)=ACCLRN
             GPU(I)=GU0(I)
         ELSE
             GPU(I)=GU0(I)
         ENDIF
 250     GU0(I)=GLF(I)
C
         DIFF=0.0
         SOLN=0.0
         DO 260 I=1,NEQ
         SOLN=SOLN+GU0(I)*GU0(I)
 260     DIFF=DIFF+(GLF(I)-GPU(I))**2
         PRCNT=DIFF/SOLN
         IF(PRCNT.LE.TOLRNS)THEN
             STOP
         ELSE
             IF(INTVL.LE.0)INTVL=1
             NTEN=(NT/INTVL)*INTVL
             IF(NTEN.EQ.NT)THEN
                 WRITE(IT,600) TIME, NT
                 WRITE(IT,590)
                 WRITE(IT,540) (GU0(I),I=1,NEQ)
                 IF(ITEM.NE.1) THEN
                     WRITE(IT,540) (GU1(I),I=1,NEQ)
                     WRITE(IT,540) (GU2(I),I=1,NEQ)
                 ENDIF
                 NT=NT+1
                 TIME=TIME+DT
             ELSE
                 NT=NT+1
                 TIME=TIME+DT
                 GOTO 150
             ENDIF
         ENDIF
      ENDIF
C
C
C              P O S T - P R O C E S S O R   U N I T
C
C
      IF(NPRNT.LE.1)THEN
         IF(MODEL.EQ.1)THEN
             WRITE(IT,530)
         ELSE
             IF(MODEL.EQ.4)THEN
                 WRITE(IT,630)
             ENDIF
             WRITE(IT,520)
         ENDIF
C
         IF(MODEL.EQ.1)THEN
             IF(NTYPE.EQ.0)THEN
                 WRITE(IT,610)
             ELSE
                 WRITE(IT,620)
             ENDIF
         ENDIF
C
         IF(MODEL.EQ.2 .OR. MODEL.EQ.3)THEN
             IF(NTYPE.EQ.0)THEN
                 WRITE(IT,650)
             ELSE
                 WRITE(IT,660)
             ENDIF
         ENDIF
C
         IF(MODEL.EQ.4)THEN
             IF(NTYPE.EQ.0)THEN
                 WRITE(IT,680)
             ELSE
                 WRITE(IT,670)
             ENDIF
         ENDIF
```

```
C
          IF(MODEL.EQ.1)THEN
              WRITE(IT,530)
          ELSE
              WRITE(IT,520)
          ENDIF
C
          IF(MODEL.LE.3)THEN
C
              CALL PSTPRC(F3,GLF,GLX,NOD,AX0,IELEM,NPE,MODEL,NTYPE,ITEM,
     *                    MXELM,MXNEQ,MXNOD,NEM,NDF)
          ELSE
              CALL REACTN(MXELM,MXNEQ,NDF,NEM,NOD,NPE,NTYPE,PR,GLF,
     *                    SE,SL,SA,SI,CS,SN,CNT,SNT,HF,VF,PF,XB)
          ENDIF
C
          IF(MODEL.EQ.1)THEN
              WRITE(IT,530)
          ELSE
              WRITE(IT,520)
          ENDIF
      ENDIF
C
      IF(ITEM.EQ.0)STOP
      IF(NT.LT.NTIME)THEN
          IF(PRCNT.GT.TOLRNS)THEN
              GOTO 150
          ENDIF
      ELSE
          WRITE(IT,710)
      ENDIF
C
C     ------------------------------------------------------------------
C                       F    O    R    M    A    T    S
C     ------------------------------------------------------------------
C
 300 FORMAT(20A4)
 310 FORMAT(4X,'OUTPUT FROM PROGRAM   FEM1DV2  BY  J. N. REDDY')
 320 FORMAT(/,4X,'*** ANALYSIS OF MODEL',I2,', AND TYPE',I2,
     *       ' PROBLEM ***',/,15X,'(see the code below)',/,
     *       /,4X,'MODEL=1,NTYPE=0: A problem described by MODEL EQ. 1',
     *       /,4X,'MODEL=1,NTYPE=1: A circular DISK (PLANE STRESS) ',
     *       /,4X,'MODEL=1,NTYPE>1: A circular DISK (PLANE STRAIN) ',
     *       /,4X,'MODEL=2,NTYPE=0: A Timoshenko BEAM (RIE) problem',
     *       /,4X,'MODEL=2,NTYPE=1: A Timoshenko PLATE (RIE) problem',
     *       /,4X,'MODEL=2,NTYPE=2: A Timoshenko BEAM (CIE) problem',
     *       /,4X,'MODEL=2,NTYPE>2: A Timoshenko PLATE (CIE) problem',
     *       /,4X,'MODEL=3,NTYPE=0: A Euler-Bernoulli BEAM problem',
     *       /,4X,'MODEL=3,NTYPE>0: A Euler-Bernoulli Circular plate',
     *       /,4X,'MODEL=4,NTYPE=0: A plane TRUSS problem',
     *       /,4X,'MODEL=4,NTYPE=1: A Euler-Bernoulli FRAME problem',
     *       /,4X,'MODEL=4,NTYPE=2: A Timoshenko (CIE) FRAME problem',/)
 330 FORMAT(/,4X,'TIME-DEPENDENT (TRANSIENT) ANALYSIS ',/)
 340 FORMAT(/,4X,'E I G E N V A L U E   A N A L Y S I S',/)
 350 FORMAT(/,10X, 'Element type (0, Hermite,>0, Lagrange)..=',I4,/,
     *         10X, 'No. of deg. of freedom per node, NDF....=',I4,/,
     *         10X, 'No. of elements in the mesh, NEM........=',I4,/,
     *         10X, 'No. of total DOF in the model, NEQ......=',I4,/,
     *         10X, 'No. of specified primary DOF, NSPV......=',I4,/,
     *         10X, 'No. of specified secondary DOF, NSSV....=',I4,/,
     *         10X, 'No. of specified Newton B. C.: NNBC.....=',I4)
 360 FORMAT(/,3X,'Element coefficient matrix, [ELM]:',/)
 370 FORMAT(/,3X, 'Initial conditions on the primary variables:',/)
 380 FORMAT(/,3X, 'Initial cond. on time der. of primary variables:',/)
 390 FORMAT(/,10X,'Coefficient, CT0........................=',E12.4,/,
     *         10X,'Coefficient, CT1........................=',E12.4,/,
     *         10X,'Parameter, ALFA.........................=',E12.4,/,
     *         10X,'Parameter, GAMA.........................=',E12.4,/,
     *         10X,'Time increment, DT......................=',E12.4,/,
     *         10X,'No. of time steps, NTIME................=',I4,/,
     *         10X,'Time-step interval to print soln., INTVL=',I4,/)
 400 FORMAT(/,10X,'Coefficient, CT0........................=',E12.4,/,
     *         10X,'Coefficient, CT1........................=',E12.4,/)
 410 FORMAT(/,3X,'Global coordinates of the nodes, {GLX}:',/)
```

```
420 FORMAT(/,3X,'Coefficients of the differential equation:',/)             F1D06320
430 FORMAT(/,5X,'Properties of Element =',I3,//,                            F1D06330
   *          10X,'XA  =',E12.4,5X,'XB  =',E12.4)                           F1D06340
440 FORMAT(  10X,'AX0 =',E12.4,5X,'AX1 =',E12.4,/,                          F1D06350
   *          10X,'BX0 =',E12.4,5X,'BX1 =',E12.4,/,                         F1D06360
   *          10X,'CX0 =',E12.4,5X,'CX1 =',E12.4,/,                         F1D06370
   *          10X,'FX0 =',E12.4,5X,'FX1 =',E12.4,5X,'FX2 =',E12.4,/)        F1D06380
445 FORMAT(  10X,'AX0 =',E12.4,5X,'AX1 =',E12.4,/,                          F1D06390
   *          10X,'BX0 =',E12.4,5X,'BX1 =',E12.4,/,                         F1D06400
   *          10X,'CX0 =',E12.4,5X,'CX1 =',E12.4,/)                         F1D06410
450 FORMAT(10X,'The poisson ratio,           PR........ =',E12.4,/,         F1D06420
   *       10X,'Modulus of elasticity,       SE........ =',E12.4,/,         F1D06430
   *       10X,'Length of the element,       SL........ =',E12.4,/,         F1D06440
   *       10X,'Area of cross section,       SA........ =',E12.4,/,         F1D06450
   *       10X,'Moment of inertia,           SI........ =',E12.4,/,         F1D06460
   *       10X,'Cosine of orientation,       CN........ =',E12.4,/,         F1D06470
   *       10X,'Sine of orientation,         SN........ =',E12.4,/,         F1D06480
   *       10X,'Axial body force (constant), HF........ =',E12.4,/,         F1D06490
   *       10X,'Transverse body force (cnst),VF........ =',E12.4,/,         F1D06500
   *       10X,'Internal point force,        PF........ =',E12.4,/,         F1D06510
   *       10X,'Location of PF from node 1,  XB........ =',E12.4,/,         F1D06520
   *       10X,'Orientation of PF: cosine,   CST....... =',E12.4,/,         F1D06530
   *       10X,'Orientation of PF: sine,     SNT....... =',E12.4,/,         F1D06540
   *       10X,'Nodal connectivity:          NOD(I,J).. =',2I6,/)           F1D06550
460 FORMAT(//,3X,'Element No. =', I3,/)                                     F1D06560
470 FORMAT(10X,'Modulus of elasticity,       SE........ =',E12.4,/,         F1D06570
   *       10X,'Length of the element,       SL........ =',E12.4,/,         F1D06580
   *       10X,'Area of cross section,       SA........ =',E12.4,/,         F1D06590
   *       10X,'Cosine of orientation,       CN........ =',E12.4,/,         F1D06600
   *       10X,'Sine of orientation,         SN........ =',E12.4,/,         F1D06610
   *       10X,'Axial body force (constant), HF........ =',E12.4,/,         F1D06620
   *       10X,'Nodal connectivity:          NOD(I,J).. =',2I6,/)           F1D06630
480 FORMAT(/,3X, 'Boundary information on primary variables:',/)            F1D06640
490 FORMAT(5X,2I5,2E15.5)                                                   F1D06650
500 FORMAT(/,3X, 'Boundary information on secondary variables:',/)          F1D06660
510 FORMAT(/,3X, 'Boundary information on mixed boundary cond.:',/)         F1D06670
520 FORMAT(2X,78('_'),/)                                                    F1D06680
530 FORMAT(2X,55('_'),/)                                                    F1D06690
540 FORMAT(2X,5E13.5)                                                       F1D06700
550 FORMAT(/,3X,'Element coefficient matrix, {ELK}:',/)                     F1D06710
560 FORMAT(/,3X,'Element source vector, {ELF}:',/)                          F1D06720
570 FORMAT(/,3X,'Global coefficient matrix, [GLK]:',/)                      F1D06730
575 FORMAT(/,3X,'Global coefficient matrix, [GLM]:',/)                      F1D06740
580 FORMAT(/,3X,'Global source vector, {GLF}:',/)                           F1D06750
590 FORMAT(/,1X,'SOLUTION (values of PVs) at the NODES: ',/)                F1D06760
600 FORMAT(/,1X,'TIME =',E12.4,5X,'Time step number =',I3,/)                F1D06770
610 FORMAT(7X,'  X  ',5X, 'P. Variable',2X,'S. Variable')                   F1D06780
620 FORMAT(7X,'  X  ',5X, 'Displacemnt',2X,'Radial Strs',2X,                F1D06790
   *       'Hoop Stress')                                                   F1D06800
630 FORMAT(/,9X,'Generalized forces in the element coordinates',/,          F1D06810
   * 5X,'(second line gives the results in the global coordinates)')        F1D06820
650 FORMAT(7X,'  X  ',6X, 'Deflect.',5X,'Rotation',5X,'B. Moment',          F1D06830
   *       3X,'Shear Force')                                                F1D06840
660 FORMAT(7X,'  X  ',6X, 'Deflect.',5X,'Rotation',4X,'Moment, Mr',         F1D06850
   *       3X,'Moment, Mt',3X,'Shear Force')                                F1D06860
670 FORMAT(3X,  'Ele  Force, H1  Force, V1  Moment, M1  Force, H2           F1D06870
   *Force, V2  Moment, M2')                                                 F1D06880
680 FORMAT(3X,  'Ele  Force, H1   Force, V1   Force, H2  Force, V2')        F1D06890
690 FORMAT(/,5X,'Number of rotations taken in JACOBI =',I2,/)               F1D06900
700 FORMAT(/,5X,'EIGENVALUE(',I2,') = ',E14.6,2X,'SQRT(EGNVAL) = ',         F1D06910
   *        E13.5,/,5X,'EIGENVECTOR:')                                      F1D06920
710 FORMAT(/,5X,'***** Number of time steps exceeded NTIME *****',/)        F1D06930
    STOP                                                                    F1D06940
    END                                                                     F1D06950
```

```
      SUBROUTINE ASSMBL(NOD,MXELM,MXNEQ,NDF,NPE,NE,ITEM,GLK,GLM,GLF)
C     ______________________________________________________________________
C
C       The subroutine calls subroutines to compute element matrices
C           and assembles them in a upper banded matrix form
C
C        {ELF}.... Element source vector, {F}
C        {ELK}.... Element coefficient matrix, [K]
C        {ELM}.... Element coefficient matrix, [M]
C        [NOD].... Connectivity matrix
C     ______________________________________________________________________
C
      IMPLICIT REAL*8 (A-H,O-Z)
      DIMENSION  GLK(MXNEQ,MXNEQ),GLM(MXNEQ,MXNEQ),GLF(MXNEQ),
     *           NOD(MXELM,4)
      COMMON/STF1/ELK(9,9),ELM(9,9),ELF(9),ELX(4),ELU(9),ELV(9),ELA(9)
      IF(ITEM.LE.2)THEN
C
C     Assemble element coefficient matrix ELK and source vector ELF
C
         DO 50 I = 1, NPE
         NR = (NOD(NE,I) - 1)*NDF
         DO 40 II = 1, NDF
         NR = NR + 1
         L = (I-1)*NDF + II
         GLF(NR) = GLF(NR) + ELF(L)
         DO 30 J = 1, NPE
         NCL = (NOD(NE,J)-1)*NDF
         DO 20 JJ = 1, NDF
         M = (J-1)*NDF + JJ
         NC = NCL-NR+JJ+1
         IF(NC)20,20,10
   10    GLK(NR,NC) = GLK(NR,NC) + ELK(L,M)
   20    CONTINUE
   30    CONTINUE
   40    CONTINUE
   50    CONTINUE
      ELSE
C
C
C     ASSEMBLE ELEMENT MATRICES INTO FULL GLOBAL MATRICES
C
         DO 100 I=1,NPE
         NR=(NOD(NE,I)-1)*NDF
         DO 90 II=1,NDF
         NR=NR+1
         L=(I-1)*NDF+II
         DO 80 J=1,NPE
         NC=(NOD(NE,J)-1)*NDF
         DO 70 JJ=1,NDF
         M=(J-1)*NDF+JJ
         NC=NC+1
         GLK(NR,NC)=GLK(NR,NC)+ELK(L,M)
   60    GLM(NR,NC)=GLM(NR,NC)+ELM(L,M)
   70    CONTINUE
   80    CONTINUE
   90    CONTINUE
  100    CONTINUE
      ENDIF
      RETURN
      END

      SUBROUTINE AXLBX(N,A,B,XX,X,NEGN,NR,MXNEQ)
C     ______________________________________________________________________
C
C      Subroutine to solve the EIGENVALUE PROBLEM:
C
C                             [A]{X} = Lambda.[B]{X}
C
C      The program can be used only for positive-definite [B] matrix
C       The dimensions of V, VT, W, and IH should be equal to MXNEQ
C     ______________________________________________________________________
C
      IMPLICIT REAL*8 (A-H,O-Z)
      DIMENSION  A(MXNEQ,MXNEQ),B(MXNEQ,MXNEQ),XX(MXNEQ),X(MXNEQ,MXNEQ)
      DIMENSION  V(50,50),VT(50,50),W(50,50),IH(50)
C
C     Call JACOBI to diagonalize [B]
C
      CALL JACOBI (N,B,NEGN,NR,V,XX,IH,MXNEQ)
C
C     Make diagonalized [B] symmetric
C
      DO 10 I=1,N
      DO 10 J=1,N
   10 B(J,I)=B(I,J)
C
C     Check (to make sure) that [B] is positive-definite
C
      DO 30 I=1,N
      IF (B(I,I))20,30,30
   20 WRITE(6,80)
      STOP
   30 CONTINUE
C
C     The eigenvectors of [B] are stored in array V(I,J)
C     Form the transpose of [V] as [VT]
C
      DO 40 I=1,N
      DO 40 J=1,N
   40 VT(I,J)=V(J,I)
C
C     Find the product [F]=[VT][A][V] and store in [A] to save storage
C
      CALL MTRXML (VT,N,N,A,N,W)
      CALL MTRXML (W,N,N,V,N,A)
C
C     Get [GI] from diagonalized [B], but store it in [B]
C
      DO 50 I=1,N
   50 B(I,I)=1.0/DSQRT(B(I,I))
C
C     Find the product [Q]=[GI][F][GI]=[B][A][B] and store in [A]
C
      CALL MTRXML (B,N,N,A,N,W)
      CALL MTRXML (W,N,N,B,N,A)
C
C     We now have the form [Q]{Z}=Lamda{Z}. Diagonalize [Q] to obtain
C     the eigenvalues by calling JACOBI.
C
      CALL JACOBI (N,A,NEGN,NR,VT,XX,IH,MXNEQ)
C
C     The eigenvalues are returned as diag [A].
C
      DO 60 J=1,N
   60 XX(J)=A(J,J)
C
C     The eigenvectors are computed from the relation,
C                     {X}=[V][GI]{Z}=[V][B]{VT}
C     since {Z} is stored in [VT].
C
      CALL MTRXML (V,N,N,B,N,W)
      CALL MTRXML (W,N,N,VT,N,X)
C
   80 FORMAT(/'*** Matrix [GLM] is NOT positive-definite ***')
      RETURN
      END

      SUBROUTINE BONDRY(NEQ,NEQR,NHBW,NSPV,NSSV,NNBC,NDF,DT,ITEM,ALFA,
     *                  IBDY,ISPV,ISSV,INBC,UREF,VSPV,VSSV,VNBC,
     *                  GLK,GLM,GLF,GU0,MXEBC,MXNBC,MXMBC,MXNEQ)
C     ________________________________________________________________
C
C     The subroutine is used to implement specified boundary conditions
C            on the assembled system of finite element equations
C     ________________________________________________________________
C
      IMPLICIT REAL*8 (A-H,O-Z)
      DIMENSION  ISPV(MXEBC,2),ISSV(MXNBC,2),INBC(MXMBC,2),IBDY(MXEBC)
      DIMENSION  UREF(MXMBC),VSPV(MXEBC),VSSV(MXNBC),VNBC(MXMBC)
      DIMENSION  GLK(MXNEQ,MXNEQ),GLM(MXNEQ,MXNEQ),GLF(MXNEQ),GU0(MXNEQ)
C
C     Impose boundary conditions for STATIC and TIME-DEPENDENT problems
C
      IF(ITEM.LE.2)THEN
C
C     Include specified PRIMARY degrees of freedom
C
         IF(NSPV.NE.0)THEN
            DO 30 NB = 1,NSPV
            IE=(ISPV(NB,1)-1)*NDF+ISPV(NB,2)
            IT=NHBW-1
            I=IE-NHBW
            DO 10 II=1,IT
            I=I+1
            IF(I .GE. 1)THEN
               J=IE-I+1
               GLF(I)=GLF(I)-GLK(I,J)*VSPV(NB)
               GLK(I,J)=0.0
            ENDIF
   10       CONTINUE
            GLK(IE,1)=1.0
            GLF(IE)=VSPV(NB)
            I=IE
            DO 20 II=2,NHBW
            I=I+1
            IF(I .LE. NEQ)THEN
               GLF(I)=GLF(I)-GLK(IE,II)*VSPV(NB)
               GLK(IE,II)=0.0
            ENDIF
   20       CONTINUE
   30       CONTINUE
         ENDIF
C
         IF(NSSV.NE.0)THEN
C
C     Include specified SECONDARY degrees of freedom
C
            DO 40 NF = 1,NSSV
            NB=(ISSV(NF,1)-1)*NDF+ISSV(NF,2)
            IF(ITEM.EQ.1)GLF(NB)=GLF(NB)+VSSV(NF)*DT
   40       IF(ITEM.NE.1)GLF(NB)=GLF(NB)+VSSV(NF)
         ENDIF
C
         IF(NNBC.NE.0)THEN
C
C     Include specified MIXED boundary conditions
C
            DO 50 IC=1,NNBC
            NC=(INBC(IC,1)-1)*NDF+INBC(IC,2)
            IF(ITEM.EQ.1)THEN
               GLK(NC,1)=GLK(NC,1)+ALFA*DT*VNBC(IC)
               GLF(NC)=GLF(NC)+DT*VNBC(IC)*(UREF(IC)
     *                          -(1.0-ALFA)*GU0(NC))
            ELSE
               GLK(NC,1)=GLK(NC,1)+VNBC(IC)
               GLF(NC)=GLF(NC)+VNBC(IC)*UREF(IC)
            ENDIF
   50       CONTINUE
         ENDIF
      ELSE
         IF(NNBC.NE.0)THEN
C
C     Include specified MIXED boundary conditions
C
            DO 70 IC=1,NNBC
            NC=(INBC(IC,1)-1)*NDF+INBC(IC,2)
            GLK(NC,NC)=GLK(NC,NC)+VNBC(IC)
   70       CONTINUE
         ENDIF
C
C        Impose boundary conditions for EIGENVALUE problems
C
```

```
         IF(NSPV.NE.0)THEN
              DO 80 IB=1,NSPV
   80         IBDY(IB)=(ISPV(IB,1)-1)*NDF+ISPV(IB,2)
              DO 120 I=1,NSPV
              IMAX=IBDY(I)
              DO 110 J=I,NSPV
              IF(IBDY(J).GE.IMAX)THEN
                   IMAX=IBDY(J)
                   IKEPT=J
              ENDIF
  110         CONTINUE
              IBDY(IKEPT)=IBDY(I)
              IBDY(I)=IMAX
  120         CONTINUE
              NEQR = NEQ
              DO 180 I=1,NSPV
              IB=IBDY(I)
              IF(IB .LT. NEQR)THEN
                   NEQR1=NEQR-1
                   DO 160 II=IB,NEQR1
                   DO 140 JJ=1,NEQR
                   GLM(II,JJ)=GLM(II+1,JJ)
  140              GLK(II,JJ)=GLK(II+1,JJ)
                   DO 150 JJ=1,NEQR
                   GLM(JJ,II)=GLM(JJ,II+1)
  150              GLK(JJ,II)=GLK(JJ,II+1)
  160              CONTINUE
              ENDIF
              NEQR=NEQR-1
  180         CONTINUE
         ENDIF
      ENDIF
      RETURN
      END

      SUBROUTINE COEFNT(IELEM,ITEM,MODEL,NDF,NPE,TIME,NTYPE,NE,F3,MXELM)
C
C     ________________________________________________________________
C
C     The subroutine computes the coefficient matrices and source vector
C           for the model problem described by Eqn. (1) (see MAIN)
C
C        X.........  Global (i.e., problem) coordinate
C        XI .......  Local (i.e., element) coordinate
C        H.........  Element length
C        {SF}......  Element interpolation (or shape) functions
C        {GDSF}....  First derivative of SF w.r.t. X
C        {GDDSF}...  Second derivative of SF w.r.t. X
C        GJ........  Jacobian of the transformation
C        [GAUSPT]..  4x4 matrix of Gauss points: N-th column corresponds
C                    to the N-point Guass rule
C        [GAUSWT]..  4x4 matrix of Gauss weights (see the comment above)
C        [A],[B],..  Element matrices needed to compute ELK
C        [ELK].....  Element coefficient matrix [K]
C        [ELM].....  Element 'mass' matrix [M]
C     ________________________________________________________________
C
      IMPLICIT REAL*8(A-H,O-Z)
      COMMON/STF1/ELK(9,9),ELM(9,9),ELF(9),ELX(4),ELU(9),ELV(9),ELA(9)
      COMMON/STF2/A1,A2,A3,A4,A5,AX0,AX1,BX0,BX1,CX0,CX1,CT0,CT1,FX0,
     *            FX1,FX2
      COMMON/SHP/SF(4),GDSF(4),GDDSF(4),GJ
      DIMENSION GAUSPT(5,5),GAUSWT(5,5),F3(MXELM)
C
      DATA GAUSPT/5*0.0D0,-.57735027D0,.57735027D0,3*0.0D0,-.77459667D0,
     * 0.0D0,.77459667D0,2*0.0D0,-.86113631D0,-.33998104D0,.33998104D0,
     *.86113631D0,0.0D0,-.906180D0,-.538469D0,0.0D0,.538469D0,.906180D0/
C
      DATA GAUSWT/2.0D0,4*0.0D0,2*1.0D0,3*0.0D0,.55555555D0,.88888888D0,
     * 0.55555555D0,2*0.0D0,.34785485D0,2*.65214515D0,.34785485D0,0.0D0,
     * 0.236927D0,.478629D0,.568889D0,.478629D0,.236927D0/
C
      NN=NDF*NPE
      H = ELX(NPE) - ELX(1)
      IF(IELEM .EQ. 0)THEN
          NGP=4
      ELSE
          NGP = IELEM+1
      ENDIF
C
      DO 10 J=1,NN
      IF(ITEM.LE.2)THEN
          ELF(J) = 0.0
      ENDIF
      DO 10 I=1,NN
      IF(ITEM.GT.0)THEN
          ELM(I,J)=0.0
      ENDIF
   10 ELK(I,J)=0.0
C
      IF(MODEL.NE.2)THEN
C
C     DO-LOOP on number of Gauss points begins here
C
          DO 100 NI=1,NGP
          XI = GAUSPT(NI,NGP)
C
C     Call subroutine SHP1D to evaluate the interpolation functions
C          and their global derivatives at the Gauss point XI
C
          CALL SHP1D(H,IELEM,NPE,XI)
C
          CONST = GJ*GAUSWT(NI,NGP)
          IF(IELEM.EQ.0)THEN
              X = ELX(1) + 0.5*H*(1.0+XI)
          ELSE
              X = 0.0
              DO 30 J=1,NPE
   30         X = X + SF(J)*ELX(J)
          ENDIF
C
C     Compute coefficient matrices and vectors for vaious model problems
C         governed by single second-order and fourth-order equations
C                       (MODEL = 1 or 3; NTYPE = 0 or 1)
C
          CX=CX0+CX1*X
          IF (ITEM.NE.3) THEN
              FX=FX0+FX1*X+FX2*X*X
          ENDIF
          IF (ITEM.GT.0)THEN
              CT=CT0+CT1*X
          ENDIF
          IF (MODEL.EQ.1)THEN
C
C         Coefficients for ALL SINGLE-VARIABLE PROBLEMS (MODEL=1)
C
              IF (NTYPE.EQ.0)THEN
C
C             All problems governed by MODEL EQUATION (3.1) (NTYPE=0)
C
                  AX=AX0+AX1*X
                  DO 50 J = 1,NN
                  IF (ITEM.LE.2)THEN
                      ELF(J) = ELF(J) + CONST*SF(J)*FX
                  ENDIF
                  DO 50 I = 1,NN
                  IF (ITEM.NE.0)THEN
                      ELM(I,J) = ELM(I,J) + CONST*SF(I)*SF(J)*CT
                  ENDIF
                  AIJ = CONST*GDSF(I)*GDSF(J)
                  CIJ = CONST*SF(I)*SF(J)
   50             ELK(I,J)=ELK(I,J) + AX*AIJ + CX*CIJ
              ELSE
C
C             RADIALLY SYMMETRIC ELASTICITY problems (MODEL=1, NTYPE>0)
C             AX0=E1, AX1=E2, BX0=NU12, BX1=H, thickness
C
                  ANU21=BX0*AX0/AX1
                  IF (NTYPE.EQ.1)THEN
```

```
                      C11=BX1*AX0/(1.0-BX0*ANU21)
                      C22=C11*(AX1/AX0)
                      C12=BX0*C22
                  ELSE
                      DENOM=1.0-BX0-ANU21
                      C11=BX1*AX0*(1.0-BX0)/(1.0+BX0)/DENOM
                      C22=BX1*AX1*(1.0-ANU21)/(1.0+ANU21)/DENOM
                      C12=BX0*C22
                  ENDIF
                  DO 60 J=1,NN
                  IF (ITEM.LE.2)THEN
                      ELF(J) = ELF(J) + CONST*SF(J)*FX*X
                  ENDIF
                  DO 60 I=1,NN
                  IF (ITEM.NE.0)THEN
                      ELM(I,J) = ELM(I,J) + CONST*SF(I)*SF(J)*CT*X
                  ENDIF
                  AIJ = CONST*GDSF(I)*GDSF(J)*C11*X
                  CIJ = CONST*SF(I)*SF(J)*CX*X
                  DIJ = CONST*(GDSF(I)*SF(J)+SF(I)*GDSF(J))*C12
                  EIJ = CONST*SF(I)*SF(J)*C22/X
   60             ELK(I,J)=ELK(I,J) + AIJ + CIJ + DIJ + EIJ   /
              ENDIF
          ELSE
C
C         Coefficients for the EULER-BERNOULLI theory (MODEL=2)
C
              IF (NTYPE.EQ.0)THEN
C
C             The Euler-Bernoulli BEAM element (MODEL=1 and NTYPE=0)
C
                  BX=BX0+BX1*X
                  CX=CX0+CX1*X
                  DO 70 J = 1,NN
                  IF (ITEM.LE.2)THEN
                      ELF(J) = ELF(J) + CONST*SF(J)*FX
                  ENDIF
                  DO 70 I = 1,NN
                  IF (ITEM.NE.0)THEN
                      ELM(I,J) = ELM(I,J) + CONST*SF(I)*SF(J)*CT
                  ENDIF
                  BIJ = CONST*GDDSF(I)*GDDSF(J)
                  CIJ = CONST*SF(I)*SF(J)
   70             ELK(I,J)=ELK(I,J) + BX*BIJ + CX*CIJ
              ELSE
C
C             The E-B CIRCULAR PLATE element (MODEL=1 and NTYPE>0)
C
                  ANU21=BX0*AX0/AX1
                  DI=(BX1**3)/12.0
                  D11=DI*AX0/(1.0-BX0*ANU21)
                  D22=D11*(AX1/AX0)
                  D12=BX0*D22
                  DO 80 J=1,NN
                  IF (ITEM.LE.2)THEN
                      ELF(J) = ELF(J) + CONST*SF(J)*FX*X
                  ENDIF
                  DO 80 I=1,NN
                  BIJ = CONST*GDDSF(I)*GDDSF(J)*D11*X
                  CIJ = CONST*SF(I)*SF(J)*CX*X
                  DIJ = CONST*(GDDSF(I)*GDSF(J)+GDSF(I)*GDDSF(J))*D12
                  EIJ = CONST*GDSF(I)*GDSF(J)*D22/X
   80             ELK(I,J)=ELK(I,J) + BIJ + CIJ + DIJ + EIJ
              ENDIF
          ENDIF
  100     CONTINUE
      ELSE
C
C     Coefficients for the TIMOSHENKO beam and circular plate (MODEL=2)
C         Full integration for bending coefficients
C
          DO 160 NI=1,NGP
          XI=GAUSPT(NI,NGP)
C
          CALL SHP1D(H,IELEM,NPE,XI)
```

```
C
      CONST=GJ*GAUSWT(NI,NGP)
      X = 0.0
      DO 110 J=1,NPE
  110 X = X + SF(J)*ELX(J)
      IF(NTYPE.EQ.0 .OR. NTYPE.EQ.2)THEN
C
C     The Timoshenko BEAM element (MODEL=2 and NTYPE=0 OR 2)
C
         BX=BX0+BX1*X
         CX=CX0+CX1*X
         FX=FX0+FX1*X+FX2*X*X
         JJ=1
         DO 130 J=1,NPE
         IF(ITEM.LE.2)THEN
            ELF(JJ)=ELF(JJ)+FX*SF(J)*CONST
         ENDIF
         II=1
         DO 120 I=1,NPE
         CIJ=SF(I)*SF(J)*CONST
         BIJ=GDSF(I)*GDSF(J)*CONST
         ELK(II,JJ)    =ELK(II,JJ)    +CX*CIJ
         ELK(II+1,JJ+1)=ELK(II+1,JJ+1)+BX*BIJ
         IF(ITEM.NE.0)THEN
            ELM(II,JJ)    =ELM(II,JJ)    +CT0*CIJ
            ELM(II+1,JJ+1)=ELM(II+1,JJ+1)+CT1*CIJ
         ENDIF
  120    II=NDF*I+1
  130    JJ=NDF*J+1
      ELSE
C
C     Timoshenko CIRCULAR PLATE element (MODEL=2 and NTYPE=1 or 3)
C         AX0=E1, AX1=E2, BX0=ANU12, BX1=H, FX2=G13*AREA*AK
C
         ANU21=BX0*AX0/AX1
         CX=CX0+CX1*X
         FX=FX0+FX1*X
         DI=(BX1**3)/12.0
         D11=DI*AX0/(1.0-BX0*ANU21)
         D22=D11*(AX1/AX0)
         D12=BX0*D22
         JJ=1
         DO 150 J=1,NPE
         IF(ITEM.LE.2)THEN
            ELF(JJ)=ELF(JJ)+FX*SF(J)*CONST*X
         ENDIF
         II=1
         DO 140 I=1,NPE
         BIJ = CONST*GDSF(I)*GDSF(J)*D11*X
         CIJ = CONST*SF(I)*SF(J)*X
         DIJ = CONST*(GDSF(I)*SF(J)+SF(I)*GDSF(J))*D12
         EIJ = CONST*SF(I)*SF(J)*D22/X
         ELK(II,JJ)    =ELK(II,JJ)     + CX*CIJ
         ELK(II+1,JJ+1)=ELK(II+1,JJ+1) + BIJ + DIJ + EIJ
         IF(ITEM.NE.0)THEN
            ELM(II,JJ)    =ELM(II,JJ)    +CT0*CIJ
            ELM(II+1,JJ+1)=ELM(II+1,JJ+1)+CT1*CIJ
         ENDIF
  140    II=NDF*I+1
  150    JJ=NDF*J+1
      ENDIF
  160 CONTINUE
C
C   Reduced integration is used to evaluate the transverse shear terms
C
      LGP=NGP-1
      DO 230 NI=1,LGP
      XI=GAUSPT(NI,LGP)
C
      CALL SHP1D(H,IELEM,NPE,XI)
      CONST=GJ*GAUSWT(NI,LGP)
C
      X = 0.0
      DO 170 J=1,NPE
  170 X = X + SF(J)*ELX(J)
      IF(NTYPE.EQ.0 .OR. NTYPE.EQ.2)THEN
```

```
C                                                                       F1D12150
C         The Timoshenko BEAM element (MODEL=2 and NTYPE=0 or 2)        F1D12160
C         AX = GAK = AX0 + AX1*X  (reduced integration)                 F1D12170
C                                                                       F1D12180
              AX=AX0+AX1*X                                              F1D12190
              JJ=1                                                      F1D12200
              DO 190 J=1,NPE                                            F1D12210
              II=1                                                      F1D12220
              DO 180 I=1,NPE                                            F1D12230
              B11=GDSF(I)*GDSF(J)*CONST                                 F1D12240
              B01=SF(I)*GDSF(J)*CONST                                   F1D12250
              B10=GDSF(I)*SF(J)*CONST                                   F1D12260
              B00=SF(I)*SF(J)*CONST                                     F1D12270
              ELK(II,JJ)    =ELK(II,JJ)    +AX*B11                      F1D12280
              ELK(II,JJ+1)  =ELK(II,JJ+1)  +AX*B10                      F1D12290
              ELK(II+1,JJ)  =ELK(II+1,JJ)  +AX*B01                      F1D12300
              ELK(II+1,JJ+1)=ELK(II+1,JJ+1)+AX*B00                      F1D12310
  180         II=I*NDF+1                                                F1D12320
  190         JJ=J*NDF+1                                                F1D12330
          ELSE                                                          F1D12340
C                                                                       F1D12350
C         Timoshenko CIRCULAR PLATE element (MODEL=2 and NTYPE=1 or 3)  F1D12360
C                     BX1=H, FX2=G13*AREA*K (reduced integration)       F1D12370
C                                                                       F1D12380
              A33=BX1*FX2                                               F1D12390
              JJ=1                                                      F1D12400
              DO 210 J=1,NPE                                            F1D12410
              II=1                                                      F1D12420
              DO 200 I=1,NPE                                            F1D12430
              BIJ = CONST*GDSF(I)*GDSF(J)*X                             F1D12440
              CIJ = CONST*SF(I)*SF(J)*X                                 F1D12450
              DIJ = CONST*GDSF(I)*SF(J)*X                               F1D12460
              DJI = CONST*SF(I)*GDSF(J)*X                               F1D12470
              ELK(II,JJ)    =ELK(II,JJ)     + A33*BIJ                   F1D12480
              ELK(II,JJ+1)  =ELK(II,JJ+1)   + A33*DIJ                   F1D12490
              ELK(II+1,JJ)  =ELK(II+1,JJ)   + A33*DJI                   F1D12500
              ELK(II+1,JJ+1)=ELK(II+1,JJ+1) + A33*CIJ                   F1D12510
  200         II=NDF*I+1                                                F1D12520
  210         JJ=NDF*J+1                                                F1D12530
          ENDIF                                                         F1D12540
  230     CONTINUE                                                      F1D12550
          IF(ITEM.EQ.0 .AND. NTYPE.GT.1)THEN                            F1D12560
              CALL TMSFRC(ELF,ELX,FX0,FX1,FX2,H,NTYPE,NE,F3,MXELM)      F1D12570
          ENDIF                                                         F1D12580
      ENDIF                                                             F1D12590
          IF(ITEM.GT.2)RETURN                                           F1D12600
      IF(ITEM.EQ.1 .OR. ITEM.EQ.2)THEN                                  F1D12610
C                                                                       F1D12620
C     Equivalent coefficient matrices for TIME-DEPENDENT problems       F1D12630
C                                                                       F1D12640
          IF(ITEM .EQ. 1)THEN                                           F1D12650
C                                                                       F1D12660
C         Alfa-family of time approximation for PARABOLIC equations     F1D12670
C                                                                       F1D12680
              DO 250 J=1,NN                                             F1D12690
              SUM=0.0                                                   F1D12700
              DO 240 I=1,NN                                             F1D12710
              SUM=SUM+(ELM(I,J)-A2*ELK(I,J))*ELU(I)                     F1D12720
  240         ELK(I,J)=ELM(I,J)+A1*ELK(I,J)                             F1D12730
  250         ELF(J)=(A1+A2)*ELF(J)+SUM                                 F1D12740
          ELSE                                                          F1D12750
C                                                                       F1D12760
C         Newmark-family of approximation for HYPERBOLIC equations      F1D12770
C                                                                       F1D12780
              IF(TIME.EQ.0.0)THEN                                       F1D12790
                  DO 260 J=1,NN                                         F1D12800
                  DO 260 I=1,NN                                         F1D12810
                  ELF(J)=ELF(J)-ELK(I,J)*ELU(I)                         F1D12820
  260             ELK(I,J)=ELM(I,J)                                     F1D12830
              ELSE                                                      F1D12840
                  DO 270 J=1,NN                                         F1D12850
                  DO 270 I=1,NN                                         F1D12860
                  ELF(J)=ELF(J)+ELM(I,J)*(A3*ELU(I)+A4*ELV(I)+A5*ELA(I))F1D12870
  270             ELK(I,J)=ELK(I,J)+A3*ELM(I,J)                         F1D12880
              ENDIF                                                     F1D12890
```

```
         ENDIF
      ENDIF
      RETURN
      END

      SUBROUTINE ECHO(IN,IT)
      IMPLICIT REAL*8(A-H,O-Z)
C
      DIMENSION AA(20)
      WRITE(IT,40)
   10 CONTINUE
      READ(IN,30,END=20) AA
      WRITE(IT,60) AA
      GO TO 10
   20 CONTINUE
      REWIND(IN)
      WRITE(IT,50)
      RETURN
   30 FORMAT(20A4)
   40 FORMAT(5X,'*** ECHO OF THE INPUT DATA STARTS ***',/)
   50 FORMAT(5X,'**** ECHO OF THE INPUT DATA ENDS ****',/)
   60 FORMAT(1X,20A4)
      END

      SUBROUTINE JACOBI (N,Q,JVEC,M,V,X,IH,MXNEQ)
C
C     ------------------------------------------------------------------
C
C       PURPOSE: To diagonalize matrix [Q] by successive rotations
C
C       DESCRIPTION OF THE VARIABLES:
C
C         N    .... Order of the real, symmetric matrix [Q] (N > 2)
C        [Q]   .... The matrix to be diagonalized (destroyed)
C        JVEC  .... 0, when only eigenvalues alone have to be found
C        [V]   .... Matrix of eigenvectors
C         M    .... Number of rotations performed
C     ------------------------------------------------------------------
C
      IMPLICIT REAL*8 (A-H,O-Z)
      DIMENSION Q(MXNEQ,MXNEQ),V(MXNEQ,MXNEQ),X(MXNEQ),IH(MXNEQ)
      EPSI=1.0D-08
C
      IF(JVEC)10,50,10
   10 DO 40 I=1,N
      DO 40 J=1,N
      IF(I-J)30,20,30
   20 V(I,J)=1.0
      GO TO 40
   30 V(I,J)=0.0
   40 CONTINUE
   50 M=0
      MI=N-1
      DO 70 I=1,MI
      X(I)=0.0
      MJ=I+1
      DO 70 J=MJ,N
      IF(X(I)-DABS(Q(I,J)))60,60,70
   60 X(I)=DABS(Q(I,J))
      IH(I)=J
   70 CONTINUE
   75 DO 100 I=1,MI
      IF(I-1)90,90,80
   80 IF(XMAX-X(I))90,100,100
   90 XMAX=X(I)
      IP=I
      JP=IH(I)
  100 CONTINUE
      IF(XMAX-EPSI)500,500,110
  110 M=M+1
      IF(Q(IP,IP)-Q(JP,JP))120,130,130
  120 TANG=-2.0*Q(IP,JP)/(DABS(Q(IP,IP)-Q(JP,JP))+DSQRT((Q(IP,IP)
     1     -Q(JP,JP))**2+4.0*Q(IP,JP)**2))
      GO TO 140
  130 TANG= 2.0*Q(IP,JP)/(DABS(Q(IP,IP)-Q(JP,JP))+DSQRT((Q(IP,IP)          F1D13610
     1      -Q(JP,JP))**2+4.0*Q(IP,JP)**2))                                 F1D13620
  140 COSN=1.0/DSQRT(1.0+TANG**2)                                           F1D13630
      SINE=TANG*COSN                                                        F1D13640
      QII=Q(IP,IP)                                                          F1D13650
      Q(IP,IP)=COSN**2*(QII+TANG*(2.*Q(IP,JP)+TANG*Q(JP,JP)))               F1D13660
      Q(JP,JP)=COSN**2*(Q(JP,JP)-TANG*(2.*Q(IP,JP)-TANG*QII))               F1D13670
      Q(IP,JP)=0.0                                                          F1D13680
      IF (Q(IP,IP)-Q(JP,JP)) 150,190,190                                    F1D13690
  150 TEMP=Q(IP,IP)                                                         F1D13700
      Q(IP,IP)=Q(JP,JP)                                                     F1D13710
      Q(JP,JP)=TEMP                                                         F1D13720
      IF(SINE) 160,170,170                                                  F1D13730
  160 TEMP=COSN                                                             F1D13740
      GOTO 180                                                              F1D13750
  170 TEMP=-COSN                                                            F1D13760
  180 COSN=DABS(SINE)                                                       F1D13770
      SINE=TEMP                                                             F1D13780
  190 DO 260 I=1,MI                                                         F1D13790
      IF (I-IP) 210,260,200                                                 F1D13800
  200 IF (I-JP) 210,260,210                                                 F1D13810
  210 IF (IH(I)-IP) 220,230,220                                             F1D13820
  220 IF (IH(I)-JP) 260,230,260                                             F1D13830
  230 K=IH(I)                                                               F1D13840
      TEMP=Q(I,K)                                                           F1D13850
      Q(I,K)=0.0                                                            F1D13860
      MJ=I+1                                                                F1D13870
      X(I)=0.0                                                              F1D13880
      DO 250 J=MJ,N                                                         F1D13890
      IF (X(I)-DABS(Q(I,J))) 240,240,250                                    F1D13900
  240 X(I)=DABS(Q(I,J))                                                     F1D13910
      IH(I)=J                                                               F1D13920
  250 CONTINUE                                                              F1D13930
      Q(I,K)=TEMP                                                           F1D13940
  260 CONTINUE                                                              F1D13950
      X(IP)=0.0                                                             F1D13960
      X(JP)=0.0                                                             F1D13970
      DO 430 I=1,N                                                          F1D13980
      IF(I-IP) 270,430,320                                                  F1D13990
  270 TEMP=Q(I,IP)                                                          F1D14000
      Q(I,IP)=COSN*TEMP+SINE*Q(I,JP)                                        F1D14010
      IF (X(I)-DABS(Q(I,IP))) 280,290,290                                   F1D14020
  280 X(I)=DABS(Q(I,IP))                                                    F1D14030
      IH(I)=IP                                                              F1D14040
  290 Q(I,JP)=-SINE*TEMP+COSN*Q(I,JP)                                       F1D14050
      IF (X(I)-DABS(Q(I,JP))) 300,430,430                                   F1D14060
  300 X(I)=DABS(Q(I,JP))                                                    F1D14070
      IH(I)=JP                                                              F1D14080
      GO TO 430                                                             F1D14090
  320 IF(I-JP) 330,430,380                                                  F1D14100
  330 TEMP=Q(IP,I)                                                          F1D14110
      Q(IP,I)=COSN*TEMP+SINE*Q(I,JP)                                        F1D14120
      IF(X(IP)-DABS(Q(IP,I)))340,350,350                                    F1D14130
  340 X(IP)=DABS(Q(IP,I))                                                   F1D14140
      IH(IP)=I                                                              F1D14150
  350 Q(I,JP)=-SINE*TEMP+COSN*Q(I,JP)                                       F1D14160
      IF (X(I)-DABS(Q(I,JP))) 300,430,430                                   F1D14170
  380 TEMP=Q(IP,I)                                                          F1D14180
      Q(IP,I)=COSN*TEMP+SINE*Q(JP,I)                                        F1D14190
      IF(X(IP)-DABS(Q(IP,I)))390,400,400                                    F1D14200
  390 X(IP)=DABS(Q(IP,I))                                                   F1D14210
      IH(IP)=I                                                              F1D14220
  400 Q(JP,I)=-SINE*TEMP+COSN*Q(JP,I)                                       F1D14230
      IF(X(JP)-DABS(Q(JP,I)))410,430,430                                    F1D14240
  410 X(JP)=DABS(Q(JP,I))                                                   F1D14250
      IH(JP)=I                                                              F1D14260
  430 CONTINUE                                                              F1D14270
      IF(JVEC)440,75,440                                                    F1D14280
  440 DO 450 I=1,N                                                          F1D14290
      TEMP=V(I,IP)                                                          F1D14300
      V(I,IP)=COSN*TEMP+SINE*V(I,JP)                                        F1D14310
  450 V(I,JP)=-SINE*TEMP+COSN*V(I,JP)                                       F1D14320
      GOTO 75                                                               F1D14330
  500 RETURN                                                                F1D14340
      END                                                                   F1D14350
      SUBROUTINE MESH1D(NEM,NNM,NPE,NOD,MXELM,MXNOD,DX,GLX)
C     ----------------------------------------------------------------
C
C          The subroutine computes the arrays {GLX} and [NOD]
C
C        {GLX}.... Vector of global coordinates
C        {DX}..... Vector of element lengths [DX(1) = node 1 coord.]
C        [NOD].... Connectivity matrix
C     ----------------------------------------------------------------
C
      IMPLICIT REAL*8 (A-H,O-Z)
      DIMENSION GLX(MXNOD),DX(MXNOD),NOD(MXELM,4)
C
C     Generate the elements of the connectivity matrix
C
      DO 10 I=1,NPE
   10 NOD(1,I)=I
      DO 20 N=2,NEM
      DO 20 I=1,NPE
   20 NOD(N,I) = NOD(N-1,I)+NPE-1
C
C     Generate global coordinates of the global nodes
C
      GLX(1)=DX(1)
      IF(NPE.EQ.2)THEN
          DO 30 I=1,NEM
   30     GLX(I+1) = GLX(I) + DX(I+1)
      ELSE
          DO 40 I=1,NEM
          II=2*I
          GLX(II) = GLX(II-1) + 0.5*DX(I+1)
   40     GLX(II+1)=GLX(II-1) + DX(I+1)
      ENDIF
      RETURN
      END

      SUBROUTINE MTRXML(A,N,M,B,L,C)
C     ----------------------------------------------------------------
C
C         COMPUTE THE PRODUCT OF MATRICES [A] AND [B]: [C]=[A][B]
C     ----------------------------------------------------------------
C
      IMPLICIT REAL*8 (A-H,O-Z)
      DIMENSION A(50,50),B(50,50),C(50,50)
      DO 10 I=1,N
      DO 10 J=1,L
      C(I,J)=0.0
      DO 10 K=1,M
   10 C(I,J)=C(I,J)+A(I,K)*B(K,J)
      RETURN
      END
      SUBROUTINE PSTPRC(F3,GLF,GLX,NOD,GA,IELEM,NPE,MODEL,NTYPE,ITEM,
     *                  MXELM,MXNEQ,MXNOD,NEM,NDF)
C     __________________________________________________________________
C
C     The subroutine computes the solution and its derivatives at five
C     points, including the nodes of the element. Note that the  post-
C     computed bending moment (BM) and shear force (VF) are as per the
C     sign convention shown in Figure 3.33 of the text; they differ in
C     sign from the element degrees of freedom.
C
C        X........ Global (i.e., problem) coordinate
C        XI ...... Local (i.e., element) coordinate
C        SF....... Element interpolation (or shape) functions
C        GDSF..... First derivative of SF w.r.t. global coordinate
C        GDDSF.... Second derivative of SF w.r.t. global coordinate
C        ELU...... Element solution vector
C        U........ Interpolated solution
C        DU....... Interpolated derivative of the solution
C        W........ Interpolated transverse deflection
C        S........ Interpolated rotation function
C        DS....... Interpolated derivative of the rotation
C        DW....... Interpolated derivative of the transverse deflection
C        DDW...... Interpolated second derivative of transverse defl.
C        DDDW..... Interpolated third derivative of transverse defl.
C     __________________________________________________________________
C
      IMPLICIT REAL*8 (A-H,O-Z)
      DIMENSION F3(MXELM),GLF(MXNEQ),GLX(MXNOD),NOD(MXELM,4)
      DIMENSION XP(9),ELX(4),ELU(9)
      COMMON/IO/IN,IT
      COMMON/SHP/SF(4),GDSF(4),GDDSF(4),GJ
      COMMON/STF2/A1,A2,A3,A4,A5,AX0,AX1,BX0,BX1,CX0,CX1,CT0,CT1,FX0,
     *            FX1,FX2
      DATA XP/-1.0D0, -0.750D0, -0.50D0, -0.250D0, 0.0D0, 0.250D0,
     *                           0.50D0,  0.750D0, 1.0D0/
C
      NPTS=9
      DO 80 NE = 1, NEM
      L=0
      DO 10 I=1,NPE
      NI=NOD(NE,I)
      ELX(I)=GLX(NI)
      LI=(NI-1)*NDF
      DO 10 J=1,NDF
      LI=LI+1
      L=L+1
   10 ELU(L)=GLF(LI)
      H = ELX(NPE) - ELX(1)
C
      DO 70 NI=1,NPTS
      XI = XP(NI)
      CALL SHP1D(H,IELEM,NPE,XI)
      IF(MODEL.EQ.3)THEN
          W=0.0
          DW=0.0
          DDW=0.0
          XC=ELX(1)+0.5*H*(1.0+XI)
          DO 20 I=1,4
          W  =W  + SF(I)*ELU(I)
          DW =DW + GDSF(I)*ELU(I)
   20     DDW=DDW+ GDDSF(I)*ELU(I)
          DDDW=((ELU(1)-ELU(3))*2.0/H-(ELU(4)+ELU(2)))*6.0/(H*H)
          ROT=-DW
          IF(NTYPE.EQ.0)THEN
              BM=(BX0+XC*BX1)*DDW
              VF=(BX0+XC*BX1)*DDDW + BX1*DDW
              WRITE(IT,90)XC,W,ROT,BM,VF
          ELSE
              ANU21=BX0*AX0/AX1
              DI=(BX1**3)/12.0
              D11=DI*AX0/(1.0-BX0*ANU21)
              D22=D11*(AX1/AX0)
              D12=BX0*D22
              BMR=D11*DDW*XC+D12*DW
              BMT=D12*DDW*XC+D22*DW
              IF(XC.NE.0.0)THEN                                         F1D15610
                  SFV=D11*(XC*DDDW+DDW)-D22*DW/XC                       F1D15620
                  WRITE(IT,90)XC,W,ROT,BMR,BMT,SFV                      F1D15630
              ELSE                                                      F1D15640
                  WRITE(IT,90)XC,W,ROT,BMR,BMT                          F1D15650
              ENDIF                                                     F1D15660
          ENDIF                                                         F1D15670
      ELSE                                                              F1D15680
          XC=0.0                                                        F1D15690
          DO 30 I=1,NPE                                                 F1D15700
   30     XC=XC+SF(I)*ELX(I)                                            F1D15710
          IF(MODEL.EQ.1)THEN                                            F1D15720
              U=0.0                                                     F1D15730
              DU=0.0                                                    F1D15740
              DO 40 I=1,NPE                                             F1D15750
              U=U+SF(I)*ELU(I)                                          F1D15760
   40         DU=DU+GDSF(I)*ELU(I)                                      F1D15770
              IF(NTYPE.EQ.0)THEN                                        F1D15780
                  SV=(AX0+AX1*XC)*DU                                    F1D15790
                  WRITE(IT,90)XC,U,SV                                   F1D15800
              ELSE                                                      F1D15810
                  ANU21=BX0*AX0/AX1                                     F1D15820
                  IF(NTYPE.EQ.1)THEN                                    F1D15830
                      C11=BX1*AX0/(1.0-BX0*ANU21)                       F1D15840
                      C22=C11*(AX1/AX0)                                 F1D15850
                      C12=BX0*C22                                       F1D15860
                  ELSE                                                  F1D15870
                      DENOM=1.0-BX0-ANU21                               F1D15880
                      C11=BX1*AX0*(1.0-BX0)/(1.0+BX0)/DENOM             F1D15890
                      C22=BX1*AX1*(1.0-ANU21)/(1.0+ANU21)/DENOM         F1D15900
                      C12=BX0*C22                                       F1D15910
                  ENDIF                                                 F1D15920
                  IF(XC.NE.0.0)THEN                                     F1D15930
                      SR=C11*DU+C12*U/XC                                F1D15940
                      ST=C12*DU+C22*U/XC                                F1D15950
                      WRITE(IT,90)XC,U,SR,ST                            F1D15960
                  ELSE                                                  F1D15970
                      WRITE(IT,90)XC,U,DU                               F1D15980
                  ENDIF                                                 F1D15990
              ENDIF                                                     F1D16000
          ELSE                                                          F1D16010
C         MODEL.EQ.2  Calculations                                      F1D16020
              IF(ITEM.EQ.0 .AND. NTYPE.GT.1)THEN                        F1D16030
                  H=ELX(NPE)-ELX(1)                                     F1D16040
                  CALL TMSTRS(GA,ELU,XI,W,DW,S,DS,NE,F3,H,MXELM)        F1D16050
              ELSE                                                      F1D16060
                  W=0.0                                                 F1D16070
                  DW=0.0                                                F1D16080
                  S = 0.0                                               F1D16090
                  DS=0.0                                                F1D16100
                  DDS=0.0                                               F1D16110
                  DO 50 I=1,NPE                                         F1D16120
                  L=2*I-1                                               F1D16130
                  W = W + SF(I)*ELU(L)                                  F1D16140
                  DW=DW+GDSF(I)*ELU(L)                                  F1D16150
                  S = S + SF(I)*ELU(L+1)                                F1D16160
                  DS=DS+GDSF(I)*ELU(L+1)                                F1D16170
   50             DDS=DDS+GDDSF(I)*ELU(L+1)                             F1D16180
              ENDIF                                                     F1D16190
                  IF(NTYPE.EQ.0 .OR. NTYPE.EQ.2)THEN                    F1D16200
                      BM=-(BX0+BX1*XC)*DS                               F1D16210
                      VF=-(AX0+AX1*XC)*(DW+S)                           F1D16220
                      WRITE(IT,90)XC,W,S,BM,VF                          F1D16230
                  ELSE                                                  F1D16240
                      ANU21=BX0*AX0/AX1                                 F1D16250
                      DI=(BX1**3)/12.0                                  F1D16260
                      D11=DI*AX0/(1.0-BX0*ANU21)                        F1D16270
                      D22=D11*(AX1/AX0)                                 F1D16280
                      D12=BX0*D22                                       F1D16290
                      BMR=-(D11*DS*XC+D12*S)                            F1D16300
                      BMT=-(D12*DS*XC+D22*S)                            F1D16310
                      SFV=-FX2*(DW+S)*XC                                F1D16320
                      WRITE(IT,90)XC,W,S,BMR,BMT,SFV                    F1D16330
                  ENDIF                                                 F1D16340
          ENDIF                                                         F1D16350
      ENDIF                                                             F1D16360
   70 CONTINUE                                                          F1D16370
   80 CONTINUE                                                          F1D16380
      RETURN                                                            F1D16390
   90 FORMAT (2X,6E13.5)                                                F1D16400
      END                                                               F1D16410

      SUBROUTINE REACTN(MXELM,MXNEQ,NDF,NEM,NOD,NPE,NTYPE,PR,GLF,       F1D16420
     *                  SE,SL,SA,SI,CS,SN,CNT,SNT,HF,VF,PF,XB)          F1D16430
                                                                        F1D16440
C     __________________________________________________________________F1D16450
C                                                                       F1D16460
C     The subroutine computes the generalized reaction forces in each  F1D16470
C         element of the truss (NDF=2) or frame (NDF=3) structure      F1D16480
C                                                                       F1D16490
C     __________________________________________________________________F1D16500
C                                                                       F1D16510
      IMPLICIT REAL*8(A-H,O-Z)                                          F1D16520
      DIMENSION  PR(MXELM),SE(MXELM),SL(MXELM),SA(MXELM),SI(MXELM)      F1D16530
      DIMENSION  CS(MXELM),SN(MXELM),CNT(MXELM),SNT(MXELM)              F1D16540
      DIMENSION  HF(MXELM),VF(MXELM),PF(MXELM),XB(MXELM)                F1D16550
      DIMENSION  NOD(MXELM,4),GLF(MXNEQ)                                F1D16560
      DIMENSION  ELR(6),TRM(6,6),TMPK(6,6)                              F1D16570
      COMMON/STF1/ELK(9,9),ELM(9,9),ELF(9),ELX(4),ELU(9),ELV(9),ELA(9)  F1D16580
C                                                                       F1D16590
      NN=NPE*NDF                                                        F1D16600
      DO 140 N=1,NEM                                                    F1D16610
      CN1=CS(N)                                                         F1D16620
      SN1=SN(N)                                                         F1D16630
C                                                                       F1D16640
C     Call TRSFRM to compute element stiffness matrix and force vector  F1D16650
C                                                                       F1D16660
      L=0                                                               F1D16670
      DO 100 I=1,NPE                                                    F1D16680
      NI=NOD(N,I)                                                       F1D16690
      LI=(NI-1)*NDF                                                     F1D16700
      DO 100 J=1,NDF                                                    F1D16710
      LI=LI+1                                                           F1D16720
      L=L+1                                                             F1D16730
  100 ELU(L)=GLF(LI)                                                    F1D16740
      CALL TRSFRM (MXELM,MXNEQ,N,NTYPE,PR,SE,SL,SA,SI,CS,SN,            F1D16750
     *             CNT,SNT,HF,VF,PF,XB)                                 F1D16760
C                                                                       F1D16770
C     Compute the FORCE and MOMENT RESULTANTS                           F1D16780
C                                                                       F1D16790
      DO 120 I=1,NN                                                     F1D16800
      ELR(I) = 0.0                                                      F1D16810
      DO 110 J=1,NN                                                     F1D16820
  110 ELR(I) =  ELR(I) + ELK(I,J)*ELU(J)                                F1D16830
  120 ELR(I) =  ELR(I) - ELF(I)                                         F1D16840
      ELF(1) =  ELR(1)*CN1+ELR(2)*SN1                                   F1D16850
      ELF(2) = -ELR(1)*SN1+ELR(2)*CN1                                   F1D16860
      IF(NTYPE.NE.0) THEN                                               F1D16870
          ELF(3) =  ELR(3)                                              F1D16880
          ELF(4) =  ELR(4)*CN1+ELR(5)*SN1                               F1D16890
          ELF(5) = -ELR(4)*SN1+ELR(5)*CN1                               F1D16900
          ELF(6) =  ELR(6)                                              F1D16910
      ELSE                                                              F1D16920
          ELF(3) =  ELR(3)*CN1+ELR(4)*SN1                               F1D16930
          ELF(4) = -ELR(3)*SN1+ELR(4)*CN1                               F1D16940
      ENDIF                                                             F1D16950
      WRITE(6,150)N, (ELF(I),I=1,NN)                                    F1D16960
      WRITE(6,160)   (ELR(I),I=1,NN)                                    F1D16970
  140 CONTINUE                                                          F1D16980
      RETURN                                                            F1D16990
  150 FORMAT (3X,I2,6E12.4)                                             F1D17000
  160 FORMAT (5X,6E12.4,/)                                              F1D17010
      END                                                               F1D17020
      SUBROUTINE SHP1D(H,IELEM,NPE,XI)                                   F1D17030
C     ___________________________________________________________________F1D17040
C                                                                        F1D17050
C     The subroutine computes shape functions and their derivatives for F1D17060
C      Hermite cubic and Lagrange linear, quadratic and cubic elements   F1D17070
C                                                                        F1D17080
C        X.........  Global (i.e., problem) coordinate                   F1D17090
C        XI .......  Local (i.e., element) coordinate                    F1D17100
C        H.........  Element length                                      F1D17110
C        {SF}......  Interpolation (or shape) functions                  F1D17120
C        {DSF}.....  First derivative of SF w.r.t. XI                    F1D17130
C        {DDSF}....  Second derivative of SFH w.r.t. XI                  F1D17140
C        {GDSF}....  First derivative of SF w.r.t. X                     F1D17150
C        {GDDSF}...  Second derivative of SFH w.r.t. X                   F1D17160
C        GJ........  Jacobian of the transformation                      F1D17170
C     ___________________________________________________________________F1D17180
C                                                                        F1D17190
      IMPLICIT REAL*8 (A-H,O-Z)                                          F1D17200
      COMMON/SHP/SF(4),GDSF(4),GDDSF(4),GJ                               F1D17210
      DIMENSION DSF(4),DDSF(4)                                           F1D17220
      IF(IELEM.EQ.0)THEN                                                 F1D17230
C                                                                        F1D17240
C     HERMITE interpolation functions (for the Euler-Bernoulli theory)   F1D17250
C                                                                        F1D17260
          NET=4                                                          F1D17270
          SF(1) = 0.25*(2.0-3.0*XI+XI**3)                                F1D17280
          SF(2) =  -H*(1.0-XI)*(1.0-XI*XI)/8.0                           F1D17290
          SF(3) = 0.25*(2.0+3.0*XI-XI**3)                                F1D17300
          SF(4) =   H*(1.0+XI)*(1.0-XI*XI)/8.0                           F1D17310
          DSF(1) = -0.75*(1.0-XI*XI)                                     F1D17320
          DSF(2) =  H*(1.0+2.0*XI-3.0*XI*XI)/8.0                         F1D17330
          DSF(3) =  0.75*(1.0-XI*XI)                                     F1D17340
          DSF(4) =  H*(1.0-2.0*XI-3.0*XI*XI)/8.0                         F1D17350
          DDSF(1) = 1.5*XI                                               F1D17360
          DDSF(2) = 0.25*H*(1.0-3.0*XI)                                  F1D17370
          DDSF(3) = -1.5*XI                                              F1D17380
          DDSF(4) =-0.25*(1.0+3.0*XI)*H                                  F1D17390
      ELSE                                                               F1D17400
          NET=NPE                                                        F1D17410
          IF(IELEM.EQ.1)THEN                                             F1D17420
C                                                                        F1D17430
C     LAGRANGE interpolation functions used for linear, quadratic and    F1D17440
C              cubic approximation of second-order equations             F1D17450
C                                                                        F1D17460
C     LINEAR interpolation functions                                     F1D17470
C                                                                        F1D17480
              SF(1) = 0.5*(1.0-XI)                                       F1D17490
              SF(2) = 0.5*(1.0+XI)                                       F1D17500
              DSF(1) = -0.5                                              F1D17510
              DSF(2) = 0.5                                               F1D17520
              DDSF(1) = 0.0                                              F1D17530
              DDSF(2) = 0.0                                              F1D17540
          ELSE                                                           F1D17550
              IF(IELEM.EQ.2)THEN                                         F1D17560
C                                                                        F1D17570
C     QUADRATIC interpolation functions                                  F1D17580
C                                                                        F1D17590
                  SF(1) = -0.5*XI*(1.0-XI)                               F1D17600
                  SF(2) = 1.0-XI*XI                                      F1D17610
                  SF(3) = 0.5*XI*(1.0+XI)                                F1D17620
                  DSF(1) = -0.5*(1.0-2.0*XI)                             F1D17630
                  DSF(2) = -2.0*XI                                       F1D17640
                  DSF(3) = 0.5*(1.0+2.0*XI)                              F1D17650
                  DDSF(1) = 1.0                                          F1D17660
                  DDSF(2) = -2.0                                         F1D17670
                  DDSF(3) = 1.0                                          F1D17680
              ELSE                                                       F1D17690
C                                                                        F1D17700
C     CUBIC interpolation functions                                      F1D17710
C                                                                        F1D17720
                  SF(1) = 0.0625*(1.0-XI)*(9.0*XI*XI-1.)                 F1D17730
                  SF(2) = 0.5625*(1.0-XI*XI)*(1.0-3.0*XI)                F1D17740
                  SF(3) = 0.5625*(1.0-XI*XI)*(1.0+3.0*XI)                F1D17750
                  SF(4) = 0.0625*(9.0*XI*XI-1.0)*(1.0+XI)                F1D17760
                  DSF(1) = 0.0625*(1.0+18.0*XI-27.0*XI*XI)               F1D17770
                  DSF(2) = 0.5625*(-3.0-2.0*XI+9.0*XI*XI)               F1D17780
                  DSF(3) = 0.5625*(3.0-2.0*XI-9.0*XI*XI)                F1D17790
                  DSF(4) = 0.0625*(18.0*XI+27.0*XI*XI-1.0)              F1D17800
                  DDSF(1) = 0.0625*(18.0-54.0*XI)                       F1D17810
                  DDSF(2) = 0.5625*(-2.0+18.0*XI)                       F1D17820
                  DDSF(3) = 0.5625*(-2.0-18.0*XI)                       F1D17830
                  DDSF(4) = 0.0625*(18.0+54.0*XI)                       F1D17840
              ENDIF                                                     F1D17850
          ENDIF                                                         F1D17860
C                                                                       F1D17870
C     Compute derivatives of the interpolation functions w.r.t. X       F1D17880
C                                                                       F1D17890
      ENDIF                                                             F1D17900
   80 GJ =  H*0.5                                                       F1D17910
      DO 90 I = 1,NET                                                   F1D17920
      GDSF(I) = DSF(I)/GJ                                               F1D17930
   90 GDDSF(I) = DDSF(I)/GJ/GJ                                          F1D17940
      RETURN                                                            F1D17950
      END                                                               F1D17960

      SUBROUTINE SOLVER(NRM,NCM,NEQNS,NBW,BAND,RHS,IRES)                F1D17970
C     ------------------------------------------------------------------F1D17980
C                                                                       F1D17990
C     The subroutine solves a  banded,  symmetric,  system of algebraic F1D18000
C     equations using the Gauss elimination method:  [BAND]{U} = {RHS}. F1D18010
C     The coefficient matrix is input as BAND(NEQNS,NBW) and the column F1D18020
C     vector is input as  RHS(NEQNS),  where NEQNS is the actual number F1D18030
C     of equations and NBW is the half band width.  The true dimensions F1D18040
C     of the matrix [BAND] in the calling program, are NRM by NCM. When F1D18050
C     IRES is greater than zero, the right hand elimination is skipped. F1D18060
C     ------------------------------------------------------------------F1D18070
C                                                                       F1D18080
      IMPLICIT REAL*8(A-H,O-Z)                                          F1D18090
      DIMENSION BAND(NRM,NCM),RHS(NRM)                                  F1D18100
C                                                                       F1D18110
      MEQNS=NEQNS-1                                                     F1D18120
      IF(IRES.LE.0) THEN                                                F1D18130
          DO 30 NPIV=1,MEQNS                                            F1D18140
          NPIVOT=NPIV+1                                                 F1D18150
          LSTSUB=NPIV+NBW-1                                             F1D18160
          IF(LSTSUB.GT.NEQNS) THEN                                      F1D18170
              LSTSUB=NEQNS                                              F1D18180
          ENDIF                                                         F1D18190
C                                                                       F1D18200
          DO 20 NROW=NPIVOT,LSTSUB                                      F1D18210
          NCOL=NROW-NPIV+1                                              F1D18220
          FACTOR=BAND(NPIV,NCOL)/BAND(NPIV,1)                           F1D18230
          DO 10 NCOL=NROW,LSTSUB                                        F1D18240
          ICOL=NCOL-NROW+1                                              F1D18250
          JCOL=NCOL-NPIV+1                                              F1D18260
   10     BAND(NROW,ICOL)=BAND(NROW,ICOL)-FACTOR*BAND(NPIV,JCOL)        F1D18270
   20     RHS(NROW)=RHS(NROW)-FACTOR*RHS(NPIV)                          F1D18280
   30     CONTINUE                                                      F1D18290
      ELSE                                                              F1D18300
   40     DO 60 NPIV=1,MEQNS                                            F1D18310
          NPIVOT=NPIV+1                                                 F1D18320
          LSTSUB=NPIV+NBW-1                                             F1D18330
          IF(LSTSUB.GT.NEQNS) THEN                                      F1D18340
              LSTSUB=NEQNS                                              F1D18350
          ENDIF                                                         F1D18360
          DO 50 NROW=NPIVOT,LSTSUB                                      F1D18370
          NCOL=NROW-NPIV+1                                              F1D18380
          FACTOR=BAND(NPIV,NCOL)/BAND(NPIV,1)                           F1D18390
   50     RHS(NROW)=RHS(NROW)-FACTOR*RHS(NPIV)                          F1D18400
   60     CONTINUE                                                      F1D18410
      ENDIF                                                             F1D18420
C                                                                       F1D18430
C     Back substitution                                                 F1D18440
C                                                                       F1D18450
      DO 90 IJK=2,NEQNS                                                 F1D18460
      NPIV=NEQNS-IJK+2                                                  F1D18470
      RHS(NPIV)=RHS(NPIV)/BAND(NPIV,1)                                  F1D18480
      LSTSUB=NPIV-NBW+1                                                 F1D18490
      IF(LSTSUB.LT.1) THEN                                              F1D18500
          LSTSUB=1                                                      F1D18510
      ENDIF                                                             F1D18520
      NPIVOT=NPIV-1                                                     F1D18530
      DO 80 JKI=LSTSUB,NPIVOT                                           F1D18540
      NROW=NPIVOT-JKI+LSTSUB                                            F1D18550
      NCOL=NPIV-NROW+1                                                  F1D18560
      FACTOR=BAND(NROW,NCOL)                                            F1D18570
   80 RHS(NROW)=RHS(NROW)-FACTOR*RHS(NPIV)                              F1D18580
   90 CONTINUE                                                          F1D18590
      RHS(1)=RHS(1)/BAND(1,1)                                           F1D18600
      RETURN                                                            F1D18610
      END                                                               F1D18620

      SUBROUTINE TMSFRC(ELF,ELX,FX0,FX1,FX2,H,NTYPE,NE,F3,MXELM)        F1D18630
C     __________________________________________________________________F1D18640
C                                                                       F1D18650
C      The subroutine computes element force vector for the consistent  F1D18660
C                interpolation Timoshenko element (CIE)                 F1D18670
C     __________________________________________________________________F1D18680
C                                                                       F1D18690
      IMPLICIT REAL*8(A-H,O-Z)                                          F1D18700
      COMMON/SHP/SF(4),GDSF(4),GDDSF(4),GJ                              F1D18710
      DIMENSION GAUSPT(5,5),GAUSWT(5,5),ELF(9),ELX(4),EX(3),F3(MXELM)   F1D18720
C                                                                       F1D18730
      DATA GAUSPT/5*0.0D0,-.57735027D0,.57735027D0,3*0.0D0,-.77459667D0,F1D18740
     * 0.0D0,.77459667D0,2*0.0D0,-.86113631D0,-.33998104D0,.33998104D0, F1D18750
     *.86113631D0,0.0D0,-.906180D0,-.538469D0,0.0D0,.538469D0,.906180D0/F1D18760
C                                                                       F1D18770
      DATA GAUSWT/2.0D0,4*0.0D0,2*1.0D0,3*0.0D0,.55555555D0,.88888888D0,F1D18780
     * 0.55555555D0,2*0.0D0,.34785485D0,2*.65214515D0,.34785485D0,0.0D0,F1D18790
     * 0.236927D0,.478629D0,.568889D0,.478629D0,.236927D0/              F1D18800
C                                                                       F1D18810
      NPE=3                                                             F1D18820
      IEL=2                                                             F1D18830
      NDF=2                                                             F1D18840
      NGP=IEL+1                                                         F1D18850
      DO 10 I=1,6                                                       F1D18860
10    ELF(I)=0.0                                                        F1D18870
C                                                                       F1D18880
      EX(1)=ELX(1)                                                      F1D18890
      EX(2)=ELX(1)+0.5*H                                                F1D18900
      EX(3)=ELX(2)                                                      F1D18910
C                                                                       F1D18920
      DO 50 NI=1,NGP                                                    F1D18930
      XI=GAUSPT(NI,NGP)                                                 F1D18940
      CALL SHP1D(H,IEL,NPE,XI)                                          F1D18950
      CONST=GJ*GAUSWT(NI,NGP)                                           F1D18960
      X = 0.0                                                           F1D18970
      DO 20 J=1,NPE                                                     F1D18980
20    X = X + SF(J)*EX(J)                                               F1D18990
C                                                                       F1D19000
C     Compute the polynomial variation of FX                            F1D19010
C                                                                       F1D19020
      IF(NTYPE.EQ.2)THEN                                                F1D19030
          FX=FX0+(FX1+FX2*X)*X                                          F1D19040
      ELSE                                                              F1D19050
          FX=(FX0+FX1*X)*X                                              F1D19060
      ENDIF                                                             F1D19070
C                                                                       F1D19080
C     Element force vector for the consistent interpolation beam elementF1D19090
C                                                                       F1D19100
25    II=1                                                              F1D19110
      DO 40 I=1,NPE                                                     F1D19120
      ELF(II)=ELF(II)+FX*SF(I)*CONST                                    F1D19130
40    II=NDF*I+1                                                        F1D19140
50    CONTINUE                                                          F1D19150
C                                                                       F1D19160
C     Rearrange the element coefficients                                F1D19170
C                                                                       F1D19180
      F3(NE)=ELF(3)                                                     F1D19190
      ELF(1)=ELF(1)+0.5*F3(NE)                                          F1D19200
      ELF(2)=-0.125*F3(NE)*H                                            F1D19210
      ELF(3)=ELF(5)+0.5*F3(NE)                                          F1D19220
      ELF(4)= 0.125*F3(NE)*H                                            F1D19230
      RETURN                                                            F1D19240
      END                                                               F1D19250
      SUBROUTINE TMSTRS(GA,ELU,XI,W,DW,S,DS,NE,F3,H,MXELM)              F1D19260
C     __________________________________________________________________F1D19270
C                                                                       F1D19280
C     The subroutine computes the solution and its global derivatives atF1D19290
C      the nine points (including the nodes) of the Timoshenko element  F1D19300
C                                                                       F1D19310
C        XC........ Global (i.e., problem) coordinate                   F1D19320
C        XI ....... ocal (i.e. element) coordinate                      F1D19330
C        SFL, SFQ.. Lagrange linear and quadratic shape functions       F1D19340
C        DSFL,DSFQ: First derivative of SF w.r.t. global coordinate     F1D19350
C        ELU....... Column vector of generalized displacements          F1D19360
C        W, DW..... Transverse deflection and its derivative            F1D19370
C        S, DS..... Rotation and its derivative                         F1D19380
C                                                                       F1D19390
C     __________________________________________________________________F1D19400
      IMPLICIT REAL*8 (A-H,O-Z)                                         F1D19410
      COMMON/IO/IN,IT                                                   F1D19420
      DIMENSION ELU(9),SFL(2),SFQ(3),DSFL(2),DSFQ(3),F3(MXELM)          F1D19430
C                                                                       F1D19440
      GJ =  H*0.5                                                       F1D19450
C                                                                       F1D19460
C     Interpolation functions for the Lagrange LINEAR element           F1D19470
C                                                                       F1D19480
      SFL(1) = 0.5*(1.0-XI)                                             F1D19490
      SFL(2) = 0.5*(1.0+XI)                                             F1D19500
      DSFL(1) = -0.5/GJ                                                 F1D19510
      DSFL(2) = 0.5/GJ                                                  F1D19520
C                                                                       F1D19530
C     Interpolation functions for the Lagrange QUADRATIC element        F1D19540
C                                                                       F1D19550
      SFQ(1) = -0.5*XI*(1.0-XI)                                         F1D19560
      SFQ(2) = 1.0-XI*XI                                                F1D19570
      SFQ(3) = 0.5*XI*(1.0+XI)                                          F1D19580
      DSFQ(1) = -0.5*(1.0-2.0*XI)/GJ                                    F1D19590
      DSFQ(2) = -2.0*XI/GJ                                              F1D19600
      DSFQ(3) = 0.5*(1.0+2.0*XI)/GJ                                     F1D19610
C                                                                       F1D19620
      W3=(3.0*H*F3(NE)/GA + 8.0*(ELU(1)+ELU(3))                         F1D19630
     *                    + 2.0*(ELU(4)-ELU(2))*H)/16.0                 F1D19640
      W =  SFQ(1)*ELU(1) + SFQ(2)*W3 + SFQ(3)*ELU(3)                    F1D19650
      DW= DSFQ(1)*ELU(1) +DSFQ(2)*W3 +DSFQ(3)*ELU(3)                    F1D19660
      S =  SFL(1)*ELU(2) + SFL(2)*ELU(4)                                F1D19670
      DS= DSFL(1)*ELU(2) +DSFL(2)*ELU(4)                                F1D19680
C                                                                       F1D19690
      RETURN                                                            F1D19700
      END                                                               F1D19710


      SUBROUTINE TRSFRM (MXELM,MXNEQ,N,NTYPE,PR,SE,SL,SA,SI,CS,SN,      F1D19720
     *                   CNT,SNT,HF,VF,PF,XB)                           F1D19730
C     __________________________________________________________________F1D19740
C                                                                       F1D19750
C     The subroutine computes stiffness matrix and force vector for the F1D19760
C                truss (NDF=2) and frame (NDF=3) elements               F1D19770
C                                                                       F1D19780
C     SE......Young's modulus                                           F1D19790
C     SL......Element length                                            F1D19800
C     SA......Cross-sectional area                                      F1D19810
C     SI......Moment of inertia                                         F1D19820
C     CS......Cosine of the angle of orientation                        F1D19830
C     SN......Sine of the angle of orientation                          F1D19840
C     HF......Distributed force along the length of the element         F1D19850
C     VF......Distributed force transverse to the element               F1D19860
C     PF......Point force at point other than nodes                     F1D19870
C     XB......Distance along the length from node 1 of the element      F1D19880
C             of the location of the point force, PF                    F1D19890
C     CNT,SNT:Direction cosines of the point force's line of applicationF1D19900
C     __________________________________________________________________F1D19910
C                                                                       F1D19920
     .IMPLICIT REAL*8(A-H,O-Z)                                          F1D19930
      DIMENSION  PR(MXELM),SE(MXELM),SL(MXELM),SA(MXELM),SI(MXELM)      F1D19940
      DIMENSION  CS(MXELM),SN(MXELM),CNT(MXELM),SNT(MXELM)              F1D19950
      DIMENSION  HF(MXELM),VF(MXELM),PF(MXELM),XB(MXELM)                F1D19960
      DIMENSION  ELR(6),TRM(6,6),TMPK(6,6)                              F1D19970
      COMMON/STF1/ELK(9,9),ELM(9,9),ELF(9),ELX(4),ELU(9),ELV(9),ELA(9)  F1D19980
```

```
C                                                                       F1D19990
      CN1=CS(N)                                                         F1D20000
      SN1=SN(N)                                                         F1D20010
      CN2=CN1*CN1                                                       F1D20020
      SN2=SN1*SN1                                                       F1D20030
      CSN=CN1*SN1                                                       F1D20040
C                                                                       F1D20050
C     Element coefficients                                              F1D20060
C                                                                       F1D20070
      IF(NTYPE.EQ.0) THEN                                               F1D20080
C                                                                       F1D20090
C         The plane TRUSS element                                       F1D20100
C                                                                       F1D20110
          NN=4                                                          F1D20120
          C1=SA(N)*SE(N)/SL(N)                                          F1D20130
          ELK(1,1) = C1*CN2                                             F1D20140
          ELK(2,1) = C1*CSN                                             F1D20150
          ELK(2,2) = C1*SN2                                             F1D20160
          ELK(3,1) = -ELK(1,1)                                          F1D20170
          ELK(3,2) = -ELK(2,1)                                          F1D20180
          ELK(3,3) =  ELK(1,1)                                          F1D20190
          ELK(4,1) = -ELK(2,1)                                          F1D20200
          ELK(4,2) = -ELK(2,2)                                          F1D20210
          ELK(4,3) = -ELK(3,2)                                          F1D20220
          ELK(4,4) =  ELK(2,2)                                          F1D20230
C                                                                       F1D20240
          DO 10 I=1,NN                                                  F1D20250
          DO 10 J=I,NN                                                  F1D20260
   10     ELK(I,J) = ELK(J,I)                                           F1D20270
C                                                                       F1D20280
C         Contribution of the point force to nodal forces               F1D20290
C                                                                       F1D20300
          XI=XB(N)/SL(N)                                                F1D20310
          SFL1 = 1.0-XI                                                 F1D20320
          SFL2 = XI                                                     F1D20330
C                                                                       F1D20340
          F1=0.5*HF(N)*SL(N)                                            F1D20350
          F3=0.5*HF(N)*SL(N)                                            F1D20360
          ELF(1) = F1*CN1                                               F1D20370
          ELF(2) = F1*SN1                                               F1D20380
          ELF(3) = F3*CN1                                               F1D20390
          ELF(4) = F3*SN1                                               F1D20400
      ELSE                                                              F1D20410
          NN=6                                                          F1D20420
          IF(NTYPE.EQ.1)THEN                                            F1D20430
C                                                                       F1D20440
C         The EULER-BERNOULLI FRAME element                             F1D20450
C                                                                       F1D20460
              AMU=0.5*SA(N)*SL(N)*SL(N)/SI(N)                           F1D20470
              C1=2.0*SE(N)*SI(N)/(SL(N)**3)                             F1D20480
              C2=6.0*SE(N)*SI(N)/(SL(N)*SL(N))                          F1D20490
              C3=C1*(AMU*CN2+6.0*SN2)                                   F1D20500
              C4=C1*(AMU-6.0)*CSN                                       F1D20510
              C5=C1*(AMU*SN2+6.0*CN2)                                   F1D20520
              C6=4.0*SE(N)*SI(N)/SL(N)                                  F1D20530
C                                                                       F1D20540
              ELK(1,1) = C3                                             F1D20550
              ELK(2,1) = C4                                             F1D20560
              ELK(2,2) = C5                                             F1D20570
              ELK(3,1) = C2*SN1                                         F1D20580
              ELK(3,2) =-C2*CN1                                         F1D20590
              ELK(3,3) = C6                                             F1D20600
              ELK(4,1) =-C3                                             F1D20610
              ELK(4,2) =-C4                                             F1D20620
              ELK(4,3) =-C2*SN1                                         F1D20630
              ELK(4,4) = C3                                             F1D20640
              ELK(5,1) =-C4                                             F1D20650
              ELK(5,2) =-C5                                             F1D20660
              ELK(5,3) = C2*CN1                                         F1D20670
              ELK(5,4) = C4                                             F1D20680
              ELK(5,5) = C5                                             F1D20690
              ELK(6,1) = C2*SN1                                         F1D20700
              ELK(6,2) =-C2*CN1                                         F1D20710
              ELK(6,3) = 0.5*C6                                         F1D20720
              ELK(6,4) =-C2*SN1                                         F1D20730
              ELK(6,5) = C2*CN1                                         F1D20740
              ELK(6,6) = C6                                             F1D20750
C                                                                       F1D20760
              DO 20 I=1,NN                                              F1D20770
              DO 20 J=I,NN                                              F1D20780
   20         ELK(I,J) = ELK(J,I)                                       F1D20790
C                                                                       F1D20800
C         Contribution of the point force to nodal generalized forces  F1D20810
C                                                                       F1D20820
              XI=XB(N)/SL(N)                                            F1D20830
              TF=PF(N)*SNT(N)                                           F1D20840
              AF=PF(N)*CNT(N)                                           F1D20850
              SFL1 = 1.0-XI                                             F1D20860
              SFL2 = XI                                                 F1D20870
              SFH1 = 1.0 - 3.0*XI*XI + 2.0*(XI**3)                      F1D20880
              SFH2 = -XI*(1.0+XI*XI-2.0*XI)*SL(N)                       F1D20890
              SFH3 = 3.0*XI*XI - 2.0*(XI**3)                            F1D20900
              SFH4 = -XI*(XI*XI - XI)*SL(N)                             F1D20910
C                                                                       F1D20920
              F1=0.5*HF(N)*SL(N)         + SFL1*AF                      F1D20930
              F2=0.5*VF(N)*SL(N)         + SFH1*TF                      F1D20940
              F3=-VF(N)*SL(N)*SL(N)/12.0 + SFH2*TF                      F1D20950
              F4=0.5*HF(N)*SL(N)         + SFL2*AF                      F1D20960
              F5=0.5*VF(N)*SL(N)         + SFH3*TF                      F1D20970
              F6=VF(N)*SL(N)*SL(N)/12.0  + SFH4*TF                      F1D20980
              ELF(1) = F1*CN1-F2*SN1                                    F1D20990
              ELF(2) = F1*SN1+F2*CN1                                    F1D21000
              ELF(3) = F3                                               F1D21010
              ELF(4) = F4*CN1-F5*SN1                                    F1D21020
              ELF(5) = F4*SN1+F5*CN1                                    F1D21030
              ELF(6) = F6                                               F1D21040
          ELSE                                                          F1D21050
C                                                                       F1D21060
C         The TIMOSHENKO FRAME element (shear coefficient=5/6)          F1D21070
C                                                                       F1D21080
              SG=5.0*SE(N)/(1.0+PR(N))/12.0                             F1D21090
              C1=SA(N)*SE(N)/SL(N)                                      F1D21100
              C2=SG*SA(N)/SL(N)                                         F1D21110
              C3=0.5*SG*SA(N)                                           F1D21120
              C4=0.25*SG*SA(N)*SL(N)                                    F1D21130
              C5=SE(N)*SI(N)/SL(N)                                      F1D21140
              ELK(1,1)=C1                                               F1D21150
              ELK(2,1)=0.0                                              F1D21160
              ELK(2,2)=C2                                               F1D21170
              ELK(3,1)=0.0                                              F1D21180
              ELK(3,2)=-C3                                              F1D21190
              ELK(3,3)=C4+C5                                            F1D21200
              ELK(4,1)=-C1                                              F1D21210
              ELK(4,2)=0.0                                              F1D21220
              ELK(4,3)=0.0                                              F1D21230
              ELK(4,4)=C1                                               F1D21240
              ELK(5,1)=0.0                                              F1D21250
              ELK(5,2)=-C2                                              F1D21260
              ELK(5,3)=C3                                               F1D21270
              ELK(5,4)=0.0                                              F1D21280
              ELK(5,5)=C2                                               F1D21290
              ELK(6,1)=0.0                                              F1D21300
              ELK(6,2)=-C3                                              F1D21310
              ELK(6,3)=C4-C5                                            F1D21320
              ELK(6,4)=0.0                                              F1D21330
              ELK(6,5)=C3                                               F1D21340
              ELK(6,6)=C4+C5                                            F1D21350
C                                                                       F1D21360
              DO 25 I=1,NN                                              F1D21370
              DO 25 J=1,NN                                              F1D21380
   25         TRM(J,I)=0.0                                              F1D21390
C                                                                       F1D21400
              TRM(1,1)=CN1                                              F1D21410
              TRM(1,2)=SN1                                              F1D21420
              TRM(2,1)=-SN1                                             F1D21430
              TRM(2,2)=CN1                                              F1D21440
              TRM(3,3)=1.0                                              F1D21450
              TRM(4,4)=CN1                                              F1D21460
              TRM(4,5)=SN1                                              F1D21470
              TRM(5,4)=-SN1                                             F1D21480
              TRM(5,5)=CN1
              TRM(6,6)=1.0
C
              DO 30 I=1,NN
              DO 30 J=I,NN
   30         ELK(I,J) = ELK(J,I)
C
              DO 40 I=1,NN
              DO 40 J=1,NN
              TMPK(I,J)=0.0
              DO 40 K=1,NN
   40         TMPK(I,J)=TMPK(I,J)+TRM(K,I)*ELK(K,J)
C
              DO 50 I=1,NN
              DO 50 J=1,NN
              ELK(I,J)=0.0
              DO 50 K=1,NN
   50         ELK(I,J)=ELK(I,J)+TMPK(I,K)*TRM(K,J)
C
C         Contribution of the point force to nodal generalized forces
C
              XI=XB(N)/SL(N)
              TF=PF(N)*SNT(N)
              AF=PF(N)*CNT(N)
              SFL1 = 1.0-XI
              SFL2 = XI
              SFQ1 = (1.0-XI)*(1.0-2.0*XI)
              SFQ2 = -XI*(1.0-2.0*XI)
              SFQ3 = 4.0*XI*(1.0-XI)
C
              F1=0.5*HF(N)*SL(N)          + SFL1*AF
              F2=0.5*VF(N)*SL(N)          + (SFQ1+0.5*SFQ3)*TF
              F3=-VF(N)*SL(N)*SL(N)/12.0 - 0.125*SFQ3*SL(N)*TF
              F4=0.5*HF(N)*SL(N)          + SFL2*AF
              F5=0.5*VF(N)*SL(N)          + (SFQ2+0.5*SFQ3)*TF
              F6=VF(N)*SL(N)*SL(N)/12.0  + 0.125*SFQ3*SL(N)*TF
              ELF(1) = F1*CN1-F2*SN1
              ELF(2) = F1*SN1+F2*CN1
              ELF(3) = F3
              ELF(4) = F4*CN1-F5*SN1
              ELF(5) = F4*SN1+F5*CN1
              ELF(6) = F6
          ENDIF
      ENDIF
      RETURN
      END
```

APPENDIX
2

COMPUTER PROGRAM FEM2DV2

```
C      Program name: FEM2DV2                         Length: 2740 lines   F2D00010
C      * * * * * * * * * * * * * * * * * * * * * * * * * * * * * * * *   F2D00020
C      *                    Program  FEM2DV2                         *   F2D00030
C      *   (AN IN-CORE FINITE ELEMENT ANALYSIS COMPUTER PROGRAM)     *   F2D00040
C      * * * * * * * * * * * * * * * * * * * * * * * * * * * * * * * *   F2D00050
C     . . . . . . . . . . . . . . . . . . . . . . . . . . . . . . . . .  F2D00060
C     .                                                               .  F2D00070
C     .     This  is  a  finite  element  computer  program  for  the .  F2D00080
C     . analysis of two-dimensional problems governed by second-order .  F2D00090
C     . partial  differential  equations  arising in:  heat transfer, .  F2D00100
C     . electrical engineering, fluid dynamics, and solid mechanics.  .  F2D00110
C     .                                                               .  F2D00120
C     .     The  program  uses  linear and quadratic,  triangular and .  F2D00130
C     . rectangular, elements with isoparametric formulations. Meshes .  F2D00140
C     . of only one type of element are allowed for a problem  (i.e., .  F2D00150
C     . two different types of elements cannot be used in a problem). .  F2D00160
C     .                                                               .  F2D00170
C     .     Many  field  problems  of engineering and applied science .  F2D00180
C     . can be analyzed using this program.  In  particular,  FEM2DV2 .  F2D00190
C     . can be used in the finite element analysis of problems in the .  F2D00200
C     . following fields:                                             .  F2D00210
C     .                                                               .  F2D00220
C     .     1.  Heat conduction and convection                        .  F2D00230
C     .     2.  Flows of viscous incompressible fluids (by penalty    .  F2D00240
C     .         function formulation)                                 .  F2D00250
C     .     3.  Plane elasticity problems                             .  F2D00260
C     .     4.  Plate bending problems using rectangular elements     .  F2D00270
C     .         based on the classical and first-order (or Mindlin)   .  F2D00280
C     .         plate theory.                                         .  F2D00290
C     .                                                               .  F2D00300
C     .     The main objective of this  program  is to illustrate how .  F2D00310
C     . finite element formulations developed in  Chapters  8 thru 12 .  F2D00320
C     . can be implemented on a computer  and used in the analysis of .  F2D00330
C     . engineering problems.  Modeling of large and complex problems .  F2D00340
C     . was not an objective of the program.  The program or parts of .  F2D00350
C     . it can be modified to analyze field problems not discussed in .  F2D00360
C     . the book.                                                     .  F2D00370
C     . . . . . . . . . . . . . . . . . . . . . . . . . . . . . . . . .  F2D00380
C                                                                        F2D00390
```

```
C          DESCRIPTION OF SOME KEY VARIABLES USED IN THE PROGRAM
C          (See Table 13.1 for a description of other variables)
C
C     [CMAT]      Matrix of stiffnesses in elasticity and plate bending
C                 problems (computed  in  the  program from engineering
C                 constants, E1, E2, G12, ANU12, etc. and thickness)
C
C     {ELA}       Vector of elemental nodal accelerations
C     {ELF}       Vector of element nodal source (or force) vector
C     [ELK]       Element coefficient (or stiffness) matrix
C     {ELU}       Vector of element nodal values of primary variables
C     {ELV}       Vector of elemental nodal velocities
C     {ELXY}      Vector of elemental global coordinates:
C                 ELXY(I,1)=x-coordinate;  ELXY(I,2)=y-coordinate
C     {GLA}       Vector of global nodal accelerations
C     {GLF}       Vector of global nodal source (or force) vector
C     [GLK]       Global coefficient (or stiffness) matrix
C     {GLU}       Vector of global nodal values of primary variables
C     {GLV}       Vector of global nodal velocities
C
C     NDF         Number of degrees of freedom per node:
C                 NDF=1, For SINGLE VARIABLE problems
C                 NDF=2, For ELASTICITY and VISCOUS FLUID FLOW
C                 NDF=3, For PLATE BENDING when FSDT or CST(N)
C                        elements are used
C                 NDF=4, For PLATE BENDING when CST(C) element
C                        is used
C
C     NEQ         Total number of equations in the problem (=NNM*NDF)
C     NHBW        Half band width of the global coefficient matrix, GLK
C     NN          Total number of degrees of freedom per element
C     -----------------------------------------------------------------
C
C          DESCRIPTION OF PARAMETERS USED TO DIMENSION THE ARRAYS
C
C     MAXCNV... Maximum number of elements with convection B.C.
C     MAXELM... Maximum number of elements allowed in the program
C     MAXNOD... Maximum number of nodes allowed in the program
C     MAXNX.... Maximum number of allowed subdivisions DX(I) along x
C     MAXNY.... Maximum number of allowed subdivisions DY(I) along y
C     MAXSPV... Maximum number of specified primary variables
C     MAXSSV... Maximum number of specified secondary variables
C     NCMAX.... Actual column dimension of: [GLK],[GLM],{GLU},{GLV},
C               {GLA}, and {GLF}
C
C               The actual row dimension of the assembled coefficient
C               matrix  should be greater than or equal to  the total
C               number of algebraic equations in the FE model.
C
C     NRMAX.... Actual row dimension of: [GLK] and [GLM]
C
C               The actual column-dimension of  assembled coefficient
C               matrix  should be greater than or equal to  the  half
C               bandwidth for static analysis or the total  number of
C               equations for the dynamic analysis.
C
C     NOTE:_____The  values  of NRMAX, NCMAX, MAXELM, MAXNOD, MAXCNV,
C               MAXSSV and MAXSPV in the 'PARAMETER' statement should
C               modified as required by the size of the problem.
C     -----------------------------------------------------------------
C                      SUBROUTINES USED IN THE PROGRAM
C
C      BOUNRY, CNCTVT, EGNBOU, INVRSE, ECHO*, ELKMFR, ELKMFT, MSH2DG,
C          MSH2DR, PSTPRC, QUADRT, SHPRCT, SHPTRI, SOLVER*, TIMER
C
C     Subroutines IWKIN and DGVCSP are the system subroutines used to
C     calculate  eigenvalues and eigenvectors.  Any other subroutines
C     (e.g.,  AXLBX  and  JACOBI  from FEM1DV2) can be used in place.
C   ___________________________________________________________________
C
      IMPLICIT REAL*8(A-H,O-Z)
      PARAMETER (NRMAX=310, NCMAX=310, MAXELM=250, MAXNOD=200,
     1           MAXSPV=200, MAXSSV=50, MAXCNV=20, MAXNX=25, MAXNY=25)
C
      DIMENSION ISPV(MAXSPV,2),VSPV(MAXSPV),ISSV(MAXSSV,2),VSSV(MAXSSV)
      DIMENSION IBN(MAXCNV),INOD(MAXCNV,3),BETA(MAXSPV),TINF(MAXSSV)
      DIMENSION GLF(NRMAX),TITLE(20),IBS(3),IBP(3),GLM(NRMAX,NRMAX)
      DIMENSION GLK(NRMAX,NCMAX),GLU(NRMAX),GLV(NRMAX),GLA(NRMAX)
      DIMENSION NOD(MAXELM,9),GLXY(MAXNOD,2),DX(MAXNX),DY(MAXNY)
      DIMENSION EGNVAL(NRMAX),EGNVEC(NRMAX,NRMAX),IBDY(MAXSPV)
C
      COMMON/STF/ELF(27),ELK(27,27),ELM(27,27),ELXY(9,2),ELU(27),
     1           ELV(27),ELA(27),A1,A2,A3,A4,A5
      COMMON/PST/A10,A1X,A1Y,A20,A2X,A2Y,A00,C0,CX,CY,F0,FX,FY,
     1           C44,C55,AMU,PENLTY,CMAT(3,3)
      COMMON/PNT/IPDF,IPDR,NIPF,NIPR
      COMMON/IO/IN,ITT
      COMMON/WORKSP/RWKSP
      REAL RWKSP(228000)
      CALL IWKIN(228000)
C
C     * * * * * * * * * * * * * * * * * * * * * * * * * * * * * * * *
C     *                                                             *
C     *              P R E P R O C E S S O R   U N I T              *
C     *                                                             *
C     * * * * * * * * * * * * * * * * * * * * * * * * * * * * * * * *
C
      IN=5
      ITT=6
      CALL ECHO(IN,ITT)
      ICONV=0
      INTIAL=0
      NSSV=0
      NFLAG=1
C
C     R E A D I N   T H E   I N P U T   D A T A   H E R E
C
      READ(IN,400) TITLE
C
C     Read problem and analysis type
C
      READ(IN,*)ITYPE,IGRAD,ITEM,NEIGN
      IF(ITEM.EQ.0) NEIGN=0
      IF(NEIGN.NE.0) THEN
          IF(ITYPE.LE.3 .AND. NEIGN.GT.1) THEN
              WRITE(ITT,991)
              STOP
          ELSE
              READ(IN,*) NVALU,NVCTR
          ENDIF
      ENDIF
C
C     Read finite element mesh information
C
      READ(IN,*) IELTYP,NPE,MESH,NPRNT
      IF(ITYPE.GE.3 .AND. IELTYP.EQ.0) THEN
          WRITE(ITT,990)
          STOP
      ENDIF
      IF(NPE.LE.4) THEN
          IEL=1
      ELSE
          IEL=2
      ENDIF
      IF(MESH.NE.1) THEN
          READ(IN,*) NEM,NNM
          IF(MESH.EQ.0)THEN
C
C     If mesh CANNOT be generated by the program, read the mesh data in
C     the next three statements
C
              DO 10 N=1,NEM
   10         READ(IN,*) (NOD(N,I),I=1,NPE)
              READ(IN,*) ((GLXY(I,J),J=1,2),I=1,NNM)
          ELSE
C
C     When mesh is to be generated by the program for more complicated
C     geometries, call MSH2DGeneral (which reads pertinent data there)
C
              CALL MSH2DG(NEM,NNM,NOD,MAXELM,MAXNOD,GLXY)
          ENDIF                                                         F2D01900
      ELSE                                                              F2D01910
C                                                                       F2D01920
C     When mesh is to be generated for rectangular domains, call programF2D01930
C     MSH2DRectangular, which requires the following data:              F2D01940
C                                                                       F2D01950
          READ(IN,*) NX,NY                                              F2D01960
          READ(IN,*) X0,(DX(I),I=1,NX)                                  F2D01970
          READ(IN,*) Y0,(DY(I),I=1,NY)                                  F2D01980
          CALL MSH2DR (IEL,IELTYP,NX,NY,NPE,NNM,NEM,NOD,DX,DY,X0,Y0,    F2D01990
     *                 GLXY,MAXELM,MAXNOD,MAXNX,MAXNY)                  F2D02000
      ENDIF                                                             F2D02010
C                                                                       F2D02020
      IF(ITYPE.EQ.0) THEN                                               F2D02030
          NDF = 1                                                       F2D02040
      ELSE                                                              F2D02050
          IF(ITYPE.GE.3) THEN                                           F2D02060
              NDF = 3                                                   F2D02070
          ELSE                                                          F2D02080
              NDF = 2                                                   F2D02090
          ENDIF                                                         F2D02100
      ENDIF                                                             F2D02110
      IF(ITYPE.EQ.5) NDF=4                                              F2D02120
C                                                                       F2D02130
      NEQ=NNM*NDF                                                       F2D02140
      NN=NPE*NDF                                                        F2D02150
      IF(NEIGN.EQ.0) THEN                                               F2D02160
C                                                                       F2D02170
C     Compute the half bandwidth of the global coefficient matrix       F2D02180
C                                                                       F2D02190
          NHBW=0                                                        F2D02200
          DO 20 N=1,NEM                                                 F2D02210
          DO 20 I=1,NPE                                                 F2D02220
          DO 20 J=1,NPE                                                 F2D02230
          NW=(IABS(NOD(N,I)-NOD(N,J))+1)*NDF                            F2D02240
   20     IF (NHBW.LT.NW) NHBW=NW                                       F2D02250
      ELSE                                                              F2D02260
          NHBW=NEQ                                                      F2D02270
      ENDIF                                                             F2D02280
C                                                                       F2D02290
C     Read specified primary and secondary degrees of freedom: node     F2D02300
C     number, local degree of freedom number, and specified value.      F2D02310
C                                                                       F2D02320
      READ(IN,*) NSPV                                                   F2D02330
      IF(NSPV.NE.0) THEN                                                F2D02340
          READ(IN,*) ((ISPV(I,J),J=1,2),I=1,NSPV)                       F2D02350
          IF(NEIGN.EQ.0) THEN                                           F2D02360
              READ(IN,*) (VSPV(I),I=1,NSPV)                             F2D02370
          ENDIF                                                         F2D02380
      ENDIF                                                             F2D02390
      IF(NEIGN.EQ.0) THEN                                               F2D02400
          READ(IN,*) NSSV                                               F2D02410
          IF(NSSV.NE.0) THEN                                            F2D02420
              READ(IN,*) ((ISSV(I,J),J=1,2),I=1,NSSV)                   F2D02430
              READ(IN,*) (VSSV(I),I=1,NSSV)                             F2D02440
          ENDIF                                                         F2D02450
      ENDIF                                                             F2D02460
C                                                                       F2D02470
      WRITE(ITT,400) TITLE                                              F2D02480
      WRITE(ITT,910)                                                    F2D02490
      WRITE(ITT,890)                                                    F2D02500
      WRITE(ITT,910)                                                    F2D02510
      IF(ITYPE.EQ.0) THEN                                               F2D02520
C                                                                       F2D02530
C     Heat transfer and like problems:__________________________________F2D02540
C                                                                       F2D02550
          WRITE(ITT,410)                                                F2D02560
C                                                                       F2D02570
C     Read the coefficients of the differential equation modeled       F2D02580
C                                                                       F2D02590
C     A11 = A10 + A1X*X + A1Y*Y; A22 = A20 + A2X*X + A2Y*Y; A00=CONST.  F2D02600
C                                                                       F2D02610
          READ(IN,*)A10,A1X,A1Y                                         F2D02620
          READ(IN,*)A20,A2X,A2Y                                         F2D02630
          READ(IN,*)A00                                                 F2D02640
          WRITE(ITT,420) A10,A1X,A1Y,A20,A2X,A2Y,A00                    F2D02650
          READ(IN,*)ICONV                                               F2D02660
          IF(ICONV.NE.0) THEN                                           F2D02670
              READ(IN,*) NBE                                            F2D02680
              READ(IN,*) (IBN(I),BETA(I),TINF(I),I=1,NBE)               F2D02690
              READ(IN,*) ((INOD(I,J),J=1,2),I=1,NBE)                    F2D02700
              WRITE(ITT,440) NBE                                        F2D02710
              DO 30 I=1,NBE                                             F2D02720
  30          WRITE(ITT,860) IBN(I),(INOD(I,J),J=1,2),BETA(I),TINF(I)   F2D02730
          ENDIF                                                         F2D02740
      ELSE                                                              F2D02750
          IF(ITYPE.EQ.1) THEN                                           F2D02760
C                                                                       F2D02770
C     Viscous incompressible flows:_____________________________________F2D02780
C                                                                       F2D02790
              WRITE(ITT,450)                                            F2D02800
              READ(IN,*)AMU,PENLTY                                      F2D02810
              WRITE(ITT,460) AMU,PENLTY                                 F2D02820
          ELSE                                                          F2D02830
              IF(ITYPE.EQ.2) THEN                                       F2D02840
C                                                                       F2D02850
C     Plane elasticity problems:________________________________________F2D02860
C                                                                       F2D02870
                  READ(IN,*) LNSTRS                                     F2D02880
                  WRITE(ITT,470)                                        F2D02890
                  READ(IN,*) E1,E2,ANU12,G12,THKNS                      F2D02900
                  WRITE(ITT,520) THKNS,E1,E2,ANU12,G12                  F2D02910
C                                                                       F2D02920
C     Compute the material coefficient matrix, CMAT(I,J), I,J=1,2,3.    F2D02930
C                                                                       F2D02940
                  ANU21=ANU12*E2/E1                                     F2D02950
                  DENOM=1.0-ANU12*ANU21                                 F2D02960
                  CMAT(3,3)=G12*THKNS                                   F2D02970
                  IF(LNSTRS.EQ.0) THEN                                  F2D02980
C                                                                       F2D02990
C     Plane strain  (ANU23 = ANU12)                                     F2D03000
C                                                                       F2D03010
                      WRITE(ITT,490)                                    F2D03020
                      S0=(1.0-ANU12-2.0*ANU12*ANU21)                    F2D03030
                      CMAT(1,1)=THKNS*E1*(1.0-ANU12)/S0                 F2D03040
                      CMAT(1,2)=THKNS*E1*ANU21/S0                       F2D03050
                      CMAT(2,2)=THKNS*E2*DENOM/S0/(1.0+ANU12)           F2D03060
                  ELSE                                                  F2D03070
C                                                                       F2D03080
C     Plane stress                                                      F2D03090
C                                                                       F2D03100
                      WRITE(ITT,510)                                    F2D03110
                      CMAT(1,1)=THKNS*E1/DENOM                          F2D03120
                      CMAT(1,2)=ANU21*CMAT(1,1)                         F2D03130
                      CMAT(2,2)=E2*CMAT(1,1)/E1                         F2D03140
                  ENDIF                                                 F2D03150
C                                                                       F2D03160
              ELSE                                                      F2D03170
C                                                                       F2D03180
C     Plate bending problems:___________________________________________F2D03190
C                                                                       F2D03200
                  WRITE(ITT,500)                                        F2D03210
                  IF(ITYPE.EQ.3) THEN                                   F2D03220
                      WRITE(ITT,505)                                    F2D03230
                  ELSE                                                  F2D03240
                      WRITE(ITT,506)                                    F2D03250
                  ENDIF                                                 F2D03260
                  READ(IN,*) E1,E2,ANU12,G12,G13,G23,THKNS              F2D03270
                  WRITE(ITT,520) THKNS,E1,E2,ANU12,G12                  F2D03280
                  WRITE(ITT,530) G13,G23                                F2D03290
                  ANU21=ANU12*E2/E1                                     F2D03300
                  DENOM=1.0-ANU12*ANU21                                 F2D03310
                  CMAT(1,1)=(THKNS**3)*E1/DENOM/12.0D0                  F2D03320
                  CMAT(1,2)=ANU21*CMAT(1,1)                             F2D03330
                  CMAT(2,2)=E2*CMAT(1,1)/E1                             F2D03340
                  CMAT(3,3)=G12*(THKNS**3)/12.0D0                       F2D03350
                  SCF=5.0D0/6.0D0                                       F2D03360
                  C44=SCF*G23*THKNS                                     F2D03370
                  C55=SCF*G13*THKNS                                     F2D03380
              ENDIF                                                     F2D03390
```

```
C
              CMAT(1,3)=0.0
              CMAT(2,3)=0.0
              CMAT(2,1)=CMAT(1,2)
              CMAT(3,1)=CMAT(1,3)
              CMAT(3,2)=CMAT(2,3)
C
          ENDIF
      ENDIF
      IF(NEIGN.EQ.0) THEN
          READ(IN,*)F0,FX,FY
          WRITE(ITT,430) F0,FX,FY
      ENDIF
C
      IF(ITEM.NE.0) THEN
          READ(IN,*) C0,CX,CY
          IF(ITYPE.GT.1) THEN
              IF(ITYPE.EQ.2)THEN
                  C0=THKNS*C0
                  CX=THKNS*CX
                  CY=THKNS*CY
              ELSE
                  IF(NEIGN.LE.1) THEN
                      C0=THKNS*C0
                      CX=(THKNS**2)*C0/12.0D0
                      CY=CX
                  ENDIF
              ENDIF
          ENDIF
C
          IF(NEIGN.NE.0) THEN
              WRITE(ITT,810)
              WRITE(ITT,540) C0,CX,CY
          ELSE
              WRITE(ITT,820)
              WRITE(ITT,540) C0,CX,CY
C
C     Read the necessary data for time-dependent problems
C
              READ(IN,*) NTIME,NSTP,INTVL,INTIAL
              IF(INTVL.LE.0)INTVL=1
              READ(IN,*) DT,ALFA,GAMA,EPSLN
              A1=ALFA*DT
              A2=(1.0-ALFA)*DT
              WRITE(ITT,550) DT,ALFA,GAMA,NTIME,NSTP,INTVL
              IF(ITEM.EQ.1) THEN
                  IF(NSSV.NE.0) THEN
                      DO 40 I=1,NSSV
  40                  VSSV(I)=VSSV(I)*DT
                  ENDIF
                  IF(INTIAL.NE.0) THEN
                      READ(IN,*) (GLU(I),I=1,NEQ)
                  ELSE
                      DO 50 I=1,NEQ
  50                  GLU(I)=0.0
                  ENDIF
              ELSE
                  DT2=DT*DT
                  A3=2.0/GAMA/DT2
                  A4=A3*DT
                  A5=1.0/GAMA-1.0
                  IF(INTIAL.NE.0) THEN
                      READ(IN,*) (GLU(I),I=1,NEQ)
                      READ(IN,*) (GLV(I),I=1,NEQ)
                      DO 60 I=1,NEQ
  60                  GLA(I)=0.0
                  ELSE
                      DO 70 I=1,NEQ
                      GLU(I)=0.0
                      GLV(I)=0.0
  70                  GLA(I)=0.0
                  ENDIF
              ENDIF
          ENDIF
      ELSE
          WRITE(ITT,830)
      ENDIF
C
C     *****      E N D   O F   T H E   D A T A   I N P U T        *****
C
      IF(IELTYP.EQ.0) THEN
          WRITE(ITT,790)
      ELSE
          WRITE(ITT,800)
      ENDIF
C
      WRITE(ITT,560) IELTYP,NPE,NDF,NEM,NNM,NEQ,NHBW
      IF(MESH.EQ.1) WRITE(ITT,570) NX,NY
      WRITE(ITT,710)NSPV
      IF(NSSV.NE.0) THEN
          WRITE(ITT,715)NSSV
          WRITE(ITT,720)
          DO 80 IB=1,NSSV
   80     WRITE(ITT,960) (ISSV(IB,JB),JB=1,2),VSSV(IB)
      ENDIF
C
      IF(NPRNT.EQ.1) THEN
          WRITE(ITT,700)
          DO 100 I=1,NEM
  100     WRITE(ITT,900) I,(NOD(I,J),J=1,NPE)
      ENDIF
C
      WRITE(ITT,910)
      WRITE(ITT,580)
      WRITE(ITT,910)
      DO 150 IM=1,NNM
      DO 110 K=1,NDF
      IBP(K)=0
  110 IBS(K)=0
      IF(NSPV.NE.0) THEN
          DO 120 JP=1,NSPV
          NODE=ISPV(JP,1)
          NDOF=ISPV(JP,2)
          IF(NODE.EQ.IM) THEN
              IBP(NDOF)=NDOF
          ENDIF
  120     CONTINUE
      ENDIF
C
      IF(NSSV.NE.0) THEN
          DO 140 JS=1,NSSV
          NODE=ISSV(JS,1)
          NDOF=ISSV(JS,2)
          IF(NODE.EQ.IM) THEN
              IBS(NDOF)=NDOF
          ENDIF
  140     CONTINUE
      ENDIF
C
      IF(NDF.EQ.1) THEN
          WRITE(ITT,870)IM,(GLXY(IM,J),J=1,2),(IBP(K),K=1,NDF),
     *                  (IBS(K),K=1,NDF)
      ELSE
          IF(NDF.EQ.2) THEN
              WRITE(ITT,920)IM,(GLXY(IM,J),J=1,2),(IBP(K),K=1,NDF),
     *                      (IBS(K),K=1,NDF)
          ELSE
              IF(NDF.EQ.3) THEN
                  WRITE(ITT,880)IM,(GLXY(IM,J),J=1,2),(IBP(K),K=1,NDF),
     *                          (IBS(K),K=1,NDF)
              ELSE
                  WRITE(ITT,885)IM,(GLXY(IM,J),J=1,2),(IBP(K),K=1,NDF),
     *                          (IBS(K),K=1,NDF)
              ENDIF
          ENDIF
      ENDIF
  150 CONTINUE
      WRITE(ITT,910)
C
```

```
C     Define the polynomial degree and number of integration points
C     (based on the assumed variation of the coefficients AX, BX, etc.)
C
      IPDR = IEL
      NIPR = IPDR+IEL-1
      IF(IELTYP.EQ.0) THEN
          IF(ITYPE.EQ.0) THEN
              IPDF = 2*IEL+1
              NIPF = IPDF+IEL
          ELSE
              IF(ITEM.NE.0) THEN
                  IPDF = 2*IEL+1
                  NIPF = IPDF+IEL
              ELSE
                  IPDF = IEL+1
                  NIPF = IPDF+1
              ENDIF
          ENDIF
          ISTR = 1
          NSTR = 1
          WRITE(ITT,480) IPDF,NIPF,IPDR,NIPR,ISTR,NSTR
      ELSE
          IF(ITYPE.GE.4) THEN
              IPDF = 4
              ISTR = 2
          ELSE
              IPDF = IEL+1
              ISTR = IEL
          ENDIF
          WRITE(ITT,485) IPDF,IPDR,ISTR
      ENDIF
C
C     * * * * * * * * * * * * * * * * * * * * * * * * * * * * * * * *
C     *                                                             *
C     *                  P R O C E S S O R   U N I T                *
C     *                                                             *
C     * * * * * * * * * * * * * * * * * * * * * * * * * * * * * * * *
C
      IF(ITEM.NE.0) THEN
          TIME=0.0
      ENDIF
C
C     Counter on number of TIME steps begins here
C
      NT = 0
      NCOUNT=0
  170 NCOUNT=NCOUNT+1
      IF(ITEM.NE.0 .AND. NEIGN.EQ.0) THEN
          IF(NCOUNT.GE.NSTP) THEN
              F0=0.0
              FX=0.0
              FY=0.0
          ENDIF
      ENDIF
C
C     Initialize the global coefficient matrices and vectors
C
      DO 180 I=1,NEQ
      GLF(I)=0.0
      DO 180 J=1,NHBW
      IF(NEIGN.NE.0) GLM(I,J)=0.0
  180 GLK(I,J)=0.0
C
C     Do-loop on the number of ELEMENTS to compute element matrices
C     and their assembly begins here
C
      DO 250 N=1,NEM
      DO 200 I=1,NPE
      NI=NOD(N,I)
      ELXY(I,1)=GLXY(NI,1)
      ELXY(I,2)=GLXY(NI,2)
      IF(NEIGN.EQ.0) THEN
          IF(ITEM.NE.0) THEN
              LI=(NI-1)*NDF
              L = (I-1)*NDF
              DO 190 J=1,NDF
              LI=LI+1
              L=L+1
              ELU(L)=GLU(LI)
              IF(ITEM.EQ.2) THEN
                  ELV(L)=GLV(LI)
                  ELA(L)=GLA(LI)
              ENDIF
  190         CONTINUE
          ENDIF
      ENDIF
  200 CONTINUE
C
C     Call subroutine ELKMFT (for Triangular elements) or ELKMFR (for
C     Rectangular elements) to compute the ELement [K], {M] and {F}.
C
      IF(IELTYP.EQ.0) THEN
          CALL ELKMFT (NCOUNT,NEIGN,NPE,NN,ITYPE,ITEM)
      ELSE
          CALL ELKMFR (NCOUNT,NEIGN,NPE,NN,ITYPE,ITEM)
      ENDIF
C
      IF(ICONV.NE.0) THEN
C
C     Add the convective terms for CONVECTION type boundary conditions
C     (exact for straight sided elements; otherwise approximate values)
C
          DO 210 M = 1,NBE
          IF(IBN(M).EQ.N) THEN
              M1  = INOD(M,1)
              M2  = INOD(M,2)
              NM1 = NOD(N,M1)
              NM2 = NOD(N,M2)
              DL  = DSQRT((GLXY(NM2,1)-GLXY(NM1,1))**2
     *                 +(GLXY(NM2,2)-GLXY(NM1,2))**2)
              BL  = BETA(M)*DL
              TF  = TINF(M)*DL
              IF(IEL.EQ.1)THEN
                  ELK(M1,M1)=ELK(M1,M1)+BL/3.0
                  ELK(M1,M2)=ELK(M1,M2)+BL/6.0
                  ELK(M2,M1)=ELK(M2,M1)+BL/6.0
                  ELK(M2,M2)=ELK(M2,M2)+BL/3.0
                  ELF(M1)=ELF(M1)+0.5*TF
                  ELF(M2)=ELF(M2)+0.5*TF
              ELSE
                  IF(NPE.GE.8) THEN
                      NPEL=4
                  ELSE
                      NPEL=3
                  ENDIF
                  M3=M1+NPEL
                  ELK(M1,M1)=ELK(M1,M1)+4.0*BL/30.0
                  ELK(M1,M3)=ELK(M1,M3)+2.0*BL/30.0
                  ELK(M1,M2)=ELK(M1,M2)-BL/30.0
                  ELK(M3,M1)=ELK(M3,M1)+2.0*BL/30.0
                  ELK(M3,M3)=ELK(M3,M3)+16.0*BL/30.0
                  ELK(M2,M3)=ELK(M2,M3)+2.0*BL/30.0
                  ELK(M2,M1)=ELK(M2,M1)-BL/30.0
                  ELK(M3,M2)=ELK(M3,M2)+2.0*BL/30.0
                  ELK(M2,M2)=ELK(M2,M2)+4.0*BL/30.0
                  ELF(M1)=ELF(M1)+TF/6.0
                  ELF(M3)=ELF(M3)+4.0*TF/6.0
                  ELF(M2)=ELF(M2)+TF/6.0
              ENDIF
          ENDIF
  210     CONTINUE
      ENDIF
C
      IF(NCOUNT.EQ.1) THEN
          IF(NPRNT.EQ.1 .OR. NPRNT.EQ.3) THEN
              IF(N.EQ.1) THEN
C
C     Print element matrices and vectors (only when NPRNT=1 or NPRNT=3)
C
                  WRITE(ITT,610)
                  DO 220 I=1,NN                                          F2D06390
  220             WRITE(ITT,930) (ELK(I,J),J=1,NN)                       F2D06400
                  IF(NEIGN.EQ.0) THEN                                    F2D06410
                      WRITE(ITT,630)                                     F2D06420
                      WRITE(ITT,930) (ELF(I),I=1,NN)                     F2D06430
                  ELSE                                                   F2D06440
                      WRITE(ITT,620)                                     F2D06450
                      DO 230 I=1,NN                                      F2D06460
  230                 WRITE(ITT,930) (ELM(I,J),J=1,NN)                   F2D06470
                  ENDIF                                                  F2D06480
              ENDIF                                                      F2D06490
          ENDIF                                                          F2D06500
      ENDIF                                                              F2D06510
C                                                                        F2D06520
      IF(NEIGN.EQ.0) THEN                                                F2D06530
          IF(ITEM.NE.0) THEN                                             F2D06540
C                                                                        F2D06550
C     Compute the element coefficient matrices [K-hat] and {F-hat}       F2D06560
C     (i.e., after time approximation) in the transient analysis:_______ F2D06570
C                                                                        F2D06580
              CALL TIMER(NCOUNT,INTIAL,ITEM,NN)                          F2D06590
          ENDIF                                                          F2D06600
      ENDIF                                                              F2D06610
C                                                                        F2D06620
C     ASSEMBLE element matrices to obtain global matrices:______________ F2D06630
C                                                                        F2D06640
      DO 240 I=1,NPE                                                     F2D06650
      NR=(NOD(N,I)-1)*NDF                                                F2D06660
      DO 240 II=1,NDF                                                    F2D06670
      NR=NR+1                                                            F2D06680
      L=(I-1)*NDF+II                                                     F2D06690
      IF(NEIGN.EQ.0) THEN                                                F2D06700
          GLF(NR)=GLF(NR)+ELF(L)                                         F2D06710
      ENDIF                                                              F2D06720
      DO 240 J=1,NPE                                                     F2D06730
      IF(NEIGN.EQ.0) THEN                                                F2D06740
          NCL=(NOD(N,J)-1)*NDF                                           F2D06750
      ELSE                                                               F2D06760
          NC=(NOD(N,J)-1)*NDF                                            F2D06770
      ENDIF                                                              F2D06780
      DO 240 JJ=1,NDF                                                    F2D06790
      M=(J-1)*NDF+JJ                                                     F2D06800
      IF(NEIGN.EQ.0) THEN                                                F2D06810
          NC=NCL+JJ+1-NR                                                 F2D06820
          IF(NC.GT.0) THEN                                               F2D06830
              GLK(NR,NC)=GLK(NR,NC)+ELK(L,M)                             F2D06840
          ENDIF                                                          F2D06850
      ELSE                                                               F2D06860
          NC=NC+1                                                        F2D06870
          GLK(NR,NC)=GLK(NR,NC)+ELK(L,M)                                 F2D06880
          GLM(NR,NC)=GLM(NR,NC)+ELM(L,M)                                 F2D06890
      ENDIF                                                              F2D06900
  240 CONTINUE                                                           F2D06910
  250 CONTINUE                                                           F2D06920
C                                                                        F2D06930
C     Print global matrices when NPRNT > 2                               F2D06940
C                                                                        F2D06950
      IF(NCOUNT.LE.1) THEN                                               F2D06960
          IF(NPRNT.GE.2) THEN                                            F2D06970
              WRITE(ITT,640)                                             F2D06980
              DO 260 I=1,NEQ                                             F2D06990
  260         WRITE(ITT,930) (GLK(I,J),J=1,NHBW)                         F2D07000
              IF(NEIGN.EQ.0) THEN                                        F2D07010
                  WRITE(ITT,650)                                         F2D07020
                  WRITE(ITT,930) (GLF(I),I=1,NEQ)                        F2D07030
              ENDIF                                                      F2D07040
          ENDIF                                                          F2D07050
      ENDIF                                                              F2D07060
C                                                                        F2D07070
C     Impose BOUNDARY CONDITIONS on primary and secondary variables      F2D07080
C                                                                        F2D07090
      IF(NEIGN.NE.0) THEN                                                F2D07100
          CALL EGNBOU(GLK,GLM,IBDY,ISPV,MAXSPV,NDF,NEQ,NEQR,NSPV,NRMAX)  F2D07110
C                                                                        F2D07120
C     Call SYSTEM subroutine ‘DGVCSP’ to solve the EIGENVALUE PROBLEM    F2D07130
```

```
C     to compute the eigenvalues and eigenvectors, and print them:
C
C      EGNVAL(I)   = Ith eigenvalue
C      EGNVEC(I,J) = Jth component of the Ith eigenvector
C
         CALL DGVCSP(NEQR,GLK,NRMAX,GLM,NRMAX,EGNVAL,EGNVEC,NRMAX)
C
         WRITE(ITT,660)
         IF(NVALU.GT.NEQR)NVALU=NEQR
         DO 270 I=1,NVALU
         IF(ITYPE.GE.2 .AND. NEIGN.EQ.1) THEN
             VALUE = DSQRT(EGNVAL(I))
             WRITE(ITT,840)I,EGNVAL(I),VALUE
         ELSE
             WRITE(ITT,845)I,EGNVAL(I)
         ENDIF
         IF(NVCTR.NE.0) THEN
             WRITE(ITT,850)
             WRITE(ITT,930)(EGNVEC(J,I),J=1,NEQR)
         ENDIF
  270    CONTINUE
         STOP
      ELSE
         CALL BOUNRY(ISPV,ISSV,MAXSPV,MAXSSV,NDF,NCMAX,NRMAX,NEQ,NHBW,
     *               NSPV,NSSV,GLK,GLF,VSPV,VSSV,NCOUNT,INTIAL)
C
C     Call subroutine  SOLVE  to solve the system of algebraic equations
C     The solution is returned in the array GLF
C
         IRES=0
         CALL SOLVER(NRMAX,NCMAX,NEQ,NHBW,GLK,GLF,IRES)
C
         IF(ITEM.NE.0) THEN
C
C     For nonzero initial conditions, GLF in the very first solution
C     is the acceleration, {A}=[MINV]({F}-[K]{U})
C
             IF(NCOUNT.EQ.1 .AND. INTIAL.NE.0) THEN
               IF(ITEM.EQ.2) THEN
                 DO 280 I=1,NEQ
  280            GLA(I)=GLF(I)
                 WRITE(ITT,600) TIME
                 WRITE(ITT,930) (GLA(I),I=1,NEQ)
                 GOTO 170
               ENDIF
             ELSE
                 NT = NT + 1
                 TIME=TIME+DT
             ENDIF
         ENDIF
C
C     Compute the difference between solutions at two consecutive times,
C     and calculate new velocities and accelerations
C
         DIFF=0.0
         SOLN=0.0
         DO 290 I=1,NEQ
         IF(ITEM.NE.0) THEN
             SOLN=SOLN+GLF(I)*GLF(I)
             DIFF=DIFF+(GLF(I)-GLU(I))*(GLF(I)-GLU(I))
         ENDIF
         IF(ITEM.EQ.2) THEN
             GLU(I)=A3*(GLF(I)-GLU(I))-A4*GLV(I)-A5*GLA(I)
             GLV(I)=GLV(I)+A1*GLU(I)+A2*GLA(I)
             GLA(I)=GLU(I)
         ENDIF
  290    GLU(I)=GLF(I)
         IF(ITEM.NE.0 .AND. NT.GT.1) THEN
             NFLAG=0
             PERCNT=DSQRT(DIFF/SOLN)
             IF(PERCNT.LE.EPSLN) THEN
                 WRITE(ITT,980)
                 STOP
             ELSE
                 INTGR=(NT/INTVL)*INTVL
```

```
                  IF(INTGR.EQ.NT) NFLAG=1
              ENDIF
          ENDIF
          IF(NFLAG.NE.0) THEN
C
C     Print the solution (i.e., nodal values of the primary variables)
C
              IF(ITEM.NE.0) THEN
                  WRITE(ITT,590) TIME,NT
              ENDIF
              WRITE(ITT,660)
              IF(NDF.LE.3) THEN
                  MDF=NDF
              ELSE
                  MDF=3
                  WRITE(ITT,666)
                  WRITE(ITT,930)(GLU(J),J=NDF,NEQ,NDF)
              ENDIF
              IF(ITYPE.EQ.0) THEN
                  WRITE(ITT,940)
              ELSE
                  WRITE(ITT,970)
              ENDIF
              IF(NDF.EQ.1)WRITE(ITT,670)
              IF(NDF.EQ.2)WRITE(ITT,680)
              IF(NDF.GE.3)WRITE(ITT,690)
              IF(ITYPE.EQ.0) THEN
                  WRITE(ITT,940)
              ELSE
                  WRITE(ITT,970)
              ENDIF
              DO 300 I=1,NNM
              II=NDF*(I-1)+1
              JJ=II+MDF-1
  300         WRITE(ITT,950)I,(GLXY(I,J),J=1,2),(GLU(J),J=II,JJ)
              WRITE(ITT,970)
          ENDIF
C
          IF(IGRAD.NE.0) THEN
              IF(NFLAG.EQ.1) THEN
C
C     * * * * * * * * * * * * * * * * * * * * * * * * * * * * * * * *
C     *                                                             *
C     *            P O S T P R O C E S S O R   U N I T              *
C     *                                                             *
C     * * * * * * * * * * * * * * * * * * * * * * * * * * * * * * * *
C
                  IF(ITYPE.LE.1) THEN
                      WRITE(ITT,970)
                  ELSE
                      WRITE(ITT,940)
                  ENDIF
                  IF(ITYPE.LE.0) THEN
                      WRITE(ITT,730)
                      IF(IGRAD.EQ.1) THEN
                          WRITE(6,740)
                      ELSE
                          WRITE(6,750)
                      ENDIF
                  ELSE
                      IF(ITYPE.EQ.1)WRITE(ITT,760)
                      IF(ITYPE.GE.2)WRITE(ITT,770)
                      IF(ITYPE.EQ.3)WRITE(ITT,780)
                  ENDIF
                  IF(ITYPE.LE.1) THEN
                      WRITE(ITT,970)
                  ELSE
                      WRITE(ITT,940)
                  ENDIF
C
C     Compute the GRADIENT of the solution for single-variable problems
C     or STRESSES for viscous flows, plane elasticity and plate bending
C
                  DO 320 N=1,NEM
                  DO 310 I=1,NPE
                  NI=NOD(N,I)
                  ELXY(I,1)=GLXY(NI,1)
                  ELXY(I,2)=GLXY(NI,2)
                  LI=(NI-1)*NDF
                  L=(I-1)*NDF
                  DO 310 J=1,NDF
                  LI=LI+1
                  L=L+1
                  ELU(L)=GLU(LI)
 310              CONTINUE
 320              CALL PSTPRC(ELXY,ITYPE,IELTYP,IGRAD,NDF,NPE,THKNS,
     *                        ELU,ISTR,NSTR)
                  IF(ITYPE.LE.1) THEN
                      WRITE(ITT,970)
                  ELSE
                      WRITE(ITT,940)
                  ENDIF
              ENDIF
          ENDIF
C
          IF(ITEM.NE.0) THEN
              IF(NT.GE.NTIME) THEN
                  STOP
              ELSE
                  GOTO 170
              ENDIF
          ENDIF
      ENDIF
      STOP
C
C                       F  O  R  M  A  T  S
C
  400 FORMAT(20A4)
  410 FORMAT (/,16X,'ANALYSIS  OF   A  POISSON/LAPLACE  EQUATION')
  420 FORMAT (/,5X,'COEFFICIENTS OF THE DIFFERENTIAL EQUATION:',//,
     *        8X,'Coefficient, A10 ......................=',E12.4,/,
     *        8X,'Coefficient, A1X ......................=',E12.4,/,
     *        8X,'Coefficient, A1Y ......................=',E12.4,/,
     *        8X,'Coefficient, A20 ......................=',E12.4,/,
     *        8X,'Coefficient, A2X ......................=',E12.4,/,
     *        8X,'Coefficient, A2Y ......................=',E12.4,/,
     *        8X,'Coefficient, A00 ......................=',E12.4,/)
  430 FORMAT (/,5X,'CONTINUOUS SOURCE COEFFICIENTS:',//,
     *        8X,'Coefficient, F0  ......................=',E12.4,/,
     *        8X,'Coefficient, FX  ......................=',E12.4,/,
     *        8X,'Coefficient, FY  ......................=',E12.4,/)
  440 FORMAT (/,5X,'CONVECTIVE HEAT TRANSFER DATA:',//,
     *        8X,'Number of elements with convection, NBE .=',I4,/,
     *        8X,'Elements, their LOCAL nodes and convective',/,
     *        8X,'heat transfer data:',/,
     *        8X,'Ele. No.',4X,'End Nodes',8X,'Film Coeff.',6X,
     *            'T-Infinity',/)
  450 FORMAT (/,16X,'A  VISCOUS INCOMPRESSIBLE FLOW IS ANALYZED')
  460 FORMAT (/,5X,'PARAMETERS OF THE FLUID FLOW PROBLEM:',//,
     *        8X,'Viscosity of the fluid, AMU .............=',E12.4,/,
     *        8X,'Penalty parameter, PENLTY ...............=',E12.4,/)
  470 FORMAT (/,16X,'A  2-D  ELASTICITY   PROBLEM  IS  ANALYZED')
  480 FORMAT (/,5X,'NUMERICAL INTEGRATION DATA:',//,
     *        8X,'Full Integration polynomial degree, IPDF =',I4,/,
     *        8X,'Number of full integration points,  NIPF =',I4,/,
     *        8X,'Reduced Integration polynomial deg.,IPDR =',I4,/,
     *        8X,'No.  of reduced integration points, NIPR =',I4,/,
     *        8X,'Integ. poly. deg. for stress comp., ISTR =',I4,/,
     *        8X,'No. of integ. pts. for stress comp.,NSTR =',I4,/)
  485 FORMAT (/,5X,'NUMERICAL INTEGRATION DATA:',//,
     *        8X,'Full quadrature (IPDF x IPDF) rule, IPDF =',I4,/,
     *        8X,'Reduced quadrature (IPDR x IPDR),   IPDR =',I4,/,
     *        8X,'Quadrature rule used in postproc.,  ISTR =',I4,/)
  490 FORMAT (9X,'**PLANE STRAIN assumption is selected by user**',/)
  500 FORMAT (/,16X,'A  PLATE   BENDING   PROBLEM  IS  ANALYZED')
  505 FORMAT (16X,  '*** using the shear deformation theory ***')
  506 FORMAT (16X,  '**** using the classical plate theory ****')
  510 FORMAT (/,8X,'***PLANE STRESS assumption is selected by user**',/)
  520 FORMAT (/,5X,'MATERIAL PROPERTIES OF THE SOLID ANALYZED:',//,
     *        8X,'Thickness of the body, THKNS ...........=',E12.4,/,
     *        8X,'Modulus of elasticity, E1 ...............=',E12.4,/,  F2D09390
     *        8X,'Modulus of elasticity, E2 ...............=',E12.4,/,  F2D09400
     *        8X,'Poisson s ratio, ANU12 ..................=',E12.4,/,  F2D09410
     *        8X,'Shear modulus, G12 ......................=',E12.4)    F2D09420
  530 FORMAT (8X,'Shear modulus, G13 ......................=',E12.4,/,  F2D09430
     *        8X,'Shear modulus, G23 ......................=',E12.4,/)  F2D09440
  540 FORMAT (/,5X,'PARAMETERS OF THE DYNAMIC ANALYSIS:',//,            F2D09450
     *        8X,'Coefficient, C0 .........................=',E12.4,/,  F2D09460
     *        8X,'Coefficient, CX .........................=',E12.4,/,  F2D09470
     *        8X,'Coefficient, CY .........................=',E12.4)    F2D09480
  550 FORMAT (8X,'Time increment used, DT .................=',E12.4,/,  F2D09490
     *        8X,'Parameter, ALFA .........................=',E12.4,/,  F2D09500
     *        8X,'Parameter, GAMA .........................=',E12.4,/,  F2D09510
     *        8X,'Number of time steps used, NTIME ........=',I4,/,     F2D09520
     *        8X,'Time step at which load is removed, NSTP.=',I4,/,     F2D09530
     *        8X,'Time interval at which soln. is printed..=',I4,/)     F2D09540
  560 FORMAT (/,5X,'FINITE ELEMENT MESH INFORMATION:',//,               F2D09550
     *        8X,'Element type: 0 = Triangle; >0 = Quad.)..=',I4,/,     F2D09560
     *        8X,'Number of nodes per element, NPE ........=',I4,/,     F2D09570
     *        8X,'No. of primary deg. of freedom/node, NDF =',I4,/,     F2D09580
     *        8X,'Number of elements in the mesh, NEM .....=',I4,/,     F2D09590
     *        8X,'Number of nodes in the mesh, NNM ........=',I4,/,     F2D09600
     *        8X,'Number of equations to be solved, NEQ ...=',I4,/,     F2D09610
     *        8X,'Half bandwidth of the matrix GLK, NHBW ..=',I4)       F2D09620
  570 FORMAT (8X,'Mesh subdivisions, NX and NY ............=',2I4,/)    F2D09630
  580 FORMAT (5X,'Node   x-coord.   y-coord.    Speci. primary & secondaF2D09640
     *ry variables',/,38X,'(0, unspecified; >0, specified)',            F2D09650
     *                 /,41X,'Primary DOF  Secondary DOF')              F2D09660
  590 FORMAT (/,5X,'*TIME* =',E12.5,5X,'Time Step Number =',I3)         F2D09670
  600 FORMAT (/,5X,'*TIME* =',E12.5,' (Initial acceleration vector:)',/)F2D09680
  610 FORMAT (/,5X,'Element coefficient matrix: ',/)                    F2D09690
  620 FORMAT (/,5X,'Element mass matrix: ',/)                           F2D09700
  630 FORMAT (/,5X,'Element source vector:',/)                          F2D09710
  640 FORMAT (/,5X,'Global coefficient matrix:',/)                      F2D09720
  650 FORMAT (/,5X,'Global source vector:',/)                           F2D09730
  660 FORMAT (/,5X,'S O L U T I O N :',/)                               F2D09740
  666 FORMAT (5X,'Nodal values of W,xy for conforming plate element:',/)F2D09750
  670 FORMAT (5X,'Node    x-coord.       y-coord.    Primary DOF')      F2D09760
  680 FORMAT (5X,'Node    x-coord.       y-coord.     Value of u',      F2D09770
     *               '  Value of v')                                    F2D09780
  690 FORMAT (5X,'Node    x-coord.       y-coord.     deflec. w',       F2D09790
     *               '    x-rotation    y-rotation')                    F2D09800
  700 FORMAT (/,5X,'Connectivity Matrix, [NOD]',/)                      F2D09810
  710 FORMAT (8X,'No. of specified PRIMARY variables, NSPV =',I4)       F2D09820
  715 FORMAT (8X,'No. of speci.  SECONDARY variables, NSSV =',I4,/)     F2D09830
  720 FORMAT (6X,'Node  DOF     Value',/)                               F2D09840
  730 FORMAT (4X,'The orientation of  gradient vector is measured from  F2D09850
     1the positive x-axis',/)                                           F2D09860
  740 FORMAT (4X,'x-coord.     y-coord.   -a11(du/dx)  -a22(du/dy)',    F2D09870
     1         3X,'Flux Mgntd  Orientation')                            F2D09880
  750 FORMAT (4X,'x-coord.     y-coord.   a22(du/dy)  -a11(du/dx)',     F2D09890
     1         3X,'Flux Mgntd  Orientation')                            F2D09900
  760 FORMAT (5X,'x-coord.     y-coord.     sigma-x      sigma-y',      F2D09910
     *'      sigma-xy    pressure')                                     F2D09920
  770 FORMAT (5X,'x-coord.     y-coord.     sigma-x      sigma-y',      F2D09930
     *'      sigma-xy')                                                 F2D09940
  780 FORMAT (5X,'                          sigma-xz     sigma-yz')     F2D09950
  790 FORMAT (/,8X,'*** A mesh of   TRIANGLES    is chosen by user ***')F2D09960
  800 FORMAT (/,8X,'*** A mesh of QUADRILATERALS is chosen by user ***')F2D09970
  810 FORMAT (/,8X,'******* An EIGENVALUE PROBLEM  is analyzed *******')F2D09980
  820 FORMAT (/,8X,'******** A TRANSIENT PROBLEM  is analyzed ********')F2D09990
  830 FORMAT (/,8X,'******* A STEADY-STATE PROBLEM is analyzed *******')F2D10000
  840 FORMAT(/,3X,'Eigenvalue(',I3,') =',E15.6,3X,'Frequency =',E13.5)  F2D10010
  845 FORMAT(5X,'E I G E N V A L U E (',I3,') =',E15.6)                 F2D10020
  850 FORMAT(/,5X,'E I G E N V E C T O R :',/)                          F2D10030
  860 FORMAT (8X,I5,5X,2I5,6X,E13.5,5X,E13.5)                           F2D10040
  870 FORMAT (5X,I3,2E12.4,8X,I9,9X,I5)                                 F2D10050
  880 FORMAT (5X,I3,2E12.4,7X,3I4,2X,3I4)                               F2D10060
  885 FORMAT (5X,I3,2E12.4,5X,4I4,2X,4I4)                               F2D10070
  890 FORMAT (12X,'OUTPUT  FROM  PROGRAM  *FEM2DV2*   BY  J. N. REDDY') F2D10080
  900 FORMAT (10X,10I5)                                                 F2D10090
  910 FORMAT (2X,70('_'),/)                                             F2D10100
  920 FORMAT (5X,I3,2E12.4,8X,2I5,4X,2I5)                               F2D10110
  930 FORMAT (8X,5E14.5)                                                F2D10120
  940 FORMAT (2X,65(' '),/)                                             F2D10130
  950 FORMAT (5X,I3,5E14.5)                                             F2D10140
  960 FORMAT (5X,I5,I4,E14.5)                                           F2D10150
  970 FORMAT (2X,77('_'),/)                                             F2D10160
  980 FORMAT (/,3X,'*** THE SOLUTION HAS REACHED  A  STEADY STATE ***') F2D10170
  990 FORMAT (/,3X,'**TRIANGULAR ELEMENTS ARE NOT ALLOWED FOR PLATES**')F2D10180
  991 FORMAT (/,3X,'*STABILITY ANALYSIS IS ONLY FOR BENDING OF PLATES*',F2D10190
     *         /,3X,'**** according to the  classical plate theory ****')F2D10200
      END                                                               F2D10210


      SUBROUTINE BOUNRY(ISPV,ISSV,MAXSPV,MAXSSV,NDF,NCMAX,NRMAX,NEQ,    F2D10220
     *                  NHBW,NSPV,NSSV,S,SL,VSPV,VSSV,NCOUNT,INTIAL)    F2D10230
C     __________________________________________________________________F2D10240
C                                                                       F2D10250
C     The subroutine implements  specified  values of the primary and   F2D10260
C     secondary variables by modifying the coefficient matrix [S] and   F2D10270
C     (banded and symmetric) and the right-hand side vector {SL}.       F2D10280
C     __________________________________________________________________F2D10290
C                                                                       F2D10300
      IMPLICIT REAL*8(A-H,O-Z)                                          F2D10310
      DIMENSION S(NRMAX,NCMAX),SL(NRMAX),ISPV(MAXSPV,2),VSPV(MAXSPV),   F2D10320
     *          ISSV(MAXSSV,2),VSSV(MAXSSV)                             F2D10330
      COMMON/IO/IN,ITT                                                  F2D10340
C                                                                       F2D10350
      IF(NSSV.NE.0) THEN                                                F2D10360
          IF(INTIAL.EQ.0 .OR. NCOUNT.NE. 1) THEN                        F2D10370
C                                                                       F2D10380
C     Implement specified values of the SECONDARY VARIABLES:____________F2D10390
C                                                                       F2D10400
              DO 10 I=1,NSSV                                            F2D10410
              II=(ISSV(I,1)-1)*NDF+ISSV(I,2)                            F2D10420
   10         SL(II)=SL(II)+VSSV(I)                                     F2D10430
          ENDIF                                                         F2D10440
      ENDIF                                                             F2D10450
C                                                                       F2D10460
C     Implement specified values of the PRIMARY VARIABLES:______________F2D10470
C                                                                       F2D10480
      IF(NSPV.NE.0) THEN                                                F2D10490
          DO 50 NB=1,NSPV                                               F2D10500
          IE=(ISPV(NB,1)-1)*NDF+ISPV(NB,2)                              F2D10510
          VALUE=VSPV(NB)                                                F2D10520
          IT=NHBW-1                                                     F2D10530
          I=IE-NHBW                                                     F2D10540
          DO 30 II=1,IT                                                 F2D10550
          I=I+1                                                         F2D10560
          IF(I.GE.1) THEN                                               F2D10570
              J=IE-I+1                                                  F2D10580
              SL(I)=SL(I)-S(I,J)*VALUE                                  F2D10590
              S(I,J)=0.0                                                F2D10600
          ENDIF                                                         F2D10610
   30     CONTINUE                                                      F2D10620
          S(IE,1)=1.0                                                   F2D10630
          SL(IE)=VALUE                                                  F2D10640
          I=IE                                                          F2D10650
          DO 40 II=2,NHBW                                               F2D10660
          I=I+1                                                         F2D10670
          IF(I.LE.NEQ) THEN                                             F2D10680
             SL(I)=SL(I)-S(IE,II)*VALUE                                 F2D10690
             S(IE,II)=0.0                                               F2D10700
          ENDIF                                                         F2D10710
   40     CONTINUE                                                      F2D10720
   50     CONTINUE                                                      F2D10730
      ENDIF                                                             F2D10740
      RETURN                                                            F2D10750
      END                                                               F2D10760
      SUBROUTINE CNCTVT(NELEM,NNODE,NODES,MAXELM,MAXNOD,GLXY)           F2D10770
C     ______________________________________________________________    F2D10780
C                                                                       F2D10790
C     Generates nodal connectivity array for a specified type of mesh   F2D10800
C                                                                       F2D10810
C     NEL1    = First element in the row of elements                    F2D10820
C     NELL    = Last element in thé row                                 F2D10830
C     IELINC  = Increment from element to the next in the row          F2D10840
C     NODINC  = Node increment from one element to the next            F2D10850
C     NPE     = Number of nodes per element                             F2D10860
C     NODE(I) = Global node numbers corresponding to the local nodes    F2D10870
C               of the first element in the row                         F2D10880
C     ______________________________________________________________    F2D10890
C                                                                       F2D10900
      IMPLICIT REAL*8(A-H,O-Z)                                          F2D10910
      DIMENSION  NODES(MAXELM,9),GLXY(MAXNOD,2),NODE(9)                 F2D10920
C                                                                       F2D10930
C     Read element data                                                 F2D10940
C                                                                       F2D10950
      READ(5,*) NRECEL                                                  F2D10960
      DO 30 IREC=1,NRECEL                                               F2D10970
      READ(5,*) NEL1,NELL,IELINC,NODINC,NPE,(NODE(I),I=1,NPE)           F2D10980
      IF(IELINC.LE.0) IELINC=1                                          F2D10990
      IF(NODINC.LE.0) NODINC=1                                          F2D11000
      IF(NELL.LE.NEL1) NELL=NEL1                                        F2D11010
      IF(NELL.GT.NELEM) THEN                                            F2D11020
          WRITE(6,60)                                                   F2D11030
          STOP                                                          F2D11040
      ELSE                                                              F2D11050
          NINC=-1                                                       F2D11060
          DO 20 N=NEL1,NELL,IELINC                                      F2D11070
          NINC=NINC+1                                                   F2D11080
          DO 10 M=1,NPE                                                 F2D11090
   10     NODES(N,M)=NODE(M)+NINC*NODINC                                F2D11100
   20     CONTINUE                                                      F2D11110
      ENDIF                                                             F2D11120
   30 CONTINUE                                                          F2D11130
C                                                                       F2D11140
      DO 50 N=1,NELEM                                                   F2D11150
      SUMX=0.0                                                          F2D11160
      SUMY=0.0                                                          F2D11170
      NEN=NPE                                                           F2D11180
      IF(NEN.NE.4) THEN                                                 F2D11190
          DO 40 M=5,NEN                                                 F2D11200
          MM=NODES(N,M)                                                 F2D11210
          IF(M.NE.9 .OR. M.NE.6) THEN                                   F2D11220
              M4=NODES(N,M-4)                                           F2D11230
              M3=NODES(N,M-3)                                           F2D11240
              IF(M.EQ.8) M3=NODES(N,1)                                  F2D11250
              IF(GLXY(MM,1).EQ.1.E20)                                   F2D11260
     *           GLXY(MM,1)=0.5*(GLXY(M4,1)+GLXY(M3,1))                 F2D11270
              IF(GLXY(MM,2).EQ.1.E20)                                   F2D11280
     *           GLXY(MM,2)=0.5*(GLXY(M4,2)+GLXY(M3,2))                 F2D11290
              IF(NEN.NE.8) THEN                                         F2D11300
                  SUMX=SUMX+GLXY(M4,1)                                  F2D11310
                  SUMY=SUMY+GLXY(M4,2)                                  F2D11320
              ENDIF                                                     F2D11330
          ELSE                                                          F2D11340
              IF(GLXY(MM,1).EQ.1.E20) GLXY(MM,1)=0.25*SUMX              F2D11350
              IF(GLXY(MM,2).EQ.1.E20) GLXY(MM,2)=0.25*SUMY              F2D11360
          ENDIF                                                         F2D11370
   40 CONTINUE                                                          F2D11380
      ENDIF                                                             F2D11390
   50 CONTINUE                                                          F2D11400
   60 FORMAT(/,'MSG from CNCTVT: Element number exceeds maximum value') F2D11410
      RETURN                                                            F2D11420
      END                                                               F2D11430
```

```
      SUBROUTINE EGNBOU(A,D,IBDY,ISPV,MXPV,NDF,NEQ,NEQR,NSPV,NRM)       F2D11440
C     ______________________________________________________________    F2D11450
C                                                                       F2D11460
C     Imposes specified homogeneous boundary conditions on the primary  F2D11470
C     variables  by  eliminating rows and columns corresponding to the  F2D11480
C     specified degrees of freedom                                      F2D11490
C     ______________________________________________________________    F2D11500
```

```
C                                                                       F2D11510
      IMPLICIT REAL*8 (A-H,O-Z)                                         F2D11520
      DIMENSION A(NRM,NRM),D(NRM,NRM),ISPV(MXPV,2),IBDY(MXPV)           F2D11530
C                                                                       F2D11540
      DO 10 I=1,NSPV                                                    F2D11550
   10 IBDY(I)=(ISPV(I,1)-1)*NDF+ISPV(I,2)                               F2D11560
      DO 30 I=1,NSPV                                                    F2D11570
      IMAX=IBDY(I)                                                      F2D11580
      DO 20 J=I,NSPV                                                    F2D11590
      IF(IBDY(J).GE.IMAX) THEN                                          F2D11600
         IMAX=IBDY(J)                                                   F2D11610
         IKEPT=J                                                        F2D11620
      ENDIF                                                             F2D11630
   20 CONTINUE                                                          F2D11640
      IBDY(IKEPT)=IBDY(I)                                               F2D11650
      IBDY(I)=IMAX                                                      F2D11660
   30 CONTINUE                                                          F2D11670
      NEQR = NEQ                                                        F2D11680
      DO 80 I=1,NSPV                                                    F2D11690
      IB=IBDY(I)                                                        F2D11700
      IF(IB .LT. NEQR) THEN                                             F2D11710
         NEQR1=NEQR-1                                                   F2D11720
         DO 60 II=IB,NEQR1                                              F2D11730
         DO 40 JJ=1,NEQR                                                F2D11740
         D(II,JJ)=D(II+1,JJ)                                            F2D11750
   40    A(II,JJ)=A(II+1,JJ)                                            F2D11760
         DO 50 JJ=1,NEQR                                                F2D11770
         D(JJ,II)=D(JJ,II+1)                                            F2D11780
   50    A(JJ,II)=A(JJ,II+1)                                            F2D11790
   60    CONTINUE                                                       F2D11800
      ENDIF                                                             F2D11810
      NEQR=NEQR-1                                                       F2D11820
   80 CONTINUE                                                          F2D11830
      RETURN                                                            F2D11840
      END                                                               F2D11850

      SUBROUTINE INVRSE(A,B)                                            F2D11860
      IMPLICIT REAL*8 (A-H,O-Z)                                         F2D11870
C     ______________________________________________________________    F2D11880
C                                                                       F2D11890
C     The subroutine computes the inverse of a 3x3 matrix,[A]; the      F2D11900
C     inverse is stored in matrix [B]                                   F2D11910
C     ______________________________________________________________    F2D11920
C                                                                       F2D11930
      DIMENSION  A(3,3), B(3,3)                                         F2D11940
C                                                                       F2D11950
      G(Z1,Z2,Z3,Z4) = Z1*Z2 - Z3*Z4                                    F2D11960
      F(Z1,Z2,Z3,Z4) = G(Z1,Z2,Z3,Z4) / DET                             F2D11970
      C1  = G(A(2,2),A(3,3),A(2,3),A(3,2))                              F2D11980
      C2  = G(A(2,3),A(3,1),A(2,1),A(3,3))                              F2D11990
      C3  = G(A(2,1),A(3,2),A(2,2),A(3,1))                              F2D12000
      DET = A(1,1)*C1 + A(1,2)*C2 + A(1,3)*C3                           F2D12010
      B(1,1) =  F(A(2,2),A(3,3),A(3,2),A(2,3))                          F2D12020
      B(1,2) = -F(A(1,2),A(3,3),A(1,3),A(3,2))                          F2D12030
      B(1,3) =  F(A(1,2),A(2,3),A(1,3),A(2,2))                          F2D12040
      B(2,1) = -F(A(2,1),A(3,3),A(2,3),A(3,1))                          F2D12050
      B(2,2) =  F(A(1,1),A(3,3),A(3,1),A(1,3))                          F2D12060
      B(2,3) = -F(A(1,1),A(2,3),A(1,3),A(2,1))                          F2D12070
      B(3,1) =  F(A(2,1),A(3,2),A(3,1),A(2,2))                          F2D12080
      B(3,2) = -F(A(1,1),A(3,2),A(1,2),A(3,1))                          F2D12090
      B(3,3) =  F(A(1,1),A(2,2),A(2,1),A(1,2))                          F2D12100
      RETURN                                                            F2D12110
      END                                                               F2D12120

      SUBROUTINE ECHO(IN,IT)                                            F2D12130
C                                                                       F2D12140
      DIMENSION AA(20)                                                  F2D12150
      WRITE(IT,40)                                                      F2D12160
   10 CONTINUE                                                          F2D12170
      READ(IN,30,END=20) AA                                             F2D12180
      WRITE(IT,30) AA                                                   F2D12190
      GO TO 10                                                          F2D12200
   20 CONTINUE                                                          F2D12210
```

```
      REWIND(IN)
      WRITE(IT,50)
      RETURN
   30 FORMAT(20A4)
   40 FORMAT(5X,'*** ECHO OF THE INPUT DATA STARTS ***',/)
   50 FORMAT(5X,'**** ECHO OF THE INPUT DATA ENDS ****',/)
      END

      SUBROUTINE ELKMFR(NCOUNT,NEIGN,NPE,NN,ITYPE,ITEM)
C     ----------------------------------------------------------------
C
C     Element  calculations based on  linear and quadratic rectangular
C     elements and  isoparametric  formulation are carried out for all
C     classes problems of the  book.  Reduced integrations are used on
C     certain terms of viscous flow and plate bending problems.
C
C     ----------------------------------------------------------------
      IMPLICIT REAL*8(A-H,O-Z)
      COMMON/STF/ELF(27),ELK(27,27),ELM(27,27),ELXY(9,2),ELU(27),
     1           ELV(27),ELA(27),A1,A2,A3,A4,A5
      COMMON/PST/A10,A1X,A1Y,A20,A2X,A2Y,A00,C0,CX,CY,F0,FX,FY,
     1           C44,C55,AMU,PENLTY,CMAT(3,3)
      COMMON/SHP/SF(9),GDSF(2,9),SFH(16),GDSFH(2,16),GDDSFH(3,16)
      COMMON/PNT/IPDF,IPDR,NIPF,NIPR
      DIMENSION  GAUSPT(5,5),GAUSWT(5,5)
      COMMON/IO/IN,ITT
C
      DATA GAUSPT/5*0.0D0, -0.57735027D0, 0.57735027D0, 3*0.0D0,
     2  -0.77459667D0, 0.0D0, 0.77459667D0, 2*0.0D0, -0.86113631D0,
     3  -0.33998104D0, 0.33998104D0, 0.86113631D0, 0.0D0, -0.90617984D0,
     4  -0.53846931D0,0.0D0,0.53846931D0,0.90617984D0/
C
      DATA GAUSWT/2.0D0, 4*0.0D0, 2*1.0D0, 3*0.0D0, 0.55555555D0,
     2    0.88888888D0, 0.55555555D0, 2*0.0D0, 0.34785485D0,
     3 2*0.65214515D0, 0.34785485D0, 0.0D0, 0.23692688D0,
     4    0.47862867D0, 0.56888888D0, 0.47862867D0, 0.23692688D0/
C
      NDF = NN/NPE
      IF(ITYPE.LE.3) THEN
          NET=NPE
      ELSE
          NET=NN
      ENDIF
C
C     Initialize the arrays
C
      DO 120 I = 1,NN
      IF(NEIGN.EQ.0) THEN
          ELF(I)   = 0.0
      ENDIF
      DO 120 J = 1,NN
      IF(ITEM.NE.0) THEN
          ELM(I,J)= 0.0
      ENDIF
  120 ELK(I,J)= 0.0
C
C     Do-loops on numerical (Gauss) integration begin here. Subroutine
C     SHPRCT (SHaPe functions for ReCTangular elements) is called here
C
      DO 200 NI = 1,IPDF
      DO 200 NJ = 1,IPDF
      XI  = GAUSPT(NI,IPDF)
      ETA = GAUSPT(NJ,IPDF)
      CALL SHPRCT (NPE,XI,ETA,DET,ELXY,NDF,ITYPE)
      CNST = DET*GAUSWT(NI,IPDF)*GAUSWT(NJ,IPDF)
      X=0.0
      Y=0.0
      DO 140 I=1,NPE
      X=X+ELXY(I,1)*SF(I)
  140 Y=Y+ELXY(I,2)*SF(I)
C
      IF(NEIGN.EQ.0) THEN
          SOURCE=F0+FX*X+FY*Y
      ENDIF
      IF(ITEM.NE.0) THEN                                                F2D12950
          IF(ITYPE.LE.2)THEN                                            F2D12960
              CT=C0+CX*X+CY*Y                                           F2D12970
          ENDIF                                                         F2D12980
      ENDIF                                                             F2D12990
      IF(ITYPE.LE.0) THEN                                               F2D13000
          A11=A10+A1X*X+A1Y*Y                                           F2D13010
          A22=A20+A2X*X+A2Y*Y                                           F2D13020
      ENDIF                                                             F2D13030
C                                                                       F2D13040
      II=1                                                              F2D13050
      DO 180 I=1,NET                                                    F2D13060
      JJ=1                                                              F2D13070
      DO 160 J=1,NET                                                    F2D13080
      IF(ITYPE.LE.3) THEN                                               F2D13090
          S00=SF(I)*SF(J)*CNST                                          F2D13100
          S11=GDSF(1,I)*GDSF(1,J)*CNST                                  F2D13110
          S22=GDSF(2,I)*GDSF(2,J)*CNST                                  F2D13120
          S12=GDSF(1,I)*GDSF(2,J)*CNST                                  F2D13130
          S21=GDSF(2,I)*GDSF(1,J)*CNST                                  F2D13140
      ENDIF                                                             F2D13150
      IF(ITYPE.EQ.0) THEN                                               F2D13160
C                                                                       F2D13170
C     Heat transfer and like problems (i.e. single DOF problems):_______F2D13180
C                                                                       F2D13190
          ELK(I,J) = ELK(I,J) + A11*S11 + A22*S22 + A00*S00             F2D13200
          IF(ITEM.NE.0) THEN                                            F2D13210
              ELM(I,J) = ELM(I,J) + CT*S00                              F2D13220
          ENDIF                                                         F2D13230
      ELSE                                                              F2D13240
          IF(ITYPE.EQ.1) THEN                                           F2D13250
C                                                                       F2D13260
C     Viscous incompressible fluids:____________________________________F2D13270
C     Compute coefficients associated with viscous terms (full integ.)  F2D13280
C                                                                       F2D13290
              ELK(II,JJ)    = ELK(II,JJ)      + AMU*(2.0*S11 + S22)     F2D13300
              ELK(II+1,JJ)  = ELK(II+1,JJ)    + AMU*S12                 F2D13310
              ELK(II,JJ+1)  = ELK(II,JJ+1)    + AMU*S21                 F2D13320
              ELK(II+1,JJ+1)= ELK(II+1,JJ+1) + AMU*(S11 + 2.0*S22)      F2D13330
              IF(ITEM.NE.0) THEN                                        F2D13340
                  ELM(II,JJ)    = ELM(II,JJ)      + CT*S00              F2D13350
                  ELM(II+1,JJ+1)= ELM(II+1,JJ+1) + CT*S00               F2D13360
              ENDIF                                                     F2D13370
          ELSE                                                          F2D13380
              IF(ITYPE.EQ.2) THEN                                       F2D13390
C                                                                       F2D13400
C     Plane elasticity problems:________________________________________F2D13410
C                                                                       F2D13420
              ELK(II,JJ)    =ELK(II,JJ)    +CMAT(1,1)*S11+CMAT(3,3)*S22 F2D13430
              ELK(II,JJ+1)  =ELK(II,JJ+1)  +CMAT(1,2)*S12+CMAT(3,3)*S21 F2D13440
              ELK(II+1,JJ)  =ELK(II+1,JJ)  +CMAT(1,2)*S21+CMAT(3,3)*S12 F2D13450
              ELK(II+1,JJ+1)=ELK(II+1,JJ+1)+CMAT(3,3)*S11+CMAT(2,2)*S22 F2D13460
              IF(ITEM.NE.0) THEN                                        F2D13470
                  ELM(II,JJ)    = ELM(II,JJ)      + CT*S00              F2D13480
                  ELM(II+1,JJ+1)= ELM(II+1,JJ+1) + CT*S00               F2D13490
              ENDIF                                                     F2D13500
              ELSE                                                      F2D13510
                  IF(ITYPE.GE.4) THEN                                   F2D13520
C                                                                       F2D13530
C     Classical plate theory:___________________________________________F2D13540
C                                                                       F2D13550
                      BM1=CMAT(1,1)*GDDSFH(1,J)+CMAT(1,2)*GDDSFH(2,J)   F2D13560
                      BM2=CMAT(1,2)*GDDSFH(1,J)+CMAT(2,2)*GDDSFH(2,J)   F2D13570
                      BM6=2.0*CMAT(3,3)*GDDSFH(3,J)                     F2D13580
                      ELK(I,J)=ELK(I,J)+CNST*(GDDSFH(1,I)*BM1+          F2D13590
     *                         GDDSFH(2,I)*BM2+2.0*GDDSFH(3,I)*BM6)     F2D13600
                      IF(ITEM.NE.0) THEN                                F2D13610
                          S00=SFH(I)*SFH(J)*CNST                        F2D13620
                          SXX=GDSFH(1,I)*GDSFH(1,J)*CNST                F2D13630
                          SYY=GDSFH(2,I)*GDSFH(2,J)*CNST                F2D13640
                          IF(NEIGN.LE.1) THEN                           F2D13650
                              ELM(I,J)=ELM(I,J) + C0*S00+CX*SXX+CY*SYY  F2D13660
                          ELSE                                          F2D13670
                              SXY=GDSFH(1,I)*GDSFH(2,J)*CNST            F2D13680
                              SYX=GDSFH(2,I)*GDSFH(1,J)*CNST            F2D13690
                              ELM(I,J)=ELM(I,J)  + C0*SXX + CX*SYY
     *                                           + CY*(SXY + SYX)
                          ENDIF
                      ENDIF
                  ELSE
C
C     Shear deformable plate theory:__________________________________
C
                      ELK(II+1,JJ+1)= ELK(II+1,JJ+1) +
     *                                CMAT(1,1)*S11+CMAT(3,3)*S22
                      ELK(II+1,JJ+2)= ELK(II+1,JJ+2) +
     *                                CMAT(1,2)*S12+CMAT(3,3)*S21
                      ELK(II+2,JJ+1)= ELK(II+2,JJ+1) +
     *                                CMAT(3,3)*S12+CMAT(1,2)*S21
                      ELK(II+2,JJ+2)= ELK(II+2,JJ+2) +
     *                                CMAT(3,3)*S11+CMAT(2,2)*S22
                      IF(ITEM.NE.0) THEN
                          IF(NEIGN.LE.1) THEN
                              ELM(II,JJ)     = ELM(II,JJ)     + C0*S00
                              ELM(II+1,JJ+1)= ELM(II+1,JJ+1)  + CX*S00
                              ELM(II+2,JJ+2)= ELM(II+2,JJ+2)  + CY*S00
                          ELSE
                              ELM(II,JJ)     = ELM(II,JJ)+C0*S11+CX*S22
     *                                                +CY*(S12+S21)
                          ENDIF
                      ENDIF
                  ENDIF
              ENDIF
          ENDIF
      ENDIF
  160 JJ = NDF*J+1
      IF(NEIGN.EQ.0) THEN
C
C     Source of the form fx = F0 + FX*X + FY*Y is assumed
C
          IF(ITYPE.LE.3) THEN
              L=(I-1)*NDF+1
              ELF(L) = ELF(L)+CNST*SF(I)*SOURCE
          ELSE
              ELF(I) = ELF(I)+CNST*SFH(I)*SOURCE
          ENDIF
      ENDIF
  180 II = NDF*I+1
  200 CONTINUE
C
      IF(ITYPE.EQ.1 .OR. ITYPE.EQ.3) THEN
C
C     Use reduced integration to evaluate coefficients associated with
C     penalty terms for flows and transverse shear terms for plates.
C
          DO 280 NI=1,IPDR
          DO 280 NJ=1,IPDR
          XI  = GAUSPT(NI,IPDR)
          ETA = GAUSPT(NJ,IPDR)
          CALL SHPRCT (NPE,XI,ETA,DET,ELXY,NDF,ITYPE)
          CNST=DET*GAUSWT(NI,IPDR)*GAUSWT(NJ,IPDR)
C
          II=1
          DO 260 I=1,NPE
          JJ = 1
          DO 240 J=1,NPE
          S11=GDSF(1,I)*GDSF(1,J)*CNST
          S22=GDSF(2,I)*GDSF(2,J)*CNST
          S12=GDSF(1,I)*GDSF(2,J)*CNST
          S21=GDSF(2,I)*GDSF(1,J)*CNST
          IF(ITYPE.EQ.1) THEN
C
C     Viscous incompressible fluids (penalty terms):____________________
C
              ELK(II,JJ)     = ELK(II,JJ)      + PENLTY*S11
              ELK(II+1,JJ)   = ELK(II+1,JJ)    + PENLTY*S21
              ELK(II,JJ+1)   = ELK(II,JJ+1)    + PENLTY*S12
              ELK(II+1,JJ+1)= ELK(II+1,JJ+1)  + PENLTY*S22
          ELSE
C
```

```
C     Shear deformable plates (transverse shear terms):___________________
C
                S00=SF(I)*SF(J)*CNST
                S10 = GDSF(1,I)*SF(J)*CNST
                S01 = SF(I)*GDSF(1,J)*CNST
                S20 = GDSF(2,I)*SF(J)*CNST
                S02 = SF(I)*GDSF(2,J)*CNST
                ELK(II,JJ)     = ELK(II,JJ)     + C55*S11+C44*S22
                ELK(II,JJ+1)   = ELK(II,JJ+1)   + C55*S10
                ELK(II+1,JJ)   = ELK(II+1,JJ)   + C55*S01
                ELK(II,JJ+2)   = ELK(II,JJ+2)   + C44*S20
                ELK(II+2,JJ)   = ELK(II+2,JJ)   + C44*S02
                ELK(II+1,JJ+1)= ELK(II+1,JJ+1) + C55*S00
                ELK(II+2,JJ+2)= ELK(II+2,JJ+2) + C44*S00
            ENDIF
  240 JJ=NDF*J+1
  260 II=NDF*I+1
  280 CONTINUE
      ENDIF
      RETURN
      END


      SUBROUTINE ELKMFT(NCOUNT,NEIGN,NPE,NN,ITYPE,ITEM)
C     ________________________________________________________________
C
C     Element  calculations based on linear and quadratic rectangular
C     elements and  isoparametric formulation are carried out for all
C     classes problems of the book.  Reduced integration  is  used on
C     penalty terms of viscous flow and plate bending problems.
C     ________________________________________________________________
C
      IMPLICIT REAL*8(A-H,O-Z)
      COMMON/STF/ELF(27),ELK(27,27),ELM(27,27),ELXY(9,2),ELU(27),
     1            ELV(27),ELA(27),A1,A2,A3,A4,A5
      COMMON/PST/A10,A1X,A1Y,A20,A2X,A2Y,A00,C0,CX,CY,F0,FX,FY,
     1            C44,C55,AMU,PENLTY,CMAT(3,3)
      COMMON/QUAD/AL1(7,5),AL2(7,5),AL3(7,5),ALWT(7,5)
      COMMON/PNT/IPDF,IPDR,NIPF,NIPR
      COMMON/SHP/SF(9),GDSF(2,9)
      COMMON/IO/IN,ITT
C
      NDF = NN/NPE
C
C     Call subroutine QUADRaTure to compute arrays of integration
C     points and weights for the given NIPF and IPDF
C
      CALL QUADRT (NIPF,IPDF)
C
C     Initialize the arrays
C
      DO 120 I = 1,NN
      IF(NEIGN.EQ.0) THEN
         ELF(I)  = 0.0
      ENDIF
      DO 120 J = 1,NN
      IF(ITEM.NE.0) THEN
         ELM(I,J)= 0.0
      ENDIF
  120 ELK(I,J)= 0.0
C
C     Do-loop on the numerical integration begins here
C
      DO 200 NI = 1,NIPF
      AC1 = AL1(NI,IPDF)
      AC2 = AL2(NI,IPDF)
      AC3 = AL3(NI,IPDF)
      CALL SHPTRI(NPE,AC1,AC2,AC3,DET,ELXY)
      CNST = 0.5D0*DET*ALWT(NI,IPDF)
      X=0.0
      Y=0.0
      DO 140 I=1,NPE
      X=X+ELXY(I,1)*SF(I)
  140 Y=Y+ELXY(I,2)*SF(I)
```

```
C                                                                        F2D15170
      IF(NEIGN.EQ.0) THEN                                                F2D15180
          SOURCE=F0+FX*X+FY*Y                                            F2D15190
      ENDIF                                                              F2D15200
      IF(ITEM.NE.0) THEN                                                 F2D15210
          CT =C0+CX*X+CY*Y                                               F2D15220
      ENDIF                                                              F2D15230
      IF(ITYPE.LE.0) THEN                                                F2D15240
          A11=A10+A1X*X+A1Y*Y                                            F2D15250
          A22=A20+A2X*X+A2Y*Y                                            F2D15260
      ENDIF                                                              F2D15270
C                                                                        F2D15280
      II=1                                                               F2D15290
      DO 180 I=1,NPE                                                     F2D15300
      JJ=1                                                               F2D15310
      DO 160 J=1,NPE                                                     F2D15320
      S00=SF(I)*SF(J)*CNST                                               F2D15330
      S11=GDSF(1,I)*GDSF(1,J)*CNST                                       F2D15340
      S22=GDSF(2,I)*GDSF(2,J)*CNST                                       F2D15350
      S12=GDSF(1,I)*GDSF(2,J)*CNST                                       F2D15360
      S21=GDSF(2,I)*GDSF(1,J)*CNST                                       F2D15370
      IF(ITYPE.EQ.0) THEN                                                F2D15380
C                                                                        F2D15390
C     Heat transfer and like problems (i.e. single DOF problems):________F2D15400
C                                                                        F2D15410
          ELK(I,J) = ELK(I,J) + A11*S11 + A22*S22 + A00*S00              F2D15420
          IF(ITEM.NE.0) THEN                                             F2D15430
              ELM(I,J) = ELM(I,J) + CT*S00                               F2D15440
          ENDIF                                                          F2D15450
      ELSE                                                               F2D15460
          IF(ITYPE.EQ.1) THEN                                            F2D15470
C                                                                        F2D15480
C     Viscous incompressible fluids:_____________________________________F2D15490
C     Compute coefficients associated with viscous terms (full integ.)   F2D15500
C                                                                        F2D15510
              ELK(II,JJ)    = ELK(II,JJ)     + AMU*(2.0*S11 + S22)       F2D15520
              ELK(II+1,JJ)  = ELK(II+1,JJ)   + AMU*S12                   F2D15530
              ELK(II,JJ+1)  = ELK(II,JJ+1)   + AMU*S21                   F2D15540
              ELK(II+1,JJ+1)= ELK(II+1,JJ+1) + AMU*(S11 + 2.0*S22)       F2D15550
              IF(ITEM.NE.0) THEN                                         F2D15560
                  ELM(II,JJ)    = ELM(II,JJ)     + CT*S00                F2D15570
                  ELM(II+1,JJ+1)= ELM(II+1,JJ+1) + CT*S00                F2D15580
              ENDIF                                                      F2D15590
          ELSE                                                           F2D15600
C                                                                        F2D15610
C     Plane elasticity problems:_________________________________________F2D15620
C                                                                        F2D15630
              ELK(II,JJ)    =ELK(II,JJ)    +CMAT(1,1)*S11+CMAT(3,3)*S22  F2D15640
              ELK(II,JJ+1)  =ELK(II,JJ+1)  +CMAT(1,2)*S12+CMAT(3,3)*S21  F2D15650
              ELK(II+1,JJ)  =ELK(II+1,JJ)  +CMAT(1,2)*S21+CMAT(3,3)*S12  F2D15660
              ELK(II+1,JJ+1)=ELK(II+1,JJ+1)+CMAT(3,3)*S11+CMAT(2,2)*S22  F2D15670
              IF(ITEM.NE.0) THEN                                         F2D15680
                  ELM(II,JJ)    = ELM(II,JJ)     + CT*S00                F2D15690
                  ELM(II+1,JJ+1)= ELM(II+1,JJ+1) + CT*S00                F2D15700
              ENDIF                                                      F2D15710
          ENDIF                                                          F2D15720
      ENDIF                                                              F2D15730
  160 JJ = NDF*J+1                                                       F2D15740
      IF(NEIGN.EQ.0) THEN                                                F2D15750
C                                                                        F2D15760
C     Source of the form fx = F0 + FX*X + FY*Y is assumed                F2D15770
C                                                                        F2D15780
          L=(I-1)*NDF+1                                                  F2D15790
          ELF(L) = ELF(L)+CNST*SF(I)*SOURCE                              F2D15800
      ENDIF                                                              F2D15810
  180 II = NDF*I+1                                                       F2D15820
  200 CONTINUE                                                           F2D15830
C                                                                        F2D15840
      IF(ITYPE.EQ.1 .OR. ITYPE.EQ.3) THEN                                F2D15850
C                                                                        F2D15860
C     Use reduced integration to evaluate coefficients associated with   F2D15870
C     penalty terms for flows and transverse shear terms for plates.     F2D15880
C                                                                        F2D15890
C     Call subroutine QUADRaTure to compute arrays of integration        F2D15900
C     points and weights for the given NIPR and IPDR                     F2D15910
```

```
C
         CALL QUADRT (NIPR,IPDR)
C
         DO 280 NI=1,NIPR
         AC1 = AL1(NI,IPDR)
         AC2 = AL2(NI,IPDR)
         AC3 = AL3(NI,IPDR)
         CALL SHPTRI(NPE,AC1,AC2,AC3,DET,ELXY)
         CNST = 0.50D0*DET*ALWT(NI,IPDR)
C
         II=1
         DO 260 I=1,NPE
         JJ = 1
         DO 240 J=1,NPE
         S11=GDSF(1,I)*GDSF(1,J)*CNST
         S22=GDSF(2,I)*GDSF(2,J)*CNST
         S12=GDSF(1,I)*GDSF(2,J)*CNST
         S21=GDSF(2,I)*GDSF(1,J)*CNST
         IF(ITYPE.EQ.1) THEN
C
C     Viscous incompressible fluids (penalty terms):___________________
C
             ELK(II,JJ)     = ELK(II,JJ)       + PENLTY*S11
             ELK(II+1,JJ)   = ELK(II+1,JJ)     + PENLTY*S21
             ELK(II,JJ+1)   = ELK(II,JJ+1)     + PENLTY*S12
             ELK(II+1,JJ+1)= ELK(II+1,JJ+1)   + PENLTY*S22
         ELSE
C
C     Shear deformable plates (transverse shear terms):________________
C
             S00=SF(I)*SF(J)*CNST
             S10 = GDSF(1,I)*SF(J)*CNST
             S01 = SF(I)*GDSF(1,J)*CNST
             S20 = GDSF(2,I)*SF(J)*CNST
             S02 = SF(I)*GDSF(2,J)*CNST
             ELK(II,JJ)     = ELK(II,JJ)       + C55*S11+C44*S22
             ELK(II,JJ+1)   = ELK(II,JJ+1)     + C55*S10
             ELK(II+1,JJ)   = ELK(II+1,JJ)     + C55*S01
             ELK(II,JJ+2)   = ELK(II,JJ+2)     + C44*S20
             ELK(II+2,JJ)   = ELK(II+2,JJ)     + C44*S02
             ELK(II+1,JJ+1)= ELK(II+1,JJ+1)   + C55*S00
             ELK(II+2,JJ+2)= ELK(II+2,JJ+2)   + C44*S00
         ENDIF
  240 JJ=NDF*J+1
  260 II=NDF*I+1
  280 CONTINUE
      ENDIF
      RETURN
      END

      SUBROUTINE MSH2DG(NELEM,NNODE,NODES,MAXELM,MAXNOD,GLXY)
C     ------------------------------------------------------------------
C
C     Generates nodal point coordinates for specified type meshes
C
C     NOD1   = First node number in the line segment
C     NODL   = Last node number in the line segment
C     NODINC= Node increment from one node to the next along the line
C     X1,Y1 = Global coordinates of the first node on the line
C     XL,YL = Global coordinates of the last node on the line
C     RATIO = The ratio of the first element to the last element
C     -------------------------------------------------------------------
C
      IMPLICIT REAL*8(A-H,O-Z)
      DIMENSION  GLXY(MAXNOD,2)
C
      DO 10 I=1,NNODE
      GLXY(I,1)=1.E20
   10 GLXY(I,2)=1.E20
C
C     Read number of the records (line segmments) and data in each line
C
      READ(5,*)NRECL
      DO 30 IREC=1,NRECL
      READ(5,*)NOD1,NODL,NODINC,X1,Y1,XL,YL,RATIO                       F2D16650
      IF(NODL.LT.NOD1) NODL = NOD1                                      F2D16660
      IF(NODL.NE.NOD1) THEN                                             F2D16670
          IF(NODINC.LE.0) NODINC = 1                                    F2D16680
          IF(RATIO.LE.0.0) RATIO=1.0                                    F2D16690
          NODIF = (NODL-NOD1)/NODINC                                    F2D16700
          XL1=XL-X1                                                     F2D16710
          YL1=YL-Y1                                                     F2D16720
          GLXY(NOD1,1)=X1                                               F2D16730
          GLXY(NOD1,2)=Y1                                               F2D16740
          ALNGTH=DSQRT(XL1*XL1+YL1*YL1)                                 F2D16750
          ALINC=(2.0*ALNGTH/NODIF)*RATIO/(RATIO+1.0)                    F2D16760
          ALRAT=ALINC/RATIO                                             F2D16770
          IF(NODIF.NE.1) DEL=(ALINC-ALRAT)/(NODIF-1)                    F2D16780
          IF(NODIF.EQ.1) DEL=0.0                                        F2D16790
          SUM=0.0                                                       F2D16800
          I=-1                                                          F2D16810
          DO 20 N=1,NODIF                                               F2D16820
          I=I+1                                                         F2D16830
          SUM=SUM+ALINC-I*DEL                                           F2D16840
          NI=NOD1+N*NODINC                                              F2D16850
          GLXY(NI,1)=X1+XL1*SUM/ALNGTH                                  F2D16860
          GLXY(NI,2)=Y1+YL1*SUM/ALNGTH                                  F2D16870
   20     CONTINUE                                                      F2D16880
      ENDIF                                                             F2D16890
   30 CONTINUE                                                          F2D16900
      CALL CNCTVT(NELEM,NNODE,NODES,MAXELM,MAXNOD,GLXY)                 F2D16910
      RETURN                                                            F2D16920
      END                                                               F2D16930

      SUBROUTINE MSH2DR(IEL,IELTYP,NX,NY,NPE,NNM,NEM,NOD,DX,DY,X0,Y0,   F2D16940
     1                  GLXY,MAXNEM,MAXNNM,MAXNX,MAXNY)                 F2D16950
C     ------------------------------------------------------------------F2D16960
C                                                                       F2D16970
C     The subroutine generates arrays [NOD] and [GLXY] for rectangular  F2D16980
C     domains. The domain is divided into NX subdivisions along the     F2D16990
C     x-direction and NY subdivisions in the y-direction. The subdivi-  F2D17000
C     sions define rectangular elements of the type required. For a     F2D17010
C     triangular element mesh, the subdivision defines two linear ele-  F2D17020
C     ments with their common diagonal being inclined to the right.     F2D17030
C                                                                       F2D17040
C     ------------------------------------------------------------------F2D17050
      IMPLICIT REAL*8 (A-H,O-Z)                                         F2D17060
      DIMENSION NOD(MAXNEM,9),GLXY(MAXNNM,2),DX(MAXNX),DY(MAXNY)        F2D17070
      COMMON/IO/IN,ITT                                                  F2D17080
C                                                                       F2D17090
      NEX1 = NX+1                                                       F2D17100
      NEY1 = NY+1                                                       F2D17110
      NXX  = IEL*NX                                                     F2D17120
      NYY  = IEL*NY                                                     F2D17130
      NXX1 = NXX + 1                                                    F2D17140
      NYY1 = NYY + 1                                                    F2D17150
      NEM  = NX*NY                                                      F2D17160
      IF(IELTYP.EQ.0)NEM=2*NX*NY                                        F2D17170
      NNM=NXX1*NYY1                                                     F2D17180
      IF(NPE.EQ.8)NNM = NXX1*NYY1 - NX*NY                               F2D17190
      IF(IELTYP.EQ.0) THEN                                              F2D17200
C                                                                       F2D17210
C     Generate the array [NOD]:_________________________________________F2D17220
C                                                                       F2D17230
C     TRIANGULAR ELEMENTS                                               F2D17240
C                                                                       F2D17250
          NX2=2*NX                                                      F2D17260
          NY2=2*NY                                                      F2D17270
          NOD(1,1) = 1                                                  F2D17280
          NOD(1,2) = IEL+1                                              F2D17290
          NOD(1,3) = IEL*NXX1+IEL+1                                     F2D17300
          IF(NPE .GT. 3) THEN                                           F2D17310
              NOD(1,4) = 2                                              F2D17320
              NOD(1,5) = NXX1 + 3                                       F2D17330
              NOD(1,6) = NXX1 + 2                                       F2D17340
          ENDIF                                                         F2D17350
C                                                                       F2D17360
          NOD(2,1) = 1                                                  F2D17370
          NOD(2,2) = NOD(1,3)                                           F2D17380
          NOD(2,3) = IEL*NXX1+1                                         F2D17390
          IF(NPE .GT. 3) THEN                                           F2D17400
              NOD(2,4) = NOD(1,6)                                       F2D17410
              NOD(2,5) = NOD(1,3) - 1                                   F2D17420
              NOD(2,6) = NOD(2,4) - 1                                   F2D17430
          ENDIF                                                         F2D17440
C                                                                       F2D17450
          K=3                                                           F2D17460
          DO 60 IY=1,NY                                                 F2D17470
          L=IY*NX2                                                      F2D17480
          M=(IY-1)*NX2                                                  F2D17490
          IF(NX.GT.1) THEN                                              F2D17500
              DO 30 N=K,L,2                                             F2D17510
              DO 20 I=1,NPE                                             F2D17520
              NOD(N,I)  = NOD(N-2,I)+IEL                                F2D17530
   20         NOD(N+1,I)= NOD(N-1,I)+IEL                                F2D17540
   30         CONTINUE                                                  F2D17550
          ENDIF                                                         F2D17560
          IF(IY.LT.NY) THEN                                             F2D17570
              DO 40 I=1,NPE                                             F2D17580
              NOD(L+1,I)=NOD(M+1,I)+IEL*NXX1                            F2D17590
   40         NOD(L+2,I)=NOD(M+2,I)+IEL*NXX1                            F2D17600
          ENDIF                                                         F2D17610
   60     K=L+3                                                         F2D17620
      ELSE                                                              F2D17630
C                                                                       F2D17640
C     RECTANGULAR ELEMENTS                                              F2D17650
C                                                                       F2D17660
          K0 = 0                                                        F2D17670
          IF (NPE .EQ. 9) K0=1                                          F2D17680
C                                                                       F2D17690
          NOD(1,1) = 1                                                  F2D17700
          NOD(1,2) = IEL+1                                              F2D17710
          NOD(1,3) = NXX1+(IEL-1)*NEX1+IEL+1                            F2D17720
          IF(NPE .EQ. 9) NOD(1,3)=4*NX+5                                F2D17730
          NOD(1,4) = NOD(1,3) - IEL                                     F2D17740
          IF(NPE .GT. 4) THEN                                           F2D17750
              NOD(1,5) = 2                                              F2D17760
              NOD(1,6) = NXX1 + (NPE-6)                                 F2D17770
              NOD(1,7) = NOD(1,3) - 1                                   F2D17780
              NOD(1,8) = NXX1+1                                         F2D17790
              IF(NPE .EQ. 9) THEN                                       F2D17800
                  NOD(1,9)=NXX1+2                                       F2D17810
              ENDIF                                                     F2D17820
          ENDIF                                                         F2D17830
C                                                                       F2D17840
          IF(NY .GT. 1) THEN                                            F2D17850
              M = 1                                                     F2D17860
              DO 110 N = 2,NY                                           F2D17870
              L = (N-1)*NX + 1                                          F2D17880
              DO 100 I = 1,NPE                                          F2D17890
  100         NOD(L,I) = NOD(M,I)+NXX1+(IEL-1)*NEX1+K0*NX               F2D17900
  110         M=L                                                       F2D17910
          ENDIF                                                         F2D17920
C                                                                       F2D17930
          IF(NX .GT .1) THEN                                            F2D17940
              DO 140 NI = 2,NX                                          F2D17950
              DO 120  I = 1,NPE                                         F2D17960
              K1 = IEL                                                  F2D17970
              IF(I .EQ. 6 .OR. I .EQ. 8)K1=1+K0                         F2D17980
  120         NOD(NI,I) = NOD(NI-1,I)+K1                                F2D17990
              M = NI                                                    F2D18000
              DO 140 NJ = 2,NY                                          F2D18010
              L = (NJ-1)*NX+NI                                          F2D18020
              DO 130 J = 1,NPE                                          F2D18030
  130         NOD(L,J) = NOD(M,J)+NXX1+(IEL-1)*NEX1+K0*NX               F2D18040
  140         M = L                                                     F2D18050
          ENDIF                                                         F2D18060
      ENDIF                                                             F2D18070
C                                                                       F2D18080
C     Generate the global coordinates of the nodes, [GLXY]:_____________F2D18090
C                                                                       F2D18100
      DX(NEX1)=0.0                                                      F2D18110
      DY(NEY1)=0.0                                                      F2D18120
      XC=X0
      YC=Y0
      IF(NPE .EQ. 8) THEN
          DO 180 NI = 1, NEY1
          I = (NXX1+NEX1)*(NI-1)+1
          J = 2*NI-1
          GLXY(I,1) = XC
          GLXY(I,2) = YC
          DO 150 NJ = 1,NX
          DELX=0.5*DX(NJ)
          I=I+1
          GLXY(I,1) = GLXY(I-1,1)+DELX
          GLXY(I,2) = YC
          I=I+1
          GLXY(I,1) = GLXY(I-1,1)+DELX
          GLXY(I,2) = YC
  150     CONTINUE
          IF(NI.LE.NY) THEN
              I = I+1
              YC= YC+0.5*DY(NI)
              GLXY(I,1) = XC
              GLXY(I,2) = YC
              DO 160 II = 1, NX
              I = I+1
              GLXY(I,1) = GLXY(I-1,1)+DX(II)
  160         GLXY(I,2) = YC
          ENDIF
  180     YC = YC+0.5*DY(NI)
C
      ELSE
          YC=Y0
          DO 200 NI = 1, NEY1
          XC = X0
          I = NXX1*IEL*(NI-1)
          DO 190 NJ = 1, NEX1
          I=I+1
          GLXY(I,1) = XC
          GLXY(I,2) = YC
          IF(NJ.LT.NEX1) THEN
              IF(IEL.EQ.2) THEN
                  I=I+1
                  XC = XC + 0.5*DX(NJ)
                  GLXY(I,1) = XC
                  GLXY(I,2) = YC
              ENDIF
          ENDIF
  190     XC = XC + DX(NJ)/IEL
          XC = X0
          IF(IEL.EQ.2) THEN
              YC = YC + 0.5*DY(NI)
              DO 195 NJ = 1, NEX1
              I=I+1
              GLXY(I,1) = XC
              GLXY(I,2) = YC
              IF(NJ.LT.NEX1) THEN
                  I=I+1
                  XC = XC + 0.5*DX(NJ)
                  GLXY(I,1) = XC
                  GLXY(I,2) = YC
              ENDIF
  195     XC = XC + 0.5*DX(NJ)
          ENDIF
  200     YC = YC + DY(NI)/IEL
      ENDIF
      RETURN
      END

      SUBROUTINE PSTPRC(ELXY,ITYPE,IELTYP,IGRAD,NDF,NPE,THKNS,ELU,
     *                  ISTR,NSTR)
C     ________________________________________________________________
C
C     Computes the derivatives of the solution for  heat transfer like
C     problems and stresses for fluid flow, plane elasticity and plate
C     bending problems.
C     ________________________________________________________________
```

```
C
      IMPLICIT REAL*8 (A-H,O-Z)
      DIMENSION  X(3),Y(3),GAMA(3),BETA(3),ELXY(9,2),ELU(27),GAUSPT(4,4)
      COMMON/PST/A10,A1X,A1Y,A20,A2X,A2Y,A00,C0,CX,CY,F0,FX,FY,
     1           C44,C55,AMU,PENLTY,CMAT(3,3)
      COMMON/SHP/SF(9),GDSF(2,9),SFH(16),GDSFH(2,16),GDDSFH(3,16)
      COMMON/QUAD/AL1(7,5),AL2(7,5),AL3(7,5),ALWT(7,5)
      COMMON/IO/IN,ITT
C
      DATA GAUSPT/4*0.0D0, -0.57735027D0, 0.57735027D0, 2*0.0D0,
     2     -0.77459667D0, 0.0D0, 0.77459667D0, 0.0D0, -0.86113631D0,
     3     -0.33998104D0, 0.33998104D0, 0.86113631D0/
C
      PI=4.0D0*DATAN(1.0D0)
      CONST=180.0D0/PI
      IF(IELTYP.EQ.0) THEN
C
C     Computation of the gradient/stresses at the reduced-integration
C     points of TRIANGULAR ELEMENTS:___________________________________
C
          CALL QUADRT (NSTR,ISTR)
C
          DO 40 NI=1,NSTR
          AC1 = AL1(NI,ISTR)
          AC2 = AL2(NI,ISTR)
          AC3 = AL3(NI,ISTR)
          CALL SHPTRI(NPE,AC1,AC2,AC3,DET,ELXY)
          XC  = 0.0
          YC  = 0.0
          DO 10 I=1,NPE
          XC  = XC+SF(I)*ELXY(I,1)
   10     YC  = YC+SF(I)*ELXY(I,2)
          IF(ITYPE.LT.3) THEN
              UX  = 0.0
              UY  = 0.0
              VX  = 0.0
              VY  = 0.0
              DO 20 I=1,NPE
              J=NDF*I-1
              IF(ITYPE.EQ.0)J=I
              UX  = UX + ELU(J)*GDSF(1,I)
              UY  = UY + ELU(J)*GDSF(2,I)
              IF(ITYPE.GE.1) THEN
                  K=J+1
                  VX  = VX + ELU(K)*GDSF(1,I)
                  VY  = VY + ELU(K)*GDSF(2,I)
              ENDIF
   20         CONTINUE
C
              IF(ITYPE.EQ.0) THEN
C
C     Single-degree-of-freedom problems:--------------------------------
C
                  SX   = -(A10+A1X*XC+A1Y*YC)*UX
                  SY   = -(A20+A2X*XC+A2Y*YC)*UY
                  VALUE= DSQRT(SX**2+SY**2)
                  IF(IGRAD.EQ.1) THEN
                      QX=SX
                      QY=SY
                  ELSE
                      QX=-SY
                      QY= SX
                  ENDIF
                  IF(QX.EQ.0.0) THEN
                      IF(QY.LT.0.0) THEN
                          ANGLE =-90.0
                      ELSE
                          ANGLE = 90.0
                      ENDIF
                  ELSE
                      ANGLE=DATAN2(QY,QX)*CONST
                  ENDIF
                  WRITE(ITT,200) XC,YC,QX,QY,VALUE,ANGLE
              ELSE
```

```
C
                  IF(ITYPE.EQ.1) THEN
C
C     Viscous incompressible flows (penalty model):----------------------
C
                      PRESSR = -PENLTY*(UX+VY)
                      STRESX = 2.0*AMU*UX-PRESSR
                      STRESY = 2.0*AMU*VY-PRESSR
                      STRSXY = AMU*(UY+VX)
                      WRITE(ITT,300) XC,YC,STRESX,STRESY,STRSXY,PRESSR
                  ELSE
C
C     Plane elasticity problems:-----------------------------------------
C
                      STRESX = (CMAT(1,1)*UX+CMAT(1,2)*VY)/THKNS
                      STRESY = (CMAT(1,2)*UX+CMAT(2,2)*VY)/THKNS
                      STRSXY = CMAT(3,3)*(UY+VX)/THKNS
                      WRITE(ITT,300) XC,YC,STRESX,STRESY,STRSXY
                  ENDIF
              ENDIF
          ENDIF
   40     CONTINUE
      ELSE
C
C     Calculation of the gradient/stresses at the reduced integration
C     gauss points of RECTANGULAR ELEMENTS:______________________________
C
          DO 100 NI=1,ISTR
          DO 100 NJ=1,ISTR
          XI  = GAUSPT(NI,ISTR)
          ETA = GAUSPT(NJ,ISTR)
          CALL SHPRCT (NPE,XI,ETA,DET,ELXY,NDF,ITYPE)
          XC  = 0.0
          YC  = 0.0
          DO 50 I=1,NPE
          XC  = XC+SF(I)*ELXY(I,1)
   50     YC  = YC+SF(I)*ELXY(I,2)
          IF(ITYPE.LT.3) THEN
              UX  = 0.0
              UY  = 0.0
              VX  = 0.0
              VY  = 0.0
              DO 60 I=1,NPE
              J=NDF*I-1
              IF(ITYPE.EQ.0)J=I
              UX  = UX + ELU(J)*GDSF(1,I)
              UY  = UY + ELU(J)*GDSF(2,I)
              IF(ITYPE.GE.1) THEN
                  K=J+1
                  VX  = VX + ELU(K)*GDSF(1,I)
                  VY  = VY + ELU(K)*GDSF(2,I)
              ENDIF
   60 CONTINUE
C
              IF(ITYPE.EQ.0) THEN
C
C     Single-degree-of-freedom problems:---------------------------------
C
                  SX   = -(A10+A1X*XC+A1Y*YC)*UX
                  SY   = -(A20+A2X*XC+A2Y*YC)*UY
                  VALUE= DSQRT(SX**2+SY**2)
                  IF(IGRAD.EQ.1) THEN
                      QX=SX
                      QY=SY
                  ELSE
                      QX=-SY
                      QY= SX
                  ENDIF
                  IF(QX.EQ.0.0) THEN
                      IF(QY.LT.0.0) THEN
                          ANGLE =-90.0
                      ELSE
                          ANGLE = 90.0
                      ENDIF
```

```
                   ELSE
                       ANGLE=DATAN2(QY,QX)*CONST
                   ENDIF
                   WRITE(ITT,200) XC,YC,QX,QY,VALUE,ANGLE
               ELSE
C
                   IF(ITYPE.EQ.1) THEN
C
C     Viscous incompressible flows (penalty model):--------------------
C
                       PRESSR = -PENLTY*(UX+VY)
                       STRESX = 2.0*AMU*UX-PRESSR
                       STRESY = 2.0*AMU*VY-PRESSR
                       STRSXY = AMU*(UY+VX)
                       WRITE(ITT,300) XC,YC,STRESX,STRESY,STRSXY,PRESSR
                   ELSE
C
C     Plane elasticity problems:---------------------------------------
C
                       STRESX = (CMAT(1,1)*UX+CMAT(1,2)*VY)/THKNS
                       STRESY = (CMAT(1,2)*UX+CMAT(2,2)*VY)/THKNS
                       STRSXY = CMAT(3,3)*(UY+VX)/THKNS
                       WRITE(ITT,300) XC,YC,STRESX,STRESY,STRSXY
                   ENDIF
               ENDIF
           ELSE
C
C     Plate bending problems:------------------------------------------
C     Stresses SGMAX, SGMAY and SGMXY are computed at the top/bottom of
C     the plate (and SGMXZ and SGMYZ are constant through thickness)
C
               PLTD=(THKNS*THKNS)/6.0D0
               SIX  = 0.0
               SIY  = 0.0
               DWX  = 0.0
               DWY  = 0.0
               DSXY = 0.0
               DSYX = 0.0
               DSXX = 0.0
               DSYY = 0.0
               IF(ITYPE.EQ.3) THEN
C
C     First-order shear deformation theory of plates:-----------------
C
                   DO 80 I=1,NPE
                   J=NDF*(I-1)+1
                   K=J+1
                   L=K+1
                   DWX  = DWX+GDSF(1,I)*ELU(J)
                   DWY  = DWY+GDSF(2,I)*ELU(J)
                   SIX  = SIX+SF(I)*ELU(K)
                   SIY  = SIY+SF(I)*ELU(L)
                   DSXX = DSXX+GDSF(1,I)*ELU(K)
                   DSXY = DSXY+GDSF(2,I)*ELU(K)
                   DSYX = DSYX+GDSF(1,I)*ELU(L)
   80              DSYY = DSYY+GDSF(2,I)*ELU(L)
                   SGMAX = (CMAT(1,1)*DSXX+CMAT(1,2)*DSYY)/PLTD
                   SGMAY = (CMAT(1,2)*DSXX+CMAT(2,2)*DSYY)/PLTD
                   SGMXY = CMAT(3,3)*(DSXY+DSYX)/PLTD
                   SGMXZ = 1.2*C55*(DWX+SIX)/THKNS
                   SGMYZ = 1.2*C44*(DWY+SIY)/THKNS
                   WRITE(ITT,300) XC,YC,SGMAX,SGMAY,SGMXY
                   WRITE(ITT,400) SGMXZ,SGMYZ
               ELSE
C
C     Classical theory of plates:--------------------------------------
C
                   NN=NPE*NDF
                   DO 90 I=1,NN
                   DSXX = DSXX+GDDSFH(1,I)*ELU(I)
                   DSYY = DSYY+GDDSFH(2,I)*ELU(I)
   90              DSXY = DSXY+GDDSFH(3,I)*ELU(I)
C
                   SGMAX =-(CMAT(1,1)*DSXX+CMAT(1,2)*DSYY)/PLTD
                   SGMAY =-(CMAT(1,2)*DSXX+CMAT(2,2)*DSYY)/PLTD
```

```
                  SGMXY =-4.0*CMAT(3,3)*DSXY/PLTD                       F2D21100
                  WRITE(ITT,300) XC,YC,SGMAX,SGMAY,SGMXY                F2D21110
              ENDIF                                                     F2D21120
          ENDIF                                                         F2D21130
 100      CONTINUE                                                      F2D21140
      ENDIF                                                             F2D21150
 200  FORMAT(5E13.4,3X,F7.2)                                            F2D21160
 300  FORMAT(6E13.4)                                                    F2D21170
 400  FORMAT(26X,2E13.4)                                                F2D21180
      RETURN                                                            F2D21190
      END                                                               F2D21200

      SUBROUTINE QUADRT(NIP,IPD)                                        F2D21210
C                                                                       F2D21220
C     ________________________________________________________________  F2D21230
C     Quadrature points and weights for triangular elements             F2D21240
C       IPD = Integrand Polynomial Degree                               F2D21250
C       NIP = Number of Integration Points                              F2D21260
C                                                                       F2D21270
C     ________________________________________________________________  F2D21280
      IMPLICIT REAL*8(A-H,O-Z)                                          F2D21290
      COMMON/QUAD/AL1(7,5),AL2(7,5),AL3(7,5),ALWT(7,5)                  F2D21300
C                                                                       F2D21310
C     Initialize arrays                                                 F2D21320
C                                                                       F2D21330
      DO 20 I = 1, NIP                                                  F2D21340
      DO 10 J = 1, IPD                                                  F2D21350
      AL1(I,J)    =  0.000000000000000                                  F2D21360
      AL2(I,J)    =  0.000000000000000                                  F2D21370
      AL3(I,J)    =  0.000000000000000                                  F2D21380
      ALWT(I,J)   =  0.000000000000000                                  F2D21390
   10 CONTINUE                                                          F2D21400
   20 CONTINUE                                                          F2D21410
C                                                                       F2D21420
C     One-point quadrature (for polynomials of order 1):________________F2D21430
C                                                                       F2D21440
      AL1(1,1)    =  0.333333333333333                                  F2D21450
      AL2(1,1)    =  0.333333333333333                                  F2D21460
      AL3(1,1)    =  0.333333333333333                                  F2D21470
      ALWT(1,1)   =  1.000000000000000                                  F2D21480
C                                                                       F2D21490
C     Three-point quadrature (for polynomials of order 2):______________F2D21500
C                                                                       F2D21510
      AL1(1,2)    =  0.000000000000000                                  F2D21520
      AL2(1,2)    =  0.500000000000000                                  F2D21530
      AL3(1,2)    =  0.500000000000000                                  F2D21540
      AL1(2,2)    =  0.500000000000000                                  F2D21550
      AL2(2,2)    =  0.000000000000000                                  F2D21560
      AL3(2,2)    =  0.500000000000000                                  F2D21570
      AL1(3,2)    =  0.500000000000000                                  F2D21580
      AL2(3,2)    =  0.500000000000000                                  F2D21590
      AL3(3,2)    =  0.000000000000000                                  F2D21600
      ALWT(1,2)   =  0.333333333333333                                  F2D21610
      ALWT(2,2)   =  0.333333333333333                                  F2D21620
      ALWT(3,2)   =  0.333333333333333                                  F2D21630
C                                                                       F2D21640
C     Four-point quadrature (for polynomials of order 3):_______________F2D21650
C                                                                       F2D21660
      AL1(1,3)    =  0.333333333333333                                  F2D21670
      AL2(1,3)    =  0.333333333333333                                  F2D21680
      AL3(1,3)    =  0.333333333333333                                  F2D21690
      AL1(2,3)    =  0.600000000000000                                  F2D21700
      AL2(2,3)    =  0.200000000000000                                  F2D21710
      AL3(2,3)    =  0.200000000000000                                  F2D21720
      AL1(3,3)    =  0.200000000000000                                  F2D21730
      AL2(3,3)    =  0.600000000000000                                  F2D21740
      AL3(3,3)    =  0.200000000000000                                  F2D21750
      AL1(4,3)    =  0.200000000000000                                  F2D21760
      AL2(4,3)    =  0.200000000000000                                  F2D21770
      AL3(4,3)    =  0.600000000000000                                  F2D21780
      ALWT(1,3)   = -0.562500000000000                                  F2D21790
      ALWT(2,3)   =  0.520833333333333                                  F2D21800
      ALWT(3,3)   =  0.520833333333333                                  F2D21810
      ALWT(4,3)   =  0.520833333333333                                  F2D21820
```

```
C                                                                       F2D21830
C     Six-point quadrature (for polynomials of order 4):________________F2D21840
C                                                                       F2D21850
      AL1(1,4)   =  0.816847572980459                                   F2D21860
      AL2(1,4)   =  0.091576213509771                                   F2D21870
      AL3(1,4)   =  0.091576213509771                                   F2D21880
      AL1(2,4)   =  0.091576213509771                                   F2D21890
      AL2(2,4)   =  0.816847572980459                                   F2D21900
      AL3(2,4)   =  0.091576213509771                                   F2D21910
      AL1(3,4)   =  0.091576213509771                                   F2D21920
      AL2(3,4)   =  0.091576213509771                                   F2D21930
      AL3(3,4)   =  0.816847572980459                                   F2D21940
      AL1(4,4)   =  0.108103018168070                                   F2D21950
      AL2(4,4)   =  0.445948490915965                                   F2D21960
      AL3(4,4)   =  0.445948490915965                                   F2D21970
      AL1(5,4)   =  0.445948490915965                                   F2D21980
      AL2(5,4)   =  0.108103018168070                                   F2D21990
      AL3(5,4)   =  0.445948490915965                                   F2D22000
      AL1(6,4)   =  0.445948490915965                                   F2D22010
      AL2(6,4)   =  0.445948490915965                                   F2D22020
      AL3(6,4)   =  0.108103018168070                                   F2D22030
      ALWT(1,4)  =  0.109951743655322                                   F2D22040
      ALWT(2,4)  =  0.109951743655322                                   F2D22050
      ALWT(3,4)  =  0.109951743655322                                   F2D22060
      ALWT(4,4)  =  0.223381589678011                                   F2D22070
      ALWT(5,4)  =  0.223381589678011                                   F2D22080
      ALWT(6,4)  =  0.223381589678011                                   F2D22090
C                                                                       F2D22100
C     Seven-point quadrature (for polynomials of order 5):______________F2D22110
C                                                                       F2D22120
      AL1(1,5)   =  0.333333333333333                                   F2D22130
      AL2(1,5)   =  0.333333333333333                                   F2D22140
      AL3(1,5)   =  0.333333333333333                                   F2D22150
      AL1(2,5)   =  0.797426985353087                                   F2D22160
      AL2(2,5)   =  0.101286507323456                                   F2D22170
      AL3(2,5)   =  0.101286507323456                                   F2D22180
      AL1(3,5)   =  0.101286507323456                                   F2D22190
      AL2(3,5)   =  0.797426985353087                                   F2D22200
      AL3(3,5)   =  0.101286507323456                                   F2D22210
      AL1(4,5)   =  0.101286507323456                                   F2D22220
      AL2(4,5)   =  0.101286507323456                                   F2D22230
      AL3(4,5)   =  0.797426985353087                                   F2D22240
      AL1(5,5)   =  0.059715871789770                                   F2D22250
      AL2(5,5)   =  0.470142064105115                                   F2D22260
      AL3(5,5)   =  0.470142064105115                                   F2D22270
      AL1(6,5)   =  0.470142064105115                                   F2D22280
      AL2(6,5)   =  0.059715871789770                                   F2D22290
      AL3(6,5)   =  0.470142064105115                                   F2D22300
      AL1(7,5)   =  0.470142064105115                                   F2D22310
      AL2(7,5)   =  0.470142064105115                                   F2D22320
      AL3(7,5)   =  0.059715871789770                                   F2D22330
      ALWT(1,5)  =  0.225000000000000                                   F2D22340
      ALWT(2,5)  =  0.125939180544827                                   F2D22350
      ALWT(3,5)  =  0.125939180544827                                   F2D22360
      ALWT(4,5)  =  0.125939180544827                                   F2D22370
      ALWT(5,5)  =  0.132394152788506                                   F2D22380
      ALWT(6,5)  =  0.132394152788506                                   F2D22390
      ALWT(7,5)  =  0.132394152788506                                   F2D22400
C                                                                       F2D22410
      RETURN                                                            F2D22420
      END                                                               F2D22430

      SUBROUTINE SHPRCT(NPE,XI,ETA,DET,ELXY,NDF,ITYPE)                  F2D22440
C     _________________________________________________________________ F2D22450
C                                                                       F2D22460
C     The subroutine evaluates the interpolation functions (SF(I)) and  F2D22470
C     their derivatives with respect to global coordinates (GDSF(I,J))  F2D22480
C     for Lagrange linear & quadratic rectangular elements, using  the  F2D22490
C     isoparametric formulation. The subroutine also evaluates Hermite  F2D22500
C     interpolation functions and their  global derivatives  using the  F2D22510
C     subparametric formulation.                                        F2D22520
C                                                                       F2D22530
C     SF(I)........Interpolation function for node I of the element     F2D22540
C     DSF(J,I).....Derivative of SF(I) with respect to XI if J=1 and    F2D22550
C                  and ETA if J=2                                       F2D22560
```

```
C     GDSF(J,I)....Derivative of SF(I) with respect to  X if J=1 and
C                  and  Y  if J=2
C     XNODE(I,J)...J-TH (J=1,2) Coordinate of node I of the element
C     NP(I)........Array of element nodes (used to define SF and DSF)
C     GJ(I,J)......Jacobian matrix
C     GJINV(I,J)...Inverse of the jacobian matrix
C
C     ________________________________________________________________
      IMPLICIT REAL*8 (A-H,O-Z)
      DIMENSION ELXY(9,2),XNODE(9,2),NP(9),DSF(2,9),GJ(2,2),GJINV(2,2)
      DIMENSION GGJ(3,3),GGINV(3,3),DDSJ(3,16),DDSF(3,4),DJCB(3,2),
     *          DSFH(3,16),DDSFH(3,16)
      COMMON/SHP/SF(9),GDSF(2,9),SFH(16),GDSFH(2,16),GDDSFH(3,16)
      COMMON/IO/IN,ITT
      DATA XNODE/-1.0D0, 2*1.0D0, -1.0D0, 0.0D0, 1.0D0, 0.0D0, -1.0D0,
     *        0.0D0, 2*-1.0D0, 2*1.0D0, -1.0D0, 0.0D0, 1.0D0, 2*0.0D0/
      DATA NP/1,2,3,4,5,7,6,8,9/
C
      FNC(A,B) = A*B
      IF(NPE.EQ.4) THEN
C
C     LINEAR Lagrange interpolation functions for FOUR-NODE element
C
          DO 10 I = 1, NPE
          XP   = XNODE(I,1)
          YP   = XNODE(I,2)
          XI0  = 1.0+XI*XP
          ETA0=1.0+ETA*YP
          SF(I)    = 0.25*FNC(XI0,ETA0)
          DSF(1,I)= 0.25*FNC(XP,ETA0)
   10     DSF(2,I)= 0.25*FNC(YP,XI0)
      ELSE
          IF(NPE.EQ.8) THEN
C
C     QUADRATIC Lagrange interpolation functions for EIGHT-NODE element
C
              DO 20 I = 1, NPE
              NI    = NP(I)
              XP    = XNODE(NI,1)
              YP    = XNODE(NI,2)
              XI0   = 1.0+XI*XP
              ETA0 = 1.0+ETA*YP
              XI1   = 1.0-XI*XI
              ETA1 = 1.0-ETA*ETA
              IF(I.LE.4) THEN
                  SF(NI)     = 0.25*FNC(XI0,ETA0)*(XI*XP+ETA*YP-1.0)
                  DSF(1,NI) = 0.25*FNC(ETA0,XP)*(2.0*XI*XP+ETA*YP)
                  DSF(2,NI) = 0.25*FNC(XI0,YP)*(2.0*ETA*YP+XI*XP)
              ELSE
                  IF(I.LE.6) THEN
                      SF(NI)     = 0.5*FNC(XI1,ETA0)
                      DSF(1,NI) = -FNC(XI,ETA0)
                      DSF(2,NI) = 0.5*FNC(YP,XI1)
                  ELSE
                      SF(NI)     = 0.5*FNC(ETA1,XI0)
                      DSF(1,NI) = 0.5*FNC(XP,ETA1)
                      DSF(2,NI) = -FNC(ETA,XI0)
                  ENDIF
              ENDIF
   20         CONTINUE
          ELSE
C
C     QUADRATIC Lagrange interpolation functions for NINE-NODE element
C
              DO 30 I=1,NPE
              NI    = NP(I)
              XP    = XNODE(NI,1)
              YP    = XNODE(NI,2)
              XI0   = 1.0+XI*XP
              ETA0 = 1.0+ETA*YP
              XI1   = 1.0-XI*XI
              ETA1 = 1.0-ETA*ETA
              XI2   = XP*XI
              ETA2 = YP*ETA
              IF(I .LE. 4) THEN
```

```
                 SF(NI)    = 0.25*FNC(XI0,ETA0)*XI2*ETA2                F2D23320
                 DSF(1,NI)= 0.25*XP*FNC(ETA2,ETA0)*(1.0+2.0*XI2)        F2D23330
                 DSF(2,NI)= 0.25*YP*FNC(XI2,XI0)*(1.0+2.0*ETA2)         F2D23340
             ELSE                                                       F2D23350
                 IF(I .LE. 6) THEN                                      F2D23360
                     SF(NI)     = 0.5*FNC(XI1,ETA0)*ETA2                F2D23370
                     DSF(1,NI) = -XI*FNC(ETA2,ETA0)                     F2D23380
                     DSF(2,NI) = 0.5*FNC(XI1,YP)*(1.0+2.0*ETA2)         F2D23390
                 ELSE                                                   F2D23400
                     IF(I .LE. 8) THEN                                  F2D23410
                         SF(NI)     = 0.5*FNC(ETA1,XI0)*XI2             F2D23420
                         DSF(2,NI) = -ETA*FNC(XI2,XI0)                  F2D23430
                         DSF(1,NI) = 0.5*FNC(ETA1,XP)*(1.0+2.0*XI2)     F2D23440
                     ELSE                                               F2D23450
                         SF(NI)     = FNC(XI1,ETA1)                     F2D23460
                         DSF(1,NI) = -2.0*XI*ETA1                       F2D23470
                         DSF(2,NI) = -2.0*ETA*XI1                       F2D23480
                     ENDIF                                              F2D23490
                 ENDIF                                                  F2D23500
             ENDIF                                                      F2D23510
  30         CONTINUE                                                   F2D23520
         ENDIF                                                          F2D23530
     ENDIF                                                              F2D23540
C                                                                       F2D23550
C    Compute the Jacobian matrix [GJ] and its inverse [GJINV]           F2D23560
C                                                                       F2D23570
     DO 40 I = 1,2                                                      F2D23580
     DO 40 J = 1,2                                                      F2D23590
     GJ(I,J)  = 0.0                                                     F2D23600
     DO 40 K = 1,NPE                                                    F2D23610
  40 GJ(I,J)  = GJ(I,J) + DSF(I,K)*ELXY(K,J)                            F2D23620
C                                                                       F2D23630
     DET = GJ(1,1)*GJ(2,2)-GJ(1,2)*GJ(2,1)                              F2D23640
     GJINV(1,1) = GJ(2,2)/DET                                           F2D23650
     GJINV(2,2) = GJ(1,1)/DET                                           F2D23660
     GJINV(1,2) = -GJ(1,2)/DET                                          F2D23670
     GJINV(2,1) = -GJ(2,1)/DET                                          F2D23680
C                                                                       F2D23690
     IF(ITYPE.LE.3) THEN                                                F2D23700
C                                                                       F2D23710
C    Compute the derivatives of the interpolation functions with        F2D23720
C    respect to the global coordinates (x,y): [GDSF]                    F2D23730
C                                                                       F2D23740
         DO 50 I  = 1,2                                                 F2D23750
         DO 50 J  = 1,NPE                                               F2D23760
         GDSF(I,J) = 0.0                                                F2D23770
         DO 50 K  = 1, 2                                                F2D23780
  50     GDSF(I,J) = GDSF(I,J) + GJINV(I,K)*DSF(K,J)                    F2D23790
     ELSE                                                               F2D23800
C                                                                       F2D23810
C    Conforming Hermite interpolation functions (four-node element)     F2D23820
C                                                                       F2D23830
         IF(NDF.EQ.4) THEN                                              F2D23840
             II = 1                                                     F2D23850
             DO 60 I = 1, NPE                                           F2D23860
             XP    = XNODE(I,1)                                         F2D23870
             YP    = XNODE(I,2)                                         F2D23880
             XI1   = XI*XP-1.0                                          F2D23890
             XI2   = XI1-1.0                                            F2D23900
             ETA1  = ETA*YP-1.0                                         F2D23910
             ETA2  = ETA1-1.0                                           F2D23920
             XI0   = (XI+XP)**2                                         F2D23930
             ETA0  = (ETA+YP)**2                                        F2D23940
             XIP0  = XI+XP                                              F2D23950
             XIP1  = 3.0*XI*XP+XP*XP                                    F2D23960
             XIP2  = 3.0*XI*XP+2.0*XP*XP                                F2D23970
             YIP0  = ETA+YP                                             F2D23980
             YIP1  = 3.0*ETA*YP+YP*YP                                   F2D23990
             YIP2  = 3.0*ETA*YP+2.0*YP*YP                               F2D24000
C                                                                       F2D24010
             SFH(II)         = 0.0625*FNC(ETA0,ETA2)*FNC(XI0,XI2)       F2D24020
             DSFH(1,II)      = 0.0625*FNC(ETA0,ETA2)*XIP0*(XIP1-4.0)    F2D24030
             DSFH(2,II)      = 0.0625*FNC(XI0,XI2)*YIP0*(YIP1-4.0)      F2D24040
             DDSFH(1,II)     = 0.125*FNC(ETA0,ETA2)*(XIP2-2.0)          F2D24050
             DDSFH(2,II)     = 0.125*FNC(XI0,XI2)*(YIP2-2.0)            F2D24060
             DDSFH(3,II)     = 0.0625*(XIP1-4.0)*(YIP1-4.0)*XIP0*YIP0   F2D24070
```

```
C
              SFH(II+1)      = -0.0625*XP*FNC(XI0,XI1)*FNC(ETA0,ETA2)
              DSFH(1,II+1)   = -0.0625*FNC(ETA0,ETA2)*XP*XIP0*(XIP1-2.0)
              DSFH(2,II+1)   = -0.0625*FNC(XI0,XI1)*XP*YIP0*(YIP1-4.)
              DDSFH(1,II+1)  = -0.125*FNC(ETA0,ETA2)*XP*(XIP2-1.0)
              DDSFH(2,II+1)  = -0.125*FNC(XI0,XI1)*(YIP2-2.0)*XP
              DDSFH(3,II+1)  = -0.0625*XP*XIP0*(XIP1-2.)*(YIP1-4.)*YIP0
C
              SFH(II+2)      = -0.0625*YP*FNC(XI0,XI2)*FNC(ETA0,ETA1)
              DSFH(1,II+2)   = -0.0625*FNC(ETA0,ETA1)*YP*XIP0*(XIP1-4.)
              DSFH(2,II+2)   = -0.0625*FNC(XI0,XI2)*YP*YIP0*(YIP1-2.)
              DDSFH(1,II+2)  = -0.125*FNC(ETA0,ETA1)*YP*(XIP2-2.)
              DDSFH(2,II+2)  = -0.125*FNC(XI0,XI2)*YP*(YIP2-1.0)
              DDSFH(3,II+2)  = -0.0625*YP*YIP0*(YIP1-2.)*(XIP1-4.0)*XIP0
C
              SFH(II+3)      = 0.0625*XP*YP*FNC(XI0,XI1)*FNC(ETA0,ETA1)
              DSFH(1,II+3)   = 0.0625*FNC(ETA0,ETA1)*XP*YP*(XIP1-2.)*XIP0
              DSFH(2,II+3)   = 0.0625*FNC(XI0,XI1)*XP*YP*(YIP1-2.)*YIP0
              DDSFH(1,II+3)  = 0.125*FNC(ETA0,ETA1)*XP*YP*(XIP2-1.)
              DDSFH(2,II+3)  = 0.125*FNC(XI0,XI1)*XP*YP*(YIP2-1.0)
              DDSFH(3,II+3)  = 0.0625*XP*YP*YIP0*XIP0*(YIP1-2.)*(XIP1-2.)
              II = I*NDF + 1
   60         CONTINUE
        ELSE
C
C     Non-conforming Hermite interpolation functions (Four-node element)
C
              II = 1
              DO 80 I = 1, NPE
              XP    = XNODE(I,1)
              YP    = XNODE(I,2)
              XI0   = XI*XP
              ETA0  = ETA*YP
              XIP1  = XI0+1
              ETAP1 = ETA0+1
              XIM1  = XI0-1
              ETAM1 = ETA0-1
              XID   = 3.0+2.0*XI0+ETA0-3.0*XI*XI-ETA*ETA-2.0*XI/XP
              ETAD  = 3.0+XI0+2.0*ETA0-XI*XI-3.0*ETA*ETA-2.0*ETA/YP
              ETAXI = 4.0+2.0*(XI0+ETA0)-3.0*(XI*XI+ETA*ETA)
     *                                -2.0*(ETA/YP+XI/XP)
C
              SFH(II) = 0.125*XIP1*ETAP1*(2.0+XI0+ETA0-XI*XI-ETA*ETA)
              DSFH(1,II)     = 0.125*XP*ETAP1*XID
              DSFH(2,II)     = 0.125*YP*XIP1*ETAD
              DDSFH(1,II)    = 0.250*XP*ETAP1*(XP-3.0*XI-1.0/XP)
              DDSFH(2,II)    = 0.250*YP*XIP1*(YP-3.0*ETA-1.0/YP)
              DDSFH(3,II)    = 0.125*XP*YP*ETAXI
C
              SFH(II+1)      = 0.125*XP*XIP1*XIP1*XIM1*ETAP1
              DSFH(1,II+1)   = 0.125*XP*XP*ETAP1*(3.0*XI0-1.0)*XIP1
              DSFH(2,II+1)   = 0.125*XP*YP*XIP1*XIP1*XIM1
              DDSFH(1,II+1)  = 0.250*XP*XP*XP*ETAP1*(3.0*XI0+1.0)
              DDSFH(2,II+1)  = 0.0
              DDSFH(3,II+1)  = 0.125*XP*XP*YP*(3.0*XI0-1.0)*XIP1
C
              SFH(II+2)      = 0.125*YP*XIP1*ETAP1*ETAP1*ETAM1
              DSFH(1,II+2)   = 0.125*XP*YP*ETAP1*ETAP1*ETAM1
              DSFH(2,II+2)   = 0.125*YP*YP*XIP1*(3.0*ETA0-1.0)*ETAP1
              DDSFH(1,II+2)  = 0.0
              DDSFH(2,II+2)  = 0.250*YP*YP*YP*XIP1*(3.0*ETA0+1.0)
              DDSFH(3,II+2)  = 0.125*XP*YP*YP*(3.0*ETA0-1.0)*ETAP1
              II = I*NDF + 1
   80         CONTINUE
        ENDIF
C
C     Compute the global first and second derivatives of the Hermite
C     interpolation functions.  The geometry is approximated using the
C     linear Lagrane interpolation functions (Subparametric formulation)
C
        DDSF(1,1) =    0.0D0
        DDSF(2,1) =    0.0D0
        DDSF(3,1) =    0.250D0
        DDSF(1,2) =    0.0D0
        DDSF(2,2) =    0.0D0
        DDSF(3,2) = -  0.250D0
```

```
         DDSF(1,3) =   0.0D0
         DDSF(2,3) =   0.0D0
         DDSF(3,3) =   0.250D0
         DDSF(1,4) =   0.0D0
         DDSF(2,4) =   0.0D0
         DDSF(3,4) = - 0.250D0
C
C     Compute global first derivatives of Hermite functions
C
         NN=NDF*NPE
         DO 110 I = 1, 2
            DO 100 J = 1, NN
            SUM = 0.0D0
            DO 90 K = 1, 2
               SUM = SUM + GJINV(I,K)*DSFH(K,J)
   90       CONTINUE
            GDSFH(I,J) = SUM
  100       CONTINUE
  110    CONTINUE
C
C     Compute global second derivatives of Hermite functions
C
         DO 140 I = 1, 3
            DO 130 J = 1, 2
            SUM = 0.0D0
            DO 120 K = 1, NPE
               SUM = SUM + DDSF(I,K)*ELXY(K,J)
  120       CONTINUE
            DJCB(I,J) = SUM
  130       CONTINUE
  140    CONTINUE
C
         DO 170 K = 1, 3
            DO 160 J = 1, NN
               SUM = 0.0D0
               DO 150 L = 1, 2
                  SUM = SUM + DJCB(K,L)*GDSFH(L,J)
  150          CONTINUE
               DDSJ(K,J) = SUM
  160       CONTINUE
  170    CONTINUE
C
C     Compute the jacobian of the transformation
C
         GGJ(1,1)=GJ(1,1)*GJ(1,1)
         GGJ(1,2)=GJ(1,2)*GJ(1,2)
         GGJ(1,3)=2.0*GJ(1,1)*GJ(1,2)
         GGJ(2,1)=GJ(2,1)*GJ(2,1)
         GGJ(2,2)=GJ(2,2)*GJ(2,2)
         GGJ(2,3)=2.0*GJ(2,1)*GJ(2,2)
         GGJ(3,1)=GJ(2,1)*GJ(1,1)
         GGJ(3,2)=GJ(2,2)*GJ(1,2)
         GGJ(3,3)=GJ(2,1)*GJ(1,2)+GJ(1,1)*GJ(2,2)
         CALL INVRSE(GGJ,GGINV)
C
         DO 200 I = 1, 3
            DO 190 J = 1, NN
               SUM = 0.0D0
               DO 180 K = 1, 3
                  SUM = SUM + GGINV(I,K)*(DDSFH(K,J)-DDSJ(K,J))
  180          CONTINUE
               GDDSFH(I,J) = SUM
  190       CONTINUE
  200    CONTINUE
      ENDIF
      RETURN
      END

      SUBROUTINE SHPTRI(NPE,AL1,AL2,AL3,DET,ELXY)
C
C     ______________________________________________________________
C
C     The subroutine computes the  Lagrangian  interpolation functions
C     and their global derivatives at quadrature points for the linear
C     and quadratic (i.e. three-node and six-node) triangular elements
```

```
C     _________________________________________________________________
C
      IMPLICIT REAL*8(A-H,O-Z)
      COMMON/SHP/SF(9),GDSF(2,9)
      DIMENSION DSF(3,9),ELXY(9,2),GJ(2,2),GJINV(2,2)
C
C     Initialize the arrays
C
      DO 10 I = 1, NPE
         DSF(1,I) = 0.0D0
         DSF(2,I) = 0.0D0
         DSF(3,I) = 0.0D0
   10 CONTINUE
C
      IF(NPE.EQ.3) THEN
C
C     Linear Lagrane interpolation for three-node element
C
   20     SF(1) =  AL1
          SF(2) =  AL2
          SF(3) =  AL3
          DSF(1,1) = 1.0D0
          DSF(2,2) = 1.0D0
          DSF(3,3) = 1.0D0
      ELSE
C
C     Quadratic Lagrange interpolation functions for six-nde element
C
          SF(1) = AL1 * (2.0D0 * AL1 - 1)
          SF(2) = AL2 * (2.0D0 * AL2 - 1)
          SF(3) = AL3 * (2.0D0 * AL3 - 1)
          SF(4) = 4.0D0 * AL1 * AL2
          SF(5) = 4.0D0 * AL2 * AL3
          SF(6) = 4.0D0 * AL3 * AL1
          DSF(1,1) = 4.0D0 * AL1 - 1
          DSF(2,2) = 4.0D0 * AL2 - 1
          DSF(3,3) = 4.0D0 * AL3 - 1
          DSF(1,4) = 4.0D0 * AL2
          DSF(2,4) = 4.0D0 * AL1
          DSF(2,5) = 4.0D0 * AL3
          DSF(3,5) = 4.0D0 * AL2
          DSF(1,6) = 4.0D0 * AL3
          DSF(3,6) = 4.0D0 * AL1
      ENDIF
C
C     Compute the global derivatives of SF(I).  Note that the special
C     form of the jacobian for area coordinates,  AL3 = 1-AL1-AL2  is
C     substituted
C
      DO 60 I = 1,2
      DO 50 J = 1,2
      SUM = 0.0D0
      DO 40 K = 1, NPE
      SUM = SUM + (DSF(I,K) - DSF(3,K))*ELXY(K,J)
   40 CONTINUE
      GJ(I,J) = SUM
   50 CONTINUE
   60 CONTINUE
C
      DET = GJ(1,1)*GJ(2,2) - GJ(1,2)*GJ(2,1)
      GJINV(1,1) = GJ(2,2)/DET
      GJINV(2,2) = GJ(1,1)/DET
      GJINV(1,2) = -GJ(1,2)/DET
      GJINV(2,1) = -GJ(2,1)/DET
      DO 100 I = 1, 2
      DO 90 J = 1, NPE
      SUM = 0.0D0
      DO 80 K = 1, 2
      SUM = SUM + GJINV(I,K) * (DSF(K,J) - DSF(3,J))
   80 CONTINUE
      GDSF(I,J) = SUM
   90 CONTINUE
  100 CONTINUE
      RETURN
      END
      SUBROUTINE SOLVER(NRM,NCM,NEQNS,NBW,BAND,RHS,IRES)                F2D26320
C     ________________________________________________________________  F2D26330
C                                                                       F2D26340
C     The subroutine solves a  banded,  symmetric,  system of algebraic F2D26350
C     equations using the Gauss elimination method:  [BAND]{U} = {RHS}. F2D26360
C     The coefficient matrix is input as BAND(NEQNS,NBW) and the column F2D26370
C     vector is input as  RHS(NEQNS),  where NEQNS is the actual number F2D26380
C     of equations and NBW is the half band width.  The true dimensions F2D26390
C     of the matrix [BAND] in the calling program, are NRM by NCM. When F2D26400
C     IRES is greater than zero, the right hand elimination is skipped. F2D26410
C                                                                       F2D26420
C     ________________________________________________________________  F2D26430
      IMPLICIT REAL*8(A-H,O-Z)                                          F2D26440
      DIMENSION BAND(NRM,NCM),RHS(NRM)                                  F2D26450
C                                                                       F2D26460
      MEQNS=NEQNS-1                                                     F2D26470
      IF(IRES.LE.0) THEN                                                F2D26480
          DO 30 NPIV=1,MEQNS                                            F2D26490
          NPIVOT=NPIV+1                                                 F2D26500
          LSTSUB=NPIV+NBW-1                                             F2D26510
          IF(LSTSUB.GT.NEQNS) THEN                                      F2D26520
              LSTSUB=NEQNS                                              F2D26530
          ENDIF                                                         F2D26540
C                                                                       F2D26550
          DO 20 NROW=NPIVOT,LSTSUB                                      F2D26560
          NCOL=NROW-NPIV+1                                              F2D26570
          FACTOR=BAND(NPIV,NCOL)/BAND(NPIV,1)                           F2D26580
          DO 10 NCOL=NROW,LSTSUB                                        F2D26590
          ICOL=NCOL-NROW+1                                              F2D26600
          JCOL=NCOL-NPIV+1                                              F2D26610
   10     BAND(NROW,ICOL)=BAND(NROW,ICOL)-FACTOR*BAND(NPIV,JCOL)        F2D26620
   20     RHS(NROW)=RHS(NROW)-FACTOR*RHS(NPIV)                          F2D26630
   30     CONTINUE                                                      F2D26640
      ELSE                                                              F2D26650
   40     DO 60 NPIV=1,MEQNS                                            F2D26660
          NPIVOT=NPIV+1                                                 F2D26670
          LSTSUB=NPIV+NBW-1                                             F2D26680
          IF(LSTSUB.GT.NEQNS) THEN                                      F2D26690
              LSTSUB=NEQNS                                              F2D26700
          ENDIF                                                         F2D26710
          DO 50 NROW=NPIVOT,LSTSUB                                      F2D26720
          NCOL=NROW-NPIV+1                                              F2D26730
          FACTOR=BAND(NPIV,NCOL)/BAND(NPIV,1)                           F2D26740
   50     RHS(NROW)=RHS(NROW)-FACTOR*RHS(NPIV)                          F2D26750
   60     CONTINUE                                                      F2D26760
      ENDIF                                                             F2D26770
C                                                                       F2D26780
C     Back substitution                                                 F2D26790
C                                                                       F2D26800
      DO 90 IJK=2,NEQNS                                                 F2D26810
      NPIV=NEQNS-IJK+2                                                  F2D26820
      RHS(NPIV)=RHS(NPIV)/BAND(NPIV,1)                                  F2D26830
      LSTSUB=NPIV-NBW+1                                                 F2D26840
      IF(LSTSUB.LT.1) THEN                                              F2D26850
          LSTSUB=1                                                      F2D26860
      ENDIF                                                             F2D26870
      NPIVOT=NPIV-1                                                     F2D26880
      DO 80 JKI=LSTSUB,NPIVOT                                           F2D26890
      NROW=NPIVOT-JKI+LSTSUB                                            F2D26900
      NCOL=NPIV-NROW+1                                                  F2D26910
      FACTOR=BAND(NROW,NCOL)                                            F2D26920
   80 RHS(NROW)=RHS(NROW)-FACTOR*RHS(NPIV)                              F2D26930
   90 CONTINUE                                                          F2D26940
      RHS(1)=RHS(1)/BAND(1,1)                                           F2D26950
      RETURN                                                            F2D26960
      END                                                               F2D26970


      SUBROUTINE TIMER(NCOUNT,INTIAL,ITEM,NN)                           F2D26980
C    _________________________________________________________________  F2D26990
C                                                                       F2D27000
C    The  subroutine computes  the algebraic equations associated with  F2D27010
C    the parabolic and hyperbolic differential equations bu using the   F2D27020
C    alfa-family and Newmark family of approximations, respectively.    F2D27030
C    _________________________________________________________________  F2D27040
```

```
C                                                                       F2D27050
      IMPLICIT REAL*8(A-H,O-Z)                                          F2D27060
      COMMON/STF/ELF(27),ELK(27,27),ELM(27,27),ELXY(9,2),ELU(27),       F2D27070
     1          ELV(27),ELA(27),A1,A2,A3,A4,A5                          F2D27080
C                                                                       F2D27090
      IF(ITEM.EQ.1) THEN                                                F2D27100
C                                                                       F2D27110
C     The alfa-family of time approximation for parabolic equations     F2D27120
C                                                                       F2D27130
         DO 20 I=1,NN                                                   F2D27140
         SUM=0.0                                                        F2D27150
         DO 10 J=1,NN                                                   F2D27160
         SUM=SUM+(ELM(I,J)-A2*ELK(I,J))*ELU(J)                          F2D27170
   10    ELK(I,J)=ELM(I,J)+A1*ELK(I,J)                                  F2D27180
   20    ELF(I)=(A1+A2)*ELF(I)+SUM                                      F2D27190
      ELSE                                                              F2D27200
C                                                                       F2D27210
C     The Newmark intergration scheme for hyperbolic equations          F2D27220
C                                                                       F2D27230
         IF(NCOUNT.EQ.1 .AND. INTIAL.NE.0) THEN                         F2D27240
            DO 40 I = 1,NN                                              F2D27250
            ELF(I)   = 0.0                                              F2D27260
            DO 40 J = 1,NN                                              F2D27270
            ELF(I)   = ELF(I)-ELK(I,J)*ELU(J)                           F2D27280
   40       ELK(I,J)= ELM(I,J)                                          F2D27290
         ELSE                                                           F2D27300
            DO 70 I = 1,NN                                              F2D27310
            SUM      = 0.0                                              F2D27320
            DO 60 J = 1,NN                                              F2D27330
            SUM      = SUM+ELM(I,J)*(A3*ELU(J)+A4*ELV(J)+A5*ELA(J))     F2D27340
   60       ELK(I,J)= ELK(I,J)+A3*ELM(I,J)                              F2D27350
   70       ELF(I)   = ELF(I)+SUM                                       F2D27360
         ENDIF                                                          F2D27370
      ENDIF                                                             F2D27380
      RETURN                                                            F2D27390
      END                                                               F2D27400
```

INDEX

Accuracy of solution, 14, 202–207
Alternative formulations, 579–594
Alpha family of approximations, 228–230, 374, 492, 504
Approximation error, 199–200
Approximation, temporal (or time) (*see* Temporal approximation)
Approximation functions, 4, 12, 40–57, 53, 78
  (*See also* Interpolation functions)
Area coordinates, 407–411
Assembly of finite elements, 7, 89–94, 109, 151–154, 168, 173, 265–267, 297, 318–322, 408–410
Axisymmetric problems, 10–12, 103–105, 132, 135, 141, 195, 272–274, 281, 288–290, 323, 345, 393, 503, 562

Backward difference method (*see* Time integration schemes)
Balance of energy (*see* Conservation of energy)
Bandwidth, 101, 265–267
Bars, 59, 63, 124, 125
Beams, 143, 198
  on elastic foundations, 59
  large deflection bending of, 595–597
  Euler–Bernoulli theory of, 37, 47, 60, 212, 272
  Timoshenko theory of, 212, 221, 240, 272
Beam elements, Euler–Bernoulli, 143–167, 238, 239, 241, 242
  Timoshenko, 177–187, 238, 239, 241, 242
Bending of beams (*see* Beams)
Bending of plates (*see* Plates)
Bilinear forms, 33–50, 76, 146, 301, 342
Boundary value problem, 21
Boundary conditions, 22, 67, 109
  convective type, 107–109, 541, 552
  Dirichlet, 99, 131, 267
  essential, 28, 30–39, 59, 71, 75, 100, 175, 267, 458, 591
  force, 75
  geometric, 75
  homogeneous, 22, 29, 67
  impositition of, 95, 154–158, 298, 321, 339, 361–363, 468, 511, 522
  mixed, 268
  non-homogeneous, 22, 29, 42, 67
  natural, 28, 30–39, 71, 75, 100, 175, 268, 458, 591
  Neumann, 132, 268, 367
  Newton, 268, 341
Boundary integral, evaluation of, 313–318, 328, 344–346, 363, 466–468
Boundary integral methods, 16
Brick element, 601
Bubnov–Galerkin method (*see* Galerkin method)
Buckling loads, 209, 213, 242

C^0 Approximation, 97
C^0 plate elements, 111
Central difference method (*see* Time integration schemes)
Classical plate theory (*see* Plate theory)
Collocation method, 16, 40, 55–57, 157, 581

Coefficient matrix, 86
Compatible elements (*see* Conforming elements)
Compatibility of elements, 442–445
Completeness of functions, 43, 50, 56, 67, 77
Computer implementation, 258–270, 533–540
Computer programs:
  applications of, 270–291, 540–575
  general purpose, 59
  FEM1D, 271
  FEM1DV2, 270–286
  FEM2D, 533
  FEM2DV2, 540–569
  PLATE, 533
Condensed equations, 95, 110, 127, 156, 161, 165, 174, 176, 328, 330, 349
Conforming elements, 406, 407, 515
Connectivity of elements (*see* Assembly)
Continuity equation (*see* Conservation of mass)
Conservation:
  of energy, 120, 133, 353, 599, 605
  of linear momentum, 119, 353, 457, 483, 605
  of mass, 119, 353, 483, 605
Consistent interpolation element (CIE), 181, 184, 191
Consistent interpolation, 179, 191
Consistent mass matrix (*see* Mass matrix)
Constant-strain triangular element, 462
Constant-average-acceleration method, 231
Constitutive equations, 457–459
Constraint equations, inclusion of, 187–191
Convective heat transfer (*see* Heat transfer)
Convergence:
  of solution, 7, 14, 77, 116, 185, 201–205, 222
  h-, 201, 222, 442–444
  p-, 201, 222, 442–444
  rate of, 201, 203, 205, 222
Coordinate:
  local (or element), 79, 83, 148, 248, 308, 312
  global, 79, 83, 248, 312
  natural (or normal), 248, 416–420
Coordinate transformation, 83, 248–250, 421–429
Cramer's rule, 78, 113
Crank–Nicolson scheme (*see* Time integration schemes)

Dirac delta function, 55, 99, 358, 581
Direction cosines, 25, 300, 345
Dirichlet boundary condition (*see* Boundary conditions)
Discrete element method (DEM), 14
Divergence theorem, 24, 300

Eigenfunctions (*see* Eigenvectors)
Eigenvalue problems, 22, 209–213, 370–384, 520–522
Eigenvalues, 22, 209, 376
Eigenvectors, 22, 209, 375
Elements (*see* Finite elements)
Energy norm, 200, 201
Equal interpolation element (EIE), 183
Equations of motion, 210–212, 225, 457, 513, 518
  (*See also* Conservation of linear momentum)
Equipotential lines, 356
Error, 199, 200, 208, 222
  approximation, 97, 99, 100, 199
  computational, 100
  quadrature and finite arithmetic, 199
  measures of, 200–201
  pointwise, 200
Error estimate, 7, 201–205, 216, 222
Euler equations, 120
Euler–Bernouilli:
  beam theory, 47, 60, 595
  frame element, 167–177
  hypothesis, 37
Eulerian description, 118
Evaluation of boundary integrals, 313–318

Finite difference method, 4, 228–231
Finite element mesh (*see* Mesh)
Finite element computer programs (*see* Computer programs)
Finite element equations for (*See also* Finite element models for):
  axisymmetric problems (*see* Axisymmetric problems)
  bar element (*see* Bars)
  beam element (*see* Beams)
  brick (*see* Brick element)
  constant-strain triangular element (CST), 405
  frame element (*see* Frame element)
  isoparametric element (*see* Isoparametric formulation)
  space–time element (*see* Space–time element)

Finite element equations for (*Contd.*):
  transition element (*see* Transition element)
  truss element (*see* Truss element)
Finite element method, basic concepts, 4–15, 58, 59
  computer applicatons of, 270–291, 540–575
Finite element model of:
  axisymmetric problems, 103–105, 323–334
  bars, 85–95
  classical plate element, 514–518
  eigenvalue problems, 213–216, 370–374, 520–522
  Euler–Bernoulli beam theory, 144–151
  frames, 178–187
  heat transfer, 108–117, 340–352
  inviscid flows, 117–123, 353–365
  membrane, 369, 381, 384
  nonlinear problems, 594–599
  one-dimensional problems, 67–141
  plane elasticity, 461–465
  shear-deformable plate element, 518–519
  three-dimensional problems, 600, 601
  Timoshenko beam element, 178–183
  time-dependent problems, 224–229, 370–375, 382–384, 465, 520–522
  torsion, 365–368
  two-dimensional problems, 301–303, 324
  viscous fluid flow, 484–494
First-order shear-deformation theory (*see* Plate theory)
Fluid mechanics, 297, 353–364
Flow about a circular cylinder, 554
Flow of:
  fluid squeezed between plates, 501, 502, 560
  viscous incompressible fluid, 60, 61, 482–507
  viscous lubricant, 497–501
Flow chart for:
  FEM1DV2, 261
  FEM2DV2, 534
Fluids:
  incompressible, 61, 121, 482, 489, 541
  ideal, 118
  Newtonian, 118, 121, 136
  viscous, 60, 67, 118, 533, 541, 573
Force vector (*see* Source vector)
Forward difference method (*see* Time integration scheme)
Fourier series, 50
Fourier components, 210
Fourier heat conduction law, 75
Frame element:
  Euler–Bernoulli, 167–177
  Timoshenko, 177–191, 272
Full integration element (FIE), 185, 187
Fully developed flows, 121
Functionals:
  bilinear, 26, 27, 33–35
  linear, 26, 33–35
  quadratic, 40, 41, 59

Galerkin method, 4, 54, 57, 581–586
Gauss points for:
  rectangular elements, 431
  triangular elements, 436
Gauss (–Legendre) quadrature (*see* Quadrature)
Generalized displacements, 147
Generalized forces, 146
Gradient theorem, 24, 25, 300
Gradient operator, 24
Groundwater flow, 132, 296, 355–359

Half-band width, 101
Half-band, upper, 265
Heat transfer, 71, 105–117, 296, 297, 340, 541, 570
  axisymmetric, 272, 278, 323
  cylindrical geometries, 323
  conductive, 105, 346–350, 384
  convective, 39, 68, 107, 341, 350–352, 384
  radiative, 346
  transient, 233–236, 376–379
Heavyside step function, 527
Hencky–Mindlin plate theory (*see* Plate theory)
Hermite interpolation functions, 148, 419, 420, 514
Homogeneous solution, 210
Hooke's law, 366
Hydrostatic pressure, 121, 573
Hyperbolic equations, 224, 230–231, 381, 564

Initial conditions, 22
Initial value problems, 21
Integral statements (*see* Weighted-integral statements)
Integration by parts, 22–24
Integration points (*see* Gauss points)
Interelement compatibility (*see* Conforming elements)
  (*See also* Compatibility of elements)

erpolation functions: 5, 77, 147–151, 404–454
  for rectangular elements, 308–311, 411–419
  for serendipity elements, 419
  for triangular elements, 304–307, 405–411
  of Hermite family, 80, 148, 207, 215, 419
  of Lagrange family, 80, 82, 169, 249, 303–311, 404–419
  properties of, 77, 84, 149, 307, 601
nviscid flow, 334, 353, 362, 541, 571
rrotational flow, 296, 353, 354, 358
Isolines, 333
Isoparametric formulations, 251, 423

Jacobian matrix, 424, 601
Jacobian of transformation, 206, 250, 425, 427

Kirchhoff plate theory (*see* Plate theory, classical)
Kirchhoff free-edge condition, 514

L_2 norm, 200
Lagrange interpolation functions, 80
  one-dimensional, 78–84, 249
  two-dimensional, 303–311, 404–420
Lagrange multiplier method, 488–491
Lagrange multipliers, 488, 489, 492
Lagrange family of finite elements, 249
Lagrangian description, 119, 123
Laplace equation, 367, 391
Laplacian operator, 24
Least-squares method, 4, 54–55, 57
Least-squares model, 40, 63, 98, 581, 582
Linear independence, 67
Lumped mass matrix (*see* Mass matrix)

Mass lumping:
  proportional, 232, 233
  row-sum, 232
Mass matrix, 214
  consistent, 229, 232
  lumped, 232
Master rectangular element, 404, 429–433
Master triangular element, 433–438
Material time derivative, 353
Membranes, 369, 381, 384
Mesh:
  effect, 524
  generation, 298, 335–339, 441–448, 527, 548–551
Mesh: (*Contd.*):
  refinement,
    h-version, 222, 442
    p-version, 222, 442
Mindlin plate theory (*see* Plate theory, shear-deformation)
Mixed formulations, 590–594
Mode shape, 211

Natural frequencies, 209
Natural vibrations, 211, 381, 473, 520
Navier–Stokes equations, 60, 120, 598
Newton–Cotes quadrature (*see* Quadrature)
Newton–Raphson method, 597
Newton's law of cooling, 107, 341, 580
Nodeless coefficients, 16
Nodeless variables, 14
Nonconforming elements, 515
Nonlinear problems, 579–606, 594, 597–598
Normal derivative operator, 25
Nuemann boundary conditions (*see* Boundary condition)
Numerical integration, 246–292, 421–438

Orthogonality conditions, 50

Parabolic equations, 224, 227, 230, 372–373, 554
Pascal's triangle, 405, 407
Penalty finite element model, 484, 488–494
Penalty parameter, 488, 491, 494
Penalty function method, 484–494
Petrov–Galerkin model, 40, 53–54, 56, 63, 581, 582, 584
Plane elasticity problems, 533, 538, 573
Plane stress assumption, 471
Plane stress problem, 456, 458
Plane strain problem, 456, 458
Plane elasticity, 455–481
  finite element model, 461
  eigenvalue and transient problems, 465
  weak form model, 464
Plane truss element, 167
Plate bending, 508–532
Plate theory, classical, 508–516, 529
  shear-deformation, 508, 509, 516–520
Poiseuille flow, 122
Poisson equation, 49, 62, 297, 325, 369, 384, 386, 554
Postprocessing of solution, 96–97, 158–160, 298, 322

Preprocessor, 259, 287, 534
Primary variables, 73–75, 90, 318, 319
Primitive variables model (*see* Velocity–pressure formulation)
Principle of virtual displacements, 123, 459
Prism elements, 602
Processor, 259, 262, 287
Program:
  FEM1D, 258, 271
  FEM1DV2, 258–270
    applications of, 270–291
    flow chart of, 231
    input for, 274–278
    source listing of (*see* Appendix 1)
  FEM1D, 533
  FEM2DV2, 533–551
    applications of, 551–575
    flow chart of, 534
    input for, 542–547
    source listing of (*see* Appendix 2)

Quadratic functional, 33–35
Quadrature points (*see* Gauss points)
Quadrature (*See also* Numerical integration):
  Gauss–Legendre, 248, 254–258, 255, 287, 421
  points, 248, 431, 436
  Newton–Cotes, 253, 255, 287
Quarter-point elements, 441

Radially symmetric problems, 103–105
Radiation, 39
Rayleigh–Ritz:
  solution, 44, 45
  method, 4, 40
Rectangular elements, 308–311, 411–420
Reduced integration element (RIE), 184, 185, 187, 191
Reduced integration, 180, 492, 519
Residual, 19
Ritz coefficients, 41, 61
Ritz method (*see* Rayleigh–Ritz method)
Ritz solution, 331

Secondary variables, 73–75, 90, 103
  balance (or equilibrium) of, 318
Seepage (*see* Groundwater flow)
Semidiscrete finite element models, 225–227, 373
Separation of variables, 210
Serendipity elements, 412, 416, 419
Shape functions (*see* Interpolation functions)
Shear correction factors, 177
Shear-deformable plate model (*see* Plates)
Shear locking, 179, 191, 519, 520
Simpson's one-third rule, 247, 253
Singular points, 339
Source vector, 86
Stability criteria, 230, 233, 375, 383
Stability of numerical schemes, 229–239, 377, 384
Stability (or geometric) stiffness matrix, 215, 521
Stiffness matrix (*See also* Coefficient matrix) of:
  bar element, 87, 126
  beam elements, 151, 181–183
  frame element, 169, 171
  plane elastic element, 464
  plate bending elements, 515, 521
  truss element, 173
Strain–displacement relations, 457
Stream function, 61, 354, 360–362, 367, 398, 504
  formulation, 360
  –Vorticity formulation, 61, 504
Stress–strain relations, 457
Subdomain method, 16, 40, 581, 582, 584
Subparametric elements (*see* Subparametric formulation)
Subparametric formulation, 251
Superparametric elements (*see* Superparametric formulation)
Superparametric formulation, 251, 423
Supmetric, 200

Tangent stiffness matrix, 595
Taylor series, 4, 204
Temperature, ambient, 342
Temporal approximations (*see* Time approximation schemes)
Tensor product, 430
Tetrahedral elements, 407
Thermal conductivity, 11, 71, 109, 216, 353
Three-dimensional problems, 579–606, 599
Time approximation schemes, 224–233, 244, 374, 375, 382, 383, 402, 465, 492, 520–522
Time-dependent problems, 21, 224–241, 370–384, 520, 554
Time integration schemes:
  backward difference, 228, 231, 375
  central difference, 231, 383, 400
  collocation, 402
  conditionally stable, 229
  constant-average-acceleration, 383

Time integration schemes: (*Contd.*):
  Crank–Nicolson, 228, 375, 377, 379
  explicit, 230
  forward difference, 228, 375
  Galerkin, 228, 231, 238, 375
  Houbolt's, 230
  linear acceleration, 231, 383
  implicit, 230
  Newmark, 382
  stable, 229
  unstable, 229
  Wilson's, 230, 402
Timoshenko beam theory, 61
Timoshenko frame element, 177
Torsion, 365–369, 398
Total potential energy principle, 35, 143, 148
Transient analysis, 227–241, 374–384, 474–476, 501–503, 527, 528
Transition elements, 299, 478
Triangular elements, 304–308, 405–410
Truss element, 167

Variational problem, 34, 76, 301
Variation, first, 27
Variational symbol, 27–28
Variational methods, 4, 13, 14, 40–59

Velocity potential, 355–358, 362–364
Velocity–pressure formulation, 484–487
Viscous incompressible flows (*see* Fluids)
Vorticity, 61, 504

Warping function, 367
Wave equation, 379
Weak form, 30–33, 40, 51, 73–76, 104, 108, 128, 214, 225, 299–301, 342–345, 380, 580, 591
  for: Euler–Bernoulli beams, 145–147, 595
    viscous flows, 484–486, 491
    Navier–Stokes equations, 598
    plane elasticity problems, 459–461
    plate bending, 513, 517
    three-dimensional problems, 600
    Timoshenko beams, 177
Weight function, 20, 29, 37, 42, 53, 74, 145, 177, 299, 461, 485, 581
Weighted-integral statements, 18–20, 28–40, 53, 57
Weighted-integral method, 4, 18
Weighted-residual methods, 51–57, 98, 580–590
Weighted-integral form (*see* Weighted-integral statements)

Pergamon

PII: S0045-7949(96)00427-0

Computers & Structures Vol. 65, No. 5, pp. 741–759, 1997
© 1997 Elsevier Science Ltd. All rights reserved
Printed in Great Britain
0045-7949/97 $17.00 + 0.00

ON THE PERFORMANCE OF HIGHER ORDER THEORIES FOR TRANSIENT DYNAMIC ANALYSIS OF SANDWICH AND COMPOSITE BEAMS

S. R. Marur† and **T. Kant**‡

† CSS Foundation for Research in Finite Elements, B4/4, Vaigai Nagar, Madurai-625 016, India
‡ Department of Civil Engineering, Indian Institute of Technology, Powai, Bombay-400 076, India

(*Received* 24 *September* 1993)

Abstract—Higher-order shear-deformable refined theories, based on isoparametric elements, are adopted for transient dynamic analysis of symmetric and unsymmetric sandwich and composite beam constructions. These shear-correction coefficient free theories model cross sectional warping using nonlinear variation of inplane displacements across the depth. They also incorporate transverse shear stress in the formulation. A special lumping scheme is employed for the evaluation of diagonal mass matrix, and a central difference scheme is used for carrying out the integration of the equation of motion, to obtain the response history. Through numerical experiments, the efficacy of higher-order models in predicting displacements and stress, resultants over from the first-order theory, with respect to time, is clearly brought out in this paper. © 1997 Elsevier Science Ltd.

1. INTRODUCTION

1.1. *The need for refined theories*

The study of laminated composite and sandwich material constructions is a fertile area of research among aero-industries and space research establishments. This is due to the ease and advantage of such materials: with a choice of different fibre materials, orientation and stacking sequences, the behaviour pattern of either isotropic or orthotropic or anisotropic material could be achieved. The resultant laminate could then be made with the required stiffness, strength to weight ratios and damage tolerance as well as superior fatigue response characteristics.

These materials, on the other hand, are not devoid of problems, such as delamination at free edges due to interlaminar normal stresses and low lamina strength, cross sectional warping including the core, transverse shear effects etc. Thus, any analysis of such constructions would only be realistic and accurate when the models employed are capable of addressing these issues and providing solutions to these problems.

1.2. *Classical theory*

In addition to the above, the literature on beam formulations reveals that the Euler–Bernoulli theory has been the most prevalent for the transient dynamic analysis of beams and arches [1] and frames [2–6]. The major handicap with this theory is that it neglects the transverse shear strain completely and hence gets restricted to sections with high aspect ratios only.

1.3. *First-order theory*

The incorporation of transverse shear deformation into the governing equation by Timoshenko [7], was the first step towards the first-order shear deformation theory. Early versions of beam finite elements with the inclusion of rotary inertia and shear effects were reported by McCallay [8] and Archer [9]. Kapur [10] proposed a Timoshenko element with independent cubic polynomials for transverse displacements due to bending and shear. Two versions of the Timoshenko element were published, with cubic variation of transverse displacement and rotation of neutral axis [11, 12].

Different orders of interpolation for w and θ were employed in the development of shear deformable elements [13, 14]. Both w and θ and their respective spatial derivatives were considered as nodal degrees of freedom by Thomas and Abbas [15] for their version of the Timoshenko element. This theory was employed for transient dynamic analysis of elastic and elastoplastic beams and frames using C^0 elements for comparison with that of Euler–Bernoulli theory using C^1 elements by Kant and Marur [16]. The shortcomings in this theory are the assumption that the shear strain remains constant across the thickness, and the need for a problem-dependent shear-correction coefficient.

1.4. *Second-, third- and fourth-order theories*

A second-order theory with two constants, one depending on the cross sectional warping and the other on the transverse direct stress, was proposed by Stephen and Levinson [17]. Heyliger and Reddy [18] proposed a third-order theory and its refined version, with transverse normal stress components, was reported later [19]. An attempt towards a fourth-order beam theory with the inclusion of transverse shear strain and warping of cross section was made by Levinson [20] and an improved version of the same was subsequently proposed by Rychter [21].

1.5. *Higher-order theory*

A higher-order model, as a further development of fourth-order theory and based on Hamilton's principle, was reported by Bickford [22] for the dynamic analysis of elastic beams. Reddy [23] also formulated a higher-order model, incorporating the transverse shear stress with C^1 elements. Kant and Gupta [24] proposed a refined higher-order model, with the inclusion of transverse shear and normal stress components with simple C^0 elements, for the static and free vibration analysis of isotropic beams. Later, the higher order models were extended to the static analysis of composite and sandwich beams, both without [25], and with [26], the transverse normal strain components.

1.6. *Higher-order theory for transient dynamics*

While the Euler–Bernoulli theory is very much restricted to thin sections, the first-order theory always requires a problem-dependent factor. Moreover, this theory cannot model the cross sectional warping, an important element in modelling composites. The second-order theory [17] needs two factors, making this theory a problem-dependent one also. The third-order theory [18] has the basic disadvantage of C^1 continuity, while the fourth-order theory [20] has been formulated exclusively for beams with narrow rectangular cross sections and, hence, cannot be directly applied to other beams with arbitrary cross sections. The higher-order theory [23] also retains the C^1 continuity.

The higher-order models of Kant and his co-workers [24–26], however, are free of all these shortcomings and are based on isoparametric elements. Moreover, they assume cubic axial strain, quadratic transverse shear strain and linear transverse normal strain components in order to capture the behaviour of composite and sandwich constructions.

While the analysis of such structures requires a tool like higher-order theory, the picture that emerges from the study of the literature clearly indicates the wider usage of Euler–Bernoulli and first-order shear deformation theories. In addition, the untapped potential of higher-order models for the exploration of transient dynamic behaviour of composites and sandwiches is indicated.

Hence, three higher-order models are proposed in this paper, in order to investigate the mechanics of composite and sandwich beams, undergoing transient dynamic deformations.

2. HIGHER-ORDER THEORIES AND FORMULATIONS

2.1. *Higher-order models*

The higher-order displacement model, based on the Taylor's series expansion [27] of the displacement components, is given by

$$u(x,z,t) = u_0(x,t) + z\theta_x(x,t) + z^2 u_0^*(x,t) + z^3\theta_x^*(x,t), \quad (1)$$

$$w(x,z,t) = w_0(x,t), \quad (2)$$

where u_0 and w_0 are axial and transverse displacements, in the x–z plane at time t, θ_x is the rotation of cross section about the y-axis, and u_0^* and θ_x^* are higher-order terms arising out of Taylor series expansion and defined at the neutral axis.

The possible variations of axial displacement given by eqn (1) are

$$u(x,z,t) = u_0(u,t) + z\theta_x(x,t) + z^2 u_0^*(x,t), \quad (3)$$

and

$$u(x,z,t) = u_0(x,t) + z\theta_x(x,t) + z^3\theta_x^*(x,t). \quad (4)$$

The models given by eqns (3), (4) and (1) can be designated as Higher Order Beam Theory 4a, HOBT4b and HOBT5, respectively, with the transverse displacement remaining the same for all the three models, as given by eqn (2). The following presentation is based on HOBT5, as the other two models are the special cases of HOBT5 itself.

2.2. *Total energy*

The total energy of a system can be given by

$$L = T - \Pi, \quad (5)$$

and

$$\Pi = U_s - W_e \quad (6)$$

where U_s is the internal strain energy, W_e is the work done by the external forces, and T is the kinetic energy.

Equation (6) can be rewritten as

$$L = \tfrac{1}{2}\int \dot{\mathbf{u}}^t \rho \dot{\mathbf{u}}\, \mathrm{d}v - [\tfrac{1}{2}\int \boldsymbol{\epsilon}^t \boldsymbol{\sigma}\, \mathrm{d}v - \int \mathbf{u}^t \mathbf{P}\, \mathrm{d}x], \quad (7)$$

where

$$\mathbf{u} = [uw]^t, \quad \dot{\mathbf{u}} = [\dot{u}\dot{w}]^t,$$

$$\boldsymbol{\epsilon} = [\epsilon_x \gamma_{xz}]^t, \quad \boldsymbol{\sigma} = [\sigma_x \tau_{xz}]^t,$$

$$\mathbf{P} = [p_x p_z]^t.$$

2.3. *Internal strain energy*

Now the displacements can be written as

$$\mathbf{u} = \underline{\boldsymbol{Z}}_d \mathbf{d} \tag{8}$$

where

$$\mathbf{u} = [uw]^t \tag{8a}$$

$$\mathbf{d} = [u_0 w_0 \theta_x u_0^* \theta_x^*]^t \tag{8b}$$

and

$$\underline{\boldsymbol{Z}}_d = \begin{bmatrix} 1 & 0 & z & z^2 & z^3 \\ 0 & 1 & 0 & 0 & 0 \end{bmatrix}. \tag{8c}$$

The strains are written as

$$\epsilon_x = \epsilon_{x0} + z^2 \epsilon_{x0}^* + zK_x + z^3 K_x^* \tag{9}$$

$$\gamma_{xz} = \phi + z^2 \phi^* + zK_{xz}, \tag{10}$$

where

$$[\epsilon_{x0} \epsilon_{x0}^* K_x K_x^*] = [u_{0,x} u_{0,x}^* \theta_{x,x} \theta_{x,x}^*] \tag{10a}$$

$$[\phi \phi^* K_{xz}] = [(w_{0,x} + \theta_x) 3\theta_x^* 2u_0^*], \tag{10b}$$

and can be expressed in the matrix form as

$$\boldsymbol{\epsilon} = \underline{\boldsymbol{Z}}_s \bar{\boldsymbol{\epsilon}} \tag{11}$$

where

$$\bar{\epsilon} = [\epsilon_{x0} \epsilon_{x0}^* K_x K_x^* | \phi \phi^* K_{xz}] \tag{11a}$$

$$\underline{\mathbf{Z}}_s = \left[\begin{array}{cccc|ccc} 1 & z^2 & z & z^3 & 0 & 0 & 0 \\ 0 & 0 & 0 & 0 & 1 & z^2 & z \end{array}\right]. \tag{11b}$$

The constitutive relation of a typical lamina is given by

$$\boldsymbol{\sigma} = \underline{\mathbf{D}} \boldsymbol{\epsilon} \tag{12}$$

where

$$\underline{\mathbf{D}} = \begin{bmatrix} E & 0 \\ 0 & G \end{bmatrix}, \tag{12a}$$

$$\boldsymbol{\sigma} = [\sigma_x \tau_{xz}]^t \tag{12b}$$

The internal strain energy, after carrying out the integration across the cross section, becomes

$$U_s = \frac{b}{2} \int_l \bar{\epsilon}^t \bar{\boldsymbol{\sigma}} \, \mathrm{d}x \tag{13}$$

where

$$\bar{\boldsymbol{\sigma}} = \underline{\bar{\mathbf{D}}} \bar{\epsilon} \tag{13a}$$

The stress resultants are given by

$$\bar{\boldsymbol{\sigma}} = [N_x N_x^* M_x M_x^* | Q Q^* S]^t \tag{14}$$

and

$$\underline{\bar{\mathbf{D}}} = \int_z \underline{\mathbf{Z}}_s^t \underline{\mathbf{D}} \underline{\mathbf{Z}}_s \, \mathrm{d}z$$

$$= \sum_{L=1}^{NL} \int_{h_{L-1}}^{h_L} \underline{\mathbf{Z}}_s^t \underline{\mathbf{D}} \underline{\mathbf{Z}}_s \, \mathrm{d}z \tag{15}$$

which appears in a matrix form as,

$$\underline{\bar{\mathbf{D}}} = \left[\begin{array}{cc|c} \underline{\mathbf{D}}_m & \underline{\mathbf{D}}_c & 0 \\ \underline{\mathbf{D}}_c^t & \underline{\mathbf{D}}_b & \\ \hline \multicolumn{2}{c|}{0} & \underline{\mathbf{D}}_s \end{array}\right] \tag{16}$$

where *NL* stands for the (total) number of layers of the cross section,

$$\underline{\mathbf{D}}_m = \sum_{L=1}^{NL} E_L \begin{bmatrix} H_1 & H_3 \\ H_3 & H_5 \end{bmatrix} \quad \underline{\mathbf{D}}_c = \sum_{L=1}^{NL} E_L \begin{bmatrix} H_2 & H_4 \\ H_4 & H_6 \end{bmatrix}$$

$$\underline{\mathbf{D}}_b = \sum_{L=1}^{NL} E_L \begin{bmatrix} H_3 & H_5 \\ H_5 & H_7 \end{bmatrix}$$

$$\underline{\mathbf{D}}_s = \sum_{L=1}^{NL} G_L \begin{bmatrix} H_1 & H_3 & H_2 \\ & H_5 & H_4 \\ \text{sym.} & & H_3 \end{bmatrix} \tag{16a}$$

and

$$H_k = (h_L^k - h_{L-1}^k)/k, \quad k = 1 \ldots 7. \tag{16b}$$

2.4. *Kinetic energy*

The kinetic energy can be expressed using eqn (8) as

$$T = \tfrac{1}{2} \int_l \dot{\mathbf{d}}^t \underline{\mathbf{m}} \dot{\mathbf{d}} \, \mathrm{d}x, \tag{17}$$

where

$$\bar{\underline{\mathbf{m}}} = b \int_z \underline{\mathbf{Z}}_d^t \rho_L \underline{\mathbf{Z}}_d \, \mathrm{d}z$$

$$= b \sum_{L=1}^{NL} \int_{h_{L-1}}^{h_L} \underline{\mathbf{Z}}_d^t \rho_L \underline{\mathbf{Z}}_d \, \mathrm{d}z. \tag{17a}$$

Here, ρ_L is the mass density of a particular layer.

The diagonal elements of the matrix given by the above equation, corresponding to any node i, can be expressed by

$$\bar{\underline{\mathbf{m}}}_{ii} = b \sum_{L=1}^{NL} \int_{h_{L-1}}^{h_L} [1 1 z^2 z^4 z^6] \rho_L \, \mathrm{d}z. \tag{18}$$

2.5. *Work potential*

Similarly, the external work done is modified using eqn (8) as

$$W_e = \int_l \mathbf{d}^t \bar{\mathbf{P}} \, \mathrm{d}x \tag{19}$$

where

$$\bar{\mathbf{P}} = \underline{\mathbf{Z}}_d^t \mathbf{P} \tag{19a}$$

or

$$\bar{\mathbf{P}} = [p_{x0} p_{z0} m_{x0} P_{x0}^* m_{x0}^*]^t. \tag{19b}$$

Now, the total energy reappears with eqns (13), (17) and (19) as

$$L = \tfrac{1}{2} \int_l \dot{\mathbf{d}}^t \bar{\underline{\mathbf{m}}} \dot{\mathbf{d}} \, \mathrm{d}x - \left[\frac{\mathrm{b}}{2} \int_l \bar{\epsilon} \bar{\sigma} \, \mathrm{d}x - \int_l \mathbf{d}^t \bar{\mathbf{P}} \, \mathrm{d}x \right]. \tag{20}$$

3. FINITE ELEMENT MODELLING

In isoparametric formulations, the displacements within an element can be expressed in terms of its nodal displacements as

$$\mathbf{d} = \underline{\mathbf{N}} \mathbf{a}_e, \tag{21}$$

where $\mathbf{a}_e$ is a vector containing nodal displacement vectors of an element, and is given by

$$\mathbf{a}_e = [\mathbf{d}_1^t \mathbf{d}_2^t \mathbf{d}_3^t \ldots \mathbf{d}_n^t]^t \tag{21a}$$

and $\underline{\mathbf{N}}$ is the shape function matrix.

Similarly, the strain within an element can be written as

$$\bar{\epsilon} = \underline{\mathbf{B}} \mathbf{a}_e \tag{22}$$

where $\underline{\mathbf{B}}$ is the strain displacement matrix.

The non-zero elements of $\underline{\mathbf{B}}$ corresponding to a particular node i can be given as

$$B_{11} = B_{24} = B_{33} = B_{45} = B_{52} = N_{i,x};$$

$$B_{53} = N_i; \quad B_{65} = 3N_i; \quad B_{74} = 2N_i. \tag{23}$$

With eqns (21) and (22), total energy can be written as

$$L = \tfrac{1}{2} \dot{\mathbf{a}}_e^t \int_l \underline{\mathbf{N}}^t \bar{\underline{\mathbf{m}}} \underline{\mathbf{N}} \, \mathrm{d}x \dot{\mathbf{a}}_e - \left[\frac{\mathrm{b}}{2} \mathbf{a}_e^t \int_l \underline{\mathbf{B}}^t \bar{\sigma} \, \mathrm{d}x - \mathbf{a}_e^t \int_l \underline{\mathbf{N}}^t \bar{\mathbf{P}} \, \mathrm{d}x \right]$$

$$= \tfrac{1}{2} \dot{\mathbf{a}}_e^t \int_l \underline{\mathbf{N}}^t \bar{\underline{\mathbf{m}}} \underline{\mathbf{N}} \, \mathrm{d}x \dot{\mathbf{a}}_e - \left[\frac{\mathrm{b}}{2} \mathbf{a}_e^t \int_l \underline{\mathbf{B}}^t \bar{\underline{\mathbf{D}}} \underline{\mathbf{B}} \, \mathrm{d}x \mathbf{a}_e \right.$$

$$\left. - \mathbf{a}_e^t \int_l \underline{\mathbf{N}}^t \bar{\mathbf{P}} \, \mathrm{d}x \right]. \tag{24}$$

Applying Hamilton's principle on L, we get the equation of motion as

$$\underline{\mathbf{M}} \ddot{\mathbf{d}} + \underline{\mathbf{K}} \mathbf{d} = \mathbf{f}(t), \tag{25}$$

where

$$\underline{\mathbf{M}} = \int_l \underline{\mathbf{N}}^t \bar{\underline{\mathbf{m}}} \underline{\mathbf{N}} \, \mathrm{d}x \tag{25a}$$

$$\underline{\mathbf{K}} = b \int_l \underline{\mathbf{B}}^t \bar{\underline{\mathbf{D}}} \underline{\mathbf{B}} \, \mathrm{d}x \tag{25b}$$

$$\mathbf{f}(t) = \int_l \underline{\mathbf{N}}^t \bar{\mathbf{P}} \, \mathrm{d}x. \tag{25c}$$

3.1. *Mass matrix evaluation*

The consistent mass matrix is evaluated as

$$\underline{\mathbf{M}}_e = \sum_{g=1}^{NG} W_g \underline{\mathbf{N}}^t \bar{\underline{\mathbf{m}}} \underline{\mathbf{N}} |J| \tag{26}$$

where NG is the (total) number of gauss points (four in this case), W_g is the weighing coefficient and $|J|$ is the determinant of Jacobian.

If the total mass of an element can be given by

$$m_t = \int_v \rho \, \mathrm{d}v, \tag{27}$$

and the sum of the diagonal coefficients of the consistent mass matrix given by eqn (26), corresponding to any translational degree of freedom alone, is termed as Σm_{ii}, then the specially lumped mass matrix can be obtained [28] by scaling all the diagonal elements of the consistent mass matrix as

$$\bar{\bar{m}}_{ii} = \bar{m}_{ii} * m_t / \Sigma m_{ii} \tag{28}$$

and making all the off-diagonal terms of the consistent mass matrix zero.

3.2. *Stiffness matrix evaluation*

The stiffness matrix can be evaluated as

$$\underline{\mathbf{K}}_e = b \sum_{g=1}^{NG} W_g \underline{\mathbf{B}}^t \underline{\bar{\mathbf{D}}} \underline{\mathbf{B}} |J| \tag{29}$$

where total number of Gauss points are four for bending and three for shear terms evaluation.

3.3. *Load vector evaluation*

The consistent load vector, due to a uniformly distributed transverse load p_0, is given by

$$\mathbf{f}(t) = \sum_{g=1}^{NG} W_g \underline{\mathbf{N}}^t \bar{\mathbf{p}} |J| \tag{30}$$

where

$$\bar{\mathbf{p}} = [0 \;\; p_0 \;\; 0 \;\; 0 \;\; 0] \quad \text{and} \quad NG = 3. \tag{30a}$$

3.4. *Solution of equation of motion*

The governing equation of motion is solved using the central difference predictor technique [29] to obtain the response history at different time steps.

4. NUMERICAL EXAMPLES

In order to test the proposed higher-order models, beams with both sandwich and composite constructions, subjected to transverse dynamic loadings, are considered in this study. Isoparametric cubic elements are employed to discretize the beams. All the experiments are carried out on an IBM compatible 486 computer on DOS in double precision.

A simply supported beam of 30 in long and unit width is discretized using four cubic elements. The length to depth ratio of the beam is five and is subjected to a transverse dynamic load of 300 lb in^{-1}. The boundary conditions used for the simply supported case are as follows:

$$u_0 = w_0 = u_0^* = 0 \quad \text{at} \quad x = 0 \quad \text{and} \quad x = L.$$

The quantities like $w(l/2, 0)$, $u(0, z)$, $Q(0)$ and $M(l/2)$ are expressed with respect to time, in their own dimensions, with $u(0, z)$ being scaled by -1, while the following are non-dimensionalized as

$$\bar{u}(0, z) = u(0, z) E_z / (-p_0)$$

$$\bar{\sigma}_x(l/2, z) = \bar{\sigma}_x(l/2, z) b / (-p_0)$$

and expressed as the variation along the depth of cross section.

Experiment 1

First, a symmetric sandwich beam with 0/90/core/90/0 configuration is studied.

Data 1

Face sheets [30]: (top/bot)

$E_x = 0.1742 \times 10^8$ psi
$E_z = 0.1147 \times 10^7$ psi
$G_{xz} = 0.7983 \times 10^6$ psi
$\rho = 0.1433 \times 10^{-3}$ lb s^2 in^{-4}
$t_f = 0.3$ in.

Core [31]:

$G_{xz} = 0.2042 \times 10^5$ psi
$\rho = 0.3098 \times 10^{-5}$ lb s^2 in^{-4}
$t_c = 4.8$ in
$t_c/t_f = 8.$

The cross section is split into six layers; top and bottom faces into two layers each and the core into two parts.

Figure 1 shows the transverse displacement response history. While HOBT5 and HOBT4b give identical values, which are almost three times higher than that of Timoshenko, the period of the response due to first-order theory is almost half its higher-order counterparts. HOBT4a predicts results which are stiffer than Timoshenko both in amplitude and period. A similar pattern is observed in the inplane response history in Fig. 2. The shear force at the left support of the simply supported beam is presented in Fig. 3. While higher order models predict higher amplitude and period than the first order model, HOBT4a is stiffer than Timoshenko. The midspan peak bending moment due to HOBT5 and HOBT4b is marginally less than Timoshenko while the higher-order period is nearly twice that of Timoshenko. HOBT4a is stiffer than Timoshenko as shown in Fig. 4.

The variation of inplane displacement along the depth is depicted in Fig. 5. While the first-order theory and HOBT4a predict the linear variation, HOBT5 and HOBT4b bring out the warping of the cross section clearly. The inplane stress variation also illustrates the difference in the predictions of Timoshenko, HOBT4a and the rest, as shown in Fig. 6.

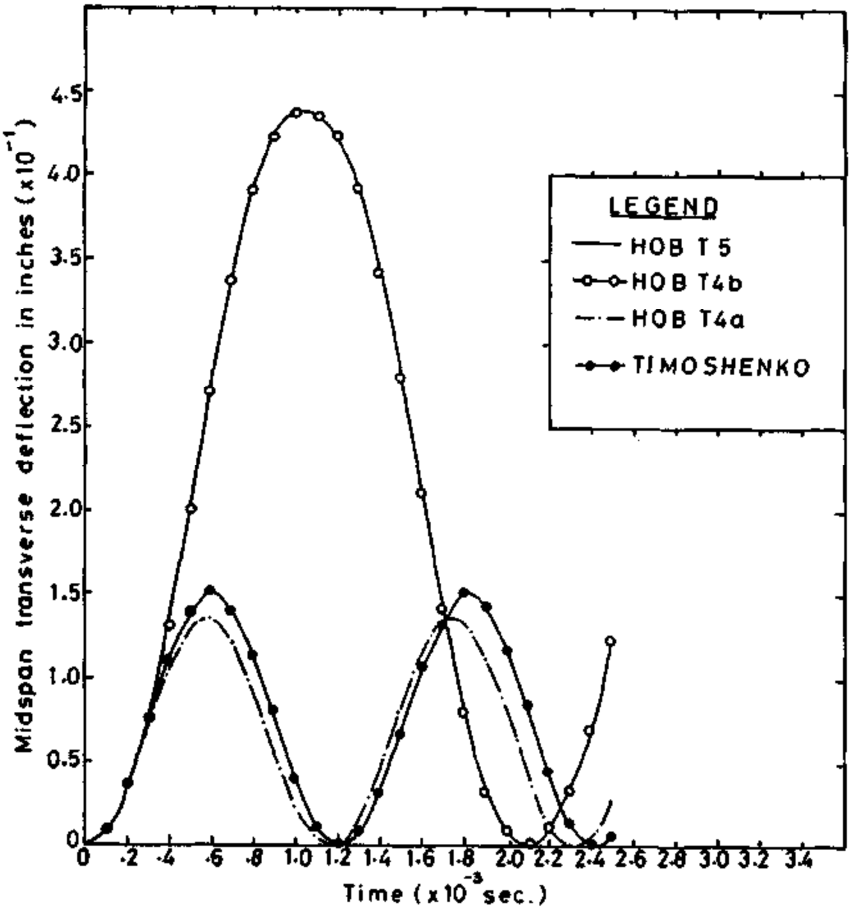

Fig. 1. Variation of midspan deflection with respect to time of symmetric sandwich beam.

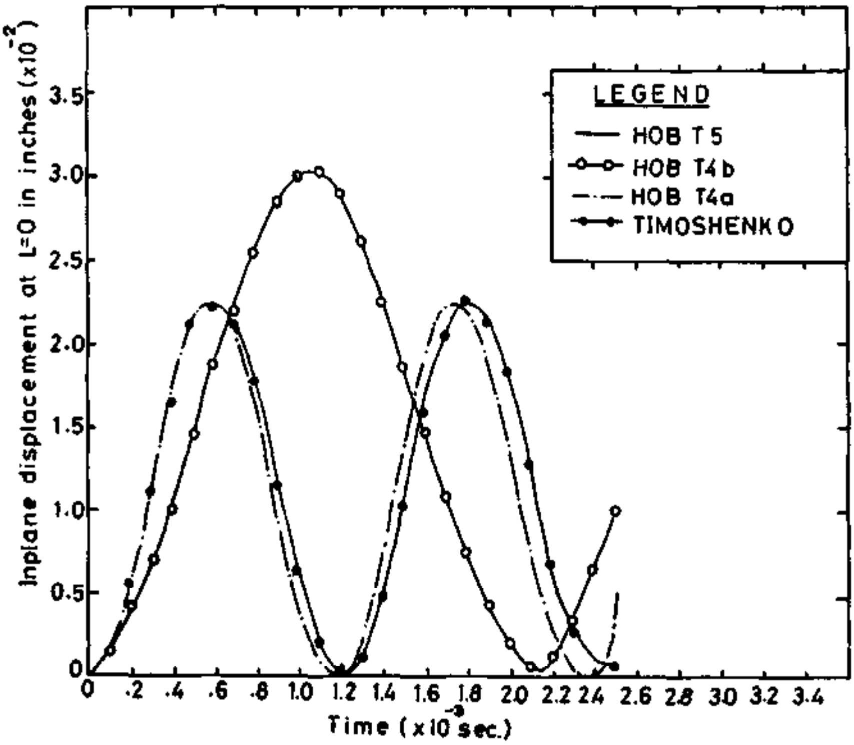

Fig. 2. Variation of inplane displacement with time of symmetric sandwich beam.

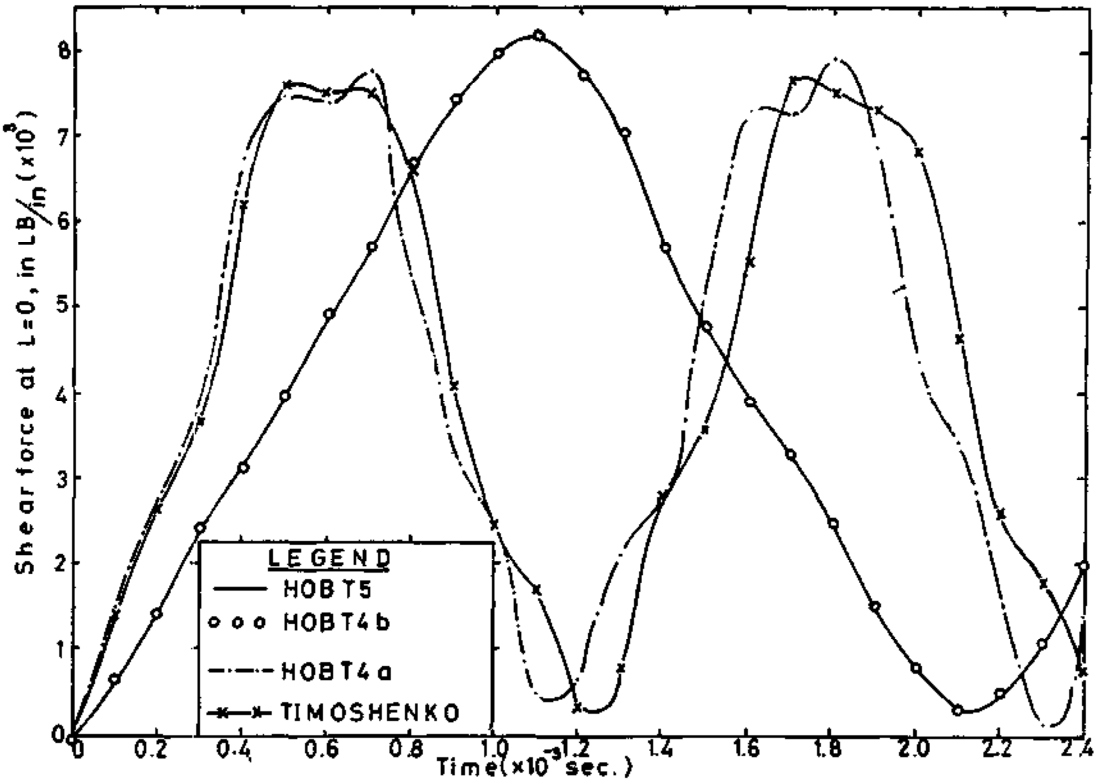

Fig. 3. Shear force variation with time of symmetric sandwich beam.

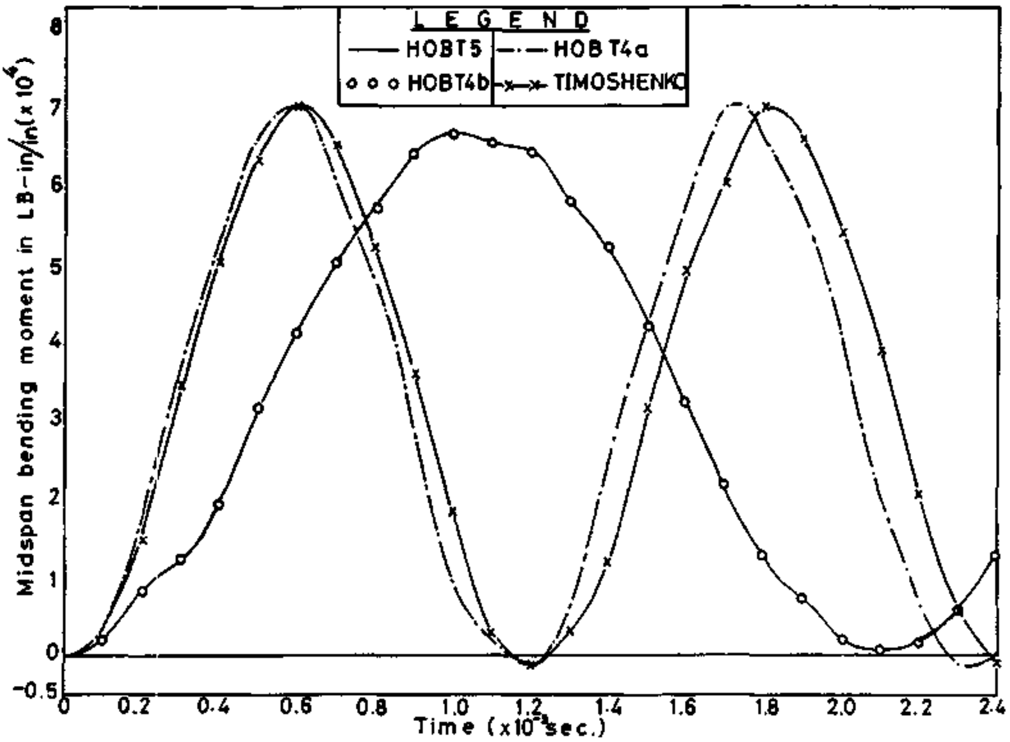

Fig. 4. Bending moment variation with time of symmetric sandwich beam.

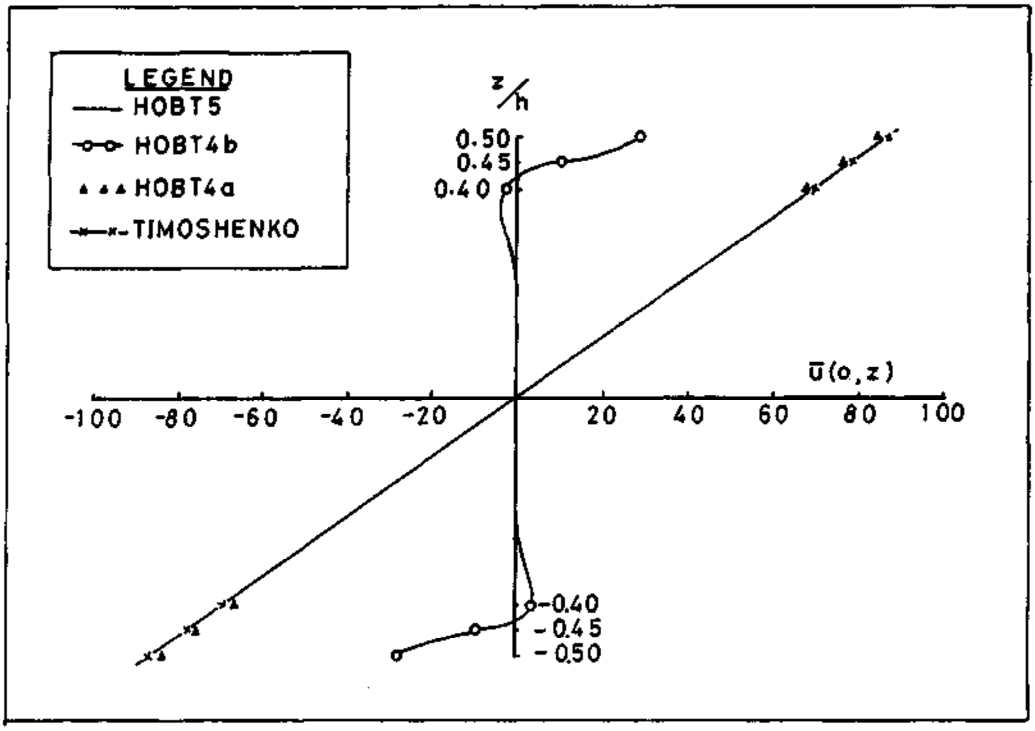

Fig. 5. Inplane displacement distribution of symmetric sandwich beam at $T = 0.18 \times 10^{-2}$ s.

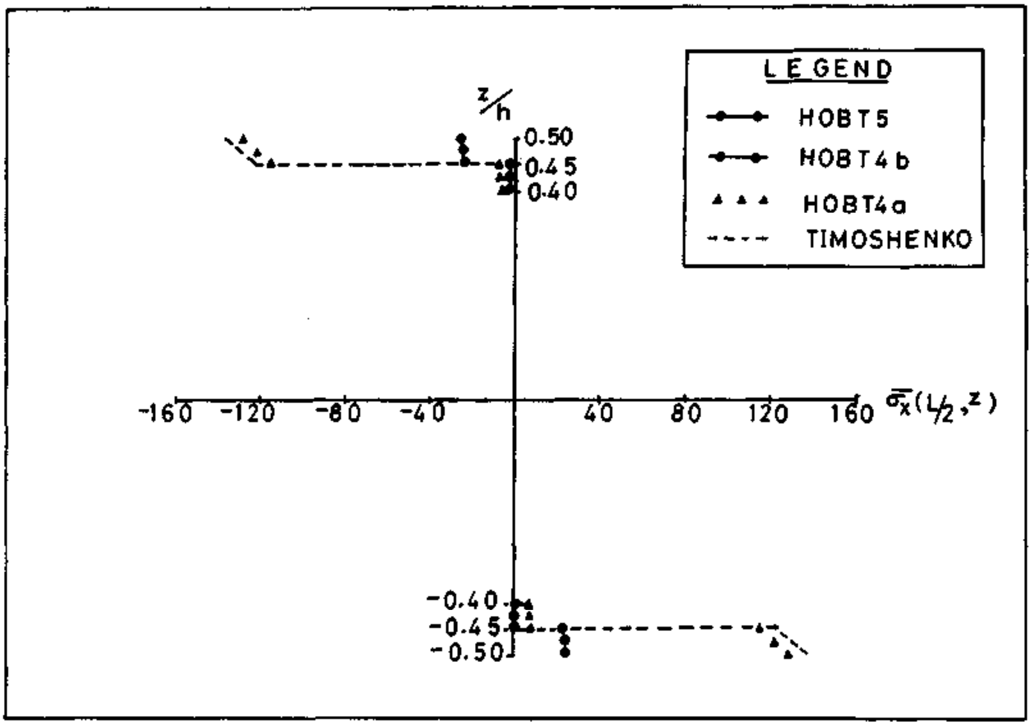

Fig. 6. Inplane stress distribution of symmetric sandwich beam at $T = 0.18 \times 10^{-2}$ s.

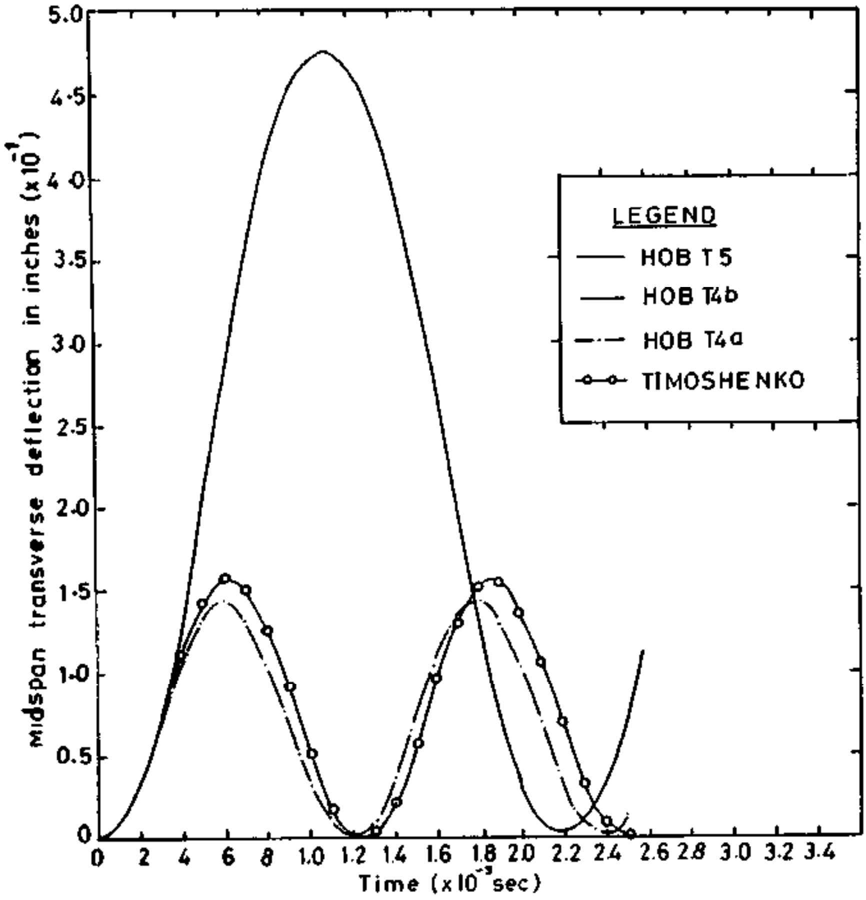

Fig. 7. Midspan transverse response history of unsymmetric sandwich beam.

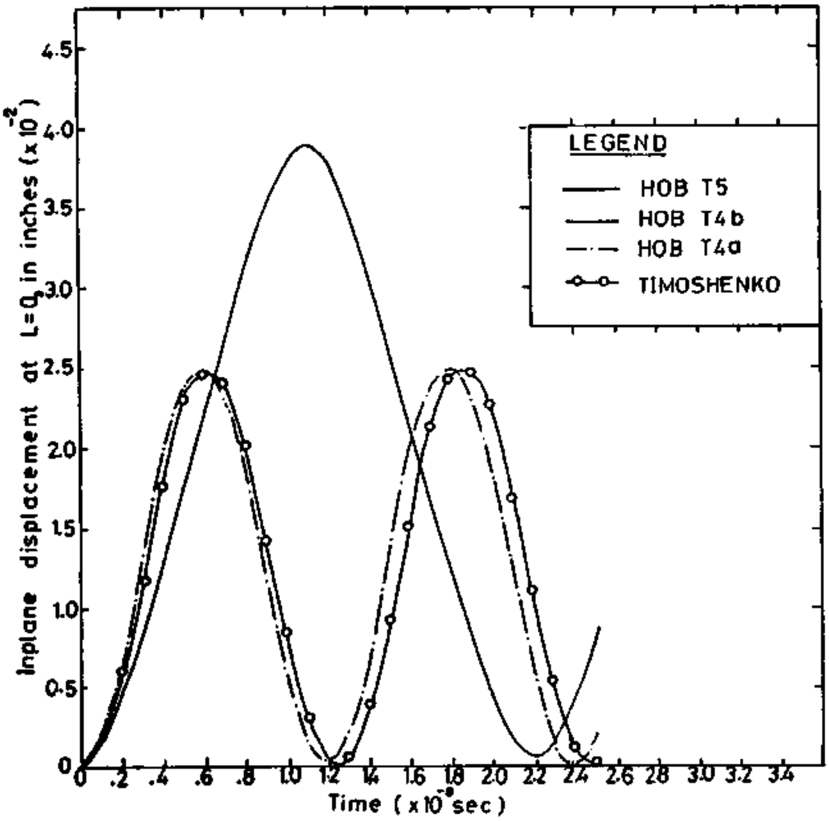

Fig. 8. Inplane displacement history with time of unsymmetric sandwich beam.

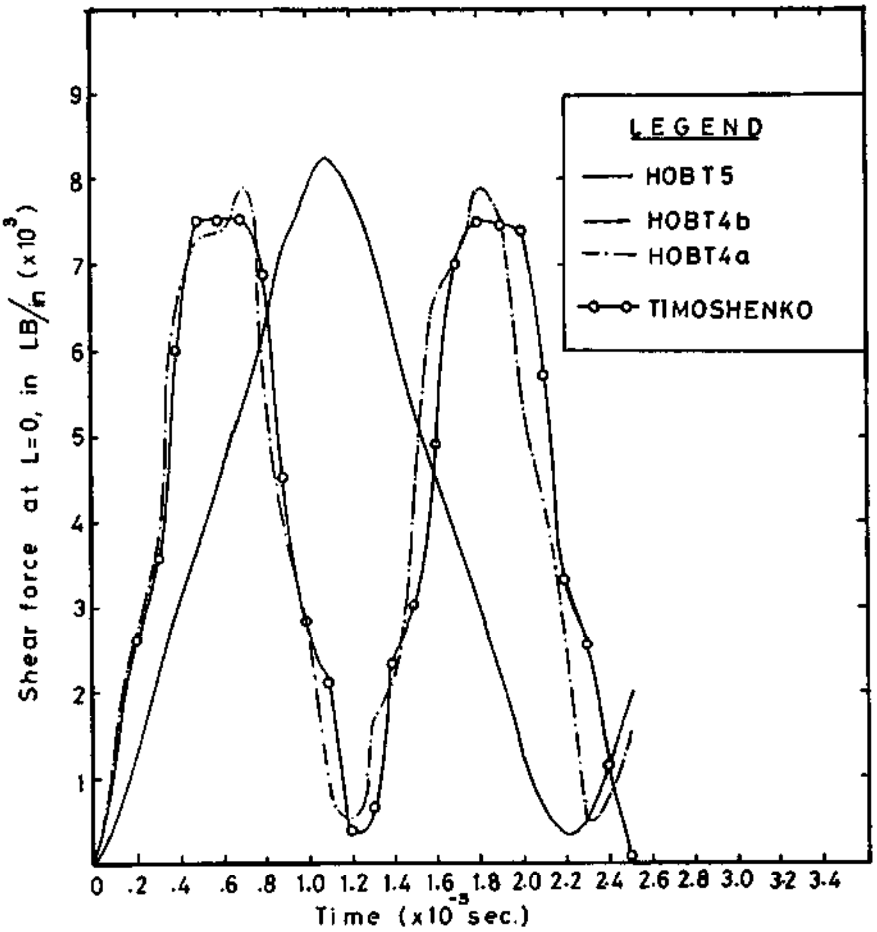

Fig. 9. Shear force variation with time of unsymmetric sandwich beam.

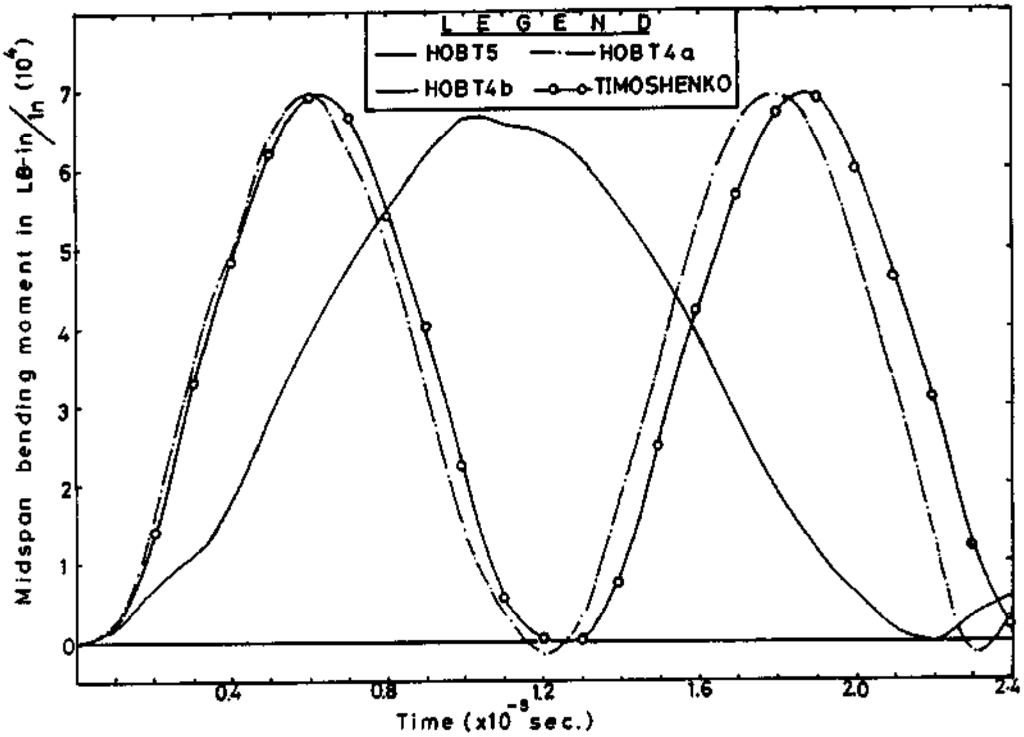

Fig. 10. Bending moment history with time of unsymmetric sandwich beam.

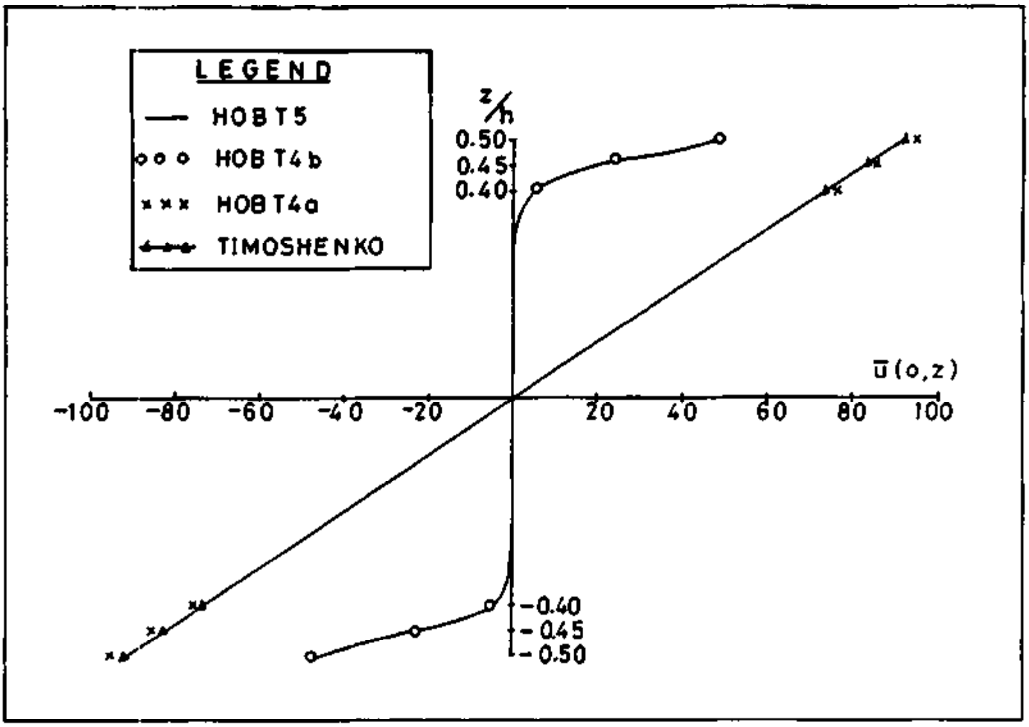

Fig. 11. Distribution of inplane displacement of unsymmetric sandwich beam at $T = 0.18 \times 10^{-2}$ s.

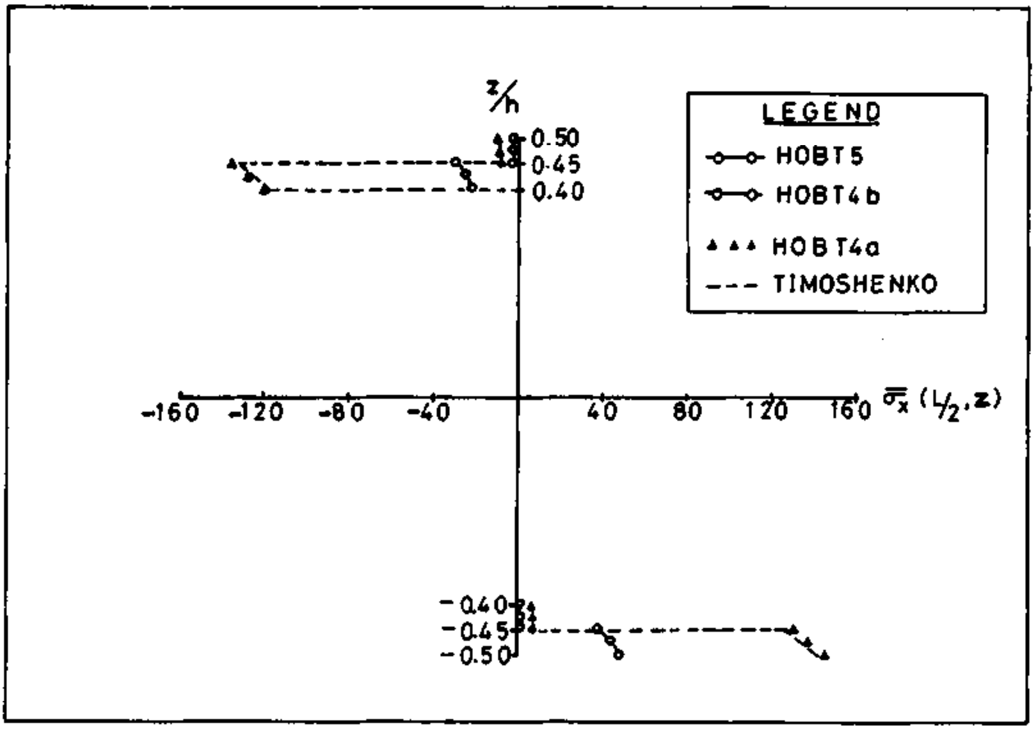

Fig. 12. Distribution of inplane stress of unsymmetric sandwich beam at $T = 0.18 \times 10^{-2}$ s.

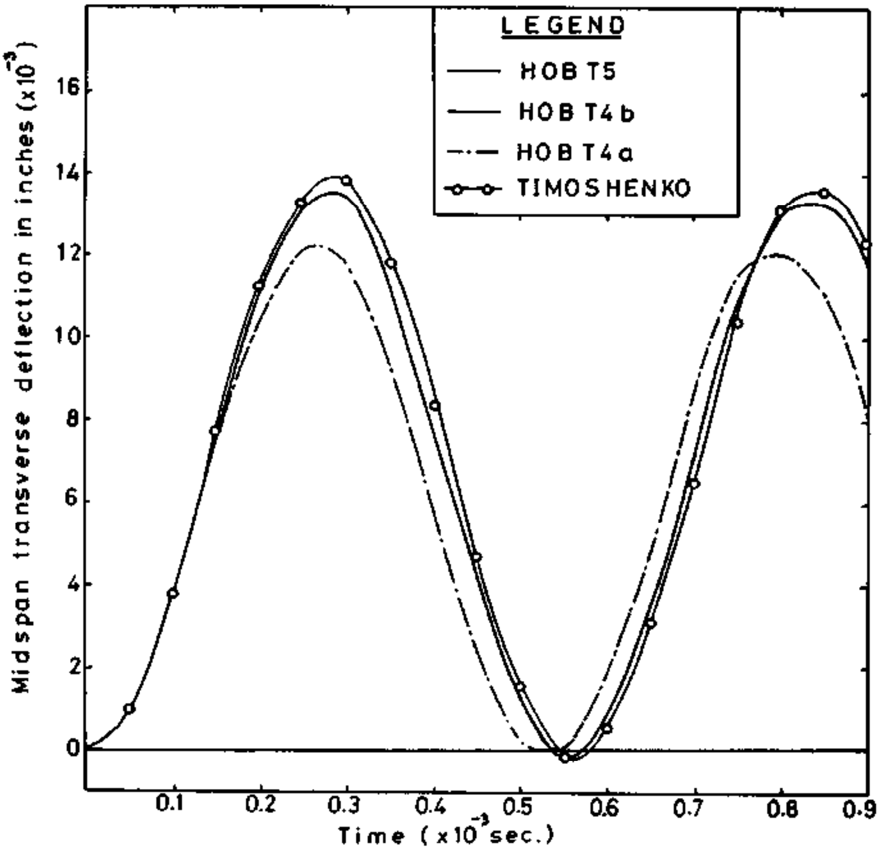

Fig. 13. Transverse deflection history of symmetric composite beam.

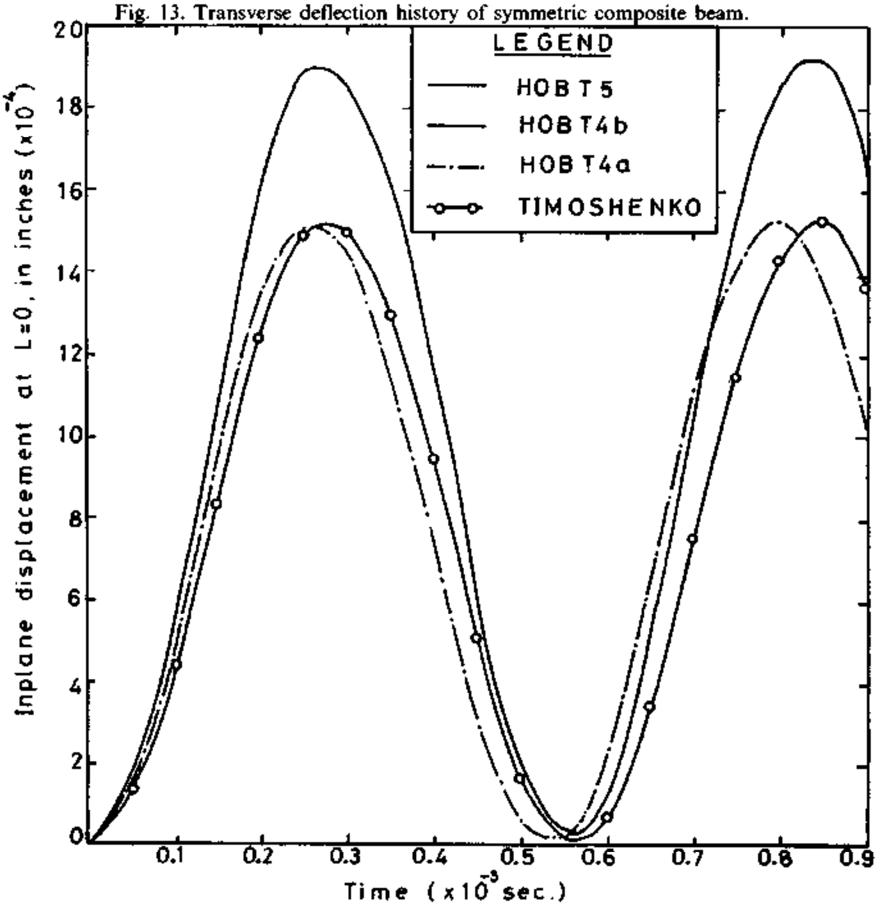

Fig. 14. Inplane displacement history of symmetric composite beam.

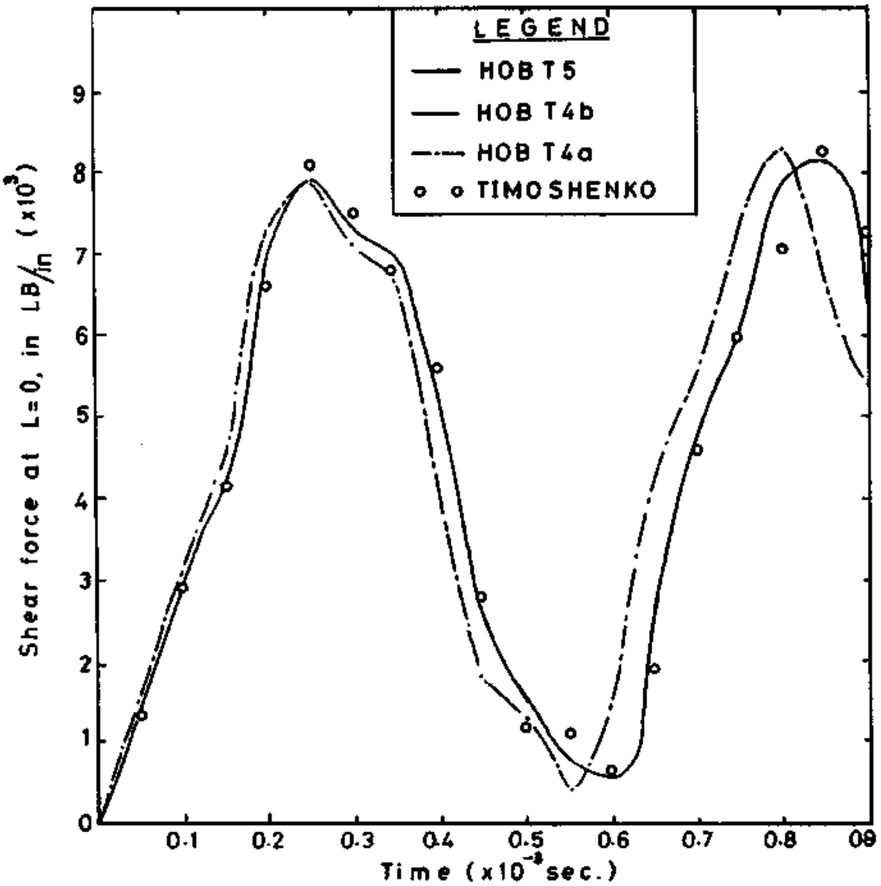

Fig. 15. Shear force history of symmetric composite beam.

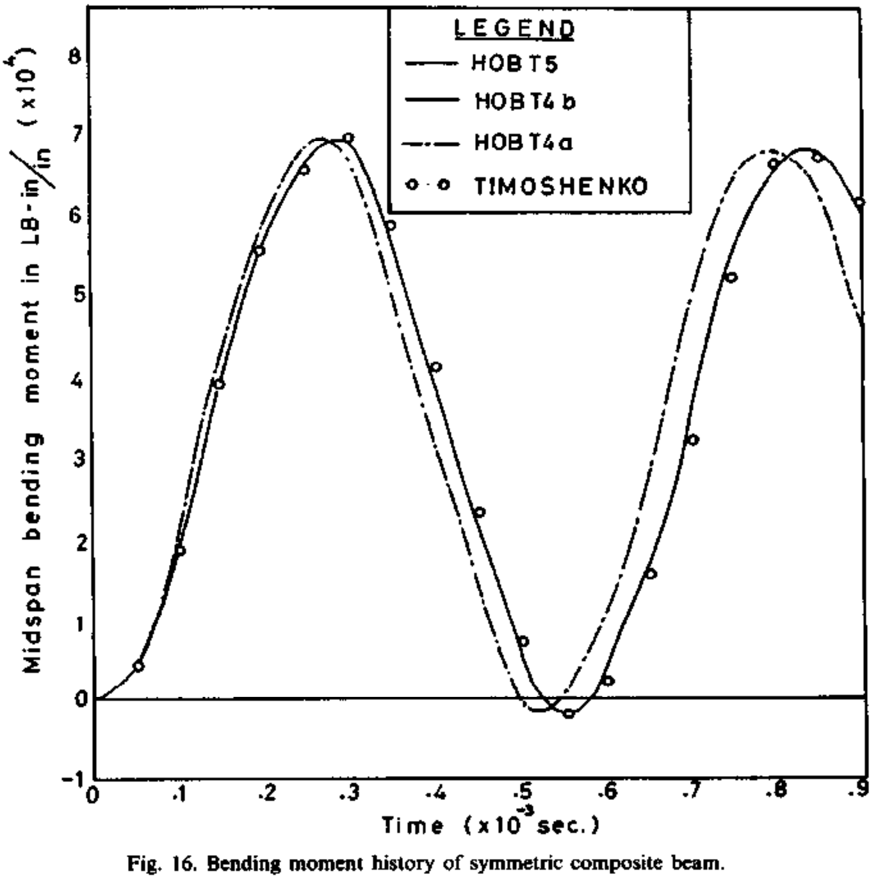

Fig. 16. Bending moment history of symmetric composite beam.

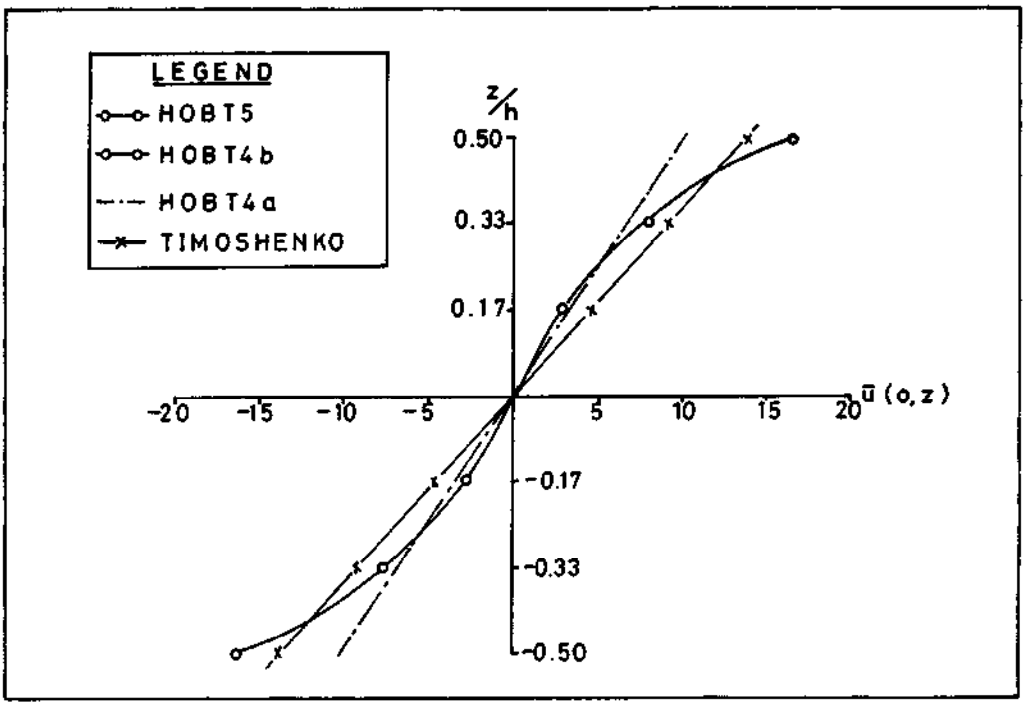

Fig. 17. Distribution of inplane displacement of symmetric composite beam at $T = 0.9 \times 10^{-3}$ s.

Experiment 2

The same data used in Experiment 1 is considered here, but with an unsymmetric configuration of 0/90/core/0/90. The transverse displacement response is shown in Fig. 7. The magnitude and period of the response of HOBT5 and HOBT4b are 3× and 2× that of Timoshenko; HOBT4a is stiffer than first-order theory. The variation of inplane displacement, shear force and bending moment are given in Figs 8–10. The magnitude of inplane displacement and the period of shear and bending moment of higher order models are nearly double those computed by first-order model and HOBT4a.

Timoshenko and HOBT4a predict only a linear

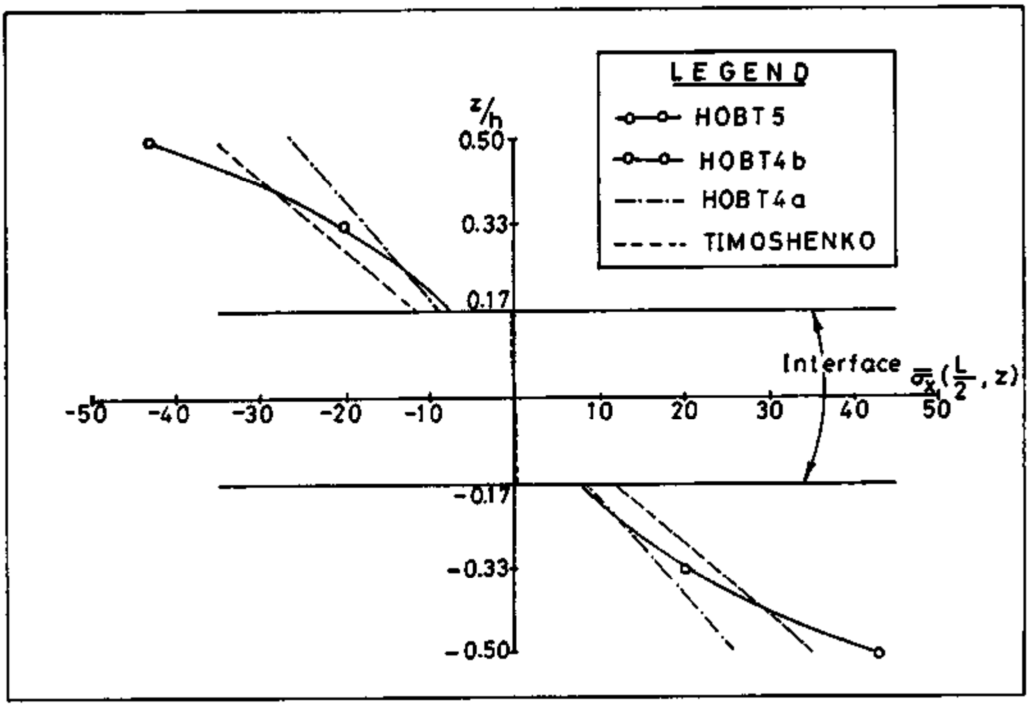

Fig. 18. Inplane stress distribution of symmetric composite beam at $T = 0.9 \times 10^{-3}$ s.

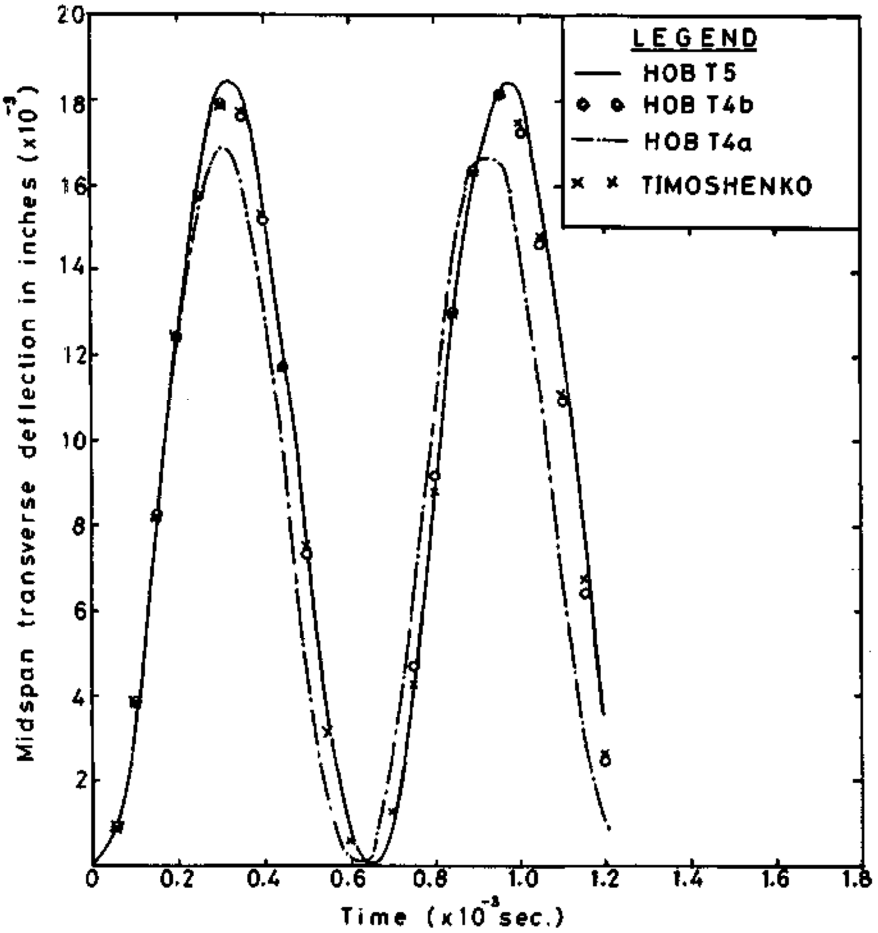

Fig. 19. Transverse deflection history of unsymmetric composite beam.

inplane displacement while higher-order models show the nonlinear variation in Fig. 11. Variation of $\bar{\sigma}_x$ is plotted in Fig. 12. The higher-order models compute stresses that are lesser than those predicted by the other two, mainly due to the fact that inplane displacement by HOBT5 and HOBT4b at $t = 0.18 \times 10^{-2}$ s, is much less than those predicted by HOBT4a and first-order theory, as can be seen in Fig. 8.

Experiment 3

Next, a symmetric composite construction of 0/0/90/90/0/0 combination with the following properties is considered [32].

Data 2

$$E_x = 0.7620 \times 10^8 \text{ psi}$$
$$E_z = 0.3048 \times 10^7 \text{ psi}$$
$$G_{xz} = 0.1524 \times 10^7 \text{ psi}$$
$$\rho = 0.7257 \times 10^{-4} \text{ lb s}^2 \text{ in}^{-4}$$
$$t_{\text{layer}} = 1 \text{ in.}$$

The transverse displacement by Timoshenko is the highest in this case followed by HOBT5 and HOBT4b, as shown in Fig. 13; HOBT4a is again the stiffest. In the case of inplane displacements, HOBT5 and HOBT4b are the highest, followed by Timoshenko and HOBT4a as in Fig. 14. This is due to the presence of various higher-order terms in the displacement function of u. From Figs 15 and 16, it can be observed that all higher-order models are marginally lesser than Timoshenko in their predictions of shear force and bending moment.

The cross sectional warping clearly brought out by higher-order models is presented in Fig. 17. Similarly, the nonlinear variation of inplane stress by higher-order models is shown in Fig. 18.

Experiment 4

The unsymmetric configuration of 0/90/0/90/0/90 with the properties given by *Data* 2, is considered in this case for time history response evaluation of the beam. From Fig. 19, it can be observed that HOBT5 predicts a transverse displacement response, which is higher than those of HOBT4b and Timoshenko (which are quite close in this case), while HOBT4a computes the stiffest results of all. The inplane displacement history, as in Fig. 20, presents a different picture. HOBT5 computes the highest, followed by HOBT4b, HOBT4a and Timoshenko in that order. In the case of shear force, HOBT4b and

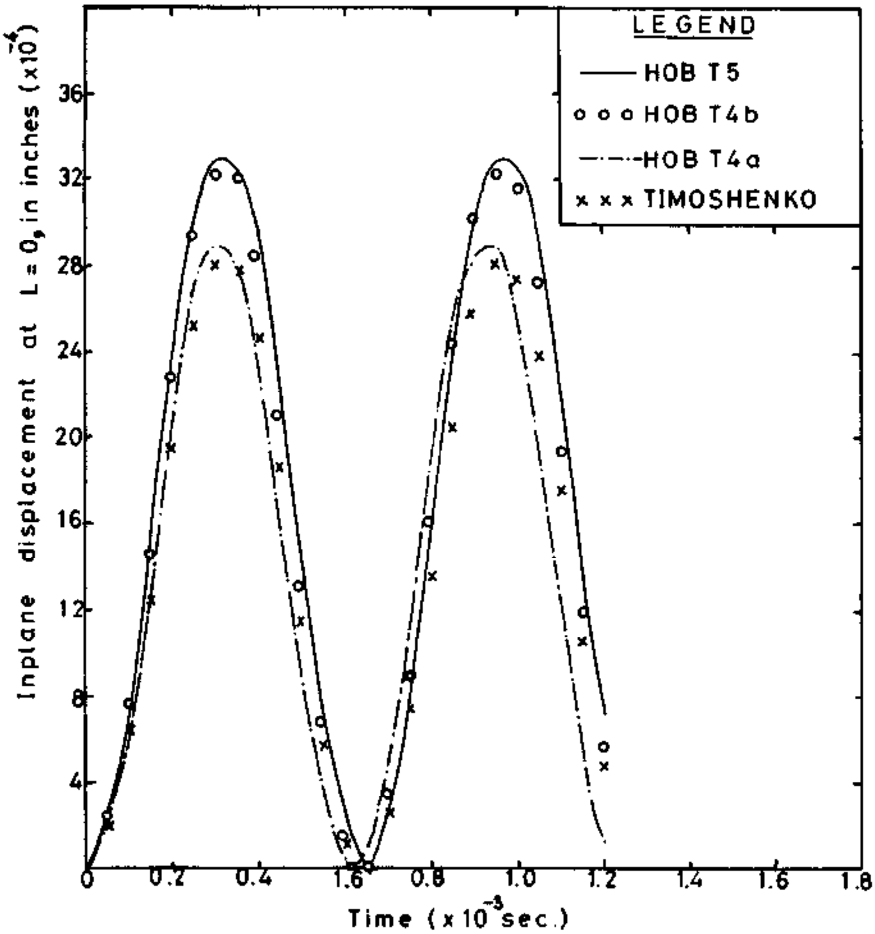

Fig. 20. Inplane displacement history of unsymmetric composite beam.

Timoshenko are much closer to HOBT5 as in Fig. 21, while HOBT4a predicts slightly higher peak values with lesser period. The bending moment by Timoshenko, HOBT4a and HOBT4b closely follow the HOBT5 moment with HOBT4a again having lesser period compared to others, as plotted in Fig. 22.

The variation of $\bar{u}$ and $\bar{\sigma}_x$ are plotted in Figs 23 and 24, which clearly brings out the nonlinear inplane displacement and inplane stress variation due to higher-order models compared to the linear predictions by HOBT4a and Timoshenko.

5. CONCLUSIONS

In our study, three refined higher-order, shear correction coefficient free models have been analysed by employing them for transient dynamic analysis of sandwich and composite beams. From the experiments conducted, it becomes apparent that the very stiff performance of HOBT4a renders it almost unusable.

The higher order models (HOBT5 and HOBT4b) predict responses which are quite high compared to Timoshenko, for both symmetric and unsymmetric sandwich constructions. The warping of cross section and nonlinear inplane distributions is vividly brought out by these higher-order models. Another interesting feature in the case of sandwiches, is that both HOBT5 and HOBT4b predict identical results.

In the case of composites, the order of difference between the higher-order and the first-order models is less compared to sandwiches. Timoshenko predicts slightly higher values in comparison with these higher-order models for symmetric composites, except for inplane displacements. For the unsymmetric composites, HOBT5 yields higher inplane and transverse displacements than those given by the rest. For both the symmetric and unsymmetric cases, the warping of the cross section and the nonlinear inplane stress distribution is brought out well by higher order models.

For sandwiches and symmetric composites, as both HOBT5 and HOBT4b are identically effective, and for unsymmetric composites as HOBT5 is better than HOBT4b, HOBT5 can well be employed as an efficient higher-order refined model for transient dynamic analysis of sandwich and composite constructions of beams.

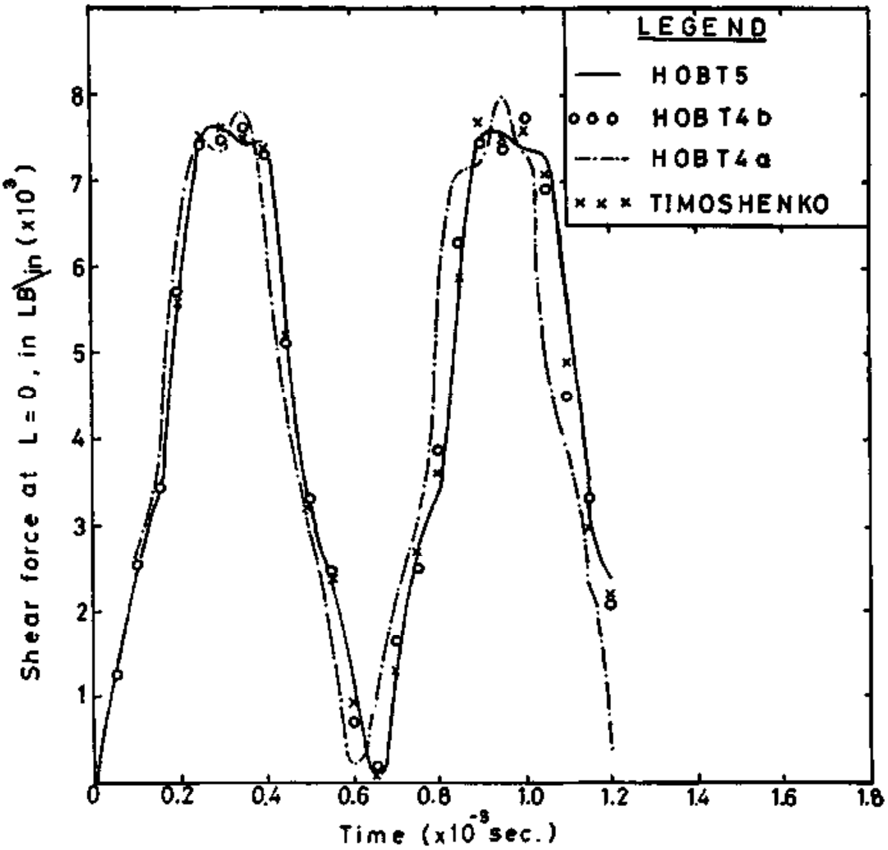

Fig. 21. Variation of shear force with time of unsymmetric composite beam.

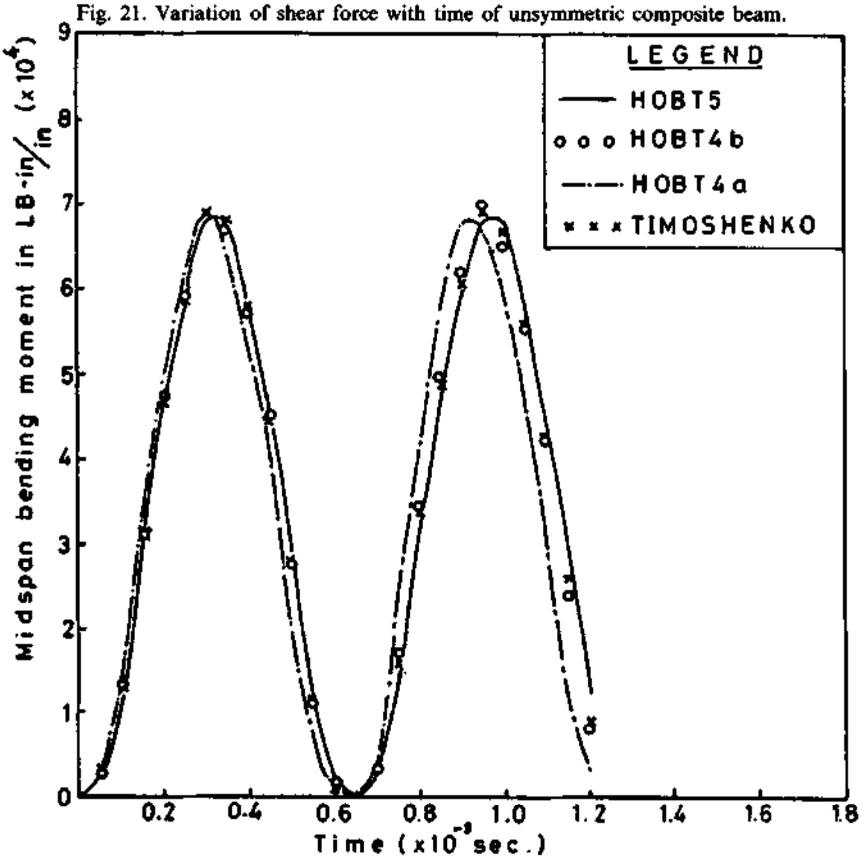

Fig. 22. Variation of bending moment with time of unsymmetric composite beam.

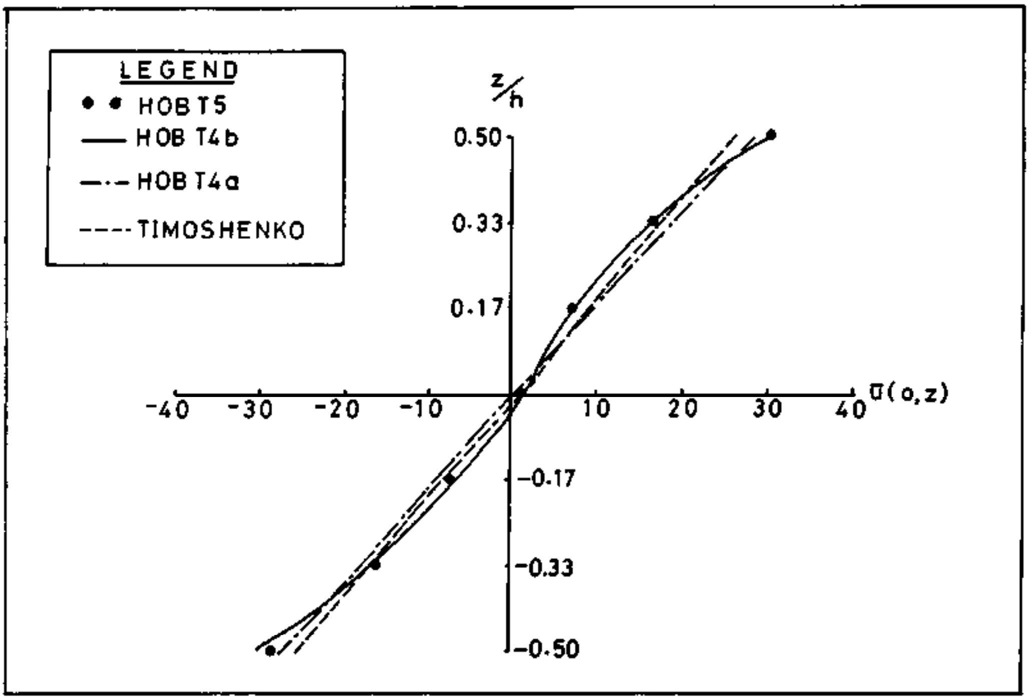

Fig. 23. Inplane displacement distribution of unsymmetric composite beam at $T = 0.9 \times 10^{-3}$ s.

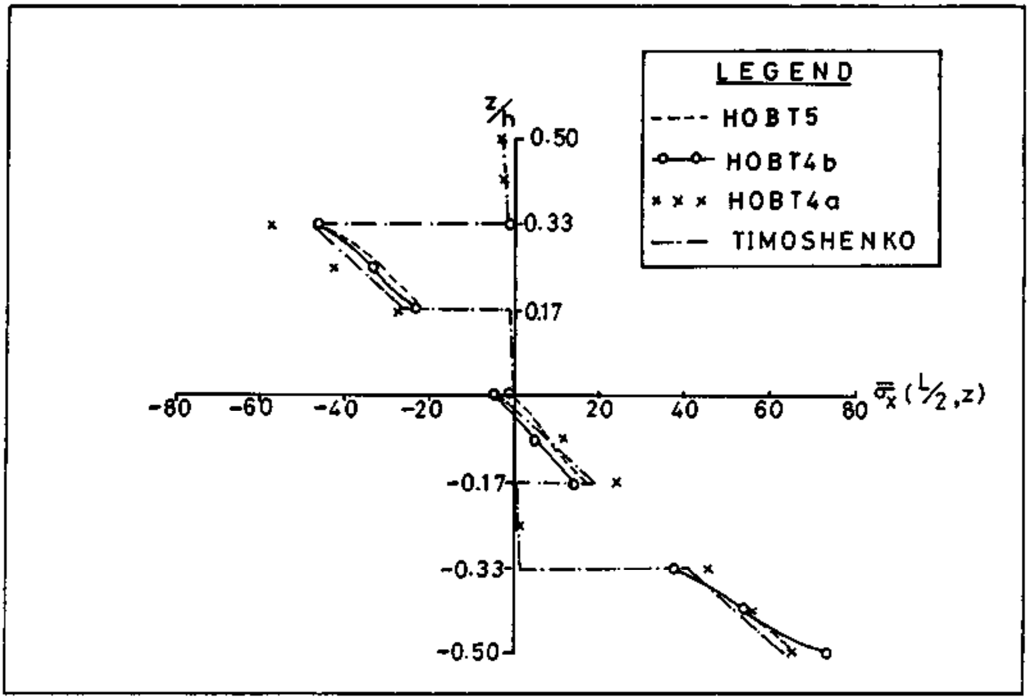

Fig. 24. Distribution of inplane stress of unsymmetric composite beam at $T = 0.9 \times 10^{-3}$ s.

REFERENCES

1. Wu, R. W. H. and Witmer, E. A., Finite element analysis of large elastic–plastic transient deformations of simple structures. *AIAA Journal*, 1971, **9**, 1719–1724.
2. Toridis, T. G. and Khozeimeh, K., Inelastic response of frames to dynamic loads. *Journal of the Structural Division of the ASCE*, 1971, **97**, 847–863.
3. Toridis, T. G. and Khozeimeh, K., Computer analysis of rigid frames. *Computers and Structures*, 1971, **1**, 193–221.
4. Mondkar, D. P. and Powell, G. H., Finite element analysis of nonlinear static and dynamic response. *International Journal of Numerical Methods in Engineering*, 1977, **11**, 499–520.
5. Hilmy, S. I. and Abel, J. F., Material and geometric

nonlinear dynamic analysis of steel frames using computer graphics. *Computers and Structures*, 1985, **21**, 825–840.

6. Kam, T. Y. and Lin, S. C., Nonlinear dynamic analysis of inelastic steel plane frames. *Computers and Structures*, 1988, **28**, 535–542.
7. Timoshenko, S. P., On the correction for shear in differential equations for transverse vibrations of prismatic bars. *Philosophical Magazine*, Series 6, 1921, **41**, 744–746.
8. McCallay, R., Rotary inertia correction for mass matrices. Report no. DIG/SA, GEC, New York, 63–73, 1963.
9. Archer, J., Consistent matrix formulations for structural analysis using finite element techniques. *AIAA Journal*, 1965, **3**, 1910–1928.
10. Kapur, K., Vibrations of a Timoshenko beam using finite element approach. *Journal of the Acoustic Society of America*, 1966, **40**, 1058–1063.
11. Carniege, W., Thomas, J. and Dokumaci, E., An improved method of matrix displacement analysis in vibration problems. *Aeronautical Quarterly*, 1969, **20**, 321–332.
12. Davis, R., Henshell, R. D. and Warburton, G. B., A Timoshenko beam element. *Journal of Sound and Vibration*, 1972, **22**, 475–487.
13. Nickel, R. and Secor, G., Convergence of consistently derived Timoshenko beam finite elements. *International Journal of Numerical Methods in Engineering*, 1972, **5**, 243–253.
14. Thomas, D. L., Wilson, J. M. and Wilson, R. R., Timoshenko beam finite elements. *Journal of Sound and Vibration*, 1973, **31**, 315–330.
15. Thomas, J. and Abbas, B. A. H., Finite element model for dynamic analysis of Timoshenko beams. *Journal of Sound and Vibration*, 1975, **41**, 291–299.
16. Kant, T. and Marur, S. R., A comparative study of C^0 and C^1 elements for linear and nonlinear transient dynamics of building frames. *Computers and Structures*, 1991, **40**, 659–678.
17. Stephen, N. G. and Levinson, M., A second-order beam theory. *Journal of Sound and Vibration*, 1979, **67**, 293–305.
18. Heyliger, P. R. and Reddy, J. N., A higher-order beam finite element for bending and vibration problems. *Journal of Sound and Vibration*, 1988, **126**, 309–326.
19. Soldatos, K. P. and Elishakoff, I., A transverse shear and normal deformable orthotropic beam theory. *Journal of Sound and Vibration*, 1992, **154**, 528–533.
20. Levinson, M., A new rectangular beam theory. *Journal of Sound and Vibration*, 1981, **74**, 81–87.
21. Rychter, Z., On the accuracy of a beam theory. *Mechanical Research Communications*, 1987, **14**, 99–105.
22. Bickford, W. B., A consistent higher-order beam theory. *Developments in Theoretical and Applied Mechanics*, 1982, **11**, 137–142.
23. Reddy, J. N., *Energy and Variational Methods in Applied Mechanics*. Wiley, New York, 1984.
24. Kant, T. and Gupta, A., A finite element model for a higher-order shear deformable beam theory. *Journal of Sound and Vibration*, 1988, **125**, 193–202.
25. Kant, T. and Manjunath, B. S., Refined theories for composite and sandwich beams with C^0 finite elements. *Computers and Structures*, 1989, **33**, 755–764.
26. Kant, T. and Manjunath, B. S., Higher-order theories for symmetric and unsymmetric fibre reinforced composite beams with C^0 finite elements. *Finite Elements in Analysis and Design*, 1990, **6**, 303–320.
27. Lo, K. H., Christensen, R. M. and Wu, E. M., A higher-order theory of plate deformation I. Homogeneous plates. *ASME Journal of Applied Mechanics*, 1977, **44**, 663–668.
28. Hinton, E., Rock, T. and Zienkiewicz, O. C., A note on mass lumping and related processes in the finite element method. *International Journal of Earthquake Engineering Structural Dynamics*, 1976, **4**, 245–249.
29. Marur, S. R. and Kant, T., A modified form of the central difference predictor scheme for damped nonlinear systems. *Computers and Structures*, 1994, **50**, 615–618.
30. Chen, J. K. and Sun, C. T., Nonlinear transient responses of initially stressed composite plates. *Computers and Structures*, 1985, **21**, 513–520.
31. Allen, H. G., *Analysis and Design of Structural Sandwich Panels*. Pergamon, London, 1969.
32. Reddy, J. N., On the solutions to forced motions of rectangular composite plates. *ASME Journal of Applied Mechanics*, 1982, **49**, 403–408.

Journal of Reinforced Plastics and Composites
http://jrp.sagepub.com/

A Review of Refined Shear Deformation Theories for Isotropic and Anisotropic Laminated Beams

Y. M. Ghugal and R. P. Shimpi

Journal of Reinforced Plastics and Composites 2001 20: 255
DOI: 10.1177/073168401772678283

The online version of this article can be found at:
http://jrp.sagepub.com/content/20/3/255

Published by:
SAGE
http://www.sagepublications.com

Additional services and information for *Journal of Reinforced Plastics and Composites* can be found at:

Email Alerts: http://jrp.sagepub.com/cgi/alerts

Subscriptions: http://jrp.sagepub.com/subscriptions

Reprints: http://www.sagepub.com/journalsReprints.nav

Permissions: http://www.sagepub.com/journalsPermissions.nav

Citations: http://jrp.sagepub.com/content/20/3/255.refs.html

>> Version of Record - Feb 1, 2001

What is This?

Downloaded from jrp.sagepub.com at UNIVERSITE LAVAL on June 13, 2014

A Review of Refined Shear Deformation Theories for Isotropic and Anisotropic Laminated Beams

Y. M. GHUGAL AND R. P. SHIMPI[1]
Department of Aerospace Engineering
Indian Institute of Technology Bombay
Powai, Mumbai—400 076, India

ABSTRACT: A review of displacement and stress based refined theories for isotropic and anisotropic laminated beams is presented. Various equivalent single layer and layerwise theories for laminated beams are discussed together with their merits and demerits. Exact elasticity solutions for the beam problems are cited, wherever available. Various critical issues, related with beam theories, based on the literature reviewed are presented.

KEY WORDS: refined beam theory, shear deformation in beams, isotropic thick beams, laminated thick beams, equivalent single layer beam theories, layerwise beam theories, elasticity solutions of beams.

INTRODUCTION

RECENT ADVANCES IN the technology of composite materials has led to the use of laminated composite beams as structural components in various engineering applications due to the superior mechanical properties of these materials. However, shear deformation effects become more pronounced in such structures due to the low transverse shear moduli as compared to inplane tensile moduli, when subjected to transverse loads. This necessitates the accurate structural analysis of laminated beams.

In this paper a review of refined shear deformation theories for the structural analysis of shear deformable isotropic and laminated beams is presented. The methods of development of refined theories are presented. More emphasis is placed on the recent advances in the modeling and analysis of laminated beams.

---

[1] Author to whom correspondence should be addressed.

1530-7964/01/03 0255–18 $10.00/0 DOI: 10.1106/N95G-ERA1-A1CM-RD7E
© 2001 Technomic Publishing Co., Inc.

Downloaded from jrp.sagepub.com at UNIVERSITE LAVAL on June 13, 2014

DIFFERENT METHODS OF DEVELOPMENT OF REFINED THEORIES

Theories of beams involve basically the reduction of a three dimensional problem of elasticity theory to a one-dimensional problem. Since the thickness dimension is much smaller than the longitudinal dimension, it is possible to approximate the distribution of the displacement, strain and stress components in the thickness dimension. The various methods of development of refined theories based on the reduction of the three dimensional problems of mechanics of elastic bodies are discussed by Gol'denveizer [1], Kil'chevskiy [2], Donnell [3], Vlasov and Leont'ev [4], and Sayir and Mitropoulos [5]. These methods are as follows:

1. Methods based on hypotheses
    (a) The semi-inverse method
    (b) The method of trigonometric functions
    (c) The method of full range Fourier series expansion
2. The method of expansion
3. The asymptotic method
4. The method of successive approximation
5. The mixed method

In all the above methods, reduction is carried out with the use of thickness coordinate. In the method of expansion, generally, Taylor series, McaLaurin series, Legendre polynomials and Bernstein polynomials are used in the thickness coordinate. However, in the method of asymptotic expansion, the small parameter such as ratio of thickness to length, i.e., the slenderness parameter, is generally used.

In this paper, theories are broadly classified as

1. the single layer (smeared) theories
2. layerwise (discrete layer) continuum theories

Necessary details (like method of development etc.) are given while discussing the theories. These theories have their roots in theories of isotropic beams, and these will be discussed first for the sake of completeness.

THEORIES OF ISOTROPIC BEAMS

Theories based on method of hypotheses and methods of relaxed hypotheses are presented in the order of their improvements. Their kinematical hypotheses are also presented.

Elementary Theory of Beam (ETB)

It is well-known that elementary theory of bending of beam based on Eu-

Downloaded from jrp.sagepub.com at UNIVERSITE LAVAL on June 13, 2014

ler-Bernoulli hypothesis disregards the effects of the shear deformation. It is also known as classical beam theory. The theory is applicable to slender beams and should not be applied to thick or deep beams since it is based on the assumption that the plane sections which are perpendicular to the neutral layer before bending remain plane and perpendicular to the neutral layer after bending, implying that the transverse shear and transverse normal strains are zero. The displacement field of the theory is as

$$u(x, z) = u_0 - z\frac{dw}{dx}$$

$$w(x, z) = w(x)$$

where u_0 is the midplane displacement component and w is the transverse displacement.

When the elementary theory of beam (ETB) is used for the analysis laminated beams, deflections are underestimated and natural frequencies and buckling loads are overestimated. This is the consequence of neglecting transverse shear deformation in ETB.

Refined theories with shear deformation effects taken into account, have been pioneered by Rankine, Bresse, Lord Rayleigh, Timoshenko, Vlasov and others. These refined theories have been fruitfully applied to both theoretical and practical solid mechanics problems.

Analysis of thick isotropic and laminated beams is complicated by the two dimensional nature of stress and strain state. The use of elasticity theory is practically unfeasible due to mathematical difficulties and the complexity of laminated systems. This led to the development of refined shear deformation theories for beams which approximate the two dimensional solutions with reasonable accuracy.

First-Order Shear Deformation Theory

This theory is an improvement over the elementary theory of beam. Rankine [6] and Bresse [7] were the first to include both the rotatory inertia and shear flexibility effects as refined dynamical effects in beam theory. This theory is, however, referred to as the Timoshenko beam theory as mentioned in the literature by Rebello et al. [8] and based upon kinematics it is known as first-order deformation theory (FSDT). The kinematics of the theory is as follows:

$$u(x, z) = u_0 + z\phi_x$$

$$w(x, z) = w(x)$$

Downloaded from jrp.sagepub.com at UNIVERSITE LAVAL on June 13, 2014

where u_0, w and ϕ_x are the unknown variables. ϕ_x is the rotation of a cross section of the beam at the neutral layer. Rayleigh [9] included the rotatory inertia effect while later the effect of shear stiffness was added by Timoshenko [10]. Timoshenko showed that the effect of shear is much greater than that of rotatory inertia for transverse vibration of prismatic beams. The first correct boundary conditions for the Timoshenko beam were derived by Kruszewski [11] and Dengler and Goland [12]. This theory is well discussed by Dym and Shames [13].

In Timoshenko beam theory transverse shear strain distribution is constant through the beam thickness and therefore requires shear correction factor to correct the strain energy of deformation. Mindlin and Deresiewicz [14] calculated this factor for variety of cross sections of beams. Cowper [15,16] and Murty [17,18] have given new expressions for this coefficient for different cross sections of the beam. History of shear coefficient is given by Kaneko [19] and critically examined by Hutchinson and Zillmer [20] and Hutchinson [21]. Further discussion on the shear coefficients in beam bending is presented by Rychter [22].

Stephen and Levinson [23] have introduced a refined theory incorporating shear curvature, transverse direct stress and rotatory inertia effects. The governing differential equation is similar in form to the Timoshenko beam equation. However, the theory requires two coefficients, one for cross sectional warping and the second dependent on the transverse direct stresses. These coefficients for various cross sections are evaluated.

Rychter [24] studied a rectangular beam bending theory which incorporates the usual mean deflection and a rotation represented in terms of the relative axial displacement of the upper and lower surfaces of the beam. Renton [25] has proposed a generalized beam theory to evaluate the shear stiffness of various cross sections.

Fan and Widera [26] and Kathnelson [27] developed an improved engineering theory for elastic isotropic uniform beam using asymptotic analysis of the variational equation of the Hellinger-Reissner principle for the three dimensional theory of elasticity. The theory gives Timoshenko type governing equations.

Zaslavsky [28] investigated the limitations of the classical shearing stress formula of the strength of material theory by applying it to the non-homogeneous sections to determine the shearing stresses.

The limitations of the elementary theory of bending (ETB) of beams and first order shear deformation theory (FSDT) for beams forced the development of higher order shear deformation theories.

Higher-Order Shear Deformation Theories

In these theories displacement distribution is represented by power series expansion in thickness coordinate to take into account shear deformation effects [29,30]. The displacement field of the general third order theory is as

Downloaded from jrp.sagepub.com at UNIVERSITE LAVAL on June 13, 2014

$$u(x,z) = u_0 + z\phi_x + z^2\psi_x + z^3\xi_x$$

$$w(x,z) = w_0 + z\phi_z + z^2\psi_z + z^3\xi_z$$

where u_0, w_0, ϕ_x, ψ_x, ξ_x, ϕ_z, ψ_z, ξ_z are unknown functions of position x. From this general third order theory, various displacement based theories can be obtained by different combination of terms.

Parabolic Shear Deformation Theories

This section deals with the refined theories giving parabolic transverse shear stress distribution through the thickness of the beam and obviating the need of shear correction factors.

Soler [31] developed the higher order theory for thick isotropic rectangular elastic beams using Legendre polynomials and Tsai and Soler [32] extended it to orthotropic beams. Effects of shear deformation and transverse normal stress are included. The interrelation between classical beam theory and higher order theories is explicitly brought out.

Essenburg [33] studied an elastic beam of rectangular section, loaded in such a manner that contact with a smooth rigid surface is included. The displacement field of the theory assumes the transverse normal component of deformation as quadratic in thickness coordinate and includes the effect of transverse shear deformation. The inplane displacement is assumed to be the linear function of thickness coordinate.

Leech [34] used the Hamilton's principle to develop a series of beam theories of increasing accuracy including parabolic shear deformation theory. The kinematics of the third order theory satisfy the zero shear strain conditions on the upper and lower edge of the beam.

Levinson [35–38] obtained the higher order beam theory providing the fourth order stiffness of differential equations, satisfying two boundary conditions at each end of the beam. No shear correction factors are required since the theory satisfies the shear stress free surface conditions on the top and bottom of the beam. The through the thickness variation of transverse shear stress is parabolic. However, Levinson's kinematic model is variationally inconsistent. The displacement field of theory is as

$$u(x,z) = u_0 + z\left[\phi_x - \frac{4}{3}\left(\frac{z}{h}\right)^2\left(\phi_x + \frac{dw}{dx}\right)\right]$$

$$w(x,z) = w(x)$$

where u_0, w and ϕ_x are the unknown functions.

Downloaded from jrp.sagepub.com at UNIVERSITE LAVAL on June 13, 2014

Bickford [39] used Hamilton's Principle to derive a consistent, higher order theory for the elastodynamics of beam based upon the kinematic and stress assumptions previously used by Levinson [35]. Bickford's variationally consistent theory consists of a sixth order system of differential equations, and satisfies three boundary conditions at each end of the beam.

Rychter [40,41] verified the consistency and accuracy of Levinson's theory by imbedding it in the two-dimensional linear theory of elasticity. It is shown that the Levinson's variationally inconsistent theory is more accurate than the variationally consistent theory of Bickford. Petrolito [42] presented a finite element solution of uniformly loaded thick beams using the Bickford's theory.

Rychter [41] has given a simple and accurate fourth-order theory for beam bending based on adequate displacement and stress distributions in the beam. This theory is an extension of Levinson's theory which incorporates transverse shear deformation, transverse normal stress, self-equilibrating axial stress and centroidal axis elongation-contraction due to Poisson's effect.

Rehfield and Murthy [43] formulated a beam theory that includes the effects of transverse normal strain, transverse shear strain, and nonclassical axial stress with the help of a plane stress elasticity solution of simply supported beam under uniform load. However, the drawback of this theory is that the stresses, derived from a specific loading condition and from which strains are estimated, are not necessarily valid for an arbitrary loading condition. Rychter [44] studied the accuracy of the Rehfield and Murthy's theory in a more general way and confirms its adequacy for anisotropic beams with increased transverse shear deformability.

Baluch et al. [45] formulated a theory which takes into account the influence of transverse shear and transverse normal strain on the bending of isotropic beams. The theory obviates the need of shear correction factor. The semi-inverse method is used to derive the refined theory. Valisetty [46] developed a refined bending theory for beams of solid circular cross section using semi-inverse approach.

Krishna Murty [47] formulated a third order beam theory including the transverse shear strain and nonclassical (nonlinear) axial stress. In this theory the parabolic transverse shear stress distribution across the depth of the beam can be obtained using constitutive relations. The displacement field of the theory is as

$$u(x,z) = u_0 - z\frac{dw}{dx} + z\left[1 - \frac{4}{3}\left(\frac{z}{h}\right)^2\right]\phi_x$$

$$w(x,z) = w_b + w_s$$

where u_0, w_b, w_s and ϕ_x are the unknown functions. The transverse deflection is considered as a sum of two partial deflections, the deflection due to bending w_b and the deflection due to transverse shearing w_s. ϕ_x is the rotation of a cross section of the beam at the neutral surface.

Downloaded from jrp.sagepub.com at UNIVERSITE LAVAL on June 13, 2014

A parabolic shear deformation beam theory assuming a higher-order variation for axial displacement has been presented by Bhimaraddi and Chandrashekhara [48]. Apart from the usual simple parabolic variation, six other shear strain variations are considered: the sinusoidal variation, cubic, quadratic, and sixth-order polynomials, and satisfy the surface constraints. A cantilever, a simply supported and clamped beams of isotropic material are solved by various theories proposed.

Irretier [49] discussed the various refined effects in dynamical theories for linear, homogeneous beams and it is shown that the shear deformation influence is the most important.

Heyliger and Reddy [50] and Kant and Gupta [51] presented finite element formulations based on higher order shear deformation theories for bending and vibration of isotropic beams.

Irschik [52] has established an analogy between refined beam theories and the classical Bernoulli-Euler theory using the principle of virtual work. The first and third order theories are used to establish the analogy for transverse deflection.

Refined Theories Using Method of Successive Approximations

Donnell [53] provided the series solution in the loading function, for the deflections and stress in continuously loaded beams of rectangular cross section in terms of the top and bottom loading. Donnell [3] also studied the effect of transverse shear strain and transverse normal stresses on the deflection of centrally loaded simply supported thick beam. Thus the transverse deflection consists of three parts, viz flexural or bending deflection, deflection due to transverse shear strain and deflection due to transverse normal stresses.

Boley and Tolins [54] calculated the stresses and deflections in rectangular beams and bars subjected to normal and shear forces varying smoothly along the span, from the two dimensional elasticity theory by an iterative procedure.

Trigonometric Shear Deformation Theories

A refined theory containing the trigonometric sine, cosine or hyperbolic sine and cosine functions in thickness coordinate, in the displacement field is termed here as trigonometric shear deformation theory (TSDT). The trigonometric functions involving thickness coordinate are associated with transverse shear deformation effects and the shear stress distribution through the thickness of the beam. This is another class of refined theories in which number of displacement variables in the simplest form can be the same as those in FSDT.

Refined beam theories with the introduction of trigonometric function in terms of thickness coordinate in kinematical assumptions are introduced by Vlasov and Leont'ev [4] and Stein [56]. It is interesting to note that in respect of plates similar trigonometric functions in thickness coordinates were used by Levy [55],

Downloaded from jrp.sagepub.com at UNIVERSITE LAVAL on June 13, 2014

Kil'chevskiy [2] and, as has been mentioned by Love [57], also by Kelvin and Tait.

The displacement field of the Vlasov and Leont'ev theory is as

$$u(x,z) = zu_1(x) + u_2(x)\sin\left(\frac{2\pi z}{h}\right)$$

$$w(x,z) = w_1(x) + v_2(x)\cos\left(\frac{\pi z}{h}\right)$$

The displacement field of Stein's theory is as

$$u(x,z) = zu_1(x) + u_2(x)\sin\left(\frac{\pi z}{h}\right)$$

$$w(x,z) = w_1(x) + v_2(x)\left(\frac{y}{b}\right)^2$$

In these displacement fields, the first right hand term represents the displacements when the sections are assumed to remain plane; the second terms are introduced to correct the inaccuracies due to this assumption and that of zero transverse elongations.

However, in these theories shear stress free boundary conditions are not satisfied on the top and bottom surfaces of the beam. This deficiency is removed by Rao [58] in a refined theory developed for beams. The theory is as simple as first order shear deformation theory. However, it is variationally inconsistent. Ghugal and Shimpi [59] developed a variationally consistent refined trigonometric shear deformation theory for flexure and free vibration of thick isotropic beams. The displacment field of the theory in its simplest form is as

$$u(x,z) = u_0(x) - z\frac{dw}{dx} + \frac{h}{\pi}\sin\left(\frac{\pi z}{h}\right)\phi_x$$

$$w(x,z) = w(x)$$

The number of displacement variables in this theory are the same as those in FSDT. The theory satisfies the zero transverse shear stress conditions on the top and bottom surfaces of the beam and thus obviates the need of shear correction factor.

Downloaded from jrp.sagepub.com at UNIVERSITE LAVAL on June 13, 2014

Elasticity Solutions

The elasticity solutions for simply supported and cantilever beams of narrow rectangular cross sections subjected to UDL and tip load respectively are given by Lekhnitskii [60] and Timoshenko and Goodier [61] using Airy's stress polynomial functions and using stress functions in the form of a Fourier series. The effects of transverse shearing force and transverse normal stress on the deflection of the beams are included.

Iyengar and Prabhakara [62] provided a three dimensional elasticity solution for the analysis of beams continuous over an infinite number of equally spaced supports. It is assumed that the beam is made of homogeneous, isotropic and perfectly elastic materials.

Neou [63] and Niedenfuhr [64] developed the method for determining the polynomial Airy stress function for homogeneous beams considered as a plane stress elasticity problem. Hasin [65] applied it to the anisotropic case.

LAMINATE BEAM THEORIES

Equivalent single layer and layerwise laminated beam theories are presented in this section. In the equivalent single layer displacement based theories one single expansion for each displacement component is used through the entire thickness of the laminate. In layerwise theories each layer is treated as a separate beam and discrete layer transverse shear effects are introduced into the assumed displacement field.

While cylindrical bending provides a convenient tool for performing a one-dimensional analysis of laminated plates, a theory for laminated, anisotropic beams is also important, beam being a basic structural element. The difference between cylindrical bending and beam bending is analogous to the difference between plane strain and plane stress in classical theory of elasticity. The major difference is in the bending stiffness term (see Whitney [66]).

Elementary Theory of Beams for Laminates

In laminated composite beams, the transverse shear deformation significantly affects the transverse displacement, the natural frequencies of vibration, and the buckling loads. The elementary theory of beam, which is based on the Bernoulli-Euler assumption that planes initially normal to the midplane remain plane and normal to the midsurface after bending, leads to high percentages of error in the analysis of anisotropic beams due to the neglect of transverse shear deformations.

Tauchert [67] examined the validity of the elementary theory of beam (ETB) for anisotropic beams. The unidirectionally reinforced composite beams with fi-

Downloaded from jrp.sagepub.com at UNIVERSITE LAVAL on June 13, 2014

bers oriented at various angles relative to the longitudinal axis of the beam are considered. The comparison of results of ETB with elasticity results showed that the ETB yields acceptable results for beams having an aspect ratio of 10 or more.

Krajcinovic [68] developed a variationally consistent layerwise shear deformation theory for composite beam. The theory is developed under the assumption that the Bernoulli's hypothesis is valid for each lamina independently but not for the entire cross section as a whole. Ojalvo [69] employed the classical Euler-Bernoulli beam theory to laminated beams.

First-Order Shear Deformation Laminate Theory

Swift and Heller [70] studied laminated beams by assuming layerwise constant shear strains and a continuous transverse displacement through the thickness. This is a layerwise application of Timoshenko beam theory. The results of a sine loaded two layered, unsymmetrically stacked graphite epoxy beam with simple supports are presented.

Shear correction coefficients for orthotropic beams are derived by Bert [71] and Dharmarajan and McCutchen [72]. Gordaninejad and Bert [73] employed the Timoshenko beam theory for the analysis of laminated beams.

Higher-Order Laminate Beam Theories

Equivalent single layer and layerwise laminated beam theories based on method of power series expansion in thickness coordinate are presented in this section.

PARABOLIC SHEAR DEFORMATION THEORIES

Ambartsumyan [74] developed a layerwise shear deformation theory for symmetric cross-ply laminates assuming the parabolic transverse shear stress distribution within each layer. The semi-inverse method is used to derive the displacement field of theory. The resulting theory is a parabolic shear deformation theory.

Krishna Murty and Shimpi [75] and Krishna Murty [76] developed the higher order shear deformation theories based on the elementary theory of beam and applied these theories for the vibration analysis of laminated beams.

Silverman [77] presented a parabolic shear deformation theory for the narrow doubly symmetrical three layer rectangular beam. The principle of minimum potential energy is used to obtain the governing equations and boundary conditions. Formulae for the deflections, bending and shear stresses have been developed for cantilever and simply supported beams.

Hu et al. [78] presented the experimental validation of parabolic refined shear deformation theory for fiber reinforced beams. The results were found to be closer to those predicted by refined theory.

Downloaded from jrp.sagepub.com at UNIVERSITE LAVAL on June 13, 2014

Khdeir and Reddy [79] presented the analysis of symmetric and antisymmetric cross-ply laminated beams using classical, first-order, second-order and third-order theories. Soldatos and Watson [80] developed a general theory for the accurate stress analysis of homogeneous and laminated composite beams which takes into consideration the effects of both transverse shear and transverse normal stress.

LO-CHRISTENSEN-WU TYPE HIGHER ORDER THEORIES

The Lo, Christensen and Wu theory [29,30] developed a consistent higher order theory for homogeneous and laminated plates including effects of transverse shear deformation, transverse normal strain and a nonlinear distribution of the inplane and transverse displacements with respect to the thickness coordinate. The theory contains eleven displacement variables. This theory is widely used by many research workers for the analyses of shear deformable beams and plates; and obtained the closed form and finite element solutions.

Kant and Manjunatha [81] and Manjunatha and Kant [82,83] developed a set of higher order theories for the analysis of composite and sandwich beams using the Lo, Christensen and Wu theory. The C^0 finite element formulation was presented for the flexural analysis of symmetric and unsymmetric composite and sandwich beams.

Maiti and Sinha [84] and Vinayak et al. [85] presented the finite element analysis of the symmetric and unsymmetric thick laminated beams based on the higher order theory of Lo et al. [29].

Soldatos and Elishakoff [86] developed a third order shear deformation theory for static and dynamic analysis of an orthotropic straight beam based on classical beam theory. The theory incorporates the effects of transverse shear and transverse normal deformation.

Recently, Murakami et al. [87] developed anisotropic beam theories with shear deformation to investigate the effect of constitutive coupling, bending, and transverse shearing deformation on the deflection of an anisotropic cantilever beam with narrow rectangular cross section. First-, second- and third-order shear deformation displacement based theories are proposed. Reissner’s mixed variational principle is used to formulate the boundary value problem. It is concluded that higher order beam theories are necessary to capture the normal shear coupling effects.

LAYERWISE THEORIES

Reddy [88] presented a more general theory for composite analysis based on a layerwise displacement field. The theory can be specialized to a number of particular theories. Assuming transverse incompressibility and layerwise representation of inplane displacement, the displacement field of a laminated beam can be written as

Downloaded from jrp.sagepub.com at UNIVERSITE LAVAL on June 13, 2014

$$u(x,z) = u_0 + U(x,z)$$

$$w(x,z) = w(x)$$

where u_0 and w are, respectively, the longitudinal and transverse displacements of a point on the reference axis of the laminate and the function $U(x,z)$ represents a layerwise inplane displacement.

Lu and Liu [89] extended Reddy's generalized laminate plate theory (GLPT) using Hermite cubic shape functions to get the continuity of interlaminar shear stresses. Results of single layered, two layered and three layered cross-ply laminate for cylindrical bending are presented. However, theory is layer dependent and computationally complicated.

Davalos et al. [90] analyzed the laminate beams with a layerwise constant shear theory. The layerwise constant shear stress obtained from constitutive relations is transformed into parabolic distribution using quadratic functions (Lagrangian Polynomials) and various numerical applications are presented using finite element method.

Elasticity Solutions

A three dimensional elasticity analysis of nonhomogeneous bars in flexure has been carried out by Muskhelishvili [91] with all layers having the same Poisson's ratio. The analysis becomes complicated when each layer is having different Poisson's ratio.

Silverman [92] presented elasticity solutions for bending of orthotropic beams under polynomial loads using Airy's stress functions. Formulas for the deflections, bending, and transverse shear stresses for simply supported and cantilever beams are given.

Lekhnitskii [60] provided the exact solutions of laminated beams using Airy's stress polynomial functions. Each layer is assumed to be specially orthotropic in the plane of bending. A more general solution for multilayered composite cantilever beam subjected to transverse load and a moment at the free end is presented and specialized it for the two layered unsymmetrically laminated cantilever beam.

Gerstner [93] developed the elasticity solution for a composite beam consisting of three isotropic elastic layers using Airy stress function. Pagano [94,95] presented exact elasticity solutions for composite laminates in cylindrical bending. A unidirectional laminate and two and three layered cross-ply laminates subjected to sinusoidal load are considered.

Rao and Ghosh [96] presented a plane stress elasticity solution of an unsymmetrically laminated beam using Airy's stress function. A simple and direct technique to choose Airy's stress function suitable to solve a laminated beam under

Downloaded from jrp.sagepub.com at UNIVERSITE LAVAL on June 13, 2014

polynomial load is presented with the help of the strength of materials theory. All the layers are of different composite materials.

Cheng et al. [97] has given a three dimensional elasticity solution for symmetrically laminated rectangular beams where each layer is assumed to be homogeneous, transversely isotropic, and unidirectionally reinforced. Only symmetrically laminated cantilever beam with tip load is considered. The solution can be applied to a simply supported or clamped beam with concentrated load at midspan using Saint Venant's Principle. The transverse normal deformation is included in the formulation.

Holt and Webber [98] provided exact solutions to sandwich beam, plate and shell problems.

COMMENTS ON LITERATURE REVIEWED

A review of the literature indicates the following points related to the refined theories where further research is required for the rational analysis of shear deformable isotropic and laminated beams.

1. Most of the research work is devoted to flexural analysis of thick isotropic beams using refined theories and comparatively less work is available on the flexural analysis of laminated beams using equivalent single layer and layerwise theories.
2. Although the layerwise theories give excellent results for displacements and stresses, they suffer from major computational drawback due to the heavy algebra involved and require reduction of displacement variables by proper modelling techniques.
3. Analysis of unsymmetric cross-ply laminated beams using layerwise theories with minimal number of displacement variables are not available.
4. Simple layerwise theories making use of constitutive relations to obtain the transverse shear stresses directly with reasonable accuracy are not available. Such theories are more suitable for the finite element analysis since the recovery of these stresses by post-processing via equilibrium equations (which is a tedious task) is avoided.
5. Use of refined shear deformation theories using trigonometric functions involving thickness coordinate is not fully explored. The layerwise shear deformation theories for the analysis of laminated beams using method trigonometric functions are not available in the literature.
6. Exact solutions for cross-ply laminated beams are not available in the literature.
7. Refined theories for the analysis of beams subjected to shear loads on the top and bottom of the beam are rarely available.
8. Refined theories for bending analysis of beams with non-rectangular cross sections are rare.

Downloaded from jrp.sagepub.com at UNIVERSITE LAVAL on June 13, 2014

REFERENCES

1. Gol'denviezer, A. L., 1968, "Methods for Justifying and Refining the Theory of Shells," *Prikladnaya Matematika I Mekhanika,* Vol. 32, No. 4, pp. 684–695. [*Journal of Applied Mathematics and Mechanics,* Vol. 32, No. 4, pp. 704–718.]
2. Kil'chevskiy, N. A., 1965, "Fundamentals of the Analytical Mechanics of Shells," NASA TT F-292, Washington, D.C., pp. 80–172.
3. Donnell, L. H., 1976. *Beams, Plates and Shells,* McGraw-Hill Book Company, New York, 453 p.
4. Vlasov, V. Z. and Leont'ev, U. N., 1960, *Beams, Plates and Shells on Elastic Foundations,* Translated from Russian by Barouch, A., and edited by Pelz, T.; Israel Program for Scientific Translations Ltd., Jerusalem, Chapter 1, pp. 1–8.
5. Sayir, M. and Mitropoulos, C., 1980, "On Elementary Theories of Linear Elastic Beams, Plates and Shells," *Zeitschrift für Angewandte Mathematik und Physik,* Vol. 31, No. 1, pp. 1–55.
6. Rankine, W. J. M., 1858, *A Manual of Applied Mechanics,* R. Griffin and Company Ltd., London, U.K., pp. 342–344.
7. Bresse, J. A. C., 1859, *Cours de Mecanique Applique,* Paris: Mallet-bacheleier, (1866 2nd ed.), Gauthier-Villars, Paris.
8. Rebello, C. A., Bert, C. W. and Gordaninejad, F., 1983, "Vibration of Bimodular Sandwich Beams with Thick Facings: A New Theory and Experimental Results," *Journal of Sound and Vibration,* Vol. 90, No. 3, pp. 381–397.
9. Lord Rayleigh, 1880, *Theory of Sound,* Macmillan Publishers, London, U.K.
10. Timoshenko, S. P., 1921, "On the Correction for Shear of the Differential Equation for Transverse Vibrations of Prismatic Bars," *Philosophical Magazine,* Series 6, Vol. 41, pp. 742–746.
11. Kruszewski, E. T., 1949, "Effect of Transverse Shear and Rotatory Inertia on the Natural Frequency of a Uniform Beam," *NACA TN* 1909.
12. Dengler, M. A. and Goland, M., 1951, "Transverse Impact of Long Beams Including Inertia and Shear Effects," *ASME Proceedings of 1st U.S. National Congress of Applied Mechanics,* New York, pp. 179–186.
13. Dym, C. L. and Shames, I. H., 1973, *Solid Mechanics: A Variational Approach,* McGraw-Hill Book Co., New York, 556 p.
14. Mindlin, R. D. and Deresiewicz, H., 1954, "Timoshenko's Shear Coefficient for Flexural Vibrations of Beams," *Proceedings of 2nd U.S. National Congress of Applied Mechanics,* ASME Publication, New York, pp. 175–178.
15. Cowper, G. R., 1966, "The Shear Coefficients in Timoshenko Beam Theory," *ASME Journal of Applied Mechanincs,* Vol. 33, pp. 335–340.
16. Cowper, G. R., 1968, "On the Accuracy of Timoshenko's Beam Theory," *ASCE Journal of the Engineering Mechanics Division,* Vol. 94, No. EM 6, pp. 1447–1453.
17. Murty, A. V. K., 1970, "Vibration of Short Beams," *AIAA Journal,* Vol. 8, pp. 34–38.
18. Murty, A. V. K., 1970, "Analysis of Short Beams," *AIAA Journal,* Vol. 8, pp. 2098–2100.
19. Kaneko, T., 1975, "On Timoshenko's Correction for Shear in Vibrating Beams," *Journal of Physics D: Applied Physics,* Vol. 8, No. 16, pp. 1927–1936.
20. Hutchinson, J. R., 1981, "Transverse Vibrations of Beams, Exact Versus Approximate Solutions," *Trans. ASME, Journal of Applied Mechanics,* Vol. 48, No. 4, pp. 923–928.
21. Hutchinson, J. R. and Zillmer, S. D., 1986. "On the Transverse Vibration of Beams of Rectangular Cross-section," *Trans. ASME, Journal of Applied Mechanics,* Vol. 53, No. 1, pp. 39–44.
22. Rychter, Z., 1987, "On the Shear Coefficient in Beam Bending," *Mechanics Research Communications,* Vol. 14, No. 5/6, pp. 379–385.
23. Stephen, N. G. and Levinson, M., 1979, "A Second Order Beam Theory," *Journal of Sound and Vibration,* Vol. 67, pp. 293–305.
24. Rychter, Z., 1988, "An Engineering Theory for Beam Bending," *Ingenieur-Archiv,* Vol. 58, No. 1, pp. 25–34.

Downloaded from jrp.sagepub.com at UNIVERSITE LAVAL on June 13, 2014

25. Renton, J. D. 1991, "Generalised Beam Theory Applied to Shear Stiffness," *International Journal of Solids and Structures,* Vol. 27, No. 15, pp. 1955–1967.
26. Fan, H. and Widera, G. E. O., 1991, "Refined Engineering Beam Theory Based on the Asymptotic Expansion Approach," *AIAA Journal,* Vol. 29, No. 3, pp. 444–449.
27. Kathnelson, A. N., 1996, "Improved Engineering Theory for Uniform Beams," *Acta Mechanica,* Note, Vol. 114, No. 1–4, pp. 225–229.
28. Zaslavsky, A., 1980, "On the Limitations of the Shearing Stress Formula," *The International Journal of Mechanical Engineering Education,* Vol. 8, pp. 13–19.
29. Lo, K. H., Christensen, R. M. and Wu, E. M., 1977, "A Higher Order Theory for Plate Deformations, Part 1: Homogeneous Plates," *ASME Journal of Applied Mechanics,* Vol. 44, pp. 663–668.
30. Lo, K. H., Christensen, R. M. and Wu, E. M., 1977, "A Higher Order Theory for Plate Deformations, Part 2: Laminated Plates," *ASME Journal of Applied Mechanics,* Vol. 44, pp. 669–676.
31. Soler, A. I., 1968, "Higher Order Effects in Thick Rectangular Elastic Beams," *International Journal of Solids and Structures,* Vol. 4, No. 7, pp. 723–739.
32. Tsai, H. and Soler, A. I., 1970, "Approximate Theory for Locally Loaded Plane Orthotropic Beams," *International Journal of Solids and Structures,* Vol. 6, No. 8, pp. 1055–1068.
33. Essenburg, F., 1975, "On the Significance of the Inclusion of the Effect of Transverse Normal Strain in Problems Involving Beams with Surface Constraint," *ASME Journal of Applied Mechanics,* Vol. 97, pp. 127–132.
34. Leech, C. M., 1977, "Beam Theories: A Variational Approach," *The International Journal of Mechanical Engineering Education,* Vol. 5, No. 1, pp. 81–87.
35. Levinson, M., 1981, "A New Rectangular Beam Theory," *Journal of Sound and Vibration,* Vol. 74, pp. 81–87.
36. Levinson, M., 1981, "Further Results of a New Beam Theory," *Journal of Sound and Vibration,* Vol. 77, pp. 440–444.
37. Levinson, M., 1985, "On Bickford's Consistent Higher Order Beam Theory," *Mechanics Research Communications,* Vol. 12, pp. 1–9.
38. Levinson, M., 1986, "Consistent and Inconsistent Higher Order Beam and Plate Theories: Some Surprising Comparisons," *Proceedings of Euromech Colloquium 219 on Refined Dynamical Theories of Beams, Plates and Shells and Their Applications,* Kassel, F.R. Germany, pp. 122–130.
39. Bickford, W. B., 1982, "A Consistent Higher Order Beam Theory," *Developments in Theoretical and Applied Mechanics, SECTAM*, 11, pp. 137–150.
40. Rychter, Z., 1987, "On the Accuracy of a Beam Theory," *Mechanics of Research Communications,* Vol. 14, No. 2, pp. 99–105.
41. Rychter, Z., 1988, "A Simple and Accurate Beam Theory," *Acta Mechanica,* Vol. 75, pp. 57–62.
42. Petrolito, J., 1995, "Stiffness Analysis of Beams Using A Higher-Order Theory," *Computers and Structures,* Vol. 55, No. 1, pp. 33–39.
43. Rehfield, L. W. and Murthy, P. L. N., 1982, "Toward a New Engineering Theory of Bending: Fundamentals," *AIAA Journal,* Vol. 20, pp. 693–699.
44. Rychter, Z., 1987, "An Error Estimate for Solutions in Beam Theory," *ZAMM. Zeitschrift für Angewandte Mathematik und Mechanic,* Vol. 67, No. 3, pp. 205–207.
45. Baluch, M. H., Azad, A. K. and Khidir, M. A., 1984, "Technical Theory of Beam with Normal Strain," *Journal of the Engineering Mechanics, Proceedings of ASCE,* Vol. 110, pp. 1233–1237.
46. Valisetty, R. R., 1990, "Refined Bending Theory for Beams of Circular Cross-section," *Proceedings of ASCE, Journal of Engineering Mechanics,* Technical Note, Vol. 116, No. 9. pp. 2072–2079.
47. Krishna Murty, A. V., 1984, "Toward a Consistent Beam Theory," *AIAA Journal,* Vol. 22, pp. 811–816.
48. Bhimaraddi, A. and Chandrashekhara, K., 1993, "Observations on Higher-Order Beam Theory," *Journal of Aerospace Engineering, Proceedings of ASCE,* Technical Note, Vol. 6, pp. 408–413.

Downloaded from jrp.sagepub.com at UNIVERSITE LAVAL on June 13, 2014

49. Irretier, H., 1986, "Refined Effects in Beam Theories and their Influence on the Natural Frequencies of Beams," *Proc. Euromech Colloquium 219, on Refined Dynamical Theories of Beams, Plates, and Shells and their Applications.* Edited by Elishakoff, I. and Irretier, H., Springer-Verlag, Berlin, pp. 163–179.
50. Heyliger, P. R. and Reddy, J. N., 1988, "A Higher Order Beam Finite Element for Bending and Vibration Problems," *Journal of Sound and Vibration,* Vol. 126, No. 2, pp. 309–326.
51. Kant, T. and Gupta, A., 1988, "A Finite Element Model for a Higher Order Shear Deformable Beam Theory," *Journal of Sound and Vibration,* Vol. 125, No. 2, pp. 193–202.
52. Irschik, H., 1991, "Analogy Between Refined Beam Theories and the Bernoulli-Euler Theory," *International Journal of Solids and Structures,* Vol. 28, No. 9, pp. 1105–1112.
53. Donnell, L. H., 1952, "Bending of Rectangular Beams," *ASME Journal of Applied Mechanics,* Vol. 74, p. 123.
54. Boley, B. A. and Tolins, I. S., 1956, "On the Stresses and Deflections of Rectangular Beams," *ASME Journal of Applied Mechanics,* Vol. 23, pp. 339–342.
55. Levy, M., 1877, "Memoire sur la Theorie des Plaques Elastiques Planes," *Journal des Mathmatiques Pures et Appliquees,* Vol. 30, pp. 219–306.
56. Stein, M., 1989, "Vibration of Beams and Plate Strips with Three-Dimensional Flexibility," *Trans. ASME, Journal of Applied Mechanics,* Vol. 56, No. 1, pp. 228–231.
57. Love, A. E. H., 1944, *The Mathematical Theory of Elasticity,* 4th ed., Dover Publications, New York, p. 462.
58. Rao, B. S., 1989, *A Refined Beam Theory,* M.Tech. Thesis, Dept. Aero. Engg., IIT. Powai, Mumbai, 29 p.
59. Ghugal, Y. M. and Shimpi, R. P., 2000, "A Trigonometric Shear Deformation Theory for Flexure and Free Vibration of Isotropic Thick Beams, *Structural Enigineering Convention, SEC-2000,* IIT Bombay, India.
60. Lekhnitskii, S. G., 1957, *Anisotropic Plates,* 2nd ed., Moscow, translated by Tsai, S. W. and Cheron, T., Gordon and Breach Science Publishers, New York.
61. Timoshenko, S. P. and Goodier, J. N., 1970, *Theory of Elasticity,* McGraw-Hill, 3rd Int. Ed., Singapore.
62. Iyengar, K. T. S. R. and Prabhakara, M. K., 1968, "Analysis of Continuous Beams: A Three-Dimensional Elasticity Solution," *International Journal of Engineering Science,* Vol. 6, pp. 193–208.
63. Neou, Y. C., 1957, "A Direct Method for Determining Airy Polynomial Stress Functions," *Trans. ASME, Journal of Applied Mechanics,* Vol. 24, pp. 387–390.
64. Niedenfuhr, F. W., 1957, "On Choosing Stress Functions in Rectangular Coordinates," *Journal of Aeronautical Sciences,* Vol. 24, pp. 460–461.
65. Hashin, Z., 1967, "Plane Anisotropic Beams," *ASME Journal of Applied Mechanics,* Vol. 34, pp. 257–262.
66. Whitney, J. M., 1987, *Structural Analysis of Laminated Anisotropic Plates,* Technomic Publishing. Co., Inc., Lancaster, PA.
67. Tauchert, T. R., 1975, "On the Validity of Elementary Bending Theory for Anisotropic Elastic Slabs," *Journal of Composite Materials,* Vol. 9, pp. 207–214.
68. Krajcinovic, D., 1972, "Sandwich Beam Analysis," *Trans. ASME, Journal of Applied Mechanics,* Vol. 39, No. 3, pp. 773–778.
69. Ojalvo, I. U., 1977, "Departures from Classical Beam Theory in Laminated, Sandwich, and Short Beams," *AIAA J.,* Vol. 15, No. 10, pp. 1518–1521.
70. Swift, G. W. and Heller, R. A., 1974, "Layered Beam Analysis," *Journal of the Engineering Mechanics Division, Proceedings of ASCE,* Vol. 100, pp. 267–282.
71. Bert, C. W., 1973, "Simplified Analysis of Static Shear Factor for Beams of Nonhomogeneous Cross Section," *Journal of Composite Materials,* Vol. 7, pp. 525–529.
72. Dharmarajan, S. and McCutchen, H. Jr., 1973, "Shear Coefficient for Orthotropic Beams," *Journal of Composite Materials,* Vol. 7, pp. 530–535.

Downloaded from jrp.sagepub.com at UNIVERSITE LAVAL on June 13, 2014

73. Gordaninejad, F. and Bert, C. W., 1989, "A New Theory for Bending of Thick Sandwich Beams," *International Journal of Mechanical Sciences,* Vol. 31, No. 11/12, pp. 925–934.
74. Ambartsumyan, S. A., 1970, *Theory of Anisotropic Plates,* J. E. Ashton, ed., Technomic Publishing Co., Inc., Lancaster, PA.
75. Krishna Murty, A. V. and Shimpi, R. P., 1974, "Vibration of Laminated Beams," *Journal of Sound and Vibration,* Vol. 36, pp. 273–284.
76. Krishna Murty, A. V., 1985, "On the Shear Deformation Theory for Dynamic Analysis of Beams," *Journal of Sound and Vibration,* Vol. 101, pp. 1–12.
77. Silverman, I. K., 1980, "Flexure of Laminated Beams," *Journal of the Structural Division, Proceedings of ASCE,* Vol. 106, pp. 711–725.
78. Hu, M. Z., Kolsky, H. and Pipkin, A. C., 1985, "Bending Theory for Fiber Reinforced Beams," *Journal of Composite Materials,* Vol. 19, pp. 235–249.
79. Khdeir, A. A. and Reddy, J. N., 1997, "An Exact Solution for the Bending of Thin and Thick Cross-ply Laminated Beams," *Composite Structures,* Vol. 37, No. 2, pp. 195–203.
80. Soldatos, K. P. and Watson, P., 1997, "A General Theory for the Accurate Stress Analysis of Homogeneous and Laminated Composite Beams," *International Journal of Solids and Structures,* Vol. 34, No. 22, pp. 2857–2885.
81. Kant, T. and Manjunatha, B. S., 1989, "Refined Theories for Composite and Sandwich Beams with C^0 Finite Elements," *Computers and Structures,* Vol. 33, pp. 755–764.
82. Manjunatha, B. S. and Kant, T., 1993a, "New Theories for Symmetric/Unsymmetric Composite and Sandwich Beams with C^0 Finite Elements," *Composite Structures,* Vol. 23, pp. 61–73.
83. Manjunatha, B. S. and Kant, T., 1993b, "Different Numerical Techniques for the Estimation of Multiaxial Stresses in Symmetric/Unsymmetric Composite and Sandwich Beams with Refined Theories," *Journal of Reinforced Plastics and Composites,* Vol. 12, pp. 2–27.
84. Maiti, D. K. and Sinha, P. K., 1994, "Bending and Free Vibration Analysis of Shear Deformable Laminated Composite Beams by Finite Element Method," *Composite Structures,* Vol. 29, pp. 421–431.
85. Vinayak, R. U., Prathap, G. and Naganarayana, B. P., 1996, "Beam Elements Based on a Higher Order Theory—I: Formulation and Analysis of Performance," *Computers and Structures,* Vol. 58, pp. 775–789.
86. Soldatos, K. P. and Elishakoff, I., 1992, "A Transverse Shear and Normal Deformable Orthotropic Beam Theory," *Journal of Sound and Vibration,* Vol. 154, No. 3, pp. 528–533.
87. Murakami, H., Reissner, E. and Yamakawa, J., 1996, "Anisotropic Beam Theories with Shear Deformation," *Trans. ASME, Journal of Applied Mechanics,* Vol. 63, pp. 660–668.
88. Reddy, J. N., 1987, "A Generalization of Two Dimensional Theories of Laminated Composite Plates," *Communications in Applied Numerical Methods,* Vol. 3, pp. 173–180.
89. Lu, X. and Liu, D., 1992, "An Interlaminar Shear Stress Continuity Theory for both Thin and Thick Composite Laminates," *ASME Journal Applied Mechanics,* Vol. 59, pp. 502–509.
90. Davalos, J. F., Kim, Y. and Barbero, E. J., 1994, "Analysis of Laminated Beams with a Layerwise Constant Shear Theory," *Composite Structures,* Vol. 28, pp. 241–253.
91. Muskhelishvili, N. I., 1963, *Some Basic Problems of the Mathematical Theory of Elasticity,* English Translation of 4th Ed., Noordhoff, Groningen, The Netherlands, Chap. 25.
92. Silverman, I. K., 1964, "Orthotropic Beams under Polynomial Loads," *Journal of the Engineering Mechanics Division, Proceedings of ASCE,* Vol. 90, pp. 293–319.
93. Gerstner, R. W., 1968, "Stresses in a Composite Cantilever," *Journal of Composite Materials,* Vol. 2, pp. 498–501.
94. Pagano, N. J., 1969, "Exact Solution for Composite Laminates in Cylindrical Bending," *Journal of Composite Materials,* Vol. 3, pp. 398–411.
95. Pagano, N. J., 1970, "Influence of Shear Coupling in Cylindrical Bending of Anisotropic Laminates," *Journal of Composite Materials,* Vol. 4, pp. 330–343.

Downloaded from jrp.sagepub.com at UNIVERSITE LAVAL on June 13, 2014

96. Rao, K. M. and Ghosh, B. G., 1979, "Exact Analysis of Unsymmetric Laminated Beam," *Journal of the Structural Division, ASCE,* Vol. 105, pp. 2313–2325.
97. Cheng, S., Wei, X. and Jiang, T., 1989, "Stress Distribution and Deformation of Adhesive-bonded Laminated Composite Beams," *Journal of Engineering Mechanics, ASCE,* Vol. 115, pp. 1150–1162.
98. Holt, P. J. and Webber, J. B. H., 1982, "Exact Solutions to Some Honeycomb Sandwich Beam, Plate and Shell Problems," *The Journal of Strain Analysis for Engineering Design,* Vol. 17, No. 1, pp. 1–8.

Downloaded from jrp.sagepub.com at UNIVERSITE LAVAL on June 13, 2014

Available online at www.sciencedirect.com

SCIENCE DIRECT

Journal of Sound and Vibration 270 (2004) 379–401

JOURNAL OF SOUND AND VIBRATION

www.elsevier.com/locate/jsvi

Development of an exact dynamic stiffness matrix for free vibration analysis of a twisted Timoshenko beam

J.R. Banerjee*

School of Engineering and Mathematical Sciences, City University, Northampton Square, London EC1V 0HB, UK

Received 9 September 2002; accepted 19 December 2002

Abstract

An exact dynamic stiffness matrix for a twisted Timoshenko beam is developed in this paper in order to investigate its free vibration characteristics. First the governing differential equations of motion and the associated natural boundary conditions of a twisted Timoshenko beam undergoing free natural vibration are derived using Hamilton's principle. The inclusion of a given pretwist together with the effects of shear deformation and rotatory inertia, gives rise in free vibration to four coupled second order partial differential equations of motion involving bending displacements and bending rotations in two planes. For harmonic oscillation these four partial differential equations are combined into an eighth order ordinary differential equation, which is identically satisfied by all components of bending displacements and bending rotations. This difficult task has become possible only with the help of symbolic computation. Next the exact solution of the differential equation is obtained in completely general form in terms of eight arbitrary constants. This is followed by application of boundary conditions for displacements and forces. The procedure leads to the formation of the dynamics stiffness matrix of the twisted Timoshenko beam relating harmonically varying forces with harmonically varying displacements at its ends. The resulting dynamic stiffness matrix is used with particular reference to the Wittrick–Williams algorithm to compute the natural frequencies and mode shapes of a twisted Timoshenko beam with cantilever end condition. The exact results from the present theory are compared with numerically simulated results using simpler theories, and some conclusions are drawn.

© 2003 Elsevier Ltd. All rights reserved.

1. Introduction

There is a considerable amount of published literature on the free vibration analysis of twisted beams [1–17]. Recently, the present author has made a contribution to this literature [18] by investigating the free vibration characteristics of a twisted beam by using the dynamic stiffness

---

*Tel.: +44-20-70408924; fax: +44-20-70408566.

E-mail address: j.r.banerjee@city.ac.uk (J.R. Banerjee).

0022-460X/$ - see front matter © 2003 Elsevier Ltd. All rights reserved.

doi:10.1016/S0022-460X(03)00633-3

method for the first time. It is evident from the research reported in the literature that prior to the emergence of the popular finite element method, there were some outstanding works on the subject using exact analytical methods which are based on the solution of classical differential equations of motion. In particular, the works of Troesch et al. [2] and Diprima and Handelman [3] need special mention. These developments are no-doubt significant and they are as relevant today as they were at the time, particularly when solving bench mark problems and validating the finite element and other approximate methods [10,11]. However, a striking shortcoming of these classical analytical works is that they are essentially based on Bernoulli–Euler assumptions and therefore, do not account for the effects of shear deformation and rotatory inertia on the free vibratory motion of the twisted beam.

As the search for refined beam theories has continued over the years the incorporation of the effects of shear deformation and rotatory inertia has progressively become more and more difficult. When developing a refined beam theory the inclusion of these terms is undoubtedly an increased and additional complexity. (Clearly the level of complexity increases as the beam theory becomes more and more refined.) Since Timoshenko implemented the effects of shear deformation and rotatory inertia on a simple Bernoulli–Euler beam in the earlier part of last century [19], research workers have recognized the importance of these effects. These are particularly important for natural frequencies of non-slender beams where the length-to-depth ratios are generally small, and also when higher natural frequencies are required [20]. The term "Timoshenko beam" (which represents a beam theory which accounts for shear deformation and rotatory inertia) is now universally accepted and has featured in literally hundreds of papers, covering amongst others, bending-torsion coupled (metallic) beams [21] and composite beams [22].

It appears that no one has made a serious analytical approach to investigate the free vibration characteristics of a twisted Timoshenko beam of the type analyzed here. It would seem that the expressions needed to derive the governing differential equations for the problem have proved to be too daunting. The problem is further compounded by the fact that even after the governing differential equations have been derived considerable difficulties would unavoidably arise in obtaining an explicit solution in closed analytical form. Clearly, the algebraic expressions for the solution are expected to be extensive and may possibly assume unmanageable proportions. This predominantly algebraic problem can now be overcome because a powerful tool has become available. This is, of course, symbolic computation that has made significant advances in recent years and these have taken place in different directions. It is now considered to be a break through in solid mechanics [23] and there are a number of diverse and wide-ranging symbolic computing packages currently available [24,25].

Against the above background this paper sets out to develop an exact dynamic stiffness matrix for a twisted Timoshenko beam, and then uses it to investigate its free vibration characteristics. It will be shown later that the dynamic stiffness formulation for a twisted Timoshenko beam is considerably more difficult than that of its Bernoulli–Euler counterpart [18]. A secondary object of this paper is to demonstrate a worthwhile application of symbolic computation in solving complex dynamical problems.

The structure analyzed in this paper is a twisted beam, in which the effects of transverse shear in two planes are included. This structure will necessarily undergo torsional deformation as it flexes, but in this paper this induced torsional deformation is ignored. This is a reasonable assumption for beams with doubly symmetric cross-section for which the shear centre and centroid are coincident and as a result the torsional deformation may be assumed to be uncoupled from flexure. However, the present method imposes a serious restriction when analyzing many practical twisted beams such as idealized compressor, turbine and helicopter blades for which the shear centre and centroid are not coincident. In this respect the twisted beam analyzed in this paper exists as an academic concept with limited applications, but has no doubt the merit of introducing structural effects of such complexity that successful analysis is possible only by the use of symbolic computation. Of course, the inclusion of induced twisting response further increases the complexity of the analysis very considerably. For the purpose of demonstrating the make-or-break contribution of the symbolic computation, the simplified twisted beam model that has been chosen—however unreal—is felt justified. The present investigation is considered to be a major step towards developing a more refined theory for twisted beams.

The investigation proceeds with the fundamental assumptions of allowable displacements of a twisted Timoshenko beam in coupled flexural motion. The kinetic and potential energy expressions are derived to formulate the Lagrangian. Hamilton's principle is then applied to derive the governing differential equations in free vibration. The expressions for the shear forces and bending moments at any cross-section of the beam are recovered from the natural boundary conditions, which emerge routinely from the Hamiltonian formulation. By assuming harmonic oscillation the governing partial differential equations are reduced to ordinary differential equations, and are combined into one ordinary differential equation by making substantial use of symbolic computation. The final differential equation is of eighth order and solved in closed analytical form. The boundary conditions for bending displacements, bending rotations, shear forces and bending moments are imposed on the general solution. This enables the elimination of the arbitrary constants from the general solution, leading to the formation of the dynamic stiffness matrix of the twisted Timoshenko beam. Finally using the Wittrick–Williams algorithm [26] the resulting dynamic stiffness matrix is processed to obtain natural frequencies of some chosen examples. The results are discussed and some conclusions are drawn.

2. Theory

A twisted beam of length L is shown in Fig. 1 in a right handed Cartesian co-ordinate system. The global co-ordinate axes XYZ are shown at the left-hand end of the beam whereas the local co-ordinate axes xyz (in lower cases) which vary along the length, as a result of the twist, are shown on the right-hand side. The local y and global Y axes are coincident, both passing through the centroid, and are perpendicular to the beam cross-section, and therefore, represent the axis of

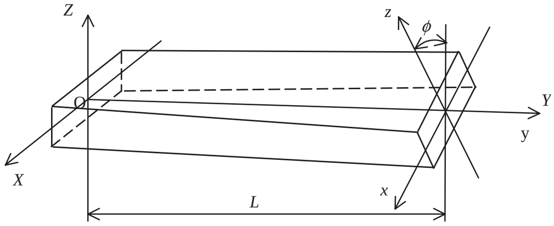

Fig. 1. Axis system and notation used for a twisted Timoshenko beam.

twist of the beam. The rate of twist k is assumed to be constant along the length. Thus, if the twist is zero at the left-hand end, and φ (in radian) at the right-hand end, then $k = \varphi/L$. The area of cross-section of the beam is A and the two principal second moment of areas are I_x and I_z, respectively.

The derivation of the governing (partial) differential equations of motion of a twisted beam (see Fig. 1) undergoing free natural vibration is of some considerable complexity, particularly when the effects of shear deformation and rotatory inertia are taken into account. This is achieved by applying Hamilton's principle (see Appendix A for details). The resulting differential equations in free vibration are presented here for the first time as follows:

$$-\rho A\ddot{u} + k_x AGu'' - k^2 k_z AGu + kAG(k_x + k_z)w' + k_x AG\psi' - kk_z AG\theta = 0, \tag{1}$$

$$-\rho A\ddot{w} + k_z AGw'' - k^2 k_x AGw - kAG(k_x + k_z)u' - kk_x AG\psi - k_z AG\theta' = 0, \tag{2}$$

$$-\rho I_x\ddot{\theta} + EI_x\theta'' - k^2 EI_z\theta - k_z AG\theta - kk_z AGu + k_z AGw' + k(EI_x + EI_z)\psi' = 0, \tag{3}$$

$$-\rho I_x\ddot{\psi} + EI_z\psi'' - k^2 EI_x\psi - k_x AG\psi - kk_x AGw - k_x AGu' - k(EI_x + EI_z)\theta' = 0, \tag{4}$$

where u and w are displacements in the x and z directions of a point lying on the centroidal axis and located at a distance y from the origin, θ and ψ are the corresponding bending rotations about the local x and y axes, ρ, E and G are respectively the density, Young's modulus and modulus of rigidity (shear modulus) of the beam material, ρA is the mass per unit length, EI_x, EI_z, $k_z AG$ and $k_x AG$ are the bending and shear rigidities in the principal planes with k_x and k_z being the shear correction (or shape) factors, and a prime and an over dot represent differentiation with respect to distance y and time t, respectively.

If harmonic variation of u, w, θ, and ψ with circular (angular) frequency ω is assumed then

$$\left.\begin{aligned} u(y,t) &= U(y)\mathrm{e}^{\mathrm{i}\omega t} \\ w(y,t) &= W(y)\mathrm{e}^{\mathrm{i}\omega t} \\ \theta(y,t) &= \Theta(y)\mathrm{e}^{\mathrm{i}\omega t} \\ \psi(y,t) &= \Psi(y)\mathrm{e}^{\mathrm{i}\omega t} \end{aligned}\right\}, \tag{5}$$

where $U(y)$, $W(y)$, $\Theta(y)$ and $\Psi(y)$ are the amplitudes of u, w, θ, and ψ in free vibration.

Substituting Eq. (5) into Eqs. (1)–(4) gives

$$k_x AGU'' - (k^2 k_z AG - \rho A\omega^2)U + kAG(k_x + k_z)W' - kk_z AG\Theta + k_x AG\Psi' = 0, \tag{6}$$

$$-kAG(k_x + k_z)U' + k_z AGW'' - (k^2 k_x AG - \rho A\omega^2)W - k_z AG\Theta' - kk_x AG\Psi = 0, \tag{7}$$

$$-kk_z AGU + k_z AGW' + EI_x\Theta'' - (k^2 EI_z + k_z AG - \rho I_x\omega^2)\Theta + k(EI_x + EI_z)\Psi' = 0, \tag{8}$$

$$-k_x AGU' - kk_x AGW - k(EI_x + EI_z)\Theta' + EI_z\Psi'' - (k^2 EI_x + k_x AG - \rho I_z\omega^2)\Psi = 0. \tag{9}$$

Introducing the non-dimensional variable ξ (in place of y) where

$$\xi = yk = y\frac{\phi}{L}. \tag{10}$$

Eqs. (6)–(9) can be written in the following form:

$$k(D^2 - \mu + b_z^2 s_z^2)U + k(1 + \mu)DW - \mu\Theta + D\Psi = 0, \tag{11}$$

$$k(1+\mu)DU - k(\mu D^2 + b_z^2 s_z^2 - 1)W + \mu D\Theta + \Psi = 0, \tag{12}$$

$$-\mu kU + \mu kDW + (\mu s_x^2 D^2 + b_z^2 r_x^2 s_z^2 - s_z^2 - \mu)\Theta + (\mu s_x^2 + s_z^2)D\Psi = 0, \tag{13}$$

$$kDU + kW + (\mu s_x^2 + s_z^2)D\Theta - (s_z^2 D^2 + b_z^2 r_z^2 s_z^2 - \mu s_x^2 - 1)\Psi = 0, \tag{14}$$

where

$$\mu = \frac{k_z}{k_x}, \quad b_x^2 = \frac{\rho A\omega^2}{EI_x k^4}, \quad b_z^2 = \frac{\rho A\omega^2}{EI_z k^4}, \tag{15}$$

$$s_x^2 = \frac{EI_x k^2}{k_z AG}, \quad s_z^2 = \frac{EI_z k^2}{k_x AG}, \quad r_x^2 = \frac{I_x k^2}{A}, \quad r_z^2 = \frac{I_z k^2}{A} \tag{16}$$

and

$$D = \frac{\mathrm{d}}{\mathrm{d}\xi}. \tag{17}$$

By carrying out an extensive amount of symbolic computation using REDUCE [24], Eqs. (11)–(14) can be combined into one differential equation by eliminating all but one of the variables U, W, Θ or Ψ to obtain, after a lot of simplification, the following eighth order differential equation:

$$(D^8 + C_1 D^6 + C_2 D^4 + C_3 D^2 + C_4)H = 0, \tag{18}$$

where

$$H = U, W, \Theta \quad \text{or } \Psi \tag{19}$$

and

$$C_1 = 4 + b_x^2(r_x^2 + s_x^2) + b_z^2(r_z^2 + s_z^2), \tag{20}$$

$$\begin{aligned} C_2 = {} & (6 - b_x^2 - b_z^2) + b_x^2 r_x^2(1 + b_x^2 s_x^2) + b_z^2 r_z^2(1 + b_z^2 s_z^2) + b_z^2(r_z^2 + s_z^2) \\ & \times \{1 + b_x^2(r_x^2 + s_x^2)\} + b_x^2(r_x^2 + s_x^2) - (b_z^2 r_x^2 + b_x^2 r_z^2), \end{aligned} \tag{21}$$

$$\begin{aligned} C_3 = {} & (4 + 6b_x^2 + 6b_z^2) - (r_x^2 + r_z^2)(b_z^4 s_z^2 + b_x^4 s_x^2) - 2(b_z^2 r_x^2 + b_x^2 r_z^2) \\ & + b_z^2(r_z^2 - s_z^2)(1 + b_x^2 r_x^2) - b_x^2 b_z^2(r_x^2 + s_x^2)(1 - b_z^2 r_z^2 s_z^2) \\ & + b_x^2(r_x^2 - s_x^2)(1 + b_z^2 r_z^2) - b_x^2 b_z^2(r_z^2 + s_z^2)(1 - b_x^2 r_x^2 s_x^2) \\ & - b_x^2 b_z^2\{s_x^2(r_x^2 - s_z^2) + s_z^2(r_z^2 - s_x^2)\}, \end{aligned} \tag{22}$$

$$\begin{aligned} C_4 = {} & (1 - b_x^2)(1 - b_z^2) + b_x^2 b_z^2 r_x^2(1 - b_z^2 r_z^2 s_z^2) + b_z^2(1 - b_x^2 r_x^2 s_x^2)(b_x^2 r_z^2 + b_z^2 s_z^2 - b_z^2 b_x^2 s_z^2 r_z^2) \\ & + b_z^2 s_z^2(b_z^2 r_x^2 + b_x^2 r_z^2) - (1 - b_x^2 s_x^2)(b_z^2 s_z^2 + b_z^2 r_x^2 + b_x^2 r_z^2) - b_x^2 s_x^2(1 - b_x^2) \\ & + b_x^2 b_z^2(r_x^2 r_z^2 - b_x^2 s_x^2 r_x^2 - b_x^2 s_x^2 s_z^2 r_z^2). \end{aligned} \tag{23}$$

The differential Eq. (18) is linear with constant coefficients so that the solution for H (and hence for U, W, Θ and Ψ) can be sought in the form

$$H = \mathrm{e}^{\lambda\xi}. \tag{24}$$

Substituting Eq. (24) into Eq. (18) yields the auxiliary (or characteristic) equation

$$\lambda^8 + C_1\lambda^6 + C_2\lambda^4 + C_3\lambda^2 + C_4 = 0. \tag{25}$$

The eighth order polynomial in λ above, can be reduced to a quartic as follows:

$$p^4 + C_1 p^3 + C_2 p^2 + C_3 p + C_4 = 0, \tag{26}$$

where

$$p = \lambda^2 \quad \text{or} \quad \lambda = \pm\sqrt{p}. \tag{27}$$

The roots of p (and hence of λ) can now be obtained by using standard procedure [27], for example, by factorizing the quartic of Eq. (26) into two quadratics. Note that the roots of p (or λ) can be real or complex depending on the coefficients of the quartic.

Thus the solutions for U, W, Θ and Ψ can be written as

$$U(\xi) = \sum_{j=1}^{8} P_j \mathrm{e}^{\lambda_j \xi} = P_1 \mathrm{e}^{\lambda_1 \xi} + P_2 \mathrm{e}^{\lambda_2 \xi} + P_3 \mathrm{e}^{\lambda_3 \xi} + P_4 \mathrm{e}^{\lambda_4 \xi} + P_5 \mathrm{e}^{\lambda_5 \xi} + P_6 \mathrm{e}^{\lambda_6 \xi} + P_7 \mathrm{e}^{\lambda_7 \xi} + P_8 \mathrm{e}^{\lambda_8 \xi}, \tag{28}$$

$$W(\xi) = \sum_{j=1}^{8} Q_j \mathrm{e}^{\lambda_j \xi} = Q_1 \mathrm{e}^{\lambda_1 \xi} + Q_2 \mathrm{e}^{\lambda_2 \xi} + Q_3 \mathrm{e}^{\lambda_3 \xi} + Q_4 \mathrm{e}^{\lambda_4 \xi} + Q_5 \mathrm{e}^{\lambda_5 \xi} + Q_6 \mathrm{e}^{\lambda_6 \xi} + Q_7 \mathrm{e}^{\lambda_7 \xi} + Q_8 \mathrm{e}^{\lambda_8 \xi}, \tag{29}$$

$$\Theta(\xi) = \sum_{j=1}^{8} R_j \mathrm{e}^{\lambda_j \xi} = R_1 \mathrm{e}^{\lambda_1 \xi} + R_2 \mathrm{e}^{\lambda_2 \xi} + R_3 \mathrm{e}^{\lambda_3 \xi} + R_4 \mathrm{e}^{\lambda_4 \xi} + R_5 \mathrm{e}^{\lambda_5 \xi} + R_6 \mathrm{e}^{\lambda_6 \xi} + R_7 \mathrm{e}^{\lambda_7 \xi} + R_8 \mathrm{e}^{\lambda_8 \xi} \tag{30}$$

and

$$\Psi(\xi) = \sum_{j=1}^{8} S_j \mathrm{e}^{\lambda_j \xi} = S_1 \mathrm{e}^{\lambda_1 \xi} + S_2 \mathrm{e}^{\lambda_2 \xi} + S_3 \mathrm{e}^{\lambda_3 \xi} + S_4 \mathrm{e}^{\lambda_4 \xi} + S_5 \mathrm{e}^{\lambda_5 \xi} + S_6 \mathrm{e}^{\lambda_6 \xi} + S_7 \mathrm{e}^{\lambda_7 \xi} + S_8 \mathrm{e}^{\lambda_8 \xi}, \tag{31}$$

where $\lambda_j (j = 1, 2, \ldots, 8)$ are the eight roots of the auxiliary Eq. (25) and P_j, Q_j, R_j, and S_j are four different sets of constants.

It can be shown by substituting Eqs. (28)–(31) into Eqs. (11)–(14) that the constants P_j, Q_j, R_j, and S_j are related as follows:

$$Q_j = \alpha_j P_j, \quad R_j = (\phi\beta_j/L)P_j, \quad S_j = (\phi\gamma_j/L)P_j, \tag{32}$$

where

$$\alpha_j = -\lambda_j A_j/B_j, \quad \beta_j = -A_j/C_j, \quad \gamma_j = -D_j/(\lambda_j C_j) \tag{33}$$

with

$$A_j = b_z^2 s_z^2(-\mu\eta_1 + \mu\varsigma_j + \eta_3) + \mu\rho_j(1 - \eta_1 + \varsigma_j - \eta_3), \tag{34}$$

$$B_j = b_z^2 s_z^2(\mu\eta_1 - \mu\varsigma_j + \eta_3\lambda_j^2) + \mu\rho_j(1 - \eta_1 + \varsigma_j + \eta_3\lambda_j^2), \tag{35}$$

$$C_j = b_z^2 s_z^2(\mu\eta_1 r_x^2 + \eta_2 r_z^2) - \eta_4(\tau_j + \sigma_j + \mu s_x^2 s_z^2 \rho_j^2) - 2\mu\eta_3\kappa_j, \tag{36}$$

$$D_j = b_z^2 s_z^2(\eta_2 + \mu\eta_3\lambda_j^2 - \varepsilon_j) + \mu\rho_j(\mu - \eta_2 + \varepsilon_j + \eta_3\lambda_j^2), \tag{37}$$

$$\eta_1 = 1 - b_z^2 r_z^2 s_z^2, \quad \eta_2 = \mu - b_z^2 r_x^2 s_z^2, \quad \eta_3 = \mu s_x^2 + s_z^2, \quad \eta_4 = \mu + 1, \tag{38}$$

$$\varsigma_j = s_z^2\lambda_j^2 - \mu s_x^2, \quad \rho_j = 1 + \lambda_j^2, \quad \kappa_j = 1 - \lambda_j^2, \tag{39}$$

$$\tau_j = \mu b_z^2 s_x^2 s_z^2(r_z^2\lambda_j^2 - r_x^2), \quad \sigma_j = b_z^2 s_z^4(r_x^2\lambda_j^2 - r_z^2), \quad \varepsilon_j = \mu s_x^2\lambda_j^2 - s_z^2. \tag{40}$$

The expressions for shear force and bending moment in the local axis system (see Appendix A) for harmonic oscillation of the beam, are given by

$$\begin{aligned}V_x &= -EI_zk^2[\Psi'' - r\Psi - (r+1)\Theta' + b_z^2r_z^2\Psi] \\ &= -EI_zk^2\left[\sum_{j=1}^{8}\lambda_j^2S_j\mathrm{e}^{\lambda_j\xi} - r\sum_{j=1}^{8}S_j\mathrm{e}^{\lambda_j\xi} - (r+1)\sum_{j=1}^{8}\lambda_jR_j\mathrm{e}^{\lambda_j\xi} + b_z^2r_z^2\sum_{j=1}^{8}S_j\mathrm{e}^{\lambda_j\xi}\right] \\ &= -EI_zk^3\sum_{j=1}^{8}[\gamma_j(\lambda_j^2 - r + b_z^2r_z^2) - (r+1)\beta_j\lambda_j]P_j\mathrm{e}^{\lambda_j\xi},\end{aligned} \tag{41}$$

$$\begin{aligned}V_z &= \frac{EI_x}{r}k^2[r\Theta'' - \Theta + (r+1)\Psi' + b_z^2r_x^2\Theta] \\ &= \frac{EI_x}{r}k^2\left[r\sum_{j=1}^{8}\lambda_j^2R_j\mathrm{e}^{\lambda_j\xi} - \sum_{j=1}^{8}R_j\mathrm{e}^{\lambda_j\xi} + (r+1)\sum_{j=1}^{8}\lambda_jS_j\mathrm{e}^{\lambda_j\xi} + b_z^2r_x^2\sum_{j=1}^{8}R_j\mathrm{e}^{\lambda_j\xi}\right] \\ &= \frac{EI_x}{r}k^3\sum_{j=1}^{8}[\beta_j(r\lambda_j^2 - 1 + b_z^2r_x^2) + (r+1)\gamma_j\lambda_j]P_j\mathrm{e}^{\lambda_j\xi}\end{aligned} \tag{42}$$

and

$$M_x = -EI_xk(\Theta' + \Psi) = -EI_xk\left[\sum_{j=1}^{8}\lambda_jR_j\mathrm{e}^{\lambda_j\xi} + \sum_{j=1}^{8}S_j\mathrm{e}^{\lambda_j\xi}\right] = -EI_xk^2\sum_{j=1}^{8}(\beta_j\lambda_j + \gamma_j)P_j\mathrm{e}^{\lambda_j\xi}, \tag{43}$$

$$M_z = -EI_zk(\Psi' - \Theta) = -EI_zk\left[\sum_{j=1}^{8}\lambda_jS_j\mathrm{e}^{\lambda_j\xi} - \sum_{j=1}^{8}R_j\mathrm{e}^{\lambda_j}\right] = -EI_zk^2\sum_{j=1}^{8}(\gamma_j\lambda_j - \beta_j)P_j\mathrm{e}^{\lambda_j\xi}, \tag{44}$$

where a prime now denotes differentiation with respect to ξ and

$$r = \frac{EI_x}{EI_z}. \tag{45}$$

The dynamic stiffness matrix of the twisted beam can now be obtained by applying the boundary condition for displacements and forces at its ends.

The boundary conditions for the bending displacement and bending rotation are:

At the left-hand end:

$$y = 0\,(\xi = 0)\colon\ U = U_{x1},\quad W = W_{z1},\quad \Theta = \Theta_{x_1},\quad \Psi = \Psi_{z_1}. \tag{46}$$

At the right-hand end:

$$y = L\,(\xi = \phi = kL)\colon\ U = U_{x2},\quad W = W_{z2},\quad \Theta = \Theta_{x_2},\quad \Psi = \Psi_{z2}. \tag{47}$$

The boundary conditions for the shear force and bending moment are:

At the left-hand end:

$$y = 0\,(\xi = 0)\colon\ V_x = V_{x1}, V_z = V_{z1}, M_x = M_{x1}, M_z = M_{z1} \tag{48}$$

At the right-hand end:

$$y = 0\,(\xi = \phi = kL)\colon\ V_x = -V_{x2}, V_z = -V_{z2}, M_x = -M_{x2}, M_z = -M_{z2} \tag{49}$$

Substituting Eqs. (46) and (47) into Eqs. (28)–(31) gives

$$U_{x1} = U(0) = \sum_{j=1}^{8} P_j, \tag{50}$$

$$W_{z1} = W(0) = \sum_{j=1}^{8} \alpha_j P_j, \tag{51}$$

$$\Theta_{x1} = \Theta(0) = k \sum_{j=1}^{8} \beta_j P_j, \tag{52}$$

$$\Psi_{z1} = \Psi(0) = k \sum_{j=1}^{8} \gamma_j P_j \tag{53}$$

and

$$U_{x2} = U(\phi) = \sum_{j=1}^{8} P_j \mathrm{e}^{\lambda_j \phi}, \tag{54}$$

$$W_{z2} = W(\phi) = \sum_{j=1}^{8} \alpha_j P_j \mathrm{e}^{\lambda_j \phi}, \tag{55}$$

$$\Theta_{x2} = \Theta(\phi) = k \sum_{j=1}^{8} \beta_j P_j \mathrm{e}^{\lambda_j \phi}, \tag{56}$$

$$\Psi_{z2} = \Psi(\phi) = k \sum_{j=1}^{8} \gamma_j P_j \mathrm{e}^{\lambda_j \phi}, \tag{57}$$

Eqs. (50) and (57) can be written in matrix form as follows:

$$\begin{bmatrix} U_{x1} \\ W_{z1} \\ \Theta_{x1} \\ \Psi_{z1} \\ U_{x2} \\ W_{z2} \\ \Theta_{x2} \\ \Psi_{z2} \end{bmatrix} = \begin{bmatrix} R_{11} & R_{12} & R_{13} & R_{14} & R_{15} & R_{16} & R_{17} & R_{18} \\ R_{21} & R_{22} & R_{23} & R_{24} & R_{25} & R_{26} & R_{27} & R_{28} \\ R_{31} & R_{32} & R_{33} & R_{34} & R_{35} & R_{36} & R_{37} & R_{38} \\ R_{41} & R_{42} & R_{43} & R_{44} & R_{45} & R_{46} & R_{47} & R_{48} \\ R_{51} & R_{52} & R_{53} & R_{54} & R_{55} & R_{56} & R_{57} & R_{58} \\ R_{61} & R_{62} & R_{63} & R_{64} & R_{65} & R_{66} & R_{67} & R_{68} \\ R_{71} & R_{72} & R_{73} & R_{74} & R_{75} & R_{76} & R_{77} & R_{78} \\ R_{81} & R_{82} & R_{83} & R_{84} & R_{85} & R_{86} & R_{87} & R_{88} \end{bmatrix} \begin{bmatrix} P_1 \\ P_2 \\ P_3 \\ P_4 \\ P_5 \\ P_6 \\ P_7 \\ P_8 \end{bmatrix} \tag{58}$$

or

$$\boldsymbol{\delta} = \mathbf{RP}, \tag{59}$$

where the elements of $\mathbf{R}$ (for $j = 1, 2, 3 \ldots 8$) are given by

$$R_{1j} = 1, \tag{60}$$

$$R_{2j} = \alpha_j, \tag{61}$$

$$R_{3j} = k\beta_j, \tag{62}$$

$$R_{4j} = k\gamma_j, \tag{63}$$

$$R_{5j} = \mathrm{e}^{\lambda_j \phi}, \tag{64}$$

$$R_{6j} = \alpha_j \mathrm{e}^{\lambda_j \phi}, \tag{65}$$

$$R_{7j} = k\beta_j \mathrm{e}^{\lambda_j \phi}, \tag{66}$$

$$R_{8j} = k\gamma_j \mathrm{e}^{\lambda_j \phi}. \tag{67}$$

Substituting Eqs. (48)–(49) into Eqs. (41)–(44), gives

$$V_{x1} = V_x(0) = -EI_z k^3 \sum_{j=1}^{8} [\gamma_j(\lambda_j^2 + b_z^2 r_z^2 - r) - (r+1)\beta_j \lambda_j] P_j, \tag{68}$$

$$V_{z1} = V_z(0) = \frac{EI_x}{r} k^3 \sum_{j=1}^{8} [\beta_j(r\lambda_j^2 + b_z^2 r_x^2 - 1) + (r+1)\gamma_j \lambda_j] P_j, \tag{69}$$

$$M_{x1} = M_x(0) = -EI_x k^2 \sum_{j=1}^{8} (\beta_j \lambda_j + \gamma_j) P_j, \tag{70}$$

$$M_{z1} = M_z(0) = -EI_z k^2 \sum_{j=1}^{8} (\gamma_j \lambda_j - \beta_j) P_j \tag{71}$$

and

$$V_{x2} = V_x(\phi) = EI_z k^3 \sum_{j=1}^{8} [\gamma_j(\lambda_j^2 + b_z^2 r_z^2 - r) - (r+1)\beta_j \lambda_j] P_j \mathrm{e}^{\lambda_j \phi}, \tag{72}$$

$$V_{z2} = V_z(\phi) = -\frac{EI_x}{r} k^3 \sum_{j=1}^{8} [\beta_j(r\lambda_j^2 + b_z^2 r_x^2 - 1) + (r+1)\gamma_j \lambda_j] P_j \mathrm{e}^{\lambda_j \phi}, \tag{73}$$

$$M_{x2} = M_x(\phi) = EI_x k^2 \sum_{j=1}^{8} (\beta_j \lambda_j + \gamma_j) P_j \mathrm{e}^{\lambda_j \phi}, \tag{74}$$

$$M_{z2} = M_z(\phi) = EI_z k^2 \sum_{j=1}^{8} (\gamma_j \lambda_j - \beta_j) P_j \mathrm{e}^{\lambda_j \phi}, \tag{75}$$

Eqs. (68)–(75) can be written in matrix form as follows:

$$\begin{bmatrix} V_{x_1} \\ V_{z_1} \\ M_{x_1} \\ M_{z_1} \\ V_{x2} \\ V_{z2} \\ M_{x2} \\ M_{z2} \end{bmatrix} = \begin{bmatrix} Q_{11} & Q_{12} & Q_{13} & Q_{14} & Q_{15} & Q_{16} & Q_{17} & Q_{18} \\ Q_{21} & Q_{22} & Q_{23} & Q_{24} & Q_{25} & Q_{26} & Q_{27} & Q_{28} \\ Q_{31} & Q_{32} & Q_{33} & Q_{34} & Q_{35} & Q_{36} & Q_{37} & Q_{38} \\ Q_{41} & Q_{42} & Q_{43} & Q_{44} & Q_{45} & Q_{46} & Q_{47} & Q_{48} \\ Q_{51} & Q_{52} & Q_{53} & Q_{54} & Q_{55} & Q_{56} & Q_{57} & Q_{58} \\ Q_{61} & Q_{62} & Q_{63} & Q_{64} & Q_{65} & Q_{66} & Q_{67} & Q_{68} \\ Q_{71} & Q_{72} & Q_{73} & Q_{74} & Q_{75} & Q_{76} & Q_{77} & Q_{78} \\ Q_{81} & Q_{82} & Q_{83} & Q_{84} & Q_{85} & Q_{86} & Q_{87} & Q_{88} \end{bmatrix} \begin{bmatrix} P_1 \\ P_2 \\ P_3 \\ P_4 \\ P_5 \\ P_6 \\ P_7 \\ P_8 \end{bmatrix} \tag{76}$$

or

$$\mathbf{F} = \mathbf{QP}, \tag{77}$$

where the elements of $\mathbf{Q}$ (for $j = 1, 2, \ldots, 8$) are given by

$$Q_{1j} = -EI_z k^3[\gamma_j(\lambda_j^2 + b_z^2 r_z^2 - r) - (r+1)\beta_j\lambda_j], \tag{78}$$

$$Q_{2j} = \frac{EI_x}{r} k^3[\beta_j(r\lambda_j^2 + b_z^2 r_x^2 - 1) + (r+1)\gamma_j\lambda_j], \tag{79}$$

$$Q_{3j} = -EI_x k^2(\beta_j\lambda_j + \gamma_j), \tag{80}$$

$$Q_{4j} = -EI_z k^2(\gamma_j\lambda_j - \beta_j) \tag{81}$$

and

$$Q_{5j} = EI_z k^3[\gamma_j(\lambda_j^2 + b_z^2 r_z^2 - r) - (r+1)\beta_j\lambda_j]\mathrm{e}^{\lambda_j\phi}, \tag{82}$$

$$Q_{6j} = -\frac{EI_x}{r} k^3[\beta_j(r\lambda_j^2 + b_z^2 r_x^2 - 1) + (r+1)\gamma_j\lambda_j]\mathrm{e}^{\lambda_j\phi}, \tag{83}$$

$$Q_{7j} = EI_x k^2(\beta_j\lambda_j + \gamma_j)\mathrm{e}^{\lambda_j\phi}, \tag{84}$$

$$Q_{8j} = EI_z k^2(\gamma_j\lambda_j - \beta_j)\mathrm{e}^{\lambda_j\phi}. \tag{85}$$

The constant vector $\mathbf{P}$ can now be eliminated from Eqs. (59) and (77) to give

$$\mathbf{F} = \mathbf{QR}^{-1}\boldsymbol{\delta} = \mathbf{K}\boldsymbol{\delta}, \tag{86}$$

where

$$\mathbf{K} = \mathbf{QR}^{-1} \tag{87}$$

is the required dynamic stiffness matrix.

When computing the dynamic stiffness matrix $\mathbf{K}$, it should be noted that the roots of p and hence for λ, see Eqs. (25) and (26), can be complex and as a consequence, the elements of matrices $\mathbf{Q}$ and $\mathbf{R}$ can be complex. Therefore, the matrix inversion and multiplication steps of Eq. (87) must be carried out using complex arithmetic. The resulting dynamic stiffness matrix $\mathbf{K}$ will, of course, be symmetric and real, with imaginary parts of each element being zero.

Thus, the force displacement relationship at the nodes of the harmonically vibrating twisted Timoshenko beam is given by

$$\begin{bmatrix} V_{x1} \\ V_{z_1} \\ M_{x_1} \\ M_{z_1} \\ V_{x2} \\ V_{z2} \\ M_{x2} \\ M_{z2} \end{bmatrix} = \begin{bmatrix} K_{11} & K_{12} & K_{13} & K_{14} & K_{15} & K_{16} & K_{17} & K_{18} \\ & K_{22} & K_{23} & K_{24} & K_{25} & K_{26} & K_{27} & K_{28} \\ & & K_{33} & K_{34} & K_{35} & K_{36} & K_{37} & K_{38} \\ & & & K_{44} & K_{45} & K_{46} & K_{47} & K_{48} \\ & & & & K_{55} & K_{56} & K_{57} & K_{58} \\ & S & Y & M & & K_{66} & K_{67} & K_{68} \\ & & & & & & K_{77} & K_{78} \\ & & & & & & & K_{88} \end{bmatrix} \begin{bmatrix} U_{x1} \\ W_{z1} \\ \Theta_{x_1} \\ \Psi_{z1} \\ U_{x2} \\ W_{z2} \\ \Theta_{x_2} \\ \Psi_{z_2} \end{bmatrix}. \tag{88}$$

It is now necessary to transform the above relationship to global co-ordinates using an appropriate transformation. Clearly, the displacements and forces at the left-hand end of the twisted beam are already in global co-ordinates, whereas the corresponding displacements and forces at the right-hand end are in local co-ordinates (see Figs. 1 and 2).

Referring to Fig. 2, the shear forces and bending moments at the right hand of the element can be resolved from global to local co-ordinates as follows. (Note that the lower and upper cases have been respectively used for the suffices of shear forces and bending moments to indicate whether they correspond to local or global co-ordinates.)

$$V_{x_2} = V_{X_2}\cos\phi - V_{Z_2}\sin\phi, \tag{89}$$

$$V_{z_2} = V_{X_2}\sin\phi + V_{Z_2}\cos\phi, \tag{90}$$

$$M_{x_2} = M_{X_2}\cos\phi - M_{Z_2}\sin\phi, \tag{91}$$

$$M_{z_2} = M_{X_2}\sin\phi + M_{Z_2}\cos\phi. \tag{92}$$

Thus, the relationships for the shear force and bending moment between the global and local co-ordinates at both ends of the beam element can be expressed as

$$\begin{bmatrix} V_{x_1} \\ V_{z_1} \\ M_{x_1} \\ M_{z1} \\ V_{x_2} \\ V_{z_2} \\ M_{x_2} \\ M_{z_2} \end{bmatrix} = \begin{bmatrix} 1 & 0 & 0 & 0 & 0 & 0 & 0 & 0 \\ 0 & 1 & 0 & 0 & 0 & 0 & 0 & 0 \\ 0 & 0 & 1 & 0 & 0 & 0 & 0 & 0 \\ 0 & 0 & 0 & 1 & 0 & 0 & 0 & 0 \\ 0 & 0 & 0 & 0 & c & -s & 0 & 0 \\ 0 & 0 & 0 & 0 & s & c & 0 & 0 \\ 0 & 0 & 0 & 0 & 0 & 0 & c & -s \\ 0 & 0 & 0 & 0 & 0 & 0 & s & c \end{bmatrix} \begin{bmatrix} V_{X_1} \\ V_{Z_1} \\ M_{X_1} \\ M_{Z_1} \\ V_{X_2} \\ V_{Z_2} \\ M_{X_2} \\ M_{Z_2} \end{bmatrix}, \tag{93}$$

where

$$c = \cos\phi \tag{94}$$

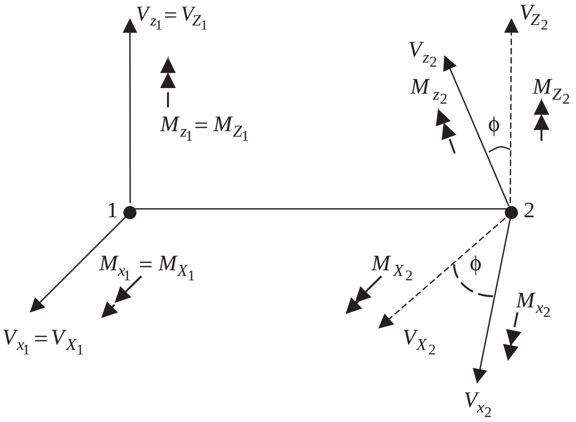

Fig. 2. Shear forces and bending moments at the ends of the twisted Timoshenko beam shown in local and global co-ordinates.

and

$$s = \sin\phi. \tag{95}$$

The displacements can be transformed from the global to local co-ordinates exactly in the same way as the forces by making use of the above transformation matrix **T**, given by

$$\mathbf{T} = \begin{bmatrix} 1 & 0 & 0 & 0 & 0 & 0 & 0 & 0 \\ 0 & 1 & 0 & 0 & 0 & 0 & 0 & 0 \\ 0 & 0 & 1 & 0 & 0 & 0 & 0 & 0 \\ 0 & 0 & 0 & 1 & 0 & 0 & 0 & 0 \\ 0 & 0 & 0 & 0 & c & -s & 0 & 0 \\ 0 & 0 & 0 & 0 & s & c & 0 & 0 \\ 0 & 0 & 0 & 0 & 0 & 0 & c & -s \\ 0 & 0 & 0 & 0 & 0 & 0 & s & c \end{bmatrix}. \tag{96}$$

In this way the stiffness matrix of the twisted beam in global co-ordinates $\tilde{\mathbf{K}}$ can now be formulated as

$$\tilde{\mathbf{K}} = \mathbf{T}'\mathbf{K}\mathbf{T}, \tag{97}$$

where $\mathbf{T}'$ denotes the transpose of the transformation matrix **T**.

3. Application of Wittrick–Williams algorithm

The dynamic stiffness matrix of Eq. (88) can now be used to compute the natural frequencies and mode shapes of twisted Timoshenko beams with various end conditions. A non-uniform twisted Timoshenko beam can also be analyzed for its free vibration characteristics by idealizing it as an assemblage of many uniform twisted Timoshenko beams. An accurate and reliable method of calculating the natural frequencies and mode shapes of a structure using the dynamic stiffness method is to apply the well-known algorithm of Wittrick and Williams [26] which has featured in numerous papers [28,29]. Before applying the algorithm the dynamic stiffness matrices of all individual elements in a structure are to be assembled to form the overall dynamic stiffness matrix $\mathbf{K}_f$ of the final (complete) structure, which may, of course, consist of a single element. The algorithm monitors the Sturm sequence condition of $\mathbf{K}_f$ in such a way that there is no possibility of missing a frequency (or mode) of the structure. This is, of course, not possible in the conventional finite element method. The algorithm (unlike its proof) is very simple to use and because of its extensive coverage in the literature the procedure is not repeated here, but interested investigators are recommended to read Refs. [28,29].

4. Scope of the theory and restrictions

The twisted beam considered in this paper is assumed to behave according to the Timoshenko theory which accounts for the effects of shear deformation and rotatory inertia, but the beam has a constant rate of twist along its length and is assumed to exhibit coupling between bending displacements only. These displacements are considered to be uncoupled with torsional and/or extensional deformations. Also the cross-section of the beam is not allowed to warp. These assumptions are quite legitimate for many twisted beams with doubly symmetric cross-section, but they can be severe for many other (practical) twisted beams such as helicopter or turbine blades for which coupling between bending, torsional and extensional deformations and the rotational speed can have significant effects. The dynamic stiffness development of such complex twisted beams involves much more difficulty requiring additional insights.

5. Results and discussion

The dynamic stiffness theory developed above for a twisted Timoshenko beam is applied to a cantilever blade taken from the literature [13,18]. This example is particularly suitable for investigating the degenerate case when the effects of shear deformation and rotatory inertia are ignored so that the results become directly comparable with published results. However, in order to validate the theory and demonstrate the accuracy of results using the Timoshenko theory, the well-established computer program BUNVIS-RG [30,31] that evaluates the dynamic stiffness method for untwisted Timoshenko beam elements is used. When modelling a twisted beam and preparing data for BUNVIS-RG a large number of untwisted beam elements with an appropriate orientation of each was utilized. The example blade [13,18] has a length $L = 3.048\,\text{m}$ with a substantial angle of twist which is zero at the root and 40° at the tip so that the rate of twist $k = \phi/L = 0.22905\,\text{radian/m}$. The structural and other properties used are: (i) $E = 70 \times 10^9\,\text{N/m}^2$, (ii) $G = 27 \times 10^9\,\text{N/m}^2$, (iii) $\rho = 2700\,\text{kg/m}^3$, (iv) $A = 0.0127667\,\text{m}^2$, (vi) $EI_x = 2869.7\,\text{N}\,\text{m}^2$, (vii) $EI_z = 57393\,\text{N}\,\text{m}^2$, (vii) $k_x = 2/3$, and (viii) $k_z = 5/8$.

The first five natural frequencies of the blade obtained from the present theory are shown in Table 1 together with those obtained from the Bernoulli–Euler theory [18]. Shear deformation and rotatory inertia have had very little effect on the natural frequencies of this particular blade. This is because the blade is extremely slender and the key parameters r_x, r_z, s_x and s_z which principally affect the natural frequencies when using the Timoshenko theory are very small for the problem. These are $r_x = 0.00041$, $r_z = 0.00184$, $s_x = 0.00081$, and $s_z = 0.00362$. The slenderness ratios of the

Table 1
Natural frequencies of a twisted blade [13,18] with cantilever end condition

Frequency number	Natural frequency (rad/s)	
	Bernoulli–Euler theory [18]	Present theory
1	3.4717	3.4715
2	13.347	13.340
3	25.171	25.165
4	56.372	56.363
5	103.26	103.20

blade in the two principal planes ($(L/\sqrt{I_x/A})$ and $(L/\sqrt{I_z/A})$) being, respectively, around 1700 and 380 are thus very large. Of course, the shear deformation and rotatory inertia are not expected to have any major effect on the natural frequencies of such a very slender blade. However, the results of Table 1 indicate that when the effects of shear deformation and rotatory inertia are taken into account, the natural frequencies decrease as expected.

A more appropriate comparison is made with the same illustrative example as above, but with the bending rigidities EI_x and EI_z increased by a factor of 5000. This gives the Timoshenko beam parameters $r_x = 0.029$, $r_z = 0.130$, $s_x = 0.057$, and $s_z = 0.256$. The first three natural frequencies of the twisted cantilever beam obtained using the present theory are shown in Table 2 alongside the results obtained using the Bernoulli–Euler theory [18]. The significant difference in results between the Timoshenko and the Bernoulli–Euler theories is apparent, particularly for the second and third natural frequencies of the twisted beam. Similar results were obtained using BUNVIS-RG [30,31] with a large number of untwisted beam elements. It has earlier been established [18,32] that approximate results of a discretized structure using a number of uniform straight elements converge almost parabolically to the exact result with increasing number of elements. The first three natural frequencies for the cantilever obtained from BUNVIS-RG [30,31] using 10 and 20 elements and their parabolic limits are shown in Table 3 using both the Bernoulli–Euler and the Timoshenko theories. A comparison of results illustrated in Tables 2 and 3 shows good agreement, and they clearly indicate that the parabolic limit of the approximate natural frequencies agrees to five-figure accuracy to the exact ones which is in accord with earlier investigations [18,32].

The final set of results using the present theory was obtained to demonstrate the effects of slenderness ratio on the natural frequencies of a twisted Timoshenko beam. Using a cantilever twisted Timoshenko beam with the same rate of twist as above, a comparison of natural frequencies was made between this beam and that of an untwisted beam. For both twisted and untwisted beams the computed natural frequencies with the inclusion of the effects of shear deformation and rotatory inertia (ω_n^T) are compared with those (ω_n^B) obtained when using the Bernoulli–Euler theory [18]. The percentage difference in the result $((\omega_n^B - \omega_n^T)/\omega_n^B) \times 100\%$ is plotted against the slenderness ratio (L/r_G) of the twisted beam, where the radius of gyration r_G is defined as $r_G = \sqrt[4]{(I_x I_z/A^2)}$. The plot for the first three natural frequencies ($n = 1$, 2 and 3) for the twisted beam is shown in Fig. 3 by solid lines whereas the corresponding results for the untwisted beam are shown by broken lines. These results demonstrate that the effects of shear deformation and rotatory inertia on the natural frequencies of a twisted beam are similar to those encountered in an untwisted beam. However, the effects are seen to be marginally more pronounced in the case

Table 2
Effects of shear deformation and rotatory inertia on the natural frequencies of a cantilever twisted beam

Frequency number	Natural frequency (rad/s)		
	Bernoulli–Euler theory [18] $r_x = r_z = s_x = s_z = 0$	Present theory $r_x = 0.029$, $r_z = 0.130$, $s_x = 0.057$, $s_z = 0.256$	% difference
1	245.50	239.09	2.61
2	943.38	769.77	18.40
3	1779.6	1425.5	19.90

Table 3
Natural frequencies of a twisted beam computed by BUNVIS-RG [30,31] using straight untwisted beam elements

Frequency number	Natural frequency (rad/s)					
	Bernoulli–Euler theory			Timoshenko theory		
	10 elements	20 elements	Parabolic limit	10 elements	20 elements	Parabolic limit
1	245.47	245.49	245.50	239.06	239.08	239.09
2	946.26	944.10	943.38	771.01	770.08	769.77
3	1769.7	1777.1	1779.6	1421.9	1424.6	1425.5

of a twisted beam than that of an untwisted one. As expected the effects are more significant for higher natural frequencies and smaller slenderness ratios.

6. Conclusions

The governing differential equations of motion of a twisted Timoshenko beam undergoing free natural vibration are derived applying Hamilton's principle. These are subsequently used to develop the dynamic stiffness matrix of the twisted Timoshenko beam. The application of the dynamic stiffness matrix is demonstrated by numerical results with particular reference to the Wittrick–Williams algorithm. The exact results from the present theory are validated by predicting the parabolic limit of approximate results obtained from the idealization of a twisted Timoshenko beam using a large number of untwisted beam elements. The shear deformation and rotatory inertia have similar effects on the natural frequencies of a twisted beam as they have on an untwisted beam. The research presented in this paper can be used as an aid to validate the finite element and other approximate methods, and is expected to stimulate further research on the dynamic stiffness development of complex structural elements.

Appendix A. Derivation of the governing differential equations of motion of a twisted Timoshenko beam

Hamiltonian mechanics is used to derive the governing differential equations of motion of a freely vibrating twisted Timoshenko beam, which has a uniform rate of twist along its length.

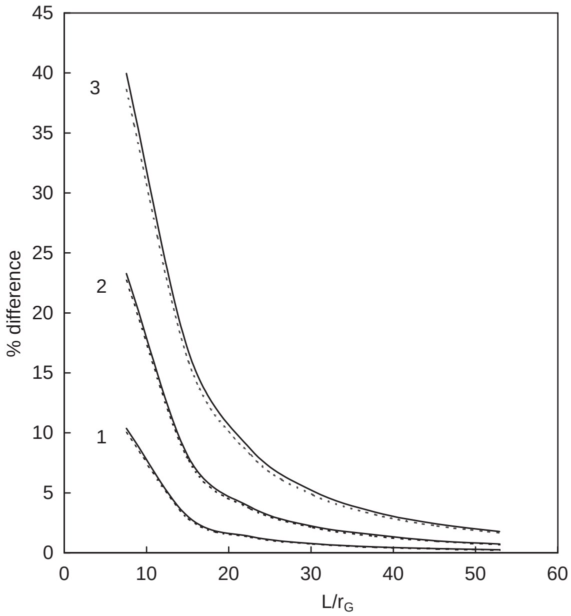

Fig. 3. The effects of shear deformation and rotatory inertia on the variation of the first three natural frequencies of a twisted and an untwisted beams as a function of slenderness ratio. —— twisted beam ($\phi = 40°$, $k = 0.22905\,\text{rad/m}$), ----- untwisted beam ($\phi = 0°$, $k = 0\,\text{rad/m}$).

A set of allowable displacements and rotations is used as the starting point to form the system of direct and shearing strains. The expressions for strain energy and kinetic energy are then derived and subsequently used when applying Hamilton's principle.

In Fig. 4, $O(X, Y, Z)$ is an inertial frame, with OY along the line of centroids of the undeflected beam cross-sections. Let G be the centroid at $Y = y$, and Gx and Gz principal axes in bending of the cross-section. The two-dimensional axis system in the plane of the cross-section represented by $G(x, z)$ has a right handed rotation ϕ about OY, so that the angle between Gx and OX (and also between Gz and OZ) is ϕ as shown. This is the angle of twist at y so that the rate of twist k (which is assumed to be constant) is $\partial\phi/\partial y$.

Let the local displacements be u along Gx and w along Gz, and θ and ψ be the rotations of the cross-section about the x- and z-axis, respectively. Now consider an adjacent section at $Y = y + \mathrm{d}y$, and let $\bar{G}(\bar{x}, \bar{z})$ be the corresponding axis system, see Fig. 5. Allowing for the relative rotation $\mathrm{d}\phi = k\,\mathrm{d}y$ of the element $\mathrm{d}y$, the axial and shearing strains of a point P on the Gxz-plane due to bending and shearing actions can be derived by identifying the elastic distortion of an element of sides $\mathrm{d}y$, $\mathrm{d}x$ and $\mathrm{d}z$ as follows.

A.1. Expression for shearing strains and strain energy due to shear

Since the displacements at G are u along Gx and w along Gz, the corresponding displacements at $\bar{G}$ are $u + (\partial u/\partial y)\,\mathrm{d}y$ along $\bar{G}\bar{x}$ and $w + (\partial w/\partial y)\,\mathrm{d}y$ along $\bar{G}\bar{z}$. Now to examine the shearing strains γ_{xy} and γ_{zy} at P (see Fig. 5) it is necessary to determine the change in the right angle formed

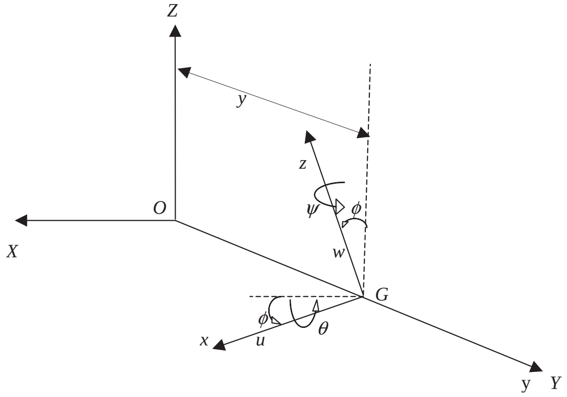

Fig. 4. Displacements and rotations of the centroid G at a distance y from the origin of the twisted Timoshenko beam shown in local co-ordinates.

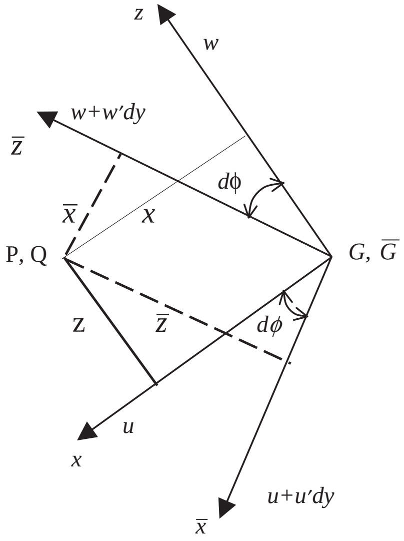

Fig. 5. Displacements of the centroids G and $\bar{G}$ at the left and right-hand ends of an elemental length dy of the twisted Timoshenko beam shown in local co-ordinates.

by lines drawn through P parallel to Gx and Gy for the evaluation of γ_{xy} and lines drawn parallel to Gz and Gy for the evaluation of γ_{zy}.

The displacements $u + (\partial u/\partial y)\,\mathrm{d}y$ along $\bar{G}\bar{x}$ and $w + (\partial w/\partial y)\,\mathrm{d}y$ along $\bar{G}\bar{z}$ will have the following components (see Fig. 5):

$$\left(u + \frac{\partial u}{\partial y}\mathrm{d}y\right)\cos(\mathrm{d}\phi) + \left(w + \frac{\partial w}{\partial y}\mathrm{d}y\right)\sin(\mathrm{d}\phi) \quad \text{along } Gx$$

and

$$-\left(u + \frac{\partial u}{\partial y}\mathrm{d}y\right)\sin(\mathrm{d}\phi) + \left(w + \frac{\partial w}{\partial y}\mathrm{d}y\right)\cos(\mathrm{d}\phi) \quad \text{along } Gz.$$

Using the general rules for infinitesimal calculus and neglecting higher order terms so that $\cos(\mathrm{d}\varphi) \cong 1$ and $\sin(\mathrm{d}\varphi) \cong \mathrm{d}\varphi$ in the limit, the above components can now be written as

$$u + \frac{\partial u}{\partial y}\mathrm{d}y + w\frac{\partial \phi}{\partial y}\mathrm{d}y, \quad \text{along } Gx$$

and

$$-u\frac{\partial \phi}{\partial y}\mathrm{d}y + w + \frac{\partial w}{\partial y}\mathrm{d}y, \quad \text{along } Gz.$$

Thus, the relative displacements in planes $\bar{G}\bar{x}\bar{z}$ and Gxz are

$$\left(\frac{\partial u}{\partial y} + w\frac{\partial \phi}{\partial y}\right)\mathrm{d}y = \left(\frac{\partial u}{\partial y} + kw\right)\mathrm{d}y, \quad \text{along } Gx$$

and

$$\left(-u\frac{\partial \phi}{\partial y} + \frac{\partial w}{\partial y}\right)\mathrm{d}y = \left(-ku + \frac{\partial w}{\partial y}\right)\mathrm{d}y, \quad \text{along } Gz,$$

where $k = (\partial\phi/\partial y)$ is the rate of twist.

Therefore, the contributions to the shearing strains γ_{xy} and γ_{zy} as a result of the above displacements are respectively, given by

$$\left(\frac{\partial u}{\partial y} + kw\right) \quad \text{and} \quad \left(-ku + \frac{\partial w}{\partial y}\right).$$

The effect of the right-handed rotation θ about Gx (or Px) and ψ about Gz (or Pz) is to modify the shearing strains, and we have, defining the shear strain as the reduction in a right angle in a defined plane, the final expressions for the shearing strains γ_{xy} and γ_{zy} as follows (see Fig. 6)

$$\gamma_{xy} = \psi + \frac{\partial u}{\partial y} + kw \tag{A.1}$$

and

$$\gamma_{zy} = -\theta + \frac{\partial w}{\partial y} - ku. \tag{A.2}$$

From these identified shearing strains, the expression for the strain energy $\mathscr{U}_S$ due to transverse shear can now be written as

$$\begin{aligned}\mathscr{U}_S =& \frac{1}{2}\int\int_V\int G(\gamma_{xy}^2 + \gamma_{yz}^2)\,\mathrm{d}v = \int_0^L \int_A G(k_x\gamma_{xy}^2 + k_z\gamma_{yz}^2)\,\mathrm{d}A\,\mathrm{d}y \\ =& \frac{1}{2}\int_0^L \{k_xGA(\gamma_{xy})^2 + k_zGA(\gamma_{yz})^2\}\,\mathrm{d}y \\ =& \frac{1}{2}\int_0^L \{k_xGA(\psi + u' + kw)^2 + k_zGA(-\theta + w' - ku)^2\}\,\mathrm{d}y,\end{aligned} \tag{A.3}$$

where a prime denotes differentiation with respect to y.

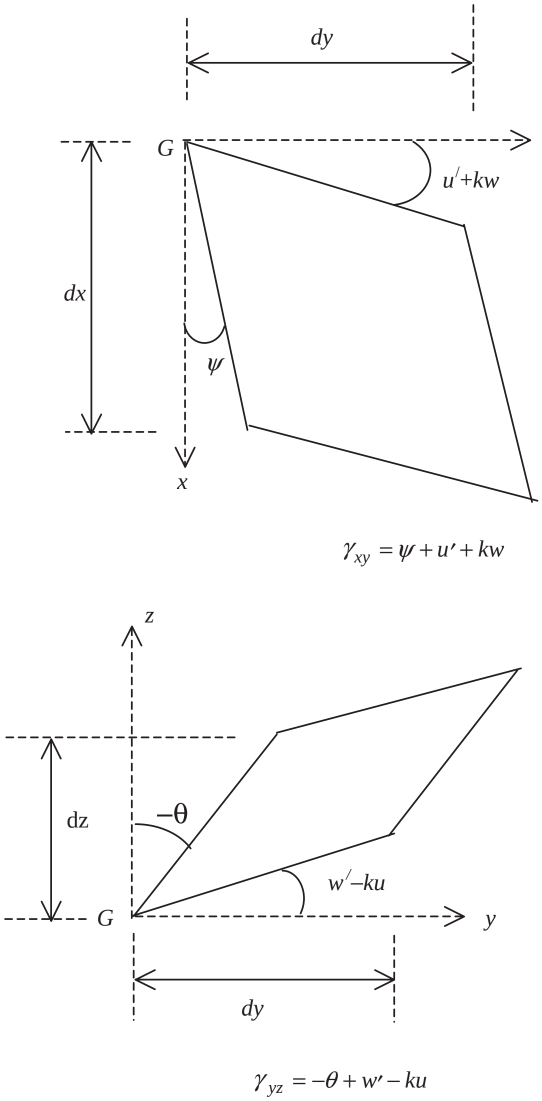

$\gamma_{xy} = \psi + u' + kw$

$\gamma_{yz} = -\theta + w' - ku$

Fig. 6. Shearing strains of an infinitesimal element dy in the xy and yz planes.

A.2. Expression for normal strain and strain energy due to normal strain

In order to determine the axial strain ε_y at P in the Gxz plane as a result of bending actions, consider a line through P, parallel to OY, which meets the section $\bar{G}\bar{x}\bar{z}$ at Q, say (see Fig. 5), then PQ for the undeformed beam is of length dy. Now if one finds the relative displacements of Q to P in the Y direction, the normal strain at P follows at once, as follows.

The co-ordinates of P in the Gxz and $\bar{G}\bar{x}\bar{z}$ axis systems are, respectively, (x, z) and $(x - kz\,\mathrm{d}y, kx\,\mathrm{d}y + z)$, see Fig. 5. The bending rotations of the plane Gxz about the axes Gx and Gz being θ and ψ, the corresponding bending rotations of the plane $\bar{G}\bar{x}\bar{z}$ about $\bar{G}\bar{x}$ and $\bar{G}\bar{z}$ are $\theta + \theta'\,\mathrm{d}y$ and $\psi + \psi'\,\mathrm{d}y$, respectively.

In section Gxz the displacement of P in the Y direction is $-z\theta + x\psi$ whereas in section $\bar{G}\bar{x}\bar{z}$ the displacement of Q in the Y direction is $-\bar{z}(\theta + \theta' \mathrm{d}y) + \bar{x}(\psi + \psi' \mathrm{d}y)$.

Thus the axial displacement of Q is

$$\begin{aligned} &-(z + kx\,\mathrm{d}y)(\theta + \theta'\mathrm{d}y) + (x - kz\,\mathrm{d}y)(\psi + \psi'\mathrm{d}y) \\ &\quad = -z\theta + x\psi + (-kx\theta - z\theta' - kz\psi + x\psi')\,\mathrm{d}y. \end{aligned}$$

Noting that the axial displacement of P is $-z\theta + x\psi$, the normal strain ε_y at P can now be written as

$$\varepsilon_y = -kx\theta - z\theta' - kz\psi + x\psi' = x(\psi' - k\theta) - z(\theta' + k\psi). \tag{A.4}$$

Therefore, the strain energy $\mathcal{U}_B$ due to axial strain resulting from bending actions is given by

$$\mathcal{U}_B = \frac{1}{2}\int\int_V\int E\varepsilon_y^2\,\mathrm{d}v = \frac{1}{2}\int_0^L\int_A E\varepsilon_y^2\,\mathrm{d}A\,\mathrm{d}y = \frac{1}{2}\int_0^L\left[E\int_A\{x(\psi' - k\theta) - z(\theta' + k\psi)\}^2\mathrm{d}A\right]\mathrm{d}y. \tag{A.5}$$

Noting that Gx and Gz are principal axes so that $\int\int_A xz\,\mathrm{d}A = 0$, the above expression simplifies to

$$\mathcal{U}_B = \frac{1}{2}\int_0^L\{EI_x(\theta' + k\psi)^2 + EI_z(\psi' - k\theta)^2\}\,\mathrm{d}y, \tag{A.6}$$

where I_x and I_z are the second moment of areas of the cross-section about the principal axes Gx and Gz, respectively, and defined in the usual notation as follows:

$$I_x = \int\int_A z^2\,\mathrm{d}A, \quad I_z = \int\int_A x^2\,\mathrm{d}A. \tag{A.7}$$

A.3. Total strain energy due to bending and shearing actions

The total strain energy $\mathcal{U}$ can now be obtained by adding the strain energy due to shearing strain resulting from the shear load and strain energy due to normal strain resulting from bending actions, given by Eqs. (A.3) and (A.6), respectively. Thus,

$$\begin{aligned} \mathcal{U} = \mathcal{U}_B + \mathcal{U}_S = \frac{1}{2}\int_0^L &[\{EI_x(\theta' + k\psi)^2 + EI_z(\psi' - k\theta)^2\} \\ &+ \{k_xAG(\psi + u' + kw)^2 + k_zAG(-\theta + w' - ku)^2\}]\,\mathrm{d}y \end{aligned} \tag{A.8}$$

A.4. Expression for the kinetic energy

The kinetic energy of the twisted Timoshenko beam can be formulated from the velocity components of the point P on the Gxz-plane as follows. These velocity components can be obtained by taking the time derivative of the displacements of P in the Gx, Gy and Gz directions. Clearly the velocity of the point P along Gx, Gy and Gz are $\dot{u}$, $-z\dot{\theta} + x\dot{\psi}$, and $\dot{w}$, respectively, with an over dot representing the time derivative.

So the kinetic energy $\mathscr{J}$ of the twisted beam can be formulated as

$$\mathscr{J}=\frac{1}{2}\int\int_V\int \rho\{\dot{u}^2+(-z\dot{\theta}+x\dot{\psi})^2+(\dot{w})^2\}\,\mathrm{d}v=\frac{1}{2}\int_0^L\{\rho A(\dot{u}+\dot{w})+\rho I_x\dot{\theta}^2+\rho I_z\dot{\psi}^2\}\,\mathrm{d}y, \quad (A.9)$$

where ρ is the density of the beam material.

A.5. Application of Hamilton's principle and derivation of the governing differential equations

Using the expressions for potential and kinetic energies $\mathscr{U}$ and $\mathscr{J}$ of the twisted beam (see Eqs. (A.8) and (A.9)) Hamilton's principle can now be applied to derive the governing differential equations of motion in free vibration.

Hamilton's principle states that

$$\delta\int_{t_1}^{t_2}\mathscr{L}\,\mathrm{d}t=0, \quad (A.10)$$

where $\mathscr{L}=\mathscr{J}-\mathscr{U}$ is the Lagrangian, and the integration is taken between arbitrary intervals of time t_1 and t_2 for a dynamic trajectory.

Substituting the expressions for $\mathscr{U}$ and $\mathscr{J}$ from Eqs. (A.8) and (A.9) for the Lagrangian $\mathscr{L}$ in Eq. (A.10) and using the δ operator, integrating by parts and noting that δu, δw, $\delta\theta$ and $\delta\psi$ are completely arbitrary, the governing differential equations of motion of the twisted Timoshenko beam are derived. As a by product of the Hamiltonian formulation the associated natural boundary conditions which give the expressions for shear forces and bending moments are also obtained. The whole procedure for the present problem is tedious, but merely a mathematical process. The derivation is routinely carried out by successive integrations, the details of which are too extensive to report. The final expressions are given as follows.

A.6. Governing differential equations of motion in free vibration

$$-\rho A\ddot{u}+k_xAGu''-k^2k_zAGu+kAG(k_x+k_z)w'+k_xAG\psi'-kk_zAG\theta=0, \quad (A.11)$$

$$-\rho A\ddot{w}+k_zAGw''-k^2k_xAGw-kAG(k_x+k_z)u'-kk_xAG\psi-k_zAG\theta'=0, \quad (A.12)$$

$$-\rho I_x\ddot{\theta}+EI_x\theta''-k^2EI_z\theta-k_zAG\theta-kk_zAGu+k_zAGw'+k(EI_x+EI_z)\psi'=0, \quad (A.13)$$

$$-\rho I_z\ddot{\psi}+EI_z\psi''-k^2EI_x\psi-k_xAG\psi-kk_xAGw-k_xAGu'-k(EI_x+EI_z)\theta'=0, \quad (A.14)$$

A.7. Natural boundary conditions

Shear force in the x direction:

$$V_x=-k_xAGu'-k_xAG\psi-kk_xAGw. \quad (A.15)$$

Shear force in the z direction:

$$V_z=-k_zAGw'+k_zAG\theta+kk_zAGu. \quad (A.16)$$

Bending moment about the x-axis:

$$M_x = -EI_x\theta' - kEI_x\psi. \tag{A.17}$$

Bending moment about the z-axis:

$$M_z = -EI_z\psi' + kEI_z\theta. \tag{A.18}$$

With the help of the governing differential Eqs. (A.13) and (A.14), the expressions for the shear forces V_x and V_z in Eqs. (A.15) and (A.16) can be written in the following alternative forms:

$$V_x = -EI_z\psi'' + k^2EI_x\psi + k(EI_x + EI_z)\theta' + \rho I_z\ddot{\psi}, \tag{A.19}$$

$$V_z = EI_x\theta'' - k^2EI_z\theta + k(EI_x + EI_z)\psi' - \rho I_x\ddot{\theta}. \tag{A.20}$$

References

[1] D.D. Rosard, Natural frequencies of twisted cantilever beams, *Journal of Applied Mechanics* 20 (1953) 241–244.

[2] A. Troesch, M. Anliker, H. Ziegler, Lateral vibrations of twisted rods, *Quarterly of Applied Mathematics* 12 (1954) 163–173.

[3] R.C. Diprima, G.H. Handelman, Vibrations of twisted beams, *Quarterly of Applied Mathematics* 12 (1954) 241–259.

[4] W. Carnegie, Vibration of pre-twisted cantilever blading, *Proceedings of the Institution of Mechanical Engineers, London* 173 (1959) 343–346.

[5] H.A. Slyper, Coupled bending vibrations of pretwisted cantilever beams, *Journal of Mechanical Engineering Science* 4 (1962) 365–379.

[6] M. Anliker, B.A. Troesch, Lateral vibrations of pretwisted rods with various boundary conditions, *Zeitschrift fuer Angewandte Mathematik und Physik* 14 (1963) 218–236.

[7] B. Dawson, Coupled bending vibrations of pretwisted cantilever blading treated by Rayleigh–Ritz method, *Journal of Mechanical Engineering Science* 10 (1968) 381–386.

[8] W. Carnegie, J. Thomas, The coupled bending-bending vibration of pre-twisted tapered blading, *Journal of Engineering for Industry, American Society of Mechanical Engineers* 94 (1972) 255–266.

[9] S.M. Lin, Vibrations of elastically restrained nonuniform beams with arbitrary pretwist, *American Institute of Aeronautics and Astronautics Journal* 35 (1977) 1681–1687.

[10] R.S. Gupta, J.S. Rao, Finite element eigenvalue analysis of tapered and twisted Timoshenko beams, *Journal of Sound and Vibration* 56 (1978) 187–200.

[11] F. Sisto, A.T. Chang, A finite element for vibration analysis of twisted blades based on beam theory, *American Institute of Aeronautics and Astronautics Journal* 22 (1984) 1646–1651.

[12] Z. Celep, D. Turham, On the influence of pretwisting on the vibration of beams including the shear and rotary inertia effects, *Journal of Sound and Vibration* 110 (1986) 523–528.

[13] A. Rosen, R.G. Loewy, B. Mathew, Use of twisted principal coordinates and non-physical coordinates in blade analysis, *Vertica* 11 (1987) 541–572.

[14] A. Rosen, Structural and dynamic behaviour of pretwisted rods and beams, *Applied Mechanics Reviews* 44 (1991) 483–515.

[15] O. Onipede, S.B. Dong, J.B. Kosmatka, Natural vibrations and waves in pretwisted rods, *Composites Engineering* 4–5 (1994) 487–502.

[16] A.S. Balhaddad, D. Onipede Jr., Three-dimensional free vibration of pretwisted beams, *American Institute of Aeronautics and Astronautics Journal* 36 (1998) 1524–1528.

[17] E. Petrov, M. Geradin, Finite element theory for curved and twisted beams based on exact solutions for three dimensional solids. Part 1: Beam concept and geometrically exact nonlinear fomulation, Part 2: anisotropic and advanced beam models, *Computer Methods in Applied Mechanics and Engineering* 165 (1998) 43–127.

[18] J.R. Banerjee, Free vibration analysis of a twisted beam using the dynamic stiffness method, *International Journal of Solids and Structures* 38 (2001) 6703–6722.

[19] S.P. Timoshenko, On the transverse vibration of bars of uniform cross-section, *Philosophical Magazine* 43 (1922) 125–131.

[20] R.W. Clough, On the importance of higher modes of vibration in the earthquake response of a tall building, *Bulletin of Seismological Society of America* 45 (1955) 289–301.

[21] J.R. Banerjee, F.W. Williams, Coupled bending-torsional dynamic stiffness matrix for Timoshenko beam elements, *Computers and Structures* 42 (1992) 301–310.

[22] J.R. Banerjee, F.W. Williams, Exact dynamic stiffness matrix for composite Timoshenko beams with applications, *Journal of Sound and Vibration* 194 (1996) 573–585.

[23] A.I. Beltzer, Engineering analysis via symbolic computation – a break-through paper, *Applied Mechanics Reviews* 43 (1990) 119–127.

[24] A.C. Hearn, *REDUCE User's Manual Version 3.5*, Rand Publication, Santa Monica, CA, 1993.

[25] S. Wolfram, *Mathematica*, 2nd Edition, Addison-Wesley, New York, 1991.

[26] W.H. Wittrick, F.W. Williams, A general algorithm for computing natural frequencies of elastic structures, *Quarterly Journal of Mechanics and Applied Mathematics* 24 (1971) 263–284.

[27] W.P. Press, B.P. Flannery, S.A. Teukolsky, W.T. Vetterling, *Numerical Recipes*, Cambridge University Press, Cambridge, 1986.

[28] F.W. Williams, W.H. Wittrick, Exact buckling and frequency calculations surveyed, *Journal of Structural Engineering, American Society of Civil Engineers* 109 (1983) 169–187.

[29] F.W. Williams, Review of exact buckling and frequency calculations with optimal multi-level substructuring, *Computers and Structures* 48 (1993) 547–552.

[30] M.S. Anderson, F.W. Williams, J.R. Banerjee, B.J. Durling, C.L. Herstorm, D. Kennedy, D.B. Warnaar, User manual for BUNVIS-RG: an exact buckling and vibration program for lattice structures, with repetitive geometry and substructuring options, NASA Technical Memorandum 87669, 1986.

[31] M.S. Anderson, F.W. Williams, BUNVIS-RG: exact frame buckling and vibration program, with repetitive geometry and substructuring, *Journal of Spacecraft and Rockets* 24 (1987) 353–361.

[32] J.R. Banerjee, Free vibration of centrifugally stiffened uniform and tapered beams using the dynamic stiffness method, *Journal of Sound and Vibration* 233 (2000) 857–875.

Shock and Vibration 15 (2008) 179–192
IOS Press

A spectral finite element model for vibration analysis of a beam based on general higher-order theory

Jiao Sujuan, Li Jun, Hua Hongxing and Shen Rongying
Vibration, Shock & Noise Institute, Shanghai Jiao Tong University, 800 Dongchuan Road, Shanghai 200240, P.R. China

Received 1 July 2006
Revised 2007

Abstract. The spectral element matrix is derived for a straight and uniform beam element having an arbitrary cross-section. The general higher-order beam theory is used, which accurately accounts for the transverse shear deformation out of the cross-sectional plane and antielastic-type deformation within the cross-sectional plane. Two coupled equations of motion are derived by use of Hamilton's principle along with the full three-dimensional constitutive relations. The theoretical expressions of the spectral element matrix are formulated from the exact solutions of the coupled governing equations. The developed spectral element matrix is directly applied to calculate the exact natural frequencies and mode shapes of the illustrative examples. Numerical results of the thick isotropic beams with rectangular and elliptical cross-sections are presented for a wide variety of cross-section aspect ratios.

Keywords: Beam, higher-order, shear deformation, dynamic analysis, spectral element matrix

1. Introduction

Beam members are basic structural components widely used in many types of structures within the fields of mechanical, aeronautical, automobile and civil engineering. Because of the practical importance, a large number of investigators have made efforts to deal with the static and dynamic analyses of the beams. The analyses of slender beams have been performed mostly using the elementary Bernoulli-Euler theory. This theory assumes that the plane sections of the cross-section remain plane and particular to the beam axis.

A more refined beam theory is Timoshenko beam theory which accounts for the shear deformation and rotary inertia that are neglected in the elementary theory. In Timoshenko beam theory the distribution of the transverse shear strain is constant through the beam thickness and therefore requires the shear correction factor to correct the strain energy of deformation. Timoshenko [1] first developed a theory which allowed one to study the vibrational behavior of the thick beams by approximately accounting for transverse shear deformation and rotary inertia, where the cross-section remained undistorted and the in-plane stresses were zero. Mindlin and Deresiewicz [2] calculated the shear correction factor for a variety of cross-sections of the beams. The dynamic shear strain distribution may differ significantly from the parabolic form of the static shear strain distribution. Cowper [3] presented a method to determine the shear correction factor based on the static three-dimensional elasticity theory along with Saint-Venant's static flexure warping function. Hutchinson [4] investigated the behavior of the shear coefficient for a rectangular Timoshenko beam by comparison of the Timoshenko beam solution with a three-dimensional solution for a simply-supported beam. It was found that a shear coefficient would have to be a function of the wave length as well as the aspect ratio.

ISSN 1070-9622/08/$17.00 © 2008 – IOS Press and the authors. All rights reserved

The limitations of the elementary Bernoulli-Euler beam theory and first-order Timoshenko shear deformation beam theory force the development of higher-order shear deformation beam theories. Stephen and Levinson [5] developed a second-order model for studying the beam vibrations with two governing differential equations having two independent coefficients. The first coefficient was similar to the Timoshenko's shear correction factor, which depended upon Saint-Venant's static flexure warping function, while the second coefficient depended upon the transverse shear stress state. Levinson [6] developed the higher-order shear deformable theory for beams with thin rectangular cross-sections that correctly accounted for the stress free boundary conditions on the upper and lower surfaces as well as the parabolic shear strain distribution through the thickness without the need for a shear correction factor. This was accomplished by expanding the axial displacement to include a cubic distribution through the thickness. This additional displacement was identical to the Saint-Venant's static flexure warping function for thin rectangular cross-sections, but for general cross-section shapes the correct expansion should be an infinite series of transcendental functions. Bickford [7] considered a shear deformation theory for rectangular beams that correctly accounted for the stress free boundary conditions on the upper and lower surfaces of the beam while retaining the parabolic distribution of the transverse shear strain. Murty [8] formulated a third-order beam theory including the transverse shear strain and nonclassical axial stress. In this theory the parabolic transverse shear stress distribution across the thickness of the beam could be obtained using the constitutive relations. Levinson [9] obtained the higher-order beam theory with the fourth-order differential equations, satisfying two boundary conditions at each end of the beam. No shear correction factors were required since the theory satisfied the shear stress free surface conditions on the top and bottom of the beam. Rychter [10] verified the consistency and accuracy of Levinson's theory by imbedding it in the two-dimensional linear theory of elasticity. It was shown that the Levinson's variationally inconsistent theory was more accurate than the variationally consistent theory of Bickford. Heyliger and Reddy [11] used a higher-order theory and noted the inadequacy of the shear correction factor in predicting the natural frequencies. Petrolito [12] presented a finite element solution of uniformly loaded thick beams using the Bickford's theory. Kathnelson [13] developed an improved engineering theory for elastic isotropic uniform beam using the asymptotic analysis of the variational equation of Hellinger-Reissner principle for the three-dimensional theory of elasticity. Wang et al. [14] discussed the derivation and comparison of the Bernoulli-Euler, Timoshenko, and Reddy-Bickford beam theories extensively. Reddy et al. [15] gave solutions to the Levinson beams in terms of the classical beam solutions. Ghugal and Shimpi [16] presented a review of the displacement and stress based refined theories for isotropic and anisotropic laminated beams. Aalami [17] studied the vibrational behavior of a general prismatic beam with an arbitrary cross-section by using a Rayleigh-Ritz energy approach to the general three-dimensional problem. His numerical and graphical results clearly illustrated the presence and importance of both the out-of-plane shear deformation and in-plane deformation for extremely high vibrational modes. Ie and Kosmatka [18] developed a static theory for a general cylindrical or prismatic beam that incorporated both out-of-plane shear and in-plane deformation functions, where these functions were assumed known. In fact, these functions could be determined exactly for simple cross-sections by solving Saint-Venant's bending and flexure problems, and approximately for an arbitrary cross-section by applying either a two-dimensional finite element approach or a power series approach. Kosmatka [19] presented a new beam theory for studying the static and vibration behaviors of the cylindrical or prismatic beam-type structures having an arbitrary cross-section. This general higher-order theory accurately accounted for the transverse shear deformation out of the cross-sectional plane and antielastic-type deformation within the cross-sectional plane.

A review of the literature indicates that the refined theories for dynamic analysis of the beams with non-rectangular cross-sections are rare. Most of the research work related to the dynamic analysis of thick isotropic beams assumes that the in-plane cross-sectional stresses are negligible and the cross-section does not deform in its own plane and comparatively less work is available on incorporating both out-of-plane shear and in-plane deformation in a unified manner. The objective of this paper is to develop an exact spectral element matrix for a general higher-order beam element with an arbitrary cross-section, which has not still been reported in literature. Although several researchers have investigated and elaborated the spectral element method [20,21], it should be noted that there are differences in the way they compute the spectral elements from the way used in this paper. The explicit analytical expressions for the entries of the spectral element matrix are derived in the paper. The spectral element method is often referred to as an exact method as it is based on the exact shape functions obtained from the exact solutions of the element differential equations. The usefulness of the method becomes apparent when higher frequencies and better accuracies of the results are required.

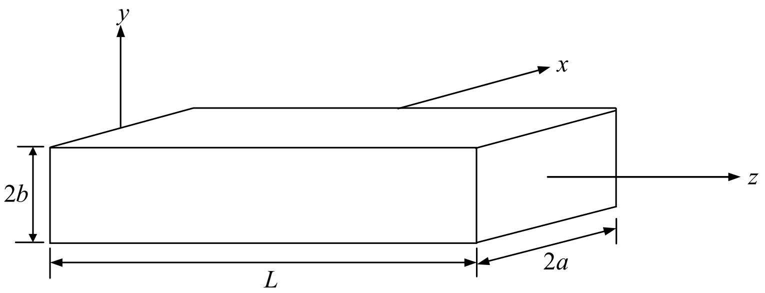

Fig. 1. A prismatic isotropic beam.

In this paper, the spectral finite element formulation for a thick isotropic beam having an arbitrary cross-section is presented. The general higher-order beam theory is employed [19], which considers both out-of-plane shear dependent warping and in-plane deformations. The theoretical expressions of the spectral element matrix for the general higher-order beam element are derived from the exact solutions of the governing differential equations. The application of the derived spectral element matrix to calculate the natural frequencies and mode shapes of the particular beams uses the automated Muller root search algorithm [22]. Numerical results are presented and compared with the available solutions in literature to validate the accuracy and efficiency of the current approach.

2. Mathematical formulation

A prismatic isotropic beam with a general homogeneous cross-section, as shown in Fig. 1, is considered in this paper. A Cartesian co-ordinate system (x, y, z) is defined on the beam, where x and y are coincident with the principal axes of the beam cross-section and z is coincident with the centroidal axis. The current development is further restricted to the study of vibrational behavior in the $y - z$ plane only, and the displacement relations are defined as [19]

$$u_1(x, y, z, t) = \partial\theta(z, t)/\partial z\psi_x(x, y) \tag{1a}$$

$$u_2(x, y, z, t) = v(z, t) + \partial\theta(z, t)/\partial z\psi_y(x, y) \tag{1b}$$

$$u_3(x, y, z, t) = y\theta(z, t) + [\partial v(z, t)/\partial z + \theta(z, t)]\psi_z(x, y) \tag{1c}$$

where (u_1, u_2, u_3) are the displacements of a point along the (x, y, z) coordinates, $v(z, t)$ represents the time-dependent y direction displacement and $\theta(z, t)$ the time-dependent rotation about the x axis. The three functions $\psi_x(x, y)$, $\psi_y(x, y)$, and $\psi_z(x, y)$, which are assumed to be known, can be determined exactly for simple cross-sections by solving Saint-Venant's bending and flexure problems, or approximately for arbitrary cross-sections using either a two-dimensional finite element approach or a power series approach [19].

The time-dependent strain-displacement relationships of the beam are defined as

$$\varepsilon_{xx} = \partial\theta/\partial z\partial\psi_x/\partial x \tag{2a}$$

$$\varepsilon_{yy} = \partial\theta/\partial z\partial\psi_y/\partial y \tag{2b}$$

$$\varepsilon_{zz} = y\partial\theta/\partial z + \partial(\partial v/\partial z + \theta)/\partial z\psi_z \tag{2c}$$

$$\gamma_{yz} = (\partial v/\partial z + \theta)(1 + \partial\psi_z/\partial y) + \partial^2\theta/\partial z^2\psi_y \tag{2d}$$

$$\gamma_{xz} = (\partial v/\partial z + \theta)\partial\psi_z/\partial x + \partial^2\theta/\partial z^2\psi_x \tag{2e}$$

$$\gamma_{xy} = \partial\theta/\partial z(\partial\psi_x/\partial y + \partial\psi_y/\partial x) \tag{2f}$$

where ε_{xx}, ε_{yy} and ε_{zz} are the normal strains in the x, y and z directions, respectively, and γ_{yz}, γ_{xz} and γ_{xy} are the shear strains.

The general constitutive relations are given as

$$\sigma_{xx} = (\lambda + 2G)\varepsilon_{xx} + \lambda\varepsilon_{yy} + \lambda\varepsilon_{zz} \tag{3a}$$

$$\sigma_{yy} = \lambda\varepsilon_{xx} + (\lambda + 2G)\varepsilon_{yy} + \lambda\varepsilon_{zz} \tag{3b}$$

$$\sigma_{zz} = \lambda\varepsilon_{xx} + \lambda\varepsilon_{yy} + (\lambda + 2G)\varepsilon_{zz} \tag{3c}$$

$$\tau_{yz} = G\gamma_{yz} \tag{3d}$$

$$\tau_{xz} = G\gamma_{xz} \tag{3e}$$

$$\tau_{xy} = G\gamma_{xy} \tag{3f}$$

Here, λ and G are defined as Lame's constants.

$$\lambda = E\nu/(1+\nu)(1-2\nu) \quad G = E/2(1+\nu)$$

where E is Young's modulus and ν is Poisson ratio.

The total strain energy $U$of the beam shown in Fig. 1 is given by

$$U = \frac{1}{2}\int_0^L \int_A (\sigma_{xx}\varepsilon_{xx} + \sigma_{yy}\varepsilon_{yy} + \sigma_{zz}\varepsilon_{zz} + \tau_{yz}\gamma_{yz} + \tau_{xz}\gamma_{xz} + \tau_{xy}\gamma_{xy})dAdz \tag{4a}$$

Substituting σ_{xx}, σ_{yy}, σ_{zz} and τ_{yz}, τ_{xz}, τ_{xy} from Eqs (3a)–(3f) into Eq. (4a) yields

$$\begin{aligned} U = \frac{1}{2}\int_0^L \int_A \big[&(\lambda+2G)\varepsilon_{xx}^2 + (\lambda+2G)\varepsilon_{yy}^2 + (\lambda+2G)\varepsilon_{xx}^2 + G\gamma_{yz}^2 + G\gamma_{xz}^2 + G\gamma_{xy}^2 \\ &+ 2\lambda\varepsilon_{xx}\varepsilon_{yy} + 2\lambda\varepsilon_{xx}\varepsilon_{zz} + 2\lambda\varepsilon_{yy}\varepsilon_{zz}\big]\, dAdz \end{aligned} \tag{4b}$$

The total kinetic energy T of the beam is defined by

$$T = \frac{1}{2}\int_0^L \int_A \rho(\dot{u}_1^2 + \dot{u}_2^2 + \dot{u}_3^2)dAdz \tag{5a}$$

where ρ is the mass density per unit volume of the beam and the superscript dot represents a derivative with respect to time t.

Substituting u_1, u_2 and u_3 from Eq. (1) into Eq. (5a) results in

$$T = \frac{1}{2}\int_0^L \int_A \rho\{(\dot{\theta}'\psi_x)^2 + (\dot{v} + \dot{\theta}'\psi_y)^2 + [y\dot{\theta} + (\dot{v'} + \dot{\theta})\psi_z]^2\}dAdz \tag{5b}$$

where the superscript prime refers to a partial derivative with respect to z co-ordinate.

The governing equations of motion and boundary conditions for the displacement relations given by Eq. (1) can be obtained conveniently by means of Hamilton's principle, which can be stated in the form

$$\begin{aligned} &\int_{t_1}^{t_2} (\delta T - \delta U)\, dt = 0 \\ &\delta v = \delta\theta = \delta v' = \delta\theta' = 0 \ \text{ at } t = t_1, t_2 \end{aligned} \tag{6}$$

Herein δU and δT are the variations of the strain and kinetic energies, respectively.

Substituting Eq. (2) into Eq. (4b), then substituting the resulting equation and Eq. (5b) into Eq. (6) and performing the variational operations yields the following governing differential equations of motion for the beam based on general higher-order theory

$$D_{12}\theta''' + D_{22}v'''' - A_{11}(v'' + \theta') - A_{12}\theta''' + m\ddot{v} + J_1\ddot{\theta}' - (J_z\ddot{v}'' + J_2\ddot{\theta}') = 0 \tag{7a}$$

$$\begin{aligned}&-(D_{11}\theta'' + D_{12}v''') + A_{11}(v' + \theta) + A_{12}\theta'' + A_{12}(v''' + \theta'')\\&\quad +A_{22}\theta'''' + J_2\ddot{v}' + I_p\ddot{\theta} - (J_1\ddot{v}' + J_p\ddot{\theta}'') = 0\end{aligned} \tag{7b}$$

where

$$m = \int_A \rho dA \quad I_p = \int_A \rho(y + \psi_z)^2 dA \quad J_1 = \int_A \rho\psi_y dA$$

$$J_p = \int_A \rho(\psi_x^2 + \psi_y^2)dA \quad J_z = \int_A \rho\psi_z^2 dA \quad J_2 = \int_A \rho(y + \psi_z)\psi_z dA$$

$$\begin{aligned}D_{11} &= \int_A (\lambda + 2G)\{(y + \psi_z)^2 + (\partial\psi_x/\partial x)^2 + (\partial\psi_y/\partial y)^2\}\\&\quad +2\lambda\{(y + \psi_z)(\partial\psi_x/\partial x + \partial\psi_y/\partial y) + \partial\psi_x/\partial x\partial\psi_y/\partial y\} + G(\partial\psi_x/\partial y + \partial\psi_y/\partial x)^2 dA\\D_{12} &= \int_A \{(\lambda + 2G)(y + \psi_z) + \lambda(\partial\psi_x/\partial x + \partial\psi_y/\partial y)\}\psi_z dA\\D_{22} &= \int_A (\lambda + 2G)\psi_z^2 dA \quad A_{11} = \int_A G\{(1 + \partial\psi_z/\partial y)^2 + (\partial\psi_z/\partial x)^2\}dA\\A_{12} &= \int_A G\{(1 + \partial\psi_z/\partial y)\psi_y + \partial\psi_z/\partial x\psi_x\}dA \quad A_{22} = \int_A G\{\psi_x^2 + \psi_y^2\}dA\end{aligned}$$

The associated boundary conditions at the ends of beam ($z = 0, L$) are obtained as follows

$$\left[-D_{12}\theta'' - D_{22}v''' + A_{11}(v' + \theta) + A_{12}\theta'' + J_z\ddot{v}' + J_2\ddot{\theta}\right]\delta v = 0 \tag{8a}$$

$$\left[D_{11}\theta' + D_{12}v'' - A_{12}(v'' + \theta') - A_{22}\theta''' + J_1\ddot{v} + J_p\ddot{\theta}'\right]\delta\theta = 0 \tag{8b}$$

$$[D_{12}\theta' + D_{22}v'']\,\delta v' = 0 \tag{8c}$$

$$[A_{12}(v' + \theta) + A_{22}\theta'']\delta\theta' = 0 \tag{8d}$$

3. Spectral finite element

It can be shown that Eq. (7) have solutions that are separable in time and space, and that the time dependence is harmonic. Letting

$$v(z,t) = V(z)\sin\omega t \tag{9a}$$

$$\theta(z,t) = \Theta(z)\sin\omega t \tag{9b}$$

where ω is the angular frequency, $V(z)$ and $\Theta(z)$ are the amplitudes of the sinusoidally varying transverse displacement and normal rotation, respectively.

Introducing Eq. (9) into Eq. (7), the following differential eigenvalue equations are obtained

$$\begin{aligned}&D_{12}\Theta''' + D_{22}V'''' - A_{11}(V'' + \Theta') - A_{12}\Theta'''\\&\quad -m\omega^2 V - J_1\omega^2\Theta' + J_z\omega^2 V'' + J_2\omega^2\Theta' = 0\end{aligned} \tag{10a}$$

$$\begin{aligned}&-D_{11}\Theta'' - D_{12}V''' + A_{11}(V' + \Theta) + A_{12}\Theta'' + A_{12}(V''' + \Theta'')\\&\quad +A_{22}\Theta'''' - J_2\omega^2 V' - I_p\omega^2\Theta + J_1\omega^2 V' + J_p\omega^2\Theta'' = 0\end{aligned} \tag{10b}$$

The solutions to Eq. (10) can be expressed as

$$V(z) = \tilde{A}e^{\kappa z} \tag{11a}$$

$$\Theta(z) = \tilde{B}e^{\kappa z} \tag{11b}$$

Substituting Eq. (11) into Eq. (10), the equivalent algebraic eigenvalue equations are obtained and the equations have nontrivial solutions when the determinant of the coefficient matrix of $\tilde{A}$ and $\tilde{B}$ vanishes. Setting the determinant equal to zero yields the characteristics equation, which is an eighth-order polynomial equation in κ

$$\eta_4\kappa^8 + \eta_3\kappa^6 + \eta_2\kappa^4 + \eta_1\kappa^2 + \eta_0 = 0 \tag{12}$$

where

$$\begin{aligned}
\eta_4 &= A_{22}D_{22}\\
\eta_3 &= A_{12}^2 - A_{11}A_{22} - 2A_{12}D_{12} + D_{12}^2 + 2A_{12}D_{22} - D_{11}D_{22} + (D_{22}J_p + A_{22}J_z)\omega^2\\
\eta_2 &= A_{11}(D_{11} - 2D_{12} + D_{22}) + J_pJ_z\omega^4\\
&\quad -(D_{22}I_p + 2(-A_{12} + D_{12})(J_1 - J_2) + A_{11}J_p + (-2A_{12} + D_{11})J_z + A_{22}m)\omega^2\\
\eta_1 &= \omega^2(A_{11}(I_p + 2J_1 - 2J_p + J_z) - 2A_{12}m + D_{11}m\\
&\quad +((J_1 - J_2)^2 - I_pJ_z - J_pm)\omega^2)\\
\eta_0 &= -A_{11}m\omega^2 + I_pm\omega^4
\end{aligned}$$

Therefore the fourth-order polynomial equation for the roots $\chi = \kappa^2$ must be solved. The solutions can be found in close-form as follows.

Equation (12) can be rewritten as

$$\chi^4 + a_1\chi^3 + a_2\chi^2 + a_3\chi + a_4 = 0 \tag{13}$$

where

$$a_1 = \eta_3/\eta_4 \quad a_2 = \eta_2/\eta_4 \quad a_3 = \eta_1/\eta_4 \quad a_4 = \eta_0/\eta_4$$

The fourth-order Eq. (13) can be factorized as

$$(\chi^2 + p_1\chi + q_1)(\chi^2 + p_2\chi + q_2) = 0$$

where

$$\begin{Bmatrix} p_1 \\ p_2 \end{Bmatrix} = \frac{1}{2}[a_1 \pm \sqrt{a_1^2 - 4a_2 + 4\lambda_1}] \quad \begin{Bmatrix} q_1 \\ q_2 \end{Bmatrix} = \frac{1}{2}\left[\lambda_1 \pm \frac{a_1\lambda_1 - 2a_3}{\sqrt{a_1^2 - 4a_2 + 4\lambda_1}}\right]$$

and λ_1 is a real root of the following cubic equation

$$\lambda^3 - a_2\lambda^2 + (a_1a_3 - 4a_4)\lambda + (4a_2a_4 - a_3^2 - a_1^2a_4) = 0 \tag{14}$$

Then the four roots of the fourth-order Eq. (13) can be written as

$$\begin{Bmatrix} \chi_1 \\ \chi_2 \end{Bmatrix} = -\frac{p_1}{2} \pm \sqrt{\frac{p_1^2}{4} - q_1} \quad \begin{Bmatrix} \chi_3 \\ \chi_4 \end{Bmatrix} = -\frac{p_2}{2} \pm \sqrt{\frac{p_2^2}{4} - q_2} \tag{15}$$

If the discriminant of cubic Eq. (14), $\bar{D}$, is negative, then Eq. (14) has usually three real roots, which can be written as

$$\lambda_1 = a_2/3 + 2\sqrt{-\bar{Q}}\cos(\vartheta/3) \quad \lambda_2 = a_2/3 + 2\sqrt{-\bar{Q}}\cos((\vartheta + 2\pi)/3)$$

$$\lambda_3 = a_2/3 + 2\sqrt{-\bar{Q}}\cos((\vartheta + 4\pi)/3)$$

where

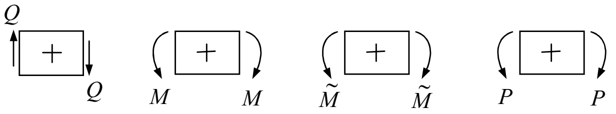

Fig. 2. Sign convention for positive shear force $Q(z)$, bending moment $M(z)$, generalized moment$\tilde{M}(z)$ and higher-order moment $P(z)$.

$$\vartheta = \cos^{-1}(\bar{R}\Big/\sqrt{-\bar{Q}^3}) \quad \bar{Q} = -\frac{1}{9}(a_2^2 - 3a_1a_3 + 12a_4)$$

$$\bar{R} = \frac{1}{54}(2a_2^3 - 9a_1a_2a_3 + 27a_3^2 + 27a_1^2a_4 - 72a_2a_4) \quad \bar{D} = \bar{Q}^3 + \bar{R}^2$$

Whichever of the three roots is chosen, the same solutions are obtained.

The general solutions to Eq. (10) are given by

$$\begin{aligned} V(z) &= A_1e^{\kappa_1 z} + A_2e^{-\kappa_1 z} + A_3e^{\kappa_2 z} + A_4e^{-\kappa_2 z} + A_5e^{\kappa_3 z} + A_6e^{-\kappa_3 z} + A_7e^{\kappa_4 z} + A_8e^{-\kappa_4 z} \\ &= \sum_{j=1}^{4}(A_{2j-1}e^{\kappa_j z} + A_{2j}e^{-\kappa_j z}) \end{aligned} \tag{16a}$$

$$\begin{aligned} \Theta(z) &= B_1e^{\kappa_1 z} + B_2e^{-\kappa_1 z} + B_3e^{\kappa_2 z} + B_4e^{-\kappa_2 z} + B_5e^{\kappa_3 z} + B_6e^{-\kappa_3 z} + +B_7e^{\kappa_4 z} + B_8e^{-\kappa_4 z} \\ &= \sum_{j=1}^{4}(B_{2j-1}e^{\kappa_j z} + B_{2j}e^{-\kappa_j z}) \end{aligned} \tag{16b}$$

$$V'(z) = \sum_{j=1}^{4}\kappa_j(A_{2j-1}e^{\kappa_j z} - A_{2j}e^{-\kappa_j z}) \tag{16c}$$

$$\Theta'(z) = \sum_{j=1}^{4}t_j\kappa_j(A_{2j-1}e^{\kappa_j z} + A_{2j}e^{-\kappa_j z}) \tag{16d}$$

where $\kappa_1 = \sqrt{\chi_1}$,$\kappa_2 = \sqrt{\chi_2}$,$\kappa_3 = \sqrt{\chi_3}$,$\kappa_4 = \sqrt{\chi_4}$. In the solution of Eq. (13), if any of the χ_j's are zero or are repeated, the solutions to the differential Eq. (10) will be modified according to the well-known methods for ordinary differential equations with constant coefficients, for those particular values of χ_j.

From Eq. (16), only eight of the sixteen constants are independent. The relationship among the constants is given by

$$B_{2j-1} = t_jA_{2j-1}$$

$$B_{2j} = -t_jA_{2j}$$

where

$$t_j = (-A_{11}\kappa_j^2 + D_{22}\kappa_j^4 + (-m + J_z\kappa_j^2)\omega^2)\big/\Delta_j$$

$$\Delta_j = \kappa_j(A_{11} + (A_{12} - D_{12})\kappa_j^2 + (J_1 - J_2)\omega^2)(j = 1 \sim 4)$$

According to the sign convention shown in Fig. 2, the expressions of shear force $Q(z)$, bending moment $M(z)$, generalized moment $\tilde{M}(z)$ and higher-order moment $P(z)$ can be obtained from Eqs (8) and (16) as follows

$$\begin{aligned} Q(z) = \sum_{j=1}^{4} &\left[D_{12}t_j\kappa_j^2 + D_{22}\kappa_j^3 - A_{11}(\kappa_j + t_j) - A_{12}t_j\kappa_j^2\right. \\ &\left.+\omega^2J_z\kappa_j + \omega^2J_2t_j\right](A_{2j-1}e^{\kappa_j z} - A_{2j}e^{-\kappa_j z}) \end{aligned} \tag{17a}$$

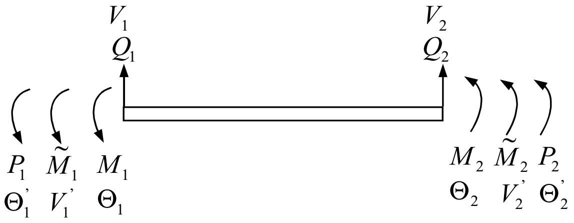
V_1
Q_1
V_2
Q_2
P_1 $\tilde{M}_1$ M_1
Θ_1' V_1' Θ_1
M_2 $\tilde{M}_2$ P_2
Θ_2 V_2' Θ_2'

Fig. 3. Boundary conditions for displacements and forces of beam element.

$$M(z)=\sum_{j=1}^{4}\left[-D_{11}t_j\kappa_j-D_{12}\kappa_j^2+A_{12}\kappa_j^2+A_{12}t_j\kappa_j+A_{22}t_j\kappa_j^3\right.$$
$$\left.+\omega^2J_1+\omega^2J_pt_j\kappa_j\right]\left(A_{2j-1}e^{\kappa_jz}+A_{2j}e^{-\kappa_jz}\right) \tag{17b}$$

$$\tilde{M}(z)=\sum_{j=1}^{4}\left[-D_{12}t_j\kappa_j-D_{22}\kappa_j^2\right](A_{2j-1}e^{\kappa_jz}+A_{2j}e^{-\kappa_jz}) \tag{17c}$$

$$P(z)=\sum_{j=1}^{4}\left[-A_{12}\kappa_j-A_{12}t_j-A_{22}t_j\kappa_j^2\right](A_{2j-1}e^{\kappa_jz}-A_{2j}e^{-\kappa_jz}) \tag{17d}$$

Refer to Fig. 3, the boundary conditions for displacements and forces of the beam element are, respectively,

$$\begin{aligned}z=0:&\quad V=V_1\quad\Theta=\Theta_1\quad V'=V_1'\quad\Theta'=\Theta_1'\\ z=L:&\quad V=V_2\quad\Theta=\Theta_2\quad V'=V_2'\quad\Theta'=\Theta_2'\end{aligned} \tag{18a}$$

$$\begin{aligned}z=0:&\quad Q=Q_1\quad M=M_1\quad\tilde{M}=\tilde{M}_1\quad P=P_1\\ z=L:&\quad Q=-Q_2\quad M=-M_2\quad\tilde{M}=-\tilde{M}_2\quad P=-P_2\end{aligned} \tag{18b}$$

Substituting Eq. (18a) into Eq. (16), the nodal displacements defined in Fig. 3 can be expressed in terms of A_i as

$$\{D\}=[R]\{A\} \tag{19}$$

where $\{D\}$ is the nodal degree-of-freedom vector defined by

$$\{D\}=\left\{V_1\;\Theta_1\;V_1'\;\Theta_1'\;V_2\;\Theta_2\;V_2'\;\Theta_2'\right\}^T$$

$$\{A\}=\left\{A_1\;A_3\;A_5\;A_7\;A_2\;A_4\;A_6\;A_8\right\}^T$$

$$[R]=\begin{bmatrix}1&1&1&1&1&1&1&1\\ t_1&t_2&t_3&t_4&-t_1&-t_2&-t_3&-t_4\\ \kappa_1&\kappa_2&\kappa_3&\kappa_4&-\kappa_1&-\kappa_2&-\kappa_3&-\kappa_4\\ t_1\kappa_1&t_2\kappa_2&t_3\kappa_3&t_4\kappa_4&t_1\kappa_1&t_2\kappa_2&t_3\kappa_3&t_4\kappa_4\\ e^{\kappa_1L}&e^{\kappa_2L}&e^{\kappa_3L}&e^{\kappa_4L}&e^{-\kappa_1L}&e^{-\kappa_2L}&e^{-\kappa_3L}&e^{-\kappa_4L}\\ t_1e^{\kappa_1L}&t_2e^{\kappa_2L}&t_3e^{\kappa_3L}&t_4e^{\kappa_4L}&-t_1e^{-\kappa_1L}&-t_2e^{-\kappa_2L}&-t_3e^{-\kappa_3L}&-t_4e^{-\kappa_4L}\\ \kappa_1e^{\kappa_1L}&\kappa_2e^{\kappa_2L}&\kappa_3e^{\kappa_3L}&\kappa_4e^{\kappa_4L}&-\kappa_1e^{-\kappa_1L}&-\kappa_2e^{-\kappa_2L}&-\kappa_3e^{-\kappa_3L}&-\kappa_4e^{-\kappa_4L}\\ t_1\kappa_1e^{\kappa_1L}&t_2\kappa_2e^{\kappa_2L}&t_3\kappa_3e^{\kappa_3L}&t_4\kappa_4e^{\kappa_4L}&t_1\kappa_1e^{-\kappa_1L}&t_2\kappa_2e^{-\kappa_2L}&t_3\kappa_3e^{-\kappa_3L}&t_4\kappa_4e^{-\kappa_4L}\end{bmatrix}$$

Substituting Eq. (18b) into Eq. (17), the nodal forces defined in Fig. 3 also can be expressed in terms of A_i as

$$\{F\}=[H]\{A\} \tag{20}$$

where $\{F\}$ is the nodal force vector defined by

$$\{F\} = \left\{ Q_1 \; M_1 \; \tilde{M}_1 \; P_1 \; Q_2 \; M_2 \; \tilde{M}_2 \; P_2 \right\}^T$$

$$[H] = \begin{bmatrix} \bar{t}_1 & \bar{t}_2 & \bar{t}_3 & \bar{t}_4 & -\bar{t}_1 & -\bar{t}_2 & -\bar{t}_3 & -\bar{t}_4 \\ \hat{t}_1 & \hat{t}_2 & \hat{t}_3 & \hat{t}_4 & \hat{t}_1 & \hat{t}_2 & \hat{t}_3 & \hat{t}_4 \\ \tilde{t}_1 & \tilde{t}_2 & \tilde{t}_3 & \tilde{t}_4 & \tilde{t}_1 & \tilde{t}_2 & \tilde{t}_3 & \tilde{t}_4 \\ \bar{\bar{t}}_1 & \bar{\bar{t}}_2 & \bar{\bar{t}}_3 & \bar{\bar{t}}_4 & -\bar{\bar{t}}_1 & -\bar{\bar{t}}_2 & -\bar{\bar{t}}_3 & -\bar{\bar{t}}_4 \\ -\bar{t}_1 e^{\kappa_1 L} & -\bar{t}_2 e^{\kappa_2 L} & -\bar{t}_3 e^{\kappa_3 L} & -\bar{t}_4 e^{\kappa_4 L} & \bar{t}_1 e^{-\kappa_1 L} & \bar{t}_2 e^{-\kappa_2 L} & \bar{t}_3 e^{-\kappa_3 L} & \bar{t}_4 e^{-\kappa_4 L} \\ -\hat{t}_1 e^{\kappa_1 L} & -\hat{t}_2 e^{\kappa_2 L} & -\hat{t}_3 e^{\kappa_3 L} & -\hat{t}_4 e^{\kappa_4 L} & -\hat{t}_1 e^{-\kappa_1 L} & -\hat{t}_2 e^{-\kappa_2 L} & -\hat{t}_3 e^{-\kappa_3 L} & -\hat{t}_4 e^{-\kappa_4 L} \\ -\tilde{t}_1 e^{\kappa_1 L} & -\tilde{t}_2 e^{\kappa_2 L} & -\tilde{t}_3 e^{\kappa_3 L} & -\tilde{t}_4 e^{\kappa_4 L} & -\tilde{t}_1 e^{-\kappa_1 L} & -\tilde{t}_2 e^{-\kappa_2 L} & -\tilde{t}_3 e^{-\kappa_3 L} & -\tilde{t}_4 e^{-\kappa_4 L} \\ -\bar{\bar{t}}_1 e^{\kappa_1 L} & -\bar{\bar{t}}_2 e^{\kappa_2 L} & -\bar{\bar{t}}_3 e^{\kappa_3 L} & -\bar{\bar{t}}_4 e^{\kappa_4 L} & \bar{\bar{t}}_1 e^{-\kappa_1 L} & \bar{\bar{t}}_2 e^{-\kappa_2 L} & \bar{\bar{t}}_3 e^{-\kappa_3 L} & \bar{\bar{t}}_4 e^{-\kappa_4 L} \end{bmatrix}$$

in which

$$\bar{t}_j = D_{12} t_j \kappa_j^2 + D_{22} \kappa_j^3 - A_{11}(\kappa_j + t_j) - A_{12} t_j \kappa_j^2 + \omega^2 J_z \kappa_j + \omega^2 J_2 t_j$$

$$\hat{t}_j = -D_{11} t_j \kappa_j - D_{12} \kappa_j^2 + A_{12} \kappa_j^2 + A_{12} t_j \kappa_j + A_{22} t_j \kappa_j^3 + \omega^2 J_1 + \omega^2 J_p t_j \kappa_j$$

$$\tilde{t}_j = -D_{12} t_j \kappa_j - D_{22} \kappa_j^2$$

$\bar{\bar{t}}_j = -A_{12}\kappa_j - A_{12} t_j - A_{22} t_j \kappa_j^2 \; (j = 1 \sim 4)$

Eliminating the coefficients A_i from Eqs (19) and (20) gives the following relationship between the nodal forces and nodal displacements

$$\{F\} = [H][R]^{-1}\{D\} = [K]\{D\} \tag{21}$$

where $[K]$ is the spectral element matrix. It should be mentioned that the explicit analytical expressions for the terms of the spectral element matrix could be derived using the symbolic manipulator software such as Maple [23], although the expressions are too lengthy to list in the paper.

4. Muller root search method

Once the spectral element matrix is obtained, the appropriate boundary conditions for the particular beam under consideration are applied to obtain the frequency characteristic determinant, which equals zero when an eigenvalue of the beam is found. Obviously the resulting frequency characteristic equation is a transcendental function of frequency, which allows an infinite number of natural frequencies to be accounted for. Although more advanced algorithms and more complex procedures may be used to determine the frequency values of the characteristic equation, a simple automated Muller root search method [22] is adopted in the present study to determine all the natural frequencies in a given frequency band. The mode shapes corresponding to the natural frequencies can be found in the usual way by making an arbitrary assumption about one unknown variable of the beam and then calculating the remaining variables in terms of the arbitrarily chosen one.

Let us denote the frequency characteristic determinant by $f(\omega)$ and consider the solution of $f(\omega) = 0$ by Muller's method. Muller's method uses a quadratic approximation to the function f by interpolating a quadratic polynomial through the last three computed points and then determining where this curve crosses the ω axis. The following algorithm is an implementation of Muller's method. This algorithm terminates when a prescribed error tolerance on $|f(\omega)|$ has been achieved or a maximum number of iterations has been performed.

(1) Pick three distinct values of ω, i.e., $\omega_0, \omega_1, \omega_2$. Set $i = 1$ and compute

$$h_i = \omega_i - \omega_{i-1}; \quad h_{i+1} = \omega_{i+1} - \omega_i; \quad \delta_i = (f(\omega_i) - f(\omega_{i-1}))/h_i;$$

$$\delta_{i+1} = (f(\omega_{i+1}) - f(\omega_i))/h_{i+1}; \quad d_i = (\delta_{i+1} - \delta_i)/(h_{i+1} + h_i).$$

(2) Compute

$$b_i = \delta_{i+1} + h_{i+1} d_i; \quad D_i = \left(b_i^2 - 4f(\omega_{i+1}) d_i\right)^{1/2}.$$

Table 1
Comparison of natural frequencies (in Hz) of Simply-Supported rectangular section beam

Mode No.	$b/a = 1000$		$b/a = 1$		$b/a = 0.5$		Third-order	Timoshenko
	Present	Ref. [19]	Present	Ref. [19]	Present	Ref. [19]		
1	123.11	123.10	122.62	122.61	123.68	123.69	119.60	118.70
2	159.01	159.02	159.37	159.38	160.55	160.57	158.38	159.32
3	303.65	N/A	296.85	296.85	252.28	252.29	281.47	271.70
4	310.53	310.39	303.18	N/A	310.93	N/A	313.70	314.58
5	503.48	N/A	465.28	N/A	388.38	N/A	454.82	421.05
6	532.62	N/A	518.96	N/A	487.06	N/A	549.09	549.77

Note: N/A denotes the result not available.

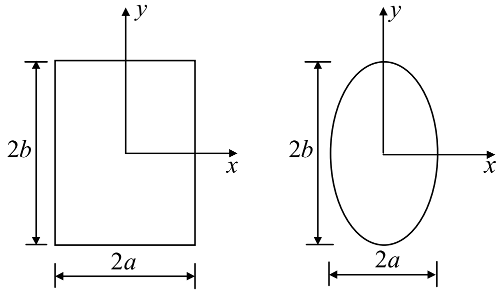

Fig. 4. A rectangular section used in example 1 and an elliptical section used in example 2.

(3) If $|b_i - D_i| < |b_i + D_i|$ then set $E_i = b_i + D_i$; else set $E_i = b_i - D_i$

(4) Set $h_{i+2} = -2f(\omega_{i+1})/E_i$; $\omega_{i+2} = \omega_{i+1} + h_{i+2}$.
where ω_{i+2} is the new approximation of the root ω_{i+1}. The process is continued until a desired accuracy is obtained. The rate of convergence is high and may be increased if an estimate of the eigenvalue is available. Previously roots may be removed from $f(\omega)$ by dividing it by $\prod_{k=1}^{p}(\omega - \omega_k)$, where ω_k $(k = 1, 2, \cdots, p)$ are the first p roots.

5. Numerical results and discussion

Two example problems are considered to demonstrate the accuracy of the spectral finite element model based on general higher-order beam theory.

The first example is of a rectangular cross-section beam shown in Fig. 4. The geometrical and physical properties of the beam are $E = 2.1 \times 10^{11}$Pa, $\nu = 0.333$, $\rho = 7860$ kg/m^3 , $L = 10$ m, $b = 5$ m.

First, the vibration behavior of the Simply-Supported beam is studied for three cross-section aspect ratios b/a. To validate the correctness and accuracy of the proposed formulation, the present results are given in Table 1 and compared with the previously published solutions [19] whenever possible. The numerical results based on third-order shear deformation and Timoshenko beam theories are also shown in Table 1, the shear correction factor is taken as 5/6 for Timoshenko beam theory. It can be seen from Table 1 that the present results are excellent agreement with the existing solutions. As a further validation of the current spectral element model, Aalami [17] predicted the fundamental frequency for a beam with $L = 10$ m having a square cross-section with $a = b = 5$ m using a Rayleigh-Ritz energy approach on the full three-dimensional problem, which is 122.09 Hz. This value is very close to the present solution 122.62 Hz.

Then, the spectral finite element model of the beam based on the general higher-order theory is used to compute the natural frequencies of the beam with a variety of aspect ratios. Five different aspect ratios, i.e., $b/a = 1000$, $b/a = 10$, $b/a = 2$, $b/a = 1$ and $b/a = 0.5$ are considered. In order to investigate the effect of the aspect ratio on the vibration frequencies, the first six natural frequencies of the beam are calculated and the percentage variations are plotted against the aspect ratio in Fig. 5. The percentage variation is defined as percentage variation $= 100(\omega - \omega_0)/\omega_0$,

Table 2
Natural frequencies (in Hz) of Simply-Supported rectangular cross-section beam

Aspect ratio b/a	Mode No.					
	1	2	3	4	5	6
1000	123.11	159.01	303.65	310.53	503.48	532.62
10	123.10	159.01	303.65	310.41	503.64	531.85
2	122.91	159.15	303.39	307.33	507.15	513.93
1	122.62	159.37	296.85	303.18	465.28	518.96
0.5	123.68	160.55	252.28	310.93	388.38	487.06

Table 3
Natural frequencies (in Hz) of Clamped-Free rectangular cross-section beam

Aspect ratio b/a	Mode No.					
	1	2	3	4	5	6
1000	55.37	166.37	268.87	415.29	452.59	641.79
10	55.38	166.31	268.91	415.01	452.56	641.68
2	55.72	164.83	269.76	407.97	451.97	631.06
1	56.98	161.37	272.15	383.04	451.91	545.12
0.5	61.83	156.30	271.12	299.43	402.43	490.40

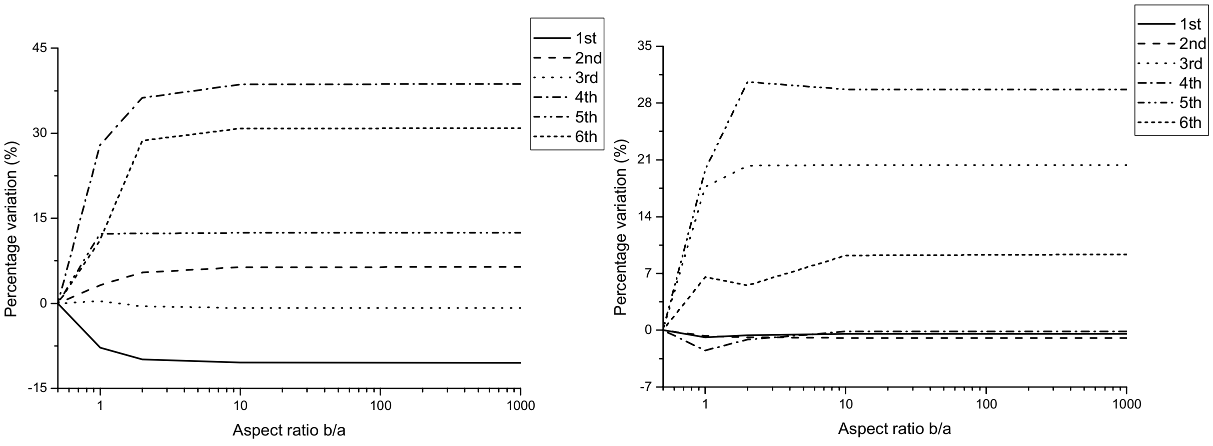

(a) (b)

Fig. 5. Percentage variations of first six frequencies versus aspect ratio for (a) Clamped-Free and (b) Simply-Supported rectangular section beams.

where ω_0 is the natural frequency of the beam with the aspect ratio $b/a = 0.5$. The numerical values of the first six natural frequencies are also shown in Tables 2 and 3. For the Simply-Supported boundary condition, the calculations of the analytical solutions using the expressions given by Kosmatka [19] are also performed. However, the analytical solutions are not displayed in Table 2 because they are complete agreement with the results predicted by the present formulation. It can be noticed from Fig. 5 that the effect of aspect ratio b/a on the natural frequencies of the beam is rather complex, it depends upon the particular boundary condition and mode number. There is a tendency that the aspect ratio has a pronounced effect on the higher frequencies. For the Clamped-Free end condition, increasing the aspect ratio from 0.5 to 1000 yields an increase in the frequency approximately -10.45%, 6.44%, -0.83%, 38.69%, 12.46% and 30.87% for the first, second, third, fourth, fifth and sixth modes, respectively.

For the Clamped-Free boundary condition, the first six normal mode shapes of the beam with cross-section aspect ratio $b/a = 1000$ are computed and the numerical results are plotted in Fig. 6.

The second example is a beam with elliptical cross-section, as shown in Fig. 4. The numerical data for this example is the same as the previous one. The first six natural frequencies of the beam with five different cross-section aspect ratios, i.e., $b/a = 1000$, $b/a = 10$, $b/a = 2$, $b/a = 1$ and $b/a = 0.5$ are also calculated and the numerical results are given in Tables 4 and 5. The percentage variations of the natural frequencies are plotted against aspect

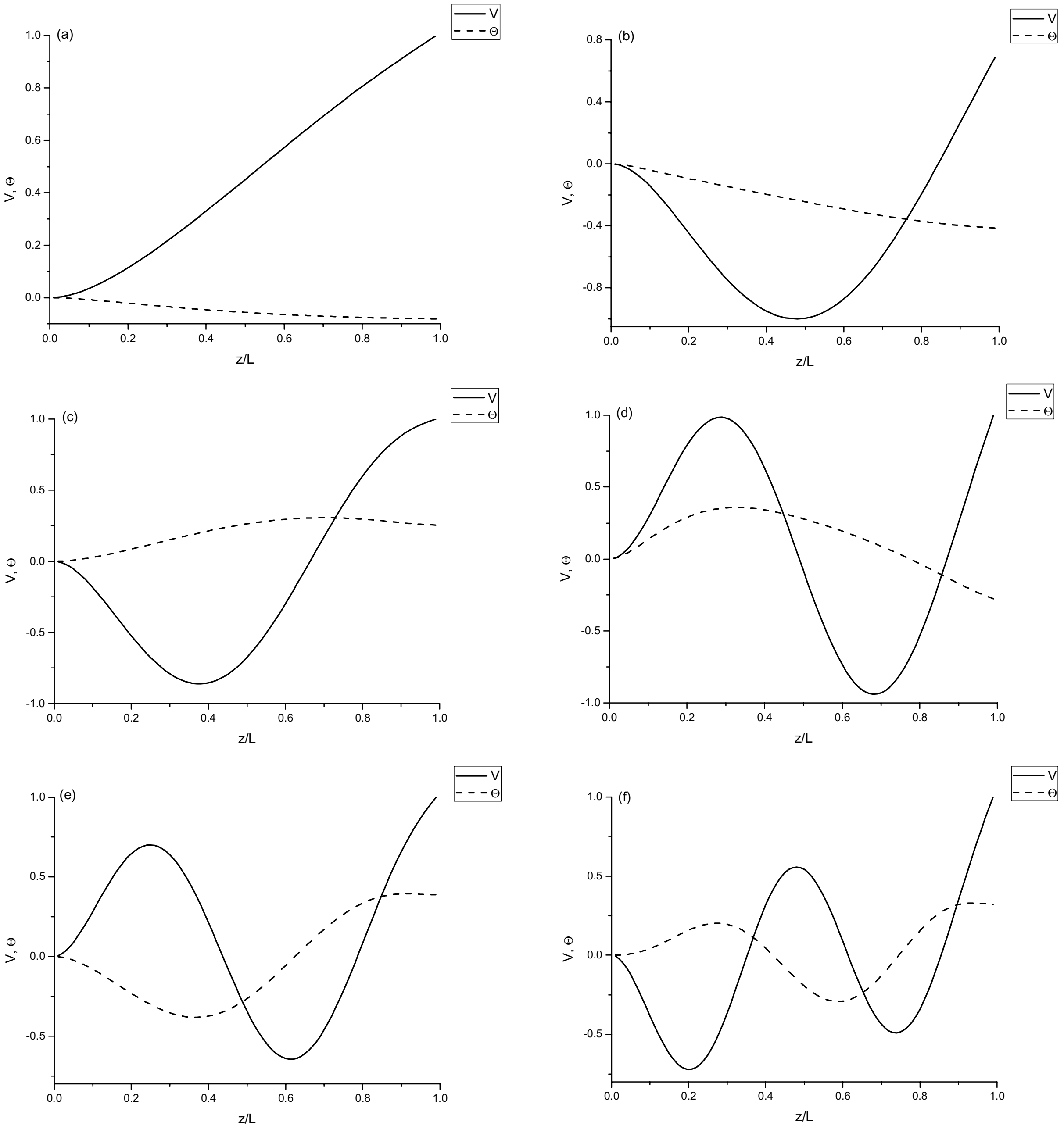

Fig. 6. First six normal mode shapes of Clamped-Free rectangular cross-section beam with aspect ratio $b/a = 1000$: (a) mode 1; (b) mode 2; (c) mode 3; (d) mode 4; (e) mode 5; (f) mode 6.

ratio in Fig. 7. The analytical solutions for the Simply-Supported end condition are also computed and they are found to be in perfect agreement with the present solutions. Figure 7 shows that the effect of aspect ratio on the natural frequency of elliptical section beam is different from that of rectangular section beam and the effect of aspect ratio on the higher frequencies can be significant. For the Clamped-Free boundary condition, changing the aspect ratio from 0.5 to 1000 increases the natural frequency by about -10.30%, -1.67%, -0.86%, 26.71%, 12.58% and 21.33% for the first, second, third, fourth, fifth and sixth modes, respectively.

Table 4
Natural frequencies (in Hz) of Simply-Supported elliptical cross-section beam

Aspect ratio b/a	Mode No.					
	1	2	3	4	5	6
1000	118.01	191.15	291.87	331.23	479.03	546.37
10	118.00	191.05	291.80	331.03	478.92	545.73
2	117.94	189.91	291.56	326.79	479.04	530.21
1	117.93	186.77	294.15	312.45	478.06	493.59
0.5	119.82	179.25	262.05	317.61	412.93	488.40

Table 5
Natural frequencies (in Hz) of Clamped-Free elliptical cross-section beam

Aspect ratio b/a	Mode No.					
	1	2	3	4	5	6
1000	51.89	161.04	280.61	391.45	463.26	612.91
10	51.89	161.02	280.53	391.36	462.99	612.86
2	52.08	161.03	279.80	390.13	457.81	614.53
1	52.88	161.53	279.38	384.48	447.46	569.00
0.5	57.85	163.78	283.05	308.94	411.51	505.18

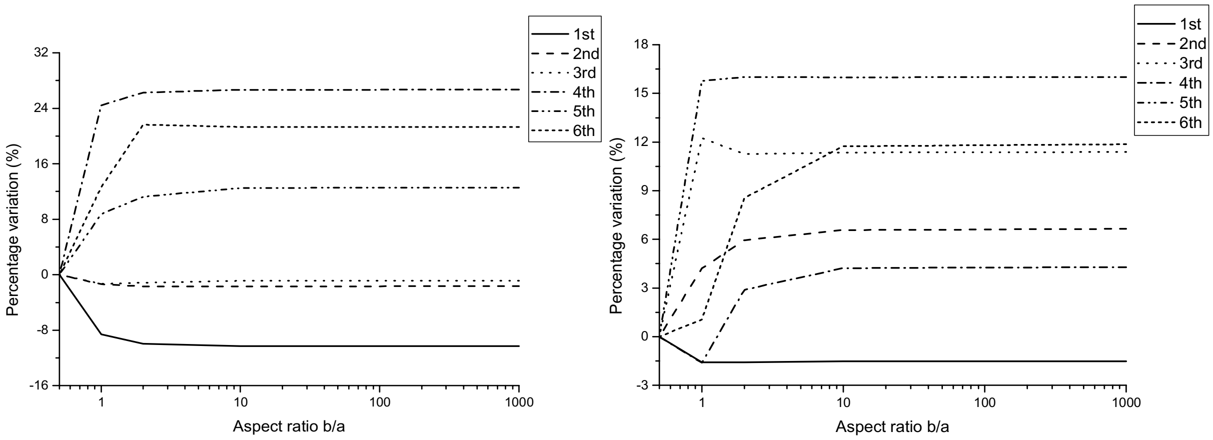

Fig. 7. Percentage variations of first six frequencies versus aspect ratio for (a) Clamped-Free and (b) Simply-Supported elliptical section beams.

6. Conclusions

A spectral element matrix has been developed for an isotropic beam with an arbitrary cross-section. The general higher-order beam theory is used, which considers both out-of-plane shear-dependent warping and in-plane deformations. The theoretical expressions of the spectral element matrix are formulated from the exact solutions of the governing differential equations of motion of the beam element. Application of the spectral element matrix enables exact prediction of the natural frequencies and mode shapes of the isotropic beams or of simple structures containing them. Two illustrative examples show exact agreement with the existing published results.

Acknowledgment

The authors thank the anonymous referees for their helpful comments.

References

[1] S.P. Timoshenko, On the correction for shear of the differential equation for transverse vibrations of prismatic beams, *Philosophical Magazine* **41** (1921), 744–746.

[2] R.D. Mindlin and H. Deresiewicz, *Timoshenko's Shear Coefficient for Flexural Vibrations of Beams*, Proceedings of 2nd US National Congress of Applied Mechanics, ASME Publication, New York, 1954, 175–178.
[3] G.R. Cowper, The shear coefficient in Timoshenko's beam theory, *Journal of Applied Mechanics* **33** (1966), 335–340.
[4] J.R. Hutchinson, On Timoshenko beams of rectangular cross-section, *Journal of Applied Mechanics* **71** (2004), 359–367.
[5] N.G. Stephen and M. Levinson, A second order beam theory, *Journal of Sound and Vibration* **67** (1979), 293–305.
[6] M. Levinson, A new rectangular beam theory, *Journal of Sound and Vibration* **74** (1981), 81–87.
[7] W.B. Bickford, A consistent high-order beam theory, *Developments in Theoretical and Applied Mechanics* **11** (1982), 137–150.
[8] A.V. Murty, Toward a consistent beam theory, *AIAA Journal* **22** (1984), 811–816.
[9] M. Levinson, On Bickford's consistent higher order beam theory, *Mechanics Research Communications* **12** (1985), 1–9.
[10] Z. Rychter, On the accuracy of a beam theory, *Mechanics of Research Communications* **14** (1987), 99–105.
[11] P.R. Heyliger and J.N. Reddy, A higher order beam finite element for bending and vibration problems, *Journal of Sound and Vibration* **126** (1988), 309–326.
[12] J. Petrolito, Stiffness analysis of beams using a higher-order theory, *Comput Struct* **55** (1995), 33–39.
[13] A.N. Kathnelson, Improved engineering theory for uniform beams, *Acta Mechanica* **114** (1996), 225–229.
[14] C.M. Wang, J.N. Reddy and K.H. Lee, *Shear Deformable Beams and Plates*, New York: Elsevier, 2000.
[15] J.N. Reddy, C.M. Wang, G.T. Lim and K.H. Ng, Bending solutions of the Levinson beams and plates in terms of the classical theories, *Int J Solids Struct* **38** (2001), 4701–4720.
[16] Y.M. Ghugal and R.P. Shimpi, A review of refined shear deformation theories for isotropic and anisotropic laminated beams, *Journal of Reinforced Plastics and Composites* **20** (2001), 255–272.
[17] B. Aalami, Waves in prismatic guides of arbitrary cross-section, *Journal of Applied Mechanics* **40** (1973), 1067–1072.
[18] C. Ie and J.B. Kosmatka, On the analysis of prismatic beams using first-order warping functions, *International Journal of Solids and Structures* **29** (1992), 879–891.
[19] J.B. Kosmatka, Transverse vibrations of shear-deformable beams using a general higher order theory, *Journal of Sound and Vibration* **160** (1993), 259–277.
[20] J.F. Doyle, *Wave Propagation in Structure*, New York: Springer-Verlag, 1989.
[21] U. Lee, *Spectral Element Method in Structural Dynamics*, Inha University, Incheon, Korea: Inha University Press, 2004.
[22] R.L. Burden and J.D. Faires, *Numerical Analysis*, Boston: Pws-Kent Publishing Company; 1989.
[23] B.W. Char, K.O. Geddes, G.H. Gonnet, M.B. Monagan and S.M. Watt, *Maple Reference Manual*, Department of Computer Science, University of Waterloo, Canada: Symbolic Computation Group and Waterloo Maple Publishing, 1990.

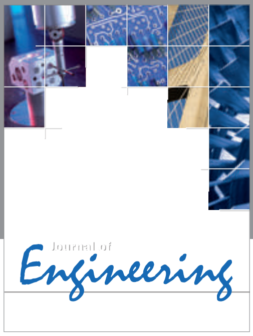

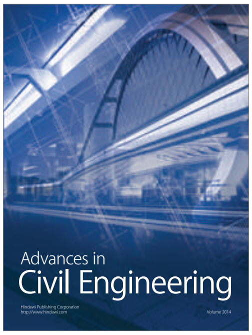

Hindawi

Submit your manuscripts at
http://www.hindawi.com

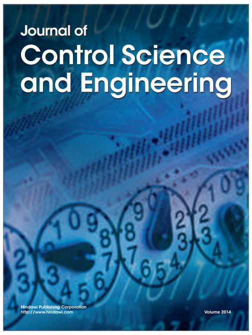

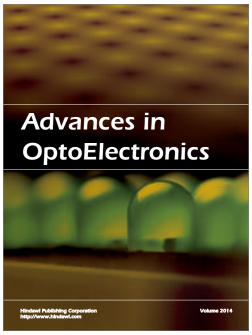

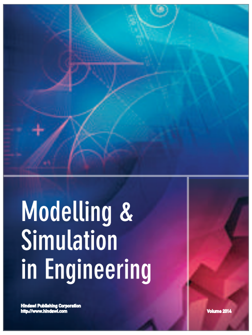

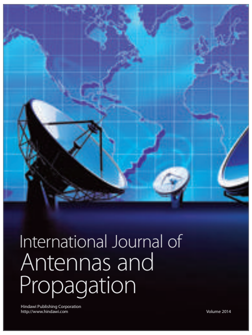

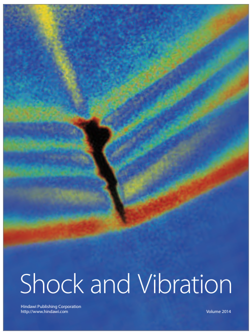

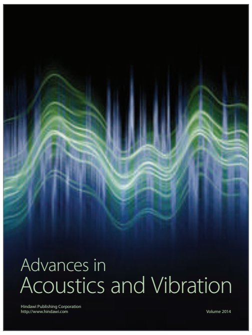

Shock and Vibration 15 (2008) 179–192
IOS Press

A spectral finite element model for vibration analysis of a beam based on general higher-order theory

Jiao Sujuan, Li Jun, Hua Hongxing and Shen Rongying
Vibration, Shock & Noise Institute, Shanghai Jiao Tong University, 800 Dongchuan Road, Shanghai 200240, P.R. China

Received 1 July 2006
Revised 2007

Abstract. The spectral element matrix is derived for a straight and uniform beam element having an arbitrary cross-section. The general higher-order beam theory is used, which accurately accounts for the transverse shear deformation out of the cross-sectional plane and antielastic-type deformation within the cross-sectional plane. Two coupled equations of motion are derived by use of Hamilton's principle along with the full three-dimensional constitutive relations. The theoretical expressions of the spectral element matrix are formulated from the exact solutions of the coupled governing equations. The developed spectral element matrix is directly applied to calculate the exact natural frequencies and mode shapes of the illustrative examples. Numerical results of the thick isotropic beams with rectangular and elliptical cross-sections are presented for a wide variety of cross-section aspect ratios.

Keywords: Beam, higher-order, shear deformation, dynamic analysis, spectral element matrix

1. Introduction

Beam members are basic structural components widely used in many types of structures within the fields of mechanical, aeronautical, automobile and civil engineering. Because of the practical importance, a large number of investigators have made efforts to deal with the static and dynamic analyses of the beams. The analyses of slender beams have been performed mostly using the elementary Bernoulli-Euler theory. This theory assumes that the plane sections of the cross-section remain plane and particular to the beam axis.

A more refined beam theory is Timoshenko beam theory which accounts for the shear deformation and rotary inertia that are neglected in the elementary theory. In Timoshenko beam theory the distribution of the transverse shear strain is constant through the beam thickness and therefore requires the shear correction factor to correct the strain energy of deformation. Timoshenko [1] first developed a theory which allowed one to study the vibrational behavior of the thick beams by approximately accounting for transverse shear deformation and rotary inertia, where the cross-section remained undistorted and the in-plane stresses were zero. Mindlin and Deresiewicz [2] calculated the shear correction factor for a variety of cross-sections of the beams. The dynamic shear strain distribution may differ significantly from the parabolic form of the static shear strain distribution. Cowper [3] presented a method to determine the shear correction factor based on the static three-dimensional elasticity theory along with Saint-Venant's static flexure warping function. Hutchinson [4] investigated the behavior of the shear coefficient for a rectangular Timoshenko beam by comparison of the Timoshenko beam solution with a three-dimensional solution for a simply-supported beam. It was found that a shear coefficient would have to be a function of the wave length as well as the aspect ratio.

ISSN 1070-9622/08/$17.00 © 2008 – IOS Press and the authors. All rights reserved

The limitations of the elementary Bernoulli-Euler beam theory and first-order Timoshenko shear deformation beam theory force the development of higher-order shear deformation beam theories. Stephen and Levinson [5] developed a second-order model for studying the beam vibrations with two governing differential equations having two independent coefficients. The first coefficient was similar to the Timoshenko's shear correction factor, which depended upon Saint-Venant's static flexure warping function, while the second coefficient depended upon the transverse shear stress state. Levinson [6] developed the higher-order shear deformable theory for beams with thin rectangular cross-sections that correctly accounted for the stress free boundary conditions on the upper and lower surfaces as well as the parabolic shear strain distribution through the thickness without the need for a shear correction factor. This was accomplished by expanding the axial displacement to include a cubic distribution through the thickness. This additional displacement was identical to the Saint-Venant's static flexure warping function for thin rectangular cross-sections, but for general cross-section shapes the correct expansion should be an infinite series of transcendental functions. Bickford [7] considered a shear deformation theory for rectangular beams that correctly accounted for the stress free boundary conditions on the upper and lower surfaces of the beam while retaining the parabolic distribution of the transverse shear strain. Murty [8] formulated a third-order beam theory including the transverse shear strain and nonclassical axial stress. In this theory the parabolic transverse shear stress distribution across the thickness of the beam could be obtained using the constitutive relations. Levinson [9] obtained the higher-order beam theory with the fourth-order differential equations, satisfying two boundary conditions at each end of the beam. No shear correction factors were required since the theory satisfied the shear stress free surface conditions on the top and bottom of the beam. Rychter [10] verified the consistency and accuracy of Levinson's theory by imbedding it in the two-dimensional linear theory of elasticity. It was shown that the Levinson's variationally inconsistent theory was more accurate than the variationally consistent theory of Bickford. Heyliger and Reddy [11] used a higher-order theory and noted the inadequacy of the shear correction factor in predicting the natural frequencies. Petrolito [12] presented a finite element solution of uniformly loaded thick beams using the Bickford's theory. Kathnelson [13] developed an improved engineering theory for elastic isotropic uniform beam using the asymptotic analysis of the variational equation of Hellinger-Reissner principle for the three-dimensional theory of elasticity. Wang et al. [14] discussed the derivation and comparison of the Bernoulli-Euler, Timoshenko, and Reddy-Bickford beam theories extensively. Reddy et al. [15] gave solutions to the Levinson beams in terms of the classical beam solutions. Ghugal and Shimpi [16] presented a review of the displacement and stress based refined theories for isotropic and anisotropic laminated beams. Aalami [17] studied the vibrational behavior of a general prismatic beam with an arbitrary cross-section by using a Rayleigh-Ritz energy approach to the general three-dimensional problem. His numerical and graphical results clearly illustrated the presence and importance of both the out-of-plane shear deformation and in-plane deformation for extremely high vibrational modes. Ie and Kosmatka [18] developed a static theory for a general cylindrical or prismatic beam that incorporated both out-of-plane shear and in-plane deformation functions, where these functions were assumed known. In fact, these functions could be determined exactly for simple cross-sections by solving Saint-Venant's bending and flexure problems, and approximately for an arbitrary cross-section by applying either a two-dimensional finite element approach or a power series approach. Kosmatka [19] presented a new beam theory for studying the static and vibration behaviors of the cylindrical or prismatic beam-type structures having an arbitrary cross-section. This general higher-order theory accurately accounted for the transverse shear deformation out of the cross-sectional plane and antielastic-type deformation within the cross-sectional plane.

A review of the literature indicates that the refined theories for dynamic analysis of the beams with non-rectangular cross-sections are rare. Most of the research work related to the dynamic analysis of thick isotropic beams assumes that the in-plane cross-sectional stresses are negligible and the cross-section does not deform in its own plane and comparatively less work is available on incorporating both out-of-plane shear and in-plane deformation in a unified manner. The objective of this paper is to develop an exact spectral element matrix for a general higher-order beam element with an arbitrary cross-section, which has not still been reported in literature. Although several researchers have investigated and elaborated the spectral element method [20,21], it should be noted that there are differences in the way they compute the spectral elements from the way used in this paper. The explicit analytical expressions for the entries of the spectral element matrix are derived in the paper. The spectral element method is often referred to as an exact method as it is based on the exact shape functions obtained from the exact solutions of the element differential equations. The usefulness of the method becomes apparent when higher frequencies and better accuracies of the results are required.

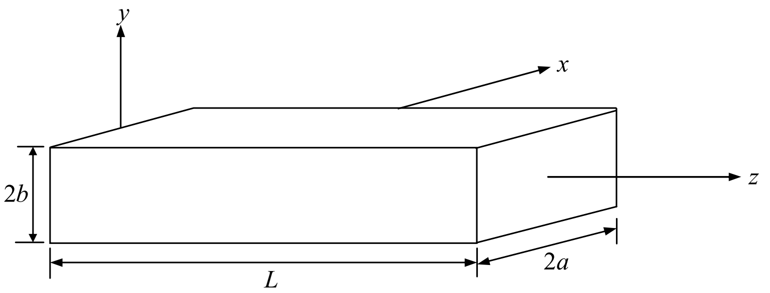

Fig. 1. A prismatic isotropic beam.

In this paper, the spectral finite element formulation for a thick isotropic beam having an arbitrary cross-section is presented. The general higher-order beam theory is employed [19], which considers both out-of-plane shear dependent warping and in-plane deformations. The theoretical expressions of the spectral element matrix for the general higher-order beam element are derived from the exact solutions of the governing differential equations. The application of the derived spectral element matrix to calculate the natural frequencies and mode shapes of the particular beams uses the automated Muller root search algorithm [22]. Numerical results are presented and compared with the available solutions in literature to validate the accuracy and efficiency of the current approach.

2. Mathematical formulation

A prismatic isotropic beam with a general homogeneous cross-section, as shown in Fig. 1, is considered in this paper. A Cartesian co-ordinate system (x, y, z) is defined on the beam, where x and y are coincident with the principal axes of the beam cross-section and z is coincident with the centroidal axis. The current development is further restricted to the study of vibrational behavior in the $y - z$ plane only, and the displacement relations are defined as [19]

$$u_1(x, y, z, t) = \partial\theta(z, t)/\partial z\psi_x(x, y) \tag{1a}$$

$$u_2(x, y, z, t) = v(z, t) + \partial\theta(z, t)/\partial z\psi_y(x, y) \tag{1b}$$

$$u_3(x, y, z, t) = y\theta(z, t) + [\partial v(z, t)/\partial z + \theta(z, t)]\psi_z(x, y) \tag{1c}$$

where (u_1, u_2, u_3) are the displacements of a point along the (x, y, z) coordinates, $v(z, t)$ represents the time-dependent y direction displacement and $\theta(z, t)$ the time-dependent rotation about the x axis. The three functions $\psi_x(x, y)$, $\psi_y(x, y)$, and $\psi_z(x, y)$, which are assumed to be known, can be determined exactly for simple cross-sections by solving Saint-Venant's bending and flexure problems, or approximately for arbitrary cross-sections using either a two-dimensional finite element approach or a power series approach [19].

The time-dependent strain-displacement relationships of the beam are defined as

$$\varepsilon_{xx} = \partial\theta/\partial z\partial\psi_x/\partial x \tag{2a}$$

$$\varepsilon_{yy} = \partial\theta/\partial z\partial\psi_y/\partial y \tag{2b}$$

$$\varepsilon_{zz} = y\partial\theta/\partial z + \partial(\partial v/\partial z + \theta)/\partial z\psi_z \tag{2c}$$

$$\gamma_{yz} = (\partial v/\partial z + \theta)(1 + \partial\psi_z/\partial y) + \partial^2\theta/\partial z^2\psi_y \tag{2d}$$

$$\gamma_{xz} = (\partial v/\partial z + \theta)\partial\psi_z/\partial x + \partial^2\theta/\partial z^2\psi_x \tag{2e}$$

$$\gamma_{xy} = \partial\theta/\partial z(\partial\psi_x/\partial y + \partial\psi_y/\partial x) \tag{2f}$$

where ε_{xx}, ε_{yy} and ε_{zz} are the normal strains in the x, y and z directions, respectively, and γ_{yz}, γ_{xz} and γ_{xy} are the shear strains.

The general constitutive relations are given as

$$\sigma_{xx} = (\lambda + 2G)\varepsilon_{xx} + \lambda\varepsilon_{yy} + \lambda\varepsilon_{zz} \tag{3a}$$

$$\sigma_{yy} = \lambda\varepsilon_{xx} + (\lambda + 2G)\varepsilon_{yy} + \lambda\varepsilon_{zz} \tag{3b}$$

$$\sigma_{zz} = \lambda\varepsilon_{xx} + \lambda\varepsilon_{yy} + (\lambda + 2G)\varepsilon_{zz} \tag{3c}$$

$$\tau_{yz} = G\gamma_{yz} \tag{3d}$$

$$\tau_{xz} = G\gamma_{xz} \tag{3e}$$

$$\tau_{xy} = G\gamma_{xy} \tag{3f}$$

Here, λ and G are defined as Lame's constants.

$$\lambda = E\nu/(1+\nu)(1-2\nu) \quad G = E/2(1+\nu)$$

where E is Young's modulus and ν is Poisson ratio.

The total strain energy $U$of the beam shown in Fig. 1 is given by

$$U = \frac{1}{2}\int_0^L \int_A (\sigma_{xx}\varepsilon_{xx} + \sigma_{yy}\varepsilon_{yy} + \sigma_{zz}\varepsilon_{zz} + \tau_{yz}\gamma_{yz} + \tau_{xz}\gamma_{xz} + \tau_{xy}\gamma_{xy})dAdz \tag{4a}$$

Substituting σ_{xx}, σ_{yy}, σ_{zz} and τ_{yz}, τ_{xz}, τ_{xy} from Eqs (3a)–(3f) into Eq. (4a) yields

$$\begin{aligned} U = \frac{1}{2}\int_0^L \int_A \big[&(\lambda + 2G)\varepsilon_{xx}^2 + (\lambda + 2G)\varepsilon_{yy}^2 + (\lambda + 2G)\varepsilon_{xx}^2 + G\gamma_{yz}^2 + G\gamma_{xz}^2 + G\gamma_{xy}^2 \\ &+2\lambda\varepsilon_{xx}\varepsilon_{yy} + 2\lambda\varepsilon_{xx}\varepsilon_{zz} + 2\lambda\varepsilon_{yy}\varepsilon_{zz}\big]\, dAdz \end{aligned} \tag{4b}$$

The total kinetic energy T of the beam is defined by

$$T = \frac{1}{2}\int_0^L \int_A \rho(\dot{u}_1^2 + \dot{u}_2^2 + \dot{u}_3^2)dAdz \tag{5a}$$

where ρ is the mass density per unit volume of the beam and the superscript dot represents a derivative with respect to time t.

Substituting u_1, u_2 and u_3 from Eq. (1) into Eq. (5a) results in

$$T = \frac{1}{2}\int_0^L \int_A \rho\{(\dot{\theta}'\psi_x)^2 + (\dot{v} + \dot{\theta}'\psi_y)^2 + [y\dot{\theta} + (\dot{v}' + \dot{\theta})\psi_z]^2\}dAdz \tag{5b}$$

where the superscript prime refers to a partial derivative with respect to z co-ordinate.

The governing equations of motion and boundary conditions for the displacement relations given by Eq. (1) can be obtained conveniently by means of Hamilton's principle, which can be stated in the form

$$\begin{gathered} \int_{t_1}^{t_2} (\delta T - \delta U)\, dt = 0 \\ \delta v = \delta\theta = \delta v' = \delta\theta' = 0 \ \text{ at } t = t_1, t_2 \end{gathered} \tag{6}$$

Herein δU and δT are the variations of the strain and kinetic energies, respectively.

Substituting Eq. (2) into Eq. (4b), then substituting the resulting equation and Eq. (5b) into Eq. (6) and performing the variational operations yields the following governing differential equations of motion for the beam based on general higher-order theory

$$D_{12}\theta''' + D_{22}v'''' - A_{11}(v'' + \theta') - A_{12}\theta''' + m\ddot{v} + J_1\ddot{\theta}' - (J_z\ddot{v}'' + J_2\ddot{\theta}') = 0 \tag{7a}$$

$$\begin{aligned}&-(D_{11}\theta'' + D_{12}v''') + A_{11}(v' + \theta) + A_{12}\theta'' + A_{12}(v''' + \theta'')\\ &\quad +A_{22}\theta'''' + J_2\ddot{v}' + I_p\ddot{\theta} - (J_1\ddot{v}' + J_p\ddot{\theta}'') = 0\end{aligned} \tag{7b}$$

where

$$m = \int_A \rho dA \quad I_p = \int_A \rho(y+\psi_z)^2 dA \quad J_1 = \int_A \rho\psi_y dA$$

$$J_p = \int_A \rho(\psi_x^2 + \psi_y^2) dA \quad J_z = \int_A \rho\psi_z^2 dA \quad J_2 = \int_A \rho(y+\psi_z)\psi_z dA$$

$$\begin{aligned}D_{11} &= \int_A (\lambda + 2G)\{(y+\psi_z)^2 + (\partial\psi_x/\partial x)^2 + (\partial\psi_y/\partial y)^2\}\\ &\quad +2\lambda\{(y+\psi_z)(\partial\psi_x/\partial x + \partial\psi_y/\partial y) + \partial\psi_x/\partial x\partial\psi_y/\partial y\} + G(\partial\psi_x/\partial y + \partial\psi_y/\partial x)^2 dA\\ D_{12} &= \int_A \{(\lambda+2G)(y+\psi_z) + \lambda(\partial\psi_x/\partial x + \partial\psi_y/\partial y)\}\psi_z dA\\ D_{22} &= \int_A (\lambda+2G)\psi_z^2 dA \quad A_{11} = \int_A G\{(1+\partial\psi_z/\partial y)^2 + (\partial\psi_z/\partial x)^2\}dA\\ A_{12} &= \int_A G\{(1+\partial\psi_z/\partial y)\psi_y + \partial\psi_z/\partial x\psi_x\}dA \quad A_{22} = \int_A G\{\psi_x^2 + \psi_y^2\}dA\end{aligned}$$

The associated boundary conditions at the ends of beam ($z = 0, L$) are obtained as follows

$$\left[-D_{12}\theta'' - D_{22}v''' + A_{11}(v' + \theta) + A_{12}\theta'' + J_z\ddot{v}' + J_2\ddot{\theta}\right]\delta v = 0 \tag{8a}$$

$$\left[D_{11}\theta' + D_{12}v'' - A_{12}(v'' + \theta') - A_{22}\theta''' + J_1\ddot{v} + J_p\ddot{\theta}'\right]\delta\theta = 0 \tag{8b}$$

$$[D_{12}\theta' + D_{22}v'']\,\delta v' = 0 \tag{8c}$$

$$[A_{12}(v' + \theta) + A_{22}\theta'']\delta\theta' = 0 \tag{8d}$$

3. Spectral finite element

It can be shown that Eq. (7) have solutions that are separable in time and space, and that the time dependence is harmonic. Letting

$$v(z,t) = V(z)\sin\omega t \tag{9a}$$

$$\theta(z,t) = \Theta(z)\sin\omega t \tag{9b}$$

where ω is the angular frequency, $V(z)$ and $\Theta(z)$ are the amplitudes of the sinusoidally varying transverse displacement and normal rotation, respectively.

Introducing Eq. (9) into Eq. (7), the following differential eigenvalue equations are obtained

$$\begin{aligned}&D_{12}\Theta''' + D_{22}V'''' - A_{11}(V'' + \Theta') - A_{12}\Theta'''\\ &\quad -m\omega^2 V - J_1\omega^2\Theta' + J_z\omega^2 V'' + J_2\omega^2\Theta' = 0\end{aligned} \tag{10a}$$

$$\begin{aligned}&-D_{11}\Theta'' - D_{12}V''' + A_{11}(V' + \Theta) + A_{12}\Theta'' + A_{12}(V''' + \Theta'')\\ &\quad +A_{22}\Theta'''' - J_2\omega^2 V' - I_p\omega^2\Theta + J_1\omega^2 V' + J_p\omega^2\Theta'' = 0\end{aligned} \tag{10b}$$

The solutions to Eq. (10) can be expressed as

$$V(z) = \tilde{A}e^{\kappa z} \tag{11a}$$

$$\Theta(z) = \tilde{B}e^{\kappa z} \tag{11b}$$

Substituting Eq. (11) into Eq. (10), the equivalent algebraic eigenvalue equations are obtained and the equations have nontrivial solutions when the determinant of the coefficient matrix of $\tilde{A}$ and $\tilde{B}$ vanishes. Setting the determinant equal to zero yields the characteristics equation, which is an eighth-order polynomial equation in κ

$$\eta_4\kappa^8 + \eta_3\kappa^6 + \eta_2\kappa^4 + \eta_1\kappa^2 + \eta_0 = 0 \tag{12}$$

where

$$\begin{aligned}
&\eta_4 = A_{22}D_{22}\\
&\eta_3 = A_{12}^2 - A_{11}A_{22} - 2A_{12}D_{12} + D_{12}^2 + 2A_{12}D_{22} - D_{11}D_{22} + (D_{22}J_p + A_{22}J_z)\omega^2\\
&\eta_2 = A_{11}(D_{11} - 2D_{12} + D_{22}) + J_pJ_z\omega^4\\
&\qquad -(D_{22}I_p + 2(-A_{12} + D_{12})(J_1 - J_2) + A_{11}J_p + (-2A_{12} + D_{11})J_z + A_{22}m)\omega^2\\
&\eta_1 = \omega^2(A_{11}(I_p + 2J_1 - 2J_p + J_z) - 2A_{12}m + D_{11}m\\
&\qquad +((J_1 - J_2)^2 - I_pJ_z - J_pm)\omega^2)\\
&\eta_0 = -A_{11}m\omega^2 + I_pm\omega^4
\end{aligned}$$

Therefore the fourth-order polynomial equation for the roots $\chi = \kappa^2$ must be solved. The solutions can be found in close-form as follows.

Equation (12) can be rewritten as

$$\chi^4 + a_1\chi^3 + a_2\chi^2 + a_3\chi + a_4 = 0 \tag{13}$$

where

$$a_1 = \eta_3/\eta_4 \quad a_2 = \eta_2/\eta_4 \quad a_3 = \eta_1/\eta_4 \quad a_4 = \eta_0/\eta_4$$

The fourth-order Eq. (13) can be factorized as

$$(\chi^2 + p_1\chi + q_1)(\chi^2 + p_2\chi + q_2) = 0$$

where

$$\begin{Bmatrix} p_1 \\ p_2 \end{Bmatrix} = \frac{1}{2}[a_1 \pm \sqrt{a_1^2 - 4a_2 + 4\lambda_1}] \quad \begin{Bmatrix} q_1 \\ q_2 \end{Bmatrix} = \frac{1}{2}\left[\lambda_1 \pm \frac{a_1\lambda_1 - 2a_3}{\sqrt{a_1^2 - 4a_2 + 4\lambda_1}}\right]$$

and λ_1 is a real root of the following cubic equation

$$\lambda^3 - a_2\lambda^2 + (a_1a_3 - 4a_4)\lambda + (4a_2a_4 - a_3^2 - a_1^2a_4) = 0 \tag{14}$$

Then the four roots of the fourth-order Eq. (13) can be written as

$$\begin{Bmatrix} \chi_1 \\ \chi_2 \end{Bmatrix} = -\frac{p_1}{2} \pm \sqrt{\frac{p_1^2}{4} - q_1} \quad \begin{Bmatrix} \chi_3 \\ \chi_4 \end{Bmatrix} = -\frac{p_2}{2} \pm \sqrt{\frac{p_2^2}{4} - q_2} \tag{15}$$

If the discriminant of cubic Eq. (14), $\bar{D}$, is negative, then Eq. (14) has usually three real roots, which can be written as

$$\lambda_1 = a_2/3 + 2\sqrt{-\bar{Q}}\cos(\vartheta/3) \quad \lambda_2 = a_2/3 + 2\sqrt{-\bar{Q}}\cos((\vartheta + 2\pi)/3)$$

$$\lambda_3 = a_2/3 + 2\sqrt{-\bar{Q}}\cos((\vartheta + 4\pi)/3)$$

where

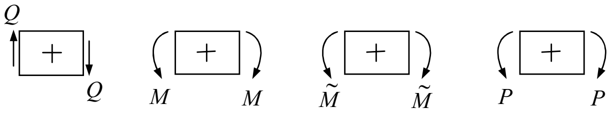

Fig. 2. Sign convention for positive shear force $Q(z)$, bending moment $M(z)$, generalized moment$\tilde{M}(z)$ and higher-order moment $P(z)$.

$$\vartheta = \cos^{-1}(\bar{R}\Big/\sqrt{-\bar{Q}^3}) \quad \bar{Q} = -\frac{1}{9}(a_2^2 - 3a_1a_3 + 12a_4)$$

$$\bar{R} = \frac{1}{54}(2a_2^3 - 9a_1a_2a_3 + 27a_3^2 + 27a_1^2a_4 - 72a_2a_4) \quad \bar{D} = \bar{Q}^3 + \bar{R}^2$$

Whichever of the three roots is chosen, the same solutions are obtained.

The general solutions to Eq. (10) are given by

$$\begin{aligned} V(z) &= A_1e^{\kappa_1 z} + A_2e^{-\kappa_1 z} + A_3e^{\kappa_2 z} + A_4e^{-\kappa_2 z} + A_5e^{\kappa_3 z} + A_6e^{-\kappa_3 z} + A_7e^{\kappa_4 z} + A_8e^{-\kappa_4 z} \\ &= \sum_{j=1}^{4}(A_{2j-1}e^{\kappa_j z} + A_{2j}e^{-\kappa_j z}) \end{aligned} \tag{16a}$$

$$\begin{aligned} \Theta(z) &= B_1e^{\kappa_1 z} + B_2e^{-\kappa_1 z} + B_3e^{\kappa_2 z} + B_4e^{-\kappa_2 z} + B_5e^{\kappa_3 z} + B_6e^{-\kappa_3 z} + +B_7e^{\kappa_4 z} + B_8e^{-\kappa_4 z} \\ &= \sum_{j=1}^{4}(B_{2j-1}e^{\kappa_j z} + B_{2j}e^{-\kappa_j z}) \end{aligned} \tag{16b}$$

$$V'(z) \ = \sum_{j=1}^{4}\kappa_j(A_{2j-1}e^{\kappa_j z} - A_{2j}e^{-\kappa_j z}) \tag{16c}$$

$$\Theta'(z) \ = \sum_{j=1}^{4}t_j\kappa_j(A_{2j-1}e^{\kappa_j z} + A_{2j}e^{-\kappa_j z}) \tag{16d}$$

where $\kappa_1 = \sqrt{\chi_1}$,$\kappa_2 = \sqrt{\chi_2}$,$\kappa_3 = \sqrt{\chi_3}$,$\kappa_4 = \sqrt{\chi_4}$. In the solution of Eq. (13), if any of the χ_j's are zero or are repeated, the solutions to the differential Eq. (10) will be modified according to the well-known methods for ordinary differential equations with constant coefficients, for those particular values of χ_j.

From Eq. (16), only eight of the sixteen constants are independent. The relationship among the constants is given by

$$B_{2j-1} = t_jA_{2j-1}$$

$$B_{2j} = -t_jA_{2j}$$

where

$$t_j = (-A_{11}\kappa_j^2 + D_{22}\kappa_j^4 + (-m + J_z\kappa_j^2)\omega^2)\big/\Delta_j$$

$$\Delta_j = \kappa_j(A_{11} + (A_{12} - D_{12})\kappa_j^2 + (J_1 - J_2)\omega^2)(j = 1 \sim 4)$$

According to the sign convention shown in Fig. 2, the expressions of shear force $Q(z)$, bending moment $M(z)$, generalized moment $\tilde{M}(z)$ and higher-order moment $P(z)$ can be obtained from Eqs (8) and (16) as follows

$$\begin{aligned} Q(z) = \sum_{j=1}^{4} &\left[D_{12}t_j\kappa_j^2 + D_{22}\kappa_j^3 - A_{11}(\kappa_j + t_j) - A_{12}t_j\kappa_j^2 \right. \\ &\left. +\omega^2J_z\kappa_j + \omega^2J_2t_j\right](A_{2j-1}e^{\kappa_j z} - A_{2j}e^{-\kappa_j z}) \end{aligned} \tag{17a}$$

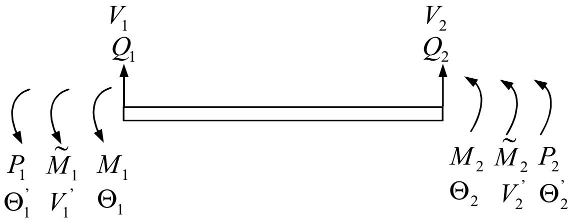
V_1
Q_1
V_2
Q_2
P_1 $\tilde{M}_1$ M_1
Θ'_1 V'_1 Θ_1
M_2 $\tilde{M}_2$ P_2
Θ_2 V'_2 Θ'_2

Fig. 3. Boundary conditions for displacements and forces of beam element.

$$M(z) = \sum_{j=1}^{4} \left[-D_{11} t_j \kappa_j - D_{12} \kappa_j^2 + A_{12} \kappa_j^2 + A_{12} t_j \kappa_j + A_{22} t_j \kappa_j^3 \right. \\ \left. + \omega^2 J_1 + \omega^2 J_p t_j \kappa_j \right] \left(A_{2j-1} e^{\kappa_j z} + A_{2j} e^{-\kappa_j z} \right) \tag{17b}$$

$$\tilde{M}(z) = \sum_{j=1}^{4} \left[-D_{12} t_j \kappa_j - D_{22} \kappa_j^2 \right] \left(A_{2j-1} e^{\kappa_j z} + A_{2j} e^{-\kappa_j z} \right) \tag{17c}$$

$$P(z) = \sum_{j=1}^{4} \left[-A_{12} \kappa_j - A_{12} t_j - A_{22} t_j \kappa_j^2 \right] \left(A_{2j-1} e^{\kappa_j z} - A_{2j} e^{-\kappa_j z} \right) \tag{17d}$$

Refer to Fig. 3, the boundary conditions for displacements and forces of the beam element are, respectively,

$$\begin{aligned} z = 0: &\quad V = V_1 \quad \Theta = \Theta_1 \quad V' = V'_1 \quad \Theta' = \Theta'_1 \\ z = L: &\quad V = V_2 \quad \Theta = \Theta_2 \quad V' = V'_2 \quad \Theta' = \Theta'_2 \end{aligned} \tag{18a}$$

$$\begin{aligned} z = 0: &\quad Q = Q_1 \quad M = M_1 \quad \tilde{M} = \tilde{M}_1 \quad P = P_1 \\ z = L: &\quad Q = -Q_2 \quad M = -M_2 \quad \tilde{M} = -\tilde{M}_2 \quad P = -P_2 \end{aligned} \tag{18b}$$

Substituting Eq. (18a) into Eq. (16), the nodal displacements defined in Fig. 3 can be expressed in terms of A_i as

$$\{D\} = [R]\{A\} \tag{19}$$

where $\{D\}$ is the nodal degree-of-freedom vector defined by

$$\{D\} = \left\{ V_1 \; \Theta_1 \; V'_1 \; \Theta'_1 \; V_2 \; \Theta_2 \; V'_2 \; \Theta'_2 \right\}^T$$

$$\{A\} = \left\{ A_1 \; A_3 \; A_5 \; A_7 \; A_2 \; A_4 \; A_6 \; A_8 \right\}^T$$

$$[R] = \begin{bmatrix} 1 & 1 & 1 & 1 & 1 & 1 & 1 & 1 \\ t_1 & t_2 & t_3 & t_4 & -t_1 & -t_2 & -t_3 & -t_4 \\ \kappa_1 & \kappa_2 & \kappa_3 & \kappa_4 & -\kappa_1 & -\kappa_2 & -\kappa_3 & -\kappa_4 \\ t_1\kappa_1 & t_2\kappa_2 & t_3\kappa_3 & t_4\kappa_4 & t_1\kappa_1 & t_2\kappa_2 & t_3\kappa_3 & t_4\kappa_4 \\ e^{\kappa_1 L} & e^{\kappa_2 L} & e^{\kappa_3 L} & e^{\kappa_4 L} & e^{-\kappa_1 L} & e^{-\kappa_2 L} & e^{-\kappa_3 L} & e^{-\kappa_4 L} \\ t_1 e^{\kappa_1 L} & t_2 e^{\kappa_2 L} & t_3 e^{\kappa_3 L} & t_4 e^{\kappa_4 L} & -t_1 e^{-\kappa_1 L} & -t_2 e^{-\kappa_2 L} & -t_3 e^{-\kappa_3 L} & -t_4 e^{-\kappa_4 L} \\ \kappa_1 e^{\kappa_1 L} & \kappa_2 e^{\kappa_2 L} & \kappa_3 e^{\kappa_3 L} & \kappa_4 e^{\kappa_4 L} & -\kappa_1 e^{-\kappa_1 L} & -\kappa_2 e^{-\kappa_2 L} & -\kappa_3 e^{-\kappa_3 L} & -\kappa_4 e^{-\kappa_4 L} \\ t_1\kappa_1 e^{\kappa_1 L} & t_2\kappa_2 e^{\kappa_2 L} & t_3\kappa_3 e^{\kappa_3 L} & t_4\kappa_4 e^{\kappa_4 L} & t_1\kappa_1 e^{-\kappa_1 L} & t_2\kappa_2 e^{-\kappa_2 L} & t_3\kappa_3 e^{-\kappa_3 L} & t_4\kappa_4 e^{-\kappa_4 L} \end{bmatrix}$$

Substituting Eq. (18b) into Eq. (17), the nodal forces defined in Fig. 3 also can be expressed in terms of A_i as

$$\{F\} = [H]\{A\} \tag{20}$$

where $\{F\}$ is the nodal force vector defined by

$$\{F\} = \left\{ Q_1 \; M_1 \; \tilde{M}_1 \; P_1 \; Q_2 \; M_2 \; \tilde{M}_2 \; P_2 \right\}^T$$

$$[H] = \begin{bmatrix} \bar{t}_1 & \bar{t}_2 & \bar{t}_3 & \bar{t}_4 & -\bar{t}_1 & -\bar{t}_2 & -\bar{t}_3 & -\bar{t}_4 \\ \hat{t}_1 & \hat{t}_2 & \hat{t}_3 & \hat{t}_4 & \hat{t}_1 & \hat{t}_2 & \hat{t}_3 & \hat{t}_4 \\ \tilde{t}_1 & \tilde{t}_2 & \tilde{t}_3 & \tilde{t}_4 & \tilde{t}_1 & \tilde{t}_2 & \tilde{t}_3 & \tilde{t}_4 \\ \bar{\bar{t}}_1 & \bar{\bar{t}}_2 & \bar{\bar{t}}_3 & \bar{\bar{t}}_4 & -\bar{\bar{t}}_1 & -\bar{\bar{t}}_2 & -\bar{\bar{t}}_3 & -\bar{\bar{t}}_4 \\ -\bar{t}_1 e^{\kappa_1 L} & -\bar{t}_2 e^{\kappa_2 L} & -\bar{t}_3 e^{\kappa_3 L} & -\bar{t}_4 e^{\kappa_4 L} & \bar{t}_1 e^{-\kappa_1 L} & \bar{t}_2 e^{-\kappa_2 L} & \bar{t}_3 e^{-\kappa_3 L} & \bar{t}_4 e^{-\kappa_4 L} \\ -\hat{t}_1 e^{\kappa_1 L} & -\hat{t}_2 e^{\kappa_2 L} & -\hat{t}_3 e^{\kappa_3 L} & -\hat{t}_4 e^{\kappa_4 L} & -\hat{t}_1 e^{-\kappa_1 L} & -\hat{t}_2 e^{-\kappa_2 L} & -\hat{t}_3 e^{-\kappa_3 L} & -\hat{t}_4 e^{-\kappa_4 L} \\ -\tilde{t}_1 e^{\kappa_1 L} & -\tilde{t}_2 e^{\kappa_2 L} & -\tilde{t}_3 e^{\kappa_3 L} & -\tilde{t}_4 e^{\kappa_4 L} & -\tilde{t}_1 e^{-\kappa_1 L} & -\tilde{t}_2 e^{-\kappa_2 L} & -\tilde{t}_3 e^{-\kappa_3 L} & -\tilde{t}_4 e^{-\kappa_4 L} \\ -\bar{\bar{t}}_1 e^{\kappa_1 L} & -\bar{\bar{t}}_2 e^{\kappa_2 L} & -\bar{\bar{t}}_3 e^{\kappa_3 L} & -\bar{\bar{t}}_4 e^{\kappa_4 L} & \bar{\bar{t}}_1 e^{-\kappa_1 L} & \bar{\bar{t}}_2 e^{-\kappa_2 L} & \bar{\bar{t}}_3 e^{-\kappa_3 L} & \bar{\bar{t}}_4 e^{-\kappa_4 L} \end{bmatrix}$$

in which

$$\bar{t}_j = D_{12} t_j \kappa_j^2 + D_{22} \kappa_j^3 - A_{11}(\kappa_j + t_j) - A_{12} t_j \kappa_j^2 + \omega^2 J_z \kappa_j + \omega^2 J_2 t_j$$

$$\hat{t}_j = -D_{11} t_j \kappa_j - D_{12} \kappa_j^2 + A_{12} \kappa_j^2 + A_{12} t_j \kappa_j + A_{22} t_j \kappa_j^3 + \omega^2 J_1 + \omega^2 J_p t_j \kappa_j$$

$$\tilde{t}_j = -D_{12} t_j \kappa_j - D_{22} \kappa_j^2$$

$\bar{\bar{t}}_j = -A_{12}\kappa_j - A_{12} t_j - A_{22} t_j \kappa_j^2 \; (j = 1 \sim 4)$

Eliminating the coefficients A_i from Eqs (19) and (20) gives the following relationship between the nodal forces and nodal displacements

$$\{F\} = [H][R]^{-1}\{D\} = [K]\{D\} \tag{21}$$

where $[K]$ is the spectral element matrix. It should be mentioned that the explicit analytical expressions for the terms of the spectral element matrix could be derived using the symbolic manipulator software such as Maple [23], although the expressions are too lengthy to list in the paper.

4. Muller root search method

Once the spectral element matrix is obtained, the appropriate boundary conditions for the particular beam under consideration are applied to obtain the frequency characteristic determinant, which equals zero when an eigenvalue of the beam is found. Obviously the resulting frequency characteristic equation is a transcendental function of frequency, which allows an infinite number of natural frequencies to be accounted for. Although more advanced algorithms and more complex procedures may be used to determine the frequency values of the characteristic equation, a simple automated Muller root search method [22] is adopted in the present study to determine all the natural frequencies in a given frequency band. The mode shapes corresponding to the natural frequencies can be found in the usual way by making an arbitrary assumption about one unknown variable of the beam and then calculating the remaining variables in terms of the arbitrarily chosen one.

Let us denote the frequency characteristic determinant by $f(\omega)$ and consider the solution of $f(\omega) = 0$ by Muller's method. Muller's method uses a quadratic approximation to the function f by interpolating a quadratic polynomial through the last three computed points and then determining where this curve crosses the ω axis. The following algorithm is an implementation of Muller's method. This algorithm terminates when a prescribed error tolerance on $|f(\omega)|$ has been achieved or a maximum number of iterations has been performed.

(1) Pick three distinct values of ω, i.e., $\omega_0, \omega_1, \omega_2$. Set $i = 1$ and compute

$$h_i = \omega_i - \omega_{i-1}; \quad h_{i+1} = \omega_{i+1} - \omega_i; \quad \delta_i = (f(\omega_i) - f(\omega_{i-1}))/h_i;$$

$$\delta_{i+1} = (f(\omega_{i+1}) - f(\omega_i))/h_{i+1}; \quad d_i = (\delta_{i+1} - \delta_i)/(h_{i+1} + h_i).$$

(2) Compute

$$b_i = \delta_{i+1} + h_{i+1} d_i; \quad D_i = \left(b_i^2 - 4f(\omega_{i+1}) d_i\right)^{1/2}.$$

Table 1
Comparison of natural frequencies (in Hz) of Simply-Supported rectangular section beam

Mode No.	$b/a = 1000$		$b/a = 1$		$b/a = 0.5$		Third-order	Timoshenko
	Present	Ref. [19]	Present	Ref. [19]	Present	Ref. [19]		
1	123.11	123.10	122.62	122.61	123.68	123.69	119.60	118.70
2	159.01	159.02	159.37	159.38	160.55	160.57	158.38	159.32
3	303.65	N/A	296.85	296.85	252.28	252.29	281.47	271.70
4	310.53	310.39	303.18	N/A	310.93	N/A	313.70	314.58
5	503.48	N/A	465.28	N/A	388.38	N/A	454.82	421.05
6	532.62	N/A	518.96	N/A	487.06	N/A	549.09	549.77

Note: N/A denotes the result not available.

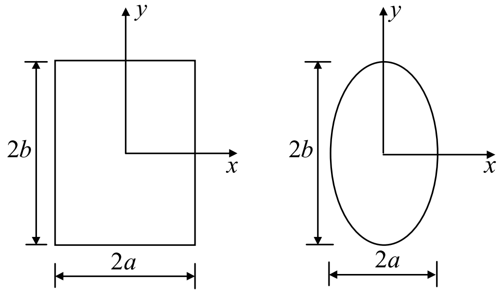

Fig. 4. A rectangular section used in example 1 and an elliptical section used in example 2.

(3) If $|b_i - D_i| < |b_i + D_i|$ then set $E_i = b_i + D_i$; else set $E_i = b_i - D_i$

(4) Set $h_{i+2} = -2f(\omega_{i+1})/E_i$; $\omega_{i+2} = \omega_{i+1} + h_{i+2}$.
where ω_{i+2} is the new approximation of the root ω_{i+1}. The process is continued until a desired accuracy is obtained. The rate of convergence is high and may be increased if an estimate of the eigenvalue is available. Previously roots may be removed from $f(\omega)$ by dividing it by $\prod_{k=1}^{p}(\omega - \omega_k)$, where ω_k $(k = 1, 2, \cdots, p)$ are the first p roots.

5. Numerical results and discussion

Two example problems are considered to demonstrate the accuracy of the spectral finite element model based on general higher-order beam theory.

The first example is of a rectangular cross-section beam shown in Fig. 4. The geometrical and physical properties of the beam are $E = 2.1 \times 10^{11}$Pa, $\nu = 0.333$, $\rho = 7860$ kg/m^3 , $L = 10$ m, $b = 5$ m.

First, the vibration behavior of the Simply-Supported beam is studied for three cross-section aspect ratios b/a. To validate the correctness and accuracy of the proposed formulation, the present results are given in Table 1 and compared with the previously published solutions [19] whenever possible. The numerical results based on third-order shear deformation and Timoshenko beam theories are also shown in Table 1, the shear correction factor is taken as 5/6 for Timoshenko beam theory. It can be seen from Table 1 that the present results are excellent agreement with the existing solutions. As a further validation of the current spectral element model, Aalami [17] predicted the fundamental frequency for a beam with $L = 10$ m having a square cross-section with $a = b = 5$ m using a Rayleigh-Ritz energy approach on the full three-dimensional problem, which is 122.09 Hz. This value is very close to the present solution 122.62 Hz.

Then, the spectral finite element model of the beam based on the general higher-order theory is used to compute the natural frequencies of the beam with a variety of aspect ratios. Five different aspect ratios, i.e., $b/a = 1000$, $b/a = 10$, $b/a = 2$, $b/a = 1$ and $b/a = 0.5$ are considered. In order to investigate the effect of the aspect ratio on the vibration frequencies, the first six natural frequencies of the beam are calculated and the percentage variations are plotted against the aspect ratio in Fig. 5. The percentage variation is defined as percentage variation $= 100(\omega - \omega_0)/\omega_0$,

Table 2
Natural frequencies (in Hz) of Simply-Supported rectangular cross-section beam

Aspect ratio b/a	Mode No.					
	1	2	3	4	5	6
1000	123.11	159.01	303.65	310.53	503.48	532.62
10	123.10	159.01	303.65	310.41	503.64	531.85
2	122.91	159.15	303.39	307.33	507.15	513.93
1	122.62	159.37	296.85	303.18	465.28	518.96
0.5	123.68	160.55	252.28	310.93	388.38	487.06

Table 3
Natural frequencies (in Hz) of Clamped-Free rectangular cross-section beam

Aspect ratio b/a	Mode No.					
	1	2	3	4	5	6
1000	55.37	166.37	268.87	415.29	452.59	641.79
10	55.38	166.31	268.91	415.01	452.56	641.68
2	55.72	164.83	269.76	407.97	451.97	631.06
1	56.98	161.37	272.15	383.04	451.91	545.12
0.5	61.83	156.30	271.12	299.43	402.43	490.40

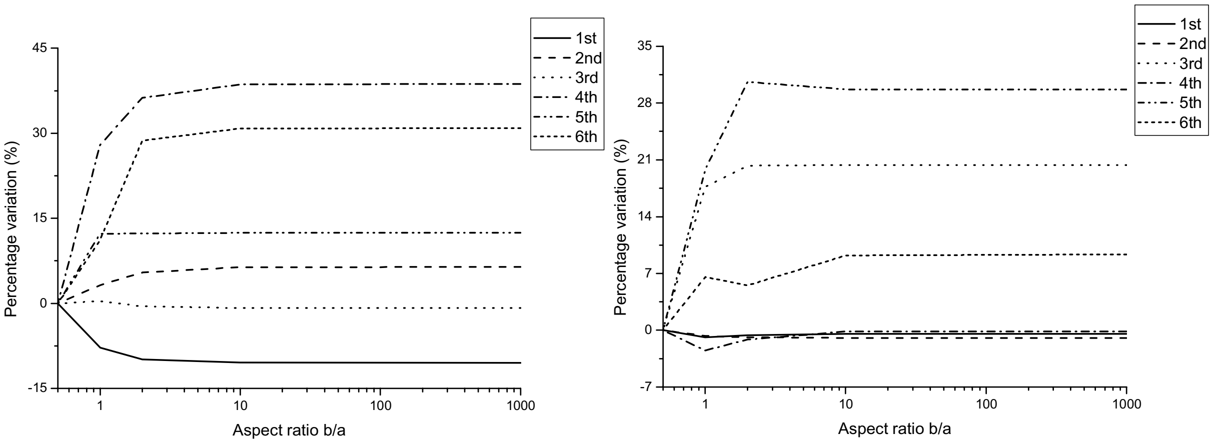

(a) (b)

Fig. 5. Percentage variations of first six frequencies versus aspect ratio for (a) Clamped-Free and (b) Simply-Supported rectangular section beams.

where ω_0 is the natural frequency of the beam with the aspect ratio $b/a = 0.5$. The numerical values of the first six natural frequencies are also shown in Tables 2 and 3. For the Simply-Supported boundary condition, the calculations of the analytical solutions using the expressions given by Kosmatka [19] are also performed. However, the analytical solutions are not displayed in Table 2 because they are complete agreement with the results predicted by the present formulation. It can be noticed from Fig. 5 that the effect of aspect ratio b/a on the natural frequencies of the beam is rather complex, it depends upon the particular boundary condition and mode number. There is a tendency that the aspect ratio has a pronounced effect on the higher frequencies. For the Clamped-Free end condition, increasing the aspect ratio from 0.5 to 1000 yields an increase in the frequency approximately -10.45%, 6.44%, -0.83%, 38.69%, 12.46% and 30.87% for the first, second, third, fourth, fifth and sixth modes, respectively.

For the Clamped-Free boundary condition, the first six normal mode shapes of the beam with cross-section aspect ratio $b/a = 1000$ are computed and the numerical results are plotted in Fig. 6.

The second example is a beam with elliptical cross-section, as shown in Fig. 4. The numerical data for this example is the same as the previous one. The first six natural frequencies of the beam with five different cross-section aspect ratios, i.e., $b/a = 1000$, $b/a = 10$, $b/a = 2$, $b/a = 1$ and $b/a = 0.5$ are also calculated and the numerical results are given in Tables 4 and 5. The percentage variations of the natural frequencies are plotted against aspect

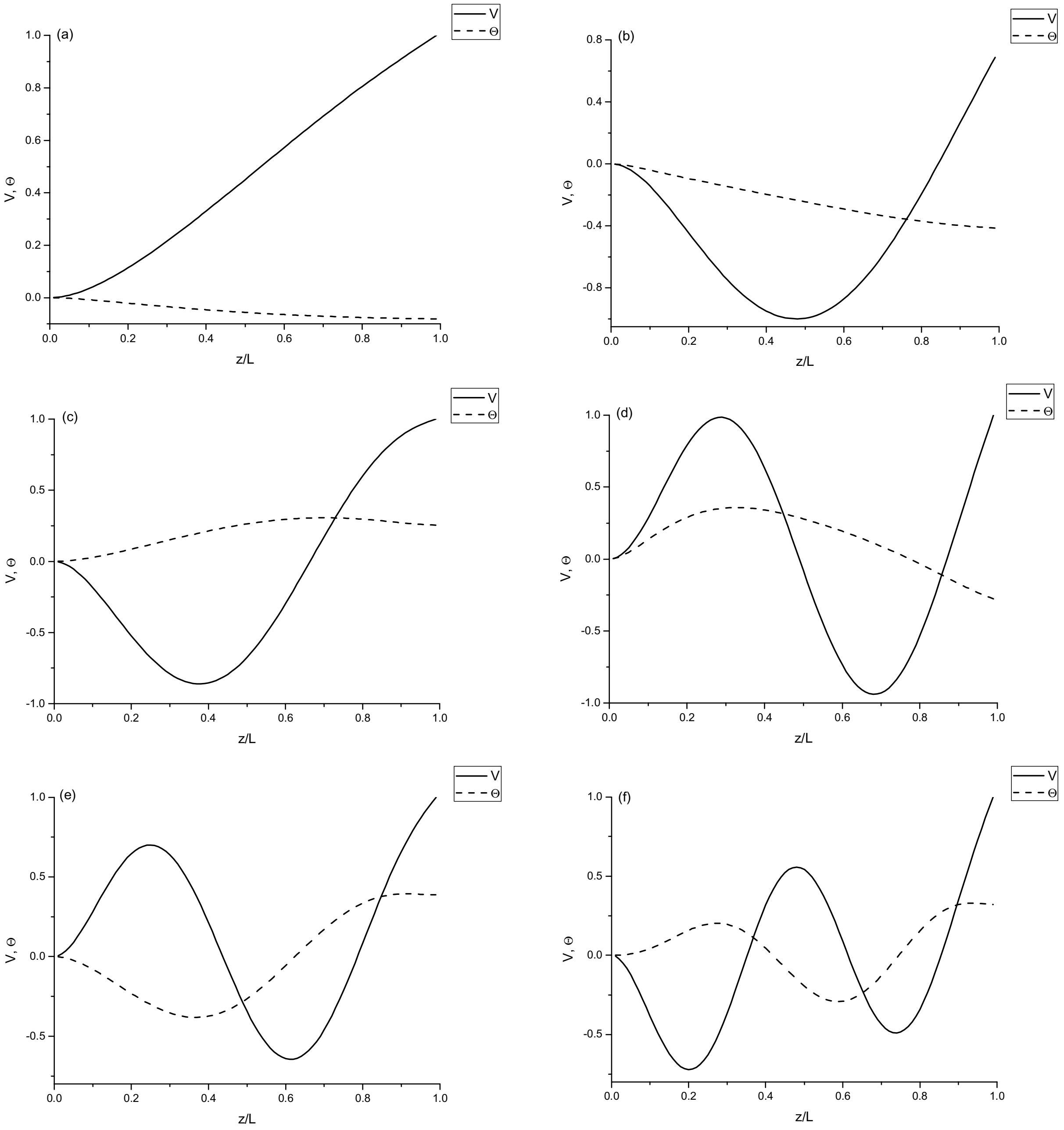

Fig. 6. First six normal mode shapes of Clamped-Free rectangular cross-section beam with aspect ratio $b/a = 1000$: (a) mode 1; (b) mode 2; (c) mode 3; (d) mode 4; (e) mode 5; (f) mode 6.

ratio in Fig. 7. The analytical solutions for the Simply-Supported end condition are also computed and they are found to be in perfect agreement with the present solutions. Figure 7 shows that the effect of aspect ratio on the natural frequency of elliptical section beam is different from that of rectangular section beam and the effect of aspect ratio on the higher frequencies can be significant. For the Clamped-Free boundary condition, changing the aspect ratio from 0.5 to 1000 increases the natural frequency by about -10.30%, -1.67%, -0.86%, 26.71%, 12.58% and 21.33% for the first, second, third, fourth, fifth and sixth modes, respectively.

Table 4
Natural frequencies (in Hz) of Simply-Supported elliptical cross-section beam

Aspect ratio b/a	Mode No.					
	1	2	3	4	5	6
1000	118.01	191.15	291.87	331.23	479.03	546.37
10	118.00	191.05	291.80	331.03	478.92	545.73
2	117.94	189.91	291.56	326.79	479.04	530.21
1	117.93	186.77	294.15	312.45	478.06	493.59
0.5	119.82	179.25	262.05	317.61	412.93	488.40

Table 5
Natural frequencies (in Hz) of Clamped-Free elliptical cross-section beam

Aspect ratio b/a	Mode No.					
	1	2	3	4	5	6
1000	51.89	161.04	280.61	391.45	463.26	612.91
10	51.89	161.02	280.53	391.36	462.99	612.86
2	52.08	161.03	279.80	390.13	457.81	614.53
1	52.88	161.53	279.38	384.48	447.46	569.00
0.5	57.85	163.78	283.05	308.94	411.51	505.18

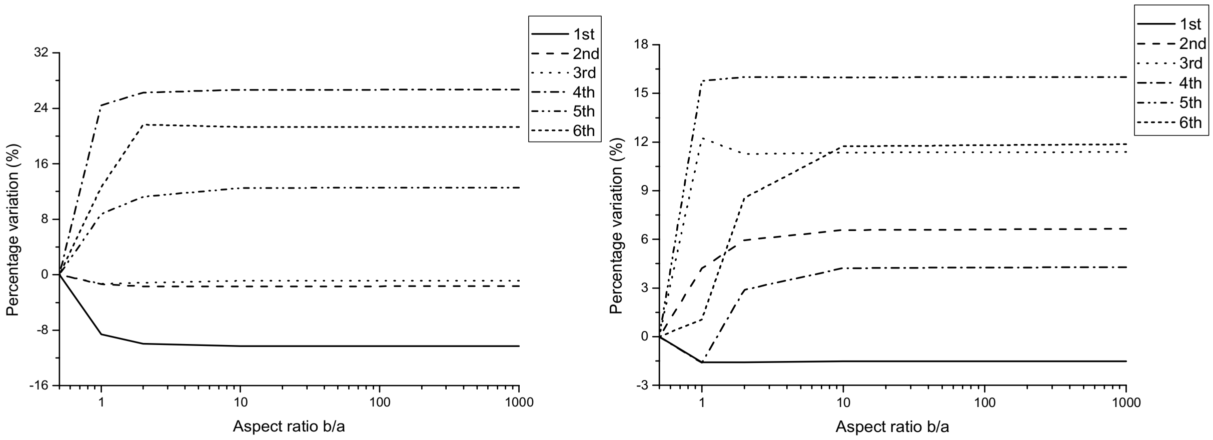

Fig. 7. Percentage variations of first six frequencies versus aspect ratio for (a) Clamped-Free and (b) Simply-Supported elliptical section beams.

6. Conclusions

A spectral element matrix has been developed for an isotropic beam with an arbitrary cross-section. The general higher-order beam theory is used, which considers both out-of-plane shear-dependent warping and in-plane deformations. The theoretical expressions of the spectral element matrix are formulated from the exact solutions of the governing differential equations of motion of the beam element. Application of the spectral element matrix enables exact prediction of the natural frequencies and mode shapes of the isotropic beams or of simple structures containing them. Two illustrative examples show exact agreement with the existing published results.

Acknowledgment

The authors thank the anonymous referees for their helpful comments.

References

[1] S.P. Timoshenko, On the correction for shear of the differential equation for transverse vibrations of prismatic beams, *Philosophical Magazine* **41** (1921), 744–746.

[2] R.D. Mindlin and H. Deresiewicz, *Timoshenko's Shear Coefficient for Flexural Vibrations of Beams*, Proceedings of 2nd US National Congress of Applied Mechanics, ASME Publication, New York, 1954, 175–178.
[3] G.R. Cowper, The shear coefficient in Timoshenko's beam theory, *Journal of Applied Mechanics* **33** (1966), 335–340.
[4] J.R. Hutchinson, On Timoshenko beams of rectangular cross-section, *Journal of Applied Mechanics* **71** (2004), 359–367.
[5] N.G. Stephen and M. Levinson, A second order beam theory, *Journal of Sound and Vibration* **67** (1979), 293–305.
[6] M. Levinson, A new rectangular beam theory, *Journal of Sound and Vibration* **74** (1981), 81–87.
[7] W.B. Bickford, A consistent high-order beam theory, *Developments in Theoretical and Applied Mechanics* **11** (1982), 137–150.
[8] A.V. Murty, Toward a consistent beam theory, *AIAA Journal* **22** (1984), 811–816.
[9] M. Levinson, On Bickford's consistent higher order beam theory, *Mechanics Research Communications* **12** (1985), 1–9.
[10] Z. Rychter, On the accuracy of a beam theory, *Mechanics of Research Communications* **14** (1987), 99–105.
[11] P.R. Heyliger and J.N. Reddy, A higher order beam finite element for bending and vibration problems, *Journal of Sound and Vibration* **126** (1988), 309–326.
[12] J. Petrolito, Stiffness analysis of beams using a higher-order theory, *Comput Struct* **55** (1995), 33–39.
[13] A.N. Kathnelson, Improved engineering theory for uniform beams, *Acta Mechanica* **114** (1996), 225–229.
[14] C.M. Wang, J.N. Reddy and K.H. Lee, *Shear Deformable Beams and Plates*, New York: Elsevier, 2000.
[15] J.N. Reddy, C.M. Wang, G.T. Lim and K.H. Ng, Bending solutions of the Levinson beams and plates in terms of the classical theories, *Int J Solids Struct* **38** (2001), 4701–4720.
[16] Y.M. Ghugal and R.P. Shimpi, A review of refined shear deformation theories for isotropic and anisotropic laminated beams, *Journal of Reinforced Plastics and Composites* **20** (2001), 255–272.
[17] B. Aalami, Waves in prismatic guides of arbitrary cross-section, *Journal of Applied Mechanics* **40** (1973), 1067–1072.
[18] C. Ie and J.B. Kosmatka, On the analysis of prismatic beams using first-order warping functions, *International Journal of Solids and Structures* **29** (1992), 879–891.
[19] J.B. Kosmatka, Transverse vibrations of shear-deformable beams using a general higher order theory, *Journal of Sound and Vibration* **160** (1993), 259–277.
[20] J.F. Doyle, *Wave Propagation in Structure*, New York: Springer-Verlag, 1989.
[21] U. Lee, *Spectral Element Method in Structural Dynamics*, Inha University, Incheon, Korea: Inha University Press, 2004.
[22] R.L. Burden and J.D. Faires, *Numerical Analysis*, Boston: Pws-Kent Publishing Company; 1989.
[23] B.W. Char, K.O. Geddes, G.H. Gonnet, M.B. Monagan and S.M. Watt, *Maple Reference Manual*, Department of Computer Science, University of Waterloo, Canada: Symbolic Computation Group and Waterloo Maple Publishing, 1990.

Hindawi

Submit your manuscripts at
http://www.hindawi.com

International Journal of Computational Methods
Vol. 6, No. 4 (2009) 585–604
© World Scientific Publishing Company

Int. J. Comput. Methods 2009.06:585-604. Downloaded from www.worldscientific.com
by QUEENSLAND UNIVERSITY OF TECHNOLOGY on 10/13/14. For personal use only.

A HYPERBOLIC SHEAR DEFORMATION THEORY FOR FLEXURE AND VIBRATION OF THICK ISOTROPIC BEAMS

YUWARAJ MAROTRAO GHUGAL* and RAJNEESH SHARMA

Department of Applied Mechanics
Government College of Engineering
Aurangabad-431005, Maharashtra, India
**ghugal@rediffmail.com*

Received 6 September 2008
Accepted 13 April 2009

A Hyperbolic Shear Deformation Theory taking into account transverse shear deformation effects, is presented for the static flexure and free flexural vibration analysis of thick isotropic beams. The displacement field of the theory contains two variables and does not require shear correction factor. The hyperbolic sine function is used in the displacement field in terms of thickness coordinate to represent shear deformation. The most important feature of the theory is that the transverse shear stress can be obtained directly from the use of constitutive relation, satisfying the stress free boundary conditions at top and bottom of the beam. Hence, the theory obviates the need of shear correction factor. Governing differential equations and boundary conditions of the theory are obtained using the principle of virtual work. Results obtained for flexure and free vibration of simply supported uniform, isotropic beams are compared with those of elementary, refined, and exact beam theories to validate the accuracy of the theory.

Keywords: Shear deformation; thick isotropic beam; static flexure; transverse shear stress; free vibration; hyperbolic shear deformation theory.

1. Introduction

It is well-known that classical Euler–Bernoulli theory of beam bending, also known as elementary theory of bending (ETB), disregards the effects of the shear deformation. The theory is suitable for slender beams and is not suitable for thick or deep beams since it is based on the assumption that the transverse normal to the neutral axis remains so during bending and after bending, implying that the transverse shear strain is zero. Since the theory neglects the transverse shear deformation, it underestimates deflections and overestimates the natural frequencies in case of thick beams, where shear deformation effects are significant.

---

*Corresponding author.

Int. J. Comput. Methods 2009.06:585-604. Downloaded from www.worldscientific.com
by QUEENSLAND UNIVERSITY OF TECHNOLOGY on 10/13/14. For personal use only.

Bresse [1859], Rayleigh [1880], and Timoshenko [1921] were the pioneer investigators to include refined effects such as the rotatory inertia and shear deformation in the beam theory. Timoshenko showed that the effect of transverse shear is much greater than that of rotatory inertia on the response of transverse vibration of prismatic bars. This theory is now widely referred to as Timoshenko beam theory or first-order shear deformation theory (FSDT) in the literature. In this theory, transverse shear strain distribution is assumed to be constant through the beam thickness and thus requires shear correction factor to appropriately represent the strain energy of deformation.

Cowper [1966] has given refined expressions for the shear correction factor for different cross-sections of the beam. The accuracy of Timoshenko beam theory for transverse vibrations of simply supported beam in respect to the fundamental frequency is verified by Cowper [1968] with a plane stress exact elasticity solution.

To remove the discrepancies in the classical theory and FSDT, higher-order or equivalent refined shear deformation theories were developed and are available in the open literature for static and vibration analysis of beams.

Levinson [1981], Bickford [1982], Rehfield and Murthy [1982], Krishna Murty [1984], Baluch *et al.* [1984], and Bhimaraddi and Chandrashekhara [1993] presented parabolic shear deformation theories (PSDTs) assuming a higher variation of axial displacement in terms of thickness coordinate. These theories satisfy shear stress free boundary conditions on the top and bottom surfaces of the beam and thus obviate the need of shear correction factor. Irretier [1986], Kant and Gupta [1988], and Heyliger and Reddy [1988] presented higher-order shear deformation theories (HSDFTs) for the static and free vibration analyses of shear deformable uniform rectangular beams.

There is another class of refined theories which includes trigonometric functions to represent the shear deformation effects through the thickness. Vlasov and Leont'ev [1966] and Stein [1989] developed refined shear deformation theories for thick beams including sinusoidal function in terms of thickness coordinate in the displacement field. However, with these theories shear stress free boundary conditions are not satisfied at top and bottom surfaces of the beam. This discrepancy is removed by Rao [1989] in a refined theory developed for beam. However, formulation of the theory is variationally inconsistent. Ghugal and Shimpi [2000] developed a variationally consistent refined trigonometric shear deformation theory (TSDT) for flexure and free vibration of thick isotropic beams. Sonawane and Ghugal [2006] studied the effect of transverse normal strain on flexural response of thick beams. Recently, Ghugal [2007] developed the single variable PSDT to study the response of thick beams in flexure. Theory developed yields very good results for displacements, stresses, and frequencies.

In this paper, a variationally consistent hyperbolic shear deformation theory (HPSDT) for thick beams is developed. The theory is applied to simply supported uniform isotropic solid beam of rectangular cross-section for both static and free vibration analysis. A general solution is obtained. The results obtained are compared

Int. J. Comput. Methods 2009.06:585-604. Downloaded from www.worldscientific.com
by QUEENSLAND UNIVERSITY OF TECHNOLOGY on 10/13/14. For personal use only.

with those of elementary, refined, and exact beam theories available in the literature. The credibility of the present theory is established by accurate evaluation of displacements, stresses, and frequencies.

2. Theoretical Formulation

The theoretical formulation of a uniform isotropic thick beam based on certain kinematical and physical assumptions is presented. The variationally correct forms of differential equations and boundary conditions, based on the assumed displacement field are obtained using the principle of virtual work. The beam under consideration occupies the region:

$$0 \leq x \leq L; \quad -b/2 \leq y \leq b/2; \quad -h/2 \leq z \leq h/2,$$

where x, y, z are Cartesian coordinates, L is the length, b is the width, and h is the total depth of beam. The beam is subjected to transverse load of intensity $q(x)$ per unit length of the beam. The beam can have any meaningful boundary conditions.

2.1. *Assumptions made in the theoretical formulation*

(1) The axial displacement consists of two parts:
  (a) displacement given by ETB of beam;
  (b) displacement due to shear deformation, which is assumed to be hyperbolic in the nature with respect to thickness coordinate, such that maximum shear stress occurs at neutral axis as predicted by the ETB of beam.

(2) The axial displacement u is such that the resultant of axial stress σ_x acting over cross-section should result in only bending moment and should not result in force in x-direction.

(3) The transverse displacement w is assumed to be a function of longitudinal length coordinate of beam.

(4) The displacements are small as compared to the beam thickness.

(5) The body forces are ignored in the analysis. (The body forces can be effectively taken into account by adding them to the external forces.)

(6) One-dimensional constitutive laws are used.

(7) The beam is subjected to transverse load only.

2.2. *The displacement field*

Based on the above-mentioned assumptions, the displacement field of the present beam theory is given by:

$$u(x,z,t) = -z\frac{\partial w(x,t)}{\partial x} + \left[z\cosh\left(\frac{1}{2}\right) - h\sinh\left(\frac{z}{h}\right)\right]\phi(x,t), \tag{1}$$

$$w(x,t) = w(x,t). \tag{2}$$

Here u and w are the axial and transverse displacements of the beam center line in the x and z directions, respectively, and t denotes time. The hyperbolic function

Int. J. Comput. Methods 2009.06:585-604. Downloaded from www.worldscientific.com
by QUEENSLAND UNIVERSITY OF TECHNOLOGY on 10/13/14. For personal use only.

is assigned according to the shearing stress distribution through the thickness of the beam. The function $\phi(x, t)$ is an unknown function to be determined and is associated with the rotation of the cross-section of the beam at neutral axis due to shear.

Normal strain

$$\varepsilon_x = \frac{\partial u}{\partial x} = -z\frac{\partial^2 w}{\partial x^2} + \left[z\cosh\left(\frac{1}{2}\right) - h\sinh\left(\frac{z}{h}\right)\right]\frac{\partial \phi}{\partial x}. \tag{3}$$

Shear strain

$$\gamma_{xz} = \frac{\partial u}{\partial z} + \frac{\partial w}{\partial x} = \left[\cosh\left(\frac{1}{2}\right) - \cosh\left(\frac{z}{h}\right)\right]\phi. \tag{4}$$

Stresses

According to assumption (6), one-dimensional constitutive laws are used to obtain the normal bending (axial) and transverse shear stresses. These stresses are given by:

$$\sigma_x = E\varepsilon_x, \quad \tau_{xz} = G\gamma_{xz}, \tag{5}$$

where E and G are the elastic constants of beam material.

2.3. *Governing equations and boundary conditions*

Using Eqs. (3)–(5) for strains and stresses and dynamic version of principle of virtual work, variationally consistent governing differential equations and boundary conditions for the beam under consideration are obtained. The principle of virtual work when applied to the beam leads to:

$$\begin{aligned} &b\int_{x=0}^{x=L}\int_{z=-h/2}^{z=h/2}(\sigma_x\delta\varepsilon_x + \tau_{xz}\delta\gamma_{xz})dzdx \\ &\quad + \rho b\int_{x=0}^{x=L}\int_{z=-h/2}^{z=h/2}\left(\frac{\partial^2 u}{\partial t^2}\delta u + \frac{\partial^2 w}{\partial t^2}\delta w\right)dzdx - \int_{x=0}^{x=L} q\delta w dx = 0, \end{aligned} \tag{6}$$

where the symbol δ denotes the variational operator. Employing Green's theorem in Eq. (6) successively, we obtain the coupled Euler–Lagrange equations which are the governing differential equations of the beam and the associated boundary conditions of the beam. The governing differential equations obtained are as follows:

$$EI\left(\frac{\partial^4 w}{\partial x^4} - A_0\frac{\partial^3 \phi}{\partial x^3}\right) - \rho I\left(\frac{\partial^4 w}{\partial x^2\partial t^2} - A_0\frac{\partial^3 \phi}{\partial x\partial t^2}\right) + \rho A\frac{\partial^2 w}{\partial t^2} = q(x,t), \tag{7}$$

$$EI\left(A_0\frac{\partial^3 w}{\partial x^3} - B_0\frac{\partial^2 \phi}{\partial x^2}\right) - \rho I\left(A_0\frac{\partial^3 w}{\partial x\partial t^2} - B_0\frac{\partial^2 \phi}{\partial t^2}\right) + GAC_0\phi = 0, \tag{8}$$

where A_0, B_0, and C_0 are the constants as given in Appendix. The associated boundary conditions obtained are as follows:

$$EI\left(\frac{\partial^3 w}{\partial x^3} - A_0\frac{\partial^2 \phi}{\partial x^2}\right) - \rho I\left(\frac{\partial^3 w}{\partial x\partial t^2} - A_0\frac{\partial^2 \phi}{\partial t^2}\right) = 0 \quad \text{or} \quad w \text{ is prescribed}, \tag{9}$$

$$EI\left(\frac{\partial^2 w}{\partial x^2} - A_0\frac{\partial \phi}{\partial x}\right) = 0 \quad \text{or} \quad \frac{\partial w}{\partial x} \text{ is prescribed,} \tag{10}$$

$$EI\left(A_0\frac{\partial^2 w}{\partial x^2} - B_0\frac{\partial \phi}{\partial x}\right) = 0 \quad \text{or} \quad \phi \text{ is prescribed.} \tag{11}$$

Thus, the variationally consistent governing differential equations and the associated boundary conditions are obtained. The static (flexural) and dynamic (vibration) behavior of beam is given by the solution of these equations and simultaneously satisfaction of the associated boundary and/or initial conditions.

Int. J. Comput. Methods 2009.06:585-604. Downloaded from www.worldscientific.com by QUEENSLAND UNIVERSITY OF TECHNOLOGY on 10/13/14. For personal use only.

2.4. *The general solution for static flexure of beams*

The governing equations for static flexure of beam can be obtained from Eqs. (7) and (8) by discarding the terms containing time (t) derivatives. Using these equations, general solution for $w(x)$ and ϕ(x) can be obtained. By integrating and rearranging the first governing equation (Eq. (7)), one can get following equation:

$$\frac{d^3 w}{dx^3} - A_0\frac{d^2\phi}{dx^2} = \frac{Q(x)}{EI}, \tag{12}$$

where $Q(x) = \int q dx + C_1$ is the generalized shear force resulting from the support and loading conditions for the beam under consideration and the second governing equation (Eq. (8)) can be written as:

$$\frac{d^3 w}{dx^3} - \frac{B_0}{A_0}\frac{d^2\phi}{dx^2} + \beta\phi = 0. \tag{13}$$

Using Eqs. (12) and (13), a single differential equation in terms of ϕ can be obtained as follows:

$$\frac{d^2\phi}{dx^2} - \lambda^2\phi = \frac{Q(x)}{\alpha EI}, \tag{14}$$

where the constants α, β, and λ used in Eqs. (13) and (14) are given in Appendix. The general solution of above Eq. (14) is given by:

$$\phi = C_2\cosh\lambda x + C_3\sinh\lambda x - \frac{Q(x)}{\beta EI}. \tag{15}$$

The general solution for transverse displacement (w) can be obtained by substituting the expression for ϕ in Eq. (13) and integrating thrice with respect to x. The solution is

$$\begin{aligned} EIw(x) = {} & \iiiint q dx dx dx dx + \frac{C_1 x^3}{6} + \frac{A_0}{\lambda} EI[C_2\cosh\lambda x + C_3\sinh\lambda x] \\ & + \frac{C_4 x^2}{2} + C_5 x + C_6, \end{aligned} \tag{16}$$

where C_1–C_6 are the arbitrary constants of integration and can be obtained by imposing natural (forced) and kinematic (geometric) boundary conditions of beam.

Int. J. Comput. Methods 2009.06:585-604. Downloaded from www.worldscientific.com
by QUEENSLAND UNIVERSITY OF TECHNOLOGY on 10/13/14. For personal use only.

2.5. *Axial stress*

Final solutions for $w(x)$ and $\phi(x)$ can be obtained using Eqs. (15) and (16) depending upon the loading and boundary conditions of the beams. Substituting the final solution for $w(x)$ and $\phi(x)$ in the displacement field, the final displacements can be obtained. Finally, the axial stress σ_x could be obtained by using stress–strain relation (constitutive relation) as given in Eq. (5).

2.6. *Transverse shear and transverse normal stresses*

The transverse shear stress τ_{xz} can be obtained either by using the constitutive relation or by integrating equilibrium equation with respect to the thickness coordinate. Two-dimensional elasticity equilibrium equations by ignoring body forces can be used to obtain transverse shear and transverse normal stresses. These equations are:

$$\frac{\partial \sigma_{xx}}{\partial x} + \frac{\partial \tau_{xz}}{\partial z} = 0, \tag{17}$$

$$\frac{\partial \tau_{xz}}{\partial x} + \frac{\partial \sigma_{zz}}{\partial z} = 0. \tag{18}$$

Integrating Eq. (17), with respect to the thickness coordinate z and imposing the following boundary condition at bottom surface of the beam

$$[\tau_{xz}]_{z=h/2} = 0$$

expression for τ_{xz} can be obtained satisfying the requirement of zero shear stress conditions on the top and bottom surfaces of the beam.

By substituting the expression obtained for transverse shear stress into Eq. (18) and integrating it with respect to the thickness coordinate z and then imposing the following boundary condition at bottom of the beam

$$[\sigma_{zz}]_{z=h/2} = 0$$

expression for σ_{zz} can be obtained satisfying the requirement of surface constraints at the top and bottom of the beam.

3. Illustrative Examples

3.1. *Example 1: Simply supported beam with uniformly distributed load q*

A simply supported beam with rectangular cross-section ($b \times h$) is subjected to uniformly distributed load (UDL) q over the span L at surface $z = -h/2$ acting in the downward z direction. The origin of beam is taken at left end support, i.e. at $x = 0$. The boundary conditions associated with simply supported beam are as

Int. J. Comput. Methods 2009.06:585-604. Downloaded from www.worldscientific.com
by QUEENSLAND UNIVERSITY OF TECHNOLOGY on 10/13/14. For personal use only.

follows:

$$EI\frac{d^3w}{dx^3} = EI\frac{d^2\phi}{dx^2} = \frac{dw}{dx} = \phi = 0 \quad \text{at} \quad x = \frac{L}{2}, \tag{19}$$

and

$$EI\frac{d^2w}{dx^2} = EI\frac{d\phi}{dx} = w = 0 \quad \text{at} \quad x = 0, L. \tag{20}$$

The boundary condition, $\phi = 0$ at $x = L/2$ is used from the condition of symmetry of deformation, in which the middle cross-section of the beam must remain plane without warping [Gere and Timoshenko (1986)]. From the general solution of beam, expressions for ϕ and w are obtained as follows:

$$\phi(x) = \frac{qL}{2\beta EI}\left[\left(1 - 2\frac{x}{L}\right) - \frac{\sinh\lambda(L/2 - x)}{(\lambda L/2)\cosh(\lambda L/2)}\right], \tag{21}$$

$$\begin{aligned} w(x) = {} & \frac{qL^4}{24EI}\left[\left(\frac{x}{L}\right)^4 - 2\left(\frac{x}{L}\right)^3 + \frac{x}{L}\right] \\ & + \frac{3}{5}\frac{qL^2}{GA}\left[\frac{x}{L}\left(1 - \frac{x}{L}\right) - \frac{2}{(\lambda L)^2}\left(1 - \frac{\cosh\lambda(L/2 - x)}{\cosh(\lambda L/2)}\right)\right]. \end{aligned} \tag{22}$$

The displacements and stresses (static flexural response) of the beam can now be obtained using this solution. The results of simply supported beam subjected to UDL, for maximum nondimensional transverse displacement, axial or normal bending stress and transverse shear stress are presented in Tables 1 and 2.

3.2. *Example 2: Simply supported beam with central concentrated load P*

A simply supported beam with rectangular cross-section $(b \times h)$ is subjected to concentrated load P at mid span, i.e. at $x = L/2$ at surface $z = -h/2$. The origin beam is taken at left end support, i.e. at $x = 0$. The boundary conditions associated

Table 1. Nondimensional maximum transverse displacement $(\bar{w})$, axial stress $(\bar{\sigma}_x)$, and transverse shear stresses $(\bar{\tau}_{xz})$ for simply supported beam subjected to uniformly distributed load (UDL) with aspect ratio, $S = 4$ (Example: 1).

Source	Model	$\bar{w}$	$\bar{\sigma}_x$	$\bar{\tau}_{xz}^{\mathrm{CR}}$	$\bar{\tau}_{xz}^{\mathrm{EE}}$
Present	HPSDT	1.806	12.258	3.074	2.709
Euler–Bernoulli	ETB	1.563	12.000	—	3.000
Timoshenko [1921]	FSDT	1.766	12.000	2.000	3.000
Heyliger and Reddy [1988]	HSDT	1.806	12.260	2.917	2.726
Ghugal and Shimpi [2000]	TSDT	1.805	12.277	3.005	2.721
Ghugal [2007]	PSDT	1.808	12.436	2.980	2.225
Sonawane and Ghugal [2006]	TSDT	1.781	12.440	2.946	2.551
Timoshenko and Goodier [1970]	Exact	1.785	12.200	3.000	—

Int. J. Comput. Methods 2009.06:585-604. Downloaded from www.worldscientific.com
by QUEENSLAND UNIVERSITY OF TECHNOLOGY on 10/13/14. For personal use only.

Table 2. Nondimensional maximum transverse displacement ($\bar{w}$), axial stress ($\bar{\sigma}_x$), and transverse shear stresses ($\bar{\tau}_{xz}$) for simply supported beam subjected to uniformly distributed load (UDL) with aspect ratio, $S = 10$ (Example: 1).

Source	Model	$\bar{w}$	$\bar{\sigma}_x$	$\bar{\tau}_{xz}^{\mathrm{CR}}$	$\bar{\tau}_{xz}^{\mathrm{EE}}$
Present	HPSDT	1.602	75.258	7.560	7.209
Euler–Bernoulli	ETB	1.563	75.000	—	7.499
Timoshenko [1921]	FSDT	1.595	75.000	4.999	7.499
Heyliger and Reddy [1988]	HSDT	1.601	75.246	7.416	7.250
Ghugal and Shimpi [2000]	TSDT	1.601	75.277	7.644	7.246
Ghugal [2007]	PSDT	1.601	75.246	7.491	6.726
Sonawane and Ghugal [2006]	TSDT	1.596	76.529	7.584	7.058
Timoshenko and Goodier [1970]	Exact	1.598	75.200	7.500	—

with simply supported beam can be obtained from Eqs. (19) and (20). Thus, the general solutions for ϕ and w are obtained as follows.

$$\phi(x) = \frac{P}{2\beta EI}\left[1 - \frac{\cosh \lambda x}{\cosh(\lambda L/2)}\right], \tag{23}$$

$$w(x) = \frac{PL^3}{48EI}\left[3\frac{x}{L} - 4\left(\frac{x}{L}\right)^3\right] + \frac{3}{5}\frac{PL}{GA}\left[\frac{x}{L} - \frac{\sinh \lambda x}{\lambda L \cosh(\lambda L/2)}\right]. \tag{24}$$

The results of simply supported beam subjected to concentrated load, for maximum nondimensional transverse displacement, axial or normal bending stress and transverse shear stress are presented in Tables 3 and 4. The values of axial stress are presented at $x = \alpha_0 L$ from left end support.

3.3. *Example 3: Free flexural vibration of beam*

A simply supported beam in Example 1 is considered for free flexural vibration. The material properties used are as follows:

$$E = 210\,\mathrm{GPa}, \quad \mu = 0.3 \quad \text{and} \quad \rho = 7800\,\mathrm{Kg/m^3}$$

Table 3. Nondimensional maximum transverse displacement ($\bar{w}$), axial stress ($\bar{\sigma}_x$ at $x = \alpha_0 L$), and transverse shear stresses ($\bar{\tau}_{xz}$) for simply supported beam subjected to concentrated load with aspect ratio, $S = 4$ (Example: 2).

Source	Model	$\bar{w}$	$\bar{\sigma}_x$	$\bar{\tau}_{xz}^{\mathrm{CR}}$	$\bar{\tau}_{xz}^{\mathrm{EE}}$
Present	HPSDT	2.974	5.734	0.748	0.75
Euler–Bernoulli	ETB	2.500	6.000	—	0.75
Timoshenko [1921]	FSDT	2.986	5.976	0.584	0.75
Ghugal [2007]	TSDT	2.973	5.735	0.774	0.75
Silverman [1980]	HSDT	2.974	—	—	—
Timoshenko and Goodier [1970]	Exact	2.913	5.734	0.75	—

Note: The values of α_0 for present (HPSDT) and Ghugal (TSDT) are 0.46377 and 0.4779, respectively, and that for ETB, FSDT and exact theory is 0.5 for aspect ratio 4.

Int. J. Comput. Methods 2009.06:585-604. Downloaded from www.worldscientific.com
by QUEENSLAND UNIVERSITY OF TECHNOLOGY on 10/13/14. For personal use only.

Table 4. Nondimensional maximum transverse displacement ($\bar{w}$), axial stress ($\bar{\sigma}_x$ at $x = \alpha_0 L$), and transverse shear stresses ($\bar{\tau}_{xz}$) for simply supported beam subjected to concentrated load with aspect ratio, $S = 10$ (Example: 2).

Source	Model	$\bar{w}$	$\bar{\sigma}_x$	$\bar{\tau}_{xz}^{\mathrm{CR}}$	$\bar{\tau}_{xz}^{\mathrm{EE}}$
Present	HPSDT	2.577	14.733	0.748	0.75
Euler–Bernoulli	ETB	2.500	15.000	—	0.75
Timoshenko [1921]	FSDT	2.578	14.939	0.584	0.75
Ghugal [2007]	TSDT	2.570	14.733	0.774	0.75
Silverman [1980]	HSDT	2.576	—	—	—
Timoshenko and Goodier [1970]	Exact	2.569	14.734	0.75	—

Note: The values of α_0 for present (HPSDT) and Ghugal (TSDT) are 0.4855 and 0.4911, respectively, and that for ETB, FSDT and exact theory is 0.5 for aspect ratio 10.

where E is the Young's modulus, ρ is the density, and μ is the Poisson's ratio of beam material. The governing equations for free flexural vibration of simply supported beam can be obtained by setting the applied transverse load equal to zero in Eqs. (7) and (8). A solution to resulting governing equations which satisfies the associated boundary or initial conditions is of the form:

$$w(x,t) = W_m \sin\frac{m\pi x}{L}\sin\,\omega_m t, \tag{25}$$

$$\phi(x,t) = \phi_m \cos\frac{m\pi x}{L}\sin\omega_m t, \tag{26}$$

where W_m and ϕ_m are the amplitudes of translation and rotation, and ω_m is natural frequency of the mth mode of vibration. Substitution of this solution form into the governing equations of free vibration of beam results in a standard eigenvalue problem $([K] - \omega_m^2[M])\{\Delta\} = 0$ the solution of which is well known. The elements of $[K]$, $[M]$ matrices and vector $\{\Delta\}$ are given in Appendix. From this solution, lowest natural frequencies at $m = 1$ or the fundamental frequencies for various aspect ratios of beam can be obtained.

Results of simply supported beam for maximum nondimensional free vibration frequencies in flexural and thickness-shear modes are presented in Tables 5 and 6, respectively.

4. Results

4.1. *Nondimensional displacements and stresses*

The results for transverse displacement ($\bar{w}$), axial stress ($\bar{\sigma}_{xx}$) and transverse shear stress ($\bar{\tau}_{xz}$), and fundamental frequencies ($\bar{\omega}$) are presented in the following nondimensional form for the purpose of presenting the results in this paper.

Example 1.

$$\bar{w} = \frac{10Ebh^3 w(L/2,0)}{ql^4} \quad \bar{\sigma}_{xx} = \frac{b\sigma_{xx}(L/2,h/2)}{q} \quad \bar{\tau}_{xz} = \frac{b\tau_{xz}(0,0)}{q}$$

Int. J. Comput. Methods 2009.06:585-604. Downloaded from www.worldscientific.com
by QUEENSLAND UNIVERSITY OF TECHNOLOGY on 10/13/14. For personal use only.

Table 5. Comparison of nondimensional fundamental frequency ($\bar{\omega}_w$) of flexural mode of vibration (Example: 3).

Source	Model	For $S = 4$		For $S = 10$	
		$\bar{\omega}_w$	% error[a]	$\bar{\omega}_w$	% error[a]
Present	HPSDT	2.655	2.04	2.813	0.32
Euler–Bernoulli	ETB	2.779	6.80	2.838	1.21
Timoshenko [1921]	FSDT	2.624	0.85	2.808	0.14
Heyliger and Reddy [1988]	HSDT	2.596	−0.23	2.802	−0.07
Ghugal and Shimpi [2000]	TSDT	2.596	−0.23	2.803	−0.04
Ghugal [2007]	PSDT	2.700	3.77	2.824	0.71
Sonawane and Ghugal [2006]	TSDT	2.065	0.12	2.807	0.11
Cowper [1968]	Exact	2.602	0.00	2.804	0.00

[a] Percentage error quoted is with respect to the corresponding value of exact elasticity solution by Cowper [1968].

Table 6. Comparison of nondimensional fundamental frequency ($\bar{\omega}_\phi$) of thickness-shear mode (Example: 3).

Source	Model	$\bar{\omega}_\phi$	
		$S = 4$	$S = 10$
Present	HPSDT	34.295	198.280
Timoshenko [1921]	FSDT	37.320	198.616
Heyliger and Reddy [1988]	HSDT	34.250	198.235
Ghugal and Shimpi [2000]	TSDT	34.238	198.108
Sonawane and Ghugal [2006]	TSDT	34.096	197.961

Example 2.

$$\bar{w} = \frac{10Ebh^3 w(L/2,0)}{Pl^3} \quad \bar{\sigma}_{xx} = \frac{bh\sigma_{xx}(\alpha_0 L, h/2)}{P} \quad \bar{\tau}_{xz} = \frac{bh\tau_{xz}(0,0)}{P}$$

Example 3.

$$\omega = \omega_m \left(\frac{L^2}{h}\right)\sqrt{\frac{\rho}{E}}.$$

In case of Example 2, the variation of σ_x at top and bottom surfaces of beam differs at mid span ($x = L/2$) due to the effect of heavy stress concentration under the concentrated load [Timoshenko and Goodier (1970)]. However, in the vicinity of concentrated load at $x = \alpha_0 L = (0.5 - \varepsilon h)L$ and when $(0.5 - \varepsilon h)L \to L/2$, this stress distribution, according to present theory, matches with the exact solution. The value of α_0 is not unique for all the theories. The values of α_0 are given in Tables 3 and 4.

Further, it may be noted that transverse shear stress $\bar{\tau}_{xz}$ when obtained by constitutive relation is indicated by $\bar{\tau}_{xz}^{\mathrm{CR}}$ and when it is obtained by using equilibrium equation, is indicated by $\bar{\tau}_{xz}^{\mathrm{EE}}$. The percentage error in results obtained by models of other researchers with respect to the corresponding results obtained by theory of elasticity is calculated as follows:

$$\%\ \text{error} = \frac{\text{value by a particular model} - \text{ value by exact elasticity solution}}{\text{value by exact elasticity solution}} \times 100.$$

5. Discussion

The results obtained from the present theory are compared with the ETB, FSDT of Timoshenko [1921], HSDT of Heyliger and Reddy [1988], TSDT of Ghugal and Shimpi [2000], a single variable PSDT of Ghugal [2007], TSDT of Sonawane and Ghugal [2006], TSDT of Ghugal [2007], HSDT of Silverman [1980], and exact elasticity solutions given by Cowper [1968] for free vibration and Timoshenko and Goodier [1970] for static flexure of beams.

5.1. *Transverse displacement ($\bar{w}$)*

The results of maximum nondimensional transverse displacements for the aspect ratios of 4 and 10 are presented in Tables 1 and 2 for a simply supported beam subjected to UDL. The values of transverse displacement given by present HPSDT and Reddy's third-order shear deformation theory (HSDT) [1988] are exactly same and are closer to the exact values. The results of TSDTs of Ghugal and Shimpi [2000] and Sonawane and Ghugal [2006] are much closer to the exact solution. A recently developed single variable PSDT by Ghugal [2007] predicts the deflection with very good accuracy.

Present theory and the theory of Heyliger and Reddy [1988] overestimate the maximum deflection for a beam subjected to UDL by 1.17% and 0.25% as compared to exact solution [1970] for aspect ratio 4 and 10, respectively, as seen from Tables 1 and 2. The FSDT underestimates the value of maximum transverse deflection by 1.07% and 0.20% for aspect ratio 4 and 10, respectively, whereas ETB underestimates the same by 12.44% and 2.20% as compared to exact value due to the neglect of transverse shear deformation effect. However, the theory of Ghugal and Shimpi [2000] overestimates it by 1.12% and 0.18%, respectively, for aspect ratio 4 and 10. The TSDT of Sonawane and Ghugal [2006] is in close agreement with exact theory since it underpredicts the deflection with very small error 0.22% for aspect ratio 4 and 0.13% for aspect ratio 10 due to the inclusion of transverse normal stain effect in the theory. The variation of transverse displacement with aspect ratio (S) is shown in Fig. 1. It approaches to the results of classical beam theory (ETB) at higher aspect ratios.

The transverse displacement results of beam with central concentrated load are presented in Tables 3 and 4. The error in transverse displacement of beam subjected to this load is varying from 2.06 to 2.09% in the present theory and theories of Ghugal (TSDT) [2007] and Silverman [1980], whereas ETB underestimates it by the values 14.17% and 2.69% for aspect ratio 4 and 10, respectively. The present and

Int. J. Comput. Methods 2009.06:585-604. Downloaded from www.worldscientific.com
by QUEENSLAND UNIVERSITY OF TECHNOLOGY on 10/13/14. For personal use only.

Int. J. Comput. Methods 2009.06:585-604. Downloaded from www.worldscientific.com
by QUEENSLAND UNIVERSITY OF TECHNOLOGY on 10/13/14. For personal use only.

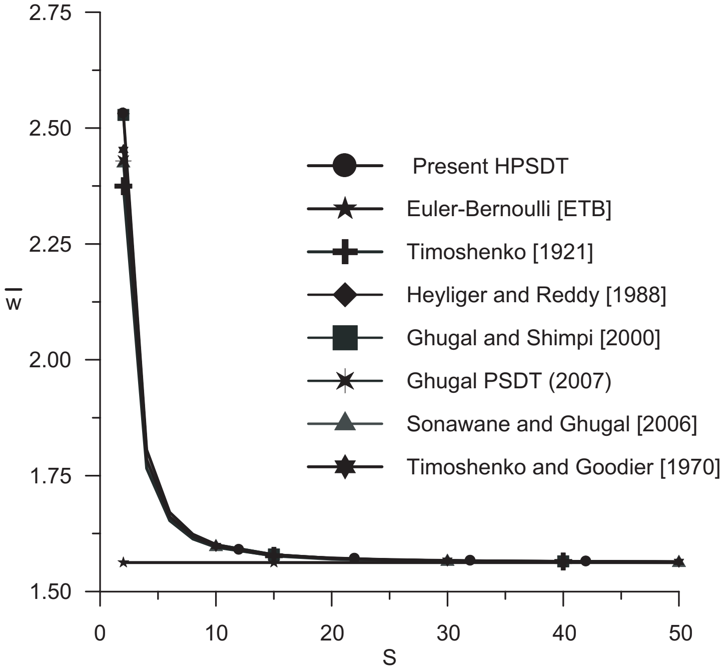

Fig. 1. Variation of maximum transverse displacement ($\bar{w}$) at ($x = L/2, z = 0$) with aspect ratio S of simply supported beam subjected to uniformly distributed load.

Silverman's theories overestimate the value by 2.09% for aspect ratio 4, whereas for aspect ratio 10 present theory and TSDT of Ghugal [2007] overestimate the value by 0.31%. The variation of transverse displacement with aspect ratio (S) is shown in Fig. 2 and this variation according to all refined theories approaches to that of classical beam theory (ETB) at higher aspect ratios.

5.2. *Axial stress ($\bar{\sigma}_x$)*

The results of maximum nondimensional axial stresses obtained by the present theory and other refined theories are presented in Tables 1 and 2 for UDL and in Tables 3 and 4 for concentrated load, for the aspect ratios of 4 and 10, respectively. It can be seen from the results that for UDL, the maximum values of axial stress obtained from the present and Heyliger and Reddy's theories are in good agreement with those of exact solution. The error in this stress is 0.48% and 0.08% for the aspect ratio 4 and 10 when compared with the exact solution. However, in the theories of Ghugal and Shimpi (TSDT), Ghugal (PSDT), and Sonawane and Ghugal (TSDT) the error in this stress is 0.63, 1.93, and 1.96%, respectively, for aspect ratio 4. The error reduces drastically for aspect ratio 10 for all the theories. The ETB and FSDT underestimate the value of this stress by 1.64% and 0.27% for aspect ratios

Int. J. Comput. Methods 2009.06:585-604. Downloaded from www.worldscientific.com
by QUEENSLAND UNIVERSITY OF TECHNOLOGY on 10/13/14. For personal use only.

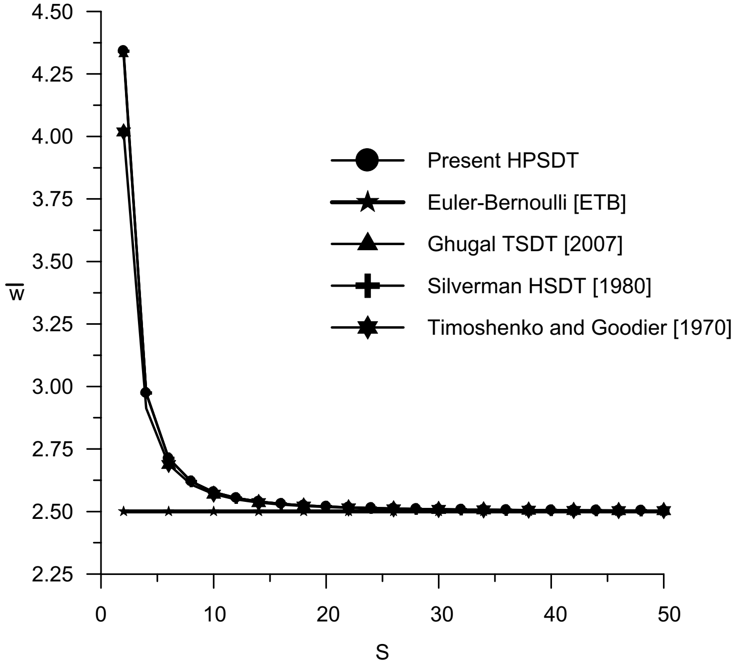

Fig. 2. Variation of maximum transverse displacement ($\bar{w}$) at ($x = L/2, z = 0$) with aspect ratio S of simply supported beam subjected to concentrated load.

4 and 10, respectively. This stress varies linearly through the thickness of beam as shown in Fig. 3.

The results of maximum nondimensional axial stress for beam subjected to concentrated load by present theory at $0.46377L$ from the support matches to exact value for aspect ratio 4 and same matches to exact value for aspect ratio 10 at $0.4855L$ from the support as seen from Tables 3 and 4. TSDT of Ghugal [2007] yields exact value of this stress at locations $0.4779L$ and $0.4911L$ from the support for aspect ratio 4 and 10, respectively. The variation of this stress is linear through the thickness for aspect ratio 4 in the vicinity of load ($\alpha_0 L$); however, it is nonlinear under the load (at $L/2$) due to heavy stress concentration as shown in Fig. 4.

5.3. *Transverse shear stress* ($\bar{\tau}_{xz}$)

The transverse shear stresses are obtained directly by constitutive relation and, alternatively, by integration of equilibrium equation of two-dimensional theory of elasticity and are denoted by ($\bar{\tau}_{xz}^{\mathrm{CR}}$) and ($\bar{\tau}_{xz}^{\mathrm{EE}}$), respectively. The transverse shear stress satisfies the stress free boundary conditions on the top ($z = -h/2$) and bottom ($z = +h/2$) surfaces of the beam when these stresses are obtained by both the above-mentioned approaches.

Int. J. Comput. Methods 2009.06:585-604. Downloaded from www.worldscientific.com
by QUEENSLAND UNIVERSITY OF TECHNOLOGY on 10/13/14. For personal use only.

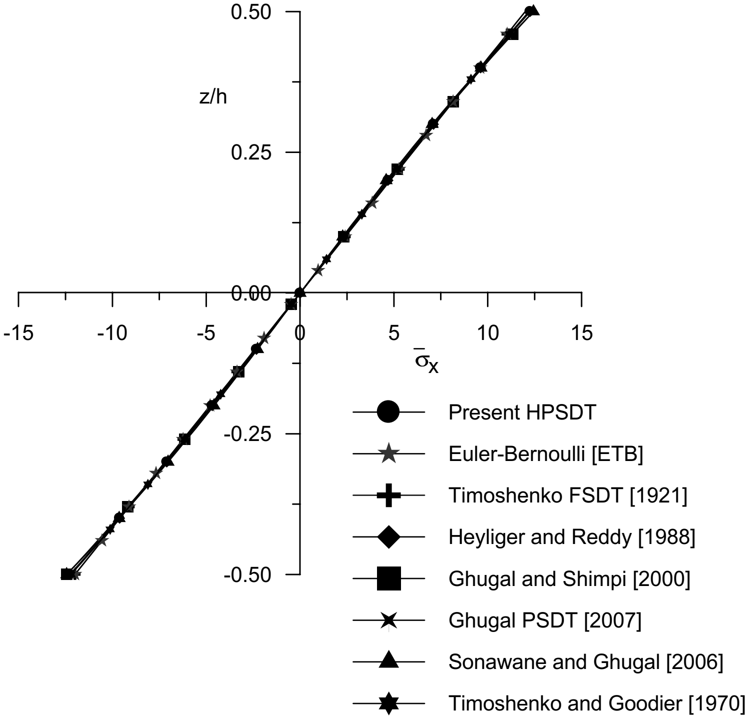

Fig. 3. Variation of axial stress ($\bar{\sigma}x$) through the thickness of simply supported beam at ($x = L/2, z$) when subjected to uniformly distributed load for $S = 4$.

For beam subjected to UDL maximum nondimensional transverse shear stresses obtained by the present theory and other refined theories are presented in Tables 1 and 2 for the aspect ratio of 4 and 10, respectively. The present theory overestimates the transverse shear stress by the value 2.47% when obtained by constitutive law and underestimate this stress by value 9.7% when obtained by equilibrium equation for aspect ratio 4. Whereas for aspect ratio 10 the value of this stress obtained by constitutive relation is closer to the exact value and value obtained by equilibrium equation underestimates it by 3.88%. The theories of Heyliger and Reddy [1988], PSDT of Ghugal [2007], and TSDT of Sonawane and Ghugal [2006] underpredict the transverse shear stress ($\bar{\tau}_{xz}^{\mathrm{CR}}$) by 2.77, 0.67, and 1.8%, respectively, for aspect ratio 4 when obtained by constitutive relation. However, TSDT of Ghugal and Shimpi [2000] gives the value of transverse shear stress closer to the exact value when obtained by constitutive law. All the refined theories underestimate the value of shear stress by more than 9% and 3% for aspect ratios 4 and 10, respectively, when obtained by equilibrium equation. The FSDT of Timoshenko [1921] overpredicts it by more than 33% when obtained by constitutive law and yields exact values when obtained by equilibrium equation for both the aspect ratios. Similarly, ETB gives the exact value of this stress when obtained by equilibrium equation for both the

Int. J. Comput. Methods 2009.06:585-604. Downloaded from www.worldscientific.com
by QUEENSLAND UNIVERSITY OF TECHNOLOGY on 10/13/14. For personal use only.

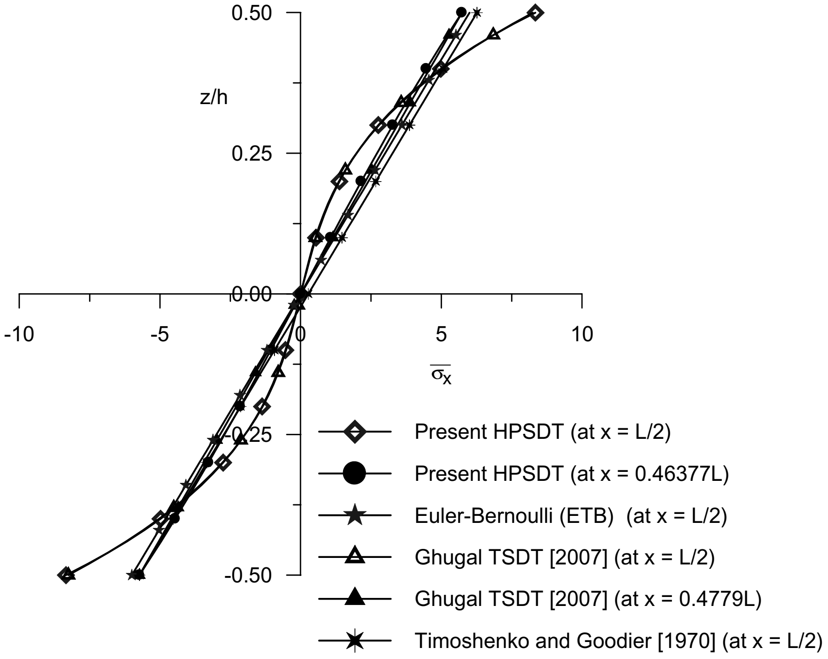

Fig. 4. Variation of axial stress ($\bar{\sigma}x$) through the thickness of simply supported beam subjected to concentrated load at $(x = \alpha_0 L, z)$ for aspect ratio $S = 4$.

aspect ratios. The through thickness variation of this stress is given in Fig. 5 for aspect ratio 4.

The maximum nondimensional transverse shear stress obtained by the present theory and other refined theories for beam with central concentrated load is presented in the Tables 3 and 4 for the aspect ratio of 4 and 10, respectively. The value of shear stress obtained by present theory is in close agreement with exact value as the error in the value is very small (0.27%), when obtained using constitutive relation and matches to the exact value when obtained from integration equilibrium equation for both aspect ratios. The TSDT of Ghugal [2007] overpredicts the value by 3.20%, when obtained by constitutive relation and matches to the exact value when obtained from the equilibrium equation for both aspect ratios. ETB and FSDT give exact value of this stress when obtained using equilibrium equations. The through thickness variation of this stress according to various theories is given in Fig. 6 for aspect ratio 4.

5.4. *Fundamental frequency ($\bar{\omega}_w$) of flexural mode*

The fundamental frequencies obtained by present theory, and other refined theories are presented in Table 5. Theories of Timoshenko [1921], Heyliger and Reddy [1988], Ghugal and Shimpi [2000], and Ghugal and Sonawane [2006] predict the

Int. J. Comput. Methods 2009.06:585-604. Downloaded from www.worldscientific.com
by QUEENSLAND UNIVERSITY OF TECHNOLOGY on 10/13/14. For personal use only.

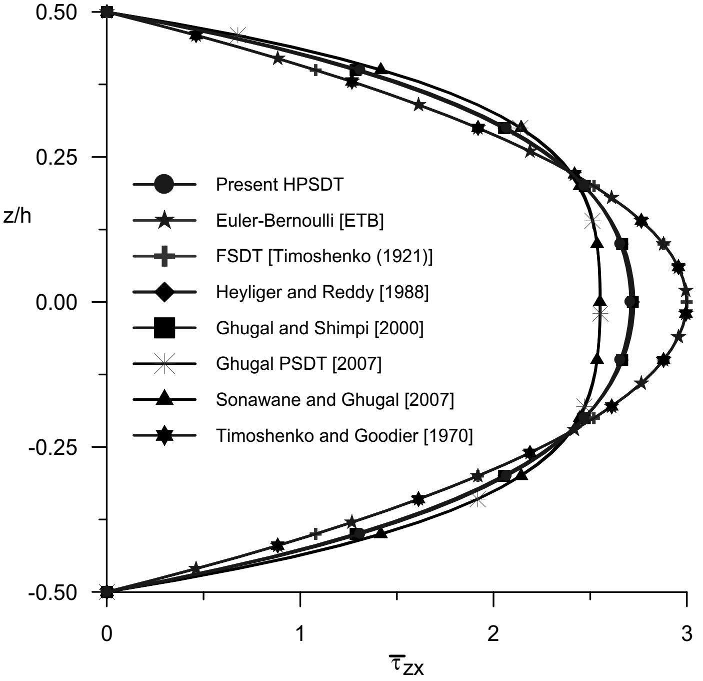

Fig. 5. Variation of transverse shear stress ($\bar{\tau}_{zx}$) through the thickness of simply supported beam at $(x = 0, z)$ when subjected to uniformly distributed load and obtain using equilibrium equation for aspect ratio 4.

values fundamental frequency in flexural mode of vibration which are in excellent agreement with that of exact solution as seen from Table 5. The ETB overestimates the fundamental frequency by 6.80% and 1.21% for the aspect ratios 4 and 10, respectively, due to neglect of shear deformation in the theory. The PSDT of Ghugal [2007] overestimates the value of this frequency by 3.37% and 0.71% for aspect ratios 4 and 10, respectively. The present theory overestimates the value by 2.04% for aspect ratio 4 and by 0.32% for the aspect ratio 10. All the refined theories predict the value of this frequency more accurately for aspect ratio 10 as seen from Table 5 since the error is within 1%.

5.5. *Fundamental frequency of thickness-shear mode* ($\bar{\omega}_\phi$)

The results of this frequency of free vibration of thick beam according to FSDT and HSDT are not available in the literature and same are generated using computer programs. Similarly, the exact solution for comparison is also not available for the frequencies of thickness-shear mode. It is seen from Table 6 that the value of this frequency predicted by all the refined theories are in excellent agreement with each other for both the aspect ratios; however, the value predicted by FSDT for aspect ratio 4 is considerably higher compared to other refined theories.

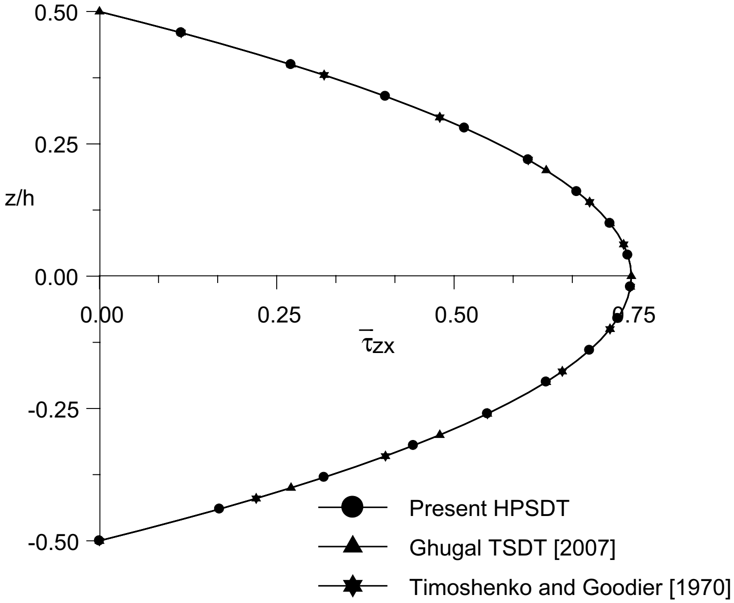

Fig. 6. Variation of transverse shear stress ($\bar{\tau}_{zx}$) through the thickness of simply supported beam at $(x = 0, z)$ when subjected to concentrated load and obtain using equilibrium equation for aspect ratio $S = 4$.

Int. J. Comput. Methods 2009.06:585-604. Downloaded from www.worldscientific.com
by QUEENSLAND UNIVERSITY OF TECHNOLOGY on 10/13/14. For personal use only.

6. Conclusions

In this paper, a HPSDT has been presented for thick homogeneous, isotropic beams. The theory has the following features:

(a) It is a displacement-based theory which includes the transverse shear effects.
(b) The number of unknown variables is same as that of FSDT.
(c) Constitutive relations are satisfied in respect of axial stress and transverse shear stress.
(d) Transverse shear stress satisfies zero shear stress boundary conditions on top and bottom surfaces of the beam perfectly.
(e) The theory obviates the need of shear correction factor.

A theory having above features is used for the static flexural and free flexural vibration analysis of thick isotropic beams. From this analysis, following conclusions are drawn.

(1) The use of present theory gives good results in respect of transverse displacements. Results of available higher-order and refined shear deformation theories for the transverse displacement are in tune with the results of the present theory.
(2) The results of axial stress obtained by the present theory are in excellent agreement with those of exact solution and those of other higher-order theories.

(3) The maximum value of transverse shear stress obtained by constitutive relation is in excellent agreement with that of exact elasticity solution in case of beam subjected to UDL. However, integration of equilibrium equation yields much better value of transverse shear stress, closer to value of exact elasticity solution in case of beam subjected to concentrated load.

(4) The fundamental frequencies in flexural mode, obtained from free flexural vibration are in good agreement with those of exact solution and the frequencies of thickness-shear mode are in excellent agreement with other refined theories.

(5) The governing differential equations and the associated boundary conditions are variationally consistent.

The use of present theory gives very good results as seen from the numerical examples studied, which validates the efficacy and credibility of the HPSDT.

Int. J. Comput. Methods 2009.06:585-604. Downloaded from www.worldscientific.com
by QUEENSLAND UNIVERSITY OF TECHNOLOGY on 10/13/14. For personal use only.

Nomenclature

A	Cross-sectional area of beam;
b	Width of beam in y-directions;
E, G, μ	Elastic constants of the material;
E	Young's modulus;
G	Shear modulus;
h	Thickness of beam;
I	Moment of inertia of beam;
$[K]$	Stiffness matrix;
L	Span of the beam;
$[M]$	Mass matrix;
m	A positive integer;
q	Intensity of uniformly distributed transverse load;
S	$= L/h =$ aspect ratio of beam;
t	Time;
u	Axial displacement in x-direction;
$\bar{u}$	Nondimensional axial displacement;
w	Transverse displacement in z-direction;
$\bar{w}$	Nondimensional transverse displacement in z-direction;
x, y, z	Rectangular Cartesian coordinates;
μ	Poisson's ratio of the beam material;
ρ	Density of beam material;
σ_x	Axial stress in x-direction;
$\bar{\sigma}_x$	Nondimensional axial stress in x-direction;
τ_{xz}	Transverse shear stress in zx-plane;
$\bar{\tau}_{xz}^{\mathrm{CR}}$	Nondimensional transverse shear stress via constitutive relation;
$\bar{\tau}_{xz}^{\mathrm{EE}}$	Nondimensional transverse shear stress via equilibrium equations;

ϕ	Unknown function associated with the shear slope;
ω	Natural frequency of vibration;
$\bar{\omega}_w$	Nondimensional natural frequency of vibration in flexural mode;
$\bar{\omega}_\phi$	Nondimensional frequency of free vibration in thickness-shear mode.

Abbreviations

ETB	Elementary Theory of Beam Bending
FSDT	First-order Shear Deformation Theory
HSDT	Higher-order Shear Deformation Theory
PSDT	Parabolic Shear Deformation Theory
TSDT	Trigonometric Shear Deformation Theory
HPSDT	Hyperbolic Shear Deformation Theory

Int. J. Comput. Methods 2009.06:585-604. Downloaded from www.worldscientific.com
by QUEENSLAND UNIVERSITY OF TECHNOLOGY on 10/13/14. For personal use only.

Appendix

The constants A_0, B_0, and C_0 appeared in governing differential equations (Eqs. (7) and (8)) are as follows:

$$\begin{aligned}
A_0 &= \cosh(1/2) - 12[\cosh(1/2) - 2\sinh(1/2)],\\
B_0 &= \cosh^2(1/2) + 6[\sinh(1) - 1] - 24\cosh(1/2)[\cosh(1/2) - 2\sinh(1/2)],\\
C_0 &= \cosh^2(1/2) + (1/2)[\sinh(1) + 1] - 4\cosh(1/2)\sinh(1/2).
\end{aligned}$$

The constants α, β, and λ appeared in general solution of differential equations Eqs. (13)–(15) are as follows:

$$\alpha = \frac{B_0}{A_0} - A_0, \quad \beta = \frac{GAC_0}{EIA_0}, \quad \lambda^2 = \frac{\beta}{\alpha}.$$

The elements of stiffness matrix $[K]$ are given below:

$$K_{11} = \frac{EI(m\pi)^4}{L^4}, \quad K_{12} = K_{21} = -\frac{EIA_0(m\pi)^3}{L^3}, \quad K_{22} = \frac{EIB_0(m\pi)^2}{L^2} + GAC_0.$$

The elements of mass matrix $[M]$ are as follows:

$$M_{11} = \frac{\rho I(m\pi)^2}{L^2} + \rho A, \quad M_{12} = M_{21} = \frac{\rho I A_0 m\pi}{L}, \quad M_{22} = \rho I B_0,$$

and the vector $\{\Delta\}^T = \{W_m, \phi_m\}$, where W_m is the amplitude of translation and ϕ_m is the amplitude of rotation.

References

Baluch, M. H., Azad, A. K. and Khidir, M. A. [1984] Technical theory of beams with normal strain, *ASCE, J. Eng. Mech.* **110**(8), 1233–1237.

Bickford, W. B. [1982] A consistent higher order beam theory, *Dev. Theor. Appl. Mech.* SECTAM **11**, 137–150.

Bhimaraddi, A. and Chandrashekhara, K. [1993] Observations on higher order beam theory, *ASCE, J. Aerosp. Eng.* **6**(4), 408–413.

Bresse, J. A. C. [1859] *Cours de Mecanique Applique* (Mallet-Bachelier, Paris).

Cowper, G. R. [1966] The Shear coefficients in Timoshenko beam theory, *ASME, J. Appl. Mech.* **33**(2), 335–340.

Cowper, G. R. [1968] On the accuracy of Timoshenko beam theory, *ASCE, J. Eng. Mech. Div.* **94**(EM6), 1447–1453.

Gere, J. M. and Timoshenko, S. P. [1986] *Mechanics of Materials*, 2nd edition, Chapter 7 (CBS Publishers and Distributors, New Delhi, India), pp. 407–414.

Ghugal, Y. M. and Shimpi, R. P. [2000] A trigonometric shear deformation theory for flexure and free vibration of isotropic thick beams, *Structural Engineering Convention*, SEC-2000, IIT Bombay, India, pp. 255–263.

Ghugal, Y. M. [2006] A two-dimensional exact elasticity solution of thick beam, *Departmental Report, No. 1, Department of Applied Mechanics*, Government Engineering College Aurangabad, India, pp. 1–96.

Ghugal, Y. M. [2007] A single variable parabolic shear deformation theory for flexure and flexural vibration of thick isotropic beams, *Proc. 3rd Int. Conf. Structural Engineering, Mechanics and Computation,* University of Cape Town South Africa, Paper No. SEMC 2007/708.

Ghugal, Y. M. [2007] A trigonometric shear deformation theory for flexure and free vibration of thick isotropic beams, *Departmental Report, No. 4, Department of Applied Mechanics,* Government College of Engineering, Aurangabad, India, pp. 1–95.

Heyliger, P. R. and Reddy, J. N. [1988] A higher order beam finite element for bending and vibration problems, *J. Sound Vib.* **126**(2), 309–326.

Irretier, H. [1986] Refined effects in beam theories and their influence on the natural frequencies of beams, *Proc. Euromech Colloquium 219, on Refined Dynamical Theories of Beam, Plates, and Shells and their Applications*, eds. Elishakoff, I. and Irretier, H. (Springer-Verlag, Berlin), pp. 163–179.

Kant, T. and Gupta, A. [1988] A finite element model for a higher order shear deformable beam theory, *J. Sound Vib.* **125**(2), 193–202.

Krishna Murty, A. V. [1984] Towards a consistent beam theory, *AIAA J.* **22**(6), 811–816.

Levinson, M. [1981] A new rectangular beam theory, *J. Sound Vib.* **74**(1), 81–87.

Rao, B. S. [1989] A refined beam theory, *M. Tech. Thesis, Dept. Aero. Eng.*, IIT Bombay, Powai, Mumbai, India.

Rayleigh, J. W. S. Lord. [1880] *The Theory of Sound* (Macmillan Publishers, London).

Rehfield, L. W. and Murthy, P. L. N. [1982] Toward a new engineering theory of bending: fundamentals, *AIAA J.* **20**(5), 693–699.

Silverman, I. K. [1980] Flexure of laminated beams, *ASCE J. Struct. Div.* **106**(ST3), 711–725.

Sonawane, S. J. and Ghugal, Y. M. [2006] Flexural analysis of thick beam including transverse shear and transverse flexibility, *M.E. Dissertation, Department of Applied Mechanics,* Government Engineering College, Aurangabad, India, pp. 1–95.

Stein, M. [1989] Vibration of beams and plate strips with three dimensional flexibility, *ASME, J. App. Mech.* **56**(1), 228–231.

Timoshenko, S. P. [1921] On the correction for shear of the differential equation for transverse vibrations of prismatic bars, *Philosophical Magazine*, Series **6**, pp. 742–746.

Timoshenko, S. P. and Goodier, J. N. [1970] *Theory of Elasticity*, 3rd edition (McGraw-Hill, Singapore).

Vlasov, V. Z. and Leont'ev, U. N. [1966] *Beams, Plates, and Shells on Elastic Foundations*, Moskva, Translated from the Russian by Barouch, A. and Pelz, T., Israel Program for Scientific Translation Ltd., Jerusalem, Chapter 1.

Int. J. Comput. Methods 2009.06:585-604. Downloaded from www.worldscientific.com
by QUEENSLAND UNIVERSITY OF TECHNOLOGY on 10/13/14. For personal use only.

This article was downloaded by: [McGill University Library]
On: 23 March 2013, At: 12:00
Publisher: Taylor & Francis
Informa Ltd Registered in England and Wales Registered Number: 1072954 Registered office: Mortimer House, 37-41 Mortimer Street, London W1T 3JH, UK

Mechanics Based Design of Structures and Machines: An International Journal
Publication details, including instructions for authors and subscription information:
http://www.tandfonline.com/loi/lmbd20

Variationally Consistent Higher-Order Analysis of Harmonic Vibrations of Laminated Beams

Li Jun [a] & Hua Hongxing [a]

[a] Institute of Vibration, Shock & Noise, Shanghai Jiao Tong University, Shanghai, People's Republic of China

Version of record first published: 10 Aug 2009.

To cite this article: Li Jun & Hua Hongxing (2009): Variationally Consistent Higher-Order Analysis of Harmonic Vibrations of Laminated Beams, Mechanics Based Design of Structures and Machines: An International Journal, 37:3, 299-326

To link to this article: http://dx.doi.org/10.1080/15397730902932608

PLEASE SCROLL DOWN FOR ARTICLE

Full terms and conditions of use: http://www.tandfonline.com/page/terms-and-conditions

This article may be used for research, teaching, and private study purposes. Any substantial or systematic reproduction, redistribution, reselling, loan, sub-licensing, systematic supply, or distribution in any form to anyone is expressly forbidden.

The publisher does not give any warranty express or implied or make any representation that the contents will be complete or accurate or up to date. The accuracy of any instructions, formulae, and drug doses should be independently verified with primary sources. The publisher shall not be liable for any loss, actions, claims, proceedings, demand, or costs or damages whatsoever or howsoever caused arising directly or indirectly in connection with or arising out of the use of this material.

Mechanics Based Design of Structures and Machines, 37: 299–326, 2009
Copyright © Taylor & Francis Group, LLC
ISSN 1539-7734 print/1539-7742 online
DOI: 10.1080/15397730902932608

Downloaded by [McGill University Library] at 12:00 23 March 2013

Variationally Consistent Higher-Order Analysis of Harmonic Vibrations of Laminated Beams[#]

Li Jun and Hua Hongxing

Institute of Vibration, Shock & Noise, Shanghai Jiao Tong University,
Shanghai, People's Republic of China

Abstract: An exact dynamic stiffness matrix is formulated for a generally layered composite beam on the basis of third-order shear deformation theory. The Poisson effect and the couplings among the axial, torsion, and bending deformations are incorporated in the one-dimensional beam model. The dynamic stiffness matrix is derived by using the analytical solutions of the governing differential equations of the beams in free vibration. The application of the dynamic stiffness method to investigate the influences of Poisson effect, material anisotropy, slenderness, and boundary condition upon the free vibration characteristics of the laminated beams is demonstrated.

Keywords: Composite beams; Dynamic stiffness method; Free vibration; Generally layered beams; Poisson effect; Third-order shear deformation theory.

INTRODUCTION

Laminated composite beams composed of fiber-reinforced composite materials have found increasing applications in a variety of engineering fields such as aerospace, civil, and marine during the recent decades. It becomes an obvious trend that more and more composite beams will be used in the design of structural components such as aircraft wings, helicopter blades, vehicle axles, and robot arms due to their excellent

Received August 1, 2008; Accepted November 29, 2008

[#] Communicated by S. Kaliszky.

Correspondence: Li Jun, Institute of Vibration, Shock & Noise, Shanghai Jiao Tong University, 800 Dongchuan Road, Shanghai 200240, People's Republic of China; E-mail: LJY60023@yahoo.com

Downloaded by [McGill University Library] at 12:00 23 March 2013

engineering properties such as high strength-to-weight and stiffness-to-weight ratios and favorable fatigue characteristics. The dynamic analyses of laminated beams help to optimize the design and avoid future repair costs. It is important for design engineers to use a satisfactory structural model together with a proper solution method to obtain reliable dynamic characteristics of laminated composite beams. Because of the substantial benefits and promise for future applications in various industries, composite beams have aroused continuing research interest and many structural models have been developed for the dynamic analysis of such beams.

Free vibration analysis of simple laminated composite beams without the effects of shear deformation and rotary inertia started only in the 1970s. It is evident from the reported studies that the classical laminated beam theory fails to accurately predict the natural frequencies of reasonably thick laminated beams. Since the ratio of extensional modulus to transverse shear modulus is high for fiber composites, the effect of transverse shear deformation must be considered in the dynamic analysis. Therefore, first-order shear deformation beam theory, which considers a constant transverse shear strain over the thickness of the beam, has been developed. This is the equivalent of isotropic Timoshenko beam theory.

Kapania and Raciti (1989) presented a literature survey on the vibration analysis of laminated composite beams. Chandrashekhara et al. (1990) presented the exact solutions for the free vibration of symmetrically laminated composite beam with the shear deformation and rotary inertia included. Krishnaswamy et al. (1992) presented analytical solutions to free vibration of generally layered, moderately thick composite beams by the Lagrange multipliers method. Rotary inertia and shear deformation effects were included in the formulation. Abramovich and Livshits (1994) studied the free vibration of nonsymmetric cross-ply composite Timoshenko beams. Eisenberger et al. (1995) utilized the dynamic stiffness approach to study the free vibration of laminated beams using first-order shear deformation theory. Teboub and Hajela (1995) adopted the symbolic computation technique to analyze the free vibration of generally layered composite beam on the basis of first-order shear deformation theory. Banerjee and Williams (1996) presented an exact dynamic stiffness matrix for a composite beam, with the effects of shear deformation, rotary inertia, and coupling between the bending and torsional deformations included. Yildirim et al. (1999) investigated the influences of rotary inertia and axial and shear deformations on the in-plane free vibration of symmetric cross-ply laminated beams. Yildirim (2000) used the stiffness method to study the in-plane free vibration problem of symmetric cross-ply laminated beams, with the effects of rotary inertia and axial and transverse shear deformations included. Chakraborty et al. (2002) presented a refined first-order shear deformable beam element and demonstrated its utility in solving the free vibration and wave propagation problems in laminated composite beam structures with symmetric as well as asymmetric ply stacking. Mahapatra and Gopalakrishnan (2003) presented a spectral finite element model for analysis of axial-flexural-shear coupled wave propagation in thick laminated composite beams. Ruotolo (2004) developed a spectral element for anisotropic laminated composite beams. The axial-bending coupled equations of motion were derived under the assumption of first-order shear deformation theory.

The first-order shear deformation beam theory, which assumes the constant shear strain distribution throughout the beam thickness, violates the shear traction-free condition on the top and bottom surfaces of the beam. The shear correction factor is then employed to correct the discrepancy between the results derived from the exact theory and the solutions obtained via first-order shear deformation theory. Therefore, various higher-order shear deformation beam theories have been developed to improve the first-order theory by assuming a higher-order displacement field through the beam thickness.

Bhimaraddi and Chandrashekhara (1991) modeled the laminated beams by a systematic reduction of the constitutive relations of the three-dimensional anisotropic body and obtained the basic equations of the beam theory based on parabolic shear deformation theory. Soldatos and Elishakoff (1992) developed a third-order shear deformation theory for static and dynamic analyses of an orthotropic beam incorporating the effects of transverse shear and transverse normal deformations. Chandrashekhara and Bangera (1992) studied the free vibration characteristics of laminated beams using a finite element method and third-order beam theory. Singh and Abdelnassar (1992) worked out the free and forced vibration problems of laminated beams based on third-order shear deformation theory. Khdeir and Reddy (1994) employed the transfer matrix method for the free vibration analysis of cross-ply laminated beams based on various shear deformation theories. Marur and Kant (1997) investigated the effect of higher-order shear deformation theories on the transient response of composite beams. Kant et al. (1997) presented an analytical method for the dynamic analysis of laminated beams using higher-order refined theory. Song and Waas (1997) studied the buckling and free vibration of stepped laminated composite beams using simple higher-order theory that assumed a cubic distribution for the displacement field through the beam thickness. Shimpi and Ainapure (1999) studied the free vibration of two-layered laminated cross-ply beams using a variationally consistent layerwise trigonometric shear deformation theory. Shi and Lam (1999) presented a new finite element formulation for the free vibration analysis of composite beams based on third-order beam theory. Shimpi and Ainapure (2001) presented a simple one-dimensional

Downloaded by [McGill University Library] at 12:00 23 March 2013

Downloaded by [McGill University Library] at 12:00 23 March 2013

beam finite element on the basis of a variationally consistent layerwise trigonometric shear deformation theory. Ghugal and Shimpi (2001) presented a review of displacement- and stress-based refined theories for isotropic and anisotropic laminated beams and discussed various equivalent single layer and layerwise theories for laminated beams. Rao et al. (2001) proposed a higher-order mixed theory for determining the natural frequencies of a diversity of simply supported laminated beams. Matsunaga (2001) studied the natural frequencies, buckling stresses, and interlaminar stresses of simply supported composite beams using a global higher-order theory. Arya et al. (2002) developed a zigzag model for symmetric laminated beams in which a sine term was used to represent the nonlinear displacement field across the thickness as compared to a third-order polynomial term in conventional higher-order theories. Karama et al. (2003) presented a new multilayered composite beam model by using a exponential function to predict the mechanical behavior of composite beams. Murthy et al. (2005) developed a refined two-node, four-degree-of-freedom/node beam element based on higher-order shear deformation theory for asymmetrically stacked composite beams. Aydogdu (2005) and Aydogdu (2006), using the Ritz method with different sets of boundary conditions, carried out vibration analyses of cross-ply and angle-ply laminated beams, respectively. The analysis was based on a three-degree-of-freedom shear deformable beam theory. Subramanian (2006) performed free vibration analyses of laminated beams using two higher-order displacement-based shear deformation theories. Both theories assume a quintic and quartic variation of in-plane and transverse displacements in the thickness coordinates of the beam, respectively, and a non-parabolic variation of transverse shear stress across the thickness of the beams is assumed for the first theory while a parabolic variation is assumed for the second theory. Tahani (2007) developed a new layerwise composite beam theory for generally laminated beams. Analytical solutions were obtained for the static bending and free vibration of cross-ply and angle-ply laminated beams by using the state space method.

A review of the literature indicates that most of the research is devoted to dynamic analysis of cross-ply composite beams using elementary and first-order shear deformation theories and only a few works have been done on the vibration analysis of generally laminated beams based on higher-order shear deformation theories. An attempt to derive the dynamic stiffness matrix of an arbitrary ply-stacking composite beam based on third-order shear deformation theory, which assumes a cubic displacement field making the straight normal to the centroidal line deform parabolically and shear-free traction conditions at the top and bottom beam surfaces, has not still been reported. This article addresses this problem. The dynamic stiffness method to solve the free or forced vibration problems of the structural elements has received

Downloaded by [McGill University Library] at 12:00 23 March 2013

much attention in recent years. Some advantages of this method are well known, particularly when higher frequencies and better accuracy are required. This method is often referred to as an exact method. A single element can be used to calculate any number of exact natural frequencies and modes of a uniform structure to any desirable accuracy.

This article formulates the dynamic stiffness matrix to analyze the free vibration characteristics of generally layered composite beams based on third-order shear deformation theory. The Poisson effect and the couplings among the axial, torsion, and bending deformations are incorporated in the one-dimensional beam model. The derivation of the governing differential equations of laminated beams is accomplished by applying Hamilton's principle. These equations are quite difficult to solve, in sharp contrast to those of laminated beams based on first-order shear deformation theory. The difficulty would appear to arise mainly due to the extensional-bending-torsional coupling and higher-order shear deformation effects, which lead to the formulation of higher-order governing differential equations. The dynamic stiffness matrix is found directly from the general solutions of the governing differential equations of motion of the beam in free vibration. The dynamic stiffness method is demonstrated by several illustrative examples of composite beams for which some published results are available. The influences of the Poisson effect, material anisotropy, slenderness, and boundary condition upon the natural frequencies of laminated beams are studied.

MATHEMATICAL FORMULATIONS

A laminated composite beam, as shown in Fig. 1, is considered. The laminated beam is made of many orthotropic layers, and the principal material directions of each layer need not be aligned with the x axis. In the right-handed Cartesian coordinate system, the x axis is coincident with the beam axis and the origin is on the midplane of the beam. The

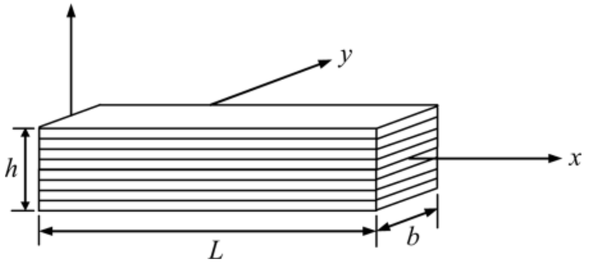

Figure 1. Coordinate axes and notation for a laminated composite beam.

Downloaded by [McGill University Library] at 12:00 23 March 2013

length, breadth, and thickness of the beam are represented by L, b and h, respectively.

To develop the equations of motion for a generally layered composite beam, the displacement field proposed in a third-order shear deformation theory is assumed to be the following:

$$u_1(x, z, t) = u(x, t) + z\left[\phi - \frac{4}{3}\left(\frac{z}{h}\right)^2\left(\phi + \frac{\partial w}{\partial x}\right)\right] \tag{1a}$$

$$u_2(x, z, t) = z\left[\psi - \frac{4}{3}\left(\frac{z}{h}\right)^2\psi\right] \tag{1b}$$

$$u_3(x, z, t) = w(x, t), \tag{1c}$$

where u_1, u_2, and u_3 are the displacements of an arbitrary point in the beam domain along the x, y, and z coordinates, respectively; u and w are the longitudinal and transverse displacements of a point on the beam midplane along the x and z directions, respectively; ϕ and ψ are the rotations of the normal to the midplane about the y and x axes, respectively. This displacement field provides a parabolic variation of the transverse shear stress that is zero at the top and bottom surfaces of the beam.

Based on the foregoing displacement field, these are the strain-displacement relations:

$$\varepsilon_x^0 = \frac{\partial u}{\partial x} \quad \kappa_x^0 = \frac{\partial \phi}{\partial x} \quad \kappa_x^2 = -\frac{4}{3h^2}\left(\frac{\partial \phi}{\partial x} + \frac{\partial^2 w}{\partial x^2}\right) \tag{2a}$$

$$\kappa_{xy}^0 = \frac{\partial \psi}{\partial x} \quad \kappa_{xy}^2 = -\frac{4}{3h^2}\frac{\partial \psi}{\partial x}$$

$$\varepsilon_{xz}^0 = \left(\phi + \frac{\partial w}{\partial x}\right) \quad \kappa_{xz}^2 = -\frac{4}{h^2}\left(\phi + \frac{\partial w}{\partial x}\right) \tag{2b}$$

These are the constitutive equations of laminated plate based on third-order shear deformation theory (Reddy, 2004):

$$\begin{Bmatrix} N_x \\ N_y \\ N_{xy} \\ M_x \\ M_y \\ M_{xy} \\ P_x \\ P_y \\ P_{xy} \end{Bmatrix} = \begin{bmatrix} A_{11} & A_{12} & A_{16} & B_{11} & B_{12} & B_{16} & E_{11} & E_{12} & E_{16} \\ A_{12} & A_{22} & A_{26} & B_{12} & B_{22} & B_{26} & E_{12} & E_{22} & E_{26} \\ A_{16} & A_{26} & A_{66} & B_{16} & B_{26} & B_{66} & E_{16} & E_{26} & E_{66} \\ B_{11} & B_{12} & B_{16} & D_{11} & D_{12} & D_{16} & F_{11} & F_{12} & F_{16} \\ B_{12} & B_{22} & B_{26} & D_{12} & D_{22} & D_{26} & F_{12} & F_{22} & F_{26} \\ B_{16} & B_{26} & B_{66} & D_{16} & D_{26} & D_{66} & F_{16} & F_{26} & F_{66} \\ E_{11} & E_{12} & E_{16} & F_{11} & F_{12} & F_{16} & H_{11} & H_{12} & H_{16} \\ E_{12} & E_{22} & E_{26} & F_{12} & F_{22} & F_{26} & H_{12} & H_{22} & H_{26} \\ E_{16} & E_{26} & E_{66} & F_{16} & F_{26} & F_{66} & H_{16} & H_{26} & H_{66} \end{bmatrix} \begin{Bmatrix} \varepsilon_x^0 \\ \varepsilon_y^0 \\ \varepsilon_{xy}^0 \\ \kappa_x^0 \\ \kappa_y^0 \\ \kappa_{xy}^0 \\ \kappa_x^2 \\ \kappa_y^2 \\ \kappa_{xy}^2 \end{Bmatrix}, \tag{3}$$

Downloaded by [McGill University Library] at 12:00 23 March 2013

where N_x, N_y, and N_{xy} are the in-plane forces, M_x, M_y, and M_{xy} the bending and twisting moments, P_x, P_y, and P_{xy} the higher-order bending and twisting moments, ε_x^0, ε_y^0, and ε_{xy}^0 the midplane strains, κ_x^0, κ_y^0, and κ_{xy}^0 the bending and twisting curvatures, κ_x^2, κ_y^2, and κ_{xy}^2 the higher-order bending and twisting curvatures, and A_{ij}, B_{ij}, D_{ij}, E_{ij}, F_{ij}, and H_{ij} $(i, j = 1, 2, 6)$ the stiffness coefficients.

In the case of the laminated composite beams, one can neglect in-plane forces N_y, N_{xy}, bending moment M_y, and higher-order moment P_y everywhere in the laminates because the laminates are so narrow that these generalized stress components are insignificant. The previous results have shown that narrow laminates can reasonably cover a range of laminates of large aspect ratio. It may be mentioned that how to define the range of narrow laminates realistically is beyond the scope of present manuscript. The midplane strains ε_y^0 and ε_{xy}^0, the bending curvature κ_y^0, and the higher-order bending curvature κ_y^2 in Eq. (3) are assumed to be nonzero. Thus, Eq. (3) may be rewritten as

$$\begin{Bmatrix} N_x \\ M_x \\ M_{xy} \\ P_x \\ P_{xy} \end{Bmatrix} = \begin{bmatrix} \overline{A}_{11} & \overline{B}_{11} & \overline{B}_{16} & \overline{E}_{11} & \overline{E}_{16} \\ \overline{B}_{11} & \overline{D}_{11} & \overline{D}_{16} & \overline{F}_{11} & \overline{F}_{16} \\ \overline{B}_{16} & \overline{D}_{16} & \overline{D}_{66} & \overline{F}_{16} & \overline{F}_{66} \\ \overline{E}_{11} & \overline{F}_{11} & \overline{F}_{16} & \overline{H}_{11} & \overline{H}_{16} \\ \overline{E}_{16} & \overline{F}_{16} & \overline{F}_{66} & \overline{H}_{16} & \overline{H}_{66} \end{bmatrix} \begin{Bmatrix} \varepsilon_x^0 \\ \kappa_x^0 \\ \kappa_{xy}^0 \\ \kappa_x^2 \\ \kappa_{xy}^2 \end{Bmatrix} \tag{4}$$

where

$$\begin{bmatrix} \overline{A}_{11} & \overline{B}_{11} & \overline{B}_{16} & \overline{E}_{11} & \overline{E}_{16} \\ \overline{B}_{11} & \overline{D}_{11} & \overline{D}_{16} & \overline{F}_{11} & \overline{F}_{16} \\ \overline{B}_{16} & \overline{D}_{16} & \overline{D}_{66} & \overline{F}_{16} & \overline{F}_{66} \\ \overline{E}_{11} & \overline{F}_{11} & \overline{F}_{16} & \overline{H}_{11} & \overline{H}_{16} \\ \overline{E}_{16} & \overline{F}_{16} & \overline{F}_{66} & \overline{H}_{16} & \overline{H}_{66} \end{bmatrix}$$

$$= \begin{bmatrix} A_{11} & B_{11} & B_{16} & E_{11} & E_{16} \\ B_{11} & D_{11} & D_{16} & F_{11} & F_{16} \\ B_{16} & D_{16} & D_{66} & F_{16} & F_{66} \\ E_{11} & F_{11} & F_{16} & H_{11} & H_{16} \\ E_{16} & F_{16} & F_{66} & H_{16} & H_{66} \end{bmatrix} - \begin{bmatrix} A_{12} & A_{16} & B_{12} & E_{12} \\ B_{12} & B_{16} & D_{12} & F_{12} \\ B_{26} & B_{66} & D_{26} & F_{26} \\ E_{12} & E_{16} & F_{12} & H_{12} \\ E_{26} & E_{66} & F_{26} & H_{26} \end{bmatrix}$$

$$\times \begin{bmatrix} A_{22} & A_{26} & B_{22} & E_{22} \\ A_{26} & A_{66} & B_{26} & E_{26} \\ B_{22} & B_{26} & D_{22} & F_{22} \\ E_{22} & E_{26} & F_{22} & H_{22} \end{bmatrix}^{-1} \begin{bmatrix} A_{12} & B_{12} & B_{26} & E_{12} & E_{26} \\ A_{16} & B_{16} & B_{66} & E_{16} & E_{66} \\ B_{12} & D_{12} & D_{26} & F_{12} & F_{26} \\ E_{12} & F_{12} & F_{26} & H_{12} & H_{26} \end{bmatrix}$$

The transverse shear force-strain relations are given by

$$\begin{Bmatrix} Q_{xz} \\ R_{xz} \end{Bmatrix} = \begin{bmatrix} A_{55} & D_{55} \\ D_{55} & F_{55} \end{bmatrix} \begin{Bmatrix} \varepsilon^0_{xz} \\ \kappa^2_{xz} \end{Bmatrix} \tag{5}$$

The laminate stiffness coefficients A_{ij}, B_{ij}, D_{ij}, E_{ij}, F_{ij}, and H_{ij}, and the transverse shear stiffnesses A_{55}, D_{55}, and F_{55}, which are functions of laminate ply orientation, material property, and stack sequence, are as follows:

$$\left(A_{ij}\ B_{ij}\ D_{ij}\ E_{ij}\ F_{ij}\ H_{ij} \right) = \int_{-\frac{h}{2}}^{\frac{h}{2}} \overline{Q}_{ij}(1, z, z^2, z^3, z^4, z^6)dz \tag{6a}$$

$$\left(A_{55}\ D_{55}\ F_{55} \right) = \int_{-\frac{h}{2}}^{\frac{h}{2}} \overline{Q}_{55}(1, z^2, z^4)dz \tag{6b}$$

The stiffnesses in Eq. (6a) are defined for $i, j = 1, 2, 6$.

The transformed reduced stiffness constants $\overline{Q}_{ij}$ $(i, j = 1, 2, 6)$ and $\overline{Q}_{55}$ are obtained by the following:

$$\overline{Q}_{11} = Q_{11}\cos^4\vartheta + 2(Q_{12} + 2Q_{66})\sin^2\vartheta\cos^2\vartheta + Q_{22}\sin^4\vartheta \tag{7a}$$

$$\overline{Q}_{12} = (Q_{11} + Q_{22} - 4Q_{66})\sin^2\vartheta\cos^2\vartheta + Q_{12}(\sin^4\vartheta + \cos^4\vartheta) \tag{7b}$$

$$\overline{Q}_{22} = Q_{11}\sin^4\vartheta + 2(Q_{12} + 2Q_{66})\sin^2\vartheta\cos^2\vartheta + Q_{22}\cos^4\vartheta \tag{7c}$$

$$\begin{aligned}\overline{Q}_{16} = {} & (Q_{11} - Q_{12} - 2Q_{66})\sin\vartheta\cos^3\vartheta + (Q_{12} - Q_{22} + 2Q_{66}) \\ & \times \sin^3\vartheta\cos\vartheta \end{aligned} \tag{7d}$$

$$\begin{aligned}\overline{Q}_{26} = {} & (Q_{11} - Q_{12} - 2Q_{66})\sin^3\vartheta\cos\vartheta + (Q_{12} - Q_{22} + 2Q_{66}) \\ & \times \sin\vartheta\cos^3\vartheta \end{aligned} \tag{7e}$$

$$\begin{aligned}\overline{Q}_{66} = {} & (Q_{11} + Q_{22} - 2Q_{12} - 2Q_{66})\sin^2\vartheta\cos^2\vartheta + Q_{66} \\ & \times(\sin^4\vartheta + \cos^4\vartheta) \end{aligned} \tag{7f}$$

$$\overline{Q}_{55} = G_{13}\cos^2\vartheta + G_{23}\sin^2\vartheta \tag{7g}$$

where ϑ is the angle between the fiber direction and longitudinal axis of the beam and the reduced stiffness constants Q_{11}, Q_{22}, Q_{12} and Q_{66} can be obtained in terms of the engineering constants Jones (1976):

$$Q_{11} = \frac{E_1}{1 - \nu_{12}\nu_{21}} \quad Q_{12} = \frac{\nu_{12}E_2}{1 - \nu_{12}\nu_{21}} = \frac{\nu_{21}E_1}{1 - \nu_{12}\nu_{21}}$$

$$Q_{22} = \frac{E_2}{1 - \nu_{12}\nu_{21}} \quad Q_{66} = G_{12}$$

Downloaded by [McGill University Library] at 12:00 23 March 2013

Downloaded by [McGill University Library] at 12:00 23 March 2013

DYNAMIC STIFFNESS MATRIX

The total strain energy V of the generally laminated composite beam shown in Fig. 1 is given as

$$V = \frac{b}{2}\int_0^L \left[N_x\varepsilon_x^0 + M_x\kappa_x^0 + P_x\kappa_x^2 + M_{xy}\kappa_{xy}^0 + P_{xy}\kappa_{xy}^2 + Q_{xz}\varepsilon_{xz}^0 + R_{xz}\kappa_{xz}^2\right]dx \tag{8}$$

Substituting N_x, M_x, P_x, M_{xy}, P_{xy}, Q_{xz}, and R_{xz} from Eqs. (4) and (5) into Eq. (8) yields

$$V = \frac{b}{2}\int_0^L \left[\begin{array}{l} \overline{A}_{11}\left(\varepsilon_x^0\right)^2 + 2\overline{B}_{11}\varepsilon_x^0\kappa_x^0 + 2\overline{B}_{16}\varepsilon_x^0\kappa_{xy}^0 + 2\overline{E}_{11}\varepsilon_x^0\kappa_x^2 + 2\overline{E}_{16}\varepsilon_x^0\kappa_{xy}^2 \\ + \overline{D}_{11}\left(\kappa_x^0\right)^2 + 2\overline{D}_{16}\kappa_x^0\kappa_{xy}^0 + 2\overline{F}_{11}\kappa_x^0\kappa_x^2 + 2\overline{F}_{16}\kappa_x^0\kappa_{xy}^2 \\ + 2\overline{F}_{16}\kappa_x^2\kappa_{xy}^0 + \overline{H}_{11}\left(\kappa_x^2\right)^2 + 2\overline{H}_{16}\kappa_x^2\kappa_{xy}^2 + \overline{D}_{66}\left(\kappa_{xy}^0\right)^2 + 2\overline{F}_{66}\kappa_{xy}^0\kappa_{xy}^2 \\ + \overline{H}_{66}\left(\kappa_{xy}^2\right)^2 + A_{55}\left(\varepsilon_{xz}^0\right)^2 + 2D_{55}\varepsilon_{xz}^0\kappa_{xz}^2 + F_{55}\left(\kappa_{xz}^2\right)^2 \end{array}\right]dx \tag{9}$$

The total kinetic energy T of generally laminated composite beam can be written as

$$T = \frac{b}{2}\int_0^L\int_{-\frac{h}{2}}^{\frac{h}{2}} \rho\left[(\dot{u}_1)^2 + (\dot{u}_2)^2 + (\dot{u}_3)^2\right]dzdx \tag{10}$$

where ρ is the mass density per unit volume. The over dot represents the derivative with respect to time t.

Substituting u_1, u_2, and u_3 from Eqs. (1) into Eq. (10) results in

$$T = \frac{b}{2}\int_0^L\int_{-\frac{h}{2}}^{\frac{h}{2}} \rho \left\{\left(\dot{u} + z\left[\dot{\phi} - \frac{4}{3}\left(\frac{z}{h}\right)^2\left(\dot{\phi} + \frac{\partial\dot{w}}{\partial x}\right)\right]\right)^2 + \left(z\left[\dot{\psi} - \frac{4}{3}\left(\frac{z}{h}\right)^2\dot{\psi}\right]\right)^2 + \dot{w}^2\right\}dzdx \tag{11}$$

The governing equations of motion and associated boundary conditions of generally laminated beams will be derived using Hamilton's principle, which can be stated in this form:

$$\int_{t_1}^{t_2}(\delta T - \delta V)dt = 0 \tag{12}$$

$$\delta u = \delta w = \delta\phi = \delta\psi = \delta(\partial w/\partial x) = 0 \text{ at } t = t_1, t_2$$

where δ is the first variation, t_1 and t_2 are two arbitrary time variables.

Downloaded by [McGill University Library] at 12:00 23 March 2013

Substituting Eq. (2) into Eq. (9), then substituting the resulting equation and Eq. (11) into Eq. (12) and following the standard procedures of the variational techniques, we obtain the following equations of motion for generally layered composite beams:

$$\begin{aligned}&-I_1\ddot{u} + \left(\frac{4}{3h^2}I_4 - I_2\right)\ddot{\phi} + \frac{4}{3h^2}I_4\frac{\partial\ddot{w}}{\partial x} + \overline{A}_{11}\frac{\partial^2 u}{\partial x^2} + \left(\overline{B}_{11} - \frac{4}{3h^2}\overline{E}_{11}\right)\frac{\partial^2\phi}{\partial x^2}\\&\quad + \left(\overline{B}_{16} - \frac{4}{3h^2}\overline{E}_{16}\right)\frac{\partial^2\psi}{\partial x^2} - \frac{4}{3h^2}\overline{E}_{11}\frac{\partial^3 w}{\partial x^3} = 0\end{aligned} \tag{13a}$$

$$\begin{aligned}&-I_1\ddot{w} - \frac{4}{3h^2}I_4\frac{\partial\ddot{u}}{\partial x} + \left(\frac{16}{9h^4}I_7 - \frac{4}{3h^2}I_5\right)\frac{\partial\ddot{\phi}}{\partial x} + \frac{16}{9h^4}I_7\frac{\partial^2\ddot{w}}{\partial x^2}\\&\quad + \frac{4}{3h^2}\overline{E}_{11}\frac{\partial^3 u}{\partial x^3} + \left(\frac{4}{3h^2}\overline{F}_{11} - \frac{16}{9h^4}\overline{H}_{11}\right)\frac{\partial^3\phi}{\partial x^3} + \left(\frac{4}{3h^2}\overline{F}_{16} - \frac{16}{9h^4}\overline{H}_{16}\right)\frac{\partial^3\psi}{\partial x^3}\\&\quad - \frac{16}{9h^4}\overline{H}_{11}\frac{\partial^4 w}{\partial x^4} + \left(A_{55} - \frac{8}{h^2}D_{55} + \frac{16}{h^4}F_{55}\right)\left(\frac{\partial\phi}{\partial x} + \frac{\partial^2 w}{\partial x^2}\right) = 0\end{aligned} \tag{13b}$$

$$\begin{aligned}&-\left(I_2 - \frac{4}{3h^2}I_4\right)\ddot{u} - \left(I_3 + \frac{16}{9h^4}I_7 - \frac{8}{3h^2}I_5\right)\ddot{\phi} + \left(\frac{4}{3h^2}I_5 - \frac{16}{9h^4}I_7\right)\frac{\partial\ddot{w}}{\partial x}\\&\quad + \left(\overline{B}_{11} - \frac{4}{3h^2}\overline{E}_{11}\right)\frac{\partial^2 u}{\partial x^2} + \left(\overline{D}_{16} - \frac{8}{3h^2}\overline{F}_{16} + \frac{16}{9h^4}\overline{H}_{16}\right)\frac{\partial^2\psi}{\partial x^2}\\&\quad + \left(\overline{D}_{11} - \frac{8}{3h^2}\overline{F}_{11} + \frac{16}{9h^4}\overline{H}_{11}\right)\frac{\partial^2\phi}{\partial x^2} + \left(\frac{16}{9h^4}\overline{H}_{11} - \frac{4}{3h^2}\overline{F}_{11}\right)\frac{\partial^3 w}{\partial x^3}\\&\quad + \left(\frac{8}{h^2}D_{55} - A_{55} - \frac{16}{h^4}F_{55}\right)\left(\phi + \frac{\partial w}{\partial x}\right) = 0\end{aligned} \tag{13c}$$

$$\begin{aligned}&-\left(I_3 + \frac{16}{9h^4}I_7 - \frac{8}{3h^2}I_5\right)\ddot{\psi} + \left(\overline{B}_{16} - \frac{4}{3h^2}\overline{E}_{16}\right)\frac{\partial^2 u}{\partial x^2}\\&\quad + \left(\overline{D}_{16} - \frac{8}{3h^2}\overline{F}_{16} + \frac{16}{9h^4}\overline{H}_{16}\right)\frac{\partial^2\phi}{\partial x^2} + \left(\frac{16}{9h^4}\overline{H}_{16} - \frac{4}{3h^2}\overline{F}_{16}\right)\frac{\partial^3 w}{\partial x^3}\\&\quad + \left(\overline{D}_{66} - \frac{8}{3h^2}\overline{F}_{66} + \frac{16}{9h^4}\overline{H}_{66}\right)\frac{\partial^2\psi}{\partial x^2} = 0\end{aligned} \tag{13d}$$

where

$$(I_1, I_2, I_3, I_4, I_5, I_7) = \int_{-\frac{h}{2}}^{\frac{h}{2}} \rho(1, z, z^2, z^3, z^4, z^6)dz$$

The boundary conditions at the ends of beam ($x = 0, L$) are

$$\begin{aligned}&\left[-\overline{A}_{11}\frac{\partial u}{\partial x} + \left(\frac{4}{3h^2}\overline{E}_{11} - \overline{B}_{11}\right)\frac{\partial\phi}{\partial x} + \frac{4}{3h^2}\overline{E}_{11}\frac{\partial^2 w}{\partial x^2}\right.\\&\quad \left. + \left(\frac{4}{3h^2}\overline{E}_{16} - \overline{B}_{16}\right)\frac{\partial\psi}{\partial x}\right]\delta u = 0\end{aligned} \tag{14a}$$

Downloaded by [McGill University Library] at 12:00 23 March 2013

$$\begin{aligned}&\Bigg[\frac{4}{3h^2}I_4\ddot{u}+\left(\frac{4}{3h^2}I_5-\frac{16}{9h^4}I_7\right)\ddot{\phi}-\frac{16}{9h^4}I_7\frac{\partial\ddot{w}}{\partial x}-\frac{4}{3h^2}\overline{E}_{11}\frac{\partial^2 u}{\partial x^2}\\&\quad+\left(\frac{16}{9h^4}\overline{H}_{11}-\frac{4}{3h^2}\overline{F}_{11}\right)\frac{\partial^2\phi}{\partial x^2}+\frac{16}{9h^4}\overline{H}_{11}\frac{\partial^3 w}{\partial x^3}+\left(\frac{16}{9h^4}\overline{H}_{16}-\frac{4}{3h^2}\overline{F}_{16}\right)\frac{\partial^2\psi}{\partial x^2}\\&\quad+\left(\frac{8}{h^2}D_{55}-A_{55}-\frac{16}{h^4}F_{55}\right)\left(\phi+\frac{\partial w}{\partial x}\right)\Bigg]\delta w=0\end{aligned}\tag{14b}$$

$$\begin{aligned}&\Bigg[\left(-\overline{B}_{11}+\frac{4}{3h^2}\overline{E}_{11}\right)\frac{\partial u}{\partial x}+\left(\frac{8}{3h^2}\overline{F}_{16}-\overline{D}_{16}-\frac{16}{9h^4}\overline{H}_{16}\right)\frac{\partial\psi}{\partial x}\\&\quad+\left(\frac{8}{3h^2}\overline{F}_{11}-\overline{D}_{11}-\frac{16}{9h^4}\overline{H}_{11}\right)\frac{\partial\phi}{\partial x}\\&\quad+\left(\frac{4}{3h^2}\overline{F}_{11}-\frac{16}{9h^4}\overline{H}_{11}\right)\frac{\partial^2 w}{\partial x^2}\Bigg]\delta\phi=0\end{aligned}\tag{14c}$$

$$\begin{aligned}&\Bigg[\left(\frac{4}{3h^2}\overline{E}_{16}-\overline{B}_{16}\right)\frac{\partial u}{\partial x}+\left(\frac{4}{3h^2}\overline{F}_{16}-\frac{16}{9h^4}\overline{H}_{16}\right)\\&\quad\frac{\partial^2 w}{\partial x^2}+\left(\frac{8}{3h^2}\overline{F}_{16}-\frac{16}{9h^4}\overline{H}_{16}-\overline{D}_{16}\right)\frac{\partial\phi}{\partial x}\\&\quad+\left(\frac{8}{3h^2}\overline{F}_{66}-\overline{D}_{66}-\frac{16}{9h^4}\overline{H}_{66}\right)\frac{\partial\psi}{\partial x}\Bigg]\delta\psi=0\end{aligned}\tag{14d}$$

$$\begin{aligned}&\Bigg[\frac{4}{3h^2}\overline{E}_{11}\frac{\partial u}{\partial x}+\left(\frac{4}{3h^2}\overline{F}_{11}-\frac{16}{9h^4}\overline{H}_{11}\right)\\&\quad\frac{\partial\phi}{\partial x}+\left(\frac{4}{3h^2}\overline{F}_{16}-\frac{16}{9h^4}\overline{H}_{16}\right)\frac{\partial\psi}{\partial x}-\frac{16}{9h^4}\overline{H}_{11}\frac{\partial^2 w}{\partial x^2}\Bigg]\delta w'=0\end{aligned}\tag{14e}$$

It can be shown that Eqs. (13) have solutions that are separable in time and space and that the time dependence is harmonic. Letting

$$\left\{\,u(x,t)\;w(x,t)\;\phi(x,t)\;\psi(x,t)\,\right\}=\left\{\,U(x)\;W(x)\;\Phi(x)\;\Psi(x)\,\right\}e^{i\omega t},\tag{15}$$

where ω is the angular frequency, $U(x)$, $W(x)$, $\Phi(x)$, and $\Psi(x)$ are the amplitudes of the harmonically varying longitudinal displacement, bending displacement, bending rotation and torsional rotation, respectively.

Introducing Eqs. (15) into Eqs. (13), the following differential eigenvalue problem is obtained

$$\begin{aligned}&I_1\omega^2 U-\left(\frac{4}{3h^2}I_4-I_2\right)\omega^2\Phi-\frac{4}{3h^2}I_4\omega^2\frac{\partial W}{\partial x}+\overline{A}_{11}\frac{\partial^2 U}{\partial x^2}\\&\quad+\left(\overline{B}_{11}-\frac{4}{3h^2}\overline{E}_{11}\right)\frac{\partial^2\Phi}{\partial x^2}+\left(\overline{B}_{16}-\frac{4}{3h^2}\overline{E}_{16}\right)\frac{\partial^2\Psi}{\partial x^2}-\frac{4}{3h^2}\overline{E}_{11}\frac{\partial^3 W}{\partial x^3}=0\end{aligned}\tag{16a}$$

Downloaded by [McGill University Library] at 12:00 23 March 2013

$$
\begin{aligned}
&I_1\omega^2 W + \frac{4}{3h^2}I_4\omega^2\frac{\partial U}{\partial x} - \left(\frac{16}{9h^4}I_7 - \frac{4}{3h^2}I_5\right)\omega^2\frac{\partial \Phi}{\partial x} - \frac{16}{9h^4}I_7\omega^2\frac{\partial^2 W}{\partial x^2} \\
&\quad \frac{4}{3h^2}\overline{E}_{11}\frac{\partial^3 U}{\partial x^3} + \left(\frac{4}{3h^2}\overline{F}_{11} - \frac{16}{9h^4}\overline{H}_{11}\right)\frac{\partial^3 \Phi}{\partial x^3} + \left(\frac{4}{3h^2}\overline{F}_{16} - \frac{16}{9h^4}\overline{H}_{16}\right)\frac{\partial^3 \Psi}{\partial x^3} \\
&\quad -\frac{16}{9h^4}\overline{H}_{11}\frac{\partial^4 W}{\partial x^4} + \left(A_{55} - \frac{8}{h^2}D_{55} + \frac{16}{h^4}F_{55}\right)\left(\frac{\partial \Phi}{\partial x} + \frac{\partial^2 W}{\partial x^2}\right) = 0
\end{aligned}
\tag{16b}
$$

$$
\begin{aligned}
&\left(I_2 - \frac{4}{3h^2}I_4\right)\omega^2 U + \left(I_3 + \frac{16}{9h^4}I_7 - \frac{8}{3h^2}I_5\right)\omega^2\Phi - \left(\frac{4}{3h^2}I_5 - \frac{16}{9h^4}I_7\right) \\
&\quad \omega^2\frac{\partial W}{\partial x} + \left(\overline{B}_{11} - \frac{4}{3h^2}\overline{E}_{11}\right)\frac{\partial^2 U}{\partial x^2} + \left(\overline{D}_{16} - \frac{8}{3h^2}\overline{F}_{16} + \frac{16}{9h^4}\overline{H}_{16}\right)\frac{\partial^2 \Psi}{\partial x^2} \\
&\quad + \left(\overline{D}_{11} - \frac{8}{3h^2}\overline{F}_{11} + \frac{16}{9h^4}\overline{H}_{11}\right)\frac{\partial^2 \Phi}{\partial x^2} + \left(\frac{16}{9h^4}\overline{H}_{11} - \frac{4}{3h^2}\overline{F}_{11}\right)\frac{\partial^3 W}{\partial x^3} \\
&\quad + \left(\frac{8}{h^2}D_{55} - A_{55} - \frac{16}{h^4}F_{55}\right)\left(\Phi + \frac{\partial W}{\partial x}\right) = 0
\end{aligned}
\tag{16c}
$$

$$
\begin{aligned}
&\left(I_3 + \frac{16}{9h^4}I_7 - \frac{8}{3h^2}I_5\right)\omega^2\Psi + \left(\overline{B}_{16} - \frac{4}{3h^2}\overline{E}_{16}\right)\frac{\partial^2 U}{\partial x^2} \\
&\quad + \left(\overline{D}_{16} - \frac{8}{3h^2}\overline{F}_{16} + \frac{16}{9h^4}\overline{H}_{16}\right)\frac{\partial^2 \Phi}{\partial x^2} \\
&\quad + \left(\frac{16}{9h^4}\overline{H}_{16} - \frac{4}{3h^2}\overline{F}_{16}\right)\frac{\partial^3 W}{\partial x^3} \\
&\quad + \left(\overline{D}_{66} - \frac{8}{3h^2}\overline{F}_{66} + \frac{16}{9h^4}\overline{H}_{66}\right)\frac{\partial^2 \Psi}{\partial x^2} = 0
\end{aligned}
\tag{16d}
$$

The solutions to Eqs. (16) are given by

$$
\left\{ U(x)\ W(x)\ \Phi(x)\ \Psi(x) \right\} = \left\{ \tilde{A}\ \tilde{B}\ \tilde{C}\ \tilde{D} \right\} e^{\kappa x}
\tag{17}
$$

When Eqs. (17) are substituted into Eqs. (16), the equivalent algebraic eigenvalue equations are obtained, and the equations have nontrivial solutions when the determinant of the coefficient matrix of $\tilde{A}$, $\tilde{B}$, $\tilde{C}$, and $\tilde{D}$ vanishes. Setting the determinant equal to zero yields the following characteristics equation:

$$
\eta_5\kappa^{10} + \eta_4\kappa^8 + \eta_3\kappa^6 + \eta_2\kappa^4 + \eta_1\kappa^2 + \eta_0 = 0
\tag{18}
$$

Therefore, the fifth-order polynomial equation for the roots χ must be solved, where $\chi = \kappa^2$ has substituted into Eq. (18) to explicitly reduce it into a fifth-order polynomial equation.

$$
\eta_5\chi^5 + \eta_4\chi^4 + \eta_3\chi^3 + \eta_2\chi^2 + \eta_1\chi + \eta_0 = 0,
\tag{19}
$$

Downloaded by [McGill University Library] at 12:00 23 March 2013

where the coefficients η_5, η_4, η_3, η_2, η_1, and η_0 are easily obtained by using the symbolic manipulator Mathematica (Wolfram, 1991) but are not presented here because of their length.

The general solutions to Eqs. (16) are given by

$$\begin{aligned} U(x) &= A_1 e^{\kappa_1 x} + A_2 e^{-\kappa_1 x} + A_3 e^{\kappa_2 x} + A_4 e^{-\kappa_2 x} + A_5 e^{\kappa_3 x} + A_6 e^{-\kappa_3 x} \\ &\quad + A_7 e^{\kappa_4 x} + A_8 e^{-\kappa_4 x} + A_9 e^{\kappa_5 x} + A_{10} e^{-\kappa_5 x} \\ &= \sum_{j=1}^{5} \left(A_{2j-1} e^{\kappa_j x} + A_{2j} e^{-\kappa_j x}\right) \end{aligned} \tag{19a}$$

$$\begin{aligned} W(x) &= B_1 e^{\kappa_1 x} + B_2 e^{-\kappa_1 x} + B_3 e^{\kappa_2 x} + B_4 e^{-\kappa_2 x} + B_5 e^{\kappa_3 x} \\ &\quad + B_6 e^{-\kappa_3 x} + B_7 e^{\kappa_4 x} + B_8 e^{-\kappa_4 x} + B_9 e^{\kappa_5 x} + B_{10} e^{-\kappa_5 x} \\ &= \sum_{j=1}^{5} \left(B_{2j-1} e^{\kappa_j x} + B_{2j} e^{-\kappa_j x}\right) \end{aligned} \tag{19b}$$

$$\begin{aligned} \Phi(x) &= C_1 e^{\kappa_1 x} + C_2 e^{-\kappa_1 x} + C_3 e^{\kappa_2 x} + C_4 e^{-\kappa_2 x} + C_5 e^{\kappa_3 x} \\ &\quad + C_6 e^{-\kappa_3 x} + C_7 e^{\kappa_4 x} + C_8 e^{-\kappa_4 x} + C_9 e^{\kappa_5 x} + C_{10} e^{-\kappa_5 x} \\ &= \sum_{j=1}^{5} \left(C_{2j-1} e^{\kappa_j x} + C_{2j} e^{-\kappa_j x}\right) \end{aligned} \tag{19c}$$

$$\begin{aligned} \Psi(x) &= D_1 e^{\kappa_1 x} + D_2 e^{-\kappa_1 x} + D_3 e^{\kappa_2 x} + D_4 e^{-\kappa_2 x} + D_5 e^{\kappa_3 x} \\ &\quad + D_6 e^{-\kappa_3 x} + D_7 e^{\kappa_4 x} + D_8 e^{-\kappa_4 x} + D_9 e^{\kappa_5 x} + D_{10} e^{-\kappa_{54} x} \\ &= \sum_{j=1}^{5} \left(D_{2j-1} e^{\kappa_j x} + D_{2j} e^{-\kappa_j x}\right) \end{aligned} \tag{19d}$$

where $\kappa_j = \sqrt{\chi_j}$ $(j = 1 \sim 5)$. In the solution of Eq. (19), if any χ_j is zero or repeated from another solution, the solutions to Eqs. (16) will be modified according to the well-known methods for ordinary differential equations with constant coefficients for those particular values of χ_j. From Eqs. (16), only ten of the forty constants are independent. The relations among the constants are given here:

$$\begin{aligned} B_{2j-1} &= t_j A_{2j-1} \quad B_{2j} = -t_j A_{2j} \\ C_{2j-1} &= \bar{t}_j A_{2j-1} \quad C_{2j} = \bar{t}_j A_{2j} \\ D_{2j-1} &= \hat{t}_j A_{2j-1} \quad D_{2j} = \hat{t}_j A_{2j} (j = 1 \sim 5), \end{aligned}$$

where the lengthy expressions of the coefficients t_j, $\bar{t}_j$, and $\hat{t}_j$, which may be obtained using Mathematica (Wolfram, 1991) via symbolic computation, are not given here due to space limitations.

According to the sign convention shown in Fig. 2, the expressions of normal force $N_x(x)$, shear force $Q_{xz}(x)$, bending moment $M_x(x)$, torque

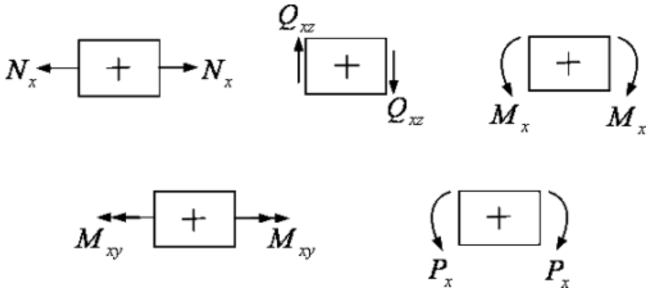

Figure 2. Sign convention for positive normal force $N_x(x)$, shear force $Q_{xz}(x)$, bending moment $M_x(x)$, torque $M_{xy}(x)$, and higher-order moment $P_x(x)$.

$M_{xy}(x)$, and higher-order moment $P_x(x)$ can be obtained from Eqs. (14) and (20) as follows:

$$N_x(x) = \sum_{j=1}^{5}\left[\overline{A}_{11}\kappa_j - \left(\frac{4}{3h^2}\overline{E}_{11} - \overline{B}_{11}\right)\kappa_j\bar{t}_j - \frac{4}{3h^2}\overline{E}_{11}\kappa_j^2 t_j - \left(\frac{4}{3h^2}\overline{E}_{16} - \overline{B}_{16}\right)\kappa_j\hat{t}_j\right]\left(A_{2j-1}e^{\kappa_j x} - A_{2j}e^{-\kappa_j x}\right) \tag{21a}$$

$$\begin{aligned}Q_{xz}(x) = \sum_{j=1}^{5}\Bigg[&-\frac{4}{3h^2}I_4\omega^2 - \left(\frac{4}{3h^2}I_5 - \frac{16}{9h^4}I_7\right)\omega^2\bar{t}_j + \frac{16}{9h^4}I_7\omega^2\kappa_j t_j \\ &-\frac{4}{3h^2}\overline{E}_{11}\kappa_j^2 + \left(\frac{16}{9h^4}\overline{H}_{11} - \frac{4}{3h^2}\overline{F}_{11}\right)\kappa_j^2\bar{t}_j + \frac{16}{9h^4}\overline{H}_{11}\kappa_j^3 t_j \\ &+\left(\frac{16}{9h^4}\overline{H}_{16} - \frac{4}{3h^2}\overline{F}_{16}\right)\kappa_j^2\hat{t}_j + \left(\frac{8}{h^2}D_{55} - A_{55} - \frac{16}{h^4}F_{55}\right) \\ &\left(\bar{t}_j + \kappa_j t_j\right)\Bigg]\left(A_{2j-1}e^{\kappa_j x} + A_{2j}e^{-\kappa_j x}\right)\end{aligned} \tag{21b}$$

$$\begin{aligned}M_x(x) = \sum_{j=1}^{5}\Bigg[&\left(-\overline{B}_{11} + \frac{4}{3h^2}\overline{E}_{11}\right)\kappa_j + \left(\frac{8}{3h^2}\overline{F}_{16} - \overline{D}_{16} - \frac{16}{9h^4}\overline{H}_{16}\right)\kappa_j\hat{t}_j \\ &+\left(\frac{8}{3h^2}\overline{F}_{11} - \overline{D}_{11} - \frac{16}{9h^4}\overline{H}_{11}\right)\kappa_j\bar{t}_j + \left(\frac{4}{3h^2}\overline{F}_{11} - \frac{16}{9h^4}\overline{H}_{11}\right)\kappa_j^2 t_j\Bigg] \\ &\times\left(A_{2j-1}e^{\kappa_j x} - A_{2j}e^{-\kappa_j x}\right)\end{aligned} \tag{21c}$$

$$\begin{aligned}M_{xy}(x) = \sum_{j=1}^{5}\Bigg[&-\left(\frac{4}{3h^2}\overline{F}_{16} - \frac{16}{9h^4}\overline{H}_{16}\right)\kappa_j^2 t_j \\ &-\left(\frac{8}{3h^2}\overline{F}_{16} - \frac{16}{9h^4}\overline{H}_{16} - \overline{D}_{16}\right)\kappa_j\bar{t}_j\end{aligned}$$

Downloaded by [McGill University Library] at 12:00 23 March 2013

Downloaded by [McGill University Library] at 12:00 23 March 2013

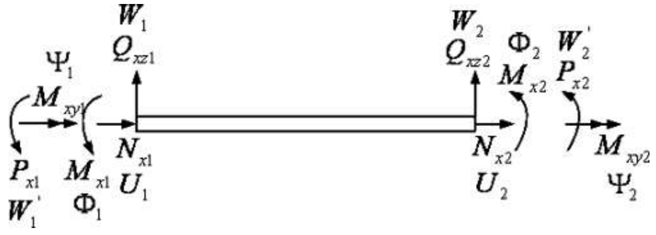

Figure 3. Boundary conditions for displacements and forces of composite beam.

$$-\left(\frac{4}{3h^2}\overline{E}_{16}-\overline{B}_{16}\right)\kappa_j-\left(\frac{8}{3h^2}\overline{F}_{66}-\overline{D}_{66}-\frac{16}{9h^4}\overline{H}_{66}\right)\kappa_j\hat{t}_j\Bigg]$$
$$\times(A_{2j-1}e^{\kappa_j x}-A_{2j}e^{-\kappa_j x}) \tag{21d}$$

$$P_x(x)=\sum_{j=1}^{5}\left[\frac{4}{3h^2}\overline{E}_{11}\kappa_j+\left(\frac{4}{3h^2}\overline{F}_{11}-\frac{16}{9h^4}\overline{H}_{11}\right)\kappa_j\bar{t}_j\right.$$
$$\left.+\left(\frac{4}{3h^2}\overline{F}_{16}-\frac{16}{9h^4}\overline{H}_{16}\right)\kappa_j\hat{t}_j-\frac{16}{9h^4}\overline{H}_{11}\kappa_j^2 t_j\right]$$
$$\times(A_{2j-1}e^{\kappa_j x}-A_{2j}e^{-\kappa_j x}) \tag{21e}$$

Referring to Fig. 3, the boundary conditions for displacements and forces of laminated beam are, respectively,

$$\text{At } x=0: U=U_1 \quad W=W_1 \quad \Phi=\Phi_1 \quad \Psi=\Psi_1 W'=W_1'$$
$$\text{At } x=L: U=U_2 \quad W=W_2 \quad \Phi=\Phi_2 \quad \Psi=\Psi_2 W'=W_2' \tag{22a}$$

$$\text{At } x=0: N_x=-N_{x1} \quad Q_{xz}=Q_{xz1} \quad M_x=M_{x1} \quad M_{xy}=-M_{xy1} \quad P_x=P_{x1}$$
$$\text{At } x=L: N_x=N_{x2} \quad Q_{xz}=-Q_{xz2} \quad M_x=-M_{x2} \quad M_{xy}=M_{xy2}$$
$$P_x=-P_{x2}, \tag{22b}$$

where the superscript primes denote the partial derivatives with respect to x.

Substituting Eqs. (22) into Eqs. (20), the nodal displacements defined in Fig. 3 can be expressed in terms of A_i as follows:

$$\{D\}=[R]\{A\} \tag{23}$$

where $\{D\}$ is the nodal degree-of-freedom vector defined by

$$\{D\}=\left\{U_1\ W_1\ \Phi_1\ \Psi_1\ W_1'\ U_2\ W_2\ \Phi_2\ \Psi_2\ W_2'\right\}^T$$

$$\{A\}=\left\{A_1\ A_3\ A_5\ A_7\ A_9\ A_2\ A_4\ A_6\ A_8\ A_{10}\right\}^T$$

Downloaded by [McGill University Library] at 12:00 23 March 2013

$$[R] = \left[\begin{matrix} 1 & 1 & 1 & 1 & 1 \\ t_1 & t_2 & t_3 & t_4 & t_5 \\ \bar{t}_1 & \bar{t}_2 & \bar{t}_3 & \bar{t}_4 & \bar{t}_5 \\ \hat{t}_1 & \hat{t}_2 & \hat{t}_3 & \hat{t}_4 & \hat{t}_5 \\ \kappa_1 t_1 & \kappa_2 t_2 & \kappa_3 t_3 & \kappa_4 t_4 & \kappa_5 t_5 \\ e^{\kappa_1 L} & e^{\kappa_2 L} & e^{\kappa_3 L} & e^{\kappa_4 L} & e^{\kappa_5 L} \\ t_1 e^{\kappa_1 L} & t_2 e^{\kappa_2 L} & t_3 e^{\kappa_3 L} & t_4 e^{\kappa_4 L} & t_5 e^{\kappa_5 L} \\ \bar{t}_1 e^{\kappa_1 L} & \bar{t}_2 e^{\kappa_2 L} & \bar{t}_3 e^{\kappa_3 L} & \bar{t}_4 e^{\kappa_4 L} & \bar{t}_5 e^{\kappa_5 L} \\ \hat{t}_1 e^{\kappa_1 L} & \hat{t}_2 e^{\kappa_2 L} & \hat{t}_3 e^{\kappa_3 L} & \hat{t}_4 e^{\kappa_4 L} & \hat{t}_5 e^{\kappa_5 L} \\ \kappa_1 t_1 e^{\kappa_1 L} & \kappa_2 t_2 e^{\kappa_2 L} & \kappa_3 t_3 e^{\kappa_3 L} & \kappa_4 t_4 e^{\kappa_4 L} & \kappa_5 t_5 e^{\kappa_5 L} \end{matrix}\right.$$

$$\left.\begin{matrix} 1 & 1 & 1 & 1 & 1 \\ -t_1 & -t_2 & -t_3 & -t_4 & -t_5 \\ \bar{t}_1 & \bar{t}_2 & \bar{t}_3 & \bar{t}_4 & \bar{t}_5 \\ \hat{t}_1 & \hat{t}_2 & \hat{t}_3 & \hat{t}_4 & \hat{t}_5 \\ \kappa_1 t_1 & \kappa_2 t_2 & \kappa_3 t_3 & \kappa_4 t_4 & \kappa_5 t_5 \\ e^{-\kappa_1 L} & e^{-\kappa_2 L} & e^{-\kappa_3 L} & e^{-\kappa_4 L} & e^{-\kappa_5 L} \\ -t_1 e^{-\kappa_1 L} & -t_2 e^{-\kappa_2 L} & -t_3 e^{-\kappa_3 L} & -t_4 e^{-\kappa_4 L} & -t_5 e^{-\kappa_5 L} \\ \bar{t}_1 e^{-\kappa_1 L} & \bar{t}_2 e^{-\kappa_2 L} & \bar{t}_3 e^{-\kappa_3 L} & \bar{t}_4 e^{-\kappa_4 L} & \bar{t}_5 e^{-\kappa_5 L} \\ \hat{t}_1 e^{-\kappa_1 L} & \hat{t}_2 e^{-\kappa_2 L} & \hat{t}_3 e^{-\kappa_3 L} & \hat{t}_4 e^{-\kappa_4 L} & \hat{t}_5 e^{-\kappa_5 L} \\ \kappa_1 t_1 e^{-\kappa_1 L} & \kappa_2 t_2 e^{-\kappa_2 L} & \kappa_3 t_3 e^{-\kappa_3 L} & \kappa_4 t_4 e^{-\kappa_4 L} & \kappa_5 t_5 e^{-\kappa_5 L} \end{matrix}\right]$$

With Eqs. (26b) substituted into Eqs. (21), the nodal forces defined in Fig. 3 can be expressed in terms of A_i as

$$\{F\} = [H]\{A\} \tag{24}$$

where $\{F\}$ is the nodal force vector defined by

$$\{F\} = \left\{N_{x1}\ Q_{xz1}\ M_{x1}\ M_{xy1}\ P_{x1}\ N_{x2}\ Q_{xz2}\ M_{x2}\ M_{xy2}\ P_{x2}\right\}^T$$

$$[H] = \left[\begin{matrix} -\tilde{t}_1 & -\tilde{t}_2 & -\tilde{t}_3 & -\tilde{t}_4 & -\tilde{t}_5 \\ \bar{\bar{t}}_1 & \bar{\bar{t}}_2 & \bar{\bar{t}}_3 & \bar{\bar{t}}_4 & \bar{\bar{t}}_5 \\ \hat{\hat{t}}_1 & \hat{\hat{t}}_2 & \hat{\hat{t}}_3 & \hat{\hat{t}}_4 & \hat{\hat{t}}_5 \\ -\tilde{\tilde{t}}_1 & -\tilde{\tilde{t}}_2 & -\tilde{\tilde{t}}_3 & -\tilde{\tilde{t}}_4 & -\tilde{\tilde{t}}_5 \\ \hat{\bar{t}}_1 & \hat{\bar{t}}_2 & \hat{\bar{t}}_3 & \hat{\bar{t}}_4 & \hat{\bar{t}}_5 \\ \tilde{t}_1 e^{\kappa_1 L} & \tilde{t}_2 e^{\kappa_2 L} & \tilde{t}_3 e^{\kappa_3 L} & \tilde{t}_4 e^{\kappa_4 L} & \tilde{t}_5 e^{\kappa_5 L} \\ -\bar{\bar{t}}_1 e^{\kappa_1 L} & -\bar{\bar{t}}_2 e^{\kappa_2 L} & -\bar{\bar{t}}_3 e^{\kappa_3 L} & -\bar{\bar{t}}_4 e^{\kappa_4 L} & -\bar{\bar{t}}_5 e^{\kappa_5 L} \\ -\hat{\hat{t}}_1 e^{\kappa_1 L} & -\hat{\hat{t}}_2 e^{\kappa_2 L} & -\hat{\hat{t}}_3 e^{\kappa_3 L} & -\hat{\hat{t}}_4 e^{\kappa_4 L} & -\hat{\hat{t}}_5 e^{\kappa_5 L} \\ \tilde{\tilde{t}}_1 e^{\kappa_1 L} & \tilde{\tilde{t}}_2 e^{\kappa_2 L} & \tilde{\tilde{t}}_3 e^{\kappa_3 L} & \tilde{\tilde{t}}_4 e^{\kappa_4 L} & \tilde{\tilde{t}}_5 e^{\kappa_5 L} \\ -\hat{\bar{t}}_1 e^{\kappa_1 L} & -\hat{\bar{t}}_2 e^{\kappa_2 L} & -\hat{\bar{t}}_3 e^{\kappa_3 L} & -\hat{\bar{t}}_4 e^{\kappa_4 L} & -\hat{\bar{t}}_5 e^{\kappa_5 L} \end{matrix}\right.$$

Downloaded by [McGill University Library] at 12:00 23 March 2013

$$\left.\begin{matrix}
\tilde{t}_1 & \tilde{t}_2 & \tilde{t}_3 & \tilde{t}_4 & \tilde{t}_5 \\
\bar{\bar{t}}_1 & \bar{\bar{t}}_2 & \bar{\bar{t}}_3 & \bar{\bar{t}}_4 & \bar{\bar{t}}_5 \\
-\hat{\hat{t}}_1 & -\hat{\hat{t}}_2 & -\hat{\hat{t}}_3 & -\hat{\hat{t}}_4 & -\hat{\hat{t}}_5 \\
-\tilde{\tilde{t}}_1 & -\tilde{\tilde{t}}_2 & -\tilde{\tilde{t}}_3 & -\tilde{\tilde{t}}_4 & -\tilde{\tilde{t}}_5 \\
-\hat{\bar{t}}_1 & -\hat{\bar{t}}_2 & -\hat{\bar{t}}_3 & -\hat{\bar{t}}_4 & -\hat{\bar{t}}_5 \\
-\tilde{t}_1 e^{-\kappa_1 L} & -\tilde{t}_2 e^{-\kappa_2 L} & -\tilde{t}_3 e^{-\kappa_3 L} & -\tilde{t}_4 e^{-\kappa_4 L} & -\tilde{t}_5 e^{-\kappa_5 L} \\
-\bar{\bar{t}}_1 e^{-\kappa_1 L} & -\bar{\bar{t}}_2 e^{-\kappa_2 L} & -\bar{\bar{t}}_3 e^{-\kappa_3 L} & -\bar{\bar{t}}_4 e^{-\kappa_4 L} & -\bar{\bar{t}}_5 e^{-\kappa_5 L} \\
\hat{\hat{t}}_1 e^{-\kappa_1 L} & \hat{\hat{t}}_2 e^{-\kappa_2 L} & \hat{\hat{t}}_3 e^{-\kappa_3 L} & \hat{\hat{t}}_4 e^{-\kappa_4 L} & \hat{\hat{t}}_5 e^{-\kappa_5 L} \\
-\tilde{\tilde{t}}_1 e^{-\kappa_1 L} & -\tilde{\tilde{t}}_2 e^{-\kappa_2 L} & -\tilde{\tilde{t}}_3 e^{-\kappa_3 L} & -\tilde{\tilde{t}}_4 e^{-\kappa_4 L} & -\tilde{\tilde{t}}_5 e^{-\kappa_5 L} \\
\hat{\bar{t}}_1 e^{-\kappa_1 L} & \hat{\bar{t}}_2 e^{-\kappa_2 L} & \hat{\bar{t}}_3 e^{-\kappa_3 L} & \hat{\bar{t}}_4 e^{-\kappa_4 L} & \hat{\bar{t}}_5 e^{-\kappa_5 L}
\end{matrix}\right]$$

where

$$\tilde{t}_j = \overline{A}_{11}\kappa_j - \left(\frac{4}{3h^2}\overline{E}_{11} - \overline{B}_{11}\right)\kappa_j\bar{t}_j - \frac{4}{3h^2}\overline{E}_{11}\kappa_j^2 t_j - \left(\frac{4}{3h^2}\overline{E}_{16} - \overline{B}_{16}\right)\kappa_j\hat{t}_j$$

$$\begin{aligned}
\bar{\bar{t}}_j = {} & -\frac{4}{3h^2}I_4\omega^2 - \left(\frac{4}{3h^2}I_5 - \frac{16}{9h^4}I_7\right)\omega^2\bar{t}_j + \frac{16}{9h^4}I_7\omega^2\kappa_j t_j - \frac{4}{3h^2}\overline{E}_{11}\kappa_j^2 \\
& + \left(\frac{16}{9h^4}\overline{H}_{11} - \frac{4}{3h^2}\overline{F}_{11}\right)\kappa_j^2\bar{t}_j + \frac{16}{9h^4}\overline{H}_{11}\kappa_j^3 t_j + \left(\frac{16}{9h^4}\overline{H}_{16} - \frac{4}{3h^2}\overline{F}_{16}\right)\kappa_j^2\hat{t}_j \\
& + \left(\frac{8}{h^2}D_{55} - A_{55} - \frac{16}{h^4}F_{55}\right)\left(\bar{t}_j + \kappa_j t_j\right)
\end{aligned}$$

$$\begin{aligned}
\hat{\hat{t}}_j = {} & \left(-\overline{B}_{11} + \frac{4}{3h^2}\overline{E}_{11}\right)\kappa_j + \left(\frac{8}{3h^2}\overline{F}_{16} - \overline{D}_{16} - \frac{16}{9h^4}\overline{H}_{16}\right)\kappa_j\hat{t}_j \\
& + \left(\frac{8}{3h^2}\overline{F}_{11} - \overline{D}_{11} - \frac{16}{9h^4}\overline{H}_{11}\right)\kappa_j\bar{t}_j + \left(\frac{4}{3h^2}\overline{F}_{11} - \frac{16}{9h^4}\overline{H}_{11}\right)\kappa_j^2 t_j
\end{aligned}$$

$$\begin{aligned}
\tilde{\tilde{t}}_j = {} & -\left(\frac{4}{3h^2}\overline{E}_{16} - \overline{B}_{16}\right)\kappa_j - \left(\frac{4}{3h^2}\overline{F}_{16} - \frac{16}{9h^4}\overline{H}_{16}\right)\kappa_j^2 t_j \\
& - \left(\frac{8}{3h^2}\overline{F}_{16} - \frac{16}{9h^4}\overline{H}_{16} - \overline{D}_{16}\right)\kappa_j\bar{t}_j - \left(\frac{8}{3h^2}\overline{F}_{66} - \overline{D}_{66} - \frac{16}{9h^4}\overline{H}_{66}\right)\kappa_j\hat{t}_j
\end{aligned}$$

$$\begin{aligned}
\hat{\bar{t}}_j = {} & \frac{4}{3h^2}\overline{E}_{11}\kappa_j + \left(\frac{4}{3h^2}\overline{F}_{11} - \frac{16}{9h^4}\overline{H}_{11}\right)\kappa_j\bar{t}_j + \left(\frac{4}{3h^2}\overline{F}_{16} - \frac{16}{9h^4}\overline{H}_{16}\right)\kappa_j\hat{t}_j \\
& - \frac{16}{9h^4}\overline{H}_{11}\kappa_j^2 t_j
\end{aligned}$$

$$(j = 1 \sim 5)$$

Eliminating the coefficients A_i from Eqs. (23) and (24) gives the following relationship between the nodal forces and nodal displacements:

$$\{F\} = [H][R]^{-1}\{D\} = [K]\{D\}, \tag{25}$$

where $[K]$ is the frequency-dependent dynamic stiffness matrix. Because matrix $[R]$ is a 10×10 matrix, it is very difficult to obtain the closed form of the inverse of $[R]$ directly using a personal computer. However, the inverse of $[R]$ can be determined in partitioned form. First, matrix $[R]$ is partitioned into $\begin{bmatrix} [R_1] & [R_2] \\ [R_3] & [R_4] \end{bmatrix}$, with $[R_i]$ a 5×5 matrix. Then,

$$[R]^{-1} = \begin{bmatrix} [I]_5 & -[R_1]^{-1}[R_2] \\ [0]_{5\times5} & [I]_5 \end{bmatrix} \begin{bmatrix} [R_1]^{-1} & [0]_{5\times5} \\ [0]_{5\times5} & ([R_4] - [R_3][R_1]^{-1}[R_2])^{-1} \end{bmatrix} \times \begin{bmatrix} [I]_5 & [0]_{5\times5} \\ -[R_3][R_1]^{-1} & [I]_5 \end{bmatrix}$$

where $[I]_5$ is a 5×5 identity matrix and $[0]_{5\times5}$ is a 5×5 matrix composed entirely of 0s. An advantage of using the above equation to evaluate the inverse of the 10×10 matrix $[R]$ is that the matrices to be inverted have orders only of five, and their closed forms can be obtained using Mathematica (Wolfram, 1991) via symbolic computation. Once the closed form of $[R]^{-1}$ is determined, the closed form of the dynamic stiffness matrix $[K] = [H][R]^{-1}$ can be obtained directly. Although the expressions of the elements of dynamic stiffness matrix $[K]$ are obtained by using the symbolic manipulator Mathematica, they are not presented here because of their length.

NEWTON'S EIGENVALUE ITERATION METHOD

Once the dynamic stiffness matrix is obtained, the appropriate boundary conditions for the particular composite beam under consideration are applied to obtain the transcendental eigenvalue problem $[\bar{K}(\omega)]\{\overline{D}\} = 0$. A simple Newton's eigenvalue iteration method Singh and Ram (2002) is adopted in present study to determine all the natural frequencies in a given frequency band. A visual method involving plotting the characteristic determinant curve to visually approximate where the value of the determinant equals zero is also implemented.

Now consider the problem of determining the nontrivial solutions ω and $\{\overline{D}\} \neq 0$ of $[\bar{K}(\omega)]\{\overline{D}\} = 0$ by means of Newton's eigenvalue iteration method, where the elements of matrix $[\bar{K}]$ are transcendental functions in ω and $\{\overline{D}\}$ is a constant eigenvector. Following Yang (1983), we define $[\underline{\bar{K}}(\omega)] = -\frac{d[\bar{K}(\omega)]}{d\omega}$. Newton's eigenvalue iteration algorithm can be summarized as follows: (a) choose an initial guess

Downloaded by [McGill University Library] at 12:00 23 March 2013

Downloaded by [McGill University Library] at 12:00 23 March 2013

$\omega^{(0)}$; (b) compute the eigenvalues of $\left[[\bar{K}(\omega^{(i-1)})] - \lambda[\bar{\bar{K}}(\omega^{(i-1)})]\right]\{\overline{D}^{(i)}\} = 0$ based upon the initial guess $\omega^{(0)}$; (c) assign the minimum eigenvalue to ε; (d) compute the new estimate $\omega^{(1)} = \omega^{(0)} + \varepsilon$; (e) compute the matrices $[\bar{K}(\omega)]$ and $[\bar{\bar{K}}(\omega)]$ by substituting $\omega = \omega^{(1)}$; (f) repeat steps (b)–(e) until the mth iteration until $|\varepsilon|$ is less than the prescribed tolerance for convergence; (g) store the value of $\omega^{(m)}$; (h) repeat steps (a)–(g) to evaluate another $\omega^{(m)}$ for different initial value $\omega^{(0)}$. In order to ensure that no natural frequencies of the structure being analyzed are missed, the solutions obtained by the Newton's eigenvalue iteration method are checked using the Sturm sequence property of the dynamic stiffness matrix, which states that the number of natural frequencies that are less than a specific value ω_0 is equal to the number of negative elements on the main diagonal of the matrix $[\bar{K}(\omega_0)]$, which has been triangulated by means of Gauss elimination without interchanges. When the natural frequency is located, the corresponding eigenvector can be obtained by inverse iteration.

NUMERICAL RESULTS AND DISCUSSIONS

In order to demonstrate the correctness and accuracy of the proposed dynamic stiffness formulation, the free vibration characteristics of several generally laminated composite beams are investigated.

The following five boundary conditions: clamped-clamped, clamped–simply supported, free-free, clamped-free and simply supported are considered in this section.

$$\text{Clamped edge}: U = W = \Phi = \Psi = W' = 0$$

$$\text{Simply supported edge}: U = W = \Psi = M_x = P_x = 0$$

$$\text{Free edge}: N_x = Q_{xz} = M_x = M_{xy} = P_x = 0$$

The first illustrative example chosen to compute the numerical results is that of a glass-polyester laminated composite beam of rectangular cross-section with lay-up scheme [45°/45°/45°/45°]. The properties of the beam are given as follows:

$$E_1 = 37.41 \times 10^9\,\text{Pa}, \quad E_2 = 13.67 \times 10^9\,\text{Pa}, \quad G_{12} = 5.478 \times 10^9\,\text{Pa},$$
$$G_{13} = 6.03 \times 10^9\,\text{Pa}$$
$$G_{23} = 6.666 \times 10^9\,\text{Pa}, \quad \nu_{12} = 0.3 \quad \rho = 1968.9\,\text{kg/m}^3$$
$$L = 0.111798\,\text{m}, \quad b = 12.7 \times 10^{-3}\,\text{m}, \quad h = 3.38 \times 10^{-3}\,\text{m}$$

The first four natural frequencies of the beam with various boundary conditions are computed and the numerical results are displayed in

Table 1. Natural frequencies (in Hz) of glass-polyester beam

			Free-free				
Mode no.	Clamped-clamped	Clamped–simply supported	Present	Teboub and Hajela (1995)	Ritchie et al. (1975)	Clamped-free	Simply supported
1	763.6	530.1	765.4	765.4	767.9	120.6	348.1
2	2089.0	1701.5	2097.4	2097.3	2091.9	752.8	1346.8
3	4054.1	3516.2	4075.7	4075.5	4155.9	2094.0	3018.8
4	6617.9	5941.1	6662.4	6662.1	6762.7	4064.4	5287.9

Tables 1 and 2, along with the numerical solutions of the first-order shear deformation beam model of Teboub and Hajela (1995) and the experimental results of Ritchie et al. (1975). The Poisson effect is considered in Table 1 but ignored in Table 2.

It can be seen from the comparison shown in Table 1 that present results agree very well with the numerical solutions of first-order shear deformation theory of Teboub and Hajela (1995) and the experimental results of Ritchie et al. (1975). Table 1 also shows the effect of boundary condition on the first four natural frequencies of the beam. Of the five boundary conditions considered, the clamped-free beam exhibits the lowest frequencies, as expected. It can be observed from Tables 1 and 2 that the Poisson effect is seen to have a relatively important influence on the natural frequencies of this particular beam for all the boundary conditions. The comparison indicates that the maximum relative error of the natural frequencies obtained by neglecting Poisson effect is about 11%.

In order to investigate the effect of slenderness on the natural frequencies of generally layered composite beams, a variety of results are presented for a [30°/50°/30°/50°] laminated beam for which some available solutions exist. Unless mentioned otherwise, the mechanical

Table 2. Natural frequencies (in Hz) of glass-polyester beam without Poisson effect included

			Free-free			
Mode no.	Clamped-clamped	Clamped–simply supported	Present	Teboub and Hajela (1995)	Clamped-free	Simply supported
1	822.0	575.2	824.2	823.7	129.9	390.8
2	2246.0	1834.2	2256.5	2255.0	810.4	1448.9
3	4352.2	3780.3	4378.5	4375.4	2252.0	3261.2
4	7091.4	6369.6	7146.2	7140.8	4364.3	5661.4

Downloaded by [McGill University Library] at 12:00 23 March 2013

Downloaded by [McGill University Library] at 12:00 23 March 2013

Table 3. Natural frequencies (in Hz) of [30°/50°/30°/50°] composite beam with $L = 0.381\,\mathrm{m}$

	Clamped-clamped					
Mode no.	Present	Chandrashekhara and Bangera (1992)	Clamped–simply supported	Free-free	Clamped-free	Simply supported
1	638.4	640.5	467.4	654.9	105.3	353.5
2	1651.6	1666.8	1392.4	1718.9	635.2	1114.1
3	3013.5	3059.5	2690.8	3129.2	1680.8	2433.3
4	3932.6	3397.8	3775.6	3987.1	1981.7	3461.7
5	4619.1	4712.5	4377.5	4838.3	2496.0	4263.5

properties of the beam used for this analysis are those shown below:

$$E_1 = 144.80 \times 10^9\,\mathrm{Pa}, \quad E_2 = 9.65 \times 10^9\,\mathrm{Pa},$$
$$G_{12} = G_{13} = 4.14 \times 10^9\,\mathrm{Pa}, \quad \nu_{12} = 0.3$$
$$G_{23} = 3.45 \times 10^9\,\mathrm{Pa}, \quad \rho = 1389.23\,\mathrm{kg/m^3},$$
$$b = 25.4 \times 10^{-3}\,\mathrm{m},\ h = 25.4 \times 10^{-3}\,\mathrm{m}$$

The free vibration behavior of the beam is studied for two different beam lengths $L = 0.381$ m and $L = 0.572$ m. The dynamic stiffness model is used to compute the natural frequencies of the beam with a variety of support conditions. The computed values of the first five natural frequencies of the beam are shown in Tables 3 and 4, along with the available solutions for the clamped-clamped boundary condition.

As can be seen from Table 3, the natural frequencies predicted by present method are in good agreement with the available results for the clamped-clamped beam except for the fourth natural frequency. The author believes that the fourth frequency of Chandrashekhara and Bangera (1992) is misprinted. It can be observed from Tables 3 and 4

Table 4. Natural frequencies (in Hz) of [30°/50°/30°/50°] composite beam with $L = 0.572$ m

Mode no.	Clamped-clamped	Clamped–simply supported	Free-free	Clamped-free	Simply supported
1	291.8	211.3	295.4	46.9	158.4
2	779.6	648.4	795.4	288.8	512.4
3	1470.2	1296.9	1504.6	787.2	1150.5
4	2323.5	2100.3	2391.2	1315.0	1863.3
5	2629.1	2588.4	2634.0	1491.1	2578.4

Downloaded by [McGill University Library] at 12:00 23 March 2013

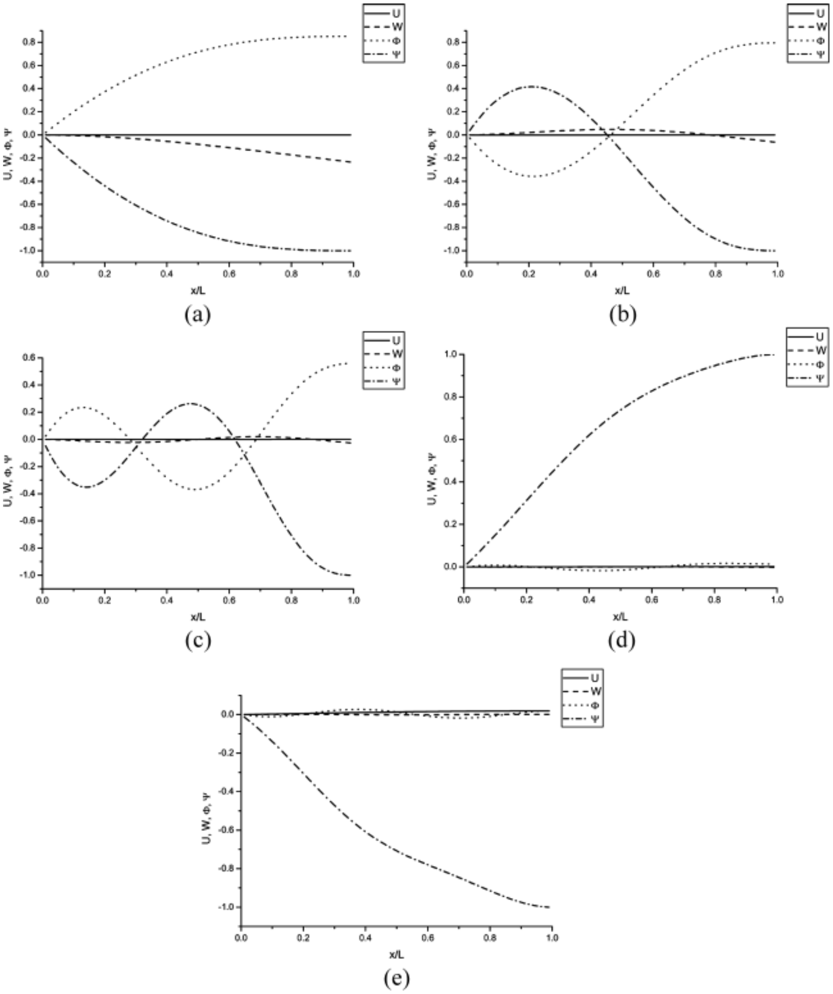

(a)

(b)

(c)

(d)

(e)

Figure 4. First five normal mode shapes of clamped-free composite beam with $L = 0.381$ m: (a) mode 1; (b) mode 2; (c) mode 3; (d) mode 4; (e) mode 5.

that the slenderness has a significant effect on the natural frequencies of the beam for all the boundary conditions. The natural frequencies decrease with the increase of beam length, as expected. The difference will tend to decrease in the higher modes of vibration.

For the clamped-free boundary condition, the first five normal mode shapes of the composite beam with $L = 0.381\,\text{m}$ and $L = 0.572\,\text{m}$ are computed and the numerical results are plotted in Figs. 4 and 5, respectively. The effect of slenderness on the mode shapes of the composite beam is obvious, especially for the third and fifth mode shapes.

Downloaded by [McGill University Library] at 12:00 23 March 2013

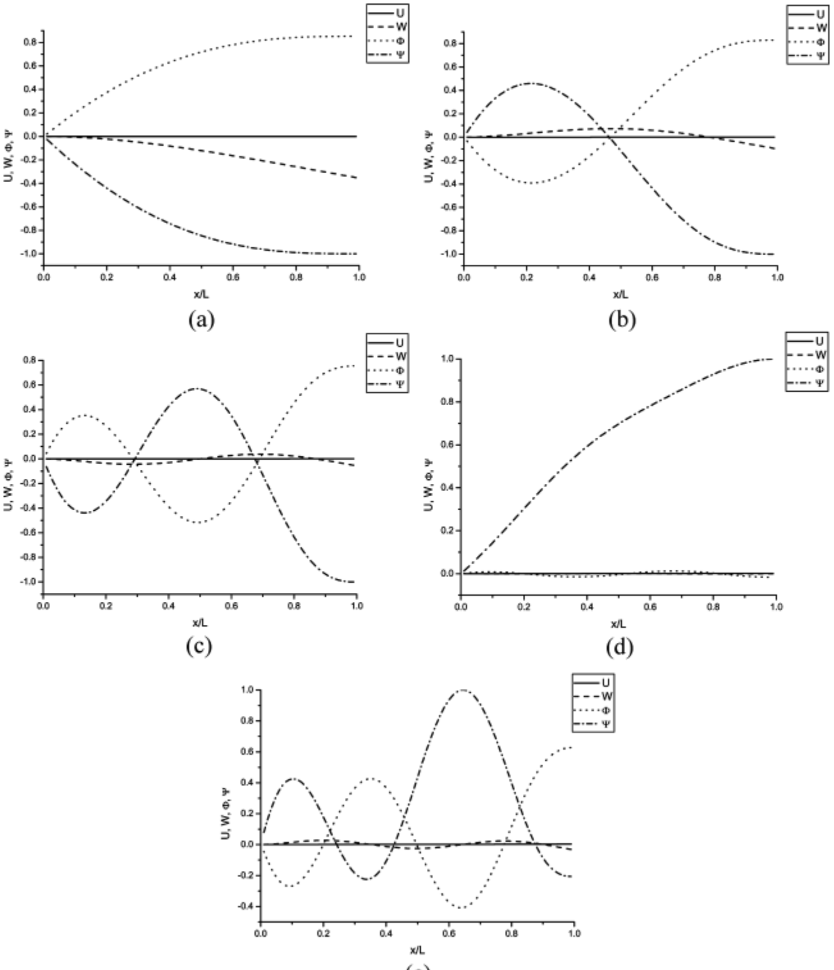

(a) (b) (c) (d) (e)

Figure 5. First five normal mode shapes of clamped-free composite beam with $L = 0.572\text{m}$: (a) mode 1; (b) mode 2; (c) mode 3; (d) mode 4; (e) mode 5.

The third example is a laminated composite beam with lay-up sequence [30°/−60°/30°/−60°], which is known to be hygrothermally curvature stable. The geometric and material properties of the beam are given below:

$$E_2 = 6.9 \times 10^9\,\text{Pa}, \quad G_{12} = 4.8 \times 10^9\,\text{Pa}, \quad G_{13} = 4.14 \times 10^9\,\text{Pa},$$

$$G_{23} = 3.45 \times 10^9\,\text{Pa}$$

$$v_{12} = 0.3 \quad \rho = 1550.1\,\text{kg/m}^3, \quad \text{L} = 0.381\,\text{m}, b = 25.4 \times 10^{-3}\,\text{m},$$

$$h = 25.4 \times 10^{-3}\,\text{m}$$

Table 5. Natural frequencies (in Hz) of composite beam with $E_1 = 138 \times 10^9$ Pa

	Clamped-clamped					
Mode no.	Present	Teboub and Hajela (1995)	Clamped–simply supported	Free-free	Clamped-free	Simply supported
1	614.0	600.9	450.4	632.4	101.5	341.6
2	1587.5	1554.0	1343.1	1660.6	612.2	1078.7
3	2895.0	2832.3	2601.2	3042.3	1622.4	2350.0
4	4425.6	5138.3	4057.9	4525.5	2262.5	3657.0
5	4522.7	N/A	4514.1	4686.5	2612.6	4505.9
6	5210.9	N/A	5108.1	5219.4	2979.7	5079.9

Note: N/A denotes the result not available.

In order to illustrate the effect of material anisotropy on the natural frequencies of the beam, two different numerical values of E_1, that is, $E_1 = 138 \times 10^9$ Pa and $E_1 = 303 \times 10^9$ Pa, are investigated.

In Table 5, the first six natural frequencies of the beam with $E_1 = 138 \times 10^9$ Pa are displayed. Five different boundary conditions are considered. The numerical results for clamped-clamped beam compare well with the results reported in Teboub and Hajela (1995), except for the fourth natural frequency. An apparent discrepancy exists between the fourth frequency predicted by Teboub and Hajela (1995) and the one predicted by present method. It is believed that the result of Teboub and Hajela (1995), obtained by first-order shear deformation theory, is a mistake. It seems that the fourth frequency of Teboub and Hajela (1995) should be the sixth one.

The first six natural frequencies of the composite beam with $E_1 = 303 \times 10^9$ Pa are shown in Table 6. Good correlation exists between the values

Table 6. Natural frequencies (in Hz) of composite beam with E_1=303×10^9 Pa

	Clamped-clamped					
Mode no.	Present	Teboub and Hajela (1995)	Clamped–simply supported	Free-free	Clamped-free	Simply supported
1	647.9	629.2	498.1	668.4	107.6	420.9
2	1666.7	1617.4	1432.7	1747.2	646.3	1134.1
3	3026.6	2931.1	2740.3	3184.2	1704.9	2528.7
4	4618.3	4459.7	4278.2	4884.0	2505.1	3833.4
5	5009.4	N/A	5004.7	5009.8	3089.5	4999.9
6	6375.4	N/A	5894.4	6530.3	3512.1	5792.0

Downloaded by [McGill University Library] at 12:00 23 March 2013

available in Teboub and Hajela (1995) and those calculated with the present method, as can be seen from the second and third columns of Table 6. It can be noticed from the results displayed in Tables 5 and 6 that increasing the in-plane tensile modulus will result in an increase in the natural frequency for all the boundary conditions. Changing the in-plane tensile modulus from $E_1 = 138 \times 10^9$ Pa to $E_1 = 303 \times 10^9$ Pa increases the fundamental frequency of the simply supported beam by approximately 20%.

Downloaded by [McGill University Library] at 12:00 23 March 2013

CONCLUSIONS

The dynamic stiffness method has been introduced for the free vibration analysis of generally laminated composite beams using third-order shear deformation theory. An exact dynamic stiffness matrix has been formulated by directly solving the governing differential equations of motion of the beam in free vibration. Although the expressions of the elements of the dynamic stiffness matrix have been obtained in partitioned form by using the symbolic manipulator Mathematica, they are not presented here because of their length. A Mathematica code has been developed to generate the closed form of the dynamic stiffness and to solve for the transcendental eigenvalue problem using Newton's eigenvalue iteration method. The validity of the results obtained from the present method has been established by comparing with the existing solutions in the literature. The importance of the Poisson effect on the analysis of one-dimensional laminated beams has been demonstrated. Also, various results have been presented to show the effects of slenderness, boundary condition, and material anisotropy on the natural frequencies of generally layered composite beams. It is expected that the present method will enable both free and forced vibration analyses of both an individual composite beam and an assembly of composite beams.

ACKNOWLEDGMENT

The authors would like to thank the reviewers for their helpful and important comments and suggestions.

REFERENCES

Abramovich, H., Livshits, A. (1994). Free vibration of non-symmetric cross-ply laminated composite beams. *Journal of Sound and Vibration* 176:597–612.

Arya, H., Shimpi, R. P., Naik, N. K. (2002). A zigzag model for laminated composite beams. *Composite Structures* 56:21–24.

Aydogdu, M. (2005). Vibration analysis of cross-ply laminated beams with general boundary conditions by Ritz method. *International Journal of Mechanical Sciences* 47:1740–1755.

Aydogdu, M. (2006). Free vibration analysis of angle-ply laminated beams with general boundary conditions. *Journal of Reinforced Plastics and Composites* 25:1571–1583.

Banerjee, J. R., Williams, F. W. (1996). Exact dynamic stiffness matrix for composite Timoshenko beams with applications. *Journal of Sound and Vibration* 194:573–585.

Bhimaraddi, A., Chandrashekhara, K. (1991). Some observations on the modeling of laminated composite beams with general lay-ups. *Composite Structures* 19:371–380.

Chakraborty, A., Mahapatra, D. R., Gopalakrishnan, S. (2002). Finite element analysis of free vibration and wave propagation in asymmetric composite beams with structural discontinuities. *Composite Structures* 55:23–36.

Chandrashekhara, K., Bangera, K. M. (1992). Free vibration of composite beams using a refined shear flexible beam element. *Computers and Structures* 43:719–727.

Chandrashekhara, K., Krishnamurthy, K., Roy, S. (1990). Free vibration of composite beams including rotary inertia and shear deformation. *Composite Structures* 14:269–279.

Eisenberger, M., Abramovich, H., Shulepov, O. (1995). Dynamic stiffness analysis of laminated beams using first order shear deformation theory. *Composite Structures* 31:265–271.

Ghugal, Y. M., Shimpi, R. P. (2001). A review of refined shear deformation theories for isotropic and anisotropic laminated beams. *Journal of Reinforced Plastics and Composites* 20:255–272.

Jones, R. M. (1976). *Mechanics of Composite Materials*. New York: McGraw-Hill.

Kant, T., Marur, S. R., Rao, G. S. (1997). Analytical solution to the dynamic analysis of laminated beams using higher order refined theory. *Composite Structures* 40:1–9.

Kapania, R. K., Raciti, S. (1989). Recent advances in analysis of laminated beams and plates: Part I. Shear effects and buckling; Part II. Vibrations and wave propagation. *AIAA Journal* 27:923–946.

Karama, M., Afaq, K. S., Mistou, S. (2003). Mechanical behaviour of laminated composite beam by the new multi-layered laminated composite structures model with transverse shear stress continuity. *International Journal of Solids and Structures* 40:1525–1546.

Khdeir, A. A., Reddy, J. N. (1994). Free vibration of cross-ply laminated beams with arbitrary boundary conditions. *International Journal of Engineering Science* 32:1971–1980.

Downloaded by [McGill University Library] at 12:00 23 March 2013

Downloaded by [McGill University Library] at 12:00 23 March 2013

Krishnaswamy, S., Chandrashekhara, K., Wu, W. Z. B. (1992). Analytical solutions to vibration of generally layered composite beams. *Journal of Sound and Vibration* 159:85–99.

Mahapatra, D. R., Gopalakrishnan, S. (2003). A spectral finite element model for analysis of axial-flexural-shear coupled wave propagation in laminated composite beams. *Composite Structures* 59:67–88.

Marur, S. R., Kant, T. (1997). On the performance of higher order theories for transient dynamic analysis of sandwich and composite beams. *Computers and Structures* 65:741–759.

Matsunaga, H. (2001). Vibration and buckling of multilayered composite beams according to higher order deformation theories. *Journal of Sound and Vibration* 246:47–62.

Murthy, M. V. V. S., Mahapatra, D. R., Badarinarayana, K., Gopalakrishnan, S. (2005). A refined higher order finite element for asymmetric composite beams. *Composite Structures* 67:27–35.

Rao, M. K., Desai, Y. M., Chitnis, M. R. (2001). Free vibrations of laminated beams using mixed theory. *Composite Structures* 52:149–160.

Reddy, J. N. (2004). *Mechanics of Laminated Composite Plates and Shells: Theory and Analysis*, 2nd ed. Boca Raton, Florida: CRC Press

Ritchie, I. G., Rosinger, H. E., Shillinglaw, A. J., Fleury, W. H. (1975). The dynamic elastic behaviour of a fiber reinforced composite sheet: Part I. The precise experimental determination of the principal elastic moduli. *Journal of Physics D - Applied Physics* 8:1733–1749.

Ruotolo, R. (2004). A spectral element for laminated composite beams: Theory and application to pyroshock analysis. *Journal of Sound and Vibration* 270:149–169.

Shi, G., Lam, K. Y. (1999). Finite element vibration analysis of composite beams based on higher-order beam theory. *Journal of Sound and Vibration* 219:707–721.

Shimpi, R. P., Ainapure, A. V. (1999). Free vibration analysis of two layered cross-ply laminated beams using layer-wise trigonometric shear deformation theory. *Communications in Numerical Methods in Engineering* 15:651–660.

Shimpi, R. P., Ainapure, A. V. (2001). A beam finite element based on layerwise trigonometric shear deformation theory. *Composite Structures* 53:153–162.

Singh, M. P., Abdelnassar, A. S. (1992). Random response of symmetric cross-ply composite beams with arbitrary boundary conditions. *AIAA Journal* 30:1081–1088.

Singh, R. V., Ram, Y. M. (2002). Transcendental eigenvalue problem and its applications. *AIAA Journal* 40:1402–1407.

Soldatos, K. P., Elishakoff, I. (1992). A transverse shear and normal deformable orthotropic beam theory. *Journal of Sound and Vibration* 154:528–533.

Song, S. J., Waas, A. M. (1997). Effects of shear deformation on buckling and free vibration of laminated composite beams. *Composite Structures* 37:33–43.

Subramanian, P. (2006). Dynamic analysis of laminated composite beams using higher order theories and finite elements. *Composite Structures* 73:342–353.

Tahani, M. (2007). Analysis of laminated composite beams using layerwise displacement theories. *Composite Structures* 79:535–547.

Teboub, Y., Hajela, P. (1995). Free vibration of generally layered composite beams using symbolic computations. *Composite Structures* 33:123–134.

Wolfram, S. (1991). *Mathematica: A System for Doing Mathematics by Computer*, 2nd ed. Reading, Massachusetts: Addison-Wesley.

Yang, W. H. (1983). A method for eigenvalues of the sparse $\lambda-$matrices. *International Journal for Numerical Methods in Engineering* 19:943–948.

Yildirim, V., Sancaktar, E., Kiral, E. (1999). Comparison of the in-plane natural frequencies of symmetric cross-ply laminated beams based on the Bernoulli-Euler and Timoshenko Beam theories. *Journal of Applied Mechanics ASME* 66:410–417.

Yildirim, V. (2000). Effect of the longitudinal to transverse moduli ratio on the in-plane natural frequencies of symmetric cross-ply laminated beams by the stiffness method. *Composite Structures* 50:319–326.

Downloaded by [McGill University Library] at 12:00 23 March 2013

Vibration of multilayered beams using sinus finite elements with transverse normal stress.

P. Vidal, O. Polit

▶ To cite this version:

P. Vidal, O. Polit. Vibration of multilayered beams using sinus finite elements with transverse normal stress.. Composite Structures, 2010, 92 (6), pp.1524-1534. 10.1016/j.compstruct.2009.10.009 . hal-01366979

HAL Id: hal-01366979
https://hal.science/hal-01366979

Submitted on 5 Jan 2018

HAL is a multi-disciplinary open access archive for the deposit and dissemination of scientific research documents, whether they are published or not. The documents may come from teaching and research institutions in France or abroad, or from public or private research centers.

L'archive ouverte pluridisciplinaire **HAL**, est destinée au dépôt et à la diffusion de documents scientifiques de niveau recherche, publiés ou non, émanant des établissements d'enseignement et de recherche français ou étrangers, des laboratoires publics ou privés.

Vibration of multilayered beams using sinus finite elements with transverse normal stress

P. Vidal *, O. Polit

LEME, Université Paris Ouest, 50 rue de Sèvres, 92410 Ville d'Avray, France

ABSTRACT

A family of sinus models is presented for the analysis of laminated beams in the framework of free vibration. A three-noded finite element is developed with a sinus distribution with layer refinement. The transverse shear strain is obtained by using a cosine function avoiding the use of shear correction factors. This kinematic accounts for the interlaminar continuity conditions on the interfaces between the layers, and the boundary conditions on the upper and lower surfaces of the beam. A conforming FE approach is carried out using Lagrange and Hermite interpolations. It is important to notice that the number of unknowns is independent of the number of layers. Vibration mechanical tests for thin and thick laminated and sandwich beams are presented in order to evaluate the capability of these new finite elements to give accurate results with respect to elasticity or finite element reference solutions. Both convergence velocity and accuracy are discussed and these new finite elements yield very accurate results at a low computational cost for various boundary conditions. In particular, the two models including the transverse normal effect have the capability to take into account the thickness mode shape.

1. Introduction

Considering the increasing applications of composite and sandwich structures in the industrial field due to their high specific strength and stiffness, it is important to develop advanced and accurate models to design. In this framework, accurate knowledge of deflection and stresses is required to take into account effects of the transverse shear deformation due to the low ratio of transverse shear modulus to axial modulus, or failure due to delamination… In fact, they can play an important role on the behaviour of structures in services, which leads to evaluate precisely their influence on local stress fields in each layer or on natural frequencies.

The aim of this paper is to construct and evaluate a family of finite elements to analyze laminated beams in elasticity in relation to small displacements, so as to obtain the accurate predictions of frequencies in free vibration case. In particular, we put the emphasis on the influence of transverse normal effects, especially for very thick beams.

According to published research, various theories in vibrational mechanics for composite or sandwich structures (beams and plates for the present scope) have been developed. The following classification is associated with the dependency on the number of degrees of freedom (dofs) with respect to the number of layers:

- The Equivalent Single Layer approach (ESL): the number of unknowns is independent of the number of layers, but the transverse shear and normal stresses continuity on the interfaces between layers are often violated. The first work for one-layer isotropic plates was proposed in [1]. Then, we can distinguish the classical laminate theory [2] (it is based on the Euler–Bernoulli hypothesis and leads to inaccurate results for composites and moderately thick beams, because both transverse shear and normal strains are neglected), the first order shear deformation theory [3–9], and higher order theories [10]. In this later, hyperbolic [11], exponential [11,12], parabolic [13], cubic [14–16,13,17], polynomial functions [18–20] are used in the expansion of the in-plane displacement component. Some of these theories also include the transverse normal effect with non-constant polynomial expressions of the out-of-plane displacement [21,19,22,17]. Most of these approaches are based on a displacement formulation; nevertheless, mixed formulations are also carried out. In this framework, finite element [14,21,10,16,13], analytical [11,15,17,12], or state-space [5,23] solution are carried out.
- The Layerwise approach (LW): The number of dofs depends on the number of layers. This theory aims at overcoming the restriction of the ESL concerning the discontinuity of out-of-plane stresses on the interface layers. This approach was introduced in [24,25], and also used in [26–28]. In recent contributions, various orders of expansion for the in-plane displacement are chosen: trigonometric [29], linear [30], quadratic

---

* Corresponding author. Tel./fax: +33 1 40 97 98 23.
E-mail address: philippe.vidal@u-paris10.fr (P. Vidal).

[31], cubic [32,33]. Some of them take into account the transverse normal effect [32] with a mixed approach. Special studies dedicated to the sandwich beam can be cited [34,35]. The transverse displacement is constant in faces and quadratic in core. See also [36].

In this framework, refined models have been developed in order to improve the accuracy of ESL models avoiding the additional computational cost of LW approach. Based on physical considerations and after some algebraic transformations, the number of unknowns becomes independent of the number of layers. [27] has extended the work of [37] for symmetric laminated composites with arbitrary orientation and a quadratic variation of the transverse stresses in each layer. A family of models, denoted zig-zag models, was first employed in [38], then in [39,31,40]. More recently, it was also modified and improved by some authors [41–46] with different order of kinematics assumptions, taking into account the transverse normal strain.

This above literature deals with only some aspects of the broad research activity about models for layered structures and corresponding finite element formulations. An extensive assessment of different approaches has been made in [47–51]. About the particular point of the evaluation of transverse normal stresses, see [52,53]. A survey of developments in the vibration analysis of laminated composite beams is compiled in [54], see also [55].

In this work, a family of finite elements for rectangular laminated beam analysis is built, in order to have a low cost tool, efficient and simple to use. In fact, our approach is associated with the ESL theory. These elements are totally free of shear locking and are based on a refined shear deformation theory [56] avoiding the use of shear correction factors for laminates. Our elements are based on the sinus model [57] and the important feature is the capability of the model to include the transverse normal effect. So, the transverse displacement is written under a second order expansion which avoids the Poisson locking mechanism (see [58]). For the in-plane displacement, the double superposition hypothesis from [59] is used: three local functions are added to the sinus model. Finally, this process yields to only six or seven independent generalized displacements. It should be noted that all interface and boundary conditions are exactly satisfied for displacements and transverse shear stress. Therefore, this approach takes into account physical meaning.

As far as the interpolation of these finite elements is concerned, our elements are C^0-continuous except for the transverse displacement associated with bending which is C^1.

In this article, the mechanical formulation for the different models is described. For each of these approaches, the associated finite element is given. They are illustrated by numerical tests which have been performed upon various laminated and sandwich beams. A parametric study is given to show the effects of different parameters such as length to thickness ratio and number of degrees of freedom. The accuracy of computations are also evaluated by comparisons with an exact 2D elasticity solution, two-dimensional computations using commercial finite element software, three other sinus models [60] and also results available in literature. Different boundary conditions are also evaluated. Through these examples, the influence of transverse normal effect is highlighted.

2. Resolution of the mechanical problem

2.1. The governing equations

Let us consider a beam occupying the domain $\mathscr{B}=[0,L]\times[-\frac{h}{2}\leqslant z\leqslant\frac{h}{2}]\times[-\frac{b}{2}\leqslant x_2\leqslant\frac{b}{2}]$ in a Cartesian coordinate (x_1,x_2,z). The beam has a rectangular uniform cross section of height h, width b and is assumed to be straight. The beam is made of NC layers of different linearly elastic materials. Each layer may be assumed to be orthotropic in the beam axes. The x_1 axis is taken along the central line of the beam whereas x_2 and z are the two axes of symmetry of the cross section intersecting at the centroid, see Fig. 1. As shown in this figure, the x_2 axis is along the width of the beam. This work is based upon a displacement approach for geometrically linear elastic beams.

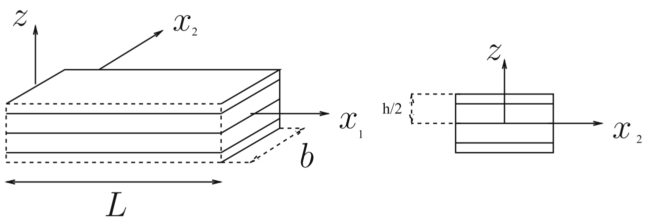

Fig. 1. The laminated beam and coordinate system.

2.1.1. Constitutive relation

Each layer of the laminate is assumed to be orthotropic. Using matrix notation, the elastic stress–strain law of the kth layer is given by:

$$\begin{bmatrix}\sigma_{11}^{(k)}\\ \sigma_{33}^{(k)}\\ \sigma_{13}^{(k)}\end{bmatrix}=\begin{bmatrix}C_{11}^{(k)} & C_{13}^{(k)} & 0\\ & C_{33}^{(k)} & 0\\ symm & & C_{55}^{(k)}\end{bmatrix}\begin{bmatrix}\varepsilon_{11}^{(k)}\\ \varepsilon_{33}^{(k)}\\ \varepsilon_{13}^{(k)}\end{bmatrix}\ \text{i.e.}\ [\sigma^{(k)}]=[C^{(k)}][\varepsilon^{(k)}] \tag{1}$$

where we denote: the stress tensor $[\sigma]$; the strain tensor $[\varepsilon]$; C_{ij} are the three-dimensional stiffness coefficients.

2.1.2. The weak form of the boundary value problem

Using the above matrix notation and for admissible virtual displacement $\vec{u}^*\in U^*$, the variational principle is given by:

find $\vec{u}\in U$ (space of admissible displacements) such as:

$$-\int_{\mathscr{B}}[\varepsilon(\vec{u}^*)]^T[\sigma(\vec{u})]d\mathscr{B}+\int_{\mathscr{B}}[u^*]^T[f]d\mathscr{B}+\int_{\partial\mathscr{B}_F}[u^*]^T[F]d\partial\mathscr{B}$$
$$=\int_{\mathscr{B}}\rho[u^*]^T[\ddot{u}]d\mathscr{B}\quad\forall\vec{u}^*\in U^* \tag{2}$$

where $[f]$ and $[F]$ are the prescribed body and surface forces applied on $\partial\mathscr{B}_F$. $\varepsilon(\vec{u}^*)$ is the virtual strain, and ρ is the mass density.

The variational principle Eq. (2) provides a convenient framework to develop finite element approximations.

2.2. The displacement field for laminated beams

Based on the sinus function (see [61,62]), two models which take into account the transverse normal deformation are presented in this section.

In the following, we can distinguish:

- The refined sinus model with 2nd order expansion for the transverse displacement (denoted SinRef-6p) where the refinement is added in each layer.
- The refined sinus model (denoted SinRef-7p) with one more unknown than the previous one for the in-plane displacement.

They are based on both

- Various works on beams, plates and shells, cf. Ref. [63,56,57,61,64–66] concerning the refined theory.
- The so-called 1,2-3 double-superposition theory developed by Li and Liu [59].

It also follows works about local–global approach studied in [67–69].

These refined models (see [60]) take into account the continuity conditions between layers of the laminate for both displacements and transverse shear stress, and the free conditions on the upper and lower surfaces owing to the Heaviside function.

The kinematics of the two models ([70]) is assumed to be of the following particular form:

(1) The SinRef-6p model:

$$\begin{cases} u_1(x_1,x_2,z) = u(x_1) - z\, w_0(x_1)_{,1} + f(z)(\omega_3(x_1) + w_0(x_1)_{,1}) \\ \qquad + \sum_{k=1}^{NC} \left(\bar{u}^{(k)}_{loc}(x_1,z) + \hat{u}^{(k)}_{loc}(x_1,z)\right)(H(z-z_k) - H(z-z_{k+1})) \\ u_3(x_1,x_2,z) = w_0(x_1) + z w_1(x_1) + z^2 w_2(x_1) \end{cases} \tag{3}$$

(2) The SinRef-7p model:

$$\begin{cases} u_1(x_1,x_2,z) = u(x_1) + z\, v(x_1) + f(z)(\omega_3(x_1) + w_0(x_1)_{,1}) \\ \qquad + \sum_{k=1}^{NC} \left(\bar{u}^{(k)}_{loc}(x_1,z) + \hat{u}^{(k)}_{loc}(x_1,z)\right)(H(z-z_k) - H(z-z_{k+1})) \\ u_3(x_1,x_2,z) = w_0(x_1) + z w_1(x_1) + z^2 w_2(x_1) \end{cases} \tag{4}$$

where H is the Heaviside function defined by

$$\begin{cases} H(z-z_k) = 1 & \text{if } z \geqslant z_k \\ H(z-z_k) = 0 & \text{if not} \end{cases} \tag{5}$$

In the classic approach, w_0 is the bending deflection following the z direction, while u is associated with the uniform extension of the cross section of the beam along the central line, and ω_3 is the shear bending rotation around the x_2 axis.

It should be noted that the kinematic constraint concerning the relation with the derivative of the deflection $(v(x_1) = -w_0(x_1)_{,1})$ is relaxed in the SinRef-7p model.

The local functions $\bar{u}^{(k)}_{loc}$ and $\hat{u}^{(k)}_{loc}$ based on the Legendre polynomial can be written as:

$$\begin{cases} \bar{u}^{(k)}_{loc}(x_1,z) = \zeta_k u^k_{31}(x_1) + \left(-\frac{1}{2} + \frac{3\zeta_k^2}{2}\right) u^k_{32}(x_1) \\ \hat{u}^{(k)}_{loc}(x_1,z) = \left(-\frac{3\zeta_k}{2} + \frac{5\zeta_k^3}{2}\right) u^k_{33}(x_1) \end{cases} \tag{6}$$

The coordinate system is precised on Fig. 2. A non-dimensional coordinate is introduced by: $\zeta_k = a_k z - b_k,\ a_k = \frac{2}{z_{k+1}-z_k},\ b_k = \frac{z_{k+1}+z_k}{z_{k+1}-z_k}$.

In the context of the sinus model, we have:

$$f(z) = \frac{h}{\pi} \sin \frac{\pi z}{h} \tag{7}$$

and the derivative of this function will represent the transverse shear strain distribution due to bending.

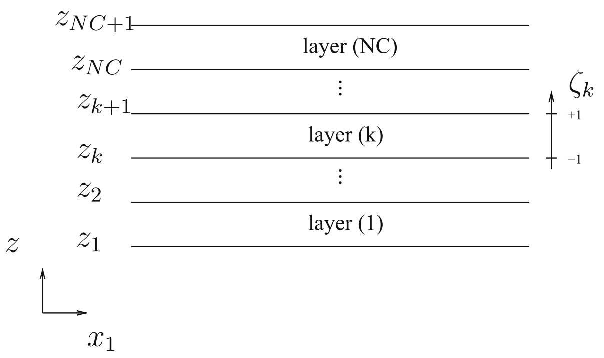

Fig. 2. Coordinate system of laminated beam.

Remarks: from Eq. (3), classical beam models can be deduced without the local functions and the two higher-order terms of the transverse displacement:

- Euler–Bernoulli

  $f(z) = 0$
- Timoshenko

  $f(z) = z$
- Sinus model

  $f(z) = \frac{h}{\pi} \sin \frac{\pi z}{h}$

Hence, it is not necessary to introduce transverse shear correction factors.

At this stage, $3 \times NC + 5$ and $3 \times NC + 6$ generalized displacements are included in Eqs. (3) and (6) (sinRef-6p model) and Eqs. (4) and (6) (sinRef-7p model), respectively.

The following part is dedicated to the obtention of relations between kinematic unknowns from

- Lateral boundary conditions.
- Interlaminar continuity conditions (displacement, transverse shear stress).

In the following, we only focus on the SinRef-7p model. The same procedure can be carried out for the SinRef-6p model by setting $v(x_1) = -w_0(x_1)_{,1}$.

2.2.1. Continuity conditions and free conditions

From the displacement field Eq. (4), some continuity conditions on displacements and interlaminar stress must be imposed. For an interface layer $k \in \{2, \ldots, NC\}$, we have

- Displacement continuity conditions as in [67] i.e.:

$$\bar{u}^{(k)}_{loc}(x_1, z_k) = \bar{u}^{(k-1)}_{loc}(x_1, z_k) \quad k = 2, \ldots, NC \tag{8}$$

$$\hat{u}^{(k)}_{loc}(x_1, z_k) = \hat{u}^{(k-1)}_{loc}(x_1, z_k) \quad k = 2, \ldots, NC \tag{9}$$

- Transverse shear stress continuity between two adjacent layers:

$$\sigma^{(k)}_{13}(x_1, z_k^+) = \sigma^{(k-1)}_{13}(x_1, z_k^-) \quad k = 2, \ldots, NC \tag{10}$$

So, $3 \times (NC - 1)$ conditions are imposed, which allow to reduce the number of unknowns to nine generalized displacements.

Free conditions of the transverse shear stress on the upper and lower surfaces must also be verified. So, we have:

$$\sigma^{(1)}_{13}\left(x_1, z = -\frac{h}{2}\right) = 0 \quad \text{and} \quad \sigma^{(NC)}_{13}\left(x_1, z = \frac{h}{2}\right) = 0 \tag{11}$$

Finally, the number of generalized displacements is reduced to seven, which is independent of the number of layers.

2.2.2. Relation between the generalized displacements

Using the displacement notation introduced in Eq. (6), the conditions Eqs. (8)–(11) can be written under a linear system which yields relations between $u^j_{31}(j \neq 1),\ u^j_{32},\ u^j_{33},\ j = 1, \ldots, NC$ and u^1_{31}. This relation can be written under the following form:

$$\begin{aligned} u^j_{3i}(x_1) = {} & \beta^j_i(\omega_3(x_1) + w_0(x_1)_{,1}) + \eta^j_i(v(x_1) + w_0(x_1)_{,1}) + \delta^j_i u^1_{31}(x_1) \\ & + \lambda^j_i w_1(x_1)_{,1} + \mu^j_i w_2(x_1)_{,1},\ j = 1, \ldots, NC \quad i = 1,2,3 \\ & \text{with } \delta^1_1 = 1,\ \beta^1_1 = \eta^1_1 = \lambda^1_1 = \mu^1_1 = 0 \end{aligned} \tag{12}$$

where $\beta_i^j,\ \delta_i^j,\ \lambda_i^j,\ \mu_i^j$, and $\eta_i^j (i = 1,2,3)$ are the coefficients deduced from this linear system.

Finally, the seven unknowns become $u,\ w_0,\ \omega_3,\ v,\ w_1,\ w_2$ and u_{31}^1. It is to be noted that the SinRef-6p model involves six unknowns $(u,\ w_0,\ \omega_3,\ w_1,\ w_2$ and $u_{31}^1)$.

2.2.3. Matrix expression for the weak form

From the weak form of the boundary value problem Eq. (2), and using Eq. (14), an integration throughout the cross section is performed analytically in order to obtain an unidimensional formulation. Therefore, the right term of Eq. (2) can be written under the following:

$$\int_{\mathscr{B}} \rho [u^*]^T [\ddot{u}] d\mathscr{B} = \int_0^L \left[\mathscr{E}_u^*\right]^T [m] \left[\ddot{\mathscr{E}}_u\right] dx_1$$

$$\text{with } [m] = \int_{\Omega} \rho [F_u(z)]^T \, [F_u(z)] \, d\Omega \tag{13}$$

where Ω represents the cross section $\left[-\frac{h}{2} \leqslant z \leqslant \frac{h}{2}\right] \times \left[-\frac{b}{2} \leqslant x_2 \leqslant \frac{b}{2}\right]$,

$$[u]^T = [F_u(z)][\mathscr{E}_u] \quad \text{with } [\mathscr{E}_u]^T$$
$$= \left[u \vdots w_0 w_{0,1} \vdots \omega_3 \vdots u_{31}^1 \vdots v \vdots w_1 w_{1,1} \vdots w_2 w_{2,1}\right] \tag{14}$$

and $[F_u(z)]$ is a matrix which only depends on the transverse displacement component and is deduced from Eqs. (12), (3) and (4).

Same calculations for the first left term of Eq. (2) are carried out to calculate the stiffness matrix, it is detailed in Appendix A.

In Eq. (13), the matrix $[m]$ is the integration throughout the cross section of the material characteristics of the beam. The interest of the choice of the Legendre polynomials can be emphasized in the calculation of the matrix $[m]$ owing to their properties of orthogonality.

2.3. The finite element approximation

This section is dedicated to the finite element approximation of the generalized displacement, see matrices $[\mathscr{E}_u]$, and $[\mathscr{E}_u^*]$, Eq. (14). It is briefly described, and the reader can obtain a detailed description in [57,60].

2.3.1. The geometric approximation

Given the displacement field constructed above for sandwich and laminated beams, a corresponding finite element is developed in order to analyze the behaviour of laminated beam structures under combined loads. Let us consider the eth element L_e^h of the mesh $\cup L_e^h$. This element has three nodes, denoted by $(g_j)_{j=1,2,3}$, see Fig. 3. A point with coordinate x_1 on the central line of the beam will be as follows:

$$x_1(\xi) = \sum_{j=1}^{2} Nl_j(\xi)\, x_1^e(g_j) \tag{15}$$

where $Nl_j(\xi)$ are Lagrange linear interpolation functions and $x_1^e(g_j)$ are Cartesian coordinates (measured along the x_1 axis) of the node g_j of the element L_e^h. ξ is an isoparametric or reduced coordinate and its variation domain is $[-1,1]$.

2.3.2. Interpolation for the beam element

The finite element approximations of the assumed displacement field components are hereafter symbolically written as $u_i^h(x_1,x_2,z)$ where the superscript h refers to the mesh $\cup L_e^h$.

From the kinematics (see Eq. (4)), the transverse displacement w_0^h must be C^1–continuous; whereas the rotation ω_3^h, the extension displacement u^h, v^h and u_{31}^1 can be only C^0–continuous. Therefore, the generalized displacement w_0^h, w_1^h, and w_2^h are interpolated by the Hermite cubic functions $Nh_j(\xi)$.

According to the transverse shear locking phenomena, the other shear bending generalized displacements, rotation ω_3^h, are interpolated by Lagrange quadratic functions denoted $Nq_j(\xi)$. This choice allows the same order of interpolation for both $w_{0,1}^h$ and ω_3^h in the corresponding transverse shear strain components due to bending, thus avoiding transverse shear locking according to the field compatibility approach [71].

Finally, traction u^h, v^h and u_{31}^1 are interpolated by Lagrange quadratic functions.

2.3.3. Elementary matrices

In the previous section, the finite element approximations were defined, and elementary mass $[M_{uu}^e]$ matrix can be deduced from Eq. (13). It has the following expression:

$$\left[M_{uu}^e\right] = \int_{L_e} [N]^T \, [m] \, [N] dL_e \tag{16}$$

where $[N]$ are deduced expressing the generalized displacement vectors, see Eq. (14), from the elementary vector of degrees of freedom (dof) denoted $[q_e]$ by:

$$[\mathscr{E}_u] = [N] \, [q_e] \tag{17}$$

The matrix $[N]$ contains only the interpolation functions.

The same technique can be used defining the elementary mechanical load vector and the elementary rigidity matrix, denoted $[B_u^e]$ and $[K_{uu}^e]$ respectively, but it is not detailed here.

3. Numerical examples: free vibration tests

Some examples of sandwich and laminated beams are used to evaluate these finite elements. It should be noted that this sinus family has been already evaluated in the static case [70]. It has shown good features for all the standard requirements: it has a proper rank without any spurious energy modes, and it does not imply shear locking.

Here, we focus on the dynamic analyses which are carried out in the free vibration case. It concerns large variety of boundary conditions with wide range of length to thickness ratios for symmetric, unsymmetric and different types of sandwich beams. These examples are taken from [12,72,73,18,36]. The results are compared with the ANSYS solution with a very refined mesh, exact 2D solution or theories available from the literature. Some of these

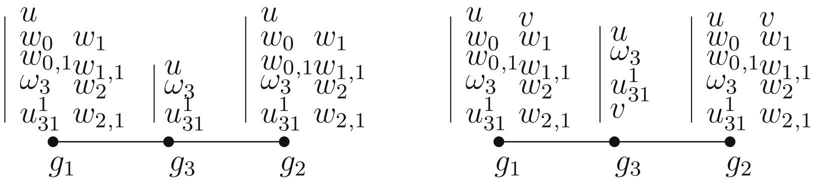

Fig. 3. Description of the laminated beam finite element d.o.f. – SinRef-6p (left) – SinRef-7p (right).

examples are extended to a very thick beam to assess these finite elements.

3.1. Convergence study for the SinRef-7p model [73]

First, a convergence study with respect to the mesh is carried out. A symmetric three layers beam is considered with an aspect ratio $S = 10$. It is detailed below:

Geometry: composite cross-ply beam (0°/90°/0°) and length to thickness ratio $S = 10$, three layers of equal thickness.
Boundary conditions: simply supported beam.
Material properties:

$$E_L = 181\text{ GPa},\quad E_T = 10.3\text{ GPa},\quad G_{LT} = 7.17\text{ GPa},$$
$$G_{TT} = 2.87\text{ GPa},\quad \nu_{LT} = 0.25,\quad \nu_{TT} = 0.33$$

where L and T refer to the fiber and transverse direction respectively.

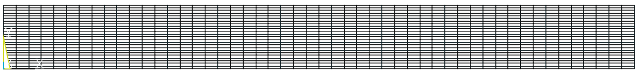

Fig. 4. Mesh with 1275 dofs (ANSYS).

Table 1
Table of principal notation.

$[\sigma]$	Stress tensor
$[\varepsilon]$	Strain tensor
C_{ij}	Elastic stiffness modulus
$[M^e_{uu}]$	Elementary mass matrix
$[\mathscr{E}_u],\ [\mathscr{E}_s]$	Generalized displacement vector
$[N]$	Interpolation functions vector
$[q_e]$	Degrees of freedom elementary vector
$\vec{u}$	Displacement vector
L	Length of the beam
b	Width of the beam
$h,\ h_f,\ h_c$	Height of the beam, face, and core respectively
NC	Number of layers
N	Number of elements
t	Time
S	Length to thickness ratio
α_k	Continuity coefficients for the Sin-c model
$\left(\delta_i^k,\ \beta_i^k\right)_{i=1,2,3}$	Continuity coefficients for the SinRef-c model
Sin	Sinus model without continuity requirements [61]
Sin-c	Sinus model with continuity requirements
SinRef-c	Refined sinus model with continuity requirements
SinRef-6p	Refined sinus model with continuity requirements including six unknowns
SinRef-7p	Refined sinus model with continuity requirements including seven unknowns

The same study is carried out with the commercial code ANSYS [74]. A very refined mesh with a 2D approach is considered as a reference. The mesh of 1275 dofs is shown in Fig. 4.

Table 2 shows the quick convergence, and a $N = 8$ mesh seems to be sufficient to model the laminated composite beam for a dynamic analysis. The % error is very low for the first six frequencies.

3.2. symmetric laminated composite [12,72]

The example is issued from [12] and [72]. It deals with a symmetric laminated composite with the following characteristics:

Geometry: the beam studied has a length of $L = 6.35$ m, and a thickness $h = 0.2794$ m (thin $S \approx 22.7$), and $h = 2.794$ m (thick $S \approx 2.2$). It possesses three layers at (90°/0°/90°), with thickness (0.25 h/0.5 h/0.25 h).
Boundary conditions: simply supported beam.
Material properties: The material used is boron epoxy which has the following mechanical properties:

$$E_{11} = 241.5\text{ GPa},\quad E_{22} = E_{33} = 18.89\text{ GPa},\quad G_{12} = G_{13} = 5.18\text{ GPa}$$
$$G_{23} = 3.45\text{ GPa},\quad \nu_{12} = \nu_{13} = 0.24,\quad \nu_{23} = 0.25,\quad \rho = 2015\text{ kg/m}^3.$$

Mesh: N = 8.
Results: the mode shapes are precised as: bend, sh, t/c, thic for bending, shear, axial traction/compression and thickness mode respectively.The notation of sinus models are given in Table 1.

Tables 3 and 4 present numerical values of frequencies for the thin and very thick beam. These results show the excellent agreement with reference values for eight and seven natural frequencies. Results of the SinRef-c model are better than those of the Sin and Sin-c models, especially for the thick beam. The maximal % error does not exceed 2.9, whereas the two others have an error of 17% and 14% respectively. The SinRef-7p model seems to be the best model among the sinus family with a maximal % error equal to 1.6 regardless of the slenderness.

Table 2
Mesh convergence study for the SinRef-7p model – natural frequencies – three-layers (0°/90°/0°) – $S = 10$.

N	Frequencies (Hz)					
	2 (38 dofs)	Error (%)	4 (66 dofs)	Error (%)	8 (122 dofs)	Error (%)
Bend	38.15	0.4	38.04	0.1	38.04	0.1
Bend	115.67	4.4	110.99	0.2	110.81	0.0
Bend	211.29	11.8	190.07	0.6	188.99	0.0
Bend	–	–	275.97	2.5	269.12	0.0
Bend	345.01	1.8	365.80	4.1	351.50	0.0
t/c	391.33	2.6	389.96	2.3	389.86	2.2

Table 3
Natural frequencies – three-layers (90°/0°/90°) – $S \approx 22.7$.

	Frequencies (Hz) thin beam										
	Sin	Error (%)	Sin-c	Error (%)	SinRef-c	Error (%)	SinRef-6p	Error (%)	SinRef-7p	Error (%)	Ansys
Bend	14.97	0.2	14.98	0.3	14.97	0.2	14.97	0.2	14.96	0.2	14.93
Bend	57.85	0.3	57.94	0.4	57.80	0.2	57.83	0.3	57.69	0.0	57.67
Bend	123.55	0.5	123.96	0.8	123.33	0.3	123.45	0.4	122.90	0.0	122.90
Bend	206.18	0.8	207.23	1.3	205.65	0.5	205.95	0.7	204.59	0.0	204.50
Bend	300.71	0.9	302.75	1.8	299.77	0.8	300.39	1.1	297.90	0.2	297.23
Bend	403.60	1.5	406.91	2.4	402.29	1.2	403.35	1.5	399.56	0.6	397.28
Bend	512.67	2.	517.43	3.	511.15	1.7	512.78	2.1	507.72	1.1	502.19
sh	640.06	1.5	632.94	0.4	634.37	0.6	634.37	0.7	634.37	0.7	630.25

Table 4
Natural frequencies – three-layers (90°/0°/90°) – $S \approx 2.2$.

	Frequencies (Hz) thick beam										
	Sin	Error (%)	Sin-c	Error (%)	SinRef-c	Error (%)	SinRef-6p	Error (%)	SinRef-7p	Error (%)	Ansys
Bend	82.81	0.7	83.66	1.	82.78	0.7	83.11	1.1	82.36	0.2	82.17
Bend	195.62	0.2	195.67	0.3	195.83	0.3	196.82	0.8	196.45	0.6	195.22
sh	277.98	1.3	274.94	0.2	274.31	0.	274.31	0.0	274.29	0.0	274.31
Bend	319.36	2.9	313.36	1.	311.73	0.5	312.92	0.9	312.91	0.9	310.07
Bend	460.18	8.4	442.07	4.1	428.96	1.	429.48	1.2	429.43	1.2	424.311
Bend	515.41	17.4	501.47	14.2	451.63	2.9	450.69	2.7	439.22	0.1	438.81
Bend	621.47	15.6	585.51	8.9	547.42	1.8	546.29	1.7	546.14	1.6	537.42

It should be noted that the values of the natural frequencies are always overestimated when compared to ANSYS finite element solution.

3.3. Free vibration of symmetric and anti-symmetric lay-up [73]

In this section, two stacking sequences of laminated composite are considered.

Geometry: composite cross-ply beam (0°/90°/0°), (0°/90°) and length to thickness ratio $S = 2$, $S = 5$, $S = 10$, $S = 20$.
Boundary conditions: free vibration of a simply supported beam.
Material properties: same material properties as in Section 3.1.
Results: the results are presented under a non-dimensional natural frequency as follows: $\bar{\omega} = \omega LS(\rho/Y_0)^{1/2}$, with $Y_0 = 10.3\ \text{GPa},\ \rho = 1578\ \text{kg/m}^3$.

They are compared with exact two-dimensional elasticity solution from [73] and results computed from ANSYS.

The shape modes for the thick symmetric and anti-symmetric beams are illustrated in Figs. 5 and 6.

It can be noticed that the natural frequencies given in Table 5 by the refined models for the symmetric lay-up are in excellent agreement with the reference solution for $S \geqslant 5$. The errors are less than 2%, excepted for thickness mode frequencies. The SinRef-c model improves results computed from the Sin and Sin-c models regardless of the length to thickness ratio. However, it is also observed that the two later models provide satisfactory results for moderately thick cases.

The effect of the transverse normal stress is significant for the very thick beam. On the one hand, the SinRef-6p and SinRef-7p models give accurate results for $S = 2$ compared with the SinRef-c model. On the other hand, they allow to exhibit thickness-stretch modes even if the corresponding error seems high. In fact, Fig. 5 shows that the fifth mode shape is symmetrical.

As far as the anti-symmetric lay-up (0°/90°) is concerned, the errors given in Table 6 vary from 0.% to 1.8% for the SinRef-7p

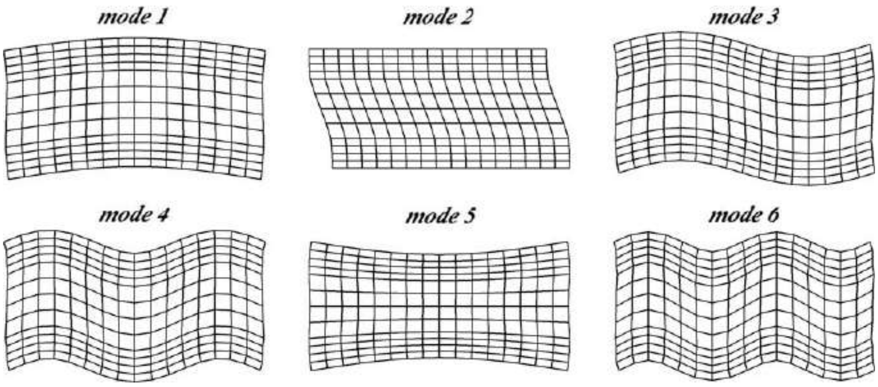

Fig. 5. Shape modes for the symmetric beam (0°/90°/0°) – $S = 2$ – SinRef-7p.

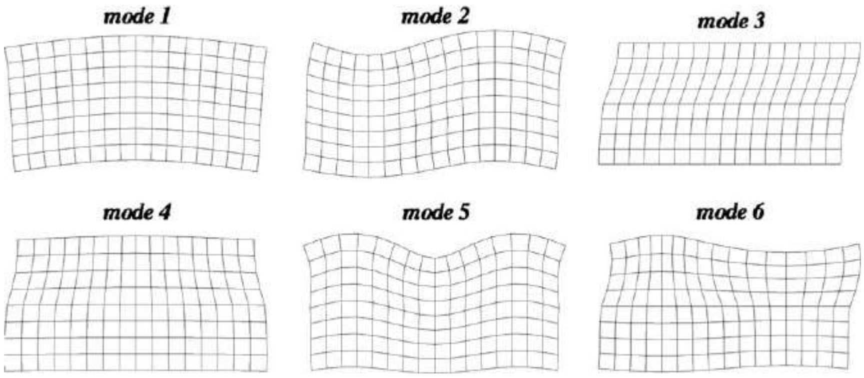

Fig. 6. Shape modes for the unsymmetric beam (0°/90°) – $S = 2$ - SinRef-7p.

Table 5
Natural frequencies – (0°/90°/0°).

S	Natural frequencies $\bar{\omega}$												
		Sin	Error (%)	Sin-c	Error (%)	SinRef-c	Error (%)	SinRef-6p	Error (%)	SinRef-7p	Error (%)	Ansys	Exact 2D [73]
2	Bend	3.50	1.6	3.55	3.4	3.53	2.4	3.45	0.2	3.45	0.1	3.45	–
	sh	7.48	6.7	7.03	0.3	11.08	58.1	7.01	0.0	7.01	0.0	7.01	–
	Bend	8.17	6.3	9.10	18	8.16	6.2	7.70	0.2	7.69	0.1	7.68	–
	Bend	14.31	19.2	17.11	42	13.02	8.5	12.08	0.7	12.08	0.6	12.00	–
	Thic	–	–	–	–	–	–	14.59	0.0	14.59	0.0	14.59	–
	Bend	22.19	37	27.62	70	18.03	11.3	16.48	1.7	16.45	1.6	16.20	–
	Thic	–	–	–	–	–	–	17.22	9.1	17.22	9	18.94	–
5	Bend	6.94	1.9	6.82	0.2	6.81	0.2	6.82	0.3	6.81	0.1	6.81	6.806
	Bend	16.80	1.6	16.79	1.6	16.54	0.1	16.56	0.2	16.53	0.0	16.52	16.515
	Bend	27.17	1.6	28.07	5.	26.73	0.04	26.75	0.1	26.72	0.0	26.72	26.688
	Bend	38.51	3.1	41.35	10.7	37.32	0.02	37.34	0.0	37.31	0.0	37.33	37.255
	Thic	–	–	–	–	–	–	47.87	9.4	47.87	9.4	43.75	–
	sh	46.76	6.7	43.93	0.3	43.80	0.01	43.80	0.0	43.79	0.0	43.80	–
	Bend	47.86	0.6	47.86	0.6	48.18	0.4	48.21	0.1	48.18	0.0	48.18	48.035
	Bend	51.24	13.3	57.13	3.3	59.26	0.2	59.25	0.2	59.22	0.2	59.11	58.876
10	Bend	9.44	1.	9.34	0.	9.36	0.1	9.36	0.2	9.36	0.1	9.34	9.343
	Bend	27.76	1.9	27.29	0.1	27.25	0.1	27.30	0.2	27.25	0.0	27.24	27.224
	Bend	47.36	1.9	46.78	0.6	46.53	0.1	46.56	0.2	46.48	0.0	46.47	46.416
	Bend	67.29	1.6	67.23	1.6	66.25	0.1	66.30	0.2	66.19	0.0	66.19	66.058
	Bend	87.77	1.5	89.13	3.1	86.51	0.1	86.57	0.2	86.45	0.0	86.43	86.169
	t/c	95.73	2.	95.73	2.	95.90	2.2	95.88	2.2	95.88	2.2	93.78	–
	Bend	–		113.04	5.4	107.38	0.1	107.45	0.2	107.33	0.1	107.20	106.75
20	Bend	10.67	0.2	10.64	0.	10.65	0.1	10.66	0.2	10.65	0.1	10.64	10.64
	Bend	37.78	1.	37.39	0.	37.45	0.1	37.46	0.2	37.43	0.1	37.40	37.374
	Bend	72.98	1.5	71.87	0.	71.94	0.1	71.97	0.2	71.87	0.0	71.85	71.744
	Bend	111.23	1.9	109.35	0.1	109.30	0.1	109.37	0.2	109.18	0.0	109.15	108.89
	Bend	150.57	2.	148.21	0.4	147.83	0.2	147.94	0.3	147.67	0.1	147.54	147.04
	Bend	190.54	2.1	188.26	0.9	187.19	0.3	187.31	0.4	186.97	0.2	186.53	185.68
	t/c	191.47	0.4	191.47	0.4	191.81	0.6	191.81	0.7	191.81	0.7	190.52	–

Table 6
Natural frequencies – anti-symmetric lay-up (0°/90°).

S	Natural frequencies $\bar{\omega}$											
		Sin	Error (%)	Sin-c	Error (%)	SinRef-c	Error (%)	SinRef-6p	Error (%)	SinRef-7p	Error (%)	Ansys
2	Bend	3.50	9	3.55	11	3.24	1.2	3.25	1.6	3.22	0.7	3.20
	Bend	7.48	1.5	9.10	23	7.87	6.8	7.67	4.0	7.58	2.9	7.37
	sh	14.31	84	7.03	9	7.76	0.0	7.76	0.0	7.76	0.0	7.76
	Bend	19.18	116	19.18	116	8.94	1.1	8.90	0.6	8.89	0.5	8.85
	Bend	25.16	129	27.62	152	12.87	17.7	11.63	6.3	11.50	5.1	10.94
	Thic	–	–	–	–	–	–	14.46	13.6	14.33	12.6	12.73
	Thic	–	–	–	–	–	–	14.00	2.2	13.97	1.9	13.71
5	Bend	4.83	1	4.87	2	4.78	0.2	4.80	0.4	4.78	0.2	4.77
	Bend	15.19	4	15.60	6	14.71	0.6	14.78	1.1	14.67	0.4	14.61
	Bend	27.30	7	28.64	12	25.87	1.8	25.90	1.9	25.65	0.9	25.40
	tc	38.12	7	36.39	3	35.56	0.4	35.52	0.3	35.45	0.1	35.42
	Bend	40.29	12	43.09	19	37.42	4	37.09	3.0	36.68	1.8	36.02
	sh	54.15	11	50.29	3	48.52	0.	48.53	0.0	48.51	0.0	48.52
10	Bend	5.30	0.3	5.32	0.5	5.29	0.1	5.30	0.2	5.30	0.1	5.29
	Bend	19.33	1	19.49	2	19.14	0.1	19.20	0.4	19.14	0.1	19.12
	Bend	38.67	2	39.33	4	37.87	0.2	38.03	0.7	37.83	0.1	37.77
	Bend	60.91	4	62.57	7	58.97	0.6	59.24	1.1	58.81	0.4	58.60
	Bend	84.87	6	88.13	9	81.26	1	81.53	1.6	80.81	0.7	80.22
	tc	90.06	2	88.92	0.5	88.65	0.2	88.63	0.2	88.55	0.1	88.44
20	Bend	5.45	<0.1	5.46	0.1	5.45	0.1	5.46	0.1	5.46	0.1	5.45
	Bend	21.23	0.3	21.28	0.4	21.20	0.1	21.22	0.2	21.20	0.1	21.18
	Bend	45.86	0.7	46.08	1	45.62	0.1	45.71	0.3	45.63	0.2	45.55
	Bend	77.58	1	78.23	2	76.81	0.3	77.03	0.6	76.80	0.3	76.59
	Bend	114.86	2	116.31	3	113.11	0.6	113.52	1.0	113.05	0.6	112.40
	Bend	156.58	3	159.32	5	153.29	1	153.95	1.6	153.13	1.1	151.48
	tc	188.63	0.4	188.09	0.1	188.26	0.2	188.25	0.2	188.20	0.2	187.89

model. The improvement is really significant compared with the four other models, especially for the very thick beam where the Sin and Sin-c models give very poor results. Nevertheless, the SinRef-7p results are very close to the SinRef-6p frequencies. Again, only two models have the capability to represent thickness mode shape (cf. Fig. 6) as they assume quadratic variation of transverse displacement through the thickness. The fifth and sixth modes clearly illustrate the effect of transverse normal deformation. It can be noticed that these modes are not symmetrical.

3.4. Free vibration of sandwich beam

3.4.1. Three-layer sandwich beam [73]

The first example of sandwich beam has the following characteristics:

Geometry: the three-layer sandwich beam has graphite-epoxy faces and a soft core with thickness 0.1 h/0.8 h/0.1 h and length to thickness ratio S = 2, S = 5, S = 10, S = 20.
Boundary conditions: simply supported beam.
Material properties: Face: $E_{11} = 131.1$ GPa, $E_{22} = E_{33} = 6.9$ GPa $G_{12} = 3.588$ GPa, $G_{13} = 3.088$ GPa, $G_{23} = 2.3322$ GPa, $\nu_{12} = \nu_{13} = 0.32$, $\nu_{23} = 0.49$, $\rho_f = 1000$ kg/m^3. Core : $E_{11} = 0.2208$ MPa, $E_{22} = 0.2001$ MPa, $E_{33} = 2760$ MPa$G_{12} = 16.56$ MPa, $G_{13} = 545.1$ MPa, $G_{23} = 455.4$ MPa, $\nu_{12} = 0.99$, $\nu_{13} = 0.00003$, $\nu_{23} = 0.00003$, $\rho_c = 70$ kg/m^3.
Results: results are presented under a non-dimensional natural frequency as follows:

$\bar{\omega} = \omega L S(\rho_f / Y_0)^{1/2}$ with $Y_0 = 6.9$GPa – *Cf*. Table 7

As far as the sandwich beam with $S \geqslant 5$ is concerned, Table 7 shows that the refined sinus models yield accurate results in all cases. The magnitude of the relative error never exceed 3.6% and 5.8 % for the three refined sinus and sinus models respectively.

Then, the five models are able to estimate accurately the natural frequencies of a sandwich beam. In our case, the SinRef-7p model gives the best results. For example, the % error is less than 0.2 for $S = 5$, and is equal to 4% for the thickness mode. We can also put the emphasis on the effect of the relation between $w_0(x_1)_{,1}$ and $v(x_1)$ for the SinRef-7p and SinRef-6p models. The accuracy on frequencies is improved with one more unknown.

For $S = 2$, remarks of Section 3.3 are identical. It should be noted that the Sin and Sin-c models allow to estimate correctly the first three frequencies. Nevertheless, the estimation of frequencies is improved owing to the transverse normal effect in the SinRef-6p and SinRef-7p models.

Fig. 7 illustrates three thickness mode shapes occurring in this very thick case. Moreover, these models are shown to provide better accuracy than the zig-zag model described in [73]. In this reference, we also notice the difficulty to estimate the frequencies of thickness modes.

Finally, it can be observed that the use of more unknown functions in the formulation seems to make the beam more flexible.

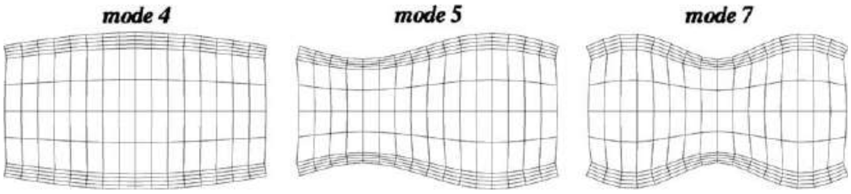

Fig. 7. Thickness mode shape for the sandwich beam – S = 2 – SinRef-7p.

Table 7
Natural frequencies – sandwich beam.

S	Natural frequencies $\bar{\omega}$												
		Sin	Error (%)	Sin-c	Error (%)	SinRef-c	Error (%)	SinRef-6p	Error (%)	SinRef-7p	Error (%)	Ansys	Exact 2D [73]
2	Bend	3.67	4	3.57	1.3	3.65	3.5	3.64	3	3.53	0.2	3.53	–
	sh	5.54	3.7	5.34	0.0	5.48	2.5	5.48	2.5	5.34	0.1	5.34	–
	Bend	7.99	5.4	8.03	5.9	7.88	3.8	7.74	2	7.60	0.2	7.58	–
	Thic	–	–	–		–	–	11.07	4	11.07	4	11.61	–
	Thic	–	–	–		–	–	9.40	19	9.40	19	11.66	–
	Bend	13.22	10	13.77	14	12.46	3.9	12.08	0.7	11.97	0.2	11.99	–
	Thic	–	–	–	–	–	–	15.00	24	15.00	24	12.09	–
	Bend	19.61	18	21.08	27	17.22	4.1	16.49	0.3	16.45	0.5	16.53	–
5	Bend	8.09	3.4	7.85	0.3	8.04	2.7	8.05	2.9	7.83	0.1	7.82	7.82
	Bend	17.96	3.9	17.43	0.8	17.86	3.3	17.83	3.2	17.31	0.1	17.28	17.27
	Bend	28.01	4.	27.42	1.8	27.88	3.5	27.71	2.9	26.97	0.2	26.93	26.90
	sh	34.66	3.7	33.42	0.	34.22	2.4	34.22	2.5	33.37	0.1	33.40	–
	Bend	38.62	4.3	38.27	3.4	38.35	3.6	37.91	2.4	37.06	0.1	37.01	36.93
	Bend	50.06	5.2	50.32	5.8	49.31	3.6	48.46	1.9	47.58	0.1	47.55	47.39
	Thic	–	–	–	–	–	–	55.39	4	55.39	4	58.02	–
10	Bend	12.49	2.1	12.25	0.1	12.45	1.7	12.47	1.9	12.26	0.1	12.23	12.23
	Bend	32.37	3.4	31.41	0.3	32.16	2.7	32.21	2.9	31.33	0.1	31.30	31.29
	Bend	52.17	3.8	50.53	0.5	51.82	3.1	51.84	3.1	50.31	0.1	50.26	50.21
	Bend	71.90	3.8	69.77	0.8	71.48	3.2	71.37	3.1	69.26	0.1	69.21	68.09
	Bend	91.88	3.9	89.52	1.2	91.43	3.4	91.08	3.0	88.51	0.1	88.41	88.18
	Bend	112.43	4.	110.11	1.9	111.91	3.5	111.20	2.9	108.25	0.2	108.02	107.61
	t/c	121.04	0.8	121.04	0.8	121.36	1.1	121.11	0.9	121.11	0.9	120.03	–
20	Bend	15.50	0.8	15.39	0.	15.51	0.8	15.52	0.9	15.41	0.2	15.38	15.38
	Bend	49.99	2.	49.04	0.1	49.82	1.7	49.88	1.8	49.04	0.1	48.98	48.94
	Bend	89.53	2.8	87.18	0.2	89.03	2.3	89.16	2.5	87.07	0.1	87.01	86.90
	Bend	169.56	3.6	164.26	0.4	168.41	2.9	168.55	3.0	163.69	0.1	163.58	163.12
	Bend	209.45	3.8	202.88	0.6	208.08	3.1	208.10	3.2	201.94	0.1	201.64	200.87
	t/c	242.08	0.2	242.06	0.2	242.73	0.4	242.64	0.4	240.59	0.4	241.61	–

3.4.2. Five-layer sandwich beam [18]

In this part, a five-layer sandwich beam is concerned. It is described in the following.

Geometry: the five-layer sandwich beam with three stiff isotropic layers at top/bottom/middle and two soft cores sandwiched in between (face/core/face/core/face): $h_c = 10.16$ mm, $h_f = 0.508$ mm – $L = 508$ mm, width $= 25.4$ mm, $h = 21.844$ mm– $S \approx 2.5,\ 5,\ 25$
Boundary conditions: simply supported beam.
Material properties: isotropic face: $E_f = 68.97 \times 10^3$ MPa, $\nu = 0.3$ $\rho = 2.7155 \times 10^2$ kg/m^3; isotropic core: $G_c = 34.485$ MPa, $\nu = 0.3$, $\rho = 67.8840$ kg/m^3.

The natural frequencies obtained from the present investigation are compared in Table 8 with two reference solutions (from [18] and the commercial code). Again, the SinRef-7p model yields very accurate results even for a very thick case. The main improvement occurs between the SinRef-6p and SinRef-7p models what shows the importance of the additional unknown $v(x_1)$. For this example, we also observe the necessity to satisfy the continuity of the transverse shear stress at the layer interfaces. This effect is particularly high (Cf Sin and Sin-c results).

3.5. Influence of boundary conditions

Free vibrations of beams with arbitrary boundary conditions are studied. Under the considerations of Sections 3.2, 3.3 and 3.4, only the SinRef-7p model is applied for the determination of frequencies, namely the most accurate theory among the ones already tested. These results are compared with higher-order shear deformation theory from [11]. It should be noted that these theories do not ensure the continuity of the transverse shear stress on the interfaces between the layers for the unsymmetric beam. This limitation does not exist in our approach.

The considered test has the following characteristics:

Geometry: composite cross-ply beam (0°/90°/0°) and (0°/90°) with $S = 5$, and layers of equal thickness.
Boundary conditions: clamped/clamped (CC), free/free (FF), simply supported/free (SF), clamped/simply supported (CS), simply supported/simply supported (SS), clamped/free (CF) beam.
Material properties:

$$E_1/E_2 = 40, \quad G_{12} = G_{13} = 0.6E_2, \quad G_{23} = 0.5E_2,$$
$$\nu_{12} = 0.25$$

Results: the natural frequencies are normalized as $\bar{\omega} = \omega L^2\sqrt{(\rho/E_2)}/h$. A comparison with the published numerical results from [11] is carried out. It implies two models:
HSDBT Hyperbolic shear deformation beam theory
PSDBT Parabolic shear deformation beam theory
the indices *ds* or *cs* stand for discontinuity and continuity interlaminar stress respectively.

The results for different stacking sequences are given in Table 9. As one can observe for the symmetric beam, the frequencies for the SinRef-7p model are always upper than these of the two other models, excepted for the CC condition. Concerning the unsymmetric case, results are always lower than the two other discontinuous models, and the difference is about 10%. This fact is already observed by [11] between continuous and discontinuous models. Nevertheless, as for Section 3.3, we can say that the present model exhibits the most reliable performance.

Table 8
Frequencies – five-layer sandwich beam [18].

S	Frequencies (Hz)											
	Sin	Error (%)	Sin-c	Error (%)	SinRef-c	Error (%)	SinRef-6p	Error (%)	SinRef-7p	Error (%)	ANSYS	Ref. [18]
≈2.5	931.13	344	203.25	2.9	225.17	7.6	226.03	8.0	203.55	2.8	209.31	–
	2366.8	451	417.42	2.7	468.20	9.1	468.20	9.1	419.67	2.2	429.12	–
	2519.5	442	482.77	4	469.70	1.2	475.62	2.5	463.90	0.0	464.01	–
	2769.3	318	645.38	2.5	739.50	11.7	757.36	14.4	652.69	1.4	661.86	–
≈5	297.24	200	97.91	1.5	107.32	7.9	107.47	8.1	97.96	1.5	99.45	–
	931.32	350	203.25	1.6	225.17	9.0	226.04	9.4	203.55	1.5	206.67	–
	1259.8	300	309.13	1.6	345.07	9.8	347.72	10.7	310.13	1.3	314.16	–
	1647.8	288	417.43	1.5	468.20	10.5	468.20	10.5	419.86	0.9	423.80	–
	2366.9	410	482.77	4	470.01	1.3	475.95	2.6	463.86	0.0	464.01	–
	2519.6	369	529.24	1.4	602.06	12.2	613.15	14.2	534.28	0.4	536.69	–
	2769.3	323	645.49	1.3	743.36	13.7	761.76	16.5	655.11	0.2	653.79	–
≈25	13.43	23	11.26	3	11.58	6	11.59	6	11.26	3.2	10.90	10.91
	52.80	65	32.58	1.7	34.64	7	34.66	7	32.59	1.2	32.02	32.20
	115.59	113	54.74	1	59.21	8	59.25	8	54.77	0.2	54.23	54.65
	198.34	160	76.50	0.5	83.50	8	83.59	8	76.58	0.2	76.09	76.74
	251.95	158	97.92	0.3	107.49	9	107.65	9	98.10	0.4	97.61	98.47
	297.39	150	119.13	0.1	131.37	9	131.63	9	119.52	0.4	118.94	119.96

Table 9
Comparison of frequencies for composite beams with (0°/90°/0°) and (0°/90°) layouts.

	Models	FF	CC	SF	CS	SS	CF
(0°/90°/0°)	PSDBT$_{cs}$ [11]	18.976	11.446	13.206	10.032	8.968	4.158
	HSDBT$_{cs}$ [11]	18.955	11.427	13.195	10.021	8.964	4.157
	SinRef-7p	19.123	11.100	13.472	10.000	9.201	4.189
(0°/90°)	PSDBT$_{ds}$ [11]	13.000	10.103	9.221	8.068	6.144	2.384
	HSDBT$_{ds}$ [11]	12.849	10.059	9.162	8.037	6.124	2.383
	SinRef-7p	11.709	8.743	8.413	7.153	5.671	2.289

Table 10
Comparison of non-dimensional frequencies for soft core sandwich beam (0°/90°/core/0°/90°).

S	Models	$\bar{\omega}$				
4	GLHT	0.638	1.800	3.631	6.133	9.276
	ZZT	0.616	1.772	3.621	6.186	9.464
	HSDT-33	1.495	3.277	5.497	7.735	10.182
	HSDT-Reddy	2.249	4.682	7.293	10.176	13.396
	SinRef-7p	0.645	1.819	3.674	6.223	9.463
10	GLHT	1.346	2.993	5.126	7.860	11.250
	ZZT	1.282	2.874	4.970	7.685	11.075
	HSDT-33	3.468	7.355	11.402	15.748	20.481
	HSDT-Reddy	5.012	11.075	17.051	23.089	29.263
	SinRef-7p	1.361	3.026	5.183	7.961	11.442

In all cases, the highest frequencies occur for the FF boundary condition.

3.6. Comparison with results available in the literature

In this paragraph, the most enriched model (SinRef-7p) is compared with results available in the literature. Unsymmetric beams are chosen from [20].

The finite element is tested with a deep laminated sandwich beam composed of two face sheets of (0/90) lay-up at the top and bottom with core sandwiched in between (0°/90°/core/0°/90°).

Geometry: five-layer sandwich beam with soft core: $h_c/h_f = 10$.
Boundary conditions: simply supported beam.
Material properties:
Face sheets: $E_{1f} = 131$ GPa, $E_{2f} = E_{3f} = 10.34$ GPa, $\nu_{12} = \nu_{13} = 0.22$, $\nu_{23} = 0.49$, $G_{12f} = G_{23f} = 6.895$ GPa, $G_{13f} = 6.205$ GPa, $\rho_f = 1627$ kg/m^3.
Isotropic core: $G_c = 3.45$ MPa, $\nu = 0.$, $E_c = 6.89$ MPa, $\rho_c = 97$ kg/m^3.

Results: the natural frequencies are normalized as $\bar{\omega} = \omega L^2 \sqrt{(\rho_f/E_{2f})}/h$. The results of four other models are given from [20]:

- GLHT (6 parameters) analytical results based on global–local higher order theory [59].
- ZZT (3 parameters) zig-zag theory satisfying the continuity of transverse shear stress at interfaces [40].
- HSDT-33 third order theory for in-plane and transverse displacements.
- HSDT-Reddy (3 parameters) Reddy's model.

The comparison of non-dimensional frequencies with the available results from [20] are given in Table 10 for thick and semi-thick beams. In all cases, we observe that the SinRef-7p models give results very close to the GLHT model which is considered as a reference in [20]. We can also notice that the increasing of the order expansion of the transverse displacement is not sufficient to get good results. In fact, the frequencies of the HSDT-33 model are very overestimated. It is more important to ensure the continuity of the transverse shear stress.

4. Conclusion

In the framework of a sinus family, two numerical models have been presented and assessed through a wide variety of stacking sequences, length to thickness ratios, and boundary conditions in free vibration analysis. Special attention is pointed towards the transverse normal stress effect which plays an important role in thick cases. It is a three-node multilayered beam finite element with a parabolic distribution of transverse displacement. Based on sinus equivalent single layer model, a third order kinematic per layer is added, improving the shear bending description for thick beams. There is no need for transverse shear correction factors and all the interface and boundary conditions are exactly satisfied. So, this approach has a strong physical meaning. Finally, the number of unknowns is independent of the number of layers.

All these different examples prove the efficiency of the family of refined sinus models for laminated composite and sandwich beams in the field of finite element. Few elements are needed to obtain good results. The new models have very good capability for a wide area of applications. In particular, for the very thick case ($S = 2$), the SinRef-7p model which take into account the transverse normal effect yields very accurate results for both frequencies and mode shapes. Nevertheless, for the thin beam, it seems that the Sin-c model presents a good compromise between the accuracy and the computational cost.

A. Matrix expression for the weak form

The expressions of the strains can be described using a matrix notation:

$$[\varepsilon] = [F_s(z)][\mathscr{E}_s]$$
$$\text{with } [\mathscr{E}_s]^T = \Big[u_{,1} \ \vdots\ w_{0,1}\ w_{0,11} \ \vdots\ \omega_3\ \omega_{3,1} \ \vdots\ u^1_{31}\ u^1_{31,1} \ \vdots\ v\ v_{,1} \ \vdots\ w_1\ w_{1,1}\ w_{1,11} \ \vdots\ w_2\ w_{2,1}\ w_{2,11}\Big] \quad \text{(A.1)}$$

and $[F_s(z)]$ depends on the normal coordinate z.

From the weak form of the boundary value problem Eq. (2), and using Eq. (A.1), an integration throughout the cross section is performed analytically in order to obtain an unidimensional formulation. Therefore, the first left term of Eq. (2) can be written under the following form:

$$\int_{\mathscr{B}} [\varepsilon(\vec{u}^*)]^T [\sigma(\vec{u})] d\mathscr{B} = \int_0^L [\mathscr{E}_s^*]^T [k][\mathscr{E}_s] dx_1 \quad \text{with}$$
$$[k] = \int_{\Omega} [F_s(z)]^T [C][F_s(z)] d\Omega \quad \text{(A.2)}$$

where $[C]$ is the constitutive law given in Section 2.1.1.

In Eq. (A.2), the matrix $[k]$ is the integration throughout the cross section of the beam material characteristics.

References

[1] Basset AB. On the extension and flexure of cylindrical and spherical thin elastic shells. Philos Trans Roy Soc (London) Ser A 1890;181:433–80.
[2] Tanigawa Y, Murakami H, Ootao Y. Transient thermal stress analysis of a laminated composite beam. J Therm Stress 1989;12:25–39.
[3] Nabi SM, Ganesan N. A generalized element for the free vibration analysis of composite beams. Compos Struct 1994;51(1):607–10.
[4] Eisenberger M, Abramovich H, Shulepov O. Dynamic stiffness analysis of laminated beams using a first order shear deformation theory. Compos Struct 1995;31:265–71.
[5] Teboub Y, Hajela P. Free vibration of generally layered composite beams using symbolic computations. Compos Struct 1995;33:123–34.
[6] Yildirim V. Effect of the longitudinal to transverse moduli ratio on the in-plane natural frequencies of symmetric cross-ply laminated beams by the stiffness method. Compos Struct 2000;50:319–26.
[7] Chakraborty A, Roy Mahapatra R, Gopalakrishnan S. Finite element analysis of free vibration and wave propagation in asymmetric composite beams with structural discontinuities. Compos Struct 2002;55:23–36.
[8] Goyal VK, Kapania RK. A shear-deformable beam element for the analysis of laminated composites. Finite Elements Anal Des 2007;43:463–77.
[9] Jun L, Hongxing H, Rongying S. Dynamic finite element method for generally laminated composite beams. Int J Mech Sci 2008;50:466–80.
[10] Chandrashekhara K, Bangera KM. Free vibration of composite beams using a refined shear flexible beam element. Comput Struct 1992;43:719–27.

[11] Aydogdu M. Vibration analysis of cross-ply laminated beams with general boundary conditions by Ritz method. Int J Mech Sci 2005;47:1740–55.

[12] Karama M, Afaq KS, Mistou S. Mechanical behaviour of laminated composite beam by the new multi-layered laminated composite structures model with transverse shear stress continuity. Int J Solids Struct 2003;40:1525–46.

[13] Marur SR, Kant T. Free vibration analysis of fiber reinforced composite beams using higher order theories and finite element modelling. J Sound Vib 1996;194:337–51.

[14] Murthy MVVS, Roy Mahapatra D, Badarinarayana K, Gopalakrishnan S. A refined higher order finite element for asymmetric composite beams. Compos Struct 2005;67(1):27–35.

[15] Soldatos KP, Elishakoff I. A transverse shear and normal deformable orthotropic beam theory. J Sound Vib 1992;155(3):528–33.

[16] Shi G, Lam KY. Finite element vibration analysis of composite beams based on higher-order beam theory. J Sound Vib 1999;219:707–21.

[17] Kant T, Marur SR, Rao GS. Analytical solution to the dynamic analysis of laminated beams using higher order refined theory. Compos Struct 1998;40(1):1–9.

[18] Kameswara Rao M, Desai YM, Chitnis MR. Free vibrations of laminated beams using mixed theory. Comput Struct 2001;52:149–60.

[19] Matsunaga H. Vibration and buckling of multilayered composite beams according to higher order deformation theories. J Sound Vib 2001;246(1):47–62.

[20] Zhen W, Wanji C. An assessment of several displacement-based theories for the vibration and stability analysis of laminated composite and sandwich beams. Compos Struct 2008;84:337–49.

[21] Subramanian P. Dynamic analysis of laminated composite beams using higher order theories and finite elements. Compos Struct 2006;73:342–53.

[22] Rao MK, Desai YM, Chitnis MR. Free vibrations of laminated beams using mixed theory. Compos Struct 2001;52:149–60.

[23] Chen WQ, Lv CF, Bian ZG. Elasticity solution for free vibration of laminated beams. Compos Struct 2003;62:75–82.

[24] Heller RA, Swift GW. Solutions for the multilayer timoshenko beam. In: Report N VPI-E-71-12. Virginia Polytechnic Institute, Blacksburg, VA; 1971.

[25] Swift GW, Heller RA. Layered beam analysis. J Eng Mech ASCE 1974;100:267–82.

[26] Srinivas S. A refined analysis of laminated composites. J Sound Vib 1973:495–507.

[27] Whitney JM. The effect of transverse shear deformation in the bending of laminated plates. J Comput Mater 1969;3:534–47.

[28] Pagano NJ. Exact solutions for composite laminates in cylindrical bending. J Comput Mater 1969;3:398–411.

[29] Shimpi RP, Ainapure AV. A beam finite element based on layerwise trigonometric shear deformation theory. Compos Struct 2001;53:153–62.

[30] Tahani M. Analysis of laminated composite beams using layerwise displacement theories. Compos Struct 2007;79(4):535–47.

[31] Lee C-Y, Liu D, Lu X. Static and vibration analysis of laminated composite beams with an interlaminar shear stress continuity theory. Int J Num Meth Eng 1992;33:409–24.

[32] Ramtekkar GS, Desai YM, Shah AH. Natural vibrations of laminated composite beams by using mixed finite element modelling. J Sound Vib 2002;257:635–51.

[33] Plagianakos TS, Saravanos DA. High-order layerwise mechanics and finite element for the damped dynamic characteristics of sandwich composite beams. Int J Solids Struct 2004;41:6853–71.

[34] Baber TT, Maddox RA, Orozco CE. A finite element model for harmonically excited viscoelastic sandwich beams. Comput Struct 1998;66:105–13.

[35] Bekuit J-JRB, Oguamanam DCD, Damisa O. A quasi-2D finite element formulation for the analysis of sandwich beams. Finite Elements Anal Des 2007;43:1099–107.

[36] Banerjee JR, Sobey AJ. Dynamic stiffness formulation and free vibration analysis of a three-layered sandwich beam. Int J Solids Struct 2005;42:2181–97.

[37] Ambartsumyan SA. Theory of anisotropic plates. In: Cheron T, Ashton JE, editors. Technomic Publishing Co.; 1969 [translated from russian].

[38] Di Sciuva M. Bending, vibration and buckling of simply supported thick multilayered orthotropic plates: an evaluation of a new displacement model. J Sound Vib 1986;105:425–42.

[39] Bhaskar K, Varadan TK. Refinement of higher-order laminated plate theories. AIAA J 1989;27:1830–1.

[40] Cho M, Parmerter R. Efficient higher-order composite plate theory for general lamination configurations. AIAA J 1993;31:1299–306.

[41] Averill RC, Yip YC. Thick beam theory and finite element model with zig-zag sublaminate approximations. AIAA J 1996;34(8):1627–32.

[42] Aitharaju VR, Averill RC. C^0 zig-zag finite element for analysis of laminated composite beams. J Eng Mech ASCE 1999;125:323–30.

[43] Di Sciuva M, Icardi U. Numerical assessment of the core deformability effect on the behavior of sandwich beams. Compos Struct 2001;52:41–53.

[44] Gaudenzi P, Barboni R, Mannini A. A finite element evaluation of single-layer and multi-layer theories for the analysis of laminated plates. Compos Struct 1995;30:427–40.

[45] Gherlone M, Di Sciuva M. Thermo-mechanics of undamaged and damaged multilayered composite plates: a sub-laminates finite approach. Comput Struct 2007;81:125–36.

[46] Kapuria S, Dumir PC, Ahmed A. An efficient higher order zigzag theory for composite and sandwich beams subjected to thermal loading. Int J Solids Struct 2003;40:6613–31.

[47] Carrera E. Historical review of zig-zag theories for multilayered plates and shells. Appl Mech Rev 2003;56(3):287–308.

[48] Noor AK, Burton WS. Assessment of computational models for multilayered composite shells. Appl Mech Rev 1990;43(4):67–97.

[49] Reddy JN. Mechanics of laminated composite plates – theory and analysis. Boca Raton (FL): CRC Press; 1997.

[50] Carrera E. Theories and finite elements for multilayered, anisotropic, composite plates and shells. Arch Comput Meth Eng 2002;9:87–140.

[51] Zhang YX, Yang CH. Recent developments in finite elements analysis for laminated composite plates. Compos Struct 2009;88:147–57.

[52] Mittelstedt C, Beckerm W. Free-edge effects in composite laminates. Appl Mech Rev 2007;60:217–44.

[53] Kant T, Swaminathan K. Estimation of transverse/interlaminar stresses in laminated composites – a selective review and survey of current developments. Compos Struct 2000;49:65–75.

[54] Kapania RK, Raciti S. Recent advances in analysis of laminated beams and plates, part II: vibrations and wave propagation. AIAA J 1989;27:935–46.

[55] Ghugal YM, Shimpi RP. A review of refined shear deformation theories for isotropic and anisotropic laminated beams. J Reinf Palst Compos 2001;20:255–72.

[56] Touratier M. A generalization of shear deformation theories for axisymmetric multilayered shells. Int J Solids Struct 1992;29:1379–99.

[57] Ganapathi M, Patel BP, Polit O, Touratier M. A C^1 finite element including transverse shear and torsion warping for rectangular sandwich beams. Int J Num Meth Eng 1999;45:47–75.

[58] Carrera E, Brischetto E. Analysis of thickness locking in classical, refined and mixed multilayered plate theories. Compos Struct 2008;82:549–62.

[59] Li X, Liu D. Generalized laminate theories based on double superposition hypothesis. Int J Num Meth Eng 1997;40:1197–212.

[60] Vidal P, Polit O. A family of sinus finite elements for the analysis of rectangular laminated beams. Compos Struct 2008;84:56–72. doi:10.1016/j.compstruct.2007.06.009.

[61] Touratier M. An efficient standard plate theory. Int J Eng Sci 1991;29:901–16.

[62] Dau F, Polit O, Touratier M. C^1 plate and shell finite elements for geometrically nonlinear analysis of multilayered structures. Comput Struct 2006;84:1264–74.

[63] Polit O, Touratier M. A multilayered/sandwich triangular finite element applied to linear and nonlinear analysis. Compos Struct 2002;58:121–8.

[64] Touratier M. A refined theory of laminated shallow shells. Int J Solids Struct 1992;29(11):1401–15.

[65] Vidal P, Polit O. A thermomechanical finite element for the analysis of rectangular laminated beams. Finite Elements Anal Des 2006;42(10):868–83.

[66] Vidal P, Polit O. Assessment of the refined sinus model for the non-linear analysis of composite beams. Compos Struct 2009;87:370–81. doi:10.1016/j.compstruct.2008.02.007.

[67] Sze KY, Chen R, Cheung YK. Finite element model with continuous transverse shear stress for composite laminates in cylindrical bending. Finite Elements Anal Des 1998;31:153–64.

[68] Wu Z, Chen R, Chen W. Refined laminated composite plate element based on global–local higher-order shear deformation theory. Compos Struct 2005;70(2):135–52.

[69] Zhen W, Wanji C. Refined global–local higher-order theory and finite element for laminated plates. Int J Num Meth Eng 2007;69:1627–70.

[70] Vidal P, Polit O. A refined sinus finite element with transverse normal deformation for the analysis of laminated beams under thermomechanical loads. J Mech Mater Struct 2009;4(6):1127–55.

[71] Polit O, Touratier M, Lory P. A new eight-node quadrilateral shear-bending plate finite element. Int J Num Meth Eng 1994;37:387–411.

[72] Karama M, Abou Harb B, Mistou S, Caperaa S. Bending buckling and free vibration of laminated composite with a transverse shear stress continuity model. Compos Part B: Eng J 1998;29:223–34.

[73] Kapuria S, Dumir PC, Jain NK. Assessment of zigzag theory for static loading, buckling, free and forced response of composite and sandwich beams. Compos Struct 2004;64:317–27.

[74] Ansys I. Ansys theoretical manual. Swanson Analysis Inc.; 1986.

Mechanics Research Communications 38 (2011) 388–392

Contents lists available at ScienceDirect

Mechanics Research Communications

journal homepage: www.elsevier.com/locate/mechrescom

Higher-order shear beam theories and enriched continuum

N. Challamel*

Université Européenne de Bretagne, INSA de Rennes – LGCGM, 20, avenue des Buttes de Coësmes, 35708 Rennes cedex 7, France

ARTICLE INFO

Article history:
Received 3 January 2011
Received in revised form 15 March 2011
Available online 24 May 2011

Keywords:
Higher-order beam theories
Nonlocal mechanics
Shear models
Buckling
Variational arguments
Gradient elasticity model
Composite beams
Microstructure

ABSTRACT

The buckling of higher-order shear beam-columns is studied in the light of enriched continuum. We show the equivalence between the enriched kinematics of usual higher-order shear beam theories with the nonlocal and gradient nature of the associated constitutive law. These equivalences are useful for a hierarchical classification of usual beam theories comprising Euler–Bernoulli beam theory, Timoshenko and third-order shear beam theories. A consistent variationnally presentation is derived for all generic theories, leading to meaningful buckling solutions. It is shown that Timoshenko or some other higher-order shear theories can be considered as nonlocal or gradient Euler–Bernoulli theories. The buckling problem of a third-order shear beam-column is analytically studied and treated in the framework of gradient elasticity Timoshenko theory. Some different gradient elasticity Timoshenko models are presented at the end of the paper with available buckling solutions for repetitive structures and microstructured beams.

© 2011 Elsevier Ltd. All rights reserved.

1. Introduction

Since the beginning of the XXIth century, there has been a considerable interest in the modelling of small-scale structures comprising micro and nanostructures. These small-scale structures present some scale effects that can be captured using nonlocal mechanics (Wang et al., 2010a). Therefore, many recent researches in theoretical mechanics have been focused on the development of theoretical solutions of structural stability (and dynamics) problems, with some additional scale parameters introduced in the nonlocal constitutive law. Some reference nonlocal solutions have been published for beam, plate, shell structural models (see for instance (Wang et al., 2010a)). In a certain sense, one could say that the mechanics community has investigated the small-scale world with specific constitutive laws generally issued of nonlocal mechanics, including gradient or integral-based nonlocal models. On the other hand, it has been also recently shown that some generic structural models used for mechanical or civil engineering problems belong to the class of nonlocal mechanics. Challamel and Wang (2008) used a nonlocal mechanics model to highlight some specific scale effects for a micro and nano-cantilever elastic structural case. This beam model has also been used at the macroscale level for composite beams or sandwich elastic beams (see also (Zhang et al., 2010) or (Challamel and Girhammar, 2011)). Therefore, nonlocality has a wide range of applications from small-scale structures to large-scale structures, even if the source of nonlocality is physically and inherently different. We do not discuss here the nonlocal inelasticity models (plasticity or damage) used for macroscale or microscale structures in presence of softening (see (Bažant and Cedolin, 2003) or more recently (Challamel et al., 2010a) or (Challamel, 2010)). In the present paper, we discuss the buckling of higher-order shear beam-columns in the light of enriched continuum, namely nonlocal and gradient mechanics. We show the equivalence between the enriched kinematics of usual higher-order beam theories with the nonlocal and gradient nature of the associated constitutive law. These equivalences are useful for a hierarchical classification of usual beam theories comprising Euler–Bernoulli beam theory, Timoshenko and third-order shear beam theories.

With respect to integral-based elasticity nonlocal model, Eringen's based nonlocal model (Eringen, 1983) has been shown to be efficient to take into account scale effects at the beam scale for most structural cases (see for instance Peddieson et al. (2003) for the bending problem, or more recently Challamel and Wang (2008). Sudak (2003) obtained the buckling solution for some Euler–Bernoulli beam problems including Eringen's nonlocal terms. These results have been extended to Timoshenko nonlocal columns (see for instance (Wang et al., 2006); (Reddy, 2007)). Wang et al. (2009) investigated the post-buckling problem of cantilevered nano rods/tubes under an end concentrated load. Reddy (2010) gave the general nonlinear formulation of higher-order beam models with Eringen's constitutive law. Challamel and Wang (2010) studied the lateral-torsional buckling problem of Eringen's based

---

* Tel.: +33 2 23 23 84 78; fax: +33 2 23 23 84 91.
E-mail address: noel.challamel@insa-rennes.fr

0093-6413/$ – see front matter © 2011 Elsevier Ltd. All rights reserved.
doi:10.1016/j.mechrescom.2011.05.004

nonlocal beams. Challamel et al. (2010b) studied the buckling of elastic beams on nonlocal foundation, or the buckling of beam systems with nonlocal elastic connections (Challamel et al., in press). Another family of enriched continuum is the so-called gradient models where the constitutive law also depends on the gradients of the state variables. The in-plane buckling of gradient elasticity Euler–Bernoulli column has been studied by Papargyri-Beskou et al. (2003). Lam et al. (2003) also developed a gradient elasticity Euler–Bernoulli beam and show the stiffening effect of small length terms. Lazopoulos (2003) studied the post-buckling behaviour of gradient elasticity columns. Park and Gao (2006) developed a modified couple stress theory for Euler–Bernoulli kinematics. Kong et al. (2009) developed a general gradient elasticity theory including the modified couple stress theory for the Euler–Bernoulli beam models. Ma et al. (2008) extended the modified couple stress theory of Park and Gao (2006) to Timoshenko beam models. These models are included in the gradient elasticity Timoshenko beam models of Wang et al. (2010b).

2. Euler–Bernoulli beam mechanics

The energy functional for the buckling of "local" Euler–Bernoulli columns is given by:

$$U[w] = \int_0^L \frac{1}{2} EIw''^2 - \frac{1}{2} Pw'^2 dx \tag{1}$$

where L is the length of the column, P is the axial load, w is the deflection, EI is the bending stiffness. The Euler–Bernoulli beam mechanics is based on the one-dimensional constitutive law:

$$M = EI\chi \quad \text{with} \quad \chi = -w'' \tag{2}$$

where M is the bending moment, and χ is the curvature. The stationarity of the energy functional $\delta U = 0$ leads to the differential equations:

$$EIw^{(4)} + Pw'' = 0 \tag{3}$$

with the natural and essential boundary conditions:

$$\left[EIw''\delta w'\right]_0^L = 0 \quad \text{and} \quad \left[-(EIw''' + Pw')\delta w\right]_0^L = 0 \tag{4}$$

For instance, for the pinned-pinned case, the Euler buckling formulae is simply:

$$P = P^E \quad \text{with} \quad P^E = EI\left(\frac{\pi}{L}\right)^2 \tag{5}$$

3. Timoshenko beam mechanics

This part is devoted to the "local" Timoshenko theory that can be understood as a nonlocal Euler–Bernoulli beam theory. In the hierarchical classification, the Timoshenko model can be considered as a superior model that includes the Euler–Bernoulli one when the shear effect can be neglected. In presence of axial loads, Engesser and Haringx's type models have to be distinguished (see Bažant and Cedolin (2003) for instance). A discussion about the hyperelastic formulation of generic Timoshenko models can be found in Reissner (1982), Bažant (2003), Hodges et al. (2006) or Attard and Hunt (2008). The energy functional of Engesser-type Timoshenko column is given by:

$$U[\psi, w] = \int_0^L \frac{1}{2} EI\psi'^2 + \frac{\kappa GA}{2}(w' - \psi)^2 - \frac{1}{2} Pw'^2 dx \tag{6}$$

where ψ is the rotation, G is the shear modulus, A is the total area, κ is the so-called shear coefficient, a dimensionless factor. It should be noted that asymptotic methods may provide a more consistent way to determine the shear stiffnesses without assuming shear correction factors or plane sections remain plane (Yu and Hodges, 2005). The Timoshenko beam mechanics is based on the two-dimensional constitutive law:

$$\begin{pmatrix} M \\ V \end{pmatrix} = \begin{pmatrix} EI & 0 \\ 0 & \kappa GA \end{pmatrix} \begin{pmatrix} \hat{\chi} \\ \gamma \end{pmatrix} \quad \text{with} \quad \begin{pmatrix} \hat{\chi} \\ \gamma \end{pmatrix} = \begin{pmatrix} -\psi' \\ w' - \psi \end{pmatrix} \tag{7}$$

where M is the bending moment, V is the shear force, $\hat{\chi}$ is the pseudo-curvature and γ is the shear strain. The stationarity of the energy functional $\delta U = 0$ leads in this case to:

$$\begin{cases} -\kappa GA(w'' - \psi') + Pw'' = 0 \\ EI\psi'' + \kappa GA(w' - \psi) = 0 \end{cases} \tag{8}$$

with the natural and essential boundary conditions:

$$\left[EI\psi'\delta\psi\right]_0^L = 0 \quad \text{and} \quad \left[(-EI\psi'' - Pw')\delta w\right]_0^L = 0 \tag{9}$$

The characteristic length l_c can be introduced as:

$$l_c = \sqrt{\frac{EI}{\kappa GA}} \tag{10}$$

The system of differential equations is now written with such a characteristic length as:

$$\begin{cases} -EI(w'' - \psi') + Pl_c{}^2 w'' = 0 \\ \psi - l_c{}^2 \psi'' = w' \end{cases} \tag{11}$$

The second equation shows that the rotation ψ is the nonlocal spatial average variable of the slope angle w':

$$\psi = \overline{w'} \quad \text{with} \quad \overline{w'} - l_c{}^2 \overline{w'}'' = w' \tag{12}$$

The Timoshenko theory is clearly a nonlocal Euler–Bernoulli beam theory where the rotation ψ of the cross section is the nonlocal spatial average variable of the slope angle w'. A similar conclusion could be anticipated from the paper of Falsone and Settineri (2011) even if the nonlocal mechanics has not been explicitly used. Furthermore, Eq. (11) leads to the uncoupled differential equation:

$$(EI - Pl_c^2)\psi''' + P\psi' = 0 \quad \text{or} \quad (EI - Pl_c^2)w^{(4)} + Pw'' = 0 \tag{13}$$

leading to the well-known Engesser formulae for most boundary conditions except for instance the fixed-pinned conditions (see Plantema (1966), Ziegler (1982) or Wang et al. (2005)):

$$P^T = \frac{P^E}{1 + P^E/\kappa GA} = \frac{P^E}{1 + (P^E/EI)l_c^2} \tag{14}$$

For instance, for the pinned-pinned case, the Engesser formulae is simplified in:

$$\frac{P^T}{P^E} = \frac{1}{1 + \pi^2(l_c/L)^2} \quad \text{with} \quad P^E = EI\left(\frac{\pi}{L}\right)^2 \tag{15}$$

This is also the formula of the in-plane and out-of-plane buckling problem of Euler–Bernoulli beam model with Eringen's nonlocal law (see for instance Challamel and Wang (2010)). In fact, the nonlocal Euler–Bernoulli constitutive law is written as:

$$M - l_c^2 M'' = EI\chi \quad \text{or equivalently} \quad M = EI\overline{\chi} \quad \text{with} \quad \overline{\chi} - l_c^2 \overline{\chi}'' = \chi \tag{16}$$

with χ as the curvature (one can choose $\chi = -w''$). This nonlocal constitutive law can be also presented in an integral format using the Green's operator associated with this differential equation:

$$M(x) = \int_0^L G(x, y)\chi(y)dy \tag{17}$$

The elastic energy of the nonlocal Euler–Bernoulli column can be expressed in the following form (see Challamel and Wang (2008); Zhang et al. (2010)):

$$U[w] = \int_0^L \frac{1}{2}EI\chi\overline{\chi} - \frac{1}{2}Pw'^2 dx \tag{18}$$

Eq. (18) is also equivalent to the double integral representation of the nonlocal beam problem, generally considered for integral nonlocal elasticity problems:

$$U[w] = \int_0^L \int_0^L \frac{1}{2}EIG(x,y)\chi(x)\chi(y)\,dxdy - \int_0^L \frac{1}{2}Pw'^2 dx \tag{19}$$

which is also equivalent to:

$$U[w] = \int_0^L \frac{1}{2}(EI - Pl_c^2)w''^2 - \frac{1}{2}Pw'^2 dx \tag{20}$$

The differential equation of the buckling of nonlocal Euler–Bernoulli column is obtained from application of the variational principle, and is given for instance by Zhang et al. (2010):

$$(EI - Pl_c^2)w^{(4)} + Pw'' = 0 \tag{21}$$

which is exactly the differential equation of the Timoshenko column (see Eq. (13)). Zhang et al. (2010) already mentioned the analogy between the vibrations problem of nonlocal Euler–Bernoulli beams and the vibrations problem of Rayleigh beams. It is shown in the present paper that the buckling problem of "local" Timoshenko column is equivalent to the one of the nonlocal Euler–Bernoulli column. Therefore, Timoshenko buckling formulae will be strictly equivalent to nonlocal Euler–Bernoulli buckling formulae if the same boundary conditions at the beam extremity are equivalent. The Timoshenko model degenerates into the local Euler–Bernoulli model when the length scale l_c is vanishing (infinite shear stiffness).

4. Higher-order shear beam mechanics

The Timoshenko beam model requires shear correction factors to compensate for the error due to the constant shear stress assumption. Some higher-order shear beam theories have been developed to enrich the simplified kinematics of Timoshenko model, with a polynomial compensation. In this enriched theory, the transverse shear strain (and shear stress) is vanishing on the top and bottom planes of the beam. Bickford–Reddy's theory typically belongs to this class of enriched beam kinematics (see (Levinson, 1981; Bickford, 1982; Reddy, 1984; Levinson, 1985)). The buckling of Bickford–Reddy column is studied by Wang et al. (2000). The theory of Shi and Voyiadjis (2011) (see also (Voyiadjis and Shi, 1991)) has been developed in a variationnally consistent framework, and is slightly different from the theory of Bickford–Reddy, even if it is a third-order shear theory. The energy functional of Shi and Voyiadjis-type column is given by:

$$\begin{aligned} U[\psi, w] = \int_0^L & \frac{1}{2}EI\psi'^2 + \frac{\kappa GA}{2}(w' - \psi)^2 \\ & + a^2\frac{\kappa GA}{2}(w'' - \psi')^2 - \frac{1}{2}Pw'^2 dx \end{aligned} \tag{22}$$

This is clearly a gradient elasticity Timoshenko model with an additional length scale denoted by a. The shear stiffness and the additional gradient term are obtained from:

$$\kappa GA = \frac{25}{16}\int_S G\left(1 - 4\frac{y^2}{h^2}\right)^2 dS \quad \text{and} \quad a = \sqrt{\frac{1}{84}\frac{EI}{\kappa GA}} \tag{23}$$

The modified gradient Timoshenko beam model is based on the three-dimensional constitutive law:

$$\begin{pmatrix} M \\ V \\ M^* \end{pmatrix} = \begin{pmatrix} EI & 0 & 0 \\ 0 & \kappa GA & 0 \\ 0 & 0 & \kappa GAa^2 \end{pmatrix} \begin{pmatrix} \hat{\chi} \\ \gamma \\ \gamma' \end{pmatrix} \quad \text{with} \quad \begin{pmatrix} \hat{\chi} \\ \gamma \\ \gamma' \end{pmatrix} = \begin{pmatrix} -\psi' \\ w' - \psi \\ w'' - \psi' \end{pmatrix} \tag{24}$$

M^* can be considered as a higher-order moment (see also (Wang et al., 2000)). The stationarity of the energy functional $\chi U = 0$ leads in this case to the principle of virtual work of this gradient system:

$$\delta U = \int_0^L M\delta\hat{\chi} + V\delta\gamma + M^*\delta\gamma' - Pw'\delta w'\,dx = 0 \tag{25}$$

The usual format of the principle of virtual work of gradient elasticity systems is clearly recognized in Eq. (25) (see more generally (Germain, 1973)). The stationarity principle leads to the system of differential equations:

$$\begin{cases} -\kappa GA(w'' - \psi') + Pw'' + a^2\kappa GA(w^{(4)} - \psi''') = 0 \\ EI\psi'' + \kappa GA(w' - \psi) - a^2\kappa GA(w''' - \psi'') = 0 \end{cases} \tag{26}$$

with the natural and essential boundary conditions:

$$\begin{aligned} & \left[(EI\psi' - a^2\kappa GA(w'' - \psi'))\delta\psi\right]_0^L \\ & \quad = 0, \ \left[(\kappa GA(w' - \psi) - a^2\kappa GA(w''' - \psi'') - Pw')\delta w\right]_0^L \\ & \quad = 0 \quad \text{and} \quad \left[a^2\kappa GA(w'' - \psi')\delta w'\right]_0^L = 0 \end{aligned} \tag{27}$$

As detailed by Shi and Voyiadjis (2011) (see also (Wang et al., 2000) for Reddy–Bickford theory), these six boundary conditions are clearly related to the higher-order nature of this shear theory (namely the gradient theory). The last additional condition that does not appeared in the "local" Timoshenko theory is also written as:

$$[M^*\delta w']_0^L = 0 \tag{28}$$

By derivative the second equation of Eq. (26) and adding to the first equation, the following simplification can be made:

$$EI\psi''' + Pw'' = 0 \tag{29}$$

The sixth-order differential equation can be obtained for the deflection:

$$a^2w^{(6)} + \left(\frac{Pl_c^2}{EI} - 1 + \frac{Pa^2}{EI}\right)w^{(4)} - \frac{P}{EI}w'' = 0 \quad \text{with} \quad l_c = \sqrt{\frac{EI}{\kappa GA}} \tag{30}$$

The buckling solution of Shi and Voyiadjis-type column is then obtained for the pinned-pinned case ($w = M = M^* = 0$ for $x = 0$ and $x = L$):

$$\frac{P^{SV}}{P^E} = \frac{1 + \pi^2(a/L)^2}{1 + \pi^2\left[(l_c/L)^2 + (a/L)^2\right]} \quad \text{with} \quad P^E = EI\left(\frac{\pi}{L}\right)^2 \tag{31}$$

Note that considering some other higher-order boundary conditions such as $w = M = w' = 0$ for $x = 0$ and $x = L$ would lead to some exponential solutions different from Eq. (31). More generally, the following formulae can be shown for usual boundary conditions (except of course the clamped-pinned case, for the same reasons as that developed for the Timoshenko beam):

$$\frac{P^{SV}}{P^E} = \frac{1 + (P^E/EI)a^2}{1 + (P^E/EI)(l_c^2 + a^2)} \tag{32}$$

This formulae is similar to the one presented by Wang et al. (2000) for buckling of Bickford–Reddy column, even if the present higher-order shear model is different in principle from the Bickford–Reddy theory. This higher-order shear model is a generalization of Euler–Bernoulli or Timoshenko models. It is worth mentioning that the present model is different from the gradient Timoshenko model recently developed by Wang et al. (2010b), where some other additional gradient terms have been considered.

5. Some other Timoshenko gradient elasticity models

Another application of gradient elasticity is the model of Hans and Boutin (2008) applied to repetitive frame structures, and obtained using homogeneization considerations. This model is based on the energy functional:

$$U[w,\psi]=\int_0^L \frac{1}{2}EI\psi'^2+\frac{1}{2}\kappa GA(w'-\psi)^2+\frac{1}{2}EI_w w''^2-\frac{1}{2}Pw'^2dx \tag{33}$$

where EI_w is an additional inner bending stiffness. This model belongs to the class of gradient Timoshenko beam model, based on the three-dimensional constitutive law:

$$\begin{pmatrix} M \\ V \\ M^* \end{pmatrix}=\begin{pmatrix} EI+EI_w & 0 & -EI_w \\ 0 & \kappa GA & 0 \\ -EI_w & 0 & EI_w \end{pmatrix}\begin{pmatrix} \hat{\chi} \\ \gamma \\ \gamma' \end{pmatrix} \quad \text{with} \quad \begin{pmatrix} \hat{\chi} \\ \gamma \\ \gamma' \end{pmatrix}=\begin{pmatrix} -\psi' \\ w'-\psi \\ w''-\psi' \end{pmatrix} \tag{34}$$

The stationarity of the energy functional $\delta U=0$ leads to the system of differential equations:

$$\begin{cases} -EI\psi''-\kappa GA(w'-\psi)=0 \\ -\kappa GA(w''-\psi')+EI_w w^{(4)}+Pw''=0 \end{cases} \tag{35}$$

The sixth-order differential equation can be obtained for the deflection:

$$\frac{EI_w}{EI}l_c^2 w^{(6)}+\left(\frac{Pl_c^2}{EI}-1-\frac{EI_w}{EI}\right)w^{(4)}-\frac{P}{EI}w''=0 \quad \text{with} \quad l_c=\sqrt{\frac{EI}{\kappa GA}} \tag{36}$$

leading to the buckling solution in the pinned-pinned case:

$$\frac{P^{HB}}{P^E}=\frac{1+EI_w/EI\left[1+\pi^2(l_c/L)^2\right]}{1+\pi^2(l_c/L)^2} \tag{37}$$

An other natural generalization of the gradient elasticity Timoshenko model applied to microstructured beams would be based on the four-dimensional constitutive law:

$$\begin{pmatrix} M \\ \Gamma \\ V \\ M^* \end{pmatrix}=\begin{pmatrix} EI & 0 & 0 & 0 \\ 0 & EIb^2 & 0 & 0 \\ 0 & 0 & \kappa GA & 0 \\ 0 & 0 & 0 & \kappa GAa^2 \end{pmatrix}\begin{pmatrix} \hat{\chi} \\ \hat{\chi}' \\ \gamma \\ \gamma' \end{pmatrix} \quad \text{with} \quad \begin{pmatrix} \hat{\chi} \\ \hat{\chi}' \\ \gamma \\ \gamma' \end{pmatrix}=\begin{pmatrix} -\psi' \\ -\psi'' \\ w'-\psi \\ w''-\psi' \end{pmatrix} \tag{38}$$

with two additional length scales (a,b) that can be eventually merged. Γ can be considered as a higher-order bending term. This gradient elasticity model is associated with the following functional for Engesser type column:

$$U\left[\psi,w\right]=\int_0^L \frac{1}{2}EI\psi'^2+\frac{\kappa GA}{2}(w'-\psi)^2+a^2\frac{\kappa GA}{2}(w''-\psi')^2+b^2\frac{EI}{2}\psi''^2-\frac{1}{2}Pw'^2dx \tag{39}$$

leading to the following system of differential equations:

$$\begin{cases} -\kappa GA(w''-\psi')+Pw''+a^2\kappa GA(w^{(4)}-\psi''')=0 \\ EI\psi''-b^2EI\psi^{(4)}+\kappa GA(w'-\psi)-a^2\kappa GA(w'''-\psi'')=0 \end{cases} \tag{40}$$

with the natural and essential boundary conditions:

$$\begin{gathered} \left[(EI\psi'-a^2\kappa GA(w''-\psi')-EIb^2\psi''')\delta\psi\right]_0^L=0 \\ \left[(\kappa GA(w'-\psi)-a^2\kappa GA(w'''-\psi'')-Pw')\delta w\right]_0^L \\ =0,\ \left[a^2\kappa GA(w''-\psi')\delta w'\right]_0^L=0 \text{ and} \\ \left[b^2EI\psi''\delta\psi'\right]_0^L=0 \end{gathered} \tag{41}$$

In this case, a height-order differential equation is obtained for the deflection $w(x)$ as:

$$-a^2b^2w^{(8)}+\left(b^2+a^2-\frac{Pb^2}{\kappa GA}\right)w^{(6)}+\left(\frac{P}{\kappa GA}-1+\frac{Pa^2}{EI}\right)w^{(4)}-\frac{P}{EI}w''=0 \tag{42}$$

The buckling solution of gradient elasticity Engesser-type Timoshenko column is then obtained for the pinned-pinned case ($w=M=M^*=\psi'''=0$ for $x=0$ and $x=L$), as a generalization of Shi and Voyiadjis-type column:

$$\frac{P^{TG}}{P^E}=\frac{1+\pi^2\left[(a/L)^2+(b/L)^2\right]+\pi^4\frac{(ab)^2}{L^4}}{1+\pi^2\left[(a/L)^2+(l_c/L)^2\right]+\pi^4\frac{(l_cb)^2}{L^4}} \quad \text{with} \quad P^E=EI\left(\frac{\pi}{L}\right)^2 \quad \text{and} \quad l_c=\sqrt{\frac{EI}{\kappa GA}} \tag{43}$$

Considering now the Haringx-type column with the gradient elasticity Timoshenko model, the following functional can be considered:

$$U[\psi,w]=\int_0^L \frac{1}{2}EI\psi'^2+\frac{\kappa GA}{2}(w'-\psi)^2+a^2\frac{\kappa GA}{2}(w''-\psi')^2+b^2\frac{EI}{2}\psi''^2-\frac{1}{2}Pw'^2+\frac{1}{2}P(w'-\psi)^2dx \tag{44}$$

leading to the following system of differential equations:

$$\begin{cases} -\kappa GA(w''-\psi')+P\psi'+a^2\kappa GA(w^{(4)}-\psi''')=0 \\ EI\psi''-b^2EI\psi^{(4)}+(\kappa GA+P)(w'-\psi)-a^2\kappa GA(w'''-\psi'')=0 \end{cases} \tag{45}$$

with the natural and essential boundary conditions:

$$\begin{gathered} \left[(EI\psi'-a^2\kappa GA(w''-\psi')-EIb^2\psi''')\delta\psi\right]_0^L=0 \\ \left[(\kappa GA(w'-\psi)-a^2\kappa GA(w'''-\psi'')-P\psi)\delta w\right]_0^L \\ =0,\ \left[a^2\kappa GA(w''-\psi')\delta w'\right]_0^L=0 \text{ and} \\ \left[b^2EI\psi''\delta\psi'\right]_0^L=0 \end{gathered} \tag{46}$$

In this case, a height-order differential equation is also obtained for the deflection $w(x)$ as:

$$-a^2b^2w^{(8)}+(b^2+a^2)w^{(6)}+\left(-1+\frac{Pa^2}{EI}\right)w^{(4)}-\frac{P}{EI}\left(1+\frac{P}{\kappa GA}\right)w''=0 \tag{47}$$

The buckling solution of gradient elasticity Haringx-type Timoshenko column is then obtained for the pinned-pinned case ($w = M = M^* = \psi''' = 0$ for $x = 0$ and $x = L$) as:

$$\pi^2\left(\frac{l_c}{L}\right)^2\left(\frac{P^{TG}}{P^E}\right)^2+\frac{P^{TG}}{P^E}\left[1+\pi^2\left(\frac{a}{L}\right)^2\right]-1-\pi^2\left[\left(\frac{a}{L}\right)^2+\left(\frac{b}{L}\right)^2\right]-\pi^4\left(\frac{a}{L}\right)^2\left(\frac{b}{L}\right)^2=0 \text{ with} \qquad (48)$$

$$P^E = EI\left(\frac{\pi}{L}\right)^2 \text{ and } l_c=\sqrt{\frac{EI}{\kappa GA}}$$

6. Concluding remarks

The buckling of higher-order shear beam-columns is studied in the light of enriched continuum. We show the equivalence between the enriched kinematics of usual higher-order beam theories with the nonlocal and gradient nature of the associated constitutive law. These equivalences are useful for a hierarchical classification of usual beam theories comprising Euler–Bernoulli beam theory, Timoshenko and third-order shear beam theories. The Timoshenko theory appears to be a Eringen's based nonlocal Euler–Bernoulli beam model. Shi and Voyadjis theory appears to be a gradient Timoshenko beam theory. This last theory is a generalization of the two previous ones, namely the Timoshenko theory and the Euler–Bernoulli theory. These theories belong to the general gradient elasticity Timoshenko beam framework.

References

Attard, M.M., Hunt, G.W., 2008. Column buckling with shear deformations – a hyperelastic formulation. Int. J. Solids Struct. 45, 4322–4339.

Bažant, Z.P., 2003. Shear buckling of sandwich, fiber composite and lattice columns, bearing and helical springs: paradox resolved. J. Appl. Mech. 70 (1), 75–83.

Bažant, Z.P., Cedolin, L., 2003. Stability of structures – Elastic, Inelastic, Fracture and Damage Theories. Dover Publications, Inc., New York.

Bickford, W.B., 1982. A consistent higher order beam theory. Dev. Theor. Appl. Mech. 11, 137–150.

Challamel, N., 2010. A variationally-based nonlocal damage model to predict diffuse microcracking evolution. Int. J. Mech. Sci. 52, 1783–1800.

Challamel, N., Girhammar, U.A., 2011. Boundary layer effect in composite beams with interlayer slip. J. Aerospace Engineering, ASCE 24 (2), 199–209.

Challamel, N., Wang, C.M., 2008. The small length scale effect for a non-local cantilever beam: a paradox solved. Nanotechnology 19, 345703.

Challamel, N., Wang, C.M., 2010. On lateral-torsional buckling of non-local beams. Adv. Appl. Math. Mech. 3, 389–398.

Challamel, N., Lanos, C., Casandjian, C., 2010a. On the propagation of localization in the plasticity collapse of hardening-softening beams. Int. J. Eng. Sci. 48 (5), 487–506.

Challamel, N., Meftah, S.A., Bernard, F., 2010b. Buckling of elastic beams on nonlocal foundation: a revisiting of Reissner model. Mech. Res. Commun. 37, 472–475.

Challamel, N., Mechab, I., Elmeiche, N., Krour, B., Buckling of composite nonlocal or gradient connected beams, Int. J. Struct. Stab. Dynamics, in Press.

Eringen, A.C., 1983. On differential equations of nonlocal elasticity and solutions of screw dislocation and surface waves. J. Appl. Phys. 54, 4703–4710.

Falsone, G., Settineri, D., 2011. An Euler–Bernoulli-like finite element method for Timoshenko beams. Mech. Res. Comm. 38, 12–16.

Germain, P., 1973. La méthode des puissances virtuelles en mécanique des milieux continus – première partie: Théorie du second gradient. J. Mécanique 12, 235–274.

Hans, S., Boutin, C., 2008. Dynamics of discrete framed structures: a unified homogenized description. J. Mech. Mater. Struct. 3 (9), 1709–1739.

Hodges, D.H., Saberi, H., Ormiston, R.A., 2006. On tension buckling in shear-flexible composite beams. AIAA J. 44 (8), 1909–1911.

Kong, S., Zhou, S., Nie, Z., Wang, K., 2009. Static and dynamic analysis of micro beams based on strain gradient elasticity theory. Int. J. Eng. Sci. 47, 487–498.

Lam, D.C.C., Yang, F., Chong, A.C.M., Wang, J., Tong, P., 2003. Experiments and theory in strain gradient elasticity. J. Mech. Phys. Solids 51, 1477–1508.

Lazopoulos, K.A., 2003. Post-buckling problems for long elastic beams. Acta Mech. 164, 189–198.

Levinson, M., 1981. A new rectangular beam theory. J. Sound Vibr. 74 (6), 343–350.

Levinson, M., 1985. On bickford's consistent higher-order beam theory. Mech. Res. Commun. 12 (1), 1–9.

Ma, H.M., Gao, X.L., Reddy, J.N., 2008. A microstructure-dependent Timoshenko beam model based on a modified couple stress theory. J. Mech. Phys. Solids 56, 3379–3391.

Papargyri-Beskou, S., Tsepoura, K.G., Polyzos, D., Beskos, D.E., 2003. Bending and stability analysis of gradient elastic beams. Int. J. Solids Struct. 40, 385–400.

Park, S.K., Gao, X.L., 2006. Bernoulli–Euler beam model based on a modified couple stress theory. J. Micromech. Microeng. 16, 2355–2359.

Peddieson, J., Buchanan, G.G., McNitt, R.P., 2003. Application of nonlocal continuum models to nanotechnology. Int. J. Eng. Sci. 41, 305–312.

Plantema, F.J., 1966. Sandwich Construction. John Wiley & Sons, New York.

Reddy, J.N., 1984. A simple higher-order theory for laminated composite plates. J. Appl. Mech. 51, 745–752.

Reddy, J.N., 2007. Nonlocal theories for bending, buckling and vibration of beams. Int. J. Eng. Sci. 45, 288–307.

Reddy, J.N., 2010. Nonlocal nonlinear formulations for bending of classical and shear deformation theories of beams and plates. Int. J. Eng. Sci. 48, 1507–1518.

Reissner, E., 1982. Some remarks on the problem of Euler buckling. Ing. Arch. 52, 115–119.

Shi, G., Voyiadjis, G.Z., 2011. A sixth-order theory of shear deformable beams with variational consistent boundary conditions. J. Appl. Mech. 78 (021019), 1–11.

Sudak, L.J., 2003. Column buckling of multiwalled carbon nanotubes using nonlocal continuum mechanics. J. Appl. Phys. 94, 7281–7287.

Voyiadjis, G.Z., Shi, G., 1991. A refined two-dimensional theory for thick cylindrical shells. Int. J. Solids Struct. 27 (3), 261–282.

Wang, C.M., Reddy, J.N., Lee, K.H., 2000. Shear Deformable Beams and Plates: Relationships with Classical Solutions. Elsevier, Oxford, UK.

Wang, C.M., Wang, C.Y., Reddy, J.N., 2005. Exact solutions for buckling of structural members. In: CRC Series in Computational Mechanics and Applied Analysis. Boca Raton, Florida.

Wang, C.M., Zhang, Y.Y., Ramesh, S.S., Kitipornchai, S., 2006. Buckling analysis of micro- and nano-rods/tubes based on nonlocal Timoshenko beam theory. J. Phys. D: Appl. Phys. 39, 3904–3909.

Wang, C.M., Xiang, Y., Kitipornchai, S., 2009. Postbuckling of nano rods/tubes based on nonlocal beam theory. Int. J. Appl. Mech. 1 (2), 259–266.

Wang, C.M., Zhang, Y.Y., Xiang, Y., Reddy, J.N., 2010a. Recent studies on buckling of carbon nanotubes. Appl. Mech. Rev. 63 (030804), 1–18.

Wang, B., Zhao, J., Zhou, S., 2010b. A micro scale Timoshenko beam model based on strain gradient elasticity theory. Eur. J. Mech. A/Solids 29, 591–599.

Yu, W., Hodges, D.H., 2005. Generalized Timoshenko theory of the variational asymptotic beam sectional analysis. J. Am. Helicopter Soc. 50 (1), 46–55.

Zhang, Y.Y., Wang, C.M., Challamel, N., 2010. Bending, buckling and vibration of hybrid nonlocal beams. J. Eng. Mech. 136 (5), 562–574.

Ziegler, H., 1982. Arguments for and against Engesser's buckling formulas. Ing. Arch. 52, 105–113.

Latin American Journal of Solids and Structures
www.lajss.org

A refined shear deformation theory for flexure of thick beams

Abstract

A Hyperbolic Shear Deformation Theory (HPSDT) taking into account transverse shear deformation effects, is used for the static flexure analysis of thick isotropic beams. The displacement field of the theory contains two variables. The hyperbolic sine function is used in the displacement field in terms of thickness coordinate to represent shear deformation. The transverse shear stress can be obtained directly from the use of constitutive relations, satisfying the shear stress-free boundary conditions at top and bottom of the beam. Hence, the theory obviates the need of shear correction factor. Governing differential equations and boundary conditions of the theory are obtained using the principle of virtual work. General solutions of thick isotropic simply supported, cantilever and fixed beams subjected to uniformly distributed and concentrated loads are obtained. Expressions for transverse displacement of beams are obtained and contribution due to shear deformation to the maximum transverse displacement is investigated. The results of the present theory are compared with those of other refined shear deformation theories of beam to verify the accuracy of the theory.

Keywords

hyperbolic shear deformation theory, static flexure, general solution of beams, shear contribution factor.

Yuwaraj M. Ghugal* **and**
Rajneesh Sharma

Department of Applied Mechanics, Government College of Engineering, Aurangabad-431005, Maharashtra State – India

Received 20 Dec 2010;
In revised form 21 Dec 2010

* Author email: ghugal@rediffmail.com

1 INTRODUCTION

The Bernoulli-Euler elementary theory of bending (ETB) of beam disregards the effect of the shear deformation. The theory is suitable for slender beams and is not suitable for thick or deep beams since it is based on the assumption that the transverse normal to the neutral axis remains so during bending and after bending, implying that the transverse shear strain is zero. Since the theory neglects the transverse shear deformation, it underestimates deflections and overestimates the natural frequencies in case of thick beams, where shear deformation effects are significant.

The first order shear deformation theory (FSDT) of Timoshenko [14] includes refined effects such as the rotatory inertia and shear deformation in the beam theory. Timoshenko showed

NOMENCLATURE

A	Cross sectional area of beam;
b	Width of beam in y direction;
E, G, μ	Elastic constants of the material;
E	Young's modulus;
G	Shear modulus;
h	Thickness of beam;
I	Moment of inertia of cross section of beam;
L	Span of the beam;
q	Intensity of uniformly distributed transverse load;
u	Axial displacement in x direction;
w	Transverse displacement in z direction;
x, y, z	Rectangular Cartesian coordinates;
μ	Poisson's ratio of the beam material;
σ_x	Axial stress in x direction;
τ_{xz}	Transverse shear stress in zx plane;
ϕ	Unknown function associated with the shear slope.

ABBREVIATIONS

ETB	Elementary Theory of Beam-bending
FSDT	First-order Shear Deformation Theory
HSDT	Higher-order Shear Deformation Theory
TSDT	Trigonometric Shear Deformation Theory
PSDT	Parabolic Shear Deformation Theory
HPSDT	Hyperbolic Shear Deformation Theory
UDL	Uniformly distributed load

that the effect of transverse shear is much greater than that of rotatory inertia on the response of transverse vibration of prismatic bars. In this theory transverse shear strain distribution is assumed to be constant through the beam thickness and thus requires shear correction factor to appropriately represent the strain energy of deformation. Cowper [4] has given refined expression for the shear correction factor for different cross-sections of the beam.

The discrepancies in the elementary theory of beam bending and first order shear deformation theory forced the development of higher order or equivalent refined shear deformation theories. Levinson [11], Bickford [3], Rehfield and Murthy [12], Krishna Murty [10], Baluch, et.al [1], Bhimaraddi and Chandrashekhara [2] presented parabolic shear deformation theories assuming a higher variation of axial displacement in terms of thickness coordinate. These theories satisfy shear stress free boundary conditions on the top and bottom surfaces of the beam and thus obviate the need of shear correction factor. Kant and Gupta [9], and Heyliger and Reddy [8] presented higher order shear deformation theories for the static and free vibration analyses of shear deformable uniform rectangular beams.

The theories based on trigonometric and hyperbolic functions to represent the shear deformation effects through the thickness is the another class of refined theories. Vlasov and Leont'ev [18] and Stein [13] developed refined shear deformation theories for thick beams including sinusoidal function in terms of thickness coordinate in the displacement field. However, with these theories shear stress free boundary conditions are not satisfied at top and bottom surfaces of the beam. This discrepancy is removed by Ghugal and Shimpi [7] and developed a variationally consistent refined trigonometric shear deformation theory for flexure and free vibration of thick isotropic beams. Ghugal and Nakhate [5] obtained the general bending solutions for thick beams using variationally consistent refined trigonometric shear deformation theory. Ghugal and Sharma [6] developed the variationally consistent hyperbolic shear deformation theory for flexural analysis of thick beams and obtained the displacements, stresses and fundamental frequencies of flexural mode and thickness shear modes from free vibration of simply supported beams.

In this paper, a variationally consistent hyperbolic shear deformation theory previously developed by Ghugal and Sharma [6] for thick beams is used to obtain the general bending solutions for thick isotropic beams. The theory is applied to uniform isotropic solid beams of rectangular cross-section for static flexure with various boundary and loading conditions. The results are compared with those of elementary, refined and exact beam theories available in the literature to verify the credibility of the present shear deformation theory.

2 THEORETICAL FORMULATION

The variationally correct forms of differential equations and boundary conditions, based on the assumed displacement field are obtained using the principle of virtual work. The beam under consideration occupies the following region:

$$0 \le x \le L; \quad -b/2 \le y \le b/2; \quad -h/2 \le z \le h/2$$

where x, y, z are Cartesian coordinates, L is the length, b is the width and h is the total depth of beam. The beam is subjected to transverse load of intensity $q(x)$ per unit length of the beam. The beam can have any meaningful boundary conditions.

2.1 The displacement field

The displacement field of the present beam theory is of the form [6]

$$u\left(x,z\right) = -z\frac{dw}{dx} + \left[z\cosh\left(\frac{1}{2}\right) - h\sinh\left(\frac{z}{h}\right)\right]\varphi\left(x\right) \tag{1}$$

$$w\left(x,z\right) = w\left(x\right) \tag{2}$$

Here u and w are the axial and transverse displacements of the beam center line in the x and z directions respectively. The first term in Eqn (1) is the axial displacement according to the elementary theory of beam bending (ETB) due to Bernoulli-Euler which is linear through the thickness of the beam the second term in the bracket is the displacement due to transverse shear deformation, which is assumed to be hyperbolic sine function in terms of thickness coordinate, which is non-linear in nature through the thickness of beam. The hyperbolic sine function is assigned according to the shearing stress distribution through the thickness of the beam. The $\varphi(x)$ is an unknown function to be determined and is associated with the rotation of the cross-section of the beam at neutral axis.

$$\text{Normal strain:} \quad \varepsilon_x = \frac{\partial u}{\partial x} = -z\frac{d^2 w}{dx^2} + \left[z\cosh\left(\frac{1}{2}\right) - h\sinh\left(\frac{z}{h}\right)\right]\frac{d\varphi}{dx} \tag{3}$$

$$\text{Shear strains:} \quad \gamma_{xz} = \frac{\partial u}{\partial z} + \frac{dw}{dx} = \left[\cosh\left(\frac{1}{2}\right) - \cosh\left(\frac{z}{h}\right)\right]\varphi \tag{4}$$

Stresses

One dimensional constitutive laws are used to obtain normal bending and transverse shear stresses. These stresses are given by

$$\sigma_x = E\varepsilon_x, \quad \tau_{xz} = G\gamma_{xz} \tag{5}$$

where E and G are the elastic constants of beam material.

2.2 Governing equations and boundary conditions

Using the expressions (3) through (5) for strains and stresses and dynamic version of principle of virtual work, variationally consistent governing differential equations and boundary conditions for the beam under consideration are obtained. The principle of virtual work when applied to the beam leads to

$$b\int_{x=0}^{x=L}\int_{z=-h/2}^{z=h/2}\left(\sigma_x\delta\varepsilon_x + \tau_{xz}\delta\gamma_{xz}\right)dxdz - \int_{x=0}^{x=L} q\delta w dx = 0 \tag{6}$$

where the symbol δ denotes the variational operator. Employing Green's theorem in Eqn. (6) successively, we obtain the coupled Euler-Lagrange equations which are the governing differential equations of the beam and the associated boundary conditions of the beam. The governing differential equations obtained are as follows:

$$EI\frac{d^4 w}{dx^4} - EIA_0\frac{d^3\varphi}{dx^3} = q \tag{7}$$

$$EIA_0\frac{d^3 w}{dx^3} - EIB_0\frac{d^2\varphi}{dx^2} + GAC_0\varphi = 0 \tag{8}$$

where A_0, B_0 and C_0 are the constants as given in Appendix and the associated boundary conditions obtained are as follows:

$$\text{Either } EI\frac{d^3 w}{dx^3} - EIA_0\frac{d^2\varphi}{dx^2} = 0 \quad \text{or } w \text{ is prescribed} \tag{9}$$

$$\text{Either } EI\frac{d^2w}{dx^2} - EIA_0\frac{d\varphi}{dx} = 0 \quad \text{or } \frac{dw}{dx} \text{ is prescribed} \tag{10}$$

$$\text{Either } EIA_0\frac{d^2w}{dx^2} - EIB_0\frac{d\varphi}{dx} = 0 \quad \text{or } \phi \text{ is prescribed} \tag{11}$$

Thus the variationally consistent governing differential equations and the associated boundary conditions are obtained. The static flexural behavior of beam is given by the solution of these equations and simultaneous satisfaction of the associated boundary conditions.

2.3 The general solution for the static flexure of beam

Using the governing equations (7) and (8) for static flexure of beam, the general solution for $w(x)$ and ϕ(x) can be obtained. By integrating and rearranging the first governing equation (Eqn. 7) one can get following equation

$$\frac{d^3w}{dx^3} - A_0\frac{d^2\varphi}{dx^2} = \frac{Q(x)}{EI} \tag{12}$$

where $Q(x)$ is the generalized shear force for the beam under consideration and it is given by $Q(x) = \int q\,dx + C_1$. The second governing equation (Eqn. 8) can be written as

$$\frac{d^3w}{dx^3} - \frac{A_0}{B_0}\frac{d^2\varphi}{dx^2} + \beta\varphi = 0 \tag{13}$$

Using Eqn. (12) and Eqn. (13), a single differential equation in terms of ϕ can be obtained as follows.

$$\frac{d^2\varphi}{dx^2} - \lambda^2\varphi = \frac{Q(x)}{\alpha EI} \tag{14}$$

where the constant α, β and λ used in Eqn. (13) and Eqn. (14) are given in Appendix. The general solution of above Eqn. (14) is given by:

$$\varphi(x) = C_2\cosh\lambda x + C_3\sinh\lambda x - \frac{Q(x)}{\beta EI} \tag{15}$$

The general solution for transverse displacement (w) can be obtained by substituting the expression for $\varphi(x)$ in Eqn. (13) and integrating thrice with respect to x. The solution is

$$\begin{aligned} EIw(x) = &\int\int\int\int q\,dx\,dx\,dx\,dx + \frac{C_1x^3}{6} + \frac{A_0EI}{\lambda}\left(C_2\sinh\lambda x + C_3\cosh\lambda x\right) \\ &+ C_4\frac{x^2}{2} + C_5x + C_6 \end{aligned} \tag{16}$$

where $C_1 - C_6$ are the arbitrary constants of integration and can be obtained by imposing natural (forced) and kinematic (geometric) boundary conditions of beams.

3 ILLUSTRATIVE EXAMPLES

3.1 Example 1: Simply supported beam with uniformly distributed load q

A simply supported beam with rectangular cross section ($b\times\ h$) is subjected to uniformly distributed load q over the span L at surface $z = -h/2$ acting in the downward z direction. The origin of beam is taken at left end support *i.e.* at $x = 0$. The boundary conditions associated with simply supported beam are as follows.

$$EI\frac{d^3w}{dx^3} = EI\frac{d^2\varphi}{dx^2} = \frac{dw}{dx} = \varphi = 0 \quad \text{at } x = \frac{L}{2} \quad \text{and} \tag{17}$$

$$EI\frac{d^2w}{dx^2} = EI\frac{d\varphi}{dx} = w = 0 \quad \text{at } x = 0, L \tag{18}$$

The boundary condition, $\phi = 0$ at $x = L/2$ is used from the condition of symmetry of deformation, in which the middle cross section of the beam must remain plane without warping (see Timoshenko [15]). Applying appropriate boundary conditions from (19) and (20) in general solutions of the beam the final expressions for $\phi(x)$ and $w(x)$ are obtained as follows:

$$\varphi(x) = \frac{qL}{2\beta EI}\left[1 - 2\frac{x}{L} + \frac{2}{\lambda L}\frac{\sinh(\lambda x - \lambda L/2)}{\cosh(\lambda L/2)}\right] \tag{19}$$

$$w(x) = \frac{qL^4}{24EI}\left(\frac{x^4}{L^4} - 2\frac{x^3}{L^3} + \frac{x}{L}\right) + \frac{3}{5}\frac{qL^2}{GA}\left[\frac{x}{L} - \frac{x^2}{L^2} - \frac{2}{(\lambda L)^2}\left(1 - \frac{\cosh(\lambda x - \lambda L/2)}{\cosh(\lambda L/2)}\right)\right] \tag{20}$$

The maximum transverse displacement at $x = L/2$ obtained from Eqn. (20) is

$$w(L/2) = \frac{5qL^4}{384EI}\left[1 + 1.92(1+\mu)\frac{h^2}{L^2}\right] \tag{21}$$

3.2 Example 2: Simply supported beam with central concentrated load P

A simply supported beam with rectangular cross section ($b \times h$) subjected to concentrated load P at mid span *i.e.* at $x = L/2$ at surface $z = -h/2$. The origin beam is taken at left end support *i.e.* at $x = 0$. The boundary conditions associated with simply supported beam with a concentrated load are given as:

$$EI\frac{dw}{dx} = \varphi = 0 \text{at} x = \frac{L}{2} \quad \text{and} \quad EI\frac{d^2w}{dx^2} = EI\frac{d\varphi}{dx} = w = 0 \text{at} x = 0, L \tag{22}$$

From the condition of symmetry, the middle cross-section of the beam must remain normal and plane, hence shear rotation, $\phi = 0$ at $x = L/2$ [15]. Using these boundary conditions, in the region ($0 = x = L/2$) of beam, the general expressions for $\phi(x)$ and $w(x)$ are obtained as follow:

$$\varphi(x) = \frac{P}{2\beta EI}\left[1 - \frac{\cosh(\lambda x)}{\cosh(\lambda L/2)}\right] \tag{23}$$

$$w(x)=\frac{PL^3}{48EI}\left(3\frac{x}{L}-4\frac{x^3}{L^3}\right)+\frac{3}{5}\frac{PL}{GA}\left(\frac{x}{L}-\frac{\sinh\lambda x}{\lambda L\cosh\left(\lambda L/2\right)}\right) \tag{24}$$

The maximum transverse displacement at $x = L/2$ obtained from Eqn. (24) is

$$w\left(L/2\right)=\frac{PL^3}{48EI}\left[1+2.4\left(1+\mu\right)\frac{h^2}{L^2}\right] \tag{25}$$

3.3 Example 3: Cantilever beam with uniformly distributed load q

A cantilever beam with rectangular cross section ($b \times h$) is subjected to uniformly distributed load q at surface $z = -h/2$ acting in the z direction. The origin of beam is taken at free end *i.e.* at $x = 0$ and it is fixed or clamped at $x = L$. The boundary conditions associated with cantilever beam are as given:

$$\begin{gathered} EI\frac{d^3w}{dx^3}=EI\frac{d^2\varphi}{dx^2}=EI\frac{d^2w}{dx^2}=EI\frac{d\varphi}{dx}=0 \quad \text{at } x=0 \text{ and} \\ \frac{dw}{dx}=\varphi=w=0 \quad \text{at } x=L \end{gathered} \tag{26}$$

Using these boundary conditions the general expressions for $\phi(x)$ and $w(x)$ are obtained from the general solution as follows:

$$\varphi\left(x\right)=\frac{qL}{\beta EI}\left[\frac{\cosh\lambda x}{\cosh\lambda L}-\frac{\sinh\lambda\left(L-x\right)}{\lambda L\cosh\lambda L}-\frac{x}{L}\right] \tag{27}$$

$$w\left(x\right)=\frac{qL^4}{24EI}\left(\frac{x^4}{L^4}-4\frac{x}{L}+3\right)+\frac{3}{5}\frac{qL^2}{GA}\left[1-\frac{x^2}{L^2}-\frac{2\left(\sinh\lambda L-\sinh\lambda x\right)}{\lambda L\cosh\lambda L}+\frac{2\cosh\lambda\left(L-x\right)}{\left(\lambda L\right)^2\cosh\lambda L}\right] \tag{28}$$

The maximum transverse displacement at free end ($x = 0$) obtained from Eqn. (28) is

$$w\left(0\right)=\frac{qL^4}{8EI}\left[1+0.8\left(1+\mu\right)\frac{h^2}{L^2}\right] \tag{29}$$

3.4 Example 4: Cantilever beam with concentrated load P at free end

A cantilever beam with rectangular cross section ($b \times h$) is subjected to concentrated load P at free end *i.e.* at $x = L$ at surface $z = -h/2$ acting in the z direction. The origin of the beam is taken at fixed end *i.e.* at $x = 0$. The boundary conditions associated with cantilever beam are as given:

$$EI\frac{d^2w}{dx^2}=EI\frac{d\varphi}{dx}=0 \quad \text{at } x=L \text{ and} \frac{dw}{dx}=w=\varphi=0 \text{at} x\text{=}0 \tag{30}$$

Using these boundary conditions in general solution of the beam, the general expressions for $\phi(x)$ and $w(x)$ are obtained as follows:

$$\phi(x) = \frac{P}{\beta EI}\left(\sinh \lambda x - \cosh \lambda x + 1\right) \tag{31}$$

$$w(x) = \frac{PL^3}{6EI}\left(3\frac{x^2}{L^2} - \frac{x^3}{L^3}\right) + \frac{6}{5}\frac{PL}{GA}\left(\frac{x}{L} + \frac{\cosh \lambda x - \sinh \lambda x - 1}{\lambda L}\right) \tag{32}$$

The maximum transverse displacement at free end ($x = L$) obtained from Eqn. (32) is

$$w\left(L\right) = \frac{PL^3}{3EI}\left[1 + 0.6\left(1+\mu\right)\frac{h^2}{L^2}\right] \tag{33}$$

3.5 Example 5: Fixed-fixed (Clamped-clamped) beam with uniformly distributed load q

A fixed-fixed beam with rectangular cross section ($b \times h$) is subjected to uniformly distributed load q at surface $z = -h/2$. The origin of the beam is taken at left end fixed/clamped support *i.e.* $x = 0$. The boundary conditions associated with this beam are as follows:

$$\begin{aligned} EI\frac{d^3w}{dx^3} = EI\frac{d^2\varphi}{dx^2} = EI\frac{dw}{dx} = \varphi = 0 \quad &\text{at } x = \frac{L}{2}; \\ \phi = w = EI\frac{dw}{dx} = 0 \quad &\text{at } x = 0, L \text{ and} \\ \frac{d^2w}{dx^2} = \frac{d\phi}{dx} = \frac{qL^2}{12EI} \quad &\text{at } x = 0 \end{aligned} \tag{34}$$

Using the appropriate boundary conditions, from the set given by Eqn. (34), in general solution of the beam, the general expressions for $\phi(x)$ and $w(x)$ are obtained as follows:

$$\varphi(x) = \frac{qL}{2\beta EI}\left[\frac{\sinh \lambda(L/2 - x)}{\sinh\left(\lambda L/2\right)} - \left(1 - 2\frac{x}{L}\right)\right] \tag{35}$$

$$w(x) = \frac{qL^4}{24EI}\left(\frac{x^4}{L^4} - 2\frac{x^3}{L^3} + \frac{x^2}{L^2}\right) + \frac{3}{5}\frac{qL^2}{GA}\left[\frac{x}{L} - \frac{x^2}{L^2} - \frac{\left(\cosh\left(\lambda L/2\right) - \cosh \lambda\left(L/2 - x\right)\right)}{\lambda L \sinh\left(\lambda L/2\right)}\right] \tag{36}$$

The maximum transverse displacement at center of the beam ($x = L/2$) obtained from Eqn. (36) is

$$w\left(L/2\right) = \frac{qL^4}{384EI}\left[1 + 9.6\left(1+\mu\right)\frac{h^2}{L^2}\right] \tag{37}$$

3.6 Example 6: Fixed-fixed beam with central concentrated load P

A fixed-fixed beam with rectangular cross section ($b \times h$) is subjected to concentrated load P at mid span at surface $z = -h/2$. The origin of the beam is taken at left end fixed/clamped support *i.e.* $x = 0$. The boundary conditions associated with this beam are as follows:

$$EI\frac{dw}{dx} = \phi = 0 \text{at} x = 0, \frac{L}{2}; w = 0 \quad \text{at } x = 0 \text{ and}$$
$$\frac{d^2w}{dx^2} = \frac{d\phi}{dx} = -\frac{PL}{8EI} \quad \text{at } x = 0 \tag{38}$$

Using these boundary conditions, in the region ($0 = x = L/2$) of beam, the general expressions for $\phi(x)$ and $w(x)$ are obtained as follow:

$$\varphi(x) = \frac{P}{2\beta EI}\left(1 + \sinh\lambda x - \cosh\lambda x - \frac{\sinh\lambda x}{\sinh\left(\lambda L/2\right)}\right) \tag{39}$$

$$w(x) = \frac{PL^3}{48EI}\left(3\frac{x^2}{L^2} - 4\frac{x^3}{L^3}\right) + \frac{3}{5}\frac{PL}{GA}\left(\frac{x}{L} + \frac{\cosh\lambda x - \sinh\lambda x - 1}{\lambda L}\right) \tag{40}$$

The maximum transverse displacement at center of the beam ($x = L/2$) obtained from Eqn. (40) is

$$w\left(L/2\right) = \frac{PL^3}{192EI}\left[1 + 9.6\left(1 + \mu\right)\frac{h^2}{L^2}\right] \tag{41}$$

While obtaining the expressions for maximum transverse displacement (deflection) in the above examples it is observed that the quantity λL is very large and therefore $\tanh\lambda L \simeq 1$, $1/\lambda L \simeq 1/\left(\lambda L\right)^2 \simeq 0$ and $\sinh\lambda L \simeq \cosh\lambda L$. For problems of practical interest this is a very good approximation.

4 RESULTS

In expressions of maximum transverse displacement the first term in the bracket is the displacement contribution according to the classical Bernoulli-Euler beam theory and the second term represents the effect of transverse shear deformation. These expressions can be written in the generalized form as follows:

$$w = w_C\left[1 + w_S\left(1 + \mu\right)\left(\frac{h}{L}\right)^2\right] \tag{42}$$

In the above equation w_c is the transverse displacement according to the classical Bernoulli-Euler beam theory and w_s is the proportionality constant due to transverse shear deformation effect. In Tables 1 through 3 the values of w_s for different beam problems are compared with those of other refined theories.

Table 1 Values of proportionality constant (w_s) for simply supported beams.

Source	Model	Uniform Load	Concentrated Load
Present	HPSDT	1.92	2.4
Timoshenko [14]	FSDT	1.92	2.4
Levinson [11]	HSDT	1.92	—
Bhimaraddi and Chandrashekhara [2]	PSDT	1.92	—
Ghugal and Nakhate [5]	TSDT	1.92	2.4
Timoshenko and Goodier [16]	Exact	1.93846	—

Table 2 Values of proportionality constant (w_s) for cantilever beams.

Source	Model	Uniform Load	Concentrated Load
Present	HPSDT	0.8	0.6
Timoshenko [14]	FSDT	0.8	0.6
Levinson [11]	HSDT	1.2	0.75
Bhimaraddi and Chandrashekhara [2]	PSDT	0.8	0.6
Ghugal and Nakhate [5]	TSDT	0.8	0.6
Timoshenko and Goodier [16]	Exact	—	0.75
Venkatraman and Patel [17]	Exact	0.68	—

Table 3 Values of proportionality constant (w_s) for fixed-fixed beams.

Source	Model	Uniform Load	Concentrated Load
Present	HPSDT	9.6	9.6
Timoshenko [14]	FSDT	9.6	9.6
Levinson [11]	HSDT	12.0	—
Bhimaraddi and Chandrashekhara [2]	PSDT	9.6	—
Ghugal and Nakhate [5]	TSDT	9.6	9.6

The numerical results shown in Table 1 for simply supported beam with uniform load and concentrated load indicate that the results of proportionality constant (w_s) due to shear deformation effect according to present theory (HPSDT) are identical to those of beam theories of Timoshenko (FSDT), Levinson (HSDT), Bhimaraddi and Chandrashekhara (PSDT), and Ghugal and Nakhate (TSDT). The results of these theories are closed to exact value in case of simply supported beam with uniform load. In case of cantilever and fixed-fixed beams with uniform load Levinson's variationally inconsistent beam theory yields higher values of w_s

than those obtained by present theory and other refined theories as shown in Tables 2 and 3. However, for cantilever beam with concentrated load Levinson's theory gives the exact value of this constant (see Table 2). In case of beam with both the ends fixed, it is observed that the constant of proportionality due to shear deformation is independent of loading conditions.

5 CONCLUSIONS

In this paper a hyperbolic shear deformation theory has been used to obtain the bending solutions for thick homogeneous, isotropic, statically determinate and indeterminate beams. General solutions for the transverse displacement and rotation are presented for transversely loaded beams with various end conditions. Expressions for maximum transverse displacements are deduced from the general solutions of the thick beams. The effect of transverse shear deformation on the bending solutions of thick beams can be readily observed from the analytical expressions presented for the transverse displacement. The values of transverse displacement contribution (w_s) due to transverse shear deformation effect obtained by present theory are found to be identical to those of first order shear deformation theory of Timoshenko with the shear correction factor equal to 5/6. The present theory requires no shear correction factor. The accuracy of present theory is verified by comparing the results of other refined theories and the exact theory.

References

[1] M. H. Baluch, A. K. Azad, and M. A. Khidir. Technical theory of beams with normal strain. *J. Engg. Mech., ASCE*, 110(8):1233–1237, 1984.

[2] A. Bhimaraddi and K. Chandrashekhara. Observations on higher order beam theory. *J. Aerospace Engineering, ASCE*, 6(4):408–413, 1993.

[3] W. B. Bickford. A consistent higher order beam theory. *Dev. in Theoretical and Applied Mechanics, SECTAM*, 11:137–150, 1982.

[4] G. R. Cowper. The shear coefficients in Timoshenko beam theory. *J. Applied Mechanics, ASME*, 33(2):335–340, 1966.

[5] Y. M. Ghugal and V. V. Nakhate. Flexure of thick beams using trigonometric shear deformation theory. *The Bridge and Structural Engineer*, 39(1):1–17, 2009.

[6] Y. M. Ghugal and R. Sharma. A hyperbolic shear deformation theory for flexure and free vibration of thick beams. *International Journal of Computational Methods*, 6(4):585–604, 2009.

[7] Y. M. Ghugal and R. P. Shimpi. A trigonometric shear deformation theory for flexure and free vibration of isotropic thick beams. In *Structural Engineering Convention, SEC-2000*, pages 255–263, Bombay, India, 2000. IIT.

[8] P. R. Heyliger and J. N. Reddy. A higher order beam finite element for bending and vibration problems. *J. Sound and Vibration*, 126(2):309–326, 1988.

[9] T. Kant and A. Gupta. A finite element model for a higher order shear deformable beam theory. *J. Sound and Vibration*, 125(2):193–202, 1988.

[10] A. V. Krishna Murty. Towards a consistent beam theory. *AIAA Journal*, 22(6):811–816, 1984.

[11] M. Levinson. A new rectangular beam theory. *J. Sound and Vibration*, 74(1):81–87, 1981.

[12] L. W. Rehfield and P. L. N. Murthy. Toward a new new engineering theory of bending: fundamentals. *AIAA J.*, 20(5):693–699, 1982.

[13] M. Stein. Vibration of beams and plate strips with three dimensional flexibility. *J. App. Mech., ASME*, 56(1):228–231, 1989.

[14] S. P. Timoshenko. On the correction for shear of the differential equation for transverse vibrations of prismatic bars. *Philosophical Magazine Series*, 6:742–746, 1921.

[15] S. P. Timoshenko. *Strength of Materials, Part 1 – Elementary Theory and Problem.* CBS Publishers and distributors, New Delhi, India, 3rd edition, 1986. Chapter 5.

[16] S. P. Timoshenko and J. N. Goodier. *Theory of Elasticity.* McGraw-Hill, Singapore, 3rd edition, 1970.

[17] B. Venkatraman and S. A. Patel. *Structural Mechanics with Introduction to Elasticity and Plasticity.* McGraw-Hill Book Company, New York, 1970. Chapter 11.

[18] V. Z. Vlasov and U. N. Leont'ev. *Beams, Plates, and Shells on Elastic Foundations.* Moskva, 1966. Translated from the Russian by Barouch, A., and Pelz, T., Israel Program for Scientific Translation Ltd., Jerusalem, Chapter 1.

APPENDIX

The constants A_0, B_0 and C_0 appeared in governing equations (7) and (8) and boundary conditions given by equations (9) – (11) are as follows:

$$A_0 = \cosh\left(\frac{1}{2}\right) - 12\left[\cosh\left(\frac{1}{2}\right) - 2\sinh\left(\frac{1}{2}\right)\right]$$

$$B_0 = \cosh^2\left(\frac{1}{2}\right) + 6\left[\sinh(1) - 1\right] - 24\cosh\left(\frac{1}{2}\right)\left[\cosh\left(\frac{1}{2}\right) - 2\sinh\left(\frac{1}{2}\right)\right]$$

$$C_0 = \cosh^2\left(\frac{1}{2}\right) + \left(\frac{1}{2}\right)\left[\sinh(1) + 1\right] - 4\cosh\left(\frac{1}{2}\right)\sinh\left(\frac{1}{2}\right)$$

The constants α, β and λ appeared in Eqns. (13) and (14) are as follows:

$$\alpha = \frac{B_0}{A_0} - A_0, \quad \beta = \frac{GAC_0}{EIA_0}, \quad \lambda^2 = \frac{\beta}{\alpha}$$

Applied and Computational Mechanics 5 (2011) 217–230

Comparison of various refined beam theories for the bending and free vibration analysis of thick beams

A. S. Sayyad[a,*]

[a] Department of Civil Engineering, SRES's College of Engineering, Kopargaon-423601, M.S., India.

Received 22 September 2011; received in revised form 19 December 2011

Abstract

In this paper, unified shear deformation theory is used to analyze simply supported thick isotropic beams for the transverse displacement, axial bending stress, transverse shear stress and natural frequencies. This theory enables the selection of different in-plane displacement components to represent shear deformation effect. The numbers of unknowns are same as that of first order shear deformation theory. The governing differential equations and boundary conditions are obtained by using the principle of virtual work. The results of displacement, stresses, natural bending and thickness shear mode frequencies for simply supported thick isotropic beams are presented and discussed critically with those of exact solution and other higher order theories. The study shows that, while the transverse displacement and the axial stress are best predicted by the models 1 through 5 whereas models 1 and 2 are overpredicts the transverse shear stress. The model 4 predicts the exact dynamic shear correction factor $(\pi^2/12 = 0.822)$ whereas model 1 overpredicts the same.

© 2011 University of West Bohemia. All rights reserved.

Keywords: Thick beam, shear deformation, principle of virtual work, bending analysis, transverse shear stress, free flexural vibration, natural frequencies, dynamic shear correction factor

---

1. Introduction

Beams are common structural elements in most structures and they are analyzed using classical or refined shear deformation theories to evaluate static and dynamic characteristics. Elementary theory of beam bending underestimates deflections and overestimates the natural frequencies since it disregards the transverse shear deformation effect. Timoshenko [24] was the first to include refined effects such as rotatory inertia and shear deformation in the beam theory. This theory is now widely referred to as Timoshenko beam theory or first order shear deformation theory. In this theory transverse shear strain distribution is assumed to be constant through the beam thickness and thus requires problem dependent shear correction factor. The accuracy of Timoshenko beam theory for transverse vibrations of simply supported beam in respect of the fundamental frequency is verified by Cowper [6, 7] with a plane stress exact elasticity solution.

The limitations of elementary theory of beam and first order shear deformation theory led to the development of higher order shear deformation theories. Many higher order shear deformation theories are available in the literature for static and dynamic analysis of beams [2–5, 11, 15]. Levinson [17] has developed a new rectangular beam theory for the static and dynamic analysis of beam. Reddy [18] has developed well known third order shear deformation theory for the non-linear analysis of plates with moderate thickness. The trigonometric shear deformation theories are presented by Touratier [25], Vlasov and Leont'ev [26] and Stein [20] for thick

---

[*] Corresponding author. Tel.: +91 97 63 567 881, e-mail: attu_sayyad@yahoo.co.in.

beams. However, with these theories shear stress free boundary conditions are not satisfied at top and bottom surfaces of the beam. Ghugal and Shipmi [9] and Ghugal [10] has developed a trigonometric shear deformation theory which satisfies the shear stress free condition at top and bottom surfaces of the beam. Soldatos [22] has dveloped hyperbolic shear deformation theory for homogeneous monoclinic plates. Recently Ghugal and Sharma [8] employed hyperbolic shear deformation theory for the static and dynamic analysis of thick isotropic beams. A study of literature [1,12–14,19] indicates that the research work dealing with flexural analysis of thick beams using refined shear deformation theories is very scant and is still in infancy. Sayyad [21] has carried out comparison of various shear deformation theories for the free vibration analysis of thick isotropic beams.

In the present study, various shear deformation theories are used for the bending and free vibration analysis of simply supported thick isotropic beams.

2. Beam under consideration

Consider a beam made up of isotropic material as shown in Fig. 1. The beam can have any boundary and loading conditions. The beam under consideration occupies the region given by

$$0 \le x \le L, \qquad -b/2 \le y \le b/2, \qquad -h/2 \le z \le h/2, \tag{1}$$

where x, y, z are Cartesian co-ordinates, L is length, b is width and h is the total depth of the beam. The beam is subjected to transverse load of intensity $q(x)$ per unit length of the beam.

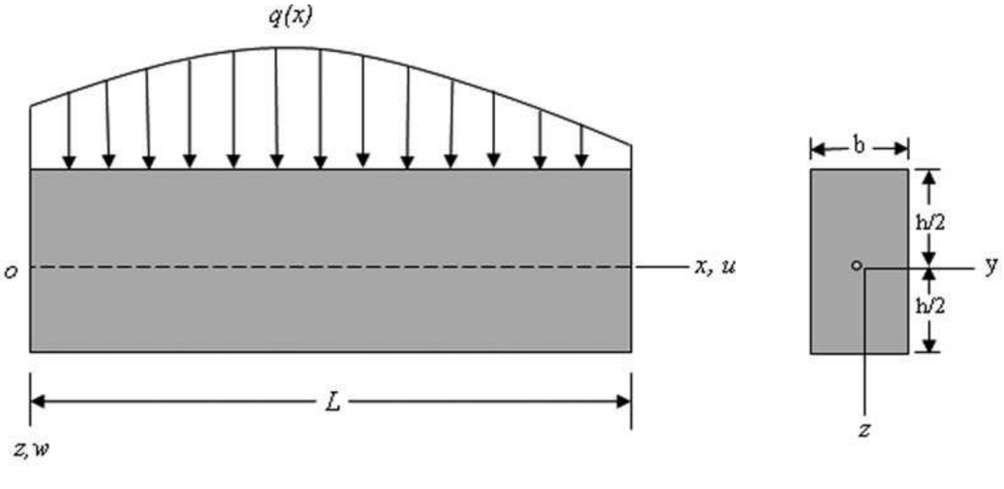

Fig. 1. Beam under bending in $x - z$ plane

2.1. Assumptions made in theoretical formulation

1. The in-plane displacement u in x direction consists of two parts:
   (a) A displacement component analogous to displacement in elementary beam theory of bending;
   (b) Displacement component due to shear deformation which is assumed to be parabolic, sinusoidal, hyperbolic and exponential in nature with respect to thickness coordinate.

2. The transverse displacement w in z direction is assumed to be a function of x coordinate.
3. One dimensional constitutive law is used.
4. The beam is subjected to lateral load only.

2.2. The displacement field

Based on the before mentioned assumptions, the displacement field of the present unified shear deformation theory is given as below

$$u(x,z,t) = -z\frac{\partial w}{\partial x} + f(z)\phi(x,t), \tag{2}$$

$$w(x,z,t) = w(x,t). \tag{3}$$

Here u and w are the axial and transverse displacements of the beam center line in x and z-directions respectively and t is the time. The ϕ represents the rotation of the cross-section of the beam at neutral axis which is an unknown function to be determined. The functions $f(z)$ assigned according to the shearing stress distribution through the thickness of the beam are given in Table 1.

Table 1. Functions $f(z)$ for different shear stress distribution

Model	Author	Function $f(z)$
Model 1	(Ambartsumian [2])	$f(z) = \left[\frac{z}{2}\left(\frac{h^2}{4} - \frac{z^2}{3}\right)\right]$
Model 2	(Kruszewski [15])	$f(z) = \left[\frac{5z}{4}\left(1 - \frac{4z^2}{3h^2}\right)\right]$
Model 3	(Reddy [18])	$f(z) = z\left[1 - \frac{4}{3}\left(\frac{z}{h}\right)^2\right]$
Model 4	(Touratier [25])	$f(z) = \frac{h}{\pi}\sin\frac{\pi z}{h}$
Model 5	(Soldatos [22])	$f(z) = \left[z\cosh\left(\frac{1}{2}\right) - h\sinh\left(\frac{z}{h}\right)\right]$
Model 6	(Karama et al. [14])	$f(z) = z\exp\left[-2\left(\frac{z}{h}\right)^2\right]$
Model 7	(Akavci [1])	$f(z) = \frac{3\pi}{2}\left[h\tanh\left(\frac{z}{h}\right) - z\sec^2\mathrm{h}\left(\frac{1}{2}\right)\right]$

2.3. Necessity of refined theories

The shear deformation effects are more pronounced in the thick beams than in the slender beams. These effects are neglected in elementary theory of beam (ETB) bending. In order to describe the correct bending behavior of thick beams including shear deformation effects and the associated cross sectional warping, shear deformation theories are required. This can be accomplished by selection of proper kinematics and constitutive models. The functions $f(z)$ is included in the displacement field of higher order theories to take into account effect of transverse shear deformation and to get the zero shear stress conditions at top and bottom surfaces of the beam.

2.4. Strain-displacement relationship

Normal strain and transverse shear strain for beam are given by

$$\begin{aligned} \varepsilon_x &= \frac{\partial u}{\partial x} = -z\frac{\partial^2 w}{\partial x^2} + f(z)\frac{\partial \phi}{\partial x}, && (4)\\ \gamma_{zx} &= \frac{\partial u}{\partial z} + \frac{\partial w}{\partial x} = f^{'}(z)\phi. && (5) \end{aligned}$$

2.5. Stress-Strain relationship

According to one dimensional constitutive law, the axial stress/normal bending stress and transverse shear stress are given by

$$\begin{aligned} \sigma_x &= E\varepsilon_x = E\left[-z\frac{\partial^2 w}{\partial x^2} + f(z)\frac{\partial \phi}{\partial x}\right], && (6)\\ \tau_{zx} &= G\gamma_{zx} = Gf'(z)\phi. && (7) \end{aligned}$$

3. Governing equations and boundary conditions

Using Eqns. (4) through (7) and the principle of virtual work, variationally consistent governing differential equations and boundary conditions for the beam under consideration can be obtained. The principle of virtual work when applied to the beam leads to

$$\begin{aligned} &\int_0^L \int_{-h/2}^{+h/2} (\sigma_x \delta\varepsilon_x + \tau_{zx}\delta\gamma_{zx})\,\mathrm{d}z\,\mathrm{d}x + && (8)\\ \rho \int_0^L \int_{z-h/2}^{+h/2} \left(\frac{\partial^2 u}{\partial t^2}\delta u + \frac{\partial^2 w}{\partial t^2}\delta w\right)\mathrm{d}z\,\mathrm{d}x - \int_0^L q\delta w\,\mathrm{d}x &= 0, \end{aligned}$$

where the symbol δ denotes the variational operator. Integrating the preceding equations by parts, and collecting the coefficients of δw and $\delta\phi$, the governing equations in terms of displacement variables are obtained as follows

$$\begin{aligned} A_0\frac{\partial^4 w}{\partial x^4} - B_0\frac{\partial^3 \phi}{\partial x^3} - \frac{\rho A_0}{E}\frac{\partial^4 w}{\partial x^2 \partial t^2} + \frac{\rho B_0}{E}\frac{\partial^3 \phi}{\partial x \partial t^2} + \rho h\frac{\partial^2 w}{\partial t^2} &= q, && (9)\\ B_0\frac{\partial^3 w}{\partial x^3} - C_0\frac{\partial^2 \phi}{\partial x^2} + D_0\phi - \frac{\rho B_0}{E}\frac{\partial^3 w}{\partial x \partial t^2} - \frac{\rho C_0}{E}\frac{\partial^2 \phi}{\partial t^2} &= 0 && (10) \end{aligned}$$

and the associated boundary conditions obtained are of following form

$$\begin{aligned} -A_0\frac{\partial^3 w}{\partial x^3} + B_0\frac{\partial^2 \phi}{\partial x^2} + \frac{\rho A_0}{E}\frac{\partial^3 w}{\partial x \partial t^2} - \frac{\rho B_0}{E}\frac{\partial^2 \phi}{\partial t^2} &= 0 \quad \text{or } w \text{ is prescribed} && (11)\\ A_0\frac{\partial^2 w}{\partial x^2} - B_0\frac{\partial \phi}{\partial x} &= 0 \quad \text{or } \frac{\mathrm{d}w}{\mathrm{d}x} \text{ is prescribed} && (12)\\ -B_0\frac{\partial^2 w}{\partial x^2} + C_0\frac{\partial \phi}{\partial x} &= 0 \quad \text{or } \phi \text{ is prescribed} && (13) \end{aligned}$$

where A_0, B_0, C_0 and D_0 are the stiffness coefficients given as follows

$$\begin{aligned} &A_0 = E\int_{-h/2}^{+h/2} z^2\,\mathrm{d}z, \quad B_0 = E\int_{-h/2}^{+h/2} zf(z)\,\mathrm{d}z, && (14)\\ &C_0 = E\int_{-h/2}^{+h/2} f^2(z)\,\mathrm{d}z, \quad D_0 = G\int_{-h/2}^{+h/2} [f'(z)]^2\,\mathrm{d}z. \end{aligned}$$

3.1. Illustrative examples

In order to prove the efficacy of the present theories, the following numerical examples are considered. The following material properties for beam are used

$$E = 210\ \text{GPa}, \qquad \mu = 0.3, \qquad G = \frac{E}{2(1+\mu)} \text{ and } \rho = 7\,800\ \text{kg/m}^3, \tag{15}$$

where E is the Young's modulus, ρ is the density, and μ is the Poisson's ratio of beam material.

Example 1: Bending analysis of beam

A simply supported uniform beam shown in Fig. 2 subjected to uniformly distributed load $q(x) = \sum_{m=1}^{m=\infty} q_m \sin\left(\frac{m\pi x}{L}\right)$ acting in the z-direction, where q_m is the coefficient of single Fourier expansion of load. The value of q_m for uniformly distributed load given as follows

$$\begin{aligned} q_m &= \frac{4q_0}{m\pi}\ , \quad m = 1, 3, 5, \ldots, \\ q_m &= 0 \quad\ \ , \quad m = 2, 4, 6, \ldots, \end{aligned} \tag{16}$$

where q_0 is the intensity of uniformly distributed load.

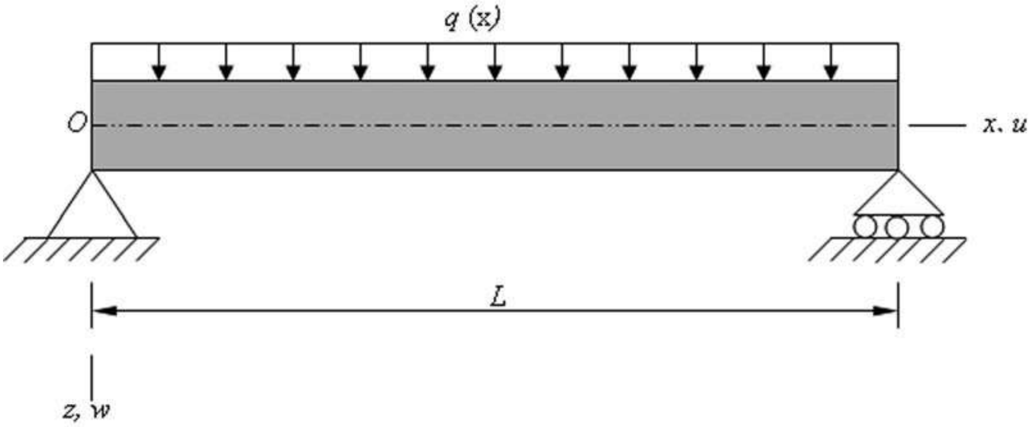

Fig. 2. Simply supported beam subjected to uniformly distributed load

The governing equations for bending analysis of beam (static flexure), discarding all the terms containing time derivatives become

$$A_0 \frac{\mathrm{d}^4 w}{\mathrm{d}x^4} - B_0 \frac{\mathrm{d}^3 \phi}{\mathrm{d}x^3} = q, \tag{17}$$

$$B_0 \frac{\mathrm{d}^3 w}{\mathrm{d}x^3} - C_0 \frac{\mathrm{d}^2 \phi}{\mathrm{d}x^2} + D_0 \phi = 0. \tag{18}$$

The following is the solution form assumed for $w(x)$ and $\phi(x)$ which satisfies the boundary conditions exactly

$$w(x) = \sum_{m=1}^{\infty} w_m \sin\frac{m\pi x}{L}, \qquad \phi(x) = \sum_{m=1}^{\infty} \phi_m \cos\frac{m\pi x}{L}, \tag{19}$$

where w_m and ϕ_m are the unknown coefficients of the respective Fourier expansion and m is the positive integer. Substituting this form of solution and the load $q(x)$ into governing equations, yields the following two algebraic simultaneous equations

$$\left(A_0\frac{m^4\pi^4}{L^4}\right)w_m - \left(B_0\frac{m^3\pi^3}{L^3}\right)\phi_m = q_m, \tag{20}$$

$$-\left(B_0\frac{m^3\pi^3}{L^3}\right)w_m + \left(C_0\frac{m^2\pi^2}{L^2} + D_0\right)\phi_m = 0. \tag{21}$$

Solving Eqns. (20) and (21) simultenously to determine unknowns w_m and ϕ_m

$$w_m = \frac{q_m\left(C_0\frac{m^2\pi^2}{L^2} + D_0\right)}{\left(C_0\frac{m^2\pi^2}{L^2} + D_0\right)\left(A_0\frac{m^4\pi^4}{L^4}\right) - \left(B_0\frac{m^3\pi^3}{L^3}\right)\left(B_0\frac{m^3\pi^3}{L^3}\right)}, \tag{22}$$

$$\phi_m = \frac{q_m\left(B_0\frac{m^3\pi^3}{L^3}\right)}{\left(C_0\frac{m^2\pi^2}{L^2} + D_0\right)\left(A_0\frac{m^4\pi^4}{L^4}\right) - \left(B_0\frac{m^3\pi^3}{L^3}\right)\left(B_0\frac{m^3\pi^3}{L^3}\right)}. \tag{23}$$

Using Eqns. (22) and (23) substitute Eqn. (19) in the displacement field [Eqns. (2) and (3)] and stress-strain relationships [Eqns. (6) and (7)] to obtain expressions for axial displacement, transverse displacement, axial bending stress and transverse shear stress

Axial displacement:
$$u = \left[-z\frac{m\pi}{L}w_m + f(z)\phi_m\right]\cos\frac{m\pi x}{L}. \tag{24}$$

Transverse displacement:
$$w = w_m \sin\frac{m\pi x}{L}. \tag{25}$$

Axial bending stress:
$$\sigma_x = E\left[z\frac{m^2\pi^2}{L^2}w_m - f(z)\frac{m\pi}{L}\phi_m\right]\sin\frac{m\pi x}{L}. \tag{26}$$

Transverse shear stress:
$$\tau_{zx} = Gf'(z)\phi_m\cos\frac{m\pi x}{L}. \tag{27}$$

Example 2: Free flexural vibration of beam

The governing equations for free flexural vibration of simply supported beam can be obtained by setting the applied transverse load equal to zero in Eqns. (9) and (10). A solution to resulting governing equations, which satisfies the associated initial conditions, is of the form

$$w = w_m\sin\frac{m\pi x}{L}\sin\omega_m t, \tag{28}$$

$$\phi = \phi_m\cos\frac{m\pi x}{L}\sin\omega_m t, \tag{29}$$

where w_m and ϕ_m are the amplitudes of translation and rotation respectively, and ω_m is the natural frequency of the m^{th} mode of vibration. Substitution of this solution form into the governing equations of free vibration of beam results in following algebraic equations

$$\left[\left(A_0\frac{m^4\pi^4}{L^4}\right)w_m - \left(B_0\frac{m^3\pi^3}{L^3}\right)\phi_m\right] - \omega^2\left[\left(\frac{\rho A_0}{E}\frac{m^2\pi^2}{L^2} + \rho h\right)w_m - \frac{\rho B_0}{E}\frac{m\pi}{L}\phi_m\right] = 0, \tag{30}$$

$$\left[-B_0\frac{m^3\pi^3}{L^3}w_m + \left(C_0\frac{m^2\pi^2}{L^2} + D_0\right)\phi_m\right] - \omega^2\left[-\left(\frac{\rho B_0}{E}\frac{m\pi}{L}\right)w_m + \frac{\rho C_0}{E}\phi_m\right] = 0. \tag{31}$$

The Eqns. (30) and (31) can be written in the following matrix form

$$\left(\begin{bmatrix} K_{11} & K_{12} \\ K_{12} & K_{22} \end{bmatrix} - \omega^2 \begin{bmatrix} M_{11} & M_{12} \\ M_{12} & M_{22} \end{bmatrix}\right) \begin{Bmatrix} w_m \\ \phi_m \end{Bmatrix} = 0. \tag{32}$$

Above Eqn. (32) can be written in following more compact form

$$([K] - \omega_m^2 [M])\{\Delta\} = 0, \tag{33}$$

where $\{\Delta\}$ denotes the vector, $\{\Delta\}^T = \{W_m, \phi_m\}$. The $[K]$ and $[M]$ are symmetric matrices. The elements of the coefficient matrix $[K]$ are given by

$$K_{11} = \left(A_0 \frac{m^4\pi^4}{L^4}\right), \quad K_{12} = K_{21} = -\left(B_0 \frac{m^3\pi^3}{L^3}\right), \quad K_{22} = \left(C_0 \frac{m^2\pi^2}{L^2} + D_0\right). \tag{34}$$

The elements of the coefficient matrix $[M]$ are given by

$$M_{11} = \left(\frac{\rho A_0}{E} \frac{m^2\pi^2}{L^2} + \rho h\right), \qquad M_{12} = M_{21} = -\frac{\rho B_0}{E} \frac{m\pi}{L}, \qquad M_{22} = \frac{\rho C_0}{E}. \tag{35}$$

For nontrivial solution of Eqn. (33), $\{\Delta\} \neq 0$, the condition expressed by

$$([K] - \omega_m^2 [M]) = 0, \tag{36}$$

yields the eigen-frequencies ω_m. From this solution natural frequencies of beam for various modes of vibration can be obtained.

4. Numerical results

The results for transverse displacement (w), axial bending stress (σ_x), transverse shear stress (τ_{zx}) and fundamental frequency ω_m are presented in the following non-dimensional form

$$\bar{w} = \frac{10Ebh^3 w}{q_0 L^4}, \quad \bar{\sigma}_x = \frac{b\sigma_x}{q_0}, \quad \bar{\tau}_{zx} = \frac{b\tau_{zx}}{q_0}, \quad \bar{\omega} = \omega_m \left(\frac{L^2}{h}\right)\sqrt{\frac{\rho}{E}}, \quad S = \frac{L}{h}, \tag{37}$$

where S is the aspect ratio.

The percentage error in results obtained by theories/models of various researchers with respect to the corresponding results obtained by theory of elasticity is calculated as follows

$$\text{error} = \left(\frac{\text{value by a particular model} - \text{value by exact elasticity solution}}{\text{value by exact elasticity solution}}\right) \times 100\,\%. \tag{38}$$

The results obtained for the above examples (static and dynamics) solved in this paper are presented in Tables 2 through 5.

5. Discussion of results

The results obtained from the present theories are compared with the elementary theory of beam (ETB), first order shear deformation theory (FSDT) of Timoshenko [24], higher order shear deformation theories of Heyliger and Reddy [12], Ghugal [10] and exact elasticity solutions given by Timoshenko and Goodier [23] and Cowper [7]. The value of dynamic shear correction factor is compared with its exact value given by Lamb [16]:

a) **Transverse Displacement ($\bar{w}$):** The comparison of maximum transverse displacement for the simply supported thick isotropic beams subjected to uniformly distributed load is presented in Table 2. The maximum transverse displacement predicted by models 5 and 6 is in excellent agreement with the exact solution for all the aspect ratios whereas the error in predicting transverse displacement by other models decreases with increase in aspect ratio. The FSDT overestimates the maximum transverse displacement whereas ETB underestimates the same for all the aspect ratios as compared to that of exact solution.

b) **Axial Bending Stress ($\bar{\sigma}_x$):** Table 2 shows the comparison of axial bending stress for the simply supported thick isotropic beams subjected to uniformly distributed load. Among all the models, model 6 overestimates the value of axial bending stress for all the aspect ratios as compared to that of exact solution whereas axial bending stress predicted by rest of the models is in excellent agreement with that of exact solution. The values of axial

Table 2. Comparison of transverse displacement $\bar{w}$ at ($x = L/2$, $z = 0$), axial bending stress $\bar{\sigma}_x$ at ($x = L/2$, $z = \pm h/2$) and transverse shear stress $\bar{\tau}_{zx}$ at ($x = 0$, $z = 0$) for isotropic beam subjected to uniformly distributed load

S	Theory	$\bar{w}$	% Error	$\bar{\sigma}_x$	% Error	$\bar{\tau}_{zx}$	% Error
2	Model 1 [2]	2.357	-3.913	3.210	0.312	1.156	-22.93
	Model 2 [15]	2.515	2.527	3.261	1.906	1.333	-11.13
	Model 3 [18]	2.532	3.220	3.261	1.906	1.415	-5.667
	Model 4 [25]	2.529	3.098	3.278	2.437	1.451	-3.267
	Model 5 [22]	2.513	2.445	3.206	0.187	1.442	-3.866
	Model 6 [14]	2.510	2.323	3.322	3.812	1.430	-4.667
	Model 7 [1]	2.523	2.853	3.253	1.656	1.397	-6.866
	Timoshenko [FSDT] [24]	2.538	3.465	3.000	-6.250	0.984	-34.40
	Bernoulli-Euler [ETB]	1.563	-3.628	3.000	-6.250	—	—
	Timoshenko and Goodier [Exact] [23]	2.453	0.000	3.200	0.000	1.500	0.000
4	Model 1 [2]	1.762	-1.288	12.212	0.098	2.389	-20.36
	Model 2 [15]	1.805	1.120	12.262	0.508	2.836	-5.466
	Model 3 [18]	1.806	1.176	12.263	0.516	2.908	-3.066
	Model 4 [25]	1.805	1.120	12.280	0.655	2.993	-0.233
	Model 5 [22]	1.802	0.952	12.207	0.057	2.982	-0.600
	Model 6 [14]	1.801	0.896	12.324	1.016	2.957	-1.433
	Model 7 [1]	1.804	1.064	12.254	0.442	2.882	-3.933
	Timoshenko [FSDT] [24]	1.806	1.176	12.000	-1.639	1.969	-34.36
	Bernoulli-Euler [ETB]	1.563	-12.43	12.000	-1.639	—	—
	Timoshenko and Goodier [Exact] [23]	1.785	0.000	12.200	0.000	3.000	0.000
10	Model 1 [2]	1.595	-0.187	75.216	0.021	6.066	-19.12
	Model 2 [15]	1.602	0.250	75.266	0.087	7.328	-2.293
	Model 3 [18]	1.602	0.250	75.268	0.090	7.361	-1.853
	Model 4 [25]	1.601	0.187	75.284	0.111	7.591	1.213
	Model 5 [22]	1.601	0.187	75.211	0.014	7.576	1.013
	Model 6 [14]	1.601	0.187	75.330	0.172	7.513	0.173
	Model 7 [1]	1.601	0.187	75.259	0.078	7.312	-2.506
	Timoshenko [FSDT] [24]	1.602	0.250	75.000	-0.265	4.922	-34.37
	Bernoulli-Euler [ETB]	1.563	-2.190	75.000	-0.265	—	—
	Timoshenko and Goodier [Exact] [23]	1.598	0.000	75.200	0.000	7.500	0.000

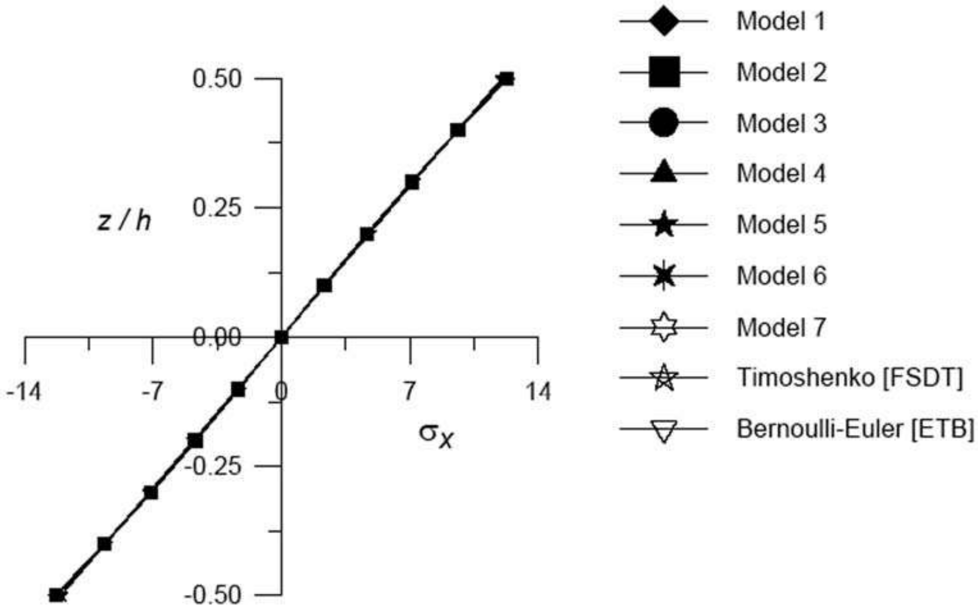

Fig. 3. Variation of axial bending stress ($\bar{\sigma}_x$) through thickness of beam subjected to uniformly distributed load for aspect ratio 4 at ($x = L/2$, z)

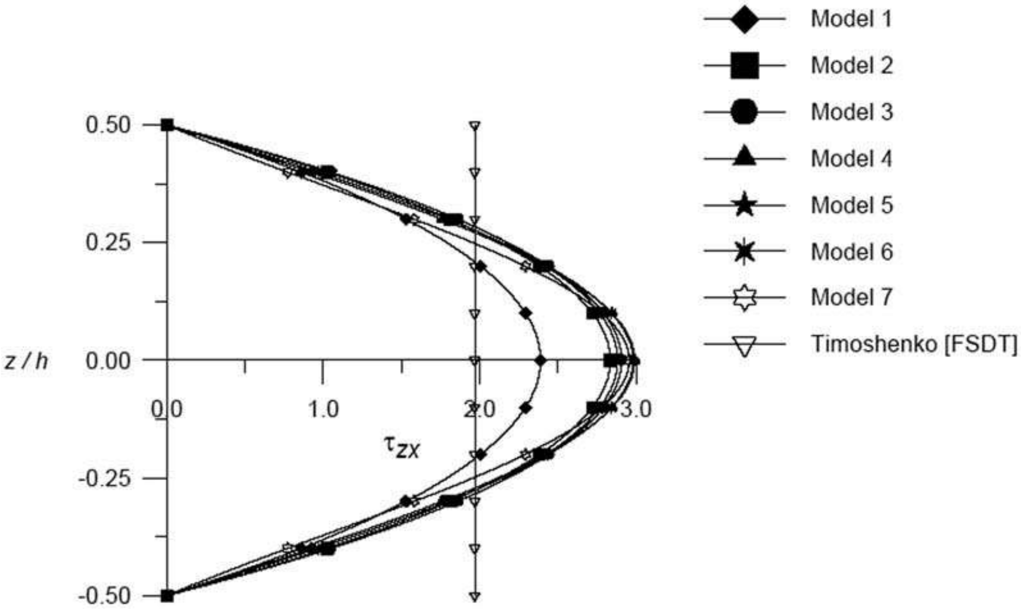

Fig. 4. Variation of transverse stress ($\bar{\tau}_{zx}$) through thickness of beam subjected to uniformly distributed load for aspect ratio 4 at ($x = 0$, z)

bending stress predicted by FSDT and ETB are identical for all the aspect ratios. The through thickness variation of axial bending stress is non-linear in nature as shown in Fig. 3.

c) **Transverse Shear Stress ($\bar{\tau}_{zx}$):** The comparison of maximum transverse shear stress for the simply supported thick isotropic beams subjected to uniformly distributed load is presented in Table 2. The transverse shear stress is obtained using constitutive relation. Examination of Table 2 reveals that model 1 overestimates the value of transverse shear

Table 3. Comparison of non-dimensional fundamental ($m = 1$) flexural and thickness shear mode frequencies of the isotropic beam

Model	$S = 4$			$S = 10$		
	$\bar{\omega}_w$	% Error	$\bar{\omega}_\phi$	$\bar{\omega}_w$	% Error	$\bar{\omega}_\phi$
Model 1 [2]	2.625	0.884	37.237	2.808	0.143	217.439
Model 2 [15]	2.597	−0.192	33.704	2.802	−0.071	194.752
Model 3 [18]	2.596	−0.230	34.259	2.802	−0.071	198.109
Model 4 [25]	2.596	−0.230	34.238	2.802	−0.071	198.109
Model 5 [22]	2.596	−0.230	34.263	2.802	−0.071	198.258
Model 6 [14]	2.608	0.230	34.711	2.805	0.036	201.290
Model 7 [1]	2.598	−0.154	33.748	2.803	−0.036	195.055
Bernoulli-Euler [ETB]	2.779	6.802	—	2.838	1.212	—
Timoshenko [FSDT] [24]	2.624	0.845	34.320	2.808	0.143	198.616
Ghugal [10]	2.602	0.000	34.135	2.804	0.000	198.105
Heyliger and Reddy [12]	2.596	−0.230	34.250	2.802	−0.071	198.235
Cowper [7]	2.602	0.000	—	2.804	0.000	—

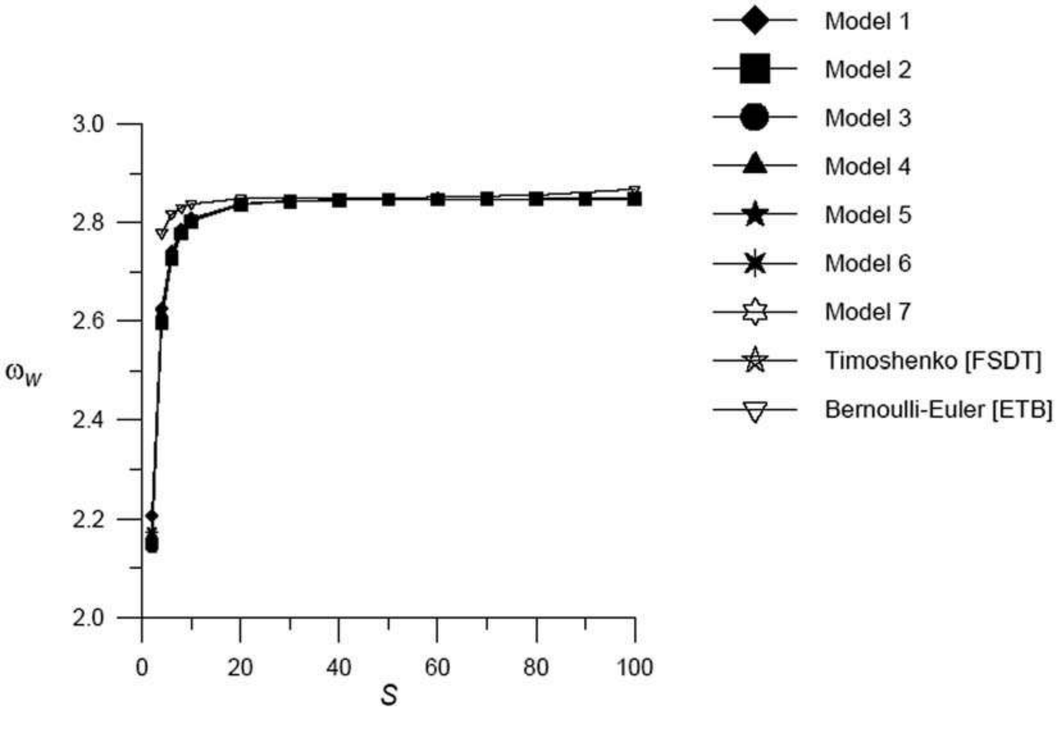

Fig. 5. Variation of fundamental bending frequency ($\bar{\omega}_w$) of beam with aspect ratio

stress whereas it is in excellent agreement when predicted by models 3 through 7 as compared to that of exact solution for all the aspect ratios. The transverse shear stress is overpredicted by models 1 and 2. Fig. 4 shows the through thickness variation of transverse shear stress for the thick isotropic beam subjected to uniformly distributed load for aspect ratio 4.

d) **Fundamental Flexural mode frequency ($\bar{\omega}_w$):** The comparison of lowest natural frequency in flexural mode is shown in Table 3. Observation of Table 2 shows that, Model 1

Table 4. Comparison of non-dimensional flexural frequency $(\bar{\omega}_w)$ of the isotropic beam for various modes of vibration

S	Model	Modes of vibration				
		$m = 1$	$m = 2$	$m = 3$	$m = 4$	$m = 5$
4	Model 1 [2]	2.625	8.823	16.491	24.713	33.165
	Model 2 [15]	2.597	8.598	15.957	23.923	32.304
	Model 3 [18]	2.596	8.569	15.793	23.435	31.240
	Model 4 [25]	2.596	8.573	15.811	23.483	31.339
	Model 5 [22]	2.596	8.569	15.791	23.429	31.228
	Model 6 [14]	2.608	8.691	16.202	24.357	32.935
	Model 7 [1]	2.598	8.612	16.004	24.027	32.493
	Cowper [7]	2.602	—	—	—	—
10	Model 1 [2]	2.808	10.791	22.903	37.999	55.142
	Model 2 [15]	2.802	10.711	22.582	37.228	53.740
	Model 3 [18]	2.802	10.709	22.566	37.164	53.557
	Model 4 [25]	2.802	10.710	22.570	37.175	53.583
	Model 5 [22]	2.802	10.709	22.566	37.163	53.554
	Model 6 [14]	2.805	10.742	22.708	37.537	54.317
	Model 7 [1]	2.803	10.715	22.598	37.271	53.827
	Cowper [7]	2.804	—	—	—	—

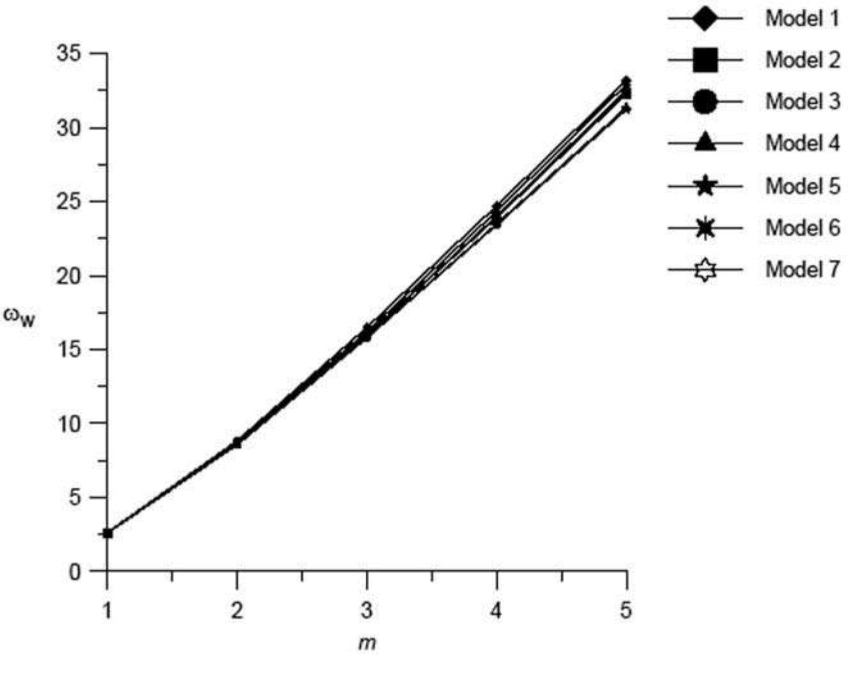

Fig. 6. Variation of fundamental bending frequency $(\bar{\omega}_w)$ of beam with various modes of vibration (m)

overestimates the lowest natural frequencies, in flexural mode by 0.884 % and 0.143 % for aspect ratios 4 and 10 respectively. The fundamental frequencies, in flexural mode predicted by models 2 through 6 is identical and in excellent agreement with that of exact solution Ghugal [10] yields the exact value of lowest natural frequencies, in flexural mode for aspect ratios 4 and 10. FSDT of Timoshenko overestimates the flexural mode

Table 5. Comparison of non-dimensional fundamental frequency of thickness shear mode ($\bar{\omega}_\phi$) of the isotropic beam for various modes of vibrations

S	Model	Modes of vibration				
		$m = 1$	$m = 2$	$m = 3$	$m = 4$	$m = 5$
4	Model 1 [2]	37.237	44.378	53.547	63.736	74.521
	Model 2 [15]	33.704	41.042	50.402	60.787	71.772
	Model 3 [18]	34.259	41.593	50.941	61.302	72.257
	Model 4 [25]	34.238	41.571	50.917	61.279	72.235
	Model 5 [22]	34.263	41.597	50.945	61.306	72.261
	Model 6 [14]	34.711	41.968	51.251	61.562	72.478
	Model 7 [1]	33.748	41.078	50.431	60.811	71.792
10	Model 1 [2]	217.439	226.391	240.105	257.416	277.363
	Model 2 [15]	194.752	204.080	218.272	236.080	256.514
	Model 3 [18]	198.235	207.555	221.739	239.539	259.959
	Model 4 [25]	198.109	207.425	221.606	239.401	259.819
	Model 5 [22]	198.258	207.578	221.763	239.563	259.984
	Model 6 [14]	201.290	210.468	224.467	242.071	262.302
	Model 7 [1]	195.055	204.368	218.539	236.327	256.740

frequency by 0.845 % and 0.143 % for aspect ratios 4 and 10 respectively whereas ETB overestimates the same by 6.802 % and 1.212 % due to neglect of shear deformation in the theory. The variation of lowest natural frequency in flexural mode with the aspect ratios is shown in Fig. 5. The comparison of flexural frequency for various modes of vibration (m) is shown in Table 4. The examination of Table 4 reveals that, the flexural frequencies obtained by various models are in excellent agreement with each other. The variation of flexural frequencies with various modes of vibration (m) is shown in Fig. 6.

e) **Fundamental frequency ($\bar{\omega}_\phi$):** Table 3 shows comparison of lowest natural frequency in thickness shear mode. Exact solution for the lowest natural frequency in thickness shear mode is not available in the literature. From the Table 3 it is observed that, thickness shear mode frequencies predicted by models 2 through 6 are in excellent agreement with each other whereas model 1 overestimates the same. Table 5 shows comparison of thickness shear mode frequencies for various modes of vibration and found in good agreement with each other. The solution for the circular frequency of thickness shear mode ($m = 0$) for thin rectangular beam is given by

$$\omega_\phi = \sqrt{\frac{K_{22}}{M_{22}}} = \sqrt{K_d \frac{GA}{\rho I}}, \tag{39}$$

where K_d is dynamic shear correction factor.

Table 6. Dynamic shear correction factors

Model	Model 1	Model 2	Model 3	Model 4	Model 5	Model 6	Model 7	Exact
K_d	0.995	0.794	0.824	0.822	0.824	0.850	0.797	0.822
% Error	21.046	−3.406	0.243	0.000	0.243	3.406	−3.041	0.000

Dynamic shear correction predicted by model 4 is same as the exact solution given by Lamb [16]. The corresponding values of shear factor for $m = 0$ according to models 3 and 5 is identical. The model 1 yields the higher value of dynamic shear correction factor whereas model 7 shows lower value for the same, Table 6.

6. Conclusions

From the study of comparison of various shear deformation theories for the bending and free vibration analysis of thick isotropic beams following conclusions are drawn.

1. The maximum transverse displacement predicted by all the models is in excellent agreement as compared to that of exact solution.
2. The axial bending stress predicted by the models 1 through 5 and 7 is in tune with exact solution whereas model 6 overestimates it for all the aspect ratios.
3. Through thickness variation of axial bending stress is non-linear in nature.
4. The maximum transverse shear stress predicted by models 3 through 7 is in excellent agreement as compared to that of exact solution whereas model 1 and 2 overestimates the value of transverse shear stress for all the aspect ratios.
5. Results of lowest natural frequencies for flexural mode predicted by models 3 through 5 are identical and in excellent agreement with that of exact solution. Model 1 overestimates the flexural mode frequency as compared to that of exact solution. Flexural mode frequencies predicted by models 2 and 7 are in tune with the exact solution.
6. The results of thickness shear mode frequencies are in excellent agreement with each other for all modes of vibration.
7. Model 4 yields the exact value of dynamic shear correction factor and it is in excellent agreement when predicted by models 3 and 5.

References

[1] Akavci, S. S., Buckling and free vibration analysis of symmetric and anti-symmetric laminated composite plates on an elastic foundation, Journal of Reinforced Plastics and Composites 26 (18) (2007) 1 907–1 919.

[2] Ambartsumyan, S. A., On the theory of bending plates, Izv Otd Tech Nauk AN SSSR 5 (1958) 69–77.

[3] Baluch, M. H., Azad, A. K., Khidir, M. A., Technical theory of beams with normal strain, Journal of Engineering Mechanics Proceedings ASCE 110 (1984) 1 233–1 237.

[4] Bhimaraddi, A., Chandrashekhara, K., Observations on higher-order beam theory, Journal of Aerospace Engineering Proceeding ASCE Technical Note 6 (1993) 408–413.

[5] Bickford, W. B., A consistent higher order beam theory. Development of Theoretical and Applied Mechanics, SECTAM 11 (1982) 137–150.

[6] Cowper, G. R., The shear coefficients in Timoshenko beam theory, ASME Journal of Applied Mechanics 33 (1966) 335–340.

[7] Cowper, G. R., On the accuracy of Timoshenko's beam theory, ASCE Journal of Engineering Mechanics Division 94 (6) (1968) 1 447–1 453.

[8] Ghugal, Y. M., Sharma, R., Hyperbolic shear deformation theory for flexure and vibration of thick isotropic beams, International Journal of Computational Methods 6 (4) (2009) 585–604.

[9] Ghugal, Y. M., Shimpi, R. P., A review of refined shear deformation theories for isotropic and anisotropic laminated beams, Journal of Reinforced Plastics and Composites 21 (2002) 775–813.

[10] Ghugal, Y. M., A simple higher order theory for beam with transverse shear and transverse normal effect, Department Report 4, Applied of Mechanics Department, Government College of Engineering, Aurangabad, India, 2006.

[11] Hildebrand, F. B., Reissner, E. C., Distribution of stress in built-in beam of narrow rectangular cross section, Journal of Applied Mechanics 64 (1942) 109–116.

[12] Heyliger, P. R., Reddy, J. N., A higher order beam finite element for bending and vibration problems, Journal of Sound and Vibration 126 (2) (1988) 309–326.

[13] Krishna Murty, A. V., Toward a consistent beam theory, AIAA Journal 22 (1984) 811–816.

[14] Karama, M., Afaq, K. S., Mistou, S., Mechanical behavior of laminated composite beam by new multi-layered laminated composite structures model with transverse shear stress continuity, International Journal of Solids and Structures, 40 (2003) 1525–1546.

[15] Kruszewski, E. T., Effect of transverse shear and rotatory inertia on the natural frequency of a uniform beam, NACATN (1909).

[16] Lamb, H., On waves in an elastic plates, Proceeding of Royal Society London Series A. 93 (1917) 114–128.

[17] Levinson, M., A new rectangular beam theory, Journal of Sound and Vibration 74 (1981) 81–87.

[18] Reddy, J. N., A general non-linear third order theory of plates with moderate thickness, International Journal of Non-linear Mechanics 25 (6) (1990) 677–686.

[19] Rehfield, L. W., Murthy, P. L. N., Toward a new engineering theory of bending: fundamentals, AIAA Journal 20 (1982) 693–699.

[20] Stein, M., Vibration of beams and plate strips with three-dimensional flexibility, Transaction ASME Journal of Applied Mechanics 56 (1) (1989) 228–231.

[21] Sayyad, A. S., Comparison of various shear deformation theories for the free vibration of thick isotropic beams, International Journal of Civil and Structural Engineering 2 (1) (2011) 85–97.

[22] Soldatos, K. P., A transverse shear deformation theory for homogeneous monoclinic plates, Acta Mechanica 94 (1992) 195–200.

[23] Timoshenko, S. P., Goodier, J. N., Theory of Elasticity, McGraw-Hill 3rd Int. ed. Singapore 1970.

[24] Timoshenko, S. P., On the correction for shear of the differential equation for transverse vibrations of prismatic bars, Philosophical Magazine 41 (6) (1921) 742–746.

[25] Touratier, M., An efficient standard plate theory, International Journal of Engineering Science 29 (8) (1991) 901–916.

[26] Vlasov, V. Z., Leont’ev, U. N., Beams, Plates and Shells on Elastic foundation, (Translated from Russian) Israel Program for Scientific Translation Ltd. Jerusalem 1996.

ResearchGate

See discussions, stats, and author profiles for this publication at: https://www.researchgate.net/publication/281775462

A Trigonometric Shear Deformation Theory for Thick Beam

Article · July 2012

CITATIONS
2

READS
71

2 authors:

Ajay Dahake
G. H. Raisoni College of Engineering & Management

48 PUBLICATIONS **130** CITATIONS

SEE PROFILE

Yuwaraj Marotrao Ghugal
Government Engineering College, Karad, Maharashtra State, India

152 PUBLICATIONS **3,284** CITATIONS

SEE PROFILE

Some of the authors of this publication are also working on these related projects:

Project Stability of Plates and Shells View project

Project Refined shear deformation theory View project

All content following this page was uploaded by Ajay Dahake on 24 June 2017.

The user has requested enhancement of the downloaded file.

A TRIGONOMETRIC THEORY FOR THICK BEAM

[1]AJAY G. DAHAKE, [2] Dr. YUWARAJ M. GHUGAL

[1] Research Scholar, Department of Applied Mechanics, GEC, Aurangabad, India -431005

[2] Professor, Department of Applied Mechanics, GEC, Karad, MS, India-410125

E-mail: ajaydahake@gmail.com, ghugal@rediffmail.com,

ABSTRACT

A trigonometric shear deformation theory for flexure of thick beams, taking into account transverse shear deformation effects, is developed. The number of variables in the present theory is same as that in the first order shear deformation theory. The sinusoidal function is used in displacement field in terms of thickness coordinate to represent the shear deformation effects. The noteworthy feature of this theory is that the transverse shear stresses can be obtained directly from the use of constitutive relations with excellent accuracy, satisfying the shear stress free conditions on the top and bottom surfaces of the beam. Hence, the theory obviates the need of shear correction factor. Governing differential equations and boundary conditions are obtained by using the principle of virtual work. The thick simply supported isotropic beams are considered for the numerical studies to demonstrate the efficiency of the. Results obtained are discussed critically with those of other theories.

Keywords: *Trigonometric shear deformation, thick beam, flexure, principle of virtual work, equilibrium equations, stress*

1. INTRODUCTION

It is well-known that elementary theory of bending of beam based on Euler-Bernoulli hypothesis disregards the effects of the shear deformation and stress concentration. The theory is suitable for slender beams and is not suitable for thick or deep beams since it is based on the assumption that the transverse normal to neutral axis remains so during bending and after bending, implying that the transverse shear strain is zero. Since theory neglects the transverse shear deformation, it underestimates deflections in case of thick beams where shear deformation effects are significant.

Bresse [1], Rayleigh [2] and Timoshenko [3] were the pioneer investigators to include refined effects such as rotatory inertia and shear deformation in the beam theory. Timoshenko showed that the effect of transverse vibration of prismatic bars. This theory is now widely referred to as Timoshenko beam theory or first order shear deformation theory (FSDT) in the literature. In this theory transverse shear strain distribution is assumed to be constant through the beam thickness and thus requires shear correction factor to appropriately represent the strain energy of deformation. Cowper [4] has given refined expression for the shear correction factor for different cross-sections of beam. The accuracy of Timoshenko beam theory for transverse vibrations of simply supported beam in respect of the fundamental frequency is verified by Cowper [5] with a plane stress exact elasticity solution. To remove the discrepancies in classical and first order shear deformation theories, higher order or refined shear deformation theories were developed and are available in the open literature for static and vibration analysis of beam.

Levinson [6], Bickford [7], Rehfield and Murty [8], Krishna Murty [9], Baluch, Azad and Khidir [10], Bhimaraddi and Chandrashekhara [11] presented parabolic shear deformation theories assuming a higher variation of axial displacement in terms of thickness coordinate. These theories satisfy shear stress free boundary conditions on top and bottom surfaces of beam and thus obviate the need of shear correction factor. Irretier [12] studied the refined dynamical effects in linear, homogenous beam according to theories, which exceed the limits of the Euler-Bernoulli beam theory. These effects are rotary inertia, shear deformation, rotary inertia and shear deformation, axial pre-stress, twist and coupling between bending and torsion.

Kant and Gupta [13], Heyliger and Reddy [14] presented finite element models based on higher order shear deformation uniform rectangular beams. However, these displacement based finite element models are not free from phenomenon of shear locking (Averill and Reddy [15], Reddy [16]).

There is another class of refined theories, which includes trigonometric functions to represent the shear deformation effects through the thickness. Vlasov and Leont'ev [17], Stein [18] developed refined shear deformation theories for thick beams including sinusoidal function in terms of thickness coordinate in displacement field. However, with these theories shear stress free boundary conditions are not satisfied at top and bottom surfaces of the beam. A study of literature by Ghugal and Shimpi [19] indicates that the research work dealing with flexural analysis of thick beams using refined trigonometric and hyperbolic shear deformation theories is very scarce and is still in infancy. In this paper development of theory and its application to thick fixed beams is presented.

2. DEVELOPMENT OF THEORY

The beam under consideration as shown in Fig. 1 occupies in $0-x-y-z$ Cartesian coordinate system the region:

$$0 \le x \le L\ ; \quad 0 \le y \le b\ ; \quad -\frac{h}{2} \le z \le \frac{h}{2}$$

where *x*, *y*, *z* are Cartesian coordinates, *L* and *b* are the length and width of beam in the x and *y* directions respectively, and *h* is the thickness of the beam in the z-direction. The beam is made up of homogeneous, linearly elastic isotropic material.

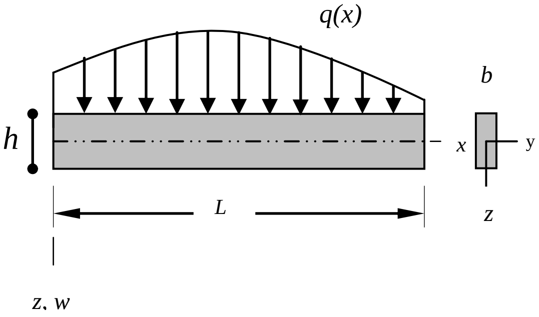

Fig. 1 Beam under bending in *x*-*z* plane

2.1 The displacement field

The displacement field of the present beam theory is of the form:

$$\begin{aligned} u(x,z) &= -z\frac{dw}{dx} + \frac{h}{\pi}\sin\frac{\pi z}{h}\phi(x) \\ w(x,z) &= w(x) \end{aligned} \tag{1}$$

where u is the axial displacement in *x* direction and *w* is the transverse displacement in *z* direction of the beam. The sinusoidal function is assigned according to the shear stress distribution through the thickness of the beam. The function ϕ represents rotation of the beam at neutral axis, which is an unknown function to be determined. The normal and shear strains obtained within the framework of linear theory of elasticity using displacement field given by "(1)" are as follows.

Normal strain:

$$\varepsilon_x = \frac{\partial u}{\partial x} = -z\frac{d^2 w}{dx^2} + \frac{h}{\pi}\sin\frac{\pi z}{h}\frac{d\phi}{dx} \tag{2}$$

Shear strain: $\gamma_{zx} = \dfrac{\partial u}{\partial z} + \dfrac{dw}{dx} = \cos\dfrac{\pi z}{h}\phi$ (3)

The stress-strain relationships used are as follows:

$$\sigma_x = E\varepsilon_x,\ \tau_{zx} = G\gamma_{zx} \tag{4}$$

2.2 Governing Equations and Boundary Conditions

"Using (2) through (4)" and using the principle of virtual work, variationally consistent governing differential equations and boundary conditions for the beam under consideration can be obtained. The principle of virtual work when applied to the beam leads to:

$$\begin{aligned} & b\int_{x=0}^{x=L}\int_{z=-h/2}^{z=+h/2}\left(\sigma_x\delta\varepsilon_x + \tau_{zx}\,\delta\gamma_{zx}\right)dx\,dz \\ & -\int_{x=0}^{x=L} q(x)\,\delta w\,dx = 0 \end{aligned} \tag{5}$$

where the symbol δ denotes the variational operator. "Employing Green's theorem to (4) successively", we obtain the coupled Euler-Lagrange equations which are the governing differential equations and associated boundary conditions of the beam. The governing differential equations obtained are as follows:

$$EI\,\frac{d^4 w}{dx^4} - \frac{24}{\pi^3}\,EI\,\frac{d^3\phi}{dx^3} = q(x) \tag{6}$$

$$\frac{24}{\pi^3}\,EI\,\frac{d^3 w}{dx^3} - \frac{6}{\pi^2}EI\,\frac{d^2\phi}{dx^2} + \frac{GA}{2}\phi = 0 \tag{7}$$

The associated consistent natural boundary conditions obtained are of following form:

At the ends $x = 0$ and $x = L$

$$V_x = EI\,\frac{d^3w}{dx^3} - \frac{24}{\pi^3}\,EI\,\frac{d^2\phi}{dx^2} = 0$$

$$\text{or } w \text{ is prescribed} \tag{8}$$

$$M_x = EI\,\frac{d^2w}{dx^2} - \frac{24}{\pi^3}\,EI\,\frac{d\phi}{dx} = 0$$

$$\text{or } \frac{dw}{dx} \text{ is prescribed} \tag{9}$$

$$M_a = EI\,\frac{24}{\pi^3}\,\frac{d^2w}{dx^2} - \frac{6}{\pi^2}\,EI\,\frac{d\phi}{dx} = 0$$

$$\text{or } \phi \text{ is prescribed} \tag{10}$$

Thus the boundary value problem of the beam bending is given by the above variationally consistent governing differential equations and boundary conditions.

2.3 The General Solution of Governing Equilibrium Equations of the Beam

The general solution for transverse displacement $w(x)$ and warping function $\phi(x)$ is obtained using "(6) and (7)" using method of solution of linear differential equations with constant coefficients. Integrating and rearranging "(6)", we obtain the following expression

$$\frac{d^3w}{dx^3} = \frac{24}{\pi^3}\frac{d^2\phi}{dx^2} + \frac{Q(x)}{EI} \tag{11}$$

where $Q(x)$ is the generalized shear force for beam and it is given by $Q(x) = \int_0^x q\,dx + C_1$.

Now "(7)" is rearranged in the following form:

$$\frac{d^3w}{dx^3} = \frac{\pi}{4}\frac{d^2\phi}{dx^2} - \beta\phi \tag{12}$$

A single equation in terms of ϕ is now obtained using "(11) and (12)" as:

$$\frac{d^2\phi}{dx^2} - \lambda^2\phi = \frac{Q(x)}{\alpha EI} \tag{13}$$

where constants α, β and λ in "(12) and (13)" are as follows

$$\alpha = \left(\frac{\pi}{4} - \frac{24}{\pi^3}\right),\ \beta = \left(\frac{\pi^3}{48}\frac{GA}{EI}\right) \text{and } \lambda^2 = \frac{\beta}{\alpha}$$

The general solution of "(13)" is as follows:

$$\phi(x) = C_2\cosh\lambda x + C_3\sinh\lambda x - \frac{Q(x)}{\beta EI} \tag{14}$$

The equation of transverse displacement $w(x)$ is obtained by substituting the expression of $\phi(x)$ in "(12)" and then integrating it thrice with respect to x. The general solution for $w(x)$ is obtained as follows

$$\begin{aligned} EI\,w(x) &= \iiiint q\,dx\,dx\,dx\,dx + \frac{C_1x^3}{6} \\ &+ \left(\frac{\pi}{4}\lambda^2 - \beta\right)\frac{EI}{\lambda^3}\left(C_2\sinh\lambda x + C_3\cosh\lambda x\right) \\ &+ C_4\frac{x^2}{2} + C_5x + C_6 \end{aligned} \tag{15}$$

where C_1, C_2, C_3, C_4, C_5 and C_6 are arbitrary constants and can be obtained by imposing boundary conditions of beam.

3. ILLUSTRATIVE EXAMPLES

In order to prove the efficacy of the present theory, the following numerical examples are considered. The following material properties for beam are used

E = 210 GPa, μ = 0.3 and ρ = 7800 kg/m^3, where E is the Young's modulus, ρ is the density, and μ is the Poisson's Units

3.1 Simply supported beam subjected to parabolic load, $q(x) = q_0\left(\frac{x}{L}\right)^2$

The simply supported beam is having its origin at left support and is simply supported at x = 0 and x =L. The beam is subjected to parabolic load, on surface $z = +h/2$ acting in the downward z direction with maximum intensity of load q_0.

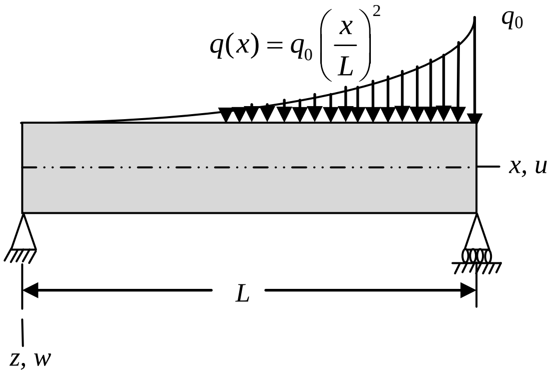

Fig. 2: Simply supported beam with parabolic load

General expressions obtained for $w(x)$ and $\phi(x)$ are as follows:

$$w(x)=\frac{q_0L^4}{120EI}\left[\begin{array}{l}\frac{1}{3}\frac{x^6}{L^6}-\frac{5}{3}\frac{x^3}{L^3}+\frac{4}{3}\frac{x}{L}\\-\frac{10}{\pi^2}\frac{E}{G}\frac{h^2}{L^2}\left(\frac{x^4}{L^4}-\frac{x}{L}\right)\end{array}\right] \tag{16}$$

$$\phi(x)=\frac{q_0L}{\beta EI}\left(\frac{1}{12}-\frac{1}{3}\frac{x^3}{L^3}+\frac{\cosh\lambda x}{\lambda L\sinh\lambda L}\right) \tag{17}$$

The axial displacement and stresses obtained based on above solutions are as follows

$$u=\frac{q_0h}{Eb}\left\{\begin{array}{l}-\frac{1}{10}\frac{z}{h}\frac{L^3}{h^3}\left[\begin{array}{l}2\frac{x^5}{L^5}-5\frac{x^2}{L^2}+\frac{4}{3}\\-\frac{10}{\pi^2}\frac{E}{G}\frac{h^2}{L^2}\left(4\frac{x^3}{L^3}-1\right)\end{array}\right]\\+\frac{48}{\pi^4}\sin\frac{\pi z}{h}\frac{E}{G}\frac{L}{h}\left(-3\frac{x^3}{L^3}+\frac{1}{12}\right)\end{array}\right\} \tag{18}$$

$$\sigma_x=\frac{q_0}{b}\left[\begin{array}{l}-\frac{1}{10}\frac{z}{h}\frac{L^2}{h^2}\left(\begin{array}{l}10\frac{x^4}{L^4}-10\frac{x}{L}\\-\frac{120}{\pi^2}\frac{E}{G}\frac{h^2}{L^2}\frac{x^2}{L^2}\end{array}\right)\\-\frac{48}{\pi^4}\sin\frac{\pi z}{h}\frac{E}{G}\frac{x^2}{L^2}\end{array}\right] \tag{19}$$

$$\tau_{zx}^{CR}=\frac{48}{\pi^3}\frac{q_0}{b}\frac{L}{h}\cos\frac{\pi z}{h}\left(\begin{array}{l}\frac{1}{3}\frac{x^3}{L^3}-\frac{1}{12}\\+\frac{\cosh\lambda x}{\lambda L\sinh\lambda L}\end{array}\right) \tag{20}$$

$$\tau_{zx}^{EE}=\frac{q_0L}{80bh}\left(4\frac{z^2}{h^2}-1\right)\left[\begin{array}{l}40\frac{x^3}{L^3}-10\\-\frac{240}{\pi^2}\frac{E}{G}\frac{h^2}{L^2}\frac{x}{L}\end{array}\right]-\frac{96}{\pi^5}\cos\frac{\pi z}{h}\frac{E}{G}\frac{q_0h}{bL}\frac{x}{L} \tag{21}$$

3.2 Simply supported beam subjected to parabolic load, $q(x)=q_0\left(1-\frac{x^2}{L^2}\right)$

The simply supported beam is having its origin at left support and is simply supported at *x* = 0 and *x* =*L*. The beam is subjected to parabolic load, on surface *z* = +*h*/2 acting in the downward *z* direction with maximum intensity of load q_0.

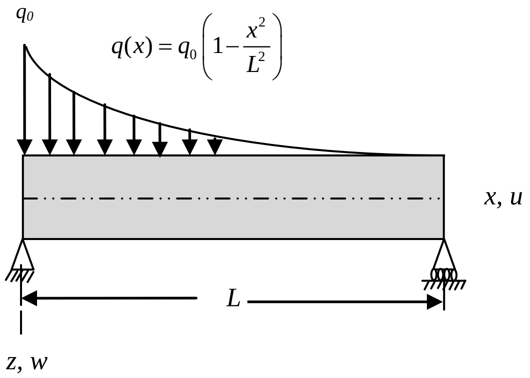

Fig. 3: Simply supported beam with parabolic load

General expressions obtained for $w(x)$ and $\phi(x)$ are as follows:

$$w(x)=\frac{q_0L^4}{120EI}\left[\begin{array}{l}5\frac{x^4}{L^4}-\frac{1}{3}\frac{x^6}{L^6}-\frac{25}{3}\frac{x^3}{L^3}+\frac{11}{3}\frac{x}{L}\\+\frac{120}{\pi^2}\frac{E}{G}\frac{h^2}{L^2}\left(\frac{1}{12}\frac{x^4}{L^4}-\frac{1}{12}\frac{x^2}{L^2}\right)\\+\frac{11520}{\pi^6}\frac{E}{G}\frac{h^2}{L^2}\left(\frac{1}{2}\frac{x}{L}-\frac{1}{2}\frac{x^2}{L^2}\right)\end{array}\right] \tag{22}$$

$$\phi(x)=\frac{q_0L}{\beta EI}\left(\begin{array}{l}\frac{5}{12}-\frac{x}{L}+\frac{1}{3}\frac{x^3}{L^3}\\+\frac{\sinh\lambda x-\cosh\lambda x}{\lambda L}\end{array}\right) \tag{23}$$

The axial displacement and stresses obtained based on above solutions are as follows

$$u=\frac{q_0h}{Eb}\left[\begin{array}{l}-\frac{1}{10}\frac{z}{h}\frac{L^3}{h^3}\left(\begin{array}{l}20\frac{x^3}{L^3}-\frac{1}{2}\frac{x^5}{L^5}-25\frac{x^2}{L^2}+\frac{11}{3}\\+\frac{120}{\pi^2}\frac{E}{G}\frac{h^2}{L^2}\left(\frac{1}{3}\frac{x^3}{L^3}-\frac{1}{12}\right)\\+\frac{11520}{\pi^6}\frac{E}{G}\frac{h^2}{L^2}\left(\frac{1}{2}-\frac{x}{L}\right)\end{array}\right)\\+\frac{48}{\pi^4}\sin\frac{\pi z}{h}\frac{E}{G}\frac{L}{h}\left(\begin{array}{l}\frac{5}{12}-\frac{x}{L}+\frac{1}{3}\frac{x^3}{L^3}\\+\frac{\sinh\lambda x-\cosh\lambda x}{\lambda L}\end{array}\right)\end{array}\right] \tag{24}$$

$$\sigma_x=\frac{q_0}{b}\left[\begin{array}{l}-\frac{1}{10}\frac{z}{h}\frac{L^2}{h^2}\left(\begin{array}{l}60\frac{x^2}{L^2}-\frac{5}{2}\frac{x^4}{L^4}-50\frac{x}{L}\\+\frac{120}{\pi^2}\frac{E}{G}\frac{h^2}{L^2}\frac{x^2}{L^2}\\-\frac{11520}{\pi^6}\frac{E}{G}\frac{h^2}{L^2}\end{array}\right)\\+\frac{48}{\pi^4}\sin\frac{\pi z}{h}\frac{E}{G}\left(\begin{array}{l}\frac{x^2}{L^2}-1\\+\cosh\lambda x-\sinh\lambda x\end{array}\right)\end{array}\right] \tag{25}$$

$$\tau_{zx}^{CR}=\frac{48}{\pi^3}\frac{q_0}{b}\frac{L}{h}\cos\frac{\pi z}{h}\left(\begin{array}{l}\frac{5}{12}+\frac{1}{3}\frac{x^3}{L^3}-\frac{x}{L}\\+\frac{\sinh\lambda x-\cosh\lambda x}{\lambda L}\end{array}\right) \tag{26}$$

$$\begin{array}{l}\tau_{zx}^{EE}=\frac{q_0L}{80\,bh}\left(4\frac{z^2}{h^2}-1\right)\left[\begin{array}{l}120\frac{x}{L}-10\frac{x^3}{L^3}-50\\+\frac{240}{\pi^2}\frac{E}{G}\frac{h^2}{L^2}\frac{x}{L}\end{array}\right]\\ \quad+\frac{48}{\pi^5}\cos\frac{\pi z}{h}\frac{E}{G}\frac{q_0h}{bL}\\ \quad\left(2\frac{x}{L}+\lambda L(\sinh\lambda x-\cosh\lambda x)\right)\end{array} \tag{27}$$

4. NUMERICAL RESULTS

In this paper, the results for inplane displacement, transverse displacement, inplane and transverse stresses are presented in the following non dimensional form for the purpose of presenting the results in this work.

For beams subjected to parabolic load, *q(x)*

$$\bar{u}=\frac{Ebu}{q_0h},\quad \bar{w}=\frac{10Ebh^3w}{q_0L^4},$$

$$\bar{\sigma}_x=\frac{b\sigma_x}{q_0},\quad \bar{\tau}_{zx}=\frac{b\tau_{zx}}{q_0}$$

Table 1: Non-Dimensional Axial Displacement ($\bar{u}$) at (x = 0.75L, z = h/2), Transverse Deflection ($\bar{w}$) at (x = 0.75L, z =0.0), Axial Stress ($\bar{\sigma}_x$) at (x = 0.75L, z = h/2) Maximum Transverse Shear Stresses $\bar{\tau}_{zx}^{CR}$ and $\bar{\tau}_{zx}^{EE}$ (x = 0, z = 0.0) of the Simply Supported Beam Subjected to Parabolic Load for Aspect Ratio 4 (Example 1)

Source	Model	$\bar{u}$	$\bar{w}$	$\bar{\sigma}_x$	$\bar{\tau}_{zx}^{CR}$	$\bar{\tau}_{zx}^{EE}$
Present	TSDT	-3.2832	0.4276	-3.6371	-0.5150	0.5000
Ghugal and Sharma	HPSDT	-3.2767	0.4272	-3.6211	-0.4984	0.5000
Krishna Murty	HSDT	-3.2784	0.4275	-3.6254	-0.5000	0.5000
Timoshenko	FSDT	-3.2146	0.5294	-3.4688	-0.3663	0.5000
Bernoulli-Euler	ETB	-3.2146	0.3562	-3.4688	—	0.5000

Table 2: Non-Dimensional Axial Displacement ($\bar{u}$) at (x = 0.75L, z = h/2), Transverse Deflection ($\bar{w}$) at (x = 0.75L, z =0.0), Axial Stress ($\bar{\sigma}_x$) at (x = 0.75L, z = h/2) Maximum Transverse Shear Stresses $\bar{\tau}_{zx}^{CR}$ and $\bar{\tau}_{zx}^{EE}$ (x = 0, z = 0.0) of the Simply Supported Beam Subjected to Parabolic Load for Aspect Ratio 10 (Example 1)

Source	Model	$\bar{u}$	$\bar{w}$	$\bar{\sigma}_x$	$\bar{\tau}_{zx}^{CR}$	$\bar{\tau}_{zx}^{EE}$
Present	TSDT	-50.3994	0.3676	-21.8481	-1.2901	1.2500
Ghugal and Sharma	HPSDT	-50.3831	0.3676	-21.8320	-1.2461	1.2500
Krishna Murty	HSDT	-50.3875	0.3676	-21.8364	-1.2500	1.2500
Timoshenko	FSDT	-50.2278	0.3893	-21.6796	-0.5723	1.2500
Bernoulli-Euler	ETB	-50.2278	0.3562	-21.6796	—	1.2500

Table 3: Non-Dimensional Axial Displacement ($\bar{u}$) at (x = 0.25L, z = h/2), Transverse Deflection ($\bar{w}$) at (x = 0.25L, z =0.0), Axial Stress ($\bar{\sigma}_x$) at (x = 0.25L, z = h/2) Maximum Transverse Shear Stresses $\bar{\tau}_{zx}^{CR}$ and $\bar{\tau}_{zx}^{EE}$ (x = 0, z = 0.0) of the Simply Supported Beam Subjected to Parabolic Load for Aspect Ratio 4 (Example 2)

Source	Model	$\bar{u}$	$\bar{w}$	$\bar{\sigma}_x$	$\bar{\tau}_{zx}^{CR}$	$\bar{\tau}_{zx}^{EE}$
Present	TSDT	7.9147	0.9479	-7.2656	-2.4845	-4.1066
Ghugal and Sharma	HPSDT	7.9055	0.9484	-7.2493	-2.4238	-6.3828
Krishna Murty	HSDT	7.9047	0.9483	-7.2504	-2.4167	-4.8125
Timoshenko	FSDT	7.7317	0.9487	-7.0078	-2.3462	-2.5000
Bernoulli-Euler	ETB	7.7317	0.8059	-7.0078	—	-2.5000

Table 4: Non-Dimensional Axial Displacement ($\bar{u}$) at (x = 0.25L, z = h/2), Transverse Deflection ($\bar{w}$) at (x = 0.25L, z =0.0), Axial Stress ($\bar{\sigma}_x$) at (x = 0.25L, z = h/2) Maximum Transverse Shear Stresses $\bar{\tau}_{zx}^{CR}$ and $\bar{\tau}_{zx}^{EE}$ (x = 0, z = 0.0) of the Simply Supported Beam Subjected to Parabolic Load for Aspect Ratio 10 (Example 2)

Source	Model	$\bar{u}$	$\bar{w}$	$\bar{\sigma}_x$	$\bar{\tau}_{zx}^{CR}$	$\bar{\tau}_{zx}^{EE}$
Present	TSDT	121.2663	0.8286	-44.0566	-6.3547	-0.3566
Ghugal and Sharma	HPSDT	121.2432	0.8287	-44.0403	-6.1621	-2.6328
Krishna Murty	HSDT	121.2413	0.8287	-44.0414	-6.1667	-1.0625
Timoshenko	FSDT	120.8089	0.8287	-43.7988	-1.4663	-6.2500
Bernoulli-Euler	ETB	120.8089	0.8059	-43.7988	—	-6.2500

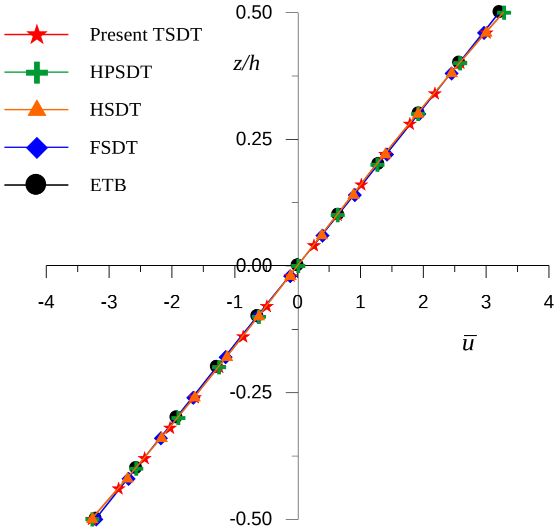

Fig. 4: Variation of axial displacement ($\bar{u}$) through the thickness of beam at (x = 0.75L, z) for aspect ratio 4. (Example 1)

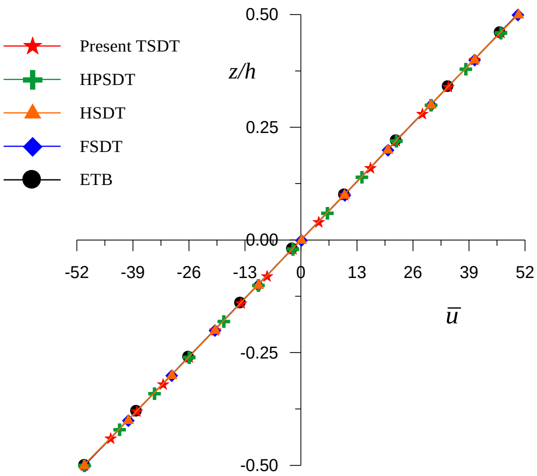

Fig. 5: Variation of axial displacement ($\bar{u}$) through the thickness beam at (x = 0.75L, z = 0) for aspect ratio 10. (Example 1)

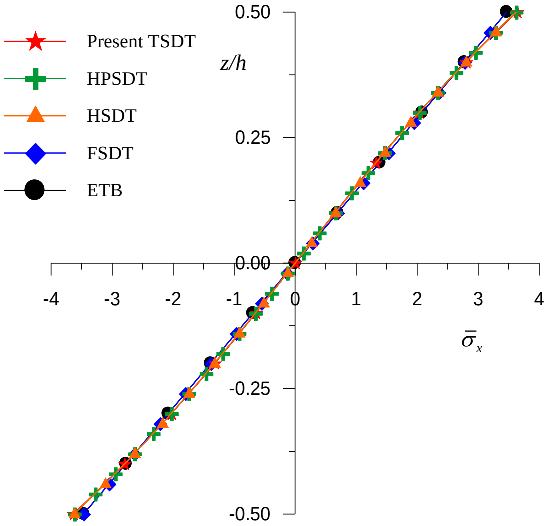

Fig. 6: Variation of axial stress ($\bar{\sigma}_x$) through the thickness beam at (x = 0.75L, z) for aspect ratio 4. (Example 1)

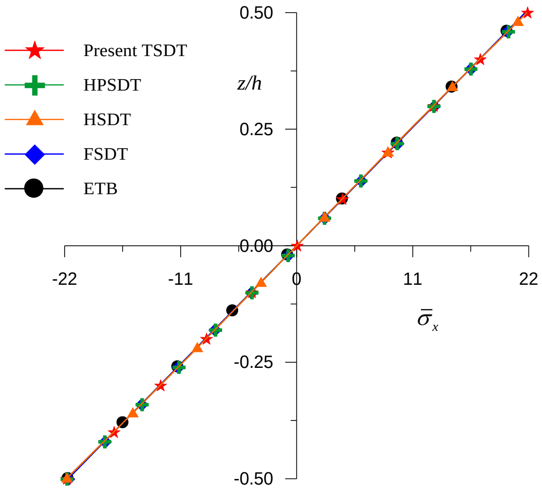

Fig. 7: Variation of axial stress ($\bar{\sigma}_x$) through the thickness of beam at (x = 0.75L, z) for aspect ratio 10. (Example 1)

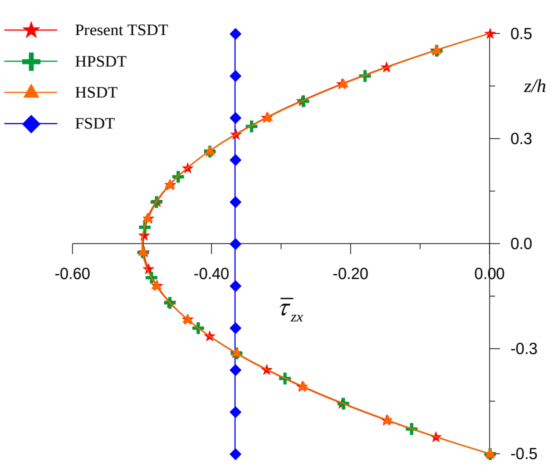

Fig. 8: Variation of transverse shear stress ($\bar{\tau}_{zx}$) through the thickness of beam at (*x* = 0, *z*) obtain using constitutive relation for aspect ratio 4. (Example 1)

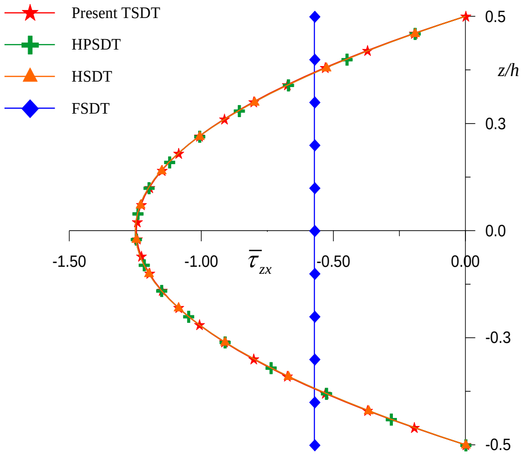

Fig. 9: Variation of transverse shear stress ($\bar{\tau}_{zx}$) through the thickness of beam at (*x* = 0, *z*) obtain using constitutive relation for aspect ratio 4. (Example 1)

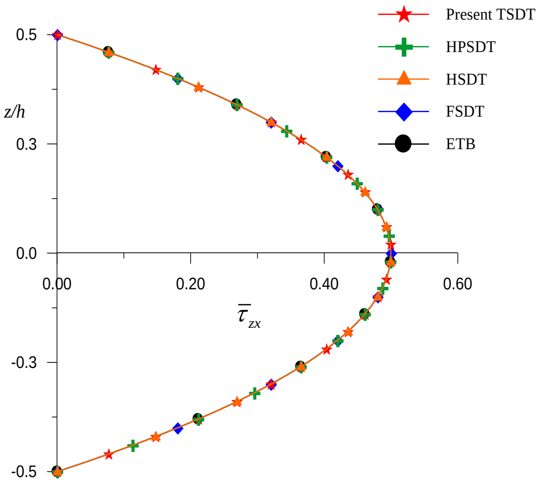

Fig. 10: Variation of transverse shear stress ($\bar{\tau}_{zx}$) through the thickness of beam at (*x* = 0, *z*) obtain using equilibrium equation for aspect ratio 4. (Example 1)

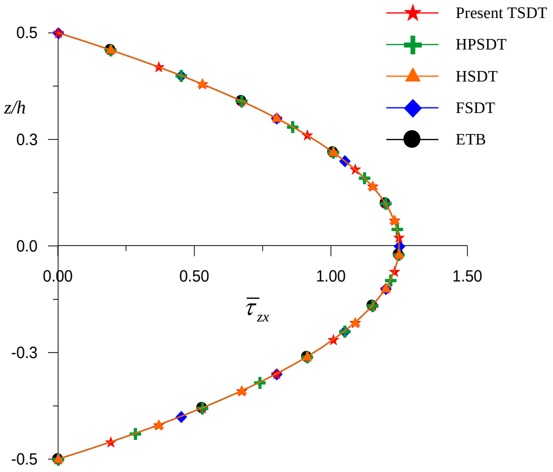

Fig. 11: Variation of transverse shear stress ($\bar{\tau}_{zx}$) through the thickness of beam at (*x* = 0, *z*) obtain using equilibrium equation for aspect ratio 10. (Example 1)

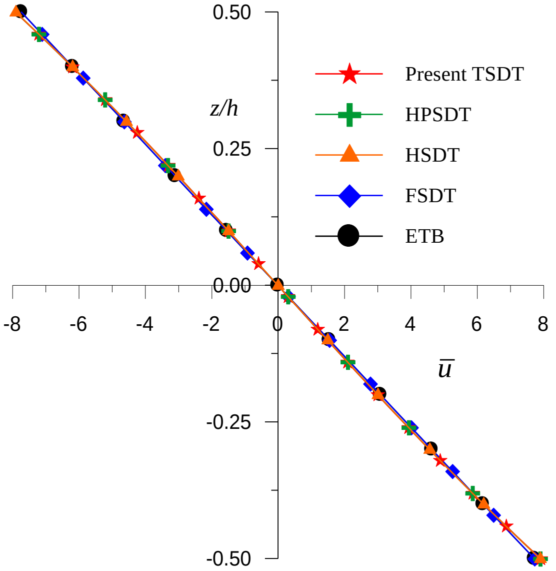

Fig. 12: Variation of axial displacement ($\bar{u}$) through the thickness of beam at (x = 0.25L, z) for aspect ratio 4. (Example 2)

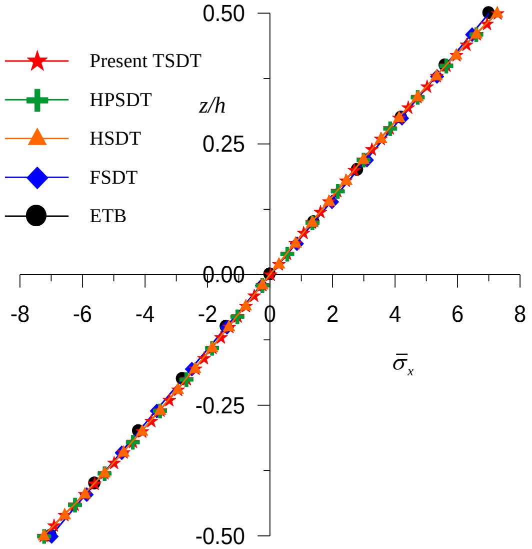

Fig. 14: Variation of axial stress ($\bar{\sigma}_x$) through the thickness of beam at (x = 0.25L, z) for aspect ratio 4. (Example 2)

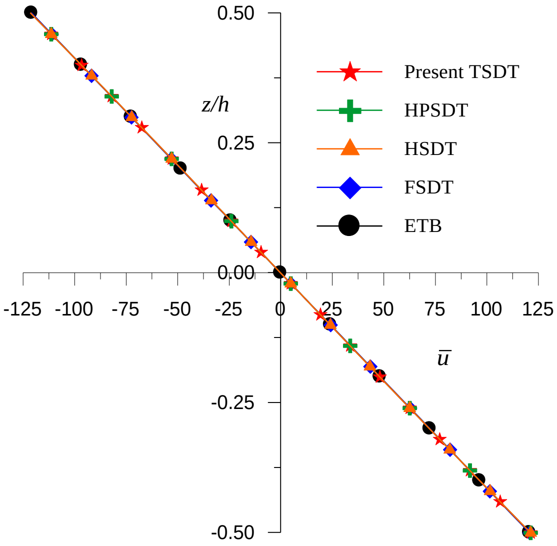

Fig. 13: Variation of axial displacement ($\bar{u}$) through the thickness of beam at (x = 0.25L, z) for aspect ratio 10. (Example 2)

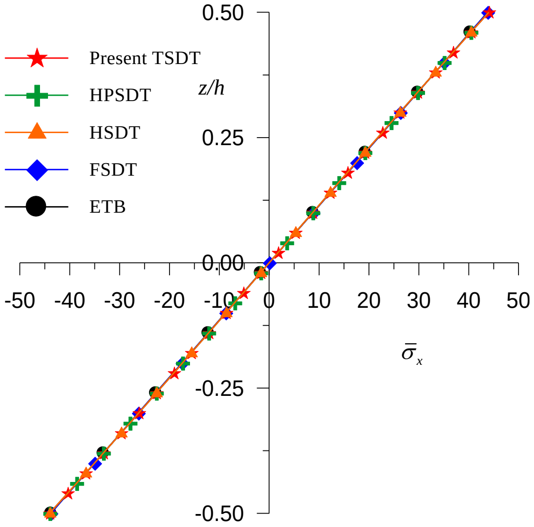

Fig. 15: Variation of axial stress ($\bar{\sigma}_x$) through the thickness of beam at (x = 0.25L, z) aspect ratio 10. (Example 2)

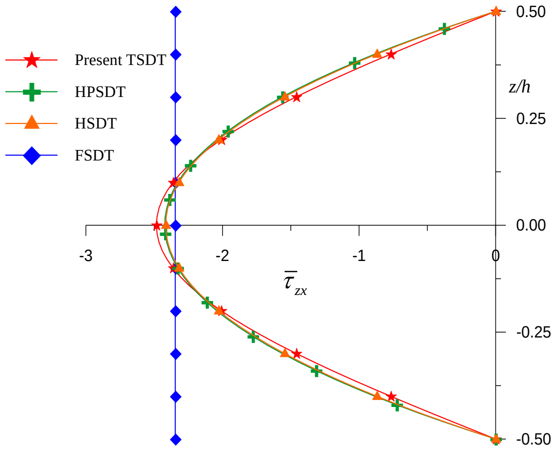

Fig. 16: Variation of transverse shear stress ($\bar{\tau}_{zx}$) through the thickness of beam at (x = 0.01L, z) obtain using constitutive relation for aspect ratio 4. (Example 2)

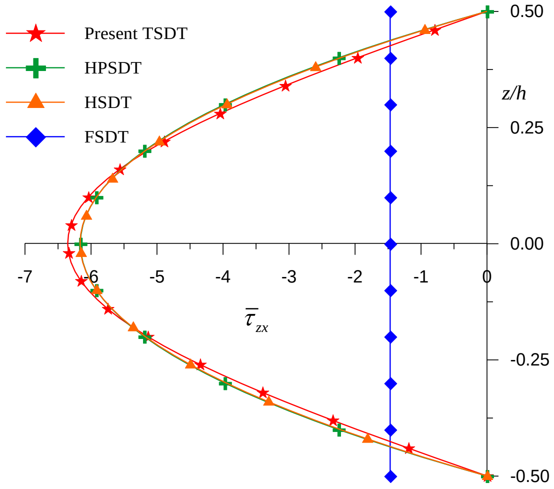

Fig. 17: Variation of transverse shear stress ($\bar{\tau}_{zx}$) through the thickness of beam at (x = 0.01L, z) obtain using constitutive relation for aspect ratio 4. (Example 2)

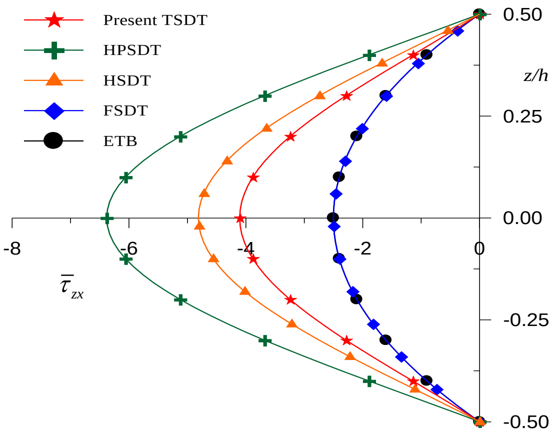

Fig. 18: Variation of transverse shear stress ($\bar{\tau}_{zx}$) through the thickness of beam at (x = 0, z) obtain using equilibrium equation for aspect ratio 4. (Example 2)

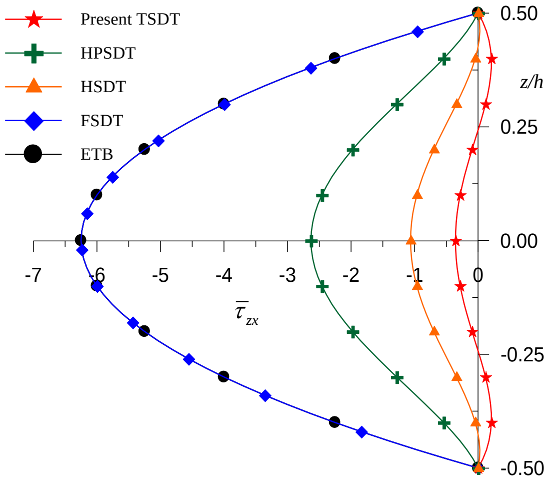

Fig. 19: Variation of transverse shear stress ($\bar{\tau}_{zx}$) through the thickness of beam at (x = 0, z) obtain using equilibrium equation for aspect ratio 10. (Example 2)

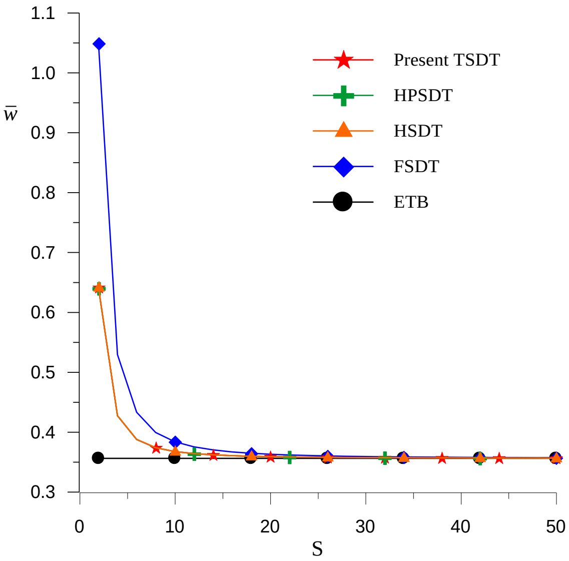

Fig. 20: Variation of maximum transverse displacement ($\bar{w}$) of beam at (x = 0.75L, z = 0) with aspect ratio S. (Example 1)

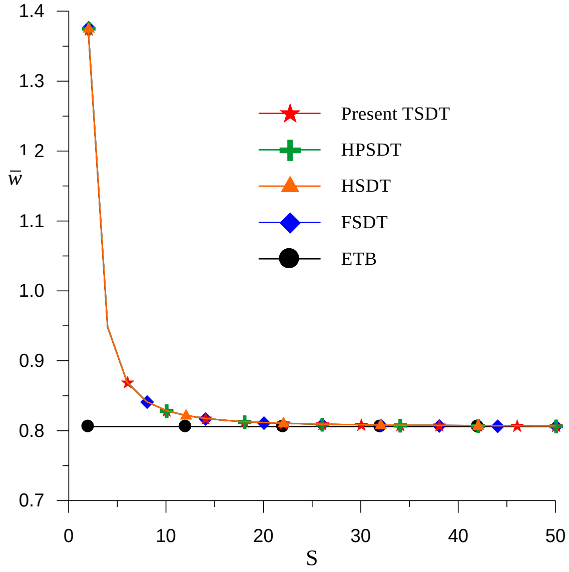

Fig. 21: Variation of maximum transverse displacement ($\bar{w}$) of beam at (x = 0.25L, z = 0) with aspect ratio S. (Example 2)

5. DISCUSSION OF RESULTS

The comparison of results of maximum non-dimensional axial displacement ($\bar{u}$) for the aspect ratios of 4 and 10 is presented in Tables 1 through 4 for simply supported beams subjected to parabolic loads (see Figs. 3 and 4). The values of axial displacement given by present theory are in close agreement with the values of other refined theories for aspect ratio 4 and 10. The through thickness distribution of this displacement obtained by present theory is in close agreement with other refined theories as shown in Figs. 4,5, 12 and 13 for aspect ratio 4 and 10.

The results of axial stress ($\bar{\sigma}_x$) are shown in Tables 1 through 4 for aspect ratios 4 and 10. The axial stresses given by present theory are compared with other higher order shear deformation theories. It is observed that the results by present theory are in excellent agreement with other refined theories as well as ETB and FSDT. The through the thickness variation of this stress given by all the theories is linear at x = 0.75L and x = 0.25L . The variations of this stress are shown in Figs. 6, 7, 14 and 15.

The comparison of maximum non-dimensional transverse shear stress for simple beams with varying and parabolic loads obtained by the present theory and other refined theories is presented in Tables 1 through 4 for aspect ratio of 4 and 10 respectively. The maximum transverse shear stress obtained by present theory using constitutive relation is in good agreement with that of higher order theories for aspect ratio 4 and for aspect ratio 10. The through thickness variation of this stress obtained via constitutive relation are presented graphically in Figs. 8, 9, 16 and 17 and those obtained via equilibrium equation are presented in Figs. 10, 11, 18 and 19. The through thickness variation of this stress when obtained by various theories via equilibrium equation shows the excellent agreement with each other. The maximum value of this stress occurs at the neutral axis.

The comparison of results of maximum non-dimensional transverse displacement ($\bar{w}$) for the aspect ratios of 4 and 10 is presented in Tables 1 through 4 for simply supported beams subjected to parabolic load. The values of present theory are in excellent agreement with the values of other refined theories for aspect ratio 4 and 10 except those of classical beam theory (ETB) and FSDT of Timoshenko. The variation of $\bar{w}$ with aspect ratio (S) is shown in Figs. 20 and 21. The refined theories converge to the values of classical beam theory for the higher aspect ratios.

6. CONCLUSION

The variationally consistent theoretical formulation of the theory with general solution technique of governing differential equations is presented. The general solutions for beams with parabolic loads are obtained in case of thick simply supported beams. The displacements and stresses obtained by present theory are in excellent agreement with those of other equivalent refined and higher order theories.

The present theory yields the realistic variation of axial displacement and stresses through the thickness of beam. Thus the validity of the present theory is established.

7. REFERENCES:

[1] J.A.C. Bresse, “Cours de Mechanique Applique”, Mallet-Bachelier, Paris, 1859.

[2] J.W.S. Lord Rayleigh, “The Theory of Sound”, Macmillan Publishers, London, 1877.

[3] S.P. Timoshenko, J. N. Goodier, “Theory of Elasticity”, Third International Edition, McGraw-Hill, Singapore. 1970.

[4] G.R. Cowper, “The shear coefficients in Timoshenko beam theory”, *ASME Journal of Applied Mechanic*, Vol. 33, No. 2, 1966, pp. 335-340.

[5] G.R. Cowper, “On the accuracy of Timoshenko beam theory”, *ASCE J. of Engineering Mechanics Division*. Vol. 94, No. EM6, pp. 1447-1453, 1968.

[6] M. Levinson, “A new rectangular beam theory”, *Journal of Sound and Vibration*, Vol. 74, No.1, 1981, pp. 81-87.

[7] W.B. Bickford, “A consistent higher order beam theory”, *International Proceeding of Development in Theoretical and Applied Mechanics* (SECTAM), Vol. 11, 1982, pp. 137-150,

[8] L.W. Rehfield, P.L.N. Murthy, “Toward a new engineering theory of bending: fundamentals”, *AIAA Journal*, Vol. 20, No. 5, 1982, pp. 693-699.

[9] A.V. Krishna Murty, “Towards a consistent beam theory”, *AIAA Journal*, Vol. 22, No. 6, 1984, pp. 811-816.

[10] M.H. Baluch, A.K. Azad, and M.A. Khidir, “Technical theory of beams with normal strain”, *ASCE Journal of Engineering Mechanics*, Vol. 110, No. 8, 1984, pp. 1233-1237.

[11] A. Bhimaraddi, K. Chandrashekhara, “Observations on higher order beam Theory”, *ASCE Journal of Aerospace Engineering*, Vol. 6, No. 4, 1993, pp. 408-413,

[12] H. Irretier, “Refined effects in beam theories and their influence on natural frequencies of beam”, *International Proceeding of Euromech Colloquium*, 219, on Refined Dynamical Theories of Beam, Plates and Shells and Their Applications, Edited by I. Elishak off and H. Irretier, Springer-Verlag, Berlin, 1986, pp. 163-179.

[13] T. Kant, A. Gupta, “A finite element model for higher order shears deformable beam theory*”, Journal of Sound and Vibration*, Vol. 125, No. 2, , 1988, pp. 193-202.

[14] P.R. Heyliger, J.N. Reddy, “A higher order beam finite element for bending and vibration problems”, *Journal of Sound and Vibration*, Vol. 126, No. 2, 1988. pp. 309-326.

[15] R.C. Averill, J.N. Reddy, “An assessment of four-noded plate finite elements based on a generalized third order theory”, *International Journal of Numerical Methods in Engineering*, Vol. 33, 1992, pp. 1553-1572.

[16] J.N. Reddy, “An Introduction to Finite Element Method”. 2nd Ed., McGraw-Hill, Inc., New York, 1993.

[17] V.Z. Vlasov, U.N. Leont’ev, “Beams, Plates and Shells on Elastic Foundations” Moskva, Chapter 1, 1-8. Translated from the Russian by A. Barouch and T. Plez *Israel Program for Scientific Translation Ltd., Jerusalem*, 1966.

[18] M. Stein, “Vibration of beams and plate strips with three dimensional flexibility”, *ASME J. of Applied Mechanics*, Vol. 56, No. 1, 1989, pp. 228-231.

[19] Y.M. Ghugal, R.P. Shmipi, “A review of refined shear deformation theories for isotropic and anisotropic laminated beams”, *Journal of Reinforced Plastics and Composites*, Vol. 20, No. 3, , 2001, pp. 255-272.

[20] Y.M. Ghugal, R. Sharma, “A hyperbolic shear deformation theory for flexure and vibration of thick isotropic beams”, *International Journal of Computational Methods*, Vol. 6, No. 4, 2009, pp. 585-604.

[21] F.B. Hildebrand, E.C. Reissner, “Distribution of Stress in Built-In Beam of Narrow Rectangular Cross Section”, *Journal of Applied Mechanics*, Vol. 64, 1942, pp. 109-116.

[22] S.P. Timoshenko, “On the correction for shear of the differential equation for transverse vibrations of prismatic bars”, *Philosophical Magazine*, Vol. 41, No. 6, 1921, pp. 742-746.

View publication stats

Applied and Computational Mechanics 6 (2012) 163–172

Flexural analysis of deep beam subjected to parabolic load using refined shear deformation theory

Y. M. Ghugal[a,*], A. G. Dahake[b]

[a]Applied Mechanics Department, Govt. College of Engineering, Karad – 415 124, MS, India
[b]Applied Mechanics Department, Govt. College of Engineering, Aurangabad – 431 005, MS, India

Received 30 July 2012; received in revised form 21 December 2012

Abstract

A trigonometric shear deformation theory for flexure of thick or deep beams, taking into account transverse shear deformation effects, is developed. The number of variables in the present theory is same as that in the first order shear deformation theory. The sinusoidal function is used in displacement field in terms of thickness coordinate to represent the shear deformation effects. The noteworthy feature of this theory is that the transverse shear stresses can be obtained directly from the use of constitutive relations with excellent accuracy, satisfying the shear stress free conditions on the top and bottom surfaces of the beam. Hence, the theory obviates the need of shear correction factor. Governing differential equations and boundary conditions are obtained by using the principle of virtual work. The thick isotropic beams are considered for the numerical studies to demonstrate the efficiency of the theory. It has been shown that the theory is capable of predicting the local effect of stress concentration due to fixity of support. The fixed isotropic beams subjected to parabolic loads are examined using the present theory. Results obtained are discussed critically with those of other theories.

© 2012 University of West Bohemia. All rights reserved.

Keywords: thick beam, trigonometric shear deformation, principle of virtual work, equilibrium equations, displacement, stress

---

1. Introduction

It is well-known that elementary theory of bending of beam based on Euler-Bernoulli hypothesis disregards the effects of the shear deformation and stress concentration. The theory is suitable for slender beams and is not suitable for thick or deep beams since it is based on the assumption that the sections normal to neutral axis before bending remain so during bending and after bending, implying that the transverse shear strain is zero. Since theory neglects the transverse shear deformation, it underestimates deflections in case of thick beams where shear deformation effects are significant.

Bresse [5], Rayleigh [16] and Timoshenko [20] were the pioneer investigators to include refined effects such as rotatory inertia and shear deformation in the beam theory. Timoshenko showed that the effect of transverse shear is much greater than that of rotatory inertia on the response of transverse vibration of prismatic bars. This theory is now widely referred to as Timoshenko beam theory or first order shear deformation theory (FSDT) in the literature. In this theory transverse shear strain distribution is assumed to be constant through the beam thickness and thus requires shear correction factor to appropriately represent the strain energy of deformation. Cowper [6] has given refined expression for the shear correction factor for different

---

[*] Corresponding author. Tel.: +91 93 70 353 722, e-mail: ghugal@rediffmail.com.

cross-sections of beam. The accuracy of Timoshenko beam theory for transverse vibrations of simply supported beam in respect of the fundamental frequency is verified by Cowper [7] with a plane stress exact elasticity solution. To remove the discrepancies in classical and first order shear deformation theories, higher order or refined shear deformation theories were developed and are available in the open literature for static and vibration analysis of beam.

Levinson [15], Bickford [4], Rehfield and Murty [18], Krishna Murty [14], Baluch et al. [2], Bhimaraddi and Chandrashekhara [3] presented parabolic shear deformation theories assuming a higher variation of axial displacement in terms of thickness coordinate. These theories satisfy shear stress free boundary conditions on top and bottom surfaces of beam and thus obviate the need of shear correction factor. Irretier [12] studied the refined dynamical effects in linear, homogenous beam according to theories, which exceed the limits of the Euler-Bernoulli beam theory. These effects are rotary inertia, shear deformation, axial pre-stress, twist and coupling between bending and torsion.

Hilderbrand and Reissner [11] have given the distribution of stress in built-in beam of narrow rectangular cross section using Airy's stress function and the principle of least work. Timoshenko and Goodier [21] presented the elasticity solutions for simply supported and cantilever beams using Airy's stress polynomial functions and using stress functions in the form of a Fourier series.

Kant and Gupta [13], Heyliger and Reddy [10] presented finite element models based on higher order shear deformation uniform rectangular beams. However, these displacement based finite element models are not free from phenomenon of shear locking (Averill and Reddy [1]; Reddy [17]).

There is another class of refined theories, which includes trigonometric functions to represent the shear deformation effects through the thickness. Vlasov and Leont'ev [22], Stein [19] developed refined shear deformation theories for thick beams including sinusoidal function in terms of thickness coordinate in displacement field. However, with these theories shear stress free boundary conditions are not satisfied at top and bottom surfaces of the beam. A study of literature by Ghugal and Shimpi [8] indicates that the research work dealing with flexural analysis of thick beams using refined trigonometric and hyperbolic shear deformation theories is very scarce and is still in infancy.

In this paper development of theory and its application to thick fixed beams is presented.

2. Development of theory

The beam under consideration as shown in Fig. 1 occupies in $0-x-y-z$ Cartesian coordinate system the region:

$$0 \le x \le L, \qquad 0 \le y \le b, \qquad -\frac{h}{2} \le z \le \frac{h}{2},$$

where x, y, z are Cartesian coordinates, L and b are the length and width of beam in the x and y directions respectively, and h is the thickness of the beam in the z-direction. The beam is made up of homogeneous, linearly elastic isotropic material.

2.1. The displacement field

The displacement field of the present beam theory is of the form:

$$\begin{aligned} u(x,z) &= -z\frac{\mathrm{d}w}{\mathrm{d}x} + \frac{h}{\pi}\sin\frac{\pi z}{h}\phi(x), \\ w(x,z) &= w(x), \end{aligned} \tag{1}$$

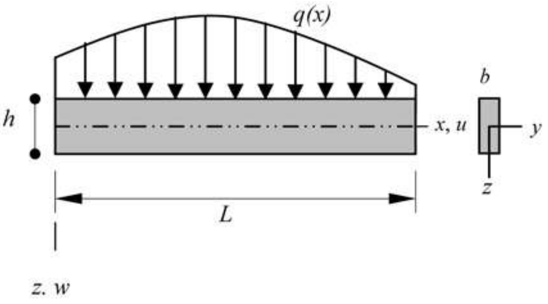

Fig. 1. Beam under bending in x–z plane

where u is the axial displacement in x direction and w is the transverse displacement in z direction of the beam. The sinusoidal function is assigned according to the shear stress distribution through the thickness of the beam. The function ϕ represents rotation of the beam at neutral axis, which is an unknown function to be determined. The normal and shear strains obtained within the framework of linear theory of elasticity using displacement field given by Eq. (1) are as follows:

$$\text{Normal strain: } \varepsilon_x = \frac{\partial u}{\partial x} = -z\frac{\mathrm{d}^2 w}{\mathrm{d}x^2} + \frac{h}{\pi}\sin\frac{\pi z}{h}\frac{\mathrm{d}\phi}{\mathrm{d}x}, \tag{2}$$

$$\text{Shear strain: } \gamma_{zx} = \frac{\partial u}{\partial z} + \frac{\mathrm{d}w}{\mathrm{d}x} = \cos\frac{\pi z}{h}\phi. \tag{3}$$

The stress-strain relationships used are as follows:

$$\sigma_x = E\varepsilon_x, \qquad \tau_{zx} = G\gamma_{zx}. \tag{4}$$

2.2. Governing equations and boundary conditions

Using the expressions for strains and stresses (2) through (4) and using the principle of virtual work, variationally consistent governing differential equations and boundary conditions for the beam under consideration can be obtained. The principle of virtual work when applied to the beam leads to:

$$b\int_{x=0}^{x=L}\int_{z=-h/2}^{z=+h/2}(\sigma_x\delta\varepsilon_x + \tau_{zx}\delta\gamma_{zx})\mathrm{d}x\,\mathrm{d}z - \int_{x=0}^{x=L} q(x)\delta w\,\mathrm{d}x = 0, \tag{5}$$

where the symbol δ denotes the variational operator. Employing Green's theorem in Eq. (4) successively, we obtain the coupled Euler-Lagrange equations which are the governing differential equations and associated boundary conditions of the beam. The governing differential equations obtained are as follows:

$$EI\frac{\mathrm{d}^4 w}{\mathrm{d}x^4} - \frac{24}{\pi^3}EI\frac{\mathrm{d}^3\phi}{\mathrm{d}x^3} = q(x), \tag{6}$$

$$\frac{24}{\pi^3}EI\frac{\mathrm{d}^3 w}{\mathrm{d}x^3} - \frac{6}{\pi^2}EI\frac{\mathrm{d}^2\phi}{\mathrm{d}x^2} + \frac{GA}{2}\phi = 0. \tag{7}$$

The associated consistent natural boundary conditions obtained are of following form:

At the ends $x = 0$ and $x = L$

$$V_x = EI\frac{\mathrm{d}^3 w}{\mathrm{d}x^3} - \frac{24}{\pi^3}EI\frac{\mathrm{d}^2\phi}{\mathrm{d}x^2} = 0 \quad \text{or } w \text{ is prescribed,} \tag{8}$$

$$M_x = EI\frac{\mathrm{d}^2 w}{\mathrm{d}x^2} - \frac{24}{\pi^3}EI\frac{\mathrm{d}\phi}{\mathrm{d}x} = 0 \quad \text{or } \frac{\mathrm{d}w}{\mathrm{d}x} \text{ is prescribed,} \tag{9}$$

$$M_a = EI\frac{24}{\pi^3}\frac{\mathrm{d}^2 w}{\mathrm{d}x^2} - \frac{6}{\pi^2}EI\frac{\mathrm{d}\phi}{\mathrm{d}x} = 0 \quad \text{or } \phi \text{ is prescribed.} \tag{10}$$

Thus the boundary value problem of the beam bending is given by the above variationally consistent governing differential equations and boundary conditions.

2.3. The general solution of governing equilibrium equations of the beam

The general solution for transverse displacement $w(x)$ and warping function $\phi(x)$ is obtained using Eqs. (6) and (7) using method of solution of linear differential equations with constant coefficients. Integrating and rearranging the first governing Eq. (6), we obtain the following equation

$$\frac{\mathrm{d}^3 w}{\mathrm{d}x^3} = \frac{24}{\pi^3}\frac{\mathrm{d}^2\phi}{\mathrm{d}x^2} + \frac{Q(x)}{EI}, \tag{11}$$

where $Q(x)$ is the generalized shear force for beam and it is given by $Q(x) = \int_0^x q\,\mathrm{d}x + C_1$.

Now the second governing Eq. (7) is rearranged in the following form:

$$\frac{\mathrm{d}^3 w}{\mathrm{d}x^3} = \frac{\pi}{4}\frac{\mathrm{d}^2\phi}{\mathrm{d}x^2} - \beta\phi. \tag{12}$$

A single equation in terms of ϕ is now obtained using Eqs. (11) and (12) as

$$\frac{\mathrm{d}^2\phi}{\mathrm{d}x^2} - \lambda^2\phi = \frac{Q(x)}{\alpha EI}, \tag{13}$$

where constants α, β and λ in Eqs. (12) and (13) are as follows

$$\alpha = \left(\frac{\pi}{4} - \frac{24}{\pi^3}\right), \qquad \beta = \left(\frac{\pi^3}{48}\frac{GA}{EI}\right) \quad \text{and} \quad \lambda^2 = \frac{\beta}{\alpha}.$$

The general solution of Eq. (13) is as follows:

$$\phi(x) = C_2\cosh\lambda x + C_3\sinh\lambda x - \frac{Q(x)}{\beta EI}. \tag{14}$$

The equation of transverse displacement $w(x)$ is obtained by substituting the expression of $\phi(x)$ in Eq. (12) and then integrating it thrice with respect to x. The general solution for $w(x)$ is obtained as follows:

$$\begin{aligned} EIw(x) = {} & \iiiint q\,\mathrm{d}x\,\mathrm{d}x\,\mathrm{d}x\,\mathrm{d}x + \frac{C_1 x^3}{6} + \\ & \left(\frac{\pi}{4}\lambda^2 - \beta\right)\frac{EI}{\lambda^3}(C_2\sinh\lambda x + C_3\cosh\lambda x) + C_4\frac{x^2}{2} + C_5 x + C_6, \end{aligned} \tag{15}$$

where C_1, C_2, C_3, C_4, C_5 and C_6 are arbitrary constants and can be obtained by imposing boundary conditions of beam.

3. Illustrative example

In order to prove the efficacy of the present theory, the following numerical example is considered. The material properties for beam used are: $E = 210$ GPa, $\mu = 0.3$ and $\rho = 7\,800$ kg/m^3, where E is the Young's modulus, ρ is the density, and μ is the Poisson's ratio of beam material.

A fixed-fixed beam has its origin at left hand side support and is fixed at $x = 0$ and L. The beam is subjected to parabolic load $q(x) = q_0\left(\frac{x}{L}\right)^2$ on surface $z = -h/2$ acting in the downward z direction with maximum intensity of load q_0 as shown in Fig. 2. The boundary conditions associated with this beam at fixed ends are: $\frac{\mathrm{d}w}{\mathrm{d}x} = \phi = w = 0$ at $x = 0$ and L.

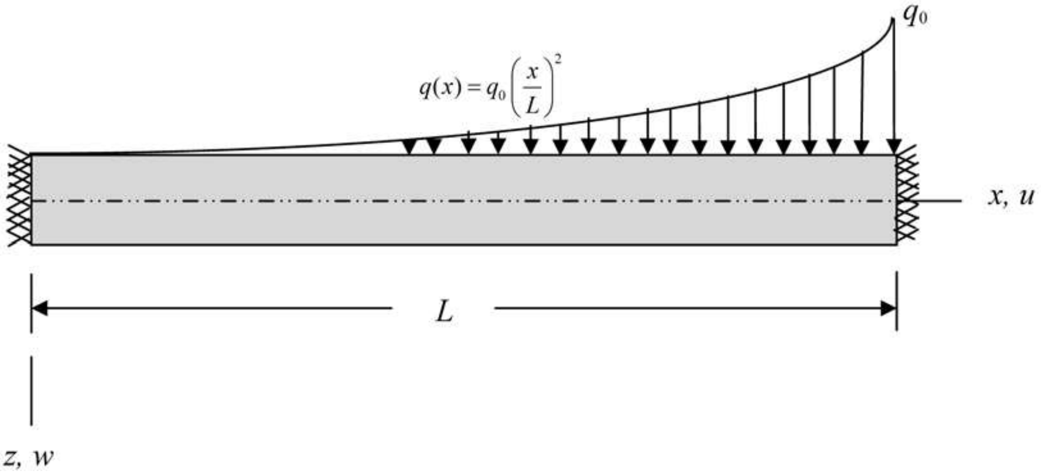

Fig. 2. Fixed beam with parabolic load

General expressions obtained for $w(x)$ and $\phi(x)$ are as follows:

$$w(x) = \frac{q_0L^4}{120EI}\left[\frac{1}{3}\frac{x^6}{L^6}+\frac{x^2}{L^2}-\frac{4}{3}\frac{x^3}{L^3}-\frac{12}{\pi^2}\frac{E}{G}\frac{h^2}{L^2}\left(\frac{5}{6}\frac{x^4}{L^4}-\frac{5}{3}\frac{x^2}{L^2}\right)-\frac{4}{5}\frac{E}{G}\frac{h^2}{L^2}\left(-\frac{x}{L}+\frac{1}{2}\frac{x^2}{L^2}+\frac{\sinh\lambda x-\cosh\lambda x+1}{\lambda L}\right)\right], \tag{16}$$

$$\phi(x) = \frac{1}{15}\frac{q_0L}{\beta EI}\left(1+5\frac{x^3}{L^3}+\sinh\lambda x-\cosh\lambda x\right). \tag{17}$$

The expression for axial displacement u is obtained by substituting Eqs. (16) and (17) into the first equation in (1) and it is as follows:

$$u = \frac{q_0h}{Eb}\left[-\frac{1}{10}\frac{z}{h}\frac{L^3}{h^3}\left(2\frac{x^5}{L^5}+2\frac{x}{L}-4\frac{x^2}{L^2}-\frac{40}{\pi^2}\frac{E}{G}\frac{h^2}{L^2}\left(\frac{x^3}{L^3}-\frac{x}{L}\right)-\frac{4}{5}\frac{E}{G}\frac{h^2}{L^2}\left(-1+\frac{x}{L}+\cosh\lambda x-\sinh\lambda x\right)\right)-\frac{16}{5\pi^4}\sin\frac{\pi z}{h}\frac{E}{G}\frac{L}{h}\left(-1+5\frac{x^3}{L^3}+\cosh\lambda x-\sinh\lambda x\right)\right]. \tag{18}$$

The expression for axial stress is obtained using Eqs. (2), (4), (16) and (17) as follows:

$$\begin{aligned}\sigma_x = \frac{q_0}{b}\Bigg\{ &-\frac{1}{10}\frac{z}{h}\frac{L^2}{h^2}\left[10\frac{x^4}{L^4} + 2 - 4\frac{x}{L} - \frac{120}{\pi^2}\frac{E}{G}\frac{h^2}{L^2}\left(\frac{x^2}{L^2} - \frac{1}{3}\right) - \right.\\ &\left.\frac{4}{5}\frac{E}{G}\frac{h^2}{L^2}\big(1 + \lambda L(\sinh\lambda x - \cosh\lambda x)\big)\right] - \\ &\frac{16}{5\pi^4}\sin\frac{\pi z}{h}\frac{E}{G}\left(15\frac{x^2}{L^2} + \lambda L(\sinh\lambda x - \cosh\lambda x)\right)\Bigg\}.\end{aligned} \tag{19}$$

The expressions for transverse shear stress is obtained using constitutive relation (4) and using Eq. (17) as follows:

$$\tau_{zx}^{CR} = \frac{16}{5\pi^3}\frac{q_0}{b}\frac{L}{h}\cos\frac{\pi z}{h}\left(1 - 5\frac{x^3}{L^3} + \sinh\lambda x - \cosh\lambda x\right). \tag{20}$$

Expression for transverse shear stress τ_{zx}^{EE} obtained from equilibrium equation

The alternate approach to determine the transverse shear stress is the use of equilibrium equations. The first stress equilibrium equation of two dimensional theory of elasticity is as follows:

$$\frac{\partial\sigma_x}{\partial x} + \frac{\partial\tau_{zx}}{\partial z} = 0. \tag{21}$$

Substituting expression for σ_x into Eq. (21) and integrating it with respect to the thickness coordinate $z$and imposing the boundary condition $\tau_{zx} = 0$ at the bounding surfaces $z = \pm h/2$ of the beam one can obtain the final expression of transverse shear stress, which is follows:

$$\begin{aligned}\tau_{zx}^{EE} = \frac{q_0 L}{80bh}\left(4\frac{z^2}{h^2} - 1\right)&\left[40\frac{x^3}{L^3} - 4 - \frac{240}{\pi^2}\frac{x}{L} - \frac{4}{5}\frac{E}{G}\frac{h^2}{L^2}\lambda^2L^2(\cosh\lambda x - \sinh\lambda x)\right] - \\ &\frac{16}{5\pi^5}\cos\frac{\pi z}{h}\frac{E}{G}\frac{q_0 h}{bL}\left(30\frac{x}{L} + \lambda^2L^2(\cosh\lambda x - \sinh\lambda x)\right).\end{aligned} \tag{22}$$

Results are obtained using expressions (16) through (22) for displacements and stresses. The numerical results are presented in Table 1 and graphically presented in Figs. 3 – 11.

Table 1. Non-dimensional axial displacement ($\bar{u}$) at ($x = 0.75L$, $z = h/2$), transverse deflection ($\bar{w}$) at ($x = 0.75L$, $z = 0.0$), axial stress ($\bar{\sigma}_x$) at ($x = 0$, $z = h/2$), maximum transverse shear stresses $\bar{\tau}_{zx}^{CR}$ and $\bar{\tau}_{zx}^{EE}$ ($x = 0.01L$, $z = 0.0$) of the beam for slenderness ratio (S) 4 and 10

Source	S	$\bar{u}$	$\bar{w}$	$\bar{\sigma}_x$	$\bar{\tau}_{zx}^{CR}$	$\bar{\tau}_{zx}^{EE}$
Present	4	0.293 2	0.251 3	3.227 3	0.196 9	−0.442 1
Ghugal and Sharma [9]		0.295 5	0.251 1	3.527 7	0.232 5	−0.455 4
Krishna Murthy [14]		0.297 9	0.251 4	3.270 2	0.205 3	−0.283 4
Timoshenko [20]		−0.881 2	0.110 7	1.600 0	0.048 2	0.399 9
Bernoulli-Euler		−0.881 2	0.059 3	1.600 0	—	0.399 9
Present	10	−10.833 1	0.090 2	13.433 9	0.827 8	−0.087 3
Ghugal and Sharma [9]		−10.827 5	0.090 2	14.189 1	0.885 1	0.425 1
Krishna Murthy [14]		−10.821 5	0.090 2	13.542 2	0.834 7	0.419 7
Timoshenko [20]		−13.769 5	0.067 5	10.000 0	0.753 8	0.999 9
Bernoulli-Euler		−13.769 5	0.059 3	10.000 0	—	0.999 9

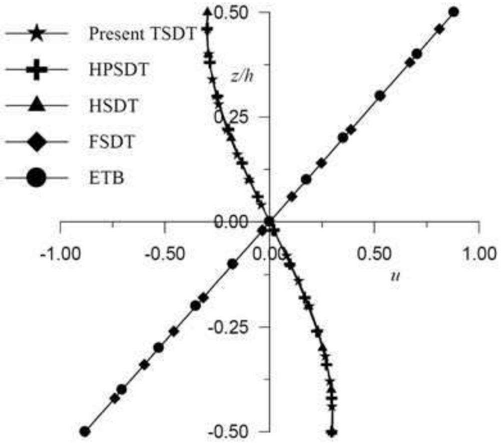

Fig. 3. Variation of axial displacement ($\bar{u}$) through the thickness of fixed-fixed beam at ($x = 0.75L$, z) for slenderness ratio 4

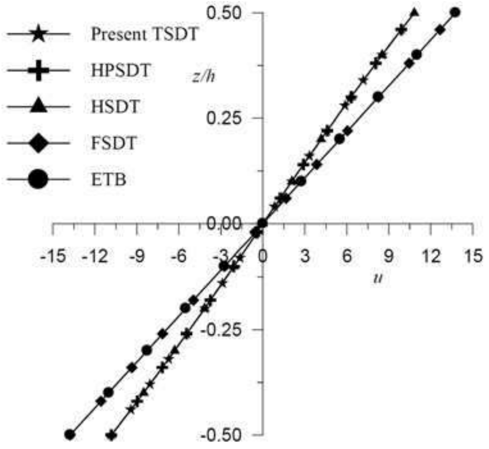

Fig. 4. Variation of axial displacement ($\bar{u}$) through the thickness of fixed-fixed beam at ($x = 0.75L$, z) for slenderness ratio 10

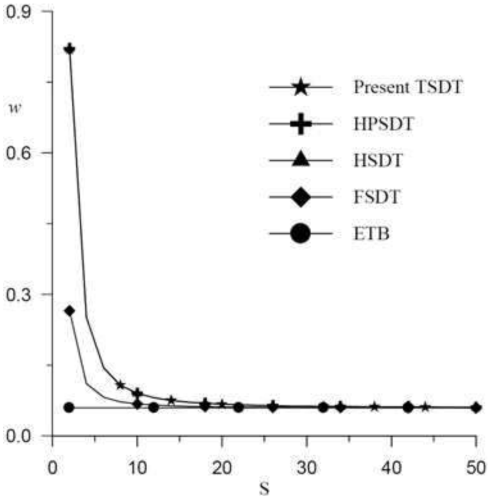

Fig. 5. Variation of maximum transverse displacement ($\bar{w}$) of fixed-fixed beam at ($x = 0.75L$, $z = 0$) with slenderness ratio S

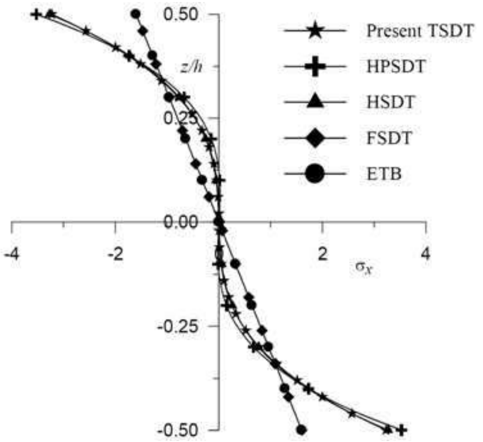

Fig. 6. Variation of axial stress ($\bar{\sigma}_x$) through the thickness of fixed-fixed beam at ($x = 0$, z) for slenderness ratio 4

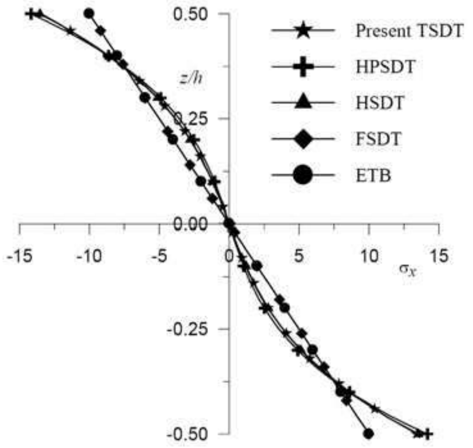

Fig. 7. Variation of axial stress ($\bar{\sigma}_x$) through the thickness of fixed-fixed beam at ($x = 0$, z) for slenderness ratio 10

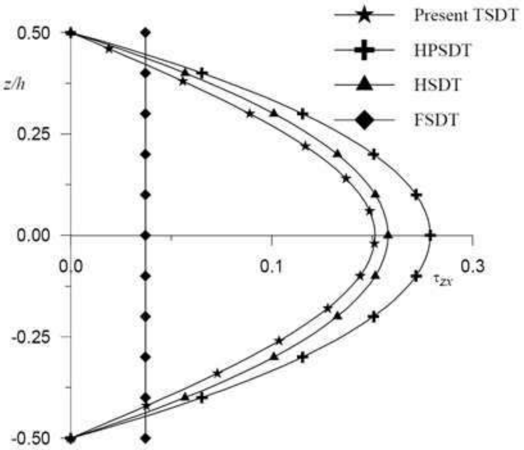

Fig. 8. Variation of transverse shear stress ($\bar{\tau}_{zx}$) through the thickness of fixed-fixed beam at ($x = 0.01L$, z) obtained using constitutive relation for slenderness ratio 4

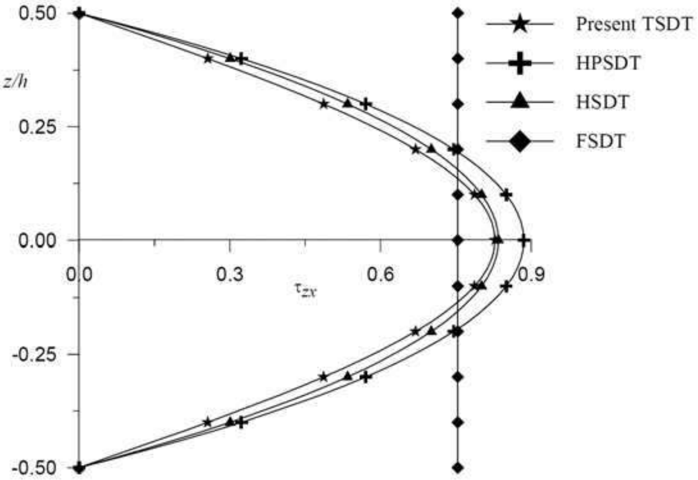

Fig. 9. Variation of transverse shear stress ($\bar{\tau}_{zx}$) through the thickness of fixed-fixed beam at ($x = 0.01L$, z) obtained using constitutive relation for slenderness ratio 4

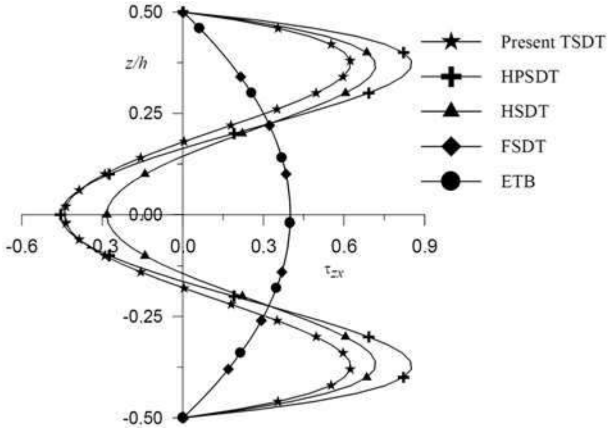

Fig. 10. Variation of transverse shear stress ($\bar{\tau}_{zx}$) through the thickness of fixed-fixed beam at ($x = 0.01L$, z) obtained using equilibrium equation for slenderness ratio 4

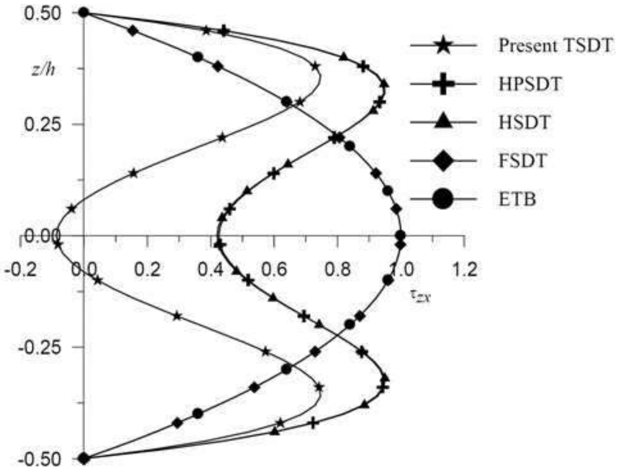

Fig. 11. Variation of transverse shear stress ($\bar{\tau}_{zx}$) through the thickness of fixed-fixed beam at ($x = 0.01L$, z) obtained using equilibrium equation for slenderness ratio 10

4. Results

The results for inplane displacement, transverse displacement, axial and transverse stresses are presented in the following non dimensional form for the purpose of presenting the results in this paper:

$$\bar{u} = \frac{Ebu}{q_0 h}, \qquad \bar{w} = \frac{10Ebh^3 w}{q_0 L^4}, \qquad \bar{\sigma}_x = \frac{b\sigma_x}{q_0}, \qquad \bar{\tau}_{zx} = \frac{b\tau_{zx}}{q_0}, \qquad S = \frac{L}{h}.$$

The numerical results for displacements and stresses are obtained using FORTRAN programs developed based on the non-dimensional expressions for these quantities.

5. Discussion and conclusion

The variationally consistent theoretical formulation of the theory with general solution technique of governing differential equations is presented. The general solutions for beam with parabolic load is obtained in case of thick fixed beams. The displacements and stresses obtained by present theory are in excellent agreement with those of other equivalent refined and higher order theories. The present theory yields the realistic variation of axial displacement and stresses through the thickness of beam. The theory is shown to be capable of predicting the effects of stress concentration on the axial and transverse stresses in the vicinity of the built-in end of the beam which is the region of heavy stress concentration. Thus the validity of the present theory is established.

References

[1] Averill, R. C., Reddy, J. N., An assessment of four-noded plate finite elements based on a generalized third order theory, International Journal of Numerical Methods in Engineering 33 (1992) 1 553–1 572.

[2] Baluch, M. H., Azad, A. K., Khidir, M. A., Technical theory of beams with normal strain, ASCE Journal of Engineering Mechanics 110 (8) (1984) 1 233–1 237.

[3] Bhimaraddi, A., Chandrashekhara, K., Observations on higher order beam theory, ASCE Journal of Aerospace Engineering 6 (4) (1993) 408–413.

[4] Bickford, W. B., A consistent higher order beam theory, Development in Theoretical Applied Mechanics (SECTAM).11 (1982) 137–150.

[5] Bresse, J. A. C., Course of applied mechanics, Mallet-Bachelier, Paris, 1859. (in French)

[6] Cowper, G. R., The shear coefficients in Timoshenko beam theory, ASME Journal of Applied Mechanic 33(2) (1966) 335–340.

[7] Cowper, G. R., On the accuracy of Timoshenko beam theory, ASCE Journal of Engineering Mechanics Division 94 (EM6) (1968) 1 447–1 453.

[8] Ghugal, Y. M., Shmipi, R. P., A review of refined shear deformation theories for isotropic and anisotropic laminated beams, Journal of Reinforced Plastics And Composites 20(3) (2001) 255–272.

[9] Ghugal, Y. M., Sharma, R., A hyperbolic shear deformation theory for flexure and vibration of thick isotropic beams, International Journal of Computational Methods 6(4) (2009) 585–604.

[10] Heyliger, P. R., Reddy, J. N., A higher order beam finite element for bending and vibration problems, Journal of Sound and Vibration 126(2) (1988) 309–326.

[11] Hildebrand, F. B., Reissner, E. C., Distribution of stress in built-in beam of narrow rectangular cross section, Journal of Applied Mechanics 64 (1942) 109–116.

[12] Irretier, H., Refined effects in beam theories and their influence on natural frequencies of beam, International Proceeding of Euromech Colloquium 219 – Refined Dynamical Theories of Beam, Plates and Shells and Their Applications, Edited by I. Elishakoff and H. Irretier, Springer-Verlag, Berlin, (1986), pp. 163–179.

[13] Kant, T., Gupta, A., A finite element model for higher order shears deformable beam theory, Journal of Sound and Vibration 125(2) (1988) 193–202.

[14] Krishna Murthy, A. V., Towards a consistent beam theory, AIAA Journal 22(6) (1984) 811–816.

[15] Levinson, M., A new rectangular beam theory, Journal of Sound and Vibration 74(1) (1981) 81–87.

[16] Lord Rayleigh, J. W. S., The theory of sound, Macmillan Publishers, London, 1877.

[17] Reddy, J. N., An Introduction to finite element method. Second edition, McGraw-Hill, Inc., New York, 1993.

[18] Rehfield, L. W., Murthy, P. L. N., Toward a new engineering theory of bending: fundamentals, AIAA Journal 20(5) (1982) 693–699.

[19] Stein, M., Vibration of beams and plate strips with three dimensional flexibility, ASME Journal of Applied Mechanics 56(1) (1989) 228–231.

[20] Timoshenko, S. P., On the correction for shear of the differential equation for transverse vibrations of prismatic bars, Philosophical Magazine 41(6) (1921) 742–746.

[21] Timoshenko, S. P., Goodier, J. N., Theory of elasticity. Third international edition, McGraw-Hill, Singapore. 1970.

[22] Vlasov, V. Z., Leont'ev, U. N., Beams, plates and shells on elastic foundations, Moskva, Chapter 1, 1–8. Translated from the Russian by Barouch A. and Plez T., Israel Program for Scientific Translation Ltd., Jerusalem, 1966.

Nomenclature

A	Cross sectional area of beam $= bh$
b	Width of beam in y-direction
E, G, μ	Elastic constants of the beam material
h	Thickness of beam
I	Moment of inertia of cross-section of beam
L	Span of the beam
q_0	Intensity of parabolic transverse load
S	Slenderness ratio of the beam $= L/h$
w	Transverse displacement in z-direction
$\bar{w}$	Non-dimensional transverse displacement
$\bar{u}$	Non-dimensional axial displacement
x, y, z	Rectangular Cartesian coordinates
$\bar{\sigma}_x$	Non-dimensional axial stress in x-direction
$\bar{\tau}_{zx}^{CR}$	Non-dimensional transverse shear stress via constitutive relation
$\bar{\tau}_{zx}^{EE}$	Non-dimensional transverse shear stress via equilibrium equation
$\phi(x)$	Unknown function associated with the shear slope

List of abbreviations

CR	Constitutive Relations
EE	Equilibrium Equations
TSDT	Trigonometric Shear Deformation Theory
HPSDT	Hyperbolic Shear Deformation Theory
HSDT	Third Order Shear Deformation Theory
FSDT	First Order Shear Deformation Theory
ETB	Elementary Theory of Beam

ResearchGate

See discussions, stats, and author profiles for this publication at: https://www.researchgate.net/publication/262525766

A new beam element for structural analysis

Conference Paper · May 2012

CITATIONS
9

READS
479

1 author:

Yucheng Liu
South Dakota State University

264 PUBLICATIONS 2,206 CITATIONS

SEE PROFILE

Some of the authors of this publication are also working on these related projects:

Alternative Energy View project

Mechanical Systems Design View project

All content following this page was uploaded by Yucheng Liu on 23 May 2014.

The user has requested enhancement of the downloaded file.

A New Beam Element for Structural Analysis

Yucheng Liu

***Abstract*—**This paper presents an isotropic beam element based on a sinusoidal shear deformation theory. The element shape functions are found directly from the solutions of the governing differential equations that describe the deformations of the cross section based on the high order theory. The presented beam element is used for stiffness analysis and the results are compared with the solutions obtained from classical beam theory, elasticity theory, and Petrolito beam theory.

***Keywords*—**beam, Touratier theory, shear deformation theory, stiffness analysis, analytical solution.

I. INTRODUCTION

Classical beam theory was based on the Bernoulli-Euler law, which assumes that plain sections of the cross section remain plain and perpendicular to the beam axis and neglects shear deformation. This theory correctly calculates the load-carrying and deflection characteristics of thin beams. However, for thick beams in which shear deformation is important, the Bernoulli-Euler theory yields some errors in describing such beam's behaviors. This defect was overcome by Timoshenko's beam theory, which takes into account shear deformation and rotational inertia effects [1]. In Timoshenko beam theory, the resulting stress field no longer satisfies the usual shear free boundary condition on the top and bottom surfaces of the beam. Therefore, in this theory, it is necessary to include a Timoshenko shear coefficient into the integrated shear constitutive equation. This problem was solved by Levinson [2], who developed a high order shear deformation theory based on a cubic in-plane displacement approximation that relaxes the restriction on the warping of the cross section. In Levinson's theory, the equilibrium equations of the classical plate theory was used for the derivation, which is variational inconsistent with the kinematics of displacements. By using the cubic displacement field of Levinson, Bickford [3], Heyliger and Reddy [4] developed variationally consistent high order beam theories, separately.

Different beam elements have been developed based on these beam theories and even plate theories. Heyliger and Reddy [4] presented a high order beam element for the static and dynamic behavior of rectangular beams by using the variationally consistent higher order plate theory of Reddy [5, 6]. Petrolito [7] used Bickford beam theory to perform exact stiffness analysis of thick beams. He derived solutions of the governing differential equations as well as the beam element's shape functions. The accuracy of Petrolito's beam element was verified by comparing with elasticity theory and classical beam theory. Eisenberger [8] continued to derive the exact stiffness matrix for the high order beam element and present an exact beam element. Examples showed that with such exact beam element, the exact results could be obtained independent of the number of elements.

Besides the aforementioned high order shear deformation theories, Touratier [9] developed a new plate theory that accounts for cosine shear stress distribution and free boundary conditions for shear stress on the top and bottom surfaces of the plate. This theory also rectifies the defect of Timoshenko's theory and was proved being more efficient than other refined plate theories, in which the shear deformation is represented by a sinusoidal function. Even Touratier theory is a plate theory, it can also be employed to define beam element. In this paper, a new beam element is presented based on Touratier theory. An illustrative example shows that the presented beam element is efficient for stiffness analysis and accurately describes the deflection behaviors of thick beams. By using Touratier theory, the beam element can be developed without using shear correction factors and independent of material behavior in the kinematics.

II. GOVERNING EQUATIONS

A typical beam element is shown in Fig. 1. Assuming that there are no loads applied along the X direction, the deformation of the beam is described by the displacements along X and Z directions, u and w, and the rotation about Y direction, θ. According to Touratier's theory, the displacement field of the present beam element takes the form

$$\begin{aligned} &w = w(x) \\ &\theta = \theta(x) \\ &u = u(x,z) = \frac{h}{\pi}\sin\left(\frac{\pi z}{h}\right)\left(\theta + \frac{\partial w}{\partial x}\right) - z\frac{\partial w}{\partial x} \end{aligned} \tag{1}$$

The strain components are

$$\begin{aligned} \varepsilon_x &= \frac{\partial u}{\partial x} = \frac{h}{\pi}\sin\left(\frac{\pi z}{h}\right)\left(\frac{\partial \theta}{\partial x} + \frac{\partial^2 w}{\partial x^2}\right) - z\frac{\partial^2 w}{\partial x^2} \\ \gamma_{xz} &= \frac{\partial u}{\partial z} + \frac{\partial w}{\partial x} = \cos\left(\frac{\pi z}{h}\right)\left(\theta + \frac{\partial w}{\partial x}\right) \end{aligned} \tag{2}$$

The stress-strain relationships are

$$\sigma x = E\varepsilon x \text{ and } \tau xz = G\gamma xz \tag{3}$$

where E is Young's modulus, G = E/2(1 + υ) is the shear modulus and υ is Poisson's ratio. Here this beam element is assumed as isotropic.

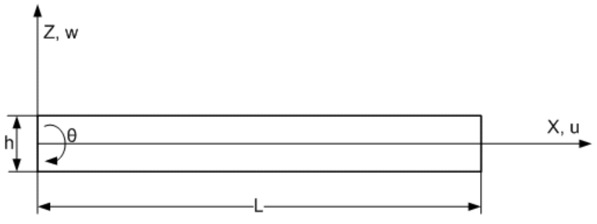

Dr. Yucheng Liu is with the University of Louisiana, Lafayette, LA 70504 USA (phone: 337-482-5822; fax: 337-482-1129; e-mail: yxl5763@ Louisiana.edu).

Fig. 1. Typical beam element

The equilibrium equations for the beam element are obtained using Hamilton's principle [4] based on Eqs. (1) to (3), which can be expressed as

$$\int_{-h/2}^{h/2}\int_0^b\int_0^L\left(\sigma_x\delta\varepsilon_x+\tau_{xz}\delta\gamma_{xz}\right)dxdydz-\int_0^L q\delta w dx=0 \qquad (4)$$

where b is the width of the beam and q is the distributed transverse load acting on the beam.

Substituting Eqs. (1) to (3) into Eq. (4) and we can have the equilibrium equations for the beam as

$$\left[\left(\frac{2h^3}{\pi^3}-\frac{h^3}{2\pi^2}\right)Eb\theta'-\left(\frac{h^3}{2\pi^2}-\frac{4h^3}{\pi^3}+\frac{h^3}{12}\right)Ebw''\right]''+\left[0.5Gbh(\theta+w')\right]'+q=0$$

$$\left[\left(\frac{2h^3}{\pi^3}-\frac{h^3}{2\pi^2}\right)Ebw''-\frac{h^3}{2\pi^2}Eb\theta'\right]'+0.5Gbh(\theta+w')=0 \qquad (5)$$

Taking the beam's cross-sectional area A = bh and the second moment of the cross-sectional area I = bh3/12, Eq. (5) can be simplified as

$$\left[0.166EI\theta'-0.06EIw''\right]''+\left[0.5GA(\theta+w')\right]'+q=0$$

$$\left[0.166EIw''-0.648EI\theta'\right]'+0.5GA(\theta+w')=0 \qquad (6)$$

where EI is the beam's bending rigidity, GA is the beam's shear rigidity, and the prime denotes d/dx.

From Eq. (6), the generalized forces appropriate for this beam element can be defined as

$$F_1=0.166EI\theta''-0.06EIw'''+0.5GA(\theta+w')$$

$$F_2=0.06EIw''-0.166EI\theta'$$

$$F_3=0.648EI\theta'-0.166EIw'' \qquad (7)$$

where the F1 is a generalized shear force, while F2 and F3 are generalized moments.

According to Petrolito [7], in order to fully determine the boundary conditions for the beam, either quantity in the following three pairs needs to be specified

w or F1;
w' or F2;
θ or F3.

So far, the beam theory has been entirely presented, which includes a sinusoidal displacement field from Touratier' theory (Eq. (1)), two equilibrium equations (Eq. (6)), and three pairs of associated boundary conditions at each end of the beam. In following sections, the equilibrium equations (Eq. (6)) are solved to determine the lateral deflection of the beam, w, and the rotation of a normal to the axis of the beam, θ in a linear bending problem.

III. GENERAL SOLUTIONS OF EQ. (6)

The coupled differential equations (Eq. (6)) can be solved and the solutions include two parts: homogeneous solutions and particular solutions. For the homogeneous solutions, assuming there is no applied transverse load, q = 0, Eq. (6) can be decoupled as

$$w^{(6)}-\lambda^2w^{(5)}=0 \text{ and } \theta^{(5)}-\lambda^2\theta^{(3)}=0 \qquad (8)$$

with

$$\lambda^2=\frac{46GA}{EI}=\frac{276}{h^2(1+\nu)} \qquad (9)$$

Such problem (Eq. (8)) has been solved by Petrolito [7] and Eisenberger [8] and the solution is

$$w=C_1+C_2x+C_3x^2+C_4x^3+C_5\sinh(\lambda x)+C_6\cosh(\lambda x)$$

$$\theta=\frac{-9.768EIC_4}{GA}-C_2-2C_3x-3C_4x^2+0.226\lambda C_6\sinh(\lambda x)+0.226\lambda C_5\cosh(\lambda x) \qquad (10)$$

Particular solutions need to be derived according to the applied loads or moments. If the applied load q(x) is linearly distributed along the beam length L with the maximum magnitude Q

$$q(x)=\frac{x}{L}Q_1 \qquad (11)$$

The particular solution of Eq. (6) is obtained as

$$w_1(x)=\frac{0.008x^5}{EIL}Q_1$$

$$\theta_1(x)=-\left(\frac{0.04x^4}{EIL}+\frac{0.78x^2}{GAL}+\frac{2.03EI}{(GA)^2L}\right)Q_1 \qquad (12)$$

Else if the applied load is given by

$$q(x)=\frac{x}{L}Q_1+\left(1-\frac{x}{L}\right)Q_2 \qquad (13)$$

The particular solution is

$$w_2(x)=w_1(x)+\frac{Q_2}{Q_1}w_1(L-x)$$

$$\theta_2(x)=\theta_1(x)-\frac{Q_2}{Q_1}\theta_1(L-x) \qquad (14)$$

Obviously, if the applied load is constant, q(x) = Q, the particular solution can be obtained from Eq. (14) by assuming Q1 = Q2 = Q.

IV. ELEMENT FORMULATION

Based on above demonstration, a typical beam element, e, can be presented. Fig. 2 plots this beam element and the element has two nodes each with three degrees of freedom w, w', and θ.

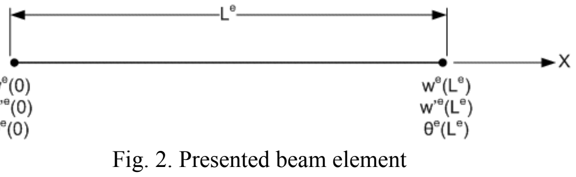

Fig. 2. Presented beam element

The beam element formulation, which is similar to that developed by Petrolito [7], is represented as

$$w^e(x)=A_1^e(x)(B^{-1})^e(d^e-d_0^e)=N_1^e(x)d^e+w_f^e(x)$$

$$\theta^e(x)=A_2^e(x)(B^{-1})^e(d^e-d_0^e)=N_2^e(x)d^e+\theta_f^e(x) \qquad (15)$$

where the shape function matrices N1(x) and N2(x) are

$$N_1(x)=A_1(x)B^{-1},\ N_2(x)=A_2(x)B^{-1} \qquad (16)$$

and wf(x) and θf(x) are fixed end solutions according to the applied loading on the element

$$w_f(x)=-A_1(x)B^{-1}d_0,\ \theta_f(x)=-A_2(x)B^{-1}d_0 \qquad (17)$$

Notations in Eq. (15) to (17) are defined as

$$A_1(x) = [1, x, x^2, x^3, \sinh(\lambda x), \cosh(\lambda x)]$$
$$A_2(x) = [0, -1, -2x, -\left(\frac{9.768EI}{GA} + 3x^2\right), 0.226\lambda\cosh(\lambda x), 0.226\lambda\sinh(\lambda x)]$$
$$B = [A_1(0), A_1'(0), A_2(0), A_1(L), A_1'(L), A_2(L)]$$
$$d_0 = [w_0(0), w_0'(0), \theta_0(0), w_0(L), w_0'(L), \theta_0(L)]$$
$$d^e = [w^e(0), w'^e(0), \theta^e(0), w^e(L^e), w'^e(L^e), \theta^e(L^e)] \tag{18}$$

where Le is the length of the beam element, d0 and de are degrees of freedom of the beam element.

From Eq. (7) and Eq. (15), the generalized forces for the element are

$$F_1^e(x) = S_1^e(x)d^e + S_{f1}^e(x)$$
$$F_2^e(x) = S_2^e(x)d^e + S_{f2}^e(x)$$
$$F_3^e(x) = S_3^e(x)d^e + S_{f3}^e(x) \tag{19}$$

where S1(x), S2(x), and S3(x) are generalized force matrices

$$S_1(x) = 0.166EIN_2''(x) - 0.06EIN_1'''(x) + 0.5GA\left(N_2(x) + N_1'(x)\right)$$
$$S_2(x) = 0.06EIN_1''(x) - 0.166EIN_2'(x)$$
$$S_3(x) = 0.648EIN_2'(x) - 0.166EIN_1''(x) \tag{20}$$

while Sf1(x), Sf2(x), and Sf3(x) are generalized fixed end forces

$$S_{f1}(x) = 0.166EI\theta_f''(x) - 0.06EIw_f'''(x) + 0.5GA\left(\theta(x) + w_f'(x)\right)$$
$$S_{f2}(x) = 0.06EIw_f''(x) - 0.166EI\theta_f'(x)$$
$$S_{f3}(x) = 0.648EI\theta_f'(x) - 0.166EIw_f''(x) \tag{21}$$

Also, from Petrolito's theorem, the stiffness equations for a beam which is composed of E beam elements are given by

$$\sum_{e=1}^{E}\left(K^e d^e - R^e\right) = 0 \tag{22}$$

where Ke denotes the element stiffness matrix, which is symmetric, and Re is the element load vector

$$R = \int_0^L pN_1^T dx \tag{23}$$

V. ILLUSTRATIVE EXAMPLE

A beam problem is solved in this section using the present beam element. The results are compared with the solutions obtained using Petrolito's beam theory [7], elasticity theory [10], and classical beam theory (the Timoshenko beam). In this example, the aspect ratio of the beam L/h varies from 1 to 100 and Poisson's ratio υ is set as 0.3.

Example: simply supported beam subjected to a uniform load

In this example, a simply supported beam with length L and depth h (Fig. 1) is subjected to a uniform load q = Q1/L (Fig. 3). This beam is analyzed using the present element and because of its symmetry, the beam is meshed with two elements where each element represents a half beam.

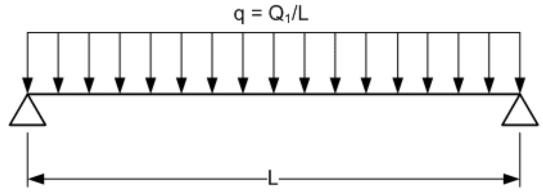

Fig. 3. Simply supported beam subjected to a uniform load

The central displacement w and maximum stress σx for the simply supported beams with different L/h are calculated using the present beam theory. The results are normalized with respect to the results obtained from the classical beam theory and are compared to the normalized elasticity solution and Petrolito's solution (as listed in table 1, the normalized elasticity solution and petrolito's results were presented in [7]).

The results listed in table 1 indicate that the present beam formulation agrees very well to the elasticity theory and Petrolito's beam model. Evident errors are observed compare to the classical solution when L/h < 5, in which cases the models cannot be considered as beams. As the ratio L/h increases, all the results tend toward the classical solution. The accuracy of the present beam formulation is therefore verified.

Table I

NORMALIZED CENTRAL DISPLACEMENT, W, NORMALIZED MAXIMUM STRESS, ΣX FOR EXAMPLE

L/h	Displacement			Stress		
	Present	Elasticity	Petrolito	Present	Elasticity	Petrolito
1	3.412	3.399	3.434	1.309	1.271	1.347
2	1.621	1.622	1.620	1.079	1.067	1.087
3	1.276	1.278	1.277	1.036	1.030	1.039
4	1.156	1.157	1.156	1.012	1.017	1.022
5	1.100	1.100	1.100	1.009	1.011	1.014
10	1.025	1.025	1.025	1.003	1.003	1.003
25	1.004	1.004	1.004	1.001	1.000	1.001
50	1.001	1.001	1.001	1.000	1.000	1.000
100	1.000	1.000	1.000	1.000	1.000	1.000

VI. CONCLUSIONS

In this paper, a new beam formulation based on Touratier's sinusoidal beam theory is presented. The governing differential equations for such beam are derived and solved. The present beam formulation can be used to correctly solve regular beam problems and by using this formulation, only the minimum number of elements are required to mesh the beam, enabling the problem to be solved rapidly. Developed based on Touratier's beam theory, such beam formulation does not require a shear correction factor and is very suitable for modeling composite beams.

REFERENCES

[1] S. P. Timoshenko, "On the correction for shear of the differential equation for transverse vibrations of prismatic bars", Philosophical Magazine 1921; 41: 744-746.
[2] M. Levinson, "A new rectangular beam theory", Journal of Sound and Vibration 1981; 74(1): 81-87.
[3] W. B. Bickford, "A consistent higher order beam theory", Developments in Theoretical and Applied Mechanics 1982; 11: 137-150
[4] P. R. Heyliger and J. N. Reddy, "A higher order beam finite element for bending and vibration problems", Journal of Sound and Vibration 1988; 126(2): 309-326.

[5] J. N. Reddy, “A simple higher-order theory for laminated composite plates”, ASME Journal of Applied Mechanics 1984; 54: 745-752.
[6] J. N. Reddy, “A refined nonlinear theory of plates with transverse shear deformation”, International Journal of Solids and Structures 1984; 20: 881-896.
[7] J. Petrolito, “Stiffness analysis of beams using a higher-order theory”, Computers & Structures 1995; 55(1): 33-39.
[8] M. Eisenberger, “An exact high order beam element”, Computers & Structures 2003; 81: 147-152.
[9] M. Touratier, “An efficient standard plate theory”, International Journal of Engineering Science 1991; 29(8): 901-916.
[10] J. Petrolito, “A modified ACM element for thick plate analysis”, Computers & Structures 1989; 31: 553-565.

Yucheng Liu PhD, PE is an Assistant Professor of Mechanical Engineering at the University of Louisiana at Lafayette. Dr. Liu’s research interests focus on numerical analysis and methods, computer modeling and simulation, applied mathematics, structural mechanics, and crashworthiness analysis. To date, he has authored and co-authored over 80 publications in his areas and has been the PI or Co-PI of numerous research projects with total funds over 2 million dollars. Dr. Liu serves as the editorial board member of an international journal and has reviewed proposals and papers for US Department of Energy, 19 peer reviewed journals, and 5 international conferences. Dr. Liu is a registered Professional Engineer and holds active membership in ASME, ASEE, and SAE.

View publication stats

International Journal of Engineering Research and Development
e-ISSN: 2278-067X, **p**-ISSN: 2278-800X, www.ijerd.com
Volume 6, Issue 10 (April 2013), PP. 09-14

Flexure of Thick Cantilever Beam using Third Order Shear Deformation Theory

Ajay Dahake[1], Rupa Walunj[2], Manjushree Dhongade[3] and Jaya Sawarkar[4]
[1]Professor, [2,3,4]UG Student,
Civil Engineering Department, Shreeyash College of Engineering and Technology, Aurangabad, M.S. , India.

Abstract:- The number of variables in the present theory is same as that in the first order shear deformation theory. A third order shear deformation theory for flexure of thick beams, taking into account transverse shear deformation effects, is developed. The sinusoidal function is used in displacement field in terms of thickness coordinate to represent the shear deformation effects. The noteworthy feature of this theory is that the transverse shear stresses can be obtained directly from the use of constitutive relations with excellent accuracy, satisfying the shear stress free conditions on the top and bottom surfaces of the beam. Hence, the theory obviates the need of shear correction factor. The thick cantilever isotropic beams are considered for the numerical studies to demonstrate the efficiency of theory. Results obtained are discussed critically with those of other theories.

Keywords:- Thick beam, displacements, stresses, , third order shear deformation, flexure.

I. INTRODUCTION

It is well-known that elementary theory of bending of beam based on Euler-Bernoulli hypothesis disregards the effects of the shear deformation and stress concentration. The theory is suitable for slender beams and is not suitable for thick or deep beams since it is based on the assumption that the transverse normal to neutral axis remains so during bending and after bending, implying that the transverse shear strain is zero. Since theory neglects the transverse shear deformation, it underestimates deflections in case of thick beams where shear deformation effects are significant.

Bresse [1], Rayleigh [2] and Timoshenko [3] were the pioneer investigators to include refined effects such as rotatory inertia and shear deformation in the beam theory. Timoshenko showed that the effect of transverse vibration of prismatic bars. This theory is now widely referred to as Timoshenko beam theory or first order shear deformation theory (FSDT) in the literature. In this theory transverse shear strain distribution is assumed to be constant through the beam thickness and thus requires shear correction factor to appropriately represent the strain energy of deformation. Cowper [4] has given refined expression for the shear correction factor for different cross-sections of beam. The accuracy of Timoshenko beam theory for transverse vibrations of cantilever beam in respect of the fundamental frequency is verified by Cowper [5] with a plane stress exact elasticity solution. To remove the discrepancies in classical and first order shear deformation theories, higher order or refined shear deformation theories were developed and are available in the open literature for static and vibration analysis of beam.

Levinson [6], Bickford [7], Rehfield and Murty [8], Krishna Murty [9], Baluch, Azad and Khidir [10], Bhimaraddi and Chandrashekhara [11] presented cosine shear deformation theories assuming a higher variation of axial displacement in terms of thickness coordinate. These theories satisfy shear stress free boundary conditions on top and bottom surfaces of beam and thus obviate the need of shear correction factor. Irretier [12] studied the refined dynamical effects in linear, homogenous beam according to theories, which exceed the limits of the Euler-Bernoulli beam theory. These effects are rotary inertia, shear deformation, rotary inertia and shear deformation, axial pre-stress, twist and coupling between bending and torsion.

Vlasov and Leont'ev [13] developed refined shear deformation theories for thick beams including sinusoidal function in terms of thickness coordinate in displacement field. However, with these theories shear stress free boundary conditions are not satisfied at top and bottom surfaces of the beam. In this paper development of theory and its application to thick cantilever beam is presented.

II. SYSTEM DEVELOPMENT

The beam under consideration as shown in Fig. 1 occupies in $0-x-y-z$ Cartesian coordinate system the region:

$$0 \le x \le L \ ; \quad 0 \le y \le b \ ; \quad -\frac{h}{2} \le z \le \frac{h}{2}$$

Where *x*, *y*, *z* are Cartesian coordinates, *L* and *b* are the length and width of beam in the x and *y* directions respectively, and *h* is the thickness of the beam in the z-direction. The beam is made up of homogeneous, linearly elastic isotropic material.

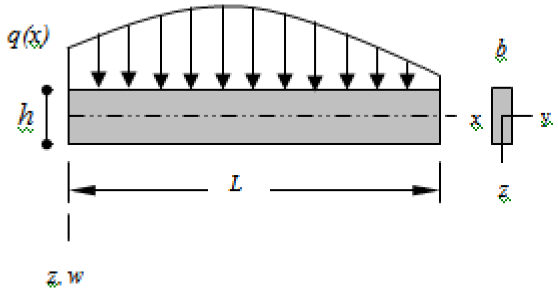

Fig.1: Beam under bending in *x-z* plane

A. *The Displacement Field*

The displacement field of the present beam theory is of the form:

$$u(x,z) = -z\frac{dw}{dx} + z\left(1 - \frac{4}{3}\frac{z^2}{h^2}\right)\phi(x) \tag{1}$$

$$w(x,z) = w(x)$$

Where u is the axial displacement in x direction and w is the transverse displacement in z direction of the beam. The sinusoidal function is assigned according to the shear stress distribution through the thickness of the beam. The function ϕ represents rotation of the beam at neutral axis, which is an unknown function to be determined. The stress-strain relationships used are as follows:

$$\sigma_x = E\varepsilon_x,\ \tau_{zx} = G\gamma_{zx} \tag{2}$$

B. *Governing Equations and Boundary Conditions*

Using the principle of virtual work, variationally consistent governing differential equations and boundary conditions for the beam under consideration can be obtained. The principle of virtual work when applied to the beam leads to:

$$b\int_{x=0}^{x=L}\int_{z=-h/2}^{z=+h/2}\left(\sigma_x\delta\varepsilon_x + \tau_{zx}\,\delta\gamma_{zx}\right)dx\,dz - \int_{x=0}^{x=L} q(x)\,\delta w\,dx = 0 \tag{3}$$

where the symbol δ denotes the variational operator.

The associated consistent natural boundary conditions obtained are of following form:

At the ends *x* = 0 and *x* = *L*

$$V_x = EI\frac{d^3w}{dx^3} - \frac{24}{\pi^3}EI\frac{d^2\phi}{dx^2} = 0 \quad \text{or } w \text{ is prescribed} \tag{4}$$

$$M_x = EI\frac{d^2w}{dx^2} - \frac{24}{\pi^3}EI\frac{d\phi}{dx} = 0 \quad \text{or } \frac{dw}{dx} \text{ is prescribed} \tag{5}$$

$$M_a = EI\frac{24}{\pi^3}\frac{d^2w}{dx^2} - \frac{6}{\pi^2}EI\frac{d\phi}{dx} = 0 \text{ or } \phi \text{ is prescribed} \tag{6}$$

Thus the boundary value problem of the beam bending is given by the above variationally consistent governing differential equations and boundary conditions.

C. *The General Solution of Governing Equilibrium Equations of Beam*

The general solution for transverse displacement w(x) and warping function ϕ (x) is obtained using "(6) and (7)" using method of solution of linear differential equations with constant coefficients. Integrating and rearranging "(6)", we obtain the following expression

$$\frac{d^3w}{dx^3} = \frac{24}{\pi^3}\frac{d^2\phi}{dx^2} + \frac{Q(x)}{EI} \tag{7}$$

Where Q(x) is the generalized shear force for beam and it is given by $Q(x) = \int_0^x q\,dx + C_1$.

III. ILLUSTRATIVE EXAMPLE

In order to prove the efficacy of the present theory, the following numerical examples are considered. The following material properties for beam are used

E = 210 GPa, μ = 0.3 and ρ = 7800 kg/m^3, where E is the Young's modulus, ρ is the density, and μ is the Poisson's Units

Cantilever beam subjected to cosine load

The cantilever beam is having its origin at left at x = 0 and free at x =L. The beam is subjected to cosine load, on surface z = +h/2 acting in the downward z direction with maximum intensity of load q_0.

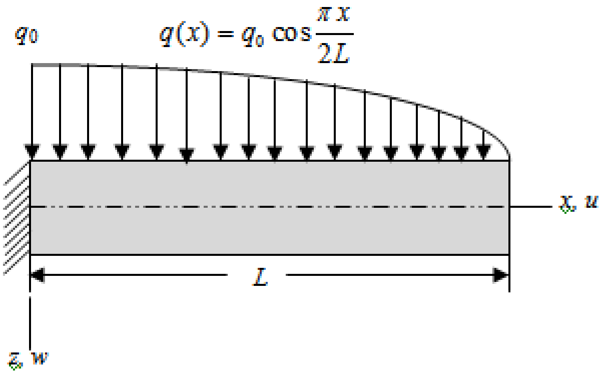

Fig.2: Cantilever beam with cosine load

General expressions obtained for $w(x)$ and $\phi(x)$ are as follows:

$$\phi(x) = \frac{2}{\pi}\frac{A_0}{C_0}\frac{q_0 L}{Gbh}\left(1-\sin\frac{\pi x}{2L}+\sinh\lambda x-\cosh\lambda x\right) \tag{8}$$

$$w(x) = \frac{q_0 L^4}{120EI}\left[\begin{aligned}&\frac{240}{\pi}\left(\frac{8}{\pi^3}\left(\cos\frac{\pi x}{2L}-1\right)-\frac{1}{6}\frac{x^3}{L^3}+\frac{1}{2}\frac{x^2}{L^2}\right)+\frac{40}{\pi^2}\frac{B_0}{C_0}\frac{E}{G}\frac{h^2}{L^2}\left(\cos\frac{\pi x}{2L}-1\right)\\&-\frac{20}{\pi}\frac{A_0^2}{C_0}\frac{E}{G}\frac{h^2}{L^2}\left(\frac{\sinh\lambda x-\cosh\lambda x+1}{\lambda L}-\frac{x}{L}\right)\end{aligned}\right] \tag{9}$$

The axial displacement and stresses obtained based on above solutions are as follows

$$u = \frac{q_0 h}{Eb}\left\{\begin{aligned}&-\frac{1}{10}\frac{z}{h}\frac{L^3}{h^3}\left[\begin{aligned}&\frac{240}{\pi}\left(\frac{4}{\pi^2}\sin\frac{\pi x}{2L}\right)-\frac{1}{2}\frac{x^2}{L^2}+\frac{x}{L}-\frac{40}{\pi^2}\frac{B_0}{C_0}\frac{E}{G}\frac{h^2}{L^2}\left(\frac{\pi}{2}\sin\frac{\pi x}{2L}\right)\\&-\frac{20}{\pi}\frac{A_0^2}{C_0}\frac{E}{G}\frac{h^2}{L^2}(\cosh\lambda x-\sinh\lambda x-1)\end{aligned}\right]\\&+\frac{z}{h}\left[1-\frac{4}{3}\frac{z^2}{h^2}\right]\frac{2}{\pi}\frac{E}{G}\frac{A_0}{C_0}\frac{L}{h}\left(\sinh\lambda x-\cosh\lambda x+1-\sin\frac{\pi x}{2L}\right)\end{aligned}\right\} \tag{10}$$

$$\sigma_x = \frac{q_0}{b}\left\{\begin{aligned}&-\frac{1}{10}\frac{z}{h}\frac{L^2}{h^2}\left[\frac{240}{\pi}\left(-\frac{2}{\pi}\cos\frac{\pi x}{2L}+1-\frac{x}{L}\right)-10\frac{B_0}{C_0}\frac{E}{G}\frac{h^2}{L^2}\cos\frac{\pi x}{2L}-\frac{20}{\pi}\frac{A_0^2}{C_0}\frac{E}{G}\frac{h^2}{L^2}(\lambda L\sinh\lambda x-\lambda L\cosh\lambda x)\right]\\&+\frac{z}{h}\left[1-\frac{4}{3}\frac{z^2}{h^2}\right]\frac{2}{\pi}\frac{E}{G}\frac{A_0}{C_0}\left(-\frac{\pi}{2}\cos\frac{\pi x}{2L}+\lambda L\cosh\lambda x-\lambda L\sinh\lambda x\right)\end{aligned}\right\} \tag{11}$$

$$\tau_{zx}^{CR} = \frac{q_0}{b}\frac{2}{\pi}\frac{A_0}{C_0}\frac{L}{h}\left(1-4\frac{z^2}{h^2}\right)\left(1-\sin\frac{\pi x}{2L}+\sinh\lambda x-\cosh\lambda x\right) \tag{12}$$

$$\begin{aligned}\tau_{zx}^{EE} = \frac{q_0 L}{80bh}\left(1-4\frac{z^2}{h^2}\right)&\left[\frac{240}{\pi}\left(1-\sin\frac{\pi x}{2L}\right)-5\pi\frac{B_0}{C_0}\frac{E}{G}\frac{h^2}{L^2}\sin\frac{\pi x}{2L}+\frac{20}{\pi}\frac{A_0^2}{C_0}\frac{E}{G}\frac{h^2}{L^2}\lambda^2L^2(\cosh\lambda x-\sinh\lambda x)\right].\\&-\frac{2}{\pi}\frac{E}{G}\frac{A_0}{C_0}\frac{h}{L}\left(\frac{1}{2}\frac{z^2}{h^2}-\frac{1}{3}\frac{z^4}{h^4}-\frac{5}{48}\right)\left(\lambda^2L^2\sinh\lambda x-\lambda^2L^2\cosh\lambda x+\frac{\pi^2}{4}\sin\frac{\pi x}{2L}\right)\end{aligned} \tag{13}$$

IV. RESULTS

In this paper, the results for inplane displacement, transverse displacement, inplane and transverse stresses are presented in the following non dimensional form for the purpose of presenting the results in this work.

For beams subjected to cosine load, *q(x)*

$$\bar{u} = \frac{Ebu}{q_0 h}, \quad \bar{w} = \frac{10Ebh^3 w}{q_0 L^4}, \bar{\sigma}_x = \frac{b\sigma_x}{q_0}, \quad \bar{\tau}_{zx} = \frac{b\tau_{zx}}{q_0}$$

Table I: Non-Dimensional Axial Displacement at (*x* = *L*, *z* = *h*/2), Transverse Deflection at (*x* = *L*, *z* =0.0), Axial Stress at (x = 0, z = h/2) Maximum Transverse Shear Stresses (x = 0.01L, z = 0.0) for Aspect Ratio 4

Model	$\bar{u}$	$\bar{w}$	$\bar{\sigma}_x$	$\bar{\tau}_{zx}^{CR}$	$\bar{\tau}_{zx}^{EE}$
HSDT	-71.15	6.17	37.00	1.90	-2.76
FSDT	23.15	6.54	22.21	0.31	3.76
ETB	23.15	5.75	22.21	-	3.76

Table II: Non-Dimensional Axial Displacement at (*x* = *L*, *z* = *h*/2), Transverse Deflection at (x = L, z =0.0), Axial Stress at (*x* = 0, *z* = *h*/2) Maximum Transverse Shear Stresses (x = 0.01*L*, *z* = 0.0) for Aspect Ratio 10

Model	$\bar{u}$	$\bar{w}$	$\bar{\sigma}_x$	$\bar{\tau}_{zx}^{CR}$	$\bar{\tau}_{zx}^{EE}$
HSDT	-1064.34	5.82	171.47	7.82	3.86
FSDT	361.78	5.88	138.80	4.80	9.40
ETB	361.78	5.75	138.80	-	9.40

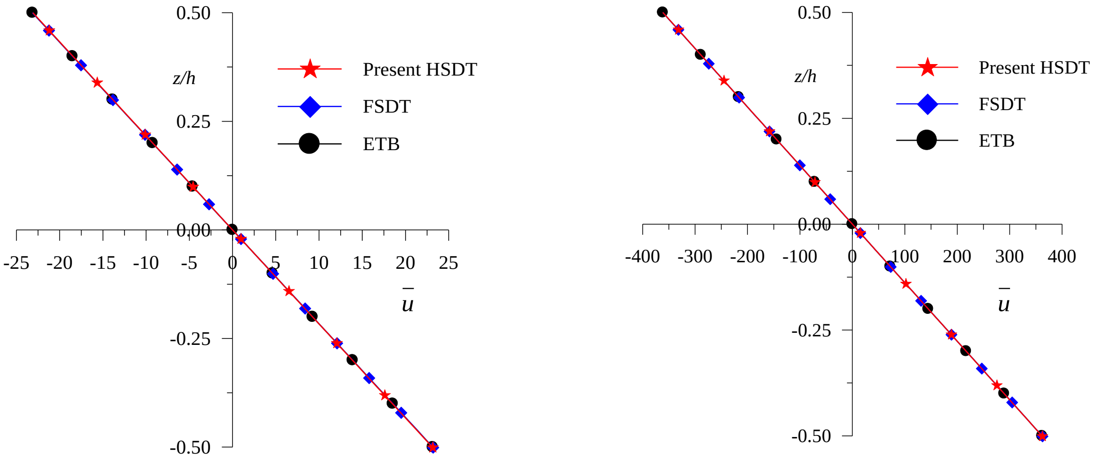

Fig. 3: Variation of axial displacement ($\bar{u}$) through the thickness of cantilever beam at (*x*=*L*, *z*) when subjected to cosine load for aspect ratio 4 and 10.

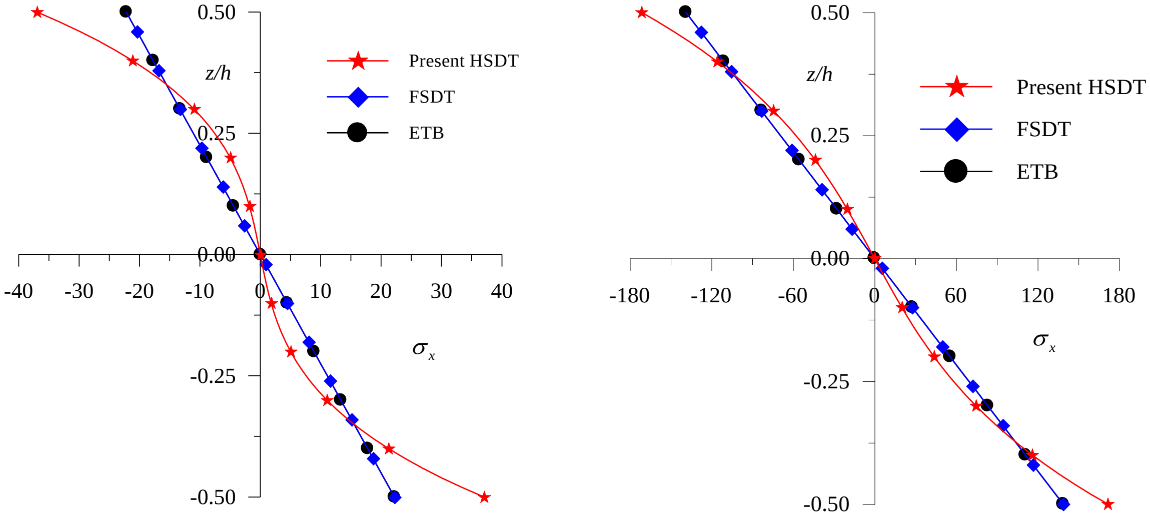

Fig. 4: Variation of axial stress (σ_x) through the thickness of cantilever beam at (*x* = 0, *z*) when subjected to cosine load for aspect ratio 4 and 10.

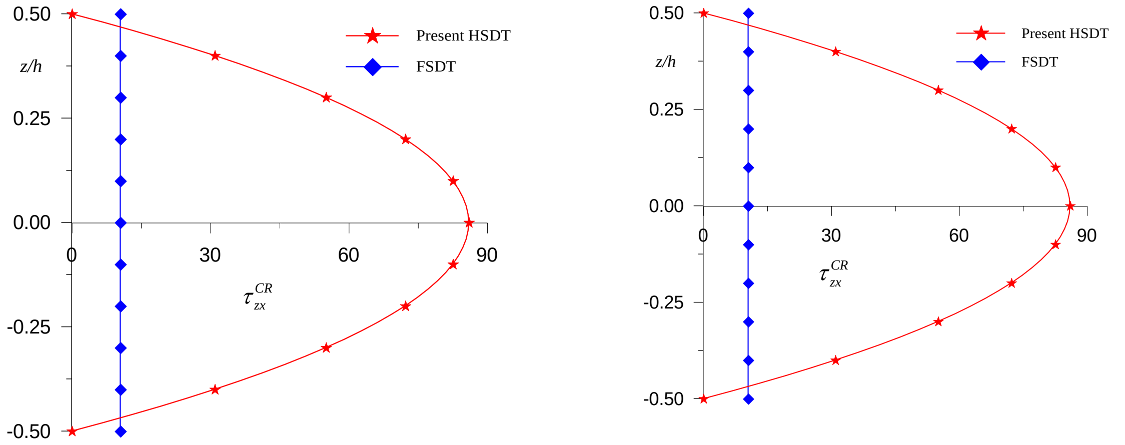

Fig. 5: Variation of transverse shear stress (τ_{zx}^{CR}) through the thickness of cantilever beam at (x = 0.01L, z) obtained via equilibrium equation when subjected to cosine load for aspect ratio 4 and 10.

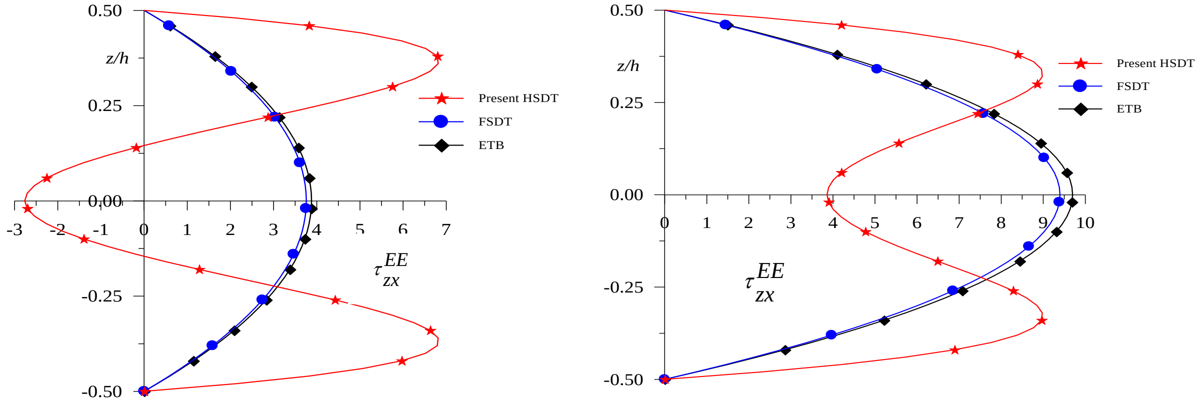

Fig. 6: Variation of transverse shear stress (τ_{zx}^{EE}) through the thickness of cantilever beam at (x = 0.01L, z) obtain via constitutive relation when subjected to cosine load for aspect ratio 4 and 10.

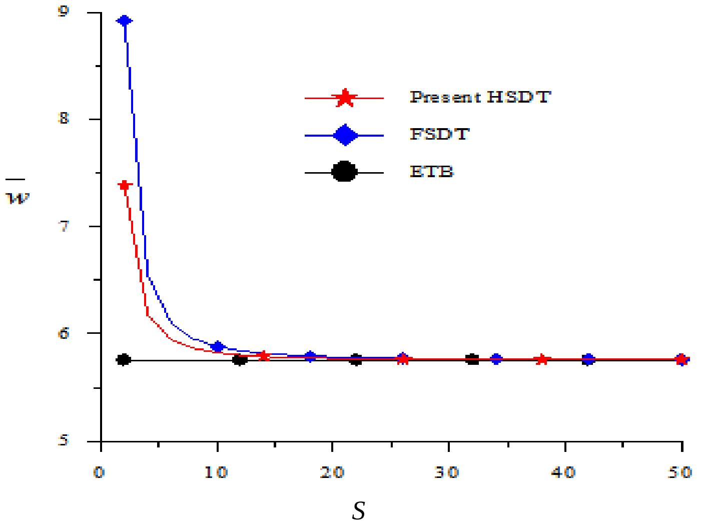

Fig. 7: Variation of displacement ($\bar{w}$) through the thickness of cantilever beam at (x = L, z) when subjected to cosine load for aspect ratio S.

V. DISCUSSION OF RESULTS

The comparison of results of maximum non-dimensional axial displacement ($\bar{u}$) for the aspect ratios of 4 and 10 is presented in Tables I and II for beam subjected to cosine loads. The values of axial displacement given by present theory are in close agreement with the values of other refined theories for aspect ratio 4 and 10.

The through thickness distribution of this displacement obtained by present theory is in close agreement with other refined theories as shown in Figs. 3 and 4 for aspect ratio 4 and 10.

The results of axial stress ($\bar{\sigma}_x$) are shown in Tables I and II for aspect ratios 4 and 10. The axial stresses given by present theory are compared with other higher order shear deformation theories. It is observed that the results by present theory are in excellent agreement with other refined theories as well as ETB and FSDT. The through the thickness variation of this stress given by all the theories is linear. The variations of this stress are shown in Figs. 5 and 6.

The comparison of maximum non-dimensional transverse shear stress for simple beams with varying and cosine loads obtained by the present theory and other refined theories is presented in Tables I and II for aspect ratio of 4 and 10 respectively. The maximum transverse shear stress obtained by present theory using constitutive relation is in good agreement with that of higher order theories for aspect ratio 4 and for aspect ratio 10. The through thickness variation of this stress obtained via constitutive relation are presented graphically in Figs. 7 and 8 and those obtained via equilibrium equation are presented in Figs. 9 and 10. The through thickness variation of this stress when obtained by various theories via equilibrium equation shows the excellent agreement with each other. The maximum value of this stress occurs at the neutral axis.

The comparison of results of maximum non-dimensional transverse displacement ($\bar{w}$) for the aspect ratios of 4 and 10 is presented in Tables I and II cantilever beam subjected to cosine load. The values of present theory are in excellent agreement with the values of other refined theories for aspect ratio 4 and 10 except those of classical beam theory (ETB) and FSDT of Timoshenko. The variation of $\bar{w}$ with aspect ratio (*S*) is shown in Fig. 11. The refined theories converge to the values of classical beam theory for the higher aspect ratios.

VI. CONCLUSION

The general solutions for beams with cosine loads are obtained in case of thick cantilever beams. The displacements and stresses obtained by present theory are in excellent agreement with those of other theories. The present theory yields the realistic variation of axial displacement and stresses through the thickness of beam. Thus the validity of the present theory is established.

REFERENCES

[1]. J.A.C. Bresse, “Cours de Mechanique Applique”, Mallet-Bachelier, Paris, 1859.

[2]. J.W.S. Lord Rayleigh, “The Theory of Sound”, Macmillan Publishers, London, 1877.

[3]. S.P. Timoshenko, J. N. Goodier, “Theory of Elasticity”, Third International Edition, McGraw-Hill, Singapore. 1970.

[4]. G.R. Cowper, “The shear coefficients in Timoshenko beam theory”, ASME Journal of Applied Mechanic, Vol. 33, No. 2, pp. 335-340, 1966.

[5]. G.R. Cowper, “On the accuracy of Timoshenko beam theory”, ASCE J. of Engineering Mechanics Division. Vol. 94, No. EM6, pp. 1447-1453, 1968.

[6]. M. Levinson, “A new rectangular beam theory”, Journal of Sound and Vibration, Vol. 74, No.1, pp. 81-8, 1981.

[7]. W.B. Bickford, “A consistent higher order beam theory”, International Proceeding of Development in Theoretical and Applied Mechanics (SECTAM), Vol. 11, pp. 137-150, 1982.

[8]. L.W. Rehfield and P.L.N. Murthy, “Toward a new engineering theory of bending: fundamentals”, AIAA Journal, Vol. 20, No. 5, pp. 693-699, 1982.

[9]. A.V. Krishna Murty, “Towards a consistent beam theory”, AIAA Journal, Vol. 22, No. 6, pp. 811-816, 1984.

[10]. M.H. Baluch, A.K. Azad, and M.A. Khidir, “Technical theory of beams with normal strain”, ASCE Journal of Engineering Mechanics, Vol. 110, No. 8, pp. 1233-1237, 1984.

[11]. A. Bhimaraddi and K. Chandrashekhara, “Observations on higher order beam Theory”, ASCE Journal of Aerospace Engineering, Vol. 6, No. 4, pp. 408-413, 1993.

[12]. H. Irretier, “Refined effects in beam theories and their influence on natural frequencies of beam”, International Proceeding of Euromech Colloquium, 219, on Refined Dynamical Theories of Beam, Plates and Shells and Their Applications, Edited by I. Elishak off and H. Irretier, Springer-Verlag, Berlin, pp. 163-179, 1986.

[13]. V.Z. Vlasov and U.N. Leont’ev, “Beams, Plates and Shells on Elastic Foundations” Moskva, Chapter 1, 1-8. Translated from the Russian by A. Barouch and T. Plez Israel Program for Scientific Translation Ltd., Jerusalem, 1966.